Denisia 35

ISSN 1608-8700

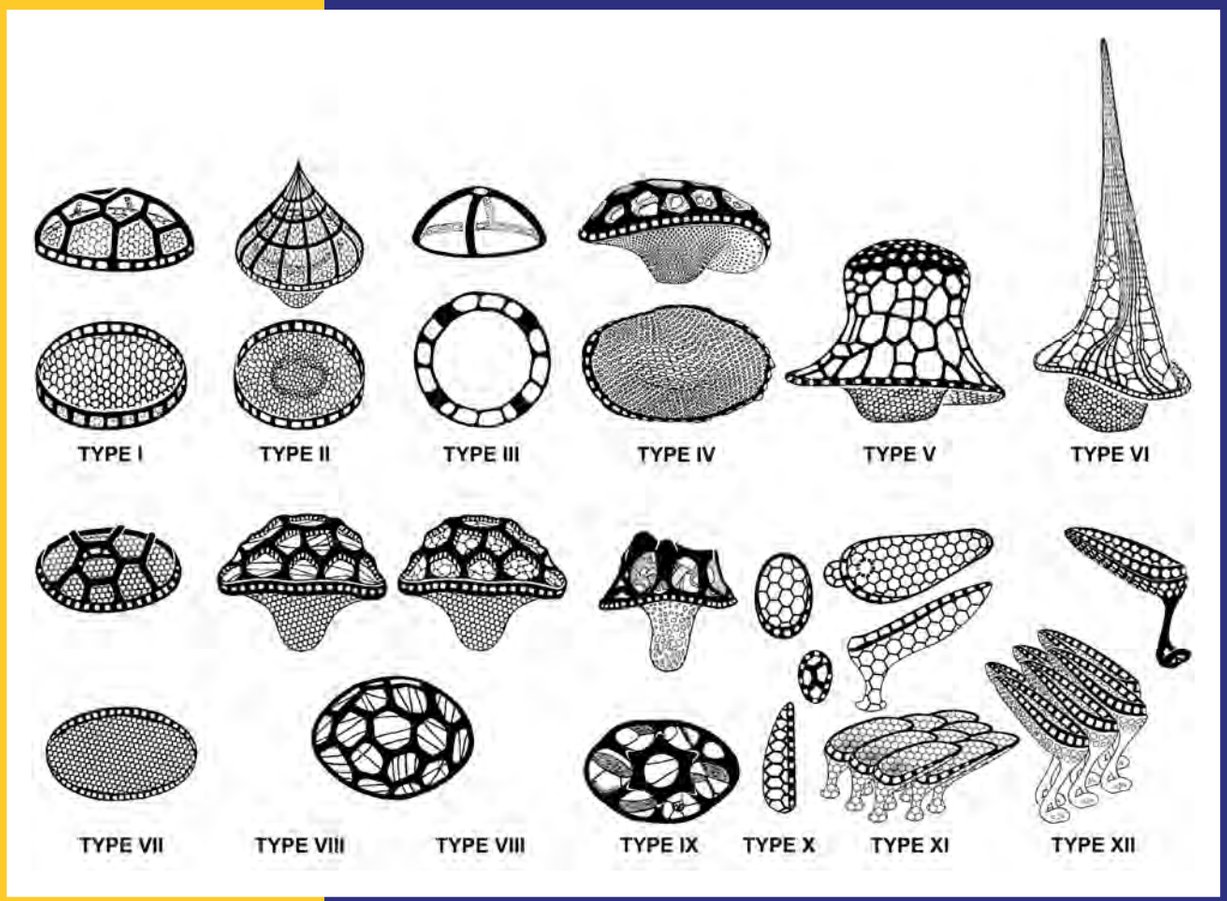

Wilhelm Foissner

Terrestrial and Semiterrestrial Ciliates (Protozoa, Ciliophora) from Venezuela and Galápagos

Terrestrial and Semiterrestrial Ciliates (Protozoa, Ciliophora) from Venezuela and Galápagos

Wilhelm FOISSNER

Denisia

35

Delivery date 30.01.2016

Preface and Acknowledgements

Tropical soil ciliates are poorly known (Foissner 1987b). Thus, I made busy holidays in Venezuela in January and February 1996 and came back to Austria with 68 well-sorted soil samples on which I worked, with some interruptions, the next five years publishing important biogeographic flagship species in individual papers (see Introduction) while the comprehensive publication had to wait. I am deeply grateful to Prof. Dr. Maurizio G. Paoletti (Padova University, Italy) who initiated the expedition, to Dr. Hugo Cerda (Caracas University, Venezuela), our wise guide in Venezuela, and to Dr. Ilse Foissner for organization and help with sampling.

Our first monograph on soil ciliate diversity in Namibia, southwest Africa (Foissner et al. 2002) has been widely acknowledged by taxonomists and ecologists. Now, we finished a monograph on soil ciliate diversity in the neotropis, i.e., Venezuela (including some samples from the unique Galápagos islands). Both monographs are unique in several ways. For the first time since the unforgotten monographs by Mueller (1786), Ehrenberg (1838), Stein (1859,1867), Penard (1922), and Kahl (1930-35), each describes more than 100 new species and each species list comprises about 400 painstakingly identified species which is by far the largest number ever published in single studies from comparatively small areas. Thus, these lists will be invaluable documents for biodiversity researchers. All species are described by a combination of classic (live observation) and modern (silver impregnation, scanning electron microscopy) methods, and many are illustrated by a multitude of micrographs. Thus, we hope that our monographs will serve as examples for ciliate community studies.

It is an increasing problem to find interested and talented students and post-docs for studies like this. Several tried but gave up after having made a few species. I added their names to the species we worked together. Thus, I had to do most work with technicians, especially with Robert Schörghofer and Andreas Zankl who excellently smoothed the micrographs with Photoshop; Michael Gruber, M. Sc., for making the morphometries and line drawings for half of the hypotrichs; Birgit Peukert, Johannes Rattey, M. Sc., and Brigitte Moser for doing SEM preparations and photographs; Dr. Wolf-Dietrich Krautgartner for ensuring the smooth operation of the electron microscopes; Mag. Barbara Harl and Dr. Heidi Bartel for typing the text into the computer; and Dr. Erna Aescht and Michaela Minich for layout and printing organization. I also thank Hans-Werner Breiner and Prof. Thorsten Stoeck (Kaiserslautern University, Germany) for making molecular sequences for some taxa mentioned previously but formally described in the present monograph. Special thanks to Dr. Remigius Geiser and Prof. Helmut Berger for help with nomenclature; I followed most advices.

Finally, I greatly appreciate the following persons for collecting soil samples containing species described in the present monograph (countries in parentheses): Prof. Dr. Karl O. Stetter (Galápagos), Prof. Dr. Eberhard Stüber (Rwanda), Dr. Hubert Blatterer (Virgin island), Prof. Dr. David Patterson (Panama), and Prof. Dr. D. G. Mueller (Chile).

Financial support was provided by the Austrian Science Fund (Project 22846-B17). Without this grant, the work would have been impossible. I am also very grateful to Hofrat Mag. Fritz Gusenleitner, director of the Biology Centre of the Upper Austrian Museum in Linz, Austria, who made it possible to publish the work in full length and excellent quality. Altogether, but without traveling and my ordinary salary, 400,000 Euro were needed for this monograph and the individual papers mentioned in the Introduction.

Denisia	**35**	1-912	30.01.2016

Terrestrial and Semiterrestrial Ciliates (Protozoa, Ciliophora) from Venezuela and Galápagos

Wilhelm Foissner

A b s t r a c t : A highly diverse ciliate community was found in 71 samples from terrestrial and semiterrestrial habitats from the western half of Venezuela (67 samples) and from Galápagos (4). The ciliates, respectively, their resting cysts, were re-activated from the air-dried samples using the non-flooded Petri dish method. Species were identified by combining live observation, silver impregnation, and scanning electron microscopy.

The faunistic and taxonomic results are summarized in chapter 3.1.1, i.e., in a detailed list of species, showing their distribution and frequency: (i) A total of 459 ciliate species is recorded in this monograph, 421 from Venezuela and Galápagos and 38 from other sites globally. Most species are new records for the areas investigated. (ii) 120 species (28%) are new to science, 82 from Venezuela including 13 from Galápagos (20%) and 38 from various sites globally; 50 species are redescribed. (iii) Based on these findings, 44 new genera and subgenera, four new families (Lingulotrichidae, Deviatidae, Urosomoididae, Apometopidae), and a new suborder (Woodruffina) are established. (iv) The ontogenesis is described for 10 species: *Platyophryides macrostoma, Cinetochilides terricola, Protospathidium salinarum, Notodeviata halophila, Idiodeviata venezuelensis, Deviata brasiliensis, Paragonostomum australiense, Gonostomum singhii, Oxytricha pulvillus,* and *Lepidothrix dorsiincisura*. (v) 656 type and voucher slides have been deposited in the Biology Centre of the Upper Austrian Museum in Linz (LI). (vi) Eight species, formerly known only by their molecular sequences, have been identified and described (Fig. 124, 294): *Maryna umbrellata, Maryna meridiana, Bursaria ovata, Platyophryides macrostoma, Sagittarides oblongistoma, Sagittaria venezuelensis, Apowoodruffia salinaria,* and *Condylostomides coeruleus.*

252 of the 459 ciliate species occur at only one or two sites, showing a patchy distribution of most species and a high proportion of rare species. No species occurred in all samples, and the euryoecious *Colpoda inflata* was most frequent occurring in 73% of samples. Only 14 species have frequences ≥ 40%, and most of them are frequent in soils globally. There is an average of 34 species/sample when the rotten rainforest samples are excluded.

Taken into account total species number and the proportion of new species, seven local ciliate diversity centres can be selected: (i) The richest sample (126 species, nine undescribed) is number (56), i.e., mud and soil from some flat, ephemeral puddles in the Morrocoy National Park on the north coast of Venezuela. (ii, iii) Samples (52) and (61) are from the rainforest in the Henri Pittier National Park with 101 and 91 species, respectively. (iv) The next richest site is number (23), i.e., a Mahadja (highly fertilized savanna soil) with 83 species, including three undescribed ones. (v) Site (54) follows, i.e., mud and soil from a highly saline coastal puddle with 78 species of which 10 were undescribed. (vi) A total of 117 species, 16 undescribed, occurred in 10 Lajas (lithotelmas on granitic outcroppings in the savanna). (vii) In the four Galápagos samples occurred 68 species of which at least 13 were undescribed. Several of the new taxa are flagship species with very likely restricted distribution.

K e y w o r d s : ciliate diversity, ciliate distribution, ciliate ecology, ciliate endemism, ciliate ontogenesis, ciliate taxonomy, methods for soil ciliates, neotropis, rainforest ciliates, saline coastal puddles, savanna ciliates.

Contents

1. Introduction

I would like to refer the reader to the introduction of the monograph on Namibian soil ciliates (Foissner et al. 2002) because I still hold the views presented at that time, viz., a decreasing interest in morphological alpha-taxonomy of protists in general and of soil ciliates in particular; the frequent misuse of grant money by ecologists doing "biodiversity studies" without identifying the species; and that there are thousands of undescribed ciliate species, one third of which very likely has a restricted distribution.

However, one important aspect should be recalled, viz., cyst genera and species. Although we emphasized this matter already in Foissner et al. (2002) and Foissner (2011), most new species and genera are still described without their resting cyst though it is the most important stage in the life cycle because the cyst protects species to become extinct locally and, possibly, even globally. For us, the time is ripe to base new genera and species on their resting cysts which are very likely better phylogenetic markers than, e.g., the presence or absence of transverse and caudal cirri in hypotrichs (Berger 1999, 2006, 2008, 2011).

The Neotropis project started in 1996 when I collected 67 soil samples from a variety of habitats in Venezuela. The investigation needed six years but a monograph could not be finished because of other projects granted for post-docs and technicians. Thus, 20 years passed before I could finalize the project in July 2015. During this time, we published several monographs and many papers containing 21 species discovered in Venezuela. They are shown in the following compilation; (X^a = new species described before this monograph with type locality in Venezuela; X^h = new species described before this monograph with type locality not in Venezuela but occurring there, e.g., *Cephalospathula brasiliensis*).

Apertospathula lajacola Foissner & Xu, 2007[a]; *Apertospathula verruculifera* Foissner, Xu & Kreutz, 2005[a]; *Apocoriplites lajacola* Oertel et al., 2008[a]; *Apofrontonia lametschwandtneri* Foissner & Song, 2002[a]; *Arcuospathidium pachyoplites* Foissner, 2003b[a]; *Armatospathula periarmata* Foissner & Xu, 2007[a]; *Cephalospathula brasiliensis* Foissner, 2003c[h]; *Drepanomonas hymenofera venezuelensis* Omar & Foissner, 2013[a]; *Drepanomonas multidentata* Foissner & Omar, 2014 in Omar & Foissner, 2014[a]; *Edaphospathula* (formerly *Sikorops*) *espeletiae* Foissner, 2000b[a]; *Enchelys lajacola* Foissner & Oertel, 2009[a]; *Fragmocirrus espeletiae* Foissner et al., 2000b[a]; *Leptopharynx brasiliensis* Foissner & Omar, 2012 in Omar & Foissner, 2012[h]; *Leptopharynx lajacola* Omar & Foissner, 2014[a]; *Longispatha elegans* Foissner, Xu & Kreutz, 2005c[a]; *Luporinophrys micelae* Foissner, 2005[a]; *Odontochlamys alpestris biciliata* Foissner, Agatha & Berger, 2002[a]; *Paracondylostoma clavistoma oligostriatum* Foissner & Kreutz, 1998[a]; *Platyophrya paoletti* Foissner, 1997[a]; *Pseudomonilicaryon gracile oviplites* Vďačný & Foissner, 2012[a]; *Sleighophrys pustulata* Foissner, 2005[a].

Finally I want to explain why I do not publish the monograph with one of the large, famous publishers. It is quite simple: they take a lot of money but lay-out and printing is usually so poor that the great effort to get nice micrographs becomes null and void.

2. Materials and Methods, Species Concept, Types

2.1 Materials

2.1.1 General Site Description

2.1.1.1 Brief Overview of Venezuela

There is no need to describe Venezuela in detail because several excellent travel guides are available (Maddicks 2011, Kaiser & Gordones 1994) and the centres of our sampling activity are treated in some detail in the following paragraphs and the site descriptions.

Venezuela (Repùblica Bolivariana de Venezuela) is on the north of South America, bordering the Caribbean Sea, between Colombia in the west and Guyana in the east and Brazil in the south (Fig.1). It extends for about 1300 km from north to south and 1500 km from west to east, i.e., between latitude 1° and 12° of the Equator and longitude 60° to 73°. Thus, the whole area is in the tropics and forms a distinct biogeographic region called Neotropis or Neogaea. Terrain and climate go from hot and sticky at sea level to icy cold on Andean peaks, although most of the land lies at under 1,000 m. Average daytime temperature: 25°C. Dry season: December – April, rainy season: May – November. About half of Venezuela is forest land and one third is Savanna dominated by *Tachypogon*, a perennial grass (Fig.2).

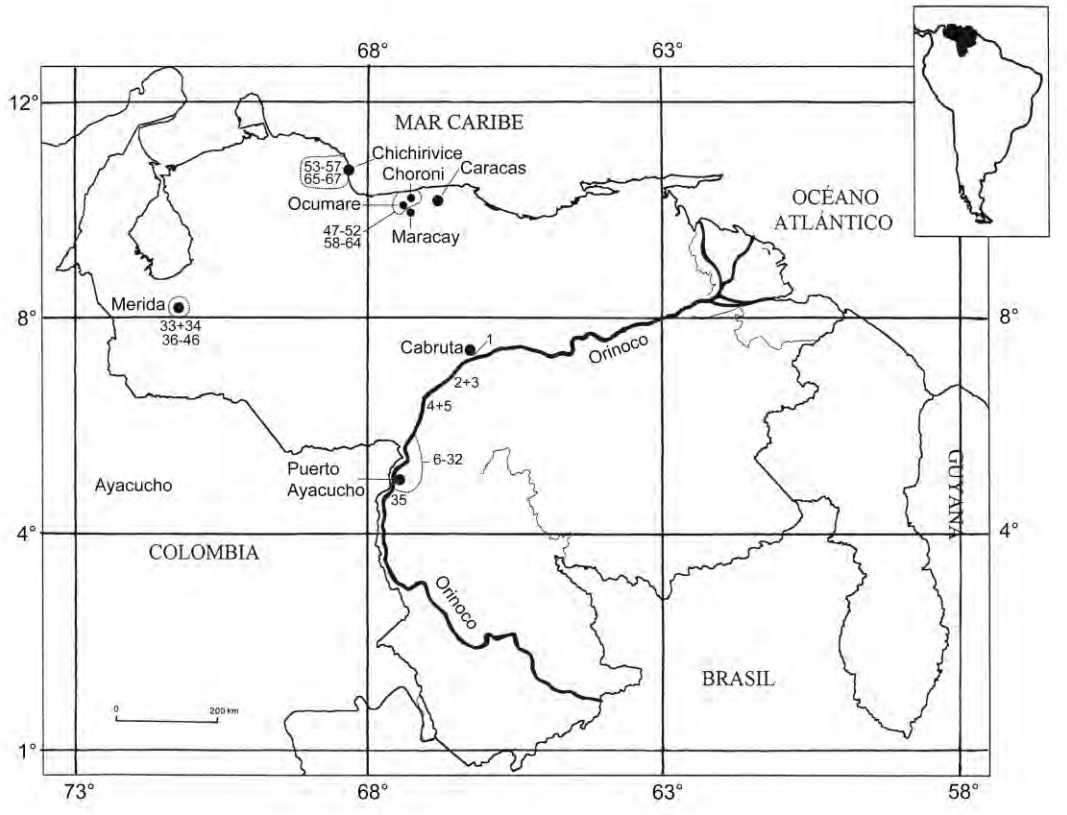

Fig. 1. Simplified map of Venezuela, showing the 67 sampling sites (based on Pèrez-Hernàndez & Lew 2001)

Fig. 2. Simplified vegetation map, showing that most of Venezuela is covered with forests and savannas (from WIKIPEDIA 1972).

Our samples represent roughly half of Venezuela´s land area, i.e., we collected only in the western half of the country the large Orinoco River forming the border (Fig. 1). We concentrated on the following regions and habitats: the north coast west of the capital Caracas, including the Henri Pittier National Park; the region around Pto. Ayacucho in the south; and the Andean rainforest around the town of Merida. Special habitats are Lajas and Mahadjas. See NETUZHILIN et al. (1999) for a detailed description of the Puerto Ayacucho area, savannas, and rainforests.

2.1.1.2 The North Coast between the Village of Chichiriviche and the Capital Caracas (Fig. 1, 3, 4)

We sampled two areas, viz., the coast sensu stricto and the Henri Pittier rainforest. Most of the coast is flat in this area and thus flooded by the sea during storms and high tides. Thus, these samples are more or less saline. The "wild" areas are grown with grass and bushes. We sampled soil and soil and mud from some of the many ephemeral pools around the village of Chichirivice, i.e., in and near the Morrocoy National Park (Fig. 1, 8, 9).

Slightly east of Chichiriviche is the Henri Pittier National Park, a small but very nice coastal cloudforest with an up to 2,426 m high mountain. On the north side, samples were taken around the coastal village of Choroni; on the south side, the samples were taken around the Biological

Station Rancho Grande at 1,100 – 1,300 m above sea level. For details on site, soil, and the invertebrate fauna, see Paoletti (1980) and Paoletti et al. (1991).

2.1.1.3 South of Venezuela, i.e., in the Outskirts of the Town of Puerto Ayacucho (Fig. 1, 2): Savannas, Mahadjas and Lajas

Puerto Ayacucho is very near to the Orinoco River and to the Equator. Thus, there is an annual precipitation of 3,000 mm and an annual mean temperature of 30°C. The soils are very sandy because the ancient, crystalline Guyana shield is superimposed by sandstone. Most samples were collected from the savanna at the right side of the Orinoco River and from the rainforest south of Pto. Ayacucho. We sampled four main habitats: savannas, Lajas, Mahadjas, and the rainforest.

The savanna at Pto. Ayacucho extends as a narrow, usually less than 30 km wide ribbon south of the Orinoco River. It is dominated by *Tachypogon*, a perennial grass, and the "Chaparro" (*Curatella americana*), a small tree that withstands the bush-fire. The lowland areas are slightly inundated when the Orinoco has high water; thus, algal crusts are frequently found on the soil surface. The savanna is used as pasture (mainly for cattle) and burnt at irregular intervals; samples were taken only from sites without signs of recent burning. The soil is very sandy, rather compact, contains few litter and humus, and was dry when collected; to get "good" samples larger humus particles and decaying litter were sieved off the sand and added to the sample in a way that sieved matter and sandy soil each provided about 50% of the sample. The soil surface becomes very hot on sunny days; on 6.2.1996, we measured 52°C at 2 o'clock.

Within the savannas there are two special habitats: Mahadjas and Lajas. Mahadjas are human-made, highly fertile fields usually near to small farms. They are usually <10,000 m^2 in size and used to grow vegetables, manioc, and fruits. The fertilizer comes from cattle and/or horses which are fenced in the area over-night so that the excrements are collected. It needs several months to become a "good" Mahadja but it can be used for 5-10 years, depending on the amount of excrements and the plants grown. Samples were taken as described in the next paragraph.

The savanna sites serving as control to the Mahadja sites were sampled as follows: 20 – 30 cores (5 cm ø, 5 cm high) of soil were taken from a transect 50 – 100 m long. Then the cores were smashed and sieved through a steel-net with 2 mm-sized meshes. The organic materials (decaying leaves, grass roots) and soil (mainly sand) particles which remained in the sieve were used to investigate ciliate diversity. This procedure enriches the organic matter and is necessary because the non-flooded Petri dish method works best when sufficient organic material is available (see above and methods).

Lajas is the indigenous name for flat, ephemeral (astatic) puddles on granitic outcroppings usually lower than 30 m (except of the famous Tepuis in eastern Venezuela which reach hundreds of meters). The Lajas are black due to a cover of filamentous and coccal cyanobacteria (Fig. 3–5, 7). Lajas have very different sizes, ranging from a few cm to 10 m or more. The larger and deeper ones are often partially or completely grown with an endemic cushion plant, Velloziaceae, that belongs to the Liliidae and accumulates dust from the air and transforms it to soil. Usually, the bottom of the Lajas is covered by some soil mixed with gravel, crust pieces of cyanobacteria, and some leaf litter from the bushes growing nearby. All Lajas were dry when sampled. Thus, we collected the litter and mud and, if present, the soil from velloziacean cushions.

Fig. 3. A granitic outcropping between the village of Cabruta and Pto. Ayacucho. It is black due to a cover of cyanobacteria.

Fig. 4. A Laja landscape in the surroundings ot the Eisenberg farm. The arrow marks a Laja covered by Velloziaeae, i. e., endemic Liliida.

Fig. 5. A Laja landscape near the airport of Pto. Ayacucho. Note the Cactaceae.

Fig. 6. Espeletia timotensis in the Páramo de Piedras Blancas, Venezuela, 4.200 m above sea-leve. This aera belongs to the Cordillera de Mérida and is about 2 km of the Pico del Ayuila.

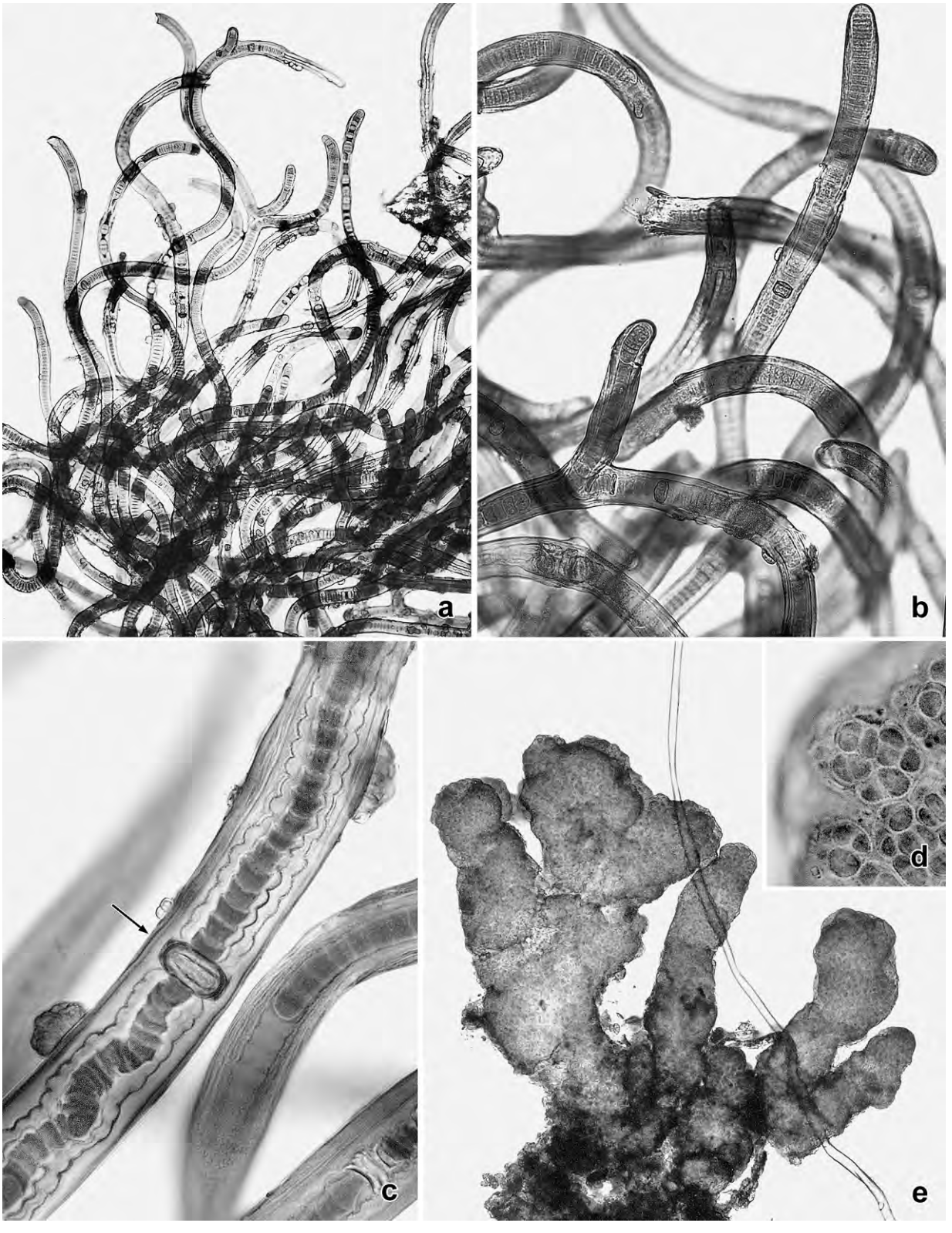

Fig. 7a-e. Filamentous (a-c) and coenobial (d, e) cyanobacteria have a thick mucous sheet and make the granitic outcroppings black. The arrow marks a heterocyst. On the top of the outcroppings are lithotelms called “Laja” by the natives.

2.1.1.4 Rainforests South of the Town of Puerto Ayacucho, in the Outskirts of the Town of Merida, and in the Henri Pittier National Park (Fig. 1, 8)

When rainforest litter and soil samples are air-dried for the non-flooded Petri dish method, then one must consider that the resting cysts of rainforest protists are much weaker than those from moderate or hot and dry regions. There is a rapid loss of species in samples older than 9 month (Foissner 1997, 2011), and new data from Venezuela show great loss within a month (see samples 35, 36, 41-46). For details on the rainforest south of Puerto Ayacucho, see Netuzhilin et al. (1999).

In Merida and Borneo (Foissner 2011), I had the opportunity to look at fresh samples. They were full of ciliates, similar as in a mesotrophic river! The negative influence of prolonged drying becomes obvious also in the samples from the Henri Pittier National Park in Venezuela (samples 47-52, 58-62, 64). Those which were investigated within a year (samples 52, 59-62) provided much more species (e.g. 101 species in sample 52) than those investigated 4-6 years after collection (e.g. 27 species in sample 64).

These observations provide two recommendations: soil and litter ciliates from everwet rainforests should be investigated on site without any culture method or within about two month after air-drying when the non-flooded Petri dish method is used. Up to one year drying is possible for rainforests whose litter and upper soil layer become dry during the dry season.

2.1.2 Description of Individual Samples

General description of main sample region, see chapter 2.1.1. Geographic coordinates are mainly from Meyer´s Atlas and from GOOGLE because GPS or detailed maps were not available. Salinity and pH were measured with a refractometer and pH paper, respectively, in samples watered for 1 hour.

Site 1: Near the village of Cabruta at ferry site over the Orinoco River, 66°14'W 7°38'N (Fig.1). Sample taken in the floodplain, i.e., about 100 m away from the riverbank. The alluvial, clayic soil has pH 5.2. Material collected: leaf litter and soil up to 10 cm depth under large Leguminosae trees; litter bound together by whitish fungal hyphae. Collected on 30.1.1996, investigated in September 2000.

Site 2: Tropical dry forest (Selva Veranera) about 100 km southwest of the village of Cabruta, along the new street to Pto. Ayacucho, 66°05'W 7°N (Fig.1). Soil stony and sandy, brownish, with sparse litter and humus, pH 6.7. Material collected: leaf litter, grass roots, and soil up to 10 cm depth. Collected on 31.1.1996, investigated in September 2000.

Site 3: As site 2: Mosses from a roadside Laja and from trees, pH 5.2. Collected on 31.1.1996, investigated in October 2000.

Site 4: Roadside Laja about 130 km southwest of the village of Cabruta, i.e., in the outskirts of the village of Raimundo, 66°55'W 7°3'N (Fig. 1, 3). Material collected: leaf litter and mud from some small Lajas partially covered with bushes, pH 5.1. Collected on 31.1.1996, investigated in May 2000.

Site 5: As site 4 but from some flat, dry ponds at the foot of the Laja. Material collected: Mud and pieces from the dry, rather thick algal and cyanobacterial crust, pH 5.2. Collected on 31.1.1996, investigated in October 2000.

Site 6: Gallery forest along a small stream at Pozo Azul, a holiday site about 10 km north of Pto. Ayacucho, 67°36'W 5°41'N (Fig. 1). Material collected: bark from various trees. Collected on 1.2.1996, investigated in April 1996. See also next site.

Site 7: As site 6. Material collected: upper 10 cm litter and soil layer composed of loosely packed fresh and decaying, dark-brown, wet leaf litter mixed with many fine roots, arthropod excrements, and mineral soil. Collected on 1.2.1996, investigated in April 1996. This looked like a very rich sample but most ciliates did not survive the two month air-drying (see rainforest in chapter 2.1.1.4).

Site 8 = Mahadja 6: Granja Cachana, i.e., the name of the farm of Mr. EISENBERG about 14 km north of Pto. Ayacucho, 67°36'W 5°41'N (Fig. 1). A 15 year old Mahadja with an organically fertilized Banana culture when the investigation took place. Soil loose, dark, humous, many fine roots in 0-3 cm, from 5 to 10 cm yellow sand, pH 6.0. Material collected: leaf litter, roots, and soil up to 10 cm depth as described in chapter 2.1.1.3. Collected on 2.2.1996, investigated in July 2001.

Site 9: As site 8. Savanna burnt three days before collection. Soil very hard, pH 5.1. Material collected: leaf litter and soil as described in chapter 2.1.1.3. Collected on 2.2.1996, investigated in November 2000.

Site 10 = control to Mahadja 6: Savanna near Mahadja 6. Soil loose, composed mainly of humus-poor, yellow sand, pH 5.2. Material collected: leaf litter and sieved soil as described in chapter 2.1.1.3. Collected on 2.2.1996, investigated in September 2000.

Site 11: As site 8, i.e., a large Laja in the surroundings of the farm (Fig. 4). Some Lajas overgrown with Velloziaceae and some moss; soil under Velloziaceae sandy and grey-brown, about 3 cm thick. Material collected: leaf litter and soil between and under Velloziaceae and some moss from the surface, pH 5.4. Collected on 2.2.1996, investigated in August 1997. This rich sample (~70 species) contained *Hemimastix amphikineta*, a Gondwanan endemic (FOISSNER et al. 1988).

Site 12: As site 11 but Lajas without Velloziaceae. Material collected: some mud and pieces of the cyanobacterial crust on the bottom of the Lajas. Collected on 2.2.1996, investigated in June 1997.

Site 13 = Mahadja 1: Farm of Dona LUISA about 10 km north of Pto. Ayacucho, 67°36'W 5°41'N (Fig. 1). In third year of cultivation with pumpkin, corn, yucca, pepper, etc; fallow when investigated. Soil grey-brown and very sandy, pH 6.0. Ten cylindric cores 5x5 cm were collected over a 50 m transect. Then, the cores were smashed and sieved through a 2 mm net; the sieve residue was used for the investigation. Collected on the 3.2.1996, investigated in April 1996.

Site 14 = control to Mahadja 1: *Tachypogon* savanna adjacent to site 13. Soil slightly more compact than at site 13, very sandy and reddish, pH 5.9. Sample taken as described for site 13. Collected on 3.2.1996, investigated in April 1996.

Site 15 = Mahadja 2: Farm of Señor Armando PEREZ about 10 km north of Pto. Ayacucho, 67°36'W 5°41'N (Fig. 1). In first year of cultivation with pumpkin, yucca, pepper, etc. Soil loose, brownish, very sandy, pH 6.1. Twenty cylindric cores 5x5 cm in size were collected over a 60 m transect. Then, the cores were smashed and sieved through a 2 mm net; the sieve residue was used for the investigation. Collected on 3.2.1996, investigated in April 1996.

Site 16 = control to Mahadja 2: *Tachypogon* savanna adjacent to Mahadja 2, used as cattle pasture. Soil more compact than in Mahadja 2, reddish, very sandy, with many fine roots, pH 6.0. Sample taken as described for site 15. Collected on 3.2.1996, investigated in April 1996.

Site 17: Lajas near Mahadja 3. Material collected: mud and pieces of the cyanobacterial crust on the bottom of some small Lajas. Collected on 6.2.1996, investigated in May 1997.

Site 18: Floodplain of a stream near Mahadja 3. Material collected: dry, small and large, spinous colonies of a freshwater sponge attached to trees, pH 5.4. Collected on 4.2.1996, investigated in October 2000.

Site 19: Crop field (conuco in the Indian language) in the evergreen, seasonal rainforest surrounding the Indian village of Pavoni about 20 km north of Pto. Ayacucho, 67°36'W 5°41'N (Fig. 1). Soil almost dry, sandy, light-brown, densely rooted, with many earthworm casts. Material collected: leaf litter, roots, and soil to a depth of 5 cm. Collected on 4.2.1996, investigated in May 1996. This looked like a "good" sample but only two ciliate species appeared in the non-flooded Petri dish culture (see rainforests in chapter 2.1.1.4).

Site 20: As site 19. Dry mosses from trees surrounding the conuco, pH 5.2. Surprisingly, 30 species were found, one of which was undescribed (*Apocoriplites lajacola*). Further, *Hemimastix amphikineta* Foissner et al., 1988, a Gondwanan endemic, was abundant three weeks after rewetting the sample. Collected on 4.2.1996, investigated in October 2000.

Site 21: Lithotelmas on large stones in the Catanjapo River just before it merges with the Orinoco River about 10 km south of the town of Pto. Ayacucho, 67°36'W 5°41N (Fig. 1). Material collected: mud from the bottom of several lithotelmas, pH 6.6. Collected on 5.2.1996, investigated in May 2000.

Site 22: Seasonal rainforest at Caño Tigre, an Indian village about 20 km south of the town of Pto. Ayacucho, 67°36'W 5°41'N (Fig. 1). Soil almost dry, brown, humous, with a 3-6 cm thick fermentation layer and a dense root-carpet in 0-3 cm, with many earthworm casts. Material collected: fresh and decaying leaf litter and soil to a depth of 5 cm. Collected on 5.2.1996, investigated in July 1996. Only two ciliate species developed in the non-flooded Petri dish culture (see rainforests in chapter 2.1.1.4).

Site 23 = Mahadja 3: Farm of Señor Pedro Cortez near the village of El Sapo about 50 km north of the town of Pto. Ayacucho and very near to the Orinoco River, 67°36'W 5°41'N (Fig. 1). A 10 year old Mahadja planted with bananas. Grey, alluvial soil (pH 6.1) with much silt and fine sand, indicating that it is inundated by high floods of the Orinoco. Material collected: 20 cylindric cores 5x5 cm in size were collected over a 50 m transect. The cores were smashed and sieved through a 2 mm net; the sieve residue was used for the investigation. Collected on 6.2.1996, investigated in May 1996.

Site 24 = control to Mahadja 3: Heavily grazed savanna about 400 m distant from the Mahadja, inundated by high floods of the Orinoco. Soil as described for site 23 but more compact, pH 5.5. Material collected as described for site 23. Collected on 6.2.1996, investigated in May 1996.

Site 25 = Mahadja 4: Another Mahadja owned by Señor Pedro Cortez about 2.5 km distant from Mahadja 3 and from the Orinoco River, about 50 km north of the town of Pto. Ayacucho; in third year of use and planted with yucca and bananas. Soil under bananas very loose and sandy, light-

brown, with many grass roots and organic matter, pH 5.6. Material collected: as in Mahadja 3. Collected on 6.2.1996, investigated in July 1996.

Site 26 = control to Mahadja 4: *Tachypogon* savanna with shrubs and some trees about 400 m distant from Mahadja 4; inundated by high floods of the Orinoco River. Soil rather compact, yellow-brown, partially covered by an algal crust, pH 5.3. Material collected as described for site 23. Collected on 6.2.1996, investigated in August 1996.

Site 27 = Mahadja 5: Farm of Señor Homero Aranguren near the village of Fundo el Desoro about 60 km north of the town of Pto. Ayacucho and about 6 km east of the Orinoco River, 67°36'W 5°41'N (Fig. 1). Mahadja in third year of use and yucca just harvested two days before our investigation. Soil rather compact, very sandy, brownish, few roots, pH 6.2. Material collected as described for site 23. Collected on 6.2.1996, investigated in August 1996.

Site 28 = control to Mahadja 5: Yearly burnt *Tachypogon* savanna adjacent to the Mahadja; not inundated by the Orinoco River. Soil very hard, few litter and humus, consists mainly of yellow-brown sand. Material collected as described for site 23. Collected on 6.2.1996, investigated in August 1996.

Site 29: A large outcropping with many Lajas between the Agricultural Research Station and the airport of the town of Pto. Ayacucho, 67°36'W 5°41'N (Fig. 1, 5). Material collected: mud and cyanobacterial crusts from several Lajas, pH 5.4, slightly saline. Collected on 6.2.1996, investigated in March 1997.

Site 30: As site 29 but only a single Laja with a diameter of about 3 m. Bottom covered by a thin, brownish crust possibly produced by the fine leaves of a plant; pH 5.4. Collected on 6.2.1996, investigated in May 1997.

Site 31: As site 29 but only a single Laja with a diameter of 30 cm. Material collected: mud and black pieces of the cyanobacterial crust covering the bottom; pH 5.4. Collected on 6.2.1996, investigated in April 1997.

Site 32: As site 29. A Laja with cushions of Velloziaceae. Material collected: mud and light-brown soil with many roots under the green part of the plant, pH 5.3. Collected on 6.2.1996, investigated in June 1997.

Site 33: Páramo de Piedras Blancas, Cordillera de Merida about 2 km east of the Pico de Aquila, 70°48'W 8°52'N at 4,200 m above sea level (Fig. 6). Material collected: Rotting *Espeletia* leaves underneath the living rosette, 5-15 year old leaves covered with a greenish algal layer; between leaves some excrements of microarthropods; pH 5.6. Collected on 10.2.1996, investigated in April 1996. For details, see Foissner (2000b).

Site 34: As site 33. Material collected: Decaying *Espeletia* leaves from dead, rotting trunks 100-150 years old. Leaves and trunk partially covered with a greenish algal layer and some small mosses; between leaves soil particles and excrements of microarthropods; pH 6.0. Collected on 10.2.1996, investigated in April 1996. For details, see Foissner (2000b).

Site 35: Secondary, evergreen, seasonal rainforest in the surroundings of Tabogán de la Selva, an Indian village about 30 km south of the town of Pto. Ayacucho, 67°36'W 5°41'N (Fig. 1). Formerly used as a crop field. Soil very sandy and humic, brown, with a 2-3 cm thick fermentation

layer, almost dry. Material collected: fresh and decaying leaf litter and soil with many fine roots to a depth of 5 cm. Collected on 7.2.1996, investigated in August 1996. No ciliates developed in the non-flooded Petri dish culture, as typical for rainforests (see chapter 2.1.1.4).

Site 36: Strongly overgrazed pasture in the surroundings of the village of Gravidia at 3,300 m above sea level, outskirts of the town of Merida, 71°9'W 8°36'N. Soil rather compact and almost black, with many grass roots, pH 5.6. *Espeletia shultzii* occurs there. Material collected: lawn, roots, and soil to a depth of 5 cm. Collected on 9.2.1996, investigated in March 1997.

Site 37-40 (poor samples and thus only briefly described; for details see Foissner (2000b): Páramo de Piedras Blancas, Cordillera de Merida about 2 km east of the Pico de Aquila, 70°48'W 8°52'N at 4,200 m above sea level (Fig. 6). Soil dark-brown, with many earthworm (?) casts and roots from dwarf cushions. Material collected: leaf litter and soil to a depth of 10 cm under and between *Espeletia* plants. Collected on 10.2.1996, investigated in April 1996.

Site 41: Sierra Nevada National Park, rainforest in the surroundings of the village of La Mucuy, about 12 km northeast of the town of Merida at 2,130 m above sea level. Material collected: fresh and decaying leaf litter, roots, and soil to a depth of 5 cm; pH 5.4. This looked like a very good sample, but only two ciliate species developed in the non-flooded Petri dish culture, as typical for rainforests (see chapter 2.1.1.4). Collected on 13.2.1996, investigated in February 1997.

Site 42: As site 41. Mosses from trees; pH 6.0. Collected on 13.2.1996, investigated in March 1997.

Site 43: As site 41. Bark with some moss from a large tree; pH 5.6. Collected on 13.2.1996, investigated in March 1997.

Site 44: As site 41. Wet soil crumbles and litter between leaves of bromeliads; pH 6.2. Collected on 13.2.1996, investigated in February 1997.

Site 45: As site 41. Slightly wet soil and many roots from bromeliads attached to trees; pH 5.0. Collected on 13.2.1996, investigated in January 1997.

Site 46: As site 41, Humboldt trail in the outskirts of the village of La Mucuy. Soil dark brown, with many roots and decaying leaf litter; pH 5.4. Material collected: litter and soil to a depth of 5 cm. Collected on 13.2.1996, investigated in January 1997.

Site 47: North border of the Henri Pittier National Park, surroundings of the village of Choroni, about 15 m distant from the sea coast and about 3 m above sea level, 67°37'W 10°30'N (Fig. 8). Material collected: litter from sieved sand up to 10 cm depth, surface grass and tree litter connected by white fungal hyphae; pH 6.7, salinity 10‰. Collected on 20.2.1996, investigated in July 2001.

Site 48: As site 47 but about 100 m distant from the sea coast. Soil covered by bushes, trees, and Cactaceae, brown, with a thin litter layer connected by white fungal hyphae; pH 6.8, salinity 10‰. Material collected: leaf litter, roots, and soil to a depth of 5 cm. Collected on 20.2.1996, investigated in March 2001.

Site 49: As site 47 but about 2 km distant from the sea coast, near a cemetery. Material collected: litter and soil particles from bundles of *Tillandsia* sp. (Bromeliaceae); pH 5.6. Collected on 20.2.1996, investigated in October 2000.

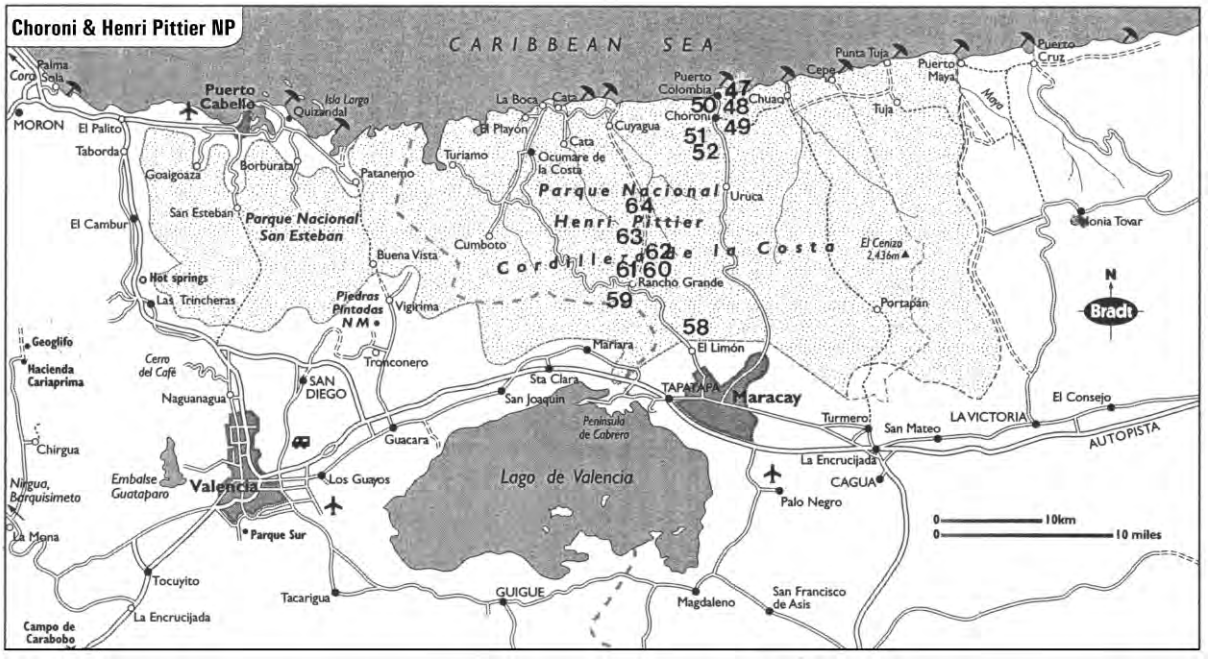

Fig. 8. North coast, Henri Pittier National Park and the village of Choroni (from MADDICKS 2011, modified).

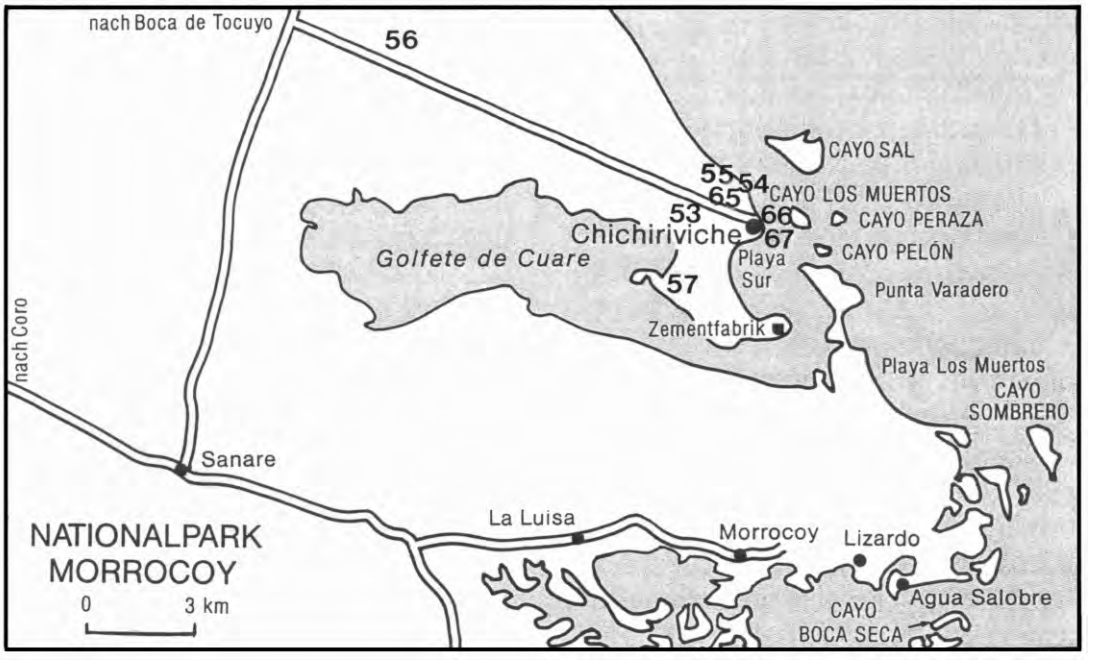

Fig. 9. Chichirivice area (from KAISER & GORDONES 1994, modified). Site 56 was the richest, i.e., we recorded 126 species nine of which were undescribed.

Site 50: As site 47, slightly west of the village of Choroni on an about 100 m high hill near the sea coast. Material collected: reddish sand up to a depth of 5 cm and litter from bushes, trees, and Cactaceae in the surroundings of the broad casting station; pH 6.7. Collected on 20.2.1996, investigated in July 1998.

Site 51: As site 47. Bark from a large tree; pH 6.0. Collected on 21.2.1996, investigated in September 2001.

Site 52: As site 47 but some km south of the village of Choroni in a gallery forest very near to a stream. Alluvial, very sandy, brown soil, pH 6.7. Material collected: fresh and rotting leaf litter and soil to a depth of 5 cm. Collected on 21.2.1996, investigated in February 1997.

Site 53: Morrocoy National Park, Pico de Chichiriviche, about 100 m above sea level, 67°13'W 11°33'N. Dry tropical forest; litter layer about 2 cm thick and with many fungal hyphae; soil yellow, with many fine roots; pH 6.7. Material collected: leaf litter, roots, and soil to a depth of 5 cm. Collected on 23.2.1996, investigated in September 2000. This and samples 54 and 55 form a short transect.

Site 54: As site 53, at foot of Pico de Chichiriviche, about 500 m distant from the sea coast. A small, saline pan with islands of halophytic plants. Soil brownish and with many fine roots; pH 7.3, salinity about 30‰. Material collected: leaf litter, algal crust, and soil to a depth of 5 cm. Collected on 23.2.1996, investigated in April 1997.

Site 55: As site 54 but about 100 m nearer to the sea coast, i.e., where the Mangrove girdle begins. Soil yellow and sandy, pH 7.2, about 100‰ salinity. Material collected: leaf litter, algal crust, and soil to a depth of 5 cm. Collected on 23.2.1996, investigated in April 1997.

Soil 56: Morrocoy National Park, about 13 km northwest of the village of Chichiriviche, 67°13'W 11°33'N (Fig. 9). This area, which is used as a cattle pasture and occasionally burnt, contains countless flat depressions which become small puddles after heavy rain. Material collected: cyanobacterial and algal crusts, mud with plant litter, and loamy brown soil from the upper 2 cm of some very flat, dry puddles covered with grass and halophytes; pH 6.0, salinity 4‰. Collected on 22.2.1996, investigated in July 2000.

Site 57: Near site 56, Golfete de Cuare, Cueva del Indio (an old coral cave). Material collected: Moss from stones and some surface soil; pH 5.7, salinity ~10‰. Collected on 22.2.1996, investigated in March 1997.

Site 58: South margin of the Henri Pittier National Park, way to the town of Ocumare, 67°37'W 10°30'N (Fig. 8). A deforested site with up to 2 m high grasses and a 2-5 cm thick litter layer interweaved by many fungal hyphae. Soil dark brown, dense, pH 5.8. Material collected: grass litter and soil up to 3 cm depth. Collected on 24.2.1996, investigated in October 2000.

Site 59: South margin of the Henri Pittier National Park, Biological Station Rancho Grande, about 1,000 m above sea level in the cloud forest, 67°37'W 10°23'N (Fig. 8). Material collected: mud and soil from four dry tank bromeliads in the surroundings of the station; pH 6.2. Collected on 24.2.1996, investigated in January 1997.

Site 60: As site 59. Material collected: moss and bark from large trees; pH 5.1. Collected on 24.2.1996, investigated in March 1997.

Site 61: As site 59, along the nature trail. Material collected: upper 5 cm of a typical rainforest soil, i.e., leaf litter layer 1-2 cm thick, followed by a moder layer 1-2 cm thick and a dense root carpet. Collected on 24.2 1996, investigated in April 1996.

Sites 62, 63: As site 59, two samples from the surroundings of the nature trail. Material collected: leaf litter, moder, and roots to a depth of 10 cm; soil sandy, brown, pH 6.3 under the root carpet. Collected on 24.2.1996, investigated in February 1997.

Site 64: As site 59, stair to the nature trail. Material collected: wall mosses from the surroundings of the stair; pH 6.6. Collected on 24.2.1996, investigated in September 2001.

Site 65: Surroundings of the village of Chichiriviche, 67°13'W 11°33'N (Fig. 9). An abandoned crop field near to the sea coast; flooded by high tides and storms. Soil loamy, brown; pH 5.8, salinity 50‰. Material collected: leaf litter from Banana and Lychee trees, surface algal crusts and moss, and soil to a depth of 5 cm. Collected on 14.10.2005, investigated in May 2011.

Site 66: As sample 65 but about 100 m distant from the sea coast. An abandoned field flooded by high tides and storms. Soil loamy, brown; salinity 63‰. Material collected: fresh and decaying leaf litter from various trees and soil to a depth of 5 cm. Collected on 14.10.2005, investigated in May 2011.

Site 67: As sample 65. Material collected: leaves and attached soil from two rotting, thick water lily trunks at the margin of a large, highly eutrophic freshwater pond. Collected on 14.10.2005, investigated in May 2011.

Galápagos samples: These were collected by Prof. Dr. Karl O. Stetter, University of Regensburg in August 2001 and investigated in November and December 2004. There were eight samples most too small for a "good" non-flooded Petri dish culture. Thus, two or three similar samples each were mixed to obtain four useable probes. The geographic coordinates of the sampling sites are from Snell et al. (1996).

Site 68 (composed of two small samples)**:** Isabela island, south coast, way to "Murode Las Lagrimas", in the surroundings of the village of Puerto Villamil, 90°57'W 0°57'S. Material collected: leaf litter and soil from the margin of a Mangrove forest and an orange-yellow, thin coat of Mangrove twigs; salinity 30‰.

Site 69 (composed of three small samples)**:** San Cristóbal island, 89°25'0"W 0°48'30"S, about 800 m above sea level; wet soil from the margin of a crater lake. San Cristóbal island, about 30 m above sea level; dry soil from the surroundings of Puerto Chino. Isabela island, about 1,300 m above sea level, near the Volcan de Azufre; dry soil from bottom of the Sierra Negra crater.

Site 70 (composed of two small samples)**:** Isabela island, Sierra Negra crater near to the Vulcan Chico, about 1,050 m above sea level; leaf litter and soil under a tree with many epiphytes. Plaze Sur about 30 m above sea level, dry soil with a salinity of 20‰.

Site 71 (a single sample)**:** Santa Cruz island, surroundings of Puerto Ayora, hotel San Fernando, 90°18'W 0°44'S. Material collected: leaf litter and soil under a *Pandanus* palm in the hotel garden; not saline.

2.2 Methods

Methods are the same as described in the monograph on Namibian soil ciliates to which the reader is thus referred to (Foissner et al. 2002). However, a few new or very important issues are described or copied from the Namibian monograph: sampling and sample processing; collection of material for preparations; and estimation of in vivo size. A recent description of the preparation methods has been published by Foissner (2014).

2.2.1 Sampling and Sample Processing

The material collected usually include mineral top soil (0-5 cm, rarely up to 10 cm depth) with fine plant roots, the humic layer, and the deciduous and/or grass litter from the soil surface. In soil with few organic materials and very sandy habitats, litter was sieved off the sand with an ordinary kitchen sieve (1 mm mesh-size), so that the final sample consisted of about 80% litter and 20% sand and gravel. Usually, 10 small subsamples were collected with a small shovel from an area of about 100 m^2 and mixed to a composite sample. Bark samples were usually taken from one to three trees. The bark was collected with a knife, selecting for regions grown with mosses or lichens and/or containing some soil. See chapter 2.1.1.3 for special methods of collecting Mahadjas and the bordering savannas. For rainforest samples, see chapter 2.1.1.4.

Generally, a "good" sample consists of 50% litter, humus and roots and 50% mineral soil. The litter and humus are very important because they release many nutrients when the sample is rewetted, stimulating growth of bacteria, fungi, flagellates, and amoeba, that is, the main food of ciliates. The nutrient increase obviously decouples microbiostasis, as explained in Foissner (1987b).

All samples were air-dried for at least one month and then sealed in plastic bags. Such samples can be stored for years without any significant loss of species, provided they are from arid or temperate environments (Foissner 1997). This is emphasized by the Namibian investigations: there is no correlation between storage time and species number; indeed, the richest samples (nos. 4, 49) are those stored for over four years (Foissner et al. 2002).

All collections were analysed with the "non-flooded Petri dish method", as described by Foissner (1987b, 1992). The technique is not perfect, but likely the best available for biodiversity assessment of soil ciliates at large. The protocol is simple:

1. Put the material in a Petri dish and spread over the bottom of the dish in at least a 1 cm, better 2 to 3 cm thick layer. As concerns the Venezuelan samples, sufficient material was available to fill a 2 cm high Petri dish 13 cm across or, rarely, a 3 cm high dish 18 cm in diameter. Basically, a large Petri dish (18 cm) is preferable because it provides more material for preparations.

2. Slightly over-saturate but do **not** flood the sample with distilled water. Water should be added to the sample until 5-20 ml will drain off when the Petri dish is tilted (45°) and the soil gently pressed with a finger. Complete saturation takes up to 12 hours, so check cultures after this time. Never flood the sample, that is make an Aufguss ("infusion") because then only a few common species will develop. Further, the material should have been dry for at least one month.

3. Cover Petri dish and pinch a clip between bottom and lid to enable gas exchange. Generally, care must be taken that the samples do not putrefy. This happens rather easily with saline material, soil containing animal excrements or, in "ordinary" samples, if the litter is very easily decomposable. In this case, change the water in the sample and do not cover it for some days so that plenty of air is available; further, slightly under-saturate sample with water. Heavily saline soil (≥ 20‰) should be "washed", if no ciliates develop. Saturate the sample

with water, as described above. After two to three days, remove the percolate and saturate again with water. Repeat two to four times, until ciliates begin to develop.

4. A distinct succession occurs in the rewetted samples. Thus, they must be inspected on days 2, 6/7, 13/14, 21/22, and 30. Later inspections usually add only few species, likely because microbiostasis (ciliatostasis; see FOISSNER 1987b) increases and metazoan (rotifers, nematods) and protozoan (mainly heliozoans!) predators often became abundant. For inspection, the Petri dish is tilted some seconds and a rather large drop (~ 0.3 ml) of the drained water ("soil percolate") taken with a Pasteur pipette and inspected for species; several such drops must be investigated from different sites of the Petri dish, until the last drop adds but few species.

2.2.2 Collection of Material for Preparations

If a "difficult" species is noted, which happens in more than 70% of the samples, material for preparations must be collected. To obtain many specimens, the Petri dish is tilted (45°) several times for a minute or so and the percolating soil water collected with a Pasteur pipette from several sites of the dish. If only little water (< 10 ml) drains from the sample and/or the species of interest is very rare, it should be sprinkled with 10-15 ml distilled water. This will cause an osmotic shock, detaching or rinsing many specimens from the soil particles and capillaries within about 10 min. Then, the procedure described above is repeated, that is, the Petri dish is tilted several times and the percolating soil water added to the first collection. Finally, the soil sample is again saturated with clean table water (e.g. Eau de Volvic) and stored for the next investigation. Certainly, these procedures strongly change the milieu, and thus a rather different ciliate community may develop, possibly containing further "difficult" species. If so, the whole procedure is repeated, and so on.

Much care must be taken to keep the percolate clean of large (> 2 µm) soil particles, which would disturb the investigation of the preparation, while particles smaller than 2 µm hardly disturb, if not too numerous. To achieve clean material, note the following advices:

1. Usually, the percolating soil water which contains the organisms will be clean because the soil particles soon become stabilized by microbial activities, mainly by fungal hyphae and bacterial mucilage. Thus, extreme care must be taken not to destroy the soil structure developed in the non-flooded Petri dish culture. Accordingly, the Petri dish must be handled gently and, if necessary, distilled water sprinkled softly on the surface. To increase percolation, mild finger pressure on the soil may be applied. Depending on the material sampled, the percolate has a light brown to orange colour (from lignins, humus colloids, etc.), which does not disturb the preparations (but see below).

2. The percolate is now gently shaken and large soil particles allowed to settle for about one minute. Then, the supernatant, which is now ready for preparations, is collected with a Pasteur pipette. Be careful not to lose bottom-dwellers. Occasionally, it may be helpful to sieve the percolate through a plankton net with 50-100 µm mesh-size or to concentrate it by mild centrifugation (max. 2000 r/min for a few seconds), especially for preparations with expensive chemicals (osmium tetroxide in CHATTON-LWOFF silver nitrate impregnation).

Other culture methods: The non-flooded Petri dish cultures, as described above, provided about 90% of the material contained in the monograph. The rest is from a variety of ordinary "limnetic" cultures. First, clone cultures were made in the usual way by transferring individual specimens into various media, preferable Eau de Volvic (French table water), either pure or mixed with soil extract in a ratio of 10:1 and enriched with a crushed and two uncrushed wheat grains to stimulate growth of indigenous food organisms, viz., bacteria and small flagellates; occasionally, selected food items were added, for instance, filamentous cyanobacteria for several nassulids. Second, 2 ml of the percolate (together with all organisms) were mixed with 8 ml Eau de Volvic and enriched with wheat grains, as described above. Of course, such cultures contain a variety of ciliates, and sometimes interesting species develop for a while. Third, a Petri dish was filled with 10-20 µm culture medium plus some wheat grains. Then some grams of soil are added as an inoculate to a small site of the Petri dish, taking care not to distribute it throughout the medium. Such cultures were sometimes helpful for strongly saline material (> 20‰), which is set up with artificial sea water. Fourth, if the sample is very saline (> 20‰), it may occur that no ciliates develop. Such samples can be "washed" every third day with fresh table water, which decreases the salt concentration. Frequently, ciliates appear after the third or fourth wash!

2.2.3 Estimation of In Vivo Size

Usually, we measure body length and width of a few contrasting specimens in vivo and without using a coverslip. As the organisms are moving, this provides only approximate values which are improved by the morphometric analysis of the preparations. The following percentages compensate preparation shrinkage; they were obtained from comparative analyses, such as shown in → *Maryna* spp.: 15% (10%-20%) for Foissner´s protargol method, 20-30% when pure ethanol was used as a fixative; 5% for Chatton-Lwoff` silver nitrate preparations; and 0% for wet preparations fixed with osmium vapours or a minute drop of osmium acid (2%). Shrinkage is highly variable in SEM preparations, ranging from near zero to 100% in very fragile structures, e.g., the lepidosomes of → trachelophyllids. The same applies for protargol methods and silver carbonate preparations that do not fix specimens on a slide before bleaching and impregnation.

3. Results

3.1 Ecology and Community Analysis

3.1.1 Species Lists

The following lists contain the 420 ciliate species and subspecies found in 67 samples from Venezuela and 4 samples from Galápagos. Further, it contains 38 new species from other localities, most supplementing a certain group of Venezuelan species. The nomenclature is adapted to Berger (1999, 2006, 2008, 2011), Foissner (1998), Foissner et al. (2002), and Vďačný & Foissner (2012). The list should be read as follows:

G = Galápagos sites (no. 68–71)

t. l. = **Type locality** of new species

V = Venezuelan sites (no. 1–67), including three species from Curacao Island

X[a] = New species with type locality in Venezuela or Galápagos and described in this monograph, e. g., *Condylostomides coeruleus* n. sp. [a]

X[b] = New species with type locality in Venezuela but published previously, e. g., *Sleighophrys pustulata* Foissner, 2005 [b]

X[c] = Here described as a new species with type locality not in Venezuela or Galápagos but occurring there, e. g., *Paroxytricha quadrinucleata* n. sp. [c]

X[d] = New species with type locality not in Venezuela or Galápagos and not found there, e. g., *Apoavestina amazonica*

X[e] = Redescription of species from a Venezuelan or a Galápagos population, e. g., *Stylonychia ammermanni* Gupta et al., 2001 [e]

X[f] = Identification questionable, e. g., *Colpoda praestans* Penard, 1922 [f]

X[g] = Redescription of species from non-Venezuelan or non-Galápagos populations, e. g., *Cladotricha australis* Blatterer & Foissner, 1993 [g]

X[h] = New species described before with type locality not in Venezuela or Galápagos but found there, e. g., *Armatospathula plurinucleata*

Afroamphisiella abdita (Foissner, 1997) Foissner, Agatha & Berger, 2002 [e]: V1; F 1.4
Afroamphisiella multinucleata Foissner, Agatha & Berger, 2002: V 54; F 1.4
Anteholosticha australis (Blatterer & Foissner, 1988) Berger, 2003: V 23, 24, 25, 52, 58, 64; F 8.5
Apertospathula lajacola Foissner & Xu, 2007 [b]: V 29, 31; F 2.8
Apertospathula verruculifera Foissner, Xu & Kreutz, 2005 [b]: V 54; F 1.4
Apoavestina amazonica n. sp. [d] (t. l. Brazil)
Apocoriplites lajacola Oertel, Wolf, Al-Rasheid & Foissner, 2008 [b]: V 3, 5, 20; F 4.2
Apofrontonia lametschwandtneri Foissner & Song, 2002 [b]: V54; F 1.4
Apogonostomum pantanalense n. sp. [d] (t. l. Brazil)
Apogonostomum vleiacola n. sp. [d] (t. l. South Africa)
Apometopoides (Apometopus) pyriformis (Levander, 1894) nov. comb. [g]
Apometopus pelobius n. sp. [d] (t. l. Dominican Rep.)
Apospathidium atypicum (Buitkamp & Wilbert, 1974) Foissner, Agatha & Berger, 2002: V 11, 12, 14, 16, 27, 50; F 8.5
Apowoodruffia salinaria n. sp. [a]: V 54, 65; F 2.8
Arcuospathidium coemeterii (Kahl, 1943) Foissner, Berger, Xu & Zechmeister-Boltenstern, 2004: V 25; F 1.4
Arcuospathidium cultriforme cultriforme (Penard, 1922) Foissner, 1984: V 8, 26, 56; F 4.2
Arcuospathidium cultriforme scalpriforme (Kahl, 1930) Foissner, 2003: V 2, 14, 16, 20, 25, 47, 52, 59, 61, 62; F 14.1
Arcuospathidium multinucleatum Foissner, 1999: V 1, 8, 14, 18, 28, 56; F 8.5
Arcuospathidium muscorum muscorum (Dragesco & Dragesco-Kernéis, 1979) Foissner, 1984: V 14, 16, 38, 52, 59; F 7.0
Arcuospathidium muscorum rhophaloplites Foissner & Xu, 2007 [h]: V 58, 63; F 2.8
Arcuospathidium namibiense namibiense Foissner, Agatha & Berger, 2002: V 20; F1.4
Arcuospathidium namibiense tristicha Foissner, Agatha & Berger, 2002: V 1, 3, 8, 10, 14, 17, 18, 23, 27, 32, 47, 52, 53, 54, 56, 59, 62; F 23.9
Arcuospathidium pachyoplites Foissner, 2003 [b]: V 47; F 1.4
Armatospathula periarmata Foissner & Xu, 2007 [b]: V 28; F 1.4
Armatospathula plurinucleata Foissner & Xu, 2007 [h]: V 32; F 1.4
Australocirrus oscitans Blatterer & Foissner, 1988: V 1, 17, 18, 24, 26, 56; F 8.5

Australothrix alwinae Blatterer & Foissner, 1988: V 11; F 1.4
Australothrix venezuelensis n. sp. [a]: V 32; F 1.4
Australothrix fraterculus n. sp. [c]: V 54; F 1.4
Australothrix steineri Foissner, 1995 [e, g]: V 54; F 1.4
Avestina ludwigi Aescht & Foissner, 1990: V 23; F 1.4
Bakuella pampinaria pampinaria Foissner, 2004 [g]
Bilamellophrya fraterculus n. sp. [d] (t. l. Dominican Rep.)
Bilamellophrya hawaiiensis Foissner, Agatha & Berger, 2002 [e]: V 24, 56; F 2.8
Birojimia (Parabirojimia) litoralis n. sp. [a]: V 47; F 1.4
Birojimia terricola Berger & Foissner, 1989 [e]: V 25; F 1.4
Bistichella chilensis n. sp. [d] (t. l. Chile)
Bistichella kenyaensis n. sp. [d] (t. l. Kenya)
Blepharisma americanum Suzuki, 1954: V 1, 26, 56; F 4.2
Blepharisma bimicronucleatum Villeneuve-Brachon, 1940: V 13, 15, 25, 61, G 68; F 7.0
Blepharisma hyalinum Perty, 1849: V 1, 2, 3, 8, 13, 15, 20, 23, 24, 25, 36, 47, 52, 53, 56, 57, 58, 59, 60, 61, 62, 63, G 71; F 32.4
Blepharisma steini Kahl, 1932: V 54, 56; F 2.8
Brachyosoma brachypoda mucosa Foissner, 1999: V 11, 12, 14, 15, 32, 52, 62; F 9.9
Bresslaua insidiatrix Claff, Dewey & Kidder, 1941: V 49, 58; F 2.8
Bresslaua vorax Kahl, 1931: V 24, 26; F 2.8
Bresslauides terricola (Foissner, 1987) Foissner, 1993: V 27, 47, 56, 61; F 5.6
Bryometopus atypicus Foissner, 1980: V 26; F 1.4
Bryometopus pseudochilodon Kahl, 1932: V 1, 2, 8, 11, 12, 13, 14, 16, 17, 18, 20, 23, 24, 25, 26, 28, 32, 56, 58, 61, 64; F 29.6
Bryometopus rostratus n. sp. [a]: V 8; F 1.4
Bryometopus sphagni (Penard, 1922) Kahl, 1932: V 11, 20, 25; F 4.2
Bryometopus triquetrus Foissner, 1993: V 3, 14, 18, 20, 25, 60; F 8.5
Bryophyllum paucistriatum Foissner, Agatha & Berger, 2002: V 20, 56, 59, 60, 62; F 7.0
Bursaria ovata Beers, 1952 [g]: V 56; F 1.4
Bursaria truncatella Mueller, 1773: V 4, 31; F 2.8
Cataphractes austriacus n. sp. [d] (t. l. Austria)
Cataphractes terricola n. sp. [a]: V 23, 25; F 2.8
Caudiholosticha halophila n. sp. [c]: V 47, 54; F 2.8
Caudiholosticha silvicola n. sp. [d] (t. l. Germany)
Caudiholosticha sylvatica (Foissner, 1982) Berger, 2003: V 13, 61; F 2.8
Caudiholosticha tetracirrata (Buitkamp & Wilbert, 1974) Berger, 2003: V 49, 56; F 2.8
Caudiholosticha virginensis n. sp. [d] (t. l. Virgin Islands)
Cephalospatula brasiliensis Foissner, 2003 [h]: V 32; F 1.4
Chilodontopsis muscorum Kahl, 1931: V 52; F 1.4
Cinetochilides monomacronucleatus n. sp.[a]: V 65; F 1.4
Cinetochilides terricola n. sp. [a]: G 68; F 1.4
Cinetochilum margaritaceum (Ehrenberg, 1830) Perty, 1852: V 3, 13, 23, 25, 50, 52, 53, 58, 61, 62; F 14.1
Circinella filiformis (Foissner, 1982) Foissner, 1994: V 23, 50, 59, 62; F 5.6
Circinella vettersi (Berger & Foissner, 1989) Foissner, 1994: V 14; F 1.4
Cladotricha australis Blatterer & Foissner, 1993 [g]: V 54; F 1.4
Cladotricha chilensis n. sp. [d] (t. l. Chile)
Cladotricha digitata n. sp. [d] (t. l. Costa Rica)
Cladotricha edaphoni Wilbert, 1995 [e]: V 65; F 1.4
Cladotricha halophila Wilbert, 1995 [e, g]: V 65; F 1.4
Clavoplites terrenum (Foissner, 1984) Foissner, Agatha & Berger, 2002: V 8, 64; F 2.8
Colpoda cucullus (Mueller, 1773) Gmelin, 1790: V 1, 2, 3, 4, 5, 8, 10, 11, 12, 13, 14, 15, 16, 17, 18, 20, 21, 23, 24, 25, 27, 28, 32, 36, 37, 38, 47, 48, 49, 50, 51, 52, 53, 54, 56, 57, 58, 59, 60, 61, 62, 63, 65, 66, 67, G 68, 69, 70, 71; F 69.0

Colpoda ecaudata (Liebmann, 1936) Foissner, Blatterer, Berger & Kohmann, 1991: V 2, 27, 28, 47, 50, 54, 61; F 9.9
Colpoda edaphoni Foissner, 1980: V 48, 52, 53, 56, 59, 61, 62, 63, G 71; F 12.7
Colpoda elliotti Bradbury & Outka, 1967: V 3, 8, 38, 47, 48, 50, 52, 59, 61, 62, 63; F 15.5
Colpoda ephemera n. sp. [c]: G 68; F 1.4
Colpoda henneguyi Fabre-Domergue, 1889: V 2, 14, 16, 18, 20, 25, 50, 52, 53, 58, 59, 61; F 16.9
Colpoda inflata (Stokes, 1884) Kahl, 1931: V 1, 2, 3, 4, 5, 8, 9, 10, 11, 12, 13, 14, 15, 16, 17, 18, 20, 23, 24, 25, 26, 27, 28, 29, 30, 32, 36, 37, 38, 41, 42, 45, 47, 48, 49, 50, 51, 52, 53, 54, 56, 57, 58, 59, 60, 61, 62, 63, 64, G 68, 70, 71; F 73.2
Colpoda lucida Greeff, 1888: V 2, 3, 4, 11, 12, 13, 14, 16, 17, 18, 20, 23, 24, 25, 26, 28, 32, 48, 50, 51, 52, 53, 56, 60, 61, 62, 63; F 38.0
Colpoda maupasi Enriques, 1908 [e, g]: V 1, 2, 3, 4, 5, 8, 9, 13, 14, 15, 16, 17, 21, 23, 24, 25, 27, 28, 29, 32, 36, 47, 48, 49, 50, 51, 52, 53, 54, 56, 57, 58, 59, 60, 61, 62, 63, 64, 65, 66, G 68, 69, 70, 71; F 62.0
Colpoda orientalis Foissner, 1993: V 15, 23, 29, 65; F 5.6
Colpoda ovinucleata Foissner, 1980: V 63; F 1.4
Colpoda praestans Penard, 1922 [f]: V 17, 52, 59, 61; F 5.6
Colpoda tripartita Kahl, 1931: V 15, 50, 52; F 4.2
Colpoda variabilis Foissner, 1980: V 3, 13, 23, 48, 58; F 7.0
Colpodidium caudatum Wilbert, 1982: V 4, 5, 11, 12, 15, 16, 24, 31, 32, 52, 54, 56, 62, G 68; F 19.7
Colpodidium microstoma Foissner, Agatha & Berger, 2002: V 8; F 1.4
Colpodidium trichocystiferum Foissner, Agatha & Berger, 2002: V 65; F 1.4
Colpodidium viridis (Mirabdullaev, 1986) Jankowski, 1992: V 24; F 1.4
Condylostomides coeruleus n. sp. [a]: V 56; F 1.4
Coriplites terricola Foissner, 1988: V 11, 12, 32; F 4.2
Coriplites tumidus n. sp. [a]: V 14; F 1.4
Coterillia bromelicola Foissner & Stoeck, 2011 [g]
Cothurnia minutissima (Penard, 1914) Kahl, 1935 [e]: V54; F 1.4
Cultellothrix atypica (Wenzel, 1953) Foissner & Xu, 2007: V 32; F 1.4
Cyclidium glaucoma Müller, 1773: V 61; F 1.4
Cyrtohymena australis Foissner, 1995: V 56, 61; F 2.8
Cyrtohymena citrina (Berger & Foissner, 1987) Foissner, 1989: V 8, 52, 56, 58, 62, 67; F 8.5
Cyrtohymena primicirrata (Berger & Foissner, 1987) Foissner, 1989: V 54; F 1.4
Cyrtohymena quadrinucleata (Dragesco & Njiné, 1971) Foissner, 1989: V 38, 47, 50, 58, 59, G 71; F 8.5
Cyrtohymena tetracirrata (Gellért, 1942) Foissner, 1989: V 63, 64; F 2.8
Cyrtolophosis mucicola Stokes, 1885: V 1, 2, 3, 4, 5, 8, 11, 13, 14, 15, 16, 17, 18, 19, 20, 22, 23, 24, 25, 26, 27, 28, 31, 32, 47, 49, 50, 52, 53, 54, 56, 58, 59, 60, 62, 63, G 68; F 52.1
Deviata bacilliformis (Gelei, 1954) Eigner, 1995: V 54; F 1.4
Deviata brasiliensis Siqueira-Castro et al., 2009 [e]: V 56, 65; F 2.8
Dileptus beersi Jones, 1956 [e]: V 23, 25, 26; F 4.2
Dileptus margaritifer (Ehrenberg, 1838) Wirnsberger, Foissner & Adam, 1984: V 56; F 1.4
Dileptus mucronatus Penard, 1922: V 8, 52, 54, 65; F 5.6
Dimacrocaryon amphileptoides (Kahl, 1931) Jankowski, 1967: V 2, 11, 32, 64; F 5.6
Dimacrocaryon amphileptoides paucivacuolatum Vďačný & Foissner, 2012 [h]: V 4, 25; F 2.8
Diplites telmatobius Foissner, 1998: V 12; F 1.4
Drepanomonas exigua bidentata Foissner, 1999: V 4, 23, 25, 52, 59; F 7.0
Drepanomonas exigua exigua Penard, 1922: V 61; F 1.4
Drepanomonas hymenofera venezuelensis Omar & Foissner, 2012 [b]: V 1; F1.4
Drepanomonas minuta Foissner & Omar, 2014 [h]: V 8, G 71; F 2.8
Drepanomonas multidentata Foissner & Omar, 2014 [b]: V 56; F 1.4
Drepanomonas muscicola Foissner, 1987: V 2, 14, 23, 25, 50, 56, 58, 60, 61; F 12.7
Drepanomonas obtusa Penard, 1922: V 11; F 1.4
Drepanomonas pauciciliata Foissner, 1987: V 1, 2, 3, 4, 5, 8, 11, 12, 13, 14, 15, 16, 17, 18, 20, 21, 23, 25, 26, 27, 28, 29, 31, 32, 48, 49, 50, 53, 56, 58, 59, 60, 61, 63, 64; F 49.3

Drepanomonas revoluta Penard, 1922: V 1, 2, 3, 8, 13, 14, 16, 24, 27, 47, 48, 50, 51, 52, 53, 56, 58, 61, 62; F 26.8
Drepanomonas sphagni Kahl, 1931: V 3, 11; F 2.8
Edaphospathula espeletiae (Foissner, 2002) Foissner & Xu, 2007 [b]: V 38; F 1.4
Edaphospathula fusioplites Foissner & Xu, 2007 [h]: V 50; F 1.4
Edaphospathula gracilis Foissner & Xu, 2007 [h]: V 57; F 1.4
Emarginatophrya aspera (Kahl, 1926) nov. comb.: V 1, 8, 13, 15, 21, 25, 36, 48, 50, 54, 56, 57, 58, G 70; F 19.7
Emarginatophrya terricola n. sp. [a]: V 56; F 1.4
Enchelariophrya wolfi n. sp. [c]: V 56; F 1.4
Enchelyodon alquasabi Foissner, Quintela-Alonso & Al-Rasheid, 2008 [h]: V 47; F 1.4
Enchelyodon armatides Foissner, Agatha & Berger, 2002 [g]
Enchelyodon floridensis n. sp. [d] (t. l. Florida)
Enchelyodon gondwanensis n. sp. [c]: V 52, 59, 62; F 4.2
Enchelyodon isostichos n. sp. [a]: V 1; F 1.4
Enchelyodon lagenula (Kahl, 1930) Blatterer & Foissner, 1988 [e, g]: V 4, 11, 20, 23, 32; F 7.0
Enchelyodon longinucleatus Foissner, 1984 [g]: V 15, 25, 47; F 4.2
Enchelyodon megastoma Foissner, Agatha & Berger, 2002 [g]
Enchelyodon monoarmatus monoarmatus n. spp. [a]: V 1; F 1.4
Enchelyodon monoarmatus pyriformis n. ssp. [d] (t. l. Botswana)
Enchelys gasterosteus Kahl, 1926: G 70; F 1.4
Enchelys geleii (Foissner, 1981) Foissner, 2000: V 23, 47, 48, 51, 52, 53, 56, 61, 62, G 71; F 14.1
Enchelys lajacola Foissner & Oertel, 2009 [b]: V5, G 71; F 2.8
Enchelys micrographica Foissner, 2010 [h]: V 56; F 1.4
Enchelys polynucleata (Foissner, 1984) Foissner, Agatha & Berger, 2002: V 4, 11, 12, 13, 17, 24, 26, 48, 52, 56; F 14.1
Enchelys terricola Foissner, 1987: V 15, 38, 62; F 4.2
Enchelys terricola lanceoplites n. spp [d] (t. l. Robinson Island)
Enchelys tumida n. sp. [c]: V 49, 61; F 2.8
Epispathidium amphoriforme (Greeff, 1888) Foissner, 1984: V 16, 50, 54, 61, G 71; F 7.0
Epispathidium ascendens (Wenzel, 1955) Foissner, 1987: V 1, 2, 13, 14, 16, 23, 31, 32, 47, 50, 52, 57, 58, 59, 61, G 68; F 22.5
Epispathidium polynucleatum Foissner, Agatha & Berger, 2002 : V 25, 50, 51, 53, 54; F 7.0
Epispathidium regium Foissner, 1984: V 52; F 1.4
Epispathidium terricola Foissner, 1987: V 3, 15, 25, 48, 52, 53, 56, 59, 60, 62; F 14.1
Epistylis alpestris Foissner, 1978 [f]: V 15, 52; F 2.8 (see *Pseudotelotrochidium epistylis*)
Erimophrya monostyla Foissner, Quintela-Alonso & Al-Rasheid, 2008 [h]: V 21; F 1.4
Erimophrya quadrinucleata Foissner, Berger, Xu & Zechmeister-Boltenstern, 2004 [h]: V 56; F 1.4
Eschaneustyla terricola Foissner, 1982: V 23, 50; F 2.8
Euplotopsis incisa Foissner, Agatha & Berger, 2002 [e]: V 54; F 1.4
Euplotopsis muscicola (Kahl, 1932) Borror & Hill, 1995: V 23, 50, 52, 54, 56; F 7.0
Exocolpoda augustini (Foissner, 1987) Foissner, Agatha & Berger, 2002: V 3, 14, 16, 50, 54, 56, 65, G 69, 70, 71; F 14.1
Fragmocirrus espeletiae Foissner, 2000 [b]: V 38, 59, 62, 63; F 5.6
Fragmospina depressa (Gellért, 1942) nov. comb. [e, g]: V 13, 14, 23, 27, 29, 56, 62; F 9.9
Frontonia angusta solea Foissner, 1987: V 32; F 1.4
Frontonia depressa (Stokes, 1886) Kahl, 1931: F 11, 23, 50, 52, 58, 59, 61; F 9.9
Frontonia terricola Foissner, 1987: V 56; F 1.4
Furgasonia theresae (Fabre-Domergue, 1889) Foissner, Agatha & Berger, 2002: V 11, 12, 29, 32; F 5.6
Fuscheria lacustris Song & Wilbert, 1989: V 8, G 71; F 2.8
Fuscheria nodosa Foissner, 1983: V 50, G 69; F 2.8
Fuscheria terricola Berger, Foissner & Adam, 1983: V 2, 15, 20, 24, 27, 52, 61, 62, 64; F 12.7
Gastronauta derouxi Blatterer & Foissner, 1992: V 15, 25; F 2.8
Gastrostyla bavariensis Foissner, Agatha & Berger, 2002: V 47; F 1.4
Gastrostyla steinii Engelmann, 1862: V 13, 15, 25, 52, 62; F 7.0

Gonostomoides bimacronucleatus n. sp. [a]: V 57; F 1.4
Gonostomoides caudatus n. sp. [d] (t. l. Chile)
Gonostomoides fraterculus n. sp.[a]: G 71; F 1.4
Gonostomoides galapagensis n. sp. [a]: V 5, 61, G 70; F 4.2
Gonostomum affine (Stein, 1859) Sterki, 1878: V 1, 2, 3, 4, 5, 8, 9, 10, 11, 12, 13, 14, 15, 16, 17, 18, 20, 21, 23, 24, 25, 26, 27, 28, 32, 38, 47, 48, 49, 50, 51, 52, 53, 54, 56, 58, 59, 60, 61, 65, G 68, 70, 71; F 60.6
Gonostomum algicola Gellért, 1942: V 48; F 1.4
Gonostomum bromelicola n. sp. [d] (t. l. Jamaica)
Gonostomum caudatulum n. sp. [d] (t. l. Brazil)
Gonostomum fraterculus n. sp. [d] (t. l. Brazil)
Gonostomum halophilum n. sp. [d] (t. l. Australia)
Gonostomum lajacola n. sp. [a]: V 32; F 1.4
Gonostomum multinucleatum n. sp. [c]: V 54, 61; F 2.8
Gonostomum namibiense Foissner, Agatha & Berger, 2002: G 68; F 1.4
Gonostomum salinarum n. sp. [d] (t. l. USA)
Gonostomum singhii Kamra & Sapra, 2008 [g]: V 24, 25; F 2.8
Gonostomum strenuum (Engelmann, 1862) Sterki, 1878 [g]: V 62, 64; F 2.8
Grossglockneria acuta Foissner, 1980: V 2, 3, 9, 11, 24, 27, 58, 60; F 11.3
Grossglockneria hyalina Foissner, 1985: V 3, 11, 48, 50, 52, 59; F 8.5
Grossglockneria lajacola n. sp. [a]: V 32; F 1.4
Halteria grandinella (Mueller, 1773) Dujardin, 1841: V 1, 13, 15, 24, 25, 29, 52, 54, 56, 57, 58, 59, 61, 63, 64, G 68; F 22.5
Haplocaulus terrenus Foissner, 1981: V 64; F 1.4
Hausmanniella discoidea (Gellért, 1956) Foissner, 1984: V 2, 3, 4, 11, 13, 14, 17, 24, 25, 28, 52, 53, 54, 56, 60, 61, 63; F 23.9
Hausmanniella patella (Kahl, 1931) Foissner, 1984: V 3, 8, 9, 15, 20, 23, 24, 26, 48, 50, 51, 53, 56, 57, 58, 59, G 69, 70, 71; F 26.8
Hemiamphisiella terricola Foissner, 1988: V 48, 50, 56, 57; F 5.6
Hemioxytricha isabelae n. sp. [a]: G 68; F 1.4
Hemisincirra gellerti gellerti (Foissner, 1982) Foissner, 1984: V 16, 25, 61; F 4.2
Hemisincirra gellerti verrucosa Foissner & Schade, 2000 in Foissner (2000): V 11, 13, 50, 62; F 5.6
Hemisincirra inquieta Hemberger, 1985: V 1, 2, 3, 4, 9, 10, 11, 13, 14, 15, 16, 18, 23, 25, 26, 28, 32, 50, 52, 53, 56, 58, 59, 61, 62, 63, G 71; F 38.0
Hemisincirra interrupta (Foissner, 1982) Foissner, 1984: V 52; F 1.4
Hemiurosoma similis (Foissner, 1982) Foissner, Agatha & Berger, 2002: V 1, 23, 56; F 4.2
Hemiurosoma terricola Foissner, Agatha & Berger, 2002: V 1; F 1.4
Heterourosomoida lanceolata (Shibuya, 1930) Singh & Kamra, 2015: V 1, 8, 15, 17, 48, 52, 54, 61, 64; F 12.7
Heterourosomoida salinarum n. sp. [d] (t. l. Costa Rica)
Holostichides chardezi Foissner, 1987: V 16, 23, 52, 56; F 5.6
Homalogastra setosa Kahl, 1926: V 2, 13,14, 15, 27, 47, 48, 50, 52, 53, 54, 56, 59, 60, 61, 62, 64, G 70; F 25.4
Idiocolpoda pelobia Foissner, 1993: V 8; F 1.4
Idiodeviata venezuelensis n. sp.[a]: V 65; F 1.4
Ileonema chobicola n. sp. [d] (t. l. Botswana)
Ilsiella palustris Foissner, 1993: V 56; F 1.4
Kahlilembus attenuatus (Smith, 1897) Foissner, Berger & Kohmann, 1994: V 2, 23, 50, 52, 59, 61, 62; F 9.9
Kamburophrys gibba (Kahl, 1935) Foissner & Oertel, 2009: V 29; F 1.4
Krassniggia auxiliaris Foissner, 1987: V 2; F 1.4
Kuehneltiella muscicola Foissner, 1993: V 23; F 1.4
Kuklikophrya ougandae (Dragesco, 1972) Foissner, 1993: V 56; F 1.4
Lagynophrya trichocystis Foissner, 1981: V 2; F 1.4
Lamtostyla australis (Blatterer & Foissner, 1988) Petz & Foissner, 1996: V 1, 8, 13, 14, 23, 24, 26, 27, 49, 54, 63, G 70; F 16.9
Lamtostyla granulifera Foissner, 1997: V 12, 25; F 2.8

Lamtostyla islandica Berger & Foissner, 1988: V 1, 2, 14, 18, 26, 28; F 8.5
Lamtostyla vitiphila (Foissner, 1987) Berger 2008: V 53; F 1.4
Lamtostylides edaphoni (Berger & Foissner, 1987) Berger, 2008: V 14, 16; F 2.8
Lamtostylides kirkeniensis (Berger & Foissner, 1988) Berger, 2008: V 3, 11; F 2.8
Lepidothrix dorsiincisura (Foissner, 1982) nov. comb [e]: V 61, G 70, 71; F 4.2
Lepidothrix reticulata Foissner, Agatha & Berger, 2002: V 47, 48; F 2.8
Leptopharynx brasiliensis Foissner & Omar, 2012 [h]: V 23, 25; F 2.8
Leptopharynx costatus gonohymen Omar & Foissner, 2012 [c]: V 56; F 1.4
Leptopharynx costatus Mermod, 1914: V 1, 2, 3, 4, 5, 9, 10, 11, 12, 13, 14, 15, 16, 17, 18, 20, 23, 24, 25, 26, 27, 28, 31, 32, 38, 47, 48, 49, 50, 51, 52, 53, 58, 59, 60, 61; F 50.7
Leptopharynx lajacola Omar & Foissner, 2014 [b]: V 11; F 1.4
Lingulothrix galapagensis n. sp. [a]: G 71; F 1.4
Litonotus muscorum (Kahl, 1931) Blatterer & Foissner, 1988: V 23, 52; F 2.8
Longispatha elegans Foissner, Xu & Kreutz, 2005 [b]: V 23, 24; F 2.8
Luporinophrys micelae Foissner, 2005 [b]: V 56; F 1.4
Mancothrix pelobia n. sp. [a]: V 21; F 1.4
Maryna lichenicola (Gelei, 1950) Foissner, 1993 [e]: V 29, 30, 32, 50, 56; F 7.0
Maryna meridiana n. sp. [c]: V 5, 12, 29, 31; F 5.6
Maryna ovata (Gelei, 1950) Foissner, 1993: V 24, 25, 56, G 68; F 5.6
Maryna umbrellata (Gelei, 1950) Foissner, 1993 [g]
Meseres corlissi Petz & Foissner, 1992: V 29, 56; F 2.8
Metathrix ellipsoidea ellipsoidea n. ssp. [a]: V 31, 56; F 2.8
Metathrix ellipsoidea oligostriata n. ssp. [d] (t. l. Brazil)
Metopus gibbus Kahl, 1927: V 1, 24; F 2.8
Metopus hasei Sondheim, 1929: V 1, 8, 11, 12, 15, 16, 17, 18, 21, 23, 24, 25, 26, 29, 30, 31, 54, 56, 65, 66, G 68, 71; F 31.0
Metopus minor Kahl, 1927: V 23, 24, 56, 65, 66; F 7.0
Metopus palaeformis Kahl, 1927: V 54, 59, G 68; F 4.2
Metopus setosus Kahl, 1927: V 29, 59; F 2.8
Microcolpoda bambicola n. sp. [d] (t. l. Jamaica)
Microdiaphanosoma arcuatum (Grandori & Grandori, 1934) Wenzel, 1953: V 9, 10, 11, 14, 16, 18, 26, 28, G 71; F 12.7
Microdiaphanosoma terricola Foissner, 1993: V 11; F 1.4
Microdileptus breviproboscis (Foissner, 1981) Vďačný & Foissner, 2012: V 25; F 1.4
Microthorax simulans (Kahl, 1926) Kahl, 1931: V 23, 52, 61; F 4.2
Monomacrocaryon polyvacuolatum (Foissner, 1989) Vďačný & Foissner, 2012: V 8, 15; F 2.8
Monomacrocaryon terrenum (Foissner, 1981) Vďačný et al., 2011: G 70; F 1.4
Monomicrocaryon crassicirratum n. sp.[c]: V 23; F 1.4
Monomicrocaryon euglenivorum fimbricirratum n. ssp. [a]: V 1; F 1.4
Monomicrocaryon granulatum n. sp. [a]: V 61; F 1.4
Mykophagophrys terricola (Foissner, 1985) Foissner, 1995: V 2, 3, 4, 5, 8, 11, 12, 13, 14, 15, 16, 18, 23, 24, 25, 26, 27, 28, 32, 49, 51, 52, 58, 59, 60, 61; F 36.6
Nassula exigua Kahl, 1931 [e]: V 54; F 1.4
Nassula ornata Ehrenberg, 1833: V 54; F 1.4
Nassula parva Kahl, 1928: V 57; F 1.4
Nassula terricola Foissner, 1989: V 54; F 1.4
Nassula tuberculata Foissner, Agatha & Berger, 2002: V 56, 65; F 2.8
Nassulides pictus (Greeff, 1888) Foissner, Agatha & Berger, 2002: V 54; F 1.4
Nivaliella plana Foissner, 1980: V 2, 3, 4, 5, 8, 9, 10, 11, 12, 13, 14, 15, 16, 17, 18, 20, 21, 26, 28, 30, 32, 42, 48, 49, 50, 53, 54, 57, 58, 59, 60; F 43.7
Notodeviata halophila n. sp. [a]: V 65; F 1.4
Notohymena antarctica Foissner, 1996 [g]: V 24, 26, 61; F 4.2
Notohymena quadrinucleata n. sp. [a]: G 71; F 1.4

Notoxoma parabryophryides Foissner, 1993: V 53, 59, 60, 61, 64; F 7.0
Nudiamphisiella illuvialis (Eigner & Foissner, 1994) Berger, 2008 [e]: V 57; F 1.4
Nudiamphisiella interrupta Foissner, Agatha & Berger, 2002 [e]: V 1, 13, 15, 16, 25, 27; F 8.5
Odontochlamys alpestris alpestris Foissner, 1981: V 27, 50, 56; F 4.2
Odontochlamys alpestris biciliata Foissner, Agatha & Berger, 2002 [b]: V 54 and Curacao; F 2.8
Odontochlamys buitkampi n. sp. [c] (t. l. Lamto)
Odontochlamys convexa (Kahl, 1931) Blatterer & Foissner, 1992: V 18; F 1.4
Odontochlamys denticulata n. sp. [a]: V 3; F 1.4
Odontochlamys gouraudi Certes, 1891: V 13, 14, 23, 25, 27; F 7.0
Opercularia curvicaule (Penard, 1922) Foissner, 1998: V 52; F 1.4
Ottowphrya dragescoi (Foissner, 1987) Foissner, Agatha & Berger, 2002 [f]: V 13, 23, 60; F 4.2
Oxytricha africana Foissner, 1999: V 18; F 1.4
Oxytricha granulifera Foissner & Adam, 1983: V 8, 13, 18, 53, 56, 59, 61, 62, 66; F 12.7
Oxytricha granulifera quadricirrata Blatterer & Foissner, 1988: V 27; F 1.4
Oxytricha lithofera n. sp. [a]: V 57; F 1.4
Oxytricha pulvillus n. sp. [a]: V 47, 65; F 2.8
Oxytrichella mahadjacola n. sp. [a]: V 23; F 1.4
Parabistichella bergeri bergeri n. ssp. [a]: V 54, 66; F 2.8
Parabistichella bergeri brevisticha n. ssp. [a]: V 67 and Curacao; F 2.8
Parabistichella variabilis Jiang et al., 2013: V 13, G 68; F 2.8
Parabryophrya penardi (Kahl, 1931) Foissner, 1985: V 52; F 1.4
Paracineta lauterborni Sondheim, 1929: V 1, 2, 13, 23, 27, 48, 52, 53, 56, 60; F 14.1
Paracolpoda lajacola n. sp. [a]: V 30, 32; F 2.8
Paracolpoda steinii (Maupas, 1883) Lynn, 1978 [g]: V 1, 2, 3, 4, 5, 8, 9, 10, 11, 12, 13, 14, 15, 16, 17, 18, 20, 21, 23, 24, 26, 28, 36, 37, 41, 42, 47, 48, 49, 50, 51, 52, 53, 54, 56, 57, 59, 60, 61, 62, 63, 64, 67, G 68, 69, 70, 71; F 66.2
Paracondylostoma clavistoma oligostriatum Foissner & Kreutz, 1998 [b]: V 11, 32; F 2.8
Paraenchelys brachyarmata Foissner, Agatha & Berger, 2002 [e]: V 24, 52, 56; F 4.2
Paraenchelys brachyoplites Foissner, Agatha & Berger, 2002: V 25; F 1.4
Paraenchelys terricola Foissner, 1984: V 3, 11, 14, 15, 18, 23, 25, 27, 32, 50, 52, 54, 58; F 18.3
Paraenchelys wenzeli Foissner, 1984: V 23; F 1.4
Parafurgasonia protectissima (Penard, 1922) Foissner, 1999: V 50, 56, 62; F 4.2
Parafurgasonia sorex (Penard, 1922) Foissner & Adam, 1981: V 24, 25, 53; F 4.2
Parafurgasonia terricola Foissner, 1999: V 2, 52, 53, 61; F 5.6
Paragastrostyla terricola (Foissner, 1988) Berger, 2006 [e]: V 11, 14, 18, 24, 27, 47, 50, 56, 57, 61, 62; F 15.5
Paragonostomum australiense n. sp. [d] (t. l. Australia)
Paragonostomum caudatum Foissner, Agatha & Berger, 2002: V 47, 54, 65, G 68, 71; F 7.0
Paramphisiella caudata (Hemberger, 1985) Foissner, 1988: V 2, 8, 13, 15, 25, 27, 52; F 9.9
Paroxytricha longigranulosa longigranulosa (Berger & Foissner, 1989) nov.comb.: V 2, 3, 20, 23, 25, 52, 56, 58; F 11.3
Paroxytricha longigranulosa imperfecta n. ssp. [a]: V 14; F 1.4
Paroxytricha longigranulosa sinensis n. ssp. [d] (t. l. China)
Paroxytricha quadrinucleata n. sp. [c]: V 59, 61, 63; F 4.2
Pattersoniella vitiphila Foissner, 1987: V 52; F 1.4
Pedohymena australiensis: V 2, 48; F 2.8
Periholosticha lanceolata Hemberger, 1985: V 25, 52; F 2.8
Periholosticha paucicirrata Foissner, Berger, Xu & Zechmeister-Boltenstern, 2004 [h]: V 14, 23, 24; F 4.2
Periholosticha sylvatica Foissner, Berger, Xu & Zechmeister-Boltenstern, 2004 [h]: V 52; F 1.4
Phacodinium metchnicoffi (Certes, 1891) Kahl, 1932: V 3, 23, 58, 61; F 5.6
Phialina binucleata Berger, Foissner & Adam, 1984: V 52, 60; F 2.8
Phialina minima (Kahl, 1927) Foissner, Agatha & Berger, 2002: V 52; F 1.4
Phialinides australis Foissner, 1988: V 50; F 1.4
Phialinides bicaryomorphus n. sp. [a]: V 1, 3, 11, 32, 56; F 7.1

Plagiocampa difficilis Foissner, 1981 [e]: V 24, 56; F 2.8
Plagiocampa monotricha n. sp. [a]: V 52; F 1.4
Plagiocampa ovata Gelei, 1954: V 4; F 1.4
Plagiocampa pentadactyla Foissner, Agatha & Berger, 2002: V 56; F 1.4
Plagiocampa rouxi Kahl, 1926 [e]: V 11, 12, 14, 15, 17, 26, 29, 30, 31, 32, 50, 54, 56, 65; F 19.7
Plagiocampides halophilus Foissner, Agatha & Berger, 2002: V 54; F 1.4
Platynematum terricola n. sp. [c]: V 4; F 1.4
Platyophrya bromelicola Foissner & Wolf, 2009 [g]
Platyophrya macrostoma Foissner, 1980: V 8, 13, 14, 25, 27, 47, 49, 56, 57, 61; F 14.1
Platyophrya paoletti Foissner, 1997 [b]: V 2, 7, 25, 31, 48, 50, 52, 67; F 11.3
Platyophrya similis (Foissner, 1980) Foissner, 1987: V 27; F 1.4
Platyophrya spumacola hexasticha Foissner, Agatha & Berger, 2002: V 20; F 1.4
Platyophrya spumacola spumacola Kahl, 1927: V 11, 27, 47, 48, 50, 52, 56, 60, 61, 62, G 70; F 15.5
Platyophrya vorax Kahl, 1926: V 1, 3, 4, 9, 10, 11, 12, 13, 14, 16, 17, 23, 24, 26, 28, 29, 32, 37, 47, 50, 53, 54, 56, 57, 58, 60, 61, 64, G 68, 69; F 42.3
Platyophryides latus (Kahl, 1930) Foissner, 1987 [e, g]: V 5, 21, 47, 66, 67, G 68; F 8.5
Platyophryides macrostoma n. sp. [c]: G 69, 70; F 2.8
Plesiocaryon elongatum (Schewiakoff, 1892) Foissner, Agatha & Berger, 2002: V 1, 2, 3, 5, 7, 8, 9, 11, 12, 13, 14, 15, 16, 18, 19, 21, 23, 24, 27, 38, 47, 48, 49, 50, 51, 52, 53, 54, 56, 57, 58, 60, 62, 63, 64, G 68, 70, 71; F 53.5
Plesiocaryon terricola Foissner, Agatha & Berger, 2002: V 8, 21, 60, 62, 65; F 7.0
Pleuroplites australis Foissner, 1988: V 2, 4, 8, 11, 23, 25, 28, 47, 52, 56, 58, 60, 63; F 18.3
Pleuroplites cavicola n. sp. [a]: V 57; F 1.4
Podophrya bivacuolata Foissner, 2004: V 1, 23, 56, 62; F 5.6
Podophrya halophila Kahl, 1934: V 54, 65; F 2.8
Podophrya tristriata Foissner, Agatha & Berger, 2002: V 8; F 1.4
Protocyclidium muscicola (Kahl, 1931) Foissner, Agatha & Berger, 2002: V 1, 2, 4, 5, 9, 11, 12, 13, 14, 20, 23, 24, 25, 26, 27, 28, 31, 32, 47, 48, 50, 51, 52, 53, 54, 56, 58, 61, 65, G 68, 69, 70; F 45.1
Protocyclidium terricola (Kahl, 1931) Foissner, Agatha & Berger, 2002: V 1, 11, 12, 17, 25, 29, 30; F 9.9
Protoplagiocampa lajacola n. sp. [a]: V 5, 11, 12, 24, 29, 31, 32; F 9.9
Protospathidium muscicola Dragesco & Dragesco-Kernéis, 1979: V 57; F 1.4
Protospathidium salinarum n. sp. [a]: V 66; F 1.4
Protospathidium serpens (Kahl, 1930) Foissner, 1981: V 1, 15, 16, 24, 26, 52, G 69; F 9.9
Protospathidium terricola Foissner, 1998: V 3; F 1.4
Pseudobirojimia muscorum (Kahl, 1932) Berger & Foissner, 1989: V 11, 13, 50, 53, 54, 56; F 8.5
Pseudocarchesium claudicans (Penard, 1922) Foissner, 1989: V 27, 61; F 2.8
Pseudochilodonopsis mutabilis Foissner, 1981: V 11, 13, 14, 15, 23, 52, 56, 61, 62; F 12.7
Pseudocohnilembus putrinus (Kahl, 1928) Foissner & Wilbert, 1981: V 11, 47; F 2.8
Pseudocyrtolophosis alpestris Foissner, 1980: V 1, 2, 3, 4, 5, 8, 10, 11, 13, 14, 15, 16, 17, 18, 20, 22, 23, 24, 25, 26, 28, 32, 38, 49, 50, 51, 52, 53, 54, 56, 57, 58, 59, 61, 62, 63; F 50.7
Pseudoholophrya minuta Foissner, Agatha & Berger, 2002: V 51; F 1.4
Pseudoholophrya terricola Berger, Foissner & Adam, 1984: V 1, 2, 8, 13, 15, 25, 27, 37, 38, 47, 48, 50, 52, 54, 56, 57, 59, 60, 61, 62, G 71; F 29.6
Pseudokreyella australis Foissner, 1993: V 56; F 1.4
Pseudomicrothorax agilis Mermod, 1914: V 11, 12, 24, 32; F 5.6
Pseudomicrothorax dubius (Maupas, 1883) Penard, 1922: V 56; F 1.4
Pseudomonilicaryon anguillula (Kahl, 1931) Vďačný & Foissner, 2012: V 14; F 1.4
Pseudomonilicaryon angustistoma Foissner, Agatha & Berger, 2002: V 60; F 1.4
Pseudomonilicaryon gracile gracile (Kahl, 1931) Foissner, 1997: V 14, 23, 25, 61; F 5.6
Pseudomonilicaryon gracile antevacuolatum Vďačný & Foissner, 2012: V 32; F 1.4
Pseudomonilicaryon gracile oviplites Vďačný & Foissner, 2012 [b]: V 11; F 1.4
Pseudomonilicaryon japonicum Foissner, Agatha & Berger, 2002 [f]: V 11, 64; F 2.8
Pseudomonilicaryon thonense (Dragesco, 1960) Vďačný & Foissner, 2012 [e]: V 29, 30, 32; F 4.2
Pseudoplatyophrya galapagensis n. sp. [a]: G 68, 69, 71; F 4.2

Pseudoplatyophrya isabelae n. sp. [a]: G 68, 69, 70; F 4.2
Pseudoplatyophrya nana (Kahl, 1926) Foissner, 1980: V 3, 4, 5, 8, 9, 10, 11, 12, 13, 14, 15, 16, 17, 20, 23, 24, 26, 27, 28, 32, 36, 37, 38, 39, 42, 47, 49, 50, 52, 57, 58, 60, 62, 63, 64; F 47.9
Pseudoplatyophrya saltans Foissner, 1988: V 1, 2, 4, 11, 12, 13, 14, 17, 24, 26, 28, 32, 48, 50, 52, 53, 56, 58, 59, 61, 62; F 29.6
Pseudoplatyophrya spinosa n. sp. [d] (t. l. Brazil)
Pseudotelotrochidium epistylis n. sp. [c]: V 1, 13, 25; F 4.2
Pseudouroleptus caudatus caudatus Hemberger, 1985: V 56; F 1.4
Pseudourostyla dimorpha n. sp. [a]: V 24; F 1.4
Pseudourostyla franzi Foissner, 1987: V 4, 50; F 2.8
Pseudovorticella sphagni Foissner & Schiffmann, 1974: V 29, 56, 61, 62; F 5.6
Quadristicha elegans (Foissner, 1999) nov. comb.: V 24, 25; F 2.8
Quadristicha opisthomuscorum (Foissner, Blatterer, Berger & Kohmann, 1991) nov. comb.: V 3, 24, 56, 57, 58, 64; F 8.5
Quadristicha setigera (Stokes, 1891) nov. comb.: V 25, 26, 52, 56; F 5.6
Renoplites venezuelensis n. sp. [a]: V 25; F 1.4
Rigidocortex octonucleatus (Foissner, 1988) Berger, 1999: V 59, 61; F 2.8
Rigidohymena candens (Kahl, 1932) Berger, 2011: V 3, 50, 51, 52, 53, 63, G 71; F 9.9
Rimaleptus alpinus (Kahl, 1931) Vďačný & Foissner, 2012: V 32; F 1.4
Rimaleptus armatus (Foissner & Schade, 2000 in Foissner (2000) Vďačný & Foissner, 2012: V 14, 58; F 2.8
Rimaleptus binucleatus (Kahl, 1931) Foissner, 1984: V 11; F 1.4
Rimaleptus canadensis Vďačný & Foissner, 2012 [h]: V 11; F 1.4
Rimaleptus tirjakovae (Vďačný & Foissner, 2008) Vďačný & Foissner, 2012 [h]: V 23; F 1.4
Rostrophrya namibiensis maldivensis Foissner, Agatha & Berger, 2002: V 54, 65; F 2.8
Rostrophryides africana africana Foissner, 1987: V 15, 23; F 2.8
Rostrophryides africana etoschensis Foissner, Agatha & Berger, 2002: G 68; F 1.4
Rostrophryides australis Blatterer & Foissner, 1988: V 11; F 1.4
Sagittaria hyalina Foissner, Czapik & Wiackowski, 1981 [e]: V 54, 65, 66, G 68; F 5.6
Sagittaria venezuelensis n. sp. [a]: V 65; F 1.4
Sagittarides oblongistoma n. sp. [a]: V 54, 65; F 2.8
Sandmannides venezuelensis n. sp. [a]: V 23; F 1.4
Sathrophilus muscorum (Kahl, 1931) Corliss, 1960: V 2, 3, 11, 12, 13, 14, 15, 18, 20, 23, 24, 25, 27, 32, 48, 50, 52, 53, 56, 58, 59, 60, 61, 64, G 70, 71; F 36.6
Saudithrix terricola Foissner, Al-Rasheid & Berger, 2006 [g, h]: V 56; F 1.4
Semiplatyophrya foissneri Wilbert & Kahan, 1986: V 8; F 1.4
Sikorops namibiensis Foissner, Agatha & Berger, 2002: V 5; F 1.4
Sleighophrys pustulata Foissner, 2005 [b]: V 56; F 1.4
Sorogena stoianovitchae Bradbury & Olive, 1980: V 23, G 69; F 2.8
Spathidium anguilla Vuxanovici, 1962: V 2, 15, 32; F 4.2
Spathidium claviforme Kahl, 1930: V 2, 4, 8, 14, 18, 23, 24, 52, 62, 64, G 70, 71; F 16.9
Spathidium curiosum n. sp. [d] (t. l. Chile)
Spathidium dispar n. sp. [a]: V 57; F 1.4
Spathidium duschli n. sp. [a]: V 13, 14, 24, 25; F 5.6
Spathidium faurefremieti Foissner, 2003: V 56; F 1.4
Spathidium inopinatum n. sp. [a]: V 14, 15; F 2.8
Spathidium multinucleatum Gellért, 1955: V 52, 65, 66; F 4.2
Spathidium muscicola Kahl, 1930: V 61, 64; F 2.8
Spathidium procerum Kahl, 1930: V 1, 12, 30, 36, 54, 58, 59, 61, 62, 65; F 14.1
Spathidium spathula (Müller, 1773) Moody, 1912: V 13, 14, 18, 23, 61; F 7.0
Spathidium stetteri n. sp. [a]: G 70, 71; F 2.8
Spathidium turgitorum Foissner, Agatha & Berger, 2002: V 11; F 1.4
Spetazoon australiense Foissner, 1994 [e, g]: V 56; F 1.4
Sphaerophrya terricola Foissner, 1986: V 47; F 1.4

Stammeridium kahli (Wenzel, 1953) Wenzel, 1969: V 2, 61; F 2.8
Sterkiella cavicola (Kahl, 1935) Foissner, Blatterer, Berger & Kohmann, 1991: V 8, 16, 17, 23, 25, 56, 57, G 71; F 11.3
Sterkiella ecuadoriana n. sp. [d] (t. l. Ecuador)
Sterkiella histriomuscorum (Foissner, Blatterer, Berger & Kohmann, 1991) Foissner, Blatterer, Berger & Kohmann, 1991: V 1, 2, 3, 4, 7, 12, 13, 15, 17, 23, 25, 26, 27, 47, 51, 52, 54, 56, 57, 58, 59, 60, 61, 62, G 68; F 35.2
Stichotricha aculeata Wrześniowski, 1866: V 56; F 1.4
Strombidinopsis minima (Gruber, 1884): V 54; F 1.4
Stylonychia ammermanni Gupta et al., 2001 [e]: V 56; F 1.4
Stylonychia gibbera n. sp. [a]: V 1; F 1.4
Stylonychia notophorides n. sp. [a]: V 24, 26; F 2.8
Suturothrix monoarmata Foissner, 2008 [h]: V 11; F 1.4
Tachysoma humicola humicola Gellért, 1957: V 2, 9, 11, 14, 47, 50, 52, 54, 58, 61, G 68; F 15.5
Tectohymena terricola Foissner, 1993: V 52; F 1.4
Terricirra livida (Berger & Foissner, 1987) Berger & Foissner, 1989: V 48; F 1.4
Terricirra matsusakai Berger & Foissner, 1989: V 8, 50; F 2.8
Terricirra viridis (Foissner, 1982) Berger & Foissner, 1989: V 56; F 1.4
Tetmemena pustulata (Mueller, 1786) Eigner, 1999 [e]: V 56, 63; F 2.8
Tetrahymena rostrata (Kahl, 1926) Corliss, 1952 [e, g]: V 13, 15, 16, 23, 25, 50, 52, 56, 61, 67; F 14.1
Tillina magna Gruber, 1879: V 54, 56, 65; F 4.2
Tillina minima Alekperov, 1985: V 24, 25, 56, G 68; F 5.6
Totothrix panamensis n. sp. [d] (t. l. Panama)
Trachelophyllides sigmoides (Kahl, 1926) nov. comb. [g]
Trachelophyllum africanum Foissner, Agatha & Berger, 2002: V 2, 51, 52; F 4.2
Trachelophyllum apiculatum (Perty, 1852) Claparède & Lachmann, 1859 [e]: V 17, 50, 54, 64, 65; F 7.0
Trachelophyllum costaricanum Foissner, Agatha & Berger, 2002: V 25; F 1.4
Trachelophyllum tachyblastum Stokes, 1884 [g]: V 52; F 1.4
Trihymena terricola Foissner, 1988: V 2, 8, 50, 52, 57, 61, 62; F 9.9
Uroleptoides magnigranulosus (Foissner, 1988) Berger, 2008: V 14, 15; F 2.8
Uroleptoides multinucleatus (Foissner, Agatha & Berger, 2002) Berger, 2008 [e]: V 9, 11, 12, 20; F 5.6
Uroleptoides polycirratus (Berger & Foissner, 1989) Berger, 2008 [g]: V 20, 23, 25; F 4.2
Uroleptus lepisma (Wenzel, 1953) Foissner, 1998: V 25, 56; F 2.8
Uroleptus notabilis (Foissner, 1982) Foissner, 1998: V 25; F 1.4
Uroleptus paranotabilis Foissner, Agatha & Berger, 2002: V 23; F 1.4
Urosoma acuminata (Stokes, 1887) Buetschli, 1889: V 56; F 1.4
Urosoma caudata (Ehrenberg, 1833) Berger, 1999: V 29; F 1.4
Urosoma gigantea (Horváth, 1933) Berger, 1999: G 68; F 1.4
Urosoma karinae Foissner, 1987: V 67; F 1.4
Urosoma macrostyla (Wrześniowski, 1866) Kahl, 1932: V 56; F 1.4
Urosomoida agiliformis Foissner, 1982: V 1, 2, 7, 8, 11, 14, 23, 25, 38, 47, 50, 51, 52, 54, 57, 58, 59, 61, G 71; F 26.8
Urosomoida galapagensis n. sp. [a]: G 68; F 1.4
Urosomoida halophila n. sp. [a]: V 65; F 1.4
Vorticella aqua-dulcis-complex: V 65, 66; F 2.8
Vorticella astyliformis Foissner, 1981: V 2, 4, 8, 11, 15, 20, 21, 23, 25, 29, 32, 47, 48, 50, 52, 53, 54, 56, 58, 59, 60, 61, 62, 63, G 68, 70; F 36.6
Vorticella infusionum Dujardin, 1841: V 15, 57, 66; F 4.2
Woodruffia australis Foissner, 1993: V 54, 65, 66, G 68; F 5.6
Woodruffia rostrata Kahl, 1931 [e]: V 65, G 68; F 2.8
Woodruffides metabolicus (Johnson & Larson, 1938) Foissner, 1987 [g]: V 23, 52, 54 62, 64; F 7.0
Woodruffides terricola Foissner, 1987: V 8, 11, 21, 47; F 5.6

Table 1. Main features of the ciliate fauna in the 71 samples investigated. Samples 1–67 Venezuela, 68–71 Galápagos, 33, 34, 35, 40 (from FOISSNER 2000a).

Samples (sites)	**1**	**2**	**3**	**4**	**5**	**6**	**7**	**8**	**9**	**10**	**11**	**12**	**13**	**14**	**15**	**16**
Number of taxa identified	45	50	42	32	21	1	4	48	16	12	66	33	52	59	50	35
Number of new taxa	4	0	2	1	3	0	1	2	0	0	3	1	2	4	1	0
Number of unidentified taxa	9	4	2	0	1	0	0	0	0	0	4	1	3	3	9	2
Number of unidentified, likely undescribed taxa	5	1	2	0	0	0	0	0	0	0	1	0	0	0	2	0
Total number of taxa	54	54	44	32	22	1	4	48	16	12	70	34	55	62	59	37

continued

Samples (sites)	**17**	**18**	**19**	**20**	**21**	**22**	**23**	**24**	**25**	**26**	**27**	**28**	**29**	**30**	**31**	**32**	**33**	**34**
Number of taxa identified	27	30	2	30	16	2	75	53	73	34	36	25	22	9	14	47	6	16
Number of new taxa	0	0	0	1	2	0	3	7	6	0	0	1	2	1	4	2	0	3
Number of unidentified taxa	0	0	0	0	0	0	8	2	5	0	1	0	1	0	1	6	0	1
Number of unidentified, likely undescribed taxa	0	0	0	0	0	0	5	0	2	0	0	0	1	0	0	3	0	1
Total number of taxa	27	30	2	30	16	2	83	55	78	34	37	25	23	9	15	53	6	17

continued

Samples (sites)	**35**	**36**	**37**	**38**	**39**	**40**	**41**	**42**	**43**	**44**	**45**	**46**	**47**	**48**	**49**	**50**	**51**	**52**	**53**
Number of taxa identified	1	7	6	16	1	0	2	4	0	2	1	0	44	35	18	64	20	90	38
Number of new taxa	0	0	0	2	0	0	0	0	0	0	0	0	4	0	1	0	0	2	0
Number of unidentified taxa	0	0	0	1	0	0	0	0	0	0	0	0	2	0	0	8	1	11	1
Number of unidentified, likely undescribed taxa	0	0	0	0	0	0	0	0	0	0	0	0	0	0	0	3	0	3	0
Total number of taxa	1	7	6	17	1	0	2	4	0	2	1	0	46	35	18	72	21	101	39

continued

Samples (sites)	**54**	**55**	**56**	**57**	**58**	**59**	**60**	**61**	**62**	**63**	**64**	**65**	**66**	**67**	**68**	**69**	**70**	**71**
Number of taxa identified	67	0	113	33	46	47	34	78	50	25	27	31	13	9	35	13	24	30
Number of new taxa	10	0	9	4	0	3	0	8	1	0	0	6	3	1	7	1	3	4
Number of unidentified taxa	11	0	13	6	0	3	0	13	1	0	0	5	0	0	7	0	1	6
Number of unidentified, likely undescribed taxa	4	0	8	3	0	1	0	7	1	0	0	4	0	0	3	0	0	2
Total number of taxa	78	0	126	39	46	50	34	91	51	25	27	36	13	9	42	13	25	36

3.1.2 Species Numbers and Local Centres of Ciliate Diversity

3.1.2.1 Large scale comparison

FOISSNER (1998) listed 643 soil ciliate species. To this must be added 143 new species from Namibia (FOISSNER et al. 2002) and 120 new species from the present study, resulting in about 900 species. This roughly doubles the number of species recorded in the present study (459), indicating a rather high percentage of species distributed over more than one main biogeographic region.

Table 2. Species recorded in 10 Laja (lithotelma) samples (no. 4, 5, 11, 12, 17, 21, 29, 30, 31, 32). Thirteen of the 118 species found were undescribed and have their type locality in these Lajas, 20 when those (n. sp.) are added which occur in the Lajas but have their type locality elsewhere in Venezuela.

Species	Species
***Apertospathula lajacola* n. sp.**	***Metathrix ellipsoidea ellipsoidea* n. ssp.**
***Apocoriplites lajacola* n. sp.**	*Metopus hasei*
Apospathidium atypicum	*Metopus setosus*
Arcuospathidium namibiense tristicha	*Microdiaphanosoma arcuatum*
***Armatospathula plurinucleata* n. sp.**	*Microdiaphanosoma terricola*
Australocirrus oscitans	*Mykophagophrys terricola*
Australothrix alwinae	*Nivaliella plana*
***Australothrix venezuelensis* n. sp.**	***Paracolpoda lajacola* n. sp.**
Brachyosoma brachypoda mucosa	*Paracolpoda steinii*
Bryometopus pseudochilodon	***Paracondylostoma clavistoma oligostriatum* n. ssp.**
Bryometopus sphagni	*Paraenchelys terricola*
Bursaria truncatella	*Paragastrostyla terricola*
***Cephalospatula brasiliensis* (n. sp.)**	***Phialinides bicaryomorphus* n. sp.**
Colpoda cucullus	*Plagiocampa ovata*
Colpoda inflata	*Plagiocampa rouxi*
Colpoda lucida	***Platynematum terricola* (n. sp.)**
Colpoda maupasi	***Platyophrya paoletti* (n. sp.)**
Colpoda orientalis	*Platyophrya spumacola spumacola*
Colpoda praestans	*Platyophrya vorax*
Colpodidium caudatum	*Platyophryides latus*
Coriplites terricola	*Plesiocaryon elongatum*
Cultellothrix atypica	*Plesiocaryon terricola*
Cyrtolophosis mucicola	*Pleuroplites australis*
Dimacrocaryon amphileptoides	*Protocyclidium muscicola*
Dimacrocaryon amphileptoides paucivacuolatum	*Protocyclidium terricola*
Diplites telmatobius	***Protoplagiocampa lajacola* n. sp.**
Drepanomonas exigua bidentata	*Pseudobirojimia muscorum*
Drepanomonas obtusa	*Pseudochilodonopsis mutabilis*
Drepanomonas pauciciliata	*Pseudocohnilembus putrinus*
Drepanomonas sphagni	*Pseudocyrtolophosis alpestris*
Emarginatophrya aspera	*Pseudomicrothorax agilis*
Enchelyodon lagenula	*Pseudomonilicaryon gracile antevacuolatum*
Enchelys lajacola n. sp.	***Pseudomonilicaryon gracile oviplites* n. ssp.**
Enchelys polynucleata	*Pseudomonilicaryon japonicum*
Epispathidium ascendens	*Pseudomonilicaryon thonense*
Erimophrya monostyla	*Pseudoplatyophrya nana*
Fragmospina depressa	*Pseudoplatyophrya saltans*
Frontonia angusta solea	*Pseudourostyla franzi*
Frontonia depressa	*Pseudovorticella sphagni*
Furgasonia theresae	*Rimaleptus alpinus*
***Gonostomoides galapagensis* (n. sp.)**	*Rimaleptus binucleatus*
Gonostomum affine	*Rimaleptus canadensis*
***Gonostomum lajacola* n. sp.**	*Rostrophryides australis*
Grossglockneria acuta	*Sathrophilus muscorum*
Grossglockneria hyalina	*Sikorops namibiensis*

continued

Species	Species
***Grossglockneria lajacola* n. sp.**	*Spathidium anguilla*
Halteria grandinella	*Spathidium claviforme*
Hausmanniella discoidea	*Spathidium procerum*
Hemisincirra gellerti verrucosa	*Spathidium turgitorum*
Hemisincirra inquieta	*Sterkiella cavicola*
Heterourosomoida lanceolata	*Sterkiella histriomuscorum*
Kamburophrys gibba	***Suturothrix monoarmata* (n. sp.)**
Lamtostyla granulifera	*Tachysoma humicola humicola*
Lamtostylides kirkeniensis	*Trachelophyllum apiculatum*
Leptopharynx costatus	*Uroleptoides multinucleatus*
***Leptopharynx lajacola* n. sp.**	*Urosoma caudata*
Maryna lichenicola	*Urosomoida agiliformis*
***Maryna meridiana* (n. sp.)**	*Vorticella astyliformis*
Meseres corlissi	*Woodruffides terricola*

We can only speculate how many soil ciliate species might be present in Venezuelan soils because we investigated only the western half of the country and most rainforest samples perished before they could be investigated. The eastern half of the country, which contains so interesting habitats as the Tepuis (high outcroppings with many endemic plants and animals) and the Orinoco estuary, were not investigated. When considered only the western half of the country, we would expect to double the number recorded, i. e., about 1000 species.

As already mentioned by Foissner et al. (2002), the high number of species found in the Namibian study makes a comparison with literature data difficult. This is corroborated by the Venezuelan results. Both studies support the conclusion of Foissner et al. (2002) that terrestrial and limnetic habitats carry a similar number of species and the estimation of only 3,000 free-living ciliate species by Finlay & Esteban (1998) is a great flaw; 30.000 are more likely (Agatha & Foissner 2000).

3.1.2.2 Local centres of ciliate diversity

There is an average of 34 species/sample when the rotten rainforest samples (19, 22, 35, 46, 53) are excluded. This matches the 28 species/sample in the Namibian study by Foissner et al. (2002). The small difference is at least partially caused by the increased knowledge of the investigator. Generally, the number of species varies highly in the individual samples, viz., from 0–126 which is not surprising considering the variety of biota investigated. The richest sample (126 species) is close to the 141 species present at the richest Namibian site (Foissner et al. 2002).

Taking into account total species number and the proportion of undescribed species, seven local ciliate diversity centres can be selected within the region investigated. Fortunately, most are in protected areas. The richest site (126 species, 9 undescribed) is number (56), i. e., mud and soil from some flat, ephemeral puddles in the Morrocoy National Park (Table 1). This diversity matches the Namibian data mentioned above and the 150 species recorded between 1982 and 2012 in an ephemeral pond in Austria (Cotterill et al. 2013).

Site (52) follows, viz., a gallery forest in the Henri Pittier National Park, where 101 species were recorded of which two (very likely five) were undescribed (Table 1). Gallery (~ floodplain) forest

Table 3. Species recorded in four samples from Galápagos. New taxa bolded.

Species	Species
Blepharisma bimicronucleatum	*Metopus palaeformis*
Blepharisma hyalinum	*Microdiaphanosoma arcuatum*
***Cinetochilides terricola* n. sp.**	*Monomacrocaryon terrenum*
Emarginatophrya aspera	***Notohymena quadrinucleata* n. sp.**
Colpoda cucullus	*Parabistichella variabilis*
Colpoda edaphoni	*Paracolpoda steinii*
***Colpoda ephemera* n. sp.**	*Paragonostomum caudatum*
Colpoda inflata	*Platyophrya spumacola spumacola*
Colpoda maupasi	*Platyophrya vorax*
Colpodidium caudatum	*Platyophryides latus*
Cyrtohymena quadrinucleata	***Platyophryides macrostoma* n. sp.**
Cyrtolophosis mucicola	*Plesiocaryon elongatum*
Drepanomonas minuta	*Protocyclidium muscicola*
***Enchelys lajacola* n. sp.**	*Protospathidium serpens*
Enchelys gasterosteus	*Pseudoholophrya terricola*
Enchelys geleii	***Pseudoplatyophrya galapagensis* n. sp.**
Epispathidium amphoriforme	***Pseudoplatyophrya isabelae* n. sp.**
Epispathidium ascendens	*Rigidohymena candens*
Exocolpoda augustini	*Rostrophryides africana etoschensis*
Fuscheria lacustris	*Sagittaria hyalina*
Fuscheria nodosa	*Sathrophilus muscorum*
***Gonostomoides fraterculus* n. sp.**	*Sorogena stoianovitchae*
***Gonostomoides galapagensis* n. sp**.	*Spathidium claviforme*
Gonostomum affine	***Spathidium stetteri* n. sp.**
Gonostomum namibiense	*Sterkiella cavicola*
Halteria grandinella	*Sterkiella histriomuscorum*
Hausmanniella patella	*Tachysoma humicola humicola*
***Hemioxytricha isabelae* n. sp.**	*Tillina minima*
Hemisincirra inquieta	*Urosoma gigantea*
Homalogastra setosa	*Urosomoida agiliformis*
Lamtostyla australis	***Urosomoida galapagensis* n. sp.**
***Lingulothrix galapagensis* n. sp.**	*Vorticella astyliformis*
Maryna ovata	*Woodruffia australis*
Metopus hasei	*Woodruffia rostrata*

soils have a high ciliate diversity globally (see Table 8 in Foissner et al. 2002 and Table 2 in Foissner et al. 2008b). This is corroborated by Foissner et al. (2005a): of 13 sites investigated in eastern Austria, the highest number of species (120) occurred in a *Pruno-Fraxinetum* floodplain.

The third rank takes site (61), i. e., rainforest soil from the surroundings of Rancho Grande in the Henri Pittier National Park (Table 1). We recorded 91 species of which eight were undescribed. This matches a sample from the Amazon rainforest, where 88 species occurred of which 13 were undescribed (Foissner 1997). These examples show – not unexpected – a high litter and soil ciliate diversity in rainforests when the samples are investigated on site or are air-dried and then investigated with the non-flooded Petri dish method within a few months (Foissner 2011).

The next richest sample is the Mahadja from site (23). We recorded 83 ciliate species three of which were undescribed (Table 1). As explained in the site description chapter, Mahadjas are

fertile, artificial savanna soils. Usually, they contain a significantly higher number of species than the neighbouring natural soil, except of Mahadja 1 (55 vs. 62 species): Mahadja 2: 59 vs. 37; Mahadja 3: 83 vs. 55; Mahadja 4: 78 vs. 34; Mahadja 5: 37 vs. 25; and Mahadja 6: 48 vs. 12 (Table 1). This is in accordance with many literature data (for reviews, see Foissner 1987b, 1999d). Obviously, fertilization increases the abundance of the "rare biopshere" so that detectable numbers develop (Weisse 2014).

Site (54) follows, i. e., mud and soil from a highly saline, ephemeral coastal puddle in the Morrocoy National Park. We recorded 78 species of which 10 were undescribed (Table 1). Saline coastal and inland puddles are poorly studied with respect to ciliates. Thus, the high number of new species is not surprising. The same can be observed in the saline Etosha Pan in Namibia (Foissner et al. 2002).

A total of 118 species occurred in the 10 Laja (Lithotelma) samples (Table 2). This matches numbers reported from ephemeral waters in Europe (for a review, see Cotterill et al. 2013). The richest Lajas were site 11 (70 species) and site 32 (53 species), both colonized by Velloziaceae (endemic Liliidae) which favour soil genesis. All other Lajas contained less than 50 species, as common in similar habitats in Europe (Cotterill et al. 2013, Dingfelder 1962). It is remarkable that nassulid ciliates, which like to feed on filamentous bluegreen bacteria and are thus divers and frequent in European ephemeral waters, are nearly absent from the Lajas – except of the cosmopolitans *Pseudomicrothorax agilis* and *Furgasonia theresae* – though a lot of bluegreens occurs there (Fig. 7a–e).

In the four small Galápagos samples 68 species were recorded, at least 13 were undescribed (Table 3). Most productive was sample (68), i. e., highly saline soil from a Mangrove forest. It contained 42 species of which seven, possibly even 10 were undescribed (Table 1). Considering the weakness of the samples, the 13 new species indicate a high number of undescribed ciliates in Galápagos soils, and rather many might be endemic.

3.1.3 Frequencies and Characteristic Species Communities

252 of the 421 ciliate species identified occur at only one or two sites, showing (i) a very patchy distribution of most species and (ii) a high proportion of possibly rare species. No species occurred in all samples, and the euryoecious *Colpoda inflata* was most frequent, occurring in 73.2% of the samples (see species list; Fig. 10). Compared to the Namibian soil ciliate community (Foissner et al. 2002), the single records are slightly higher (120 vs. 177), possibly mainly due to the increased ability of the investigator in identifying very rare or "difficult" species. However, the frequencies of the Namibian and Venezuelan soil ciliate communities are very similar to ordinary protist communities (Fenchel 1987, Foissner 2008a) and to those of plants and animals (Schwerdtfeger 1975).

Only 14 species (11 in Namibia) have frequencies ≥ 40%, viz., *Platyophrya vorax, Nivaliella plana, Protocyclidium muscicola, Pseudoplatyophrya nana, Drepanomonas pauciciliata, Leptopharynx costatus, Pseudocyrtolophosis alpestris, Cyrtolophosis mucicola, Plesiocaryon elongatum, Gonostomum affine, Colpoda maupasi, Paracolpoda steinii, Colpoda cucullus,* and *Colpoda inflata*. Most of these species are frequent in soils globally (Table 4) and feed on bacteria,

except for the obligate fungivorous *N. plana* and *P. nana*; further, most belong to the r-selected, fast-growing colpodids adapted to utilize short, wet periods in the region and habitats investigated (Foissner 1987b). *Pseudoplatyophrya nana*, a minute (25 µm) fungi and yeast feeder, is common in soils globally while the high frequency of *N. plana* is shared only with Namibia, a dry region which has almost the same C/P quotients as the region investigated (0.6 vs. 0.7) and for the most frequent species (8.0 vs. 10.0; Table 4). This shows that we investigated mainly rather extreme habitats (Foissner et al. 2002, Lüftenegger et al. 1985).

Interestingly, all Venezuelan species with a frequency of ≥ 40% dominate also in other regions of the world, suggesting that the list in Table 4 is complete or nearly complete, altogether 46 species. However, great differences occur, e. g., *Exocolpoda augustini* in Namibia and *Leptopharynx costatus* and *Plesiocaryon elongatum* in Venezuela. They are highly frequent at only one or two sites. And only two colpodids occur with high frequency in all communities, viz., *Colpoda inflata* and *Paracolpoda steinii* (Table 4); five further species occur in seven out of the eight communities investigated (Table 4): *Colpoda maupasi* (colpodids), *Protocyclidium muscicola* (hymenostomatids), *Epispathidium terricola* (haptorids, one of the few predators in Table 4), *Pseudocyrtolophosis alpestris* (colpodids), and *Pseudoplatyophrya nana* (a funigvorous colpodid). This distribution pattern shows that even euryoecious, cosmopolitan species are **not** "globally ubiquitous" as suggested by Finlay et al. (1999).

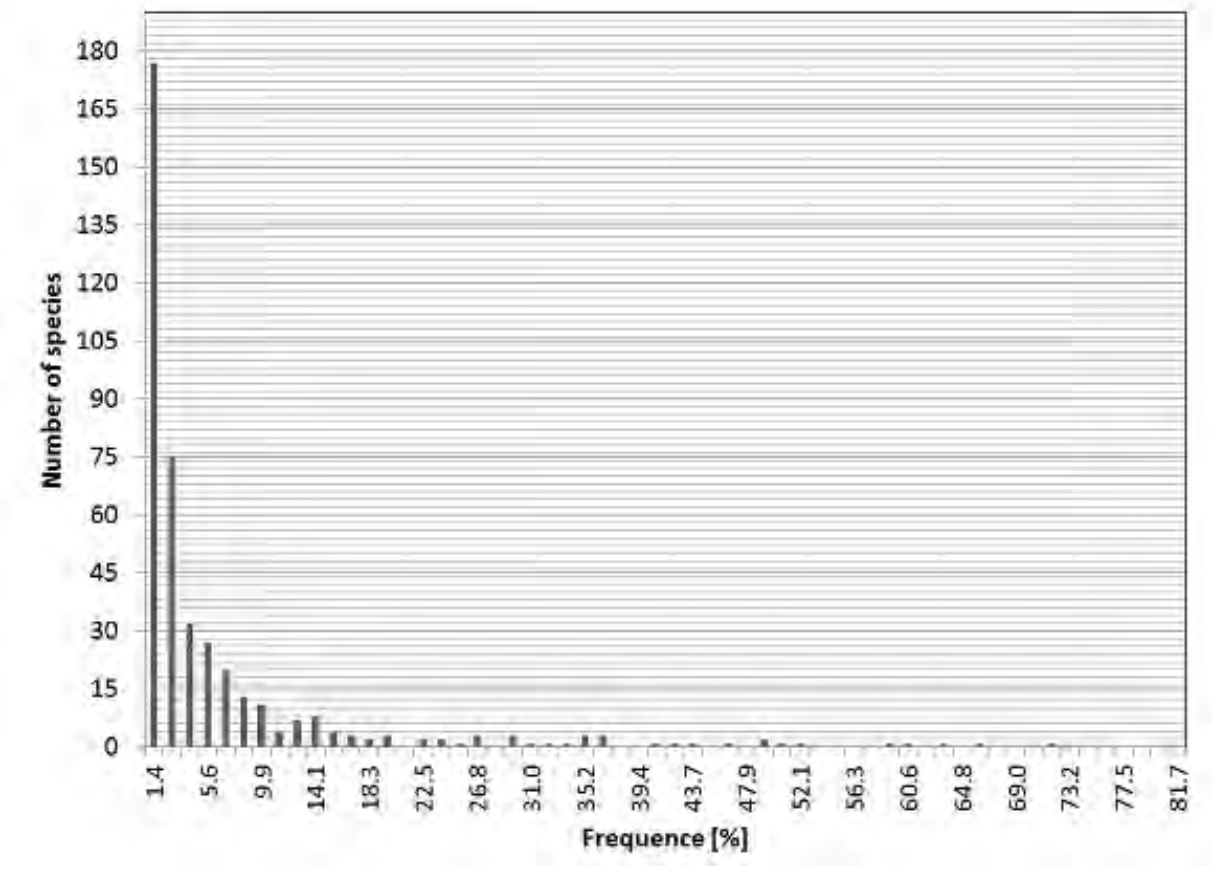

Fig. 10. Frequencies of 421 ciliate species in 71 samples from terrestrial habitats of Venezuela and Galápagos.

Table 4. Comparison of frequent (usually occurring in ≥ 40% of samples) soil ciliate species worldwide. + = present, – = absent.

Species [a]	**Namibia** [b]	**Kenya** [c]	**Australia** [d]	**Antarctica** [e]	**Germany** [f]	**Austria** [g] **Tullnerfeld**	**Austria** [h] **alpine habitats**	**South America** [i]
Anteholosticha sigmoidea	-	-	-	+	-	-	-	-
Blepharisma hyalinum	-	+	+	-	+	-	-	-
Bryometopus pseudochilodon	-	-	+	-	-	-	-	-
Caudiholosticha gracilis	-	-	-	-	-	+	-	-
Colpoda cucullus	+	+	+	-	+	+	-	+
Colpoda ecaudata	-	-	-	+	-	-	-	-
Colpoda henneguyi	-	+	+	-	-	-	-	-
Colpoda inflata	+	+	+	+	+	+	+	+
Colpoda lucida	-	-	+	-	-	-	-	-
Colpoda maupasi	+	+	+	-	+	+	-	+
Cyclidium glaucoma	-	-	-	+	-	-	-	-
Cyrtolophosis mucicola	-	+	+	+	+	-	-	+
Drepanomonas pauciciliata	-	+	+	-	-	-	-	+
Drepanomonas revoluta	-	+	-	-	+	-	-	-
Emarginatophrya aspera	-	-	-	-	-	+	+	-
Epispathidium terricola	-	+	+	+	+	+	+	-
Euplotopsis muscicola	-	-	-	-	+	-	-	-
Exocolpoda augustini	+	-	-	-	-	-	-	-
Gonostomum affine	+	-	+	-	+	+	-	+
Hemisincirra gellerti	-	-	-	-	-	+	-	-
Hemisincirra inquieta	-	-	-	-	+	-	-	-
Homalogaster setosa	+	-	+	-	+	-	-	-
Leptopharynx costatus	-	+	-	-	-	-	-	+
Microdiaphanosoma arcuatum	-	-	-	+	-	-	-	-
Mykophagophrys terricola	-	-	+	-	-	-	-	-
Nivaliella plana	+	-	-	-	-	-	-	+
Paracolpoda steinii	+	+	+	+	+	+	+	+
Paraenchelys terricola	-	+	-	-	-	-	-	-
Platyophrya macrostoma	-	-	-	-	-	+	+	-
Platyophrya vorax	-	-	+	+	+	-	+	+
Plesiocaryon elongatum	+	-	-	-	-	+	-	+
Pleuroplitoides smithi	-	-	-	+	-	-	-	-
Protocyclidium muscicola	-	+	+	+	+	-	+	+

continued

Species [a]	Namibia [b]	Kenya [c]	Australia [d]	Antarctica [e]	Germany [f]	Austria [g] Tullnerfeld	Austria [h] alpine habitats	South America [i]
Pseudochilodonopsis mutabilis	-	-	-	-	-	+	-	-
Pseudocyrtolophosis alpestris	-	+	+	+	+	-	+	+
Pseudoholophrya terricola	-	+	-	-	-	-	-	-
Pseudoplatyophrya nana	+	-	+	+	+	+	-	+
Quadristicha opisthomuscorum	-	-	-	+	-	-	-	-
Quadristicha setigera	-	+	-	-	+	+	-	-
Rimaleptus alpinus	-	-	+	-	-	-	-	-
Sathrophilus muscorum	-	+	+	-	+	+	-	-
Sterkiella histriomuscorum	-	-	+	-	+	-	-	-
Tetrahymena rostrata	-	-	+	-	+	-	-	-
Urosomoida agiliformis	-	+	-	-	-	-	-	-
Urosomoida agilis	-	-	-	-	-	+	-	-
Vorticella astyliformis	+	+	+	+	-	+	-	-
C/P quotient [j]	8.0	2.3	4.0	4.0	1.3	1.6	6.0	10.0

[a] Nomenclature adapted to FOISSNER (1998), BERGER (1999, 2006, 2008, 2011), and VĎAČNÝ & FOISSNER (2012), who also provide authorship and date for species. All data based on non-flooded Petri dish cultures.

[b] From FOISSNER et al. (2002). Species with ≥ 48% frequency are included.

[c] From FOISSNER (1999b). Nine samples containing 125 taxa from the Shimba Hills near Mombasa. Species with ≥ 55% frequency are included.

[d] From BLATTERER & FOISSNER (1988). Twenty-one samples containing 139 taxa were investigated. Species with ≥ 50% frequency are included.

[e] From FOISSNER (1996a). Fifty-nine samples containing 64 taxa were investigated. Many samples contained no or few species causing very low frequency values. Thus, species with a frequency of ≥ 5.1% are included.

[f] From FOISSNER (2000a). Twenty samples and sample groups containing 270 species were investigated. Species with ≥ 50% frequency are included.

[g] From FOISSNER et al. (1985b). Seven sites, each investigated ten times during a period of 27 months, containing 132 taxa. Species with a frequency of ≥ 50% are included.

[h] From FOISSNER (1981b). Fifteen sites, some investigated several times, containing 81 taxa. Species with ≥ 50% frequency are included.

[i] Present study, i. e., 67 samples from Venezuela and 4 samples from Galápagos. Species with ≥ 40% frequency are included.

[j] Quotient of Colpodea and Polyhymenophora (heterotrichs, oligotrichs, hypotrichs), as described by LÜFTENEGGER et al. (1985). The higher the value, the extremer the habitat.

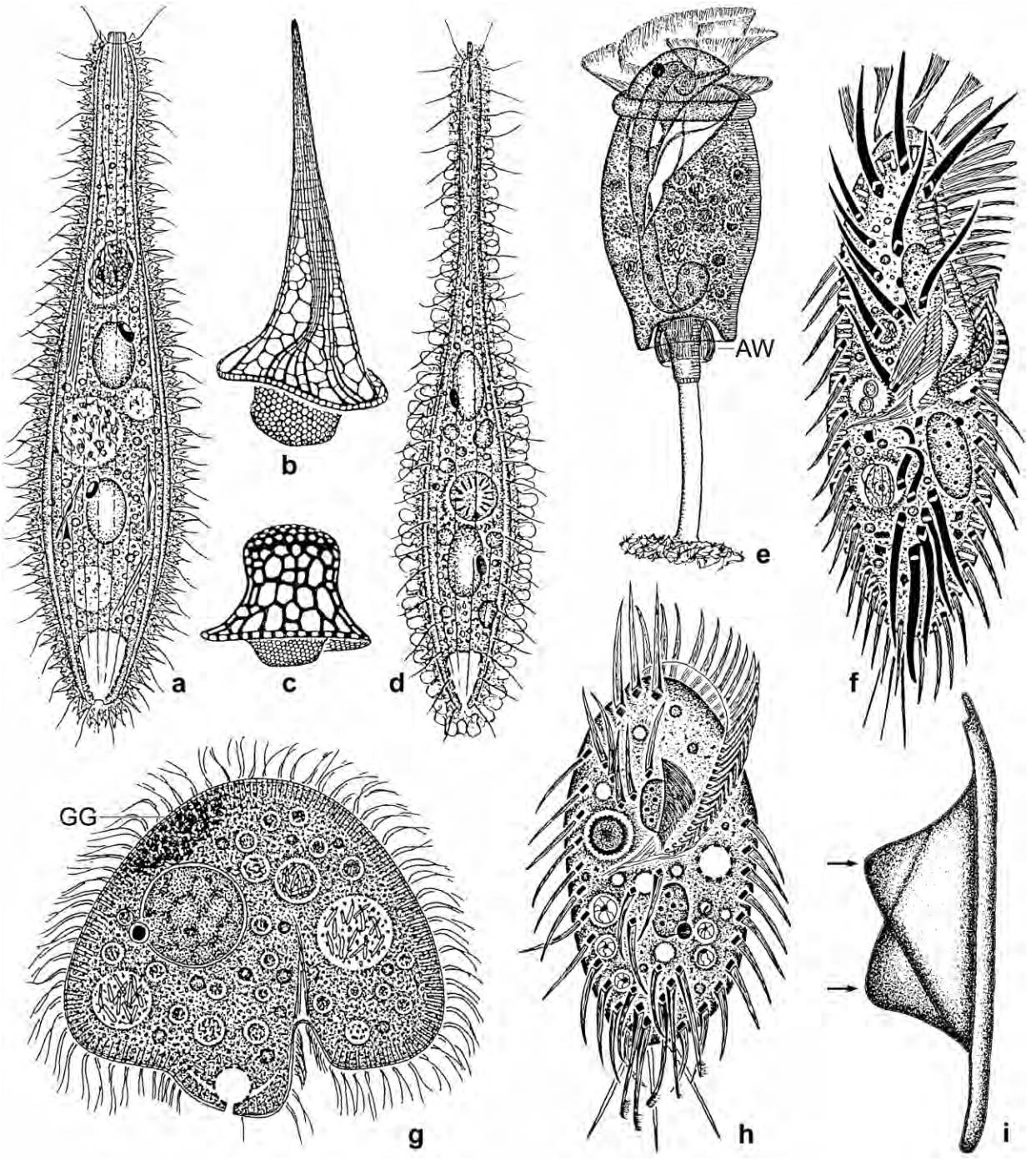

Fig. 11a–i. Supposed endemic Gondwanan "flagships" in Venezuelan soil and mud samples. **a–d:** *Luporinophrys micelae* and *Sleighophrys pustulata*, both described by FOISSNER (2005), are about 200 µm long and have unique epicortical scales (b, c) called lepidosomes. **e:** → *Pseudotelotrochidium epistylis* is about 85 µm long (without the short stalk) and has a permanent aboral ciliary wreath (AW). **f:** → *Gonostomum bromelicola* is about 100 µm long and lives in tank bromeliads. Uniquely, dorsal kinety 2 is interrupted. **g:** → *Maryna meridiana* is about 80 µm high and occurs in the Neotropis, in Africa, and in Australia. The European *M. umbrellata* has a size of about 130 µm and has 83 (vs. 46) ciliary rows. **h, i:** → *Stylonychia gibbera* is about 100 µm long and has two conspicuous humps, unique within the genus, on the dorsal side. GG – glass granules.

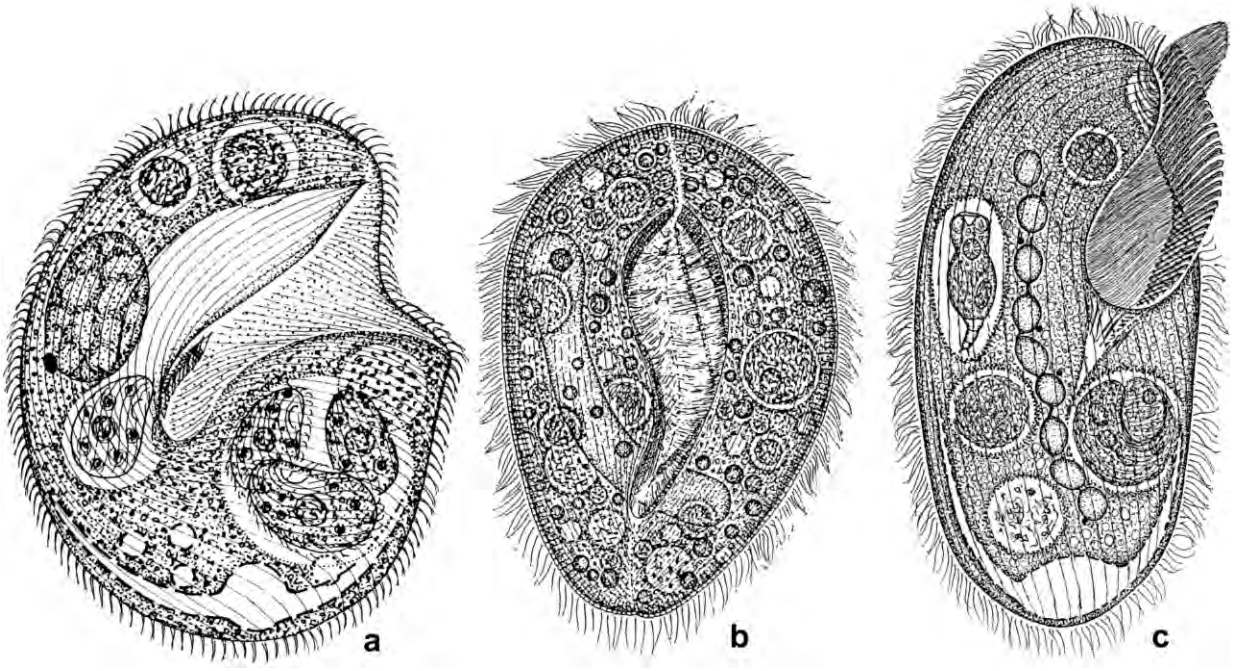

Fig. 12a– c. Supposed endemic Gondwanan "flagships" in Venezuelan soil and mud samples. **a:** → *Krassniggia auxiliaris* Foissner, 1987a is about 200 µm long and occurs in the Neotropis, in Africa, and in Australia. It has a unique oral apparatus. **b:** *Apofrontonia lametschwandtneri* Foissner & Song, 2002 has a length of about 180 µm. It differs from the German and Mediterraneum congeners by the huge body size, the number of ciliary rows, and by details of the oral apparatus. **c:** → *Condylostomides coeruleus* is about 235 µm long and has blueish cortical granules and the macronuclear nodules do not fuse in the resting cyst. The African *C. etoschensis* has citrine cortical granules and the macronuclear nodules fuse in the resting cyst (Foissner et al. 2002).

3.1.4 Not Everything is Everywhere

The distribution problem of microscopic organisms has been controversely discussed (Finlay et al. 2001, Foissner et al. 2002). Fortunately, two recent compilations of papers from a variety of microscopic organisms cleared the matter at least partially, showing endemic species embedded in a mass of cosmopolites (Foissner 2008a, Fontaneto 2011). This supports the "moderate endemicity model", i. e., that about one third of protists have restricted distribution while most are cosmopolites (Foissner 1999c, 2006, 2011).

Based on our investigations on Namibian and Venezuelan soil ciliates, as well as on global soil ciliate diversity (Chao et al. 2006), we summarize the main issues for a restricted distribution of part of the soil ciliates as follows:

(i) The main problem is undersampling, i. e., that it is practically impossible to get a complete species inventory from a certain site or from a certain region because many species are in cystic state when the investigation takes place. Further, the man power necessary is usually not available. Thus, a surrogate must be used, i. e., so-called flagship species which are so distinct that they cannot be overlooked or misidentified (see next item).

(ii) In Figures 11 and 12, we put together some putative flagship species from the Neotropis. The most impressive examples are *Condylostomides etoschensis* and → *C. coeruleus*. The first is common in the Etosha Pan of Namibia, the second occurs in Central and South

America. Both are easily distinguished by the colour of the cortical granules (citrine vs. blueish like in *Stentor coeruleus*) and the resting cyst (macronuclear nodules fused vs. not fused). In our opinion, it is highly unlikely that, if both occur globally, we found them either only in Africa or in the Neotropis.

(iii) The similarity of global ciliate communities is rather low, viz. 30% to 40 % (Table 5) and separates the Neotropis clearly from the Holarctic, Palaeotropis and Australis (Fig. 13).

(iv) Often, the wide or cosmopolitan distribution of protists is assumed to be associated with their small size and high numbers. However, this is disproved by macrofungi, mosses and ferns, many of which have small areals in spite of appropriate habitats globally and minute (< 50 µm) spores produced in high numbers (Foissner 2006, 2008a).

(v) The common Gondwanan endemic, *Hemimastix amphikineta*, a peculiar flagellate, occurs in Venezuelan samples (11, 14), i.e., in a lithotelma (Laja) and a savanna.

Table 5. Classic Jaccard similarty index for an updated world list of soil ciliates (from Chao et al. 2006).

Region	Holarctic	Paleotropis	Australis	Neotropis
Holarctic	1			
Paleotropis	0.36	1		
Australis	0.34	0.41	1	
Neotropis	0.32	0.36	0.39	1

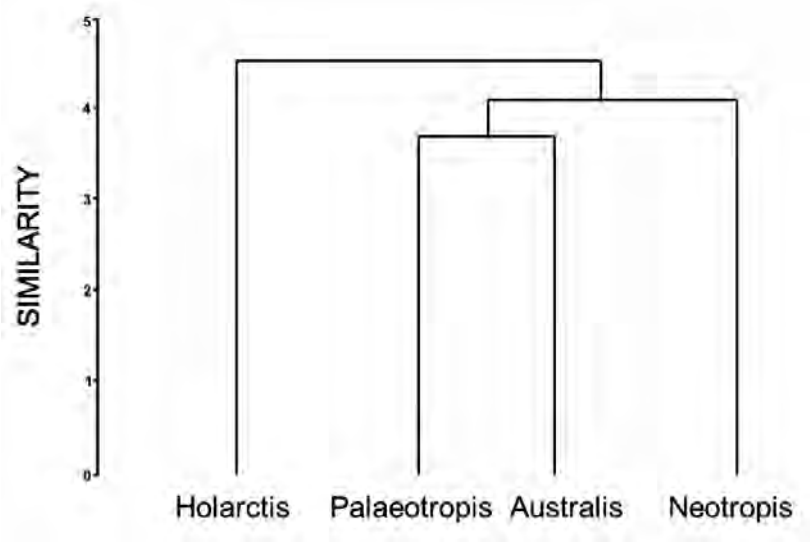

Fig. 13. Cluster analysis for the data shown in Table 5 (from Chao et al. 2006). Over 900 ciliate species were recorded in about 1000 soil samples taken globally. They make a "meaningful" grouping, that is, Gondwanan and Laurasian sites are clearly distant from the Holarctic sites, showing that not everything is everywhere, i. e., soil ciliates have a biogeography.

3.2 Description of Insufficiently Known and New Species

3.2.1 Summary of New Taxa Described in this Monograph and of Nomenclatural Acts

New suborder: Woodruffiina (p. 361).

New families: Apometopidae (p. 868), Deviatidae (p. 566), Lingulotrichidae (p. 105), Urosomoididae (p. 775).

New genera (dp = described previously with type locality in Venezuela): *Allotrichides* (p. 770), *Apoavestina* (p. 289), *Apofrontonia* (dp), *Apogonostomum* (p. 611), *Aponotohymena* (p. 769), *Apowoodruffia* (p. 369), *Armatospathula* (dp), *Cataphractes* (p. 118), *Cintetochilides* (p. 429), *Columnospatha* (p. 187), *Emarginatophrya* (p. 286), *Enchelariophrya* (p. 230), *Facetospatha* (p. 187), *Fragmospina* (p. 727), *Gastrostylides* (p. 770), *Gonostomoides* (p. 632), *Hemioxytricha* (p. 769), *Idiodeviata* (p. 578), *Lepidothrix* (p. 781), *Lingulothrix* (p. 106), *Longispatha* (dp), *Luporinophrys* (dp), *Mamillospatha* (p. 185), *Mancothrix* (p. 403), *Metagonostomum* (p. 611), *Metathrix* (p. 469), *Microcolpoda* (p. 294), *Monomicrocaryon* (p. 751), *Notodeviata* (p. 567), *Oxytrichella* (p. 776), *Paragonostomoides* (p. 610), *Paroxytricha* (p. 734), *Protoplagiocampa* (p. 452), *Pseudobirojimia* (p. 524), *Pseudotelotrochidium* (p. 474), *Quadristicha* (p. 769), *Renoplites* (p. 254), *Sagittarides* (p. 392), *Sandmannides* (p. 340), *Sleighophrys* (dp), *Totothrix* (p. 816), *Trachelophyllides* (p. 72).

New subgenera: *Apometopus* (*Apometopus*) (p. 869), *Apometopus* (*Apometopides*) (p. 874).

New species and new species described previously (dp): *Apertospathula lajacola* (dp), *Apertospathula verruculifera* (dp), *Apoavestina amazonica* (p. 290), *Apocoriplites lajacola* (dp), *Apofrontonia lametschwandtneri* (dp), *Apogonostomum pantanalense* (p. 611), *Apogonostomum vleiacola* (p. 616), *Apometopus pelobius* (p. 869), *Apowoodruffia salinaria* (p. 369), *Arcuospathidium pachyoplites* (dp), *Armatospathula periarmata* (dp), *Australothrix fraterculus* (p. 491), *Australothrix venezuelensis* (p. 497), *Bilamellophrya fraterculus* (p. 99), *Birojimia litoralis* (p. 504), *Bistichella chilensis* (p. 592), *Bistichella kenyaensis* (p. 596), *Bryometopus rostratus* (p. 344), *Cataphractes austriacus* (p. 118), *Cataphractes terricola* (p. 130), *Caudiholosticha halophila* (p. 532), *Caudiholosticha silvicola* (p. 531), *Caudiholosticha virginensis* (p. 535), *Cephalospathula brasiliensis* (dp), *Cinetochilides monomacronucleatus* (p. 440), *Cinetochilides terricola* (p. 430), *Cladotricha chilensis* (p. 541), *Cladotricha digitata* (p. 550), *Colpoda ephemera* (p. 265), *Condylostomides coeruleus* (p. 851), *Coriplites tumidus* (p. 179), *Drepanomonas multidentata* (dp), *Edaphospathula espeletiae* (dp), *Emarginatophrya terricola* (p. 287), *Enchelariophrya wolfi* (p. 231), *Enchelyodon floridensis* (p. 141), *Enchelyodon gondwanensis* (p. 136), *Enchelyodon isostichos* (p. 146), *Enchelys lajacola* (dp), *Enchelys tumida* (p. 251), *Fragmocirrus espeletiae* (dp), *Gonostomoides bimacronucleatus* (p. 637), *Gonostomoides caudatus* (p. 640), *Gonostomoides fraterculus* (p. 644), *Gonostomoides galapagensis* (p. 632), *Gonostomum bromelicola* (p. 686), *Gonostomum caudatulum* (p. 660), *Gonostomum fraterculus* (p. 696), *Gonostomum halophilum* (p. 651), *Gonostomum lajacola* (p. 676), *Gonostomum multinucleatum* (p. 679), *Gonostomum salinarum* (p. 658), *Grossglockneria lajacola* (p. 302), *Hemioxytricha isabelae* (p. 770), *Heterourosomoida salinarum* (p. 806), *Idiodeviata venezuelensis* (p. 579), *Ileonema chobicola* (p. 52), *Leptopharynx lajacola* (dp),

Lingulothrix galapagensis (p. 106), *Longispatha elegans* (dp), *Luporinophrys micelae* (dp), *Mancothrix pelobia* (p. 403), *Maryna meridiana* (p. 317), *Microcolpoda bambicola* (p. 295), *Monomicrocaryon crassicirratum* (p. 762), *Monomicrocaryon granulatum* (p. 752), *Notodeviata halophila* (p. 567), *Notohymena quadrinucleata* (p. 722), *Odontochlamys alpestris biciliata* (dp), *Odontochlamys buitkampi* (p. 429), *Odontochlamys denticulata* (p. 424), *Oxytricha lithofera* (p. 699), *Oxytricha pulvillus* (p. 704), *Oxytrichella mahadjacola* (p. 776), *Paracolpoda lajacola* (p. 275), *Paragonostomum australiense* (p. 622), *Paroxytricha quadrinucleata* (p. 735), *Phialinides bicaryomorphus* (p. 241), *Plagiocampa monotricha* (p. 459), *Platynematum terricola* (p. 411), *Platyophrya paoletti* (dp), *Platyophryides macrostoma* (p. 409), *Pleuroplites cavicola* (p. 260), *Protoplagiocampa lajacola* (p. 452), *Protospathidium salinarum* (p. 187), *Pseudomonilicaryon gracile oviplites* (dp), *Pseudoplatyophrya galapagensis* (p. 308), *Pseudoplatyophrya isabelae* (p. 304), *Pseudoplatyophrya spinosa* (p. 311), *Pseudotelotrochidium epistylis* (p. 475), *Pseudourostyla dimorpha* (p. 524), *Renoplites venezuelensis* (p. 255), *Sagittaria venezuelensis* (p. 380), *Sagittarides oblongistoma* (p. 393), *Sandmannides venezuelensis* (p. 341), *Sleighophrys pustulata* (dp), *Spathidium curiosum* (p. 204), *Spathidium dispar* (p. 217), *Spathidium duschli* (p. 207), *Spathidium inopinatum* (p. 201), *Spathidium stetteri* (p. 194), *Sterkiella ecuadoriana* (p. 810), *Stylonychia gibbera* (p. 828), *Stylonychia notophorides* (p. 835), *Totothrix panamensis* (p. 817), *Urosomoida galapagensis* (p. 800), *Urosomoida halophila* (p. 796).

New subspecies: *Drepanomonas hymenofera venezuelensis* (dp), *Enchelyodon monoarmatus monoarmatus* (p. 154), *Enchelyodon monoarmatus pyriformis* (p. 166), *Enchelys terricola terricola* (p. 246), *Enchelys terricola lanceoplites* (p. 246), *Metathrix ellipsoidea ellipsoidea* (p. 469), *Metathrix ellipsoidea oligostriata* (p. 474), *Monomicrocaryon euglenivorum euglenivorum* (p. 756), *Monomicrocaryon euglenivorum fimbricirratum* (p. 757), *Paroxytricha longigranulosa imperfecta* (p. 750), *Paroxytricha longigranulosa longigranulosa* (p. 742), *Paroxytricha longigranulosa sinensis* (p. 742), *Parabistichella bergeri bergeri* (p. 599), *Parabistichella bergeri brevisticha* (p. 606), *Paracondylostoma clavistoma oligostriatum* (dp).

Species redescribed: *Afroamphisiella abdita* (p. 823), *Amphisiella illuvialis* (p. 826), *Apometopus pyriformis* (p. 874), *Australothrix steineri* (p. 488), *Bakuella pampinaria pampinaria* (p. 524), *Bilamellophrya hawaiiensis* (p. 105), *Birojimia terricola* (p. 516), *Bursaria ovata* (p. 347), *Cladotricha australis* (p. 547), *Cladotricha edaphoni* (p. 547), *Clavoplites terrenum* (p. 258), *Colpoda maupasi* (p. 272), *Cothurnia minutissima* (p. 487), *Coterillia bromelicola* (p. 609), *Deviata brasiliensis* (p. 585), *Enchelyodon armatides* (p. 174), *Enchelyodon lagenula* (p. 179), *Enchelyodon longinucleatus* (p. 141), *Enchelyodon megastoma* (p. 154), *Enchelys lajacola* (p. 235), *Enchelys terricola* (p. 245), *Epistylis alpestris* (p. 483), *Euplotopsis incisa* (p. 845), *Fragmospina depressa* (p. 728), *Gonostomum singhii* (p. 666), *Gonostomum strenuum* (p. 647), *Krassniggia auxiliaris* (p. 299), *Lepidothrix dorsiincisura* (p. 781), *Maryna lichenicola* (p. 340), *Maryna umbrellata* (p. 328), *Notohymena antarctica* (p. 714), *Nudiamphisiella interrupta* (p. 823), *Paracolpoda steinii* (p. 284), *Paragastrostyla terricola* (p. 540), *Plagiocampa difficilis* (p. 466), *Plagiocampa rouxi* (p. 462), *Platyophrya bromelicola* (p. 407), *Platyophryides latus* (p. 422), *Sagittaria hyalina* (p. 392), *Saudithrix terricola* (p. 609), *Spetazoon australiense* (p. 62), *Stylonychia ammermanni* (p. 839), *Tetmemena pustulata* (p. 845), *Tetrahymena rostrata* (p. 445), *Trachelophyllides sigmoides* (p. 79), *Trachelophyllum apiculatum* (p. 91), *Trachelophyllum tachyblastum* (p. 93), *Uroleptoides polycirratus* (p. 821), *Woodruffia rostrata* (p. 365), *Woodruffides metabolicus* (p. 362).

Species neotypified: *Trachelophyllum tachyblastum* (p. 93).

New combinations

Amphisiella namibiensis Foissner et al., 2002 transferred to → *Parabistichella*, p. 599.
Arcuospathidium bromelicola Foissner et al., 2014 transferred to → *Columnospatha*, p. 187.
Bistichella encystica Fan et al., 2014 transferred to → *Parabistichella*, p. 599.
Cinetochilum australiensis Foissner et al., 1994 transferred to → *Cinetochilides*, p. 439.
Cinetochilum ovale Gong & Song, 1988 transferred to → *Cinetochilides*, p. 429.
Colpoda aspera Kahl, 1926 transferred to → *Emarginatophrya*, p. 286.
Gastrostyla dorsicirrata Foissner, 1982 transferred to → *Gastrostylides*, p. 770.
Holosticha geleii Wilbert, 1986 transferred to → *Monomicrocaryon*, p. 751.
Keronopsis dieckmanni Foissner, 1998 transferred to → *Parabistichella*, p. 599.
Metopus pyriformis Levander, 1834 transferred to → *Apometopus*, p. 874.
Onychodromopsis flexilis Petz & Foissner, 1996 transferred to → *Allotrichides*, p. 770.
Opisthotricha crassistilata Kahl, 1932 transferred to → *Monomicrocaryon*, p. 751.
Opisthotricha euglenivora Kahl, 1932 transferred to → *Monomicrocaryon*, p. 751.
Opisthotricha halophila Kahl, 1932 transferred to → *Monomicrocaryon*, p. 751.
Opisthotricha muscorum Kahl, 1932 transferred to → *Monomicrocaryon*, p. 751.
Opisthotricha opisthomuscorum Kahl, 1932 transferred to → *Quadristicha*, p. 751.
Oxytricha alfredi Berger, 1999 transferred to → *Monomicrocaryon*, p. 751.
Oxytricha australis Foissner & O´Donoghue, 1990 transferred to → *Aponotohymena*, p. 770.
Oxytricha balladyna Song & Wilbert, 1989 transferred to → *Monomicrocaryon*, p. 751.
Oxytricha buitkampi Dragesco & Dragesco-Kernéis,1986 transferred to → *Oxytrichella*, p. 776.
Oxytricha elegans Foissner, 1999 transferred to → *Quadristicha*, p. 751.
Oxytricha kahlovata Berger, 1999 transferred to → *Monomicrocaryon*, p. 751.
Oxytricha longigranulosa Berger & Foissner, 1989 transferred to → *Paroxytricha*, p. 735.
Oxytricha ottowi Foissner, 1996 transferred to → *Paroxytricha*, p. 735.
Oxytricha parahalophila Wang & Nie, 1935 transferred to → *Monomicrocaryon*, p. 751.
Oxytricha pseudofusiformis Dragesco & Dragesco-Kernéis, 1986 transferred to → *Monomicrocaryon*, p. 751.
Oxytricha saprobia Kahl, 1932 transferred to → *Monomicrocaryon*, p. 751.
Oxytricha setigera Stokes, 1891 transferred to → *Quadristicha*, p. 769.
Oxytricha setigera Buitkamp, 1977a transferred to → *Oxytrichella*, p. 776.
Oxytricha sphagni Kahl, 1931 transferred to → *Monomicrocaryon*, p. 751.
Paragonostomum minutum Kamra, Kumar & Sapra, 2008 transferred to → *Paragonostomoides*, p. 610.
Protospathidium lepidosomatum Foissner et al., 2014 transferred to → *Mamillospatha*, p. 187.
Pseudouroleptus procerus Berger & Foissner, 1987 transferred to → *Parabistichella*, p. 599.
Pseudouroleptus terrestris Hemberger, 1985 transferred to → *Parabistichella*, p. 599.
Spathidium cultriforme Penard, 1922 transferred to → *Facetospatha*, p. 187.
Steinia candens depressa Gellért, 1942 transferred to → *Fragmospina*, p. 727.
Tachysoma furcata Gelei, 1954 transferred to → *Monomicrocaryon*, p. 751.
Trachelochaeta gonostomoida Hemberger, 1985 transferred to → *Metagonostomum*, p. 611.
Uroleptus muscorum Kahl, 1932 transferred to → *Pseudobirojimia*, p. 524.
Urosoma longicirrata Kahl, 1932 transferred to → *Monomicrocaryon*, p. 751.

Urosomoida dorsiincisura Foissner, 1982 transferred to → *Lepidothrix,* p. 775.
Urosomoida monostyla Foissner et al., 2002 transferred to → *Oxytrichella,* p. 776.
Urosomoida perthensis Foissner & O´Donoghue, 1990 transferred to → *Oxytrichella,* p. 776.
Urosomoida reticulata Foissner, Agatha & Berger, 2002 transferred to → *Lepidothrix,* p. 781.

3.2.2 Descriptions

Gymnostomatea

The Gymnostomatea were founded by Bütschli (1889) for a group of ciliates with simple (gymnostomous) oral ciliature. Later, many other names were suggested, such as Litostomatea, Haptorida, Filicorticata, and Homotricha, for basically the same ciliates. Thus, and for reasons of stability (International Commission On Zoological Nomenclature 1999), we prefer Bütschli's time-honoured name Gymnostomatea.

Gymnostome ciliates are frequent in soils globally, i. e., they count for 18% of the global soil ciliate diversity (Foissner et al. 2002). Indeed, this is the third place in the global soil ciliate community (hypotrichs 36%, colpodids 22%). Many gymnostomes are inconspicuous and look alike at first glance. More detailed analysis, however, reveals quite a lot of organization types, especially of the circumoral ciliature and the extrusomes, which are highly evolved in this basically rapacious group of ciliates. This is emphasized by the present study, which discovered 5 new gymnostomatous genera and 24 new species. The great number of rapacious soil ciliates indicates a high and diverse number of potential food organisms, ranging from protists to small metazoans, especially rotifers. The morphologial and molecular phylogeny of the Gymnostomatea is still in its infancy, very likely due to a great number of homoplasies (Vďačný et al. 2014). For terminology, see Foissner & Xu (2007).

Suborder Trachelophyllina Grain, 1994

Diagnosis (from Foissner et al. 2002): Spathidiida Foissner & Foissner, 1988 with lepidosomes (epicortical scales).

Type family: Trachelophyllidae Kent, 1881.

Families assignable: Trachelophyllidae Kent, 1881; Lingulotrichidae nov. fam.

Nomenclature: This suborder has been established two times, viz., by Grain (1994) and Foissner et al. (2002).

Remarks: We adhere to the diagnosis given above because that of Grain (1994) is so unspecified that it embraces most haptorids. Foissner et al. (2002) established the Trachelophyllina with a single family, the Trachelophyllidae Kent, 1881, while Grain (1994) included also the Pseudotrachelocercidae Song, 1990a. However, the Pseudotrachelocercidae lack epicortical scales and have a different dorsal brush.

Here, we establish a new family for *Enchelys*-like and E*nchelyodon*-like haptorids having specific epicortical scales and a complex, multi-rowed dorsal brush. This requires an emendation of the diagnosis of the family Trachelophyllidae Kent, 1881, as defined by Foissner et al. (2002).

The data in this monograph markedly broaden the knowledge on trachelophyllid ciliates and show a considerable diversity of their lepidosomes summarized in Fig. 14 and Table 6.

Family Trachelophyllidae Kent, 1881

Improved diagnosis: Narrowly to cylindroidally (length:width ratio 3–12:1) lagenifrom and often highly contractile Trachelophyllina Grain,1994 with three-rowed dorsal brush: rows 1 and 2 dikinetal, row 3 monokinetal. Several types of three-dimensional lepidosomes: ground scales of type I or type VII; cover scales of type II, III, IV, V, VI, VIII, IX.

Type genus: *Trachelophyllum* Claparède & Lachmann,1859.

Genera assignable: *Trachelophyllum* Claparède & Lachmann, 1859: *Ileonema* Stokes, 1884b; *Spetazoon* Foissner, 1994; *Bilamellophrya* Foissner, Agatha & Berger, 2002; *Epitholiolus* Foissner, Agatha & Berger, 2002; *Luporinophrys* Foissner, 2005; *Sleighophrys* Foissner, 2005; *Trachelophyllides* nov. gen.

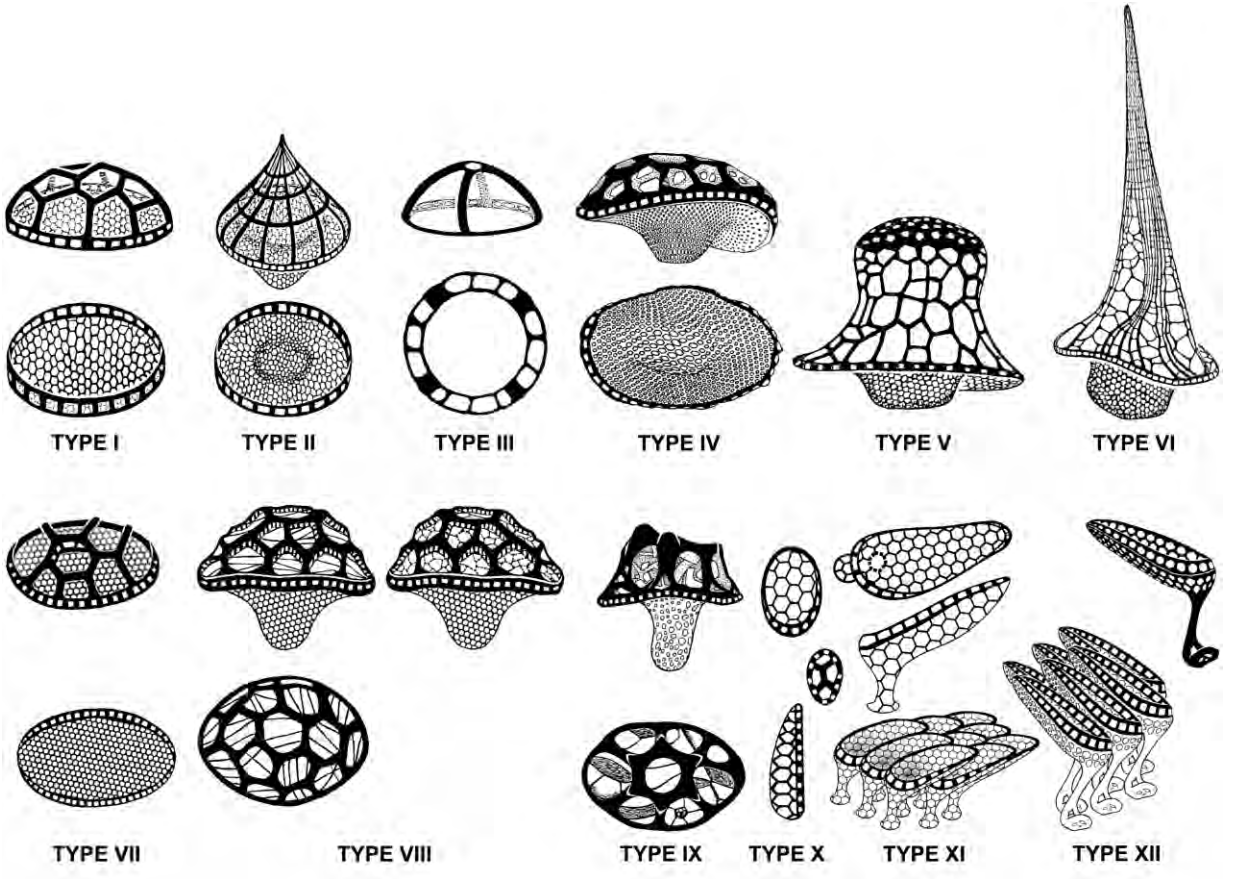

Fig. 14. Lepidosome types in the Trachelophyllina.

Table 6. Comparison of main taxonomic features in 19 well-investigated trachelophyllids.

Species[a]	Average size in vivo (µm)	Nuclear pattern[b]	Type I extrusome size and shape	Ciliary rows, number	Brush row 2 distinctly longer than 1	Oral bulge shape	Lepidosome types[c]
Bilamellophrya australiensis	200 × 30	Ordinary	Rod-shaped, > 10 µm	24	Yes	Anvil-shaped	I, II
Bilamellophrya etoschensis	140 × 15	Ordinary	Rod-shaped, < 10 µm	11	No	Conical	I, II
Bilamellophrya fraterculum	150 × 20	Ordinary	Cylindroid, < 10 µm	13	No	Conical	I, II
Bilamellophrya hawaiiensis	150 × 25	Ordinary	Acicular, > 10 µm	13	No	Cylindroidal	I, II
Cataphractes austriacus	120 × 20	Different	Acicular, > 10 µm	18	No	Discoidal	X, XII
Cataphractes terricola	120 × 20	Different	Rod-shaped, > 10 µm	13	No	Discoidal	XII
Epitholiolus chilensis	95 × 10	Different	Acicular, ~ 10 µm	9	Yes	Cylindroidal	III
Ileonema chobicola	175 × 25	Ordinary	Acicular, > 10 µm	19	Yes	Conical	I, IV
Lingulothrix galapagensis	120 × 17	Different	Rod-shaped, > 10 µm	14	No	Discoidal	X, XI
Luporinophrys micelae	200 × 35	Ordinary	Acicular, > 10 µm	21	Yes	Cylindroidal	I, II, VI
Sleighophrys pustulata	180 × 23	Ordinary	Acicular, > 10 µm	12	No	Pin-shaped	I, V
Spetazoon australiense	250 × 55	Ordinary	Acicular, > 10 µm	31	No	Conical	VII, VIII
Trachelophyllides sigmoides	350 × 65	Ordinary	Rod-shaped, > 10 µm	40	No	Discoidal	I, IV, IX
Trachelophyllum africanum	200 × 25	Ordinary	Narrowly lanceolate, < 10 µm	13	Yes	Cylindroidal	I
Trachelophyllum apiculatum	150 × 25	Ordinary	Rod-shaped, > 10 µm	13	No	Cylindroidal	I
Trachelophyllum costaricanum	180 × 15	Ordinary	Obclavate, > 10 µm	9	Yes	Cylindroidal	I
Trachelophyllum lineare	280 × 60	Ordinary	?	30	?	?	I
Trachelophyllum pannonicum	200 × 20	Ordinary	Acicular, ~ 10 µm	11	Yes	Cylindroidal	I
Trachelophyllum tachyblastum	120 × 17	Ordinary	Rod-shaped, > 10 µm	11	Yes	Conical	I

[a] Most data are from FOISSNER et al. (2002), FOISSNER (2005), and the present monograph; those on *S. australiense* are from FOISSNER (1994) and the present monograph, and those on *T. lineare* (junior synonym: *L. fornicis*; see FOISSNER 1994 and FOISSNER et al. 2002) are from NICHOLLS & LYNN (1984).

[b] Ordinary: two widely separate macronuclear nodules with a micronucleus each. Different: two narrowly spaced macronucleus nodules with a single micronucleus in between, or a single macronucleus.

[c] See Fig. 14.

Ileonema Stokes, 1884b

Improved diagnosis: Ordinarily to cylindroidally lageniform Trachelophyllidae with a conspicuous, retractable mouth process. Cortex covered with type I and type IV lepidosomes. Type I on pellicle, elliptical, baseplate finely honeycombed, superstructure dome-shaped and made of polygons. Type IV in periphery of mucilaginous layer, ampulliform, i. e., with a finely honeycombed, strongly concave baseplate and a dome-shaped superstructure containing a filamentous reticulum.

Type species: *Ileonema dispar* Stokes, 1884b.

Remarks: *Ileonema* spp. are outstanding haptorids because they have a flagellum-like cytoplasmic process associated with the oral apparatus. Although several species have been reported, a solid redescription of any species is not available. Thus, we are proud to close this gap almost 100 years after the last description of a new species by the Swiss protozoologist Penard (1922).

The type species has the mouth process structured in a thick, twisted proximal half and a thin, thread-like distal half. The other species, including that described here, lack this bipartition, indicating that they could comprise a distinct genus.

Ileonema chobicola nov. spec. (Fig. 15a–m, 16b–u, 17a–j; Table 7)

Diagnosis: Size in vivo about 175 × 25 µm; highly contractile. Very narrowly lageniform. 2 globular, distinctly separate macronuclear nodules with a globular micronucleus each. Extrusomes acicular, about 20 × 0.6 µm. On average 19 ciliary rows. Type I lepidosomes on average 1.5 × 0.75 × 0.7 µm in size and with 8 polygons in slightly convex superstructure; type IV lepidosomes ampulliform, 2.1 × 1.3 × 1 µm in size and with 20 polygons in quarter-globular superstructure.

Type locality: Soil from the dry, green bed of the Chobe River near the Muchenje Safari Lodge, Botswana, 24°40'E 18°S.

Type material: 1 holotype and 1 paratype slide with protargol-impregnated specimens have been deposited in the Biology Centre of the Upper Austrian Museum in Linz (LI). The holotype and other relevant specimens have been marked by black ink circles on the coverslip.

Etymology: The species-group name is a composite of *chobe* (the Botswanan river the species was discovered), the thematic vowel *-i-*, and the Latin verb *colere* (to live).

Description: *Ileonema chobicola* is highly variable most coefficients of variation being higher than 20%, especially continuous features. This might be caused by its pronounced contractility; however, some discrete features have also coefficients around 20% (Table 7).

Size in vivo 120–225 × 15–35 µm, usually about 175 × 25 µm, as calculated from some live measurements and the morphometric data (Table 7) adding 25% preparation and contraction shrinkage for body length (see the high variation coefficients) and 15% for body width. Body shape trachelophyllid, i. e., very narrowly lageniform with an average length:width ratio of

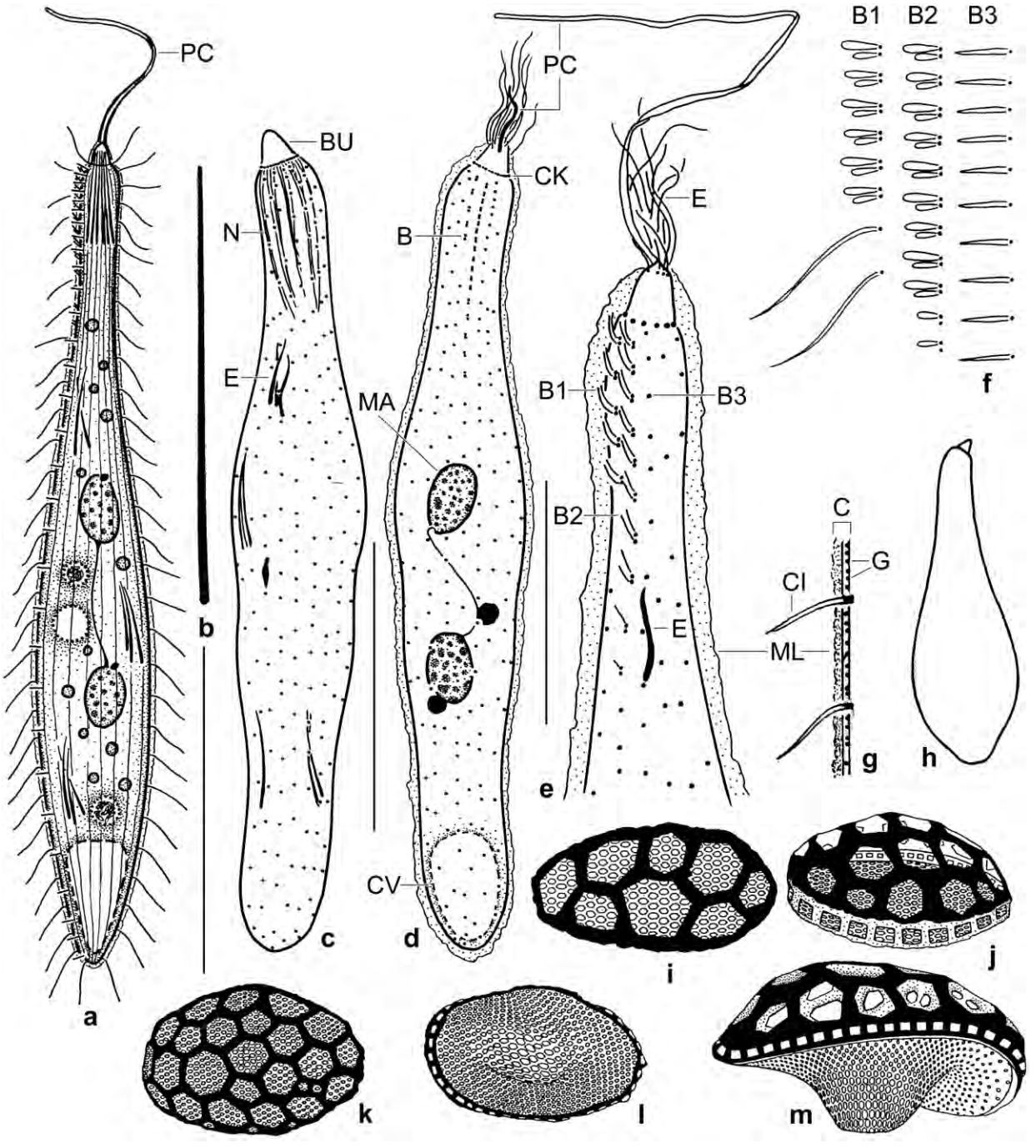

Fig. 15a–m. *Ileonema chobicola* from life (a, b, f–h), after protargol impregnation (c–e), and in the SEM (i–m). **a, b, g, h:** Lateral view of a representative specimen (a, 160 µm); an about 20 µm long acicular extrusome (b), and optical section of cortex (g). Contracted cells are about half as long as extended ones and distinctly broader (h). **c, d:** Ventral and dorsal view of holotype specimen, length 147 µm. **e, f:** Anterior region with dorsal brush (e, f), partially exploded extrusomes (e), and mouth process (e). The brush bristles are up to 3 µm long in vivo (f). **i, j:** Frontal and lateral view of a type I lepidosome (ground plate), size about 1.5 × 0.75 × 0.68 µm. **k–m:** Frontal, posterior polar, and lateral view of an ampulliform type IV lepidosome, size about 2.1 × 1.3 × 1 µm. B – dorsal brush, B1, 2, 3 – dorsal brush rows, BU – oral bulge, C – cortex, CI – ordinary somatic cilium, CK – circumoral kinety, CV – contractile vacuole, E – extrusomes, G – cortical granules, MA – macronuclear nodule, ML – mucilaginous layer, N – nematodesmata, PC – mouth process. Scale bars 20 µm (e), 50 µm (c, d), and 70 µm (a).

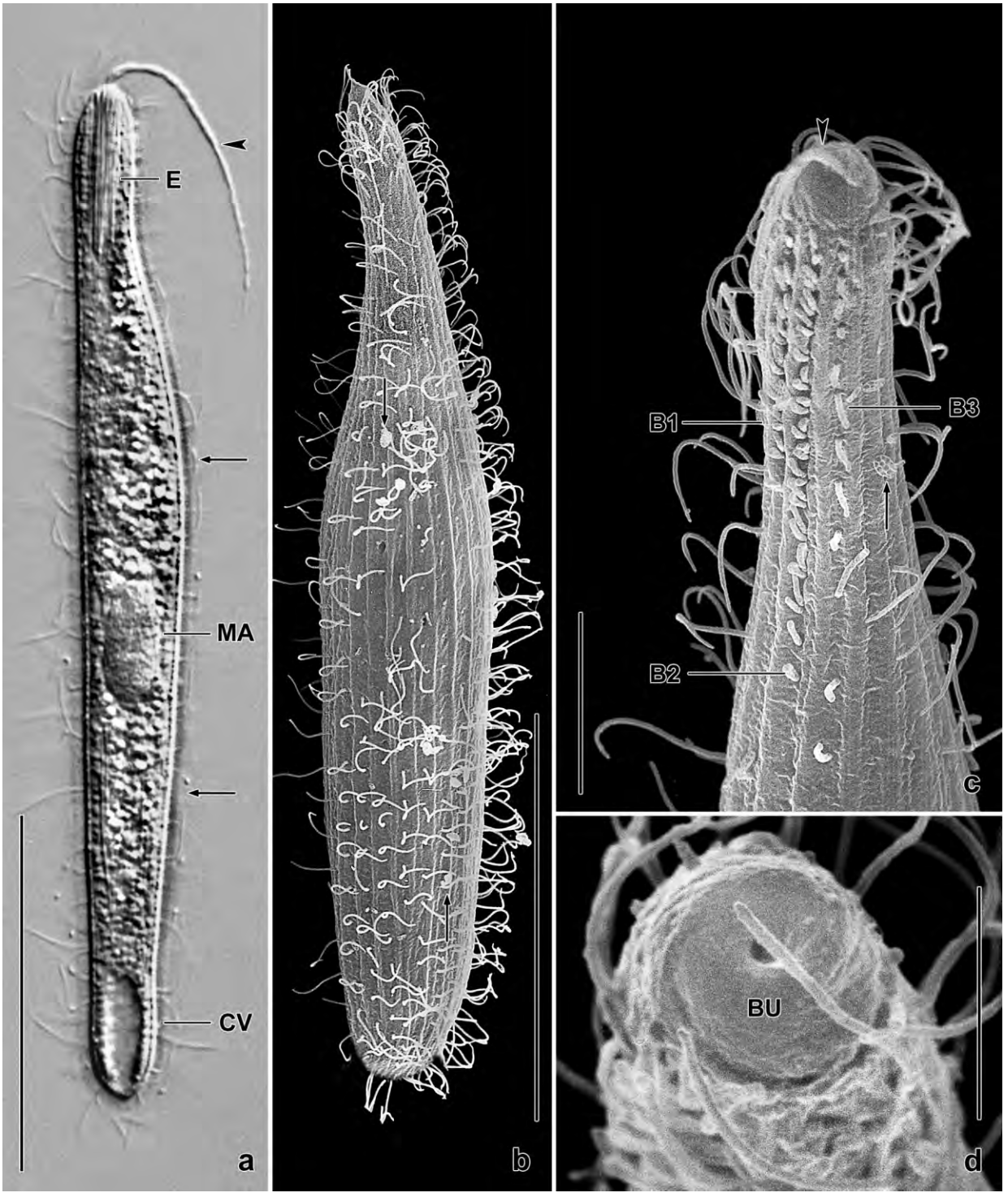

Fig. 16a–d. *Ileonema simplex* (a; from Kreutz & Foissner 2006) and *I. chobicola* (b–d) from life (a) and in the SEM (b–d). **a:** *Ileonema simplex* has only one macronuclear nodule. The arrows denote the lepidosome (mucilaginous) layer. The arrowhead marks the mouth process. **b, c:** The lepidosomes (arrows) are loosely attached to the cortex and thus usually lost in the preparations, exposing cilia and dorsal brush. The arrowhead marks the mouth process. **d:** Oblique frontal view of oral bulge, showing a central concavity from which the mouth process emerges. B1, 2, 3 – dorsal brush rows, BU – oral bulge, CV – contractile vacuole, E – extrusome bundle, MA – macronucleus. Scale bars 5 µm (d), 10 µm (c), and 50 µm (a, b).

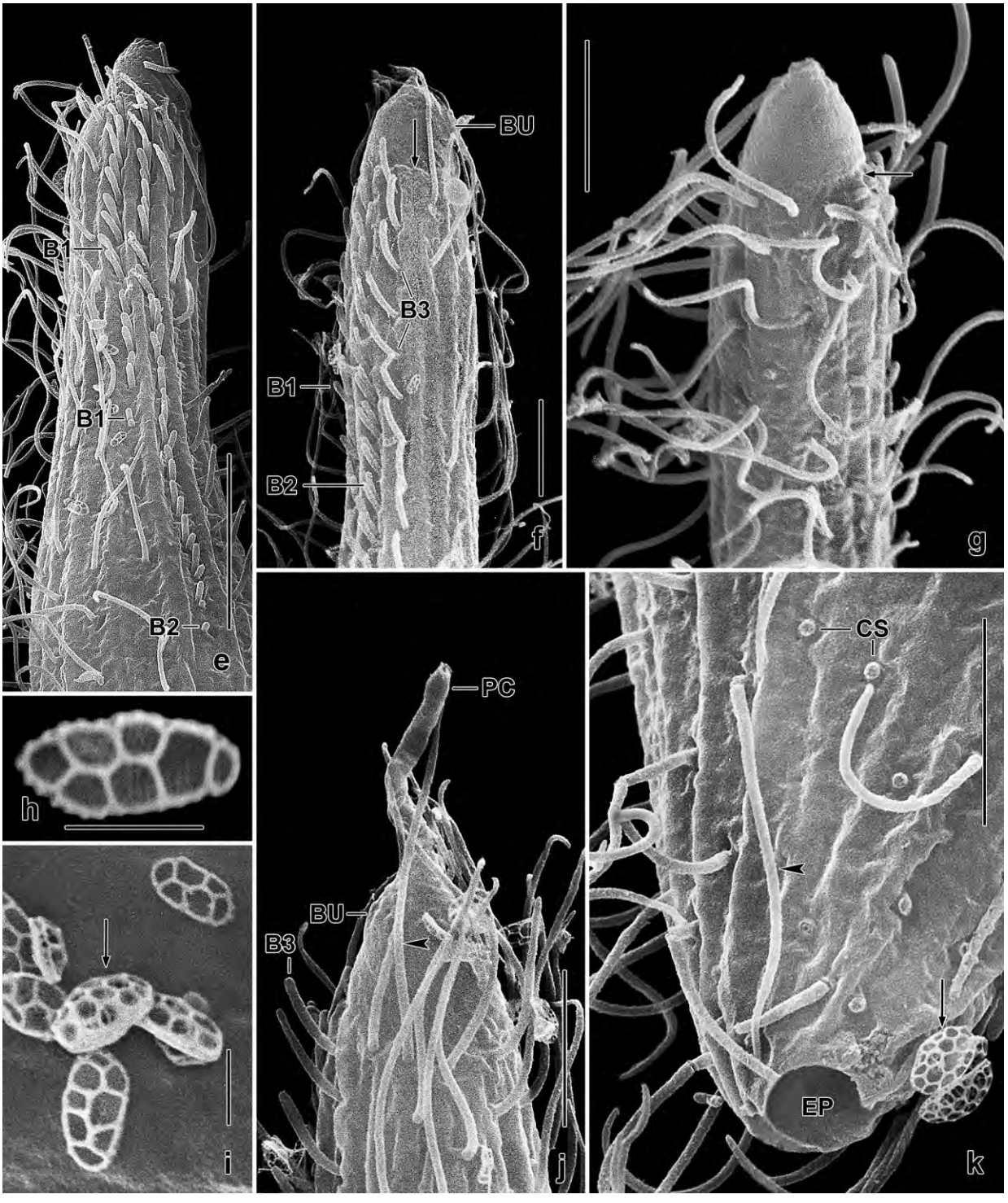

Fig. 16e–k. *Ileonema chobicola* in the SEM. **e, f, g, j**: Anterior region, showing the conical oral bulge, the absence of circumoral cilia (f, g, arrows), an almost completely retracted mouth process (j), the dorsal brush (e, f, j), and an about 12 µm long cilium (arrowhead) at begin of the ciliary rows; it is only slightly longer than the ordinary somatic cilia (10 µm, k). **h, i:** Type I lepidosomes. The arrow marks a type IV lepidosome. **k:** Posterior body end, showing the large excretory pore, two type IV lepidosomes (arrow), and a 10 µm long cilium (arrowhead). B1, 2, 3 – dorsal brush rows, BU – oral bulge, CS – ciliary stump, EP – excretory pore, PC – mouth process. Scale bars 1 µm (h, i), 5 µm (f, g, j, k), and 10 µm (e).

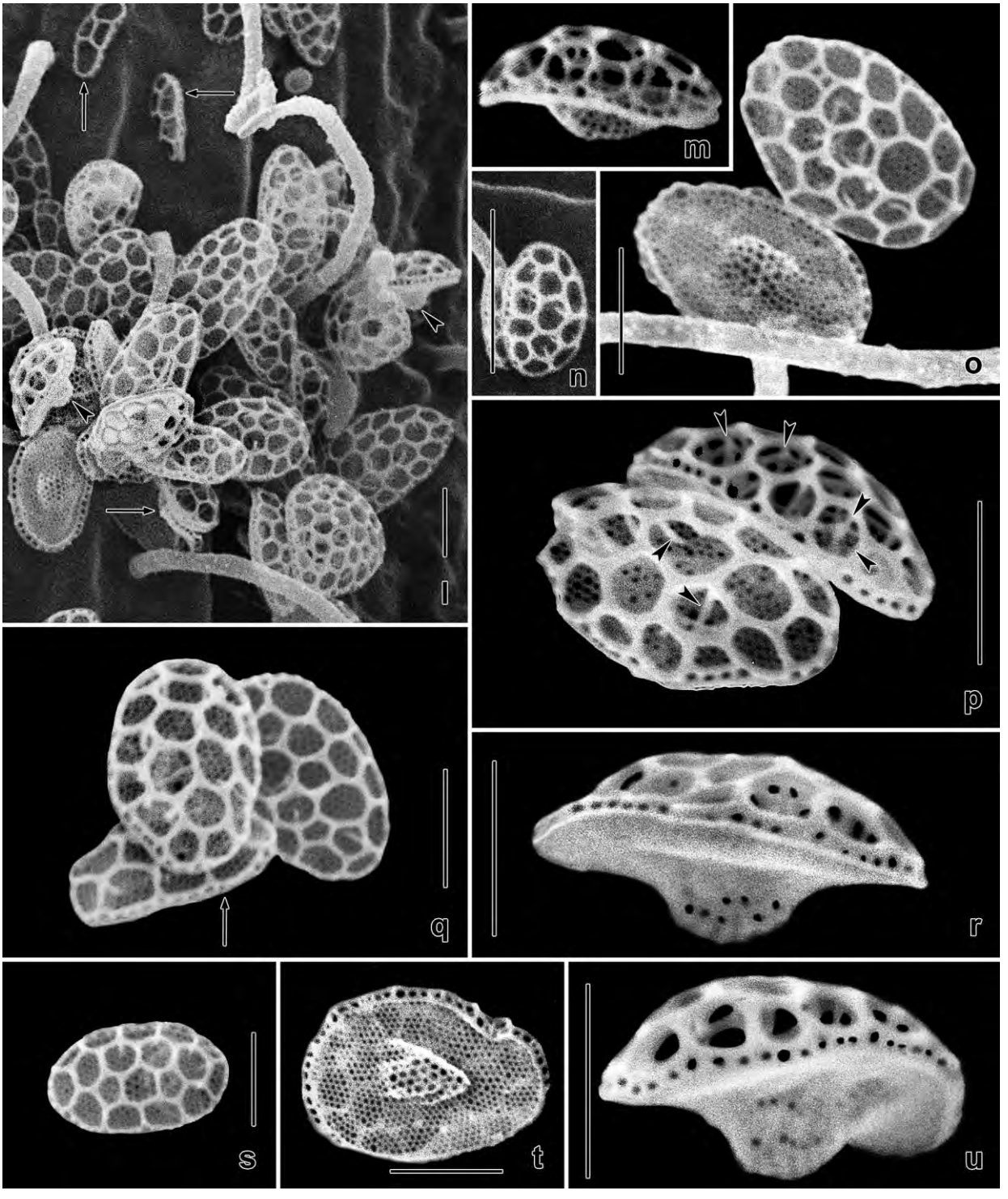

Fig. 16l–u. *Ileonema chobicola*, lepidosomes in the scanning electron microscope. Type I has an average size of 1.5 × 0.75 × 0.7 µm and seven polygons in the superstructure. For type IV the values are 2.1 × 1.3 × 1 µm and 20 polygons. **l, q:** Type I (arrows) and type IV lepidosomes in frontal and lateral (arrowheads) view. **m, r, u:** Lateral view of type IV lepidosomes. **n, s:** Frontal view of type IV lepidosomes. **p:** Frontal and lateral view of type IV lepidosomes having a filamentous reticulum in the superstructure (arrowheads, see also Fig. 15m). **o, t:** Frontal and posterior polar view of type IV lepidosomes. Scale bars 1 µm.

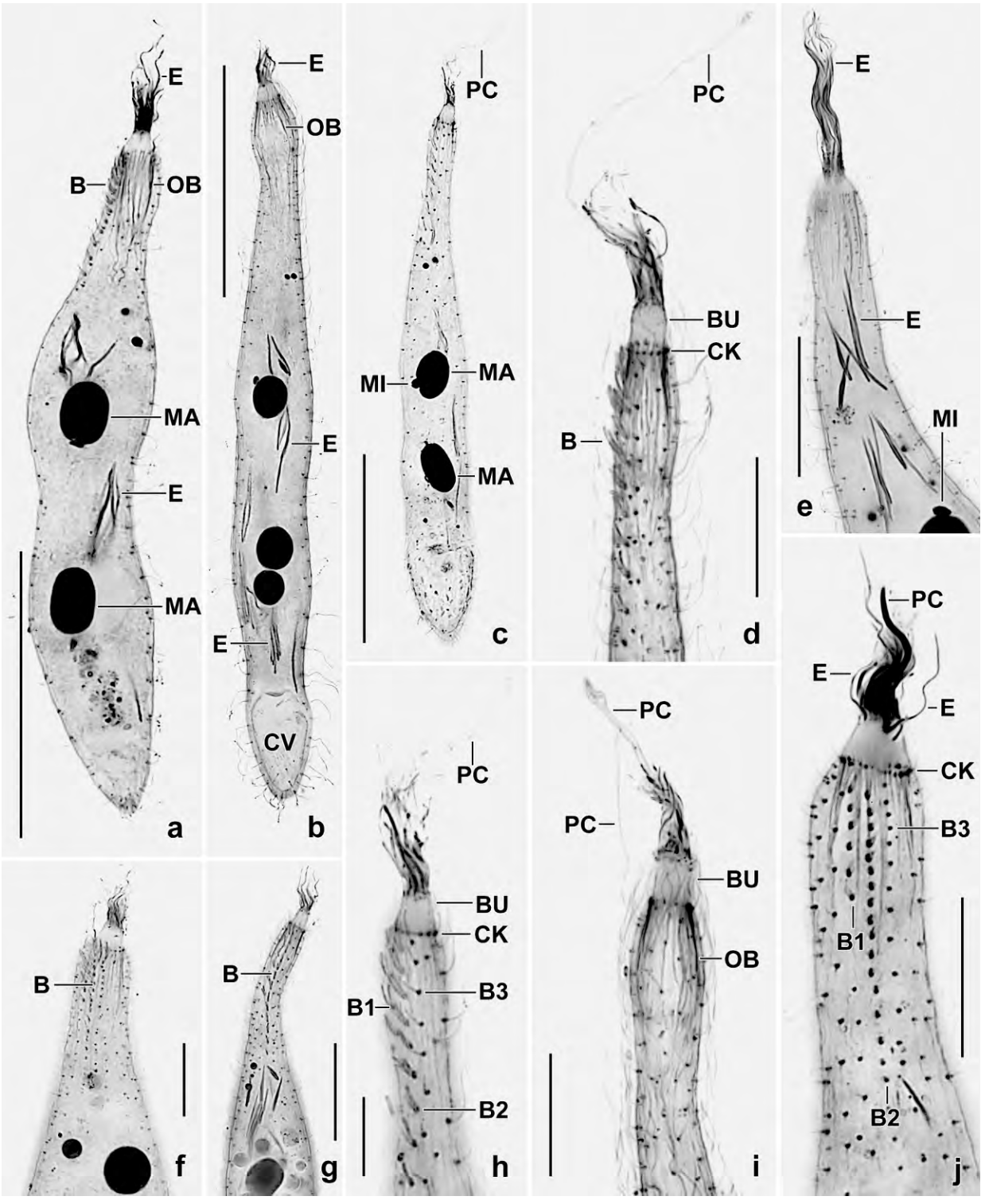

Fig. 17a–j. *Ileonema chobicola* after protargol impregnation. **a–c:** Body shape of specimens beginning contraction. **d–j:** Anterior body region of various specimens some showing the long mouth process (d, h, i). B – dorsal brush, B1, 2, 3 – dorsal brush rows, BU – oral bulge, B1, 2, 3 – dorsal brush rows, CK – circumoral kinety, CV – contractile vacuole, E – extrusomes, MA – macronuclear nodules, MI – micronuclei, OB – oral basket, PC – mouth process. Scale bars 10 μm (h), 15 μm (j), 20 μm (d–g), and 50 μm (a–c).

Table 7. Morphometric data on *Ileonema chobicola* based, if not mentioned otherwise, on mounted, protargol-impregnated, randomly selected specimens from a raw culture. Measurements in µm. CV – coefficient of variation in %, M – median, Max – maximum, Mean – arithmetic mean, Min – minimum, n – number of individuals investigated, SD – standard deviation, SE – standard error of arithmetic mean, SEM – scanning electron microscopy.

Characteristics	Mean	M	SD	SE	CV	Min	Max	n
Body, length	139.0	140.0	27.9	6.1	20.1	95.0	180.0	21
Body, width (without mucilaginous layer)	21.2	22.0	4.4	1.0	20.9	13.0	31.0	21
Body length:width, ratio	6.9	6.2	2.0	0.4	29.2	4.1	10.7	21
Mucilaginous layer, thickness	1.7	1.5	0.5	0.1	27.4	1.0	3.0	21
Body, length (SEM)	139.7	138.0	18.1	7.4	13.0	117.0	168.0	6
Body, width (SEM)	21.5	22.0	3.2	1.3	14.6	17.0	26.0	6
Body length:width, ratio (SEM)	6.6	6.5	1.3	0.5	19.1	5.1	8.4	6
Anterior body end to first macronuclear nodule, distance	55.7	55.0	15.6	3.4	27.9	25.0	83.0	21
Nuclear figure, length	44.4	45.0	13.0	2.8	29.3	19.0	70.0	21
Macronuclear nodules, distance in between	24.5	21.0	15.7	3.4	64.2	5.0	77.0	21
Anterior macronuclear nodule, length	10.5	10.0	2.6	0.6	24.6	6.0	17.0	21
Anterior macronuclear nodule, width	8.6	9.0	1.3	0.3	14.6	6.0	10.0	21
Macronuclear nodules, number	1.9	2.0	–	–	–	1.0	8.0	182
Micronuclei, length	2.4	2.0	0.6	0.1	24.7	2.0	4.0	17
Micronuclei, width	1.7	1.7	0.4	0.1	24.1	1.0	2.5	17
Micronuclei, number	1.5	2.0	0.9	0.2	57.3	0.0	3.0	21
Ciliary rows, total number in mid-body	18.9	19.0	1.0	0.2	5.3	17.0	20.0	21
Dorsal brush rows, number	3.0	3.0	0.0	0.0	0.0	3.0	3.0	21
Cilia in a ventral kinety, number	27.6	30.0	5.8	1.3	20.9	15.0	35.0	21
Dorsal brush row 1, length (beginning at circumoral kinety)	13.8	13.0	4.0	0.9	28.8	8.0	24.0	21
Dorsal brush row 1, number of dikinetids	6.1	6.0	1.3	0.3	20.8	4.0	10.0	21
Dorsal brush row 2, length (beginning at circumoral kinety)	28.8	27.0	7.8	1.7	27.1	20.0	40.0	21
Dorsal brush row 2, number of dikinetids	13.4	14.0	1.9	0.4	14.5	9.0	16.0	21
Type I lepidosomes, length (SEM)	1.5	1.5	0.3	0.1	20.3	1.1	2.2	30
Type I lepidosomes, width (SEM)	0.8	0.8	0.2	0.1	23.3	0.5	1.1	30
Type I lepidosomes, height (SEM)	0.7	0.4	0.9	0.3	137.0	0.3	3.5	11
Type I lepidosomes, number of polygons in superstructure (SEM)	6.9	6.5	2.0	0.4	29.6	4.0	11.0	30
Type IV lepidosomes, length (SEM)	2.1	2.1	0.3	0.1	12.7	1.8	2.8	16
Type IV lepidosomes, width (SEM)	1.3	1.3	0.2	0.1	13.1	1.1	1.8	16
Type IV lepidosomes, height (SEM)	1.0	1.0	–	–	–	0.7	1.2	13
Type IV lepidosomes, number of polygons in superstructure (SEM)	20.4	18.5	5.0	1.3	24.6	13.0	34.0	16

6.6:1; data from protargol preparations match well those from specimens prepared for scanning electron microscopy (osmium fixed!); laterally flattened about 2:1 (Fig. 15a, 16b, 17b, c; Table 7). Contractile up to half of body length becoming much stouter and ordinarily lageniform (Fig. 15h); contracts and retracts rather slowly, beginning in mid-body providing cell with a more or less dumbell-shaped outline (Fig. 17a–c).

Nuclear apparatus in central third of cell, may be dislocated by large food vacuoles, usually composed of two macronuclear nodules and two globular micronuclei firmly attached to macronuclear nodules (Fig. 15a, d, 17a–c, e; Table 7); number of macronuclear nodules rather variable: of 182 randomly selected specimens 12 have one nodule, 167 have two nodules, two have three nodules, and one has 8 nodules. Macronuclear nodules connected by an argyrophilic thread, distance between nodules highly variable, spherical to ellipsoidal, usually very broadly ellipsoidal, contain many minute nucleoli. Contractile vacuole in rear body end, with a single, large excretory pore (Fig. 15a, d, 16k, 17b). One type of extrusomes, when mature acicular, in vivo about 18–22 × 0.5–0.7 µm in size, form a refractive bundle attached to oral bulge, partially extruded in protargol preparations; single and bundled extrusomes 10–20 µm long scattered throughout cytoplasm (Fig. 15a, b, d, e, 17a–j).

Cortex thin and flexible, contains rows of colourless granules about 0.1 µm across; covered with an about 1 µm thick, mucilaginous layer of lepidosomes difficult to recognize in vivo and in protargol preparations (Fig 15a, d, e, g; Table 7). Mucilaginous layer composed of two types of lepidosomes lying one upon the other and so loosely attached to the cortex that most are lost during preparation (Fig 15a, g, i–m, 16b, c, e–u; Table 7). Type I lepidosomes in one layer on body surface, except for oral bulge, 1.5 × 0.75 × 0.7 µm in size and thus hardly recognizable in the light microscope, domed superstructure with eight polygons on average. Type IV lepidosomes on type I, ampulliform, 2.1 × 1.3 × 1 µm in size and with 20 polygons in quarter-globular superstructure; baseplate with stalk-like, central process creating the ampulliform shape together with the domed superstructure; about half of type IV lepidosomes with a three-dimensional filamentous reticulum within in superstructure (Fig. 15i–m, 16l–u).

Cilia about 10 µm long in vivo, loosely spaced, arranged in an average of 19 meridionally, ordinarily spaced rows, three of them differentiated to dorsal brush anteriorly (Fig. 15a, c–f, 16c, e, f, 17a, d, f–j; Table 7). Brush row 1 about half as long as row 2, composed of rather widely spaced dikinetids bearing about 2 µm long slightly clavate bristles (Fig. 15f) appearing rod-shaped and of same length in the SEM (Fig. 16c, e, f). Brush row 2 like row 1 but twice as long and composed of 14 ordinarily spaced dikinetids, those in posterior region with only one bristle shorter < 1 µm (Fig. 16e). Brush row 3 extends to near posterior body end, composed of monokinetids with 3 µm long acicular (in vivo) or oblong (SEM, protargol) bristles in some specimens narrowly spaced anteriorly. All brush rows continue posteriorly as ordinary somatic kineties.

Oral bulge in vivo rather conspicuous because about 6 × 6 µm in size, indistinctly separate from body proper and highly refractive due to the extrusomes contained; usually conical, very rarely discoidal and with distinct central opening, suggesting that this shape occurs just before or after prey ingestion; opens widely because prey is taken whole (Fig. 15a, e, 16c–g, j, 17a–j; Table 7).

Mouth process originates from centre of oral bulge, plasmatic, up to 50 µm long and about 1 µm thick near oral bulge; very likely cannot beat actively but is dragged posteriorly when cell swims and whip-like thrown anteriorly when it suddenly stops; withdrawn very rapidly when cell is disturbed, thus usually not recognizable in fixed specimens; retracts slowly or not at all, at least in the specimen we observed for half an hour (Fig. 15a, e, 16c, d, j, 17c, d, h–j).

Circumoral kinety at base of oral bulge, often composed of 25–30 unciliated (!) granules (all basal bodies?), i. e., a higher number than the 19 ciliary rows; gives rise to delicate fibres extending anteriorly into the oral bulge and to distinct nematodesmata forming the slightly, conical or obconical oral basket (Fig. 15a, c–e, 16f, g, j, 17d, h, j).

Occurrence and ecology: As yet found only at type locality where it became abundant in a raw culture. This indicates that *I. chobicola* is a limnetic species. Green river beds occur in the tropics during the dry season. The Chobe River was dry since two months when the sample was taken from the upper 5 cm of the bed, which was green by grasses and herbs. The soil and water are highly fertile because both, the wet and the dry river, are densely populated by hippos and elephants whose fecal masses are scattered over the bed. There was few litter, but the dark slightly acidic (pH 5.1 in water) and very humic soil contained many grass roots. When rewetted, the soil becomes a swampy, fine-grained mass difficult to investigate.

Remarks: In his review, Kahl (1930a) reported only three *Ileonema* species. *Ileonema dispar* Stokes, 1884b has only one (vs. two) macronuclear nodule and is much stouter than *I. chobicola* (length:width ratio about 3:1 vs. 6.6:1).

Ileonema simplex, of which Penard (1922) found only a single specimen in a *Sphagnum* upholstery, has also only one (vs. two) macronuclear nodule. This has been confirmed (Fig. 16a) by Kreutz & Mayer (2000) and Kreutz & Foissner (2006). Thus, *I. simplex* is clearly different from *I. chobicola.*

Ileonema ciliata (Roux, 1901) Kahl, 1930a resembles *I. chobicola* in body shape and in having two macronuclear nodules. However, it is much smaller (in vivo ~ 75 × 14 µm vs. ~ 160 × 25 µm) and slightly stouter (~ 5.3:1 vs. 6.6:1). Very likely, further differences exist but cannot be settled because the description of Roux (1901) is very brief. *Ileonema ciliata* has been reported by several authors, e. g., by Chorik & Vikol (1973) in a cooling plant in Moldavia and in Mexico by Ramirez De Guerrero (1970) who misidentified a small (80 × 15 µm), monomacronucleate *Ileonema* as *I. ciliata* Roux.

Spetazoon Foissner, 1994

Improved diagnosis: Trachelophyllidae Kent, 1881 with type VII and type VIII lepidosomes whose superstructure is made of pierced planks. Type VII on pellicle, composed of a finely honeycombed, elliptical baseplate from which a widely and polygonally faceted, dome-shaped superstructure emerges. Type VIII lepidosomes ampulliform, composed of a finely honeycombed, strongly concave, elliptical baseplate associated with a widely and polygonally faceted, hemispherical superstructure filled with a three-dimensional net of filaments.

Type species: *Spetazoon australiense* Foissner, 1994.

Remarks: The diagnosis has been adapted to FOISSNER (2005) and to the new results on the lepidosomes.

We rediscovered *S. australiense* in a soil sample from the floodplain of the Murray River near to the town of Albury, southern Australia while the type population has been discovered in a soil sample from the bottom of the Fogg Dam in the surroundings of the town of Darwin, northern Australia (FOISSNER 1994). The Murray River specimens were very similar to those from the type population. Thus, we reinvestigated only the epicortical scales (lepidosomes), which FOISSNER (1994) studied with an insufficient method (air-drying) and described as spherical structures composed of a hexagonally faceted external layer and a honeycombed internal layer. Critical-point drying showed much more details although the rough surface view is quite similar (cp. Fig. 22n–p with Fig. 20–22 in FOISSNER 1994).

Spetazoon australiense has type VII and type VIII lepidosomes (for types, see FOISSNER 2005 and the present study, Fig. 14). The lepidosomes are shown by a multitude of SEM micrographs (Fig. 22d, e–u, 23a–g). Thus, the description will be short.

Table 8. Morphometric data on the lepidosomes of an Australian population of *Spetazoon australiense* and of the body of *S. australiense*-like specimens from Venezuelan site (56). Lepidosome data based on about 10 critical-point dried specimens. Body data based on mounted, protargol-impregnated, and randomly selected specimens from a non-flooded Petri dish culture. Measurements in µm. CV – coefficient of variation in %, M – median, Max – maximum, Mean – arithmetic mean, Min – minimum, n – number of specimens investigated, P – protargol impregnation (FOISSNER's method), SD – standard deviation, SE – standard error of arithmetic mean, SEM – scanning electron micrographs.

Characteristics	Method	Mean	M	SD	SE	CV	Min	Max	n
Type VII lepidosomes, length	SEM	2.3	2.3	0.3	0.1	12.1	1.6	2.8	30
Type VII lepidosomes, width	SEM	1.3	1.3	0.2	0.1	16.8	0.9	1.8	30
Type VII lepidosomes, height	SEM	0.6	0.6	0.2	0.1	33.8	0.3	1.2	30
Type VII lepidosomes, number of polygons in superstructure	SEM	8.2	9.0	2.0	0.4	24.1	5.0	12.0	30
Type VIII lepidosomes, length	SEM	3.0	3.1	0.4	0.1	13.4	2.3	3.9	30
Type VIII lepidosomes, width	SEM	2.3	2.3	0.3	0.1	13.3	1.6	2.9	30
Type VIII lepidosomes, height	SEM	2.2	2.2	0.5	0.1	21.7	1.5	3.0	30
Type VIII lepidosomes, number of polygons in superstructure	SEM	19.3	18.0	4.6	0.8	23.7	13.0	32.0	30
Body, length	P	181.6	180.0	24.5	5.8	13.5	130.0	255.0	18
Body, width	P	68.5	68.5	1.0	2.4	14.6	53.0	88.0	18
Ciliary rows, number	P	23.8	24.0	0.9	0.2	3.6	23.0	26.0	19
Dikinetids, number in brush row 1	P	20.4	20.0	2.8	0.7	13.6	13.0	25.0	18

The type VII lepidosomes are elliptical, rarely broadly elliptical and lie on the pellicle in one or two layers (Fig. 22i–m). The flat baseplate is finely hexagonally faceted while the superstructure is coarsely polygonally faceted and has a feature not yet observed in the type I scales of other species: the central facete(s) is composed of pierced planks (Fig. 22l, m). The average size is 2.3 × 1.3 × 0.6 µm in the scanning electron microscope, showing that the superstructure is very flat (Fig. 23a; Table 8).

The type VIII lepidosomes, which have an average size of 3 × 2.3 × 2.2 µm (Table 8) in the SEM, are ampulliform, i. e., have a blunt stalk and a hemispherical cap resembling the type IV lepidosomes of → *Ileonema* (Fig. 22d–h, n–q, 23a–g). They lie on the type VII lepidosomes in one or two layers. The baseplate has a strongly convex central area and is finely hexagonally faceted while the hemispherical superstructure is coarsely polygonally faceted. The superstructure is made of polygons composed of pierced planks and contains a three-dimensional net of filaments recognizable only at high magnification (Fig. 22r–u, 23c, d, f, g). A reinterpretation of the lepidosomes of other species showed that the type V lepidosomes of *Sleighophrys pustulata* contain a similar net (Fig. 31–33 in Foissner 2005).

Spetazoon australiense Foissner, 1994

Improved diagnosis: Size in vivo about 265 × 60 µm, contractile by about 40% of body length. Lageniform with bluntly pointed posterior end; distinctly flattened dorsoventrally. Two ellipsoidal, widely distant macronuclear nodules with a micronucleus each. Extrusomes distinctly acicular, about 20 × 1 µm in size. On average 31 ciliary rows; dorsal brush isostichad. Type VII lepidosomes about 2.3 × 1.3 × 0.6 µm in SEM preparations, dome composed of an average of nine large polygons; type VIII lepidosomes about 3 × 2.3 × 2.2 µm in SEM preparations, baseplate with conspicuous central convexity, dome composed of an average of 19 large polygons.

Remarks: The diagnosis has been adapted to Foissner (2005) and to the new data on the lepidosomes. We did not reinvestigate the species, except of the lepidosomes, because the in vivo aspect was very similar to that of the type specimens.

However, we observed this or a similar species in sample (56) from Venezuela. These specimens looked quite similar to the Australian ones in vivo (cp. Fig. 22a, b, f–h with Fig. 1, 3, 17–19 in Foissner 1994), except of the extrusomes, which were shorter (about 15 µm vs. 20 µm) and less distinctly acicular (Fig. 22c). Protargol preparations showed (Tables 8, 10) that the Venezuelan specimens are shorter (210 µm vs. 265 µm in vivo) and have a lower, non-overlapping number of ciliary rows (24 vs. 31). Thus, we cannot exclude that the Venezuelan population is at least a distinct subspecies. Unfortunately, we studied the lepidosomes of the Venezuelan specimens only in the light microscope (Fig. 22a, b), where they appeared quite similar to those of the Australian populations.

We deposited three slides with protargol-impregnated specimens from the Venezuelan population in the Biology Centre of the Upper Austrian Museum in Linz (LI). Some well-impregnated cells are marked with black ink circles on the coverslip.

Spetazoon australiense: description of an Austrian population (Fig. 18a–m, 19a–x, 20a–k; Tables 9, 10)

Material and Remarks: *Spetazoon australiense* was found in August and November 2004 in the mud of a flooded meadow in the surroundings of the railway station "village of Selker", near to the town of Kefermarkt, Upper Austria, 48°48'N 15°14'E. This is a site of the *Meseres* study (Weisse et al. 2008). We deposited 4 voucher slides with protargol-impregnated specimens in the Biology Centre of the Upper Austrian Museum in Linz (LI).

Description: *Spetazoon australiense* is rather variable because most variation coefficients are > 15%, including those from the lepidosomes (Table 9). Part of the variability of the continuous features is very likely caused by the contractility of the cells. As usual, the number of ciliary rows is little variable (CV = 5.1%) and thus an important feature for species recognition. The description is based on slowly growing specimens from a raw culture set up with tap water and some squashed wheat kernels.

Size in vivo about 290 × 45 µm and about 290 × 65 µm in protargol slides when 25% are added for length shrinkage due to partial contraction and preparation shrinkage while only 15% for body width because cells generally tend to become slightly inflated in preparations (Table 9); in vivo contractile by about 30% of body length; length:width ratio highly variable (3–8:1; Table 9), very likely due to a more or less strong contraction when cells are fixed. Body lageniform to very slenderly lageniform both in vivo (6.3:1 on average) and in protargol preparations (4.1:1), widest in or slightly posterior of mid-body, neck distinct and usually slightly curved producing an inconspicuous shoulder, posterior end bluntly pointed even in contracted specimens (Fig. 18a, c, i–m, 19a–c, e, k; Table 9). Nuclear apparatus on average in central quarters of cell (Fig. 18a, c, 19e, k, s, t; Table 9). Macronuclear nodules in about half of specimens in slightly oblique pattern (Fig. 19e), connected by an argyrophilic strand; globular to ellipsoid, on average broadly ellipsoid, only one nodule in two out of 21 cells investigated; nucleoli granular, numerous. On average six conspicuous micronuclei near and attached to macronuclear nodules, ellipsoid, elongate ellipsoid, ovate or lageniform, usually ellipsoid (2:1) to elongate ellipsoid (≥ 3:1), in vivo bright because compact, about 11 × 4 µm in size. Contractile vacuole in posterior body end, with large subterminal excretory pore (Fig. 18a, c, j, 19g, k). Two types of extrusomes attached to oral bulge and scattered in cytoplasm (Fig. 18a, d, f, g, 19e, h, i, j, l; Table 9): type I acicular and more or less curved, on average 18 × 0.9 µm in size; type II minute, i. e., only 2–3 µm long. Cytoplasm colourless and densely granulated, contains few to many globular and irregular, highly refractive lipid droplets up to 15 µm in size (Fig. 18a, 19c, e). Feeds on *Vorticella convallaria* (Fig. 19e). Glides slowly on bottom of Petri dish or swims slowly rotating about main body axis.

Cortex highly flexible, slightly ribbed right of ciliary rows (Fig. 19p), about 1 µm thick, contains innumerable granules smaller than 0.5 µm in narrowly spaced rows (Fig. 18b, 19q), covered by a mucilaginous layer 3–5 µm thick in vivo (Fig. 18a–c, 19k, m, n, o, r). Mucilaginous layer composed of slime and two types of lepidosomes both staining with alcain blue suggesting acid mucopolysaccharides as a main component (Foissner 2009). Lepidosomes of "complex type", i. e., superstructure made of planks pierced by quadrangular or polygonal meshes. Type VII lepidosomes 1.9 × 1.1 × 0.6 µm in the scanning electron microscope, very hyaline and thus hardly recognizable in the light microscope although having about double size in vivo; composed of an elliptical, finely honeycombed baseplate and a rather flat superstructure with an average of nine polygons the central one(s) made of pierced planks (Fig. 18b, 19u–x, 20f–h, 21a, b, d, e; Table 9). Type VIII lepidosomes on type VII in two layers, 2.6 × 1.8 × 1.9 µm in the scanning electron microscope, well recognizable in the light microscope appearing spherical or hemispherical with a diameter of 3–4 µm (Fig. 18b, 19n, o, r); composed of a circular or broadly elliptical, finely honeycombed baseplate and a complex hemispherical superstructure with polygons made of planks pierced quadrangularly or polygonally; superstructure filled with a three-dimensional, irregular net made of filaments (Fig. 18b, c, 19a, b, n, o, r, 20a–d, i–k; Table 9).

Table 9. Morphometric data on an Austrian population of *Spetazoon australiense* from a raw culture. Measurements in µm. CV – coefficient of variation in %, IV – in vivo, M – median, Max – maximum, Mean – arithmetic mean, Min – minimum, n – number of individuals investigated, P – protargol impregnation, randomly selected, SD – standard deviation, SE – standard error of mean, SEM – scanning electron microscopy.

Characteristics	Method	Mean	M	SD	SE	CV	Min	Max	n
Body, length (rough values)	IV	291.4	280.0	–	–	–	260.0	320.0	7
Body, width (rough values)	IV	47.1	50.0	–	–	–	40.0	60.0	7
Body length:width, ratio (rough values)	IV	6.3	6.4	–	–	–	4.7	8.0	7
Body, length	P	230.5	226.0	37.3	8.1	16.2	165.0	295.0	21
Body, width	P	57.2	55.0	9.0	2.0	15.8	43.0	72.0	21
Body length:width, ratio	P	4.1	3.9	0.8	0.2	19.7	3.0	6.0	21
Anterior body end to first macronuclear nodule, distance	P	79.0	77.0	17.9	3.9	22.6	57.0	115.0	21
Macronuclear pattern, length	P	85.3	90.0	22.1	4.8	26.0	43.0	130.0	21
Macronuclear nodules, distance in between	P	40.4	42.0	19.6	4.3	48.6	3.0	74.0	21
Anterior macronuclear nodule, length	P	24.3	23.0	4.6	1.0	18.6	18.0	35.0	21
Anterior macronuclear nodule, width	P	19.7	20.0	2.9	0.6	14.7	11.0	25.0	21
Macronuclear nodules, number	P	2.0	2.0	0.0	0.0	0.0	2.0	2.0	21
Micronuclei, length	P	9.7	10.0	1.9	0.4	19.6	6.0	13.0	21
Micronuclei, width	P	3.8	4.0	0.7	0.1	17.2	3.0	5.0	21
Micronuclei, number	P	5.9	6.0	1.8	0.4	30.2	4.0	11.0	21
Oral bulge, width at circumoral kinety	P	7.1	7.0	0.8	0.2	11.7	6.0	9.0	21
Oral bulge, height	P	4.5	4.0	0.9	0.2	20.8	3.5	8.0	21
Ciliary rows, number including dorsal brush	P	37.0	37.0	1.9	0.6	5.1	34.0	40.0	11
Basal bodies in a ventral kinety, number	P	52.8	52.5	6.9	2.8	13.1	42.0	60.0	6
Dikinetal dorsal brush rows, number	P	2.0	2.0	0.0	0.0	0.0	2.0	2.0	21
Dorsal brush row 1, length	P	46.2	45.0	8.4	2.3	18.2	30.0	60.0	13
Dorsal brush row 1, number of dikinetids	P	24.1	24.0	2.6	0.7	10.8	19.0	29.0	13
Dorsal brush row 2, length	P	47.9	48.0	7.7	2.1	16.0	34.0	63.0	13
Dorsal brush row 2, number of dikinetids	P	30.2	30.0	4.9	1.4	16.3	21.0	38.0	13
Type 1 extrusomes, length	IV	18.1	18.0	1.8	0.5	10.0	16.0	22.0	13
Type VII lepidosomes, length	SEM	1.9	1.9	0.3	0.1	15.8	1.1	2.3	31
Type VII lepidosomes, width	SEM	1.1	1.1	0.3	0.1	24.4	0.6	1.8	31
Type VII lepidosomes, height	SEM	0.6	0.6	0.1	0.1	18.0	0.4	0.9	25
Type VII lepidosomes, number of polygons in superstructure	SEM	8.8	9.0	2.1	0.4	23.4	4.0	12.0	31
Type VIII lepidosomes, length	SEM	2.6	2.6	0.2	0.1	8.9	2.1	3.2	38
Type VIII lepidosomes, width	SEM	1.8	1.9	0.2	0.1	9.5	1.5	2.1	38
Type VIII lepidosomes, height	SEM	1.9	1.8	0.3	0.1	15.3	1.4	2.4	24
Type VIII lepidosomes, number of polygons in superstructure	SEM	24.7	25.5	6.4	1.0	25.8	14.0	39.0	38

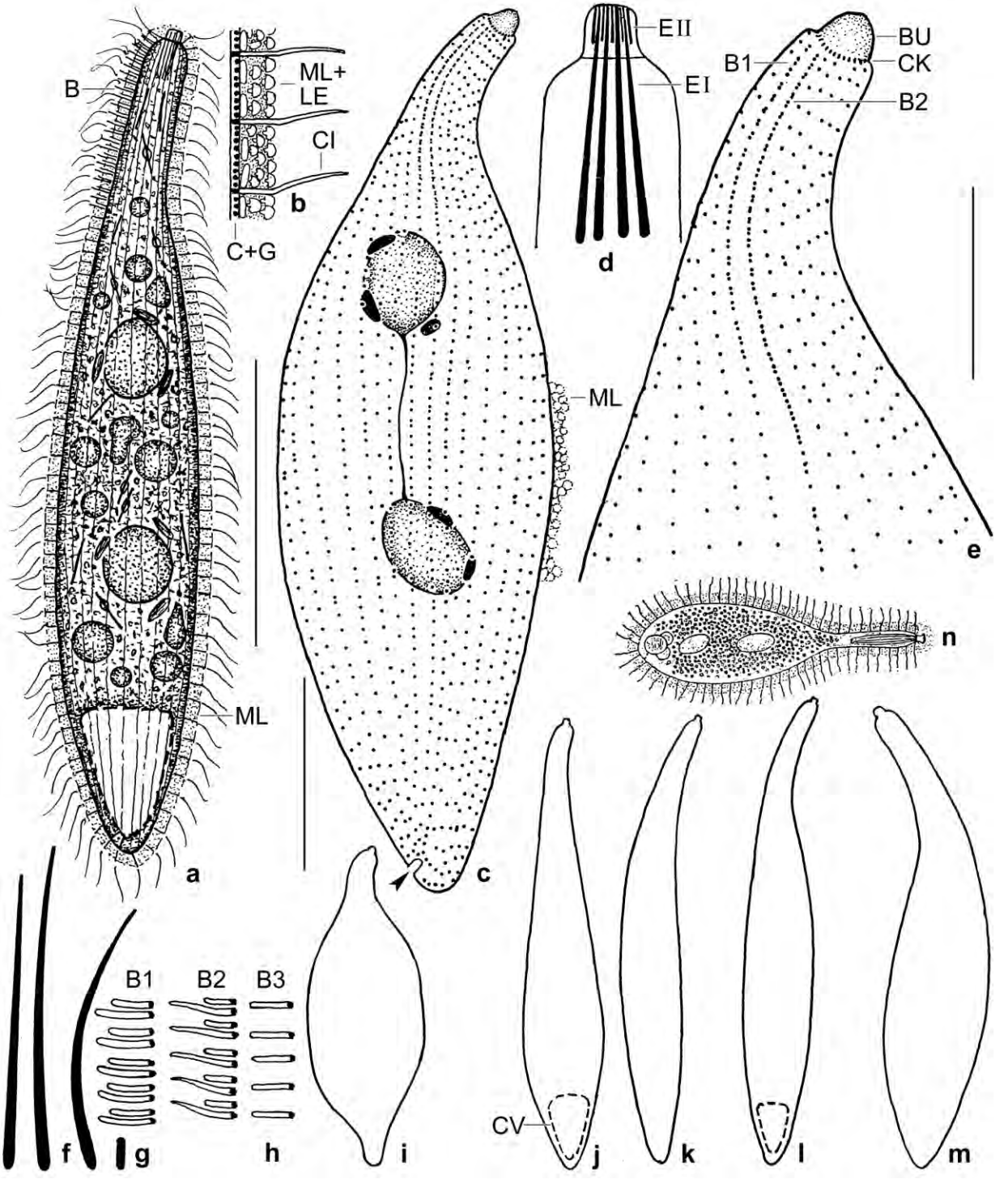

Fig. 18a–n. *Spetazoon australiense* (a–m) and *Trachelophyllum vestitum* (n). Austrian specimens from life (a, b, d, f–m) and after protargol impregnation (c, e). **a:** Left side view of a representative specimen, length 290 µm. **b:** Optical section of cell´s periphery. **c, e:** Dorsal views of main voucher specimen. **d, f, g:** *Spetazoon australiense* has long (~ 20 µm) type I and minute (~2.5 µm) type II extrusomes. **h:** Dorsal brush, longest bristles 6 µm. **i:** Contracted specimen. **j–m:** Shape variability. **n:** *Trachelophyllum vestitum*, length 250 µm (from Stokes 1884a). B – dorsal brush, BU – oral bulge, B1, 2, 3 – dorsal brush rows, C – cortex, CI – cilium, CK – circumoral kinety, CV – contractile vacuole, EI, II – extrusome types, G – cortical granules, LE – lepidosomes, ML – mucilaginous layer. Scale bars 50 µm (c, e) and 100 µm (a).

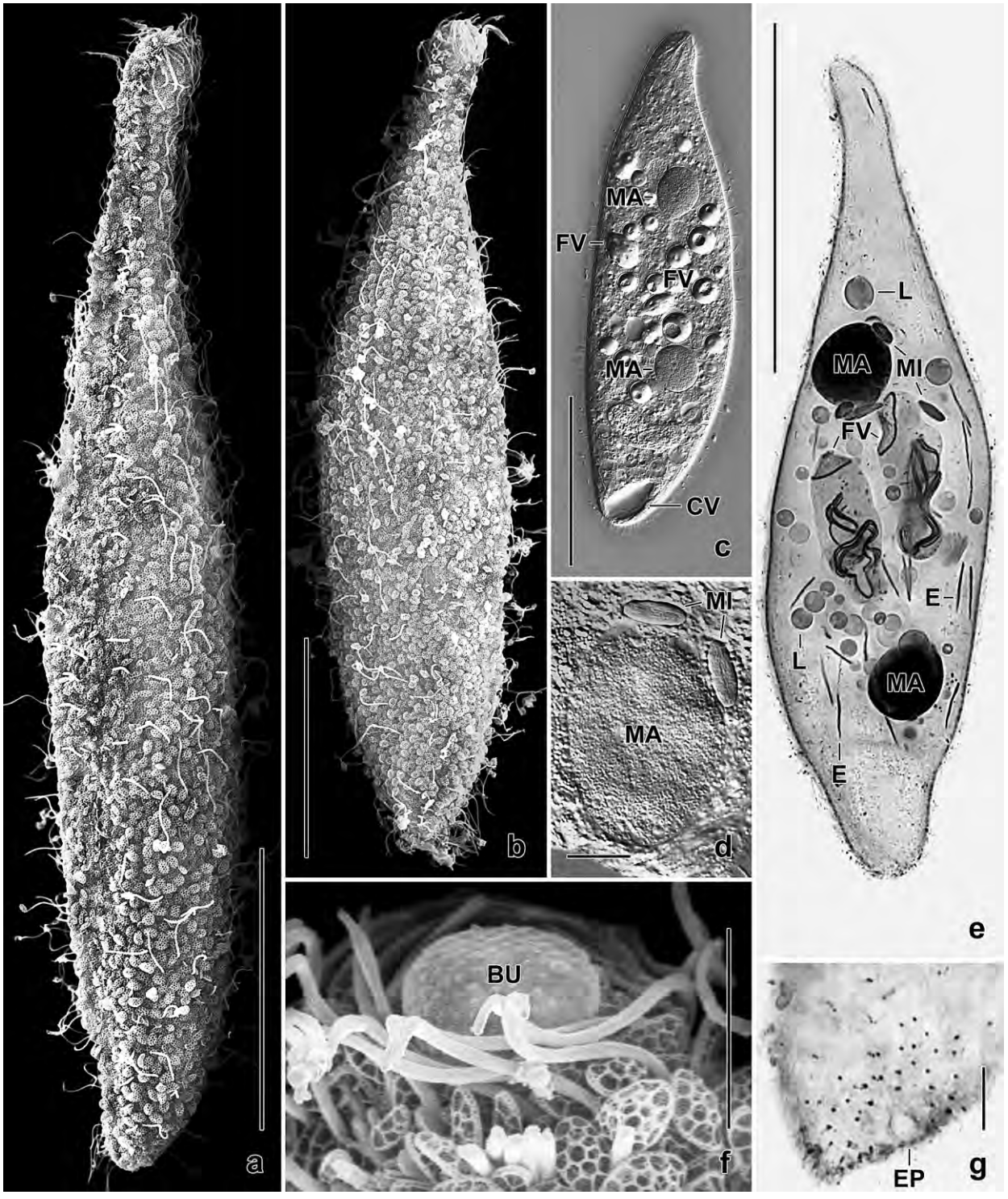

Fig. 19a–g. *Spetazoon australiense*, Austrian specimens from life (c, d), after protargol impregnation (e, g), and in the SEM (a, b, f). **a, b:** An extended (210 µm) and a moderately contracted (190 µm) specimen. **c:** A strongly contracted specimen. **d:** Nuclear apparatus. **e:** Optical section, showing food vacuoles with *Vorticella convallaria*. **f:** Oral bulge. **g:** Subterminal excretory pore. BU – oral bulge, CV – contractile vacuole, E – developing extrusomes, EP – excretory pore, FV – food vacuoles, L – lipid droplets, MA – macronuclear nodules, MI – micronuclei. Scale bars 4 µm (f), 10 µm (d, g), 50 µm (a, b), and 100 µm (c, e).

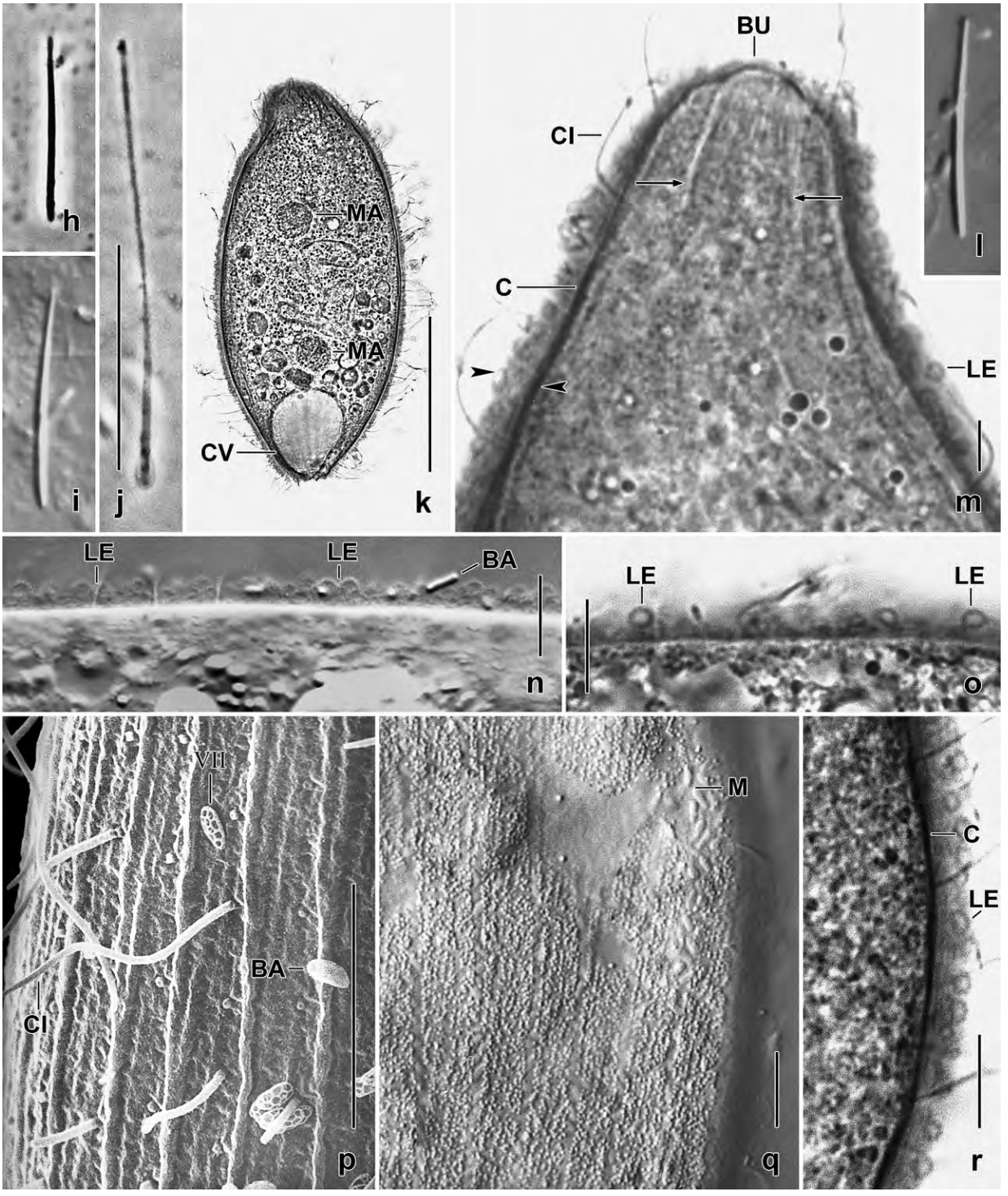

Fig. 19h–r. *Spetazoon australiense*, Austrian specimens from life (h–j, l, n, q), after alcian blue staining (k, m, o, r), and in the SEM (p). **h, i, l:** Type I extrusomes are acicular and about 20 µm long. **j:** Exploded type I extrusome, 50 µm. **k, m–o, r:** Alcian blue stains of the mucilaginous layer (m, opposed arrowheads), i. e., the slime and the lepidosomes thus having more contrast than in vivo (cp. Fig. 19o, r with Fig. 19n). Opposed arrows in (m) mark the tubular pharynx. **p, q**: Surface views, showing cortical ridges and dense cortical granulation. BA – bacteria, BU – oral bulge, CI – cilia, CV – contractile vacuole, LE – lepidosomes, M – mitochondria, MA – macronuclear nodules. Scale bars 10 µm (m–r), 25 µm (j), and 100 µm (k).

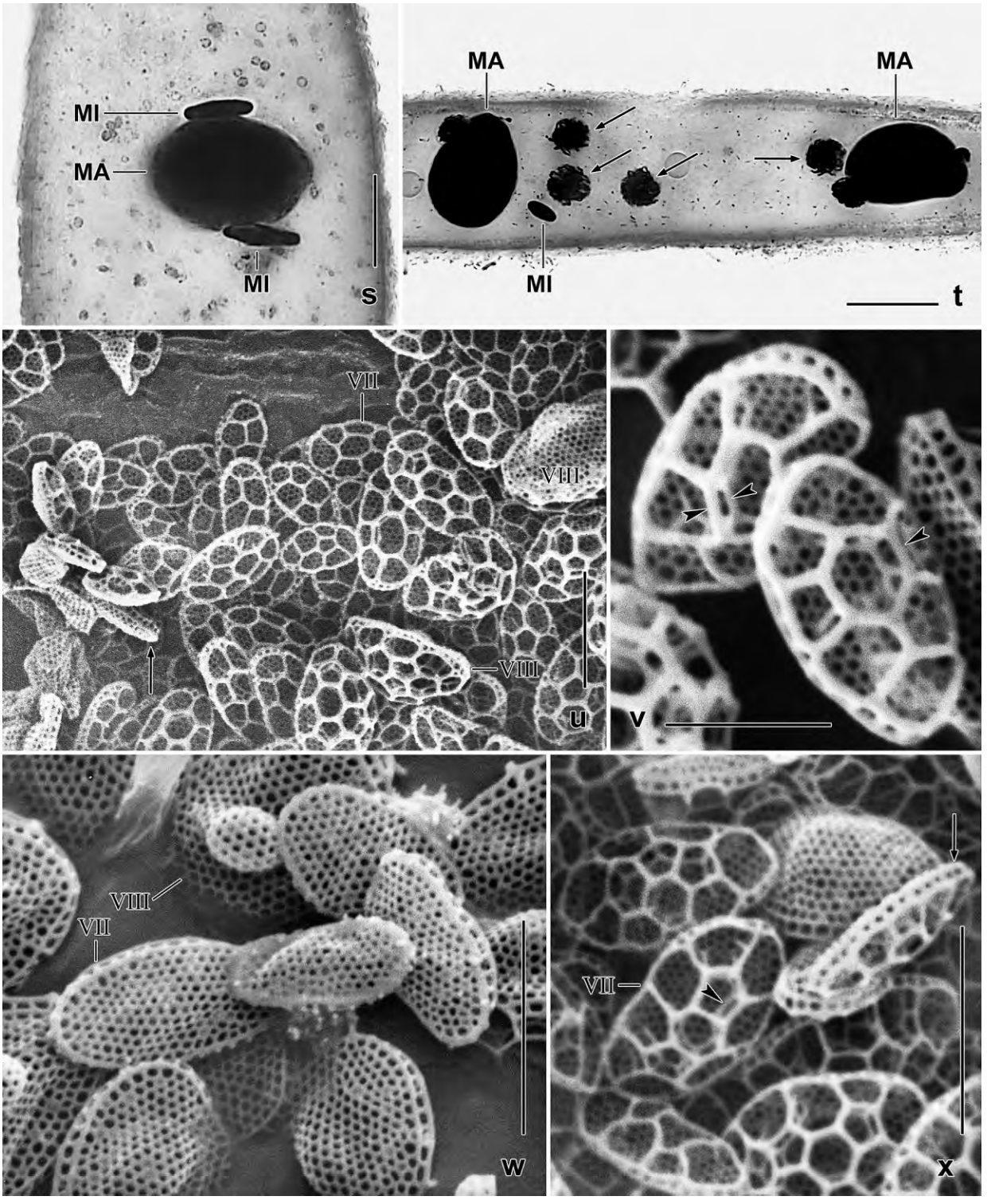

Fig. 19s–x. *Spetazoon australiense,* Austrian specimens after protargol impregnation (s, t) and in the SEM (u–x). Arrows in (u, x) mark lateral views of type VII lepidosomes. **s:** Nuclear apparatus, showing the elongate ellipsoid micronuclei. **t:** Divider with swollen micronuclei (arrows). **u, v, x:** Superstructure of type VII lepidosomes with complex central mesh (arrowheads). **w:** Posterior polar view of type VII and VIII lepidosomes. MA – macronuclear nodules, MI – micronuclei. Scale bars 1 µm (v), 2 µm (u, w, x), and 15 µm (s, t).

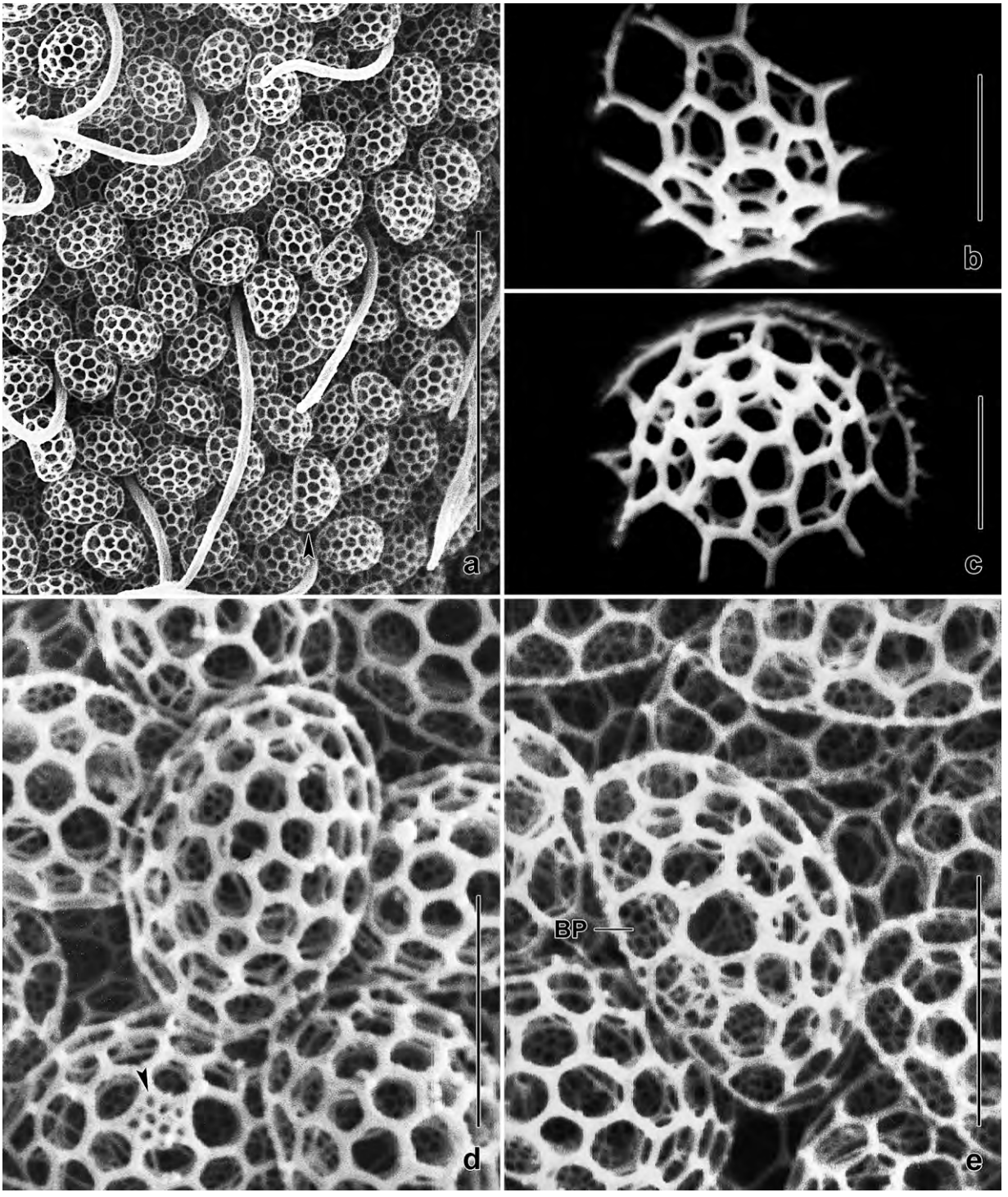

Fig. 20a–e. *Spetazoon australiense,* lepidosomes of Austrian specimens in the scanning electron microscope. **a:** Overview, showing two layers of narrowly spaced type VIII lepidosomes in the periphery of the mucilaginous layer. **b, c:** Anterior polar views, showing the complex polygons made of pierced planks. **d, e:** Anterior and oblique anterior polar view, showing the baseplate and the superstructure made of planks pierced by minute polygonal meshes. The arrowhead in (d) marks a polygon "closed" by a narrowly honeycombed membrane (?). BP – baseplate. Scale bars 1 µm (b, c), 2 µm (d, e), and 10 µm (a).

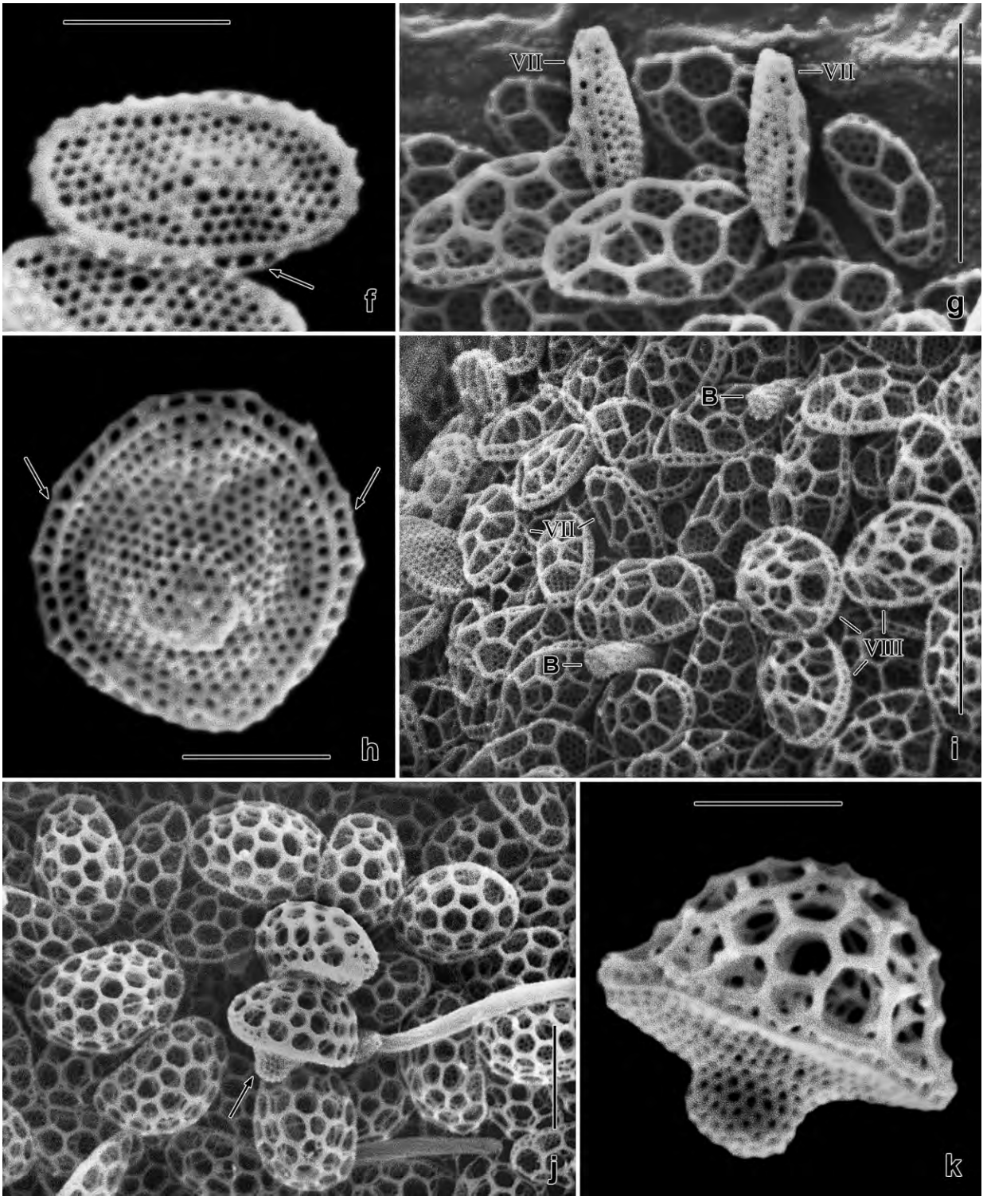

Fig. 20f–k. *Spetazoon australiense*, type VII and VIII lepidosomes of Austrian specimens in the scanning electron microscope. **f, h:** Posterior polar view of type VII and VIII with basering made of quadrangular meshes marked by arrows. **g:** Polar and lateral views of type VII. **i:** Various views of type VII and VIII. **j:** Anterior polar views and lateral view (arrow) of type VIII. **k:** Type VIII lepidosome, showing the complex polygons. B – dorsal bristles. Scale bars 1 µm (f, h, k) and 2 µm (g, i, j).

Cilia about 15 µm long in vivo, loosely spaced, proximal third motionless due to the mucilaginous layer; arranged in an average of 37 equidistantly, narrowly spaced, meridional rows two differentiated to a dikinetal dorsal brush anteriorly. Dikinetal brush rows isostichad, bristles up to 6 µm long and likely structured as shown in Fig. 18h; brush row 3 composed of monokinetids with rod-shaped bristles about 4 µm long in vivo, extends to near posterior body end (Fig. 18a, c, e, 19p; Table 9).

Oral bulge about 4 × 4 µm in vivo while 7 × 4.5 µm in protargol preparations; rectangular in vivo, bluntly conical after protargol impregnation, discoidal in SEM preparations (Fig. 18a, c, e, 19e, f; Table 9). Circumoral kinety at base of oral bulge, composed of narrowly spaced dikinetids. Pharynx tubular, slightly divergent (Fig. 19m).

Comparison of Australian and Austrian population (Table 10): It was a great surprise to find this Australian species in Austria. On the other hand, the trachelophyllids were so poorly known in 1994 that such "discoveries" have to be expected. Although we did not find really distinct differences between the Australian and Austrian populations, we provided a full description of the later because refined methods might find significant differences in future.

The data in Table 10 show a good agreement of the Australian and the Austrian population of *S. australiense* although the number of ciliary rows, which is an important feature due to its low

Table 10. Comparison of three *Spetazoon* populations. Data based on protargol-impregnated, randomly selected specimens. Arithmetic means and extremes (in parentheses) are shown.

Characteristics	Australia (Foissner 1994)	Austria (this study)	Venezuela (this study)
Body, length (µm)	229 (185–285)	230 (165–295)	182 (130–255)
Body, width (µm)	51 (38–61)	57 (43–72)	68 (53–88)
Ciliary rows, number	31 (29–34)	37 (34–40)	24 (23–26)
Dikinetids in dorsal brush row 1, number	24 (16–36)	24 (19–29)	20 (13–25)
Type I extrusomes, shape and size	acicular, ~ 20 µm	acicular, ~ 20 µm	almost rod-shaped, < 15 µm
Number of specimens investigated	12	21	18

variability (CV ≤ 5%), hardly overlaps. This is corroborated by the type VIII lepidosomes. In the Austrian specimens, they contain an irregular, filamentous reticulum (Fig. 20e, j, k, 21d) while two subtypes occur in the Australian specimens: one is very similar to the Austrian pattern (Fig. 21d, 22q, s, 23c, f) while the other occurs only in Australia and is characterized by straight, thread-like filaments (Fig. 21c, f, 22r, t, u, 23d, g). On the other hand, the Venezuelan population, which has only 24 ciliary rows and slightly different extrusomes, is very likely a distinct species.

As concerns body shape, we are convinced that Figure 1 in Foissner (1994) shows a slightly contracted specimen (Fig. 18i) because the shape of protargol-impregnated specimens is virtually identical in the Australian and the Austrian cells.

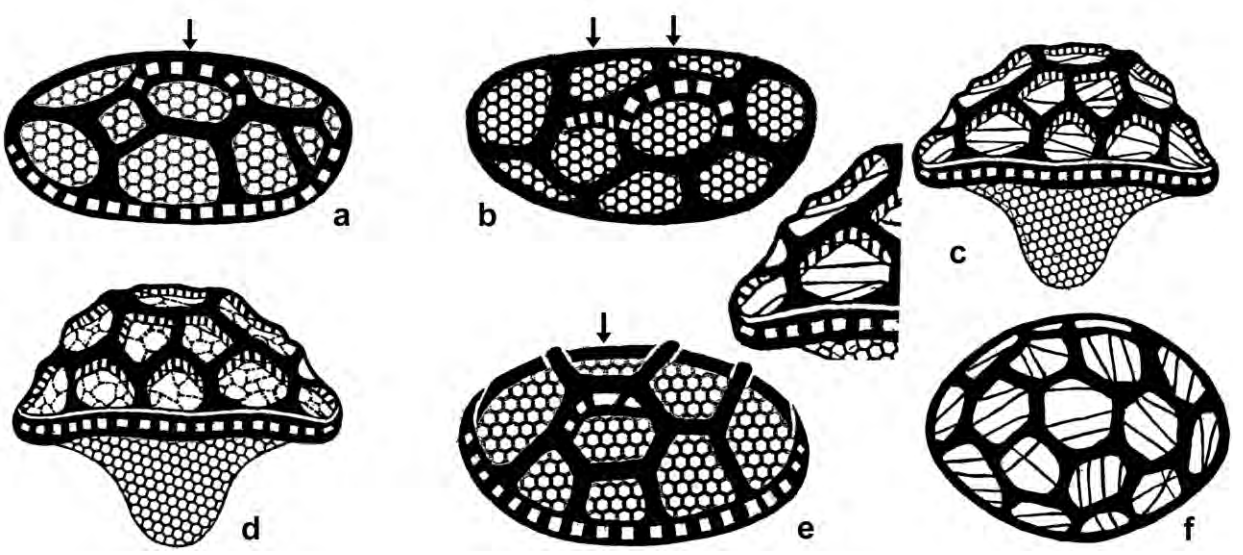

Fig. 21a–f. *Spetazoon australiense*, type VII (a, b, e) and type VIII (c, d, f) lepidosomes. Redrawn and slightly schematized from scanning electron micrographs. The arrows in the type VII lepidosomes mark the pierced planks in the central facete. For details, see text.

Splitters would possibly separate the Australian and Austrian population at subspecies level while lumpers will argue that other important features match very well, e. g., the shape and size of the extrusomes and the dorsal brush. We suggest to study further populations before separation.

***Spetazoon australiense*, a junior synonym of *Trachelophyllum vestitum* Stokes, 1884a?** The description of Stokes is rather detailed but misses, understandably, important details, such as the number of ciliary rows, the structure of the dorsal brush, and the length of the extrusomes (Fig. 18n). However, there are three features that match (Fig. 18a, d): body length in vivo (~ 290 and 250 μm), the shape of the extrusomes (acicular), and the thick mucilaginous layer. But there are two problems: body shape and extrusome length. Body shape is a difficult feature in the contractile trachelophyllids: it is clavate and 3.5:1 according to the illustration of Stokes (Fig. 18m) while the description states: "the length from four to five times the breadth". Thus, Stokes illustrated a more or less contracted specimen. However, we never saw cells with a shape like that illustrated by Stokes in the Australian and Austrian populations, suggesting that it is a different North American species. This is corroborated by the length of the extrusomes: about 58 μm according to the illustration of Stokes, only 20 μm in the Australian and Austrian cells.

Trachelophyllides nov. gen.

Diagnosis: Trachelophyllidae Kent, 1881 with type I, IV, and IX lepidosomes. Type I on pellicle, composed of a finely honeycombed, elliptical baseplate from which a widely and polygonally faceted, slightly convex superstructure emerges. Type IV mixed with type IX, ampulliform, composed of a finely honeycombed, elliptical, moderately concave baseplate from which a widely and polygonally faceted, convex superstructure emerges containing a filamentous network. Type IX on type I lepidosomes, mushroom-shaped with comparatively long and thick, finely honeycombed stalk and trapeziform cap composed of large polygons and containing a three-dimensional net of filaments and membranoid structures.

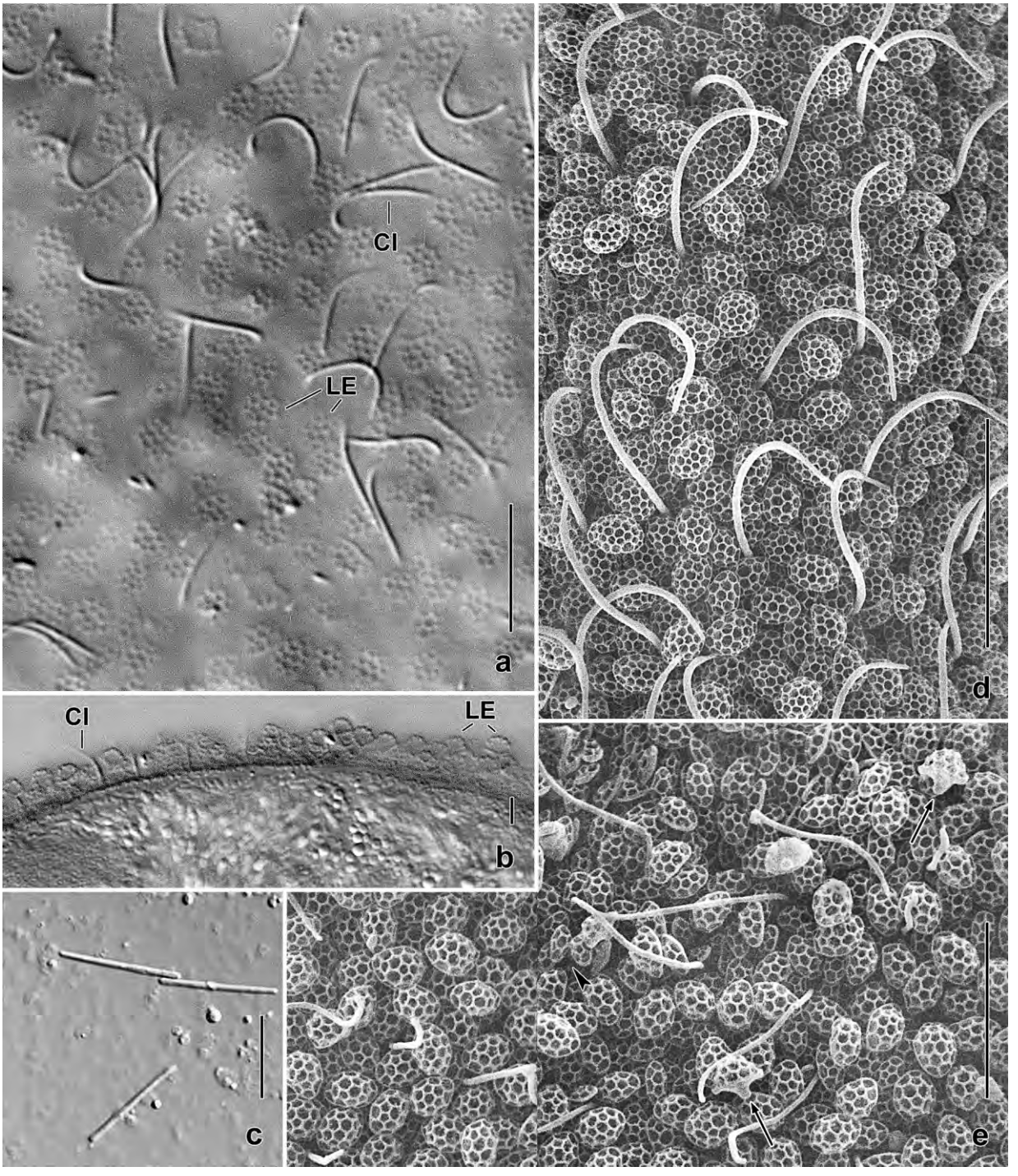

Fig. 22a–e. *Spetazoon australiense*, Venezuelan (a–c) and Australian (d, e) specimens from life (a–c) and in the scanning electron microscope. **a, b:** Surface view and optical section of cortex, showing that the lepidosomes of the Venezuelan specimens are highly similar to those of the Australian type population illustrated in Foissner (1994). **c:** The extrusomes of the Venezuelan specimens are less distinctly acicular than those from Australia (cp. Foissner 1994). **d, e:** Surface views, showing the dense layer of type VIII lepidosomes. Arrows mark side views; arrowhead denotes the smaller and simpler type VII scales. CI – somatic cilia, LE – lepidosomes. Scale bars 3 µm (b) and 10 µm (a, c–e).

Fig. 22f–h. *Spetazoon australiense*, Australian specimens in the scanning electron microscope, showing shape and size variability and the dense lepidosome cover. **f, g:** Slightly contracted specimens in narrow side view. The lepidosomes are rather loosely attached, and thus some can be found in the surroundings (arrowheads). **h:** Broad side view of a large, slightly contracted specimen, resembling those shown by Foissner (1994). Scale bars 50 µm.

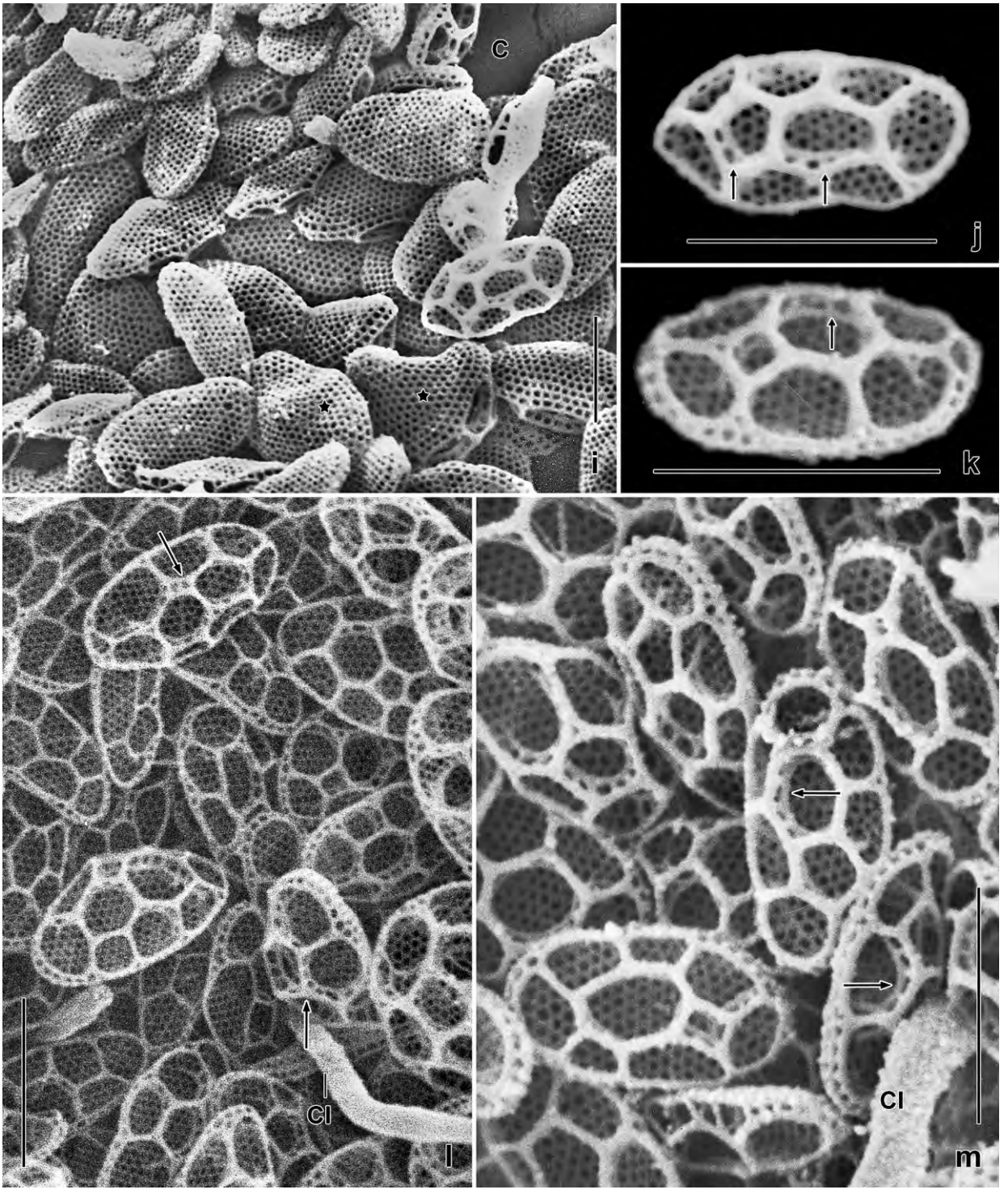

Fig. 22i–m. *Spetazoon australiense* from Australia, type VII lepidosomes in the scanning electron microscope. The type VII lepidosomes have an average size of 2.3 × 1.3 × 0.6 µm and consist of a finely perforated baseplate and an arched superstructure made of nine large polygons on average. **i:** Baseplate views. Asterisks mark baseplate of two type VIII scales (see next plates). **j–m:** Surface views, showing the arched superstructure with the central facete having a row of honeycombs (arrows). The type VII scales form one or two layers on the cell surface. C – cell cortex, CI – ordinary somatic cilia. Scale bars 2 µm.

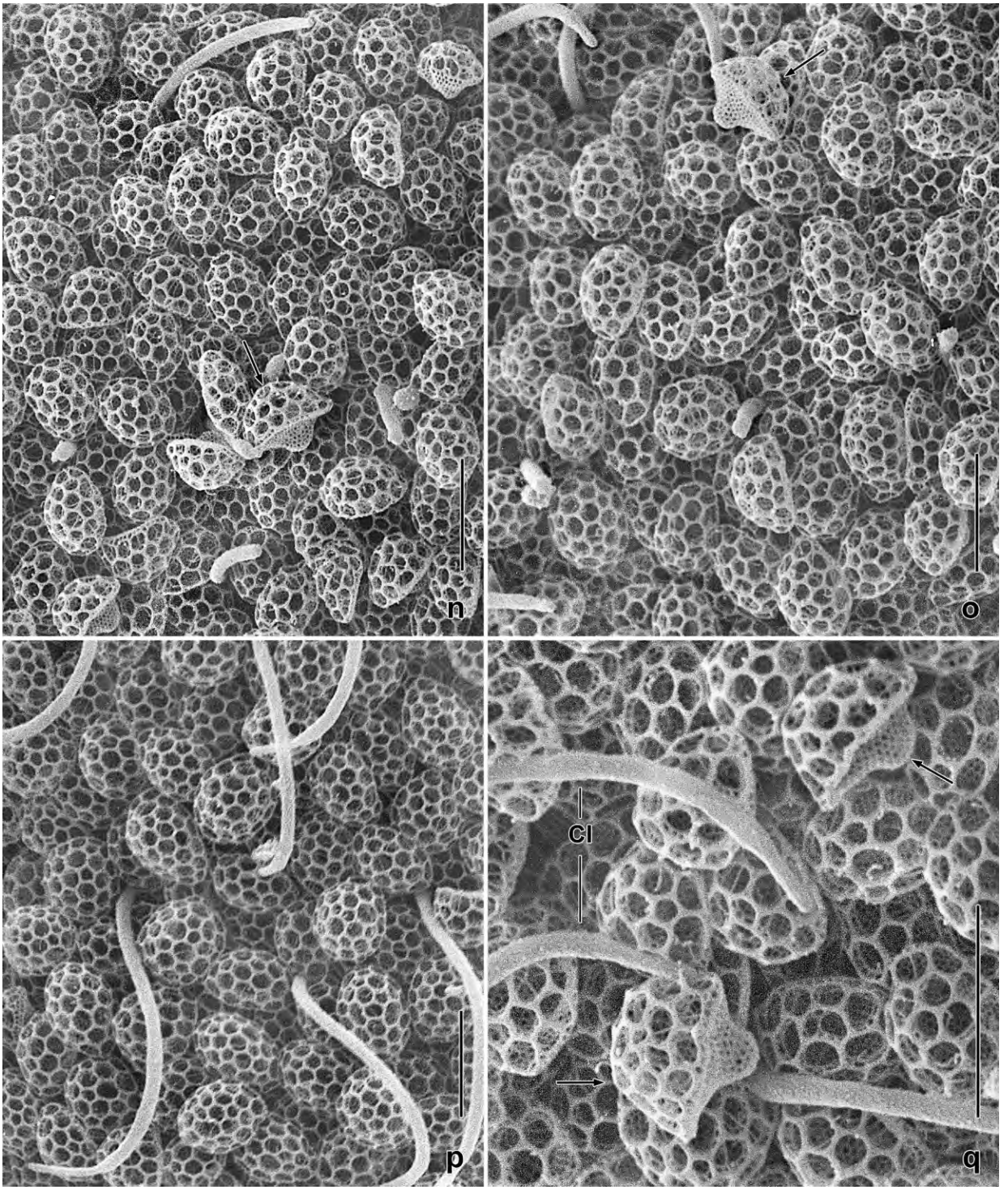

Fig. 22n–q. *Spetazoon australiense* from Australia, type VIII lepidosomes in the scanning electron microscope. The type VIII lepidosomes form one or two layers upon the type VII lepidosomes and have a highly characteristic, ampulliform shape recognizable in side view (arrows and last plate). They have an average size of 3 × 2.3 × 2.2 µm and the hemispherical superstructure consists of an average of 19 polygons while the convex baseplate is finely faceted. Within the superstructure are special filaments shown on the next plate. CI – ordinary somatic cilia. Scale bars 3 µm.

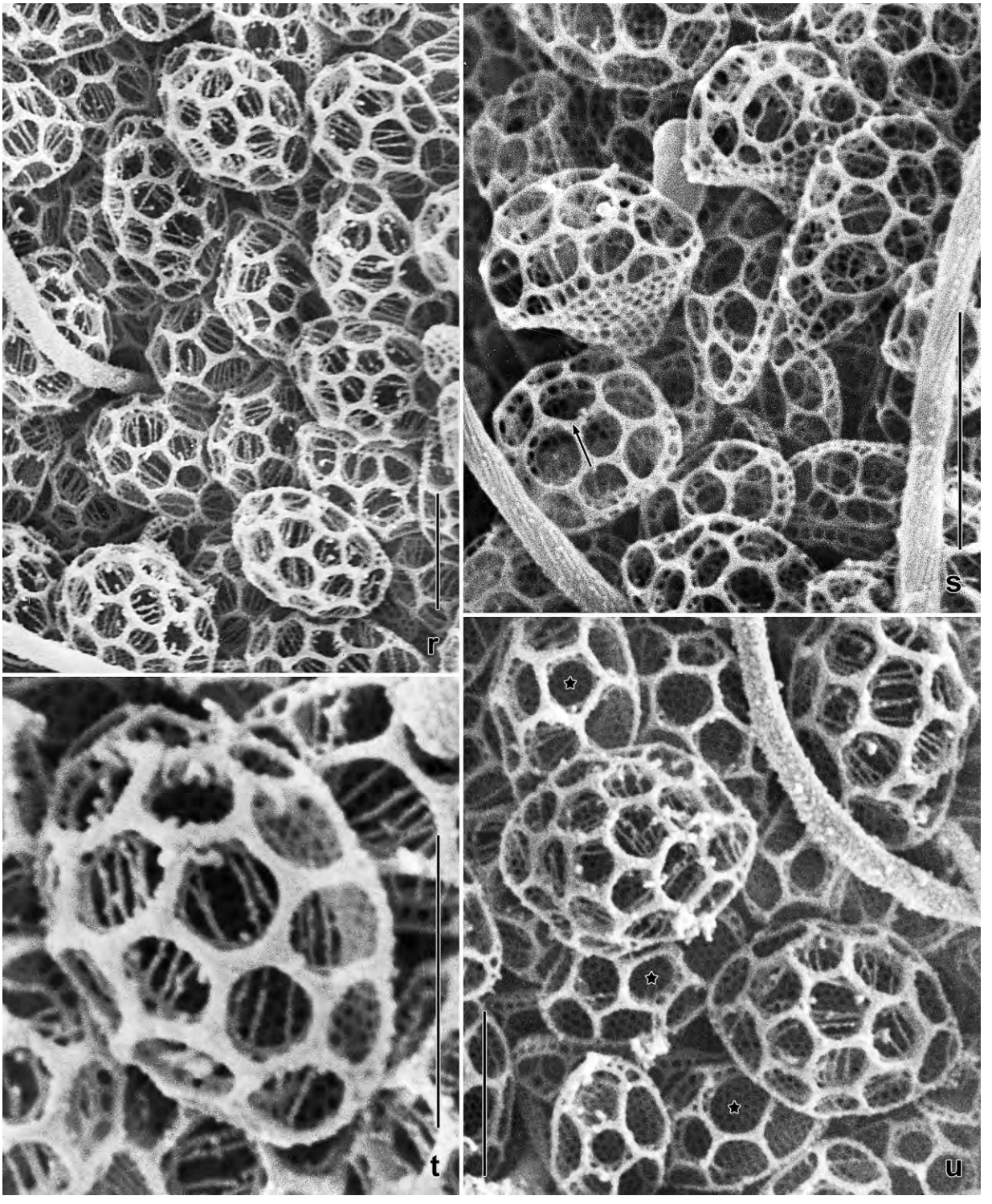

Fig. 22r–u. *Spetazoon australiense* from Australia, type VIII lepidosomes in the scanning electron microscope. When the magnification is sufficient, filamentous structures, which form a more or less distinct reticulum within the hemispherical superstructure, becomes visible. The arrow in (s) marks a polygon where its pierced planks are well recognizable. Asterisks in (u) denote type VII lepidosomes lacking these internal structures. Scale bars 2 μm.

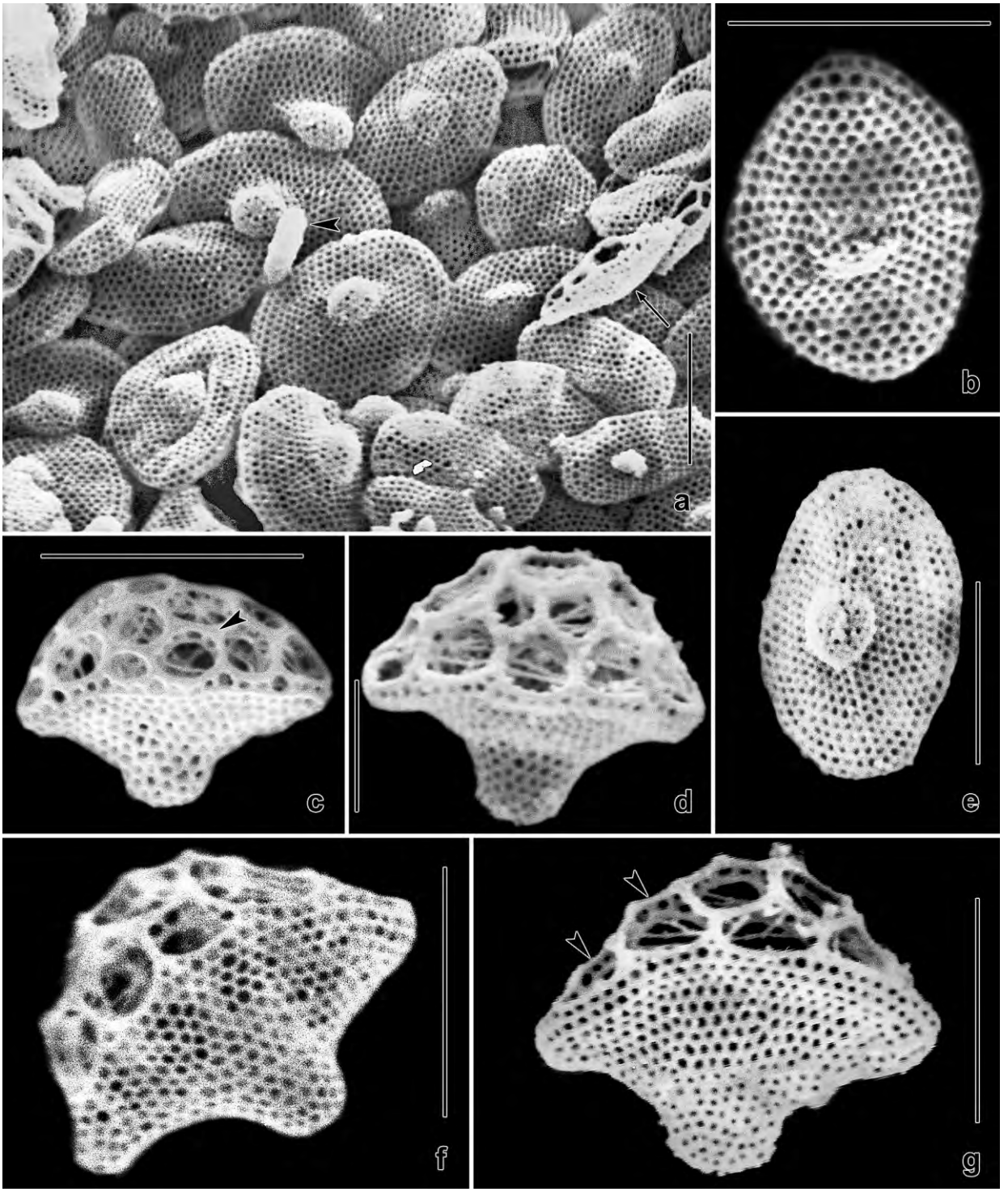

Fig. 23a–g. *Spetazoon australiense* from Australia, type VIII lepidosomes in the scanning electron microscope. **a, b, e:** Posterior polar views, showing the finely faceted baseplate. The arrow in (a) marks a flat type VII lepidosome, while the arrowhead denotes a bristle of dorsal brush row 3. **c, d, f, g:** Lateral views, showing the ampulliform (mushroom-like) shape and the three-dimensional net within the superstructure. The arrowheads in (c, g) mark the pierced planks of the polygons. Scale bars 2 µm.

Type species: *Trachelophyllum sigmoides* Kahl, 1926.

Etymology: The name is a composite of the genus-group name *Trachelophyllum* and the Greek suffix *ides* (similar), referring to the similarity with *Trachelophyllum*. Masculine gender.

Species assignable: Monotypic!

Remarks: As yet, *T. sigmoides* is the sole trachelophyllid with three types of lepidosomes, of which type IX is unique justifying a distinct genus. For further details, see **Remarks** to genus → *Spetazoon.*

Trachelophyllides **sigmoides** (Kahl, 1926) **nov. comb.** (Fig. 24a–w, 25a–v, 26a–x; Table 11)

The redescription is based on a population from a *Sphagnum* pond in the southeast of Germany (for details, see Kreutz & Foissner 2006). We thank Dr. Martin Kreutz for sending material several times. Unfortunately, this species was always very rare, as stated also by Kahl (1926, 1930a), and thus we could impregnate only a few specimens because most cells were used for live observation and scanning electron microscopy.

Improved diagnosis (contains also data from Kahl): Size in vivo about 350 × 65 µm; contractile by about 30% of body length. Asymmetrically lageniform with slightly curved anterior region and bluntly pointed posterior end; dorsoventrally flattened up to 2:1. 2 broadly ellipsoid, widely distant macronuclear nodules each with several globular to broadly ellipsoidal micronuclei. 2 types of extrusomes attached to oral bulge: type I rod-shaped and slightly curved, ~ 50 × 0.5 µm in vivo; type II rod-shaped to indistinctly acicular, ~ 5 × 0.4 µm in vivo. Usually green by symbiotic algae. About 40 ciliary rows; dorsal brush isostichad. Lepidosomes and slime produce a 5–7 µm thick mucilaginous layer easily recognizable in vivo. Type I lepidosomes discoid, in the SEM 1.6 × 0.7 × 0.5 µm and with 5 large polygons in superstructure on average; type IV ampulliform, 2.4 × 1.1 × 1.1 µm in size and with 8 polygons in superstructure; type IX mushroom-shaped, 2.5 × 1.9 × 2.4 µm in sized and with 8 polygons in superstructure.

Type locality: Sapropelic ponds in the surroundings of the town of Hamburg, Germany (Kahl 1926, 1930).

Type material: Not available. We deposited 2 voucher slides with some protargol-impregnated specimens from the Simmelried in Germany in the Biology Centre of the Upper Austrian Museum in Linz (LI). Relevant specimens have been marked by black ink circles on the coverslip.

Etymology: The Greek adjective *sigmoides* (S-shaped) refers to the curved anterior region which causes a slightly sigmoid outline (Kahl 1926).

Description: Size in vivo 250–480 × 40–90 µm matching well the 250–400 × 60–70 µm reported by Kahl (1926, 1930a); usually about 350 × 65 µm, length:width ratio thus 5.4:1 on average (Table 11); up to 10:1 according to a figure by Kahl (1926) here reproduced as Fig. 24u; contractile by about 30% of body length, e. g., 400 × 80 µm when extended and 350 × 90 µm when contracted

or 300 × 60 µm and 250 × 70 µm; contracts and extends very slowly with movements resembling euglenid metaboly (Fig. 24f). Basically lageniform but anterior region usually more or less curved making cells slightly sigmoid and asymmetric; dorsoventrally flattened up to 2:1, depending on amount of food ingested (Fig. 24a–c, 25a, b, f, h); when moderately contracted elongate quadrangular or indistinctly dumbell-shaped (Fig. 24f); fully contracted cells broadly lenticular, i. e., with a length:width ratio of about 2:1.

Nuclear apparatus in central quarters of cell (Fig. 24a, c, 25a, b, f–h, p). Macronuclear nodules connected by a fine strand, broadly ellipsoid, in vivo about 30 × 25 µm; with many minute nucleoli ≤ 1 µm across. Several micronuclei attached and near to macronuclear nodules, broadly ellipsoid or indistinctly pyramidal, about 6 × 5 µm in vivo. Contractile vacuole in posterior end, with large, tubular excretory pore in or near pole centre (Fig. 24a, f, 25a, b, d, e, f, h). Two types of extrusomes attached to oral bulge and scattered throughout cytoplasm (Fig. 24a, d, e, h, 25c, f, l, p, t, 26a–f; Table 11). Type I extrusomes filiform with rounded ends, slightly curved and very flexible, 35–65 × 0.4–0.6 µm in vivo, usually about 50 × 0.5 µm; make a thick, conspicuous bundle in oral area and thin bundles in cytoplasm; when extruded of typical toxicyst structure and about 100 µm long. Type II extrusomes rod-shaped to indistinctly acicular, make a highly refractive ring in oral bulge, 5–8 × 0.3–0.4 µm in vivo (Fig. 24a, e, h, 26c–e); produce small bundles in cytoplasm. Cytoplasm usually green due to symbiotic algae (*Chlorella* sp.) 5–6 × 4–5 µm in size and without eyespot, rarely cells without or with few symbiotic algae. Algae bleach within a few minutes in squashed *Trachelophyllides* while those of *Pseudoblepharisma* do not, indicating that the chlorellas of *T. sigmoides* could be cleptoplasts. This is corroborated by a

Table 11. Morphometric data on body and extrusome size (in vivo) and lepidosomes (SEM) of *Trachelophyllides sigmoides*. Measurements in µm. CV – coefficient of variation in %, M – median, Max – maximum, Mean – arithmetic mean, Min – minimum, n – number of individuals investigated, SD – standard deviation, SE – standard error of arithmetic mean.

Characteristics	Mean	M	SD	SE	CV	Min	Max	n
Body, length (in vivo)	353.8	350.0	72.5	25.6	20.5	250.0	480.0	8
Body, width (in vivo)	68.0	67.0	15.6	5.5	22.9	40.0	90.0	8
Body length:width, ratio (in vivo)	5.4	5.2	1.3	0.5	24.5	3.6	7.5	8
Type I extrusomes, length in vivo	49.5	50.0	7.6	1.8	15.4	35.0	65.0	19
Type I lepidosomes, length	1.6	1.5	0.2	0.1	10.2	1.4	1.9	30
Type I lepidosomes, width	0.7	0.7	0.1	0.1	13.1	0.6	0.9	30
Type I lepidosomes, height	0.5	0.4	0.2	0.1	34.2	0.3	0.8	11
Type I lepidosomes, number of polygons in superstructure	5.3	5.0	1.3	0.2	23.8	4.0	8.0	30
Type IV lepidosomes, length	2.4	2.4	0.2	0.1	7.9	2.0	2.7	11
Type IV lepidosomes, width	1.1	1.0	0.2	0.1	17.8	0.9	1.4	6
Type IV lepidosomes, height	1.1	1.2	0.3	0.1	26.2	0.7	1.5	7
Type IV lepidosomes, number of polygons in superstructure	8.2	7.5	1.5	0.6	18.0	7.0	10.0	6
Type IX lepidosomes, length	2.5	2.6	0.3	0.1	10.3	2.0	3.0	30
Type IX lepidosomes, width	1.9	1.9	0.3	0.1	13.5	1.5	2.8	30
Type IX lepidosomes, height	2.4	2.5	0.4	0.1	16.8	1.5	3.0	30
Type IX lepidosomes, number of polygons in superstructure	7.9	8.0	1.8	0.3	22.2	6.0	12.0	30

specimen where most algae were within fatty-appearing globules up to 30 µm across (Fig. 24a, 25v). Cells sometimes spotted, i. e., green and reddish when feeding on rhodobacteria colonies digested in vacuoles 20–30 µm across (Fig. 24a, 25e); feeds also on protists, such as euglenids and ciliates and thus frequently studded with lipid droplets 1–10 µm across (Fig. 24a, i, 25a–i, p, v). Glides slowly to rather rapidly on and in the *Sphagnum* mud slowly rotating about main body axis.

Cell and cortex very flexible, contains stripes composed of one to four rows of narrowly spaced, colourless granules about 0.5 µm in size (Fig. 24g, i, 25u); covered by a 5–7 µm thick, mucilaginous layer composed of slime and lepidosomes easily recognizable in vivo, even at moderate magnification (~ 250×; Fig. 24a, i, 25a–i, p, t, 26f). Three types of very fragile lepidosomes shrinking about 100% in SEM preparations (Fig. 24j–q, 25j, m–o, q, s, 26g–x; Table 11). Type I lepidosomes on pellicle, conspicuously ellipsoid and very thin, i. e., 1.6 × 0.7 × 0.5 µm on average; baseplate finely honeycombed, surrounded by a ring of quadrangular meshes, flat or slightly convex; dome (superstructure) slightly convex and composed of five large polygons on average (Fig. 24j, k, 26i–m). Type IV lepidosomes rare and mixed with type IX, ampulliform with short "stalk" and rather flat superstructure, conspicuously ellipsoid, i. e., 2.4 × 1.1 × 1.1 µm on average; baseplate finely honeycombed and moderately concave; dome quarter-globular, composed of eight polygons on average, contains a three-dimensional net of filaments (Fig. 24l, m, 25k, 26m, u, x). Type IX lepidosomes in two or more layers at periphery of mucilaginous coat, mushroom-shaped in lateral view, broadly ellipsoidal in polar views, in vivo 3–5 × 2–3 µm and thus well recognizable in the light microscope (Fig 24i, 25m–o, q, s), in SEM preparations shrunken to 2.5 × 1.9 × 2.4 µm on average. Baseplate membranoid and with conspicuous central, finely honeycombed stalk about as long as dome height; superstructure (mushroom cap) trapeziform in lateral view, composed of an average of eight polygons distally slightly projecting forming a pentagonal or hexagonal central polygon; polygons frequently "closed" by a membranoid structure; cap contains an irregular network of filaments and membranous structures (Fig. 24i, n–q, 25k, 26h, n–t, v, w).

Cilia in vivo 17–20 µm long, arranged in about 40 meridional, equidistant rows, as typical for trachelophyllids; proximal third of cilia immobile because constrained by the mucilaginous layer. Two rows anteriorly modified to an isostichad, dikinetal dorsal brush with up to 8 µm long bristles (Fig. 24r); left of dikinetal rows one (rarely possibly two) monokinetal row extending beyond mid-body with acicular, 8 µm long bristles; all brush kineties continue posteriorly as ordinary somatic ciliary rows.

Oral bulge in vivo only about 3 µm high and hardly separate from neck, emphasized also by Kahl (1926, 1930a, b), slightly concave and covered by a thin mucilaginous layer. Circumoral kinety at base of oral bulge, made of very narrowly spaced dikinetids each bearing a 20 µm long cilium. Oral basket tubular (Fig. 24a, c, h, f, 25a–c, f, h, t, 26f, g).

Occurrence and ecology: Common in sapropelic ponds in the surroundings of Hamburg, Germany, also during winter; usually rare, occasionally rather abundant and very slowly moving, possibly some sort of prolonged digestion (Kahl 1926, 1930a, b). We know *T. sigmoides* only from sapropelic ponds in the Simmelried, as mentioned in the introduction to the description. There are few reports of this species, and some might be misidentifications. Nauwerck (1996)

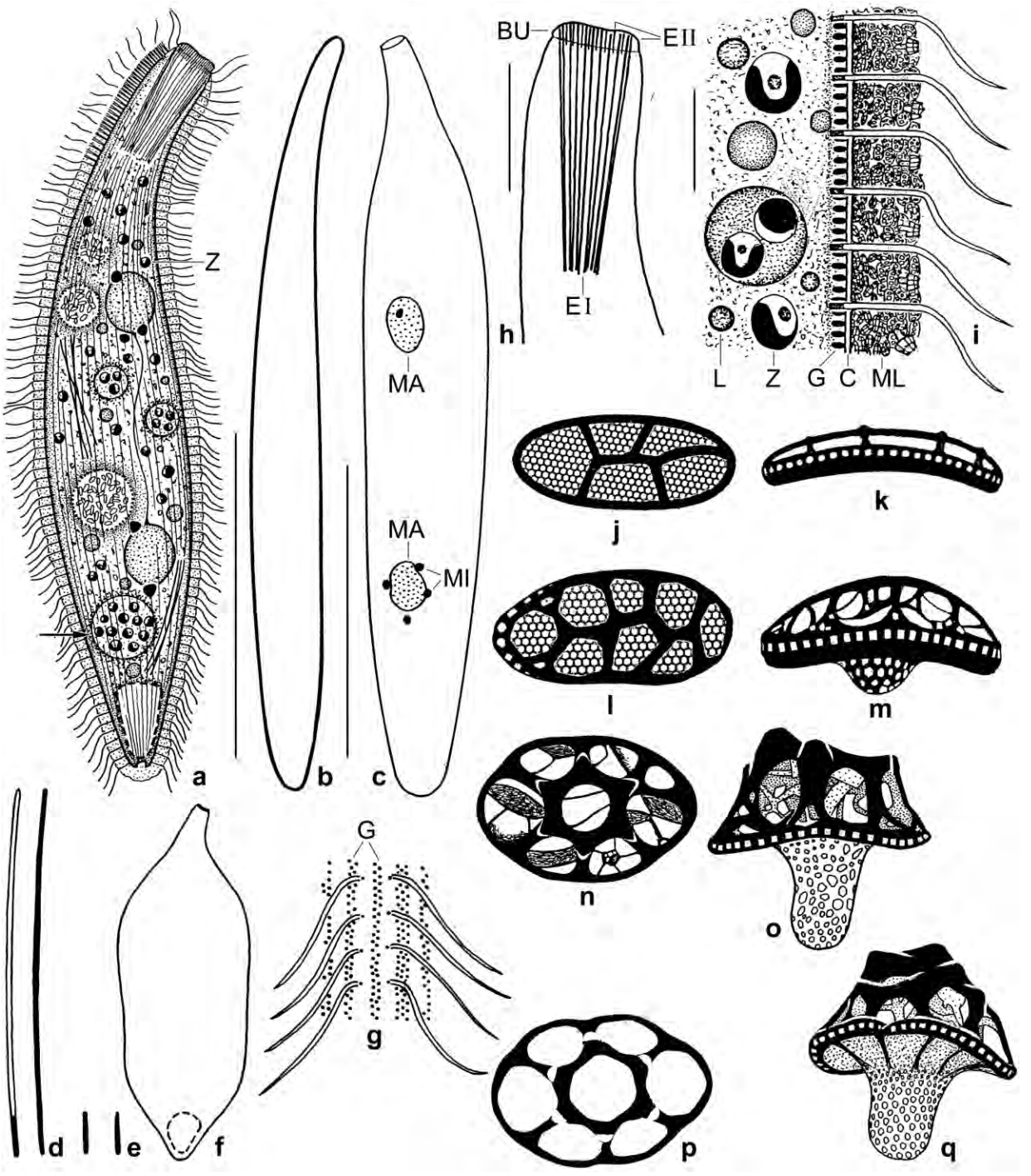

Fig. 24a–q. *Trachelophyllides sigmoides* from life (a, b, d–i), in a protargol preparation (c), and in the scanning electron microscope (j–q). **a, b:** Lateral and ventral view of a representative specimen, length 350 µm. Arrow marks a large lipid (?) droplet including many zoochlorellae. **c:** A 400 µm long specimen. **d:** Type I extrusomes without and with toxin, 50 µm. **e:** Type II extrusomes, 5 µm. **f:** A contracted specimen. **g:** Cortical granulation. **h:** Extrusomes attached to oral bulge. **i:** Optical section of periphery. **j–q:** *T. sigmoides* has three types of lepidosomes: I (j–k), IV (l, m), and IX (n–q). BU – oral bulge, C – cortex, EI, II – extrusome types, G – cortical granules, L – lipid droplets, MA – macronuclear nodules, MI – micronuclei, ML – mucilaginous layer, Z – zoochlorellae. Scale bars 10 µm (i), 25 µm (h), and 150 µm (a–c).

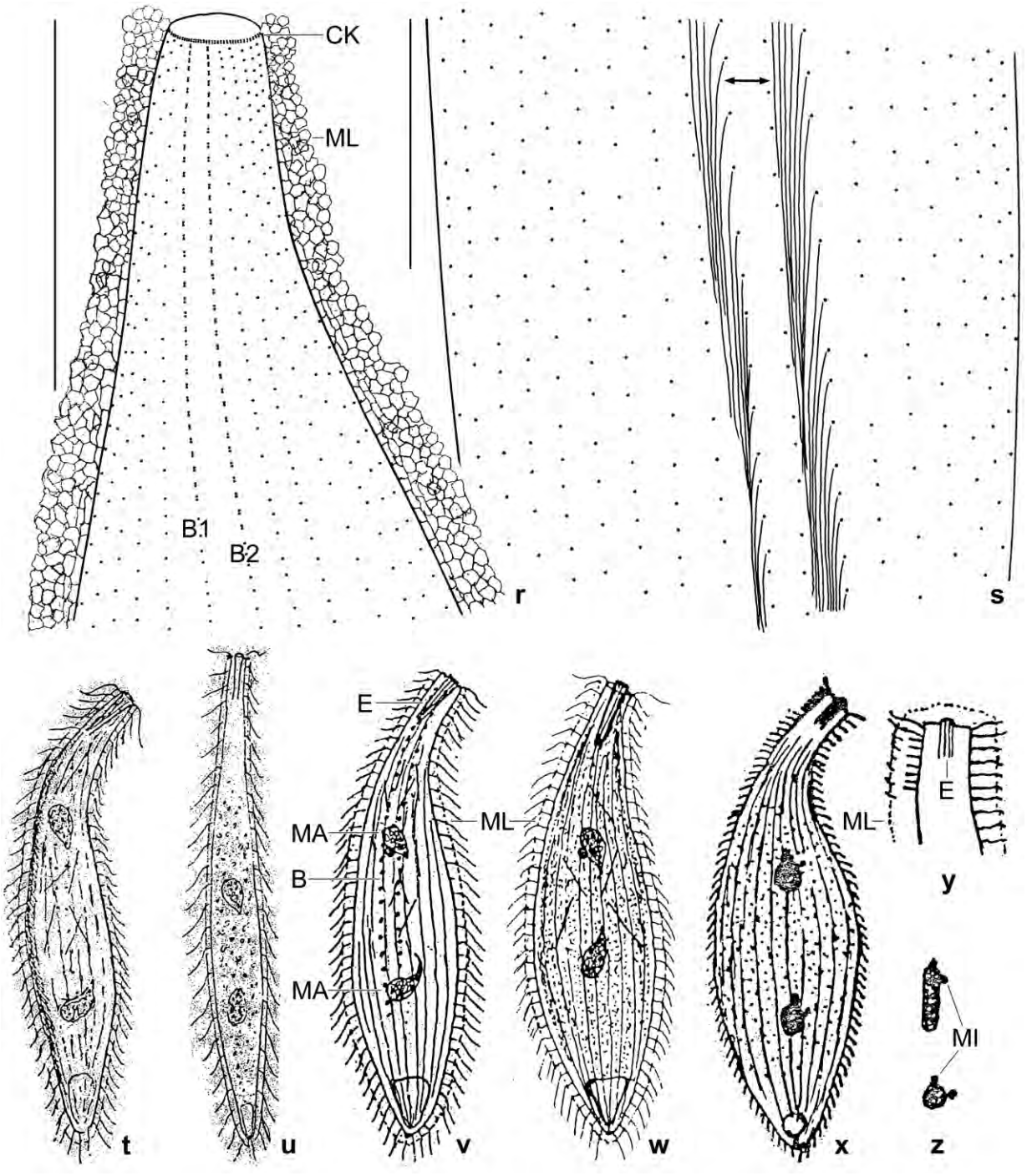

Fig. 24r–z. *Trachelophyllides sigmoides* after protargol impregnation (r, s) and from life (t–z). **r:** Dorsal side of anterior region, showing the two dikinetal isostichad brush rows. The mucilaginous layer does not cover the distal surface of the oral bulge. **s:** Ciliary rows in mid-body. The basal bodies are associated with long postciliary microtubule ribbons (arrows). **t–w:** From KAHL 1926 (t, u; 250–400 µm), KAHL 1930a (v; 400µm), and KAHL 1943 (w; 300 µm). **x–z:** From VUXANOVICI (1962). Overview (x; 32 µm?), oral detail (y), and nuclear apparatus of another specimen (z). B – dorsal brush, B1, 2 –brush rows, CK – circumoral kinety, E – extrusomes, MA – macronuclear nodules, MI – micronuclei, ML – mucilaginous layer. Scale bars 25 µm (s) and 50 µm (r).

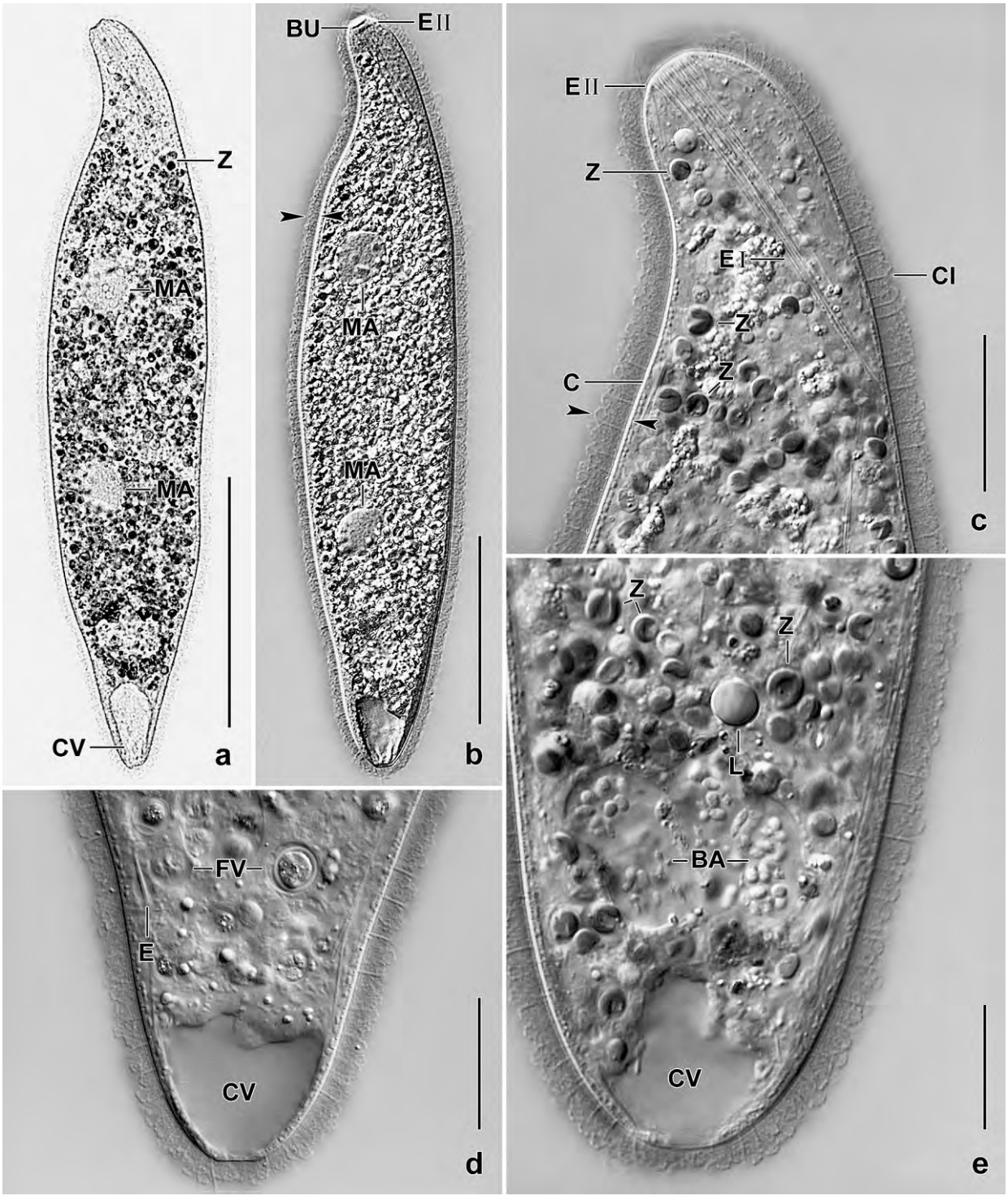

Fig. 25a–e. *Trachelophyllides sigmoides* from life. Opposed arrowheads mark cortex and mucilaginous layer. **a, b:** A possibly fully extended specimen studded with zoochlorellae in the bright field and interference contrast microscope. The type II extrusomes form a refractive transverse line (b). **c–e:** Anterior and posterior region at high magnification, showing many details, especially zoochlorellae and large food vacuoles with rhodobacteria (e). BA – bacteria, C – cortex, CI – somatic cilia, CV – contractile vacuole, E – developing extrusome, EI, II – extrusome types, FV – food vacuoles, L – lipid droplets, MA – macronuclear nodules, Z – zoochlorellae. Scale bars 25 µm (c–e) and 100 µm (a, b).

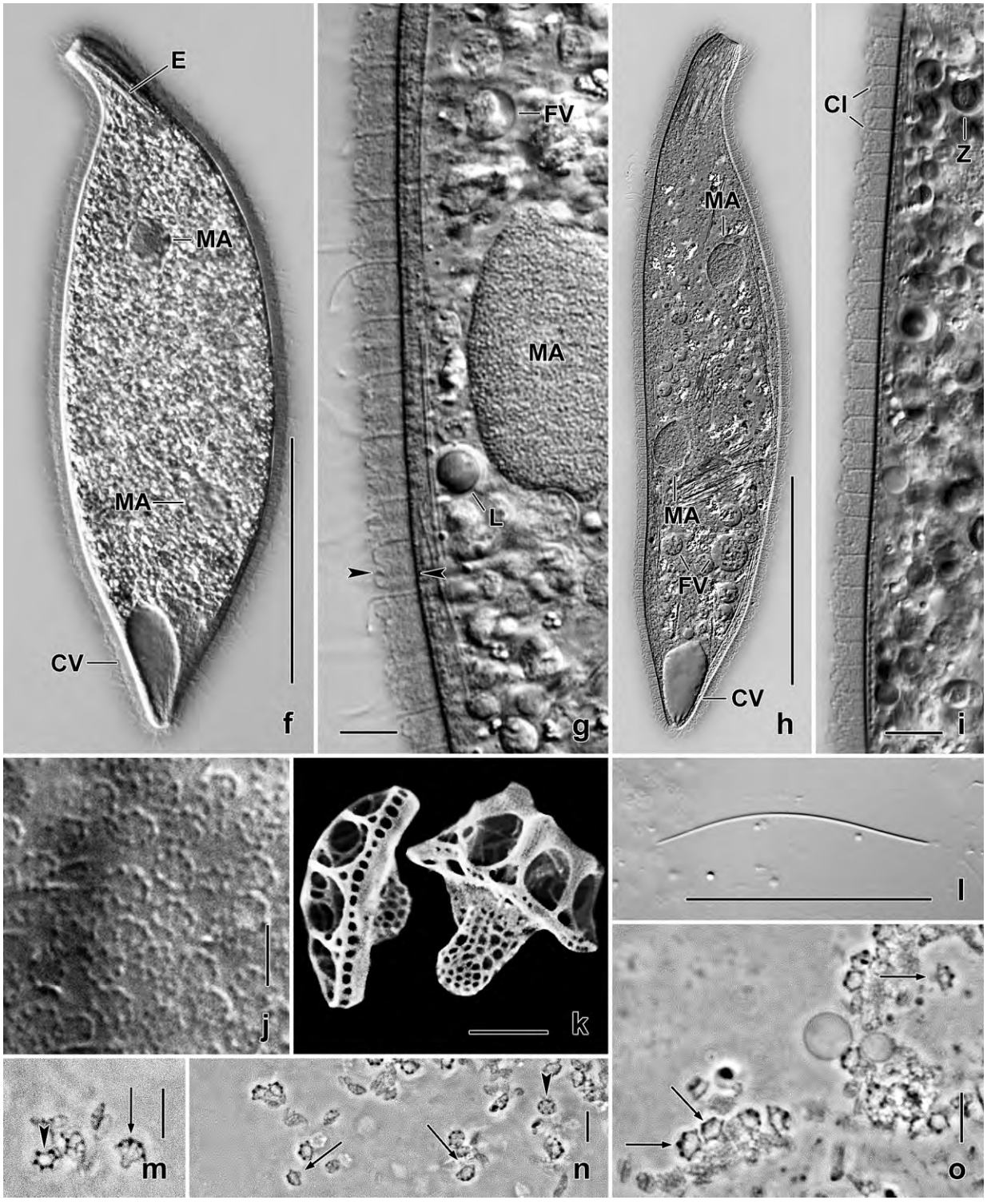

Fig. 25f–o. *Trachelophyllides sigmoides* from life (f–j, l–o) and in the SEM (k). Fig 2f, k from Kreutz & Foissner (2006). **f–i:** Overviews and details from slightly contracted specimens. Opposed arrowheads (g) mark mucilaginous layer. **j:** Surface view, showing type IX lepidosomes. **k:** A type IV and IX lepidosome. **l:** Type I extrusome. **m–o:** Type IX lepidosomes laterally (arrows) and frontally (arrowheads). CI – cilia, CV – contractile vacuole, E – extrusome bundle, FV – food vacuoles, L – lipid droplet, MA – macronuclear nodules, Z – zoochlorellae. Scale bars 1 µm (k), 5 µm (j, m–o), 10 µm (g, i), 40 µm (l), and 100 µm (f, h).

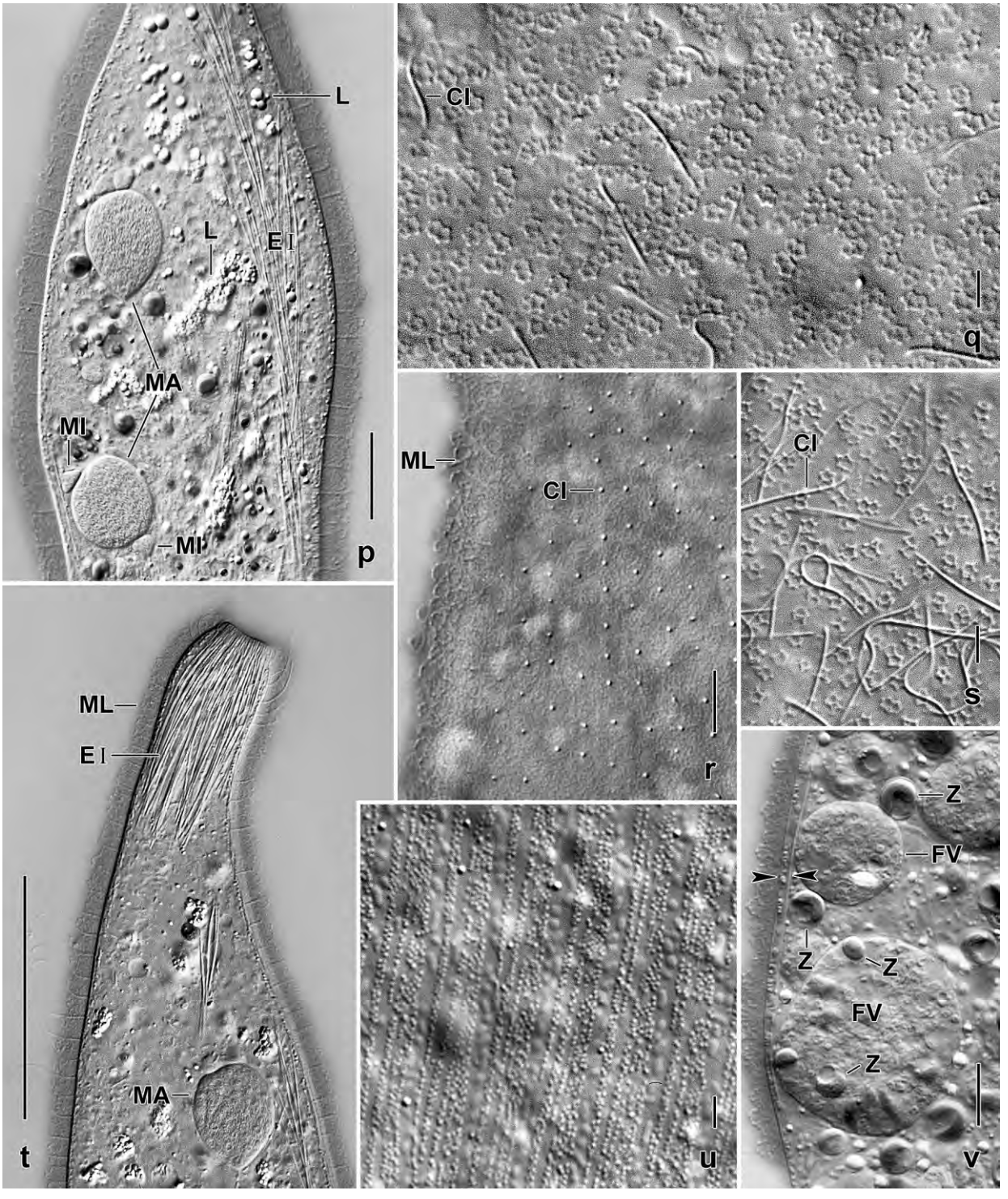

Fig. 25p–v. *Trachelophyllides sigmoides* from life. **p:** Mid-body with macronuclear nodules and pyramidal micronuclei. **q, s:** Surface views, showing type IX lepidosomes. **r:** Surface view, showing proximal end of cilia and mucilaginous layer. **t:** Anterior region. **u:** Surface view, showing cortical granulation. **v:** There are large lipid (?) droplets containing zoochlorellae. The opposed arrowheads mark the cortex and the cortical granules. CI – ordinary somatic cilia, EI – type I extrusomes, FV – food vacuoles, L – lipid droplets, MA – macronuclear nodules, MI – micronuclei, ML – mucilaginous layer, Z – zoochlorellae. Scale bars 5 µm (u), 6 µm (q, s), 10 µm (r, v), 20 µm (p), and 50 µm (t).

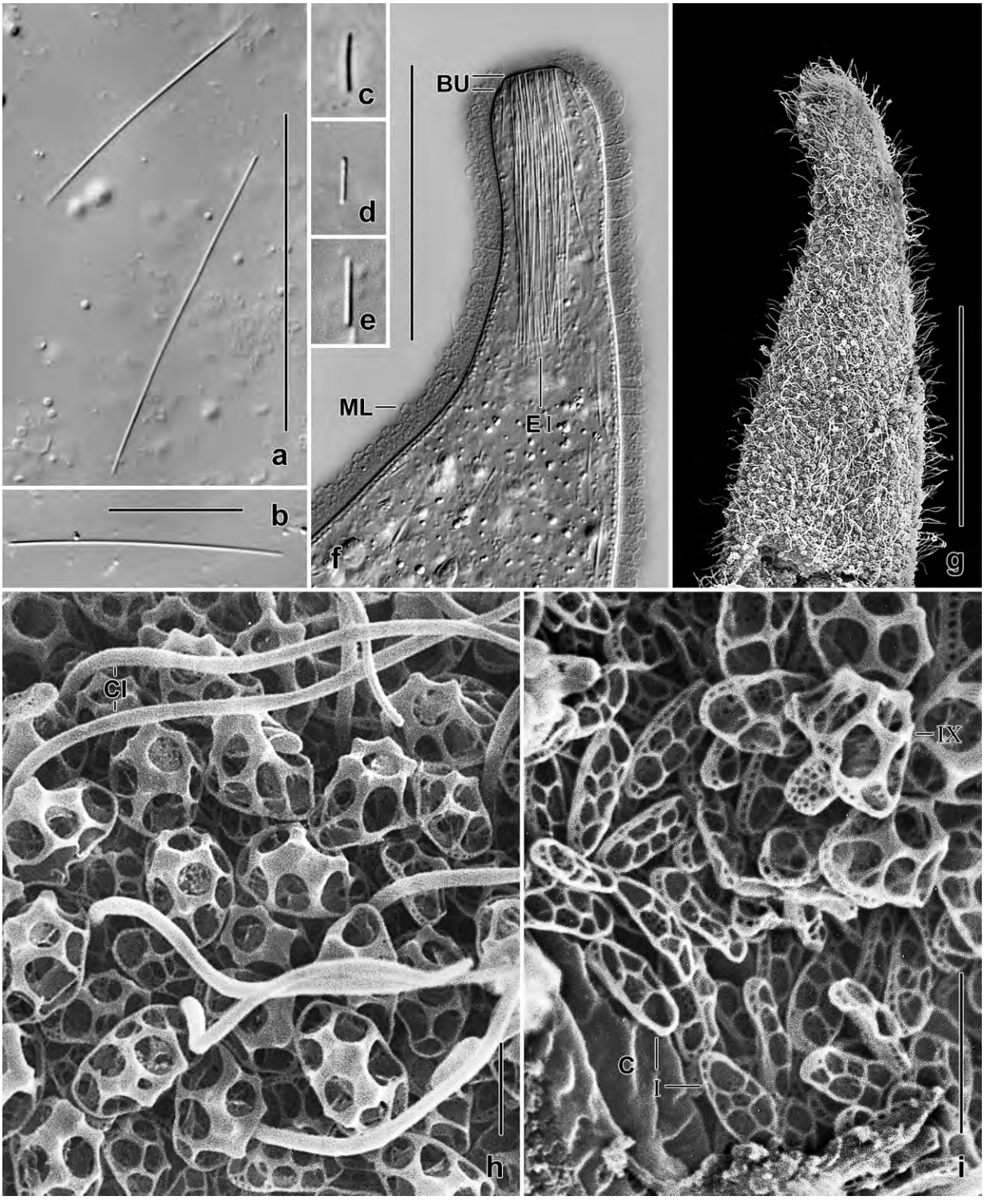

Fig. 26a–i. *Trachelophyllides sigmoides* from life (a–f) and in the scanning electron microscope (g–i). **a–e:** Type I (a, b) and type II (c–e; ~ 5 µm long) extrusomes. **f:** Oral region, showing the low oral bulge hardly separated from neck. **g:** Anterior body region. **h, i:** Type I and type IX lepidosomes. BU – oral bulge, C – cortex, CI – somatic cilia, EI – type I extrusomes. Scale bars 2 µm (h, i), 20 µm (b), 50 µm (a, f), and 80 µm (g).

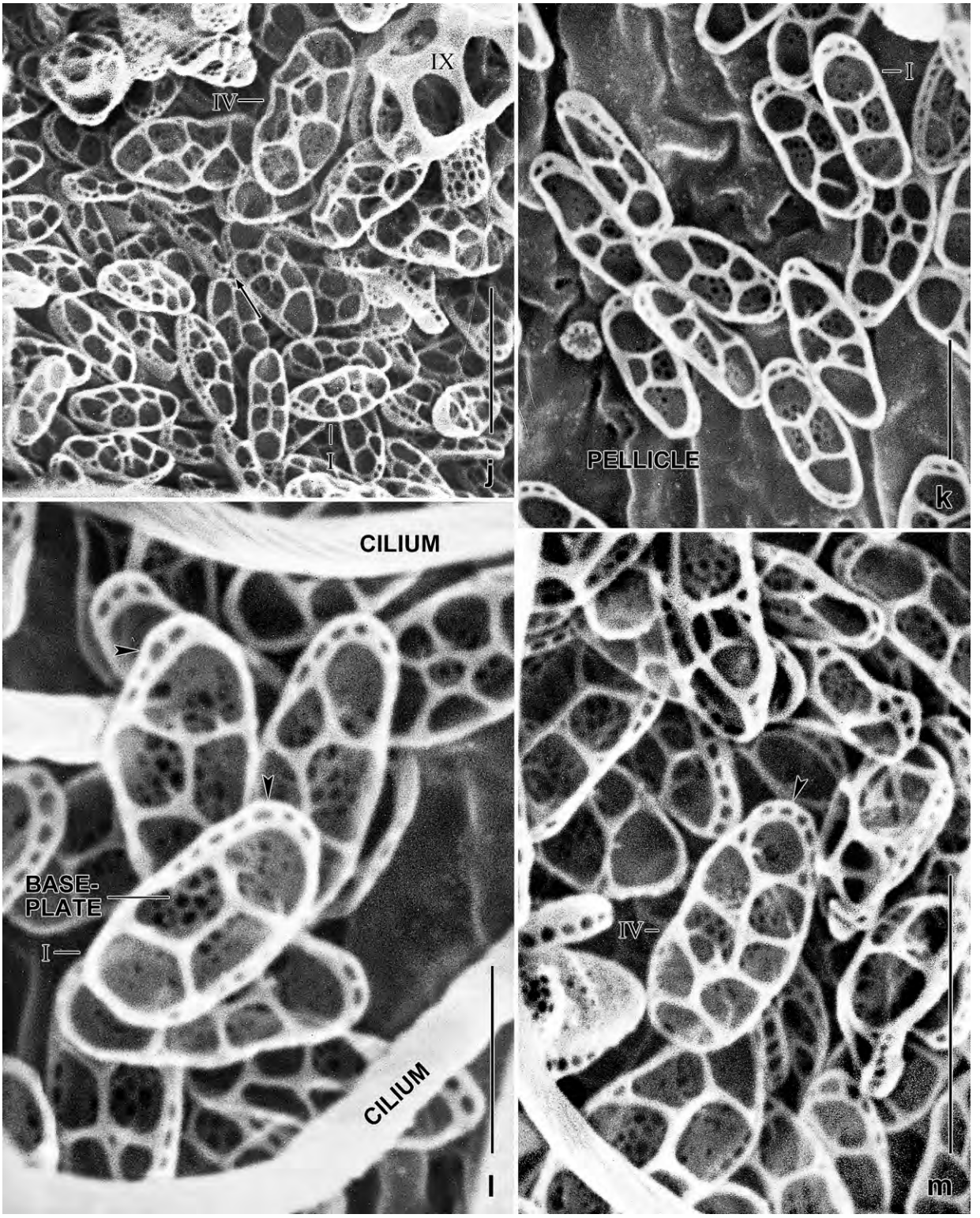

Fig. 26j–m. *Trachelophyllides sigmoides*, type I, IV, and IX lepidosomes in the scanning electron microscope. Arrow in (j) marks a type I lepidosome in lateral view. Arrowheads in (l, m) mark the ring surrounding the baseplate. Scale bars 1 µm (l) and 2 µm (j, k, m).

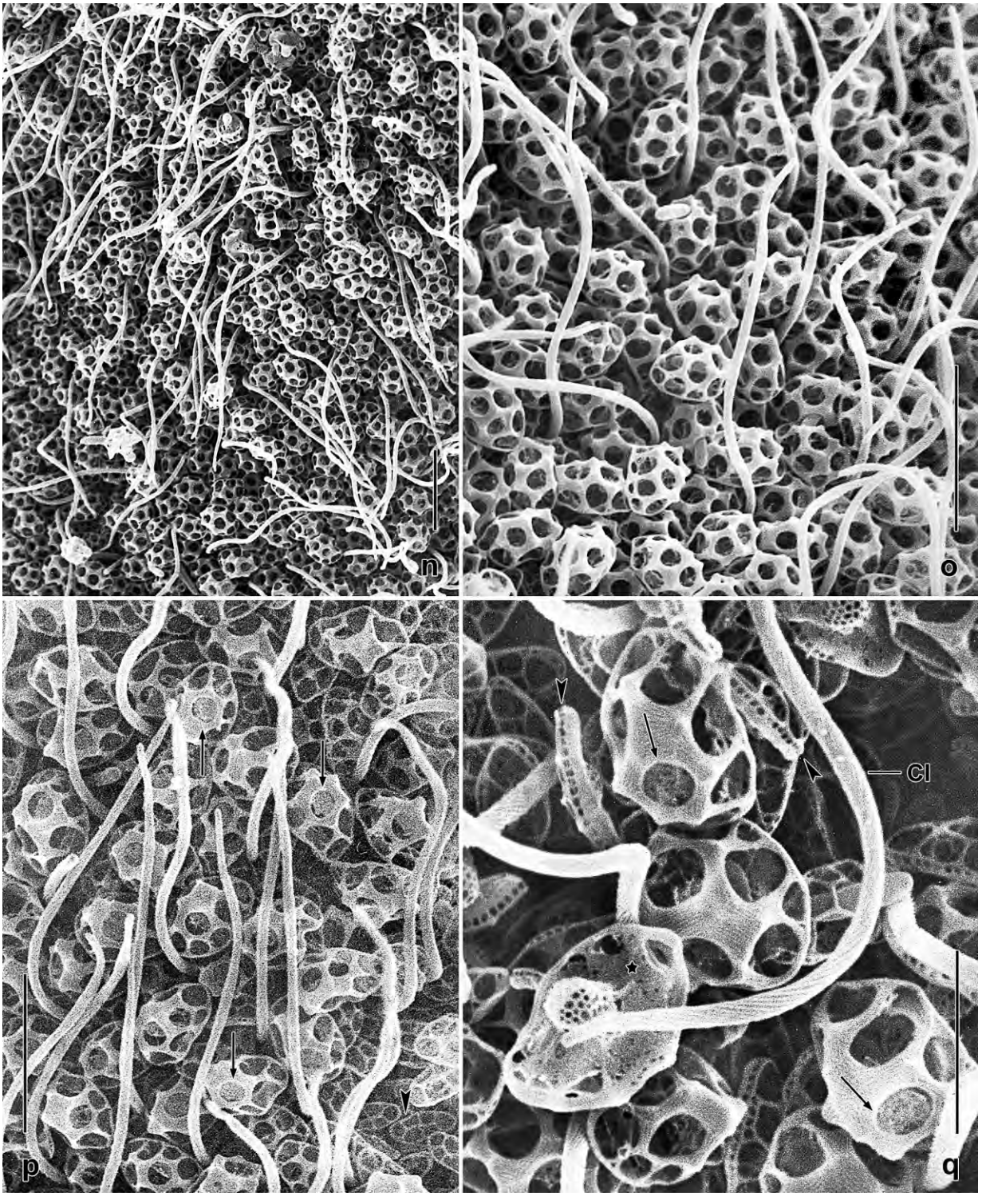

Fig. 26n–q. *Trachelophyllides sigmoides*, type I and IX lepidosomes in the scanning electron microscope. **n, o:** Overviews, showing the dense arrangement of type IX in the surface of the mucilaginous layer. **p, q:** Higher magnifications, showing part of the polygons of type IX "closed" by a membrane-like structure (arrows). The arrowheads in (q) mark lateral views of type I. The asterisk denotes a posterior polar view of type IX. CI – somatic cilium. Scale bars 3 µm (q) and 5 µm (n–p).

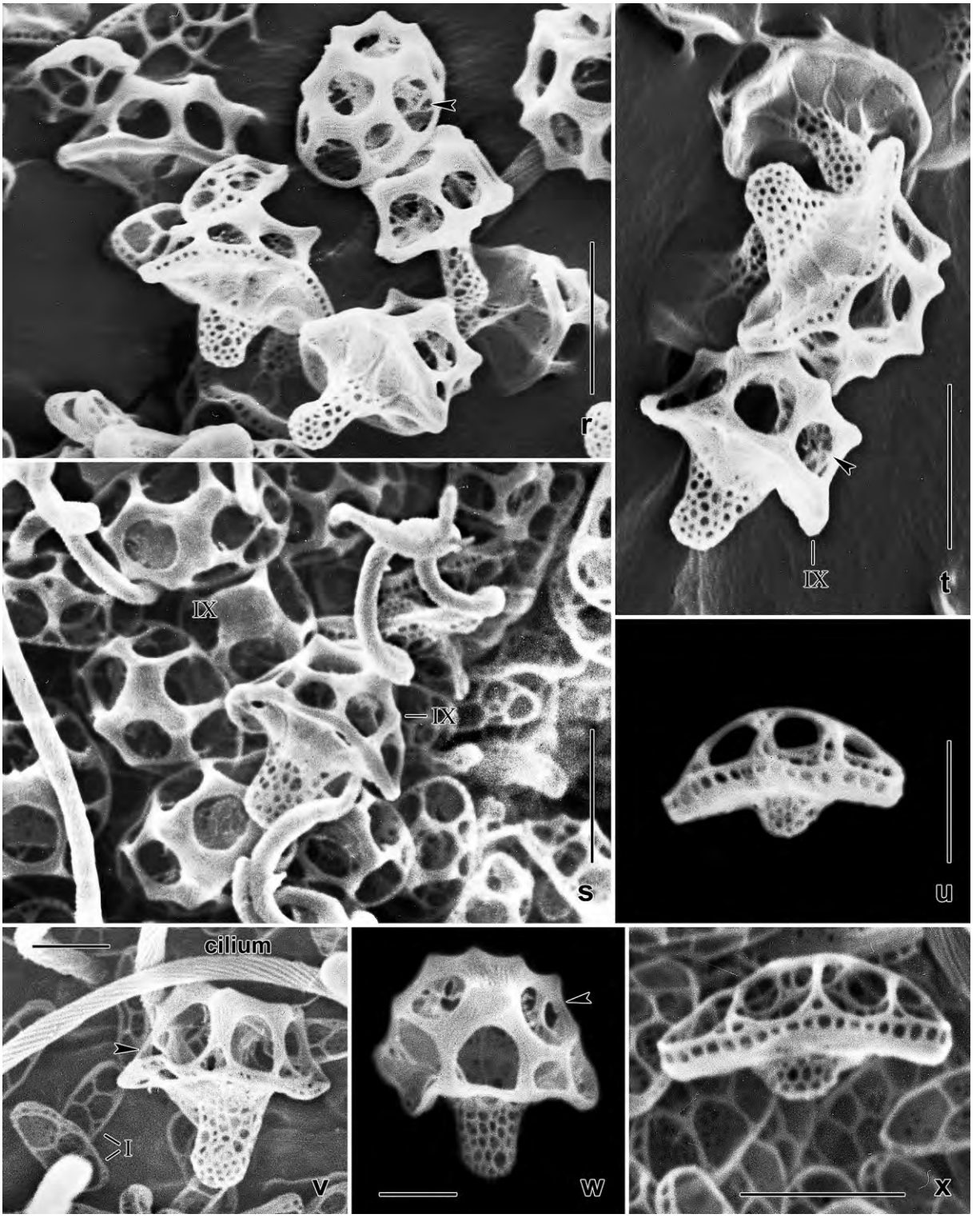

Fig. 26r–x. *Trachelophyllides sigmoides*, type I (v), IV (u, x), and IX (r– t, v, w) lepidosomes in the SEM. **r–t, v, w:** Type IX is mushroom-shaped and has slightly protruding polygon ridges. Note filaments and membrane-like structures in the superstructure (arrowheads). **u, x:** This applies also to type IV. Scale bars 1 µm (v–x) and 2 µm (r–u).

reported *T. sigmoides* from the pelagial of a small lake (Höllerersee) in Upper Austria. Muecke (1979) found it in ponds of the "Heiliges Meer" in Germany. Vuxanovici (1962) reported it from a basin of the Botanical Garden in Bucharest, Rumania (but see Remarks). Pratt et al. (1987) observed it in spring in the Flint River and Lake Blackshear impoundment, southwestern Georgia, USA. Shizheng & Zhengxue (1994) found it in one out of eleven industrial sewage plants, Qinghai province, China.

Remarks: Our observations match those of Kahl (1926, 1930a, b, 1943), who provided four slightly different figures over the years (Fig. 24t–w), almost perfectly, including the length of the type I extrusomes (~ 48 µm according to Fig. 24v). Thus we do not neotypify the species. The sole remarkable difference is the dikinetal dorsal brush which extends beyond mid-body according to Kahl (Fig. 24v) while it is only about 65 µm long in our population (Fig. 24a, r). Possibly, Kahl (1930a, b) saw only the monokinetal brush row 3 which, indeed, extends beyond mid-body.

We found only one other illustration of *T. sigmoides* in the literature (Vuxanovici 1962). Unfortunately, the figure explanation appears incorrect providing a body size of only 32 µm, and the text describes the extrusomes and the dorsal brush as only 18 µm and 15 µm long, respectively. Thus, we cannot be sure about this population although the shape of the body and oral bulge matches Kahl´s figures very well (cp. Fig. 24t–w with Fig. 24x–z).

There is only one species, → *Spetazoon australiense*, which might be confused with *T. sigmoides* because it has a similar size and shape of the body and a thick mucilaginous layer. However, it differs by the shape of the micronuclei (ellipsoid to elongate ellipsoid vs. globular to broadly ellipsoid), the shape and length of the type I extrusomes (distinctly acicular and 20 µm long vs. filiform and 50 µm long), the symbiotic algae (absent vs. present), the oral bulge (distinct vs. indistinct), and the lepidosomes (types VII, VIII vs. types I, IV, IX). As concerns *Trachelophyllum vestitum*, see → *Spetazoon australiense*.

Trachelophyllum apiculatum (Perty, 1852) Claparède and Lachmann, 1859 (Fig. 28a–g)

The Venezuelan population from mosses of the Henri Pittier National Park matches the redescription by Foissner et al. (2002) only partially and emphasizes the variability of the species. Body size about 100 × 20 µm, contractile by about 1/3; excretory pore large and in centre of posterior pole; extrusomes rod-shaped, about 16 × 0.3–0.4 µm in size (Fig. 28a); lepidosomes (Fig. 28b–d) rather similar to those of the Venezuelan site (54) neotype population described by Foissner et al. (2002), i. e., 1.3 × 0.8 × 0.7 µm (n = 15) in size and with 6 polygons in hemispherical superstructure.

There is a single, possibly important difference: the specimens of this population have not only long extrusomes but also very minute ones (~ 2 µm long) in the oral bulge (Fig. 28c). They are difficult to recognize, suggesting that they have been overlooked previously. Further, the lepidosomes, although having the same size as those from the neotype, have only 6 (vs. 11) polygons in the superstructure. See also → *T. tachyblastum*.

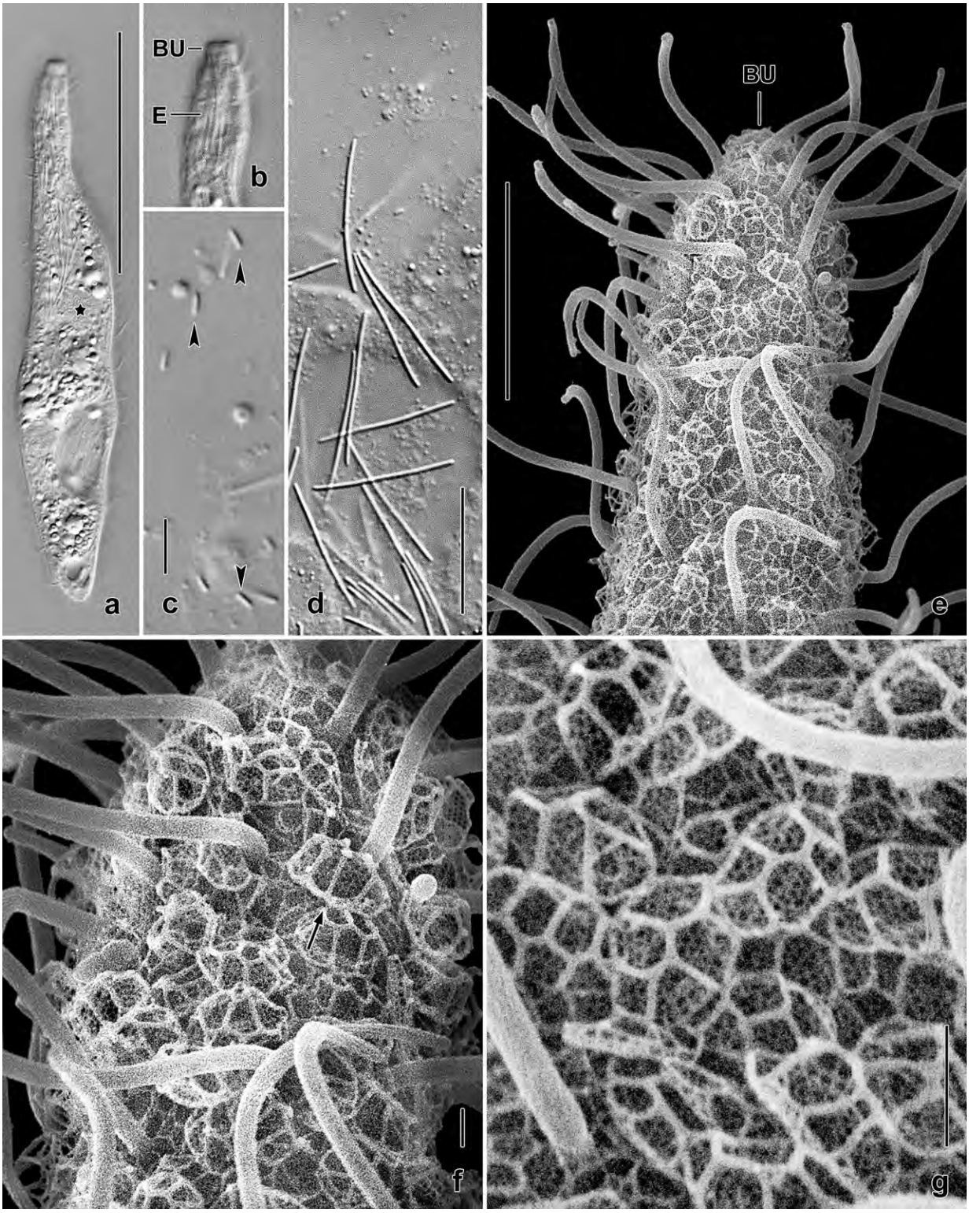

Fig. 28a–g. *Trachelophyllum apiculatum* from Venezuelan site (64) from life (a–d) and in the SEM (e–g). **a, b:** Overview and oral detail. **c, d:** Short (arrowheads) and long extrusomes. **e, f:** Anterior body portion, showing a lepidosome in lateral view (f, arrow) and the oral bulge covered with lepidosomes. **g:** Surface view showing lepidosomes. BU – oral bulge, E – extrusomes. Scale bars 1 µm (f, g), 5 µm (c), 10 µm (e), 15 µm (d), and 40 µm (a).

Trachelophyllum tachyblastum Stokes, 1884a (Fig. 29a–l, 30a–n; Table 12)

Improved diagnosis: Size in vivo about 120 × 17 µm; lageniform to slenderly lageniform. 2 broadly ellipsoid macronuclear nodules with a globular micronucleus each. Two types of extrusomes: type I rod-shaped to indistinctly acicular and slightly curved, 12–16 µm long; type II oblong, about 2 µm long. On average 11 ciliary rows; dorsal brush heterostichad, rows 1 and 2 with an average of 5 and 11 dikinetids, respectively. Lepidosomes about 1.8 × 1.2 × 1 µm and with an average of 8 polygons in hemispherical superstructure.

Neotype locality: Leaf litter and soil from the Fern Creek, Muir National Park, San Francisco, USA, W122°5' N37°5'.

Neotype material: 4 neotype slides with protargol-impregnated specimens have been deposited in the Biology Centre of the Upper Austrian Museum in Linz (LI). The neotype specimen and other relevant cells have been marked by black ink circles on the coverslip.

Etymology: The Greek *tachyblastos* means sprouting quickly (Stokes 1884a).

Description: Size in vivo 90–140 × 10–25 µm, usually about 120 × 17 µm, as calculated from some in vivo measurements and the morphometric data in Table 12 adding 15% preparation shrinkage; length:width ratio also highly variable, i. e., 5–11:1, on average around 7:1 both in vivo and in protargol preparations (Table 12); up to 2:1 flattened dorsoventrally, depending on nutrition state. Lageniform to slenderly lageniform with neck slightly widened in oral region and gradually merging into broadened trunk, both ends narrowly rounded (Fig. 29a, c, d, 30a, m). Cells very flexible but only slightly (< 20%) contractile, mainly in neck region, preserved specimens thus of similar size and shape as live ones (Fig. 29a, d). Nuclear apparatus on average in posterior half of body, i. e., in mid of trunk (Fig. 29a, d, 30m; Table 12). Macronuclear nodules globular to slenderly ellipsoidal (3:1), on average 11 × 6 µm in protargol preparations, usually distinctly apart and connected by a fine strand; very rarely almost abutting. A micronucleus each attached to macronuclear nodules, globular to broadly ellipsoidal, about 2 µm in size. Contractile vacuole in posterior body end, with tubular pore in pole centre. Two types of extrusomes attached to oral bulge, their cytoplasmic developmental stages impregnate rather deeply with protargol (Fig. 29a, e–g, 30e, h, k, l): type I conspicuous because 12–16 × ~ 0.3 µm, rod-shaped and slightly curved, in one specimen very slightly acicular; type II inconspicuous because only about 2 × 0.4 µm in size. Cytoplasm hyaline, with few to many lipid droplets up to 5 µm across, depending on nutrition state. Glides slowly on microscope slide.

Cortex flexible, contains scattered, colourless granules ≤ 0.3 µm across (Fig. 29l); and a fibre system as described in *T. apiculatum* by Foissner et al. (2002). Mucilaginous layer in vivo very hyaline, about 2 µm thick and composed of globular lepidosomes 1.5–2 µm across (Fig. 29a), impregnate rather deeply with protargol (Fig. 29d, 30i, j). Lepidosomes of *Trachelophyllum* structure (Foissner et al. 2002), on average 1.8 × 1.2 × 1 µm in size and with 8 polygons in hemispherical superstructure; baseplate and dish margin finely faceted, central area slightly concave (Fig. 29h–j, 30a–d, f, g; Table 12).

Cilia about 8 µm long in vivo, widely spaced, some non-ciliated granules (kinetids?) in line

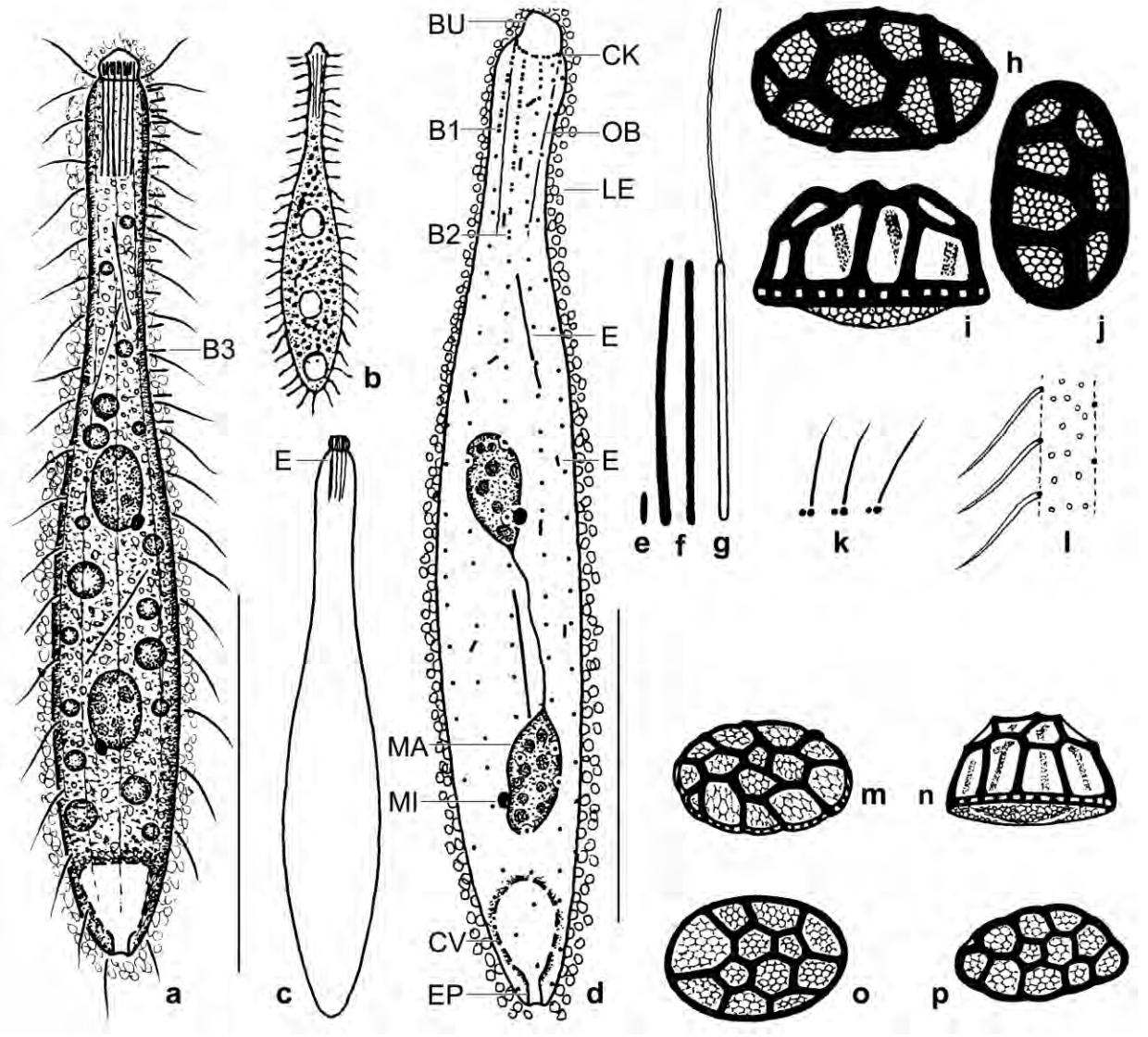

Fig. 29a–p. *Trachelophyllum tachyblastum* (a–l) and *T. apiculatum* (m–p, from Foissner et al. 2002) from life (a–c, e–g, l), after protargol impregnation (d, k), and in the scanning electron microscope (h–j, m–p). **a:** Overview of a representative specimen from neotype locality, length 120 µm. **b:** Original illustration by Stokes (1884a), length 127–152 µm. **c:** Shape variant. **d:** Dorsal view of main neotype specimen, length 95 µm, showing, inter alia, the ciliary pattern and the nuclear apparatus. **e, f:** Short, (~ 2 µm) and long (~ 16 µm) extrusomes drawn to scale. **g:** Exploded long extrusome, length ~ 30 µm. **h–j, m–p:** Surface and lateral views of lepidosomes of *T. tachyblastum* and *T. apiculatum*, drawn to scale. The lepidosomes of *T. tachyblastum* are larger (1.8 × 1.2 × 1 µm on average) than those of *T. apiculatum* (1.3 × 0.8 µm on average). **k:** The circumoral kinety consists of dikinetids, of which only the left basal body is ciliated. **l:** Sparse cortical granulation. B1–3 – dorsal brush rows, BU – oral bulge, CK – circumoral kinety, CV – contractile vacuole, E – extrusomes, EP – excretory pore of contractile vacuole, LE – lepidosomes, MA – macronucleus, MI – micronucleus, OB – oral basket. Scale bars 30 µm (d) and 50 µm (a).

with ciliated ones. On average 11 ordinarily to narrowly spaced ciliary rows meridionally and equidistantly arranged, three of them differentiated to dorsal brush anteriorly (Fig. 29a, d, 30h, m, n; Table 12). Dorsal brush heterostichad because row 1 about half as long as row 2, composed of an average of five widely spaced dikinetids; row 2 composed of 11 ordinarily to widely spaced dikinetids; bristles of both rows about 4 µm long in vivo and arranged as described by Foissner et al. (2002) in *T. costaricanum*. Brush row 3 extends to near mid-body, composed of monokinetids

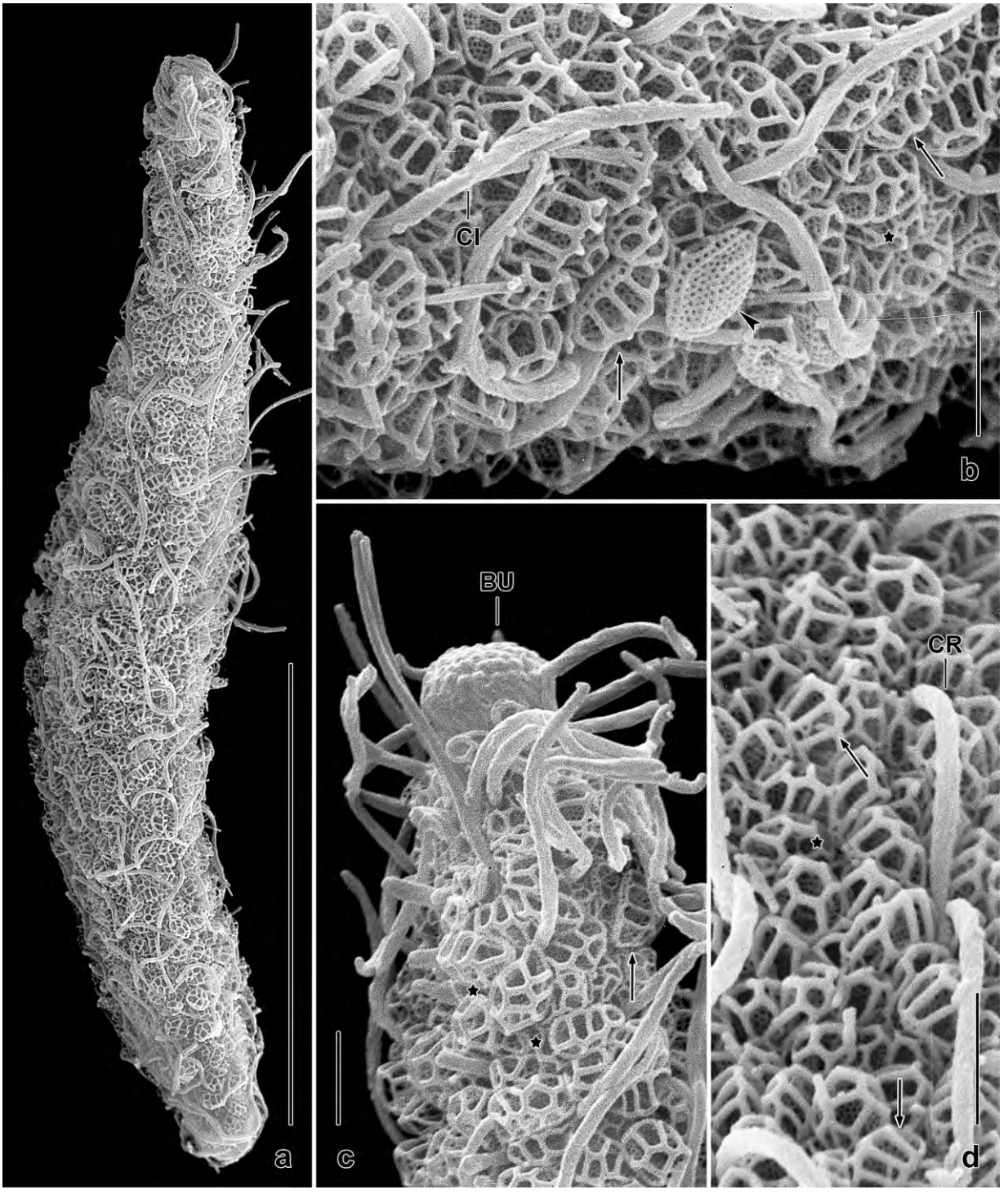

Fig. 30a–d. *Trachelophyllum tachyblastum*, North American neotype population in the scanning electron microscope. **a:** Overview, showing the body densely covered with epicortical scales (lepidosomes). **b, d:** Fine structure of the lepidosomes. Arrows mark lateral views, arrowhead denotes a baseplate view, and asterisks mark surface views. **c:** Anterior body end, showing the cylindroidal oral bulge, whose pustulate surface is caused by the extrusomes. Arrow marks a lepidosome in lateral view, asterisks denote surface views. BU – oral bulge, CI – ordinary somatic cilium, CR – ciliary row. Scale bars 2 μm (b–d) and 30 μm (a).

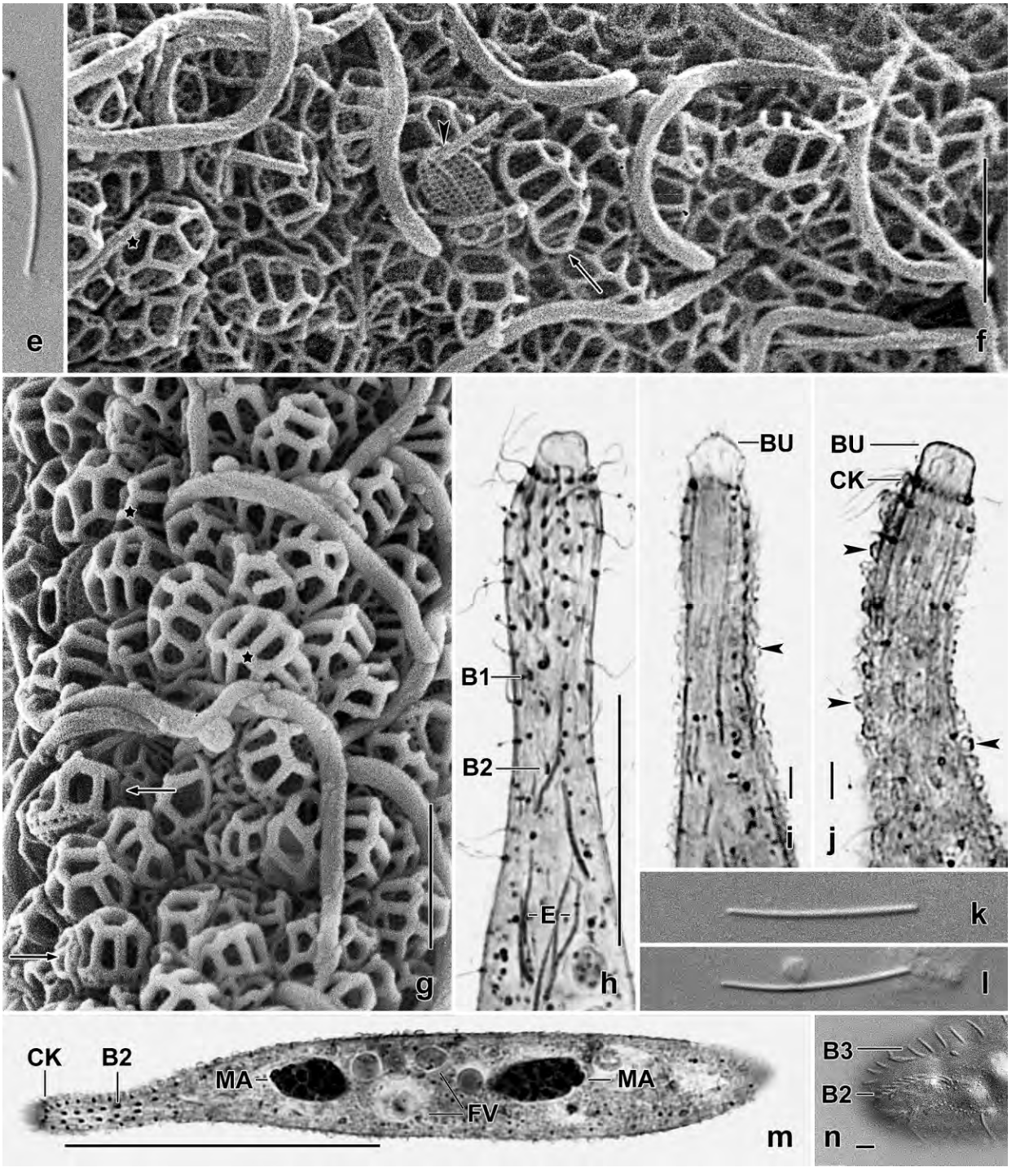

Fig. 30e–n. *Trachelophyllum tachyblastum* from life (e, k, l, n), in the scanning electron microscope (f, g), and after protargol impregnation (h–j, m). **e, k, l:** The extrusomes are indistinctly acicular and 12–16 µm long. **f, g:** Lepidosomes. Arrows mark lateral views, arrowhead denotes a baseplate view, and asterisks mark surface views. **h–j, n:** Dorsal (h, n) and lateral (i, j) views, showing dorsal brush and lepidosome cover (arrowheads). Note the highly variable shape of the oral bulge. **m:** Overview. BU – oral bulge, B1–3 – dorsal brush rows, CK – circumoral kinety, E – extrusomes, FV – food vacuoles, MA – macronuclear nodules. Scale bars 2 µm (f, g), 3 µm (n), 5 µm (i, j), 20 µm (h), and 50 µm (m).

Table 12. Morphometric data on *Bilamellophrya fraterculum* (upper line) and *Trachelophyllum tachyblastum* (lower line) based on mounted, protargol-impregnated (FOISSNER's method), and randomly selected specimens from non-flooded Petri dish cultures. Measurements in µm. CV – coefficient of variability in %, M – median, Max – maximum, Mean – arithmetic mean, Min – minimum, n – number of specimens investigated, SD – standard deviation, SE – standard error of arithmetic mean.

Characteristics	Mean	M	SD	SE	CV	Min	Max	n
Body, length	131.2	131.0	13.6	3.0	10.4	110.0	158.0	21
	105.5	105.0	12.9	2.8	12.2	87.0	133.0	21
Body, width (without scale layer at widest site)	19.9	19.0	4.1	0.9	20.5	14.0	30.0	21
	14.8	14.0	3.1	0.7	21.1	10.0	22.0	21
Body length:width, ratio	6.9	6.5	1.6	0.3	22.7	4.0	9.7	21
	7.4	7.3	1.5	0.3	20.2	5.2	11.0	21
Body, width in neck area	7.8	7.0	1.2	0.3	15.7	5.0	10.0	21
	5.9	6.0	0.7	0.2	12.4	5.0	7.0	21
Oral bulge, height	2.9	3.0	0.3	0.1	11.7	2.5	4.0	21
	3.8	4.0	0.4	0.1	10.7	3.0	4.5	21
Oral bulge, diameter (of circumoral kinety)	3.8	4.0	–	–	–	3.5	4.0	21
	5.0	5.0	0.6	0.1	11.9	4.0	6.0	21
Anterior body end to macronucleus, distance	60.6	62.0	9.9	2.2	16.4	43.0	81.0	21
	47.9	45.0	8.1	1.8	17.0	35.0	68.0	21
Circumoral kinety to last dikinetid of brush row 1	48.9	49.0	6.4	1.4	13.0	36.0	63.0	21
	12.3	12.0	2.8	0.6	22.4	7.0	17.0	21
Brush row 1, number of dikinetids	21.2	21.0	1.9	0.4	9.0	18.0	25.0	21
	5.5	5.0	0.8	0.2	14.9	4.0	7.0	21
Circumoral kinety to last dikinetid of brush row 2	49.3	50.0	6.3	1.4	12.7	36.0	63.0	21
	21.6	21.0	5.5	1.2	25.5	11.0	30.0	21
Brush row 2, number of dikinetids	23.4	23.0	2.7	0.6	11.5	17.0	29.0	21
	10.7	11.0	2.0	0.4	18.6	6.0	15.0	21
Anterior macronuclear nodule, length	13.3	13.0	2.5	0.5	18.9	9.0	18.0	21
	10.8	10.0	2.8	0.6	26.1	6.0	17.0	21
Anterior macronuclear nodule, width	9.5	9.0	1.2	0.3	12.3	7.0	12.0	21
	6.0	6.0	0.7	0.2	12.2	5.0	8.0	21
Macronuclear nodules, distance in between	17.9	19.0	7.6	1.7	42.3	5.0	28.0	21
	16.9	16.0	5.9	1.3	34.8	6.0	30.0	21
Macronuclear nodules, number	2.0	2.0	0.0	0.0	0.0	2.0	2.0	21
	2.0	2.0	0.0	0.0	0.0	2.0	2.0	21
Micronuclei, length	3.6	4.0	0.5	0.1	13.1	3.0	4.5	21
	2.0	2.0	0.3	0.1	13.7	1.5	3.0	21
Micronuclei, width	2.3	2.0	0.5	0.1	20.7	1.5	3.0	21
	1.8	2.0	0.3	0.1	18.5	1.0	2.5	21
Micronuclei, number	2.0	2.0	0.0	0.0	0.0	2.0	2.0	21
	2.0	2.0	0.0	0.0	0.0	2.0	2.0	21

continued

Characteristics	Mean	M	SD	SE	CV	Min	Max	n
Ciliary rows, number	12.7	13.0	0.6	0.1	4.6	12.0	14.0	21
	11.1	11.0	0.8	0.2	7.5	10.0	13.0	21
Ciliated kinetids in a ventral kinety, number	26.1	27.0	4.6	1.0	17.6	18.0	36.0	21
	20.3	19.0	3.7	0.8	18.3	15.0	29.0	21
Dikinetidal brush rows, number	2.0	2.0	0.0	0.0	0.0	2.0	2.0	21
	3.0	3.0	0.0	0.0	0.0	3.0	3.0	21
Type I scales, length (from SEM micrographs)	1.3	1.3	0.1	0.1	11.1	0.9	1.5	16
	1.8	1.8	0.2	0.1	10.3	1.4	2.1	28
Type I scales, width (from SEM micrographs)	0.8	0.8	0.1	0.1	18.0	0.6	1.0	16
	1.2	1.2	0.2	0.1	13.2	0.7	1.5	28
Type I scales, height (from SEM micrographs)	–	–	–	–	–	–	–	–
	1.0	1.0	0.1	0.1	15.1	0.7	1.3	32
Type I scales, number of polygons (from SEM micrographs)	6.0	5.9	1.0	0.2	16.9	4.0	8.0	16
	7.8	8.0	0.9	0.1	11.5	6.0	10.0	32
Type II scales, length (from SEM micrographs)	1.9	1.8	0.2	0.1	12.7	1.4	2.3	21
	–	–	–	–	–	–	–	–
Type II scales, width (from SEM micrographs)	1.2	1.2	0.2	0.1	15.5	0.9	1.6	21
	–	–	–	–	–	–	–	–
Type II scales, height (from SEM micrographs)	1.4	1.5	0.2	0.1	13.4	1.1	1.8	19
	–	–	–	–	–	–	–	–
Type II scales, number of polygons forming cone (from SEM micrographs)	12.0	11.6	1.8	0.4	15.6	7.0	15.0	21
	–	–	–	–	–	–	–	–

with 3–4 µm long, immobile bristles projecting at right angles from body proper (Fig. 30n).

Oral bulge rather conspicuous in vivo because about 5 × 4 µm in size and glossy due to the extrusomes attached, distinctly separate from body proper, usually covered by lepidosomes. Bulge shape highly variable (Fig. 29a, c, d, 30c, h–j; Table 12): distinctly to indistinctly pentagonal in 11 out of 21 specimens analysed and cylindroid with distal surface sometimes obliquely truncate in 10 cells; rarely button-shaped or obconical. Circumoral kinety at base of oral bulge, composed of about 10 comparatively widely spaced dikinetids each having a single cilium and a nematodesma contributing to the tubercular oral basket (Fig. 29d, k, 30j, m).

Occurrence and ecology: Stokes (1884a) discovered *T. tachyblastum* in decaying mud of shallow pools in the surroundings of the town of Trenton, Philadelphia, USA. Our neotype is from the opposite side of the continent, i. e., from the Muir National Park in San Francisco. The sample was taken above the Redwood zone on the left slope of the Fern Creek. There is mixed forest with an up to 10 cm thick leaf litter layer, which was collected together with some mineral soil; pH 6.1 in water. A further record is from Venezuelan site (52) where *T. tachyblastum* occurred in soil from a gallery forest. The specimens from this site are slightly smaller than those from the neotype locality but otherwise they match perfectly. Possibly, *T. tachyblastum* occurs also in soil from Austria, where Foissner (1984) misidentified it as *T. apiculatum* (for a brief review, see Foissner et al. 2002).

Comparison with original description and neotypification: The description and illustration of *T. tachyblastum* by Stokes (1884a) is rather meagre, showing the following features (Fig. 29b): body length 127–152 µm; body clavate, about eight to ten times as long as broad (but only 6:1 in the figure!); two macronuclear nodules and a contractile vacuole; rather long, rod-shaped extrusomes; oral bulge obtusely rounded.

We neotypify *T. tachyblastum* although the differences between *T. tachyblastum* and → *T. apiculatum* are rather prominent, especially the dorsal brush, they are not easily distinguished because they have a similar body and extrusome shape and size. Further, *T. apiculatum* possibly consists of two or more species.

Remarks: Kahl (1930a) synonymized *T. tachyblastum* with *T. apiculatum*. Indeed, these species are highly similar in vivo. However, when compared with the Venezuelan neotype established by Foissner et al. (2002), the following differences can be recognized (listed by importance): (i) dorsal brush (row 1 with 5 vs. 18 dikinetids, row 2 with 11 vs. 22 dikinetids); (ii) with vs. without short (type II) extrusomes; (iii) lepidosomes larger although the body is smaller (1.8 × 1.2 ×1 µm vs. 1.3 × 0.8 µm; 8 vs. 11 polygons in superstructure, Fig. 29h–j, m–p); (iv) body smaller (90–140 × 10–25 µm vs. 130–200 × 20–30 µm). These features, especially the small brush, are sufficient to accept both species.

Bilamellophrya fraterculus nov. spec. (Fig. 31a–e, 32a–l; Table 12)

Diagnosis: Size about 150 × 20 µm in vivo, contractile up to 30%; slenderly lageniform. 2 broadly ellipsoid macronuclear nodules widely apart and with an ellipsoid micronucleus each. Extrusomes cylindroid, about 1 µm long. On average 13 ciliary rows; dikinetal dorsal brush rows isostichad, both composed of about 22 kinetids. Mucilaginous layer 1–2 µm thick. Type I lepidosomes on average 1.3 × 0.8 µm and with 6 polygons in superstructure. Type II lepidosomes about 1.9 × 1.2 × 1.4 µm, conical superstructure composed of an average of 12 scattered polygons tapering to 1 or 2 oblong peaks.

Type locality: Upper, slightly saline (8‰) soil layer of a small grass island in the mangrove forest about 10 km west of the town of Puerto Plata, Dominican Republic, 70°35′W 19°50′N.

Type material: 1 holotype and 2 paratype slides with protargol-impregnated specimens have been deposited in the Biology Centre of the Upper Austrian Museum in Linz (LI). The holotype and other relevant specimens have been marked by black ink circles on the coverslip.

Etymology: The Latin name *fraterculus* (small brother) is a noun in apposition, referring to the similarity with *B. etoschensis* from Southwest Africa, Namibia (Foissner et al. 2002).

Description: About half of the specimens have a clear cytoplasm without food vacuoles and are thus more slender than the cells with food vacuoles. Furthermore, the macronuclear nodules are usually nearer together and more slender. Thus, the variability coefficients are high for body width, the length of the macronuclear nodules, and the distance in between the nodules. Nonetheless, we included these – possibly precystic – specimens in the morphometric analysis (Table 12).

Size 130–180 × 15–25 µm in vivo, usually about 150 × 20 µm; length: width ratio 4–9.7:1, on average 6.9:1, that is, very wide due to the slender specimens mentioned above. Shape slenderly to very slenderly lageniform, specimens without food vacuoles frequently almost rod-shaped; neck slightly widened at base of oral bulge (Fig. 31a, 32a); laterally flattened up to 3:1. Contracted cells narrowly to very narrowly ellipsoid and slightly curved (Fig. 32e). Nuclear apparatus on average posterior of mid-body, likely due to the specimens without food vacuoles where the macronuclear nodules move slightly backwards (Fig. 31a, c, 32a; Table 12). Invariably, two widely separate macronuclear nodules and two micronuclei attached to or a few µm away from nodules. Individual macronuclear nodules globular to ellipsoidal, on average broadly ellipsoidal; contain many nucleoli 1–2 µm across. Micronuclei discoidal to hemispherical (Fig. 31a, c; Table 12); three micronuclei in one out of 30 specimens. Contractile vacuole in posterior body end, with large excretory pore in pole centre (Fig. 31a, c). Extrusomes attached to oral bulge, very inconspicuous because only 1 µm long (Fig. 31a, b, 32c); do not impregnate with the protargol method used. Cytoplasm colourless, contains food vacuoles 4–8 µm across and few to many lipid droplets. Glides and swims rather rapidly.

Cortex as in congeners (Foissner et al. 2002), covered by a 1–2 µm thick layer of slime and lepidosomes, producing a slightly serrate body margin both in vivo and in protargol preparations (Fig. 31a). Mucilaginous layer contains two kinds of lepidosomes lying one upon the other (Fig. 31e, 32d–l; Table 12). Type 1 lepidosomes in one layer on body surface, circular to ellipsoidal, on average 1.3 × 0.8 µm in size and thus hardly recognizable in the light microscope, domed superstructure with 6 polygons on average. Type II lepidosomes complex and beautiful, upon and rather tightly arranged on type 1 scales, broadly ellipsoid to ellipsoid, on average 1.9 × 1.2 µm in size and 1.4 µm high with baseplate included; baseplate slightly to distinctly concave; conical superstructure composed of an average of 12 scattered polygons tapering anteriorly to one or two oblong peaks.

Somatic cilia about 10 µm long, arranged in an average of 13 bipolar, equidistant rows each having 26 cilia on average; three rows anteriorly modified to dorsal brush (Fig. 31a, c, d, 32c, Table 12). Brush rows 1 and 2 in rather deep furrows, on average of same length and structure, i. e., composed of fairly widely spaced dikinetids with V-like spread bristles about 2 µm (anterior bristle of dikinetids) and 4 µm (posterior bristle) long; bristles immobile and obliquely attached to body surface, thus entirely covered by the mucilaginous layer and invisible in the scanning electron microscope. Brush row 3 extends to mid-body, composed of monokinetids with about 3 µm long, cylindroidal, immobile bristles projecting from body proper at right angles and piercing mucilaginous layer (Fig. 31c, 32c). All rows continue posteriorly as ordinary somatic ciliary rows.

Oral bulge distinctly set off from neck, about 4 µm wide and 3 µm high in vivo, in most specimens conical, in a few cylindroidal or incus-shaped. Circumoral kinety at base of oral bulge, composed of dikinetids each with a 10 µm long cilium. Oral basket not impregnated (Fig. 31a, c, 32a–c).

Occurrence and ecology: As yet found only at type locality, where it was moderately abundant so that SEM investigations could be made. The minute extrusomes suggest a special diet. Unfortunately, we could not identify the contents of the food vacuoles, possibly because the prey is lysed outside.

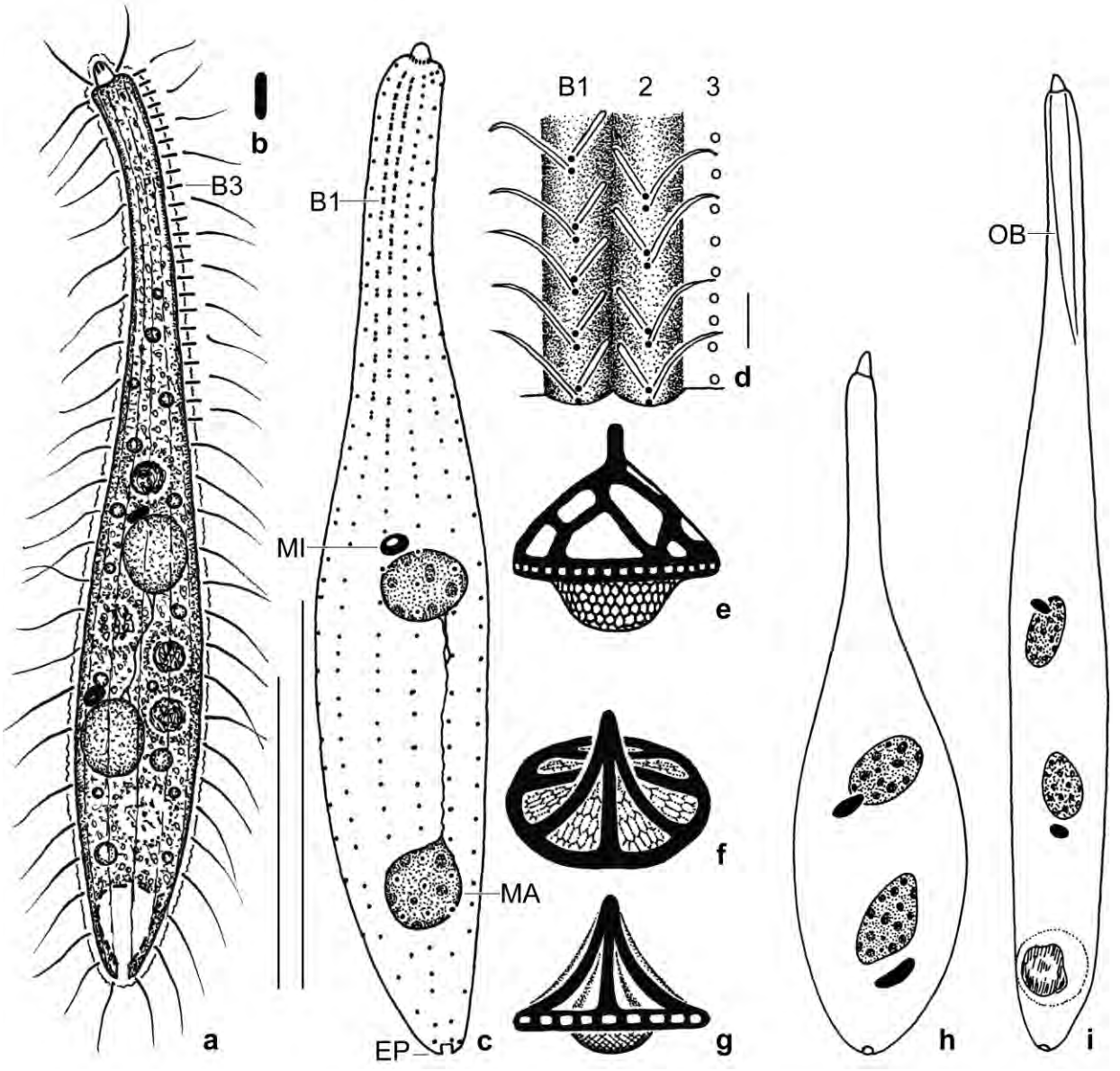

Fig. 31a–i. *Bilamellophrya fraterculus* (a–e) and *B. etoschensis* (f–i, from FOISSNER et al. 2002) from life (a, b, d), after protargol impregnation (c, h, i), and in the scanning electron microscope (e–g). **a:** Lateral view of a representative specimen, length 150 µm. **b:** Mature oral bulge extrusome, length only 1 µm (!). **c:** Dorsal view of holotype specimen, showing ciliary pattern and nuclear apparatus, length 130 µm. This specimen contains some food vacuoles and possibly has only one micronucleus (a second could be hidden by the macronuclear nodules). **d:** Part of dorsal brush (cp. Fig. 32c). Brush rows 1 and 2 extend in flat furrows; the bristles of row 3 are shown in frontal view because they spread perpendicularly from body proper, while those of rows 1 and 2 attach to the cortex. All bristles are immobile. **e–g:** The type II lepidosomes of *B. fraterculus* (e) differ by the scattered polygons in the superstructure from *B. etoschensis* which has several concave, equidistant arcs. **h, i:** *B. fraterculus* shows the same variability of body shape as *B. etoschensis*. B1–3 – dorsal brush rows, MA – macronuclear nodule, MI – micronucleus, OB – oral basket. Scale bars 2 µm (d) and 50 µm (a, c).

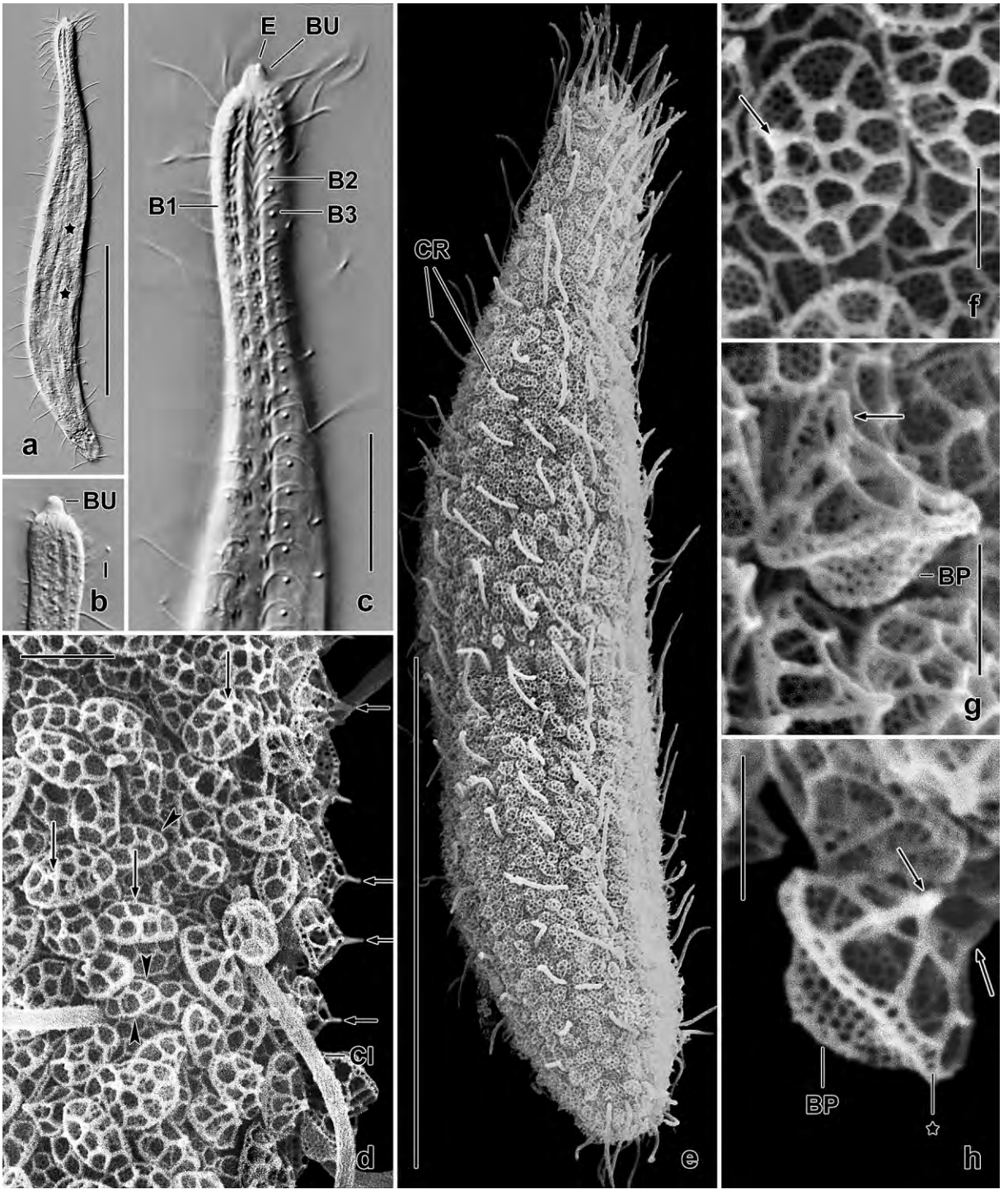

Fig. 32a–h. *Bilamellophrya fraterculus* from life (a–c) and in the SEM (d–h). Arrowheads mark type I scales, arrows denote peak of type II scales. **a, c:** Overview and dorsal brush; bristles of row 3 appear as bright dots because they are seen frontally. Asterisks mark macronucleus nodules. **b:** Anterior end with oral bulge. **d, e:** Overview of scale layer and of a contracted cell. **f–h:** Type II scales in surface (f) and lateral views (g, h). Note scale with two peaks (h). Asterisk in (h) marks the perforated margin of the baseplate. BP – baseplate, BU – oral bulge, CI – somatic cilia, CR – ciliary rows, B1–3 – dorsal brush rows, E – extrusome. Scale bars 1 µm (f–h), 2 µm (d), 5 µm (b), 10 µm (c), and 50 µm (a, e).

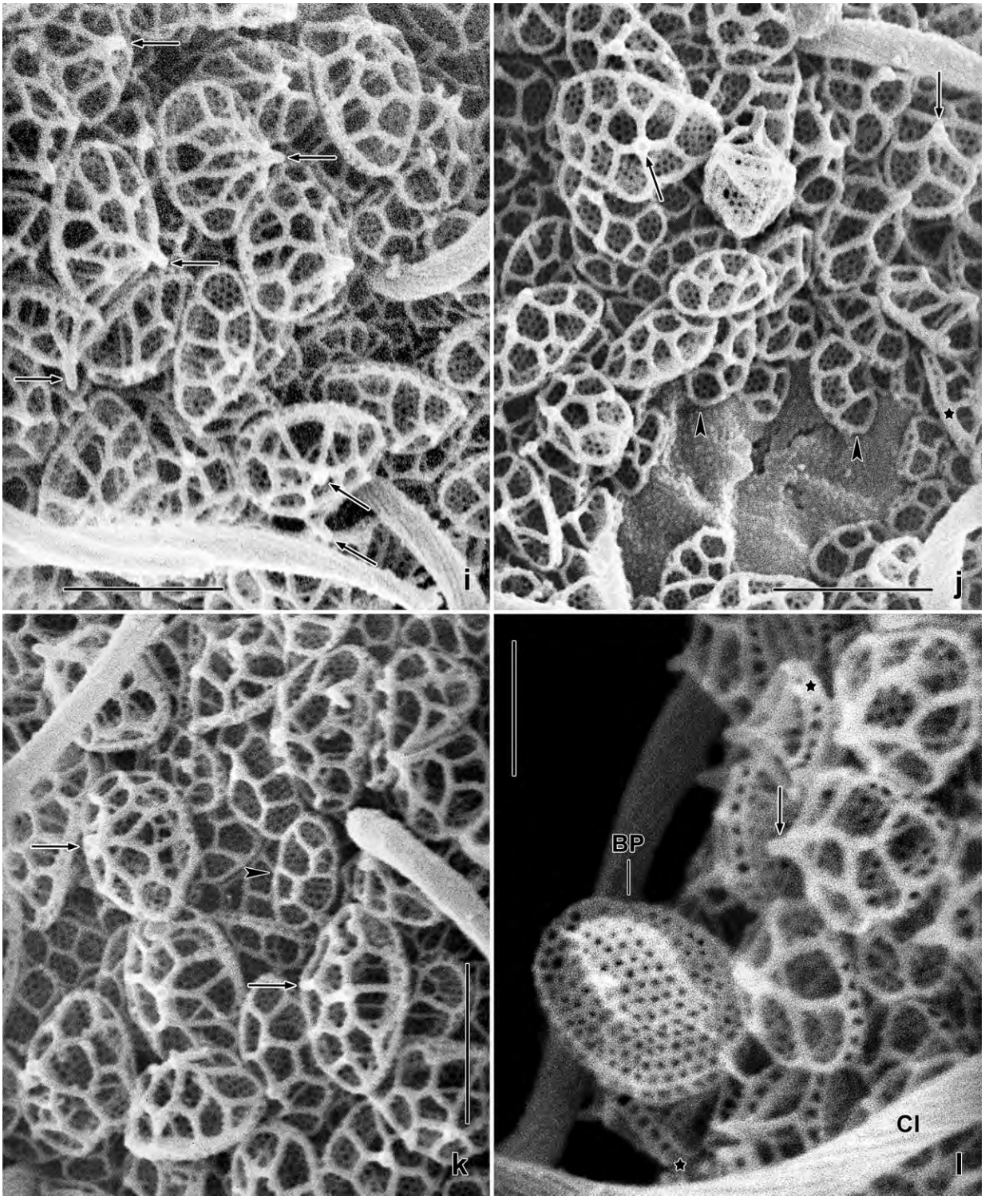

Fig. 32i–l. *Bilamellophrya fraterculus*, epicortical scales in the scanning electron microscope. Arrowheads mark type I scales, arrows denote peak of type II scales. Asterisks mark the perforated margin of the baseplates, which have a hexagonal pattern. Type I scales are on average 1.3 × 0.8 µm in size and have six polygons (j, k). Type II scales have an average size of 1.9 × 1.2 × 1.4 µm and have 12 scattered polygons, that merge into a cylindroidal peak (arrows). BP – baseplates, CI – somatic cilia. Scale bars 1 µm (l) and 2 µm (i–k).

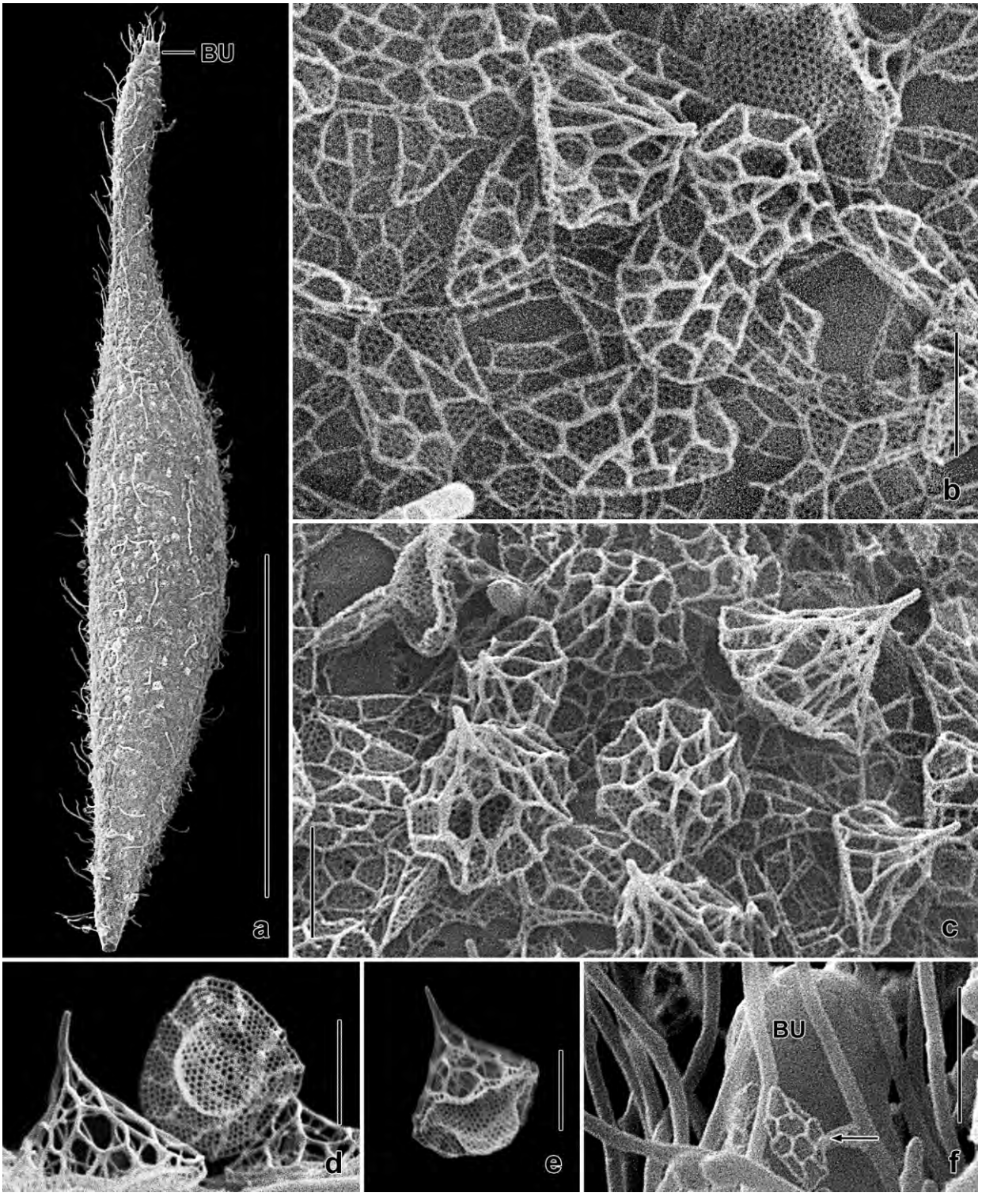

Fig. 33a–f. *Bilammelophrya hawaiiensis* from Venezuelan site (56) in the scanning electron microscope. **a:** Overview. **b, c:** Type II lepidosomes. **d, e:** Lateral and posterior polar views of type II lepidosomes. **f:** Oral bulge and a type I scale (arrow). BU – oral bulge. Scale bars 1 µm (b, c–e), 2 µm (f), and 50 µm (a).

Remarks: There are two other trachelophyllids with minute extrusomes: *Bilamellophrya etoschensis* Foissner et al., 2002 from a slightly saline soil of the Etoscha National Park in Namibia; and *Trachelophyllum africanum* Foissner et al., 2002 from soil of South Africa. *Bilamellophrya etoschensis* differs from *B. fraterculus* by the type II scales (with concave arcs vs. irregularly arranged polygons; Fig. 31e–g) and the extrusomes (4 µm long, fine rods vs. 1 µm long cylinders).

Trachelophyllum africanum differs from *B. fraterculus*, of course, by the lepidosomes (one vs. two types), while body and extrusome shape are rather similar (very narrowly cuneate and 3.5–4 µm long vs. cylindroid and 1 µm long). However, Foissner et al. (2002) described two other populations of *T. africanum*, one from Namibia (Southwest Africa) and another from Venezuela. These populations have extrusomes like *B. fraterculus*, except of the argyrophily (deeply impregnating vs. not impregnating using the same method). Unfortunately, Foissner et al. (2002) provided SEM micrographs only for the Venezuelan specimens, which differ distinctly from *B. fraterculus* in having only type I scales (confirmed by inspection of the original SEM micrographs).

Bilammelophrya hawaiiensis Foissner, Agatha & Berger, 2002 (Fig. 33a–f)

The specimens from Venezuelan site (56) match the Hawaiian type quite well. However, they are slightly larger (~ 200 µm vs. 150 µm) and have slightly more polygons in the superstructure of the type I scales (11 vs. 8). We add some scanning micrographs, especially from the hexagonally faceted baseplate of the type II scales, which were rather poorly preserved in the Hawaiian specimens (Fig. 33d, e).

Lingulotrichidae nov. fam.

Diagnosis: Oblong to narrowly obclavate, moderately to distinctly contractile Trachelophyllina Grain, 1994. Dorsal brush heteromorphic, composed of more than three rows. Two types of finely honeycombed, two-dimensional lepidosomes. Type X elliptic with upright basering; type XI and type XII tongue-shaped with concave baseplate and special structures anchoring lepidosomes to pellicle.

Type genus: *Lingulothrix* nov. gen.

Remarks: The new family is well supported by the complex dorsal brush and the unique lepidosomes. Whether or not the Lingulotrichidae belong to the → Trachelophyllina needs molecular investigations. Possibly, it is a distinct group with a different ancestor because the organization of the dorsal brush, the shape of the dikinetal brush bristles, the lepidosomes, and the nuclear apparatus are markedly different. Possibly, the genera *Enchelyotricha* and *Balantidion* (for SEM micrographs and descriptions, see Foissner 1987, Foissner et al. 1999, 2002) belong to the Lingulotrichidae because their dorsal brush and nuclear apparatus is highly similar. However, lepidosomes are absent.

The lepidosomes of the Lingulotrichidae lack the superstructure found in the → Trachelophyllidae, i. e., they consist of the baseplate only and are thus two-dimensional (vs. three-dimensional). The baseplates of the → Trachelophyllidae have a simple organization while those of the Lingulotrichidae are rather complex anchoring the lepidosomes to the pellicle. We distinguish two genera according to the shape of the anchor: *Lingulothrix* nov. gen. (anchor campanulate) and *Cataphractes* nov. gen. (anchor gooseneck-shaped).

Lingulothrix nov. gen.

Diagnosis: Lingulotrichidae with type X and type XI lepidosomes. Type XI anchored to pellicle with a short, campanulate elongation of the baseplate making lepidosomes sock-shaped in lateral view.

Type species: *Lingulothrix galapagensis* nov. spec.

Etymology: Composite of the Latin noun *lingula* (small tongue) and the Greek noun *thrix* (hair ~ ciliate), meaning a ciliate with tongue-shaped lepidosomes. Feminine gender.

Remarks: *Enchelys*-like and *Enchelyodon*-like haptorids with a slime cover were classified by Kahl (1927) into the genus *Lagynus* Quennerstedt, 1867. However, *Lagynus elegans*, type of the genus, lacks such cover (reviewed in Foissner et. al. 1995 and Aescht 2001). In 1930a, he classified slimy haptorids into the genus *Enchelys*. However, *E. farcimen*, type of the genus, and its supposed junior synonym, *E. gasterosteus* Kahl, 1927, also lack a slime cover (Kahl 1930a, Foissner and Foissner 1988, Foissner et al. 1995). Based on the following description of several slimy haptorids with tongue-shaped lepidosomes, we split *Enchelys* into *Enchelys* (dorsal brush three-rowed, without lepidosomes), → *Lingulothrix* nov. gen. (dorsal brush complex, lepidosomes sock-shaped), and → *Cataphractes* nov. gen. (dorsal brush complex, lepidosomes gooseneck-shaped).

Lingulothrix galapagensis Foissner & Stempfhuber nov. spec. (Fig. 34a–v, 35a–n, 36a–r, 37a–k; Table 13)

Diagnosis: Size about 110 × 17 µm in vivo, moderately contractile; oblong to narrowly obclavate and more or less curved. Macronucleus ellipsoid, micronucleus globular. Oral bulge indistinct, discoid. Two types of basically rod-shaped extrusomes: type I slightly curved and about 23 µm long; type II only 2–3 µm long. On average 14 ciliary rows, 5 contributing to dorsal brush: row 1 with about 9 dikinetids; rows 2 and 3 with 1–2 dikinetids anteriorly followed by an average of 15 and 4 monokinetal bristles, respectively; rows 4 and 5 composed of an average of 9 and 10 monokinetal bristles, respectively. Type X lepidosomes cuneate, on average 0.6 × 0.35 × 0.23 µm in size and with 10 hexagons in baseplate. Type XI sock-shaped in lateral view, on average 1.2 × 0.5 × 0.35 µm in size and with 36 hexagons in baseplate; anchor about 0.3 µm long and slightly to distinctly campanulate.

Type material: 1 holotype and 3 paratype slides with protargol-impregnated specimens have

been deposited in the Biology Centre of the Upper Austrian Museum in Linz (LI). Relevant specimens have been marked with black ink circles on the coverslip.

Type locality: Soil from the garden of the hotel San Fernando, Puerto Ayora, Galápagos Islands, 0°44' S 90°18' W.

Etymology: Named after the Galápagos Islands, where it was discovered.

Description: This species was difficult to impregnate with the ordinary protargol protocol. However, when ethanol (70% vol.) was used as a fixative, clear impregnations were obtained. Unfortunately, ethanol fixation usually causes strong shrinkage of the cells. According to the live measurements, *L. galapagensis* has a size of about 110 × 17 µm; specimens in the SEM have a size of 90 × 14 µm (Table 13); assuming a shrinkage of about 20%, as common in SEM preparations, we obtain an average size quite similar to that from live. In contrast, the ethanol-fixed cells measure only 70 × 14 µm, suggesting a length reduction by 37%. The length:width ratio is also rather distinctly influenced by the preparation method: about 7:1 in vivo, 6.3:1 in SEM

Table 13. Morphometric data on *Lingulothrix galapagensis* based, if not mentioned otherwise, on ethanol-fixed (70% vol.), mounted, protargol-impregnated (FOISSNER´s method), and randomly selected specimens from a non-flooded Petri dish culture. Measurements in µm. CV – coefficient of variation in %, M – Median, Max – maximum, Mean – arithmetic mean, Min – minimum, n – number of specimens investigated, SD – standard deviation, SE – standard error of arithmetic mean.

Characteristics	Mean	M	SD	SE	CV	Min	Max	n
Body, length (in vivo, rough values)	110.0	110.0	–	–	–	90.0	120.0	5
Body, length (protargol)	69.5	69.0	8.2	1.8	11.8	50.0	84.0	21
Body, length (not contracted SEM specimens)	90.6	93.0	9.1	3.5	10.1	74.0	104.0	7
Body, length (contracted SEM specimens)	67.8	68.0	6.7	3.4	9.9	61.0	74.0	4
Body, width (in vivo, rough values)	17.4	15.0	–	–	–	15.0	20.0	5
Body, width (protargol)	13.6	13.5	1.7	0.4	12.4	9.5	17.0	21
Body, width (not contracted SEM specimens)	14.9	14.0	2.7	1.0	18.4	12.0	20.0	7
Body, width (contracted SEM specimens)	23.5	23.5	4.7	2.3	19.8	18.0	29.0	4
Body length:width, ratio (in vivo)	6.5	7.3	–	–	–	4.5	8.0	5
Body length:width, ratio (protargol)	5.2	5.2	0.7	0.2	14.5	3.4	6.3	21
Body length:width, ratio (not contracted SEM specimens)	6.3	6.7	1.3	0.5	20.7	3.7	7.4	7
Body length:width, ratio (contracted SEM specimens)	3.0	3.1	0.6	0.3	19.2	2.2	3.4	4
Oral bulge, height	4.0	4.0	0.9	0.2	24.0	3.0	6.0	21
Oral bulge, width at circumoral kinety	6.4	6.5	0.9	0.2	14.0	5.0	8.0	21
Anterior body end to macronucleus, distance	30.0	29.0	5.5	1.2	18.4	21.0	40.0	21
Dorsal brush rows, number	5.0	5.0	0.0	0.0	0.0	5.0	5.0	21
Brush row 1, length	13.5	13.5	1.5	0.3	11.4	9.0	15.0	21
Dikinetids in brush row 1, number	8.8	9.0	0.5	0.1	6.2	8.0	10.0	21
Brush row 2, length	31.0	30.0	4.8	1.1	15.6	25.0	43.0	21
Dikinetids in brush row 2, number	1.2	1.0	0.4	0.1	33.8	1.0	2.0	21
Monokinetal bristles in brush row 2, number	14.8	14.0	1.3	0.3	9.0	13.0	18.0	21
Brush row 3, length	1.0	1.0	0.0	0.0	0.0	1.0	1.0	21
Dikinetids in brush row 3, number	1.8	2.0	0.5	0.1	28.3	1.0	3.0	21

continued

Characteristics	Mean	M	SD	SE	CV	Min	Max	n
Monokinetal bristles in brush row 3, number	4.3	4.0	1.2	0.3	26.8	2.5	6.5	21
Brush row 4, length	19.9	19.0	4.3	1.3	21.8	13.0	25.5	11
Monokinetal bristles in brush row 4, number	8.7	9.0	0.8	0.2	9.0	7.0	10.0	11
Brush row 5, length	19.2	19.0	2.9	0.9	15.1	15.5	25.0	11
Monokinetal bristles in brush row 5, number	10.0	10.0	1.0	0.3	10.0	8.0	12.0	11
Macronucleus, length	14.0	14.0	1.8	0.4	12.9	9.5	17.0	21
Macronucleus, width	7.2	7.0	1.1	0.2	15.4	5.5	10.0	21
Micronucleus, length	2.2	2.0	0.4	0.1	18.2	1.5	3.0	21
Micronucleus, width	1.9	2.0	0.3	0.1	15.8	1.5	2.5	21
Type I extrusomes, length	19.6	19.5	1.7	0.4	8.7	15.0	23.0	21
Somatic ciliary rows, number	13.8	14.0	0.6	0.1	4.4	13.0	15.0	21
Kinetids in a ventral kinety, number	24.9	25.0	2.3	0.5	9.3	22.0	31.0	21
Mucilaginous (epicortical scale) layer, thickness	1.5	1.5	–	–	–	1.0	2.0	21
Type X lepidosomes, length [a]	0.63	0.60	0.16	0.10	25.0	0.40	1.10	23
Type X lepidosomes, width [a]	0.34	0.33	0.06	0.01	17.5	0.22	0.40	23
Type X lepidosomes, height [a]	0.23	0.23	0.04	0.01	16.6	0.20	0.30	13
Type X lepidosomes, hexagons in baseplate, number [a]	10.0	10.0	3.60	0.75	36.1	4.0	18.0	23
Type X lepidosomes, openings in basering, number [a]	9.9	10.0	1.90	0.40	18.8	6.0	13.0	21
Type XI lepidosomes, length [a]	1.20	1.20	0.19	0.03	15.6	0.80	1.5	32
Type XI lepidosomes, width [a]	0.57	0.50	0.15	0.03	26.1	0.40	0.80	32
Type XI lepidosomes, height without anchor [a]	0.38	0.35	0.1	0.05	25.2	0.3	0.5	4
Type XI lepidosomes, height with anchor [a]	0.68	0.65	0.1	0.05	14.1	0.60	0.80	4
Type XI lepidosomes, length of anchor [a]	0.33	0.30	0.07	0.02	20.9	0.23	0.50	19
Type XI lepidosomes, width of anchorplate [a]	0.25	0.25	0.06	0.01	24.5	0.20	0.50	31
Type XI lepidosomes, hexagons in baseplate, number [a]	36.0	34.0	6.93	1.51	19.2	27.0	55.0	21
Type XI lepidosomes, quadrangular meshes in basering, number [a]	22.8	24.0	1.7	0.4	7.6	20.0	26.0	21

[a] From scanning electron micrographs.

preparations, and 5.2:1 in ethanol-fixed and protargol-impregnated specimens (Fig. 34a–c, 35f, l–n, 36a, b; Table 13). Contracted specimens distinctly stouter, i.e., with an average length:width ratio of about 3:1 (Fig. 34f, 35b, c, d, 36c; Table 13).

Body oblong to narrowly obclavate, frequently slightly curved in anterior half; not flattened; in protargol preparations usually buckled or sigmoidal (Fig. 34a–c, t, 35f, l–n, 36a, b). Contractile by about one third of body length, becomes elongate ellipsoid, rarely indistinctly obclavate (Fig. 34f, 35b–d, 36c); contracts and extends slowly with movements resembling euglenid metaboly (Fig. 35d). Nuclear apparatus in or near body centre (Fig. 34a, u, 35c, d, f, l–n; Table 13). Macronucleus ellipsoid to distinctly reniform, on average 14 × 7 µm in protargol preparations; nucleoli of ordinary size. Micronucleus attached to long side of macronucleus, usually globular, rarely ellipsoid, about 2 µm across; possibly lacking in half of specimens. Contractile vacuole in posterior end, a single excretory pore in pole centre (Fig. 34a, u, 35b, c, f, 36q). Two types of extrusomes attached to oral bulge (Fig. 34a, d, g–i, 35b, d–j, 37a; Table 13): type I forms a

conspicuous bundle, rod-shaped to indistinctly acicular, slightly curved, about 20–25 × 0.5 µm in vivo; many immature stages scattered in cytoplasm, these and the proximal, toxin-containing portion of mature extrusomes usually lightly impregnate with the protargol method used. Type II extrusomes oblong and 2–3 µm long in vivo; explode under slight coverslip pressure, do not impregnate with protargol. Cytoplasm colourless, usually studded with food vacuoles 5–8 µm across and few to many lipid droplets 0.5–10 µm in size (Fig. 34a, 35b, c, f). Swims and creeps slowly on microscope slide. Food not known but likely small ciliates as indicated by large lipid droplets.

Cortex flexible, contains rather dense rows of colourless granules 0.1–0.5 µm across (Fig. 34e, 37d); covered by a mucilaginous layer about 1 µm thick in vivo and 1.5 µm in protargol preparations. Mucilaginous layer contains type X and type XI lepidosomes, the latter recognizable in vivo as minute, anteriorly directed lines, and as blue cover in alcian blue preparations (Fig. 34m, 37a, b). Type X lepidosomes attached to pellicle; ovate, elliptic or broadly elliptic in surface view while cuneate in lateral view (Fig. 34j–l, 36l–o, 37e; Table 13): on average 0.6 × 0.35 × 0.23 µm in size and with 10 hexagons in baseplate and 10 quadrangular meshes in basering. Type XI in one layer on type X lepidosomes, of complex structure, i. e., with a tongue-shaped main part and a campanulate anchor attached to pellicle; best described as sock-shaped in lateral view and as tongue-shaped in top and back view. Tongue-shaped part in lateral view straight, slightly concave, or slightly sigmoid, narrowed end directed anteriorly, sock instep (baseplate) moderately concave; basering on surface and composed of an average of 23 quadrangular meshes; baseplate composed of an average of 36 hexagons (with anchor); anchor slightly inclined posteriorly, belongs to baseplate, length 0.33 µm on average (Fig. 34a, m, o–s, 36a–l, p, r, 37e–g, i–k; Table 13).

Cilia about 8 µm long in vivo, show spiral pattern staining with alcian blue, ordinarily spaced, arranged in an average of 14 narrowly spaced (~3 µm), bipolar rows five modified to dorsal brush anteriorly (Fig. 34a, t–v, 35a, l–n, 36a, c, i–k, 37h; Table 13). Dorsal brush heteromorphic, likely structured as shown in Fig. 34n, v; row 1 composed of an average of nine dikinetids with anterior bristles in vivo slightly inflated, 1–2 µm long, and thicker than posterior bristles 0.5–1 µm long; rows 2 and 3 each commences with a single dikinetid followed by monokinetal, acicular bristles about 3 µm long in vivo; rows 4 and 5 composed of only monokinetal bristles. All rows continue posteriorly as ordinary somatic kineties.

Oral bulge in vivo and in the SEM inconspicuous because only 2–3 µm high (Fig. 34a–c, g, 35b–f, 36a–c, k) while usually inflated to an average of 4 µm in ethanol-fixed cells (Fig. 35k–n); discoid with slightly concave centre, assumes a characteristic shape under slight coverslip pressure (Fig. 34d); rather refractive because containing type II extrusomes and anterior end of type I extrusomes. Circumoral kinety circular, composed of dikinetids, anterior basal body ciliated, posterior barren but with a pharyngeal rod contributing to the oral basket (Fig. 34a, d, g, n, t–v, 35k–n, 36a, k; Table 13).

Occurrence and ecology: To date known only from type locality, where it became abundant in the non-flooded Petri dish culture one week after rewetting.

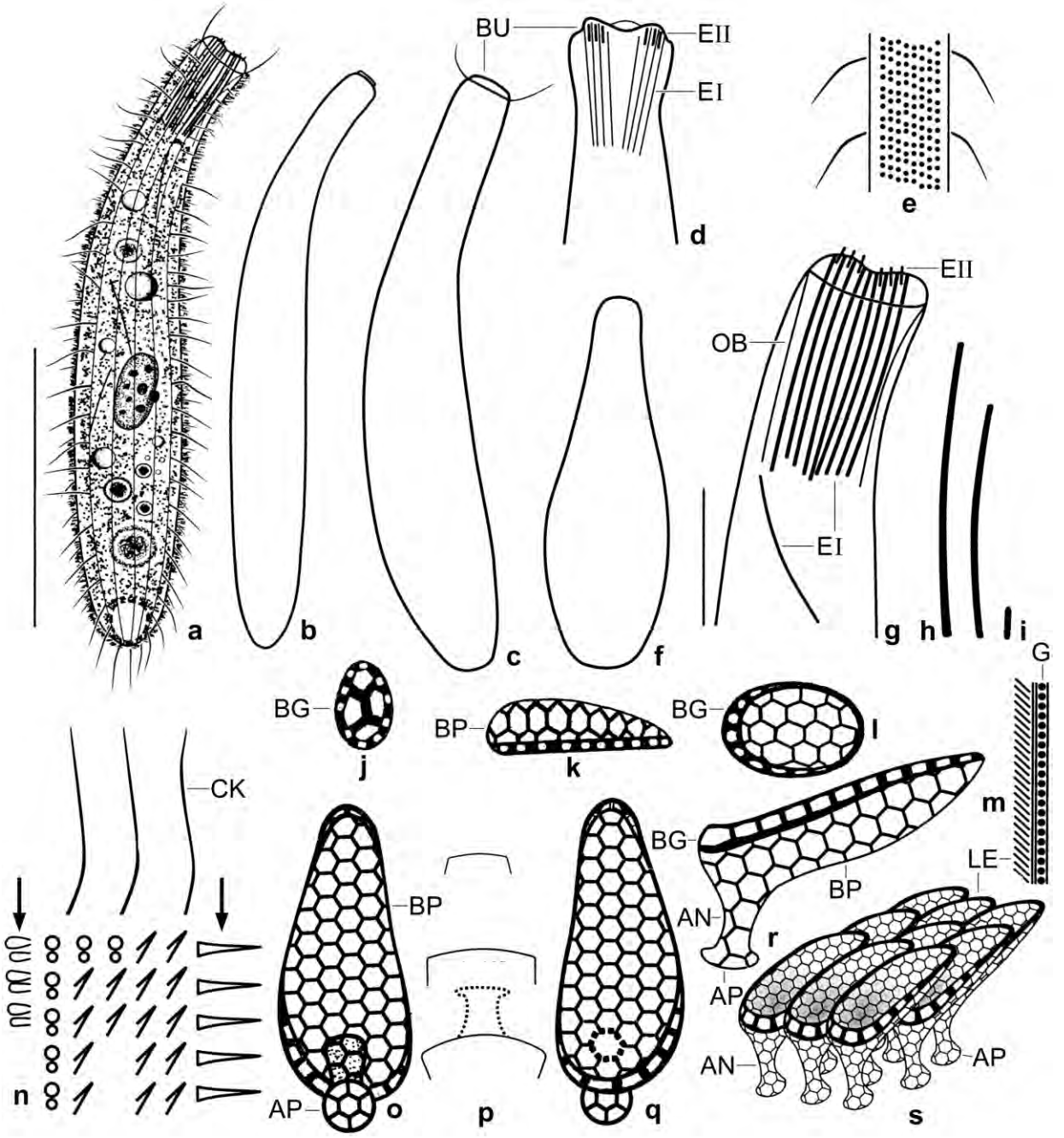

Fig. 34a–s. *Lingulothrix galapagensis* from life (a–i, m, n) and in the scanning electron microscope (j–l, o–s). **a:** A representative specimen, length 110 µm. **b, c, f:** Outline of slender (b), normal (c), and contracted (f) specimens. **d, g:** Details of anterior body region of slightly pressed specimens, showing the oral bulge and the arrangement of type I and type II extrusomes. **e:** Surface view, showing cortical granulation. **h, i:** Type I (~ 20 µm) and type II (2–3 µm) extrusomes drawn to scale. **j–l:** Type X lepidosomes, top (j), lateral (k), and back (l) view, size on average 0.63 × 0.34 × 0.23 µm (Table 13). **m:** Optical section of cortex, showing arrangement of lepidosomes and cortical granules. **n:** Distal region of dorsal brush with dikinetal (left arrow) and monokinetal (right arrow) bristles in lateral (arrows) and top view. **o–q:** Slightly schematized type XI lepidosomes in top (o) and back (q) view, and cross-sections of left lepidosome at three levels, showing the concave baseplate; size on average 1.2 × 0.57 × 0.38 µm (Table 13). **r, s:** Lateral views of type XI lepidosomes anchored to the pellicle by a short, campanulate elongation of the baseplate. AN – anchor, AP – anchorplate, BG – basering, BP – baseplate, BU – oral bulge, CK – circumoral kinety, EI, II – extrusome types, G – cortical granules, LE – lepidosomes, OB – oral basket. Scale bar 50 µm.

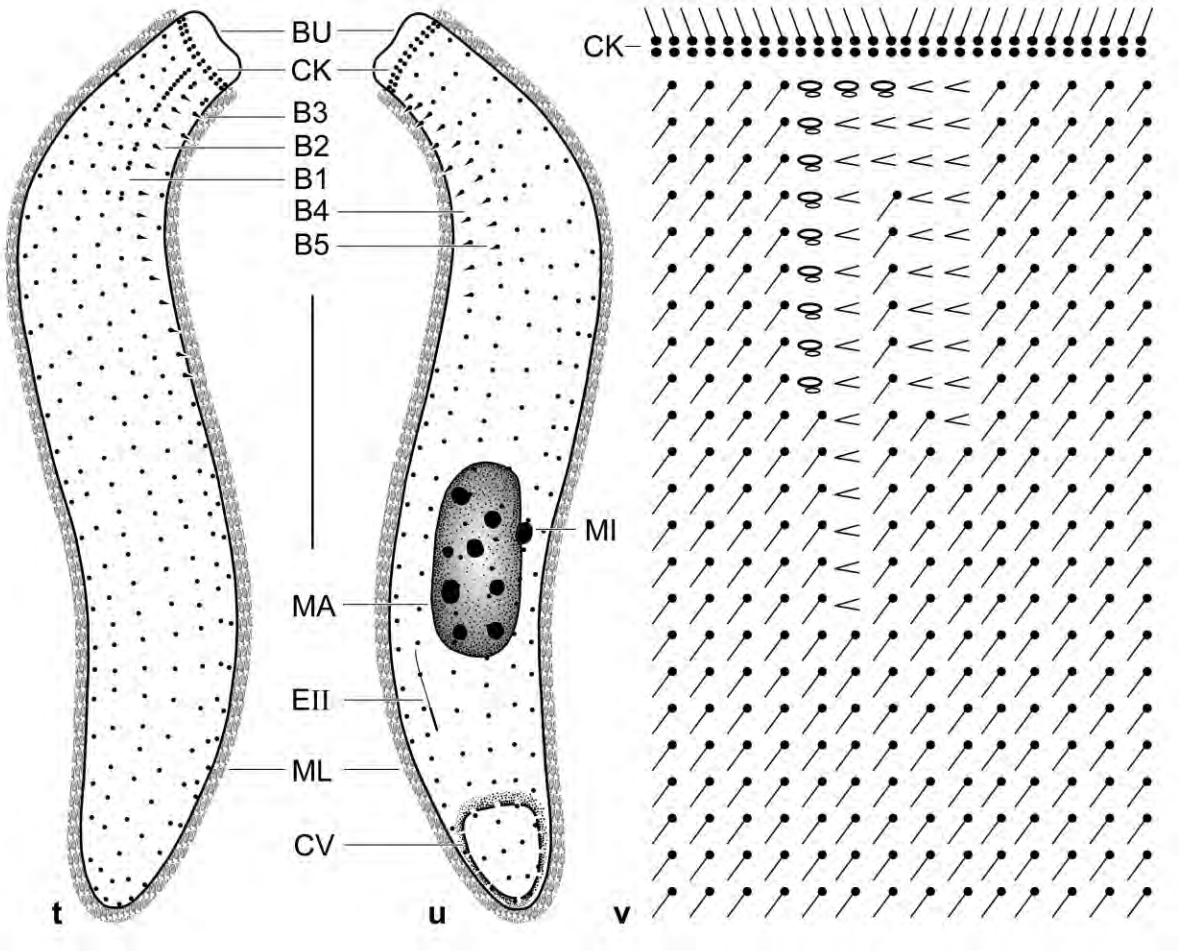

Fig. 34t–v. *Lingulothrix galapagensis* from life (v) and after protargol impregnation (t, u). **t, u:** Dorsal and ventral view of holotype specimen, showing the ciliary and nuclear pattern, length 70 µm. **v:** Scheme of oral and somatic ciliature including the complex, five-rowed dorsal brush. B1–5 – dorsal brush rows, BU – oral bulge, CK – circumoral kinety, CV – contractile vacuole, EII – developing type II extrusome, MA – macronucleus, MI – micronucleus, ML – mucilaginous layer. Scale bar 20µm.

Remarks: For a general discussion, see → *Cataphractes austriacus* which differs from *L. galapagensis* by the number of ciliary rows (18 vs. 14, extremes non-overlapping) and by the length (30 µm vs. 19 µm) and shape (acicular vs. rod-shaped) of the type I extrusomes. In contrast, → *Cataphractes terricola* is in vivo and in protargol preparations indistinguishable from *L. galapagensis.*

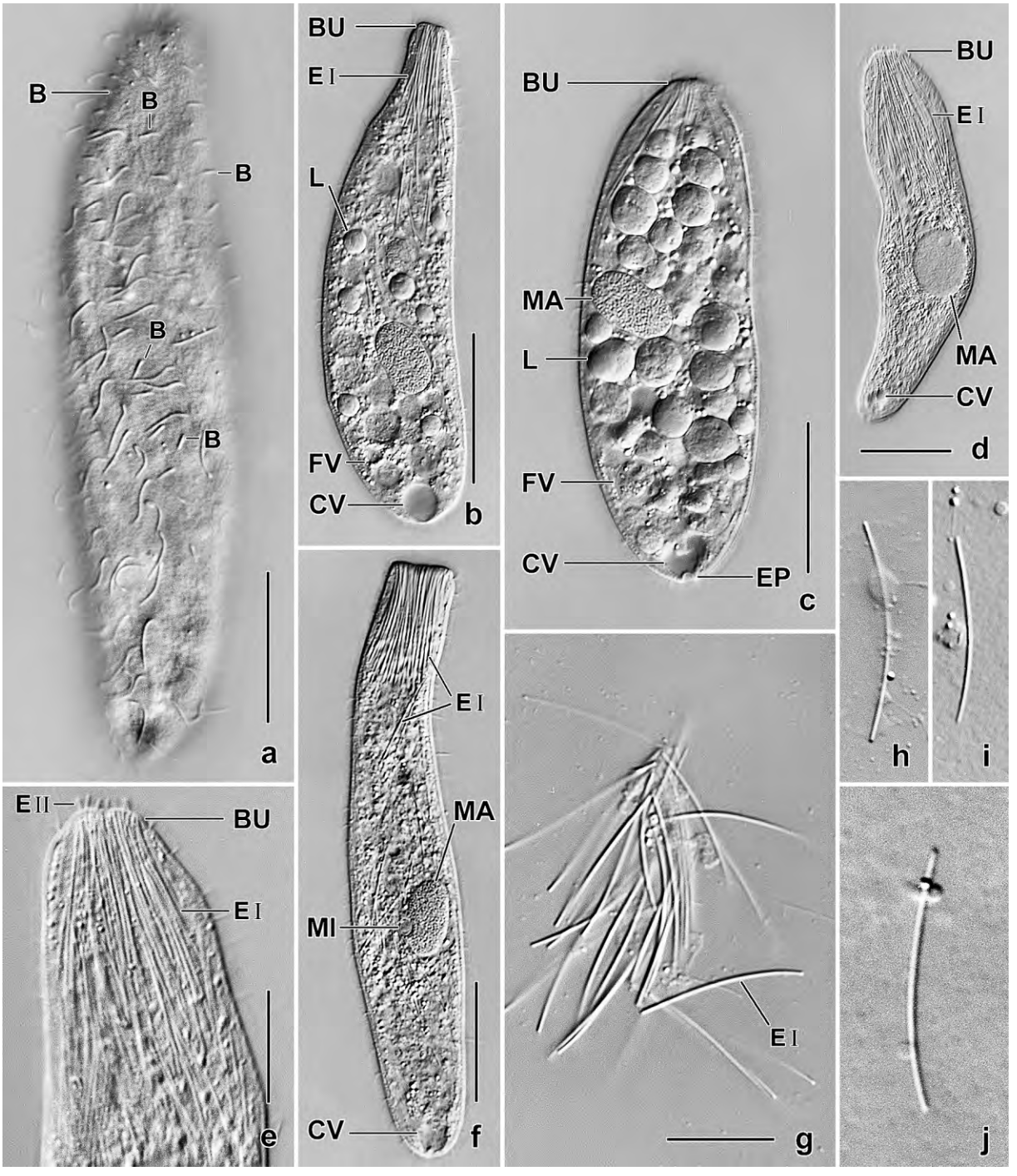

Fig. 35a–j. *Lingulothrix galapagensis* from life. **a:** Surface view, showing part of dorsal brush. **b, c:** Contracted specimens with many food vacuoles and lipid droplets. **d:** Contracting specimen, showing a kind of euglenid metaboly. **e:** Oral bulge region, showing exploded type II extrusomes. **f:** A slightly pressed specimen, showing the nuclear apparatus and the type I extrusomes which form a dense bundle. **g–j:** Mature type I extrusomes are 15–25 µm long and slightly curved. B – dorsal brush, BU – oral bulge, CV – contractile vacuole, EI, II – extrusome types, EP – excretory pore, FV – food vacuoles, L – lipid droplets, MA – macronucleus, MI – micronucleus. Scale bars 10 µm (e), 15 µm (d, g), 20 µm (f), and 25 µm (a–c).

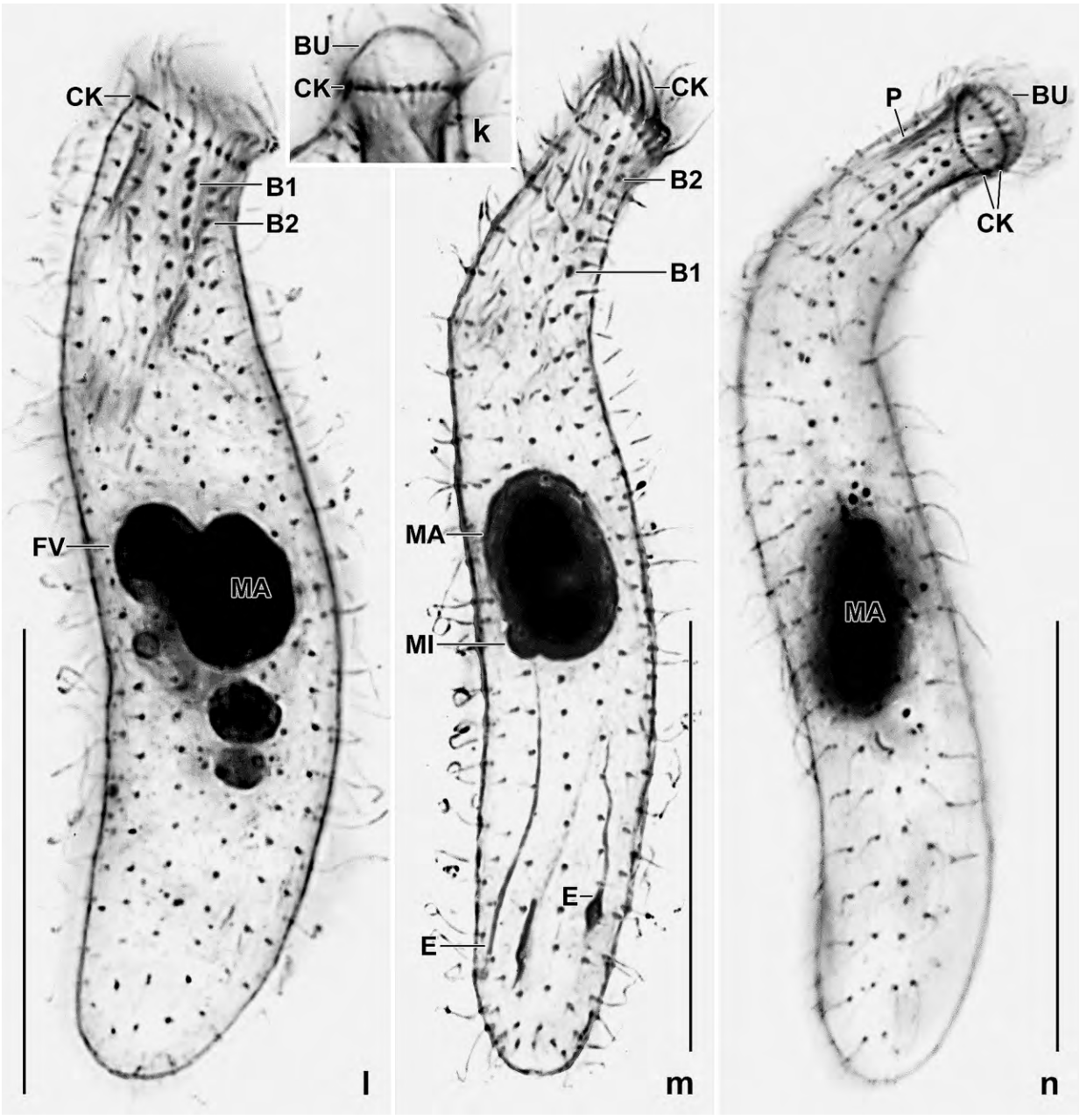

Fig. 35k–n. *Lingulothrix galapagensis* after protargol impregnation. The specimens show the variability in body shape and size as well as the inconspicuous dikinetal part of the dorsal brush. The oral bulge is usually more pronounced in the preparations (k, n) than in vivo (Fig. 35b–f), indicating a distinct inflation. BU – oral bulge, B1, 2 – dorsal brush rows, CK – circumoral kinety, E – developing type I extrusomes, FV – food vacuole, MA – macronucleus, MI – micronucleus, P – pharynx. Scale bars 30 µm.

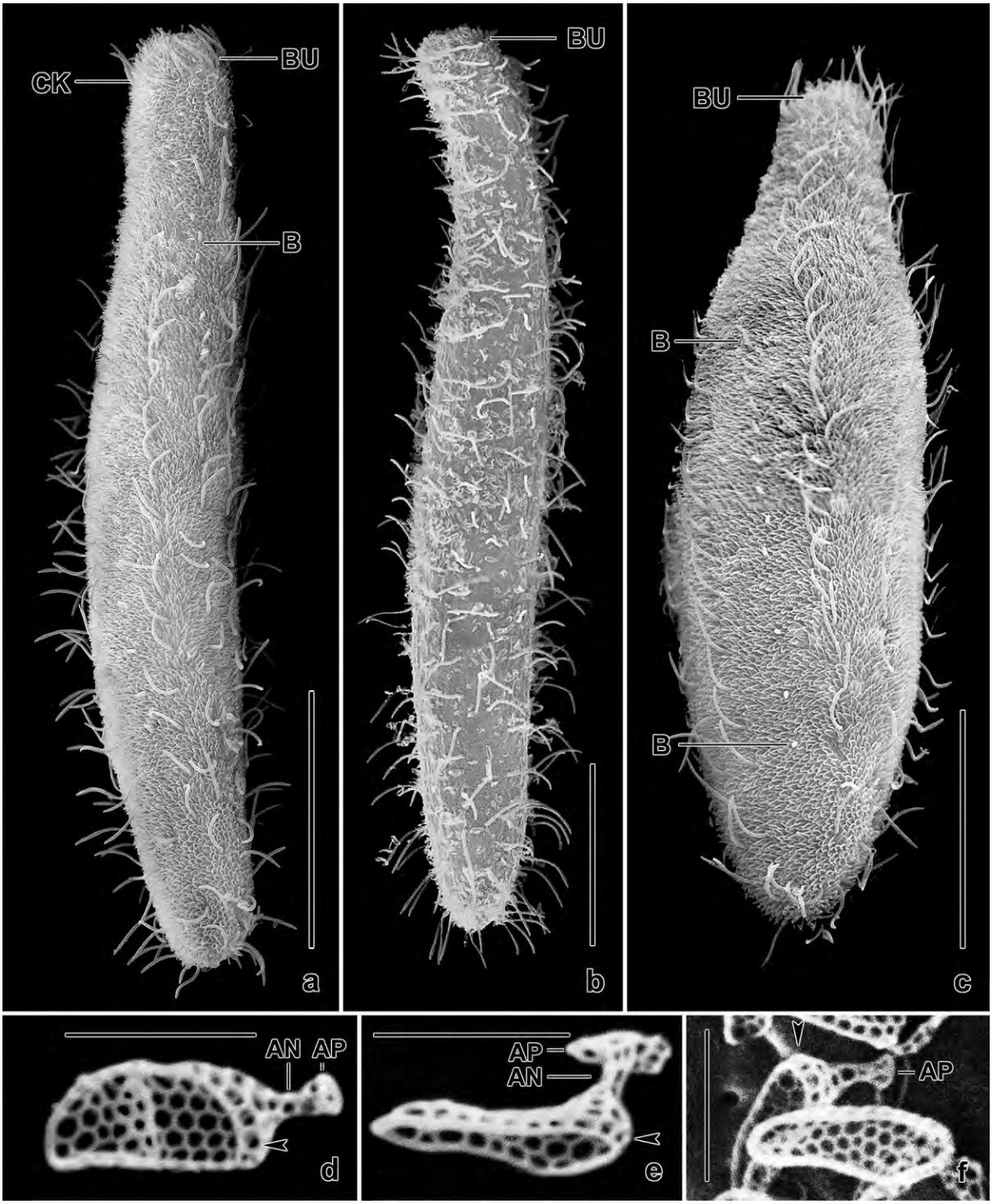

Fig. 36a–f. *Lingulothrix galapagensis* in the scanning electron microscope. **a–c:** Overviews of extended (a, b) and of contracted (c) specimens, showing countless minute tongues, i. e., type XI lepidosomes; the specimen shown in (b) lost most lepidosomes during the preparation. One of the dorsal brush rows extends to near posterior body end (c). **d–f:** Type XI lepidosomes in top (d), lateral (e), and back (f) view. Note the basering (arrowheads) and the campanulate anchor attached to the pellicle of the ciliate. AN – anchor, AP – anchorplate, B – dorsal brush rows, BU – oral bulge, CK – circumoral kinety. Scale bars 1 µm (d–f) and 20 µm (a–c).

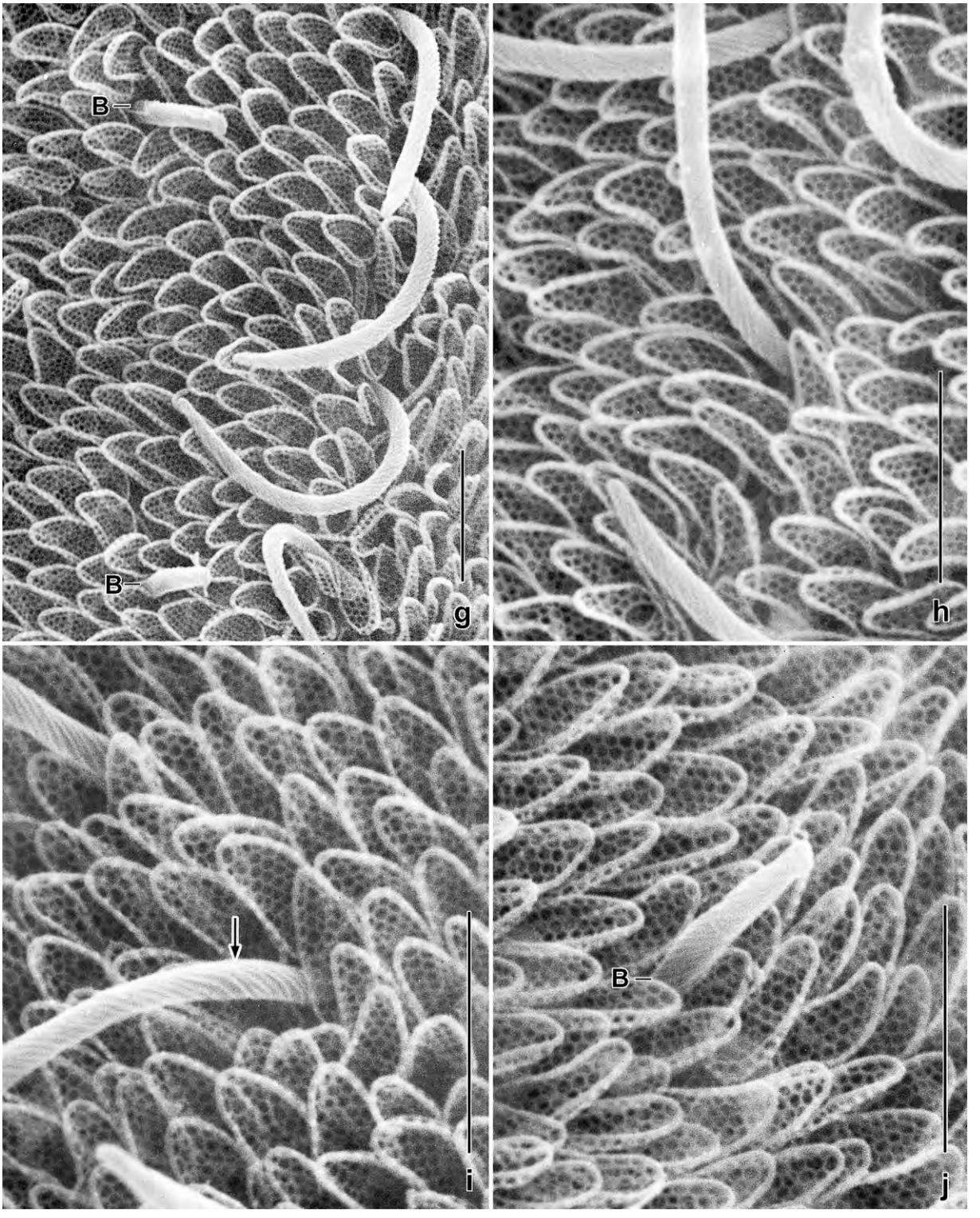

Fig. 36g–j. *Lingulothrix galapagensis*, surface views of the mucilaginous layer, showing the tongue-shaped type XI lepidosomes. Note the spiral pattern on the surface of the cilia (i, arrow) and dorsal bristles (j). B – dorsal brush bristles. Scale bars 2 µm.

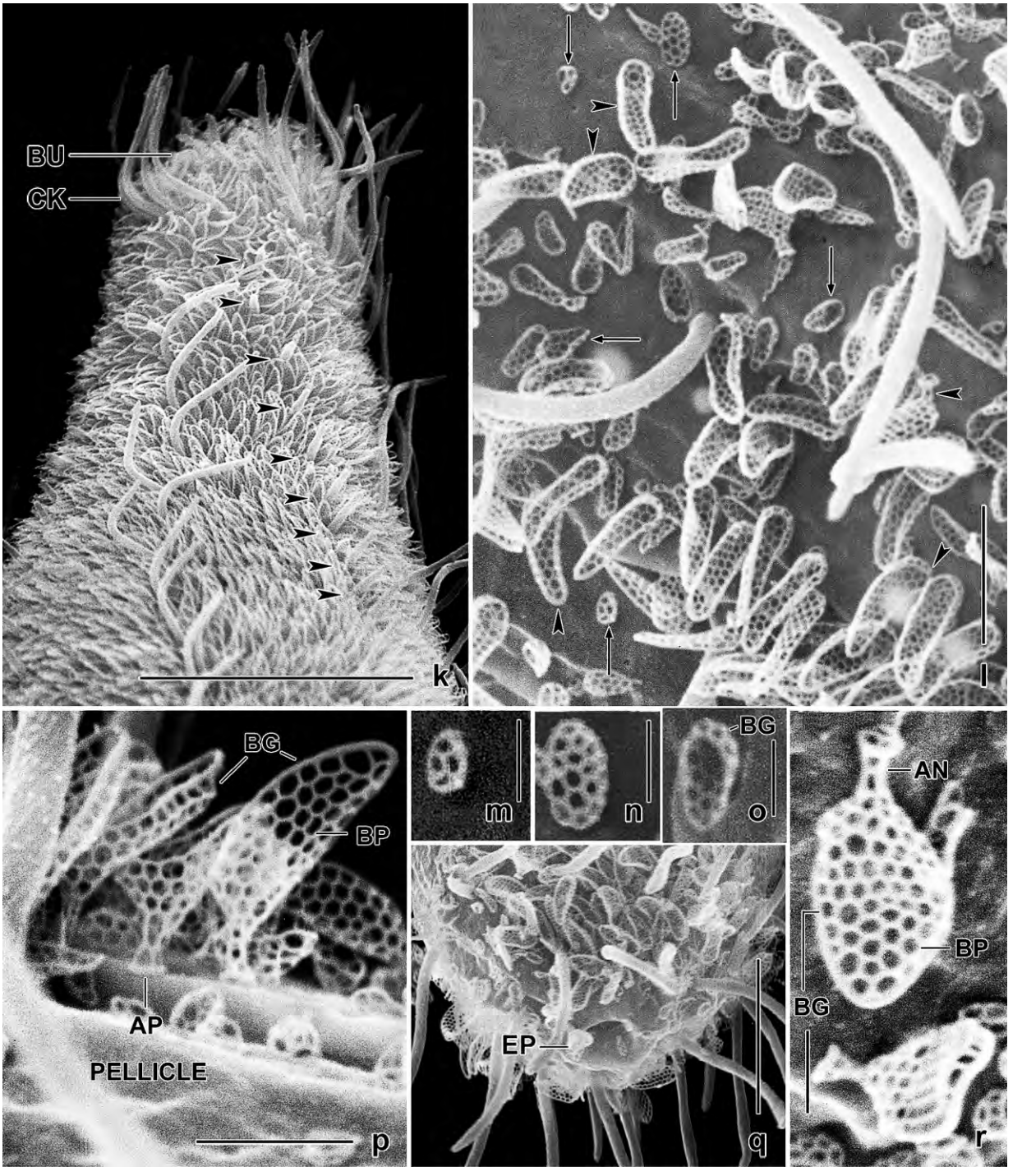

Fig. 36k–r. *Lingulothrix galapagensis* in the scanning electron microscope. **k:** Anterior body region, showing a row of dorsal brush bristles (arrowheads). **l:** Surface view of a disturbed specimen, showing type X (arrows) and type XI (arrowheads) lepidosomes on the pellicle. **m–o:** Type X lepidosomes have an average length of 0.63 µm and are hightly variable in size and in the number of polygons. **p:** Type XI lepidosomes attached to the pellicle with a campanulate anchor. **q:** Posterior body end with excretory pore. **r:** Organization of the type XI lepidosomes. AN – anchor, AP – anchorplate, BG – basering, BP – baseplate, BU – oral bulge, CK – circumoral kinety, EP – excretory pore. Scale bars 0.5 µm (r), 1 µm (p), 2 µm (l), 4 µm (q), and 10 µm (k).

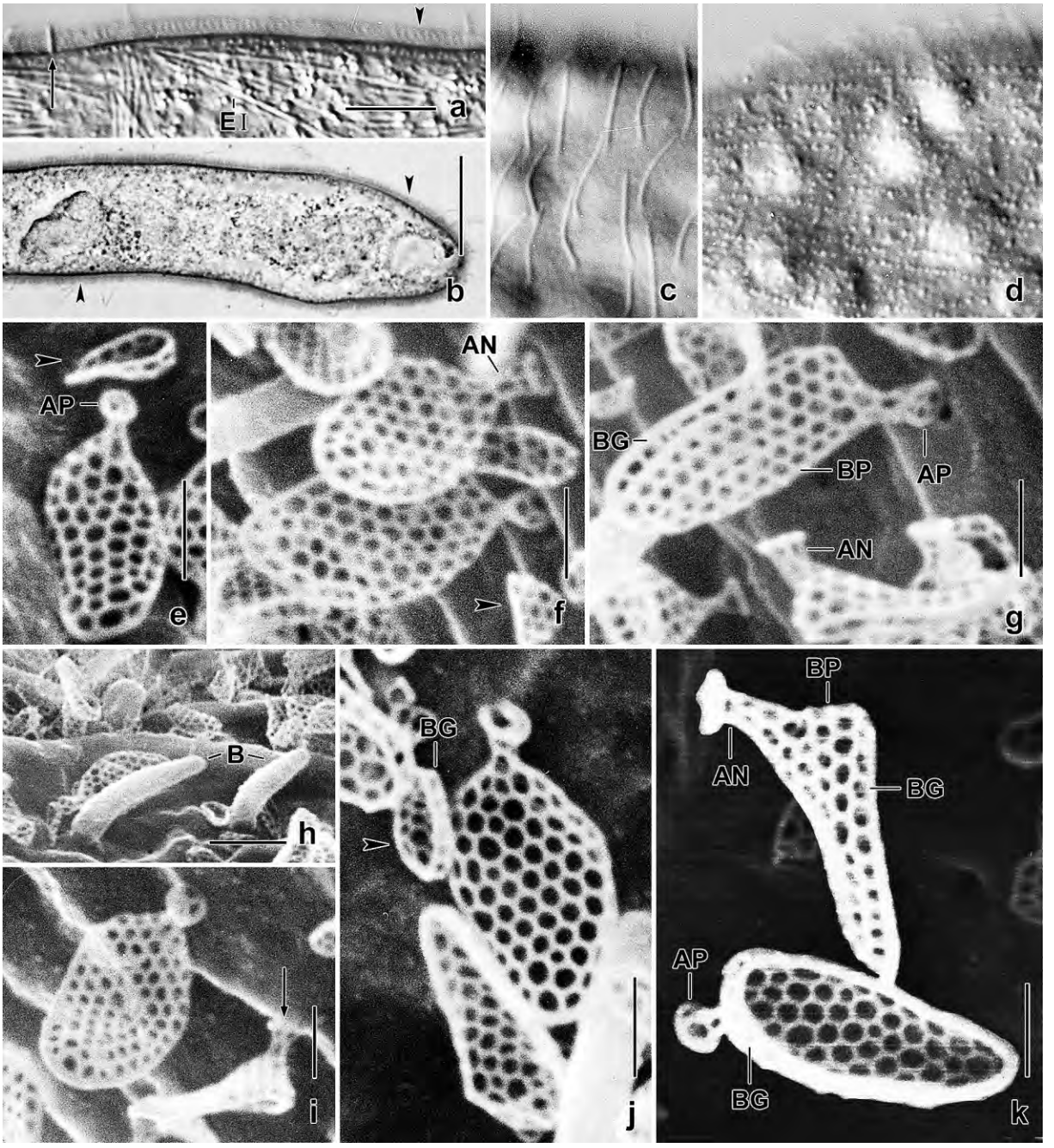

Fig. 37a–k. *Lingulothrix galapagensis* from life (a, c, d), in an alcian blue stain (b), and in the scanning electron microscope (e–k). **a, b:** The mucilaginous layer stains with alcian blue (arrowheads), showing acid mucopolysaccharids as a main component. The arrow marks a dorsal bristle. **c, d:** Surface views, showing the mucilaginous layer (c) and he cortical granulation (d). **e–g:** The minute type X lepidosomes (arrowheads) are cuneate in lateral view. The type XI lepidosomes have a campanulate anchor, a basering with quadrangular meshes (g), and a honeycombed baseplate. **h:** The monokinetal brush bristles are narrowed distally. **i:** Top view and lateral view (arrow) of type XI lepidosomes. The lateral view shows the lepidosome attached to the pellicle with the anchor. **j:** Top view of a type XI lepidosome and lateral view of a type X lepidosome (arrowhead), showing the basering. **k:** Lateral and back view of type XI lepidosomes, showing the two main orientations: in lateral view, they look like socks; in top and back view, they are tongue-shaped. AN – anchor, AP – anchorplate, BG – basering, BP – baseplate, EI –type I extrusome. Scale bars 0.5 µm (e–k), 1 µm (h), and 15 µm (a, b).

Cataphractes nov. gen.

Diagnosis: Lingulotrichidae with type X and gooseneck-shaped type XII lepidosomes anchored to pellicle with a minute plate (goosehead).

Type species: *Cataphractes austriacus* nov. spec.

Etymology: The Latin noun *cataphractes* (scale = lepidsome maker) refers to the mucilaginous cover containing minute scales. Masculine gender.

Remarks: See **Remarks** to family and to genus → *Lingulothrix*.

Cataphractes austriacus nov. spec. (Fig. 38a–x, 39a–l, 40a–t, 41a–g; Tables 14, 15)

Diagnosis (includes KAHL´s data): Size in vivo 120 × 20 µm, contractile by up to 50%. Very narrowly oblong (~7:1), elongate ellipsoid when moderately contracted. Macronucleus ellipsoid, micronucleus globular to ellipsoid. Oral bulge indistinct, discoid. Two types of extrusomes: type I slightly acicular and more or less curved, 25–30 µm long; type II only 2–3 µm long. On average 18 ciliary rows, 6 contributing to dorsal brush: row 1 composed of an average of 13 dikinetids; row 2 with three; rows 3–6 composed of monokinetids with up to 6 µm long bristles. Type X lepidosomes broadly to slenderly elliptical or ovate, with an average of 11 polygons in baseplate, 0.63 × 0.40 µm in size. Type XII lepidosomes gooseneck-shaped in lateral view, with 37 hexagons in baseplate and 4 polygons in anchorplate on average, about 1.23 × 0.55 × 0.94 µm in the scanning electron microscope.

Type locality: Water and mud from *Sphagnum* cushions of a small bog in the surroundings of the village of Überling, Salzburg country, 47°48'N 13°03'O.

Type material: 1 holotype and 3 paratype slides with protargol-impregnated specimens have been deposited in the Biology Centre of the Upper Austrian Museum in Linz (LI). The holotype and other relevant specimens have been marked by black ink circles on the coverslip.

Description: Moderately variable, i. e., coefficient of variability (CV) > 15% in only five of 18 features measured; CV < 15% in all important characteristics, such as body length (9.6%), number of ciliary rows (3.4%), and number of dikinetids in dorsal brush row 1 (13.1%). Most lepidosome features with a CV > 15%, very likely partially caused by strong preparation shrinkage (Table 14).

Size in vivo 100–140 × 17–20 µm, on average 120 × 19 µm (Table 14); protargol-prepared specimens match well when 15% preparation shrinkage is added. Body in vivo narrowly oblong (length:width ratio 4.6) to cylindroidal (9.7), on average very narrowly oblong (7.3); frequently curved, especially in anterior half; body ends narrowly rounded, rarely bluntly pointed; not flattened laterally (Fig. 38a, b, d, e, u, 39a–c). Contractile up to 50% of body length, strongly contracted cells elongate ellipsoid or more or less lageniform (Fig. 38c, w, 39d, f, i, 40b); contracts

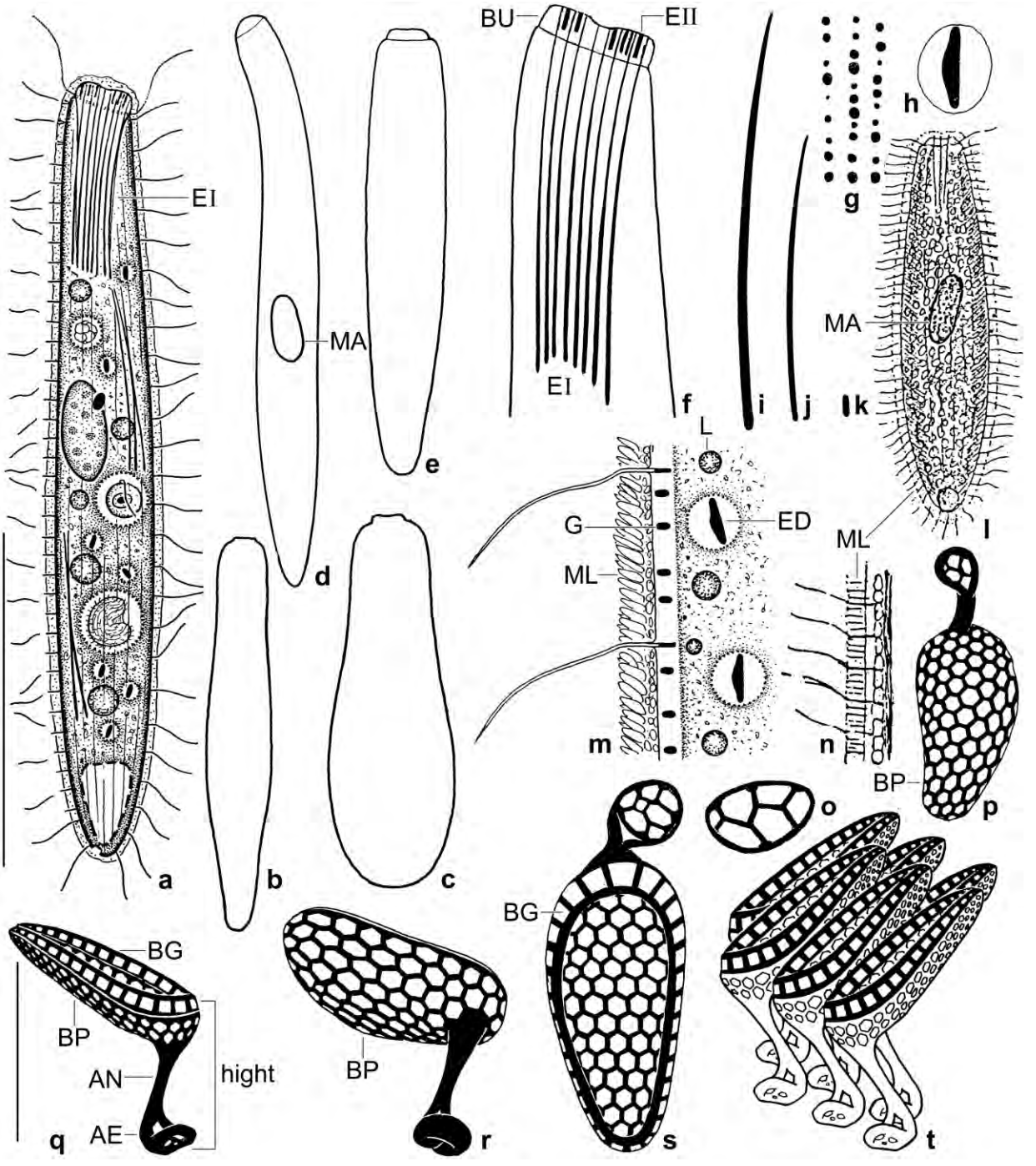

Fig. 38a–t. *Cataphractes austriacus* (a–k, m, o–t) and *Lagynus vestitus* (l, n) from life (a–n) and in the scanning electron microscope (o–t). **a:** A representative, extended specimen, length 120 µm. **b, c, e:** More or less contracted specimens. **d:** A slender specimen. **f:** Anterior body region, showing type I and type II extrusomes. **g:** Surface view, showing cortical granulation. **h:** Developing extrusome. **i:** Type I extrusomes are acicular and about 30 µm long. **j, k:** Type I and type II (2 µm) extrusomes drawn to scale. **l, n:** *Lagynus vestitus*, about 200 µm (from Kahl 1927, 1930a). **m:** Optical section of cell´s periphery. **o:** Type X lepidosome. **p–t:** Type XII lepidosomes are gooseneck-shaped when observed laterally and upside down. AE – anchorplate, AN – anchor, BG – basering, BP – baseplate, BU – oral bulge, ED – developing extrusome, EI, II – extrusome types, G – cortical granules, L – lipid droplet, MA – macronucleus, ML – mucilaginous layer. Scale bars 1 µm (q) and 50 µm (a).

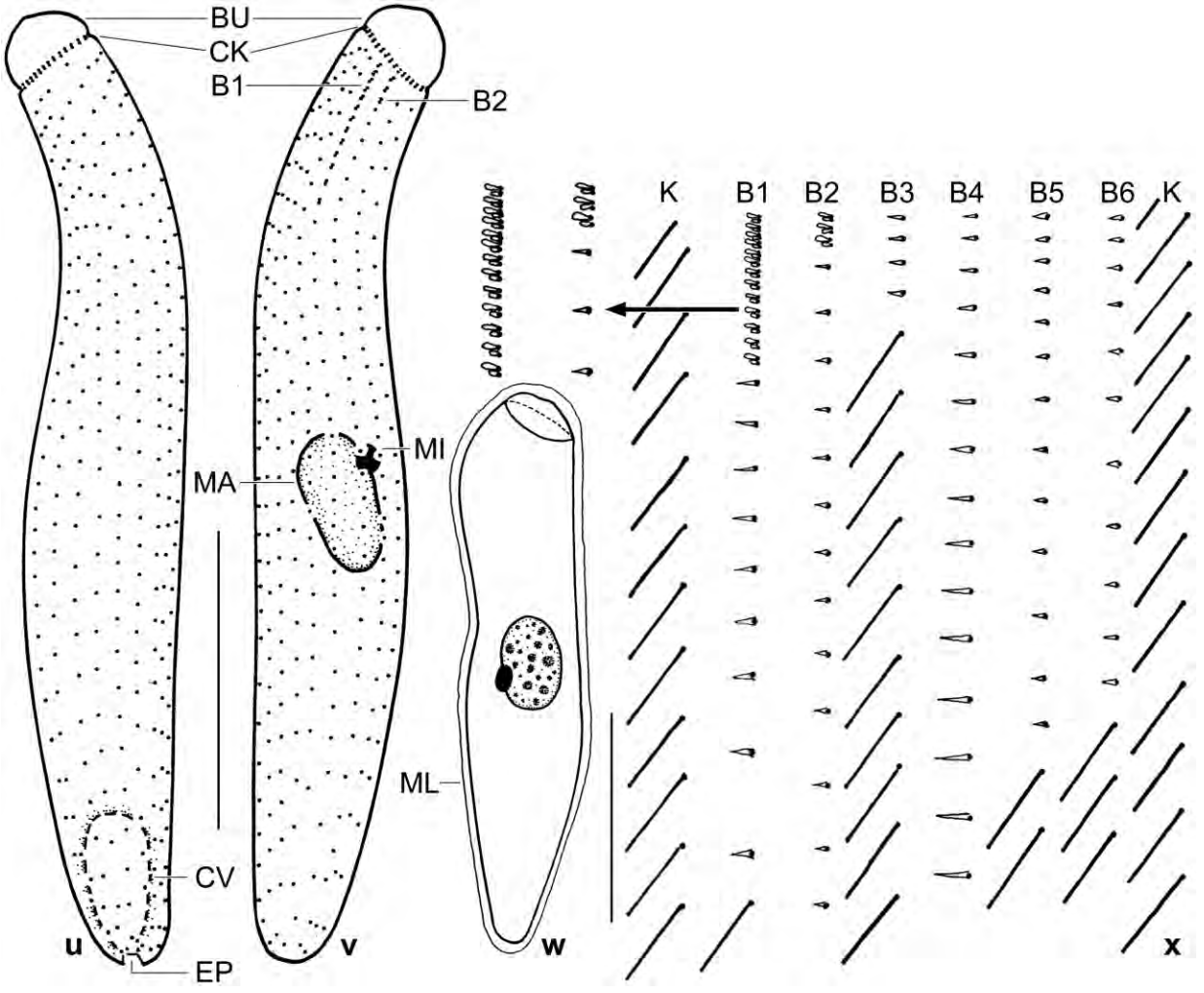

Fig. 38u–x. *Cataphractes austriacus* after protargol impregnation (u–w) and from life (x). **u, v:** Infraciliature and nuclear apparatus of holotype specimen, length 100 µm. The hemispherical oral bulge is a preparation artifact. **w:** A contracted specimen. **x:** Dorsal brush with details slightly uncertain in B3–B6. BU – oral bulge, B1–6 – dorsal brush rows, CK – circumoral kinety, CV – contractile vacuole, EP – excretory pore, K – ordinary somatic kineties, MA – macronucleus, MI – micronucleus, ML – mucilaginous layer. Scale bars 30 µm.

and retracts slowly with movements resembling euglenid metaboly (Fig. 38w). Nuclear apparatus in or near mid-body, may be strongly dislocated in overfed specimens (Fig. 38a, v, w, 39a–d, f, g; Table 14). Macronucleus globular to elongate ellipsoid, on average ellipsoid; contains many minute nucleoli. A single micronucleus attached to macronucleus in various positions, globular to ellipsoid. Contractile vacuole in posterior body end, with single excretory pore in or slightly off pole centre (Fig. 38a, u, 39c). Two types of extrusomes attached to oral bulge (Fig. 38a, f, i–k, 39g, j, k): type I forms a conspicuous bundle in oral body portion, slightly to rather distinctly acicular, more or less curved, about 30 µm long in vivo, does not impregnate with the protargol method used; type II oblong and minute, i. e., 1–2 µm long. Developing extrusomes frequent in cytoplasm, rod-shaped and curved, certain stages impregnate with protargol (Fig. 38h, m, 39k). Cytoplasm colourless, usually studded with 5–10 µm-sized lipid droplets and food vacuoles with small flagellates and ciliates (Fig. 38a, 39f, g). Glides and swims slowly rotating about main body axis.

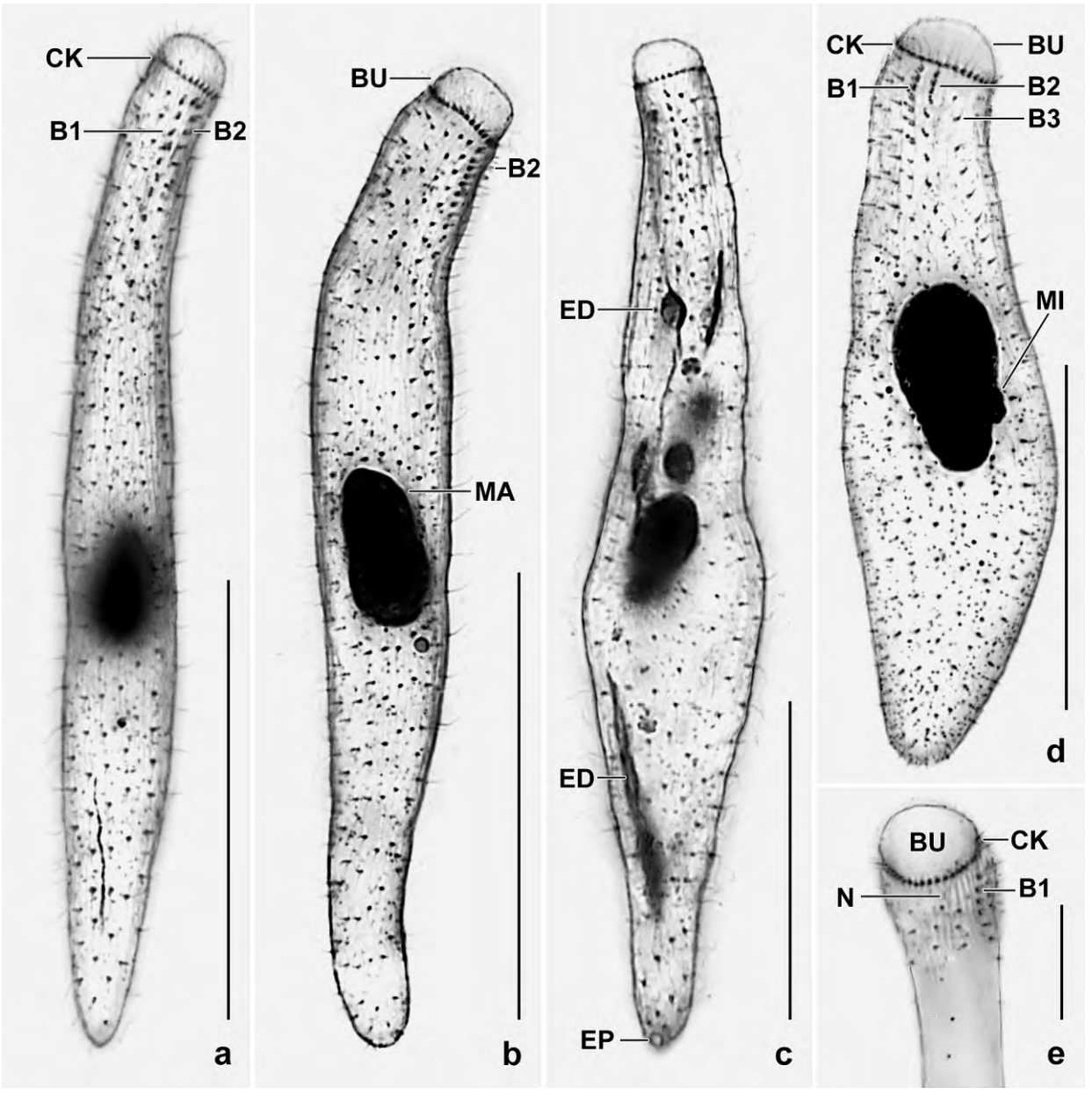

Fig. 39a–e. *Cataphractes austriacus*, infraciliature and nuclear apparatus after ethanol fixation and protargol impregnation. **a–c:** Extended specimens are very slender. The huge oral bulge is a preparation artifact. **d:** A rather distinctly contracted specimen. **e:** Oral region, showing the circular oral bulge and the nematodesmata forming the oral basket. BU – oral bulge, B1, 2, 3 – dorsal brush rows, CK – circumoral kinety, ED – developing extrusomes, EP – excretory pore of contractile vacuole, MA – macronucleus, MI – micronucleus, N – nematodesmata. Scale bars 10 µm (e), 30 µm (c, d), and 50 µm (a, b).

Cortex very flexible, contains narrowly spaced rows of granules with highly different size, i. e., about 0.3–0.8 × 0.2–0.6 µm (Fig. 38g, 39h); covered by a mucilaginous layer 1–1.5 µm thick in vivo. Mucilaginous layer composed of slime and type X and type XII lepidosomes, the latter recognizable in vivo as minute, oblique structures oriented anteriorly (Fig. 38a, m, 39g, h). Slime partially preserved in SEM preparations, appears as dense filamentous reticulum on and between type XII lepidosomes (Fig. 40d, i, j, t). Type X lepidosomes on pellicle; broadly elliptical, elliptical or ovate in top views; basering very likely absent; on average 0.63 × 0.40

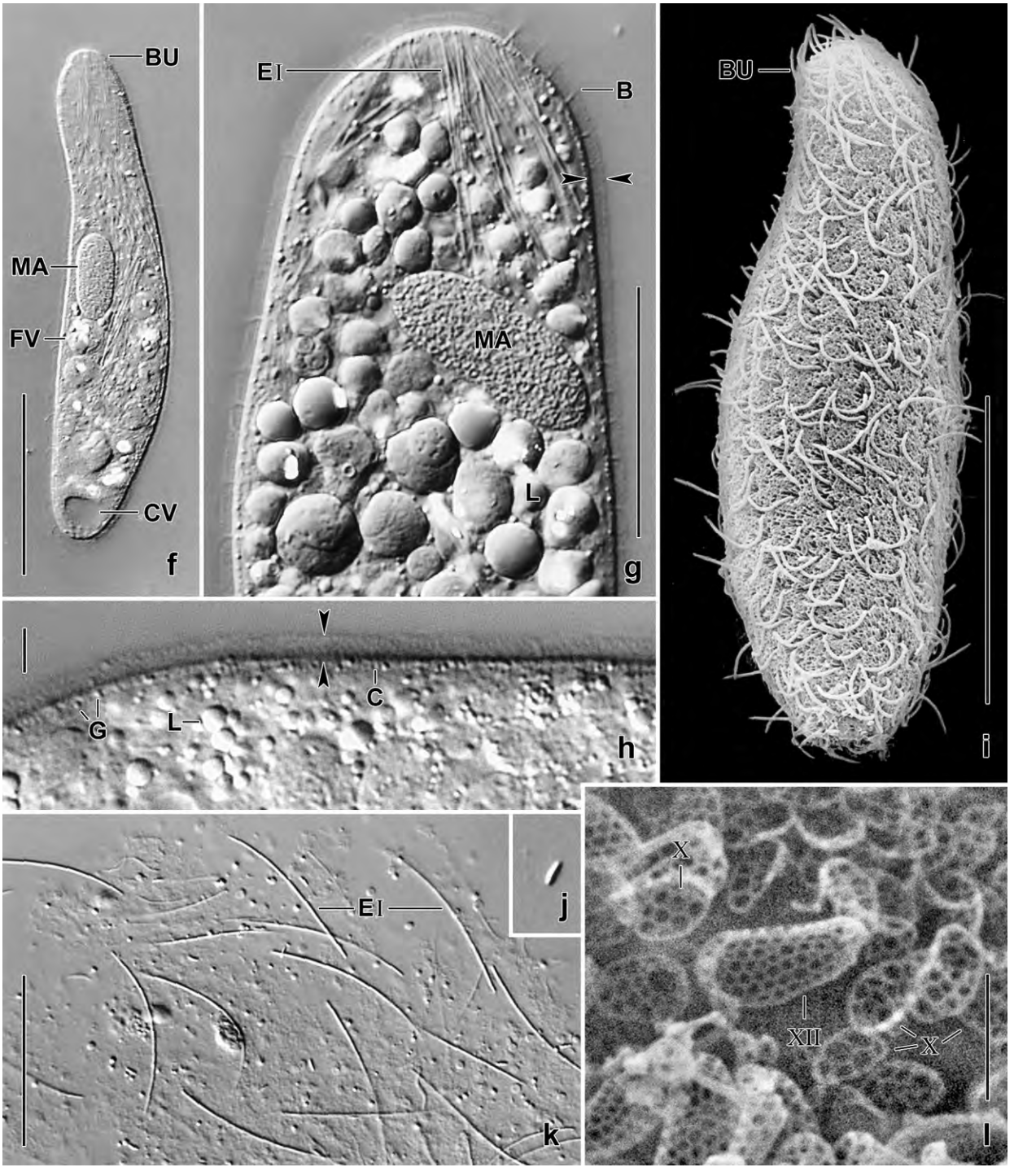

Fig. 39f–l. *Cataphractes austriacus* from life (f–h, j, k) and in the scanning electron microscope (i, l). **f:** A moderately contracted specimen, showing the general organization. **g, h:** Anterior and mid-body region, showing the 1–1.5 µm thick mucilaginous layer (opposed arrowheads) and details of the cortex and the cytoplasm. **i:** Overview. The mucilaginous layer looks like a fine fur. **j:** Type II extrusome, about 2 µm long. **k:** Cytoplasmic type I extrusomes are rod-shaped and about 25 µm long. **l:** The body surface is covered by minute type X lepidosomes. B – dorsal brush bristle, BU – oral bulge, C – cortex, CV – contractile vacuole, EI –type I extrusomes, FV – food vacuoles, G – cortical granules, L – lipid droplets, MA – macronucleus, X, XII – lepidosome types. Scale bars 1 µm (l), 3 µm (h), and 30µm (f, g, i, k).

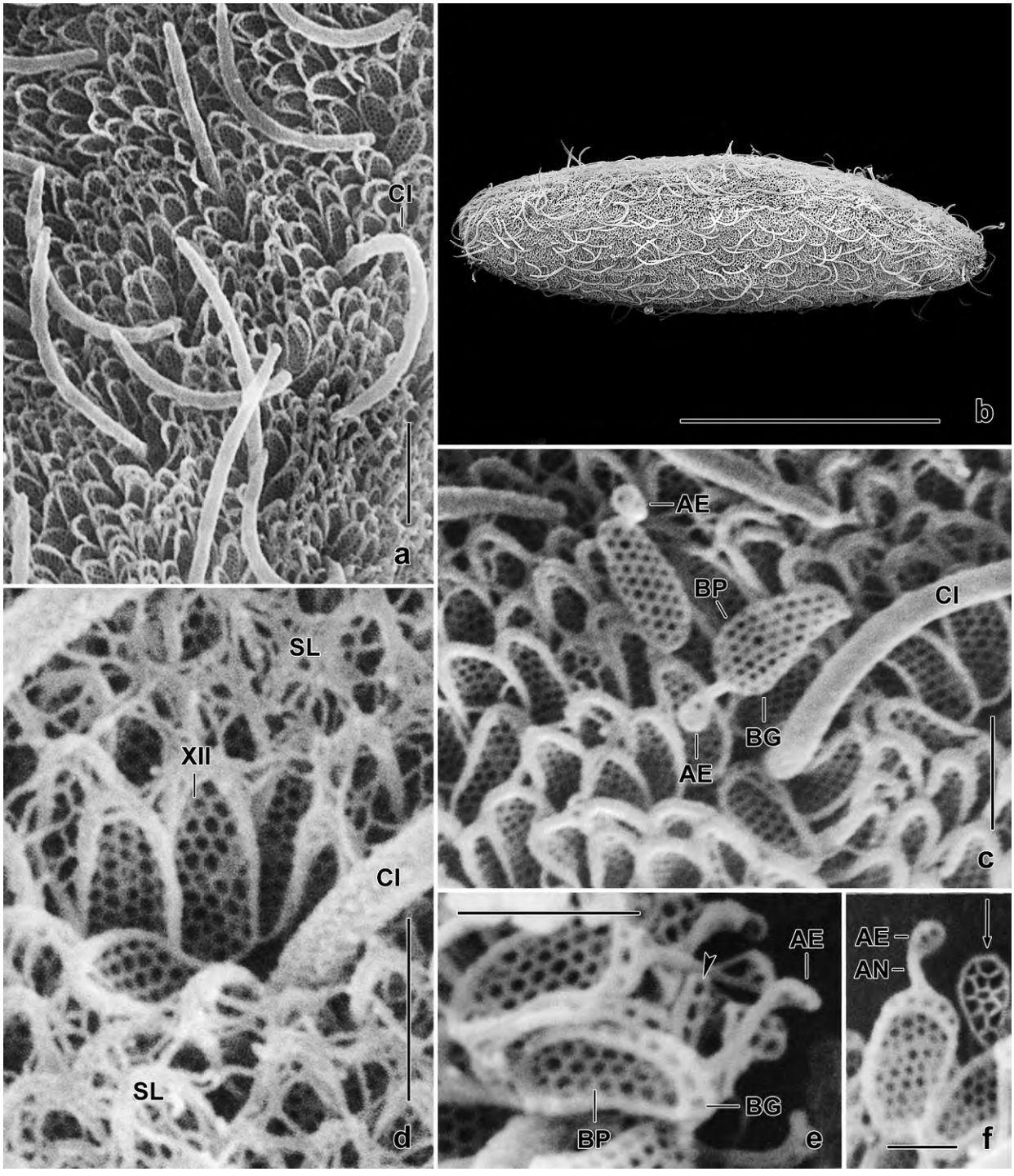

Fig. 40a–f. *Cataphractes austriacus*, type XII lepidosomes in the scanning electron microscope. **a:** The narrowly spaced lepidosomes are directed anteriorly and look like minute tongues. **b:** Strongly contracted specimens are elongate ellipsoid. **c:** Top view of two type XII lepidosomes. **d:** In some specimens the slime cover is recognizable; usually it disappears during preparation. **e, f:** Back view of type XII lepidosomes. The arrow in (f) marks a type X lepidosome; the arrowhead in (e) denotes the rectangular meshes of the basering. AE – anchorplate, AN – anchor, BG – basering, BP – baseplate, CI – cilia, SL – slime, XII – type 12 lepidosome. Scale bars 0.5 µm (f), 1 µm (c–e), and 2 µm (a, b).

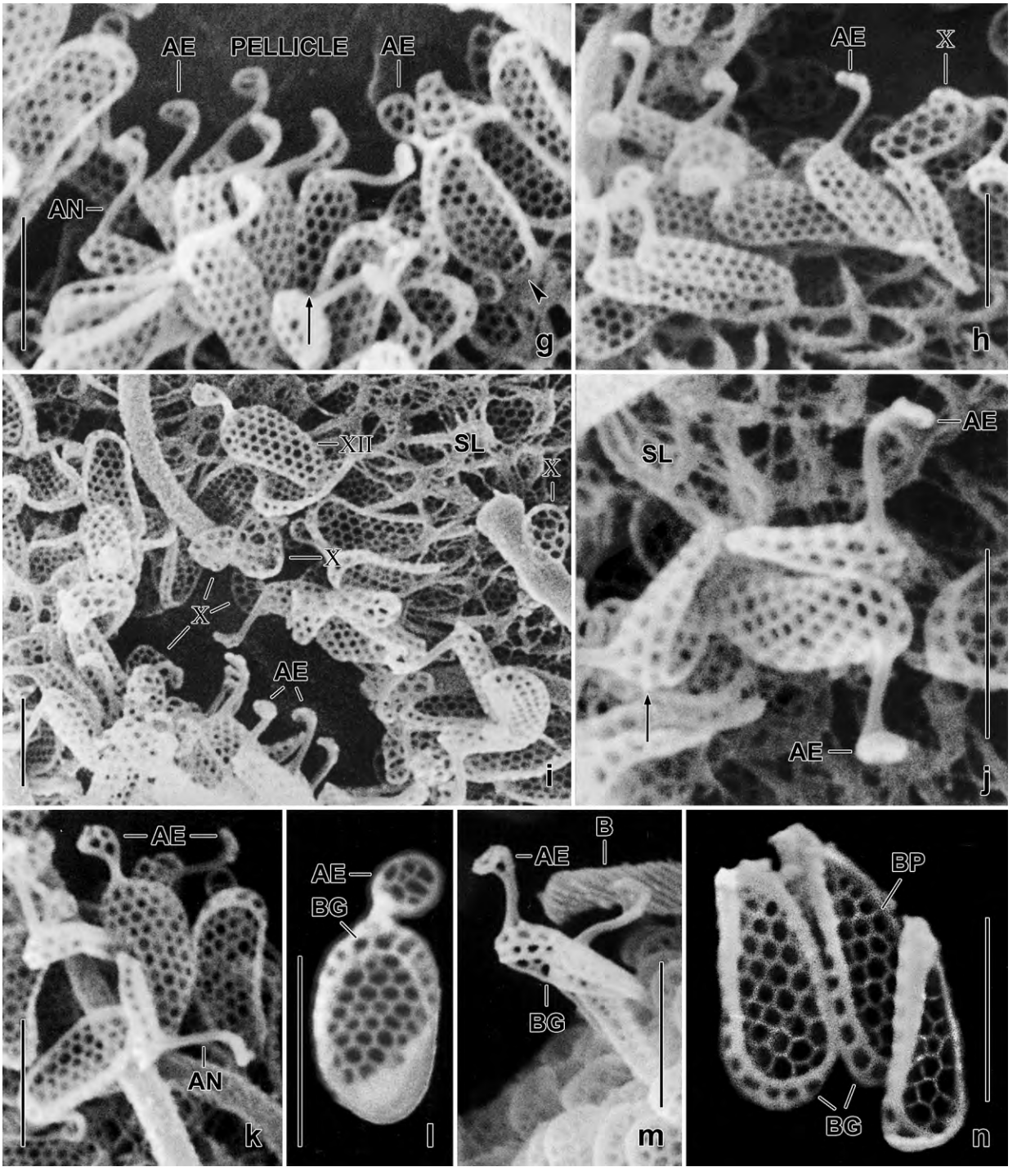

Fig. 40g–n. *Cataphractes austriacus*, lepidosomes in the SEM. **g, h:** When the mucilaginous layer is disturbed, the gooseneck shape of the type XII lepidosomes becomes visible. The arrow marks a top view, the arrowhead denotes a back view. The lepidosomes are attached to the pellicle with the anchor plate. **i:** Similar to (g, h) but some slime and a few type X lepidosomes are recognizable. **j, m:** When opposed, the goosenecks become scorpions. The upper lepidosome in (j) and that in (m) show that the anchor is a specialization of the cuneate baseplate (j; arrow). Note the spiral coat of a dorsal bristle. **k, l:** Top and lateral view (k) and a back view (l) of type XII lepidosomes. **n:** Type XII lepidosomes, showing the hexagonal meshes of the baseplate and the quadrangular meshes of the basering. AE – anchorplate, AN – anchor, B – bristle of dorsal brush, BG – basering, BP – baseplate, SL – slime. X, XII – lepidosome types. Scale bars 1 µm.

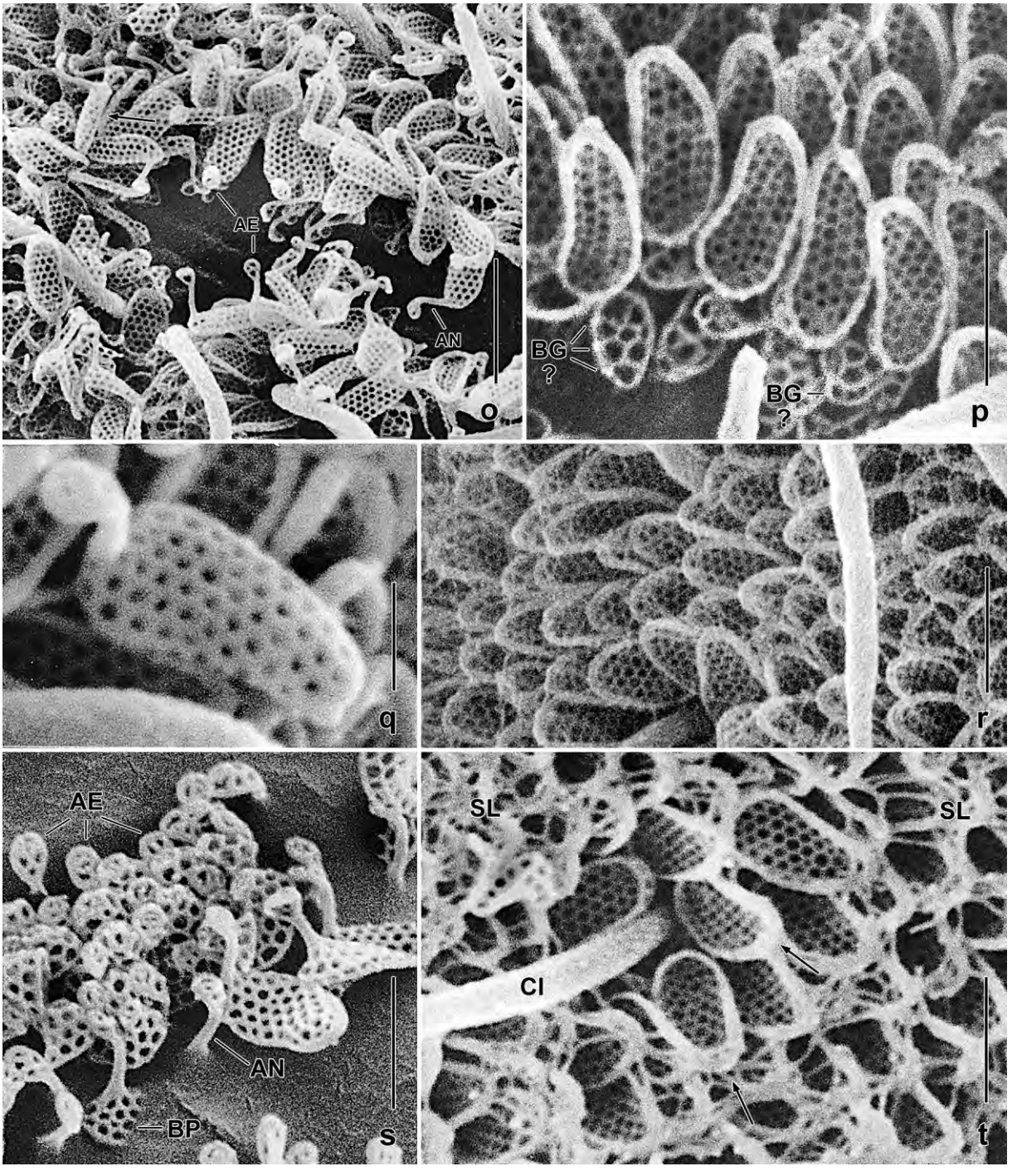

Fig. 40o–t. *Cataphractes austriacus*, lepidosomes in the SEM. **o:** When the mucilaginous layer is disturbed, the gooseneck shape of the type XII lepidosomes becomes recognizable. The lepidosomes are anchored to the pellicle with the anchor plate. The arrow marks a type XII lepidosome in lateral view. **p:** The type XII lepidosomes are tongue-shaped and slightly curved. They are distinctly larger than the type X lepidosomes which possibly have a basering. **q:** In top view the goose becomes a duck. **r:** The lepidosomes are arranged like the tiles of a roof. **s:** Most type XII lepidosomes sank into the carbon film of the SEM slide leaving back the anchor plates. **t:** Around the cilia the lepidosomes are shorter and ovate (arrows). AE – anchorplate, AN – anchor, BG – basering, BP – baseplate, CI – cilium, SL – slime. Scale bars 0.5 µm (q), 1 µm (p, r–t), and 2 µm (o).

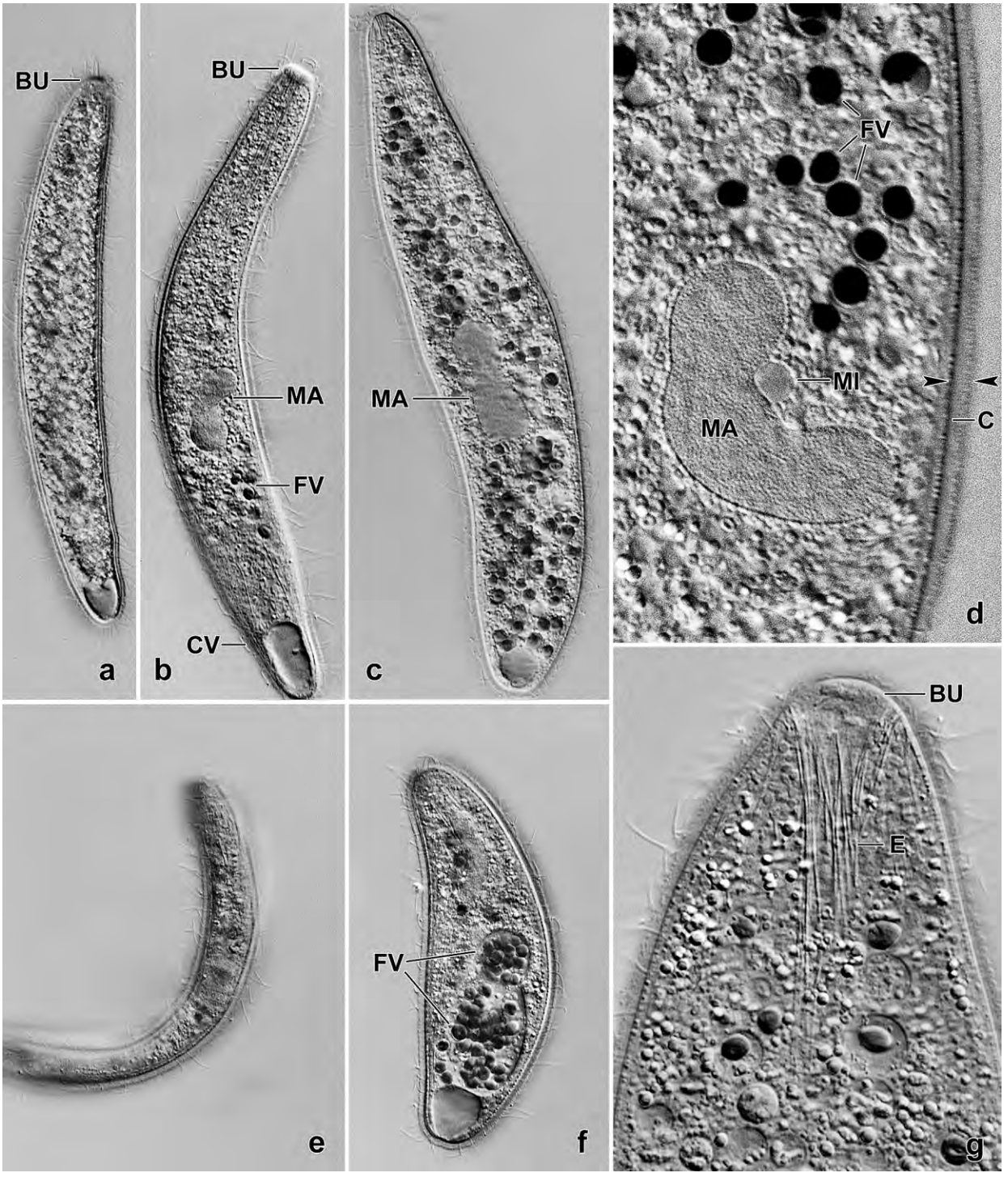

Fig. 41a–g. *Enchelys vestita* (?) from life (kindly provided by Dr. Martin KREUTZ). **a–c:** Extended specimens, length 160–270 µm. **d:** Detail showing the strongly reniform macronucleus and the 1.8–2.7 µm ($\bar{x}$ = 2.2 µm, n = 26) thick mucilaginous layer (opposed arrowheads) composed of lingulotrichid lepidosomes. **e:** This species is distinctly flattened at both sides. **f:** A contracted specimen, length ~ 150 µm, with two large food vacuoles containing coccal green algae. **g:** Anterior body region of a pressed specimen. BU – oral bulge, E – extrusomes, FV – food vacuoles, MA – macronucleus, MI – micronucleus.

Table 14. Morphometric data on *Cataphractes austriacus* (CA) from Austria and *C. terricola* (CE) from Venezuelan site (25). Data based, if not mentioned otherwise, on ethanol (CA) or mercuric chloride (CE) fixed, mounted, protargol-impregnated (FOISSNER´s method), and randomly selected specimens from freshwater (CA) and from a non-flooded Petri dish culture (CE). Measurements in µm. CV – coefficient of variation in %, M – median, Max – maximum, Mean – arithmetic mean, Min – minimum, n – number of specimens investigated, Pop – population, SD – standard deviation, SE – standard error of arithmetic mean.

Characteristics	Pop	Mean	M	SD	SE	CV	Min	Max	n
Body, length in vivo (rough values)	CA	120.9	120.0	–	–	–	100.0	140.0	11
	CE	128.0	130.0	–	–	–	120.0	140.0	5
Body, width in vivo (rough values)	CA	19.2	20.0	–	–	–	17.0	20.0	11
	CE	20.0	20.0	–	–	–	20.0	20.0	5
Body, length	CA	99.6	100.0	9.6	2.1	9.6	78.0	117.0	21
	CE	71.7	72.0	6.6	1.3	9.2	57.0	85.0	25
Body, width	CA	14.3	13.0	3.5	0.8	24.8	10.0	23.0	21
	CE	13.0	13.0	1.7	0.3	12.9	10.0	16.0	25
Body length:width, ratio	CA	7.3	7.7	1.6	0.4	22.4	4.6	9.7	21
	CE	5.6	5.5	0.8	0.2	15.1	4.1	7.1	25
Oral bulge, height	CA	5.1	5.0	0.6	0.1	12.6	4.0	7.0	21
	CE	2.6	2.8	0.4	0.1	14.5	2.0	3.5	12
Oral bulge, diameter	CA	8.6	8.5	1.5	0.3	17.7	6.0	12.0	21
	CE	5.3	5.0	0.9	0.3	17.0	4.0	7.0	13
Anterior body end to macronucleus, distance	CA	43.2	45.0	6.5	1.4	15.0	27.0	54.0	21
	CE	28.3	29.0	3.9	0.8	13.8	21.0	36.0	25
Macronucleus, length	CA	15.5	15.0	2.3	0.5	14.7	12.0	20.0	21
	CE	12.4	12.0	1.4	0.3	11.6	11.0	15.0	25
Macronucleus, width	CA	7.5	7.0	1.4	0.3	18.7	6.0	11.0	21
	CE	5.6	6.0	0.7	0.1	12.7	4.0	7.0	25
Micronucleus, length	CA	2.8	3.0	0.5	0.1	17.2	2.0	4.0	21
	CE	2.0	2.0	0.3	0.1	12.6	1.5	2.5	12
Micronucleus, width	CA	2.1	2.0	0.4	0.1	16.7	1.5	3.0	21
	CE	1.3	1.5	–	–	–	1.0	1.5	11
Somatic ciliary rows, number including brush rows	CA	17.6	18.0	0.6	0.1	3.4	17.0	19.0	21
	CE	13.3	13.0	0.9	0.2	7.0	12.0	15.0	23
Ciliated kinetids in a ventral kinety, number	CA	25.0	25.0	3.7	0.8	14.8	18.0	33.0	21
	CE	27.0	28.0	4.6	1.3	16.9	20.0	34.0	12
Dorsal brush row 1, length (from circumoral kinety)	CA	24.3	24.0	3.5	0.8	14.3	18.0	31.0	21
	CE	13.0	15.5	2.9	1.5	19.6	11.0	18.0	4
Dikinetids in dorsal brush row 1, number	CA	12.6	13.0	1.7	0.4	13.1	10.0	16.0	21
	CE	7.7	8.0	0.8	0.3	9.8	7.0	9.0	7
Dorsal brush row 2, length (rom circumoral kinety)	CA	10.1	10.0	0.9	0.2	8.6	8.0	12.0	20
	CE	7.5	7.5	–	–	–	7.0	8.0	2
Dikinetids in dorsal brush row 2, number	CA	3.1	3.0	0.4	0.1	12.6	2.0	4.0	21

continued

Characteristics	Pop	Mean	M	SD	SE	CV	Min	Max	n
	CE	2.3	2.0	0.8	0.3	35.0	2.0	4.0	6
Type X lepidosomes, length (SEM)	CA	0.63	0.62	0.1	0.1	15.3	0.38	0.77	17
Type X lepidosomes, width (SEM)	CA	0.40	0.41	0.1	0.1	18.7	0.28	0.57	17
Type X lepidosomes, polygons in baseplate (SEM)	CA	10.7	11.0	3.0	0.7	27.6	6.0	19.0	17
Type XII lepidosomes, length (SEM)	CA	1.23	1.20	0.13	0.1	10.3	1.0	1.5	30
	CE	0.98	1.0	0.17	0.1	17.6	0.6	1.2	19
Type XII lepidosomes, width (SEM)	CA	0.55	0.55	0.08	0.1	13.9	0.37	0.72	30
	CE	0.47	0.49	0.07	0.1	14.9	0.29	0.54	19
Type XII lepidosomes, height without anchor (SEM)	CA	0.37	0.35	0.11	0.1	28.6	0.17	0.53	19
	CE	0.28	0.28	0.06	0.1	22.6	0.19	0.35	8
Type XII lepidosomes, height with anchor and anchor plate (SEM)	CA	0.94	1.0	0.16	0.1	17.5	0.77	1.3	25
Type XII lepidosomes, hexagons in baseplate (SEM)	CA	36.9	37.0	6.0	1.1	16.2	22.0	45.0	30
	CE	33.7	35.0	6.0	1.4	17.7	17.0	46.0	19
Type XII lepidosomes, length of anchorplate (SEM)	CA	0.32	0.33	0.04	0.1	12.5	0.23	0.38	19
	CE	0.26	–	–	–	–	–	–	2
Type XII lepidosomes, width of anchorplate (SEM)	CA	0.27	0.03	0.26	0.1	10.8	0.23	0.32	19
	CE	0.24	–	–	–	–	–	–	2
Type XII lepidosomes, polygons in anchorplate (SEM)	CA	3.9	4.0	1.35	0.3	34.4	2.0	7.0	23
	CE	5.0	–	–	–	–	–	–	2

µm in the SEM; 11 polygons in baseplate on average (Fig. 38o, 39l, 40f, h, i; Table 14). Type XII in one layer on type X lepidosomes, of complex structure, i. e., with a tongue-shaped main part and a gooseneck-shaped anchor attached to pellicle with a minute anchorplate (goosehead); best described as swan-shaped in lateral view and as tongue-shaped in top and back view; on average 1.23 × 0.55 × 0.94 µm in size and with 37 hexagons in concave baseplate and four in flat anchorplate. Tongue-shaped part in lateral view straight, slightly concave, or slightly sigmoidal, narrowed end directed anteriorly, tongue underside slightly concave; basering on surface and composed of quadrangular meshes. Anchor belongs to baseplate, straight or slightly sigmoid, anchorplate rectangularly curved and directed backwards, on average 0.32 × 0.27 µm in size (Fig. 38m, p–t, 39i, l, 40a, c–t; Table 14).

Cilia about 8 µm long in vivo, with spiral surface pattern (Fig. 40m), ordinarily to loosely spaced, arranged in an average of 18 narrowly spaced (~3.5 µm), bipolar rows five or six modified to dorsal brush anteriorly (Fig. 38a, u, v, x, 39a–e, i, 40a, b; Table 14). Dorsal brush heteromorphic, very likely structured as shown in Figures 38v, x; row 1 composed of an average of 13 dikinetids with anterior bristles in vivo slightly inflated, about 1 µm long, and thicker than posterior bristles about 0.5 µm long, continues with monokinetal about 3 µm long bristles; row 2 composed of an average of three dikinetids quite similar to those of row 1, continues posteriorly with about 3 µm long monokinetal bristles; rows 3 to 6 with monokinetal bristles, those of row 4 gradually increasing in length from 2 µm anteriorly to 6 µm posteriorly.

Oral bulge in vivo and in SEM micrographs inconspicuous because only 2 to 3 µm high (Fig. 38a, f, 39f, i, 40b) while usually inflated to an average of 5 µm in ethanol-fixed cells (Fig. 38u, v, 39a–d; Table 14); discoidal with slightly concave centre, covered by the mucilaginous layer, rather refractive because containing type II extrusomes and anterior end of type I extrusomes. Circumoral kinety circular (Fig. 39e), composed of 30 to 40 dikinetids, anterior basal body ciliated, posterior barren but associated with a pharyngeal rod contributing to the tubular oral basket (Fig. 38a, f, u, v, 39a–g, i).

Occurrence and ecology: As yet found only at type locality. We could cultivate *C. austriacus* for a week in the original sample enriched with a few wheat kernels, providing sufficient specimens for a detailed investigation.

Remarks: Species of the genera *Lingulothrix* and *Cataphractes* are difficult to identify in vivo because they have few features and body size and shape vary distinctly due to their contractility; additionally, contraction and extension are very slow, and thus the real shape and size are difficult to fix. For comparison with similar species, see → *Lingulothrix galapagensis* and Table 15. There are haptorids from various genera which look similar to lingulotrichids, e. g., several *Enchelys* and *Enchelyodon* species (Foissner 1984, Kahl 1930a) and *Enchelyotricha* spp. (Foissner et al. 2002). However, none has a mucilaginous cover, except of the → trachelophyllids, and are thus easily separable from the lingulotrichids.

Kahl (1927) described *Lagynus vestitus* which he later transferred to *Enchelys* (Kahl 1930a). Kahl´s *Enchelys vestita* is highly similar to *Cataphractes austriacus*: both have a thin, radially striated mucilaginous layer, a single ellipsoid macronucleus, about 25 µm long toxicysts, a similar body shape, and occur in boggy habitats of Central Europe. Only one feature does not match well, viz., body length which is 200–220 µm according to Kahl (1930a) while only about 150 µm in Kahl (1927) due to a calibration error (Foissner & Wenzel 2004). Another difference concerns contractility which Kahl (1927) did not recognize ("ohne bemerkte Kontraktilität")

Table 15. Comparison of main features in four lingulotrichid populations.

Characteristics	**Method**	***Lingulothrix galapagensis* (Galápagos)**	***Cataphractes austriacus* (Austria)**	***Cataphractes terricola* (Venezuela, site 25)**	***Cataphractes* sp. (Brazil) [a]**
Body, length (µm)	in vivo	110 (n = 5) (90–120)	121 (n = 11) (100–140)	128 (n = 5) (120–140)	172 (n = 5) (150–200)
Body, length (µm)	Protargol	70 (n = 21) (50–84)	100 (n = 21) (78–117)	72 (n = 25) (57–85)	116 (n = 19) (90–134)
Ciliary rows, number	Protargol	14 (n = 21) (13–15)	18 (n = 21) (17–19)	13 (n = 23) (12–14)	27 (n = 16) (23–33)
Type I extrusomes, length (µm)	in vivo	19 (n = 14) (17–25)	30 (n = 1)	18 (n = 1)	31 (n = 11) (24–39)
Type I extrusomes, shape	in vivo	rod-shaped to indistinctly acicular	acicular	rod-shaped	rod-shaped
Main lepidosomes, shape	SEM	sock-shaped	gooseneck-shaped	gooseneck-shaped	gooseneck-shaped

[a] A freshwater species which will be described later.

while our specimens are distinctly contractile. Unfortunately, *Enchelys vestita* has never been redescribed and lacks type material.

The considerable size difference (120 µm vs. 200 µm) argues against the use of the Austrian population as a neotype for *Enchelys vestita*. Indeed, Martin Kreutz (pers. comm.) found a species in a small *Sphagnum* pond in Germany (Kreutz & Foissner 2006) that looks quite similar to *C. austriacus* (Fig. 41a–c, f) but has a size of about 200 × 35 µm (n = 26) when extended. An identification with *E. vestita* is possible if one assumes that Kahl (1927) observed only contracted specimens (Fig. 38l) and did not recognize the strongly reniform shape of the macronucleus (Fig. 38l, 41d). Our Brazilian freshwater species is also rather similar to *E. vestita* (Table 15) but body shape is clearly different and the cells are not flattened laterally (vs. flattened on one side, Kahl 1927). Obviously, much more research is needed before a neotypification can be made.

Cataphractes terricola nov. spec. (Fig. 42a–n, 43a–q; Tables 14, 15)

Diagnosis: Size in vivo about 120 × 20 µm, contractile by up to 50%. Cylindroid to lageniform, elongate ellipsoid to ellipsoid when fully contracted. Macronucleus and micronucleus ellipsoid. Oral bulge indistinct, discoid. Two types of extrusomes: type I rod-shaped and slightly curved, about 18 µm long in vivo; type II only 1.5 µm long. On average 31 ciliary rows, 5 or 6 contributing to dorsal brush: row 1 composed of an average of 8 dikinetids; row 2 of 2; rows 3–5(6) composed of monokinetids with about 2 µm long bristles. Type X lepidosomes (ground scales) very likely absent. Type XII lepidosomes gooseneck-shaped in lateral view, with 34 hexagons in baseplate and about 5 polygons in anchorplate, about 1 × 0.5 µm in the scanning electron microscope.

Type locality: Highly fertile Mahadja soil from Venezuelan site (25), about 50 km north of Pto. Ayacucho, 67°36'W 5°41'N.

Type material: 1 holotype and 4 paratype slides with protargol-impregnated specimens have been deposited in the Biology Centre of the Upper Austrian Museum in Linz (LI). The holotype and other relevant specimens have been marked by black ink circles on the coverslip.

Etymology: The Latin species-group name *terricola* (living in soil) refers to the habitat the species was discovered.

Description: The protargol preparations are mediocre because the cortical granules impregnated rather deeply. However, most main features are recognizable, e. g., the nuclear apparatus and the number of ciliary rows.

Size in vivo up to 130 × 20 µm (Fig. 43a), usually shorter, i. e., near 100 µm because rarely fully extended; in protargol preparations 66–98 × 12–18 µm, on average 83 × 15 µm when 15% preparation shrinkage is added (Table 14); contractile by up to 50%, contracts and extends slowly with movements resembling euglenoid metaboly. When extended or slightly contracted narrowly oblong (~ 5–6:1) to cylindroid (≥ 9:1) or slenderly lageniform (Fig. 42a, d–f, i, j, 43a, b, d), when moderately or strongly contracted elongate ellipsoid or ellipsoid (Fig. 43h). Nuclear apparatus in or slightly anterior of mid-body (Fig. 42a, d–f, j, 43a, b, d, j). Macronucleus ellipsoid to slightly reniform; contains many minute nucleoli. A single, ellipsoid micronucleus attached to long side

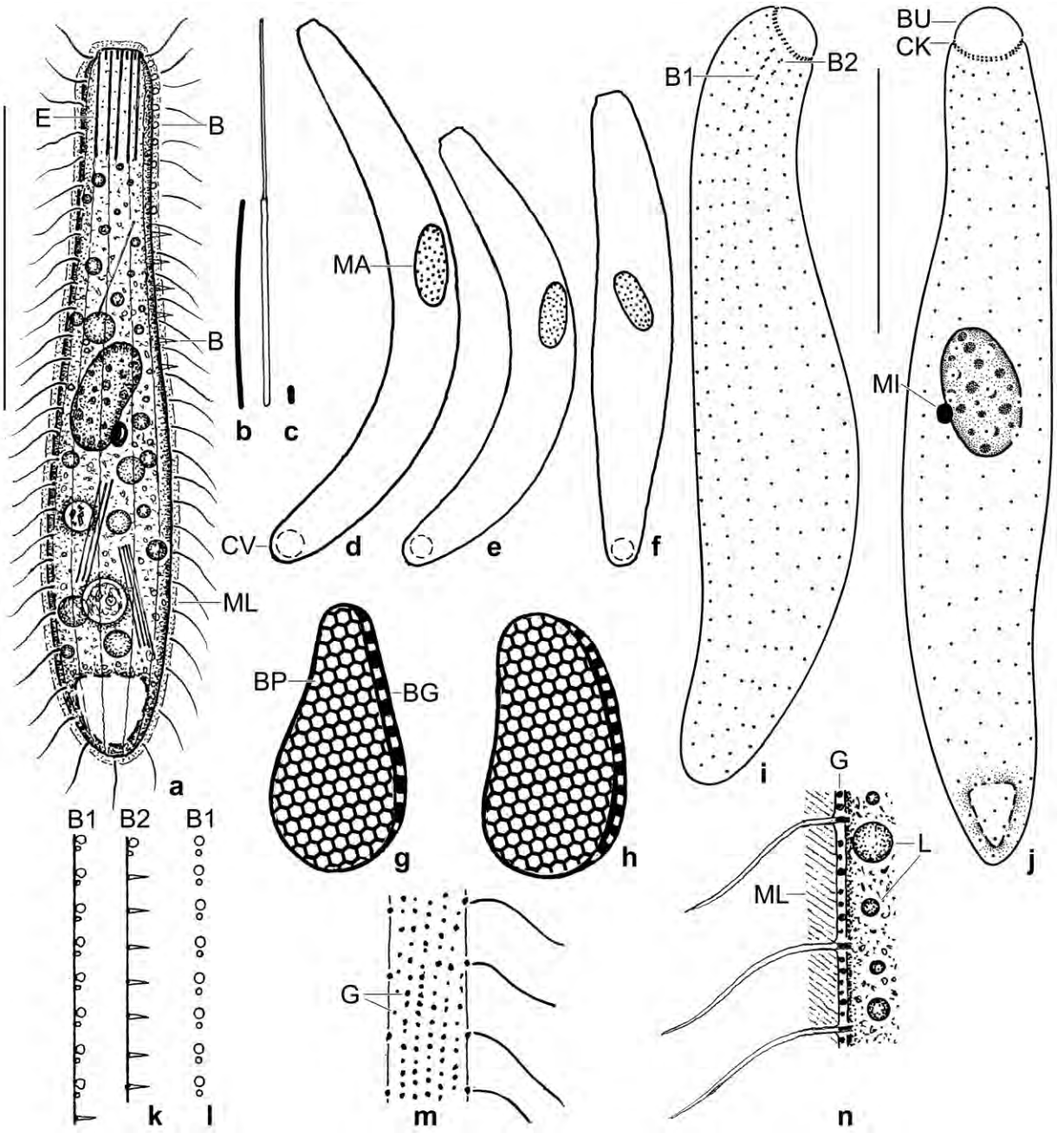

Fig. 42a–n. *Cataphractes terricola* (a–g, i–n) and → *C. austriacus* (h) from life (a–f, k–n), in the SEM (g, h), and after protargol impregnation (i, j). **a:** Right side view of a representative, possibly slightly contracted specimen, length 120 µm. **b, c:** Resting type I extrusome (a, ~ 18 µm), exploded type I extrusome (b, ~ 30 µm), and a resting type II extrusome (c, ~1.5 µm) drawn to scale. **d–f:** An extended (d, ~ 130 µm) and moderately contracted (e, f, ~ 110 µm) specimen (cp. Fig. 43a–c). **g, h:** The type XII lepidosomes (anchor not shown) of *C. terricola* (g) are narrower distally than those of *C. austriacus* (h), length ~ 1.3 µm. **i:** Ciliary pattern of dorsal side of holotype specimen, length 75 µm. **j:** Ciliary and nuclear pattern of ventral side of a paratype specimen. **k:** Anterior region of dorsal brush rows 1 and 2. **l:** Frontal view of dikinetal portion of dorsal brush row 1. The anterior bristle is thicker than the posterior. **m:** Surface view, showing cortical granules which have different size. **n:** Optical section of cell´s periphery, showing the mucilaginous layer. B – dorsal brush, B1, 2 – dorsal brush rows, BG – basering, BP – baseplate, BU – oral bulge, CK – circumoral kinety, CV – contractile vacuole, E – extrusomes, G – cortical granules, L – lipid droplets, MA – macronucleus, MI – micronucleus, ML – mucilaginous layer. Scale bars 25 µm (i, j) and 50 µm (a).

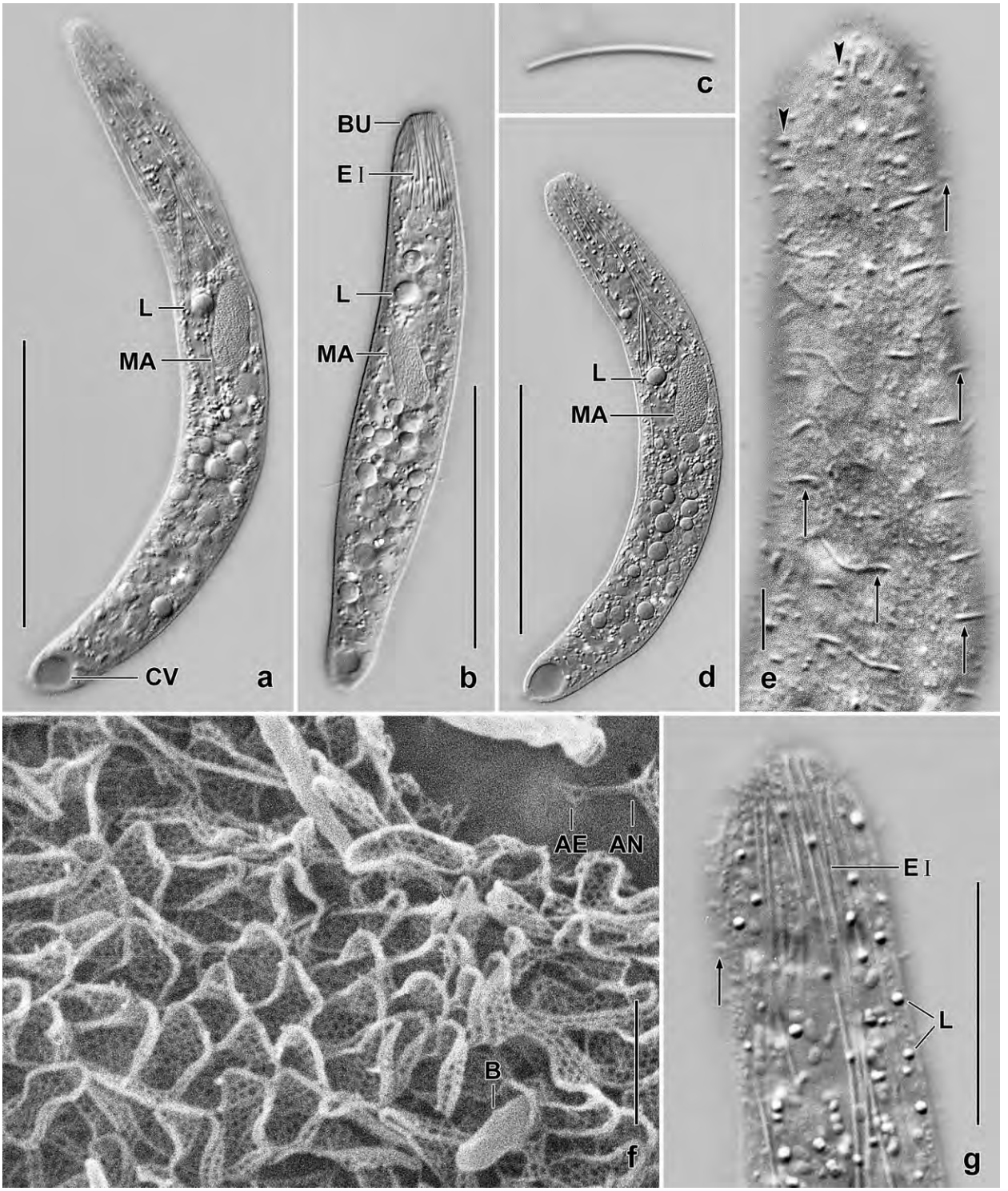

Fig. 43a–g. *Cataphractes terricola* in vivo (a–e, g) and in the SEM (f). **a, b, d:** An extended (a, ~ 130 µm) and moderately contracted (b, d, ~ 110 µm) specimen. **c:** Type I extrusome, 18 µm. **e:** Anterior region, showing dorsal brush. Arrows mark five rows with acicular bristles, arrowheads denote some minute globular bristles at begin of rows 1 and 2. **f:** The lepidosomes are attached to the pellicle with the anchorplate. **g:** Anterior body region, showing type I extrusomes and globular bristles of dorsal brush row 1 (arrow). AE – anchorplate, AN – anchor, B – dorsal brush bristle, BU – oral bulge, CV – contractile vacuole, EI –type I extrusomes, L – lipid droplets, MA – macronucleus. Scale bars 1 µm (f), 5 µm (e), 20 µm (g), and 50 µm (a, b, d).

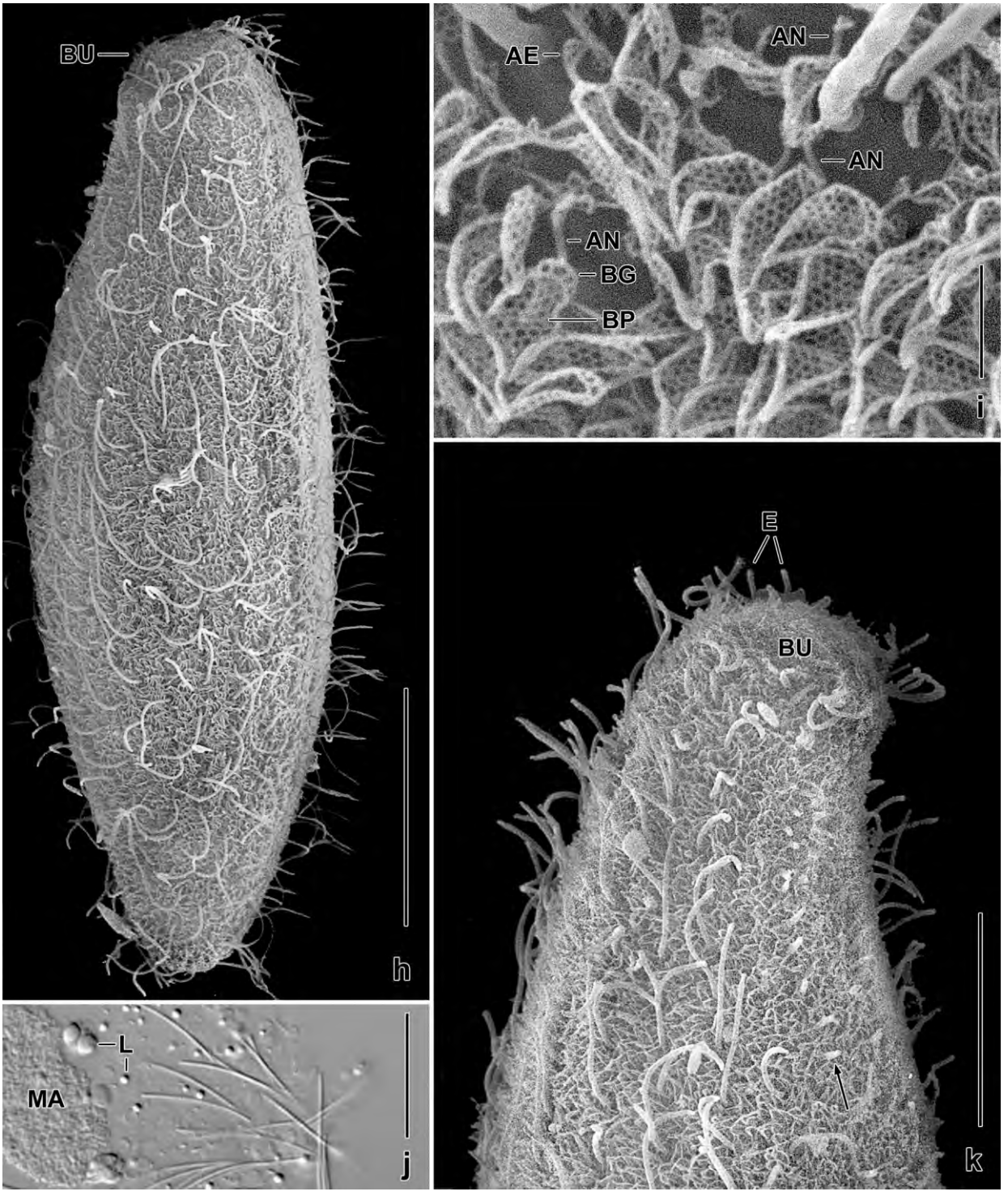

Fig. 43h–k. *Cataphractes terricola* from life (j) and in the scanning electron microscope (h, i, k). **h:** A strongly contracted specimen, length 78 µm. **i:** The gooseneck-shaped lepidosomes are composed of a tongue-shaped baseplate (BP, swan body), an upright neck (AN), and an anchorplate (AE, goosehead). **j:** Type I extrusomes are rod-shaped and about 18 µm long. **k:** Dorsolateral view of anterior body region, showing the inconspicuous oral bulge, the lepidosome (mucilaginous) layer, and row 1 of the dorsal brush (arrow). AE – anchorplate, AN – anchor, BG – basering, BP – baseplate, BU – oral bulge, E – extrusomes, L – lipid droplets, MA – macronucleus. Scale bars 1 µm (i), 10 µm (k), and 20 µm (h, j).

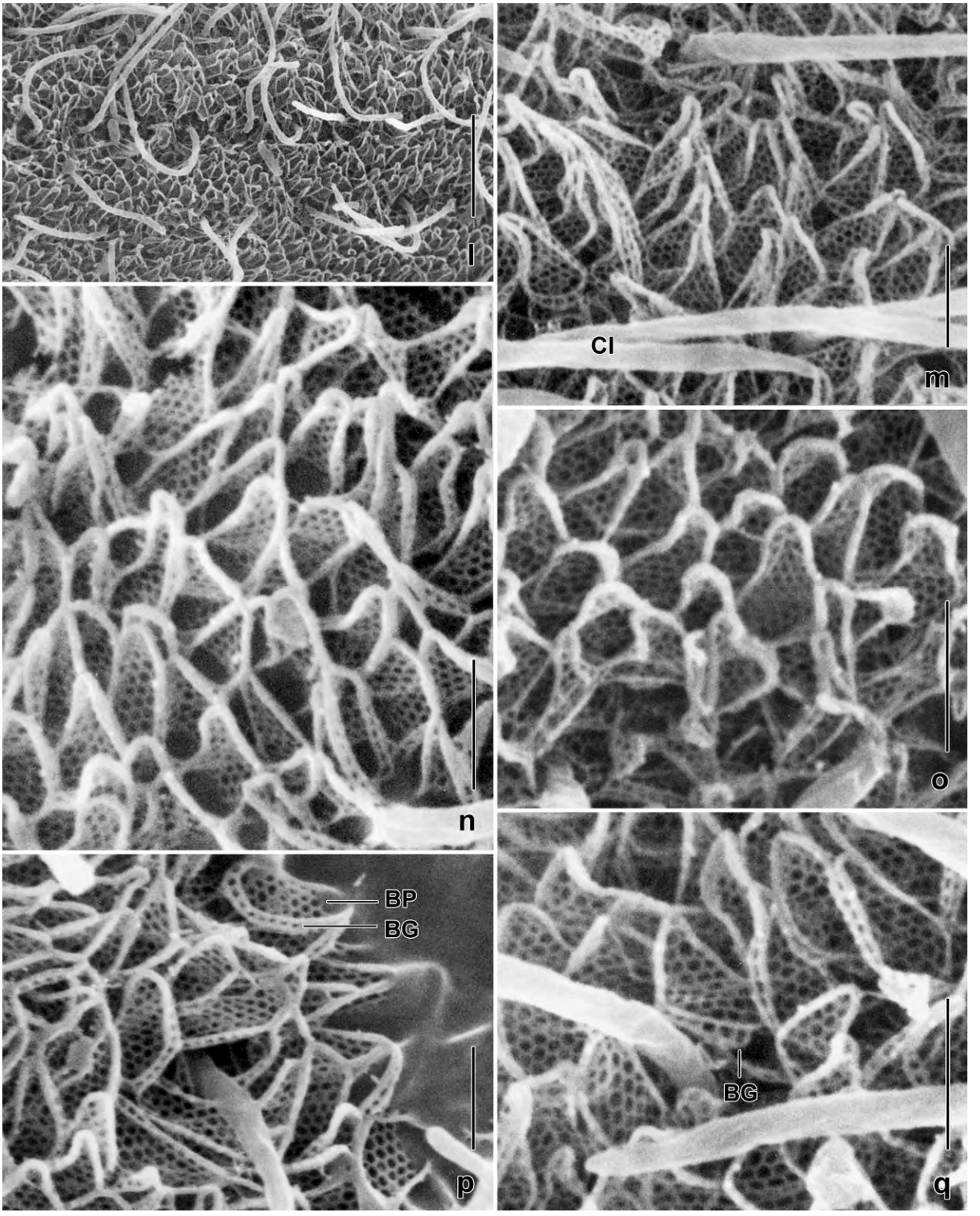

Fig. 43l–q. *Cataphractes terricola*, lepidosomes in the scanning electron microscope. **l:** Overview. **m–q:** Details showing the tongue-shaped baseplate. For anchor and anchorplate, see Figure 43i. BG – basering, BP – baseplate, CI – cilia. Scale bars 1 µm (m–q) and 4 µm (l).

of macronucleus. Contractile vacuole in posterior body end (Fig. 42a, d–f, j, 43a, b, d). Two types of extrusomes attached to oral bulge (Fig. 42a–c, 43b, c, g, j, k): type I forms a conspicuous bundle in oral body portion, rod-shaped and slightly curved, about 18 × 0.5 µm in vivo; does not impregnate with the protargol method used; type II oblong and minute, i. e., about 1.5 µm long. Developing extrusomes frequent in cytoplasm, either as singles or in small bundles, certain stages impregnate with protargol (Fig. 42a). Cytoplasm colourless, more or less studded with 0.5–10 µm-sized lipid droplets and some vacuoles with crystalline contents indicating ciliates as a main food; very likely feeds also on 10–15 µm long bacterial rods. Glides slowly on microscope slide.

Cortex very flexible, contains narrowly spaced rows of granules about 0.3–0.8 × 0.2–0.6 µm in size (Fig. 42m); covered by a mucilaginous layer about 1 µm thick and thus easily overlooked in vivo and in protargol preparations. Mucilaginous layer composed of slime and type XII lepidosomes recognizable in vivo as minute, oblique lines oriented anteriorly (Fig. 42n); type X lepidosomes, i. e., groundplates very likely absent. Type XII lepidosomes not studied in detail but sufficiently to be sure that they are very similar to those of → *C. austriacus*, i. e., gooseneck-shaped with the morphometrics shown in Table 14 (Fig. 43f, h, i, k–q); distal third narrower than in → *C. austriacus* (Fig. 42g, h) but a preparation artifact cannot be excluded.

Cilia about 8 µm long in vivo, with spiral surface pattern, ordinarily to loosely spaced, arranged in an average of 13 ordinarily spaced, bipolar rows five or six modified to dorsal brush anteriorly (Fig. 42a, i, k, l, 43e, g, k; Table 14). Dorsal brush very similar to that of → *C. austriacus*: row 1 composed of an average of 8 dikinetids with bristles as described in *C. austriacus* and shown in the Figures cited above; row 2 with two to four dikinetids anteriorly and monokinetal bristles posteriorly; rows 3–5(6) only with monokinetal bristles 2 µm long in vivo.

Oral bulge in vivo and in SEM micrographs inconspicuous because only about 2 µm high (Fig. 42a, 43b, d, h, k) while usually inflated to an average of 3 µm in protargol-prepared cells (Fig. 42i, j; Table 14); discoidal, covered by the mucilaginous layer, rather refractive because containing type II extrusomes and anterior end of type I extrusomes. Circumoral kinety composed of narrowly spaced dikinetids, anterior basal body ciliated, posterior barren but associated with a pharyngeal rod contributing to the tubular oral basket (Fig. 42a, i, j, 43k; Table 14).

Occurrence and ecology: As yet found at Venezuelan sites (23, 25), i.e., in nutrient-rich, wet soils; likely, a different species occurs at sites (56, 57). In the non-flooded Petri dish culture, *C. terricola* was first recognized 20 days after rewetting sample (25), indicating a k-selected life strategy (Foissner 1987).

Remarks: *Cataphractes terricola* and → *Lingulothrix galapagensis* are so similar that they cannot be separated in vivo or in protargol preparations (Table 15) while the lepidosomes are definitely different (gooseneck-shaped vs. sock-shaped). → *Cataphractes austriacus* has a higher, non-overlapping number of ciliary rows (18 vs. 13–14 on average) and longer type I extrusomes (~ 30 vs. 20 µm) with a different shape (acicular vs. rod-shaped). In contrast, the lepidosomes are rather similar (Tables 14, 15) although type X (ground lepidosomes) is very likely absent.

Enchelyodon gondwanensis **nov. spec.** (Fig. 44a–l, 45a–g; Table 16)

Diagnosis: Size about 200 × 30 µm in vivo; slightly clavate to almost vermiform. On average 56 ellipsoid, scattered macronuclear nodules and 14 micronuclei. Extrusomes curved-filiform, about 17 µm long in vivo. Cortex thick, studded with ellipsoid, refractive granules. On average 21 ciliary rows, three anteriorly differentiated to a distinctly heterostichad dorsal brush occupying 18% of body length and having up to 6 µm long bristles; row 1 on average with 17 dikinetids, row 2 with 23, and row 3 with 11. Oral bulge discoid, about 7 µm width and up to 3 µm high.

Type locality: Soil from a horse pasture in the surroundings of the Selva Verde Lodge, Pto. Viejo, Costa Rica, 84°6'W 10°45'N.

Type material: 1 holotype and 3 paratype slides with protargol-impregnated specimens have been deposited in the Biology Centre of the Upper Austrian Museum in Linz (LI). Relevant specimens have been marked by black ink circles on the coverslip.

Etymology: Named after the Ur-continent *Gondwana*, supposing that it originated in this area.

Description: Size 160–280 × 20–60 µm in vivo, on average about 200 × 30 µm, as calculated from some in vivo measurements and the morphometric data shown in Table 16 adding 15% preparation shrinkage. Length:width ratio 3–12:1, on average 6.4:1 (Table 16). Shape also highly variable, partially depending on nutrition state, slightly clavate, very elongate ellipsoid, or almost vermiform; not flattened (Fig. 44a, b, e–g, 45a, b; Table 16). Macronuclear nodules and micronuclei scattered in central 3/5 of cell (Fig. 44a, b, e, j, 45a–d, g; Table 16). Macronuclear nodules on average 7 × 3.4 µm in size, each containing one or two large and some granular nucleoli; usually, some rather long, moniliform pieces, resulting from incomplete fragmentation after cell division (Foissner et al. 2002). Micronuclei minute, i. e., 1.5–2 µm across in protargol preparations. Contractile vacuole occupying posterior end, without canals extending anteriorly, several excretory pores in pole centre; a rather large defecation vacuole with hyaline, flabby material ahead of contractile vacuole in about one third of specimens (Fig. 44a, c, e, g, 45a). Mature extrusomes attached to oral bulge, curved-filiform, 16–18 µm long in vivo, do not impregnate with the protargol method used; some specimens with many developing extrusomes in cytoplasm, acicular with a large subterminal blister, impregnate deeply with protargol (Fig. 44a, b, i). Cortex colourless and slightly furrowed by ciliary rows, conspicuous because 1–1.5 µm thick and the distinct *tela corticalis* impregnating with protargol (Fig. 45c, g); contains countless ellipsoid, highly refractive, about 1 µm long granules, forming oblique rows between kineties (Fig. 44a, j, k, 45g). Cytoplasm colourless, in one third of specimens packed with some large (6–10 µm) and many small (2–5 µm) globular food inclusions, possibly segregated vacuoles from large ciliate prey; most specimens rather transparent, containing small lipid droplets 1–3 µm across and some empty appearing vacuoles. Glides and swims slowly, slender specimens show considerable flexibility when wriggling between soil particles.

Cilia about 10 µm long in vivo, arranged in an average of 21 ordinarily ciliated and ordinarily spaced, meridional rows; slightly condensed in oral area while slightly dispersed in rear quarter and in anterior portion of one or two kineties left of dorsal brush (Fig. 44a–d; Table 16). Interkinetal distance slightly reduced between first kinety right and left and posterior of dorsal brush; rarely a

Table 16. Morphometric data on *Enchelyodon gondwanensis* based on mounted, protargol-impregnated (FOISSNER's method), and randomly selected specimens from a non-flooded Petri dish culture. Measurements in µm. CV – coefficient of variation in %, M – median, Max – maximum, Mean – arithmetic mean, Min – minimum, n – number of specimens investigated, SD – standard deviation, SE – standard error of arithmetic mean.

Characteristics	Mean	M	SD	SE	CV	Min	Max	n
Body, length	174.3	175.0	23.4	5.4	13.4	140.0	240.0	19
Body, width	29.0	27.0	7.4	1.7	25.5	20.0	50.0	19
Body length:width, ratio	6.4	6.1	1.9	0.4	29.7	3.2	12.0	19
Oral bulge (basket), distal width	7.1	7.0	0.7	0.2	9.3	6.0	8.0	19
Oral bulge, height	2.4	2.5	–	–	–	2.0	3.0	19
Oral basket, length	45.7	45.0	6.5	1.7	14.3	35.0	60.0	15
Anterior body end to first macronuclear nodule, distance	33.8	33.0	10.4	2.4	30.8	19.0	60.0	19
Macronuclear nodules, length [a]	7.0	6.0	3.0	0.7	42.6	3.0	13.0	19
Macronuclear nodules, width [a]	3.7	4.0	0.8	0.2	21.6	2.0	5.0	19
Macronuclear nodules, number [b]	56.0	55.0	8.8	2.0	15.7	40.0	70.0	19
Micronuclei, diameter	1.7	1.7	–	–	–	1.5	2.0	18
Micronuclei, number	14.1	13.0	4.2	1.4	29.7	7.0	20.0	9
Ciliary rows, number (including brush)	21.1	21.0	1.0	0.2	4.7	20.0	23.0	17
Kinetids in a ventral kinety, number [c]	78.2	74.0	19.8	5.5	25.3	54.0	120.0	13
Dorsal brush, number of rows	3.0	3.0	0.0	0.0	0.0	3.0	3.0	17
Circumoral kinety to end of brush row 1, distance	30.1	30.0	3.3	0.8	11.0	25.0	40.0	18
Circumoral kinety to end of brush row 2, distance	36.0	35.0	4.9	1.2	13.6	30.0	52.0	18
Circumoral kinety to end of brush row 3, distance	12.0	12.0	1.8	0.4	15.1	9.0	17.0	18
Dikinetids in brush row 1, number	16.6	16.5	2.2	0.5	13.1	14.0	20.0	18
Dikinetids in brush row 2, number	23.3	23.5	3.0	0.7	12.7	18.0	28.0	18
Dikinetids in brush row 3, number	10.6	10.5	1.1	0.3	10.4	9.0	13.0	18

[a] Moniliform pieces excluded.

[b] Moniliform pieces included.

[c] Ciliated and unciliated.

minute suture at left margin of dorsal brush, where one or two kineties can be slightly shortened (Fig. 44d). Dorsal brush three-rowed, distinctly heterostichad because row 3 shorter by 2/3 than row 2; differences less pronounced in number of dikinetids: 16, 23, 11; occupies an average of 18% of body length. Brush bristles similar in all rows: anterior bristle of dikinetids oblong and shorter by about 1/3 than slightly clavate posterior bristle; length of bristles decreases from 5–6 µm anteriorly to 2 µm posteriorly (Fig. 44a, c, d, h, 45b–f; Table 16); row 3 with a monokinetal tail extending to second body third with rather narrowly spaced, about 3 µm long bristles; anterior brush tails absent.

Oral bulge discoid, occupies about half of anterior body end, but in vivo inconspicuous because only up to 3 µm high; on average 7 µm across in protargol preparations; dorsally slightly higher than ventrally, causing a slightly oblique anterior end; surface flat to slightly convex; contains anterior end of extrusomes (Fig. 44a–d, g, l; 45g, h; Table 16). Circumoral kinety and oral basket as typical for haptorids; basket obconical and about 50 µm long, hardly recognizable in vivo; oralized somatic monokinetids absent (Fig. 44b–f, 45c, e, f; Table 16).

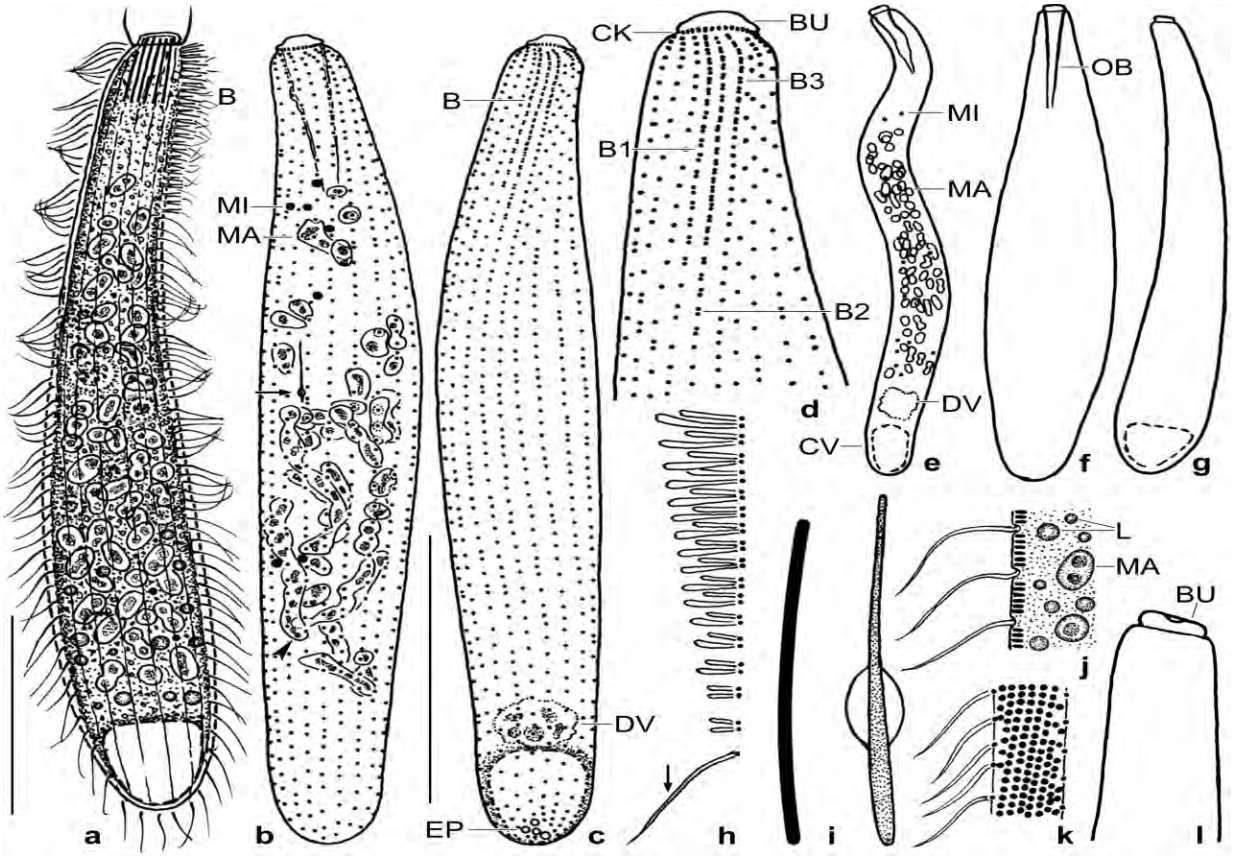

Fig. 44a–l. *Enchelyodon gondwanensis* from life (a, h–k) and after protargol impregnation (b–g, l). **a:** Left side view of a representative specimen, length 200 µm. **b–d:** Ventral and dorsal ciliary pattern and nuclear apparatus of holotype specimen, length 150 µm. The arrow marks a developing extrusome. The arrowhead denotes a moniliform piece of the macronucleus. **e–g:** Shape and size variability, length 240 µm, 160 µm, and 150 µm. **h:** Dorsal brush row 1. Arrow marks the first ordinary somatic cilium. **i:** A mature and a developing extrusome, length about 18 µm. **j, k:** Optical section and surface view of cortex, showing the arrangement of the cortical granules. **l:** Anterior region of the specimen shown in (g). The oral bulge is slightly higher dorsally than ventrally. B (1–3) – dorsal brush (rows), BU – oral bulge, CK – circumoral kinety, CV – contractile vacuole, DV – defecation vacuole, EP – excretory pores, L – lipid droplets, MA – macronuclear nodules, MI – micronuclei, OB – oral basket. Scale bars 50 µm.

Occurrence and ecology: As yet found in Costa Rica (see type locality) and in Venezuela, where it occurred at three sites in the Henri Pittier National Park, viz., in soil and bromeliad mud near Rancho Grande and in soil of a gallery forest.

Remarks: In vivo, *E. gondwanensis* highly resembles the Arabian *E. alqasabi* Foissner et al., 2008a because of many matching features, e. g., body size and shape, nuclear pattern, and extrusome shape. However, *E. gondwanensis* has doubled the number of ciliary rows ($\bar{x}$ 21 vs. 11) and has a flat (vs. globular) oral bulge. Further, details of the dorsal brush are different, e. g., the total number of dikinetids (51 vs. 26) and the absence (vs. presence) of anterior brush tails. Thus, we consider both as distinct species emphasizing, however, their similarity in all main traits, suggesting a common ancestor. Another similar species is *E. tratzi* Foissner, 1987d, an European member of the genus, which differs from *E. gondwanensis* mainly by the ordinary, weakly granulated cortex, a feature we checked in the original notes. Further, *E. tratzi* has acicular (vs. filiform) extrusomes, less macronuclear nodules ($\bar{x}$ 21 vs. 56), much shorter dorsal bristles

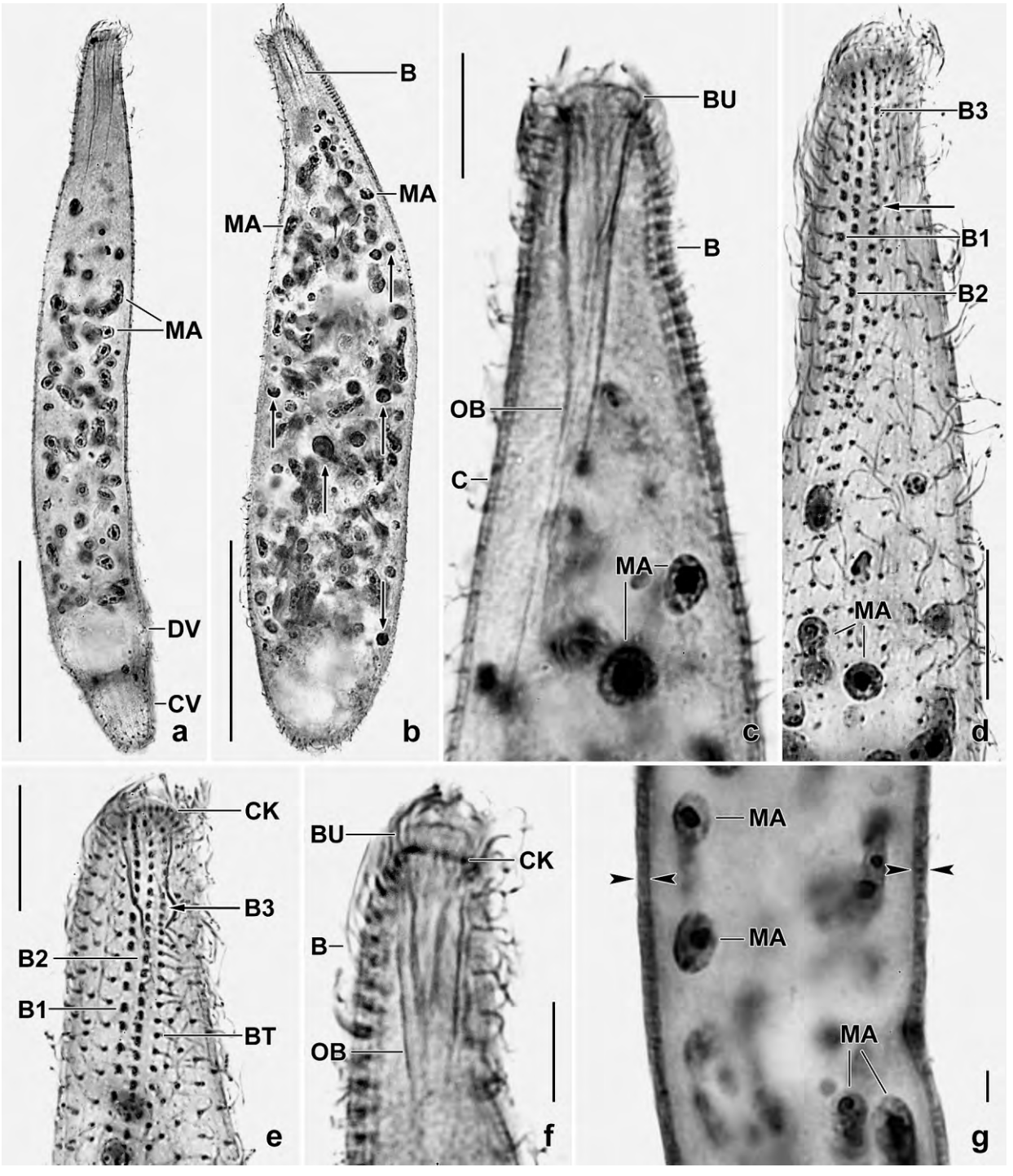

Fig. 45a–g. *Enchelyodon gondwanensis* after protargol impregnation. **a, b:** A slender and a stout specimen. Both are studded with macronuclear nodules, and the stout cell, additionally, contains many small food vacuoles (arrows). **c, f:** Optical sections, showing the inconspicuous oral bulge and the long oral basket. **d, e:** The dorsal brush is three-rowed and heterostichad because row 3 (arrows) is much shorter than rows 1 and 2. **g:** The cortex (opposed arrowheads) is conspicuously thick. B (1–3) – dorsal brush (rows), BT – monokinetidal bristle tail of brush row 3, BU – oral bulge, C – cortex, CK – circumoral kinety, CV – contractile vacuole, DV – defecation vacuole, MA – macronuclear nodules, OB – oral basket. Scale bars 5 µm (g), 10 µm (c, e, f), 20 µm (d), and 50 µm (a, b).

Table 17. Morphometric data on *Enchelyodon isostichos* (EI) and *E. floridensis* (EF) based on mounted, protargol impregnated (FOISSNER's method), and randomly selected specimens from non-flooded Petri dish cultures. Measurements in µm. CV – coefficient of variation in %, M – median, Max – maximum, Mean – arithmetic mean, Min – minimum, n – number of specimens investigated, SD – standard deviation, SE – standard error of arithmetic mean.

Characteristics	Species	Mean	M	SD	SE	CV	Min	Max	n
Body, length	EI	132.8	130.0	15.9	3.7	12.0	112.0	180.0	19
	EF	86.8	83.0	12.8	3.3	14.7	72.0	112.0	15
Body, width	EI	68.0	66.0	7.7	1.8	11.4	55.0	85.0	19
	EF	42.3	38.0	8.6	2.2	20.4	34.0	65.0	15
Body length:width, ratio	EI	2.0	1.9	0.3	0.1	14.7	1.6	2.8	19
	EF	2.1	2.0	0.3	0.1	12.4	1.7	2.5	15
Body cover, thickness	EI	7.8	8.0	1.9	0.4	24.1	5.0	10.0	19
	EF	absent							
Oral bulge, width when dorsal brush is in or near midline	EI	14.6	15.0	2.1	0.5	14.3	12.0	18.0	19
	EF	9.3	9.5	1.2	0.5	13.0	8.0	11.0	6
Oral bulge, width when dorsal brush is at margin of cell	EI	14.1	14.5	2.6	0.7	18.8	10.0	18.0	14
	EF	12.5	12.5	1.7	0.5	13.7	9.0	15.0	10
Oral bulge (basket), distal width independent of location of cell	EI	15.6	16.0	3.0	0.7	19.0	10.0	20.0	19
	EF	11.3	12.0	2.8	0.5	19.3	8.0	15.0	16
Macronucleus, length (rough values)	EI	256.8	260.0	–	–	–	180.0	330.0	19
	EF	100.3	90.0	–	–	–	50.0	160.0	15
Macronucleus, width	EI	7.3	7.0	0.8	0.2	11.1	6.0	9.0	19
	EF	7.8	8.0	0.9	0.2	11.1	7.0	10.0	15
Macronucleus, number of nodules	EI	absent							
	EF	8.3	8.0	1.6	0.4	19.1	6.0	12.0	15
Ciliary rows, number (including brush rows)	EI	71.6	70.0	7.7	2.6	10.8	63.0	87.0	9
	EF	47.1	47.0	4.5	1.5	9.6	40.0	54.0	9
Cilia in mid-body in 10 µm, number	EI	5.9	6.0	1.2	0.3	19.5	4.0	8.0	19
	EF	4.8	5.0	0.6	0.2	12.0	4.0	6.0	12
Dorsal brush, number of rows	EI	3.0	3.0	0.0	0.0	0.0	3.0	3.0	19
	EF	3.0	3.0	0.0	0.0	0.0	3.0	3.0	11
Circumoral kinety to end of brush row 1, distance	EI	53.5	53.0	4.8	1.1	9.0	45.0	62.0	19
	EF	36.1	37.0	8.4	2.8	23.3	24.0	48.0	9
Circumoral kinety to end of brush row 2, distance	EI	54.7	55.0	5.4	1.2	9.9	48.0	70.0	19
	EF	39.9	40.0	6.6	2.2	16.6	30.0	51.0	9
Circumoral kinety to end of brush row 3, distance	EI	50.1	50.0	3.7	0.9	7.3	45.0	58.0	19
	EF	31.8	30.0	5.6	1.9	17.7	24.0	43.0	9
Dikinetids in brush row 1, number	EI	51.2	50.0	4.5	1.5	8.8	45.0	58.0	9
	EF	42.6	42.0	9.2	4.1	21.6	32.0	55.0	5
Dikinetids in brush row 2, number	EI	61.4	63.0	5.0	1.7	8.1	50.0	67.0	9
	EF	45.0	43.0	10.2	5.9	22.6	36.0	56.0	3

continued

Characteristics	Species	Mean	M	SD	SE	CV	Min	Max	n
Dikinetids in brush row 3, number	EI	48.0	47.0	4.6	1.5	9.6	43.0	57.0	9
	EF	31.0	33.0	7.2	4.2	23.3	23.0	37.0	3
Dikinetids in brush row 1, number in 20 µm [a]	EI	17.9	18.0	2.1	0.5	11.4	13.0	21.0	19
	EF	21.3	22.0	2.6	0.5	12.4	16.0	24.0	9
Dikinetids in brush row 2, number in 20 µm [a]	EI	21.2	21.0	3.2	0.7	15.1	15.0	28.0	19
	EF	23.6	24.0	4.0	1.3	16.9	18.0	30.0	9
Dikinetids in brush row 3, number in 20 µm [a]	EI	16.8	17.0	2.1	0.5	12.6	12.0	21.0	19
	EF	20.2	20.0	2.5	0.8	12.6	16.0	24.0	9
Cyst spines, length [b]	EF	8.5	8.0	1.3	0.3	15.0	7.0	11.0	26
Cyst spines, base width [b]	EF	3.3	3.0	–	–	–	3.0	4.0	26

[a] Used as a proxy because total counts were possible in only few specimens. When then related to the length of the individual brush rows, the following numbers are obtained: for *E. isostichos* 48 vs. 51, 58 vs. 61, 43 vs. 48 and *E. floridensis* 38 vs. 43, 47 vs. 45, 31 vs. 32.

[b] The three longest spines per cell.

(up to 2 µm vs. 6 µm), and is contractile (vs. acontractile) by 1/3 of body length. *Enchelyodon kenyaensis* and *E. armatides*, both described by FOISSNER et al. (2002), are at first glance also very similar but have a single, tortuous macronuclear strand. The most slimy specimens (Fig. 44e) resemble *E. terrenus* FOISSNER, 1984, which, however, has acicular (vs. filiform) extrusomes and an average of 33 (vs. 21) ciliary rows and 150 (vs. 56) macronuclear nodules.

Enchelyodon longinucleatus FOISSNER, 1984 (Fig. 46h–k, 48d–i; Table 18)

The population studied is from soil at the margin of a mangrove swamp in the Dominican Republic, about 10 km west of the town of Puerto Plata. The dark, slightly saline soil (5‰) had pH 6.2. We investigated only the resting cysts, which are spherical with an average diameter of 32.4 µm (SD = 3.2, CV = 9.9, Min = 28, Max = 38, n = 8). The cyst is colourless and has a voluminous mucous coat ($\bar{x}$ = 60.6 µm, SD = 4.0, CV = 6.0, Min = 55, Max = 67, n = 8) densely populated by about 4 µm-sized bacteria with bright, refractive inclusions (Fig. 46h–k, 48d, e, g, h). The cyst wall is 1–2 µm thick, lacks any recognizable zonation (Fig. 48i), and is studded with conical spines 1–3 µm high and about 2 µm wide at base (Fig. 46h, i, 48f). The cyst's plasm is very finely granulated and dense. The macronucleus is distinctly shortened (Fig. 48g).

Enchelyodon floridensis **nov. spec.** (Fig. 46a–g, 47a–f, 48a–c; Tables 17, 18)

Diagnosis: Size about 100 × 50 µm in vivo; usually ellipsoid. Macronucleus about as long as cell, with 8 distinct nodules on average. Extrusomes rod-shaped, about 10 µm long in vivo. Cortex thick, studded with ellipsoid, refractive granules. On average 47 ciliary rows, three anteriorly differentiated to an isostichad dorsal brush occupying 46% of body length and having up to 3 µm long bristles; row 1 on average with 43 dikinetids, row 2 with 45, and row 3 with 31. Oral bulge circular to broadly elliptical, about 11 µm wide and up to 2 µm high. Cyst spines conical, about 8 × 3 µm in size.

Type locality: Soil from the Everglades in Florida, USA, Pine trail, 80°41'W 39°N.

Type material: 1 holotype and 3 paratype slides with protargol-impregnated specimens have been deposited in the Biology Centre of the Upper Austrian Museum in Linz (LI). Relevant specimens have been marked by black ink circles on the coverslip.

Etymology: Named after the country in which it was discovered.

Description: Only 18 specimens were found in the protargol slides; about half were well impregnated. Thus, the morphometry of some characteristics is incomplete, and the brush dikinetids were counted not only in total but also in 20 µm of each row.

Size 80–130 × 35–65 µm in vivo, on average about 100 × 50 µm, as calculated from some in vivo measurements and the data shown in Table 17 adding 15% preparation shrinkage. Length:width ratio 1.7–2.5:1, on average 2.1:1. Shape fairly constant, usually ellipsoidal, rarely slightly ovate or bluntly pointed posteriorly; inconspicuously flattened in anterior third (Fig. 46a, c, d, 47a–c, e, f). Macronucleus strongly and irregularly curved, about as long as cell, with an average of eight distinct nodules and globular to irregular nucleoli (Fig. 46a, c, d, 47b, c, e, f; Table 17). Micronuclei scattered throughout cell, 2–3 µm across, difficult to count because of similar cell inclusions (Fig. 46a, c, 47b, c, e). Contractile vacuole in posterior end, with several excretory pores in pole centre (Fig. 46a, c, d). Mature and developing extrusomes scattered in cytoplasm, the latter sometimes deeply impregnated and with a central convexity (Fig. 46c); when mature rod-shaped with rounded ends, in vivo about 10 × 0.4 µm in size, form a broad ring in oral bulge (Fig. 46a, b, e, 48a); exploded in silver carbonate preparations, showing an about 5 µm long, deeply impregnated, toxin-containing proximal region and a 20–30 µm long, weaker-impregnated tube (Fig. 48b, c). In silver carbonate preparations, a second type of extrusomes (?) becomes recognizable, viz., oblong structures (developing cortical granules?) 1–2 µm long. Cortex colourless and slightly furrowed by ciliary rows, flexible but not contractile, conspicuous because gelatinous and 1–1.5 µm thick, studded with ellipsoidal, highly refractive granules about

Table 18. Comparison of main features in *Enchelyodon longinucleatus* (from FOISSNER 1984 and this monograph), *E. isostichos* (this monograph), and *E. floridensis* nov. spec. (this monograph). Protargol impregnation.

Characteristics	*E. longinucleatus*	*E. isostichos*	*E. floridensis*
Body length ($\bar{x}$, µm)	62	133	87
Body width ($\bar{x}$, µm)	39	68	42
Body length:width, ratio	1.6	2.0	2.1
Body shape	elongate ellipsoid, rarely ovate	frequently slightly dumbbell-shaped	ellipsoid, rarely ovate
Macronucleus, length	~ twice body length	~ twice body length	~ body length
Macronucleus nodulated	no	no	yes ($\bar{x}$ = 8)
Extrusome length (µm)	7	8–10	10
Diameter of oral basket at distal end (µm) [a]	6	16	11
Cyst spines, length (µm)	1–3	7–10	7–11
Cyst spines, shape	conical	amphoriform	conical
Ciliary rows, number	37	72	47

[a] When dorsal brush is at cell margin.

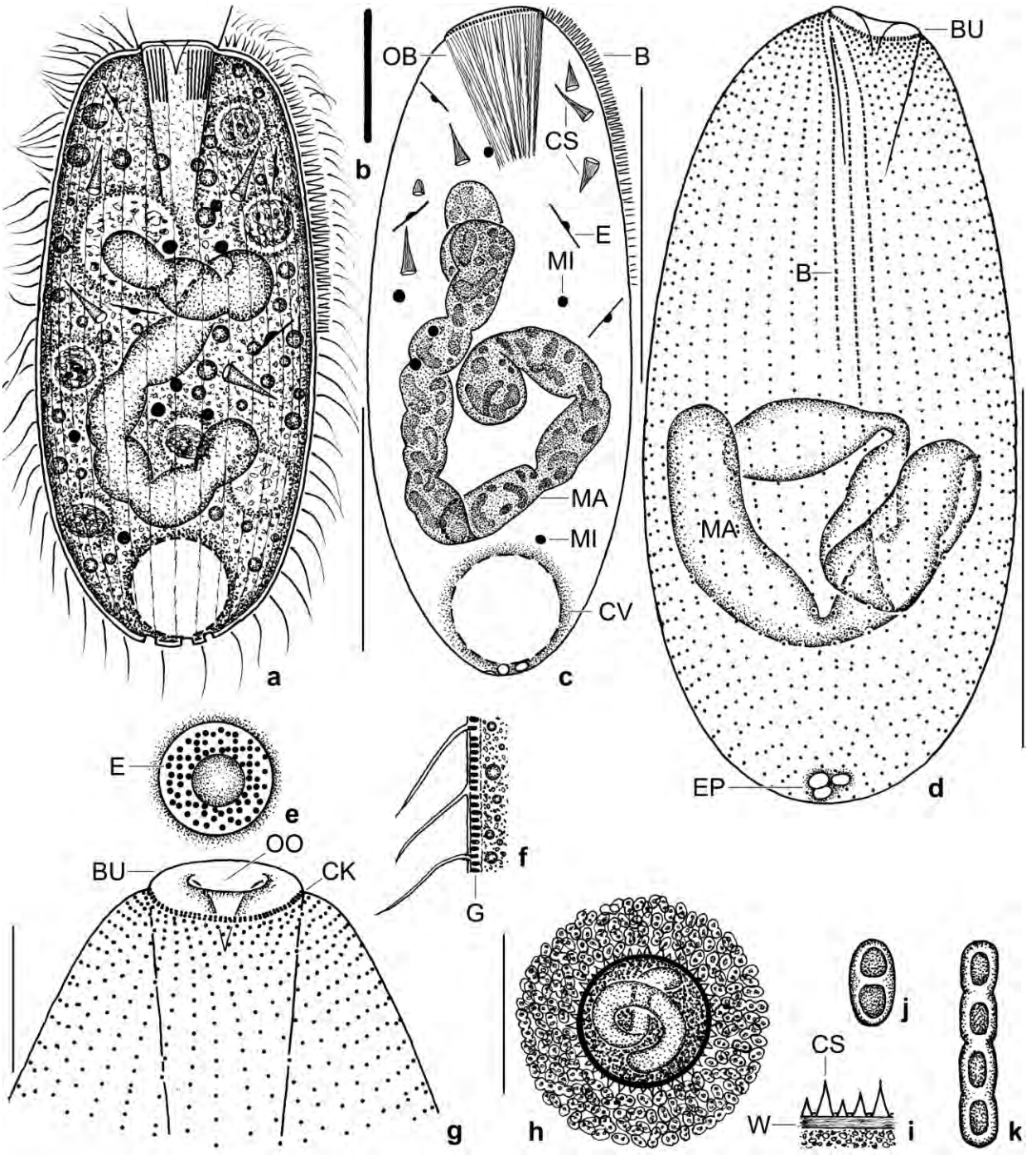

Fig. 46a–k. *Enchelyodon floridensis* (a–g) and *E. longinucleatus* (h–k) from life (a, b, e, f, h–k) and after protargol impregnation (c, d, g). **a:** Left side view of a representative specimen, length 100 µm. **b:** Mature extrusome, length 10 µm. **c:** Overview of cell organization, especially the nodulated macronucleus. **d:** Ciliary pattern of dorsal side and macronucleus of holotype specimen, length 90 µm. Note the flat oral bulge and the nodulated macronucleus. **e:** Frontal view of oral bulge, which is circular to broadly elliptical. **f:** The cortex is studded with refractive granules. **g:** Ciliary pattern of anterior ventral side. **h, j, k:** The resting cysts of *E. longinucleatus* are covered by a voluminous mucous layer densely populated by 4–5 µm long bacteria. **i:** The 1–2 µm thick cyst wall is studded with conical spines 1–3 µm high. B – dorsal brush, BU – oral bulge, CK – circumoral kinety, CS – cyst spines, CV – contractile vacuole, E – mature and developing extrusomes, EP – excretory pores, G – granules, MA – macronucleus, MI – micronuclei, OB – oral basket, OO – oral opening, W – cyst wall. Scale bars 15 µm (g) and 40 µm (a, c, d, h).

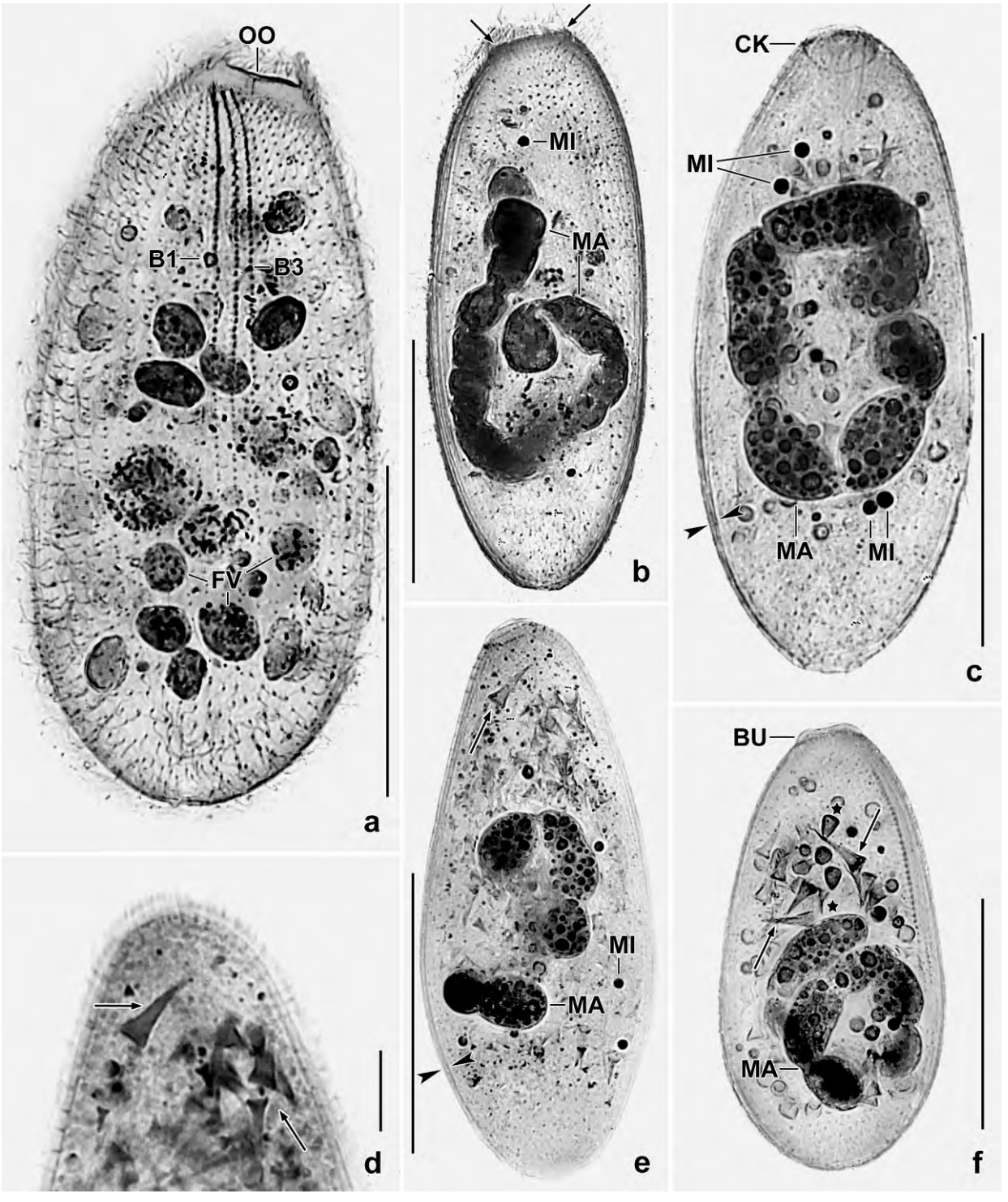

Fig. 47a–f. *Enchelyodon floridensis* after protargol impregnation. Opposed arrowheads (c, e) mark the thick cortex. **a:** Dorsal view of holotype specimen, showing the ciliary pattern and many food vacuoles. **b, c:** Overviews showing body shape, the margin of the oral bulge/basket (arrows), and the nodular macronucleus, which is a main feature of *E. floridensis*. **d–f:** One third of the specimens have developing (asterisks) and mature (arrows) cyst spines in the cytoplasm. Note the nodulated macronucleus. B 1, 3 – dorsal brush rows, BU – oral bulge, CK – circumoral kinety, FV – food vacuoles, MA – macronucleus, MI – micronuclei, OO – oral opening. Scale bars 10 µm (d) and 40 µm (a, b, c, e, f).

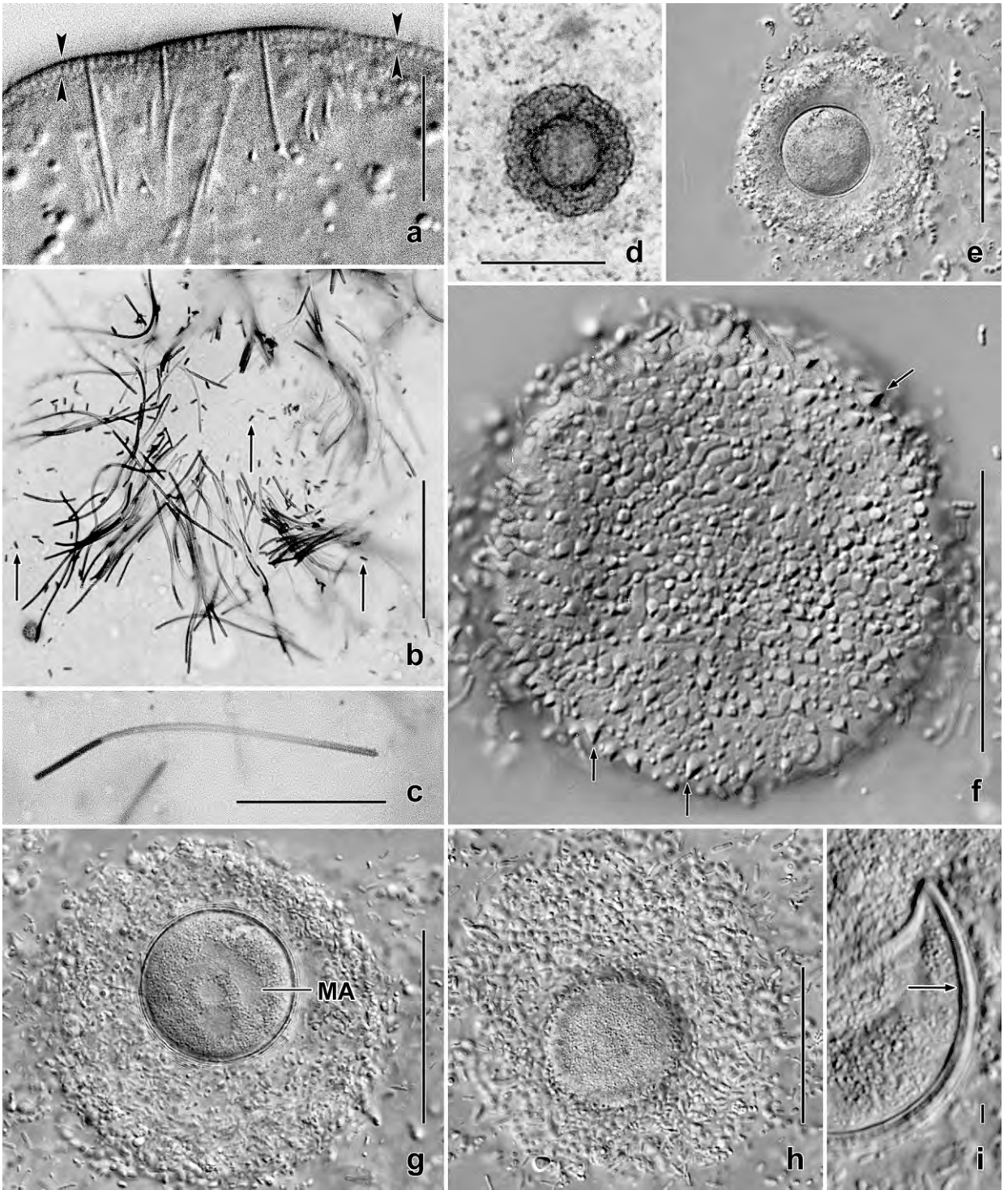

Fig. 48a–i. *Enchelyodon floridensis* (a–c) and *E. longinucleatus* (d–i) from life (a, d–i) and after silver carbonate impregnation (b, c). **a:** A squashed specimen, showing the about 10 µm long, mature extrusomes. The thick cortex (arrowheads) is studded with refractive granules. **b, c:** In silver preparations, the toxicysts explode, showing a short, deeply impregnated portion and a long, light tube. Arrows mark minute, oblong structures, possibly cortical granules. **d, e, g, h:** The cysts have a voluminous cover densely populated with bacteria. **f, i:** The cyst wall is 1–2 µm thick (i) and studded with conical spines 1–3 µm high (f, arrows). MA – macronucleus. Scale bars 2 µm (i), 10 µm (a, c), 20 µm (b, f), 40 µm (e, g, h), and 60 µm (d).

1 × 0.5 in size (Fig. 46f, 47c, e). Cytoplasm packed with compact and loose food vacuoles up to 20 µm across, few to many lipid droplets 1–5 µm in diameter, and up to 200 conical inclusions, very likely cyst spines (Foissner 2011) with an average size of 8.5 × 3.3 µm (Fig. 46a, c, 47a; Table 17); spines slightly concentrated in anterior third of body, some slightly curved, faintly impregnated; developing spines smaller and heap-shaped (Fig. 46c, 47d–f; Table 17). Swims slowly rotating about main body axis.

Cilia 8–10 µm long in vivo, arranged in an average of 47 ordinarily spaced, meridional rows abutting slightly obliquely on circumoral kinety; interkinetal distance gradually increases from anterior to posterior, rear pole area sparsely ciliated. Three isostichad, dikinetal brush rows with longest row 40 µm and thus occupying 46% of body length. Brush bristles up to 3 µm long in vivo and very narrowly spaced, brush thus difficult to investigate (Fig. 46a, c, d, g, 47a; Table 17).

Oral bulge occupies central half of anterior body end, about 11 µm wide but very inconspicuous because only 1 to 2 µm high, circular to broadly elliptical, according to the morphometric analysis (Table 17). Circumoral kinety associated with about 25 µm long nematodesmata, forming a distinct basket of which usually only the distal half is well impregnated; oralized somatic monokinetids absent (Fig. 46a, c–e, g, 47a–c, f).

Occurrence and ecology: As yet found only at type locality, i. e., in soil from the Everglades of Florida. *Enchelyodon floridensis* was rare in the non-flooded Petri dish culture because only 18 specimens were found in eight protargol slides, and one third of these was precystic having cyst spines in the cytoplasm. We cannot exclude that *E. floridensis* is a limnetic species because the sample is from swamp land.

This small and inconspicuous sample contained two further conspicuous, undescribed species: *Apocolpodidium* (*Phagoon*) *macrostoma* Foissner et al., 2002 and *Apodileptus edaphicus* Vďačný and Foissner, 2012. As yet, these three species have been found only in this sample, indicating that the region contains a high number of endemics.

Remarks: Many features of *E. floridensis* are between *E. longinucleatus* Foissner, 1984 and → *E. isostichos* (Table 18). Possibly, the nodulated macronucleus is the most characteristic feature of *E. floridensis*.

***Enchelyodon isostichos* nov. spec.** (Fig. 49a–l, 50a–z; Tables 17, 18)

Diagnosis: Size about 150 × 75 µm in vivo; usually ellipsoid and more or less dumbbell-shaped, broadest anteriorly or posteriorly. Macronucleus about two times as long as body. Extrusomes rod-shaped, about 8 µm long in vivo. Cortex thick, studded with ellipsoid, refractive granules. On average 72 ciliary rows, three anteriorly differentiated to an isostichad dorsal brush occupying 41% of body length and having up to 3 µm long bristles; row 1 on average with 51 dikinetids, row 2 with 61, and row 3 with 48. Oral bulge circular to elliptic, about 16 µm width and up to 3 µm high. Cyst spines amphoriform, 7–10 µm long.

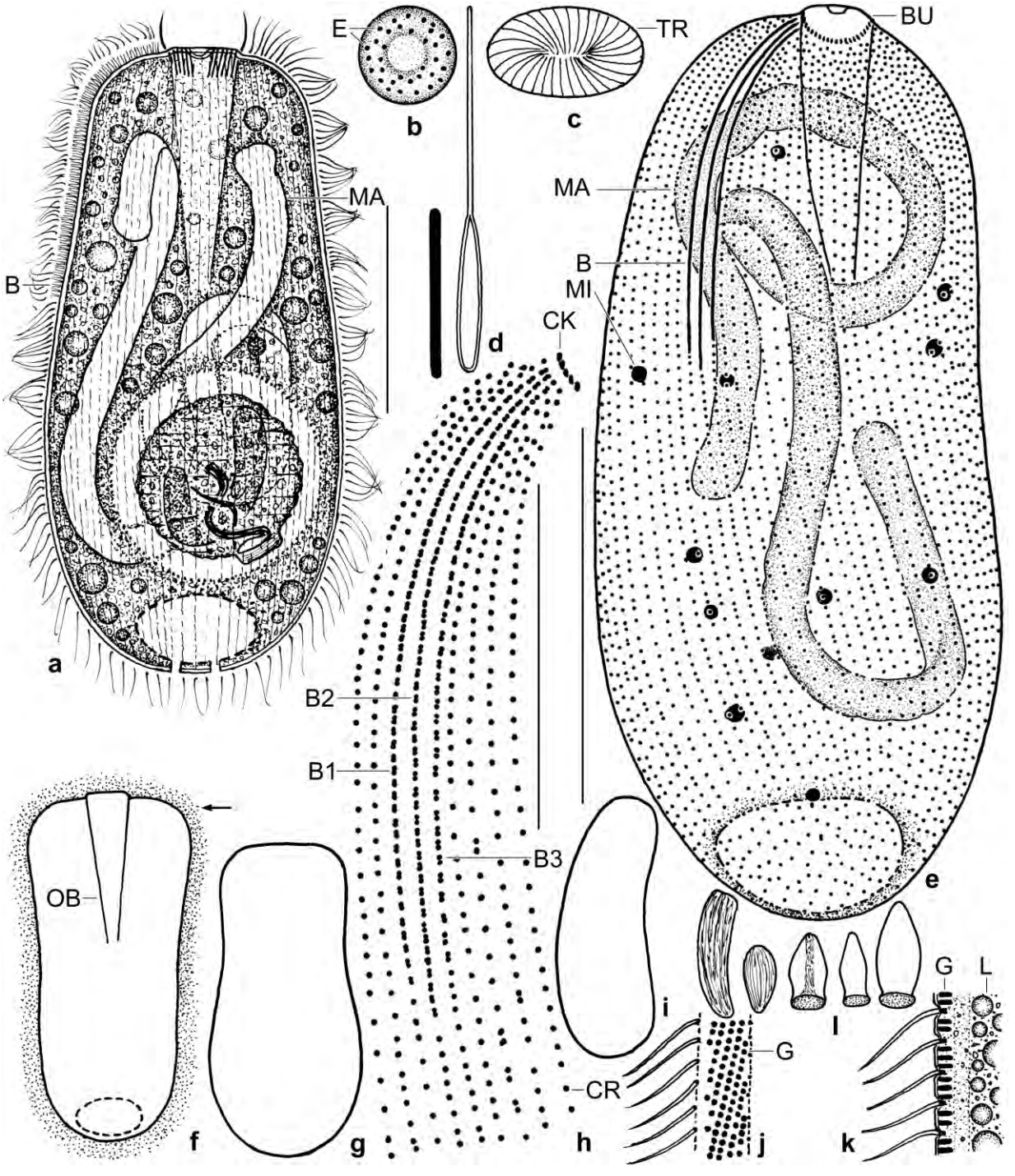

Fig. 49a–l. *Enchelyodon isostichos* from life (a–d, f, g, i–k) and after protargol impregnation (e, f, h, l). **a:** Side view of a representative specimen having ingested a zooid of *Pseudotelotrochidium epistylis*, length 150 µm. **b, c:** Shape variability of oral bulge (cp. Fig. 50w, z). **d:** Resting (8 µm) and exploded toxicyst. **e, h:** Dorsolateral view of holotype specimen, length 120 µm; (h) shows the isostichad dorsal brush. **f, g:** Shape of starved specimens. The arrow marks a structureless cover recognizable in protargol preparations. **i:** A curved specimen. **j, k:** Surface view and optical section of cortex, showing the conspicuous granules. **l:** Precursors of and mature cyst spines, 6–11 µm. B (1–3) – dorsal brush (rows), BU – oral bulge, CK – circumoral kinety, CR – ciliary row, CV – contractile vacuole, E – extrusomes, G – cortical granules, L – lipid droplets, MA – macronucleus, MI – micronucleus, OB – oral basket, TR – transverse microtubule ribbons. Scale bars 25 µm (h) and 50 µm (a, e).

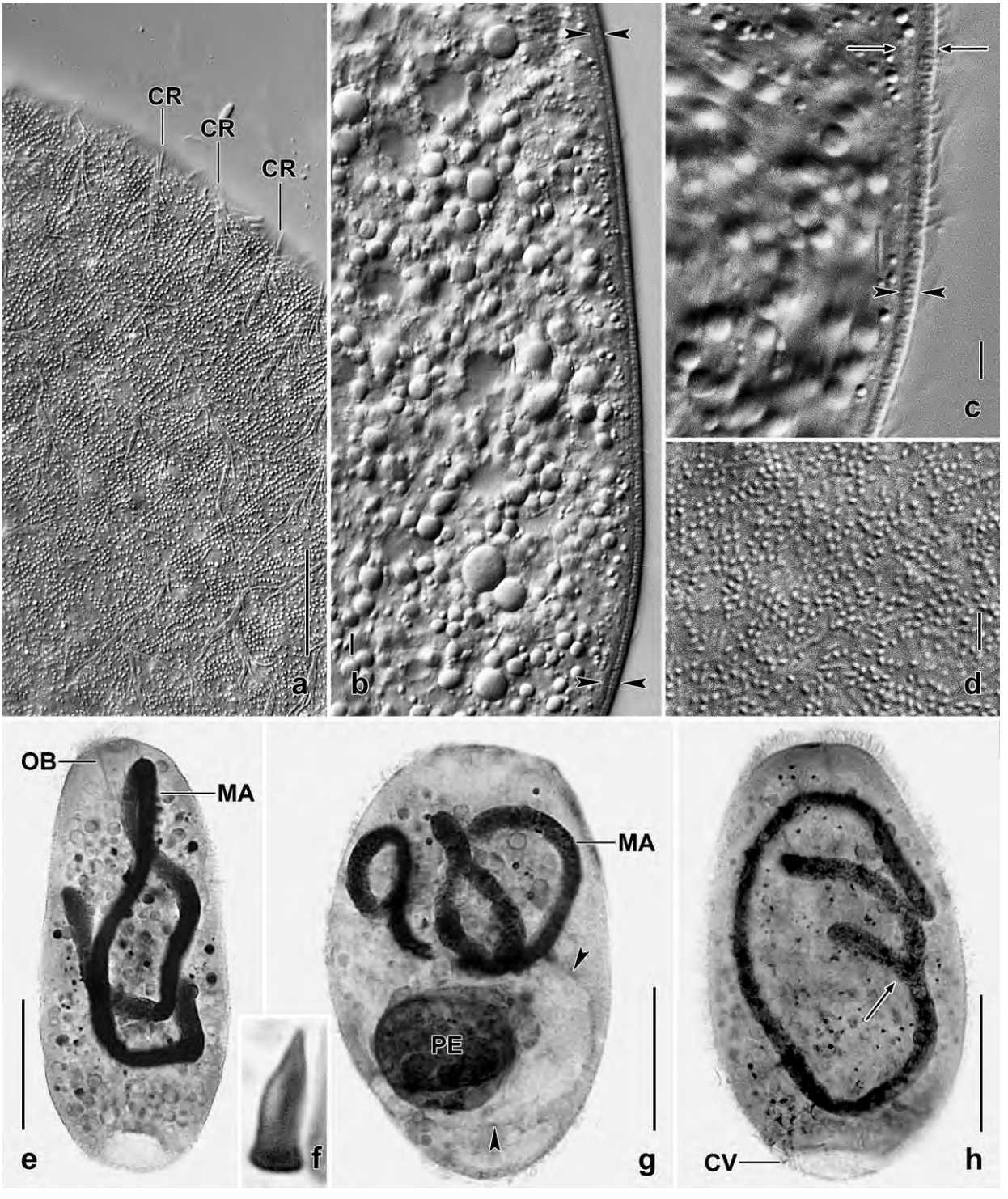

Fig. 50a–h. *Enchelyodon isostichos* from life (a–d) and after protargol impregnation (e–h). **a, d:** Surface views showing the dense, refractive cortical granulation. **b, c:** Optical sections, showing the thick cortex and the cytoplasm studded with lipid droplets. The opposed arrows in (c) mark the cortex plus a bright, gelatinous layer; the opposed arrowheads denote the about 1.5 µm thick cortex. **e, g, h:** Overviews showing the macronucleus and a large food vacuole (g, arrowheads) containing *P. epistylis*. The arrow in (h) marks a bifurcation of the macronucleus. **f:** Morphostatic specimens contain developing and mature, 7–10 µm long cyst scales. CR – ciliary rows, CV – contractile vacuole, MA – macronucleus, OB – oral basket, PE – *Pseudotelotrochidium epistylis*. Scale bars 3 µm (c, d), 5 µm (a, b), and 50 µm (e, g, h).

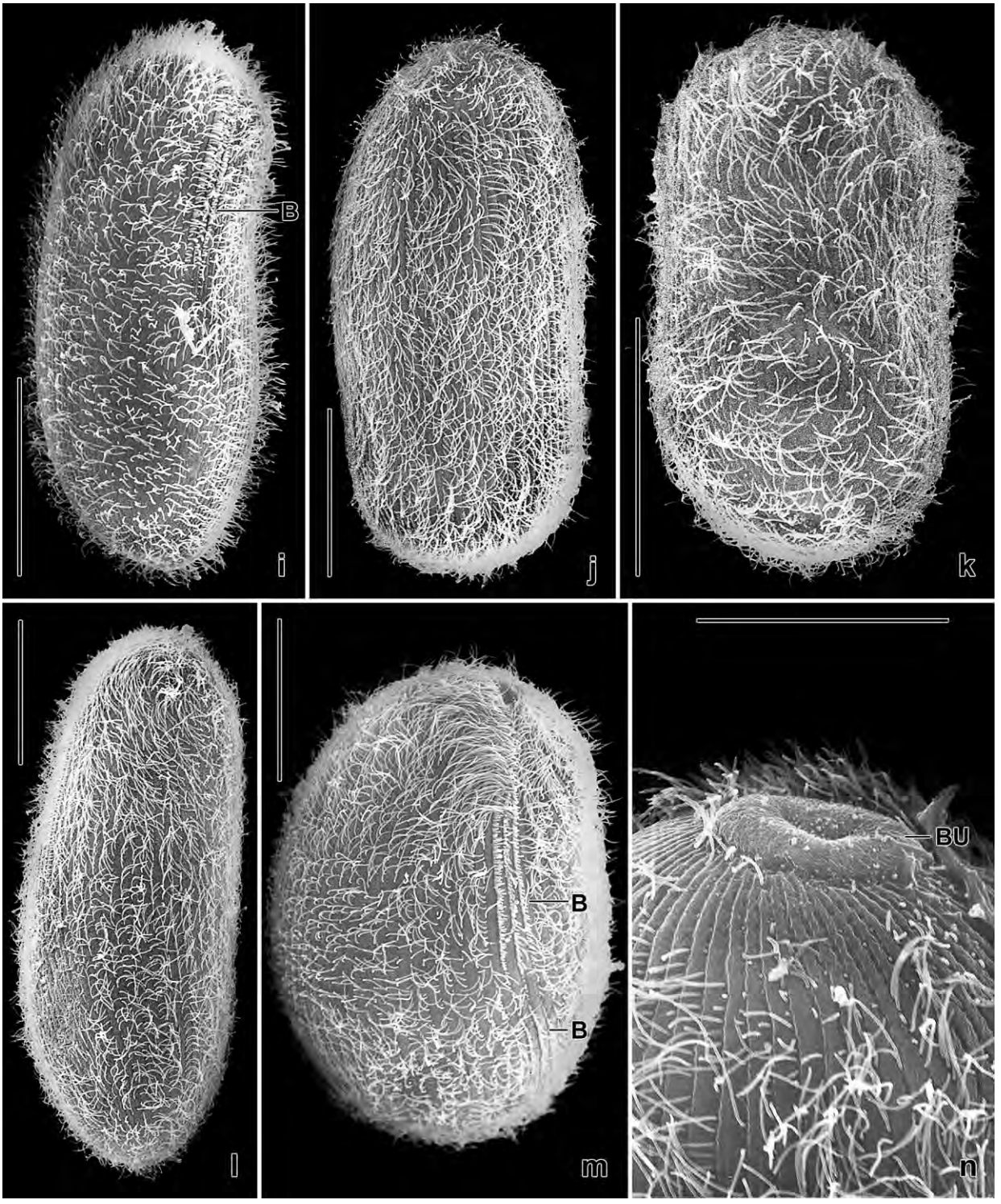

Fig. 50i–n. *Enchelyodon isostichos* in the scanning electron microscope. **i–l:** Size (80–150 µm) and shape variability of morphostatic specimens: elongate ellipsoid (j, l), slightly curved (i), and dumbbell-like (k). For details of the dorsal brush, see next plate. **m:** An early divider which already has organized the dorsal brush of the opisthe. The proter brush remains unchanged. **n:** A partially deciliated specimen, showing the thin but broad oral bulge. The ciliary rows extend in flat furrows. B – dorsal brush, BU – oral bulge. Scale bars 20 µm (n) and 40 µm (i–m).

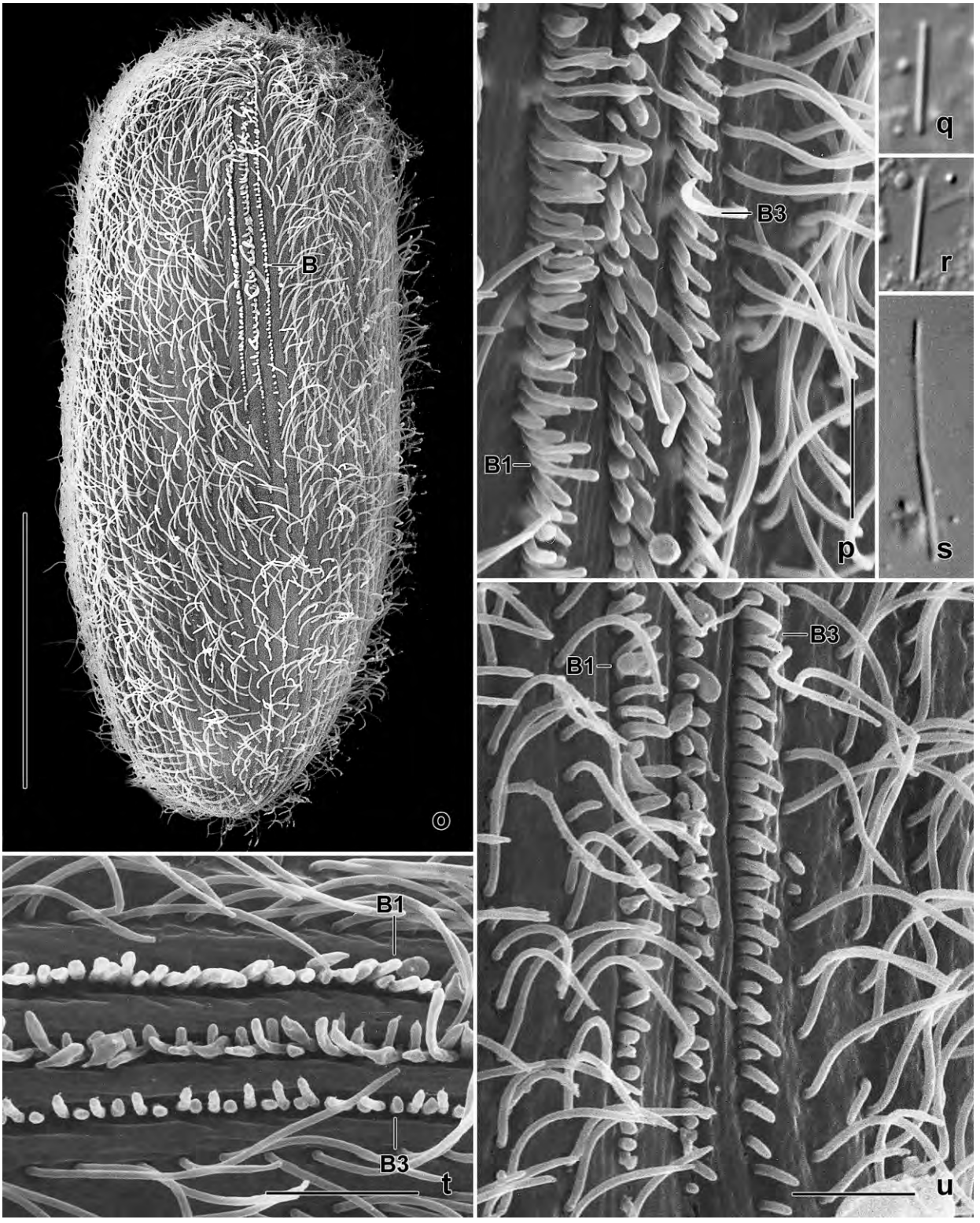

Fig. 50o–u. *Enchelyodon isostichos* in the SEM. **o:** Dorsal overview with dorsal brush. **p, t, u:** Details of dorsal brush (see text). The distally inflated row 2 bristles collapsed partially due to the preparation procedures. **q, r:** Resting toxicysts, 8–10 µm. **s:** Exploded toxicyst, 20 µm. B (1, 3) – dorsal brush (rows). Scale bars 4 µm (p, t, u) and 40 µm (o).

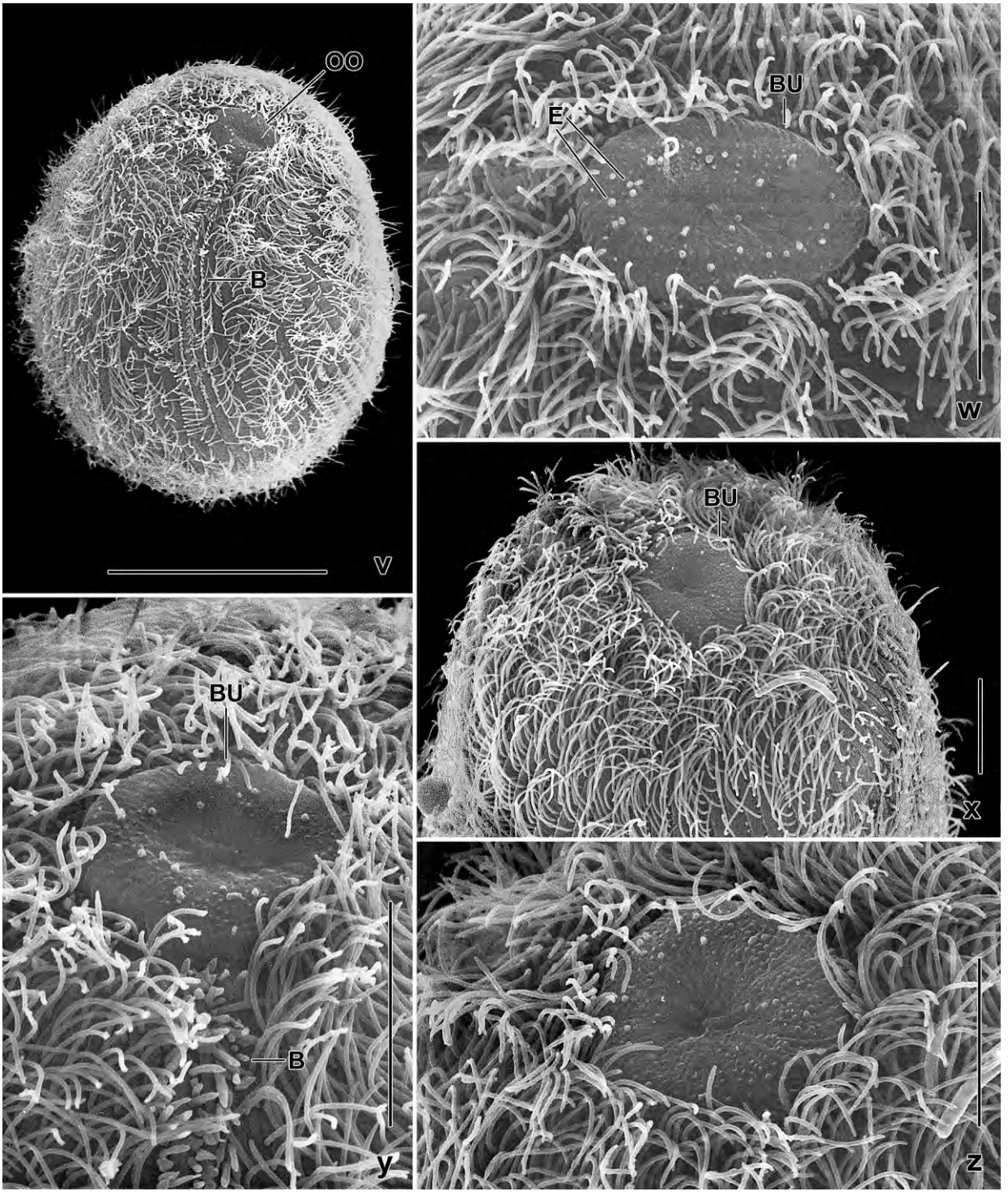

Fig. 50v–z. *Enchelyodon isostichos*, oral apparatus in the scanning electron microscope. **v:** Oblique frontal overview, showing both the oral opening (bulge) and the dorsal brush. **w:** A specimen with broadly elliptic oral bulge. The fine striation is caused by transverse microtubuli ribbons originating from the circumoral dikinetids. **x, z:** Oblique frontal view of a specimen with circular oral bulge (cp. Fig. (w)!). Note the dense ciliation of *E. isostichos*. **y:** Oblique frontal view, showing the dorsal brush extending to the slightly concave oral bulge. B – dorsal brush, BU – oral bulge, E – extrusomes leaving the cell, OO – oral opening. Scale bars 10 µm (w–z) and 40 µm (v).

Type locality: Venezuelan site (1), i. e., soil from floodplain of the Orinoco River in the surroundings of the village of Cabruta, 66°14'W 7°38'N.

Type material: 1 holotype and 3 paratype slides with protargol-impregnated specimens have been deposited in the Biology Centre of the Upper Austrian Museum in Linz (LI). Relevant specimens have been marked by black ink circles on the coverslip.

Etymology: *Isosticha* is a noun in apposition, composed of the Greek adjective *iso* (equal) and the Greek noun *stichos* (row), referring to the dorsal brush whose rows have a very similar length.

Description: The preparations of *E. isostichos* are mediocre. Thus, the number of ciliary rows and brush dikinetids could be counted in only nine specimens; the latter were counted also in 20 µm of each brush row (Table 17).

Size 130–210 × 60–100 µm in vivo, on average about 150 × 75 µm, as calculated from some in vivo measurements and the values shown in Table 17 adding 15% preparation shrinkage. Length:width ratio 1.6–2.8:1, on average 2:1. Shape also highly variable, when starved cells are included. Ordinary specimens ellipsoid to curved-ellipsoid with inconspicuous subapical narrowing making cells slightly dumbbell-shaped. Starved specimens as shown in Fig. (49f, g), i. e., rather distinctly dumbbell-shaped and broader anteriorly or posteriorly. Slightly flattened only in anterior third (Fig. 49a, e–g, i, 50e, g–m, o; Table 17). Macronucleus and micronuclei scattered throughout cell (Fig. 49a, e, 50e, g, h; Table 17). Macronucleus strongly and irregularly curved, about twice as long as cell, ends slightly inflated; with dense, three-dimensional nucleolar net; rarely broken into several pieces or bifurcate (Fig. 50h). Micronuclei 2–3 µm across, difficult to count because of many similar-sized lipid droplets; some clear cells show the following numbers: 16, 18, 20, 22, 23. Contractile vacuole occupies posterior end, during systole surrounded by small adventive vacuoles, canals extending anteriorly absent; several excretory pores in pole centre (Fig. 49a, e, f, 50h). Mature extrusomes scattered in cytoplasm and forming a broad ring in oral bulge in vivo, rod-shaped with rounded ends, about 8–10 × 0.5 µm in size, do not impregnate with the protargol method used; when exploded about 20 µm long and of typical toxicyst structure (Fig. 49d, 50q–s); many deeply impregnated, fusiform, 6–8 µm long developmental stages in cytoplasm. Cortex colourless and slightly furrowed by ciliary rows, flexible but not contractile, conspicuous because gelatinous and 1–2 µm thick, studded with ellipsoid, highly refractive granules, forming slightly oblique rows between kineties (Fig. 49j, k, 50a–d, n), covered by an about 8 µm thick, structureless substance impregnating yellowish in protargol preparations, possibly slime from extruded mucocysts (Fig. 49f). Most specimens dark under low magnification (< 100 ×) and transmitted light because packed with lipid droplets up to 7 µm across and developing or mature, amphoriform cyst wall precursors 7–10 µm long (Fig. 49l); most specimens contain one, rarely two zooids of *Pseudotelotrochidium epistylis* (Fig. 49a, 50g). Swims moderately rapid rotating about main body axis.

Cilia 8–10 µm long in vivo, arranged in an average of 72 densely ciliated and narrowly spaced, meridional to very slightly oblique rows; not condensed in oral area, slightly dispersed in posterior pole region (Fig. 49a, e, 50i–o; Table 17); do not form sutures along dorsal brush. Three

isostichad, dikinetal brush rows, each about 55 µm long and thus occupying roughly 40% of body length, extend in rather deep furrows and end with minute tails comprising a few monokinetal bristles up to 2 µm long. Brush bristles only 2–4 µm long and very narrowly spaced, making brush difficult to investigate, even in the scanning electron microscope (Fig. 49a, e, h, 50i, m, o, p, t, u, v; Table 17). Brush row 1 composed of an average of 51 dikinetids; anterior bristles rod-shaped and shorter than posterior ones being flame-shaped and about 4 µm long in anterior half of row while slightly clavate in posterior half. Brush row 2 composed of an average of 61 dikinetids, bristles similar to those of row 1 but posterior bristles flame-shaped throughout. Row 3 composed of an average of 48 dikinetids with rod-shaped bristles, anterior bristles about 2 µm long, posterior 3 µm.

Oral bulge discoid, occupies middle third to half of anterior body end, about 16 µm wide but very inconspicuous because only up to 2 µm high, circular to broadly elliptical, slightly furrowed by transverse microtubule ribbons originating from circumoral dikinetids and extending into concave bulge centre. Circumoral kinety associated with about 60 µm long nematodesmata, forming a conspicuous basket of which usually only the distal half is well recognizable; oralized somatic monokinetids absent (Fig. 49a–c, e, f, 50v–z; Table 17).

Occurrence and ecology: We found this species also in a *terra firma* soil sample from one of the many islands in the Amazon River near to the town of Manaus. *Enchelyodon isostichos* possibly feeds only on peritrichs because no other food was contained in the about 50 cells investigated. It is a massive species, indicating that it could be a contaminant in the soil sample, i. e., a freshwater species which excysted in the non-flooded Petri dish culture.

Remarks: Few *Enchelyodon* species have been well described (Foissner 1984, Foissner et al. 2002, Senler and Yildiz 2003), which limits the possibility to compare our new species. *Enchelyodon isostichos* is obviously rather closely related to an Austrian population of *E. longinucleatus* Foissner, 1984, in that it is, as yet, the sole congener with an isostichad dorsal brush; in all other well-studied species, brush row 3 is distinctly shorter than row 2. Most features of *E. isostichos* are twice or thrice as large as in *E. longinucleatus*. There is no overlap in important features, such as body length ($\bar{x}$ = 133 µm; 112–180 µm vs. 62 µm; 56–70 µm), number of ciliary rows ($\bar{x}$ = 71; 63–87 vs. $\bar{x}$ = 37; 32–43), and width of oral opening ($\bar{x}$ = 16 µm; 10–20 µm vs. $\bar{x}$ = 6.6 µm; 6–7). The values for *E. longinucleatus* have been confirmed in a population from Kenya, Africa, emphasizing the distinctness of *E. isostichos*. Further, *E. longinucleatus* has an ordinary ciliate cortex while it is thick and studded with conspicuous granules in *E. isostichos*. For distinguishing *E. isostichos* from → *E. floridensis*, see that species.

Enchelyodon isostichos shows two peculiarities. The body is covered by a yellowish-impregnating substance, possibly slime from extruded mucocysts (cortical granules). The shape of the oral bulge is rather variable (CV nearly 20%, Table 17), i. e., circular to broadly elliptic. We studied this very carefully in vivo and in the scanning electron microscope because bulge shape is an important feature that has been used also as a generic vehicle (Fig. 49b, c, 50w–z).

Enchelyodon megastoma Foissner, Agatha and Berger, 2002 (Table 19)

Remarks: We found this species in floodplain soil from Botswana, with features very similar to those described by Foissner et al. (2002), especially the large body (~ 200 µm) and the two extrusome size types. Thus, we improved the morphometry (Table 19) and deposited seven voucher slides with protargol-impregnated specimens in the repository mentioned below.

Foissner et al. (2002) described the oral bulge of the Namibian specimens as circular, which would be a rather distinct difference to the populations from Botswana and Venezuela described below. A re-inspection of the original notes on *E. megastoma* showed that a circular oral bulge is definitely mentioned in vivo and in two out of 10 prepared specimens. Further, a circular oral bulge is usual in this genus, but this may be variable (→ *E. isostichos*). In spite of these data, we doubt the observation of Foissner et al. (2002) because the preparations from the Botswanan specimens of *E. megastoma* show that the oral bulge is circular to elliptic, i. e., one can recognize a long and a short bulge axis in some specimens (Table 19).

Enchelyodon monoarmatus nov. spec.

Diagnosis (includes two subspecies): Size of cultivated specimens about 150 × 100 µm in vivo. Body broadly ellipsoid to slightly dumbbell-shaped or obovate to pyriform. Macronucleus a tortuous strand about twice as long as cell; many micronuclei. Extrusomes rod-shaped, in vivo about 12 × 0.5 µm. Cortex ~ 1 µm or ~ 2 µm thick, studded with granules about 0.8 × 0.2 µm or 1.5–2 µm in size. On average 86 or 115 ciliary rows, three anteriorly differentiated to an isostichad dorsal brush occupying about half of body length and with bristles up to 5 µm long in vivo; brush row 1 on average with 52 or 64 dikinetids, row 2 with 55 or 74, and row 3 with 48 or 60. Oral bulge elliptic to slightly pyriform or ovate to pyriform, on average 52 × 36 µm or 60 × 40 µm in protargol preparations. Resting cysts spiny, wall about 1 µm or 4 µm thick.

Etymology: *Monoarmatus* is a Latin adjective composed of *mono* (single) and *armatus* (armed), referring to the single type of extrusomes compared to *E. megastoma* Foissner et al., 2002 which has two types.

Remarks: *Enchelyodon monoarmatus* is rather similar to *E. megastoma* from which it differs in having only one (vs. two) type of toxicysts, in body size (~ 150 × 100 µm vs. ~ 200 × 120 µm), and the number of ciliary rows (< 120 vs. > 120).

The neotropic and the paleotropic populations of *E. monoarmatus* differ considerably, suggesting subspecies rank for both.

Enchelyodon monoarmatus monoarmatus nov. sspec. (Fig. 51a–p, 52a–z; Table 19)

Diagnosis: Size of cultivated specimens about 160 × 100 µm in vivo; broadly ellipsoid or slightly dumbbell-shaped in broad side view. Cortex ~ 1 µm thick, studded with oblong granules about 0.8 × 0.2 µm in size. On average 86 ciliary rows; dorsal brush row 1 with 52 dikinetids, row 2

Table 19. Morphometric data on *Enchelyodon megastoma* from Namibia (EMM; from FOISSNER et al. 2002) and Botswana (EMB; original data), *E. monoarmatus monoarmatus* (EME [d]), and *E. monoarmatus pyriformis* (EMP [d]). Data based, if not mentioned otherwise, on mounted, protargol-impregnated (FOISSNER's method), and randomly selected specimens from non-flooded Petri dish cultures (EMM, EMB) or pure cultures (EME, EMP). Measurements in µm. CV – coefficient of variation in %, M – median, Max – maximum, Mean – arithmetic mean, Min – minimum, n – number of specimens investigated, Pop – population, SD – standard deviation, SE – standard error of arithmetic mean.

Characteristics	Pop.	Mean	M	SD	SE	CV	Min	Max	n
Body, length	EMM	175.9	183.5	33.4	10.6	19.0	125.0	230.0	10
	EMB	188.6	196.5	30.5	6.8	16.2	125.0	230.0	20
	EME	126.2	127.0	15.2	3.3	12.0	100.0	160.0	21
	EMP	118.9	120.0	11.8	2.6	10.0	92.0	140.0	21
Body, width	EMM	98.8	95.5	20.7	6.5	20.9	65.0	140.0	10
	EMB	119.9	118.0	17.0	3.8	14.2	85.0	150.0	20
	EME	91.0	87.0	11.3	2.5	12.4	77.0	118.0	21
	EMP	92.3	92.0	9.8	2.1	10.7	77.0	110.0	21
Body length:width, ratio	EMM	1.9	1.9	0.2	0.1	10.8	1.6	2.2	10
	EMB	1.6	1.5	0.2	0.1	15.2	1.2	2.1	20
	EME	1.4	1.4	0.2	0.1	15.2	1.2	2.0	21
	EMP	1.3	1.3	0.1	0.1	7.3	1.1	1.5	21
Body, length (silver nitrate)	EME	151.4	150.0	22.5	4.9	14.9	108.0	190.0	21
Body, width (silver nitrate)	EME	97.9	93.0	11.8	2.6	12.0	83.0	120.0	21
Body length:width, ratio (sn)	EME	1.6	1.5	0.3	0.1	16.5	1.2	2.2	21
Anterior body end to macronucleus, distance	EME	26.6	24.0	7.9	1.7	29.8	18.0	42.0	21
	EMP	24.6	25.0	10.5	2.3	42.7	10.0	55	21
Macronucleus, length (spread; approximate)	EMM	320.0	325.0	–	–	–	200.0	500.0	10
	EMB	389.5	390.0	–	–	–	250.0	530.0	20
	EME	260.0	260.0	–	–	–	200.0	320.0	21
	EMP	257.0	260.0	–	–	–	150.0	400.0	21
Macronucleus, width	EMM	9.2	9.0	0.8	0.2	8.6	8.0	10.0	10
	EMB	11.0	11.0	1.9	0.4	17.3	8.0	14.0	20
	EME	8.6	8.0	1.0	0.2	11.3	7.0	10.0	21
	EMP	8.9	9.0	1.3	0.3	14.8	6.0	12.0	21
Macronucleus, number	EMM	1.0	1.0	–	–	–	1.0	2.0	10
	EMB	1.0	1.0	–	–	–	1.0	2.0	20
	EME	1.0	1.0	0.0	0.0	0.0	1.0	1.0	21
	EMP	1.0	1.0	0.0	0.0	0.0	1.0	1.0	21
Ciliary rows, number (including brush rows)	EMM [a]	133.3	128.5	–	–	–	88.0	189.0	10
	EMB [e]	124.7	125.0	11.7	3.9	9.4	110.0	145.0	9
	EME	86.2	85.0	8.7	1.9	10.1	74.0	105.0	21
	EMP	114.9	117.0	6.3	1.4	5.5	105.0	125.0	21
Cilia in mid-body in 10 µm,	EMB	5.1	5.0	1.1	0.3	22.5	4.0	8.0	20

continued

Characteristics	Pop.	Mean	M	SD	SE	CV	Min	Max	n
number	EME	6.4	6.5	1.6	0.4	24.9	4.0	10.0	21
	EMP	4.5	4.0	0.6	0.1	13.4	4.0	6.0	21
Dorsal brush, number of rows	EMB	3.0	3.0	0.0	0.0	0.0	3.0	3.0	8
	EME	3.0	3.0	0.0	0.0	0.0	3.0	3.0	21
	EMP	3.0	3.0	0.0	0.0	0.0	3.0	3.0	21
Circumoral kinety to end of brush row 1, distance	EME	54.0	53.0	6.2	1.8	11.5	46.0	70.0	12
	EMP	53.8	54.0	4.6	1.2	8.6	45.0	60.0	14
Circumoral kinety to end of brush row 2, distance	EMB	98.8	95.0	–	–	–	75.0	130.0	4
	EME	58.2	60.0	8.2	2.4	14.2	47.0	80.0	12
	EMP	58.5	60.0	4.9	1.3	8.3	50.0	70.0	14
Circumoral kinety to end of brush row 3, distance	EME	51.7	52.5	7.0	2.0	13.6	40.0	60.0	12
	EMP	49.0	48.5	4.6	1.2	9.4	42.0	55.0	14
Dikinetids in brush row 1, number	EME	51.8	50.5	6.2	1.8	12.0	43.0	67.0	12
	EMP	64.4	64.5	6.5	1.7	10.1	47.0	70.0	14
Dikinetids in brush row 2, number	EME	55.4	54.5	8.5	2.4	15.3	43.0	72.0	12
	EMP	73.8	74.5	7.5	2.0	10.1	60.0	85.0	14
Dikinetids in brush row 3, number	EME	47.6	48.0	6.7	1.9	14.2	38.0	60.0	12
	EMP	59.6	60.5	6.1	1.6	10.3	50.0	72.0	14
Oral bulge (basket), length of long axis	EMM [b]	60.6	65.0	10.8	3.4	17.8	40.0	77.0	10
	EMB [b]	67.4	66.0	9.3	2.2	13.8	50.0	85.0	18
	EME [b]	52.2	50.0	4.7	1.0	8.9	43.0	64.0	21
	EMP [b]	59.2	60.0	7.9	1.7	13.3	45.0	76.0	21
Oral bulge (basket), length of short axis	EMB [b]	42.3	40.0	7.7	2.7	18.2	30.0	55.0	8
	EME [b]	36.0	35.0	4.2	0.9	11.7	28.0	44.0	21
	EMP [b]	39.1	40.0	7.1	1.7	18.1	25.0	50.0	17
Oral bulge, height	EME	2.5	3.0	–	–	–	2.0	3.0	11
	EMP	about 3 µm							
Oral basket, length	EMM [c]	44.0	40.0	–	–	–	35.0	70.0	10
	EMB [c]	106.7	100.0	29.6	8.6	27.8	70.0	160.0	12
	EME [c]	43.1	40.0	–	–	–	30.0	60.0	21
	EMP	69.5	70.0	14.7	3.2	21.2	50.0	110.0	21

[a] Calculated from average kinety distance and circumference of specimen.

[b] long axis = lateral view = dorsal brush near or at margin of cell; short axis = ventral or dorsal view = dorsal brush in middle third of cell.

[c] Very likely longer, but too fine to be recognizable.

[d] Data based on specimens from growing pure cultures fixed with Bouin's solution (EME) or a 1:1 mixture of concentrated ethanol and formol (EMP).

[e] When calculated from the number of rows in 20–40 µm and the circumference of the specimens, the values are as follows: $\bar{x}$ = 131.2, Median = 127, SD = 20.8, SE = 5.1, CV = 15.9, Min = 110, Max = 195, n = 17.

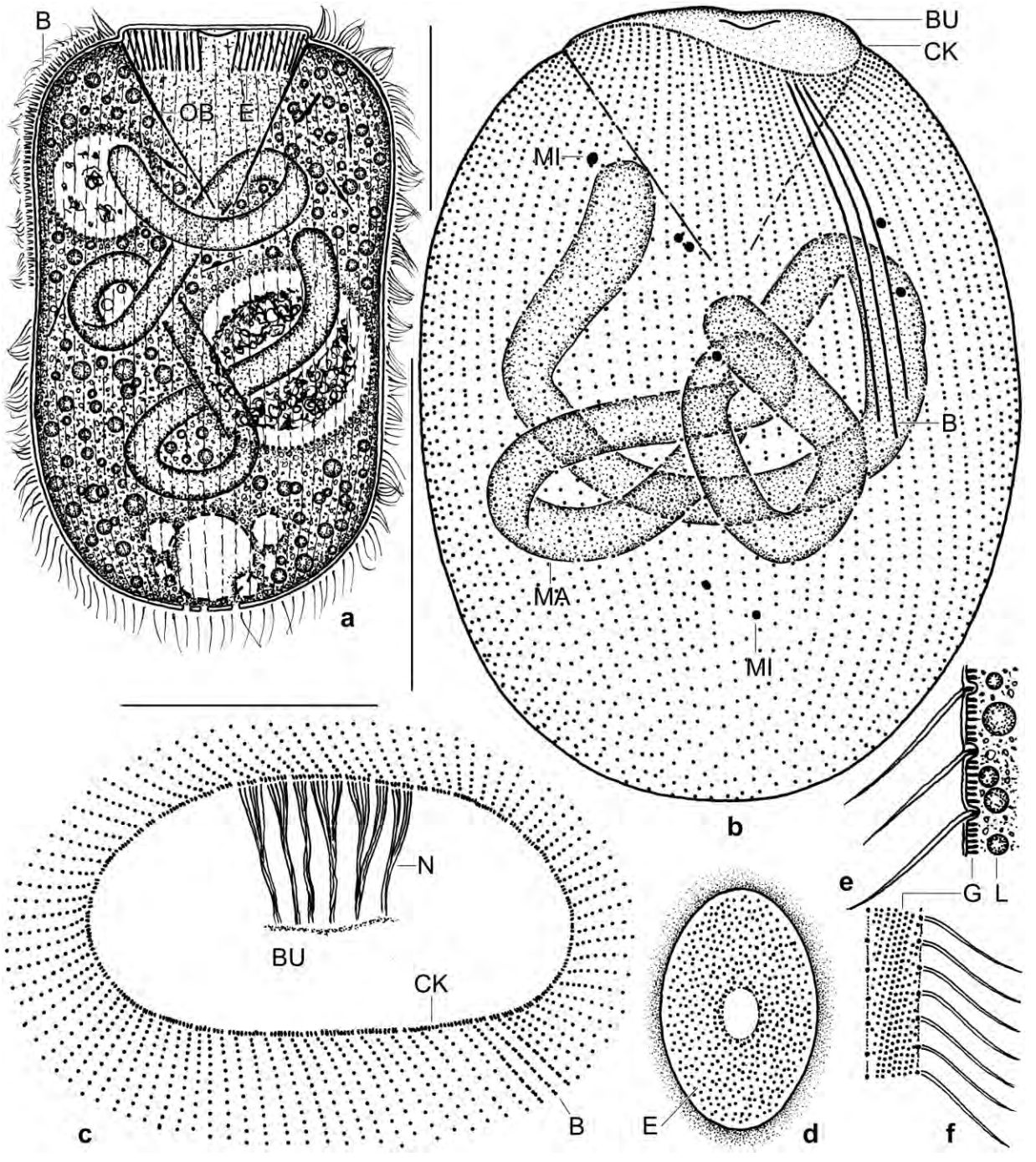

Fig. 51a–f. *Enchelyodon monoarmatus monoarmatus* from life (a, d–f) and after protargol impregnation (b, c). **a:** Right side view of a representative, slightly dumbbell-shaped specimen, length 160 µm. Note the huge oral basket and oral bulge, the tortuous macronucleus, and a large food vacuole with a decaying *Euplotes*. **b:** Dorsolateral view of holotype specimen, showing ciliary pattern and nuclear apparatus, length 120 µm. For details on dorsal brush, see Fig. 51g. **c:** Frontal view of a partially broken specimen, showing the large, elliptic oral bulge and the nematodesma bundles forming the oral basket. **d:** Frontal view of oral bulge studded with extrusomes; outline according to the values in Table 19. **e, f:** Optical section and surface view, showing cortical granulation. B – dorsal brush, BU – oral bulge, CK – circumoral kinety, E – extrusomes (toxicysts), G – cortical granulation, L – lipid droplet, MA – macronucleus, MI – micronuclei, N – nematodesmata (oral basket rods), OB – oral basket. Scale bars 25 µm (c) and 50 µm (a, b).

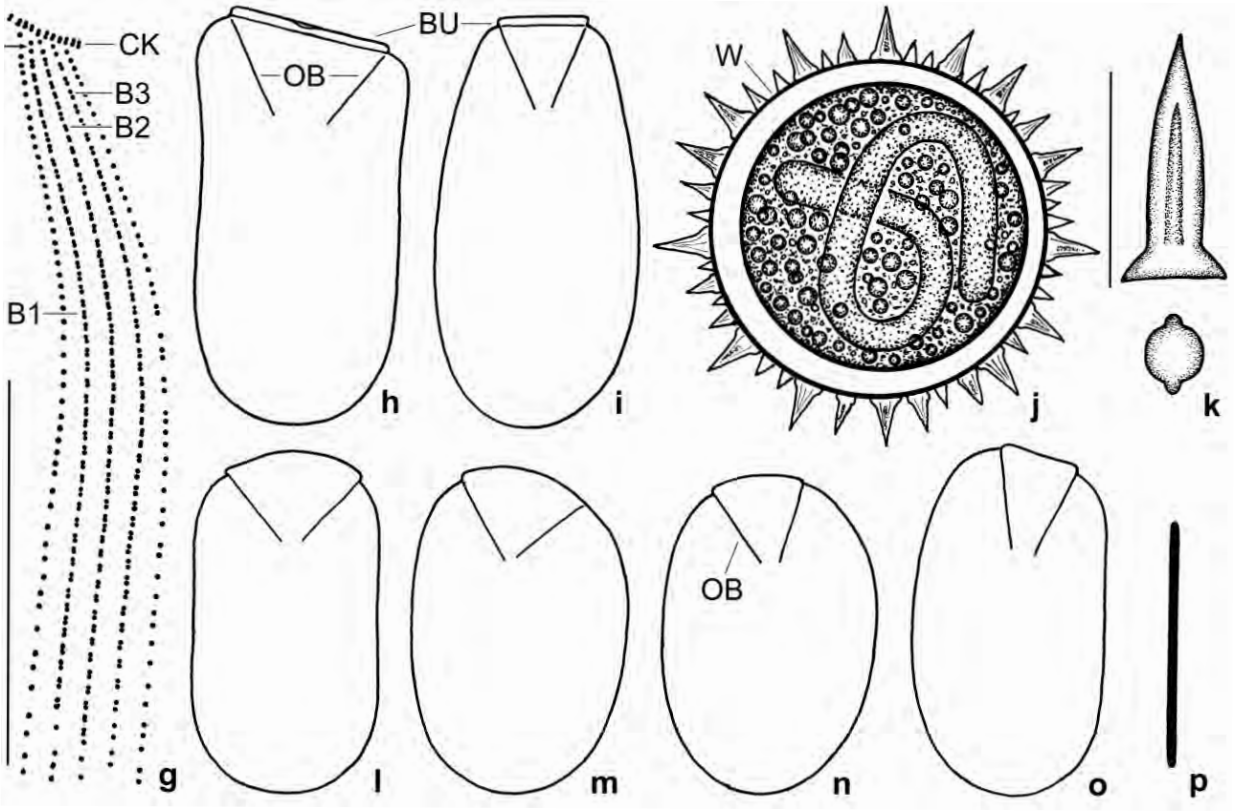

Fig. 51g–p. *Enchelyodon monoarmatus monoarmatus* from life (h, i–k, p), after protargol impregnation (g), and after silver nitrate impregnation (l–o). **g:** Dorsal brush of holotype specimen shown in Fig. 51b. The brush is three-rowed, isostichad (all rows of similar length), and composed of very narrowly spaced dikinetids. Each row has a short anterior tail of monokinetids (arrow). **h, i:** Lateral and dorsal view of same specimen, showing conspicuous shape differences and the elliptic oral bulge. **j, k:** Resting cyst. The wall is only 1–1.5 µm thick but has conspicuous spines with more or less distinct ridges. **l–o:** Lateral (l, m) and dorsal (n, o) views, showing shape variability and oral bulge which is, like the cell proper, narrowed laterally, thus becoming elliptical. **p:** Oral bulge extrusome, length 12 µm. B (1–3) – dorsal brush (rows), BU – oral bulge, CK – circumoral kinety, OB – oral basket, W – cyst wall. Scale bars 30 µm (g) and 40 µm (j).

with 55, and row 3 with 48. Oral bulge on average 52 × 36 µm in protargol preparations, usually broadly elliptic. Resting cyst wall about 1 µm thick.

Type locality: Venezuelan site (1), i. e., soil from the floodplain of the Orinoco River in the surroundings of the village of Cabruta, 66°14'W 7°38' N.

Type material: 1 holotype and 3 paratype slides with protargol-impregnated specimens have been deposited in the Biology Centre of the Upper Austrian Museum in Linz (LI). Further, we deposited 4 paratype slides with silver nitrate-impregnated specimens (Chatton-Lwoff method). Relevant specimens have been marked by black ink circles on the coverslip.

Description: The live observations were based on specimens from a non-flooded Petri dish culture, while morphometry and ciliary pattern were studied in cells from pure cultures set up in Eau de Volvic with crashed wheat grains and some ml of the Petri dish culture. This caused strong growth of *Euplotes muscicola*, the preferred food of *Enchelyodon monoarmatus monoarmatus*.

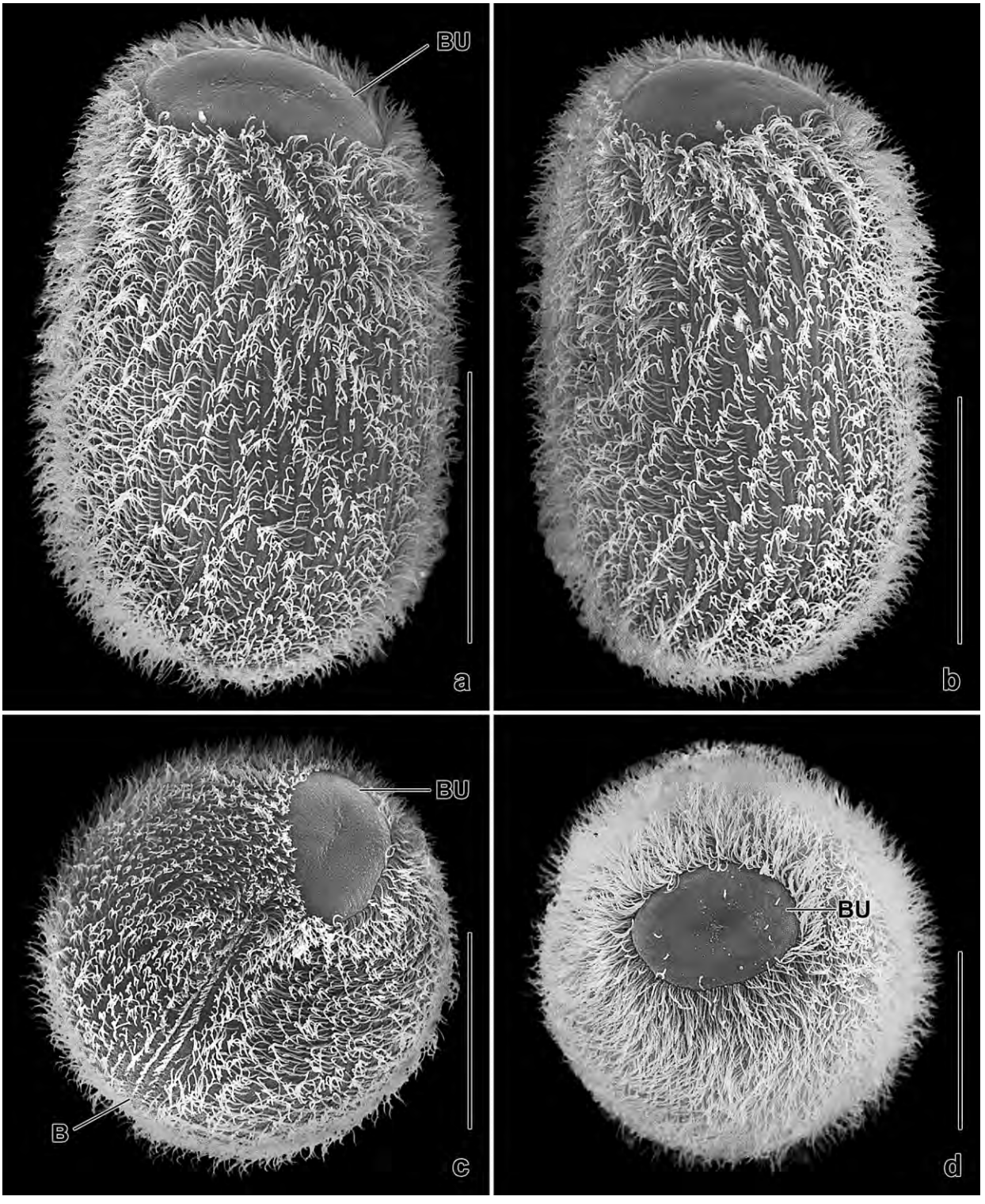

Fig. 52a–d. *Enchelyodon monoarmatus monoarmatus* in the scanning electron microscope. **a, b:** Right side views, showing the massive body, the ovate oral bulge, and metachronal ciliary waves, which are distinct due to the dense ciliation. **c:** Oblique frontal view, showing the ovate oral bulge and the dorsal brush. **d:** Frontal view of a specimen with broadly elliptic oral bulge (see Fig. 52g for a higher magnification). Note the dense ciliation. B – dorsal brush, BU – oral bulge. Scale bars 40 µm (c, d) and 50 µm (a, b).

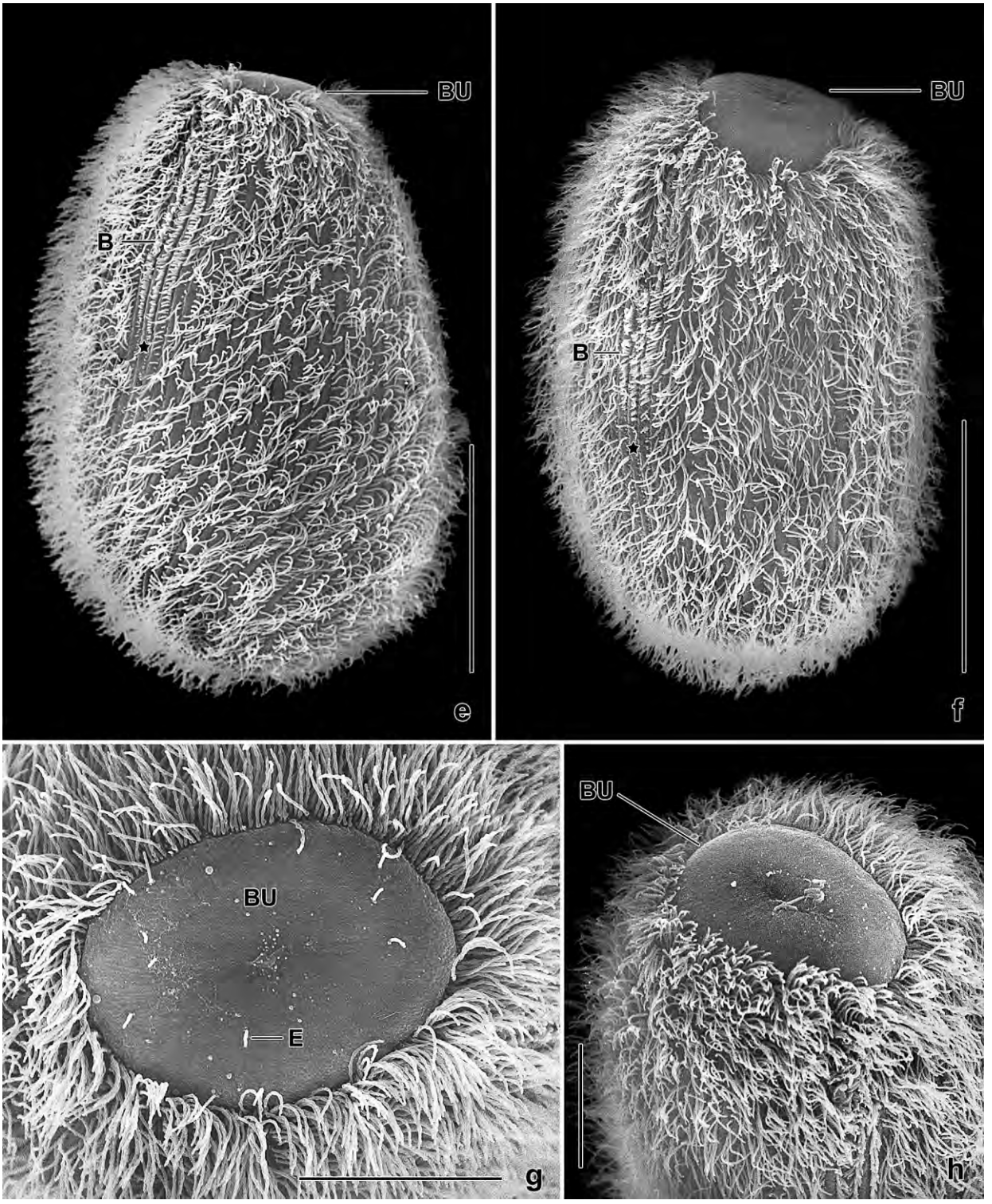

Fig. 52e–h. *Enchelyodon monoarmatus monoarmatus* in the scanning electron microscope. **e, f:** Dorsal views showing an almost circular oral bulge (f) and the dorsal brush (B) posterior of which is a short, barren stripe (asterisks). The oral bulge, which is flat (e) and about 3 µm high in vivo, becomes more or less convex (inflated) due to the preparation procedures (f, h). **g, h:** The shape of the oral bulge is highly variable, viz., circular (f), broadly elliptic (g), or ovate (h). Note the dense ciliation (g). B – dorsal brush, BU – oral bulge, E – extrusomes. Scale bars 20 µm (g, h) and 50 µm (e, f).

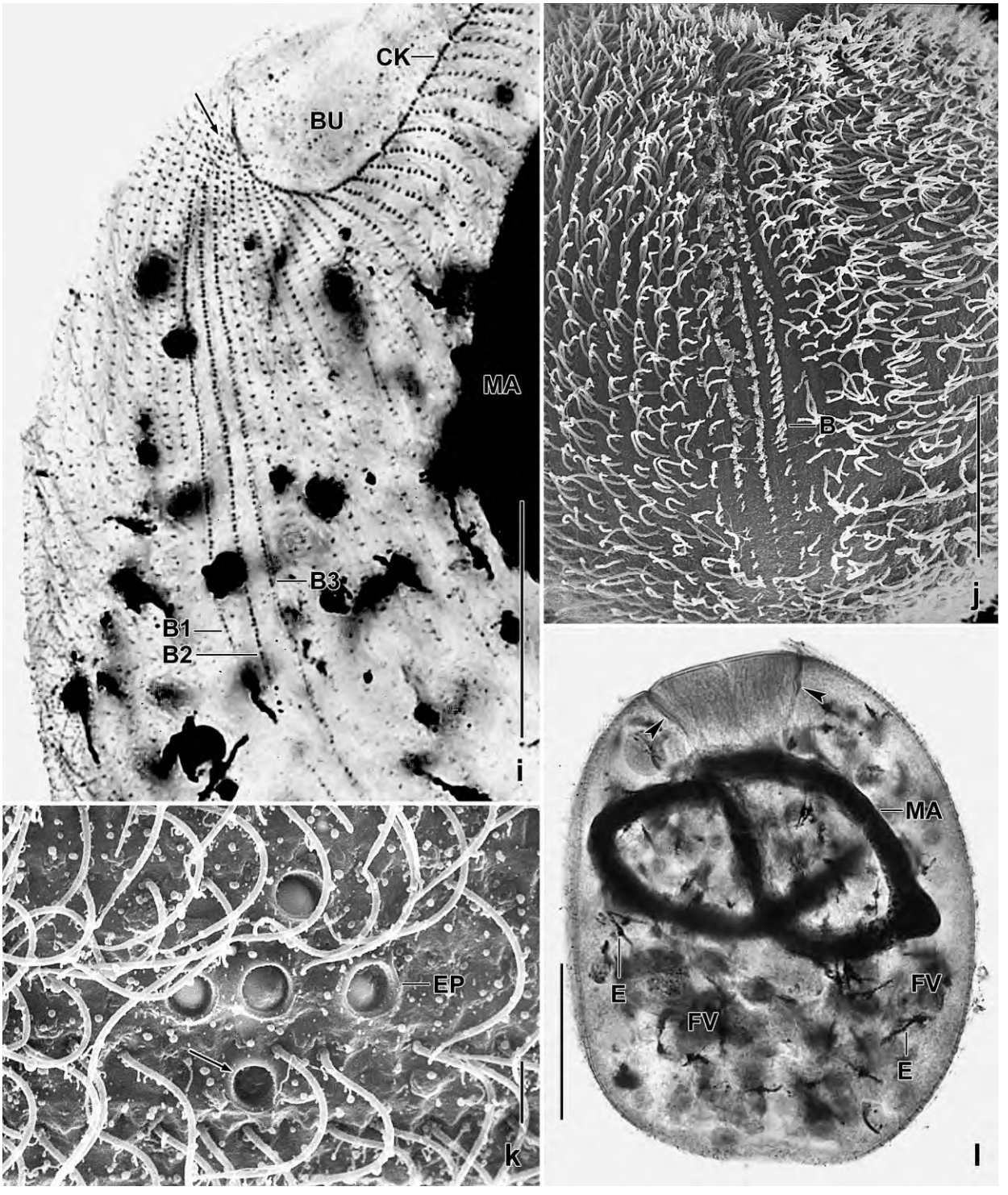

Fig. 52i–l. *Enchelyodon monoarmatus monoarmatus* after protargol impregnation (i, l) and in the scanning electron microscope (j, k). **i, j:** Anterior body half, showing oral apparatus (i) and dorsal brush (i, j). Anteriorly, each brush row has a short tail of ordinary cilia (i, arrow). **k:** Posterior polar view, showing the excretory pores of the contractile vacuole. The pores are closed by a membrane, except of that marked with an arrow. **l:** Overview showing the large oral basket (arrowheads) and the tortuous macronucleus. Developing extrusomes are fusiform. B (1–3) – dorsal brush (rows), BU – oral bulge, CK – circumoral kinety, E – developing extrusomes, EP – excretory pores, FV – food vacuoles, MA – macronucleus. Scale bars 2 µm (k), 20 µm (j), 30 µm (i), and 50 µm (l).

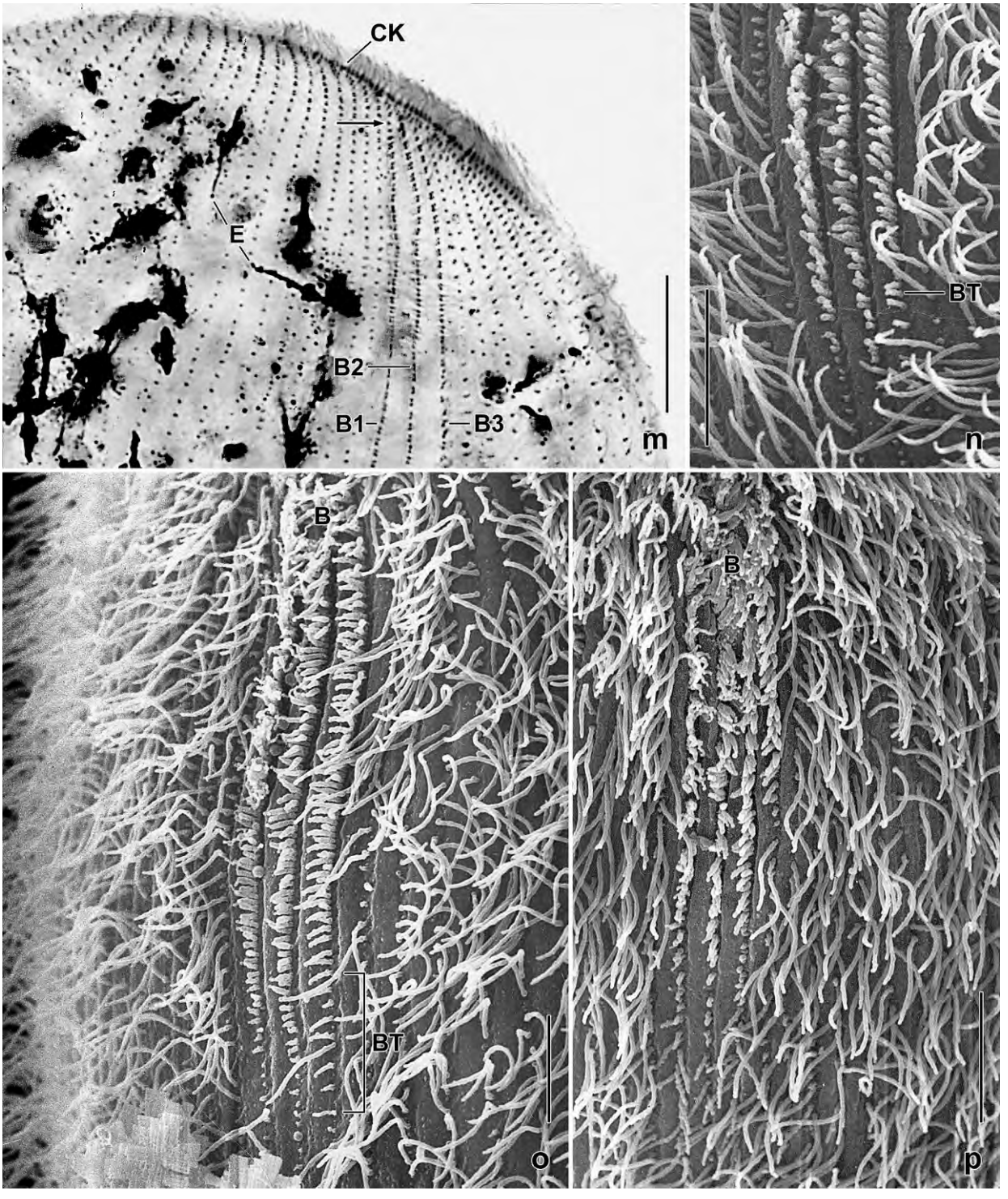

Fig. 52m–p. *Enchelyodon monoarmatus monoarmatus*, dorsal brush after protargol impregnation (m) and in the scanning electron microscope (n–p). The brush consists of three rows of very narrowly spaced dikinetids (m) associated with up to 4 µm long, slightly clavate bristles (n–p). Anteriorly, the rows have a short, monokinetal tail of ordinary cilia (m, arrow). Posteriorly, the bristles strongly decrease in length and row 3 shows a short, monokinetal bristle tail (n, o); then, the rows proceed with ordinary cilia to posterior body end (p). B (1–3) – dorsal brush (rows), BT – monokinetal bristle tail, CK – circumoral kinety, E – developing extrusomes. Scale bars 10 µm.

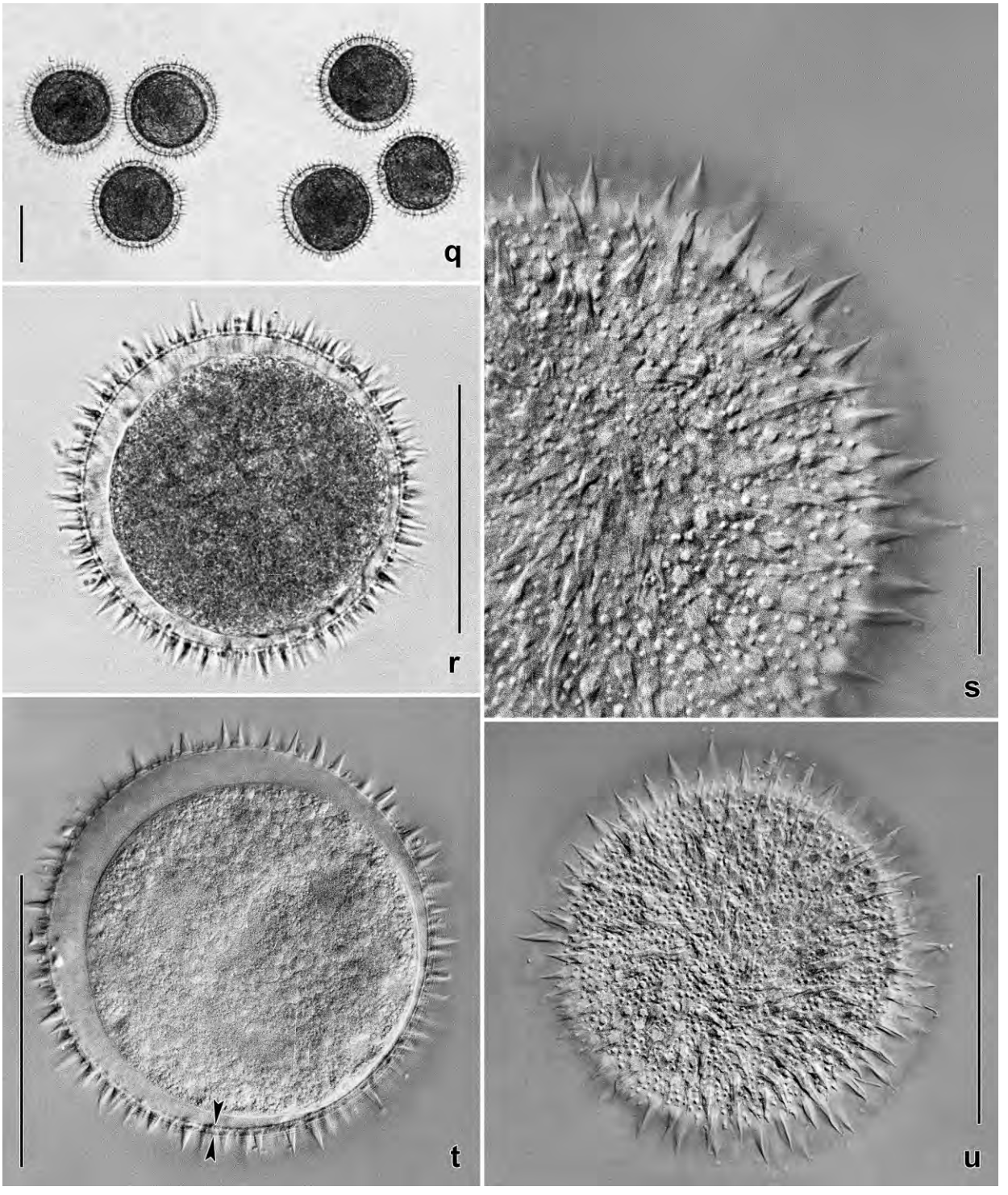

Fig. 52q–u. *Enchelyodon monoarmatus monoarmatus*, mature resting cysts from life under the bright field (q, r) and interference contrast microscope (s–u). The cysts have a diameter of about 80 µm and an about 1.5 µm thick wall (t, arrowheads) studded with 1–12 µm long spines; they are colourless but appear dark under low magnification due to the compact contents (q, r). When mature, the cyst contents shrinks, producing a hyaline area between wall and specimen (r, t). The hyaline area appears as a bright ring in the bright field microscope (q). The cyst contents is composed of the cell organelles and countless lipid droplets up to 5 µm across. Scale bars 10 µm (s) and 50 µm (q, r, t, u).

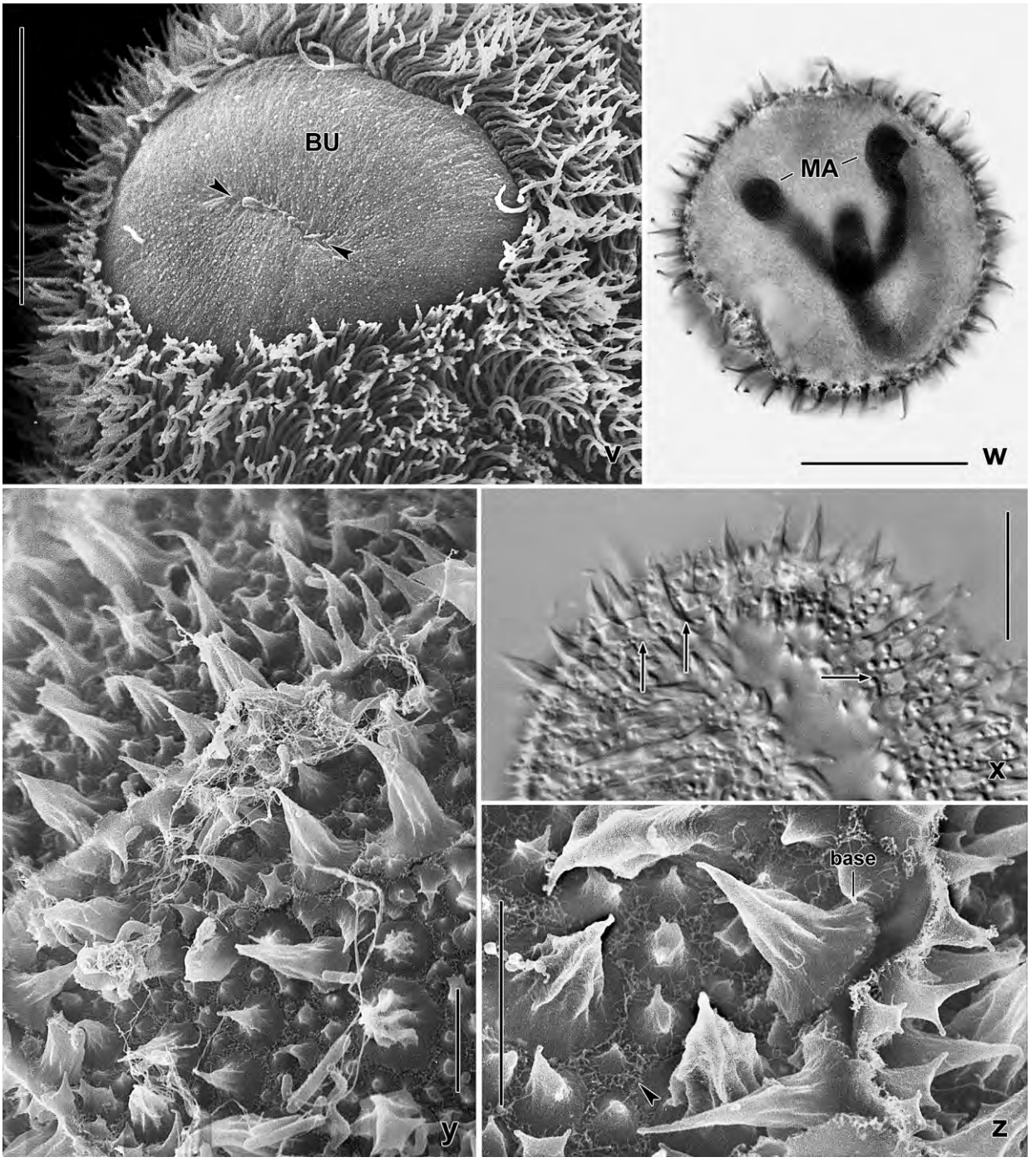

Fig. 52v–z. *Enchelyodon monoarmatus monoarmatus* from life (x), after protargol impregnation (w), and in the scanning electron microscope (v, y, z). **v:** Frontal view, showing the ovate oral bulge surrounded by a very dense ciliature. The arrowheads mark the line where the bulge opens, i. e., where the postciliary microtubule ribbons, which originate from the circumoral dikinetids, plunge into the oral basket. **w:** Resting cyst, showing the macronucleus shortened by about 50% relative to the trophic specimen. The cyst spines impregnate distinctly. **x:** In optical section, the long cyst spines are quadrangular (arrows). **y, z:** The spines, which are up to 12 µm long and have a broad base (z), are sharp like needles and show distinct ribs and furrows recognizable also with interference contrast (x). The surface of the cyst wall is covered by reticulate, likely slimy material (z, arrowhead). BU – oral bulge, MA – macronucleus. Scale bars 5 µm (y, z), 20 µm (v, x), and 40 µm (w).

However, growth was slow and strongly decreased after some weeks. Likewise, protargol impregnation was difficult due to the thick cortex and the cortical granulation. Of the many preparations made with various fixatives and methods, only a handful good slides remained. Thus, we made also Chatton-Lwoff silver nitrate preparations, where cell shape and size as well as, in some well-impregnated specimens, even kinety number could be counted.

Size 115–200 × 85–125 µm in vivo, on average about 160 × 100 µm, as calculated from some in vivo measurements and the values shown in Table 19 adding 5% preparation shrinkage in the silver nitrate prepared specimens; protargol-impregnated cells smaller by ~ 15% due to the weaker fixation. Length:width ratio 1.2–2.2:1, on average 1.6:1. Shape also highly variable and partially depending on side viewed (Fig. 51a, h, i, l–o, 52a, b, e, f, l; Table 19): ellipsoid to broadly ellipsoid and more or less flattened anteriorly when viewed dorsally or ventrally (dorsal brush in or near midline of cell) while oblong, slightly ovate or dumbbell-shaped when viewed laterally (dorsal brush at cell margin). Anterior body end transverse truncate, rarely more or less oblique, posterior broadly rounded. Macronucleus in central three fifths of cell, strongly and irregularly curved, about twice as long as cell, with many scattered nucleoli occasionally forming a three-dimensional reticulum; rarely broken in two pieces. Micronuclei difficult to identify due to many similar-sized and impregnated cell inclusions (Fig. 51a, b; Table 19). Contractile vacuole in posterior end, during systole surrounded by small adventive vacuoles, canals extending anteriorly absent. Several excretory pores in pole centre (Fig. 51a, 52k). Mature extrusomes scattered in oral bulge, except of bulge centre, very numerous, rod-shaped with narrowed, rounded ends, 12–15 × 0.4 µm in vivo (Fig. 51a, p), do not impregnate with the protargol method used; many developing, deeply impregnating fusiform extrusomes in cytoplasm (Fig. 52i, l, m). Cortex colourless, very flexible, hardly furrowed by ciliary rows, 1–1.5 µm thick, contains countless granules forming oblique rows between kineties; individual granules very fine, i. e., about 0.8–1 × 0.2 µm in size, impregnate more or less deeply with protargol (Fig. 51e, f). Specimens usually dark under low magnification (< 100 ×) and transmitted light because packed with lipid droplets, food residues and, sometimes, with a big food vacuole containing a *Euplotes muscicola* or, rarely, a *Vorticella* sp. (Fig. 51a). Swims rather slowly by rotation about main body axis.

Cilia about 10 µm long in vivo, arranged in an average of 86 loosely ciliated and narrowly to ordinarily spaced, meridional rows distinctly condensed in oral region while scattered in posterior pole area; abut to circumoral kinety in or in nearly right angles; some rows shortened anteriorly and/or posteriorly; do not form sutures along dorsal brush (Fig. 51a–c, g, 52a, b, d, e–h, i, m; Table 19). Three isostichad, dikinetal brush rows, each about 55 µm long and thus occupying roughly 43% of body length; each row with some ordinary cilia anteriorly and a minute tail posteriorly, especially row 3, composed of 1 µm long bristles; posterior of brush a small non-ciliated area in some cells; specimens with broken or irregular brush rows very rare. Brush bristles only up to 3 µm long in vivo, their length gradually decreasing to less than 1 µm posteriorly; oblong to slightly clavate and very narrowly spaced, making brush difficult to investigate, even with the scanning electron microscope (Fig. 51a–c, g, 52c, e, f, i, j, m–p; Table 19). Brush row 1 composed of an average of 52 dikinetids. Brush row 2 composed of an average of 55 dikinetids. Brush row 3 composed of an average of 48 dikinetids, posterior bristle of dikinetids shortened by about 50% (Fig. 52o; Table 19).

Oral bulge very large, i. e., on average 52 × 34 µm in protargol preparations, but inconspicuous in lateral view because only 2–3 µm high (Table 19). Shape highly variable, according to the SEM micrographs: usually broadly elliptical, rarely ovate, slightly pyriform, or almost circular (Fig. 51c, d, 52a–h, v); slightly furrowed by transverse microtubule ribbons originating from circumoral dikinetids and extending into the slightly concave bulge centre (Fig. 51c, 52v). Circumoral kinety associated with about 50 µm long nematodesmata, forming a conspicuous, obconical basket studded with extrusomes (Fig. 51a–d, h, 52g, i, m; Table 19).

Resting cyst (Fig. 51j, k, 52q–u, w–z): The cysts are spherical with an average diameter of 80.1 µm when the spines are included (M = 80, SD = 6, SE = 1.1, CV = 7.4, Min = 70, Max = 95, n = 27). The yellowish, spinose wall is – for this kind of ciliates – conspicuously thin, viz., 1–1.5 µm. There are two size types of spines: the large type is 4–12 µm long, conical to elongate conical, and has an up to 5 µm wide baseplate while the spine proper is quadrangular and shows two to several flat ridges in optical section; the small type is up to 4 µm long, conical, and smooth.

The cyst contents is colourless and mainly composed of lipid droplets 0.5–5 µm across. The tortuous macronucleus is shortened by about 50%. When cysts became older, the contents separates from the wall (Fig. 51j, 52q, r, t).

Occurrence and ecology: This species occurred in the same sample as → *E. isostichos,* i. e., in alluvial, clayic, rather acidic (pH 5.2) soil covered with a thin litter layer visibly bound together by whitish fungal hyphae. The sample was taken under a few leguminose trees about 100 m off the river bank. The body shape indicates that *E. monoarmatus monoarmatus* is not a soil ciliate but a floodplain "contaminate".

Remarks: See *E. monoarmatus pyriformis* for discussion.

Enchelyodon monoarmatus pyriformis **nov. sspec.** (Fig. 53a–y, 54a–i, 55a–v; Table 19)

Diagnosis: Size of cultivated specimens about 140 × 100 µm; obovate or pyriform in broad side view. Cortex 1.5–2 µm thick, studded with granules about 2 × 0.3 µm in size. On average 115 ciliary rows; dorsal brush row 1 with 64 dikinetids, row 2 with 74, and row 3 with 60. Oral bulge on average 60 × 40 µm in protargol preparations, usually ovate or pyriform. Resting cyst wall about 4 µm thick.

Type locality: Soil from the Chobe River, Kabolebole Peninsula, southern Africa, 17°50' E 25°S.

Type material: 1 holotype and 3 paratype slides with protargol-impregnated specimens have been deposited in the Biology Centre of the Upper Austrian Museum in Linz (LI). Relevant specimens have been marked by black ink circles on the coverslip.

Etymology: *pyriformis* (pear-shaped) refers to body shape.

Description and **Remarks**: Instead of providing an ordinary description, as for *E. monoarmatus monoarmatus*, we emphasize the differences of the two subspecies. Further, the rich illustration

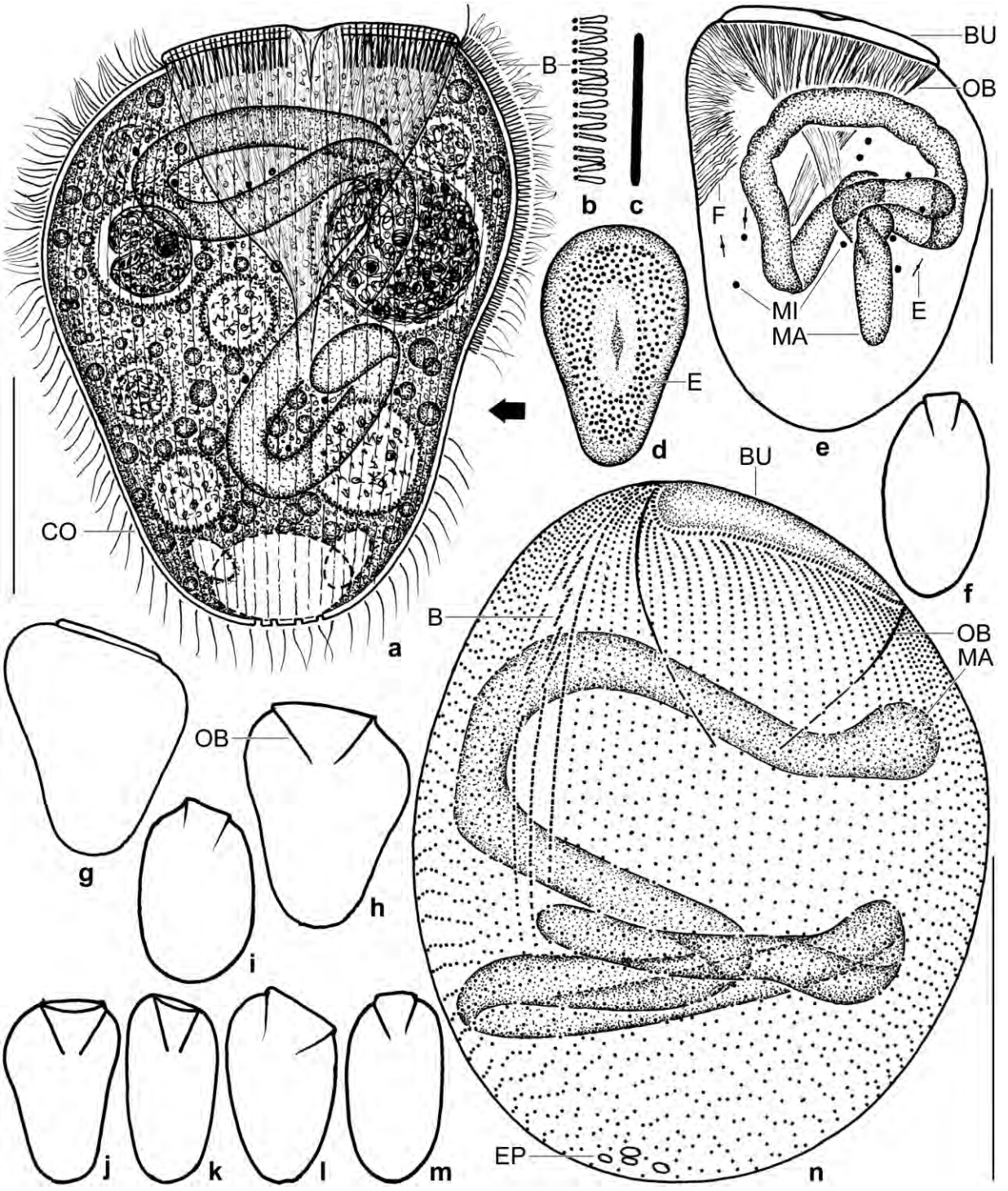

Fig. 53a–n. *Enchelyodon monoarmatus pyriformis* from life (a–d, f–m) and after protargol impregnation (e, n). **a:** Left side view of a representative specimen, length 140 µm. The arrow marks the unciliated post-brush area. **b:** Part of dorsal brush with 4 µm long bristles. **c:** Extrusome, 10 µm. **d:** Frontal view of oral bulge. **e:** Nuclear apparatus and fibres. **f–m:** Live shapes redrawn from micrographs; (j, k) show the same specimen in lateral and dorsal view. **n:** Ciliary pattern of right side and macronucleus of holotype specimen, length 108 µm. B − dorsal brush, BU – oral bulge, CO – cortex, E – extrusomes, EP – excretory pores, F – fibres, MA – macronucleus, MI – micronuclei, OB – oral basket. Scale bars 50 µm.

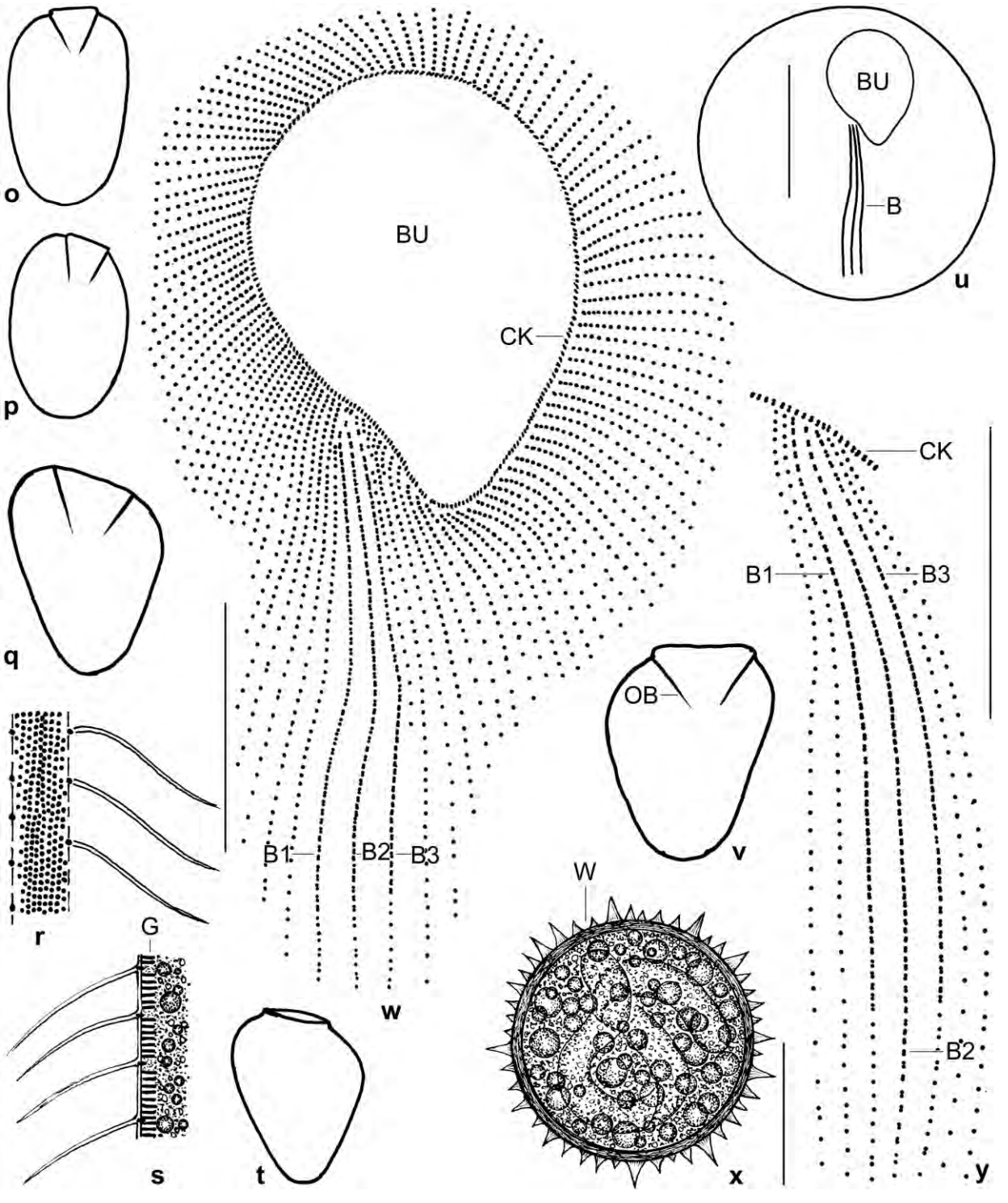

Fig. 53o–y. *Enchelyodon monoarmatus pyriformis* from life (o–t, v, x) and after protargol impregnation (u, w, y). **o–q, t, v:** Live shapes redrawn from micrographs. **r, s:** Surface view and optical section of cortex, showing the dense granulation. **u, w:** Oblique frontal view, showing the pyriform oral bulge and the dorsal brush. **x:** The spiny resting cysts are about 100 µm across and have a 4 µm thick wall. **y:** Circumoral kinety and isostichad dorsal brush, both composed of dikinetids. B (1–3) – dorsal brush (rows), BU – oral bulge, CK – circumoral kinety, G – cortical granules, OB – oral basket, W – cyst wall. Scale bars 25 µm (w, y) and 50 µm (u, x).

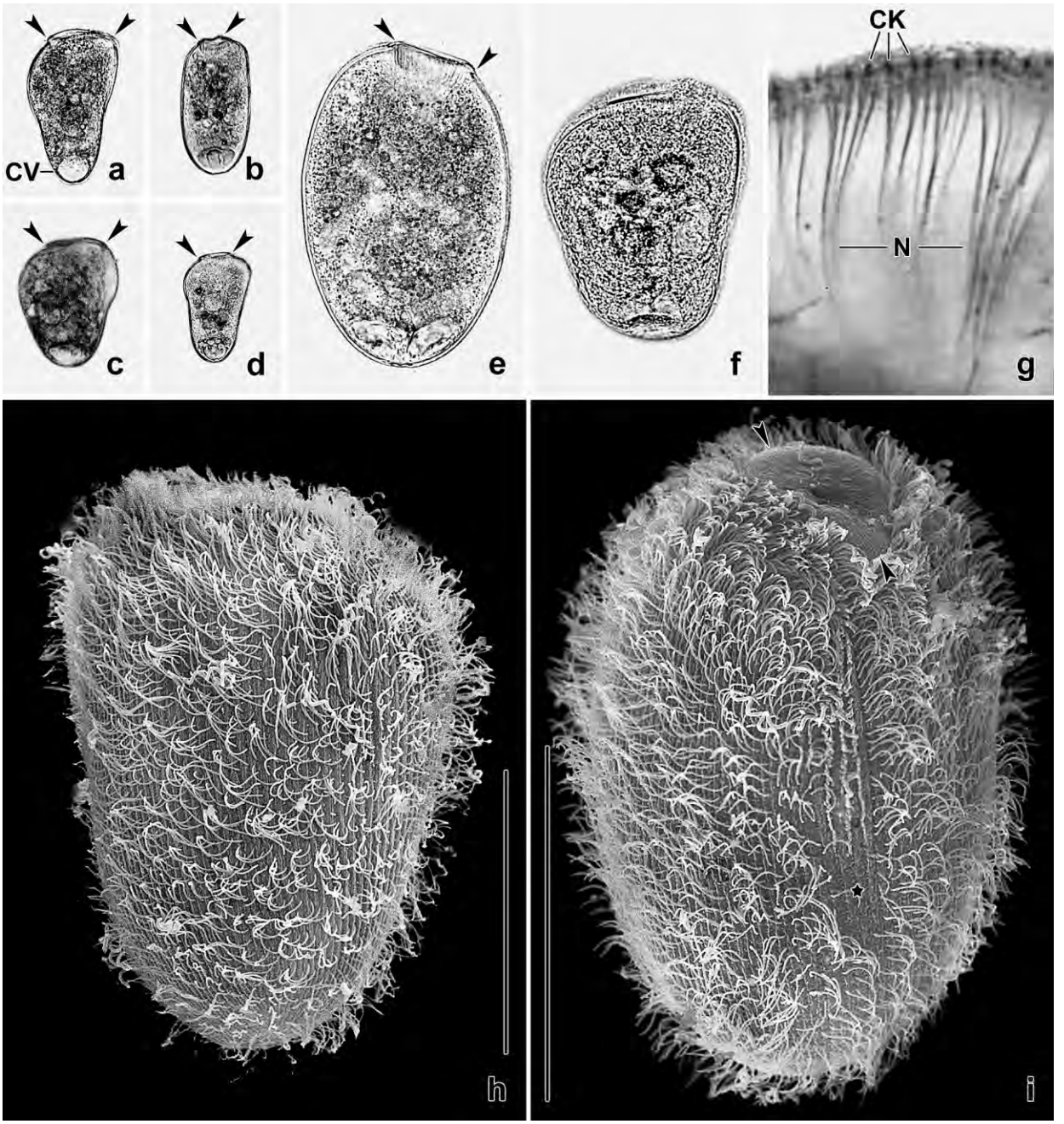

Fig. 54a–i. *Enchelyodon monoarmatus pyriformis* from life (a–e; 100–160 µm), after fixation with osmium vapours (f), after protargol impregnation (g), and in the scanning electron microscope (h, i). **a, b:** This subspecies is distinctly asymmetric: pyriform in lateral view, while ellipsoid in ventral and dorsal view. Likewise, the oral bulge has a long and a short axis (arrowheads). **c, d, f:** Many cells are slightly to distinctly pyriform, becoming ellipsoidal in protargol preparations (Fig. 55b, c) and obovate in the SEM (Fig. 55a). Arrowheads mark the pyriform oral bulge. **e:** Disturbed cells become ellipsoidal and open the oral bulge (arrowheads). **g:** Long nematodesmata originate from the dikinetal circumoral kinety and form a large oral basket (Fig. 55b, c, e). **h:** Lateral view of an obovate specimen (possibly pyriform in live). **i:** In dorsal view, *E. monoarmatus pyriformis* is ellipsoid. Note the barren post-brush area (asterisk) and the pyriform oral bulge (opposed arrowheads). CK – circumoral kinety, CV – contractile vacuole, N – nematodesmata (oral basket rods). Scale bars 60 µm (h, i).

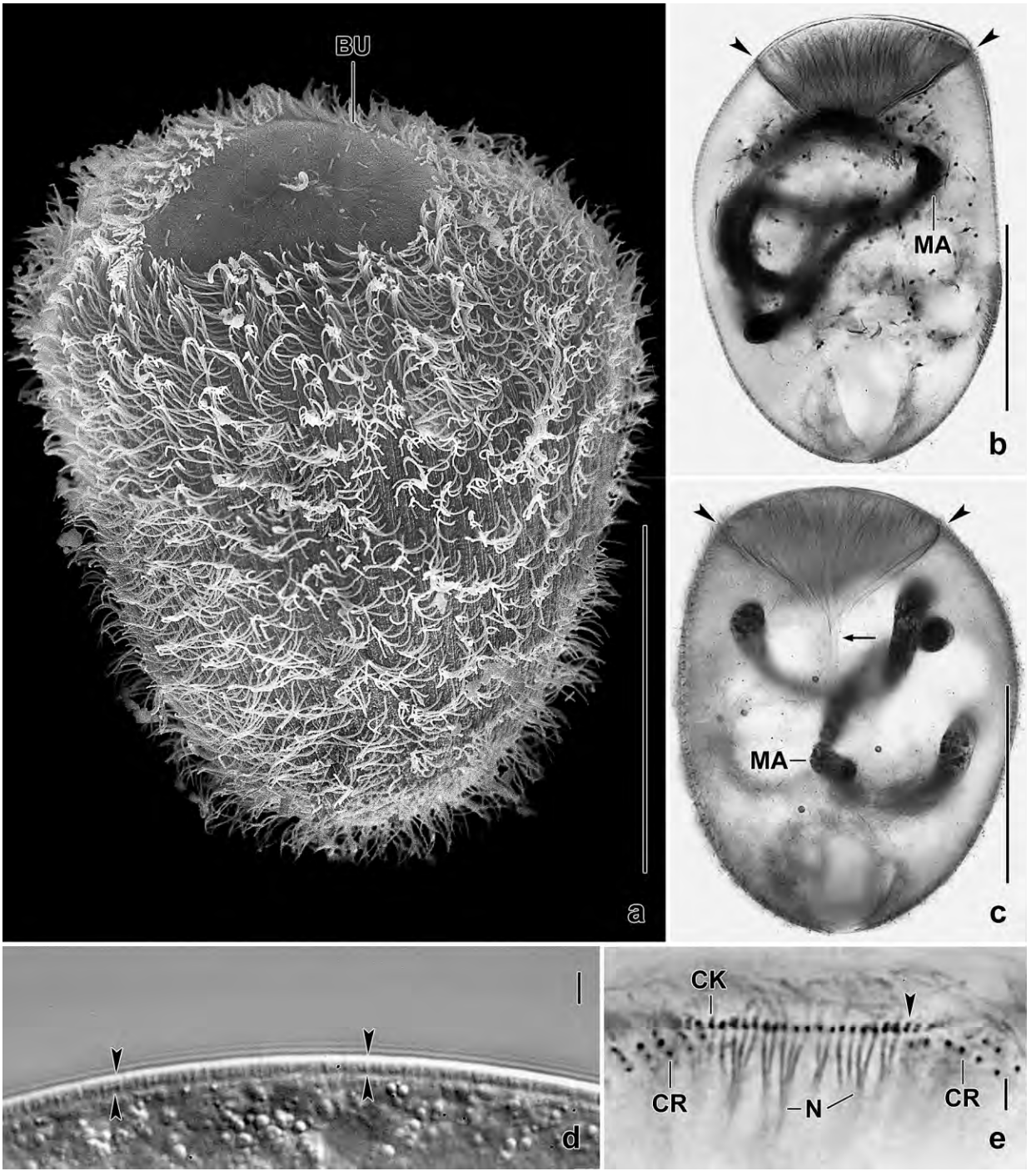

Fig. 55a–e. *Enchelyodon monoarmatus pyriformis* from life (d), after protargol impregnation (b, c, e), and in the scanning electron microscope (a). **a:** Lateral view of a typical specimen with obovate body and pyriform oral bulge. **b, c:** Lateral overviews, showing the enormous oral basket (arrowheads) and the tortuous macronucleus. The arrow (c) marks the mushroom-like narrowing of the proximal region of the oral basket. **d:** Optical section, showing the about 2 µm thick cortex (opposed arrowheads) and the oblong cortical granules. **e:** Part of the circumoral kinety, which is composed of obliquely arranged dikinetids (arrowhead) producing nematodesmata (oral basket rods). BU – oral bulge, CK – circumoral kinety, CR – ciliary rows, L – lipid droplets, MA – macronucleus, N – nematodesmata. Scale bars 5 µm (d, e) and 50 µm (a–e).

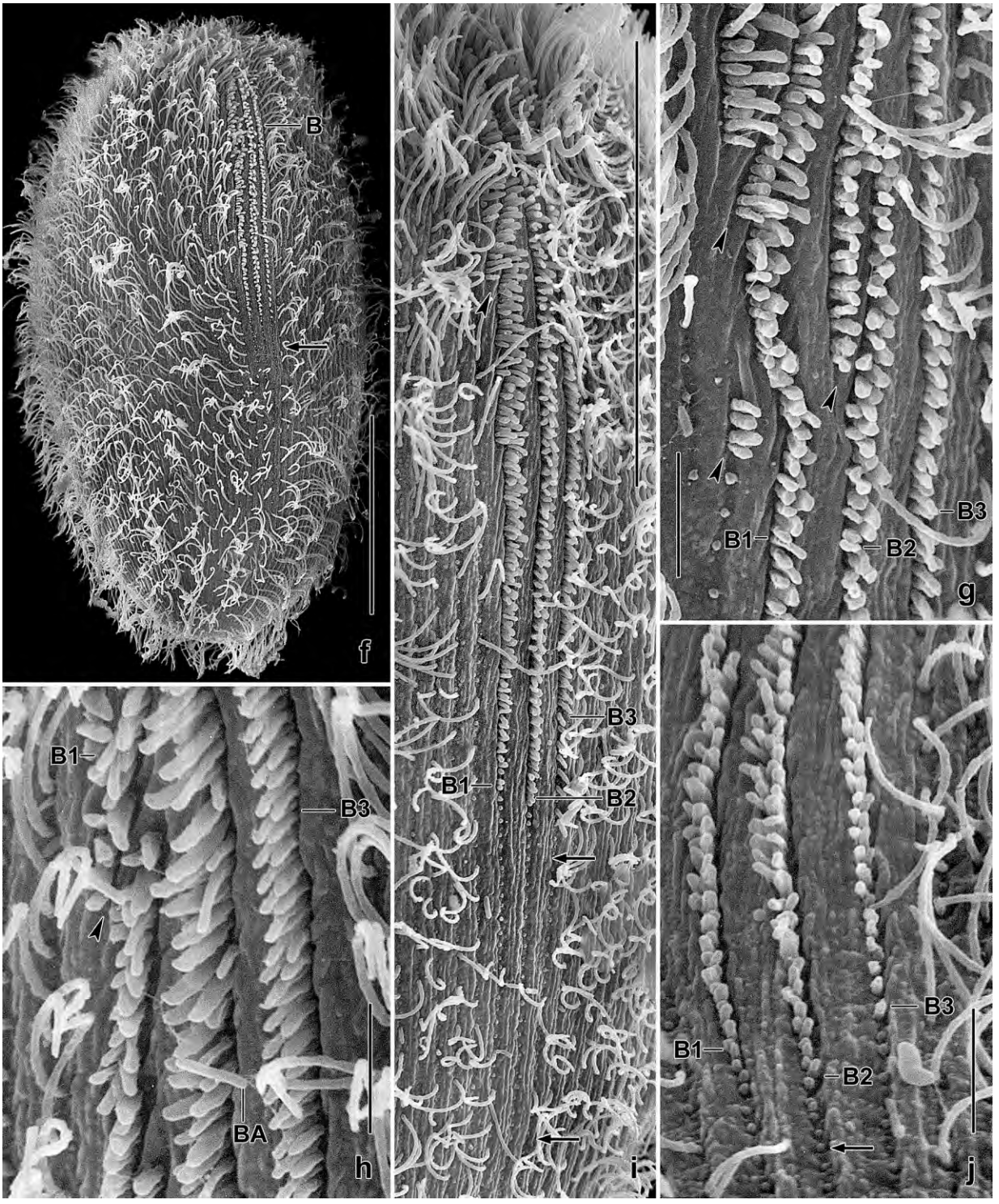

Fig. 55f–j. *Enchelyodon monoarmatus pyriformis*, dorsal brush in the SEM. The brush consists of three isostichad rows of very narrowly spaced dikinetids with up to 5 µm long bristles, which gradually decrease to 1 µm long stumps posteriorly. **f, i:** Overview and dorsal brush with barren post-brush area marked by arrows. **g, h:** Anterior brush region, frequently showing broken rows (arrowheads). **j:** Posterior brush region merging into barren post-brush area (arrow). BA – bacterium, B(1–3) – dorsal brush (rows). Scale bars 5 µm (g, h, j) and 40 µm (a, i).

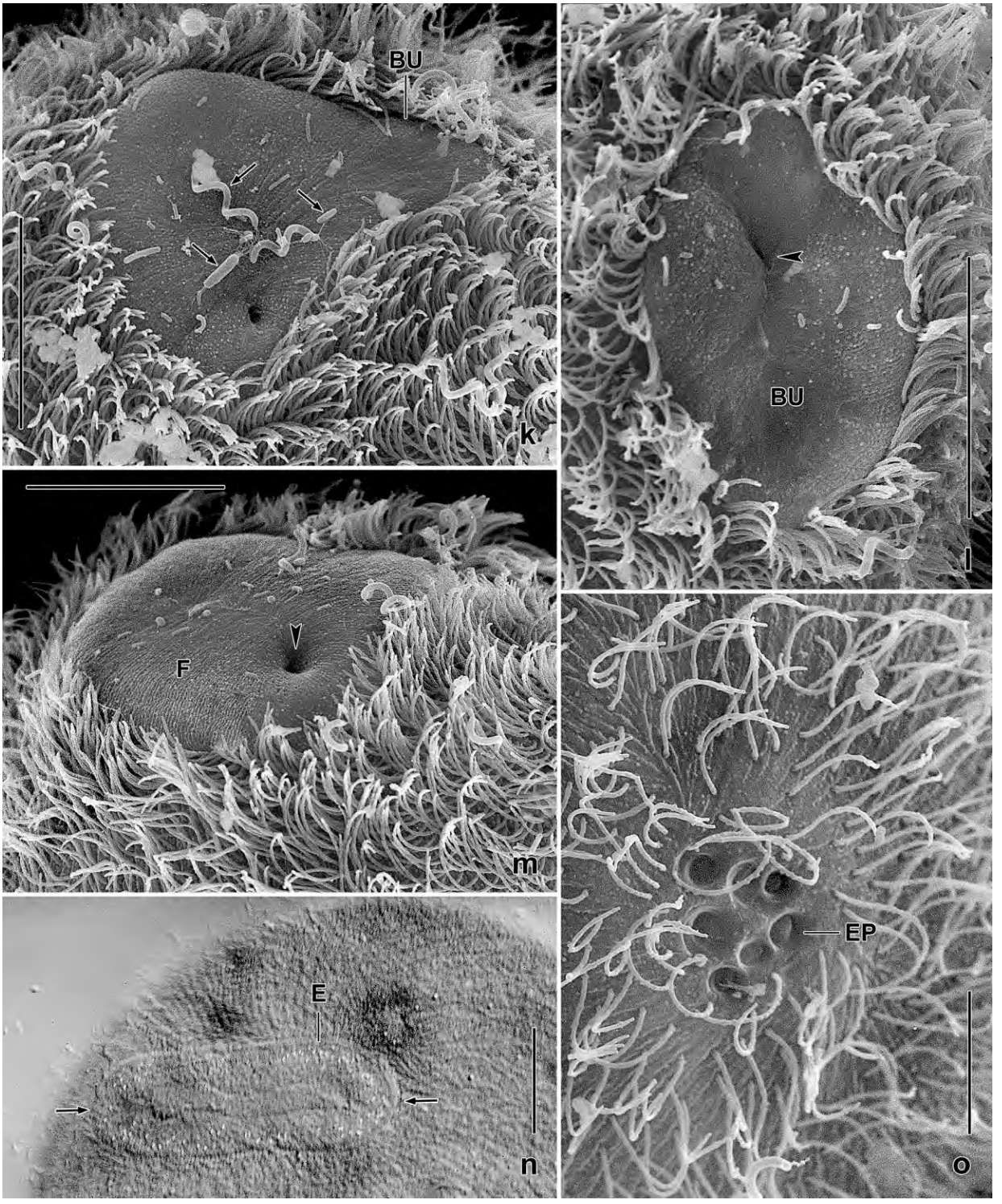

Fig. 55k–o. *Enchelyodon monoarmatus pyriformis* from life (n) and in the SEM (k–m, o). **k–m:** The oral bulge is pyriform (k), elliptic (l), or roughly circular (m). Arrows mark bacteria, arrowheads denote bulge centre. **n:** When disturbed by mild coverslip pressure, the oral bulge becomes elongate elliptic (arrows). **o:** Six excretory pores are in posterior pole centre; some are closed by a membrane while others appear open. BU – oral bulge, E – extrusomes, EP – excretory pores, F – fibres. Scale bars 10 µm (o) and 20 µm (k–n).

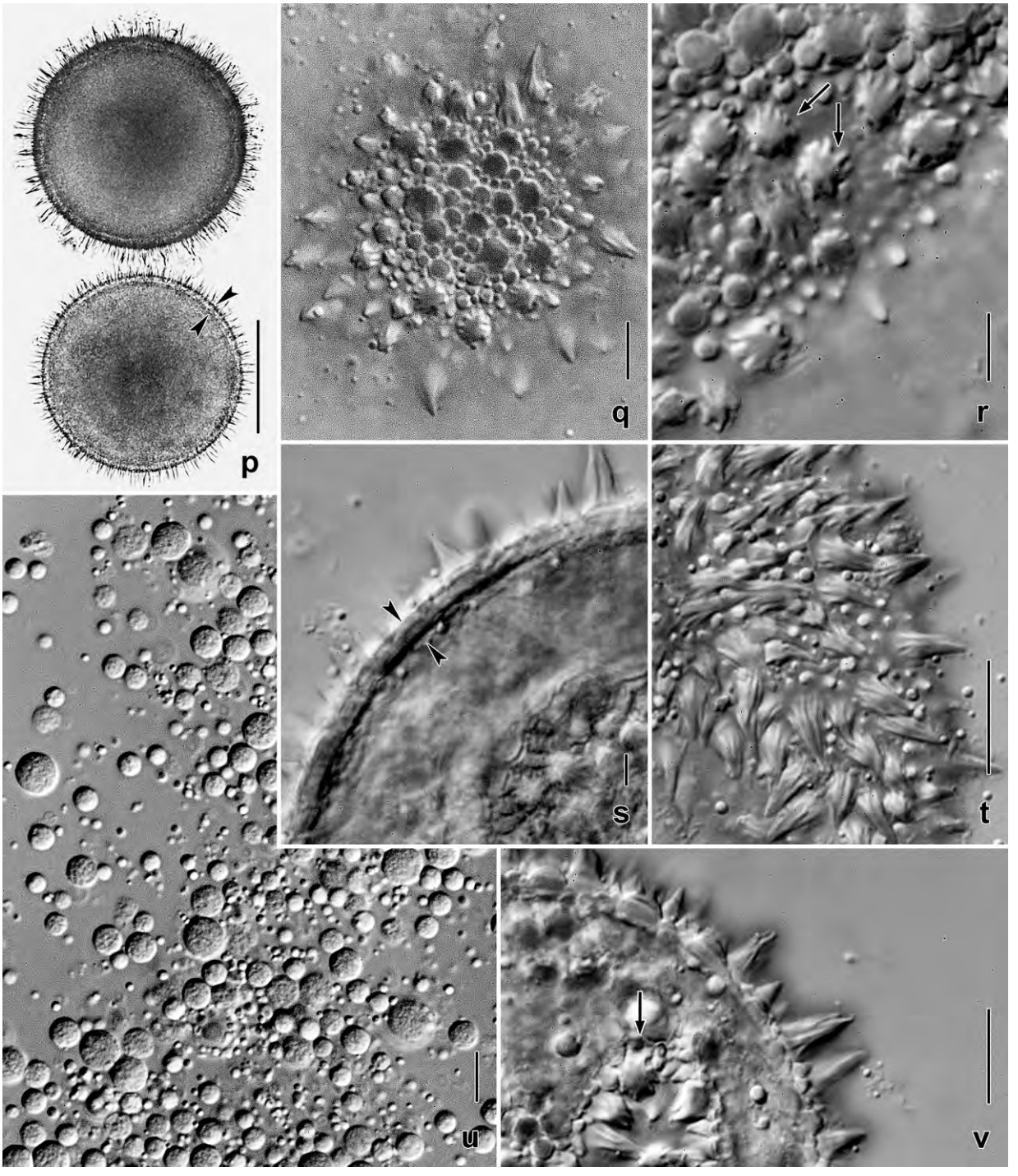

Fig 55p–v. *Enchelyodon monoarmatus pyriformis*, resting cysts from life. **p:** Optical section under bright field illumination. The cysts are spherical, spiny, and have an about 4 µm thick wall (opposed arrowheads). **q:** Surface view, showing the circular transverse view and the very different diameter and length of the spines. **r, t, v:** The cyst spines appear star-like in transverse optical section (r, v) because they have deep furrows. **s:** The cyst wall (opposed arrowheads) is about 4 µm thick. **u:** The cyst's plasm contains countless globular inclusions up to 10 µm in size; the larger globules might be autophagous vacuoles. Scale bars 5 µm (r, s), 10 µm (q, t–v) and 50 µm (p).

should help in identification. There are three main and three minor differences between *E. monoarmatus monoarmatus* and *E. monoarmatus pyriformis*.

(i) Although body shape is sometimes a weak character and frequently poorly preserved in preparations of large species, the differences are too conspicuous to be neglected. Both subspecies are flattened laterally, i. e., when the dorsal brush is in or near the midline of the cell. In this orientation, both are ellipsoidal to broadly ellipsoidal and have a transverse truncate anterior end and a comparatively narrow oral basket (Fig. 53f, i, k, m, o, p, 54b, d, i, 55f). In broad side view, when the dorsal brush is near or at cell margin, *E. monoarmatus pyriformis* is usually obovate or distinctly pyriform and has a more or less oblique anterior end and a wide oral basket (Fig. 53a, e, g, h, j, l, n, q, v, t, 54a, c, f, h, 55a) while *E. monoarmatus monoarmatus* is ovate to ellipsoid and slightly dumbbell-shaped and has a roughly transverse truncate anterior end (Fig. 53a, b, h, i, l–o, 54a, b, e, f). Thus, the length:width ratio is higher in *monoarmatus* than *pyriformis* (1.4:1 vs. 1.3:1; Table 19).

(ii) The cyst wall is about 4 µm thick in *E. monoarmatus pyriformis* (Fig. 55p, s) while only about 1 µm in *E. monoarmatus monoarmatus* (Fig. 54r, t). Although the thickness of the cyst wall may depend on environmental factors (Foissner 2011), this does not apply to the two subspecies of *E. monoarmatus*, both having been isolated from floodplain soil and cultivated with the same method. Further, the spines are more ribbed in *E. monoarmatus pyriformis* than in *E. monoarmatus monoarmatus*.

(iii) The median of the number of ciliary rows is 115 in *E. monoarmatus pyriformis* while 85 in *E. monoarmatus monoarmatus*, corresponding to a difference of 35%. Although there is some overlap, the averages argue for separation of the populations (Table 19).

(iv) The oral bulge is usually more or less pyriform, rarely elliptic, obovate or roughly circular in *E. monoarmatus pyriformis* (Fig. 53d, u, 54i, 55a, k–n) while usually elliptic, rarely indistinctly pyriform, ovate, or roughly circular in *E. monoarmatus monoarmatus*.

(v) The cortex is 1.5–2 µm thick and studded with granules about 2 × 0.3 µm in size in *E. monoarmatus pyriformis* (Fig. 53r, s, 55d) while about 1 µm thick and studded with granules about 0.8 × 0.2 µm in size in *E. monoarmatus monoarmatus* (Fig. 53e, f).

(vi) The barren post-brush area is distinctly larger in *E. monoarmatus pyriformis* (Fig. 54i, 55f, i, j) than in *E. monoarmatus monoarmatus* (Fig. 54e, j, n, p)

Enchelyodon armatides Foissner, Agatha and Berger, 2002 (Fig. 56a–j)

Material: Dominican Republic, site 21 (soil from margin of a mangrove swamp).

Supplementary observations: The Dominican specimens match well the three populations investigated by Foissner et al. (2002). For instance, they have acicular extrusomes and 13–18 ciliary rows ($\bar{x}$ 15.7, M 15.5, SD 1.4, CV 9.0). Here, we supplement the description with scanning electron micrographs, showing some other important features, such as the shape of the oral bulge and details of the dorsal brush.

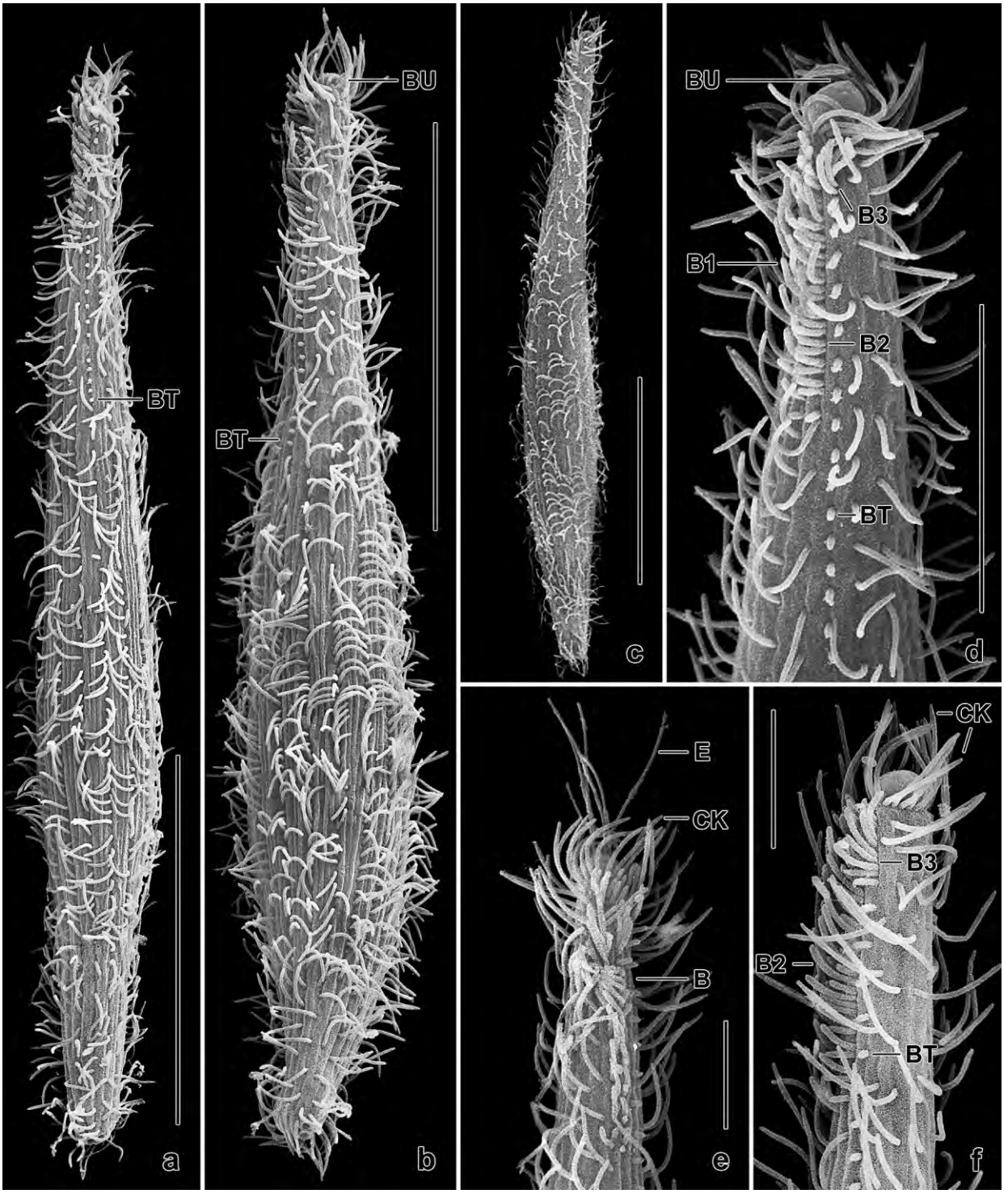

Fig. 56a–f. *Enchelyodon armatides* in the scanning electron microscope. **a–c:** Dorsal overviews, showing shape variability and the monokinetal bristles of dorsal brush row 3 (a, b, BT). **d, f:** Anterior body portion, showing details of the dorsal brush, the circumoral kinety, and the oral bulge. Note the monokinetal bristle tail of brush row 3, which has only a few dikinetids anteriorly (for overviews, see Fig. 56a, b). **e:** Anterior body region, showing exploding toxicysts and the dorsal brush. B (1–3) – dorsal brush (rows), BT – monokinetal bristle tail of brush row 3, BU – oral bulge, CK – circumoral kinety, E – extrusomes (toxicysts). Scale bars 10 µm (f), 20 µm (d, e), and 50 µm (a–c).

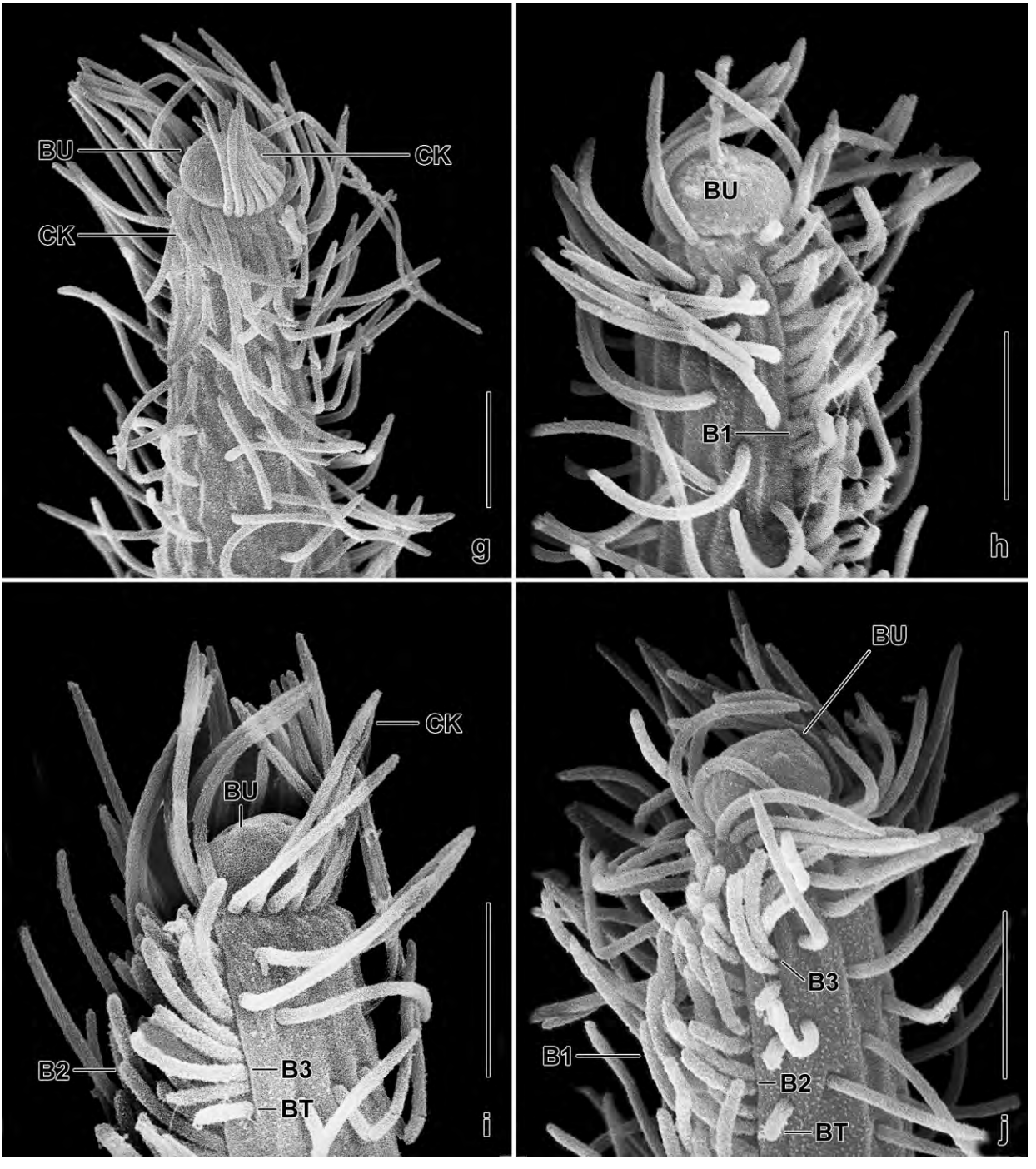

Fig. 56g–j. *Enchelyodon armatides*, anterior region in the scanning electron microscope. Overviews for Fig. (i) and (j), see Fig. (f) and (d) on plate before, respectively. The shape of the oral bulge varies from discoid (g) to hemispheric (j). The bulge is surrounded by narrowly spaced cilia, forming the circumoral kinety (g, i). The cilia, which are not elongated, originate from the dikinetal circumoral kinety whose kinetids have ciliated only one basal body. The dorsal brush consists of three rows with up to 5 μm long bristles (h–j). Row 3 is composed of a short dikinetal portion anteriorly and a long monokinetal tail of minute bristles (i, j and a, b, f of previous plate). B (1–3) – dorsal brush (rows), BT – monokinetal tail of brush row 3, BU – oral bulge, CK – circumoral kinety. Scale bars 5 μm.

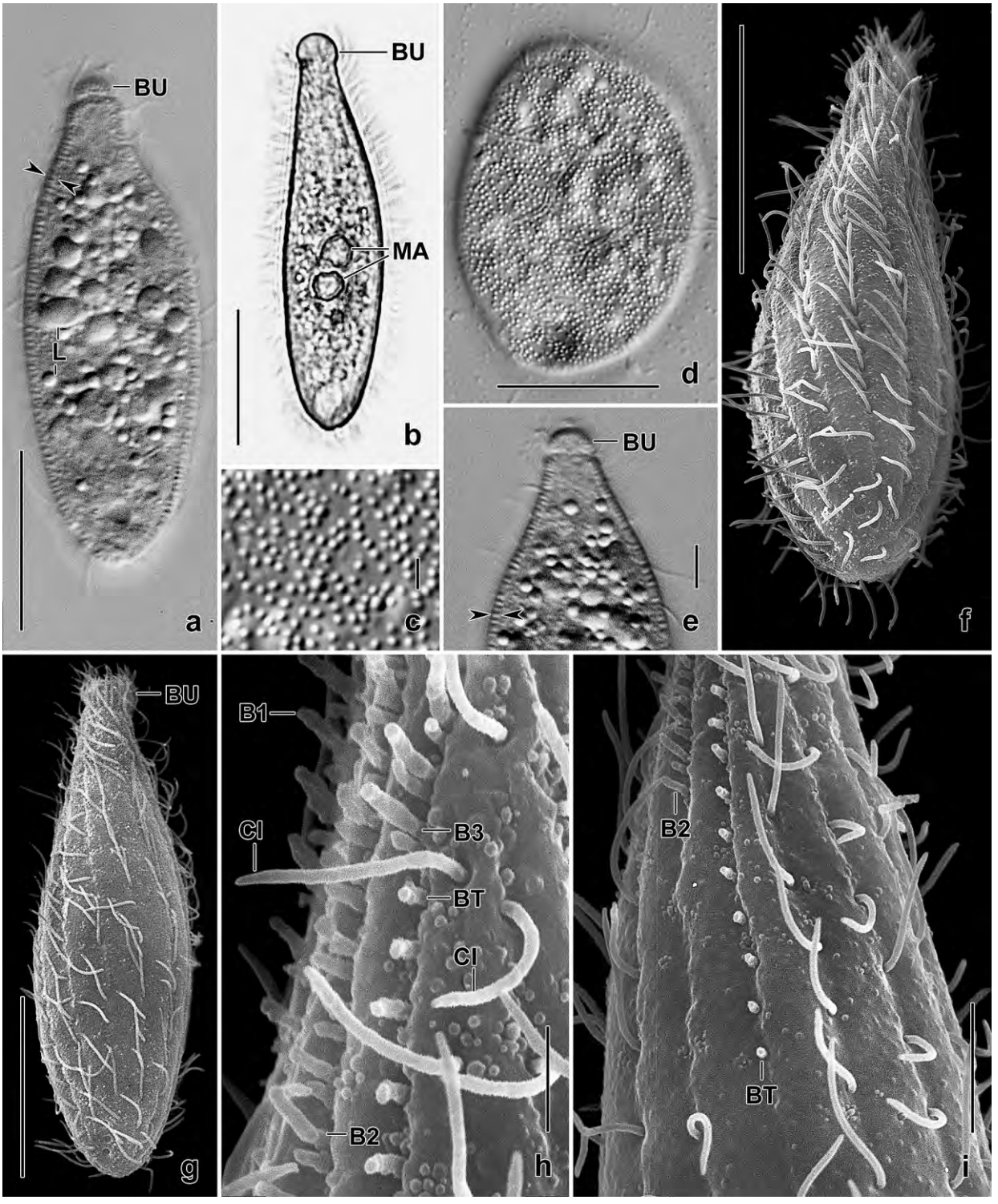

Fig. 57a–i. *Enchelyodon lagenula*, Jamaican (a–e) and Venezuelan (f–i) specimens from life (a–e) and in the SEM (f–i). **a–e:** This ciliate has a hemispheric oral bulge (a, b, e), paired macronuclear nodules (b), and a conspicuous cortical granulation recognizable both, in optical sections (a, e, opposed arrowheads) and in surface views (c, d). **f, g:** Ventral overviews. **h, i:** Details of dorsal brush. B1–3 – dorsal brush rows, BT – tail of brush row 3, BU – oral bulge, CI – ordinary somatic cilia, L – lipid droplets, MA – macronuclear nodules,. Scale bars 2 µm (h), 5 µm (c, e, i), and 20 µm (a, b, d, f, g).

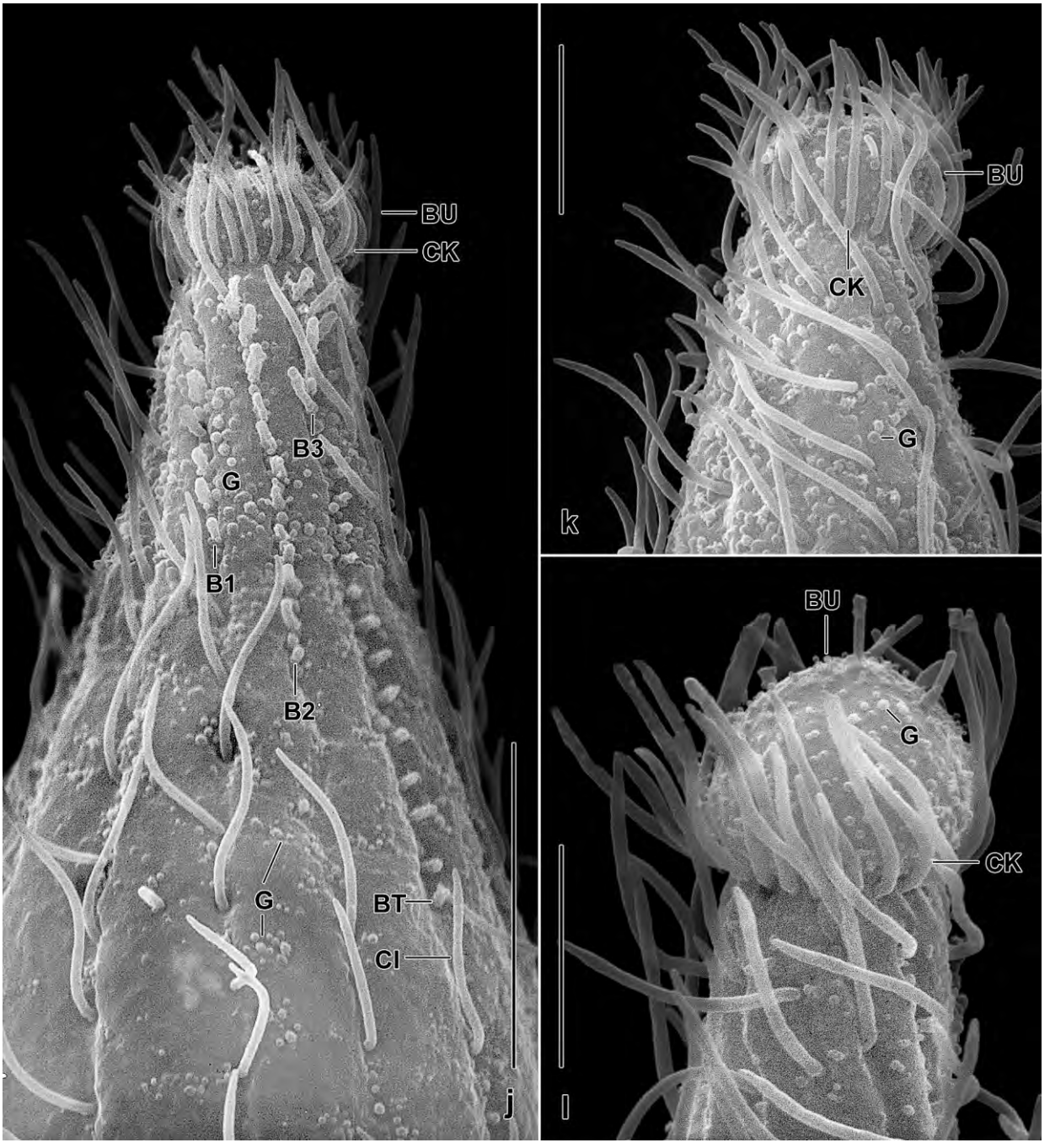

Fig. 57j–l. *Enchelyodon lagenula*, Venezuelan specimens in the scanning electron microscope. **j, k:** Dorsal and ventral view of oral body portion. The circumoral kinety, which consists of dikinetids (Blatterer and Foissner 1988), has ciliated only one basal body of each pair. The dorsal brush consists of three rows of paired bristles; row 3, additionally, has a moderately long posterior tail of monokinetal bristles. Note the massive, hemispheric oral bulge and exploding cortical granules. **l:** A specimen with slightly conic oral bulge. B1–3 – dorsal brush rows, BT – posterior tail of dorsal brush row 3, BU – oral bulge, CI – ordinary somatic cilium, CK – circumoral kinety, G – exploding cortical granules. Scale bars 5 µm (k, l) and 10 µm (j).

The shape of the oral bulge varies from discoid (g) to hemispheric (j). The general structure of the dorsal brush matches the description by Foissner et al. (2002): rows 1 and 2 have a very similar length while the dikinetal portion of row 3 is distinctly shorter. We could not see clearly the bristles of row 1; likely, they are similar to those of row 2 but slightly longer (Fig. 56d, i, j). The middle portion of row 2 is composed of dikinetids with the anterior bristles shorter by about 40% than the about 4 µm long, slightly clavate posterior bristles; at the anterior and posterior end of the row, both bristles are about 2 µm long and oblong (Fig. 56d, f, i, j). Brush row 3 consists of a short dikinetal portion anteriorly, followed by an about 40 µm long tail of monokinetal, about 1 µm long bristles (Fig. 56a, b, d, f, j); the posterior bristle of the dikinetids is slightly shorter than the 3–4 µm long anterior bristle (Fig. 56d, f, i, j).

Occurrence and ecology: *Enchelyodon armatides* occurs not only in the neotropics but also globally. It has been reported from Australia, Namibia, and Tenerife (Foissner et al. 2002) as well as from Austria (Foissner et al. 2005) and Saudi Arabia (Foissner et al. 2008). The habitats range from sand dunes to mangrove soil, suggesting that it is an euryoecious cosmopolite.

Enchelyodon lagenula (Kahl, 1930) Blatterer and Foissner, 1988 (Fig. 57a–l)

Supplementary observations: The specimens from soil of the floodplain of the Pedro River in Jamaica and from soil of Venezuelan site (20) match very well the original description and the redescription by Blatterer and Foissner (1988). Thus, only some micrographs are provided, showing important features of the species, such as the hemispheric (Fig. 57b, e, g, j, k) to conical (Fig. 57l) oral bulge, the paired macronuclear nodules (Fig. 57b), the dense and conspicuous cortical granulation (Fig. 57a, c, d), and the three-rowed dorsal brush having inconspicuous bristles (Fig. 57h–j).

Occurrence and ecology: *E. lagenula* occurs in various terrestrial habitats globally, i. e., is an euryoecious cosmopolite (Foissner 1998) which is, however, rather infrequent and possibly absent from large regions, e. g., Namibia (Foissner et al. 2002).

Coriplites tumidus **nov. spec.** (Fig. 58a–p, 59a–m; Table 20)

Diagnosis (based on three populations): Size about 110 × 20 µm in vivo. Body narrowly obclavate or elongate lenticular and with conspicuous, bulbous anterior end; posterior end narrowly rounded. 2 ellipsoid macronuclear nodules with a micronucleus in between. On average 9–11 ciliary rows, three anteriorly differentiated to a heterostichad dorsal brush occupying 20–27% of body length; brush row 3 shorter than row 2 by about 60% and composed of an average of 6 dikinetids. Oral bulge discoid to hemispheric, comparatively conspicuous because in vivo 4–6 µm high and slightly wider than neck.

Type locality: Needle litter and red surface soil (pH 6) from a small mountain in the outskirts of the town of Alice Springs, Australia, 133°E 24°S.

Type material: 1 holotype and 4 paratype slides with protargol-impregnated specimens have been deposited in the Biology Centre of the Upper Austrian Museum in Linz (LI). Further, 4 and 5 voucher slides each from the Brazilian and the North American populations have been

Table 20. Morphometric data on *Coriplites tumidus* from Australia (AUS, type), Brazil (BRA), and North America (USA). Data based on mounted, protargol-impregnated, and randomly selected specimens from non-flooded Petri dish cultures. Measurements in µm. CV – coefficient of variation in %, M – median, Max – maximum, Mean – arithmetic mean, Min – minimum, n – number of individuals investigated, SD – standard deviation, SE – standard error of arithmetic mean.

Characteristics	Site	Mean	M	SD	SE	CV	Min	Max	n
Body, length	AUS	93.1	91.0	12.1	2.6	13.0	70.0	115.0	21
	BRA	99.9	98.0	14.9	4.5	14.9	75.0	123.0	11
	USA	93.2	95.0	12.8	3.9	13.7	73.0	110.0	11
Body, maximum width	AUS	20.0	19.0	3.8	0.8	19.0	15.0	29.0	21
	BRA	15.8	16.0	2.5	0.8	15.7	11.0	20.0	11
	USA	12.9	12.0	2.1	0.6	16.1	11.0	17.0	11
Body, narrowest neck width	AUS	6.3	7.0	1.1	0.2	16.8	4.0	8.0	21
	BRA	5.6	6.0	1.2	0.4	21.4	4.0	8.0	11
	USA	5.2	5.0	1.0	0.3	18.9	4.0	8.0	11
Body length:width, ratio	AUS	4.8	4.8	0.8	0.2	15.8	2.6	6.0	21
	BRA	6.5	6.2	1.4	0.4	22.0	4.7	9.2	11
	USA	7.4	7.5	1.4	0.4	18.7	5.0	9.2	11
Oral bulge, width	AUS	7.6	7.0	1.1	0.2	14.2	6.0	10.0	21
	BRA	6.5	6.5	1.2	0.4	18.5	4.5	9.0	11
	USA	5.4	5.0	1.3	0.4	23.4	4.0	8.0	11
Oral bulge, height	AUS	4.6	5.0	1.2	0.3	25.5	3.0	8.0	21
	BRA	4.0	3.5	1.2	0.4	29.6	3.0	7.0	11
	USA	3.4	3.0	0.8	0.2	24.5	3.0	6.0	11
Anterior body end to nuclear apparatus	AUS	49.3	49.0	7.5	1.7	15.3	33.0	61.0	21
	BRA	52.0	52.0	9.1	2.7	17.5	36.0	66.0	11
	USA	48.6	47.0	9.5	2.9	19.6	33.0	64.0	11
Macronucleus figure, length	AUS	13.0	13.0	3.0	0.7	23.1	8.0	22.0	21
	BRA	16.8	17.0	2.6	0.8	15.2	14.0	21.0	11
	USA	16.6	18.0	2.5	0.8	15.1	13.0	20.0	11
Macronuclear nodules, length	AUS	8.6	9.0	1.5	0.3	17.4	6.0	11.0	21
	BRA	10.3	10.0	2.4	0.7	23.5	7.0	14.0	11
	USA	10.8	12.0	2.1	0.6	19.3	7.0	14.0	11
Macronuclear nodules, width	AUS	5.3	5.0	0.7	0.2	13.7	4.0	7.0	21
	BRA	5.7	6.0	0.9	0.3	15.8	4.0	7.0	11
	USA	5.3	6.0	0.9	0.3	17.2	4.0	6.0	11
Macronuclear nodules, number	AUS	2.0	2.0	0.0	0.0	0.0	2.0	2.0	21
	BRA	2.0	2.0	0.0	0.0	0.0	2.0	2.0	11
	USA	2.0	2.0	0.0	0.0	0.0	2.0	2.0	11
Micronucleus, length	AUS	1.7	1.5	0.6	0.1	34.0	1.1	3.5	21
	BRA	2.1	2.0	0.5	0.2	23.1	1.5	3.0	10
	USA	1.9	1.8	–	–	–	1.8	2.0	3

continued

Characteristics	Site	Mean	M	SD	SE	CV	Min	Max	n
Micronucleus, width	AUS	1.4	1.3	0.4	0.1	29.8	1.1	3.0	21
	BRA	1.4	1.5	0.5	0.2	37.8	0.8	2.5	10
	USA	1.6	1.8	–	–	–	1.0	2.0	3
Micronucleus, number	AUS	1.0	1.0	0.0	0.0	0.0	1.0	1.0	21
	BRA	1.0	1.0	0.0	0.0	0.0	1.0	1.0	14
	USA	1.0	1.0	–	–	–	1.0	1.0	3
Ciliary rows, number	AUS	10.6	11.0	0.6	0.1	5.7	9.0	11.0	21
	BRA	9.5	9.0	0.5	0.2	5.5	9.0	10.0	11
	USA	10.2	10.0	0.4	0.1	4.0	10.0	11.0	11
Ciliated kinetids in a ventral kinety, number	AUS	29.1	28.0	4.9	1.1	16.9	22.0	40.0	21
	BRA	31.9	33.0	3.6	1.2	11.3	27.0	36.0	11
	USA	26.1	27.0	4.0	1.9	15.2	20.0	31.0	11
Dorsal brush row 1, length (from circumoral kinety to last dikinetid)	AUS	22.7	22.0	3.1	0.7	13.5	17.0	27.0	21
	BRA	19.1	19.0	2.7	0.8	14.3	15.0	25.0	11
	USA	16.4	15.0	3.4	1.0	20.5	11.0	22.0	11
Dorsal brush row 1, number of dikinetids	AUS	12.9	13.0	1.3	0.3	10.2	10.0	16.0	21
	BRA	10.6	10.0	1.8	0.5	16.6	8.0	13.0	11
	USA	10.4	11.0	1.6	0.5	15.1	7.0	12.0	11
Dorsal brush row 2, length	AUS	25.6	25.0	4.5	1.0	17.5	18.0	39.0	21
	BRA	21.7	21.0	2.6	0.8	12.0	18.0	27.0	11
	USA	18.5	19.0	3.9	1.2	21.0	12.0	25.0	11
Dorsal brush row 2, number of dikinetids	AUS	15.9	16.0	1.8	0.4	11.2	12.0	19.0	21
	BRA	13.0	13.0	1.5	0.5	11.4	11.0	16.0	11
	USA	13.4	14.0	1.8	0.5	13.1	10.0	16.0	11
Dorsal brush row 3, length	AUS	10.9	10.0	2.1	0.5	19.2	8.0	15.0	21
	BRA	9.0	9.0	1.3	0.4	14.9	7.0	11.0	11
	USA	8.5	8.0	2.3	0.7	27.7	6.0	14.0	11
Dorsal brush row 3, number of dikinetids	AUS	6.6	6.0	1.1	0.2	16.4	5.0	9.0	21
	BRA	6.2	6.0	1.0	0.3	15.9	5.0	8.0	11
	USA	5.7	6.0	0.9	0.3	15.8	4.0	7.0	11
Dorsal brush rows, number	AUS	3.0	3.0	0.0	0.0	0.0	3.0	3.0	21
	BRA	3.0	3.0	0.0	0.0	0.0	3.0	3.0	11
	USA	3.0	3.0	0.0	0.0	0.0	3.0	3.0	11

deposited in the same repository. The holotype and other relevant specimens have been marked by black ink circles on the coverslip.

Etymology: The Latin adjective *tumidus* (swollen) refers to the bulbous oral bulge.

Description: We investigated three populations, whose morphology and morphometrics match so well that conspecificity is beyond reasonable doubt. Thus, we merge all data, except when deviating more than usual.

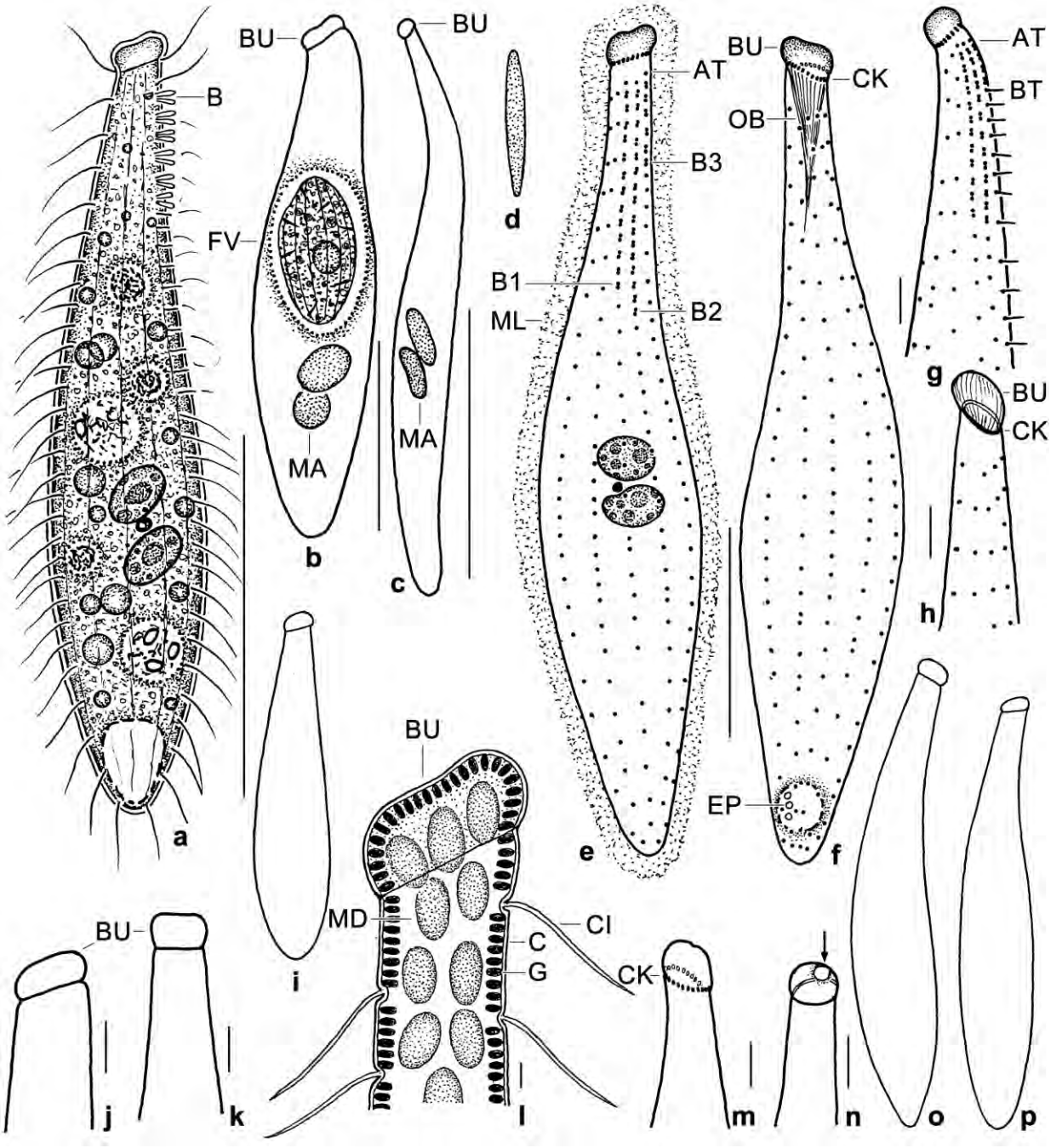

Fig. 58a–p. *Coriplites tumidus* from life (a, d, i, l, o, p) and after protargol impregnation (b, c, e–h, j, k, m, n). **a:** Left side view of a representative, slightly claviform specimen, length 110 µm. **b:** A Brazilian specimen having just ingested a *Sathrophilus muscorum*. **d:** Exploded mucocyst, 10 µm. **e, f:** Dorso- and ventrolateral view of Australian holotype specimen, length 100 µm. **g:** Dorsolateral view of a Brazilian specimen. **h:** Ventrolateral view of an Australian specimen, showing the elliptical circumoral kinety. **i, o, p:** Outline of specimens from Brazil, Australia, and the Robinson Island, length 80 µm, 100 µm, 100 µm. **j, k:** Oral bulge of an Australian and a Brazilian specimen. **l:** Slightly schematized view of anterior body portion, showing the highly refractive cortical granules and the absence of oral bulge toxicysts; their space is occupied by pale mitochondria. **m, n:** Oral bulge of Australian specimens; arrow marks central concavity. AT – anterior tail of brush rows, B(1–3) – dorsal brush (rows), BT – posterior tail of brush row 3, BU – oral bulge, C – cortex, CK – circumoral kinety, CI – somatic cilium, EP – excretory pores, FV – food vacuole, G – cortical granules, MA – macronuclear nodules, MD – mitochondrium, ML – mucous layer, OB – oral basket,. Scale bars 2 µm (l), 5 µm (g, h, j, k, m, n), 25 µm (b, e, f) and 50 µm (a, c).

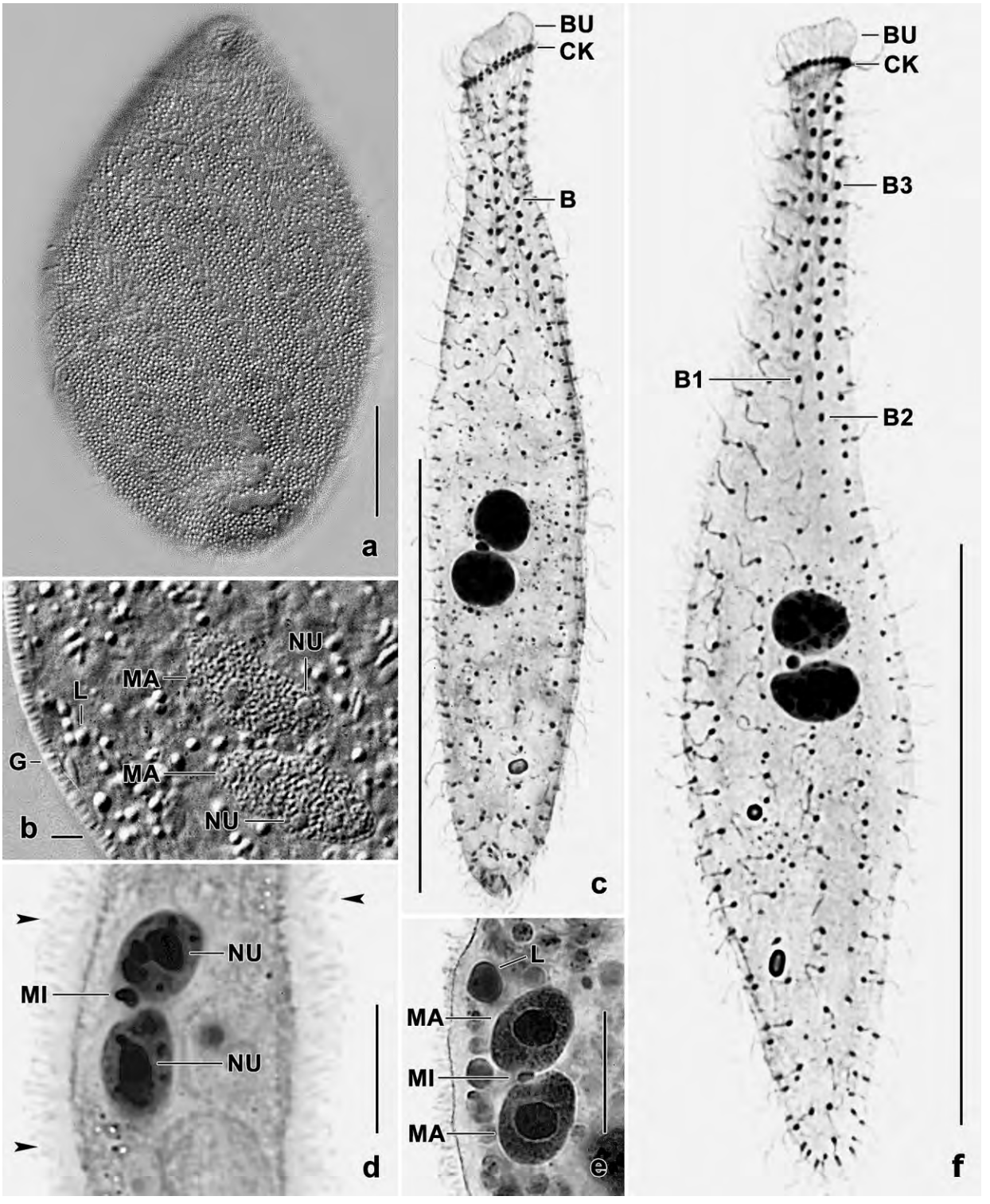

Fig. 59a–f. *Coriplites tumidus* from life (a, b) and after protargol impregnation (c–f). **a, b:** Surface view and optical section, showing the strongly refractive cortical granules and the two macronuclear nodules. **d, e:** Nuclear apparatus, showing a reniform micronucleus in left specimen. Arrowheads mark mucous coat. **c, f:** Dorsolateral overviews. B(1–3) – dorsal brush (rows), BU – oral bulge, CK – circumoral kinety, G – cortical granules, L – lipid droplets, MA – macronuclear nodules, MI – micronucleus, NU – nucleoli. Scale bars 5 µm (b), 10 µm (d, e), 20 µm (a), and 50 µm (c, f).

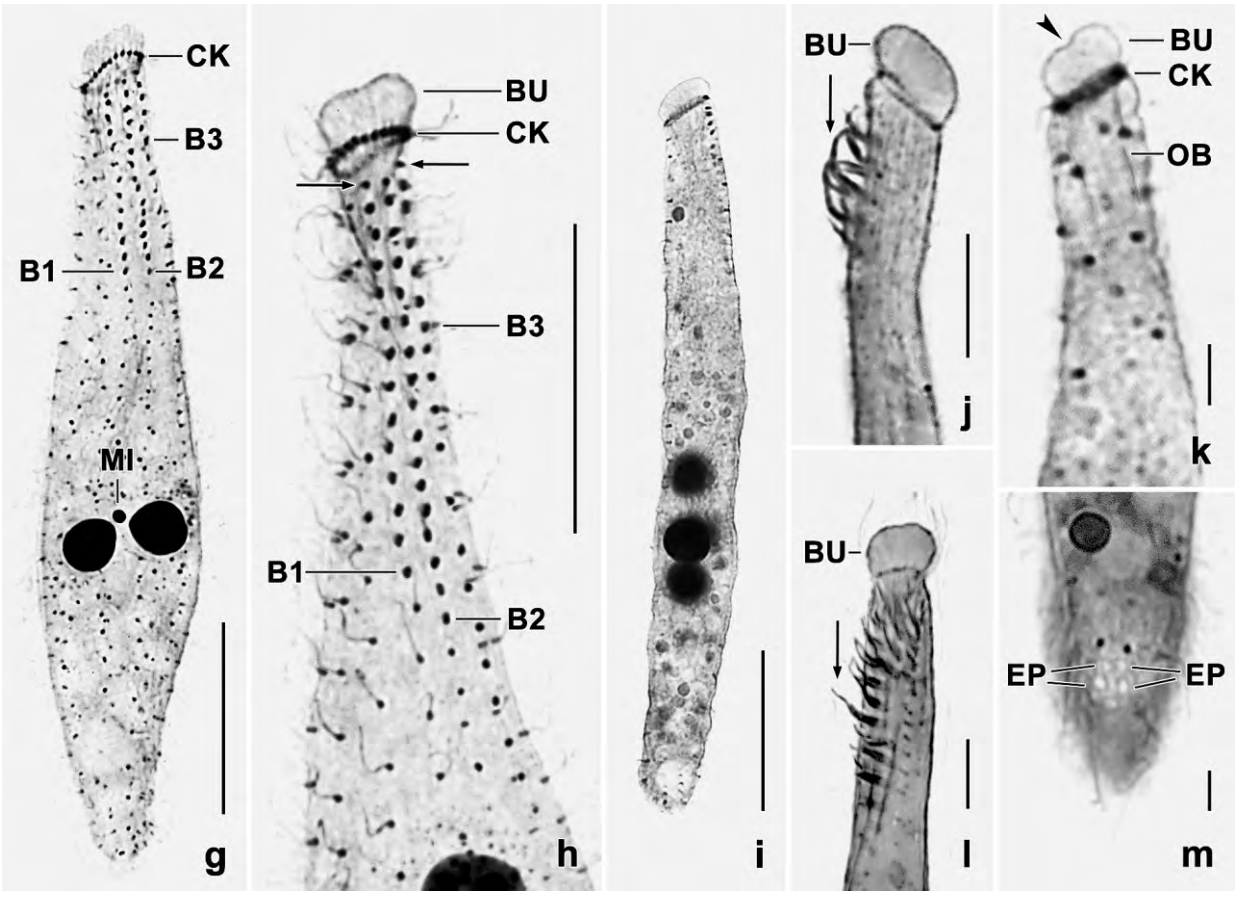

Fig. 59g–m. *Coriplites tumidus* after protargol impregnation. **g:** Overview of a lenticular Australian specimen with transversely arranged, globular macronuclear nodules; the micronucleus is in the vertex of the nodules. Dorsal brush row 3 is much shorter than rows 1 and 2. **h:** Higher magnification of the holotype specimen shown in Fig. 59f. The arrows mark the single monokinetid at the anterior end of the dorsal brush rows. Brush row 3 is much shorter than rows 1 and 2, a main difference to *C. terricola*. The oral bulge is very conspicuous because it is about 4 µm high and slightly wider than the neck. The circumoral kinety is indistinctly ∞- shaped. **i:** A cylindroidal post-conjugate with four globular macronuclear nodules. **j, l:** Very slender North American specimens with the oral bulge about 5 × 3.5 µm in size. The arrows mark bristles of the dorsal brush. **k:** A specimen with faintly impregnated oral basket and a minute concavity in the centre of the oral bulge (arrowhead). **m:** Subterminal excretory pores of the contractile vacuole. B1–3 – dorsal brush rows, BU – oral bulge, CK – circumoral kinety, EP – excretory pores, MI – micronucleus, OB – oral basket. Scale bars 5 µm (k–m), 10 µm (j), and 20 µm (g–i).

Size in vivo 80–130 × 15–35 µm, usually about 110 × 20 µm, as calculated from some live measurements and the values in Table 20 adding 15% preparation shrinkage; Australian cells distinctly broader than those from Brazil and North America while body length is highly similar; up to 30% contractile, especially neck. Length:width ratio 4.8–7.4 on average, body thus narrowly to very narrowly obclavate or elongate lenticular and with conspicuous, bulbous anterior end (= oral bulge) and narrowly rounded or acute posterior end (Fig. 58a, e, i, o, p, 59c, f, g; Table 20); slightly flattened laterally; usually slightly curved, rarely serpentine (Fig. 58c). Nuclear apparatus in various positions (CV 15–20%), on average slightly posterior to mid-body; invariably composed of two macronuclear nodules and a single micronucleus in between; macronuclear nodules irregularly arranged, nuclear figure thus highly variable (Fig. 58a, c, e, 59c, f, g; Table 20). Nodules globular to very narrowly ellipsoid, usually ellipsoid to broadly ellipsoid, rarely reniform or C-shaped with micronucleus in C-centre; not separated into pairs in two out of

about 50 Australian specimens; about 10 × 6 µm in vivo and in protargol preparations; with large central nucleolus and several small nucleoli in about 1/3 of specimens (Fig. 59d, e), others with medium-sized and minute nucleoli. Micronucleus usually in between macronuclear nodules, very rarely in vortex of nodules or attached laterally to a nodule; shape highly variable, viz., globular, ellipsoid or broadly ellipsoid, rarely reniform (Fig. 58a, e, 59c–g; Table 20); frequently not or only lightly impregnated with protargol. Some post-conjugants with typical nuclear pattern, i. e., four globular macronuclear nodules, present in each population (Fig. 59i). Contractile vacuole in posterior body end with several subterminal excretory pores (Fig. 58a, f, 59m). Cytopyge next to contractile vacuole, fecal mass loose. Cortex colourless and flexible, conspicuously thick due to innumerable, ellipsoid extrusomes (mucocysts) about 1–1.3 × 0.5 µm in size. Extrusomes strongly refractive thus appearing as minute, bright dots in surface view, form about eight rows between adjacent kineties, present also in oral bulge cortex; bluntly fusiform and about 10 µm long when exploded, swell to a 3–6 µm thick coat impregnating yellowish in some specimens (Fig. 58a, d, e, l, 59a, b, d). Cytoplasm colourless, neck hyaline, trunk more or less turbid by lipid droplets 1–7 µm across and food vacuoles 5–10 µm in diameter (Fig. 58a, b, 59b, e). Likely feeds on flagellates and ciliates, Brazilian specimens ingest whole *Sathrophilus muscorum* possibly contracting neck during food uptake (Fig. 58b). Glides and swims slowly.

Somatic cilia 8–10 µm long in vivo, arranged in an average of 9–11 meridional, ordinarily to narrowly (USA) spaced rows each composed of about 30 ordinarily spaced cilia on average; cilia slightly wider spaced in neck and rear region, frequently absent posterior of circumoral kinety (Fig. 58a, e, f, 59c, f–h; Table 20). Dorsal brush three- rowed and isomorphic, on average occupies 20–27% of body length; heterostichad in Australian and Brazilian specimens, distinctly heterostichad in USA population; each row with a minute anterior tail composed of a single (very rarely two) monokinetid (Fig. 58a, e, g, 59c, f–h; Table 20). Brush dikinetids frequently oriented slightly obliquely to main kinety axis, widely spaced except of ordinarily spaced kinetids in row 2 of North American specimens. Brush row 1 composed of an average of 19 dikinetids, slightly shorter than row 2 composed of 22 dikinetids on average; row 3 shorter than row 2 by about 60%, composed of an average of six dikinetids followed by a tail composed of about 10 monokinetal bristles 1–2.5 µm long. Bristles not studied in detail, slightly clavate and up to 3 µm long in vivo while up to 5 µm in protargol preparations (Fig. 58a, 59j, l; Table 20).

Oral bulge without toxicysts, as typical for genus, checked in about 10 populations; contains pale mitochondria 2–4 × 1–3 µm in size; slightly to distinctly obliquely arranged to main body axis and slightly higher dorsally than ventrally; in frontal view broadly elliptic and with small central concavity; shape and size highly variable, discoid to hemispheric, usually conspicuous in vivo and in protargol preparations because about 7 × 5 µm in size and thus slightly wider than neck (Fig. 58a, c, e, g–p, 59c, f–h, j–l; Table 20). Circumoral kinety broadly elliptic, ∞- shaped due to oblique position on neck, composed of narrowly spaced, oblique dikinetids (Fig. 58a, e–h, 59g, h). Oral basket hardly recognizable in vivo and rarely distinctly impregnated with protargol, about 20–30 µm long (Fig. 58f, 59k); oralized somatic monokinetids invisible, even in darkly impregnated cells.

Occurrence and ecology: *Coriplites tumidus* is rather common in Australia, where it has been found at several sites. It is also widespread in South America, where it occurs in Brazil, at Venezuelan site (14), and at site (2) of the Isla Robinson Crusoe. In North America, *C. tumidus*

has been found in Idahoe, that is, in the outskirts of the town of St. Anthony, where it was moderately abundant in a moos and litter collection (pH 6.8) from a sandy bushland. In Africa, we found *C. tumidus* in red soil from the Agricultural Research Station of the Benin University (coll. Jean Dragesco) and in surface soil (pH 6.1) from the Koël Bay, Cape Peninsula, Republic of South Africa. As yet, we do not have a record from Europe. Most of the sites are sandy, which matches the slender shape of the organism. In the non-flooded Petri dish cultures, the abundance of *C. tumidus* is low to moderate.

Remarks: *Coriplites tumidus* has a highly characteristic nuclear pattern: two macronuclear nodules and a micronucleus in between. However, the same pattern is found in two congeners (Oertel et al. 2008) and in at least six further haptorid genera (Blatterer & Foissner 1988, Foissner et al. 2002, Foissner & Xu 2007): *Apocoriplites lajacola*, *Apoenchelys bamforthi*, *Arcuospathidium vermiforme*, *Cultellothrix spp.*, *Enchelys binucleata*, → *E. lagenula*, and *Epitholiolus chilensis*. Thus, this feature is an identification mean only in context with a conspicuous oral bulge lacking toxicysts.

Instead of a circumstantial comparison of *C. tumidus* with its congeners, we update the key provided by Oertel et al. (2008), showing that *C. tumidus* differs mainly by the large oral bulge and the organization of the dorsal brush from its supposed nearest relative, *C. terricola*. The last feature has been studied in two *C. terricola* and three *C. tumidus* populations, respectively, showing a remarkable stability.

1 Two globular or ellipsoid macronuclear nodules with a micronucleus in between 2

– One macronucleus ..... *Coriplites proctori*

2 Body length ≤ 110 µm in vivo 3

– Body length ≥ 130 µm, usually about 180 µm .....*Coriplites grandis*

3 Two dorsal brush rows ..... *Apocoriplites lajacola*

– Three dorsal brush rows 4

4 Size about 60 × 13 µm in vivo. Dorsal brush row 3 about as long as row 2 and composed of an average of 11 dikinetids. Oral bulge inconspicuous, i. e., flat and up to 3 µm high in vivo, does not project from neck ..... *Coriplites terricola*

– Size about 110 × 20 µm in vivo. Dorsal brush row 3 shorter than row 2 by about 60% and composed of an average of six dikinetids. Oral bulge conspicuous in vivo because 3–5 µm high, slightly wider than neck, and discoidal to hemispherical .... *Coriplites tumidus*

Family Spathidiidae

Mamillospatha nov. gen.

Diagnosis:Spathidiida Foissner & Foissner, 1988 with protospathidid ciliary pattern and nipple-shaped lepidosomes on resting cyst surface.

Type species: *Mamillospatha lepidosomatum* (Foissner et al., 2014c) nov. comb. (basionym: *Protospathidium lepidosomatum* Foissner et al., 2014c). Monotypic!

Etymology: Composite of the Latin nouns *mamilla* (nipple) and *spatha* (spatula) connected by the thematic vowel *-o*, referring to the nipple-shaped lepidosomes of the resting cyst surface. Feminine gender.

Remarks: This and the following genus are based on the study by Foissner et al. (2014c), i. e., on the resting cysts that have highly characteristic lepidosomes with shapes quite different from those of the → *Trachelophyllina*, another group of haptorids. Further, this step takes into account the molecular data that show many not yet named evolutionary traits within the Spathidiida and Haptorida in general (Vďačný et al. 2014c).

Columnospatha nov. gen.

Diagnosis:Spathidiida Foissner & Foissner, 1988 with arcuospathidid ciliary pattern and pillar-shaped lepidosomes on resting cyst surface.

Type species: *Columnospatha bromelicola* (Foissner et al., 2014) nov. comb. (basionym: *Arcuospathidium bromelicola* Foissner et al., 2014). Monotypic!

Etymology: Composite of the Latin nouns *columna* (pillar) and *spatha* (spatula) connected by the thematic vowel *-o*, referring to the pillar-shaped lepidosomes of the resting cyst surface. Feminine gender.

Remarks: See → *Mamillospatha*

Facetospatha nov. gen.

Diagnosis:Spathidiida Foissner & Foissner, 1988 with arcuospathidid ciliary pattern and thick, faceted cyst wall.

Type species: *Facetospatha cultriforme* (Penard, 1922) nov. comb. (basionyms: *Spathidium cultriforme* Penard, 1922 and *Arcuospathidium cultriforme* (Penard, 1922) Foissner, 1984.

Etymology: Composite of the French noun *facette* (facet) and the Latin noun *spatha* (spatula) connected by the thematic vowel *-o*, referring to the faceted wall of the resting cyst.

Remarks: The faceted resting cyst has been described by Foissner & Xu (2007). The genus is supported by the molecular data where *F. cultriforme* forms a separate clade with moderate statistical support (BI = 0.97, ML = 60, MP –) together with three *Spathidium* species and *Teuthophrys trisulca* (Vďačný et al. 2014).

Protospathidium salinarum nov. spec. (Fig. 60a–m, 61a–v; Table 21)

Diagnosis: Size in vivo about 150 × 20 µm. Very narrowly spathulate with oblique oral bulge about half as width as broadest trunk region. Macronucleus a tortuous, more or less nodulated strand. Usually, a lenticular micronucleus each near anterior and posterior end of macronucleus. Extrusomes fine and rod-shaped, about 5 µm long. On average 13 ciliary rows, 3 anteriorly

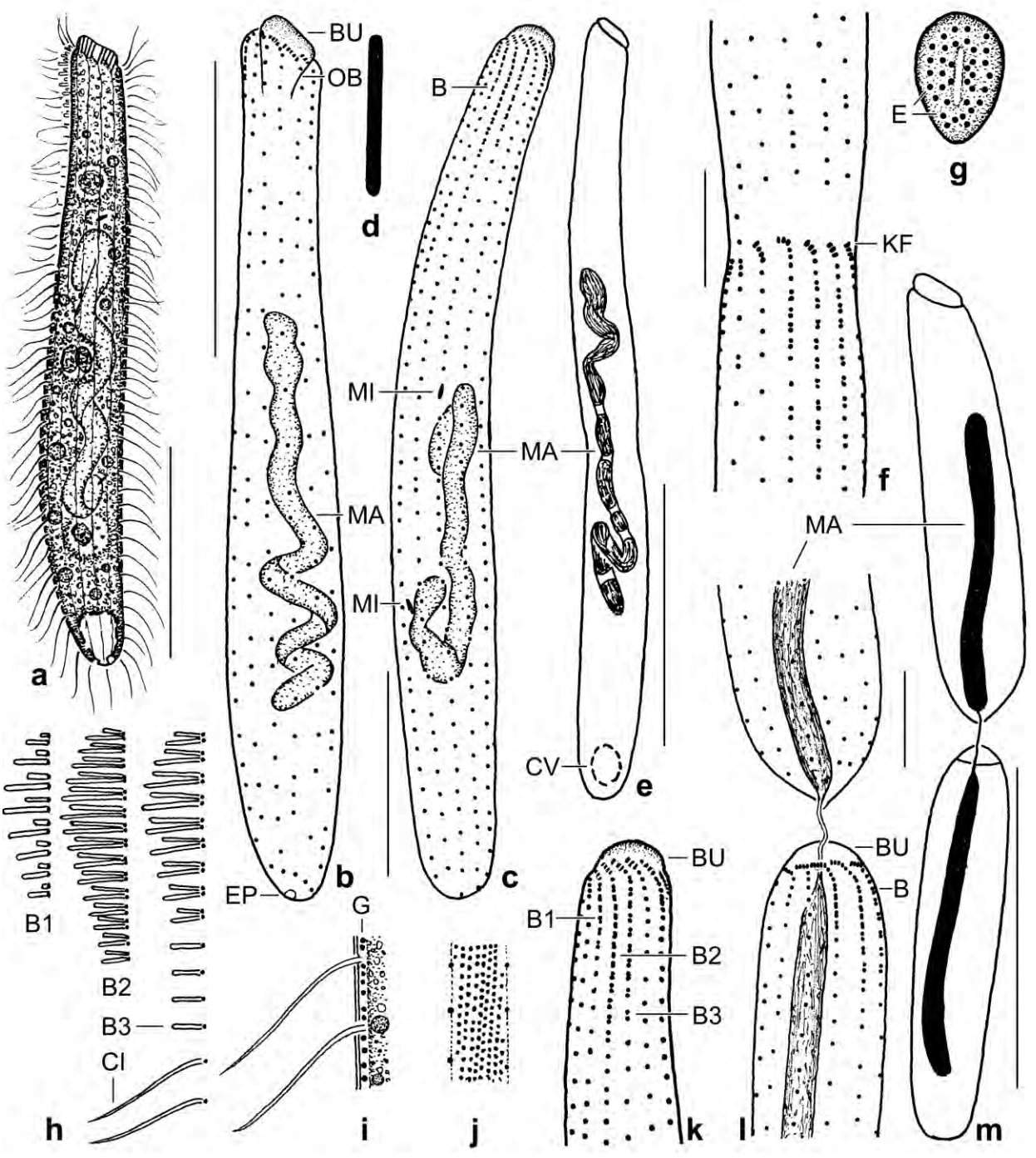

Fig. 60a–m. *Protospathidium salinarum*, morphostatic (a–d, g–k) and dividing (e, f, l, m) specimens from life (a, d, g, h–j), after protargol impregnation (b, c, e, f, k–m), and in the SEM (h). **a:** Right side view of a representative specimen, length 150 µm. **b:** Ciliary pattern of right side. **c, k:** Ciliary pattern of dorsal side and nuclear apparatus of holotype specimen, length 128 µm. Note the two micronuclei. **d:** Mature extrusome, 5 µm. **e, f:** Late early divider showing the "true" shape of the macronucleus, the slight indentation in the prospective fission area, and forming kinetofragments. **g:** Ventral view of oral bulge. **h:** Dorsal brush, slightly schematized. **i, j:** Optical section and surface view, showing the cortical granulation. **l, m:** Very late divider with opisthe's oral bulge not yet fully developed. B(1–3) – dorsal brush (rows), BU – oral bulge, CI – ordinary somatic cilia, CV – contractile vacuole, E – extrusomes, EP – excretory pore, G – cortical granules, KF – kinetofragments, MA – macronucleus, MI – micronuclei, OB – oral basket. Scale bars 10 µm (f, l), 30 µm (b, c), and 50 µm (a, e, m).

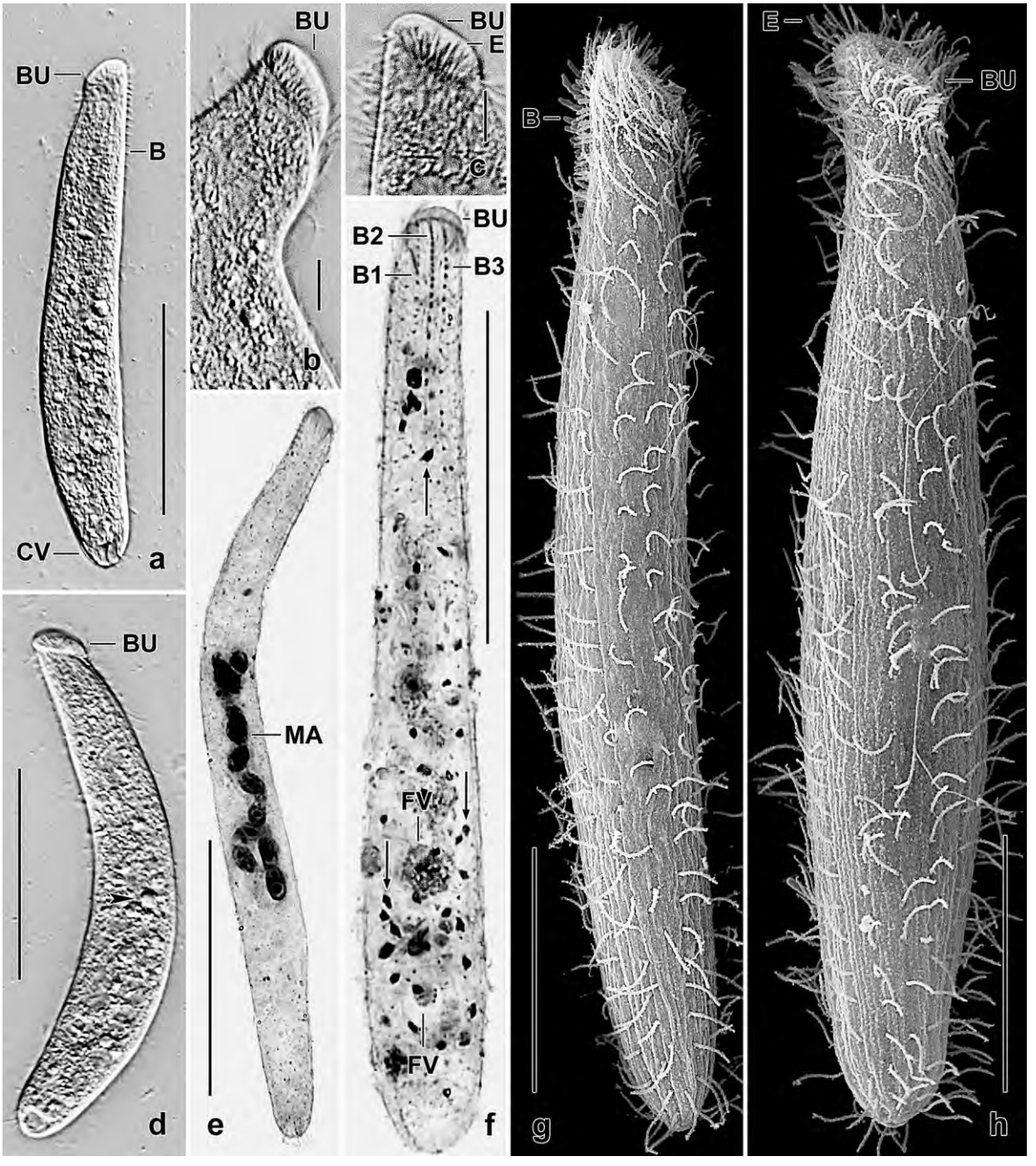

Fig. 61a–h. *Protospathidium salinarum* from life (a–d), after protargol impregnation (e, f), and in the scanning electron microscope (g, h). **a, d, e–h:** The body shape is rather variable, i. e., very narrowly spathulate and more or less curved (a, d, e, g), very elongate lenticular (h), or rod-like (f). Usually, the length:width ratio is near 7:1. The cytoplasm is densely granulated (a–d); the arrowhead in (d) marks small, moderately refractive (lipid?) inclusions. Arrows in (f) denote minute, deeply impregnating structures, i. e., developing extrusomes and, possibly, cyst wall precursors. Note the moniliform macronucleus in the very slender specimen shown in (e). **b, c:** The oral bulge is fairly distinct and striated by the rod-shaped extrusomes contained. B(1–3) – dorsal brush (rows), BU – oral bulge, CV – contractile vacuole, E – extrusomes, FV – food vacuoles, MA – macronucleus. Scale bars 5 µm (b, e), 25 µm (g, h), and 50 µm (a, b, e, f).

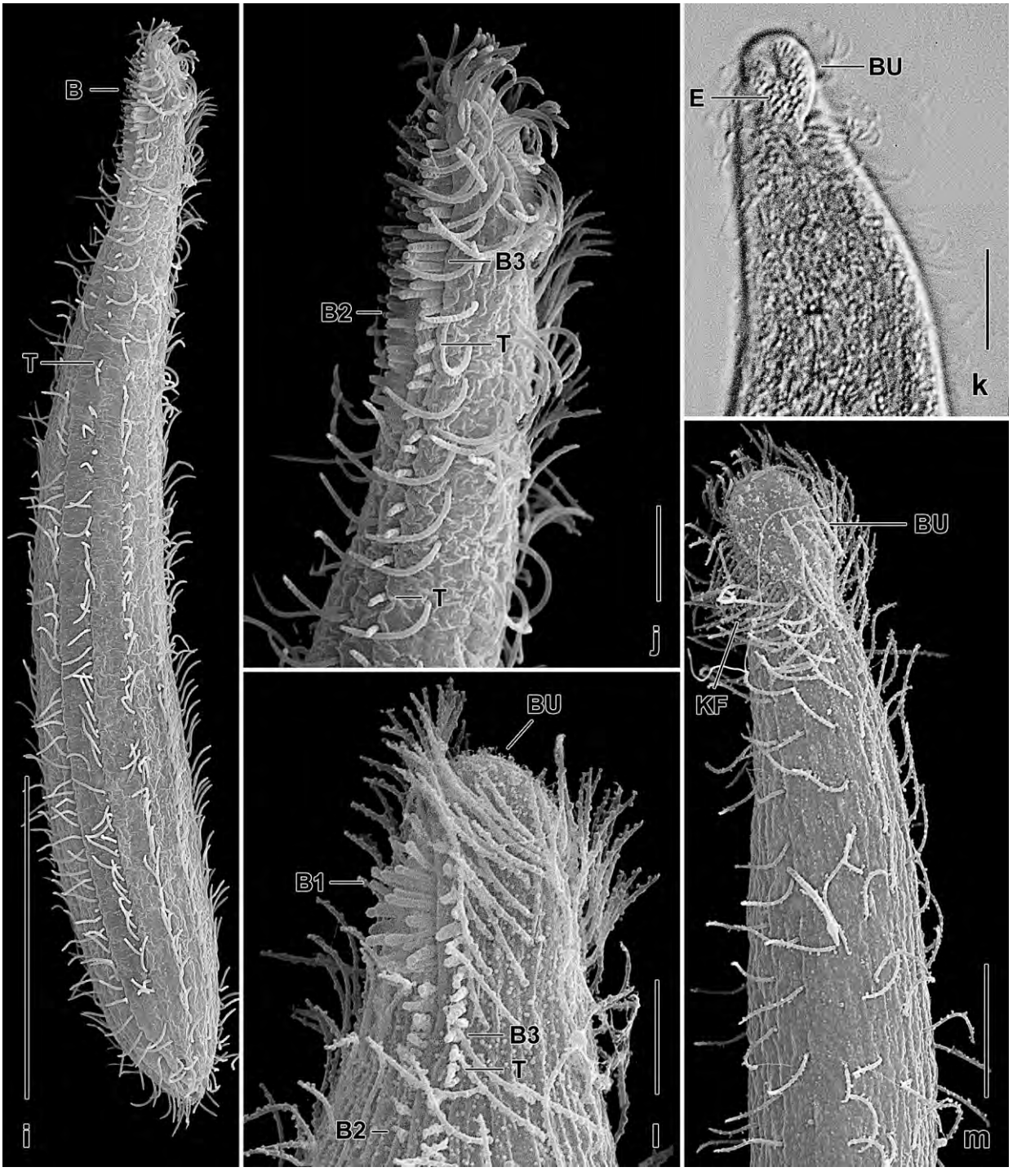

Fig. 61i–m. *Protospathidium salinarum* from life (k) and in the scanning electron microscope (i, j, l, m). **i, j:** A very narrowly spatulate and slightly obclavate specimen, showing dorsal brush rows 2 and 3, the later having a rather long monokinetal bristle tail. **k, m:** Ventral views, showing the obovate oral bulge studded with extrusomes (k). **l:** The dorsal brush consists of three rows with the longest bristles in the second quarter. The monokinetal bristle tail of brush row 3 is short in this specimen. B(1–3) – dorsal brush (rows), BU – oral bulge, E – extrusomes, KF – kinetofragments, T – tail of brush row 3. Scale bars 5 μm (j, l), 10 μm (k, m), and 40 μm (i).

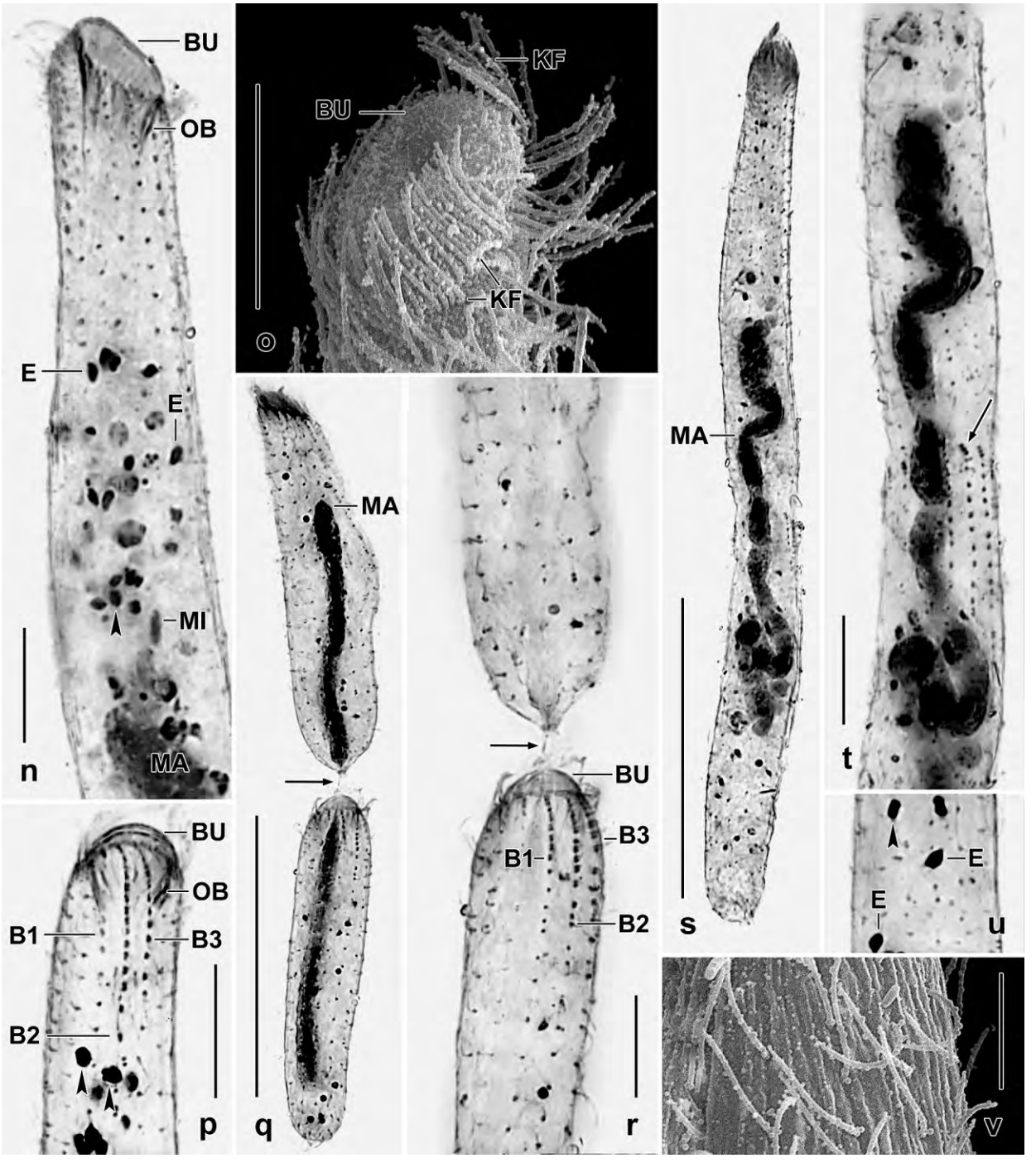

Fig. 61n–v. *Protospathidium salinarum*, morphostatic (n–p, u, v) and dividing (q–t) specimens after protargol impregnation (n, p–u) and in the scanning electron microscope (o, v). **n, p, u:** Right side and dorsal view, showing developing extrusomes (E) and, possibly, cyst wall precursors (arrowheads). **o:** Ventrolateral view of oral area. **q, r:** The opisthe oral bulge is not yet shaped in this very late divider connected by a fine strand of nuclear material (arrows). **s, t:** A late early divider, showing the new oral kinetofragments (arrow), the indentation in the prospective fission area, and the "true" shape of the macronucleus, i. e., a tortuous, slightly nodulated strand (s). **v:** The longitudinal striation of the cortex is caused by postciliary microtubule ribbons. B1–3 – dorsal brush rows, BU – oral bulge, E – developing extrusomes, KF – kinetofragments, MA – macronucleus, MI – micronucleus, OB – oral basket. Scale bars 5 µm (v), 10 µm (n–p, r, t), and 50 µm (q, s).

Table 21. Morphometric data on *Protospathidium salinarum* from a non-flooded Petri dish culture. Data based on mounted, protargol-impregnated specimens selected as indicated in the description. Measurements in µm. CV – coefficient of variation in %, M – median, Max – maximum, Mean – arithmetic mean, Min – minimum, n – number of specimens investigated, SD – standard deviation, SE – standard error of arithmetic mean.

Characteristics	Mean	M	SD	SE	CV	Min	Max	n
Body, length	125.8	125.0	20.8	4.5	16.5	92.0	180.0	21
Body, width	15.8	16.0	2.4	0.5	14.9	11.0	20.0	21
Body length:width, ratio	8.1	7.8	1.8	0.4	22.0	5.4	13.0	21
Anterior body end to macronucleus, distance	38.6	36.0	13.6	3.0	35.2	19.0	67.0	21
Oral bulge, width	9.5	10.0	1.3	0.3	13.1	7.0	12.0	21
Oral bulge, height	2.7	2.5	0.4	0.1	15.9	2.0	4.0	21
Oral basket rods, length [a]	18.5	20.0	–	–	–	12.0	25.0	21
Oral kinetofragments, number of dikinetids	6.1	6.0	1.6	0.3	25.9	3.0	9.0	21
Macronuclear figure, length	54.5	55.0	11.6	2.5	21.4	40.0	90.0	21
Macronucleus, estimated total length [b]	75.2	75.0	–	–	–	50.0	110.0	21
Macronucleus, width	4.8	5.0	0.8	0.2	17.5	4.0	7.0	21
Micronuclei, length	2.6	2.5	0.4	0.1	14.8	2.0	3.0	13
Micronuclei, width [a]	1.0	1.0	–	–	–	0.5	1.5	13
Micronuclei, number [a]	2.5	2.0	–	–	–	2.0	4.0	10
Ciliary rows, total number	13.1	13.0	1.1	0.2	8.4	11.0	15.0	21
Ventral ciliary rows, number of ciliated kinetids	48.4	47.0	8.5	1.9	17.5	35.0	70.0	21
Dorsal brush rows, number	3.0	3.0	0.0	0.0	0.0	3.0	3.0	21
Brush row 1, length	9.7	9.0	2.4	0.5	25.2	6.0	13.0	21
Brush row 1, number of dikinetids	8.8	8.0	1.9	0.4	21.4	6.0	13.0	21
Brush row 2, length	15.7	15.0	2.7	0.6	16.9	12.0	22.0	21
Brush row 2, number of dikinetids	14.0	15.0	2.9	0.6	20.7	8.0	19.0	21
Brush row 3, length	12.0	13.0	2.3	0.5	18.8	6.0	15.0	21
Brush row 3, number of dikinetids	9.3	9.0	2.3	0.5	25.0	5.0	13.0	21

[a] Rough values because incompletely impregnated or difficult to measure.

[b] When uncoiled.

differentiated to an inconspicuous, heterostichad dorsal brush occupying 13% of body length and comprising up to 4 µm long bristles: brush row 1 composed of an average of 9 dikinetids, row 2 of 14, and row 3 of 9 dikinetids followed by a short monokinetal bristle tail. Right side oral kinetofragments composed of about 6 dikinetids each.

Type locality: Venezuelan site (66), i. e., highly saline soil from the north coast, Morrocoy National Park, surroundings of the village of Chichiriviche, 67°13'W 11°33'N.

Type material: 1 holotype and 3 paratype slides with protargol-impregnated specimens have been deposited in the Biology Centre of the Upper Austrian Museum in Linz (LI). Relevant specimens have been marked by black ink circles on the coverslip.

Etymology: The specific name is a noun in plural genetive and thus does not change the gender when combined with, e. g., a masculine genus; it refers to the habitat, i. e., growing or living in saline environment.

Description: This species was discovered in a highly saline (~50–70‰) soil sample, and thus it did not fix well. Further, the sample was fixed after a mass conjugation, and thus the slides contain many post-conjugates with four globular macronuclear nodules, as typical for haptorids (Foissner and Xu 2007). These and poorly preserved specimens were excluded; however, we cannot entirely exclude that some very late post-conjugates with an "ordinary" macronucleus were included in the morphometric analysis. The SEM micrographs are from cultivated specimens which differ from the non-flooded Petri dish cells in having frequently a disordered brush and a less dense ciliation (Fig. 61g, h). Size in vivo 110–210 × 15–25 µm, on average about 150 × 20 µm, as calculated from live and the morphometric data in Table 21 adding 15% preparation shrinkage; length:width ratio on average 6:1 (3.3–11:1, n = 16) in vivo, 8:1 in protargol preparations (Table 21), and 6.8:1 (3.4–8.9:1, n = 22) in SEM micrographs. Body usually very narrowly spathulate or very elongate lenticular, rarely rod-like or very elongate obclavate, straight to distinctly curved; slightly flattened laterally in oral region (Fig. 60a–c, 61a, d–i; Table 21). Nuclear apparatus in central quarters of cell and rather poorly preserved in the protargol preparations (Fig. 60a, b, c, e, 61e, n, s; Table 21). Macronucleus a tortuous more or less nodulated strand in 30 out of 40 specimens analysed and in late early dividers (Fig. 61s); moniliform in six cells (Fig. 61e), and rod-like in four specimens; frequently partially or completely spiralized with ends curved proximally; nucleoli indistinct. Micronuclei not or poorly recognizable in two thirds of protargol-impregnated cells, frequently difficult to distinguish from similar-sized, developing extrusomes and, possibly, from cyst wall precursors; remarkable because of the lenticular shape (on average 2.6 × 1 µm) and the special location: usually one each at or near ends of macronuclear strand; when three or four micronuclei, some scattered along macronucleus (Fig. 60a, c, 61n; Table 21). Contractile vacuole in posterior body end, with several pores in pole area. Mature extrusomes scattered around centre of oral bulge, rod-shaped, 4–5 × about 0.5 µm in vivo, do not impregnate with the protargol method used (Fig. 60a, d, g, 61c, k); many developing extrusomes and other lenticular or conical, deeply impregnated structures (cyst wall precursors?) scattered throughout cytoplasm (Fig. 61f, n, p, s, u). Cortex very flexible, colourless, slightly furrowed by ciliary rows and postciliary microtubule ribbons, studded with minute (~ 0.2 µm) granules forming about eight rows between two kineties each (Fig. 60i, j, 61h, v). Cytoplasm densely granulated, contains few to many moderately refractive, 2–5 µm-sized (lipid?) inclusions and some up to 10 µm-sized food vacuoles with rather compact contents, likely flagellates. Burrows between soil particles but swims also rather rapidly.

Cilia about 8 µm long in vivo, arranged in an average of 13 equidistant, ordinarily spaced and ciliated rows modified to short, slightly oblique kinetofragments producing dense ciliation at base of oral bulge; right side kinetofragments composed of three to nine dikinetids (Fig. 60a–c, 61g–i, m, o; Table 21). Dorsal brush three-rowed, heterostichad, isomorphic, and composed of ordinarily spaced dikinetids, except of anterior tails each comprising about four very narrowly spaced monokinetids; inconspicuous because occupying only 13% of body length and bristles merely up to 4 µm long in second quarter of rows (Fig. 60a, c, h, k, 61a, f, i, j, l, p; Table 21). Brush row 1 shortest, composed of an average of nine dikinetids having up to 3 µm and 1 µm long posterior and anterior bristles, respectively. Brush row 2 longest, composed of an average of 14 dikinetids with posterior and anterior bristles up to 4 µm and 3 µm long, respectively. Brush row 3 shorter than row 2, composed of an average of nine dikinetids with bristles similar to those of row 2; posterior tail composed of 2 to 20 monokinetal bristles 2–3 µm long.

Oral bulge flat and slightly higher on dorsal than ventral side of cell, obliquely truncate by 30° to 60° ($\bar{x}$ = 40°), obovate in ventral view, centre slightly concave (Fig. 60a–c, e, g, k, 61a–h, k, m–p; Table 21); inconspicuous because about half as width as broadest trunk region and only 3–5 µm high. Oral basket rods well recognizable only in over-impregnated specimens, originate from circumoral kinetofragments and extend about 20 µm into the cell. Ontogenesis: Some key stages were found in the protargol preparations, showing (i) a slight indentation in mid-body in late early dividers when the oral kinetofragments are assembled (Fig. 60e, f, 61s, t), (ii) a distinct widening in mid-body of early mid-dividers, and (iii) a still incomplete opisthe oral bulge when the sisters separate (Fig. 60l, m, 61q, r). See Foissner and Xu (2007) and Foissner et al. (2014b) for a comparison with other spathidiids.

Occurrence and ecology: As yet found only at type locality, i. e., a highly saline (50–70‰) coastal soil from Venezuela. *Protospathidium salinarum* could be cultivated for a short time by adding some squashed wheat grains to the soil eluate.

Remarks: All genera and species mentioned in the following comparisons are reviewed in the monograph of Foissner and Xu (2007). The population investigated belongs to *Protospathidium* because, in contrast to *Edaphospathula*, the extrusomes are longer (≥ 4 µm vs. ≤ 4 µm) and rod-shaped (vs. ovate and massive), and the right side oral kinetofragments are composed of ≥ three dikinetids (vs. ≤ 3).

Protospathidium salinarum resembles *P. namibicola, P. vermiforme, P. serpens,* and *P. fraterculum*. It differs from *P. namibicola* by body size (150 × 20 µm vs. 210 × 20 µm), the number and shape of the micronuclei (up to 4, lenticular vs. many and ellipsoidal), and the number of ciliary rows (on average 13 vs. only 9 although being considerably larger). *Protospathidium salinarum* differs from *P. vermiforme*, an incompletely described species from the Austrian Central Alps, by body size (150 × 20 µm vs. 120 × 10 µm) and the number of dikinetids in dorsal brush row 1 (8 vs. 3). *Protospathidium serpens* and *P. fraterculum* differ from *P. salinarum* by body size (90 × 15 vs. 150 × 20), the shape of the micronuclei (globular vs. lenticular), and the number of dikinetids in brush row 1 (3 vs. 8). Some *Edaphospathula* species also resemble *P. salinarum* but differ by the features mentioned above. Do not confuse *P. salinarum* with *Arcuospathidium namibiense*, which has a similar size and shape but possesses about 20 macronuclear nodules; minute, ovate extrusomes; and some 15–20 µm long dorsal bristles.

Most *Protospathidium* and *Edaphospathula* species have been not recorded from saline habitats, except of *P. serpens* and *E. minor* (Foissner and Xu 2007). Thus, the halophily of *P. salinarum* can be considered as a further species character.

Spathidium stetteri Foissner & Xu **nov. spec.** (Fig. 62a–o, 63a–o; Table 22)

Diagnosis: Size in vivo about 210 × 30 µm. Very narrowly spatulate with oblique to strongly oblique, cuneate oral bulge about 80% as long as widest trunk region. Macronucleus long and tortuous; multimicronucleate. Oral extrusomes in vivo rod-shaped and slightly curved, about 6 × 0.3 µm in size. One size type of cortical granules. On average 17 ciliary rows, 3 anteriorly modified to an isostichad dorsal brush with longest row 2 occupying about 20% of body length;

Table 22. Morphometric data on *Spathidium stetteri* based on mounted, protargol-impregnated (FOISSNER's method), and randomly selected specimens from a non-flooded Petri dish culture. Measurements in µm. CK – circumoral kinety, CV – coefficient of variation in %, M – median, Max – maximum, Mean – arithmetic mean, Min – minimum, n – number of individuals investigated, SD – standard deviation, SE – standard error of arithmetic mean.

Characteristics	Mean	M	SD	SE	CV	Min	Max	n
Body, length	184.3	185.0	18.1	4.0	9.8	152.0	230.0	21
Body, width	25.7	25.0	3.6	0.8	13.8	21.0	35.0	21
Body length:width, ratio	7.3	7.4	1.1	0.2	14.9	4.7	9.2	21
Oral bulge, length	18.8	19.0	1.7	0.4	9.0	15.0	22.0	21
Oral bulge (circumoral kinety), width	6.0	6.0	0.5	0.2	8.9	5.0	7.0	8
Oral bulge, height	3.5	3.5	0.4	0.1	10.8	3.0	4.0	21
Oral bulge length:body width, ratio	0.7	0.8	0.1	–	12.3	0.5	0.9	21
CK to last dikinetid of brush row 1, distance	31.3	31.0	3.6	0.8	11.4	24.0	38.0	21
CK to last dikinetid of brush row 2, distance	36.0	37.0	4.6	1.0	12.8	28.0	45.0	21
CK to last dikinetid of brush row 3, distance	34.2	35.0	4.0	0.9	11.7	25.0	40.0	21
Anterior body end to macronucleus, distance	60.0	58.0	13.4	2.9	22.3	36.0	88.0	21
Macronucleus Figure, length	95.6	98.0	19.4	4.2	20.3	43.0	130.0	21
Macronucleus, length (spread and thus approximate)	168.6	150.0	–	–	–	120.0	300.0	21
Macronucleus, width in mid	5.3	5.0	1.3	0.3	24.8	3.0	9.0	21
Macronucleus, number	1.0	1.0	0.0	0.0	0.0	1.0	1.0	21
Micronuclei, across	2.3	2.0	0.4	0.1	15.8	2.0	3.0	17
Micronuclei, number	6.5	6.0	1.3	0.3	20.1	4.0	9.0	15
Somatic kineties, number	16.7	17.0	1.1	0.2	6.3	15.0	19.0	21
Basal bodies in a right side kinety, number	86.3	84.0	19.2	4.2	22.2	60.0	145.0	21
Dorsal brush rows, number	3.0	3.0	0.0	0.0	0.0	3.0	3.0	21
Dikinetids in brush row 1, number	25.5	25.0	3.6	0.8	13.9	20.0	33.0	21
Dikinetids in brush row 2, number	30.0	30.0	3.6	0.8	12.2	25.0	37.0	21
Dikinetids in brush row 3, number	23.1	23.0	3.0	0.7	12.9	17.0	28.0	21

brush row 3 with heteromorphic tail. Resting cyst about 40 µm across, wall smooth and covered by a thick mucous layer.

Type locality: Site (71), i. e., surface soil under a *Pandanus* palm in the garden of the hotel San Fernando, Puerto Ayora, Santa Cruz Island, Galápagos, 0°37'S 90°21'W.

Type material: 1 holotype and 2 paratype slides with protargol-impregnated specimens have been deposited in the Biology Centre of the Upper Austrian Museum in Linz (LI). Relevant specimens have been marked by black ink circles on the coverslip.

Dedication: We dedicate this species to em. Prof. Dr. Karl O. STETTER, University of Regensburg, Germany, who collected the Galápagos samples.

Description: Size in vivo 170–260 × 25–40 µm, usually about 210 × 30 µm, as calculated from some in vivo measurements and the morphometric data in Table 22 adding 15% preparation shrinkage; length:width ratio also highly variable, viz., 4.7–9.2:1, on average near 7:1 both in vivo

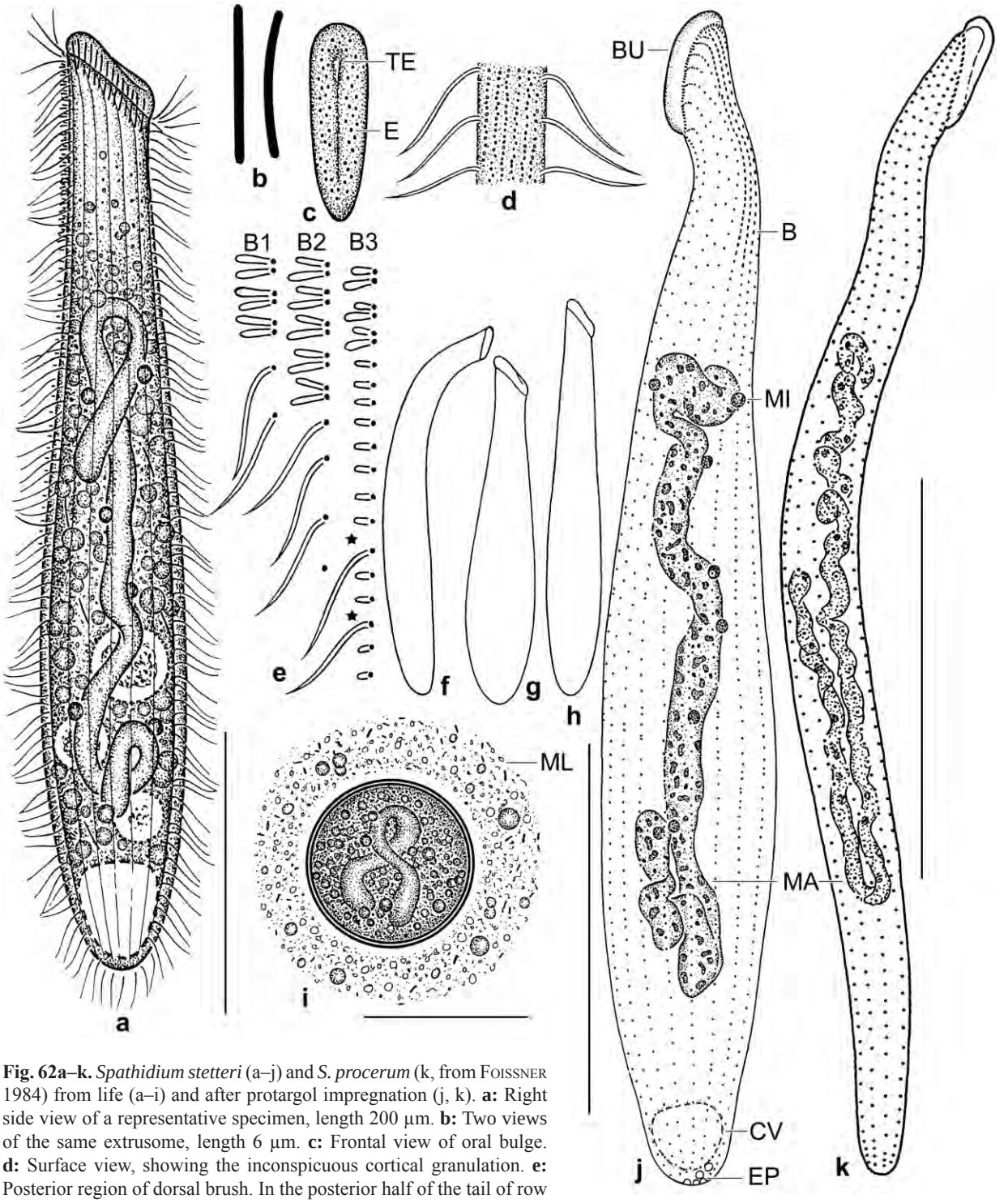

Fig. 62a–k. *Spathidium stetteri* (a–j) and *S. procerum* (k, from FOISSNER 1984) from life (a–i) and after protargol impregnation (j, k). **a:** Right side view of a representative specimen, length 200 µm. **b:** Two views of the same extrusome, length 6 µm. **c:** Frontal view of oral bulge. **d:** Surface view, showing the inconspicuous cortical granulation. **e:** Posterior region of dorsal brush. In the posterior half of the tail of row 3, bristles alternate with ordinary somatic cilia (asterisks), and thus the row is heteromorphic. **f–h:** Shape variants. **i:** Resting cyst, 40 µm in diameter without mucous layer. **j:** Left side view of holotype specimen, showing the ciliary and nuclear pattern (for details, see next plate). **k:** Right side view, showing that *S. procerum* is much more slender and has fewer ciliary rows than *S. stetteri*. B(1, 2, 3) – dorsal brush (rows), BU – oral bulge, CV – contractile vacuole, E – extrusomes, EP – excretory pores, MA – macronucleus, MI – micronuclei, ML – mucous coat, TE – temporary cytostome. Scale bars 40 µm (i) and 60 µm (a, j, k).

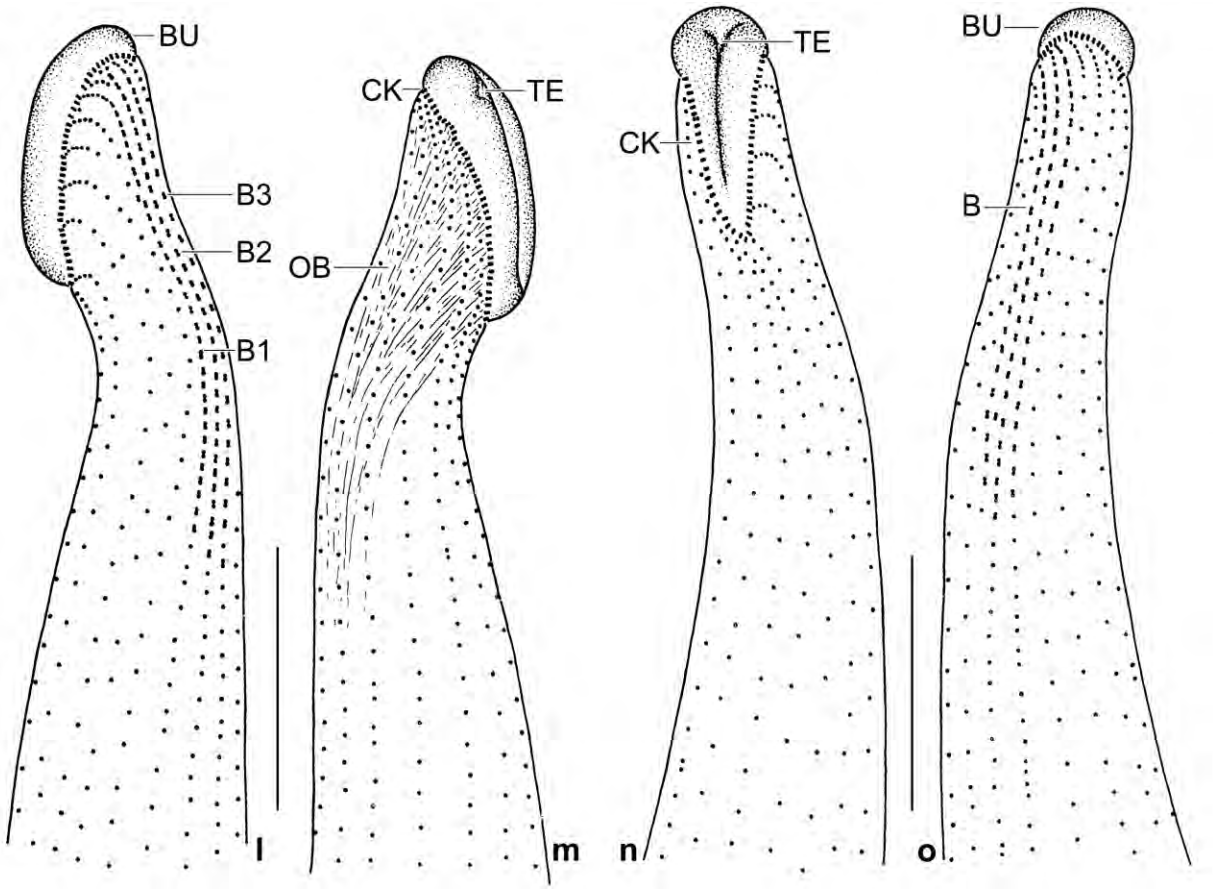

Fig. 62l–o. *Spathidium stetteri*, ciliary pattern in anterior body region after protargol impregnation. **l, m:** Left and right side view of holotype specimen (for an overview, see Fig. 62j). Note the spathidid ciliary pattern. **n, o:** Ventral and dorsal view, showing the cuneate circumoral kinety and the isostichad dorsal brush. B(1, 2, 3) – dorsal brush (rows), BU – oral bulge, CK – circumoral kinety, OB – oral basket, TE – temporary cytostome. Scale bars 20 µm.

and in protargol preparations. Shape narrowly spatulate to almost cylindroid, neck moderately distinct, slender specimens can curve anterior body region (Fig. 62f, j); anterior end distinctly oblique, posterior rounded, widest in or slightly posterior of mid-body (Fig. 62a, f–h, j, 63a, c; Table 22). Macronucleus in central quarters of body, a long and highly tortuous, slightly flattened strand frequently coiled and/or with slightly inflated ends; rarely more or less moniliform or in two pieces (observed in only two out of 40 specimens); studded with nucleoli up to 7 µm across. On average six globular micronuclei near and attached to macronuclear strand (Fig. 62a, j; Table 22). Contractile vacuole and some excretory pores in rear end (Fig. 62a, j). Mature extrusomes studded in oral bulge, rod-shaped and slightly curved, in vivo 6–7 × 0.3–0.4 µm in size (Fig. 62a–c, 63f, k, l, o); do not impregnate with the protargol method used while some fusiform cytoplasmic developmental stages impregnate deeply. Cortex flexible; cortical granules difficult to recognize because only ~ 0.2 µm across and colourless, form about six rows between each two kineties (Fig. 62d). Cytoplasm colourless, contains numerous lipid droplets up to 7 µm across and some food vacuoles mainly in posterior body half, usually hyaline in anterior quarter (Fig. 62a). Food not known. Swims and creeps rather rapidly.

Somatic cilia about 10 µm long in vivo, arranged in an average of 17 ordinarily spaced, mostly

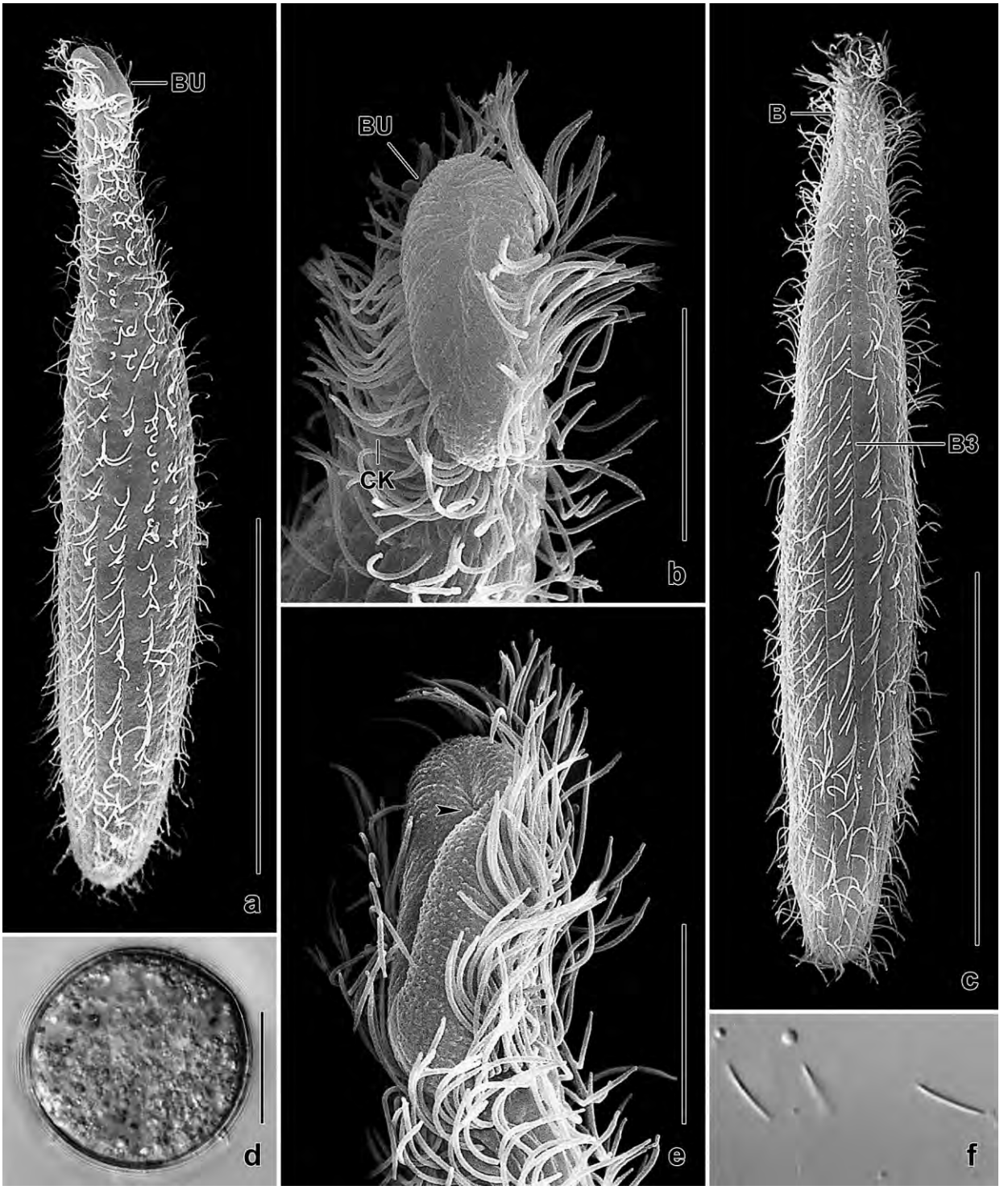

Fig. 63a–f. *Spathidium stetteri* from life (d, f) and in the scanning electron microscope (a–c, e). **a:** Ventrolateral view, showing body shape and short oral bulge. **b:** Frontal view of the cuneate oral bulge. **c:** Dorsal overview, showing brush row 3 which is heteromorphic in the posterior half, where bristles and ordinary cilia alternate. **d:** Resting cyst without mucous coat. The cyst wall is smooth and thin. **e:** Ventrolateral view of oral bulge, showing the temporary cytostome (arrowhead). **f:** Mature extrusomes, length 6–7 µm. B(3) – dorsal brush (row), BU – oral bulge, CK – circumoral kinety. Scale bars 10 µm (b, e), 20 µm (d), and 60 µm (a, c).

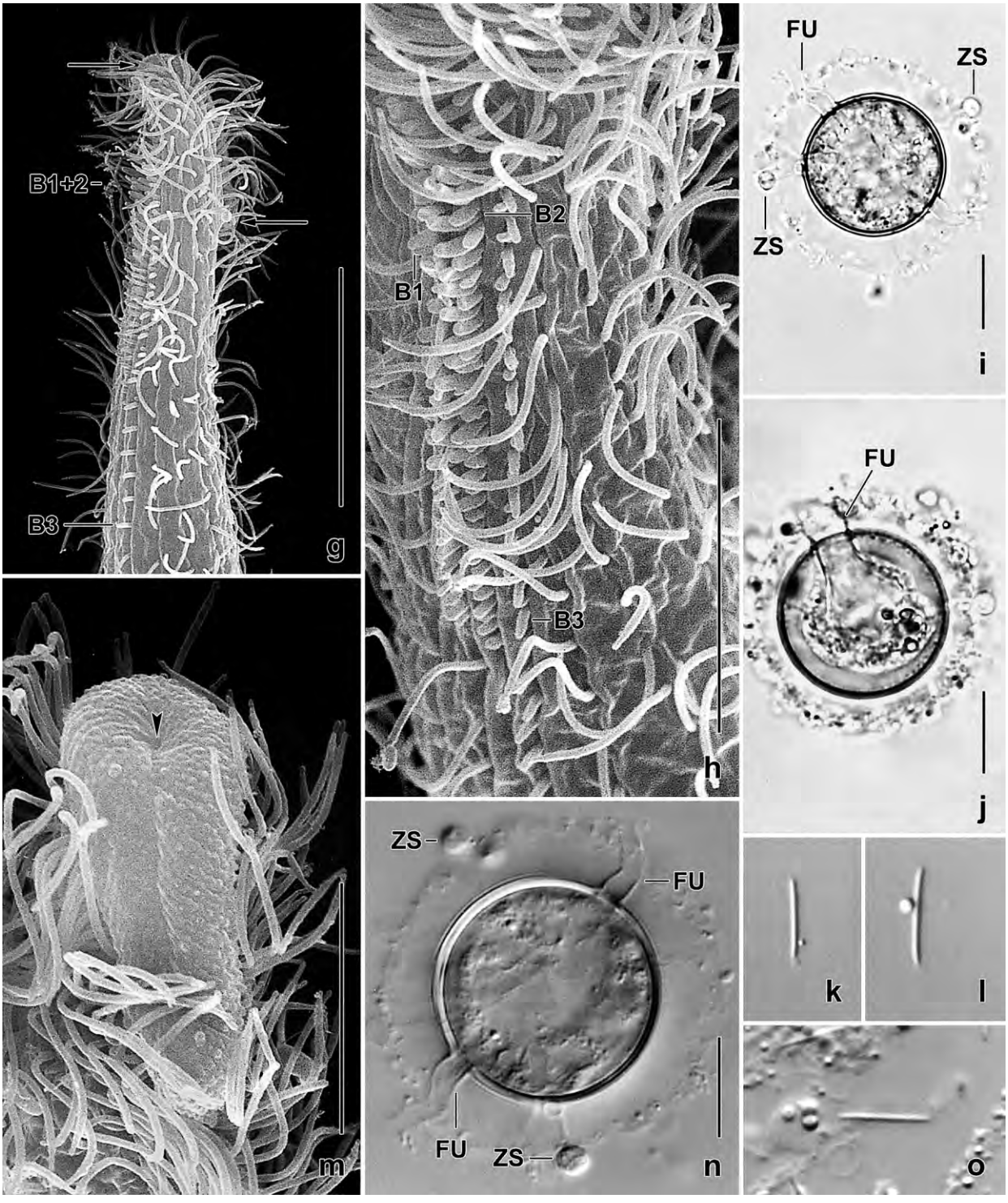

Fig. 63g–o. *Spathidium stetteri* from life (i, j–l, n, o) and in the scanning electron microscope (g, h, m). **g:** Right side view of anterior body region. Arrows mark oral bulge. **h:** Dorsal view, showing the three rows of the dorsal brush. **i, j, n:** Resting cysts infected by a fungus. Some zoospores are on the mucus coat. **k, l, o:** Mature extrusomes, length 6–7 µm. Depending on the side viewed, they are straight or slightly curved. **m:** Frontal view of oral bulge, which is cuneate and has a emporary cytostome (arrowhead) near the dorsal end. B1, 2, 3 – dorsal brush rows, FU – fungus, ZS – zoospores. Scale bars 10 µm (h, m) and 20 µm (g, i, j, n).

bipolar and ordinarily ciliated rows abutting on circumoral kinety in typical *Spathidium* pattern; anterior end of kineties densely ciliated; occasionally some irregularities, such as minute breaks and/or short, supernumerary rows (Fig. 62a, j, l–o, 63a, c; Table 22). Dorsal brush slightly dorsolateral, isostichad, dikinetal and three-rowed, inconspicuous because occupying only about 20% of body length and bristles merely up to 3 µm long in vivo; all rows commence at circumoral kinety with some ordinary cilia and end at similar level posteriorly continuing as ordinary somatic kineties, except of row 3 (Fig. 62a, e, j, l, o, 63c, g, h; Table 22). Brush row 1 slightly shorter than rows 2 and 3, composed of an average of 25 dikinetids associated with about 3 µm long, slightly inflated bristles. Longest brush row 2 composed of an average of 30 dikinetids associated with about 2.5 µm long anterior bristles and 3 µm long posterior bristles. Brush row 3 composed of an average of 23 dikinetids more loosely spaced (~ 1.5 µm) than those of rows 1 and 2 (~ 1.2 µm), anterior bristle of dikinetids about 1.5 µm long, posterior 2 µm; with monokinetal tail extending to mid-body, posterior half of tail heteromorphic comprising about 1.5 µm long bristles mixed with ordinary cilia (Fig. 62a, e, 63c, g, h; Table 22).

Oral bulge occupies anterior body end slanted 45°–60°, on average 80% as long as widest trunk region; moderately distinct because slightly ∞-shaped in lateral view and about 4 µm high. Surface flat to slightly convex, concave only at temporary cytostome near dorsal bulge end; cuneate or narrowly obovate in frontal view (Fig. 62a, c, f–h, j, l, m, 63a, b, e, g, m; Table 22). Circumoral kinety cuneate, slightly rugged by somatic ciliary rows, composed of ordinarily spaced dikinetids each associated with a cilium and a faintly impregnated nematodesma. Oral basket hardly recognizable in vivo but fairly distinct in protargol preparations (Fig. 62j, l–n, 63b; Table 22).

Resting cyst: Mature resting cysts globular and colourless, covered by an about 7 µm thick, solid mucous layer colonized by various bacteria. Cyst proper on average 40.3 µm across (M = 40.0, SD = 3.4, CV = 8.4, Min = 35.0, Max = 45.0, n = 15). Cyst wall smooth, bipartite, about 1.5 µm thick. Cytoplasm packed with macronucleus and lipid droplets (Fig. 62i, 63d). Cysts soon became parasitized by a fungus (Fig. 63i, j, n), possibly a *Ciliatomyces* species, as described by Foissner & Foissner (1986, 1995).

Occurrence and ecology: As yet found at type locality and in sample (70), where it became abundant five and 12 days, respectively, after setting up the non-flooded Petri dish cultures. The slender shape and the occurrence in sample (70) indicate that *P. stetteri* is a "true" soil ciliate tolerating brackish conditions.

Remarks: *Spathidium stetteri* resembles *S. procerum* (Fig. 62k), as redescribed by Foissner (1984). They differ in two main features: body shape (length:width ratio 7:1 vs. 12:1 on average) and number of ciliary rows (17 vs. 10 on average). The values for → *S. procerum* have been confirmed in a population from the Dominican Republic. Possibly, there is a further different feature which, however, has not yet been investigated in *S. procerum*: the heteromorphic bristle tail of brush row 3 (Fig. 62a, e, 63c). *Spathidium stetteri* is easily confused with *S. ascendens*, as redesribed by Foissner (1987c). They differ by the length of the extrusomes (6 vs. 8–12 µm), the number of ciliary rows (17 vs. 21), the length of the oral bulge (19 vs. 26 µm) and, especially, by the resting cyst (wall smooth vs. spiny).

Spathidium inopinatum **nov. spec.** (Fig. 64a–h, j–m; Table 23)

Diagnosis: Size in vivo about 135 × 18 µm. Very narrowly spatulate with oblique, oblong oral bulge about as long as widest trunk region. Macronucleus oblong, on average 26 × 5 µm in protargol preparations; micronucleus discoidal. Mature extrusomes in vivo slightly curved rods about 6 × 0.5 µm in size. One size type of cortical granules. On average 9 ciliary rows, 3 anteriorly modified to a heterostichad dorsal brush with longest row 2 occupying 16% of body length on average; row 1 longer than row 3.

Type locality: Venezuelan site (14), i. e., soil from a *Tachypogon* savanna in the outskirts of the town of Puerto Ayacucho, 67°36'W 5°41'N.

Type material: 1 holotype and 4 paratype slides with protargol-impregnated specimens have been deposited in the Biology Centre of the Upper Austrian Museum in Linz (LI). Relevant specimens have been marked with black ink circles on the coverslip.

Etymology: The Latin adjective *inopinatus* (unexpected) refers to the unexpectedly short macronucleus in this long and slender species.

Description: Size in vivo 110–180 × 15–25 µm, usually about 135 × 18 µm, as calculated from some in vivo measurements and the morphometric data in Table 23 adding 15% preparation shrinkage; length:width ratio also highly variable, viz., 5.3–10.2:1, on average about 7.8:1 in protargol preparations (Table 23). Body narrowly spatulate to cylindroidal, unflattened, neck indistinct in very slender cells; both ends narrowly rounded, widest in or slightly posterior to mid-body (Fig. 64a, e, j, l, m; Table 23). Nuclear apparatus in or near mid-body (Fig. 64a, e, l; Table 23). Macronucleus oblong to cylindroidal, very rarely spiral, 40 × 5 µm in a live specimen, in protargol preparations 26 × 5 µm on average; with many small nucleoli. One micronucleus attached to macronucleus, discoidal, in vivo about 4–5 × 2–3 × 1–2 µm; does not impregnate in one third of specimens. Contractile vacuole in posterior body end, some excretory pores in pole area (Fig. 64f). Mature extrusomes form a row each in right and left half of oral bulge; slightly curved rods with rounded ends and a size of 5–6 × 0.4–0.6 µm in vivo (Fig. 64a–c, m); do not impregnate with the protargol method used. Cortex flexible, contains about five rows of colourless, narrowly spaced granules between two kineties each; granules usually impregnating with protargol blurring trunk ciliary pattern (Fig. 64d). Cytoplasm colourless, contains few to many lipid droplets up to 5 µm across (Fig. 64a). Swims rather rapidly, showing great flexibility between soil particles.

Somatic cilia in vivo about 8 µm long, arranged in an average of nine ordinarily spaced, bipolar rows abutting on circumoral kinety in *Spathidium* pattern (Fig. 64a, e, f, h, j, k; Table 23). Dorsal brush dorsolaterally located, three-rowed each with a distinct monokinetal anterior tail, heterostichad because row 3 shorter by about 33% than longest row 2 occupying 16% of body length on average. Brush bristles up to 5 µm long in vivo, not studied in detail. Brush rows 1 and 2 of similar length, composed of 12–13 dikinetids on average; dikinetal portion of row 3 only half as long as in rows 1 and 2, composed of an average of 8 kinetids followed by a monokinetal tail extending to second body third with 1–2 µm long bristles (Fig. 64a, h, k; Table 23).

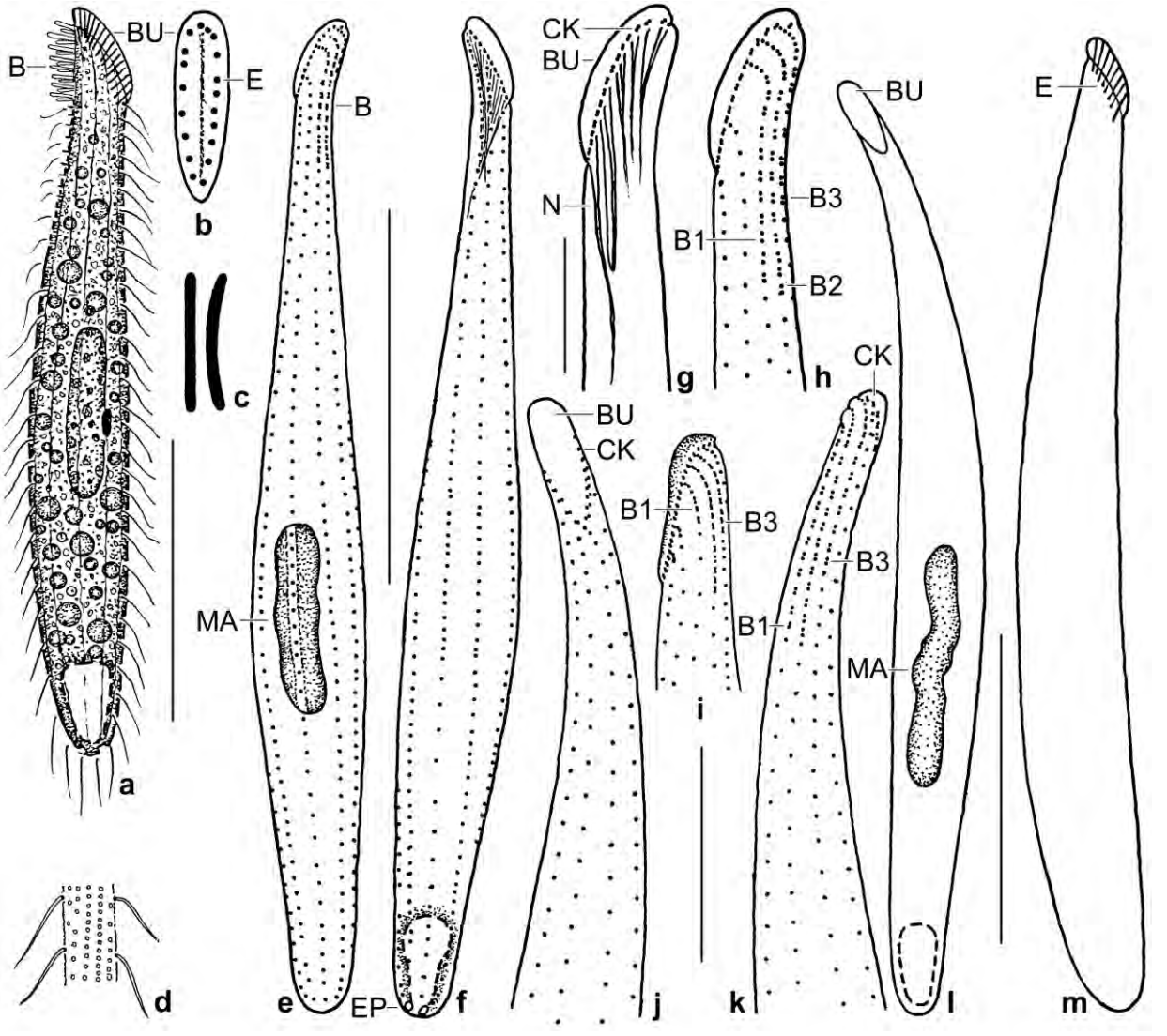

Fig. 64a–m. *Spathidium inopinatum* (a–h, j–m) and *S. etoschense* (i, from Foissner et al. 2002) from life (a–d, m) and after protargol impregnation (e–l). **a:** Right side view of a representative specimen, length 135 µm. **b:** Frontal view of oral bulge. **c:** Two views of the same extrusome, length 6 µm. **d:** Surface view, showing cortical granulation. **e–h:** Left and right side view of the slender holotype specimen, length 135 µm. **i:** Brush row 1 of *S. etoschense* is shorter than row 3, which contrasts *S. inopinatum* (h, k), and is thus a main distinguishing feature. **j–k, l:** Overview (l) and details (j, k), showing the shape of the oral bulge and the dorsal brush. **m:** A specimen with inconspicuous neck. B(1–3) – dorsal brush (rows), BU – oral bulge, CK – circumoral kinety, E – extrusomes, EP – excretory pores of the contractile vacuole, MA – macronucleus, N – nematodesmata. Scale bars 10 µm (g, h), 20 µm (j, k), and 50 µm (a, e, f, l).

Oral bulge occupies anterior body end slanted by about 45°, about as long as widest trunk region, slightly convex, oblong with bluntly pointed ventral end; inconspicuous in vivo because short and only 3–4 µm high (Fig. 64a, b, e–h, j–m; Table 23). Circumoral kinety of same shape as oral bulge, continuous, that is, not interrupted by somatic kineties; composed of an average of 31 comparatively widely spaced dikinetids each associated with a cilium, a fibre extending into the pharynx, and an oral basket rod. Oral basket short compared to body length, of ordinary structure (Fig. 64f, g, j, l; Table 23).

Occurrence and ecology: As yet, found at type locality and in a sample nearby. It appeared two weeks after rewetting the samples and remained sparse in the non-flooded Petri dish cultures. Very likely, *S. inopinatum* is a "true" soil inhabitant because it is slender and has a moderate size.

Remarks: There is only one species, *S. etoschense* FOISSNER at al., 2002, which can be confused with *S. inopinatum* because it has a similar shape of body and macronucleus and a similar number of ciliary rows (Table 23). However, *S. etoschense* has acicular (vs. rod-shaped) extrusomes and row 1 of the dorsal brush is shorter (vs. longer) than row 3. Further, the macronucleus of *S. etoschense* is considerably longer than in *S. inopinatum* (ratio body length: macronucleus length 2.6 vs. 5.2; Table 23); likewise, the oral bulge of *S. etoschense* is distinctly longer than in *S. inopinatum* (23 vs. 12 µm; Table 23).

There is also some similarity with *Apospathidium atypicum* which, inter alia, has a similar body size and number of ciliary rows as well as the same macronucleus type (for a review, see FOISSNER et al. 2002). However, *A. atypicum* has the posterior body region distinctly narrowed (vs. slightly) and the contractile vacuole far subterminal (vs. terminal). Further, it has somatic extrusomes absent from *S. inopinatum*.

Table 23. Morphometric data on *Spathidium inopinatum* and *S. etoschense* (from FOISSNER et al. 2002) based on mounted, protargol-impregnated (FOISSNER's method), and randomly selected specimens from non-flooded Petri dish cultures. Measurements in µm. CV – coefficient of variation in %, M – median, Max – maximum, Mean – arithmetic mean, Min – minimum, n – number of individuals investigated, SD – standard deviation, SE – standard error of arithmetic mean.

Characteristics	Mean	M	SD	SE	CV	Min	Max	n
Body, length	117.2	112.0	15.3	3.4	13.1	97.0	152.0	21
	145.0	145.0	15.9	5.3	10.9	123.0	180.0	9
Body, width	15.3	15.0	2.1	0.5	13.7	13.0	20.0	21
	22.7	22.0	4.9	1.6	21.8	17.0	32.0	9
Body length:width, ratio	7.8	7.5	1.4	0.3	17.3	5.3	10.2	21
	6.7	6.7	1.4	0.5	20.3	4.1	8.2	9
Oral bulge, length	12.3	12.0	1.4	0.3	11.3	9.0	15.0	21
	22.7	23.0	4.1	1.4	17.9	16.0	29.0	9
Circumoral kinety to last dikinetid of brush row 1, distance	16.8	16.0	3.1	0.9	18.4	12.0	22.0	13
	8.0	7.0	3.8	1.4	54.7	4.0	14.0	7
Circumoral kinety to last dikinetid of brush row 2, distance	18.3	17.0	3.5	1.0	19.0	14.0	25.0	13
	18.1	17.0	3.0	1.1	16.4	14.0	23.0	7
Circumoral kinety to last dikinetid of brush row 3, distance	12.3	12.0	2.8	0.8	22.8	8.0	18.0	13
	13.3	13.0	4.0	1.5	30.0	7.0	20.0	7
Nuclear figure, length	26.9	26.0	3.6	0.8	13.4	21.0	35.0	21
	42.7	39.0	14.5	4.8	33.9	24.0	76.0	9
Macronucleus, estimated total length when uncoiled (rough data)	26.9	26.0	3.6	0.8	13.4	21.0	35.0	21
	57.1	55.0	–	–	–	44.0	90.0	9
Body length:macronucleus total length, ratio	5.2	4.4	3.6	0.8	69.5	3.3	6.1	21
	2.6	2.7	0.5	0.2	18.6	2.0	3.3	9
Macronucleus, width	5.0	5.0	0.5	0.1	8.9	4.0	6.0	21

continued

Characteristics	Mean	M	SD	SE	CV	Min	Max	n
	5.0	5.0	0.7	0.2	13.1	4.0	6.0	15
Micronuclei, number	1.0	1.0	0.0	0.0	0.0	1.0	1.0	11
	several							
Somatic kineties, number	8.6	8.5	0.7	0.2	7.8	8.0	10.0	12
	10.4	11.0	1.1	0.4	10.9	9.0	12.0	9
Ciliated kinetids in a right side kinety, number	not counted							
	64.0	68.0	9.1	3.7	14.2	46.0	70.0	6
Dorsal brush rows, number	3.0	3.0	0.0	0.0	0.0	3.0	3.0	13
	3.1	3.0	–	–	–	3.0	4.0	7
Dikinetids in brush row 1, number	12.6	12.0	1.9	0.5	14.7	11.0	17.0	13
	5.4	6.0	2.1	0.7	39.8	3.0	8.0	7
Dikinetids in brush row 2, number	13.9	13.0	1.9	0.5	13.8	12.0	19.0	13
	17.6	19.0	3.9	1.5	22.0	12.0	21.0	7
Dikinetids in brush row 3, number	8.0	8.0	1.2	0.3	15.3	7.0	11.0	13
	12.3	12.0	2.0	0.7	16.1	9.0	15.0	7
Circumoral dikinetids, number	30.9	32.0	2.9	0.8	9.3	25.0	35.0	13
	not counted							
Anterior body end to macronucleus, distance	52.4	50.0	10.3	2.2	19.6	40.0	84.0	21
	not measured							

We consider the African *S. etoschense* and the South American *S. inopinatum* as an impressive example of geographic speciation. For details, see chapter 3.1.5a.

Spathidium curiosum Foissner & Xu **nov. spec.** (Fig. 65a–j; Table 24)

Diagnosis: Size in vivo about 120 × 30 µm. Narrowly spatulate with oblique, oblong oral bulge about two thirds as long as widest trunk region. Macronucleus long and tortuous; multimicronucleate. Oral extrusomes in vivo about 15 × 1 µm, rod-shaped to indistinctly acicular, with conspicuous subterminal lenticular inflation. One size type of cortical granules. On average 21 ciliary rows, 3 anteriorly modified to a heterostichad dorsal brush with longest row 2 occupying 23% of body length on average.

Type locality: Surface soil of a savanna in the Parque Nacional Torres del Paine, Lago de Oros, Chile, 73°26'W 51°0'S.

Type material: 1 holotype and 4 paratype slides with protargol-impregnated specimens have been deposited in the Biology Centre of the Upper Austrian Museum in Linz (LI). Relevant specimens have been marked by black ink circles on the coverslip.

Etymology: The Latin adjective *curiosus* (curious) refers to the drumstick-shaped extrusomes.

Description: Size in vivo 100–170 × 20–40 µm, usually about 120 × 30 µm, as calculated from some in vivo measurements and the morphometric data in Table 24 adding 15% preparation shrinkage; length:width ratio 3.1–5.8:1, on average near 4:1 both in vivo and in protargol preparations (Table 24). Size and shape similar to *Epispathidium terricola* Foissner, 1987c

Table 24. Morphometric data on *Spathidium curiosum* based on mounted, protargol-impregnated (FOISSNER's method), and randomly selected specimens from a non-flooded Petri dish culture. Measurements in µm. CV – coefficient of variation in %, CK – circumoral kinety, M – median, Max – maximum, Mean – arithmetic mean, Min – minimum, n – number of individuals investigated, SD – standard deviation, SE – standard error of arithmetic mean.

Characteristics	Mean	M	SD	SE	CV	Min	Max	n
Body, length	107.3	102.0	16.7	3.6	15.6	88.0	148.0	21
Body, width	25.7	23.0	4.9	1.1	18.9	20.0	35.0	21
Body length:width, ratio	4.2	4.2	0.6	0.1	14.7	3.1	5.8	21
Oral bulge, length	17.8	18.0	2.6	0.6	14.5	13.0	22.0	21
Oral bulge, width	6.3	6.0	0.5	0.2	7.4	6.0	7.0	8
Oral bulge, height	3.5	3.0	0.6	0.1	16.7	3.0	5.0	21
Oral bulge length:body width, ratio	0.7	0.7	0.1	–	19.4	0.5	1.0	21
CK to last dikinetid of brush row 1, distance	24.5	24.0	4.4	1.2	17.7	17.0	33.0	13
CK to last dikinetid of brush row 2, distance	25.0	25.0	4.5	1.2	17.9	18.0	34.0	13
CK to last dikinetid of brush row 3, distance	12.7	12.0	3.0	0.8	23.9	10.0	20.0	13
Anterior body end to macronucleus, distance	36.1	35.0	8.6	1.9	23.9	25.0	55.0	21
Macronucleus figure, length	51.1	50.0	11.9	2.6	23.2	30.0	75.0	21
Macronucleus, length (spread and thus approximate)	111.0	110.0	–	–	–	70.0	200.0	21
Macronucleus, width in middle third	4.6	5.0	0.7	0.2	16.0	3.0	6.0	21
Micronuclei, length	5.0	5.0	1.2	0.3	24.3	3.0	8.0	21
Micronuclei, width	1.9	2.0	0.3	0.1	14.3	1.5	2.5	21
Micronuclei, number	2.3	2.0	0.6	0.1	24.5	1.0	3.0	21
Macronucleus-associated inclusions, length	6.8	7.0	1.8	0.4	26.1	4.0	10.0	21
Macronucleus-associated inclusions, width	4.1	4.0	1.7	0.4	40.8	2.0	8.0	21
Macronucleus-associated (including micronucleus-like) inclusions, number	8.4	7.0	3.5	0.8	41.0	4.0	17.0	21
Somatic kineties, number	21.0	21.0	1.1	0.3	5.1	19.0	23.0	15
Dikinetids in brush row 1, number	23.3	22.0	4.3	1.2	18.3	17.0	33.0	13
Dikinetids in brush row 2, number	24.0	24.0	4.7	1.3	19.8	18.0	33.0	13
Dikinetids in brush row 3, number	10.2	10.0	2.4	0.7	23.7	7.0	16.0	13

but usually narrowly spatulate to slightly obclavate with rather indistinct neck flattened up to 2:1; anterior end oblique, posterior rounded, widest posterior of mid-body (Fig. 65a, c, d, i, j; Table 24). Macronucleus in middle quarters of cell, long and tortuous, contains many globular nucleoli up to 2 µm across; in all specimens seen surrounded by more or less flattened, variform structures, possibly decaying macronuclear material and/or micronuclei, with an average size of 7 × 4 µm and with many argyrophilic granules causing a dotted appearance. Several micronuclei near and attached to macronuclear strand, about 5 × 2 µm in size (Fig. 65a, c, d, g, i, j; Table 24). Contractile vacuole in posterior body end, some excretory pores in pole area. Mature oral bulge extrusomes in vivo about 15 × 0.7–1 µm in size, rod-shaped to slightly acicular and indistinctly curved, with conspicuous subterminal lenticular inflation; rarely impregnate lightly with the protargol method used while cytoplasmic developmental stages of various shapes and up to 15 µm in length impregnate deeply; in oral region 2–3 µm long, deeply impregnating rods, possibly a small type of extrusomes overlooked in vivo (Fig. 65a, b, f, g, j). Cortex flexible, contains

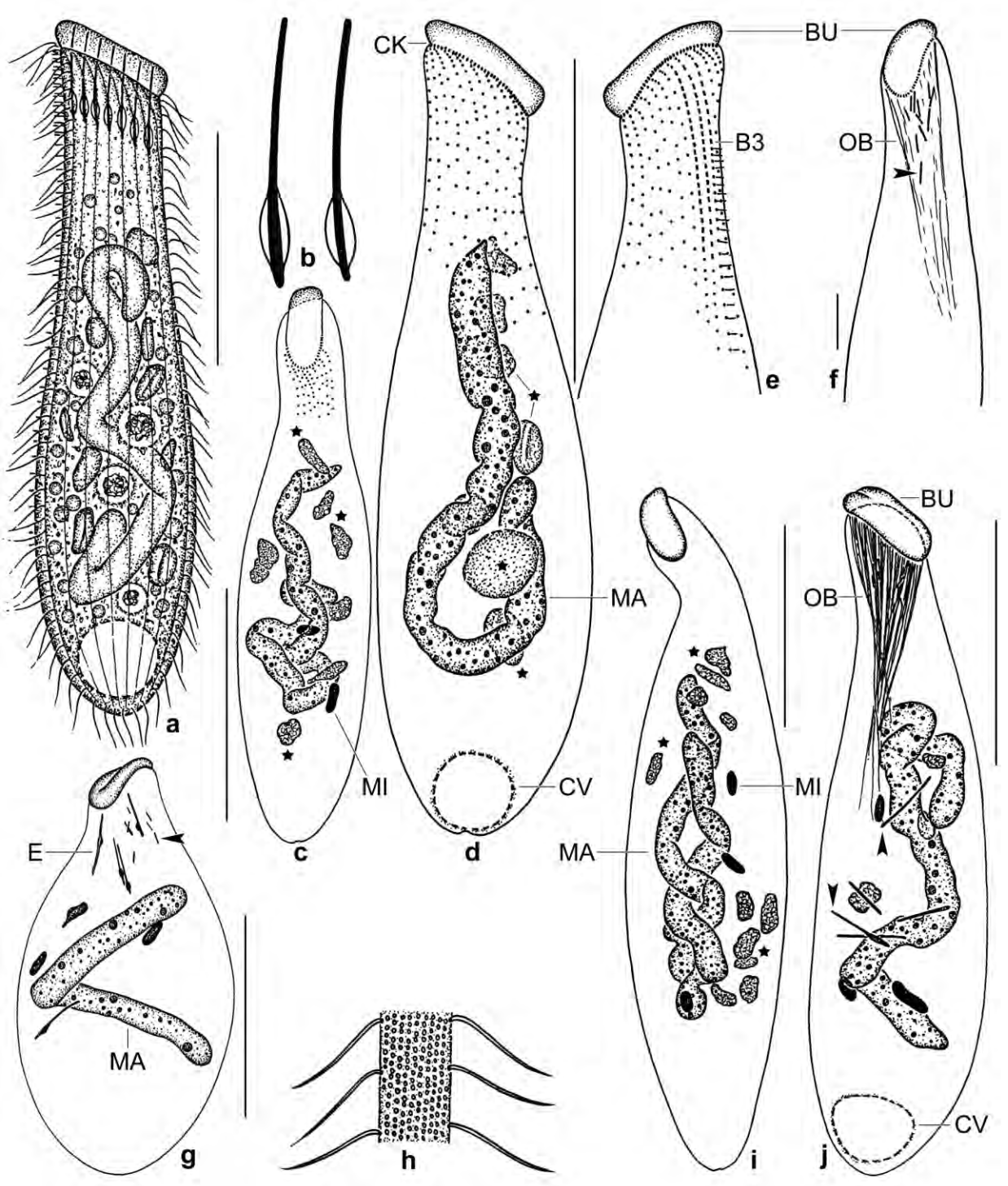

Fig. 65a–j. *Spathidium curiosum* from life (a, b, h) and after protargol impregnation (c–g, i, j). Asterisks denote decaying (?) macronuclear pieces and, possibly, micronuclei. **a:** Right side view of a representative specimen, length 120 µm. **b:** Oral bulge extrusomes, about 15 × 0.7–1 µm. **c, f, j:** Frontal views, showing the oblong oral bulge, the tortuous macronucleus, and the long oral basket. Arrowheads mark cytoplasmic extrusomes. **d, e:** Right and left side view of holotype specimen, length 100 µm. **g, i:** Size and shape variability. Arrowhead marks a minute extrusome. **h:** Surface view, showing cortical granulation. BU – oral bulge, B3 – dorsal brush row 3, CK – circumoral kinety, CV – contractile vacuole, E – extrusomes, MA – macronucleus, MI – micronucleus, OB – oral basket. Scale bars 10 µm (f) and 40 µm (a, c–g, i, j).

about ten rows of colourless, narrowly spaced granules – usually impregnating with protargol and blurring ciliary pattern between each two ciliary rows (Fig. 65h). Cytoplasm colourless, contains some lipid droplets as well as small and up to 40 µm-sized food vacuoles with remnants of amoebae, flagellates and ciliates (Fig 65a). Swims rather rapidly.

Somatic cilia about 8 µm long in vivo, arranged in an average of 21 ordinarily spaced, bipolar, ordinarily ciliated rows abutting on circumoral kinety in typical *Spathidium* pattern (Fig. 65a, c, d, e; Table 24). Dorsal brush dorsolaterally located, three-rowed, heterostichad because row 3 shorter by about 50% than longest row 2 occupying 23% of body length on average; all rows commence with some ordinary cilia, and rows 1 and 2 continue as somatic kineties posteriorly. Brush bristles minute, length increases from about 2 µm anteriorly to 3 µm posteriorly. Brush rows 1 and 2 end at same level on average, composed of an average of 23 and 24 dikinetids, respectively; dikinetal portion of row 3 only half as long as in rows 1 and 2, composed of an average of 10 dikinetids followed by a monokinetal tail extending to near body end with 1–2 µm long bristles (Fig. 65a, e; Table 24).

Oral bulge occupies anterior body end slanted by about 45°, rather conspicuous, though only about two thirds as long as widest trunk region, because up to 5 µm high and distinctly separate from body proper; flat to slightly convex, oblong with both ends broadly rounded (Fig. 65a, c–g, i, j; Table 24). Circumoral kinety slightly ∞-shaped in lateral view while oblong when seen frontally, ventral end broadly, rarely narrowly rounded, continuous, composed of ordinarily spaced dikinetids each associated with a cilium, a fibre extending into the pharynx, and a long oral basket rod. Nematodesmata (oral basket rods) rather conspicuous in the protargol preparations because bundled and extending to mid-body (Fig. 65c, f, j).

Occurrence and ecology: At type locality, *S. curiosum* was very rare in the non-flooded Petri dish culture. We found it also in Australia, viz., in soil from sugar cane fields in the outskirts of the towns of Cairns and Eubenangee.

Remarks: *Spathidium curiosum* differs from all described spathidids by the curious shape of the extrusomes (toxicysts). We carefully checked this feature in three populations (see above) because they are similar to developing extrusomes in several other spathidids. There is a considerable overall similarity of *S. curiosum* with *Epispathidium terricola* Foissner, 1987c. They differ in the number of ciliary rows (21 vs. 39), the ciliary pattern (*Spathidium* vs. indistinct *Epispathidium* pattern), and the length of the extrusomes (15 µm vs. 40 µm).

Spathidium duschli nov. spec. (Fig. 66a–p, 67a–u; Table 25)

Diagnosis: Size in vivo about 200 × 35 µm. Narrowly to very narrowly spatulate with oblique, cuneate oral bulge approximately as long as widest trunk region. About 100 ellipsoid, scattered macronuclear nodules; multimicronucleate. Oral extrusomes asymmetrically obclavate, circa 7 × 0.8 µm, proximal end strongly argyrophilic. One size type of cortical granules. About 20 ciliary rows, those in dorsal half of right side attached to circumoral kinetofragments, as in *Protospathidium*; dorsal brush inconspicuous, isostichad and of ordinary length occupying 25% of body length.

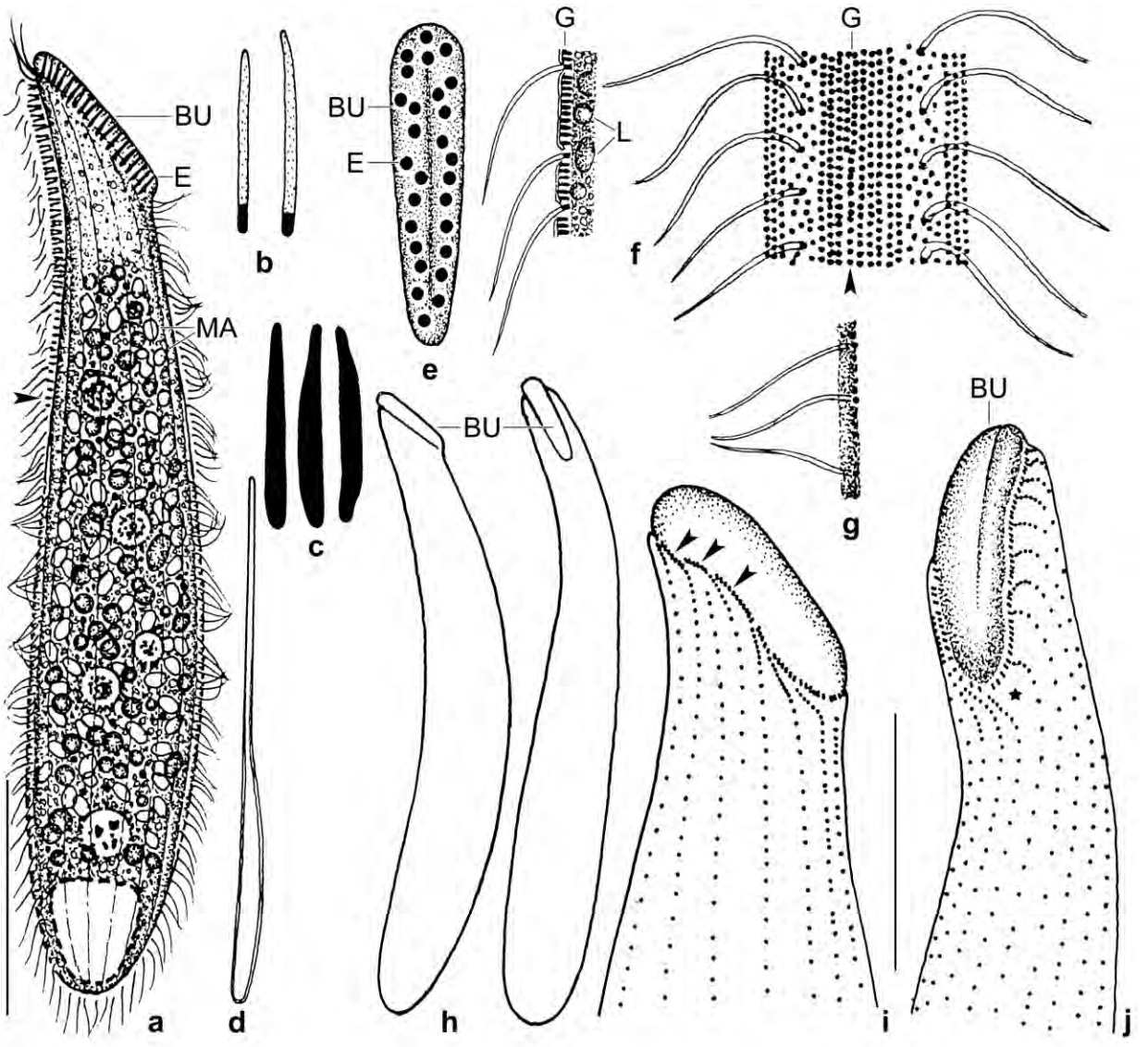

Fig. 66a–j. *Spathidium duschli* from life (a, c–f, h) and after protargol impregnation (b, g, i, j). **a:** Right side view of a representative specimen, length 200 µm. Arrowhead marks posterior end of bristle tail of brush row 3. **b:** Oral bulge extrusomes, length 6 µm. Occasionally, the anterior end is also argyrophilic. **c:** Resting oral bulge extrusomes, length 6–7 µm. The left two Figures show the same extrusome from the symmetrical and asymmetrical side. **d:** Exploded extrusome, length 17 µm. **e:** Frontal view of oral bulge. **f:** Optical section and surface view of cortex. Arrowhead marks a bifurcated granule row. **g:** Optical section showing mucous layer on cortex. **h:** A slender specimen seen from right and ventral side. The anterior portion is curved dorsally and right laterally. **i:** Ciliary pattern of a specimen with protospathidiid circumoral kinety (arrowheads) in dorsal half of cell, length of oral bulge 28 µm. **j:** Ventral view, length of oral bulge, 28 µm. Asterisk marks an inconspicuous inflation between last ventral and first left lateral kinety. BU – oral bulge, E – extrusomes, G – cortical granules, L – lipid droplets, MA – macronuclear nodules. Scale bars 50 µm.

Type locality: Venezuelan site (14), i. e., highly fertile field (Mahadja) soil from the surroundings of Pto. Ayacucho, 67°36'W 5°41'N.

Type material: 1 holotype, 3 paratype, and 4 voucher slides with protargol-impregnated specimens have been deposited in the Biology Centre of the Upper Austrian Museum in Linz (LI). The holotype and other relevant specimens have been marked by black ink circles on the coverslip.

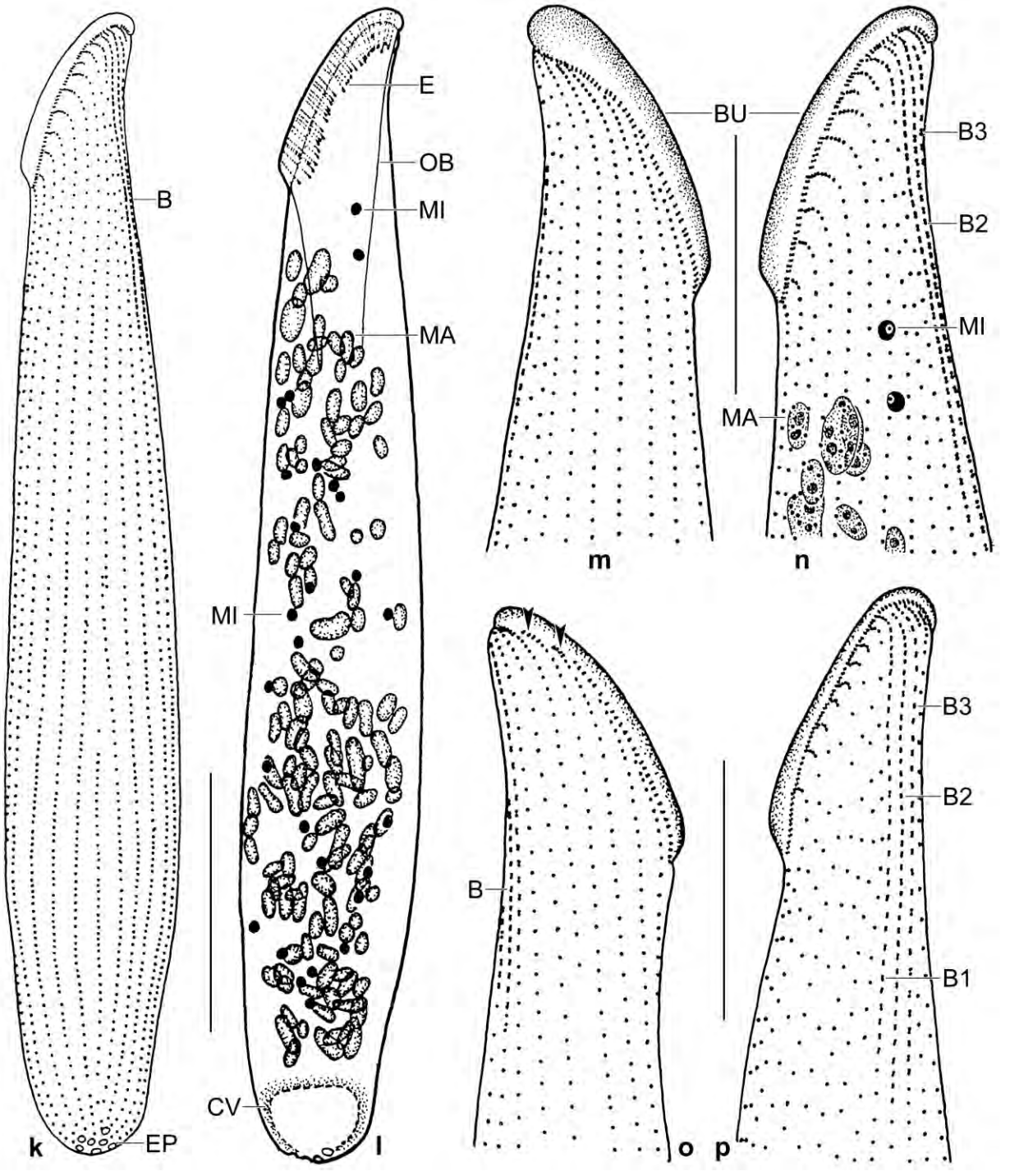

Fig. 66k–p. *Spathidium duschli*, ciliary pattern of type locality specimens after protargol impregnation. **k–n:** Left and right side views of holotype specimen, which has 135 macronuclear nodules and 27 micronuclei, length 220 µm. The proximal end of the oral bulge extrusomes is rather deeply impregnated. **o, p:** Ventro- and dorsolateral view of a specimen with protospathidiid circumoral kinetofragments (arrowheads) in right dorsal portion, bulge 36 µm. Note the isostichad dorsal brush with dikinetids wider spaced in row 3 than in rows 1 and 2. B(1–3) – dorsal brush (rows), BU – oral bulge, CV – contractile vacuole, E – extrusomes, EP – excretory pores, OB – oral basket, MA – macronuclear nodules, MI – micronuclei. Scale bars 30 µm (o, p), 40 µm (m, n), and 50 µm (k, l).

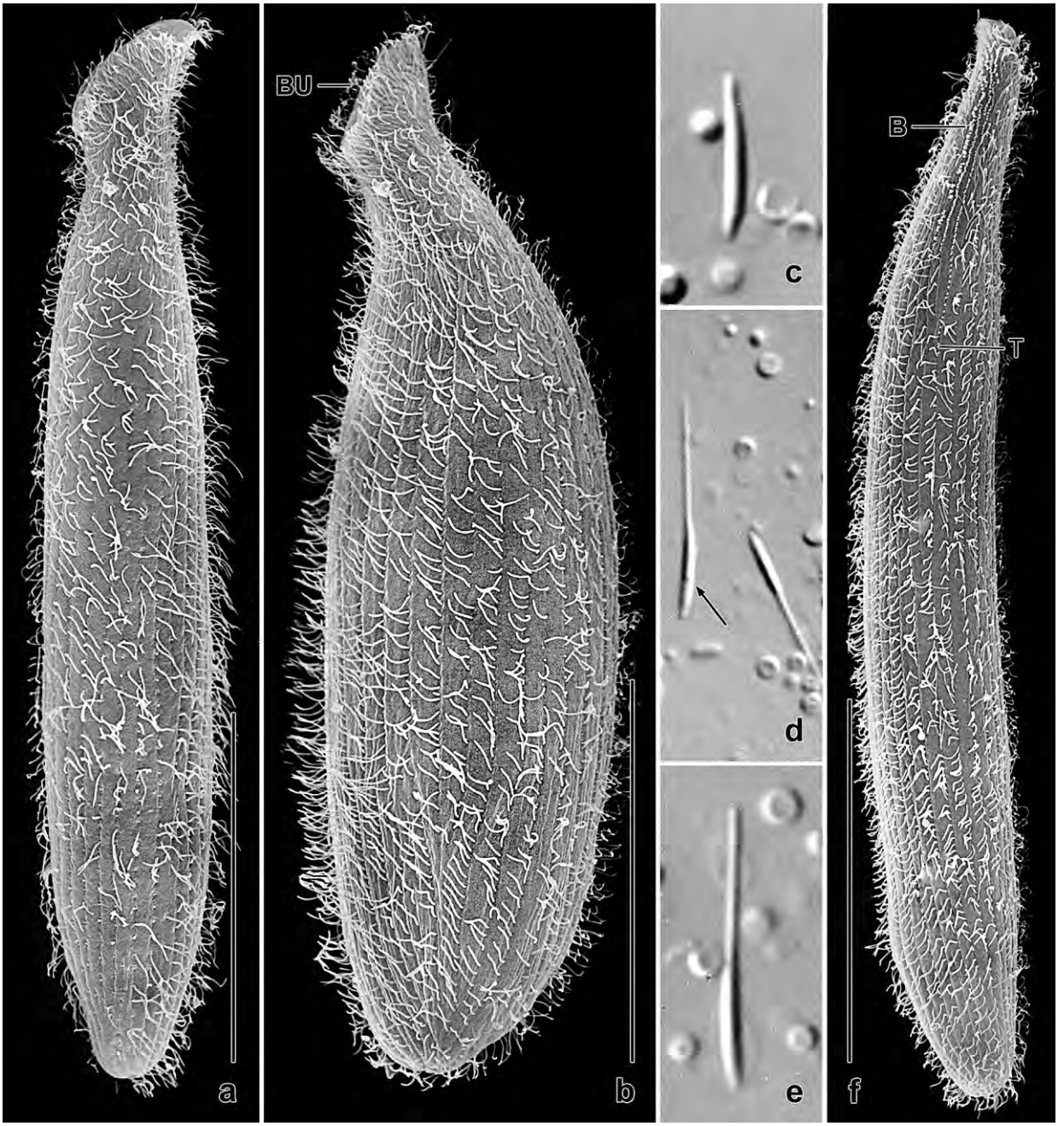

Fig. 67a–f. *Spathidium duschli*, Morrocoy National Park specimens in the scanning electron microscope (a, b, f) and from life (c–e). **a, b:** Left side views of an ordinary and of a fat specimen. **c:** Resting extrusome, length 7 µm. **d, e:** Exploded extrusomes, 10–17 µm long. Arrow marks an extrusome with partially extruded contents. **f:** Dorsal view, showing flattened left side and end of monokinetal bristle tail (T) of dorsal brush row 3. B – dorsal brush, BU – oral bulge. Scale bars 50 µm (a, b) and 70 µm (f).

Dedication: We dedicate this species to Univ.-Prof. Dr. Albert Duschl, Vice Rector of Salzburg University, for supporting our research group.

Description: The two populations studied in vivo and in protargol preparations are very similar, except for the number of macronuclear nodules and micronuclei (both doubled in type population specimens) and the length of the brush rows while the number of dikinetids composing the brush is

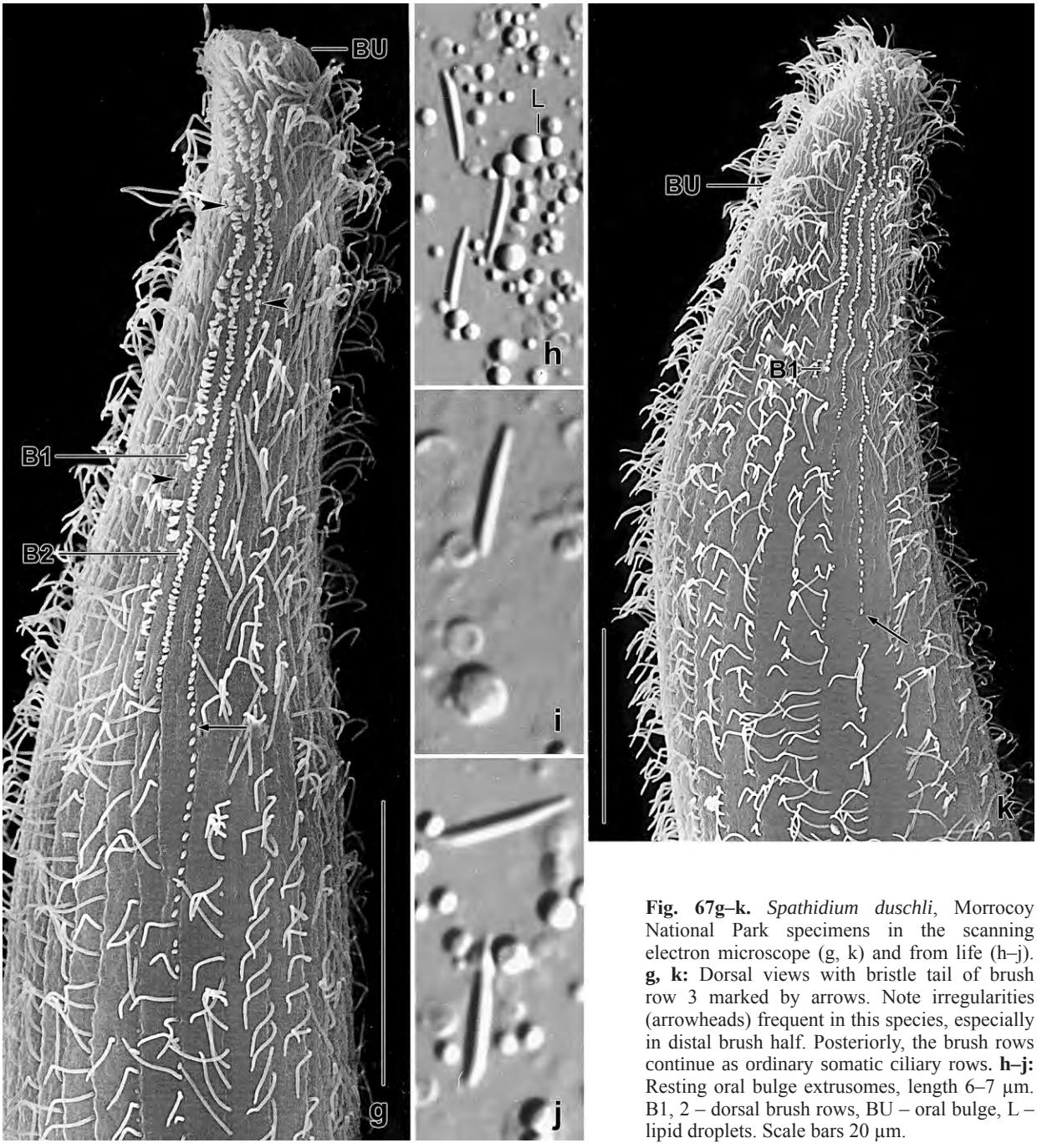

Fig. 67g–k. *Spathidium duschli*, Morrocoy National Park specimens in the scanning electron microscope (g, k) and from life (h–j). **g, k:** Dorsal views with bristle tail of brush row 3 marked by arrows. Note irregularities (arrowheads) frequent in this species, especially in distal brush half. Posteriorly, the brush rows continue as ordinary somatic ciliary rows. **h–j:** Resting oral bulge extrusomes, length 6–7 µm. B1, 2 – dorsal brush rows, BU – oral bulge, L – lipid droplets. Scale bars 20 µm.

almost identical, suggesting the length differences as culture effect. Thus, the diagnosis includes both populations, emphasizing, however, the type. The scanning electron micrographs are based on cultivated specimens of a third population found in the Morrocoy National Park.

Size highly variable, viz., 120–300 × 20–45 µm in vivo, usually about 200 × 35 µm, as calculated from some in vivo measurements and the morphometric data in Table 25 adding 15% preparation shrinkage; length:width ratio 3.5–8:1, on average near 6:1 both in vivo and in protargol-impregnated specimens while about 5:1 in SEM preparations (n = 8). Narrowly to very narrowly

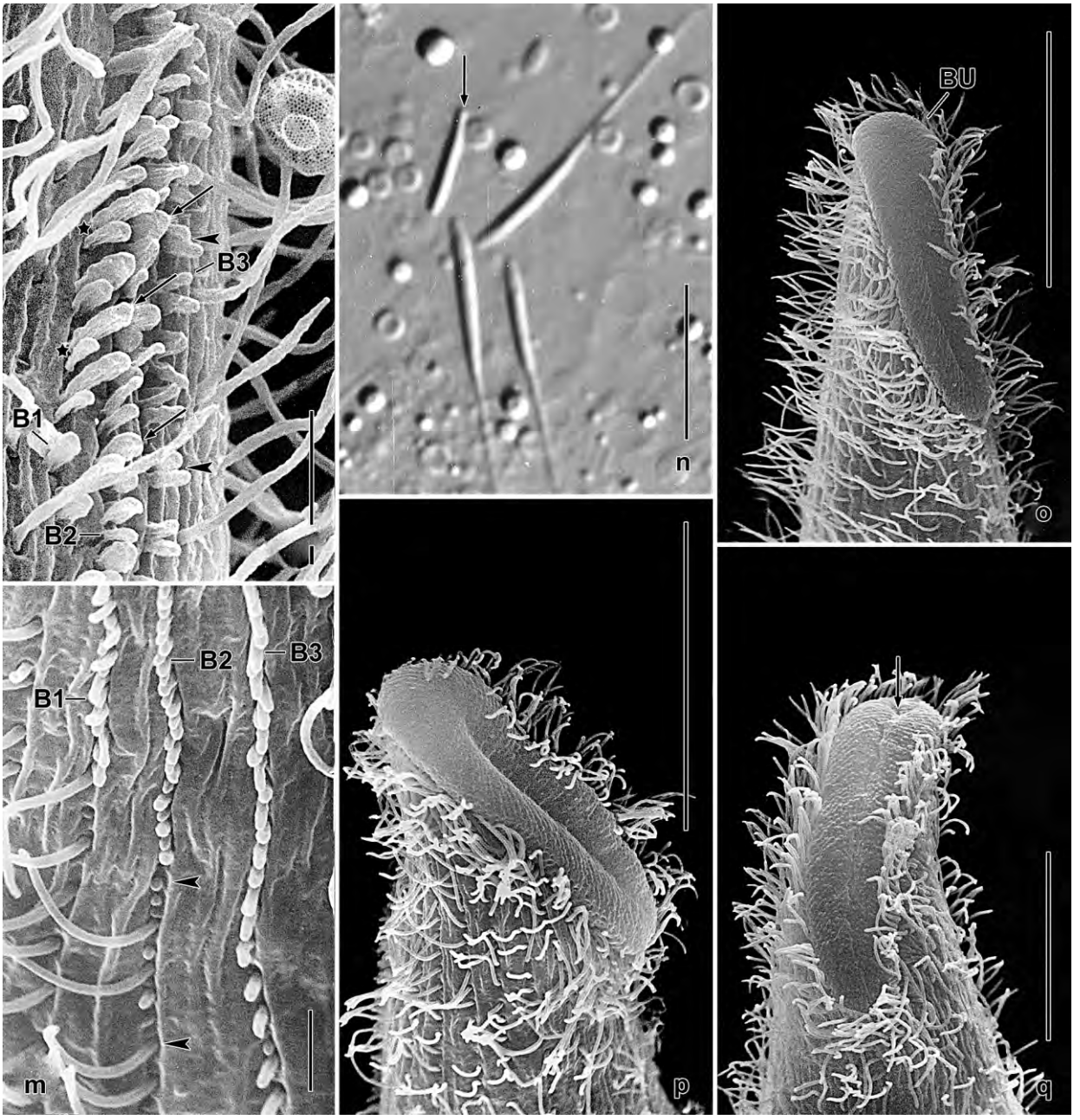

Fig. 67l–q. *Spathidium duschli*, Morrocoy National Park specimens from live (n) and in the scanning electron microscope (l, m, o–q). **l:** Middle portion of dorsal brush; clavate bristles wrinkled by the preparation procedures. The bristles, which are up to 4 µm long in vivo, are clavate (arrows) in rows 1 and 2 while rod-shaped (arrowheads) in row 3. The posterior bristle (asterisks) is distinctly shorter than the anterior in row 1; the bristles of row 2 have similar length while the anterior bristle (arrowheads) is slightly shorter than the posterior in row 3. **m:** Posterior end of dorsal brush, where the bristles decrease in length to 1 µm. Arrowheads mark heteromorphic end of row 2, where bristles and cilia alternate irregularly. **n:** Resting (arrow) and exploded extrusomes. **o, q:** Ventral views showing the cuneate oral bulge (BU) and the cyrtopharyngeal entrance (arrow). **p:** Right side view of a specimen with partially opened oral bulge. BU – oral bulge, B(1–3) – dorsal brush (rows). Scale bars 2 µm (m), 10 µm (n, q), and 20 µm (o, p).

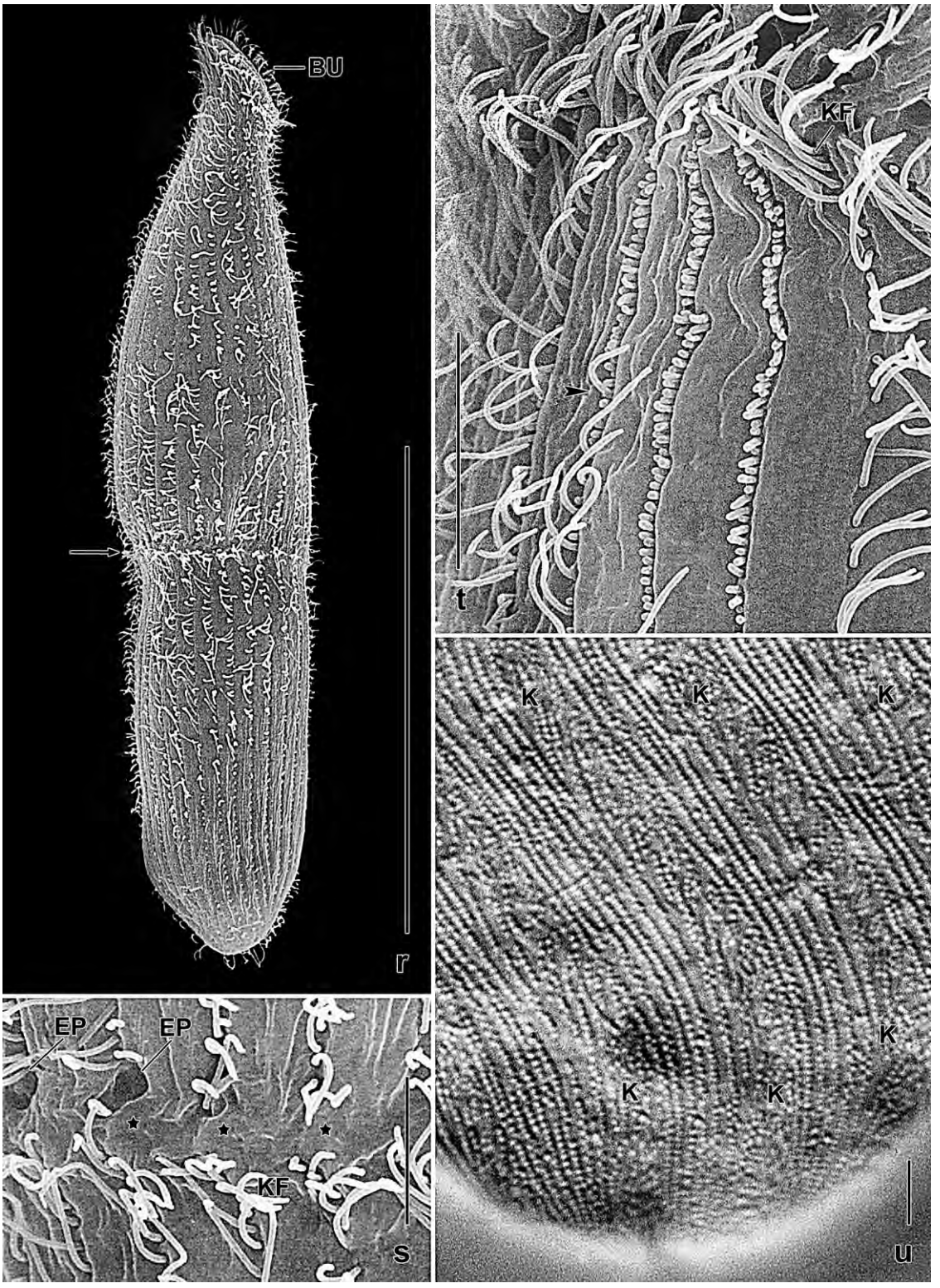

Fig. 67r–u. *Spathidium duschli*, Morrocoy National Park specimens in the SEM (r–t) and from life (u). **r, s:** Early divider showing indentation in prospective fission area (arrow) and division blebs (asterisks). **t:** Dorsal brush of an early divider. The parental cilia are replaced by bristles in row 1 (arrowhead). **u:** The cortical granulation is conspicuous. BU – oral bulge, EP – excretory pores, K – kineties, KF – circumoral kinetofragments. Scale bars 10 µm (s–u) and 100 µm (r).

spatulate with oblique anterior (oral) end, rather distinct neck, and rounded posterior end, widest usually in middle third of body; flattened only in hyaline oral region. Slender, almost parallel-sided specimens frequent and anteriorly curved dorsally and right laterally; thus, swimming and longitudinally rotating specimens describe a wide circle with anterior body region, looking like some asymmetric *Enchelyodon* species or a swimming cone (Fig. 66a, h, k, 67a, b, f). Macronuclear nodules and micronuclei scattered throughout body, except for oral and contractile vacuole region; nodules globular to oblong, on average ellipsoid, about 8 × 4 µm in protargol preparations; nucleoli of ordinary size and number. Micronuclei globular to broadly ellipsoid, about 3 µm across, usually impregnate deeply and thus well distinguishable from more faintly stained other cell inclusions (Fig. 66a, l, n; Table 25). Contractile vacuole in rear end, on average seven excretory pores scattered in pole area (Fig. 66a, k, l; Table 25). Mature extrusomes in vivo asymmetrically obclavate and 6–8 × 0.7–1 µm in size; rod-shaped to slightly acicular and faintly impregnated in protargol preparations, except for deeply impregnated anterior and/or posterior end, forming a dotted line each in and underneath oral bulge (Fig. 66a–c, e, l, 67c, h–j, n; Table 25). Released extrusomes of typical toxicyst structure, on average (n = 8) 13.1 µm (10–17) long in vivo (Fig. 66d, 67d, e, n). Cortex colourless and flexible, rather distinctly furrowed by ciliary rows, about 1 µm thick and jelly-like due to compact granules forming about ten conspicuous, sometimes bifurcated rows between each two kineties (Fig. 66f, 67u); individual granules highly refractive, about 0.8 × 0.4 µm in size, do not stain with methyl green-pyronin but slowly disappear, likely releasing a very hyaline substance forming an 1–3 µm thick, yellowish layer in protargol preparations, a rare feature in spathidiids (Fig. 66g). Cytoplasm packed with macronuclear nodules and lipid droplets 0.5–4 µm across. Feeds on various middle-sized ciliates, such as *Gonostomum affine*, and likely also on heterotrophic flagellates digested in 5–50 µm-sized vacuoles (Fig. 66a). Swims moderately rapid by rotation about main body axis, looking like a swimming cone as described above.

Cilia 10 µm long in vivo, arranged in an average of about 20 equidistant, frequently slightly disturbed (broken, shortened etc.), densely ciliated rows abutting on circumoral kinety in typical *Spathidium* pattern. Right side ciliary rows anteriorly distinctly curved dorsally and touching circumoral kinety, rarely still attached to the individual kinetofragments, forming protospathidiid pattern in dorsal half; left side rows densely ciliated anteriorly and abutting on continuous circumoral kinety; leftmost ventral and first left side kinety curved anteriorly, producing a slightly widened area (Fig. 66a, i–p; 67a, b, f; Table 25). Dorsal brush occupies about 25% of body length, inconspicuous because bristles only up to 4 µm long; isostichad with rows 1 and 3 slightly shorter than row 2, all rows with anterior tail and more or less irregular in over 50% of specimens, that is, have overlapping or non-overlapping breaks and lacking or supernumerary dikinetids forming short rows (Fig. 66a, m–p, 67f, g, k–m; Table 25). Further details recognizable in scanning electron micrographs (Fig. 67f, g, k–m): bristles become shorter posteriorly, where rows 1and 2 are often slightly heteromorphic; bristles of rows 1 and 2 distinctly clavate, those of row 3 inflated only in anterior portion; posterior bristle of dikinetids shorter by up to 50% in rows 1 and 3; posterior tail of row 3 short, consisting of only 13–16 (n = 3) minute (~ 1 µm) bristles (seen also in type locality specimens).

Oral bulge occupies anterior body end slanted by 40–70° ($\bar{\times}$ = 52°, n = 12), on average about as long as widest trunk region, moderately distinct, that is, slightly separate from body

Table 25. Morphometric data on *Spathidium duschli* from type locality (upper line) and from a site in the surroundings (lower line). Data based on mounted, protargol-impregnated (FOISSNER's method), and randomly selected specimens from a non-flooded Petri dish culture (voucher population) and a "dirty" pure culture with various food ciliates (type population). Measurements in µm. CV – coefficient of variation in %, M – median, Max – maximum, Mean – arithmetic mean, Min – minimum, n – number of individuals investigated, SD – standard deviation, SE – standard error of arithmetic mean.

Characteristics	Mean	M	SD	SE	CV	Min	Max	n
Body, length	186.6	180.0	26.2	7.9	14.0	140.0	230.0	11
	179.8	184.5	38.5	11.1	21.4	105.0	260.0	12
Body, width	34.0	35.0	6.1	1.8	17.8	24.0	42.0	11
	32.3	32.5	7.1	2.1	21.9	19.0	45.0	12
Body length:width, ratio	5.6	5.8	0.9	0.3	15.5	4.2	6.6	11
	5.6	5.5	1.0	0.3	16.9	4.2	7.6	12
Oral bulge (circumoral kinety), length	33.3	34.0	4.5	1.4	13.6	25.0	40.0	11
	28.8	29.5	5.0	1.5	17.5	20.0	37.0	12
Oral bulge length:body width, ratio	1.0	1.1	0.2	0.1	19.9	0.6	1.2	11
	0.9	1.0	0.1	0.1	15.9	0.7	1.1	12
Oral bulge, height	3.4	3.0	–	–	–	3.0	4.0	9
	3.5	3.0	0.7	0.2	19.9	3.5	5.0	11
Oral bulge, width (maximum distance between circumoral kinety)	5.4	5.0	–	–	–	4.0	7.0	5
	6.9	7.0	0.7	0.3	10.1	6.0	8.0	7
Circumoral kinety to last dikinetid of brush row 1, distance	44.6	46.0	13.6	4.1	30.4	25.0	70.0	11
	34.9	35.0	10.4	3.1	29.8	20.0	48.0	11
Circumoral kinety to last dikinetid of brush row 2, distance	51.1	52.0	13.1	3.9	25.5	31.0	75.0	11
	40.8	39.0	9.7	2.9	23.8	27.0	54.0	11
Circumoral kinety to last dikinetid of brush row 3, distance	46.6	50.0	13.3	4.0	28.5	29.0	70.0	11
	33.8	29.0	11.8	3.6	35.0	20.0	52.0	11
Anterior body end to first macronuclear nodule, distance	33.5	33.0	6.2	1.9	18.6	23.0	45.0	11
	39.8	38.5	12.4	3.6	31.0	20.0	57.0	12
Macronuclear nodules, length	7.7	7.0	2.9	0.9	37.1	4.0	15.0	11
	9.0	9.0	4.0	1.2	44.8	3.5	17.0	12
Macronuclear nodules, width	3.6	4.0	0.7	0.2	18.5	3.0	5.0	11
	4.0	4.0	0.9	0.3	22.7	3.0	6.0	12
Macronuclear nodules, number (rough values)	104.5	105.0	–	–	–	60.0	140.0	10
	64.1	65.0	–	–	–	30.0	90.0	12
Micronuclei, length	2.9	3.0	0.5	0.2	16.9	2.2	4.0	11
	2.7	2.8	0.6	0.2	23.6	2.0	4.0	11
Micronuclei, width	2.7	2.8	–	–	–	2.2	3.0	11
	2.4	2.5	–	–	–	2.0	3.0	11
Micronuclei, number	30.2	30.0	6.2	2.0	20.6	20.0	41.0	10
	17.9	20.0	5.7	1.7	32.0	8.0	25.0	11
Ciliary rows, number	22.6	23.0	1.8	0.5	7.8	19.0	25.0	11

continued

Characteristics	Mean	M	SD	SE	CV	Min	Max	n
	17.0	18.0	2.4	0.7	14.0	13.0	20.0	12
Ciliated kinetids in a right side kinety, number	86.4	80.0	15.5	4.7	18.0	60.0	120.0	11
	98.4	95.5	30.4	9.6	30.9	50.0	146.0	10
Dorsal brush rows, number	3.0	3.0	0.0	0.0	0.0	3.0	3.0	11
	3.0	3.0	0.0	0.0	0.0	3.0	3.0	12
Dikinetids in brush row 1, number	29.6	30.0	7.0	2.1	23.4	20.0	40.0	11
	28.6	30.0	10.5	3.2	36.9	12.0	43.0	11
Dikinetids in brush row 2, number	38.7	40.0	7.3	2.2	18.8	24.0	46.0	11
	36.2	34.0	11.4	3.3	31.4	18.0	52.0	12
Dikinetids in brush row 3, number	26.9	27.0	4.7	1.4	17.5	18.0	35.0	11
	26.5	26.0	7.7	2.2	28.9	14.0	38.0	12
Excretory pores, number	4.9	5.0	1.5	0.9	31.4	3.0	7.0	9
	4.3	4.0	0.7	0.2	16.3	3.0	5.0	9
Oral bulge extrusomes, length	6.7	7.0	0.9	0.3	13.5	5.0	8.0	11
	6.5	6.0	1.4	0.6	21.2	5.0	9.0	6

proper and up to 5 µm high in vivo; surface flat to moderately convex, in frontal view oblong to rather distinctly cuneate (length:width ratio 3–4:1, n = 6) and frequently slightly curved to left side. Cytopharyngeal opening not impregnated with protargol but recognizable as a minute concavity near dorsal bulge end in scanning electron micrographs. Circumoral kinety of same shape as oral bulge, basically continuous (but see above), composed of narrowly spaced dikinetids each associated with a cilium, an oral basket rod, and a faintly impregnated fibre extending into oral bulge. Nematodesmata fairly distinct and bundled, forming a rather conspicuous basket in protargol-impregnated specimens (Fig. 66a, e, i–p, 67a, b, o–q, Table 25). Ontogenesis: Some dividers were observed in the scanning electron microscope (Fig. 67r–t). Early dividers show a slight indentation in the prospective fission area; division blebs; and the gradual replacement of parental somatic cilia by brush bristles during opisthe dorsal brush formation.

Occurrence and ecology: As yet found only in Venezuela, viz., in soil of two Mahadjas (organically fertilized fields) from the surroundings of Pt. Ayacucho and in the soil/mud mixture from very flat, slightly saline (4‰) grassland puddles on the north coast (Morrocoy National Park). The type locality Mahadja was fertilized three years ago and out of use in the year when the sample was taken. The second site is in the neighbourhood of the type locality. This Mahadja was in the first year of use and cultivated with pepper, pumpkin, and yucca. The material collected was a mixture of soil and litter sieved off the fine-grained soil to a depth of 10 cm. In the Morrocoy National Park, *S. duschli* occurred with two other peculiar ciliates, viz., *Sleighophrys pustulata* and *Luporinophrys micelae*, both described by Foissner (2005). *Spathidium duschli* is a large but rather slender ciliate; nonetheless, with an average width of 35 µm, it can live only in large soil pores; likely, it is a semiterrestrial litter species, as indicated by the occurrence in the soil/mud mixture of grassland ponds. We could cultivate *S. duschli* some weeks in Eau de Volvic enriched with a few squashed wheat grains to stimulate growth of food organisms, that is, the native flagellate and ciliate community. Abundances were low in the non-flooded Petri dish cultures and the dirty pure culture from type locality while considerable numbers developed in the dirty pure culture from the Morrocoy National Park.

Remarks: *Spathidium duschli* is easily distinguished from the other members of the *elongatum* group (will be described in Vol. II of the revision of the spathidiids) by the macronuclear pattern (scattered nodules vs. a tortuous strand). Scattered macronuclear nodules occur also in some other *Spathidium* species which, however, lack the argyrophilic extrusome end and are much stouter (*S. seppelti*, *S. multinucleatum*) and/or have fewer ciliary rows (*S. turgitorum*).

Spathidium dispar FOISSNER & XU **nov. spec**. (Fig. 68a–n, 69a–o, 70a–i, 71a–x; Table 26)

Diagnosis (based on Venezuelan type and an Austrian population): Size about 300 × 35 µm in vivo. Slenderly spatulate to cylindroid with strongly oblique, slightly cuneate oral bulge about 1.2 times as long as widest trunk region. Macronucleus long and tortuous; multimicronucleate. Oral extrusomes acicular, about 7 × 0.8 µm in size, ends deeply argyrophilic. One type of cortical granules. On average 23 ciliary rows, those in dorsal half of right side attached to the circumoral kinetofragments in *Protospathidium* pattern; dorsal brush inconspicuous, isostichad and of ordinary length occupying 24% of body length.

Type locality: Venezuelan site (57), i. e., moss on stones and soil from the Cueva del Indio, a small cave near the village of Chichiriviche, north coast of the Morrocoy National Park, 67°13'W 11°33'N.

Type material: 1 holotype, 2 paratype, and 3 voucher slides with protargol-impregnated specimens have been deposited in the Biology Centre of the Upper Austrian Museum in Linz (LI). The holotype and other relevant specimens have been marked by black ink circles on the coverslip.

Etymology: The Latin adjective *dispar* (unlike) expresses that this species is different from a similar, not yet described species.

Description: This species was independently discovered and studied from two widely separate sites, viz., Venezuela (type) and Austria. None the less, the populations match very well, even in a curious feature, that is, the *Protospathidium*-like ciliary pattern on the dorsal half of the right side. Thus, conspecificity is beyond reasonable doubt, and the diagnosis includes both populations; however, the different shape of the micronuclei (lenticular vs. broadly elliptic) could be a subspecific character. The morphometry is incomplete because the species was rare at both sites.

Size highly variable, viz., 220–350 × 30–40 µm in vivo, usually near 270 × 30 µm in Venezuelan population and 200–450 × 30–55 µm, frequently about 320 × 45 µm in Austrian specimens, as calculated from some in vivo measurements and the morphometric data in Table 26 adding 10% preparation shrinkage; prepared cells somewhat inflated and thus wider. Slenderly spatulate to cylindroid with considerably varying length:width ratio of about 5–10:1, on average 8:1 in protargol-impregnated cells of both populations; live specimens, however, frequently stouter in Austrian (approx. 7:1) than Venezuelan (approx. 9:1) population. Neck of ordinary distinctness, more pronounced in Venezuelan than in Austrian specimens, trunk widest in or posterior to mid-body, flattened only in oral region. Anterior (oral) body end steeply (about 60°) truncate and

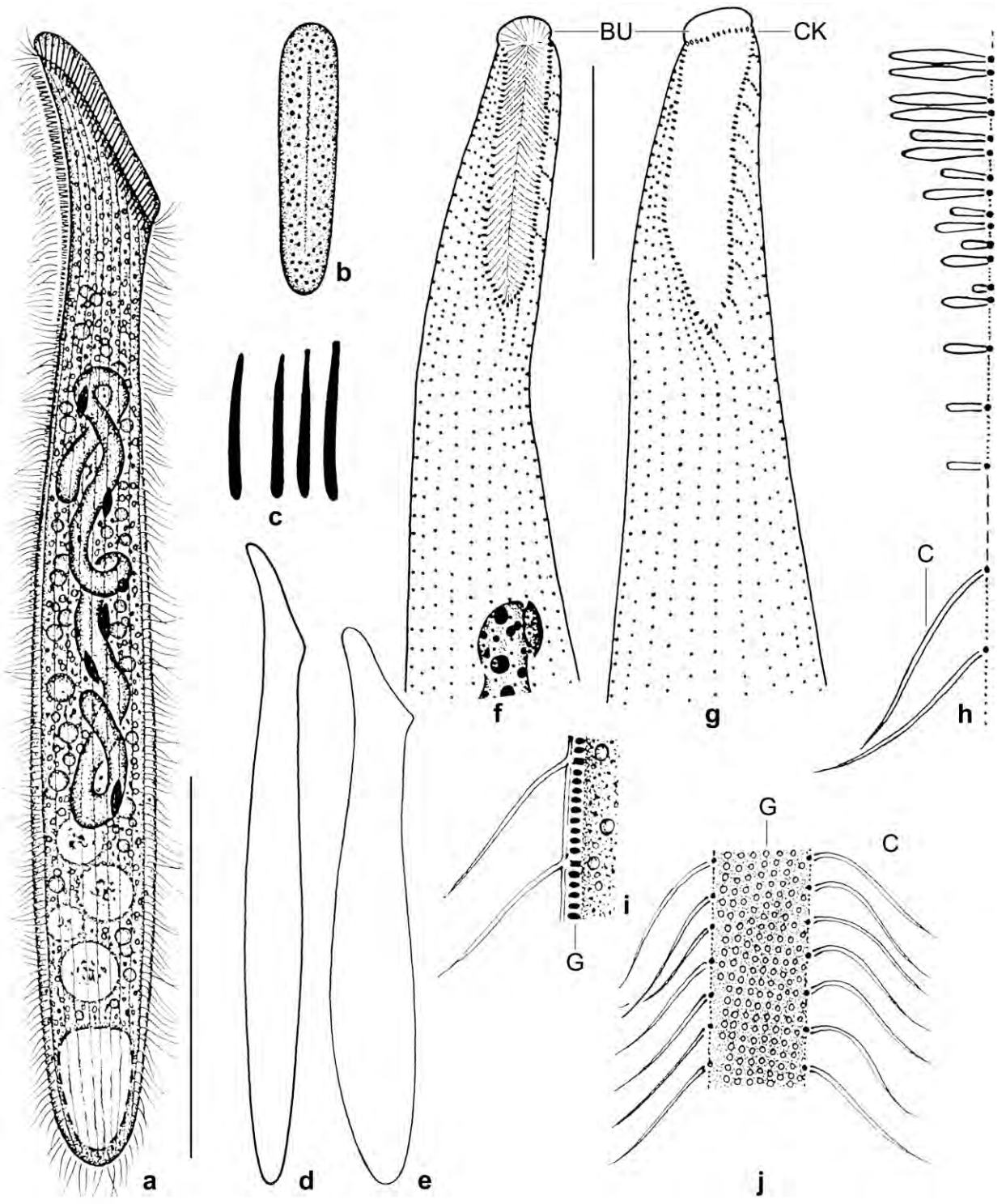

Fig. 68a–j. *Spathidium dispar,* Venezuelan specimens from life (a–e, h–j) and after protargol impregnation (f, g). **a:** Right side view of a representative specimen, length 300 µm. **b:** Frontal view of oral bulge studded with extrusomes. **c:** Oral bulge extrusomes, 6–7 × 0.8 µm. **d, e:** Size and shape variants, length 350 µm and 250 µm. **f, g:** Ventral views, showing oral and somatic ciliary pattern in anterior body portion. Fibres originate from the circumoral dikinetids and extend into the oral bulge, where they form an arrow-like pattern. **h:** Posterior portion of dorsal brush row 3, longest bristles 4 µm. **i, j:** Optical section and surface view showing cortical granulation. BU – oral bulge, C – ordinary somatic cilia, CK – circumoral kinety, G – cortical granules. Scale bars 20 µm (f, g) and 100 µm (a).

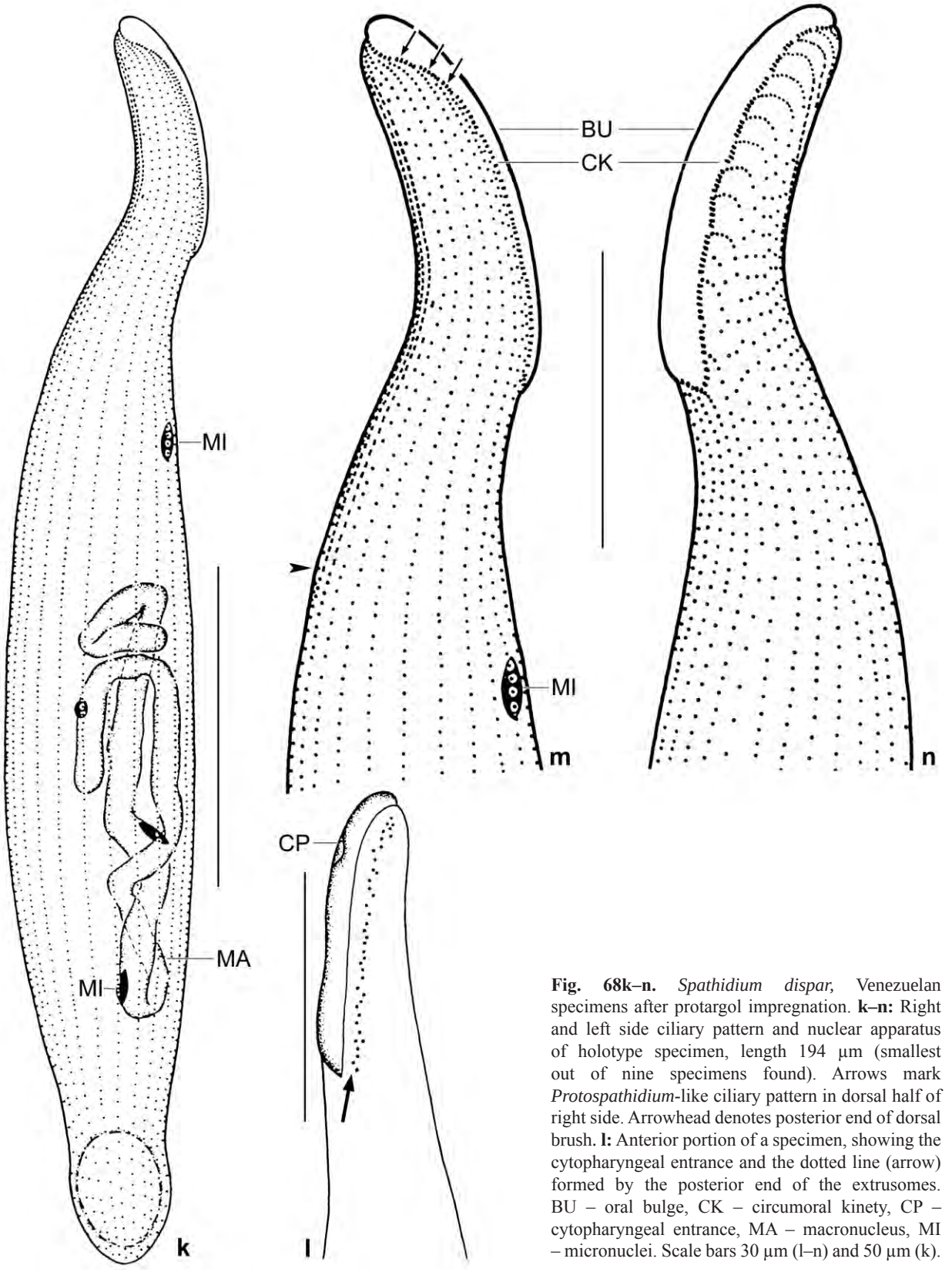

Fig. 68k–n. *Spathidium dispar,* Venezuelan specimens after protargol impregnation. **k–n:** Right and left side ciliary pattern and nuclear apparatus of holotype specimen, length 194 µm (smallest out of nine specimens found). Arrows mark *Protospathidium*-like ciliary pattern in dorsal half of right side. Arrowhead denotes posterior end of dorsal brush. **l:** Anterior portion of a specimen, showing the cytopharyngeal entrance and the dotted line (arrow) formed by the posterior end of the extrusomes. BU – oral bulge, CK – circumoral kinety, CP – cytopharyngeal entrance, MA – macronucleus, MI – micronuclei. Scale bars 30 µm (l–n) and 50 µm (k).

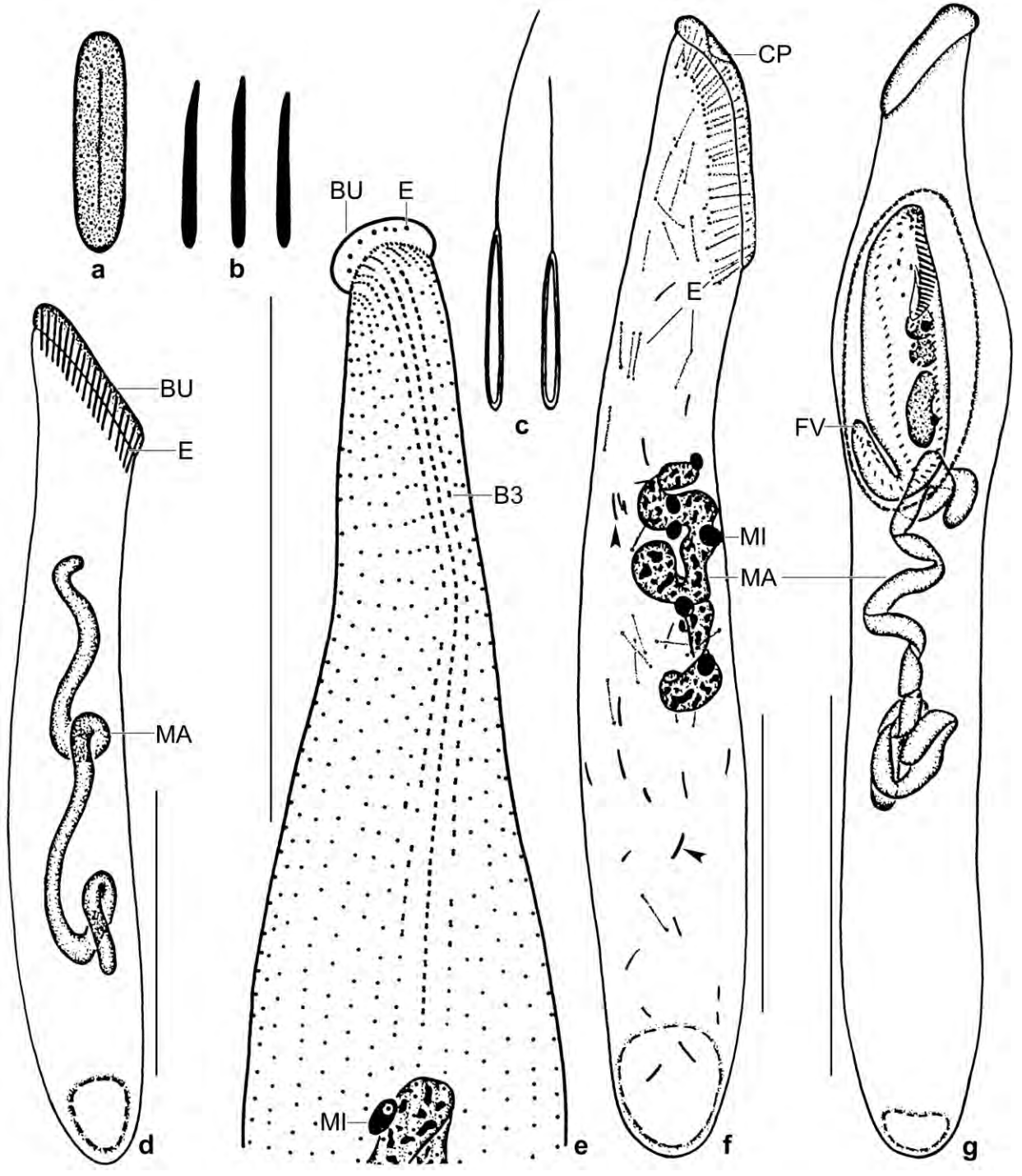

Fig. 69a–g. *Spathidium dispar*, Austrian specimens from life (a–d) and after protargol impregnation (e–g). **a:** Frontal view of oral bulge studded with extrusomes. **b:** Oral bulge extrusomes, 8–10 × 0.8 µm. **c:** Exploded extrusomes, length 12–20 µm. **d:** Outline of a representative specimen. **e:** Ciliary pattern of dorsal anterior portion. Note the dorsal brush with middle row 2 slightly longer than marginal rows 1 and 3, which have slight irregularities (some dikinetids lacking). **f:** Extrusomes are studded in oral bulge and scattered in cytoplasm; in this species, they impregnate with protargol, especially the ends. Arrowheads mark developing extrusomes, which are shorter and more deeply impregnated. **g:** A specimen having just ingested a large hypotrich ciliate. BU – oral bulge, B3 – dorsal brush row 3, CP – cytopharyngeal entrance, E – extrusomes, FV – food vacuole, MA – macronucleus, MI – micronucleus. Scale bars 50 µm (e, f) and 100 µm (d, g).

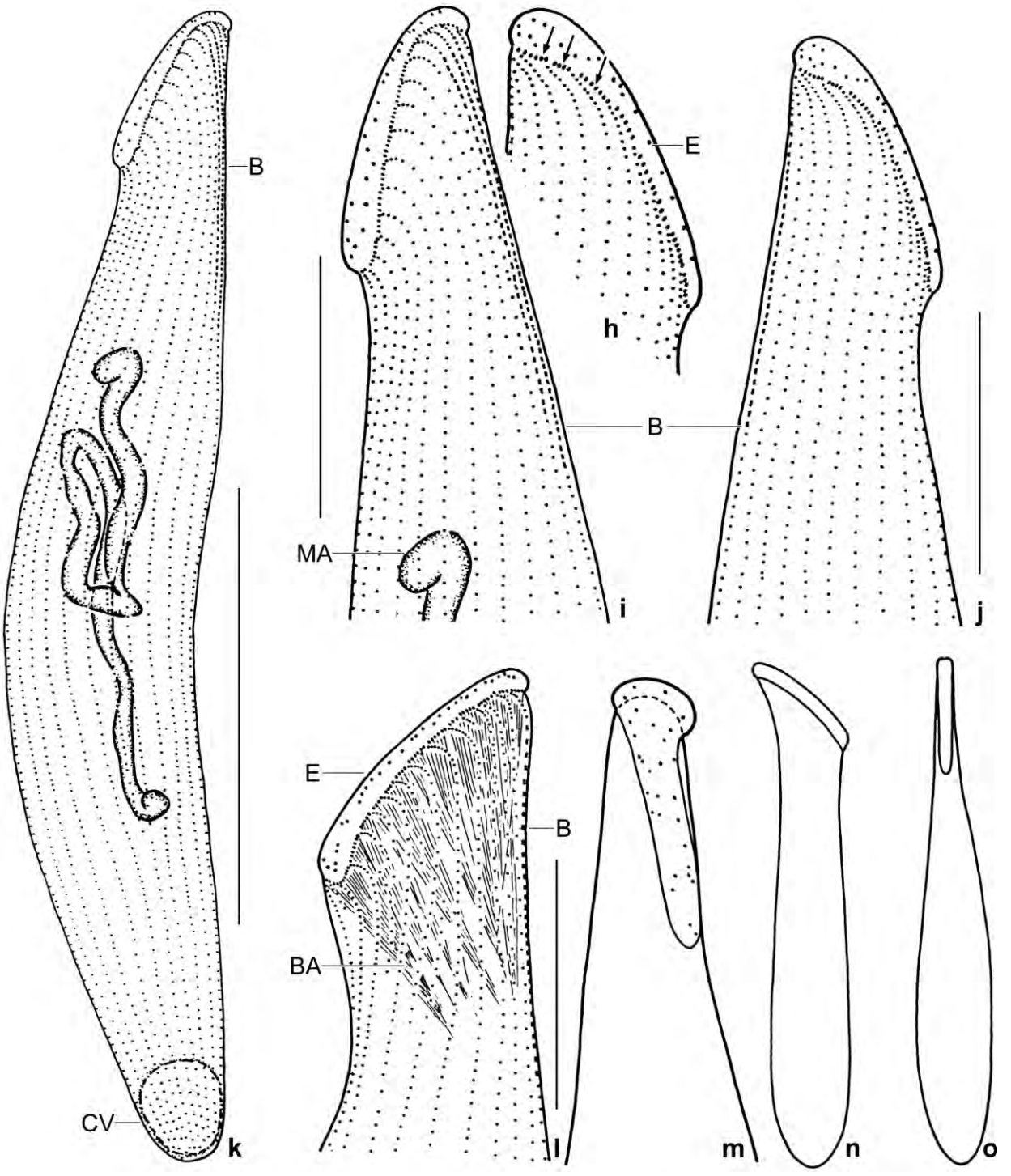

Fig. 69h–o. *Spathidium dispar*, Austrian specimens after protargol impregnation (h–m) and from life (n, o). **h–k:** Ciliary pattern of right and left side and macronucleus of main voucher specimen, length 264 µm. Arrows mark *Protospathidium*-like ciliary pattern in dorsal half of right side, a highly characteristic feature found also in the Venezuelan type specimens. **l:** Ventrolateral view of another specimen, oral bulge length 46 µm. Note the impregnated anterior end of the extrusomes. **m:** Ventrolateral view of a specimen with cuneate oral bulge and circumoral kinety. **n, o:** Right side and ventral view of same specimen, showing flattened oral area. B – dorsal brush, BA – oral basket, CV – contractile vacuole, E – anterior end of extrusomes, MA – macronucleus. Scale bars 30 µm (i, j), 40 µm (l), and 100 µm (k).

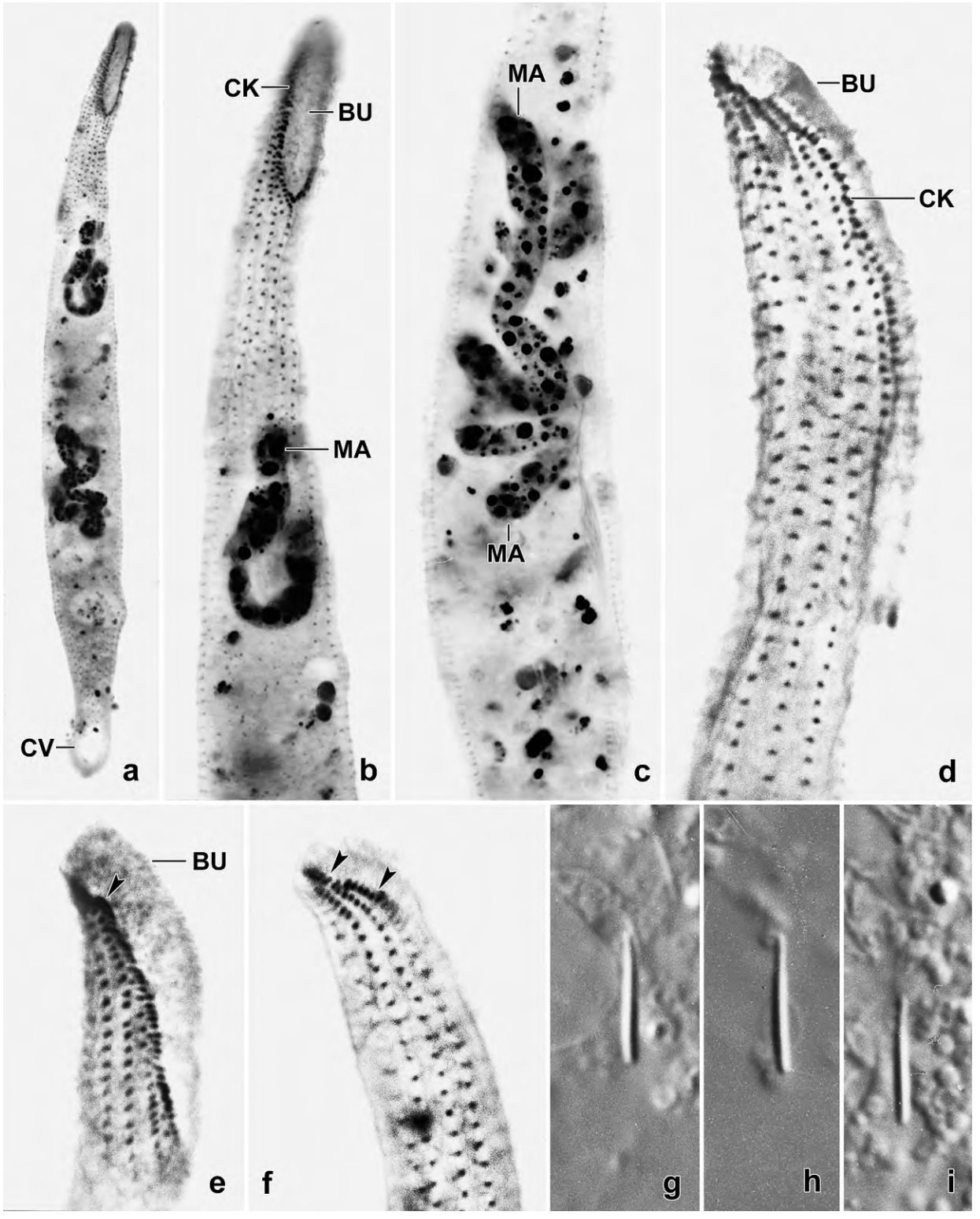

Fig. 70a–i. *Spathidium dispar*, Venezuelan specimens after protargol impregnation (a–f) and from life (g–i). **a, b:** Ventral overview and detail of a specimen with macronucleus broken into two tortuous pieces. Note the elliptic oral bulge and the circumoral kinety bluntly pointed ventrally. **c:** Mid-body region showing the tortuous macronucleus. **d–f:** Ciliary pattern in anterior region of right side. In the dorsal area, the ciliary rows adhere to the oral kinetofragments (arrowheads). Figure (e) is an oblique view, where the oral bulge appears cuneate and much higher dorsally than ventrally. **g–i:** Mature oral bulge extrusomes are slightly acicular and about 7 µm long. BU – oral bulge, CK – circumoral kinety, CV – contractile vacuole, MA – macronucleus.

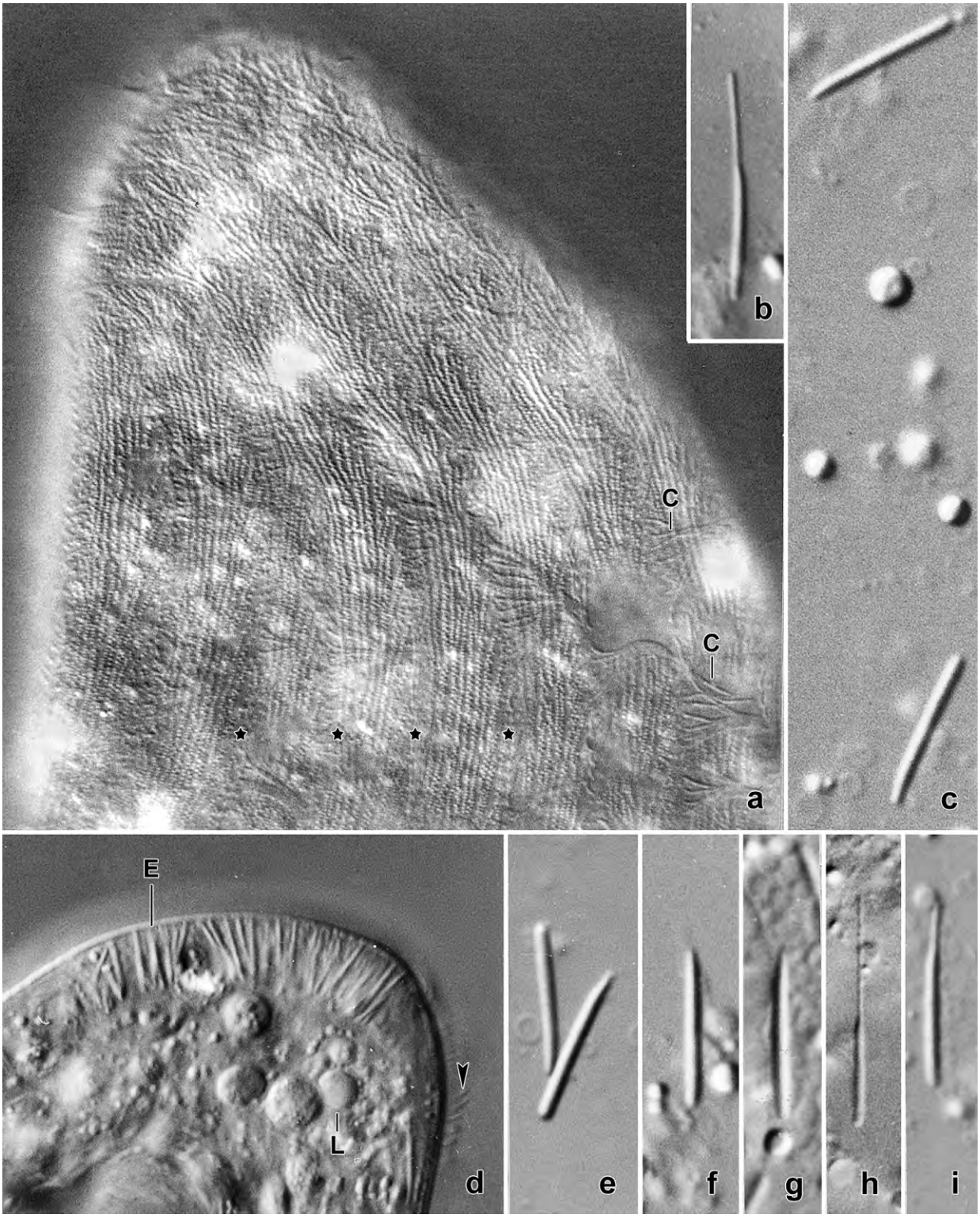

Fig. 71a–i. *Spathidium dispar*, Austrian specimens from life. **a:** Lateral view of anterior body portion, showing the distinct cortical granulation. The granules form rows commencing right of the kineties (asterisks) and extend obliquely posteriorly. **b, h:** Exploded toxicysts, length 15–20 µm. **c, e–g:** Resting oral bulge extrusomes are 8–10 µm long and less distinctly acicular than in the Venezuelan specimens (Fig. 70g–i). **d:** A squashed specimen. The extrusomes appear rod-shaped at low magnification and slightly acicular at high magnification (c, e–g). Arrowhead marks the short bristles of the dorsal brush. **i:** Partially exploded extrusome. C – ordinary somatic cilia, E – extrusomes, L – lipid droplets.

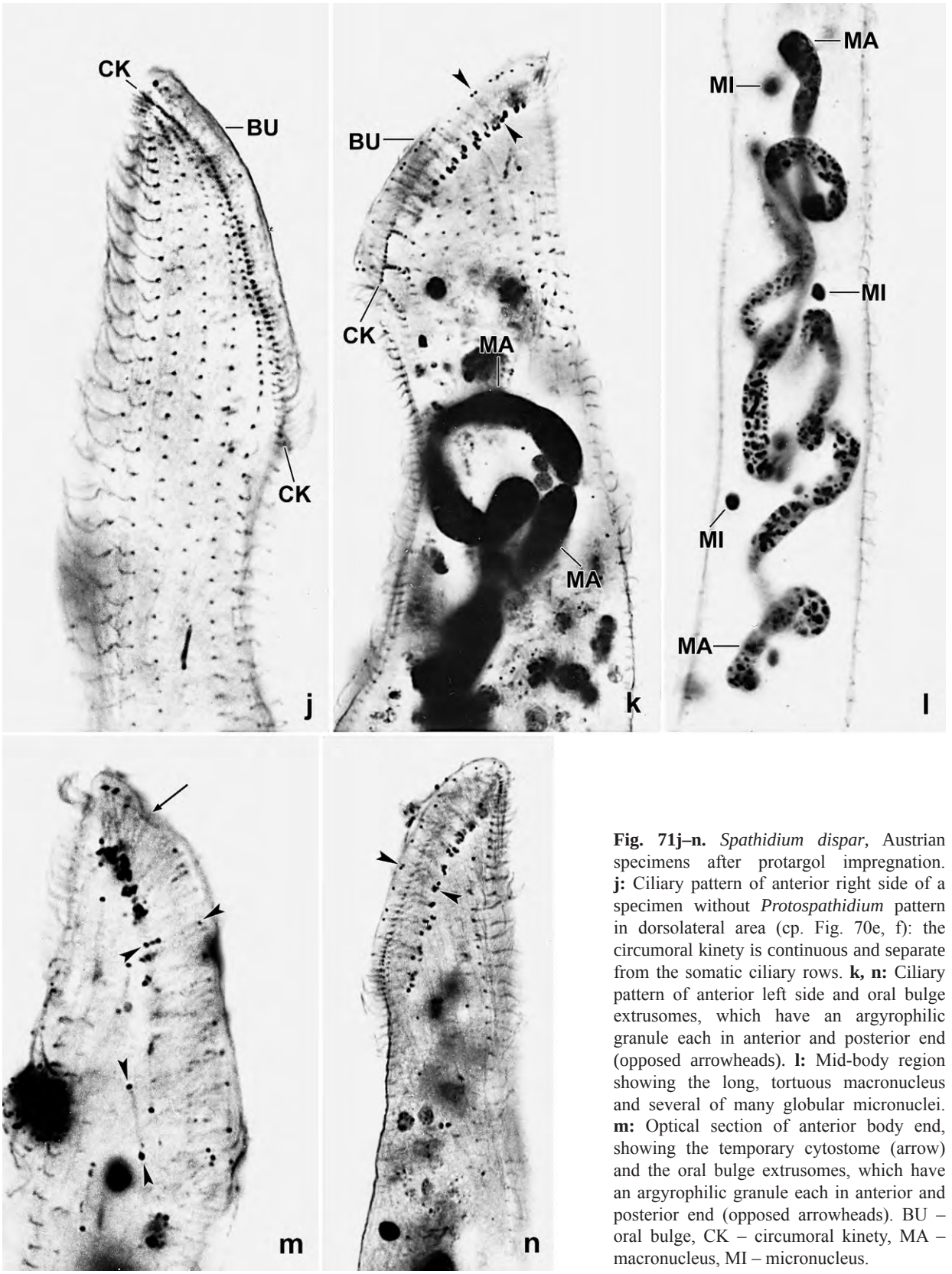

Fig. 71j–n. *Spathidium dispar*, Austrian specimens after protargol impregnation. **j:** Ciliary pattern of anterior right side of a specimen without *Protospathidium* pattern in dorsolateral area (cp. Fig. 70e, f): the circumoral kinety is continuous and separate from the somatic ciliary rows. **k, n:** Ciliary pattern of anterior left side and oral bulge extrusomes, which have an argyrophilic granule each in anterior and posterior end (opposed arrowheads). **l:** Mid-body region showing the long, tortuous macronucleus and several of many globular micronuclei. **m:** Optical section of anterior body end, showing the temporary cytostome (arrow) and the oral bulge extrusomes, which have an argyrophilic granule each in anterior and posterior end (opposed arrowheads). BU – oral bulge, CK – circumoral kinety, MA – macronucleus, MI – micronucleus.

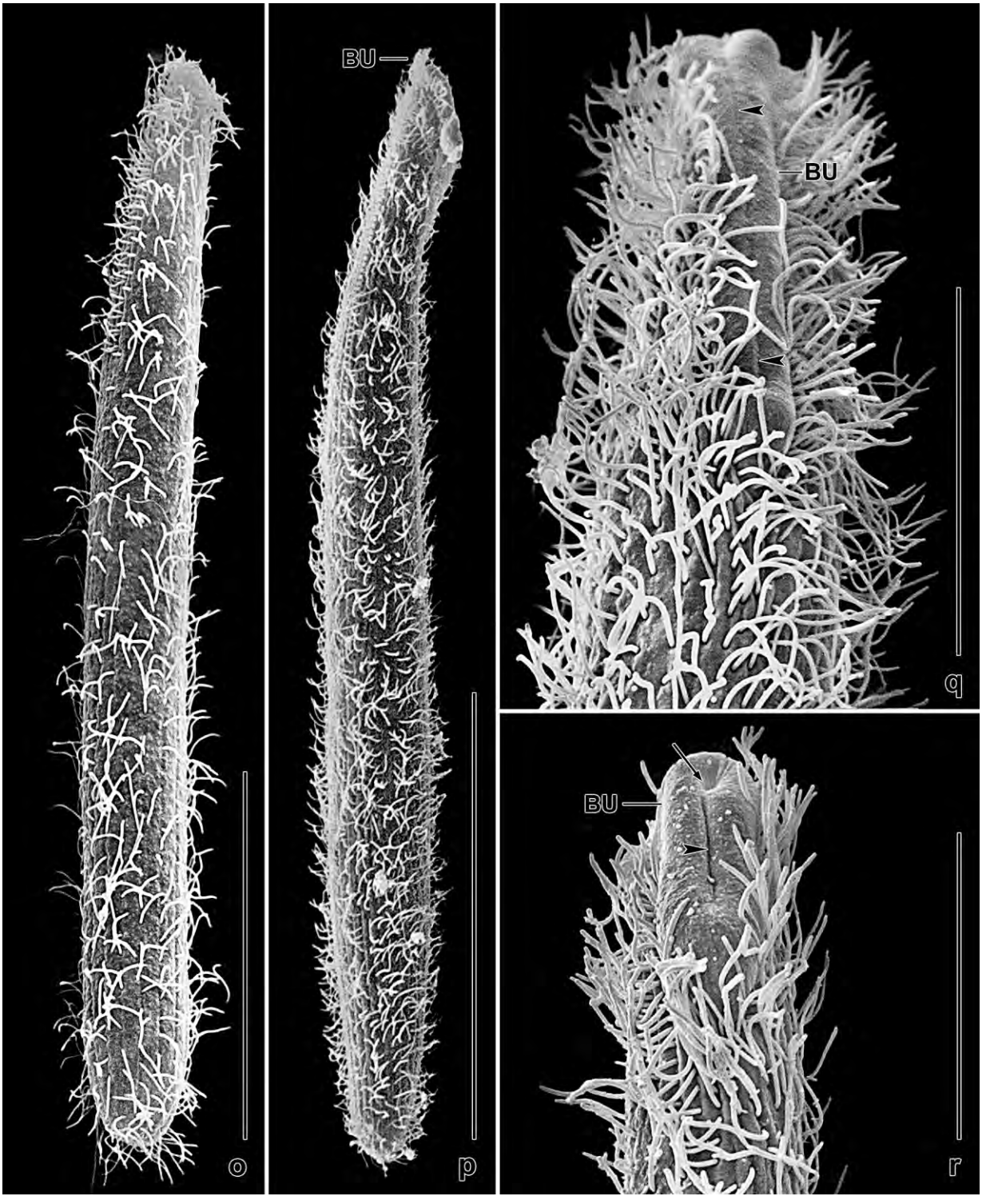

Fig. 71o–r. *Spathidium dispar*, scanning electron micrographs of Austrian specimens. **o, p:** Overviews showing the slender body shape typical for the *procerum* group. **q, r:** Ventral views of oral bulge, showing the slight depression in midline (arrowheads), where the right and left bulge half abut. Arrow marks temporary cytostome, that is, a minute, obconical depression near dorsal bulge end. BU – oral bulge. Scale bars 20 µm (q, r), 50 µm (o), and 100 µm (p).

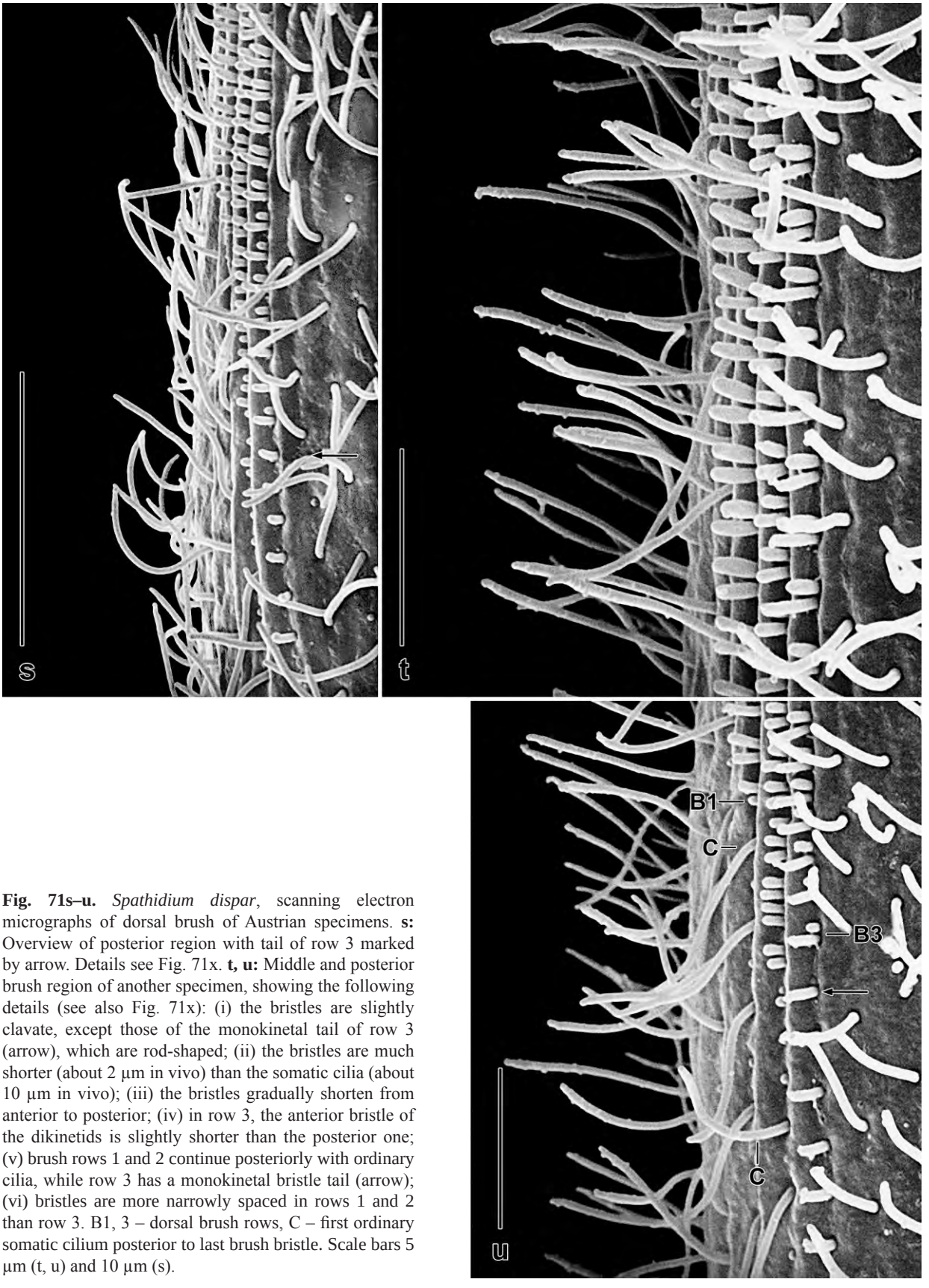

Fig. 71s–u. *Spathidium dispar*, scanning electron micrographs of dorsal brush of Austrian specimens. **s:** Overview of posterior region with tail of row 3 marked by arrow. Details see Fig. 71x. **t, u:** Middle and posterior brush region of another specimen, showing the following details (see also Fig. 71x): (i) the bristles are slightly clavate, except those of the monokinetal tail of row 3 (arrow), which are rod-shaped; (ii) the bristles are much shorter (about 2 µm in vivo) than the somatic cilia (about 10 µm in vivo); (iii) the bristles gradually shorten from anterior to posterior; (iv) in row 3, the anterior bristle of the dikinetids is slightly shorter than the posterior one; (v) brush rows 1 and 2 continue posteriorly with ordinary cilia, while row 3 has a monokinetal bristle tail (arrow); (vi) bristles are more narrowly spaced in rows 1 and 2 than row 3. B1, 3 – dorsal brush rows, C – first ordinary somatic cilium posterior to last brush bristle. Scale bars 5 µm (t, u) and 10 µm (s).

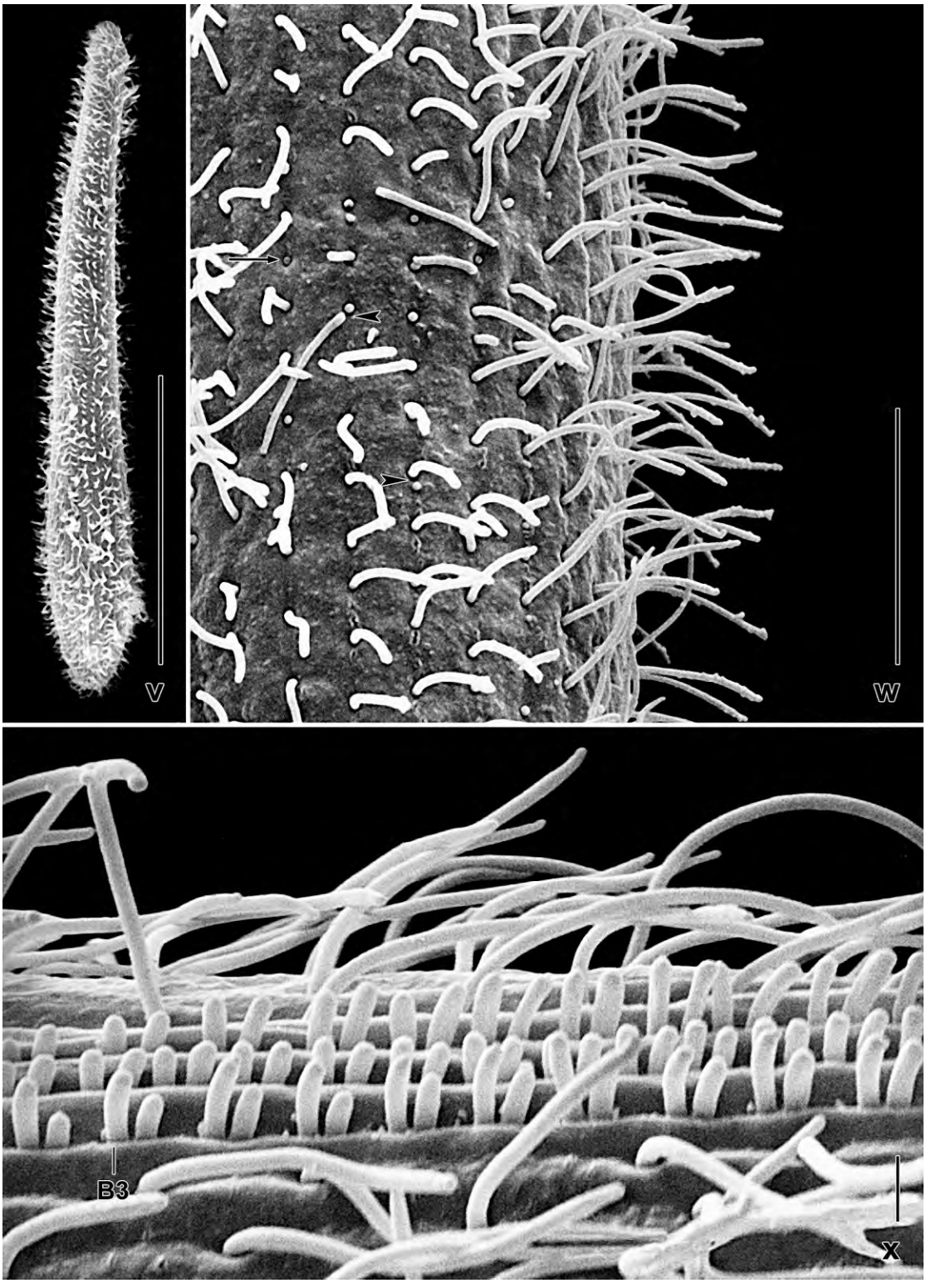

Fig. 71v–x. *Spathidium dispar*, scanning electron micrographs of Austrian specimens. **v:** Overview of a comparatively stout, obclavate specimen. **w:** Somatic ciliature in mid-body. Arrow marks a bare kinetid between two ciliated kinetids. Arrowheads denote dikinetids (?) with either the anterior or posterior cilium lacking. **x:** Posterior region of brush shown in overview in Fig. 71s. The anterior bristle of the dikinetids of row 3 is shorter than the posterior one. Further details, see explanation to Fig. 71t, u. B3 – dorsal brush row 3. Scale bars 1 µm (x), 10 µm (w), and 100 µm (v).

distinctly sigmoid in live Venezuelan specimens while flat to moderately convex in Austrian and prepared Venezuelan cells; posterior end narrowly to moderately broadly rounded and frequently bulbous and/or wrinkled due to the contractile vacuole contained (Fig. 68a, d, e, k, 69d, f, k, n, o, 71o, p; Table 26). Macronucleus extends in middle quarters of cell, basically a long, tortuous, irregularly nodulated strand with many up to 2.5 µm-sized nucleoli; occasionally in two long pieces. Many micronuclei attached and near to macronucleus, exact number not recognizable due to many similar-sized and impregnated cytoplasmic inclusions; individual micronuclei lenticular (6 × 2.5 µm) in Venezuelan and broadly ellipsoid (3 × 2.5 µm) in Austrian specimens (Fig. 68a, k, 69d, f, g, k, 70a–c, 71k, l; Table 26). Contractile vacuole in rear body end, several excretory pores scattered in pole area; definitely, no second contractile vacuole in anterior body half. Oral bulge extrusomes very similar in both populations, viz., acicular to almost rod-shaped with obliquely truncate distal portion, of ordinary thickness, in vivo approximately 6–7 × 0.8 µm in Venezuelan and 8–10 × 0.8 µm in Austrian specimens; impregnate more or less deeply with the protargol method used, especially the ends (only the proximal end in Venezuelan cells), producing a dotted line each on and posterior of oral bulge. Exploded extrusomes of typical toxicyst structure, 12–20 µm long in vivo. Developing cytoplasmic extrusomes of same shape and impregnation capability

Table 26. Morphometric data on *Spathidium dispar* from Venezuela (SD1) and *S. dispar* from Austria (SD2). Data based on mounted and protargol-impregnated (FOISSNER's method) specimens from non-flooded Petri dish cultures. Measurements in µm. CV – coefficient of variation in %, M – median, Max – maximum, Mean– arithmetic mean, Min – minimum, n – number of individuals investigated, Pop – population, SD – standard deviation, SE – standard error of arithmetic mean.

Characteristics	Pop	Mean	M	SD	SE	CV	Min	Max	n
Body, length	SD1	240.4	240.0	35.0	11.7	14.5	194.0	296.0	9
	SD2	292.3	290.0	60.9	18.4	20.8	185.0	390.0	11
Body, width	SD1	29.6	30.0	2.5	0.8	8.3	24.0	32.0	9
	SD2	37.6	38.0	6.7	2.0	17.7	28.0	50.0	11
Body length:width, ratio	SD1	8.2	8.1	1.2	0.4	15.2	6.5	10.2	9
	SD2	7.9	7.9	1.5	0.5	19.6	5.1	10.0	11
Oral bulge (circumoral kinety), length	SD1	36.0	34.0	5.8	1.9	16.0	30.0	45.0	9
	SD2	39.9	40.0	6.5	2.0	16.2	30.0	52.0	11
Oral bulge length:body width, ratio	SD1	1.2	1.2	0.2	0.1	15.2	0.9	1.6	9
	SD2	1.1	1.0	0.2	0.1	17.7	0.8	1.5	11
Circumoral kinety to last dikinetid of brush row 1, distance	SD1	49.0	46.0	6.9	2.6	14.1	44.0	63.0	7
	SD2	61.4	60.0	8.2	3.1	13.3	54.0	75.0	7
Circumoral kinety to last dikinetid of brush row 2, distance	SD1	57.3	56.0	9.4	3.6	16.5	49.0	76.0	7
	SD2	70.3	70.0	7.4	2.8	10.6	60.0	80.0	7
Circumoral kinety to last dikinetid of brush row 3, distance	SD1	57.9	55.0	9.3	3.5	16.0	50.0	76.0	7
	SD2	59.4	60.0	7.3	2.8	12.3	51.0	73.0	7
Anterior body end to macronucleus, distance	SD1	84.0	75.0	18.1	6.0	21.5	68.0	120.0	9
	SD2	87.0	90.0	18.6	5.6	21.3	55.0	107.0	11
Macronuclear figure, length	SD1	94.0	91.0	29.7	9.9	31.6	58.0	150.0	9
	SD2	147.9	135.0	59.7	18.0	40.4	42.0	260.0	11
Macronucleus, length (spread; rough values)	SD1	211.7	220.0	–	–	–	120.0	300.0	9

continued

Characteristics	Pop	Mean	M	SD	SE	CV	Min	Max	n
	SD2	256.8	250.0	–	–	–	90.0	410.0	11
Macronucleus, width in mid	SD1	5.8	6.0	0.7	0.2	11.5	5.0	7.0	9
	SD2	5.4	5.0	0.8	0.2	15.1	4.0	7.0	11
Micronuclei, length	SD1	6.0	6.0	0.5	0.2	8.3	5.0	7.0	9
	SD2	3.3	3.0	–	–	–	3.0	4.0	7
Micronuclei, width	SD1	2.3	2.5	–	–	–	2.0	2.5	9
	SD2	2.4	2.5	–	–	–	2.0	2.5	7
Ciliary rows, number	SD1	22.2	22.0	1.5	0.5	6.7	21.0	25.0	9
	SD2	24.2	24.0	2.1	0.6	8.6	20.0	27.0	11
Ciliated kinetids in a right side kinety, number	SD1	178.1	169.0	29.5	9.8	16.6	138.0	221.0	9
	SD2	134.9	128.0	36.8	11.1	27.2	71.0	186.0	11
Dorsal brush rows, number	SD1	3.0	3.0	0.0	0.0	0.0	3.0	3.0	7
	SD2	3.0	3.0	0.0	0.0	0.0	3.0	3.0	11
Dikinetids in brush row 1, number	SD1	51.4	54.0	5.5	2.5	10.7	45.0	57.0	5
	SD2	43.0	43.0	4.6	1.9	10.6	37.0	48.0	6
Dikinetids in brush row 2, number	SD1	61.0	63.0	8.3	3.7	13.6	50.0	69.0	5
	SD2	61.8	64.5	9.3	3.8	15.0	46.0	70.0	6
Dikinetids in brush row 3, number	SD1	51.2	54.0	4.7	2.1	9.1	44.0	55.0	5
	SD2	39.7	39.0	5.9	2.4	14.8	33.0	47.0	6

as mature oral bulge toxicysts, but only 3–5 × 0.5 µm in size (Fig. 68a–c, l, 69a–d, f, h, l, m, 70g–i, 71b–i, k, m, n). Cortex very flexible, contains about eight rows of colourless, brilliant granules between each two kineties; individual granules about 1 × 0.5 µm in Venezuelan and 0.8 × 0.3 µm in Austrian cells (Fig. 68i, j, 71a). Cytoplasm colourless, usually packed with developing and mature extrusomes, lipid droplets up to 10 µm across, and some food vacuoles with remnants of various ciliates, e. g., *Halteria grandinella*; an Austrian specimen contained a just ingested, still intact, over 100 µm-sized oxytrichid hypotrich (Fig. 69g); subterminal frequently a large vacuole with indigestible debris. Swims and glides rather rapidly, showing worm-like flexibility.

Cilia about 10 µm long in vivo, arranged in an average of 22 (Venezuela) or 24 (Austria) equidistant, mostly bipolar, densely ciliated (average ciliary distance 1.5 µm, Table 26) rows abutting on circumoral kinety in typical *Spathidium* pattern, except in dorsal half of right side, where most specimens have a *Protospathidium*-like pattern because the circumoral kinetofragments are separated by minute gaps and adhere to the ciliary rows, similar to the left side, where the kineties are very densely ciliated anteriorly (Fig. 68a, k, m, n, 69h, i, k, l, 70d–f, 71o–r, v, w; Table 26). Dorsal brush inconspicuous in both populations because occupying only 24% of body length and bristles merely up to 4 µm long and only slightly inflated in vivo; dikinetids more widely spaced in Austrian than in Venezuelan specimens, as shown by the lower total number (144 vs. 164) in spite of the larger cell size (292 vs. 240 µm, Table 26). Details of rows and bristles very similar in Venezuelan and Austrian specimens: all rows commence with some ordinary cilia anteriorly and end posteriorly at nearly same level, with middle row 2 slightly longer than rows 1 and 3; row 3 with a monokinetal tail of 2 µm long, rod-shaped bristles extending to mid-body; bristles indistinctly clavate and about 4 µm long in anterior three quarters of brush, gradually decrease to

2 µm in posterior quarter, anterior bristle of pairs decreases in length to < 0.5 µm (Fig. 68a, h, k, m, 69e, k, i, 71s–u, w, x; Table 26).

Oral bulge occupies anterior body end strongly slanted by an angle of about 60°, in vivo approximately 1.5 times as long as widest trunk region, while on average only slightly longer than trunk width in protargol preparations (Table 26), likely because cells became inflated by the preparation and few specimens were available; distinct in live Venezuelan specimens because about 6 µm high and often neatly sigmoidal, while usually convex or flat in prepared cells and in Austrian specimens; in frontal view elongate elliptic or slightly cuneate in both populations, dorsal end conspicuously widened in some Austrian specimens; with minute, obconical depression (cytopharyngeal entrance) near dorsal end distinct in only few specimens (Fig. 68a, b, d–g, k, 69a, d, e, f, 70a, b, d–f, 71j, k, m–r). Circumoral kinety of same shape as oral bulge, basically continuous, except of dorsal half of right side where individual fragments are separated by minute gaps, as described above; composed of narrowly spaced dikinetids each associated with a cilium, an oral basket rod, and a faintly impregnated fibre extending into oral bulge. Nematodesmata and oral basket of usual structure (Fig. 68f, g, m, n, 69i–l, 70a, b, d–f, 71j, k, o–r; Table 26).

Occurrence and ecology: To date found in mosses from Venezuela (type locality) and in Austria, where it occurred in slightly saline grassland soil (pH 8.1) from the surroundings of the town of Illmitz, Burgenland, 47°45'N 16°48'E. The species was rare in the non-flooded Petri dish cultures from both sites, that is, less than 15 specimens were found in eight protargol slides each. However, the Austrian population became rather abundant in the non-flooded Petri dish culture after one month, and thus could be studied in the scanning electron microscope. With its slender, highly flexible body, *S. dispar* can exploit even small soil pores.

Remarks: The large size, the slender body, the long and tortuous macronucleus, the acicular extrusomes, and the circumoral ciliary pattern distinguish *S. dispar* from all described congeners.

Enchelariophrya nov. gen.

Diagnosis: Spathidiida (?) with ciliary rows slightly curved anteriorly; 3 rows anteriorly differentiated to a dorsal brush. Oral bulge small; oral basket made of nematodesmata originating exclusively from first (di?) kinetid of each ciliary row.

Type species: *Enchelariophrya wolfi* nov. spec.

Etymology: Composite of the generic name *Enchelys* (~ eel), the Latin suffix *arius* (similar to the genus *Enchelaria*), and the Greek noun *ophrya* (eyebrow ~ cilia ~ ciliate), meaning a ciliate resembling the genus *Enchelaria* Foissner et al., 2002.

Remarks: The two new species assigned to *Enchelariophrya* have the same oral apparatus as *Enchelaria* Foissner et al., 2002 but have three (vs. two) dorsal brush rows, a feature significant at genus level (Oertel et al. 2008). Otherwise, the problems are the same as mentioned by Foissner et al. (2002): "*Enchelariophrya* has an atypical circumoral kinety made of the anterior kinetid of each somatic ciliary row. This and the anteriorly curved kineties resemble the → Acropisthiidae. However, *Enchelariophrya* lacks oralized somatic monokinetids, although we cannot entirely

exclude that the anterior kinetid is an oralized somatic kinetid. If so, *Enchelariophrya* still is a distinct genus because then it would lack the haptorid oral dikinetids so typical for the → Acropisthiidae and → Fuscheriidae. On the other hand, a lack of oral dikinetids would relate *Enchelaria* and *Enchelariophrya* to the Enchelyidae which, however, invariably have oralized monokinetids at the anterior region of the ciliary rows".

The general appearance of, especially, → *E. galapagensis* resembles genera like *Sikorops* Foissner, 2000 and → *Enchelyodon*. However, the latter has straight ciliary rows and a circumoral kinety composed of many more dikinetids than ciliary rows. Thus, we propose that *Enchelariophrya* is related to the Spathidiidae which not only have anteriorly curved ciliary rows but also contain genera with tuberculate oral bulge (several → *Protospathidium* and *Arcuospathidium* species). Further, most genera of the Spathidiidae have three dorsal brush rows and much more circumoral dikinetids than ciliary rows, including *Semispathidium*, which highly resembles *Enchelaria* and *Enchelariophrya*. To sum up, *Enchelariophrya* represents a distinct genus, no matter the familial classification. Figure 72a–g summarizes this discussion.

Enchelariophrya wolfi nov. spec. (Fig. 73a–f, 74a–m; Table 27)

Diagnosis: Size about 75 × 15 µm in vivo. Shape narrowly oblong, rarely slightly obclavate. On average 45 globular to narrowly ellipsoid macronuclear nodules and 8 globular micronuclei. Extrusomes narrowly ovate, about 4 × 0.8 µm. 23 ciliary rows on average, three anteriorly differentiated to a distinctly heterostichad dorsal brush occupying about 21% body length. Oral bulge tuberculate, about 4 × 2 µm in size.

Type locality: Humous surface soil (0–5 cm) from an *Aechmea paniculigera* (Bromeliacea) site in the surroundings of the village of Quick Step in Cockpit Country, Jamaica, 77°41'W 18°17'N.

Type material: 1 holotype and 4 paratype slides with protargol-impregnated specimens have been deposited in the Biology Centre of the Upper Austrian Museum in Linz (LI). The holotype and other relevant specimens have been marked by black ink circles on the coverslip.

Dedication: We dedicate this new species to Dr. habil. Klaus Wolf, Electron Microscopy Unit at the University of the West Indies, Kingston, Jamaica, who made it possible to collect in this area.

Description: Size in vivo about 60–90 × 10–25 µm, usually about 75 × 15 µm, as calculated from some live measurements and the morphometric data compiled in Table 27 adding 15% preparation shrinkage. Body often narrowly oblong, sometimes obclavate (length:width ratio 3.6–5:1), anterior region frequently slightly bulbous; rather distinctly flattened laterally (Fig. 73a, d, f, 74a–c, h–j; Table 27). Nuclear apparatus in central three fifths of cell (Fig. 73a, e, 74h–j; Table 27). On average about 45 globular to narrowly ellipsoid macronuclear nodules 3–4 µm in size in vivo and 3.8 × 1.8 µm in protargol preparations, difficult to count because close together; contain globular and ellipsoid nucleoli. On average eight micronuclei scattered among macronuclear nodules, about 1.5 µm across in prepared specimens. Contractile vacuole in rear body end; one large excretory pore out of pole centre (Fig. 73a, f, 74a–c, j, m). Mature extrusomes attached to oral bulge and studded in cytoplasm, narrowly ovate to indistinctly lenticular, 3–5 × 0.8 µm in size, do not impregnate with the protargol method used; many lenticular developing

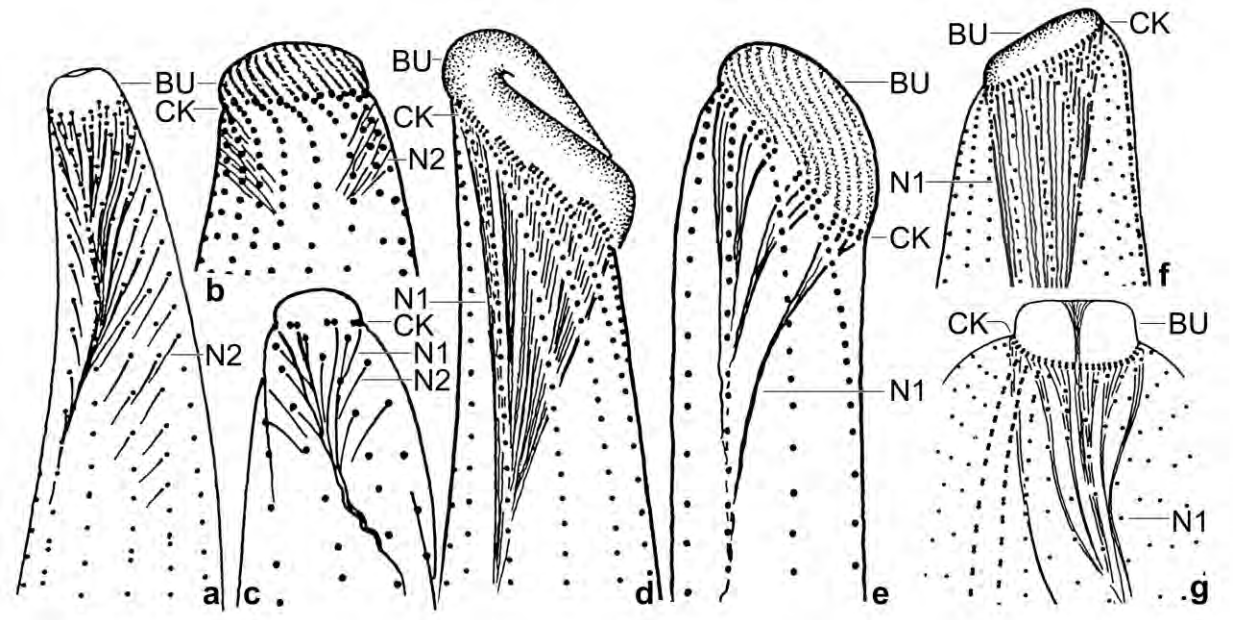

Fig. 72a–g. Oral structures and anterior somatic kinety pattern of some haptorid ciliates (from Foissner 1984 and Foissner et al. 2002, 2010a). **a:** *Apoenchelys* has straight somatic kineties. The oral basket is made of nematodesmata originating from oralized somatic monokinetids because circumoral dikinetids are absent. **b:** *Sikorops* has curved somatic kineties. The oral basket is made of nematodesmata originating from dikinetids of a special circumoral kinety and of nematodesmata originating from oralized somatic monokinetids. **c:** *Diplites* has straight somatic kineties. The oral basket is made of nematodesmata originating from the widely spaced dikinetids of the circumoral kinety and of nematodesmata originating from oralized somatic monokinetids. **d, e:** *Spathidium* and *Protospathidium* have curved somatic kineties. The oral basket is made of nematodesmata originating from the circumoral dikinetids that form a more or less closed circumoral kinety (*Spathidium*) or dikinetal circumoral fragments (*Protospathidium*). **f:** *Semispathidium* has curved somatic kineties. The oral basket is made of nematodesmata originating from the circumoral dikinetids (kinety) that are usually much more numerous than the somatic kineties. **g:** *Enchelyodon* has straight somatic kineties. The oral basket is made of nematodesmata originating from the circumoral dikinetids (kinety) that are usually much more numerous than the somatic kineties. *Enchelariophrya* is different from all (Fig. 72f): the somatic kineties are curved and the anteriormost (di?) kinetid of each somatic kinety produces a nematodesma contributing to the oral basket. BU – oral bulge, CK – circumoral kinety, N1 – nematodesmata originating from circumoral dikinetids (kinety), N2 – nematodesmata originating from oralized somatic monokinetids.

extrusomes in cytoplasm (Fig. 73c, 74d–g). Cortex colourless, about 1 µm thick, contains several rows of broadly ellipsoid granules about 0.7 × 0.5 µm in size between each two kineties (Fig. 73b). Cytoplasm colourless, without peculiarities. Food not observed and not recognizable in the preparations. Swims rapidly by rotation about main body axis, showing pronounced flexibility.

Somatic cilia about 8 µm long in vivo, arranged in an average of 23 meridional, narrowly spaced rows slightly curved at anterior end; on average 52 narrowly spaced kinetids per row, more densely spaced in oral area (Fig. 73a, d, f, 74h, i, k; Table 27). Dorsal brush composed of three rows, occupies on average 21% of body length, distinctly heterostichad: row 1 slightly longer than row 2; row 3 shorter than row 1 by about 60% and with a monokinetal tail extending to rear body end with 1 µm long bristles; dikinetids too close together to be counted; no suture, neither left or right of dorsal brush (Fig. 73a, d, 74h, k; Table 27).

Oral bulge minute, tuberculate, about 4 × 2 µm in vivo and thus difficult to recognize (Fig. 73a, d, f, 74b, c, h–j, k, l). No circumoral kinety recognizable, oral basket rods originate from first kinetid of each ciliary row. Oral basket obconical, in protargol-impregnated specimens about 15 µm long (Fig.73f, 74j, l).

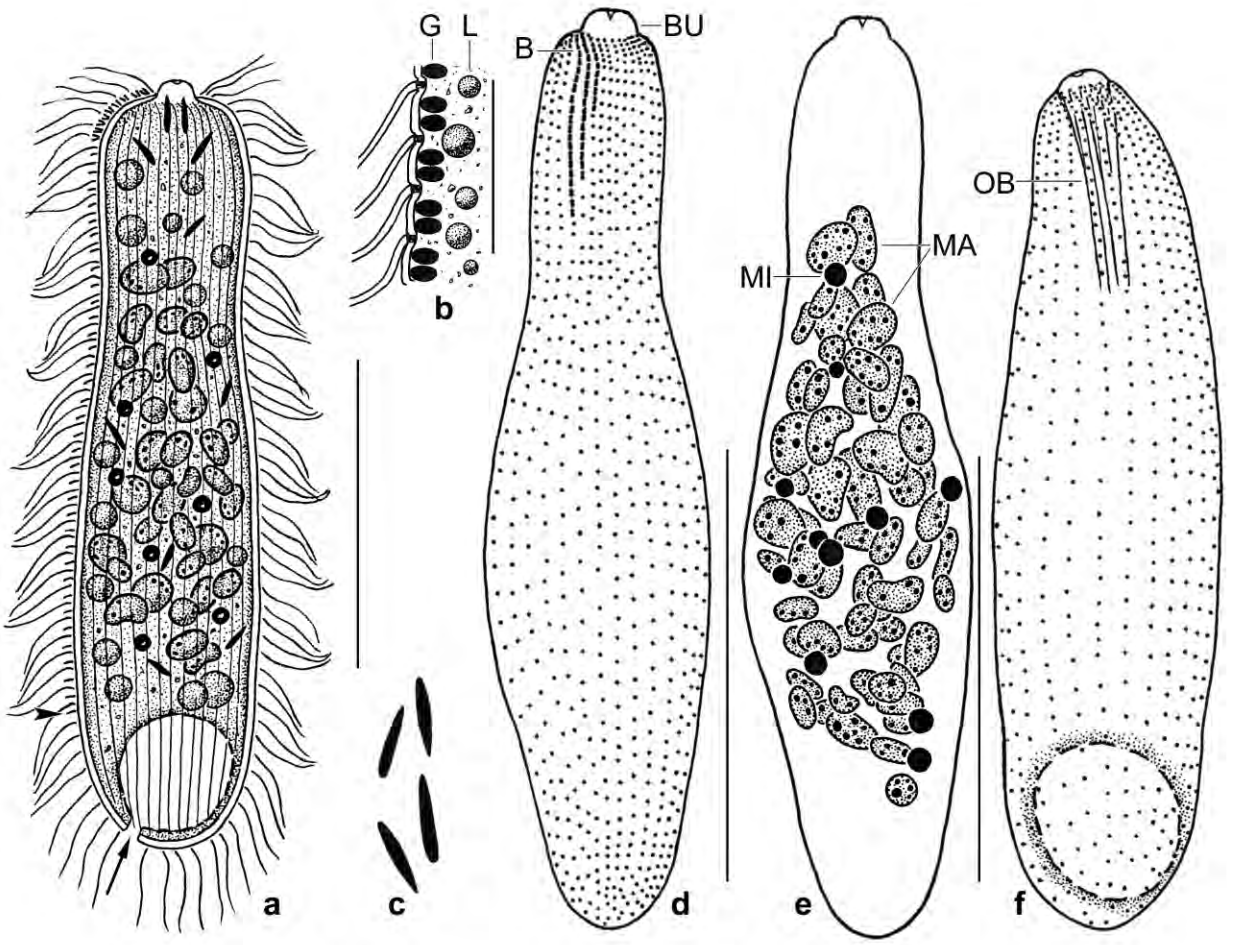

Fig. 73a–f. *Enchelariophrya wolfi* from life (a–c) and after protargol impregnation (d–f). **a:** Right side view of a representative, oblong specimen, showing the slightly bulbous anterior portion, length 75 µm. The dikinetids in dorsal brush row 3 do not represent the real number but only their position. The arrowhead marks the end of the monokinetal tail of brush row 3. The arrow denotes the excretory pore of the contractile vacuole. **b:** Optical section showing the cortical granules. **c:** Extrusomes, 3-5 µm long**. d:** Dorsal view of holotype specimen, showing body shape and ciliary pattern, length 65 µm. **e:** Nuclear apparatus of holotype specimen**,** showing 56 macronuclear nodules and 11 micronuclei. **f:** Ventral view of a paratype specimen, length 60 µm. B – dorsal brush, BU – oral bulge, G – cortical granules, L – lipid droplet, MA – macronuclear nodules, MI – micronucleus, OB – oral basket. Scale bars 5 µm (b) and 30 µm (a, d–f).

Occurrence and ecology: To date found only at type locality and at Venezuelan site (56).

Remarks: Regarding similar species, *E. wolfi* is distinct from *Enchelaria multinucleata* Foissner et al., 2002 in body shape (oblong or obclavate vs. lageniform or cylindroidal), body size (75 × 15 µm vs. 160 × 20 µm), the number of macronuclear nodules (on average 45 vs. 127), and the number of ciliary rows (on average 24 vs. 17). Within the genus *Enchelyodon,* there are very few multinucleate species, all distinctly different from *E. wolfi*. Perhaps *E. granosus* Lepsi, 1957 should be mentioned because it resembles *E. wolfi* in size and shape. However, it has a broad oral bulge and a rod-shaped axial structure. Unfortunately, Lepsi (1957) could not observe the nuclear apparatus and based the description on a single specimen from decaying *Sphagnum*.

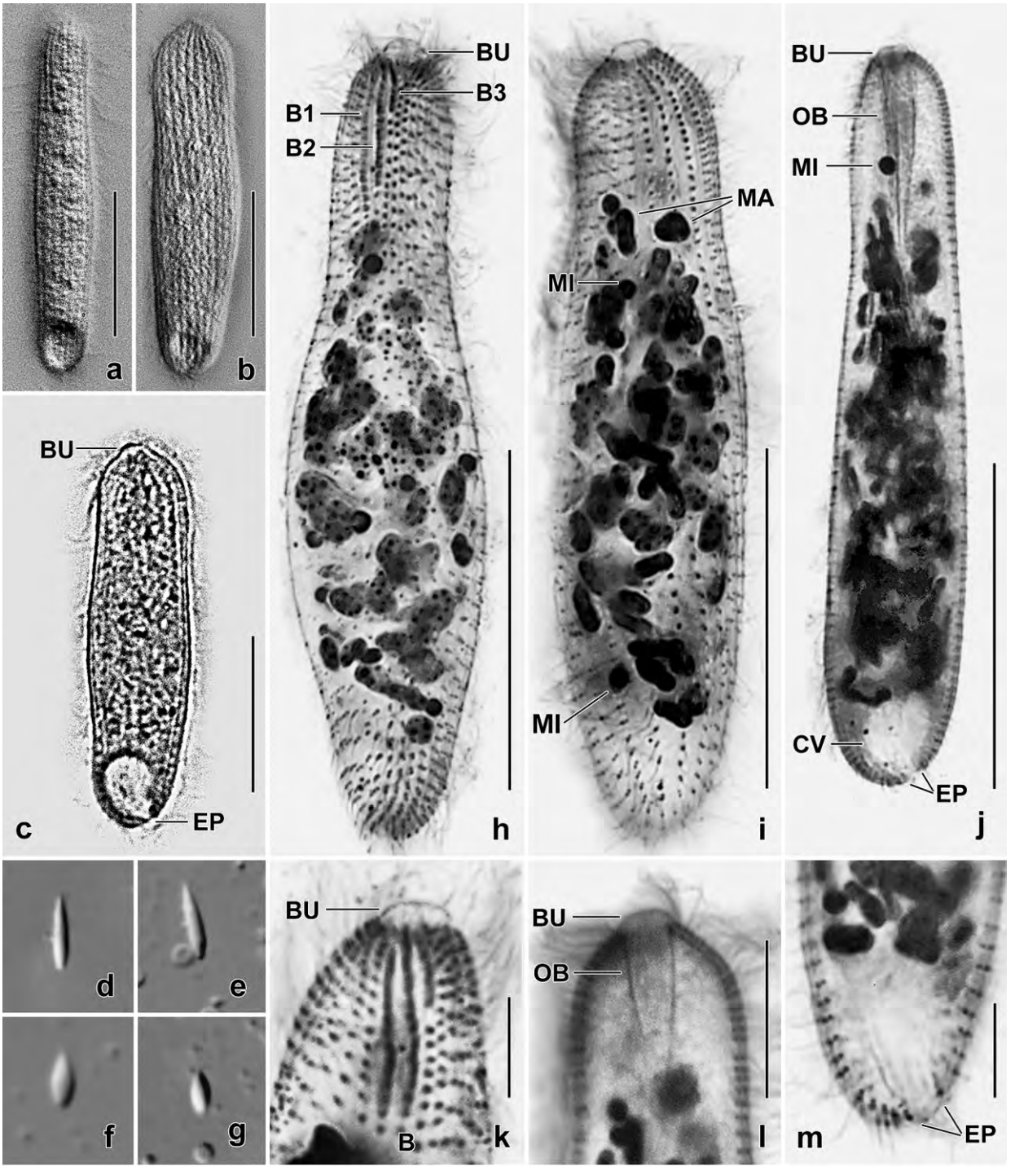

Fig. 74a–m. *Enchelariophrya wolfi* from life (a–g) and after protargol impregnation (h–m). **a, b:** Narrow- and broad-side view of same specimen, showing lateral flattening. **c:** Broad side overview. **d–g:** Mature (d, e; 3–5 µm long) and developing (f, g; 2–3 µm long) extrusomes. **h:** Dorsal overview of holotype, length 65 µm. Note the tuberculate oral bulge. **i:** Ventral overview of a paratype specimen, showing the nuclear apparatus. **j, l:** When focused to body centre, the minute oral bulge and the oral basket become recognizable. **k:** Dorsal brush and oral bulge of a paratype specimen. **m:** Enlarged detail from (j) to show the large excretory pore. B(1–3) – dorsal brush (rows), BU – oral bulge, CV – contractile vacuole, EP – excretory pore, MA – macronuclear nodules, MI – micronuclei, OB – oral basket. Scale bars 5 µm (m), 10 µm (k, l), and 30 µm (a–c, h–j).

Table 27. Morphometric data on *Enchelariophrya wolfi* based on mounted, protargol-impregnated, and randomly selected Jamaican specimens from a non-flooded Petri dish culture. Measurements in µm. CV – coefficient of variation in %, M – median, Max – maximum, Mean – arithmetic mean, Min – minimum, n – number of individuals investigated, SD – standard deviation, SE – standard error of arithmetic mean.

Characteristics	Mean	M	SD	SE	CV	Min	Max	n
Body, length	64.3	64.0	8.9	1.9	13.8	51.0	78.0	21
Body, width	14.2	14.0	1.9	0.4	13.7	11.0	20.0	21
Body length:width, ratio	4.6	4.4	0.6	0.1	12.2	3.6	6.2	21
Macronuclear nodules, length	3.8	4.0	0.7	0.2	19.1	3.0	5.0	21
Macronuclear nodules, width	1.8	1.5	0.4	0.1	20.9	1.5	3.0	21
Macronuclear nodules, number	45.1	44.0	6.9	1.5	15.3	36.0	59.0	21
Micronuclei, diametre	1.4	1.5	0.2	0.0	10.4	1.0	1.5	21
Micronuclei, number	7.6	7.0	2.0	0.4	26.3	4.0	12.0	21
Ciliary rows, number	23.3	24.0	1.2	0.3	4.9	21.0	25.0	21
Kinetids in a kinety, number	52.3	54.0	7.5	1.6	14.4	36.0	65.0	21
Dorsal brush row 1, length	13.2	14.0	1.8	0.4	14.0	10.0	16.0	19
Dorsal brush row 2, length	12.1	12.0	2.0	0.5	16.9	9.0	15.0	19
Dorsal brush row 3, length	5.5	5.0	1.6	0.5	30.0	4.0	9.0	11
Oral bulge, width	3.5	3.5	0.6	0.1	16.6	3.0	5.0	21
Oral bulge, height	1.6	1.5	0.3	0.1	18.2	1.0	2.0	21

Enchelys lajacola FOISSNER & OERTEL, 2009 (Fig. 75a–m, r, 76a–x; Table 28)

Improved diagnosis (includes type population): Size in vivo about 125 × 40 µm; narrowly (theronts) to broadly (trophonts) lageniform or obclavate. Macronuclear strand tortuous, 60 µm long on average. Extrusomes form a ring in oral bulge, rod-shaped, about 10 × 0.5 µm. On average 18 ciliary rows, 3 differentiated to a distinctly heterostichad dorsal brush with longest row 2 occupying about 22% of body length. Oral bulge about 7 × 3 µm in protargol preparations.

Voucher locality: Galápagos site (71), i. e., surface soil under a *Pandanus* palm in the garden of the hotel San Fernando, Puerto Ayora, Santa Cruz Island, S 90°18'W 0°44'.

Voucher material: 4 voucher slides with protargol-impregnated specimens have been deposited in the Biology Centre of the Upper Austrian Museum in Linz (LI). Relevant specimens have been marked by black ink circles on the coverslip.

Description: Details of the oral apparatus are difficult to investigate because the oral bulge extrusomes impregnate deeply, hidding most of the ciliary pattern. Thus, some data are vague. Further, the protargol preparations are mediocre because all specimens are studded with more or less deeply impregnated food vacuoles.

Size in vivo 100–180 × 30–80 µm, usually about 130 × 40 µm, as calculated from some in vivo measurements and the morphometric data in Table 28 adding 15% preparation shrinkage. Body shape highly variable, i. e., indistinctly to distinctly and very slenderly to broadly obclavate,

Table 28. Morphometric data on *Enchelariophrya lajacola* based on mounted, protargol-impregnated (FOISSNER's method), and randomly selected specimens from a non-flooded Petri dish culture. Measurements in µm. CV – coefficient of variation in %, M – median, Max – maximum, Mean – arithmetic mean, Min – minimum, n – number of individuals investigated, SD – standard deviation, SE – standard error of arithmetic mean.

Characteristics	Mean	M	SD	SE	CV	Min	Max	n
Body, length	112.9	107.0	18.8	4.1	16.7	85.0	160.0	21
Body, width	48.4	48.0	8.6	1.8	17.8	38.0	73.0	21
Body, subapical width	9.8	10.0	1.3	0.3	13.3	8.0	13.0	21
Body length:width, ratio	2.4	2.2	0.4	0.1	16.8	1.7	3.2	21
Anterior body end to macronucleus, distance	49.3	50.0	14.4	3.2	29.3	22.0	75.0	21
Macronucleus, length (~)	73.3	70.0	–	–	–	45.0	120.0	21
Macronucleus, width	6.5	6.0	0.9	0.2	14.3	5.0	8.0	21
Excretion pores, number (~)	8.6	8.0	–	–	–	6.0	12.0	15
Extrusomes, length	10.0	10.0	0.5	0.1	4.7	9.0	11.0	21
Oral bulge, width	7.1	7.0	0.7	0.2	9.9	6.0	8.0	11
Oral bulge, height	3.4	3.0	1.2	0.4	35.9	2.0	6.0	11
Ciliary rows, total number	19.5	19.0	1.8	0.4	9.3	17.0	24.0	23
Dorsal brush rows, number	3.0	3.0	0.0	0.0	0.0	3.0	3.0	17
Dorsal brush row 1, length	18.7	20.0	2.5	0.6	13.5	13.0	22.0	19
Dorsal brush row 1, number of dikinetids [a]	15.1	15.0	–	–	–	10.0	20.0	19
Dorsal brush row 2, length	24.7	25.0	3.3	0.8	13.4	18.0	30.0	19
Dorsal brush row 2, number of dikinetids [a]	20.1	20.0	–	–	–	14.0	27.0	19
Dorsal brush row 3, length	6.6	6.0	0.8	0.2	12.5	6.0	8.0	19
Dorsal brush row 3, number of dikinetids [a]	7.9	8.0	–	–	–	6.0	9.0	19

[a] Approximate values because difficult to recognize in the subapical area.

partially depending on amount of food ingested (Fig. 75a, d, g–j, k, l, 76d–g, j, k, l, n, p); when transferred to the microscope slide and under slight coverslip pressure contractile by about one third of body length, especially anterior body half (Fig. 75f, 76d–g). Anterior body portion ("neck"), in contrast, little variable, viz., about 10 µm in diameter irrespective of width in mid-body (Fig. 75a, d, g–j, k, l, 76d–g, j, k, l, n–p; Table 28). Macronucleus in central quarters of cell, a highly tortuous strand about 70 × 7 µm in protargol preparations; nucleoli reticulate (Fig. 75a, k, l, 76f, j, k, l; Table 28). Likely several micronuclei but not unequivocally separable from food inclusions. Contractile vacuole and cytopyge in posterior body end, several excretory pores (Fig. 75a, l, 76f, g, i, j; Table 28). Extrusomes rod-shaped with rounded ends, 10–11 × ~ 0.5 µm in size both in vivo and in protargol preparations, form a ring in oral bulge and scattered in anterior body half, impregnate deeply with the protargol method used; cytoplasmic extrusomes occasionally acicular (Fig. 75a, b, d, e, k, 76a, b, h, j, l, m, p; Table 28). Exploded extrusomes of typical toxicyst structure, about 30 µm long (Fig. 75e, 76c). Cortex very flexible, contains countless minute granules (~ 0.2 µm), forming about 10 slightly oblique rows between two ciliary rows each (Fig. 75c). Cytoplasm colourless but dark at low magnification (≤ 100×) due to many food inclusions and lipid droplets up to 10 µm across. Of four *Colpoda* species present (*C. steinii*, *C. maupasi*, *C. inflata*, *C. cuccullus*), only *C. inflata* was ingested whole, showing strict food selection and an extraordinarily extensibility of the thin neck (Fig. 75d, 76n, p). The large food

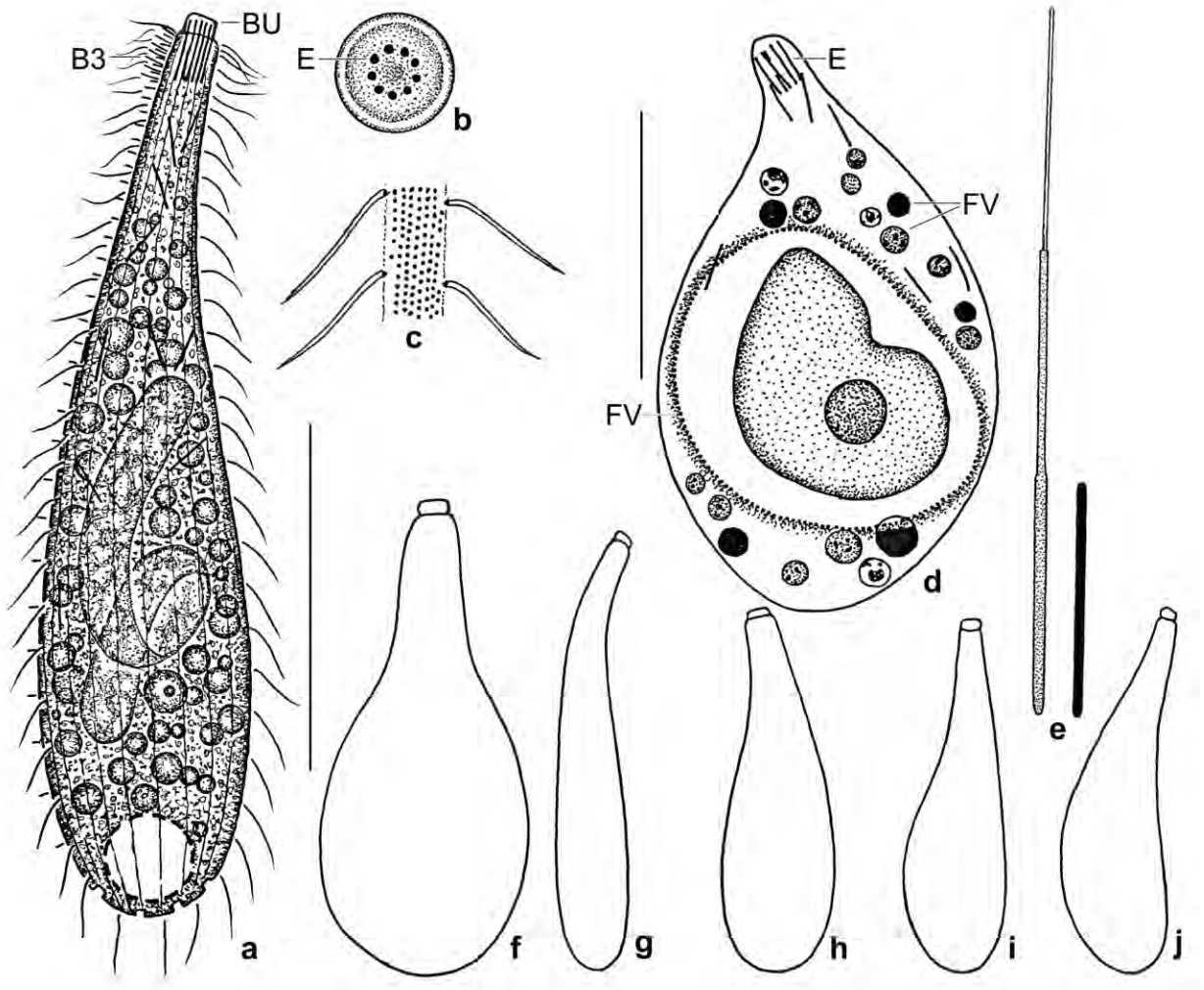

Fig. 75a–j. *Enchelys lajacola* from life (a–c, e–j) and after protargol impregnation (d). **a:** A representative specimen with many globular food inclusions, length 130 µm. **b:** Frontal view, showing the extrusome ring. **c:** Surface view, showing the cortical granulation. **d:** A specimen having just ingested a *Colpoda inflata*. The food globules have different affinity to protargol, likely because they contain different materials (food segregation). **e:** An exploded (30 µm) and a resting (10 µm) toxicyst. **f:** A contracted specimen just put on the microscope slide. **g–j:** Shape variability of ordinarily nourished specimens. B3 – dorsal brush row 3, BU – oral bulge, E – extrusomes, FV – food vacuoles. Scale bars 50 µm.

vacuoles disintegrate into many small globules with different affinity to protargol, suggesting food segregation (Fig. 75a, d, 76b, d–g, i–n). Swims rapidly moving oral portion slightly to and fro possibly sensing for food.

Cilia in vivo 9 µm long, arranged in an average of 19 meridional, widely spaced rows composed of loosely spaced cilia; anterior portion of rows slightly curved and densely ciliated. Dorsal brush distinctly heterostichad and isomorph, longest row 2 occupies 22% of body length on average; all rows possibly with a short anterior tail of ciliated monokinetids; row 3 extends to posterior body end with monokinetal, about 2 µm long bristles (Fig. 75a, k, m, r, 76l, m, o; Table 28).

Oral bulge discoid, about 7 × 3 µm in protargol preparations, slightly oblique, contains a circular

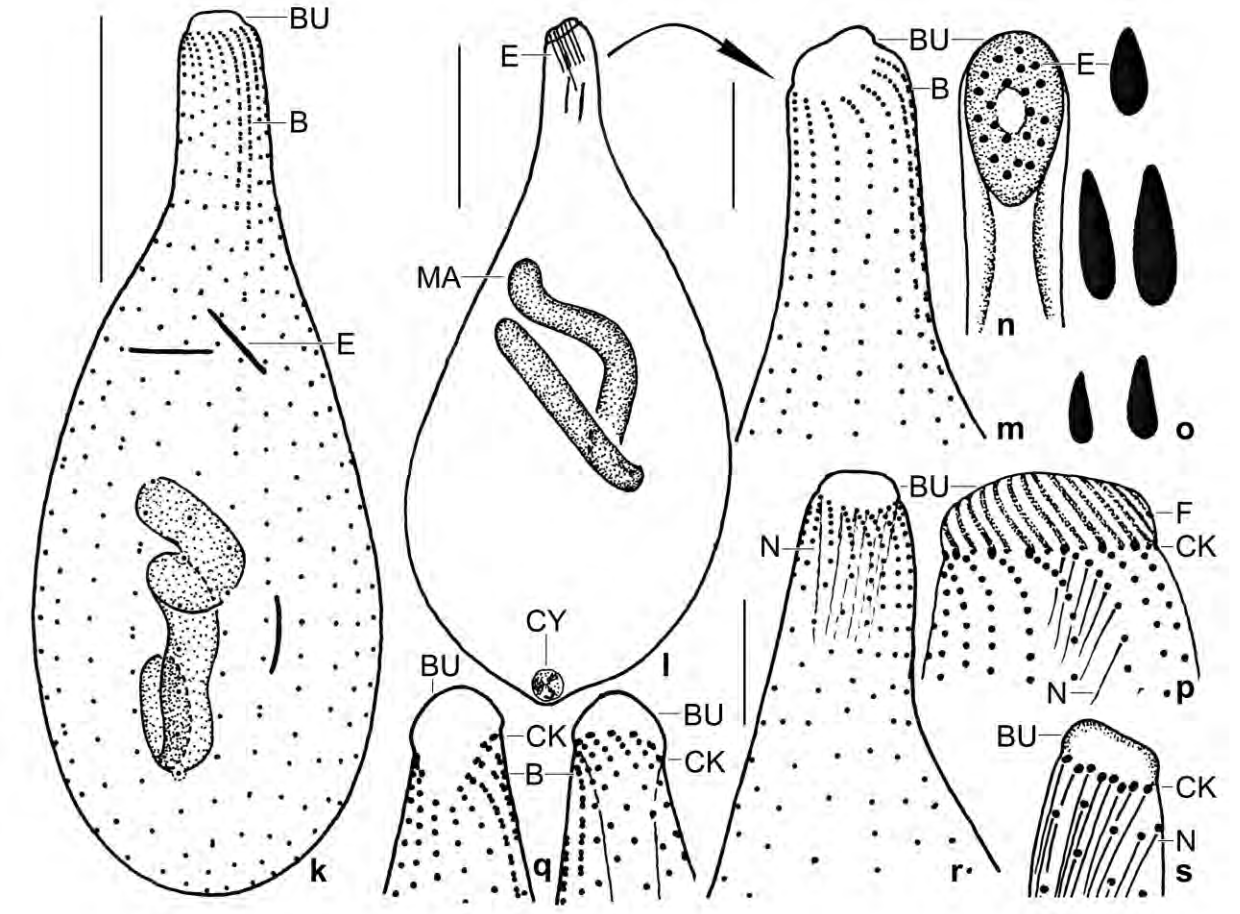

Fig. 75k–s. *Enchelys lajacola* (k, l, m, r), *Sikorops namibiensis* (n, o, p; from Foissner et al. 2002), *S. woronowiczae* (s; from Foissner 1999b), and *S. espeletiae* (q; from Foissner 2000b) from life (n, o) and after protargol impregnation (k–m, p–s). **k:** Dorsolateral view of holotype specimen, length 100 µm. **l, m, r:** Outline and ciliary pattern in anterior body region. Note the curved anterior portion of the ciliary rows and very fine oral basket rods originating from the first or several kinetids of the kineties (r). **n, q:** Ventral and dorsal views of oral region, showing the obovate oral bulge and supposed dikinetids forming an indistinct circumoral kinety. **o:** Extrusome shape in three species. **p, s:** Anterior body region, showing oral basket rods originating from the first (di?) kinetid of each ciliary row and from the following somatic monokinetids. B – dorsal brush, BU – oral bulge, CK – circumoral (di?) kinetids (kinety), CY – cytopyge, E – extrusomes, F – fibres, N – nematodesmata = oral basket rods. Scale bars 10 µm (m, r) and 30 µm (k, l).

array of toxicysts. Circumoral kinety absent. Nematodesmata very fine, originate from anterior kinetids of each ciliary row (Fig. 75a, b, d, k–m, r, 76j, m, o; Table 28).

Occurrence and ecology: At the type locality it was numerous in the non-flooded Petri dish culture three days after rewetting the sample. Likewise, it was numerous in the Galápagos sample six days after re-wetting the sample.

Remarks: Ciliates of this type are very difficult to classify and to identify because they have few characters. The observations match those of Foissner & Oertel (2009). Although there are several similar genera, only *Sikorops* Foissner, 1999b has the same constellation of characters. However, the three *Sikorops* species (Foissner 1999b, 2000b, Foissner & Xu 2007, Foissner et

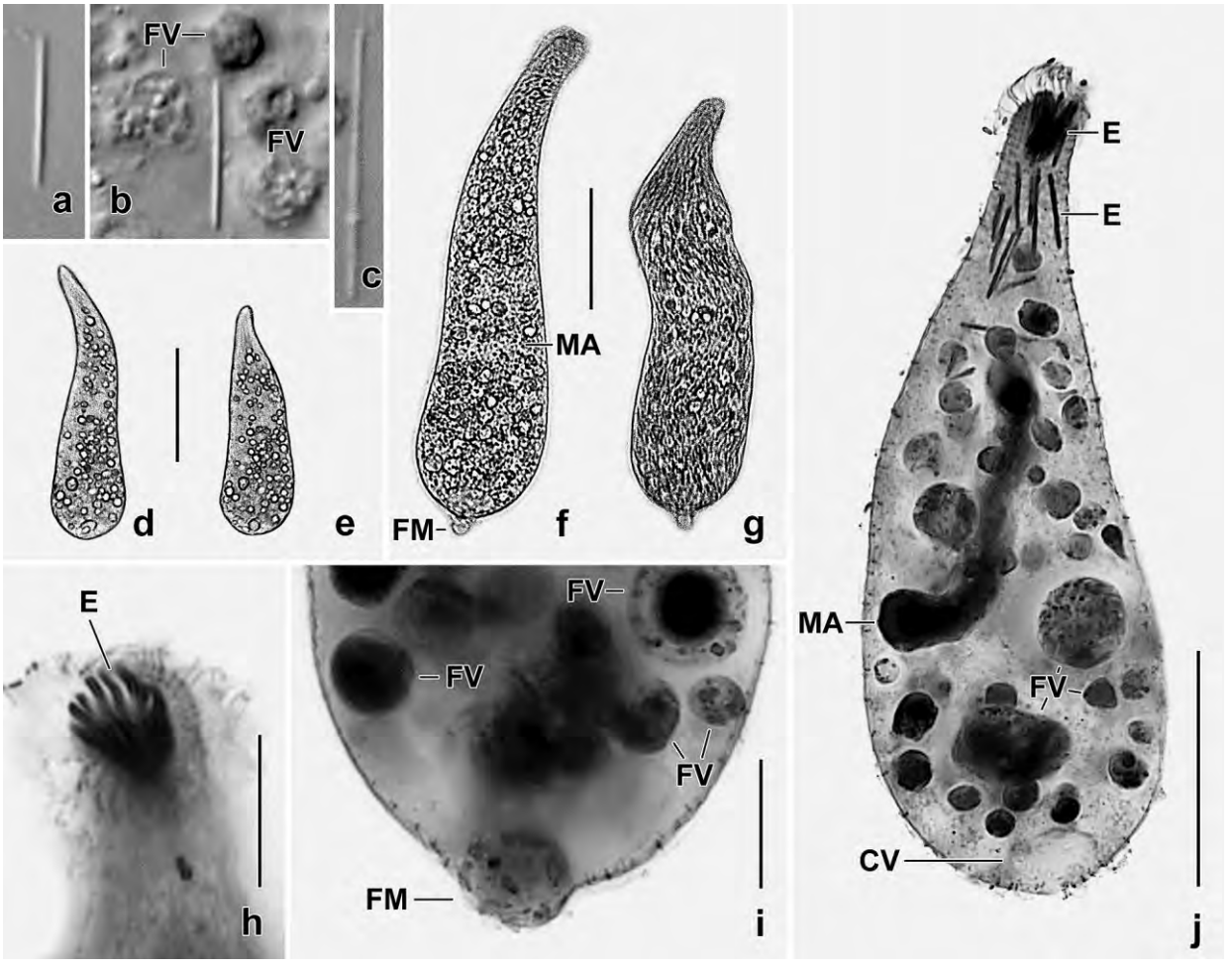

Fig. 76a–j. *Enchelys lajacola* from life (a–g) and after protargol impregnation (h–j). **a, b:** Resting extrusomes, length 10 µm. Note the different structure of the food vacuoles, indicating food segregation. **c:** An exploded toxicyst, length about 30 µm. **d, e:** The same specimen extended and slightly contracted. The bright globules are food vacuoles. **f, g:** The same specimen extended and just contracting. Note fecal mass leaving cell through the cytopyge. **h:** Oblique frontal view, showing the circular arrangement of the oral bulge extrusomes. **i:** Posterior body region, showing a globular fecal mass leaving the cell in pole centre. Note the different structure of the food vacuoles. **j:** Overview. The size, shape, and protargol-affinity of the food vacuoles (globules) are very different, indicating food segregation, i. e., the various prey organelles are collected and digested in specific vacuoles. CV – contractile vacuole, E – extrusomes, FM – fecal mass, FV – food vacuoles, MA – macronucleus. Scale bars 10 µm (h, i), 30 µm (j), and 50 µm (d–g).

al. 2002) have an obovate (Fig. 75n, q) vs. circular (Fig. 75b) oral bulge and ovate (Fig. 75o) vs. rod-shaped (Fig. 75e) extrusomes.

As far as we know, such a population has not been described, although several of the old species look quite similar in vivo, especially from the genera *Enchelys* and *Enchelyodon*. All described *Enchelys* species have a single, short macronucleus (vs. an about 70 µm long strand) or several small nodules (Kahl 1930a). *Enchelyodon elegans* var. *striatus* Kahl, 1930a, b, which resembles *E. galapagensis* in the shape and size of the body, the macronucleus, and the oral bulge, is a limnetic species with about 30 ciliary rows (vs. terrestrial and 19 ciliary rows); the extrusomes are not known.

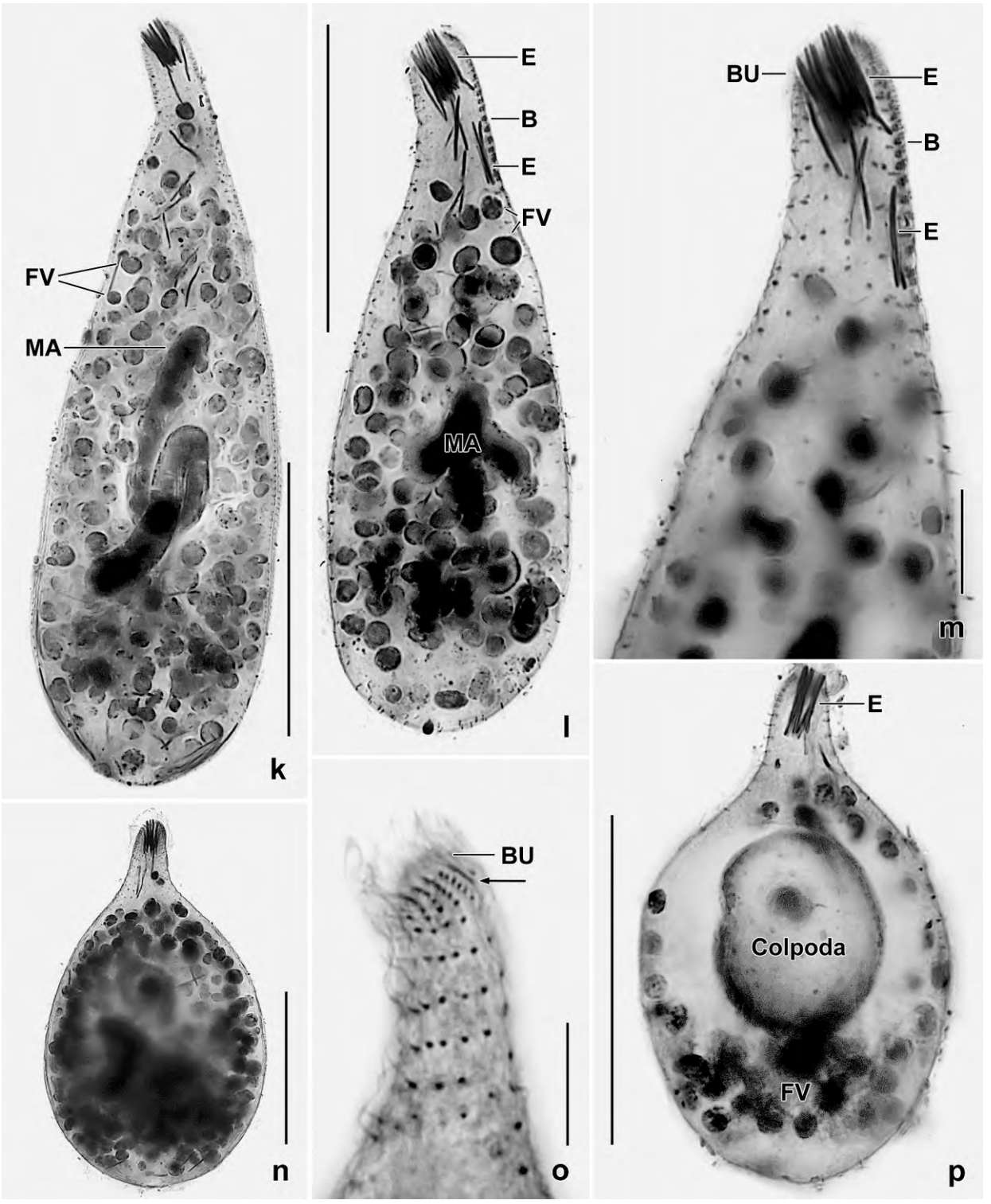

Fig. 76k–p. *Enchelys lajacola* after protargol impregnation. **k:** Overview of a well-nourished specimen, showing the pharyngeal extrusome bundle and the long, tortuous macronucleus. **l, m:** Overview and detail, showing parts of the ciliary pattern. **n, p:** Specimens having just ingested a *Colpoda inflata* become almost globular. **o:** Anterior body region, showing the ciliary pattern and the absence of a circumoral kinety. The arrow marks the perioral, closely spaced monokinetids. B – dorsal brush, BU – oral bulge, E – extrusomes, FV – food vacuoles, MA – macronucleus. Scale bars 10 µm (m, o) and 50 µm (k, l, n, p).

Phialinides bicaryomorphus **nov. spec.** (Fig. 77a–i, 78a–f; Table 29)

Diagnosis: Size in vivo about 110 × 25 µm, can contract half of body length becoming almost globular. In vivo slightly clavate, when swimming rapidly and in protargol preparations narrowly to very narrowly ellipsoid. Macronucleus discoid, strongly flattened in middle third, narrow side view thus dumbbell-shaped. Micronucleus in terminal concavity of macronucleus. Contractile vacuole and excretory pores subterminal. Extrusomes rod-shaped, about 16 × 1 µm in size. On average 23 ciliary rows. Oral bulge discoid to hemispheric.

Type locality: Venezuelan site (56), i. e., slightly saline surface mud and soil from temporary grassland puddles in the surroundings of the village of Chichiriviche, Morrocoy National Park, about 13 km inshore from the north coast, 67°13' W 11°33' N.

Type material: 1 holotype and 3 paratype slides with protargol-impregnated specimens have been deposited in the Biology Centre of the Upper Austrian Museum in Linz (LI). Relevant specimens have been marked by black ink circles on the coverslip.

Etymology: Composite of the Greek words *bi* (two), *caryon* (nucleus), and *morphé* (shape), referring to the special shape of the macronucleus.

Description: Size of extended cells in vivo 90–120 × 20–30 µm, on average about 110 × 25 µm, as calculated from some in vivo measurements and the morphometric data in Table 29 adding 15% preparation shrinkage. Length:width ratio 3.6–5.5:1, on average 4.5:1. Can contract to about half of body length, especially under mild coverslip pressure. Distinctly contracted cells in protargol preparations 59–75 × 22–30 µm, on average 67 × 26 µm, i. e., length considerably decreases (67 µm vs. 110 µm) while width slightly increases (22–30 µm vs. 17–26 µm). Length:width ratio 2.1–2.9:1, on average 2.6:1, and thus much narrower than in extended cells (4.5:1). Contraction and extension occur slowly, body length thus possibly underestimated because slightly contracted specimens are indistinguishable from fully extended ones; however, length error likely small as indicated by the low variability coefficients (~ 10%, Table 29).

Extended specimens in vivo indistinctly to rather distinctly clavate with widest region posterior of neck (Fig. 77a); widening lost in protargol-impregnated specimens, very likely due to some contraction making cells narrowly to very narrowly ellipsoid (Fig. 77b, e, f, 78a, b, e, f); oral bulge plus head form conspicuous hemispherical protrusion in vivo (Fig. 77a, b, e, g, h). When swimming rapidly, cells become very narrowly ellipsoid (Fig. 77g). Moderately to distinctly contracted specimens elongate ellipsoid in vivo (Fig. 77h, 78e), strongly contracted cells almost globular (Fig. 77i).

Nuclear apparatus slightly posterior of mid-body on average (Table 29). Macronucleus conspicuously dimorphic because discoidally flattened by about 30% (Table 29), in middle third even by about 50%; outline in broad side view elliptic to broadly elliptic (Fig. 77a, e, f, 78c, f; Table 29) while more or less dumbbell-shaped in narrow side view (Fig. 77b, h, 78a, b, d); nucleoli numerous but inconspicuous because ≤ 1 µm in size (Fig. 77a, 78c). Micronucleus in small concavity of anterior or posterior end of macronucleus, roughly lenticular, on average 2.2

Table 29. Morphometric data on extended (upper line) [a] and contracted (lower line) [a] *Phialinides bicaryomorphus* based on mounted, protargol-impregnated (FOISSNER's method), and randomly selected specimens from a non-flooded Petri dish culture. Measurements in µm. CV – coefficient of variation in %, M – median, Max – maximum, Mean – arithmetic mean, Min – minimum, n – number of specimens investigated, SD – standard deviation, SE – standard error of arithmetic mean.

Characteristics	Mean	M	SD	SE	CV	Min	Max	n
Body, total length	93.7	98.0	8.1	1.8	8.6	81.0	105.0	21
	67.5	67.0	6.0	2.5	8.9	59.0	75.0	6
Body, width	21.1	21.0	2.3	0.5	10.7	17.0	26.0	21
	25.8	26.0	2.8	1.1	10.8	22.0	30.0	6
Body length:width, ratio	4.5	4.5	0.5	0.1	11.5	3.6	5.5	21
	2.6	2.7	0.3	0.1	12.3	2.1	2.9	6
Oral bulge plus head, height	10.7	11.0	0.6	0.1	6.0	10.0	12.0	21
	8.0	8.0	1.6	0.6	19.4	6.0	10.0	6
Oral bulge, height	4.8	5.0	0.5	0.1	10.6	4.0	6.0	21
	2.9	2.3	1.3	0.5	43.9	2.0	5.0	6
Oral bulge, width	8.3	8.0	0.7	0.2	8.7	7.0	10.0	21
	7.5	7.5	1.1	0.4	14.0	6.0	9.0	6
Head, width	11.7	12.0	0.7	0.2	6.3	11.0	13.0	21
	12.0	12.5	1.8	0.7	14.9	9.0	14.0	6
Anterior body end to macronucleus, distance	43.4	42.0	6.5	1.4	15.1	32.0	59.0	21
	27.7	27.0	6.0	2.4	21.7	19.0	36.0	6
Anterior body end to somatic kineties on trunk, distance	14.2	14.0	1.3	0.3	8.9	12.0	17.0	21
	10.0	10.0	2.0	0.8	20.0	7.0	13.0	6
Macronucleus, length	21.8	22.0	2.2	0.4	10.1	17.0	26.0	28
Macronucleus, width (broad side view)	11.9	11.5	1.1	0.4	9.5	11.0	14.0	8
Macronucleus, width (narrow side view) [b]	8.7	8.0	1.3	0.3	15.0	7.0	12.0	20
Micronucleus, length	2.2	2.0	–	–	–	2.0	3.0	10
Micronucleus, width	1.6	1.7	–	–	–	1.0	2.0	10
Ciliary rows, number	22.6	23.0	0.8	0.2	3.3	20.0	23.0	21
	22.7	22.5	0.8	0.3	3.6	22.0	24.0	6
Brush pairs or triplets in a kinety, number	4.7	5.0	1.2	0.3	24.7	3.0	7.0	21
	4.8	5.0	0.8	0.3	15.6	4.0	6.0	6
Kinetids in a ciliary row, number [c]	38.7	36.0	7.4	1.6	19.1	28.0	57.0	21
	43.2	43.0	7.0	2.9	16.3	32.0	54.0	6
Phialinides ciliary wreath, number of kinetids	13.2	14.0	1.9	0.4	14.5	9.0	17.0	21

[a] According to the morphometric data and live observations, cells longer than 75 µm were classified as extended (however, they are very likely also contracted by up to 10%) while those smaller than 75 µm were considered distinctly contracted.

[b] Maximum width measured.

[c] Brush dikinetids and trikinetids as well as somatic, pair-like kinetids each counted as (1) kinetid.

× 1.6 µm in protargol-impregnated cells (Fig. 77a, e, f, 78c, e, f; Table 29). Contractile vacuole in posterior end, with three or more subterminal excretory pores recognizable in vivo and in deeply impregnated cells (Fig. 77a, e, f, 78b). Extrusomes form conspicuous bundle in oral bulge and head, rod-shaped, 11–20 × 0.8–1.2 µm in vivo, on average (n 9) 16 × 1 µm (Fig. 77a, c); extrusome bundle frequently dislocated into cytoplasm in squeezed specimens; do not impregnate with the protargol method used. Cortex very flexible, colourless, contains many narrowly spaced granule

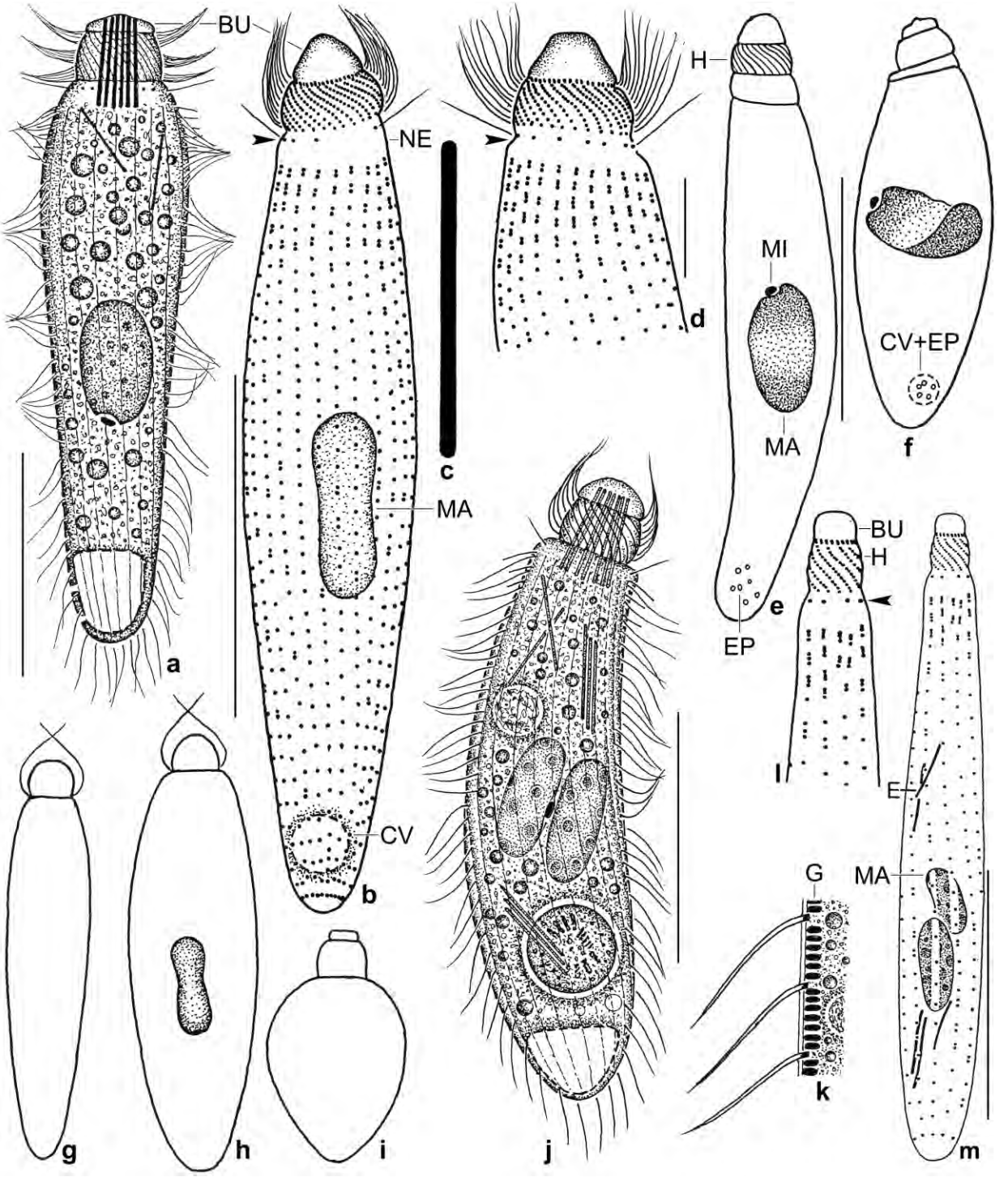

Fig. 77a–m. *Phialinides bicaryomorphus* (a–i), *P. muscicola* (j, k; from Foissner & Wenzel 2004), and *P. australis* (l, m; from Foissner 1988a) from life (a, c, g–k) and after protargol impregnation (b, d–f, l, m). **a, j:** Representative specimens, length 110 µm and 100 µm. **b, d:** Holotype specimen (b), length 100 µm, and anterior third of a paratype specimen (d). Arrowheads denote the phialinid ciliary wreath. **c:** Extrusome, length 15 µm. **e, f:** Extended and contracted specimen drawn to scale. **g:** A very rapidly swimming cell. **h, i:** A slightly and a strongly contracted cell. **k:** Cortical granulation in *P. bicaryomorphus* and *P. muscicola*. **l, m:** Holotype specimen, length 105 µm. Arrowhead marks phialinid ciliary wreath. BU – oral bulge, CV – contractile vacuole, E – extrusomes, EP – excretory pores, G – cortical granules, H – head, MA – macronucleus, MI – micronucleus, NE – neck. Scale bars 10 µm (d) and 40 µm (a, b, e, f, j, m).

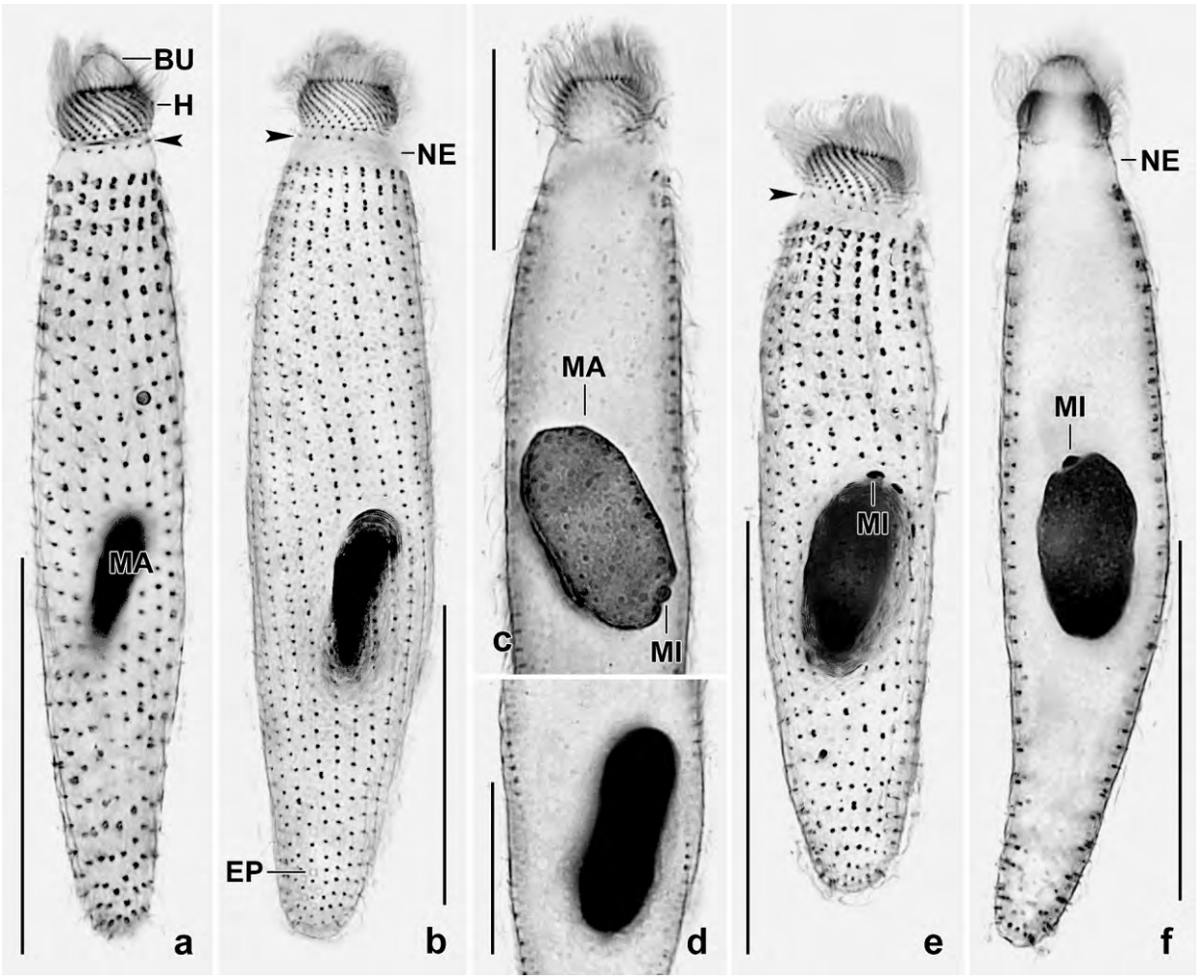

Fig. 78a–f. *Phialinides bicaryomorphus*, ciliary and nuclear pattern after protargol impregnation. The arrowheads mark the phialinid ciliary wreath posterior of the densely ciliated head. **a:** A slender specimen with meridionally extending ciliary rows and conical oral bulge. Note dikinetids in anterior region of kineties. The macronucleus shows the narrow side. **b, d:** A typical specimen with hemispheric oral bulge and slightly spiralling ciliary rows commencing with dikinetids. The macronucleus is distinctly flattened, especially in the middle third, and is thus dumbbell-shaped in narrow side view (d). **c:** Anterior half of a specimen, showing the broad side of the macronucleus. The micronucleus is in a minute concavity at the end of the macronucleus. **e:** A rather strongly contracted specimen with almost meridional ciliary rows. **f:** A slender specimen, showing the nuclear apparatus, the hemispheric oral bulge, and the unciliated neck. BU – oral bulge, EP – excretory pores of contractile vacuole, H – head, MA – macronucleus, MI – micronucleus, NE – neck. Scale bars 20 µm (c, d) and 40 µm (a, b, e, f).

rows; individual granules strongly refractive, about 0.8 × 0.2 µm in size (Fig. 77k). Cytoplasm colourless, not dark at low magnification but sometimes studded with lipid droplets up to 5 µm across, most 1–2 µm. Food not known. Swims rapidly to very rapidly pushing to and fro.

Cilia about 10 µm long in vivo, arranged in an average of 23 narrowly to ordinarily spaced rows extending meridionally to slightly spirally from neck to posterior body end, forming a dense wreath on head; course of rows independent of contraction and extension state of body (Fig. 78e). Kineties composed of 39 ordinarily spaced kinetids on average, commence with an average of five di- and trikinetids with anterior cilium shortened to about 4 µm. Phialinid ciliary wreath composed of an average of 13 ciliated monokinetids (Fig. 77a, b, d, 78a, b, e; Table 29).

Oral bulge plus head conspicuously hemispherical in vivo, on average about 11 µm high both in vivo and in protargol preparations (Fig. 77a, g; Table 29). Oral bulge discoid with slightly convex surface in vivo (Fig. 77a) while discoidal, conical or hemispherical in protargol-impregnated specimens (Fig. 77b, d, e, f, 78a, b, f), very likely due to some changes during fixation, as indicated by the high variability coefficient of 44% (Table 29). Head ciliature as typical for genus and family, cilia about 10 µm long, forming metachronal waves during forward swimming. Oral basket not impregnated.

Occurrence and ecology: As yet found in five ephemeral habitats (see chapter 3.1.1). *Phialinides bicaryomorphus* was moderately abundant in the non-flooded Petri dish culture three weeks after rewetting sample (56).

Remarks: The genus *Phialinides* Foissner, 1988a differs from *Phialina* Bory de St. Vincent, 1824 in having an isolated ciliary wreath on the short neck, i. e., posterior to the head (Fig. 77a, d, l, 78a, b, e). Although this feature is not always distinct, it is very likely reliable (Foissner et al. 1999).

Lacrymariids of the *Lacrymaria*/*Phialina*/*Phialinides* type are very difficult to identify because of a lot of poorly described species. Our attempts to identify the Venezuelan population with one of the *Lacrymaria*/*Phialina* species reviewed by Kahl (1926, 1930a) failed. Likewise, we did not find it in more recent publications, e. g., Vuxanovici (1959). As concerns body size and shape as well as the number of ciliary rows and macronuclear nodules, the Venezuelan population is possibly most similar to *Phialina vertens* (Stokes, 1885), as redescribed by Kahl (1926, 1930a), Foissner (1983), and Song & Wilbert (1989). Unfortunately, it is possible that each of the redescriptions represents a different species. Kahl's authoritative redescription shows a semicircular macronucleus with the micronucleus in curve centre. The *P. vertens* of Song & Wilbert (1989) has an ellipsoid or indistinctly reniform macronucleus with the micronucleus attached to various sites. The population of Foissner (1983) has the same nuclear pattern as *P. bicaryomorphus* but is slightly smaller (in vivo 60–85 µm vs. 90–120 µm), has fewer ciliary rows (15–20 vs. 20–25), and likely lacks the phialinid ciliary wreath.

Of the three *Phialinides* species described by Foissner (1988a, Fig. 77l, m), Foissner et al. (2002), and Foissner & Wenzel (2004, Fig. 77j, k), *P. bicaryomorphus* is unique, inter alia, by the number (1 vs. 2 or more) and shape (dimorph vs. monomorph) of the macronuclear nodules.

Enchelys terricola Foissner, 1987c

Improved diagnosis: Length in vivo about 115–130 µm; theronts slenderly obclavate, about 30 µm wide, trophonts obclavate, about 40 µm wide. Many macronuclear nodules. Contractile vacuole in rear end. Mature extrusomes either rod-shaped and about 5 µm long or lanceolate and 6 µm long. On average 16–17 ciliary rows with curved anterior end. Dorsal brush heterostichad, rows 1 and 2 of similar length, row 3 shorter than longest row 2 by about 60%. Oral bulge about 7 µm wide, oblique with slightly convex surface.

Remarks: The body's length:width ratio was calculated from the original data (Foissner 1987c). The diagnosis was adapted to the modern standard.

We split *E. terricola* into two subspecies, differing mainly in the shape of the extrusomes (rod-like vs. lanceolate). We consider the extrusome shape as an important feature possibly involved in prey selection. When the extrusome shape of two or more populations is very different (e. g., rod-like vs. ellipsoidal), then we consider the populations as different species (Foissner et al. 002, Gabilondo & Foissner 2009).

Enchelys terricola terricola Foissner, 1987c **nov. stat.**

Diagnosis: As given above; extrusomes rod-shaped.

Type locality: Grassland soil in the outskirts of the town of Salzburg, Austria.

Description: See Foissner (1987c) and Table 30.

Enchelys terricola lanceoplites **nov. sspec.** (Fig. 79a–l, 80a–k; Table 30)

Diagnosis: As given above; extrusomes lanceolate.

Type locality: Litter and soil from a forest on the Robinson Crusoe Island, 82°W 34°S.

Type material: 1 holotype and 4 paratype slides with protargol-impregnated specimens have been deposited in the Biology Centre of the Upper Austrian Museum in Linz (LI). Relevant specimens have been marked by black ink circles on the coverslip.

Etymology: Composite of the Latin nouns *terricola* (living in soil) and *lancea* (lance), and the Greek noun *hoplites* (soldiers ~ extrusomes). Thus, *lanceoplites* means a ciliate with lanceolate extrusomes.

Description: This species has a distinct life cycle with slender theronts and inflated trophonts. When not separated in the morphometric analyses, several features get a high variation coefficient, e. g., 30% for the ratio of body length:width (Table 30).

Size in vivo 90–150 × 25–55 µm, usually about 115 × 30 µm (theronts) or 115 × 40 µm (trophonts), as calculated from some in vivo measurements and the morphometric data in Table 30 adding 15% preparation shrinkage. Body length:width ratio on average 3:1 in protargol preparations (Table 30), about 5:1 in theronts and 2:1 in trophonts (data not shown). Body slenderly obclavate (theronts) to obclavate (trophonts), neck usually slightly curved ventrally, likely unflattened (Fig. 79a, d, f, i, 80a, g, k). Ten to 30 globular to elongate ellipsoid macronuclear nodules, each with a large central nucleolus, accumulated in third quarter of cell. Micronuclei not unequivocally identified due to many similar cytoplasmic inclusions (Fig. 79a, e, f, 80a, k). Contractile vacuole in posterior body end, very likely several excretory pores (Fig. 79a, i). Mature extrusomes attached to oral bulge, in vivo lanceolate and about 6–7 × 0.8–1.2 µm in size; impregnate lightly to

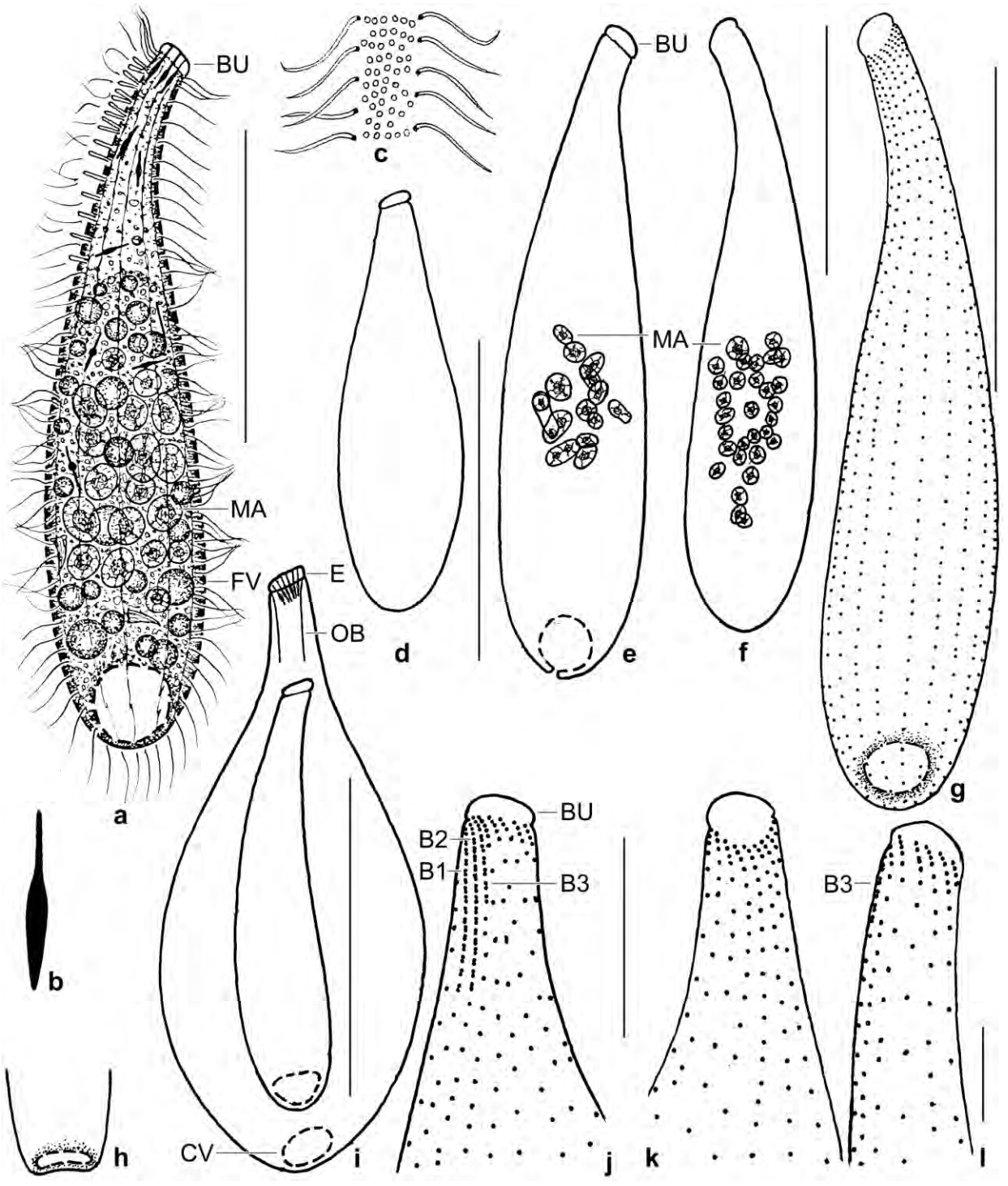

Fig. 79a–l. *Enchelys terricola lanceoplites* from life (a–d, h) and after protargol impregnation (e–g, i–l). **a:** A representative theront, length 115 µm. **b:** Mature extrusome, 6 µm. **c:** Cortical granulation. **d:** Shape of a specimen becoming a trophont. **e:** Macronuclear pattern. **f, g, l:** Ciliary and nuclear pattern of holotype specimen, length 125 µm. **h:** Posterior body end after function of the contractile vacuole. **i:** Size relation of theront and trophont. **j, k:** Ciliary pattern in anterior body region of a paratype specimen. BU – oral bulge, B1–3 – dorsal brush rows, CV – contractile vacuole, E – extrusomes, FV – food vacuole, MA – macronuclear nodules, OB – oral basket. Scale bars 10 µm (l), 15 µm (j, k), and 50 µm (a, e–g, i).

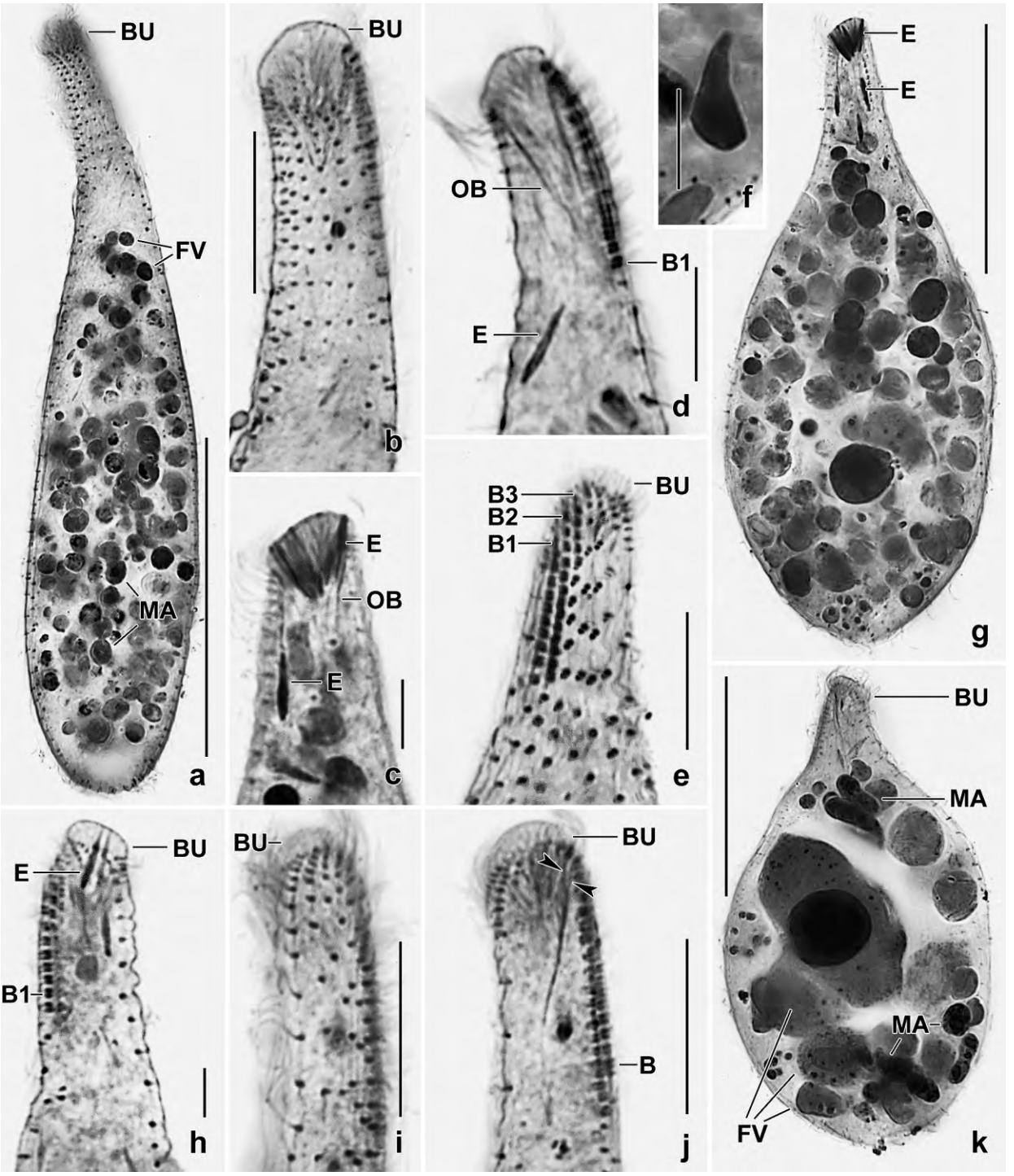

Fig. 80a–k. *Enchelys terricola lanceoplites* after protargol impregnation. **a, b:** Ventral overview and oral detail of a theront developing into a trophont. The ciliary rows are curved anteriorly. **c, h:** Anterior body region, showing mature, lanceolate extrusomes attached to the oblique oral bulge. **d, j:** Anterior body region, showing the oral basket made of nematodesmata originating from one to three oralized somatic monokinetids (j; opposed arrowheads). **e:** Dorsal view, showing the heterostichad dorsal brush. **f:** Likely, this is the precursor of a cyst spine. **i:** Dorsolateral view, showing the condensed ciliature around the oral opening. **g, k:** Trophonts are studded with food vacuoles, that shown in (k) just ingested a *Colpoda inflata*. BU – oral bulge, B(1–3) – dorsal brush (rows), E – extrusomes, FV – food vacuoles, MA – macronuclear nodules, OB – oral basket. Scale bars 5 µm (c, f, h), 10 µm (b, e, i, j), 40 µm (g, k), and 50 µm (a).

deeply with the protargol method used, maintaining shape and size; many mature and developing extrusomes in cytoplasm (Fig. 79a, b, i, 80c, d, g, h; Table 30). Cortex very flexible, contains several granule rows between two kineties each; granules colourless and hyaline, about 0.7 × 0.5 µm in size, thus not forming a distinct fringe (Fig. 79c). Cytoplasm colourless, in trophonts dark at low magnification (≤ ×100), except of hyaline neck, due to many food inclusions. Feeds on middle-sized ciliates, viz., *Colpoda inflata* recognizable in one specimen (Fig. 80k); prey not identifiable in 30 other specimens, suggesting outside lysis by the extrusomes. Large food vacuoles disintegrate into hundreds of globules 4–10 µm across and with different contents and protargol affinity, suggesting prey segregation (Fig. 79a, 80a, g, k). Swims slowly rotating about main body axis.

Cilia in vivo 9 µm long, arranged in an average of 17 meridional, ordinarily (theronts) to widely (trophonts) spaced rows composed of ordinarily (neck) to narrowly (trunk) spaced cilia; anterior portion of rows rather distinctly curved and densely ciliated. Dorsal brush heterostichad and isomorphic, rows 1 and 2 of almost same length with longest row 2 occupying 11% of body length; row 3 extends to second body third with monokinetal bristles about 3 µm long; all rows with a short anterior tail of ciliated monokinetids (Fig. 79a, g, j–l, 80a, e, h, j; Table 30). Brush

Table 30. Morphometric data on *Enchelys terricola terricola* from Austria (FOISSNER 1987c; type locality; upper line) and *Enchelys terricola lanceoplites* from the Robinson Island (lower line). Data based on mounted, protargol-impregnated (FOISSNER's method), and randomly selected specimens from non-flooded Petri dish cultures. Measurements in µm. CV – coefficient of variation in %, M – median, Max – maximum, Mean – arithmetic mean, Min – minimum, n – number of individuals investigated, SD – standard deviation, SE – standard error of arithmetic mean.

Characteristics	Mean	M	SD	SE	CV	Min	Max	n
Body, length	115.0	110.0	18.0	5.7	15.7	91.0	143.0	10
	98.6	100.0	13.6	2.5	13.8	78.0	130.0	29
Body, width	39.8	39.0	7.8	2.5	19.6	31.0	58.0	10
	33.3	32.0	6.8	1.3	20.3	23.0	47.0	29
Body length:width, ratio	3.0	3.0	0.6	0.2	19.4	2.4	4.1	10
	3.1	2.9	0.9	0.2	30.0	2.0	5.2	29
Oral bulge, width	6.2	6.0	0.9	0.3	14.8	4.0	7.0	10
	7.3	8.0	1.0	0.2	13.7	5.0	9.0	19
Oral bulge, height	not measured							
	3.0	3.0	0.6	0.1	19.5	2.0	4.0	19
Oral basket length (approximate because poorly impregnated)	not measured							
	18.2	18.0	–	–	–	13.0	25.0	19
Anterior body end to first macronuclear nodule, distance	not measured							
	44.1	43.0	9.6	2.2	21.9	25.0	65.0	19
Macronuclear nodules, length	8.8	8.5	2.2	0.7	25.6	6.0	13.0	10
	6.7	6.0	2.6	0.6	39.0	3.0	12.0	19
Macronuclear nodules, width	7.5	7.5	1.7	0.5	22.9	5.0	11.0	10
	4.5	5.0	1.0	0.2	21.6	3.0	6.0	19
Macronuclear number (approximate)	11.9	11.5	2.4	0.8	19.8	9.0	15.8	8
	18.4	17.0	–	–	–	10.0	30.0	19

continued

Characteristics	Mean	M	SD	SE	CV	Min	Max	n
Somatic kineties, number	15.6	15.5	1.6	0.6	10.2	14.0	19.0	8
	16.5	17.0	0.9	0.2	5.5	15.0	18.0	19
Kinetids (granules) in a ventral ciliary row, number	65.7	67.5	17.6	7.2	26.8	42.0	90.0	6
	55.2	55.0	10.6	2.4	19.1	38.0	75.0	19
Dorsal brush, number of rows	3.0	3.0	0.0	0.0	0.0	3.0	3.0	7
	3.4	3.0	–	–	–	3.0	4.0	19
Oral bulge base to end of brush row 1, distance	13.1	13.0	1.1	0.4	8.4	11.0	14.0	7
	10.0	10.0	2.1	0.7	21.2	7.0	13.0	9
Dorsal brush row 1, number of dikinetids	not counted							
	10.8	12.0	1.6	0.5	15.2	8.0	12.0	9
Oral bulge base to end of brush row 2, distance	14.0	14.0	0.6	0.2	4.3	13.0	15.0	7
	11.4	11.0	2.7	0.9	23.3	8.0	16.0	9
Dorsal brush row 2, number of dikinetids	not counted							
	13.6	14.0	2.6	0.9	19.1	9.0	18.0	9
Oral bulge base to end of brush row 3, distance	6.1	6.0	0.4	0.1	6.2	6.0	7.0	7
	5.3	5.5	1.2	0.4	22.8	3.0	7.9	9
Dorsal brush row 3, number of dikinetids	not counted							
	5.3	5.0	0.7	0.2	13.3	4.0	6.0	9
Oral bulge (mature) extrusomes, length	not measured							
	5.4	5.0	0.6	0.1	11.2	5.0	7.0	19
Oral bulge (mature) extrusomes, width	not measured							
	0.7	0.7	–	–	–	0.5	1.0	19

malformed in about half of specimens, i. e., with supernumerary dikinetids forming a more or less distinct fourth row.

Oral bulge circular, filled with extrusomes, about 8 × 3 µm in vivo, slightly to distinctly oblique (20–40°), surface flat to slightly convex. Circumoral kinety absent. Oral basket rods fine, about 18 µm long, originate from one to three oralized somatic monokinetids, forming an indistinct basket (Fig. 79a, e–g, i–l, 80b, d, g–k; Table 30).

Occurrence and ecology: As yet found only at type locality; appeared with low abundance in the non-flooded Petri dish culture 17 days after rewetting the sample.

Remarks: *Enchelys terricola lanceoplites* differs from the European nominal subspecies only by the shape of the extrusomes, as discussed above. This could result from the very wide spatial separation of the populations.

The overall appearance of *E. terricola terricola* and *E. terricola lanceoplites* is quite similar to several congeners and other haptorid genera shown in this monograph and in Foissner et al. (2002), for instance, *Enchelaria* (three vs. two dorsal brush rows), *Enchelariophrya* (with vs. without oralized somatic monokinetids), *Enchelyodon* (ciliary rows curved vs. not curved anteriorly), *Sikorops* (without vs. with oral dikinetids), and *Protospathidium* (without vs. with dikinetal oral kinetofragments).

Enchelys tumida **nov. spec.** (Fig. 81a–l, 82a–c; Table 31)

Diagnosis: Size in vivo about 200 × 70 µm. Narrowly bursiform with distinct oral bulge containing about 15 µm long, rod-shaped extrusomes. Macronucleus curved-cylindroid, usually 30% shorter than body; several globular micronuclei. Cortical granulation dense, plate-like. About 37 ciliary rows each with 5 to 8 oralized somatic monokinetids. Dorsal brush three-rowed, occupies 22% of body length, distinctly heterostichad because row 3 shorter by two thirds than rows 1 and 2.

Type locality: Mould litter and humous soil (pH 6.0) under a *Casuarina* (Beef-wood) tree between the town of Erldunda and the Ayers Rock, Australia, about 27° S 132°E.

Type material: 1 holotype and 1 paratype slide with protargol-impregnated specimens have been deposited in the Biology Centre of the Upper Austrian Museum in Linz (LI). The holotype and other relevant specimens have been marked by black ink circles on the coverslip.

Etymology: The Latin adjective *tumidus* (swollen) refers to the bulbous oral bulge.

Description: This species was very rare, both at the Australian type locality and at Venezuelan sites (49) and (61). Thus the morphometric data are very incomplete (Table 31).

Large, in vivo 155–225 × 50–90 µm, usually about 200 × 70 µm, as calculated from some live measurements and the values in Table 31 adding 15% preparation shrinkage. Body bursiform to elongate bursiform, oral region neck-like narrowed, anterior end transverse-truncate, posterior broadly rounded; slightly flattened in oral region (Fig. 81a, d, i, 82b, c). Macronucleus usually in central quarters of body, rod-shaped and about 16% shorter than cell, more or less tortuous;

Table 31. Morphometric data on the Australian *Enchelys tumida* based on mounted, protargol-impregnated specimens from a non-flooded Petri dish culture. Measurements in µm. CV – coefficient of variation in %, M – median, Max – maximum, Mean – arithmetic mean, Min – minimum, n – number of specimens investigated, SD – standard deviation, SE – standard error of arithmetic mean.

Characteristics	Mean	M	SD	SE	CV	Min	Max	n
Body, length	174.3	188.5	25.2	11.3	14.5	136.0	194.0	5
Body, width	58.8	55.0	12.7	5.7	21.6	45.0	78.0	5
Body length:width, ratio	3.0	3.0	0.5	0.2	17.4	2.5	3.6	5
Anterior body end to macronucleus, distance	50.2	40.0	24.2	10.8	48.3	34.0	93.0	5
Nuclear figure, length	89.8	101.0	21.2	9.5	23.6	66.0	111.0	5
Macronucleus, length (rough values)	146.4	126.0	–	–	–	105.0	219.0	5
Macronucleus, width	8.8	9.0	1.2	0.5	13.1	7.0	10.0	5
Somatic ciliary rows, number	37.0	37.0	–	–	–	33.0	41.0	2
Dorsal brush row 1, length	33.5	33.5	–	–	–	31.0	36.0	2
Dorsal brush row 1, number of dikinetids	32.5	32.5	–	–	–	27.0	38.0	2
Dorsal brush row 2, length	37.5	37.5	–	–	–	36.0	39.0	2
Dorsal brush row 2, number of dikinetids	41.0	–	–	–	–	–	–	1
Dorsal brush row 3, length	12.3	12.3	–	–	–	10.0	15.0	2
Dorsal brush row 3, number of dikinetids	13.0	–	–	–	–	–	–	1
Oral bulge, width	19.7	18.5	4.8	2.1	24.3	14.0	27.0	5
Oral bulge, height	4.5	4.5	0.5	0.3	11.1	4.0	5.0	3

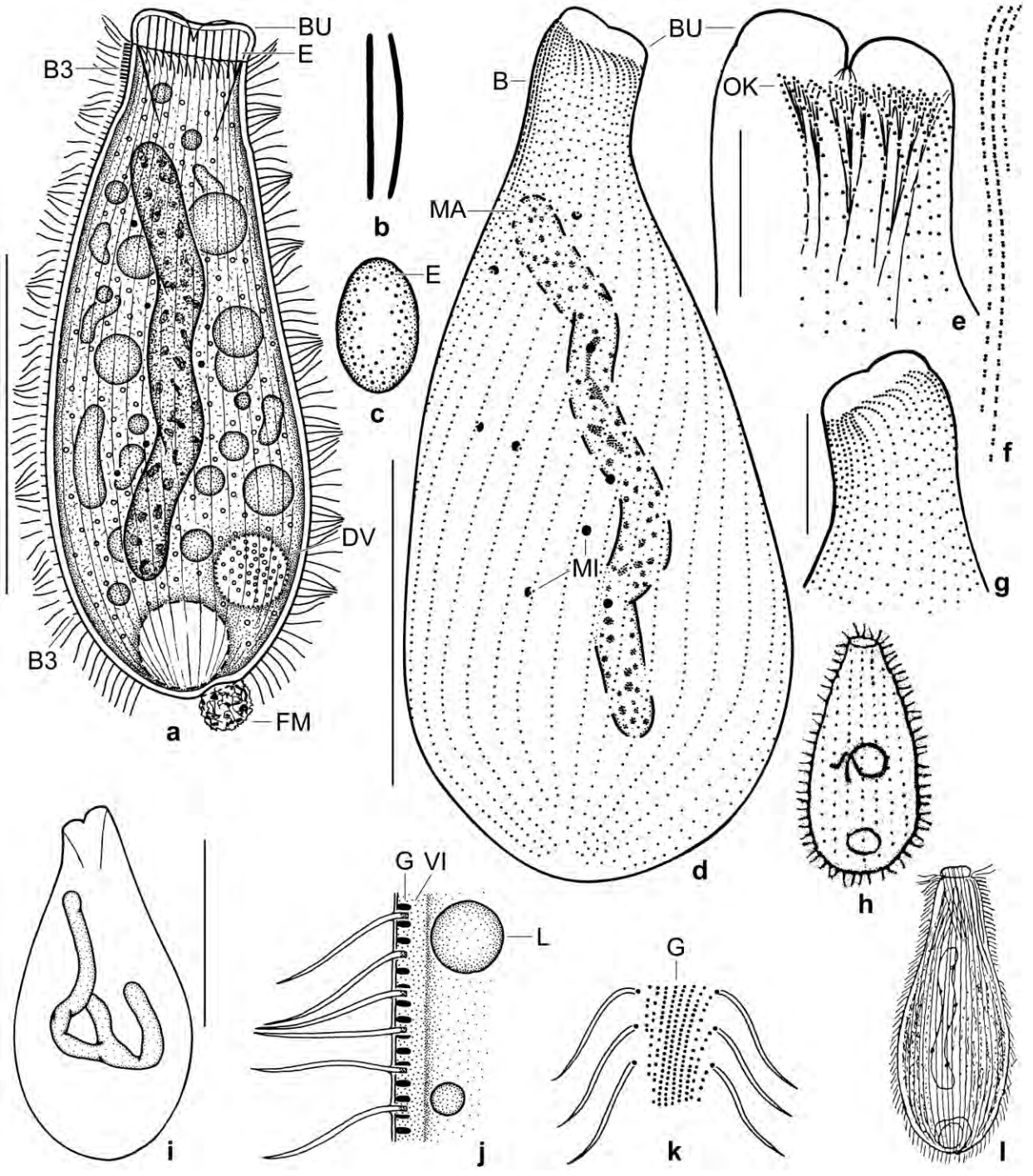

Fig. 81a–l. *Enchelys tumida* (a–g, i–k) and similar species (h, l). **a:** Right side view of a representative specimen, length 200 µm. The monokinetal tail of dorsal brush row 3 extends to near body end. **b:** Two views of the same extrusome, 15 µm. **c:** Frontal view of oral bulge. **d, g:** Right and left side view, showing ciliary and nuclear pattern of holotype specimen, length 160 µm. **e, i:** Detail with oralized somatic monokinetids (e) and overview (i), showing the bifurcate macronucleus of the main paratype specimen. **f:** Dorsal brush row 3 is strongly shortened**. h, k:** *Holophrya curvilata* (160 µm, from SMITH 1897) and *Enchelyodon elegans* (180 µm, from KAHL 1930a) are similar to *E. tumida* (see text). **j, k:** Optical section and surface view, showing cortical granulation. B – dorsal brush, B3 – dorsal brush row 3, BU – oral bulge, DV – defecation vacuole, E – extrusomes, FM – fecal mass, G – cortical granules, L – lipid droplet, MA – macronucleus, MI – micronuclei, OK – oralized somatic monokinetids, VI – viscous layer. Scale bars 20 µm (e, g), 60 µm (d), and 100 µm (a, i).

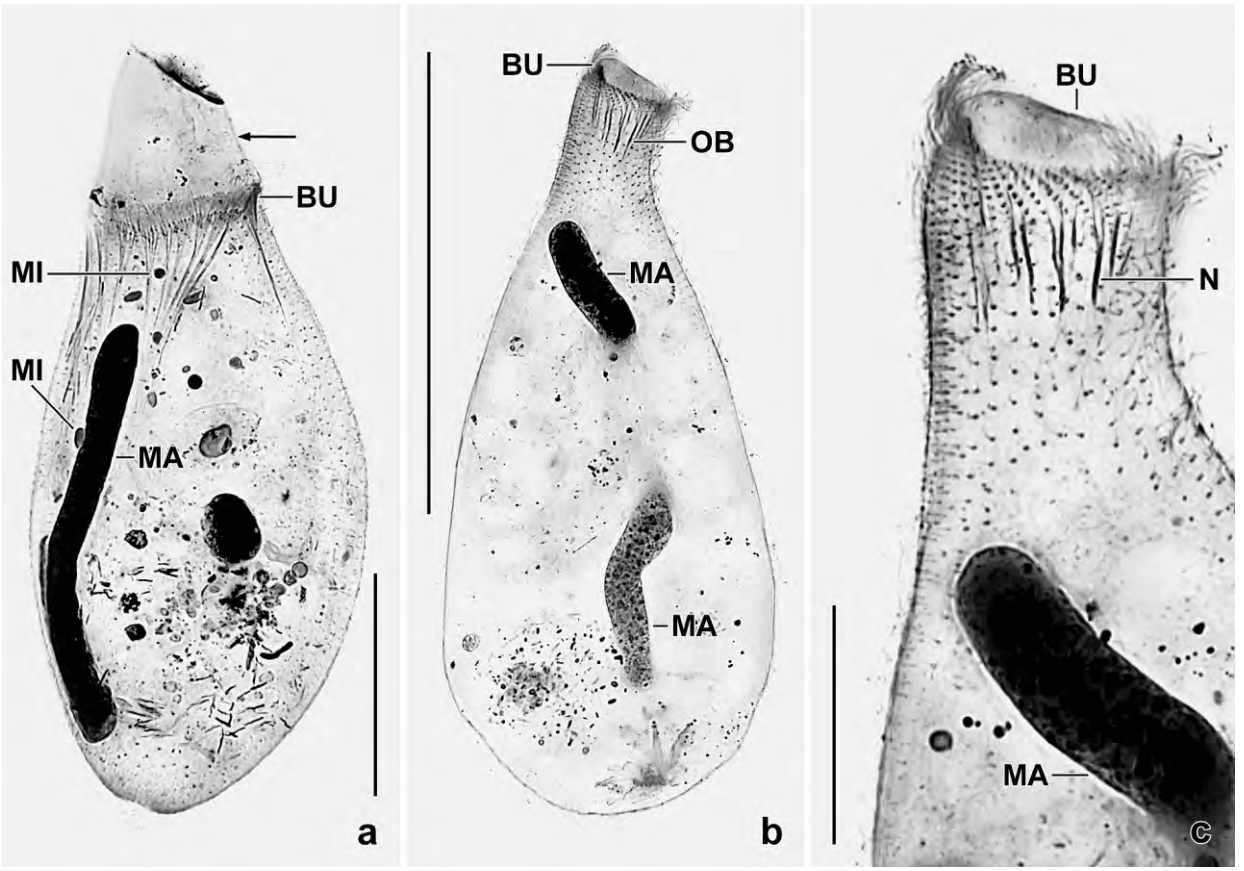

Fig. 82a–c. *Enchelys tumida* after protargol impregnation. **a:** A specimen just ingesting a hypotrich ciliate (arrow). **b, c:** Right side views of holotype specimen, showing the long macronucleus and the absence of a circumoral kinety. The oral basket rods (nematodesmata) originate from oralized somatic monokinetids at begin of the ciliary rows. BU – oral bulge, MA – macronucleus, MI – micronuclei, N – nematodesmata, OB – oral basket. Scale bars 20 µm (c), 50 µm (a), and 100 µm (b).

studded with minute nucleoli. Very likely many globular micronuclei attached to macronucleus and scattered in cytoplasm (Fig. 81a, d, 82a–c). Contractile vacuole in posterior body end, with about 10 excretory pores; defecation vacuole subterminal, contains granular inclusions, about 20 µm across; cytopyge near contractile vacuole, fecal mass slimy and with granular inclusions mentioned above (Fig. 81a). Mature extrusomes attached to marginal half of oral bulge, rod-shaped and slightly curved, about 13–15 × 0.5 µm in size (Fig. 81a–c). Cortex colourless and flexible, bipartite in a granular zone and a viscous layer each about 1 µm thick; contains countless granules about 1 × 0.5 µm in size, forming about 10 narrowly spaced rows between two kineties each (Fig. 81a, j, k). Cells brownish at low magnification (≤ 100×), very likely because thick and studded with rather refractive cortical granules. Cytoplasm studded with granules 1 µm across and with few to many globular and irregular lipid inclusions 5–20 µm in size (Fig. 81a). Feeds on middle-sized ciliates, e. g., *Gonostomum affine* ingested whole (Fig. 82a).

Somatic cilia 8–10 µm long in vivo, arranged in about 37 meridional, ordinarily spaced rows curved anteriorly. Ciliary rows more or less shortened in posterior pole area; each row comprises 5 to 10 narrowly spaced cilia anteriorly followed by about 100 ordinarily spaced cilia. Dorsal brush three-rowed and distinctly heterostichad, occupies about 22% of body length, bristles 2–4

µm long; rows 1 and 2 of similar length, row 3 strongly shortened but with a monokinetal tail extending to near body end (Fig. 81a, d, g, 82b, c; Table 31).

Oral bulge rather conspicuous because separated from neck by a flat furrow and 7–10 µm high in vivo, can open widely when ingesting large prey (Fig. 82a); slightly flattened laterally and thus elliptic to broadly elliptic in vivo; centre slightly concave, marginal area studded with extrusomes. Circumoral kinety absent, oral basket thus made of 5–10 oralized somatic monokinetids at begin of ciliary rows (Fig. 81a, c–e, g, 82b, c; Table 31).

Occurrence and ecology: As yet found in three soil samples, viz., the Australian type locality and in Venezuelan samples (49) and (61), showing a wide range from desert soil over bromeliad mud to rainforest soil.

Remarks: *Enchelys tumida* resembles *Holophrya curvilata* Smith, 1897 and *Enchelyodon elegans* Kahl, 1930a in size and shape of body and macronucleus. *Holophrya curvilata* has been described superficially. Smith (1897) did not describe or illustrate (Fig. 81h) any oral bulge, suggesting that *H. curvilata* is a different, probably North American species. *Enchelyodon elegans* is distinctly flattened (vs. unflattened), contractile (vs. not contractile), and has about 50 µm (vs. 15 µm) long extrusomes associated with the oral bulge (Fig. 81l).

According to Kahl (1930a), the genera *Enchelys* and *Enchelyodon* are separated by the oral bulge (absent or inconspicuous vs. conspicuous). The present and other species, e. g., *Enchelys polynucleata* (Foissner 1984, Foissner et al. 2002) show that this feature, although often useful, might guide to the wrong genus because the real feature separating *Enchelys* and *Enchelyodon* is the absence vs. presence of a circumoral kinety. In the former, the oral basket is made of nematodesmata originating from oralized somatic monokinetids, in the latter it is made from the circumoral dikinetids.

Renoplites nov. gen.

Diagnosis: Fuscheriidae with comparatively minute, reniform extrusomes and two dorsal brush rows.

Type species: *Renoplites venezuelensis* nov. spec.

Etymology: Composite of the Latin noun *ren* (kidney) and the Greek noun *hoplites* (soldier), referring to the reniform extrusomes. Masculine gender.

Remarks: Foissner et al. (2002) briefly reviewed this kind of haptorids and classified them into two families: Fuscheriidae (with enchelyodonid general shape) and Acropisthiidae (with spathidiid general organization). *Renoplites* matches the fuscheriid pattern because the ciliary rows abut on the circumoral kinety at right angles.

Foissner et al. (2002) classified the Fuscheriidae into four genera: *Fuscheria*, *Actinorhabdos*, *Diplites*, and *Dioplitophrya*. Gabilondo & Foissner (2009) added *Fuscheriides* and *Aciculoplites*.

All these genera were defined with two main features: the shape of the extrusomes and the number of dorsal brush rows, i. e., two or three, the later occurring only in *Dioplitophrya*. *Renoplites* is unique in having reniform extrusomes. See FOISSNER et al. (2002) and GABILONDO and FOISSNER (2009) for a discussion of generic features.

Renoplites venezuelensis nov. spec. (Fig. 83a, b, d–f, 84a–h; Table 32)

Diagnosis: Size in vivo about 75 × 25 µm; narrowly ovate. Macronucleus oblong to slightly reniform; single micronucleus. Extrusomes 1–1.5 µm long. On average 13 bipolar ciliary rows, 2 anteriorly modified to an isomorphic, heterostichad dorsal brush with up to 3 µm long bristles; brush row 1 with an average of 6 dikinetids, row 2 with 3. Oral bulge discoid to hemispheric.

Type locality: Venezuelan site (25), i. e., highly fertile field (Mahadja) soil from the surroundings of the village of El Sapo, about 50 km north of Pto. Ayacucho, 67°36'W 5°41'N.

Type material: 1 holotype and 4 paratype slides with protargol-impregnated specimens have been deposited in the Biology Centre of the Upper Austrian Museum in Linz (LI). Relevant specimens have been marked with black ink circles on the coverslip.

Etymology: Named after the country (Venezuela) where it was discovered.

Table 32. Morphometric data on *Renoplites venezuelensis* based on mounted, protargol-impregnated (FOISSNER's method), randomly selected specimens from a non-flooded Petri dish culture. Measurements in µm. CV – coefficient of variation in %, M – median, Max – maximum, Mean – arithmetic mean, Min – minimum, n – number of individuals investigated, SD – standard deviation, SE – standard error of arithmetic mean.

Characteristics	Mean	M	SD	SE	CV	Min	Max	n
Body, length	65.5	65.0	9.3	2.0	14.2	51.0	84.0	21
Body, maximum width	21.4	22.0	3.1	0.7	14.5	14.0	26.0	21
Body length:width, ratio	3.2	3.1	0.7	0.2	22.9	2.1	5.6	21
Anterior body end to macronucleus, distance	25.9	26.0	9.5	2.1	36.6	12.0	52.0	21
Oral bulge, width	5.1	5.0	0.6	0.1	11.6	4.0	7.0	21
Oral bulge, height	3.5	4.0	1.1	0.2	30.3	2.0	5.0	21
Macronucleus, length	15.1	13.0	3.5	0.8	23.3	11.0	24.0	21
Macronucleus, width	6.1	6.0	0.9	0.2	14.8	4.0	8.0	21
Micronucleus, length	2.6	2.5	0.3	0.1	9.7	2.0	3.0	19
Micronucleus, width	2.0	2.0	0.4	0.1	18.6	1.5	2.5	19
Ciliary rows, number	13.5	13.0	1.4	0.3	10.4	12.0	17.0	21
Ciliated kinetids in a ventral kinety, number	22.3	21.0	4.1	0.9	18.3	16.0	30.0	21
Oralized somatic kinetids, number/kinety	2.4	2.0	0.6	0.2	25.8	1.0	3.0	17
Dorsal brush rows, number	2.0	2.0	0.0	0.0	0.0	2.0	2.0	21
Brush row 1, length	8.0	7.0	1.9	0.4	23.4	6.0	13.0	21
Brush row 1, number of dikinetids	5.7	5.0	1.7	0.4	30.2	3.0	9.0	21
Brush row 2, length	4.4	4.0	0.8	0.2	18.4	3.0	6.0	21
Brush row 2, number of dikinetids	3.3	3.0	0.7	0.2	21.8	2.0	5.0	21
Excretory pores, number	2.0	2.0	0.0	0.0	0.0	2.0	2.0	8

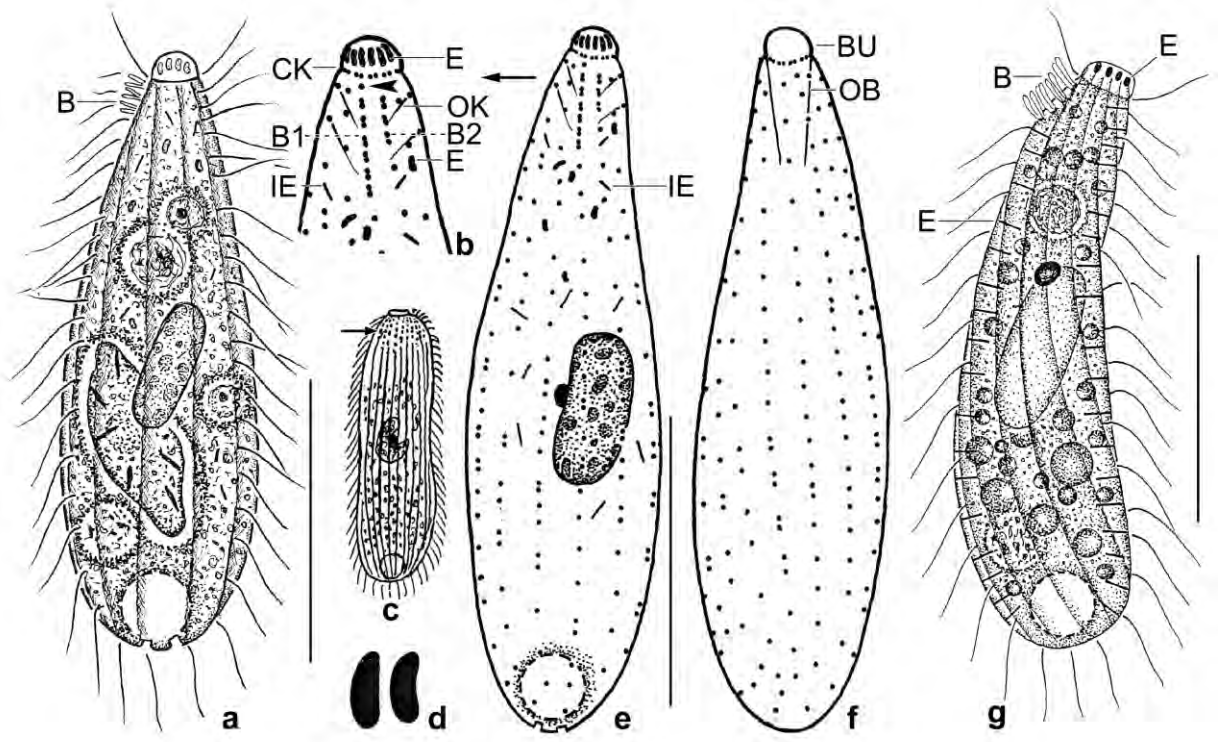

Fig. 83a–g. *Renoplites venezuelensis* (a, b, d–f), *Enchelyodon californicus* (c, from KAHL 1935), and *Diplites arenicola* (g, from FOISSNER et al. 2002) from life (a, c, d, g) and after protargol impregnation (b, e, f). **a:** Overview of a representative specimen, length 75 µm. Note the large food vacuole containing a *Leptopharynx costatus*. **b, e, f:** Dorsal and ventral view of holotype specimen, length 60 µm. Note the oralized somatic monokinetids and the single monokinetid at anterior end of dorsal brush row 1 (arrowhead). **c:** *Enchelyodon californicus* has highly refractive cortical granules subapically (arrow) and is 120–130 µm long. **d:** Mature oral bulge extrusomes, 1–1.5 µm long. **g:** On superficial observation, *D. arenicola* from the Namib Desert (Southwest Africa) is highly similar to *R. venezuelensis* but has oblong body extrusomes and ellipsoid oral extrusomes. B(1, 2) – dorsal brush (rows), BU – oral bulge, CK – circumoral kinety, E – extrusomes, IE – immature (developing) extrusomes, OB – oral basket, OK – oralized somatic monokinetids. Scale bars 25 µm (e–g) and 35 µm (a).

Description: This species is very variable, as shown by some high coefficients of variation (Table 32). However, most of the high coefficients can be explained, for instance, the location of the macronucleus, which is sometimes dislocated by food inclusions (Fig. 84h). Others are more difficult, especially the high variability of macronucleus length and oral bulge height; for the later, it is not only the height but also the shape (discoidal to hemispherical), indicating that two species are mixed or the oral bulge is very sensitive to preparation artifacts.

Size in vivo 60–100 × 15–30 µm, on average 75 × 25 µm, as calculated from some in vivo measurements and the protargol-impregnated specimens in Table 32 adding 15% preparation shrinkage; laterally not flattened. Body narrowly ovate, rarely very narrowly ovate, ovate, or indistinctly obclavate (Fig. 83a, e, 84a–c; Table 32). Nuclear apparatus in or near body centre, may be dislocated by large food inclusions (Fig. 83a, e, 84a, b, d, h; Table 32). Macronucleus on average 15 × 6 µm in protargol preparations, oblong to slightly reniform in 75% of specimens, rarely ellipsoid or C-shaped; studded with small and middle-sized nucleoli. Micronucleus attached to macronucleus, broadly ellipsoid to ellipsoid, possibly lacking in half of specimens. Contractile vacuole in posterior end, with two excretory pores. Extrusomes in oral bulge and

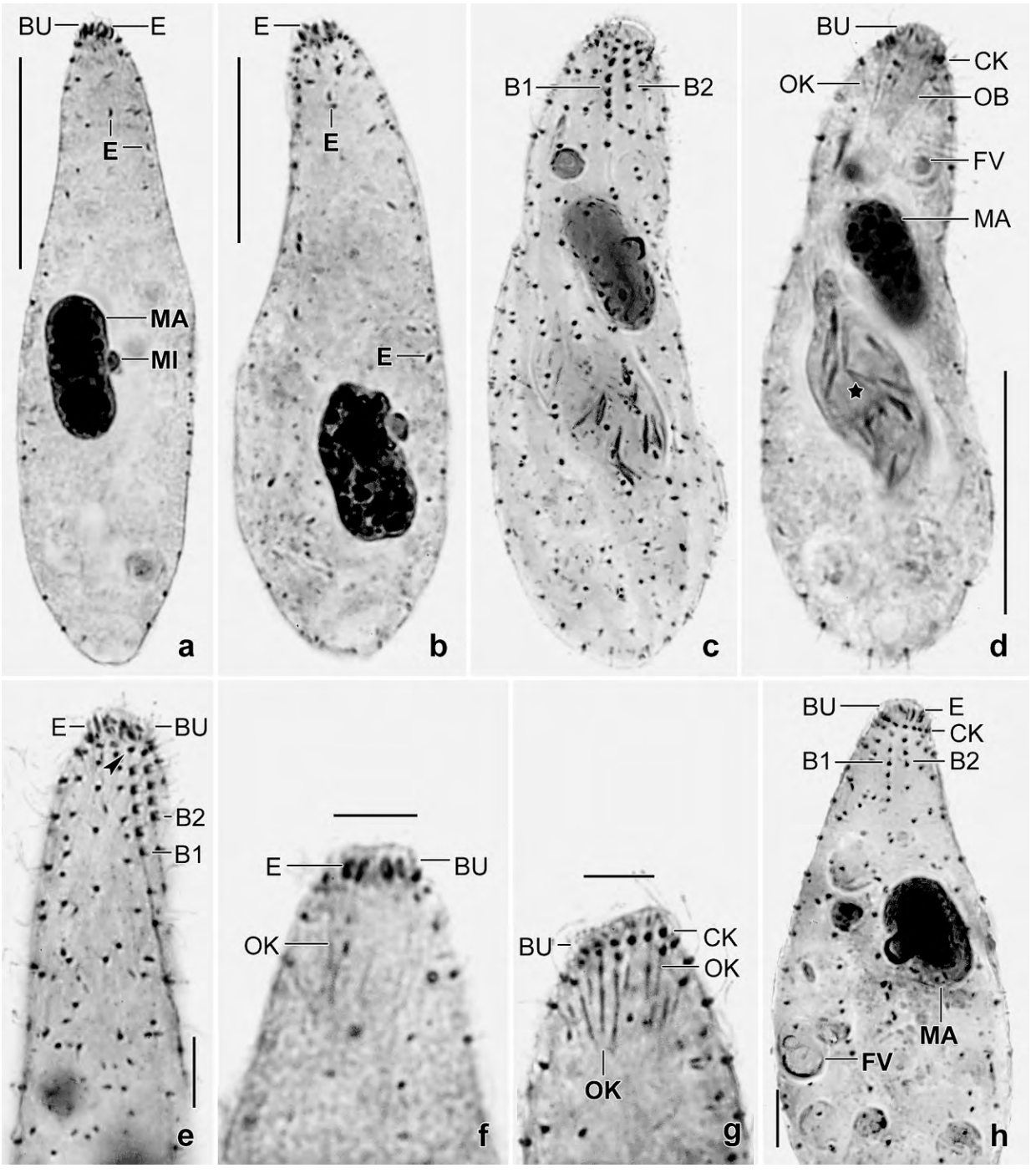

Fig. 84a–h. *Renoplites venezuelensis* after protargol impregnation. The oral bulge (BU) of this species can be low and discoid (e–g) or high and hemispherical (a, d, h). **a, b:** Overviews showing body shape and some main organelles. **c, d:** Surface view and optical section of a specimen having ingested a *Leptopharynx costatus* with deeply impregnated extrusomes (d, asterisk). The dorsal brush consists of two short rows. **e:** Anterior region, showing the two dorsal brush rows and the single monokinetid (arrowhead) at the anterior end of brush row 1. **f, g:** Optical sections of anterior body region, showing oralized somatic monokinetids. **h:** Dorsal view, showing the two-rowed dorsal brush consisting of six and three dikinetids, respectively. B(1, 2) – dorsal brush (rows), BU – oral bulge, CK – circumoral kinety, E – extrusomes, FV – food vacuoles, MA – macronucleus, MI – micronucleus, OB – oral basket, OK – oralized somatic monokinetids. Scale bars 5 µm (e–h) and 20 µm (a–d).

scattered in pharyngeal and somatic plasm, usually impregnate with the protargol method used (Fig. 83a, b, d, e, 84a, b, e, f, h). Mature oral bulge extrusomes reniform in vivo, some indistinctly narrowed anteriorly, minute (~ 1–1.5 µm) and thus difficult to recognize. Immature cytoplasmic extrusomes fine and about 2 µm long. Cortex distinctly furrowed by ciliary rows, ridges right of rows, contain thick bundles of postciliary microtubule ribbons. Cytoplasm colourless, usually studded with food vacuoles 5–10 µm across. Feeds on the heterotrophic flagellate *Polytoma* and the ciliate *Leptopharynx costatus* (Fig. 83a, 84c, d, h).

On average 13 ordinarily spaced, bipolar ciliary rows with ordinarily spaced cilia; two rows anteriorly modified to an inconspicuous, isomorphic and heterostichad dorsal brush with up to 3 µm long bristles: row 1 about twice as long as row 2, on average composed of 6 and 3 dikinetids, respectively; row 1 commences with a single monokinetid (Fig. 83a, e, f, 84c, e, h; Table 32). One to three, usually two oralized somatic monokinetids per kinety, often difficult to recognize (Fig. 83b, e, 84d, f, g).

Oral bulge occupies anterior body end, highly variable, i. e., low and flat (discoid) or high and hemispherical (Fig. 83a, b, 84a, b, d–h; Table 32). Circumoral kinety composed of dikinetids, left basal body ciliated, right barren but with a rather distinct pharyngeal rod, forming the oral basket together with the nematodesmata from the oralized somatic monokinetids (Fig. 83a, e, f, 84c, d, f, g, h).

Notes on ontogenesis: A very late divider showed that shaping of the oral bulge and circumoral kinety occurs post-divisionally.

Occurrence and ecology: As yet found only at type locality, i. e., in a very fertile soil, where it was moderately abundant in the non-flooded Petri dish culture for about three weeks.

Remarks: The old literature often does not provide exact data on the extrusomes and dorsal brush, two main features of the haptorids. We did not find a described ciliate that could be identical with *R. venezuelensis*. But there are some similar species, especially from the genus *Enchelyodon*, for instance, *E. muscicola* (Kahl, 1927) Kahl, 1930a, which, however, has "distinct, converging extrusomes". This has been confirmed by Vuxanovici (1959). *Enchelyodon californicus* Kahl, 1935, a 120–130 µm long moss species, seemingly lacks extrusomes but has highly refractive granules, likely mucocysts, in the subapical cortex (Fig. 83c). Our species is smaller (up to 100 µm) and lacks such granules but we cannot exclude that Kahl (1927, 1930a) could not see so minute extrusomes as present in *R. venezuelensis*. *Diplites arenicola* (Fig. 83g) from the Namib Desert is highly similar to *R. venezuelensis* but has oblong body extrusomes (vs. absent) and ellipsoid (vs. reniform) oral extrusomes.

This kind of haptorids has very few distinct features and is thus difficult to identify. The best characters for in vivo identification are the size and shape of the extrusomes and the body.

Clavoplites terrenum (Foissner, 1984) Foissner, Agatha & Berger, 2002 (Fig. 85a–i, 86 a–i)

Observations: This species occurred at Venezuelan sites (8) and (62). We could not make

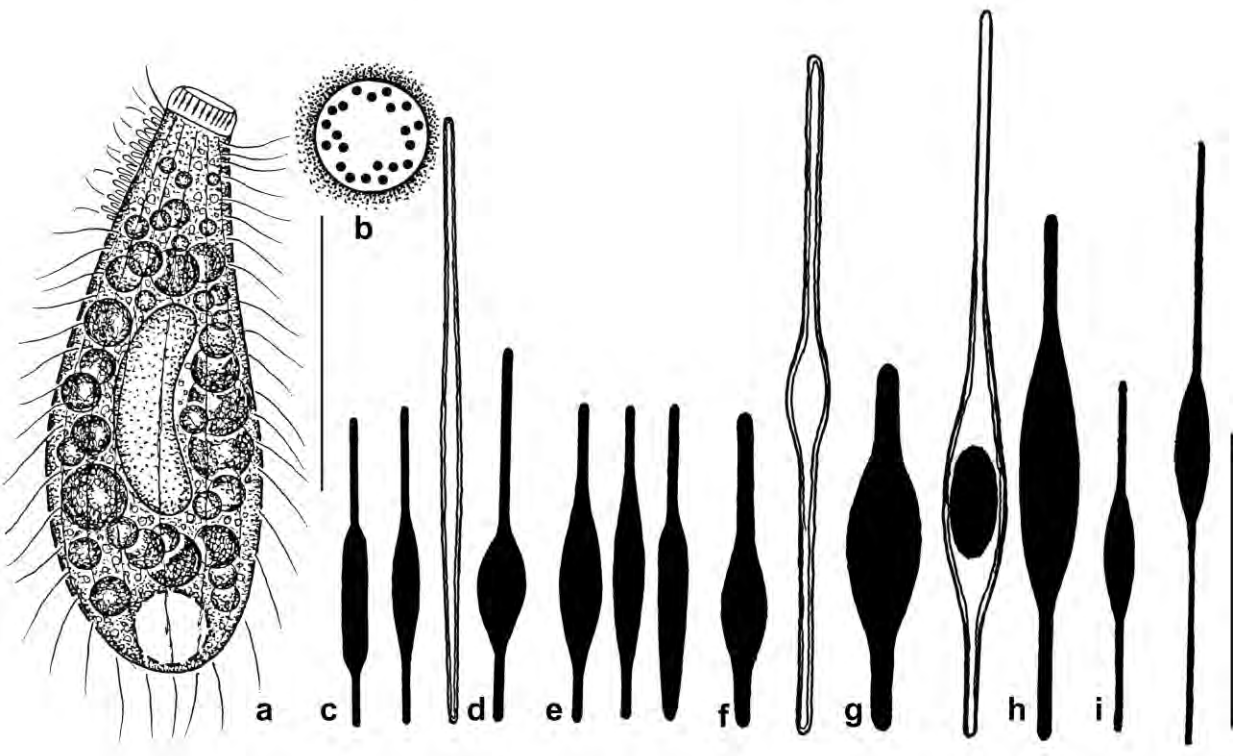

Fig. 85a–i. *Clavoplites terrenum* from live. Extrusomes drawn to scale, 4 µm (bar at right end of series). **a–c:** Venezuelan site (8) specimens, right side overview (a, bar 40 µm), frontal view showing arrangement of extrusomes (b) as well as resting and exploded extrusomes (c), length 5–6 µm and 10–12 µm. **d:** Resting extrusome of a specimen from Thailand, length 6–7 µm. **e:** Resting extrusomes of Austrian (Salzburg) specimens, length 5–6 µm. **f:** A resting and an exploded extrusome of a specimen from the Republic of South Africa, length 4 µm and 10–15 µm. **g:** A resting and an exploded extrusome from a specimen of the USA, length 5 µm and 12 µm. **h:** Resting extrusome of a specimen from Venezuelan site (62), length 8 µm. **i:** A resting and an exploded extrusome from the Austrian type population, length 5 µm and 8 µm (from Foissner 1984).

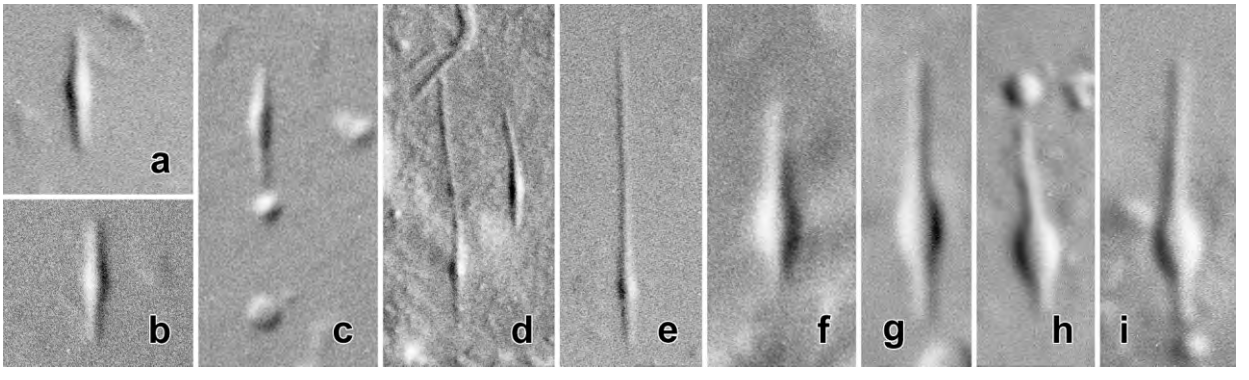

Fig. 86a–i. *Clavoplites terrenum*, extrusomes from life. **a–e:** Resting (a–c) and exploded (d, e) extrusomes from USA specimens, length 5 µm and 12 µm. **f:** A resting extrusome from a South African specimen, length 4 µm. **g–i:** Resting extrusomes from Thailand specimens, length 6–7 µm.

preparations because of the low abundance. Size in vivo about 70–100 × 25–35 µm, unflattened. Shape bluntly obclaviform or indistinctly bursiform, depending on nutrition state (Fig. 85a). Macronucleus elongate reniform. Extrusomes in margin of oral bulge (Fig. 85b), 5–6 × 0.6–1 µm in size, pseudofusiform, i. e., with a quadrangular or slenderly ellipsoid mid, posterior part of shaft shorter than anterior one; when exploded, about 10–12 × 1 µm (Fig. 85c). Somatic cilia about 10 µm long, arranged in about 15 rows. Oral bulge about 10 × 5 µm in size.

Comparison with type population: The Venezuelan specimens differ by the number of ciliary rows (about 15 vs. 22 on average) and the slightly different shape of the extrusomes (cp. Fig. 85c, h with Fig. 85i). However, extrusome shape is rather variable in this species (see below) and the number of ciliary rows has been not studied in preparations. Thus, the Venezuelan populations are considered to fall into the ordinary variability of the species.

Extrusomes of various populations: Over the years, we studied extrusomes from seven populations (Fig. 85c–i, 86a–i). There is a considerable variability in shape and size. However, one feature is stable and distinguishes *C. terrenum* from *C. edaphicus* and *C. australiensis* both described by Foissner et al. (2002): the extrusomes have a central or subcentral convexity, which is at the anterior or posterior end in the other species. See figure explanations for sites, shape, and size.

***Pleuroplites cavicola* nov. spec.** (Fig. 87a–j, 88a–f; Table 33)

Diagnosis: Size in vivo about 55 × 37 µm. Theronts slenderly ellipsoid to ellipsoid, trophonts usually broadly ovate. Macronucleus globular. Extrusomes rod-shaped, about 7 µm long. On average 23 ciliary rows, about 10 modified to dorsal brush in anterior half.

Type locality: Venezuelan site (57), i. e., moss on stones and soil from the Cueva del Indio, a small cave near the village of Chichiriviche, north coast of the Morrocoy National Park, 67°13'W 11°33'N.

Type material: 1 holotype and 1 paratype slide with protargol-impregnated specimens have been deposited in the Biology Centre of the Upper Austrian Museum in Linz (LI). The holotype and other relevant specimens have been marked by black ink circles on the coverslip.

Etymology: The species name is a composite of the Latin noun *cavum* (cave), the thematic vowel ·*i*-, and the Latin verb *colere* (to live in). It refers to the habitat the species was discovered.

Description: Size in vivo 45–65 × 25–45 µm, usually about 55 × 37 µm, as calculated from some live measurements and the values shown in Table 33 adding 15% preparation shrinkage; length:width ratio 1.2–2.1:1, body width more variable (CV = 17.2%) than body length (CV = 10.5%) because theronts and trophonts occur (Table 33). Theronts slenderly ellipsoid to ellipsoid (Fig. 87c, h, 88d, e), rarely obpyriform (Fig. 87d); trophonts ovate to broadly ovate (Fig. 87a, i, 88a–c), rarely ellipsoid (Fig. 88f) or almost globular (Fig. 87e); not flattened laterally. Nuclear apparatus on average slightly posterior to body centre (Table 33). Macronucleus spheric to slightly ellipsoid, on average 10.1 × 9.8 µm in protargol preparations (Fig. 87a, c–e, h, i, 88a–f); nucleoli about 0.5 µm distant from nuclear membrane, numerous, 0.5–2 µm across. Micronucleus attached to macronucleus, with distinct membrane, 2.5 × 2.2 µm in protargol preparations (Fig. 87a, h, i,

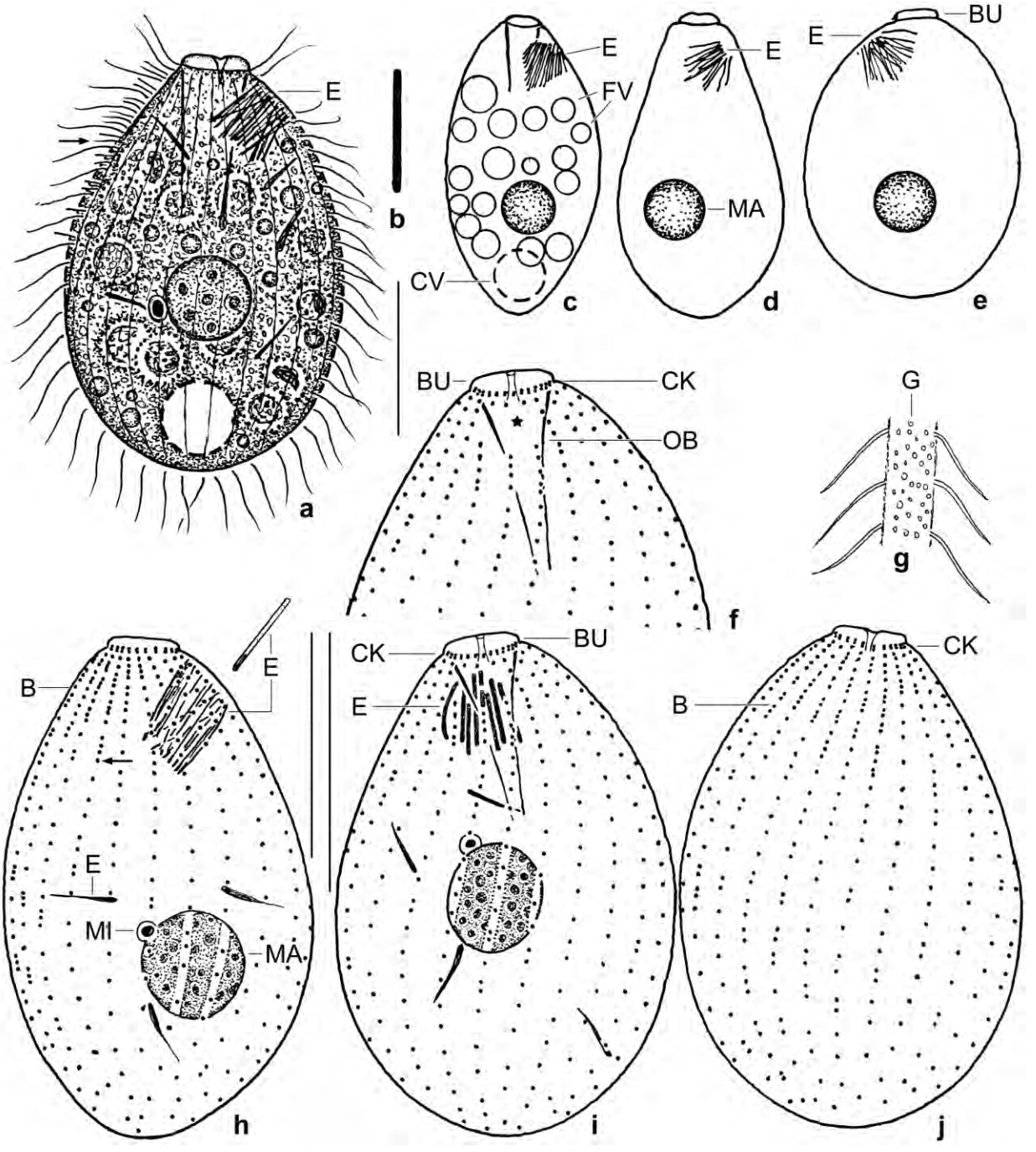

Fig. 87a–j. *Pleuroplites cavicola* from life (a, b, g) and after protargol impregnation (c–f, h–j). **a:** Right side view of a representative specimen, length 55 µm. The arrow marks a dorsal brush row. **b:** Extrusome, 7 µm. **c–e:** Variability of body shape. **f:** Ventral anterior body portion of holotype specimen, showing the absence of basal bodies (cilia) in the area of the extrusome bundle (asterisk). **g:** Cortical granulation. **h:** Right side view of a paratype specimen. The arrow marks the last row with heteromorphic cilia in anterior half. **i, j:** Ventral and dorsal view of holotype specimen (see also Fig. 87f), length 40 µm. The extrusome bundle is on the ventral side while the brush occupies the dorsal side and consists of about 10 rows with heteromorphic cilia in the anterior half (cp. Fig. 87a). Note the distinct micronuclear membrane. B – dorsal brush, BU – oral bulge, CK – circumoral kinety, CV – contractile vacuole, E – extrusomes, FV – food vacuoles, G – cortical granules, MA – macronucleus, MI – micronucleus, OB – oral basket. Scale bars 20 µm.

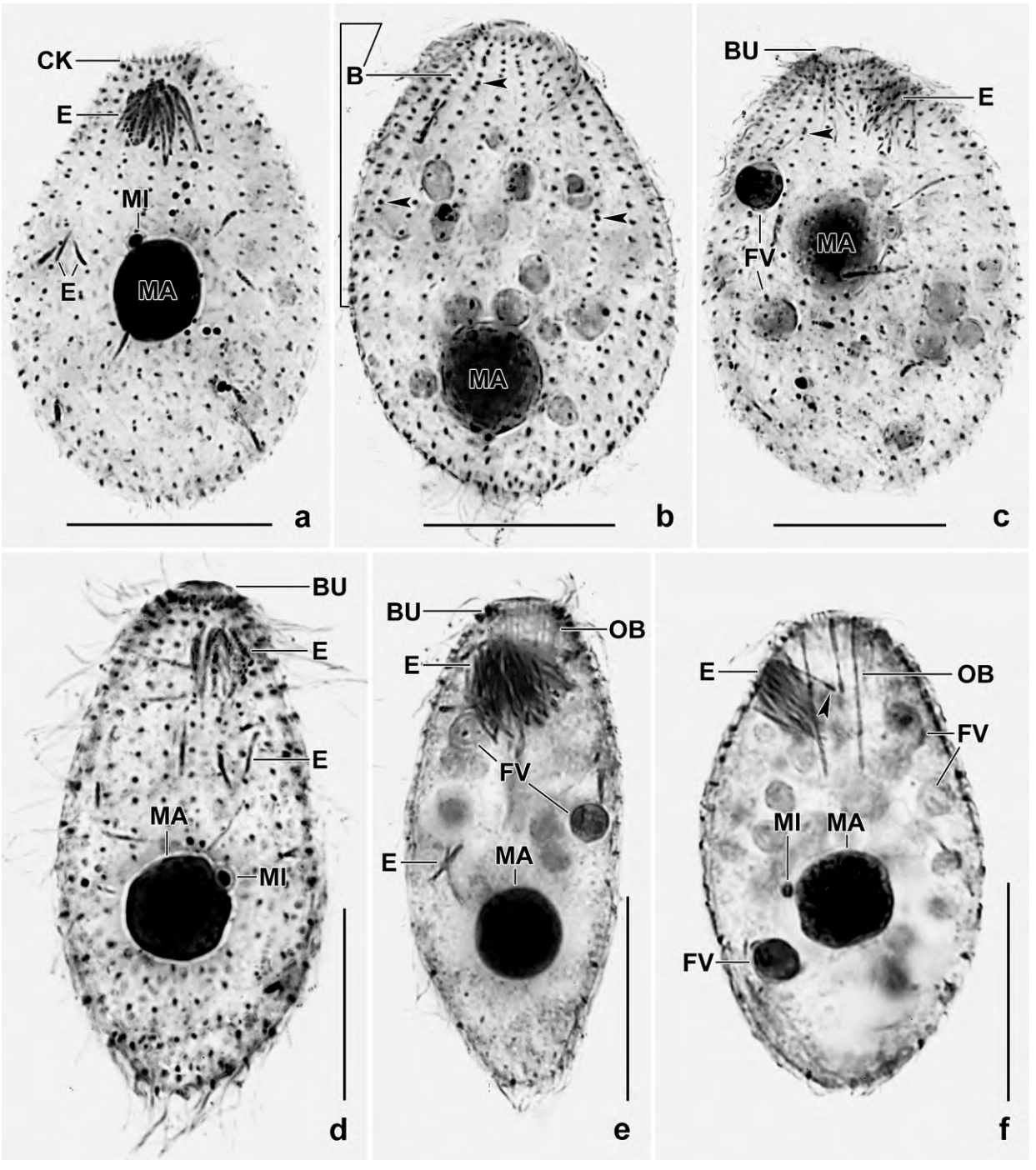

Fig. 88a–f. *Pleuroplites cavicola* after protargol impregnation. **a–c:** Ventral, dorsal, and right lateral view of trophonts with many small food vacuoles. Note the prominent, subapical extrusome bundle (a, c), the globular macronucleus, and the dorsal brush (b, c), which consists of about 10 kineties the anterior half of which contains triads of basal bodies (b, c, arrowheads): the two anterior basal bodies of a triad have short, bristle-like cilia while the posterior basal body has an ordinary cilium. Note the acicular cytoplasmic extrusomes. **d:** Ventral view of a slender specimen, showing the conspicuous micronuclear membrane. **e:** Ventral view of a very slender specimen with a large extrusome bundle. Note the flat, thin oral bulge and the oral basket. **f:** Lateral view of an ordinary specimen. The arrowhead marks the strongly argyrophilic posterior sixth of an extrusome. B – dorsal brush, BU – oral bulge, CK – circumoral kinety, E – extrusomes, FV – food vacuoles, MA – macronucleus, MI – micronucleus, OB – oral basket. Scale bars 20 μm.

88a, d, f). Contractile vacuole in posterior body end. Extrusome bundle subapical in ventral side, usually slightly divergent, rarely cylindroid, composed of about 20 rods 6–7 × 0.5–0.7 µm in size (Fig. 87a–e, h, i, 88a, c, d–f; Table 33); impregnate with the protargol method used, especially the proximal sixth (Fig. 87h, 88f). Developing extrusomes scattered throughout cytoplasm, cuneate to acicular, 4–6 µm long (Fig. 87a, h, i, 88a, d). Cortex flexible, in theronts slightly furrowed by ciliary rows; cortical granules about 0.7 µm across, loosely arranged, inconspicuous (Fig. 87g). Depending on life cycle, few (early theronts; Fig. 88e) to many (trophonts; Fig. 87a, 88b, c, f) food vacuoles 3–7 µm across, i. e., comparatively small each containing very likely only a single, heterotrophic flagellate. Swims rather rapidly, especially the theronts.

Somatic cilia about 8 µm long in vivo, arranged in an average of 23 meridional to slightly spiral, ordinarily spaced rows composed of 26 cilia on average; cilia narrower spaced in anterior than posterior third of rows (Fig. 87a, h–j, 88a–d; Table 33). Ciliary rows bipolar except of three ventral rows shortened anteriorly at site of extrusome bundle (Fig. 87f, i, 88a, d). About 10 ciliary rows modified to a heteromorphic dorsal brush in anterior half, composed of single basal bodies with ordinary cilia, dyads with 3–4 µm long bristles, and triads with two bristles and one ordinary cilium (Fig. 87a, h, j, 88b, c).

Table 33. Morphometric data on *Pleuroplites cavicola* based on mounted, protargol-impregnated, and randomly selected specimens from a non-flooded Petri dish culture. Measurements in µm. CV – coefficient of variation in %, M – median, Max – maximum, Mean– arithmetic mean, Min – minimum, n – number of individuals investigated, SD – standard deviation, SE – standard error of arithmetic mean.

Characteristics	Mean	M	SD	SE	CV	Min	Max	n
Body, length	47.2	47.0	5.0	1.1	10.5	38.0	56.0	21
Body, width	31.6	34.0	5.4	1.2	17.2	22.0	40.0	21
Body length:width, ratio	1.5	1.5	0.2	0.1	14.8	1.2	2.1	21
Anterior body end to macronucleus, distance	21.2	21.0	6.6	1.4	30.8	15.0	37.0	21
Macronucleus, length	10.1	10.0	1.4	0.3	14.0	6.0	12.0	21
Macronucleus, width	9.8	10.0	1.5	0.3	14.8	6.0	12.0	21
Micronucleus, length	2.5	2.5	–	–	–	2.0	3.0	21
Micronucleus, width	2.2	2.0	–	–	–	1.5	3.0	21
Oral bulge, width	6.2	6.0	0.8	0.2	13.1	5.0	8.0	21
Oral bulge, height	1.2	1.0	–	–	–	1.0	2.0	21
Anterior body end to end of oral basket, distance [a]	17.3	18.0	–	–	–	10.0	30.0	21
Anterior body end to extrusome bundle, distance [a]	2.7	3.0	–	–	–	1.0	4.0	21
Extrusomes in bundle, length	6.7	7.0	–	–	–	6.0	7.0	21
Extrusomes in bundle, number [a]	19.1	20.0	–	–	–	4.0	30.0	21
Ciliary rows, number	22.6	23.0	0.9	0.2	4.1	21.0	25.0	21
Ciliary rows, number modified to dorsal brush [a]	9.8	10.0	–	–	–	8.0	12.0	17
Anterior body end to end of longest modified ciliay row, distance [a]	26.7	25.0	–	–	–	20.0	42.0	21
Kinetids in an ordinary ciliary row, number	26.2	25.0	5.8	1.3	22.2	18.0	40.0	21

[a] Approximate values because difficult to measure or to count.

Oral bulge inconspicuous because only about 1 μm high and 6 μm width in protargol preparations; in frontal view circular with a shallow central concavity caused by the fine internal oral basket (Fig. 87a, d–f, h, i, 88c–e; Table 33). Circumoral kinety composed of slightly oblique dikinetids (Fig. 87f, h–j, 88a). Oral basket hardly recognizable in vivo and only faintly impregnated with protargol, about half as long as body (Fig. 87a, c, i, 88e, f; Table 33); oralized somatic monokinetids absent or not impregnated.

Occurrence and ecology: As yet found only at type locality where it was abundant in the non-flooded Petri dish culture three weeks after rewetting the sample.

Remarks: The Pleuroplitidae Foissner, 1996a are unique in having the extrusomes not within the oral basket, as all other haptorids, but in a subapical, extracytostomal bundle. The family contains two genera: *Pleuroplites* Foissner, 1988a (with heteromorphic dorsal brush) and *Pleuroplitoides* Foissner, 1996a (with isomorphic dorsal brush). Both genera are monotypic.

The Venezuelan population has a heteromorphic dorsal brush, and thus it belongs to the genus *Pleuroplites*. It differs from the Australian, Japanese, and Antarctic populations of *P. australis*, described by Foissner (1988a, 1996a, 2000a) and Esteban et al. (2000), in the length (~ 7 μm vs. ≤ 3μm) and shape (rod-like vs. narrowly ovate) of the extrusomes and the number of ciliary rows (on average 23 vs. 14, 15, 14, 18). As concerns the extrusomes, the most important feature of the new species, which appear highly variable (or due to cryptic species!) in *P. australis* (Foissner 2000a), they are rod-shaped also in a Kenyan population of *P. australis* but their length is quite different (~ 7 μm vs. 3 μm). The limnetic population of *P. australis* has 17–19 ciliary rows (Esteban et al. 2000) and thus resembles *P. cavicola*. In contrast, the extrusomes are as minute as in the other populations and thus clearly different from those of *P. cavicola.*

Colpodea

The Colpodea were reviewed by Foissner (1993a). He recognized 55 genera with a total of 170 species. Seven new genera and nine new species were described between 1994 and 2001. In Namibia, we discovered four new genera and 17 new species (Foissner et al. 2002). Three new genera and five new species were described between 2003 and 2014: *Colpoda brasiliensis* Foissner, 2003a; *Pseudomaryna australiensis* Foissner, 2003a; *Platyophrya bromelicola* Foissner & Wolf, 2009; *Sandmanniella terricola* Foissner & Stoeck, 2009; *Bromeliothrix metopoides* Foissner, 2010a; and *Apocyrtolophosis minor* (Vuxanovici, 1963) Foissner et al., 2014b. Further, three genera were resurrected (Foissner et al. 2011, 2014b): *Tillina, Paracolpoda,* and *Repoma*. In the present monograph, we describe 7 new colpodean genera and 17 new species; the description of eight further species is improved. Thus, there are now 80 colpodean genera (45% increase since 1993) with 218 species (28% increase).

Molecular data, mainly the nuclear small subunit rDNA, are available from 35 genera and 58 species (Foissner et al. 2011, 2014b). They greatly improved our understanding of the colpodean phylogeny and showed that the core genus, *Colpoda,* performed an intense adaptive radiation producing many new genera and species. However, several clades are still paraphyletic or have poor statistical support, even some of the most complex and characteristic genera, such as *Jaroschia* and *Kalometopia.*

Colpoda ephemera nov. spec. (Fig. 89a–h, 90a–s, 91a–e; Table 34)

Diagnosis: Size in vivo about 70 × 45 µm. Body ellipsoid to broadly ellipsoid with distinct concavity at oral opening in anterior third of body; outline usually distinctly bulged by a mass of food vacuoles. Nuclear apparatus in first to second quarter of body; macro- and micronucleus broadly ellipsoidal. Cortex with scattered, minute extrusomes, rough because usually bulged by a mass of food vacuoles. On average 15 ciliary rows with ciliature condensed right and left of preoral suture. Left oral polykinetid quadrangular, composed of an average of 9 kineties. Appears 1 day after rewetting the sample and encysts after 2 to 3 days. Resting cysts 45 µm in diameter on average, wall 1.5–2.5 µm thick, ectocyst membranous and wrinkled, cytoplasm with food vacuoles likely containing viable bacteria.

Table 34. Comparison of morphometric data on *Colpoda ephemera* (CE), *C. maupasi* (CM) from Venezuelan site (52), and *C. maupasi* from an Austrian coniferous forest (CA). Data based on mounted, randomly selected specimens from non-flooded Petri dish cultures. Measurements in µm. CHL – CHATTON-LWOFF silver nitrate impregnation, CV – coefficient of variation in %, M – median, Max – maximum, Me – method, Mean – arithmetic mean, Min – minimum, n – number of individuals investigated, P – protargol, Pop – population, SC – silver carbonate, SD – standard deviation, SE – standard error of arithmetic mean.

Characteristics	Pop	Me	Mean	M	SD	SE	CV	Min	Max	n
Body, length	CE	CHL	66.7	66.0	10.6	2.4	15.9	45.0	82.0	19
	CM	CHL	61.1	64.0	6.4	1.8	10.5	45.0	69.0	13
	CA	CHL	45.6	45.0	3.6	1.0	7.8	41.0	53.0	13
Body, width	CE	CHL	45.2	44.0	8.3	1.9	18.3	30.0	60.0	19
	CM	CHL	38.2	40.0	5.2	1.4	13.6	26.0	44.0	13
	CA	CHL	24.6	25.0	2.6	0.7	10.7	20.0	29.0	13
Body length:width, ratio	CE	CHL	1.5	1.5	0.2	0.1	9.9	1.3	1.8	19
	CM	CHL	1.6	1.6	0.2	0.1	8.5	1.3	1.8	13
	CA	CHL	1.9	1.8	0.2	0.1	7.4	1.7	2.2	13
Body, length	CE	P	57.0	57.0	7.8	1.8	13.7	44.0	80.0	19
Body, width	CE	P	40.8	38.0	6.8	1.6	17.1	27.0	58.0	19
Body length:width, ratio	CE	P	1.4	1.4	0.1	0.1	8.0	1.3	1.6	19
Anterior body end to macronucleus, distance	CE	P	15.8	17.0	5.7	1.3	35.9	7.0	27.0	18
	CM	CHL	23.9	28.0	8.1	2.2	33.7	8.0	32.0	13
	CA	CHL	23.9	23.0	4.3	1.2	17.9	16.0	34.0	13
Macronucleus, length	CE	P	12.0	11.0	2.7	0.6	22.2	8.0	18.0	19
	CM	CHL	9.3	10.0	1.3	0.4	14.1	7.0	11.0	13
	CA	CHL	8.2	8.0	1.3	0.4	15.8	6.0	10.0	13
Macronucleus, width	CE	P	10.8	10.0	2.5	0.6	22.8	7.0	15.0	19
	CM	CHL	8.9	9.0	1.3	0.4	14.8	6.0	11.0	13
	CA	CHL	7.1	7.0	1.3	0.4	17.7	5.0	10.0	13
Micronucleus, length	CE	P	3.6	3.5	0.9	0.4	25.6	2.5	5.0	6
Micronucleus, width	CE	P	2.8	3.0	0.4	0.2	15.2	2.0	3.0	6
Anterior body end to right oral polykinetid, distance	CE	CHL	14.4	14.0	3.1	0.7	21.1	10.0	21.0	19
	CM	CHL	13.2	13.0	1.3	0.4	10.2	11.0	15.0	13

continued

Characteristics	Pop	Me	Mean	M	SD	SE	CV	Min	Max	n
	CA	CHL	8.4	8.0	–	–	–	8.0	9.0	13
Anterior body end to left oral polykinetid, distance	CE	CHL	18.9	18.0	3.3	0.7	17.2	13.0	27.0	19
	CM	CHL	17.7	18.0	1.5	0.4	8.4	15.0	21.0	13
	CA	CHL	12.5	12.0	0.8	0.2	6.2	12.0	14.0	13
Left oral polykinetid, length	CE	CHL	5.7	6.0	0.9	0.2	15.6	4.0	7.0	19
	CM	CHL	5.8	6.0	–	–	–	5.0	6.0	13
	CA	CHL	4.7	5.0	–	–	–	4.0	5.0	13
Left oral polykinetid, width	CE	CHL	2.8	3.0	–	–	–	2.0	3.0	19
	CM	CHL	2.9	3.0	–	–	–	2.0	3.0	13
	CA	CHL	2.0	2.0	–	–	–	1.5	2.5	13
Left oral polykinetid, number of ciliary rows	CE	SC	8.8	9.0	1.4	0.3	16.1	6.0	11.0	19
	CM	CHL	11.0	11.0	–	–	–	11.0	11.0	3
	CA	CHL	9.6	10.0	–	–	–	9.0	10.0	10
Excretory pore of contractile vacuole, diameter	CE	CHL	3.5	3.5	–	–	–	3.0	4.0	19
	CM	CHL	2.8	3.0	–	–	–	2.0	3.0	13
	CA	CHL	1.8	2.0	–	–	–	1.5	2.0	13
Ciliary rows, number	CE	CHL	15.6	15.0	1.6	0.4	10.3	13.0	19.0	19
	CM	CHL	18.1	18.0	1.1	0.3	6.2	17.0	20.0	13
	CA	CHL	14.3	14.0	1.0	0.3	6.6	13.0	16.0	13
Dikinetids in ciliary row 4, total number	CE	CHL	15.5	16.0	2.4	0.6	15.4	12.0	19.0	19
	CM	CHL	21.2	22.0	3.2	0.9	15.3	17.0	26.0	13
	CA	CHL	13.3	14.0	1.5	0.4	11.2	10.0	15.0	13
Dikinetids in ciliary row 5, total number	CE	CHL	15.5	16.0	2.3	0.5	14.5	12.0	19.0	19
	CM	CHL	21.3	21.0	3.5	1.0	16.2	17.0	26.0	13
	CA	CHL	13.5	14.0	1.1	0.3	7.8	11.0	15.0	13
Dikinetids in ciliary row 4 in mid-body, number in 20 µm	CE	CHL	3.4	3.0	1.0	0.2	29.7	2.0	6.0	19
	CM	CHL	5.0	5.0	1.0	0.3	19.4	4.0	7.0	13
	CA	CHL	4.3	4.0	0.6	0.2	14.6	3.0	5.0	13
Silverlines between ciliary rows 4 and 5, total number	CE	CHL	33.0	34.0	5.1	1.2	15.5	26.0	44.0	19
	CM	CHL	30.5	30.0	3.9	1.1	12.7	23.0	36.0	13
	CA	CHL	21.6	21.0	1.4	0.4	6.4	20.0	24.0	13

continued

Type locality: Floodplain soil from the Matjula River in the surroundings of the Berg-en-dal Lodge near to the southern border of the Krueger National Park, Republic of South Africa, 31°28'E 25°20'S.

Type and voucher slides: 1 holotype and 3 paratype slides with Chatton-Lwoff silver nitrate-impregnated specimens have been deposited in the Biology Centre of the Upper Austrian Museum in Linz (LI). Additionally, we deposited 5 slides with protargol- impregnated specimens. The holotype and other relevant specimes have been marked by black ink circles on the coverslip. At the same locality, we deposited a voucher slide each with Chatton-Lwoff silver nitrate-impregnated *C. maupasi* from Venezuela and Austria used for comparison with *C. ephemera* (Table 34).

Characteristics	Pop	Me	Mean	M	SD	SE	CV	Min	Max	n
Silverlines between ciliary rows 4 and 5 in mid-body, number in 20 µm	CE	CHL	8.0	8.0	1.2	0.3	14.8	6.0	11.0	19
	CM	CHL	7.8	7.0	2.4	0.7	31.2	3.0	13.0	13
	CA	CHL	6.9	7.0	0.9	0.2	12.5	5.0	8.0	13
Dikinetids in central row of left side, total number	CE	CHL	13.7	14.0	4.1	1.1	29.6	9.0	25.0	19
	CM	CHL	20.8	22.0	2.9	0.8	13.8	17.0	25.0	13
	CA	CHL	13.6	13.0	4.6	1.3	33.5	9.0	23.0	13
Dikinetids in central row of left side, number in 20 µm	CE	CHL	3.1	3.0	0.4	0.1	14.0	2.0	4.0	17
	CM	CHL	4.5	4.0	0.7	0.2	14.6	4.0	6.0	13
	CA	CHL	4.5	4.0	1.5	0.4	33.8	3.0	8.0	13
Silverlines between two central rows of left side, total number	CE	CHL	27.3	27.0	4.1	1.1	15.2	21.0	37.0	19
	CM	CHL	29.8	30.0	3.2	0.9	10.6	24.0	38.0	13
	CA	CHL	19.5	20.0	4.5	1.2	22.9	14.0	32.0	13
Silverlines between two central rows of left side in mid-body, number in 20 µm	CE	CHL	7.7	8.0	1.0	0.2	13.0	6.0	9.0	17
	CM	CHL	7.4	7.0	1.3	0.4	17.1	6.0	10.0	13
	CA	CHL	7.5	7.0	1.3	0.4	16.8	6.0	10.0	13
Ciliary rows 4 and 5, distance in mid-body	CE	CHL	7.8	8.0	1.1	0.2	13.7	6.0	10.0	19
	CM	CHL	4.9	5.0	0.9	0.3	18.8	3.5	6.0	13
	CA	CHL	4.6	5.0	0.5	0.1	10.8	4.0	5.0	13
Central ciliary rows of left side, distance in mid-body	CE	CHL	7.8	8.0	1.0	0.2	13.2	6.0	10.0	19
	CM	CHL	5.2	5.0	0.8	0.2	15.9	4.0	7.0	13
	CA	CHL	4.7	5.0	–	–	–	4.0	5.0	13

Etymology: The Latinized adjective *ephemera* (ephemeral) refers to the short periods of activity.

Description: Size in vivo 50–90 × 30–65 µm, usually about 70 × 45 µm, as calculated from some in vivo measurements and the morphometric data adding 5% and 15% preparation shrinkage for silver nitrate and protargol-impregnated specimens, respectively (Table 34). Body ellipsoid to broadly ellipsoid, hardly flattened laterally, with distinct concavity at oral opening in anterior body third, preoral region occasionally slightly rostrate, ovate to broadly ovate when viewed ventrally or dorsally (Fig. 89a, c, 90a–d, f–h, l, m). Nuclear apparatus usually between first and second quarter of cell, in rather many specimens dislocated into posterior body half and/or compressed by a mass of food vacuoles (Fig. 89a, g, 90a, b, e, g; Table 34). Macronucleus and micronucleus broadly ellipsoidal; macronucleus 12 × 11 µm in protargol preparations, with a single, lobed nucleolus or several globular nucleoli. Contractile vacuole in posterior end of cell, excretory pore in or near pole centre, 3–4 µm in diameter (Fig. 89a, c, 90i, l). Cortex flexible and bright, contains minute (~ 0.5 µm) extrusomes hardly recognizable in vivo but distinct in some silver nitrate-impregnated specimens, appearing as about 0.5 µm-sized rings and granules when attached or extruded, respectively (Fig. 89h); usually distinctly bulged by an enormous number of food vacuoles (Fig. 89a, 90d, f, m). Cytoplasm colourless but dark at low magnification (≤ 100×) because studded with lipid droplets 1–3 µm across and compact food vacuoles, except of clear and thus bright anterior end (Fig. 89a). Food vacuoles covered with a protargol-affine substance; in two types both containing bacterial rods (Fig. 90p, s), rarely small ciliates such as *Protocyclidium terricola* (Fig. 90d, f, g, m): type 1 mainly subcortical, ellipsoid, about 5–8 × 3–4

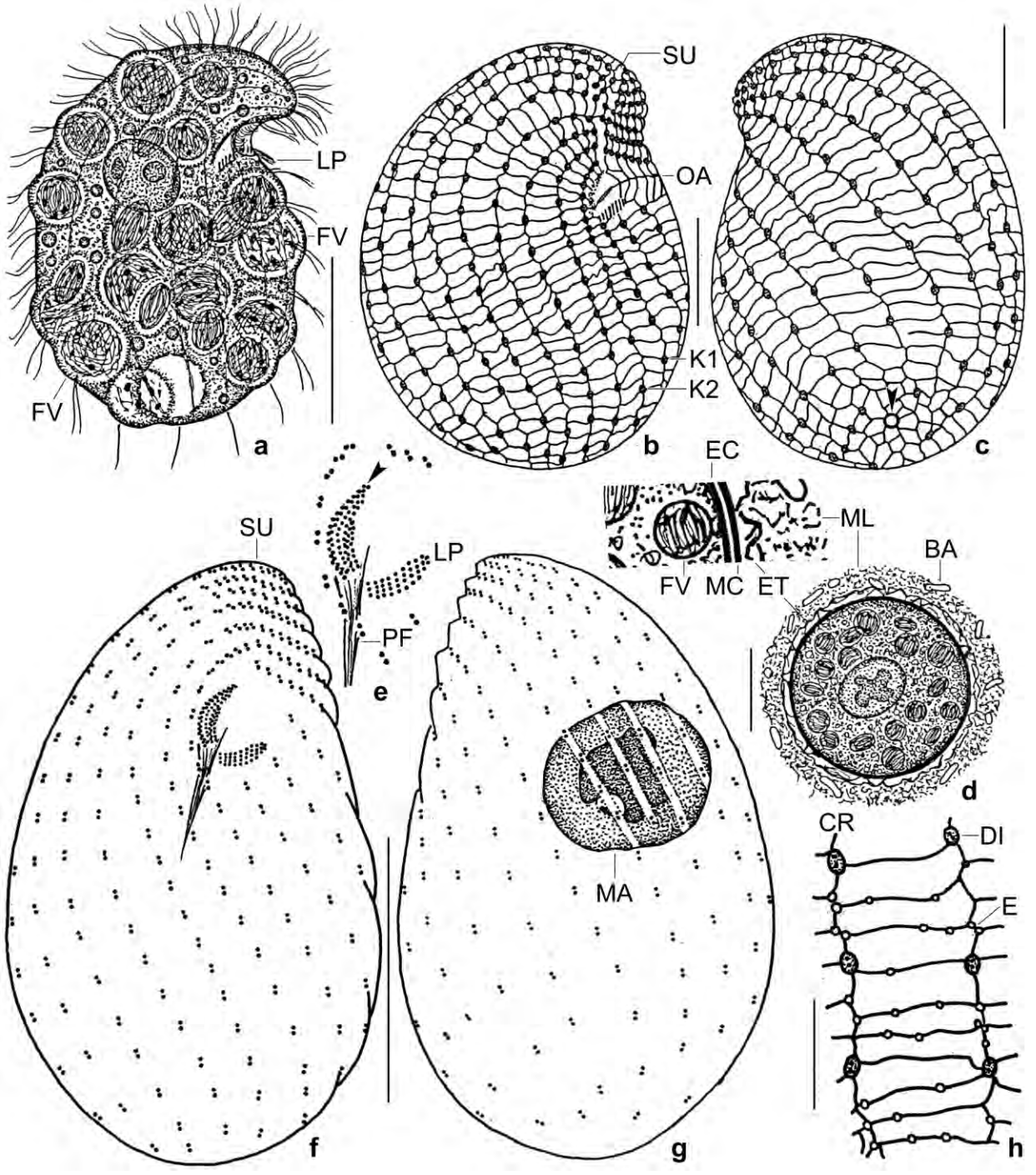

Fig. 89a–h. *Colpoda ephemera* from life (a, d), in Chatton-Lwoff silver nitrate preparations (b, c, h), and after protargol impregnation (e–g). **a:** Right side view of a representative specimen with many ordinary and large food vacuoles bulging the surface, length 70 µm. **b, c:** Right and left side view, showing the kinetid and silverline pattern. The arrowhead in (c) marks the excretory pore. **d:** Even mature resting cysts contain many food vacuoles with bacteria. **e–g:** Ventral and left lateral view of oral and somatic kinetid pattern of holotype specimen, length 60 µm. The arrowhead in (e) marks a row of dikinetids on the dorsal margin of the right oral polykinetid. **h:** Detail of silverline pattern with extrusomes surrounded by minute silverline rings. BA – bacteria, CR – ciliary row, DI – dikinetid, E – extrusomes, EC – endocyst, ET – ectocyst, FV – food vacuoles, K1,2 – kineties, LP – left oral polykinetid, MC – mesocyst, MA – macronucleus, ML – mucilaginous layer, OA – oral apparatus, PF – pharyngeal fibres, SU – preoral suture. Scale bars 15 µm (h), 20 µm (b, c, d), and 30 µm (a, f, g).

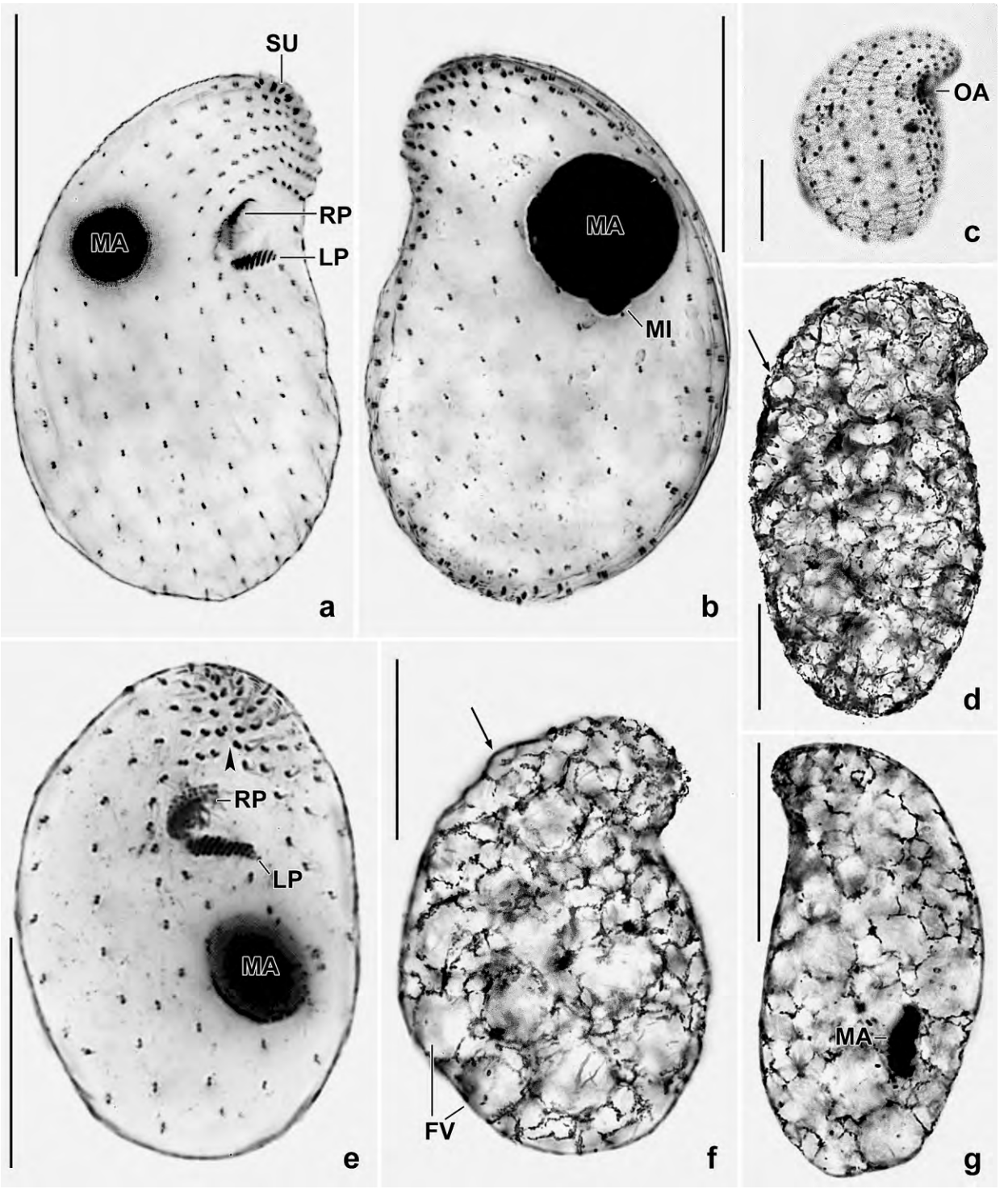

Fig. 90a–g. *Colpoda ephemera* after protargol (a, b, d–g) and Chatton-Lwoff silver nitrate (c) impregnation. **a, b:** Right and left side view of kinetid pattern. **c:** A thick, rostrate specimen. **e:** Oblique anterior polar view, showing the narrowly spaced kinetids right and left of the preoral suture (arrowhead). **d, f, g:** Shape variability of specimens studded with food vacuoles covered by protargol precipitations. Note the bulged surface (arrows) and the compressed macronucleus (g). FV – food vacuoles, LP – left oral polykinetid, MA – macronucleus, MI – micronucleus, OA – oral apparatus, RP – right oral polykinetid, SU – preoral suture. Scale bars 15 µm (d) and 30 µm (a–c, e–g).

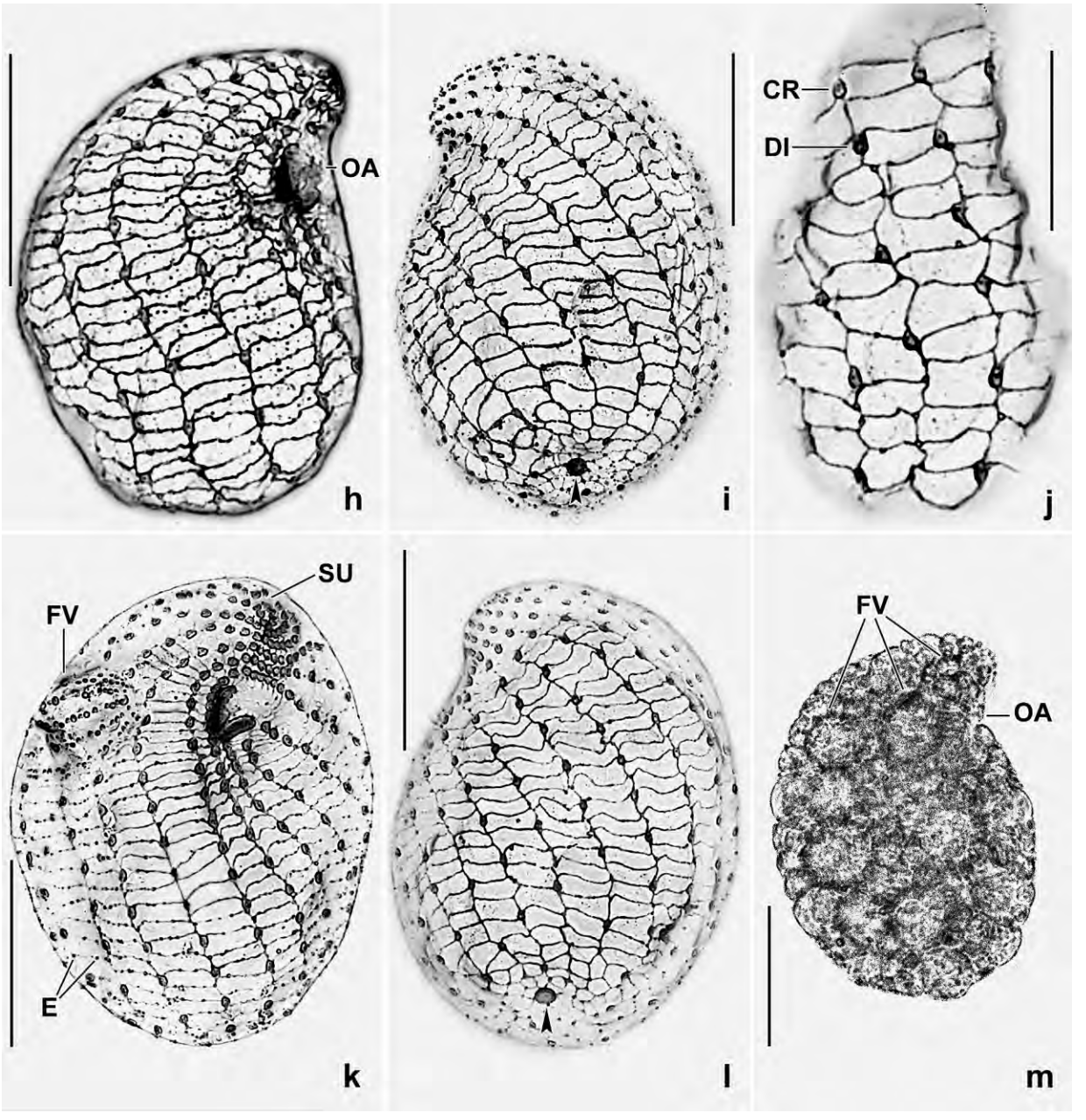

Fig. 90h–m. *Colpoda ephemera* in Chatton-Lwoff silver nitrate preparations (h–l) and from life (m). **h–l:** Right and left side views (h, i, l), dorsal view (j), and oblique anterior polar view (k) of kinetid (ciliary) and silverline pattern. Arrowheads mark the excretory pore of the contractile vacuole. There are two to three transverse silverlines between two kinetids each. Thus, the silverline pattern of *C. ephemera* is "narrower" than that of *C. maupasi* which has one to two transverse silverlines (Fig. 91a–e). The dikinetids are very narrowly spaced left of the preoral suture (k) and the excretory pore of the contractile vacuole (arrowheads) is surrounded by minute polygonal silverline meshes. Note a *Protocyclidium terricola* in a food vacuole of the specimen shown in (k). **m:** In vivo (bright field), *C. ephemera* has a very characteristic appearance because it is usually so studded with ordinary and large food vacuoles that the body surface becomes bulged. CR – ciliary row, DI – dikinetid, E – extrusomes, FV – food vacuoles, OA – oral apparatus, SU – preoral suture. Scale bars 20 µm (j) and 30 µm (h, i, k–m).

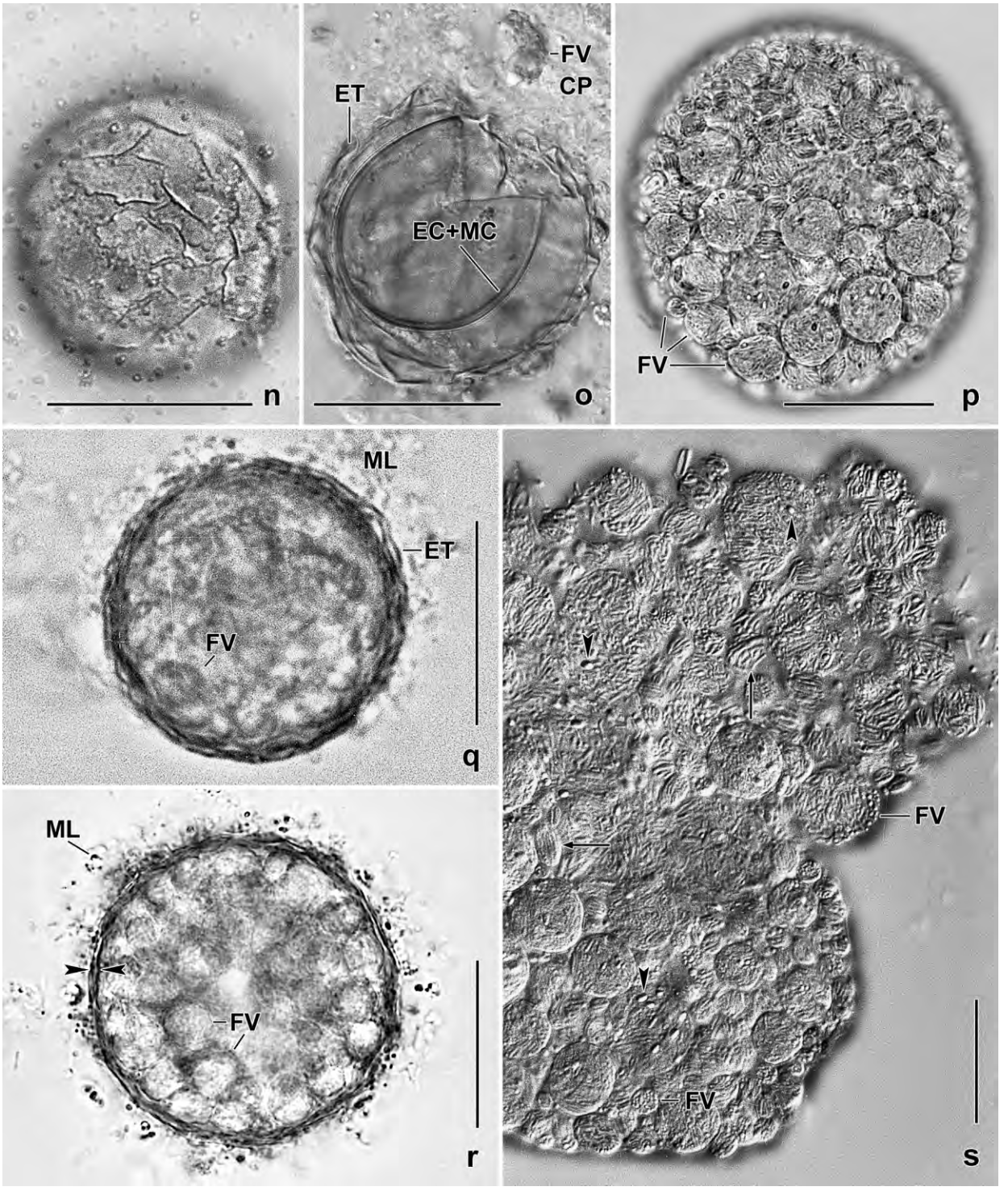

Fig. 90n–s. *Colpoda ephemera,* resting cysts from South African (n–q, s) and North American (r) specimens. **n:** Surface view, showing the wrinkled ectocyst. **o:** Optical section of a squashed cyst, showing wall details. **p, s:** An encysting, slightly squashed specimen studded with small and large food vacuoles containing bacteria. Arrows mark small, ellipsoid food vacuoles; arrowheads denote spores of bacteria. **q, r:** Optical sections, showing wall and large food vacuoles. Opposed arrowheads mark meso- and endocyst. CP – cytoplasm, EC – endocyst, ET – ectocyst, FV – food vacuoles, MC – mesocyst, ML – mucilaginous layer. Scale bars 20 µm (s) and 30 µm (n–r).

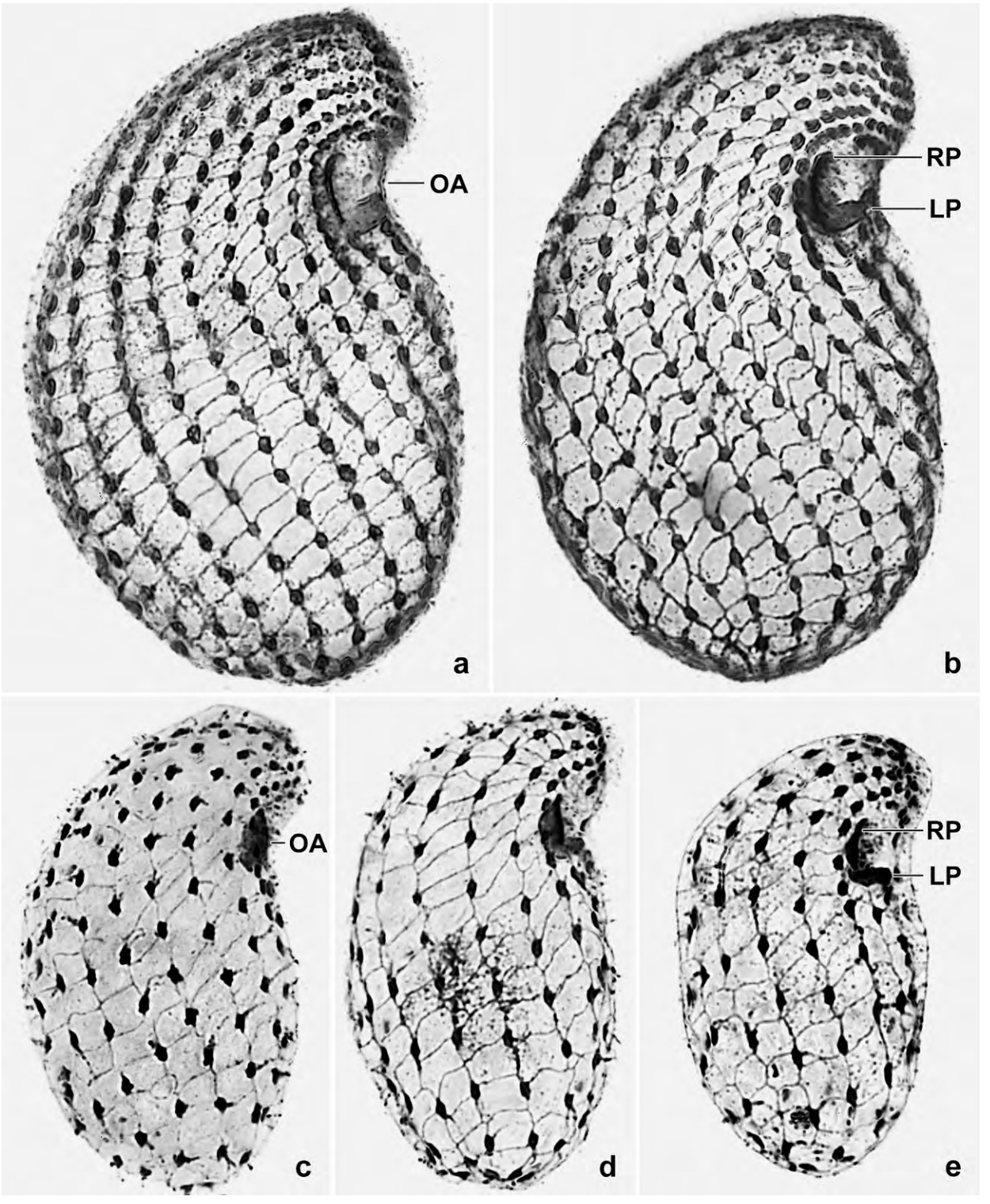

Fig. 91a–e. *Colpoda maupasi,* kinetid and silverline pattern after Chatton-Lwoff silver nitrate impregnation (for comparison with C. *ephemera,* Fig. 90h–l and Table 34). **a, b:** Right side views of large Venezuelan specimens, length about 65 µm. The silverline pattern appears "wider" than in *C. ephemera* mainly because the ciliary rows are narrower spaced (Table 34). **c–e:** Right side views of small Austrian specimens, length about 45 µm. LP – left oral polykinetid, OA – oral apparatus, RP – right oral polykinetid.

µm in size; type 2 scattered throughout cell, globular and up to 20 µm in size frequently bulging cortex. Swims slowly by rotation about main body axis.

Somatic cilia about 10 µm long in vivo, paired except of dikinetids in posterior quarter of rows lacking anterior cilium; arranged in 13–19, usually 15 equidistant, moderately spiral, widely spaced (6–10 µm, on average 8 µm) rows commencing right and left of preoral suture except for three postoral rows (Fig. 89a–c, f, g, 90a–c, e, h, i, k, l; Table 34). Dikinetids within rows ordinarily to widely spaced, those in preoral region narrowly spaced right and left of preoral suture; number of dikinetids/row slightly lower on left (14) than right (16) side of cell; elongated caudal cilia absent.

Silverline pattern colpodid, usually slightly wrinkled due to the bulging food vacuoles. Two to three transverse silverlines between two dikinetids each, meshes thus narrowly quadrangular, on average 34 silverlines between ciliary rows 4 and 5 while 27 between central rows of left side. Meshes small and polygonal around excretory pore of contractile vacuole (Fig. 89b, c, 90h–l; Table 34).

Oral apparatus in a distinct concavity of anterior body third (Fig. 89a, b, f, 90a, c–h, m; Table 34). Buccal cavity funnel-shaped, small compared to body size, viz., about 8 µm wide and 10 µm deep. Right oral polykinetid curved-cuneate, about 8 µm long, composed of three to four kineties with 3 µm long cilia and a row of dikinetids at dorsal margin (Fig. 90e, f). Left oral polykinetid quadrangular, rarely elliptic, 4–7 × 2–3 µm in size, composed of an average of nine rows with 4 µm long cilia projecting from body proper but not forming a distinct beard.

Resting cyst: We investigated the resting cysts of specimens from the type locality and from Idahoe, North America (see Occurrence section). They were highly similar and are thus described together. The cysts were studied four days after isolation of ordinary specimens from the non-flooded Petri dish cultures. They did not show any movement of the cytoplasm. However, when they were slightly pressed with the coverslip, the encysted specimens commenced rotation after about 1 min, indicating that cilia were still present and the cysts were possibly not mature.

The most conspicuous feature of the cyst of *C. ephemera* are in both populations a mass of food vacuoles likely packed with viable bacteria (Fig. 89d, 90p–s), as do the cysts of *Pseudomaryna australiensis* Foissner, 2003 and *Sandmanniella terricola* Foissner & Stoeck, 2009. Otherwise, the cysts of *C. ephemera* are highly similar to those of *C. maupasi* (see micrographs 73q, r in Foissner 1993a) except for the size which is much larger in *C. ephemera* (45–58 µm, averages from two populations) than in *C. maupasi* (25–30 µm, averages from two populations, see Foissner 1993a).

Globular, size in type population on average 46.5 µm (M = 45 µm, SD = 5.5, SE = 1.3, CV = 11.8, Min = 40, Max = 60, n = 17), in North American specimens 58.4 µm (55–60 µm, n = 5). Cyst wall light brown or yellowish, 2–3 µm thick, composed (from outside to inside, Fig. 89d, 90n, o, q, r) of an up to 10 µm thick mucous coat colonized by various bacteria and disappearing in old cysts; ectocyst 1–1.5 µm thick, wrinkled producing a pustulate appearance of the mesocyst; mesocyst indistinctly separate from ectocyst, about 0.8 µm thick; endocyst close to mesocyst, about 0.6

µm thick. Mesocyst and endocyst elastic because becoming smaller when wall is broken (Fig. 90o). Cytoplasm colourless, with many globular and ellipsoid food vacuoles 5–15 µm in size (see above) and many lipid droplets 0.5–3 µm across. Macronucleus in cyst centre, broadly ellipsoid.

Occurrence and ecology: As yet, we found *C. ephemera* in the upper 10 cm soil layer of an active flood plain in the Republic of South Africa (see type locality); in Galápagos sample (68), i. e., in soil from a mangrove forest at a salinity of 30‰ (!); and in the upper soil layer from a flood-irrigated grass lawn in Boise, Idahoe, USA (43°38'10.82"N 116°13'50.5"W, elev. 813 m; sample kindly supplied by Dr. Bill Bourland). These habitats are ephemeral, suggesting that *C. ephemera* belongs to the ephemeral ciliate community. This is sustained by the curious life cycle (see next paragraph).

Independent whether *C. ephemera* is or is not a distinct species (see **Remarks**), we never met a *C. ephemera*-like ciliate in many soil samples from Austria and Germany, suggesting restricted distribution, especially in Gondwanan areas.

Colpoda ephemera appeared in the three samples one day after rewetting and disappeared on days two or three, i. e., made resting cysts with food vacuoles. Such behaviour has been described also in two other colpodids, viz., *Pseudomaryna australiensis* Foissner, 2003a and *Sandmanniella terricola* Foissner & Stoeck, 2009. To put part of growth into the resting cyst may be interpreted as a pronounced r-selected survival strategy.

Remarks: The most similar species, *C. maupasi*, has an enormous variability when literature data and those from Table 34 are compared (for a review, see Foissner 1993a). Part of this variability might be caused by the preparation methods used, the exactness of the observations and, possibly, by mixing different species. Thus, we compared *C. ephemera* with two *C. maupasi* populations cultivated (non-flooded Petri dish method), impregnated (Chatton-Lwoff silver nitrate), and analyzed with the same methods (Table 34).

Morphological and ecological comparison: *Colpoda maupasi* (~ 60 × 30 µm in vivo, 16 ciliary rows, left oral polykinetid with nine to ten kineties) is a frequent cosmopolitan (Foissner 1993a, Foissner et al. 2002) and is possibly the ancestor of *C. ephemera* (~ 70 × 45 µm, cortex bulged by a mass of ordinary and large food vacuoles, 15 ciliary rows, left oral polykinetid composed of nine kineties), *C. brasiliensis* Foissner, 2003 (~ 33 × 18 µm, body covered with a mineral envelope, 12 ciliary rows, left oral polykinetid with five kineties), *Apocolpoda africana* Foissner, 1993a (~ 40 × 25 µm, with curved preoral ridge and kinety, 12 ciliary rows, left oral polykinetid composed of 14 kineties), *Cosmocolpoda naschbergeri* Foissner, 1993a (~ 60 × 47 µm, with cortical crests forming a ladder-like pattern between ciliary rows, 16 ciliary rows, left oral polykinetid with seven kineties), *Idiocolpoda pelobia* Foissner, 1993b (~ 35 × 19 µm, oral apparatus on left side of body, 12 ciliary rows, left oral polykinetid composed of eight kineties), and *Dragescozoon terricola* Foissner et al., 2002 (~ 40 × 27 µm, somatic ciliary rows in special preoral pattern, 10 ciliary rows, left oral polykinetid composed of 5 kineties). These species, which have a similar size and organization, are comparatively rare and look like variants of *C. maupasi*, for instance, *Cosmocolpoda naschbergeri* which has the same "dense" silverline pattern as *Colpoda ephemera*. Thus, *C. ephemera* can be diagnosed only by a combination of morphological and ecological

features: life cycle (appears soon after rewetting and disappears after two days while *C. maupasi* usually appears when *C. ephemera* is declining or had disappeared); the enormous number and size of food vacuoles bulging the cortex (has been never observed in *C. maupasi*); the resting cysts which contain food vacuoles with bacteria, as do *Pseudomaryna australiensis* Foissner, 2003 and *Sandmanniella terricola* Foissner & Stoeck, 2009; and the biogeographic distribution (very likely absent from Central Europe where *C. maupasi* is very frequent).

Morphometric comparison (Table 34, Fig. 91a–e): Most morphometric features of *C. ephemera* highly overlap with those of the two very different *C. maupasi* populations investigated and with literature data (for a review, see Foissner 1993a); or they appear correlated with body size, e. g., the interkinetal distance which is distinctly larger in *C. ephemera* than in *C. maupasi*, very likely because *C. ephemera* is inflated by the high number of food vacuoles. Actually, there remains only one rather reliable feature, viz., the "dense" silverline pattern which results from the wide interkinetal distance and a slightly higher number (8 vs. 7 in 20 µm, Table 34) of transverse silverlines between the kineties (cp. Fig. 89b, c, 90h–l, 91a–e). Statistically, this is poorly supported but usually there is one transverse silverline between two kinetids in *C. maupasi* while two in *C. ephemera*.

Finally, *Colpoda brasiliensis* Foissner, 2003a should be mentioned because it looks like a miniaturized *C. ephemera*. They differ by body size (about 33 × 18 µm vs. 70 × 45 µm in vivo), the presence vs. absence of a mineral envelope, the somatic ciliary pattern (kineties 2 and 3 spread vs. not spread anteriorly), and the number of ciliary rows (12 vs. 15 on average) and of kineties in the left oral polykinetid (5 vs. 9). Thus, these species are easily distinguished both in vivo and in silver preparations.

Unfortunately, we failed to obtain pure cultures, in contrast to *C. maupasi* which grows easily. Further, our effort to separate *C. ephemera* from *C. maupasi* by morphometric features failed either because they are the same species or because of the high variability of *C. maupasi*. Thus, we recommend to use the morphological and ecological features, especially the numerous and extraordinarily large food vacuoles bulging the cortex and the presence of food vacuoles in the resting cyst.

***Paracolpoda lajacola* nov. spec.** (Fig. 92a–j, 93a–q, 94a–s, 95a–p; Table 35)

Diagnosis: Size in vivo about 25 × 18 µm, up to 2:1 flattened laterally. Body outline ovate or semicircular. Nuclear apparatus in posterior ventral quadrant of cell: macronucleus broadly ellipsoidal and with central nucleolus; micronucleus discoidal, about 4 µm across and 2 µm thick. Minute granular intrakinetal extrusomes. Usually 12 ciliary rows with an average total of 53 dikinetids: rows 2, 5, 6 complete, right side rows 3 and 4 and all ventral and left side rows distinctly shortened; last dikinetid of row 2 with two caudal cilia about 15 µm long. Oral apparatus in anterior third of cell, upper margin with distinct bulge. Left oral polykinetid spatulate, usually composed of 10 kineties. Resting cysts on average 12 µm across, ectocyst distinctly separate from endocyst.

Type locality: Venezuelan site (30), i. e., mud from an ephemeral lithotelma (Laja) on granitic

Table 35. Comparison of morphometric data on *Paracolpoda lajacola* (PL) and a Salzburg population of *P. steinii* (PS, conifer litter from the surroundings of the village of Michelbeuern, Salzburg). Data based on mounted, silver-impregnated, randomly selected specimens from non-flooded Petri dish cultures. Measurements in µm. CV – coefficient of variation in %, M – median, Max – maximum, Mean – arithmetic mean, Min – minimum, n – number of individuals investigated, P – protargol impregnation, PL – *Paracolpoda lajacola*, PS – *Paracolpoda steinii*, SD – standard deviation, SE – standard error of arithmetic mean, SN – Chatton-Lwoff silver nitrate impregnation.

Characteristics	Species	Method	Mean	M	SD	SE	CV	Min	Max	n
Body, length	PL	SN	24.3	24.0	2.2	0.5	9.0	22.0	31.0	21
	PS	SN	30.0	31.0	3.8	1.2	12.7	23.0	37.0	11
Body, width	PL	SN	17.2	17.0	1.4	0.3	8.4	15.0	20.0	21
	PS	SN	19.0	19.0	1.8	0.6	9.7	16.0	22.0	11
Body length:width, ratio	PL	SN	1.4	1.4	0.1	0.1	6.4	1.3	1.6	21
	PS	SN	1.6	1.6	0.1	0.1	7.9	1.4	1.7	11
Body, length	PL	P	23.1	23.0	2.8	0.6	11.9	18.0	29.0	21
Body, width	PL	P	15.6	16.0	1.7	0.4	10.9	12.0	18.0	21
Body length:width, ratio	PL	P	1.5	1.5	0.1	0.1	8.9	1.3	1.8	21
Body, thickness	PL	SN	11.1	11.0	1.7	0.4	15.1	7.0	14.0	21
	PS	SN	12.2	12.0	1.8	0.6	15.1	10.0	15.0	11
Anterior body end to macronucleus, distance	PL	P	10.4	10.0	1.6	0.3	15.1	7.0	14.0	21
	PS	SN	13.9	14.0	1.9	0.6	13.4	11.0	17.0	11
Macronucleus, length	PL	P	7.1	7.0	1.1	0.2	14.9	5.0	9.0	21
	PS	SN	6.8	7.0	0.9	0.3	12.8	5.0	8.0	11
Macronucleus, width	PL	P	5.5	5.0	0.9	0.2	15.7	4.0	7.0	21
	PS	SN	5.5	5.0	–	–	–	5.0	6.0	11
Large nucleoli, number	PL	P	1.1	1.0	–	–	–	1.0	2.0	21
	PS	SN	1.0	1.0	0.0	0.0	0.0	1.0	1.0	11
Central nucleolus, length	PL	P	2.4	2.3	–	–	–	2.0	3.0	21
	PS	SN	2.8	3.0	–	–	–	2.0	3.5	11
Central nucleolus, width	PL	P	2.3	2.1	–	–	–	1.5	3.0	21
	PS	SN	2.3	2.2	–	–	–	2.0	2.5	11
Micronucleus, diameter	PL	P	3.3	3.0	–	–	–	3.0	4.0	21
	PS	SN	3.3	3.0	–	–	–	3.0	4.0	11
Micronucleus, thickness	PL	P	1.5	1.5	–	–	–	1.0	2.0	21
	PS	SN	1.6	1.5	–	–	–	1.0	2.0	21
Anterior body end to left oral polykinetid, distance	PL	SN	8.1	8.0	0.8	0.2	10.4	7.0	10.0	21
	PS	SN	9.6	10.0	1.0	0.3	10.9	7.0	11.0	11
Buccal cavity, depth	PL	SN	6.4	7.0	0.9	0.2	13.6	5.0	8.0	21
	PS	SN	7.4	7.0	1.2	0.4	16.4	6.0	10.0	11
Left oral polykinetid, length	PL	SN	4.9	5.0	–	–	–	4.0	5.0	21
	PS	SN	5.6	6.0	–	–	–	5.0	6.0	11
Left oral polykinetid, width	PL	SN	2.8	3.0	–	–	–	2.0	3.0	21
	PS	SN	3.0	3.0	0.0	0.0	0.0	3.0	3.0	11
Left oral polykinetid, number of ciliary rows	PL	SN	10.1	10.0	–	–	–	10.0	11.0	11
	PS	SN	11.6	12.0	0.8	0.3	7.3	10.0	13.0	11
Somatic ciliary rows, number	PL	SN	11.7	12.0	–	–	–	11.0	12.0	21
	PS	SN	12.0	12.0	0.6	0.2	5.3	11.0	13.0	11

continued

Characteristics	Species	Method	Mean	M	SD	SE	CV	Min	Max	n
Somatic ciliary row 1, number of dikinetids [a]	PL	SN	3.0	3.0	0.0	0.0	0.0	3.0	3.0	21
	PS	SN	4.7	5.0	0.8	0.2	16.7	4.0	6.0	11
Somatic ciliary row 2, distance from anterior body end to end of row	PL	SN	24.2	24.0	2.4	0.5	9.9	20.0	31.0	21
	PS	SN	29.4	30.0	3.9	1.2	13.3	23.0	37.0	11
Somatic ciliary row 2, number of dikinetids [b]	PL	SN	10.1	10.0	1.1	0.2	10.7	8.0	12.0	21
	PS	SN	15.3	15.0	2.1	0.6	13.8	13.0	20.0	11
Somatic ciliary row 3, distance from anterior body end to end of row	PL	SN	12.9	13.0	2.8	0.6	21.5	8.0	18.0	21
	PS	SN	25.4	28.0	5.0	1.5	19.6	17.0	32.0	11
Somatic ciliary row 3, number of dikinetids [b]	PL	SN	5.0	5.0	0.7	0.2	13.5	4.0	6.0	21
	PS	SN	9.3	9.0	1.4	0.4	15.3	7.0	12.0	11
Somatic ciliary row 4, distance from anterior body end to end of row	PL	SN	9.9	10.0	2.3	0.5	23.0	6.0	14.0	21
	PS	SN	20.4	20.0	3.2	1.0	15.7	16.0	27.0	11
Somatic ciliary row 4, number of dikinetids [b]	PL	SN	6.2	6.0	0.9	0.2	15.0	5.0	8.0	21
	PS	SN	9.4	9.0	1.3	0.4	13.7	7.0	11.0	11
Somatic ciliary row 5, distance from anterior body end to end of row	PL	SN	22.9	23.0	2.1	0.5	9.3	21.0	29.0	21
	PS	SN	29.0	29.0	3.6	1.1	12.5	23.0	35.0	11
Somatic ciliary row 5, number of dikinetids [b]	PL	SN	9.4	9.0	1.7	0.4	17.6	6.0	13.0	21
	PS	SN	11.7	12.0	1.7	0.5	14.8	8.0	14.0	11
Somatic ciliary row 6, distance from anterior body end to end of row	PL	SN	21.5	21.0	2.7	0.6	12.6	16.0	27.0	21
	PS	SN	26.2	25.0	3.9	1.2	14.8	20.0	33.0	11
Somatic ciliary row 6, number of dikinetids [b]	PL	SN	8.4	9.0	1.0	0.2	11.6	7.0	10.0	21
	PS	SN	10.7	11.0	1.7	0.5	15.7	8.0	14.0	11
Somatic ciliary row 7, distance from anterior body end to end of row	PL	SN	10.1	10.0	3.2	0.7	31.9	6.0	19.0	21
	PS	SN	21.5	22.0	5.1	1.5	23.8	15.0	32.0	11
Somatic ciliary row 7, number of dikinetids [b]	PL	SN	4.8	5.0	0.9	0.2	19.3	3.0	7.0	21
	PS	SN	9.3	8.0	2.1	0.6	22.2	7.0	12.0	11
Somatic ciliary row 8, distance from anterior body end to end of row	PL	SN	5.8	5.0	1.7	0.4	29.6	4.0	10.0	21
	PS	SN	14.9	12.0	5.5	1.7	36.9	8.0	25.0	11
Somatic ciliary row 8, number of dikinetids [b]	PL	SN	1.7	1.0	0.8	0.2	47.8	1.0	3.0	21
	PS	SN	6.6	6.0	1.7	0.5	25.9	4.0	9.0	11
Somatic ciliary row 9, distance from anterior body end to end of row	PL	SN	6.0	6.0	1.0	0.2	16.7	4.0	8.0	21
	PS	SN	11.6	10.0	3.9	1.2	33.9	8.0	18.0	11
Somatic ciliary row 9, number of dikinetids [b]	PL	SN	1.1	1.0	–	–	–	1.0	2.0	21
	PS	SN	3.6	3.0	1.3	0.4	35.4	2.0	7.0	11
Somatic ciliary row 10, number of dikinetids [b]	PL	SN	1.5	2.0	–	–	–	1.0	2.0	21
	PS	SN	2.0	2.0	0.8	0.2	38.7	1.0	4.0	11
Somatic ciliary row 11, number of dikinetids [b]	PL	SN	2.5	3.0	–	–	–	2.0	3.0	21
	PS	SN	3.5	3.0	1.2	0.4	34.6	2.0	6.0	11
Somatic ciliary row 12, number of dikinetids [b]	PL	SN	1.4	1.0	–	–	–	1.0	2.0	16
	PS	SN	4.2	4.0	1.0	0.3	23.4	3.0	6.0	11
Somatic dikinetids, total number [b]	PL	SN	53.5	53.0	4.8	1.0	8.9	44.0	62.0	21
	PS	SN	87.1	89.0	10.6	3.2	12.2	72.0	105.0	11

[a] This is the rightmost postoral row (FOISSNER 1993).

[b] Selected for specimens with 12 ciliary rows.

outcroppings between the Agricultural Research Institute and the airport of Pto. Ayacucho, 67°36'W 5°41'N.

Type and voucher slides: 1 holotype and 1 paratype slide with Chatton-Lwoff silver nitrate-impregnated specimens have been deposited in the Biology Centre of the Upper Austrian Museum in Linz (LI). Additionally, we deposited 4 and 2 slides with protargol and Klein-Foissner silver nitrate impregnated specimens, respectively. The holotype and other relevant specimens have been marked by black ink circles on the coverslip. At the same locality, we deposited 2 slides with Chatton-Lwoff silver nitrate-impregnated *P. steinii*, used for comparison with *P. lajacola* (Table 35).

Etymology: The name is a composite of *Laja* (indigenous name for an ephemeral puddle on granitic outcroppings) and the Latin verb *colere* (to live in) referring to the habitat the species was discovered.

Description: Size in vivo 20–30 × 15–20 µm, usually about 25 × 18 µm, as calculated from some in vivo measurements and the morphometric data adding 5% for preparation shrinkage; values for protargol-impregnated specimens similar (Table 35); up to 2:1 flattened laterally, right side flat, left more or less convex (Fig. 92, g, 93h). Body outline broadly elliptical, rarely reniform or semicircular, preoral region receding, posterior end rounded, rarely bluntly pointed (Fig. 92b–d, h–j, 93a, e, g, i, 94a, b, n, p). Nuclear apparatus invariably in left posterior quadrant of cell (Fig. 92b, 94a–c, f; Table 35). Macronucleus broadly ellipsoidal, rarely ellipsoidal, about 7 × 5 µm in vivo and in protargol preparations; nuclear plasm hyaline except for a conspicuous central nucleolus 2–3 µm across and composed of argyrophilic granules. Micronucleus attached to macronucleus, discoidal, in live about 4 µm across and 2 µm thick, easy to see in vivo because rather refractive. Contractile vacuole in posterior end of cell, excretory pore in or near pole centre; surrounded by crystals of various shape and size, most 1.5–2 µm, appear dark at low magnification (≤ 100x) and bright field illumination (Fig. 92b, e, h, 94s). Cytopyge anterior of excretory pore (Fig. 94s). Cortex flexible, contains many intrakinetal, protargol-affine granules (likely a sort of mucocysts) ≤ 1 µm across (Fig. 94a–c); granules not recognizable in vivo and in methyl green-pyronin stains, appear as granules or rings in silver nitrate preparations (Fig. 92j, 94p). Cytoplasm colourless, contains few to many lipid droplets 1–2 µm in size and 3–5 µm-sized food vacuoles with loose contents, some with only one bacterial rod (Fig. 92b). Moves moderately fast, swims, glides, and climbs on microscope slides and soil particles, respectively.

Cilia in vivo about 7 µm long, arranged in 12, rarely in 11 ordinarily to widely spaced, slightly spiral rows distributed as follows (Fig. 92b, c, e, g–j, 93a–h, j, k, 94e–s; Table 35): rows 2–4 on right side; rows 5 and 6 on margins of dorsal side; rows 7–9 on left side, 8 and 9 often difficult to recognize because consisting of only 1–3 dikinetids, one of these rows lacking in specimens with only 11 rows; rows 10, 11, and 1 postoral on ventral side. Rows 2, 5, and 6 unshortened, the rest shortened anteriorly (postoral rows) or posteriorly; rows 3 and 4 strongly shortened (but see

Remarks), 3 usually ends slightly posterior of mid-body, 4 usually slightly anterior of mid-body (Fig. 92c, i, j, 93a–d, 94k–p; Table 35). Dikinetal distances gradually increase from anterior to posterior, those of row 2 condensed in oral region; total number of dikinetids 44–62, on average

53 (Table 35). Two caudal cilia very likely associated with last dikinetid of row 2, about 15 µm long with filamentous distal half (Fig. 92b, j, 93i).

Silverline pattern colpodid. Meshes of right body side transverse-quadrangular, even in unciliated areas; those of left side quadrangular or slightly polygonal (Fig. 92e, g–j, 93a–h, 94k–s).

Oral apparatus in anterior third of cell, buccal cavity funnel-shaped, about 7 µm deep, usually with distinct preoral bulge closing preoral suture (Fig. 92b, c, i; and SEM micrographs of a *P. steinii*-like population, Fig. 95i, j, m, o). Right oral polykinetid lunate, composed of about seven convex rows of 3 µm long cilia, very likely without dikinetal row at dorsal margin. Left oral polykinetid about 5 × 3 µm in size, spatulate, usually composed of 10 ciliary rows with 6 µm long cilia forming a distinct beard (Fig. 92a, b, j, 93a, b, i, j, 94e–h; Table 35).

Resting cyst: Resting cysts colourless to yellowish, globular, on average 12.3 × 11.6 µm in size (M = 12/12, SD = 1.4/1.3, SE = 0.3/0.3, CV = 11.2/10.8, Min = 10/10, Max = 14/14, n = 19). Wall composed of three distinct layers (Fig. 92f, 93l–q): ectocyst about 0.3 µm thick, slightly to distinctly yellowish, surface slightly wrinkled and indistinctly pustulate. Endocyst compact and rather refractive, about 0.5 µm thick, colourless. Between ecto- and endocyst a clear, 1–2 µm wide zone, possibly the mesocyst. Cytoplasm studded with about 0.5 µm-sized granules covering the macronucleus and rather many pale globules about 2 µm across, possibly autophagous vacuoles. Central nucleolus of macronucleus maintained, ciliary rows likely resorbed.

Remarks: The most similar species, *P. steinii,* has an enormous variability when literature data are compared (for a review, see Foissner 1993a). Part of this variability might be caused by the preparation methods used, the exactness of the observations and, possibly, by mixing different species. Thus, we compared *P. lajacola* with a *P. steinii* population cultivated (non-flooded Petri dish method), impregnated (Chatton-Lwoff silver nitrate), and analyzed with the same methods (Table 35).

Morphological comparison: There is only one species, *P. steinii* (reviewed in Foissner 1993a), that strongly resembles *P. lajacola*, i. e., has a similar body size and nuclear apparatus, 12 somatic kineties and two elongated caudal cilia, and a spatulate left oral polykinetid. Indeed, there is only one distinct morphological difference, viz., the preoral bulge which is absent from the described populations of *P. steinii*. However, we found a supposed *P. steinii* population with a distinct bulge in Austria (Fig. 95i–p). These specimens are also almost fully ciliated, suggesting that they belong to an undescribed species.

A second feature is the resting cyst which is different from that of *P. steinii* when compared with most literature data and Figure 70f in Foissner (1993a) where the wall consists of two tightly spaced, compact zones while endocyst and ectocyst are separated by a wide space in *P. lajacola* (Fig. 93l–q). However, Ruthmann & Kuck (1985) described a cyst wall highly similar to that of *P. lajacola* in a German population of *P. steinii.* Unfortunately, the interphase morphology of the Ruthmann population is unknown.

Morphometric comparison (Table 35): Most morphometric features of *P. lajacola* are very similar to those of *P. steinii*, e. g., the number of ciliary rows on body and in the left oral polykinetid as

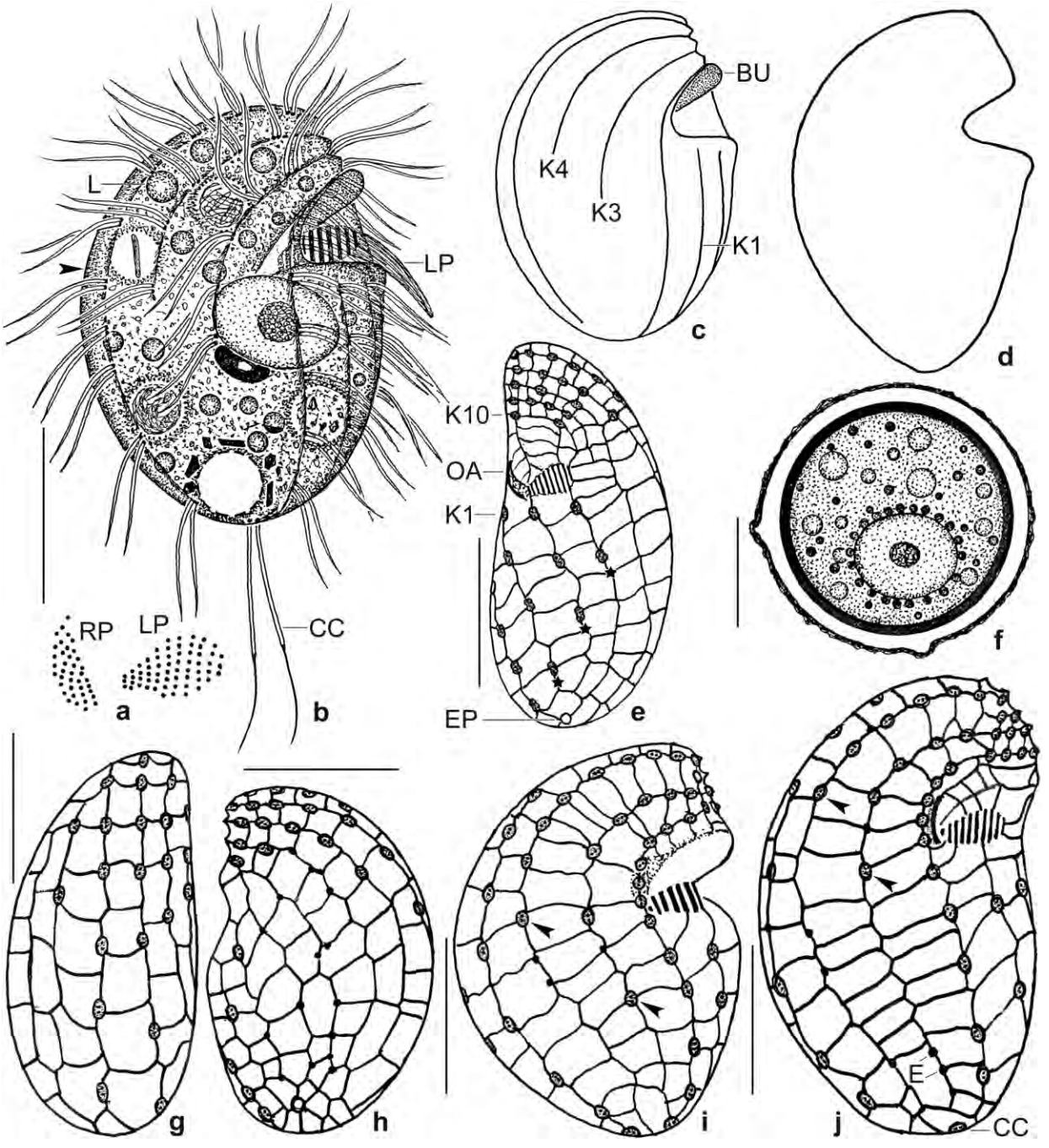

Fig. 92a–j. *Paracolpoda lajacola* from life (b, c, f) and after silver carbonate (a) and Chatton-Lwoff silver nitrate (e, g–j) impregnation. **a:** Oral polykinetids redrawn from Fig. 94e, h. **b, c:** Right side overviews of a representative specimen, length 25 µm. Frequently, some food vacuoles contain only a single bacterial rod (arrowhead). Kineties 3 and 4 are strongly shortened. **d:** A specimen bluntly pointed posteriorly. **e:** Ventral view, showing the three postoral kineties (asterisks). **f:** A four-weeks-old resting cyst. The macronucleus is frequently covered by refractive lipid droplets. **g, h:** Dorsal and left side kinetid and silverline pattern. **i:** Right side kinetid and silverline pattern of holotype specimen, length 26 µm. Kineties 3 and 4 are distinctly shortened (arrowheads). **j:** Ventrolateral view of a large specimen with strongly shortened kineties 3 and 4 (arrowheads). CC – caudal cilia, BU – bulge, E – extrusomes, EP – excretory pore, K1, 3, 4, 10 – somatic kineties, L – lipid droplet, LP – left oral polykinetid, OA – oral apparatus, RP – right oral polykinetid. Scale bars 5 µm (f) and 10 µm (b, c, e, g–j).

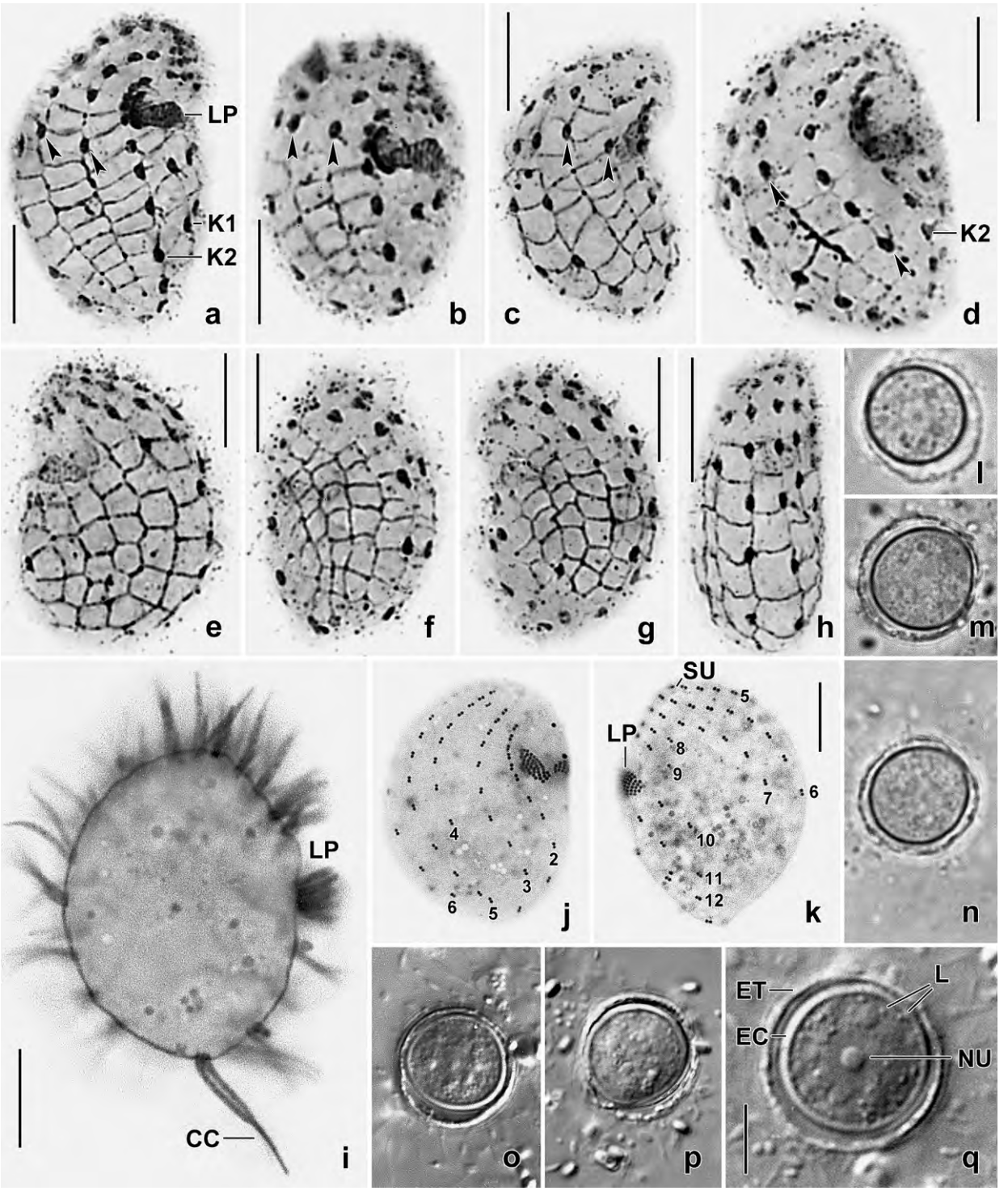

Fig. 93a–q. *Paracolpoda lajacola* from life (l–q) and in Chatton-Lwoff silver nitrate (a–h) and slightly squashed silver carbonate (i–k) preparations. **a–d:** Right side views, showing the silverline pattern and the strongly shortened kineties 3 and 4 (arrowheads). **e–g:** The left side is only marginally ciliated. **h:** Dorsal view, showing cell flattening. **i:** Caudal cilia**. j, k:** Kinetid pattern. Kineties 3 and 4 are longer than in silver nitrate preparations (a–d; see text). **l–q:** Four-weeks-old resting cysts. CC – caudal cilia, EC – endocyst, ET – ectocyst, K(1–12) – kineties, L – lipid droplets, LP – left oral polykinetid, NU – nucleolus, SU – preoral suture. Scale bars 5 µm (q) and 10 µm (a–k).

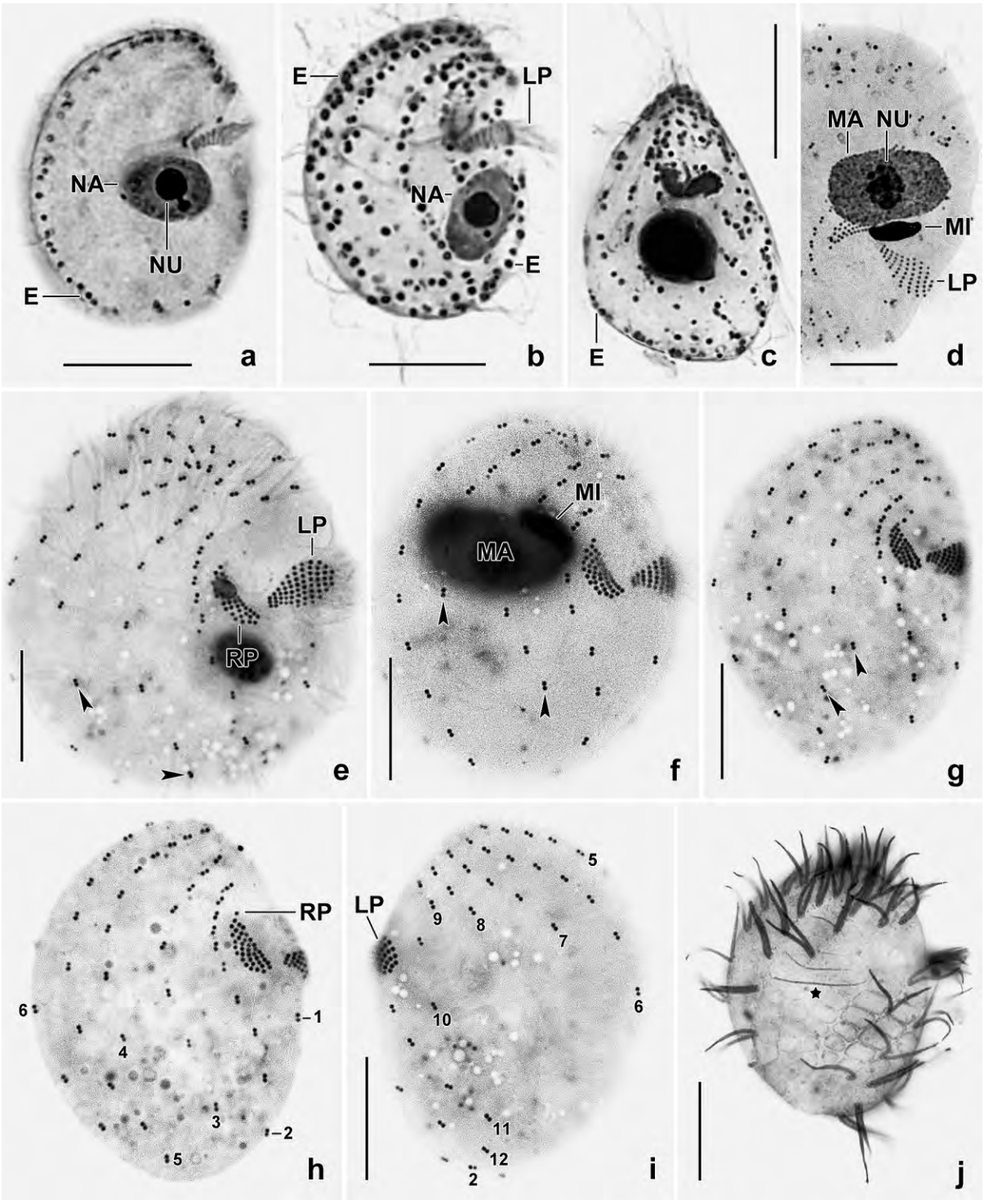

Fig. 94a–j. *Paracolpoda lajacola* after protargol preparation (a–c) and in pressed silver carbonate (d–j) impregnations. **a–d:** Right side (a, b, d) and ventral (c) views, showing nuclear and extrusome pattern. **e–g, j:** Right side kinetid and ciliary pattern. Arrowheads mark end of kineties 3 and 4 whose last kinetids are not ciliated causing a large, barren area (j, asterisk). **h, i:** Right and left side kinetid pattern with kineties numbered. E – extrusomes, K1–12 – somatic kineties, LP – left polykinetid, MA – macronucleus, MI – micronucleus, NA – nuclear apparatus, NU – nucleolus, RP – right polykinetid. Scale bars 10 µm.

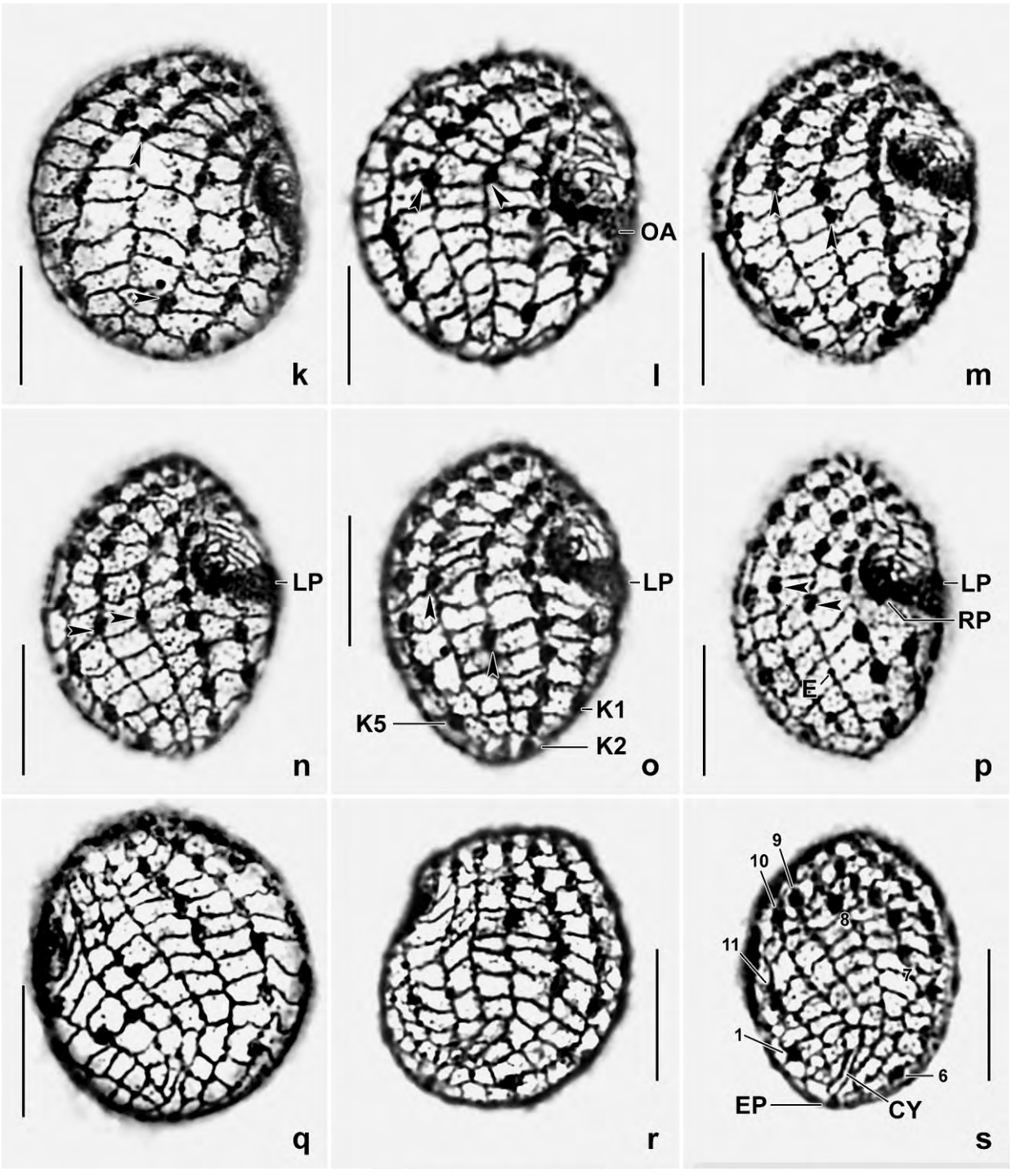

Fig. 94k–s. *Paracolpoda lajacola* after Klein-Foissner silver nitrate impregnation. Numerals denote somatic ciliary rows (kineties). **k–p:** Right side views, showing the colpodid silverline pattern and the distinctly shortened kineties 3 and 4 marked by arrowheads, except for specimens shown in (k, o) which have kinety 3 only slightly shortened. **q–s:** Left side views, showing the silverline pattern and the strongly shortened kineties 7–11 (s), producing a large, barren area. CY – cytopyge, EP – excretory pore of contractile vacuole, K(1–11) – somatic kineties (ciliary rows), LP – left oral polykinetid, OA – oral apparatus, RP – right oral polykinetid. Scale bars 10 µm.

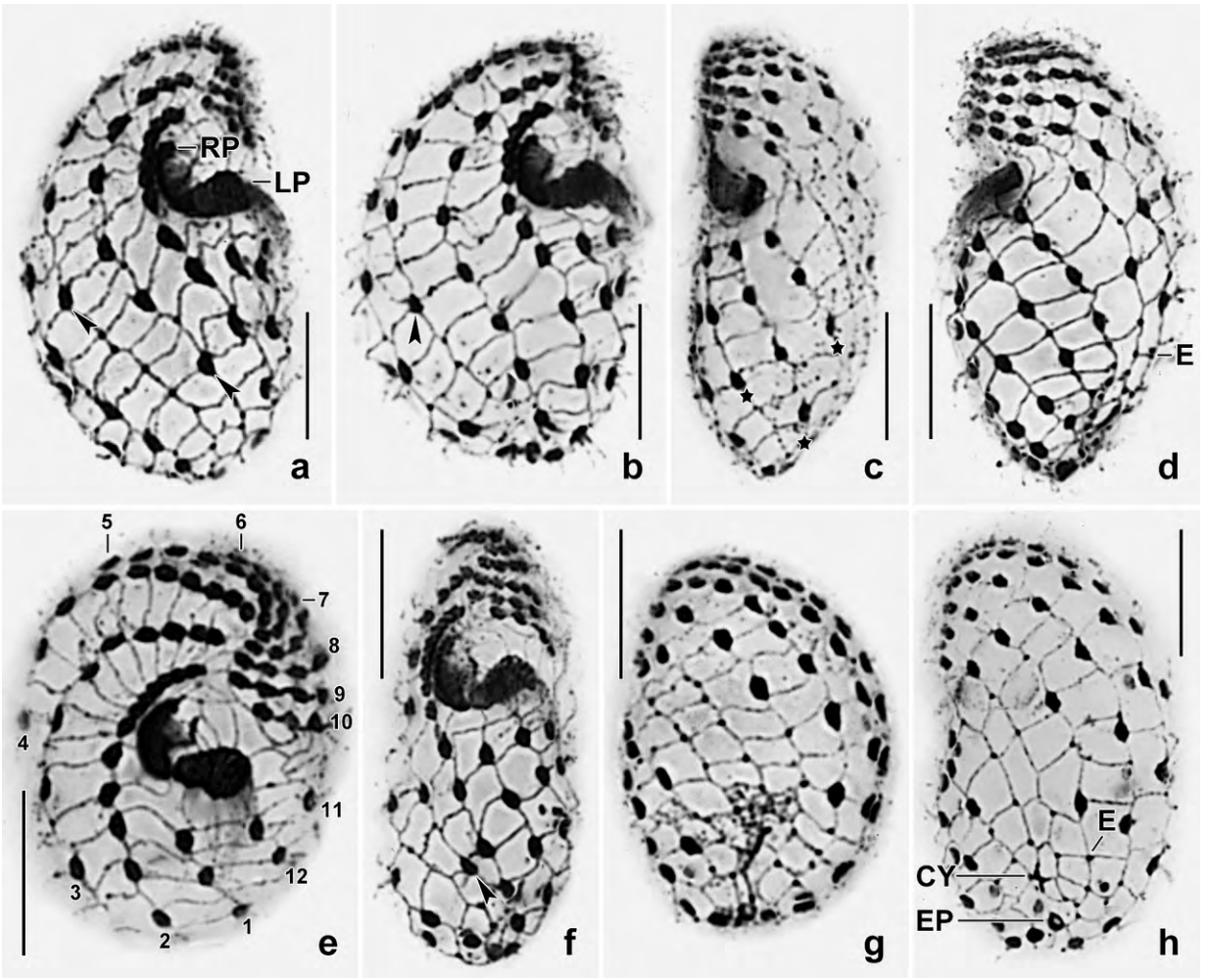

Fig. 95a–h. *Paracolpoda steinii* after Chatton-Lwoff silver nitrate impregnation. **a, b:** Right side views with shortened kineties marked by arrowheads. The (b) specimen has an unshortened row 3. **c, d:** Ventrolateral views, showing the three postoral kineties (asterisks) **e:** Oblique anterior polar view, showing the 12 ciliary rows (numerals). **f:** Ventral view of a specimen with slightly shortened kinety 3 (arrowhead). **g, h:** Left side views. CY – cytopyge, E – extrusomes, EP – excretory pore of contractile vacuole, LP – left oral polykinetid, RP – right oral polykinetid. Scale bars 10 µm.

well as the structure and size of the macronucleus and micronucleus. Actually, we found only three rather different features, viz., body size, the total number of somatic dikinetids, and the number of shortened right side kineties. Body size (~ 25 × 18 µm vs. 30 × 19 µm) and length:width ratio (1.4:1 vs. 1.6:1) are smaller in *P. lajacola* than in *P. steinii,* which is corroborated by literature data (Foissner 1993a). This applies also to distances and sizes correlated with body size, viz., distance from anterior body end to nuclear apparatus and to posterior end of ciliary rows, depth of buccal cavity, and length and width of left oral polykinetid. The number of dikinetids is clearly different in most ciliary rows, and thus also the total number (53 vs. 89, 68%; Table 35). This is recognizable also in the literature (Foissner 1993a). *Paracolpoda lajacola* has kineties 3 and 4 strongly shortened posteriorly while *P. steinii* has shortened only row 4 (Foissner 1993a). However, in silver carbonate preparations of *P. lajacola*, kineties 3 and 4 are less distinctly shortened than in protargol and silver nitrate preparations (cp. Fig. 93e–h vs. 92b–d, 93k–p). Thus, the additional kinetids are not ciliated, producing a large barren area on right side (Fig. 94j).

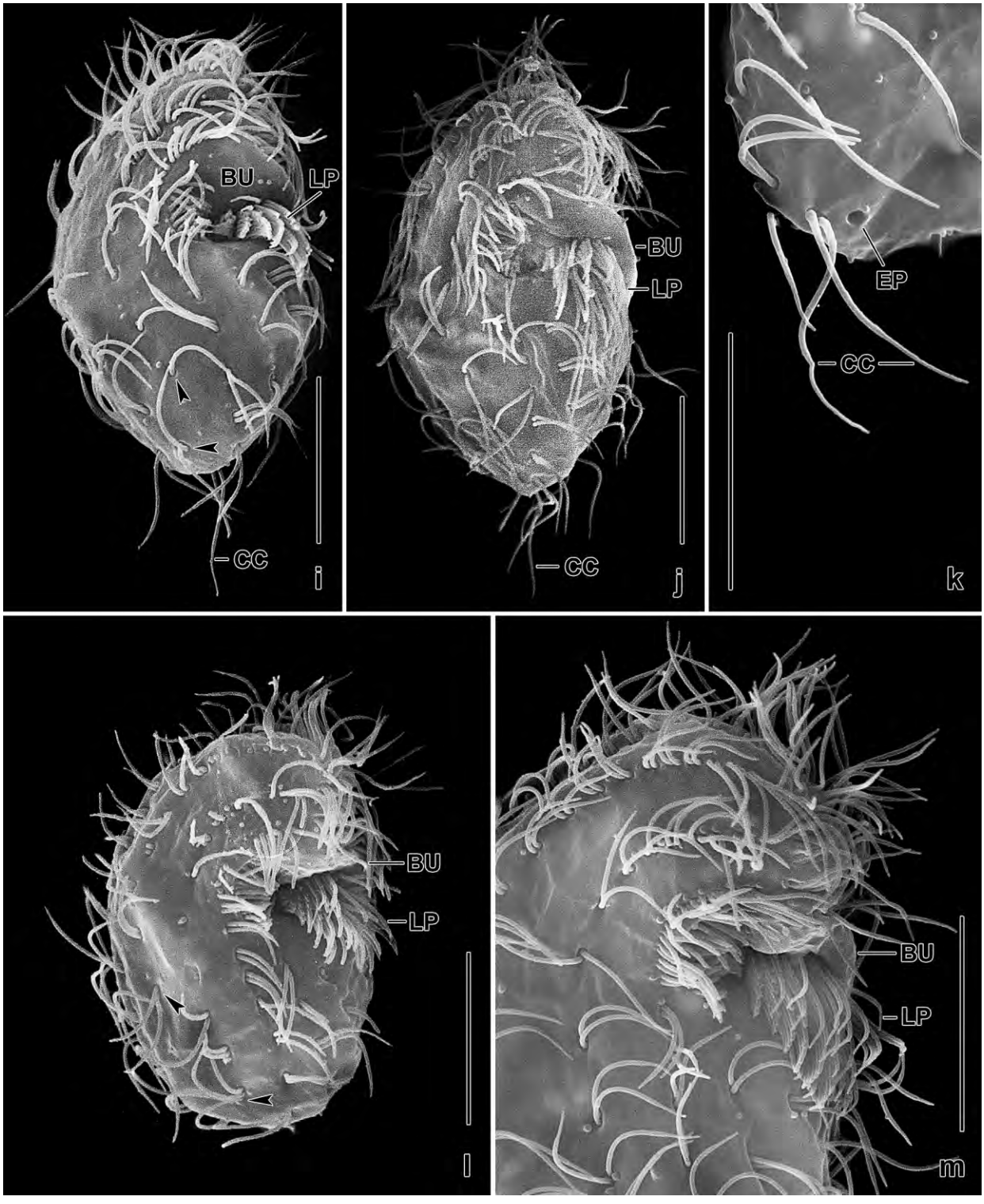

Fig. 95i–m. *Paracolpoda steinii* (?) in the scanning electron microscope. This population, which is from the surroundings of the village of Hüttschlag in Salzburg, has a distinct preoral bulge and equally long caudal cilia (k), as *P. lajacola*. Kineties 3 and 4 are shortened or unshortened (arrowheads; see also Fig. 95o). BU – oral bulge, CC – caudal cilia, EP – excretory pore of contractile vacuole, LP – left oral polykinetid. Scale bars 10 µm.

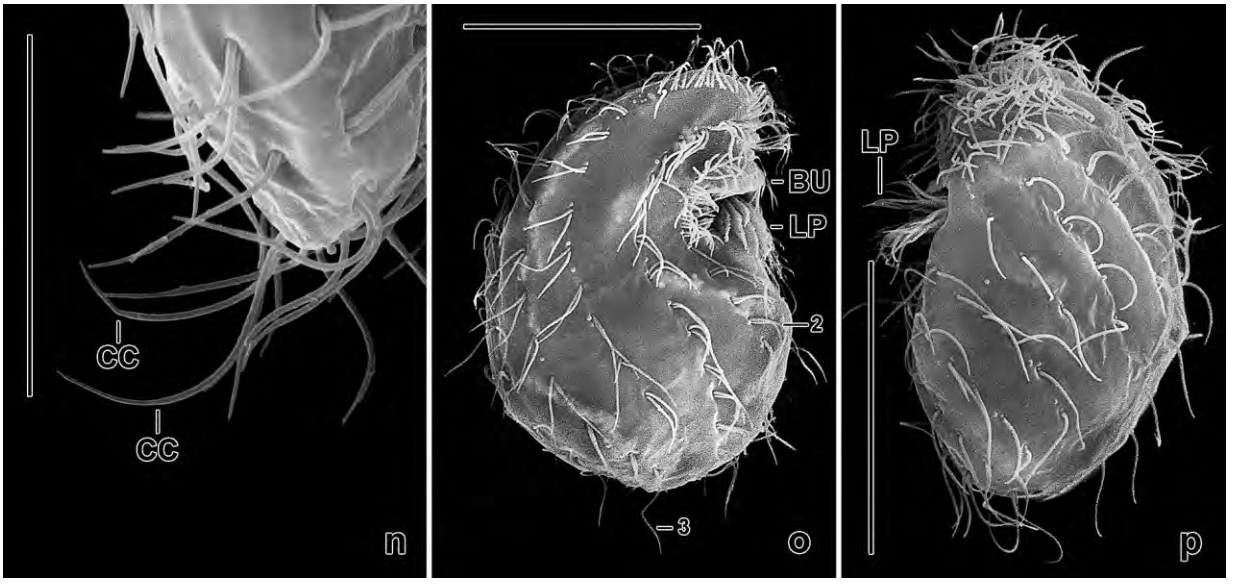

Fig. 95n–p. *Paracolpoda steinii* (?), Hüttschlag population in the scanning electron microscope. **n:** The two caudal cilia have the same length. **o:** Right side view of a specimen with unshortened kineties 3 and 4. **p:** The left side is almost completely ciliated. The distinct oral bulge and the hardly reduced ciliature suggest this population as an undescribed species. BU – preoral bulge, CC – caudal cilia, LP – left oral polykinetid, 2, 3 – kineties. Scale bars 10 µm (n) and 20 µm (o, p).

To sum up, *P. lajacola* and *P. steinii* differ in the following features: body size (usually about 25 × 18 vs. 30 × 19 µm); the preoral bulge (present vs. usually absent or indistinct); the length of the individual ciliary rows (most strongly reduced posteriorly vs. some strongly reduced), especially of kineties 3 (distinctly shortened vs. unshortened) and 4 (ends anterior vs. posterior of mid-body, Fig. 92c); and the total number of somatic dikinetids (53 vs. 89, Table 35). In spite of these differences, we cannot exclude that *P. lajacola* is a variation of *P. steinii*, which is either highly variable or is a complex of cryptic species.

Occurrence and ecology: As yet found only at type locality, i. e., an ephemeral lithotelma.

Emarginatophrya nov. gen.

Diagnosis: Hausmanniellidae with distally emarginated left oral polykinetid.

Type species: *Emarginatophrya terricola* nov. spec.

Species assignable: *Emarginatophrya aspera (*Kahl, 1926) nov. comb. (basionym: *Colpoda aspera* Kahl, 1926), *E. terricola* nov. spec.

Etymology: *Emarginatophrya* is a composite of the Latin adjective e*marginatus* (shallowly notched usually at tip) and the Greek noun *ophrya* (eyebrow ~ cilia ~ ciliate), referring to the emarginated left oral polykinetid. Feminine gender.

Remarks: There are now two species with an emarginated left oral polykinetid: *Emarginatophrya aspera* (Fig. 96c, d) and *E. terricola* (Fig. 96a, b, 97a, b). The first is likely a cosmopolitan while the second has been found as yet only in Venezuela.

The classification of *Emarginatophrya* into the Hausmanniellidae is based on Foissner et al. (2011, 2014b), who assume a fast radiation of *Colpoda*, several species of which then evolved independently, forming new species and genera. Possibly, *Colpoda elliotti* belongs also to this clade because it unites with *E. aspera* in trees made of only colpodids s. str. (Foissner et al. 2011). Morphologically, *C. elliotti* is very similar to *E. aspera* but its left oral polykinetid is not emarginated (Foissner 1993a).

Emarginatophrya terricola nov. spec. (Fig. 96a, b, 97a–c; Table 36)

Diagnosis: Size in vivo about 45 × 28 µm; ellipsoid. Single macronucleus and micronucleus. On average 19 slightly spiral somatic ciliary rows, kinety 2 with a perioral ciliary condensation. Right oral polykinetid composed of about 20 kineties, left of an average of 14 kineties of which 4 are emarginated.

Type locality: Venezuelan site (56), i. e., mud and soil from temporary grassland puddles in the surroundings of the village of Chichiriviche, Morrocoy National Park, 67°13'W 11°33'N.

Type material: 1 holotype and 2 paratype slides with a total of 4 protargol-impregnated specimens, marked by black ink circles on the coverslip, have been deposited in the Biology Centre of the Upper Austrian Museum in Linz (LI).

Table 36. Morphometric data on *Emarginatophrya terricola* based on mounted and protargol-impregnated specimens from a non-flooded Petri dish culture. Measurements in µm. CV – coefficient of variation in %, M – median, Max – maximum, Mean – arithmetic mean, Min – minimum, n – number of individuals investigated, SD – standard deviation, SE – standard error of arithmetic mean.

Characteristics	Mean	M	SD	SE	CV	Min	Max	n
Body, length	38.3	38.0	5.9	2.9	15.3	32.0	45.0	4
Body, width	24.0	23.5	3.7	1.9	15.6	20.0	29.0	4
Body length:width, ratio	1.6	1.6	0.3	0.2	20.7	1.3	2.0	4
Anterior body end to right oral polykinetid, distance	9.8	9.5	1.0	0.5	9.8	9.0	11.0	4
Anterior body end to end of right oral polykinetid, distance	17.3	17.0	2.2	1.1	12.8	15.0	20.0	4
Anterior body end to macronucleus, distance	17.5	17.0	5.0	2.5	28.6	12.0	24.0	4
Macronucleus, length	11.0	11.5	1.4	0.7	12.9	9.0	12.0	4
Macronucleus, width	7.8	7.5	1.0	0.5	12.3	7.0	9.0	4
Micronucleus, large axis	2.1	2.1	–	–	–	2.0	2.3	4
Ciliary rows, number	19.0	19.0	0.8	0.4	4.3	18.0	20.0	4
Somatic kinety 3, number of dikinetids	25.3	24.0	6.4	3.2	25.3	20.0	33.0	4
Mouth, width [a]	10.8	10.5	1.0	0.5	8.9	10.0	12.0	4
Left oral polykinetid, number of long rows	10.3	10.5	1.0	0.5	9.3	9.0	11.0	4
Left oral polykinetid, number of short rows	3.8	4.0	–	–	–	3.0	4.0	4
Left oral polykinetid, total number of ciliary rows	14.0	14.0	0.8	0.4	5.8	13.0	15.0	4

[a] Distance from right margin of right polykinetid to left margin of left polykinetid.

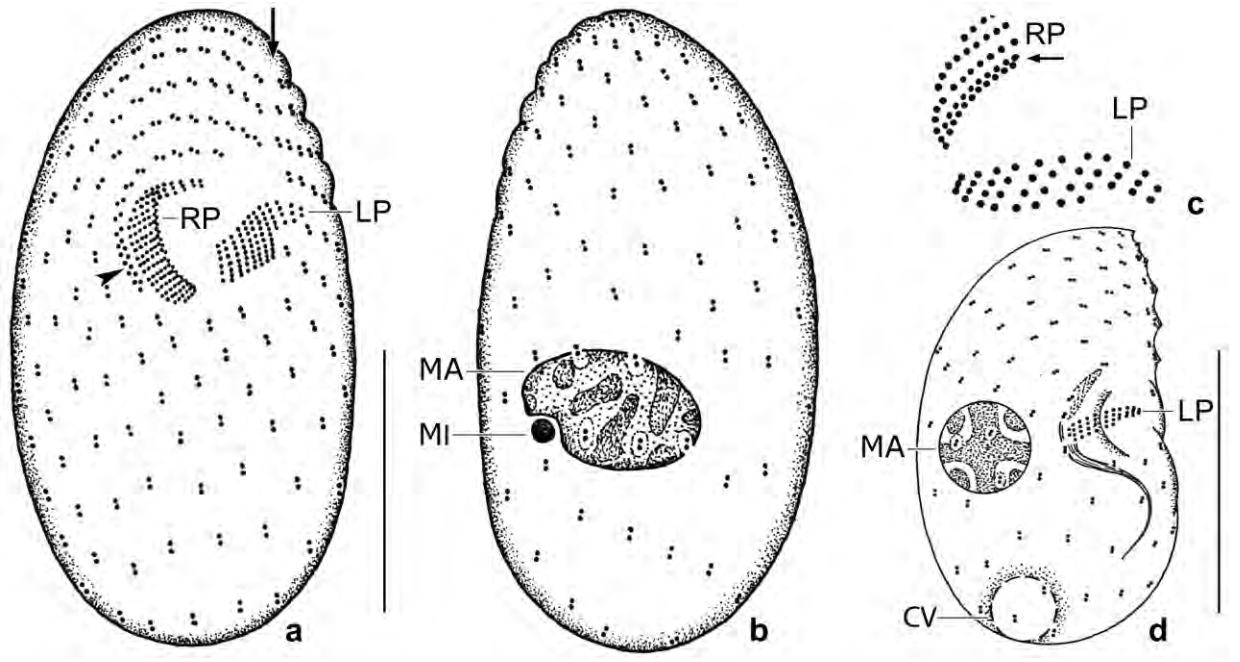

Fig. 96a–d. *Emarginatophrya terricola* (a, b) and *E. aspera* (c, d; from Foissner 1993a, modified) after protargol impregnation. **a, b:** Ventral and dorsal view of holotype specimen, length 36 µm. Note the dikinetal row at the dorsal margin of the right oral polykinetid and the conspicuous emargination in the left polykinetid. The arrow marks the preoral suture; the arrowhead denotes the perioral ciliary condensation. **c:** Oral structures of *E. aspera* with dorsal dikinetal row marked by arrow. **d:** Right side overview. CV – contractile vacuole, LP – left oral polykinetid, MA – macronucleus, MI – micronucleus, RP – right oral polykinetid. Scale bars 15 µm.

Etymology: The Latin species-group name *terricola* (living in soil) refers to the habitat the species was discovered.

Description: We found only four specimens in the protargol slides, and we did not recognize the species in the non-flooded Petri dish culture. Thus, in vivo observations are lacking. In spite of this, we describe this population because (i) it has a clear identity, (ii) the chance is small that this rare species is refound, and (iii) the preparation is excellent.

Size in vivo about 37–52 × 23–33 µm, on average 45 × 28 µm, when adding 15% preparation shrinkage (Table 36). Body broadly ellipsoid to indistinctly ovate; unflattened (Fig. 96a, 97a, b). Nuclear apparatus on average in mid-body (Fig. 96b, 97a, b; Table 36). Macronucleus globular to broadly ellipsoid, with oblong nucleoli up to 5 µm in size. Micronucleus attached to macronucleus, globular. Cytoplasm studded with argyrophilic granules 1–2 µm across, especially in posterior body region (Fig. 97a–c).

Somatic ciliature typical colpodid, i. e., composed of dikinetids forming an average of 19 slightly spiral rows commencing at preoral suture and postorally; first ciliary row right of oral apparatus with a perioral ciliary condensation (Fig. 96a, b, 97a–c; Table 36).

Oral apparatus also typical colpodid, i. e., in anterior body half and with two conspicuous polykinetids (Fig. 96a, 97a, b; Table 36). Right polykinetid composed of about 20 slightly oblique, short rows dorsally limited by a row of dikinetids. Left polykinetid composed of an average

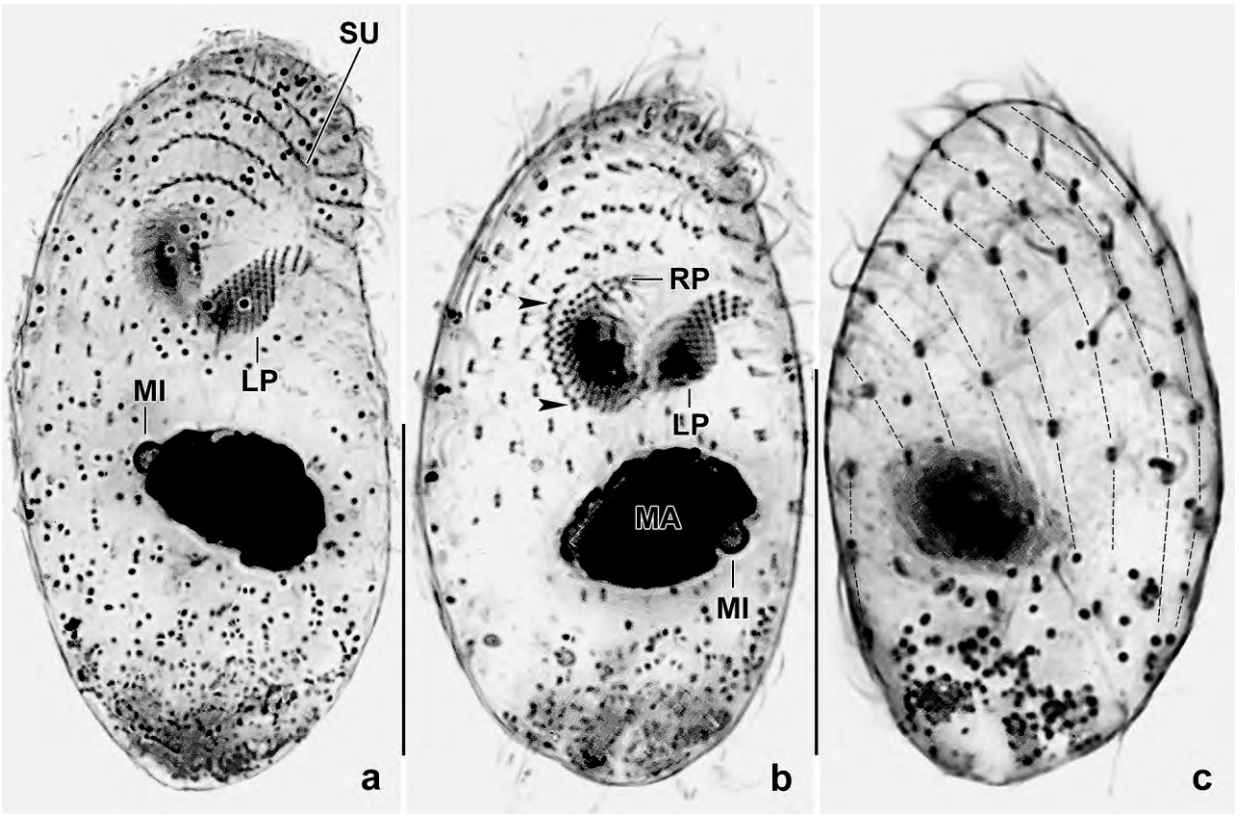

Fig. 97a–c. *Emarginatophrya terricola* after protargol impregnation. The specimens are studded with argyrophilic granules some of which have been removed to clear the ciliary pattern. **a:** Ventral view of a paratype specimen, showing the emarginated left oral polykinetid. **b, c:** Ventral and dorsal view of holotype specimen, length 36 µm. Note the oral polykinetids and the perioral ciliary condensation (arrowheads). LP – left oral polykinetid, MA – macronucleus, MI – micronucleus, RP – right oral polykinetid, SU – preoral suture. Scale bars 20 µm.

of 14 comparatively long ciliary rows of which 3–4 are shortened, producing the emarginate appearance of the organelle (Fig. 96a, 97a, b). Oral cavity large but shallow.

Occurrence and ecology: As yet found only at type locality where it was very rare. As the sample includes dry mud from the ephemeral ponds, we cannot exclude that *E. terricola* occurs also in limnetic and/or semiterrestrial habitats.

Remarks: This is a very distinct species due to the emarginated left oral polykinetid. Nothing similar has been described before (for a review, see Foissner 1993a).

Apoavestina nov. gen.

Diagnosis: Very small Hausmanniellidae (?) with slightly concave, open oral field and bipartite, staggered left oral polykinetid. Right oral polykinetid composed of slightly disordered basal bodies and a row of dikinetids. Pharyngeal fibres extend laterally and anteriorly.

Type species: *Apoavestina amazonica* nov. spec.

Etymology: Composite of *apo* (derived from) and the generic name *Avestina*. Feminine gender.

Remarks: Of all members of the order Colpodida, *A. amazonica* is unique in having a bipartite, staggered left oral polykinetid. Further, the proximal ribbon of the left polykinetid is unique in having two distinctly elongated rows of monokinetids (Foissner 1993a, Foissner et al. 2002). These features are so outstanding that generic separation is natural. There is some similarity with *Bardeliella pulchra* in which the long left polykinetid consists of a bryometopid anterior portion and a colpodid posterior portion, i. e., the polykinetid is bipartite structurally (Foissner et al. 2011).

Family classification of *Apoavestina* is difficult but we are rather sure that it belongs either to the Hausmanniellidae, the Colpodidae, or to still undefined families embracing either *Paracolpoda steinii* and *Bromeliothrix metopoides* Foissner, 2010 or → *Emarginatophrya aspera,* → *Microcolpoda bambicola,* and *Hausmanniella*. This is suggested by morphological similarities and gene sequence data (Foissner et al. 2011). *Paracolpoda steinii*, *Bromeliothrix metopoides*, and *A. amazonica* have a similar somatic ciliary pattern, a central nucleolus in the macronucleus, extrusomes invisible in vivo, and anteriorly extending pharyngeal fibres. → *Emarginatophrya aspera*, *Hausmanniella discoidea*, and *A. amazonica* have a similar ciliary pattern and, if *Avestina* and → *Microcolpoda bambicola* are included, a flat, open oral field and a minute body size. See Foissner (1993a) for the genera mentioned.

Apoavestina amazonica nov. spec. (Fig. 98a–h, 99a–i; Table 37)

Diagnosis: On average 25 × 18 µm in vivo. Outline semicircular with slightly sigmoidal or convex ventral side, preoral suture with 4 distinct teeth. Macronucleus broadly elliptic, about 6 × 4 µm in vivo, very transparent, with minute central nucleolus. Micronucleus lenticular, compact, about 4 × 2 µm in size. Extrusomes intrakinetal, about 1 µm across, recognizable only in preparations. On average10 ciliary rows, ciliature anteriorly condensed in kineties 2–4; 2 slightly elongated caudal cilia. Proximal ribbon of left oral polykinetid composed of 6 kineties, forming a cuneate pattern due to 2 distinctly elongated distal rows; distal ribbon of polykinetid slightly convex, composed of 5 rows slightly decreasing in length distally.

Type locality: Soil from the Anavilhanas peninsula in the Rio Negro, vicinity of Ariau lodge, Manaus, Brazil, 60°W 4°S.

Etymology: Named after the region (Amazon) the species was discovered.

Type slides: 1 holotype and 3 paratype slides with protargol-impregnated specimens have been deposited in the Biology Centre of the Upper Austrian Museum in Linz (LI). The holotype and other relevant specimens have been marked by black ink circles on the coverslip.

Description: We found merely 13 specimens in 8 protargol slides, and only some were well impregnated. However, together with the detailed live observations the species could be well defined.

Table 37. Morphometric data on *Apoavestina amazonica* based on mounted and protargol-impregnated (FOISSNER's method) specimens from a non-flooded Petri dish culture. Measurements in µm. CV – coefficient of variation in %, M – median, Max – maximum, Mean – arithmetic mean, Min – minimum, n – number of specimens investigated, SD – standard deviation, SE – standard error of mean.

Characteristics	Mean	M	SD	SE	CV	Min	Max	n
Body, length	24.0	24.0	2.8	0.8	11.6	20.0	28.0	11
Body, width	16.7	16.0	2.3	0.7	13.7	13.0	21.8	11
Body length:width, ratio	1.5	1.4	0.2	0.1	10.4	1.3	1.8	11
Anterior end to right oral polykinetid, distance	7.7	8.0	0.8	0.3	11.0	6.0	9.0	11
Anterior end to end of right oral polykinetid, distance	12.0	12.0	1.7	0.5	14.4	10.0	15.0	11
Anterior end to proximal end of proximal ribbon of left oral polykinetid, distance	13.9	14.0	1.3	0.4	9.4	2.0	16.0	11
Anterior end to distal ribbon of left oral polykinetid, distance	8.1	8.0	0.6	0.2	7.1	7.0	9.0	11
Anterior end to macronucleus, distance	12.0	12.0	1.8	0.5	14.9	10.0	15.0	11
Macronucleus, length	5.4	5.5	0.9	0.3	16.7	4.0	7.0	11
Macronucleus, width	3.5	3.5	–	–	–	3.0	4.0	11
Somatic cilia, length	7.4	7.0	–	–	–	7.0	8.0	9
Caudal cilia, length	10.3	10.0	1.0	0.4	10.0	9.0	12.0	6
Ciliary rows, number	10.3	10.0	1.0	0.4	9.3	9.0	12.0	7
Dikinetids, number in kinety 2	16.7	17.0	2.6	1.0	15.7	13.0	20.0	7
Dikinetids, number in kinety 3	11.0	11.0	0.8	0.4	7.4	10.0	12.0	4
Kineties in proximal ribbon of left polykinetid, number	6.0	6.0	0.0	0.0	0.0	6.0	6.0	10
Kineties in distal ribbon of left oral polykinetid, number	5.0	5.0	0.0	0.0	0.0	5.0	5.0	5

Size in vivo 22–30 × 15–25 µm, usually about 25 × 18 µm, as calculated from some in vivo measurements and the morphometric data in Table 37 adding 15% preparation shrinkage. Shape inconspicuous, i. e., outline roughly semicircular or semielliptic with slightly sigmoidal ventral side; preoral suture with four distinct teeth (Fig. 98a, b, g, h, 99e–g). Nuclear apparatus usually posterior to mid-body (Fig. 98a, c, 99c–e, i; Table 37). Macronucleus about 6 × 4 µm in vivo, remarkable because very transparent and with a minute (~ 1.5 µm) central nucleolus, easily dislocated under slight coverslip pressure (Fig. 99c, d); often strongly distorted in protargol preparations being ellipsoid and wrinkled in 9 out of 13 specimens analysed; nucleoplasm with a diffuse reticulum. Micronucleus attached to macronucleus, comparatively large, viz., 4 × 2 µm and compact, thus more easily recognized than the macronucleus in vivo; lenticular, side attached to macronucleus slightly flattened; does not impregnate with the protargol method used. Contractile vacuole in posterior body end, excretory pore in pole centre (Fig. 98a, 99d). Extrusomes, likely a special kind of mucocysts, invisible in vivo but distinct in protargol preparations disturbing analysis of ciliary pattern; most within ciliary rows, discoidal with a diameter of about 1 µm (Fig. 99f); highly similar to those of *Paracolpoda steinii* and *Bromeliothrix metopoides* (FOISSNER 1993a, 2010a). Cytoplasm colourless, well-fed specimens dark at low magnification (× 100) because studded with food vacuoles 2–4 µm across; some minute crystals around contractile vacuole and some small lipid droplets scattered throughout plasm (Fig. 98a, 99a–d). Cytopyge not observed but fecal remnants frequently adhere to posterior pole area in well-fed specimens (Fig. 98g, h). Feeds on bacteria. Glides rapidly to and fro on microscope slide.

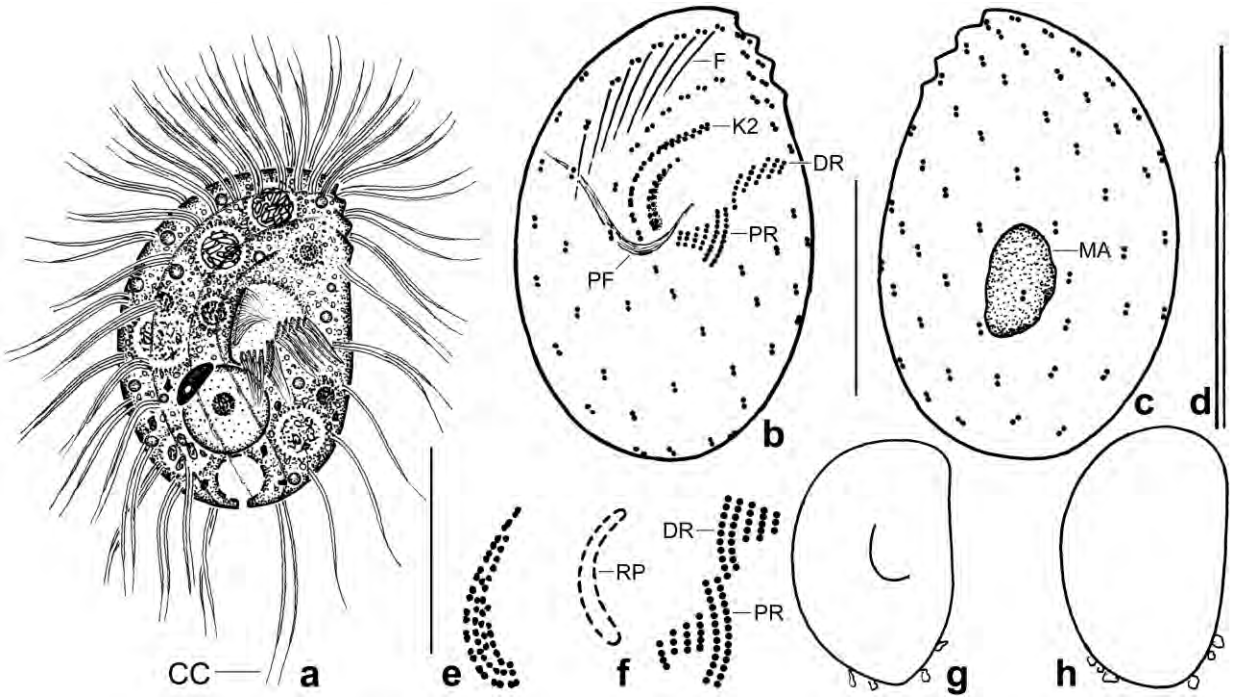

Fig. 98a–h. *Apoavestina amazonica* from life (a, d, e, g, h) and after protargol impregnation (b, c, f). **a:** Right side view of a representative specimen, length 25 µm. Note the nuclear apparatus, consisting of a lenticular, compact micronucleus and a transparent, globular macronucleus with a minute central nucleolus. **b, c:** Ciliary pattern of right and left side and macronucleus of holotype specimen, length 21 µm. The micronucleus is not impregnated and the macronucleus is rather strongly distorted. Note the anteriorly directed pharyngeal fibres. **d:** The somatic cilia have a long, fine process. **e:** Right oral polykinetid, according to careful live observations. **f:** The oral infraciliature consists of a right polykinetid and a left polykinetid uniquely in two staggered parts: the proximal and the distal ribbon. **g, h:** Outline drawings of specimens packed with food vacuoles. Note fecal remnants adhering to the posterior pole area. CC – caudal cilia, DR – distal ribbon of left oral polykinetid, F – fibres, K2 – kinety 2, MA – macronucleus, PF – pharyngeal fibres, PR – proximal ribbon of left oral polykinetid, RP – right oral polykinetid. Scale bars 10 µm (b, c) and 15 µm (a).

Cilia in vivo about 10 µm long and thus almost half of body length, with a rather long and fine distal portion, usually arranged in 10 equidistant rows of which three to four originate postorally, last kinetid of kinety 2 with two slightly elongated caudal cilia; both the long somatic cilia and the caudal cilia confirmed in protargol preparations (Fig. 98a–c, 99a, e; Table 37). Kineties in typical *Colpoda* pattern, densely ciliated anteriorly, especially rows 2 to 4 having ciliated both basal bodies of the dikinetids throughout; postoral kineties and posterior half of left side kineties have ciliated only the posterior basal bodies; distances between kinetids gradually and distinctly increasing from anterior to posterior in all kineties Fig. 98b, c, 99a, b, e). Distinct, oblique fibres, very likely transverse microtubule ribbons, originate from anterior kinetids of kinety 4 (Fig. 98b, 99e).

Oral apparatus in middle third of cell and usually left of body´s midline, forming a roughly circular pattern about 5–7 µm across. Oral field without lip and thus open, slightly concave (Fig. 98a, b, 99a, b, e; Table 37). Cilia of polykinetids about 4 µm long in vivo. Right oral polykinetid narrow, colpodid according to careful live observations, i. e., composed of a row of dikinetids dorsally and of slightly disordered rows of monokinetids ventrally (Fig. 98e). Left oral polykinetid composed of two staggered ribbons: proximal ribbon within trough of oral field, distal ribbon on its margin and ahead of proximal one. Proximal ribbon invariably composed of

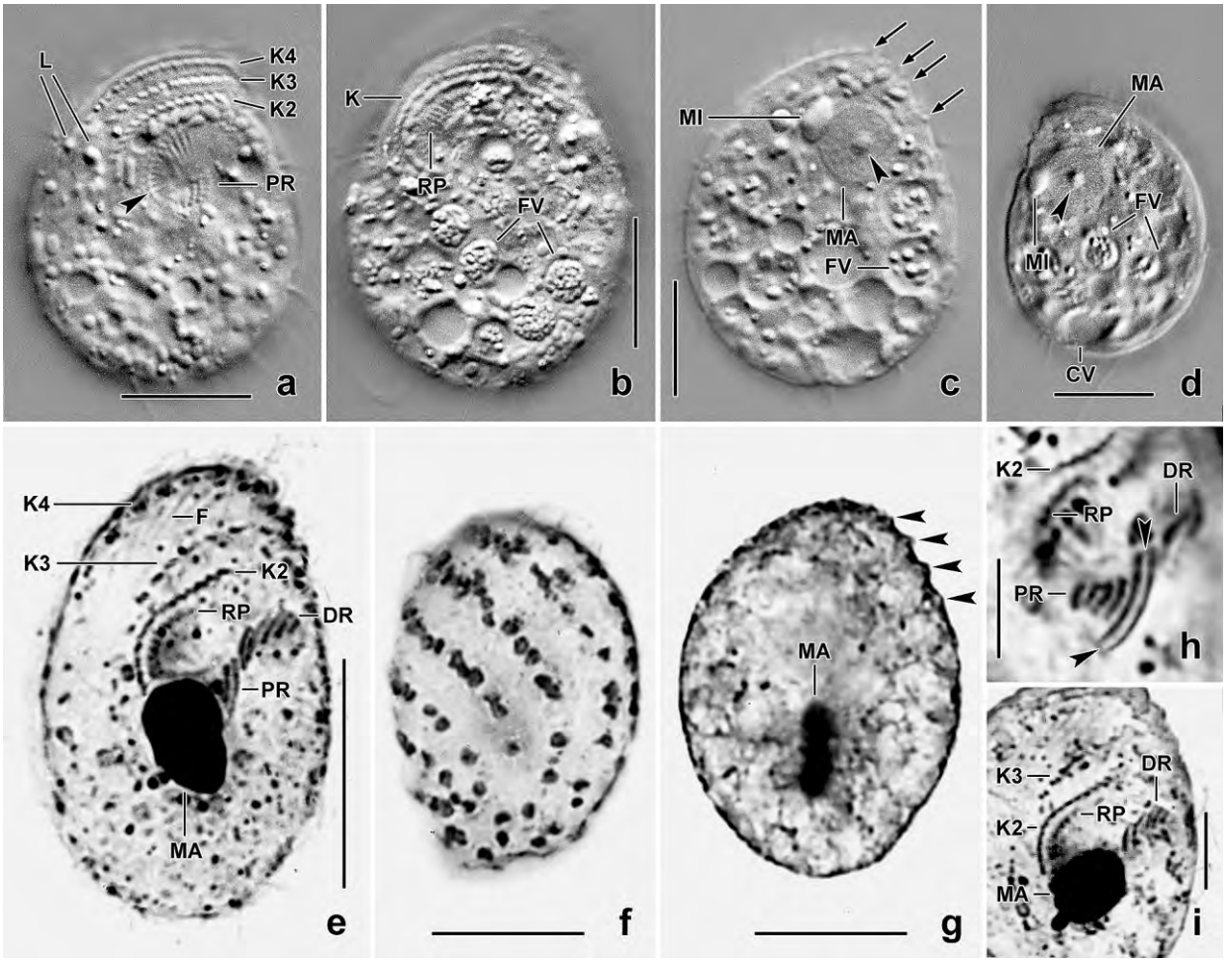

Fig. 99a–i. *Apoavestina amazonica* from life (a–d) and after protargol impregnation (e–i). **a, b:** Right side surface views of specimens slightly pressed by coverslip, showing part of the somatic and oral ciliary pattern. The arrowhead marks the right margin of the oral trough. **c, d:** Slightly pressed specimens, showing the remarkable nuclear apparatus dislocated anteriorly by coverslip pressure. The macronucleus is very transparent and has a minute central nucleolus (arrowheads) while the micronucleus is compact and comparatively large. **e, h, i:** Holotype (e) and paratype (h, i) specimens, showing the somatic and oral ciliary pattern of the right side. Note especially, the bipartite, staggered left oral polykinetid (e, h). The arrowheads in (h) limit the two elongated kineties of the proximal ribbon of the left oral polykinetid. **f:** Extrusome (mucocyst) pattern of left side. **g:** A broadly ellipsoid specimen, showing the four teeth of the preoral suture (arrowheads). CV – contractile vacuole, DR – distal ribbon of left oral polykinetid, F – fibres, FV – food vacuoles, K(2–4) – somatic kineties, L – lipid droplets, LP – left oral polykinetid, MA – macronucleus, MI – micronucleus, PR – proximal ribbon of left oral polykinetid, RP – right oral polykinetid. Scale bars 5µm (h, i), 10 µm (a–d), and 20 µm (e–g).

six rows of monokinetids: kineties 1–4 slightly and gradually increase in length from proximal to distal, kineties 5 and 6 distinctly elongated and slightly convex; distal ribbon slightly convex and invariably composed of five kineties decreasing in length from proximal to distal (Fig. 98a, b, f, 99a, b, e, h, i; Table 37). Pharyngeal fibres commencing in or near centre of oral cavity, first extend horizontally and then anteriorly, as in *Paracolpoda steinii* and *Bromeliothrix metopoides* (Fig. 98b; Foissner 1993a, 2010a).

Occurrence and ecology: As yet found only at type locality, i. e., in a seasonally flooded rainforest on a peninsula of the Rio Negro, just before it merges with the Rio Solimoes to become the great Amazon River. The sample consisted of about 50% leaf litter mixed with soil and fine roots from the root carpet extending in 5–7 cm soil depth. Soil brownish, crumbly, pH 5.1 in water.

Apoavestina amazonica and many other ciliate species were present already 48 h after rewetting the air-dried sample. The entire soil percolate from the non-flooded Petri dish culture was used for preparations; then the percolate was replaced by tap water. *Apoavestina amazonica* did not reappear, although many other species did and some new ones developed. Thus, *A. amazonica* is possibly an r-selected species. Further investigations are required to find out whether *A. amazonica* is a local or Gondwanan endemic.

Remarks: We did not find a described species that could be identical with *A. amazonica*. This species is so minute that live identification is very difficult, especially because it superficially resembles rather many small colpodeans, for instance, *Colpoda ecaudata*, → *Emarginatophrya aspera*, *Paracolpoda steinii*, *Avestina ludwigi*, *Orthokreyella schiffmanni*, *Kreyella muscicola*, *Microdiaphanosoma terricola*, and *Pseudokreyella* spp. (see Foissner 1993a for description of species). Thus, the identification should be checked in silver preparations.

Microcolpoda nov. gen.

Diagnosis: Minute, *Hausmanniella*-like ciliates with ventrolateral oral apparatus in anterior half of body. Somatic ciliary rows 2 and 3 very densely ciliated in anterior half, curve semicircularly around anterior margin of oral apparatus. Oral field moderately concave and open (without roof), ciliature thus exposed; right oral ciliary field composed of a single row of dikinetids, left of a typical polykinetid extending transversely to main body axis; with a long, basket-like pharynx commencing at right margin of oral ciliature. Silverline pattern colpodid.

Type species: *Microcolpoda bambicola* nov. spec.

Etymology: Composite of the Greek adjective *mikrós* (small) and the generic name *Colpoda* (bosom-shaped). Feminine gender.

Remarks: This minute ciliate is difficult to classify but likely more closely related to the Colpodina than to any other higher colpodean taxon. Within the Colpodina, *M. bambicola* resembles the Hausmanniellidae in having the mouth located ventro-laterally while it is on the right side in *Avestina*, a supposed hausmanniellid (Foissner 1993a). Further, *Avestina* spp. have the left oral polykinetid oriented obliquely to the main body axis while that of *M. bambicola* extends transversely, as in most small *Colpoda* species. Very likely, *Microcolpoda* and *Avestina* are closely related.

The phylogenetic position of *Microcolpoda* is difficult to find because it has a main feature each from the Hausmanniellidae (general organization, see Foissner 1993a) and the Sandmanniellidae Foissner & Stoeck, 2009 (a basket-like pharynx; see also → *Sandmannides venezuelensis*). The molecular analysis (Dunthorn et al. 2012, as *Kreyella*-like undesc. gen. & sp.) supports a hausmanniellid relationship because *Microcolpoda* forms a cluster with *Hausmanniella discoidea* and the minute → *Emarginatophrya aspera*. Thus, an oral basket-like pharynx is possibly plesiomorphic and remained in at least five groups: *Sandmanniella*, → *Sandmannides*, *Microcolpoda*, *Notoxoma*, and *Pseudochlamydonella* (for genera see → *Sandmannides* and Foissner 1993a).

Microcolpoda bambicola **nov. spec.** (Fig. 100a–l, 101a–l; Table 38)

Diagnosis: Size in vivo about 20 × 15 µm. Body outline semicircular to broadly reniform. Macro- and micronucleus globular. On average 11 somatic ciliary rows extending slightly spirally. Left oral polykinetid narrow, composed of an average of 9 ciliary rows.

Type locality: Mud from a bamboo stump along the Bowden Hill Road to the Hermitage dam, north of the town of Kingston, Jamaica, 79°46'W 18°5'N.

Type material: 1 holotype slide and 3 paratype slides with protargol-impregnated specimens, 6 paratype slides with Chatton-Lwoff silver nitrate-prepared cells, and 2 paratype slides with Klein-Foissner silver nitrate-impregnated specimens have been deposited in the Biology Centre of the Upper Austrian Museum in Linz (LI). The holotype and other relevant specimens have been marked by black ink circles on the coverslip.

Etymology: Composite of the generic name *Bambus*, the thematic vowel *i*, and the Latin verb *colere* (to live in), referring to the habitat the species was discovered.

Table 38. Morphometric data on *Microcolpoda bambicola* based on mounted, silver-impregnated specimens from a raw culture. Measurements in µm. CV – coefficient of variation in %, M – median, Max – maximum, Mean – arithmetic mean, Min – minimum, n – number of individuals investigated, P – protargol (FOISSNER's method), SD – standard deviation, SE – standard error of arithmetic mean, SN – silver nitrate after CHATTON-LWOFF.

Characteristics	Method	Mean	M	SD	SE	CV	Min	Max	n
Body, length	SN	19.3	20.0	1.9	0.4	9.7	15.0	22.0	21
Body, width	SN	14.6	15.0	1.8	0.4	12.0	11.0	17.0	21
Body length:width, ratio	SN	1.3	1.3	0.1	0.1	7.3	1.2	1.5	21
Body, length	P	16.0	16.0	1.7	0.4	10.5	12.0	18.0	21
Body, width	P	12.1	13.0	1.2	0.3	9.8	9.0	13.0	21
Body length:width, ratio	P	1.3	1.3	0.1	0.1	10.6	1.0	1.7	21
Anterior body end to macronucleus, distance	P	8.8	9.0	1.1	0.3	13.0	7.0	10.0	21
Anterior body end to right oral polykinetid, distance	P	4.5	4.5	1.0	0.2	23.3	2.0	6.0	21
Anterior body end to end of right polykinetid, distance	P	8.9	9.0	1.3	0.3	14.4	6.0	10.0	21
Right oral polykinetid, length	P	4.5	5.0	0.6	0.1	13.4	3.0	5.0	21
Anterior body end to left oral polykinetid, distance	P	7.3	7.0	1.1	0.2	15.0	5.0	9.0	21
Left oral polykinetid, length	P	4.5	4.5	0.5	0.1	12.0	3.5	5.0	21
Left oral polykinetid, width	P	1.1	1.0	–	–	–	1.0	1.5	21
Left oral polykinetid, number of ciliary rows	P	9.0	9.0	0.7	0.2	7.5	8.0	10.0	21
Macronucleus, length	P	4.2	4.0	0.6	0.1	15.3	3.0	5.0	21
Macronucleus, width	P	4.1	4.0	0.6	0.1	14.4	3.0	5.0	21
Micronucleus, length	P	2.1	2.0	–	–	–	1.5	2.5	21
Micronucleus, width	P	1.9	1.8	–	–	–	1.5	2.5	21
Ciliary rows, number	P	10.8	11.0	0.6	0.1	5.6	10.0	12.0	21
Dikinetids in kinety 3, number	P	18.3	18.0	1.8	0.4	9.8	15.0	21.0	21
Dikinetids in a left side kinety, number	P	8.9	9.0	0.7	0.2	8.2	8.0	10.0	21

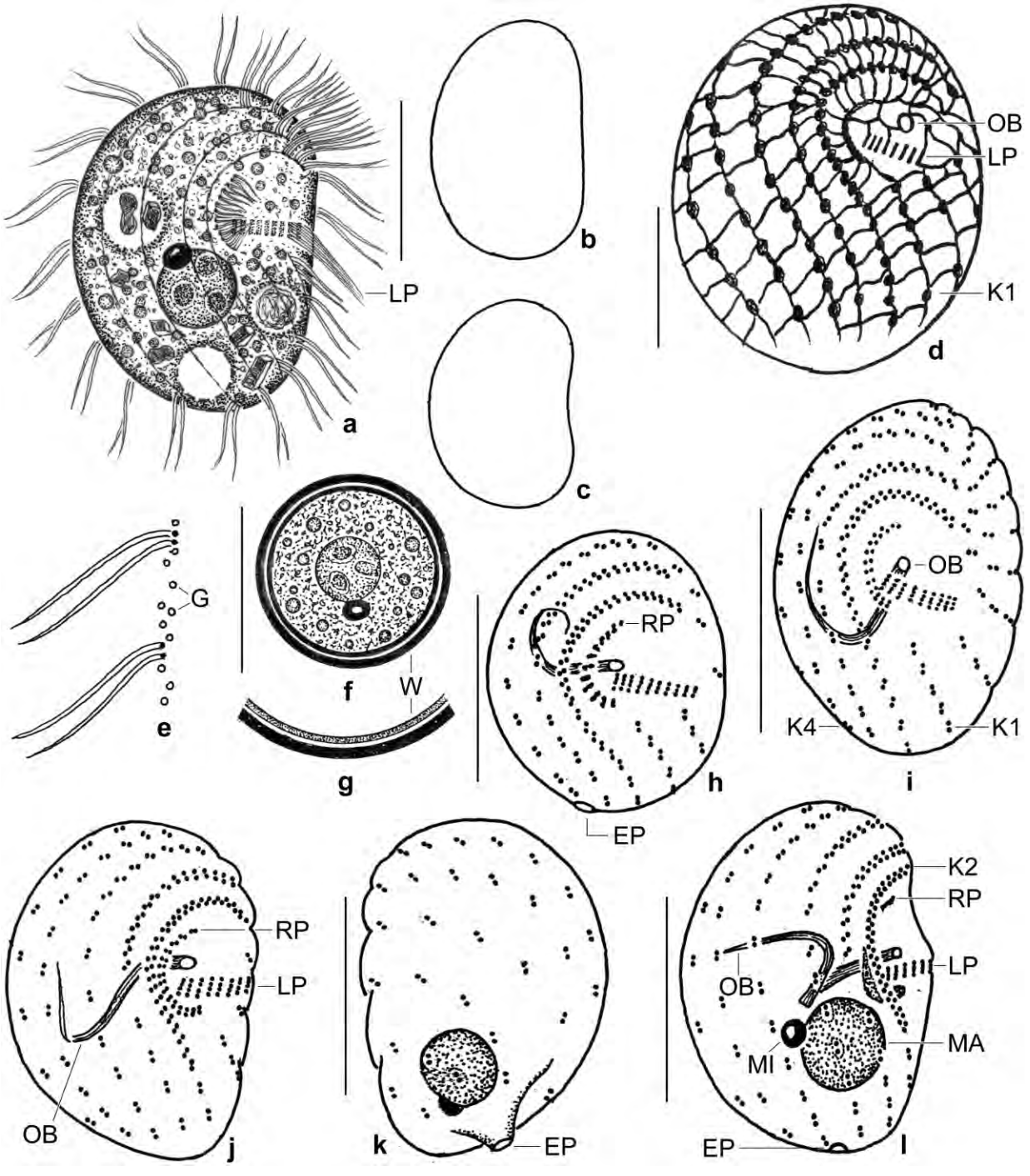

Fig. 100a–l. *Microcolpoda bambicola* from life (a–c, e–g), in a Klein-Foissner silver nitrate preparation (d), and after protargol impregnation (h–l). **a:** Right side view of a representative specimen, length 20 µm. **b:** Frequent shape variant. **c:** Most swimming specimens are slightly reniform. **d:** Right side view, showing the colpodid silverline pattern. **e:** Intrakinetal cortical granulation. **f, g:** Resting cyst, 12 µm. **h, i:** Ventral views, showing somatic and oral dikinetid pattern. Note the very narrowly spaced dikinetids in anterior half of kineties 2 and 3. **j, k:** Right and left side view of holotype specimen, length 17 µm. Note the oral basket and the very narrowly spaced dikinetids in kineties 2 and 3. **l:** Right side view of infraciliature and nuclear apparatus. EP – excretory pore of contractile vacuole, G – cortical granules, K1–4 – somatic kineties, LP – left oral polykinetid, MA – macronucleus, MI – micronucleus, OB – oral basket, RP – right oral polykinetid, W – cyst wall. Scale bars 10 µm.

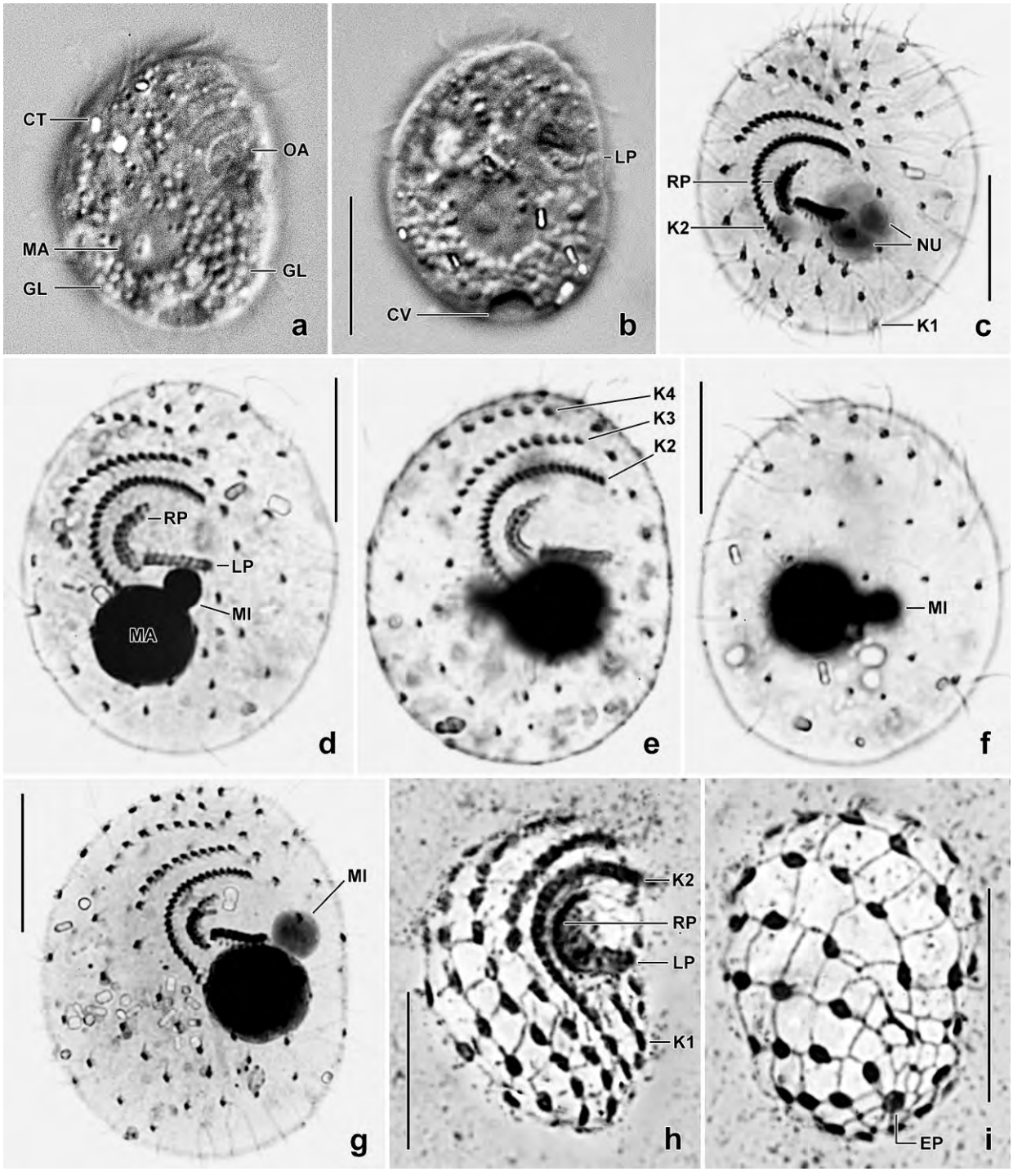

Fig. 101a–i. *Microcolpoda bambicola* from life (a,b), after silver carbonate impregnation (c–g, specimens heavily flattened by coverslip pressure), and in Chatton-Lwoff silver nitrate preparations (h,i). **a, b:** Right side view at two focal planes. **c:** Oblique anterior polar view of infraciliature. **d, g:** Ventral views of infraciliature and nuclear apparatus. **e, f:** Ventro- and dorsolateral view of same specimen. **h:** Ventrolateral view, showing the dikinetid pattern and the colpodid silverline pattern. **i:** Oblique posterior polar view, showing the silverline pattern and the excretory pore. CT – cytoplasmic crystal, CV – contractile vacuole, EP – excretory pore, K1–4 – somatic kineties, GL – cytoplasmic globules, LP – left oral polykinetid, MA – macronucleus, MI – micronucleus, NU – nucleoli, OA – oral apparatus, RP – right oral polykinetid. Scale bars 10 μm.

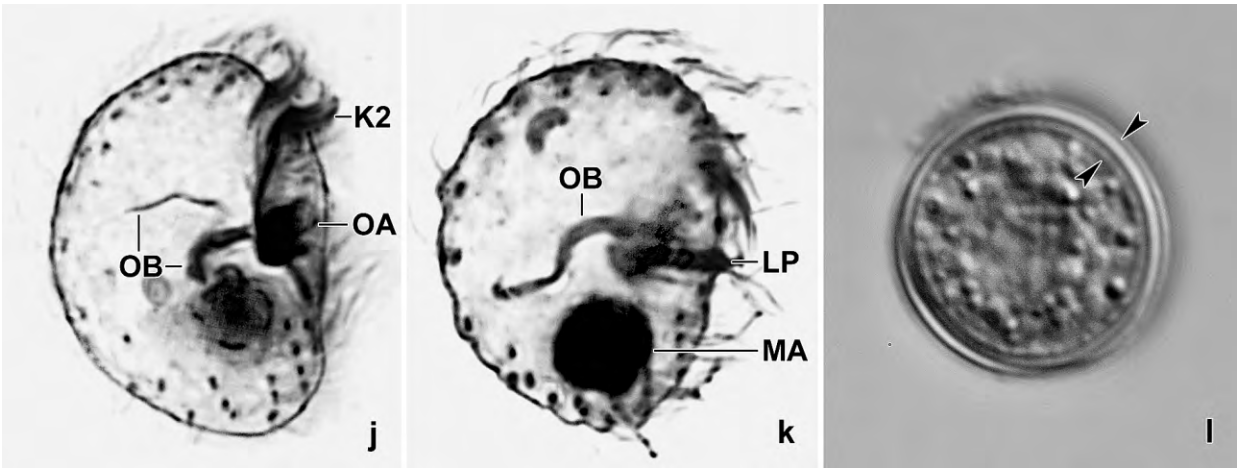

Fig. 101j–l. *Microcolpoda bambicola* from life (l) and after protargol impregnation (j, k). **j, k:** Oral basket in two specimens. **m:** Resting cyst with wall marked by opposed arrowheads. K2 – somatic kinety 2, MA – macronucleus, LP – left oral polykinetid, OA – oral apparatus, OB – oral basket. Scale bars 10 µm.

Description: Size in vivo 16–25 × 12–18 µm, usually about 20 × 15 µm, as calculated from some in vivo measurements and the Chatton-Lwoff silver nitrate-impregnated specimens adding 5% preparation shrinkage (Table 38). Protargol-impregnated specimens considerably smaller because fixed with alcohol-formalin and thus shrunken by about 20% (Table 38). Body outline semicircular (Fig. 100a, b, 101a, b), usually slightly narrowed posteriorly (Fig. 100a, j), rarely anteriorly; in vivo indistinctly flattened laterally, slightly convex on right side, strongly on left (Fig. 100i, 101j, k). Swimming specimens broadly reniform caused by concave oral field (Fig. 100c, l). Nuclear apparatus in or slightly posterior of mid-body (Fig. 100a, k, l, 101a–g; Table 38). Macronucleus globular, rarely very broadly ellipsoid; with few, comparatively large nucleoli (Fig. 100a, 101c). Micronucleus as macronucleus, very likely not in perinuclear space because simply attached to macronucleus (Fig. 100a, k, l, 101d, g). Contractile vacuole and excretory pore in or near centre of posterior pole, rather prominent in protargol preparations; surrounded by highly refractive crystals of various shape and 1–2 µm in size, likely originate from prey because present also in food vacuoles (Fig. 100a, h, k, l, 101a, b, i). Cortex flexible, contains intrakinetal granules about 0.3 µm in size, very likely a sort of mucocysts (Fig. 100e). Cytoplasm colourless, densely granulated by pale globules about 1 µm across, contains some crystals described above and food vacuoles with loose contents, likely bacteria and heterotrophic flagellates (Fig. 100a, 101a, b). Swims rather rapidly rotating about main body axis, glides on microscope slides and mud accumulations.

Somatic cilia paired, in vivo about 6 µm long, anterior cilium lacking in dikinetids of left posterior half of cell, arranged in 10–12 slightly spiral rows more narrowly spaced on right than left side, especially rows 2 and 3 having dikinetids so narrowly spaced in semicircular anterior half that a zigzag pattern is produced; intrakinetal distances of left side about twice as wide as those in right side row 3, right side thus much more ciliated than left; preoral suture very narrow; elongated caudal cilia absent (Fig. 100a, d, h–l, 101c–i; Table 38).

Silverline pattern wide-meshed, typical colpodid, indistinguishable from that of other small colpodids s.str. (Fig. 100d, 101h, i).

Oral apparatus ventrolateral in second quarter of body, structures exposed because not roofed over by a buccal lip (Fig. 100a, j, l, 101a, b, d, e, g, h; Table 38). Oral field about 5 µm across in vivo, moderately concave, contains three important structures (Fig. 100a, d, h–j, l, 101b–e, g, h; Table 38): (i) a right ciliary field very likely composed of a row of dikinetids with 2–3 µm long cilia, a third row possibly occurs in posterior half of some specimens (Fig. 100h, 101c); (ii) a left polykinetid extending transversely from right margin of oral field to ventral side, about 5 × 1 µm in size, composed of an average of nine monokinetal rows with about 6 µm long cilia; and (iii) an oral basket-like pharynx commencing near proximal end of left polykinetid and extending to dorsal side of body (Fig. 100d, h–j, l, 101j, k).

Resting cyst: Resting cysts globular and colourless, without mucous coat, in vivo 12.4 µm across on average (M = 12 µm, SD = 1.5, SE = 0.4, CV = 12.1, Min = 11, Max = 16, n = 15). Cyst wall composed of two tightly spaced layers 0.7–1 µm thick together (Fig. 100f, g, 101l). Cytoplasm with some lipid droplets 0.5–1 µm in diameter; macronucleus in cyst centre, about 5 µm across.

Occurrence and ecology: As yet found only at type locality. A raw culture was obtained from the wet bamboo mud, tap water and some squashed wheat grains.

Remarks: *Microcolpoda bambicola* belongs to the very small colpodeans having a body length of 10–30 µm (Foissner 1993a). There are rather many of such species, all reviewed in Foissner (1993a). In vivo, body size and shape of *M. bambicola* resemble *Colpoda ecaudata*, → *Emarginatophrya aspera* and → *Paracolpoda* spp. (mouth on ventral side, without perioral ciliary condensations); *Pseudoplatyophrya* spp. and *Nivaliella plana* (with minute, subapical feeding tube); *Apocyrtolophosis minor* (without perioral ciliary condensations); *Microdiaphanosoma arcuatum*, *Orthokreyella schiffmanni*, and *Kreyella minuta* (left side ciliated only along anterior margin).

Krassniggia auxiliaris Foissner, 1987a (Fig. 102a–k)

This conspicuous ciliate, which belongs to the Colpodidae, occurred in sample (2) from Venezuela and matches very well the original description (for a review, see Foissner 1993a). Thus, we provide only a few micrographs and deposit four slides with silver nitrate-impregnated specimens in the Biology Centre of the Upper Austrian Museum in Linz (LI). As yet, this species has been recorded only from Gondwanan localities: Kenya (Africa), Australia, and now South America.

The overall appearance of *K. auxiliaries* is rather similar to another gigantic colpodid, *Bresslauides discoideus*, as described by Foissner (1993a). However, this species has different oral structures and thus belongs to the Hausmanniellidae.

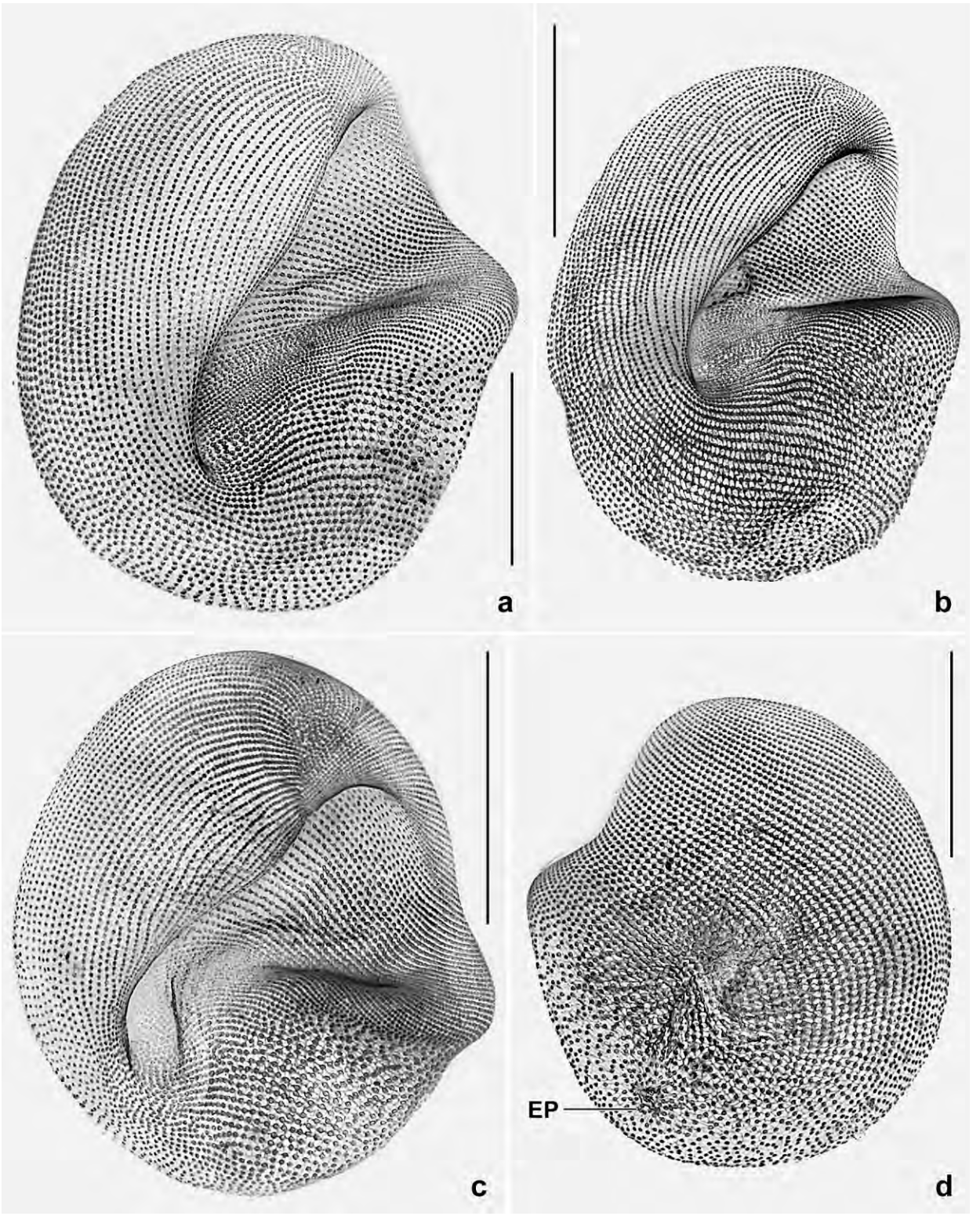

Fig. 102a–d. *Krassniggia auxiliaris*, body shape and ciliary pattern after silver nitrate impregnation. **a, b:** Right side views, showing the margin of the right wall of the buccal cavity extending utricle-like posteriorly. **c:** Slightly oblique ventrolateral view, showing the gigantic mouth. **d:** Left side view. EP – excretory pore. Scale bars 50 µm (a) and 70 µm (b–d).

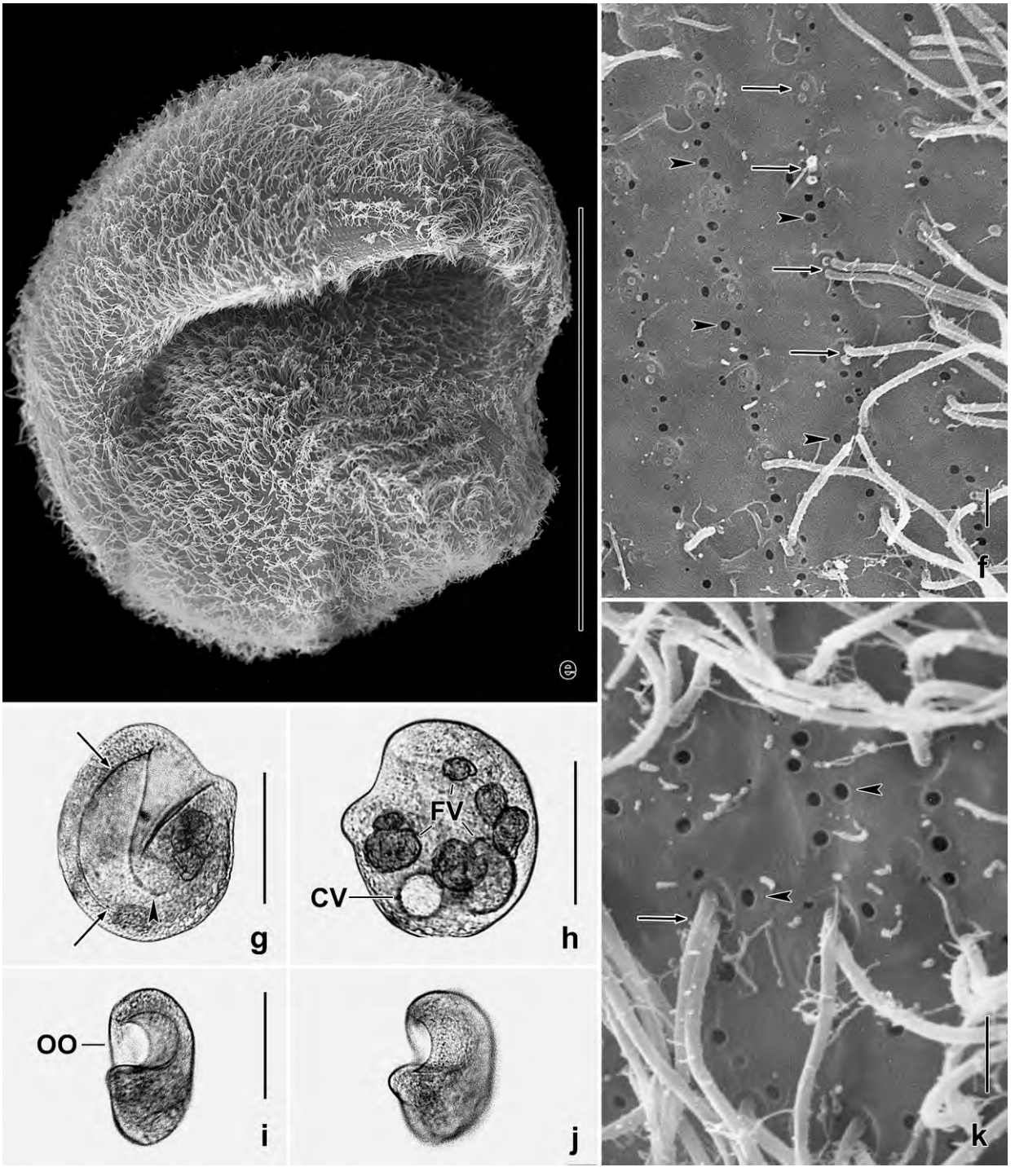

Fig. 102e–k. *Krassniggia auxiliaris* from life (g–j) and in the scanning electron microscope (e, f, k). **e:** Ventral view, showing the table-like bottom of the buccal cavity. **f, k:** Surface views of a partially deciliated specimen, showing the dikinetal ciliary rows (arrows) and the holes from just extruded mucocysts (arrowheads) within the ciliary rows. **g:** Right side overview, showing the posterior end of the right wall of the buccal cavity (arrowhead) and its huge size with the dorsal margin marked by arrows. **h:** Left side overview of a specimen with seven large food vacuoles. **i, j:** Two views of a specimen turning from ventrolateral (i) to ventral (j), showing the lateral flattening (cp. g, h). CV – contractile vacuole, FV – food vacuoles, OO – oral opening. Scale bars 1 µm (f, k) and 100 µm (e, g–j).

Grossglockneria lajacola **nov. spec.** (Fig. 103a, b, 104a–d)

Diagnosis: As *G. acuta* but with a 15–20 µm long caudal cilium.

Type locality: Venezuelan site (32), i. e., ephemeral puddles (Lajas) on granitic outgroppings between the Agricultural Research Institute and the airport of Pto. Ayacucho, 68°W 6°N.

Type material: 1 holotype and 2 paratype slides with a total of 4 protargol-impregnated specimens have been deposited in the Biology Centre of the Upper Austrian Museum in Linz (LI). The specimens have been marked by black ink circles on the coverslip.

Etymology: The species name is a composite of *Laja* (native term for ephemeral puddles on granitic outcroppings) and the Latin verb *colere* (to live in), the habitat *G. lajacola* was discovered.

Description: This species was very rare. We found only five poorly impregnated cells in the protargol slides (Fig. 104a–d). Thus, we cannot provide morphometric data and base the description mainly on the live observations. The identity of the species is very clear due to the unique caudal cilium. Nonetheless, the species needs a more detailed investigation also with respect to the micronucleus and the number of ciliary rows.

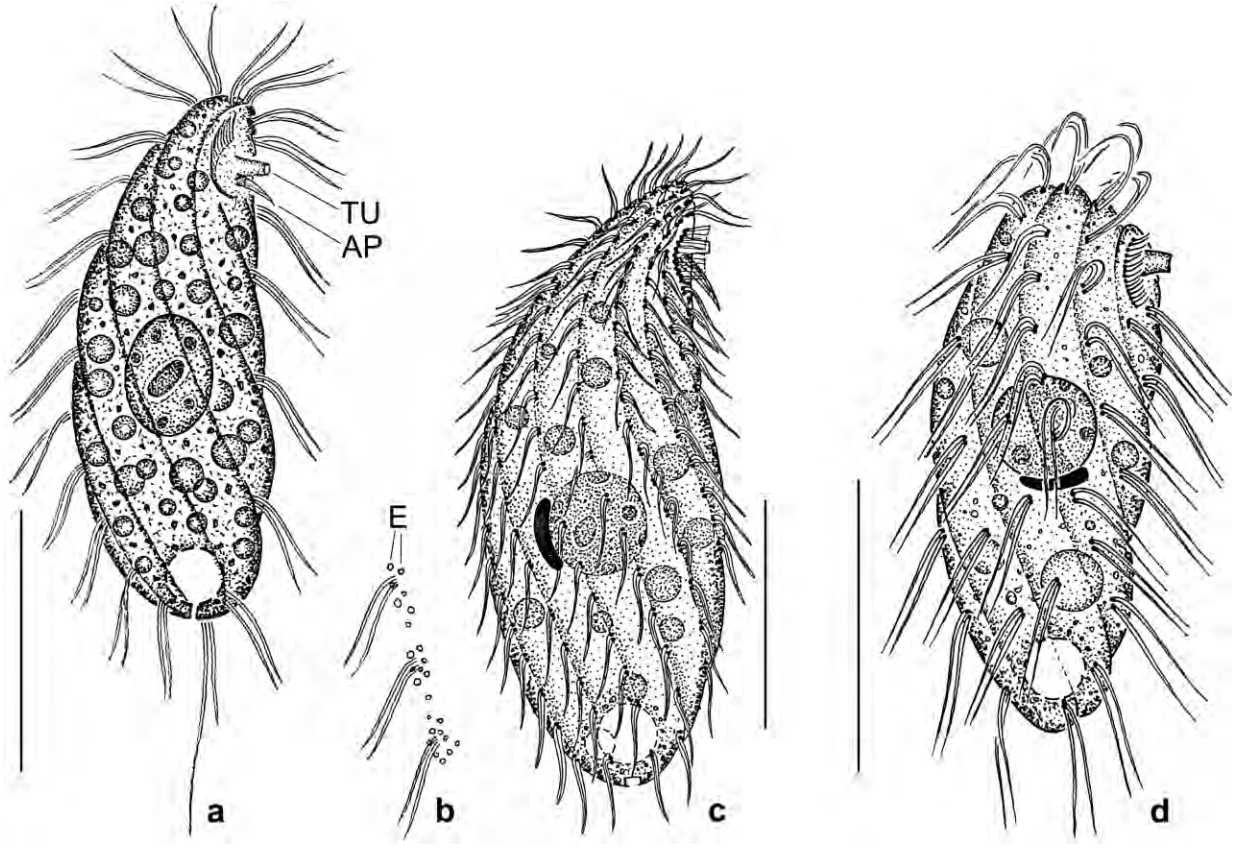

Fig. 103a–d. *Grossglockneria* species, right side views from life. **a, b:** *G. lajacola*, overview and part of a ciliary row, showing minute extrusomes mainly around the kinetids. **c:** *G. acuta* (from Foissner 1980). **d:** *G. hyalina* (from Foissner 1985). AP – adoral polykinetid, E – extrusomes, TU – feeding tube. Scale bars 20 µm.

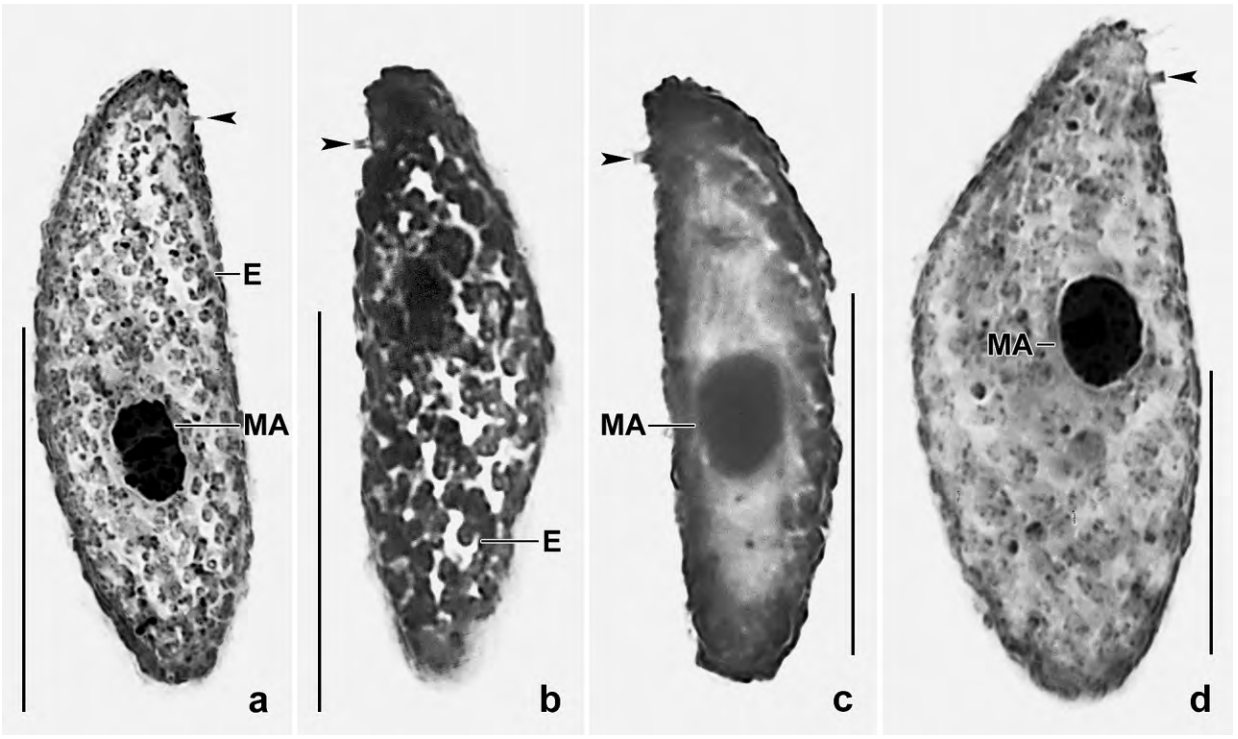

Fig. 104a–d. *Grossglockneria lajacola* after protargol impregnation. The arrowheads mark the minute feeding tube, the main diagnostic feature of the grossglockneriids. **a:** Right side view of holotype specimen, length 32 µm. **b, c:** Left side views. Note the swollen extrusomes hidding the ciliary pattern. **d:** Right side view of the largest specimen found, length 47 µm. It highly resembles a "typical" *G. acuta*. E – extrusomes, MA – macronucleus. Scale bars 20 µm.

Size in vivo 30–50 × 10–20 µm, usually about 40 × 15 µm, as calculated from some in vivo measurements and the five prepared specimens adding 15% preparation shrinkage. Slenderly ovate (Fig. 103a), slenderly ellipsoid (Fig. 104a–c) or ellipsoid (Fig. 104d); anterior end bluntly pointed, posterior slightly narrowed and rounded. Macronucleus slightly anterior or posterior of mid-body, broadly ellipsoid, 6–10 × 4–6 µm in vivo; frequently with an enlarged, central nucleolus surrounded by several small nucleoli 1–2 µm across (Fig. 103a, 104a–d). Micronucleus not studied and not impregnated. Contractile vacuole in posterior end, with tubular excretory pore close to caudal cilium. Cortex colourless, very flexible, distinctly furrowed by ciliary rows; contains minute (~ 0.4 µm) extrusomes mainly around dikinetids, swollen to 1–2 µm-sized, deeply impregnating structures in protargol preparations as in *G. acuta* (Fig. 103b, 104a, b). Cytoplasm hyaline, contains many minute (~ 0.5 µm) crystals sparkling under interference contrast illumination and globular food droplets 1–3 µm across, usually about 2 µm. Swims rather rapidly, never rests.

Nine or 10 ciliary rows extend spirally from anterior to posterior end of cell (Fig. 103a, 104a,b). Cilia 7–8 µm long in vivo, paired except for left posterior region covered with single cilia. In or near centre of posterior pole a dikinetid with an ordinary anterior cilium and an elongated posterior cilium 15–20 µm long in vivo; distal half of caudal cilium difficult to recognize because very fine and strongly beating (Fig. 103a).

Oral apparatus grossglockneriid, i. e., subapical and small. Feeding tube about 2 µm long in vivo (Fig. 103a, 104a–d). Cilia of paroral membrane and adoral polykinetid about 2.5 µm long in vivo (Fig. 103a).

Occurrence and ecology: As yet found only at type locality, a special habitat to which it is probably restricted.

Remarks: This species, which we supposed to be a small *Grossglockneria acuta* (Fig. 103c), came to our attention by the rather small size and the hyaline cytoplasm. First, we recognized a rather large central nucleolus in the macronucleus and then we saw the elongated caudal cilium, showing that it was an undescribed species.

Three *Grossglockneria* species have been described: *G. acuta* Foissner, 1980a (Fig. 103c); *G. hyalina* Foissner, 1985 (Fig. 103d); and *G. ovata* Foissner, 1999a. None has an elongated caudal cilium. All other features are highly similar to *G. acuta*.

In vivo, *G. lajacola* is easily confused with *G. acuta* (without caudal cilium) and *Trihymena terricola* Foissner, 1988a (with minute but distinct adoral polykinetids; see Foissner 1993a). The great similarity of *G. lajacola* and *G. acuta* requires that in future all *G. acuta*-like populations are checked for the absence of a caudal cilium!

Pseudoplatyophrya isabelae nov. spec. (Fig. 105a–d, 106a–d; Table 39)

Diagnosis: Size in vivo about 23 × 15 µm. Body outline elliptic or oval, anterior end obliquely truncate in ~ 1/3 of specimens. Macronucleus globular, micronucleus ellipsoid. Minute extrusomes within ciliary rows. 9 somatic kineties with a total of about 40 dikinetids: kinety 1 extends postorally, composed of an average of five dikinetids, last dikinetid associated with an elongated caudal cilium; kinety 2 extends to or slightly posterior to mid-body, usually composed of three widely spaced dikinetids; kinety 3 extends in anterior body half and curves around anterior body end, usually composed of five or six dikinetids. Oral apparatus grossglockneriid, adoral polykinetid minute.

Type locality: Galápagos sample (68), i. e., highly saline (~ 30‰) soil and tree bark from a mangrove forest near the village of Puerto Villamil, south coast of Isabela Island, 0°57'S 90°57'W.

Type material: 1 holotype slide with protargol-impregnated specimens has been deposited in the Biology Centre of the Upper Austrian Museum in Linz (LI). Relevant specimens have been marked by black ink circles on the coverslip.

Etymology: Named after the island it was discovered, i. e., Isabela Island of the Galápagos archipelago.

Description: In vivo, we misidentified this species as *P. nana*. Thus, we did not study it in detail and cannot provide live observations (see also → *P. galapagensis*).

Size in vivo 20–27 × 11–17 µm, usually about 23 × 15 µm when 15% preparation shrinkage are added to values shown in Table 39. Body outline roughly elliptic (Fig. 105a, 106a, c) or ovate (Fig.

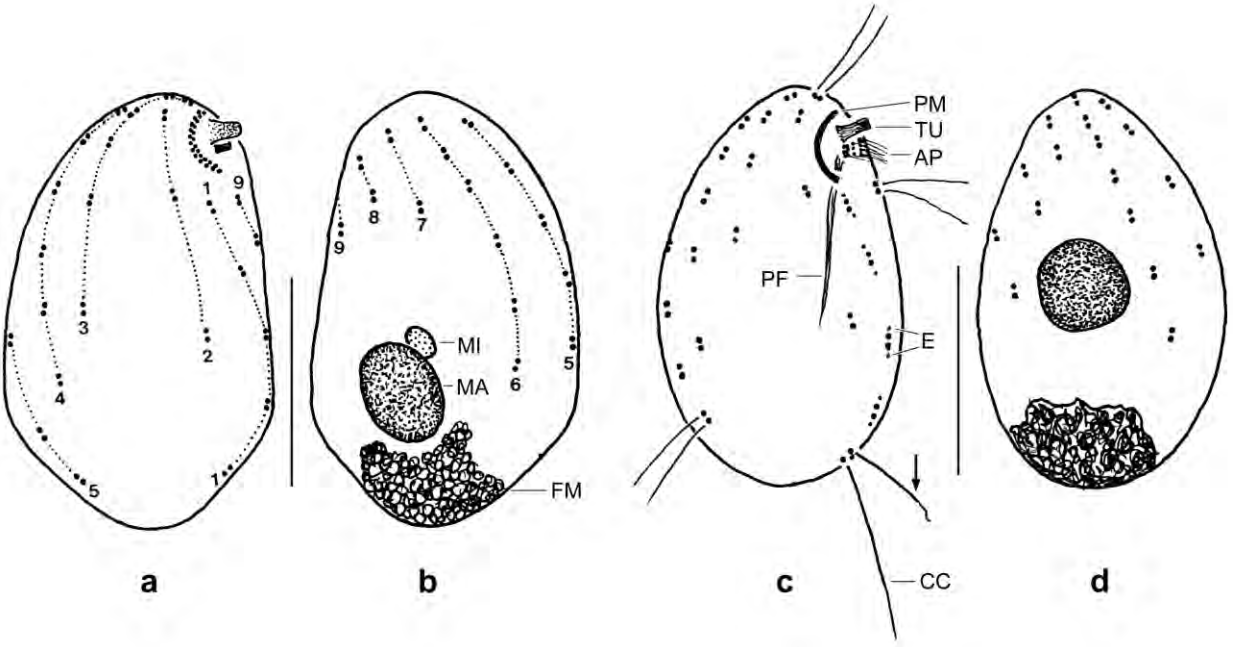

Fig. 105a–d. *Pseudoplatyophrya isabelae* after protargol impregnation. **a, b:** Dikinetid pattern of right and left side and nuclear apparatus of holotype specimen, length 20 µm. Dikinetids of proposed ciliary rows (numerals) connected by dotted lines. Note row 3 which curves around the anterior body end. **c, d:** Dikinetid pattern of right and left side of an ovate paratype specimen. The anterior basal body of the last dikinetid of row 1 has an ordinary somatic cilium (arrow) while the posterior basal body has an elongated caudal cilium (see also Fig. 106d). Minute extrusomes are associated with the dikinetids. AP – adoral polykinetid, CC – caudal cilium, E – extrusomes, FM – fecal mass, MA – macronucleus, MI – micronucleus, PF – pharyngeal fibres, PM – paroral membrane, TU – feeding tube, 1–9 – somatic ciliary rows. Scale bars 10 µm.

105c, 106d), anterior end slightly oblique in about 1/3 of specimens (Fig. 105a, 106a, c); slightly to distinctly (~ 2:1) flattened laterally. Nuclear apparatus in or posterior to mid-body on average (Fig. 105b, d, 106b–d; Table 39). Macronucleus globular to broadly ellipsoid, about 5 µm across in protargol preparations. Micronucleus attached to macronucleus, ellipsoid to elongate ellipsoid (3:1), possibly slightly flattened (Fig. 105b, 106b, c). Contractile vacuole not recognizable in the preparations, very likely in posterior end studded with deeply impregnating granular material, possibly fecal mass (Fig. 105b, d, 106a–d). Within ciliary rows minute (< 0.5 µm) argyrophilic granules, very likely extrusomes of the mucocyst type. Food vacuoles impregnate lightly, up to 5 µm in size.

Ordinary somatic cilia 6–7 µm long, caudal cilium 11–14 µm in protargol preparations; arranged in nine meridional, ordinarily spaced rows commencing apically and ending at different length of body, distance between rows 2 and 3 distinctly increased; anterior basal body of dikinetids usually barren in posterior half of left side (Fig. 105a–d, 106a–d; Table 39). Ciliary row 1 on ventral side, usually composed of five dikinetids, last dikinetid associated with an ordinary cilium anteriorly and an elongated caudal cilium posteriorly (for numbering of rows, see Fig. 105a, b and 106a, b, d); row 2 on right side of cell, composed of three dikinetids, ends slightly posterior to mid-body; row 3 on right side of cell, usually composed of six dikinetids, curves around anterior body end and terminates in or near mid-body; row 4 on right side of cell, composed of five to six dikinetids, extends to last third of body; row 5 on dorsal side of body, composed of about eight dikinetids,

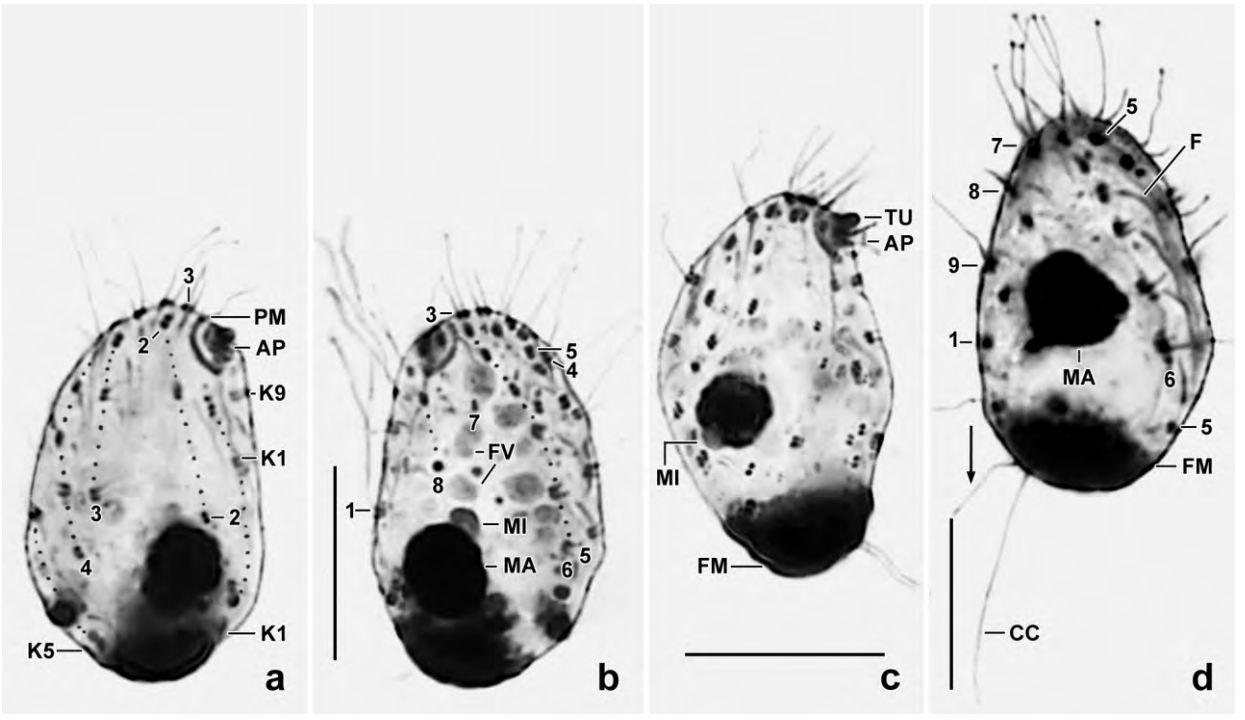

Fig. 106a–d. *Pseudoplatyophrya isabelae* after protargol impregnation. **a, b:** Dikinetid pattern of right and left side and nuclear apparatus of holotype specimen, length 20 µm. Dikinetids of proposed ciliary rows (numerals) connected by dotted lines. Note row 2 which consists of three dikinetids, and row 3 which curves around the anterior body end. **c:** An ellipsoid paratype specimen with broadly ellipsoid micronucleus. **d:** Left side view of a paratype specimen, showing the ciliary pattern and, especially, the 14 µm long caudal cilium which is associated with an ordinary cilium (arrow). Numerals denote ciliary rows. AP – adoral polykinetid, CC – caudal cilium, FM – fecal mass, FV – food vacuoles, K(1–9) – somatic ciliary rows, MA – macronucleus, MI – micronucleus, PM – paroral membrane, TU – feeding tube. Scale bars 10 µm.

extends whole body length; row 6 on left side of body, composed of 5–7 dikinetids, extends to last third of cell; rows 7 and 8 on left side of body, usually composed of two dikinetids each, extend to second third of body; row 9 on ventral side, usually composed of three dikinetids, ends in or slightly anterior to mid-body. In total about 40 dikinetids (Fig. 105a–d, 106a–d; Table 39).

Oral apparatus grossglockneriid, i. e., minute and slightly subapical; cilia only 2.5–3 µm long in protargol preparations. Paroral membrane moderately curved, likely composed of dikinetids. Adoral polykinetid close posterior to feeding tube, likely composed of three kineties with three cilia each. Feeding tube about 2 µm long and about 1 µm across at distal end. Pharyngeal fibres extend vertically to mid-body (Fig. 105a, c, 106a, c; Table 39).

Occurrence and ecology: See → *P. galapagensis*!

Remarks: As explained in → *P. galapagensis*, these minute ciliates are difficult to study, even when the protargol preparations are excellent. Thus, misinterpretations cannot be excluded, for instance, the caudal cilium is possibly associated with kinety 2, not with kinety 1 as described above.

Pseudoplatyophrya isabelae differs from → *P. galapagensis* mainly by somatic kinety 2, which is composed of three (vs. one) dikinetids. Further, it is slightly broader (length:width ratio 1.9 vs. 1.6) and larger in most features, for instance, the total number of dikinetids (~ 40 vs. ~ 30) and the number of dikinetids composing kinety 4 (five vs. four). The main feature, viz., kinety 2, appears

Table 39. Morphometric data on *Pseudoplatyophrya galapagensis* (upper line) and *Pseudoplatyophrya isabelae* (lower line). Data based on mounted, protargol-impregnated, well-prepared specimens from a non-flooded Petri dish culture. Measurements in µm. CV – coefficient of variation in %, M – median, Max – maximum, Mean – arithmetic mean, Min – minimum, n – number of individuals investigated, SD – standard deviation, SE – standard error of arithmetic mean.

Characteristics	Mean	M	SD	SE	CV	Min	Max	n
Body, length	19.2	20.0	1.3	0.4	6.9	17.0	21.0	11
	20.4	21.0	1.6	0.4	7.6	17.0	23.0	15
Body, width	10.9	9.0	1.3	0.4	13.4	9.0	13.0	11
	12.7	13.4	1.6	0.4	12.8	10.0	15.0	15
Body length:width, ratio	1.9	1.9	0.2	0.1	11.1	1.5	2.2	11
	1.6	1.6	0.2	0.1	12.5	1.4	2.2	15
Anterior body end to paroral membrane, distance	0.9	1.0	0.3	0.1	33.2	0.5	1.5	11
	0.8	0.5	0.3	0.1	41.7	0.5	1.5	15
Anterior body end to end of paroral membrane, distance	3.8	4.0	0.5	0.1	12.4	3.0	4.5	11
	4.3	4.5	0.4	0.1	9.6	3.5	5.0	15
Paroral membrane, length	2.9	3.0	–	–	–	2.5	3.0	11
	3.5	3.5	–	–	–	3.0	4.0	15
Anterior body end to macronucleus, distance	7.6	8.0	1.4	0.4	17.8	5.0	10.0	11
	9.1	8.0	2.6	0.7	28.0	5.0	14.0	15
Macronucleus, length	5.3	5.0	0.9	0.3	17.2	4.0	7.0	11
	5.2	5.0	0.5	0.1	8.7	4.5	6.0	15
Macronucleus, width	4.6	5.0	0.7	0.2	15.1	3.0	5.0	11
	4.9	5.0	0.5	0.1	10.0	4.0	6.0	15
Micronucleus, length	2.2	2.0	–	–	–	2.0	3.0	6
	2.5	2.5	–	–	–	2.0	3.0	15
Micronucleus, width	1.4	1.5	–	–	–	1.0	2.0	6
	1.1	1.0	–	–	–	1.0	1.5	15
Feeding tube, length	1.4	1.5	–	–	–	1.0	1.5	11
	1.8	1.8	–	–	–	1.5	2.0	15
Ciliary rows, number	9.0	9.0	0.0	0.0	0.0	9.0	9.0	11
	9.0	9.0	0.0	0.0	0.0	9.0	9.0	15
Ciliary row 1, number of dikinetids	3.9	4.0	–	–	–	3.0	4.0	11
	4.9	5.0	–	–	–	4.0	5.0	15
Ciliary row 2, number of dikinetids	1.0	1.0	0.0	0.0	0.0	1.0	1.0	9
	3.0	3.0	0.0	0.0	0.0	3.0	3.0	12
Ciliary row 4, number of dikinetids	4.0	4.0	0.8	0.2	19.4	3.0	5.0	11
	5.3	5.0	–	–	–	5.0	6.0	15
Ciliary row 7, number of dikinetids	2.1	2.0	–	–	–	2.0	3.0	11
	2.0	2.0	0.0	0.0	0.0	2.0	2.0	15

not impressive but its invariability might justify a distinct species. For the species mentioned in the next paragraph, see FOISSNER (1993a).

Pseudoplatyophrya nana differs from *P. isabelae* by the shape of the micronucleus (~ 5 µm across and strongly flattened vs. ~ 3 µm and only slightly flattened), the number of dikinetids in row 2 (~ eight vs. three), and the total number of somatic dikinetids (usually ~ 60 vs. ~ 40; Fig. 106f–j). *Pseudoplatyophrya saltans* differs from *P. isabelae* by the shape of the micronucleus (distinctly vs. slightly flattened), the body size (< 20 µm vs. > 20 µm), the higher number of dikinetids in rows 7 and 8 (≥ five vs. two), and, very likely, it does not jump (vs. sudden jumps in *P. saltans*). *Nivaliella plana* differs from *P. isabelae* by the shape of the micronucleus (distinctly vs. slightly flattened), the number of dikinetids in ciliary rows 3 and 4 (≤ three vs. ≥ five), and the total number of dikinetids (25–30 vs. 40; see also FOISSNER et al. 2002).

Pseudoplatyophrya galapagensis nov. spec. (Fig. 107a–d, 108a–e; Table 39)

Diagnosis: Size in vivo about 22 × 12 µm. Body ellipsoid to quadrangular with rounded corners, anterior end usually slightly obliquely truncate. Macronucleus and micronucleus broadly ellipsoid. 9 somatic kineties with a total of about 30 dikinetids: kinety 1 extends postorally, usually composed of four dikinetids, last dikinetid associated with an elongated caudal cilium; kinety 2 composed of only one dikinetid slightly right and posterior of oral apparatus; kinety 3 extends in anterior quarter of body, usually composed of two dikinetids; kinety 5 extends whole body length and curves around anterior body end, composed of about nine dikinetids. Oral apparatus grossglockneriid, adoral polykinetid minute.

Type locality: Galápagos sample (68), i. e., highly saline (~ 30‰) soil and tree bark from a mangrove forest near the village of Puerto Villamil, south coast of Isabela Island, 0°57'S 90°57'W.

Type material: 1 holotype and 1 paratype slide with protargol-impregnated specimens have been deposited in the Biology Centre of the Upper Austrian Museum in Linz (LI). Relevant specimens have been marked by black ink circles on the coverslip.

Etymology: Named after the country it was discovered, i. e., the Galápagos archipelago.

Description (see **Remarks** for the in vivo aspect): Size in vivo 20–25 × 10–15 µm, usually about 22 × 12 µm when 15% preparation shrinkage are added to the values shown in Table 39. Body shape highly dependent on amount of food ingested, i. e., quadrangular with rounded ends and leaf-like flattened when starving (Fig. 107d, 108c, d) while ellipsoid when moderately filled with food droplets (Fig. 107a, c, 108a); anterior body end usually slightly oblique. Nuclear apparatus in mid-body on average, macronucleus and micronucleus broadly ellipsoid on average, micronucleus only faintly impregnated (Fig. 107b, 108a–e; Table 39). Contractile vacuole not recognizable in the preparations, very likely in rear end usually studded with deeply impregnating granules, possibly fecal mass (Fig. 107b, c, 108a–c). Extrusomes not recognizable in protargol preparations. Cytoplasm colourless, studded with 2–10 µm-sized food droplets in ellipsoid specimens, rare in starving quadrangular cells.

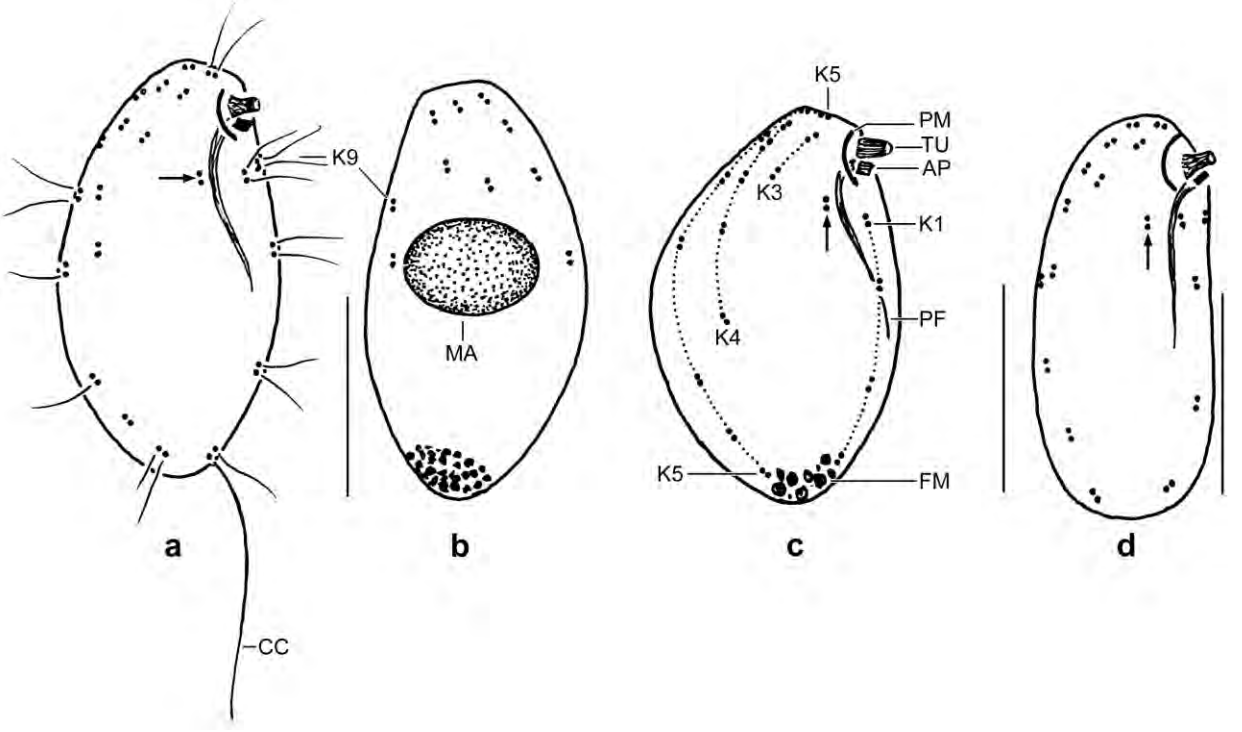

Fig. 107a–d. *Pseudoplatyophrya galapagensis* after protargol impregnation. **a, b:** Right and left side view of holotype specimen, length 20 µm. Arrow marks kinety 2 which consists of a single dikinetid and is thus the most important feature of the species. **c:** Right side view of a well-fed specimen. Arrow marks the single dikinetid of kinety 2. Kinetids of rows connected by dotted lines. Left side ciliary pattern as in Figure 107b. **d:** Right side view of a starving specimen with quadrangular outline and so strongly flattened that kineties 4, 5 and 6 are difficult to separate. Arrow marks kinety 2, which consists of a single dikinetid. AP – adoral polykinetid, CC – caudal cilium, FM – fecal mass, K1–5, K9 – ciliary rows, MA – macronucleus, PF – pharyngeal fibres, PM – paroral membrane, TU – feeding tube. Scale bars 10 µm.

Ordinary somatic cilia 5–6 µm long in protargol preparations, caudal cilium about half of body length; arranged in nine meridional, ordinarily spaced rows commencing apically and ending at different length of body, distance between rows 2 and 3 distinctly increased; anterior basal body of left side dikinetids barren in posterior dikinetids (Fig. 107a–d, 108a–e; Table 39). Ciliary row 1 on ventral side, usually composed of four dikinetids, last dikinetid associated with an ordinary cilium anteriorly and an elongated caudal cilium posteriorly (for numbering of rows, see Fig. 107c, 108a, b); row 2 on right side of cell, composed of one, very rarely two dikinetids slightly right and posterior of oral apparatus; row 3 extends in anterior quarter of body, usually composed of two dikinetids; row 4 on right side of cell, extends to mid-body, composed of an average of four dikinetids; row 5 on dorsal side of cell, extends whole body length and curves around anterior body end, composed of about nine dikinetids; row 6 on left side of cell, extends to mid-body, usually composed of four dikinetids; rows 7 and 8 on left side of cell, each composed of only two dikinetids and thus ending in anterior third of body; row 9 on ventral side, extends to mid-body, usually composed of three dikinetids. In total about 30 dikinetids (Fig. 107a–d, 108a–e; Table 39).

Oral apparatus grossglockneriid, i. e., minute and slightly subapical; cilia up to 3 µm long

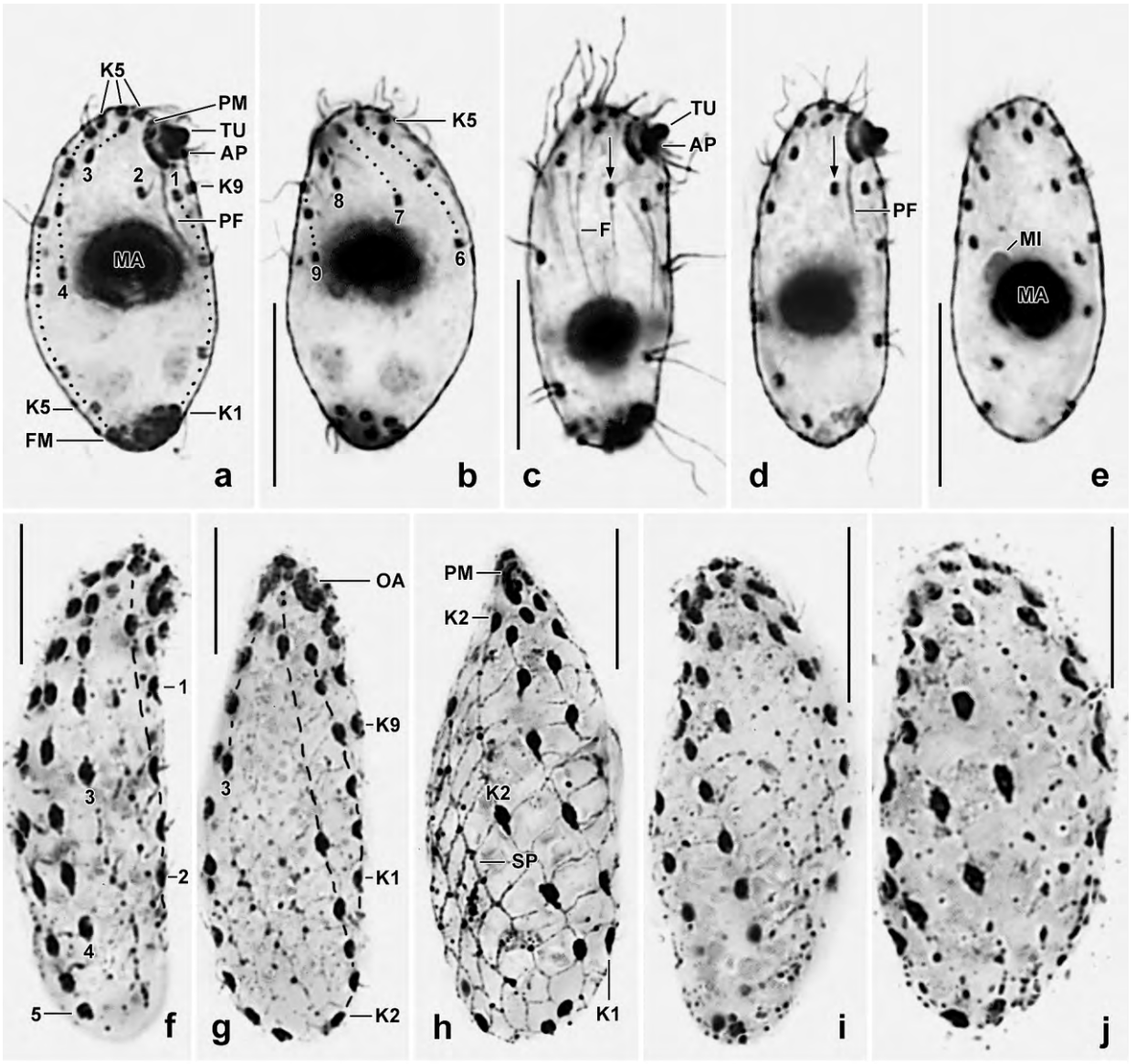

Fig. 108a–j. *Pseudoplatyophrya galapagensis* (a–e) and a large-sized *P. nana* (f–j) from Austria after protargol (a–e) and Chatton-Lwoff silver nitrate (f–j) impregnation. **a, b:** Right and left side view of holotype specimen with dikinetids of ciliary rows connected by dotted lines. Kinety 2 consists of only a single dikinetid which is the most prominent feature in *P. galapagensis*. **c–e:** Right (c, d) and left (e) side views of starving and thus quadrangular specimens. Arrows mark the single dikinetid comprising kinety 2. Note the broadly ellipsoidal and comparatively small micronucleus (e) which is distinctly different from the large, strongly flattened micronucleus of *P. nana* (Foissner 1993a). **f–j:** Right side (f), ventro-lateral (g), ventral (h), and left side (i, j) views of the dikinetid pattern of *P. nana*. This species differs from *P. galapagensis* and *P. isabelae* not only by the shape of the micronucleus but also by kinety 2, marked by hatched lines, which consists of more than one dikinetid. Generally, *P. nana* has more dikinetids (~ 60) than *P. galapagensis* (~ 30) and *P. isabelae* (~ 40). AP – adoral polykinetid, F – fibres originating from dikinetids, FM – fecal mass, K(1–9) – kineties, MA – macronucleus, MI – micronucleus, OA – oral apparatus, PF – pharyngeal fibres, PM – paroral membrane, SP – colpodid silverline pattern, TU – feeding tube. Scale bars 10 µm.

after protargol impregnation. Paroral membrane moderately curved, very likely composed of dikinetids. Adoral polykinetid close posterior to feeding tube, likely composed of three kineties with three cilia each. Feeding tube 1.5–2 µm long and about 1 µm across at distal end. Pharyngeal fibres extend vertically to mid-body (Fig. 107a, c, 108a, c, d; Table 39).

Occurrence and ecology: *Pseudoplatyophrya galapagensis* and → *P. isabelae* occurred in the non-flooded Petri dish culture of the same sample but sequentially and each for a few days only. Both were very rare, possibly due to the high salt concentration (30‰). Basically, both are candidates for Galápagense or neotropic endemics. However, the in vivo misidentification shows that the species might have a broader, as yet unrecognized distribution. See also next paragraph.

Remarks: *Pseudoplatyophrya galapagensis* and → *P. isabelae* were discovered in a highly saline (~ 30‰) soil and bark sample from a mangrove forest on the Galápagos archipelago. They did not appear at the same time but sequentially in the non-flooded Petri dish culture. Both were rare and were in vivo misidentified as *P. nana* Foissner, 1980a with which they have a lot in common, especially body shape and size and the elongated caudal cilium. However, the protargol preparations showed a different ciliary pattern and a stouter micronucleus. The misidentification caused that we did not study the live aspect in detail. In spite of this, we describe these species because they have a clear identity and the in vivo aspect was at least checked.

Ciliates of this small size and with strongly reduced ciliature are difficult to observe even when the protargol preparations are excellent. Thus, some interpretation mistakes cannot be excluded, for instance, ciliary row 4, not row 5 might curve around the anterior body end in *P. galapagensis* and the caudal cilium might be associated with kinety 2, not kinety 1 in both species.

See → *P. isabelae* for distinguishing it from *P. galapagensis*. From the other congeners, viz., *P. nana* (Fig. 108f–j), *P. saltans,* and *P. terricola*, all reviewed in Foissner (1993a), *P. galapagensis* differs mainly by the number of dikinetids in kinety 2 (one vs. ≥ three). The most similar species is *Nivaliella plana*, also reviewed in Foissner (1993a) and Foissner et al. (2002), which, however, has 10 (vs. 9) ciliary rows, possesses at least two (vs. one) dikinetids in kinety 2, and is usually broader (length:width ratio 1.5:1 in two populations vs. 1.9:1; see Table 39, Foissner 1993a, and Foissner et al. 2002).

The generic classification of *P. galapagensis* and → *P. isabelae* is uncertain, i. e., they could belong to *Nivaliella* due to the strongly reduced, hardly spiralling ciliature while body shape (length:width ratio) match *Pseudoplatyophrya* (see above).

***Pseudoplatyophrya spinosa* nov. spec.** (Fig. 109a–l, 110a–m; Table 40)

Diagnosis: Size in vivo about 30 × 20 µm. Ellipsoid or slightly ovate, with complex cortical ridges producing two ventral spines; posteriorly, a tubular process containing an ellipsoid granule. Macronucleus globular, micronucleus discoidal and up to 4 µm across. Minute extrusomes within ciliary rows. 10 somatic kineties with a total of about 34 dikinetids: kinety 1 extends postorally, composed of two dikinetids; kinety 2 extends right of oral apparatus, usually composed of three widely spaced dikinetids, last dikinetid with a caudal cilium almost as long as body; kinety 3 composed of one dikinetid; kineties 5–7 bipolar; kineties 8–10 strongly shortened extending in anterior half of body. Oral apparatus grossglockneriid, adoral polykinetid minute.

Type locality: Brazil, i. e., litter and soil from the rain forest around the Ariau Lodge on the Anavilhanas archipelago about 40 km west of the town of Manaus, 60°W 4°S.

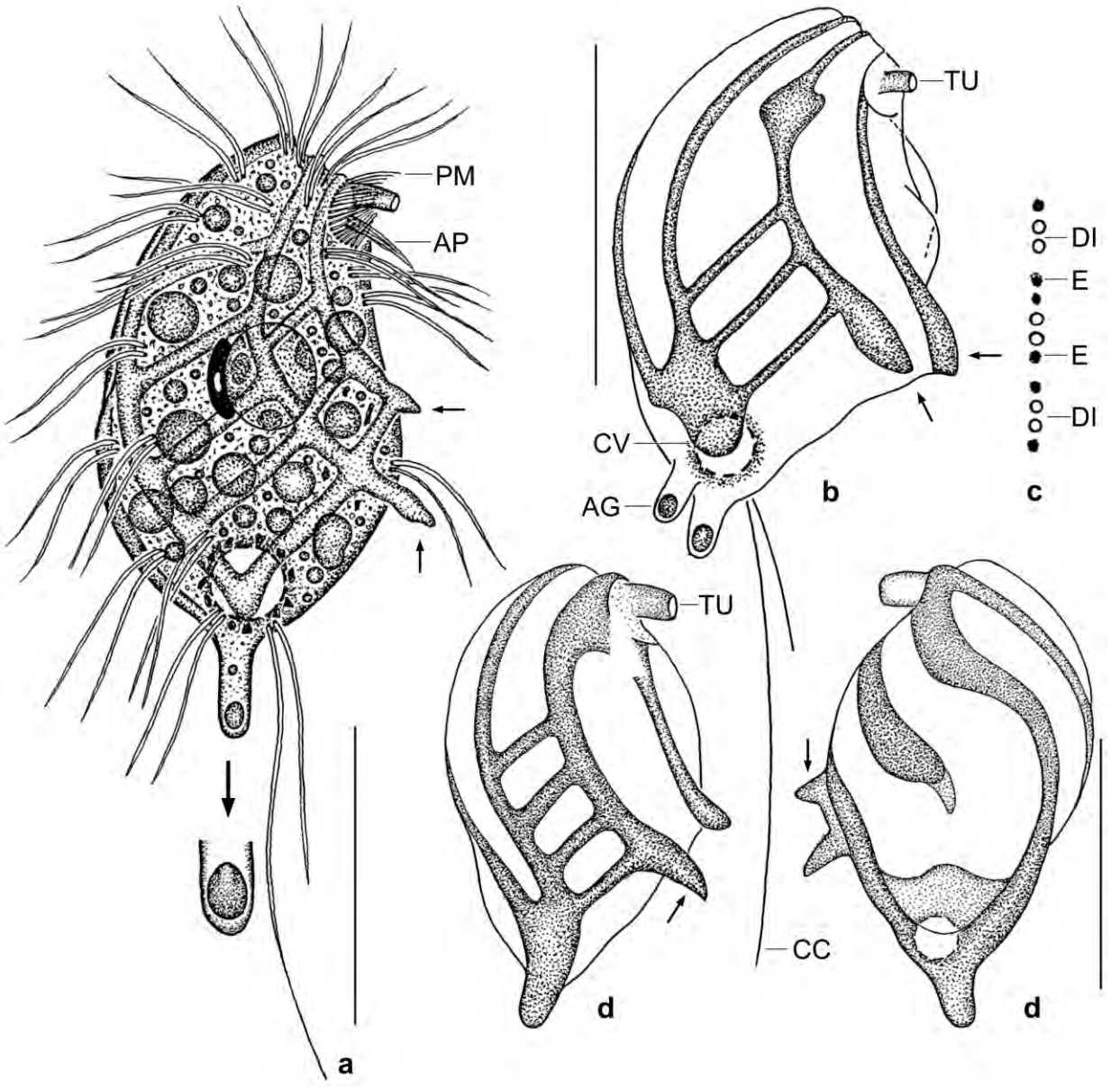

Fig. 109a–d. *Pseudoplatyophrya spinosa,* live illustrations from video records. Arrows mark ventral spines. **a:** Right side view of a representative specimen, length 30 µm. **b:** A specimen with two posterior appendages both containing an ellipsoid granule. **c:** Part of a ciliary row, showing the localization of the extrusomes. **d:** Right and left side view, showing the ridge pattern. AP – adoral polykinetid, AG – posterior appendage, CC – caudal cilium, CV – contractile vacuole, DI – dikinetids, E – extrusomes, PM – paroral membrane, TU – feeding tube. Scale bars 15 µm (a) and 20 µm (b, d).

Type material: 1 holotype and 3 paratype slides with protargol-impregnated specimens have been deposited in the Biology Centre of the Upper Austrian Museum in Linz (LI). Relevant specimens have been marked by black ink circles on the coverslip.

Etymology: The Latin adjective *spinosa* (spiny, thorny) refers to the spinous body.

Description: *Pseudoplatyophrya spinosa* has three processes of which those in mid-body are true "spines" related to cortex ridges. The tubular posterior process contains an ellipsoid granule resembling microsporidian cysts. We call this the "posterior appendage".

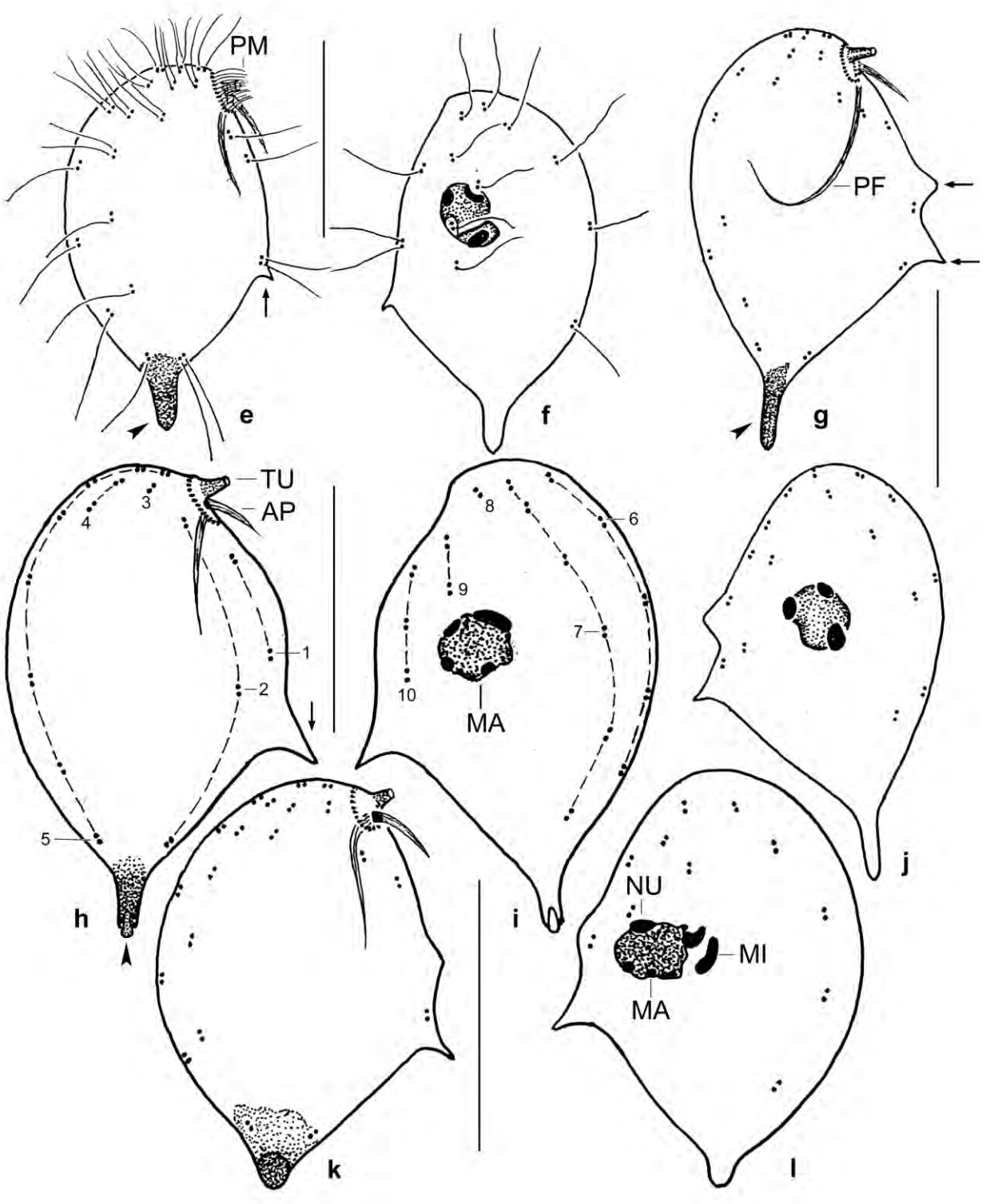

Fig. 109e–l. *Pseudoplatyophrya spinosa,* kinetid and nuclear pattern after protargol impregnation. Arrows mark ventral spines; arrowheads denote the argyrophilic posterior appendage. **e, f; g, j; h, i; k, l:** Right and left side view of four specimens. The supposed arrangement of the ciliary rows is shown in (h, i). Posteriorly, the cilia are slightly elongated and the anterior basal body of a pair is barren (e). AP – adoral polykinetid, MA – macronucleus, MI – micronucleus (?), NU – nucleolus, PF – pharyngeal fibres, PM – paroral membrane, TU – feeding tube, 1–10 – somatic kineties. Scale bars 15 μm.

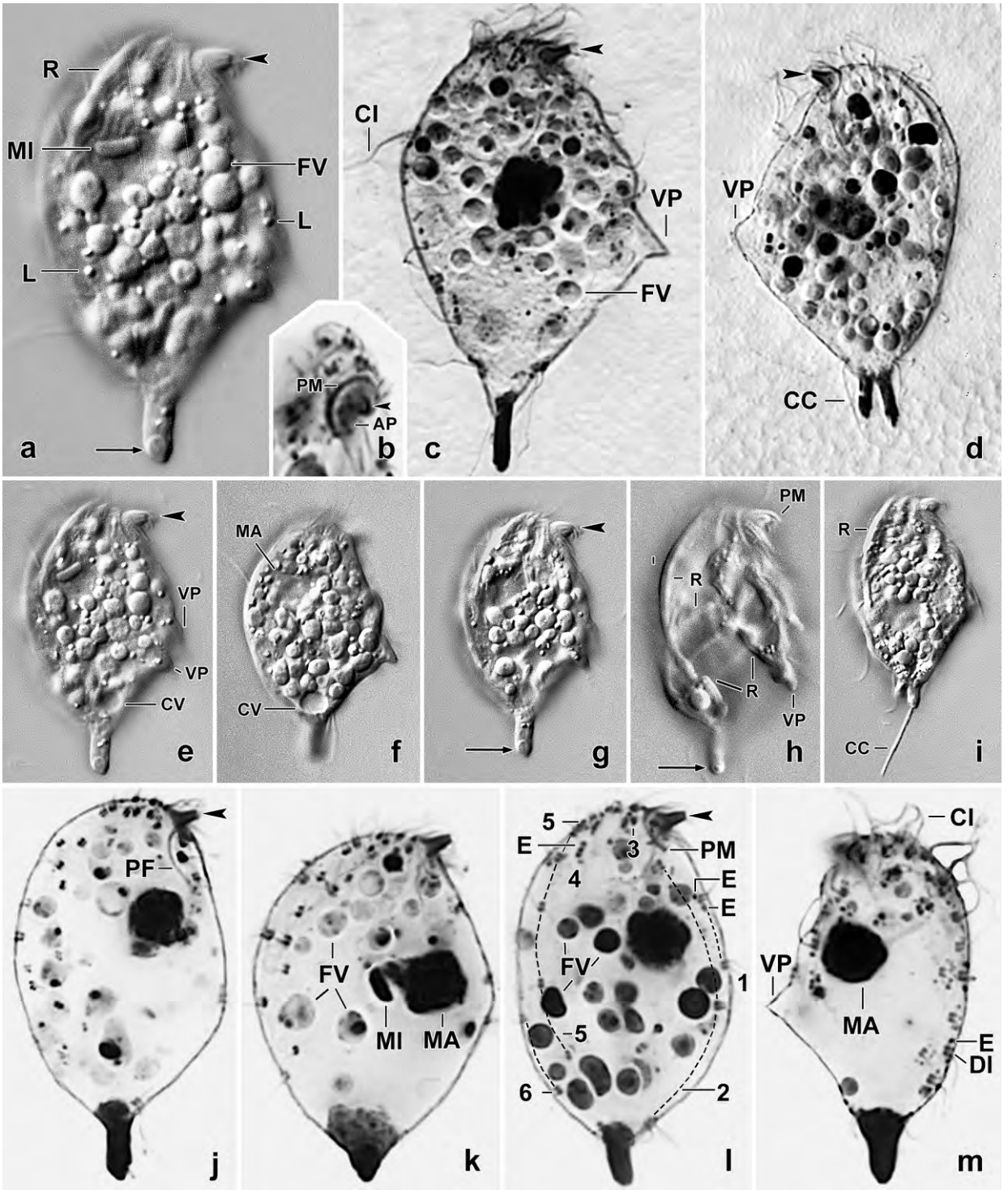

Fig. 110a–m. *Pseudoplatyophrya spinosa* from life (a, e–i) and after protargol impregnation (b–d, j–m). Arrows denote a granule in the posterior appendage which is, like the feeding tube (arrowheads) deeply impregnated. Right side kinety pattern shown in (l). AP – adoral polykinetid, CC – caudal cilium, CI – cilia, CV – contractile vacuole, E – extrusomes, FV – food vacuoles, L – lipid droplets, MA – macronucleus, MI – micronucleus, PF – pharyngeal fibres, PM – paroral membrane, R – cortical ridges, VP – ventral spines, 1–6 – somatic kineties. Length of cells with posterior appendage 25–35 µm.

Table 40. Morphometric data on *Pseudoplatyophrya spinosa* based on mounted, protargol-impregnated, well-prepared specimens from a non-flooded Petri dish culture. Measurements in µm. CV – coefficient of variation in %, M – median, Max – maximum, Mean – arithmetic mean, Min – minimum, n – number of individuals investigated, SD – standard deviation, SE – standard error of arithmetic mean.

Characteristics	Mean	M	SD	SE	CV	Min	Max	n
Body, length (with posterior appendage)	28.2	28.0	3.0	0.6	10.4	22.0	33.0	21
Body, width (with spines)	18.7	18.0	2.1	0.5	11.3	15.0	22.0	21
Body length:width, ratio	1.5	1.6	0.1	0.1	8.6	1.3	1.7	21
Anterior body end to paroral membrane, distance	3.9	4.0	0.6	0.1	15.4	3.0	5.0	21
Anterior body end to macronucleus, distance	7.8	8.0	2.2	0.5	28.2	3.0	13.0	21
Macronucleus, length	5.2	5.0	0.6	0.1	12.0	4.0	6.0	21
Macronucleus, width	4.3	4.0	0.5	0.1	10.7	4.0	5.0	21
Posterior appendage, length	4.2	4.0	0.9	0.2	21.0	2.0	6.0	21
Main spine on ventral side, height	2.3	2.0	0.6	0.1	25.5	1.0	3.0	21
Feeding tube, length	2.0	2.0	0.2	0.1	7.9	1.5	2.5	21
Dikinetids in kinety 1, number	2.0	2.0	0.0	0.0	0.0	2.0	2.0	12
Dikinetids in kinety 2, number	3.0	3.0	–	–	–	2.0	3.0	12
Dikinetids in kinety 3, number	1.0	1.0	0.0	0.0	0.0	1.0	1.0	12
Dikinetids in kinety 4, number	2.3	2.0	–	–	–	2.0	3.0	12
Dikinetids in kinety 5, number	7.7	8.0	0.7	0.2	8.5	6.0	8.0	12
Dikinetids in kinety 6, number	4.5	4.5	–	–	–	4.0	5.0	12
Dikinetids in kinety 7, number	5.0	5.0	0.7	0.2	14.8	4.0	6.0	12
Dikinetids in kinety 8, number [a]	1.3	1.0	–	–	–	1.0	2.0	12
Dikinetids in kinety 9, number [a]	2.7	2.0	1.1	0.3	40.2	2.0	5.0	12
Dikinetids in kinety 10, number [a]	2.3	2.5	0.8	0.2	33.4	1.0	3.0	12
Dikinetids, total number	33.9	34.0	1.2	0.3	3.4	32.0	36.0	12

[a] Approximate values because difficult to count.

Pseudoplatyophrya spinosa is moderately variable in most important features (CV ≤ 15%; Table 40) except of spine height (CV = 25.5%), the length of the posterior appendage (CV = 21%), and the number of kinetids in the "difficult" kineties 9 and 10 (CV = 30–40%).

Size in vivo 25–40 × 15–25 µm, usually about 30 × 20 µm with posterior appendage, as calculated from some in vivo measurements and the morphometric data in Table 40 adding 15% preparation shrinkage. Body ellipsoid to broadly ellipsoid with a length:width ratio of up to 1.7:1; rarely slightly ovate; laterally flattened up to 3:1. Anterior body end slightly to distinctly obliquely truncate, gradually narrowed to posterior appendage (Fig. 109a–l, 110a–m). Nuclear apparatus slightly anterior to mid-body on average (Fig. 109a, f, i, j, l, 110a, f, k, m; Table 40). Macronucleus globular to broadly ellipsoid, on average 5 × 4 µm in protargol preparations, with about five peripheral nucleoli 1–3 µm in size. Micronucleus in vivo about 3–4 × 1–2 µm, i. e., discoidal and comparably large as in *P. nana* (FOISSNER 1993a), stains blue with methyl green-pyronin but very rarely impregnates and distinctly shrinks in protargol preparations (Fig. 109l, 110k). Contractile vacuole in rear body end, i. e., anterior to posterior appendage, surrounded by sparkling crystals ≤ 1 µm in size. Minute (≤ 0.5 µm) cortical granules, very likely extrusomes of the mucocyst type, recognizable in protargol preparations, usually one granule anterior and posterior to dikinetids

(Fig. 109c, 110l, m). Cytoplasm colourless, usually packed with globular, rarely irregular, bright inclusions 0.5–3 µm in size, i. e., the contents of fungal hyphae and/or spores; inclusions of different protargol affinity, very likely depending on stage of digestion; contains also many sparkling crystals 0.5–1 µm in size (Fig. 109a, 110a, c–l). Glides rather rapidly on microscope slide and soil particles.

Cortex about 1 µm thick, glossy, supported by a complex ridge pattern forming two small ventrolateral spines in and slightly posterior to mid-body; anterior spine usually smaller than posterior; ridge height increases posteriorly. Ridge pattern rather variable but middle third of right side usually occupied by a faceted area in posterior half (Fig. 109a–d, 110c, d–f, h, m). Posterior appendage conspicuous in vivo and in protargol preparations because about 5 µm long and so deeply impregnated that the distal granule becomes indiscernible; tubular distal region occupied by an ellipsoid or broadly ovate granule 1–2 µm in size and occasionally with a rather bright area in anterior half; two such appendages in three out of 27 specimens investigated (Fig. 109a–d, e, g, h, k, 110a, c–e, g, h, m; Table 40).

Cilia in vivo about 10 µm long in upper thirds of body, about 13 µm in posterior third; caudal cilium about as long as body, distal third very fine; arranged in 10 rows of which rows 2, 5, 6, and 7 are bipolar while the others are distinctly shortened; in total about 34 dikinetids (Fig. 109a, e–l, 110j–m Table 40).

Oral apparatus grossglockneriid, i. e., minute and slightly subapical with feeding tube about 3 µm long in vivo. Paroral membrane semicircular, cilia about 4 µm long in vivo. Adoral polykinetid close posterior to feeding tube, likely composed of a row with three cilia and a second row with one cilium, cilia 4–5 µm long in vivo, form a beating bundle. Pharyngeal fibres distinct, extend vertically to mid-body (Fig. 109a, b, d, e, g, h, k, 110a–e, g–l; Table 40).

Occurrence and ecology: In the year 1996, we discovered this unusual ciliate in rain forest soil from a small island in the Rio Negro (see type locality and Foissner 1997), where it was very rare in the non-flooded Petri dish culture. We collected litter, soil and roots from 0–8 cm; litter layer up to 5 cm thick, followed by a 3–5 cm thick root-carpet mixed with brown, humic soil; mineral soil under root carpet loamy, brown, pH 5.1 in water.

It was a great surprise to find this conspicuous ciliate later in eastern Austria (Foissner et al. 2005a, *Pseudoplatyophrya sp.*), viz., in soil from a beech forest in the surroundings of the town of Dürnstein, 48°24’ N 15°32’ E; in vivo, it was indistinguishable from the Brazilian specimens. Like in Brazil, *P. spinosa* was very rare in the non-flooded Petri dish culture and could not be found in the protargol slides. The site we found it was investigated four times a year but *P. spinosa* appeared at only one occasion indicating special needs.

Remarks: *Pseudoplatyophrya spinosa* is unique among all colpodids described in having a cortical ridge pattern that forms two short spines on ventral side. If this pattern is inherent to the species, then it is easily identified. But we cannot exclude that the posterior appendage contains a microsporidian parasite – as described in a platyophryid colpodid by Foissner & Foissner (1995a, b) – that causes the cortical ridges. For this case, we provide a detailed comparison with the ciliary patterns of the congeners *P. nana*, → *P. isabelae*, and → *P. galapagensis*, as well as *Nivaliella*

plana (see FOISSNER 1993a for *P. nana* and *N. plana*). Ahead of this, we need to emphasize that some misinterpretations of the ciliary pattern cannot be excluded because these ciliates are so tiny and complex (e. g., caudal cilium associated with kinety 1 or 2, number of kinetids in a certain kinety, 9 or 10 ciliary rows).

Pseudoplatyophrya nana, type of the genus and the most common fungivorous ciliate has much more kinetids than *P. spinosa* (~ 60 vs. 34) and lacks argyrophilic material in the posterior body end. → *Pseudoplatyophrya isabelae* differs from *P. spinosa* by ciliary rows 3 (composed of six vs. one kinetid) and 7 (composed of five vs. two kinetids). → *Pseudoplatyophrya galapagensis* differs from *P. spinosa* by ciliary row 4 (composed of four vs. two kinetids) and by rows 6 and 7 which end posterior vs. anterior to mid-body. *Nivaliella plana,* which has 10 ciliary rows like *P. spinosa* (FOISSNER 1993a, FOISSNER et al. 2002), lacks a posterior accumulation of argyrophilic material and ciliary rows 5 and 7 end in or near mid-body vs. extend to posterior body end.

Except of *P. nana,* all *Pseudoplatyophrya* species and *Grossglockneria hyalina* have deeply impregnating material in the posterior body end, possibly fecal mass. However, the feeding tube impregnates usually also deeply in all grossglockneriids, possibly due to the enzymes contained. Thus, the deeply impregnating posterior material could contain similar enzymes as the feeding tube.

Maryna meridiana nov. spec. (Fig. 111a–g, 112a–s, 113b, d, e, 124; Table 41)

2002 *Maryna umbrellata* (GELEI, 1950) FOISSNER, 1993 – FOISSNER, AGATHA & BERGER, Denisia 5: 945 (misidentification; description and neotypification of a Costa Rican population).

Diagnosis (includes Costa Rican and Jamaican populations): Size about 100 µm or 65 µm in vivo, slightly broader than high. Calix very broadly conical or globular, uvula moderately conspicuous. Macro- and micronucleus globular to broadly ellipsoid. Contractile vacuole with short collecting canals. Extrusomes within ciliary rows, rod-shaped, 3–4 µm long. About 46 ciliary rows and 20 kineties in left oral polykinetid. Resting cysts 57 µm across on average. Cyst wall about 1 µm thick in vivo, covered by an up to 5 µm thick layer of glass granules 1–7 µm in size, most about 2 µm.

Type locality: In tanks of *Guzmania monostachia* (Bromeliaceae) along the road from the village of Quick Step to the Aberdeen House, Jamaica, St. Elisabeth, about 77°33'W 21°30' N.

Type material: 1 holotype and 1 paratype slide with protargol-impregnated specimens and 5 paratype slides with Chatton-Lwoff silver nitrate-impregnated cells have been deposited in the Biology Centre of the Upper Austrian Museum in Linz (LI). The holotype and other relevant specimens have been marked by black ink circles on the coverslip.

Etymology: *Meridiana* (south, southern) is a Latin adjective that refers to the supposed restricted Gondwanan (southern) distribution.

Description of Jamaican type population: The data are based on cultivated specimens from the type locality (tape water and some crashed wheat grains). Although having well-impregnated silver nitrate specimens (Table 41), we describe only protargol-impregnated cells fixed with ~

Table 41. Morphometric data on *Maryna umbrellata* from Austria (MU, from FOISSNER 2009), *M. meridiana* from Jamaican bromeliads (MJ, original data), and *M. meridiana* from Costa Rica (MC, from FOISSNER et al. 2002). Measurements in µm. Data based on randomly selected specimens from pure cultures. AU – Australian population, CHL – Chatton-Lwoff silver nitrate impregnation, CV – coefficient of variation in %, IV – in vivo, M – median, Max – maximum, Mean – arithmetic mean, Min – minimum, n – number of specimens investigated, P – protargol impregnation (FOISSNER method), Pop – population, PW – protargol impregnation (WILBERT method), SC – silver carbonate, SD – standard deviation, SE – standard error of arithmetic mean, SEM – scanning electron microscopy, TEM – transmission electron microscopy.

Characteristics	Pop	Method	Mean	M	SD	SE	CV	Min	Max	n
Body width, lateral view	MU	Osmium [a]	95.6	95.0	14.2	3.1	14.9	75	130	21
	MJ	Osmium [a]	62.3	65.0	6.4	1.4	10.3	50	70	21
Body height, lateral view	MU	Osmium [a]	89.2	90.0	10.3	2.2	11.5	75	110	21
	MJ	Osmium [a]	65.6	70.0	6.2	1.4	9.5	50	73	21
Body width, lateral view	MU	CHL	131.9	132.0	10.7	2.3	8.1	110	145	21
	MJ	CHL	63.0	62.0	6.2.	1.4	9.8	48	72	21
	MC	CHL	84.3	85.0	5.6	1.2	6.7	74	96	21
Body height, lateral view	MU	CHL	109.8	112.0	11.1	2.4	10.1	87	132	21
	MJ	CHL	57.8	55.0	6.5	1.4	11.2	50	73	21
	MC	CHL	71.9	70.0	6.3	1.4	8.7	76	104	21
Body width, transverse view (long axis)	MU	CHL	133.7	135.0	17.1	3.7	12.8	95	165	21
	MJ	CHL	63.1	65.0	5.3	1.2	8.5	52	72	21
	MC	CHL	79.0	80.0	4.3	0.9	5.5	70	86	21
Body width, transverse view (short axis)	MU	CHL	129.7	132.0	17.0	3.7	13.1	92	160	21
	MJ	CHL	58.1	60.0	4.6	1.0	7.9	47	65	21
Body width, lateral view	MU	P	128.5	128.0	16.0	3.5	12.5	93	160	21
	MJ	P	57.8	57.0	6.1	1.3	10.6	48	68	21
Body height, lateral view	MU	P	113.7	110.0	16.4	3.6	14.4	80	150	21
	MJ	P	59.4	58.0	6.2	1.3	10.4	52	70	21
Body width, transverse view (long axis)	MU	P	128.4	127.0	15.2	3.3	11.9	105	160	21
	MJ	P	59.8	60.0	6.1	1.3	10.1	50	68	21
Body width, transverse view (short axis)	MU	P	118.5	120.0	13.4	2.9	11.3	96	140	21
	MJ	P	58.4	60.0	5.9	1.3	10.1	50	67	21
Anterior body end to macronucleus, distance	MU	P	57.1	58.0	15.5	3.4	27.2	30	95	21
	MJ	P	27.0	27.0	6.2	1.4	23.2	17	38	21
	MC	CHL	36.0	35.0	6.6	1.4	18.4	20	47	21
Anterior body end to oral opening, distance	MU	P	100.8	100.0	13.6	3.8	13.5	80	120	13
	MJ	P	46.3	45.0	6.5	1.4	14.0	37	57	21
	MC	P	54.3	55.0	9.6	2.1	17.7	35	75	21
Macronucleus, length	MU	P	35.5	35.0	3.1	0.7	8.9	30	42	21
	MJ	P	17.1	17.0	1.9	0.4	10.9	13	20	21
	MC	PW	25.7	26.0	3.0	0.7	11.8	17	30	21
Macronucleus, width	MU	P	31.9	32.0	3.4	0.7	10.6	25	37	21
	MJ	P	14.0	13.0	1.5	0.3	11.0	12	17	21
	MC	PW	24.4	25.0	2.3	0.5	9.5	20	29	21
Micronucleus, length (with membrane)	MU	P	6.0	6.0	0.6	0.1	9.7	5	7	21
	MJ	P	3.3	3.0	0.4	0.1	13.2	2	4	21

continued

Characteristics	Pop	Method	Mean	M	SD	SE	CV	Min	Max	n
Micronucleus, width (with membrane)	MU	P	4.1	4.0	0.6	0.1	13.6	3	5	21
	MJ	P	3.0	3.0	0.4	0.1	13.0	2	4	21
Somatic kineties, total number	MU	P	83.1	83.0	9.7	1.7	11.6	72	110	31
	MJ	P	46.4	46.0	2.5	0.6	5.5	43	50	20
	MC	CHL	46.9	47.0	3.0	0.7	6.3	42	52	21
Postoral kineties, number	MU	P	5.9	6.0	0.8	0.1	13.6	5	8	35
	MJ	P	4.0	4.0	0.6	0.1	16.2	3	5	20
	MC	CHL	4.4	4.0	–	–	–	4	5	21
Buccal cavity, depth	MU	P	21.6	22.0	2.0	0.4	9.2	18	27	21
	MJ	P	13.4	13.0	1.5	0.3	11.5	10	15	21
Left oral polykinetid, length	MU	P	16.0	16.0	2.5	0.5	15.5	12	20	21
	MJ	P	10.3	10.0	0.6	0.1	5.5	9	11	21
	MC	PW	10.6	11.0	1.4	0.4	13.6	8	13	12
Left oral polykinetid, width	MU	P	6.8	7.0	1.2	0.3	18.1	5	9	21
	MJ	P	3.6	3.5	0.6	0.1	15.6	3	5	21
	MC	PW	5.5	5.0	0.7	0.2	12.3	5	7	12
Left oral polykinetid, number of kineties	MU	P	32.8	33.0	2.4	0.5	7.4	28	37	21
	MJ	P	19.4	20.0	1.5	0.3	7.7	16	22	21
	MC	PW	21.4	21.0	0.9	0.2	4.1	20	23	13
	VE	SC	16.4	16.0	1.1	0.4	6.9	15	19	9
Right oral polykinetid, length	MU	P	21.9	22.0	2.2	0.5	10.2	18	27	21
	MJ	P	13.1	13.0	1.2	0.3	9.4	9	15	21
	MC	PW	19.9	19.0	3.5	1.0	17.6	16	26	12
Right oral polykinetid, width	MU	P	9.9	10.0	1.2	0.3	11.9	8	12	21
	MJ	P	4.9	5.0	0.6	0.1	12.1	4	6	21
	MC	PW	8.0	8.0	1.1	0.3	14.1	6	10	12
Resting cyst, diameter	MU	IV	102.5	100.0	8.8	1.9	8.6	90	120	21
	MJ	IV	57.2	58.0	3.8	0.9	6.7	52	65	19
	AU	IV	66.1	64.0	5.0	1.1	7.5	59	76	21
Resting cyst, wall thickness without glass layer	MU	TEM	9.3	8.7	3.1	1.0	32.0	5	14	9
	MJ	TEM	1.5	1.6	0.3	0.1	19.6	1.2	1.9	14
Resting cyst, diameter of glass granules	MU	SEM	0.8	0.8	0.3	0.1	3.3	0.17	1.3	129
	MJ	SEM	1.9	1.9	0.6	0.1	32.3	1.0	2.9	43
	AU	IV	2.8	3.0	1.6	0.3	56.0	1.0	6.0	29

[a] Taken as in vivo size.

70% ethanol because silver nitrate prepared cells were used for the description of the Costa Rican population (FOISSNER et al. 2002). Together, these preparations provide a very detailed morphology.

Maryna meridiana has a moderate variability with all important features having variation coefficients ≤ 15% (Table 41).

Size very similar with the three methods used, in vivo 50–73 × 48–72 µm, usually about 60

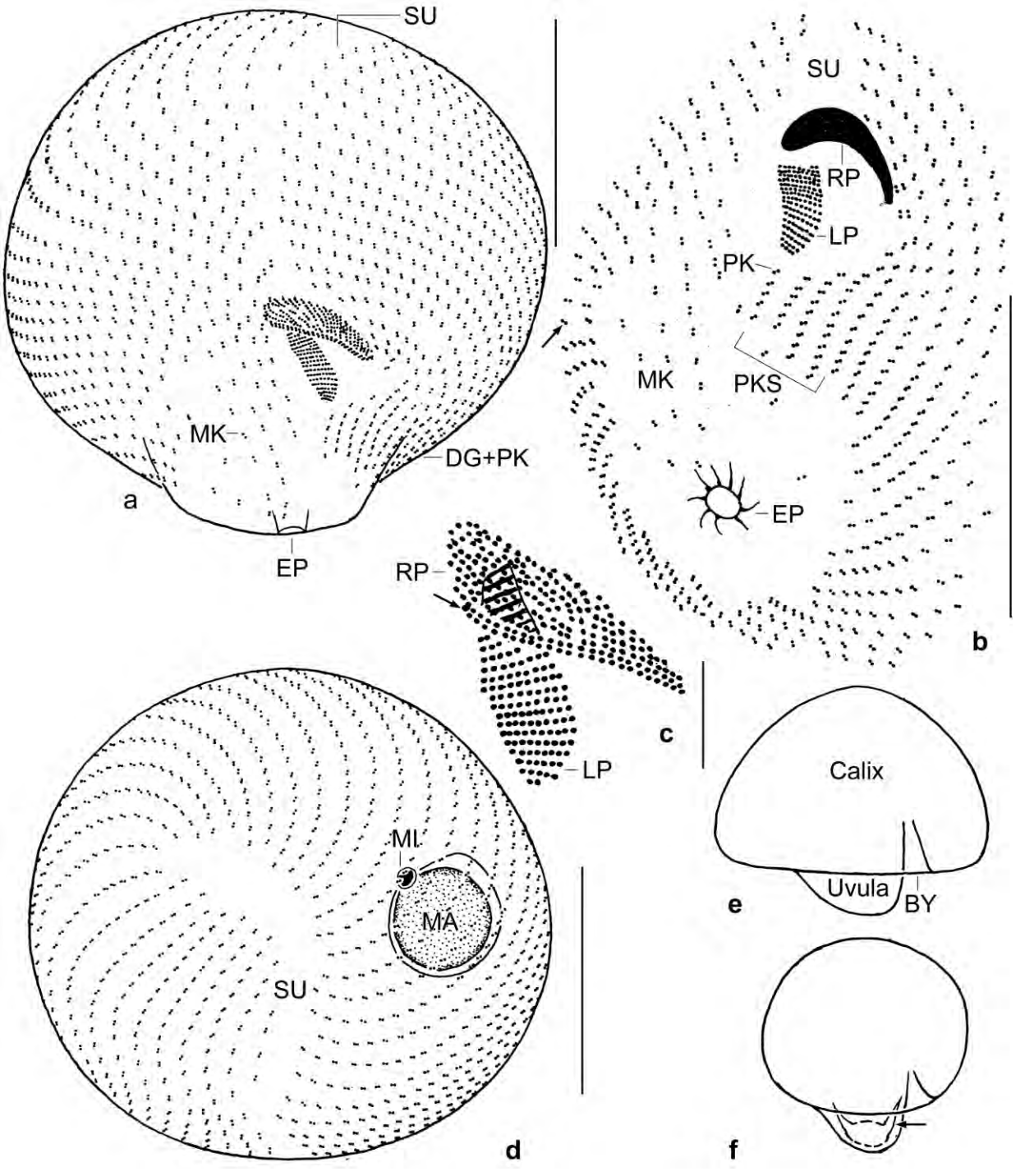

Fig. 111a–f. *Maryna meridiana* from life (e, f) and after protargol impregnation (a–d). **a:** Ventral view of holotype specimen, ~ 60 µm. Note the globular shape. **b:** Oblique posterior polar view. The postoral kineties s. str. (PKS) are those that extend posterior of the oral opening while the postoral kineties s. l. (PK) extend in the diagonal groove with last kinety marked by an arrow. **c:** Oral polykinetids. The arrow marks a row of dikinetids on dorsal margin of the right polykinetid. **d:** Anterior polar view. **e, f:** Two frequent body shapes in the environmental sample. The arrow marks a collecting canal of the contractile vacuole. BY – buccal cavity, DG – diagonal groove, EP – excretory pore, LP – left oral polykinetid, MA – macronucleus, MK – mycteral kineties, MI – micronucleus, PK – postoral kineties s. l., PKS – postoral kineties s. str., RP – right oral polykinetid, SU – suture. Scale bars 5 µm (c) and 25 µm (a, b, d).

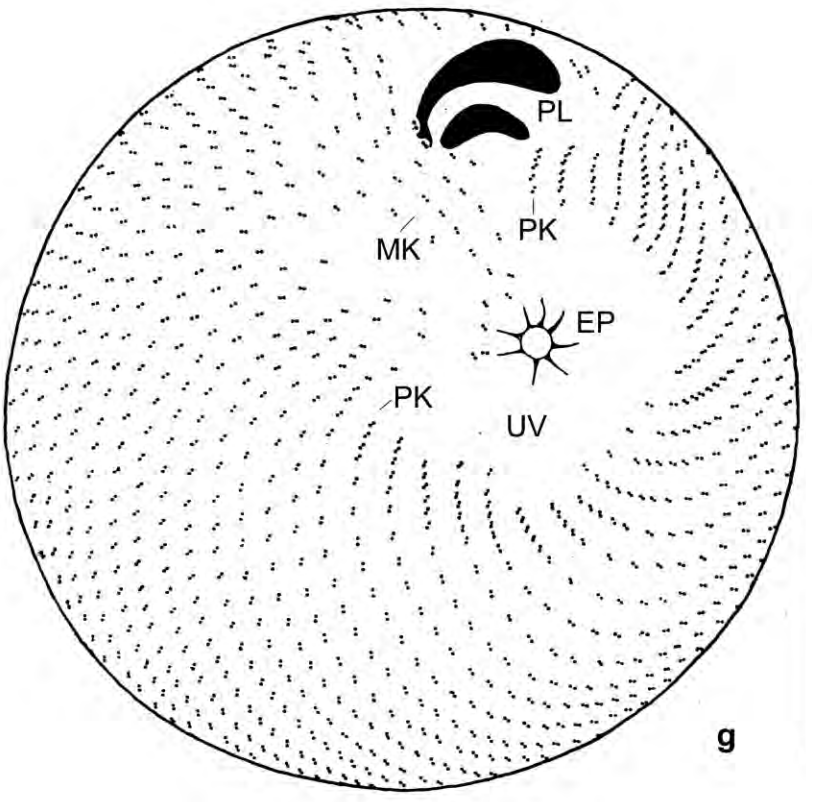

Fig. 111g. *Maryna meridiana*, posterior polar view after protargol impregnation. The ciliature, which consists of dikinetids, is highly ordered. The uvula is free of cilia except of the mycteral kineties that extend to the excretory pore of the contractile vacuole. The postoral kineties extend in the diagonal (postoral) groove and have a condensed ciliature. The excretory pore of the contractile vacuole is anchored by fibres. For the structure of the oral polykinetids, see Figures 111a, c, 112j, m, n. EP – excretory pore, MK – mycteral kineties, PK – postoral kineties, PL – oral polykinetids, UV – uvula. Scale bar 25 µm.

µm high and 65 µm wide (Table 41). Calix (cap) usually broadly conical (Fig. 111e, 112a, i, 113d), becomes easily globular under oxygen stress and in preparations (Fig. 111a, f), ventrally indistinctly flattened and with a shallow groove containing preoral suture. Uvula (trunk) rather conspicuous because projecting distinctly from body proper, roughly triangular in lateral view because merging into dorsal side, diagonal (postoral) groove comparatively flat (Fig. 111a, e, f, 112a, b, d, e, i, 113d; Table 41). Nuclear apparatus in or near mid-body on average (Fig. 111d, k, l, 113d; Table 41). Macronucleus globular to broadly ellipsoid, in vivo about 20 µm across, with a 1 µm thick membrane and reticulate nucleolus. Micronucleus attached to macronucleus, globular to broadly ellipsoid, with distinct membrane separated from contents. Contractile vacuole in uvula, with inconspicuous collecting canals and single excretory pore in centre of uvula surface; excretory pore about 3 µm across, anchored to cell with short fibres (Fig. 111a, b, f, g, 112a, c–e, 113d). Cortex very flexible, gelatinous and about 1 µm thick, punctated by ciliary pits, in optical section rather distinctly striated by the extrusomes (Fig. 112a, b, o, 113d). Extrusomes numerous and scattered within ciliary rows, rod-shaped and fine, in vivo about 2–3 × < 0.5 µm, form an indistinct cortical fringe, stain purple and become extruded, but do not explode when methyl green-pyronin is applied (Fig. 112b, n, 113d); belong to the mucocyst type (Foissner, unpubl.). Cytoplasm packed with inclusions: (i) numerous food vacuoles 3–6 µm and 10–20 µm in size in the acid and alkaline phase, respectively; most filled with short bacterial rods, some with about 8 µm long, coiled bacteria (Fig. 112f, 113d); (ii) lipid droplets 1–4 µm, usually 2–3 µm across (Fig. 112f, 113d); (iii) glass granules about 1 µm in size and forming a brownish spot in anterior half of dorsal side, conspicuously sparkling under interference contrast while colourless under transmitted light (Fig. 112g, h, 113b, d). Does not feed on *Polytomella* sp. even when present in

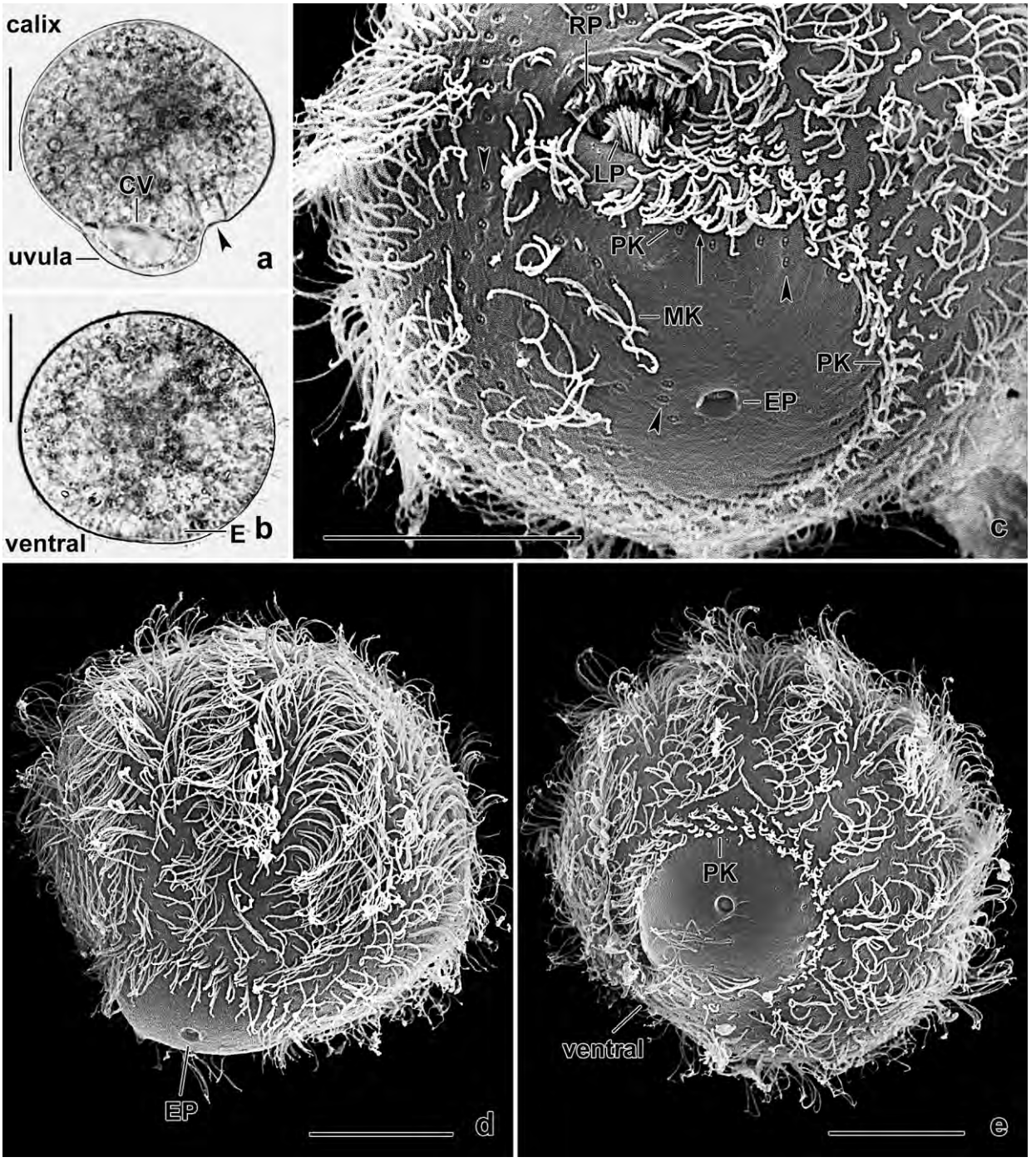

Fig. 112a–e. *Maryna meridiana* osmium fixed (a, b) and in the scanning electron microscope (c–e). **a:** Right side view, showing general organization. The arrowhead marks the oral funnel. **b:** Transverse view, showing a slight flattening of the ventral side. **c:** Oblique posterior polar view, showing the oral apparatus and the different length of the ordinary somatic cilia, the mycteral cilia, the minute postoral cilia, and the slightly longer postoral cilia (arrow) left of the oral opening and posterior of the ordinary postoral cilia. Arrowheads mark unciliated dikinetids. **d:** Lateral view, showing nice metachronal ciliary waves and the naked uvula. **e:** Posterior polar view, showing nice metachronal ciliary waves and the minute postoral cilia in the diagonal groove. CV – contractile vacuole, EP – excretory pore of the contractile vacuole, LP – left oral polykinetid, MK – mycteral cilia, PK – postoral kineties, RP – right oral polykinetid. Scale bars 20 μm (c–e) and 30 μm (a, b).

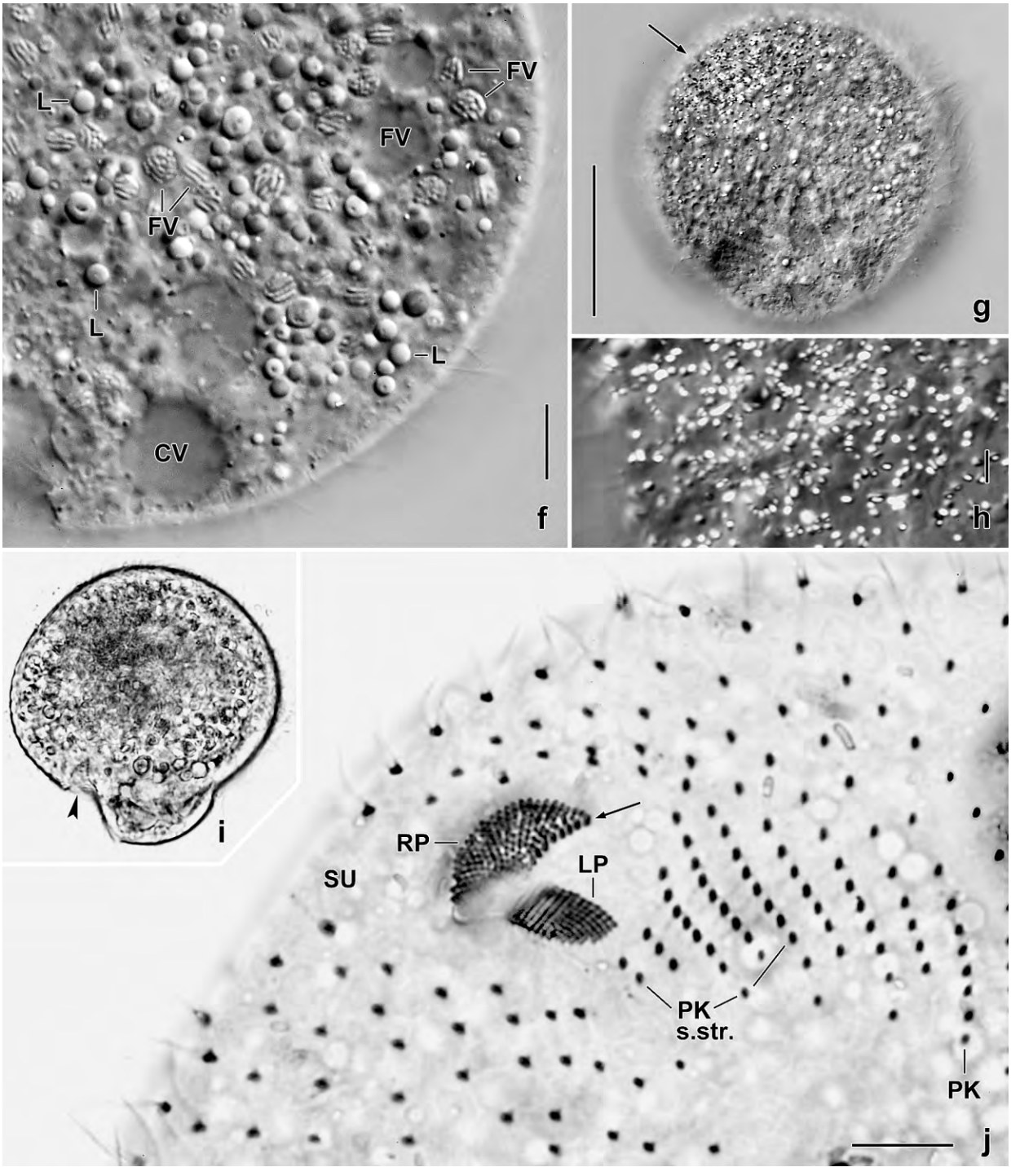

Fig. 112f–j. *Maryna meridiana* from life (f–h), osmium fixed (i), and protargol-impregnated (j). **f:** Posterior region, showing the cytoplasm crammed with lipid droplets and small food vacuoles containing bacterial rods. **g, h:** Oblique posterior polar view, showing a spot (g, arrow) of glass granules conspicuously sparkling under interference contrast (h). **i:** A globular cell with distinct uvula. The arrowhead marks the oral opening. **j:** Oral area, showing parts of the oral polykinetids and the narrowly spaced dikinetids of the postoral kineties which extend anteriorly. The arrow marks a row of dikinetids on dorsal edge of the right polykinetid. CV – contractile vacuole, FV – food vacuoles, L – lipid droplets, LP – left oral polykinetid, PK – postoral kineties, RP – right oral polykinetid, SU – preoral suture. Scale bars 5 µm (h), 10 µm (f, j), 30 µm (g), and 40 µm (i).

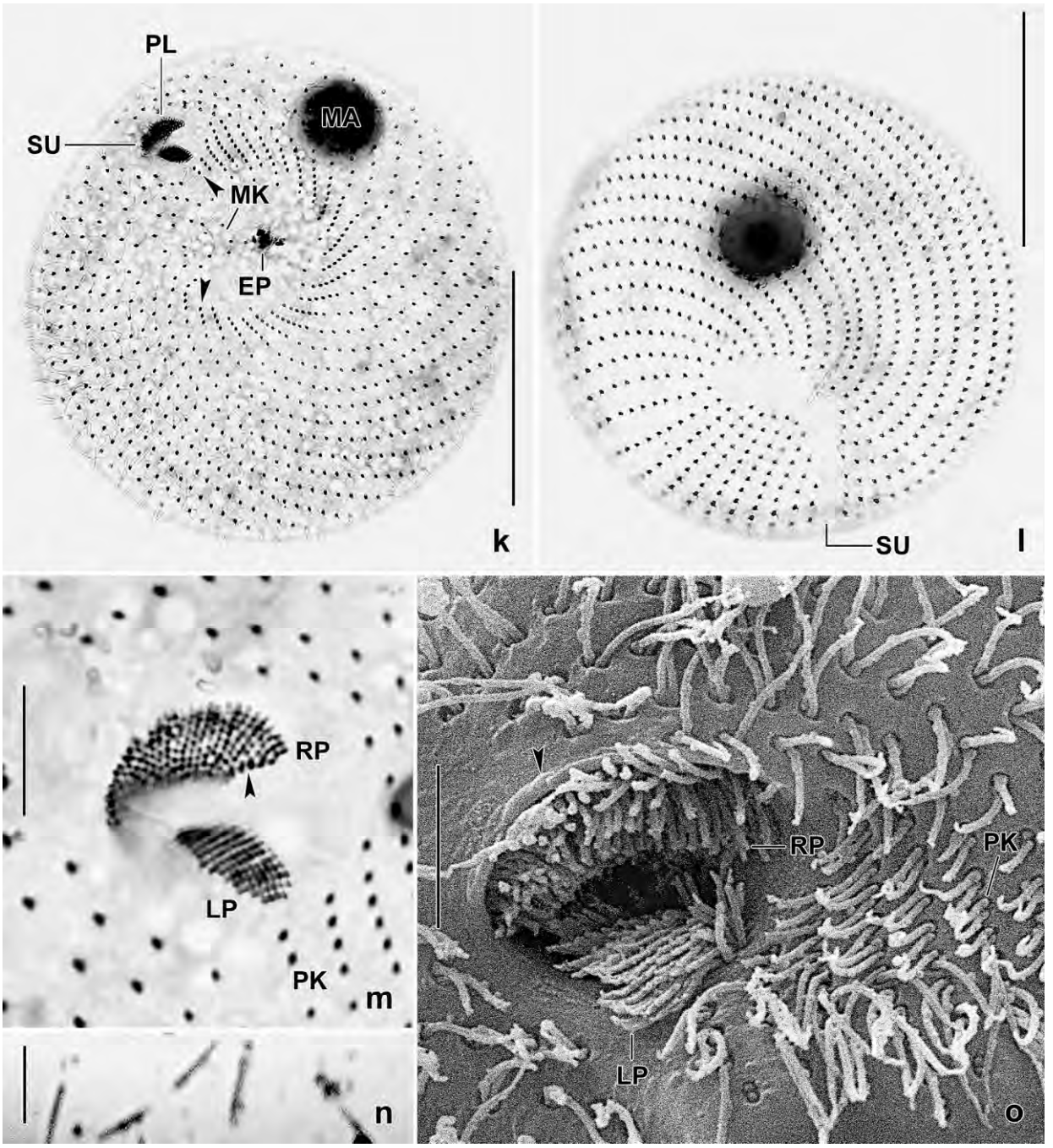

Fig. 112k–o. *Maryna meridiana* after protargol impregnation (k–m), in a methyl green-pyronin stain (n), and in the SEM (o). **k, l:** Posterior and anterior polar view, showing the highly ordered somatic basal bodies. There is a spoon-shaped ventral suture extending from the oral apparatus to the anterior pole where it broadens. The arrowheads denote the first and the last postoral kinety s. l. where the dikinetids are condensed. **m:** The buccal cavity contains two distinct polykinetids. The left polykinetid is made of short, equidistantly spaced kineties while some irregularities occur in the right polykinetid which has a row of dikinetids on the dorsal edge (arrowhead). **n:** When methyl green-pyronin is applied, the extrusomes are discharged but do not elongate. **o:** The anterior margin of the oral opening is slightly thickened. The two oral polykinetids and the postoral kineties have short, about 3 µm long cilia. EP – excretory pore of the contractile vacuole, LP – left oral polykinetid, MA – macronucleus, MI – micronucleus, MK – mycteral kineties, PK – postoral kineties, PL – oral polykinetds, RP – right oral polykinetid, SU – ventral suture. Scale bars 3 µm (n), 10 µm (m), 25 µm (o), and 40 µm (k, l).

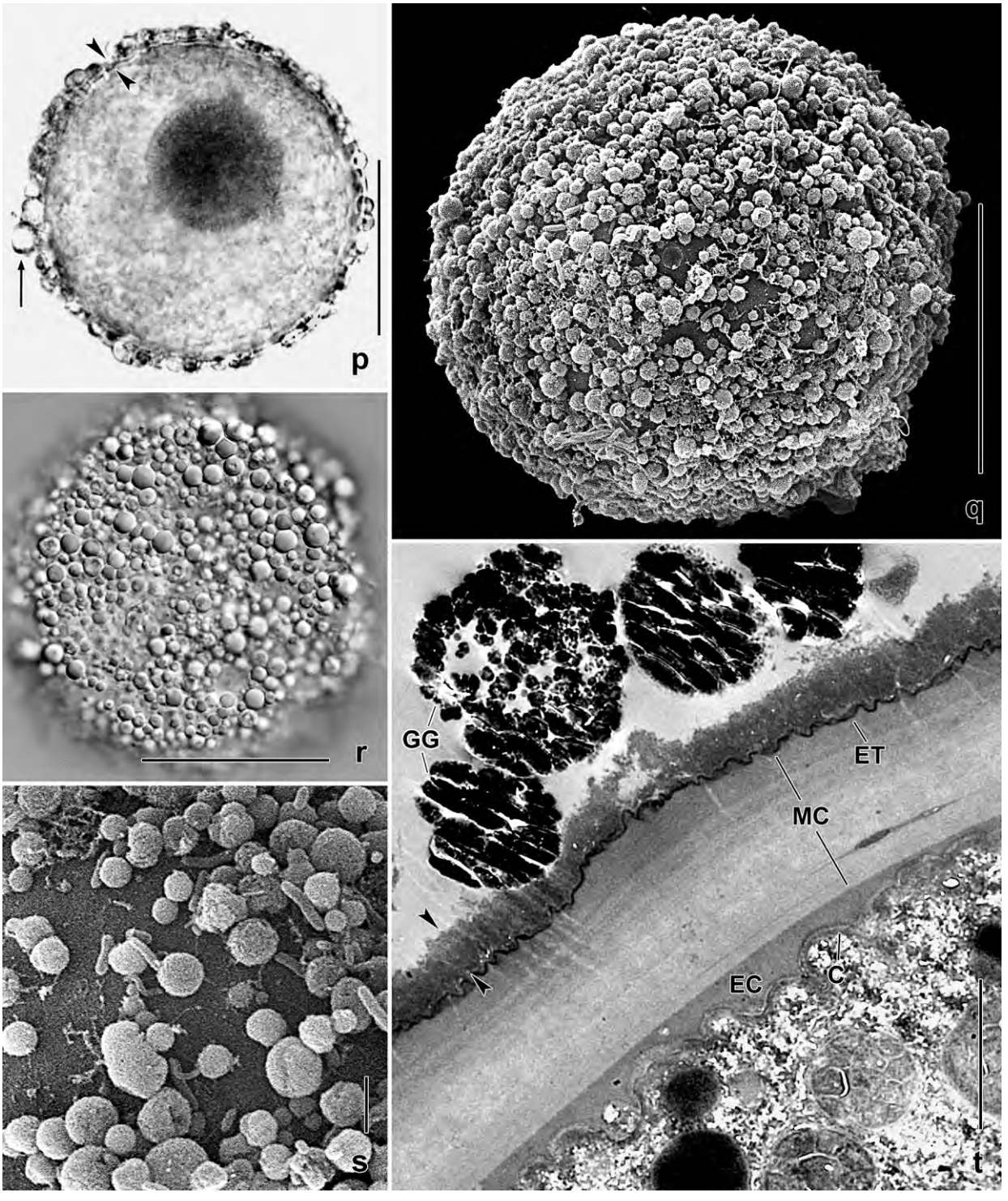

Fig. 112p–t. *Maryna meridiana,* resting cysts from life (p, r) and in the scanning (q, s) and transmission (t) electron microscope. **p:** Optical section, showing the thin cyst wall (opposed arrwoheads) and some large glass granules (arrow). **q–s:** Surface views, showing the glass granules most having a diameter of 2–3 µm. **t:** The structure of the cyst wall is highly similar to that of *M. umbrellata* but the wall is much thinner (1.5 vs. 9.3 µm; Table 41). The opposed arrowheads denote the basal layer. C – cortex, EC – endocyst, ET – ectocyst, L – lepidosomes (glass granules), MA – macronucleus, MC – mesocyst. Scale bars 1 µm (t), 3 µm (s), and 30 µm (p–r).

masses. Swims rapidly in narrow spirals. Does not build dwelling tubes neither in environmental samples or in pure cultures grown at various conditions.

Somatic and oral ciliary pattern as typical for *Maryna* (Foissner 1993a). Silverline pattern also as in congeners and described for a Costa Rican population by Foissner et al. (2002). All kinetids paired, anterior cilium lacking in some mycteral kinetids. Cilia sprout from elliptic pits, of very different length in vivo and in the scanning electron microscope: those on calix 10–12 µm long, produce nice metachronal waves; mycteral and postoral s. str. cilia about 7 µm long; those in diagonal (postoral) groove only 3–4 µm long; elongated caudal cilia definitely absent (Fig. 111d, 112c–e, o, 113d). Cilia arranged in an average of 46 rows including four postoral kineties s. str.; rows extend spirally from anterior pole into diagonal groove with last kinetids distinctly condensed, separated in a right and a left portion by a distinct preoral suture performing a sharp right-turn anteriorly and widens on pole area; postoral suture also distinct because in a "stripe contrast" zone, that is, the region where the loosely ciliated mycteral kineties right of the oral opening abut in sharp angles on the more densely ciliated postoral kineties. Uvula surface barren except of a few mycteral kineties extending to or near to excretory pore of contractile vacuole (Fig. 111a, b, d, g, 112c–e, j–l, o; Table 41).

Oral apparatus between calix and uvula, small compared to size of cell (Table 41). Buccal cavity conical, about 15 µm deep in vivo, extends obliquely to body centre. Oral opening elliptic, margin of right half thickened, aboral side merges into diagonal groove (Fig. 111a, b, e, g, 112a, c, i, o, 113d). Cilia of oral polykinetids 3–4 µm long in vivo, left polykinetid on bottom of buccal cavity, elongate elliptic, i. e., 10 × 3.6 µm in protargol preparations, composed of an average of 19 monokinetal rows decreasing gradually in length at both ends. Right oral polykinetid on roof of buccal cavity, cuneate with broad end proximally, composed of a proximal row of dikinetids and of slightly irregular oblique rows of monokinetids. Pharyngeal fibres not impregnated but as distinct as in *M. umbrellata* in specimens fixed with mercuric chloride (Fig. 111a–c, g, 112c, j, k, n, o, 113d; Table 41).

Resting cyst (Fig. 112p–t, 113e; Table 41; for TEM details, see Foissner 2009): Highly similar to that of Costa Rican population studied by Foissner et al. (2002). Globular, 57 µm across on average and with glass layer, colourless but dark at low magnification (≤ 100×) due to the thick layer of glass granules and the dense cytoplasm. Cyst wall composed of two distinct layers: internal layer in vivo 0.5–1 µm thick while 1.5 µm in TEM micrographs because basal layer and endocyst not recognizable in vivo; external layer slimy, up to 5 µm thick, composed of colourless to yellowish glass granules 1–7 µm across in vivo while 1.9 µm in SEM micrographs (Fig. 112q, s; Table 41), make small heaps producing a rough cyst outline (Fig. 112q), homogenous to ring-shaped in the light microscope.

Extrusomes maintained, attached to the strongly crenelated cortex. Nuclear apparatus in or near cyst centre, covered by an up to 2 µm thick layer of glass granules becoming reddish under transmitted light and moderate magnification (250×), conspicuously sparkling under interference contrast. Cytoplasm packed with lipid (?) droplets 1–3 µm across and some glass granules.

Molecular phylogeny (Foissner et al. 2014 and Fig. 124): We expected that *M. meridiana* would

make a clade with the similar → *M. umbrellata* or with *M. ovata*. However, *M. meridiana* makes a well-supported clade (0.99/1.00) with a Botswanan *Pseudomaryna* that has a rather different morphology (Foissner, unpubl.).

Occurrence and ecology: As yet found at four sites in Namibia (Foissner et al. 2002, misidentified as *M. umbrellata*): granitic and dolomitic rock-pools, Okerfontein water-hole in the Etosha Pan); Botswana (soil from a dry part of the Chobe River); Australia (lithotelma); Costa Rica (rock-pools in the surroundings of the ranch house "La Casona", Santa Rosa National Park), Jamaica (tank bromeliad, see type locality), and Venezuelan sites 41, 42, 66, 70 (rock pools on granitic outcroppings). Obviously, *M. meridiana* is restricted to ephemeral Gondwanan habitats. Very likely feeds exclusively on bacteria.

Comparison of populations: There is only one remarkable difference between the Jamaican population and those studied by Foissner et al. (2002), viz., body size in vivo: 50–75 µm in the Jamaican type population while 80–110 µm in the Costa Rican specimens, 70–120 µm in the Australian cells, and 70–90 µm in the Namibian specimens. Such differences are recognizable also in silver nitrate-impregnated cells (Table 41): body width 48–72 µm vs. 74–96 µm in the Costa Rican specimens. In contrast, the number of ciliary rows on body and in the left oral polykinetid is very similar (Table 41). Thus, we consider the size differences of minor importance and emphasize the other features, including the very similar resting cysts known, however, only from the Jamaican and Australian populations.

Comparison with → *M. umbrellata* (Table 41): Although there is some overlap in body size, *M. umbrellata* is on average considerably larger than *M. meridiana* (body width 132 µm vs. 63 µm in silver nitrate preparations, 96 µm vs. 62 µm in Osmium fixed cells, and 129 µm vs. 58 µm in protargol preparations). Further, the numbers of ciliary rows on body (83 vs. 46) and in the left oral polykinetid (33 vs. 19) are markedly different. This applies also to the size of the resting cysts (103 µm vs. 57 µm) and the thickness of the cyst wall (9.3 µm vs. 1.5 µm) while the glass granules are distinctly smaller in *M. umbrellata* than in *M. meridiana* (0.8 µm vs. 1.9 µm). These are massive morphometric differences justifying both as distinct species which is corroborated by the molecular data discussed above.

Comparison with other congeners: Among the species reviewed by Foissner (1993a) and (re) described by Foissner et al. (2002) only *M. atra* (Gelei, 1950) Foissner, 1993a has some similarity with *M. meridiana*. They differ by the macronucleus (ellipsoid vs. globular), the extrusomes (not recognizable vs. 3 µm long rods), the cytoplasm (dark vs. opaque at low magnification), the left oral polykinetid (composed of about 14 vs. 19 kineties), and the cyst wall (6–8 µm thick with brown crystals in ectocyst vs. up to 2 µm thick and with conspicuous glass granules 1–7 µm across).

The false neotypification of *M. umbrellata* (Gelei, 1950) Foissner, 1993a by Foissner et al. (2002): Foissner et al. (2002) misidentified *M. meridiana* as *M. umbrellata*, assuming that Gelei´s data on body size and number of ciliary rows were incorrect. Now we know that this was premature because another population matches Gelei´s description much better except for the short collecting canals of the contractile vacuole (see redescription of → *M. umbrellata*).

Maryna umbrellata (Gelei, 1950) Foissner, 1993a (Fig. 113a–c, f–o, 114a–s, 115a–m, 124; Table 41)

1950 *Mycterothrix umbrellata* Gelei, Hidrol. Közl., 30: 112.

1993 *Maryna umbrellata* (Gelei, 1950) nov. comb.– Foissner, Colpodea: 339 (revision).

2002 *Maryna umbrellata* (Gelei, 1950) Foissner, 1993 – Foissner, Agatha & Berger, Denisia 5: 945 (misidentification, see → *Maryna meridiana).*

2009 *Maryna umbrellata* (Gelei, 1950) Foissner, 1993 – Foissner, Weissenbacher, Krautgartner & Lütz-Meindl, J. Eukaryot. Microbiol., 56: 519 (description of glass granules in morphostatic and cystic specimens).

2009 *Maryna umbrellata* (Gelei, 1950) Foissner, 1993 – Foissner, Acta Protozool., 48: 223 (detailed description of resting cyst).

Improved diagnosis (includes Hungarian type population and the Austrian specimens described here): Size about 130 × 115 µm in vivo, slightly broader than high. Calix broadly conical, uvula inconspicuous. Macro- and micronucleus globular to broadly ellipsoid. Contractile vacuole with short collecting canals or small collecting vesicles. Extrusomes within ciliary rows, rod-shaped, about 6 × 0.3 µm in size. On average 83 ciliary rows and 33 kineties in left oral polykinetid. Resting cysts about 100 µm across on average. Cyst wall about 13 µm thick in vivo, including an about 4 µm thick glass cover with glass granules ≤ 1 µm in size.

Type locality: Hungary, possibly in the surroundings of the town of Szeged (20°05'E 46°10'N). The population investigated here is from an ephemeral grassland pond in the town of Salzburg, Austria (13°02'40''E 47°47''30.7''N; see Cotterill et al. 2013 for a detailed description).

Voucher material: 7 and 9 voucher slides with protargol and silver nitrate-impregnated (Chatton-Lwoff method) specimens, respectively, have been deposited in the Biology Centre of the Upper Austrian Museum in Linz (LI). Relevant specimens have been marked by black ink circles on the coverslip.

Etymology: Not given in the original description. The Latin noun *umbrella* (sunshade, bell-shaped) obviously refers to the umbrella-shaped calix.

Redescription: Most data are based on specimens cultivated on Eau de Volvic (French mineral water) supplemented with some crushed wheat grains. This provides flourishing cultures.

Maryna umbrellata is ordinarily variable with most variation coefficients ≤ 15% (Table 41). The high variability of the thickness of cyst wall (CV = 32%) is caused by a technical reason, i. e., when the cyst is not sectioned in the middle quarter then the wall becomes more or less obliquely sectioned increasing its thickness.

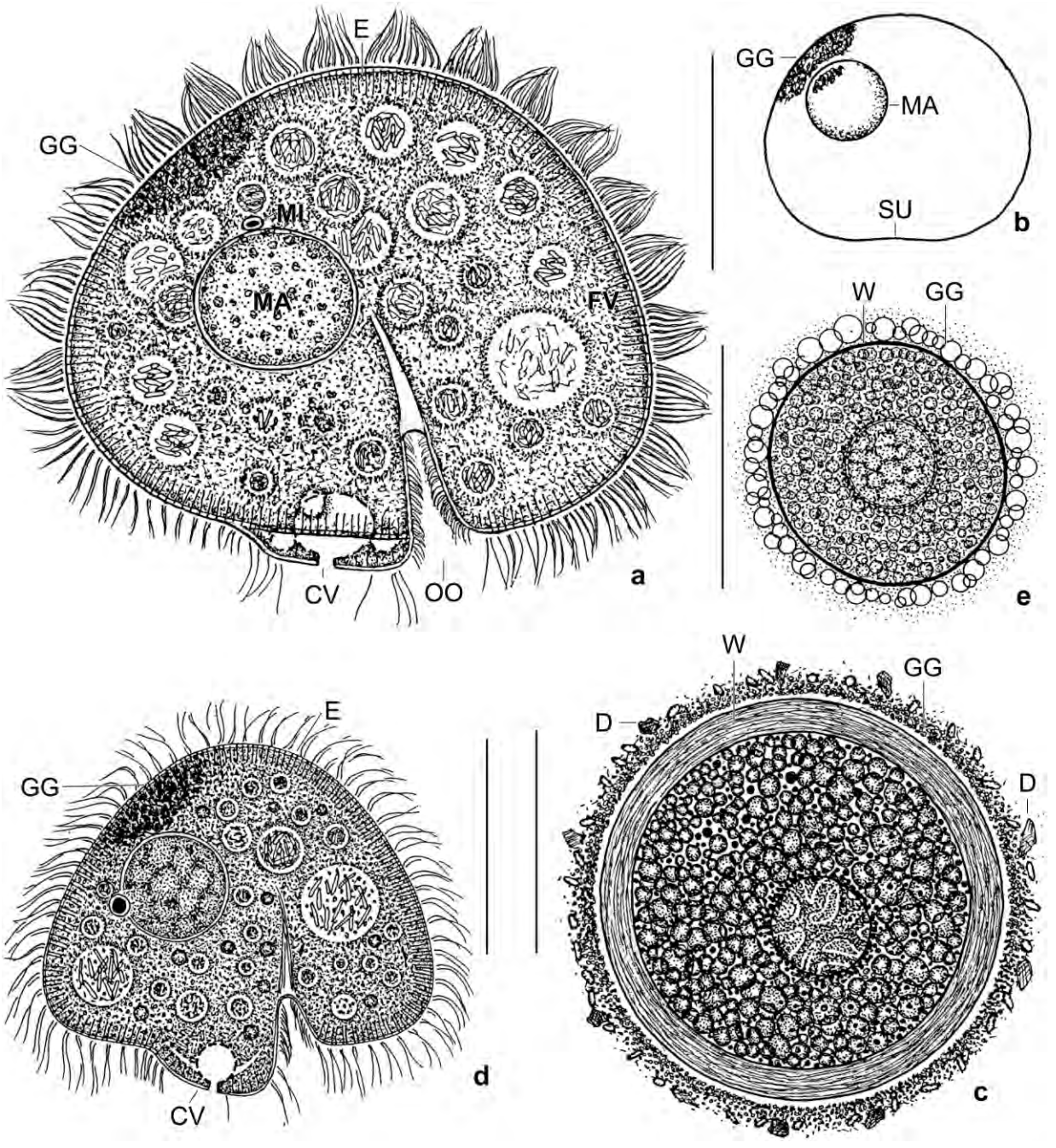

Fig. 113a–e. *Maryna umbrellata* (a–c) and *M. meridiana* (d, e; from Foissner et al. 2002, refined to include Jamaican population) from life and drawn to scale. **a, d:** The morphostatic specimens are in vivo very similar in body shape and structure but differ distinctly in body size (~ 130 µm vs. 65 µm to 100 µm; Foissner et al. 2002). In silver preparations, the number of ciliary rows on body (~83 vs. 46) and in the left oral polykinetid (~ 33 vs. 19) is markedly different (Table 41). **b:** Transverse view, showing a slight dorsoventral flattening and the spot of glass granules. **c, e:** The resting cysts are quite different in size (~ 100 µm vs. 60 µm, Table 41) and structure: cyst wall without glass cover ~ 9 µm vs. 1 µm thick in vivo, glass granules ~ 2 µm (up to 7 µm) vs. 1 µm across on average. CV – contractile vacuole and excretory pore, D – debris, E – extrusomes form a rather distinct fringe, FV – food vacuoles, GG – glass granules, forming a brownish, dorsolateral spot in the morphostatic specimens and a dense external layer in the resting cysts, MA – macronucleus, MI – micronucleus, OO – oral opening, SU – preoral suture, W – cyst wall without glass layer. Scale bars 50 µm.

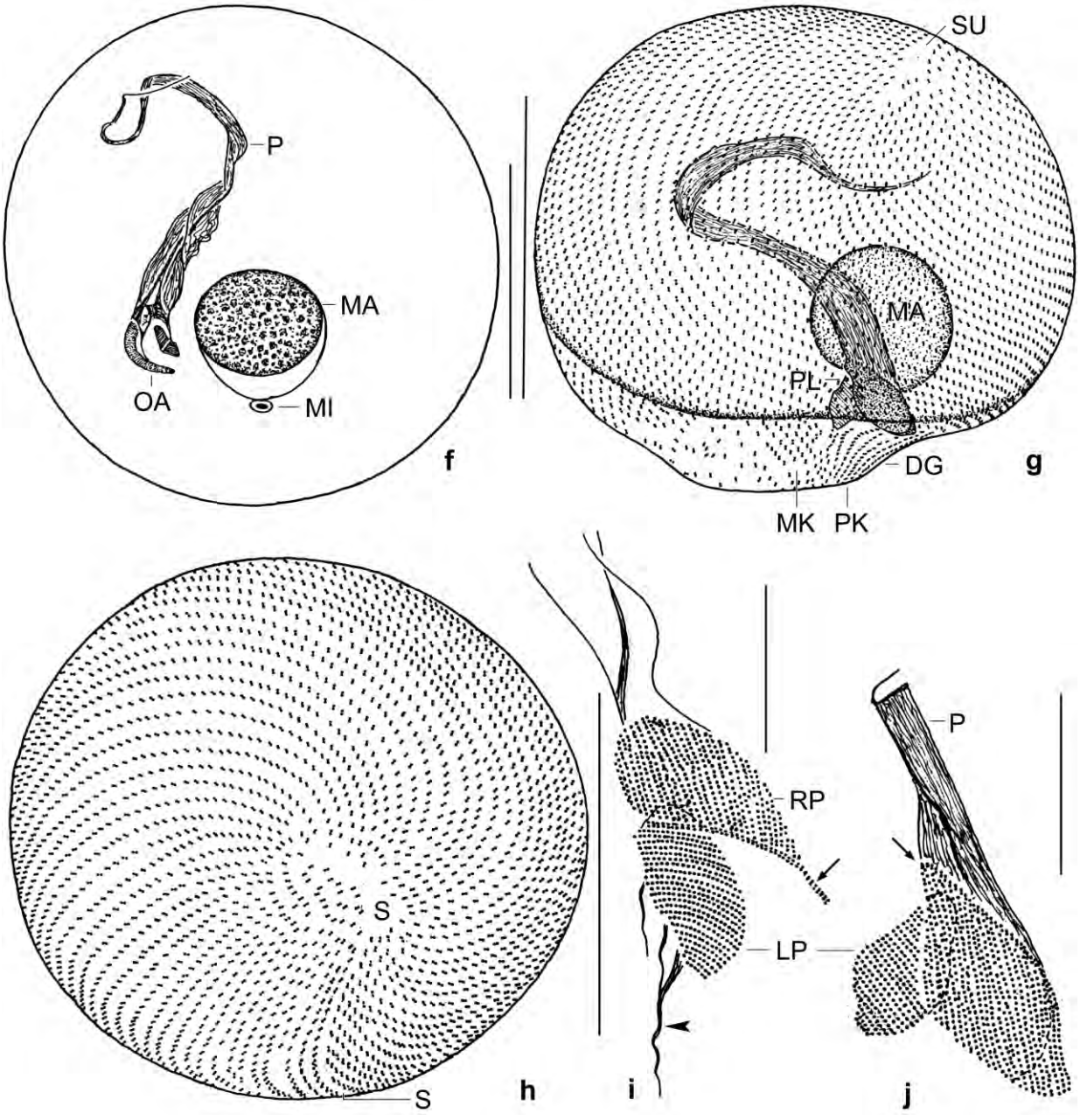

Fig. 113f–j. *Maryna umbrellata* after protargol impregnation. The entire ciliary pattern consists of dikinetids most having ciliated both basal bodies**. f, g:** Oblique posterior polar and ventral view, showing the large pharynx extending anteriorly, the narrow preoral suture, and the ciliary pattern. The pharynx originates from the right oral polykinetid. **h:** Anterior polar view, showing the narrow preoral suture and some irregularities in the ciliary pattern. **i, j:** Oral apparatus. The arrows mark a row of dikinetids associated with the right polykinetid, the arrowhead denotes a fibre bundle in the postoral suture. DG – diagonal groove, LP – left oral polykinetid, MA – macronucleus, MI – micronucleus, MK – mycteral kineties, OA – oral apparatus, P – pharynx, PK – postoral kineties in diagonal (postoral) groove, PL – oral polykinetids, RP – right oral polykinetid, SU – preoral suture. Scale bars 15 µm (i, j) and 70 µm (f–h).

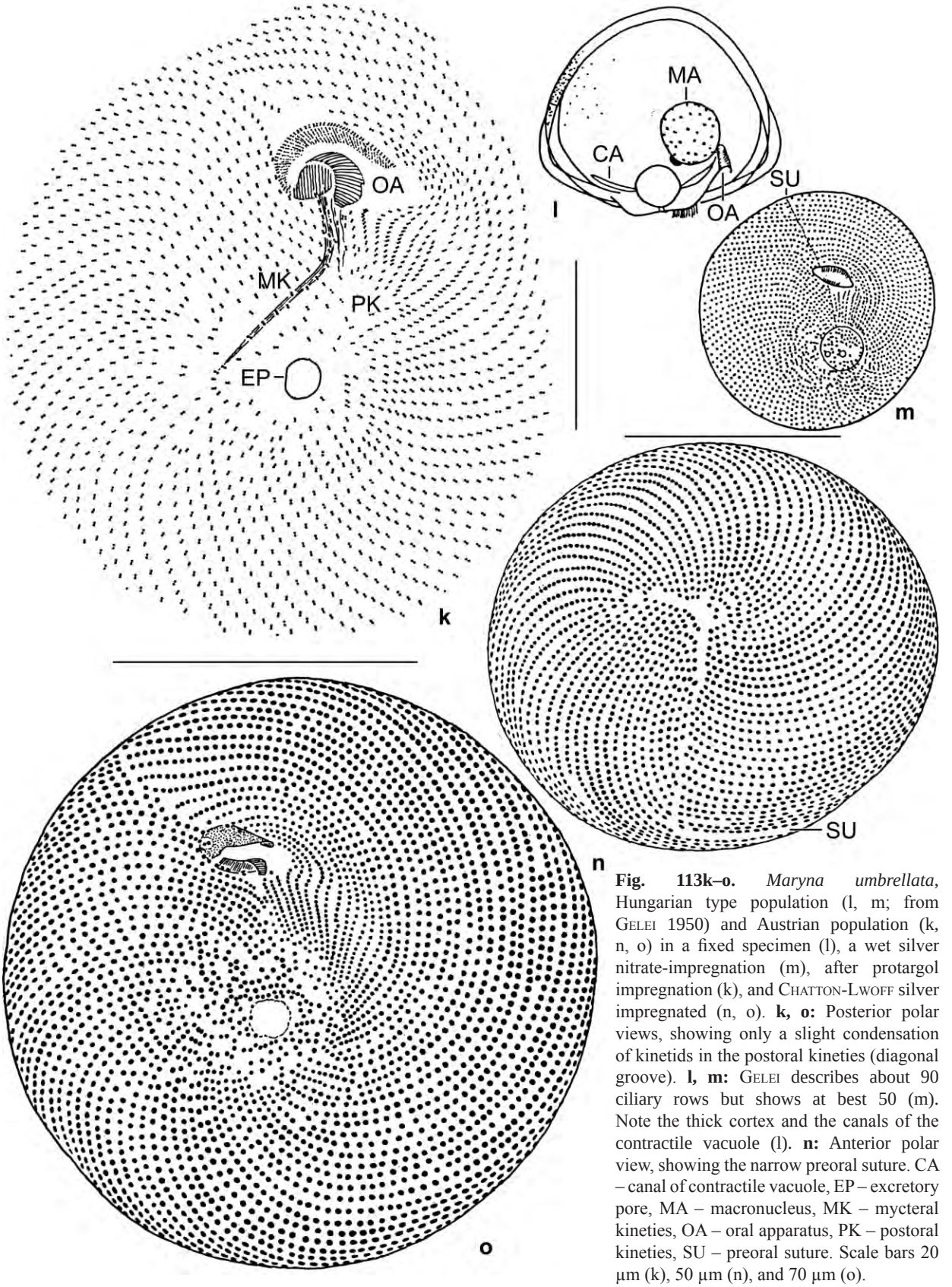

Fig. 113k–o. *Maryna umbrellata*, Hungarian type population (l, m; from Gelei 1950) and Austrian population (k, n, o) in a fixed specimen (l), a wet silver nitrate-impregnation (m), after protargol impregnation (k), and Chatton-Lwoff silver impregnated (n, o). **k, o:** Posterior polar views, showing only a slight condensation of kinetids in the postoral kineties (diagonal groove). **l, m:** Gelei describes about 90 ciliary rows but shows at best 50 (m). Note the thick cortex and the canals of the contractile vacuole (l). **n:** Anterior polar view, showing the narrow preoral suture. CA – canal of contractile vacuole, EP – excretory pore, MA – macronucleus, MK – mycteral kineties, OA – oral apparatus, PK – postoral kineties, SU – preoral suture. Scale bars 20 µm (k), 50 µm (n), and 70 µm (o).

Size highly dependent on culture conditions and growth phase, difficult to measure in vivo because cells swim incessantly and rapidly. In the three preparations made, the cells have a size of 75–130 (width) × 75–130 µm (height), 110–145 × 87–132 µm, and 93–160 × 80–150 µm (Table 41) or 75–130 × 75–110 µm, 127–167 × 100–152 µm, and 107–184 × 92–173 µm when preparation shrinkage is added (0% for osmium, 5% for Chatton-Lwoff sliver nitrate, 15% for protargol). Taking the averages, an in vivo size of about 130 × 115 µm is obtained.

Calix broadly conical or hemiellipsoid, slightly broader than high; uvula broad but hardly projecting from body proper because partially covered by posterior margin of calix. Ventral side slightly flattened and with a shallow groove at site of preoral suture (Fig. 113a, 114a–i, k, 115d; Table 41). Location of nuclear apparatus highly variable (CV = 27%), on average slightly anterior to mid-body. Macronucleus and micronucleus very broadly elliptic to globular, both with a distinct membrane; nucleoli granular, numerous (Fig. 113a, n, 114f, r; Table 41). Contractile vacuole in uvula, during diastole surrounded by some collecting vesicles never forming short canals (checked in three specimens). Excretory pore in centre of uvula surface, about 4 µm across (Fig. 113a, d, h, 114b, l). Cortex very flexible, gelatinous and about 1 µm thick, punctated by deep ciliary pits, and in optical section indistinctly striated by the extrusomes (Fig. 113a, 114a–h). Extrusomes scattered within ciliary rows, numerous, rod-shaped, in vivo about 6 × 0.3 µm in size, belong to the mucocyst type (Foissner, unpubl.). Cytoplasm colourless, turbid because crammed with hundreds of food vacuoles most 5–10 µm in size, up to 30 µm in the alkaline phase. In anterior half of dorsal side a brownish spot of glass granules about 1 µm in size; some granules scattered throughout cytoplasm, conspicuously sparkling under interference contrast (Fig. 113a, b, 114b, f). Feeds exclusively on 3–5 µm long bacterial rods, even when masses of flagellates (*Polytomella*) are present. Dances rapidly in wide spirals within a globular area; positive phototactic concentrating at bright side of Petri dish and on decaying wheat grains. Divides in cysts with up to four tomites (Fig. 114m, n). Does not build dwelling tubes neither in environmental samples or in pure cultures grown under various conditions.

Somatic and oral ciliature and silverline pattern as typical for *Maryna* (Foissner 1993a). All kinetids paired, cilia sprout from deep, elliptic pits containing white spots when deeply impregnated (Fig. 114s), of very different length in vivo and in the scanning electron microscope: those on calix about 15 µm long and producing nice metachronal waves, cilia in diagonal (postoral) groove only 5 µm long; elongated caudal cilia definitely absent (Fig. 113a, 114i–l). Cilia arranged in an average of 83 spiral rows including about six postoral kineties; very densely spaced throughout, polymerization in postoral groove thus inconspicuous; separated in a right and left portion by a very narrow preoral suture difficult to recognize in one third of specimens; postoral suture distinct because in a "stripe contrast" zone, that is, the region where the mycteral kineties right of the oral opening abut in sharp angles on the slightly denser ciliated postoral kineties. Uvula surface loosely and irregularly ciliated (Fig. 113a, g, h, k, n, o, 114k, l, o–r, 115a, c–m; Table 41).

Oral apparatus between calix and uvula, small compared to body size (Table 41). Buccal cavity about 25 µm deep in vivo, extends slightly obliquely to body centre. Oral opening elliptic, margin of right half slightly thickened, aboral side merges into diagonal groove (Fig. 113a, g, 114a, h, k, l, 115a, c; Table 41). Cilia of oral polykinetids about 4 µm long in vivo, left polykinetid on bottom of buccal cavity, elliptic, i. e., 16 × 7 µm on average after protargol-impregnation, composed of

an average of 33 slightly oblique kineties gradually decreasing in length at both ends, associated with some fibre bundles the strongest extending in postoral suture. Right oral polykinetid on roof of buccal cavity, obliquely rectangular, composed of a proximal row of dikinetids and of slightly irregular, oblique rows of monokinetids; associated with a long pharynx extending to anterior pole and possibly U-shaped proximally (Fig. 113a, f, g, i, j, 114p, r, 115b, c, f–m; Table 41).

Resting cyst: This has been described by Foissner (2009) and Foissner et al. (2009b). Briefly, the cyst has a diameter of about 100 µm of which the external 13 µm are made by the thick wall including an about 4 µm thick glass cover with glass granules about 0.8 µm in size (Fig. 113c; Table 41).

Molecular phylogeny: Of the 25 marynids described so far only three have been investigated for gene sequences (Fig. 124). *Maryna umbrellata* makes a well-supported clade (0.86/1.00) with *M. meridiana* and *Pseudomaryna* sp. while *M. ovata* produces a separate clade.

Occurrence and ecology: Few reliable records of *M. umbrellata* are known and all are from ephemeral habitats of Europe suggesting that it might be restricted to Laurasia (Foissner 1993a, Cotterill et al. 2013). Very likely feeds exclusively on bacteria.

Comparison with original description: Except of one feature all observations match the original description of Gelei (1950) who provided the following "hard" facts (Fig. 113l, m): Size in vivo 110–150 × 100–140 µm, depending on nutrition and growth phase; umbrella-shaped with width usually slightly greater than height; uvula broad but short; cortex remarkably thick, indicating extrusomes; with a spot of refractive granules on dorsal side; without dwelling tube; about 90 ciliary rows (the illustration shows only 50 at best, Fig. 113m); polymerization of ciliature in diagonal groove indistinct; hard facts on oral apparatus and cyst lacking. The sole difference to the Austrian population is the contractile vacuole which has collecting vesicles instead of canals (Fig. 113a, l). The significance of this feature might be greater than it appears because canals or vesicles are independent of body size (see → *M. meridiana*) and the gene sequence data do not show *M. umbrellata* as nearest relative of → *M. meridiana* (with canals).

Comparison with → *M. meridiana* and other congeners: As concerns → *M. meridiana*, see that species. Two other species have a considerable similarity in size and shape with *M. umbrellata*. The most similar congener is *M. cardioides* (Gelei, 1950) Foissner, 1993a, which shows a cordate shape when sitting in its short dwelling tube absent from *M. umbrellata*. However, the most valuable feature is the macronucleus (globular vs. ellipsoid). The second, less similar species is *M. galeata* Gelei, 1950. It is larger than *M. umbrellata* (in vivo about 200 µm vs. 130 µm), has a helmet-shaped calix (vs. posterior edge of calix not crimped), a dwelling tube (vs. without), and about 200 vs. 80 ciliary rows.

Neotypification: Cotterill et al. (2013) suggested neotypification of *M. umbrellata* with the Austrian population described here. Basically, this is recommendable because the morphostatic cells are difficult to distinguish from → *M. meridiana*. However, this would be premature

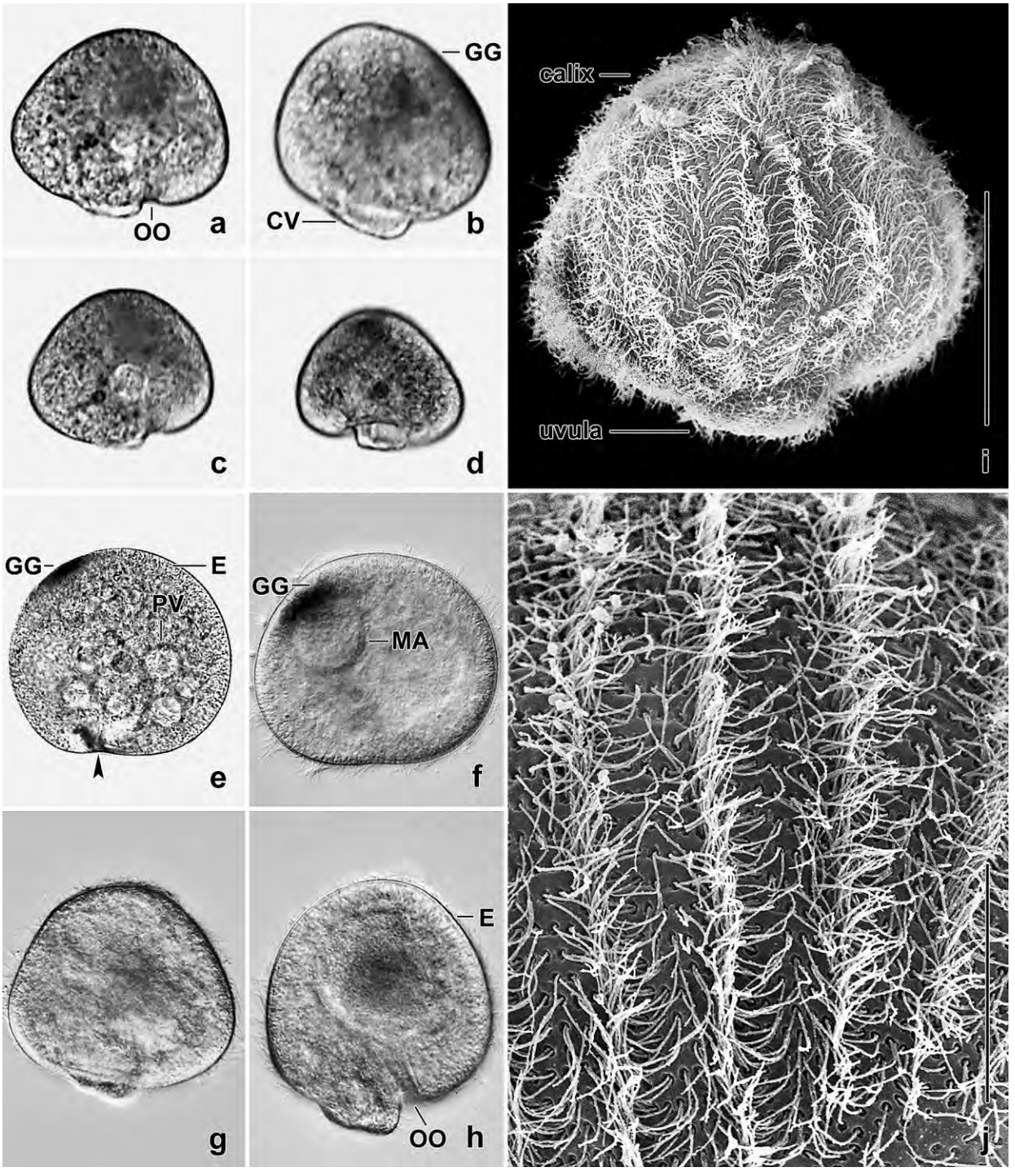

Fig. 114a–j. *Maryna umbrellata* from life (a–e), osmium fixed (f–h), and in the scanning electron microscope (i, j). **a–d, g–i:** Lateral views of freely motile specimens (a–d), showing the broadly conical shape of the calix, the inconspicuous uvula, and the brownish spot of glass granules dorsolaterally. The cilia form nice metachronal waves (i). **e, f:** Transverse views, showing the slight dorsoventral flattening and the minute concavity containing the preoral suture (arrowhead). In the alkaline phase, the food vacuoles have a diameter of 15–20 µm (e). **j:** Metachronal ciliary waves on calix. CV – contractile vacuole, E – extrusome fringe, FV – food vacuoles, GG – glass granules, MA – macronucleus, OO – oral opening, Scale bar 20 µm (j) and 40 µm (i). Figures (a–h): width 90–140 µm.

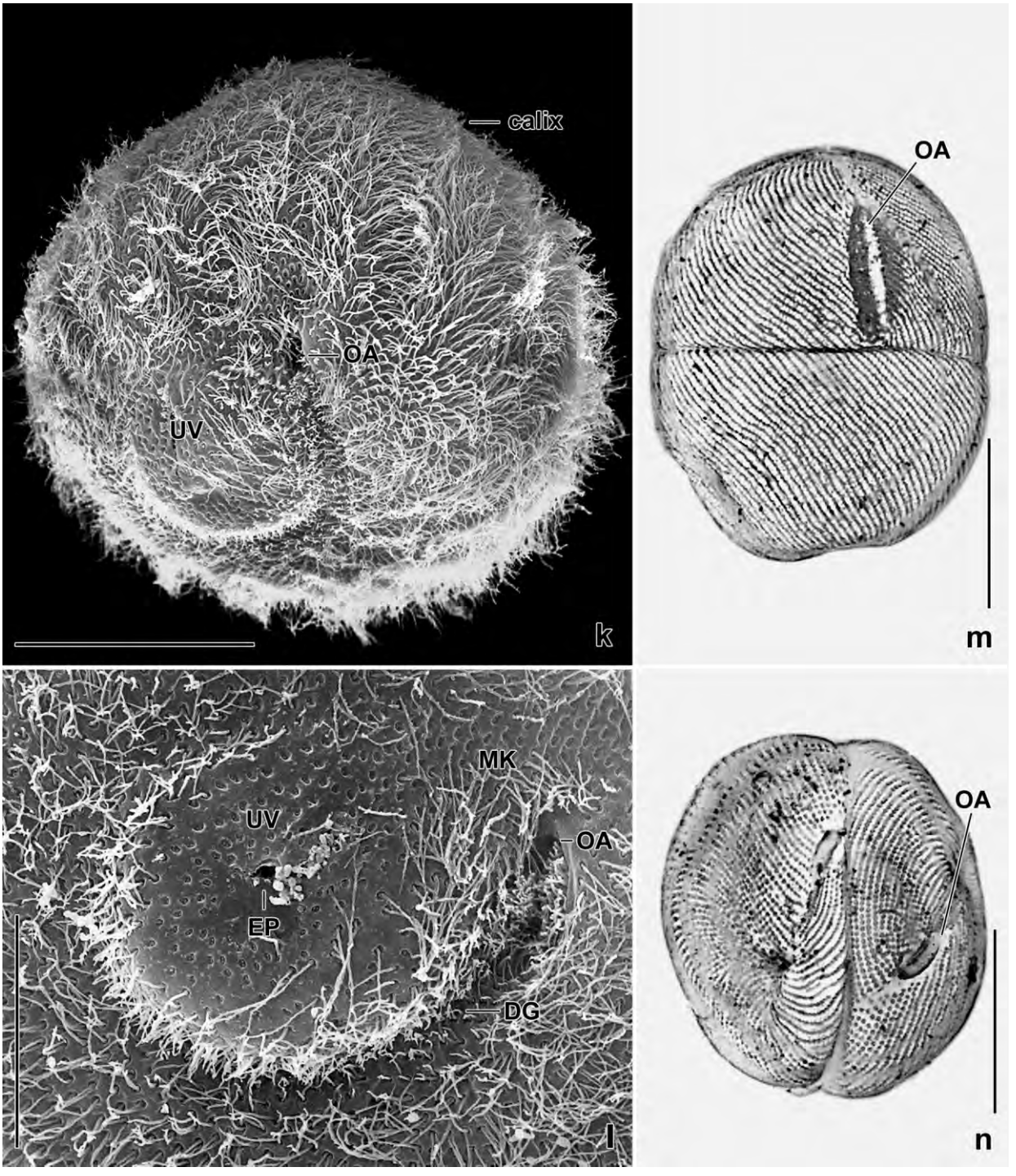

Fig. 114k–n. *Maryna umbrellata* in the scanning electron microscope (k, l) and after Chatton-Lwoff silver nitrate impregnation (m, n). **k:** Oblique posterior polar view. The uvula and the oral apparatus are small compared to the calix. **l:** Posterior polar view, showing the uvula lacking cilia while they are slightly condensed in the diagonal (postoral) groove. The entrance to the buccal cavity is minute compared to the size of the cell. **m, n:** Two early dividers, showing a typical colpodid ontogenesis, i. e., it occurs in division cysts and the new oral polykinetids originate from the ends of somatic kineties. DG – diagonal (postoral) groove, EP – excretory pore of contractile vacuole, MK – mycteral kineties, OA – entrance to buccal cavity, UV – uvula. Scale bars 20 µm (l), 30 µm (k), and 50 µm (m, n).

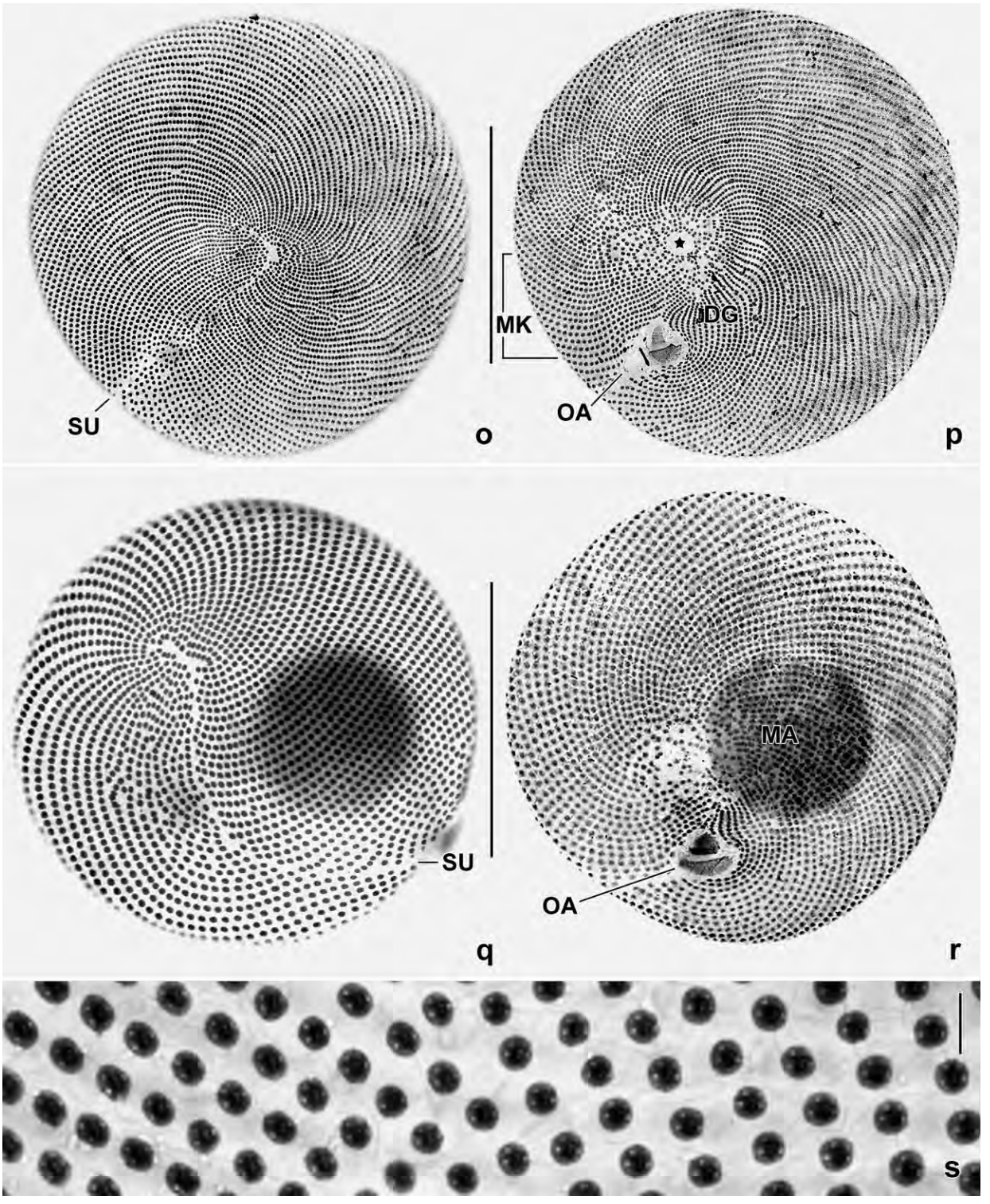

Fig. 114o–s. *Maryna umbrellata*, basal body pattern after protargol impregnation. **o, p:** Anterior and posterior polar view of a specimen with 90 kineties, showing the preoral suture and the ciliature which is so dense that the very narrowly spaced kinetids in the diagonal groove become inconspicuous. The asterisk marks the excretory pore. **q, r:** As (o, p) but in a slightly different orientation and only 72 ciliary rows. **s:** High magnification of calix dikinetids. DG – diagonal groove, MA – macronucleus, MK – mycteral kineties, OA – oral apparatus, SU – preoral suture. Scale bars 3 µm (s) and 70 µm (o–r).

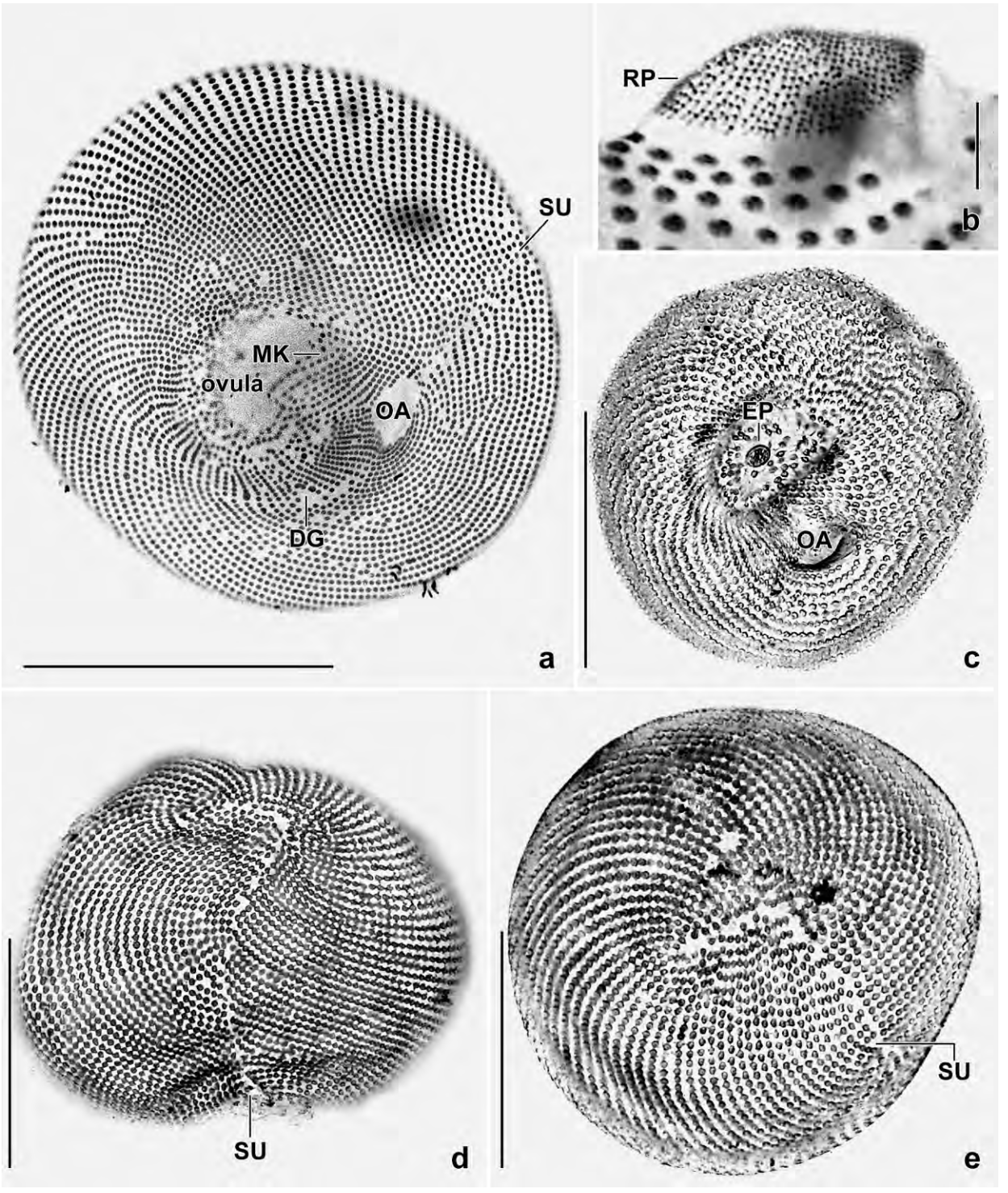

Fig. 115a–e. *Maryna umbrellata*, basal body (ciliary) pattern after protargol (a, b) and CHATTON-LWOFF silver nitrate (c–e) impregnation. **a:** Posterior polar view of a specimen with 100 ciliary rows. The calix dikinetids are so narrowly spaced that the very narrowly spaced kinetids in the diagonal (postoral) groove become inconspicuous. **b:** Part of right oral polykinetid consisting of monokinetids. **c:** Posterior polar view. **d, e:** Ventral and anterior polar view, showing the kinety pattern and the narrow preoral suture. DG – diagonal (postoral) groove, EP – excretory pore, MK – mycteral kineties, OA – oral apparatus, RP – right oral polykinetid, SU – preoral suture. Scale bars 10 µm (b) and 70 µm (a, c–e).

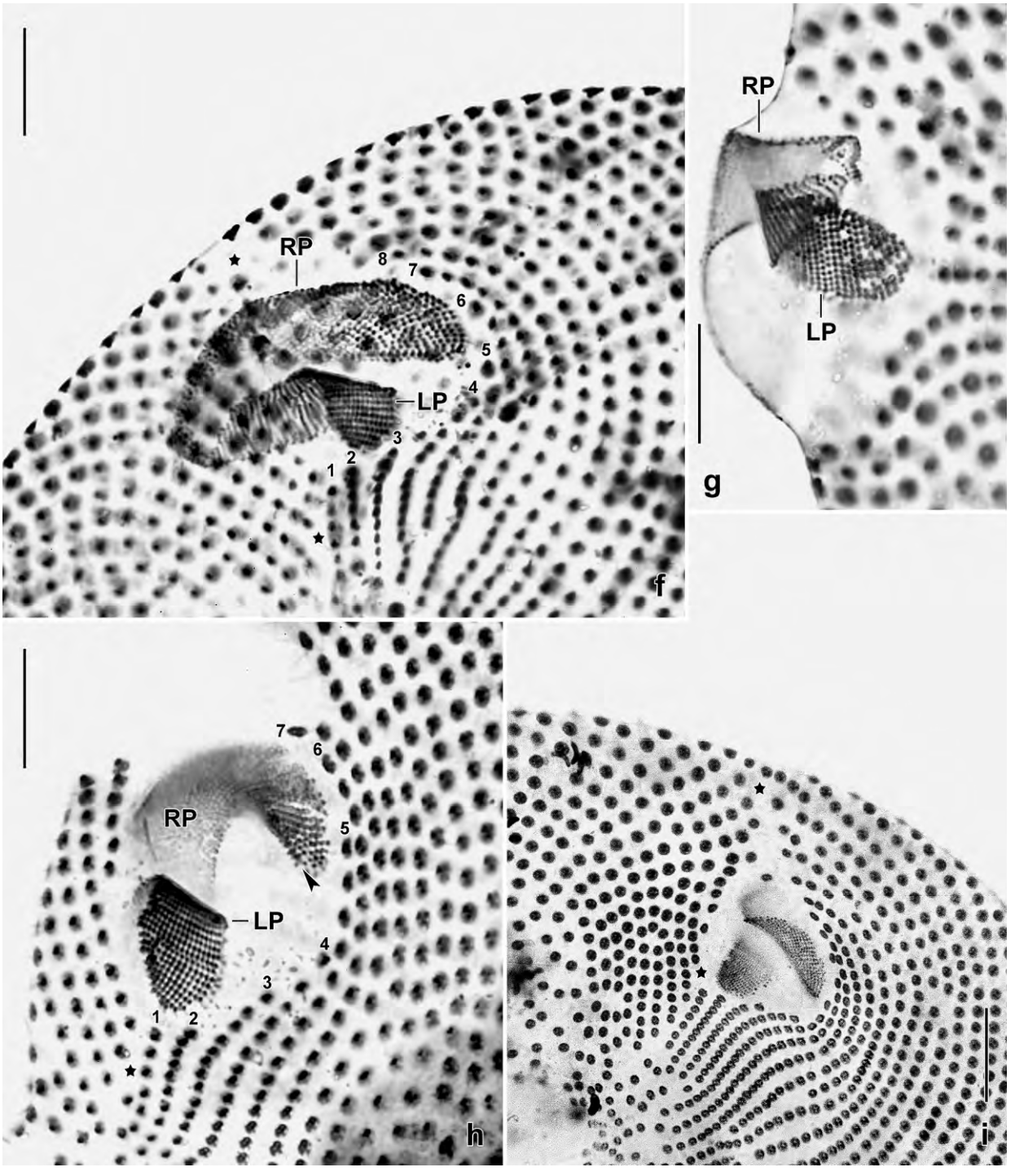

Fig. 115f–i. *Maryna umbrellata*, oral and perioral basal body (ciliary) pattern after ethanol fixation and protargol impregnation (preparations pressed by coverslip). The asterisks mark the preoral and postoral suture where the ciliary rows of the right and left side abut. The numerals denote the postoral kineties s. str. There are two oral polykinetids in the buccal cavity. The left polykinetid is on the bottom of the cavity and consists of an average of 33 kineties. The right polykinetid is on the roof of the buccal cavity and consists of many kineties some of which are slightly disordered; on the dorsal margin is a row of dikinetids (h, arrowhead). LP – left oral polykinetid, RP – right oral polykinetid. Scale bars 10 μm (f–h) and 20 μm (i).

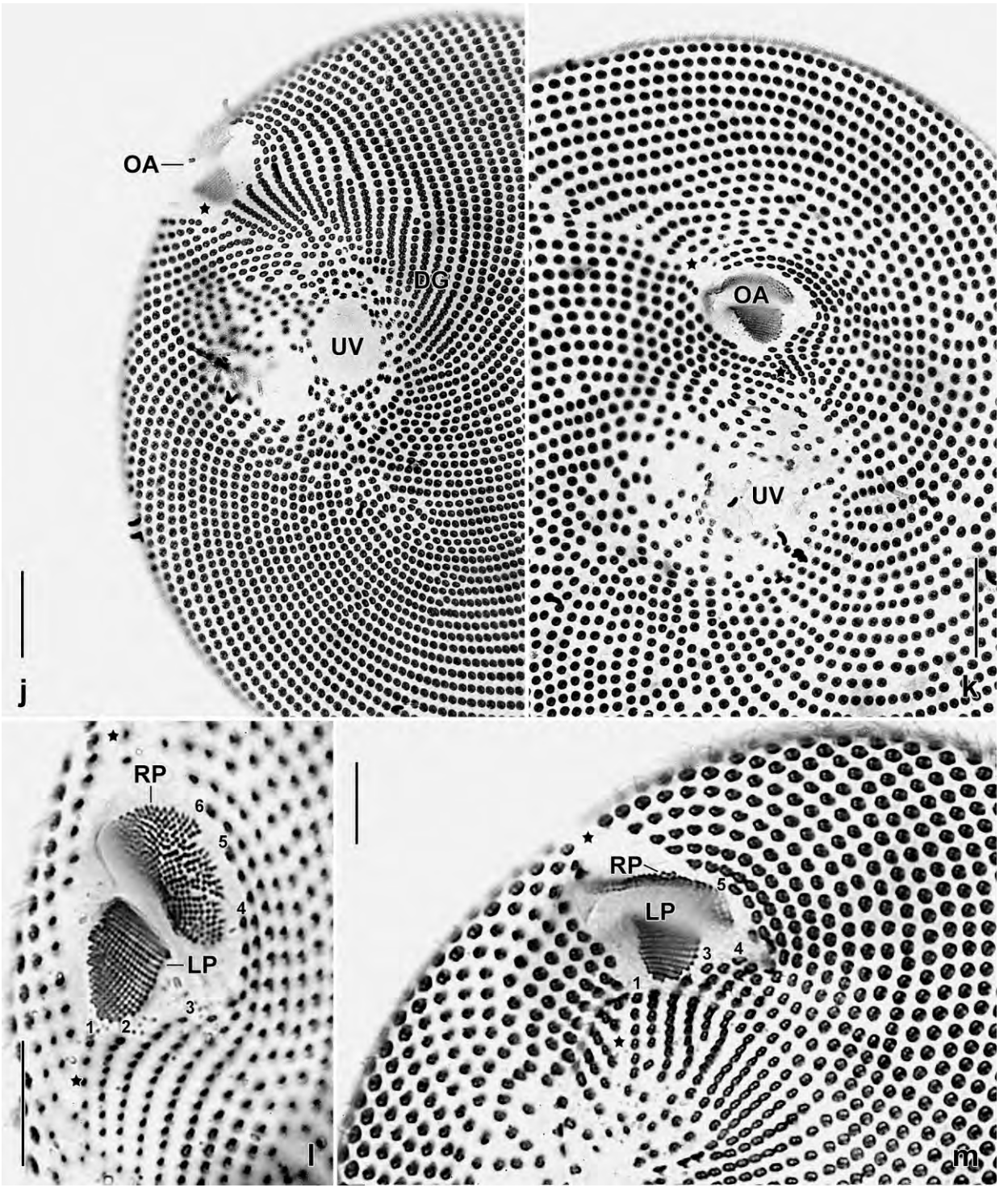

Fig. 115j–m. *Maryna umbrellata*, oral and perioral basal body (ciliary) pattern after ethanol fixation and protargol impregnation (preparations pressed by coverslip). The asterisks mark the preoral and postoral suture. The numerals denote the postoral kineties s. str. **j, k:** Posterior polar views, showing the loosely ciliated uvula and the inconspicuous diagonal (postoral) groove where the dikinetids are especially narrowly spaced, which is hardly recognizable in the specimen shown in (k). **l, m:** Two views of the oral polykinetids and the perioral ciliature. DG – diagonal (postoral) groove, LP – left oral polykinetid, OA – oral apparatus, RP – right oral polykinetid, UV – uvula. Scale bars 10 µm (l, m) and 20 µm (j, k).

considering the difference in the contractile vacuole (see above). Thus, neotypification should await data from other populations.

Maryna lichenicola (Gelei, 1950) Foissner, 1993a (Fig. 116a–c)

Material: Venezuelan sample (29). Two voucher slides with Chatton-Lwoff silver nitrate-impregnated specimens have been deposited in the Biology Centre of the Upper Austrian Museum in Linz (LI). Some relevant specimens have been marked by black ink circles on the coverslip.

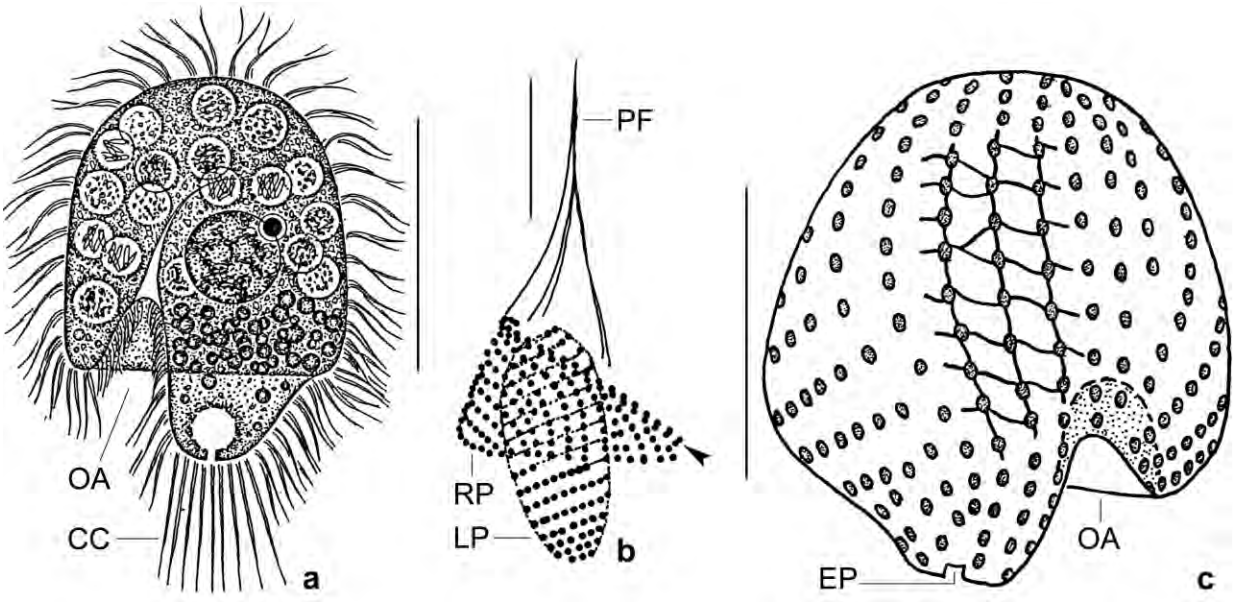

Fig. 116a–c. *Maryna lichenicola* from life (a), after protargol impregnation (b), and in a Chatton-Lwoff silver nitrate preparation (c). **a:** Left lateral optical section at level of oral apparatus of a representative specimen packed with food vacuoles (from Foissner et al. 2002). **b:** Oral apparatus in a left laterally oriented specimen. The arrowhead marks a row of dikinetids at the proximal margin of the right polykinetid (from Foissner et al. 2002) **c:** Right side view of a well preserved specimen, showing body shape, ciliary rows, and silverline pattern in midline of cell. CC – caudal cilia, EP – excretory pore of contractile vacuole, LP – left oral polykinetid, OA – oral apparatus, PF – pharyngeal fibres, RP - right oral polykinetid. Scale bars 5 µm (b) and 20 µm (a, c).

Remarks: This species has been carefully redescribed by Foissner et al. (2002), using live observation and protargol impregnation (Fig. 116a, b). Here, we add a silver nitrate-impregnated specimen with well preserved body shape and silverline pattern (Fig. 116c).

Sandmannides nov. gen.

Diagnosis: Small Sandmanniellidae with almost circular right oral polykinetid open slightly right and posterior of preoral suture. Several minute adoral polykinetids at right margin of preoral suture and anterior of right oral polykinetid.

Type species: *Sandmannides venezuelensis* nov. spec.

Etymology: *Sandmannides* is a composite of the personal name *Sandmann* and the Latin suffix

ides (similar), indicating a similarity with the genus *Sandmanniella* Foissner & Stoeck, 2009a. Masculine gender.

Remarks: Foissner & Stoeck (2009a) described a curious Colpodean from Africa, *Sandmanniella terricola,* with a very narrow oral basket resembling the basket of the nassulids. It was a great surprise to find a ciliate with the same feature in Venezuela. The Venezuelan species resembles the genus *Notoxoma* Foissner, 1993a, which forms a clade with *Sandmanniella* in most molecular trees (Foissner et al. 2011). Thus, we reinvestigated *Notoxoma parabryophryides* (Fig. 117b) which has, indeed, an oral basket similar to that of *Sandmanniella* and *Sandmannides*. The basket is very narrow and has been overlooked by Foissner (1993a).

Sandmannides differs from *Notoxoma* by the orientation of the opening of the right oral polykinetid (almost in main body axis vs. left lateral; Fig. 117a, b, 118a, d) and the location of the adoral polykinetids (outside the circle formed by the right polykinetid, right of the preoral suture vs. between the ends of the right polykinetid; Fig. 117a, b, d, 118a, d, e). *Sandmannides* differs from *Sandmanniella* by the shape of the right oral polykinetid (circular vs. lunate; Fig. 117a, c, e, f), the location of the left oral polykinetids (right of the preoral suture vs. vis a vis of the right polykinetid posterior to the preoral suture; Fig. 117a, c, e, f), and the absence (vs. presence) of a perioral ciliary condensation right of the oral apparatus (Fig. 117a, c, e, f, 118e). *Parabryophrya* Foissner, 1993a, is similar to *Notoxoma* but has a deeper oral cavity with vestibular kineties absent from *Sandmanniella* and *Sandmannides*. We reinvestigated excellently impregnated specimens from Austria and could not find an oral basket, indicating that it is not congeneric.

Sandmannides venezuelensis nov. spec. (Fig. 117a, d, 118a–e)

Diagnosis: Size in vivo about 60 × 35 µm; ellipsoid. On average 22 ciliary rows extending spirally from anterior to posterior. Right oral polykinetid composed of about 25–30 short kineties. About 5 adoral polykinetids each composed of dikinetids.

Type locality: Venezuelan site (23), i. e., field (Mahadja) soil from the surroundings of the village of El Sapo and the Orinoco River, that is, about 50 km north of Pto. Ayachuco, Venezuela, 67°36'°W 5°41'N.

Type material: 1 holotype slide with three protargol-impregnated specimens, marked by black ink circles on the coverslip, has been deposited in the Biology Centre of the Upper Austrian Museum in Linz (LI).

Etymology: Named after the country in which it was discovered.

Description: We found only three specimens in the protargol slides, and we did not recognize the species in the non-flooded Petri dish culture. Thus, in vivo observations are lacking. In spite of this, we describe this population because (i) it has a clear identity, (ii) the preparation is excellent, and (iii) because it is phylogenetically very important (see Remarks to genus).

Size in vivo 47–63 × 30–38 µm, usually about 60 × 35 µm when adding 15% shrinkage to the protargol preparation. Body ellipsoid to slightly ovate (Fig. 117a, 118a, d). Macronucleus in central third of cell, globular to slightly ellipsoid, after protargol impregnation 14 × 13 µm in size. Micronucleus, contractile vacuole, and cytoplasm not impregnated.

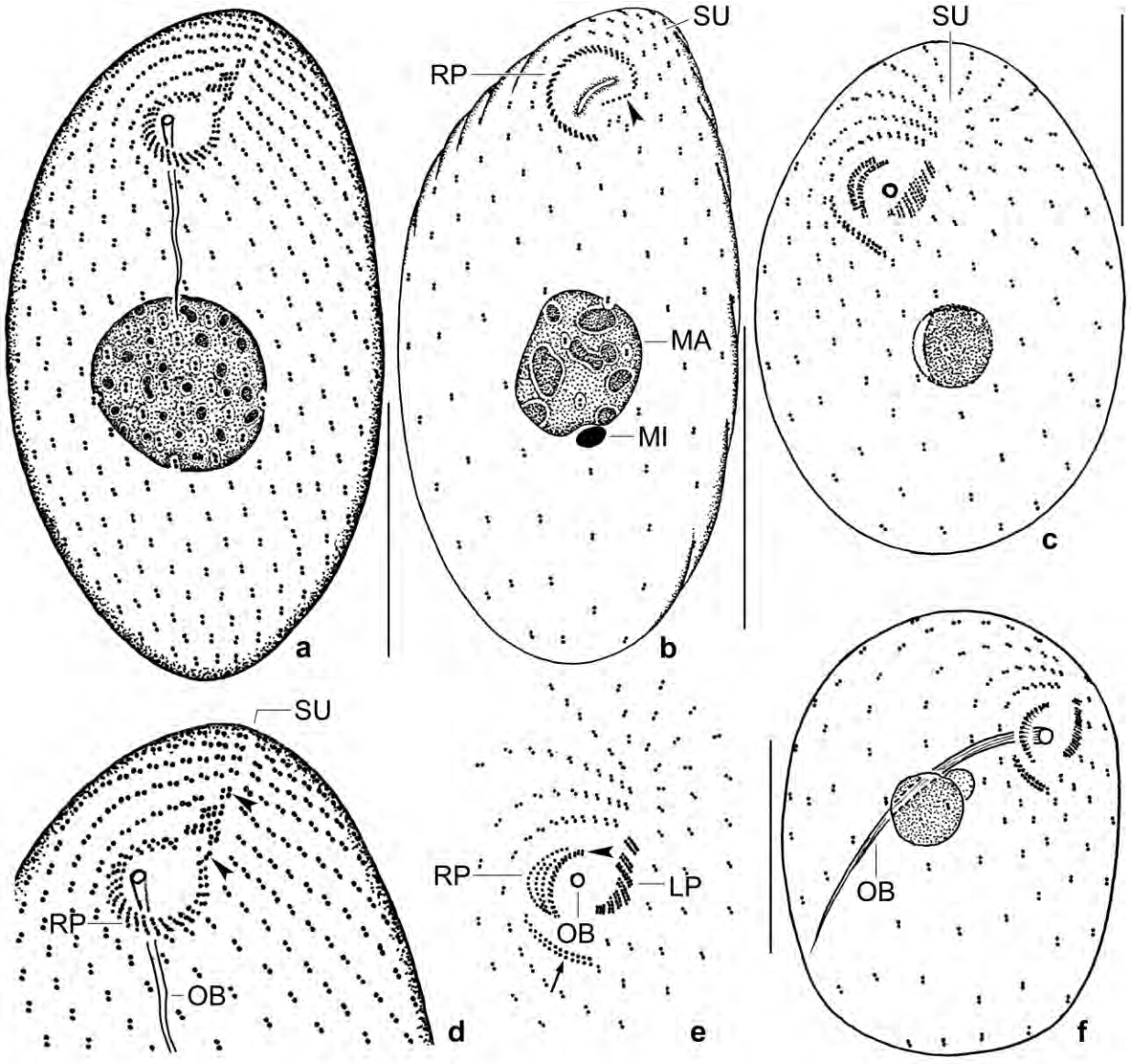

Fig. 117a–f. Sandmanniellid ciliates, infraciliature after protargol impregnation. **a, d:** *Sandmannides venezuelensis,* ventral views of holotype specimen, length 55 µm. Arrowheads in (d) limit five adoral polykinetids each consisting of a row of dikinetids. **b:** *Notoxoma parabryophryides,* ventral view of holotype specimen, length 45 µm (from Foissner 1993a, oral basked overlooked). The arrowhead denotes the single adoral organelle. **c, e, f:** *Sandmanniella terricola,* ventral (c, e) and lateral (f) views (from Foissner & Stoeck 2009a). The arrow marks the perioral ciliary condensation; the arrowhead denotes a row of dikinetids at the dorsal margin of the right oral polykinetid. Note the very narrow oral basket (OB), a highly specific feature of the sandmanniellids, present also in *Sandmannides* (a, d) and *Notoxoma* (b). LP – left oral polykinetid, MA – macronucleus, MI – micronucleus, OB – oral basket, RP – right oral polykinetid, SU – preoral suture. Scale bars 20 µm (a–c, f).

Somatic ciliature colpodid, i. e., composed of dikinetids forming about 22 ciliary rows in each of the three specimens found; rows commence at preoral suture and postorally and extend spirally to posterior body end; third kinety right of oral apparatus with an average of 35 dikinetids (Fig. 117a, 118a–d).

Oral apparatus about 8 µm subapical, conspicuous in protargol preparations because right polykinetid forms a strongly impregnated circle composed of about 25–30 minute ciliary rows

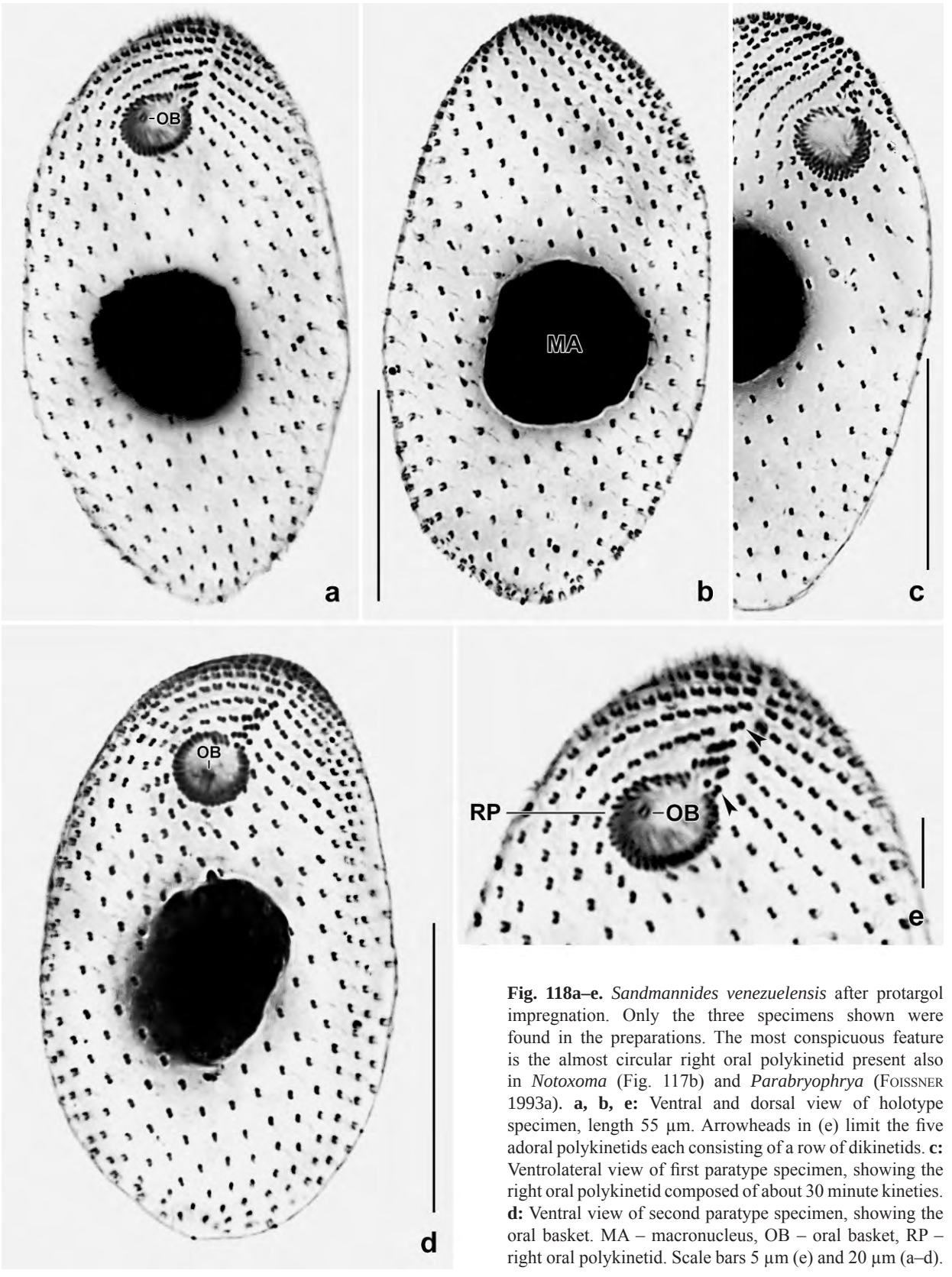

Fig. 118a–e. *Sandmannides venezuelensis* after protargol impregnation. Only the three specimens shown were found in the preparations. The most conspicuous feature is the almost circular right oral polykinetid present also in *Notoxoma* (Fig. 117b) and *Parabryophrya* (Foissner 1993a). **a, b, e:** Ventral and dorsal view of holotype specimen, length 55 µm. Arrowheads in (e) limit the five adoral polykinetids each consisting of a row of dikinetids. **c:** Ventrolateral view of first paratype specimen, showing the right oral polykinetid composed of about 30 minute kineties. **d:** Ventral view of second paratype specimen, showing the oral basket. MA – macronucleus, OB – oral basket, RP – right oral polykinetid. Scale bars 5 µm (e) and 20 µm (a–d).

with length gradually decreasing at ends of polykinetid (Fig. 117a, d, 118a, c, d). Oral cavity about 3 µm deep, in or near centre a basket only 1 µm across and extending to mid-body (Fig. 117a, d, 118a, d, e). Right polykinetid about 6 µm across, opens slightly right of oblique preoral suture right of which insert about five dikinetal adoral organelles of different length (Fig. 117a, d, 118e). We cannot exclude the presence of a dikinetal row along the dorsal margin of the right polykinetid.

Occurrence and ecology: As yet found only at type locality, i. e., in very fertile soil.

Remarks: This is a very distinct species which, however, in vivo can be easily confused with *Notoxoma parabryophryides* (more slender, i. e., 2.8 vs. 2:1) and *Parabryophrya penardi* (without vs. with distinct vestibular kineties recognizable also in vivo). The identification should be checked in silver carbonate or protargol preparations.

Bryometopus rostratus nov. spec. (Fig. 119a–d, 120a–e)

Diagnosis: Size in vivo about 70 × 30 µm; rostrate. Single micronucleus. Contractile vacuole far subterminal. Oral apparatus on ventral side, occupies about one quarter of body length,

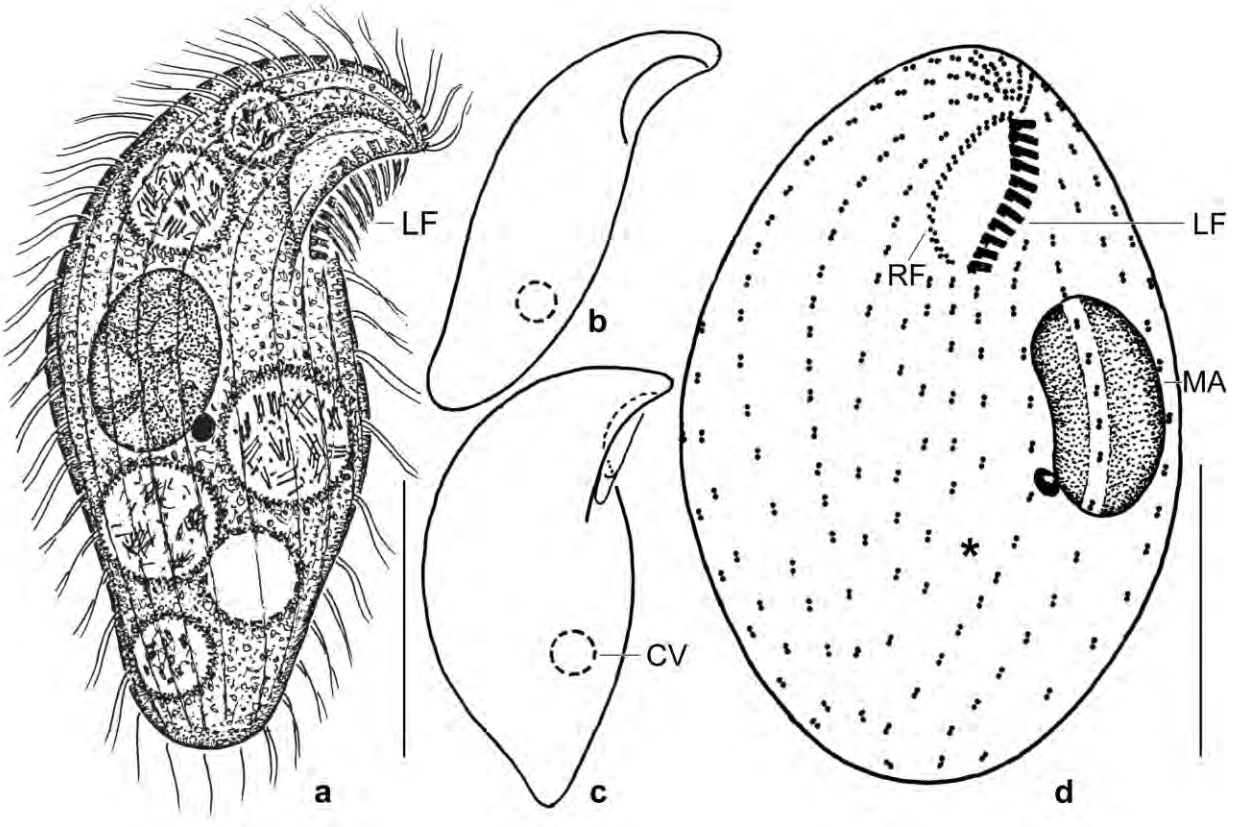

Fig. 119a–d. *Bryometopus rostratus*, specimens from Venezuelan type population (a, c, d) and from Brazil (b) in vivo (a–c) and after silver carbonate impregnation (d). **a, c:** Right side view of representative specimens, length about 70 µm. Note the considerable difference in body shape and the far subterminal contractile vacuole, an important difference to *B. balantidioides*, which has it in the posterior end. **b:** The Brazilian specimens are slightly longer and narrower than those from Venezuela. **d:** Ventral view of a moderately pressed specimen, showing the oral and somatic ciliary pattern as well as the nuclear apparatus. The asterisk marks shortened postoral kineties. CV – contractile vacuole, LF – left oral ciliary field, MA – macronucleus, RF – right oral ciliary field. Scale bars 30 µm.

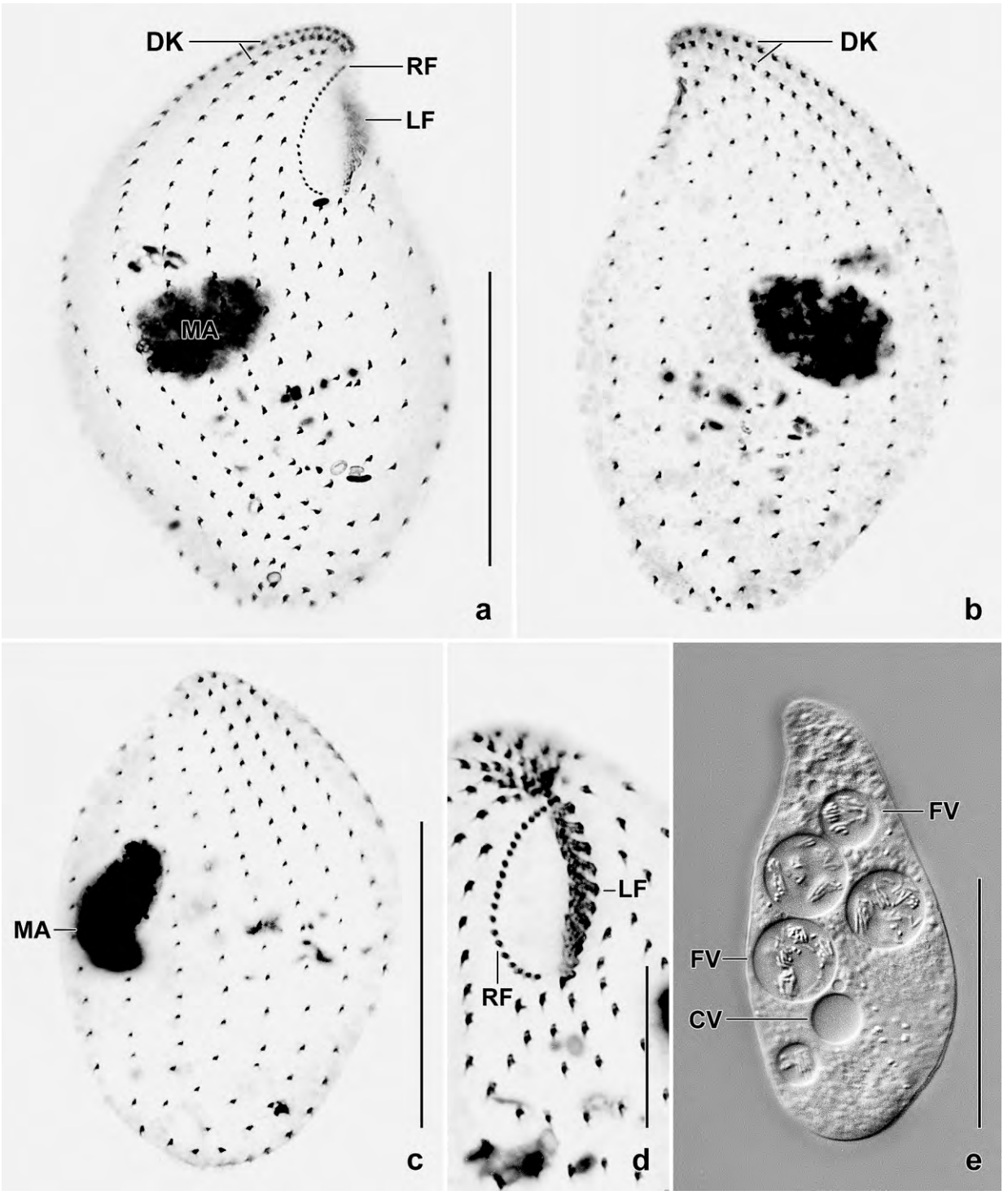

Fig. 120a–e. *Bryometopus rostratus*, specimens from type locality in vivo (e) and after silver carbonate impregnation (a–d). **a, b:** Right and left side view of a moderately pressed specimen, still showing the rostrate anterior body portion. Note the comparatively small oral apparatus. **c, d:** Dorsal and ventral ciliary pattern of a slightly pressed specimen, showing the ciliary pattern. **e:** Left side view of a moderately pressed specimen, showing the large food vacuoles and the far subterminal contractile vacuole. CV – contractile vacuole, DK – dorsal kineties, FV – food vacuoles, LF – left oral ciliary field, MA – macronucleus, RF – right oral ciliary field. Scale bars 15 µm (d) and 40 µm (a–c, e).

parallel to longitudinal axis of body, right wall of oral cavity overhangs left. On average (n = 5) 17 somatic kineties, 11 adoral polykinetids, and 22 dikinetids in right oral ciliary field.

Type locality: Soil and litter from an organically farmed banana plantation at the farm (Ganja Cochama) of Mr. Eisenberg, about 50 km NE of Puerto Ayacucho, Venezuela, 67°36'W 5°41'N.

Type material: Not available.

Etymology: The Latin adjective *rostratus* refers to the rostrate anterior body end.

Description: This species was present only during the second day after rewetting the sample. The abundance was very low, and thus we could prepare and morphometrically analyze only five silver carbonate-impregnated specimens.

Size of specimens from type locality 60–85 × 25–35 µm in vivo, usually about 70 × 30 µm; Brazil specimens larger and narrower, i. e., 80–100 × 20–30 µm (Fig. 119b). Body shape highly variable, basically bluntly fusiform with rostrate anterior portion; posterior end acute to narrowly rounded (Fig. 119a–c, 120a, b); only slightly flattened laterally. Nuclear apparatus in mid-body (Fig. 119a, d, 120a–c). Macronucleus ellipsoid to broadly ellipsoid and with reticular nucleolus. Micronucleus attached to macronucleus, broadly ellipsoid, 2–3 µm in size. Contractile vacuole distinctly subterminal near margin of ventral and right side (Fig. 119a–c, 120e). Cortex slightly furrowed by ciliary rows. Particular cortical granules or extrusomes not recognizable in vivo and in silver carbonate preparations. Food vacuoles comparatively conspicuous because up to 15 µm across, contain bacteria and their undigested spores (Fig. 119a, 120e). Swims rapidly rotating about main body axis.

Somatic cilia paired throughout, about 7 µm long in vivo, arranged in an average of 17 (16–19) rows all commencing around oral aperture and most extending slightly spirally to posterior body end; postoral rows rather irregular, shortened posteriorly sometimes forming a suture-like pattern. On average 34 (29–44) kinetids in longest dorsal kinety, narrowly spaced anteriorly in the four dorsal kineties (Fig. 119a, d, 120a–c).

Oral apparatus on ventral side in longitudinal axis of body, in lateral view partially covered by overhanging right body side; small, i. e., occupies about one quarter of body length and possesses only 11 (10–11) adoral polykinetids on average. Right oral ciliary field a single, convex row composed of an average of 22 (20–24) dikinetids (Fig. 119a, c, d, 120a, d).

Occurrence and ecology: As mentioned above, *B. rostratus* disappeared three days after rewetting the sample, indicating an *r*-selected life strategy, as most colpodids (Foissner 1987b). A second population was found in the Pantanal, Brazil. Like the Venezuelan specimens, it was present only during day two after rewetting. Considering these records and the absence in over 1000 soil samples investigated globally, *B. rostratus* might be endemic to the Neotropis.

Remarks: Of the 10 *Bryometopus* species described (Foissner 1993a), only the Australian *B. balantidioides* resembles *B. rostratus* in some main morphometrics: on average 15 vs. 17 somatic ciliary rows and 25 vs. 22 dikinetids in the right oral ciliary field. These species share also another

important feature, viz., the ventral location of the oral apparatus. Nevertheless, *B. balantidioides* and *B. rostratus* can be easily distinguished by body shape (reniform vs. rostrate), the location of the contractile vacuole (in posterior end vs. distinctly subterminal), and the number of adoral polykinetids (25 vs. 11 on average).

Bursaria ovata Beers, 1952 (Fig. 121a–k, 122a–x, 123a–v; Table 42)

Material: This species occurred at Venezuelan site (56). Here, we describe a population from Botswana, i. e., from floodplain soil near to the Kwai River Lodge (23°45'E 19°5'S). The soil, which is very fine and almost black, is covered with *Sphaeranthus incisus* and a dry, paper-thick algal layer; pH 5.3 in water. *Bursaria ovata* was cultivated in tap water enriched with some ml eluate from the non-flooded Petri dish culture and some squashed wheat grains to stimulate bacterial production and growth of indigenous protists and of *Colpidium colpoda* which was added as food (Fig. 121a, 122e, s). Six and five voucher slides with Chatton-Lwoff silver nitrate and protargol-impregnated specimens, respectively, have been deposited in the Biology Centre of the Upper Austrian Museum in Linz (LI). Relevant specimens have been marked by black ink circles on the coverslip.

Description: The Botswanan population is very similar to the North American specimens described by Beers (1952). Thus, we describe mainly new and/or deviating observations and refer to the opulent illustration, the morphometric analysis, and to Foissner (1993a) who fully cites the description of Beers (1952).

Body size on average highly similar in three cultures and preparations (Table 42): 535 × 307 µm (1.7:1) in vivo, 521 × 323 µm (1.6:1) in Chatton-Lwoff silver nitrate preparations, and 511 × 330 µm (1.6:1) in protargol slides, and thus distinctly smaller than Beers' cells (500–1000 × 250–475 µm); laterally flattened up to 2:1 (Fig. 121c, 122n). Body shape rather variable and indistinguishable from that of *B. truncatella,* i. e., bursiform with anterior end transversely truncate and posterior bluntly pointed (Fig. 122b, h, i, k, l, 123m) to broadly rounded, especially when full of food (Fig. 121a, b, 122a, o); left body margin usually less convex than right. Precystic specimens distinctly narrowed posteriorly (Fig. 121g, 122c, d, g). Macronucleus as described by Beers. Micronuclei numerous, in vivo about 10 µm across and composed of an about 5 µm wide, compact central body surrounded by a distinct membrane 2.5 µm distant from central body (Fig. 121f), as described by Schmähl (1926) for *B. truncatella.*

Extrusomes misinterpreted by Beers as alveolar layer, form conspicuous rows composed of granules about 2 µm across in surface view (Fig. 121e, 122p, r); in optical section about 20 × 2 µm and very hyaline, producing a bright, smooth fringe (Fig. 121h, 122q, 123c, j); when disturbed, contract (?) to about 10 µm becoming a compact, radially striated fringe (Fig. 121i, 122o, s, t); continued disturbance causes extrusome release and size increase to about 20 µm without loosening the compact structure (Fig. 121j); then, the extrusomes elongate to 30–60 µm long, curved, rather hyaline rods (Fig. 121j, 122u, w) that eventually become long (> 100 µm) filaments forming a thick envelope (Fig. 121k, 122v, x, 123v). Extrusome holes prominent in silver preparations (Fig. 123a, h, u) and in scanning electron micrographs (Fig. 123b, d).

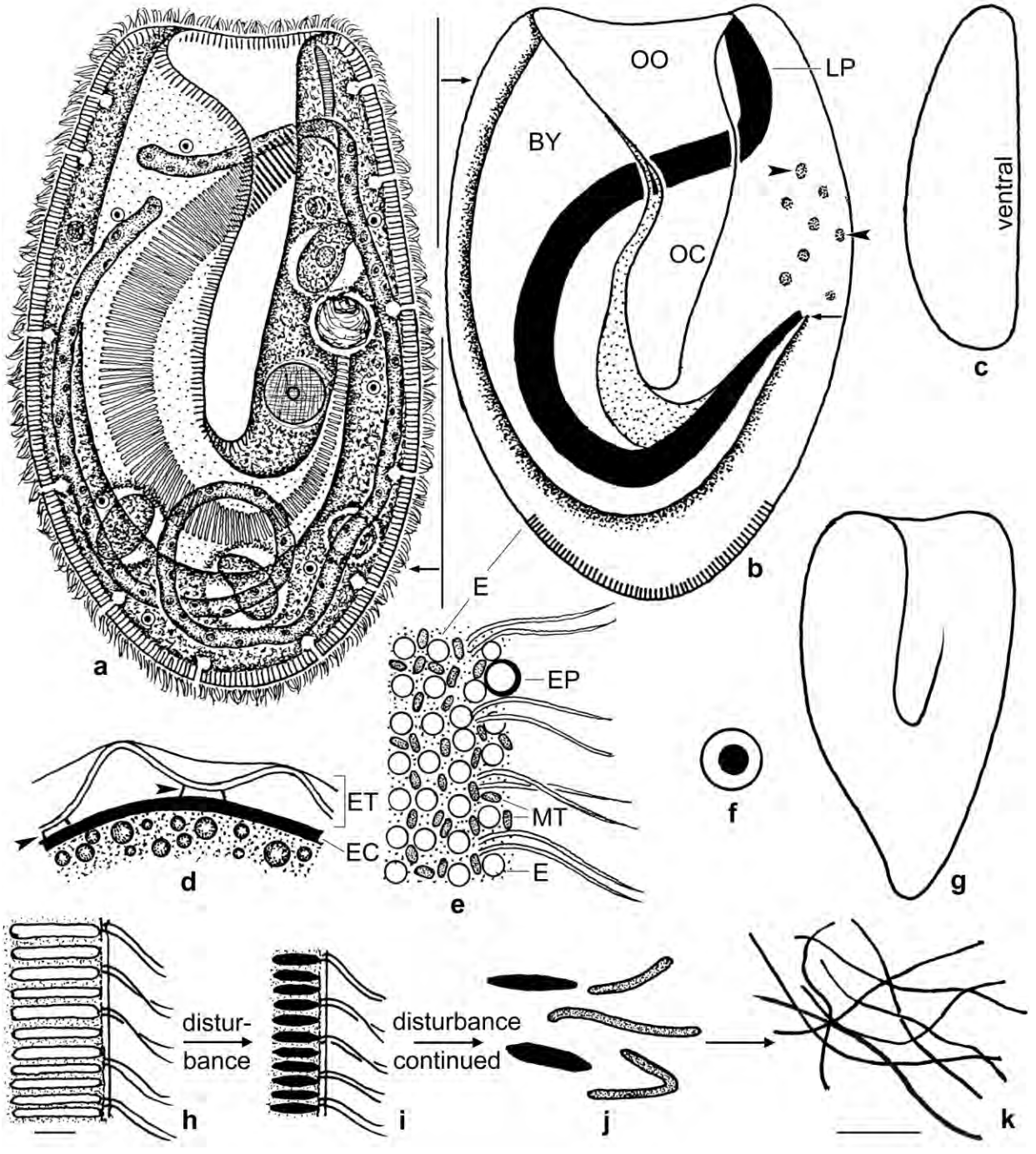

Fig. 121a–k. *Bursaria ovata* from life (a, c–j), after protargol impregnation (b), and stained with methyl green-pyronin (j, k). **a, b:** Ventral views of representative specimens with disturbed extrusomes shortened to about 10 µm and forming a distinct, striated fringe; length about 500 µm. The specimen shown in (a) has been constructed with the averages shown in Table 42. The oral apparatus recurves posteriorly and ends on average in mid-body left of midline (arrow). The arrowheads mark granular, protargol-affine blisters. **c:** Lateral view. **d:** Part of resting cyst with bridges (arrowheads) connecting ecto- and endocyst. **e:** Surface view of cortex. **f:** Micronucleus. **g:** A precystic specimen distinctly narrowed posteriorly. **h–k:** Resting (h) and disturbed (i) extrusomes which are released (j) and become long filaments (k). BY – buccal cavity, E – extrusomes, EC – endocyst, EP – excretory pore of a contractile vacuole, ET – ectocyst, LP – left oral polykinetid, MT – mitochondria, OC – oral cleft, OO – oral opening. Scale bars 10 µm (h–j), 20 µm (k), and 200 µm (a, b).

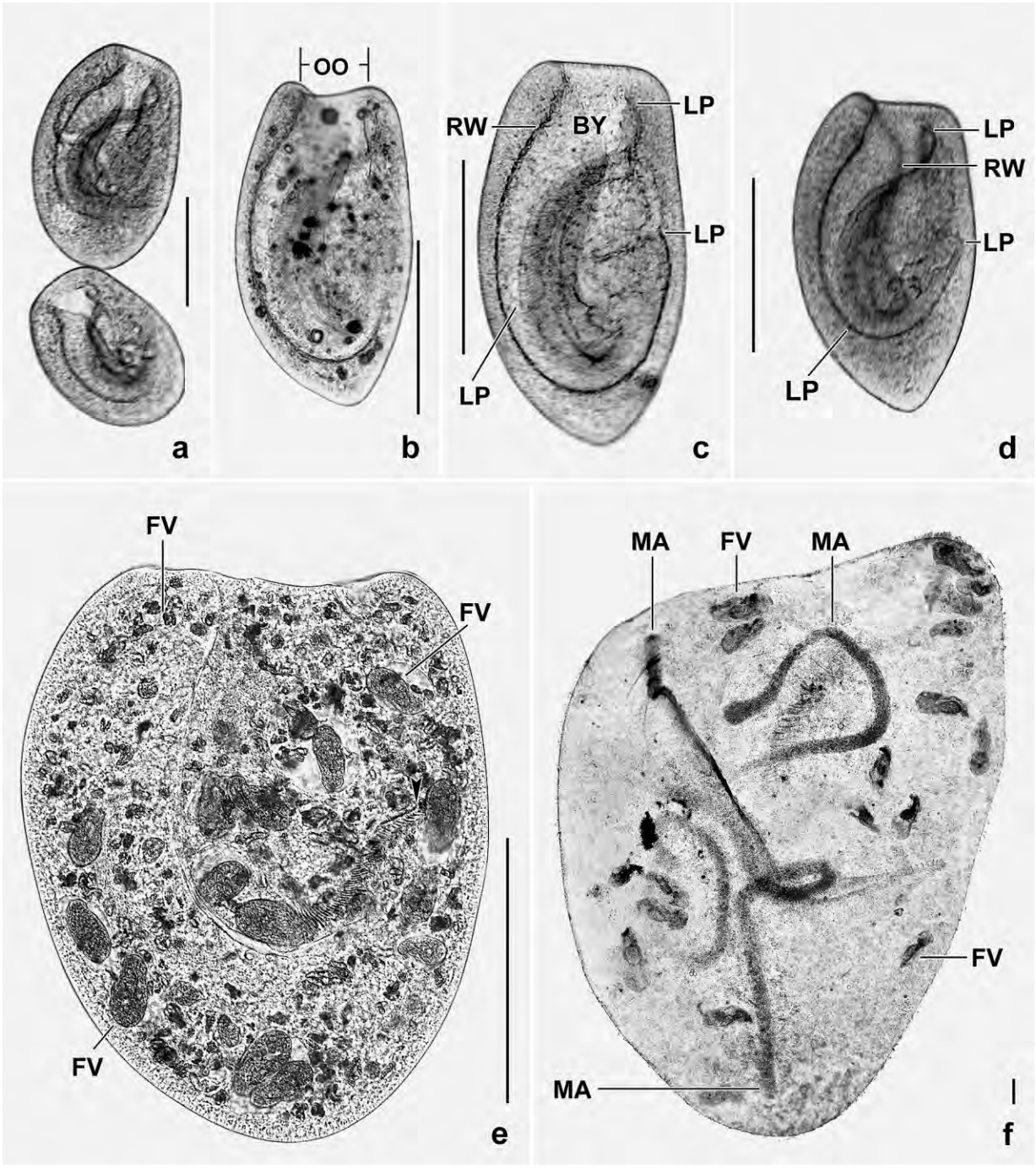

Fig. 122a–f. *Bursaria ovata,* cultivated Botswanan specimens from life (a–e, a–d starved) and after protargol impregnation (f). **a:** Freely motile specimens at begin of starvation. The cells are broadly rounded posteriorly. **b–d:** Ventral view of freely motile specimens. When starved for some hours, the specimens become bluntly acute posteriorly. Note the U-shaped buccal cavity and left oral polykinetid, a main feature of this species. **e:** A specimen fed with *Colpidium colpoda* and heterotrophic flagellates (pressed to show the details mentioned). The arrowhead marks the posterior end of the left oral polykinetid. **f:** A pressed specimen showing the long, vermiform macronucleus. BY – buccal cavity, FV – food vacuoles, LP – left oral polykinetid, MA – macronucleus, OO – oral opening, RW – right wall and margin of buccal cavity. Scale bars 30 µm (f) and 300 µm (a–e).

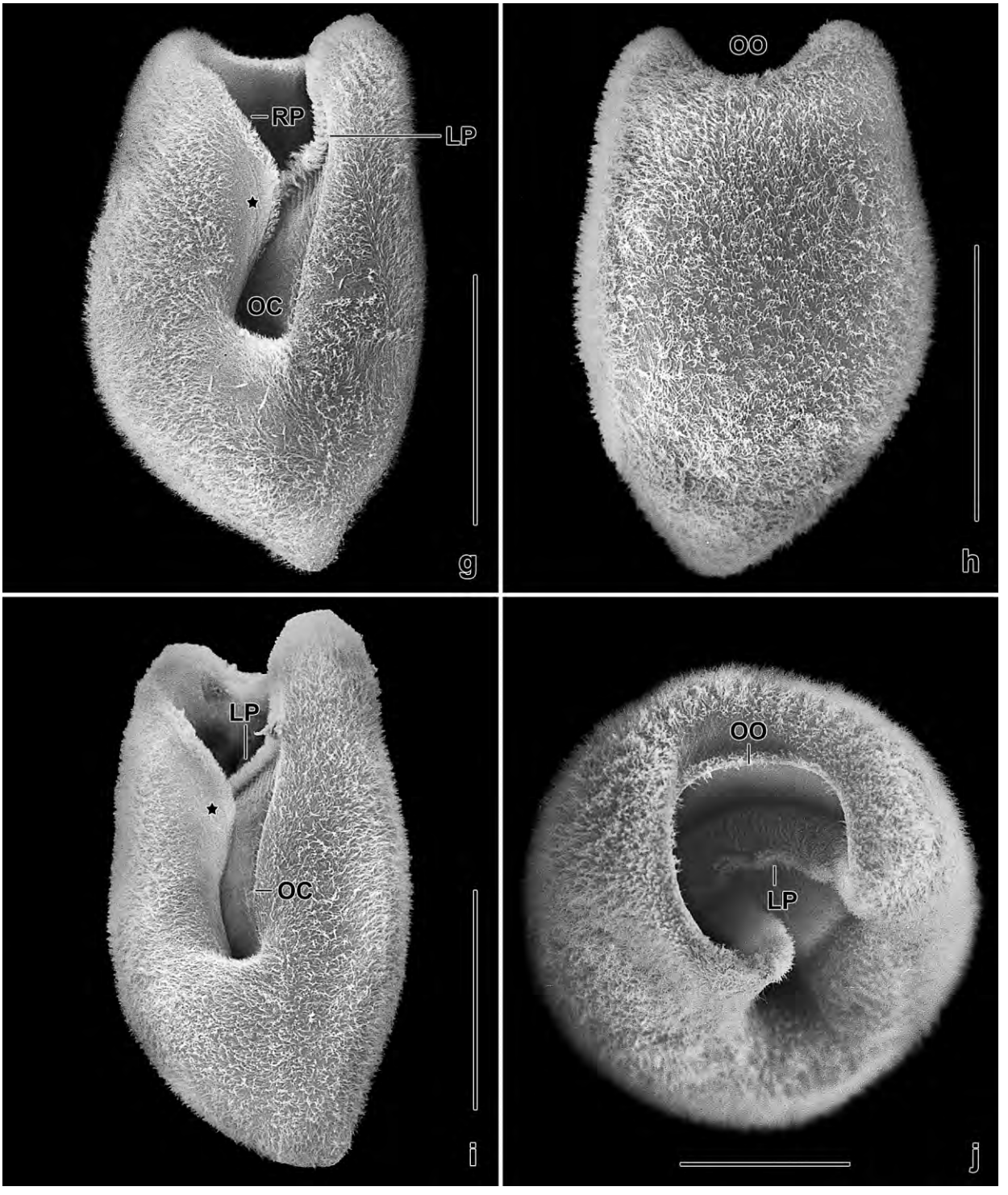

Fig. 122g–j. *Bursaria ovata*, cultivated Botswanan specimens in the scanning electron microscope. The specimens have been starved for some hours and have thus a bluntly pointed posterior body end. **g, i:** Ventral views, showing the long oral cleft and the non-ciliated stripe (asterisks) right of the right oral polykinetid. **h:** Dorsal view. **j:** Anterior polar view, showing the circular oral opening. LP – left oral polykinetid, OC – oral cleft, OO – oral opening, RP – right oral polykinetid. Scale bars 100 μm (j) and 200 μm (g–i).

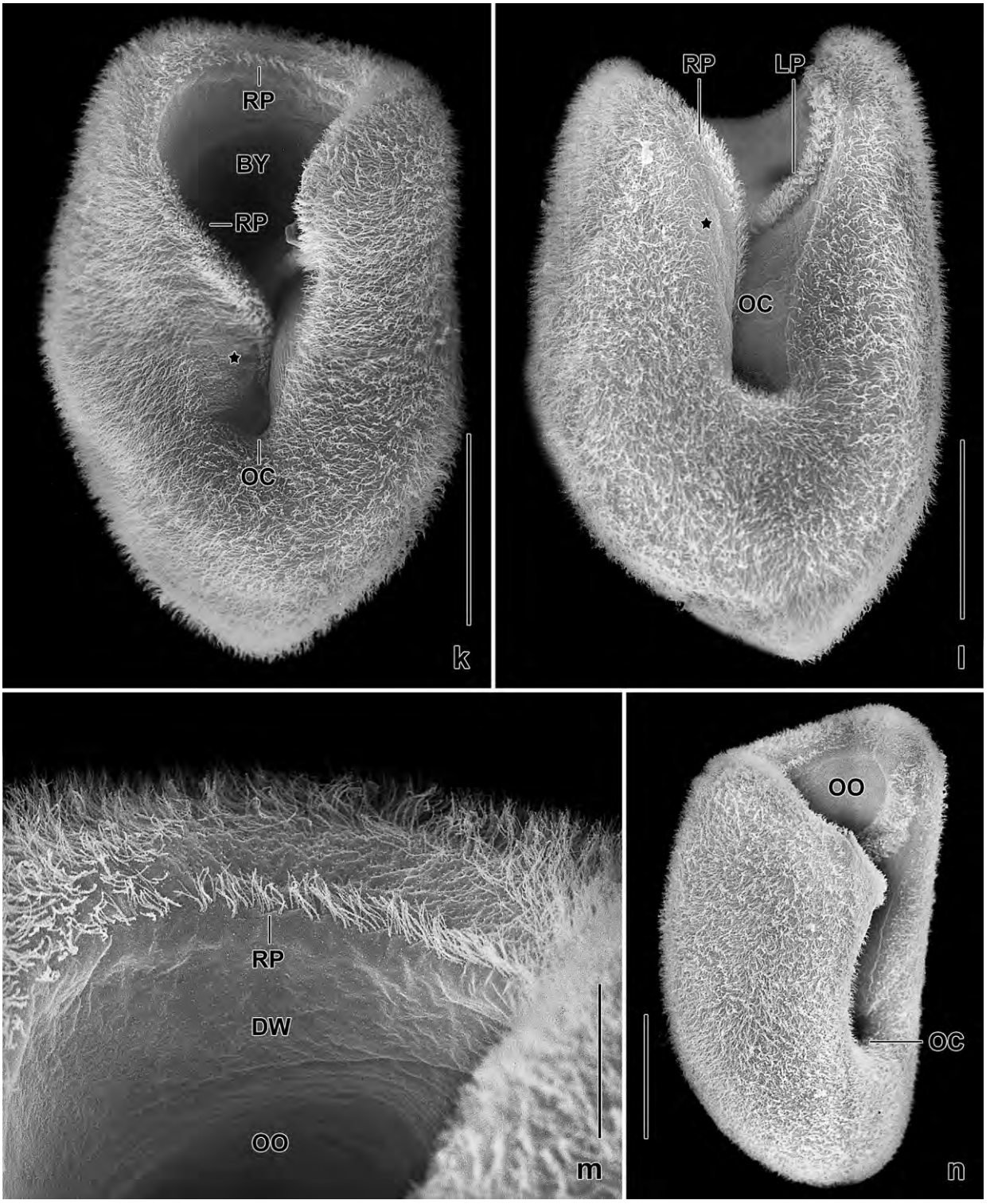

Fig. 122k–n. *Bursaria ovata*, cultivated Botswanan specimens in the scanning electron microscope. **k, m:** Oblique ventral view of a specimen in which the oral cleft almost disappeared due to the preparation procedures. The asterisk marks the non-ciliated stripe right of the right oral polykinetid which extends to the left wall of the buccal cavity (m). **l:** Ventral view with non-ciliated stripe marked by an asterisk. **n:** Lateral view, showing ventral flattening and dorsal convexity. DW – dorsal wall of buccal cavity, LP – left oral polykinetid, OC – oral cleft, OO – oral opening, RP – right oral polykinetid. Scale bars 25 µm (m) and 100 µm (k, l, n).

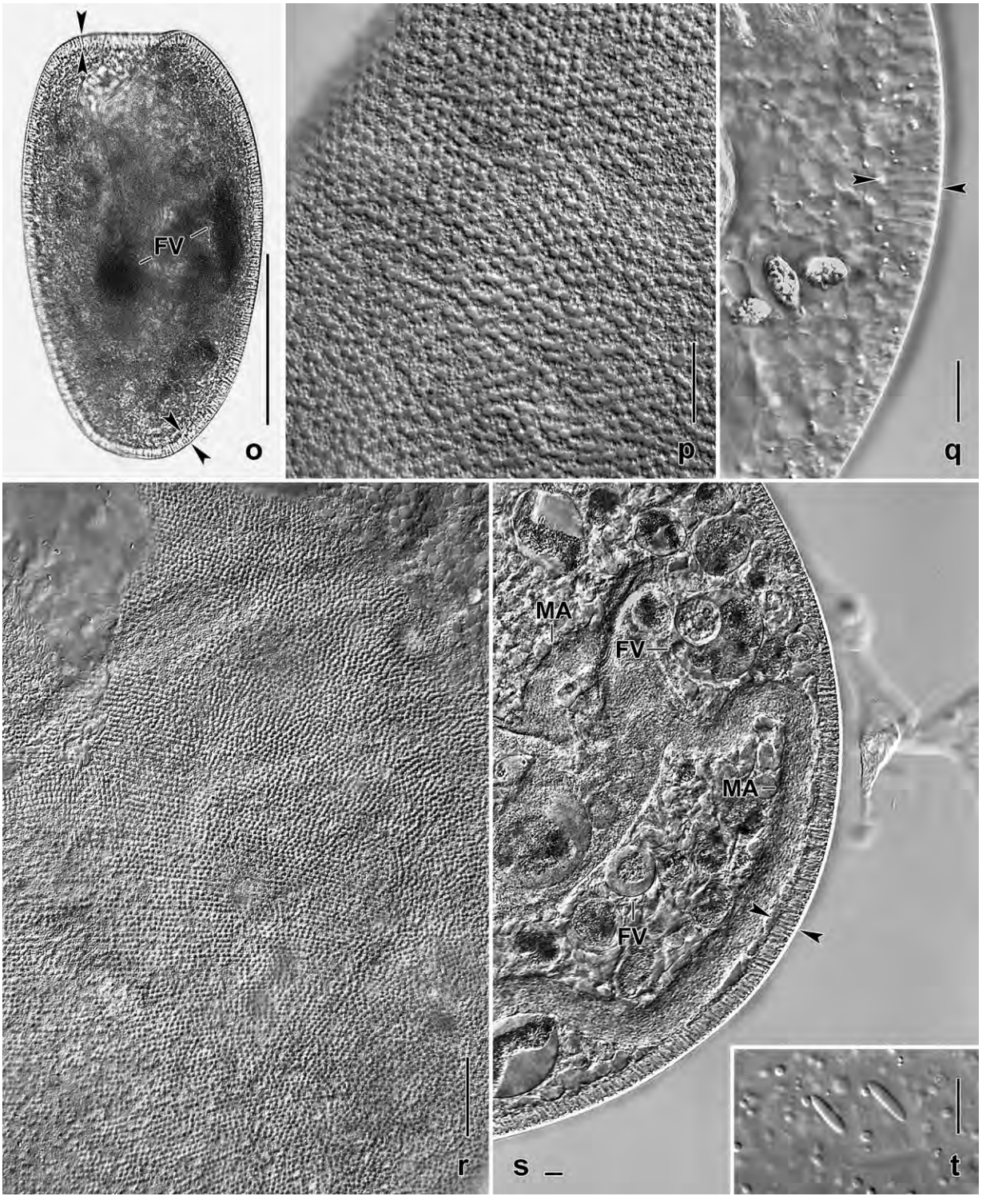

Fig. 122o–t. *Bursaria ovata*, cultivated Botswanan specimens from life. The opposed arrowheads delimit the extrusome fringe. **o, s, t:** Just before the extrusomes are released, they shorten from about 20 µm (q) to 10 µm and become compact (t), making the fringe striated (o, s). **p, r:** Surface views at high and low magnification, showing the dense rows of extrusomes. **q:** Optical section of cortex, showing undisturbed extrusomes with very low refractivity (see also Fig. 123c). FV – food vacuoles, MA – macronucleus. Scale bars 10 µm (s, t), 20 µm (p, q, r), and 200 µm (o).

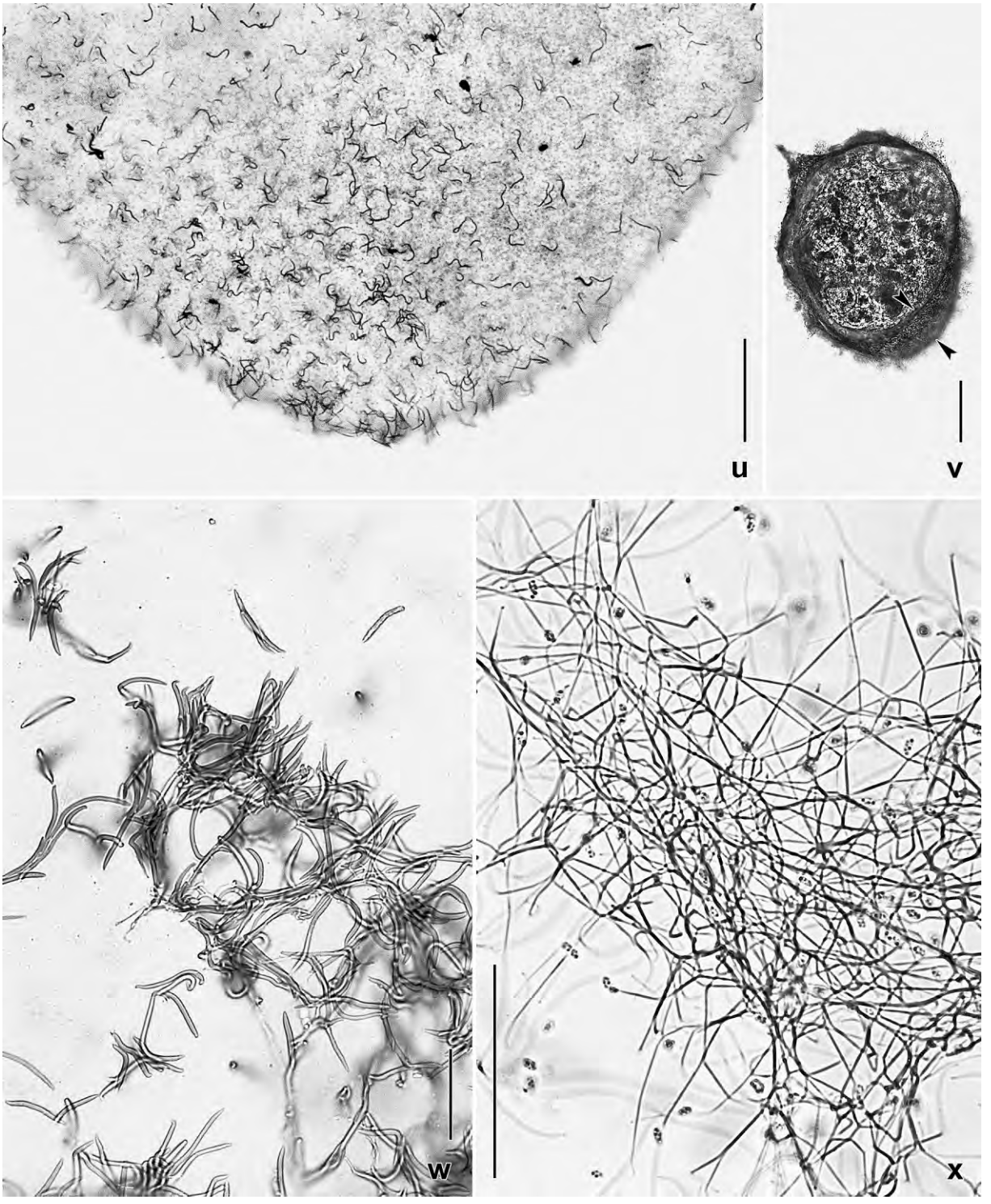

Fig. 122u–x. *Bursaria ovata*, cultivated Botswanan specimens after methyl green-pyronin staining, showing the extrusomes. **u, w:** Overview and detail, showing just extruded, vermiform, compact extrusomes. **v:** When fully exploded, the extrusomes form a thick, mucous layer (opposed arrowheads). **x:** Fully exploded extrusomes are filamentous and form a dense, three-dimensional reticulum. Scale bars 30 µm (w) and 100 µm (u, v, x).

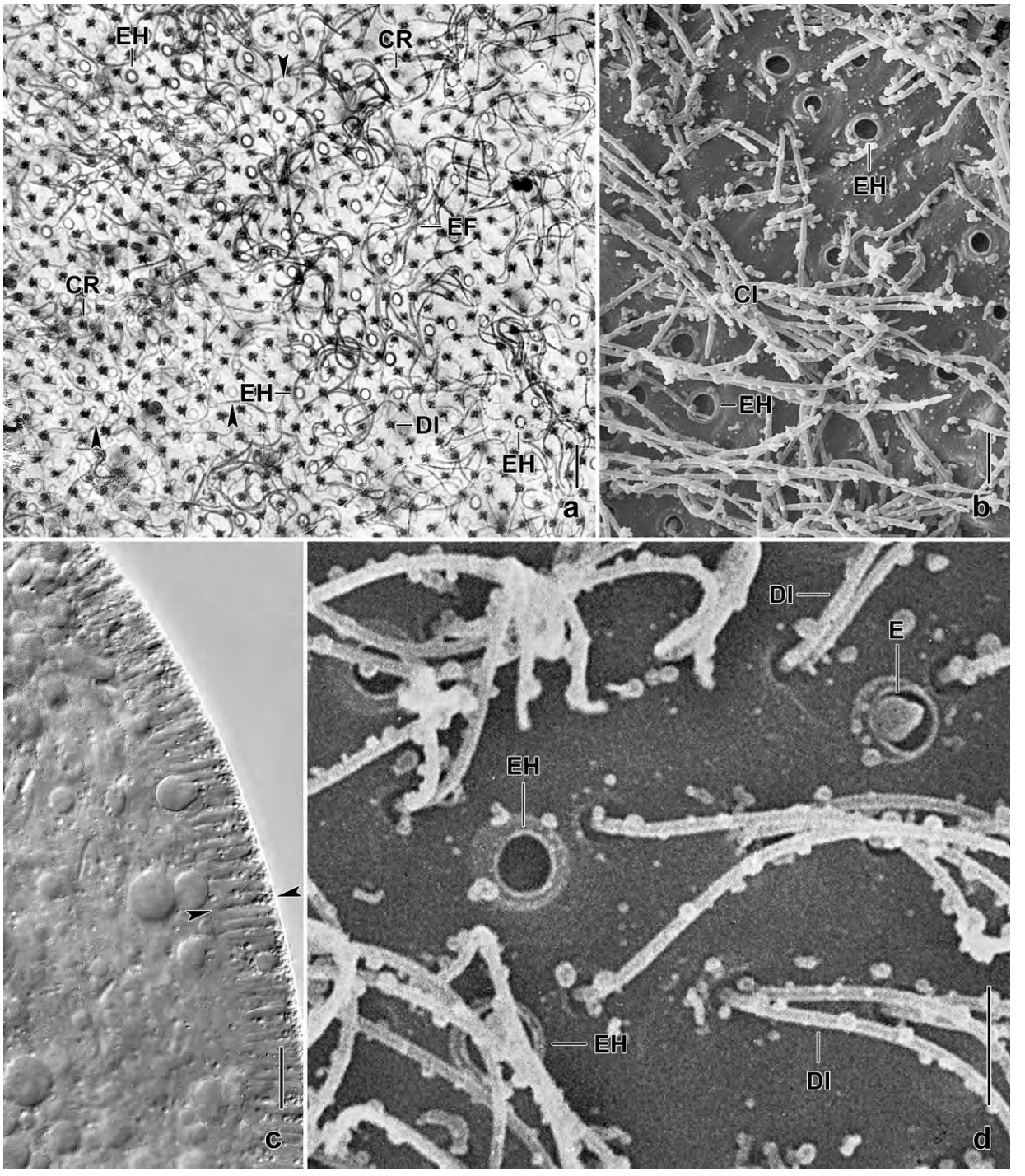

Fig. 123a–d. *Bursaria ovata*, cultivated specimens from life (c), after silver carbonate impregnation (a), and in the scanning electron microscope (b, d). **a:** Surface view of cortex, showing the basal bodies of the ciliary rows; exploded, filamentous extrusomes; and many extrusome holes, i. e., minute openings where extrusomes have been released. The arrowheads mark fading extrusome holes which become closed by the pellicular membranes. **b, d:** Extrusome holes in the SEM. Note an extrusome just leaving the cell (d, E) and the ciliated dikinetids. **c:** When undisturbed, the extrusomes are about 20 µm long and very hyaline, forming an indistinct fringe (opposed arrowheads). CI – cilia, CR – ciliary rows, DI – dikinetids, E – extrusome leaving the cell, EF – exploded, filamentous extrusomes, EH – extrusome holes. Scale bars 2 µm (b, d), 5 µm (a), and 20 µm (c).

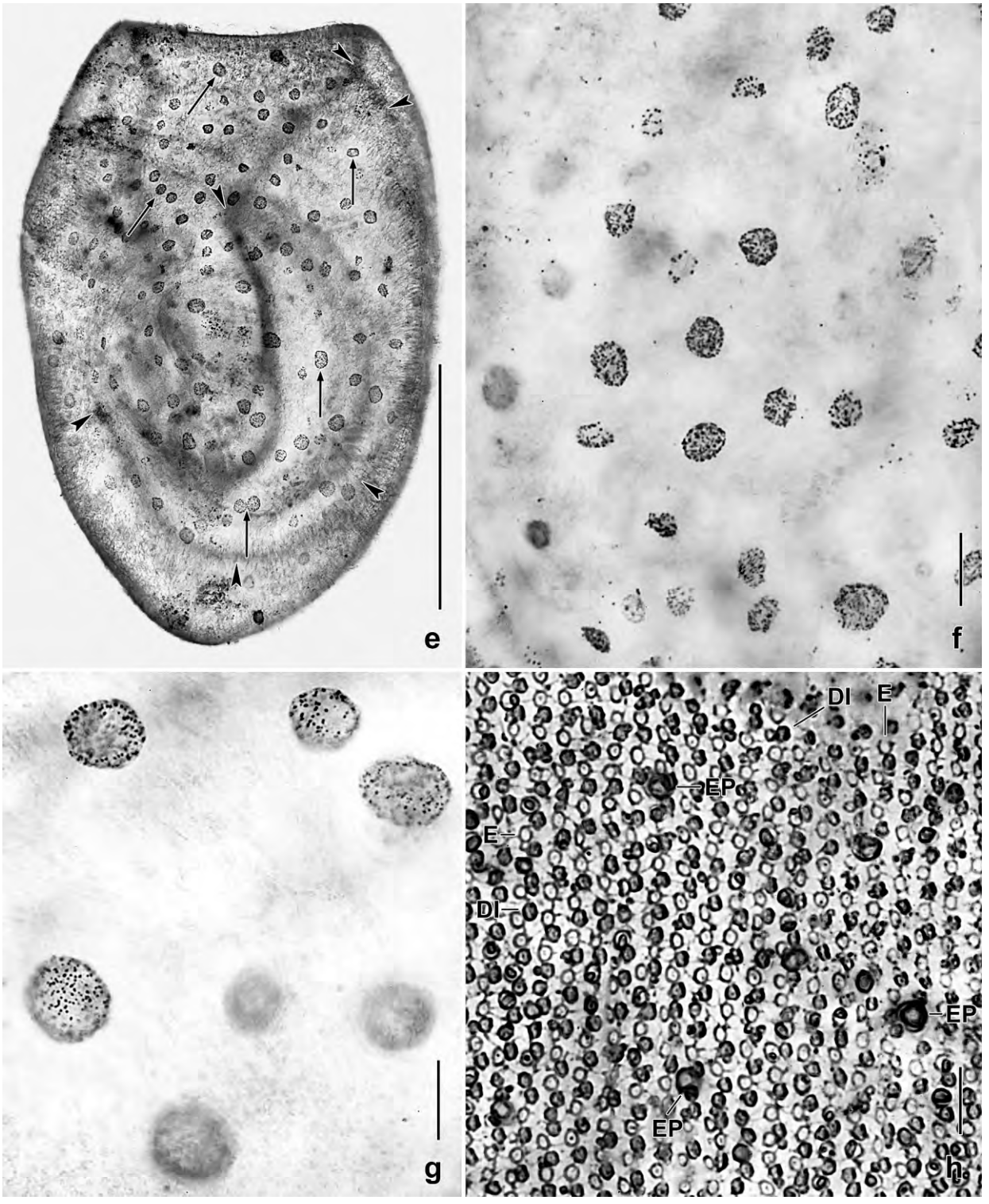

Fig. 123e–h. *Bursaria ovata*, cultivated Botswanan specimens after protargol (e–g) and CHATTON-LWOFF silver nitrate (h) impregnation. **e, f, g:** There are numerous subcortical vacuoles (e, arrows) with granular contents (f, g). The arrowheads mark the horn-shaped buccal cavity. **h:** Surface view of cortex, showing dikinetids (dark circles), extrusomes (bright circles), and the narrowly-meshed silverline pattern. DI – dikinetids, E – extrusomes, EP – excretory pores. Scale bars 6 µm (h), 10 µm (g), 20 µm (f), and 200 µm (e).

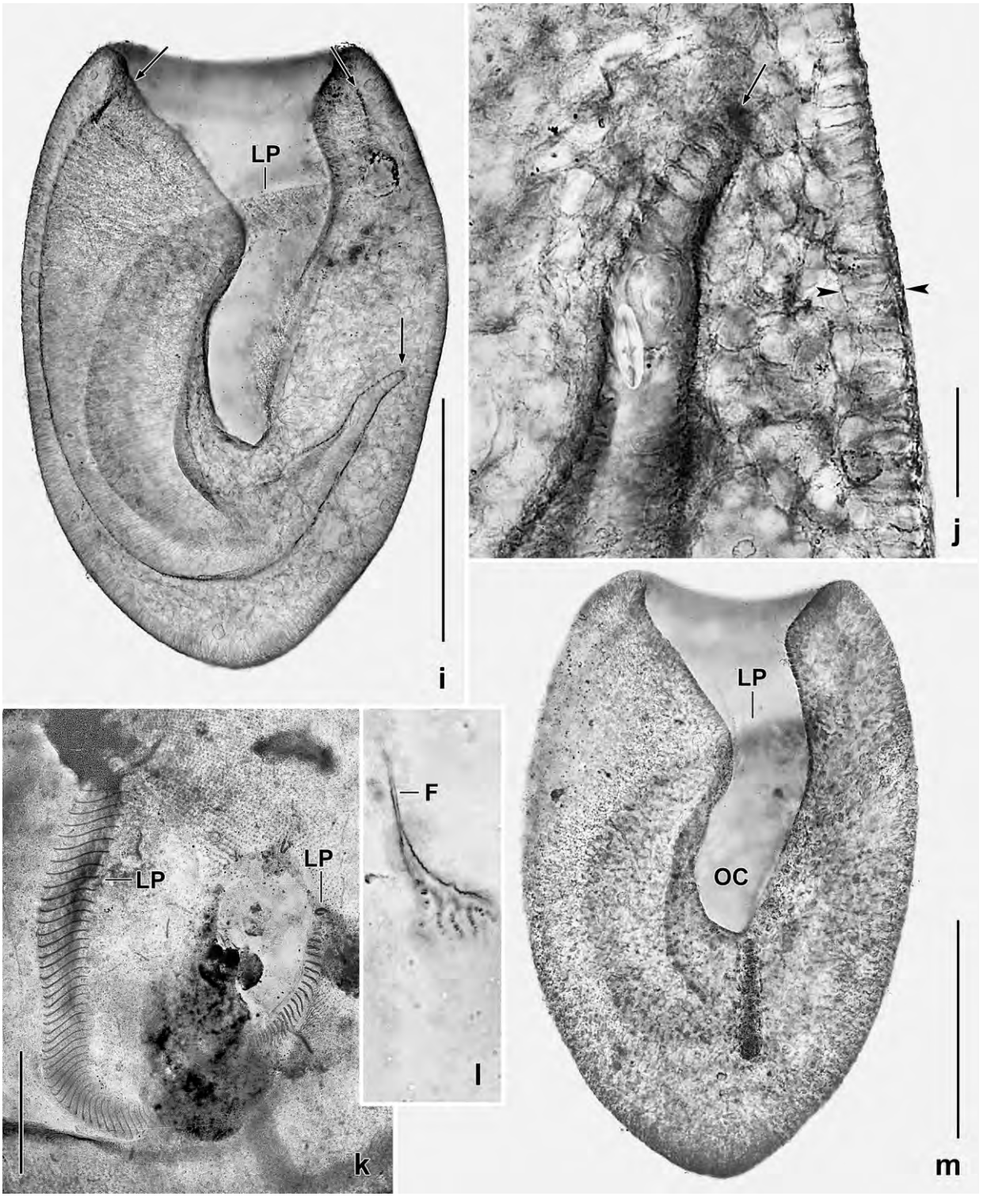

Fig. 123i–m. *Bursaria ovata*, cultivated Botswanan specimens after protargol impregnation. **i, j, m:** Overviews and detail, showing body shape and begin and end of the horn-shaped buccal cavity (i, j, marked by arrows). Opposed arrowheads mark extrusome fringe (j). **k:** Left oral polykinetid. **l:** Proximal end of buccal cavity and polykineties. F – fibres, LP – left oral polykinetid, OC – oral cleft. Scale bars 30 µm (j), 60 µm (k), and 200 µm (i, m).

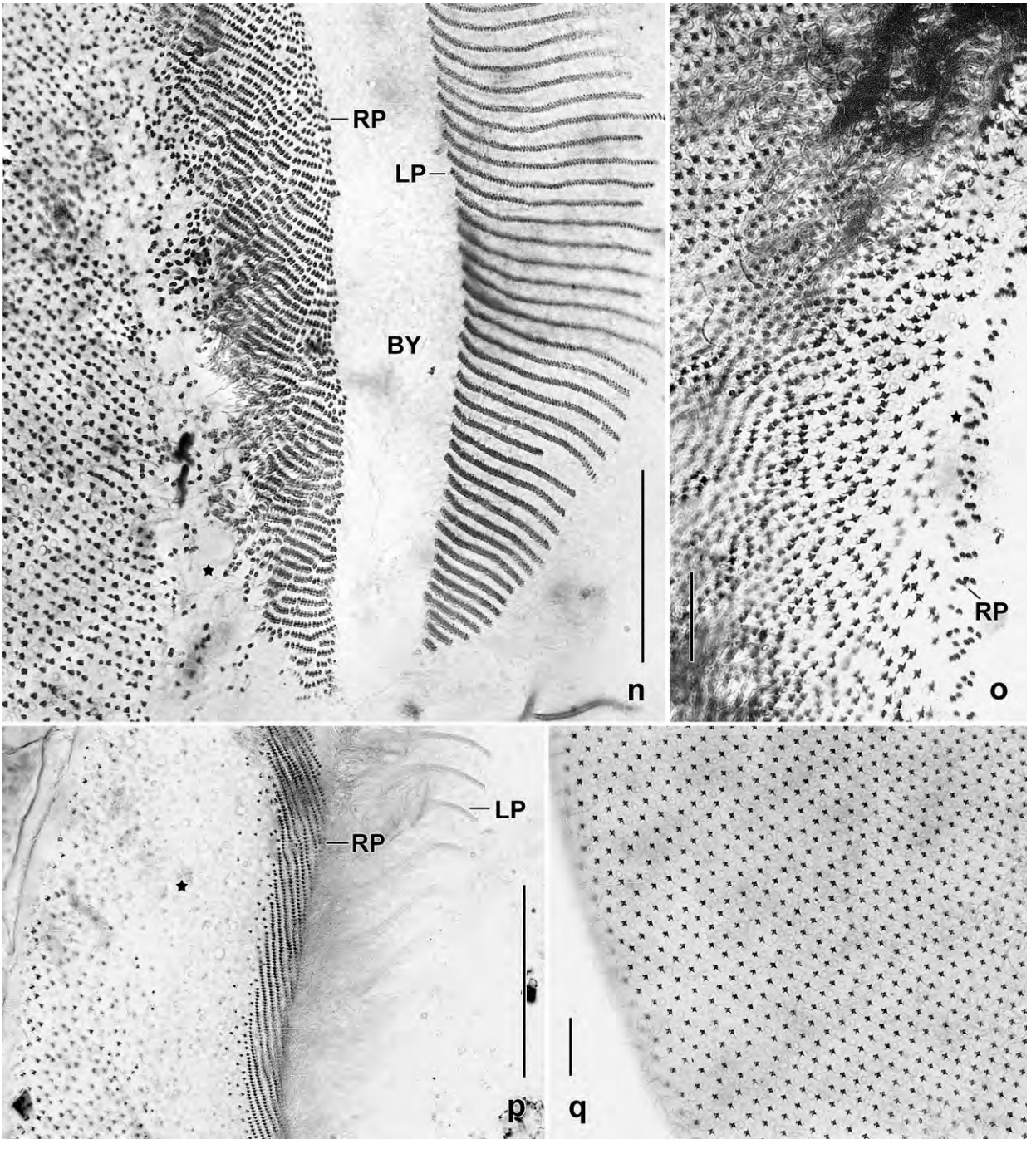

Fig. 123n–q. *Bursaria ovata,* cultivated Botswanan specimens after silver carbonate impregnation. **n:** Proximal end of the oral polykinetids. The non-ciliated stripe (asterisk) right of the right polykinetid extends to the end of the buccal cavity. The individual polykinetids of the left polykinety consist of short oblique kineties with three basal bodies each. **o:** Anterior end (right) of the buccal cavity (oral opening), showing the non-ciliated stripe (asterisk) right of the right oral polykinetid. **p:** Mid of right oral polykinetid where the kineties are well ordered. The asterisk marks a broad, non-ciliated stripe right of the right polykinetid; its function is not known. **q:** Part of the somatic ciliary pattern which consists of highly ordered dikinetids. BY – buccal cavity, LP – left oral polykinetid, RP – right oral polykinetid. Scale bars 10 µm (p), 20 µm (n), and 30 µm (m, o).

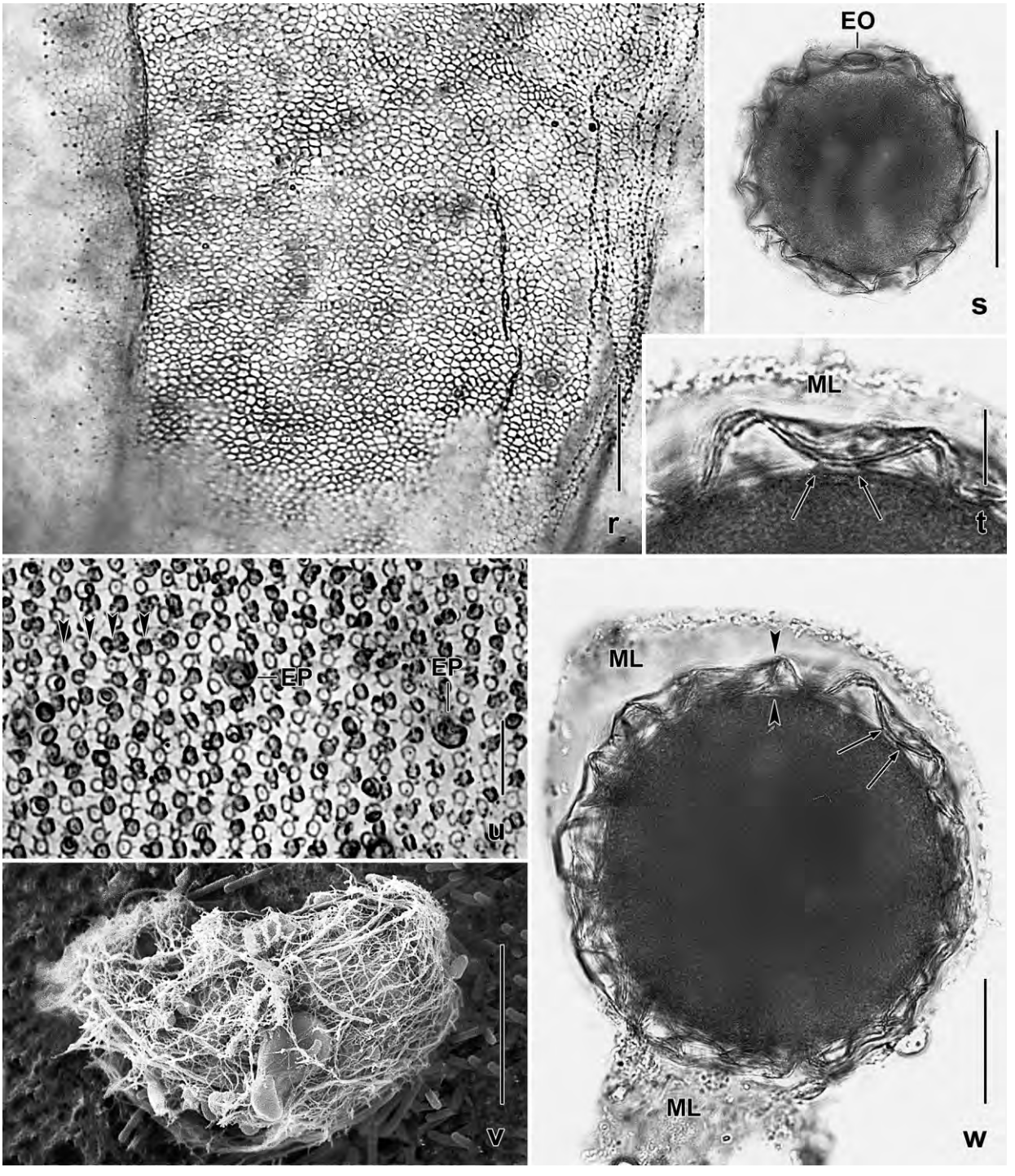

Fi**g. 123r–w.** *Bursaria ovata,* cultivated Botswanan specimens from life (s, t, w), in the SEM (v), and after Chatton-Lwoff silver nitrate impregnation (u). **r:** The wall of the buccal cavity contains a narrowly-meshed silverline pattern. **s:** Resting cyst, overview. **t, w:** Resting cyst. The external and internal wall (arrowheads) are connected by bridges (arrows), which are difficult to recognize because they are only about 1 µm high. **u:** Surface view of cortex, showing ciliary rows (arrowheads) composed of darkly impregnated dikinetids; bright rings associated with the extrusomes; excretory pores of the contractile vacuoles; and a narrowly-meshed silverline pattern which connects all cortical organelles. **v:** Filamentous reticulum produced by the extrusomes. EO – escape opening, EP – excretory pores, ML – mucus layer. Scale bars 10 µm (r, u), 20 µm (t), 50 µm (w), and 100 µm (s, v).

Table 42. Morphometric data on *Bursaria ovata* from Botswana based on mounted, randomly selected specimens from pure cultures. Measurements in µm. CV – coefficient of variation in %, IV – in vivo, M – median, Max – maximum, , Mean – arithmetic mean, Min – minimum, n – number of individuals investigated, P – protargol impregnation, SD – standard deviation, SE – standard error of arithmetic mean, SN – Chatton-Lwoff silver nitrate impregnation.

Characteristics	Method	Mean	M	SD	SE	CV	Min	Max	n
Body, length	IV	535.0	512.5	100.8	31.9	18.8	400.0	700.0	10
Body, width	IV	307.5	312.5	39.2	12.4	12.5	250.0	350.0	10
Body length:width, ratio	IV	1.7	1.8	0.2	0.1	10.4	1.4	2.0	10
Body, length	SN	521.0	500.0	54.7	17.3	10.5	440.0	600.0	10
Body, width	SN	323.0	325.0	29.1	9.2	9.0	270.0	360.0	10
Body length:width, ratio	SN	1.6	1.6	0.1	0.1	7.5	1.4	1.8	10
Body, length	P	511.0	510.0	54.5	14.1	10.7	400.0	590.0	15
Body, width	P	330.7	330.0	32.6	8.4	9.9	270.0	380.0	15
Body length:width, ratio	P	1.6	1.5	0.1	0.1	7.4	1.3	1.8	15
Anterior body end to end of oral cleft, distance	SN	333.0	345.0	40.8	12.9	12.3	270.0	390.0	10
Anterior body end to end of left polykinetid, distance	SN	256.7	250.0	20.8	12.0	8.1	240.0	280.0	3
Posterior body end to deepest point of left polykinetid	SN	95.5	92.5	13.4	4.3	14.1	70.0	120.0	10
Oral opening, width	SN	106.0	110.0	18.4	5.8	17.3	80.0	130.0	10
Oral cleft, maximum width	SN	35.3	36.5	8.4	2.6	23.7	20.0	50.0	10
Ciliary rows, number	SN	288.0	285.0	30.8	9.8	10.7	250.0	350.0	10
Dikinetids, number in 20 µm in mid-body	SN	8.0	8.0	1.6	0.5	19.5	5.0	10.0	10
Anterior body end to end of oral cleft, distance	P	300.0	320.0	39.4	10.2	13.1	220.0	350.0	15
Anterior body end to end of left polykinety, distance	P	246.0	250.0	46.0	11.9	18.7	170.0	350.0	15
Oral opening, width	P	162.0	160.0	16.6	4.3	10.2	140.0	200.0	15
Oral cleft, maximum width	P	75.3	70.0	20.7	5.3	27.4	50.0	120.0	15
Macronucleus, width	P	16.1	15.0	2.7	0.7	18.7	12.0	22.0	15
Extrusome fringe, height	P	14.3	15.0	2.3	0.6	15.8	10.0	17.0	15
Left oral polykinetids, maximum length	P	33.4	34.0	3.1	0.9	9.2	30.0	40.0	15
Left oral polykinetids, maximum distance in between	P	5.4	5.0	1.1	0.1	19.8	4.0	7.0	19
Left oral polykinetids, number	P	147.9	150.0	10.8	4.1	7.3	130.0	160.0	7
Resting cyst, diameter with wall	IV	193.2	198.0	12.6	3.2	6.5	176.0	212.0	16
Resting cyst, diameter without wall	IV	165.9	168.0	8.6	2.1	5.2	152.0	180.0	16
Resting cyst bridges, width	IV	13.0	12.0	5.4	1.2	41.0	5.0	26.0	19
Resting cyst escape opening, diameter	IV	34.6	36.0	4.3	1.1	12.4	30.0	42.0	14

Underneath extrusome layer many curious vesicles 5–10 µm across and filled with argyrophilic granules (Fig. 121b, 123e–g); not identical with contractile vacuoles.

Omnivorous, i. e., feeding on flagellates, testate amoebae (*Arcella*), and a variety of ciliates, e. g., *Colpidium colpoda*. Food depletion causes encystment (Fig. 121a, 122b, e, f, s).

Somatic cilia 15 µm long in vivo, paired, arranged in an average of about 288 ordinarily spaced

rows (~ 2.7 µm, Table 42); ciliary pattern indistinguishable from that of *B. truncatella*, including a triangular field of unciliated basal bodies at margin of right wall of buccal cavity (Fig. 122g–i, k, l, 123a, b, h, q). Silverline pattern irregular reticulate, both on body (Fig. 123h, u) and in wall of buccal cavity (Fig. 123r).

Oral opening circular (Fig. 122j), with a narrow ventral cleft extending 60% of body length on average (Fig. 121a, b, 122a, g, i, k, l, n, 123i, m; Table 42). Buccal cavity and oral polykinetids almost U-shaped, i. e., extend from anterior to near posterior body end and then recurves anteriorly left of body´s midline to mid-body on average, as already described by Beers (Fig. 121a, b, 122a–d, 123e, i–m; Table 42). Oral polykinetids as in *B. truncatella*.

Resting cysts basically as in *B. truncatella* but height of bridges between ectocyst and endocyst only about 1 µm, bridges thus difficult to recognize (Fig. 123s, t, w); considerably smaller than described by Beers (Table 42): 176–212 µm vs. 230–280 µm (with wall); young cysts with distinct mucous envelope (Fig. 123w).

Identification: Our observations basically match the description of Beers (1952), except of the resting cyst and the extrusomes, which Beers did not recognize as such: "The ectoplasm is clearly differentiated as a radially striated alveolar layer which bears a superficial pellicle and contains the basal bodies of the cilia". Unfortunately, Beers (1952) did not provide measurements. However, his illustrations indicate that the "striated alveolar layer" is 8–9 µm thick which matches our data in the striated explosion phase (Fig. 121a, b, i, 122o, s).

For the resting cysts, Beers (1952) states: "Bridges uniting ectocyst and endocyst, as in *B. truncatella*, are absent". In contrast, bridges are present in our population (Fig. 123t, w). However, they are often difficult to recognize because they are only 1 µm high. Thus, we assume that Beers (1952) overlooked the bridges. The same happened Sergejeva (1989) who first missed bridges but later found them (Sergejeva et al. 1995).

Comparison with *B. truncatella*: Beers (1952) distinguished *B. ovata* from *B. truncatella* by the U-shaped oral apparatus and the lack of bridges in the resting cyst. The second feature is very likely a misobservation (see above) but can be replaced by the extrusomes which are clearly different: 1–5 µm in *B. truncatella* (Foissner 1993a and unpubl.) while about 20 µm in *B. ovata* (Fig. 122o–t, u–x, 123c). The U-shaped oral structures are in some specimens not very pronounced (Table 42) and might thus overlap with some specimens of *B. truncatella* (Foissner 1993a, Fig. 185b, e). However, usually it is a reliable character, especially in connection with the unique extrusomes.

There is no doubt that *B. ovata* and *B. truncatella* are closely related. This is corroborated by the very similar 18rDNA (Fig. 124). Further, there is no doubt that several *Bursaria* species exist (Fig. 124). However, their identity is threatened by several more or less incorrect descriptions of *B. truncatella* (for a review, see Foissner 1993a). Both, the European and the North American *B. truncatella* need careful redescription because they are possibly different species, as indicated by their 18rDNA (Fig. 124).

Occurrence and ecology: As yet found in temporary habitats of the USA, Russia, Belgium, Botswana (Southern Africa, present population), and Venezuelan site (56).

Woodruffiina nov. subordo

The Colpodea were revised by Foissner et al. (2011, 2014b). These authors recognized four well supported molecular clades (Fig. 124), one of which is the order Platyophryida, containing the suborders Platyophryina and Sorogenina as well as the families Platyophryidae, Woodruffiidae, Sagittariidae, and Reticulowoodruffiidae.

Here, we describe two new genera, *Apowoodruffia* and *Sagittariides*, which form a strongly supported molecular clade with the genera *Woodruffides* and *Sagittaria* (Fig. 124). We classify

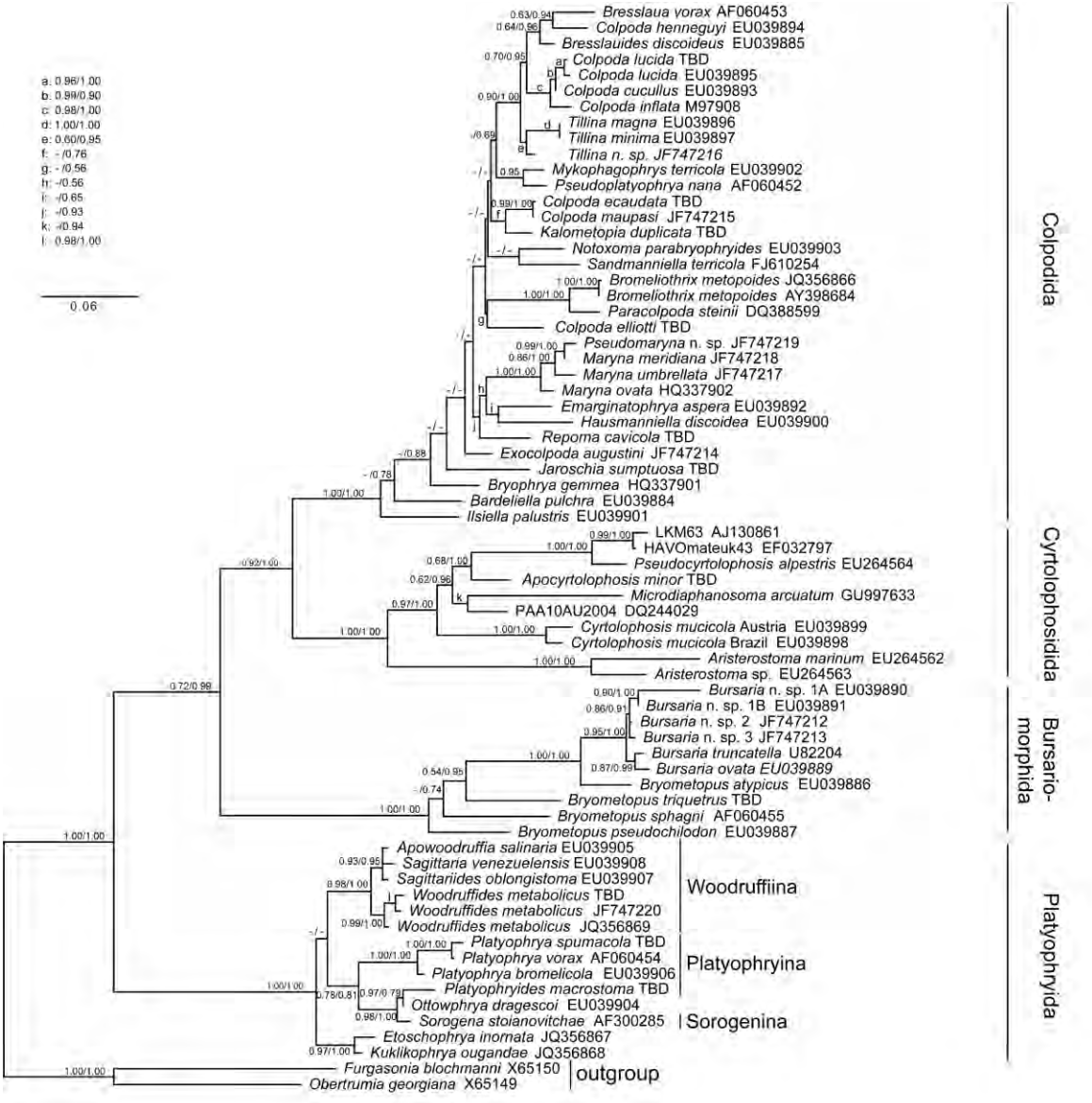

Fig. 124. Nuclear SSU-rDNA molecular tree of the Colpodea (from Foissner et al. 2011, 2014b), showing the classification of the new genera *Apowoodruffia* ("*Platyophrya*-like" in Foissner et al. 2011) and *Sagittariides* ("*Rostrophrya* sp." in Foissner et al. 2011) as well as of the species *Sagittaria venezuelensis* ("*Sagittaria* sp." in Foissner et al. 2011), *Platyophryides macrostoma* (*Platyophryides* n. sp. in Foissner et al. 2013b), *Bursaria ovata* ("*Bursaria muco*" in Foissner et al. 2013b), and *Maryna meridiana* ("*Maryna* sp." in Foissner et al. 2013b).

this clade as a distinct suborder, not only due to the molecular distinctness but also because of the resting cysts, which are distinctly different from those of the Platyophryina and Sorogenina (for a review see Foissner 1993a; Fig. 125, 126): The wall is tripartite and of an orange colour in the former (this monograph), while a simple, colourless, 1–3 µm thick layer in the latter (Fig. 125m). The suborder is classified into two families: the Woodruffiidae Gelei, 1954 (containing *Woodruffides* and possibly several other genera, such as *Rostrophrya*, *Rostrophryides*, and *Kuklikophrya*) and the Sagittariidae Grandori & Grandori, 1934, containing the genera *Sagittaria*, *Apowoodruffia*, and *Sagittariides*, all described in the following chapters.

Diagnosis: Small to large (~ 30–300 µm), oblong to rostrate Platyophryina with circular to slit-like oral opening at anterior pole or the rostrate portion. Micronucleus in perinuclear space of macronucleus. Silverline pattern platyophryid or colpodid. Postoral pseudomembrane absent. Divides in freely motile condition or in division cysts. Resting cysts conspicuously orange, with thin, yellowish ectocyst; thick, orange-coloured mesocyst; and thin, colourless endocyst.

Type family: Woodruffiidae Gelei, 1954.

Taxa assignable: Woodruffiidae Gelei, 1954 and Sagittariidae Grandori & Grandori, 1934.

Remarks: The position of the Reticulowoodruffiidae Foissner, 1993a, a monotypic family and genus, remains unknown. The best feature to distinguish the Woodruffiina from the Platyophryina and Sorogenina are the resting cysts. All other characteristics occur in all suborders but with different frequency. For instance, the postoral pseudomembrane, which is absent from all Woodruffiina and in *Sorogena* as well as in some genera of the Platyophryina, viz., in *Ottowphrya*, *Rostrophrya*, and *Kuklikophrya*. However, the molecular position of the last mentioned genera is still unknown.

Woodruffides metabolicus (Johnson and Larson, 1938) Foissner, 1993a (Fig. 124, 125a–l, 126a)

Our observations match those of previous authors (reviewed by Foisser 1993a), especially in the strong pigmentation of the mature cyst. However, the illustrations available are meagre and micrographs are lacking at all. Thus, we redescribe the cyst, based on Japanese specimens from soil of a rice field in the surroundings of the Lake Biwa museum (Fig. 125a, 126a).

The young cyst (Fig. 126b, c): Young cysts are colourless to yellowish and have an up to 20 µm wide, bright cover that contains many granular accumulations, i. e., extruded cytoplasmic and/or nuclear material, as have many other colpodids (Foissner 1993a). This conspicuous, hyaline layer, which does not stain with alcian blue, is followed by an about 2 µm thick, colourless, compact cover, the endocyst. The cyst contents is colourless and coarse-grained (Fig. 125b, c).

The mature cyst (Fig. 125d–l, 126a): Cysts are mature, i. e., do not change further after a week. They are remarkable in being so strongly pigmented that details can be studied only in pressed (flattened) and crushed specimens (Fig. 125d, f, g). The cysts, which are globular to slightly ellipsoid, have an average size of 71.9 × 71 µm (M = 70 × 68 µm, SD = 9.2/9.5 µm, CV =

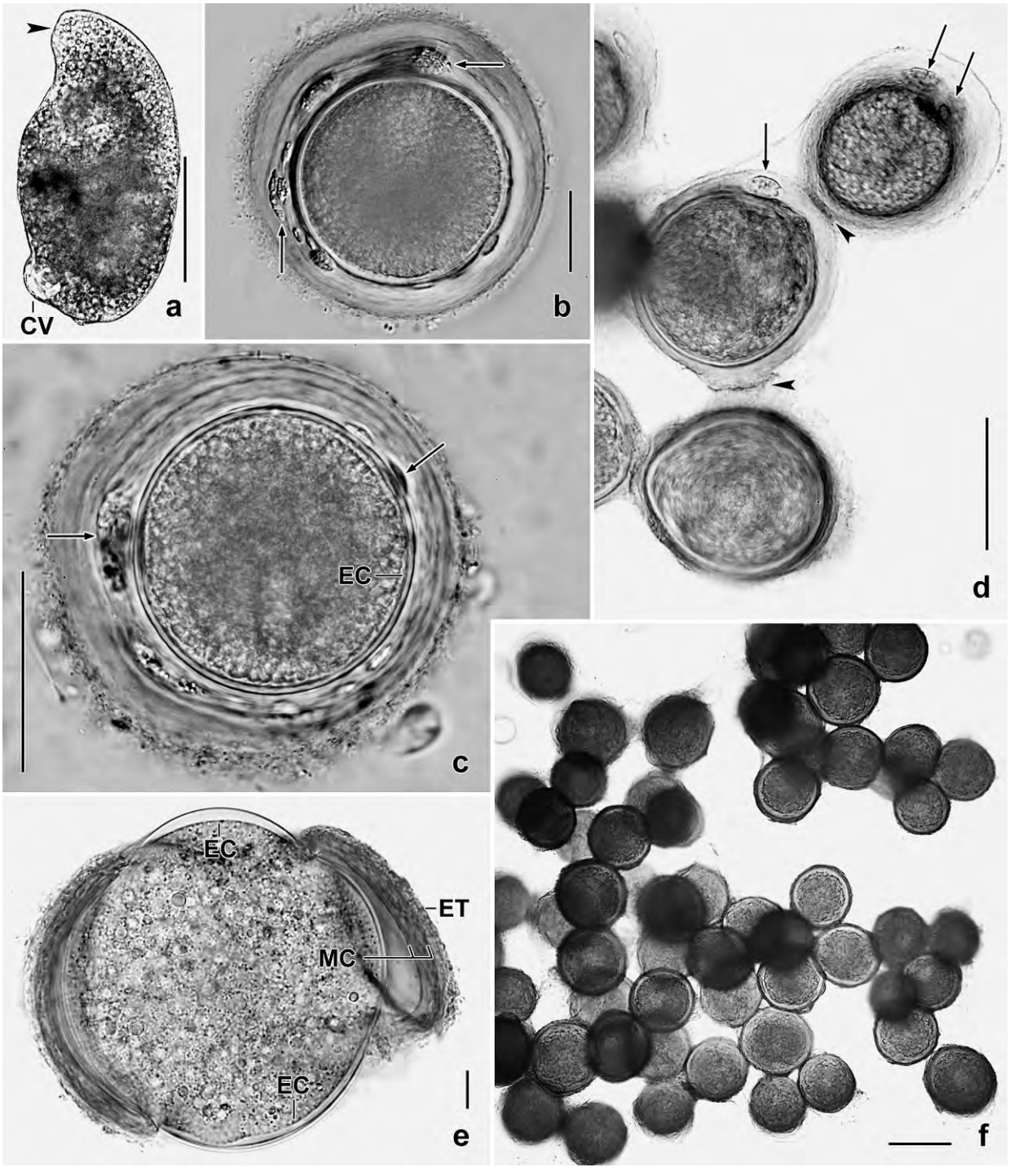

Fig. 125a–f. *Woodruffides metabolicus*, immature (b, c) and mature (d–f) resting cysts from Japanese specimens. Arrows mark extruded cytoplasmic and/or nuclear material. The dark appearance of the mature cysts is caused by the deep orange pigmentation. **a:** Left side view of a vegetative specimen with obliquely truncate anterior body end (arrowhead) and distinct contractile vacuole (CV). **b, c:** Young cysts show two distinct wall layers. The thick, hyaline external layer is yellowish and later forms the ecto- and mesocyst. The thin, colourless endocyst is distinct because it is highly refractive. **d, f:** Mature cysts at moderate and low magnification. When encysting, the cells accumulate and become loosely connected by the ectocyst (d, arrowheads). **e:** Crushed cyst, showing the colourless endocyst (EC) and the strongly pigmented ecto- and mesocyst (ET, MC). Scale bars 5 µm (e), 25 µm (b), 50 µm (c, d), 75 µm (f), and 100 µm (a).

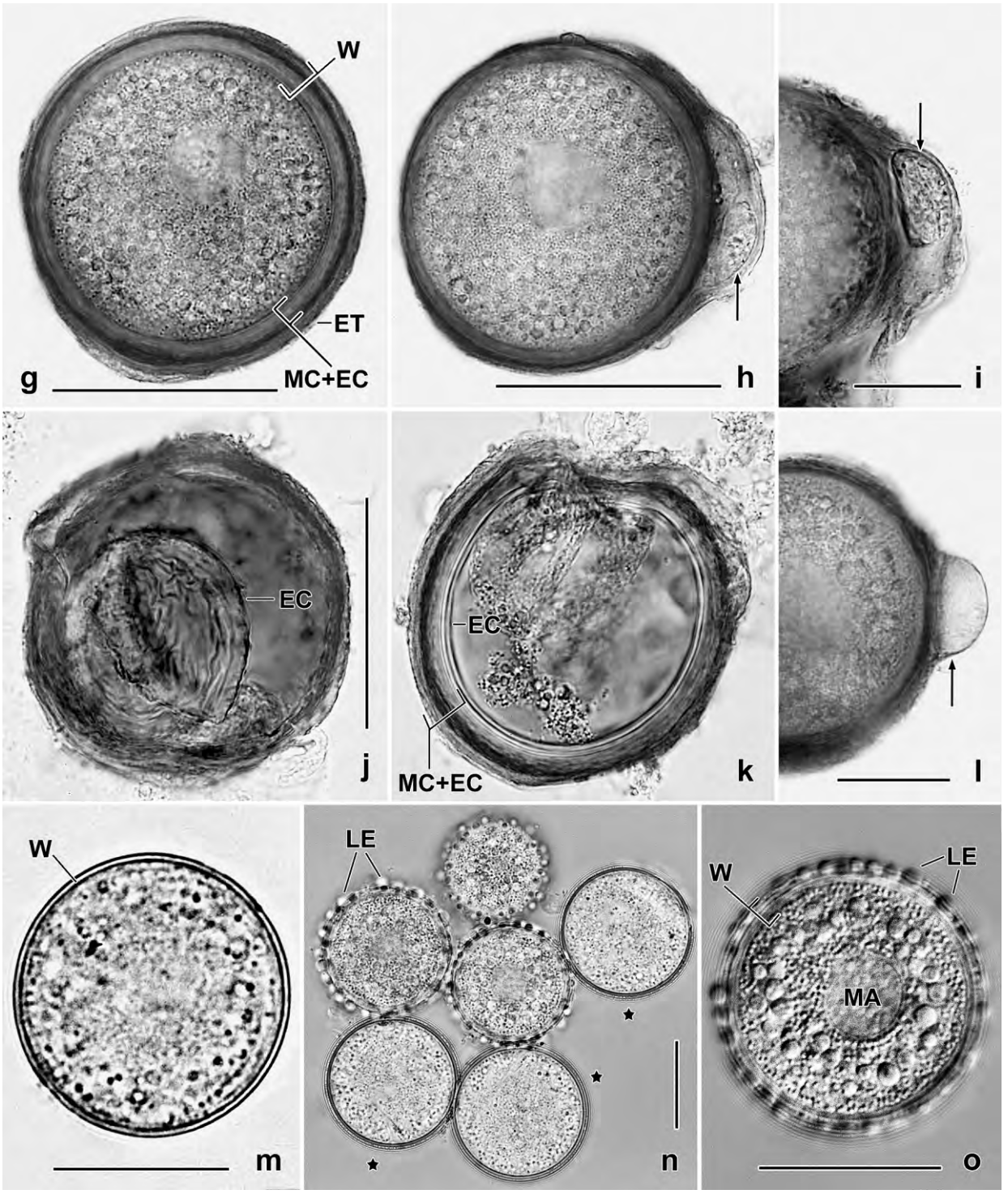

Fig. 125g–o. Mature resting cysts of *Woodruffides metabolicus* (g–l), *Platyophrya spumacola* (m), and *Ottophrya dragescoi* (n, o). **g, h:** Typical cysts. The arrow in (h) marks extruded material within a large blister made of the ecto- and mesocyst. Most of the pigment is in the dark brown surface area of the mesocyst. **i, l:** Wall blisters with and without contents; the latter resembling an escape apparatus. **j, k:** Squashed cysts showing the colourless endocyst and the deep pigmentation of the ecto- and mesocyst. **m:** Mature resting cyst of *Platyophrya spumacola* (from Foissner 1993). **n, o:** Mature and immature (starred) resting cysts of *Ottowphrya dragescoi* from Belgium (Foissner, unpubl.). The cyst wall is covered by many spheres (lepidosomes) 1.5–3 µm across. EC – endocyst, ET – ectocyst, LE – lepidosomes, MA – macronucleus, MC – mesocyst, W – cyst wall. Scale bars 20 µm (m), 25 µm (i, l, n, o), and 50 µm (g, h, j, k).

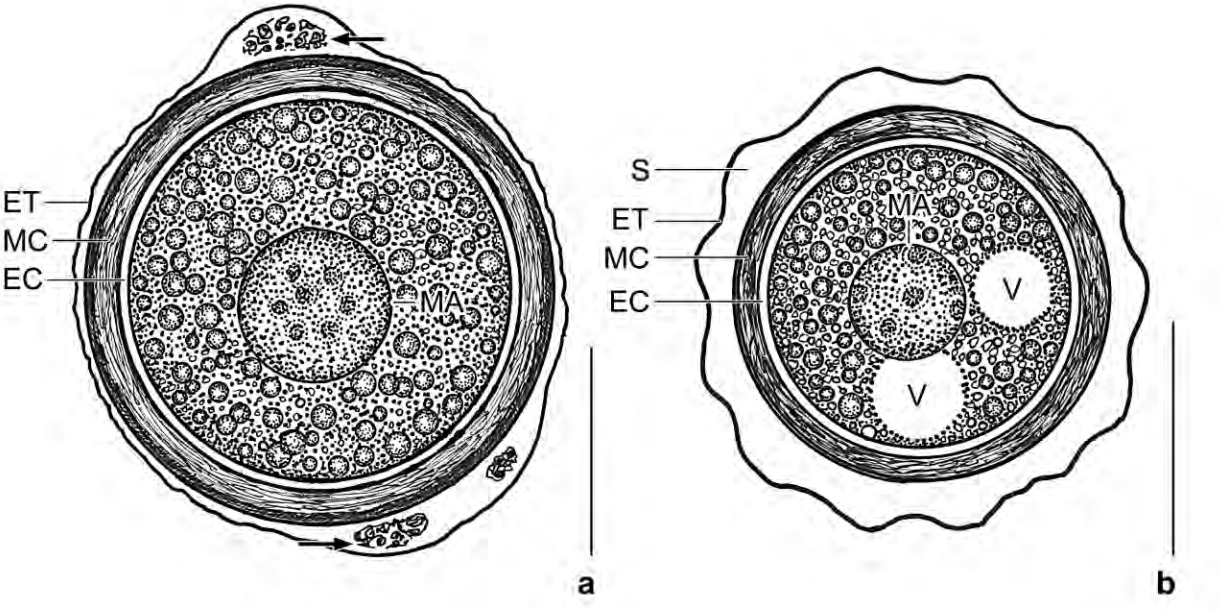

Fig. 126a, b. *Woodruffides metabolicus* and *Woodruffia rostrata*, mature resting cysts. The cysts have three distinct layers (EC, ET, MC), an average diameter of 70 µm and 57 µm, respectively, and are orange to dark brown. EC – endocyst, ET – ectocyst, MA – macronucleus, MC – mesocyst, S – space between ectocyst and mesocyst, V – vacuoles. Scale bars 30 µm.

12.7/13.4%, Min–Max = 62/97 µm, n = 13) and are deep orange to dark brown, resembling insect cuticulas (Fig. 125d, f–l). However, the Van Wisselingh chitin test, as described by Foissner et al. (2005b), is negative, i. e., the cysts dissolve completely in KOH, while cysts of *Blepharisma,* fungal spores, and cellulose remain and give clear reactions. The cyst wall is on average 5.2 µm thick (M = 5 µm, SD = 0.6 µm, CV = 11.5%, Min–Max = 4–7 µm, n = 13) and composed of three layers. The external layer (ectocyst?) is brownish, 1–2 µm thick, and attaches to the middle layer (mesocyst?), which is orange to dark brown, 2–3 µm thick, and structureless (Fig. 125d, e, g, h, 126a). Extruded cytoplasmic and/or nuclear material occurs between the external and middle layer, forming more or less distinct protrusions (Fig. 125d, h, i, l). The middle layer originates by shrinkage of the thick coat covering young cysts (Fig. 125d, e, g–l, 126a). The inner layer (endocyst?) is colourless, about 1.5 µm thick and structureless (Fig. 125e, j, k, 126a). The cytoplasm is colourless and packed with lipid (?) droplets 2–4 µm across and countless granules less than 0.5 µm in size. The macronucleus is about 20 µm across and in the centre of the cyst (Fig. 125d, e, g, h, k, 126a).

Woodruffia rostrata Kahl, 1931 (Fig. 126b, 127a–g, 128a-h)

Material: Site (68), i. e., Isabela Island, Galápagos (silver preparations) and Venezuelan site (65; SEM micrographs and resting cysts). Two voucher slides (one protargol-impregnated, the other Chatton-Lwoff silver nitrate-impregnated) have been deposited in the Biology Centre of the Upper Austrian Museum in Linz (LI). Some relevant specimens have been marked by black ink circles on the coverslip.

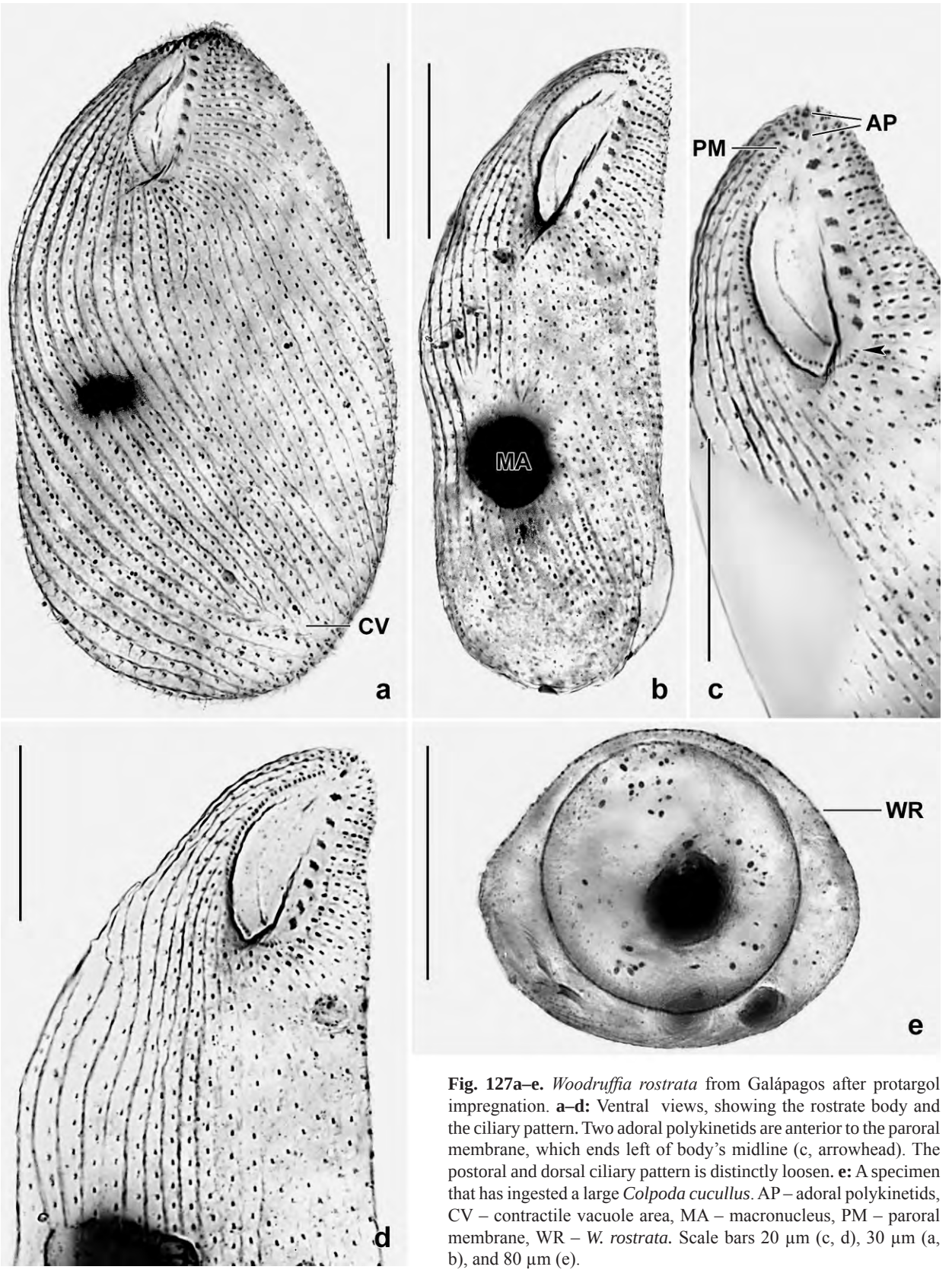

Fig. 127a–e. *Woodruffia rostrata* from Galápagos after protargol impregnation. **a–d:** Ventral views, showing the rostrate body and the ciliary pattern. Two adoral polykinetids are anterior to the paroral membrane, which ends left of body's midline (c, arrowhead). The postoral and dorsal ciliary pattern is distinctly loosen. **e:** A specimen that has ingested a large *Colpoda cucullus*. AP – adoral polykinetids, CV – contractile vacuole area, MA – macronucleus, PM – paroral membrane, WR – *W. rostrata*. Scale bars 20 µm (c, d), 30 µm (a, b), and 80 µm (e).

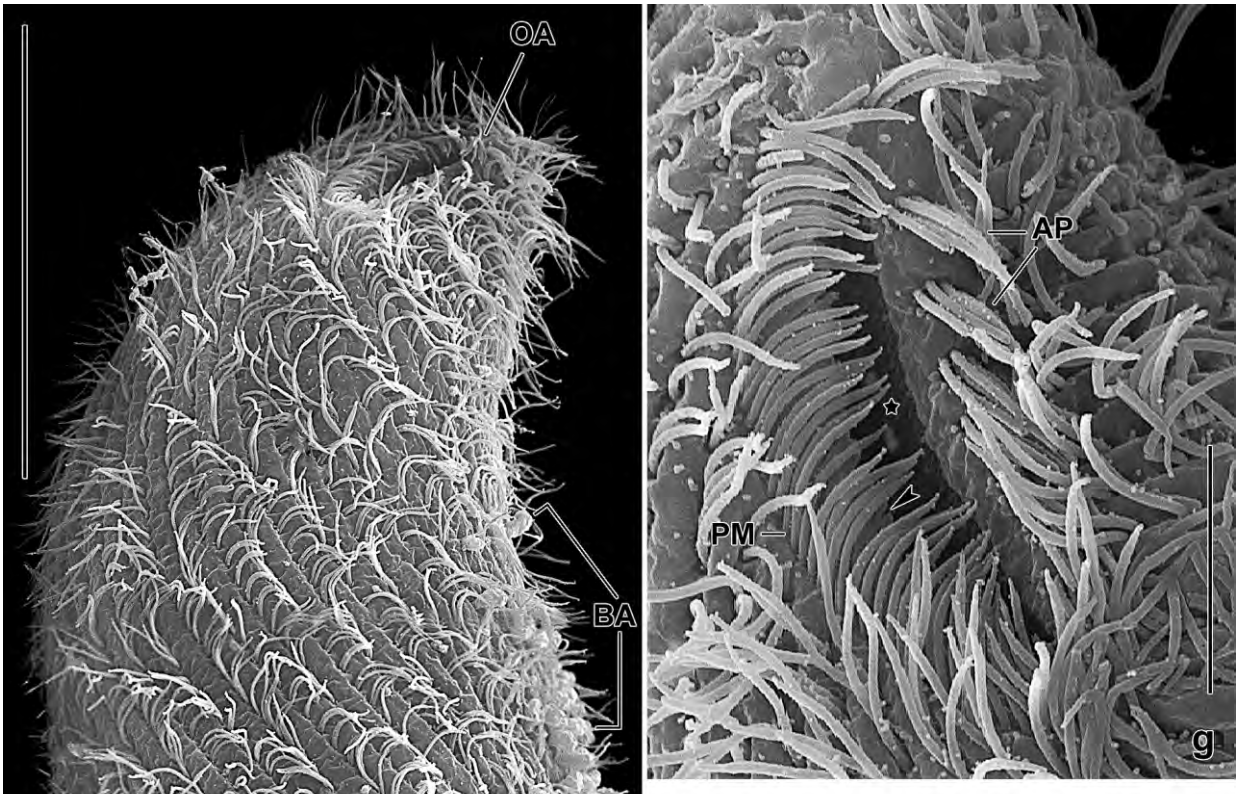

Fig. 127f, g. *Woodruffia rostrata*, Venezuelan specimens in the scanning electron microscope. **f:** A representative specimen, showing the rostrate body and the slightly spiral ciliary rows composed of ciliated dikinetids. The cortex is distinctly furrowed by the ciliary rows and is partially covered with bacteria, as usual in saline soil habitats. **g:** Oral apparatus. The paroral membrane covers the buccal lip (arrowhead) and consists of a single row of needle-shaped cilia. The adoral polykinetids are composed of short, dull cilia with different length. The asterisk marks the oral slit which can open widely to ingest even large prey (Fig. 127e). AP – adoral polykinetids, BA – epicortical bacteria, OA – oral apparatus, PM – paroral membrane. Scale bars 5 μm (g) and 40 μm (f).

Resting cyst: The mature resting cyst of specimens from highly saline coastal soil of Venezuelan site (65) is remarkable in being so strongly pigmented that details can be studied only in pressed (flattened) and/or crushed cysts (Fig. 128e–h). The cysts have an average total diameter of 57 μm (52–63 μm, n = 6) and are orange, dark brown, or russet. The cyst wall is 5–10 μm thick, depending on the width of the space between ectocyst and mesocyst, and consists of three layers. The external layer (ectocyst?) is yellowish to brownish, 0.5–1 μm thick, and usually strongly wrinkled and widely separate from the middle layer (Fig. 126b, 128a–d, g). The middle layer (mesocyst?) is orange to russet, 2–4 μm thick, and compact (Fig. 126b, 128b–d, g, h). The internal layer (endocyst?) is colourless, 1–2 μm thick, structureless, and elastic (Fig. 126b, 128c, e, g). About half of the specimens have two internal layers: when squeezed, one layer comes out of the cyst, forming a small sphere, while the other layer remains within the cyst (Fig. 128f, h).

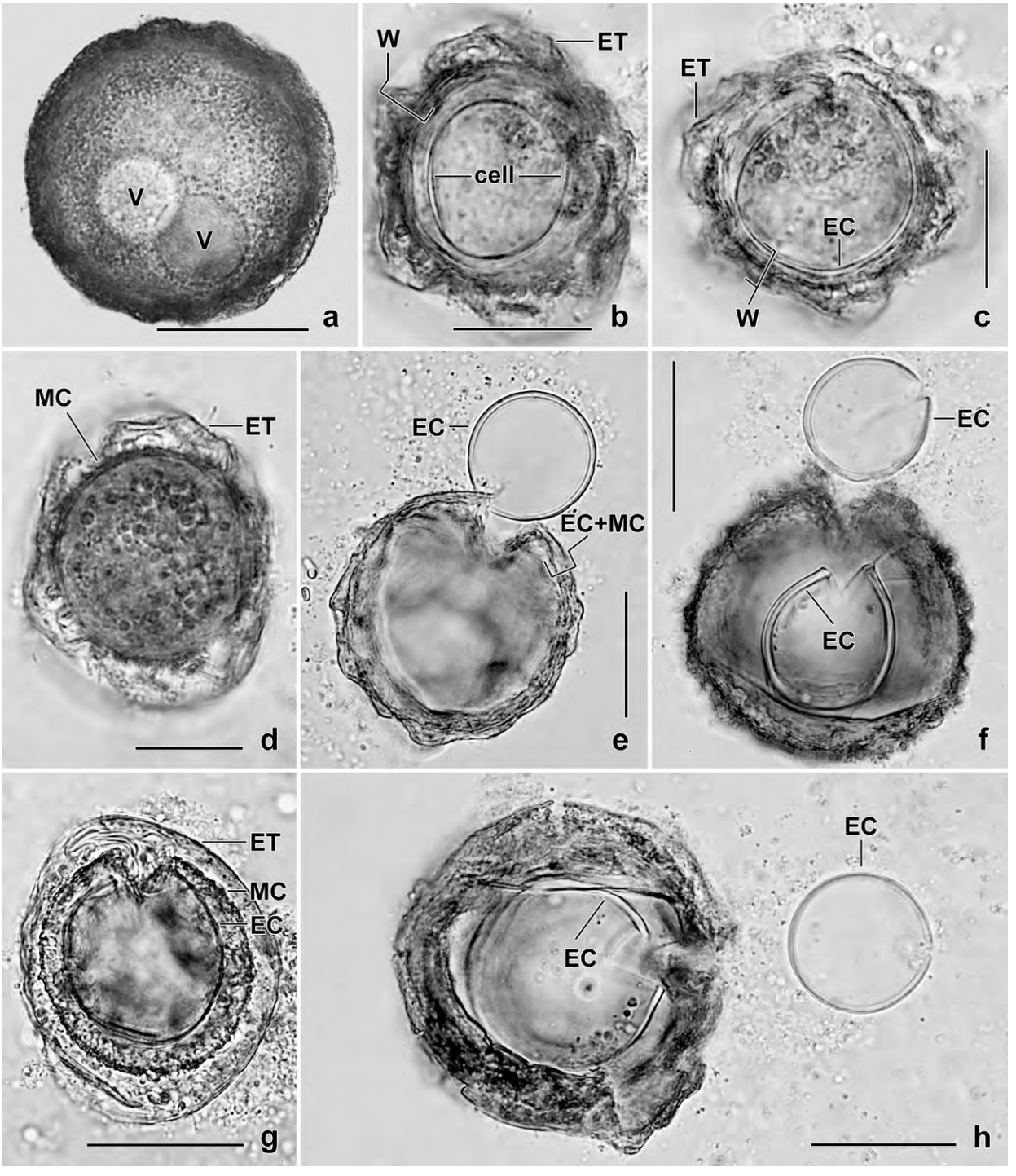

Fig. 128a–h. *Woodruffia rostrata*, mature resting cysts under bright field illumination. The dark appearance of the cysts is caused by the deep orange to dark brown pigmentation of the mesocyst. **a:** A typical cyst with russet colour and two large vacuoles in the cytoplasm. **b–d:** Typical cysts, showing the thin, distinctly wrinkled ectocyst; the thick, strongly pigmented mesocyst; and the thin, colourless endocyst. **e:** When slightly pressed, the cyst wall breaks and the elastic, colourless endocyst comes out of the cyst. **f, h:** As Figure (e) but with two endocyst-like structures, one each outside and inside the cyst. **g:** Squashed cyst, showing the three wall layers. EC – endocyst, ET – ectocyst, MC – mesocyst, V – vacuoles, W – cyst wall. Scale bars 30 µm.

The cyst's cytoplasm is colourless and contains two 10–20 µm-sized vacuoles with invisible contents (Fig. 128a); an about 15 µm wide macronucleus; and countless 0.5–3 µm-sized granules (Fig. 126b, 128b–d).

Remarks: *Woodruffia rostrata* has been reported from the Holarctis, the Palaeotropis, and the Australis (Foissner et al. 2002). Now, we found it also in the Neotropis, showing that it is a cosmopolitan preferring slightly to highly saline coastal habitats. It is a voracious predator feeding on ciliates ingested whole (Fig. 127e).

Foissner (1987a, 1993a) redescribed *W. rostrata* from the Cape Verde Island Santo Vicente. The Galápagos and Venezuelan specimens are highly similar, i. e., have about 35 ciliary rows and 10 adoral polykinetids, of which two insert anterior to the paroral membrane (Fig. 127a–d, f, g). The silverline pattern is colpodid. Scanning electron microscopy shows a "typical" platyophryid somatic and oral ciliary pattern (Fig. 127f, g).

Apowoodruffia Foissner & Buosi **nov. gen.**

Diagnosis: Small to moderately small Woodruffiina with oral apparatus on right side of body and slanted to left of main body axis. Adoral polykinetids brick-shaped, one usually in line or anterior of distal end of hooked right oral ciliary field (dikinetal paroral membrane). Silverline pattern colpodid. Resting cyst woodruffid.

Type species: *Apowoodruffia salinaria* nov. spec.

Etymology: Composite of the Greek prefix *apo* (derived from) and the generic name *Woodruffia*, meaning a ciliate genus similar to *Woodruffia*. Feminine gender.

Remarks: At first glance, *Apowoodruffia* resembles *Platyophrya* due to the shape of the body and oral apparatus. However, *Platyophrya* has the oral apparatus slanted to the right of the main body axis. The colpodid silverline pattern separates *Apowoodruffia* from *Woodruffides* which has a platyophryid silverline pattern. → *Sagittaria* and → *Sagittariides*, which have the same silverline pattern as *Apowoodruffia*, have a polar oral opening. This unique character constellation justifies separation at genus level. For family classification, see discussion of the new suborder Woodruffiina.

Apowoodruffia salinaria Foissner & Buosi **nov. spec.** (Fig. 129a–j, 130a–r, 131a–q, 132a–j; Table 43)

Diagnosis: Size about 75 × 30 µm in vivo. Usually elongate reniform with slightly narrowed anterior region. Contractile vacuole in posterior body end with excretory pore in pole centre. On average 18 somatic ciliary rows. Oral apparatus with 4–5 adoral polykinetids and an about 6 µm long, hooked paroral membrane comprising 20 dikinetids on average.

Type locality: Venezuelan site (65), i. e., highly saline soil from the north coast of Venezuela,

Morrocoy National Park, surroundings of the village of Chichiriviche, 67°13'W 11°33'N.

Etymology: The adjective *salinaria* (saline environments) refers to the saline habitat the species was discovered.

Type slides: 1 holotype and 3 paratype and voucher slides with CHATTON-LWOFF silver nitrate-impregnated specimens and 3 paratype slides with protargol-impregnated cells have been deposited in the Biology Centre of the Upper Austrian Museum in Linz (LI). Relevant specimens have been marked by black ink circles on the coverslip.

Description: To obtain sufficient material, we re-wetted and dried the sample several times. This showed a considerable variability in body shape and size in the preparations, mainly due to the widening of the cells in CHATTON-LWOFF silver nitrate-impregnated specimens (Table 43). *Apowoodruffia salinaria* was difficult to impregnate with ordinary methods; however, when fixed with DA FANO's fluid, beautiful protargol preparations were obtained.

Size 60–85 × 25–50 µm in vivo, usually about 75 × 30 µm, as calculated from in vivo measurements and values shown in Table 43; length:width ratio 1.7–3.3:1, usually 2.4:1 in protargol preparations;

Table 43. Morphometric data on *Apowoodruffia salinaria* based on silver-impregnated, randomly selected specimens from a non-flooded Petri dish culture. Measurements in µm. CHL – CHATTON-LWOFF silver nitrate impregnation, CV – coefficient of variation in %, IV – in vivo, M – median, Max – maximum, Mean – arithmetic mean, Min – minimum, n – number of specimens investigated, P – protargol impregnation (FOISSNER's method), SD – standard deviation, SE – standard error of mean, SEM – scanning electron microscope.

Characteristics	Method	Mean	M	SD	SE	CV	Min	Max	n
Body length, first re-wetting	P	55.9	55.0	7.4	1.6	13.2	40.0	68.0	23
Body length, second re-wetting	IV	73.7	70.0	7.4	2.6	10.1	70.0	90.0	8
	CHL	64.5	64.0	6.6	1.4	10.2	55.0	78.0	23
Body length, last re-wetting	CHL	61.6	60.8	6.2	1.3	10.1	48.0	78.0	23
Body width, first re-wetting	P	23.7	24.0	3.2	0.7	13.6	19.0	30.0	23
Body width, second re-wetting	IV	28.7	30.0	3.5	1.2	12.3	25.0	35.0	8
	CHL	34.5	33.0	4.0	0.8	11.6	29.0	45.0	23
Body width, last re-wetting	CHL	31.5	31.2	2.9	0.6	9.3	26.0	37.0	23
Body length: width ratio, first re-wetting	P	2.4	2.3	0.4	0.1	18.1	1.7	3.3	23
Body length: width ratio, second re-wetting	IV	2.6	2.6	0.4	0.1	15.7	2.0	3.2	8
	CHL	1.9	1.9	0.2	0.1	10.2	1.6	2.4	23
Body length: width ratio, last re-wetting	CHL	2.0	1.9	0.2	0.1	10.6	1.6	2.4	23
	SEM	2.8	2.8	0.2	0.1	7.1	2.4	3.2	12
Body length: width, ratio in micrographs	IV	2.6	2.6	0.4	0.1	13.8	2.1	3.4	15
Body, width in oral area	P	12.9	13.0	1.7	0.4	13.2	9.0	16.0	23
	CHL	19.5	19.0	3.3	0.7	16.7	15.0	28.0	23
Anterior body end to macronucleus, distance	P	22.8	23.0	3.2	0.7	14.2	15.6	28.0	23
Anterior body end to anterior end of right oral ciliary field, distance	P	1.4	1.6	–	–	–	0.8	2.3	23
Anterior body end to posterior end of right oral ciliary field, distance	P	7.6	7.8	0.8	0.2	10.5	5.5	8.6	23

continued

Characteristics	Method	Mean	M	SD	SE	CV	Min	Max	n
Oral field, length	P	7.1	7.0	0.7	0.2	9.9	6.2	8.6	23
Oral field, widest site	P	4.6	4.7	0.6	0.1	13.2	3.0	5.5	23
Macronucleus, length	P	8.4	8.6	0.8	0.2	9.1	7.0	10.0	23
Macronucleus, width	P	7.7	7.8	0.6	0.1	8.1	6.2	8.6	23
Micronucleus, length	P	2.4	2.3	–	–	–	1.6	3.0	9
Micronucleus, width	P	1.4	1.2	–	–	–	0.8	2.3	9
Right oral ciliary field, length	P	6.1	6.2	0.7	0.1	11.6	4.7	7.8	23
Distance between right side ciliary rows in mid-body	P	2.5	2.3	0.5	0.1	21.0	1.2	3.5	23
Distance between left side ciliary rows in mid-body	P	3.7	3.5	–	–	–	3.0	4.4	23
Somatic ciliary rows, number	P	18.1	18.0	1.3	0.3	7.4	15.0	21.0	23
Dikinetids in right oral ciliary field, number	P	20.1	20.0	2.1	0.4	10.3	16.0	24.0	21
Adoral polykinetids, number	P	4.1	4.0	0.4	0.1	10.2	3.0	5.0	23
Cysts, length without ectocyst	IV	25.7	26.0	2.8	0.6	11.1	17.0	30.0	25
Cysts, width without ectocyst	IV	25.4	25.0	2.8	0.6	10.7	17.0	30.0	25
Cysts, length with wrinkled ectocyst	IV	35.4	35.0	2.3	1.0	6.5	32.0	38.0	5
Cysts, width with wrinkled ectocyst	IV	36.0	35.0	3.1	1.4	8.6	32.0	40.0	5

1.6–2.4:1, usually 1.9:1 in silver nitrate preparations; and about 2.6:1 in vivo (Table 43). In protargol preparations with specimens from first re-wetting shape rather variable, that is, 22 out of 50 specimens elongate ovate with a shallow postoral concavity making it more or less reniform or *Colpoda maupasi*-shaped (Fig. 129a, h, 130a, e, r); 20 specimens elongate ellipsoid with a more or less concave ventral side, making it sausage-shaped (Fig. 129d, h, 130a, c, o, 132a, b, i); rarely ellipsoid or ovate (Fig. 129g, h, 132h); in Chatton-Lwoff silver nitrate preparations with specimens from second re-wetting, shape basically as in protargol preparations, but broader (Fig. 129g, i); specimens from first re-wetting usually sausage-shaped, those from last re-wetting usually elongate ovate or ellipsoidal with slightly concave left margin, making them sausage-shaped or slightly reniform both in vivo and in SEM (Fig. 129a, d, 130a, c, e, 132a, b, i, j); shape fairly dependent on nutritional state, that is, hungry specimens slender and up to 2:1 flattened laterally (Fig 129d, 130d, f). Nuclear apparatus in or near centre of cell on average (Fig. 129a, f, 130l, o, r; Table 43). Macronucleus about 8 µm across in preparations, contains some small nucleoli. Micronucleus hemispherical, attached to macronucleus by flattened side, about 2.5 × 1.5 µm (Fig 129a, 130o, p; Table 43). Contractile vacuole in posterior end with excretory pore near pole centre (Fig. 129a, i, 130e–h, 131b, e). Cortex distinctly furrowed by somatic kineties, contains numerous bright, colourless granules (possibly mucocysts) about 0.4 µm across; usually rather densely covered by bacteria (Fig 129b, c, 130h–k, 132c, f–h). Cytoplasm without specific inclusions, often studded with lipid droplets 2–6 µm across; likely feeds on bacteria and fungal spores (Fig. 129a, 130b, e, g). Swims rather rapidly by rotation about main body axis. Division occurs in freely-motile (non-encysted) condition.

Somatic cilia about 8 µm long in vivo, paired in anterior body third, anterior cilium absent in middle and posterior third. On average 18 slightly sigmoid ciliary rows all commencing around

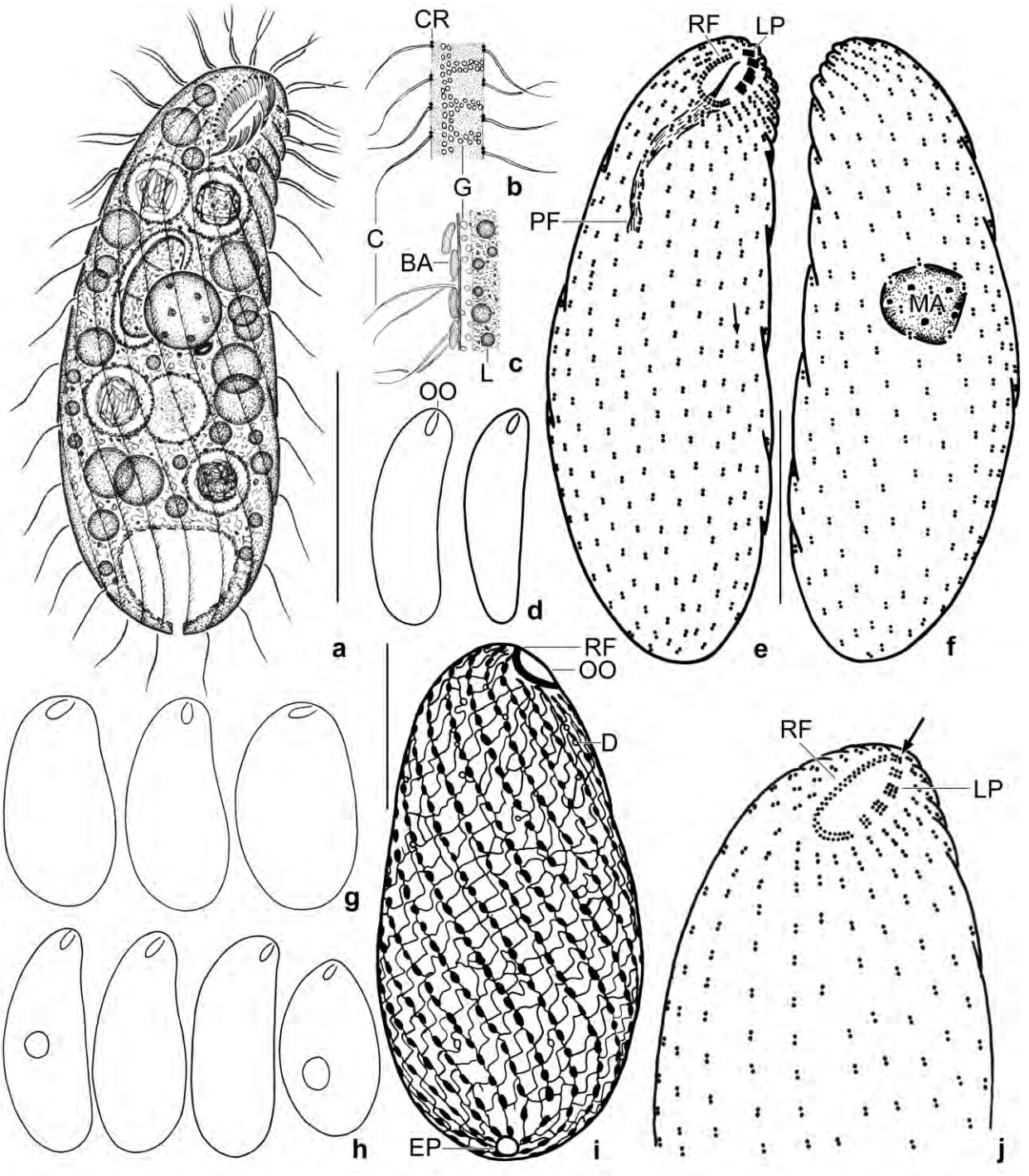

Fig. 129a–j. *Apowoodruffia salinaria* from life (a–d) and after protargol (e, f, h, j) and silver nitrate (g, i) impregnation. **a:** Right side view of a representative specimen, length 75 µm. **b, c:** Surface view and optical section of cortex. **d:** Outline of specimens from first re-wetting. **e, f:** Ciliary pattern of right and left side of an elongate reniform specimen. Arrow marks a kinety commencing in mid-body. **g, h:** Outline of silver nitrate (g) and protargol-impregnated (h) specimens. **i:** Lateral view of holotype specimen, showing the silverline pattern, length 64 µm. **j:** Oral ciliary pattern. Arrow denotes a polykinetid in line with right oral ciliary field. BA – bacteria, C – somatic cilia, CR – somatic ciliary row, D – docked extrusome, EP – excretory pore, G – cortical granules, L – lipid droplet, LP – left oral polykinetids, MA – macronucleus, OO – oral opening, PF – pharyngeal fibres, RF – right oral ciliary field (paroral membrane). Scale bars 10 µm (j) 20 µm (e, f, i, j), and 30 µm (a).

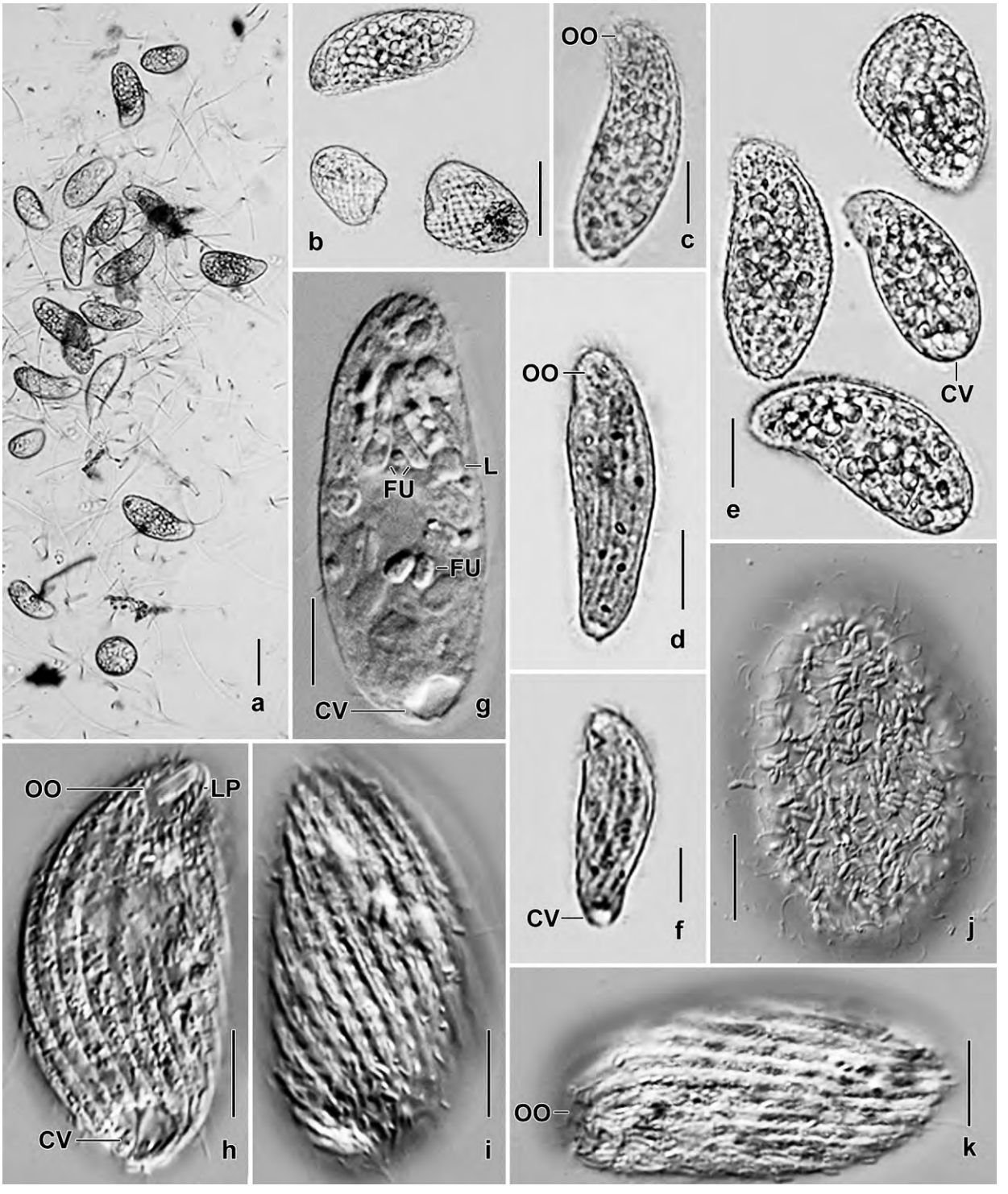

Fig. 130a–k. *Apowoodruffia salinaria* from life, specimens from last re-wetting. a–f: Overviews showing the considerable shape variability, especially the Cyrtolophosis-like cells in Figures (d, f). The lower half of Figure (b) shows two specimens of → Sagittaria venezuelensis. g: Right side view of a specimen, showing the cytoplasm packed with lipid droplets and fungal spores. h–k: Right and left side views of slightly pressed specimens, showing the distinctly furrowed cortex and the bacterial cover (j). CV – contractile vacuole, FU – fungal spores, L – lipid droplets, LP – left oral polykinetids, OO – oral opening. Scale bars 15 µm (g–k), 20 µm (c–f), 30 µm (b), and 50 µm (a).

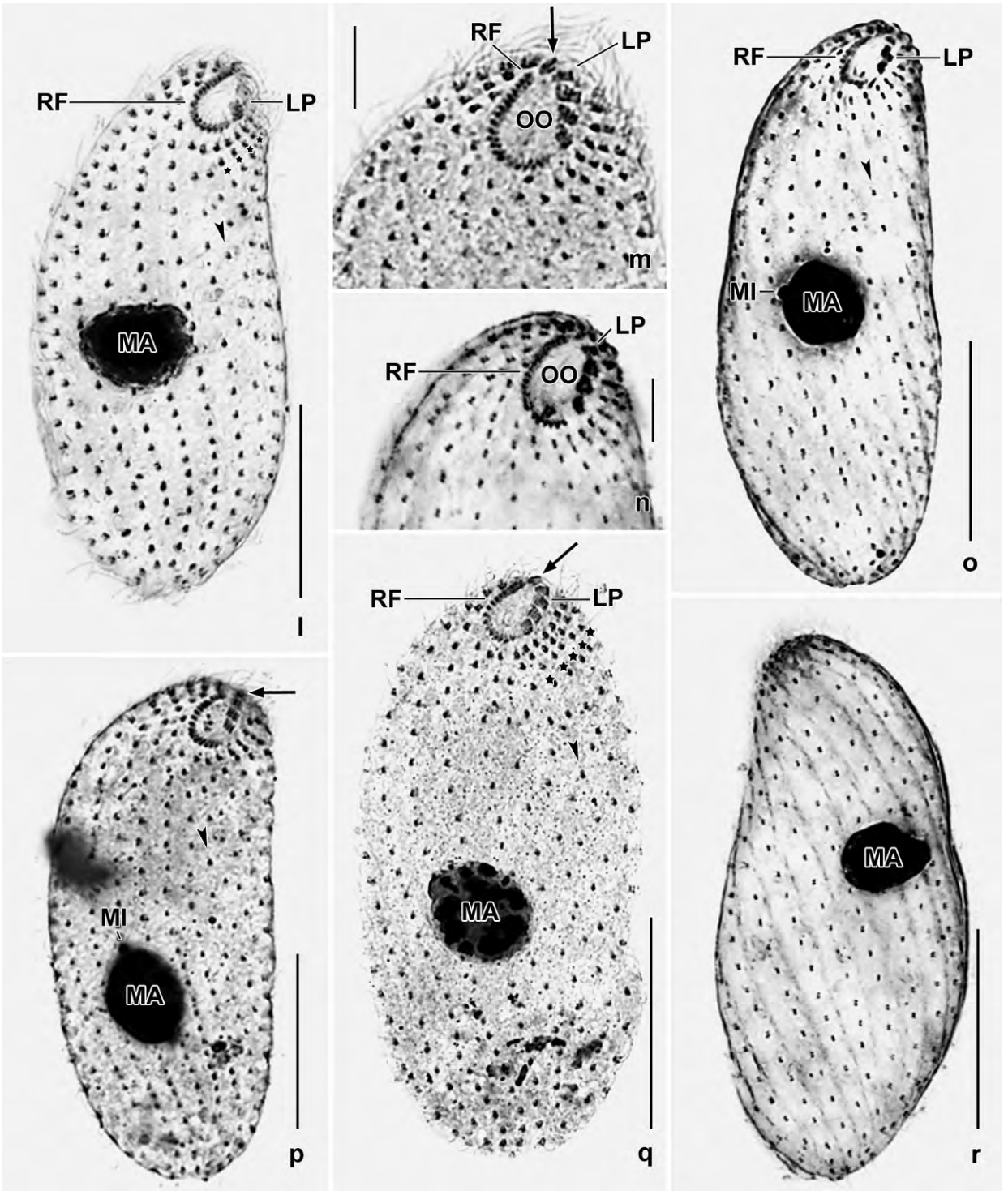

Fig. 130l–r. *Apowoodruffia salinaria* after silver carbonate (l, m, p, q) and protargol (n, o, r) impregnation. Arrows mark an adoral polykinetid anterior of distal end of right oral ciliary field (paroral membrane). Arrowheads denote a kinety commencing slightly above mid-body. **l, p, q:** Right side views, showing the ciliary pattern. Asterisks (g) mark narrowly spaced kinetids – appearing like a "postoral pseudomembrane" – in the postoral kineties. **m, n:** Details of oral area. **o, r:** Right and left side view, showing somatic and oral ciliary pattern. LP – left oral ciliaty field, MA – macronucleus, MI – micronucleus, OO – oral opening, RF – right oral ciliary field. Scale bars 5 µm (m, n) and 20 µm (l, o–r).

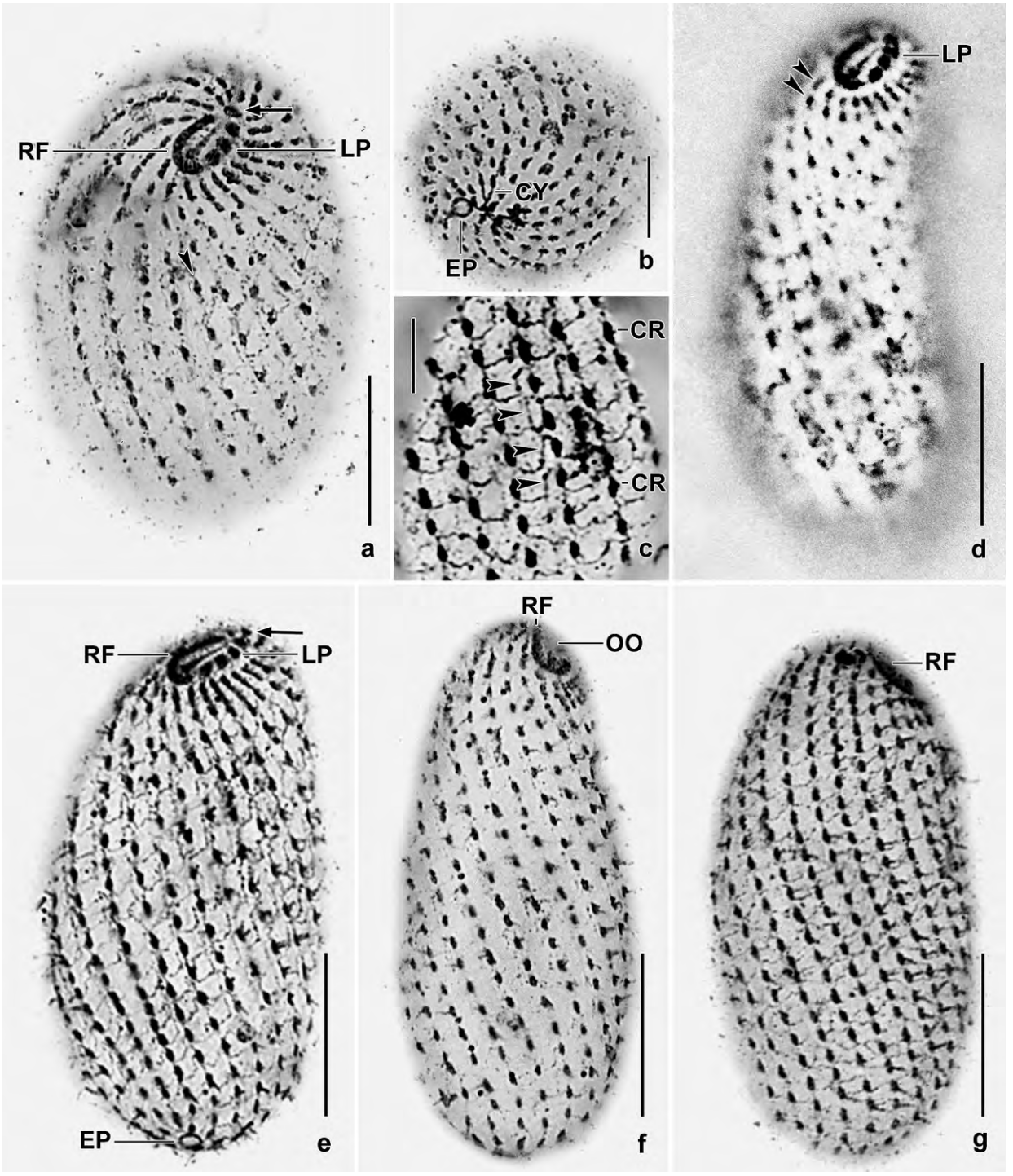

Fig. 131a–g. *Apowoodruffia salinaria* after silver nitrate impregnation. **a, e:** Oblique frontal and ventral view of specimens with one polykinetid anterior to distal end of right oral ciliary field (arrows). Arrowhead marks a kinety commencing slightly above mid-body. **b:** Posterior polar view showing cytopyge and excretory pore. **c:** Silverline pattern with stair-shaped transverse silverlines (arrowheads). **d:** Right side view of a specimen with postoral kinetids arranged in a pseudomembrane-like pattern (arrowheads) **e–g:** Ventral and lateral views, showing the colpodid silverline pattern. CR – somatic ciliary rows, CY – cytopyge, EP – excretory pore, LP – left oral polykinetid, OO – oral opening, RF – right oral ciliary field. Scale bars 5 µm (c), 10 µm (b), and 20 µm (a, d–g).

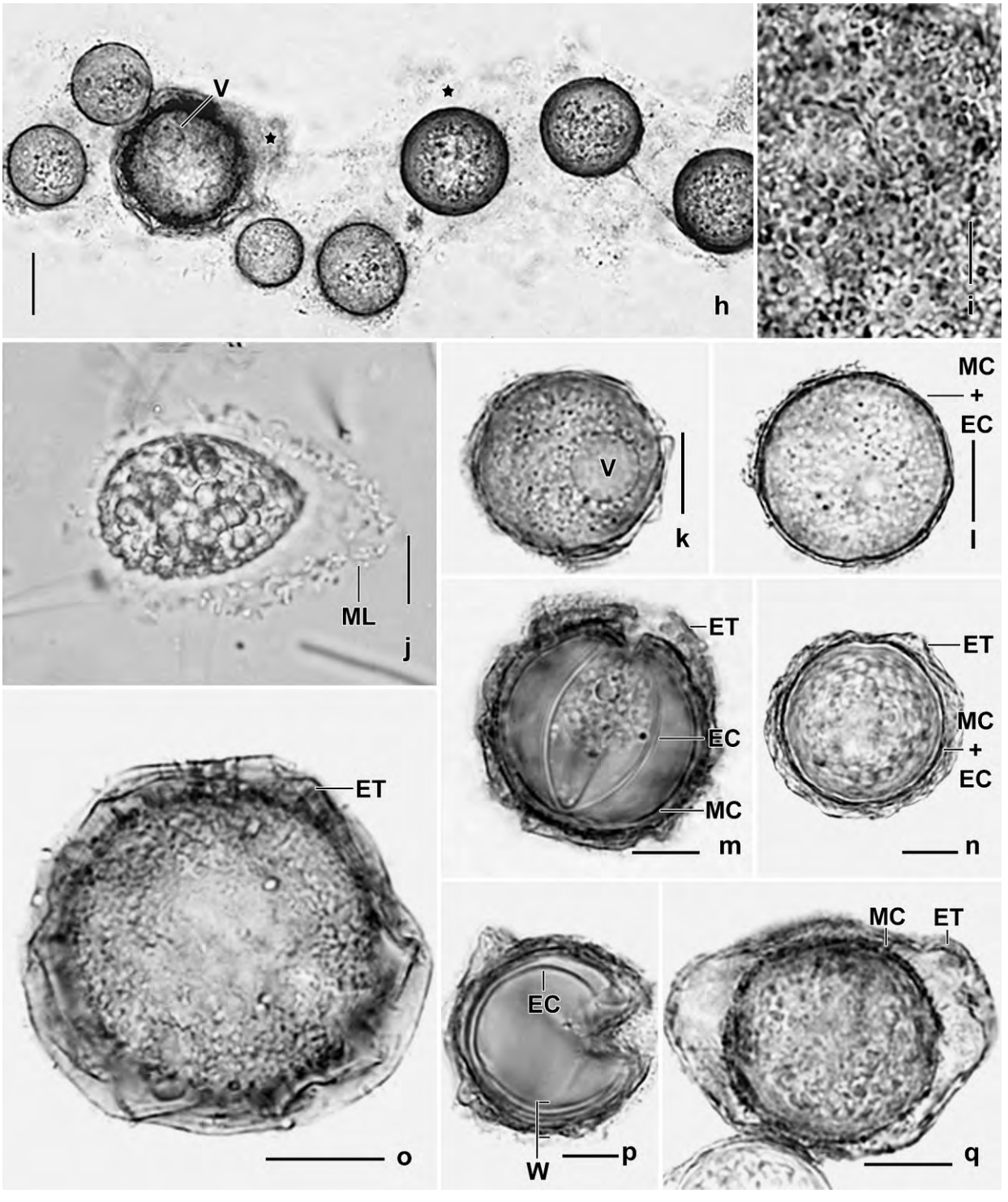

Fig. 131h–q. *Apowoodruffia salinaria*, resting cysts from life. **h:** Several young and two mature (asterisks) cysts each surrounded by a mucous layer. **i:** Ectocyst with orange platelets possibly from the environment. **j:** When encysting, the cell becomes ovate and secretes a mucous cover. **k, l:** Young cysts with a single vacuole (k). **m, p:** When mature cysts are pressed, the inner and outer layers produce a 4 µm thick wall and the endocyst becomes visible. **n, o, q:** Mature cysts, showing the wrinkled ectocyst. EC – endocyst, ET – ectocyst, MC – mesocyst, ML – mucous layer, V – vacuole, W – cyst wall. Scale bars 5 µm (i), 10 µm (k–q), and 15 µm (h, j).

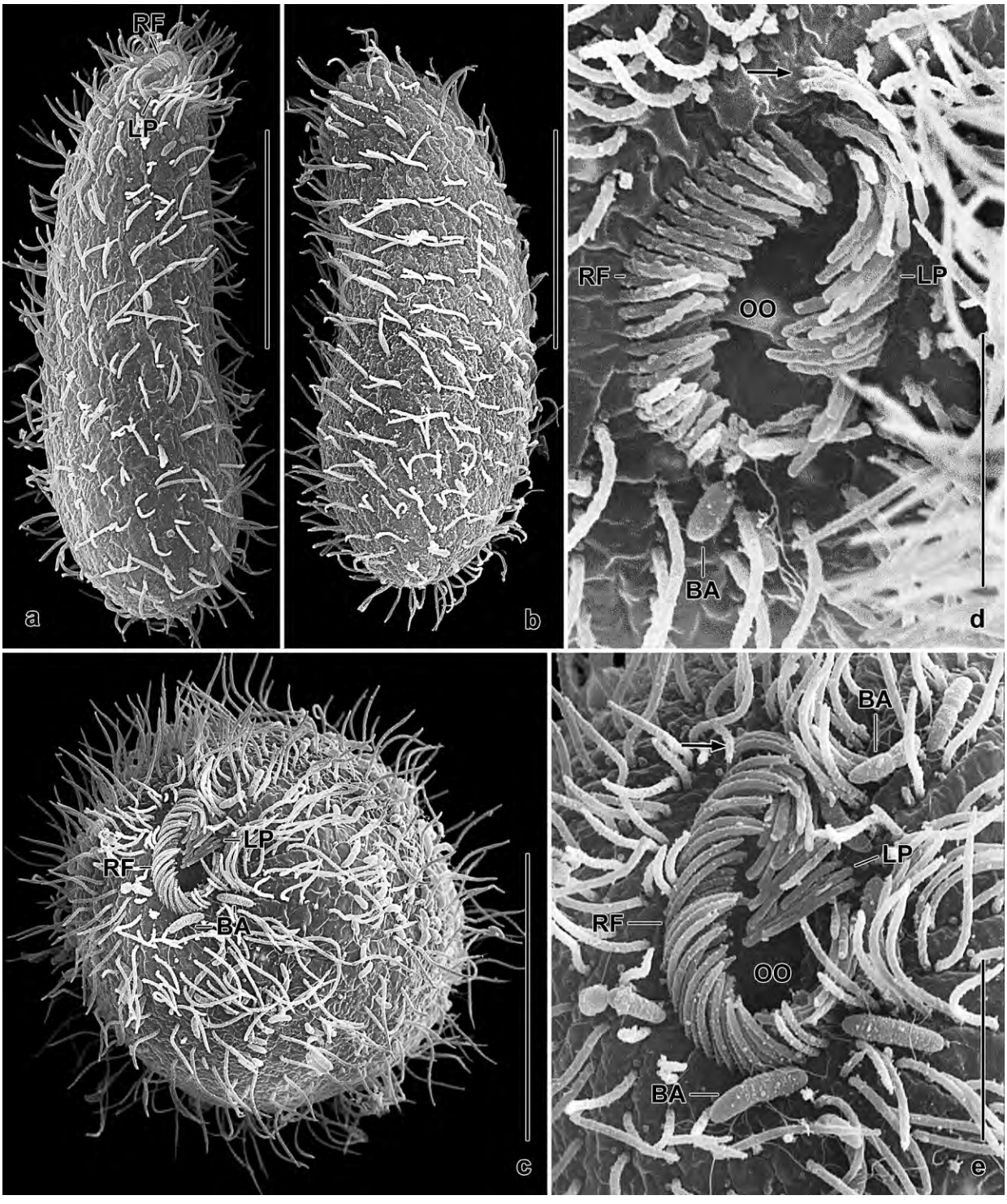

Fig. 132a–e. *Apowoodruffia salinaria* in the scanning electron microscope. **a, b:** Right and left side view of slightly reniform specimens, showing the ciliary pattern. **c, e:** Frontal views from same specimen at low (c) and high (e) magnification, showing the location and structure of the oral apparatus. Arrow marks an adoral polykinetid anterior to distal end of right oral ciliary field. The cortex surface is partially covered with bacteria. **d:** Details of oral ciliary pattern. Arrow marks a polykinetid anterior to distal end of right oral ciliary field which consists of a row of ciliated dikinetids. BA – bacteria, LP – left oral polykinetids, OO – oral opening, RF – right oral ciliary field. Scale bars 5 μm (d, e) and 20 μm (a–c).

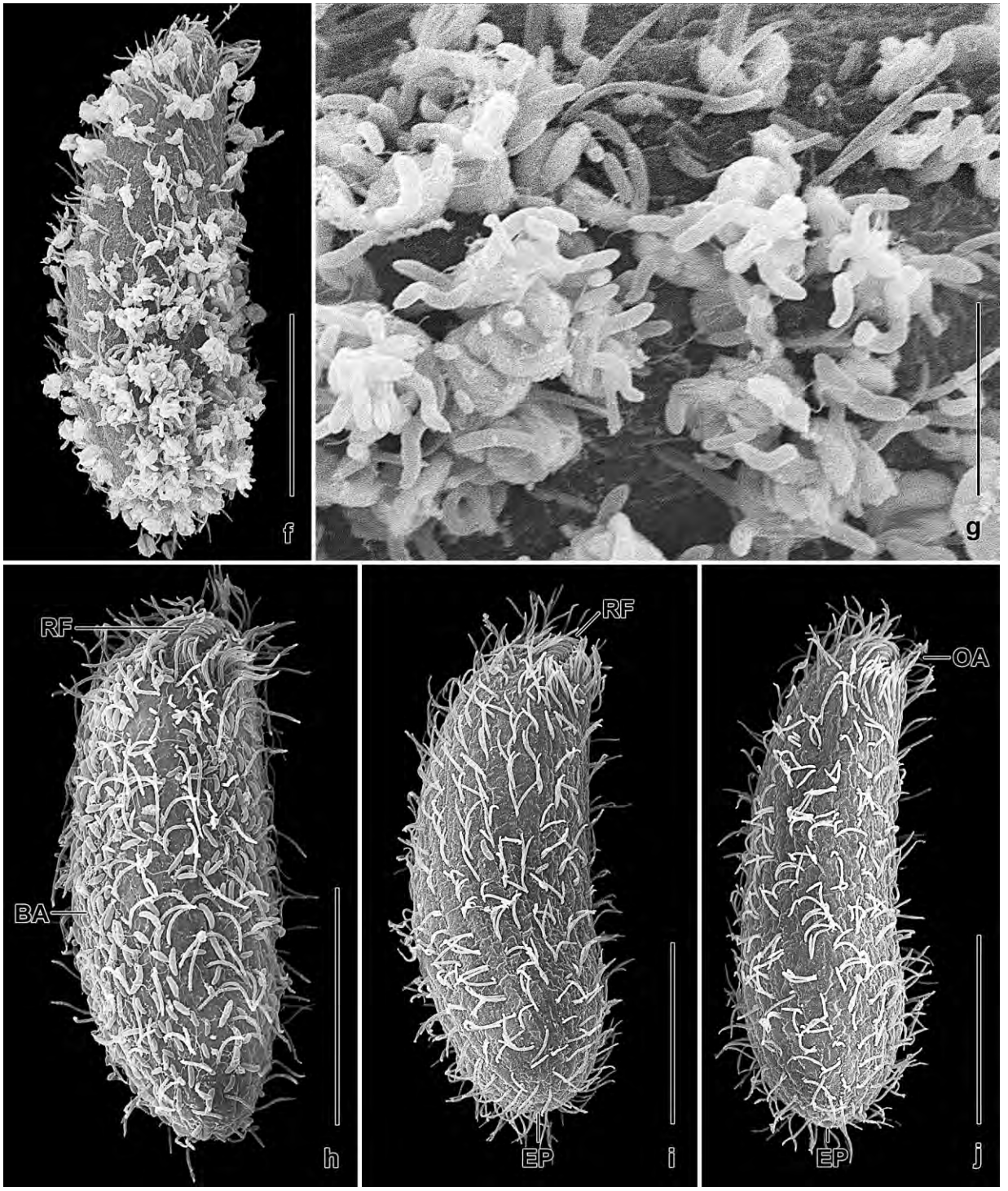

Fig. 132f–j. *Apowoodruffia salinaria* in the scanning electron microscope. **f, g:** Right side views of a specimen having the cortex densely colonized with various bacteria. **h:** Right side view of an elongate ellipsoidal specimen, showing the cell surface rather densely colonized with bacteria. **i, j:** Right side view of slightly reniform specimens, showing the somatic and oral ciliary pattern and the excretory pore of the contractile vacuole in the centre of the posterior pole, an important difference to, e. g., *Platyophrya,* which has the pore subterminally on the right side. BA – bacteria, EP – excretory pore, OA – oral apparatus, RF – right oral ciliary field. Scale bars 5 μm (g) and 20 μm (f, h–j).

oral apparatus and ending in posterior pole area, except of a single postoral kinety usually commencing near mid-body; interkinetal distances of left side slightly larger than those of right side; posterior of left mouth margin ciliary rows commence with 2–4, usually 3 closely spaced dikinetids not forming a postoral pseudomembrane (Fig 129a, e, f, j, 130h, i, l, o, q, r, 131a, d, 132a, b, e, i, j; Table 43).

Oral opening subapical, occupies on average 35% of anterior body width; elliptical to broadly elliptical, on average 7.1 × 4.6 µm in protargol preparations (Fig. 129a, e, j, 130h, n, o, 131a, d, 132c–e, h–j; Table 43). Right oral ciliary field hooked, about 6 µm long in preparations, composed of a single row of 20 ciliated dikinetids on average; cilia 3–4 µm long and invariably curved to oral slit in SEM preparations, basal bodies associated with fibres forming right half of pharyngeal basket (Fig 129a, e, j, 130l–q, 131a, e, 132c–e; Table 43). On average four small, rectangular adoral polykinetids on left mouth margin, one usually in line with or anterior and slightly right of right oral ciliary field; individual polykinetids obliquely oriented to main mouth axis, distal polykinetid often perpendicularly orientated, composed of two rows with three basal bodies each; cilia 3 – 4 µm long and invariably curved posteriorly in SEM preparations, absent from one of the two rows in at least the most distal polykinetid (Fig 129a, e, j, 130h, l–q, 131a, e, 132c–e; Table 43). Pharyngeal basket extends to mid-body, formed by fibres originating from right ciliary field and adoral polykinetids (Fig. 129e, j).

Silverline pattern colpodid throughout, meshes often rather irregular (Fig. 129i, 131a, c, e, g). Transverse silverlines between ciliary rows usually originating from longitudinal silverlines connecting kinetids of kineties; often stair-shaped, likely due to strong cortex furrowing, creating a sort of line between each two ciliary rows, i. e., a platyophryid-like pattern (Fig. 129i, 131a, c, e). Nevertheless, an ordinary colpodid pattern occurs in several specimens, as well as combined with a platyophryid-like pattern (Fig. 131g). Silverlines also surround excretory pore and docked extrusomes (Fig. 129i, 131b, e).

Resting cysts globular, about 26 × 25 µm in vivo without ectocyst and 36 × 35 µm on average with wrinkled ectocyst (Table 43). Overall structure and colour as in → *Woodruffia rostrata*, to which the reader is referred to (Fig. 131h–q). During encystment, cells become ovate and covered by an up to 5 µm thick mucus layer populated by bacteria (Fig. 131h, j). Usually only one (two in *W. rostrata*) vacuole.

Occurrence and ecology: To date only found at type locality, i. e., soil from a highly saline, abandoned field on the north coast of Venezuela. The species can be cultivated on squeezed wheat grains and artificial sea water with a salinity of 20–60‰.

Remarks: See Foissner (1993a) and Foissner, Agatha & Berger (2002) for detailed descriptions of the species mentioned in the following discussion.

Apowoodruffia salinaria resembles some *Platyophrya* and *Rostrophryides* species, such as *P. vorax, P. sphagni, P. spumacola*, and *R. africana*, not only due to body shape and size but also because of some narrowly spaced kinetids – which may be mistaken as a postoral pseudomembrane – posterior to the adoral polykinetids. Further, silver nitrate preparations are required to reveal the silverline pattern, which is colpodid in *A. salinaria* while platyophryid in *Rostrophryides*

and in *Platyophrya*. Nevertheless, the stair-shaped silverlines of *A. salinaria* create a sort of line between each two ciliary rows, and may thus be easily confused with a median silverline, i. e. the main feature of the platyophryid silverline pattern. *Apowoodruffia* and *Platyophrya* can be separated also on careful live observation by the orientation of the oral apparatus: slanted to left vs. right.

Apowoodruffia salinaria also resembles *Semiplatyophrya acrostoma* and *Platyophryides latus*. The former species is similar to *A. salinaria* in the shape of the body and in the number of adoral polykinetids while the latter is similar in body size and shape, the number of adoral polykinetids, and the silverline pattern. However, *S. acrostoma* has a minute, apically located oral apparatus and a platyophryid silverline pattern on the left side, and *P. latus* has the adoral polykinetids parallel to the right oral ciliary field and its oral apparatus is oriented to the right of the main body axis.

***Sagittaria venezuelensis* nov. spec.** (Fig. 124, 133a–c, f–l, 134a–y, 135a–l; Table 44)

Diagnosis: Size in vivo about 35 × 25 µm; obovate to bursiform. 1 globular macronucleus and 1 micronucleus. Contractile vacuole in posterior end, with single excretory pore in or near pole centre. On average 22 spiral ciliary rows distinctly furrowing cortex. Oral opening broadly elliptical; paroral membrane composed of an average of 21 ciliated dikinetids with interkinetidal spaces gradually increasing from ventral to dorsal side of cell; on average 6 minute adoral polykinetids most composed of 3 rows with 3–5 basal bodies each.

Type locality: Venezuelan sample (65), i.e., highly saline soil from the north coast of the Morrocoy National Park, surroundings of the village of Chichiriviche, 67°13'W 11°33'N.

Type material: 1 holotype and 4 paratype slides with protargol-impregnated cells and 3 slides with Chatton-Lwoff silver nitrate-prepared specimens have been deposited in the Biology Centre of the Upper Austrian Museum in Linz (LI). Relevant specimens have been marked by black ink circles on the coverslip.

Etymology: Named after the country where it was discovered, i. e., Venezuela.

Description: To get clear protargol preparations, the species was fixed with ethanol. This caused about 20% shrinkage and widening of body and of the oral field, as evident from a comparison of the length:width ratios in vivo and in well-fixed material used for SEM (Table 44).

Size in vivo 30–42 × 24–38 µm, usually about 35 × 25 µm, as calculated from some in vivo measurements and values shown in Table 44 adding 20% preparation shrinkage due to ethanol fixation. Body shape rather variable, ordinarily to broadly obovate (Fig. 133a, b, 134a, b) or bursiform (Fig. 134c, e, q, r), depending on amount of food ingested and culture conditions; unflattened (Fig.133c, 134j, s, x). Anterior body end usually slightly obliquely truncate, rarely transversely truncate, posterior end rounded to bluntly pointed (Fig. 133a, b, 134a–e, q). Nuclear apparatus usually anterior of mid-body (Fig. 133a, 134f, g, m; Table 44). Macronucleus globular, hyaline, with comparatively large, oblong nucleoli, about 10 µm across in protargol preparations.

Micronucleus attached to macronucleus, possibly in its perinuclear space, globular to broadly ellipsoidal, 2–2.5 µm after protargol impregnation. Contractile vacuole in posterior body end (Fig. 133a, b, 134b, f, g, 135d, j), with single excretory pore in or near pole centre (Fig. 135d, j). Cortex very flexible, colourless, usually distinctly furrowed by ridges right of ciliary rows, distinctness depending on amount of food ingested and culture conditions; often studded with bacteria (Fig. 133a, 134a–i); cortical granules not detectable neither in vivo or silver preparations. Cytoplasm colourless, contains few to many globular to broadly ellipsoid food vacuoles with sporolating bacteria 2–5 µm in size; some small lipid droplets; and sometimes a large defecation vacuole containing many highly refractile bacterial spores and fluffy material (Fig. 133a, b, 134a–i). Swims rapidly, never rests, does not build a case.

Somatic cilia in vivo about 8 µm long, arranged in an average of 22 narrowly or ordinarily spaced rows commencing around oral opening and extending spirally to barren posterior pole. Ciliature composed of dikinetids slightly more densely spaced in perioral area and in left half of cell, anterior cilium lacking posterior of perioral dikinetids. Without postoral pseudomembrane (Fig. 133a, f, h, j, l, 134m–r; Table 44).

Silverline pattern colpodid, i. e., composed of rectangular meshes extending between ciliary rows (Fig. 134k, l).

Oral opening occupies about half of anterior pole area, elliptical to broadly elliptical, slightly deepened (Fig. 133a–c, f, j, 134b–d, m–w; Table 44). Paroral membrane on right margin of oral opening, C-shaped, composed of an average of 21 dikinetids with about 5 µm long, pointed cilia; distance between dikinetids distinctly increasing from ventral to dorsal end of oral opening;

Table 44. Morphometric data on *Sagittaria venezuelensis* based, if not mentioned otherwise, on mounted, protargol-impregnated, and randomly selected specimens from a non-flooded Petri dish culture. Measurements in µm. CV – coefficient of variation in %, M – median, Max – maximum, Mean– arithmetic mean, Min – minimum, n – number of individuals investigated, SD – standard deviation, SE – standard error of arithmetic mean.

Characteristics	Mean	M	SD	SE	CV	Min	Max	n
Body, length	27.6	27.0	2.8	0.6	10.2	24.0	35.0	21
Body, width	24.1	23.0	3.0	0.7	12.4	20.0	32.0	21
Body length:width, ratio (protargol)	1.1	1.2	–	–	–	1.1	1.2	21
Body length:width, ratio (in vivo)	1.4	1.4	0.1	0.1	10.4	1.2	1.9	30
Anterior body end to macronucleus, distance	5.3	5.0	2.1	0.5	39.5	2.0	9.0	21
Macronucleus, length	10.4	10.0	1.0	0.2	9.9	9.0	12.0	21
Macronucleus, width	9.6	10.0	1.2	0.3	12.1	7.0	12.0	21
Micronucleus, large axis	2.1	2.0	–	–	–	2.0	2.5	12
Somatic ciliary rows, number	22.1	22.0	1.0	0.2	4.3	21.0	24.0	23
Oral opening, length	9.4	9.0	1.0	0.2	11.0	8.0	12.0	23
Oral opening, widest site	7.5	8.0	0.9	0.2	11.3	6.0	9.0	23
Oral opening length:width, ratio (protargol)	1.3	1.3	0.2	0.1	13.4	1.0	1.5	23
Oral opening length:width, ratio (SEM)	1.7	1.7	0.2	0.1	13.6	1.4	2.0	17
Adoral polykinetids, number	6.0	6.0	0.4	0.1	6.1	5.0	7.0	23
Paroral dikinetids, number	21.5	21.0	2.0	0.4	9.1	19.0	26.0	23

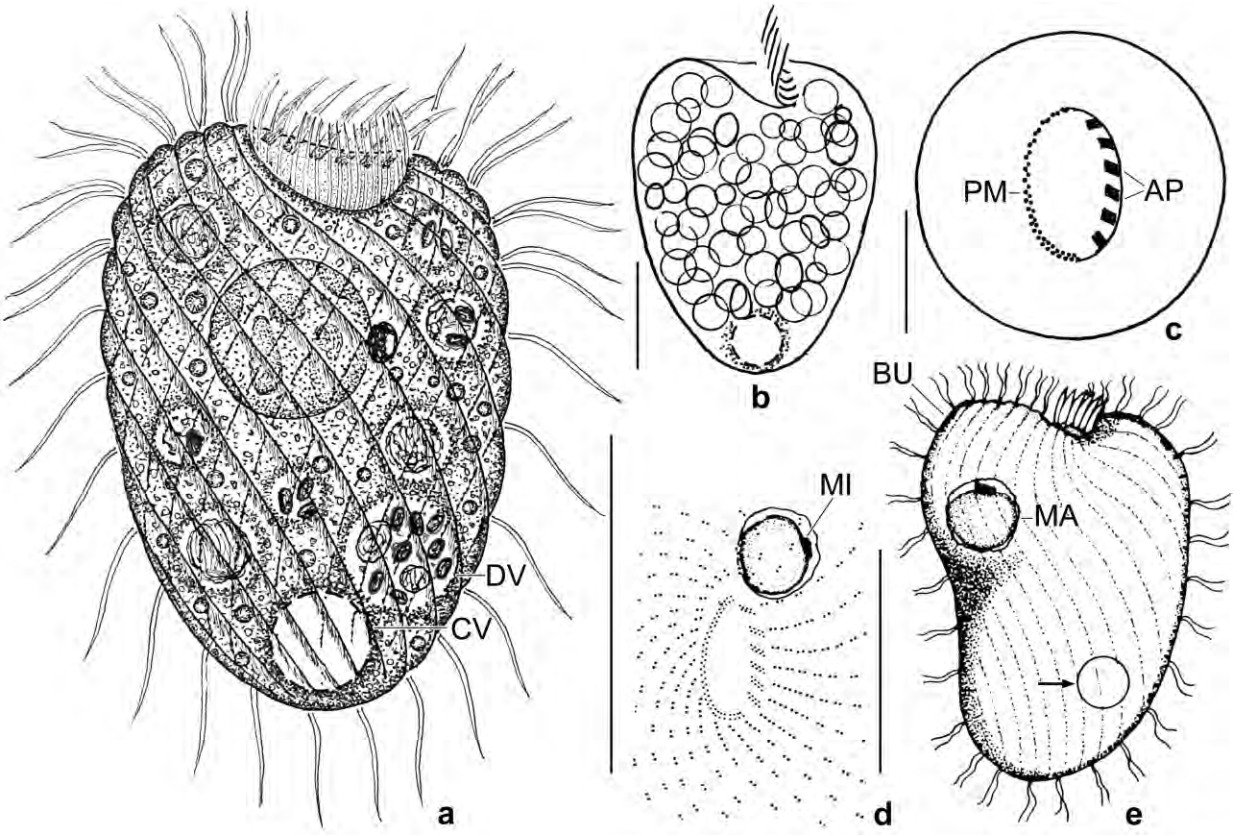

Fig. 133a–e. *Sagittaria venezuelensis* (a–c) and *S. australis* (d, e; from Pomp & Wilbert 1988) from life (a, b, e), after protargol impregnation (d), and (c) idealized according to the protargol preparations (outline diameter, oral structures) and SEM (outline of oral opening). **a:** Lateral view of a representative specimen, length 35 µm. **b:** A specimen studded with food vacuoles. **c:** Frontal view, showing shape and size of the oral opening in relation to the diameter of the body. **d:** Oral infraciliature. **e:** A representative specimen with a projecting bulge and a far subterminal contractile vacuole (arrow). AP – adoral polykinetids, BU – bulge, CV – contractile vacuole, DV – defecation vacuole, MA – macronucleus, MI – micronucleus, PM – paroral membrane. Scale bars 10 µm (b, c) and 20 µm (a, e).

external row of cilia active, internal row likely passive because cilia appear immobile in SEM micrographs (Fig. 133a, c, f, j, 134m–p, s–x; Table 44). On average six adoral polykinetids on left margin of oral opening; individual polykinetids rhomboid, composed of three, rarely of two rows with three to five basal bodies each, about two thirds of basal bodies barren, according to SEM. Most adoral cilia only 2–3 µm long and with blunt end, especially in ventral half of polykinetids; some cilia up to 5 µm long and pointed, mainly in dorsal half of polykinetids (Fig. 133a, f, g, i–k, 134f, g, i, m–p, s–x; Table 44).

Ontogenesis: This was followed in the scanning electron microscope. It commences with the resorption of the external ciliary row of the paroral membrane and a shortening of the adoral cilia (Fig. 134x, y). Next the internal row of the paroral membrane and the somatic cilia are resorbed to stumps while a stump grows out from the barren anterior basal body of the dikinetids (Fig. 135a, b). Finally, the oral opening and the entire oral and somatic ciliature have been resorbed (Fig. 135c). When furrowing commences, new cilia and a new oral apparatus become recognizable in proter and opisthe, clearly showing that the paroral membrane consists of two ciliary rows (Fig. 135e–h). During these processes, the opisthe rotates slightly relative to the proter, as recognizable by the oral apparatus (Fig. 135i, j). When the cells separate, the ciliature is usually fully developed

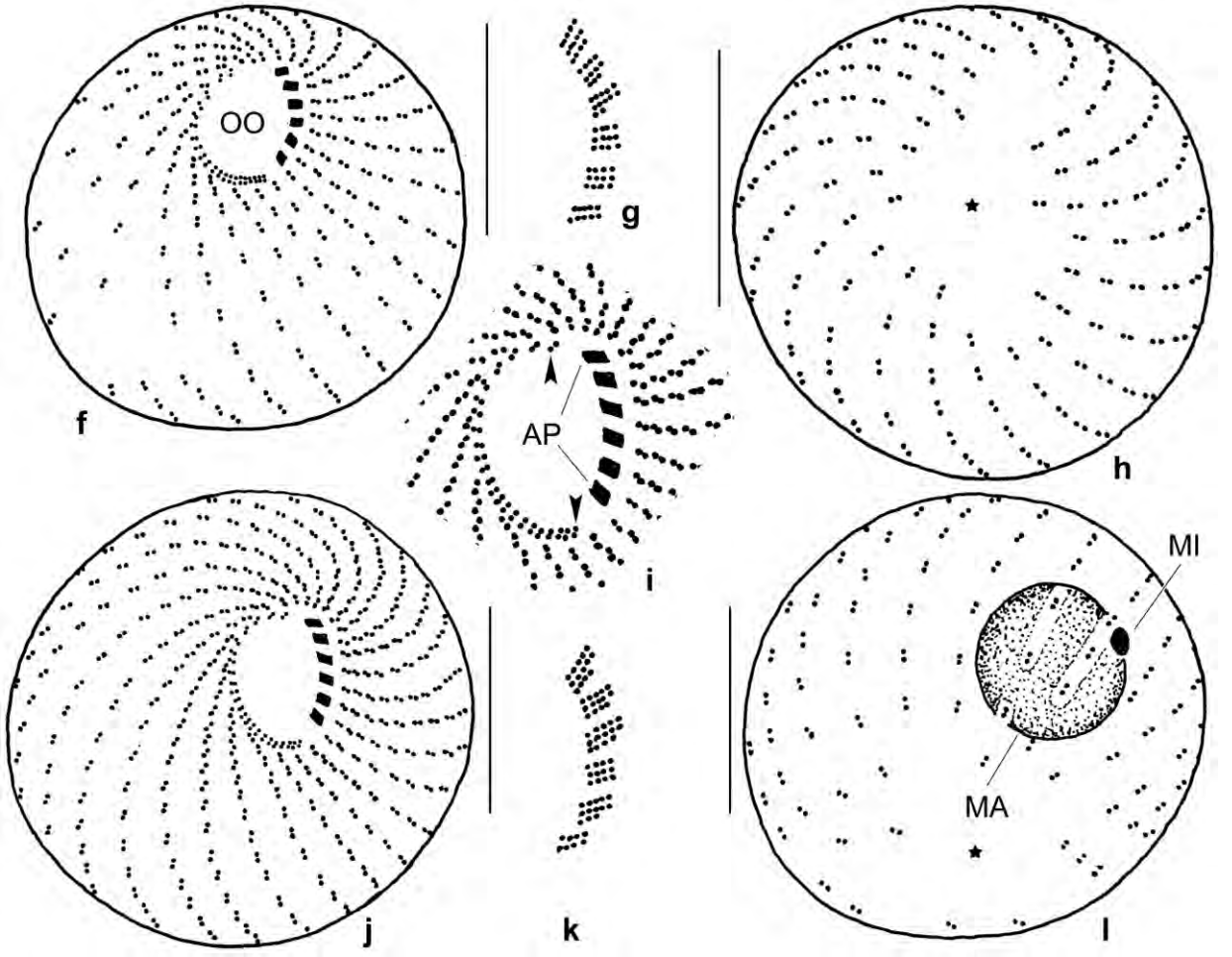

Fig. 133f–l. *Sagittaria venezuelensis*, infraciliature and nuclear apparatus after protargol impregnation. **f, h:** Anterior and posterior polar view of different specimens. The asterisk in (h) marks the unciliated posterior pole area. **g, k:** Details of the adoral polykinetids**. i, j, l:** Anterior and posterior polar view of same specimen. The asterisk in (l) marks the unciliated posterior pole area. The arrowheads in (i) denote the paroral membrane whose dikinetids become gradually narrower spaced ventrally. AP – adoral polykinetids, MA – macronucleus, MI – micronucleus, OO – oral opening. Scale bars 15 µm (f, h, j, l).

(Fig. 135i, j), rarely the cilia are still growing (Fig. 135k, l).

Molecular phylogeny (Fig. 124): The molecular tree shows *S. venezuelensis* within a clade containing *Apowoodruffia salinaria*, *Sagittariides oblongistoma,* and *Woodruffides metabolicus*. This is corroborated by distinct morphological similarities mentioned in the diagnosis of the → Woodruffina.

Occurrence and ecology: As yet found only at type locality. Moderate numbers developed in the non-flooded Petri dish culture one to two days after re-wetting; then it disappeared. When the sample was air-dried several times, the same cycle was performed, indicating that *S. venezuelensis* is more r- than k-selected.

Remarks: There is only one similar species, viz., *Sagittaria australis* Pomp & Wilbert, 1988 (Fig. 133d, e), which has the contractile vacuole far subterminal (vs. terminal), possesses a distinct hump (vs. absent), and has the paroral membrane composed of equidistantly spaced dikinetids (vs. gradually increasing from ventral to dorsal) and the adoral polykinetids built of two (vs.

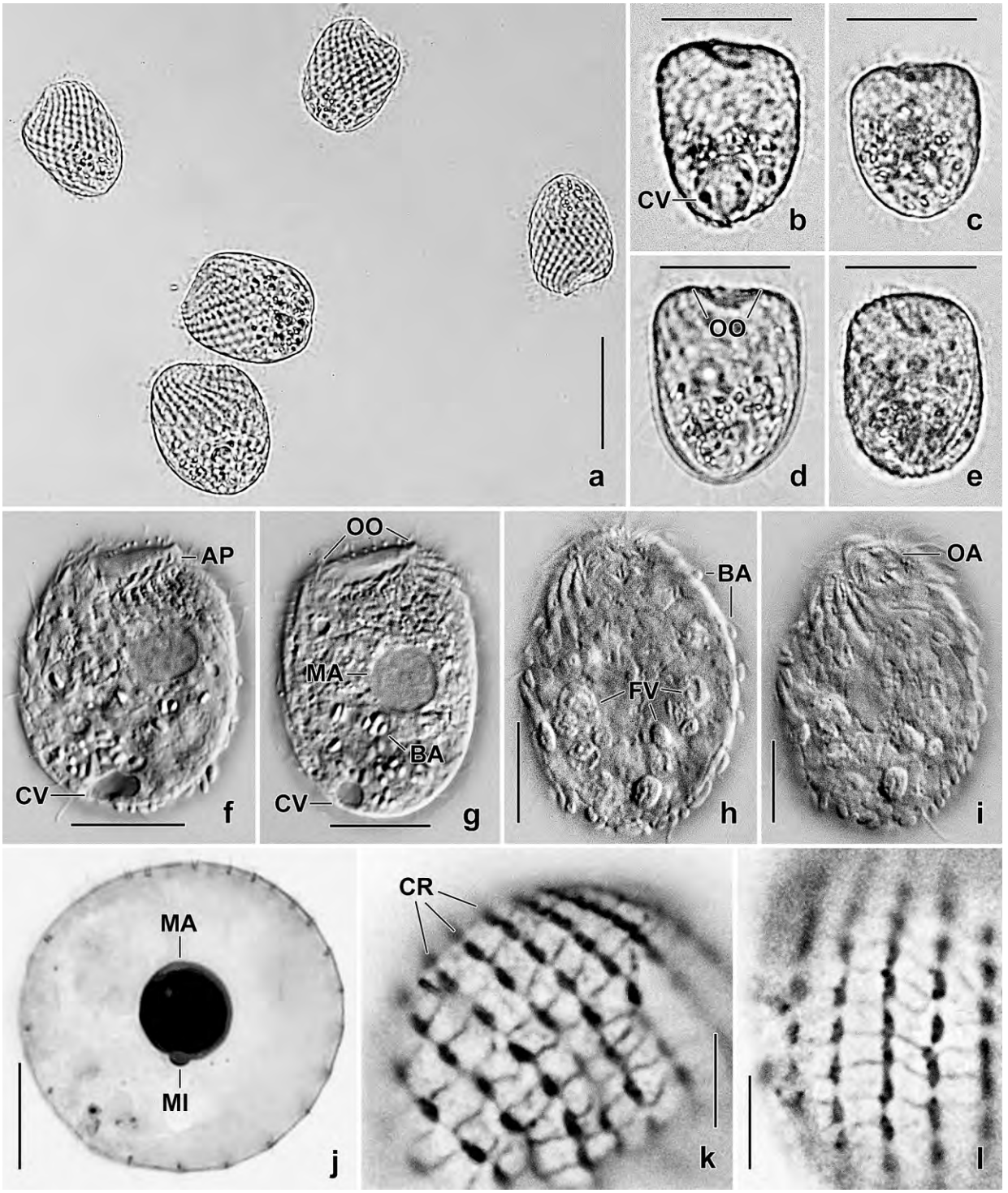

Fig. 134a–l. *Sagittaria venezuelensis* from life (a–i), after protargol impregnation (j), and in CHATTON-LWOFF silver nitrate preparations (k, l). **a–e:** Overviews of freely motile specimens in bright field (a) and interference contrast (b-e). Note the distinct, spiral furrowing. **f–i:** Slightly pressed specimens, showing details. **j:** Nuclear apparatus. **k, l:** Colpodid silverline pattern. AP – adoral polykinetids, BA – bacteria attached to cell surface and bacterial spores in food vacuoles, CR – ciliary rows, CV – contractile vacuole, FV – food vacuoles, MA – macronucleus, MI – micronucleus, OA – oral apparatus, OO – oral opening. Scale bars 10 µm (j, k, l), 15 µm (f–i), 25 µm (b–e), and 30 µm (a).

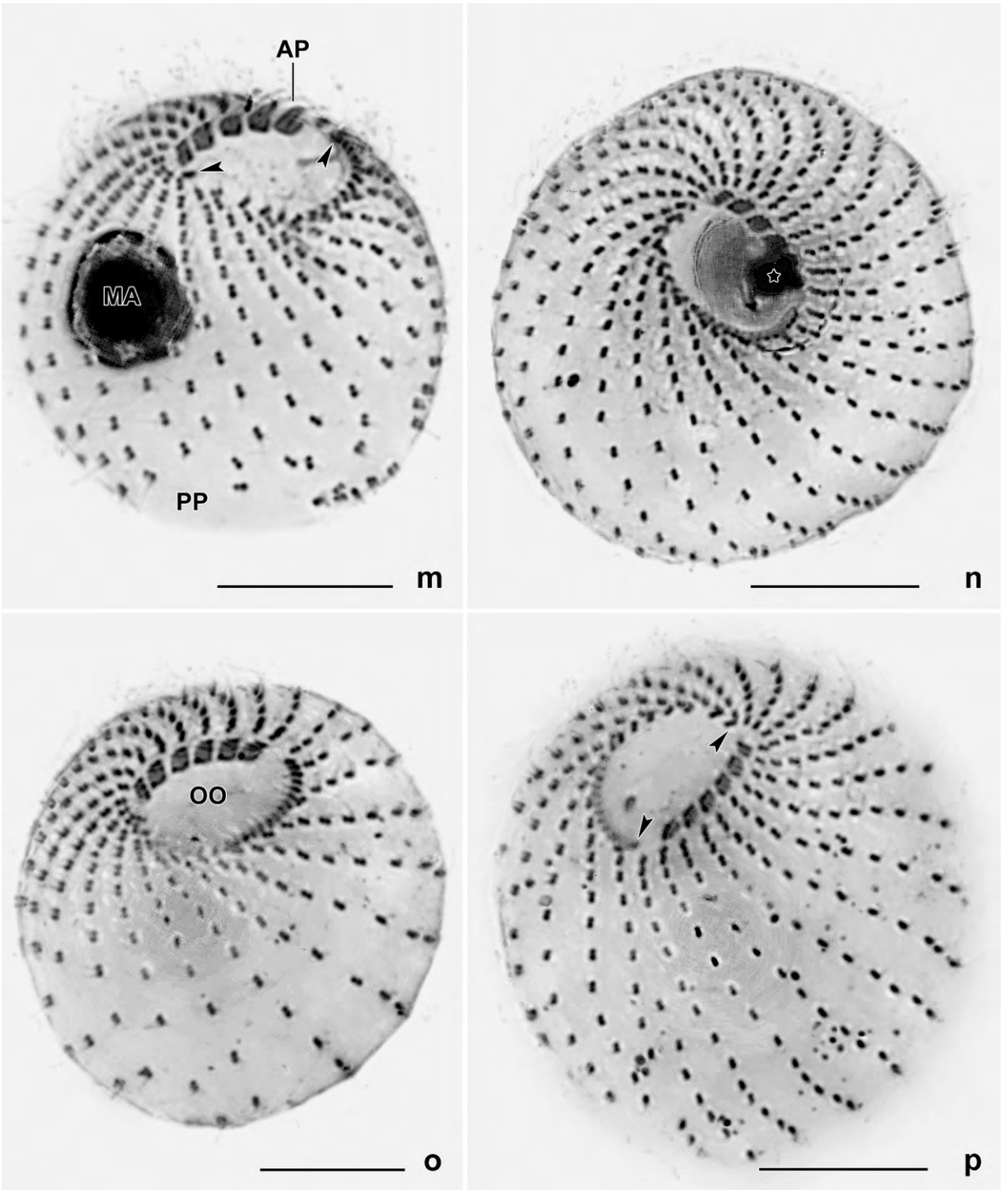

Fig. 134m–p. *Sagittaria venezuelensis*, ethanol-preserved and protargol-impregnated. These are anterior polar views, showing the number of ciliary rows, the distinctly spiraling ciliary rows, the gradual increase of kinetid distance from anterior to posterior, the ellipsoid to broadly ellipsoid oral opening, the five (m) to six (n–p) adoral polykinetids, and the paroral membrane whose dikinetal distances strongly increase from ventral to dorsal (m, p, arrowheads). The asterisk in (n) marks impregnated debris. AP – adoral polykinetids, MA – macronucleus, OO – oral opening, PP – posterior pole. Scale bars 10 μm.

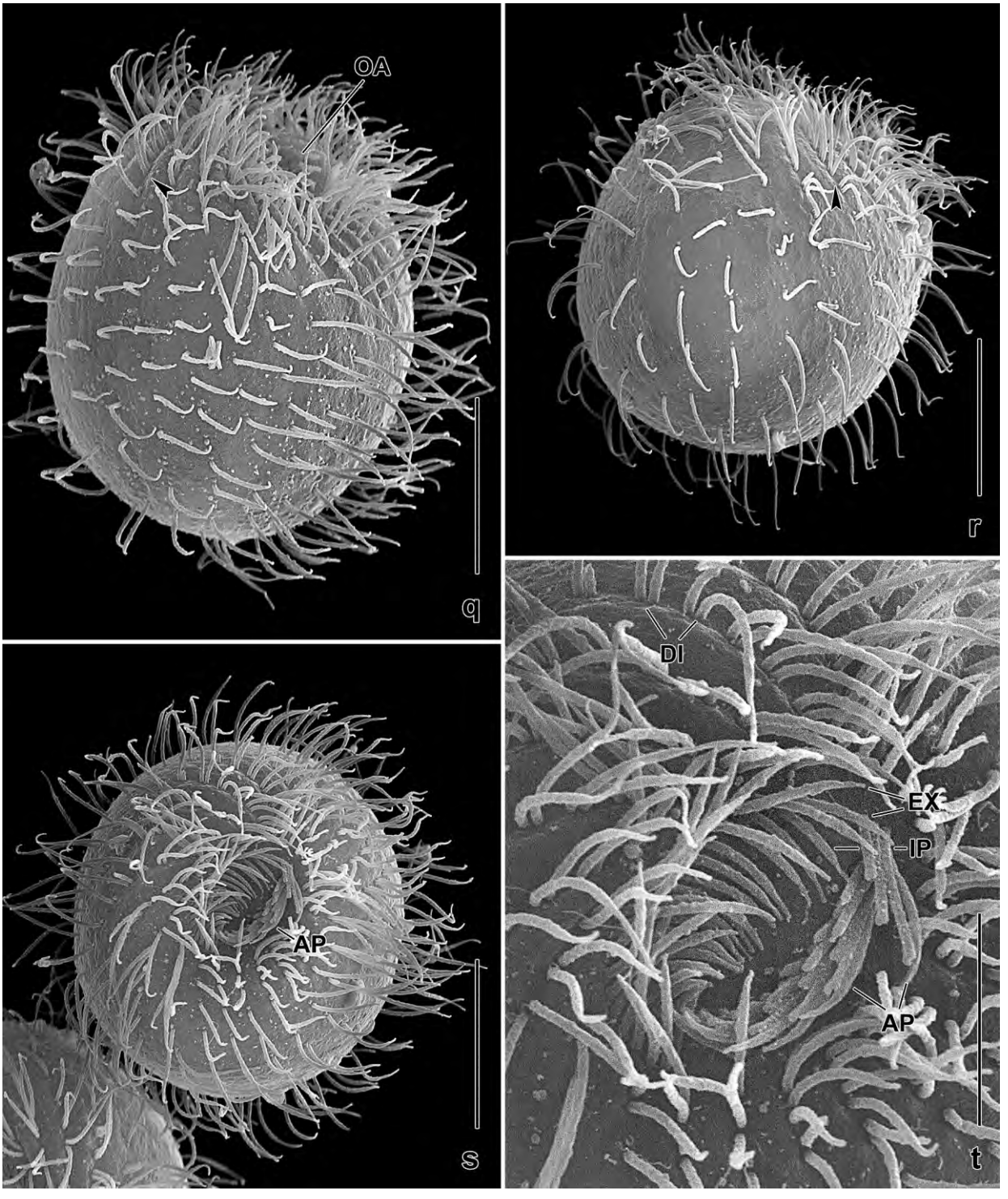

Fig. 134q–t. *Sagittaria venezuelensis* in the scanning electron microscope. **q, r:** Lateral view of bursiform specimens. Ciliated dikinetids (arrowheads) occur only in the oral region. **s, t:** Anterior polar views, showing the broadly elliptic oral field, overview and detail. At its left margin are six adoral polykinetids with cilia increasing in length from right to left. At the right margin is a paroral membrane composed of ciliated dikinetids. AP – adoral polykinetids, DI – ciliated dikinetids, EX – external paroral membrane, IP – internal paroral membrane, OA – oral apparatus. Scale bars 5 μm (t) and 10 μm (q–s).

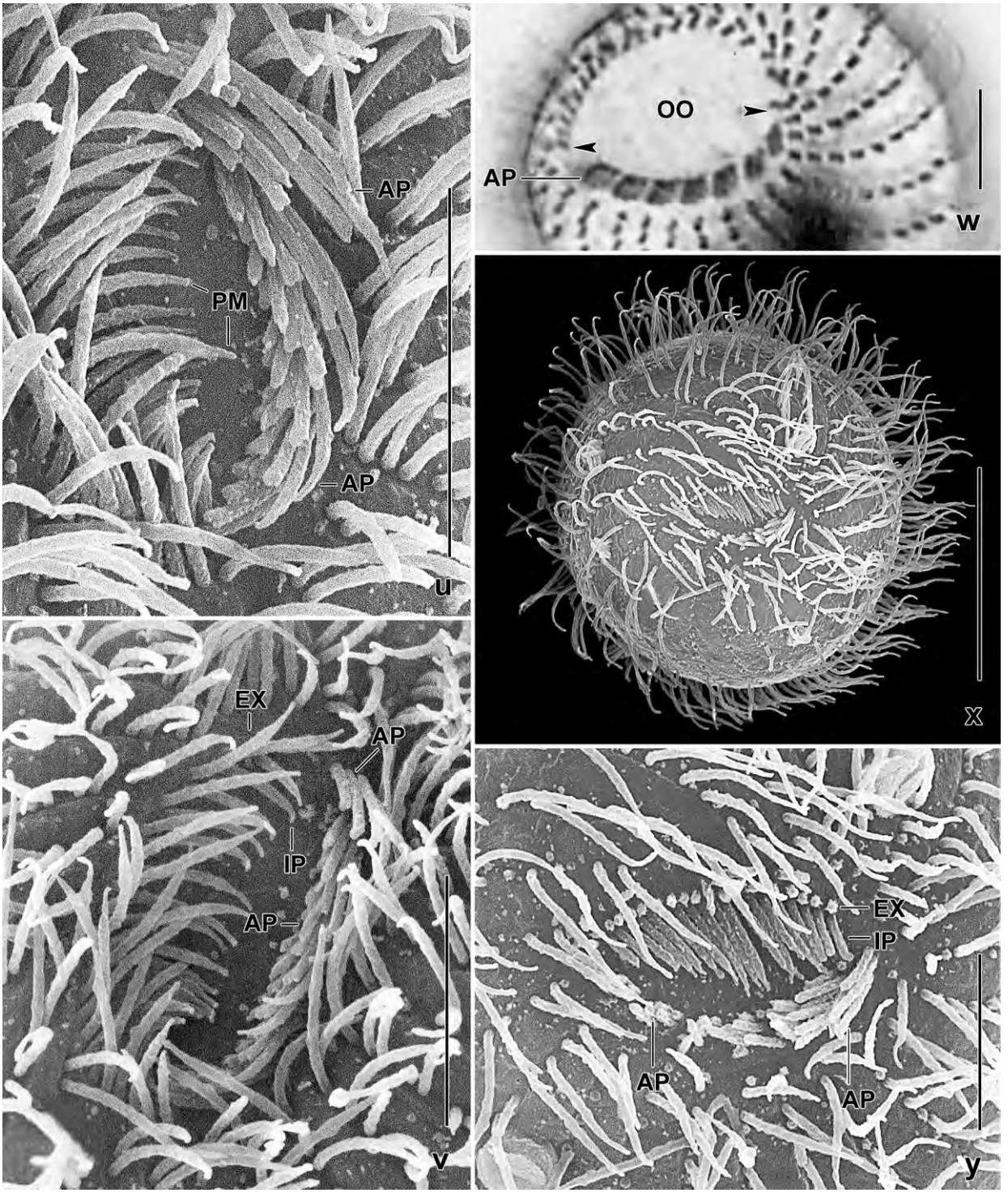

Fig. 134u–y. *Sagittaria venezuelensis*, morphostatic specimens (u–w) and a very early divider (x, y) in the scanning electron microscope (u, v, x, y) and after protargol impregnation (w). **u–w:** Anterior polar views, showing the oral structures. The left margin of the oral opening is occupied by 5–7 adoral polykinetids, on the right margin are ciliated dikinetids whose distances decrease from dorsal to ventral (w, arrowheads). **x, y:** Very early dividers first resorb the external paroral membrane and shorten the cilia of the adoral polykinetids. AP – adoral polykinetids, EX – external paroral membrane, IP – internal paroral membrane, OO – oral opening, PM – paroral membrane. Scale bars 5 µm (u, v, x, y) and 15 µm (w).

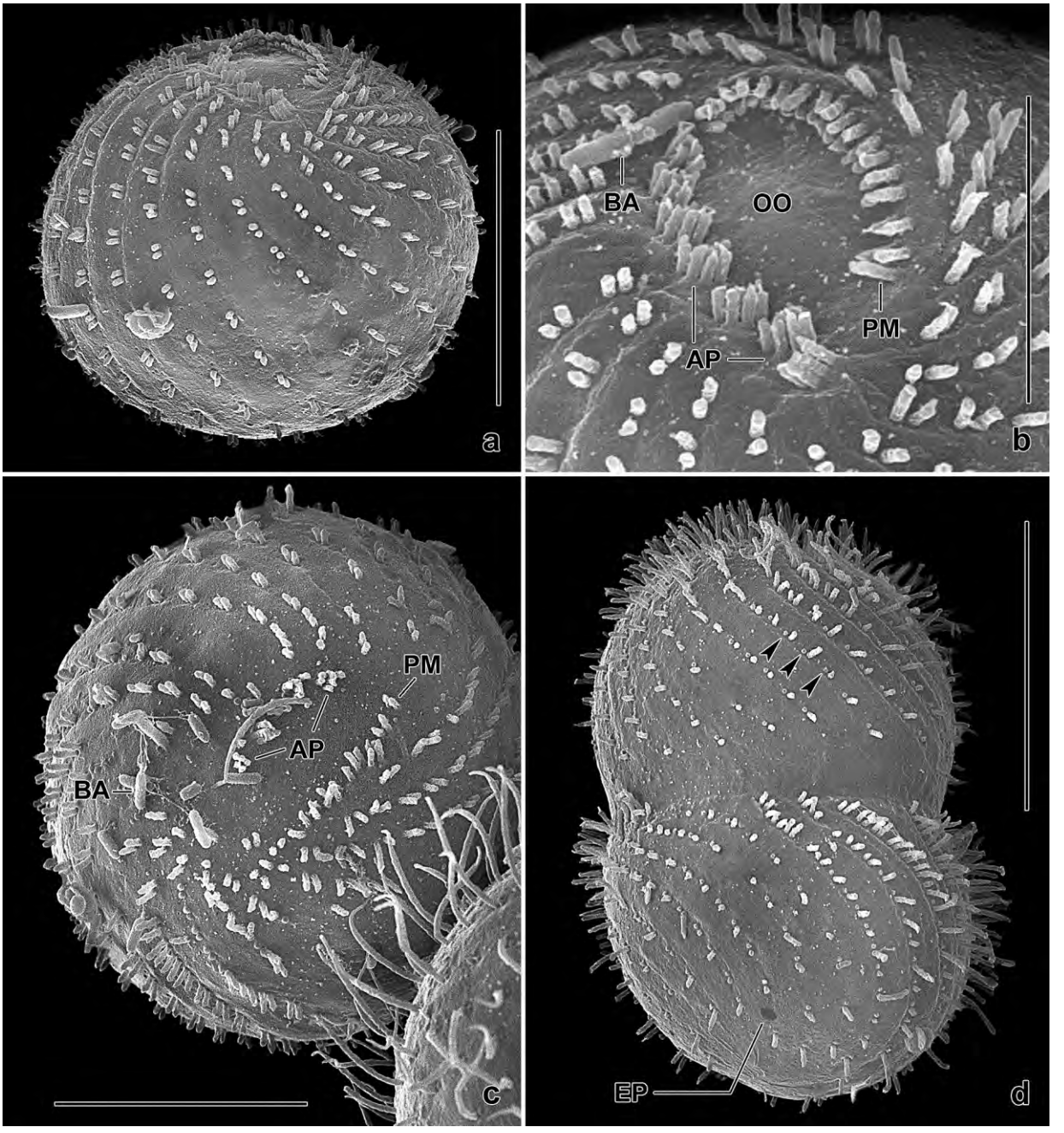

Fig. 135a–d. *Sagittaria venezuelensis,* dividers in the scanning electron microscope. **a, b:** Late stage of resorption of somatic and oral ciliature, overview and detail. Both basal bodies of all somatic dikinetids have ciliary stumps while the anterior basal body is barren posterior of the ciliated perioral dikinetids in the morphostatic condition (Fig. 134q, r). Both basal bodies of the paroral dikinetids are ciliated while some basal bodies of the adoral polykinetids are barren (cp. Fig. 133g, k). **c:** Resorption maximum, where the parental oral apparatus is difficult to recognize. **d:** Early late divider with division furrow and sprouting cilia originating from the posterior basal body of the dikinetids while the anterior stump is resorbed (arrowheads). AP – adoral polykinetids, BA – epicortical bacteria, EP – excretory pore of the contractile vacuole, OO – oral opening, PM – paroral membrane. Scale bars 5 μm (b), 10 μm (a, c), and 15 μm (d).

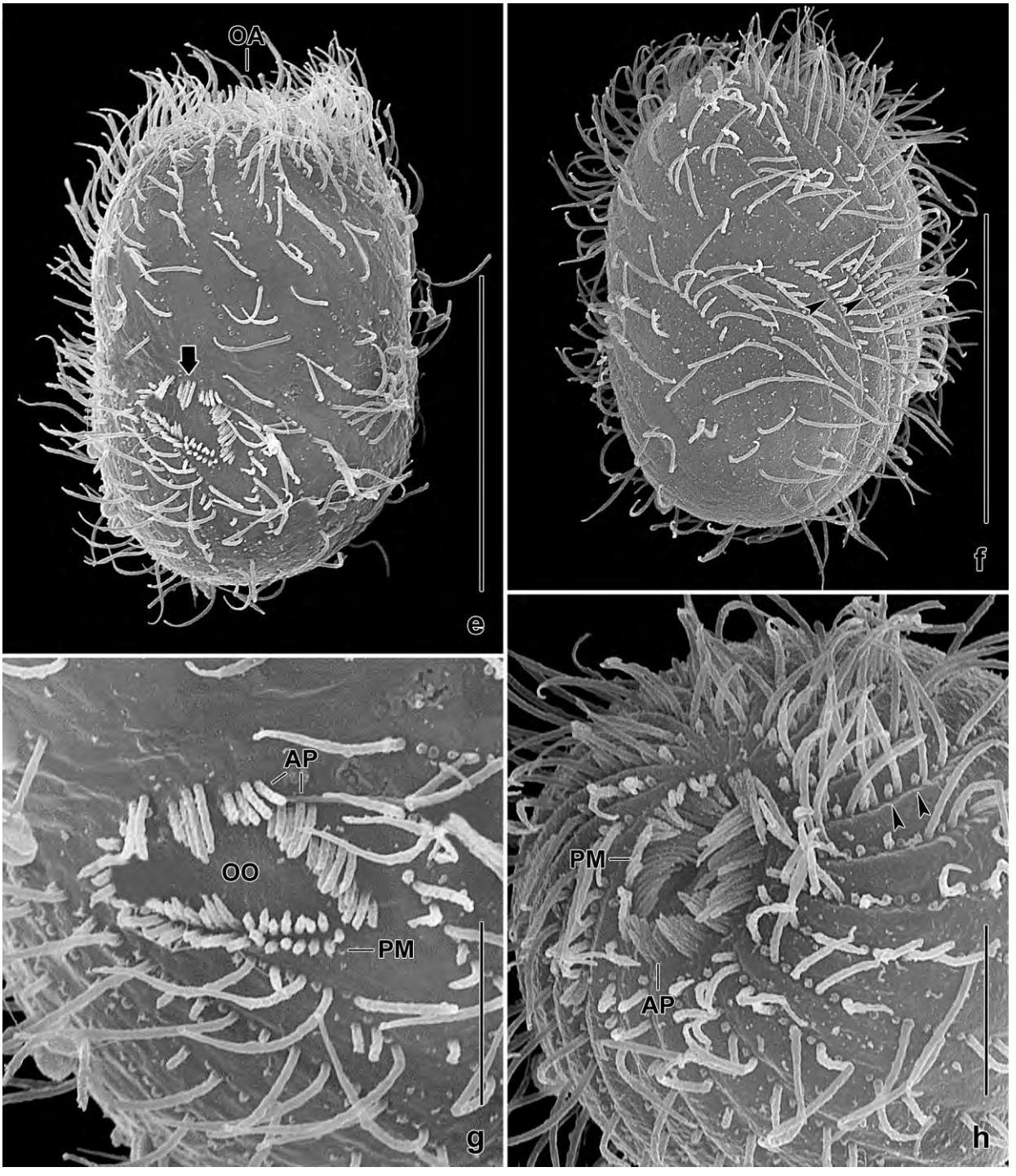

Fig. 135e–h. *Sagittaria venezuelensis,* late dividers in the scanning electron microscope. **e, g:** Middle or late divider, overview and oral detail (e, arrow). The somatic cilia regrow and the opisthe oral ciliature becomes recognizable (e, arrow). The paroral consists of ciliated dikinetids. The adoral polykinetids have less cilia than basal bodies (cp. Fig. 133g, k). **f:** A late divider constructing the perioral ciliature, i. e., the ciliated dikinetids where the anterior cilium is still a stump (arrowheads). **h:** The reorganizing proter oral apparatus is highly similar to the growing oral apparatus of the opisthe (left). Arrowheads mark growing anterior cilia of the perioral dikinetids. AP – adoral polykinetids, OA – oral apparatus, OO – oral opening, PM – paroral membrane. Scale bars 5 µm (g, h) and 20 µm (e, f).

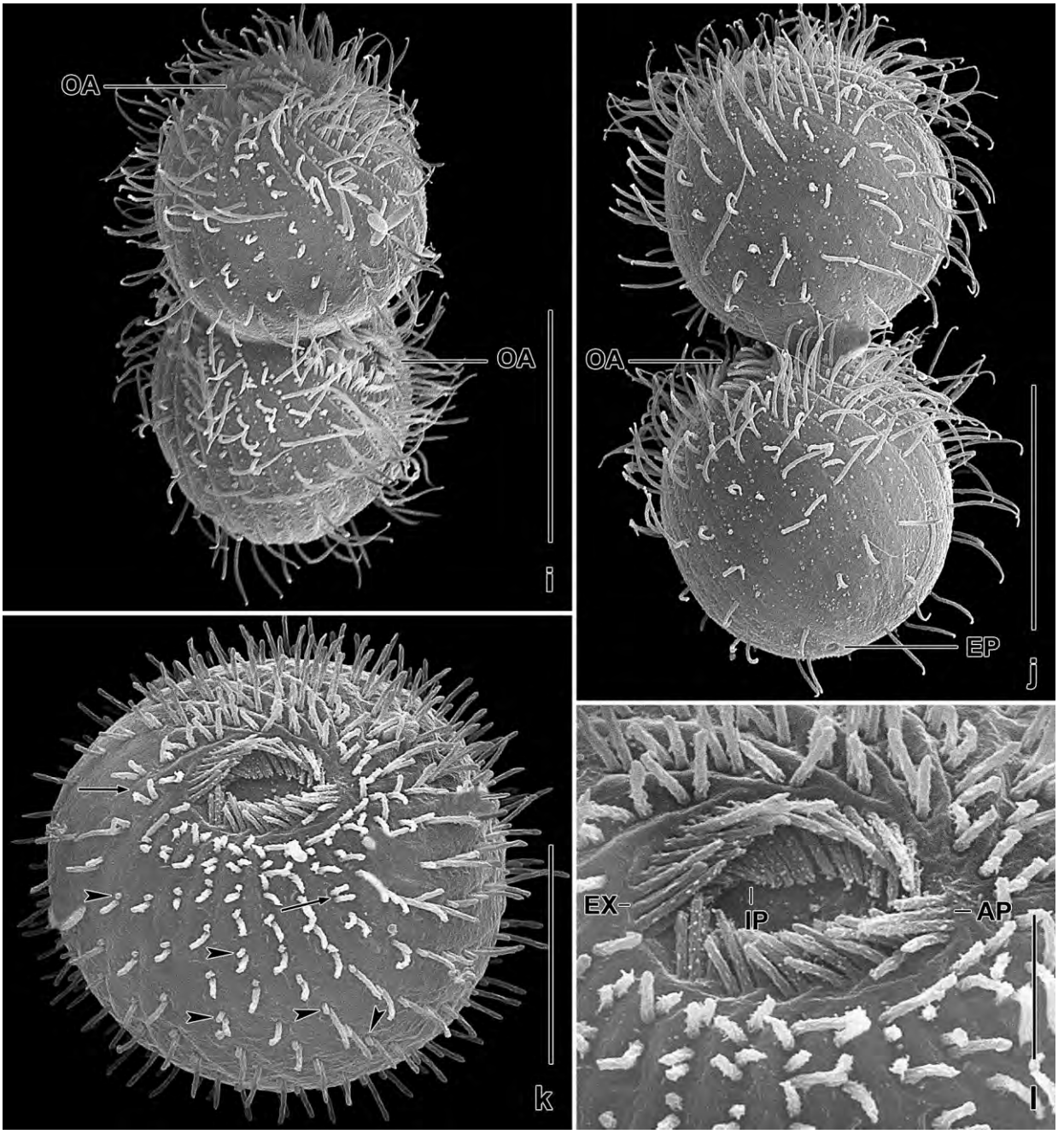

Fig. 135i–l. *Sagittaria venezuelensis*, very late dividers and a post-divider in the scanning electron microscope. **i:** The proter and opisthe oral apparatus are not in line but rotated by about 180°, as typical for platyophryid colpodids (FOISSNER et al. 2002). Still, many cilia are growing, especially in the perioral area. **j:** Similar to the specimen shown in (i). The anterior cilium of the perioral dikinetids is still growing. The excretory pore of the contractile vacuole is in the posterior pole area while far subterminal in *S. australis* (Fig. 133e). **k, l:** A post-divider with growing oral and somatic cilia. Arrows mark ciliated perioral dikinetids while arrowheads denote the ciliary stump in the anterior basal body of the post-perioral dikinetids. AP – adoral polykinetids, EP – excretory pore of the contractile vacuole, EX – external paroral membrane, IP – internal paroral membrane, OA – oral apparatus. Scale bars 3 µm (l), 10 µm (k), and 15 µm (i, j).

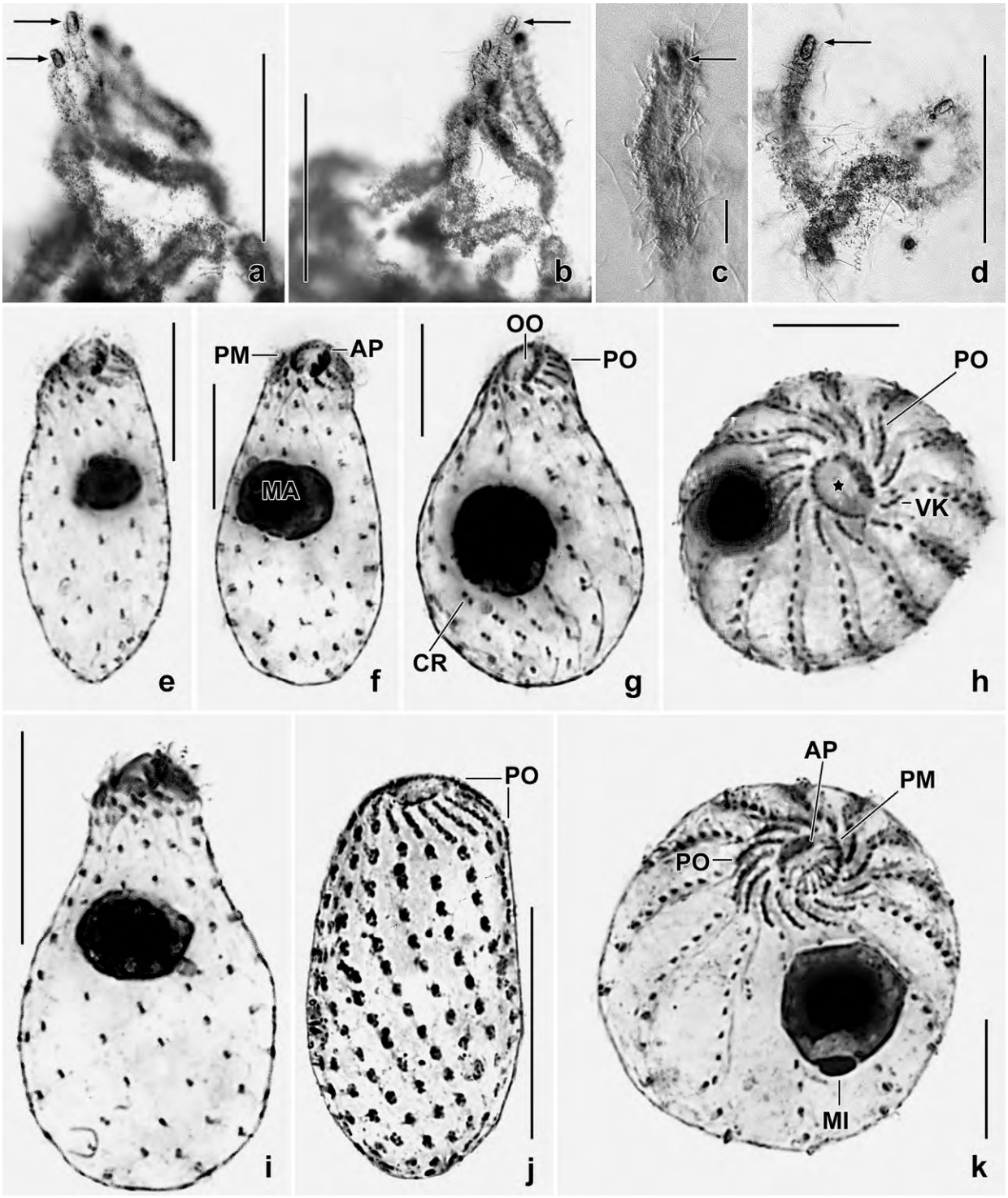

Fig. 136a–k. *Sagittaria hyalina* from life (a–d), after protargol impregnation (e–i, k), and in a Chatton-Lwoff silver nitrate preparation (j). **a–d:** Loricas with inhabitants marked by arrows. **e–g, i, j:** Ventral views, showing the spiral ciliary rows and the apical oral opening. **h, k:** Anterior polar views, showing the oral and perioral ciliary pattern. The asterisk (h) marks the oral opening. AP – adoral polykinetids, CR – ciliary rows, MA – macronucleus, MI – micronucleus, OO – oral opening, PM – paroral membrane, PO – perioral ciliature, RP - left oral polykinetid, VK – ventral kinety. Scale bars 10 µm (e–h, j, k), 20 µm (i), 30 µm (a, b, d), and 40 µm (c).

three) rows of basal bodies. In vivo, *S. venezuelensis* can be confused with → *Apowoodruffia salinaria* which, however, is usually larger (75 × 30 vs. 35 × 25 µm in vivo) and more slender (~ 2.4:1 vs. 1.4:1).

The ontogenesis is very similar to that of other platyophryids, for instance, *Platyophyrides latus*, and to that of colpodids in general, for instance, *Bromeliothrix metopoides* (Foissner 1993a, 2010a; Foissner et al. 2002). Possibly, the rotation of the opisthe is less pronounced.

Sagittaria hyalina Foissner, Czapik & Wiackowski, 1981 (Fig. 136a–k)

Material: Site (68), i. e., Galápagos (ciliary pattern) and Venezuelan site 65 (lorica).

Remarks: *Sagittaria hyalina* was discovered in a road puddle near the University of Cracow. Since then, we found indistinguishable populations in many soil samples globally, especially when they were saline (Foissner et al. 2002). Here, we show specimens from Galápagos, matching very well the Polish population (Foissner et al. 1981).

Sagittaria has a simple organization and is closely related to *Platyophrya* (Fig. 136). The figures in Foissner et al. (1981) show insufficiently the dense circumoral ciliature composed of 6–8 very narrowly spaced dikinetids, except of one or two ventral kineties which have only two to three dikinetids (Fig. 136e–k). Body size and shape are very variable, especially in highly saline habitats. The slimy lorica is rarely recognizable because the inhabitants leave it when they are transported from the sample to the microscope slide, where lorica building can be observed with some patience (Fig. 136a–d).

Sagittarides Foissner & Buosi **nov. gen.**

Diagnosis: Small to moderately small, laterally flattened Sagittariidae with narrowly elliptic oral aperture in a shallow, slightly oblique concavity of anterior body end. One or more adoral polykinetids anteriorly of hooked right oral ciliary field (paroral membrane). Silverline pattern colpodid. Resting cyst woodruffid.

Type species: *Sagittarides oblongistoma* nov. spec.

Etymology: Composite of the generic name *Sagittaria* and the Greek suffix *ides* (similar), meaning a ciliate genus similar to *Sagittaria*. Masculine gender.

Remarks: Among members of the family Sagittariidae, *Sagittarides oblongistoma* is unique in having a polar, narrowly elliptical oral opening and one or more polykinetids anterior of the right oral ciliary field. These features justify a generic separation.

Sagittarides oblongistoma has some similarities with members of the family Woodruffiidae, viz., a narrow oral aperture and polykinetids anterior of the right oral ciliary field. However, the Woodruffiidae have the oral apparatus on the ventral side, i. e., not apically as the Sagittariidae. For a revision of the families mentioned, see Foissner (1993a).

Sagittarides oblongistoma Foissner & Buosi **nov. spec.** (Fig. 124, 137a–t, 138a–y, 139a–l; Table 45)

Diagnosis: Size about 55 × 35 µm in vivo. Usually obtriangular or bursiform with transverse or obliquely truncate anterior end. On average 26 somatic ciliary rows. Oral apparatus with 7 adoral polykinetids and an about 15 µm long, hooked paroral membrane comprising 33 dikinetids on average.

Type locality: Venezuelan site (65), i. e., highly saline soil from the north coast of Venezuela, Morrocoy National Park, surroundings of the village of Chichiriviche, 67°13'W 11°33'N.

Etymology: Composite of the Latin adjective *oblongus* (oblong) and the Greek noun *stoma* (mouth), i. e., an apposition referring to the oblong shape of the mouth entrance, a main feature of the species.

Type slides: 1 holotype and 3 paratype slides with protargol-impregnated specimens and 4 paratype slides with silver nitrate-impregnated cells have been deposited in the Biology Centre of the Upper Austrian Museum in Linz (LI). Relevant specimens have been marked by black ink circles on the coverslip.

Description: When we had finished the observations, we dried the sample. After seven years we rewetted it again, and rich populations of *S. oblongistoma* and → *Apowoodruffia salinaria* developed. Three differences were recognized in *S. oblongistoma*, viz., most cells were more slender (~ 1.8:1) and hardly flattened, few specimens showed an anterior obliquity, and all cells were colourless because the cyanobacteria did not survive the long period of drought, showing that *S. oblongistoma* reproduces well on bacteria (Fig. 138a–h, k). This species impregnates very well with protargol after fixation with Da Fano's fluid as used for Chatton-Lwoff silver nitrate impregnation.

Size in vivo 40–65 × 30–45 µm, usually about 55 × 35 µm, as calculated from some in vivo measurements and values shown in Table 45 adding 15% preparation shrinkage. Body shape very variable, length:width ratio 1.6:1 on average in protargol preparations, usually obtriangular as observed in 53% (Fig. 137a, c, e, o, 138a–c, h, m, 139a, b) out of 60 specimens analyzed, bursiform in 42% (Fig. 137b, d, q, r, 138q, r), rarely ellipsoid or globular (5% of specimens; Fig. 138d, e, g, 139c); anterior body end also rather variable, that is, in 62% out of 50 protargol-impregnated specimens transverse truncate (Fig. 137b, d, r, 138c, r), in 30% obliquely to slightly obliquely truncate (Fig. 137a, e, 138a, b, h, m, q, 139a), and in 8% more or less convex (Fig. 137c, 138d–g, 139b, c); many specimens with a small obliquity at left anterior end (Fig. 137a, e, 138c, h); posterior end broadly rounded to pointed (Fig. 137a–e, 138a–h, 139a, b); laterally flattened up to 2:1. Nuclear apparatus usually in middle body third (Fig. 137a, p, q, s, t, 138m, n, q, r; Table 45). Macronucleus very hyaline in vivo, globular to broadly ellipsoid, about 12 × 9 µm in preparations, contains some small nucleoli only recognizable in faintly impregnated specimens; macronuclear contents often wrinkled and strongly shrunken in preparations. Micronucleus hemispherical, about 2 × 1.5 µm, invariably attached to macronucleus by its flattened side,

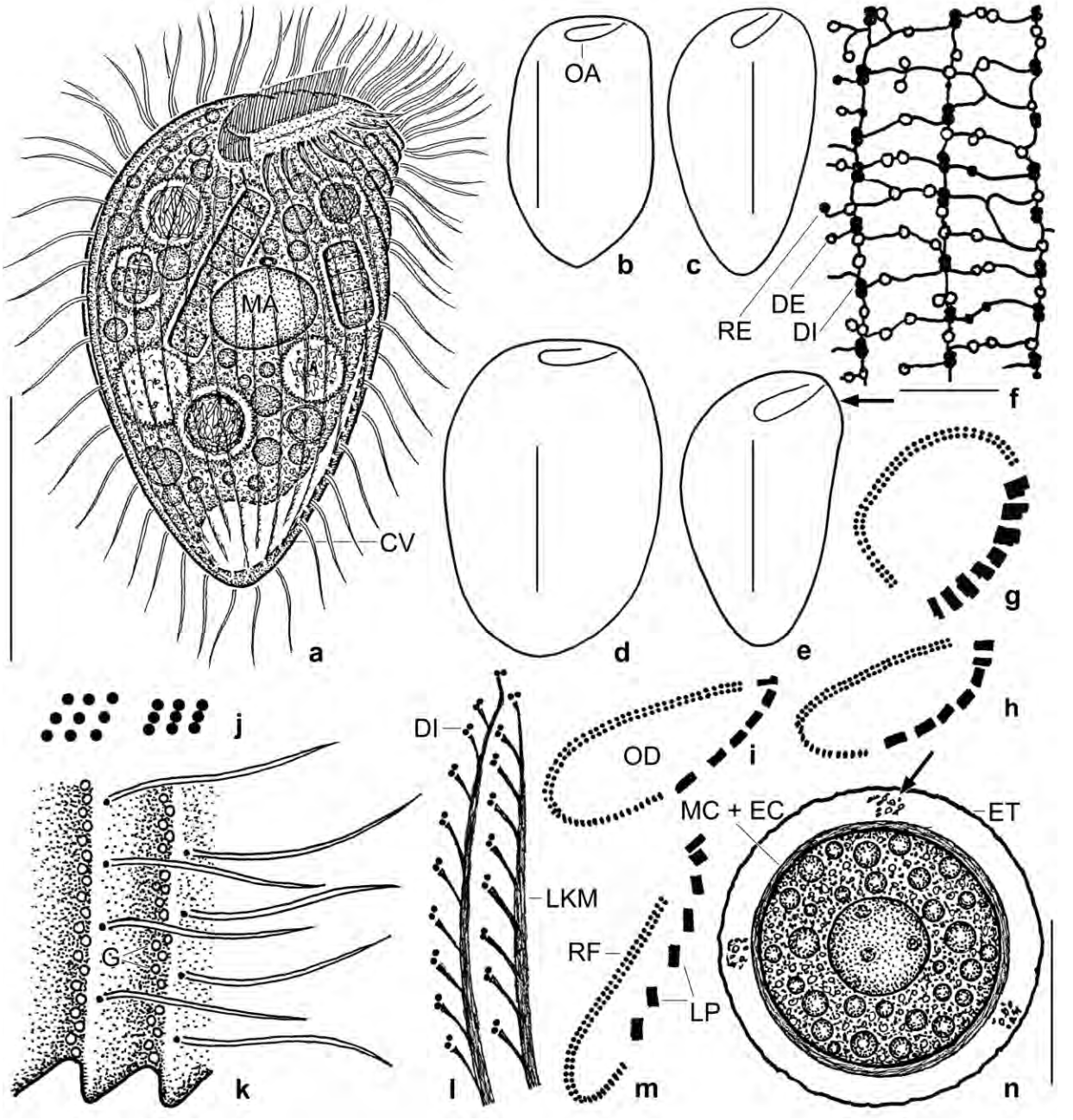

Fig. 137a–n. *Sagittarides oblongistoma* from life (a, e, j, k, n), after Chatton-Lwoff silver nitrate impregnation (f), and after protargol impregnation (b–d, g–j, l, m). **a:** Right side view of a representative specimen studded with lipid droplets and food vacuoles containing bacterial rods and "bluegreen algae". **b–e:** Variability of body shape; in vivo, the left anterior end is frequently obliquely truncate (a; e, arrow). **f:** The silverline pattern is colpodid and usually very faintly impregnated (2w–y). **g, h, i, m:** Variability of oral field and oral ciliary pattern. The specimen shown in (g) is distorted. The right oral field is a dikinetal, ciliated paroral membrane while the left field consists of 5–9 brick-shaped adoral organelles (polykinetids), of which the distalmost have a transverse orientation. **j:** Frontal and oblique view of a polykinetid. **k:** The cortex is distinctly furrowed, and the ridges contain minute granules, likely mucocysts. **l:** Part of the somatic ciliature, showing the conspicuous "left kinetodesmal fibres". **n:** The resting cyst is orange-coloured and shows extruded material between ectocyst and mesocyst (arrow). CV – contractile vacuole, DE – docked extrusome, DI – dikinetid, EC – endocyst, ET – ectocyst, G – granules, LP – left oral polykinetids, LKM – left kinetodesmal fibre, MA – macronucleus, MC – mesocyst, OA – oral apparatus, OD – oral field, RE – released extrusomes, RF – right oral ciliary field. Scale bars 5 µm (f), 15 µm (n), and 30 µm (a–e).

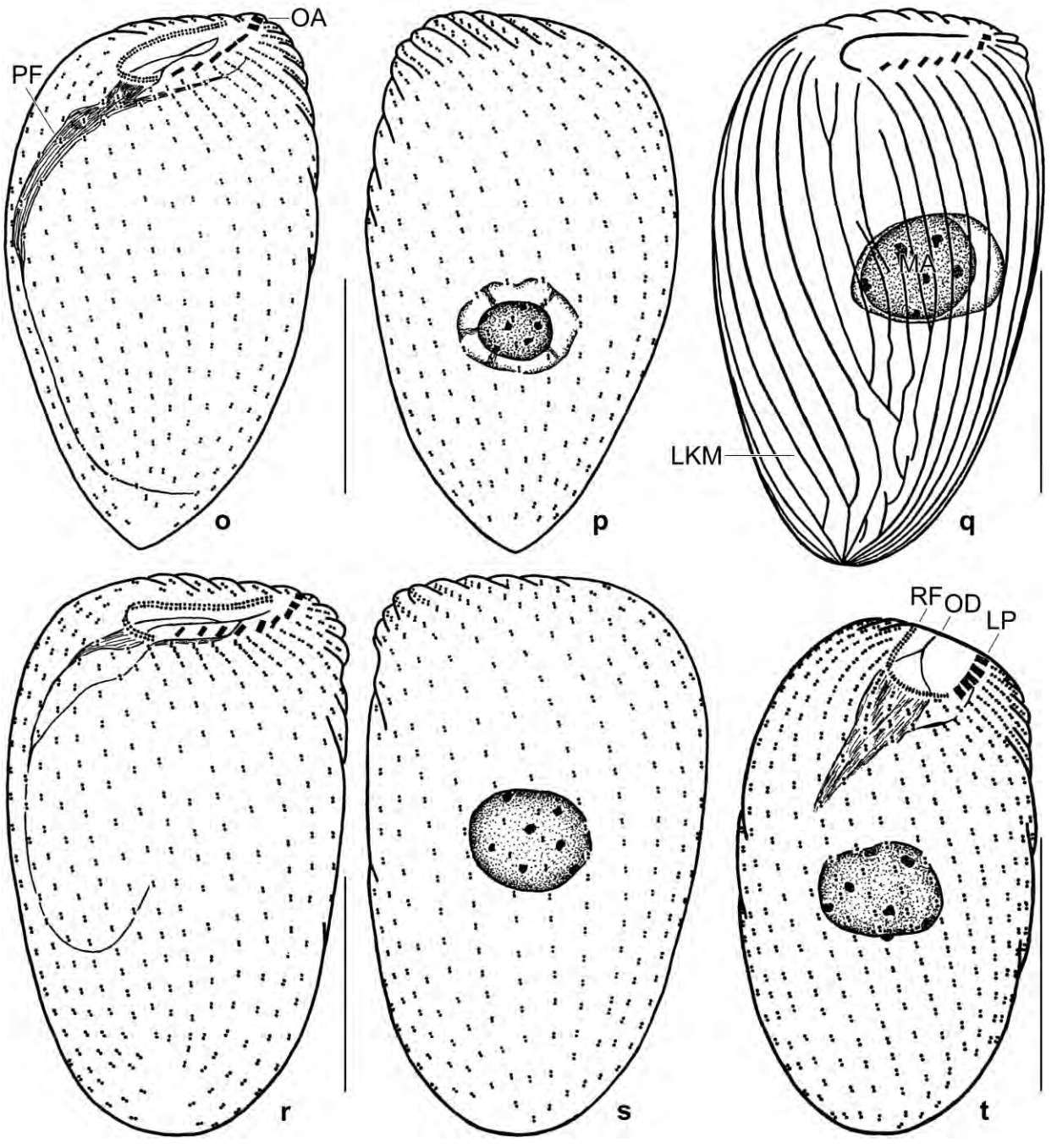

Fig. 137o–t. *Sagittarides oblongistoma*, somatic and oral ciliary pattern after protargol impregnation. **o, p:** Right and left side view of holotype specimen, showing the obtriangular body shape and the long pharyngeal fibres, length 50 µm. The nucleoplasm shrunk due to the preparation procedures, leaving fibrillar columns attached to the macronuclear membrane. **q:** Right side pattern of the "left kinetodesmal fibres" (transverse microtubule ribbons of the posterior basal body of the dikinetids; for a detail, see Fig. 137l). Note the irregularities in midline, sometimes forming a suture-like pattern. **r, s:** Right and left side view of a bursiform specimen with long, narrow oral field. **t:** Dorsal view, showing the oral apparatus in the centre of body thickness, i. e., apically. LKM – "left kinetodesmal fibres", LP – left oral polykinetids, MA – macronucleus, OA – oral apparatus, OD – oral field, PF – pharyngeal fibres, RF – right oral ciliary field. Scale bars 20 µm.

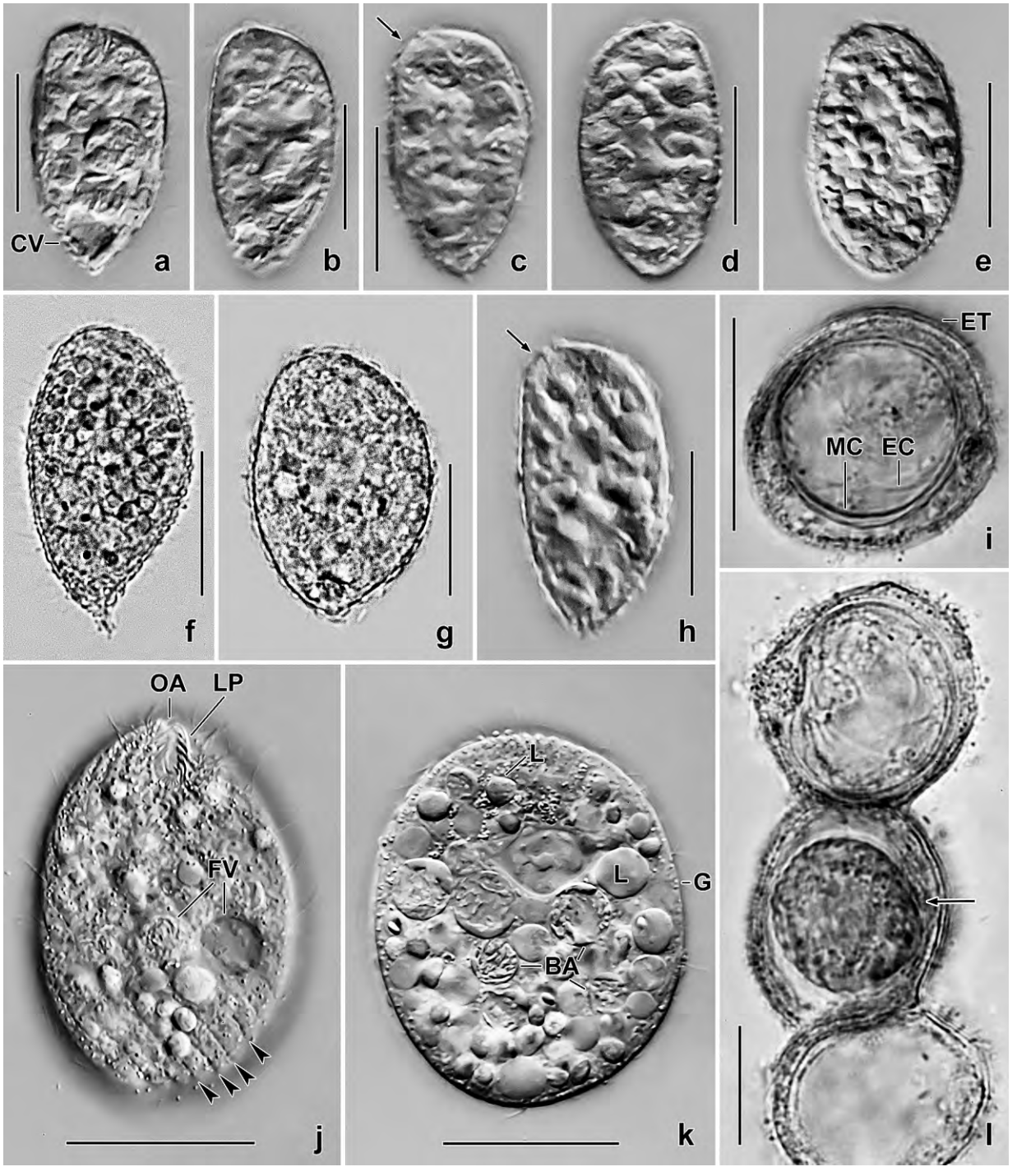

Fig. 138a–l. *Sagittarides oblongistoma*, vegetative (a–h, j, k) and cystic (i, l) specimens from life. **a–h, k:** Freely motile specimens (a–h), some showing the typical oblique truncation of the left anterior end (arrows). The cells are studded with food vacuoles and lipid droplets, well recognizable in the squashed specimen shown in (k). **j:** Ventral view, showing the deeply furrowed cortex (arrowheads) and the oral apparatus in mid of cell's thickness. **i, l:** The globular resting cysts are lightly to deeply orange-coloured. The contents was destroyed by bacteria in three out of the four cysts. BA – food vacuoles with bacteria, CV – contractile vacuole, EC – endocyst, ET – ectocyst, FV – food vacuoles, G – granules, L – lipid droplets, LP – left oral polykinetids, MC – mesocyst, OA – oral apparatus. Scale bars 15 µm (l) and 30 µm (a–k).

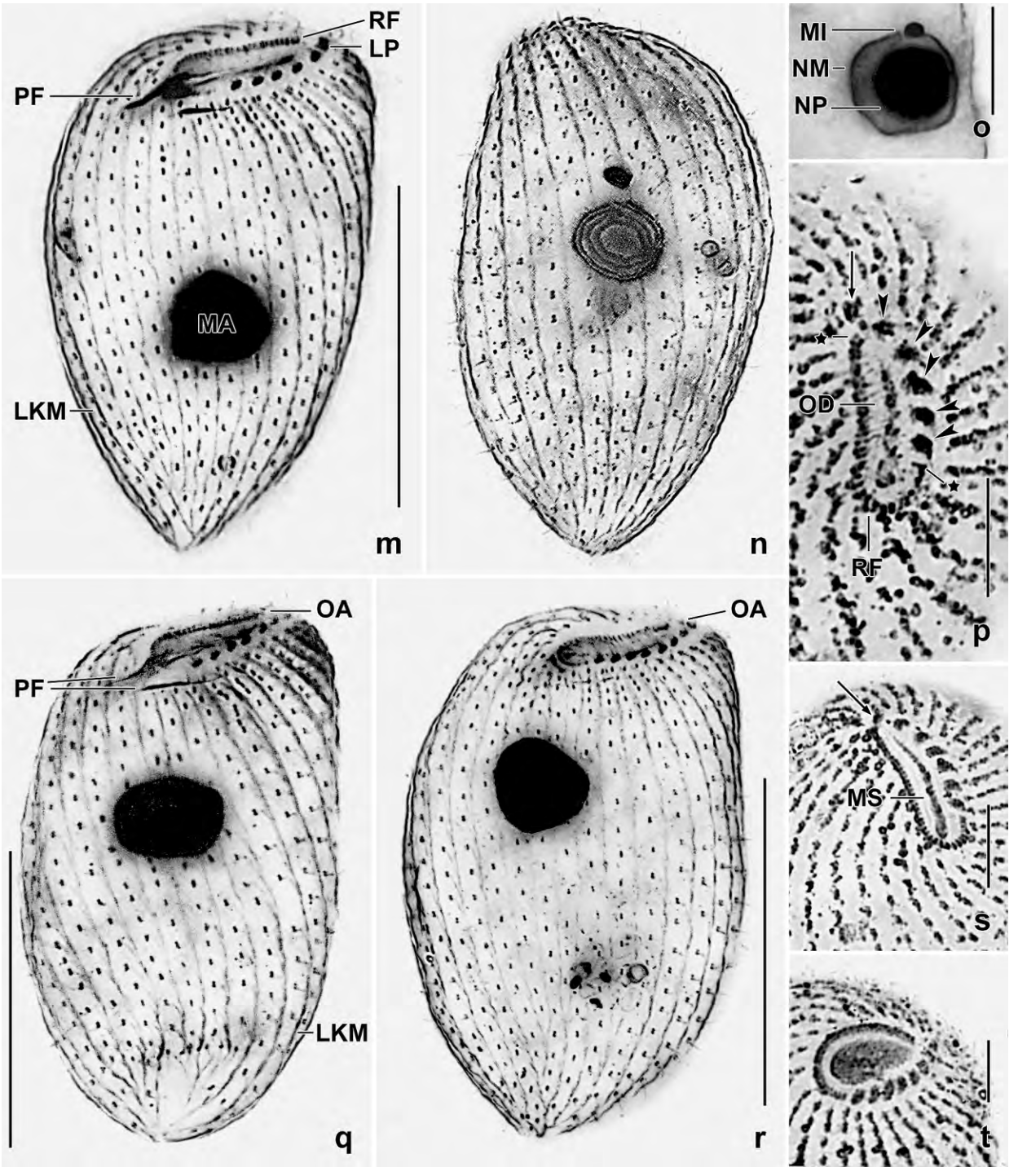

Fig. 138m–t. *Sagittarides oblongistoma*, ciliary pattern after protargol (m–o, q, r) and silver nitrate (p, s, t) impregnation. **m, n:** Right and left side view of holotype specimen, length 50 µm. Note the obtriangular body shape. **q, r:** Right side view of a bursiform and of an obovate specimen. **o:** Nuclear apparatus. **p, s:** Anterior polar views. The arrows mark a polykinetid ahead of the right oral ciliary field, whose ends are marked by asterisks. The arrowheads denote the brick-shaped left oral polykinetids. **t:** Oral structures of an early post-divider. LKM – "left kinetodesmal fibre", LP – left oral polykinetids, MA – macronucleus, MI – micronucleus, MS – mouth slit, NM – macronuclear membrane, NP – nucleoplasm, OA – oral apparatus, OD – oral field, PF – pharyngeal fibres, RF – right oral ciliary field. Scale bars 10 µm (o, p, s, t) and 30 µm (m, n, q, r).

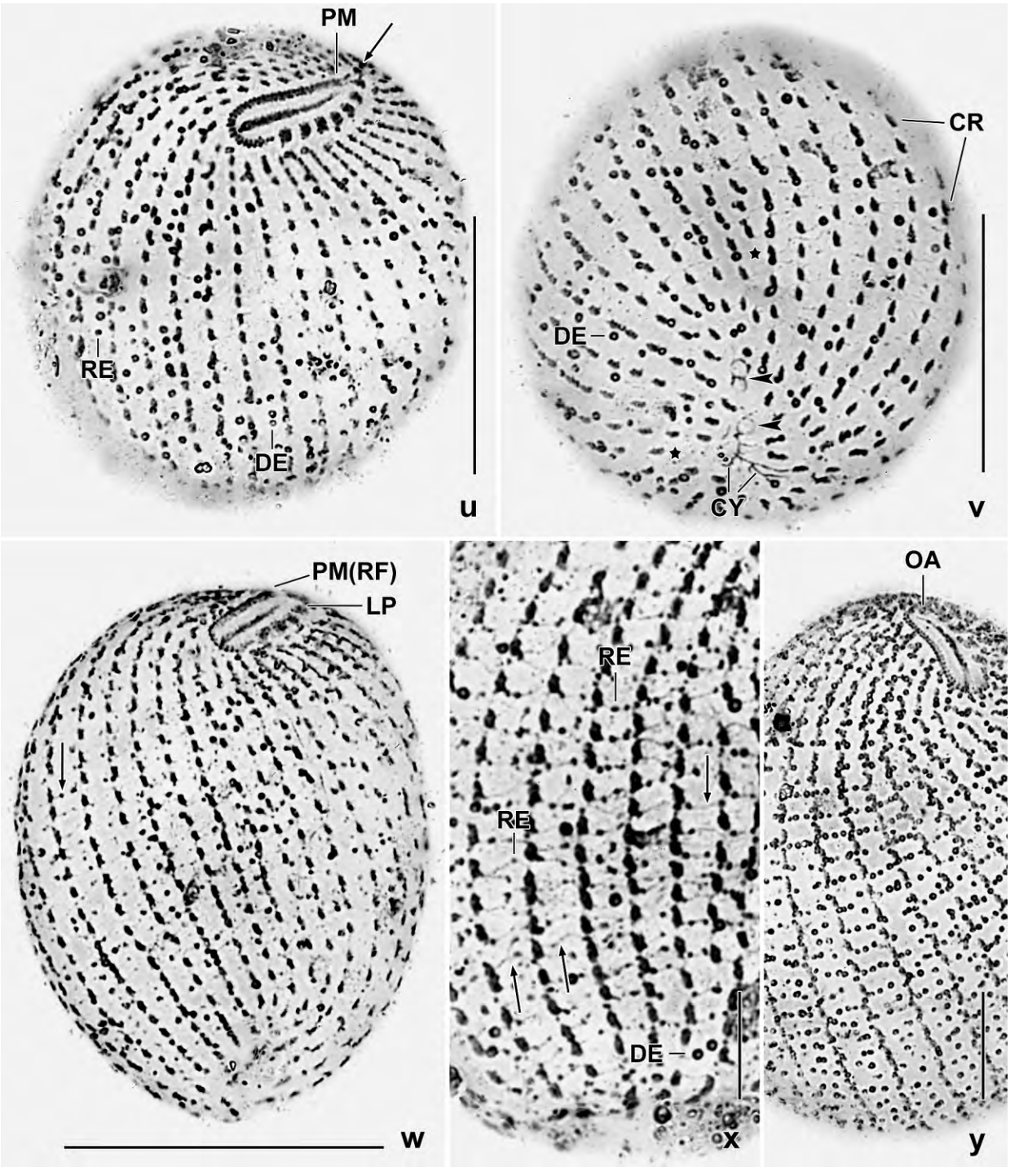

Fig. 138u–y. *Sagittarides oblongistoma*, ciliary and silverline pattern after Chatton-Lwoff silver nitrate impregnation. **u, v:** Oblique anterior and posterior polar view. The arrow marks a left oral polykinetid anterior of the right oral ciliary field (paroral membrane). The arrowheads denote excretory pores. The asterisk marks shortened ciliary rows. **w, x:** Dorsolateral views, showing the ciliary and silverline (arrows) pattern. **y:** Dorsolateral view, showing the silverlines studded with docked extrusomes. CR – ciliary rows, CY – cytopyge, DE – docked extrusomes, LP – left oral polykinetids, OA – oral apparatus, PM (RF) – paroral membrane (right oral ciliary field), RE – argyrophilic granules remaining after extrusome release. Scale bars 10 µm (x, y) and 30 (u–w).

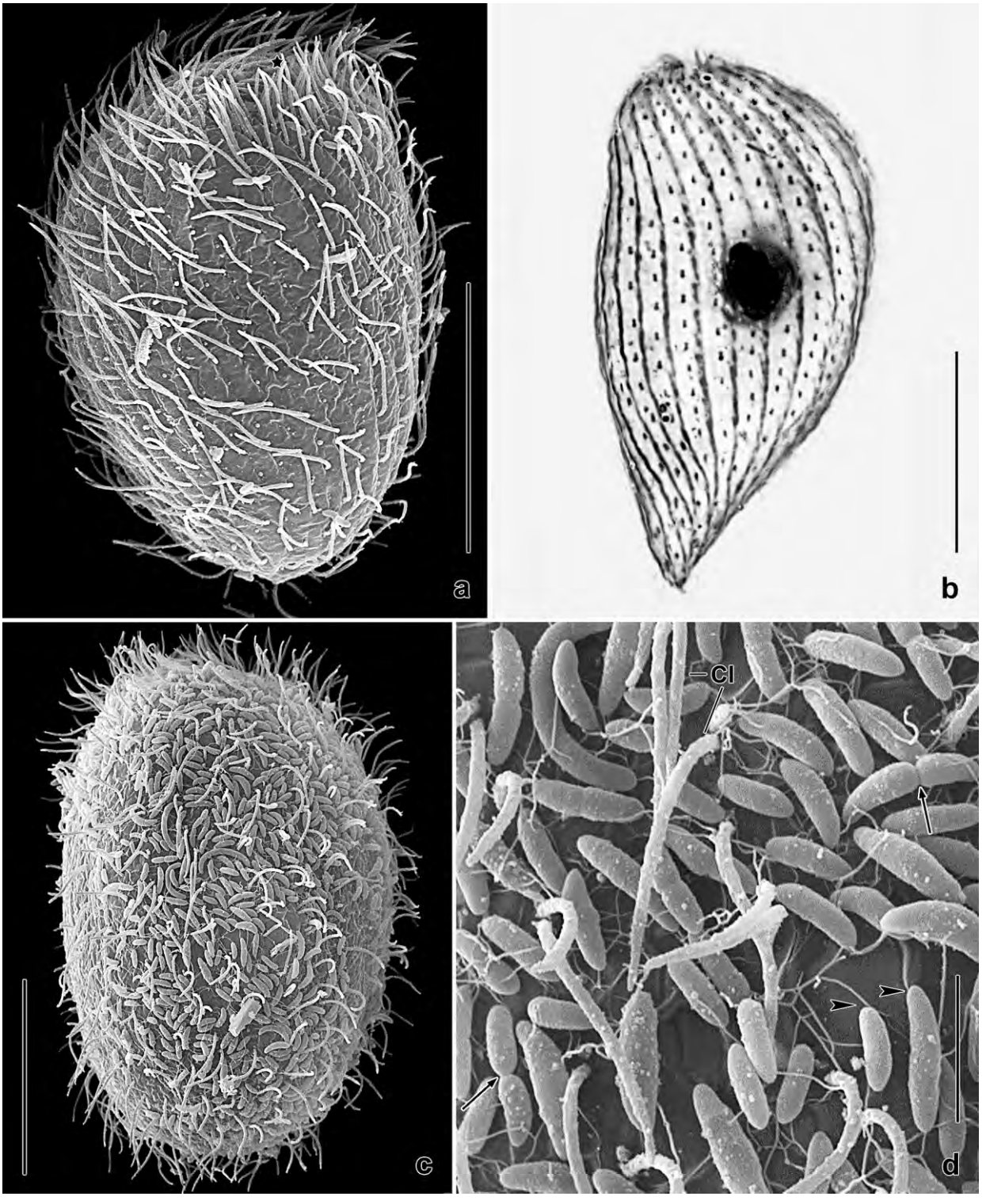

Fig. 139a–d. *Sagittarides oblongistoma* in the scanning electron microscope (a, c, d) and after protargol impregnation (b). **a, b:** Right and left side view, showing the obtriangular body shape and the distinct fibres formed by the transverse microtubule ribbons. The asterisk marks the mouth, which is hardly recognizable because of its polar localization. **c, d:** Many specimens are partially or completely covered with reniform bacteria having long flagella (arrowheads), forming reticulate structures (d). Arrows mark dividing bacteria. CI – ordinary somatic cilia. Scale bars 3 μm (d) and 20 μm (a–c).

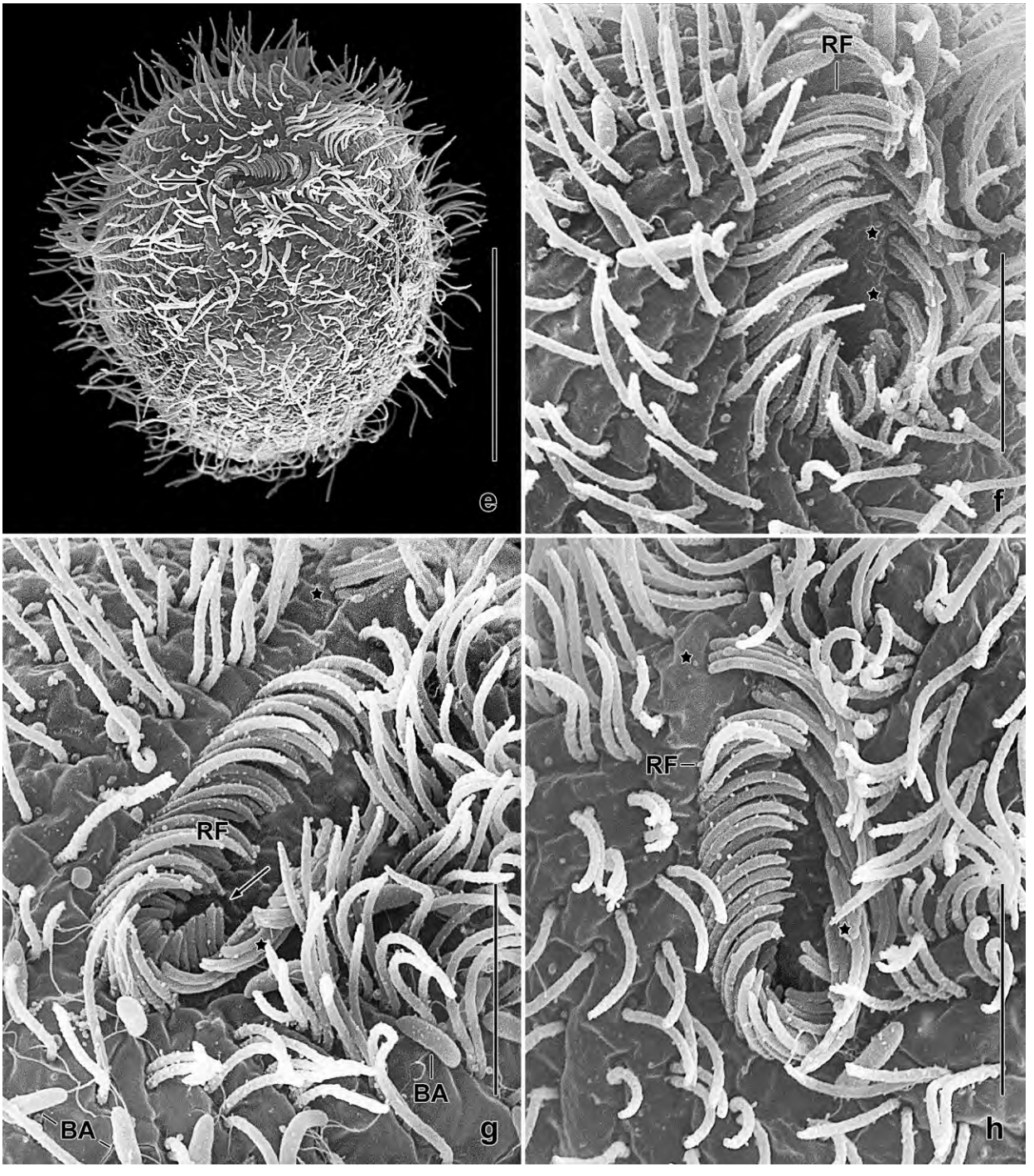

Fig. 139e–h. *Sagittarides oblongistoma* in the scanning electron microscope. **e:** Oblique frontal view, showing the mouth (arrow) oriented transversely to the main body axis. **f:** Oral structures. The asterisks mark two adoral polykinetids, each composed of only four cilia, showing that only part of the polykinetids are ciliated (cp. Fig. 137j). **g, h:** Oral structures. The right oral ciliary field is a dikinetidal, hooked (arrow) row (paroral). The left oral ciliary field consists of brick-shaped, small polykinetids (asterisks), of which the distalmost is in line with (h, anterior asterisk) or right of the anterior end of the right oral ciliary field (g, anterior asterisk). Note the curved and posteriorly directed cilia of the adoral polykinetids (asterisks) and the dense somatic ciliature around the mouth. BA – bacteria, RF – right oral ciliary field. Scale bars 5 μm (f–h) and 20 μm (e).

possibly out of perinuclear space in 24 out of 27 specimens observed (Fig. 137a, 138o; Table 45). Contractile vacuole in posterior body end with single colleting canal extending anteriorly near ventral margin of cell; excretory pores and cytopyge in central pole area (Fig. 137a, 138a, v). Cortex distinctly furrowed by somatic kineties, often covered with bacteria (Fig. 139c, d); ridges studded with granules (extrusomes) about 0.4 µm across (Fig. 137k, 138k). Cytoplasm colourless, specimens, however, may become greenish due to ingested filamentous cyanobacteria (*Oscillatoria* sp.), forming golden food vacuoles up to 15 µm across during digestion; possibly feeds mainly on cyanobacteria (Fig. 137a; but see above). Glides rather rapidly on microscope slides and soil particles, does not build a gelatinous case. Division occurs in freely motile (non-encysted) condition.

Somatic cilia about 10 µm long in vivo. On average 26 slightly spiral ciliary rows all beginning around oral entrance, ventral rows on average with 40% fewer kinetids and slightly more narrowly spaced than dorsal rows; both basal bodies of dikinetids ciliated in anterior third, while anterior basal bodies barren in middle and posterior third; first 5–10 dikinetids of ciliary rows underneath polykinetids more closely spaced, forming a densely ciliated area in left anterior quadrant of cell (Fig 137a, o, p, r, s, 138m, q, r, u–w, 139a, e, g, h; Table 45). Some kineties end subterminally, producing a rather irregular ciliary pattern in posterior pole region; rarely, a distinct ventral suture produced by irregularly shortened midline kineties (Fig. 137q). Long transverse microtubule ribbons originate from posterior basal bodies of dikinetids and extend posteriorly to form conspicuous LKm fibres left of somatic kineties (Fig. 137l, q, 138m, n, q, r, 139b).

Oral opening in a shallow, slightly oblique concavity of anterior body end, commences near ventral body margin and extends dorsally slightly right of main body axis, in or near middle third of anterior body end when viewed ventrally (Fig. 137t), occupies 40–72%, on average 57% of anterior body width; overall appearance rather variable (Fig. 137a–e, g, h, i, m, o, q, r, 138m, p–s, u, y, 139a, e–h; Table 45): elongate elliptic to elliptic in 30 out of 60 protargol-impregnated specimens, very elongate elliptic in 15 specimens, elongate ovate in 12 specimens, and circular in 3 distorted, globular specimens; in 64% out of 14 Chatton-Lwoff silver nitrate-impregnated specimens elongate elliptic to elliptic and in 36% ovate. Right oral ciliary field (paroral membrane) composed of a single row of about 33 dikinetids with curved cilia about 5 µm long in vivo, right portion strongly curved abutting on last adoral polykinetid. Six to nine, on average seven rectangular, obliquely oriented polykinetids (adoral organelles) on left mouth margin, of which 1–3 are anterior of ventral end of paroral membrane often having a perpendicular orientation; individual polykinetids composed of three ciliary rows, rarely of two, each with three basal bodies some of which may be lacking; often 1 or 2 rows of basal bodies barren; cilia curved posteriorly in SEM preparations (Fig. 137a, g, h, i, m, o, q, r, 138m, p–s, u, y, 139e–h; Table 45). Pharyngeal fibres originate from paroral and adoral kinetids, extend posteriorly near right margin of cell, and curve upwards in posterior body third (Fig. 137o, r, t, 138m, q).

Silverline pattern colpodid, i. e., composed of rather wide and regular meshes produced by short, transverse silverlines extending between longitudinal silverlines connecting kinetids of a kinety (Fig. 137f, 138w–y). Silverlines usually studded with extrusomes (Fig. 138y).

Resting cysts globular, on average 28.7 × 27.2 µm in size (M = 28 / 27.5, SD = 2.8 / 2.4, CV = 9.9 / 9, Min = 25 / 25, Max = 35 / 32, n = 9), lightly to deeply orange-coloured, contain many lipid droplets 1–3 µm across. Ectocyst smooth to slightly wrinkled, about 0.5 µm thick. Mesocyst and endocyst 1–2 µm thick, mesocyst coloured as described above, separated from ectocyst by a 3–5 µm wide space containing accumulations of granular excretes (Fig. 137n, 138i, l).

Occurrence and ecology: To date only found at type locality, i. e., in soil from a highly saline

Table 45. Morphometric data on *Sagittarides oblongistoma*. Data based on mounted, silver-impregnated, randomly selected specimens from a non-flooded Petri dish culture. Measurements in µm. CHL – Chatton-Lwoff silver nitrate impregnation, CV – coefficient of variation in %, M – median, Max – maximum, Mean – arithmetic mean, Min – minimum, n – number of specimens investigated, PA – protargol impregnation (FOISSNER's method), using DA FANO'S fluid as a fixative, SD – standard deviation, SE – standard error of mean.

Characteristics	Method	Mean	M	SD	SE	CV	Min	Max	n
Body, length	PA	49.0	50.0	5.3	1.1	10.9	36.0	59.0	23
Body, width	PA	31.0	31.0	3.1	0.7	10.0	26.0	37.0	23
Body length:width, ratio	PA	1.6	1.6	0.2	0.1	13.2	1.1	2.0	23
Anterior body end to macronucleus, distance	PA	19.0	20.0	4.0	0.8	20.5	13.5	26.0	23
Anterior body end to right end of right oral ciliary field, distance	PA	6.2	6.1	1.2	0.3	20.0	4.7	10.0	21
Anterior body end to left end of right oral ciliary field, distance	PA	1.3	1.2	0.5	0.1	38.5	0.0	2.3	21
Anterior body end to right end of left oral polykinetids, distance	PA	5.8	5.5	0.9	0.2	15.6	4.0	8.0	21
Anterior body end to left end of left oral polykinetid, distance	PA	0.3	0.0	–	–	–	0.0	1.6	21
Oral field, length [a]	PA	14.1	14.0	1.6	0.3	11.6	10.0	18.0	23
	CHL	14.6	14.5	1.9	0.5	12.8	12.0	18.0	14
Oral field, widest site	PA	4.0	4.0	1.0	0.2	24.1	3.0	8.0	23
	CHL	5.9	6.0	0.9	0.2	14.8	5.0	8.0	14
Macronucleus, length	PA	12.1	12.0	1.6	0.3	13.6	9.5	15.5	23
Macronucleus, width	PA	9.5	10.0	1.0	0.2	10.4	7.5	11.0	23
Micronucleus, length	PA	2.0	2.0	–	–	–	1.5	2.5	13
Micronucleus, width	PA	1.5	1.5	–	–	–	1.0	2.0	13
Right oral ciliary field, length [b]	PA	14.7	14.0	–	–	–	12.5	18.0	23
Left oral polykinetids, total length	PA	10.6	10.5	1.9	0.4	18.3	7.0	15.0	23
Dikinetids in right oral ciliary field, number	PA	33.5	33.0	2.4	0.6	7.2	28.0	38.0	19
Adoral organelles (polykinetids), number	PA	7.4	7.0	0.7	0.1	9.8	6.0	9.0	23
	CHL	6.6	7.0	0.7	0.2	11.2	5.0	8.0	14
Somatic kineties, number	PA	26.1	26.0	1.4	0.3	5.3	23.0	28.0	23
Dikinetids in a ventral kinety, number [c]	PA	17.7	18.0	2.4	0.5	13.5	13.0	22.0	21
Dikinetids in a midline dorsal kinety, number	PA	25.5	26.0	2.7	0.6	10.5	21.0	29.0	21

[a] Distance from right margin of curve of right oral ciliary field to leftmost adoral polykinetid.

[b] Distance from left end to curve of right ciliary field plus distance from curve to rightmost polykinetid; approximations.

[c] Kinety commencing between right end of paroral membrane and begin of adoral polykinetids.

(about 50‰), abandoned field on the north coast of Venezuela.

Remarks: See FOISSNER (1993a) and FOISSNER et al. (2002) for detailed descriptions of the families, genera and species mentioned in the following discussion.

A near relative of *Sagittarides oblongistoma* is apparently *Sagittaria australis* because it has the same location of the oral apparatus and does not build a gelatinous case present in *S. poligonalis* and *S. hyalina*. This is supported by the molecular data (Fig. 124). However, *S. australis* has a broadly elliptic oral field and a different body shape (usually bursiform vs. obtriangular), and the adoral polykinetids do not extend beyond the right oral ciliary field. Further, *S. oblongistoma* is about twice as large as *S. australis*, and thus the number of ciliary rows is also higher (on average 22 vs. 26).

In vivo, *Sagittarides oblongistoma* may be confused with *Etoschophrya oscillatoriophaga* FOISSNER, AGATHA & BERGER, 2002, which has a similar size and shape, also lives in highly saline soils, and feeds on filamentous cyanobacteria. However, the oral apparatus of *E. oscillatoriophaga* is in the left anterior quadrant of the cell, while it is in the middle third of the anterior body end in *S. oblongistoma*. Further, *S. oblongistoma* has a colpodid silverline pattern that differentiates it not only from *E. oscillatoriophaga* (right side of body with platyophryid, left side with kreyellid silverline pattern) but also from other members of the family Woodruffiidae, like *Rostrophryides* spp. and *Kuklikophrya* spp., which resemble *S. oblongistoma* in vivo but have a platyophryid silverline pattern and, in case of *Rostrophryides* spp. a postoral pseudomembrane. On the other hand, *Woodruffia* spp. have a colpodid silverline pattern like *S. oblongistoma* but the ventral position of the oral apparatus is quite different.

Mancothrix nov. gen.

Diagnosis: Small Platyophryidae without postoral pseudomembrane. Silverline pattern platyophryid. Adoral polykinetids minute, rhomboid.

Type species: *Mancothrix pelobia* nov. spec.

Etymology: Composite of the Latin adjective *mancus* (incomplete) and the Greek noun *thrix* (hair ~ ciliate), referring to the absence of a postoral pseudomembrane. Feminine gender.

Remarks: We compiled the most similar genera in Table 46. This shows that *Mancothrix* is highly similar to *Platyophrya* and *Rostrophryides* except for the lack of a postoral pseudomembrane which we consider as a generic feature.

Mancothrix pelobia nov. spec. (Fig. 140a–d, f–i, 141a–h; Table 47)

Diagnosis: Size in vivo about 45 × 15 µm. Elongate ovate with oblique and slightly curved anterior end containing the oral apparatus. 1 macronucleus and 1 micronucleus. 9–10 ciliary rows, those of left side sparsely ciliated. Oral apparatus platyophryid, 4–5 minute adoral polykinetids.

Type locality: Venezuelan site (21), i. e., mud from lithotelmas of the Cataniapo River, 67°36’W 5°36’N.

Type material: 1 holotype and 1 paratype slide with protargol-impregnated specimens and 1 slide with CHATTON-LWOFF silver nitrate-prepared cells have been deposited in the Biology Centre of the Upper Austrian Museum in Linz (LI). Relevant specimens have been marked by black ink circles on the coverslip.

Etymology: The Latinized adjective *pelobia* (living in mud) refers to the habitat the species was discovered.

Description: All preparations were made on the same day, i.e., the soil eluate was split: one half was used for protargol impregnation, the other for silver nitrate preparations. Thus, it can be excluded that different species were investigated (see oral apparatus).

Size in vivo 35–55 × 12–20 µm, usually about 45 × 15 µm, as calculated from some in vivo measurements and the morphometric data adding 15% and 5% shrinkage for the protargol and silver nitrate preparations, respectively (Table 47). Data from both preparation methods fairly similar, except for body width which is distinctly smaller (12.1 µm) in silver nitrate than protargol preparations (17.4 µm) where specimens are likely slightly inflated (Table 47). Body typically platyophryid, i. e., elongate ovate or reniform and occasionally slightly curved, oral apparatus at oblique anterior end, laterally flattened up to 2:1 (Fig. 140a–d, f–i, 141a, b, e–h). Nuclear apparatus in mid-body on average, macronucleus globular, micronucleus ellipsoid and likely in perinuclear space of macronucleus. (Fig. 140a, c, 141e–h; Table 47). Contractile vacuole

Table 47. Morphometric data on *Mancothrix pelobia* based, if not mentioned otherwise, on mounted, protargol-impregnated, and randomly selected specimens from a non-flooded Petri dish culture. Measurements in µm. CV – coefficient of variation in %, M – median, Max – maximum, Mean – arithmetic mean,Min – minimum, n – number of individuals investigated, SD – standard deviation, SE – standard error of arithmetic mean.

Characteristics	Mean	M	SD	SE	CV	Min	Max	n
Body, length (protargol)	39.9	39.0	3.7	0.9	9.3	33.0	47.0	17
Body, width (protargol)	15.1	15.0	1.8	0.4	11.7	12.0	18.0	17
Body length:width, ratio (protargol)	2.7	2.7	0.3	0.1	12.0	2.1	3.6	17
Body, length (Chatton-Lwoff silver nitrate)	41.0	40.0	3.1	0.9	7.5	35.0	45.0	11
Body, width (Chatton-Lwoff silver nitrate)	12.1	12.0	1.6	0.5	13.6	10.0	15.0	11
Body length:width, ratio (silver nitrate)	3.5	3.5	0.4	0.1	12.0	2.9	4.0	11
Anterior body end to macronucleus, distance	19.8	20.0	2.9	0.7	14.4	16.0	24.0	17
Macronucleus, length	7.4	7.0	0.9	0.2	12.7	6.0	9.0	17
Macronucleus, width	7.2	7.0	0.9	0.2	12.3	6.0	9.0	17
Micronucleus, length	2.5	2.5	–	–	–	2.0	3.0	6
Micronucleus, width	1.5	1.5	–	–	–	1.0	2.0	6
Ciliary rows, number in mid-body	9.7	10.0	–	–	–	9.0	10.0	17
Dikinetids in a right side kinety, number	23.9	23.0	3.8	0.9	15.9	18.0	35.0	17
Dikinetids in a left side kinety, number	13.0	12.0	2.0	0.5	15.6	10.0	18.0	17
Anterior body end to end of mouth, distance	4.9	5.0	–	–	–	4.0	5.0	17
Oral opening, length	4.3	4.0	0.5	0.1	10.9	3.5	5.0	17
Oral opening, width	3.2	3.0	–	–	–	3.0	4.0	17

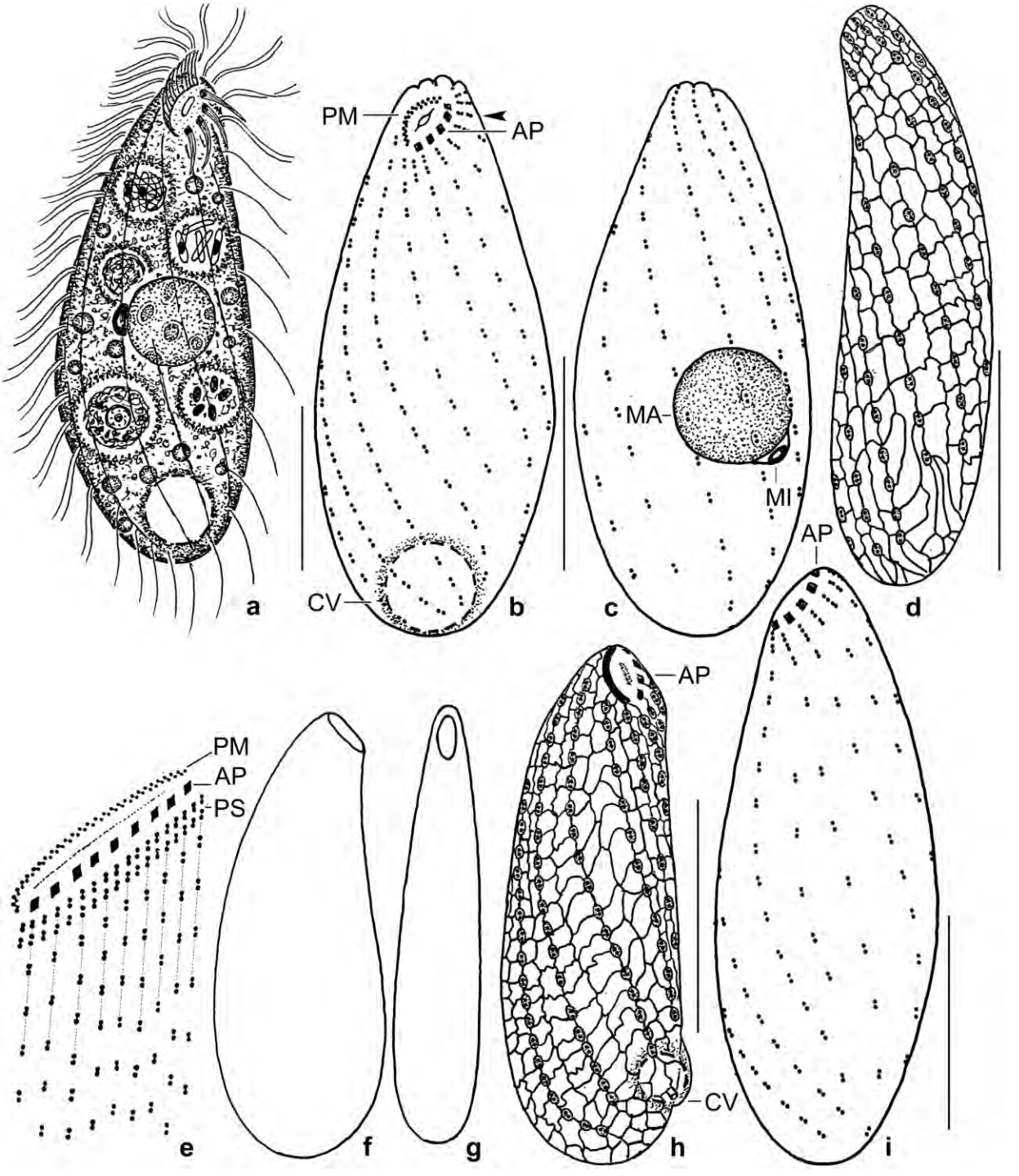

Fig. 140a–i. *Mancothrix pelobia* (a–d, f–i) and scheme of a postoral pseudomembrane (e; from Foissner et al. 2002) from life (a, f, g) and after protargol (b, c, e, i) and silver nitrate impregnation (d, h). **a:** Ventral view of a representative specimen, length 45 µm. **b, c:** Ventral and dorsal view of holotype specimen, 40 µm. Arrowhead marks a postoral condensation of two dikinetids. **d, h:** Platyophryid silverline pattern in left and right side cortex. **e:** Short, extra kineties build a "postoral pseudomembrane". **f, g:** Right side and ventral view of same specimen. **i:** The left side is more loosely ciliated than the right. AP – adoral polykinetids, CV – contractile vacuole, MA – macronucleus, MI – micronucleus, PM – paroral membrane, PS – postoral pseudomembrane. Scale bars 15 µm.

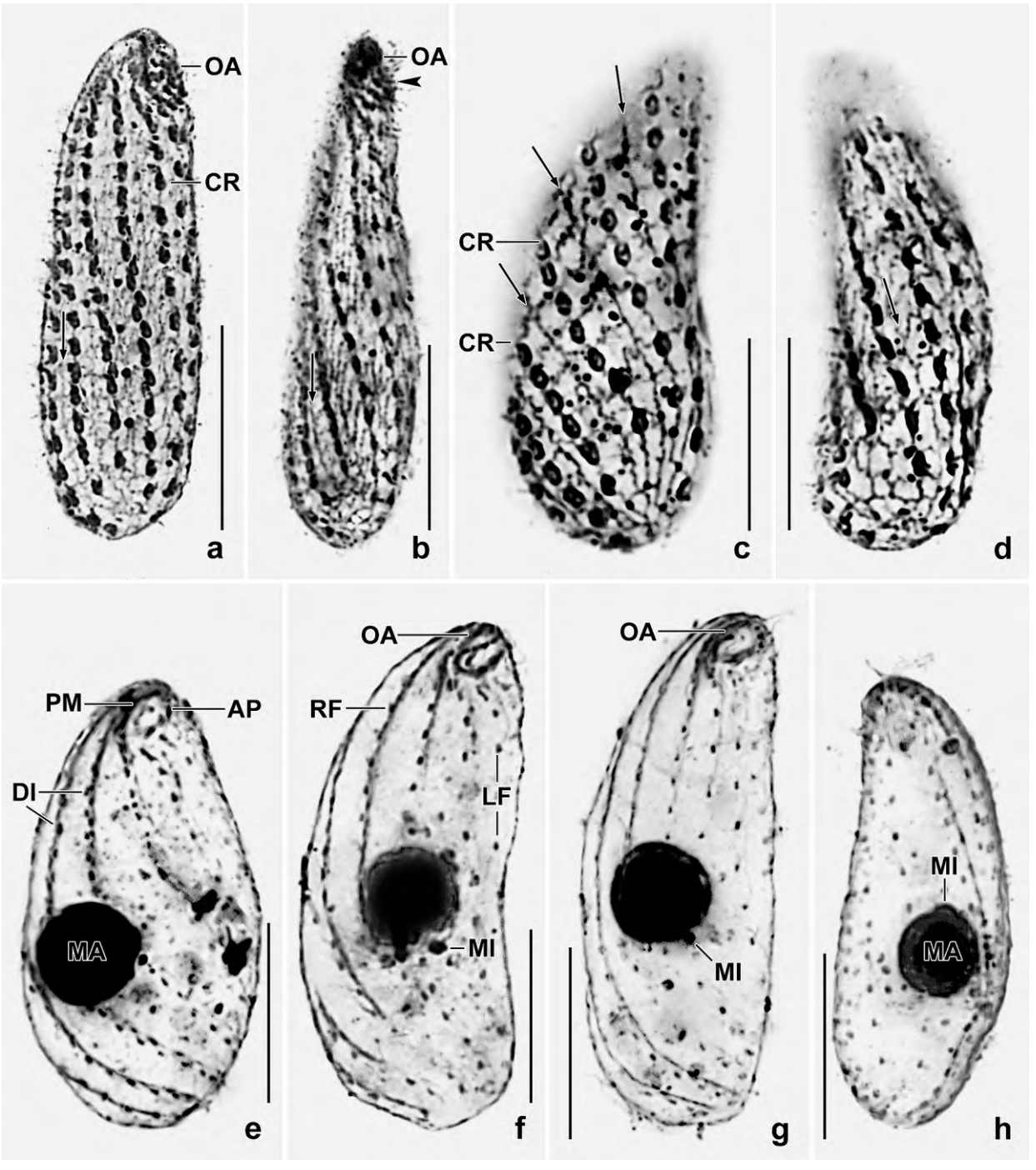

Fig. 141a–h. *Mancothrix pelobia* in Chatton-Lwoff silver nitrate preparations (a–d) and after protargol impregnation (e–h). The arrows in (a–d) mark semimedian silverlines which produce the platyophryid silverline pattern by dividing the quadrangular colpodid pattern (Foissner 1993a). **a:** Right side overview. **b:** Ventral view, showing the lateral flattening and a condensation of two postoral dikinetids (arrowhead). **c, d:** Right and left side view, showing that both sides have a platyophryid silverline pattern with semimedian silverlines marked by arrows (cp. Table 46). **e–g:** Ventral views, showing the somatic and oral ciliary pattern and the nuclear apparatus. The left side is more loosely ciliated than the right. **h:** Left side view, showing the sparse ciliature. AP – adoral polykinetids, CR – ciliary rows, DI – dikinetids, LF – left side ciliature, MA – macronucleus, MI – micronucleus, OA – oral apparatus, PM – paroral membrane, RF – right side ciliature. Scale bars 15 µm.

subterminal, approaches ventral side (Fig. 140a, b, h). Cortex very flexible, slightly furrowed by ciliary rows; cortical granules (extrusomes) not studied in vivo, possibly absent because not recognizable in the preparations. Cytoplasm colourless, contains few to rather many lipid droplets and food vacuoles up to 10 µm across (Fig. 140a). Feeds on spore-forming bacteria, heterotrophic flagellates, and naked amoebae. Usually glides on mud accumulations, showing great flexibility; swims slowly rotating about main body axis.

Somatic cilia in vivo about 8 µm long, arranged in nine or ten ordinarily spaced rows extending slightly spirally from oral apparatus to posterior body end. Right side rows densely ciliated with an average of 24 dikinetids, left side rows sparsely ciliated because composed of only 13 dikinetids most lacking the anterior cilium (Fig. 140a–d, h, i, 141a–h; Table 47). Left side rows commence close posterior of adoral polykinetids with two narrowly spaced, ciliated dikinetids but do not form a postoral pseudomembrane (Fig. 140b, i, 141b, e) shown in Figure 140e.

Silverline pattern platyophryid throughout, irregulary reticulate in posterior pole area (Fig. 140d, h, 141a–d).

Oral apparatus in oblique anterior end, composed of a curved, dikinetal paroral membrane and four to five minute, rhomboid adoral polykinetids (Fig. 140a, b, f–i, 141a,b, e–g; Table 47). Cytopharyngeal rods inconspicuous, extend to dorsal side of cell. Orientation of oral opening as in *Platyophrya* as shown by a plasticine model, i. e., obliquely extending from left to right (Fig. 140f, h); most specimens, however, ventrolaterally oriented in the preparations making the oral pattern rostrophryid, i. e., extending slightly obliquely from left to right (Fig. 141e–g).

Occurrence and ecology: As yet found only at type locality, i. e., highly fertile Mahadja soil. The abundance was low in the non-flooded Petri dish culture.

Remarks: This small, highly flexible ciliate is easily confused with the genera mentioned in Table 46. However, the absence of a postoral pseudomembrane can be recognized with interference contrast and some experience. Identifications should be checked in protargol or silver carbonate preparations.

Platyophrya bromelicola Foissner & Wolf, 2009 (Fig. 142a–n)

Material: Cultivated populations from tank bromeliads of Rio de Janeiro (cyst) and Jamaica (live, morphostatic specimens).

Remarks: *Platyophrya bromelicola* is probably confined to tank bromeliads and unique in making microstomes and macrostomes. Foissner & Wolf (2009b) could not induce cyst formation. Later, we were successful in a pure culture where resting cysts were readily produced, most in small heaps with 50–200 specimens (Fig. 142j). Further, Foissner & Wolf (2009b) did not show in vivo micrographs of the unique, bluntly clavate body (Fig. 142a–i).

The resting cysts are spherical with an average diameter of 17 µm (M = 17.0, SD = 0.5, CV = 13.2, Min = 14, Max = 21, n = 18). The cyst wall is structureless, smooth, colourless, and 0.6–1

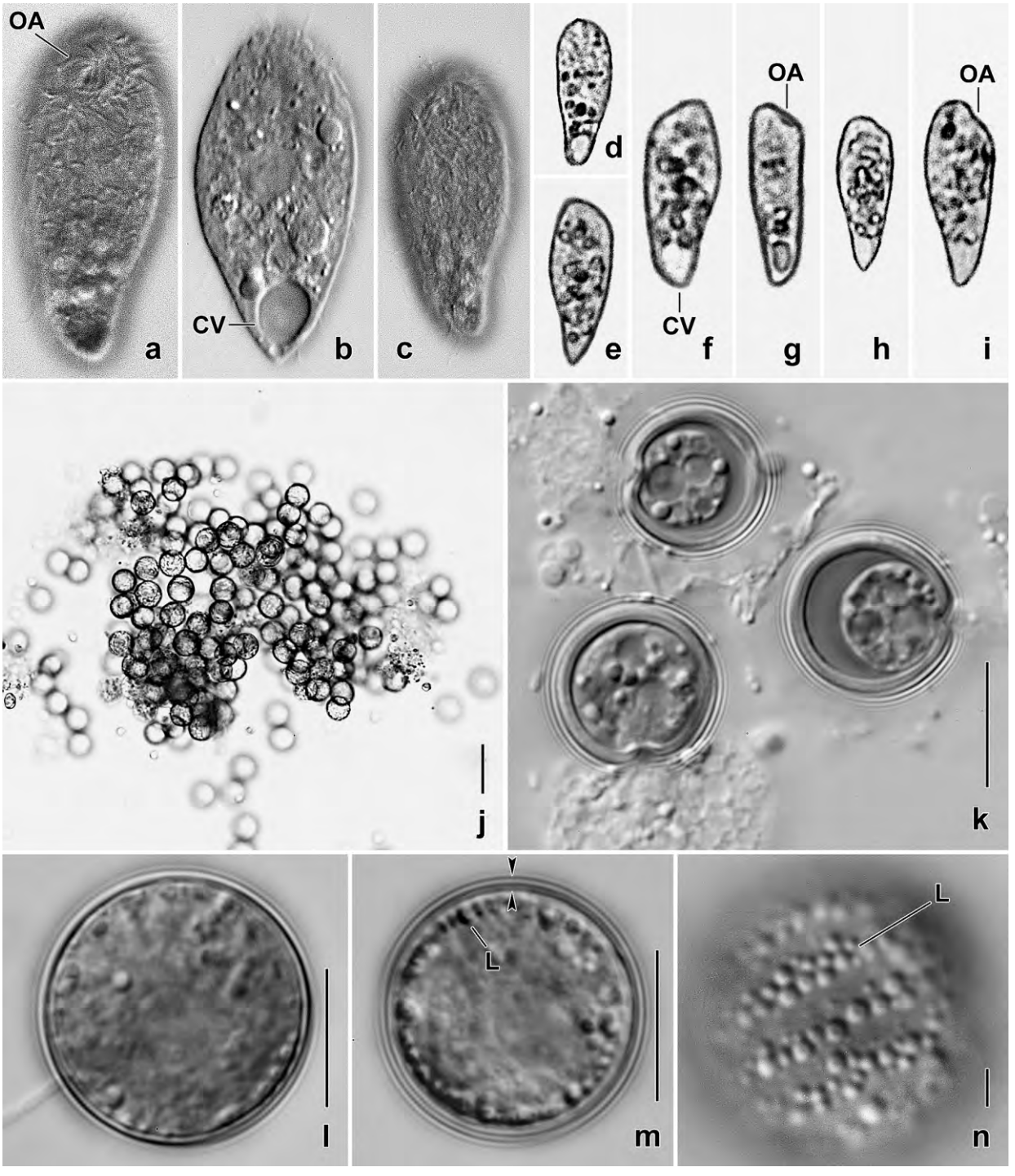

Fig. 142a–n. *Platyophrya bromelicola* from life. **a–i:** Body shape variability, length 30–70 µm. Typically, *P. bromelicola* is bluntly clavate (a, c–f, h, i) and has a subapical oral opening (a, g, i). **j:** A cyst heap on bottom of Petri dish. **k:** When the cyst contents is pressed out, the wall becomes thicker**. l, m:** Optical sections with wall limited by arrowheads (m)**. n:** In the cytoplasm and subcortically are rows of lipid (?) droplets (L). CV – contractile vacuole, L – lipid droplets, OA – oral apparatus. Scale bars 4 µm (n), 10 µm (k–m), and 40 µm (j).

µm thick (Fig. 142l, m). When the contents is pressed out, the cyst diameter decreases and the wall becomes 2–3 µm thick (Fig. 142k). Within the cyst are scattered lipid (?) droplets 0.5–2 µm across, which produce conspicuous rows subcortically (Fig. 142n). The cyst centre is occupied by the nuclear apparatus. To sum up, the resting cyst of *P. bromelicola* is highly similar to that of the common *P. spumacola* described by Foissner (1993a).

***Platyophryides macrostoma* nov. spec.** (Fig. 124, 143a–j, 144a–y, 145a–m; Table 48)

Diagnosis: Size in vivo about 120 × 80 × 50 µm. Bursiform to broadly bursiform with oral portion usually curved ventrally; right side flattened. 1 broadly ellipsoid macronucleus and 1 micronucleus. Excretory pore of contractile vacuole subterminal in midline of right body side. On average 38 slightly spiral ciliary rows, those on right side closer together and more densely ciliated than those on left side. Oral apparatus in anterior body end, oral field narrowly oblong, paroral membrane about 35 µm long, composed of dikinetids having ciliated only the left basal body. On average 6 adoral polykinetids each about 3 µm long and composed of 2 rows of basal bodies of which only the right row is ciliated.

Type locality: In mud of bamboo stumps from the Bamboo Avenue west of the town of Lacovia, Jamaica, 77°49'W 18°05'N.

Type material: 1 holotype and 4 paratype slides with protargol-impregnated specimens and 4 slides with Chatton-Lwoff silver nitrate-prepared cells have been deposited in the Biology Centre of the Upper Austrian Museum in Linz (LI). The holotype and relevant paratype specimens have been marked by black ink circles on the coverslip.

Etymology: *macrostoma* (large-mouthed) is an apposite noun composed of the Greek adjective *makrós* (large) and the Greek noun *to stóma* (mouth), referring to the large mouth.

Description: Specimens cultivated on *Tetrahymena mobilis* were used for all investigations. The morphometry is based on silver nitrate-impregnated specimens because good protargol preparations were obtained only with ethanol-fixed and thus rather strongly shrunken (~ 20%) specimens. However, we choose as holotype a protargol preparation because it shows the oral details better than the silver nitrate-impregnated specimens.

Size in vivo 85–150 × 50–100 µm, usually about 120 × 80 µm, as calculated from data in Table 48 adding 5% preparation shrinkage. Shape bursiform, oral portion about half of maximum body width and slightly to distinctly curved ventrally, producing a more or less oblique anterior end (Fig. 143a, 144a, b, d, f–i, x, y, 145k–m; Table 48). Right side flat to slightly convex, left side slightly to strongly convex depending on amount of food ingested (Fig. 144c, e). Nuclear apparatus in or near body centre on average. Macronucleus broadly ellipsoid, nucleolus reticulate. Micronucleus attached to macronucleus, broadly ellipsoid (Fig. 143a, g, 144j, l, u, 145a, e; Table 48). Contractile vacuole and excretory pore subterminal slightly left of body´s midline, with short canal extending anteriorly (Fig. 143a, 144c, f, h). Cytopyge posterior to contractile vacuole (Fig. 144a, h). Cortex very flexible, contains countless minute, protargol-affine granules (extrusomes?)

along ciliary rows of right side and in silverline pattern in left side (Fig. 145n, o). Cytoplasm densely granulated, contains small lipid droplets and up to 10 food vacuoles with *Tetrahymena* (Fig. 143a, c, 144x, y, 145k–m). Feeds also on middle-sized hypotrichs, heliozoans, and becomes cannibalistic in old cultures. Glides and swims comparatively slowly but never rests, usually gliding in and on mud accumulations, showing great flexibility.

Cilia about 10 µm long in vivo, arranged in an average of 38 ordinarily spaced, slightly spiral, bipolar rows narrower spaced and denser ciliated in right than left side of body; ordinarily spaced, except of densely ciliated oral portion both in right and left side; paired in right side, anterior cilium lacking in about half of dikinetids of left side; dikinetids obliquely arranged in trunk area; some ciliary rows more or less shortened anteriorly and/or posteriorly, especially in excretory pore area (Fig. 143a, g, h, 144a, b, d, e–l; Table 48). Silverline pattern colpodid throughout (Fig. 143i, 144v).

Oral apparatus in oblique, usually slightly concave anterior body end (Fig. 143a, c, d, g, j, 144a, d, e, f, h–j, l, o–t, w, 145a; Table 48). Oral field and oral opening very elongate oblong (Fig. 143d, j, 144e, t). Right margin of oral field occupied by a paroral membrane composed of about 75 oblique dikinetids of which only the inner (left) basal body is ciliated (see ontogenesis). Left margin of oral field occupied by an average of six adoral polykinetids each about 3 µm long and composed of two ciliary rows, of which only the inner (right) row is ciliated; length of cilia gradually increases from dorsal to ventral (Fig. 143a, c, d, g, j, 144h, j, l, o–q, t, 145a; Table

Table 48. Morphometric data on *Platyophryides macrostoma* based, if not mentioned otherwise, on cultivated, CHATTON-LWOFF silver nitrate-impregnated and randomly selected specimens. Measurements in µm. CV – coefficient of variation in %, M – median, Max – maximum, Mean – arithmetic mean, Min – minimum, n – number of individuals investigated, SD – standard deviation, SE – standard error of arithmetic mean.

Characteristics	Mean	M	SD	SE	CV	Min	Max	n
Body, length	110.7	108.0	16.3	3.7	14.7	82.0	140.0	19
Body, oral width	43.2	43.0	6.1	1.4	14.1	32.0	57.0	19
Body, maximum postoral width	75.7	78.0	13.3	3.0	17.6	48.0	96.0	19
Body length:maximal width, ratio	1.5	1.4	0.2	0.1	14.9	1.2	2.0	19
Anterior body end to macronucleus, distance	53.8	55.0	15.9	3.6	29.5	20.0	80.0	19
Macronucleus, length	24.7	25.0	3.1	0.7	12.6	20.0	33.0	19
Macronucleus, width	18.9	18.0	2.5	0.6	13.1	15.0	24.0	19
Somatic ciliary rows, number	38.0	38.5	4.0	0.7	10.6	30.0	46.0	30
Right side kineties, distance in between in mid-body	4.6	5.0	–	–	–	4.0	5.0	19
Left side kineties, distance in between in mid-body	6.4	6.0	0.7	0.2	10.7	5.0	8.0	19
Right side kineties, number of dikinetids in a median row	61.8	58.0	14.1	3.2	22.8	38.0	95.0	19
Left side kineties, number of dikinetids in a median row	44.5	45.0	8.2	1.9	18.5	32.0	67.0	19
Paroral membrane, length of straight portion	33.7	33.0	4.5	1.0	13.5	27.0	42.0	19
Adoral polykinetids, number	6.0	6.0	1.4	0.2	23.2	4.0	9.0	32
Adoral polykinetids, length of third polykinetid	2.9	3.0	0.6	0.1	19.2	2.0	4.0	17
Resting cysts, diameter in vivo	41.6	40.0	5.1	1.2	12.2	32.0	50.0	19

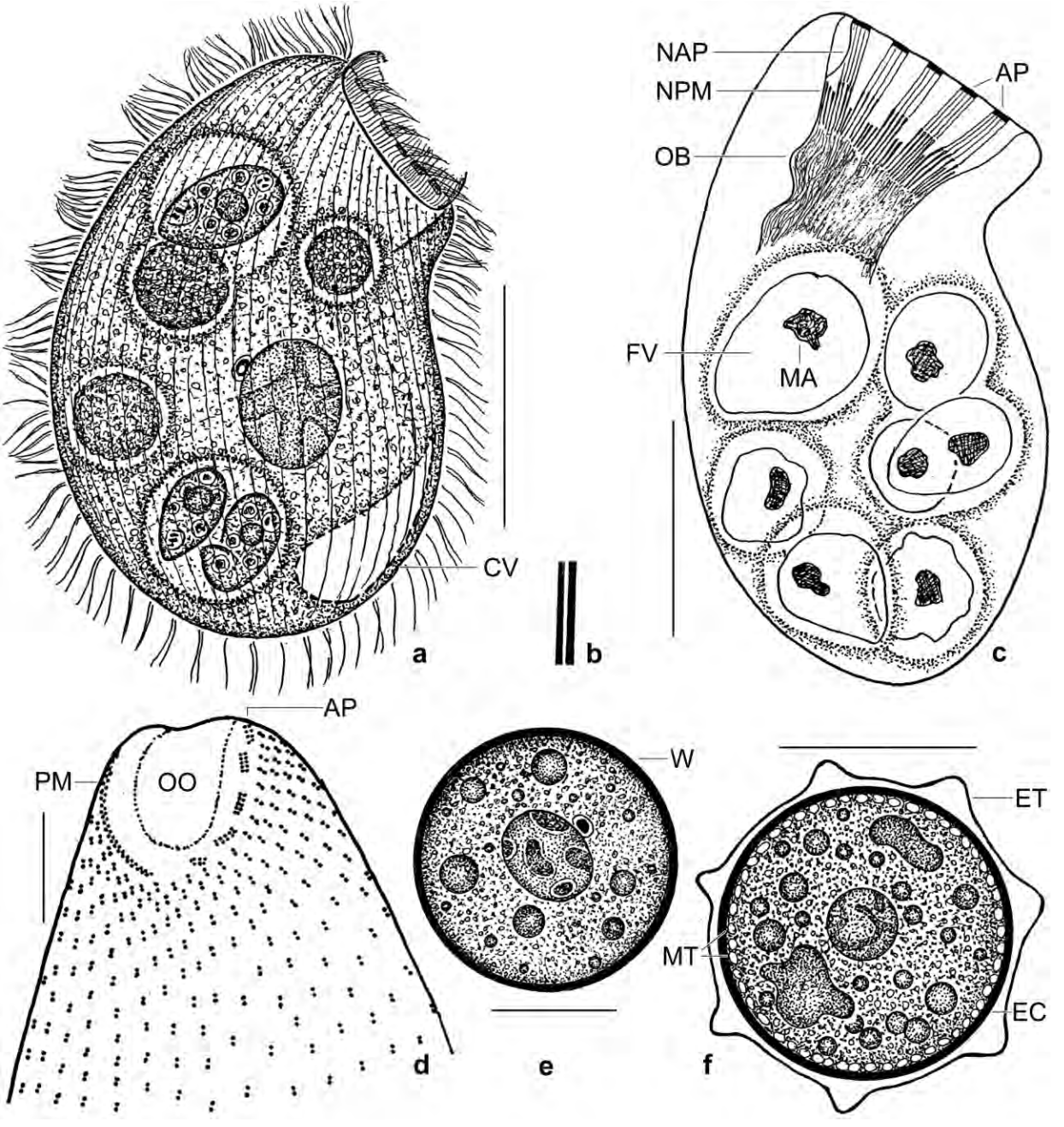

Fig. 143a–f. *Platyophryides macrostoma* (a–e) and → *P. latus* (f) from life (a, b, e, f) and after protargol impregnation (c, d). **a:** Right side view of a representative specimen fed on *Tetrahymena*, length 120 µm. **b:** Resting cyst wall, about 1.2 µm thick. **c:** Internal structures of holotype specimen having ingested seven Tetrahymenas, length 102 µm. For the ciliary pattern, see next plate. **d:** Ventral view of oral region, showing the dikinetal paroral membrane and the adoral polykinetids, which are composed of two rows of basal bodies. **e:** Resting cyst, 45 µm. The wall is smooth and composed of two layers (b) **f:** The cyst wall of → *P. latus* consists of a polygonally faceted ectocyst and a thin, smooth endocyst, diameter 35 µm. The cytoplasm contains many globular and large, irregular lipid inclusions. AP – adoral polykinetids, CV – contractile vacuole, EC – endocyst, ET – ectocyst, FV – food vacuole, MA – macronucleus, MT – mitochondria, NAP – nematodesmata of adoral polykinetids, NPM – nematodesmata of paroral dikinetids, OB – oral basket, OO – oral opening, PM – paroral membrane, W – cyst wall. Scale bars 10 µm (d), 20 µm (e, f), 30 µm (c), and 50 µm (a).

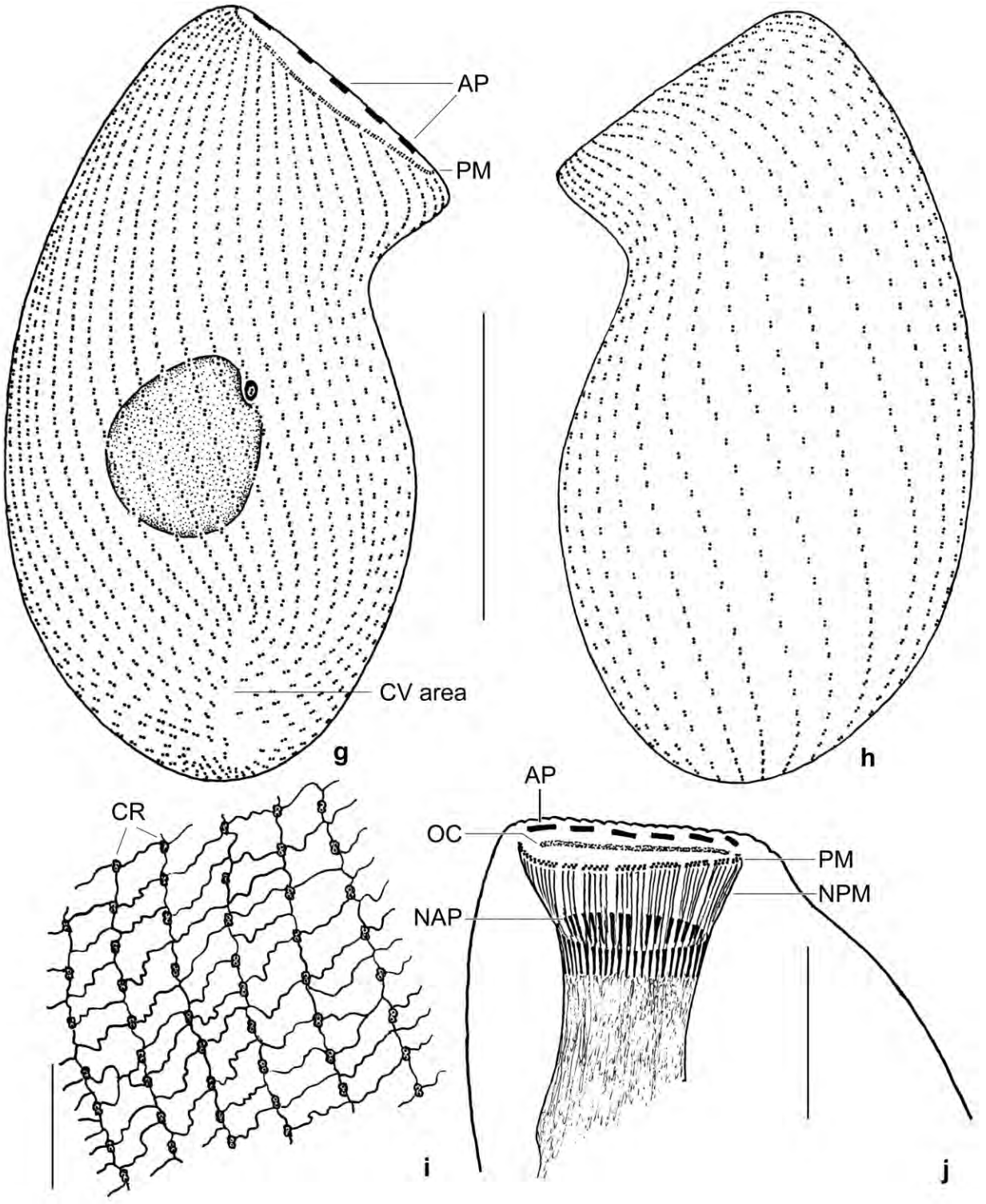

Fig. 143g–j. *Platyophryides macrostoma* after protargol (g, h, j) and CHATTON-LWOFF silver nitrate (i) impregnation. **g, h:** Right and left side view of holotype, length 102 µm. The excretory pore of the contractile vacuole is not impregnated. **i:** Colpodid silverline pattern. **j:** Oral apparatus. AP – adoral polykinetids, CR – ciliary rows, CV – contractile vacuole, NAP, NPM – nematodesmata of adoral polykinetids and of paroral dikinetids, OC – oral cleft, PM – paroral membrane. Scale bars 10 µm (i), 20 µm (j), and 40 µm (g, h).

Fig. 144a–e. *Platyophryides macrostoma* from life (c) and in the scanning electron microscope. **a, b:** Right and left side view of broad specimens. The right side is more densely ciliated than the left. A fecal mass is just leaving the cell (a). **c:** Lateral view, showing flattening of right side. **d:** Right side view of a slender specimen. **e:** Ventral view, showing the convex left side. CV – contractile vacuole, CY – cytopyge, OO – oral opening. Scale bars 40 µm.

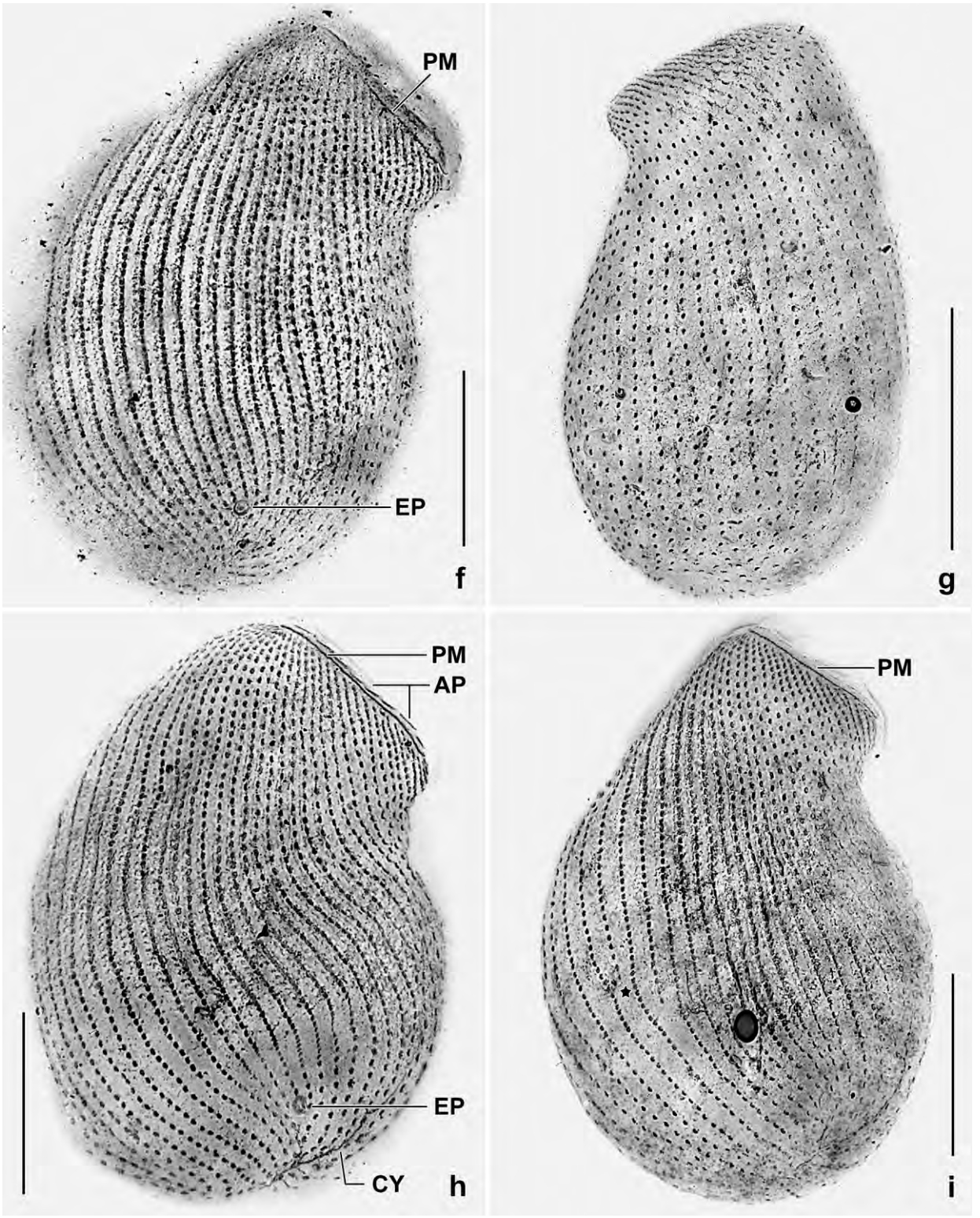

Fig. 144f–i. *Platyophryides macrostoma,* ciliary pattern after CHATTON-LWOFF silver nitrate impregnation. **f, h, i:** Right side views. Asterisk (i) marks a shortened kinety. **g:** Left side view. AP – adoral polykinetids, CY – cytopyge. EP – excretory pore of contractile vacuole, PM – paroral membrane. Scale bars 40 μm.

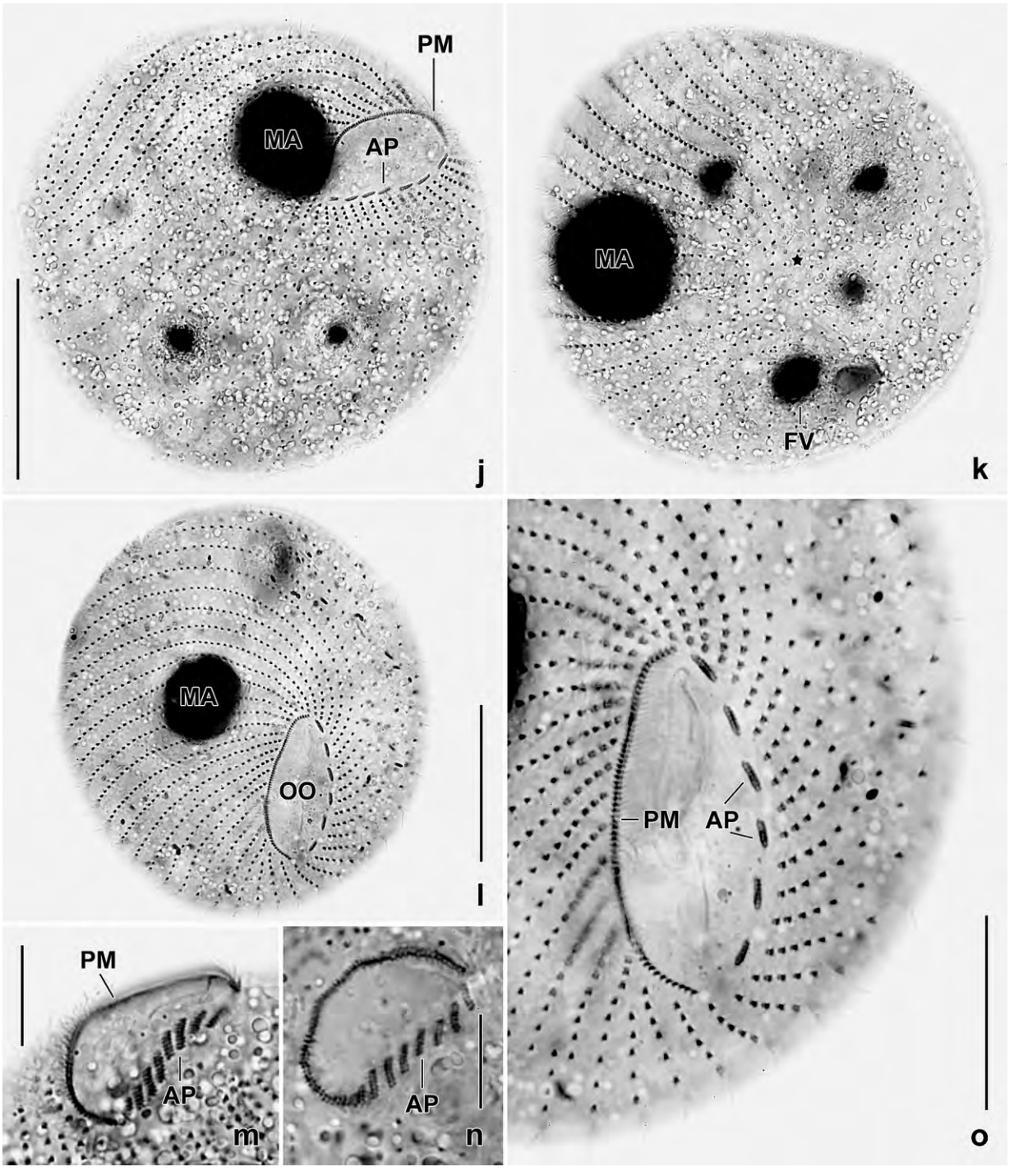

Fig. 144j–o. *Platyophryides macrostoma*, somatic and oral ciliary pattern after silver carbonate impregnation. **j, k:** Oblique anterior and posterior polar view of same specimen, showing the sparse ciliation in the posterior pole area (asterisk) and in the left side kineties. The food vacuole contains a just ingested *Tetrahymena* whose mouth and macronucleus are recognizable. **l, o:** Anterior polar view, overview and oral detail. The ciliature is condensed around the mouth opening and the adoral polykinetids are composed of two rows of basal bodies. **m, n:** Opisthe and proter mid-dividers have the adoral polykinetids obliquely oriented and composed of three rows of basal bodies. AP – adoral polykinetids, FV – food vacuoles, MA – macronucleus, OO – oral opening, PM – paroral membrane. Scale bars 10 µm (m, n), 20 µm (o), and 40 µm (j–l).

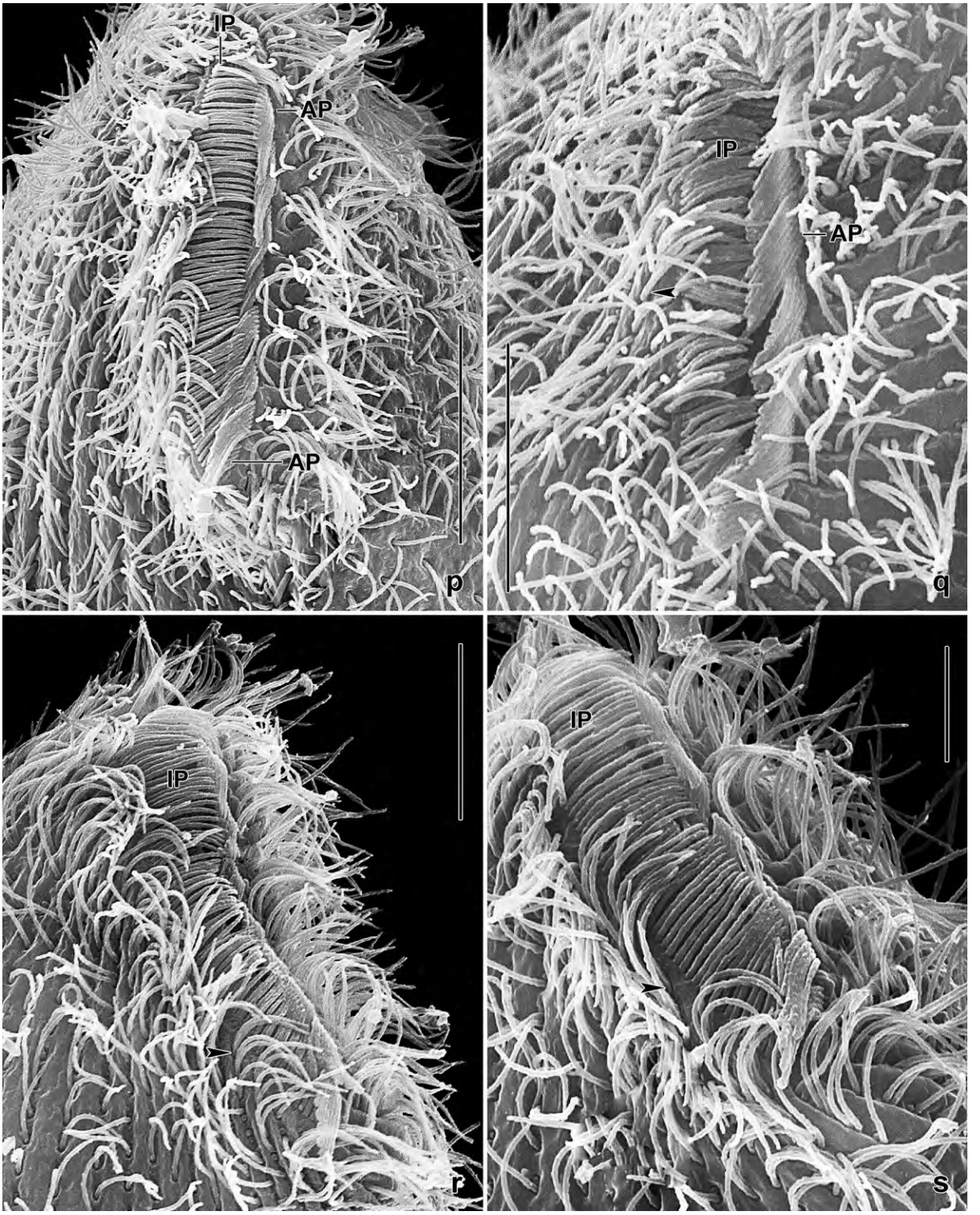

Fig. 144p–s. *Platyophryides macrostoma*, oral ciliature in the SEM. Arrowheads mark anterior end of ciliary rows. Figure 144q is from a late post-divider with short (5 µm vs. 10 µm) and slightly disordered paroral cilia. AP – adoral polykinetids, IP – internal paroral membrane (see ontogenesis). Scale bars 10 µm (r, s) and 15 µm (p, q).

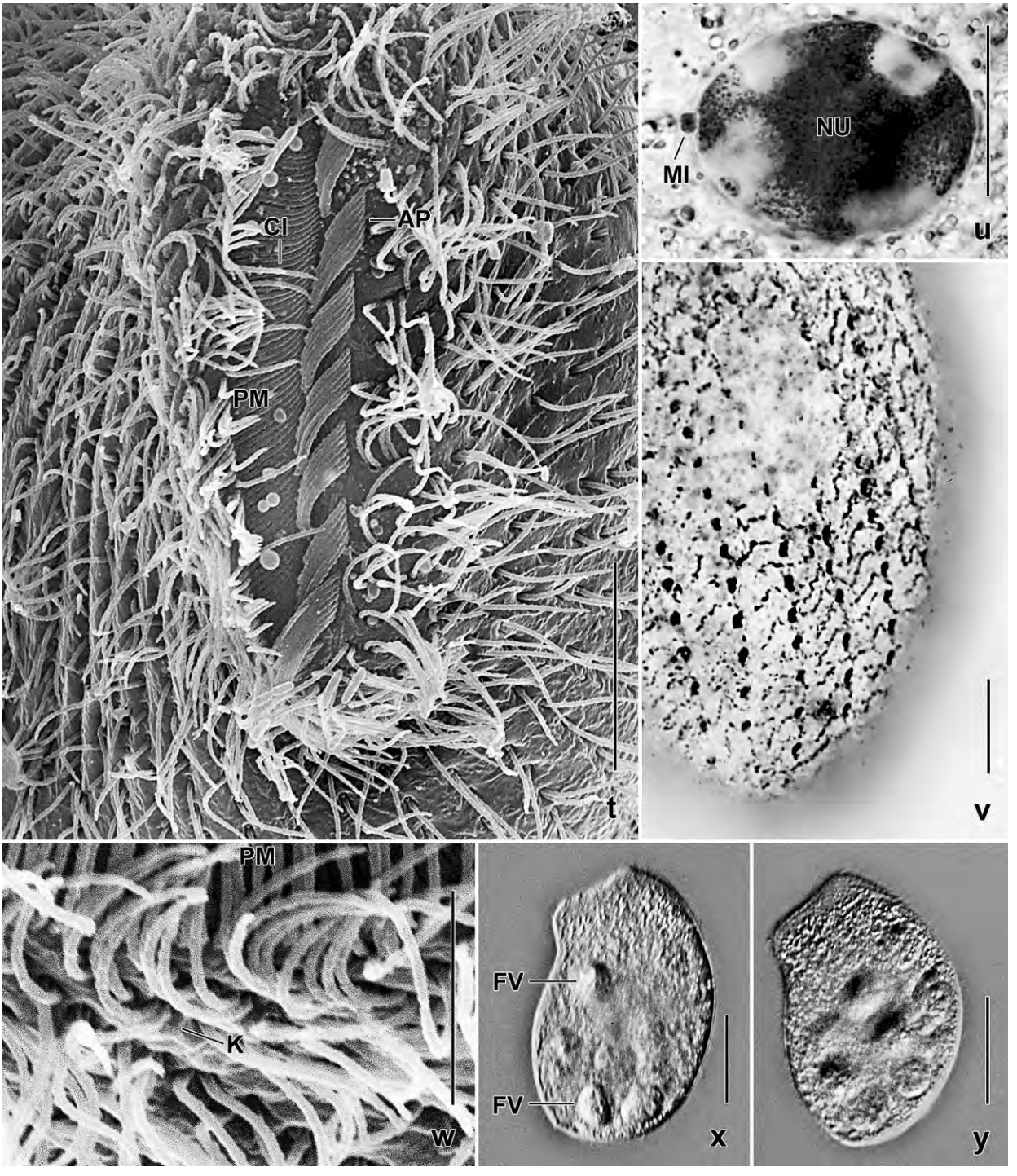

Fig. 144t–y. *Platyophryides macrostoma* from life (x, y), in the scanning electron microscope (t, w), after silver carbonate impregnation (u), and in a CHATTON-LWOFF silver nitrate preparation (v). **t:** Anterior polar view of a specimen with seven adoral polykinetids each composed of a single row of cilia. **u:** Nuclear apparatus with reticulate nucleolus in the macronucleus. **v:** Colpodid silverline pattern (partially bleached). **w:** Right side view, showing anterior end of somatic ciliary rows and internal paroral membrane. **x, y:** Left side views of specimens having ingested several Tetrahymenas. AP – adoral polykinetid, CI – ordinary somatic cilium, FV – food vacuoles, K – kinety, MI – micronucleus, NU – nucleolus, PM – paroral membrane. Scale bars 5 µm (w), 10 µm (t, v), 15 µm (u), and 40 µm (x, y).

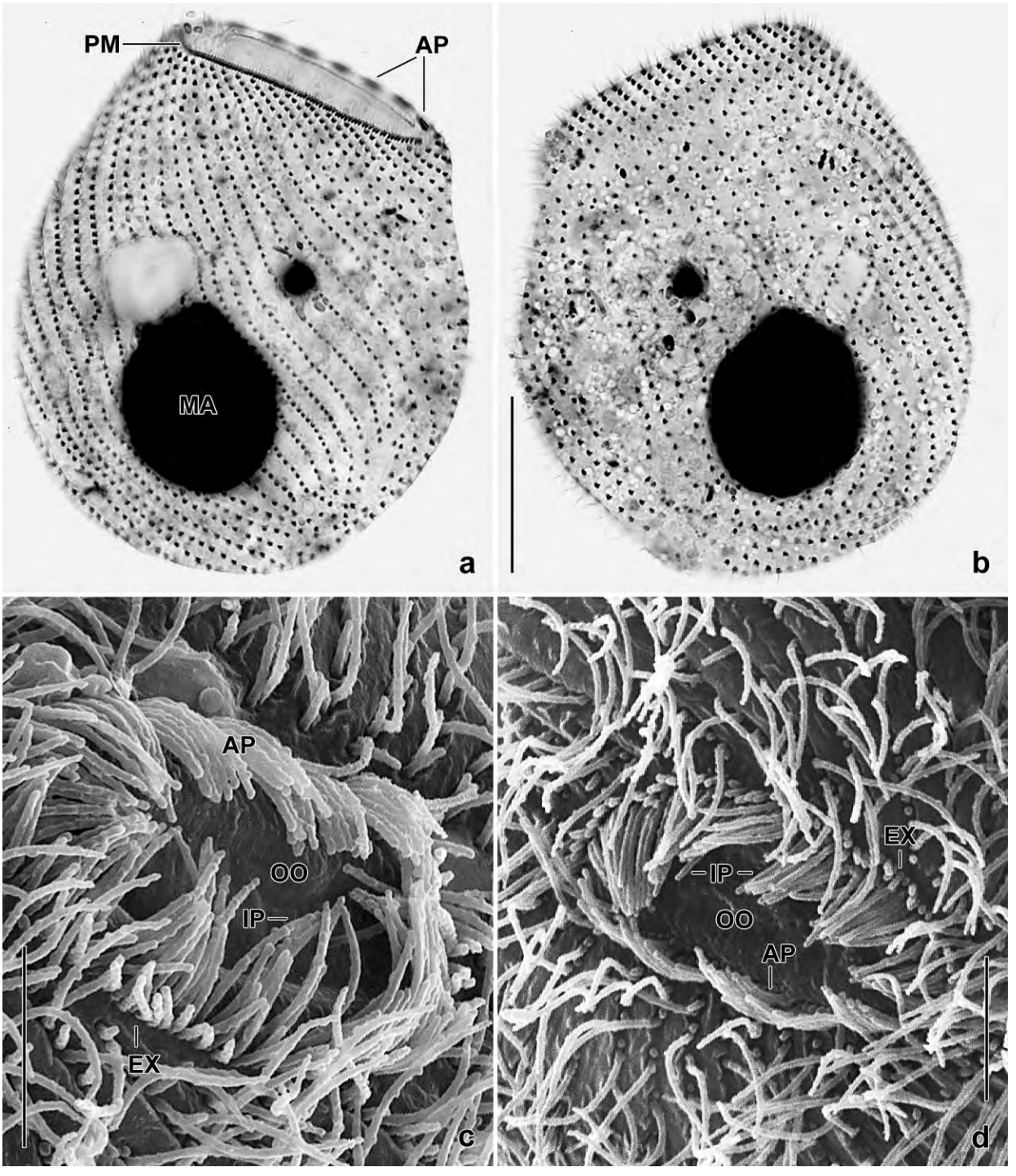

Fig. 145a–d. *Platyophryides macrostoma* after silver carbonate impregnation (a, b) and in the scanning electron microscope (c, d). **a, b:** Right and left side infraciliature of a specimen flattened by coverslip pressure and thus distinctly broadened. It has eight adoral polykinetids. **c, d:** Dividing specimens, showing the reorganizing proter oral apparatus (overview for Fig. 145c, see Fig. 145g). During this process, two paroral membranes become recognizable, an external one with very short cilia and an internal membrane with comparatively long cilia; the same occurs along the adoral polykinetids (for details, see text). AP – adoral polykinetids, EX – external paroral membrane, IP – internal paroral membrane, MA – macronucleus, OO – oral opening, PM – paroral membrane. Scale bars 5 μm (c, d) and 40 μm (a, b).

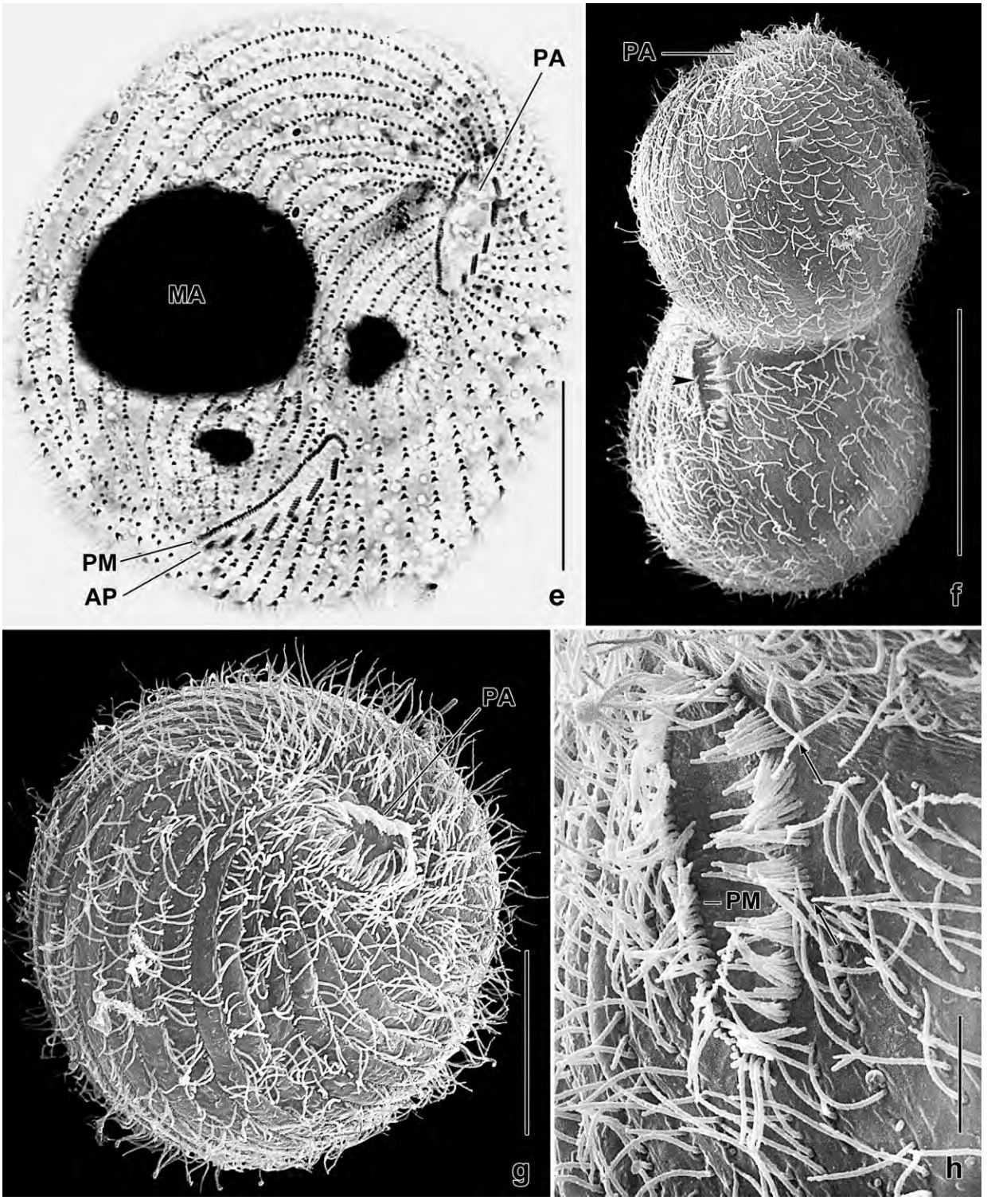

Fig. 145e–h. *Platyophryides macrostoma*, dividers after silver carbonate impregnation (e) and in the SEM (f–h). **e, f, h:** Late dividers with almost finished opisthe oral apparatus (f, arrowhead) shown at higher magnification in (h). The adoral polykinetids are composed of two ciliary rows (arrows). **g:** Late divider with reorganizing proter oral apparatus (for details, see Fig. 145c). AP – adoral polykinetids, MA – macronucleus, PA – parental oral apparatus, PM – new paroral membrane. Scale bars 5 μm (h), 20 μm (g), and 40 μm (e, f).

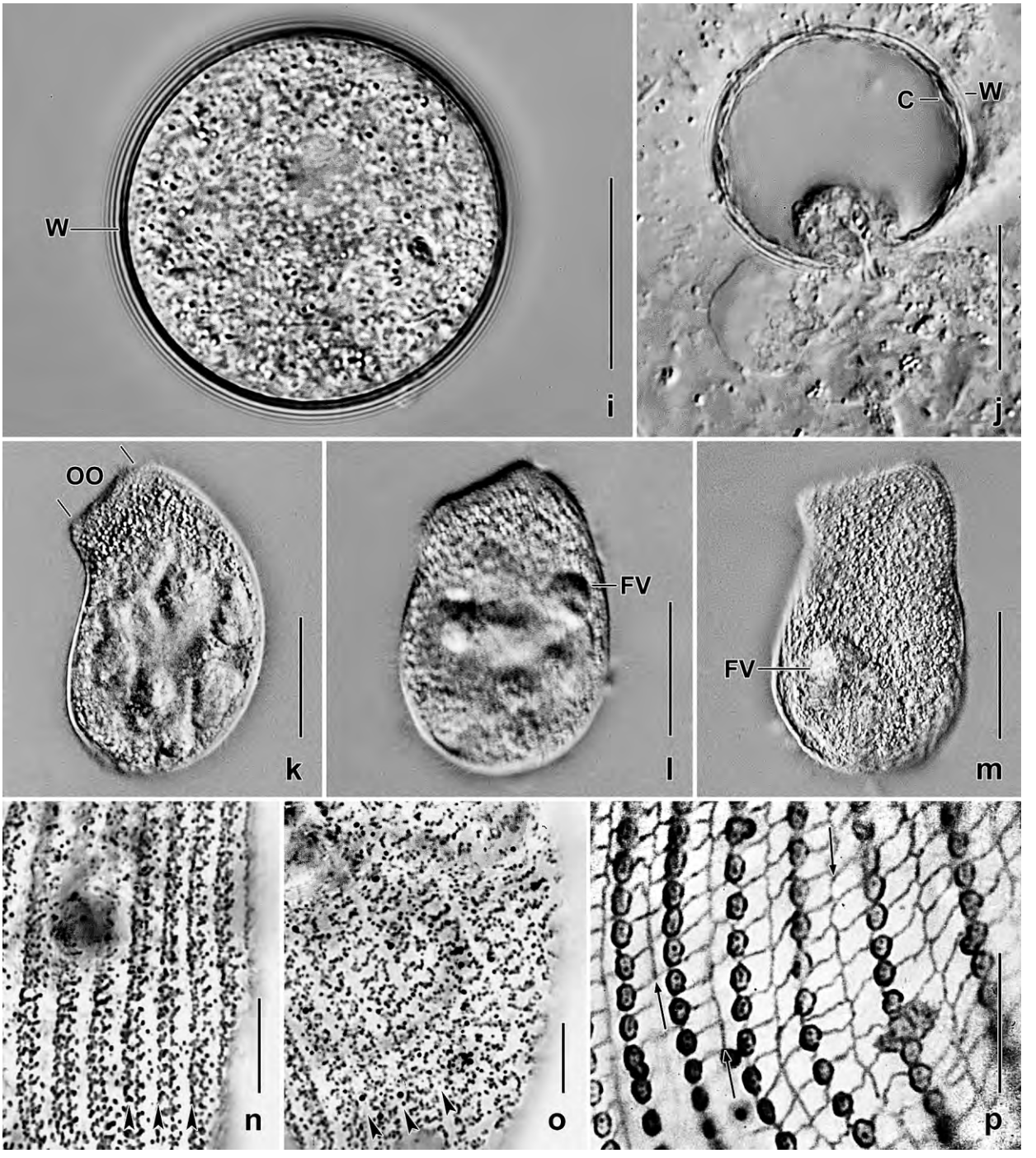

Fig. 145i–p. *Platyophryides macrostoma* (i–o) and *Ottowphrya dragescoi* (p; from Foissner et al. 2002) from life (i–m), after protargol impregnation (n, o), and in a Chatton-Lwoff silver nitrate preparation (p). **i:** Resting cyst. Note the thin, smooth wall. **j:** Squashed resting cyst to show the thin wall. **k–m:** Left side views of morphostatic specimens. **n, o:** Cortical granule pattern in right and left side; arrowheads mark ciliary rows. **p:** Platyophryid silverline pattern of *Ottowphrya*. Arrows mark semimedian silverlines which characterize the platyophryid silverline pattern. *Platyophryides macrostoma*, in contrast, has a colpodid silverline pattern without semimedian silverlines (Fig. 143i). C – cortex of cell, FV – food vacuoles, OO – oral opening, W – cyst wall. Scale bars 10 µm (n–p), 20 µm (i, j), and 50 µm (k–m).

48). Oral basket prominent in protargol preparations, made of nematodesmata originating from paroral dikinetids and adoral polykinetids; nematodesmata thickened in mid of length and then transformed to a smooth tube (Fig. 143a, c, j; Table 48).

Resting cyst (Fig. 143b, e, 145i, j; Table 48): One-week-old cysts globular, in vivo 41.5 µm across on average, colourless, without peculiarities. Wall about 1.2 µm thick, composed of two layers very near together, surface smooth. Cytoplasm densely granulated, contains some inclusions up to 6 µm across. Contractile vacuole and ciliary rows disappeared.

Ontogenesis: Division is highly similar to that of *P. latus* described by Foissner et al. (2002) and to platyophryids in general (Foissner 1993a). In the SEM preparations, we found five dividers reorganizing the proter oral apparatus (Fig. 145c, d, g) and a late divider developing the opisthe oral apparatus (Fig. 145f, h). The following details can be recognized on the photographs:

1. The parental (proter) oral apparatus is reorganized, i. e., the cilia are resorbed. When the division furrow appears, cilia sprout from the basal bodies. In the paroral and adoral anlagen appear two rows of cilia in proter and opisthe, viz., an external row with very short cilia and an internal row with longer cilia (Fig. 145c, d, g). The external row is obviously resorbed in very late dividers and post-dividers to obtain the single row typical for the morphostatic specimens (Fig. 144p–t);

2. The newly formed adoral polykinetids are obliquely oriented in proter and opisthe (Fig. 144m, n, 145e–h). The genus-specific linear arrangement (Fig. 144j, o) is obtained in very late dividers and in post-dividers.

The interpretation of these observations is difficult but the development of a second row of cilia in the paroral and adoral ciliature is very likely a plesiomorphic feature because they are resorbed in late dividers and in post-dividers. This is sustained by observations on *Reticulowoodruffia terricola* which has both paroral kineties ciliated (Foissner et al. 2002).

Except of *Platyophryides* and *Ottowphrya*, all platyophryids and woodruffids have the adoral polykinetids obliquely oriented (Foissner 1993a, Foissner et al. 2002). In *Platyophryides*, an oblique orientation occurs only during ontogenesis (Foissner et al. 2002; Fig. 144m, n, 145e–h). Thus, the linear arrangement, which occurs only in morphostatic cells (Fig. 144j, o), is very likely an apomorphic state.

Molecular phylogeny: The 18 SSU-rDNA of *P. macrostoma* has been sequenced by Foissner et al. (2014b) under the name *Platyophryides* sp. (Fig. 124). It is quite similar to that of *Ottowphrya* and *Sorogena*, which matches morphology but not the unique life cycle of *Sorogena* (for a review, see Foissner 1993a).

Occurrence and ecology: Bamboo stumps are an interesting habitat for protists because competition is reduced due to the short times they are filled with water and the small surface restricting distribution of potential predators. As yet, we did not find *P. macrostoma* in tank bromeliads but it occurred in soil samples (69) and (70) from Galápagos, showing wide distribution in terrestrial and semiterrestrial habitats. Possibly, it occurs also in Venezuela where we identified *Ottowphrya dragescoi* in samples (13), (23), and (26). We cannot exclude that these were *P. macrostoma* because we did not check the silverline pattern and the resting cyst.

Platyophryides macrostoma is easily cultivated with tap water and the middle-sized ciliate *Tetrahymena mobilis*. But it feeds also on other protists and becomes cannibalistic in old cultures when *Tetrahymena* prey disappears and large *Platyophryides* feed on small ones.

Remarks: *Platyophryides macrostoma* is easily distinguished from → *P. latus,* the single congener redescribed and neotypified by Foissner et al. (2002) and here shown by a multitude of micrographs (Fig. 146). *Platyophryides latus* is more slender than *P. macrostoma* (34 µm vs. 76 µm on average) and thus has a lower number of ciliary rows (23 vs. 38 on average) and a much smaller oral width (15 µm vs. 43 µm on average). In contrast, body shape and size of *P. macrostoma* are highly similar to *Ottowphrya* spp. reviewed in Foissner et al. (2002). They can be reliably distinguished only by the silverline pattern: colpodid in *Platyophryides* (Fig. 143i, 144v) while platyophryid in *Ottowphrya* (Fig. 145p). The structure of the cyst wall is also different (Fig. 143e, f). Generally, the cyst of *P. macrostoma* is highly similar to that of *Platyophrya spumacola* (Foissner 1993a).

Platyophryides latus (Kahl, 1930) Foissner, 1987 (Fig. 143f, 146a–p)

Material: Venezuelan sample (5, live observation) and moss from Jamaica (silverline pattern).

Remarks: *Platyophryides latus* has been carefully redescribed by Foissner et al. (2002). Thus, we mention only some live observations from the Venezuelan population and provide a description of the resting cyst not investigated by Foissner et al. (2002).

The morphostatic specimens are highly similar to the Jordanian and Namibian populations studied by Foissner et al. (2002). Size in vivo about 80–100 × 30–50 µm (n = 6). Bursiform to slenderly bursiform with flattened oral area more or less curved ventrally; about 0.5:1 flattened laterally; anterior third slightly contractile (Fig. 146a–d, f–l). Contractile vacuole subterminal in ventral side. Right side cortex rather distinctly furrowed by ciliary rows. Cortical granules about 0.2 µm across, roughly in silverline pattern. Feeds on bacteria digested in food vacuoles about 7 µm across. Ciliary and silverline pattern (Fig. 146b, c) as described by Foissner et al. (2002). Oral field elongate oblong, about 15 × 5 µm, paroral and adoral cilia about 6 µm long in vivo (Fig. 146e, m). A distinct fibre (?) associated with each paroral dikinetid extends into the buccal lip.

Resting cysts colourless and on average 35.6 µm in diameter (M = 36, SD = 1.4, SE = 0.4, CV = 4.1, Min = 32, Max = 38, n = 13). Ectocyst membranous, polygonally faceted, 2–4 µm distant from the about 1 µm thick, structureless endocyst followed by a dense layer of mitochondria. Cytoplasm densely granulated, contains many globular and polymorphic lipid inclusions up to 15 µm in size (Fig. 143f, 146n–p). No slime cover, contractile vacuole and cilia not recognizable.

Cyrtophorida, Hymenostomata, Protostomatida, Peritrichia

Odontochlamys denticulata **nov. spec.** (Fig. 147a–d, 148a–h; Table 49)

Diagnosis: Size in vivo about 35 × 28 µm; very broadly ovate. Dorsal hump cog wheel-shaped. Left ciliary field composed of 6 kineties; leftmost kinety comprising an average of 2 cilia.

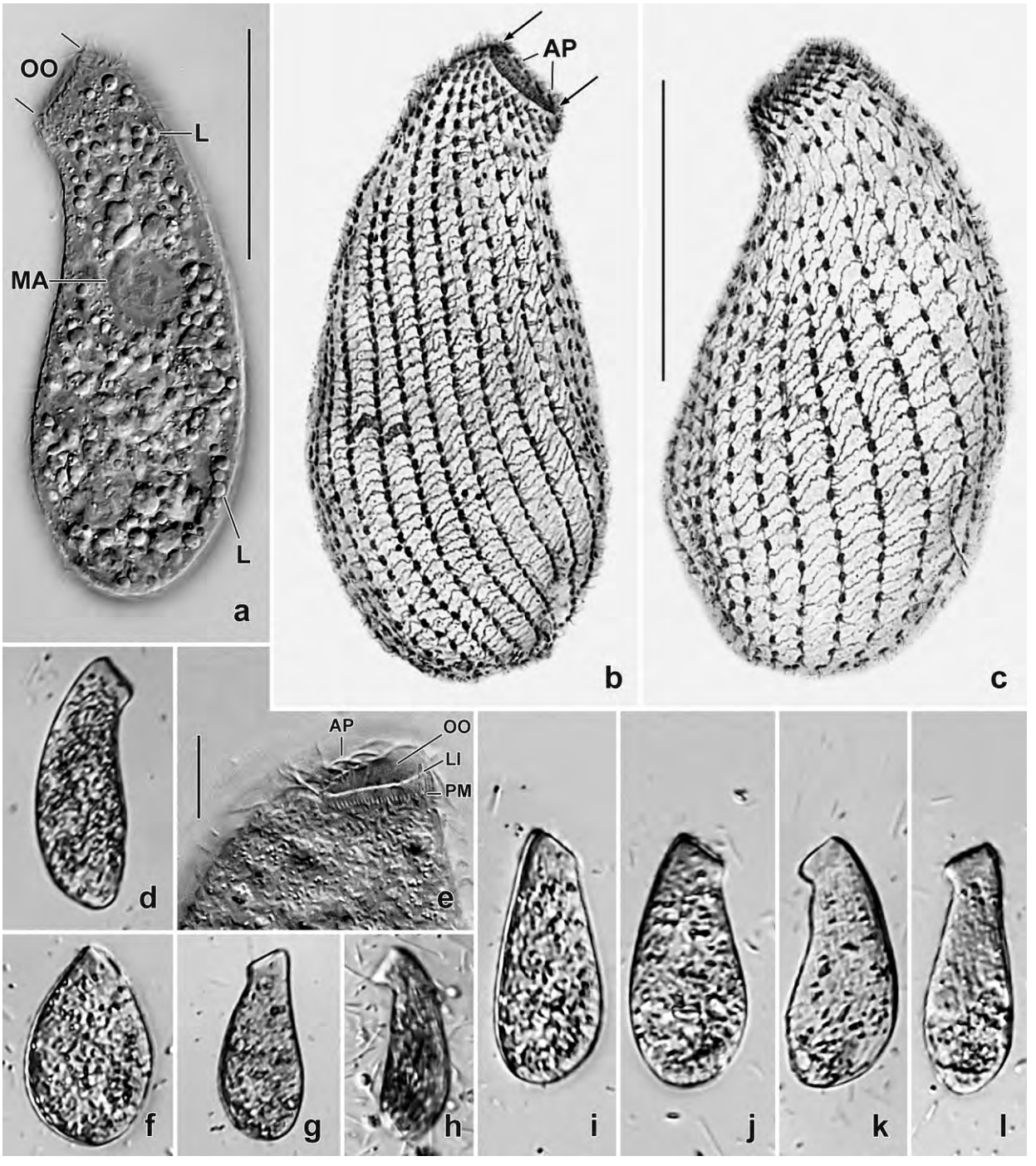

Fig. 146a–l. *Platyophryides latus* from life (a, d–l) and after Chatton-Lwoff silver nitrate impregnation (b, c). **a:** Left side view of a representative specimen studded with lipid droplets from *Tetrahymena* prey. **b, c:** Right and left side view of kinetid and colpodid silverline pattern, showing that *P. latus* has much fewer ciliary rows than → *P. macrostoma.* Arrows mark oral opening. The right side is denser ciliated than the left. **d, f–l:** Variability of body shape in freely motile specimens, length 80–100 µm. Very characteristic are specimens which have the oral area marked by a sharp, ventral bend (h, k, l). **e:** Oral apparatus (see also next plate). AP – adoral polykinetids, L – lipid droplets, LI – lip, MA – macronucleus, OO – oral opening, PM – paroral membrane. Scale bars 10 µm (e) and 40 µm (a–c).

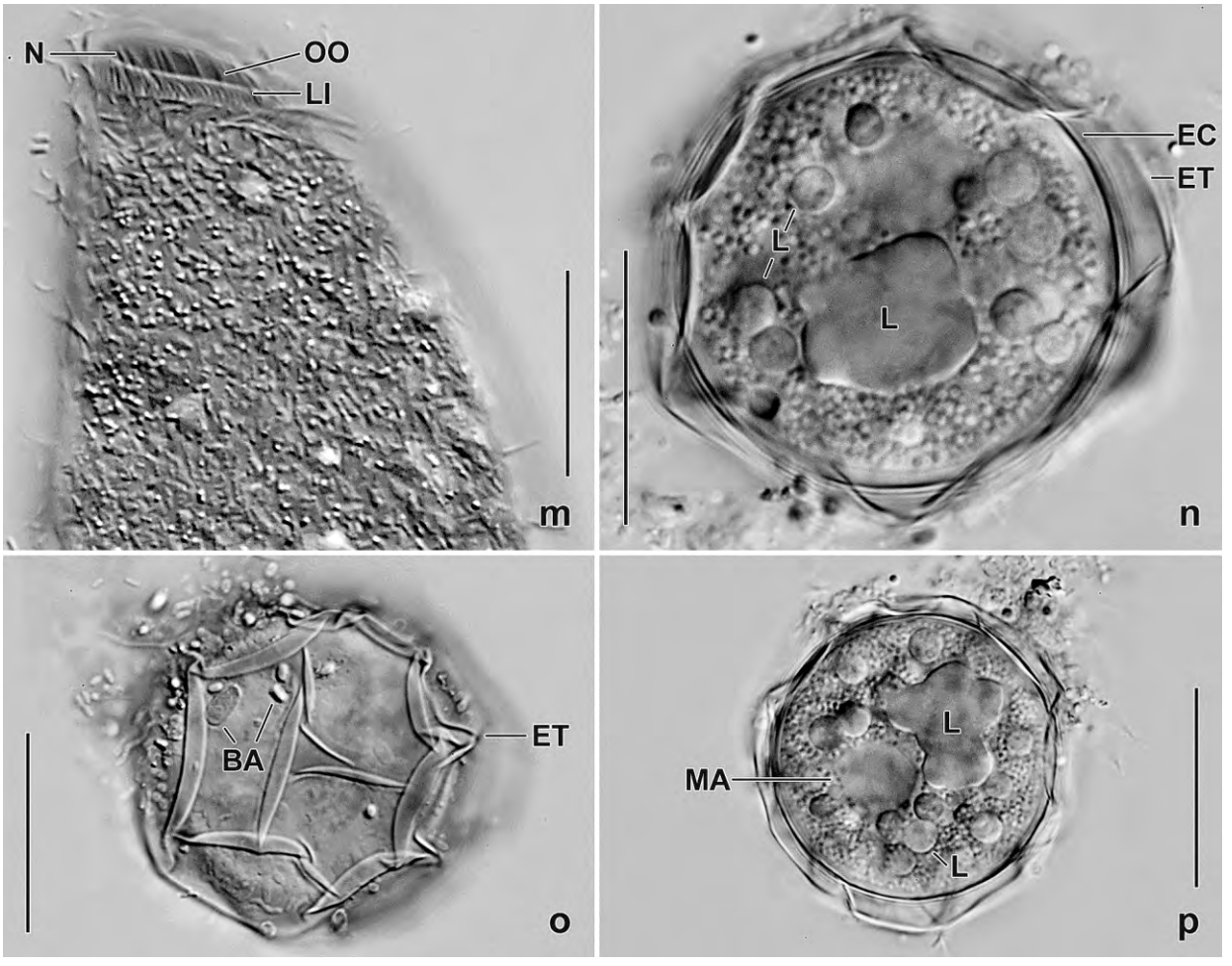

Fig. 146m–p. *Platyophryides latus* from life. **m:** Oral apparatus. **n–p:** Resting cysts, surface view (o) and optical sections (n, p). The ectocyst is polygonally faceted. The cytoplasm is densely granulated and contains globular and large, polymorphic lipid inclusions. BA – bacteria, EC – endocyst, ET – ectocyst, L – lipid droplets, LI – lip, MA – macronucleus, N – nematodesmata originating from adoral polykinetids, OO – oral opening. Scale bars 20 µm.

Type locality: Venezuelan site (3), i. e., mosses from a roadside Laja (granitic rock-pool) and from neighbouring trees of a tropical dry forest (Selva Veranera) about 150 km NE of Puerto Ayacucho, 66°50'E 7°N.

Type material: 1 holotype and 3 paratype slides with 9 protargol-impregnated specimens have been deposited in the Biology Centre of the Upper Austrian Museum in Linz (LI). All specimens have been marked with black ink circles on the coverslip.

Etymology: *Denticulata* (with very small teeth) is a Latin adjective and refers to the denticulated dorsal hump.

Description: Size in vivo 28–40 × 22–34 µm, usually about 35 × 28 µm, as calculated from some in vivo measurements and the morphometric data in Table 49 adding 15% preparation shrinkage; length:width ratio rather stable, i. e., 1.1–1.4:1 with an average of 1.2:1 (Table 49). Broadly ovate, left margin slightly concave at level of oral basket opening (Fig. 147a, 148b, c, g). Postoral

ventral region distinctly concave. Dorsal hump densely granulated, conspicuous because having 10–15 refractive processes forming a perfect cog wheel in the 15 live and protargol-impregnated specimens observed; cogs also recognizable in protargol preparations (Fig. 147a, c, 148a, b, c, f, h). Nuclear apparatus in middle third of cell and slightly left of midline (Fig. 147c, 148e–g; Table 49). Macronucleus globular to almost ellipsoid, on average 11 × 8 µm after protargol impregnation; nucleoli or chromatin bodies mainly in periphery, four out of 11 specimens with a faintly impregnated globule in macronucleus centre. Several specimens with a large, fluffy body posterior of macronucleus, possibly a nuclear anlage. Micronucleus 3–4 µm across, distinct in vivo, faintly impregnated with protargol, usually 1–2 µm distant from macronucleus. Invariably two contractile vacuoles in typical diagonal position and with an excretory pore each (Fig. 147a, b, 148a, e, g; Table 49). Cytoplasm hyaline, contains many granules 0.5–2 µm in size; food vacuoles absent or not impregnated. Lively gliding on microscope slide and soil particles, showing considerable flexibility.

Encysts very fast, as does *O. gouraudi* (FOISSNER 2011). Ontogenesis commences as in *Chilodonella uncinata*, i. e., an anlage develops at right margin of right ciliary field.

Table 49. Morphometric data on *Odontochlamys denticulata* (upper line) and *O. gouraudi* (lower line; from FOISSNER 1988) based on mounted, protargol-impregnated, randomly selected specimens from non-flooded Petri dish cultures. Measurements in µm. CV – coefficient of variation in %, M – median, Max – maximum, Mean – arithmetic mean, Min – minimum, SD – standard deviation, SE – standard error of arithmetic mean.

Characteristics	Mean	M	SD	SE	CV	Min	Max	n
Body, length	30.0	29.0	3.7	1.1	12.5	25.0	36.0	11
	32.2	33.0	4.3	1.2	13.3	25.0	39.0	13
Body, width	24.7	23.0	4.0	1.2	16.0	20.0	31.0	11
	25.0	24.0	3.8	1.1	15.3	20.0	31.0	13
Body length:width, ratio	1.2	1.2	0.1	0.1	6.3	1.1	1.4	11
	1.3	1.3	0.1	0.1	7.7	1.2	1.5	13
Anterior body end to inner circumoral kinety, distance	7.6	7.0	0.9	0.3	12.4	6.0	9.0	11
	5.3	5.6	0.5	0.1	9.7	4.0	6.0	13
Anterior body end to macronucleus, distance	9.1	9.0	2.1	0.6	22.8	6.0	12.0	11
	9.2	8.5	1.0	0.3	10.9	8.0	11.0	13
Anterior body end to anterior excretory pore, distance	9.6	10.0	1.5	0.5	15.6	8.0	12.0	11
	9.0	9.0	1.1	0.3	2.0	8.0	11.0	13
Anterior body end to posterior excretory pore, distance	17.7	18.0	2.4	0.7	13.6	13.0	21.0	11
	21.2	20.0	2.4	0.7	11.6	16.0	25.0	13
Macronucleus, length	10.7	11.0	0.7	0.2	6.0	10.0	12.0	11
	12.1	12.0	2.2	0.6	18.0	9.0	18.0	13
Macronucleus, width	7.7	7.0	1.5	0.5	19.3	6.0	11.0	11
	6.0	6.0	1.0	0.3	16.6	4.0	8.0	13
Oral basket, diameter at distal end	3.1	3.0	–	–	–	3.0	3.5	9
	2.9	2.9	–	–	–	2.0	3.0	13
Non-ciliated postoral area, maximum	7.0	6.0	1.7	0.5	24.7	5.0	10.0	11

continued

Characteristics	Mean	M	SD	SE	CV	Min	Max	n
width	10.7	11.0	2.1	0.6	19.9	8.0	14.0	13
Chord of dorsal brush, length	11.8	12.0	0.6	0.2	5.1	11.0	13.0	11
	10.9	10.6	2.6	0.7	23.9	9.0	19.0	13
Somatic kineties in right ciliary field, number	5.0	5.0	0.0	0.0	0.0	5.0	5.0	11
	5.0	5.0	0.0	0.0	0.0	5.0	5.0	13
Somatic kineties in left ciliary field, number	6.0	6.0	0.0	0.0	0.0	6.0	6.0	11
	6.0	6.0	0.0	0.0	0.0	6.0	6.0	13
Circumoral kineties, number	2.0	2.0	0.0	0.0	0.0	2.0	2.0	11
	2.0	2.0	0.0	0.0	0.0	2.0	2.0	13
Preoral kineties, number	1.0	1.0	0.0	0.0	0.0	1.0	1.0	11
	1.0	1.0	0.0	0.0	0.0	1.0	1.0	13
Basal bodies in innermost kinety of left ciliary field, number	10.3	10.0	7.4	2.2	71.6	4.0	30.0	11
	15.3	14.0	5.4	1.5	35.3	8.0	24.0	13
Basal bodies in leftmost kinety of left ciliary field, number	1.8	2.0	1.0	0.3	54.0	1.0	4.0	11
	19.6	20.0	6.8	1.9	34.5	10.0	35.0	13
Dorsal brush cilia, number	8.1	8.0	0.7	0.2	8.7	7.0	9.0	11
	13.6	14.0	1.1	0.3	8.2	11.0	15.0	13
Oral basket rods, number	9.0	9.0	0.0	0.0	0.0	9.0	9.0	8
	about 12–15							13

Somatic and oral ciliature as described by FOISSNER (1988) in *O. gouraudi*, with the following differences (Fig. 147b, d, 148e–g; Table 49): (i) fewer basal bodies (cilia), especially in leftmost kinety of left ciliary field and (ii) fewer dorsal bristles (9 vs. 12–15). Dorsal brush along anterior and left subapical margin of cell, bristles in vivo about 8 µm long with very fine distal half. At right end of preoral kinety or anterior circumoral kinety a deeply impregnating granule (dikinetid?). Oral basket inconspicuous because only 3 µm across and composed of nine thin rods.

Remarks: FOISSNER (1988b) discussed the problems associated with *O. gouraudi*, type of the genus. In this species spines occur only in the posterior half of the dorsal hump. This has been found in four studies (CERTES 1891, KAHL 1931, WENZEL 1953, FOISSNER 1988b) and in an unpublished population from tanks of a Mexican bromeliad (Fig. 148i–m). Thus, it should be considered as a constant feature, although there is a considerable variability in the size and distinctness of the spines.

BUITKAMP (1977a) described an African (Ivory Coast) population with a cog wheel-shaped dorsal hump, matching the Venezuelan specimens. However, the African population has only five (vs. six) ciliary rows in the left ciliary field and the leftmost kinety of this field is composed of much more cilia than in the Venezuelan specimens (~ 15 vs. 1–4). Thus, we consider the African population as a distinct species described below.

We consider the cog wheel-shaped dorsal hump as the main feature of the Venezuelan population, i. e., of *O. denticulata*. This is supported by the evidence discussed above and by the following side-features (Table 49): the number of oral basket rods (9 in *O. denticulata* vs. 12–15 in *O.*

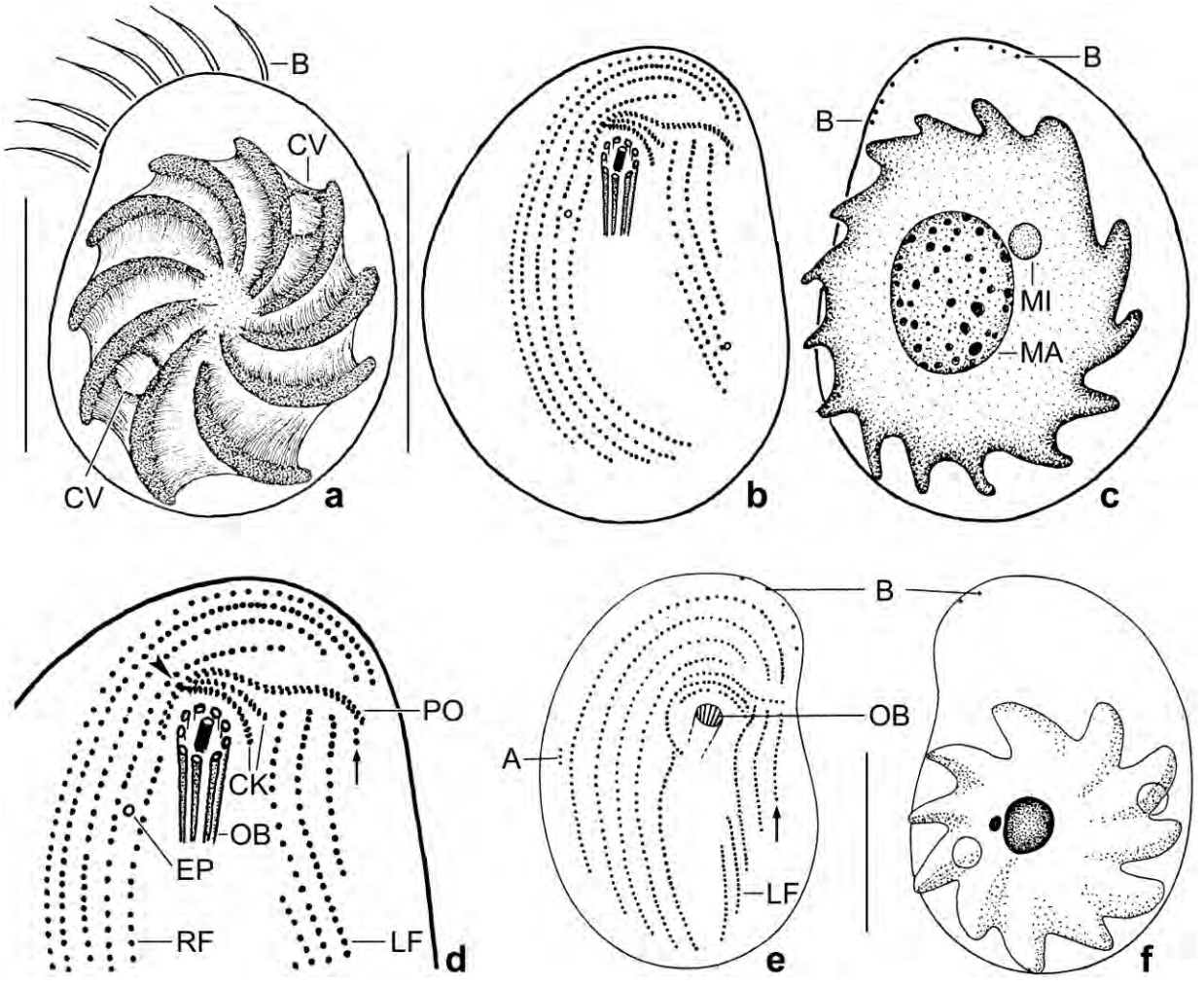

Fig. 147a–f. *Odontochlamys denticulata* (a–d) and *O. buitkampi* (e, f) from life (a) and after protargol impregnation (b–f). **a:** Dorsal view, showing the cog wheel-shaped dorsal hump and the dorsal bristles. **b–d:** Ventral and dorsal view of holotype specimen, length 32 µm. Note the cog wheel-shaped dorsal hump (c) and the left ciliary field whose leftmost kinety consists of only two basal bodies (arrow). The arrowhead in (d) marks a deeply impregnated granule (dikinetid ?). **e, f:** *Odontochlamys buitkampi* differs from *O. denticulata* by the left ciliary field, which consists of only five (vs. six) kineties, and by the much longer leftmost kinety (arrow). A – ontogenetic anlage, B – dorsal brush, CK – circumoral kineties, CV – contractile vacuoles, EP – excretory pore, LF – left ciliary field, MA – macronucleus, MI – micronucleus, OB – oral basket, PO – preoral kinety, RF – right ciliary field. Scale bars 10 µm (e, f) and 20 µm (a–c).

gouraudi), the number of dorsal bristles (8 vs. 13), and the number of cilia in the leftmost kinety of the left ciliary field (1–4 vs. 10–35). These differences are not size-related because the average body size is very similar in *O. denticulata* (30 × 25 µm) and *O. gouraudi* (32 × 25 µm). Further, the macronucleus is ellipsoid in *O. gouraudi* (12 × 6 µm), while broadly ellipsoidal to globular in the Venezuelan (11 × 8 µm; Table 49) and African (Buitkamp 1977a) populations.

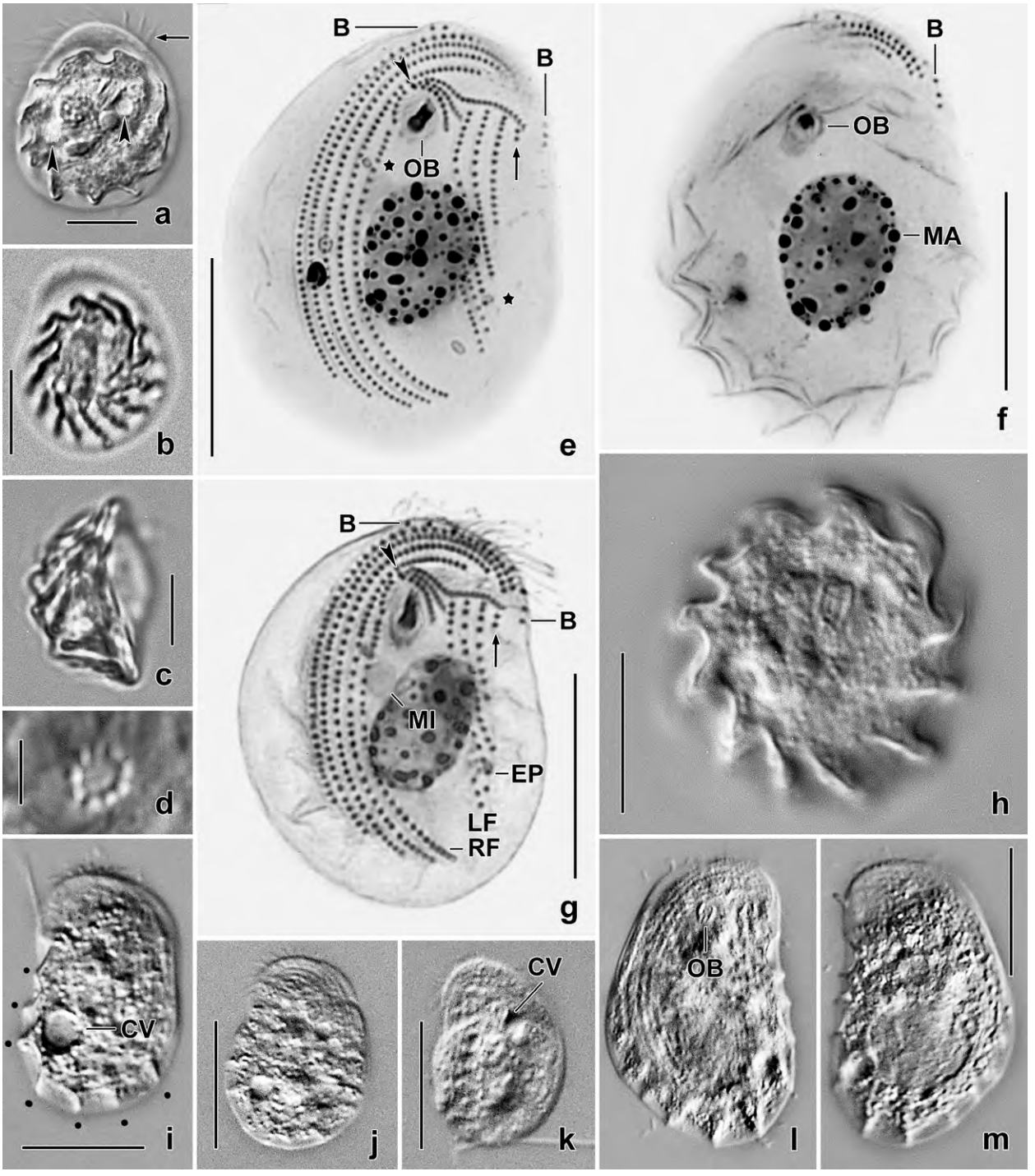

Fig. 148a–m. *Odontochlamys denticulata* (a–h) and *O. gouraudi* (i–m) from a Mexican tank bromeliad from life (a–d, h–m) and after protargol impregnation (e–g). **a:** Dorsal view of a slightly squashed specimen, showing the contractile vacuoles (arrowheads) and the proximal half of some dorsal bristles (arrow). **b, h:** Freely motile specimens, showing the cog wheel-shaped dorsal hump. **c:** Optical section. **d:** The oral basket consists of nine rods. **e–g:** Ventral (e, g) and dorsal (f) views, showing the ciliary pattern and the nuclear apparatus. The leftmost kinety (arrows) of the left ciliary field consists of only two basal bodies. The arrowheads mark a deeply impregnated dikinetid (?). The asterisks denote the excretory pores. **i–m:** The hump of *O. gouraudi* lacks spines (dots) in the dorsal anterior half, and the spines may be minute (j, k). B – dorsal brush, CV – contractile vacuole, EP – excretory pore, LF – left ciliary field, MA – macronucleus, MI – micronucleus, OB – oral basket, RF – right ciliary field. Scale bars 3 µm (d), 15 µm (a–c, e–h), and 20 µm (i–m).

Odontochlamys buitkampi nov. spec. (Fig. 147e, f)

Diagnosis: Length (in vivo?) 20–22 µm; very broadly reniform. Dorsal hump cog wheel-shaped. Left ciliary field composed of 5 kineties; leftmost kinety with > 10 cilia.

Type locality: Soil from the surroundings of the town of Sangrobo, Ivory Coast (Côte d'Ivoire), 6°N 4°50'W.

Type material: Slide(s) with protargol-impregnated specimens have been deposited at the Institut für Landwirtschaftliche Zoologie, Universität Bonn (Buitkamp 1977a).

Dedication: We dedicate this species to Dr. Ulrich Buitkamp (Germany), the discoverer.

Description: See Buitkamp (1977a) and the diagnoses of *O. buitkampi* and of→ *O. denticulata*.

Cinetochilides nov. gen.

Diagnosis: Cinetochilidae (?) with kinetids membrane-like polymerized in anterior quarter of somatic kineties 1 and 2. Two rounds of basal body production between paroral membrane and kinety 1 generate, together with the scutica, the paroral membrane and the adoral membranelles of the opisthe; protomembranelle 1 elongated and sigmoid, its right third very likely incorporated into paroral membrane. The second round produces the new scutica for proter and opisthe.

Type species: *Cinetochilides terricola* nov. spec.

Etymology: *Cinetochilides* is a composite of the genus-group name *Cinetochilum* and the Greek suffix *-ides* (similar, especially in shape), referring to the similarity with *Cinetochilum*. Masculine gender.

Species assignable: *Cinetochilides terricola* nov. spec. (type); *C. monomacronucleatus* nov. spec.; *C. australiensis* (Foissner et al., 1994) nov. comb. (basionym: *Cinetochilum australiense* Foissner et al., 1994; for the homonym *Cinetochilum marinum* Pomp & Wilbert, 1988; if *Cinetochilum marinum* Kahl, 1931 is a member of the genus *Cinetochilides*, the species name given by Pomp & Wilbert (1988) should be activated: *Cinetochilides marinus*); and *Cinetochilides ovale* (Gong & Song, 2008) nov. comb. (basionym: *Cinetochilum ovale* Gong & Song, 1988).

The species transferred to *Cinetochilides* match the morphostatic morphology of *C. terricola*, i. e., all have polymerized kinetids in the anterior portion of somatic kineties 1 and 2 while *Cinetochilum margaritaceum*, type of the genus (Aescht 2001), lacks such a distinct condensation (Foissner et al. 1994, Gelei 1940, Puytorac et al. 1974). Unfortunately, ontogenetic data are not available for the species transferred.

Remarks: We establish the genus *Cinetochilides* with a morphostatic (polymerization of anterior kinetids in kineties 1 and 2) and two ontogenetic (two rounds of basal body production along the paroral membrane; protomembranelle 1 elongated and sigmoid) features. A distinct kinetid polymerization is absent from *Cinetochilum margaritaceum*, type of the genus (Fig. 152a, b; Aescht 2001, Foissner et al. 1994, Gelei 1940, Puytorac et al. 1974). The ontogenesis of C.

margaritaceum has been studied by PUYTORAC et al. (1974). There is neither an elongated, sigmoid protomembranelle 1 or a second round of basal body production along the paroral membrane. Thus, a generic separation of *Cinetochilum margaritaceum* and *Cinetochilides terricola* is appropriate.

The molecular data show that *Cinetochilides ovalis* makes a clade with *Platynematum salinarum* (FOISSNER et al. 2013). Very likely, *Cinetochilides terricola* belongs to this clade because it has the same peculiarities in protomembranelle 1 (cp. Fig. 149h, i). Unfortunately, a molecular sequence is not available from *Cinetochilum margaritaceum.*

***Cinetochilides terricola* nov. spec.** (Fig. 149a–h, j–x, 150k–w, 151a–f, 152a–c; Table 50)

Diagnosis: Size in vivo about 27 × 23 µm; broadly ellipsoid. 2 globular macronuclear nodules; extrusomes cuneate, about 3 µm long. 11 ciliary rows with several caudal cilia 15–20 µm long in vivo; 4 preoral dikinetids in specific pattern. Oral apparatus extends to 63% of body length on average; oral opening roughly triangular; adoral membranelles each composed of 3 rows of basal

Table 50. Morphometric data on *Cinetochilides terricola* from Galápagos (upper line) and *Cinetochilides monomacronucleatus* from Venezuela (lower line) based on mounted, protargol-impregnated, randomly selected specimens from raw cultures. Measurements in µm. CV – coefficient of variation in %, M – median, Max – maximum, Mean – arithmetic mean, Min – minimum, n – number of individuals investigated, SD – standard deviation, SE – standard error of arithmetic mean.

Characteristics	Mean	M	SD	SE	CV	Min	Max	n
Body, length	22.8	23.0	1.7	0.4	7.3	20.0	25.0	19
	18.2	18.0	1.5	0.4	8.0	16.0	20.0	13
Body, width	19.2	19.0	1.7	0.4	8.9	17.0	22.0	19
	14.0	14.0	1.3	0.4	9.2	12.0	17.0	13
Body length:width, ratio	1.2	1.2	0.1	0.1	5.6	1.1	1.3	19
	1.3	1.3	0.1	0.1	6.6	1.2	1.4	13
Anterior body end to adoral membranelle 1, distance	5.6	5.0	1.3	0.3	23.0	4.0	8.5	19
	4.8	4.5	1.5	0.4	31.1	3.0	7.0	13
Anterior body end to adoral membranelle 3, distance	10.1	10.0	1.2	0.3	12.2	8.0	13.0	19
	9.1	9.0	1.2	0.3	13.0	7.0	11.0	13
Anterior body end to proximal end of paroral membrane, distance	14.2	14.0	1.8	0.4	12.5	11.0	19.0	19
	11.5	12.0	1.6	0.4	13.6	9.0	14.0	13
Anterior body end to proximal end of paroral membrane, % distance	62.5	63.0	8.7	2.0	13.9	48.5	80.0	19
	63.3	63.0	7.8	2.2	12.3	50.0	75.0	13
Adoral membranelle 1, length	3.3	3.5	–	–	–	3.0	3.5	19
	2.8	3.0	–	–	–	2.5	3.0	13
Adoral membranelle 2, length	3.0	3.0	–	–	–	3.0	3.5	19
	2.4	2.5	–	–	–	2.0	2.5	13
Adoral membranelle 3, length	1.5	1.5	–	–	–	1.5	2.0	19
	1.5	1.5	–	–	–	1.0	2.0	13
Paroral membrane, length of chord	6.6	6.5	–	–	–	6.0	7.0	19

continued

Characteristics	Mean	M	SD	SE	CV	Min	Max	n
	5.2	5.0	0.6	0.2	10.8	4.0	6.0	13
Anterior body end to macronucleus, distance	9.5	10.0	1.7	0.4	18.2	6.0	12.0	19
	8.4	8.0	1.6	0.4	19.2	6.0	10.0	13
Macronuclear nodule, length	7.3	8.0	1.2	0.3	16.7	4.0	9.0	19
	6.7	7.0	0.8	0.2	11.2	6.0	8.0	13
Macronuclear nodule, width	6.7	7.0	1.3	0.3	19.3	4.0	9.0	19
	5.7	5.0	0.7	0.2	13.1	5.0	7.0	13
Macronuclear nodules, number	2.0	2.0	0.0	0.0	0.0	2.0	2.0	19
	1.0	1.0	0.0	0.0	0.0	1.0	1.0	13
Somatic kineties, number (without postoral kineties)	11.0	11.0	0.0	0.0	0.0	11.0	11.0	19
	11.1	11.0	–	–	–	11.0	12.0	13
Somatic kinety n, number of basal bodies	8.2	8.0	0.9	0.2	11.2	6.0	10.0	19
	no data							
Somatic kinety n-2, number of basal bodies	17.6	17.0	1.1	0.3	6.1	16.0	20.0	19
	14.5	15.0	1.8	0.5	12.5	12.0	18.0	13
Somatic kinety 1, number of polymerized kinetids	10.1	10.0	0.7	0.2	7.3	9.0	12.0	19
	no data							
Somatic kinety 1, length of polymerized portion	4.1	4.0	0.4	0.1	8.9	3.5	5.0	19
	2.7	3.0	–	–	–	2.5	3.5	13
Somatic kinety 2, length of polymerized portion	2.7	2.5	–	–	–	2.0	3.5	19
	3.6	4.0	–	–	–	3.0	4.0	13
Preoral dikinetids, number	4.0	4.0	0.0	0.0	0.0	4.0	4.0	19
	4.0	4.0	0.0	0.0	0.0	4.0	4.0	13
Postoral kineties, number	2.3	2.0	–	–	–	2.0	3.0	19
	2.0	2.0	0.0	0.0	0.0	2.0	2.0	7

bodies; 2–3 minute postoral kineties.

Type locality: Galápagos site (68), i. e., saline soil (~ 30‰) from the surroundings of the village of Puerto Villamil, south coast of Isabela Island, 0°57’S 90°57’W.

Type material: 1 holotype and 5 paratype slides with protargol-impregnated morphostatic and dividing specimens have been deposited in the Biology Centre of the Upper Austrian Museum in Linz (LI). The holotype and other relevant morphostatic and dividing specimens have been marked by black ink circles on the coverslip.

Etymology: The Latin species-group name *terricola* (living in soil) refers to the habitat the species was discovered.

Description: Size in vivo 24–30 × 20–26 µm, usually about 27 × 23 µm, as calculated from some live measurements and the morphometric data in Table 50 adding 20% preparation shrinkage due to ethanol fixation. Body shape inconspicuous, i. e., broadly ellipsoid or slightly ovate or obovate, preorally distinctly furrowed by ciliary rows (Fig. 149a, b, 150l, o; Table 50); laterally

flattened about 2:1. Macronuclear nodules in or slightly posterior to mid-body and in or near body´s midline, side by side or one upon the other (Fig. 150), globular to broadly elliptic (Fig. 149a, c, 150m, o, q, t, w; Table 50); one of 100 randomly selected specimens with only one nodule. Micronucleus (ei?) not impregnated with the protargol method used, not even in dividers. Contractile vacuole in posterior end in body´s midline or slightly neighbored ventral side, excretory pore not impregnated; contracts rarely, very likely due to the high salt concentration (Fig. 149a). Extrusomes within ciliary rows, crenelate cortex because slightly protruding, oriented obliquely to transverse axis of cell, slenderly cuneate with broad end attached to cortex, in vivo about 3 × 0.5 µm in size (Fig. 149a, d, 150k, n, s). Cytoplasm colourless, contains one to three bright crystals of various shape and 1–3 µm in size, and few to many food vacuoles 3–4 µm across and studded with minute bacteria (Fig. 149a, 150k, m, n). Glides rather rapidly on microscope slides and bottom of culture dishes; swims clumsily.

Cilia in vivo 6–8 µm long, arranged in eleven ordinarily and equidistantly spaced rows extending in deep furrows and following body contour, i. e., curved on ventral and left side while slightly oblique on right (Fig. 149a–c, g, 150k, l, o–r, w; Table 50). Most ciliary rows bipolar anteriorly leaving blank an obovate area; all begin with a dikinetid having ciliated only the posterior basal body except of SKn–1 and SKn–2 each commencing with two ciliated "preoral" dikinetids widely spaced in SKn–1. Cilia more widely spaced in posterior region of rows, about five modified to 15–20 µm long caudal cilia difficult to recognize because beating rather rapidly and very fine in distal half. Anterior region of kineties 1 and 2 each with about 10 very narrowly spaced cilia forming a membrane-like structure. Two, occasionally possibly three minute postoral kineties each composed of three to four kinetids between SKn and proximal end of paroral membrane. Kinety SKn extends along posterior half of left mouth margin, composed of an average of eight kinetids forming two or three dikinetids anteriorly (Fig. 149a–c, g, 150k, l, o–t, w; Table 50).

Oral apparatus in mid-body, oral opening roughly triangular (Fig. 149a, b, g, 150k, m, o, p, r; Table 50). Three minute adoral membranelles each composed of three rows of basal bodies with about 5 µm long cilia in vivo. Membranelle 1 longest, slightly convex, anterior row of basal bodies slightly shortened at left end. Membranelle 2 slightly shorter than membranelle 1, separated by a minute cleft in a long left and a short right portion. Membranelle 3 roughly quadrangular, composed of six or nine basal bodies. Paroral membrane distinctly curved, likely composed of dikinetids but usually appears as a single row of basal bodies. Scutica extends along proximal region of paroral membrane, composed of two short rows of basal bodies (Fig. 149a, b, g, 150k, m, o, p, r; Table 50).

Ontogenesis (Fig. 149e–h, j–x, 150u, v, 151a–f): The preparations do not show the structure of the paroral membrane with sufficient clarity. Thus, we show it as a single row of basal bodies throughout although it is very likely dikinetal in some stages. Likewise, the adoral membranelles are too unclear. Thus, we show them as black bars; very likely, there is some internal reorganization.

Cinetochilides terricola has a complex ontogenesis. The earliest stage observed shows disordered basal bodies right of the paroral membrane and a distinct growth of the postoral kineties and SKn (Fig. 149e). Next, the scutica, the basal bodies right of the paroral membrane, and possibly also some postoral basal bodies produce three protomembranelles each composed of two rows of basal

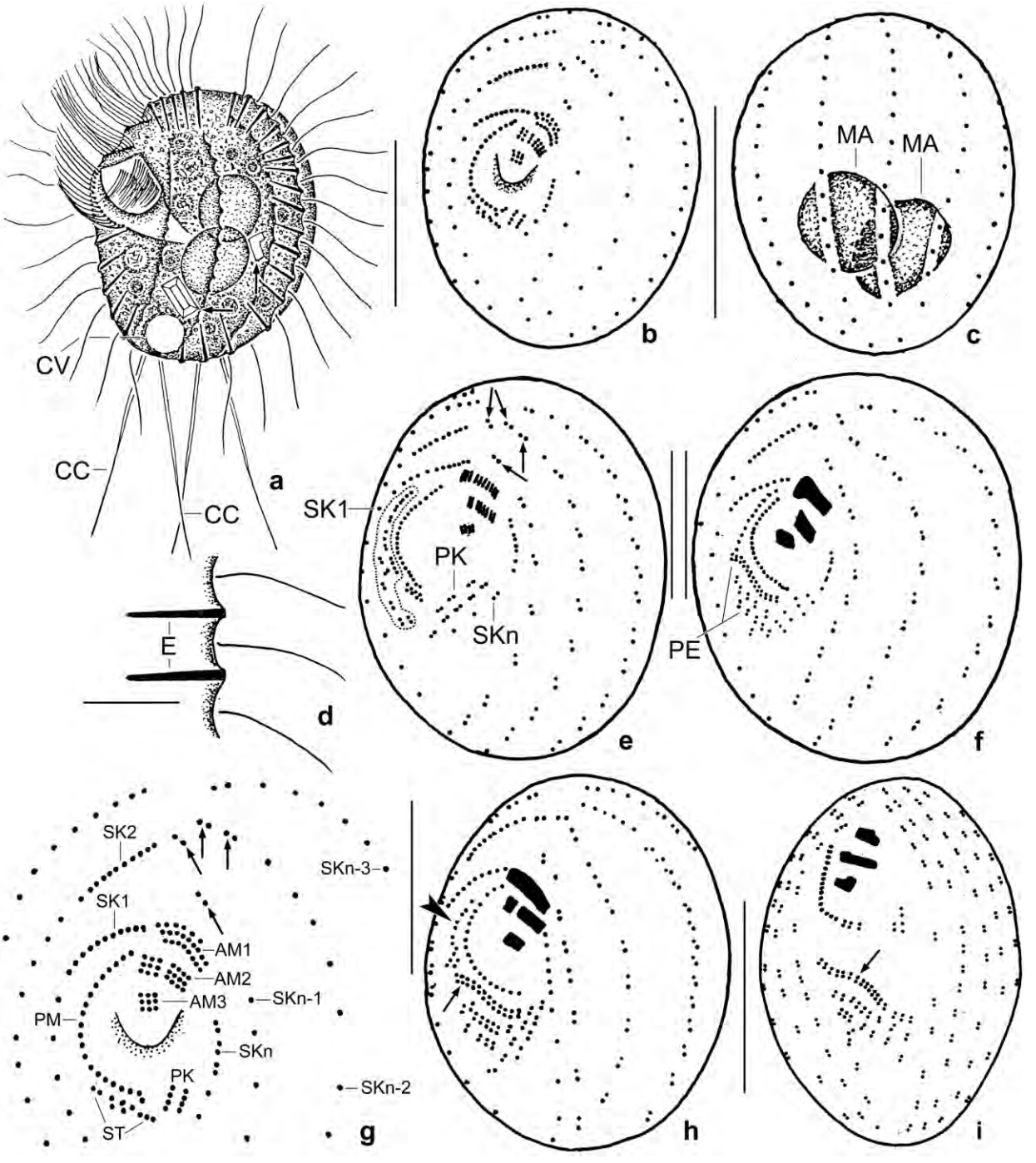

Fig. 149a–i. *Cinetochilides terricola* (a–h) and *Platynematum salinarum* (i) from life (a, d) and after protargol impregnation (b, c, e–i). **a:** Ventrolateral view of a representative specimen, length 25 µm. Arrows mark crystals. **b, c, g:** Ventral and dorsal view of holotype specimen, length 24 µm. Arrows in (g) mark four preoral dikinetids. **d:** Extrusomes are attached with the broad end. **e, f:** Early dividers with preoral dikinetids marked by arrows (e). The dotted area in (e) shows basal bodies developing to oral structures in the opisthe (f). **h, i:** Three protomembranelles developed, of which membranelle 1 (arrows) is distinctly longer and sigmoid. The arrowhead marks a row of basal bodies that will become the paroral of the opisthe together with the right third of protomembranelle 1, as shown by Foissner et al. (2014) in *P. salinarum* (i). AM1, 2, 3 – adoral membranelles, CC – caudal cilia, CV – contractile vacuole, E – extrusomes, MA – macronuclear nodules, PE – protomembranelles, PK – postoral kineties, PM – paroral membrane, SK1, 2 – somatic ciliary rows, SKn – last somatic kinety, SKn1, 2, 3 – penultimate kineties, ST – scutica. Scale bars 3 µm (d), 10 µm (e, f, h), and 15 µm (a–c, i).

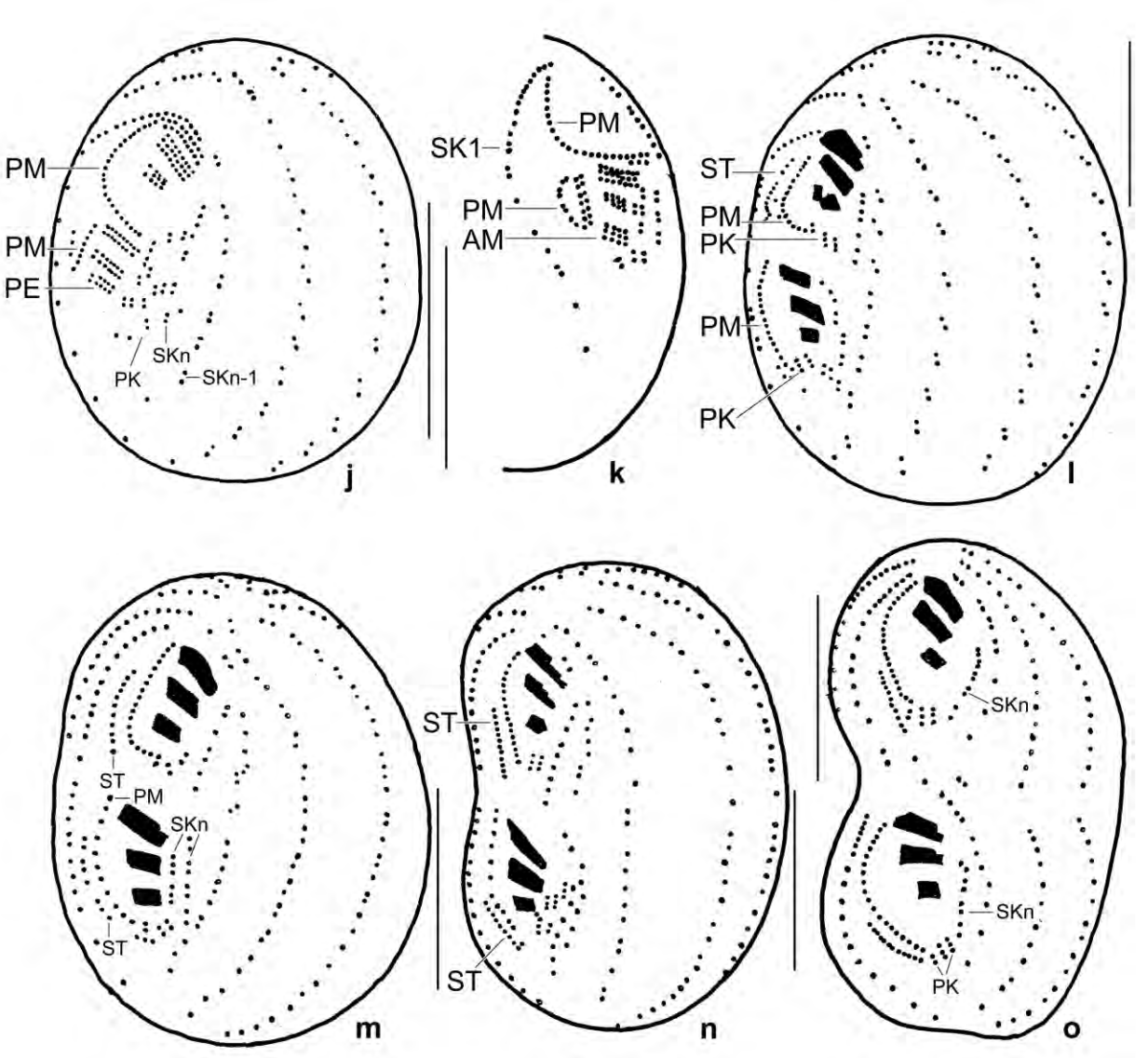

Fig. 149j–o. *Cinetochilides terricola*, ventral and ventrolateral views of protargol-impregnated dividers. **j, k:** The paroral membrane of the opisthe is generated very likely from two sources: the right third of protomembranelle 1 and from the kinetids right of the proter paroral membrane (Fig. 149h, i) because these kinetids disappeared leaving a blank stripe between the parental paroral and kinety 1. Note also the accumulation of kinetids left of the new adoral membranelles. **l, m, u:** A new kinety, very likely the later scutica, is generated right of the paroral membrane of proter and opisthe. The kinetids left of the adoral membranelles organize to postoral kineties and a new somatic kinety n (SKn). The macronuclear nodules are slightly swollen (u, on next page). **n, o, v:** The new scutica, the new postoral kineties, and the new SKn are now well recognizable. The macronuclear nodules have elongated (v, on next page) and the division furrow becomes recognizable. AM – adoral membranelles, PE – protomembranelles, PK – postoral kineties, PM – paroral membrane, SK1 – somatic kinety 1, SKn – kinety SKn, SKn-1 – kinety SKn-1, ST – scutica. Scale bars 10 μm (l–o) and 15 μm (j, k).

bodies (Fig. 149f, h, 150v). Protomembranelle 1 is distinctly longer than protomembranelles 2 and 3 and slightly sigmoid, a highly characteristic feature found also in *Platynematum* (Fig. 149i).

Next, the opisthe paroral membrane is generated and the adoral membranelles become three-rowed (Fig. 149j, k, 151a). The paroral is built from basal bodies right of the parental paroral and, very likely as in *Platynematum* (Fig. 149i), from the right portion of protomembranelle 1 whose

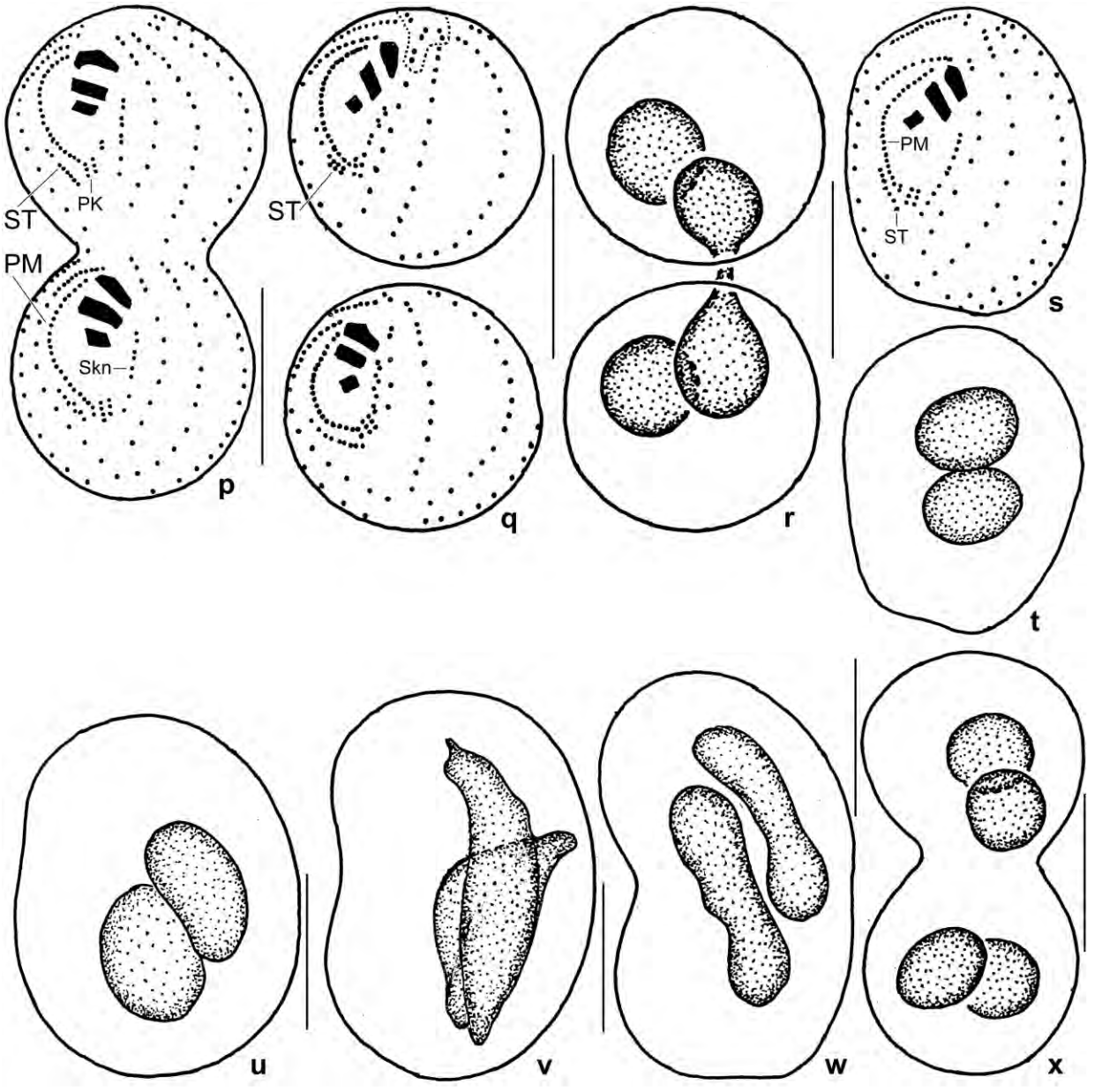

Fig. 149p–x. *Cinetochilides terricola*, ventral views of dividers (p, q, s) and genesis of the macronucleus (r, t–x); explanations for (u, v, w) see previous page. **p, x:** A late divider with fully developed infraciliature and macronucleus. **q, r:** A very late divider hold together by a dividing macronuclear nodule. The dotted area includes the four apical dikinetids. **s, t:** A 18 µm long post-divider with fully developed infraciliature and macronucleus. PK – postoral kineties, PM – paroral membrane, SKn – kinety SKn, ST – scutica. Scale bars 10 µm.

length distinctly decreased. In this stage, all basal bodies disappear right of the parental paroral, respectively, have been used to build the oral structures of the opisthe (Fig. 149j, k, 151a). In late early dividers, a second round of basal body production occurs along the parental (proter) paroral membrane and a first round along the new paroral of the opisthe (Fig. 149l, 150u, 151b). These basal bodies become a new scutica in proter and opisthe (Fig. 149m, n, 151c, d). Concomitantly, new postoral kineties and many somatic kinetids are generated and the macronuclear nodules begin to swell (Fig. 149l, m, u, 150u, 151b, c).

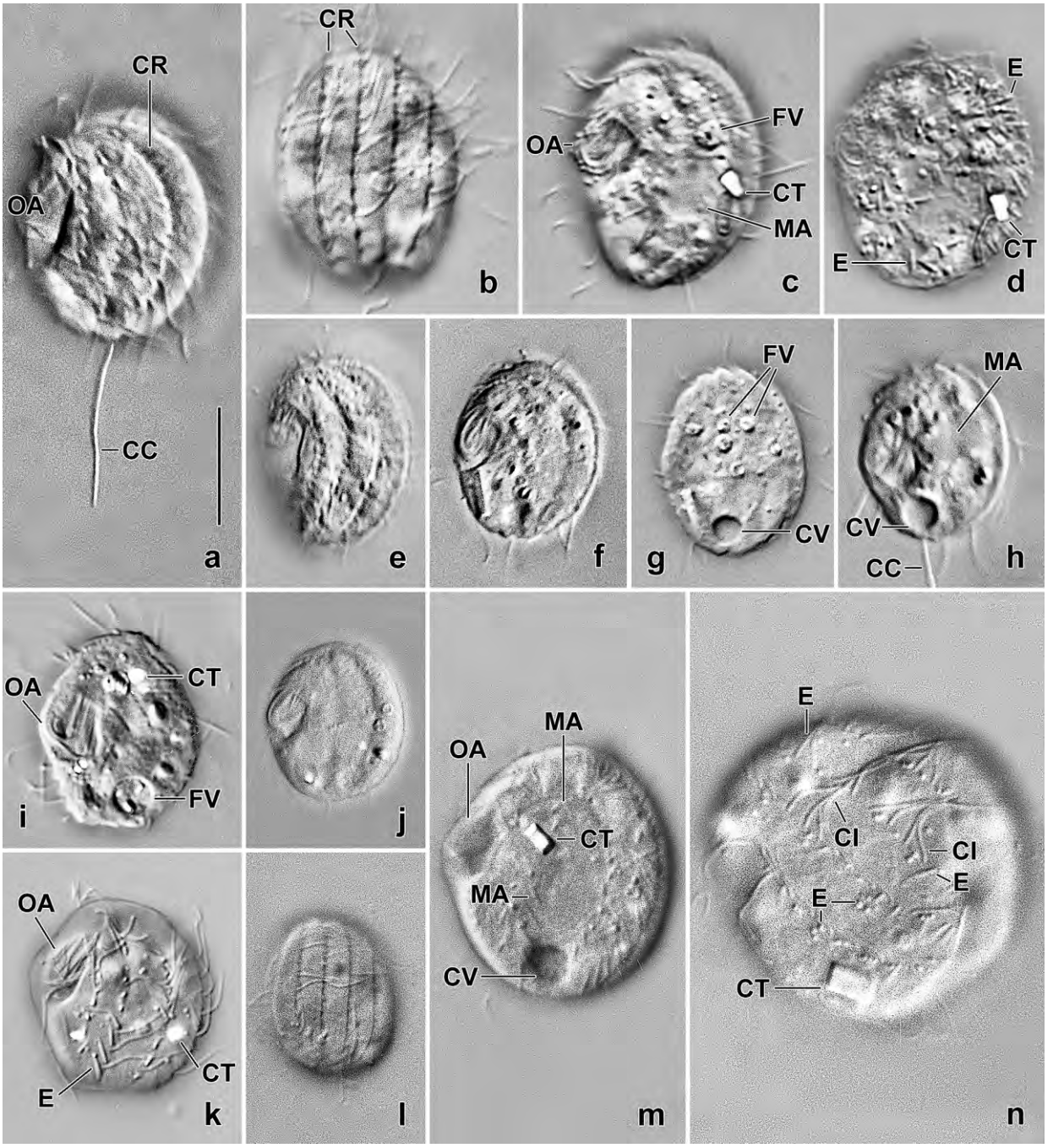

Fig. 150a–n. *Cinetochilides monomacronucleata* from Venezuela (a–h), *Cinetochilides* sp. from Namibia (i, j), and *C. terricola* from Galápagos (k–n), live views in interference contrast. The three populations match in all features except of the macronucleus: one nodule in the Venezuelan and Namibian specimens, two nodules in the specimens from Galápagos. Left side (a, c–k, m, n) and right side (b, l) views. Length of cells in vivo usually 20–25 µm; scale bar (10 µm) shown only in (a). **a–h:** Freely motile (a–c, e–h) and a squashed specimen (d), showing variability of body shape and of location of oral apparatus in or slightly anterior or posterior to mid-body. Note the caudal cilia (a, h; only one of several in focal plane!), the deep cortical furrows produced by the ciliary rows, the cytoplasmic crystals (c, d), and the contractile vacuole (g, h). **i, j:** Freely motile Namibian specimens. **k–n:** Freely motile (l) and more or less squashed specimens from Galápagos (k, m, n) to show the cuneate, 3 µm long extrusomes (k, n), the deep cortical furrows where the ciliary rows extend (l), and the cytoplasmic crystals (k, m, n). CC – caudal cilia, CI – cilia, CR – ciliary rows, CT – crystals, CV – contractile vacuole, E – extrusomes, FV – food vacuoles, MA – macronucleus, OA – oral apparatus.

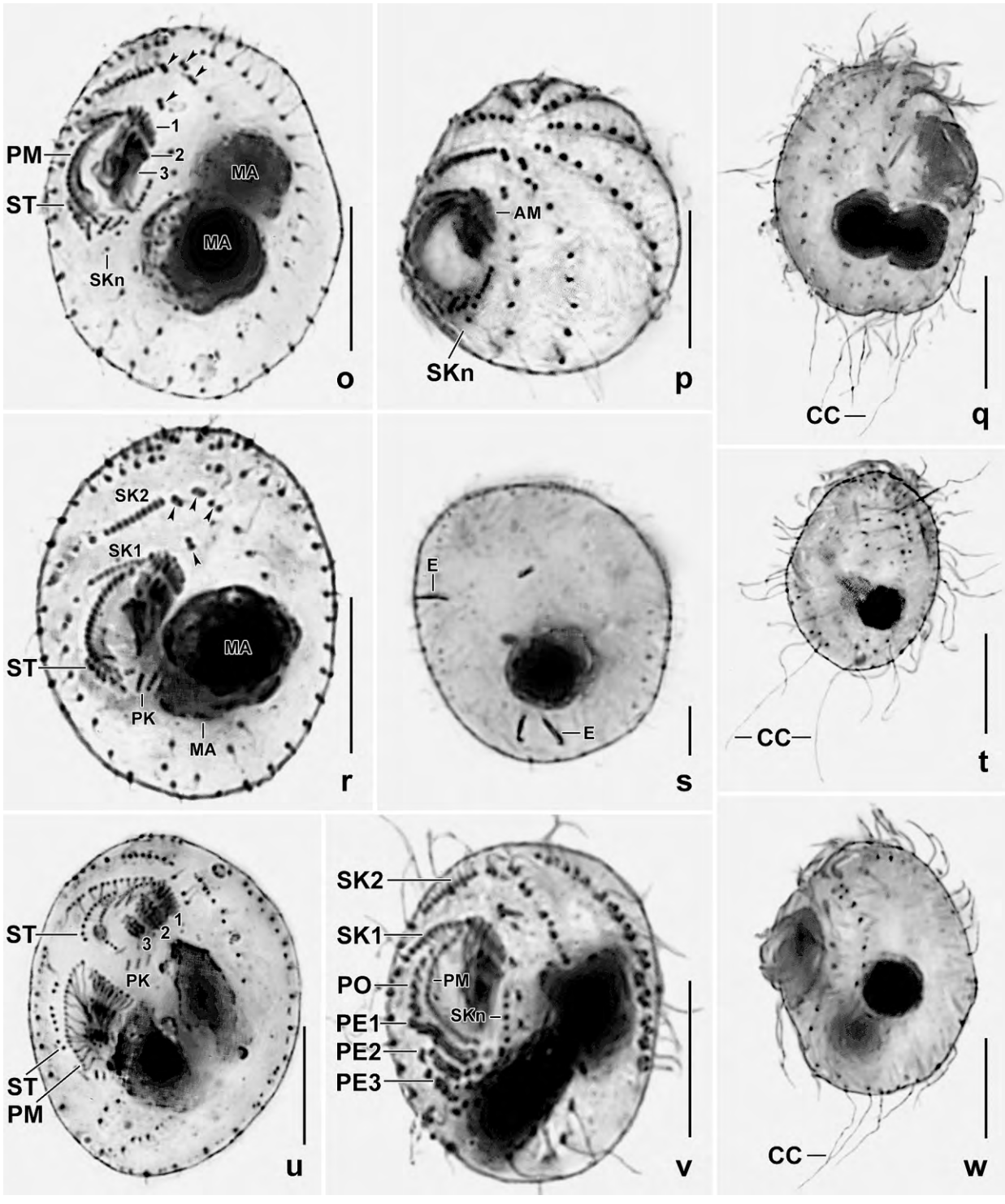

Fig. 150o–w. *Cinetochilides terricola* after protargol impregnation. **o, p, r:** Ventrolateral, oblique anterior polar, and ventral view of morphostatic specimens. Arrowheads mark the four preoral dikinetids. **q, t, w**: Caudal cilia. **s:** Extrusomes. **u:** An early mid-divider with proter and opisthe oral apparatus almost completed. Note the new scutica (ST). **v:** Early divider with sigmoid protomembranelle 1. Note anlage for the paroral membrane of the opisthe (PO). AM – adoral membranelles, CC – caudal cilia, E – extrusomes, MA – macronuclear nodules, PE 1, 2, 3 – protomembranelles, PK – postoral kineties, PM – paroral membrane, SK1, 2 – somatic kineties, SKn – kinety SKn, ST – scutica, 1, 2, 3 – adoral membranelles. Scale bars 10 µm.

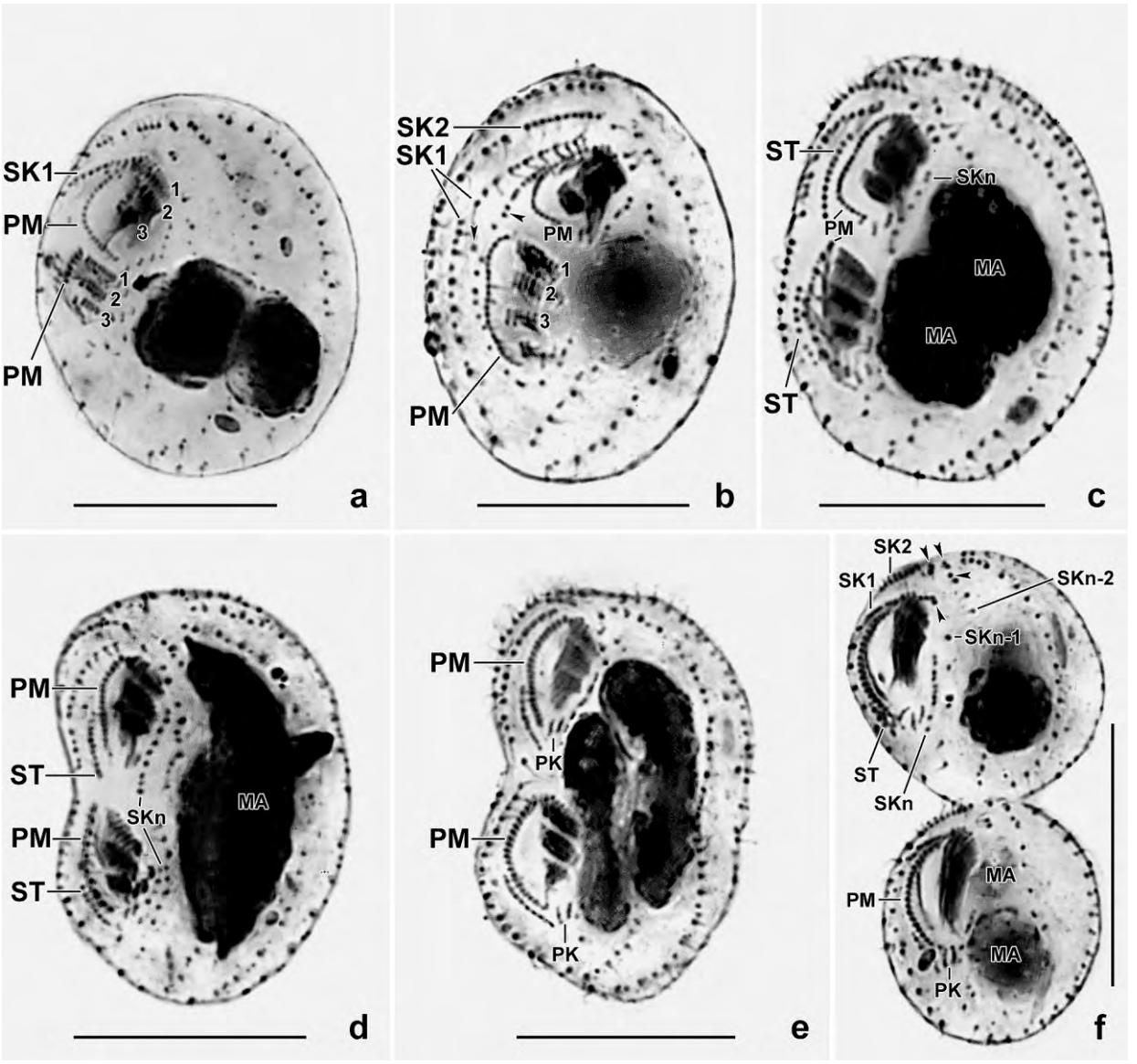

Fig. 151a–f. *Cinetochilides terricola*, protargol-impregnated dividers. **a:** An early mid-divider having assembled the opisthe paroral membrane from kinetids between the proter paroral and somatic kinety 1 and the right third of protomembranelle 1, and thus there are no kinetids between paroral and kinety 1 of the proter, in contrast to a slightly earlier stage (Fig. 150v). The protomembranelles each consist of two rows of basal bodies. **b:** Slightly later than the stage shown in (a) because the adoral membranelles are composed of three rows of basal bodies, as in morphostatic specimens. A new scutica (arrowheads) has been generated between paroral membrane and somatic kinety 1 both in proter and opisthe. **c:** An early mid-divider with swollen macronuclear nodules and distinct scutica in proter and opisthe. **d, e:** Mid-dividers with elongated macronuclear nodules and beginning cytokinesis. The oral apparatus has been completed in both proter and opisthe, and the paroral membrane very likely became dikinetal (e). **f:** A late divider, showing that the four preoral dikinetids belong to somatic kineties SKn-1 and SKn-2. MA – macronuclear nodules, PK – postoral kineties, PM – paroral membrane, SKn – last somatic kinety, SKn-1, SKn-2 – penultimate somatic kineties, SK1, 2 – ordinary somatic kineties, ST – scutica, 1, 2, 3 – adoral membranelles. Scale bars 15 μm.

Mid-dividers elongate the macronuclear nodules and organize details of the new infraciliature, especially SKn and SKn-1 (Fig. 149n, 151d, e). In early late dividers, these processes continue and cytokinesis commences (Fig. 149o, w, 151e). Late dividers have a deep division furrow and have divided the macronuclear nodules (Fig. 149p, x, 151f). Very late dividers are globular and

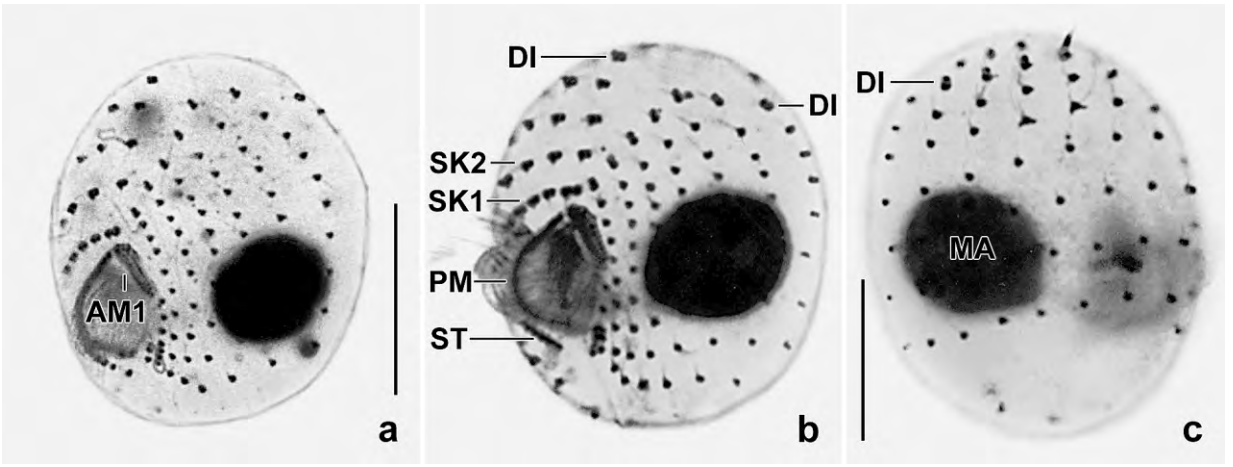

Fig. 152a–c. *Cinetochilum margaritaceum*, protargol-impregnated specimens from the Amper River in Bavaria. Figures (b, c) show both sides of a single specimen. *Cinetochilum margaritaceum* differs from *Cinetochilides terricola* by many features: one vs. two macronuclear nodules; oral apparatus distinctly vs. slightly posterior to mid-body; 15–18 vs. 11 somatic ciliary rows; somatic kineties 1 and 2 indistinct vs. with distinct polymerization of kinetids anteriorly; somatic kineties distinctly shortened vs. unshortened posteriorly; without vs. with four preoral dikinetids. AM1 – adoral membranelle 1, DI – dikinetid on anterior end of all ciliary rows, MA – macronucleus, PM – paroral membrane, SK1, 2 – somatic kineties, ST – scutica. Scale bars 10 µm (a) and 15 µm (b, c).

organize the four preoral dikinetids (Fig. 149q, r). Early post- dividers look like morphostatic cells but are slightly smaller (Fig. 149s, t).

Remarks: There are three similar species to compare with *C. terricola*: *Cinetochilum marinum* Kahl, 1931; *C. australiense* Foissner et al., 1994 (for the homonym *C. marinum* Pomp & Wilbert, 1988); and *C. ovale* Gong & Song, 2008. The two last-mentioned species have been transferred to *Cinetochilides* above. The following comparison excludes extrusomes (not described but likely present in the three species mentioned) and caudal cilia (difficult to observe).

Cinetochilum marinum has been not yet investigated with modern methods making a sound comparison difficult. It differs from → *Cinetochilides terricola* by body shape (slightly triangular vs. broadly elliptic); the macronucleus (one vs. two nodules); the location of the oral apparatus (in posterior body half vs. slightly posterior to mid-body); and the caudal cilia (short vs. about 15 µm; but see above).

Cinetochilides australiense differs from *C. terricola* by body shape (sharply notched posteriorly in body´s midline vs. smoothly rounded); the absence (vs. presence) of isolated preoral dikinetids; and the absence (vs. presence) of caudal cilia (but see above). Obviously these species are rather similar.

Cinetochilides ovale differs from *C. terricola* by the macronucleus (one vs. two nodules); the shape of the oral opening (ellipsoid vs. roughly triangular); the structure of adoral membranelle 1 (composed of two vs. three rows of basal bodies); and the pattern of preoral dikinetids (two dikinetids in an oblique vs. vertical row and dikinetids on begin of SKn-1 side by side vs. one after the other).

Cinetochilides monomacronucleatus **nov. spec.** (Fig. 150a–h; Table 50)

Diagnosis: As *Cinetochilides terricola* but with only 1 macronuclear nodule.

Type locality: Venezuelan site (65), i. e., highly saline (~ 50‰) coastal soil from the surroundings of the village of Chichirivice, Morrocoy National Park, 67°13'W 11°33'N.

Type material: 1 holotype and 5 paratype slides with protargol- and silver nitrate-impregnated specimens have been deposited in the Biology Centre of the Upper Austrian Museum in Linz (LI). Relevant specimens have been marked by black ink circles on the coverslip.

Etymology: The species name is a composite of the Greek numeral *mono* (single), the Greek adjective *macros* (large), and the Latin noun *nucleus* (nucleus), referring to the single macronuclear nodule characterizing this species.

Description: We do not provide a conventional description because *C. monomacronucleatus* is indistinguishable from → *C. terricola* except of the single (vs. two) macronuclear nodule (Fig. 150a–h; Table 50).

In vivo *C. monomacronucleatus* has a size about 15–25 × 10–20 μm while it is slightly smaller than → *C. terricola* in the protargol preparations; this, of course, also influences the distances measured (Table 50). A single micronucleus is attached to the globular macronucleus and about 1 μm in size. The food vacuoles contain minute (~ 1 μm) bacteria. The ordinary somatic cilia are 6–7 μm long while the caudal cilia are about 15 μm long in vivo.

Occurrence and ecology: As yet found only at type locality. Occurs, according to live observations, also in Namibia (dune 45 at road to Sossus Vlei; not saline; Foissner et al. 2002) and in Australia (highly saline mangrove soil in the surroundings of the town of Cairns).

Remarks: There are two similar species, i. e., with one macronuclear nodule: *Cinetochilum marinum* Kahl, 1931 and *Cinetochilides ovale* (Gong & Song, 2008). The following comparison excludes extrusomes (not described but likely present in the species mentioned) and caudal cilia (difficult to observe).

Cinetochilum marinum has been not yet investigated with modern methods making a reliable comparison difficult. It differs from *Cinetochilides monomacronucleatus* by body outline (triangular vs. broadly elliptic); the location of the oral apparatus (in posterior body half vs. slightly posterior to mid-body); and the caudal cilia (short vs. about 15 μm long; but see above).

Cinetochilides ovale differs from *C. monomacronucleatus* by the shape of the oral opening (ellipsoid vs. roughly triangular); the structure of adoral membranelle 1 (composed of two vs. three rows of basal bodies); and the pattern of preoral dikinetids (two dikinetids in an oblique vs. vertical row and dikinetids on begin of SKn-1 side by side vs. one after the other).

Platynematum terricola **nov. spec.** (Fig. 153a–h, 154a–g; Table 51)

Diagnosis: Size in vivo about 33 × 19 µm. Body slightly ovate, inconspicuously to up to 2:1 flattened laterally; frontal plate obovate. Nuclear apparatus posterior to mid-body. Contractile vacuole subterminal with excretory pore between kineties 2 and 3. Extrusomes, very likely a sort of trichocysts, within ciliary rows, cuneate, 2–3 µm long. Cortex thick, with distinct ciliary pits. On average 18 ciliary rows most commencing with two ciliated dikinetids; Kn–1 without dikinetids; a single caudal cilium about as long as body. Oral apparatus distinctly subapical, tetrahymenid.

Type locality: Soil surrounding roots of bulbs from *Prospero*, Antalya, Cakilli Gecidi, about 11 km SE of the town of Cevizli, 1200 NN, Anatolia, Turkey, 31°45'O 37°45'N.

Type material: 1 holotype and 2 paratype slides with protargol-impregnated specimens have been deposited in the Biology Centre of the Upper Austrian Museum in Linz (LI). Relevant specimens have been marked by black ink circles on the coverslip.

Etymology: The Latin species-group name *terricola* (living in soil) refers to the habitat the species was discovered.

Description: Size in vivo 25–40 × 15–23 µm, usually about 33 × 19 µm, as calculated from measurements of live and prepared specimens adding 15% for preparation shrinkage (Table 51). Shape slightly ovate with a shallow concavity in mouth area, laterally slightly to distinctly (~ 2:1) flattened, frontal plate obovate and easily recognizable (Fig. 153a–e, 154c, g); spines or notches definitely absent. Nuclear apparatus posterior to mid-body, without peculiarities (Fig. 153a, c, e, 154b, c, e; Table 51). Macronucleus globular, finely granulated and about 7 µm across in vivo. Micronucleus about 1.5 µm across, attached to macronucleus. Contractile vacuole subterminal, i. e., on average 6 µm distant from posterior pole; excretory pore with long, oblique canal opening between kineties 2 and 3 (Fig. 153a, b, 154b; Table 51). Extrusomes numerous, very likely a kind of trichocysts, most within ciliary rows, cuneate, 2–3 µm long, impregnate lightly with the protargol method used (Fig. 153a, f, h, 154d, f, g). Cortex about 1 µm thick, ciliary pits distinct, without conspicuous ridges (Fig. 153a, h, 154e). Cytoplasm colourless, specimens, however, dark at low magnification (≤ ×100) because usually studded with ring-shaped granules, especially in anterior half; individual granules with minute to wide central hole, moderately refractive, globular to broadly ellipsoid, about 1 µm in size, dissolve during protargol impregnation (Fig. 153a, h, 154a, b, e). Most food vacuoles in middle body third, 3–5 µm across in vivo, contain bacteria and their spores. Swims rapidly and incessantly rotating about main body axis.

Somatic cilia in vivo about 7 µm long. Caudal cilium in centre of pole, about as long as body, proximal thirds as thick as somatic cilia, distal third very fine and more or less curved (Fig. 153a, b, 154a). On average 18 meridional, equidistant, basically monokinetal ciliary rows most commencing posterior of frontal plate and ending in posterior pole area (Fig. 153a–c, e, g, 154c, d, g; Table 51). Kinety 1 commences with about three dikinetids posterior and right of paroral membrane. Kinety 2 slightly shortened anteriorly, commences with six narrowly spaced, ciliated basal bodies and then extends right of paroral membrane to rear body end. Kineties 3–16

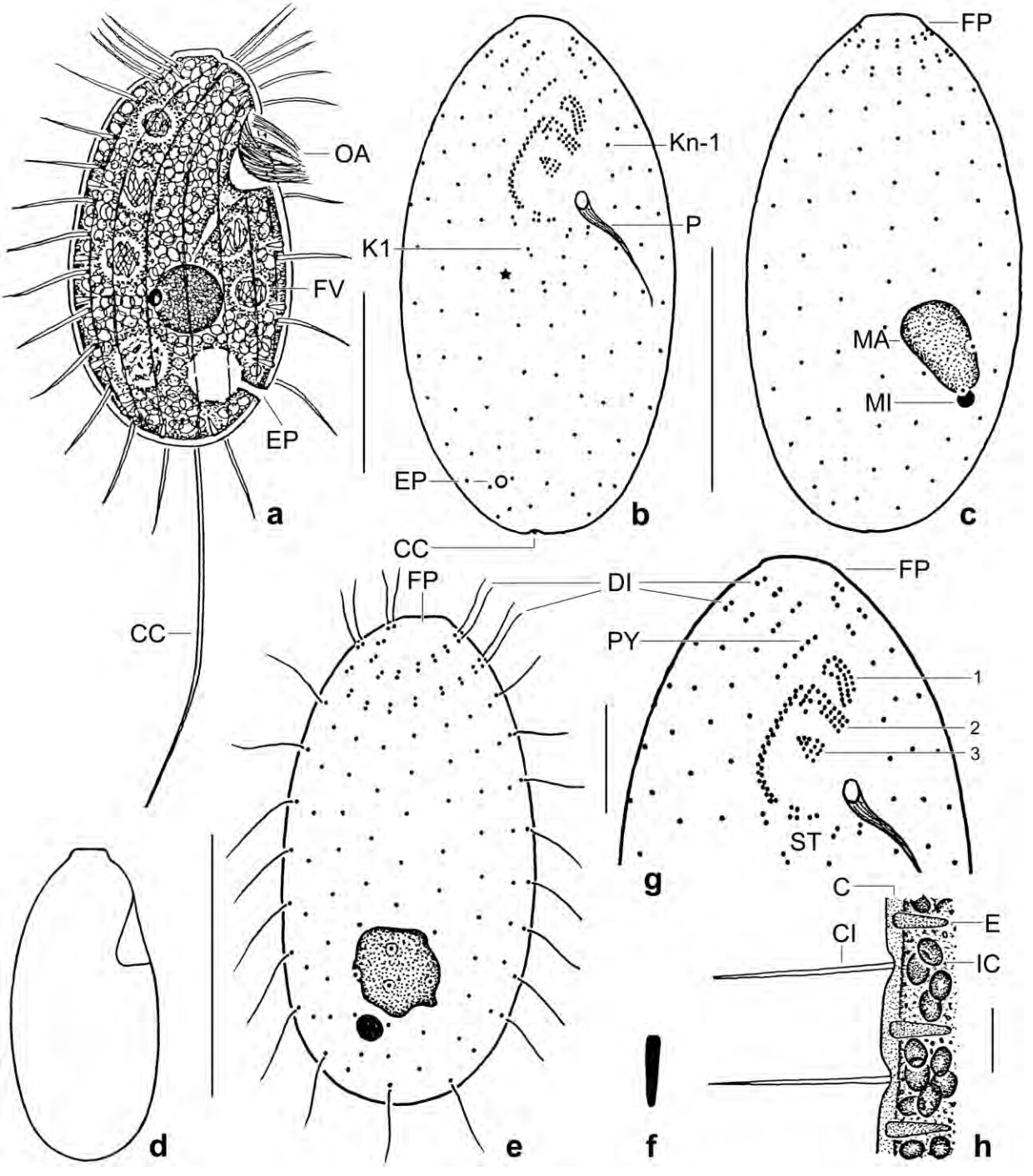

Fig. 153a–h. *Platynematum terricola* from life (a, d, h) and after protargol impregnation (b, c, e, g). **a:** Right side overview of a representative specimen studded with cytoplasmic inclusions, length 33 µm. **b, c, g:** Ventral and dorsal view of holotype specimen, length 32 µm. Note the subterminal contractile vacuole and the absence of dikinetids in Kn–1, a main feature of this species. The asterisk marks an additional ciliary row present only in this specimen. **d:** A slender specimen. **e:** A paratype specimen, showing the barren frontal plate and the two ciliated dikinetids at begin of the ciliary rows. **f:** Extrusome, 2.5 µm long. **h:** Optical section. C – cortex, CC – caudal cilium, CI – ordinary somatic cilium, DI – dikinetids, E – extrusome, EP – excretion pore of contractile vacuole, FP – frontal plate, FV – food vacuole, IC – cytoplasmic inclusions, K1 – somatic kinety, Kn–1 – somatic kinety, MA – macronucleus, MI – micronucleus, OA – oral apparatus, P – pharynx, PY – ciliary polymerization, ST – scutica, 1, 2, 3 – adoral membranelles. Scale bars 3 µm (h), 5 µm (g), and 15 µm (a–c, e).

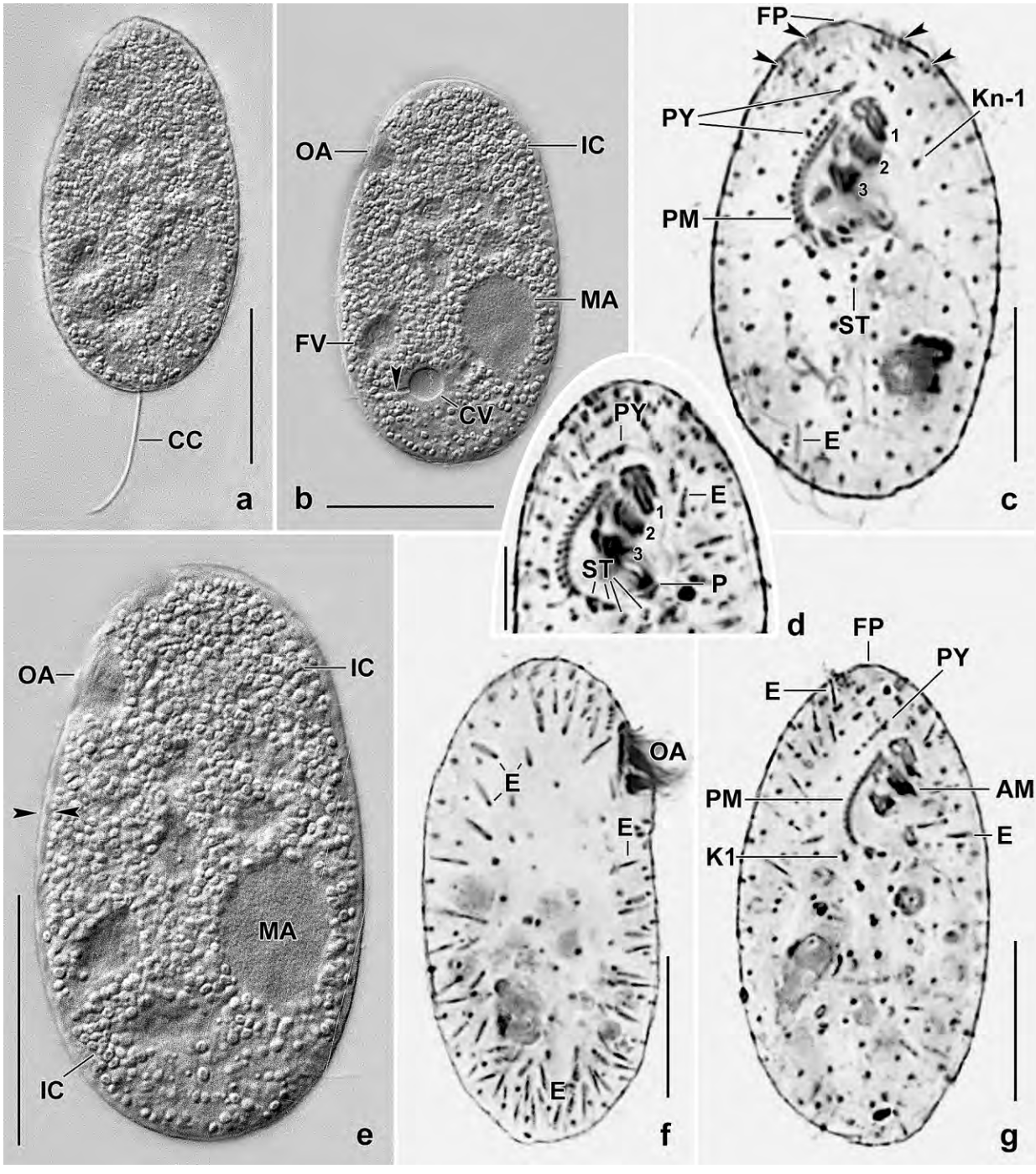

Fig. 154a–g. *Platynematum terricola* from life (a, b, e) and after protargol impregnation (c, d, f, g). **a:** Left side overview of a slightly pressed specimen, showing the proximal half of the caudal cilium. **b, e:** Same specimen as in (a) but stronger pressed to show the macronucleus and the ring-shaped cytoplasmic inclusions. The arrowhead in (b) marks the canal of the contractile vacuole. The opposed arrowheads in (e) denote the thick cortex. **c, d, g:** Ventral views, showing the somatic and oral kinetid pattern. The arrowheads in (c) mark the two dikinetids at begin of the ciliary rows. **f:** Optical section, showing the extrusomes. AM – adoral membranelles, CC – caudal cilium, CV – contractile vacuole, E – extrusomes, FP – frontal plate, FV – food vacuole, IC – cytoplasmic inclusions, K1 – kinety 1, Kn–1 – kinety n-1, MA – macronucleus, OA – oral apparatus, P – pharynx, PM – paroral membrane, PY – ciliary polymerization, ST – scuticus, 1, 2, 3 – adoral membranelles. Scale bars 5 µm (d), 10 µm (c, f, g), and 15 µm (a, b, e).

Table 51. Morphometric data on *Platynematum terricola* based on mounted, protargol-impregnated, and randomly selected specimens from a non-flooded Petri dish culture. Measurements in µm. CV – coefficient of variation in %, M – median, Max – maximum, Mean – arithmetic mean, Min – minimum, n – number of individuals investigated, SD – standard deviation, SE – standard error of arithmetic mean.

Characteristics	Mean	M	SD	SE	CV	Min	Max	n
Body, length	29.0	28.0	3.3	0.9	11.4	23.0	36.0	15
Body, width	16.3	16.0	1.8	0.5	11.0	13.0	20.0	15
Body length:width, ratio	1.8	1.8	0.1	0.1	4.9	1.6	1.9	15
Anterior body end to macronucleus, distance	18.7	18.0	1.9	0.5	10.3	16.0	22.0	15
Anterior body end to end of paroral, distance	11.6	12.0	0.9	0.2	10.8	10.3	13.0	15
Anterior body end to excretory pore, distance	23.1	23.5	2.4	0.7	10.4	18.0	27.0	12
Macronucleus, length	5.2	5.0	0.6	0.1	10.8	4.0	6.0	15
Macronucleus, width	4.6	5.0	–	–	–	4.0	5.0	15
Micronucleus, length	1.4	1.2	–	–	–	1.1	2.0	15
Micronucleus, width	1.3	1.2	–	–	–	1.0	2.0	15
Ciliary rows in mid-body, number	17.8	18.0	–	–	–	17.0	18.0	15
Kinetids in a dorsal kinety, number (dikinetid = 1 kinetid)	12.2	12.0	1.2	0.3	9.4	11.0	15.0	15
Ciliary row 2, number of polymerized kinetids	6.0	6.0	0.0	0.0	0.0	6.0	6.0	15
Scutica, number of basal bodies (1 dikinetid = 2 basal bodies)	9.1	9.0	0.9	0.2	9.8	8.0	11.0	15

commence posterior of frontal plate with two ciliated dikinetids. Kinety 17 (= Kn–1) commences at level of second adoral membranelle, monokinetal throughout. Kinety 18 commences at posterior margin of buccal cavity with one or two dikinetids. Scutica along and posterior of buccal vertex, composed of 8–11 basal bodies, most as dikinetids (Fig. 153a–c, e, g, 154 c, d, g; Table 51).

Oral apparatus in a shallow, subapical concavity with paroral membrane extending to 40% of body length in protargol preparations; structure and shape tetrahymenid (Fig. 153a, b, d, g, 154a–e, g; Table 51). Oral opening triangular, paroral membrane moderately curved, composed of about 15 narrowly spaced dikinetids in zigzag pattern; proximal third associated with lightly impregnated oral ribs, forming a distinct pharynx extending obliquely to mid-body. Adoral membranelles short and thick, each likely composed of three rows of basal bodies, details slightly variable and difficult to recognize; some scattered basal bodies right of membranelle 2 (Fig. 153a, b, d, g, 154 c, d, g; Table 51).

Occurrence and ecology: As yet found in Turkey (type locality); Indonesia; Venezuelan sample (4), i. e., in the mud of a lithotelma; and in the Pantanal, Brazil. Thus, it is possibly a cosmopolitan.

Remarks: *Platynematum terricola* is highly similar to *P. salinarum* recently described by Foissner et al. (2013) from a hypersaline (~ 120‰) solar saltern in Portugal. Actually, there are only two clearly different features: the number of ciliary rows (17–18 vs. 21–22) which is very stable in both populations (CV < 5%), and the absence (vs. presence) of dikinetids in the anterior third of kinety n–1. Very likely, the extrusomes are also different but they could be not seen in *P. salinarum*. Furthermore, the Portuguese specimens lack the prominent cytoplasmic inclusions of the Turkish cells; however, this could be caused by the very different habitats.

According to the molecular data, *Platynematum* belongs to the Cinetochilidae which, however, are paraphyletic (FOISSNER et al. 2014a).

Tetrahymena rostrata (KAHL, 1926) CORLISS, 1952 (Fig. 155a–m; Table 52)

Material: Over the years, we studied this species from a variety of terrestrial habitats globally.

Tetrahymena rostrata is not easily identified because its life cycle includes slender, fast-swimming theronts and broad, ordinarily swimming trophonts. Further, the short caudal cilium (~ 15 µm,

Table 52. Morphometric data on *Tetrahymena rostrata* from Venezuela (VE) and Austria (AU, from FOISSNER 1987) based on mounted, protargol-impregnated, and randomly selected specimens from non-flooded Petri dish cultures. Measurements in µm. CV – coefficient of variation in %, M – median, Max – maximum, Mean – arithmetic mean, Min – minimum, n – number of specimens investigated, Pop – population, SD – standard deviation, SE – standard error of arithmetic mean.

Characteristics	Pop	Mean	M	SD	SE	CV	Min	Max	n
Body, length	VE	55.4	55.0	5.3	1.2	9.6	46.0	65.0	21
	AU	55.0	53.0	8.9	2.8	16.3	42.0	70.0	10
Body, width	VE	14.4	14.0	2.7	0.6	18.4	10.0	19.0	21
	AU	28.4	28.0	4.8	1.5	17.0	24.0	40.0	10
Body length:width, ratio	VE	2.0	1.9	0.5	0.2	26.6	1.3	2.8	21
	AU	2.0	1.9	0.5	0.2	26.6	1.3	2.8	10
Anterior body end to 1st adoral membranelle, distance	VE	7.1	7.0	0.8	0.2	10.8	13.0	18.0	21
	AU	3.9	4.0	0.6	0.2	15.2	3.0	5.0	10
Anterior body end to proximal end of paroral membrane, distance	VE	15.1	15.0	1.4	0.3	18.4	13.0	18.0	21
	AU	14.7	15.0	1.3	0.4	8.5	13.0	17.0	10
Anterior body end to 1st macronuclear nodule, distance	VE	20.9	20.0	2.3	0.5	11.0	18.0	25.0	21
	AU	19.9	19.0	6.4	2.0	32.3	12.0	31.0	10
Anterior body end to 2nd macronuclear nodule, distance	VE	28.7	28.0	2.7	0.6	10.0	25.0	35.0	21
	AU	absent							10
Anterior body end to excretory pore of contractile vacuole, distance	VE	46.0	47.0	4.4	1.5	9.5	38.0	53.0	9
	AU	41.3	42.0	3.3	1.1	8.1	35.0	46.0	10
Macronulear figure, length	VE	15.0	15.0	1.8	0.4	11.9	12.0	18.0	21
Anterior macronuclear nodule, length	VE	6.5	7.0	0.8	0.2	12.9	5.0	8.0	21
	AU	16.8	16.5	2.3	0.7	14.0	14.0	21.0	10
Anterior macronuclear nodule, width	VE	5.6	6.0	–	–	–	5.0	6.0	21
	AU	14.1	14.0	1.1	0.3	7.8	12.0	16.0	10
Micronucleus, length	VE	2.8	3.0	–	–	–	2.5	3.0	21
	AU	2.8	2.8	0.4	0.1	15.5	2.0	4.0	10
Micronucleus, width	VE	2.7	2.5	–	–	–	2.5	3.0	21
	AU	2.6	2.5	0.4	0.1	16.4	2.0	4.0	10
Macronuclear nodules, number [a]	VE [a]	–	–	–	–	–	1.0	2.0	41
	AU	1.0	1.0	0.0	0.0	0.0	1.0	1.0	10
Somatic ciliary rows, number in mid-body	VE	27.9	27.5	1.5	0.4	5.2	26.0	30.0	16
	AU	29.6	29.5	0.7	0.2	2.4	29.0	31.0	10

[a] Of 41 specimens investigated, 11 (27%) had one macronuclear nodule and 30 (73%) had two nodules (Fig. 155b, f, g, j–m).

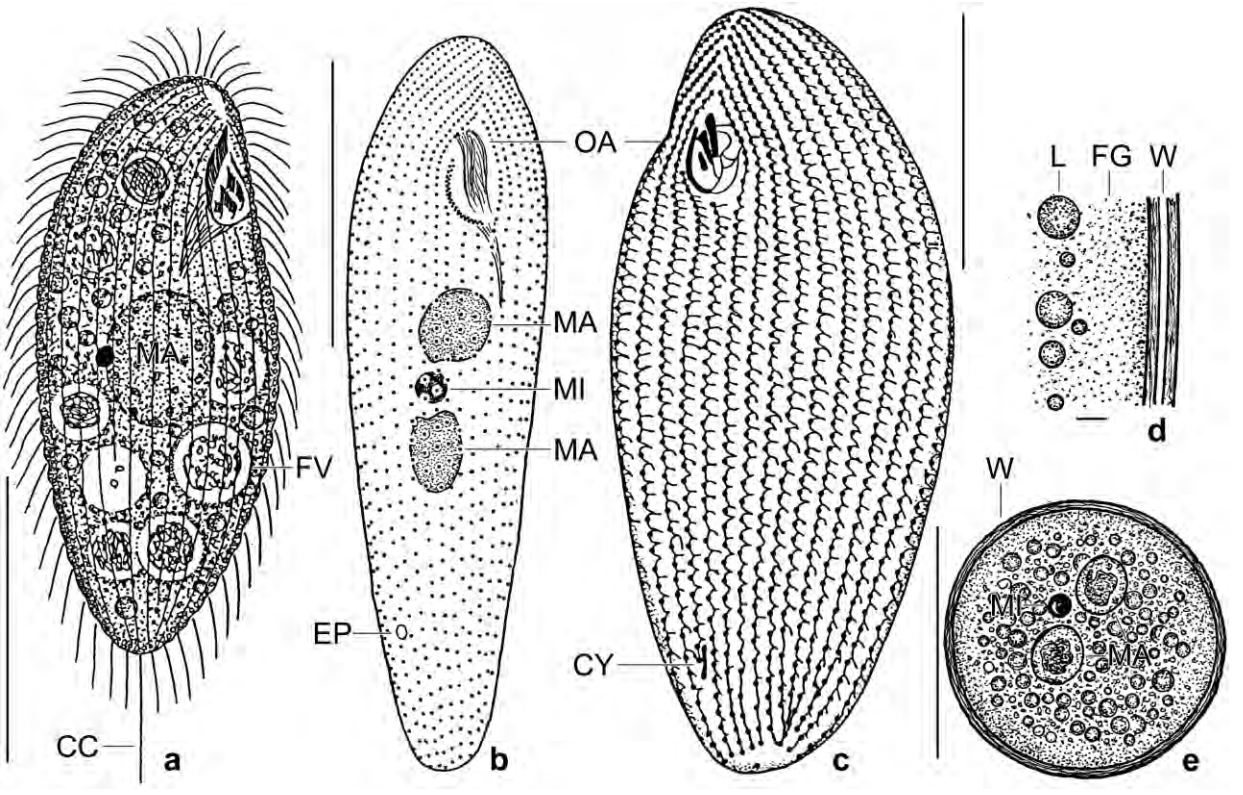

Fig. 155a–e. *Tetrahymena rostrata*, Austrian (Burgenland; a, c), Venezuelan (b), and Namibian (d, e) populations from life (a, d, e), after protargol impregnation (b), and KLEIN-FOISSNER silver nitrate impregnation (c). **a, c:** Right side view of a theront with single macro- and micronucleus (a). Figure (c) shows the silverline pattern, which has many short cross-lines that originate from the vertical silverlines connecting the basal bodies of the ciliary rows. **b:** Ventral view of ciliary- and nuclear pattern of a just excysted specimen. The ciliary pattern is as in ordinary specimens while the nuclear apparatus is composed of two macronuclear nodules and a micronucleus in between. **d, e:** The globular resting cyst has an about 1 µm thick wall (d) and two macronuclear nodules with a micronucleus in between. CC – caudal cilium, CY – cytopyge, EP – excretory pore of contractile vacuole, FG – finely granular zone, FV – food vacuole, L – lipid droplet, M – macronuclear nodules, MI – micronucleus, OA – oral apparatus, W – cyst wall. Scale bars 1 µm (d), 25 µm (b, c, e), and 40 µm (a).

i. e., twice as long as the ordinary somatic cilia) and the minute mucocysts (~ 0.5 µm) require observation with a high power oil immersion objective. Last but not least, the resting cyst should be checked because it has a peculiar nuclear pattern not described from any other *Tetrahymena* species.

Here, we mention observations from the following sites: Austria (Burgenland, grassland soil from the Seewinkel National Park; detailed site and species description in FOISSNER 1987); Austria (Salzburg, soil from alpine grassland in the Gastein area; observations on life cycle FOISSNER 1987, site description in PEER & FOISSNER 1985); USA (soil from the Arizona Desert; resting cyst from life but nuclear apparatus not checked); Africa (floodplain soil from the Bukaos River in Namibia, site 64 in FOISSNER et al. 2002; resting cyst from life and after methyl green-pyronin staining, Fig. 155d, e, j–m), and Venezuelan site 61 (rain forest soil; live observation and protargol impregnation of recently excysted specimens, Fig. 155b, f–i; four voucher slides deposited in the Biology Centre of the Upper Austrian Museum in Linz, (LI).

Morphological notes: The morphology of *T. rostrata* has been described by KAHL (1926, 1931), CORLISS (1975), and FOISSNER (1987). The Venezuelan specimens match the Austrian ones both

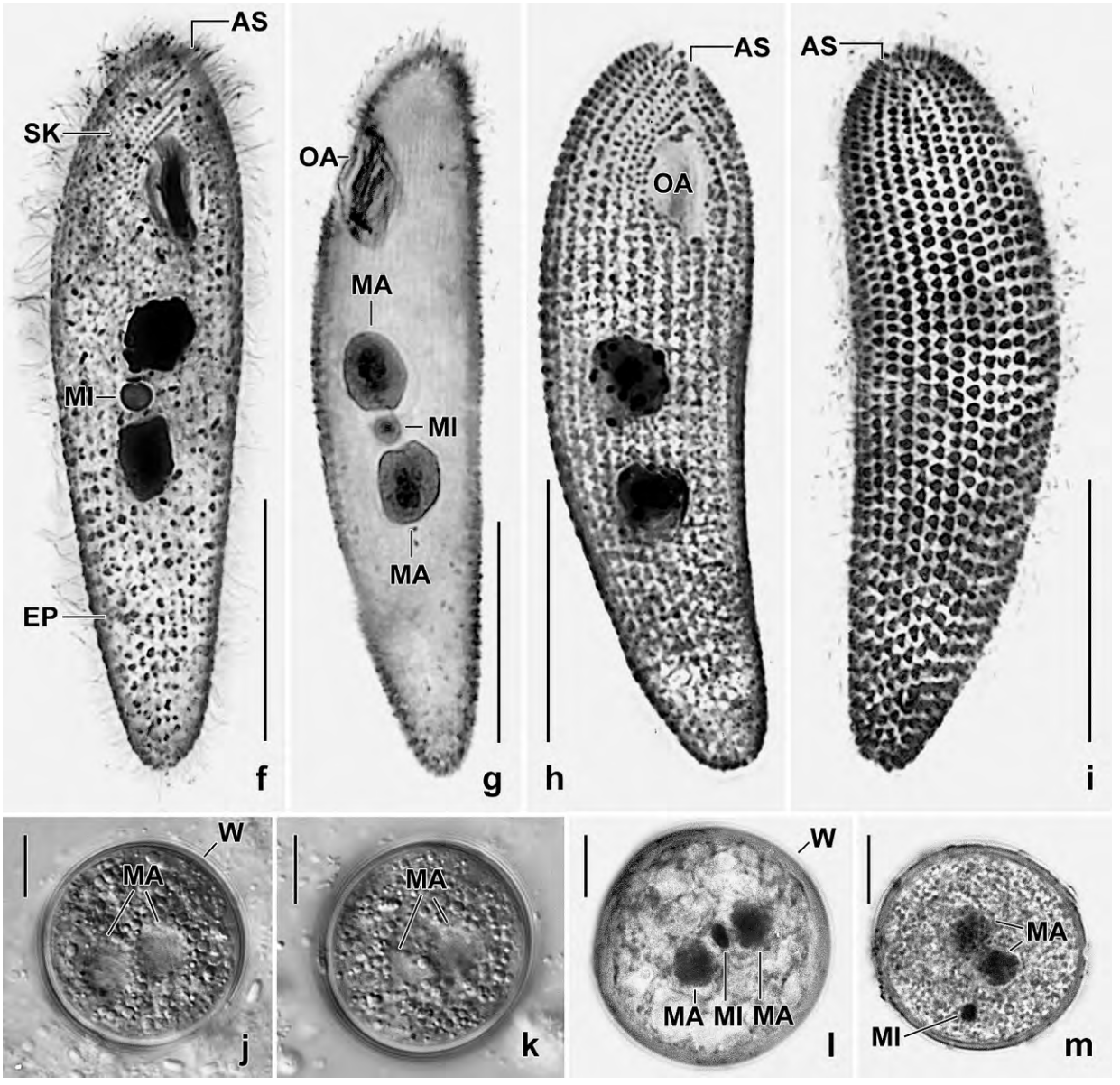

Fig. 155f–m. *Tetrahymena rostrata*, Venezuelan (f–i) and Namibian (j–m) specimens after protargol impregnation (f–i), from life (j, k), and after methyl green-pyronin staining (l, m). **f–i:** Just excysted specimens are slender and have a specific nuclear pattern, viz., two macronuclear nodules and a micronucleus in between (f–h). The ciliary pattern is as in ordinary specimens and conspicuous because the basal bodies are surrounded by minute mucocysts and thus appear comparatively large (h, i). **j–m:** Encysted specimens have a thin wall and an unusual nuclear pattern, viz., two macronuclear nodules and a single micronucleus in between (l) or scattered in the plasm (m). AS – anterior suture, EP – excretory pore of contractile vacuole, MA – macronuclear nodules, MI – micronucleus, OA – oral apparatus, SK – somatic kineties, W – cyst wall. Scale bars 10 µm (j–m) and 20 µm (f–i).

in morphology (body shape; single, short caudal cilium; ciliary and mucocyst pattern; many equidistantly spaced cross-silverlines; Fig. 155b, c, f–i) and most main morphometrics (body size, body length:width ratio, anterior body end to proximal end of paroral membrane, number of ciliary rows). The nuclear apparatus, in contrast, is different in 73% of the specimens, i. e., not composed of a single but of two macronuclear nodules and a single, about 3 µm-sized micronucleus in between or near to the nodules (Fig. 155b, f–h; Table 52). The binucleate state

is taken over from the resting cyst, suggesting that 73% of the specimens have recently excysted.

Resting cyst: Resting cysts were observed in populations from the USA, Namibia, Venezuela, and Austria. They are very similar in shape (globular), size (about 30 µm), and wall (smooth, thin, and colourless).

In the USA population, the cysts are globular with an average diameter of 28.3 µm (M = 28, SD = 3.4, SE = 0.7, CV = 12.0, Min = 20.0, Max = 32, n = 23). The cyst wall is smooth, about 1.4 µm thick, and colourless. The cytoplasm is studded with (lipid?) globules up to 5 µm across, providing the cyst with a yellow tint. The cysts of the Namibian specimens are globular with an average size of 30.8 × 30.1 µm (length/width: M = 30.5/30.0, SD = 2.2/1.7, SE = 0.5/0.4, CV = 7.0/5.7, Min = 27.0/27.0, Max = 35/33, n = 16/16). The cyst wall is smooth; 1.0–1.5 µm thick; and composed of two very thin, compact layers separated by a bright sheet. The cytoplasm is studded with colourless (lipid?) globules up to 2 µm across. The nuclear apparatus consists of two, rarely of three or more scattered macronuclear nodules with a single micronucleus in between or near to the nodules (Fig. 155d, e, j–m). Very recently, we checked an Austrian population for the cyst morphology. It is highly similar to that from Namibia.

Family Urotrichidae Small & Lynn, 1985

Improved diagnosis: Prostomatida with comparatively short oral flaps (palps) and continuous circumoral kinety. Adoral membranelles oriented more or less obliquely and inserted in anterior region of somatic ciliature; arranged one after the other, i. e., along main body axis. Oral basket complete and thus distinct. Somatic ciliary rows posteriorly shortened by 10–20%. Cortical alveoli and/or silverlines in *Urotricha* or *Parurotricha* pattern, i. e., quadrangular meshes or tetrahymenid.

Type genus: *Urotricha* Claparède & Lachmann, 1859.

Remarks: Many urotrichs and plagiocampids are small and thus difficult to investigate. Instead of an extensive discussion, we provide improved diagnoses and semischematic illustrations for distinguishing urotrichids from plagiocampids as well as for the plagiocampid genera (Fig. 156). Our main characteristics (oral flaps, location of adoral membranelles) include the cortical alveoli because they appear of considerable discriminatory value, although they are not known from all genera. The same applies to the silverline pattern, which is quite different to the alveolar pattern in some genera.

Looking at the scheme (Fig. 156) and the diagnoses, it becomes obvious that Lynn (2008) misclassified the urotrichid genus *Parurotricha* Foissner, 1983 in the Plagiocampidae.

Family Plagiocampidae Kahl, 1926

Improved diagnosis: *Prostomatida* with short or long oral flaps (palps). Circumoral kinety interrupted by adoral membranelles (brosse) side by side, i. e., oriented transversely to main body axis. Oral basket indistinct because basket rods lacking at brosse site. Somatic ciliary rows not or only slightly (≤ 10%) shortened posteriorly. Cortical alveoli in *Plagiocampa* pattern or forming minute polygonal meshes.

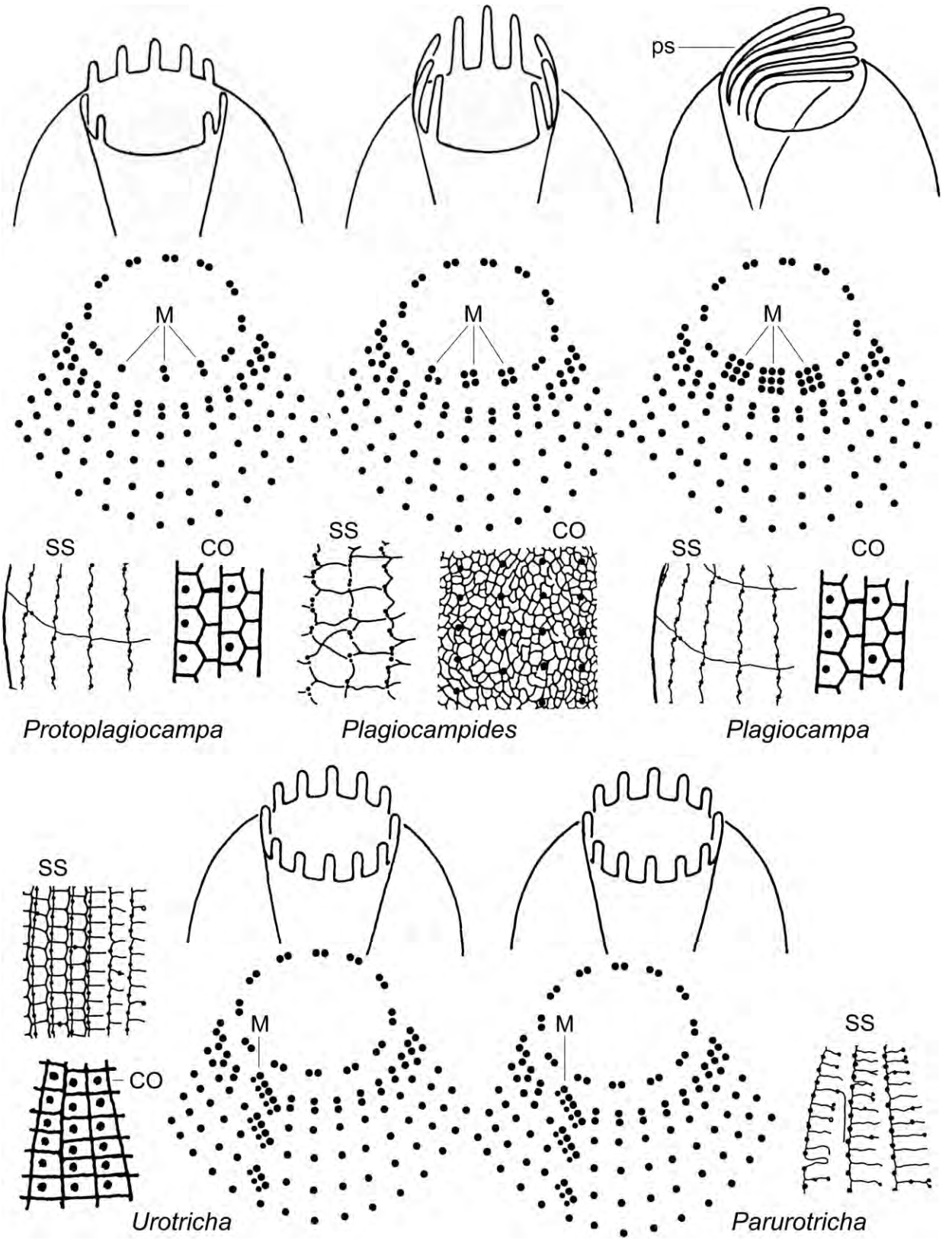

Fig. 156. Distinguishing plagiocampid and urotrichid genera by the location of the adoral membranelles (M), the structure of the cortex (CO), and the silverline pattern (SS).

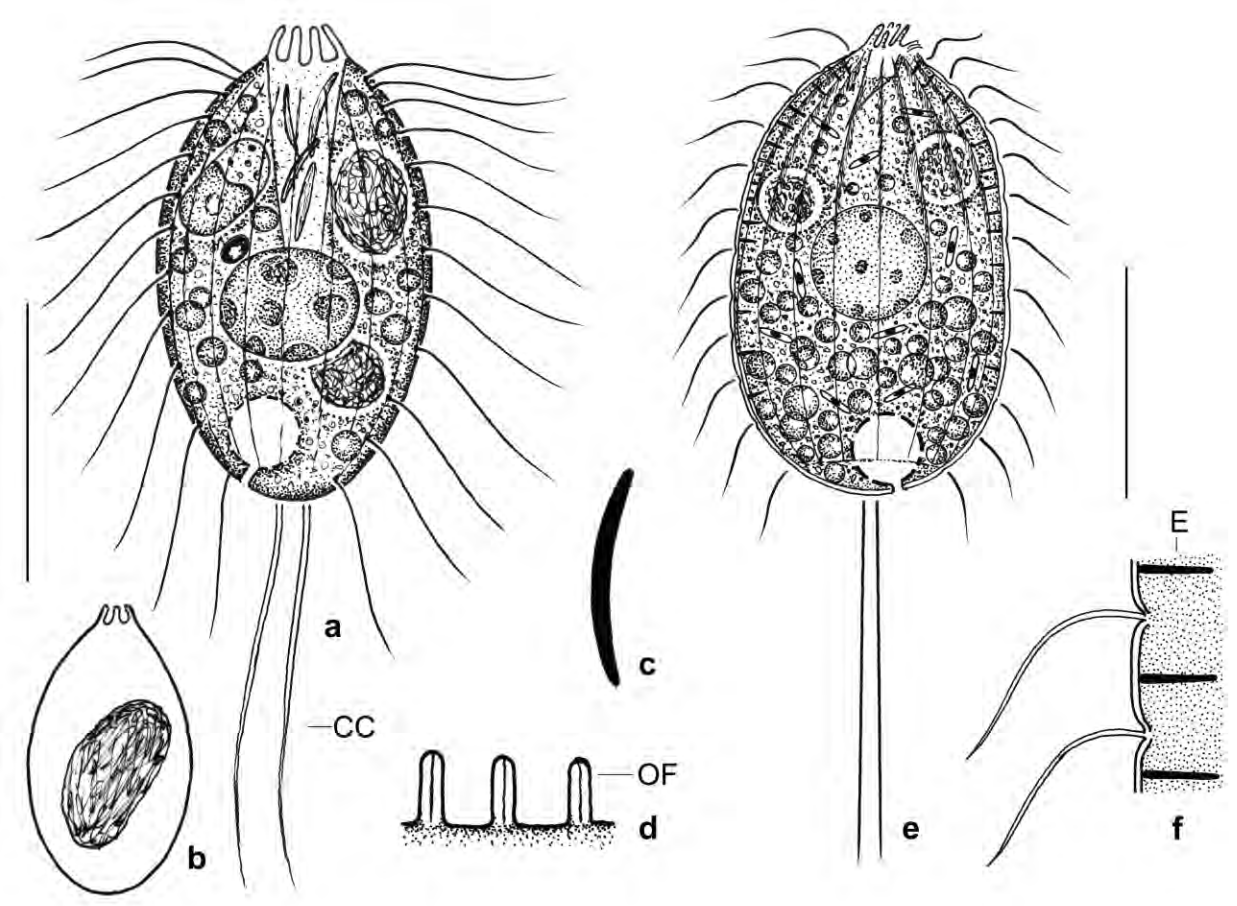

Fig. 157a–f. *Protoplagiocampa lajacola* (a–d) and *Plagiocampa pentadactyla* (e, f; from Foissner et al. 2002) from life. **a, e:** Overviews of representative specimens, length 25 µm and 30 µm. These species differ, inter alia, by the oral flaps (± motionless vs. beating up and down); the oral basket (funnel-shaped with extrusomes vs. bowl-shaped without extrusomes); and the somatic extrusomes (absent vs. present). **b:** A specimen having ingested an *Apocyclidium terricola*. **c, f:** Extrusomes, length 3 µm and 2 µm. **d:** The oral flaps each consist of two ciliary stumps. CC – caudal cilia, E – extrusomes, OF – oral flaps. Scale bars 15 µm.

Type genus: *Plagiocampa* Schewiakoff, 1893.

Remarks: As yet, this family was insufficiently separated from the Urotrichidae diagnosed above (Foissner & Pfister 1997, Lynn 2008). The discovery of a new plagiocampid genus is a good opportunity to clarify this matter by improving the diagnoses of the families and of the four plagiocampid genera.

Genus *Plagiocampa* Schewiakoff, 1893

Improved diagnosis: Plagiocampidae with oral flaps beating up and down the oral opening. Cortical alveoli in *Plagiocampa* pattern.

Type species: *Plagiocampa mutabilis* Schewiakoff, 1893.

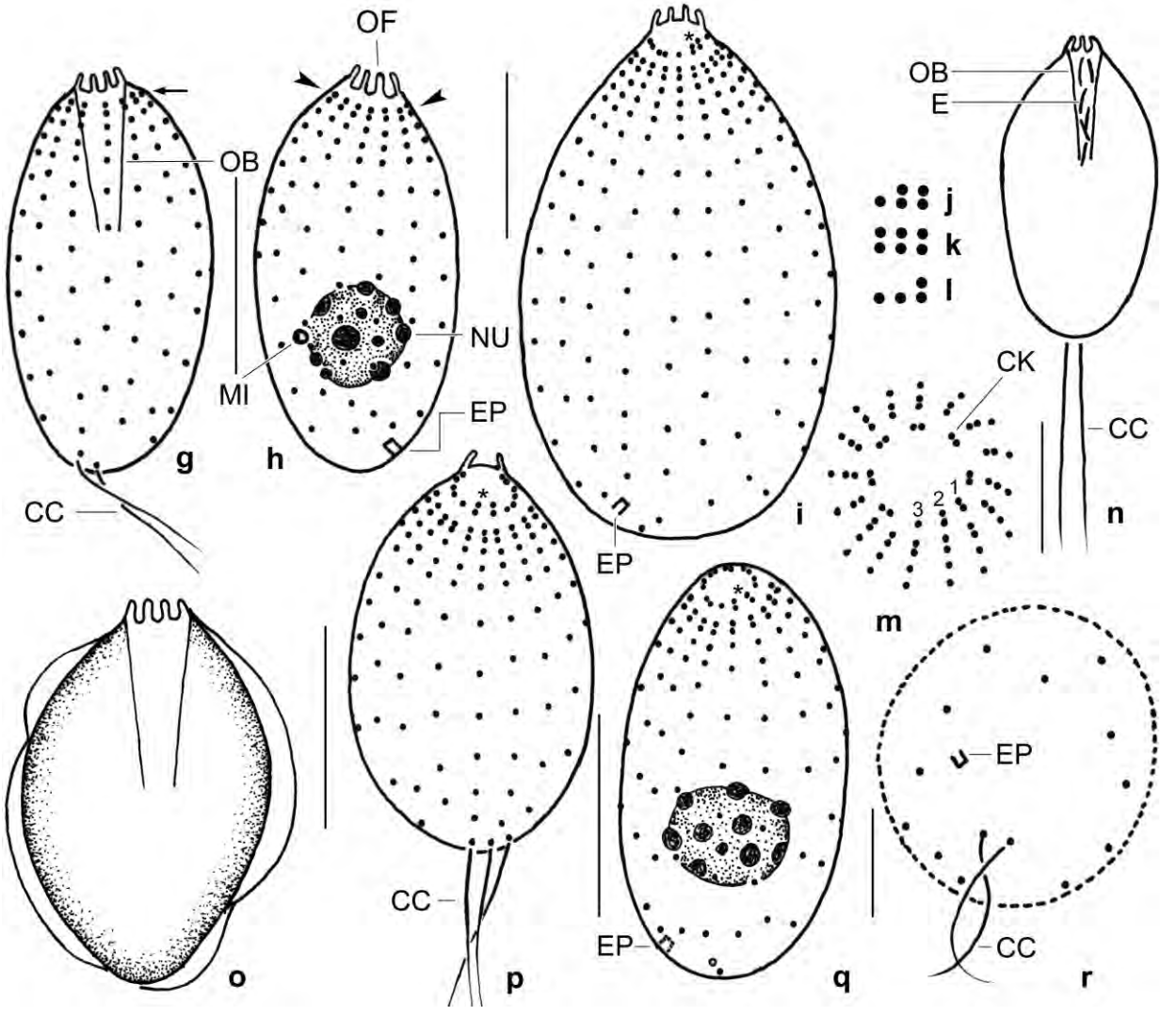

Fig. 157g–r. *Protoplagiocampa lajacola* from life (n, o) and after protargol impregnation (g–m, p–r). Figures (g–i, p, q) drawn to scale to show size variability. **g, h:** Right and left side view of holotype specimen, length 20 µm. The arrow marks the brosse side. The arrowheads denote the dikinetid at the anterior end of the ciliary rows. **i, p, q:** Ventral view of paratype specimens, showing the inconspicuous brosse (asterisks) and a cell with three caudal cilia. The excretory pore of the contractile vacuole and one of the two caudal cilia are not recognizable at this focal plan but appear when the focus is near cell centre (q). **j–l:** Structure of the adoral membranelles (brosse): 95% of the specimens have the pattern shown in (j), while (k) and (l) are very rare. **m, r:** Anterior and posterior polar view, showing the organization of the oral and somatic ciliature. Posteriorly, the ciliary rows end at slightly different level. Thus, the cilia do not form a perfect circle, in contrast to the circumoral kinety which, however, is interrupted by the adoral membranelles (numerals 1, 2, 3). **n:** A slender specimen without large food vacuoles, resembling *Urotricha farcta*. **o:** The cortex forms large blisters under slight coverslip pressure (see Fig. 158g). CC – caudal cilia, CK – circumoral kinety, E – extrusomes, EP – excretory pore of contractile vacuole, MI – micronucleus, NU – nucleolus of macronucleus, OB – oral basket, OF – oral flaps. Scale bars 5 µm (m, r) and 10 µm (g–i, p, q).

Remarks: The most remarkable features of *Plagiocampa* are the oral flaps, which beat up and down the mouth opening, and the distinct difference between cortical and silverline pattern (Fig. 156).

Genus *Chilophrya* Kahl, 1930a

At the present state of knowledge, *Chilophrya* cannot be distinguished unambiguously from *Plagiocampa*. Foissner (1984) described in detail a terrestrial *Chilophrya* species but the generic assignment remained doubtful. The terrestrial species is similar to *Plagiocampa* but has a different silverline pattern and extrusomes with anchors, like the microthoracids.

Genus *Plagiocampides* Foissner, Agatha & Berger, 2002

Improved diagnosis: Plagiocampidae with long oral flaps not beating up and down the oral opening. Cortical alveoli minute and polygonal.

Type species: *Plagiocampides halophilus* Foissner, Agatha & Berger, 2002.

Remarks: Both, the cortical alveoli and the silverline pattern are markedly different from those of the congeners (Fig. 156), emphasizing the uniqueness of the type species.

Protoplagiocampa nov. gen.

Diagnosis: Plagiocampidae with short oral flaps not beating up and down the oral opening. Cortical alveoli in *Plagiocampa* pattern.

Type species: *Protoplagiocampa lajacola* nov. spec.

Etymology: Composite of the Greek prefix *proto* (coming first) and the generic name *Plagiocampa*, supposing that *Plagiocampa* evolved from *Protoplagiocampa*. Feminine gender.

Remarks: We put together the features distinguishing the plagiocampid genera in Fig. 156, showing that *Protoplagiocampa* has minute, urotrichid oral flaps while the adoral membranelles are plagiocampid.

Protoplagiocampa lajacola nov. spec. (Fig. 157a–r, 158a–v, 159a–g; Table 53)

Diagnosis: Size about 25 × 15 µm in vivo. Shape usually broadly ellipsoid, overfed specimens broadly ovate. 1 macronucleus and 1 micronucleus. Extrusomes mainly within oral basket, 3–4 µm long rods with narrowed ends. On average 17 ciliary rows commencing subapically with a dikinetid and ending in posterior pole area; 2 caudal cilia 20–25 µm long. On average 6 circumoral dikinetids associated with 2–3 µm high oral flaps and nematodesmata, forming a comparatively distinct oral basket. 3 adoral membranelles composed of 2, 2 and 1 kinetid, respectively.

Type locality: Venezuelan site (30), viz., mud and soil from ephemeral puddles (Lajas) on granitic outcroppings between the Agricultural Research Institute and the airport of Pto. Ayacucho, 67°36‘W 5°41‘N.

Type material: 1 holotype and 1 paratype slide with protargol-impregnated specimens as well

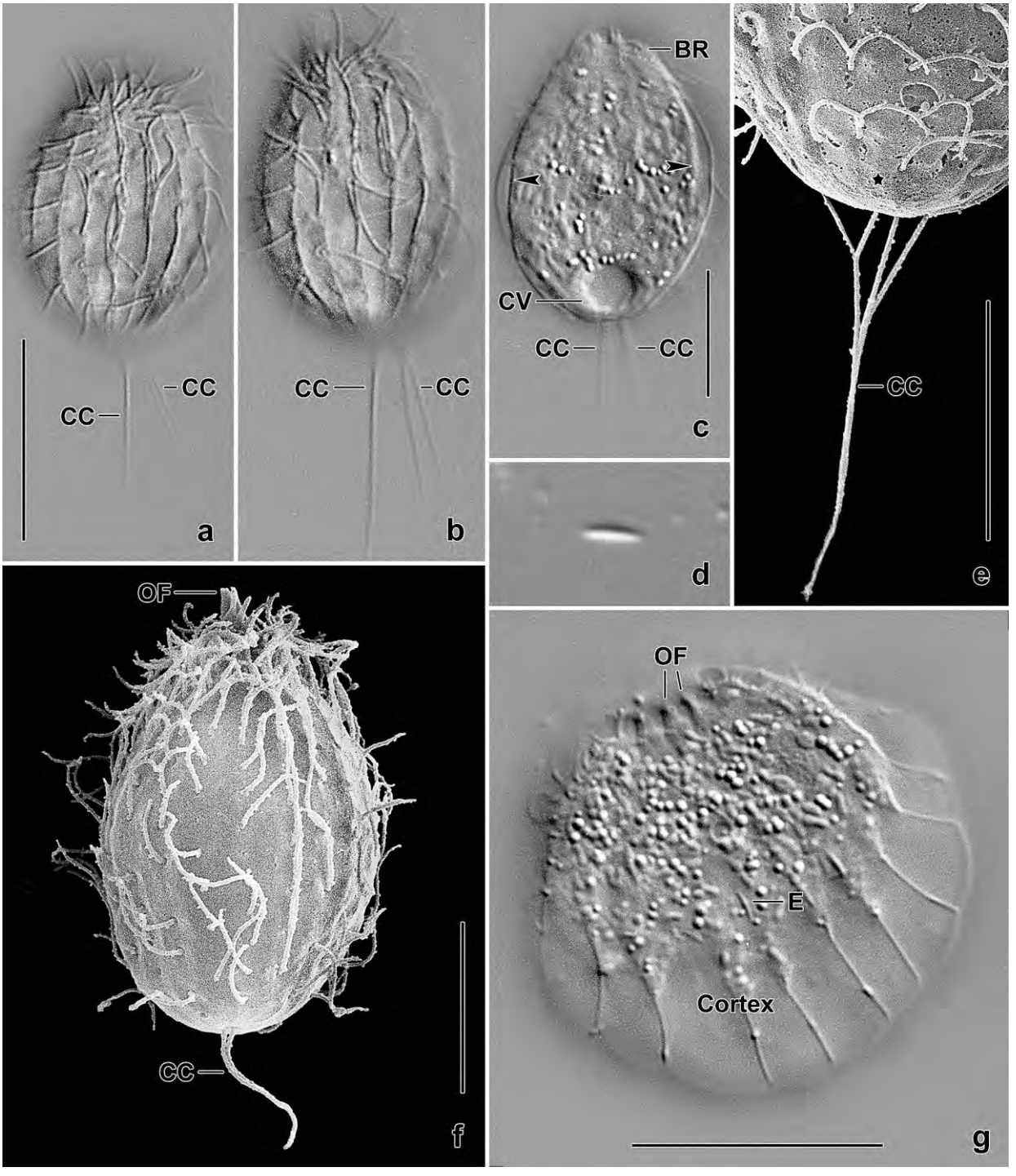

Fig. 158a–g. *Protoplagiocampa lajacola* from life (a–d, g) and in the scanning electron microscope (e, f). **a, b:** A specimen with three caudal cilia. **c, g:** When slightly pressed, large blisters appear (c, arrowheads) and the cortex is sheded (g). **d:** Extrusome, length 3 µm. **e:** A specimen with four caudal cilia. The asterisk marks the minute, non-ciliated posterior pole area. **f:** Overview of a specimen with two caudal cilia. BR – brosse, CC – caudal cilia, CV – contractile vacuole, E – extrusome, OF – oral flaps. Scale bars 10 µm (e, f) and 20 µm (a–c, g).

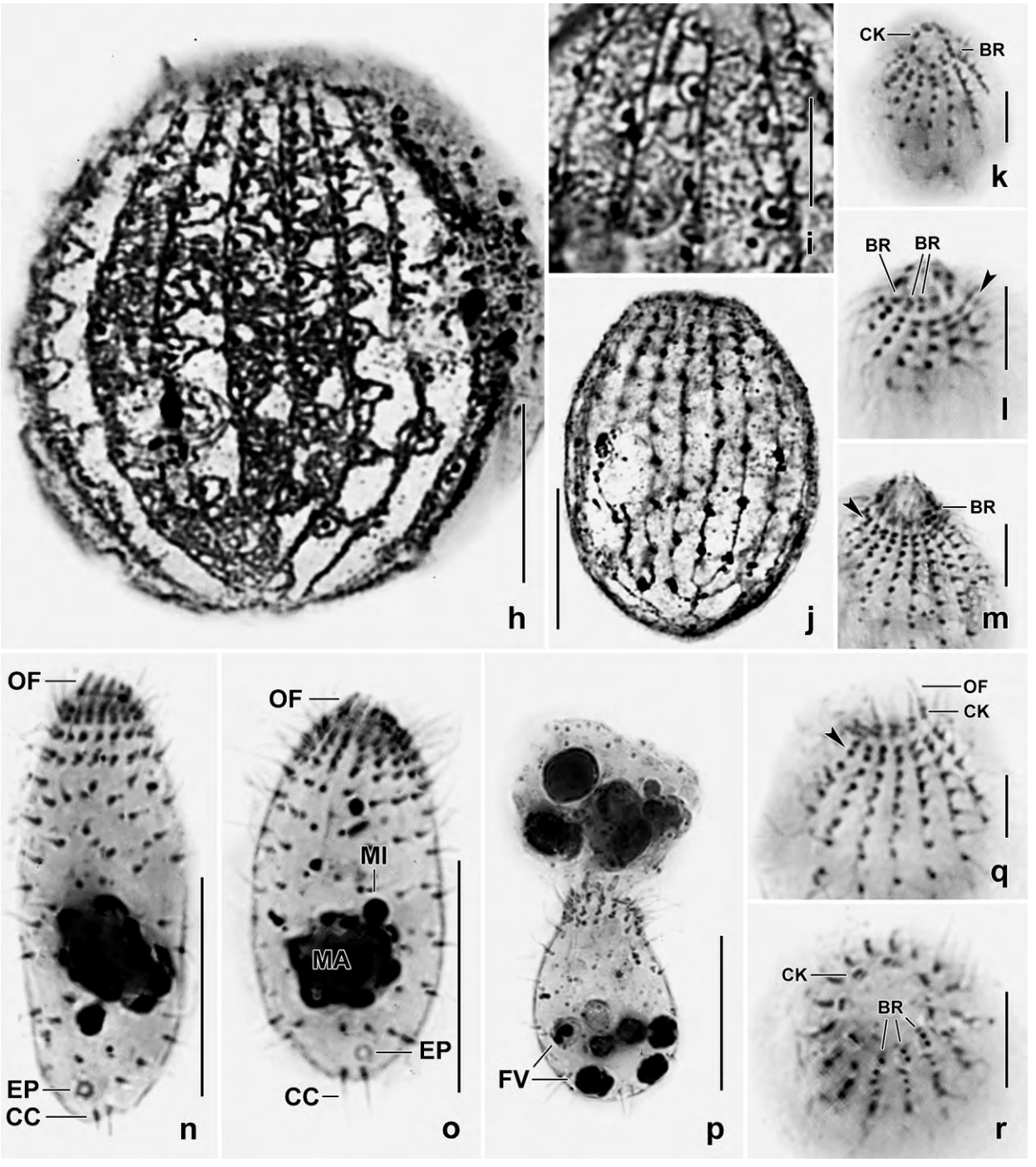

Fig. 158h–r. *Protoplagiocampa lajacola* after silver nitrate (h–j, Klein-Foissner method) and protargol (k–r) impregnation. **h, i:** Plagiocampid cortex pattern. **j:** Silverline pattern. **k–m, q, r:** Anterior and oblique anterior polar views, showing the oral and circumoral ciliature. The arrowheads in (l, m, q) mark a dikinetid at the anterior end of the ciliary rows. The minute brosse (adoral membranelles) is difficult to recognize. **n, o:** Overviews. The macronucleus is pustulate due to large nucleoli. **p:** Feeding on *Apocyclidium terricola* lysed outside the cell (cp. Fig. 159c, g). BR – brosse, CC – caudal cilia, CK – circumoral kinety, EP – excretory pore, FV – food vacuoles, MA – macronucleus, MI – micronucleus, OF – oral flaps. Scale bars 4 µm (i, k–m, q, r), 10 µm (h, j), and 15 µm (n–p).

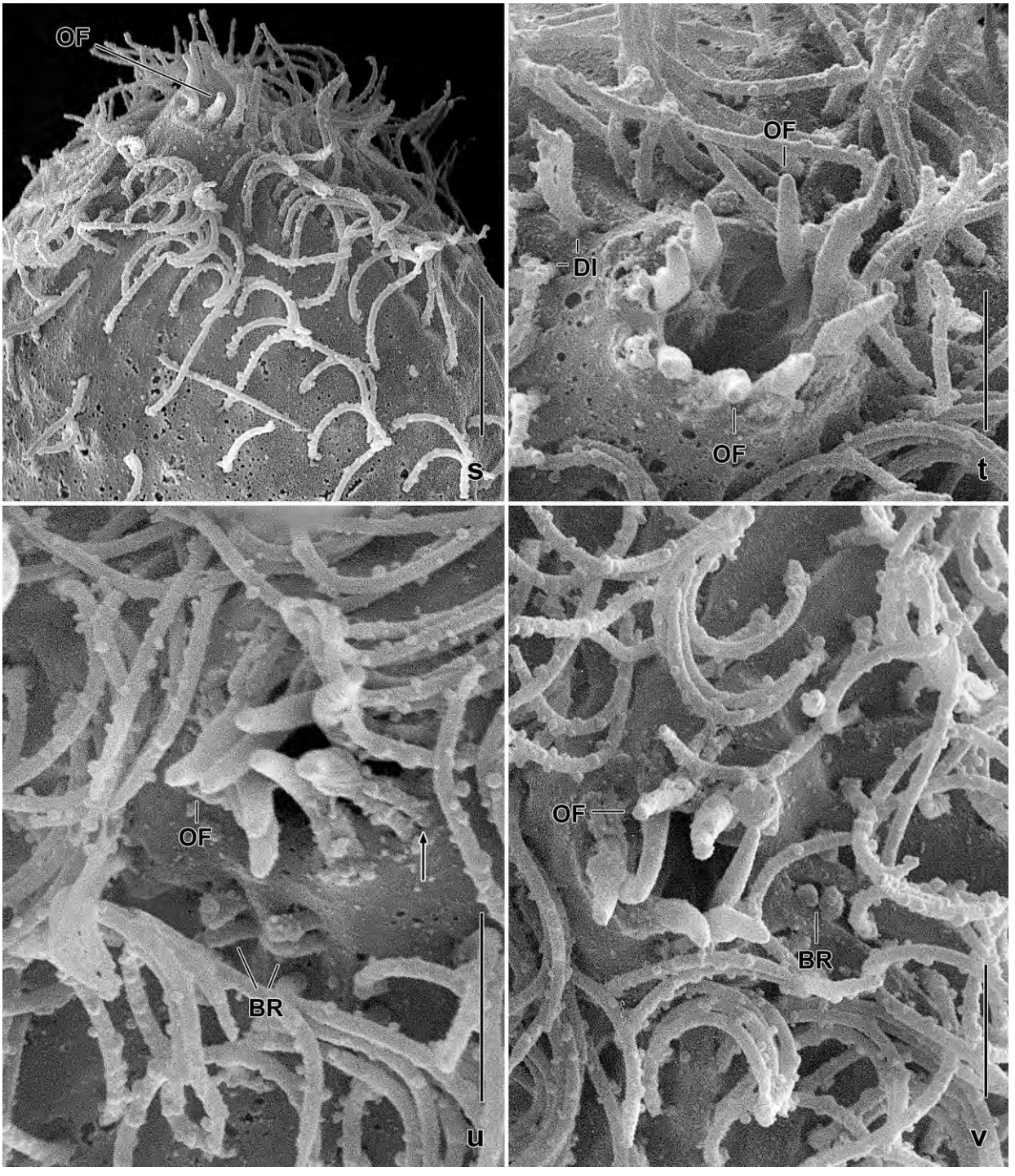

Fig. 158s–v. *Protoplagiocampa lajacola*, oral structures in the scanning electron microscope. **s:** Lateral view of anterior region. **t:** Anterior polar view, showing the mouth opening surrounded by eight oral flaps with a length of about 2 µm. **u, v:** Anterior polar views, showing the mouth opening surrounded by the oral flaps, each consisting of two minute cilia (u, arrow). Note the brosse (adoral) cilia, which are only 0.7 µm long. BR – brosse (adoral membranelles), DI – dikinetids at begin of somatic ciliary rows, OF – oral flaps. Scale bars 2 µm (t–v) and 5 µm (s).

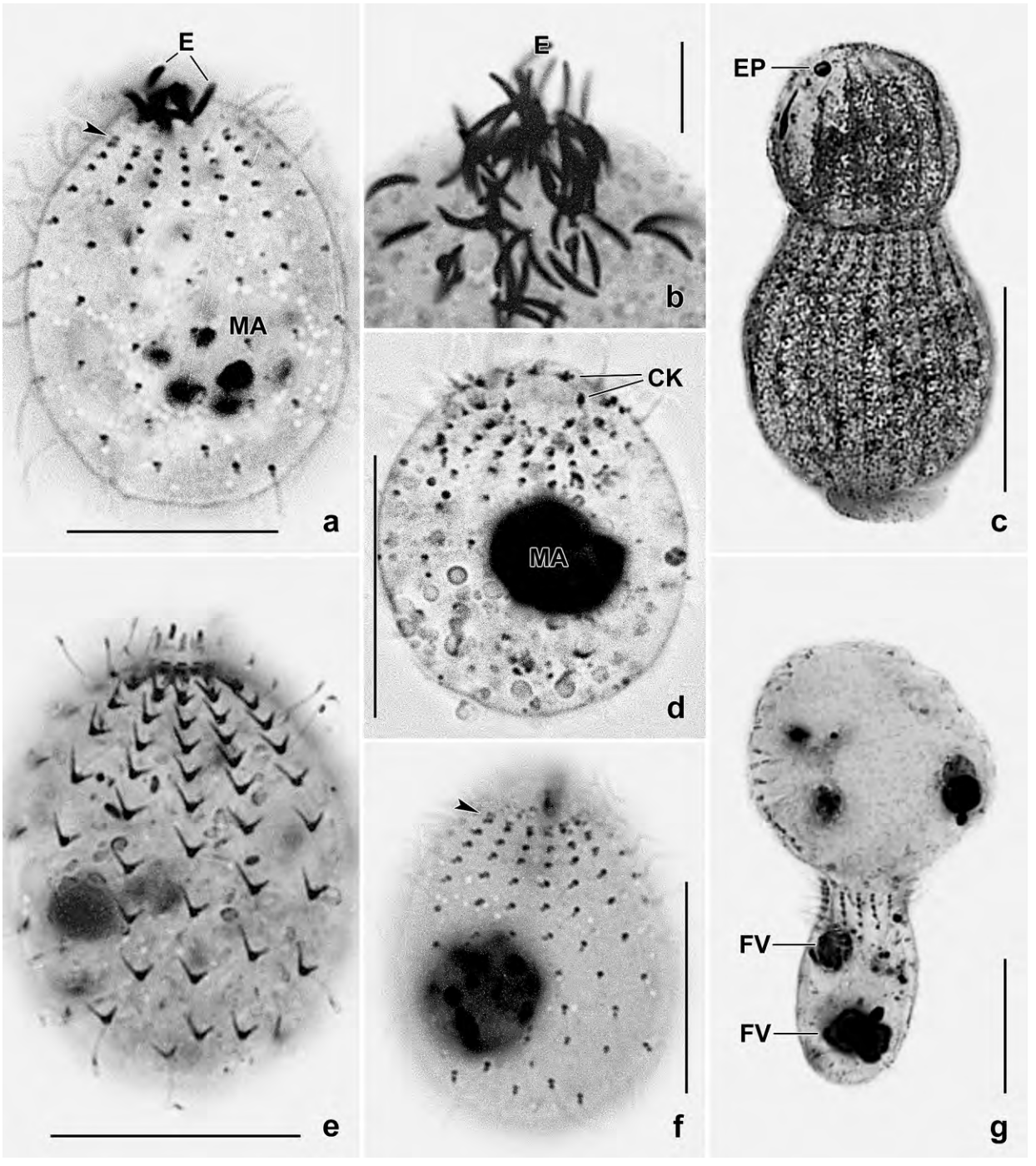

Fig. 159a–g. *Protoplagiocampa lajacola* after silver carbonate (a, b, d–f), silver nitrate (c, Chatton-Lwoff method), and protargol (g) impregnation. **a, f:** Lateral overviews, showing the dikinetid (arrowheads) at the anterior end of the somatic ciliary rows and the extrusomes restricted to the mouth (a). **b:** The cytopharynx contains many extrusomes deeply impregnating with silver carbonate. **c:** A cannibalistic specimen. **d:** Oblique anterior polar view, showing the circumoral kinety. **e:** Fibre system associated with somatic kineties. **g:** Feeding on *Apocyclidium terricola*, which is inflated and larger than *P. lajacola*. Possibly, this is an early stage where the prey is not yet lysed completely (cp. Fig. 158p). CK – circumoral kinety, E – extrusomes, EP – excretory pore, FV – food vacuoles, MA – macronucleus. Scale bars 5 µm (b), 15 µm (a, d–f), and 20 µm (c, g),

Table 53. Morphometric data on *Protoplagiocampa lajacola* based on mounted, protargol-impregnated (FOISSNER'S method), and randomly selected specimens from a non-flooded Petri dish culture. Measurements in µm. CV – coefficient of variation in %, M – median, Max – maximum, , Mean – arithmetic mean, Min – minimum, n – number of individuals investigated, SD – standard deviation, SE – standard error of mean.

Characteristics	Mean	M	SD	SE	CV	Min	Max	n
Body, length	21.5	21.0	4.5	1.0	21.1	13.0	31.0	21
Body, width	13.2	12.0	4.3	0.9	32.4	7.0	23.0	21
Body length:width, ratio	1.7	1.7	0.3	0.1	17.1	1.3	2.6	21
Anterior body end to macronucleus, distance	9.0	9.0	1.9	0.4	21.4	6.0	14.0	21
Oral field, diameter of somatic kineties	3.9	4.0	0.8	0.2	19.9	3.0	5.5	21
Oral field, diameter of circumoral kinety	2.9	2.5	0.6	0.1	21.3	2.0	4.0	21
Macronucleus, length	6.6	6.0	1.5	0.3	22.7	4.0	10.0	21
Macronucleus, width	5.8	6.0	1.4	0.3	23.9	3.0	10.0	21
Micronucleus, diameter	1.2	1.2	–	–	–	1.0	1.5	21
Ciliary rows, number	16.8	16.0	1.9	0.4	11.4	15.0	21.0	21
Basal bodies in a kinety, number	11.8	11.0	2.1	0.5	18.0	9.0	16.0	21
Caudal cilia, number	2.2	2.0	–	–	–	2.0	4.0	21
Circumoral dikinetids, number	6.3	6.0	0.7	0.1	10.4	5.0	8.0	21
Adoral membranelles, number	3.0	3.0	0.0	0.0	0.0	3.0	3.0	21

as 1 and 5 paratype slides with CHATTON-LWOFF and KLEIN-FOISSNER silver nitrate-impregnated specimens, respectively, have been deposited in the Biology Centre of the Upper Austrian Museum in Linz (LI). Further, we deposited at the same locality 2 voucher slides with specimens from Venezuelan site (12). Relevant specimens have been marked by black ink circles on the coverslip.

Etymology: The name is a composite of *Laja* (ephemeral puddles on granitic outcroppings) and the Latin verb *colere* (to live in), the habitat the species was discovered.

Description: This species impregnated poorly with silver nitrate while excellently with protargol, making it possible to study the finest details. Many features have a rather high (CV near 20%) variability (Table 53). This is associated with feeding: specimens with many food vacuoles are distinctly larger than starving cells. We could not decide whether large cells develop when food is abundant or small specimens become expanded when strongly fed; macrostome formation does not occur.

Size 15–35 × 9–27 µm in vivo, usually about 25 × 15 µm (Table 53); not contractile. Body shape and length:width ratio (1.3–2.6:1, on average 1.7:1) highly variable, depending on amount of food ingested: usually ellipsoid (Fig. 157a, b, g, h, q, 158b, f, n, o) to indistinctly ovate (Fig. 157p); narrowly ellipsoid and indistinctly pentagonal with narrowed, slightly projecting oral area when starving (Fig. 157n); broadly ovate with bluntly acute oral area when overfed (Fig. 157i); slightly asymmetrical because anterior shoulder more pronounced on brosse side (Fig. 157n). Nuclear apparatus in or near body centre. Macronucleus broadly ellipsoid to globular, in vivo about 7 µm across and with pale, up to 3 µm-sized nucleoli, making it pustulate in protargol preparations

due to shrinkage processes. Micronucleus attached to macronucleus, about 1.2 µm in protargol preparations (Fig. 157a, h, q, 158o, 159a, d; Table 53). Contractile vacuole in posterior body end slightly out of pole centre, with single excretory pore (Fig. 157a, h, i, q, r). Mature extrusomes only within oral basket, impregnate deeply with silver carbonate but not with protargol; slightly curved, 3–4 µm long, ends slightly narrowed (Fig. 157a, c, 159a, b); somatic extrusomes absent. Cortex very flexible, rather thick, of *Plagiocampa* structure, according to the silver nitrate preparations (Fig. 158h, i); easily separates from cytoplasm under slight coverslip pressure, forming large blisters showing ciliary imprints (Fig. 157o, 158c, g). Cytoplasm colourless, often contains many lipid droplets up to 2 µm across. Feeds on small ciliates, flagellates, and an 8 µm long green alga; a greedy predator containing up to six partially digested *Apocyclidium terricola* (30–40 µm long!) because prey is partially or completely lysed at mouth entrance (Fig. 158p, 159g); rarely cannebalistic (Fig. 159c). Swims in wide spirals and glides rapidly and upright, i. e., with the mouth directed to microscope slide.

Somatic cilia about 10 µm long in vivo, arranged in an average of 17 longitudinal, equidistant rows commencing subapically with a dikinetid and ending in posterior pole region; unciliated posterior pole area thus indistinct; each kinety with an average of 12 cilia. Two to four, usually two caudal cilia slightly displaced dorsally; conspicuous because 20–25 µm long in vivo and beating slowly; distal half very fine and thus not preserved in protargol preparations (Fig. 157a, g–i, n, p–r, 158a–f, n, o, s, 159a, e, f; Table 53).

Oral opening in centre of anterior pole, occupying about 22% of body width, limited by circumoral kinety composed of an average of six dikinetids each associated with a 2–3 µm high ciliary stump, forming an oral flap not beating up and down. Oral basket inconspicuous in vivo and protargol preparations, funnel-shaped, extends to mid-body, contains extrusomes as described above. Adoral membranelles (brosse) on anterior end of three somatic ciliary rows, intersect circumoral kinety, minute, i. e., membranelles 1 and 2 each composed of two minute cilia, membranelle 3 of only one basal body; some variation occurs (Fig. 157a, d, g–n, p–r158, f, g, k–v, 159a, d, f; Table 53).

Ecology and Occurrence: Common in Lajas (lithotelmas) of Venezuela; one record from savannah soil. *Protoplagiocampa lajacola* reproduced rapidly and became abundant in the non-flooded Petri dish culture, feeding mainly on the slightly larger *Apocyclidium terricola*, which is partially or completely lysed at the mouth entrance (Fig. 158p, 159g).

Remarks: *Protoplagiocampa lajacola* is a minute ciliate not easily identified. In vivo, the best feature is probably the extrusomes within the oral basket and the two caudal cilia. In protargol preparations, the unique structure of the brosse, the two caudal cilia, and the main morphometrics should produce a safe identification.

There are two *Plagiocampa* species with which *P. lajacola* can be mixed because they have a similar size and shape and two caudal cilia. *Plagiocampa pentadactyla* Foissner et al., 2002 has a rather distinct subapical shoulder, making the outline pentagonal (Fig. 157e). Further, it has 2 µm long somatic extrusomes (Fig. 157f) while *P. lajacola* has 3–4 µm long oral extrusomes (Fig. 157a, c). *Plagiocampa namibiensis* Foissner et al., 2002 is ovate, has somatic extrusomes, and

possesses only 6 (vs. 12) cilia in the somatic kineties. There are also similar *Urotricha* species, e. g., *U. furcata*, which, however, lack cilia in the posterior quarter (Foissner et al. 1999).

Plagiocampa monotricha nov. spec. (Fig. 160a–l; Table 54)

Diagnosis: Size in vivo about 35 × 25 µm; broadly ellipsoid. Oral extrusomes slightly fusiform, about 5 × 0.4 µm in size; somatic extrusomes about 1 µm long. 1 caudal cilium. On average 24 ciliary rows and 17 oral dikinetids (flaps).

Type locality: Venezuelan site (52), i. e., upper soil layer of a gallery forest some km south of the village of Choroni, 67°37' W 10°30'N.

Type material: 1 holotype and 4 paratype slides with protargol-impregnated specimens have been deposited in the Biology Centre of the Upper Austrian Museum in Linz (LI).

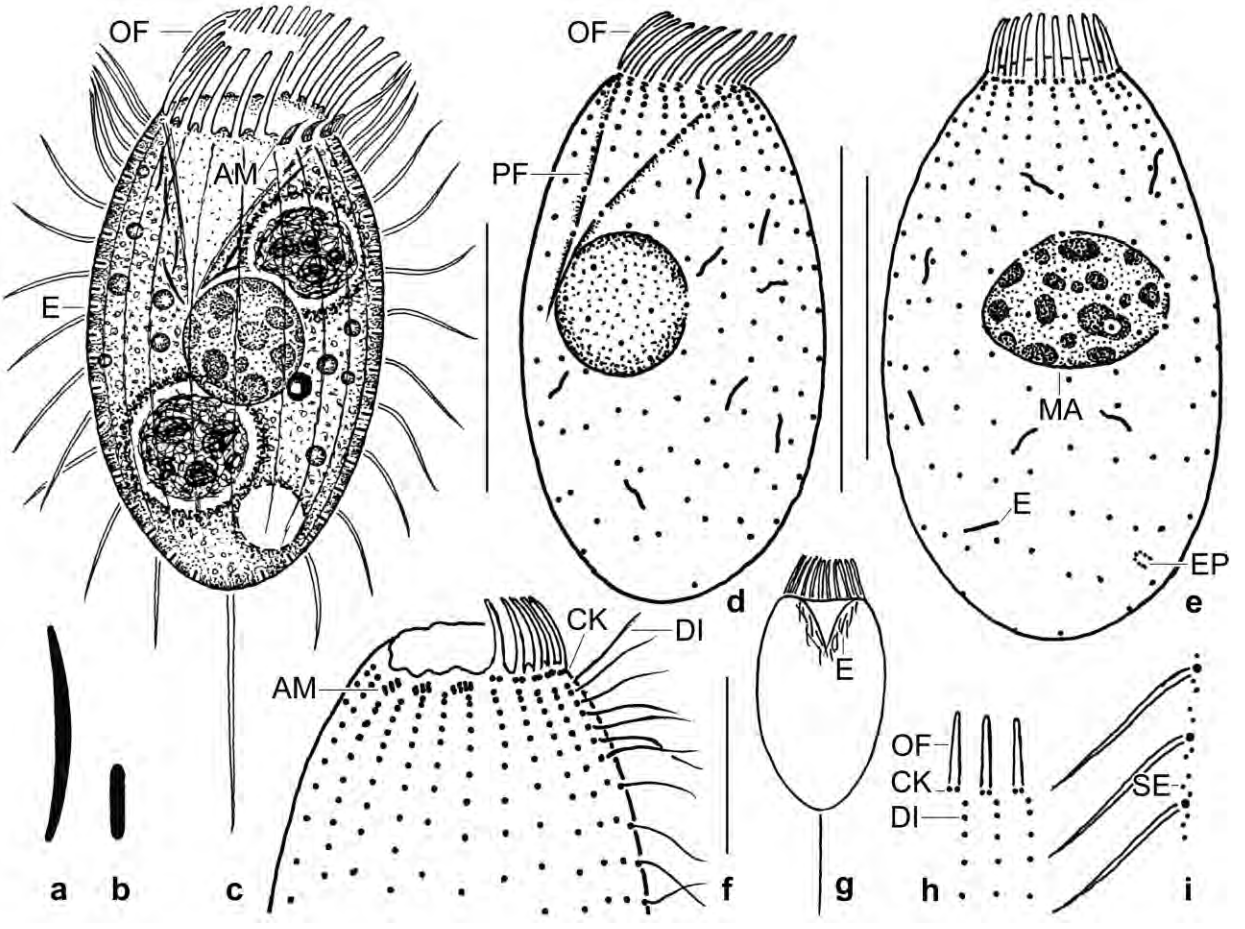

Fig. 160a–i. *Plagiocampa monotricha* from life (a–c, g–i) and after protargol impregnation (d–f). **a, b:** An oral and a somatic extrusome, length 5 µm and 1 µm. **c:** Ventrolateral view of a representative specimen, length 35 µm. **d, e:** Lateral views, showing the ciliary pattern and the macronucleus. **f:** Ventrolateral view of holotype specimen, showing the three adoral membranelles. **g:** Dorsal view, showing the obconical pharynx in the middle third of the anterior body end. **h:** Oral structures in vivo. **i:** The somatic extrusomes are within the ciliary rows. AM – adoral membranelles, CK – circumoral kinety, DI – ciliated dikinetid on begin of ciliary rows, E – extrusomes, EP – excretory pore of contractile vacuole, MA – macronucleus, OF – oral flaps, PF – pharyngeal fibres, SE – somatic extrusomes. Scale bars 10 µm (f) and 20 µm (c–e).

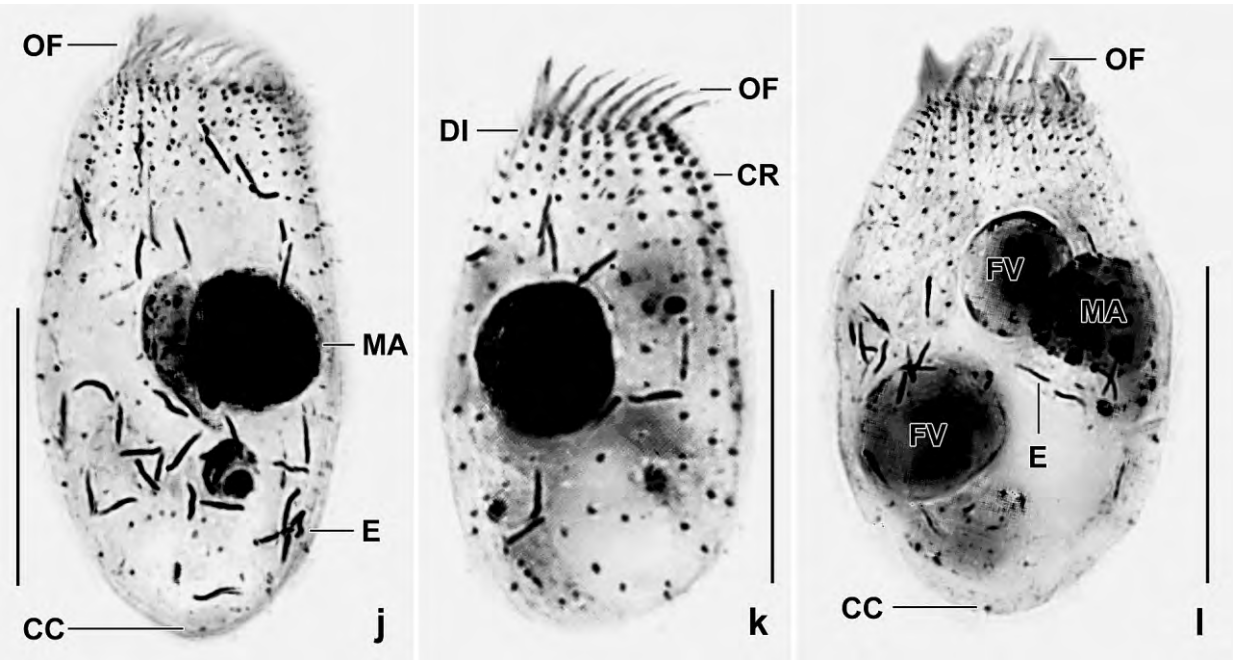

Fig. 160j–l. *Plagiocampa monotricha* after protargol impregnation. The ellipsoid body (a) becomes ovate in well-fed specimens (c). Note the ciliary pattern, the long oral flaps and the single basal body bearing the caudal cilium in centre of posterior pole. CC – caudal cilium, CR – ciliary rows, DI – dikinetid at begin of ciliary rows, E – extrusomes, FV – food vacuoles, MA – macronucleus, OF – oral flaps. Scale bars 20 µm.

Etymology: The Latinized Greek adjective *monotricha* (one hair) refers to the single caudal cilium, a main character of this species.

Description: Size in vivo 30–45 × 20–30 µm, usually about 35 × 25 µm as calculated from some live measurements and the morphometric data in Table 54 adding 15% preparation shrinkage; slightly to up to 2:1 flattened laterally. Shape ellipsoid to broadly ellipsoid, bluntly ovate when full of food (Fig. 160c–e, g, j–l; Table 54). Nuclear apparatus in or near body centre, may be dislocated by large food vacuoles (Fig. 160c–e, j–l; Table 54). Macronucleus globular to broadly ellipsoid, contains many large nucleoli. Micronucleus attached to macronucleus, about 2 µm across. Excretory pore of contractile vacuole on ventral side subterminal at boarder of ciliated/non-ciliated body portion (Fig. 160c, e). Cortex flexible, glossy; contains many minute, about 1 µm long extrusomes within ciliary rows, do not impregnate with the protargol method used (Fig. 160b, c, i). Mature oral extrusomes mainly around oral basket, slightly fusiform and about 5 × 0.4 µm in size (Fig. 160a, c, g, j–l), do not impregnate with protargol; 3 µm long, wrinkled extrusome precursors scattered throughout cytoplasm, impregnate deeply with protargol (Fig. 160d, e, j–l). Cytoplasm hyaline, glossy, usually contains some lipid droplets up to 2 µm across and one or two up to 12 µm-sized food vacuoles with *Protocyclidium terricola*, possibly the preferred food (Fig. 160a, l). Swims rapidly frequently changing direction.

Somatic cilia about 8 µm long in vivo, intrakinetal distances gradually increase strongly from anterior to posterior; caudal cilium about half body length, fragile and frequently shed when cells are immobilized by coverslip pressure. On average 24 ciliary rows, extend meridionally and equidistantly, commence posterior of oral opening with a ciliated dikinetid; slightly shortened

Table 54. Morphometric data on *Plagiocampa monotricha* (PM) and *P. bitricha* (PB, Tenerife type population; from FOISSNER 1999b) based on mounted, protargol-impregnated (FOISSNER's method), and randomly selected specimens from non-flooded Petri dish cultures. Measurements in µm. CV – coefficient of variability in %, M – median, Max – maximum, Mean – arithmetic mean, Min – minimum, n – number of specimens investigated, SD – standard deviation, SE – standard error of arithmetic mean.

Characteristics	Species	Mean	M	SD	SE	CV	Min	Max	n
Body, length	PM	32.8	32.0	4.0	1.1	12.3	27.0	41.0	13
	PB	33.1	33.0	2.1	0.6	6.3	30.0	36.0	11
Body, width (in ventral or dorsal view)	PM	21.1	20.0	3.0	0.9	14.5	17.0	27.0	11
	PB	24.7	25.0	2.4	0.7	9.6	21.0	29.0	11
Body length:width, ratio	PM	1.6	1.6	0.2	0.1	10.7	1.2	1.8	11
	PB	1.3	–	–	–	–	–	–	11
Anterior body end to macronucleus, distance	PM	9.3	10.0	2.1	0.6	23.0	6.0	12.0	13
Macronucleus, length	PM	9.8	9.0	1.5	0.4	15.4	8.0	13.0	13
	PB	10.1	10.0	0.8	0.2	8.2	9.0	11.0	11
Macronucleus, width	PM	8.1	8.0	1.6	0.4	19.2	5.0	10.0	13
	PB	8.6	9.0	0.9	0.3	10.7	7.0	10.0	11
Somatic ciliary rows, number	PM	23.9	24.0	1.3	0.4	5.5	22.0	26.0	13
	PB	18.1	18.0	0.5	0.2	3.0	17.0	19.0	11
Kinetids in a dorsal kinety, number [a]	PM	13.3	14.0	1.5	0.4	11.6	10.0	15.0	13
	PB	16.4	17.0	2.1	0.6	12.9	13.0	19.0	11
Caudal cilia	PM	1.0	1.0	0.0	0.0	0.0	1.0	1.0	13
	PB	2.0	2.0	0.0	0.0	0.0	2.0	2.0	11
Oral dikinetids (flaps), number	PM	16.8	17.0	1.2	0.3	7.4	15.0	19.0	13
	PB	14.4	14.0	–	–	–	14.0	15.0	12
Adoral membranelles, number	PM	3.0	3.0	0.0	0.0	0.0	3.0	3.0	8
	PB	3.0	3.0	0.0	0.0	0.0	3.0	3.0	11

[a] Dikinetid at begin of kineties counted as 1 kinetid.

posteriorly, producing a blank pole area with caudal cilium (Fig. 160c–e, f, j–l; Table 54).

Oral opening occupies anterior body end, almost entirely surrounded by circumoral dikinetids associated with an average of 17 flaps beating up and down, producing a digitate (undulating) membrane; individual flaps composed of two glued cilia, slightly conical, about 7 × 1.2 µm (base width) in size (Fig. 160c–e, h, j–l; Table 54). Three adoral membranelles (brosse) side by side, each very likely composed of dikinetids having 2–3 µm long cilia (Fig. 160c, f; Table 54). Pharyngeal basket oblique-conical, that is, longer ventrally than dorsally, opens on ventral (brosse) side; basket rods lightly impregnated with protargol, originate from circumoral dikinetids (Fig. 160c, d).

Occurrence and ecology: As yet found only at type locality with very low abundance.

Remarks: There is only one species similar to *P. monosticha*, viz., *P. bisticha* FOISSNER, 1999b. These species differ mainly in having one vs. two caudal cilia and the presence vs. absence of somatic extrusomes. Further, *P. monosticha* has a non-overlapping number of ciliary rows (Table 54): 22–26 ($\bar{x}$ = 23.9) vs. 17–19 ($\bar{x}$ = 18.1).

Plagiocampa rouxi KAHL, 1926 (Fig. 161a–k, 162a–n; Tables 55, 56)

Material deposited: 3 voucher slides with protargol-impregnated specimens from Venezuelan site (56) have been deposited in the Biology Centre of the Upper Austrian Museum in Linz (LI). Relevant cells have been marked by black ink circles on the coverslip.

Description of a population from Venezuelan site (56): Size in vivo 35–50 × 15–30 µm, usually about 45 × 25 µm, as calculated from some in vivo measurements and data in Table 55 adding 15% preparation shrinkage. Body shape rather variable, i. e., slightly to distinctly obovate, slightly reniform, or ellipsoid with bluntly pointed ends (Fig. 161a–d); in protargol and SEM preparations usually ellipsoid (Fig. 161e, f, 162k–m). Nuclear apparatus in or near cell centre (Fig. 161a, e, f, 162a–c, k, l; Table 55). Macronucleus small compared to body size, i. e., 5–6 µm in protargol preparations, globular to very broadly ellipsoid, contains a large central nucleolus and several small peripheral nucleoli. Micronucleus attached to macronucleus, about 1.5 µm in diameter. Contractile vacuole and excretory pore subterminal in unciliated posterior pole area between ventral and right side (Fig. 161a, e, 162a, b, k). No extrusomes recognizable. Cortex slightly flexible, not furrowed by ciliary rows, right of ciliary rows a granular line (Fig. 162e, f, m, n). Cytoplasm colourless, specimens, however, usually dark at low magnification (≤ 100×) due to compact food vacuoles up to 12 µm across, many lipid droplets mainly in posterior half of cell, and countless, ring-shaped, colourless granules in anterior half; granules 1–2 µm, usually about 1.7 µm across, rather refractive but organic in nature, ring wall thicker than ring hole, impregnate deeply with silver nitrate; developing granules without distinct wall, yellowish (Fig. 161a, 162c, d, j). Feeds on heterotrophic flagellates of the genus *Chilomonas*. Swims rather rapidly rotating about main body axis. Somatic cilia 7–8 µm long in vivo, arise from distinct pits, arranged in an average of 14 ordinarily spaced, meridional rows each comprising about 13 ordinarily spaced cilia. Ciliary rows not indented, separated from oral opening by a 2–3 µm wide perioral area, begin with a dikinetid composed of comparatively widely spaced cilia, and extend 88% of body length on average; rows posterior to adoral membranelles commence with two dikinetids; unciliated posterior pole area with an about 20 µm long caudal cilium in pole centre (Fig. 161a, e–h, 162a, b, e, g, k–n; Table 55). Oral opening and perioral zone occupy about half of anterior body width. Oral opening elliptic, dorsal margin occupied by a semicircular array of 6–8 ($\bar{x}$ = 7) paroral dikinetids associated with about 4 µm long flaps beating up and down. Three minute adoral membranelles (brosse) in small concavities on ventral margin of mouth opening; individual membranelles each composed of six basal bodies three bearing an about 2 µm long cilium; membranelles 1 and 2 in line with ciliary rows, membranelle 3 oriented obliquely. Pharynx obtriangular in lateral view, dorsal wall supported by about 4 µm long nematodesmata originating from paroral dikinetids; ventral wall supported by inconspicuous nematodesmata originating from adoral membranelles (FOISSNER 1984; Fig. 161a–i, 162a–c, e–g, i, k, l; Table 55). Silverline pattern plagiocampid, i. e., composed of two systems (Fig. 156): one consists of large, sigmoidal meshes (Fig. 162d), the other matches the cortex pattern (Fig. 162h).

Remarks: The redescription is based on a population from Venezuelan site (56) and has been supplemented, mainly the photographic documentation, by supposed

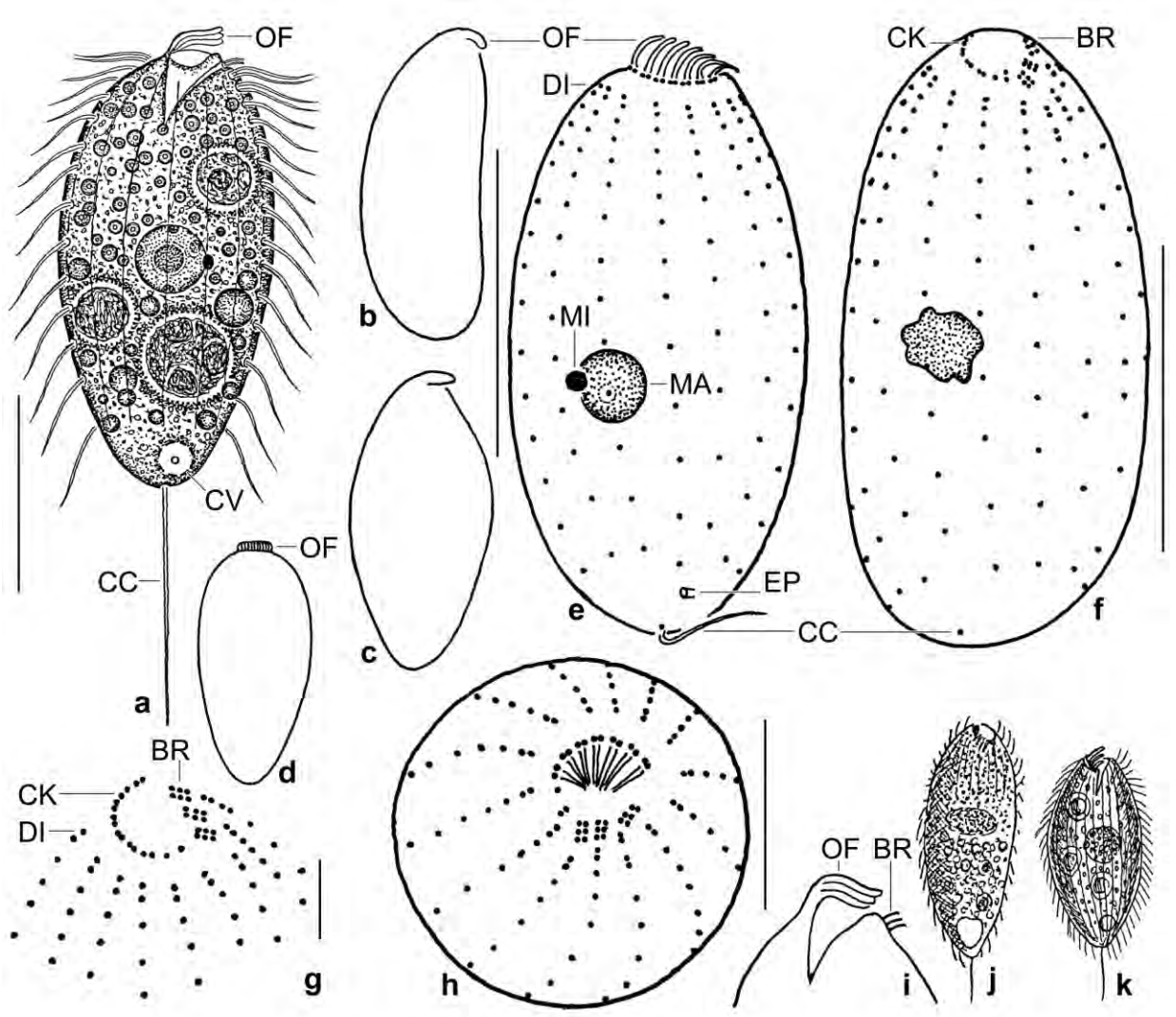

Fig. 161a–k. *Plagiocampa rouxi* from life (a–d, i–k) and after protargol impregnation (e–h). **a:** Right side view of a representative specimen, length 45 µm. The macronucleus contains a large central nucleolus. In the anterior body half occur mainly ring-shaped cytoplasmic granules while the posterior half contains mainly lipid droplets. **b–d:** Shape variants. **e, f:** Dorsal and dorsolateral view, showing the ciliary pattern and the nuclear apparatus. The macronucleus of the right specimen is strongly shrunken. **g:** Oblique frontal view, showing the oral and somatic ciliary pattern. **h:** Anterior polar view of main voucher specimen. For labels, see Fig. (g). Note the oblique arrangement of adoral membranelle 3. **i:** Lateral view of oral apparatus, showing the 4 µm long oral flaps and the about 2 µm long brosse cilia. **j, k:** Figures published by KAHL (1926) and (1930a); length 40 µm and 50–90 µm. BR – brosse (adoral membranelles), CC – caudal cilium, CK – circumoral kinety (paroral), CV – contractile vacuole, DI – dikinetid at anterior end of ciliary rows, EP – excretory pore, MA – macronucleus, MI – micronucleus, OF – oral flaps. Scale bars 5 µm (g), 10 µm (h), and 20 µm (a, e, f).

conspecifics from Salzburg, Saudi Arabia (FOISSNER et al. 2008a), and Namibia (FOISSNER et al. 2002). Very likely, *P. rouxi* is an euryoecious, cosmopolitan species occurring in limnetic and terrestrial habitats, preferring mesosaprobic environments. *Plagiocampa rouxi*-like populations are common. Thus, there are several descriptions available, all deviating more or less from each other (Table 56 and ROUX 1899, KAHL 1926, 1930a, FOISSNER 1978a, 1984). Indeed, body shape and size appear highly variable while the number of ciliary rows and circumoral dikinetids as well as the length of the oral flaps and the caudal cilium are

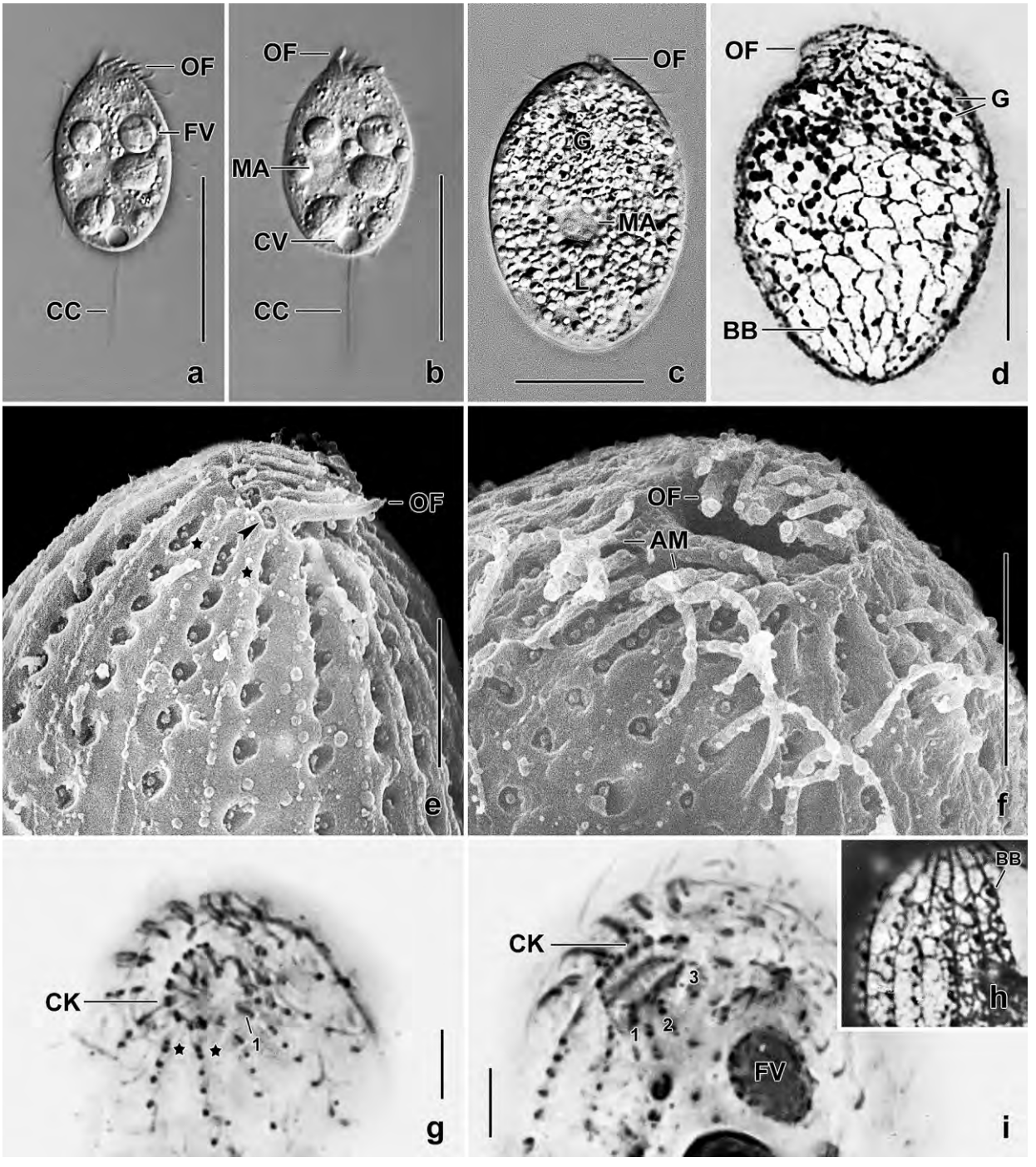

Fig. 162a–i. *Plagiocampa rouxi* from life (a–c), after dry silver nitrate (d, h) and protargol (g, h) impregnation, and in the SEM (e, f). **a, b:** Two shots of a slightly pressed Saudi Arabian specimen, showing the movement of the oral flaps and the caudal cilium. **c:** A pressed Venezuelan specimen packed with ring-shaped granules and lipid droplets. **d, h:** Silverline pattern of a Namibian and a Venezuelan specimen. **e:** Lateral view of a deciliated Salzburg specimen, showing the dikinetid at the base of the oral flaps (arrowhead) and at begin of the ciliary rows (asterisks). **f:** Ventral view of a Salzburg specimen. **g, h:** Anterior polar views. Asterisks denote a dikinetid at begin of the ciliary rows. AM – adoral membranelles (brosse), BB – basal body of a cilium, CC – caudal cilium, CK – circumoral kinety, CV – contractile vacuole, FV – food vacuole, G – cytoplasmic granules, L – lipid droplets, MA – macronucleus, OF – oral flaps, 1, 2, 3 – adoral membranelles. Scale bars 5 µm (e–g, i), 20 µm (c, d), and 30 µm (a, b).

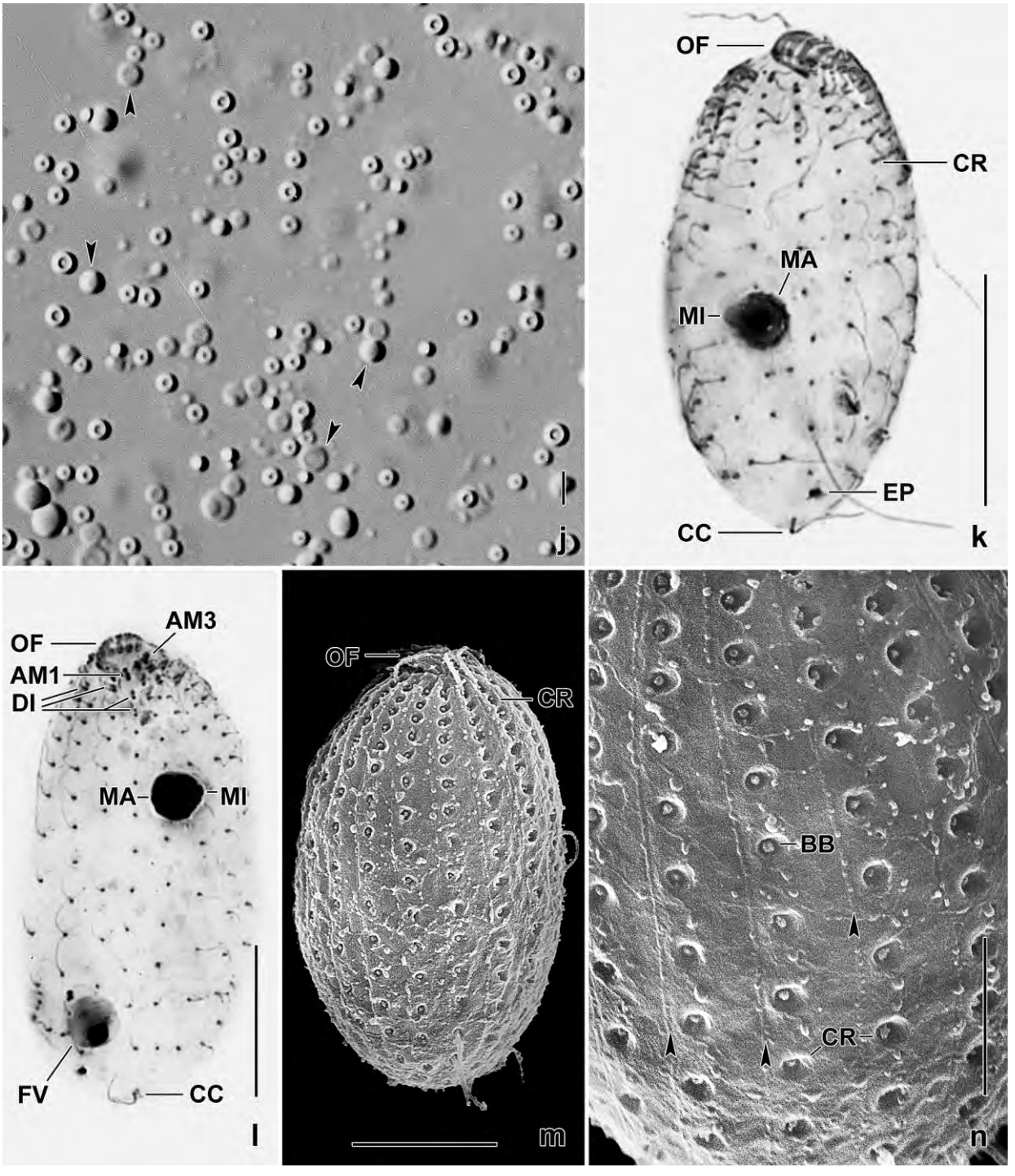

Fig. 162j–n. *Plagiocampa rouxi* from life (j), after protargol impregnation (k, l), and in the SEM (m, n). **j:** Developing (arrowheads) and mature "Ringgranula". **k, l:** Lateral and ventrolateral view of Venezuelan specimens, showing the ciliary pattern and the nuclear apparatus. The ciliary rows posterior to the adoral membranelles commence with two dikinetids. The barren posterior polar area is well recognizable. **m, n:** Deciliated Salzburg specimens, showing the pronounced ciliary pits and a granular line (arrowheads) right of the ciliary rows. AM1, 3 – adoral membranelles, BB – basal body, CC – caudal cilium, CR – ciliary rows, DI – dikinetids at begin of ciliary rows, EP – excretory pore, FV – food vacuole, MA – macronucleus, MI – micronucleus, OF – oral flaps. Scale bars 3 µm (j), 5 µm (n), 10 µm (m), 15 µm (l), and 20 µm (k).

Table 55. Morphometric data on *Plagiocampa rouxi* from Venezuelan site (56) based on mounted, protargol-impregnated (FOISSNER's method), and randomly selected specimens from a non-flooded Petri dish culture. Measurements in µm. CV – coefficient of variation in %, M – median, Max – maximum, Mean – arithmetic mean, Min – minimum, n – number of individuals investigated, SD – standard deviation, SE – standard error of arithmetic mean.

Characteristics	Mean	M	SD	SE	CV	Min	Max	n
Body, length	40.2	40.0	3.4	0.7	8.5	29.0	44.0	21
Body, width	20.8	21.0	2.9	0.6	13.8	15.0	26.0	21
Body length:width, ratio	2.0	1.9	0.3	0.1	16.4	1.6	2.9	21
Anterior body end to macronucleus, distance	19.2	20.0	4.7	1.0	24.5	10.0	29.0	21
Anterior body end to end of ciliary rows, distance	35.7	36.0	3.4	0.8	9.6	25.0	40.0	21
Oral field, diameter of paroral kinety	5.6	6.0	0.6	0.1	10.5	5.0	7.0	21
Macronucleus, length	5.3	5.0	–	–	–	5.0	6.0	21
Macronucleus, width	5.0	5.0	0.3	0.1	6.3	4.0	6.0	21
Micronucleus, diameter	1.3	1.3	–	–	–	1.0	2.0	11
Ciliary rows, number	14.1	14.0	0.6	0.1	4.2	13.0	15.0	21
Kinetids in a dorsal ciliary row, number [a]	13.3	14.0	1.5	0.3	11.0	11.0	15.0	21
Caudal cilia, number	1.0	1.0	0.0	0.0	0.0	1.0	1.0	21
Paroral dikinetids, number	7.0	7.0	0.4	0.1	5.5	6.0	8.0	21
Adoral membranelles, number	3.0	3.0	0.0	0.0	0.0	3.0	3.0	21
Nematodesmata, length	4.1	4.0	0.7	0.2	17.1	3.0	5.0	21

[a] Dikinetids counted as 1 kinetid.

fairly constant. Very likely, the macronuclear structure (with or without a central nucleolus) and the cytoplasmic granules (few or numerous, homogenous or ring-shaped) are poor features.
Based on the knowledge available, *P. rouxi* can be diagnosed as follows: Size in vivo about 40 × 20 µm; slightly to distinctly obovate or ellipsoid. Macronucleus globular. Contractile vacuole and excretory pore subterminal in unciliated pole area. Cytoplasm frequently studded with ordinary or ring-shaped rather refractive organic granules. Usually 14 ciliary rows commencing subapically with a dikinetid and extending over about 90% of body length; those posterior to adoral membranelles commence with one or two dikinetids; caudal cilium in pole centre, about half as long as body. Usually, 7–8 circumoral dikinetids associated with 3–4 µm long oral flaps. 3 minute adoral membranelles (brosse) each composed of 6 basal bodies, membranelle 3 obliquely oriented. In limnetic and terrestrial habitats. About 25 *Plagiocampa* species have been described but only a quarter has been investigated with modern methods: *P. bitricha* FOISSNER, 1999b; *P. difficilis* FOISSNER, 1981a; *P. monotricha* (this monograph); *P. namibiensis* FOISSNER et al., 2002; *P. ovata* GELEI, 1954 (redescribed by FOISSNER 2000a and FOISSNER et al. 2002); *P. pentadactyla* (FOISSNER et al. 2002), and *P. rouxi* KAHL, 1926 (redescribed several times, see Table 56). Of the seven well described species, only *P. difficilis* is possibly a junior synonym of *P. rouxi* because their features become more and more similar the more populations are investigated.

Plagiocampa difficilis FOISSNER, 1981a (Fig. 163a–d; Table 57)

Material: Venezuelan site (24), i. e., soil from the savannah surrounding the village of El Sapo about 50 km north of Puerto Ayacucho. Five voucher slides with protargol-impregnated

Table 56. Comparison of *Plagiocampa rouxi* and *P. difficilis* populations.

Characteristics	*P. rouxi* (Foissner 1978a)	*P. rouxi* (Foissner 1984)	*P. rouxi* (this study)	*P. difficilis* (Foissner 1981a)	*P. difficilis* (this study)
Body shape	obovate	obovate	obovate	ovate	ellipsoid
Body size in vivo (µm)	~ 40–50 µm	~ 38 × 20	~ 45 × 25	~ 35 × 20	~ 30 × 15
Body size in protargol preparations (µm)	?	~ 31 × 18	~ 40 × 21	~ 22 × 16	~ 27 × 12
Structure of macronucleus	several large nucleoli	many minute nucleoli	large central nucleolus	large central nucleolus	several nucleoli
Circumoral dikinetids, number	8 (8) [a]	8–9 (8.8) [a]	6–8 (7) [a]	6–8 (7.1) [a]	5–6 (6) [a]
Ciliary rows, number	17–18 (17) [a]	13–16 (14.8) [a]	13–15 (14.1) [a]	13 (13) [a]	12–14 (13) [a]
Kinetids in a dorsal kinety, number	~ 16	9–16 (12) [a]	11–15 (13.3) [a]	9–12 (10.5) [a]	10–13 (12) [a]
Locality	ephemeral alpine pool	wetland soil in lower Austria	ephemeral pool	alpine soil	savannah soil
Data base	silver nitrate (Chatton-Lwoff)	protargol	protargol	protargol	protargol
Specimens investigated, number	~ 10	15	21	12	13

[a] Extremes and arithmetic mean.

specimens have been deposited in the Biology Centre of the Upper Austrian Museum in Linz (LI). Relevant specimens have been marked by black ink circles on the coverslip.

Description: Size in vivo 27–36 × 11–17 µm, usually about 30 × 15 µm, as calculated from some in vivo measurements and values shown in Table 57 adding 15% preparation shrinkage. Body ellipsoid to elongate ellipsoid, on average 2.3:1 (Fig. 163a, c; Table 57). Nuclear apparatus in or slightly posterior to mid-body (Fig. 163a, d; Table 57). Macronucleus globular to broadly ellipsoid, with rather large nucleoli. Likely one micronucleus usually difficult to separate from cytoplasmic inclusions. Contractile vacuole in posterior body end. Cortex inconspicuous, without granules. Extrusomes not studied in vivo, not recognizable in protargol preparations. Cytoplasm colourless, contains food vacuoles 4–7 µm across; likely feeds on small, heterotrophic flagellates. Movement without peculiarities.

Somatic cilia about 8 µm long in vivo, arranged in an average of 13 meridional, ordinarily spaced rows each composed of about 12 ordinarily spaced cilia with intrarow distances distinctly increasing from anterior to posterior; each row commences with a dikinetid, central ventral rows with an additional dikinetid each. Caudal cilium about 15 µm long in vivo, inserts in or near centre of posterior pole (Fig. 163a–d; Table 57).

Oral opening occupies anterior body end (Fig. 163a–d; Table 57). Adoral membranelles on ventral margin of oral opening, minute, i. e., each composed of three to four basal bodies possibly having short cilia. Paroral membrane on dorsal margin of oral opening, composed of five to six dikinetids each associated with an about 3 µm long flap possibly containing a toxicyst (cp. Foissner 1985). Oral basket difficult to recognize, extends to mid-body.

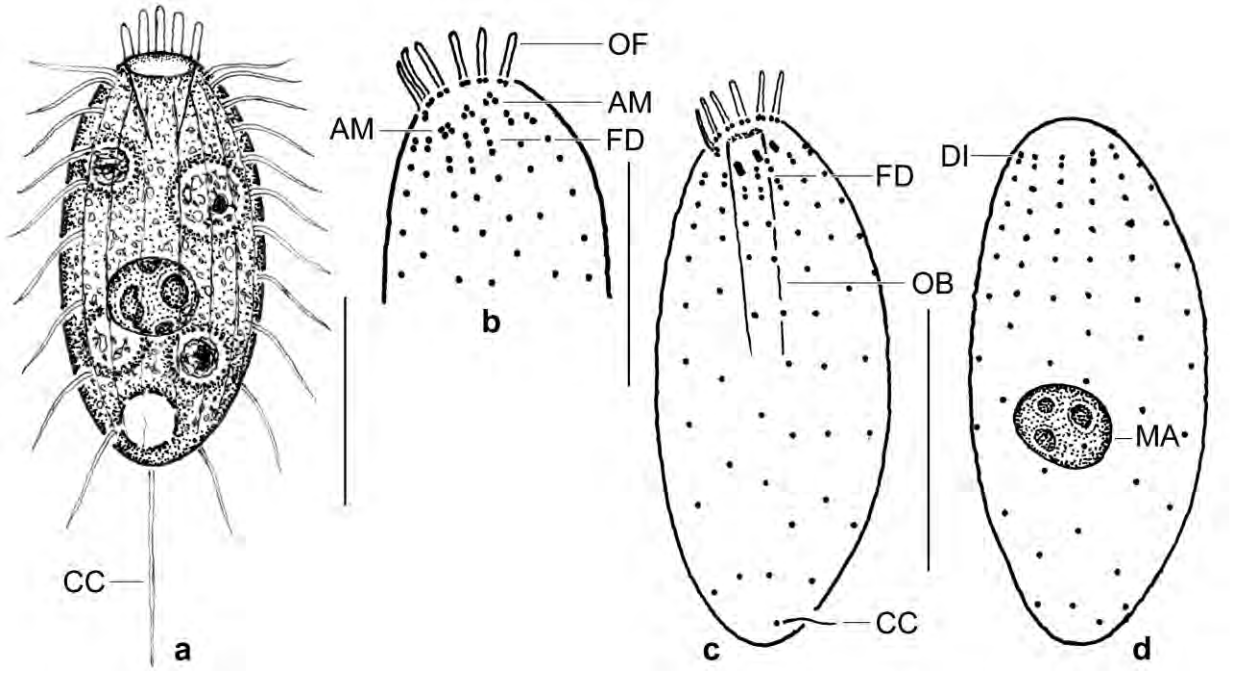

Fig. 163a–d. *Plagiocampa difficilis* from life (a) and after protargol impregnation (b–d). **a:** Ventral view of a representative specimen, length 30 µm. **b:** Ventral anterior half, showing the oral structures. The postoral field of dikinetids defines this genus. **c, d:** Ventral and dorsal view of holotype specimen, length 30 µm. AM – adoral membranelles, CC – caudal cilium, DI – dikinetid on anterior end of ciliary rows, FD – postoral field of dikinetids, MA – macronucleus, OB – oral basket, OF – oral flaps. Scale bars 10 µm (b) and 15 µm (a, c, d).

Table 57. Morphometric data on *Plagiocampa difficilis* based on mounted, protargol-impregnated, useable specimens from a non-flooded Petri dish culture. Measurements in µm. CV – coefficient of variation in %, M – median, Max – maximum, Mean – arithmetic mean, Min – minimum, n – number of individuals investigated, SD – standard deviation, SE – standard error of arithmetic mean.

Characteristics	Mean	M	SD	SE	CV	Min	Max	n
Body, length	26.9	27.0	2.5	0.7	9.2	24.0	31.0	13
Body, width	12.1	12.0	1.7	0.5	14.1	10.0	15.0	13
Body length:width, ratio	2.3	2.3	0.3	0.1	11.2	1.9	2.9	13
Anterior body end to macronucleus, distance	13.5	13.0	1.9	0.5	14.0	11.0	17.0	13
Macronucleus, length	5.2	5.0	0.9	0.3	17.4	4.0	7.0	13
Macronucleus, width	4.1	4.0	0.5	0.1	12.1	3.0	5.0	13
Oral opening, width	4.5	5.0	0.7	0.2	14.8	3.0	5.0	13
Oral flaps, length	3.3	3.0	–	–	–	3.0	4.0	13
Oral flaps, number	5.8	6.0	–	–	–	5.0	6.0	12
Ciliary rows, number	13.0	13.0	0.4	0.1	3.1	12.0	14.0	13
Kinetids in a dorsal ciliary row, number [a]	11.6	12.0	1.0	0.3	9.0	10.0	13.0	13
Caudal cilium, length	11.9	11.0	2.2	0.8	18.5	9.0	15.0	7
Somatic cilia, length	6.3	6.0	0.6	0.2	10.0	6.0	8.0	13

[a] Dikinetids counted as one kinetid.

Occurrence and ecology: *Plagiocampa difficilis* has been recorded from all main biogeographic regions, even from Antarctica (Foissner 1996a). It prefers meagre and extreme habitats.

Remarks: This population matches rather well that described by Foissner (1981a) but sligthly weakens the distance to *P. rouxi* because of the absence of a central nucleolus in the macronucleus. A close relationship of *P. rouxi* and *P. difficilis* is also indicated by the increased number of dikinetids in the kineties posterior to the adoral membranelles (Fig. 163b, c).

Metathrix nov. gen

Diagnosis: Metacystidae with contractile vacuole in mid-body and 4 perioral ciliary rings, anterior two rings composed of dikinetids. Lorica, receptacle, and terminal vacuole absent.

Type species: *Metathrix ellipsoidea* nov. spec.

Etymology: Composite of Greek prefix *meta* (associated with, changed, substituted for) and the Greek noun *thrix* (hair = ciliate s.l.), assuming that the freely motile life style was associated with the loss of a lorica. Feminine gender.

Remarks: As yet, the Metacystidae contained three genera (Kahl 1930a, Lynn 2008): *Metacystis*, *Vasicola*, and *Pelatractus*. They differ from each other by the perioral ciliary pattern: two rings each of dikinetids and monokinetids in *Vasicola* (Kreutz and Foissner 2006; the redescription of *V. ciliata* by Dragesco et al. 1974 is wrong) and *Metathrix* (Fig. 164b, 165e–g) while one ring of dikinetids and four rings of monokinetids in *Metacystis* (Fig. 164c) and *Pelatractus* (Aladro-Lubel and Martinez-Murillo 2003, Arregui et al.2010, Dragesco et al. 1974, Foissner 1984). *Vasicola* and *Metathrix* differ by the presence vs. absence of a lorica and a receptacle, i. e., a kind of oral cavity (Kahl 1930a). *Metacystis* and *Pelatractus* differ by the terminal vacuole that is unciliated in the former and ciliated in the latter (Kahl 1930a, Kreutz and Foissner 2006). The systematic position of the Metacystidae is not known. *Metathrix* possibly has a minute brush, supporting the classification into the Prostomatea (Lynn 2008).

Metathrix ellipsoidea nov. spec.

Diagnosis: Size about 35 × 22 µm in vivo; ellipsoid to broadly ellipsoid. Single macronucleus and micronucleus in or near centre of cell. On average 23 or 32 longitudinal ciliary rows, forming 5–6 transverse ciliary rings. Single caudal cilium in or near centre of pole.

Etymology: The Latinized adjective *ellipsoidea* (ellipsoid) refers to body shape.

Remarks: We split this species into two subspecies because of the distinct difference in the number of ciliary rows. Other differences, especially in the length:width ratio of the body, are possibly caused by the different preparation methods used.

Metathrix ellipsoidea ellipsoidea nov. sspec. (Fig. 164a, b, e, f, 165a–f, Table 58)

Diagnosis: With 29–35, on average 32 longitudinal ciliary rows.

Table 58. Morphometric data on *Metathrix ellipsoidea ellipsoidea* from Venezuela (upper line, protargol impregnation) and *Metathrix ellipsoidea oligostriata* from Brazil (lower line, CHATTON-LWOFF silver nitrate impregnation). Data based on mounted, silver-impregnated, and randomly selected specimen from non-flooded Petri dish cultures. Measurements in µm. CV – coefficient of variation in %, M – median, Max – maximum, Mean – arithmetic mean, Min – minimum, n – number of individuals investigated, SD – standard deviation, SE – standard error of arithmetic mean.

Characteristics	Mean	M	SD	SE	CV	Min	Max	n
Body, length	30.1	30.0	3.5	0.9	11.7	24.0	37.0	17
	31.0	31.0	2.2	0.5	7.2	27.0	35.0	21
Body, width	23.4	23.0	2.0	0.5	8.6	20.0	26.0	17
	18.8	18.0	2.7	0.6	14.1	15.0	24.0	21
Body, length:width ratio	1.3	1.3	0.1	0.1	10.8	1.1	1.7	17
	1.7	1.7	0.2	0.1	12.1	1.3	2.1	21
Anterior body end to end of perioral ciliature, distance	3.6	4.0	0.6	0.2	17.2	3.0	5.0	17
	4.4	4.0	0.6	0.1	13.5	4.0	6.0	21
Anterior body end to macronucleus, distance	11.8	12.0	3.0	0.7	25.1	7.0	18.0	17
	13.6	14.0	2.3	0.5	16.7	7.0	17.0	21
Anterior body end to excretory pore of contractile vacuole, distance	not impregnated							
	14.4	14.0	1.7	0.4	12.1	11.0	18.0	21
Posterior body end to last ring of cilia, distance	4.9	5.0	1.0	0.2	19.6	3.0	6.0	16
	4.4	4.0	0.7	0.2	15.3	3.0	6.0	21
Oral opening, diameter [a]	4.3	4.0	–	–	–	3.0	5.0	14
	4.8	5.0	–	–	–	4.0	7.0	15
Macronucleus, length	8.2	8.0	0.9	0.2	10.8	7.0	10.0	17
	5.8	6.0	0.9	0.2	15.4	5.0	8.0	21
Macronucleus, width	8.0	8.0	1.0	0.2	12.2	6.0	10.0	17
	5.6	6.0	0.6	0.1	10.7	5.0	7.0	21
Micronucleus, diameter	2.0	2.0	0.2	0.1	10.9	1.5	2.5	13
	1.5	1.5	–	–	–	1.2	1.7	3
Postoral rings of basal bodies, number [b]	5.4	5.0	–	–	–	5.0	6.0	17
	5.6	6.0	–	–	–	5.0	6.0	21
Longitudinal ciliary rows, number	31.9	32.0	1.5	0.3	4.6	29.0	35.0	18
	23.6	23.0	1.5	0.3	6.4	20.0	26.0	21
Caudal cilia, number	1.0	1.0	0.0	0.0	0.0	1.0	1.0	17
	1.0	1.0	0.0	0.0	0.0	1.0	1.0	21
Perioral rings of cilia, number	4.0	4.0	0.0	0.0	0.0	4.0	4.0	13
	4.0	4.0	0.0	0.0	0.0	4.0	4.0	21

[a] Rough values obtained from diameter of circumoral kinety.

[b] Basically, there are five rings (see description).

Type locality: Venezuelan site (31), viz., a small ephemeral puddle (Laja) on granitic outcroppings between the Agricultural Research Institute and the airport of Pto. Ayacucho, 67°36‘W 5°41‘N.

Type material: 1 holotype and 1 paratype slide with protargol-impregnated specimens have been deposited in the Biology Centre of the Upper Austrian Museum in Linz (LI). Relevant specimens

are marked by black ink circles on the coverslip. Further material is contained in the type slides of *Apertospathula lajacola* deposited at the same locality.

Description: The following description is valid for both subspecies because they differ from each other mainly by the number of ciliary rows. Different methods were applied for studying the morphology. However, there are few characters that can be recognized only by a certain method, viz., the location of the excretory pore (not recognizable in protargol-impregnated *M. ellipsoidea ellipsoidea*) and the fibres associated with some circumoral dikinetids (not recognizable in silver nitrate-impregnated *M. ellipsoidea oligostriata*).

Size 25–45 × 18–25 µm in vivo, usually about 35 × 22 µm, according to some in vivo measurements and the values shown in Table 58 adding 20% length shrinkage and 10% width inflation in the protargol preparations; length:width ratio thus distinctly lower (1.3:1) in protargol than in silver nitrate (1.7:1) prepared cells. Most specimens broadly to ordinarily ellipsoid slightly narrowing posteriorly; rarely rather distinctly ovate, slightly reniform, or almost globular; oral opening slightly projecting, posterior end broadly rounded, without terminal vacuole (Fig. 164a, 165d, g, h). Nuclear apparatus in or near body centre on average, may be displaced by food vacuoles (Fig. 164a, f, 165d; Table 58). Macronucleus about 8 µm across, with compact nucleoli 1–3 µm in size. Micronucleus attached to macronucleus, about 2 µm across. Contractile vacuole slightly anterior of body centre, excretory pore about 1.5 µm across and located as follows in 37 specimens investigated: between ciliary rings 2 and 3 or 3 and 4, or within ring 3 in 12, 2, and 2 five-ringed cells, respectively; between rings 2 and 3 or 3 and 4, or within ring 3 in 7, 12, and 2 six-ringed cells, respectively (Fig. 164a, f, g, 165a, h; Table 58). Extrusomes, very likely mucocysts, about 1 × 0.4 µm in size and thus difficult to recognize, scattered within ciliary rows and in posterior pole area (Fig. 164a, e). Cortex conspicuous because about 2 µm thick and rectangularly patterned by comparatively large alveoli indistinctly separated from cytoplasm; rectangular units with a compact granule in each corner, cilia in mid of long side of units; appears slightly transversely furrowed by kinety rings (Fig. 164a, e, 165a, b). Environmental specimens usually dark at low magnification because studded with (i) compact food vacuoles 4–7 µm across, (ii) few to many lipid droplets 1–2 µm in size, and (iii) some minute crystals sparkling under interference contrast illumination (Fig. 164a, 165c). Likely feeds on bacteria, fungal spores, and small ciliates (*Apocyclidium terricola*) lysed above mouth opening and ingesting the fluid produced. Swims rapidly rotating about main body axis. Does not build a lorica on microscope slides or in the non-flooded Petri dish culture.

Somatic ciliature monokinetal; cilia about 10 µm long in vivo, arranged in highly ordered pattern producing five or six transverse ciliary rings and an average of 32 bipolar rows; in five-ringed specimens frequently an incomplete ciliary ring between last and penultimate ring, causing five or six rings, depending on area analysed; close to inner margin of last ciliary ring three to five cilia forming a short row. Caudal cilium in or near centre of pole, about 25 µm long in vivo, distal third very fine (Fig. 164a, d, f, g, 165d, g, h; Table 58). Somatic basal bodies accompanied by a parasomal sac, making kinetids oblong in silver nitrate preparations. A granule ring each between ciliary rings; granules scattered in posterior pole region (Fig. 164g, 165g–j). Silverline pattern possibly very similar to cortical pattern (Fig. 164g).

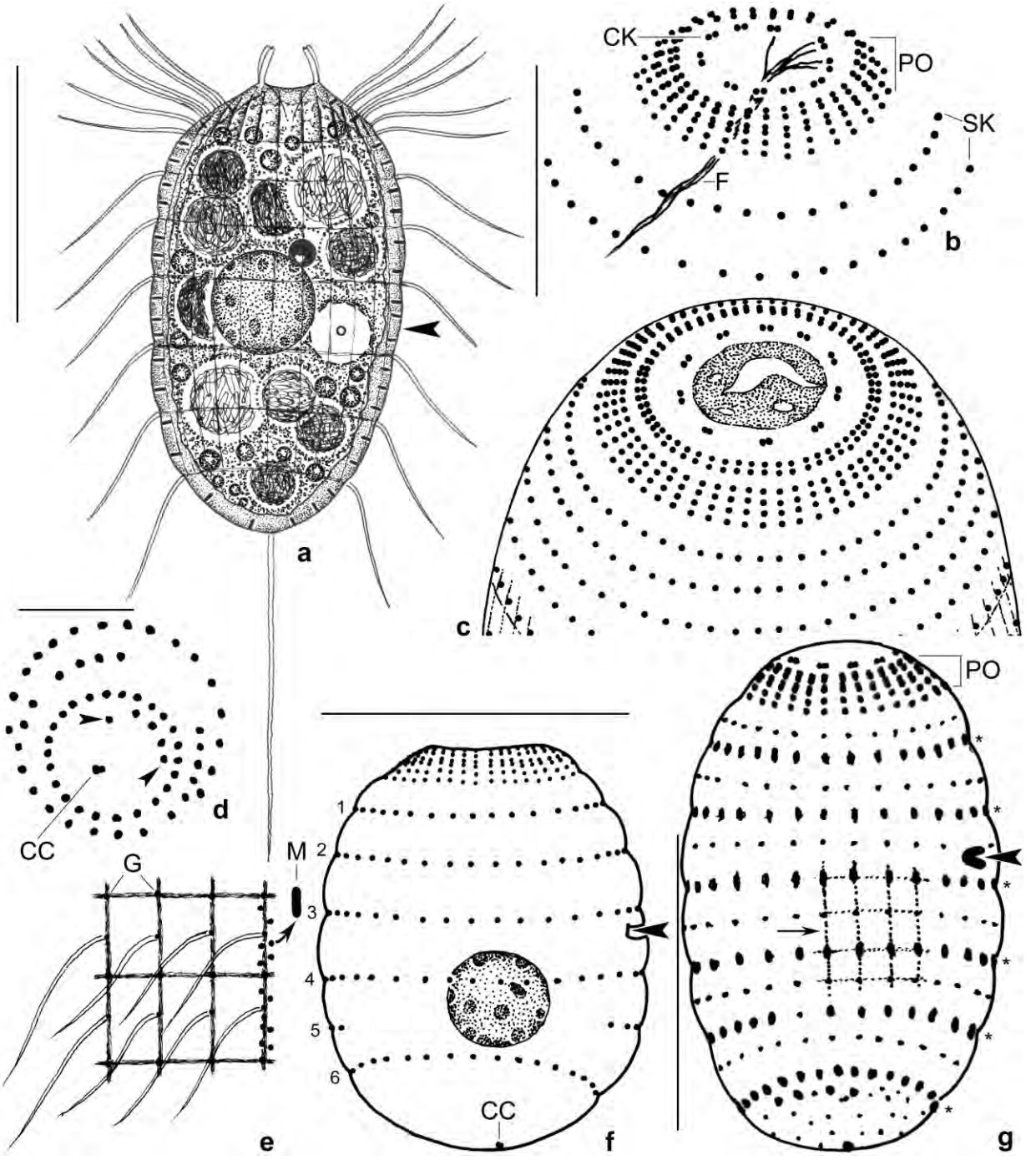

Fig. 164a–g. *Metathrix ellipsoidea ellipsoidea* (a, b, e, f), *M. ellipsoidea oligostriata* (d, g), and *Metacystis striata* (c, from FOISSNER 1984). **a:** A representative specimen, length 35 µm. Note the thick cortex. Arrowhead marks contractile vacuole. **b, c:** Differences in the perioral ciliature of *Metathrix* and *Metacystis*. **d:** Posterior polar view, showing a short kinety (arrowheads) close to last ciliary ring. **e:** The cortex shows a rectangular pattern with a granule in each corner. **f, g:** Lateral views. Numerals denote ciliary rings. Asterisks mark granule rows between ciliary rings. Arrowheads denote excretory pore of contractile vacuole. Arrow marks supposed silverline pattern. CC – caudal cilium, CK – circumoral kinety, F – fibres, G – granules in corners of cortical alveoli, M – mucocysts, PO – perioral ciliature, SK – somatic kineties. Scale bars 10 µm (b, d) and 20 µm (a, f, g).

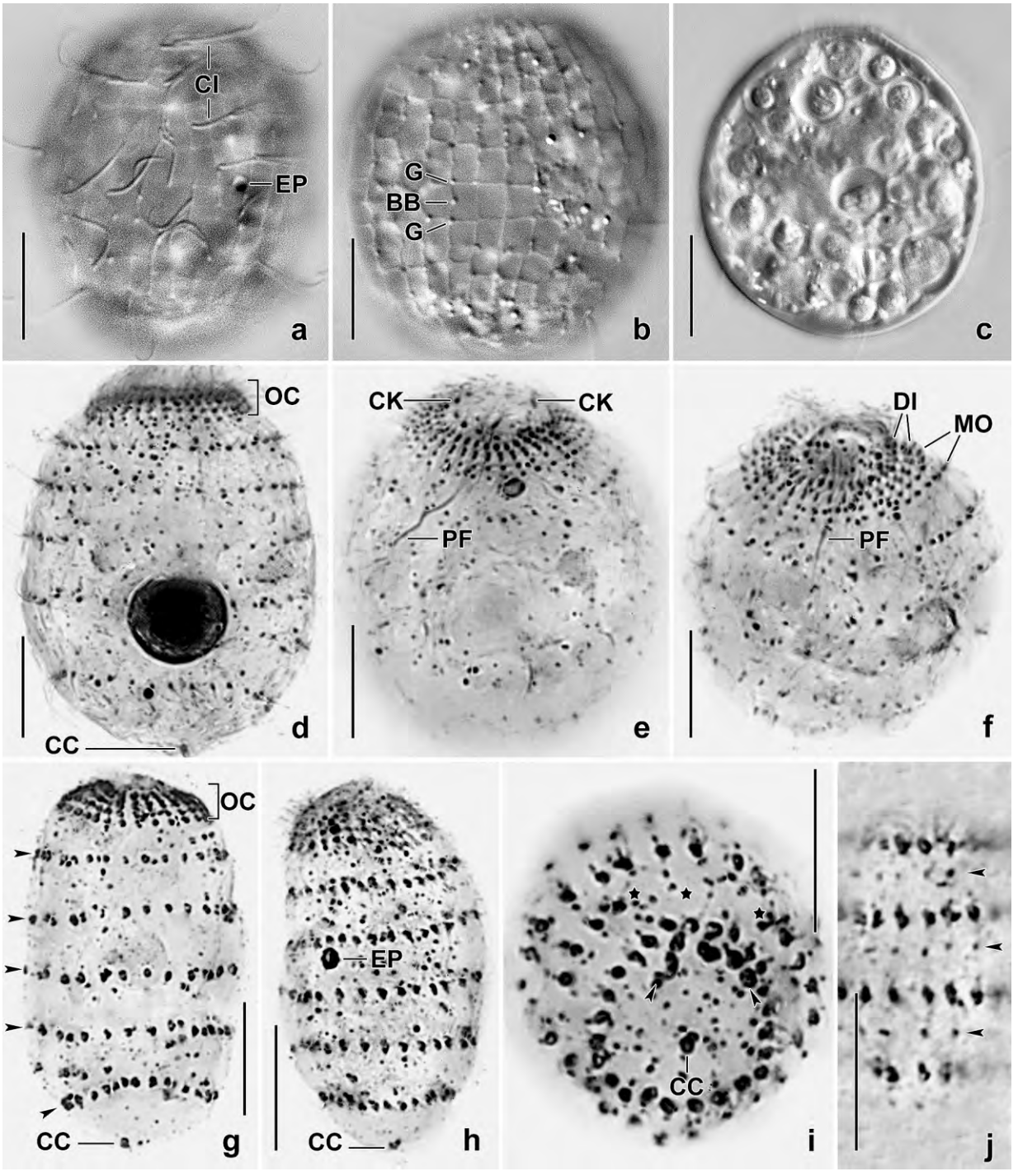

Fig. 165a–j. *Metathrix ellipsoidea ellipsoidea* (a–f) and *M. e. oligostriata* (g–j) from life (a–c) and after protargol (d–f) and silver nitrate (g–j) impregnation. **a, b:** Surface views showing cortex structure. **c:** The cytoplasm is studded with food vacuoles. **d–f:** Lateral and oblique frontal views, showing somatic and oral ciliary pattern. **g, h:** Lateral views, showing ciliary rings (arrowheads) and excretory pore. **i:** Posterior polar view. Arrowheads mark a short row of basal bodies inside of the last ciliary ring, while asterisks denote a broken ring. **j:** Arrowheads mark granule rings between ciliary rings. BB – basal body, CC – caudal cilium, CI – cilia, CK – circumoral kinety, DI – dikinetal perioral ciliary rings, EP – excretory pore, G – granules, MA – macronucleus, MO – monokinetal perioral ciliary rings, OC – oral and perioral ciliature. Scale bars 10 µm.

Oral opening in centre of anterior end, about 5 µm across, surrounded by a circumoral kinety and perioral ciliature, without receptacle. Circumoral dikinetids associated with about 3 µm long bristles resembling those of, e. g., *Urotricha*; three of them associated with long fibres obliquely extending to body midline, resembling a prostomatean brush. Perioral ciliary rows extend along distinct longitudinal ribs, forming two dikinetal and two monokinetal rings (Fig. 164a, b, f, g, 165d–g; Table 58).

Occurrence and ecology: As yet found at type locality and Venezuelan site (56), i. e., in ephemeral habitats, indicating that *M. ellipsoidea* is a limnetic species.

Remarks: We did not find a species in the literature that could be identical with *M. ellipsoidea*. However, body shape and size are similar to those of many small prostomatean and haptorian ciliates, e. g., *Urotricha* and *Enchelys*. Thus, careful observation is required, especially of the typical cortex structure, the caudal cilium, the perioral ciliature and, especially, the curious location of the contractile vacuole.

Metathrix ellipsoidea oligostriata nov. subspec. (Fig. 164d, g, 165g–j; Table 58)

Diagnosis: With 20–26, on average 23 longitudinal ciliary rows.

Type locality: Floodplain soil from the Aurelio Lagoon in the Paraná River floodplain, surroundings of the town of Maringá, State of Matu Grosso du Sul, Brazil, W53°15' S22°40'.

Type material: 1 holotype and 2 paratype slides with Chatton-Lwoff silver nitrate-impregnated specimens have been deposited in the Biology Centre of the Upper Austrian Museum in Linz (LI). Relevant specimens have been marked by black ink circles on the coverslip.

Etymology: Composite of the Latin prefix *oligo* (few) and the Latin participial adjective *striata* (striated).

Description: This subspecies differs from *M. ellipsoidea ellipsoidea* mainly (only?) by the non-overlapping number of longitudinal ciliary rows: 20–26 (23) vs. 29–35 (32). Such difference is considered as typical for subspecies (see General Section) and is frequently even used for species rank because the number of ciliary rows is an important and comparatively stable feature.

Pseudotelotrochidium nov. gen.

Diagnosis: Stalked Epistylididae with permanently ciliated aboral wreath. A row of narrowly spaced granules posterior of aboral ciliary wreath. Swarmer with open oral apparatus.

Type species: *Pseudotelotrochidium epistylis* nov. spec.

Etymology: Composite of the Greek *pseudo* (false) and the Greek generic name *Telotrochidium* (*Telotrocha* = worm-larva and *eidos* = form). Neuter gender.

Remarks: *Pseudotelotrochidium epistylis* could belong to two morphogenera: *Epistylis* (colonial) and *Rhabdostyla* (non-colonial). As the latter may form small colonies, as does *P. epistylis*, some authors synonymized *Rhabdostyla* with *Epistylis* (Stiller 1971). However, none of the described *Epistylis* and *Rhabdostyla* species have the two unique characteristics of *P. epistylis*: a permanently invaginated posterior body portion and a permanently ciliated aboral wreath. The last feature is shared with only one other peritrich ciliate, viz., *Amphiphyra ameiuri*, a fish parasite belonging to the *Scyphidiidae* (see Lom & Dykova 1992 for an excellent redescription).

The permanent aboral ciliary wreath of *P. epistylis* is identical to that found in *Telotrochidium* and *Opisthonecta*. However, these genera never develop a stalk (for reviews, see Foissner 1975b and Martin-Cereceda et al. 2007).

***Pseudotelotrochidium epistylis* nov. spec.** (Fig. 166a–j, 167a–u, 168a–v, 169a–d; Table 59)

Diagnosis: Size in vivo about 85 × 40 µm; barrel-shaped with posterior region invaginated. Macronuclear strand elongate C-shaped in longitudinal body axis. Contractile vacuole and cytopyge slightly posterior of oral bulge in dorsal wall of vestibulum. On average, 99 silverlines from anterior body end to aboral ciliary wreath and 16 silverlines from there to scopula. Oral apparatus of ordinary size, oral disc slightly convex to hemispherical. Adoral ciliary spiral performs one turn each on oral disc and in vestibulum; polykineties end in usual pattern. Stalk on average slightly shorter than body, about 4 µm across, very rarely branched. Swarmers 70–130 × 30–40 µm in size, more or less funnel-shaped and curved laterally. Resting cyst faceted; infraciliature maintained.

Type locality: Floodplain soil of the Rio Claro about 10 km upstream of the Pousada Rio Claro, northern Pantanal, Brazil, 56°62'W16°25'S.

Type material: We deposited in the Biology Centre of the Upper Austrian Museum in Linz (LI) 1 holotype slide with protargol-impregnated specimens from the type locality and 7 paratype slides with protargol-impregnated and silver nitrate-impregnated cells. Further, 4 voucher slides with silver nitrate and protargol-impregnated specimens from Jamaica were deposited in the same locality. Relevant specimens were marked with black ink circles on the coverslip.

Etymology: A noun in apposition, i. e., named after the genus *Epistylis* because of the high similarity to *Epistylis* spp.

Description of morphostatic specimens: The Jamaican specimens are highly similar to those from the Brazilian type population, both in vivo and in silver preparations (Table 59). If not mentioned otherwise, the description refers to the type population.

Body size (Table 59): In vivo, *P. epistylis* has a size of 60–100 × 30–50 µm, on average 84 × 42 µm. Both, body size and length:width ratio are moderately variable (CV up to 13%) in vivo and in protargol preparations, showing that *P. epistylis* contracts slowly and not strongly.
Body shape (Fig. 166a, 167a–c, e, f, h, j; Table 59): When extended, *P. epistylis* is barrel-shaped due to the narrowed oral region and the invaginated and thus comparatively broad posterior portion.

Table 59. Morphometric data on *Pseudotelotrochidium epistylis* based on specimens from a non-clonal raw culture. CV – coefficient of variation in %, IV – in vivo, M – median, Max – maximum, Mean – arithmetic mean, Min – minimum, n – number of individuals analysed, P – protargol impregnation, SD – standard deviation, SE – standard error, SN – silver nitrate impregnation.

Characteristics	Method	Mean	M	SD	SE	CV	Min	Max	n
Brasilian type population									
Body, length (µm)	IV	84.2	85.0	9.6	2.2	11.4	60.0	100.0	19
Body length (µm)	P	60.8	62.0	5.6	1.2	9.2	50.0	72.0	21
Body, width (µm)	IV	42.0	40.0	5.6	1.3	13.3	30.0	50.0	19
Body, length: width ratio	IV	2.0	2.0	0.2	0.1	11.5	1.7	2.5	19
Oral bulge, width (µm)	IV	32.5	30.0	3.0	0.7	9.3	30.0	40.0	19
Posterior invagination, depth (µm)	IV	15.6	15.0	2.4	0.6	15.6	10.0	20.0	19
Stalk, length (µm)	IV	63.4	70.0	–	–	–	15.0	110.0	19
Stalk, width (µm)	IV	4.0	4.0	0.9	0.2	21.5	3.0	5.0	19
Scopula, diameter (µm)	P	3.1	3.0	–	–	–	3.0	3.5	18
Macronucleus, distance from anterior end (µm)	P	3.2	3.0	2.5	0.6	78.6	0.0	9.0	20
Macronucleus, length (µm) [a]	P	47.0	47.0	5.2	1.1	11.1	33.0	55.0	21
Macronucleus, width in mid-region (µm)	P	4.5	4.0	1.1	0.3	24.8	3.0	8.0	21
Macronucleus, width in posterior region (µm)	P	6.8	7.0	1.0	0.2	14.4	5.0	9.0	21
Micronucleus, diameter with membrane (µm)	P	3.9	4.0	0.5	0.1	13.2	3.5	5.5	21
Silverlines from anterior end to aboral ciliary wreath, number	SN	98.8	98.0	3.7	0.8	3.8	92.0	106.0	21
Silverlines, number from aboral ciliary wreath to scopula [b]	SN	16.1	16.0	1.3	0.3	8.0	14.0	18.0	21
Silverlines, total number	SN	114.8	114.0	3.9	0.9	3.4	109.0	123.0	21
Cortical pores, number in 100µm^2	SN	32.4	32.0	9.1	2.0	28.0	17.0	50.0	21
Resting cysts, diameter with ridges (µm)	IV	47.8	47.0	2.6	0.6	5.5	45.0	52.0	19
Resting cysts, diameter without ridges (µm)	IV	36.5	36.0	1.8	0.4	5.0	33.0	40.0	19
Resting cysts, number of ridges when focused to the centre	IV	10.8	11.0	0.9	0.2	8.7	9.0	13.0	18
Jamaican population									
Silverlines from anterior body end to aboral ciliary wreath, number	SN	95.9	95.0	5.1	1.1	5.4	90.0	106.0	21
Silverlines from aboral ciliary wreath to scopula, number	SN	13.7	14.0	–	–	–	12.0	15.0	3

[a] Loops and curves not included.

[b] Granule row posterior of aboral ciliary wreath excluded.

The invagination is highly characteristic and is 5 to 8 µm deep, containing the region between aboral ciliary wreath and scopula; it is recognizable also in contracted specimens (Fig. 167j) but disappears in the swarmers (Fig. 167l, s). When contracted, *P. epistylis* is broadly ellipsoidal to globular (Fig. 167a) with the oral bulge slightly snout-like projecting in the Jamaican specimens (Fig. 167h).

Nuclear apparatus (Fig. 166a, c, 168a, b; Table 59): Both, in vivo and in protargol preparations the macronucleus is in the longitudinal body axis and dorsal to the oral apparatus, usually commencing in the oral disc and extending to the aboral ciliary wreath; it never extends posterior of the wreath while its anterior end may be 0–9 µm distant from body end, producing a variability of 72%.

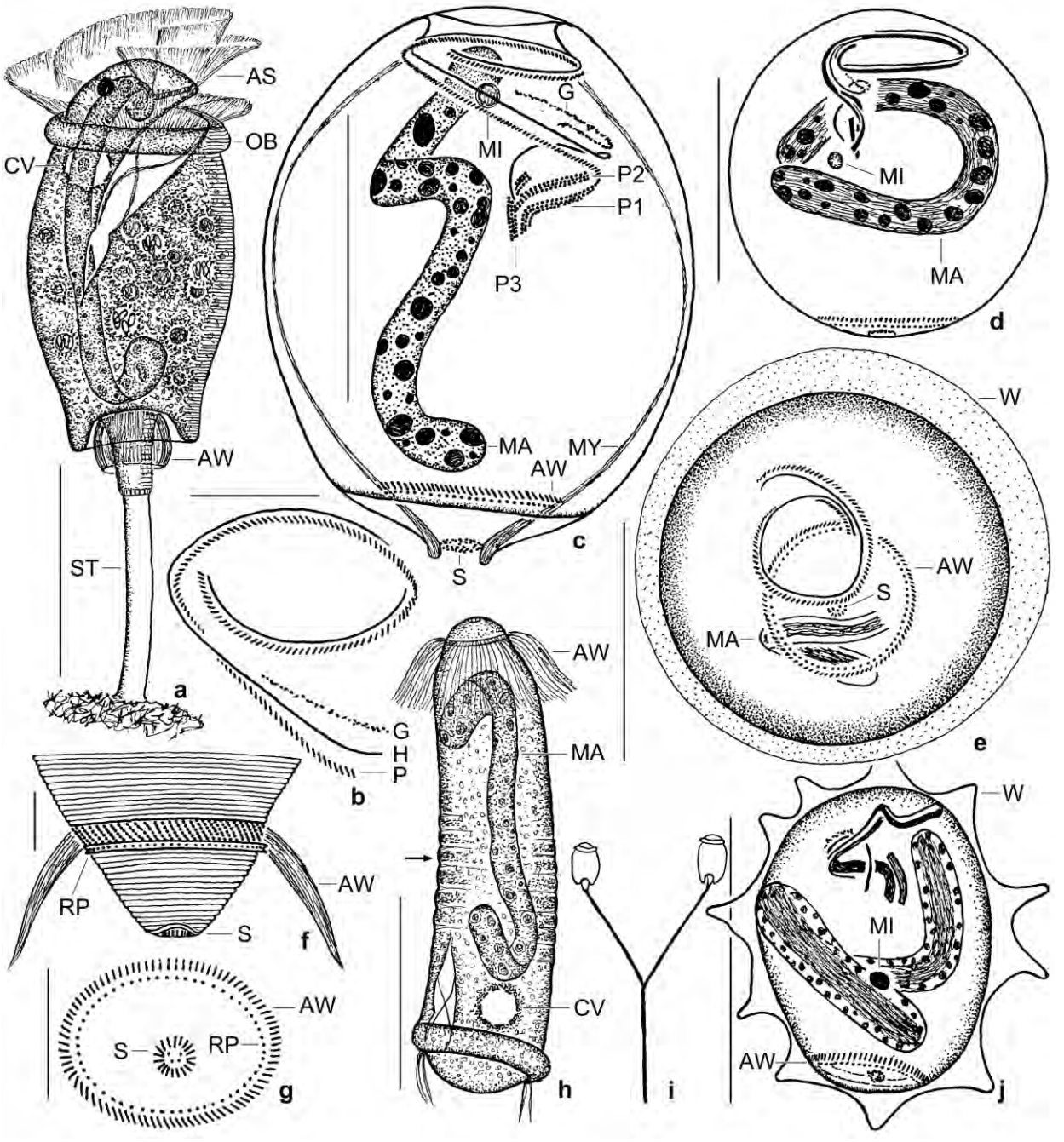

Fig. 166a–j. *Pseudotelotrochidium epistylis* from life (a, f, h, i) and after protargol impregnation (b–e, g, j). **a.** Lateral view of a representative specimen, length (without stalk) 85 µm. Note the invaginated posterior region and the ciliated aboral wreath (main genus character). **b:** External portion of the adoral ciliature, showing the absence of an epistomial membrane. **c:** Optical section, showing the oral and aboral infraciliature and the nuclear apparatus. **d, e, j:** A very young, a middle, and a mature resting cyst. The macronucleus (only partially shown in e) orients transverse to the main body axis and becomes studded with fibres. The infraciliature is maintained. **f, g:** Lateral and posterior polar view of aboral ciliary wreath. **h:** Swarmer, length 100 µm. It swims with the aboral ciliary wreath ahead and open oral apparatus. The arrow marks minute bulges in the curved central third. **i:** A bifurcate mini-colony of the Jamaican population. AS – adoral ciliary spiral, AW – aboral ciliary wreath; CV – contractile vacuole, G – germinal kinety, H – haplokinety, MA – macronucleus, MI – micronucleus, MY – myoneme, OB – oral bulge, RP – ring of pores, P(1–3) – oral polykinetids, S – scopula, ST – stalk, W – cyst wall. Scale bars 5 µm (f), 10 µm (b, g), 30 µm (c–e, j), and 40 µm (a, h).

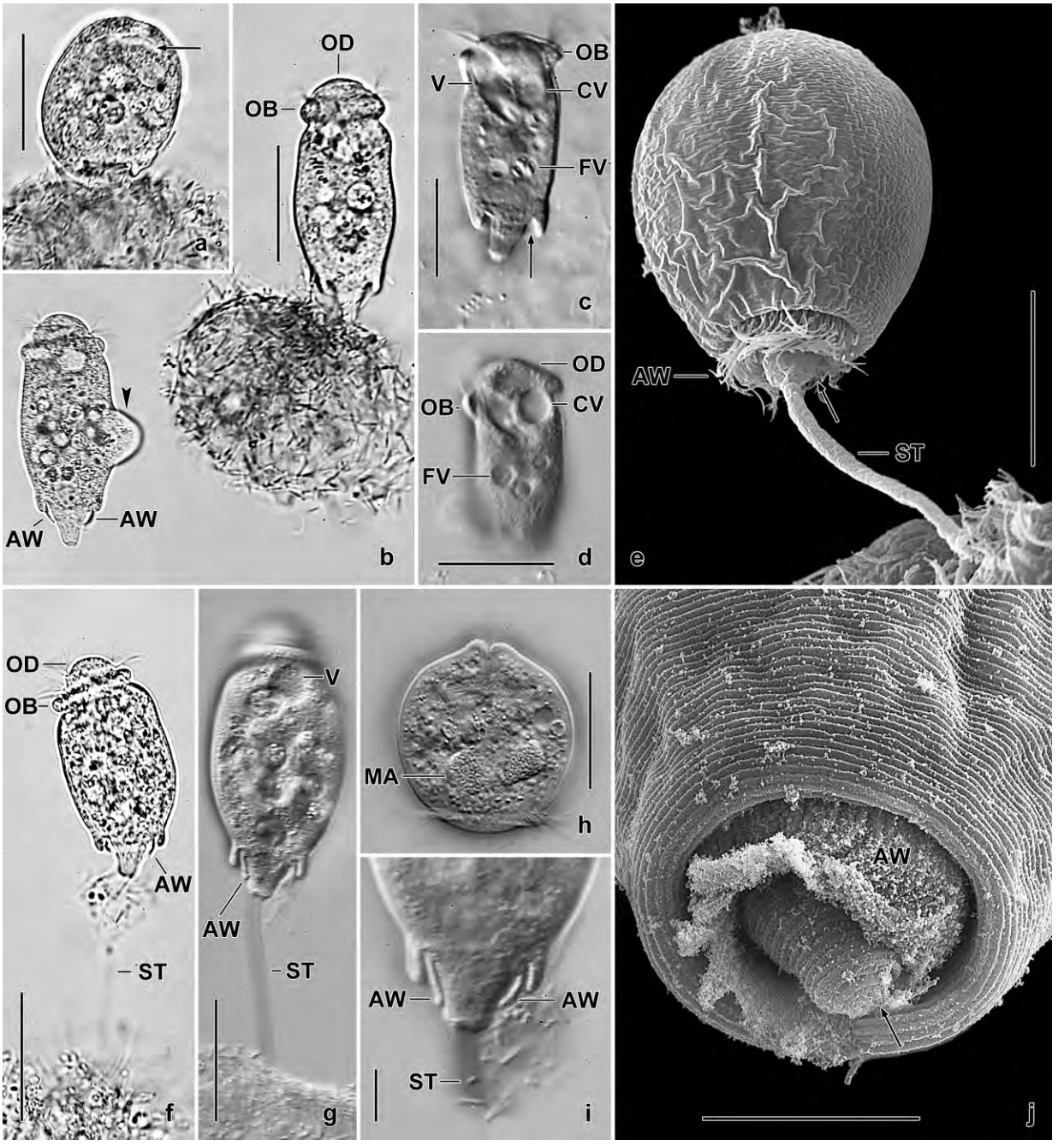

Fig. 167a–j. *Pseudotelotrochidium epistylis* from life (a–d, f–i) and in the scanning electron microscope (e, j). **a, b:** The same specimen, contracted and extended, attached to a slimy accumulation of bacteria. The oral structures (arrow) are contracted. Left a conjugation with the microgamont marked by arrowhead. **c, d:** Two specimens, showing the oral structures and the contractile vacuole on the dorsal wall of the vestibulum. The arrow marks the posterior invagination. **e, j:** The aboral ciliary wreath is present also in morphostatic specimens, which have the posterior body region invaginated (arrows). Note the short, thin stalk and the narrow striation of the cortex. **f:** A specimen with almost hemispherical oral disc. **g, i:** The same specimen in optical section at moderate and high magnification, showing the posterior invagination and the permanent aboral ciliary wreath, i.e., the main generic characteristics. **h:** A contracted Jamaican specimen. AW – aboral ciliary wreath, CV – contractile vacuoles, FV – food vacuoles, MA – macronucleus, OB – oral bulge, OD – oral disc, ST – stalk, V – vestibulum. Scale bars 10 µm (i, j), 20 µm (e), and 40 µm (a–d, f–h).

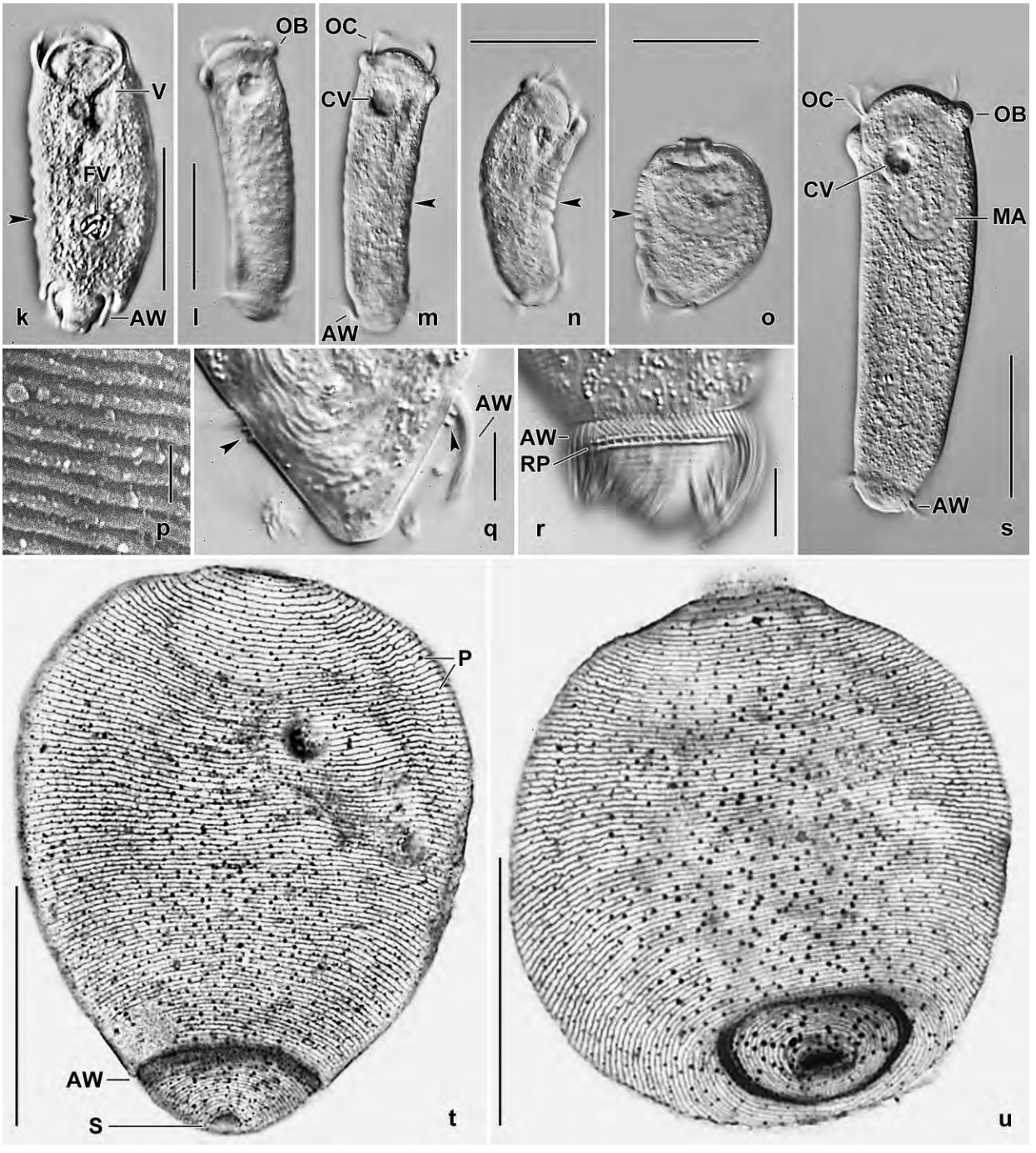

Fig. 167k–u. *Pseudotelotrochidium epistylis* from life (k–o, q–s), in the scanning electron microscope (p), and after Klein-Foissner silver nitrate impregnation (t, u). **k:** A developing swarmer with still invaginated posterior region but with characteristic bulges (arrowhead). **l–o:** The same swarmer slightly contracted (l, m), moderately contracted (n), and fully contracted (o). Note the open oral apparatus (l–n), except when fully contracted (o). Arrowheads mark the characteristic bulges. **p:** Fine cortical striation. The silverlines (t, u) are in the ridges (Foissner 1975a). **q, r:** Posterior body portion of a swarmer in optical section and in surface view. The arrowhead marks the minute ridges deliminating a row of distinct cortical pores posterior of the aboral ciliary wreath. **s:** An old, fully extended swarmer with clear cytoplasm and open oral apparatus. **t, u:** Silverline pattern. AW – aboral ciliary wreath, CV – contractile vacuole, MA – macronucleus, OB – oral bulge, OC – oral cilia, P – cortical pores, S – scopula, V – vestibulum. Scale bars 1 µm (p), 5 µm (q, r), and 40 µm (k–o, s–u).

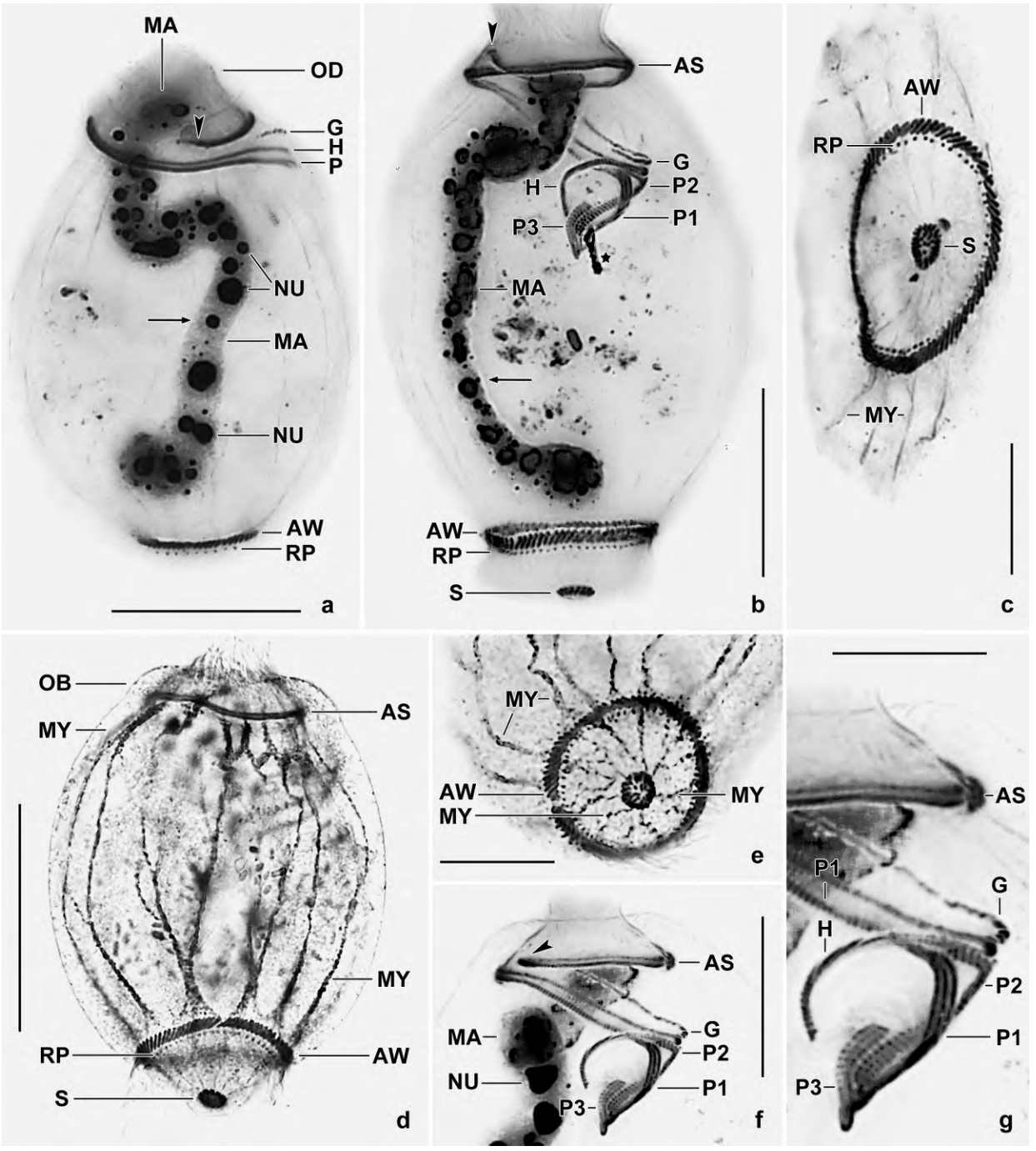

Fig. 168a–g. *Pseudotelotrochidium epistylis*, infraciliature and macronucleus after protargol impregnation. **a, b:** Lateral and ventral overview. The macronucleus extends in main body axis; the middle quarter is thinner (arrows). The arrowheads mark the begin of the adoral ciliary spiral. The asterisk denotes a debris covering the end of polykinety 1. **c, e:** Posterior polar views, showing the aboral ciliary wreath and a ring of special pores posterior of the wreath. **d, e:** The myoneme system of *P. epistylis* is comparatively simple and weakly developed. The myoneme strands originate in the scopula area and extend anteriorly to attach on the external part of the adoral ciliary spiral. **b, f, g:** *Pseudotelotrochidium epistylis* has classical peritrich oral structures. The adoral ciliary spiral (begin marked by arrowheads) makes a turn each on the peristomial disc and in the vestibulum. Note absence of an epistomial membrane. AS – adoral ciliary spiral, AW – aboral ciliary wreath, G – germinal kinety, H – haplokinety, MA – macronucleus, MY – myonemes, NU – nucleoli, OB – oral bulge, OD – oral disc, P(1–3) – oral polykinetids, RP – ring of pores, S – scopula. Scale bars 10 µm (c, e, g), 20 µm (a, b, f), and 40 µm (d).

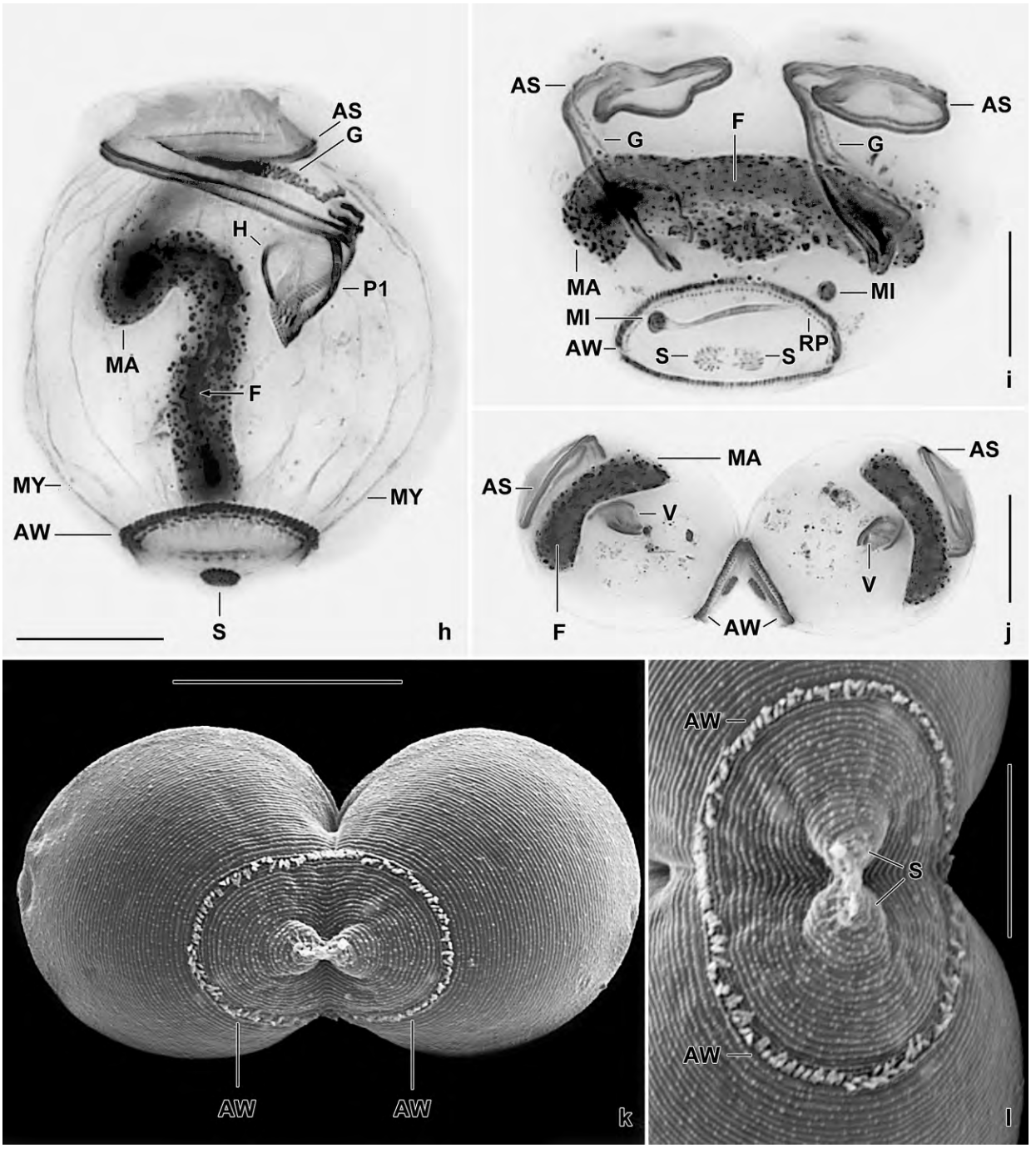

Fig. 168h–l. *Pseudotelotrochidium epistylis*, dividers in protargol preparations (h–j) and in the scanning electron microscope (k, l). **h:** Very early divider, showing that the germinal kinety develops to an anarchic field of basal bodies. The macronucleus is still in the longitudinal axis of the cell but its structure changed markedly: a fibre bundle (arrow) developed in the centre and the large nucleoli disintegrated to granular material. **i:** A late middle divider with an adoral ciliary spiral in each daughter. The macronucleus oriented transversely to the main body axis and contains a thick fibre bundle. The micronucleus and the scopula are dividing. **j–l:** Very late dividers, showing the organized oral apparatus and the reorganizing aboral ciliary wreath. Note the narrowly spaced cortical ridges which divide without a special anlage. AS – adoral ciliary spiral, AW – aboral ciliary wreath, F – fibre bundle, G – germinal kinety, H – haplokinety, MA – macronucleus, MI – micronucleus, MY – myonemes, P1 – polykinety 1, S – scopula, V – vestibulum. Scale bars 10 µm (l) and 20 µm (h–k).

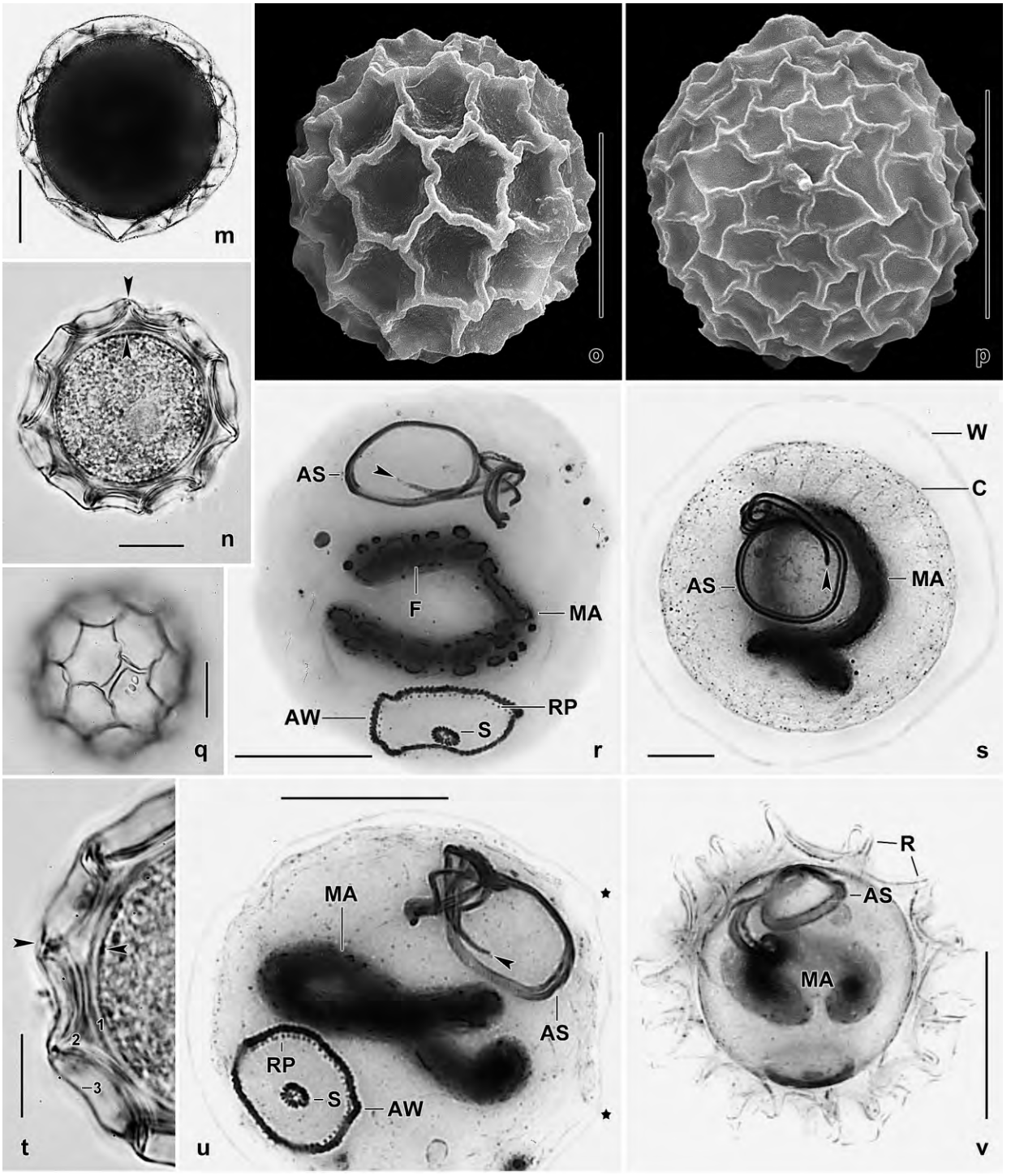

Fig. 168m–v. *Pseudotelotrochidium epistylis*, resting cysts from life (m, n, q, t), after protargol impregnation (r, s, u, v), and in the scanning electron microscope (o, p). **m:** Young cyst with thin, membranous wall and very dense cytoplasm appearing dark (strongly opaque) in the bright field microscope. **n, t:** Mature cyst, showing the about 7 µm thick wall (opposed arrowheads) consisting of three layers (from inside to outside): the about 2 µm thick internal layer (1), the about 6 µm thick, ridged middle layer (2), and the external membrane (3). **o–q:** Surface views of mature cysts, showing the ridges of the middle layer. The size of the polygons formed by the ridges is highly variable. **r–v:** Genesis of the resting cyst. Arrowheads mark the distal end of the adoral ciliary spiral which is, like the aboral ciliary wreath, maintained. The macronucleus becomes circular and transversely oriented, and has a thick fibre bundle in the centre. First, the cell rounds up (r). Second, an about 8 µm thick, hyaline wall is secreted (s).

continued vis à vis

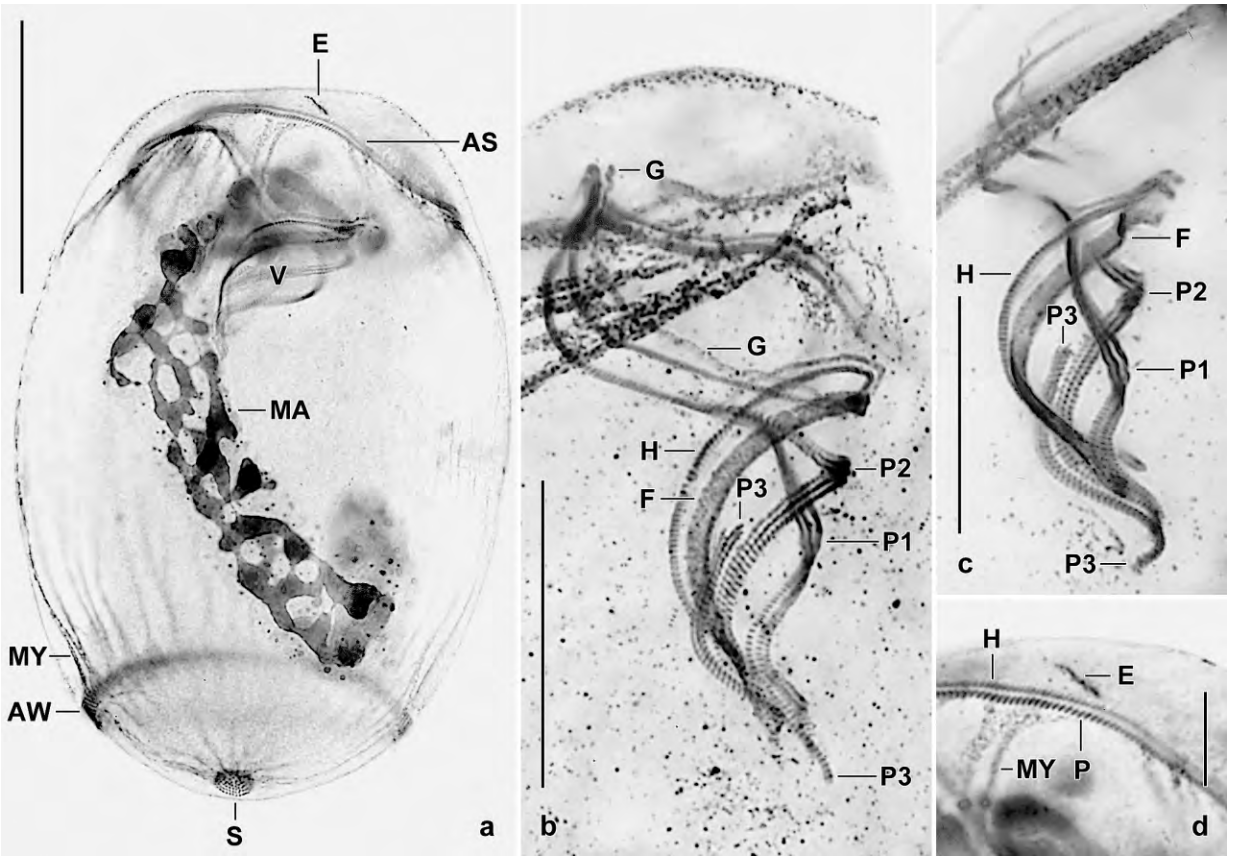

Fig. 169a–d. *Epistylis alpestris* after protargol impregnation. In vivo, *E. alpestris* resembles *Pseudotelotrochidium epistylis*, both in the morphostatic and in the swarming state. However, they differ by several important features (see **Remarks**), of which two are recognizable in these micrographs: with vs. without epistomial membrane (b, d) and with long, sigmoidal (b, c) vs. short, slightly curved (Fig. 168b, g) polykinety 3. AS, adoral ciliary spiral, AW – aboral ciliary wreath, E – basal bodies of the epistomial membrane, F – fibrous plate, G – germinal kinety, H – haplokinety, MA – macronucleus, MY – myonemes, P(1–3) – aboral polykineties, S – scopula, V – vestibulum. Scale bars 10 µm (d), 20 µm (b, c), and 50 µm (a).

The macronucleus is narrowed in the middle third and is elongate C-shaped with both ends more or less inflated and twisted; it is studded with large and small nucleoli. The micronucleus is at or near the anterior end of the macronucleus, rarely at other sites. In protargol preparations, the micronucleus shows a distinct membrane and is about 4 µm in size; frequently, it is lightly or not impregnated.

Contractile vacuole and cytopyge (Fig. 166a, 167c, d): Both are close to the posterior margin of the oral bulge at the dorsal wall of the vestibulum. The cytopyge is anterior of the contractile vacuole and releases granular food remnants.

Cortex and silverline pattern (Fig. 166a, f, 167b, c, j, p, t, u, 168k, l; Table 59): The cortex is rigid and colourless. It is transversely striated by ridges so minute that it appears smooth in the light microscope, though each ridge produces a minute convexity, as typical for epistylids (Foissner & Schiffmann 1974, Foissner 1975a) and recognizable in the scanning micrographs (Fig. 167j, p, 168k). The silverline pattern of *P. epistylis* is as typical for most sessile peritrichs, i.e., it is

Fig. 168m–v. Next, the wall condenses and begins to form ridges (u, asterisks). In the mature cyst, the ridges become very prominent (n–p, v). AS – adoral ciliary spiral, AW – aboral ciliary wreath, C – cortex of cell, F – fibre bundle, MA – macronucleus, R – ridges, RP – ring of pores, S – scopula, W – cyst wall. Scale bars 10 µm (s, t), 15 µm (n–q), and 20 µm (m, r, u, v).

composed of transverse rings with an average distance of 0.73 µm (average body length in vivo by average number of silverline rings). The number of silverline rings is conspicuously stable (CV 3–8%): on average 99 rings from the anterior body end to the aboral ciliary wreath and 16 rings from the wreath to the scopula (Fig. 167t, u, 168k, l; Table 59). In 100 µm² is an average of 32 distinct cortical pores most attached to the anterior margin of the silverlines.

Myoneme system (Fig. 168c–e): *Pseudotelotrochidium epistylis* contracts rather slowly and not very strongly, i.e., fully contracted, broadly ellipsoidal cells are shorter than extended cells by only one third (Fig. 167a, h). Indeed, the myoneme system (Fig. 168c–e) is simple when compared with that of other epistylids (Foissner 1977a, b; Foissner et al. 1985, 2009a): myonemes are lacking or inconspicuous in the oral bulge and the oral disc, and a disc retractor is absent. There extend about 13 myoneme strands from the scopula to the aboral ciliary wreath and about 20–25 strands in mid-body, most of which are attached to the external portion of the adoral ciliary spiral (Fig. 168d, e).

Cytoplasm (Fig. 166a, 167a–d, f–h, k): The cytoplasm is granular and colourless. There is no accumulation of refractive granules in the body. Depending on food, the cytoplasm contains few to many food vacuoles 3–6 µm across and accumulated in middle third of body. *Pseudotelotrochidium epistylis* feeds exclusively on ellipsoidal, about 3 µm long bacteria well recognizable in young food vacuoles (Fig. 167c, d, k).

Oral apparatus (Fig. 166a–c, 167a–d, f, g, 168a, b, f–h; Table 59): The oral apparatus is quite similar to that of many other epistylids. The oral bulge is 6–8 µm thick in vivo and narrower than mid-body by 20% on average (Fig. 166a, 167b–d, f; Table 59). The oral disc is highly variable, i.e., it is slightly convex to hemispheral and up to 10 µm high (Fig. 166a, 167b–d, f). The vestibulum is of ordinary size and extends obliquely (~ 45°) to near mid-body. The adoral ciliary spiral performs one turn each on the oral disc and in the vestibulum (Fig. 166a, 167c, d, 168a, b, f–h). The polykineties end isostichad (see Discussion). The lack of an epistomial membrane has been carefully checked in vivo and in protargol preparations in morphostatic cells and in swarmers.

Aboral ciliary wreath and scopula (Fig. 166a, c, f, g, 167b, f, g, i, j, q, r, t, u, 168c, e; Table 59): The posterior body region and the aboral ciliary wreath are invaginated as described above (Fig. 167j). The wreath is about 1 µm width in the protargol preparations while kineties are 1.5–2 µm long because they are obliquely oriented (Fig. 168b, c). The wreath is permanently ciliated with about 10 µm long, very densely spaced cilia beating slowly and only slightly, thus appearing like a membrane (Fig. 167i, j). Posterior of the wreath is a single row of distinct cortical pores between about 1 µm high ridges (Fig. 166g, 167q, r, 168c).

The scopula has 3–3.5 µm in diameter. The scopular organelles, which are about 1–1.2 µm long, are more densely arranged in the margin than the centre of the scopula (Fig. 166a, f, g, 167j, t 168b–e).

Stalk (Fig. 166a, i, 167b, e–g, i; Table 59): The stalk is inconspicuous because it has an average size of only 63 × 4 µm. It never branched in the Brazilian specimens while a few bifurcate mini-colonies were observed in the Jamaican population (Fig. 166i). The stalk, which is hyaline and structureless in the light- and scanning electron microscope, is attached to a variety of solid matters, such as soil particles and slimy bacterial masses (Fig. 167b, g, i).

Ontogenesis (Fig. 168h–l): We found some main divisional stages in the preparations. These show that: (i) the aboral ciliary wreath is reorganized (k, l), (ii) the macronucleus becomes transversely

oriented (i), and (iii) the infraciliature develops as described by Wang et al. (2012) in *Epistylis*.
Conjugation (Fig. 167b): The microgamont attaches to the macrogamont at various sites between near anterior body end and aboral ciliary wreath.

Swarmer: *Pseudotelotrochidium epistylis* can transform to a swarmer when the environmental conditions become unfavourable (Fig. 166f, h, 167k–o, q–s). The transformation needs about 10 min and is associated with the excavation of the posterior body part, the excretion of most food vacuoles, and the separation from the stalk. Young swarmers still have some food vacuoles (Fig. 167a) while the older ones show a "clear" cytoplasm studded with granules up to 1 µm across (Fig. 167s).

Mature swarmers swim very rapidly with the aboral ciliary wreath ahead and are slightly to distinctly funnel-shaped, rarely cylindroidal (Fig. 166h, 167l, m, s). They have a size of 70–130 × 30–40 µm in vivo and are slightly to distinctly curved, producing many minute bulges along the body (Fig. 167m). The aboral ciliary wreath is as in the morphostatic specimens but the cilia elongated from about 10 µm to 15 µm and are much more active (Fig. 166f, 167q–s). The oral structures are neither contracted or changed, making it difficult to separate adults and swarmers in silver preparations; an epistomial membrane is absent (Fig. 166h, 167k, m).

When contracting, the swarmer first becomes distinctly curved and bulged, especially in the middle third (Fig. 167n). Fully contracted swarmers are broadly pyriform to globular with the oral bulge forming a minute snout (Fig. 167h, o).

Encystment and resting cyst: *Pseudotelotrochidium epistylis* encysted in the raw culture. First, the cell closes the oral apparatus and becomes globular. Concomitantly, a thick fibre bundle, which is surrounded by many large and small nucleoli, develops in the centre of the macronuclear strand that becomes semicircular to circular and orients transversely to the main body axis (Fig. 166d, 168r). Next, the cell secrets an about 4 µm thick wall that is hyaline and structureless (Fig. 166e, 168s). Then, the wall slightly condenses and commences to form ridges (Fig. 168u). When the ridges are well recognizable, they are made of a thin (≤ 1 µm), membrane-like material (Fig. 166j, 168m). In this stage, the cyst contents are very dense and thus dark under bright field illumination and low to moderate magnifications (≤ 250×). In mature cysts, the wall of the ridges becomes thicker and higher, making the ridges very conspicuous (Fig. 168n–q, t). We did not observe the secretion of the internal cyst wall.

Mature cysts are spherical to slightly ellipsoidal and have an average size of 48 µm (with ridges) or 36 µm (without ridges) in vivo; thus, the ridges are about 6 µm high (Table 59). The cyst wall has three layers (Fig. 168t): a rather thick external membrane covers the yellowish ridge layer, which is composed of strongly refractive, 1–2 µm thick sheets; the internal layer, which is colourless and moderately refractive, is about 1.5 µm thick. Thus, total wall thickness is about 7 µm (Fig. 168n, t; Table 59). The ridge polygons are of rather different size in the individual cysts (Fig. 168o–q). The cyst contents and the macronucleus are distinctly condensed (Fig. 168m, n, v). The cytoplasm is moderately refractive and composed of lipid (?) globules 1–2 µm across. The contractile vacuole appears as a small blister which does not contract. The oral and aboral infraciliature is maintained, possibly including the cilia (Fig. 166j, 168r, s, u, v).
In addition to the morphometric data shown in Table 59, we calculated the following ratios:

cyst volume (with wall) in % of morphostatic cells = 49%, which is quite similar to the 51% in *Vorticella echini* but rather different from the 24% in *Opisthonecta henneguyi* (Foissner et al. 2006); cyst volume (without wall) by morphostatic cell volume = 0.26; and cyst wall thickness by cyst radius = 0.41.

Occurrence and ecology: As yet, *P. epistylis* has been found in an ephemeral habitat each in Central and South America: in the mud of a tree-hole in the campus of the University of the West Indies, Kingston, Jamaica, and in floodplain soil from the Pantanal in Brazil. Further, it occurs at Venezuelan sites (1, 13, 25), i. e., in flood plain soil of the Orinoco River and in soil from two Mahadjas.

Possibly, *P. epistylis* is restricted to Central and South America because we did not find it in Austria during our studies on stalkless peritrichs (Foissner 1975b, 1976, 1977) and in about 1000 samples of soil globally (Foissner 1998; Foissner et al. 2002), including rather many samples from floodplains, e.g., the Murray River in Australia (Foissner, unpubl.), the Niger River in West Africa (Foissner & Stoeck 2006), and the Enns River in Austria (Foissner 2004).

We did not perform ecological experiments. However, both populations developed in non-flooded Petri dish cultures and could be cultivated in tap water enriched with some squashed wheat grains and some ml of the eluate from the non-flooded Petri dish culture.

Remarks: There are few *Epistylis* and *Rhabdostyla* species that have a long macronucleus oriented in main body axis (for reviews, see Kahl 1935, Stiller 1971). Those which have such a macronucleus form colonies or have the contractile vacuole on the ventral wall of the vestibulum, e.g., *E. lacustris*, *E. pürneri*, and *E. sessilis*. Thus, *P. epistylis* is fairly easily distinguished from other epistylidids even in vivo.

However, there are two species which in vivo superficially resemble *P. epistylis*: *Epistylis alpestris* and *Telotrochidium cylindricum*, both described by Foissner (1978b). *Epistylis alpestris*, as described by Foissner (1978b) and Foissner et al. (2002) is larger than *P. epistylis* (100–140 µm vs. 60–100 µm in vivo), usually forms distinct colonies (vs. usually singly), is obconical (vs. barrel-shaped) when extended; has the oral opening of the swarmer closed (vs. open), possesses 138–160 (vs. 92–106) silverlines from the anterior body end to the aboral ciliary wreath and 35–45 (vs. 14–18) silverlines from the aboral wreath to the scopula, the adoral ciliary spiral performs 1.5 (vs. 1) turn within the vestibulum, has an epistomial membrane (Fig. 169a, d) (vs. lacking), and polykinety 3 is distinctly (vs. not) elongated posteriorly (Fig. 169b, c). These are quite a lot of differences but most are difficult to recognize in vivo.

Telotrochidium cylindricum differs from the swarmer of *P. epistylis* by body size (130–170 vs. 70–130 µm in vivo), body shape (usually cylindroidal vs. conical), the number of silverlines from the anterior body end to the aboral ciliary wreath (142–156 vs. 92–106) and from the aboral wreath to the scopula (20–28 vs. 14–18), and a row of cortical granules each anterior and posterior (vs. only posterior) of the aboral wreath. Obviously, swarmers of *P. epistylis* are difficult to distinguish from *T. cylindricum* in vivo.

Cothurnia minutissima (Penard, 1914) Kahl, 1935 (Fig. 170a–c)

Attached to soil particles from Venezuelan site (54), we found two specimens of a loricate peritrich ciliate that might have been *C. minutissima* (Fig. 170a–c). The lorica was 40–43 µm long and slightly curved, in one specimen indistinct ridges were recognizable in posterior half (Fig. 170a). The identification followed Penard (1914) and was based on the size and shape of the lorica because the inhabitant did not extend (Fig. 170a, b).

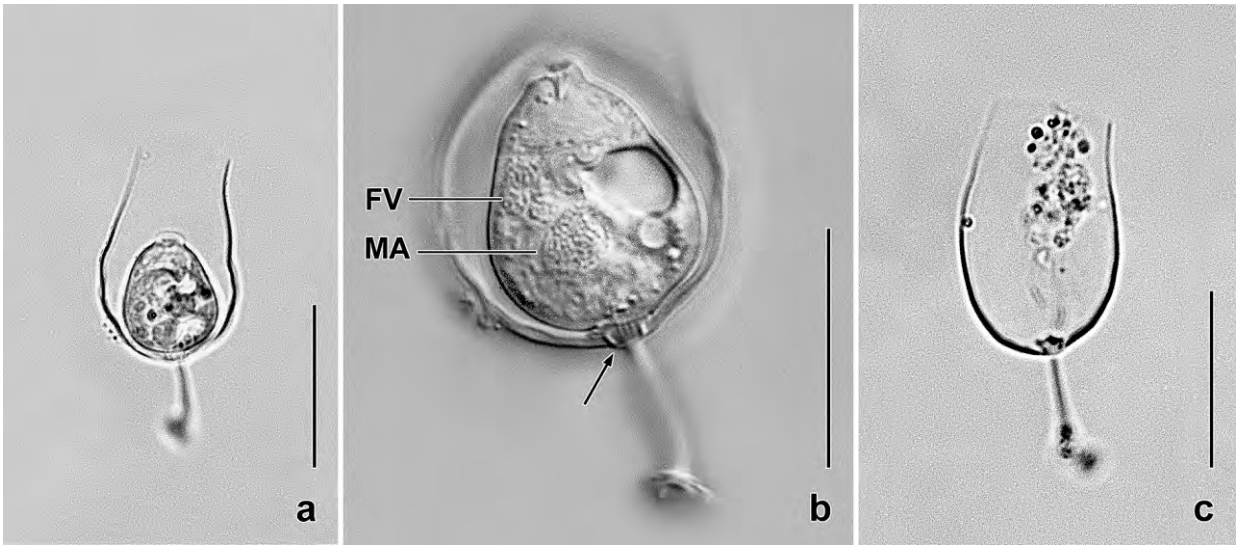

Fig. 170a–c. *Cothurnia minutissima* from life. **a, b:** A contracted specimen within the lorica under bright field and interference contrast. The arrow marks a striated structure between cell and stalk. **c:** A smooth, empty lorica. FV – food vacuole, MA – macronucleus. Scale bars 20 µm (b) and 30 µm (a, c).

Hypotrichida

"About one third of 128 new species discovered in the 73 soil samples are hypotrichs. This matches the high dominance of soil hypotrichs in general (Foissner 1998) and might be associated with the flexible, elongated body pre-adapting hypotrichs for life in microporous (soil) environments. Both saline and desert habitats are rich in new species, showing the evolutionary pressure of extreme habitats.

Many of the new species look inconspicuous, that is, are small and of ordinary shape. However, more detailed investigations show that they are not only undescribed, but also representatives of new genera. Indeed, some of the new "ontogenetic" genera established in this book are so surprising and unexplainable that hypotrich classification appears hopelessly complicated. And there is no indication that further new taxa to be discovered will clear the matter!

We still have about 200 undescribed soil hypotrichs in our notebooks, showing that the present study just touched the peak of an iceberg. It is even possible that there are more terrestrial than

(described) limnetic hypotrichs. This bewildering diversity shows that there must be thousands of hypotrich species, most still undescribed (Foissner et al. 2002)."

Twelve years after the notion by Foissner et al. (2002) little has been changed. A flood of papers by Chinese, Korean, Indian, and Austrian researchers shows the proposed high diversity of the hypotrichs. In fact, nearly half of the species described or redescribed in the present monograph belong to this group. The molecular taxonomy made little progress, although now much more sequences are available than in 2002, but shows that the small subunit (SSU) rDNA is insufficient for entangling the complex phylogeny of the hypotrichs (Foissner et al. 2014 a, Heber et al. 2014, Lynn 2008, Paiva et al. 2009, Schmidt et al. 2007a, Shao et al. 2015, Singh & Kamra 2013, 2015, Song et al. 2009, Yi & Song 2011, Yi et al. 2009a, b, 2012). More genes, detailed ontogenetic studies, and fine-tuned morphological investigations can probably provide new insights into the classification and geographic distribution of the hypotrichs.

Australothrix steineri Foissner, 1995 (Fig. 171a–l, 172a–e; Table 60)

Material: (i) Costa Rican paratype specimens from the original description. (ii) Costa Rican site (20), Santa Rosa National Park, 85°08'W 10°27'N, very near to the type locality of *A. steineri*. Tropical dry rain forest, bark (pH 7.1) from an old *Acacia* tree at the entrance to the Hacienda "La Pacifica" near to the town of Canas. Live observation with special regard to the cortical granules. (iii) Venezuelan site (54). Live observation and protargol impregnation. One voucher slide deposited in the Biology Centre of the Upper Austrian Museum in Linz (LI). (iv) Brazilian site (28): Surface litter and glayic soil from an island in the Amazon River in the outskirts of the town of Manaus; flooded during high water; 60°W 4°S. Protargol impregnation. Two voucher slides deposited. (v) Brazilian site (32): About 40 km west of Manaus, Anavilhanas archipelago in the Rio Negro, vicinity of Ariau lodge, 60°W 4°S. Blackwater inundation primary (?) rain forest on one of the many small islands of the region, flooded by the Rio Negro during high water periods. Collection of litter, soil and roots from 0–8 cm; litter layer up to 5 cm thick, followed by a 3–5 cm thick root-carpet mixed with brown, humic soil; mineral soil under root-carpet loamy, brown; pH 5.1. Three voucher slides deposited. (vi) Republic of South Africa, Cape of Good Hope Nature Reserve, 18°25'E 34°15'S. Fynbos biome, soil from margin of a small pond (Sirkelsvlei) flooded by high water. Soil sandy with many grass roots, pH 5.4 in water. Live observation and protargol impregnation. Three voucher slides deposited.

Additional observations and remarks: Over the years, we found six populations, five in Central and South America and one in South Africa. Although they do not agree in all features, we are rather sure that they are conspecific.

(i) Foissner (1995) stated the *A. steineri* lacks cortical granules, which would be a major difference to the populations described here. Thus, we reinvestigated some deeply impregnated paratype specimens. They show clear spots within the dorsal kineties (Fig. 172e). Their size and location suggest that these are cortical granules.

(ii) This is corroborated by a population found in the vicinity of the type locality. These specimens have cortical granules about 2 × 1 μm in size (Fig. 171d). See also the South African population.

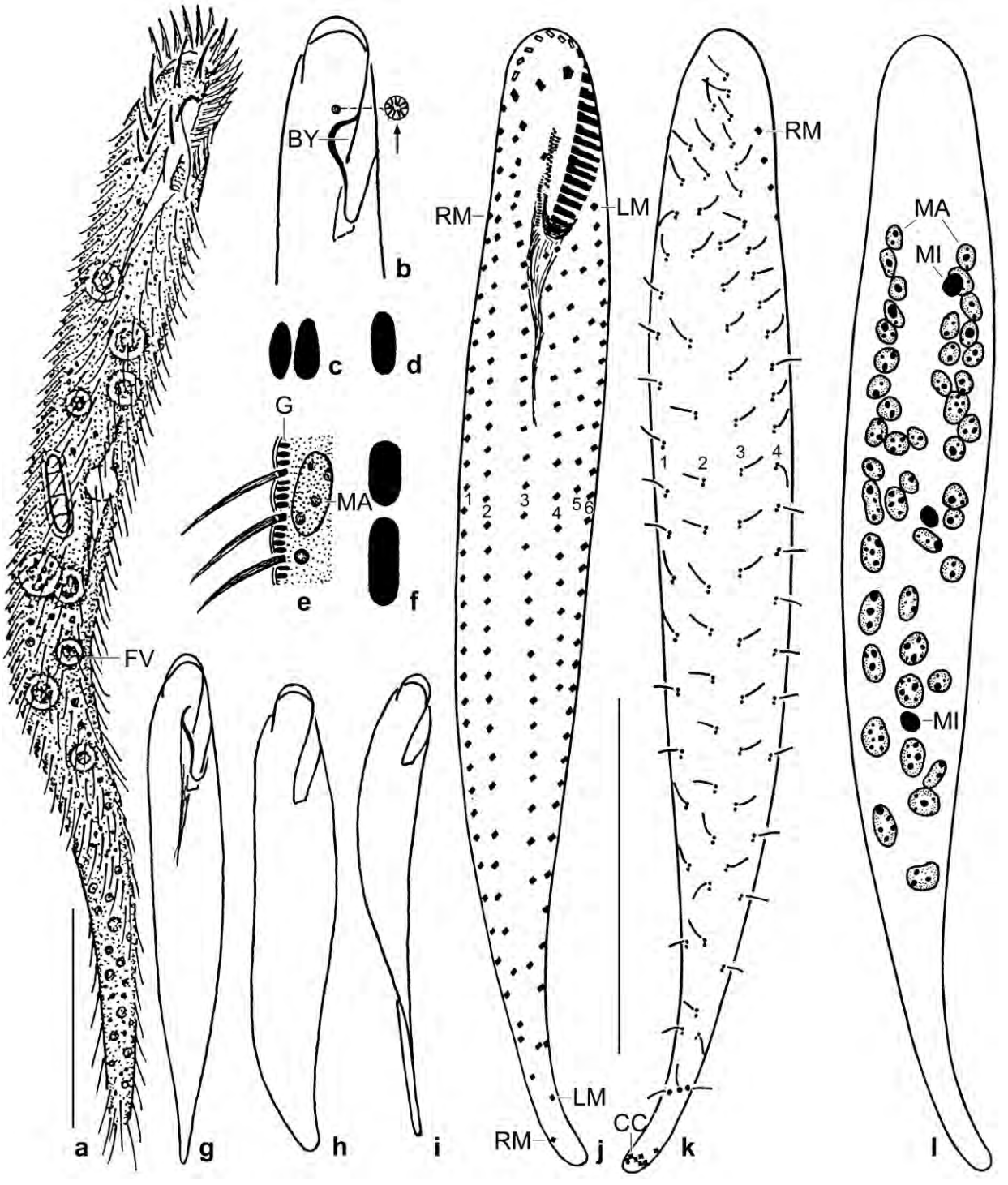

Fig. 171a–l. *Australothrix steineri* populations from life (a–i) and after protargol impregnation (j–l). **a:** From type locality (from Foissner 1995). **b:** Specimens from Venezuelan site (54) have a curious structure (arrow). **c, d:** Cortical granules from Venezuela (54) and Costa Rica (d). **e, f:** Cortical granules from South African specimens. **g–i:** Shape of South African specimens, that in (i) is contorted about the main axis. **j–l:** Main voucher specimen from Brazilian site (28). It has six cirral rows (j, numerals; rows 4 and 5 distinctly shortened) and four dorsal kineties (k, numerals). BY – buccal cavity, CC – caudal cirri, FV – food vacuole, G – cortical granules, LM – left marginal row, MA – macronuclear nodules, MI – micronuclei, RM – right marginal row. Scale bars 50 μm.

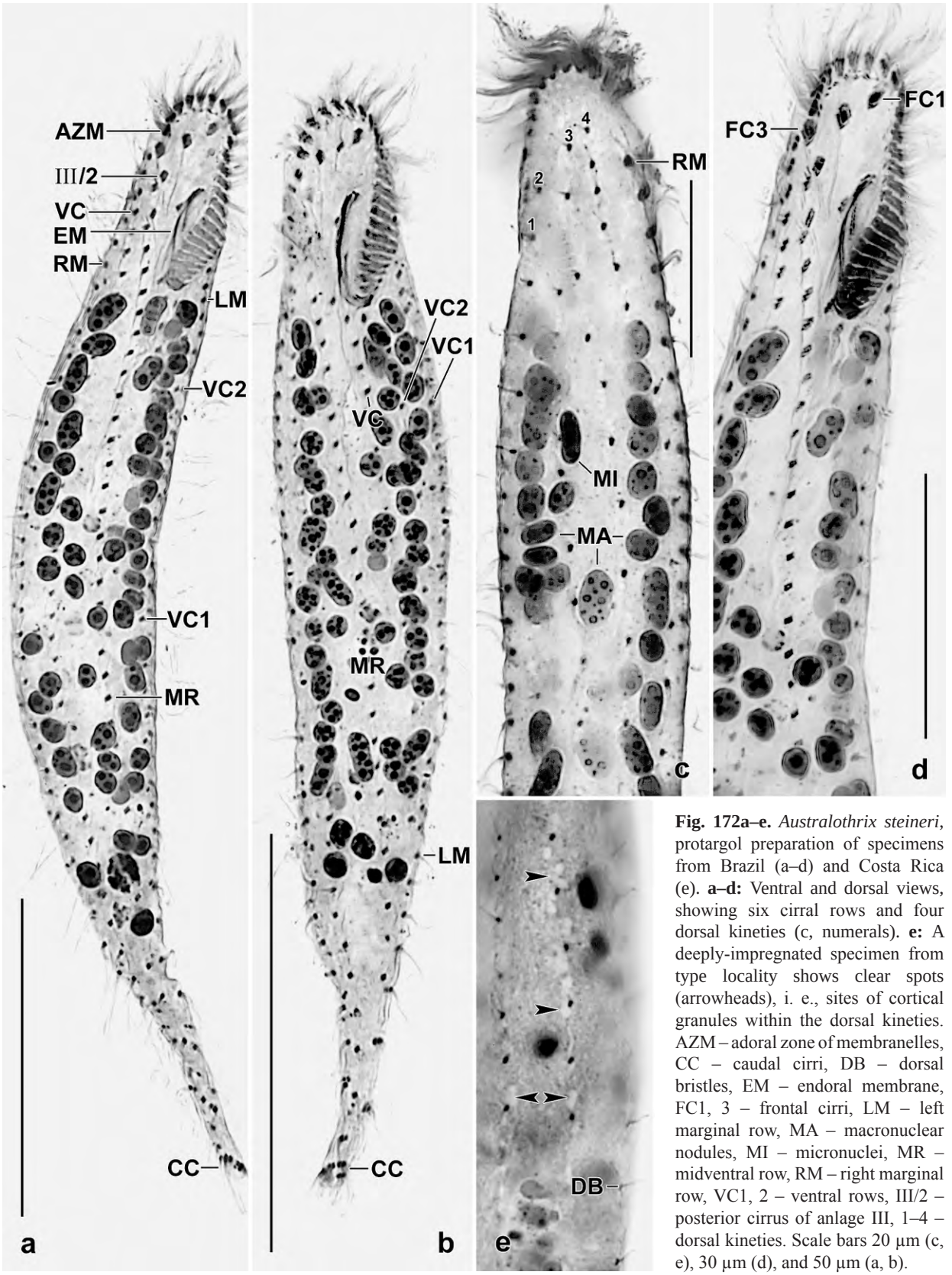

Fig. 172a–e. *Australothrix steineri*, protargol preparation of specimens from Brazil (a–d) and Costa Rica (e). **a–d:** Ventral and dorsal views, showing six cirral rows and four dorsal kineties (c, numerals). **e:** A deeply-impregnated specimen from type locality shows clear spots (arrowheads), i. e., sites of cortical granules within the dorsal kineties. AZM – adoral zone of membranelles, CC – caudal cirri, DB – dorsal bristles, EM – endoral membrane, FC1, 3 – frontal cirri, LM – left marginal row, MA – macronuclear nodules, MI – micronuclei, MR – midventral row, RM – right marginal row, VC1, 2 – ventral rows, III/2 – posterior cirrus of anlage III, 1–4 – dorsal kineties. Scale bars 20 µm (c, e), 30 µm (d), and 50 µm (a, b).

(iii) The specimens from Venezuelan site (54) differ in two features. First, they possess a curious organelle (?) anterior of the buccal cavity. It was present in the five cells studied and has a diameter of about 3 µm and contains minute rods (Fig. 171b). It does not impregnate with the protargol method used. Possibly, we overlooked this minute structure in the other populations. Second, the cortical granules are elliptic to indistinctly ovate and have a size of about 2 × 1 µm (Fig. 171c).

(iv) The morphologic and morphometric data on the two Brazilian populations match fairly well those from the type population (Fig. 171j–l, 172a–d; Table 60). On average the cells are smaller (160 µm, 198 µm vs. 236 µm) and possess less right and left marginal cirri (37 vs. 63 and ~ 35 vs. 58).

(v) The South African specimens are comparatively clumsy, most lacking a distinct tail. Thus, individual cells may be difficult to distinguish in vivo from several *Uroleptus* and *Holosticha* s. l. species. They are more or less helically contorted, just as the specimens from the neotropic populations (Fig. 171g–i; Table 60). The cortical granulation matches the Costa Rican site (20) cells in size (1–1.5 × 0.5–0.7 µm) and shape (oblong) while the yellowish shimmer is unique (Fig. 171e, f). When methyl green-pyronin is applied, the granules become inflated to about 3 µm.

Occurrence and ecology: *Australothrix steineri* is very likely restricted to Gondwana, which is supported by the two Australian species described by Blatterer & Foissner (1988); at least, we never met an *Australothrix* in central and north Europe. The genus has a wider distribution, as shown by the Chinese → *A. fraterculus*.

Except of Costa Rican site (20), all populations of *A. steineri* were found in floodplain environments, suggesting it as a semiterrestrial species rarely occurring also under mainly limnetic conditions.

Emendation of the diagnosis of *A. steineri*: Size in vivo about 180–270 × 25 µm. Very elongate cuneate and usually contorted about main body axis. About 50–150 scattered, ellipsoid macronuclear nodules and some micronuclei. Cortical granules mainly around cirri and dorsal bristles, colourless, oblong, about 1–2 × 0.5–1 µm in size. Midventral complex composed of 2–3 midventral pairs and a long midventral row composed of about 30 cirri and extending to last quarter of cell. A total of 6 cirral rows, ventral rows left of midventral row more or less shortened posteriorly. 4 dorsal kineties with 4–8 caudal cirri. Prefers floodplain environments.

Australothrix fraterculus nov. spec. (Fig. 173a–k, 174a–g; Table 60)

Diagnosis: Size in vivo about 220 × 20 µm. Very elongate cuneate and often contorted about main body axis. On average 65 scattered, ellipsoid macronuclear nodules and 3 micronuclei. Cortical granules mainly around cirri and dorsal bristles, colourless, ovate and 1–1.5 × 0.5–0.8 µm in size. Midventral complex composed of 3 midventral pairs and a long midventral row composed of about 35 cirri and extending to body end. A total of 5 cirral rows, ventral row left of midventral row ends slightly posterior to mid-body. 3 dorsal kineties and 4–6 caudal cirri. Adoral zone extends about 15% of body length, composed of an average of 23 membranelles.

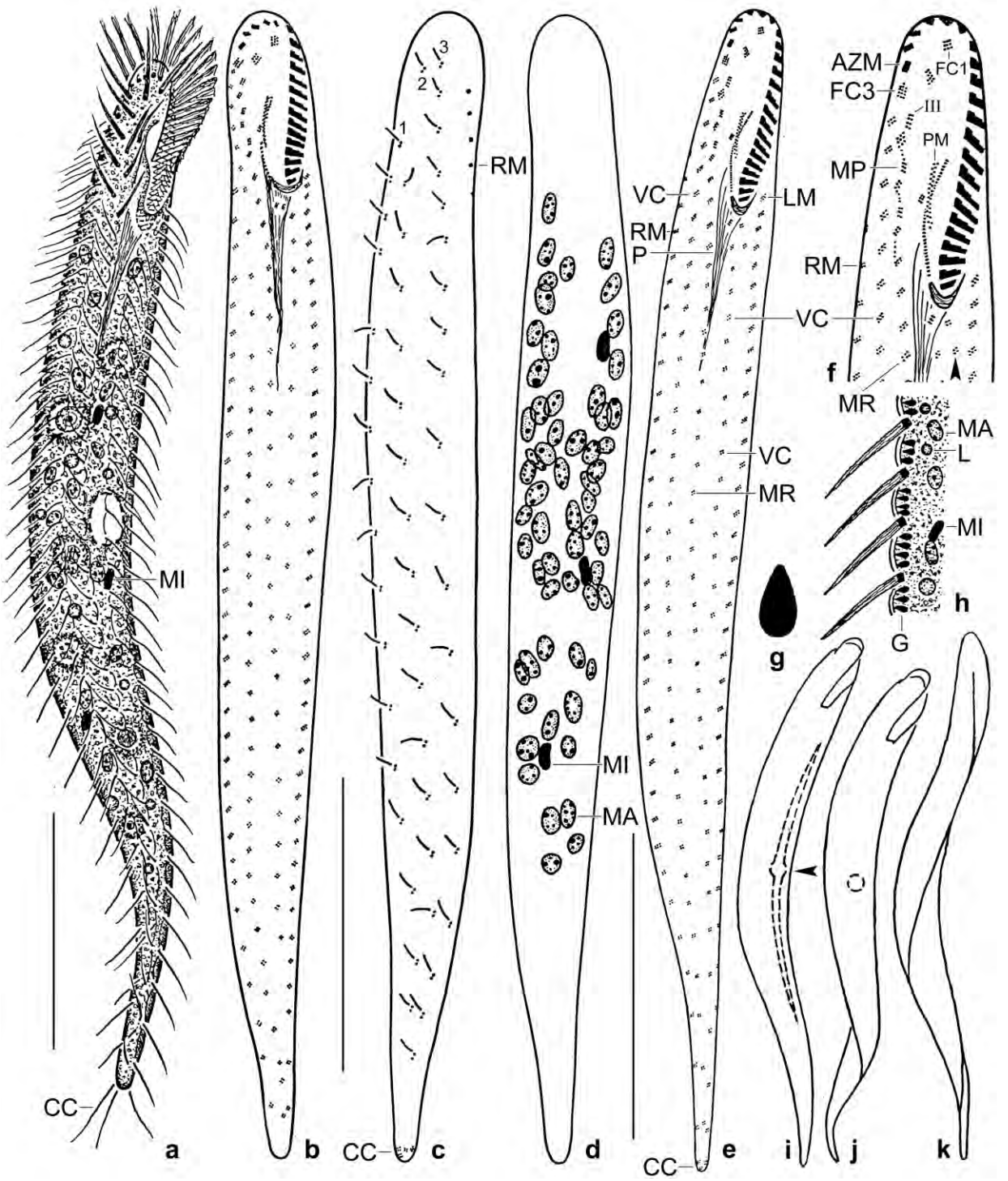

Fig. 173a–k. *Australothrix fraterculus* from life (a, g–k) and after protargol impregnation (b–f). **a:** Ventral view of a representative specimen, length 220 µm. **b–d:** Ventral and dorsal view of a paratype specimen. **e, f:** Ventral view of holotype specimen, length 193 µm. *Australothrix fraterculus* has five cirral rows and three midventral pairs (f, connected by dotted lines). Arrowhead marks two extra cirri. **g, h:** Cortical granule (~ 1 × 0.5 µm) and optical section of cortex. **i–k:** A single, swimming specimen redrawn from video records. Arrow marks contractile vacuole. AZM – adoral zone of membranelles, CC – caudal cirri, FC1, 3 – frontal cirri, G – cortical granules, L – lipid droplet, LM – left marginal row, MA – macronuclear nodules, MI – micronuclei, MP – midventral pairs, MR – midventral row, P – pharynx, PM – paroral membrane, RM – right marginal row, VC – ventral cirral row, 1, 2, 3 – dorsal kineties, III – posterior cirrus of anlage III. Scale bars 50 µm.

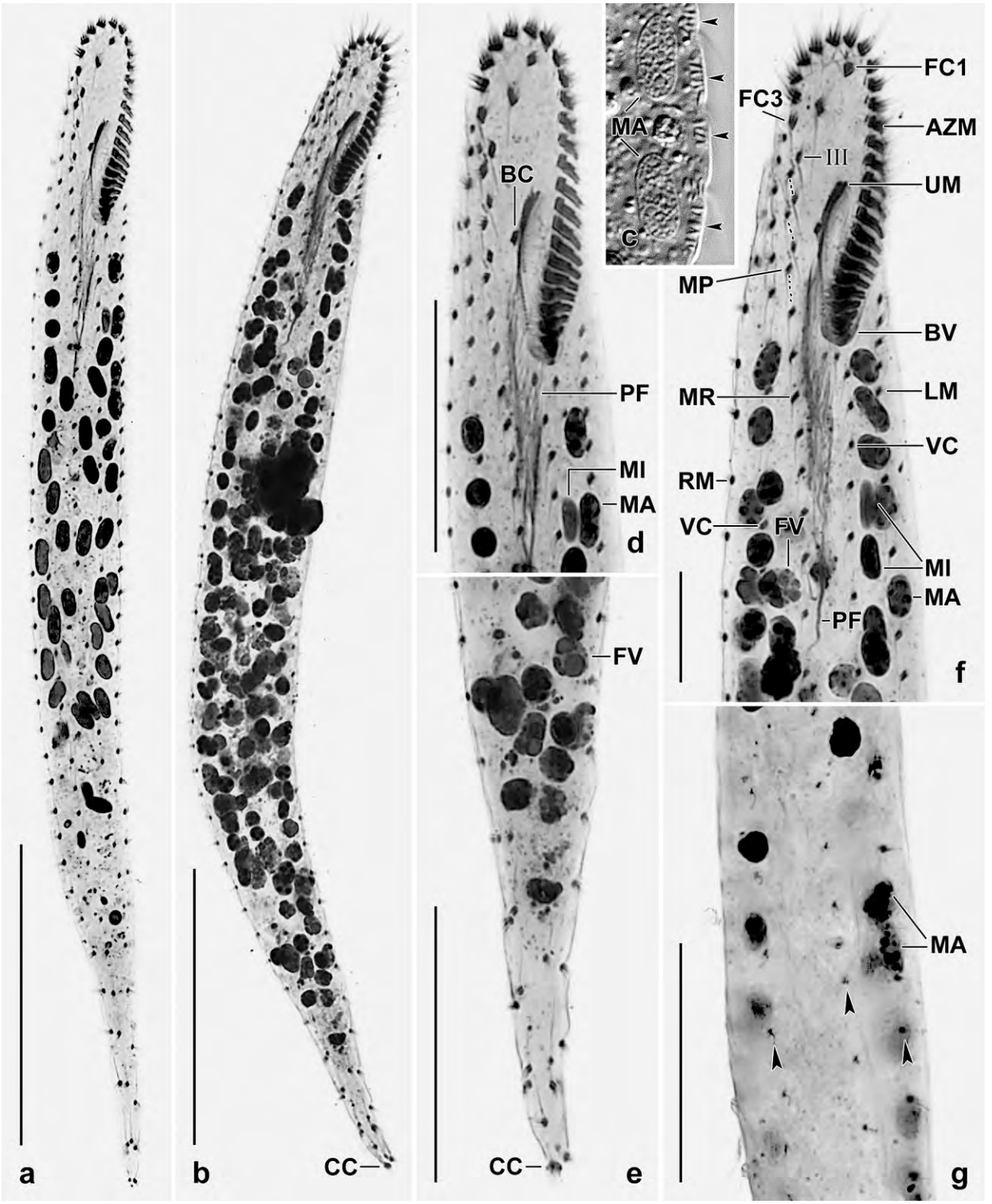

Fig. 174a–g. *Australothrix fraterculus* from life (c) and after protargol impregnation (a, b, d–g). **a, b, d–f:** Ventral views. **c:** Optical section, showing cortical granules (arrowheads). **g:** Dorsal view with kineties marked by arrowheads. AZM – adoral zone, BC – buccal cirrus, BV – buccal vertex, CC – caudal cirri, FC1, 3 – frontal cirri, FV – food vacuole, LM – left marginal row, MA – macronuclear nodules, MI – micronuclei, MP – midventral pairs, MR – midventral row, PF – pharyngeal fibres, RM – right marginal row, UM – undulating membranes, VC – ventral cirral rows, III – posterior cirrus of anlage III. Scale bars 10 µm (f), 25 µm (d, e, g), and 50 µm (a, b).

Table 60. Comparative morphometric data on *Australothrix steineri* from Costa Rica (CR; from FOISSNER 1995) and two sites from Brazil (BR28 and BR32), and *Australothrix fraterculus* from China (CH). Data based on mounted, protargol-impregnated, and randomly selected specimens from non-flooded Petri dish cultures. Measurements in µm. CV – coefficient of variation in %, M – median, Max – maximum, Mean – arithmetic mean, Min – minimum, n – number of individuals investigated, Pop – population, SD – standard deviation, SE – standard error of arithmetic mean.

Characteristics	Pop	Mean	M	SD	SE	CV	Min	Max	n
Body, length	CR	236.1	240.0	53.3	17.8	22.6	145.0	315.0	9
	BR28	160.5	158.0	25.3	5.5	15.8	117.0	220.0	21
	BR32	198.3	193.5	33.7	10.6	17.0	145.0	249.0	10
	CH	195.1	196.0	31.2	8.7	16.0	150.0	246.0	13
Body, width	CR	22.7	24.0	4.6	1.5	20.2	16.0	31.0	9
	BR28	19.9	20.0	2.0	0.4	10.1	16.0	24.0	21
	BR32	20.6	20.5	3.7	1.2	17.8	15.0	25.0	10
	CH	19.4	19.0	4.6	1.3	23.7	14.0	32.0	13
Body length:width, ratio	CR	10.4	–	–	–	–	–	–	9
	BR28	8.1	8.1	0.9	0.2	11.6	6.5	10.2	21
	BR32	9.9	9.5	2.3	0.7	23.4	6.9	13.9	10
	CH	10.5	10.5	0.8	0.2	7.6	8.9	11.7	13
Anterior body end to rear end of adoral zone of membranelles, distance	CR	31.6	32.0	2.2	0.7	7.1	28.0	35.0	9
	BR28	28.9	29.0	2.3	0.5	8.0	25.0	33.0	21
	BR32	32.6	32.8	1.4	0.5	4.4	30.0	35.0	10
	CH	30.2	30.0	4.4	1.2	14.6	24.0	37.0	13
Nuclear apparatus, length of Figure	BR28	91.2	93.0	15.9	3.5	17.4	61.0	127.0	21
	CH	116.8	119.0	24.3	6.7	20.8	84.0	166.0	13
Nuclear apparatus, width of Figure	BR28	16.6	16.0	1.7	0.4	10.2	14.5	20.0	21
	CH	15.5	16.0	2.8	0.8	18.3	11.0	19.0	13
Macronuclear nodules, length	CR	5.3	5.0	0.7	0.2	13.3	4.0	6.0	9
	BR28	4.8	4.5	0.9	0.2	19.7	3.5	7.5	21
	BR32	4.3	4.5	0.7	0.2	15.7	3.5	5.5	10
	CH	4.4	4.5	0.7	0.2	15.6	2.5	5.0	13
Macronuclear nodules, width	CR	2.6	3.0	0.5	0.2	20.6	2.0	3.0	9
	BR28	2.7	2.5	0.3	0.1	10.8	2.0	3.0	21
	BR32	2.2	2.0	0.3	0.1	11.7	2.0	2.5	10
	CH	2.3	2.0	0.4	0.1	16.6	2.0	3.0	13
Macronuclear nodules, number	BR28	54.7	55.0	6.0	1.3	11.1	43.0	65.0	21
	BR32	71.1	75.5	13.8	4.4	19.4	46.0	86.0	10
	CH	65.2	64.0	21.3	5.9	32.6	32.0	119.0	13
Micronucleus, length	BR28	3.8	4.0	0.3	0.1	9.0	3.0	4.0	21
	BR32	2.9	2.8	0.5	0.2	16.6	2.5	4.0	10
	CH	4.7	5.0	0.5	0.1	10.2	4.0	5.5	13
Micronucleus, width	BR28	2.3	2.0	0.3	0.1	15.0	2.0	3.0	21
	BR32	2.1	2.0	0.3	0.1	13.9	1.5	2.5	10
	CH	1.6	1.5	0.2	0.1	11.9	1.5	2.0	13
Micronuclei, number	BR28	2.6	3.0	0.6	0.1	23.2	2.0	4.0	21
	BR32	3.8	3.5	1.2	0.4	32.4	2.0	6.0	10
	CH	2.5	3.0	0.8	0.2	30.6	1.0	4.0	13

continued

Characteristics	Pop	Mean	M	SD	SE	CV	Min	Max	n
Adoral membranelles, number	CR	25.2	25.0	1.1	0.4	4.3	24.0	27.0	9
	BR28	23.7	24.0	1.0	0.2	4.0	21.0	25.0	21
	BR32	25.8	26.0	1.3	0.4	5.1	24.0	28.0	10
	CH	22.6	23.0	1.8	0.5	8.0	19.0	24.0	13
Frontal cirri, number	CR	3.0	3.0	0.0	0.0	0.0	3.0	3.0	8
	BR28	3.0	3.0	0.0	0.0	0.0	3.0	3.0	21
	BR32	3.1	3.0	0.3	0.1	10.2	3.0	4.0	10
	CH	3.0	3.0	0.0	0.0	0.0	3.0	3.0	13
Buccal cirri, number	CR	1.0	1.0	0.0	0.0	0.0	1.0	1.0	7
	BR28	1.0	1.0	0.0	0.0	0.0	1.0	1.0	21
	BR32	1.0	1.0	0.0	0.0	0.0	1.0	1.0	10
	CH	1.0	1.0	0.0	0.0	0.0	1.0	1.0	13
Ventral cirral rows, number (ex. marginal rows)	CR	4.8	5.0	0.9	0.3	18.1	4.0	6.0	11
	BR28	4.0	4.0	0.0	0.0	0.0	4.0	4.0	21
	BR32	4.0	4.0	0.0	0.0	0.0	4.0	4.0	10
	CH	3.0	3.0	0.0	0.0	0.0	3.0	3.0	13
Anterior body end to last midventral pair, distance	CR	24.3	25.0	3.1	1.2	12.7	21.0	30.0	7
	BR28	21.4	22.0	4.5	1.0	21.1	5.0	28.5	21
	BR32	21.9	22.3	1.9	0.6	8.7	17.5	24.5	10
	CH	24.6	26.0	3.6	1.1	14.6	17.0	29.5	11
Midventral pairs, number	CR	2.3	2.0	–	–	–	2.0	3.0	7
	BR28	2.2	2.0	0.4	0.1	19.5	2.0	3.0	21
	BR32	1.9	2.0	0.3	0.1	16.6	1.0	2.0	10
	CH	2.7	3.0	0.5	0.2	17.9	2.0	3.0	10
Posterior body end to end of midventral row, distance	BR28	2.9	3.0	0.8	0.2	28.8	1.5	4.5	16
	BR32	2.8	2.5	0.9	0.3	33.8	2.0	5.0	9
	CH	1.6	2.0	0.6	0.2	38.7	0.5	2.0	7
Midventral complex, number of cirri in right row	BR28	26.8	28.0	6.4	1.4	24.1	2.0	34.0	21
	BR32	33.9	33.0	4.2	1.4	12.5	29.0	43.0	9
	CH	35.6	35.0	4.9	1.7	13.7	29.0	43.0	8
Right marginal cirri, number	CR	63.3	75.0	20.7	7.8	32.7	35.0	85.0	7
	BR28	36.7	37.0	2.9	0.6	8.0	31.0	41.0	21
	BR32	37.4	37.5	5.3	1.7	14.2	28.0	45.0	10
	CH	41.0	39.0	5.4	1.6	13.2	32.0	48.0	11
Left marginal cirri, number	CR	58.0	56.5	19.7	7.0	34.0	36.0	82.0	8
	BR28	33.7	34.0	2.0	0.4	5.8	30.0	36.0	21
	BR32	38.0	36.5	7.6	2.4	20.1	29.0	56.0	10
	CH	40.5	38.0	5.2	1.6	12.7	35.0	51.0	11
Dorsal bristle rows, number	CR	4.0	4.0	0.0	0.0	0.0	4.0	4.0	9
	BR28	4.0	4.0	0.0	0.0	0.0	4.0	4.0	21
	BR32	4.0	4.0	0.0	0.0	0.0	4.0	4.0	10
	CH	3.0	3.0	0.0	0.0	0.0	3.0	3.0	13
Caudal cirri, number	BR28	6.1	6.0	1.1	0.2	17.7	4.0	8.0	21
	BR32	3.9	4.0	0.7	0.2	18.9	3.0	5.0	10
	CH	4.5	4.0	0.7	0.2	15.4	4.0	6.0	11

Type locality: Litter and soil from the outskirts of the town of Yungning, about 90 km northeast of Bejing, entrance to the Big Wall at Badaling, surroundings of the toilet, 116°10'E 40°20'N.

Type material: 1 holotype and 3 paratype slides with protargol-impregnated specimens have been deposited in the Biology Centre of the Upper Austrian Museum in Linz (LI). Relevant specimens have been marked by black ink circles on the coverslip.

Etymology: The Latin species name is a noun in apposition and a composite of *frater* (brother) and the diminutive *culus* (small, similar), referring to the similarity with *A. steineri*.

Description: The variability of *Australothrix* spp. is rather high, i. e., most coefficients of variation are between 15% and 20%. This is usual for large species, especially when they are slender.

Size in vivo 170–280 × 15–35 µm, usually about 220 × 20 µm, as calculated from some in vivo measurements and the morphometric data in Table 60 adding 15% preparation shrinkage; very flexible but not contractile. Body very slender, on average 10.5:1, becoming tail-like posteriorly; usually slightly to distinctly contorted about main body axis especially when just isolated from the non-flooded Petri dish culture, later the contortion becomes indistinct or vanishes; laterally flattened up to 2:1 (Fig. 173a, b, e, i–k, 174a, b; Table 60). Nuclear apparatus on average in central four sixths of cell, i. e., absent from oral and tail region as well as from pharyngeal and cortex areas. On average 65 broadly to ordinarily ellipsoid macronuclear nodules in vivo 4–7 × 3–5 µm in size; studded with minute nucleoli. Usually two to three micronuclei scattered among and as long as macronuclear nodules but narrower, compact and thus well recognizable in vivo (Fig. 173a, d, h, 174a, g; Table 60). Contractile vacuole in or slightly anterior to mid-body at left margin of cell, with long collecting canals (Fig. 173a, i). Cortex very flexible, associated with colourless granules 1–1.5 × 0.5–0.8 µm in size, mainly around bases of cirri and dorsal bristles (Fig. 173g, h, 174c); granules stain red with methyl green-pyronin but are not extruded and do not impregnate with the protargol method used. Cytoplasm colourless, studded with macronuclear nodules, some food vacuoles up to 10 µm across, and minute lipid droplets. Feeds on bacteria and small heterotrophic flagellates. Usually glides slowly on and between soil particles, rarely swims showing the contorted body.

Cirral pattern as typical for genus (Berger 2006), i. e., transverse cirri and frontoterminal cirri absent and five long cirral rows, including two marginal rows, two ventral rows, and a midventral row; most cirri in rather distinct pits, 10–12 µm long and fine, i. e., composed of four or six basal bodies in two minute rows (Fig. 173a, b, e, f, h, 174a–f; Table 60). Three thickened frontal cirri extend in slightly concave row from body`s midline to distal end of adoral zone; cirrus III/2 upon midventral complex, composed of six to eight basal bodies. Buccal cirrus at summit of paroral membrane, composed of six basal bodies. Usually three midventral pairs right of undulating membranes, cirri composed of six basal bodies; followed by midventral row extending subterminally with cirri composed of six basal bodies except of those on tail consisting of only four. Right marginal row commences subapically on dorsal side, then turns to right body margin and extends to near posterior body end, composed of cirri with six basal bodies except of those on tail consisting of only four. Left marginal row commences slightly anterior of oral vertex and extends to near body end with cirri composed as those of right row. One ventral cirral

row each right and left of midventral row, most cirri composed of only four basal bodies; right row commences slightly posterior to frontal cirrus 3 and ends subterminally, left row commences posterior to oral vertex and ends slightly posterior to mid-body (Fig. 173a, b, e, f, h, 174a–f; Table 60).

Dorsal kinetids in distinct pits, surrounded by cortical granules, bristles 3–4 µm long in vivo, arranged in three rows commencing slightly subapically and ending subterminally. Four to six caudal cirri at end of tail each composed of four, rarely two basal bodies (Fig. 173a, c, e, 174a, b, e, g).

Adoral zone very short extending only 15% of body length, composed of an average of 23 ordinary membranelles (Fig. 173a, b, e, f, 174a, b, d, f; Table 60). Buccal cavity flat and narrow, buccal lip covers some proximal membranelles. Undulating membranes slightly curved, paroral about half as long as endoral, optically intersect at level of buccal cirrus. Pharynx conspicuous possibly because containing long endoral cilia, extends to second third of cell.

Occurrence and ecology: As yet found only at type locality where it was rare in the non-flooded Petri dish culture. The locality was covered with grass and bushes. Leaf litter, soil, and roots were collected from the upper 3 cm.

Remarks: The Chinese *Australothrix* is rather similar to *A. steineri* Foissner, 1995. They differ, however, by three good features: cortical granules ovate vs. oblong; five vs. six cirral rows; and three vs. four dorsal kineties.

Australothrix venezuelensis Foissner & Heber **nov. spec.** (Fig. 175a–h, 176a–c; Tables 61, 62)

Diagnosis: Size in vivo about 230 × 65 µm; very elongate obovate, pisciform, or ellipsoid. Nuclear apparatus on average composed of 94 scattered, ellipsoid macronuclear nodules and 3 micronuclei. Cortical granules in dense rows, ellipsoid, colourless, in vivo 3–4 × 1–1.5 µm in size. Midventral complex on average composed of 7 cirral pairs and a long midventral row consisting of about 25 cirri. 1 left and 2 right marginal cirral rows, right row 1 shortened posteriorly and thus exceeded by midventral row. Usually 4 dorsal kineties and an average of 13 caudal cirri.

Type locality: Venezuelan site (32), i. e., soil under a carpet of Velloziacean plants in a Laja between the Agricultural Research Station and the airport of Puerto Ayacucho, 67°36‘W 5°41‘N.

Type material: 1 holotype slide and 3 paratype slides with protargol-impregnated specimens have been deposited in the Biology Centre of the Upper Austrian Museum in Linz (LI). Relevant specimens have been marked by black ink circles on the coverslip.

Etymology: Named after the country discovered.

Description: *Australothrix venezuelensis* is a comparatively large ciliate. Thus, several measurements may be affected by preparation artifacts, as indicated by high coefficients of

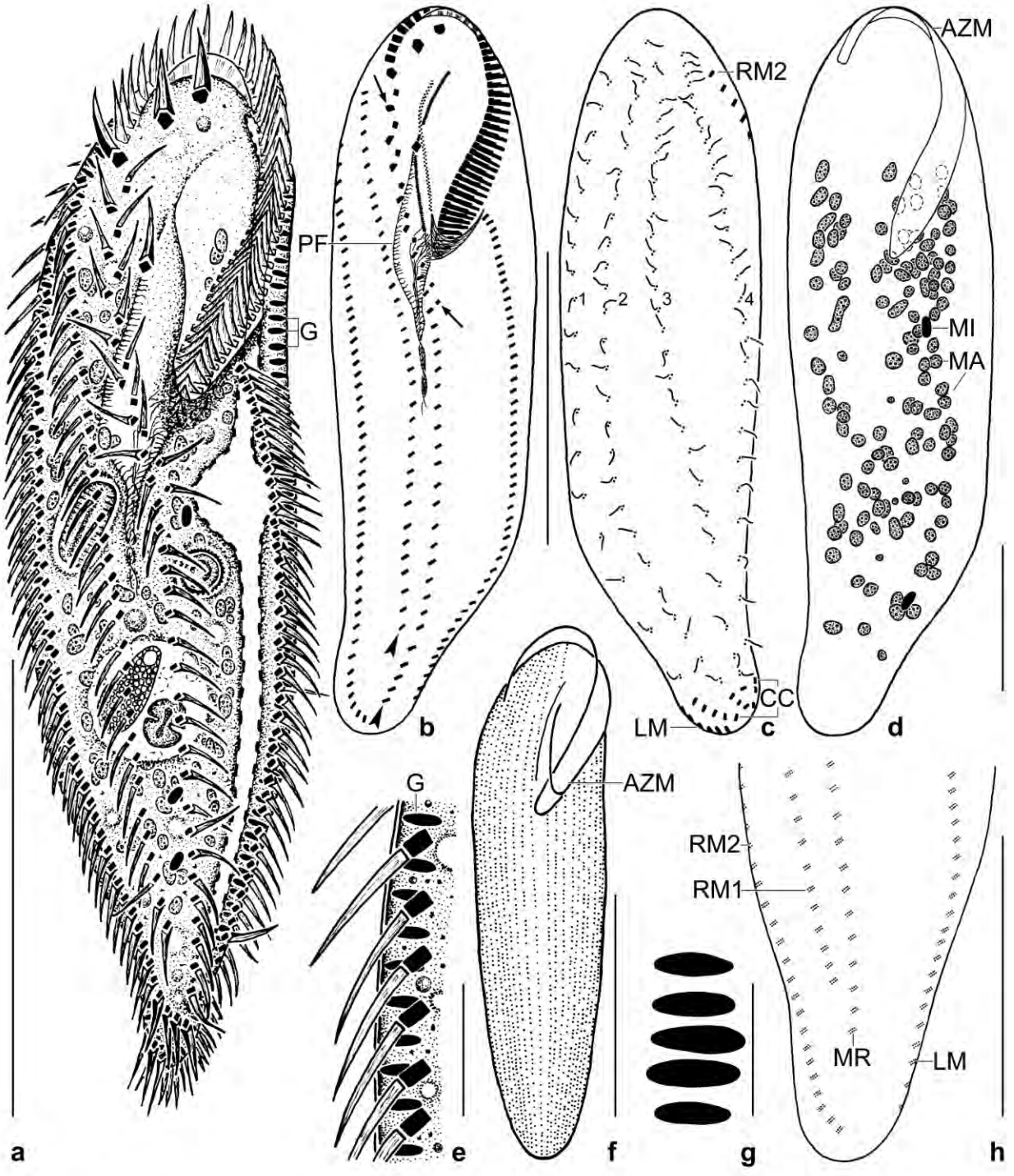

Fig. 175a–h. *Australothrix venezuelensis* from life (a, e–g) and after protargol impregnation (b–d, h). **a:** Ventral view of a representative specimen having ingested a ciliate cyst, a diatom, a desmid, and a testate amoeba, length 230 µm. **b–d:** Ventral and dorsal infraciliature and nuclear apparatus of holotype specimen, length 250 µm. Arrows mark first and last cirral pair of midventral complex, arrowheads denote posterior end of midventral and right marginal row. **e:** Optical section, showing the fringe of cortical granules. **f:** Outline and cortical granulation of a tailless specimen. **g:** Shape of cortical granules. **h:** Posterior body region, showing the absence of transverse cirri and the long midventral row. AZM – adoral zone of membranelles, CC – caudal cirri, G – cortical granules, LM – left marginal cirral row, MA – macronuclear nodules, MI – micronucleus, MR – midventral cirral row, PF – pharynx and minute oblong structures in the pharyngeal wall, RM1, RM2 – right marginal cirral rows, 1–4 – dorsal kineties. Scale bars 5 µm (g), 10 µm (e), 50 µm (d, h), and 100 µm (a–c, f).

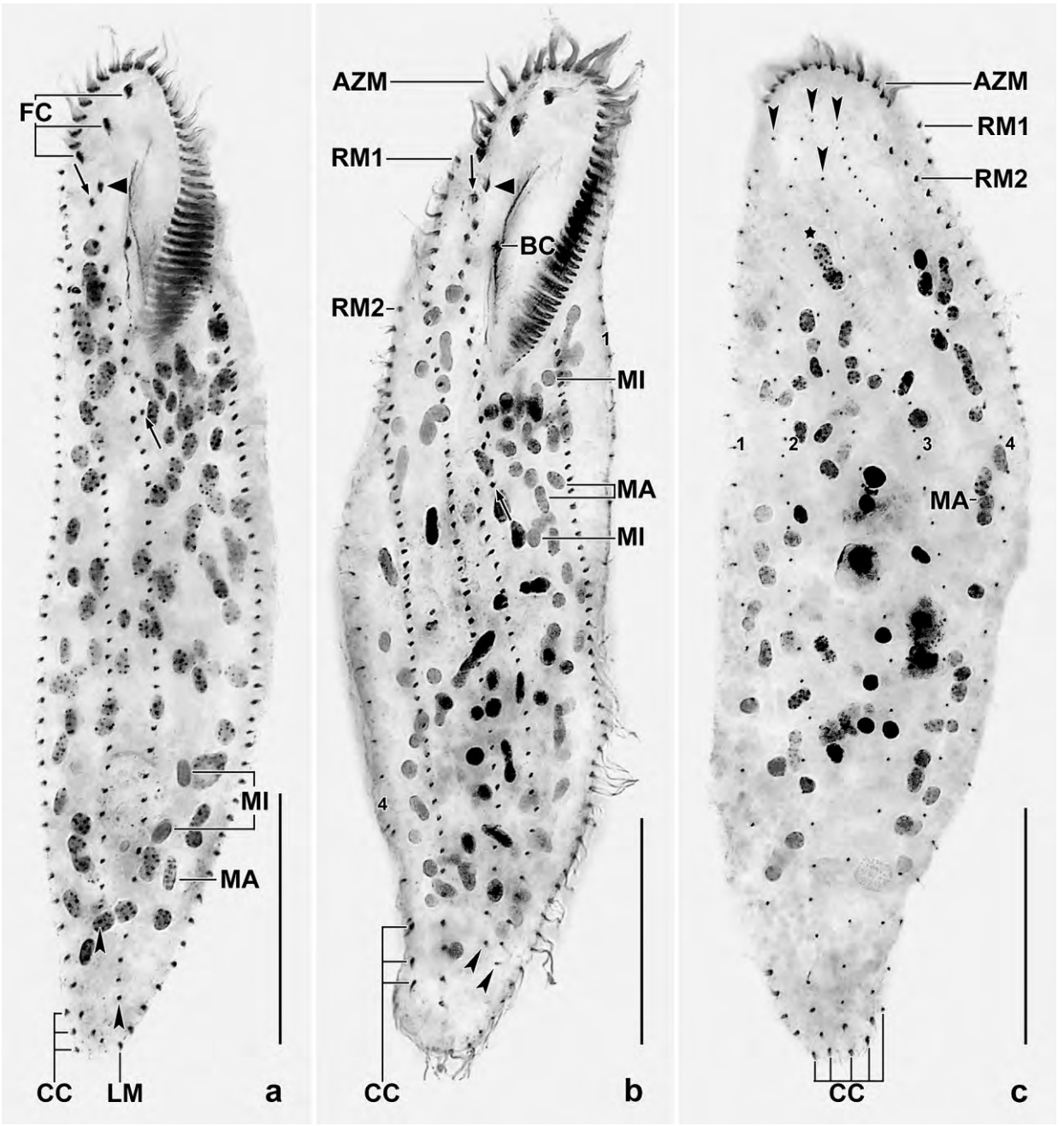

Fig. 176a–c. *Australothrix venezuelensis* after protargol impregnation. **a, b:** Ventral view of representative specimens, length 164 µm (a) and 220 µm (b). Arrows denote the anteriormost and posteriormost cirral pair of the midventral complex; triangles mark the solitary cirrus III/2; arrowheads mark the posterior end of the midventral row and the right marginal row 1; the midventral row exceeds the right marginal row 1 in length, an important diagnostic feature of this species. The caudal cirri of dorsal kinety 4 are often laterally located and thus frequently recognizable in ventral view of the cell. The micronuclei are almost as large as the macronuclear nodules. **c:** Dorsal view of a specimen with an additional fifth dorsal kinety (asterisk), length 212 µm. The arrowheads denote the anterior end of the four ordinary bristle rows. AZM – adoral zone of membranelles, BC – buccal cirrus, CC – caudal cirri, FC – frontal cirri, LM – left marginal cirral row, MA – macronuclear nodules, MI – micronuclei, RM1, RM2 – right marginal cirral rows, 1–4 – dorsal kineties. Scale bars 40 µm (a) and 50 µm (b, c).

Table 61. Morphometric data on *Australothrix venezuelensis* based on mounted, protargol-impregnated, and randomly selected specimens from a non-flooded Petri dish culture. Measurements in µm. CV – coefficient of variation in %, M – median, Max – maximum, Mean – arithmetic mean, Min – minimum, n – number of individuals investigated, SD – standard deviation, SE – standard error of arithmetic mean.

Characteristics	MEAN	M	SD	SE	CV	Min	Max	n
Body, length	203.7	203.0	29.5	6.0	14.5	152.0	264.0	24
Body, width	58.0	57.0	12.5	2.5	21.5	34.0	88.0	24
Body length:width, ratio	3.6	3.7	0.8	0.2	21.2	2.2	5.0	24
Anterior body end to anteriormost macronuclear nodule, distance	33.5	33.0	4.9	1.1	14.6	25.0	42.0	21
Posterior body end to posteriormost macronuclear nodule, distance	25.9	26.0	7.3	1.6	28.0	15.0	47.0	21
Macronuclear nodules, number	94.3	94.0	15.7	3.4	16.6	72.0	118.0	21
Anteriormost macronuclear nodule, length	6.0	6.0	1.7	0.4	27.4	3.0	9.0	21
Anteriormost macronuclear nodule, width	3.5	3.0	0.6	0.1	17.1	3.0	5.0	21
Anteriormost macronuclear nodule length:width, ratio	1.8	1.8	0.6	0.1	31.9	1.0	3.0	21
Micronuclei, number	3.0	3.0	1.1	0.2	36.3	2.0	5.0	21
Anteriormost micronucleus, length	5.0	5.0	1.1	0.2	21.2	4.0	7.0	21
Anteriormost micronucleus, width	3.0	3.0	–	–	–	3.0	4.0	21
Anteriormost micronucleus length:width, ratio	1.7	1.7	0.4	0.1	22.8	1.0	2.3	21
Anterior body end to proximal end of adoral zone, distance	59.7	59.0	6.6	1.4	11.1	48.0	70.0	21
Adoral zone, percentage of body length	29.6	29.3	2.4	0.5	8.0	25.9	34.3	21
Adoral membranelles, number	41.3	41.0	3.1	0.7	7.6	35.0	47.0	21
Adoral membranelles, length of largest membranellar basis	9.5	10.0	1.0	0.2	10.3	8.0	12.0	21
Buccal cavity, width [a]	11.8	12.0	3.0	0.6	25.1	8.0	16.0	21
Anterior body end to paroral membrane, distance	19.2	20.0	3.0	0.7	15.8	11.0	25.0	21
Paroral membrane, length	32.0	33.0	4.5	1.0	13.9	25.0	40.0	21
Anterior body end to endoral membrane, distance	17.0	18.0	3.0	0.7	17.8	9.0	22.0	21
Endoral membrane, length	35.1	36.0	6.7	1.5	19.2	22.0	44.0	21
Frontal cirri, number	3.0	3.0	0.0	0.0	0.0	3.0	3.0	24
Anterior body end to buccal cirrus, distance	33.5	35.0	5.4	1.2	16.1	21.0	44.0	21
Buccal cirri, number	1.0	1.0	0.0	0.0	0.0	1.0	1.0	24
Anterior body end to midventral complex, distance	20.1	21.0	3.8	0.8	18.7	13.0	26.0	21
Anterior body end to posteriormost cirral pair of midventral complex, distance	78.3	78.0	15.3	3.3	19.5	49.0	105.0	21
Posterior body end to midventral row, distance	16.8	15.0	6.7	1.5	40.0	8.0	32.0	21
Midventral complex, number of cirral pairs	7.4	7.0	2.1	0.5	27.8	4.0	11.0	21
Midventral complex, number of cirri in midventral row	25.1	25.0	3.6	0.8	14.1	19.0	31.0	21
Anterior body end to right marginal row 1, distance	16.5	16.0	4.7	1.0	28.4	8.0	28.0	21
Posterior body end to right marginal row 1, distance	29.2	31.0	8.1	1.8	27.7	15.0	44.0	21

continued

Characteristics	MEAN	M	SD	SE	CV	Min	Max	n
Right marginal row 1, number of cirri	39.0	38.0	4.6	1.0	11.9	32.0	47.0	21
Anterior body end to right marginal row 2, distance	16.5	18.0	4.3	0.9	26.4	8.0	25.0	21
Right marginal row 2, number of cirri	50.8	50.0	5.9	1.3	11.6	37.0	62.0	21
Anterior body end to left marginal row, distance	51.6	52.0	6.8	1.5	13.2	41.0	67.0	21
Left marginal row, number of cirri	53.3	53.0	6.5	1.4	12.2	39.0	63.0	21
Dorsal kineties, number [b]	4.1	4.0	–	–	–	4.0	5.0	21
Anterior body end to dorsal kinety 1, distance	16.0	15.0	6.3	1.4	39.3	6.0	35.0	21
Dorsal kinety 1, number of bristles	22.4	22.0	4.2	0.9	18.8	16.0	29.0	21
Anterior body end to dorsal kinety 2, distance	13.9	13.0	3.0	0.6	21.3	10.0	20.0	21
Dorsal kinety 2, number of bristles	26.2	25.0	3.8	0.8	14.5	20.0	33.0	21
Anterior body end to dorsal kinety 3, distance	26.8	26.0	6.2	1.4	23.1	15.0	38.0	21
Dorsal kinety 3, number of bristles	23.7	23.0	4.0	0.9	17.0	18.0	32.0	21
Anterior body end to dorsal kinety 4, distance	13.9	14.0	2.0	0.4	14.4	10.0	17.0	21
Dorsal kinety 4, number of bristles	29.8	29.0	4.5	1.0	15.2	24.0	41.0	21
Bristles in specimens with 4 dorsal kineties, number	102.6	100.0	14.9	3.5	14.5	82.0	133.0	18
Posterior body end to anteriormost caudal cirrus of dorsal kinety 1, distance	15.6	13.0	6.9	1.5	44.2	8.0	34.0	21
Dorsal kinety 1, number of caudal cirri	5.0	5.0	1.0	0.2	21.0	3.0	8.0	21
Posterior body end to anteriormost caudal cirrus of dorsal kinety 2, distance	10.8	10.0	2.4	0.5	22.6	6.0	15.0	21
Dorsal kinety 2, number of caudal cirri	2.3	2.0	0.6	0.1	24.7	1.0	3.0	21
Posterior body end to anteriormost caudal cirrus of dorsal kinety 3, distance	10.5	11.0	2.6	0.6	24.8	5.0	15.0	21
Dorsal kinety 3, number of caudal cirri	2.5	3.0	–	–	–	2.0	3.0	21
Posterior body end to anteriormost caudal cirrus of dorsal kinety 4, distance	15.0	15.0	4.8	1.1	32.2	5.0	27.0	21
Dorsal kinety 4, number of caudal cirri	3.0	3.0	0.6	0.1	21.1	2.0	4.0	21
Caudal cirri in specimens with 4 dorsal kineties, number	12.8	13.0	1.5	0.4	11.6	10.0	15.0	18

[a] Distance between summit of paroral membrane and right margin of adoral zone.

[b] A supernumeral dorsal bristle row between kineties 2 and 3 occurs in two out of 21 specimens investigated; they have 2 caudal cirri and 22, respectively, 18 dorsal bristles. One out of 21 specimens has a supernumeral row of caudal cirri left of dorsal kinety 1; it is composed of merely three cirri.

variation. However, most important characters, such as body length, length of adoral zone, and number of adoral membranelles, marginal, and caudal cirri have ordinary variability.

Size in vivo 170–300 × 40–100 µm, usually about 230 × 65 µm, as calculated from some in vivo measurements and the morphometric data in Table 61 adding 15 % preparation shrinkage. Body highly flexible, very elongate obovate, pisciform, or ellipsoid, anteriorly broadly rounded, posteriorly narrowly rounded or bluntly tailed; brownish at low magnification (Fig. 175a, f, 176a–c; Table 61). Nuclear apparatus within central quintiles of cell, consists of an average of 94 (72–118) scattered macronuclear nodules and 3 (2–5) micronuclei (Fig. 175a, d, 176a–c; Table 61). Nodules globular to elongate ellipsoid, on average 6 × 3.5 µm in protargol preparations; nucleoli less than 1 µm across. Micronuclei globular to ellipsoid, about 5 × 3.5 µm. Contractile vacuole at

Table 62. Comparison of main morphometrics of *Australothrix simplex* (from BERGER 2006) and *Australothrix venezuelensis*. Data based on mounted, protargol-impregnated, and randomly selected specimens from non-flooded Petri dish cultures. Measurements in µm: first value arithmetic mean; minimum and maximum in parentheses.

Characteristics	***Australothrix simplex***[a]	***Australothrix venezuelensis***
Body, length	(116–187)	204 (152–264)
Body, width	(49–77)	58 (34–88)
Body length:width, ratio (in vivo)	~ 3	~ 4[b]
Macronuclear nodules, number	(40–50)	94 (72–118)
Adoral zone, percentage of body length	~ 33	30 (26–34)
Adoral membranelles, number	~ 38	41 (35–47)
Midventral complex, number of cirral pairs	~ 11	7 (4–11)
Midventral complex, number of cirri in midventral row	~ 5	25 (19–31)
Right marginal row 1, number of cirri	~ 19	39 (32–47)
Right marginal row 2, number of cirri	~ 47	51 (37–62)
Left marginal row, number of cirri	~ 49	53 (39–63)
Caudal cirri, number	(4–5)[c]	13 (10–15)[d]
Dorsal kineties, number	5	4 (4–5)
Specimens investigated, number	no data	18–24

[a] Except of body length and width, most values likely based on few specimens.

[b] According to three live specimens.

[c] Assuming a dorsal pattern similar to that of *A. alwinae* and *A. aplosa*. Figure 140b in Berger (2006) shows five caudal cirri associated with only the rightmost dorsal kinety; thus the given value is very likely a distinct underestimation.

[d] From specimens with four dorsal kineties.

left body margin in or slightly anterior to mid-body; collecting canals extend to body ends (Fig. 175a). Cortical granules in dense rows, ellipsoid, in vivo 3–4 × 1–1.5 µm, colourless, stain deeply with methyl green-pyronin, do not impregnate with the protargol method used; become long filaments, forming a dense reticulum when extruded (Fig. 175a, e, g). Food vacuoles scattered throughout body, in vivo up to 30 µm across, contain diatoms, desmids, ciliate cysts (*Vorticella astyliformis*), and naked and testate (*Trinema lineare*) amoebae (Fig. 175a).

Cirral pattern as typical for genus (Berger 2006), i. e., transverse and frontoterminal cirri absent and more than two marginal rows (Fig. 175a, b, h, 176a, b; Table 61). Three thickened frontal cirri extend in oblique row from body´s midline to distal end of adoral zone, cirri 12–15 µm long in protargol preparations. Cirrus III/2 between right frontal cirrus and midventral complex. Buccal cirrus near optical intersection of undulating membranes, about 13 µm long. Midventral complex roughly in body´s midline, commences near right frontal cirrus and ends slightly posterior to buccal vertex, composed of an average of 7 (4–11) cirral pairs, cirri 10–12 µm long in protargol preparations, those of anterior pairs slightly enlarged; midventral row ends subterminally, composed of an average of 25 (19–31) cirri. Two right marginal rows: internal row (RM1) begins near right frontal cirrus, posteriorly shorter than midventral row, on average composed of 39 (32–47) cirri; external row (RM2) almost bipolar, anterior portion extends onto dorsal side, posteriorly usually curved to body´s midline, on average composed of 51 (37–62) cirri. Left marginal row

extends to body end, posteriormost cirri often dorsolaterally located, composed of 53 (39–63) cirri on average (Fig. 175a, b, h, 176a, b; Table 61). Two supernumerary cirri between RM1 and midventral row in one out of 24 specimens.

Dorsal bristles about 4 µm long in vivo, usually arranged in four rows with a total of 103 (82–133) bristles; rows 1, 2, and 4 bipolar, row 3 slightly shortened anteriorly (Fig 175c, 176c; Table 61). An additional kinety between rows 2 and 3 in two out of 21 specimens investigated, anteriorly shortened, associated with two caudal cirri and 22, respectively, 18 dorsal bristles (Fig. 176c). Three supernumeral caudal cirri left of dorsal row 1 in one out of 21 specimens. On average a total of 13 caudal cirri about 12 µm long in protargol preparations: five at end of bristle row 1 and two or three each in rows 2–4, cirri of rightmost row often displaced ventrolaterally and thus easily mixed with marginal cirri (Fig. 175c, 176a–c; Table 61).

Adoral zone occupies about 30 % of body length, proximal portion slightly spatulate, usually composed of 41 (35–47) ordinary membranelles with cilia up to 15 µm long in protargol preparations; bases of largest membranelles about 12 µm wide in vivo, on average 10 (8–12) µm in protargol preparations (Fig. 175a, b, 176a, b; Table 61). Buccal cavity conspicuous because wide and deep; buccal lip covers proximal portion of adoral zone. Undulating membranes moderately curved, of similar length, optically intersect near level of buccal cirrus, paroral cilia approximately 10 µm long in vivo, endoral cilia about 20 µm. Pharynx conspicuous, extends from buccal cirrus to mid-body, broadest near proximal end of adoral zone; pharyngeal wall studded with minute, oblong, argyrophilic structures as, for instance, in *Australothrix alwinae* and *Caudiholosticha notabilis* (Fig. 175a, b; for a review, see Berger 2006).

Occurrence and ecology: As yet found only at type locality. The large size and the broad body suggest *A. venezuelensis* as litter or freshwater species.

Remarks: *Australothrix zignis* and *A. gibba* are poorly described aquatic species with two macronuclear nodules (for a review, see Berger 2006). The terrestrial *Australothrix* species are so different from each other that polyphyly of the genus cannot be excluded (Blatterer & Foissner 1988). One group, including *A. australis* and *A. steineri*, has the midventral complex near the right body margin and several cirral rows left of the complex. The other group, composed of *A. alwinae, A. simplex,* and *A. venezuelensis* has the midventral complex roughly in body midline and several cirral *rows* right of the complex.

Australothrix venezuelensis is very likely most closely related to *A. simplex* Shen et al., 1992 because it shares the simplified cirral pattern clearly different from that of *A. alwinae* (invariably 4 cirral rows vs. 7–11). Unfortunately, *A. simplex* has been rather superficially described. A comparison of the morphometric data (Table 62) reveals that *A. venezuelensis* is best distinguished from *A. simplex* by the more slender body (length:width ratio in vivo 3.7–4.4 vs. 3), the higher number of macronuclear nodules (72–118 vs. 40–50), and the longer midventral row (19–31 cirri posteriorly exceeding RM1 vs. ~ 5 cirri not exceeding RM1). Further, Shen et al. (1992) did not mention cortical granules (overlooked ?), a most distinct feature of *A. venezuelensis*.

Birojimia Berger & Foissner, 1989

Improved diagnosis: Slender (> 2:1) Holostichidae with 1–2 left and 2 or more right marginal cirral rows gradually shortened and replaced by dorsal bristles from anterior to posterior. Midventral complex composed of midventral cirral pairs only. With 3 frontal cirri, frontoterminal, buccal, transverse, and caudal cirri. Adoral zone of membranelles continuous. Several dorsal kineties, forming distinct suture left of body midline.

Type species (by original designation): *Birojimia terricola* Berger & Foissner, 1989.

Remarks: Berger & Foissner (1989) overlooked the second main feature of this genus, viz., the curious arrangement of the dorsal kineties: two bipolar rows along left body margin and several shortened rows that abut on the bipolar rows in acute angles, forming a distinct suture. This has been confirmed by a reinvestigation of specimens from the type population. To our best knowledge, no other hypotrich has suture-forming dorsal kineties. Thus, this feature has been added to the diagnosis of the genus.

Birojimia matches Berger's characterization of the Holostichidae: "Urostyloidae with 3 frontal cirri and a midventral complex composed of cirral pairs only". Berger (2006) recognizes eight holostichid genera non having more than one right marginal row and suture-forming dorsal kineties.

Birojimia litoralis nov. spec. (Fig. 177a–k, 178a–z, 179a–e; Table 63)

Diagnosis: Size in vivo about 235 × 55 µm; parallel-sided with body ends broadly rounded and oral portion slightly narrowed. On average 150 macronuclear nodules and several micronuclei. Cortical granules mainly within cirral and dorsal bristle rows, colourless, about 3 × 1 µm in size. Usually 4 right and 2 left marginal rows. On average 15 midventral pairs; 2 frontoterminal, 1 buccal, and 11 transverse and pretransverse cirri; 3 caudal cirri; and 48 adoral membranelles. Usually 9 dorsal kineties, the two leftmost bipolar, the others gradually shortened anteriorly producing the dorsal suture.

Type locality: Venezuelan site (47), i. e., coastal sand and soil from the Henri Pittier National Park, surroundings of the village of Choroni, 67°37'W 10°30'N.

Type material: 1 holotype and 3 paratype slides with protargol-impregnated specimens have been deposited in the Biology Centre of the Upper Austrian Museum in Linz (LI). Relevant specimens have been marked by black ink circles on the coverslip.

Etymology: The Latin species name *litoralis* (pertaining to the sea-shore) refers to the habitat the species was discovered.

Description: Size in vivo 200–290 × 45–75 µm, usually about 235 × 55 µm, as calculated from some in vivo measurements and the morphometric data in Table 63 adding 15% preparation shrinkage; slightly contractile under mild coverslip pressure. Body shape inconspicuous, elongate

to very elongate quadrangular (average 4.3:1) even when studded with food vacuoles, oral portion slightly narrowed and inconspicuously cephalized due to last row of dorsal bristles, body ends broadly rounded; laterally flattened up to 2:1 (Fig. 177a, b, j, k, 178g, h, l, u; Table 63). Nuclear apparatus scattered throughout cytoplasm except for body ends (Fig. 177a, c, 178a, c, d, g, h, j, k; Table 63). On average 151 globular to ellipsoid macronuclear nodules in vivo 4–7 × 3–4 µm in size; each with several nucleoli of ordinary size. Most micronuclei in posterior half of cell, compact and thus rather refractive, in vivo about 4 × 3 µm, number in Table 63 possibly underestimated. Contractile vacuole at left body margin in or slightly anterior to mid-body, with long collecting canals (Fig. 177a). Cortex very flexible, colourless. Cortical granules mainly within cirral and dorsal bristle rows but also in barren areas forming long, rough rows composed of short, slightly oblique granule assemblages (Fig. 177h, i, 178b, e, f, t–z, 179b). Individual granules colourless and thus difficult to recognize, in vivo about 3 × 1 µm in size, stain red and are extruded when methyl green-pyronin is applied, becoming long filaments forming a voluminous coat (Fig. 178e, f, t, z); do not impregnate with the protargol method used; leave distinct holes in cortex when just extruded (Fig. 178y); when disturbed become broadly ellipsoid (Fig. 178b). Cytoplasm colourless, contains many lipid droplets 2–10 µm in size and large lithosome aggregates mainly in anterior

Table 63. Morphometric data on *Birojimia litoralis*. Data based on mounted, protargol-impregnated, and randomly selected specimens from a non-flooded Petri dish culture. Measurements in µm. CV – coefficient of variation in %, M – median, Max – maximum, Mean – arithmetic mean, Min – minimum, n – number of individuals investigated, SD – standard deviation, SE – standard error of arithmetic mean.

Characteristics	Mean	M	SD	SE	CV	Min	Max	n
Body, length	205.4	205.0	18.1	3.9	8.8	179.0	251.0	21
Body, width	49.5	50.0	6.4	1.4	13.0	40.0	65.0	21
Body length: width, ratio	4.2	4.2	0.5	0.1	11.9	3.3	5.2	21
Anterior body end to posterior end of adoral zone, distance	65.2	65.0	5.1	1.1	7.8	56.0	73.0	21
Body length: length of adoral zone, ratio	3.2	3.1	0.3	0.1	9.2	2.8	3.8	21
Largest adoral membranelle, length of base	8.4	8.0	1.1	0.3	13.7	6.0	10.5	21
Adoral membranelles, number	48.4	49.0	4.1	0.9	8.4	40.0	55.0	21
Anterior body end to buccal cirrus, distance	35.8	36.0	3.6	0.8	10.1	29.0	45.0	21
Anterior body end to paroral membrane, distance	16.6	16.5	2.5	0.5	14.9	11.0	20.5	21
Anterior body end to endoral membrane, distance	18.9	19.5	2.8	0.6	15.1	13.0	24.0	21
Anterior body end to right marginal row 1, distance	19.3	20.0	2.4	0.5	12.4	15.0	24.0	21
Anterior body end to posterior end of right marginal row 1, distance	181.4	178.0	19.4	4.2	10.7	154.0	239.0	21
Anterior body end to right marginal row 2, distance	39.9	40.0	6.5	1.4	16.3	29.0	54.0	21
Anterior body end to posterior end of right marginal row 2, distance	181.0	183.0	25.8	5.6	14.3	119.0	232.0	21
Anterior body end to right marginal row 3, distance	80.5	80.0	13.0	2.8	16.1	59.0	100.0	21
Anterior body end to posterior end of right marginal row 3, distance	193.3	187.0	18.0	3.9	9.3	167.0	243.0	21
Anterior body end to right marginal row 4, distance	153.5	155.0	28.4	6.4	18.5	98.0	200.0	20
Anterior body end to posterior end of right marginal row 4, distance	200.9	201.5	17.1	3.8	8.5	175.0	248.0	20
Posterior body end to left marginal row 1, distance	3.8	4.0	1.8	0.4	48.2	1.0	9.0	21
Anterior body end to left marginal row 2, distance	53.6	52.5	7.8	1.7	14.6	40.0	72.0	21
Anterior body end to posterior end of left marginal row 2, distance	202.7	202.5	18.8	4.1	9.3	174.0	249.0	21
Anterior body end to midventral complex, distance	19.1	19.0	1.9	0.4	10.1	15.0	22.0	21

continued

Anterior body end to posterior end of midventral complex, distance	121.8	125.0	23.6	5.2	19.4	78.0	177.0	21
Anterior body end to anteriormost macronuclear nodule, distance	21.3	22.0	3.0	0.6	13.9	17.0	27.0	21
Posterior body end to transverse cirri, distance	16.6	17.0	4.1	0.9	24.6	10.0	23.0	21
Right marginal row 1, number of cirri	42.1	42.0	4.1	0.9	9.8	34.0	52.0	21
Right marginal row 2, number of cirri	31.2	30.0	4.7	1.0	15.2	24.0	42.0	21
Right marginal row 3, number of cirri	20.1	20.0	4.7	1.0	23.1	10.0	28.0	21
Right marginal row 4, number of cirri	7.5	8.0	3.8	0.8	50.7	2.0	16.0	21
Left marginal row 1, number of cirri	45.5	46.0	4.6	1.0	10.0	33.0	54.0	21
Left marginal row 2, number of cirri	35.5	35.0	7.1	1.5	19.9	18.0	46.0	21
Midventral pairs, number	14.4	15.0	2.4	0.5	16.5	9.0	19.0	21
Transverse and pretransverse cirri, number	11.1	11.0	1.5	0.3	13.0	8.0	14.0	21
Anteriormost macronuclear nodule, length	5.3	5.0	0.7	0.2	13.6	4.5	7.0	21
Anteriormost macronuclear nodule, width	3.0	3.0	0.5	0.1	16.1	2.5	4.0	21
Macronuclear nodules, number	150.7	142.0	27.2	5.9	18.0	116.0	210.0	21
Anteriormost micronucleus, length	3.7	4.0	0.5	0.1	12.5	2.5	4.0	21
Anteriormost micronucleus, width	2.8	3.0	0.4	0.1	14.7	2.0	3.5	21
Micronuclei, number	5.5	5.0	2.5	0.5	45.0	1.0	12.0	21
Buccal cavity, width	24.8	24.0	3.3	0.7	13.2	19.0	30.0	21
Frontal cirri, number	3.0	3.0	0.0	0.0	0.0	3.0	3.0	21
Buccal cirri, number	1.0	1.0	0.0	0.0	0.0	1.0	1.0	21
Frontoterminal cirri, number	2.1	2.0	0.3	0.1	14.4	2.0	3.0	21
Caudal cirri, number	3.0	3.0	0.0	0.0	0.0	3.0	3.0	21
Dorsal bristle rows, number	9.1	9.0	0.6	0.1	6.5	8.0	11.0	21
Dorsal bristle row 1, number of bristles	29.4	30.0	3.6	0.8	12.1	22.0	36.0	21
Dorsal bristle row 2, number of bristles	13.4	13.0	1.8	0.4	13.0	11.0	18.0	21
Dorsal bristle row 3, number of bristles	5.1	5.0	1.1	0.2	21.4	3.0	7.0	21

body half. Lithosome aggregates composed of a central large lithosome (~ 3 µm) surrounded by many small, 1–2 µm-sized lithosomes (Fig. 178c, d). Usually studded with up to 60 µm-sized food vacuoles containing small testate amoebae (*Euglypha rotunda, Trinema lineare*), flagellates, ciliates and their cytoplasmic crystals, and remnants of fungal hyphe (Fig. 177a, 178a, c, 179a, b). Cirral pattern typical of genus and thus complex, for details see Figures and morphometry (Fig. 177a, b, e, g, 178g, h, j, l–n, 179c, d; Table 63). Three enlarged, in vivo about 30 µm long frontal cirri in oblique row, and a single, enlarged cirrus III/2 posterior of right frontal cirrus. Buccal cirrus enlarged, very close to and at summit of paroral membrane. Two inconspicuous frontoterminal cirri slightly right and posterior to right frontal cirrus. Midventral complex composed of 9–19, on average 14 midventral pairs, commences close posterior to cirrus III/2, extends slightly obliquely terminating left of body midline at 56% of body length on average; cirri slightly enlarged especially the right ones. On average two thin pretransverse and nine transverse cirri up to 30 µm long in vivo and thus slightly to distinctly projecting from body proper, forming a distinct corona together with marginal and caudal cirri around posterior body margin; thickness increases from anterior to posterior, distal end of posterior cirri fringed. Left marginal cirral row 1 commences near level of buccal vertex, row 2 begins about 18% anterior of buccal vertex, both rows extend to

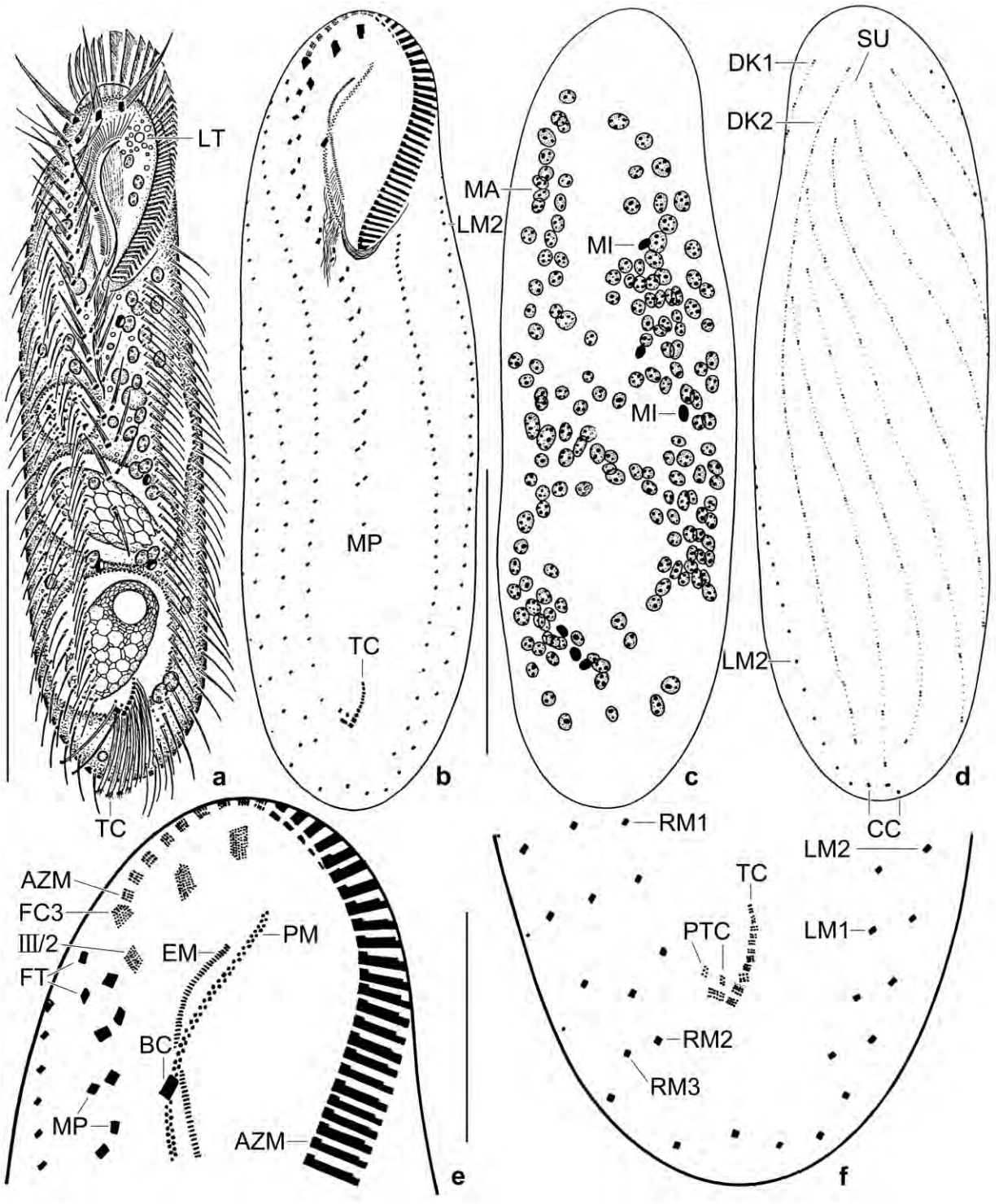

Fig. 177a–f. *Birojimia litoralis* from life (a) and after protargol impregnation (b–f). **a:** Ventral view of a representative specimen, length 240 µm. It has ingested two testate amoebae. **b–f:** Somatic and oral infraciliature and nuclear apparatus of holotype specimen, length 200 µm. AZM – adoral zone of membranelles, BC – buccal cirrus, CC – three caudal cirri, DK1, 2 – dorsal kineties, EM – endoral membrane, FC3 – frontal cirrus 3, FT – frontoterminal cirri, LM1, 2 – left marginal cirral rows, LT – lithosomes, MA – macronuclear nodules, MI – micronuclei, MP – midventral pairs, RM1–3 – right marginal cirral rows, PM – paroral membrane, PTC – pretransverse cirri, SU – suture, TC –transverse cirri, III/2 – cirrus III/2. Scale bars 25 µm (e, f), 70 µm (b–d), and 100 µm (a).

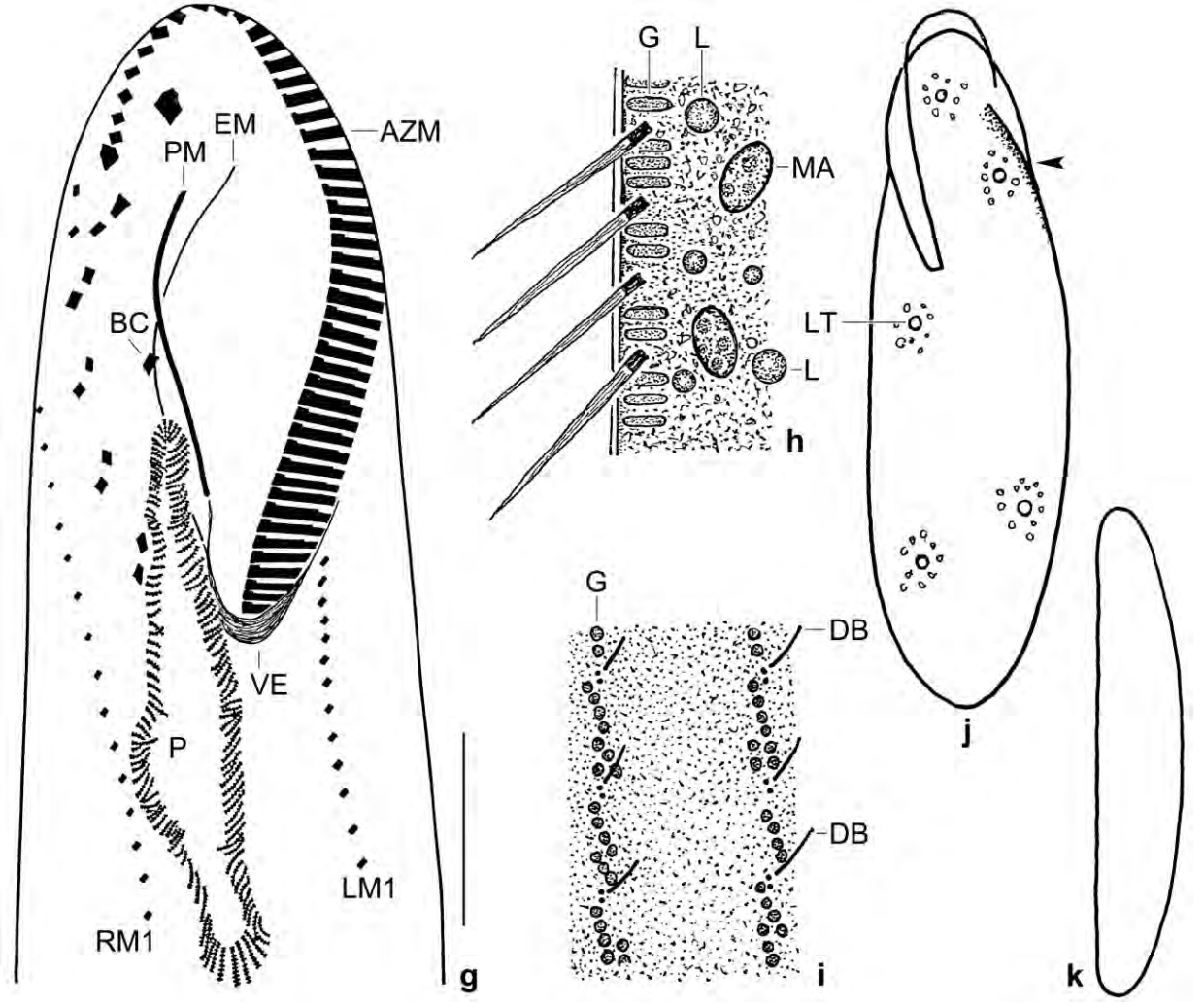

Fig. 177g–k. *Birojimia litoralis* from life (h–k) and after protargol impregnation (g). **g:** Ventral view of anterior body portion (see also Fig. 178h, j), showing many short granule rows in the pharyngeal wall. **h, i:** Optical section and surface view, showing the cortical granulation; individual granules about 3 × 0.8 µm in size. **j:** Dorsal view of a broad specimen, showing some of the lithosome aggregates. The arrowhead marks a subapical concavity caused by a sudden height increase of the dorsal body, producing a slight cephalization. **k:** Lateral view of the specimen shown in Fig. 177a. AZM – adoral zone of membranelles, BC – buccal cirrus, DB – dorsal bristles, EM – endoral membrane, G – cortical granules, L – lipid droplets, LM1 – left marginal cirral row 1, LT – lithosomes, MA – macronuclear nodules, P – pharynx, PM – paroral membrane, RM1 – right marginal cirral row 1, VE – buccal vertex. Scale bar 20 µm (g).

near posterior body end. Usually two, very rarely three or four left marginal cirral rows and four right marginal rows with thin cirri composed of two rows each with five cilia about 15 µm long in vivo; right marginal row 1 complete, i. e., without dorsal bristles anteriorly; cirri of rows 2–4 gradually replaced by dorsal bristles anteriorly (Fig. 177a, b, e, f, 178g, h, j, l–n, 179c, d; Table 63). Dorsal bristles 3 µm long in vivo, arranged in an average of 9 rows: rows 1 and 2 bipolar extending along left body margin; rows 3–9 partially associated with right marginal rows 2–4, as described in the diagnoses of the genus, and, possibly, with caudal cirri; most shortened anteriorly, forming a prominent suture with bipolar kinety 2. Invariably three inconspicuous caudal cirri (Fig. 177d, 178u, v, x, y; Table 63).

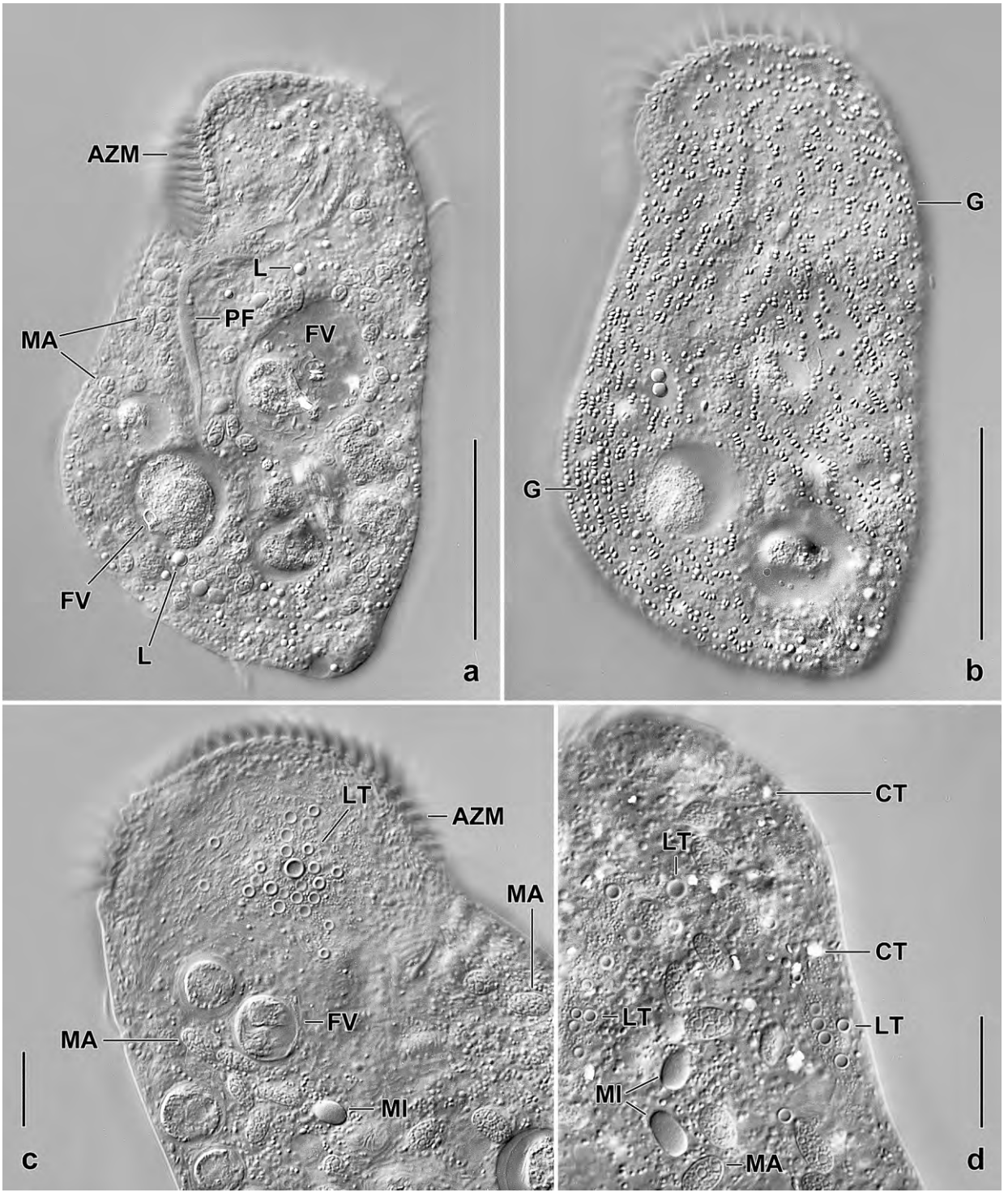

Fig. 178a–d. *Birojimia litoralis* from life, specimens strongly flattened by coverslip pressure. **a, b:** Focused to body centre and body surface, showing the pharyngeal "fibre" bundle mainly made of endoral cilia (a). The cortical granules are disturbed and thus broadly ellipsoid (b). The food vacuoles contain ciliates. **c, d:** Lithosome aggregates and nuclear apparatus. The micronuclei are as large as the macronuclear nodules and compact. AZM – adoral zone of membranelles, CT – crystals, FV – food vacuoles, G – cortical granules, L – lipid droplets, LT – lithosomes, MA – macronuclear nodules, MI – microculei, PF – pharyngeal fibres and endoral cilia. Scale bars 10 µm (c, d) and 50 µm (a, b).

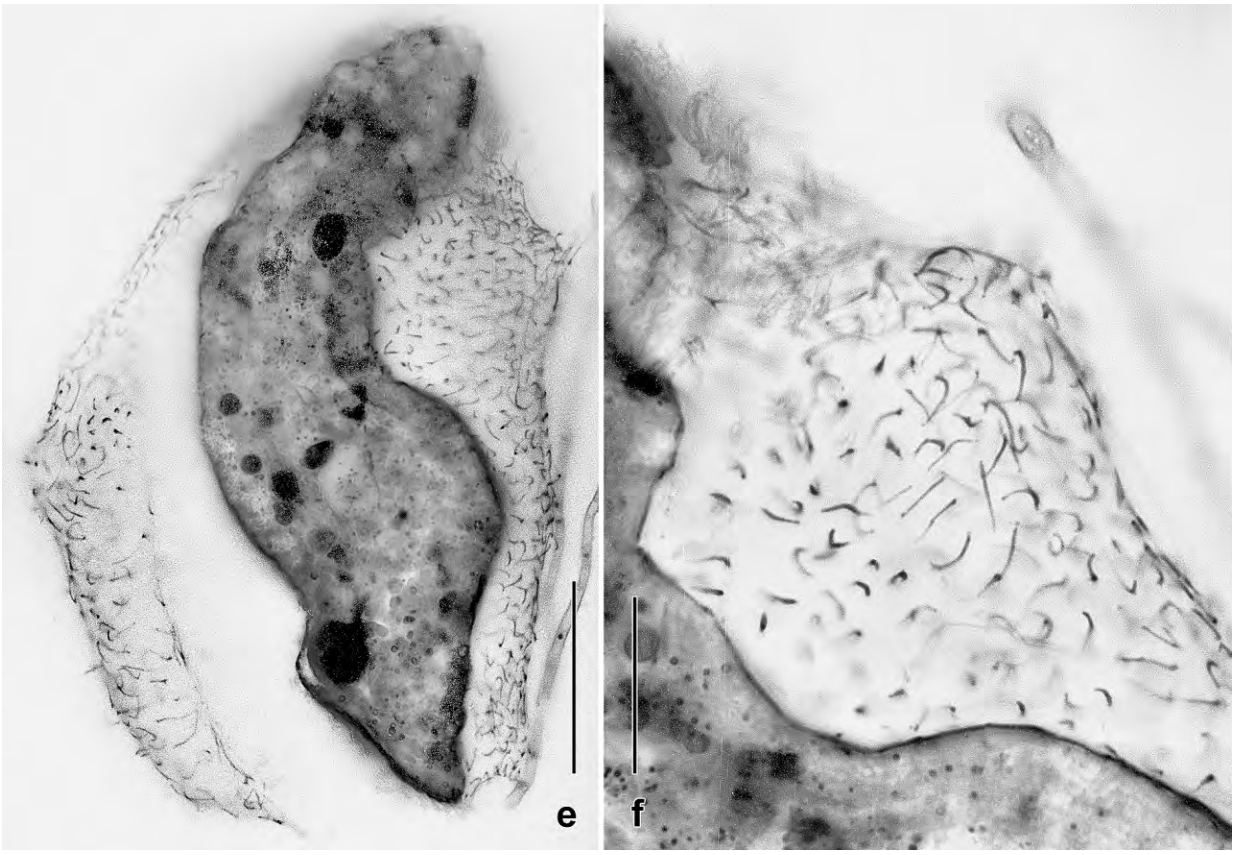

Fig. 178e, f. *Birojimia litoralis.* When methyl green-pyronin is added, the cortical granules are released and extend to long filaments, forming a voluminous coat. Scale bars 20 µm (f) and 50 µm (e).

Adoral zone of ordinary shape and structure, extends 32% of body length on average, composed of an average of 48 ordinary membranelles, bases of largest membranelles about 10 µm wide in vivo; cilia of frontal membranelles about 25 µm long in vivo; lateral membranellar cilia inconspicuous, recognizable only in posterior portion of zone (Fig. 177a, b, e, 178a, g, h, j, l, m, o, u, v, 179d; Table 63). Buccal cavity in vivo rather distinctly curved anteriorly, very deep extending to dorsal side of cell, associated with a large pharynx lined by short rows of minute, granular structures, as in *B. terricola* (Fig. 177a, g, 178g, h, j). Buccal lip of angular type (Foissner & Al-Rasheid 2006), rather broad but vertex covers only a few posterior membranelles, left margin sigmoidal and with distinct cleft containing paroral membrane composed of ciliated dikinetids with length of cilia gradually decreasing from about 12 µm anteriorly to 5 µm posteriorly (Fig. 177a, b, g, 178g, h, l, m, o–r). Endoral membrane covered by buccal seal (Foissner & Al-Rasheid 2006), optically crosses paroral membrane in mid near buccal cirrus, cilia 30–40 µm long producing a distinct bundle together with the pharyngeal fibres extending dorsally and to near mid-body (Fig. 177a, 178g, h, l, p, s; Table 63). Ontogenesis commences with minute anarchic ciliary fields left of postoral midventral pairs (Fig. 179d, e).

Occurrence and ecology: As yet found only at type locality with a salinity of 10‰. The large size suggests that *B. litoralis* is a litter species.

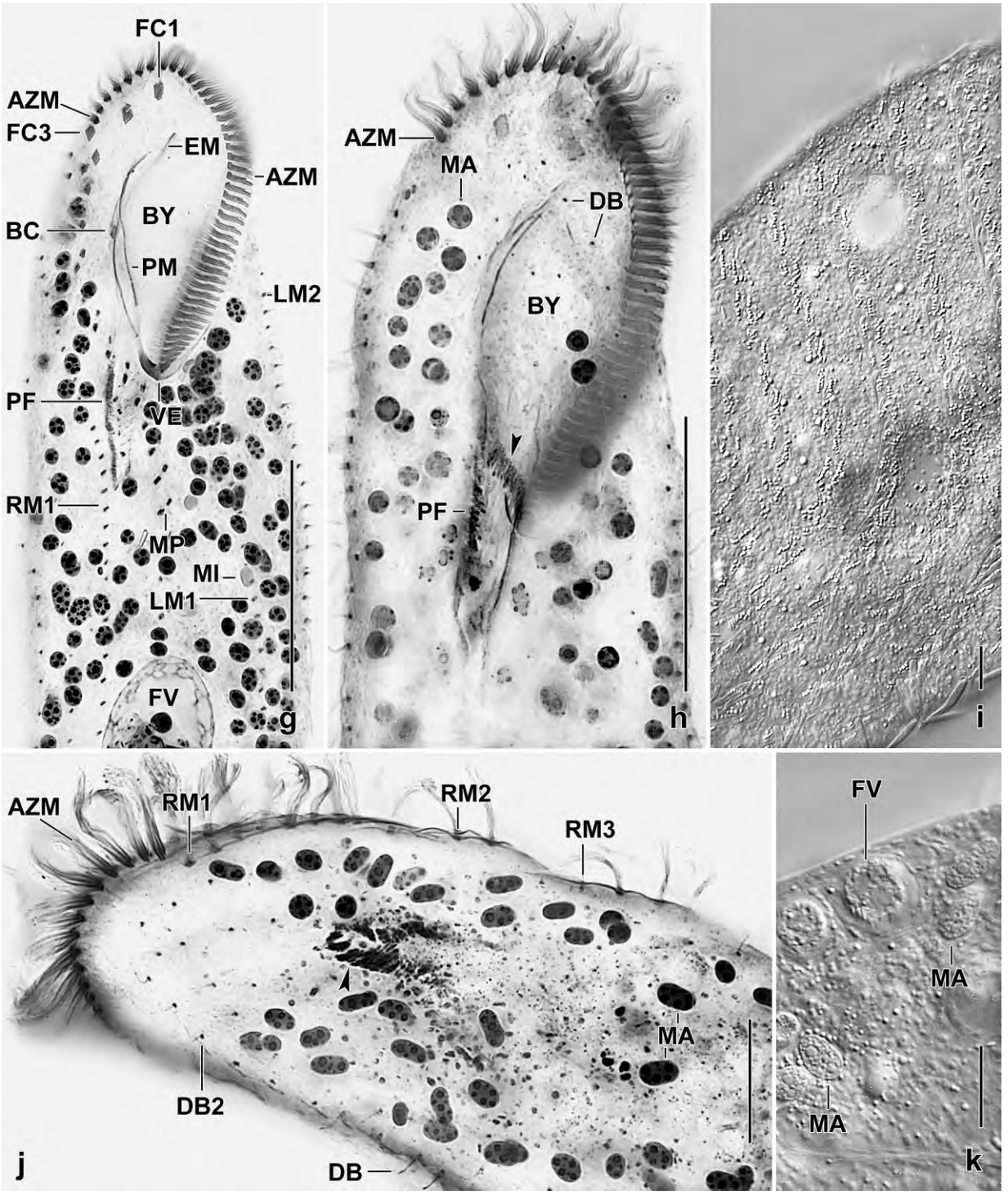

Fig. 178g–k. *Birojimia litoralis* from life (i, k) and after protargol impregnation (g, h, j). **g:** Ventral view of anterior body half, showing details of the infraciliature and nuclear apparatus. **h, j:** Anterior body half focused to body centre (h) and to near dorsal side (j), showing the pharynx extending to the dorsal side. The wall contains many short granule rows (arrowheads). **i:** Cortical granule rows. **k:** Cytoplasmic inclusions. AZM – adoral zone of membranelles, BC – buccal cirrus, BY – buccal cavity, DB(2) – dorsal bristle (row), EM – endoral membrane, FC1,3 – frontal cirri, FV – food vacuoles, LM2 – left marginal row 2, MA – macronuclear nodules, MI – micronuclei, MP – midventral pairs, PF – pharyngeal fibres and endoral cilia, PM – paroral membrane, RM1–3 – right marginal rows, VE – buccal vertex. Scale bars 10 µm (i, k), 20 µm (j), and 40 µm (g, h).

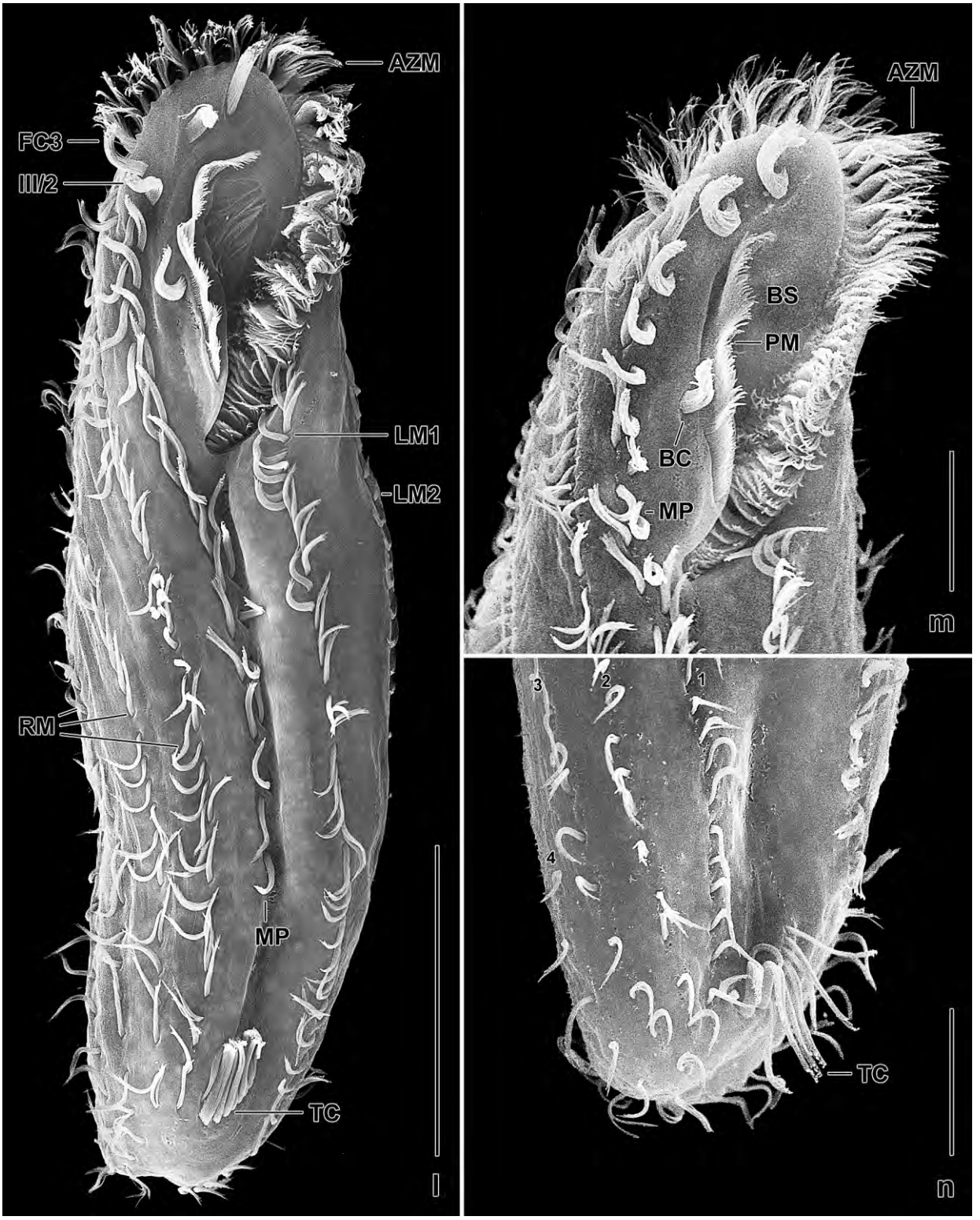

Fig. 178l–n. *Birojimia litoralis*, ventral views in the SEM. AZM – adoral zone of membranelles, BC – buccal cirrus, BS – buccal seal, FC3 – frontal cirrus 3, LM1, 2 – left marginal cirral rows, MP – midventral pairs, PM – paroral membrane, RM(1–4) – right marginal rows, TC –transverse cirri, III/2 – cirrus III/2. Scale bars 20 μm (m, n) and 50 μm (l).

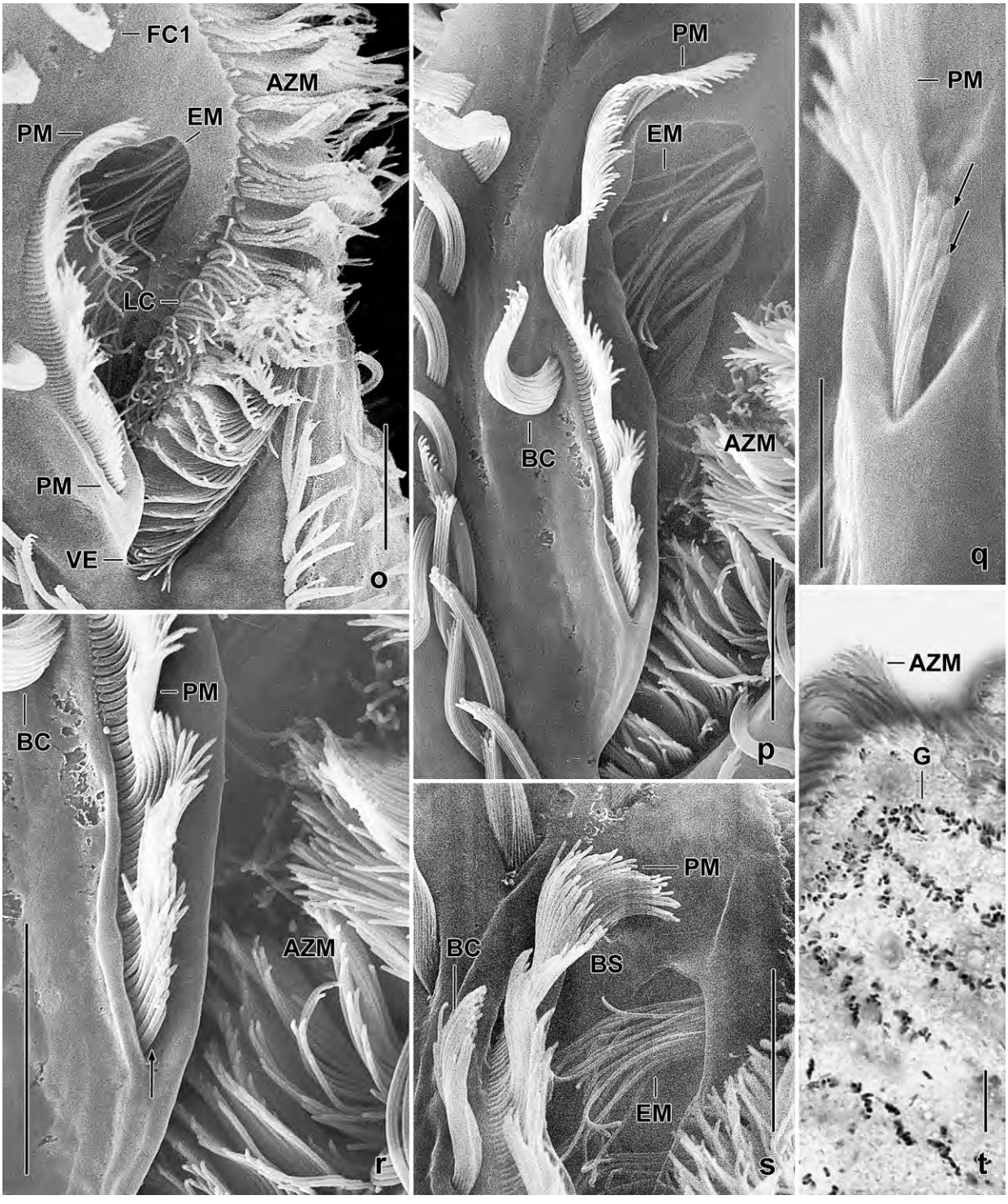

Fig. 178o–t. *Birojimia litoralis,* oral apparatus in the scanning electron microscope (o–s) and cortical granules stained with methyl green-pyronin (t). **o, s:** When the buccal seal disappears, the deep buccal cavity, endoral cilia, and lateral membranellar cilia become recognizable. **p–r:** Details showing the ciliated dikinetids (arrows) of the paroral membrane and the long endoral cilia. **t:** Intrakinetal location of dorsal cortical granules. AZM – adoral zone of membranelles, BC – buccal cirrus, BS – buccal seal, EM – endoral membrane, FC1 – frontal cirrus, G – cortical granules, LC – lateral membranellar cilia, PM – paroral membrane, VE – buccal vertex. Scale bars 4 μm (q) and 10 μm (o, p, r–t).

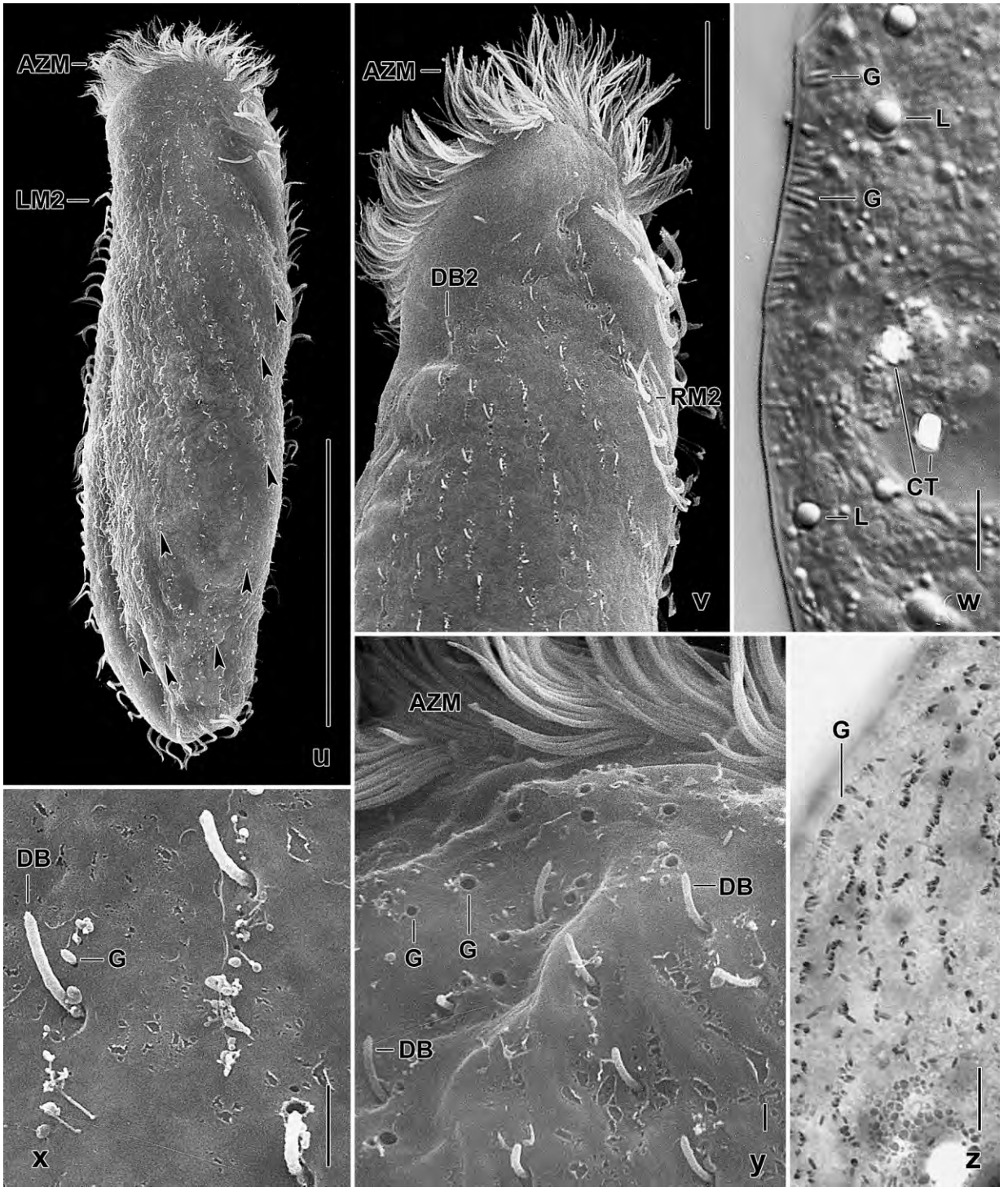

Fig. 178u–z. *Birojimia litoralis,* dorsal cortical granulation from life (w), in the SEM (u, v, x, y), and stained with methyl green-pyronin (z). **u, v, x, y:** Most cortical granules are within the dorsal kineties (arrowheads) composed of minute bristles (x, y). When the granules have been extruded, minute holes are recognizable in the cortex (y). **w, z:** The cortical granules have a size of about 3 × 0.8 µm (w) and stain red with methyl green-pyronin (z). AZM – adoral zone of membranelles, CT – crystals in a food vacuole, DB – dorsal bristles, DB2 – bristle row 2, G – cortical granules, L – lipid droplets, LM2 – left marginal cirral row, RM2 – right marginal cirral row. Scale bars 1 µm (y), 2 µm (x), 10 µm (w, z), 15 µm (v), and 80 µm (u).

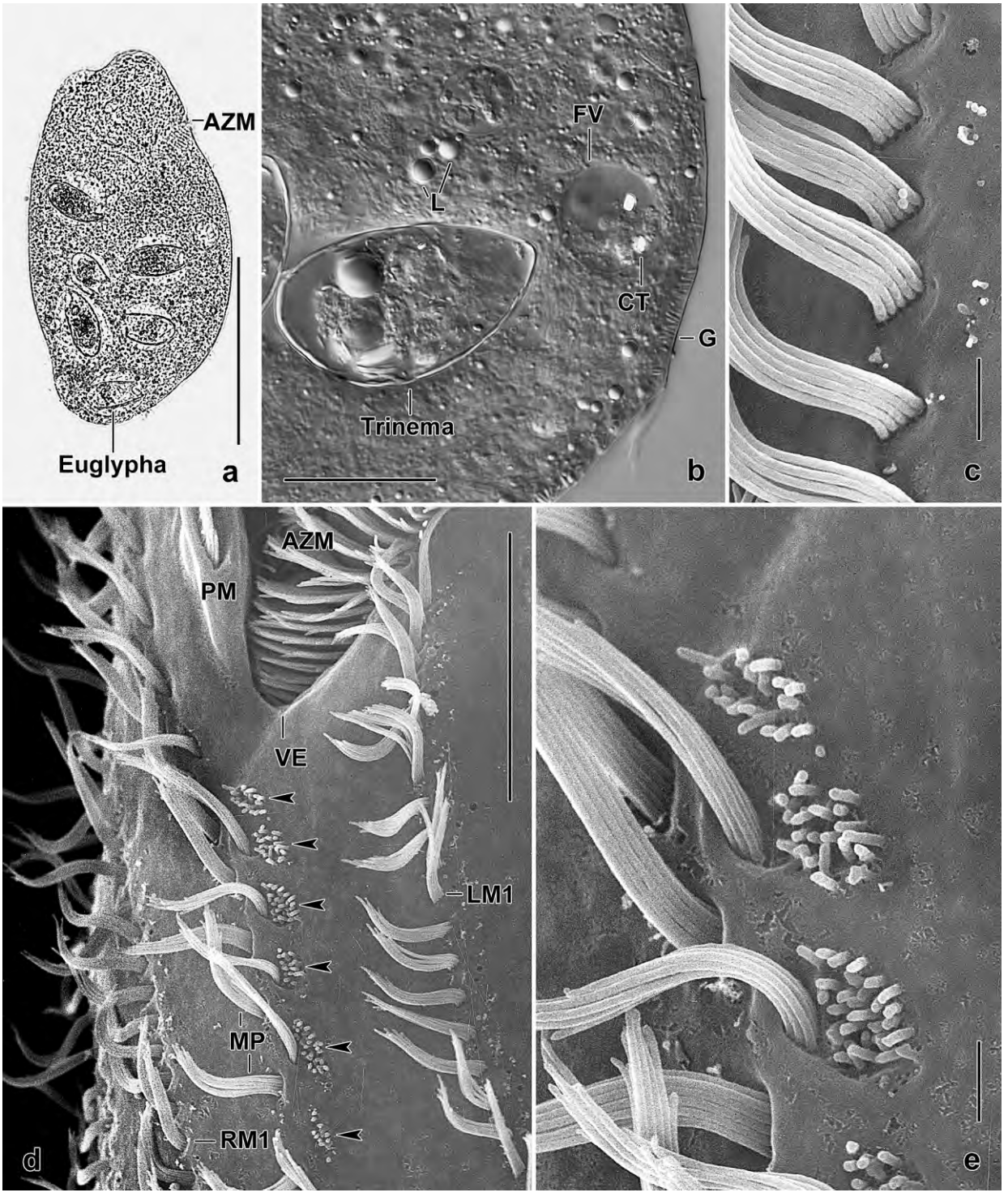

Fig. 179a–e. *Birojimia litoralis* from life (a, b) and in the SEM (c–e). **a:** A specimen having ingested an *Euglypha rotunda* and five *Trinema lineare*. **b:** When undisturbed, the cortical granules are oblong (~ 3 × 0.8 µm). A *Trinema* is digested. **c:** The right marginal cirri consist of two rows with five cilia each. **d, e:** The ontogenesis begins with small, anarchic fields of cilia left of the postoral midventral pairs (arrowheads). AZM – adoral zone of membranelles, CT – crystal, FV – food vacuole, G – cortical granules, L – lipid droplets, LM1 – left marginal cirral row 1, MP – midventral cirral pairs, PM – paroral membrane, RM1 – right marginal cirral row 1, VE – buccal vertex. Scale bars 2 µm (c, e), 10 µm (d), 20 µm (b), and 100 µm (a).

Remarks: *Birojimia litoralis* is a very distinct species differing from the three populations of → *B. terricola* by body shape (quadrangular with rounded ends, length:width ratio ~ 4.2:1 vs. very elongate ellipsoid, ~ 5:1), the number of left marginal cirral rows (2 vs. 1), and many non-overlapping or only slightly overlapping morphometric features, such as body size ($\bar{x}$ 235 × 55µm vs. 150–180 × 35–40 µm in vivo), number of macronuclear nodules (116–210 vs. 42–111), and number of adoral membranelles ($\bar{x}$ 48 vs. 37, 40–55 vs. 30–43).
→ *Pseudobirojimia muscorum* is much more slender than *B. litoralis* ($\bar{x}$ 7:1 vs. 4:1) and has many non-overlapping morphometric features, for instance, the number of dorsal kineties (4 vs. 9) and the number of adoral membranelles ($\bar{x}$ 29 vs. 48).

Birojimia terricola Berger & Foissner, 1989 (Fig. 180a–l, 181a–e; Table 64)

Improved diagnosis (includes data from the reinvestigation of the type population and from Venezuelan and Brazilian specimens): Size in vivo about 150–180 × 35–40 µm; very elongate ellipsoid (~ 5:1). Many (60–80) macronuclear nodules and several micronuclei. Cortical granules within and between cirral and bristle rows, colourless, 2–3 × 1–2 µm in size. 4 to 6 right marginal cirral rows. On average 9–13 midventral cirral pairs; 2 frontoterminal, 1 buccal, and 6–7 transverse and pretransverse cirri; 3 caudal cirri; and about 37 adoral membranelles. 5–8 dorsal kineties, the two leftmost bipolar, the others shortened forming the dorsal suture.

Description of Venezuelan site (25) population (Fig. 180a–e, i–l, 181a–e; Table 64)

Material deposited: 9 voucher slides with protargol-impregnated specimens from Venezuela have been deposited in the Biology Centre of the Upper Austrian Museum in Linz (LI). Further, 2 paratype slides and 2 voucher slides of the Japanese type population and of specimens from Manaus (Brazil), respectively, have been deposited in the same repository. The specimens figured and other relevant cells have been marked by black ink circles on the coverslip.

Description: Size in vivo 150–240 × 30–60 µm, usually about 180 × 40 µm, as calculated from some in vivo measurements and the morphometric data in Table 64 adding 15% preparation shrinkage. Shape fairly constant, i. e., very elongate ellipsoid with posterior region slightly more narrowed than anterior one, body length:width ratio 3.8–6.1, on average 4.5:1; laterally flattened up to 2:1 (Fig. 180a, b, i, j, 181a, c; Table 64). Nuclear apparatus mainly in postoral area and along right and left body margin, composed of an average of 70 macronuclear nodules and several micronuclei (Fig. 180k, 181a, c; Table 64). Macronuclear nodules globular to ellipsoid, on average 4.8 × 3.1 µm in protargol preparations, some occasionally connected by fine strands of membranous material; nucleoli globular, deeply impregnated. Likely more than 10 globular to broadly ellipsoid micronuclei scattered between macronuclear nodules, difficult to identify due to similar-sized and impregnated cytoplasmic inclusions. Contractile vacuole in left body margin slightly anterior to mid-body, with long collecting canals extending to body ends (Fig. 180a). Cortex very flexible, colourless. Cortical granules within and between cirral and bristle rows, broadly ellipsoid to lenticular, 2–3 × 1–2 µm in size but difficult to recognize in vivo because colourless and similar to small cytoplasmic lipid droplets (Fig. 180c, e); stain violet with methyl green-pyronin and become up to 5 µm long when released; do not impregnate with protargol but

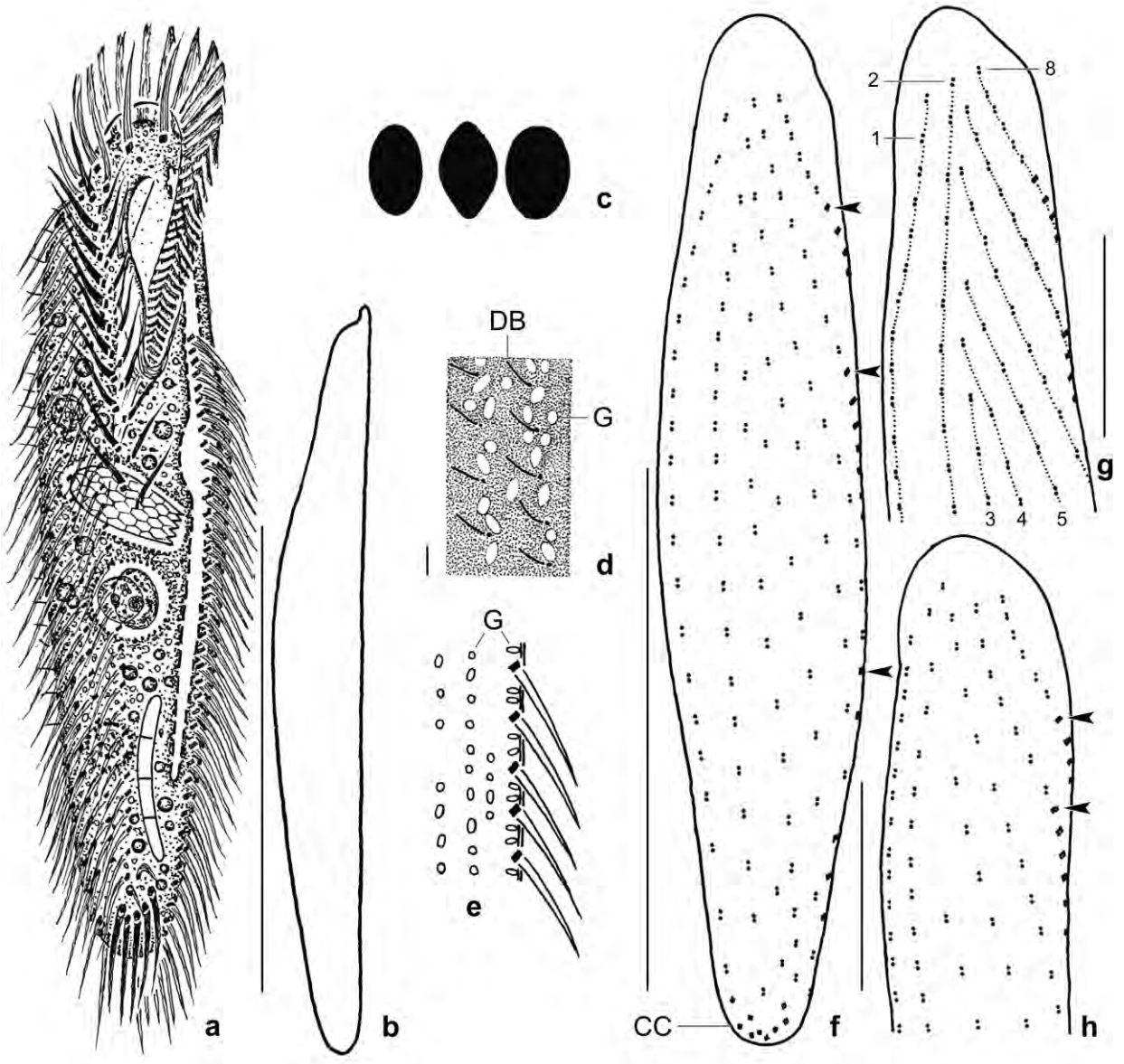

Fig. 180a–h. *Birojimia terricola*, Venezuelan specimens from life (a–c, e) and specimens from Japanese type population (d, f–h) after protargol impregnation. **a:** Ventral view of a representative specimen, length 180 µm. The cell is studded with about 70 macronuclear nodules (not shown for the sake of clarity) and food vacuoles containing testate amoebae, flagellates, and fungal spores. **b:** The cells are flattened up to 2:1. **c:** Shape of cortical granules, 2–3 × 1–2 µm in size. **d:** The cortical granules do not impregnate with the protargol method used but appear as colourless structures in the cortex of deeply impregnated cells. **e:** Surface view and optical section showing the cortical granulation. Although the granules are 2–3 × 1–2 µm in size, they are difficult to recognize because they are colourless and have a similar refractivity as several cytoplasmic inclusions, especially small lipid droplets. **f–h:** The dorsal kineties (numerals) form a distinct suture overlooked by Berger & Foissner (1989). Three of the four right side cirral rows are associated with dorsal bristles anteriorly (arrowheads). CC – caudal cirri, DB – dorsal bristles, G – cortical granules. Scale bars 3 µm (d), 40 µm (g, h), and 100 µm (a, f).

stand out as colourless (whitish) structures from cortex of deeply impregnated specimens (Fig. 180d, 181d). Cytoplasm colourless, without crystals, studded with small lipid droplets 1–3 µm in diameter and food vacuoles containing testate amoebae (*Euglypha*), heterotrophic flagellates (*Polytoma*), ciliates, colourless and brown fungal spores, and possibly also bacteria (Fig. 180a).

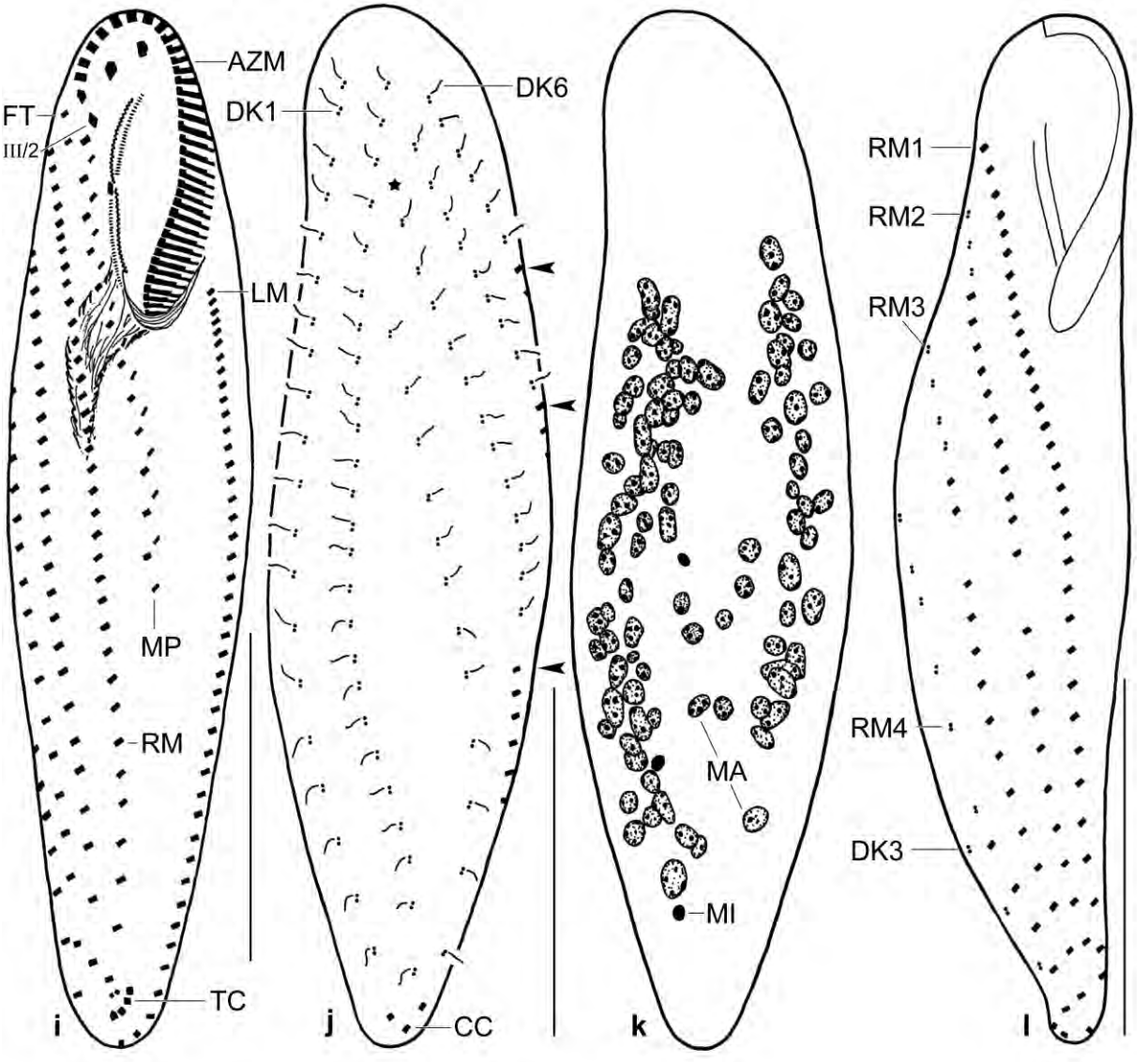

Fig. 180i–l. *Birojimia terricola*, Venezuelan specimens after protargol impregnation. **i, l:** Ventral and right side view, showing the special cirral and bristle pattern. **j, k:** Dorsal bristle pattern and nuclear apparatus of same specimen. Note the six dorsal kineties, three of which are associated with cirri posteriorly (arrowheads). The asterisk marks the suture formed by dorsal kineties 1, 2 and 3–6. AZM – adoral zone of membranelles, CC – caudal cirri, DK1, 3, 6 – dorsal kineties, FT – frontoterminal cirri, LM – left marginal row, MA – macronuclear nodules, MI – micronucleus, MP – midventral pairs, RM(1–4) – right marginal rows, TC – transverse cirri, III/2 – posterior cirrus of anlage III. Scale bars 50 µm.

Glides fairly rapidly on microscope slides and between soil particles, showing pronounced flexibility.

Cirral pattern invariable, while some distances vary highly, e. g., anterior body end to right marginal rows 1 and 4, anterior body end to posterior end of midventral complex, and posterior body end to transverse cirri. Cirri 15–20 µm long in vivo, of similar size, except of frontal cirri, most composed of two rows of basal bodies (Fig. 180a, i, j, 181a, c; Table 64). Three enlarged frontal cirri in oblique row and a single, usually slightly enlarged cirrus III/2 posterior of right

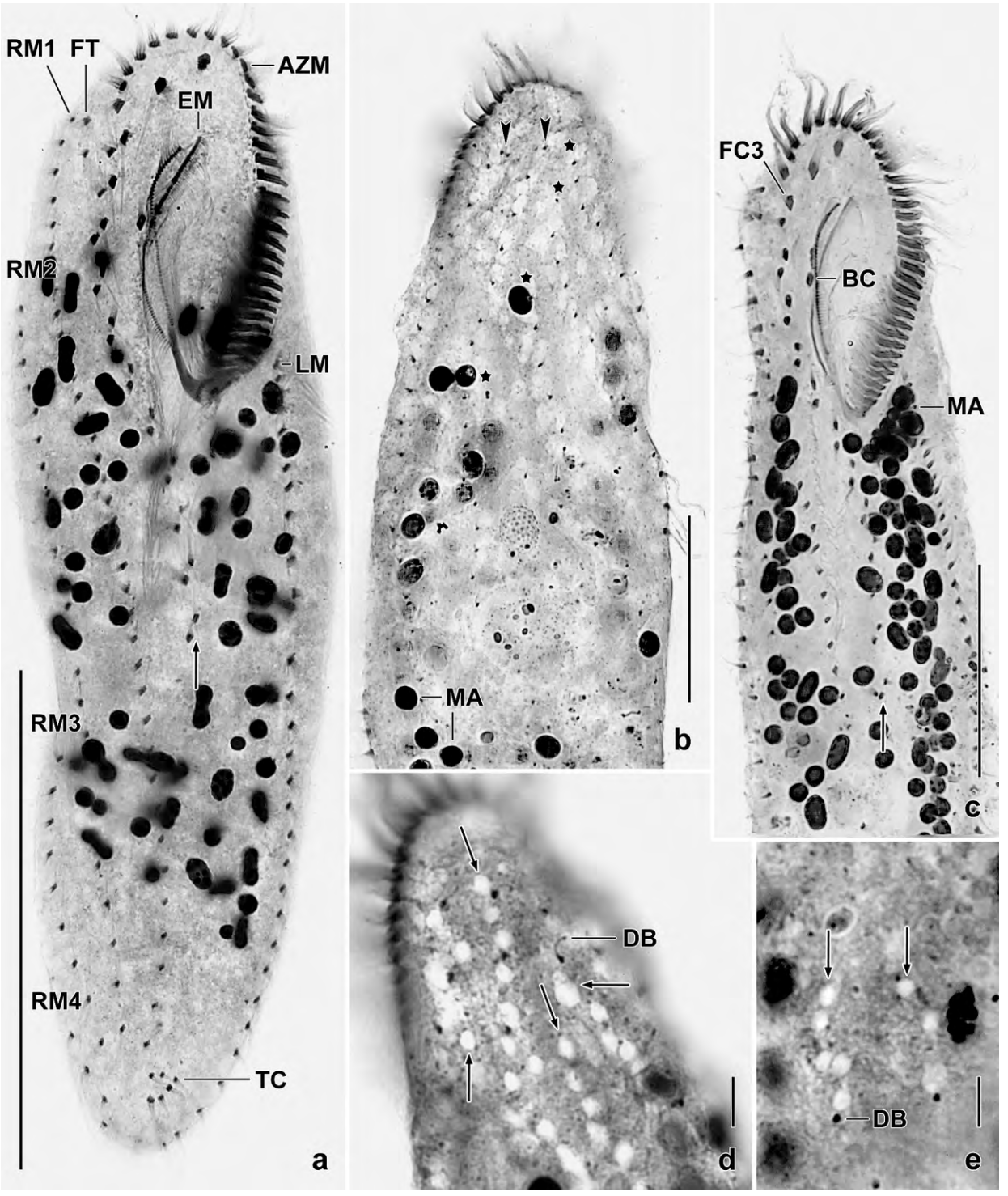

Fig. 181a–e. *Birojimia terricola*, Venezuelan (a–d) and Japanese (e) specimens after protargol impregnation. **a, c:** Ventral views, showing the four right marginal rows and the proximal end of the midventral complex (arrows). **b:** Dorsal view, showing the two bipolar kineties (arrowheads) to which some shortened kineties abut (asterisks). **d, e:** Dorsal views, showing globular and ellipsoid, colourless structures, i. e., cortical granules (arrows). AZM – adoral zone of membranelles, BC – buccal cirrus, DB – dorsal bristles, EM – endoral membrane, FC3 – frontal cirrus, LM – left marginal rows, MA – macronuclear nodules, RM(1–4) – right marginal rows, TC – transverse cirri. Scale bars 5 µm (d, e), 30 µm (b, c), and 80 µm (a).

Table 64. Morphometric data on *Birojimia terricola*, Venezuelan specimens (VE), Brazilian specimens (BR), and Japanese type population (JA, from BERGER & FOISSNER 1989). Data based on mounted, protargol-impregnated, and randomly selected specimens from non-flooded Petri dish cultures. Measurements in µm. CV – coefficient of variation in %, JA – Japanese population, M – median, Max – maximum, Mean – arithmetic mean, Min – minimum, n – number of individuals investigated, Pop – population, SD – standard deviation, SE – standard error of arithmetic mean, VE – Venezuelan population.

Characteristics	Pop	Mean	M	SD	SE	CV	Min	Max	n
Body, length	VE	162.4	158.0	25.2	5.5	15.5	133.0	217.0	21
	BR	167.9	167.0	16.6	5.2	9.7	143.0	194.0	10
	JA	180.1	186.0	26.7	7.6	14.6	126.0	215.0	12
Body, width	VE	36.8	36.0	6.3	1.4	17.1	26.0	54.0	21
	BR	31.2	30.0	3.9	1.2	12.5	27.0	38.0	10
	JA	37.2	36.5	3.8	1.1	10.3	32.0	43.0	12
Body length:width, ratio	VE	4.5	4.4	0.6	0.1	12.7	3.8	6.1	21
	BR	5.4	5.4	0.4	0.1	7.5	4.9	6.2	10
	JA	4.8	?	?	?	?	?	?	12
Anterior body end to proximal end of adoral zone of membranelles, distance	VE	48.3	46.0	6.1	1.3	12.5	40.0	64.0	21
	BR	47.2	47.0	3.8	1.2	8.1	42.5	54.0	10
	JA	54.6	55.0	5.2	1.5	9.5	46.0	63.0	12
Body length:length of adoral zone of membranelles, ratio	VE	3.4	3.3	0.3	0.1	8.9	3.0	4.0	21
	BR	2.6	2.6	0.2	0.1	8.6	2.2	3.0	10
	JA	3.3	?	?	?	?	?	?	12
Largest adoral membranelle, length of basis	VE	6.5	6.0	–	–	–	6.0	7.0	21
	BR	7.1	7.0	0.7	0.2	10.3	6.0	8.0	10
Adoral membranelles, number	VE	35.9	36.0	3.2	0.7	8.9	30.0	42.0	21
	BR	35.3	36.0	2.7	0.9	7.7	32.0	40.0	10
	JA	39.1	40.0	3.1	0.9	7.8	35.0	43.0	12
Anterior body end to buccal cirrus, distance	VE	25.0	25.0	3.7	0.8	14.8	19.0	32.0	21
	BR	25.6	24.8	3.0	1.0	11.9	22.0	33.0	10
Anterior body end to right marginal row 1, distance	VE	14.9	14.0	4.1	0.9	27.9	7.0	23.0	21
	BR	18.9	18.0	4.7	1.5	25.0	13.0	29.5	10
	JA	14.6	15.0	2.5	0.7	17.4	8.0	18.0	12
Anterior body end to posterior end of right marginal row 1, distance	VE	148.4	142.0	23.3	5.1	15.7	121.0	207.0	21
	BR	151.1	149.0	15.8	5.3	10.5	127.5	181.1	9
Right marginal row 1, number of cirri	VE	37.0	37.0	3.8	0.8	10.2	28.0	43.0	21
	BR	35.7	35.5	3.9	1.2	10.8	29.0	41.0	10
	JA	41.2	40.5	5.5	1.6	13.4	32.0	49.0	12
Anterior body end to right marginal row 2, distance	VE	37.6	37.0	6.2	1.4	16.5	30.0	55.0	21
	BR	54.6	55.0	9.5	3.0	17.4	41.0	67.5	10
	JA	44.3	43.5	11.6	3.4	26.2	29.0	63.0	12
Anterior body end to posterior end of right marginal row 2, distance	VE	146.8	143.0	23.6	5.1	16.1	115.0	195.0	21
	BR	156.2	154.0	16.4	5.5	10.5	131.0	183.0	9

continued

Characteristics	Pop	Mean	M	SD	SE	CV	Min	Max	n
Right marginal row 2, number of cirri	VE	25.5	25.0	3.6	0.8	13.9	22.0	33.0	21
	BR	24.6	25.0	3.5	1.1	14.1	20.0	29.0	10
	JA	28.9	29.0	5.0	1.4	17.2	22.0	38.0	12
Anterior body end to right marginal row 3, distance	VE	59.7	58.0	9.8	2.1	16.3	47.0	81.0	21
	BR	118.0	121.0	22.0	7.0	18.6	85.0	151.0	10
	JA	70.3	75.0	13.9	4.0	19.8	35.0	88.0	12
Anterior body end to posterior end of right marginal row 3, distance	VE	147.7	142.0	23.4	5.1	15.9	112.0	205.0	21
	BR	160.9	160.0	15.7	5.2	9.8	139.0	187.5	9
Right marginal row 3, number of cirri	VE	18.7	18.0	3.8	0.8	20.3	11.0	26.0	21
	BR	8.6	9.0	2.7	0.9	31.5	3.0	12.0	9
	JA	19.1	20.0	4.7	1.4	24.6	13.0	27.0	12
Anterior body end to right marginal row 4, distance	VE	114.0	117.0	31.2	6.8	27.4	57.0	168.0	21
	BR	155.5	154.0	14.2	4.7	9.1	138.0	183.0	9
	JA	135.4	139.0	27.6	8.0	20.3	92.0	200.0	12
Anterior body end to posterior end of right marginal row 4, distance	VE	156.6	151.0	24.9	5.4	15.9	120.0	216.0	21
	BR	165.6	164.0	17.5	5.8	10.6	139.5	191.5	9
Right marginal row 4, number of cirri	VE	8.5	7.0	4.5	1.0	52.8	3.0	19.0	21
	BR	3.0	3.0	1.1	0.4	37.3	1.0	4.0	9
	JA	6.9	7.0	3.4	1.0	48.7	3.0	13.0	12
Posterior body end to left marginal row, distance	VE	0.9	0.0	1.5	0.3	167.3	0.0	6.0	21
	BR	0.8	0.5	0.4	0.1	52.7	0.5	1.5	10
Left marginal row, number of cirri	VE	42.1	43.0	5.4	1.2	12.9	31.0	52.0	21
	BR	41.5	40.5	5.3	1.7	12.7	35.0	50.0	10
	JA	47.3	48.0	4.7	1.3	9.8	40.0	53.0	12
Anterior body end to midventral complex, distance	VE	14.0	14.0	2.5	0.5	17.9	10.0	19.0	21
	BR	17.7	17.0	2.1	0.7	11.6	16.0	21.0	10
Anterior body end to posterior end of midventral complex, distance	VE	90.7	89.0	16.6	3.6	18.3	68.0	126.0	21
	BR	95.7	95.0	13.9	4.4	14.5	77.0	126.5	10
	JA	107.2	106.0	18.3	5.3	17.1	75.0	133.0	12
Midventral pairs, number	VE	11.3	12.0	1.5	0.3	13.2	9.0	15.0	21
	BR	9.3	9.5	2.3	0.7	24.3	6.0	12.0	10
	JA	13.2	13.0	2.2	0.7	16.3	10.5	16.5	12
Posterior body end to transverse cirri, distance	VE	6.0	6.0	2.2	0.5	37.2	2.0	9.0	21
	BR	8.1	8.3	2.2	0.7	26.9	4.0	11.0	10
Transverse plus pretransverse cirri, number	VE	6.0	6.0	2.2	0.5	37.2	2.0	9.0	21
	BR	7.8	7.5	1.6	0.5	19.9	6.0	11.0	10
	JA	7.0	?	?	?	?	?	?	12
Anterior body end to first macronuclear nodule, distance	VE	33.0	34.0	4.9	1.1	14.8	21.0	40.0	21
	BR	40.3	41.5	4.9	1.5	12.1	33.0	46.0	10
Macronuclear nodules, length	VE	4.8	5.0	1.1	0.2	22.4	3.0	7.0	21
	BR	4.3	4.0	0.8	0.3	19.4	3.0	6.0	10
	JA	5.6	6.0	1.2	0.4	22.2	4.0	7.0	12

continued

Characteristics	Pop	Mean	M	SD	SE	CV	Min	Max	n
Macronuclear nodules, width	VE	3.1	3.0	0.5	0.1	16.0	2.0	4.0	21
	BR	2.9	3.0	0.3	0.1	11.8	2.5	3.5	10
	JA	4.1	4.0	0.8	0.2	19.4	3.0	5.0	12
Macronuclear nodules, number	VE	70.1	63.0	13.9	3.0	19.9	59.0	98.0	21
	BR	74.3	76.0	22.9	7.3	30.9	42.0	111.0	10
	JA	60.7	61.0	3.5	1.0	5.7	55.0	65.0	12
Micronuclei, length	VE	2.4	2.5	0.4	0.1	16.6	2.0	3.0	21
	BR	3.8	4.0	0.8	0.3	21.4	2.0	4.5	8
	JA	3.5	3.5	–	–	–	3.0	4.0	26
Micronuclei, width	VE	2.0	2.0	0.3	0.1	13.8	1.0	2.5	21
	BR	2.3	2.3	0.7	0.2	29.1	1.5	3.5	8
	JA	2.7	3.0	–	–	–	2.0	3.0	6
Micronuclei, number	BR	2.4	2.5	1.4	0.5	59.3	1.0	5.0	8
Anterior body end to paroral membrane, distance	VE	13.3	13.0	2.7	0.6	20.4	10.0	21.0	21
	BR	14.1	14.5	2.7	0.9	19.3	8.0	18.0	10
Anterior body end to endoral membrane, distance	VE	12.9	13.0	2.4	0.5	18.8	10.0	20.0	21
	BR	13.2	13.3	2.2	0.7	17.0	8.5	16.0	10
Buccal cavity, width [a]	VE	10.7	10.0	2.9	0.6	27.2	7.0	17.0	21
	BR	18.1	18.0	1.3	0.4	7.2	16.0	20.0	10
Frontal cirri, number	VE	3.0	3.0	0.0	0.0	0.0	3.0	3.0	21
	BR	3.0	3.0	0.0	0.0	0.0	3.0	3.0	10
	JA	3.0	3.0	0.0	0.0	0.0	3.0	3.0	12
Buccal cirri, number	VE	1.0	1.0	0.0	0.0	0.0	1.0	1.0	21
	BR	1.0	1.0	0.0	0.0	0.0	1.0	1.0	10
	JA	1.0	1.0	0.0	0.0	0.0	1.0	1.0	12
Frontoterminal cirri, number	VE	2.0	2.0	0.0	0.0	0.0	2.0	2.0	21
	BR	2.0	2.0	0.0	0.0	0.0	2.0	2.0	10
	JA	1.8	2.0	0.7	0.2	39.1	0.0	3.0	12
Caudal cirri, number	VE	3.0	3.0	0.0	0.0	0.0	3.0	3.0	21
	BR	1.9	2.0	0.3	0.1	16.6	1.0	2.0	10
	JA	3.6	3.0	1.6	0.5	44.0	2.0	7.0	12
Dorsal bristle rows, number	VE	6.6	7.0	–	–	–	6.0	7.0	21
	BR	5.1	5.0	0.3	0.1	5.9	5.0	6.0	11
	JA	7.7	8.0	–	–	–	7.0	8.0	5
Dorsal bristles in row 1, number	VE	19.4	19.0	3.3	0.7	17.1	15.0	27.0	21
	BR	18.9	19.0	1.9	0.6	10.1	16.0	21.0	10
Dorsal bristles in row 2, number	VE	22.0	21.0	3.5	0.8	16.1	15.0	31.0	21
	BR	22.8	23.0	2.3	0.8	10.0	20.0	26.0	9
Dorsal bristles in last row, number	VE	6.0	6.0	0.9	0.2	15.8	4.0	7.0	21
	BR	9.7	9.5	1.6	0.5	16.9	7.0	12.0	10

[a] Distance between summit of paroral membrane and right margin of adoral zone of membranelles.

frontal cirrus. Buccal cirrus at summit of paroral. Two frontoterminal cirri slightly right and posterior to right frontal cirrus. Midventral complex composed of 9–15, on average 11 midventral pairs, commences close posterior of cirrus III/2, extends slightly obliquely posteriorly, terminating left of body midline at 56% of body length on average; right cirrus of pairs larger than left one; no midventral row in 21 specimens investigated. On average six (extremes 2–9) transverse and pretransverse cirri 6 µm anterior of posterior body and, of similar size as marginal cirri. Left marginal row commences at level of buccal vertex, terminates in midline of rear body end. Four right marginal rows: row 1 complete, i. e., without dorsal bristles anteriorly; cirri of rows 2–4 gradually replaced by dorsal bristles anteriorly (Fig. 180j, l, 181a; Table 64).

Dorsal bristles 3 µm long in vivo, arranged in 6–7 rows: rows 1 and 2 bipolar extending along left body margin, likely associated with caudal cirri; rows 3–6(7) partially associated with a caudal cirrus and with right marginal rows 2–4, as described above; most shortened anteriorly, forming prominent suture with bipolar kinety 2 (Fig. 180j, 181b; Table 64). Caudal cirri inconspicuous.

Adoral zone of ordinary shape and structure, extends 30% of body length on average, composed of an average of 35 ordinary membranelles, bases of largest membranelles about 10 µm wide in vivo while 6–7 µm in protargol preparations; cilia of frontal membranelles about 20 µm long in vivo. Buccal cavity moderately deep and wide, buccal lip of usual shape and size. Undulating membranes long and slightly to moderately curved, intersect optically near or at level of buccal cirrus; paroral composed of zigzagging dikinetids with cilia 13 µm long in vivo; endoral composed of very narrowly spaced cilia 18 µm long in vivo. Pharyngeal fibres conspicuous, pharynx wall studded with minute rods in protargol preparations, as in *Caudiholosticha notabilis* (Fig. 180a, i, 181, a, c; Table 64).

Morphometry of Brazilian site (18) population (Table 64): Most morphometrics of the Venezuelan and Brazilian populations are more similar than those of the Japanese type population, indicating some biogeographic specialization, for instance, body length and the number of cirri in the marginal rows, the number and size of the macronuclear nodules, the number of midventral pairs, the number of adoral membranelles, and the number of dorsal kineties.

Occurrence and ecology: As yet found at Japanese type locality, i. e., in brown soil of a deciduous forest; at Venezuelan site (25); and at Brazilian site (18), indicating a preference for fertile habitats.

Comparison with type population: As discussed in the improved diagnosis of the genus, Berger & Foissner (1989) overlooked the specific dorsal ciliary pattern (Fig. 180f–h, 181b). Further, Berger & Foissner (1989) missed the cortical granules, as shown by a reinvestigation of specimens from the type locality, where the granules stand out as colourless (whitish) structures from the cortex of deeply impregnated specimens (Fig. 180d, 181d, e). Thus and because of some well-matching morphometric data (Table 64), we consider the Venezuelan population as conspecific with the Japanese type.

Pseudobirojimia nov. gen.

Diagnosis: Slender Bakuellidae with 1 left and 2 or more right marginal cirral rows. Midventral complex composed of cirral pairs and a midventral cirral row. With 3 frontal cirri, frontoterminal, buccal, transverse, and caudal cirri. Dorsal kineties in ordinary bipolar pattern.

Type species: *Uroleptus muscorum* Kahl, 1932.

Reference material: Foissner (1982) reinvestigated this species and deposited a slide (reg. no. 1984/79) with protargol-impregnated specimens from Austria in the Biology Centre of the Upper Austrian Museum in Linz (LI), under the name *Paruroleptus muscorum*.

Remarks: Based on the redescription by Foissner (1982), Berger & Foissner (1989) transferred *Uroleptus muscorum* Kahl, 1932 to the genus *Birojimia*. However, Berger (2006) recognized that *B. terricola* (see above) and *U. muscorum* have a different midventral complex (without vs. with a midventral row). Thus, he assigned *U. muscorum* only provisionally to *Birojimia*. The reinvestigation of → *B. terricola* showed a further main difference, viz., a suture in the dorsal kinety pattern (see above and Fig. 180f–h, 181b). As we now have two distinct differences, *U. muscorum* is referred to a new genus, *Pseudobirojimia*, differing from the *Holostichidae* by the midventral complex (midventral cirral pairs plus a midventral row vs. only midventral cirral pairs), which matches that of the Bakuellidae. However, none of the bakuellid genera matches *P. muscorum* in other features, i. e., has a left and at least two right marginal cirral rows and a continuous adoral zone of membranelles (for a review, see Berger 2006).

Bakuella pampinaria pampinaria Eigner & Foissner, 1992

Observations on Brazilian site (26) population: Body size about 160 × 45 µm in vivo and 152 × 38 µm (SD = 19 × 7 µm, CV = 13 × 17%, Min = 135 µm, Max = 180 µm, n = 12) in protargol preparations; many macronuclear nodules about 4–10 × 3–7 µm in vivo; contractile vacuole distinctly anterior to mid-body, with two conspicuous collecting canals; cortex very flexible, studded with rows of strongly refractive, slightly to distinctly yellowish granules about 0.5–1 × 0.5–0.8 µm in size; feeds on ciliates (*Gonostomum affine*), flagellates (*Polytomella* sp.), and a green alga with a mucous cover; glides rather rapidly on microscope slides; three to four oblique ventral cirral rows, four to six buccal cirri, five to eight transverse cirri about 20 µm long and thus slightly projecting from body proper; dorsal kinetids in three rows, bristles about 3 µm long in vivo; oral apparatus conspicuous, composed of $\bar{x}$ = 38 adoral membranelles (SD = 4.3 µm, CV = 11.3%, Min = 32 µm, Max = 45 µm, n = 10, protargol impregnation), a large and deep buccal cavity, and paroral and endoral cilia 10 µm and 30 µm (!) long in vivo, respectively.

This population resembles *B. pampinaria pampinaria* in body size while the number of adoral membranelles matches *B. edaphoni* (for details, see Berger 2006). Thus, these species are either synonymous or the Brazilian population represents a distinct subspecies. We do not fix any possibility because the protargol preparations are poor and the absence of cortical granules is unlikely in *B. edaphoni*.

Material deposited: 1 voucher slide with protargol-impregnated specimens has been deposited in the Biology Centre of the Upper Austrian Museum in Linz (LI). Some relevant cells have been marked by black ink circles on the coverslip.

Pseudourostyla dimorpha nov. spec. (Fig. 182a–j, 183a–e; Tables 65, 66)

Diagnosis: Exists as a broad (length:width ratio ≤ 4:1) and as a slender (> 4:1) morph with very similar morphometrics except for body size: on average 160 × 40 µm vs. 180 × 30 µm in vivo. About 120 ellipsoid macronuclear nodules and 5 micronuclei of similar size as macronuclear nodules. Cortical granules mainly around cirral and bristle rows, colourless, 1–2 × 1.5 µm in size. Midventral complex composed of an average of 8 cirral pairs and 9 cirri forming a bicorona. Right and left of midventral complex 5 cirral rows each on average. About 4 dorsal kineties and some caudal cirri. On average 2 buccal cirri and 6 transverse cirri about 10 µm distant from rear end. Adoral zone extends about 30% of body length, composed of an average of 39

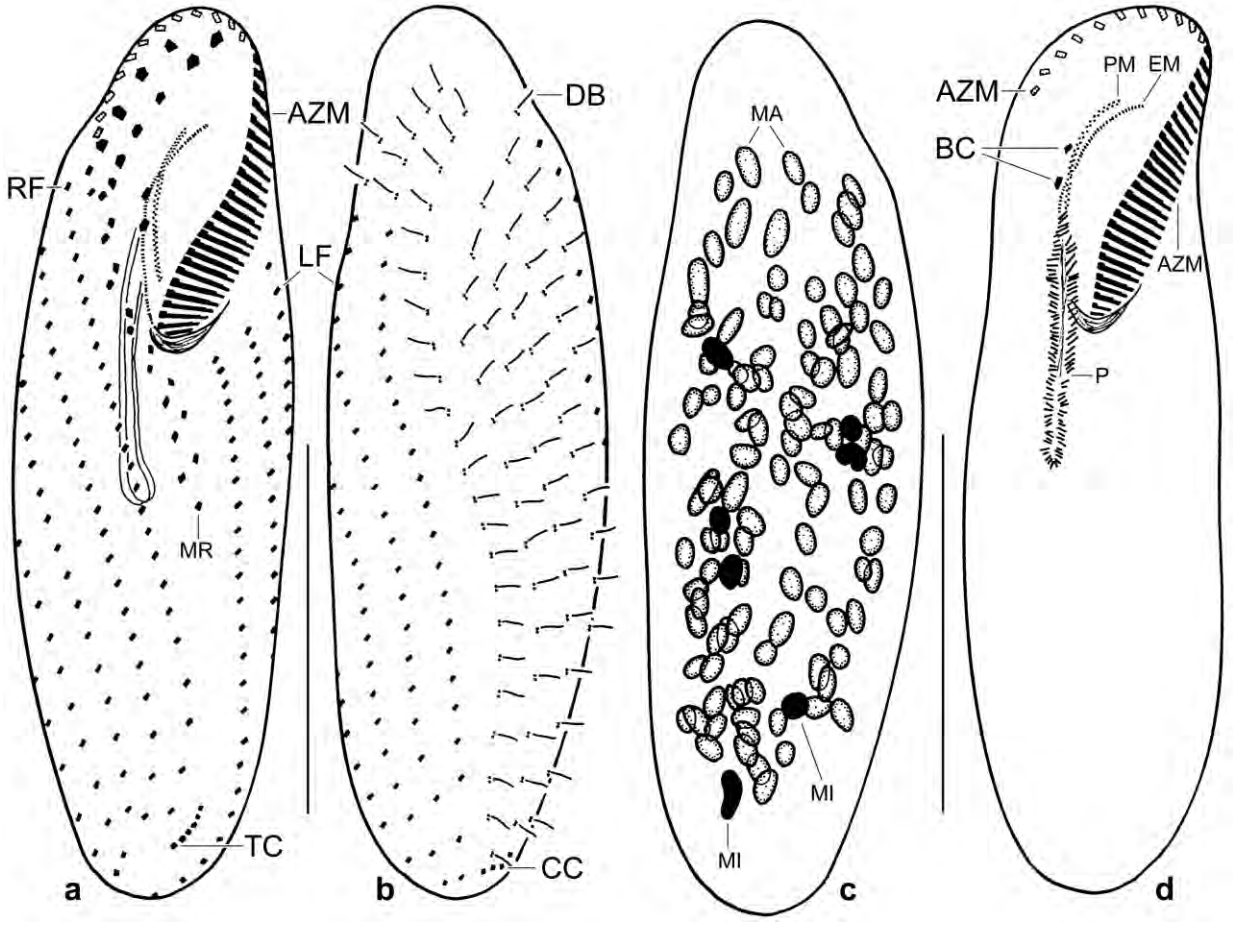

Fig. 182a–d. *Pseudourostyla dimorpha* after protargol impregnation. **a–c:** Ventral and dorsal view of infraciliature and nuclear apparatus of the hapantotype for the broad morph (length:width ≤ 4:1), length 120 µm. The micronuclei are slightly larger than the macronuclear nodules. There are five cirral rows each right and left of the midventral complex. **d:** Ventral view of a paratype specimen, showing the oral structures. The pharynx is surrounded by minute, oblong structures. AZM – adoral zone of membranelles, BC – buccal cirri, CC – caudal cirri, DB – dorsal bristles, EM – endoral membrane, LF – left cirral field, MA – macronuclear nodules, MI – micronuclei, MR – midventral rows/complex, P – pharynx, PM – paroral membrane, RF – right cirral field, TC – transverse cirri. Scale bars 50 µm.

Table 65. Morphometric data on *Pseudourostyla dimorpha*, broad morph (< 4:1, upper line) and slender morph (> 4:1, lower line) based on mounted, protargol-impregnated, and randomly selected specimens from a non-flooded Petri dish culture. Measurements in µm. CV – coefficient of variation in %, M – median, Max – maximum, Mean – arithmetic mean, Min – minimum, n – number of individuals investigated, SD – standard deviation, SE – standard error of arithmetic mean.

Characteristics	Mean	M	SD	SE	CV	Min	Max	n
Body, length	140.4	132.0	22.3	4.7	15.9	106.0	183.0	23
	154.8	154.0	22.6	4.8	14.6	115.8	198.0	22
Body, width	37.8	35.0	7.0	1.5	18.6	30.0	57.0	23
	27.4	27.0	4.4	0.9	16.1	21.0	36.0	22
Body length:width, ratio	3.7	3.7	0.2	0.1	5.7	3.1	4.0	23
	5.9	5.0	1.6	0.3	27.2	4.1	9.4	22
Anterior body end to proximal end of adoral zone of membranelles, distance	45.1	44.0	5.8	1.2	12.8	31.0	55.0	23
	44.0	44.0	3.6	0.8	8.1	38.0	52.0	21
Adoral zone of membranelles, percentage of body length	32.2	31.6	2.9	0.6	8.9	28.0	38.0	23
	29.0	29.1	2.8	0.6	9.7	22.0	34.0	21
Adoral membranelles, number	39.8	40.0	4.1	0.9	10.2	31.0	47.0	23
	38.2	39.0	3.1	0.6	8.1	33.0	45.0	24
Largest adoral membranelle, length of base	6.4	6.5	1.2	0.3	18.9	4.0	8.5	23
	6.1	6.3	0.9	0.2	14.7	4.5	7.0	20
Buccal cavity, width	11.6	11.0	2.5	0.5	21.1	9.0	17.0	23
	9.1	9.0	1.7	0.4	18.8	6.0	12.0	20
Pharynx, length	23.9	23.0	4.6	1.0	19.1	16.0	33.0	23
	23.6	23.0	3.2	0.7	13.4	18.0	29.0	20
Anterior body end to paroral membrane, distance	15.6	16.0	1.7	0.4	11.1	12.0	19.0	23
	15.5	15.0	2.1	0.5	13.4	12.0	20.0	21
Anterior body end to endoral membrane, distance	15.0	15.0	1.7	0.4	11.3	12.0	18.0	23
	14.6	14.0	2.1	0.5	14.4	10.0	19.0	21
Anterior body end to first macronuclear nodule, distance	17.7	16.0	3.6	0.8	20.5	13.0	27.0	23
	21.1	21.0	5.5	1.2	26.1	11.0	30.0	21
Nuclear figure, length	109.2	106.0	17.1	3.6	15.7	82.0	145.0	23
	123.0	123.0	19.0	4.3	15.5	89.0	156.0	20
First macronuclear nodule, length	4.7	4.5	0.6	0.1	12.7	4.0	6.0	23
	5.1	5.0	1.0	0.2	18.8	3.5	7.0	21
First macronuclear nodule, width	2.8	2.5	0.5	0.1	16.5	2.0	4.0	23
	2.3	2.5	–	–	–	2.0	3.0	21
Macronuclear nodules, number (rough values)	119.1	116.0	–	–	–	96.0	160.0	23
	115.1	119.0	–	–	–	67.0	133.0	21
First micronucleus, length	5.3	5.5	0.9	0.2	16.1	3.5	7.0	23
	5.4	5.0	0.9	0.2	16.2	3.0	7.0	21
First micronucleus, width	2.7	2.5	0.5	0.1	18.4	2.0	3.5	23
	2.2	2.0	–	–	–	2.0	2.5	21
Micronuclei, number (rough values)	5.0	5.0	–	–	–	2.0	9.0	23
	5.3	5.0	–	–	–	3.0	8.0	21
Anterior body end to last cirrus of midventral complex, distance	71.7	70.0	10.8	2.3	15.0	52.0	92.0	23
	73.7	72.0	10.0	2.2	13.6	62.0	95.0	21

continued

Characteristics	Mean	M	SD	SE	CV	Min	Max	n
Midventral complex, number of cirri	17.6	17.0	3.0	0.6	17.2	13.0	23.0	23
	16.5	17.0	1.9	0.4	11.3	13.0	21.0	21
Midventral complex, number of cirral pairs	8.2	8.0	1.5	0.3	18.3	6.0	11.0	23
	7.8	8.0	0.9	0.2	12.2	6.0	10.0	21
Right cirral field, number of rows	5.4	5.0	–	–	–	5.0	6.0	23
	5.3	5.0	0.6	0.1	10.5	4.0	6.0	23
Right cirral row 1, number of cirri	27.0	26.0	3.4	0.7	12.7	21.0	34.0	22
	26.1	26.0	3.0	0.7	11.6	18.0	31.0	21
Right cirral row 2, number of cirri	28.0	28.0	3.4	0.7	12.3	21.0	35.0	22
	27.5	27.0	3.3	0.7	12.1	20.0	24.0	21
Right cirral row 3, number of cirri	22.5	22.0	3.1	0.6	13.7	17.0	29.0	23
	21.9	21.0	3.4	0.7	15.6	12.0	28.0	21
Right cirral row 4, number of cirri	18.7	19.0	2.9	0.6	15.3	14.0	24.0	23
	17.9	18.0	3.2	0.7	17.7	10.0	23.0	21
Right cirral row 5, number of cirri	10.2	11.0	4.3	0.9	41.9	2.0	17.0	23
	10.9	11.0	3.7	0.8	34.3	3.0	17.0	20
Right cirral row 6, number of cirri	4.2	3.0	1.6	0.5	38.6	3.0	7.0	10
	3.8	3.0	1.4	0.5	37.0	3.0	7.0	8
Left cirral field, number of rows	5.2	5.0	–	–	–	5.0	6.0	22
	5.3	5.0	–	–	–	5.0	6.0	23
Left cirral row 1, number of cirri	26.4	26.0	3.5	0.8	13.4	20.0	32.0	22
	27.5	27.0	3.4	0.8	12.5	23.0	34.0	20
Left cirral row 2, number of cirri	25.6	26.0	3.2	0.7	12.6	19.0	33.0	23
	25.7	25.0	2.5	0.6	9.9	22.0	30.0	20
Left cirral row 3, number of cirri	24.8	25.0	3.3	0.7	13.2	20.0	33.0	23
	24.7	25.0	2.5	0.6	9.9	21.0	29.0	20
Left cirral row 4, number of cirri	24.4	23.0	3.8	0.8	15.6	19.0	34.0	22
	24.3	24.0	2.9	0.7	12.0	19.0	29.0	20
Left cirral row 5, number of cirri	21.6	22.0	3.8	0.8	17.4	16.0	28.0	22
	20.3	20.0	5.7	1.3	28.1	2.0	28.0	20
Left cirral row 6, number of cirri	19.4	20.0	3.9	1.8	20.2	14.0	23.0	5
	15.5	16.0	3.5	1.4	22.6	11.0	20.0	6
Anterior body end to rearmost buccal cirrus, distance	29.2	30.0	4.4	0.9	15.2	21.0	36.0	23
	28.3	29.0	3.0	0.7	10.6	21.0	36.0	21
Buccal cirri, distance in between	2.4	2.5	–	–	–	1.5	3.5	20
	2.3	2.5	–	–	–	1.5	3.0	18
Buccal cirri, number	2.1	2.0	0.5	0.1	24.7	1.0	4.0	23
	1.9	2.0	–	–	–	1.0	2.0	21
Frontal cirri, anterior bow, number of cirri	5.2	5.0	0.6	0.1	11.1	4.0	6.0	23
	5.0	5.0	0.7	0.2	14.9	3.0	6.0	21
Frontal cirri, posterior bow, number of cirri	4.1	4.0	0.5	0.1	12.6	3.0	5.0	23
	4.1	4.0	0.7	0.1	15.8	3.0	5.0	21
Frontoterminal cirri, number	2.0	2.0	0.0	0.0	0.0	2.0	2.0	23
	2.0	2.0	–	–	–	1.0	2.0	21
Transverse cirri, number	5.9	6.0	1.3	0.3	22.6	4.0	9.0	23

continued

Characteristics	Mean	M	SD	SE	CV	Min	Max	n
	5.2	5.0	0.8	0.2	15.5	4.0	7.0	22
Posterior body end to rearmost transverse cirrus, distance	10.2	10.0	3.0	0.6	28.9	6.0	17.0	23
	7.9	8.0	1.9	0.4	24.4	4.0	12.0	21
Dorsal kineties, number	2.3	2.0	–	–	–	2.0	3.0	22
	2.3	2.0	–	–	–	2.0	3.0	21

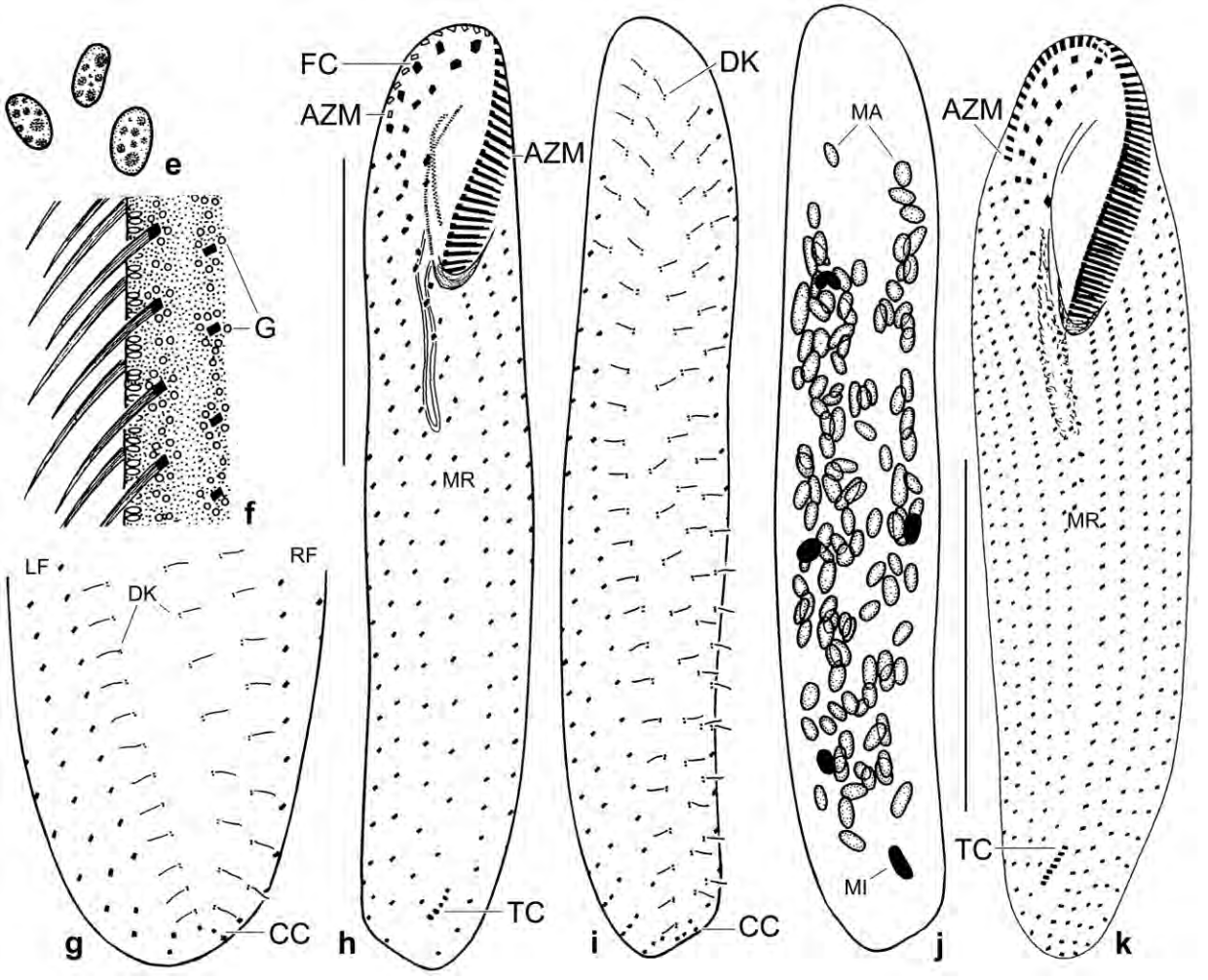

Fig. 182e–k. *Pseudourostyla dimorpha* (e, g–j) and *P. franzi* (f, k) from life (f; from Foissner 1987a) and after protargol impregnation (e, g–k). **e:** Macronuclear nodules from the specimen shown in Fig. 182c. **f:** The cortical granulation is very similar in *P. franzi* and *P. dimorpha*. **g:** Dorsal posterior region of a paratype specimen, showing caudal cirri. **h–j:** Ventral and dorsal view of infraciliature and nuclear apparatus of the hapantotype for the slender morph (length:width ratio > 4:1), length 153 µm. The slender and the broad morph (Fig. 182a–c) differ only in body width. **k:** Ventral view of *P. franzi* which differs from *P. dimorpha* by some independent non-overlapping main features, viz., body length, the number of adoral membranelles and cirral rows in the right and left cirral field, and by the location of the transverse cirri which are rather near to the rear end in *P. dimorpha* and thus project from body proper (Table 66). AZM – adoral zone of membranelles, CC – caudal cirri, DK – dorsal kineties, FC – frontal cirri, G – cortical granules, LF – left cirral field, MA – macronuclear nodules, MI – micronuclei, MR – midventral rows/complex, RF – right cirral field, TC – transverse cirri. Scale bars 50 µm (h–j) and 100 µm (k).

Table 66. Comparison of *Pseudourostyla franzi* (from FOISSNER 1987a) and → *P. dimorpha*. Based on protargol-impregnated specimens from non-flooded Petri dish cultures. Arithmetic means and extremes in parentheses.

Characteristics	***P. franzi* (n=10)**	***P. dimorpha* (< 4:1, n=23)**	***P. dimorpha* (> 4:1, n=20)**
Body length (µm)[a]	257.2 (216–308)	140.4 (106–183)	154.8 (116–198)
Body width (µm)[a]	56.0 (49–63)	37.8 (30–57)	27.4 (21–36)
Body length:width, ratio	4.6	3.7 (3.1–4)	5.9 (4.1–9.4)
Adoral zone of membranelles, percentage of body length	29.9	32.2 (28–38)	29.0 (22–34)
Adoral membranelles, number	67.1 (59–72)	39.8 (31–47)	38.2 (33–45)
Cirral rows in right field, number (includes marginal row)	8.8 (8–10)	5.4 (5–6)	5.3 (4–6)
Cirral rows in left field, number (includes marginal row)	9.4 (8–10)	5.2 (5–6)	5.3 (5–6)
Transverse cirri, number	7.7 (5–11)	5.9 (4–9)	5.2 (4–7)
Rearmost transverse cirrus to posterior body end, distance (µm)	23 (20–27)	10.2 (6–17)	7.9 (4–12)

[a] The in vivo size can be calculated by adding 15% preparation shrinkage. Broad morph: 120–210 × 35–65 µm, on average 160 × 40 µm. Slender morph: 135–230 × 25–40 µm, on average 180 × 30 µm (values generously rounded).

membranelles. Buccal cavity and undulating membranes in ordinary pattern. Pharynx surrounded by minute, oblong structures.

Type locality: Venezuelan site (24), i. e., soil from a *Tachypogon* savannah about 50 km north of the town of Puerto Ayacucho, 67°36‘W 5°41‘N.

Type material: 1 holotype and 3 paratype slides with protargol-impregnated specimens have been deposited in the Biology Centre of the Upper Austrian Museum in Linz (LI). The holotype and paratype specimens have been marked by black ink circles on the coverslip.

Etymology: The name is a composite of the Greek numeral *di* (two) and the Greek substantive *morphe* (shape), referring to the two morphs of *P. dimorpha*.

Description and remarks: The overall appearance of *P. dimorpha* is highly similar to *P. franzi* FOISSNER, 1987a (reviewed in BERGER 2006). Thus, we do not provide a live illustration and “ordinary” description but refer to the diagnosis, the Figures (182a–j, 183a–e), the detailed morphometry (Table 65), the comparison with *P. franzi* (Table 66), and the following text.

(i) *P. dimorpha* grew well in the non-flooded Petri dish culture for a month. Invariably, there were broad and slender cells. Of 100 randomly selected specimens in a protargol preparation 28 had a length:width ratio of ≤ 4:1 and 72 were slender (> 4:1). The high number of slender cells suggests them as the “typical” morph.

(ii) This is substantiated by the coefficients of variation. Of 42 usable features 28 were lower in the slender than the broad specimens.

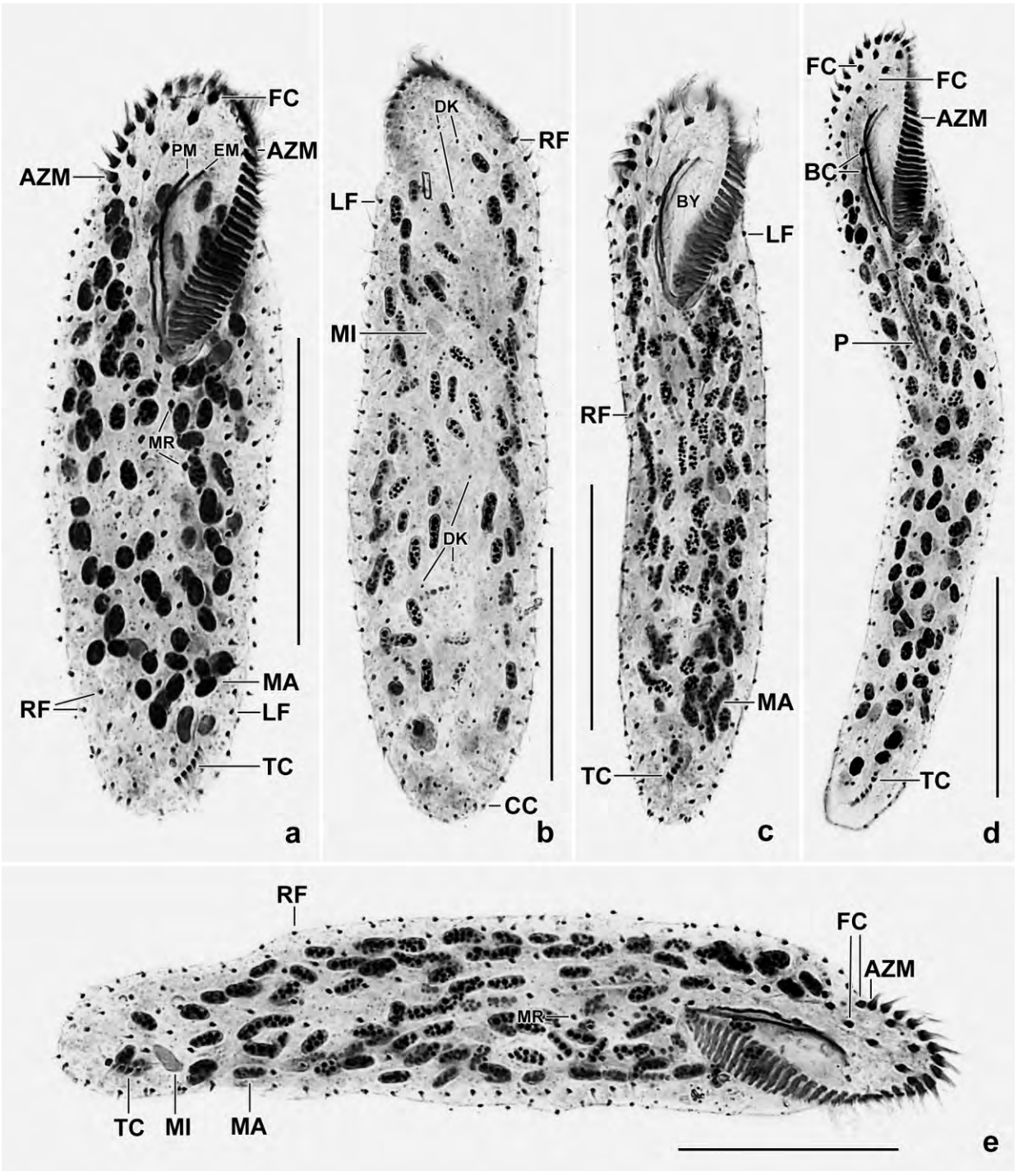

Fig. 183a–e. *Pseudourostyla dimorpha* after protargol impregnation. Note transverse cirri near body end. **a, b:** Ventral and dorsal view of broad morph (length:width ≤ 4:1). **c, d:** Ventral view of slender morph (> 4:1) which differs from the broad morph (a, b) only by body width. **e:** A specimen (transition stage) with a length:width ratio of ~ 4:1. AZM – adoral zone of membranelles, BC – buccal cirri, BY – buccal cavity, CC – caudal cirri, DK – dorsal kineties, EM – endoral membrane, FC – frontal cirral corona, LF – left cirral field, MA – macronuclear nodules, MI – micronuclei, MR – midventral rows, P – pharynx, PM – paroral membrane, RF – right cirral field, TC – transverse cirri. Scale bars 50 μm.

(iii) Except of body width, the two morphs are indistinguishable morphologically and morphometrically (Tables 65, 66).

(iv) The nearest relative of *P. dimorpha* is very likely *P. franzi* FOISSNER, 1987. However, they differ not only by the two morphs but also by some independent, non-overlapping main features, viz., body length, the number of adoral membranelles and cirral rows in the right and left cirral field, and by the location of the transverse cirri which are rather near to the posterior body end in *P. dimorpha* and thus project from body proper (cp. Fig. 182a, h with Fig. 182k; Table 66).

Caudiholosticha silvicola nov. spec. (Fig. 184d, e; Table 67)

Diagnosis: Size in vivo about 105 × 20 µm; pisciform to very narrowly obovate. On average 31 ellipsoid macronuclear nodules. Cortical granules only around bases of cirri and dorsal bristles, colourless, about 0.5 µm across. Midventral complex composed of an average of 6 cirral pairs and 1 cirrus; on average 2 transverse cirri, 2 caudal cirri, and 4 dorsal kineties with kinety 4 strongly shortened posteriorly. Adoral zone extends about 23% of body length, composed of an average of 17 membranelles. Buccal cavity wide and deep. Pharynx with minute, oblong structures.

Type locality: Needle litter and soil from a spruce forest in the surroundings of the town of Ulm, Germany, 10°E 48°23'N.

Type material: 1 holotype and 4 paratype slides with protargol-impregnated specimens have been deposited in the Biology Centre of the Upper Austrian Museum in Linz (LI). Relevant specimens have been marked by black ink circles on the coverslip.

Etymology: The species name is a composite of the Latin nouns *silva* (forest) and *incola* (inhabitant), referring to the habitat the species was discovered.

Table 67. Comparison of *Caudiholosticha notabilis*-like hypotrichs. All from protargol preparations (Foissner's method). Measurements in µm. First value: arithmetic mean, second values: extremes.

Characteristics	*Caudiholosticha notabilis*	*Caudiholosticha notabilis*	*Caudiholosticha silvicola*	*Caudiholosticha halophila*
Body, length	163 (150–180)	159 (136–198)	94 (74–110)	160 (130–215)
Adoral zone, length	33 (32–33)	40 (35–47)	21 (18–27)	40 (32–57)
Adoral membranelles, number	30 (28–35)	32 (26–36)	17 (16–18)	35 (30–42)
Midventral pairs, number	8	9 (7–14)	6 (4–8)	14 (11–19)
Midventral row, number of cirri	1	1	1	4 (2–7)
Right marginal row, no. of cirri	36 (32–42)	33 (28–41)	23 (18–25)	46 (40–53)
Left marginal row, no. of cirri	39 (32–45)	39 (32–55)	24 (22–27)	47 (39–52)
Transverse cirri, number	4 (2–6)	3 (1–4)	2 (0–2)	2 (1–2)
Dorsal kineties, number	3 (3–3)	4 (4–4)	4 (4–4)	5 (5–5)
Caudal cirri, number	3 (2–4)	3 (3–3)	2 (1–3)	6 (5–7)
Locality	Alpine pasture, Austria	Soil from pine forest, Australia	Soil from pine forest, Germany	Saline coastal soil, Venezuela
Number of specimens studied	3	11	11	14–17
References	FOISSNER (1982)	BLATTERER & FOISSNER (1988)	BERGER & FOISSNER (1987)	Present monograph

Remarks: Berger & Foissner (1987) and Berger (2006) described this population under the names *Paruroleptus notabilis* and *Caudiholosticha notabilis*, respectively. We refer to these descriptions, the diagnosis of the species, and Table 67.

Berger & Foissner (1987) doubted the identification and suggested that it might be a distinct species. This is emphasized by a Venezuelan population (see next species) which is distinctly different in most features, as shown in Table 67. Specifically, *C. silvicola* is the smallest of the three species recognized having, for instance, only half the adoral membranelles and marginal cirri as the other species. Further, dorsal kinety 4 is strongly shortened posteriorly. Be careful not to mix *C. silvicola* with *C. paranotabilis* which differs mainly by the narrow, flat buccal cavity (Foissner et al. 2002).

Caudiholosticha halophila nov. spec. (Fig. 184a–c, f, g, 185a–d; Tables 67, 68)

Diagnosis: Size in vivo about 180 × 30 µm; pisciform to very narrowly obovate. On average 68 broadly ellipsoid macronuclear nodules. Cortical granules as in *C. notabilis*. Midventral complex composed of an average of 14 cirral pairs and 4 cirri; on average 2 transverse cirri, 6 caudal cirri, and 5 dorsal kineties with kinety 4 slightly shortened anteriorly. Adoral zone extends about 25% of body length, composed of an average of 35 membranelles. Buccal cavity wide and deep. Pharynx with minute, oblong structures.

Type locality: Venezuelan site (54), i. e., saline soil from flooded coastal grassland in the Morrocoy National Park, 67°13'W 11°33'N.

Type material: 1 holotype and 2 paratype slides with protargol-impregnated specimens have been deposited in the Biology Centre of the Upper Austrian Museum in Linz (LI). Relevant specimens have been marked by black ink circles on the coverslip.

Etymology: The species name is a composite of the Greek noun *halós* (salt) and the Greek adjective *philos* (preferring), referring to the saline habitat the species was discovered.

Description: In vivo, we identified this population as "large *Uroleptus notabilis*", according to the descriptions of Foissner (1982) and Blatterer & Foissner (1988). However, the protargol impregnations show that it is a new species, for which we cannot provide a live Figure because we did not study the in vivo aspect in detail.

Size in vivo 150–250 × 25–40 µm, usually about 180 × 30 µm, as calculated from the morphometric data in Table 68 adding 15% preparation shrinkage. Body very elongate obovate (length:width ratio ~ 6:1) and frequently slightly sigmoid (Fig. 184a–c, 185a). Nuclear apparatus in central fifths of cell, composed of an average of 68 globular to elongate ellipsoid (~ 3:1) macronuclear nodules with ordinary nucleoli and about five scattered, globular to ellipsoid micronuclei (Fig. 184b, f, 185a–d; Table 68). Cortical granules present, similar to those of *C. notabilis* (see introduction to description), form an up to 8 µm thick coat in most protargol-impregnated specimens (Fig. 185a). Feeds on fungal spores, resting cysts of naked amoebae, and small ciliates (*Odontochlamys alpestris*) digested in food vacuoles up to 20 µm in diameter (Fig. 185a).

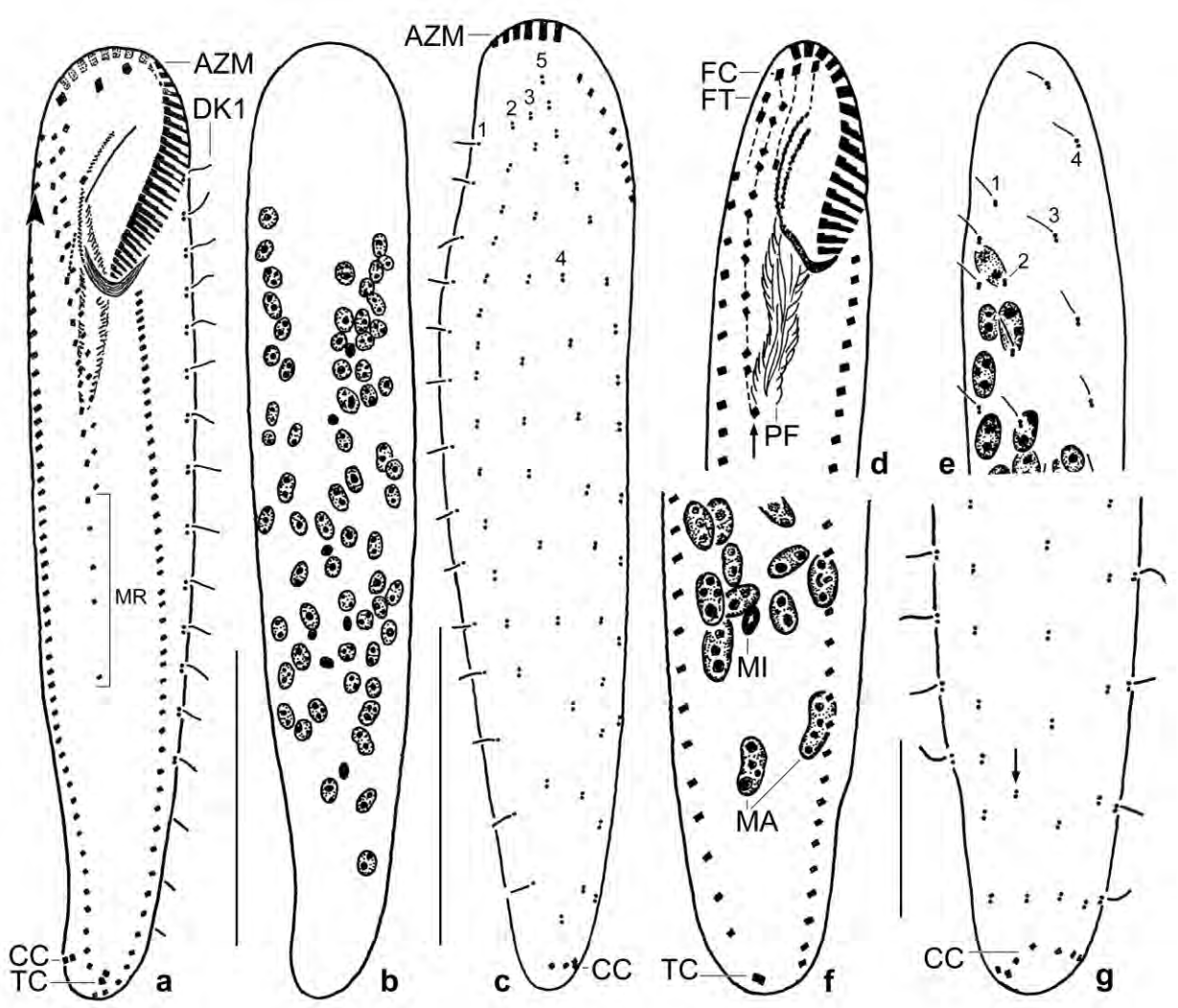

Fig. 184a–g. *Caudiholosticha halophila* (a–c, f, g) and *C. silvicola* (d, e) after protargol impregnation. **a, b:** Ventral infraciliature and nuclear apparatus of holotype specimen, length 165 µm. The arrowhead marks the three frontoterminal cirri. **c:** Dorsal bristle pattern of a paratype specimen. Note the shortened row 4. **f, g:** Ventral and dorsal view of posterior body region. The arrow marks a short additional row. **d, e** (from Berger 2006)**:** *Caudiholosticha silvicola* is much smaller than *C. halophila* and has thus only half the adoral membranelles. Note the strongly shortened dorsal kinety 4. The arrow marks the posterior end of the midventral complex. AZM – adoral zone of membranelles, CC – caudal cirri, DK1 – dorsal kinety 1, FC – frontal cirri, FT – frontoterminal cirri, MA – macronuclear nodules, MI – micronucleus, MR – midventral row, PF – pharyngeal fibres, TC – transverse cirri, 1–5 – dorsal bristle rows. Scale bars 20 µm (f, g) and 50 µm (a–c).

Cirri 10–13 µm long in protargol preparations, arranged in typical urostylid pattern (Berger 2006). Midventral complex composed of an average of 14 pairs and 4 single, widely spaced cirri forming a rather long row (Fig. 184a, 185b; Table 68). On average three distinctly enlarged frontal cirri, three frontoterminal cirri, one buccal cirrus at mid-level of buccal cavity, two transverse cirri near posterior body end, and six caudal cirri (Fig. 184a, f, 185a; Table 68). Dorsal bristles about 5 µm long in protargol preparations, arranged in five bipolar rows, except of row 4 (rarely row 3) rather distinctly shortened anteriorly (Fig. 184b, g; Table 68).

Adoral zone of ordinary shape, extends only 25% of body length on average, composed of about

35 ordinary membranelles with cilia 10–15 µm long in prepared cells. Buccal cavity wide and deep. Undulating membranes moderately curved, optically intersect slightly posterior to mid-buccal cavity, of very similar length (Fig. 184a, 185a, b). Pharynx commences slightly posterior to buccal cirrus and extends over second third of body; pharyngeal wall studded with 1–2 µm long rods, as typical for *Caudiholosticha* (Fig. 184a, 185b–d).

Occurrence and ecology: Obtained low abundance in the non-flooded Petri dish culture from the type locality while it was numerous at site (47). Both sites are saline, suggesting saline soils as the typical habitat.

Table 68. Morphometric data on *Caudiholosticha halophila* based on mounted, protargol-impregnated, randomly selected specimens from a non-flooded Petri dish culture. Measurements in µm. CV – coefficient of variation in %, M – median, Max – maximum, Mean – arithmetic mean, Min – minimum, n – number of individuals investigated, SD – standard deviation, SE – standard error of arithmetic mean.

Characteristics	Mean	M	SD	SE	CV	Min	Max	n
Body, length	159.6	155.0	22.8	5.5	14.3	130.0	215.0	17
Body, width	27.8	27.0	3.1	0.8	11.2	23.0	33.0	17
Body length:width, ratio	5.8	5.9	0.8	0.2	13.2	4.7	7.5	17
Anterior body end to proximal end of adoral zone of membranelles, distance	40.4	40.0	5.5	1.3	13.7	32.0	57.0	17
Adoral zone, % of body length	25.5	25.0	3.4	0.8	13.4	20.0	32.0	17
Adoral membranelles, number	35.0	35.0	3.4	0.9	9.7	30.0	42.0	15
Anterior body end to buccal cirrus, distance	18.5	18.0	2.7	0.7	14.8	14.0	23.0	17
Anterior end to undulating membranes, distance	11.1	11.0	1.8	0.4	16.5	8.0	15.0	17
Anterior end to end of midventral pairs, distance	76.8	75.0	11.3	2.9	14.6	60.0	98.0	15
Anterior end to end of midventral row, distance	102.3	96.0	19.8	5.3	19.4	80.0	158.0	14
Adoral cilia, length	13.0	13.0	1.4	0.4	10.9	10.0	15.0	12
Somatic cirri, length	11.3	11.5	1.1	0.3	9.5	10.3	13.0	16
Dorsal bristles, length	5.1	5.0	0.7	0.2	13.4	4.0	6.0	16
Macronuclear nodules, number	68.2	65.0	10.6	2.6	15.6	55.0	90.0	17
Macronuclear nodules, length	5.3	5.0	1.7	0.4	32.0	3.0	9.0	16
Macronuclear nodules, width	3.2	3.0	0.8	0.2	25.5	2.0	5.0	16
Micronuclei, number [a]	5.2	5.0	–	–	–	3.0	8.0	15
Micronuclei, length	2.9	3.0	0.4	0.1	14.0	2.2	4.0	16
Micronuclei, width	2.4	2.4	–	–	–	2.0	3.0	16
Midventral pairs, number	14.2	13.5	2.1	0.6	14.9	11.0	19.0	14
Midventral row, number of cirri	4.2	4.0	1.4	0.4	32.6	2.0	7.0	14
Right marginal cirri, number	45.6	45.5	4.1	1.1	9.0	40.0	53.0	14
Left marginal cirri, number	46.5	46.5	4.2	1.1	9.0	39.0	52.0	14
Frontal cirri, number	3.0	3.0	0.0	0.0	0.0	3.0	3.0	16
Buccal cirri, number	1.0	1.0	0.0	0.0	0.0	1.0	1.0	16
Frontoterminal cirri, number	3.3	3.0	–	–	–	3.0	4.0	16
Transverse cirri, number	1.6	2.0	–	–	–	1.0	2.0	12
Caudal cirri, number	5.9	6.0	0.9	0.3	15.4	5.0	7.0	13
Dorsal bristle rows, number	5.0	5.0	0.0	0.0	0.0	5.0	5.0	12

[a] Likely an under-estimation because difficult to recognize among the mass of macronuclear nodules and cell inclusions.

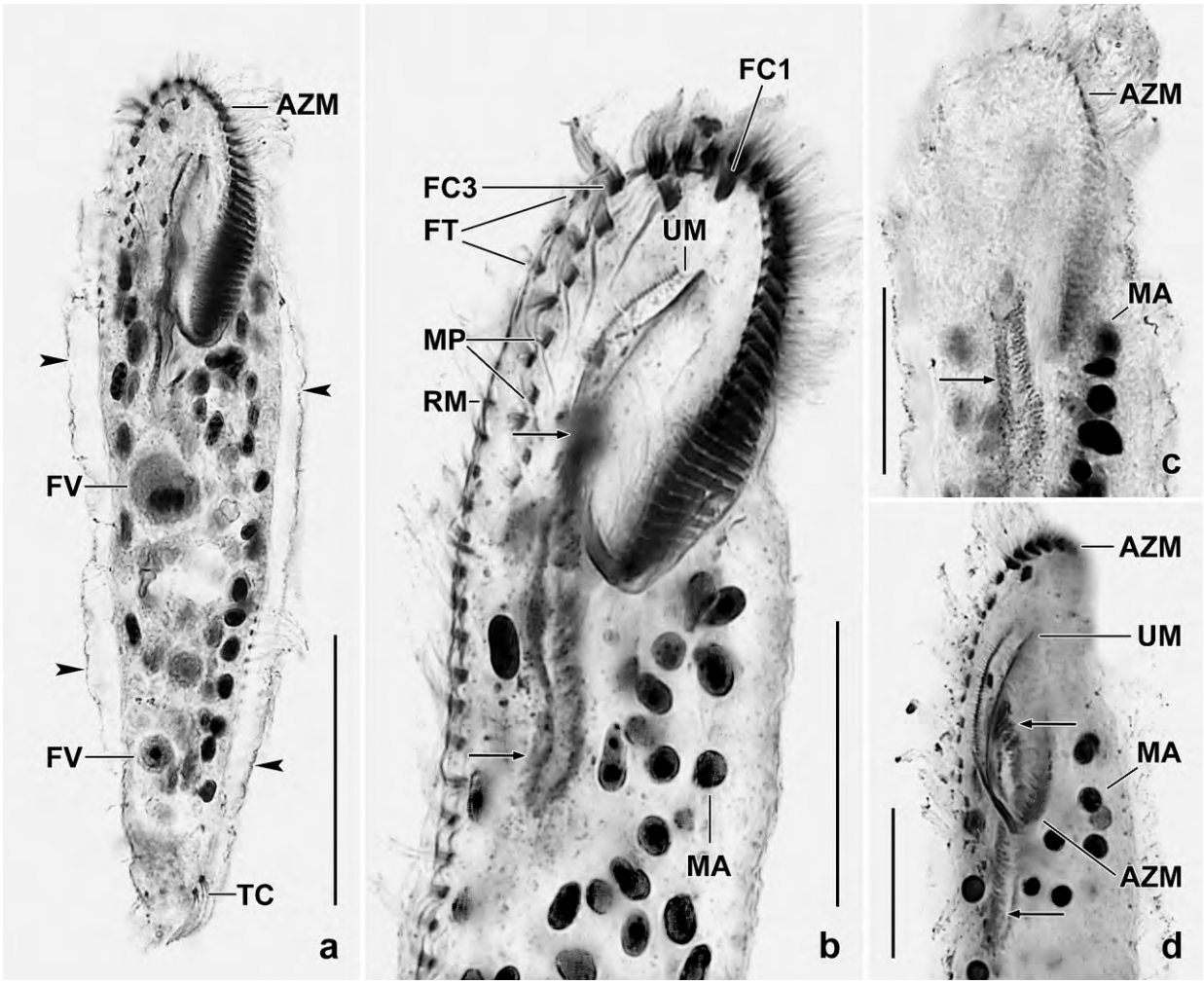

Fig. 185a–d. *Caudiholosticha halophila* after protargol impregnation. **a:** Overview focused to body centre to show the thick mucous layer (arrowheads) very likely produced by exploded cortical granules. **b–d:** Ventral overview and details. The arrows mark the long pharynx, the wall of which is studded with minute, oblong structures. AZM – adoral zone of membranelles, FC1, 3 – frontal cirri, FT – frontoterminal cirri, FV – food vacuoles, MA – macronuclear nodules, MP –midventral pairs, RM – right marginal cirral row, TC – transverse cirri, UM – undulating membranes. Scale bars 25 µm (b–d) and 50 µm (a).

Remarks: *Caudiholosticha halophila* differs significantly from the nearest known relative, *C. notabilis*, by the following morphometrics (Table 67): number of midventral cirral pairs (14 vs. 8), number of cirri in midventral row (4 vs. 1), number of dorsal kineties (5 vs. 3–4), and number of caudal cirri (6 vs. 3). Some of these features have a difference of ≥ 100%, suggesting species rank for the Venezuelan population (Foissner et al. 2002).

Caudiholosticha virginensis nov. spec. (Fig. 186a–g, 187a–h; Table 69)

Diagnosis: Size in vivo about 180 × 30 µm; very elongate rectangular. On average 18 ellipsoid macronuclear nodules and several micronuclei, forming a ribbon left of body´s midline. Cortical granules in dense rows, form distinct fringe, colourless, about 2.5 × 1 µm in vivo. Midventral complex composed of an average of 20 pairs, ends subterminally. 2 frontoterminal cirri, 1 buccal cirrus near anterior end of undulating membranes, 2 transverse cirri, 2 pretransverse cirri, 2

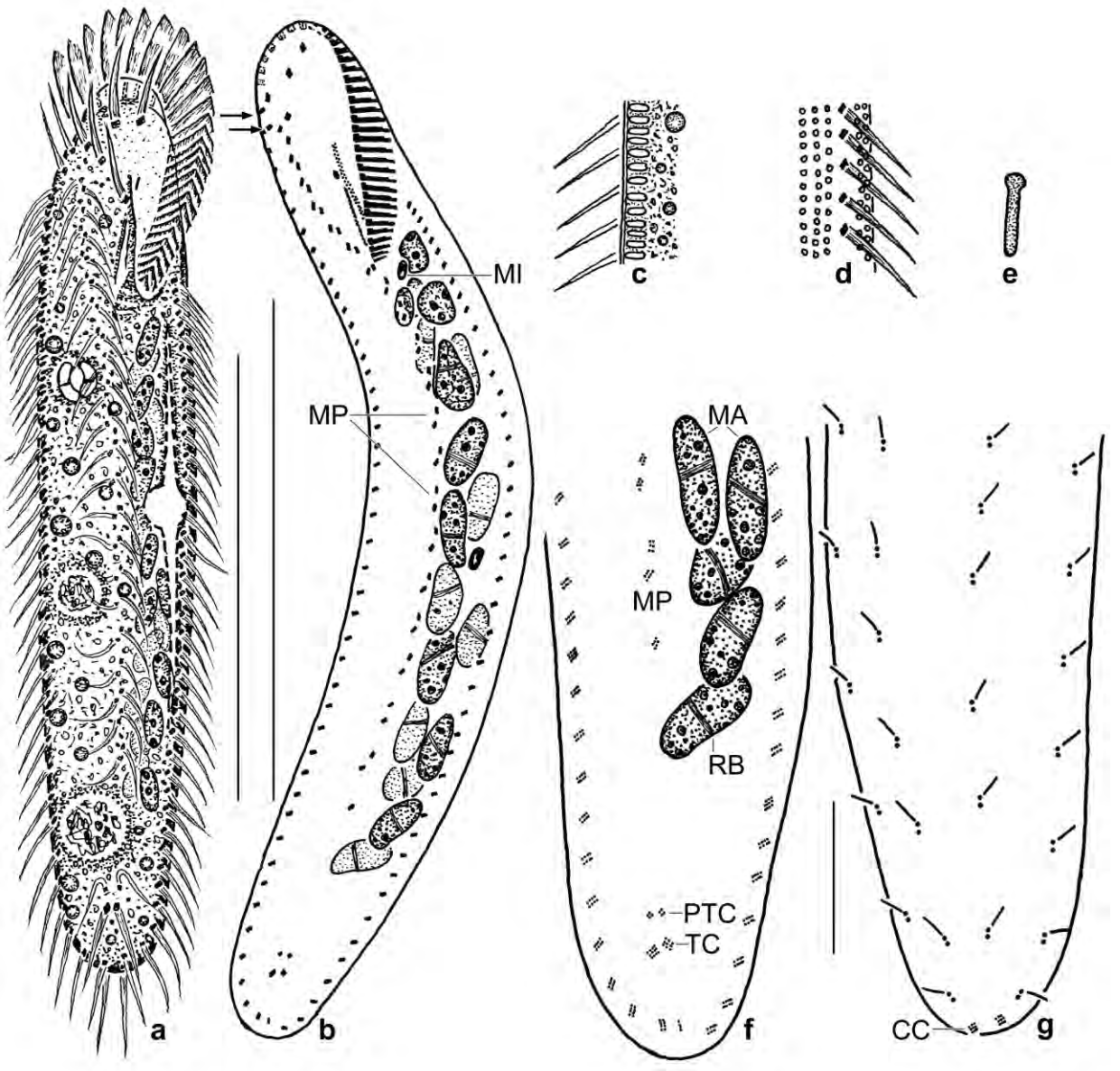

Fig. 186a–g. *Caudiholosticha virginensis* from life (a, c, d), in a methyl green-pyronin stain (e), and after protargol impregnation (b, f, g). **a:** Ventral view of a representative specimen, length 180 µm. **b, f, g:** Ventral and dorsal view of holotype specimen, length about 200 µm; figures (f, g) show the posterior region of figure (b) at higher magnification. Arrows mark frontoterminal cirri. **c, d:** Optical section and surface view of cortical granulation; individual granules colourless and about 2.5 × 1 µm in vivo. **e:** An extruded cortical granule, length 5 µm. CC – caudal cirri, MA – macronuclear nodules, MI – micronucleus, MP – midventral cirral pairs, PTC – pretransverse cirri, RB – reorganization band, TC – transverse cirri. Scale bars 20 µm (f, g) and 100 µm (a, b).

caudal cirri, and 4 dorsal kineties. Buccal cavity narrow and flat; adoral zone extends about 27% of body length, composed of 32 membranelles on average. Undulating membranes comparatively short, straight, side by side.

Type locality: Soil surface litter and decaying wood from a fallen tree in the rain forest along the Mahagani River Road, Saint Croix, Virgin Islands, 65°W 18°N.

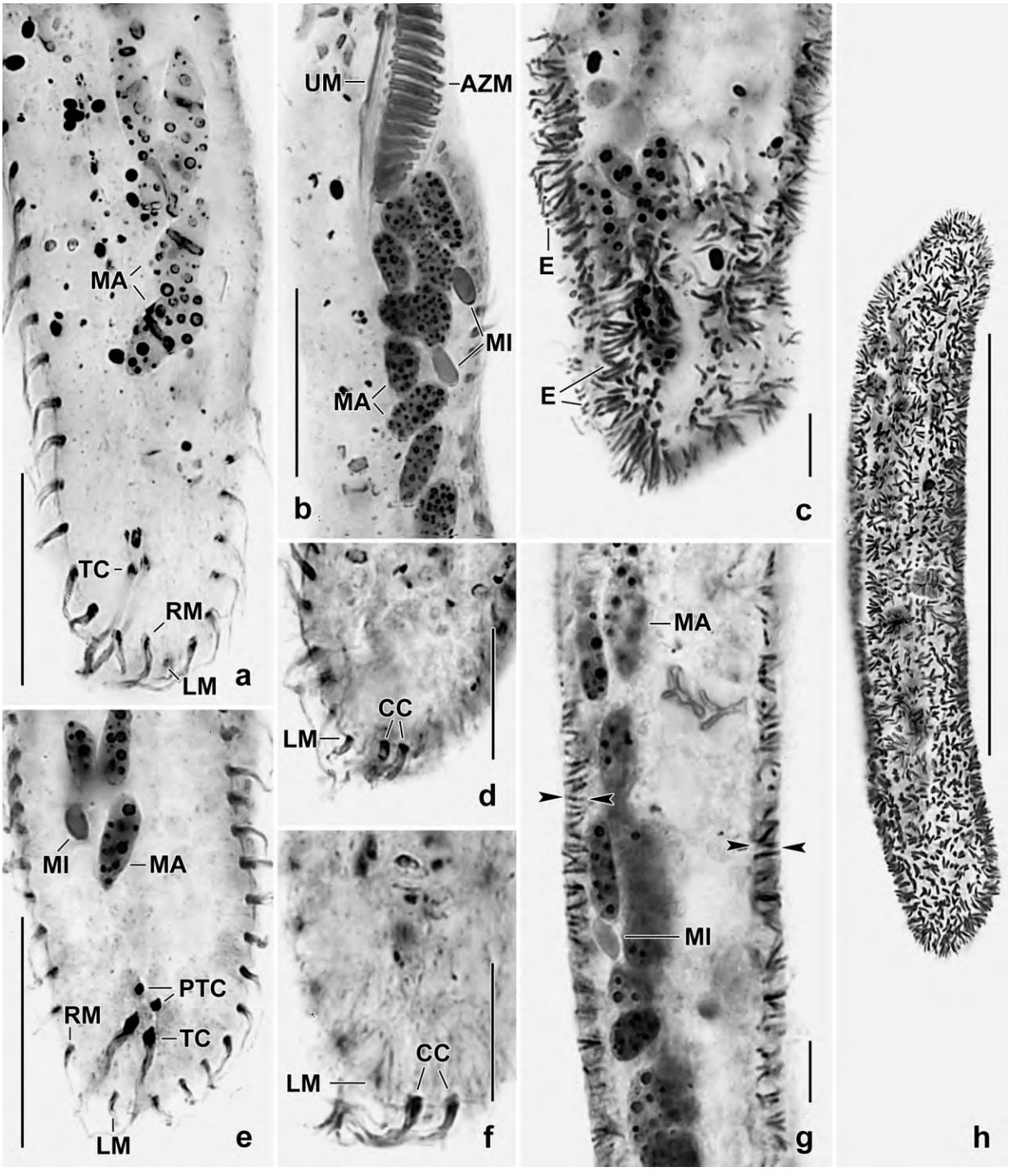

Fig. 187a–h. *Caudiholosticha virginensis* after protargol impregnation. **a, e:** Ventral views of posterior body region, showing pretransverse and transverse cirri as well as the marginal cirral rows. Note the reorganization band in the macronuclear nodules (a). **b:** The micronuclei are conspicuously large. **c, g, h:** Cortical granules extruded (c), partially extruded (h), and resting (g). The granules are numerous and comparatively long, thus forming a distinct fringe (g, opposed arrowheads). **d, f:** Dorsal views of posterior body region, showing the two distinct caudal cirri. AZM – adoral zone of membranelles, CC – caudal cirri, E – extrusomes, LM – left marginal row, MA – macronuclear nodules, MI – micronuclei, PTC – pretransverse cirri, RM – right marginal row, TC – transverse cirri, UM – undulating membranes. Scale bars 10 µm (c, g), 15 µm (d, f), 25 µm (a, b, e), and 100 µm (h).

Table 69. Morphometric data on *Caudiholosticha virginensis* based on mounted, protargol-impregnated, randomly selected specimens from a non-flooded Petri dish culture. Measurements in µm. CV – coefficient of variation in %, M – median, Max – maximum, Mean – arithmetic mean, Min – minimum, n – number of individuals investigated, SD – standard deviation, SE – standard error of arithmetic mean.

Characteristics	Mean	M	SD	SE	CV	Min	Max	n
Body, length	157.0	152.5	21.2	6.7	13.5	130.0	200.0	10
Body, width	27.7	29.0	4.5	1.4	16.3	20.0	33.0	10
Body length:width, ratio	5.8	5.7	0.8	0.3	13.8	4.8	7.0	10
Anterior body end to end of midventral rows, distance	120.5	119.0	16.7	5.3	13.8	98.0	145.0	10
Anterior body end to proximal end of adoral zone, distance	43.1	41.0	7.5	2.4	17.4	38.0	64.0	10
Adoral membranelles, number	31.6	31.5	1.6	0.5	5.2	30.0	34.0	10
Macronuclear nodules, length	11.3	11.0	2.6	0.8	22.9	8.0	16.0	10
Macronuclear nodules, width	4.0	4.0	1.1	0.3	26.4	3.0	6.0	10
Macronuclear nodules, number	18.0	17.5	2.6	0.8	14.3	15.0	23.0	10
Micronuclei, length	4.7	4.8	0.8	0.2	16.9	3.0	6.0	10
Micronuclei, width	2.4	2.3	0.5	0.1	19.1	2.0	3.0	10
Micronuclei, number	3.5	3.0	1.8	0.6	50.8	1.0	7.0	10
Right marginal row, number of cirri	42.1	42.0	3.1	1.0	7.5	37.0	46.0	10
Left marginal row, number of cirri	41.5	41.0	2.9	0.9	7.0	39.0	49.0	10
Midventral pairs, number	20.4	20.5	1.0	0.4	5.2	19.0	22.0	8
Frontal cirri, number	4.0	4.0	0.0	0.0	0.0	4.0	4.0	10
Frontoterminal cirri, number	2.0	2.0	0.0	0.0	0.0	2.0	2.0	10
Buccal cirri, number	1.0	1.0	0.0	0.0	0.0	1.0	1.0	10
Pretransverse cirri, number	2.0	2.0	0.0	0.0	0.0	2.0	2.0	13
Transverse cirri, number	2.0	2.0	0.0	0.0	0.0	2.0	2.0	13
Caudal cirri, number	2.0	2.0	0.0	0.0	0.0	2.0	2.0	7
Dorsal kineties, number	4.0	4.0	0.0	0.0	0.0	4.0	4.0	5

Type material: 1 holotype and 4 paratype slides with protargol-impregnated specimens have been deposited in the Biology Centre of the Upper Austrian Museum in Linz (LI). Relevant specimens have been marked by black ink circles on the coverslip.

Etymology: Named after the country it was discovered, i. e., the Virgin Islands in the Caribbean Sea.

Description: Size in vivo 130–230 × 20–40 µm, usually about 180 × 30 µm, as calculated from some in vivo measurements and the morphometric data in Table 69 adding 15% preparation shrinkage. Body shape very elongate rectangular or indistinctly ellipsoidal, length:width ratio 4.8–7:1, on average 5.8:1 (Fig. 186a, b, 187h; Table 69); flattened laterally about 2:1. Nuclear apparatus left of body´s midline, forms a narrow ribbon commencing near buccal vertex and extending subterminally, composed of an average of 18 globular to very elongate ellipsoid macronuclear nodules and about four ellipsoid micronuclei with a size of about 6 × 4 µm in vivo; macronuclear nodules in two rough rows one upon the other (Fig. 186a, b, f, 187a, b, e, g; Table 69). Contractile vacuole about in mid-body at left body margin, with short collecting canals

extending anteriorly and posteriorly (Fig. 186a). Cortex very flexible and colourless. Cortical granules arranged in dense rows forming a distinct, about 3 µm wide fringe, absent from cirral areas, colourless, in vivo about 2.5 × 1 µm in size (Fig. 186c, d); impregnate more or less deeply with the protargol method used, forming a 2–4 µm wide fringe (Fig. 187c, g, h); when extruded drumstick-shaped and about 5 µm long, stain blue with methyl green-pyronin (Fig. 186e). Cytoplasm hyaline with lipid droplets up to 10 µm across. Feeds on bacteria, fungal spores, and ciliates digested in food vacuoles up to 30 × 20 µm in size. Glides rather rapidly on microscope slide and soil particles, showing great flexibility.

Cirral pattern as typical for genus and of ordinary variability (Fig. 186a, b, f, g, 187a, d, e, f; Table 69). Midventral rows composed of 20 cirral pairs on average, end about 23% subterminally. Marginal cirral rows usually almost touching at posterior end, caudal cirri occasionally indistinctly separated from left marginal cirri. Invariably four slightly enlarged frontal cirri, two frontoterminal cirri, one buccal cirrus, two pretransverse cirri, two transverse cirri, two caudal cirri, and four bipolar dorsal kineties with 3–4 µm long bristles.

Adoral zone comparatively short, i. e., extends 27% of body length on average, of usual shape and structure, consists of an average of 32 ordinary membranelles, first membranelle close to third frontal cirrus. Buccal cavity narrow and flat; buccal lip inconspicuous covering some proximal membranelles. Both undulating membranes comparatively short, straight, slightly overlap in anterior quarter. Pharyngeal fibres inconspicuous in vivo and in protargol preparations (Fig. 186a, 187b; Table 69).

Occurrence and ecology: As yet found only at type locality. Appeared four weeks after rewetting the sample (pH 6.8), indicating a k-selected life strategy.

Remarks: This species has a holostichid cirral pattern and two distinct caudal cirri. Thus, it belongs to the genus *Caudiholosticha* Berger, 2003. None of the 14 species classified by Berger (2006) into this genus strongly resembles *C. virginensis*. This applies also to the genus *Holosticha*, which lacks caudal cirri. However, there are at least two *Anteholosticha* species which are quite similar, except for the lack of caudal cirri: *A. australis* (Blatterer & Foissner, 1988) and *A. distyla* (Buitkamp, 1977a). *Anteholosticha australis* further differs from *C. virginensis* by the number of transverse cirri (3–6 vs. 2). *Anteholosticha distyla*, which Buitkamp (1977a) discovered in soil from the Ivory Coast (Africa), lacks cortical granules and caudal cirri (Buitkamp: "caudal cirri totally absent"). However, Hemberger (1982) reinvestigated the type material of *A. distyla* and observed that the number of transverse cirri varies from two to four and that the three last cirri of the left marginal row could be caudal cirri. Thus, only the presence vs. absence of cortical granules remains as a distinct difference between *C. virginensis* and *A. distyla*. Unfortunately, we cannot be sure about this difference because Buitkamp (1977a) did not make detailed live observations, and thus he could have overlooked cortical granules in his species.

Paragastrostyla terricola (Foissner, 1988) Berger, 2006 (Fig. 188a–i)

The specimens from Venezuelan site (62) match well the original description. However, they are more slender: 100–130 × 10–20 µm, n = 5, 7.5:1 (vs. 80–140 × 15–30 µm, ~ 5:1) in vivo, respectively, 80–120 × 10–12 µm, n = 8, 8.5:1 (vs. 91 × 16, 5.6:1) in protargol preparations. The cortical granules are difficult to recognize because they are minute (~ 0.2–0.5 µm), colourless to slightly yellowish, and occur mainly around the bases of the cirri and dorsal bristles. The granules stain blue, but are not extruded, in methyl green-pyronin preparations. Some ordinary crystals and lipid droplets accumulated in posterior region. Feeds on bacteria digested in vacuoles 3–5 µm across.

Two voucher slides with protargol-impregnated specimens have been deposited in the Biology Centre of the Upper Austrian Museum in Linz (LI).

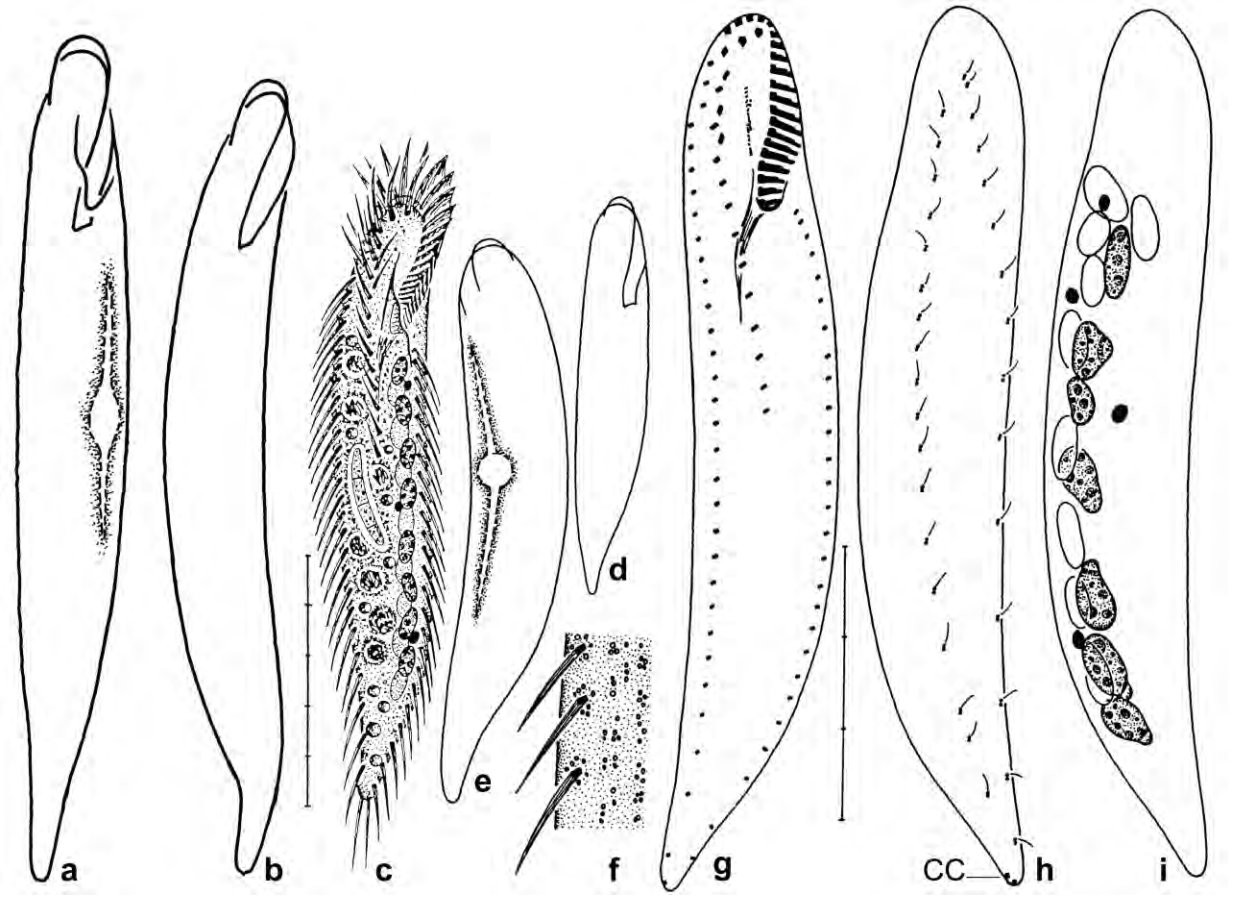

Fig. 188a–i. *Paragastrostyla terricola*, Venezuelan (a, b) and Kenyan (c–i, from Foissner 1988a) specimens from life (a–f) and after protargol impregnation (g–i). **a–e:** The Venezuelan specimens (a, b; length ~ 120 µm) are thinner than the African ones (c–e). **f:** The cortical granules are colourless to yellowish in the Venezuelan specimens while yellow to orange yellow in the Kenyan ones. **g–i:** Infraciliature of ventral and dorsal side and nuclear apparatus of Kenyan holotype specimen. The macronuclear nodules are arranged in two rough rows one upon the other. Note absence of a buccal cirrus (main generic feature). CC – caudal cirri. Scale bar division 10 µm.

Cladotricha chilensis **nov. spec.** (Fig. 188.1a–d; Table 69a)

Diagnosis: Size in vivo about 70 × 13 µm; very elongate ellipsoid with posterior region tail-like narrowed. 2 ellipsoid macronuclear nodules in middle third of cell; 1 to 2 micronuclei. 3 frontal cirri, first far subapical and distinctly enlarged; 1 buccal cirrus anterior of undulating membranes; 2 ventral cirral rows commence subapically and end at 40% and 25% of body length, respectively, composed of an average of 9 and 6 cirri, respectively. Right marginal row commences at level of buccal cirrus, composed of an average of 22 cirri, left of 16. Dorsal bristles about 3 µm long, form 3 rows, row 1 commences at level of buccal vertex; 3 caudal cirri. Adoral zone of membranelles gonostomoid, extends 36% of body length, proximal half covered by the distinctly convex buccal lip, composed of an average of 19 membranelles. Buccal cavity narrow. Paroral and endoral membrane side by side, the former composed of an average of 7 kinetids with 10 µm long cilia.

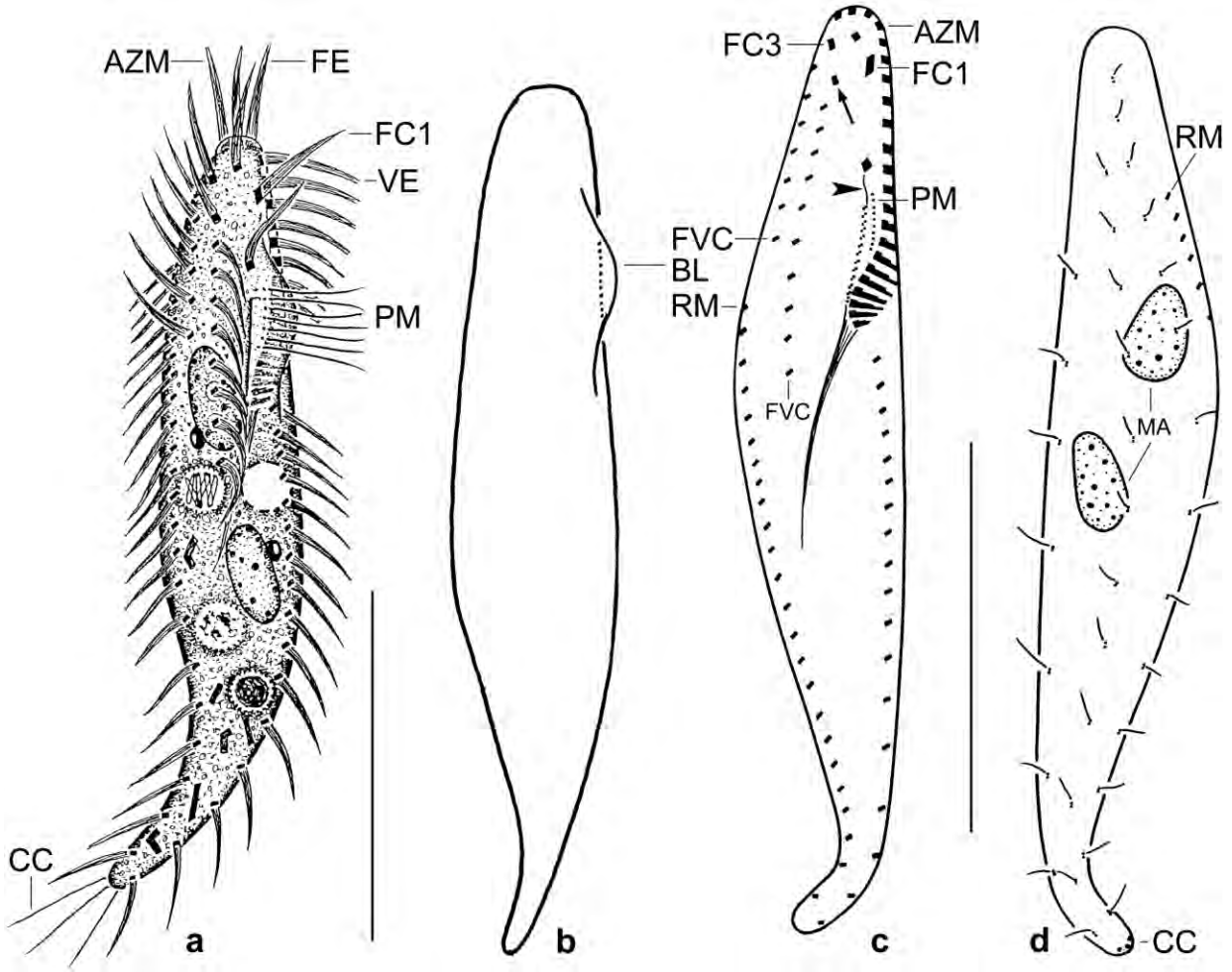

Fig. 188.1a–d. *Cladotricha chilensis* from life (a, b) and after protargol impregnation (c, d). **a:** Ventral view of a representative specimen, length 70 µm. Note the 10 µm long cilia of the paroral membrane and the tail-like posterior body region. **b:** Shape variant, showing the convex buccal lip. **c, d:** Ventral and dorsal view of holotype specimen, length 75 µm. The arrow marks cirrus III/2. The arrowhead denotes a fibre originating from the first endoral kinetid and extending to the buccal cirrus. AZM – adoral zone of membranelles, BL – buccal lip, CC – caudal cirri, FC1, 3 – frontal cirri, FE – frontal adoral membranelles, FVC – frontoventral cirral rows, MA – macronuclear nodules, PM – paroral membrane, RM – right marginal cirral row, VE – ventral adoral membranelles. Scale bars 30 µm.

Table 69a. Morphometric data on *Cladotricha chilensis* (CC), *Cladotricha australis* from Argentina (CAC), and *Cladotricha australis* from Australia (CAA; from BLATTERER & FOISSNER 1988). Data based on mounted, protargol-impregnated, and randomly selected specimens from non-flooded Petri dish cultures. Measurements in µm. CV – coefficient of variation in %, M – median, Max – maximum, Mean – arithmetic mean, Min – minimum, n – number of individuals investigated, SD – standard deviation, SE – standard error of arithmetic mean.

Characteristics	Population	Mean	M	SD	SE	CV	Min	Max	n
Body, length	CC	65.7	67.0	8.6	2.6	13.1	53.0	80.0	11
	CAC	77.5	78.0	7.8	2.2	10.1	69.0	92.0	13
	CAA	91.2	90.5	9.3	2.7	10.2	79.0	108.0	12
Body, width	CC	12.0	12.0	1.3	0.4	10.5	10.0	14.0	11
	CAC	20.9	21.0	2.3	0.6	10.8	18.0	25.0	13
	CAA	25.4	25.0	4.6	1.3	17.9	20.0	38.0	12
Body length:width, ratio	CC	5.5	5.5	0.6	0.2	11.3	4.3	6.7	11
	CAC	3.8	3.7	0.5	0.1	12.1	3.0	4.5	13
	CAA	3.6	–	–	–	–	–	–	12
Anterior body end to proximal end of adoral zone of membranelles, distance	CC	23.5	24.0	1.6	0.5	6.7	21.0	25.0	11
	CAC	24.8	25.0	2.1	0.6	8.4	21.0	29.0	13
	CAA	32.1	33.5	5.2	1.5	16.3	22.0	39.0	12
Body length:length of adoral zone of membranelles, percent	CC	36.1	37.0	3.6	1.1	10.1	31.0	43.0	11
	CAC	32.3	32.0	3.7	1.0	11.4	23.0	37.0	13
	CAA	35.2	–	–	–	–	–	–	12
Adoral membranelles, number	CC	18.7	19.0	0.9	0.3	4.8	17.0	20.0	11
	CAC	23.6	23.0	1.1	0.3	4.8	22.0	25.0	13
	CAA	24.3	25.0	2.5	0.7	10.1	20.0	27.0	12
Paroral kinetids, number	CC	6.7	7.0	1.0	0.3	14.2	5.0	8.0	7
	CAC	3.2	3.0	0.7	0.2	21.8	2.0	4.0	13
	CAA	2.0	–	–	–	–	3.0	4.0	12
Anterior body end to first macronuclear nodule, distance	CAC	7.5	7.0	2.1	0.6	28.0	5.0	12.0	13
Nuclear figure, length	CAC	53.2	53.0	5.1	1.4	9.6	47.0	62.0	13
Macronuclear nodules, number	CC	2.0	2.0	0.0	0.0	0.0	2.0	2.0	11
	CAC	21.2	18.0	7.0	1.9	32.9	14.0	34.0	13
	CAA	18.4	15.5	5.4	1.6	29.3	13.0	28.0	12
Macronuclear nodules, length	CC	9.6	10.0	1.9	0.6	19.8	7.0	12.0	11
	CAC	4.7	4.5	1.3	0.4	27.8	3.0	7.0	13
	CAA	5.1	4.5	1.8	0.5	35.0	3.0	9.0	12
Macronuclear nodules, width	CC	3.9	4.0	0.7	0.2	17.9	3.0	5.0	11
	CAC	2.0	2.0	–	–	–	2.0	3.0	13
	CAA	3.2	3.0	0.6	0.2	19.4	2.5	4.5	12
Micronuclei, number	CC	1.6	2.0	–	–	–	1.0	2.0	7
	CAC	2.4	2.0	0.7	0.2	27.3	2.0	4.0	13
	CAA	1.5	1.5	–	–	–	1.0	2.0	4
Micronuclei, length	CC	2.4	2.5	–	–	–	1.5	3.0	7
	CAC	1.7	1.5	–	–	–	1.5	2.0	13
	CAA	3.0	2.7	–	–	–	2.5	3.8	3
Micronuclei, width	CC	1.8	2.0	–	–	–	1.5	2.0	7

continued

Characteristics	Population	Mean	M	SD	SE	CV	Min	Max	n
	CAC	1.4	1.5	–	–	–	1.0	1.5	13
	CAA	1.9	1.6	–	–	–	1.5	2.7	3
Frontal cirri, number	CC	3.0	3.0	0.0	0.0	0.0	3.0	3.0	11
	CAC	3.0	3.0	0.0	0.0	0.0	3.0	3.0	13
	CAA	3.0	3.0	0.0	0.0	0.0	3.0	3.0	12
Buccal cirri, number	CC	1.0	1.0	0.0	0.0	0.0	1.0	1.0	11
	CAC	2.5	3.0	–	–	–	2.0	3.0	13
	CAA	3.3	3.0	1.0	0.3	29.7	1.0	5.0	12
Ventral row III, number of cirri	CC	1.0	1.0	0.0	0.0	0.0	1.0	1.0	11
	CAC	4.5	5.0	0.8	0.2	17.1	3.0	5.0	13
	CAA	4.3	4.0	1.1	0.3	24.6	3.0	7.0	10
Anterior body end to end of ventral row IV, distance	CC	26.5	26.0	4.4	1.3	16.7	20.0	34.0	11
Ventral row IV, number of cirri	CC	9.2	9.0	1.2	0.4	12.7	8.0	12.0	11
	CAC	18.2	18.0	2.8	0.8	15.2	12.0	22.0	13
	CAA	22.3	22.0	4.6	1.4	20.6	14.0	33.0	11
Anterior body end to end of ventral row V, distance	CC	15.1	15.0	2.6	0.8	17.4	11.0	20.0	11
Ventral row V, number of cirri	CC	6.3	6.0	0.6	0.2	10.3	5.0	7.0	11
	CAC	11.1	11.0	1.6	0.4	14.0	8.0	14.0	13
	CAA	18.3	18.0	3.7	1.1	20.1	14.0	26.0	12
Right marginal row, number of cirri	CC	22.5	22.0	1.9	0.6	8.3	20.0	26.0	11
	CAC	26.8	26.0	2.8	0.8	10.5	24.0	35.0	13
	CAA	26.2	25.5	5.0	1.4	19.1	20.0	39.0	12
Left marginal row, number of cirri	CC	15.8	16.0	1.7	0.5	10.9	14.0	18.0	11
	CAC	19.9	20.0	2.0	0.6	10.1	16.0	23.0	13
	CAA	22.3	22.0	4.6	1.4	20.6	14.0	33.0	11
Dorsal kineties, number	CC	3.0	3.0	0.0	0.0	0.0	3.0	3.0	11
	CAC	3.0	3.0	0.0	0.0	0.0	3.0	3.0	13
	CAA	3.0	3.0	0.0	0.0	0.0	3.0	3.0	11
Caudal cirri, number	CC	3.0	3.0	0.0	0.0	0.0	3.0	3.0	4
	CAC	not well recognizable, likely 3							
	CAA	2.3	3.0	1.2	0.5	51.9	0?	3.0	6

Type locality: Highly saline soil from the bank of the Rio Loa near to the town of Calama, Chile, 69°W 23°S.

Type material: 1 holotype and 2 paratype slides with protargol-impregnated specimens have been deposited in the Biology Centre of the Upper Austrian Museum in Linz (LI). The holotype and other relevant specimens have been marked by black ink circles on the coverslip.

Etymology: Named after the country in which it was discovered.

Description: *Cladotricha chilensis* was rather rare in the non-flooded Petri dish culture. Further, it was very fragile and became strongly inflated in ordinary protargol preparations. Thus, we made a second fixation with osmic acid. This stabilized the body but the infraciliature became poorly impregnated. Thus, we combined both preparations: osmic acid for body shape and related features (e. g., length of adoral zone), Stieve´s fluid for the infraciliature. But we obtained only 11 specimens for the morphological and morphometric analysis. All these drawbacks suggest a redescription based on more and better preserved specimens.

Size in vivo about 60–90 × 10–15 µm, usually about 70 × 13 µm, as calculated from some in vivo measurements and the morphometric data in Table 69a adding 10% preparation shrinkage. Body very elongate ellipsoid with broadest site slightly posterior to mid-body and tail-like narrowed posterior region; laterally not or slightly flattened (Fig. 188.1a–c; Table 69a). Nuclear apparatus in central third of body. Two broadly to ordinarily ellipsoid macronuclear nodules with many minute nucleoli. One to two micronuclei attached to macronuclear nodules, broadly ellipsoid on average, rarely impregnated with the protargol method used (Fig. 188.1a, d; Table 69a). Contractile vacuole in mid-body at left body margin (Fig. 188.1a). Cortex very flexible but not contractile, without specific granules. Cytoplasm colourless, contains some yellowish crystals mainly in tail region. Feeds on bacteria digested in vacuoles 4–6 µm across. Creeps and swims slowly rotating about main body axis.

Cirri arranged in *Cladotricha* or *Paragonostomum* pattern shown by Berger (2011), i. e., in two frontoventral rows and one right and left marginal row; most cirri 8–10 µm long in vivo and composed of two rows with three basal bodies each (Fig. 188.1a, c; Table 69a). Three enlarged frontal cirri, first distinctly subapical and markedly enlarged; cirrus III/2 slightly enlarged, on top or slightly left of left frontoventral cirral row; buccal cirrus anterior of undulating membranes. Frontoventral cirral rows right of body´s midline, commence subapically, left row extends about 40% of body length, right 25%, composed of an average of 9 and 6 cirri, respectively. Right marginal row commences at level of buccal cirrus, composed of an average of 22 cirri with intracirral distances distinctly increasing in posterior region; left marginal row as right but composed of only 16 cirri on average (Fig. 188.1a, c; Table 69a).

Dorsal bristles in vivo 3 µm long, loosely spaced, form three rows each with an about 15 µm long, fine caudal cirrus. Row 1 commences at level of buccal vertex, row 2 far subapically, and row 3 subapically (Fig. 188.1d; Table 69a).

Oral apparatus in *Gonostomum* pattern (Berger 1999), i. e., adoral zone flat and following anterior and left body margin before bending abruptly into cell at 36% of body length; zone composed of an average of 19 membranelles, frontal membranelles strongly beating, about 10 µm long, not separated from almost immobile ventral membranelles with cilia about 10 µm long in anterior half (Fig. 188.1a, c; Table 69a). Buccal cavity short and narrow, covered by the distinctly convex buccal lip. Endoral membrane on dorsal wall of buccal cavity, composed of dikinetids, anterior dikinetid with a short fibre touching buccal cirrus. Paroral membrane on convex part of buccal lip, conspicuous because composed of an average of 7 kinetids with 10 µm long cilia. Pharyngeal fibres distinct in vivo and in protargol preparations, extend slightly obliquely to mid-body, possibly mixed with long endoral cilia (Fig. 188.1a, c; Table 69a).

Table 69b. Morphometric data on *Cladotricha edaphoni* (upper line) and *Cladotricha digitata* (lower line) based on mounted, protargol-impregnated, and randomly selected specimens from non-flooded Petri dish cultures. Measurements in µm. CV – coefficient of variation in %, M – median, Max – maximum, Mean – arithmetic mean, Min – minimum, n – number of individuals investigated, SD – standard deviation, SE – standard error of arithmetic mean.

Characteristics	Mean	M	SD	SE	CV	Min	Max	n
Body, length in vivo (crude measurements)	104.0	–	–	–	–	70.0	130.0	8
	116.7	–	–	–	–	110.0	120.0	3
Body, width in vivo (crude measurements)	19.4	–	–	–	–	15.0	25.0	8
	30.0	–	–	–	–	25.0	35.0	3
Body, length	74.9	73.0	8.7	1.9	11.7	59.0	93.0	21
	79.7	78.0	8.0	1.7	10.0	66.0	94.0	21
Body, width	14.0	14.0	1.9	0.4	13.5	10.0	17.0	21
	21.8	22.0	2.2	0.5	10.1	18.0	25.0	21
Body length:width, ratio	5.4	5.4	0.6	0.1	10.8	4.5	6.5	21
	3.7	3.7	0.3	0.1	8.6	3.1	4.3	21
Anterior body end to proximal end of adoral zone of membranelles, distance	20.7	21.0	1.5	0.3	7.3	18.0	24.0	21
	24.5	25.0	1.0	0.2	4.3	22.0	27.0	21
Body length:length of adoral zone, percent	27.9	28.0	2.8	0.6	10.2	23.0	33.0	21
	31.1	31.0	3.0	0.7	9.8	26.0	38.0	21
Adoral membranelles, number	17.6	18.0	0.9	0.2	5.0	16.0	19.0	21
	23.0	23.0	1.2	0.3	5.2	21.0	25.0	21
Anterior body end to paroral membrane, distance	13.8	14.0	1.8	0.4	13.0	11.0	19.0	21
	16.3	16.5	1.2	0.3	7.4	14.0	18.0	14
Paroral membrane, number of kinetids	2.7	3.0	0.8	0.2	27.9	2.0	4.0	19
	2.9	3.0	0.8	0.2	28.3	1.0	4.0	14
Anterior body end to endoral membrane, distance	14.3	14.0	1.8	0.4	12.3	12.0	20.0	21
	17.0	17.0	1.3	0.3	7.7	15.0	19.0	16
Anterior body end to first macronuclear nodule, distance	8.0	8.0	1.6	0.3	19.5	5.0	12.0	21
	13.9	13.0	2.6	0.6	18.7	11.0	18.0	17
Anterior macronuclear nodule, length	4.1	4.0	1.5	0.3	37.9	2.0	7.0	21
	7.4	7.0	1.0	0.2	13.0	5.0	10.0	21
Anterior macronuclear nodule, width	1.7	2.0	0.4	0.1	21.6	1.0	3.0	21
	4.5	4.5	–	–	–	4.0	5.0	21
Macronuclear nodules, number	19.9	20.0	3.4	0.7	17.1	15.0	26.0	21
	4.0	4.0	0.0	0.0	0.0	4.0	4.0	21
Anteriormost micronucleus, length	1.5	1.5	–	–	–	1.0	2.0	11
	1.5	1.5	–	–	–	1.0	2.0	21
Anteriormost micronucleus, width	1.1	1.0	–	–	–	1.0	1.5	11
	1.1	1.0	–	–	–	1.0	1.5	21
Micronuclei, number	3.0	3.0	0.8	0.2	25.8	2.0	4.0	11
	1.9	2.0	0.6	0.1	32.8	1.0	4.0	21
Anterior body end to buccal cirrus, distance	11.4	11.5	0.9	0.2	7.7	9.0	14.0	20
	12.9	13.0	1.1	0.3	8.7	11.0	15.0	16
Anterior body end to end of ventral row III, distance	11.2	12.0	2.3	0.5	20.7	6.0	14.0	21
	14.3	15.0	2.0	0.5	14.2	11.0	19.0	17

continued

Characteristics	Mean	M	SD	SE	CV	Min	Max	n
Ventral row III, number of cirri	2.8	3.0	–	–	–	2.0	3.0	21
	5.0	5.0	0.5	0.1	10.1	4.0	6.0	21
Anterior body end to end of ventral row IV, distance	38.8	39.0	4.9	1.1	12.7	29.0	48.0	21
	62.7	61.0	8.7	2.1	13.9	53.0	80.0	17
Ventral row IV, number of cirri	13.7	14.0	1.4	0.3	10.4	11.0	16.0	21
	18.8	18.0	2.6	0.6	14.0	16.0	25.0	21
Anterior body end to end of ventral row V, distance	7.9	8.0	1.5	0.3	18.8	6.0	12.0	21
	10.4	10.0	1.9	0.5	18.7	7.0	15.0	17
Ventral row V, number of cirri	4.1	4.0	–	–	–	4.0	5.0	21
	3.7	4.0	–	–	–	3.0	4.0	21
Buccal cirri, number	1.0	1.0	0.0	0.0	0.0	1.0	1.0	21
	1.0	1.0	0.0	0.0	0.0	1.0	1.0	21
Frontal cirri, number	3.0	3.0	0.0	0.0	0.0	3.0	3.0	21
	3.0	3.0	0.0	0.0	0.0	3.0	3.0	21
Anterior body end to right marginal cirral row, distance	8.4	8.0	1.5	0.3	17.6	6.0	12.0	21
	9.9	10.0	1.5	0.4	15.6	6.0	12.0	17
Posterior body end to right marginal cirral row, distance	1.2	1.0	–	–	–	0.5	2.0	19
	1.6	1.0	0.8	0.2	50.1	1.0	3.0	17
Right marginal row, number of cirri	29.1	29.0	3.5	0.8	12.0	23.0	38.0	21
	25.1	25.0	2.8	0.6	11.1	21.0	31.0	21
Posterior body end to left marginal row, distance	0.5	0.5	–	–	–	0.0	1.0	19
	1.3	1.0	–	–	–	1.0	2.0	17
Left marginal row, number of cirri	22.4	22.0	3.0	0.7	13.4	17.0	29.0	21
	20.8	21.0	2.8	0.6	13.6	17.0	27.0	21
Dorsal kineties, number	3.0	3.0	0.0	0.0	0.0	3.0	3.0	21
	3.0	3.0	0.0	0.0	0.0	3.0	3.0	21
Dorsal kinety 1, number of kinetids	11.1	11.0	1.7	0.4	15.4	8.0	14.0	20
	17.9	18.0	1.5	0.4	8.6	15.0	20.0	17
Dorsal kinety 2, number of kinetids	13.5	14.0	1.6	0.4	12.2	11.0	17.0	20
	17.1	17.0	1.7	0.4	10.1	14.0	20.0	17
Dorsal kinety 3, number of kinetids	18.8	19.0	1.9	0.4	10.2	15.0	22.0	21
	24.1	24.0	2.4	0.6	9.8	18.0	29.0	16
Caudal cirri, number	3.0	3.0	0.0	0.0	0.0	3.0	3.0	18
	3.0	3.0	0.0	0.0	0.0	3.0	3.0	21

Occurrence and ecology: As yet found only at type locality. The sample consisted of highly saline (> 30‰), red, very sandy soil and some plant residues.

Remarks: The generic classification of *C. chilensis* is uncertain because the genera *Paragonostomum* and *Cladotricha* are insufficiently separated (Berger 2011). To be sure that our population represents a new species, we compared the species of both genera using the monograph of Berger (2011).

Cladotricha australis Blatterer & Foissner, 1988 (Table 69a)

Material: Highly saline (> 30‰) soil from the Atlantic coast in the surroundings of the town of San Julián, Argentina, 68°W 48°S. Three voucher slides with protargol-impregnated specimens have been deposited in the Biology Centre of the Upper Austrian Museum in Linz (LI). Relevant specimens have been marked by black ink circles on the coverslip.

Remarks: The Argentinian specimens match perfectly the Australian population in all main features. Only ventral cirral row 5 (anlage V) is distinctly shorter and has thus less cirri (mean: 11 vs. 18; extremes: 8–14 vs. 14–26; Table 69a). Considering the rather high variation coefficients (CV = 14 vs. 20%), this difference is insufficient to separate the two populations at subspecies or species level.

Cladotricha edaphoni Wilbert, 1995 (Fig. 188.2a–d, 188.3a–d; Table 69b)

Material: 4 voucher slides with protargol-impregnated specimens from Venezuelan site (65) have been deposited in the Biology Centre of the Upper Austrian Museum in Linz (LI). Relevant specimens have been marked by black ink circles on the coverslip.

Improved diagnosis (includes Wilbert´s data): Size in vivo about 100 × 17 µm. Elongate ellipsoid with posterior third distinctly narrowed. On average 17–20 scattered, ellipsoid macronuclear nodules and 3–4 micronuclei. 3 frontal cirri, first distinctly subapical and enlarged; 1 buccal cirrus far anterior of paroral membrane; 3 ventral cirral rows, rows III and V strongly shortened, each composed of 3 to 8 cirri; row IV commences far subapically and extends to mid-body, composed of 14–18 cirri on average; 3 caudal cirri. Right marginal row composed of an average of 25–29 cirri, left row of 19–22. Dorsal bristles about 2 µm long; in 3 rows, row 1 commences at level of buccal vertex. Adoral zone gonostomoid, proximal third covered by strongly convex buccal lip, extends about 28–34% of body length, composed of an average of 18–21 membranelles. Buccal cavity minute; paroral membrane composed of 2–4 kinetids.

Description: We provide a full description of the Venezuelan population because Wilbert´s description is rather incomplete (see Remarks section).

Cladotricha edaphoni has a moderate variability with most variation coefficients smaller than 15%. Up to 20% and more concern mainly distances and the nuclear apparatus.

Size in vivo 70–130 × 15–25 µm, usually about 100 × 17 µm; shrunken to 59–93 × 10–17 µm, on average 75 × 14 µm in protargol preparations, mainly due to ethanol fixation (Table 69b). Body elongate ellipsoid with widest site slightly posterior to mid-body, just before distinctly narrowing posteriorly; more or less curved and sometimes slightly contorted about main body axis, especially when just taken from soil; slightly flattened dorsoventrally (Fig. 188.2a, b, 188.3a–d; Table 69b). Nuclear apparatus in central quarters of cell. On average 20 globular to elongate ellipsoid, scattered macronuclear nodules with conspicuous nucleoli. Two to four micronuclei scattered among macronuclear nodules, broadly to ordinarily ellipsoid, rarely lightly impregnated with the protargol method used (Fig. 188.2a, d, 188.3a–d; Table 69b). Contractile vacuole not recognizable, very likely due to the high salinity. Cortex very flexible, without specific granules.

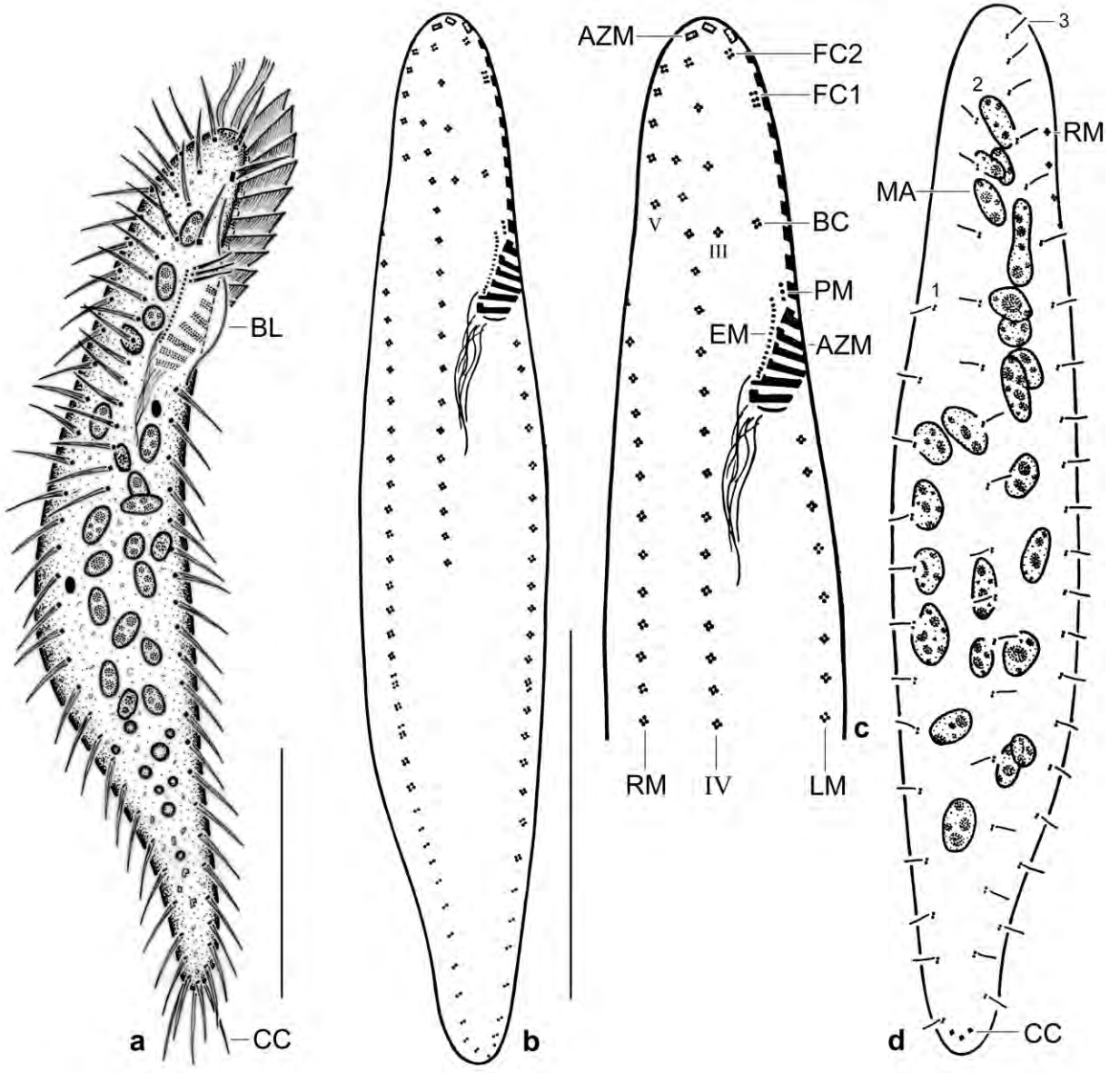

Fig. 188.2a–d. *Cladotricha edaphoni* from life (a) and after protargol impregnation (b–d). **a:** Ventral view of a representative specimen, length 100 µm. The strongly convex buccal lip projects from body proper and covers the proximal third of the adoral zone of membranelles. **b–d:** Ventral and dorsal view of holotype specimen, length 83 µm. Frontal cirrus 1 is gonostomoid (far subterminal and enlarged) and the paroral membrane consists of only three kinetids. AZM – adoral zone of membranelles, BC – buccal cirrus, BL – buccal lip, CC – caudal cirri, EM – endoral membrane, FC1, 2 – frontal cirri, LM – left marginal row, MA – macronuclear nodules, PM – paroral membrane, RM – right marginal cirral row, 1, 2, 3 – dorsal kineties, III, IV, V – ventral cirral rows originating from anlagen III, IV, and V. Scale bars 30 µm.

Cytoplasm colourless, bright, contains some small lipid droplets and crystals mainly in posterior quarter of cell; likely feeds on bacteria (Fig. 188.2a). Glides moderately rapid on microscope slides and between soil particles, showing pronounced flexibility.

Cirri arranged in *Cladotricha* pattern shown by Berger (2011), i. e., in five anlagen or rows with all cirri composed of only four cilia (basal bodies) about 7 µm long in vivo, except of frontal cirrus 1 (six basal bodies) and marginal cirri (two basal bodies) in posterior quarter of rows (Fig.

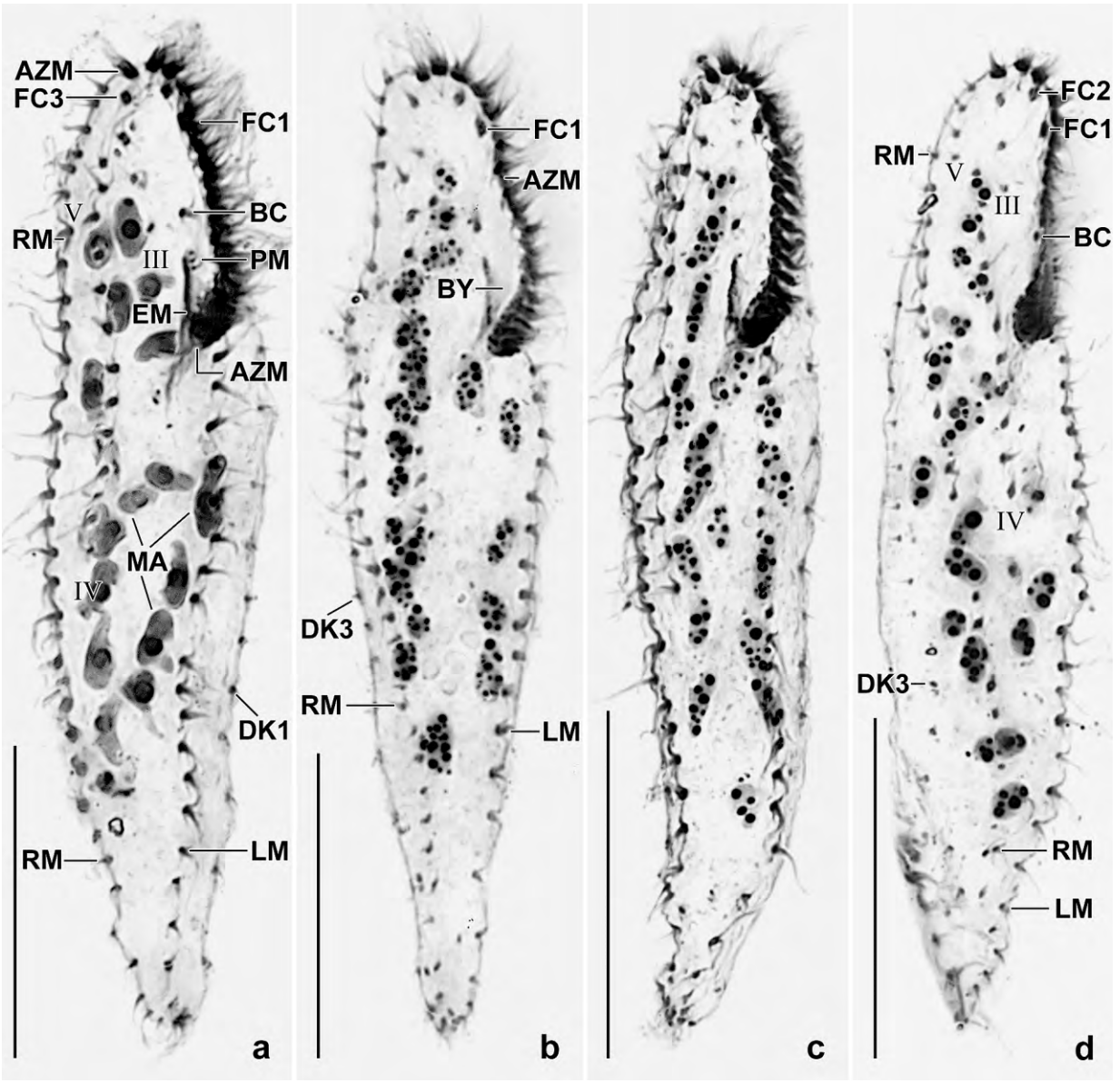

Fig. 188.3a–d. *Cladotricha edaphoni*, ventral views of protargol-impregnated specimens. Note the slender body, the many macronuclear nodules, the subapically located and enlarged frontal cirrus 1, the three ventral cirral rows (III, IV, V), the gonostomoid adoral zone, the minute buccal cavity and paroral membrane, and the absence of transverse cirri. The specimen shown in (d) is slightly contorted about the main body axis. AZM – adoral zone of membranelles, BC – buccal cirrus, BY – buccal cavity, DK1, 3 – dorsal kineties, EM – endoral membrane, FC1–3 – frontal cirri, LM – left marginal row, MA – macronuclear nodules, PM – paroral membrane, RM – right marginal cirral row, III, IV, V – ventral cirral rows originating from anlagen III, IV, and V. Scale bars 25 µm.

188.2a–c, 188.3a–d; Table 69b). Anlage I produces frontal cirrus 1 located far subapically; anlage II produces frontal cirrus 2 and a single buccal cirrus far anteriorly of undulating membranes; anlage III produces frontal cirrus 3 and two to three cirri forming a short row; anlage IV longest, composed of an average of 14 cirri, commences far subapically and ends slightly posterior of mid-body; anlage V composed of four to five cirri forming a short row commencing subapically. Right marginal row commences about 8 µm subapically and extends to posterior body end as does left row (Fig. 188.2a–c, 188.3a–d; Table 69b).

Dorsal bristles about 2 µm long in vivo, arranged in three rows each associated with a caudal cirrus composed of four, in vivo 10 µm long cilia. Row 1 commences at level of buccal vertex, row 2 subapically, and row 3 near anterior body end; all rows end subterminally (Fig. 188.2a, d, 188.3a, b, d; Table 69b).

Oral apparatus in *Gonostomum* pattern (Berger 1999), i. e., adoral zone flat and following anterior and ventral body margin before bending abruptly into cell at about 28% of body length; zone composed of an average of 18 membranelles with cilia of frontal membranelles in vivo about 10 µm long; frontal and ventral membranelles not separated by a gap (Fig. 188.2a–c, 188.3a–d; Table 69b). Buccal cavity very short and narrow, cavity and proximal third of adoral zone covered by the distinctly convex buccal lip. Endoral membrane slightly curved, composed of about 10 kinetids; paroral membrane left of anterior end of endoral, composed of only two to four kinetids. Pharyngeal fibres distinct in protargol preparations, extend vertically to mid-body (Fig. 188.2a–c, 188.3a–d; Table 69b).

Occurrence and ecology: Wilbert (1995) discovered *C. edaphoni* in the Coorong National Park between the towns of Adelaide and Kingston, Australia. The sample was from a dry salt lake with pH 8.8 and a salinity between 26 and 57‰. We found *C. edaphoni* in a highly saline (50‰, pH 5.8) soil sample (65) from the north coast of Venezuela. It became numerous in the non-flooded Petri dish culture. Obviously, *C. edaphoni* is a hypersaline species well adapted to soil by the slender and very flexible body.

Remarks: In his valuable review, Berger (2011) synonymized *Cladotricha edaphoni* Wilbert, 1995 with *C. australis* Blatterer & Foissner, 1988. We disagree mainly because of the different length of ventral row V (extends to level of buccal cirrus vs. to near posterior body end). Obviously, this feature is constant across continents.

Most morphometrics of the Australian and Venezuelan specimens match well, except of body size in vivo which is 90–125 × 32–49 µm. While the length match well, the width does not (Table 69b). In our opinion, this has two reasons: (i) Wilbert´s protargol method is excellent but tends to inflate the specimens, (ii) although stated as "in vivo" measurements in the diagnosis, the values are the same as in his Table 10 where the measurements are "based on protargol-impregnated specimens". Very likely, the same applies to his in vivo figure of *C. edaphoni*. He did not recognize the large buccal lip and the body shape appears too general.

Taken together, we are convinced about the identification because the mismatches can be explained by the sloppy observations of Wilbert (1995).

Cladotricha digitata nov. spec. (Fig. 188.4a–h, 188.5a–g; Table 69b)

Diagnosis: Size in vivo about 100 × 25 µm. Elongate ellipsoid to indistinctly pisciform with posterior fifth distinctly narrowed. 4 broadly ellipsoid macronuclear nodules in 2 pairs right of body`s midline and 2 micronuclei. Bases of cirri and dorsal bristles surrounded by colourless granules about 1× 0.5 µm in size. 3 frontal cirri, first subapical and occasionally slightly enlarged; 1 buccal cirrus anterior of undulating membranes; 3 ventral cirral rows, rows III and V short

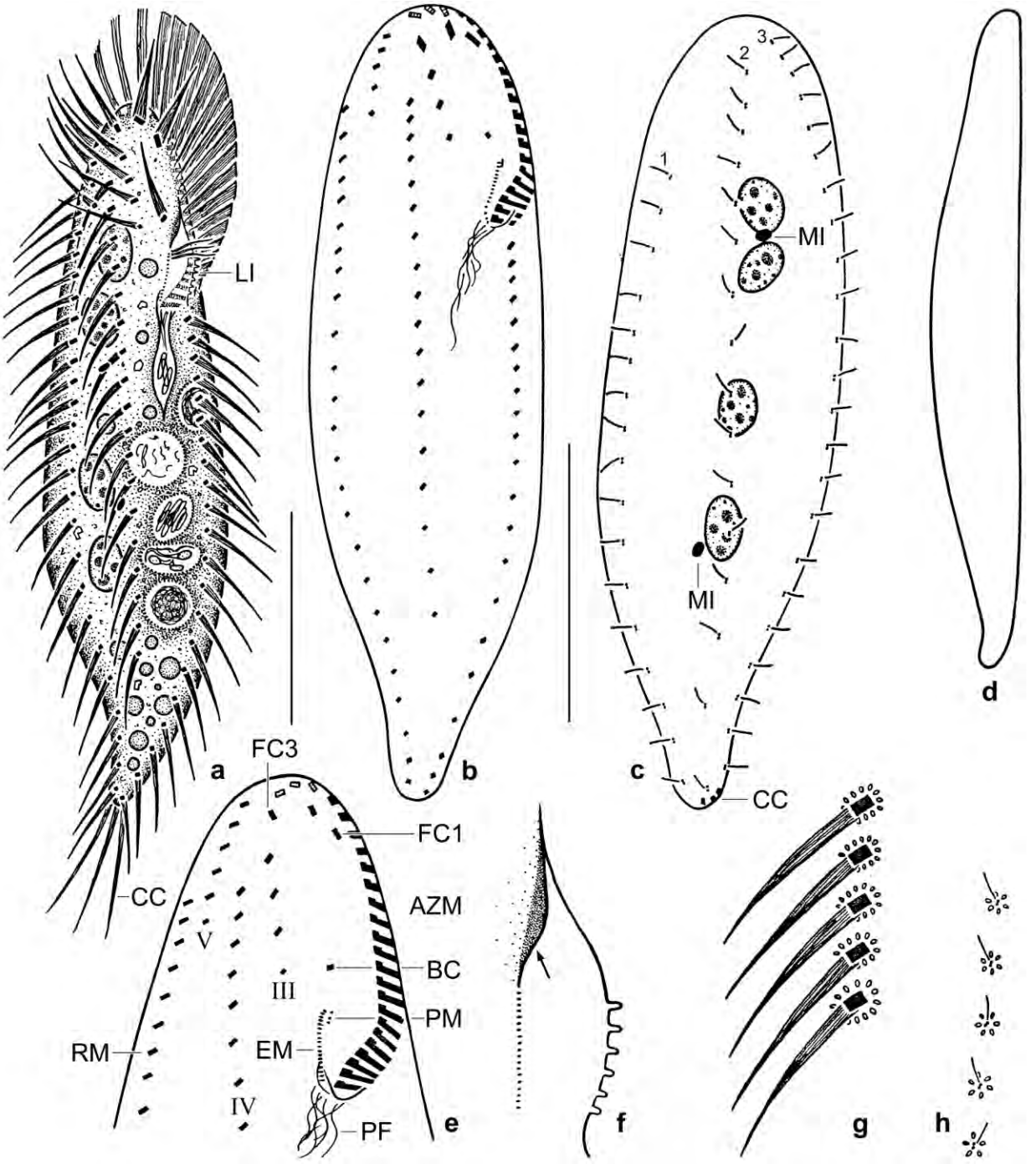

Fig. 188.4a–h. *Cladotricha digitata*, Costa Rican specimens from life (a, d, f–h) and after protargol impregnation (b, c, e). **a:** Ventral view of a representative specimen, length 100 µm. **b, c, e:** Ventral and dorsal view of holotype specimen, length 88 µm, and oral area of a paratype specimen (e). There are five frontoventral cirral rows/anlagen (III, IV, V); anlage I is the first frontal cirrus, anlage II is the second frontal cirrus and the buccal cirrus. Note the minute paroral membrane consisting of only three kinetids (e). **d:** Lateral view. **f:** The buccal lip has a digitate margin. The arrow marks a thickened, bright structure. **g, h:** The bases of cirri and dorsal bristles are surrounded by colourless granules. AZM – adoral zone of membranelles, BC – buccal cirrus, CC – caudal cirri, EM – endoral membrane, FC1, 3 – frontal cirri, LI – buccal lip, MI – micronuclei, PF – pharyngeal fibres, PM – paroral membrane, RM – right marginal cirral row, 1, 2, 3 – dorsal kineties, III, IV, V – cirral rows originating from anlagen III, IV, and V. Scale bars 30 µm.

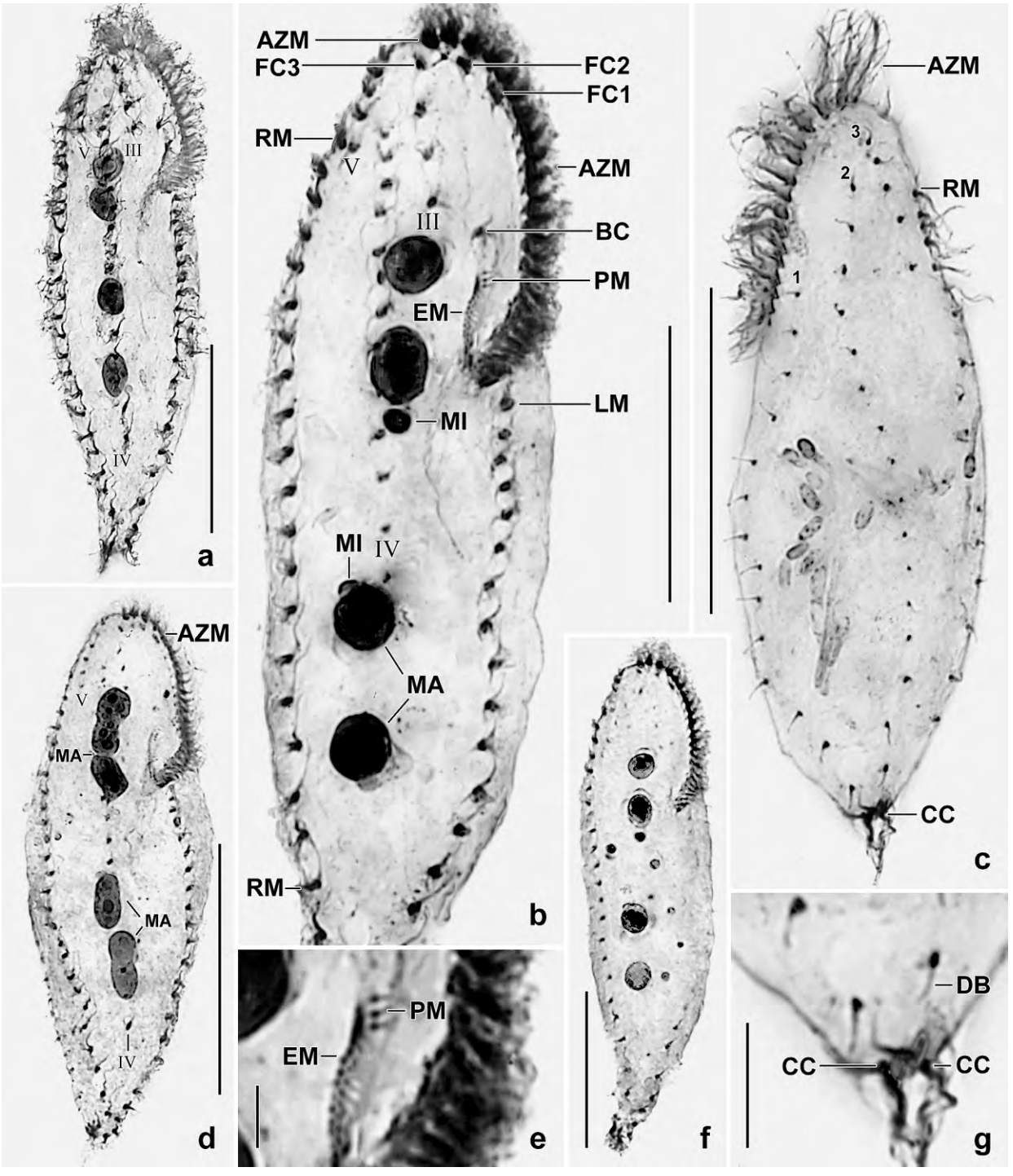

Fig. 188.5a–g. *Cladotricha digitata* after protargol impregnation. **a, d, f:** Ventral overviews, showing body shape, the gonostomoid adoral zone, the arrangement of the cirri and, especially, the four macronuclear nodules. **b, e:** Ventral overview and detail, showing, inter alia, the cirral rows III, IV, V and the minute paroral membrane. **c, g:** Dorsal overview and detail. There are three dorsal kineties each with a caudal cirrus; kinety 1 is distinctly shortened anteriorly and the right marginal row commences 10 µm subapically. AZM – adoral zone of membranelles, BC – buccal cirrus, CC – caudal cirri, DB – dorsal bristle, EM – endoral membrane, FC1–3 – frontal cirri, LM – left marginal cirral row, MA – macronuclear nodules, MI – micronuclei, PM – paroral membrane, RM – right marginal cirral row, 1, 2, 3 – dorsal kineties, III, IV, V – cirral rows originating from anlagen III, IV, and V. Scale bars 2 µm (e), 5 µm (g), 20 µm (b), and 30 µm (a, c, d, f).

each composed of about 5 cirri, row IV commences subapically and extends about 80 % of body length, composed of 18 cirri on average. Right marginal row composed of 25 cirri on average, left of 21. Dorsal bristles about 4 µm long, form 3 rows, row 1 commences at level of buccal vertex; 3 caudal cirri. Adoral zone gonostomoid, proximal quarter covered by a convex buccal lip with digitate margin, composed of an average of 23 membranelles. Buccal cavity narrow; paroral membrane composed of 3 kinetids on average.

Type locality: Highly saline (~ 100‰) soil from a dry lagoon in the Santa Rosa National Park, Costa Rica, 35°38'W 10°50'N.

Type material: 1 holotype and 2 paratype slides with protargol-impregnated specimens have been deposited in the Biology Centre of the Upper Austrian Museum in Linz (LI). The holotype and other relevant specimens have been marked by black ink circles on the coverslip.

Etymology: The Latin adjective *digitata* (finger-shaped) refers to the curious processes of the buccal lip.

Description: *Cladotricha digitata* has a moderate variability with most variation coefficients smaller than 15%. Up to 20% and more are several distances and features composed of few structures, e. g., the paroral membrane.

Size in vivo 75–120 × 20–30 µm, usually about 100 × 25 µm, as calculated from some live measurements and the morphometric data (Table 69b) adding 15% preparation shrinkage. Body shape moderately variable, basically elongate ellipsoid with posterior region distinctly narrowed and curved right, producing a pisciform outline with widest region at begin of last third, i. e., just before narrowing (Fig. 188.4a, d, 188.5a, f; Table 69b). Nuclear apparatus in central quarters of cell right of midline. Invariably four globular to ellipsoidal, on average broadly ellipsoid macronuclear nodules usually in two distinct pairs and with ordinary nucleoli. Micronuclei between and outside of macronuclear nodules, broadly ellipsoid, rarely impregnated with the method used (Fig. 188.4a, c, 188.5a, b, d, f; Table 69b). Contractile vacuole not recognizable, very likely due to the high salinity. Cortex very flexible, with bright granules around bases of adoral membranelles, cirri, and dorsal bristles; individual granules colourless and oblong with a size of about 1 × 0.5 µm in vivo (Fig. 188.4g, h); do not impregnate with the method used. Cytoplasm colourless, contains some crystals and lipid droplets both 1–4 µm in size and concentrated in posterior region. Food vacuoles globular to ellipsoid, 5–10 µm in size, most with compact contents consisting of bacteria ordered side by side in the ellipsoidal vacuoles; rarely vacuoles with loose contents (Fig. 188.4a). Glides slowly on microscope slides and between soil particles, showing high flexibility.

Cirri arranged in *Cladotricha* pattern shown by Berger (2011), i. e., in five anlagen or rows with most cirri composed of four to six cilia (basal bodies) about 12 µm long in vivo (Fig. 188.4a, b, e, 188.5a, b, d, f; Table 69b). Subapically three frontal cirri distinctly enlarged in about one third of cells. Anlage I produces frontal cirrus 1 located distinctly subapical; anlage II produces frontal cirrus 2 and a single buccal cirrus distinctly anterior of undulating membranes; anlage III generates frontal cirrus 3 and an average of five cirri forming a short row; anlage IV longest, composed of an average of 18 cirri, commences distinctly subapical and ends at 80% of body

length; anlage V composed of three to four cirri forming a short row commencing subapically and extending near right body margin. Right marginal row commences about 12 µm subapically and extends to near posterior body end as does left row (Fig. 188.4a, b, e, 188.5a, b, d, f; Table 69b).

Dorsal bristles 3–4 µm long in vivo, arranged in three rows each associated with a caudal cirrus about 20 µm long in vivo. Row 1 commences at level of buccal vertex, row 2 subapically, and row 3 near anterior body end; all rows extend to near posterior body end (Fig. 188.4c, h, 188.5c, g; Table 69b).

Oral apparatus in *Gonostomum* pattern (Berger 1999), i. e., adoral zone flat and following anterior and left body margin before bending abruptly into cell at 31% of body length; zone composed of an average of 23 membranelles with cilia of frontal membranelles about 15 µm long in vivo; frontal and ventral membranelles not separated by a gap (Fig. 188.4a, b, e, f, 188.5a, b, d–f; Table 69b). Buccal cavity short and narrow, with a bright thickening in dorsal anterior region; cavity and proximal third of adoral zone covered by a convex buccal lip with distal margin having about 1 µm long digitate processes (Fig. 188.4f). Endoral membrane short and straight; paroral membrane left of anterior end of endoral, composed of one to four, on average three kinetids with 6 µm long cilia. Pharyngeal fibres distinct in protargol preparations, extend vertically to mid-body.

Occurrence and ecology: As yet found only at type locality, a highly saline habitat containing several undescribed ciliate species.

Remarks: *Cladotricha digitata* has a special feature, viz., digitate processes on the buccal lip as yet known from only one other genus, *Schmidingerophrya* Foissner, 2012a, a very curious ciliate lacking most of the "typical" hypotrich features, even the dorsal bristles. This supports the evolutionary scenario suggested by Foissner et al. (2014a) that *Cladotricha* is sister to *Schmidingerophrya* with evolving dorsal bristles as main apomorphy. Interestingly, other *Cladotricha* species lack the processes, suggesting their loss as a further evolutionary step conducting to the gonostomatids. As the processes are difficult to recognize, we can state this only for *C. halophila* where we definitely looked for this feature.

The identity of the species *Cladotricha koltzowii* Gaievskaia, 1925 is uncertain (Berger 2011). Our specimens lack three features of the type population (see Berger 2011 for a review of all species and authors mentioned in our discussion): a needle-like tail, a row of about 10 cirri close to the adoral zone of membranelles, and two distinctly elongated frontal membranelles. Later, Ruinen (1938) redescribed *C. koltzowii*. Again, there are three mismatches with our specimens: a short but sharp tail, frontal and ventral adoral membranelles separated by a distinct gap, and two distinctly elongated frontal membranelles. Finally, Borror & Evans (1979) redescribed *C. koltzowii* using a special nigrosin stain and protargol impregnation. The cirral pattern of the North American specimens matches our data while the long paroral membrane does not. Accordingly, the Costa Rican population is a new species.

Cladotricha halophila Wilbert, 1995 (Fig. 188.6a–d, 188.7a–f, 188.8a–j, 188.9a–n; Tables 69c, d)

Material: Highly saline soils from Venezuelan site (65) and Costa Rican site (28), i. e., litter and grass roots from a highly saline, dry lagoon on the coast of the Santa Rosa National Park (35°38'W 10°50'N). Three (Venezuela) and 3 (Costa Rica) voucher slides with protargol-impregnated morphostatic and dividing specimens have been deposited in the Biology Centre of the Upper Austrian Museum in Linz (LI). The specimens illustrated and other relevant cells have been marked by black ink circles on the coverslip.

Improved diagnosis (based on three populations): Size in protargol preparations 138 × 30 µm (Australian type pop.; AU) or about 70 × 20 µm (Venezuelan and Costa Rican pop.; VE, CR).

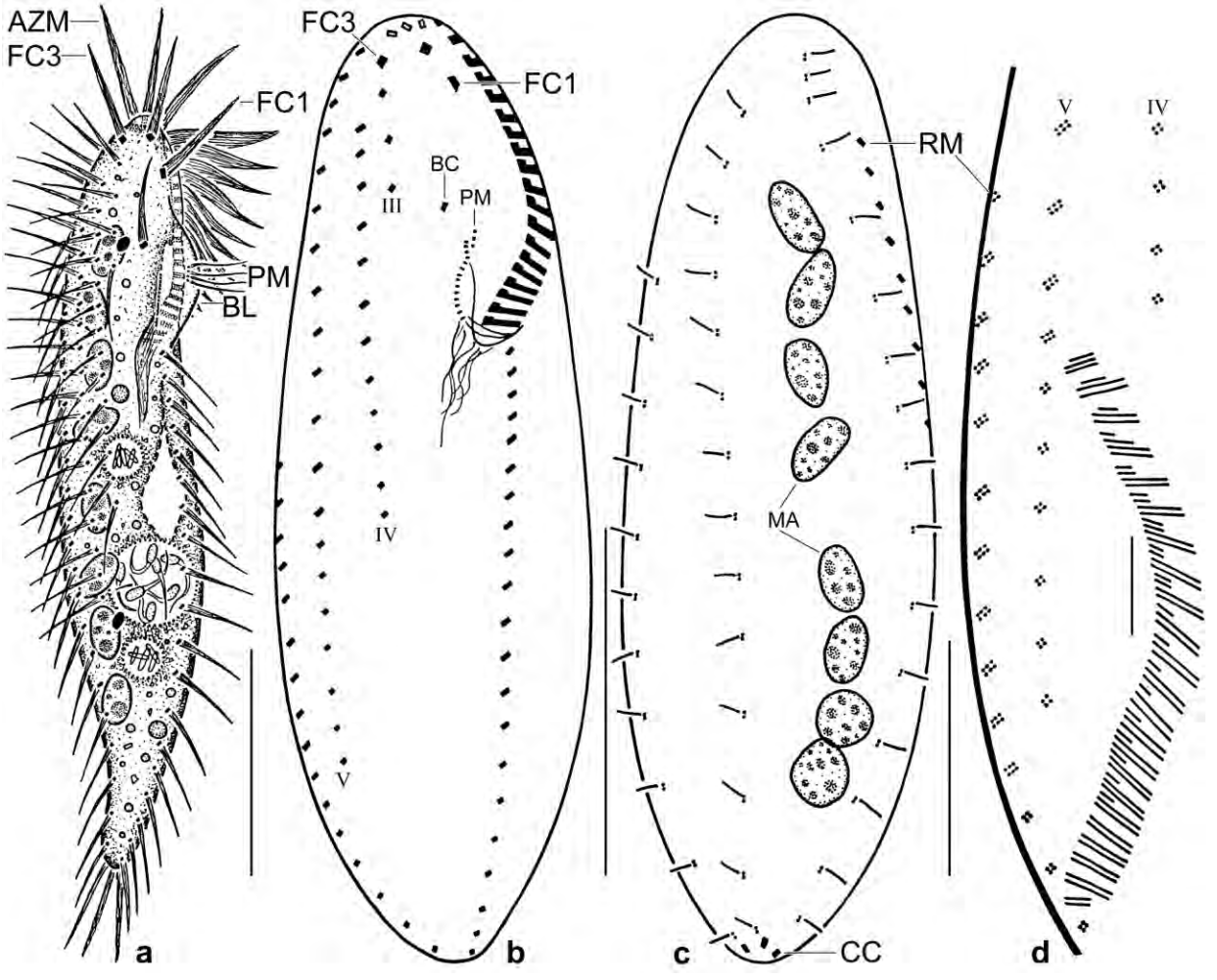

Fig. 188.6a–d. *Cladotricha halophila* from life (a) and after protargol impregnation (b–d). **a:** Ventral view of a representative specimen, length 100 µm. The buccal lip covers the proximal half of the adoral zone of membranelles and the three frontal membranelles appear like thick cirri. **b–d:** Ventral and dorsal view of holotype specimen (b, c), length 70 µm. The cirri are composed of four to six basal bodies (d) and the adoral zone of membranelles of a late divider, shown in Fig. 188.8i, is highly differentiated (d, inset). AZM – adoral zone of membranelles, BC – buccal cirrus, BL – buccal lip, CC – caudal cirri, FC1, 3 – frontal cirri, MA – macronuclear nodules, PM – paroral membrane, RM – right marginal cirral row, III, IV, V – cirral rows generated by anlagen III–V. Scale bars 5 µm (d, inset), 10 µm (d), 25 µm (b, c), and 30 µm (a).

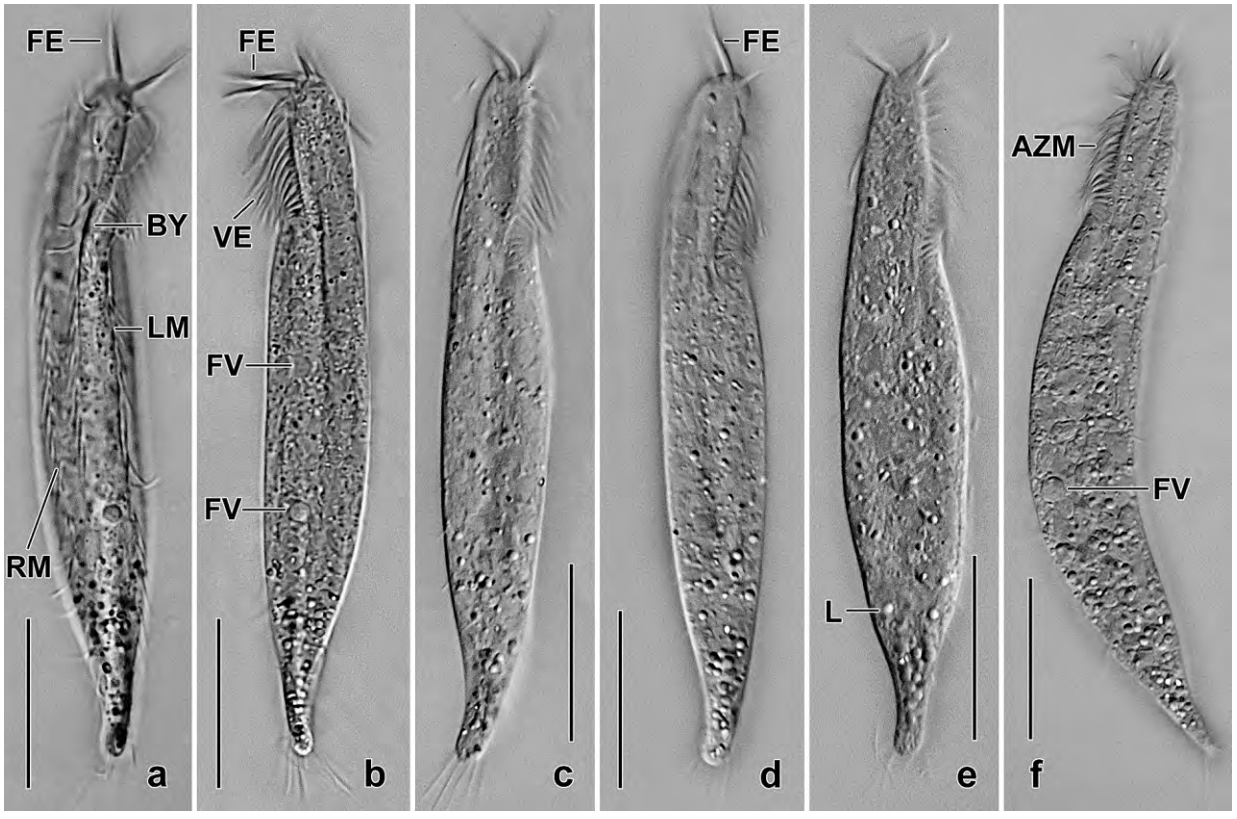

Fig. 188.7a–f. *Cladotricha halophila*, cultivated, freely motile specimens. **a, b:** Ventral and dorsal view of same specimen, showing body shape and the three frontal membranelles (FE) appearing like thick cirri. The cilia in the anterior half of the ventral membranelles have the same length as the frontal membranelles (b). Note also the very narrow buccal cavity. **c–f:** Shape variability. AZM – adoral zone of membranelles, BY – buccal cavity, FE – frontal adoral membranelles, FV – food vacuoles, L – lipid droplet, LM – left marginal cirral row, RM – right marginal cirral row, VE – ventral adoral membranelles. Scale bars 30 µm.

Very elongate ellipsoid with short, blunt tail slightly curved right. About 9 broadly ellipsoid macronuclear nodules forming a moniliform strand right of body´s midline; 2 micronuclei. 3 frontal cirri; 1 buccal cirrus anterior of undulating membranes; 3 frontoventral cirral rows/anlagen: row 3 short, does not extend beyond buccal vertex, composed of about 5 cirri; row 4 composed of an average of 19 cirri (AU) or of about 13 cirri (VE, CR), row 5 composed of an average of 28 cirri (AU) or of about 22 cirri (VE, CR). Right marginal row composed of an average of 30 cirri (AU) or of about 22 cirri (VE, CR), left row of about 20 cirri. Dorsal bristles 3 µm long; in 3 rows with a caudal cirrus each. Adoral zone of membranelles gonostomoid, proximal half covered by a convex buccal lip, extends about 36% of body length, composed of about 20–25 membranelles. Buccal cavity very narrow; paroral membrane composed of about 4 kinetids.

Description: We provide a full description of the neotropic populations because WILBERT`s description is very short and thus incomplete. Further, the Venezuelan and Costa Rican population will be described together because they are very similar in all features investigated (Tables 69c, d). The variability is moderate (CV ≤ 15%) for most diagnostic features, except for the number of paroral kinetids (CV up to 26%), the number of macronuclear nodules (CV 13 –18%), and the number of micronuclei (CV ~ 50%).

Table 69c. Morphometric data on *Cladotricha halophila* from Venezuelan site (65, upper line) and Costa Rican site (28, lower line) based on mounted, protargol-impregnated, and randomly selected specimens from non-flooded Petri dish cultures. Measurements in µm. CV – coefficient of variation in %, M – median, Max – maximum, Mean – arithmetic mean, Min – minimum, n – number of individuals investigated, SD – standard deviation, SE – standard error of arithmetic mean.

Characteristics	Mean	M	SD	SE	CV	Min	Max	n
Body, length	71.4	72.0	5.4	1.2	7.6	61.5	85.0	21
	69.1	70.0	8.5	1.9	12.3	53.0	83.0	21
Body, width	21.0	21.5	1.5	0.3	7.2	18.0	24.0	21
	20.6	21.0	2.8	0.6	13.6	17.0	29.0	21
Body length:width, ratio	3.4	3.5	0.2	0.0	5.7	3.1	3.7	21
	3.4	3.4	0.4	0.1	13.0	2.8	4.4	21
Anterior body end to proximal end of adoral zone of membranelles, distance	23.9	24.0	1.2	0.3	4.9	22.0	27.0	21
	24.2	25.0	2.3	0.5	9.4	20.0	29.0	21
Body length:length of adoral zone, percent	33.6	34.0	1.9	0.4	5.5	29.0	37.0	21
	35.2	36.0	3.6	0.8	10.2	29.0	42.0	21
Adoral membranelles, number	20.6	21.0	0.9	0.2	4.2	19.0	22.0	21
	21.5	22.0	1.1	0.3	5.2	19.0	24.0	21
Anterior body end to paroral membrane, distance	14.6	15.0	0.9	0.2	6.3	12.0	16.0	21
	13.8	13.0	2.0	0.4	14.2	11.0	18.0	21
Paroral membrane, number of kinetids	3.6	4.0	0.7	0.2	18.5	3.0	5.0	21
	3.5	3.0	0.9	0.2	25.7	2.0	5.0	20
Anterior body end to endoral membrane, distance	15.3	15.0	0.9	0.2	6.0	13.0	18.0	21
	14.9	14.5	1.9	0.4	12.9	12.0	19.0	20
Anterior body end to first macronuclear nodule, distance	10.9	11.0	1.4	0.3	12.9	8.0	14.0	21
	10.9	11.0	1.7	0.4	15.5	8.0	14.0	21
Anteriormost macronuclear nodule, length	5.3	5.0	0.6	0.1	11.9	4.0	6.0	21
	5.5	5.5	0.9	0.2	17.1	3.0	7.0	21
Anteriormost macronuclear nodule, width	3.3	3.0	0.6	0.1	19.6	2.0	4.0	21
	2.9	3.0	0.6	0.1	18.9	2.0	4.0	21
Macronuclear nodules, number	8.2	8.0	1.0	0.2	12.6	7.0	11.0	21
	8.5	8.0	1.5	0.3	18.1	6.0	13.0	21
Nuclear figure, length	45.5	44.0	5.0	1.1	11.1	38.0	61.0	21
	42.6	43.0	5.3	1.2	12.4	32.0	53.0	21
Anteriormost micronucleus, length	1.8	2.0	–	–	–	1.5	2.0	21
	1.8	2.0	–	–	–	1.5	2.0	5
Anteriormost micronucleus, width	1.3	1.5	–	–	–	1.0	1.5	21
	1.0	1.0	–	–	–	1.0	1.0	5
Micronuclei, number	1.7	2.0	0.9	0.2	49.3	1.0	4.0	21
	1.6	2.0	–	–	–	1.0	2.0	5
Anterior body end to buccal cirrus, distance	12.0	12.0	0.9	0.2	7.9	10.0	14.0	21
	11.9	12.0	1.6	0.3	13.1	9.0	14.0	21
Buccal cirri, number	1.0	1.0	0.0	0.0	0.0	1.0	1.0	21
	1.0	1.0	0.0	0.0	0.0	1.0	1.0	21
Anterior body end to end of ventral row III, distance	14.6	15.0	1.9	0.4	12.7	11.0	19.0	21
	12.9	13.0	2.6	0.6	20.2	8.0	17.0	21

continued

Ventral row III, number of cirri	4.8	5.0	0.7	0.2	14.1	4.0	7.0	21
	4.0	4.0	0.6	0.1	15.8	3.0	5.0	21
Anterior body end to end of ventral row IV, distance	38.0	38.0	3.7	0.8	9.7	31.0	47.0	21
	37.5	36.0	5.4	1.2	14.4	30.0	52.0	21
Ventral row IV, number of cirri	14.4	14.0	2.1	0.5	14.3	12.0	20.0	21
	13.2	13.0	1.6	0.4	12.2	11.0	17.0	21
Anterior body end to end of ventral row V, distance	49.7	51.0	5.8	1.3	11.7	37.0	60.0	21
	46.6	45.0	6.0	1.3	12.8	38.0	60.0	21
Ventral row V, number of cirri	20.3	20.0	2.4	0.5	11.8	16.0	26.0	21
	18.5	19.0	1.9	0.4	10.0	14.0	22.0	21
Frontal cirri, number	3.0	3.0	0.0	0.0	0.0	3.0	3.0	21
	3.0	3.0	0.0	0.0	0.0	3.0	3.0	21
Anterior body end to right marginal cirral row, distance	11.2	11.0	2.2	0.5	20.1	8.0	15.0	21
	10.1	10.0	1.9	0.4	18.5	5.0	14.0	21
Posterior body end to right marginal cirral row, distance	2.2	2.0	0.8	0.2	36.4	1.0	4.0	21
	1.4	1.0	–	–	–	1.0	2.0	20
Right marginal row, number of cirri	21.7	21.0	3.0	0.6	13.6	18.0	32.0	21
	23.1	23.0	2.5	0.6	10.9	19.0	29.0	21
Posterior body end to left marginal row, distance	1.1	1.0	0.6	0.1	50.8	0.5	2.5	21
	1.4	1.0	–	–	–	1.0	2.0	20
Left marginal row, number of cirri	19.4	19.0	2.7	0.6	13.9	15.0	28.0	21
	18.9	19.0	2.4	0.5	12.6	13.0	24.0	21
Dorsal kineties, number	3.0	3.0	0.0	0.0	0.0	3.0	3.0	21
	3.0	3.0	0.0	0.0	0.0	3.0	3.0	21
Dorsal kinety 1, number of kinetids	12.0	12.0	1.1	0.2	8.7	10.0	15.0	21
	11.3	11.0	1.4	0.3	11.9	9.0	14.0	21
Dorsal kinety 2, number of kinetids	15.7	16.0	2.0	0.4	12.5	12.0	21.0	21
	14.1	14.0	1.4	0.3	10.1	11.0	17.0	21
Dorsal kinety 3, number of kinetids	19.1	19.0	1.8	0.4	9.4	17.0	26.0	21
	15.9	16.0	2.1	0.5	13.1	12.0	19.0	21
Caudal cirri, number	3.0	3.0	0.0	0.0	0.0	3.0	3.0	21
	3.0	3.0	0.0	0.0	0.0	3.0	3.0	21

Size highly variable, depending on culture conditions: in vivo about 80 × 25 µm in ordinary non-flooded Petri dish cultures (NFP) while up to 140 × 30 µm in a flourishing semipure culture (Fig. 188.7a–f). Body shape also highly depending on culture conditions. Usually slightly sigmoid or cuneate and distinctly narrowed posteriorly, forming a blunt, short tail slightly curved right; in NFP cultures ellipsoid (up to 2.5:1) to elongate ellipsoid or cuneate (up to 4:1); in a semipure culture very elongate ellipsoid to almost rod-shaped with a length:width ratio of up to 7:1 (Fig 188.7a–f). Laterally indistinctly flattened. Difficult to preserve, i. e., specimens become distinctly inflated in protargol preparations, showing a length:width ratio of about 3.5:1 (Fig. 188.6b; Table 69c).

Nuclear apparatus in central quarters of cell right of body´s midline (Fig. 188.6a, c, 188.9a–c, l–n). On average eight broadly ellipsoid macronuclear nodules forming a moniliform strand;

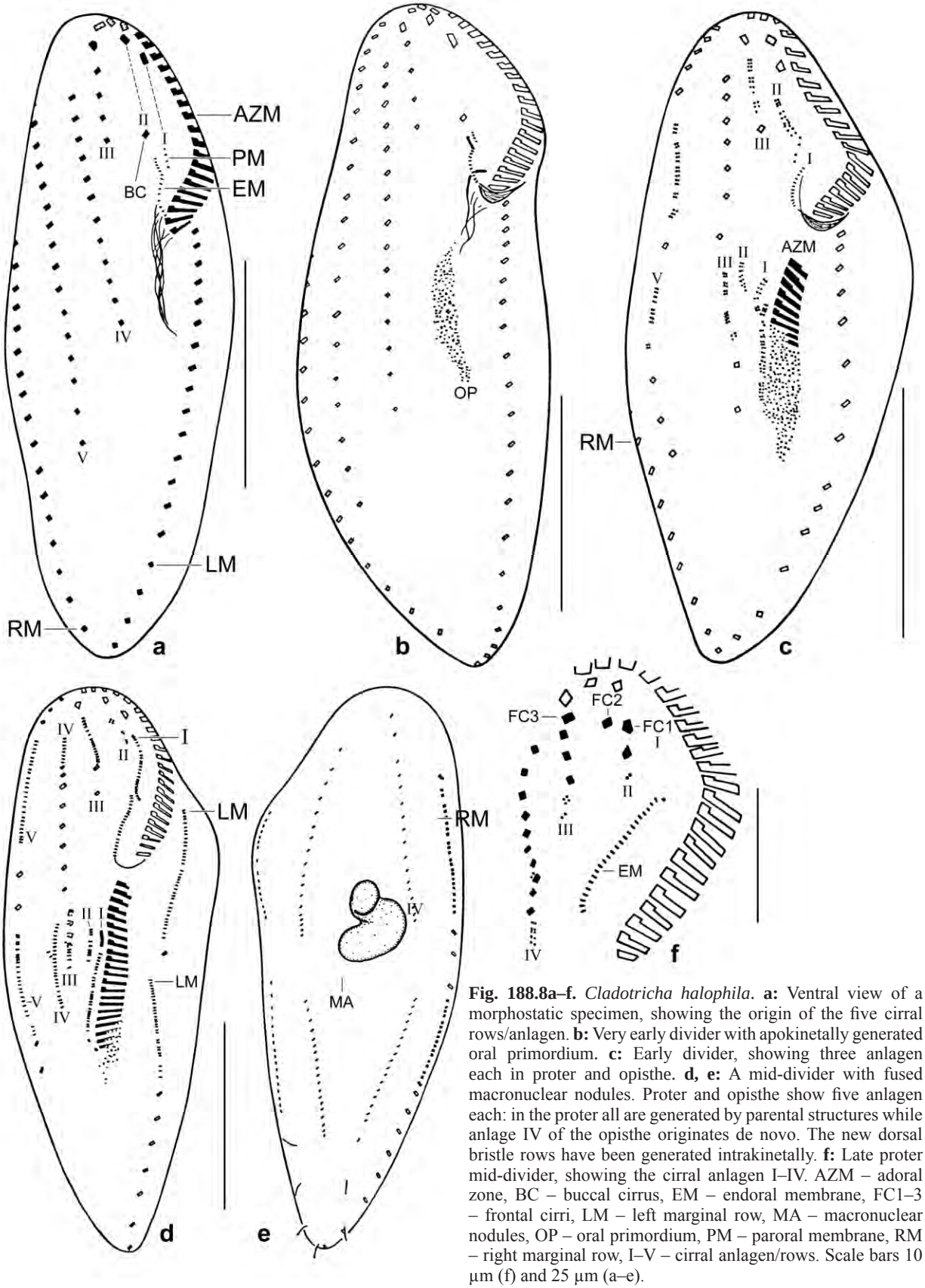

Fig. 188.8a–f. *Cladotricha halophila*. **a:** Ventral view of a morphostatic specimen, showing the origin of the five cirral rows/anlagen. **b:** Very early divider with apokinetally generated oral primordium. **c:** Early divider, showing three anlagen each in proter and opisthe. **d, e:** A mid-divider with fused macronuclear nodules. Proter and opisthe show five anlagen each: in the proter all are generated by parental structures while anlage IV of the opisthe originates de novo. The new dorsal bristle rows have been generated intrakinetally. **f:** Late proter mid-divider, showing the cirral anlagen I–IV. AZM – adoral zone, BC – buccal cirrus, EM – endoral membrane, FC1–3 – frontal cirri, LM – left marginal row, MA – macronuclear nodules, OP – oral primordium, PM – paroral membrane, RM – right marginal row, I–V – cirral anlagen/rows. Scale bars 10 µm (f) and 25 µm (a–e).

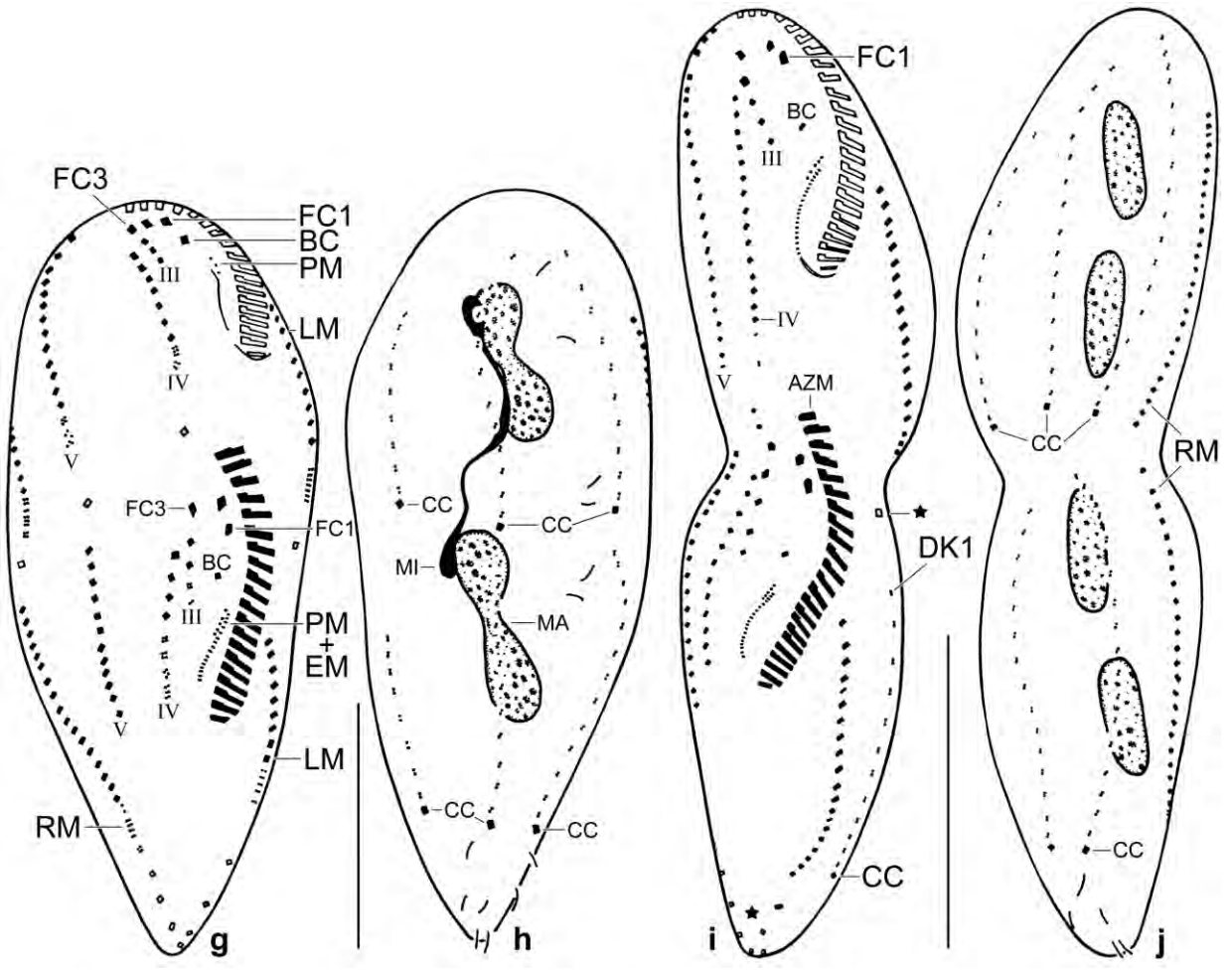

Fig. 188.8g–j. *Cladotricha halophila* after protargol impregnation. **g, h:** Ventral and dorsal view of an early late divider with cuneate body shape. The infraciliature has been renewed and the macronuclear nodules commence to divide a second time. Still, there are parental cirri, shown by contour, especially between the proter and opisthe and in the posterior portion of the marginal rows. A single parental cirrus each occurs between the proter and opisthe cirral rows/anlagen IV and V and the marginal rows. **i, j:** Ventral and dorsal view of a late divider with distinct division furrow and four macronuclear nodules. The new cirri and dorsal bristles have arranged in the species-specific pattern. Still, there are some parental cirri present (asterisk), which will be resorbed in very late dividers and during post-divisional body shaping. The parental adoral zone of membranelles did not reorganize. Details of the new opisthe adoral zone are shown in Fig. 188.6d. AZM – adoral zone of membranelles, BC – buccal cirrus, CC – caudal cirri, DK1 – dorsal kinety 1, EM – endoral membrane, FC1, 3 – frontal cirri, LM – left marginal cirral row, MA – macronuclear nodules, MI – dividing micronucleus, PM – paroral membrane, RM – right marginal cirral row, I–V – cirral anlagen/rows. Scale bars 20 µm (g, h) and 30 µm (i, j).

individual nodules globular to ellipsoid, with many ordinary nucleoli; not connected by a fibrous strand, at least with the protargol method used. On average two broadly ellipsoid micronuclei attached to various sites of macronuclear strand; rarely impregnate with the protargol method used. Contractile vacuole in or slightly anterior of mid-body near left margin of cell (Fig. 188.6a). Cortex very flexible, without specific granules. Cytoplasm colourless, opaque because studded with food vacuoles and lipid(?) droplets 0.5–1 µm in size; in tail region droplets with up to 3 µm. Some minute crystals scattered through body. Feeds on bacteria digested in vacuoles 4–6 µm across (Fig. 188.6a, 188.7a–f). Usually creeping on bottom of culture dish and in and on mud accumulations, showing great flexibility.

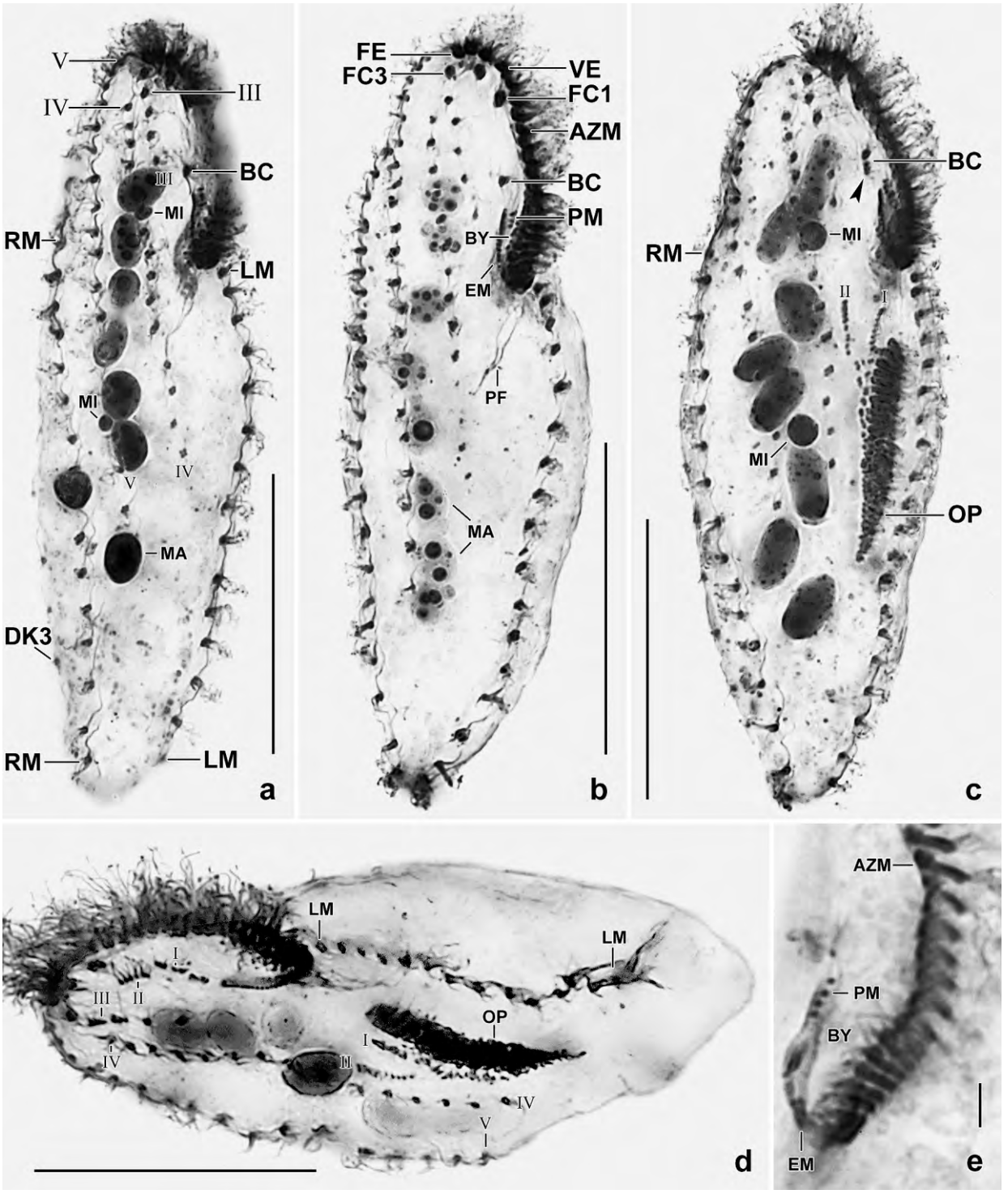

Fig. 188.9a–e. *Cladotricha halophila*, ventral views of Venezuelan (a–c, e) and Costa Rican (d) specimens after protargol impregnation. **a, b, e:** Morphostatic specimens with minute paroral membrane (e) and narrow buccal cavity (b, e). **c:** An early divider with two anlagen (I, II) in the opisthe and one in the proter posterior of the buccal cirrus (arrowhead) **d:** As (c) but slightly advanced. AZM – adoral zone of membranelles, BC – buccal cirrus, BY – buccal cavity, DK3 – dorsal kinety 3, EM – endoral membrane, FC1, 3 – frontal cirri, FE – frontal membranelles, LM – left marginal row, MA – macronuclear nodules, MI – micronuclei, OP – oral primordium, PF – pharyngeal fibres, PM – paroral membrane, RM – right marginal row, VE – ventral adoral membranelles, I–V – cirral anlagen/rows. Scale bars 2 µm (e) and 30 µm (a–d).

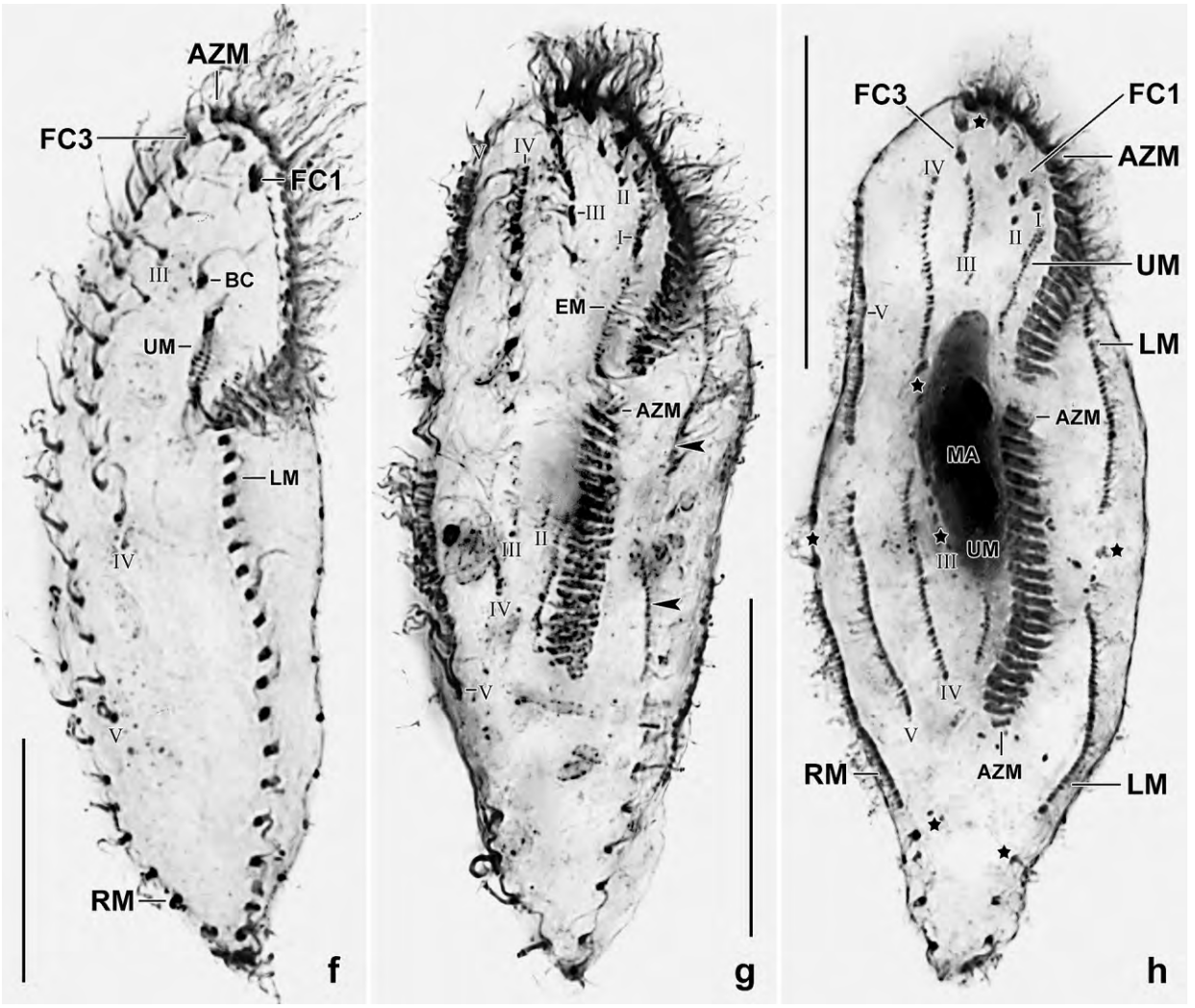

Fig. 188.9f–h. *Cladotricha halophila*, ventral views after protargol impregnation. **f:** A morphostatic specimen, showing the main features. **g:** An early mid-divider with fusing macronuclear nodules and anlagen in the ventral and marginal cirral rows. Anlage IV originates from parental row IV in the proter while de novo in the opisthe. **h:** A mid-divider with fused macronuclear nodules and fully developed cirral anlagen. Anlage IV of the opisthe developed de novo. Asterisks mark parental cirri. AZM – adoral zone of membranelles, BC – buccal cirrus, EM – endoral membrane, FC1, 3 – frontal cirri, LM – left marginal cirral row, MA – fused macronuclear nodules, RM – right marginal cirral row, UM – undulating membranes, I–V – cirral anlagen/rows. Scale bars 20 µm (f) and 30 µm (g, h).

Cirri arranged in *Cladotricha* pattern shown by Berger (2011), i. e., in frontoventral anlagen or rows with most cirri composed of four or six cilia (basal bodies) up to 15 µm long in vivo (Fig. 188.6a, b, d, 188.7a–f, 188.9a–c, f, l; Table 69c). Subapically three slightly enlarged frontal cirri about 15 µm long in vivo. Anlage I (cirral row 1) produces the undulating membranes and frontal cirrus 1; anlage II (row 2) produces frontal cirrus 2 and a single buccal cirrus slightly right and anterior of undulating membranes; anlage III (row 3) generates frontal cirrus 3 and an average of five cirri forming a short row in midline of body; anlage IV (row 4) commences far subapically and extends to mid-body on average, composed of about 14 cirri; anlage V (row 5) longest, commences at anterior body end and extends to 63% of body length on average, composed of about 19 cirri. Right marginal row commences 15% (12 µm) subapically and extends to posterior body end, composed of about 22 cirri, left row of about 19 cirri.

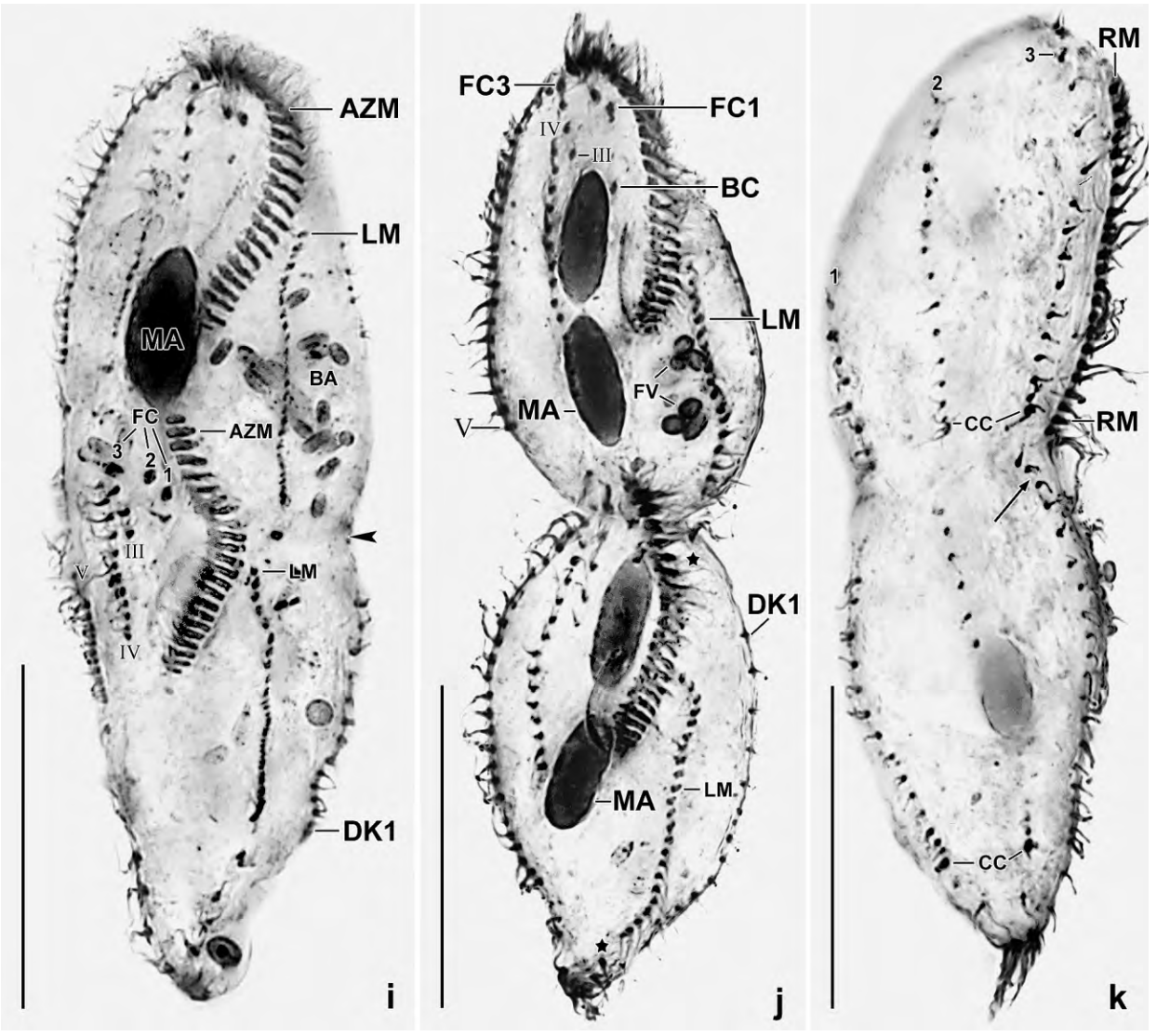

Fig. 188.9i–k. *Cladotricha halophila*, dividers after protargol impregnation. **i:** An early late divider with first round macronuclear reorganization and beginning cytokinesis (arrowhead). The new cirral rows migrate to their specific sites. **j, k:** Ventral and dorsal view of a late divider with distinct division furrow and four macronuclear nodules. The new cirri and dorsal bristles obtained the species-specific pattern. Still, there are some parental cirri present (asterisks), which will be resorbed in very late dividers and post-divisional body shaping. The parental adoral zone of membranelles did not reorganize. AZM – adoral zone of membranelles, BA – bacteria in food vacuoles, BC – buccal cirrus, CC – caudal cirri, DK1 – dorsal kinety 1, FC1– 3 – frontal cirri, FV – food vacuoles with bacterial spores, LM – left marginal cirral row, MA –macronuclear nodules, RM – right marginal cirral row, I–V – cirral anlagen/rows, 1–3 – dorsal kineties. Scale bars 30 µm.

Dorsal bristles about 3 µm long in vivo and in protargol preparations, arranged in three rows each associated with a caudal cirrus about 20 µm long in vivo. Row 1 commences at level of buccal vertex, row 2 subapically, and row 3 near anterior body end where bristles are slightly polymerized (Fig. 188.6c, 188.9k, m, n; Table 69c).

Oral apparatus in *Gonostomum* pattern (Berger 1999), i. e., adoral zone flat and following anterior and left body margin before bending abruptly into cell at about 35% of body length; zone composed

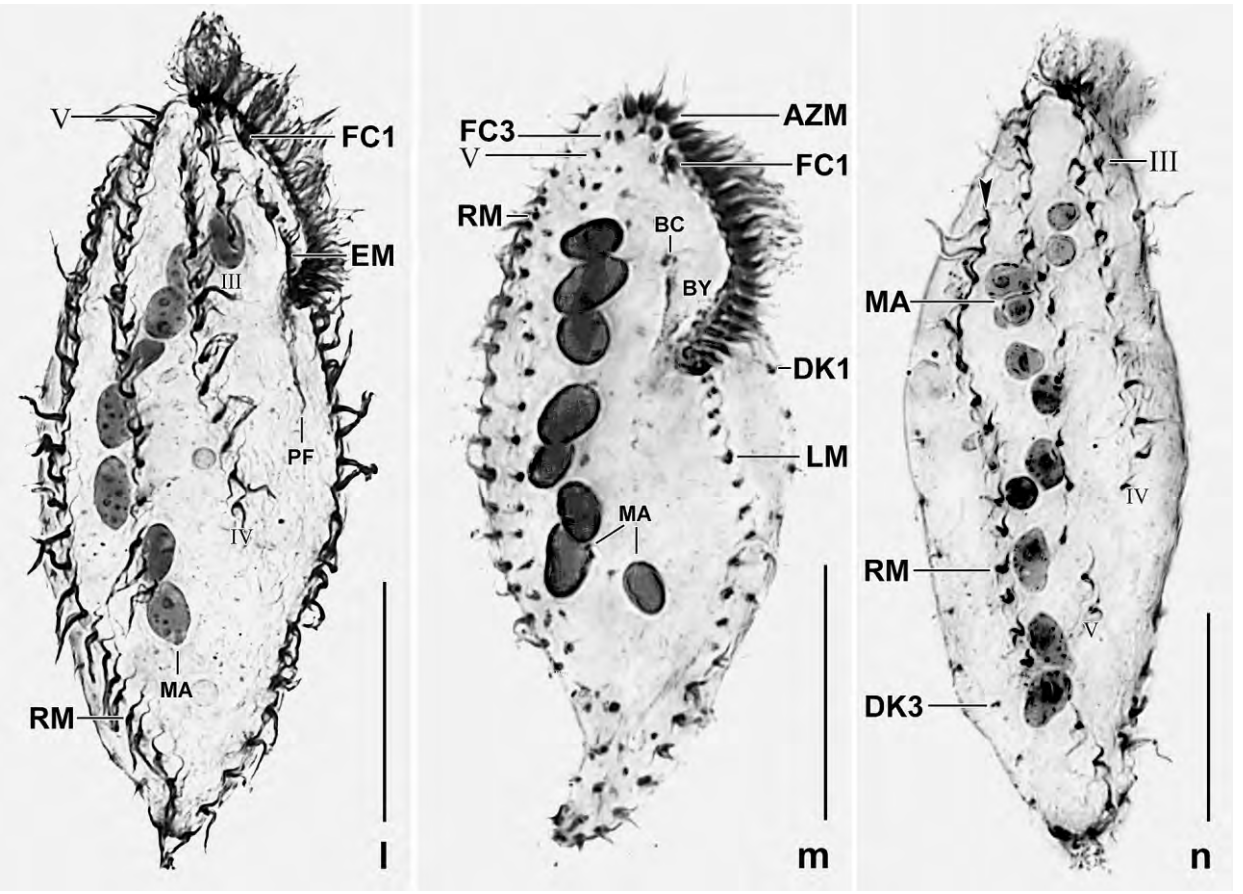

Fig. 188.9l–n. *Cladotricha halophila* after protargol impregnation. **l, m:** Ventral views of a proter and an opisthe post-divider. They have a fully developed cirral and nuclear pattern while body shape of the proter is still in work (l). **n:** Right lateral view of a morphostatic specimen, showing the subapical begin of the right marginal row (arrowhead) and cirral rows/anlagen III–V. AZM – adoral zone of membranelles, BC – buccal cirrus, BY – buccal cavity, DK1, 3 – dorsal kineties, EM – endoral membrane, FC1, 3 – frontal cirri, LM – left marginal cirral row, MA – macronuclear nodules, PF – pharyngeal fibres, RM – right marginal cirral row, III–V – cirral anlagen/rows. Scale bars 20 µm.

Table 69d. Comparison of main features in three populations of *Cladotricha halophila* based on protargol preparations.

Characteristics	**Australia (n=17) (WILBERT 1995)**	**Venezuela (n=21)**	**Costa Rica (n=21)**
Body length (µm)	138.4	71.4	69.1
Body length:width, ratio	4.6	3.4	3.4
Macronuclear nodules, number	9.6	8.2	8.5
Adoral membranelles, number	24.3	20.6	21.5
Paroral kinetids, number	4.0[a]	3.6	3.5
Frontoventral row 4, number of cirri	18.7	14.4	13.2
Frontoventral row 5, number of cirri	28.5	20.3	18.5
Right marginal row, number of cirri	29.5	21.7	23.1
Left marginal row, number of cirri	21.6	19.4	18.9

[a] According to the holotype specimen.

of an average of 21 highly differentiated membranelles (Fig. 188.6d, inset). Frontal membranelles about 15 µm long, appear like thickened cirri in vivo (Fig. 188.6a, 188.7a–f). Anterior half of ventral membranelles also about 15µm long, not separated from frontal membranelles; posterior half of membranelles covered by a distinctly convex buccal lip projecting from body proper (Fig. 188.6a). Buccal cavity short and narrow in vivo, covered by buccal lip without digitate processes. Endoral membrane short and more or less convex; paroral membrane minute, left of anterior end of endoral, composed of an average of four kinetids with about 8 µm long cilia. Pharyngeal fibres distinct in protargol preparations, extend vertically to mid-body (Fig. 188.6a, b, d, 188.7a–f, 188.8a, 188.9a, b, e, f; Table 69c).

Ontogenesis: We shall not provide a detailed description of the ontogenetic processes but restrict it to important events and refer to the line drawings and micrographs for the more common processes.

(i) The ontogenesis of *C. halophila* is apokinetal, i. e., an anarchic field of basal bodies develops posterior to the buccal vertex without any participation of parental structures (Fig. 188.8b).

(ii) In the proter develop five cirral anlagen streaks as usual (Fig. 188.8c, d, 188.9c, d, g–i): anlage I produces the new undulating membranes and frontal cirrus I; anlage II originates from the buccal cirrus and produces frontal cirrus 2 and the new buccal cirrus; anlage III originates within frontoventral cirral row 3 and produces frontal cirrus 3 and a new cirral row 3; the anlagen IV and V are also produced within the parental rows 4 and 5. The opisthe anlagen develop differently because the oral primordium generates only two cirral anlagen and cirral row 3 of the proter does not reach the opisthe (Fig. 188.8c, d, 188.9c, d, g–i): cirral anlagen I and II develop from the oral primordium and generate frontal cirri 1 and 2 as well as the buccal cirrus and the undulating membranes; anlage III is missing because the frontoventral cirral row 3 produces only for the proter. Thus, proter anlage IV becomes anlage III in the opisthe. Right of this anlage a new cirral row develops de novo becoming cirral row 4 of the opisthe; anlage V develops within the parental row.

(iii) The ontogenesis confirms the absence of transverse cirri and the presence of caudal cirri one each produced by the three dorsal kineties (Fig. 188.8g–j, 188.9h–k).

(iv) The further processes are as expected: cirri develop in the anlagen and the new cirral rows migrate to the species-specific sites; the macronuclear mass divides three times to generate eight nodules each in proter and opisthe; body shaping occurs post-divisionally, especially in the proter (Fig. 188.8g–j, 188.9i–n).

Occurrence and ecology: As yet found in Australia (Wilbert 1995), in Costa Rica, and in Venezuela (this study) indicating wide or even cosmopolitan distribution. Likely confined to highly saline coastal and inland habitats. In Venezuela it occurred only at site (65).

Remarks: The neotropic populations of *Cladotricha halophila* match the Australian type population rather well, especially when the difference in body length is partially ascribed to methodological problems (Table 69d). However, the higher number of cirri in all cirral rows shows that the Australian specimens are indeed larger than those from Venezuela and Costa Rica. On the other hand, important features such as the number of adoral membranelles, macronuclear

nodules, and paroral kinetids is quite similar (Table 69d). Thus, we do not separate the neotropic and Australian populations.

As concerns the ontogenesis neither Borror & Evans (1979) or Wilbert (1995) recognized the de novo origin of a cirral row in the opisthe, possibly because they did not find division stages like those shown in Fig. 188.8c, d and 188.9c, d, g, h.

Deviatidae nov. fam.

Diagnosis: Non-dorsomarginalian or dorsomarginalian hypotrichs with kahliellid organization, i. e., with several longitudinal cirral rows dividing intrakinetally or with multiple within anlagen. Transverse cirri absent, caudal cirri present or absent. The oral primordium originates within the first row of the right cirral field or apokinetally between right and left cirral field. Four to six frontoventral cirral anlagen partially reduced in *Notodeviata*.

Type genus: *Deviata* Eigner, 1995.

Genera assignable: *Deviata* Eigner, 1995, → *Notodeviata* nov. gen., and → *Idiodeviata* nov. gen.

Remarks: *Notodeviata* is very likely closely related to → *Idiodeviata* and *Deviata* Eigner, 1995 whose systematic position is not known, according to Berger (2011), who puts much weight on the presence/absence of dorsomarginal kineties. However, evidence is increasing that this feature evolved several times independently (see → *Idiodeviata*). This is the basis for our decision to unite *Deviata, Notodeviata* and *Idiodeviata* in a distinct family which is possibly sister to the non-dorsomarginalian Kahliellidae Tuffrau, 1979.

Notodeviata nov. gen.

Diagnosis: Non-dorsomarginalian Deviatidae with frontal, buccal, and caudal cirri. The oral primordium originates apokinetally between right and left cirral field. Four frontoventral cirral anlagen, of which anlage IV and most cirri of anlagen II and III are resorbed in late and very late dividers.

Type species: *Notodeviata halophila* nov. spec.

Etymology: *Notodeviata* is a composite of the Greek noun *ho notos* (the south) and the genus-group name *Deviata*, referring to the geographic region the type species was discovered and to its similarity to species of the genus *Deviata*. Feminine gender.

Remarks: *Notodeviata* differs from *Deviata*, as defined by Eigner (1995) and Berger (2011), by the possession of caudal cirri, the apokinetal origin of the oral primordium, and the absence of multiple within anlagen. Further, it is unique in the massive reduction of cirri in the frontoventral anlagen. Most of these features suggest that *Notodeviata* evolved from a more complex ancestor similar to *Deviata*.

Notodeviata halophila **nov. spec.** (Fig. 189a–f, 190a–x, 191a–o; Table 70)

Diagnosis: Size in vivo about 120 × 17 µm. Cultrate to very narrowly ellipsoid with slightly slanted oral region, hardly flattened laterally, very flexible. 2 macronuclear nodules and 2 micronuclei on average. 3 cirral rows right of body´s midline, 2 left; 3 frontal cirri; 1 buccal cirrus subapical of paroral membrane; 2 dorsal kineties; 2, rarely 3 caudal cirri. Adoral zone extends 18% of body length, composed of an average of 18 membranelles. Buccal cavity short and narrow, covered by

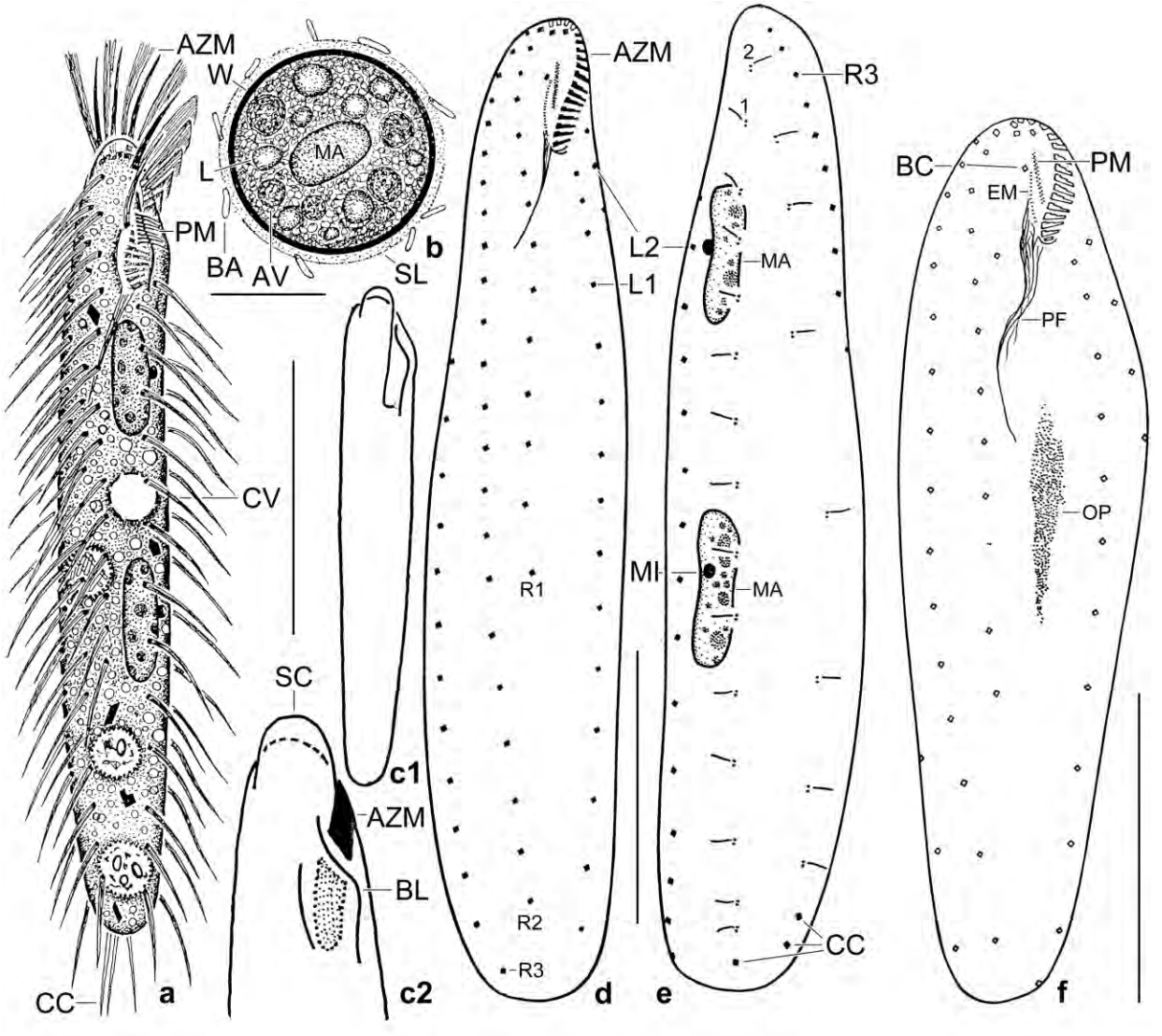

Fig. 189a–f. *Notodeviata halophila* from life (a–c) and after protargol impregnation (d–f). **a:** Ventral view of a representative specimen, length 120 µm. It is studded with lipid droplets up to 5 µm across. **b:** Resting cyst, 40 µm. The centre is occupied by the fused macronuclear nodules. **c1, c2:** A frequent shape and anterior end, showing the membranellar scutum and the convex buccal lip which covers the proximal half of the adoral zone of membranelles. **d, e:** Ventral and dorsal view of holotype specimen, length 140 µm. Note the caudal cirri, the main feature of the genus. **f:** Ventral view of a very early divider, showing the apokinetal origin of the oral primordium. AV – autophagous vacuole, AZM – adoral zone of membranelles, BA – bacterium, BC – buccal cirrus, BL – buccal lip, CC – caudal cirri, CV – contractile vacuole, EM – endoral membrane, L – lipid (?) droplet, L1, 2 – left cirral rows, MA – macronuclear nodules, MI – micronucleus, OP – oral primordium, PF – pharyngeal fibres, PM – paroral membrane, R1–3 – right cirral rows, SC – scutum, SL – slime cover, W – cyst wall, 1, 2 – dorsal kineties. Scale bars 40 µm.

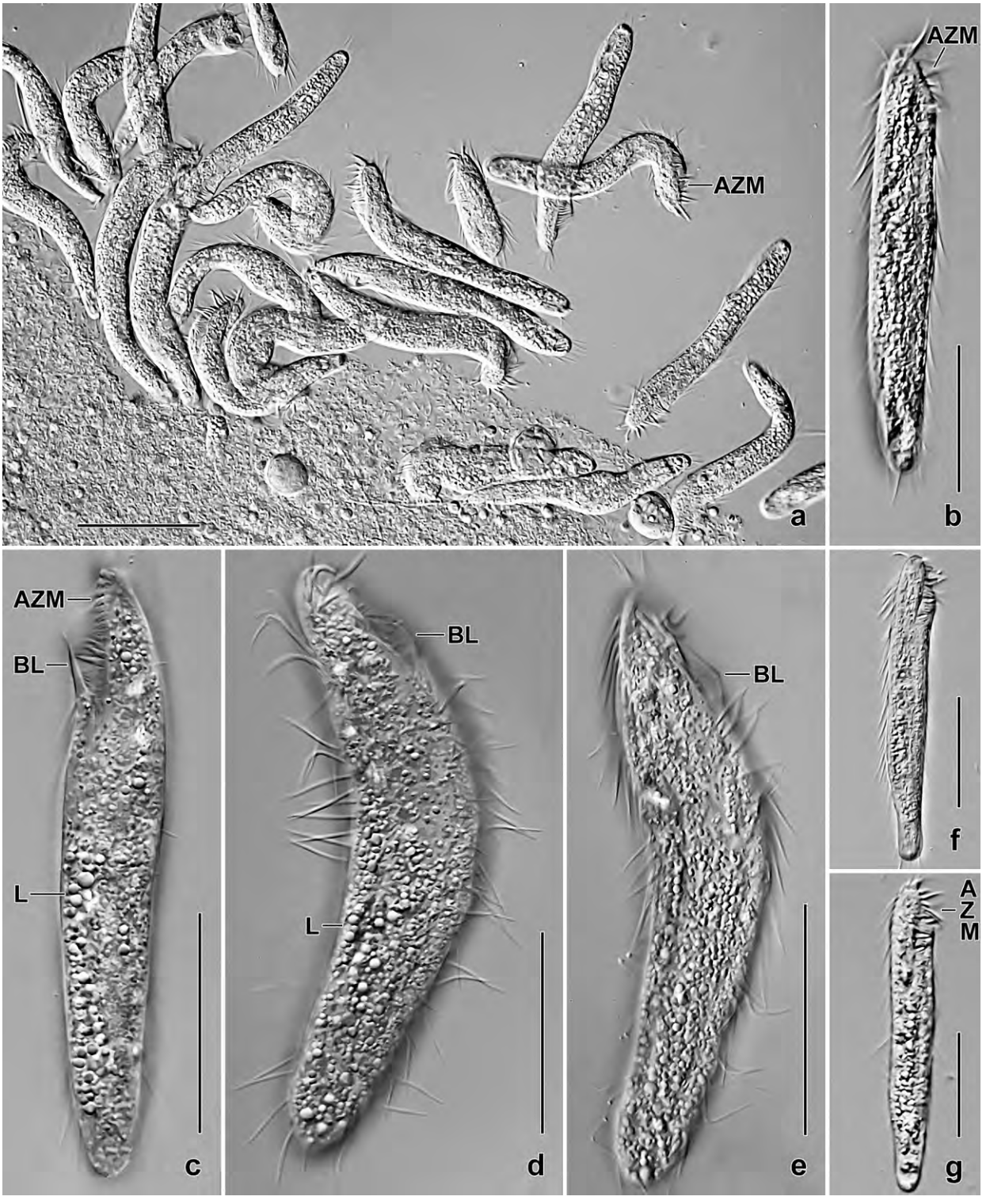

Fig. 190a–g. *Notodeviata halophila* from life. **a:** Overview of cells gathering on the surface of a bacterial flock. Note the high flexibility and the granular cytoplasm. **b, f, g:** Shape variability of freely motile specimens. Note the slanted oral area. **c:** Lateral view, showing the conspicuous buccal lip. **d, e:** Slightly pressed (by coverslip) specimens, showing the convex buccal lip, the strongly granulated cytoplasm, and the long, fine cirri. AZM – adoral zone of membranelles, BL – buccal lip, L – lipid (?) droplets. Scale bars 20 μm (a) and 40 μm (b–g).

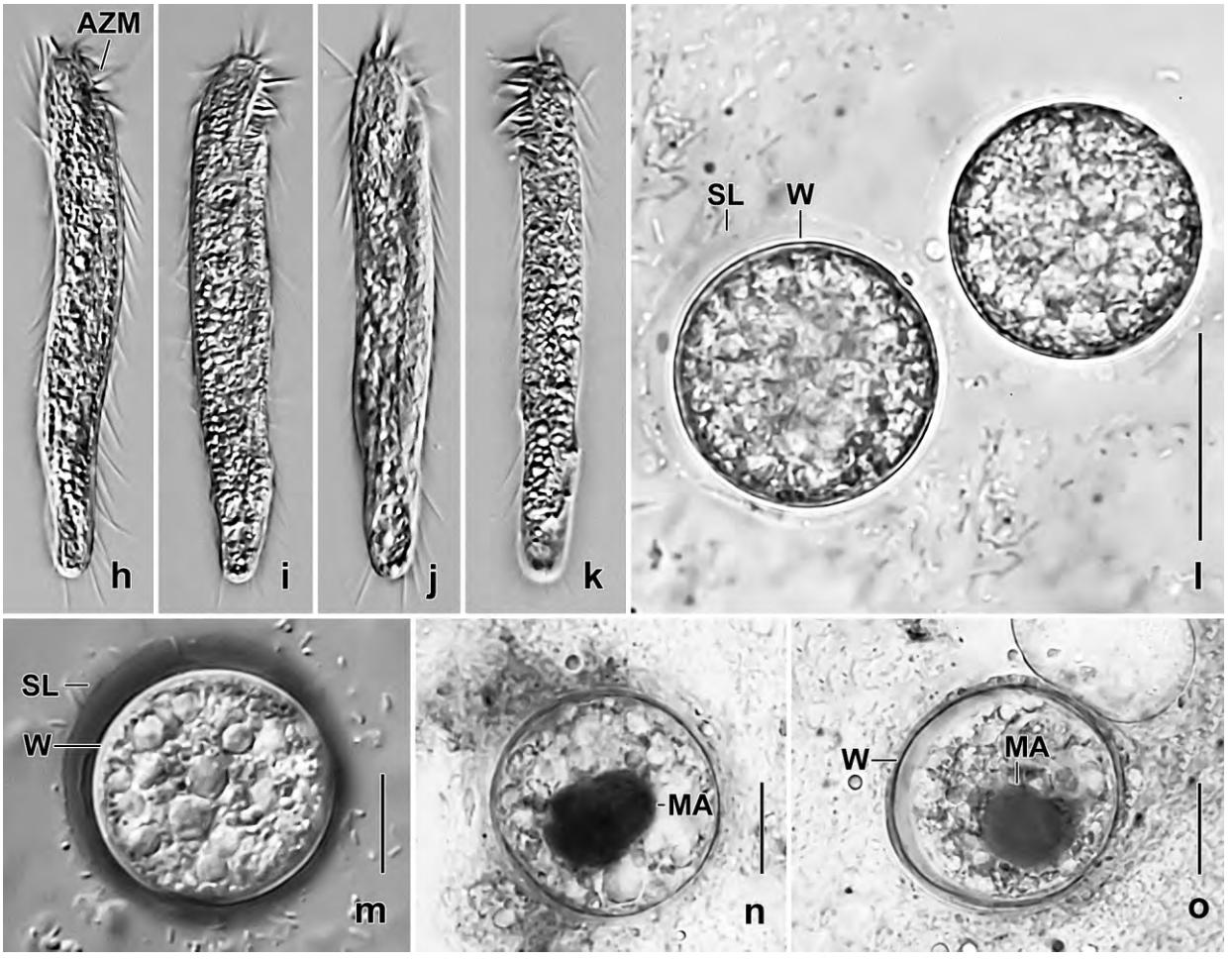

Fig. 190h–o. *Notodeviata halophila* from life (h–m) and after staining with methyl green-pyronin (n, o). **h–k:** Freely motile specimens, length 110–130 µm. **l, m:** Resting cysts are studded with globular inclusions some of which might be autophagous vacuoles while most globules resemble those found in morphostatic cells. The slime (?) cover is very hyaline (l) but becomes distinct after contrast enhancing (m). **n, o:** The two macronuclear nodules of the morphostatic cell fused to a single, globular mass. AZM – adoral zone of membranelles, MA – macronucleus, SL – slime (?) cover not staining with methyl green-pyronin, W – cyst wall. Scale bars 15 µm (m–o) and 30 µm (l).

a convex lip. Paroral and endoral membrane optically side by side but staggered by about 60%. Resting cyst wall smooth; macronuclear nodules fused.

Type locality: Venezuelan site (65), i. e., highly saline soil from the north coast, Morrocoy National Park, surroundings of the village of Chichiriviche, 67°13‘W 11°33‘N.

Type material: 1 holotype and 8 paratype slides with protargol-impregnated morphostatic and dividing specimens have been deposited in the Biology Centre of the Upper Austrian Museum in Linz (LI). The holotype, various paratypes, and the dividers shown have been marked by black ink circles on the coverslip.

Etymology: The name is a composite of the Greek noun *hals* (salt) and the Greek adjective *philos* (loving, preferring), referring to the highly saline habitat (50‰) the species was discovered.

Description: *Notodeviata halophila* is ordinarily variable, i. e., most variation coefficients are ≤ 15%, including all diagnostic features. Higher variation coefficients occur in many distances and ratios, most of which have little taxonomic value.

Size in vivo 100–160 × 15–30 µm, usually about 120 × 17 µm, as calculated from various in vivo measurements and protargol-impregnated specimens in Table 70 adding 15% preparation shrinkage; as usual, also depends on culture conditions and fixation fluid. Body in vivo cultrate to very narrowly ellipsoid (~ 7:1) with indistinctly slanted oral region, usually slightly wider anteriorly than posteriorly, in protargol preparations vice versa and width distinctly inflated; hardly flattened laterally (Fig. 189a, c1, d, 190a–k, p–t; Table 70). Nuclear apparatus in central quarters left of body´s midline (Fig. 189a, e, 190p–t; Table 70). Two, very rarely three macronuclear nodules, anterior nodule slightly posterior of adoral zone, second nodule slightly posterior of mid-body;

Table 70. Morphometric data on *Notodeviata halophila* (upper line) and *Idiodeviata venezuelensis* (lower line) based on mounted, protargol-impregnated (if not mentioned otherwise), and selected for well-looking specimens from a raw culture. Measurements in µm. CV – coefficient of variation in %, M – median, Max – maximum, Mean – arithmetic mean, Min – minimum, n – number of individuals investigated, SD – standard deviation, SE – standard error of arithmetic mean.

Characteristics	Mean	M	SD	SE	CV	Min	Max	n
Body, length in vivo	117.5	120.5	10.4	3.7	8.8	110.0	130.0	8
	not investigated							
Body, width in vivo	20.6	20.0	3.9	1.4	18.9	16.0	25.0	8
	not investigated							
Body length: width, ratio in vivo	5.9	5.6	1.2	0.4	20.4	4.4	7.6	8
	not investigated							
Body length: width, ratio from life micrographs	7.4	7.3	0.8	0.2	10.5	6.3	8.5	10
	not investigated							
Body, length	108.5	108.0	14.5	3.2	13.4	86.0	137.0	21
	86.0	84.0	10.1	2.6	11.7	75.0	116.0	15
Body, width	24.6	24.0	3.5	0.8	14.3	19.0	31.0	21
	29.1	28.0	3.1	0.8	10.5	25.0	34.0	15
Body length: width, ratio	4.5	4.5	0.8	0.2	17.0	3.3	6.3	21
	3.0	2.9	0.5	0.1	16.5	2.5	4.5	15
Anterior body end to proximal end of adoral zone, distance	18.6	18.0	2.1	0.5	11.3	15.0	22.0	21
	20.4	20.0	0.7	0.2	3.6	19.0	22.0	15
Adoral zone of membranelles, percentage of body length	17.4	18.5	2.7	0.6	15.2	13.0	21.0	21
	24.0	23.9	2.3	0.6	9.7	18.1	26.9	15
Adoral membranelles, number	18.3	18.0	0.7	0.2	3.9	17.0	19.0	16
	19.5	19.0	0.5	0.2	2.7	19.0	20.0	11
Anterior body end to paroral membrane, distance	6.9	7.0	1.3	0.3	19.1	4.0	10.0	21
	6.3	6.0	0.8	0.2	12.9	5.0	8.0	15
Anterior body end to endoral membrane, distance	9.5	9.5	1.3	0.3	13.7	7.0	12.0	21
	7.9	8.0	1.0	0.3	12.1	6.0	9.0	15
Anterior body end to first macronuclear nodule, distance	21.1	21.5	3.3	0.7	15.7	15.0	28.0	21
	15.9	15.0	1.8	0.5	11.4	13.0	20.0	15
Macronuclear nodules, distance in between	20.5	20.0	7.0	1.5	34.0	6.0	32.0	21

continued

nodules elongate ellipsoid, on average 13 × 4 µm in protargol preparations, with many minute and some ordinary nucleoli most in right half of nodule, a curious pattern (Fig. 189e, 190q, t). On average two broadly ellipsoid micronuclei usually attached to left side of macronuclear nodules; rarely impregnate with the method used. Contractile vacuole slightly anterior of mid-body (Fig. 189a). Cortex very flexible, without specific granules. Cytoplasm colourless, opaque because studded with globular to indistinctly polygonal lipid (?) droplets and some ordinary crystals both up to 4 µm in size (Fig. 189a, 190a–k). Feeds on oblong bacteria digested in vacuoles about 5 µm across, in raw cultures also ingests small starch grains. Can swim rapidly but usually burrows on and in mud and bacteria accumulations, showing great flexibility (Fig. 190a).

Characteristics	Mean	M	SD	SE	CV	Min	Max	n
	frequently in two indistinct pairs separated by a few µm							
Nuclear figure, length	49.1	52.0	8.4	1.8	17.2	31.0	60.0	21
	46.5	45.0	6.8	1.7	14.5	37.0	65.0	15
Macronuclear nodules, number	2.0	2.0	0.0	0.0	0.0	2.0	2.0	21
	3.9	4.0	0.3	0.1	6.6	3.0	4.0	15
Macronuclear nodules, length	13.2	13.0	1.7	0.4	13.0	10.0	17.0	21
	11.5	12.0	1.6	0.4	13.9	9.0	15.0	15
Macronuclear nodules, width	4.2	4.0	1.0	0.2	24.2	2.0	7.0	21
	5.6	5.0	1.1	0.3	18.9	4.0	7.0	15
Micronuclei, number	1.8	2.0	0.6	0.1	30.8	1.0	3.0	18
	1.9	2.0	0.3	0.1	13.4	1.0	2.0	15
Micronuclei, length	2.0	2.0	0.2	0.1	10.6	1.5	2.5	18
	2.6	3.0	0.5	0.1	19.5	2.0	3.0	15
Micronuclei, width	1.7	1.5	–	–	–	1.5	2.0	18
	2.1	2.0	0.3	0.1	12.5	2.0	3.0	15
Frontal cirri, number	3.0	3.0	0.0	0.0	0.0	3.0	3.0	21
	3.0	3.0	0.0	0.0	0.0	3.0	3.0	15
Anterior body end to buccal cirrus, distance	8.2	8.5	1.3	0.3	15.4	6.0	11.0	21
	8.6	9.0	1.0	0.3	11.5	7.0	11.0	15
Buccal cirri, number	1.0	1.0	0.0	0.0	0.0	1.0	1.0	21
	1.0	1.0	0.0	0.0	0.0	1.0	1.0	15
Anterior body end to end of right cirral row 1, distance	66.1	66.0	14.5	3.2	21.9	44.0	97.0	21
	28.5	27.0	3.9	1.0	13.8	22.0	36.0	15
Right cirral row 1, number of cirri	12.5	13.0	1.7	0.4	13.3	10.0	16.0	21
	8.1	9.0	1.7	0.5	21.2	6.0	12.0	15
Anterior body end to end of right cirral row 2, distance	94.2	97.0	13.7	3.0	14.6	65.0	124.0	21
	82.1	79.0	10.5	2.7	12.8	72.0	112.0	15
Right cirral row 2, number of cirri	21.3	21.0	2.6	0.6	12.2	17.0	27.0	21
	28.3	28.0	2.2	0.6	7.7	23.0	32.0	15
Anterior body end to end of right cirral row 3, distance	not measured							
	83.7	79.0	10.6	2.7	12.7	72.0	115.0	15
Posterior body end to right cirral row 3, distance	7.1	6.8	3.0	0.7	41.7	2.0	15.0	20

continued

Cirri about 15 µm long in vivo, fine because composed of only four cilia including frontal and buccal cirri; intracirral distances gradually increase from anterior to posterior, arranged in five longitudinal rows forming two fields separated by a barren stripe left of body´s midline (Fig. 189a, d, e, 190d, h, p–t; Table 70): right field composed of three rows, row 1 ends about 61% of body length, rows 2 and 3 end subterminally, row 3 extends dorsolaterally; left field composed of two rows, row 2 extends dorsolaterally. Three frontal and one buccal cirrus subapical of paroral membrane.

Dorsal bristles 3–4 µm long in vivo and in protargol preparations, arranged in two rows both with one or two caudal cirri (Fig. 189e, 190t, w, 191h, j, m; Table 70). Row 1 moderately shortened anteriorly, composed of an average of 11 equally distributed bristles. Row 2 almost bipolar, composed of an average of seven bristles more widely spaced in middle third of cell.

Oral apparatus very small compared to length of cell, in kahliellid pattern as described by Berger (2011). Adoral zone extends about 18% of body length, composed of an average of 18 membranelles 3–4 µm width and with cilia up to 15 µm long in vivo (Fig. 189a, c1, c2, d, 190a–k, p–s; Table 70). Buccal cavity short and narrow, covered by an about 4 µm wide, convex lip (Fig. 189a, c2, 190c–e). Paroral and endoral membrane straight to slightly curved, side by side but staggered by about 60%; paroral cilia about 3 µm long in vivo, endoral cilia at least 10 µm long, extend into pharyngeal funnel.

Characteristics	Mean	M	SD	SE	CV	Min	Max	n
	2.3	2.0	1.4	0.4	61.2	1.0	5.0	15
Right cirral row 3, number of cirri	18.6	19.0	1.8	0.4	9.5	15.0	23.0	21
	30.0	30.0	2.9	0.8	9.7	24.0	34.0	15
Posterior body end to left cirral row 2 (*N. halophila*) and to right cirral row 3 (*I. venezuelensis*), distance	4.5	3.8	2.7	0.6	60.3	1.0	10.0	20
	1.8	2.0	0.9	0.2	47.9	1.0	3.0	15
Left cirral row 1, number of cirri	13.7	14.0	1.5	0.3	10.6	11.0	16.0	21
	18.3	18.0	1.7	0.4	9.1	16.0	22.0	15
Left cirral row 2, number of cirri	13.4	14.0	1.6	0.4	12.2	10.0	17.0	21
	18.3	19.0	1.6	0.4	8.9	15.0	20.0	15
Left cirral row 3, number of cirri	absent							
	21.2	21.0	1.5	0.4	7.0	18.0	24.0	15
Dorsal kineties, number	2.0	2.0	0.0	0.0	0.0	2.0	2.0	21
	2.0	2.0	0.0	0.0	0.0	2.0	2.0	15
Kinetids in dorsal kinety 1, number	10.8	10.0	1.4	0.4	13.2	9.0	13.0	17
	16.0	16.0	1.4	0.4	8.5	14.0	18.0	15
Kinetids in dorsal kinety 2, number	6.7	7.0	–	–	–	6.0	7.0	15
	2.0	2.0	0.0	0.0	0.0	2.0	2.0	14
Caudal cirri, number in late dividers	2.1	2.0	–	–	–	2.0	3.0	16
	absent							
Resting cysts, diameter without slime cover	36.8	37.0	3.0	0.9	8.2	32.0	40.0	12
	not investigated							
Resting cysts, diameter with slime cover	42.3	43.0	2.8	0.8	6.6	36.0	45.0	12
	not investigated							

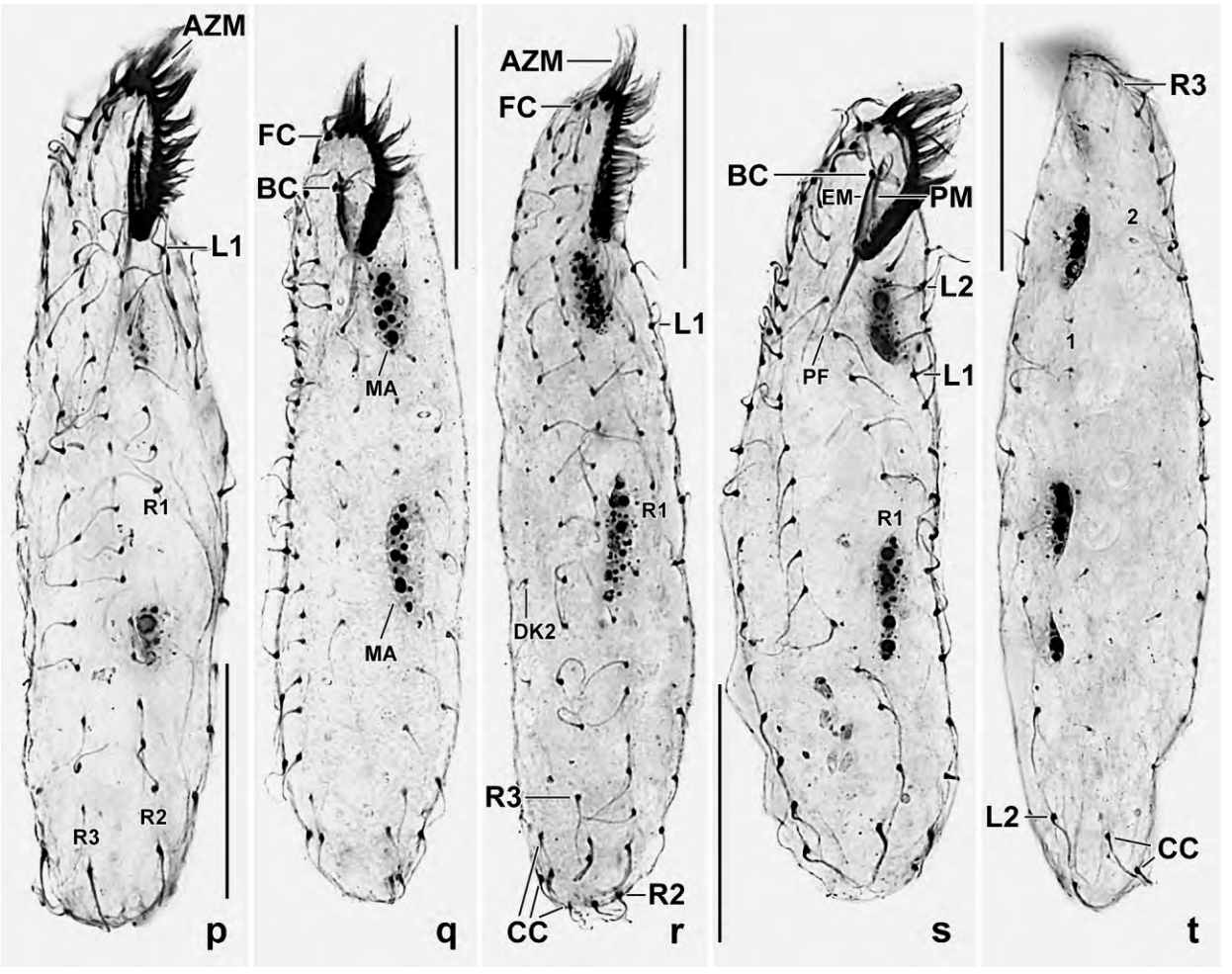

Fig. 190p–t. *Notodeviata halophila* after protargol impregnation. **p–s:** Ventral views, showing the ciliary pattern which consists of three cirral rows right (R1–3) and two left (L1, 2) of body´s midline. Further, there are three frontal cirri and one buccal cirrus. The macronuclear nodules have nucleoli mainly in the right half (see also [t]). **t:** Dorsal view, showing the two dorsal kineties each with a caudal cirrus posteriorly. AZM – adoral zone of membranelles, BC – buccal cirrus, CC – caudal cirri, DK2 – dorsal kinety 2, EM – endoral membrane, FC – frontal cirri, L1, 2 – cirral rows left of body´s midline, MA – macronuclear nodules, PF – pharyngeal fibres, PM – paroral membrane, R1–3 – cirral rows right of body´s midline, 1, 2 – dorsal kineties. Scale bars 30 µm.

Resting cyst (Fig. 189b, 190l–o; Table 70): Cysts in vivo perfectly spherical, on average 37 µm (without slime cover) or 42 µm (with slime cover) in diameter. Cyst wall 1–1.5 µm thick, structureless in the light microscope, stains pink with methyl green-pyronin; "slime" cover 1–3 µm thick, very hyaline but rigid and thus possibly the ectocyst, does not stain with methyl green-pyronin indicating a special (inorganic?) composition. Macronuclear nodules fused to a central mass (Fig. 190n, o). Cytoplasm packed with lipid (?) droplets, as morphostatic cells, and autophagous vacuoles up to 10 µm across.

Ontogenesis (Fig. 189f, 190u, v, x, 191a–o): The ontogenesis of *N. halophila* is rather simple, well illustrated, and described carefully in the Figure explanations. Thus, we concentrate on the important processes.

(v) The oral primordium originates apokinetally in mid-body between the right and the left cirral field (Fig. 189f).

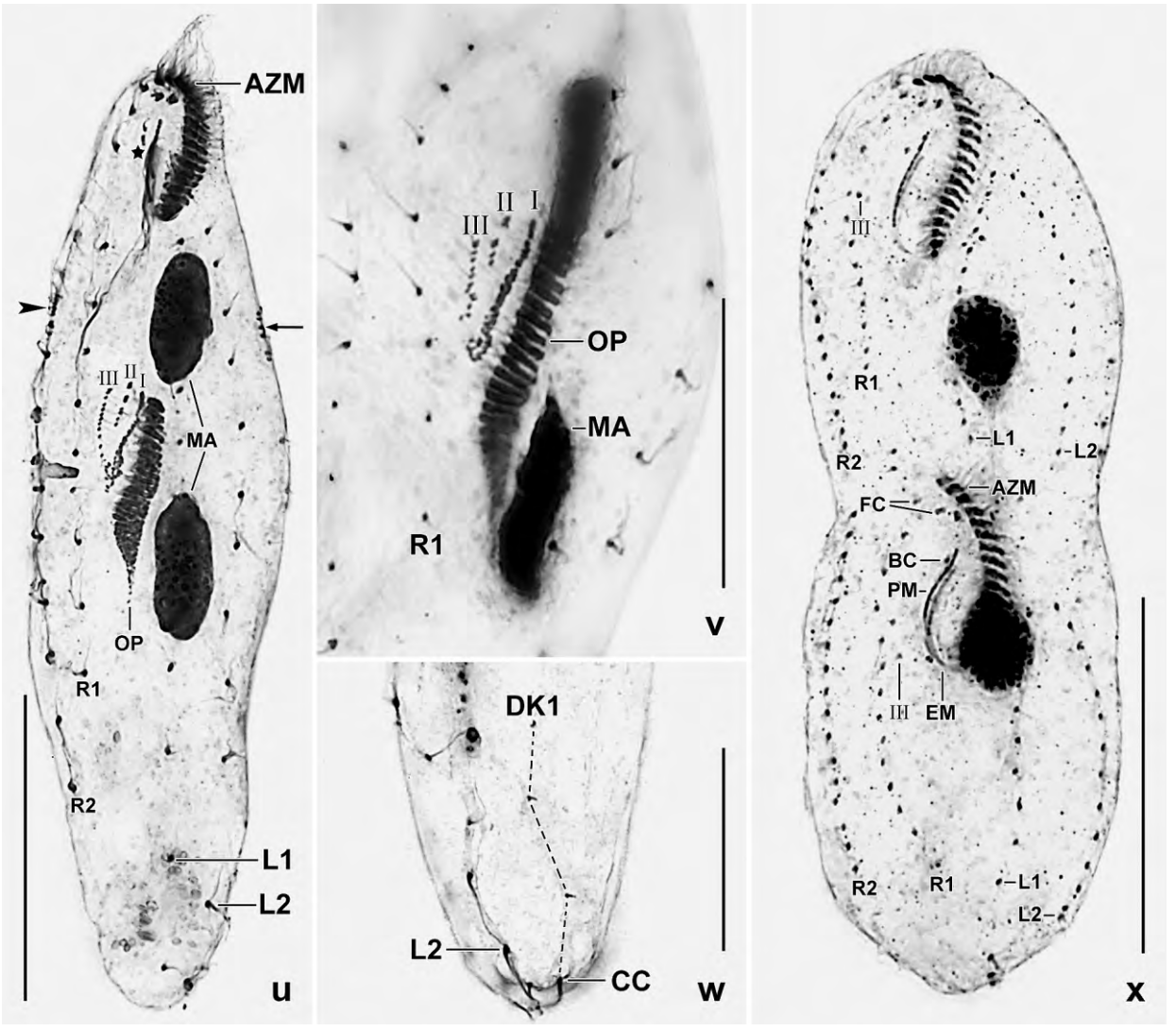

Fig. 190u–x. *Notodeviata halophila* after protargol impregnation. **u, v** (cp. Fig. 191a)**:** Ventral view of early dividers with three conspicuous cirral anlagen (I–III) in the opisthe. In the proter, the buccal cirrus becomes an anlage (asterisk). The arrowhead marks an anlage in cirral row 2 of the proter. The arrow marks an anlage in dorsal kinety 1. **w:** Dorsal view of posterior region of a morphostatic specimen. **x:** Ventral view of an early late divider which just resorbs anlage III. See Fig. 191i–k for a detailed explanation. AZM – adoral zone of membranelles, BC – buccal cirrus, CC – caudal cirri, DK1 – dorsal kinety 1, EM – endoral membrane, FC – frontal cirri, L1, 2 – cirral rows left of body´s midline, MA – macronuclear nodules, OP – oral primordium, PM – paroral membrane, R1,2 – cirral rows right of body´s midline, I–III – cirral anlagen. Scale bars 20 µm (w), 30 µm (v), and 40 µm (u, x).

(vi) Next, four cirral anlagen streaks develop in proter and opisthe. In the proter, anlage IV very likely develops de novo; the opisthe anlagen develop from the oral primordium. Concomitantly, anlagen are produced in all cirral rows and the dorsal kineties both in proter and opisthe (Fig. 190u, v, 191a–f).

(vii) In mid-dividers and early late dividers, the anlagen develop cirri and dorsal kinetids generate caudal cirri. Now, a curious process begins in the frontoventral anlagen II–IV of proter and opisthe, viz., a large-scale resorption of the just produced cirri. It culminates in the complete resorption of anlage IV and of most cirri in the anlagen II and III leaving three frontal cirri

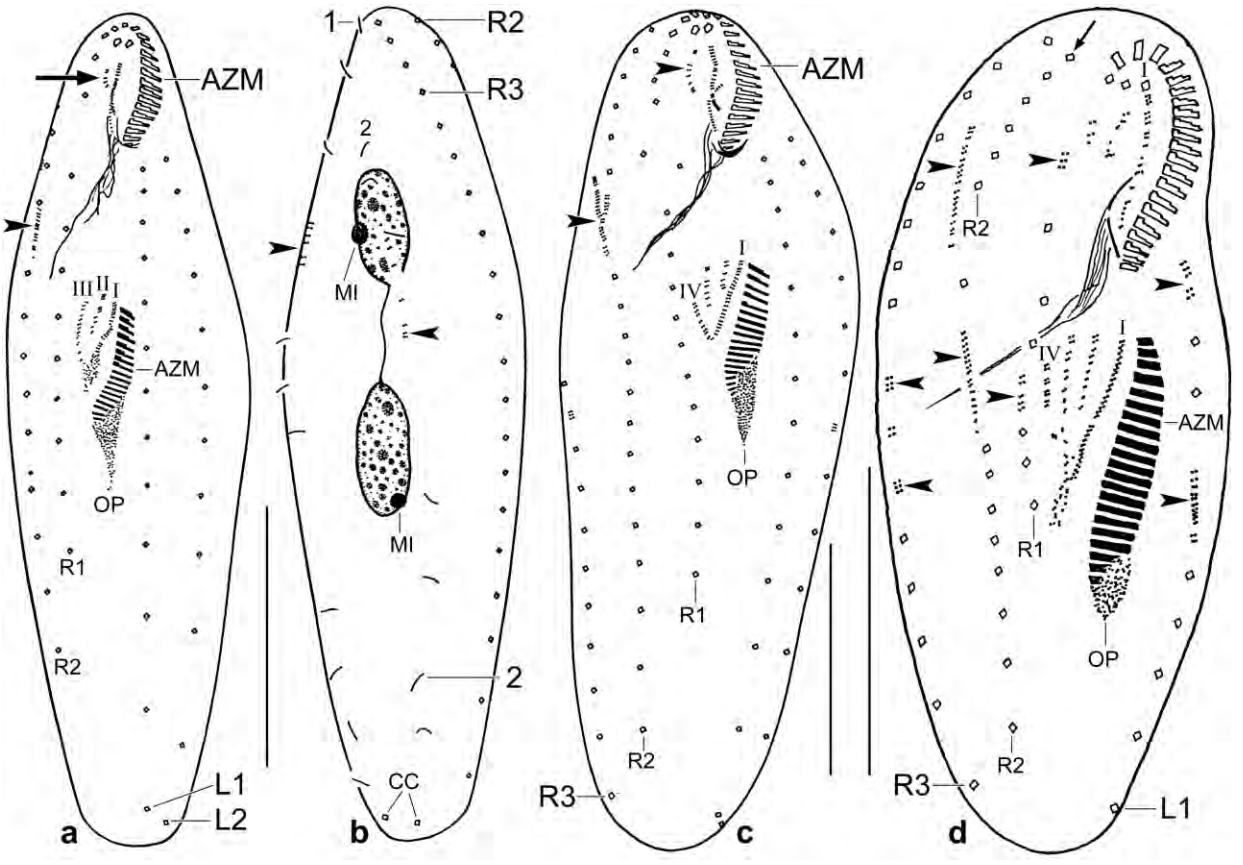

Fig. 191a–d. *Notodeviata halophila*, protargol-impregnated dividers. Parental structures shown by contour, new structures shadded black. For a very early divider, see Fig. 189f. The oral primordium originates apokinetally in body´s midline. **a, b:** Ventral and dorsal view of an early divider, showing two frontoventral anlagen (arrow, paroral membrane and buccal cirrus) in the proter and three (I-III) in the opisthe. In the proter, cirral row R2 develops an anlage (a, arrowhead). Intrakinetal anlagen develop in the dorsal kineties of the proter (b, arrowheads). **c:** Similar to (a) but a fourth cirral streak developed in the opisthe. The arrowheads mark cirral anlagen in the proter. **d:** A late early divider, showing three frontoventral cirral anlagen in the proter and four in the opisthe. The cirral rows R1, R2, R3 and L1 develop an anlage each in proter and opisthe (arrowheads). The arrow denotes the parental anterior portion of cirral row R2. AZM – adoral zone of membranelles, CC – caudal cirri, L1, 2 – cirral rows left of body´s midline, MI – micronucleus, OP – oral primordium, R1, 2, 3 – cirral rows right of body´s midline, 1, 2 – dorsal kineties, I–IV – frontoventral cirral anlagen. Scale bars 30 µm (c, d) and 40 µm (a, b).

and one buccal cirrus (Fig. 190x, 191g, j, k). On the dorsal side, the caudal cirri are formed, one or two in each kinety (Fig. 191h, l, m, o).

(viii) Late dividers have resorbed most parental cirri that were not involved in anlagen formation and most or all cirri in the frontoventral anlagen II–IV. Thus the morphostatic cirral pattern is now well recognizable (Fig. 191n, o).

Occurrence and ecology: As yet found only at type locality, a highly saline (~ 50‰) soil from the north coast of Venezuela. The slender shape indicates that *N. halophila* is a "true" soil ciliate.

Remarks: Among the deviatids and kahliellids reviewed by Berger (2011), *Notodeviata* is unique in having the frontoventral ciliature reduced to three frontal cirri and one buccal cirrus (Fig. 189a, b). Ontogenesis indicates that this is a young trait because much more cirri are produced but later resorbed. The next similar species is → *Idiodeviata venezuelensis* which possesses three frontal

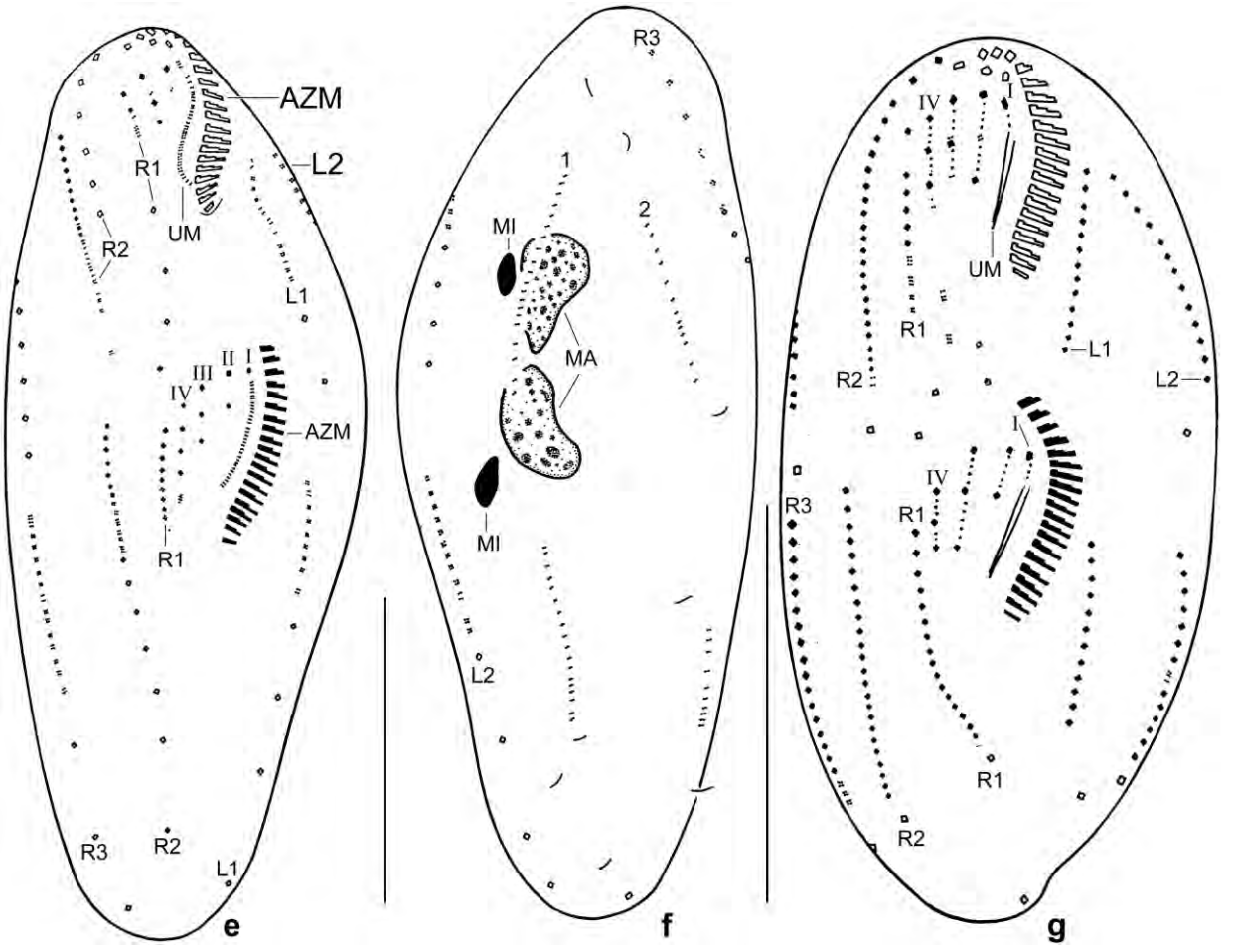

Fig. 191e–g. *Notodeviata halophila*, protargol-impregnated dividers. Parental structures shown by contour, new structures shadded black. **e, f:** Ventral and dorsal view of an early mid-divider with three frontoventral cirral anlagen in the proter and four in the opisthe. The cirral rows R1, 2, 3 and L1, 2, as well as the dorsal kineties divided intrakinetally. The anlagen for the undulating membranes have developed and the new adoral zone of membranelles has been completed. **g:** Ventral view of a mid-divider (dorsal view on next page) having four frontoventral cirral anlagen each in proter and opisthe; very likely, the fourth anlage of the proter developed from cirral row R1. The new cirral rows have been formed and some parental cirri have been resorbed. AZM – adoral zone of membranelles, L1, 2 – cirral rows left of body´s midline, MA – macronuclear nodules, MI – micronuclei, R1, 2, 3 – cirral rows right of body´s midline, UM – anlage for the undulating membranes, 1, 2 – dorsal kineties, I–IV – frontoventral cirral anlagen. Scale bars 40 µm.

cirri, cirrus III/2, and one buccal cirrus.

In vivo, *N. halophila* is easily confused with → *Idiodeviata venezuelensis* (two vs. four macronuclear nodules) and the binucleate *Deviata* species reviewed by Berger (2011): *D. abbrevescens* (macronuclear nodules ellipsoid vs. rod-shaped), *D. bacilliformis* (when binucleate; without vs. with a short row of frontoventral cirri), and *D. estevesi* (slender vs. rather broad and with four vs. many cirri in frontal area; possibly belongs to *Parastrongylidium*, see Berger 2011 for a detailed discussion).

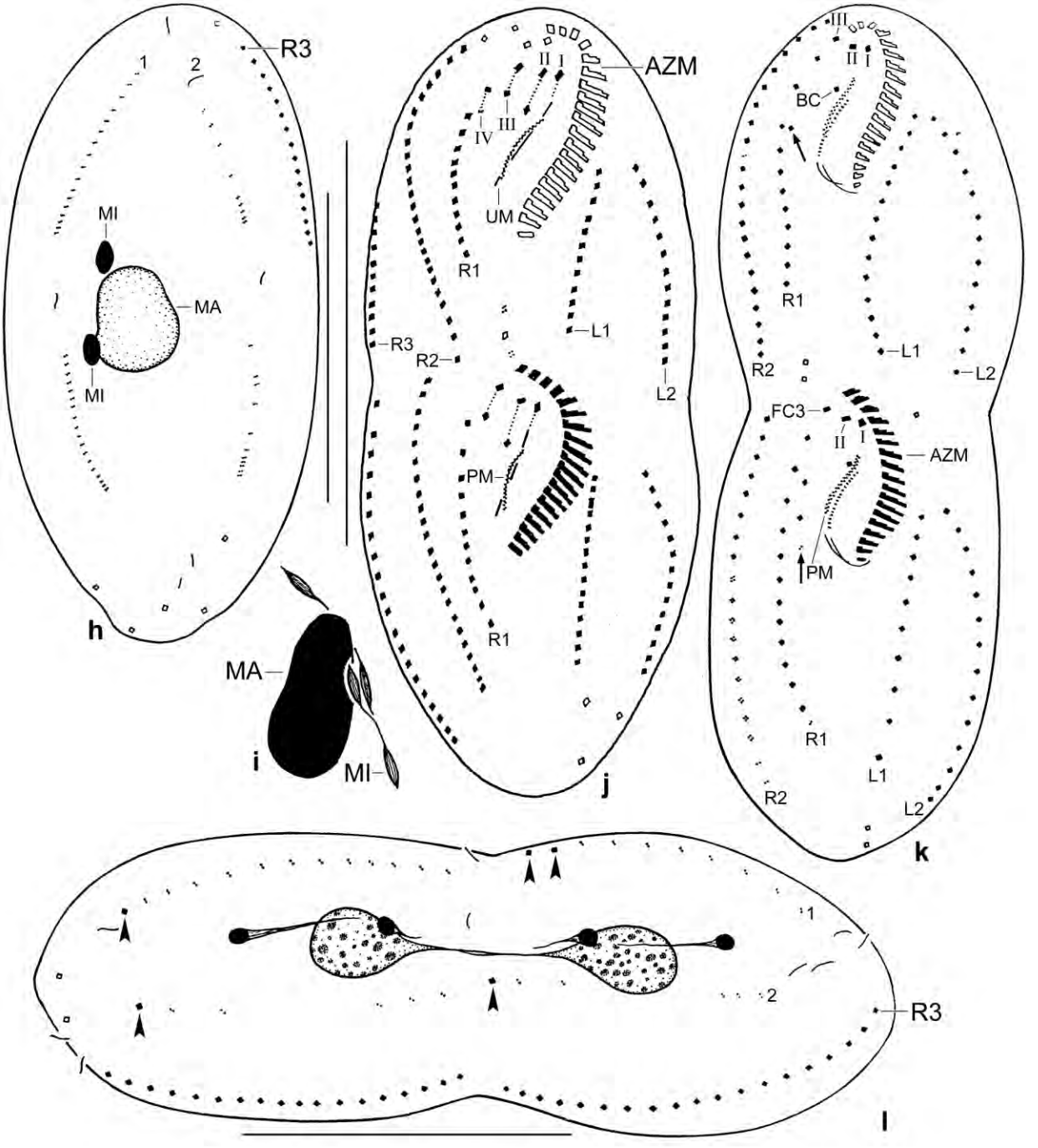

Fig. 191h–l. *Notodeviata halophila*, protargol-impregnated dividers. Parental structures shown by contour, new structures shadded black. **h:** Dorsal view of the specimen shown in Fig. 191g. The macronuclear nodules fused to a globular mass and the new dorsal dikinetids polymerize to caudal cirri posteriorly. **i, j:** Ventral view of an early late divider with beginning cytokinesis and dividing micronuclei. Now a curious process commences, viz., the resorption of most of the newly formed frontoventral cirri. Most of the parental cirri that were not involved in anlagen formation have been resorbed. **k, l:** Ventral and dorsal view of an early late divider with dividing macronuclear mass and completed micronuclear division. Half of the newly formed frontoventral cirri have been resorbed; the arrows mark the last cirrus of anlage III. Caudal cirri have been produced at posterior end of both dorsal kineties (l, arrowheads). AZM – adoral zone of membranelles, BC – buccal cirrus, FC3 – frontal cirrus 3, L1, 2 – cirral rows left of body´s midline, MA – macronucleus, MI – micronuclei, PM – paroral membrane, R1, 2, 3 – cirral rows right of body´s midline, UM –undulating membranes, 1, 2 – dorsal kineties, I–IV – frontoventral cirral anlagen. Scale bars 40 µm.

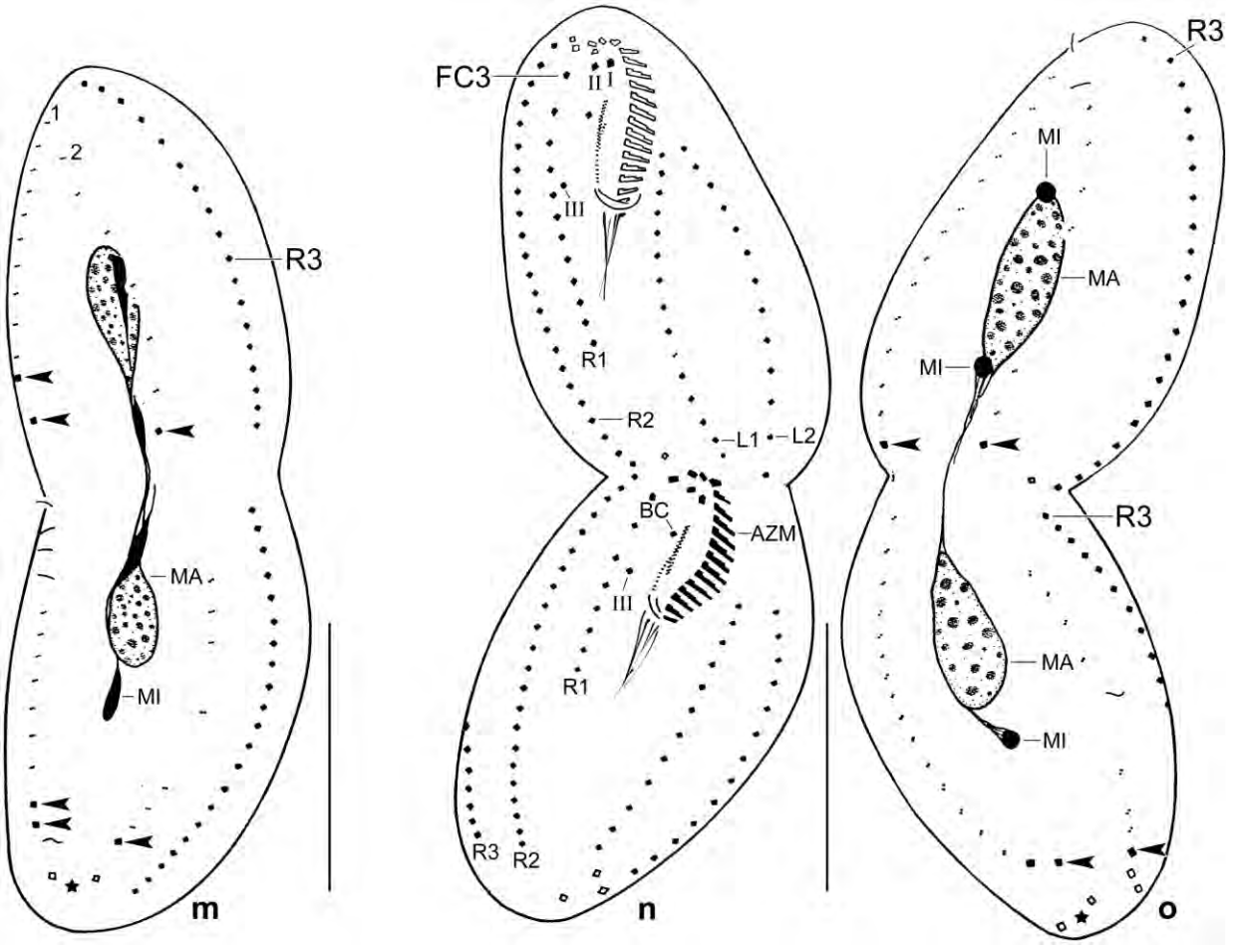

Fig. 191m–o. *Notodeviata halophila*, dividers after protargol impregnation. **m:** Dorsal view of an early late divider, showing the production of three caudal cirri each in proter and opisthe (arrowheads). The asterisk marks parental caudal cirri. **n, o:** Ventral and dorsal view of a late divider which has resorbed half of the new frontoventral cirri (cp. Fig. 191e); the last cirrus of anlage III is usually resorbed in early post-dividers, but it may also persist (Fig. 189f, 190c). Likewise, most of the parental cirri, shown by contour, have been resorbed. The asterisk in (o) denotes two parental caudal cirri while the arrowheads mark new caudal cirri, two in the proter, three in the opisthe. AZM – adoral zone of membranelles, BC – buccal cirrus, FC3 – frontal cirrus 3, L1, 2 – cirral rows left of body´s midline, MA – macronuclear nodules, MI – micronuclei, R1–3 – cirral rows right of body´s midline, 1, 2 – dorsal kineties, I–III – cirral anlagen. Scale bars 30 µm.

Idiodeviata nov. gen.

Diagnosis: Dorsomarginalian Deviatidae with frontoventral and buccal cirri. The oral primordium originates apokinetally between right and left cirral field. Four frontoventral cirral anlagen. Dorsal kinety 2 originates dorsomarginally. Caudal cirri absent.

Type species: *Idiodeviata venezuelensis* nov. spec.

Etymology: The name is a composite of the Latin preposition *idio* (following its own way, strange) and the Latin adjective *devius* (aside its way, special, curious), emphasizing the differences to → *Notodeviata*. Feminine gender.

Remarks: *Idiodeviata* is very likely closely related to → *Notodeviata*, differing by the absence of caudal cirri and an only slight resorption of newly produced cirri in the frontoventral anlagen. This combination of features, to which the apokinetal production of the oral primordium and the dorsomarginally generated dorsal kinety 2 must be added, is unique to *Idiodeviata*, separating it from all kahliellids s. l. and the deviatids reviewed by Berger (2011).

Possibly, *Deviata rositae* Küppers et al., 2007 very likely belongs to *Idiodeviata* because it has the same ciliature, including cirrus III/2. However, a transfer would need ontogenetic data on the oral primordium and dorsal kinety 2.

Idiodeviata venezuelensis nov. spec. (Fig. 192a–t, 193a–c; Table 70)

Diagnosis: Size in vivo about 100 × 20 µm. Very narrowly ellipsoid, hardly flattened laterally. 4 macronuclear nodules frequently forming two indistinct pairs each with a micronucleus between macronuclear pairs. 3 cirral rows each right and left of body´s midline; 3 frontal cirri; 1 buccal cirrus right of anterior end of paroral membrane; and with cirrus III/2. 2 dorsal kineties; kinety 1 bipolar, kinety 2 reduced to 2 subapical bristles. Adoral zone extends 24% of body length, composed of an average of 19 membranelles. Buccal cavity short and narrow. Paroral and endoral membrane optically side by side but staggered by about 30%.

Type locality: Venezuelan site (65), i. e., highly saline soil from the north coast, Morrocoy NP, surroundings of the village of Chichiriviche, 67°13‘W 11°33‘N.

Type material: 1 holotype and 5 paratype slides with protargol-impregnated morphostatic and dividing specimens have been deposited in the Biology Centre of the Upper Austrian Museum in Linz (LI). The holotype, various paratypes, and the dividers shown have been marked by black ink circles on the coverslip.

Etymology: Named after the country in which it was discovered, i. e., Venezuela.

Description: *Idiodeviata venezuelensis* occurred in the same sample as → *Notodeviata halophila* but was less abundant. Although we recognized specimens with two or four macronuclear nodules during live observation, we did not separate them because the other features were highly similar and the number of macronuclear nodules is sometimes rather variable in this group of hypotrichs (Berger 2011). However, protargol impregnation revealed two distinct species but we had already abandoned the sample. Thus, we cannot provide specific in vivo data. However, *I. venezuelensis* is in vivo very similar to → *N. halophila,* except for the number of macronuclear nodules.

The sample was fixed with ethanol which made clear protargol preparations but poorly preserved body size and shape, specifically most cells became strongly inflated. Thus, we cannot provide exact in vivo size and shape data but emphasize the overall similarity with → *N. halophila* which is likely slightly longer and thinner than *I. venezuelensis.*

Cirri about 10 µm long in protargol-impregnated cells. Frontoventral cirri and first cirri of longitudinal rows usually slightly thickened, i. e., composed of 6–8 cilia; main portion of rows with cirri composed of four cilia; most cirri of rear portion composed of only two cilia. Intracirral

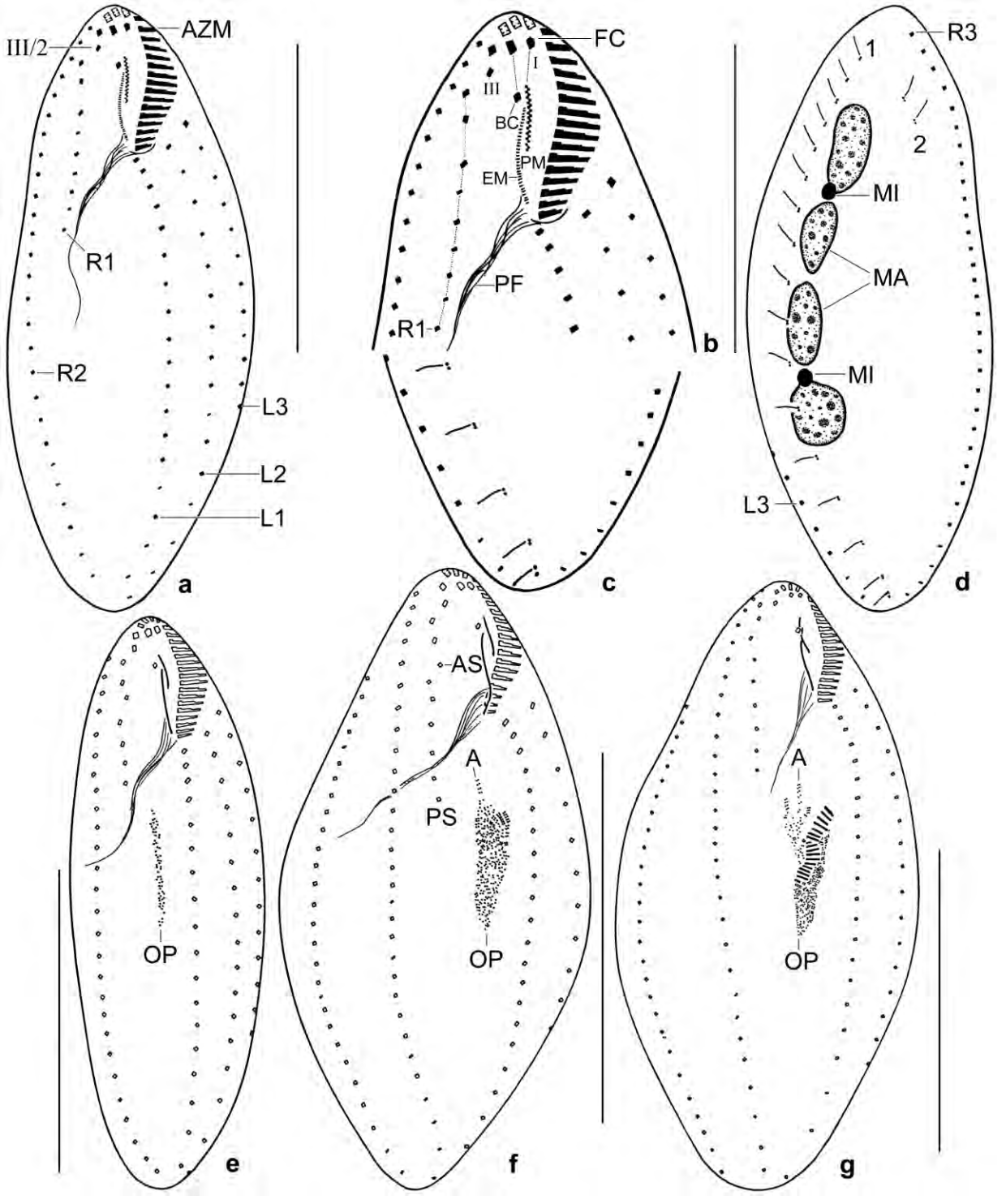

Fig. 192a–g. *Idiodeviata venezuelensis*, ventral and dorsal views of morphostatic (a–d) and dividing (e–g) specimens after protargol impregnation. **a–d:** Cirri originating from same anlage connected by dots. **e–g:** Very early and early dividers, showing the apokinetally developing oral primordium and cirral anlagen (A). AS – anterior segment of anlage IV, AZM – adoral zone of membranelles, BC – buccal cirrus, EM – endoral membrane, L1, 2, 3 – cirral rows left of body´s midline, MA – macronuclear nodules, MI – micronuclei, OP – oral primordium, PF – pharyngeal fibres, PM – paroral membrane, PS – posterior segment of anlage IV, R1, 2, 3 – cirral rows right of body´s midline, 1, 2 – dorsal kineties, I, III, IV – cirral anlagen. Scale bars 50 μm.

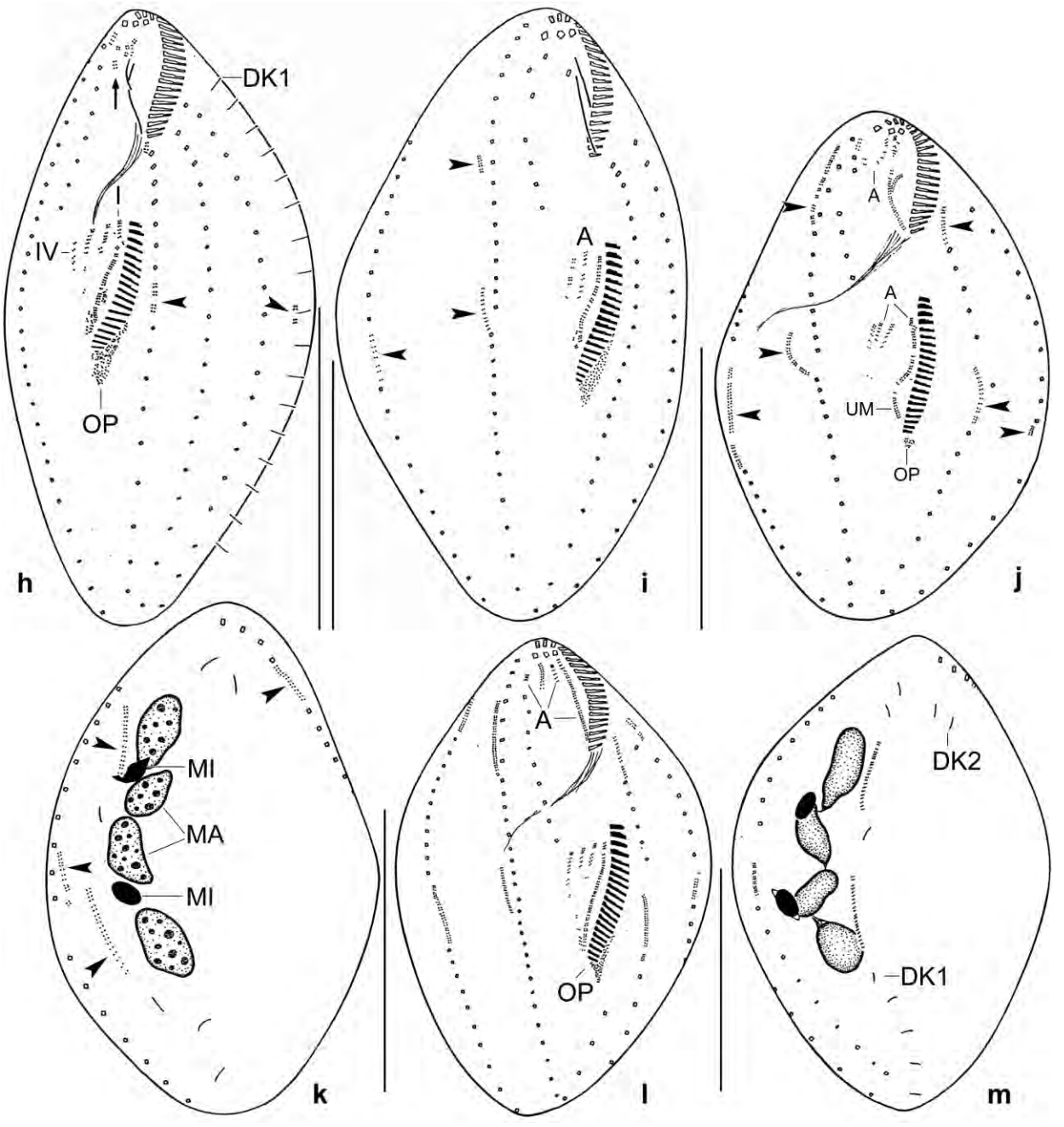

Fig. 192h–m. *Idiodeviata venezuelensis*, ventral (h–j, l) and dorsal (k, m) views of protargol-impregnated early mid-dividers characterized by the origin of anlagen (arrowheads) in the cirral rows and four frontoventral cirral anlagen. **h, i:** Two stages, showing that the ontogenetic processes may have a slightly different time-table: the specimen shown in (h) has four cirral anlagen in the opisthe and is just commencing anlagen formation in the left cirral row 1 and in dorsal kinety 1 (arrowheads); the specimen shown in (i) has only three opisthe cirral anlagen while the anlagen in the right cirral rows are already distinct (arrowheads). **j, k:** Ventral and dorsal view of same specimen. Distinct anlagen developed in proter, in all cirral rows, and in dorsal kinety 1 (arrowheads). **l, m:** Ventral and dorsal view of same specimen. Four anlagen for the frontoventral cirri and the undulating membranes developed in proter and opisthe. The macronuclear nodules dissolved the nucleoli and became connected by an argyrophilic strand. A – anlagen for the frontoventral cirri and the undulating membranes, DK – dorsal kineties, MA – macronuclear nodules, MI – micronuclei, OP – oral primordium, UM – undulating membranes, I, IV – cirral anlagen. Scale bars 40 µm.

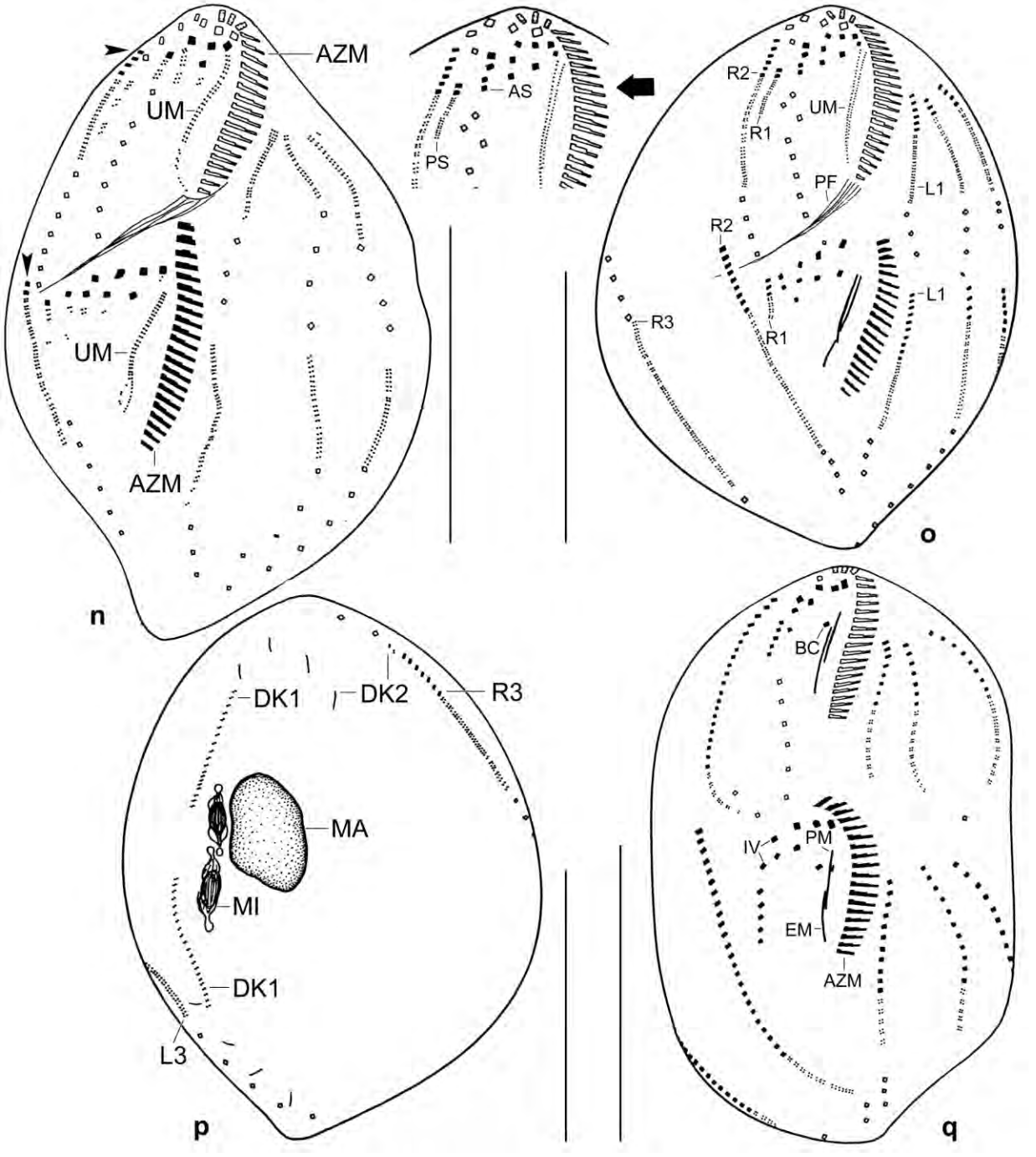

Fig. 192n–q. *Idiodeviata venezuelensis*, ventral (n, o, q) and dorsal (p) views of mid-dividers. Parental structures shown by contour, newly formed shadded black. **n:** Cirri begin to form in the frontoventral anlagen and in the anlagen of the right rows (arrowheads). **o, p:** In mid-dividers, the macronuclear nodules fuse to a globular mass. The production of cirri within the anlagen proceeds; the rightmost frontoventral cirral anlage is composed of an anterior segment and a posterior segment slightly displaced to the right. Dorsal kinety 2 is generated dorsomarginally. **q** (dorsal view, see next plate)**:** The new ciliature is almost finished and most of the cirri that were not involved in anlagen formation have been resorbed. AS – anterior segment of anlage IV, AZM – adoral zone of membranelles, BC – buccal cirrus, DK1, 2 – dorsal kineties, EM – endoral membrane, L1, 3 – cirral rows left of body´s midline, MA – macronuclear mass, MI – micronuclei, PF – pharyngeal fibres, PM – paroral membrane, PS – posterior segment of anlage IV, R1, 2, 3 – cirral rows right of body´s midline, UM – undulating membranes, IV – frontoventral cirral anlage. Scale bars 40 μm.

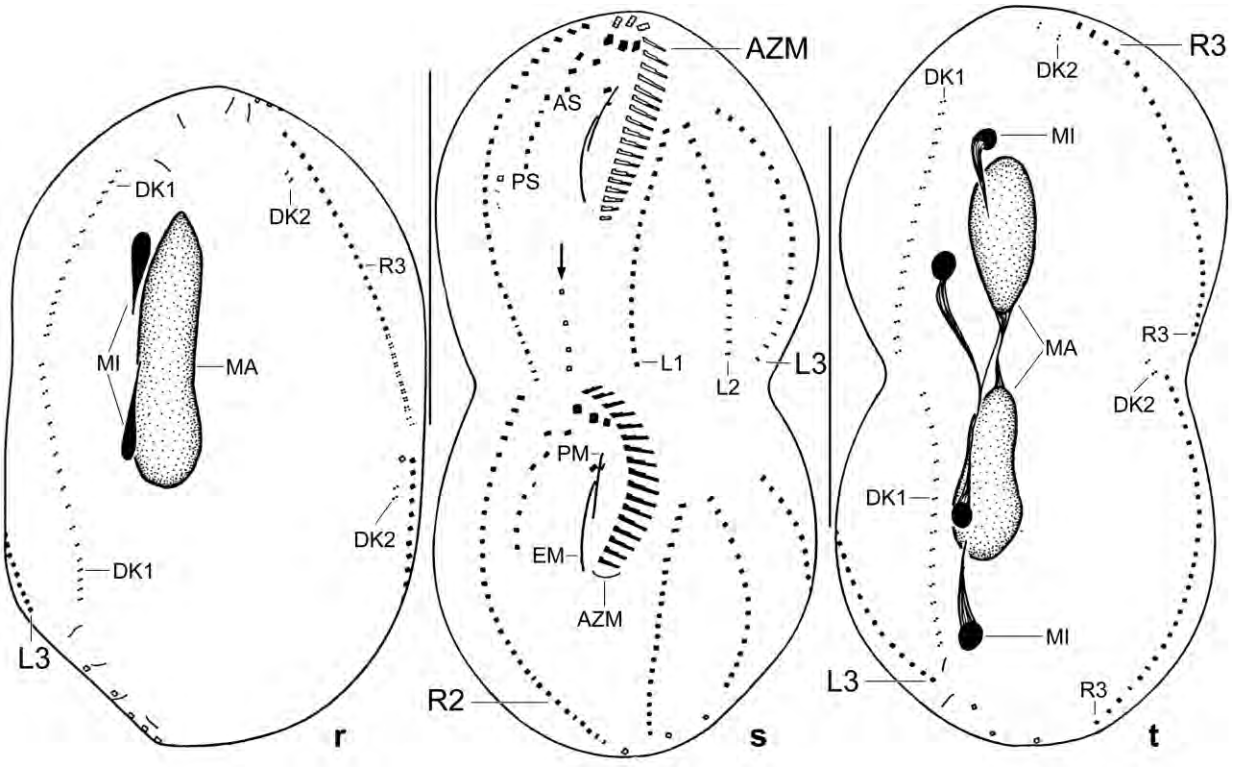

Fig. 192r–t. *Idiodeviata venezuelensis*, ventral (s) and dorsal (r, t) views of a mid-divider (r) and of a late divider (s, t). Parental structures shown by contour, newly formed shadded black. **r:** Dorsal view of the mid-divider shown in Fig. 192q. The globular macronuclear mass (Fig. 192p) elongates and the micronuclei commence division. Dorsal kinety 1 has been generated by within anlagen while kinety 2 has been produced dorsomarginally. **s, t:** Ventral and dorsal view of a late divider, showing the first round of macronuclear division and the second round of micronuclear division. The new ciliature is finished and most cirri that were not involved in anlagen formation have been resorbed. The arrow marks the posterior, not yet resorbed cirri of the parental frontoventral cirral row. AS – anterior segment of anlage IV, AZM – adoral zone of membranelles, DK1, 2 – dorsal kineties, EM – endoral membrane, L1, 2, 3 – cirral rows left of body´s midline, MA – macronuclear nodules, MI – micronuclei, PM – paroral membrane, PS – posterior segment of anlage IV, R2 – cirral row right of body´s midline. Scale bars 40 µm.

distances hardly increase from anterior to posterior. Cirri arranged in three nearly bipolar rows each right and left of a wide, barren stripe in body´s midline, except of right row 1 extending only 33% of body length on average (Fig. 192a, b, d–g, 193a–c; Table 70).

Dorsal bristles 3 µm long in protargol-impregnated cells, arranged in two rows without caudal cirri (Fig. 192c, d, 193c). Row 1 slightly shortened anteriorly, composed of an average of 16 dikinetids with intrakinetid distances slightly increasing from anterior to posterior. Row 2 distinctly subapical, composed of only two dikinetids.

Oral apparatus small compared to length of cell, i. e., adoral zone extends only 24% of body length, composed of an average of 19 ordinary membranelles with largest bases about 5 µm wide and cilia about 10 µm long in protargol preparations (Fig. 192a, b, 193a, b; Table 70). Buccal cavity short and narrow, likely covered by a convex lip. Paroral and endoral membrane slightly curved, side by side but staggered by about 30%. Pharyngeal fibres extend obliquely backwards, about 25 µm long.

Ontogenesis (Fig. 192c–t): The ontogenesis of *I. venezuelensis* is well illustrated and described in the Figure explanations. Thus, we concentrate on the diagnostic processes.

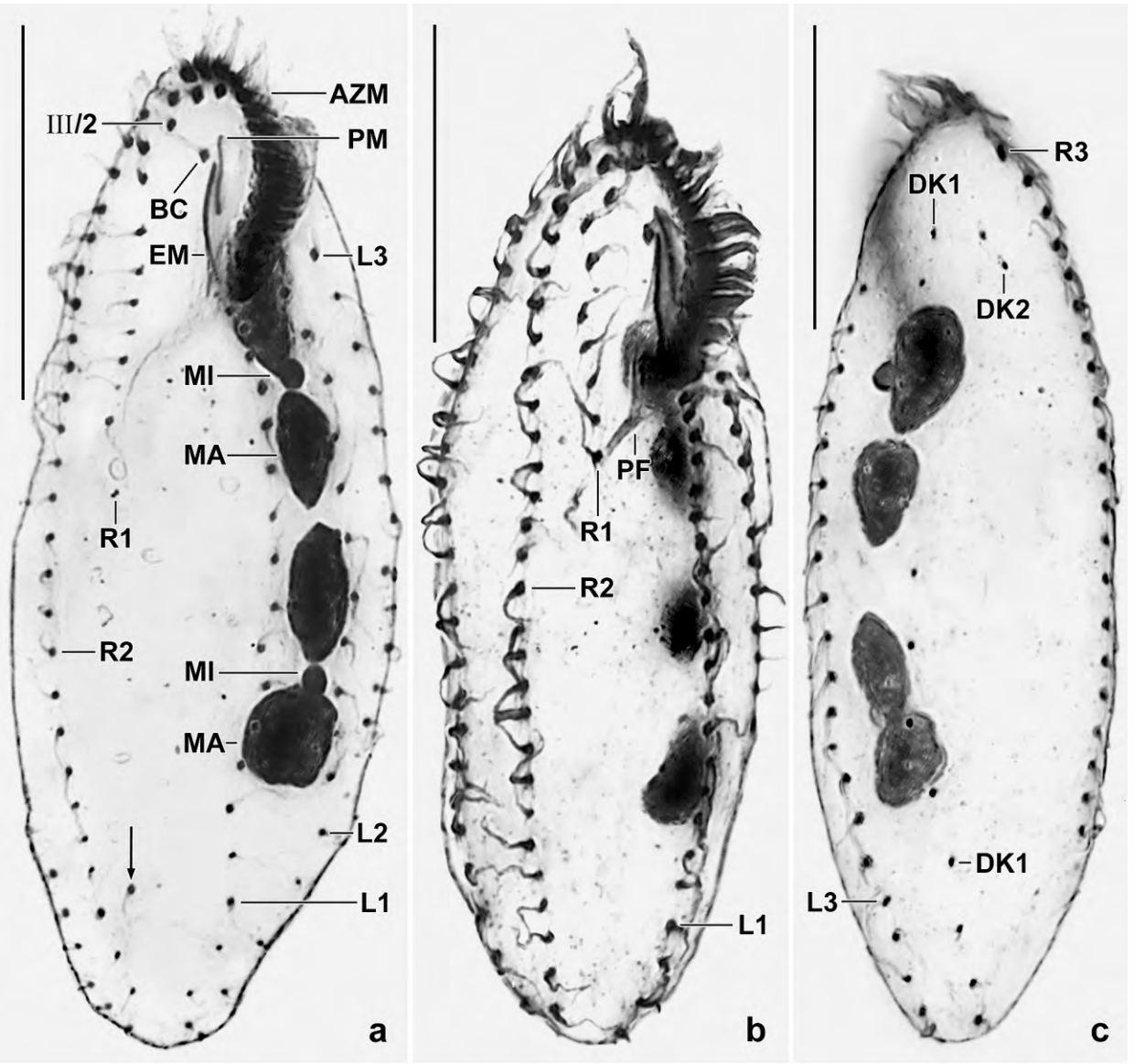

Fig. 193a–c. *Idiodeviata venezuelensis* after protargol impregnation. **a, b:** Ventral views, showing the infraciliature and the nuclear apparatus. The arrow in (a) marks a supernumerary cirrus. **c:** Dorsal infraciliature. Dorsal kinety 2 consists of only two kinetids which originate dorsomarginally. AZM – adoral zone of membranelles, BC – buccal cirrus, DK1, 2 – dorsal kineties, EM – endoral membrane, L1, 3 – cirral rows left of body´s midline, MA – macronuclear nodules, MI – micronuclei, PF – pharyngeal fibres, PM – paroral membrane, R1–3 – cirral rows right of body´s midline, III/2 – second cirrus of anlage III. Scale bars 30 µm.

(i) The oral primordium originates apokinetally in mid-body between the right and the left cirral field (Fig. 192e).

(ii) Next, four cirral anlagen each develop in proter and opisthe (Fig. 192f–j, l, n, o, q). In the proter, anlage I originates from the parental undulating membranes, anlage II develops from the buccal cirrus, anlage III very likely originates from cirrus III/2, and anlage IV is generated either de novo or from the anteriormost cirrus of right cirral row 1. In the opisthe, the four anlagen originate from the oral primordium. Anlage IV, which generates the short right cirral row 1, originates in two steps in proter and opisthe: anteriorly, three cirri from anlage IV form

an anterior segment; then, a posterior segment with four to six cirri is generated (de novo?) and usually slightly dislocated to the right, producing an inconspicuous break recognizable also in most morphostatic specimens and in early dividers (Fig. 192e, f).

(iii) Concomitantly with the production of the frontoventral cirral anlagen those of the ordinary cirral rows and of dorsal kinety 1 are generated right of the parental rows in the right field, within the rows in the left.

(iv) In middle and late dividers, dorsal kinety 2, which consists of only two kinetids, is generated dorsomarginally (Fig. 192p, r, t); however, we cannot entirely exclude a de novo origin because the minute details are very difficult to interpret.

(v) Late dividers have resorbed most parental cirri that were not involved in anlagen formation and two to four supernumerary cirri in anlagen I–III. Thus, the morphostatic cirral pattern is now well recognizable (Fig. 192s, t).

Occurrence and ecology: As yet found only at type locality, a highly saline (~ 50‰) soil from the north coast of Venezuela. The moderate size and the slender shape indicate that *I. venezuelensis* is a "true" soil ciliate.

Remarks: In vivo, *Idiodeviata venezuelensis* is very similar to → *Notodeviata halophila*, except for the number of macronuclear nodules (four vs. two). Further, *I. venezuelensis* is easily confused with several quadrinucleate *Deviata* species (see Berger 2011 for the species now mentioned): *D. bacilliformis* (6 vs. 10 postoral cirral rows), *D. quadrinucleata* (6 vs. 10 postoral cirral rows), *D. brasiliensis* (first cirral row right of body´s midline ends anterior vs. posterior of mid-body, dorsal kinety 2 reduced to two anterior dikinetids vs. bipolar), *D. spirostoma* (~ 20 vs. 45–50 adoral membranelles, body length in vivo about 100 vs. 180 µm), and *D. polycirrata* (body size in vivo about 100 × 20 µm vs. 152 × 62 µm, about 20 vs. 43 adoral membranelles, 6 vs. 9–13 postoral ciliary rows).

Generally, this type of hypotrichs is difficult to identify in vivo, and there might be further such species not yet described. Thus, the identification should be checked in protargol preparations.

Deviata brasiliensis Siqueira-Castro et al., 2009 (Fig. 194a–d, 195a–n; Table 71)

Material: 4 voucher slides with protargol-impregnated specimens from Venezuelan site (56) have been deposited in the Biology Centre of the Upper Austrian Museum in Linz (LI). Relevant specimens have been marked by black ink circles on the coverslip.

Observations and Remarks on a Venezuelan population: *Deviata brasiliensis* Siqueira-Castro et al., 2009 has been discovered in Brazil and is characterized, according to the original description, by having 4 (2–6) macronuclear nodules; 1 (1–3) parabuccal cirrus; 7 (7–11) long cirral rows of which the innermost right row (R4) is posteriorly shortened; 22 (18–31) adoral membranelles; and 2 dorsal kineties, with kinety 2 anteriorly shortened and its posterior kinetids very widely spaced.

Detailed morphometric data on *Deviata brasiliensis* from Venezuelan site (56) are presented and compared with specimens from the Brazilian type population (Table 71). The cultivated

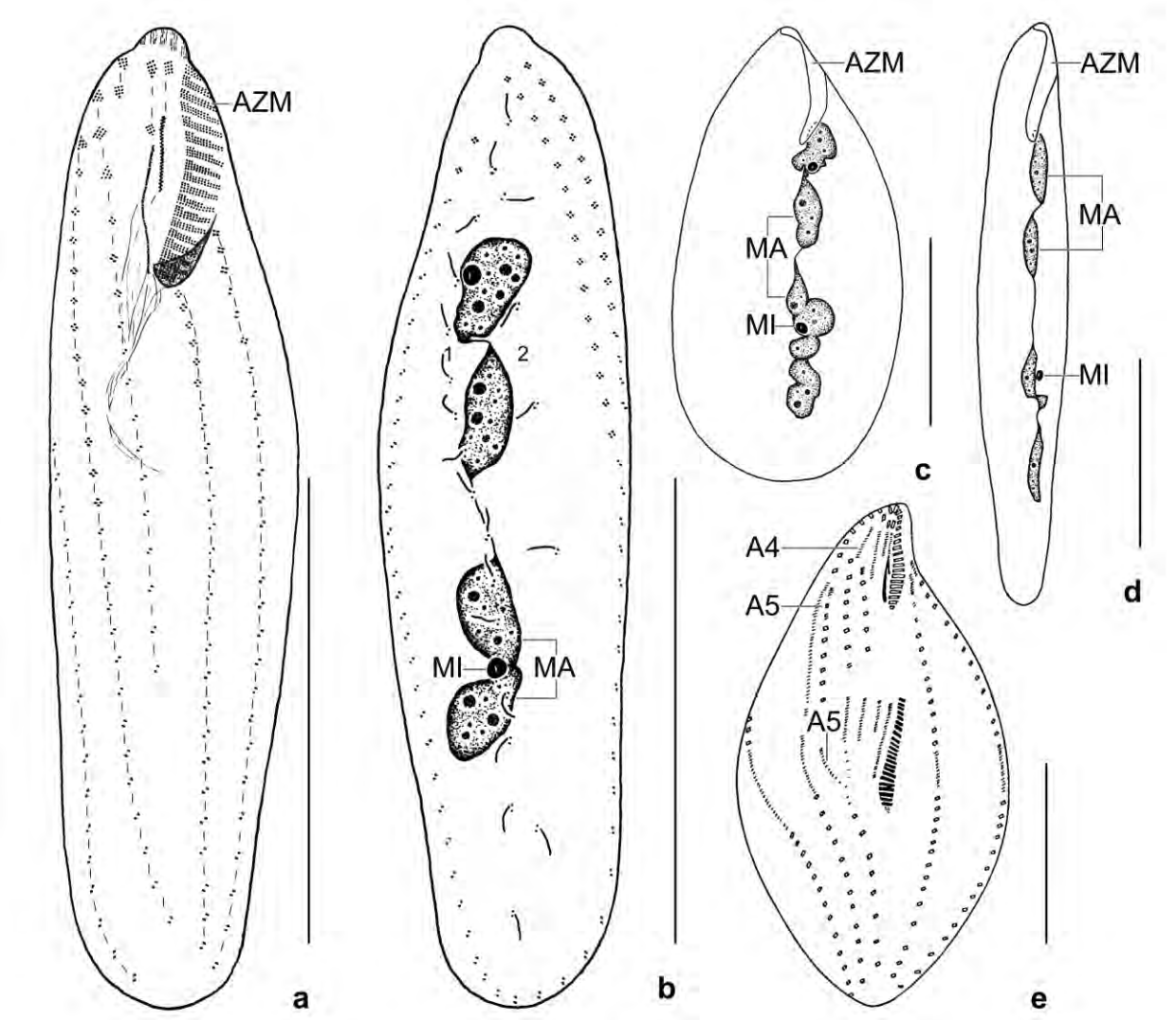

Fig. 194a–e. *Deviata brasiliensis* (a–d) from Venezuelan site (56) and *Deviata abbrevescens* from Austria (e, from EIGNER 1995) after protargol impregnation. **a, b:** Ventral and dorsal view of a representative specimen, showing the infraciliature and the nuclear apparatus, length 104 µm. Cirral rows on ventral side are emphasized by dashes. **c:** Outline and nuclear apparatus of an oblong specimen, length 116 µm. **d:** Outline and nuclear apparatus of a slender specimen, length 154 µm. **e:** Ventral view of a mid-divider of *D. abbrevescens*, showing that its ontogenetic pattern is identical with that of *D. brasiliensis* (Fig. 195e–g). 1, 2 – dorsal kineties, A4, A5 – cirral anlagen, AZM – adoral zone of membranelles, MA – macronuclear nodules, MI – micronuclei. Scale bars 50 µm.

Venezuelan specimens have a highly variable length:width ratio (Fig. 194a–d, 195a–d), depending on the amount of food ingested. Slender specimens (length:width ratio 3.8–7.8) with an ordinary number of food vacuoles make 83 % of the population (n = 393) while 17 % of the cells are studded with starch grains and are thus oblong (length:width ratio < 3.8). Besides the length:width ratios of body and macronuclear nodules, no differences occur between the slender and the oblong individuals.

In general, the Venezuelan population is less variable then the type population, as shown by the lower coefficient of variation for almost every character studied (Table 71). For example, more than one parabuccal cirrus or more than three long cirral rows left of the adoral zone are

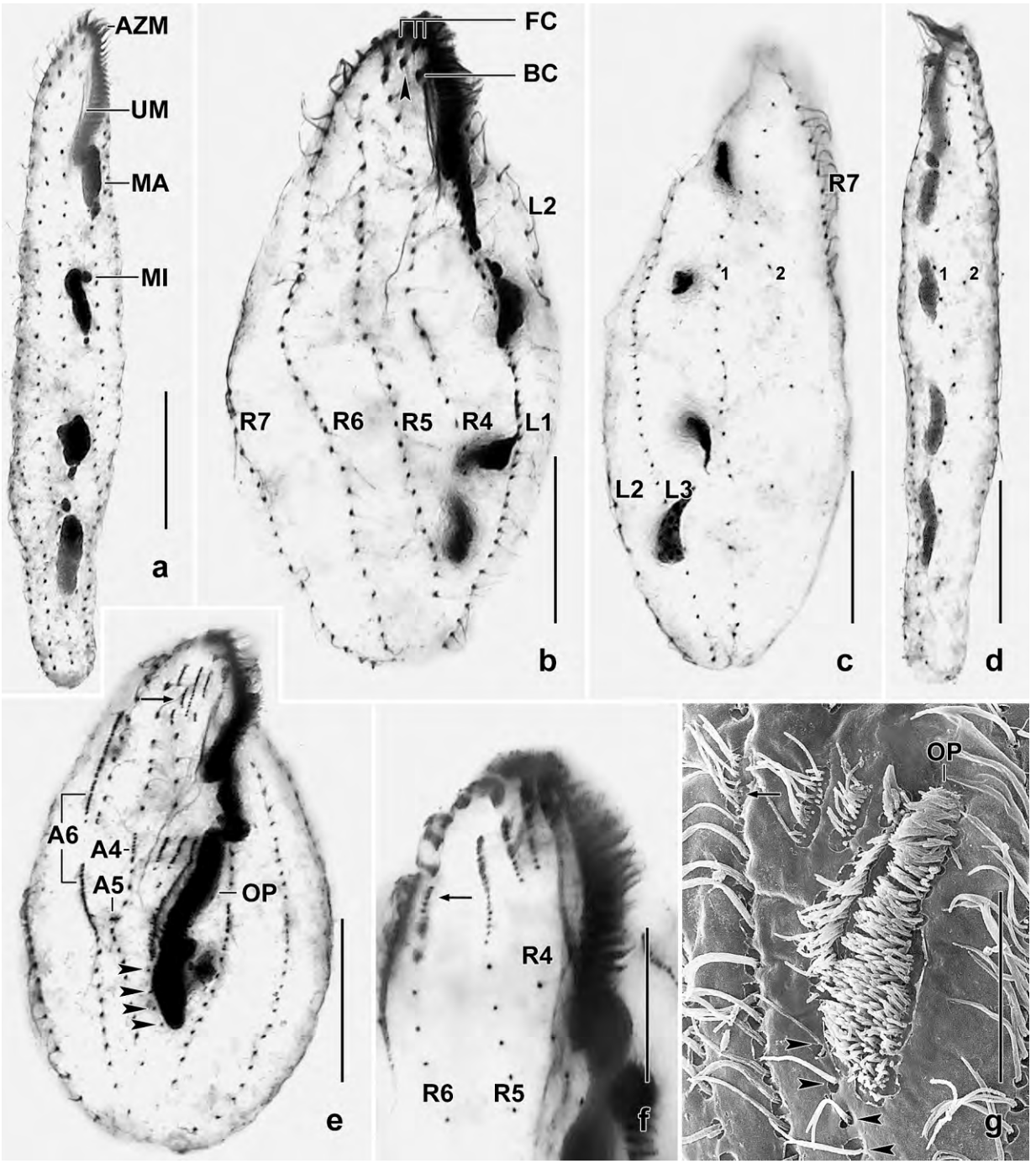

Fig. 195a–g. *Deviata brasiliensis* from Venezuelan site (56) after protargol impregnation (a–f) and in the scanning electron microscope (g). **a–d:** Ventral (a, b) and dorsal (c, d) views of slender and oblong specimens. Arrowhead denotes the parabuccal cirrus III/2. **e:** Mid-divider, showing a fragmentation of proter anlage A4 (arrow) which may cause unaligned cirri in some specimens (Fig. 195k). Arrowheads denote posterior cirri of row R4. **f:** Anterior portion of a mid-divider, showing anlage 5 of the proter (arrow) originating within row R6. **g:** Opisthe of a mid-divider, showing anlage 4 (arrow) originating within row R5 and the remaining posterior cirri of row R4 (arrowheads). AZM – adoral zone of membranelles, BC – buccal cirrus, FC – frontal cirri, L1–L3 – cirral rows left of AZM, MA – macronuclear nodule, MI – micronucleus, OP – oral primordium, R4–R7 – cirral rows right of AZM, UM – undulating membranes, 1, 2 – dorsal kineties, A4–A6 – cirral anlagen. Scale bars 15 µm (f, g) and 30 µm (a–e).

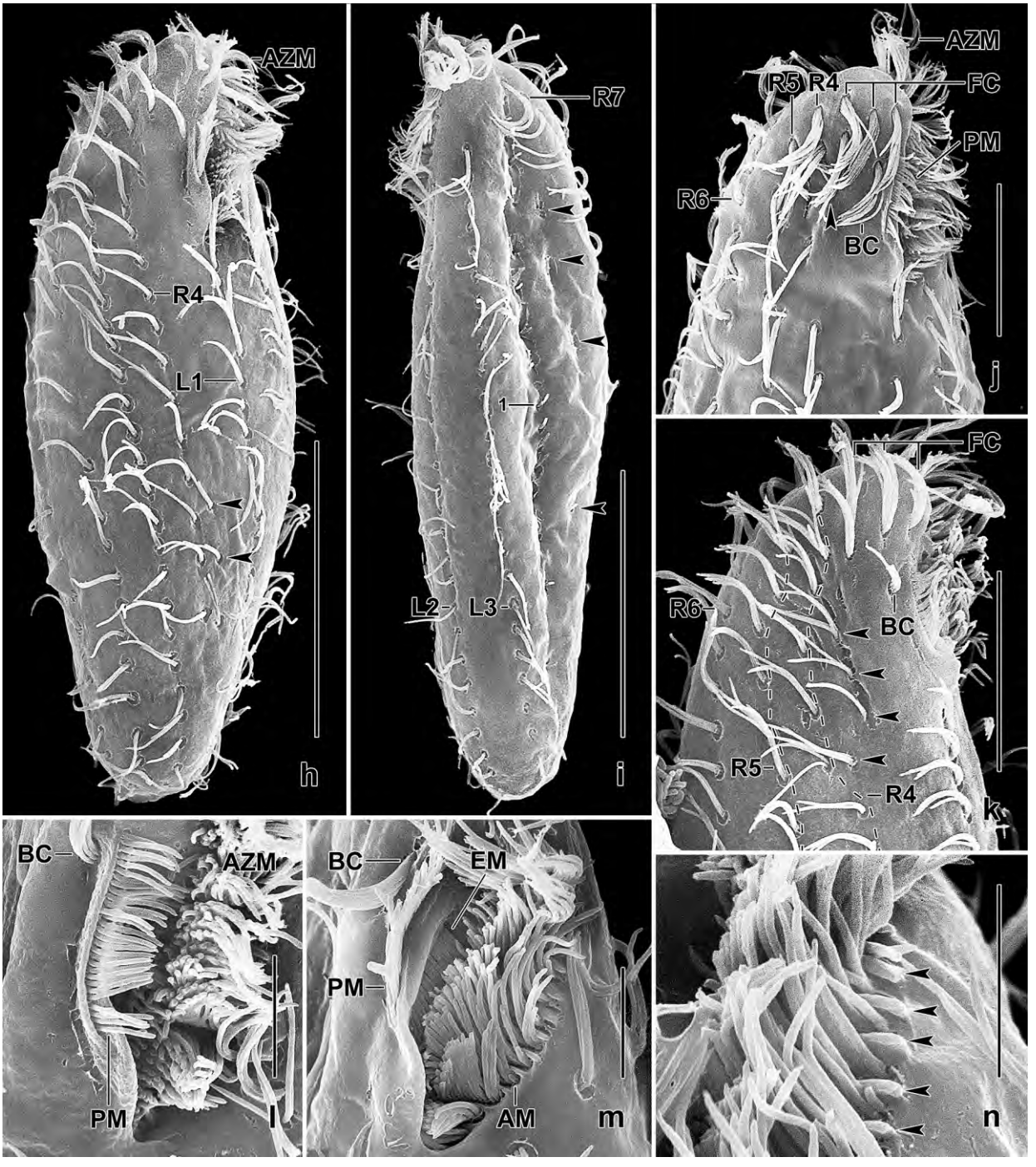

Fig. 195h–n. *Deviata brasiliensis* from Venezuelan site (56) in the scanning electron microscope. **h:** Ventral view. Arrowheads mark two supernumeral cirri between rows R4 and L1. **i:** Dorsal view, showing the bristles of dorsal kinety 2 (arrowheads). **j:** Ventral view of anterior body region, showing the ordered cirral pattern and the inconspicuous oral apparatus. The arrowhead denotes the parabuccal cirrus III/2. **k:** Anterior body region of a specimen with supernumeral cirri (arrowheads), presumably induced by a fragmentation of anlage A IV (Fig. 195e). **l:** Oral region, showing the short paroral cilia originating from a cleft in the buccal lip. **m:** Oral region, showing endoral cilia and the upright buccal lip. **n:** Mid-portion of adoral zone, showing conspicuous ridges (arrowheads) between the adoral membranelles. 1 – dorsal kinety, AM – adoral membranelles, AZM – adoral zone of membranelles, BC – buccal cirrus, EM – endoral membrane, FC – frontal cirri, L1–L3 – cirral rows left of AZM, PM – paroral membrane, R4–R6 – cirral rows right of AZM. Scale bars 5 µm (l–n), 15 µm (j, k), and 30 µm (h, i).

Table 71. Morphometric data on slender (BS) and oblong (BO) specimens of *Deviata brasiliensis* from Venezuelan site (56), and from the Brazilian type locality (BH, SIQUEIRA-CASTRO et al. 2009). Venezuelan data based on mounted, protargol-impregnated, and randomly selected specimens from a semi-pure culture. Measurements in µm. CV – coefficient of variation in %, M – median, Max – maximum, Mean – arithmetic mean, Min – minimum, n – number of individuals investigated, Pop – population, SD – standard deviation, SE – standard error of arithmetic mean.

Characteristics	Pop	Mean	M	SD	SE	CV	Min	Max	n
Body, length	BS	144.2	144.0	23.2	5.1	16.1	102.0	190.0	21
	BO	112.5	115.0	8.7	2.6	7.7	96.0	127.0	11
	BH	107.2	104.0	24.2	3.6	22.6	62.0	160.0	45
Body, width	BS	25.1	24.0	3.8	0.8	15.1	20.0	35.0	21
	BO	52.4	51.0	9.4	2.8	18.0	40.0	66.0	11
	BH	43.9	43.0	8.1	1.2	18.4	28.0	64.0	45
Body length:width, ratio	BS	5.8	6.0	1.0	0.2	17.5	3.8	7.8	21
	BO	2.2	2.3	0.3	0.1	15.5	1.7	2.6	11
	BH[a]	2.4	–	–	–	–	–	–	45
Posterior macronuclear nodule, length	BS	20.7	19.0	5.2	1.1	25.1	16.0	40.0	21
	BO	15.1	14.0	3.1	0.9	20.4	11.0	21.0	11
	BH	12.9	11.0	4.8	0.8	37.1	6.0	24.0	36
Posterior macronuclear nodule, width	BS	3.8	4.0	0.8	0.2	21.4	3.0	6.0	21
	BO	5.5	6.0	1.2	0.4	21.9	4.0	8.0	11
	BH	5.0	5.0	1.4	0.2	27.1	2.0	9.0	36
Posterior macronuclear nodule length:width, ratio	BS	5.7	5.5	2.2	0.5	38.2	3.6	13.3	21
	BO	2.9	2.7	1.0	0.3	34.0	1.4	4.5	11
	BH[a]	2.6	–	–	–	–	–	–	36
Central macronuclear nodules, distance in between	BS	12.1	12.0	4.7	1.0	38.5	2.0	24.0	21
	BO	10.2	10.0	3.7	1.1	36.2	4.0	16.0	11
	BH	10.5	10.0	3.6	0.6	34.2	4.0	17.0	37
Macronuclear nodules, number	BS	4.1	4.0	0.5	0.1	13.2	3.0	6.0	21
	BO	4.0	4.0	0.0	0.0	0.0	4.0	4.0	11
	BH	4.1	4.0	0.6	0.1	14.3	2.0	6.0	45
Micronuclei, number	BS	2.0	2.0	0.5	0.1	27.4	1.0	4.0	21
	BO	1.6	2.0	0.5	0.2	30.8	1.0	2.0	11
	BH	2.5	2.0	0.7	0.1	29.9	2.0	4.0	34
Micronuclei, length	BS	3.2	3.0	0.5	0.1	14.4	2.5	4.0	21
	BO	3.6	4.0	0.5	0.2	13.9	3.0	4.0	11
	BH	2.4	2.0	0.5	0.1	23.1	2.0	4.0	34
Micronuclei, width	BS	2.6	2.5	0.2	0.0	8.3	2.5	3.0	21
	BO	3.0	3.0	0.4	0.1	14.1	2.5	4.0	11
Adoral zone, length	BS	29.9	30.0	2.6	0.6	8.7	24.0	36.0	21
	BO	30.2	30.0	1.6	0.5	5.3	28.0	32.0	11
	BH	20.8	21.0	2.5	0.4	11.9	14.0	25.0	45
Adoral zone of membranelles, percentage of body length	BS	20.6	20.3	2.7	0.6	12.9	15.8	25.9	21
	BO	27.9	27.3	3.3	1.0	11.8	23.9	34.1	11
	BH[a]	19.4	–	–	–	–	–	–	45
Adoral zone, number of membranelles	BS	24.8	25.0	1.3	0.3	5.3	23.0	28.0	21

continued

Characteristics	Pop	Mean	M	SD	SE	CV	Min	Max	n
	BO	25.3	25.0	1.2	0.4	4.7	23.0	27.0	11
	BH	21.9	22.0	2.2	0.3	9.9	18.0	31.0	45
Pharyngeal fibres, length	BS	24.2	24.0	4.9	1.1	20.2	15.0	36.0	21
	BO	26.2	26.0	4.2	1.3	16.1	18.0	32.0	11
	BH	24.3	25.0	6.0	1.3	24.7	13.0	40.0	22
Frontal cirri, number	BS	3.0	3.0	0.0	0.0	0.0	3.0	3.0	21
	BO	3.0	3.0	0.0	0.0	0.0	3.0	3.0	11
	BH	3.0	3.0	0.0	0.0	0.0	3.0	3.0	45
Buccal cirri, number	BS	1.0	1.0	0.0	0.0	0.0	1.0	1.0	21
	BO	1.0	1.0	0.0	0.0	0.0	1.0	1.0	11
	BH	1.0	1.0	0.0	0.0	0.0	1.0	1.0	45
Parabuccal cirri, number	BS	1.0	1.0	0.0	0.0	0.0	1.0	1.0	21
	BO	1.1	1.0	0.3	0.1	27.6	1.0	2.0	11
	BH	1.4	1.0	0.5	0.1	38.8	1.0	3.0	44
Long cirral rows right (R) of adoral zone, number	BS	4.0	4.0	0.0	0.0	0.0	4.0	4.0	53
	BO	4.0	4.0	0.0	0.0	0.0	4.0	4.0	29
	BH	4.2	4.0	0.4	0.1	9.2	4.0	5.0	40
Cirral row R4, number of cirri	BS	18.9	19.0	2.6	0.6	14.0	13.0	24.0	21
	BO	18.7	19.0	2.5	0.8	13.3	13.0	21.0	11
	BH	20.2	21.0	6.4	1.0	31.7	10.0	34.0	40
Cirral row R5, number of cirri	BS	27.0	28.0	2.9	0.6	10.9	22.0	32.0	21
	BO	28.1	27.0	2.8	0.9	10.1	24.0	34.0	11
	BH	32.6	32.0	3.7	0.6	11.5	25.0	42.0	40
Cirral row R6, number of cirri	BS	33.8	33.0	4.3	0.9	12.6	26.0	42.0	21
	BO	35.5	34.0	4.2	1.3	11.8	32.0	44.0	11
	BH	36.9	36.0	4.9	0.8	13.3	26.0	46.0	39
Cirral row R7, number of cirri	BS	37.3	38.0	4.6	1.0	12.4	30.0	48.0	21
	BO	35.0	36.0	3.2	1.0	9.2	30.0	39.0	11
	BH	36.7	35.0	6.7	1.1	18.3	26.0	52.0	38
Long cirral rows left (L) of adoral zone, number [b]	BS	3.1	3.0	0.4	0.1	14.1	3.0	5.0	53
	BO	3.1	3.0	0.4	0.1	13.2	3.0	5.0	29
	BH	3.9	4.0	0.8	0.1	21.5	3.0	6.0	39
Cirral row L1, number of cirri	BS	28.3	29.0	3.8	0.8	13.3	23.0	36.0	21
	BO	28.9	30.0	4.8	1.4	16.5	20.0	37.0	11
	BH	29.5	29.0	5.5	0.9	18.6	17.0	41.0	40
Cirral row L2, number of cirri	BS	30.2	31.0	4.1	0.9	13.6	22.0	43.0	21
	BO	29.4	29.0	3.5	1.0	11.8	23.0	37.0	11
	BH	29.2	28.0	5.5	0.9	19.0	20.0	41.0	39
Cirral row L3, number of cirri	BS	33.0	33.0	4.7	1.0	14.2	23.0	43.0	21
	BO	30.7	30.0	4.6	1.4	15.1	24.0	40.0	11
	BH	30.5	28.0	7.1	1.1	23.3	19.0	48.0	39
Dorsal kineties, number	BS	2.0	2.0	0.0	0.0	0.0	2.0	2.0	21
	BO	2.0	2.0	0.0	0.0	0.0	2.0	2.0	11
	BH	2.0	2.0	0.3	0.1	12.7	1.0	2.0	32
Dorsal kinety 1, number of bristles	BS	17.4	18.0	2.1	0.5	12.2	13.0	22.0	21

continued

Characteristics	Pop	Mean	M	SD	SE	CV	Min	Max	n
	BO	19.1	19.0	1.5	0.5	7.9	17.0	22.0	11
	BH	21.6	21.0	4.2	0.7	19.3	13.0	28.0	41
Dorsal kinety 2, number of bristles	BS	6.6	7.0	1.1	0.2	16.2	4.0	8.0	21
	BO	7.1	7.0	0.9	0.3	13.3	6.0	9.0	11
	BH	8.6	9.0	1.6	0.3	19.1	5.0	12.0	38
Dorsal bristles, total number	BS	24.1	24.0	2.5	0.6	10.5	19.0	29.0	21
	BO	26.2	26.0	2.2	0.7	8.3	24.0	31.0	11
	BH[a]	30.2	–	–	–	–	–	–	38

[a] Calculated from arithmetic mean.

[b] Row L4 with 25–30 cirri was found in five slender and two oblong Venezuelan specimens (type population 13–34 cirri, $\bar{x}$ = 26, n = 25). Row L5 with 26–35 cirri was found in two slender and one oblong specimen (cirri of this row were not counted in the type population).

not uncommon in the type population but rare in the Venezuelan specimens. The Venezuelan population possesses constant characters, e. g., four long cirral rows right of the adoral zone and two dorsal kineties while both are slightly variable in the type population. The two isolated cirri between rows R4 and L1 are ciliated, contrary to the original description (Fig. 195h).

Siqueira-Castro et al. (2009) state that the oral primordium of *D. brasiliensis* usually originates within cirral row R4 and incorporates its posterior cirri. Although we cannot exclude that some cirri of row R4 contribute to the oral primordium, we found the posterior cirri still intact in mid-dividers (Fig. 195e, g). The ontogenesis (Fig. 195e–g) follows the pattern described for *D. abbrevescens* (Eigner 1995, Fig. 194e); we did not find evidence for the deviations reported by Siqueira-Castro et al. (2009): anlage IV of the proter originates at the anterior end of parental row R4 and extends obliquely to parental row R5, later incorporating its cirri (vs. incorporating only cirri of row R4); anlage V of the proter originates within parental row R6, extending through incorporation of cirri from the latter (vs. originating at anterior end of row R5). The origin of anlagen IV and V of the opisthe was not unambiguously determined by Siqueira-Castro et al. (2009). Our observations showed clearly the *D. abbrevescens* pattern, that is, anlage IV originates within parental row R5 and anlage V originates within row R6, extending to row R5 and later detaching from row R6 (Fig. 194e, 195e, g).

As yet, SEM illustrations of *D. brasiliensis* were not available. Thus, we show some overviews and details in Fig. 195h–n. For details, see figure explanations.

Occurrence and ecology: The type locality of *D. brasiliensis* is a sewage treatment plant in Rio de Janeiro (Brazil), where it was discovered in the primary settling tanks (27.8 °C, pH 7, 2.2 mgl^{-1} O_2). Siqueira-Castro et al. (2009) also reported it from ordinary limnetic samples, coexisting with *Paramecium aurelia* and testate amoebae. We found *D. brasiliensis* in slightly saline (4 ‰) soil and mud from ephemeral puddles on the north coast of Venezuela, Morrocoy National Park, 67°13’W 11°33’N.

Bistichella Berger, 2008

Improved diagnosis: Hypotricha with 2 or 3 short frontal cirral rows and 2 or 3 long frontoventral cirral rows, of which the right one may be interrupted in mid-body or reduced to a short posterior segment. 3 or 4 enlarged frontal cirri and more than one buccal cirrus. With a right and a left marginal cirral row. Adoral zone of membranelles continuous, buccal cavity conspicuous because ± *cyrtohymenid*-shaped. Dorsal kinety pattern of *Gonostomum*-type, i. e., several bipolar rows. Caudal, transverse, and postperistomial cirri lacking.

Type species (by original designation): *Paraurostyla buitkampi* Foissner, 1982.

Species assignable: *Bistichella buitkampi* (Foissner, 1982) Berger, 2008; *B. chilensis* nov. spec., *B. humicola* (Gellért, 1956) Berger, 2008; *B. kenyaensis* nov. spec.

Remarks: See genus → *Parabistichella*. Briefly, *Bistichella* and *Parabistichella* differ by the absence vs. presence of transverse cirri.

Bistichella chilensis nov. spec. (Fig. 196a–c; Table 72)

Diagnosis: Size in vivo about 140 × 50 µm; elongate ellipsoid. 2 macronuclear nodules and about 5 micronuclei. 2–3 short frontal cirral rows and 2 long frontoventral rows; right frontoventral row with a wide break in mid-body. 4 enlarged frontal cirri and an average of 9 cirri in short frontal rows. On average, 23 cirri in left frontoventral row, 15 + 10 cirri in right frontoventral row, 4 buccal cirri, 43 cirri in left and 46 cirri in right marginal row. Adoral zone short, i. e., extends about 27% of body length, composed of 30 membranelles on average. 3 dorsal kineties.

Type locality: Soil from a dry area of the Fray Jorge National Park in the surroundings of the town of Coquimbo, Chile, 72°W 30°S.

Type material: 1 holotype and 3 paratype slides with protargol-impregnated specimens have been deposited in the Biology Centre of the Upper Austrian Museum in Linz (LI). Relevant specimens have been marked by black ink circles on the coverslip.

Etymology: Named after the country where it was discovered.

Description: The species was very rare in the non-flooded Petri dish culture. Thus, only nine specimens could be analysed morphometrically in the protargol slides (Table 72).

Size in vivo 120–170 × 35–55 µm, usually about 140 × 50 µm, as calculated from some in vivo measurements and the morphometric data in Table 72 adding 15% preparation shrinkage. Body slenderly ellipsoid to almost rectangular, left margin usually slightly convex, both in vivo and in protargol preparations (Fig. 196a–c). Two, rarely three macronuclear nodules in central quarters of cell and left of body´s midline; individual nodules ellipsoid to elongate ellipsoid; with many small nucleoli. Two to nine globular to broadly ellipsoid micronuclei attached to and around macronuclear nodules (Fig. 196a, c; Table 72). Contractile vacuole in mid-body at left

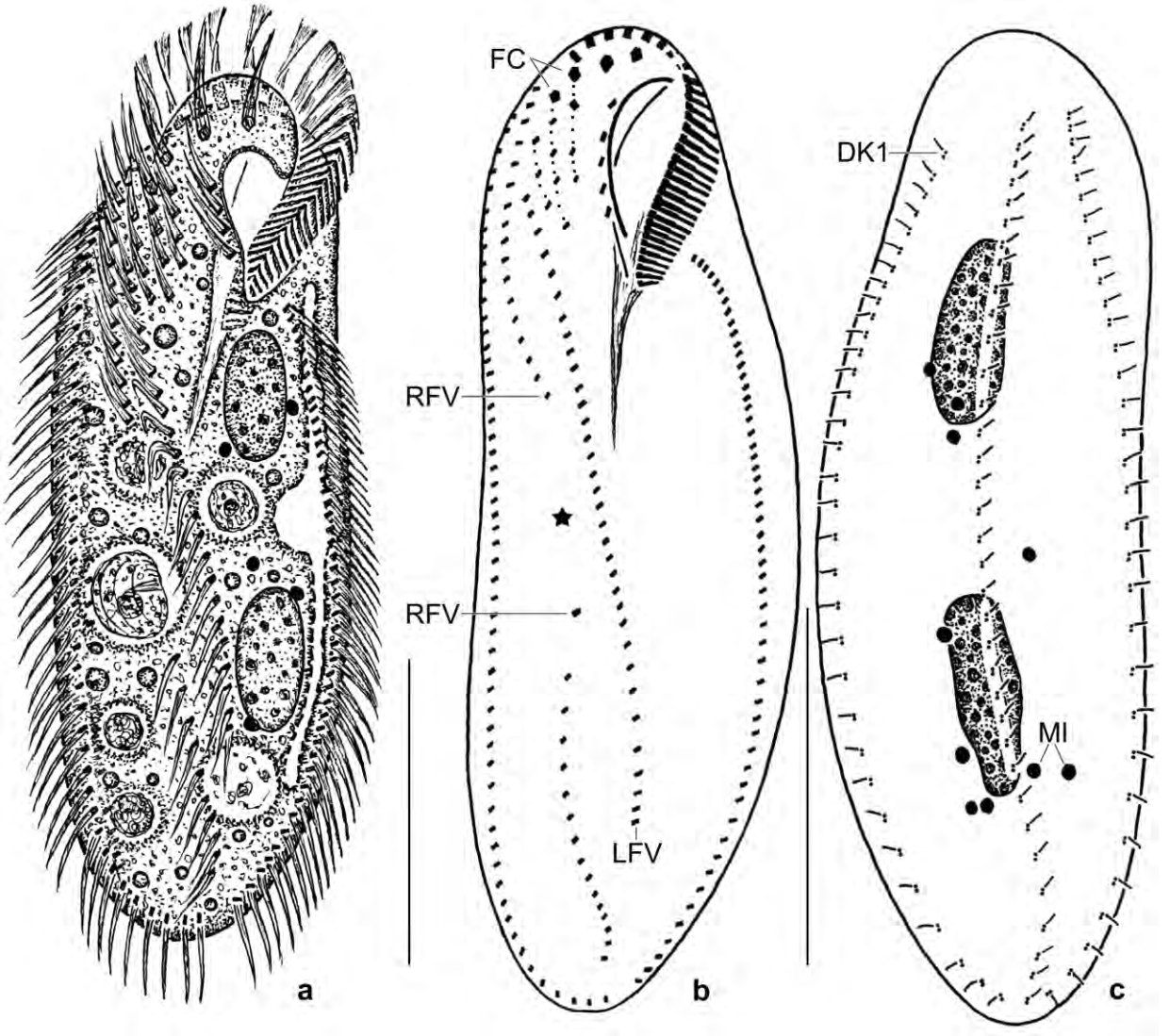

Fig. 196a–c. *Bistichella chilensis* from life (a) and after protargol impregnation (b, c). **a:** Ventral view of a representative specimen, length 140 µm. **b, c:** Infraciliature of ventral and dorsal side and nuclear apparatus of holotype species, length 142 µm. The asterisk marks the wide break in the right frontoventral row. The cirri of the three short frontal rows are connected by dotted lines. DK1 – dorsal kinety 1, FC – enlarged frontal cirri 3 and 4, LFV – left frontoventral row, MI – micronuclei, RFV – right frontoventral row. Scale bars 50 µm.

margin, with two lacunar collecting canals (Fig. 196a). Cortex very flexible, without specific granules. Cytoplasm colourless and without crystals, studded with up to 10 µm-sized lipid droplets and large food vacuoles containing flagellates (*Polytoma*) and middle-sized ciliates, e. g., *Leptopharynx costatus* and *Protocyclidium muscicola* (Fig. 196a). Moves rapidly, showing pronounced flexibility.

Cirri about 15 µm long in vivo, comparatively fine, i. e., most consisting of only two rows of basal bodies, arranged in *Bistichella* pattern, showing three peculiarities (Fig. 196a, c): (i) four enlarged frontal cirri, (ii) two to three short frontal cirral rows composed of 6–13, on average of 9 cirri, (iii) right frontoventral cirral row interrupted in mid-body, anterior segment slightly convex and composed of 12–18, on average 15 cirri; posterior segment rather distinctly curved

posteriorly and composed of 6–18, on average 10 cirri. Cirri narrowly spaced in anterior half of marginal rows, right row curves around posterior body end almost touching left row. Number of cirri within rows highly variable (CV > 15%, Table 72).

Dorsal bristles about 3 µm long in vivo, arranged in three bipolar rows commencing subapically, extend at body margin and in body midline. Caudal cirri absent (Fig. 196c; Table 72).

Adoral zone comparatively short, i. e., extends 23–31%, on average 27% of body length, of usual shape and structure, consists of an average of 30 membranelles, bases of largest membranelles about 11 µm wide in vivo, first membranelle close to third enlarged frontal cirrus. Buccal cavity conspicuous in vivo because *Cyrtohymena*-shaped, i. e., with distinctly curved anterior portion; partially covered by buccal lip with thickened margin. Both undulating membranes rather distinctly curved optically intersecting in mid of buccal cavity, kinetids very narrowly spaced. Pharyngeal fibres distinct in vivo and after protargol impregnation, of ordinary length and structure (Fig. 196a, b; Table 72).

Table 72. Morphometric data on *Bistichella chilensis* (Bc) and *Bistichella kenyaensis* (Bk). Data based on mounted, protargol-impregnated, randomly selected specimens from non-flooded Petri dish cultures. Measurements in µm. CV – coefficient of variation in %, FVR – frontoventral cirral row, M – median, Max – maximum, Mean – arithmetic mean, Min – minimum, n – number of individuals investigated, SD – standard deviation, SE – standard error of arithmetic mean.

Characteristics	Species	Mean	M	SD	SE	CV	Min	Max	n
Body, length	Bc	121.1	125.0	15.8	5.3	13.0	100.0	143.0	9
	Bk	90.3	91.0	8.1	2.3	9.0	78.0	102.0	13
Body, width	Bc	40.1	37.0	6.9	2.3	17.2	30.0	47.0	9
	Bk	36.4	36.0	4.2	1.2	11.5	27.0	42.0	13
Body length:width, ratio	Bc	3.1	3.0	0.3	0.2	10.0	2.7	3.6	9
	Bk	2.5	2.5	0.3	0.1	10.3	2.1	2.9	13
Anterior body end to proximal end of adoral zone, distance	Bc	33.3	34.0	3.7	1.2	11.1	28.0	38.0	9
	Bk	26.7	27.0	3.4	1.0	12.8	21.0	35.0	13
Body length:length of adoral zone, ratio	Bc	3.6	3.7	0.3	0.2	7.6	3.3	4.0	9
	Bk	3.4	3.4	0.4	0.2	12.6	2.3	4.0	13
Adoral membranelles, number	Bc	30.4	30.0	4.3	1.4	14.0	25.0	38.0	9
	Bk	24.5	24.0	2.3	0.6	9.4	21.0	30.0	13
Macronuclear nodules, number	Bc	2.1	2.0	–	–	–	2.0	3.0	9
	Bk	2.0	2.0	0.0	0.0	0.0	2.0	2.0	13
Macronuclear nodules, length	Bc	23.0	22.0	3.1	1.0	13.6	19.0	28.0	9
	Bk	17.0	17.0	2.0	0.6	12.0	14.0	21.0	13
Macronuclear nodules, width	Bc	9.7	10.0	1.1	0.4	11.6	8.0	12.0	9
	Bk	8.2	8.0	1.6	0.4	19.3	6.0	10.0	13
Micronuclei, number	Bc	5.4	6.0	2.4	0.8	44.2	2.0	9.0	9
	Bk	3.5	3.0	1.6	0.4	44.5	2.0	7.0	14
Micronuclei, length	Bc	2.9	3.0	0.2	0.1	7.6	2.5	3.0	9
	Bk	2.3	2.3	0.2	0.1	10.1	1.8	2.7	13
Micronuclei, width	Bc	2.7	2.5	0.2	0.1	9.1	2.5	3.0	9

continued

Characteristics	Species	Mean	M	SD	SE	CV	Min	Max	n
	Bk	2.0	2.0	0.3	0.1	14.0	1.6	2.5	13
Anterior body end to proximal end of anterior segment of right FVR, distance	Bc	45.3	50.0	8.0	2.7	17.7	35.0	53.0	9
	Bk	28.0	29.0	4.3	1.2	15.2	21.0	35.0	13
Anterior segment of right frontoventral row, number of cirri	Bc	14.6	14.5	2.1	0.8	14.6	12.0	18.0	8
	Bk	11.8	10.0	3.6	1.0	30.0	8.0	21.0	13
Posterior segment of right frontoventral row, number of cirri	Bc	10.4	9.0	3.8	1.3	36.2	6.0	18.0	9
	Bk	4.2	4.0	1.6	0.4	37.9	2.0	6.0	13
Anterior body end to begin of left frontoventral row, distance	Bc	23.6	23.5	5.3	1.9	22.3	16.0	30.0	8
	Bk	20.1	21.0	3.0	0.8	15.1	14.0	25.0	13
Anterior body end to proximal end of left frontoventral row, distance	Bc	92.3	95.0	17.0	5.7	18.4	70.0	115.0	9
	Bk	48.9	49.0	6.0	1.7	12.2	42.0	60.0	13
Left frontoventral row, number of cirri	Bc	22.6	23.0	5.2	1.8	23.0	16.0	33.0	8
	Bk	13.1	13.0	2.9	0.8	22.0	9.0	20.0	13
Enlarged frontal cirri, number	Bc	4.0	4.0	0.0	0.0	0.0	4.0	4.0	9
	Bk	3.0	3.0	0.0	0.0	0.0	3.0	3.0	13
Short frontal rows, number of cirri	Bc	8.9	8.5	2.4	0.8	26.6	6.0	13.0	8
	Bk	5.0	5.0	0.8	0.2	16.3	4.0	6.0	13
Buccal cirri, number	Bc	4.4	4.0	0.7	0.2	16.3	4.0	6.0	9
	Bk	2.5	3.0	–	–	–	2.0	3.0	13
Right marginal row, number of cirri	Bc	43.0	42.5	8.3	2.9	19.2	29.0	55.0	8
	Bk	33.7	34.0	3.1	0.9	9.3	30.0	43.0	13
Left marginal row, number of cirri	Bc	45.9	45.0	7.5	2.5	16.3	35.0	54.0	9
	Bk	33.5	32.0	4.5	1.2	13.4	29.0	47.0	13
Dorsal bristle rows, number	Bc	3.0	3.0	0.0	0.0	0.0	3.0	3.0	9
	Bk	3.0	3.0	0.0	0.0	0.0	3.0	3.0	13

Occurrence and ecology: As yet found only at type locality.

Remarks: There is only one congener similar to *B. chilensis*, viz., → *B. kenyaensis*, providing a good example for biogeographic speciation. *Bistichella kenyaensis* is smaller than *B. chilensis* (90 × 36 µm vs. 121 × 40 µm in protargol preparations, Table 72) and has thus a lower total number of cirri (107 vs. 154), while the number of adoral membranelles is rather similar (24 vs. 30); further, the frontoventral rows are more distinctly reduced: left row composed of 13 vs. 23 cirri, right row composed of 12 + 4 vs. 15 + 10 cirri (Table 72). Additionally, the posterior end of the marginal cirral rows is different: the right row curves around the body end in *B. chilensis*, while either the left row curves around the body end or both rows are shortened, leaving a wide space in → *B. kenyaensis* (Fig. 196b, 197b, c).

The cirral pattern, of course, resembles several species which, however, have four macronuclear nodules (*B. buitkampi*) or transverse cirri (*Bistichellides terrestris*, → *B. brevisticha*). In vivo, *B. chilensis* can be confused not only with → *Bistichellides* species (without vs. with transverse cirri) but also with various other massive hypotrichs, such as *Uroleptoides polycirratus* (two vs. one long frontoventral cirral rows, without vs. with transverse cirri). Thus, the identification should be controlled in protargol preparations.

Bistichella kenyaensis **nov. spec.** (Fig. 197a–f; Table 72)

Diagnosis: Size in vivo about 110 × 45 µm; ellipsoid to elongate ellipsoid. 2 macronuclear nodules and 3 micronuclei on average. 2–3 short frontal cirral rows and 2–3 long frontoventral rows; right frontoventral row with very wide break in middle quarters of body. 3 enlarged frontal cirri and an average of 5 cirri in short frontal rows. On average, 13 cirri in left frontoventral row, 11 + 4 cirri in right frontoventral row, 3 buccal cirri, and about 33 cirri each in left and right marginal row. Adoral zone extends on average 30% of body length, composed of 24 membranelles on average. 3 dorsal kineties.

Type locality: Litter and soil from the surroundings of the Kilimanjaro Lodge in Kenya, tropical Africa, 37°E 3°S.

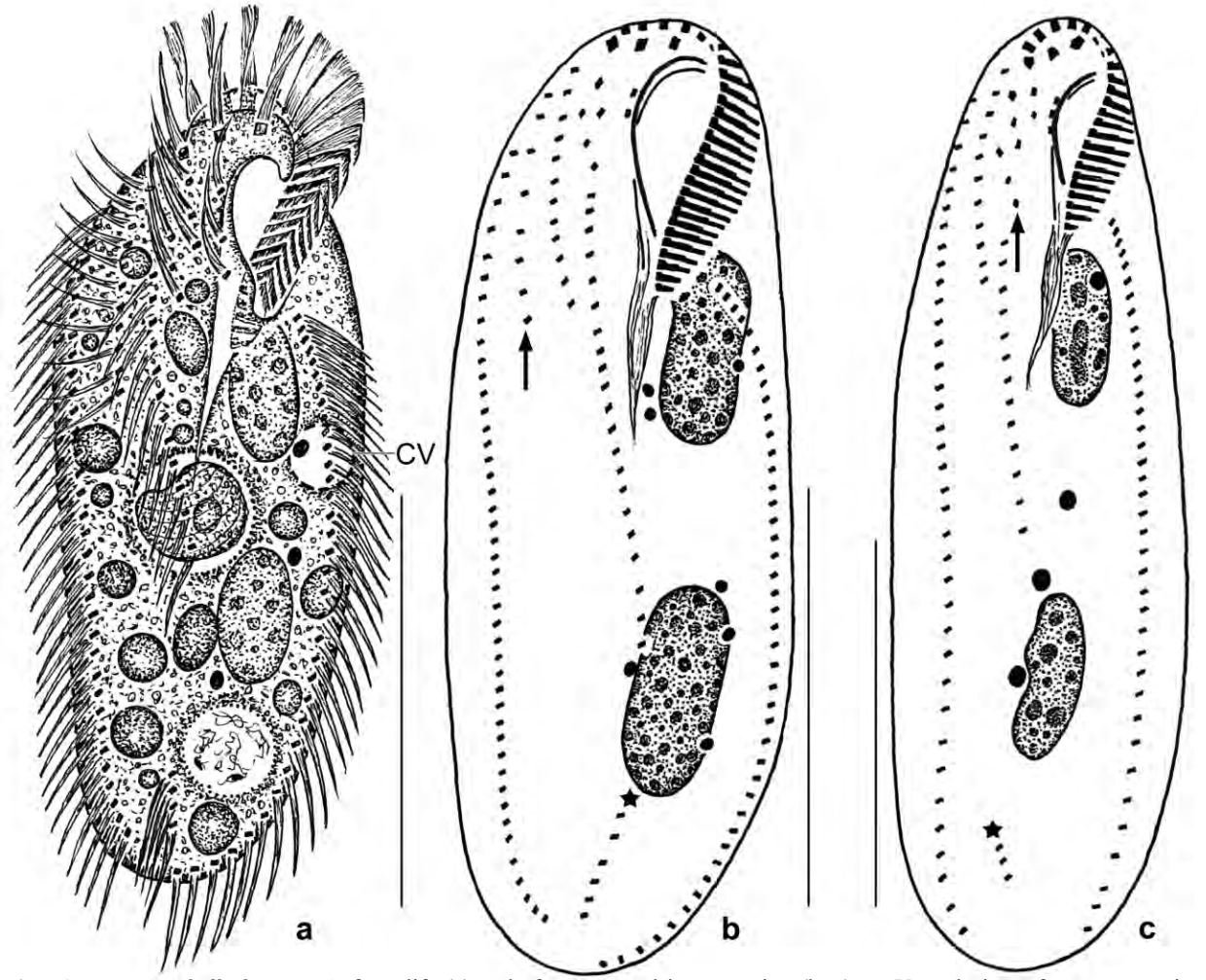

Fig. 197a–c. *Bistichella kenyaensis* from life (a) and after protargol impregnation (b, c). **a:** Ventral view of a representative specimen, length 110 µm. The up to 10 µm large, bright, lipid-like inclusions are likely ciliates in a very late stage of digestion. **b, c:** Ventral views of two rare variants: one has an additional frontoventral row (b, arrow), the other has an additional frontal row (c, arrow). The asterisks mark the short posterior segment of the right frontoventral cirral row. CV – contractile vacuole. Scale bars 40 µm (b, c) and 50 µm (a).

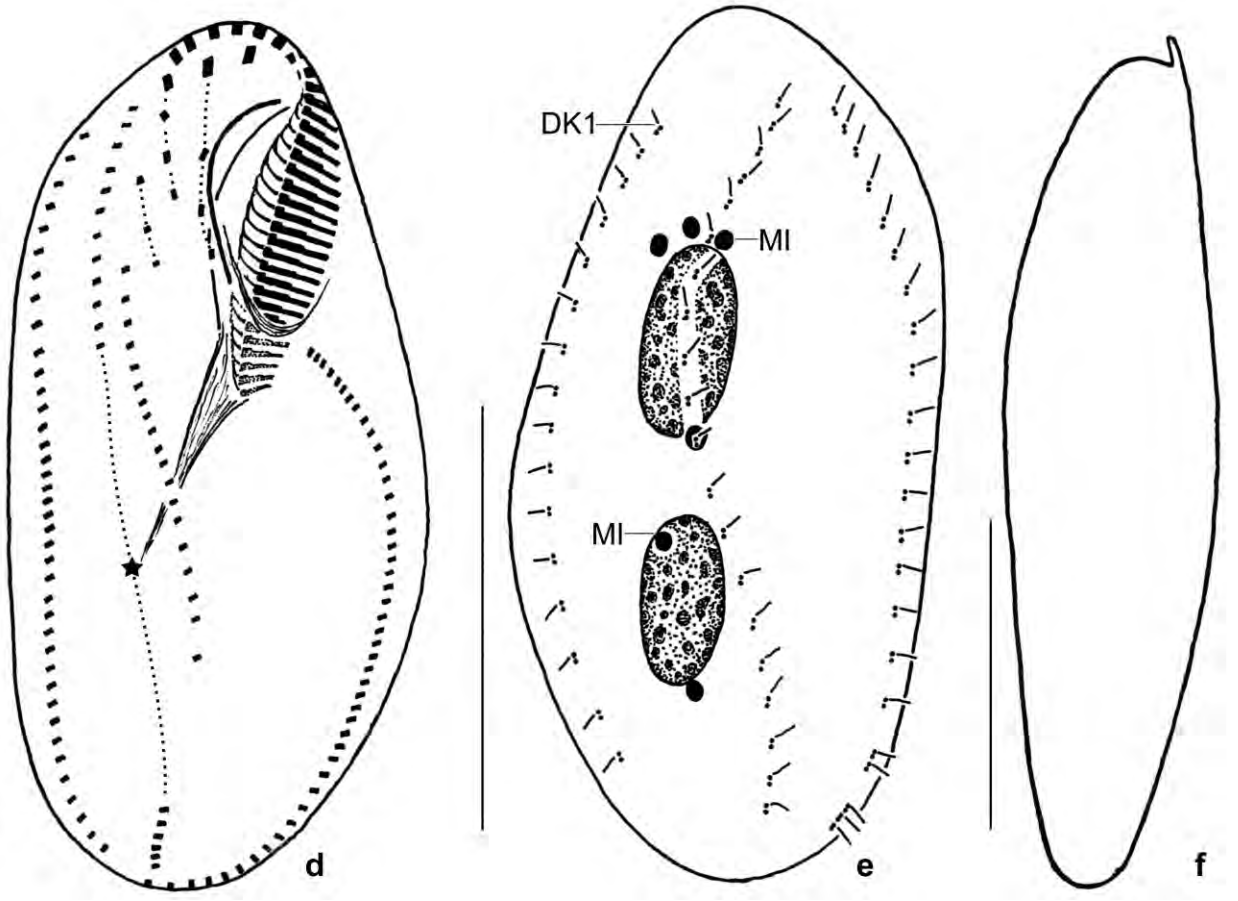

Fig. 197d–f. *Bistichella kenyaensis* from life (f) and after protargol impregnation (d, e). **d, e:** Infraciliature of ventral and dorsal side and nuclear apparatus of holotype specimen, length 82 µm. Dotted lines in (d) connect cirri likely developing from same anlage (cp. Berger 2008). The asterisk marks the very wide gape between anterior and posterior segment of the right frontoventral cirral row. Note the distinct fibres originating from the membranelles neighbouring the deep buccal cavity. **f:** Lateral view of specimen shown in Fig. 197a. DK1 – dorsal kinety 1, MI – micronuclei. Scale bars 40 µm.

Type material: 1 holotype and 3 paratype slides with protargol-impregnated specimens have been deposited in the Biology Centre of the Upper Austrian Museum in Linz (LI). Relevant specimens have been marked with black ink circles on the coverslip.

Etymology: Named after the country where it was discovered.

Description: Although the cirral pattern of most specimens looks like shown in Fig. 197d, we present also two rare variations (Fig. 197b, c) not included in the morphometric analysis.

Size in vivo 90–130 × 35–50 µm, usually about 110 × 45 µm, as calculated from some in vivo measurements and the morphometric data in Table 72 adding 15–20% preparation shrinkage. Body shape ellipsoid to slenderly ellipsoid but usually widest anterior of mid-body; left body margin frequently more convex than right; laterally flattened about 0.5:1 (Fig. 197a, d, f; Table 72). Two macronuclear nodules in central quarters of cell and left of body's midline; individual nodules broadly to slenderly ellipsoid; with many small nucleoli. Two to seven globular to broadly ellipsoid micronuclei attached to and near macronuclear nodules (Fig. 197a–c, e; Table

72). Contractile vacuole slightly anterior of mid-body. Cortex very flexible, without specific granules. Cytoplasm colourless and without crystals, studded with up to 10 µm-sized, bright inclusions and some food vacuoles containing heterotrophic flagellates and middle-sized ciliates, e. g., *Colpoda maupasi* (Fig. 197a).

Cirri about 15 µm long in vivo, comparatively fine, i. e., most consisting of only two rows of basal bodies, arranged as in → *B. chilensis*, but more variable and average total number of cirri much lower (154 vs. 107). Gap in right frontoventral cirral row much wider than in → *B. chilensis*. Distances between marginal cirri gradually increase from very narrowly anteriorly to ordinarily posteriorly. Left marginal cirral row curves around posterior body end or both marginal rows slightly shortened leaving blank body end (Fig. 197a–d; Table 72).

Dorsal bristles about 3 µm long in vivo, arranged in three bipolar rows commencing subapically and ending subterminally, extend at body margin and in body midline. Caudal cirri absent (Fig. 197e; Table 72).

Adoral zone extends 23–39%, on average 30% of body length, of usual shape and structure, consists of an average of 24 membranelles, bases of largest membranelles about 10 µm wide in vivo, first membranelle close to third enlarged frontal cirrus. Buccal cavity conspicuous in vivo because *Cyrtohymena*-shaped, i. e., with distinctly curved anterior portion; partially covered by buccal lip with thickened margin. Both undulating membranes distinctly curved optically intersecting in mid of buccal cavity, kinetids very narrowly spaced. Pharyngeal fibres distinct in vivo and after protargol impregnation, of ordinary length and structure (Fig. 197a–d; Table 72).

Notes on ontogenesis: Stomatogenesis begins with the production of basal bodies along the postoral portion of the left frontoventral row whose cirri are incorporated in the anlage.

Occurrence and ecology: As yet found only at type locality, i. e., in a mixture of grass and leaf litter and slightly alkaline soil (pH 8 in water) from the upper 5 cm. Soil grey, fine-grained, possibly of volcanic origin. Collected on 8. 7. 1985, investigated 1986.

Comparison with similar species: See → *B. chilensis*!

Parabistichella Jiang et al., 2013

Improved diagnosis: Hypotricha with 2 or 3 short frontal cirral rows and 2 or 3 long frontoventral cirral rows, of which the right one may be interrupted in mid-body or reduced to a short posterior segment. 3 or 4 enlarged frontal cirri and more than one buccal cirrus. With transverse cirri and a right and a left marginal cirral row. Adoral zone of membranelles continuous, buccal cavity conspicuous because ± cyrtohymenid. Dorsal kinety pattern of *Gonostomum*-type, i. e., several bipolar rows.

Type species (by original designation): *Parabistichella variabilis* Jiang et al., 2013.

Species assignable: Jiang et al. (2013) included only the type species in *Parabistichella*. However, there are several *Bistichella* species that match the diagnosis of Jiang et al. (2013): *Parabistichella*

encystica (Fan et al., 2014) nov. comb. (basionym: *Bistichella encystica* Fan et al., 2014); → *P. bergeri bergeri* nov. sspec.; → *P. bergeri brevisticha* nov. sspec.; *P. dieckmanni* (Foissner, 1998) nov. comb. (basionym: *Keronopsis dieckmanni* Foissner, 1998); → *P. namibiensis* (Foissner, Agatha & Berger, 2002) nov. comb. (basionym: *Amphisiella namibiensis* Foissner, Agatha & Berger, 2002); *P. procerus* (Berger & Foissner, 1987) nov. comb. (basionym: *Pseudouroleptus procerus* Berger & Foissner, 1987); *P. terrestris* (Hemberger, 1985) nov. comb. (basionym: *Pseudouroleptus terrestris* Hemberger, 1985).

Remarks: The diagnosis is adapted to the monograph of Berger (2008), who founded *Bistichella* with five species, most having transverse cirri, except of the type species (*B. buitkampi*) and the questionable *B. humicola*. We discovered two subspecies with transverse cirri. As the presence vs. absence of transverse cirri is usually considered as a generic character (Berger 1999, 2008, 2011), we classify species with transverse cirri into the genus *Parabistichella* as diagnosed above. Very likely, all *Bistichella* and *Parabistichella* species lack caudal cirri. Occasionally, there are some cirri at the posterior end but these likely belong to a ventral or marginal row (Fig. 199h).

Like Berger (2008), we do not have a solid idea about the nearest relatives of *Bistichella* and *Parabistichella*. The molecular data indicate a statistically poorly supported relationship with *Uroleptoides* and *Orthoamphisiella* (Jiang et al. 2013, Fan et al. 2014).

Parabistichella bergeri nov. spec.

Diagnosis(of two subspecies): Size of cultivated specimens in vivo about 215 × 80 µm; length:width ratio 2.4 or 3.6:1 in protargol preparations; ellipsoid. 2 macronuclear nodules and 3 micronuclei. On average 8 or 5 buccal cirri, 5 transverse cirri, 60 cirri in right marginal row, 50 in left; total number of cirri 203 or 180 on average. About 30 or 21 bristles in dorsal kinety 1. Adoral zone extends about 30% of body length, composed of an average of 50 or 38 membranelles. Buccal cavity rather wide and deep. Resting cyst globular, in vivo about 40 µm across; wall smooth.

Remarks: We split *Parabistichella bergeri* into two subspecies mainly due to the non-overlapping number of adoral membranelles.

Parabistichella bergeri bergeri nov. subspec. (Fig. 198a–d, 199a–n; Table 73)

Diagnosis: Length:width ratio about 2.4:1 in protargol preparations. On average a total of 203 cirri including 8 buccal cirri; 30 bristles in dorsal kinety 1. Adoral zone composed of an average of 50 membranelles.

Type locality: Venezuelan site (66), i. e., highly saline (63‰) soil from the outskirts of the village of Chichiriviche, 67°13’W 11°33’N.

Type material: 1 holotype and 4 paratype slides with protargol-impregnated specimens have been deposited in the Biology Centre of the Upper Austrian Museum in Linz (LI). The holotype and other relevant specimens have been marked by black ink circles on the coverslip.

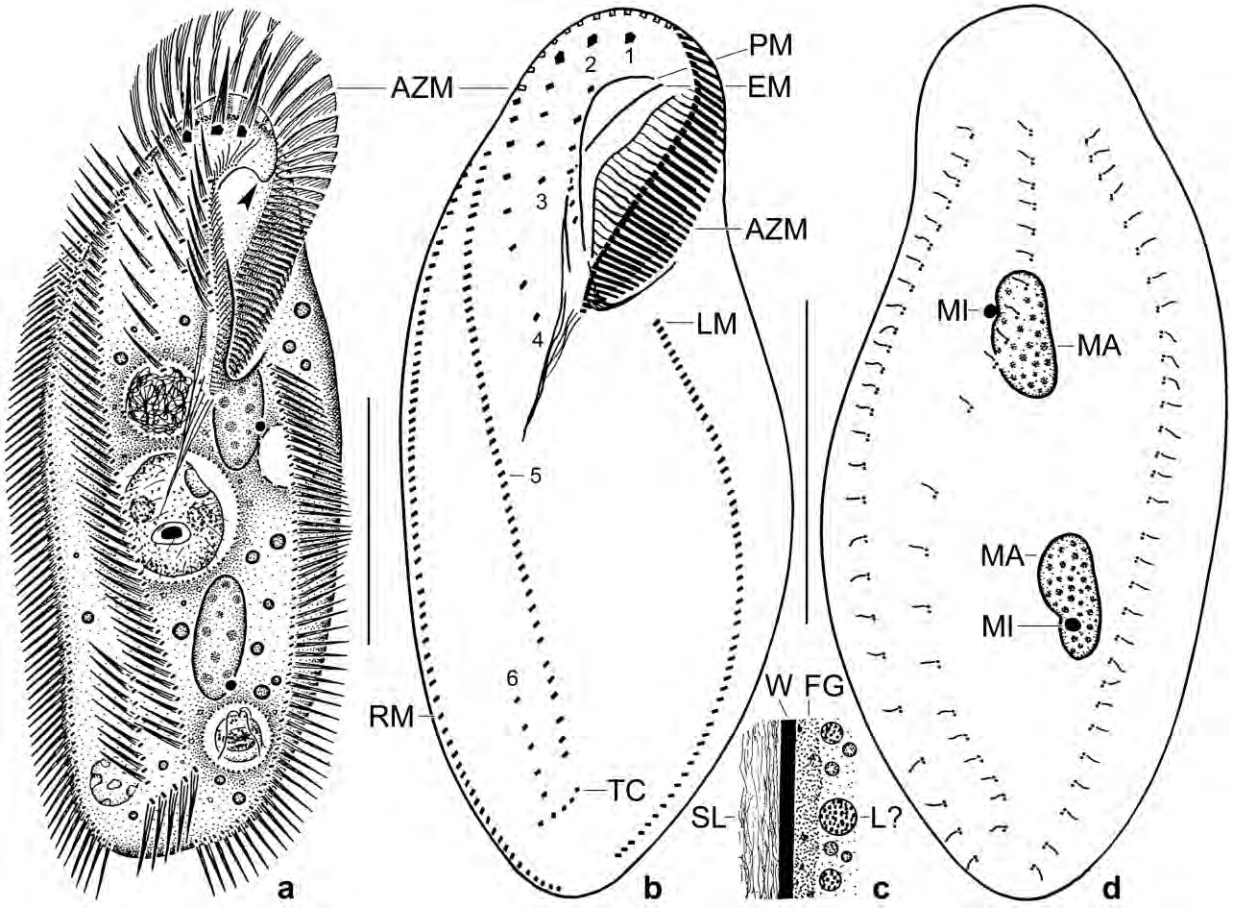

Fig. 198a–d. *Parabistichella bergeri bergeri* from life (a, c) and after protargol impregnation (b, d). **a:** Ventral view of a representative specimen, length 220 µm. The arrowhead marks the buccal horn. The cytoplasm is crammed with lipid droplets and food vacuoles containing bacteria, heterotrophic flagellates, small ciliates, and corroded wheat starch from the culture medium. **b, d:** Ventral and dorsal view of holotype specimen, length 185 µm. Note the complex oral apparatus, the transverse cirri, the six cirral rows/anlagen, and the three dorsal kineties. **c:** Cyst wall (2–3 µm thick) and cytoplasmic peculiarities. AZM – adoral zone of membranelles, EM – endoral membrane, FG – finely granular zone, L – lipid droplets, LM – left marginal cirral row, MA – macronuclear nodules, MI – micronuclei, PM – paroral membrane, RM – right marginal cirral row, SL – slime cover, TC – transverse cirri, W – cyst wall s. str., 1–6 – cirral rows/anlagen. Scale bars 70 µm.

Etymology: Dedicated to Prof. Dr. Helmut Berger, my former student, whose hypotrich monographs will live for ever.

Description: Moderately variable with most coefficients of variation ≤ 15%, especially those used in the diagnosis.

Size of cultivated specimens in vivo 180–250 × 70–100 µm, usually about 215 × 80 µm, as calculated from live measurements and the morphometric data in Table 73 adding 15% preparation shrinkage. Body basically ellipsoid, more or less deformed when studded with food vacuoles, anterior half contractile by about 10% (Fig. 198a, 199a–f). Macronuclear nodules in central quarters in or near midline of cell, widely separate; ellipsoid, rarely broadly ellipsoid both in vivo and in protargol preparations; with distinct nucleoli. Micronuclei attached to various sites of macronucleus, about 3 µm across (Fig. 198a, d, 199g, i, j; Table 73). Contractile vacuole slightly

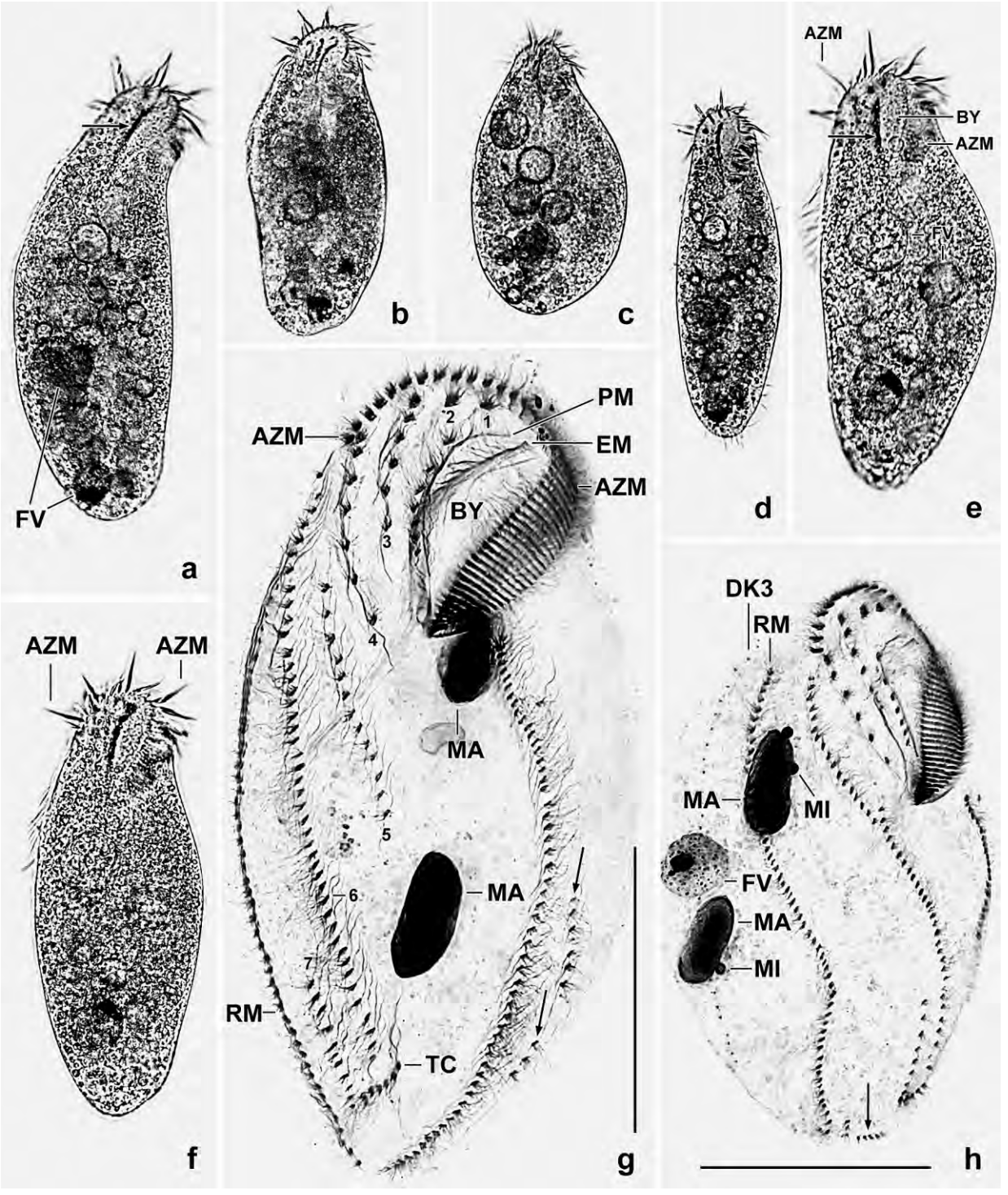

Fig. 199a–h. *Parabistichella bergeri bergeri* from life (a–f) and after protargol impregnation (g, h). **a–f:** Ventral views of freely motile specimens, length 180–250 µm. Note the high shape variability and the dorsal wall of the broad buccal cavity (arrows). **g, h:** Ventral views. The large specimen (g) has seven cirral rows/anlagen and remnants of marginal cirri (arrows). The arrow in (h) marks a broken part of the right marginal row. AZM – adoral zone of membranelles, BY – buccal cavity, DK3 – dorsal kinety 3, EM – endoral membrane, FV – food vacuoles, MA – macronuclear nodules, MI – micronuclei, PM – paroral membrane, RM – right marginal cirral row, TC – transverse cirri, 1–7 – cirral rows/anlagen. Scale bars 70 µm.

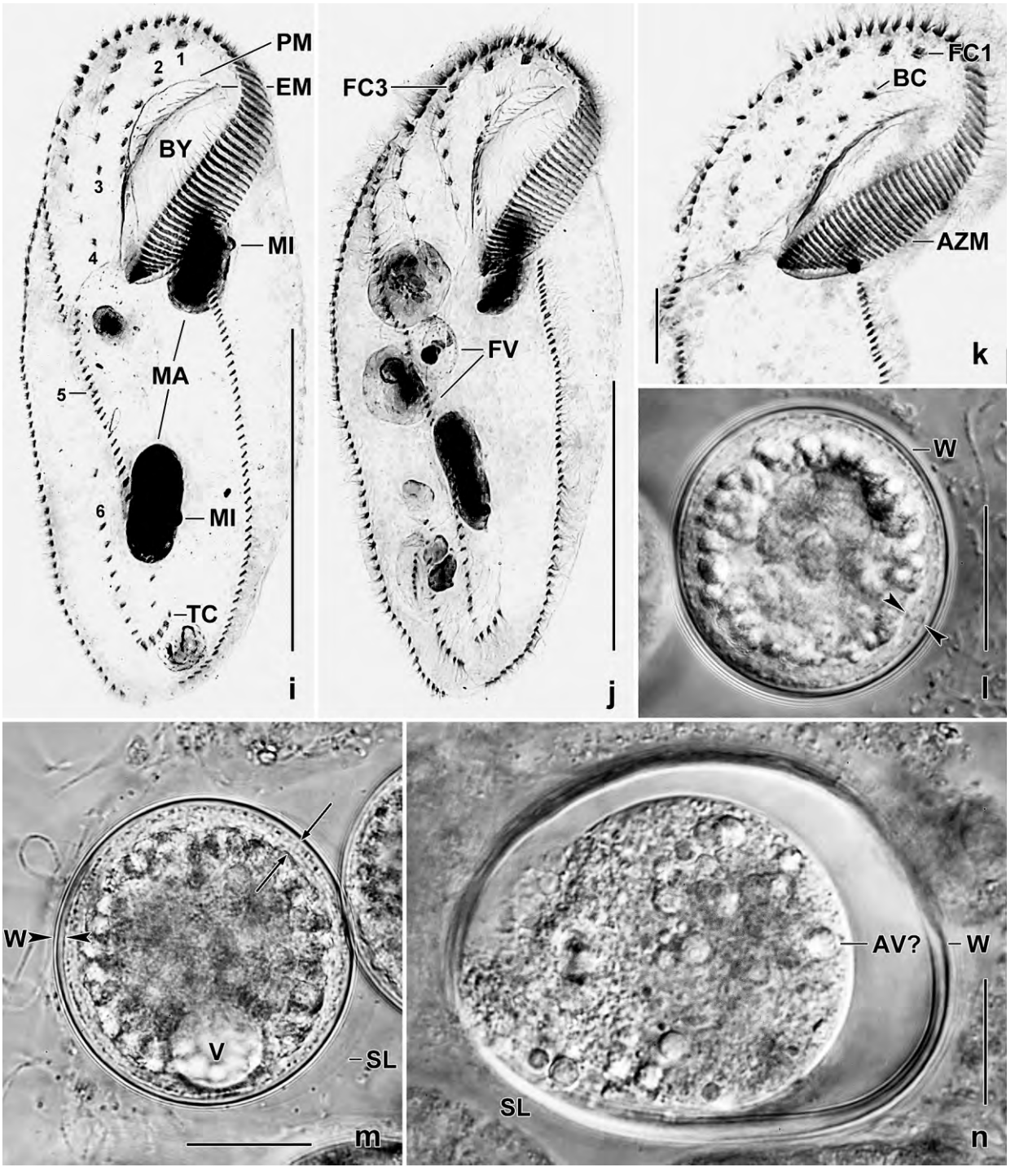

Fig. 199i–n. *P. bergeri bergeri* from life (l–n) and after protargol impregnation (i–k). **i–k:** Ventral views showing, inter alia, the lanceolate adoral zone (k), the six cirral rows/anlagen (i, j), and the transverse cirri (i). **l:** Resting cyst with finely granular zone defined by opposed arrowheads. The globular inclusions are possibly lipid droplets and/or autophagous vacuoles. **m:** Resting cyst, showing the big vacuole, the cyst wall (opposed arrowheads), and the finely granular layer (opposed arrows). **n:** Squashed resting cyst, showing details of wall and cytoplasm. AV? – autophagous vacuoles, AZM – adoral zone of membranelles, BC – buccal cirri, BY – buccal cavity, EM – endoral membrane, FC1,3 – frontal cirri, FV – food vacuoles, MA – macronuclear nodules, MI – micronuclei, PM – paroral membrane, SL – slime layer, TC – transverse cirri, V – vacuole, W – cyst wall, 1–6 – cirral rows/anlagen. Scale bars 15 µm (k), 20 µm (l–n), and 70 µm (i, j).

Table 73. Morphometric data on *Parabistichella bergeri brevisticha* (upper line; from a non-flooded Petri dish culture) and *P. bergeri bergeri* (lower line; from a semipure culture) based on mounted, protargol-impregnated, and randomly selected specimens. Measurements in µm. CV – coefficient of variation in %, M – median, Max – maximum, Mean – arithmetic mean, Min – minimum, n – number of individuals investigated, SD – standard deviation, SE – standard error of arithmetic mean.

Characteristics	Mean	M	SD	SE	CV	Min	Max	n
Body length, in vivo (raw culture)	207.0	200.0	–	–	–	170.0	250.0	3
	225.5	230.0	25.4	7.6	11.2	180.0	250.0	11
Body width, in vivo (raw culture)	71.7	70.0	–	–	–	70.0	75.0	3
	88.2	90.0	11.0	3.3	12.5	70.0	100.0	11
Body, length	169.9	167.0	13.5	4.3	7.9	154.0	196.0	10
	177.2	177.0	16.7	3.6	9.4	141.0	213.0	21
Body, width	47.3	47.0	7.4	2.3	15.6	38.0	57.0	10
	74.5	75.0	7.3	1.6	9.8	60.0	87.0	21
Body length: width, ratio	3.6	3.7	0.5	0.1	12.6	3.0	4.2	10
	2.4	2.4	0.3	0.1	11.1	1.9	2.9	21
Anterior body end to proximal end of adoral zone of membranelles, distance	47.0	47.5	2.4	0.8	5.2	42.0	50.0	10
	58.8	60.0	3.5	0.8	5.9	54.0	65.0	21
Adoral zone of membranelles, percentage of body length	27.7	26.0	3.3	1.0	11.8	24.0	34.0	10
	33.3	33.0	2.5	0.6	7.6	30.0	40.0	21
Largest membranellar bases, length	11.2	11.0	1.1	0.4	10.1	10.0	13.0	10
	12.9	13.0	1.8	0.4	13.0	10.0	17.0	21
Buccal field, width[a]	9.7	10.0	1.6	0.5	16.9	7.0	12.0	10
	13.8	13.0	1.8	0.4	13.0	10.0	17.0	21
Anterior body end to first buccal cirrus, distance	14.7	14.0	3.0	0.9	20.3	11.0	22.0	10
	14.7	15.0	1.6	0.4	11.0	12.0	17.0	21
Anterior body end to paroral membrane, distance	11.5	11.3	1.2	0.4	10.0	10.0	13.0	10
	12.9	13.0	1.5	0.3	11.5	10.0	15.0	21
Anterior body end to endoral membrane, distance	12.1	12.0	1.0	0.3	8.6	10.5	14.0	10
	13.1	13.0	1.5	0.3	11.6	10.0	16.0	21
Anterior body end to right marginal row, distance	18.3	17.5	5.4	1.7	29.6	10.0	26.0	10
	29.6	30.0	6.6	1.4	22.2	17.0	41.0	21
Anterior body end to frontal row 3, distance	10.0	9.5	2.7	0.9	27.1	6.0	14.0	10
	12.7	12.0	2.0	0.4	15.6	10.0	17.0	21
Anterior body end to end of frontal row 3, distance	28.7	26.5	5.8	1.8	20.1	23.0	43.0	10
	38.6	38.0	5.0	1.1	13.1	31.0	48.0	21
Anterior body end to frontal row 4, distance	10.3	10.0	3.1	1.0	30.0	6.0	15.0	10
	18.5	18.0	3.1	0.7	17.0	14.0	27.0	21
Anterior body end to end of frontal row 4, distance	46.9	46.5	6.2	2.0	13.2	40.0	57.0	10
	62.2	60.0	10.4	2.3	16.8	48.0	94.0	21
Anterior body end to frontoventral row 5, distance	13.5	12.0	4.1	1.3	30.5	8.0	20.0	10
	24.6	25.0	3.5	0.8	14.1	18.0	32.0	21
Anterior body end to end of frontoventral row 5, distance	148.7	149.0	12.1	3.8	8.2	132.0	169.0	10
	150.8	152.0	14.7	3.2	9.7	121.0	178.0	21
Anterior body end to ventral cirral row 6, distance	not investigated							
	123.4	125.0	16.4	3.6	13.3	88.0	159.0	21

continued

Characteristics	Mean	M	SD	SE	CV	Min	Max	n
Anterior body end to end of ventral cirral row 6, distance	not investigated							
	157.4	158.0	11.7	2.5	7.4	132.0	179.0	21
Anterior body end to first macronuclear nodule, distance	42.8	42.0	3.9	1.2	9.0	38.0	51.0	10
	48.6	49.0	5.0	1.1	10.3	36.0	56.0	21
Posterior body end to transverse cirri, distance	6.8	5.5	2.9	0.9	43.2	4.0	11.0	10
	14.7	15.0	4.8	1.0	32.8	6.0	27.0	21
Posterior body end to right marginal cirral row, distance	4.2	4.3	1.9	0.6	45.7	1.0	7.0	10
	1.6	1.5	–	–	–	6.0	21.0	21
Posterior body end to left marginal cirral row, distance	0.7	0.0	–	–	–	0.0	4.0	10
	7.0	6.0	3.8	0.8	53.9	1.0	15.0	21
Anterior macronuclear nodule, length	21.3	21.0	1.6	0.5	7.7	19.0	24.0	10
	24.6	25.0	2.8	0.6	11.5	17.0	30.0	21
Anterior macronuclear nodule, width	10.4	10.5	1.1	0.3	10.3	8.0	12.0	10
	12.9	13.0	1.0	0.2	7.7	11.0	15.0	21
Macronuclear nodules, number	2.0	2.0	0.0	0.0	0.0	2.0	2.0	10
	2.0	2.0	0.0	0.0	0.0	2.0	2.0	21
Micronuclei, length	3.2	3.0	–	–	–	3.0	3.5	10
	3.1	3.0	–	–	–	3.0	4.0	21
Micronuclei, width	3.1	3.0	–	–	–	3.0	3.5	10
	3.1	3.0	–	–	–	3.0	4.0	21
Micronuclei, number	2.7	3.0	0.7	0.2	25.0	2.0	4.0	10
	2.7	3.0	0.7	0.1	24.7	1.0	4.0	21
Adoral membranelles, number	38.0	38.0	1.8	0.6	4.6	35.0	40.0	10
	50.3	50.0	2.6	0.6	5.1	45.0	57.0	21
Frontal cirri, number	3.0	3.0	0.0	0.0	0.0	3.0	3.0	10
	3.0	3.0	0.0	0.0	0.0	3.0	3.0	21
Buccal cirri, number	5.3	5.0	0.7	0.2	12.7	4.0	6.0	10
	7.5	8.0	0.7	0.2	10.0	6.0	9.0	21
Frontal row 3, number of cirri	3.9	4.0	0.7	0.2	18.9	3.0	5.0	10
	5.2	5.0	0.7	0.2	13.4	4.0	6.0	21
Frontal row 4, number of cirri	6.1	6.0	1.2	0.4	19.6	5.0	8.0	10
	7.7	7.0	1.7	0.4	21.6	6.0	14.0	21
Frontoventral row 5, number of cirri	45.6	46.5	2.3	0.7	5.0	42.0	48.0	10
	48.5	48.0	4.2	0.9	8.6	39.0	57.0	21
Frontoventral row 6, number of cirri	not counted							
	9.3	9.0	2.7	0.6	28.8	3.0	16.0	21
Transverse cirri, number	about 5; see text							
	5.5	5.0	1.0	0.2	17.9	4.0	8.0	21
Right marginal cirri, number	55.1	55.0	1.7	0.5	3.1	53.0	58.0	10
	62.1	64.0	8.3	1.8	13.4	50.0	77.0	21
Left marginal cirri, number	48.0	49.0	3.2	1.0	6.6	40.0	52.0	10
	54.4	55.0	3.9	0.9	7.2	44.0	61.0	21
Dorsal bristle rows, number	3.0	3.0	0.0	0.0	0.0	3.0	3.0	5
	3.0	3.0	0.0	0.0	0.0	3.0	3.0	21
Dorsal row 1, number of bristles	21.4	21.0	2.3	1.0	10.8	19.0	25.0	5

continued

Characteristics	Mean	M	SD	SE	CV	Min	Max	n
	30.0	30.0	3.4	0.7	11.4	23.0	38.0	21
Dorsal row 2, number of bristles	24.0	–	–	–	–	–	–	1
	29.2	28.0	2.5	0.6	8.7	25.0	34.0	21
Dorsal row 3, number of bristles	24.5	24.5	–	–	–	23.0	26.0	2
	32.4	33.0	3.4	0.7	10.5	26.0	40.0	21
Resting cyst, diameter	not investigated							
	48.6	38.0	16.7	4.2	34.4	33.0	72.0	16

[a] Distance between centre of paroral membrane and right margin of adoral zone.

anterior of mid-body (Fig. 198a). Cortex very flexible, without specific granules. Cytoplasm colourless, usually opaque and dark at low magnification because studded with lipid droplets up to 5 µm across and up to 40 µm-sized food vacuoles containing bacteria, heterotrophic flagellates, small and middle-sized ciliates (*Paracolpoda steinii, Urosoma karinae*), and corroded starch grains from culture medium (Fig. 198a, 199a–f, j). Glides rather slowly on bottom of culture dish as well as on and between soil and mud accumulations, showing much flexibility.

Infraciliature as typical for bistichellids (Berger 2008), i. e., composed of a right and a left marginal cirral row; four frontal and two (rarely three) frontoventral cirral rows; transverse cirri; and dorsal kineties (Fig. 198a, b, d, 199g–k; Table 73). Frontal row 1 composed of frontal cirrus 1 about 20 µm long in vivo; frontal row 2 composed of frontal cirrus 2 and an average of eight buccal cirri; frontal row 3 composed of frontal cirrus 3 and an average of five cirri; frontal row 4 composed of an average of eight cirri; frontoventral row 5 extends to near transverse cirri, composed of an average of 48 cirri; and frontoventral row 6 strongly shortened to an average of nine cirri usually ending at level of transverse cirri. On average five transverse cirri forming an oblique row, about 20 µm long in vivo and inserted rather far subterminal, thus only slightly projecting from body proper. Right marginal cirral row commences about 30 µm subapically and extends to near rear body end, cirri 15 µm long in vivo. On average a total of 203 cirri. Dorsal bristles 3 µm long in vivo, in three rows commencing distinctly subapically and extending to near posterior body end. Caudal cirri absent (Fig. 198d).

Oral apparatus also as typical for bistichellids (Berger 2008). Adoral zone of membranelles conspicuous because composed of an average of 50 membranelles and lanceolate; begins far subapically on right body margin, then curves around anterior body end and extends about 33% of body length. Distal half of zone made of small membranelles (base width < 10 µm, handle of lance), then bases gradually widen to about 20 µm (lance) and, finally, base width decreases rather abruptly to 2 µm (lancehead). Cilia of frontal membranelles and lateral membranellar cilia up to 25 µm long. Buccal cavity rather wide and deep, supported by a complex fibre system described in detail by Foissner et al. (2002). Buccal lip about 7 µm wide, bears strongly curved paroral membrane with cilia gradually decreasing in length from 10 µm anteriorly to 5 µm posteriorly. Endoral membrane also distinctly curved, crosses obliquely bottom of buccal cavity, intersects optically with paroral in mid of buccal cavity. Pharynx comparatively small, extends to mid-body (Fig. 198a, b, 199d–g, i–k; Table 73).

Resting cyst (Fig. 198c, 199l–n; Table 73): When encysting several to many specimens come together, forming aggregates with individual cysts hold next to each other by their slimy cover. Cysts spherical to slightly ellipsoid, 33–72 µm in vivo, on average about 40 µm across (Table 73). Cyst wall covered by an up to 5 µm thick very hyaline slime layer; 2.5 to 3 µm thick, compact, stains purple with methyl green-pyronin. All cysts with a large, non-contracting vacuole. Cyst contents bipartite; external zone finely granular and 2–5 µm thick; internal zone contains macronuclear nodules (not fused) and many 2–6 µm-sized globules with granular fine structure, possibly autophagous vacuoles and/or lipid droplets (Fig. 198c, 199l–n). Possibly very similar to that of *Bistichella encystica* insufficiently described by Fan et al. (2014).

Occurrence and ecology: As yet found only in two samples from closely spaced sites (66, 67). The large size and the broad shape and the type locality indicate a preference for litter and/or brackish habitats. Could be cultivated for a while in saline water (50‰) with some squashed wheat kernels.

Remarks: In the species comparison, we discuss only binucleate taxa with transverse cirri and without cortical granules. These are *Parabistichella namibiensis* (cirral rows 5 and 6 vs. only row 5 extends to transverse cirri), and *Parabistichella procera and P. terrestris* (~ 2 vs. ~ 5 transverse cirri; cirral rows 5 and 6 extend to or slightly posterior of mid-body vs. row 5 extends to transverse cirri and row 6 strongly shortened ending at level of transverse cirri). See Berger (2008) for authors and dates of the species mentioned.

Parabistichella bergeri brevisticha nov. subspec. (Fig. 200a–e; Table 73)

Diagnosis: Length:width ratio about 3.6:1 in protargol preparations of environmental specimens. On average a total of 180 cirri including 5 buccal cirri; 21 bristles in dorsal kinety 1. Adoral zone composed of an average of 38 membranelles.

Type locality: Highly saline (>50‰) litter and humous soil from the coast of Caracas Bay, Curacao Island, north coast of Venezuela, 71°W 12°N.

Type material: 1 holotype and 6 paratype slides with protargol-impregnated specimens have been deposited in the Biology Centre of the Upper Austrian Museum in Linz (LI). The holotype and other relevant specimens have been marked by black ink circles on the coverslip.

Etymology: *brevisticha* is a composite of the Latin adjective *brevis* (short) and the Greek noun *stichus* (row), referring to the slightly shorter cirral rows compared to *P. bergeri bergeri*.

Description and Remarks: As mentioned above, *P. bergeri brevisticha* differs from *P. bergeri bergeri* mainly by the lower, non-overlapping number of adoral membranelles (38 vs. 50 on average). This difference is likely not caused by body length which is quite similar in both subspecies (Table 73). The other differences mentioned in the diagnosis overlap more or less and are thus of questionable value.

Body size and shape as well as somatic and oral infraciliature are highly similar in the two subspecies, especially when cultivated specimens are compared (Table 73). Thus, we do not

provide a full description but refer to the figures, the morphometrics, and the following in vivo observations.

Body shape basically ellipsoid, frequently slightly sigmoid, rarely elongate rectangular with rounded corners; usually slightly wider in anterior than posterior half; laterally flattened up to 2:1 (Fig. 200a–d; Table 73). Anterior macronuclear nodule close to proximal end of adoral zone. Micronuclei about 5 µm across. Contractile vacuole not recognizable very likely due to the highly saline environment. Cortex very flexible, specific cortical granules and cytoplasmic crystals absent, but 2 µm long rods occur in the buccal wall. Preferably feeds on various colpodids, such as *Cyrtolophosis mucicola, Paracolpoda steinii,* and even the large *Tillina minima* digested in food

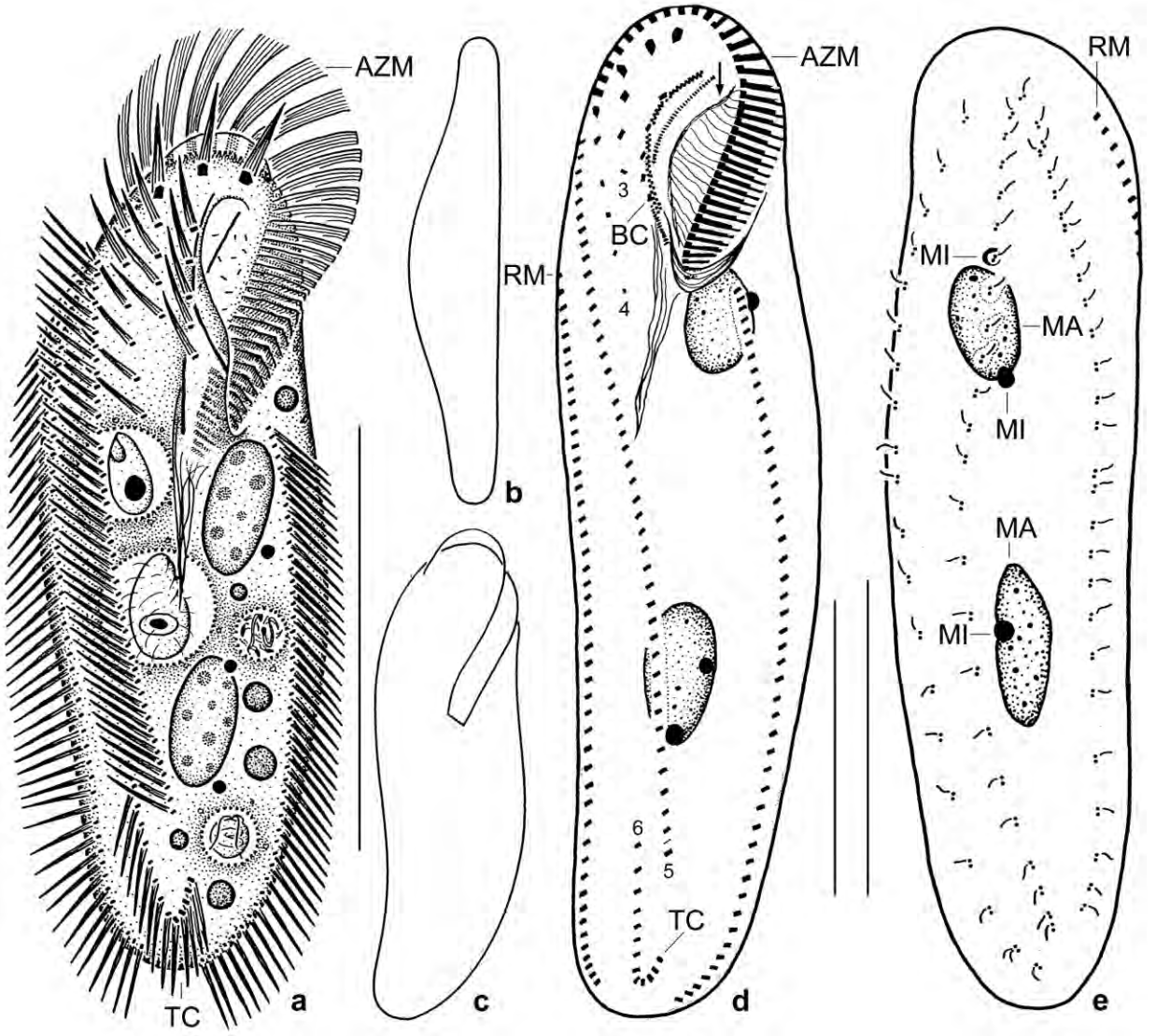

Fig. 200a–e. *Parabistichella bergeri brevisticha* from life (a– c) and after protargol impregnation (d, e). **a:** Ventral view of a representative specimen, length 200 µm. **b:** Lateral view. **c:** Slightly sigmoid shape variant. **d:** Ventral view of holotype specimen, length 170 µm. The arrow marks a thick fibre in bottom of buccal cavity. **e:** Dorsal view of a paratype specimen, showing three dorsal kineties. AZM – adoral zone of membranelles, BC – row of buccal cirri, MA – macronuclear nodules, MI – micronuclei, RM – right marginal cirral row, TC – transverse cirri, 3–6 – cirral rows. Scale bars 50 µm (d, e) and 100 µm (a).

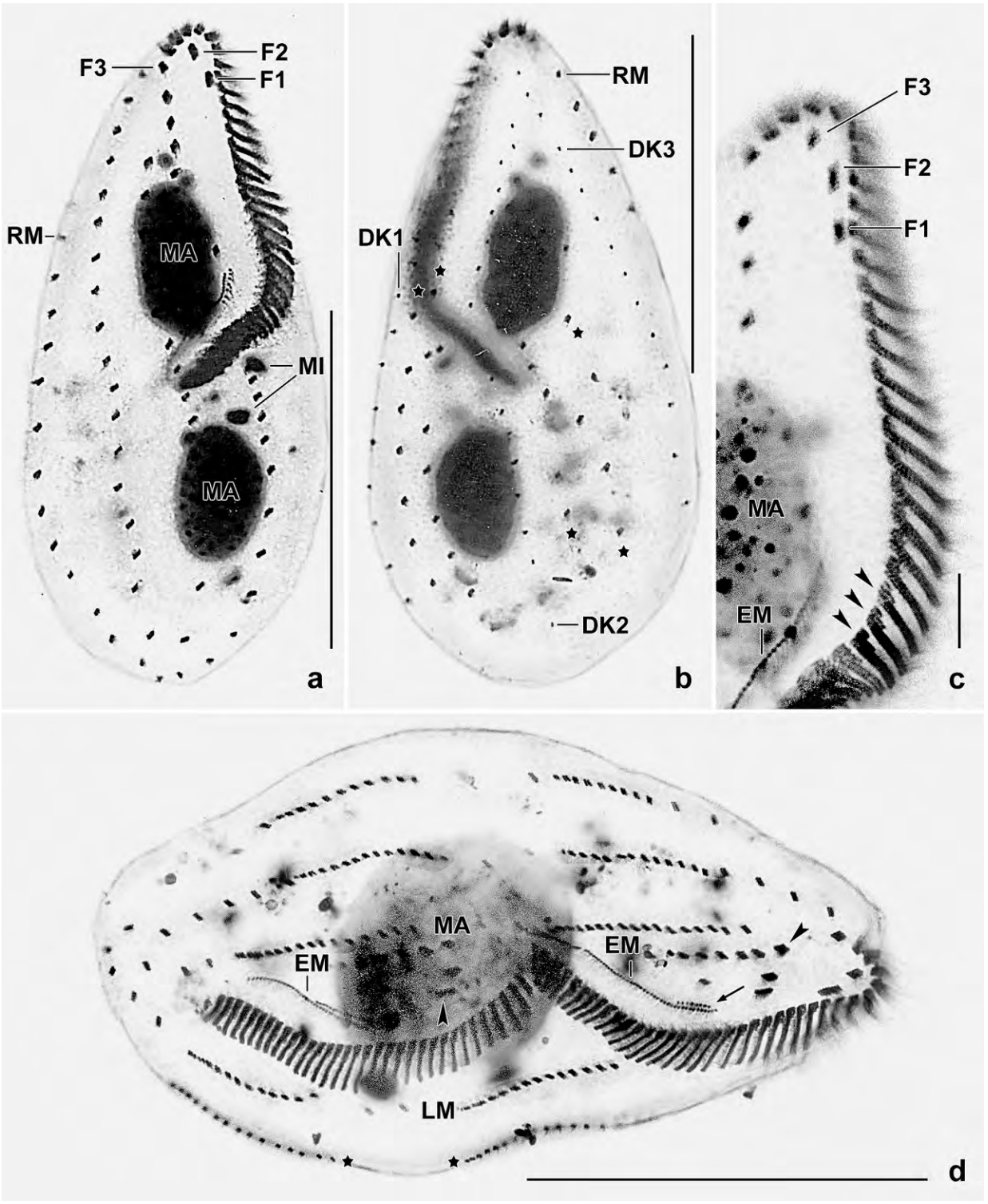

Fig. 201a–d. *Cotterillia bromelicola* from Costa Rica after protargol impregnation. **a, b:** Ventral and dorsal overview with dorsal cirral rows marked by asterisks. **c:** Oral apparatus of a specimen with misplaced frontal cirri (cp. Fig. 201a), showing the very short membranellar ciliary rows 3 and 4 (arrowheads). **d:** Ventral view of a mid-divider, showing the paroral membrane still right of the endoral (arrow); the three new frontal cirri (arrowheads); and a de novo generated dorsal kinety each in proter and opisthe (asterisks). DK1–3 – dorsal kineties, EM – endoral membrane, FC1–3 – frontal cirri, LM – left marginal cirral row, MA – macronuclear nodules, MI – micronuclei, RM – right marginal cirral row. Scale bars 5 µm (c) and 50 µm (a, b, d).

vacuoles up to 50 µm across. Frontal cirri about 20 µm long, marginal and transverse cirri about 17 µm, the latter thus only slightly projecting from body proper. Oral apparatus conspicuous; lanceolate shape of adoral zone of membranelles indistinct; largest bases of adoral membranelles about 20 µm long (Fig. 200a–d; Table 73).

Occurrence and ecology: As yet found only at type locality, a highly saline habitat (>50‰ salinity, pH 8.1). *Parabistichella bergeri brevisticha* appeared in the non-flooded Petri dish culture two days after rewetting the air-dried sample.

Cotterillia bromelicola Foissner & Stoeck, 2011 (Fig. 201a–d)

The Costa Rican population matches well the Mexican type. Thus, we provide only some figures. The species was found in moss and mud from old cacao-trees colonized by many bromeliads. Thus, it might be a bromeliad ciliate, as the type population.

We deposited two voucher slides with protargol-impregnated specimens in the Biology Centre of the Upper Austrian Museum in Linz (LI). Some excellently prepared specimens have been marked by black ink circles on the coverslip.

Saudithrix terricola Foissner, Al-Rasheid and Berger in Berger, Al-Rasheid and Foissner, 2006 (Fig. 202a–h)

This conspicuous ciliate occurred in sample (18) from Costa Rica, i. e., in the mud of a lithotelma at the bank of the Rio Corobici, near the Centro Ecologia La Pacifica. Thus, *S. terricola* is now

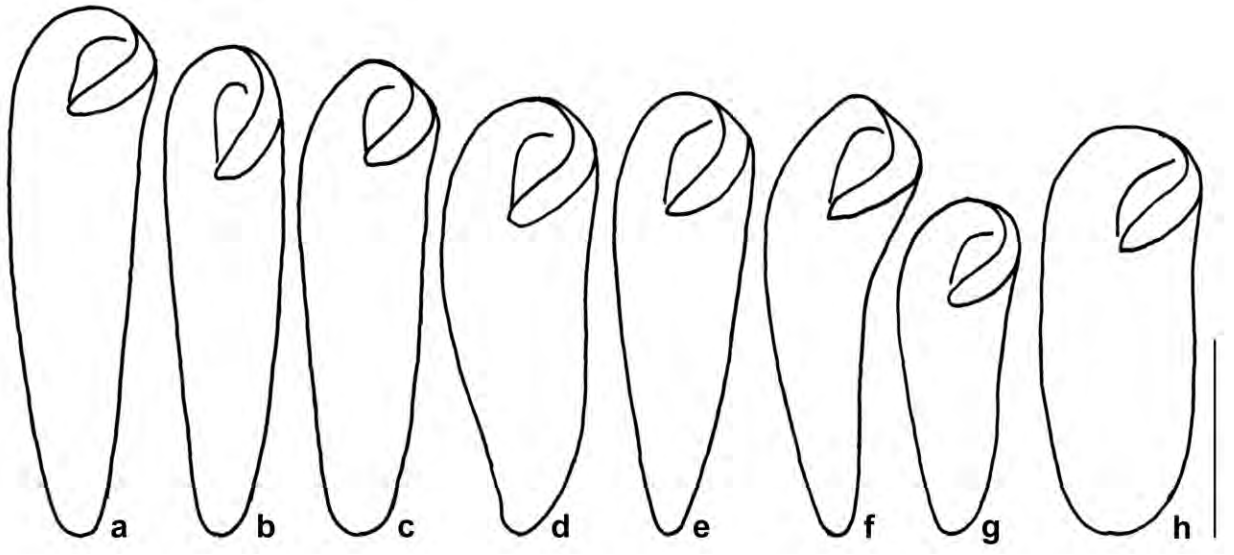

Fig. 202a–h. *Saudithrix terricola*, protargol-impregnated specimens from Costa Rica. About 90% of the specimens are distinctly narrowed posteriorly, and only few have the ellipsoid shape typical for the specimens from the type locality (h). Drawn to scale 100 µm.

known from three sites: Saudi Arabia (type), China (Foissner 2007), and Central America, indicating wide or even cosmopolitan distribution; however, we did not find it in 100 samples each from Australia and Central Europe.

The Costa Rican specimens were first similar to those from the type population (Fig. 202h). However, when abundance increased in the non-flooded Petri dish culture, about 90% of the specimens gradually narrowed posteriorly for unknown reasons (Fig. 202a–g). The cirral pattern did not change. Size about 250 × 80 µm in vivo; cortical granules absent; transverse cirri about 25 µm long slightly projecting from body proper; three dorsal kineties and scattered bristles between the rows; fed mainly on two small ciliates, viz. *Drepanomonas revoluta* and swarmers of *Pseudovorticella sphagni*.

We deposited three voucher slides with protargol-impregnated specimens in the Biology Centre of the Upper Austrian Museum in Linz (LI). The specimens illustrated are marked by black ink circles on the coverslip.

Family Gonostomatidae Small & Lynn, 1985

As an example, we include in this chapter most unpublished gonostomatids collected since 1985. These are 11 new species and four new genera which almost doubles the number of described *Gonostomum* and *Paragonostomum* species (for a review, see Berger 2001). Most of the new species were discovered in Gondwanan regions putting forward the "moderate endemicity model" discussed by Foissner (2008a) and Foissner et al. (2008b). We have many taxa like the gonostomatids in our unpublished material, suggesting an enormous number of soil ciliate species most being undescribed.

In hypotrichs, many cirral and nuclear patterns occur, and the gonostomatids are an example that all patterns are realized in a single family, for instance the presence/absence of transverse (TC) and caudal (CC) cirri: with TC and CC (*Gonostomum*), without TC and CC (*Gonostomoides* nov. gen.), with CC but without TC (*Paragonostomum*), and with TC but without CC (*Apogonostomum* nov. gen.). As concerns the nuclear apparatus, three of the four main patterns (2 macronuclear nodules, 4 nodules, many nodules, monomicrocaryon pattern) have been found. A similar series is formed by the following genera: *Paragonostomoides* nov. gen., *Metagonostomum* nov. gen., and *Apogonostomum* nov. gen. They have either the frontoterminal or the frontoventral cirri organized in long rows.

Paragonostomoides nov. gen.

Diagnosis: Gonostomatidae with caudal cirri and a long row of frontoterminal cirri.

Type species: *Paragonostomum minutum* Kamra, Kumra & Sapra, 2008.

Etymology: Composite of the generic name *Gonostomum* and the suffix *-oides* (similar), meaning a ciliate similar to *Gonostomum*. Masculine gender.

Gonostomum is neuter (Aescht 2001, Berger 2011). Thus, the type species must read *Paragonostomum minutum*. Kamra et al. (2008) used the false feminine ending "minuta".

Species assignable: Monotypic!

Remarks: Kamra et al. (2008) noted that the second right marginal row of *Paragonostomum minutum* is a long row of frontoterminal cirri. We agree although this should be substantiated by ontogenetic evidences. In any case, this feature is a strong apomorphy justifying the classification into a new genus, *Paragonostomoides.*

Metagonostomum nov. gen.

Diagnosis: Gonostomatidae with transverse and caudal cirri and a long row of frontoterminal cirri.

Type species: *Trachelochaeta gonostomoida* Hemberger, 1985.

Etymology: Composite of the Greek prefix *meta* (next to, among after) and the genus-group name *Gonostomum*, referring to the similarity with *Gonostomum* which also has transverse and caudal cirri but only a few frontoterminal cirri.

Species assignable: Monotypic! Possibly, *Trachelochaeta terrestre*, which Berger (2011) classified into *Gonostomum*, also belongs to *Metagonostomum.* But a solid redescription should be awaited because the original description by Alekperov (2005) is too weak.

Remarks: As in *Paragonostomoides*, differing from that genus by possessing transverse cirri. The type species has been redescribed by Kamra et al. (2008) and Kim and Shin (2006).

Apogonostomum nov. gen.

Diagnosis: Tailed Gonostomatidae with transverse cirri and frontoventral cirral pairs extending in body`s midline to buccal vertex or to near transverse cirri. Caudal cirri absent.

Type species: *Apogonostomum pantanalense* nov. spec.

Etymology: Composite of the Greek prefix *apo* (derived) and the genus-group name *Gonostomum.* Neuter gender.

Remarks: This new type of gonostomatids lacks caudal cirri, likely due to the thin tail. It resembles *Wallackia* (without frontoterminal cirri; for modern descriptions, see Foissner et al. 2002) and the new genera → *Paragonostomoides* and → *Metagonostomum* whose cirral rows originate by an increase of the frontoterminal cirri; in both the ventral cirral row is close to the right marginal row while the two rows of *Apogonostomum* are in midline of body.

Apogonostomum pantanalense nov. spec. (Fig. 203a–g, 204a–h; Table 74)

Diagnosis: Size in vivo about 170 × 40 µm. Very elongate ellipsoid with distinct tail. 2 ordinarily located, elongate ellipsoid macronuclear nodules and 3 comparatively large globular micronuclei. Cortical granules prominent because 6 × 1 µm in vivo, form colourless rows. 3 frontal cirri, 2 frontoterminal cirri, 1 buccal cirrus far subapical of paroral membrane, 2 frontoventral cirral rows forming an average of 8 cirral pairs, 2 pretransverse cirri in special position and 4 transverse cirri. Right marginal row composed of an average of 25 cirri, left of 16. Three dorsal kineties with

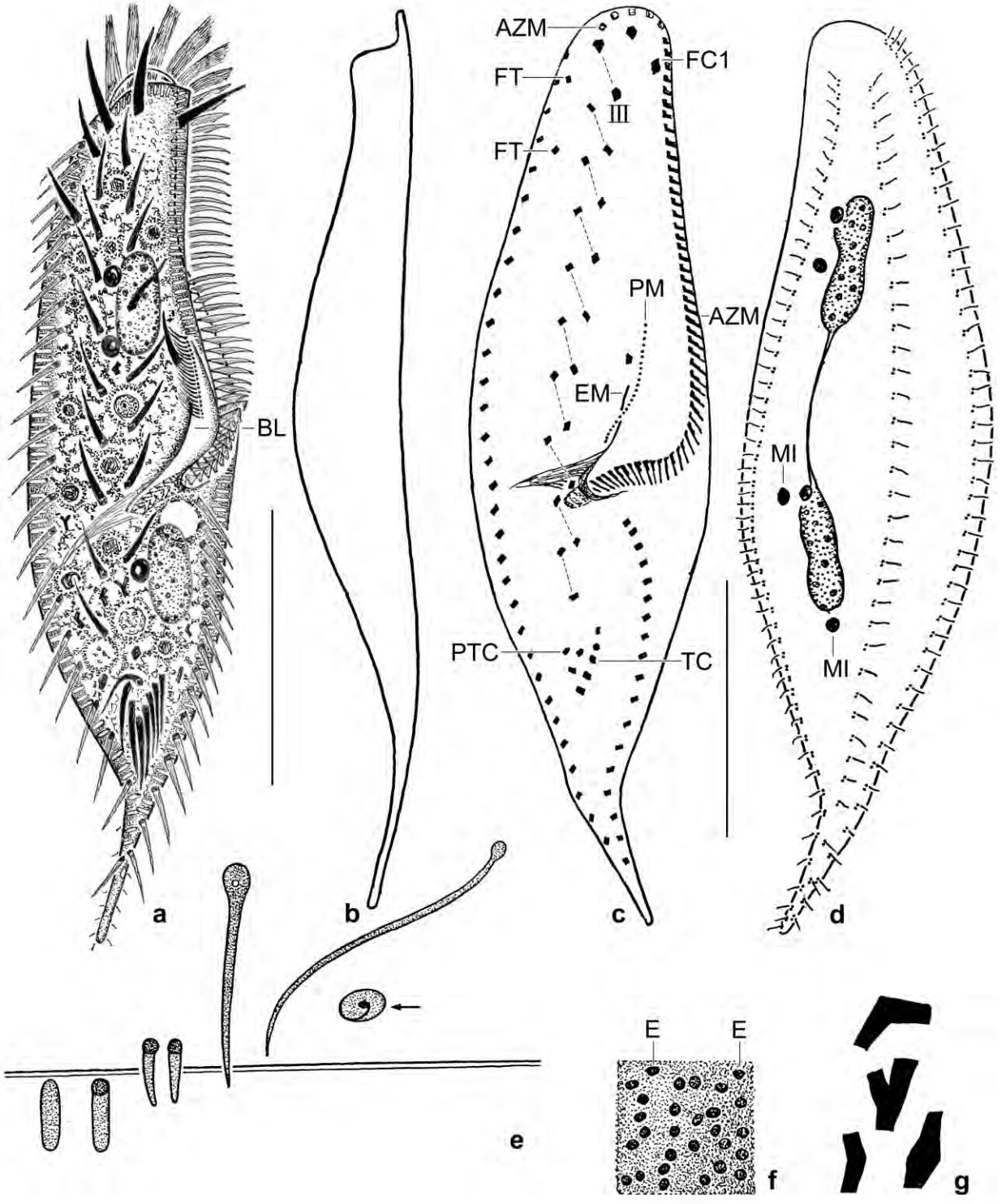

Fig. 203a–g. *Apogonostomum pantanalense* from life (a, b, e–g) and after protargol impregnation (c, d). **a:** Ventral view of a representative specimen, length 160 µm. Body shape redrawn from a micrograph; fronto-ventral-transverse cirri shadded black. Note the extrusome fringe. **b:** Lateral view. **c, d:** Ventral and dorsal view of holotype specimen, length 180 µm. **e:** Extrusome extrusion. Arrow marks an only partially exploded extrusome. **f:** Surface view, showing the extrusomes. **g:** Cytoplasmic crystals, 2–5 µm. AZM – adoral zone of membranelles, BL – buccal lip, E – extrusomes, EM – endoral membrane, FC1 – frontal cirrus 1, FT – frontoterminal cirri, MI – micronuclei, PM – paroral membrane, PTC – pretransverse cirri, TC – transverse cirri, III – posterior cirrus of anlage III. Scale bars 10 µm (e) and 50 µm (a–d).

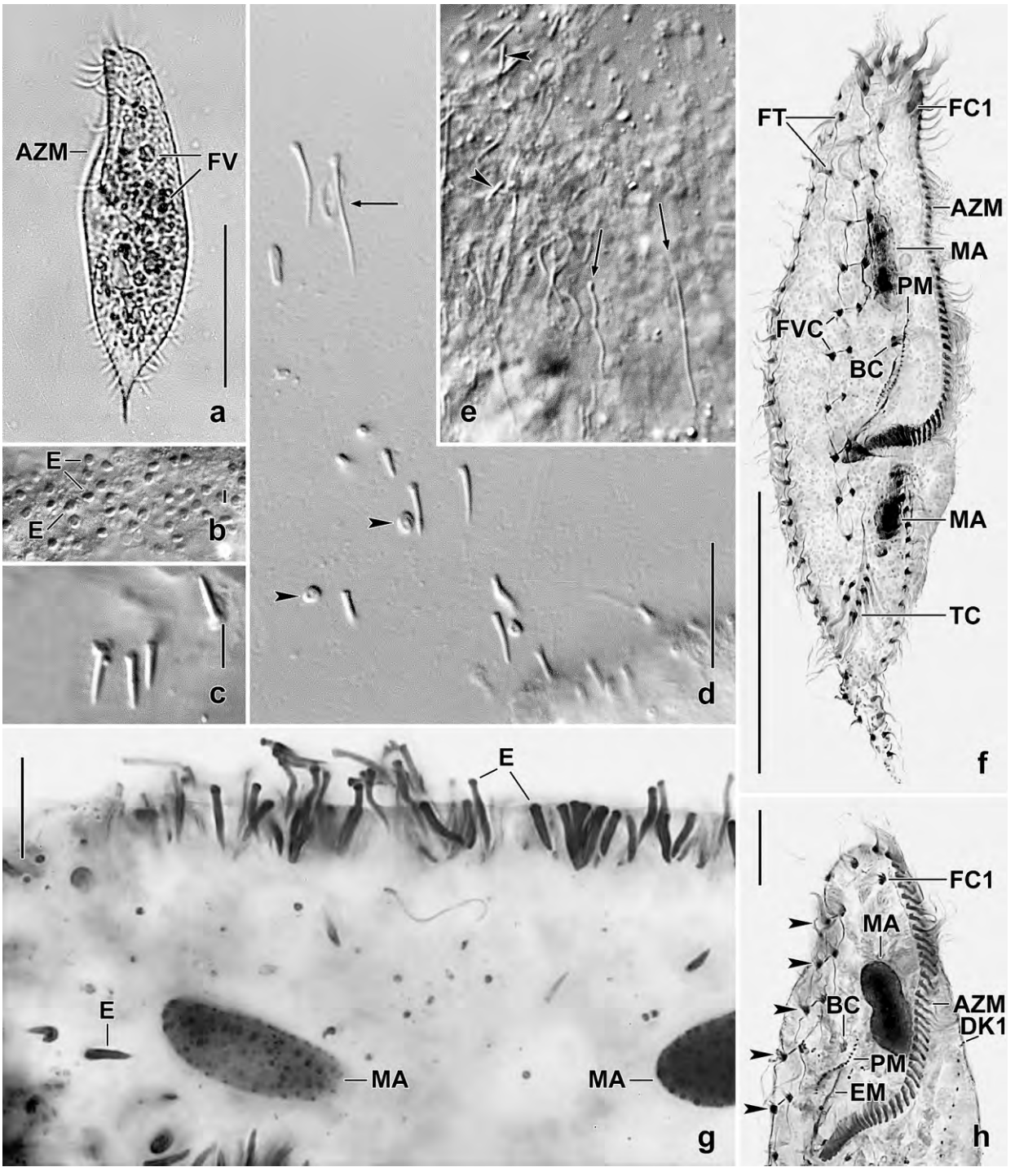

Fig. 204a–h. *Apogonostomum pantanalense* from life (a–e) and after protargol impregnation (f–h). **a:** Dorsal view of a broad specimen. **b:** Surface view, showing extrusomes in transverse view. **c:** Just released, nail-shaped extrusomes. **d:** After the explosion, the extrusomes become sperm-shaped (arrow). The arrowheads mark partially exploded extrusomes. **e:** Finally, the extrusomes become long filaments (arrows). The arrowheads mark resting extrusomes. **f:** Ventral view of holotype specimen, length 180 µm. **g:** Exploding extrusomes. **h:** Ventral view, showing the frontoventral cirral pairs (arrowheads). AZM – adoral zone, BC – buccal cirrus, DK1 – dorsal kinety 1, E – extrusomes, EM – endoral membrane, FC1 – frontal cirrus, FT – frontoterminal cirri, FV – food vacuoles, FVC – frontoventral cirri, MA – macronuclear nodules, PM – paroral membrane, TC – transverse cirri. Scale bars 1 µm (b), 10 µm (c, g), 20 µm (d, e, h), and 70 µm (a, f).

Table 74. Morphometric data on *Apogonostomum pantanalense* based on mounted, protargol-impregnated, and randomly selected specimens from a non-flooded Petri dish culture. Measurements in µm. CV – coefficient of variability in %, M – median, Max – maximum, Mean – arithmetic mean, Min – minimum, n – number of individuals investigated, SD – standard deviation, SE – standard error of arithmetic mean.

Characteristics	Mean	M	SD	SE	CV	Min	Max	n
Body, length	142.9	141.0	21.1	3.9	14.8	114.0	185.0	29
Body, width	42.4	42.0	6.2	1.2	14.5	31.0	60.0	28
Body length:width, ratio	3.3	3.4	0.8	0.2	23.6	0.8	4.8	28
Anterior body end to proximal end of adoral zone, distance	81.0	79.0	11.2	2.1	13.9	66.0	100.0	29
Adoral zone of membranelles, percentage of body length	57.1	57.0	4.1	0.8	7.2	47.0	63.0	28
Adoral membranelles, number	53.4	54.0	5.5	1.1	10.2	44.0	64.0	27
Anterior body end to paroral membrane, distance	47.2	46.0	5.8	1.4	12.3	41.0	63.0	17
Paroral kinetids, number	19.4	19.0	3.7	0.9	19.0	14.0	26.0	17
Anterior body end to endoral membrane, distance	57.8	56.0	8.1	2.0	14.0	48.0	75.0	17
Anterior body end to buccal cirrus, distance	52.2	50.0	7.0	1.7	13.5	43.0	68.0	17
Buccal cirri, number	1.0	1.0	0.0	0.0	0.0	1.0	1.0	22
Nuclear figure, length	68.4	68.0	8.8	2.1	12.9	54.0	85.0	17
Anterior body end to first macronuclear nodule, distance	31.0	31.0	4.8	0.9	15.5	23.0	38.0	29
Macronuclear nodules, length	20.9	20.0	4.0	0.7	19.2	14.0	29.0	29
Macronuclear nodules, width	8.2	8.0	1.4	0.3	16.8	6.0	11.0	29
Macronuclear nodules, number	2.0	2.0	0.0	0.0	0.0	2.0	2.0	29
Micronuclei, length	4.5	4.5	0.6	0.1	14.3	3.5	5.7	29
Micronuclei, width	3.3	3.2	0.3	0.1	9.9	2.8	4.0	29
Micronuclei, number	2.8	2.0	1.2	0.2	43.2	2.0	6.0	29
Frontal cirri, number	3.0	3.0	0.0	0.0	0.0	3.0	3.0	25
Frontoterminal cirri, number	2.0	2.0	0.0	0.0	0.0	2.0	2.0	23
Ventral cirral pairs, number	7.8	8.0	0.7	0.2	9.2	7.0	9.0	20
Pretransverse cirri, number	2.1	2.0	–	–	–	2.0	3.0	21
Transverse cirri, number	4.5	4.0	0.8	0.2	16.8	4.0	6.0	21
Right marginal cirri, number	25.6	25.0	3.5	0.7	13.7	21.0	32.0	25
Left marginal cirri, number	16.1	16.0	2.1	0.4	13.2	13.0	21.0	23
Dorsal kineties, number	3.0	3.0	0.0	0.0	0.0	3.0	3.0	30
Dorsal kinety 1, number of kinetids	45.0	45.0	5.3	1.2	11.7	37.0	56.0	18
Dorsal kinety 2, number of kinetids	35.7	35.0	4.3	1.2	12.0	30.0	44.0	13
Dorsal kinety 3, number of kinetids	37.3	37.0	5.1	1.2	13.6	30.0	46.0	18

3–4 µm long cilia. Adoral zone sigmoid, extends 57% of body length, composed of an average of 53 membranelles; paroral membrane composed of an average of 19 kinetids with 8 µm long cilia.

Type locality: Floodplain soil of the Paraná River near to the town of Maringà, Pantanal, Brazil, 53°15‘W 22°40‘S.

Type material: 1 holotype and 4 paratype slides with protargol-impregnated specimens have been deposited in the Biology Centre of the Upper Austrian Museum in Linz (LI). The holotype and relevant paratype specimens have been marked by black ink circles on the coverslip.

Etymology: The adjective *pantanalense* is a combination of the suffix *-ensis* and the region the species was discovered, i. e., the Pantanal, a famous wetland in Brazil.

Description: Size in vivo 130–215 × 35–70 µm, usually about 170 × 40 µm, as calculated from some in vivo measurements and the morphometric data in Table 74 adding 20% and 15% for length and width shrinkage of especially the tail. Body basically ellipsoid, posterior region, however, tail-like elongated and anterior end slightly beak-shaped due to the more or less narrowed and concave oral area; laterally flattened up to 2:1 (Fig. 203a–c, 204a, f; Table 74). Nuclear apparatus composed of two macronuclear nodules and two to six micronuclei (Fig. 203a, d, 204f–h; Table 74). Macronuclear nodules in usual pattern, i. e., a nodule each in anterior quarter of cell and slightly posterior of proximal region of adoral zone of membranelles; nodules ellipsoid to elongate ellipsoid, with many minute nucleoli. Micronuclei near and attached to macronuclear nodules, conspicuous in vivo because about 6 × 5 µm in size and highly refractive, globular to broadly ellipsoid. Contractile vacuole posterior of proximal region of adoral zone, moderately distant from left body margin (Fig. 203a). Cortex flexible, with rows of colourless extrusomes (cortical granules) 5–7 × 1–2 µm in size and thus forming a conspicuous fringe in vivo and in preparations, produce a spotted surface, stain with methyl green-pyronin and often impregnate deeply with the protargol method used (Fig. 203a, e, f, 204b–e, g); become extruded and nail-shaped when cell is slightly pressed, then elongate to long filaments producing a dense envelope (further details, see Figures cited above and Figure explanations). Cytoplasm colourless, usually distinctly vacuolated, contains some ordinary crystals (Fig. 203g) and many 3–10 µm-sized food vacuoles with bacteria, fungal spores, and heterotrophic flagellates (Fig. 203a, 204a). Creeps slowly on microscope slides and swims clumsily.

Cirri not in typical *Gonostomum* pattern shown by Berger (1999, 2011) and Foissner et al. (2001) because frontoventral cirri greatly increased in number, forming two rows extending in cell`s midline from near anterior body end to transverse cirri (Fig. 203a, c, 204f, h); rows rather widely spaced, form an average of eight strongly oblique cirral pairs. Three distinctly enlarged frontal cirri about 20 µm long in vivo, and one cirrus ("fourth frontal cirrus") from anlage III; two frontoterminal cirri in anterior quarter of cell and right of frontoventral cirral rows; one buccal cirrus far subapical of paroral membrane. Usually four or five thin transverse cirri far subterminal at base of tail and thus not projecting from body proper; in ordinary pattern and about 20 µm long in vivo. Pretransverse cirri in unusual position, viz., side by side opposite to transverse cirri. Marginal cirri about 17 µm long in vivo, intracirral distances slightly increasing from anterior to posterior; right row begins subapically and ends subterminally one or two cirri anterior of left marginal row (Fig. 203a, c, 204f, h).

Three dorsal kineties with cilia 3–4 µm long in vivo and in protargol preparations; rows bipolar, that in midline ending subterminally near base of tail; kinetids narrowly spaced, especially in row 1. Caudal cirri definitely absent in holotype and some marked paratype specimens, while right and left row extend to tip of tail (Fig. 203d, 204a, f, h; Table 74).

Oral apparatus in *Gonostomum* pattern (Berger 1999, 2011), i. e., adoral zone slightly sigmoid and following left body margin before bending rather abruptly inwards at about 57% of body length, on average composed of 53 ordinary membranelles with largest bases only 5 µm long in vivo (Fig. 203a, c, 204a, f, h; Table 74). Buccal cavity flat and small compared to body size; buccal lip distinctly convex, bears slightly oblique paroral membrane composed of an average of 19 kinetids with cilia about 8 µm long in vivo. Endoral membrane extends on dorsal margin of buccal cavity, cilia about 10 µm long in vivo, anteriorly distinctly shorter than paroral membrane while distinctly longer posteriorly extending to last adoral membranelle; undulating membrane pattern depending on preparation quality and angle viewed, i.e., the paroral may be partially or entirely right or left of the endoral. Pharyngeal fibres extend almost transversely to body`s main axis, originate from endoral membrane and last adoral membranelles.

Occurrence and ecology: As yet found only at type locality, viz., the floodplain of the Aurelio Lagoon associated with the Baia River which is a tributary of the large Paraná River. The dark, humic soil was mixed with much partially decomposed leave litter and had pH 5.1 in water (sample kindly provided by Dr. Felipe Machado Velho, Maringá State University, Brazil). In the non-flooded Petri dish culture, *A. pantanalense* appeared 10 days after rewetting. Considering the habitat, we cannot exclude that *A. pantanalense* is a limnetic mud-dweller.

Remarks: *Apogonostomum pantanalense* has a clear identity. There are only two species which have a notable overall similarity, viz., *Gonostomum namibiense* Foissner et al., 2002 (only 90 × 20 µm vs. 170 × 40 µm; frontoventral cirri do not extend postorally vs. extending to transverse cirri) and *Apogonostomum vleiacola* (frontoventral ciliature does not extend postorally vs. extending to transverse cirri; tail ⅓ vs. ⅕ of body length).

Apogonostomum vleiacola nov. spec. (Fig. 205a–i, 206a–k; Table 75)

Diagnosis: Size in vivo about 130 × 25 µm. Body knife-shaped with tail counting for about one third of body length. 2 ordinarily located, ellipsoid macronuclear nodules and 2 micronuclei. Cortical granules in dense rows, in vivo about 2.5 × 0.8 µm in size, distal end stains deeply with methyl green-pyronin when extruded. 3 frontal cirri, 2 frontoterminal cirri, 1 buccal cirrus subapical of paroral membrane, 4 frontoventral cirral pairs, 2 pretransverse cirri, and 5 transverse cirri at base of tail, i. e., far subterminal. Right marginal row composed of an average of 27 cirri, left of 15. 3 dorsal kineties, distal end of bristles deeply impregnated with protargol. Adoral zone of membranelles extends 41% of body length, composed of an average of 29 membranelles; buccal lip convex, covers proximal membranelles. Paroral and endoral membrane side by side, distinctly staggered, paroral membrane composed of an average of 16 kinetids with 10 µm long cilia.

Type locality: Soil from the margin of the Sirkelsvlei, Cape of Good Hope Nature Reserve, Republic of South Africa, 33°53’S 18°25’E.

Type material: 1 holotype and 2 paratype slides with protargol-impregnated specimens have been deposited in the Biology Centre of the Upper Austrian Museum in Linz (LI). The holotype and important paratype specimens have been marked by black ink circles on the coverslip.

Table 75. Morphometric data on *Apogonostomum vleiacola* based on mounted, protargol-impregnated, and selected (for complete tail) specimens from a non-flooded Petri dish culture. Measurements in µm. AZM – adoral zone of membranelles, CV – coefficient of variation in %, M – median, Max – maximum, Mean – arithmetic mean, Min – minimum, n – number of individuals investigated, SD – standard deviation, SE – standard error of arithmetic mean.

Characteristics	Mean	M	SD	SE	CV	Min	Max	n
Body, length	104.1	104.0	12.2	2.7	11.7	83.0	130.0	21
Body, width	23.1	23.0	2.9	0.6	12.5	17.0	28.0	21
Body length:width, ratio	4.6	4.5	0.6	0.1	12.5	3.7	5.8	21
Anterior body end to proximal end of AZM, distance	42.6	43.0	2.3	0.5	5.3	38.0	46.0	21
Adoral zone of membranelles, percentage of body length	41.4	41.0	4.1	0.9	9.8	35.0	51.0	21
Adoral membranelles, number	29.4	29.0	1.0	0.2	3.5	28.0	32.0	21
Anterior body end to paroral membrane, distance	19.7	20.0	1.6	0.4	8.2	16.0	22.0	21
Paroral membrane, length	12.8	13.0	1.1	0.3	8.6	11.0	15.0	20
Paroral membrane, number of kinetids	16.4	16.0	1.4	0.3	8.5	13.0	19.0	20
Anterior body end to endoral membrane, distance	26.9	27.0	1.9	0.4	6.9	23.0	30.0	21
Endoral membrane, length	15.0	15.0	1.0	0.2	6.9	13.0	17.0	21
Anterior body end to first macronuclear nodule, distance	18.0	18.0	1.9	0.4	10.4	15.0	21.0	21
Nuclear figure, length	38.6	39.0	3.8	0.8	9.9	32.0	45.0	21
Macronuclear nodules, distance in between	17.6	18.0	2.5	0.6	14.2	13.0	20.0	21
Macronuclear nodules, length	11.1	11.0	1.5	0.3	13.3	9.0	14.0	21
Macronuclear nodules, width	5.2	5.0	0.8	0.2	14.7	4.0	7.0	21
Macronuclear nodules, number	2.0	2.0	0.0	0.0	0.0	2.0	2.0	21
Micronuclei, length	2.9	3.0	0.5	0.1	16.7	2.0	4.0	21
Micronuclei, width	2.1	2.0	0.4	0.1	20.8	2.0	4.0	21
Micronuclei, number	2.1	2.0	0.2	0.1	10.7	2.0	3.0	21
Anterior body end to right marginal row, distance	10.5	10.0	1.6	0.4	15.5	8.0	14.0	21
Right marginal row, number of cirri	26.7	26.0	1.5	0.3	5.6	25.0	30.0	21
Left marginal row, number of cirri	15.0	15.0	1.3	0.3	8.7	13.0	17.0	21
Frontal cirri, number	3.0	3.0	0.0	0.0	0.0	3.0	3.0	21
Anterior body end to buccal cirrus, distance	21.8	22.0	1.6	0.4	7.5	19.0	25.0	20
Buccal cirri, number	1.0	1.0	0.0	0.0	0.0	1.0	1.0	21
Anterior body end to 2nd frontoterminal cirrus, distance	15.3	15.0	1.5	0.3	10.0	12.0	18.0	21
Frontoterminal cirri, number	2.0	2.0	0.0	0.0	0.0	2.0	2.0	21
Anterior body end to last frontoventral cirrus, distance	39.3	40.0	3.2	0.7	8.3	32.0	44.0	21
Frontoventral cirral pairs, number	4.1	4.0	–	–	–	4.0	5.0	21
Remaining frontoventral cirri, number	0.9	1.0	–	–	–	0.0	1.0	21
Anterior body end to uppermost transverse cirrus, distance	63.6	65.0	6.4	1.4	10.0	52.0	73.0	21
Pretransverse cirri, number	2.0	2.0	0.0	0.0	0.0	2.0	2.0	21
Transverse cirri, number	5.5	6.0	–	–	–	5.0	6.0	21
Dorsal kineties, number	3.0	3.0	0.0	0.0	0.0	3.0	3.0	21
Kinetids in dorsal kinety 2, number	21.6	22.0	1.8	0.5	8.2	19.0	25.0	14

Etymology: Composite of the noun *Vlei* (a shallow pond in the local dialect), the thematic vowel *-a-*, and the Latin verb *colere* (to live in), referring to the habitat the species was discovered.

Description: Although *A. vleiacola* is rather fragile, most coefficients of variation are lower than

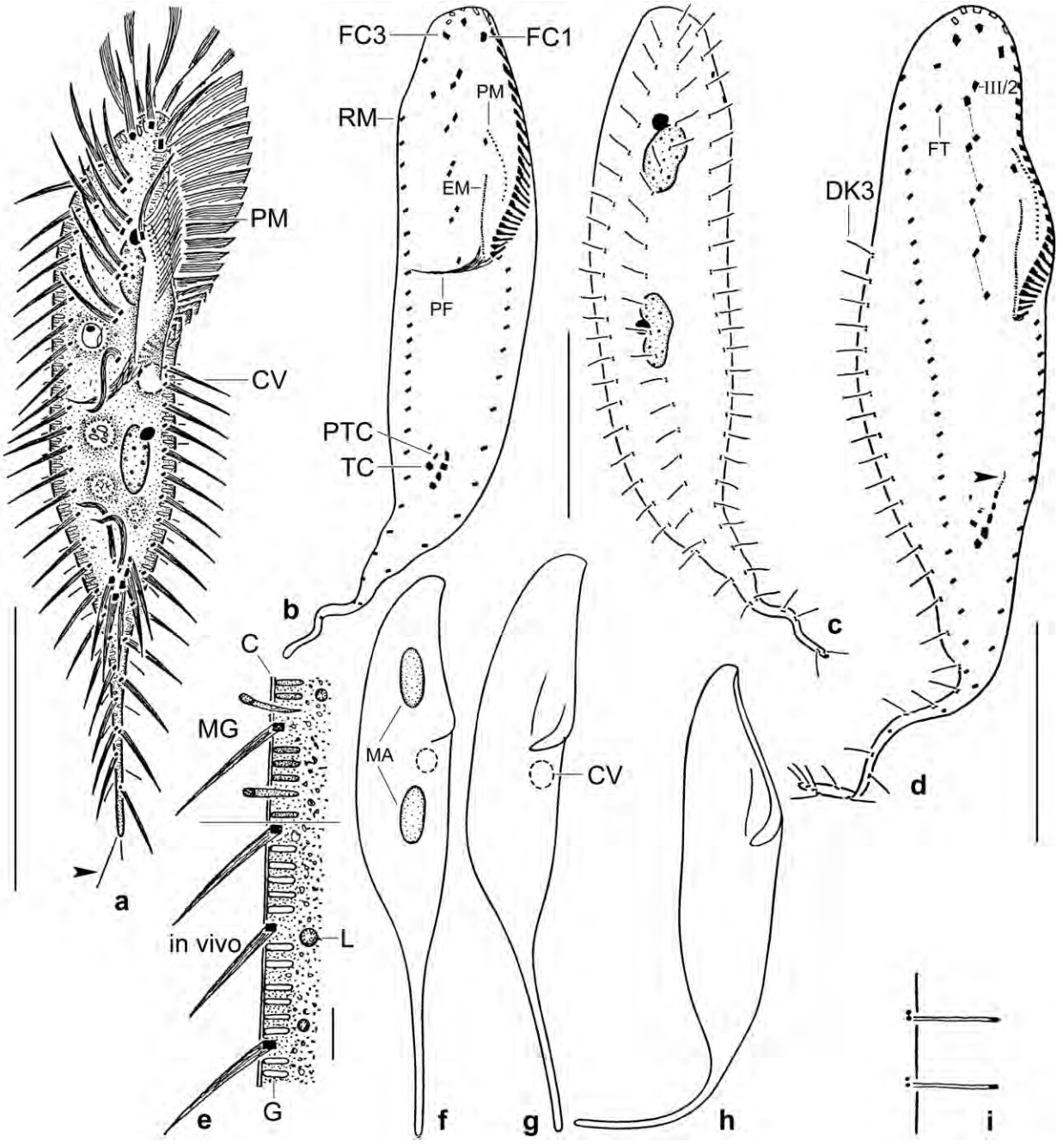

Fig. 205a–i. *Apogonostomum vleiacola* from life (a, e–h) and after protargol impregnation (b–d, i). Note the distinct tail. **a:** Ventral overview of a representative specimen, length 130 µm. The arrowhead marks an elongated dorsal bristle or a right marginal cirrus (cp. Fig. 206i). **b, c:** Ventral and dorsal view of holotype specimen, length 120 µm. **d:** A very early divider with oral primordium marked by arrowhead. The frontoventral cirri form distinct pairs (dotted lines). **e:** Optical section of cortex in vivo and after methyl green-pyronin application, which shows the extrusome nature of the cortical granules**. f–h:** Video sequence, showing the same specimen gliding, resting, and flicking away using the tail. **i:** The distal end of the dorsal bristles has an increased affinity to protargol. C – cortex, CV – contractile vacuole, DK3 – dorsal kinety 3, EM – endoral membrane, FC1, 3 – frontal cirri, FT – frontoterminal cirri, G – cortical granules, L – lipid droplet, MA – macronuclear nodules, MG – methyl green-pyronin, PF – pharyngeal fibres, PM – paroral membrane, PTC – pretransverse cirri, RM – right marginal row, TC – transverse cirri, III/2 – cirrus III/2. Scale bars 10 µm (e), 30 µm (b–d), and 50 µm (a).

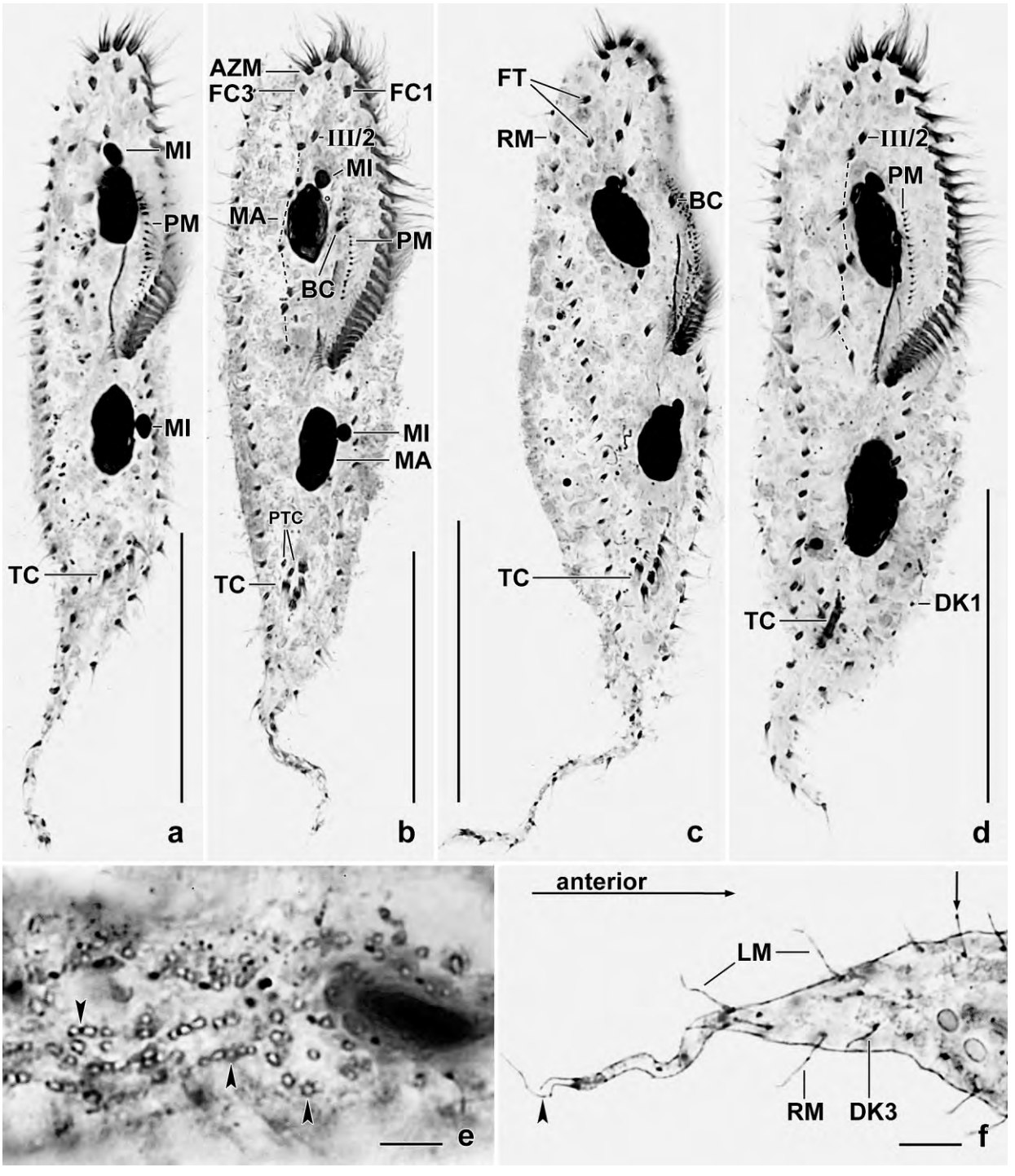

Fig. 206a–f. *Apogonostomum vleiacola* after protargol impregnation. **a–d:** Ventral overviews showing tail occupying about one third of body length (partially lost in (d)). Dotted lines in (b) and (d) mark the four pairs of frontoventral cirri. **e:** Surface view of cortex, showing the holes (arrowheads) left by exploded extrusomes. **f:** Dorsal view of distal region of tail. The arrow marks the deeply impregnating distal end of a dorsal bristle. The arrowhead denotes a long dorsal bristle or a right marginal cirrus at top of tail. AZM – adoral zone of membranelles, BC – buccal cirrus, DK1, 3 – dorsal kineties, EM – endoral membrane, FC1, 3 – frontal cirri, FT – frontoterminal cirri, LM – left marginal row, MA – macronuclear nodules, MI – micronuclei, PM – paroral membrane, RM – right marginal row, PTC – pretransverse cirri, TC – transverse cirri, III/2 – cirrus III/2. Scale bars 10 µm (e, f) and 40 µm (a–d).

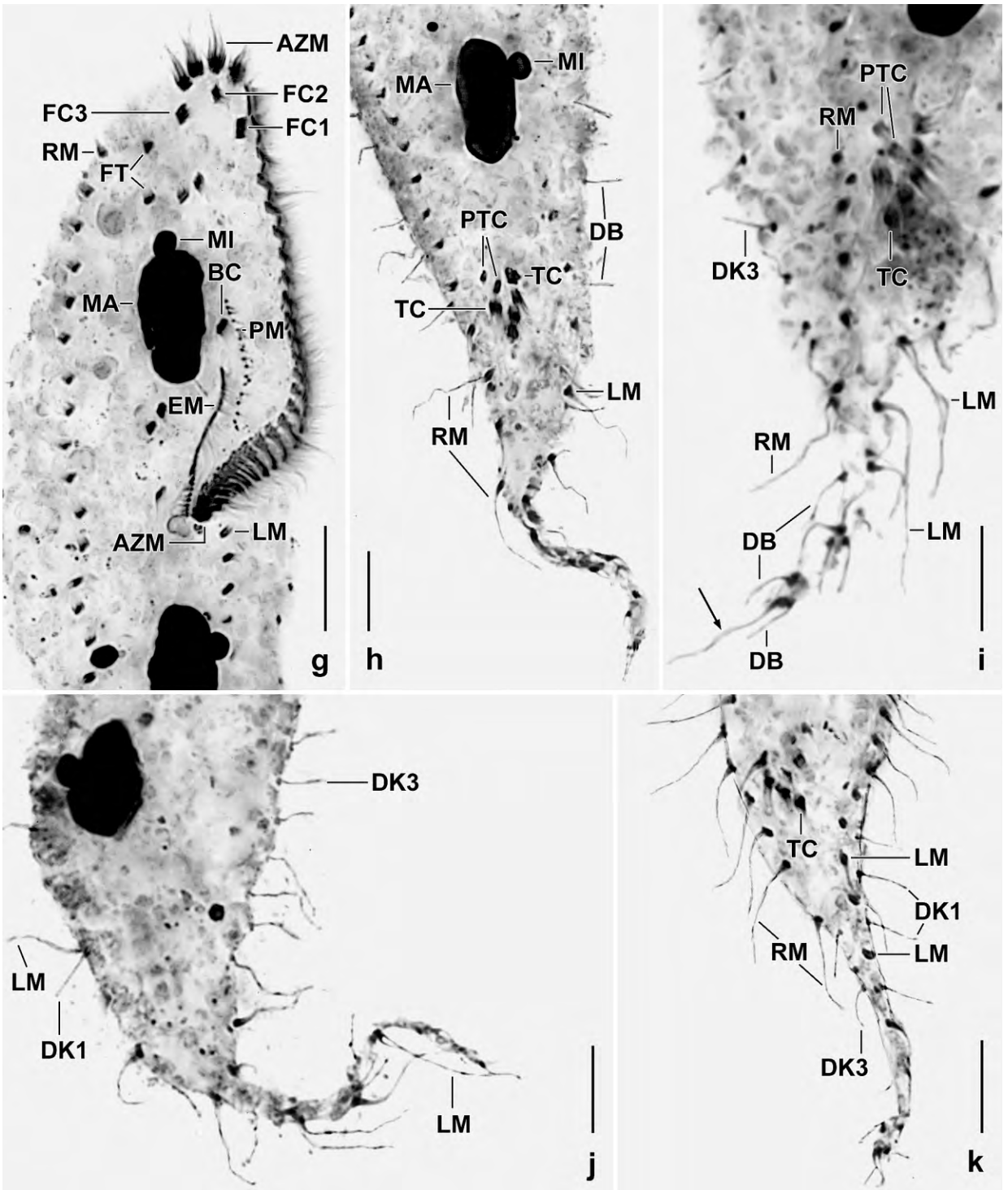

Fig. 206g–k. *Apogonostomum vleiacola*, ventral (g–i, k) and dorsal (j) views after protargol impregnation. **g:** Details in anterior body half. **h–k:** Tail region. Arrow in (i) marks an elongated dorsal bristle or a right marginal cirrus. Note the rather long dorsal bristles (i–k). AZM – adoral zone of membranelles, BC – buccal cirrus, DB – dorsal bristles, DK1, 3 – dorsal kineties, EM – endoral membrane, FC1–3 – frontal cirri, FT – frontoterminal cirri, LM – left marginal cirral row, MA – macronuclear nodules, MI – micronuclei, PM – paroral membrane, PTC – pretransverse cirri, RM – right marginal cirral row, TC – transverse cirri. Scale bars 10 μm.

15%, in the main characteristics even lower than 10%. Accordingly, similar but distinct species of this group should be easily recognizable. Only specimens with well preserved tail were used for the morphological and morphometric analyses.

Size in vivo 100–160 × 20–30 µm, on average about 130 × 25 µm, as calculated from some in vivo measurements and the morphometric data in Table 75 adding 25% length shrinkage (due to general fragility of the species, especially of the tail) and 15% width shrinkage. Body elegant because slender and with long tail; roughly knife-shaped or elongate claviform, oblong without tail; length:width ratio 3.7–5.8:1 in protargol preparations, up to 7:1 in vivo; anterior end slightly projecting ventrally; tail elongate cuneate, distal end 1.5–2.5 µm wide in vivo (Fig. 205a–d, f–h, 206a–c; Table 75). Nuclear apparatus in central quarters of cell, composed of two ellipsoid or elongate ellipsoid macronuclear nodules with many minute nucleoli and two to three globular or ellipsoid micronuclei often attached to anterior end of macronuclear nodules (Fig. 205a, c, f, 206a–d, g, h; Table 75). Contractile vacuole at proximal end of adoral zone (Fig. 205a, f). Tail and cortex fragile, studded with rows of colourless granules in vivo about 2.5 × 0.8 µm in size; granules in vivo difficult to recognize and to separate from mitochondria because pale and hidden by the opaque cytoplasm; stain blue and partially extruded when methyl green-pyronin is applied becoming about 3 µm long and cuneate with a deeply stained dot in distal end; in protargol preparations up to 6 µm long, indicating that they can elongate to long threads like those of → *A. pantanalensis* (Fig. 205a, e, 206e). Cytoplasm opaque due to countless granules, colourless. Feeds on bacteria and small heterotrophic flagellates digested in vacuoles up to 8 µm across. Glides versatily on microscope slides and between soil particles; performs a kind of jumps using the tail as flicking support (Fig. 205f–h).

Somatic ciliature dominated by four, rarely five pairs of frontoventral cirri in body`s midline, last cirrus at level of buccal vertex, cirri about 12 µm long in vivo (Fig. 205a, b, d, 206b, c, d, g; Table 75). Three slightly thickened frontal cirri about 15 µm long in vivo; two frontoterminal cirri right of first pair of frontoventral cirri, usually distinctly separate from each other and from distal end of adoral zone; one buccal cirrus subapical of paroral membrane, about 15 µm long in vivo. Transverse cirri on average 40% distant from posterior body end, i. e., at base of tail; two minute pretransverse cirri in *Gonostomum* pattern, i. e., side by side in cavity formed by transverse cirri; five to six transverse cirri, some slightly thickened, in □-like pattern, about 15 µm long in vivo. Marginal cirri composed of two ciliary rows with three cilia each, cirri in distal third of tail composed of only four cilia, rarely of only two, all about 12 µm long in vivo. Right marginal row commences about 10% posterior of anterior body end, first cirrus occasionally set off by a slightly increased intracirral distance (Fig. 205d), ends subterminally, composed of an average of 27 cirri contrasting the 15 cirri composing the left row extending to or near to tip of tail (Fig. 205a, b, d, 206b, c, d, g; Table 75).

Dorsal bristles in three rows, 4–5 µm long in vivo and in protargol preparations, distal end with increased protargol affinity (Fig. 205a, c, d, i, 206f, h–k; Table 75). Rows 1 and 3 bipolar, row 2 ends near base of tail; on tip of tail an ordinary, 4–5 µm long bristle and a second about 12 µm long bristle or a marginal cirrus made of only one cilium seen three times in vivo and two times in protargol preparations (Fig. 205a, 206f). Caudal cirri absent.

Oral apparatus gonostomoid (Berger 2011), i. e., the adoral zone follows the anterior and left body

margin and bends abruptly into the cell at about 41% of body length. Adoral zone flat to slightly sigmoid, on average composed of 29 gonostomoid membranelles with largest bases about 3.5 µm long, intramembranellar distances distinctly increase from proximal to distal, a rare feature present also in → *Gonostomum lajacola*; four frontal membranelles with about 20 µm long cilia (Fig. 205a, b, d, f–h, 206a–d, g; Table 75). Buccal cavity flat and moderately wide; buccal lip convex, covers some proximal membranelles. Paroral membrane near left margin of buccal lip and thus slightly convex, composed of an average of 16 kinetids with cilia about 10 µm long in vivo and in protargol preparations. Endoral membrane commences at level of posterior half of paroral, straight, kinetids narrower spaced anteriorly than posteriorly. Pharyngeal fibres extend at right angles to right margin of cell (Fig. 205a, b, d, f–h, 206a–d, g; Table 75).

Occurrence and ecology: As yet found only at type locality which is a semiterrestrial habitat. Thus, we cannot know the preferred environment but the slender body indicates soil (Foissner 1987b).

Remarks: *Apogonostomum vleiacola* differs from → *A. pantanalensis* mainly by the ventral cirral pairs (extending to buccal vertex vs. to transverse cirri), the length of the adoral zone (41% vs. 57% of body length), and the number (29 vs. 51) of adoral membranelles. In vivo, *Paragonostomum caudatum* Foissner et al. 2002 resembles *A. vleiacola* because it has a very similar body shape. They can be distinguished by body size (85 × 20 µm vs. 130 × 25 µm in vivo), the cortical granules (absent vs. present), and the number of transverse cirri (absent vs. five to six).

Paragonostomum australiense nov. spec. (Fig. 207a–g, 208a–f, 209a–t; Table 76)

Diagnosis: Size in vivo about 80 × 25 µm; lenticular with acute posterior region. 2 ellipsoid macronuclear nodules and 2 micronuclei. Cortical granules scattered, colourless, 1–1.5 × 0.5–0.8 µm in size. 3 frontal cirri, 4 frontoterminal cirri on average; 1 buccal cirrus slightly subapical of paroral membrane; 3 dorsal kineties and caudal cirri. Adoral zone flat, extends about 45% of body length, consists of an average of 23 membranelles. On average 12 paroral kinetids with cilia 10–12 µm long in vivo.

Type locality: Litter and soil from crevices of a small mountain in the Macdonnell Ranges slightly south of the town of Alice Springs, Australia, 134°E 23°30’S.

Type material: 1 holotype and 2 paratype slides as well as 6 voucher slides with protargol-impregnated specimens have been deposited in the Biology Centre of the Upper Austrian Museum in Linz (LI). The holotype and other relevant specimens have been marked by black ink circles on the coverslip.

Etymology: Named after the continent found, viz., Australia.

Description: We studied two populations from Australia in vivo and in protargol preparations. Although being separated by a distance of about 1.500 km, they are highly similar and thus are described together.

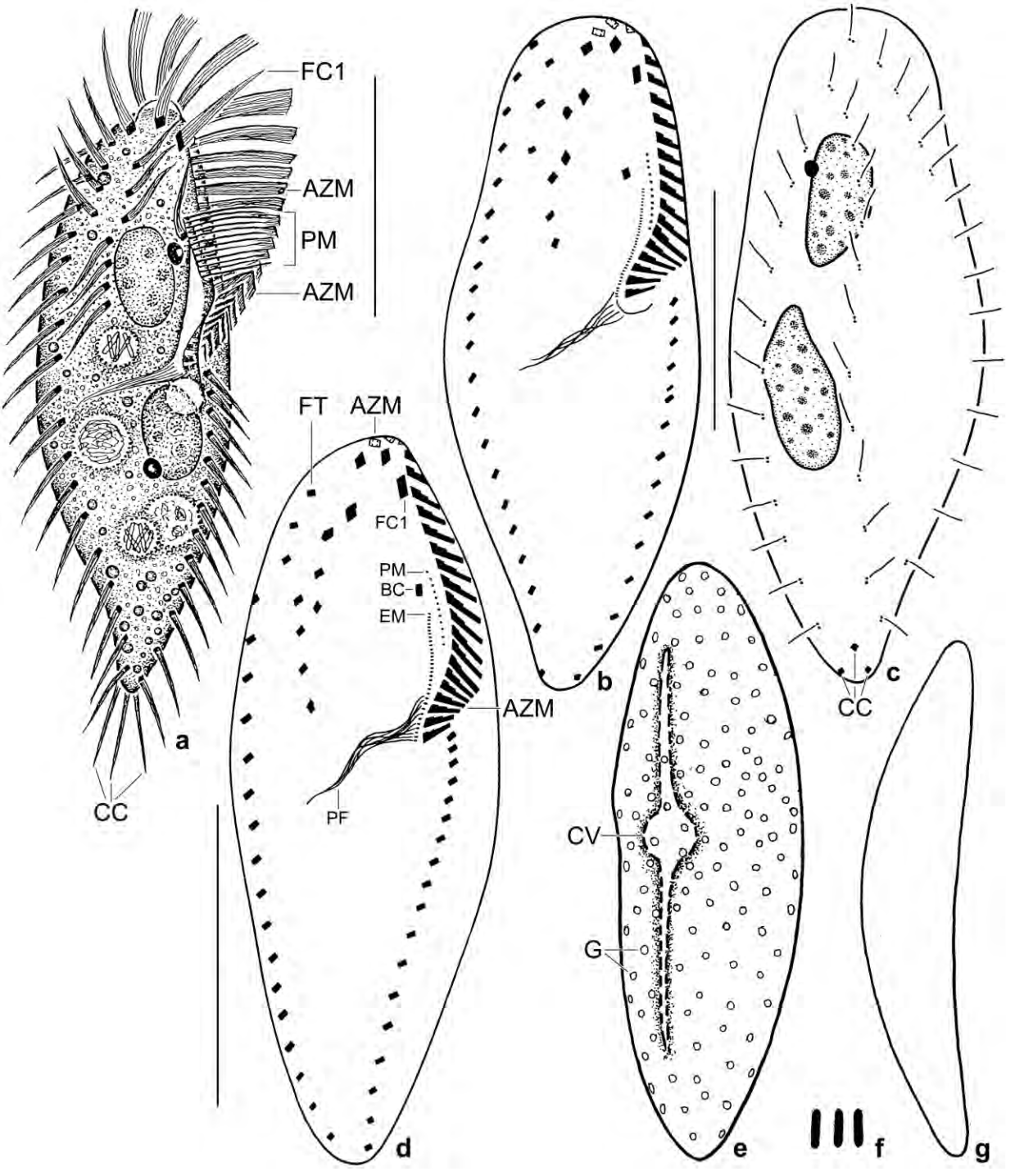

Fig. 207a–g. *Paragonostomum australiense* from life (a, e–g) and after protargol impregnation (b–d). **a:** Ventral view of a representative specimen, length 80 µm. Note the 10 µm long cilia of the paroral membrane and the lenticular body shape. **b, c:** Ventral and dorsal view of holotype specimen, length 57 µm. Note absence of transverse cirri. **d:** Ventral view of a paratype specimen. **e:** Cortical granulation of dorsal side. **f:** Cortical granules, 1–1.5 × 0.5–0.8 µm in size. **g:** Lateral view. AZM – adoral zone of membranelles, BC – buccal cirrus, CC – caudal cirri, CV – contractile vacuole, EM – endoral membrane, FC1 – frontal cirrus 1, FT – frontoterminal cirri, G – cortical granules, PF – pharyngeal fibres, PM – paroral membrane. Scale bars 20 µm (b, c) and 30 µm (a, d).

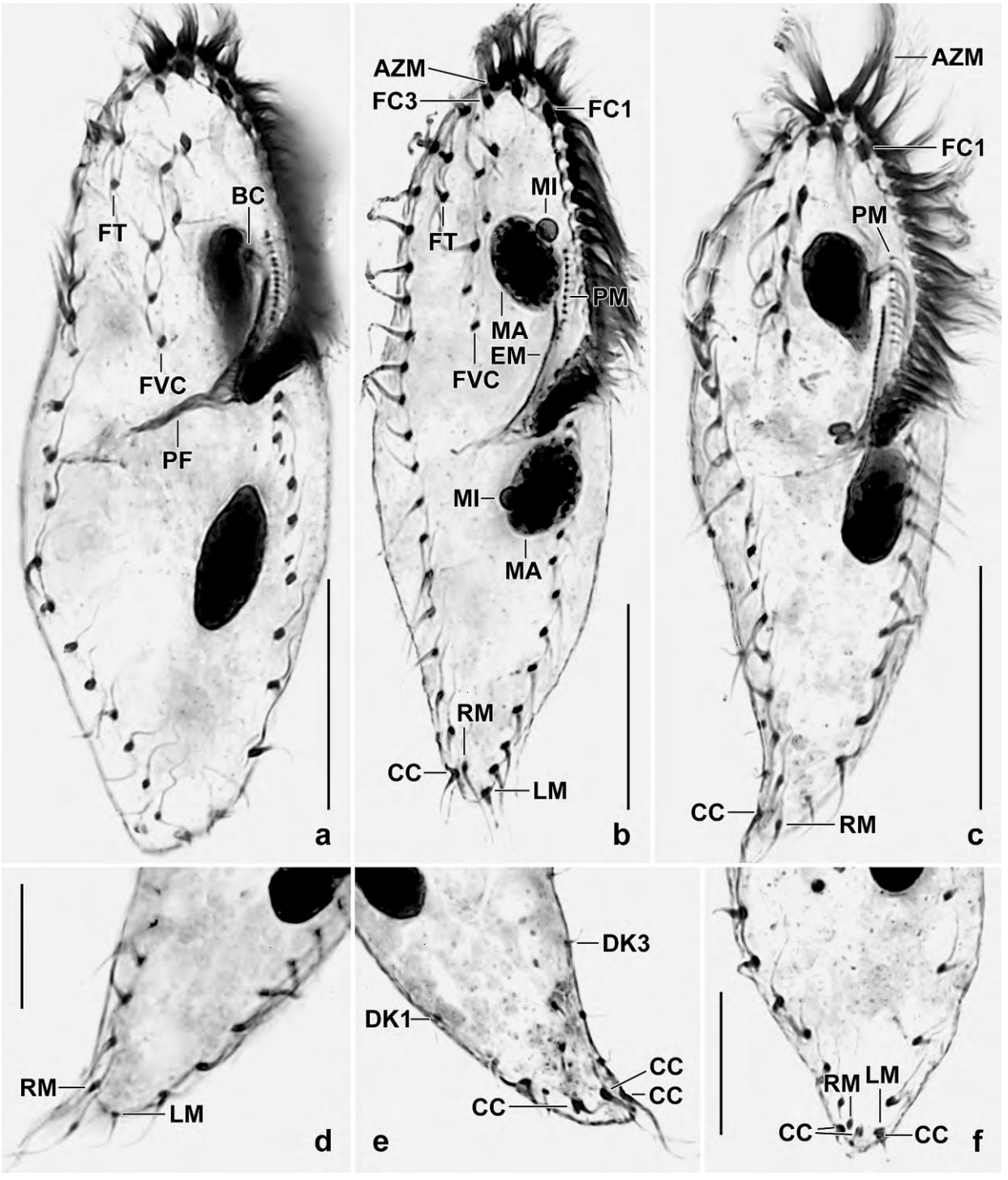

Fig. 208a–f. *Paragonostomum australiense*, infraciliature after protargol impregnation. **a–c:** Ventral views; figure (b) shows the typical body shape while (c) shows a slightly sigmoid specimen. **d, e:** Posterior body region of same specimen to show the caudal cirri on dorsal side (e) and the absence of transverse cirri (d). **f:** Ventral view of posterior region, showing marginal and caudal cirri. AZM – adoral zone of membranelles, BC – buccal cirrus, CC – caudal cirri, DK1,3 – dorsal kineties, EM – endoral membrane, FC1, 3 – frontal cirri, FT – frontoterminal cirri, FVC – frontoventral cirri, LM – left marginal cirral row, MA – macronuclear nodules, MI – micronuclei, PF – pharyngeal fibres, PM – paroral membrane, RM – right marginal cirral row. Scale bars 10 μm (e, f) and 20 μm (a–c).

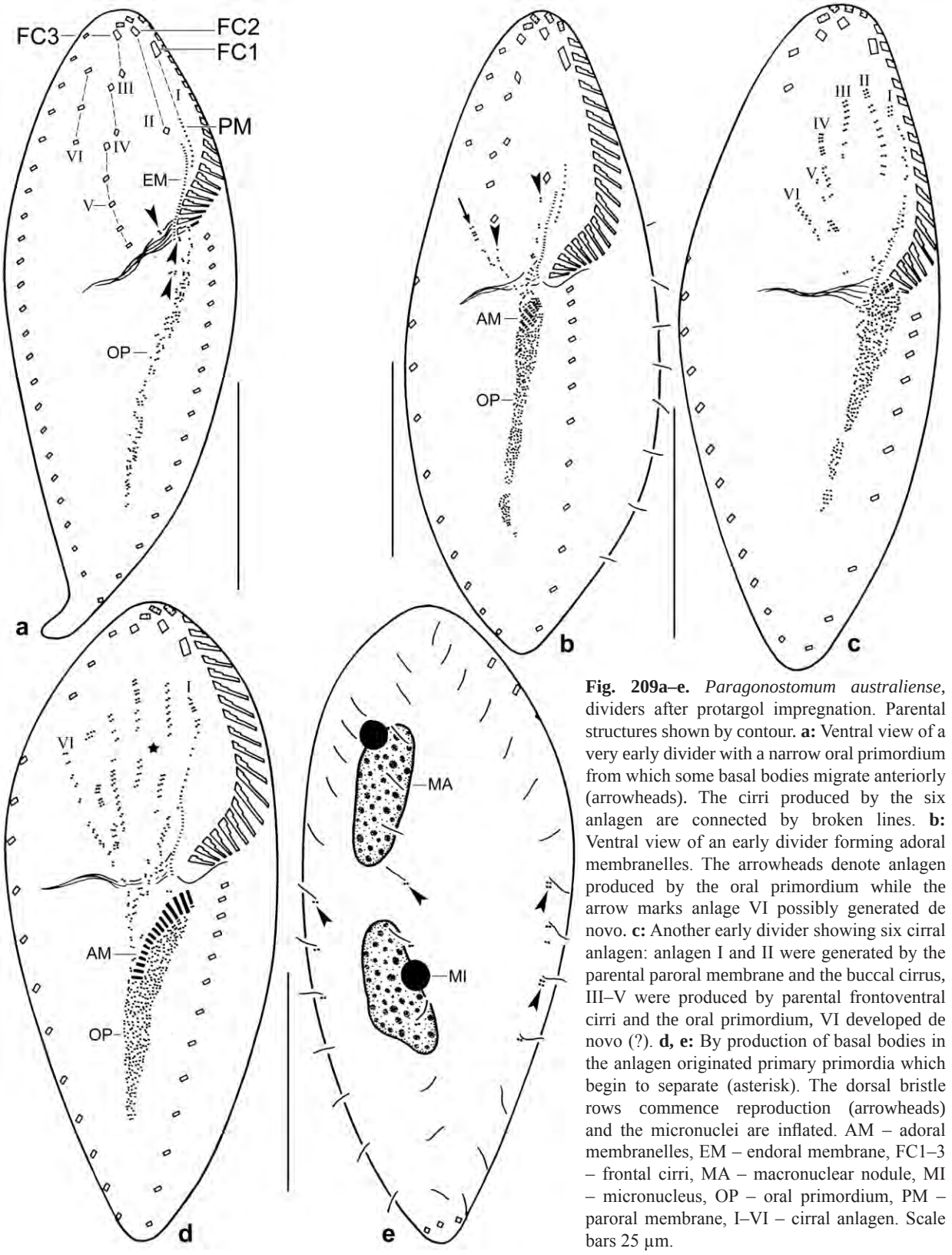

Fig. 209a–e. *Paragonostomum australiense*, dividers after protargol impregnation. Parental structures shown by contour. **a:** Ventral view of a very early divider with a narrow oral primordium from which some basal bodies migrate anteriorly (arrowheads). The cirri produced by the six anlagen are connected by broken lines. **b:** Ventral view of an early divider forming adoral membranelles. The arrowheads denote anlagen produced by the oral primordium while the arrow marks anlage VI possibly generated de novo. **c:** Another early divider showing six cirral anlagen: anlagen I and II were generated by the parental paroral membrane and the buccal cirrus, III–V were produced by parental frontoventral cirri and the oral primordium, VI developed de novo (?). **d, e:** By production of basal bodies in the anlagen originated primary primordia which begin to separate (asterisk). The dorsal bristle rows commence reproduction (arrowheads) and the micronuclei are inflated. AM – adoral membranelles, EM – endoral membrane, FC1–3 – frontal cirri, MA – macronuclear nodule, MI – micronucleus, OP – oral primordium, PM – paroral membrane, I–VI – cirral anlagen. Scale bars 25 μm.

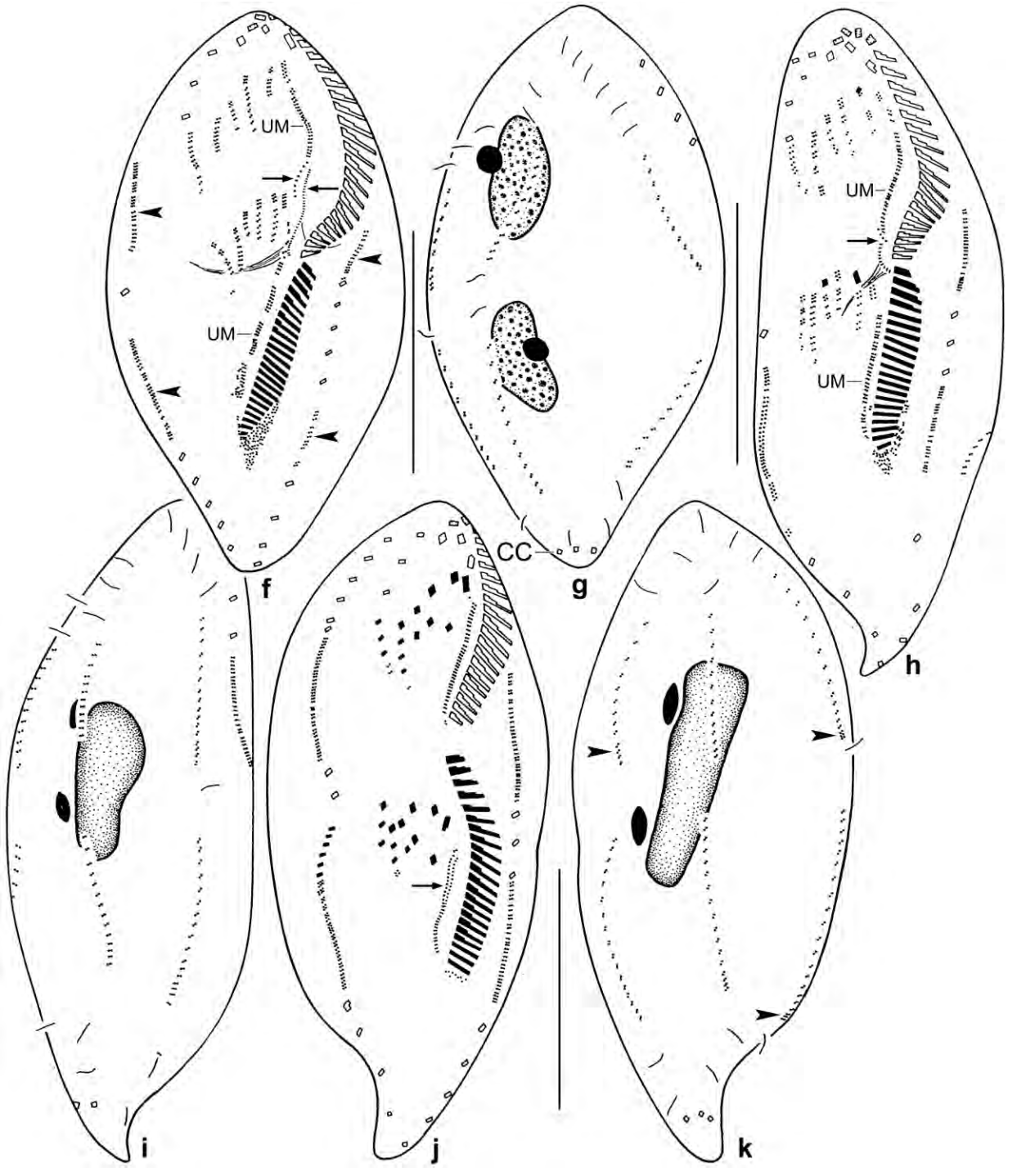

Fig. 209f–k. *Paragonostomum australiense*, dividers after protargol impregnation. Parental structures shown by contour, new structures shadded black. **f, g:** An early mid-divider, showing the separation of the primary primordia to six anlagen each in proter and opisthe; the anlagen in the marginal cirral rows (arrowheads) and dorsal kineties; and the production of an anlage for the undulating membranes each in proter and opisthe. Still, parts of the parental undulating membranes are recognizable (arrows). **h, i:** A mid-divider with fused macronuclear nodules. The arrow marks remnants of the parental undulating membranes while the new membranes are growing. Cirri are forming in the anlagen. **j, k:** A late mid-divider with elongating macronuclear mass. Cirri have formed in the streaks and the new undulating membranes become recognizable (arrow). Caudal cirri are developing in the dorsal kineties (arrowheads). CC – caudal cirri, UM – undulating membranes (paroral and endoral). Scale bars 30 µm.

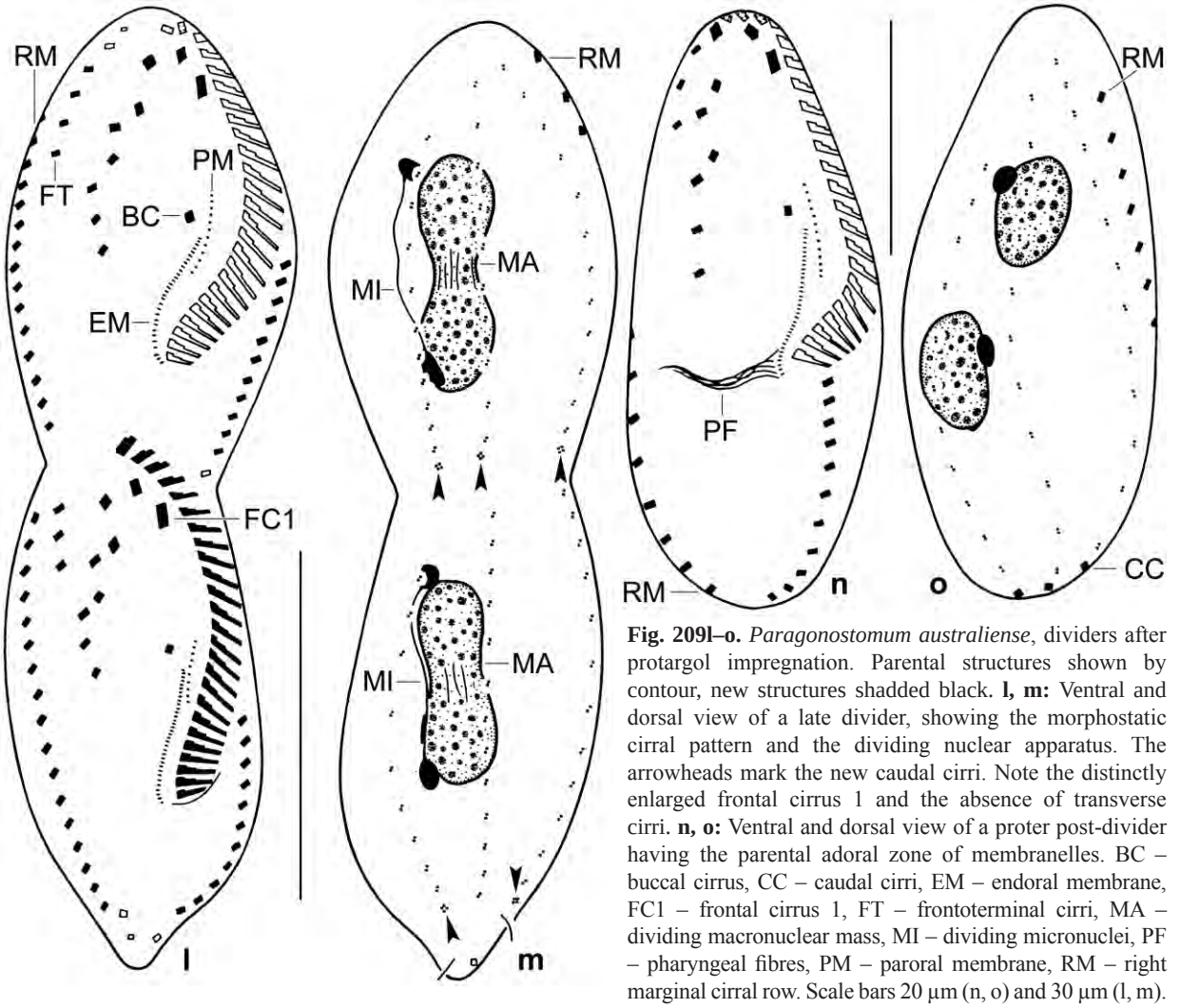

Fig. 209l–o. *Paragonostomum australiense*, dividers after protargol impregnation. Parental structures shown by contour, new structures shadded black. **l, m:** Ventral and dorsal view of a late divider, showing the morphostatic cirral pattern and the dividing nuclear apparatus. The arrowheads mark the new caudal cirri. Note the distinctly enlarged frontal cirrus 1 and the absence of transverse cirri. **n, o:** Ventral and dorsal view of a proter post-divider having the parental adoral zone of membranelles. BC – buccal cirrus, CC – caudal cirri, EM – endoral membrane, FC1 – frontal cirrus 1, FT – frontoterminal cirri, MA – dividing macronuclear mass, MI – dividing micronuclei, PF – pharyngeal fibres, PM – paroral membrane, RM – right marginal cirral row. Scale bars 20 µm (n, o) and 30 µm (l, m).

Most features of *P. australiense* have an ordinary variability (CV ≤ 15%; Table 76). The type population is more variable than the voucher specimens. Of the characteristics used in the diagnosis, the number of micronuclei (1–5, CV ~ 32%) and frontoterminal cirri (2–5, CV ~ 16%) have coefficients of variation > 15%.

Size in vivo 65–100 × 20–35 µm, usually about 80 × 25 µm, as calculated from some in vivo measurements and the morphometric data in Table 76 adding 15% preparation shrinkage. Body ordinarily to elongate lenticular or pisciform, i. e., both ends distinctly narrowed, posterior end bluntly acute, right margin usually more convex than left; laterally flattened up to 2:1 and slightly concave ventrally (Fig. 207a, b, d, e, g, 208a–c; Table 76). Nuclear apparatus in central quarters left of body´s midline. Macronuclear nodules rather close, viz., slightly anterior and posterior of proximal end of adoral zone of membranelles; anterior nodule in or slightly left of body´s midline, posterior left of midline; ellipsoid to elongate ellipsoid, with many small nucleoli. Usually two micronuclei attached to right or left side of macronuclear nodules, in type population distinctly smaller than in the second one (Fig. 207a, c, 208a–c; Table 76). Contractile vacuole very near to proximal end of adoral zone of membranelles and rather far away from left body margin, with

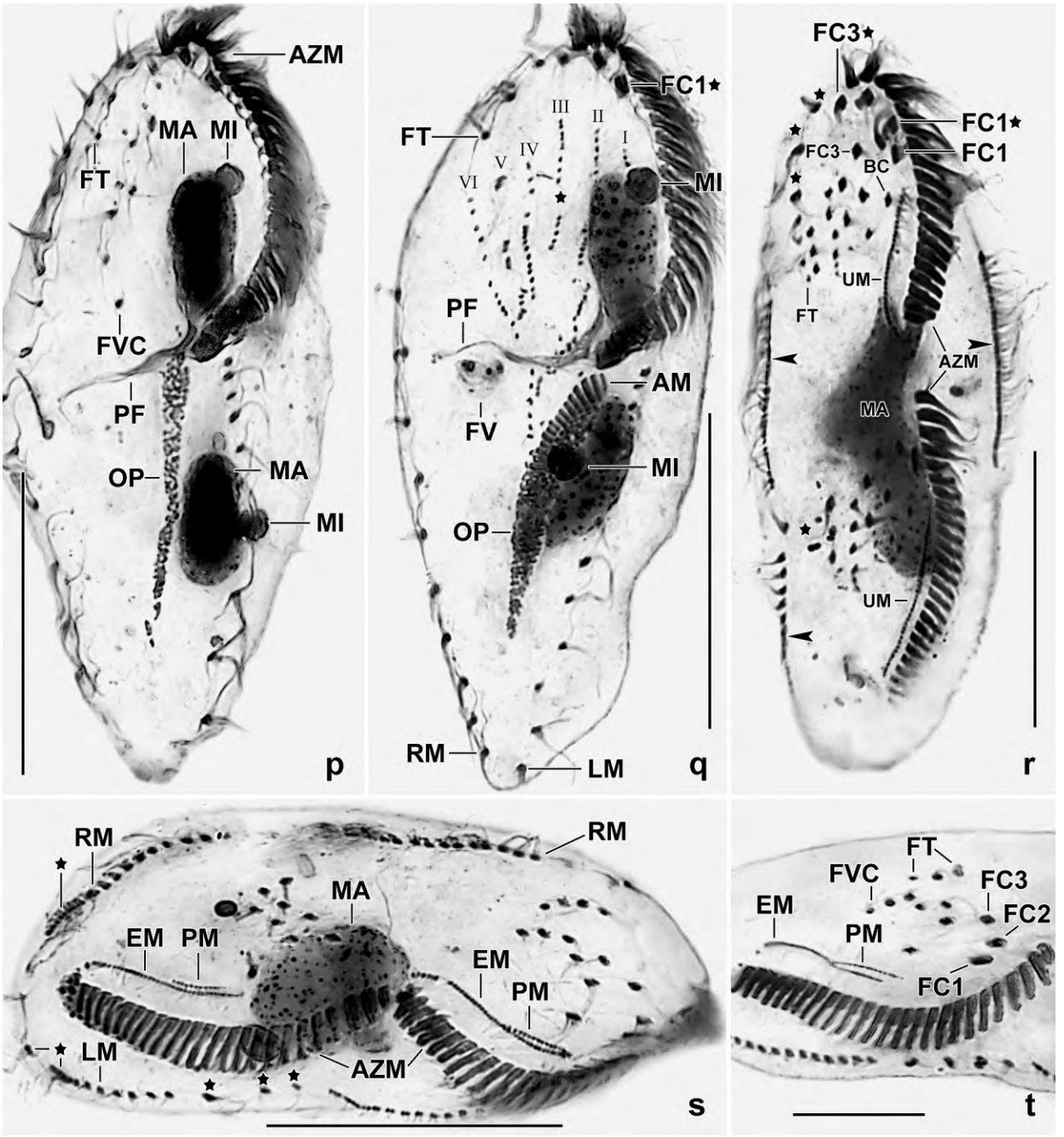

Fig. 209p–t. *Paragonostomum australiense*, ventral views of protargol-impregnated dividers. **p:** Very early divider with long, cuneate oral primordium. **q:** By production of basal bodies in the anlagen originated primary primordia which begin to separate (asterisk): the upper streaks become cirri for the proter, the lower ones become cirri for the opisthe. The oral primordium develops adoral membranelles from anterior to posterior. Note the inflated micronuclei. **r:** An early mid-divider showing parental (*) and new cirri. The arrowheads mark anlagen in the marginal cirral rows. **s, t:** Mid-dividers showing, inter alia, the split of the paroral membrane from the endoral. Asterisks mark parental cirri. AM – adoral membranelles, AZM – adoral zone of membranelles, BC – buccal cirrus, EM – endoral membrane, FC1–3 – new frontal cirri, FC1*, 3* – parental frontal cirri, FT – frontoterminal cirri, FV – food vacuole, FVC – frontoventral cirri, LM – left marginal cirral row, MA – macronuclear nodules or macronuclear mass, MI – micronuclei, OP – oral primordium, PF – pharyngeal fibres, PM – paroral membrane, RM – right marginal cirral row, UM – undulating membranes, I–VI – cirral anlagen. Scale bars 20 µm (t) and 30 µm (p–s).

Table 76. Morphometric data on two Australian populations (upper line: type locality) of *Paragonostomum australiense.* Data based on mounted, protargol-impregnated, and randomly selected specimens from non-flooded Petri dish cultures. Measurements in µm. CV – coefficient of variation in %, M – median, Max – maximum, Mean – arithmetic mean, Min – minimum, n – number of individuals investigated, SD – standard deviation, SE – standard error of arithmetic mean.

Characteristics	Mean	M	SD	SE	CV	Min	Max	n
Body, length	67.1	67.0	6.8	1.5	10.1	57.0	85.0	21
	71.7	73.0	5.4	1.2	7.5	56.0	82.0	21
Body, width	22.7	23.0	2.6	0.6	11.6	17.0	26.0	21
	24.3	24.0	2.6	0.6	10.8	19.0	30.0	21
Body length: width, ratio	3.0	2.9	0.4	0.1	12.0	2.3	3.6	21
	3.0	3.0	0.3	0.1	10.8	2.3	3.5	21
Body length: width, percent	34.0	34.7	4.1	0.9	12.1	27.9	43.3	21
	34.1	32.9	4.1	0.9	12.0	28.4	43.3	21
Anterior body end to proximal end of adoral zone of membranelles, distance	29.7	30.0	1.9	0.4	6.3	25.0	33.0	21
	33.3	33.0	2.3	0.5	6.9	29.0	39.0	21
Body length: adoral zone of membranelles length, ratio	2.3	2.3	0.2	0.0	7.7	2.0	2.8	21
	2.2	2.2	0.1	0.0	6.5	1.9	2.4	21
Anterior body end to proximal end of adoral zone of membranelles, percentage of body length	44.5	43.5	3.5	0.8	7.8	35.3	50.8	21
	46.7	46.4	2.9	0.6	6.1	41.9	51.8	21
Adoral membranelles, number	22.2	22.0	1.1	0.3	5.1	20.0	24.0	21
	23.9	24.0	1.1	0.2	4.7	22.0	26.0	21
Largest base of adoral membranelles, width	4.0	4.0	–	–	–	3.5	5.0	21
	4.1	4.0	–	–	–	4.0	5.0	18
Anterior body end to paroral membrane, distance	12.9	13.0	1.4	0.3	11.1	10.0	15.0	21
	15.9	16.0	1.2	0.3	7.5	14.0	19.0	21
Paroral membrane, length	8.0	8.0	0.9	0.2	11.2	6.0	10.0	21
	7.9	8.0	0.9	0.2	11.9	6.0	10.0	21
Paroral kinetids, number	11.2	11.0	1.4	0.3	12.8	8.0	15.0	21
	12.9	13.0	1.8	0.4	13.6	10.0	17.0	21
Anterior body end to endoral membrane, distance	17.4	18.0	1.8	0.4	10.0	13.0	20.0	21
	20.4	20.0	1.4	0.3	6.9	18.0	24.0	21
Endoral membrane, length	11.3	11.0	1.3	0.3	11.3	9.0	14.0	21
	11.9	12.0	1.2	0.3	9.9	9.0	15.0	21
Anterior body end to anterior macronuclear nodule, distance	12.4	12.0	1.4	0.3	11.0	10.0	15.0	21
	15.6	16.0	1.7	0.4	10.8	12.0	18.0	21
Nuclear figure, length	31.2	32.0	4.9	1.1	15.5	23.0	41.0	21
	33.7	34.0	3.3	0.7	9.7	27.0	40.0	21
Macronuclear nodules, distance in between	6.6	6.0	2.4	0.5	36.8	3.0	12.0	21
	9.7	10.0	2.7	0.6	27.3	4.0	14.0	21
Anterior macronuclear nodule, length	12.0	12.0	1.4	0.3	12.0	9.0	15.0	21
	12.2	12.0	2.1	0.5	17.5	9.0	16.0	21
Anterior macronuclear nodule, width	5.2	5.0	0.7	0.2	13.4	4.0	7.0	21
	5.7	6.0	0.6	0.1	9.8	5.0	7.0	21
Macronuclear nodules, number	2.0	2.0	0.0	0.0	0.0	2.0	2.0	21
	2.0	2.0	0.0	0.0	0.0	2.0	2.0	21

continued

Characteristics	Mean	M	SD	SE	CV	Min	Max	n
Micronuclei, length	1.6	1.5	–	–	–	1.0	2.0	21
	2.2	2.0	–	–	–	2.0	3.0	21
Micronuclei, width	1.1	1.0	–	–	–	1.0	1.5	21
	2.0	2.0	–	–	–	1.5	2.0	21
Micronuclei, number	2.1	2.0	0.7	0.1	30.6	1.0	4.0	21
	2.6	2.0	0.9	0.2	33.8	2.0	5.0	21
Frontal cirri, number	3.0	3.0	0.0	0.0	0.0	3.0	3.0	21
	3.0	3.0	0.0	0.0	0.0	3.0	3.0	21
Anterior body end to buccal cirrus, distance	14.5	15.0	1.3	0.3	8.9	12.0	16.0	21
	17.6	17.0	1.3	0.3	7.3	15.0	20.0	21
Buccal cirri, number	1.0	1.0	0.0	0.0	0.0	1.0	1.0	21
	1.0	1.0	0.0	0.0	0.0	1.0	1.0	21
Anterior body end to rearmost frontoterminal cirrus, distance	13.5	14.0	2.3	0.5	17.3	9.0	18.0	21
	13.8	14.0	2.0	0.4	14.7	11.0	18.0	21
Frontoterminal cirri, number	3.7	4.0	0.7	0.2	19.3	2.0	5.0	21
	3.2	3.0	–	–	–	3.0	4.0	21
Anterior body end to rearmost frontoventral cirrus, distance	23.5	23.0	3.1	0.7	13.0	17.0	27.0	21
	26.7	26.0	3.1	0.7	11.6	21.0	32.0	21
Frontoventral cirri, number	7.1	7.0	1.1	0.2	15.9	5.0	10.0	21
	6.2	6.0	0.8	0.2	13.1	4.0	8.0	21
Anterior body end to right marginal row, distance	3.2	3.0	1.1	0.2	33.8	1.0	6.0	21
	6.0	6.0	1.7	0.4	28.8	3.0	10.0	21
Posterior body end to right marginal row, distance	3.1	3.0	1.5	0.3	46.4	1.0	6.0	21
	2.7	3.0	1.0	0.2	36.2	1.0	6.0	21
Right marginal row, number of cirri	21.5	21.0	2.7	0.6	12.4	18.0	28.0	21
	18.1	17.0	3.0	0.7	16.9	14.0	24.0	21
Posterior body end to left marginal row, distance	2.8	3.0	1.3	0.3	48.5	1.0	6.0	21
	1.4	1.0	0.6	0.1	41.8	1.0	3.0	21
Left marginal row, number of cirri	14.1	14.0	2.4	0.5	17.4	11.0	19.0	21
	12.6	12.0	1.6	0.4	12.7	10.0	16.0	21
Dorsal kineties, number	3.0	3.0	0.0	0.0	0.0	3.0	3.0	21
	3.0	3.0	0.0	0.0	0.0	3.0	3.0	21
Dorsal kinety 2, number of kinetids	13.3	13.0	2.1	0.5	15.5	10.0	18.0	20
	12.1	12.0	1.4	0.3	11.7	10.0	16.0	21
Caudal cirri, number	3.0	3.0	–	–	–	2.0	3.0	19
	3.0	3.0	0.0	0.0	0.0	3.0	3.0	21

two collecting canals extending to body ends (Fig. 207a, e). Cortex very flexible, contains rather refractive, colourless, scattered granules 1–1.5 × 0.5–0.8 µm in size and staining red with methyl green-pyronin (Fig. 207e, f). Cytoplasm colourless, contains food vacuoles 5–10 µm across and, mainly in posterior third, lipid droplets 1–3 µm in size. Feeds on bacteria, naked amoebae with ingested fungal spores, small ciliates (*Protocyclidium terricola*) and flagellates (*Polytoma*), and cysts of amoebae or flagellates (Fig. 207a). Glides moderately rapid on microscope slides.

Cirri of ordinary length and thickness, arranged like in → *G. strenuum*, i. e., with comparatively long frontoterminal row and long, slightly oblique anlage V, each composed of three to five cirri (Fig. 207a, b, d, 208a–c; Table 76). Three frontal cirri about 15 µm long in vivo, cirrus 1 distinctly enlarged; second cirrus of anlage III ("fourth frontal cirrus") slightly enlarged; buccal cirrus slightly subapical of paroral membrane; transverse cirri absent. Marginal cirri 8–10 µm long in vivo and in protargol preparations, very likely composed of two rows with three cilia each in anterior thirds of rows while of two rows with two cilia each in posterior third; right marginal row commences subapically and both rows extend to near posterior body end (Fig. 207a, b, 208a–c; Table 76).

Dorsal bristle pattern without peculiarities, bristles about 3 µm long in vivo and in protargol preparations. Caudal cirri near posterior body end, about 12 µm long in vivo (Fig. 207a, c, 208b, c, e, f; Table 76).

Oral apparatus in *Gonostomum* pattern (Berger 2011), i. e., the adoral zone follows anterior and left body margin where it bends abruptly inwards at about 45% of body length (Fig. 207a, b, d, 208a–c; Table 76). Adoral zone flat, on average composed of 23 gonostomoid membranelles with largest bases about 4 µm long in vivo and in protargol preparations. Buccal cavity narrow, covered by a convex lip bearing paroral membrane composed of an average of 12 kinetids with cilia 10–12 µm long in vivo and in protargol preparations. Endoral membrane commences in mid of paroral membrane, slightly convex. Pharyngeal fibres extend slightly obliquely to right body margin.

Ontogenesis (Fig. 209a–t): This is highly similar to those of *Gonostomum affine*, *G. kuehnelti*, and *G. algicola* (reviewed in Berger 2011), except for the absence of transverse cirri which develop from anlagen V and VI or only from VI in *Gonostomum* spp. In our opinion it is still questionable whether anlage VI originates de novo or from migrating basal bodies of the oral primordium or the neighbouring anlagen.

We do not provide a detailed description of the ontogenesis of *Paragonostomum australiense* because it is so similar to that of *Gonostomum* spp. However, we provide detailed figures and figure explanations so that a comparison with other gonostomatids becomes possible.

Occurrence and ecology: Found not only in central Australia but also about 1.500 km east, i. e., in a litter and soil sample from the bushland between Mount Molley and the town of Mareeba, 45°25' E 17°S. This indicates wide distribution in Australia.

Remarks: Several congeners resemble *P. australiense*, but only one has cortical granules, viz., *P. simplex*, a species as yet recorded only from Austria. Further, *P. simplex* has a rather broadly rounded posterior end and a C-shaped macronuclear figure composed of an average of 10 nodules. *Paragonostomum caudatum* has a real tail (vs. acute end); *P. rarisetum* has also a distinct tail (vs. acute end) and a specific pattern of the frontoventral and frontoterminal cirri (vs. ordinary pattern); and *P. binucleatum* has only about 9 (vs. ~ 15) frontal and frontoventral cirri. Further, its paroral membrane is bipartite (vs. uninterrupted). See Berger (2011) for a review of all taxa mentioned.

Gonostomoides nov. gen.

Diagnosis: As *Gonostomum* and *Paragonostomum* but without transverse and caudal cirri.

Type species: *Gonostomoides galapagensis* nov. spec.

Etymology: Composite of the generic name *Gonostomum* and the Greek suffix *oides* (similar), meaning a ciliate similar to *Gonostomum*. Masculine gender.

Remarks: Gonostomatids are very common in soils globally (Foissner 1998). *Gonostomum*, which occurs also in limnetic habitats, has an ordinary cirral pattern, i. e., there are frontal, frontoventral, buccal, marginal, transverse, and caudal cirri (Berger 1999). The genus *Paragonostomum*, which was established by Foissner et al. (2002), lacks transverse cirri, and *Gonostomoides* lacks both, transverse and caudal cirri. Today, this is considered as significant at generic level (Berger 2006, 2008, 2011). It is remarkable that we found four species in the neotropis while none in the other large biogeographic regions, suggesting a restricted distribution.

Gonostomoides galapagensis nov. spec. (Fig. 210a–i, 211a–g; Table 77)

Diagnosis: Size in vivo about 75 × 25 µm; ellipsoid to slenderly obovate. On average 6 globular to ellipsoid macronuclear nodules and 2 globular to broadly ellipsoid micronuclei. Cortical granules dispersed, refractive, colourless, about 1 × 0.5 µm. On average 3 frontal cirri, 6 frontoventral cirri, 1 buccal cirrus far anteriorly of undulating membranes, 18 cirri in right marginal row and 12 in left. 3 dorsal kineties. Adoral zone extends an average of 43% of body length, composed of about 20 membranelles. Buccal cavity narrow and flat. Paroral membrane composed of 4 kinetids on average.

Type locality: Surface soil under a tree with many epiphytic orchids in the Sierra Negra Crater near the volcano "Chico", 1050 m above sea level, Isabela Island, Galápagos, 0°57'S 90°57'W.

Type material: 1 holotype and 2 paratype slides with protargol-impregnated specimens have been deposited in the Biology Centre of the Upper Austrian Museum in Linz (LI). Relevant specimens have been marked by black ink circles on the coverslip.

Etymology: Named after the archipelago where it was discovered, i. e., the Galápagos Islands.

Description: Size in vivo 60–90 × 20–30 µm, usually about 75 × 25 µm, as calculated from some in vivo measurements and the morphometric data in Table 77 adding 20% length and 10% width shrinkage due to insufficient fixation. Body in vivo slenderly obovate to slenderly ellipsoid, usually widest in anterior quarter due to a more or less pronounced convexity along right margin of cell (Fig. 210a–c, 211a, c); most prepared specimens ellipsoid to narrowly ellipsoid due to insufficient fixation (Fig. 210g–i, 211b, d, e); dorsoventrally flattened up to 2:1. Four to nine, on average six macronuclear nodules, forming a conspicuous strand in body´s midline; individual nodules globular to narrowly ellipsoid, usually ellipsoid, not connected; nucleoli inconspicuous.

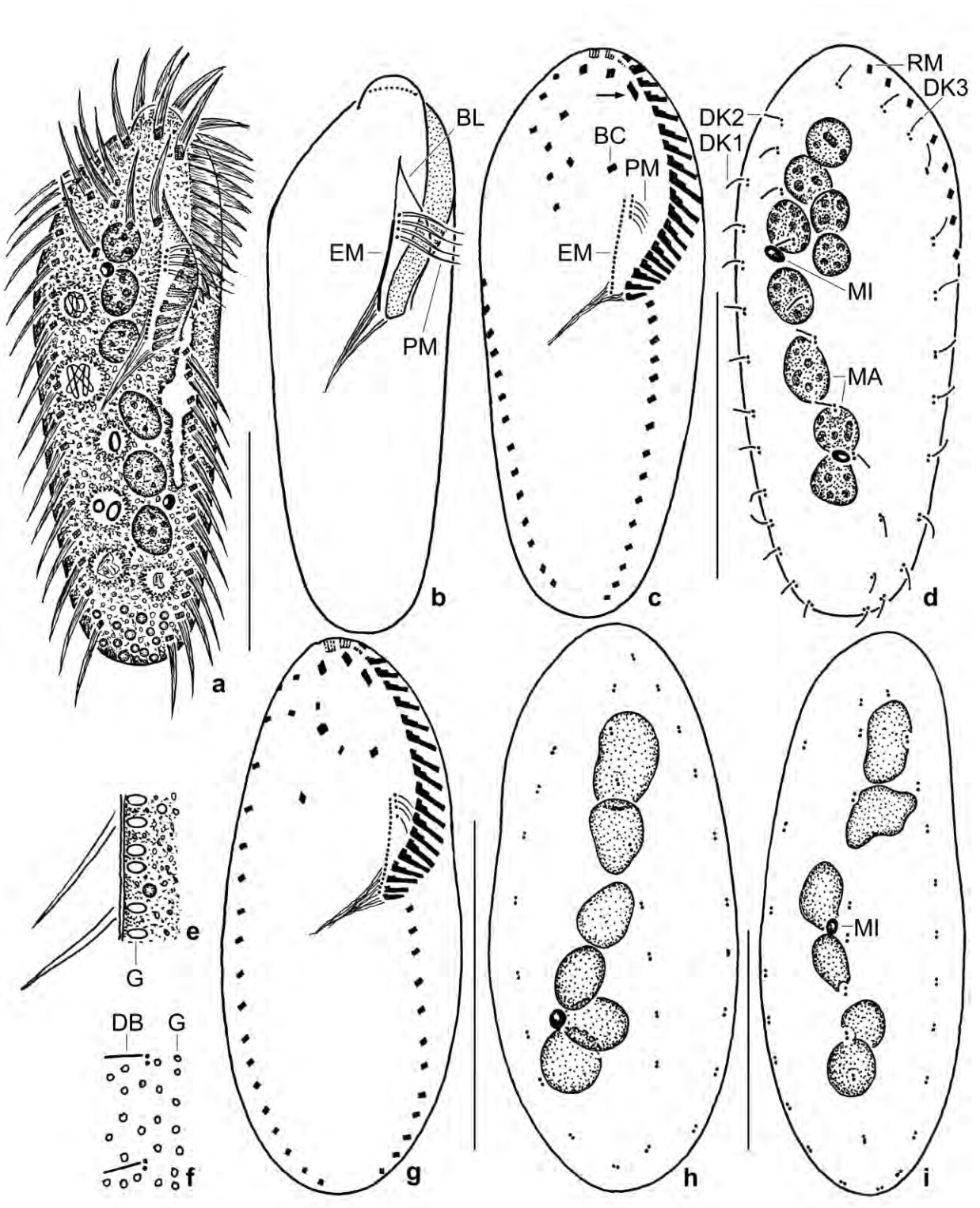

Fig. 210a–i. *Gonostomoides galapagensis* from life (a, b, e, f) and after protargol impregnation (c, d, g–i). **a, b:** Ventral views of a representative specimen, length 75 µm. Note the 10 µm long paroral cilia. **c, d:** Infraciliature of ventral and dorsal side and nuclear apparatus of holotype specimen, length 60 µm. Arrow marks enlarged first frontal cirrus. The first basal body of the paroral is barren. **e, f:** Optical section and surface view, showing the cortical granulation. **g–i:** Infraciliature and nuclear apparatus of paratype specimens. BC – buccal cirrus, BL – buccal lip, DB – dorsal bristle, DK1–3 – dorsal kineties, EM – endoral membrane, G – cortical granules, MA – macronuclear nodules, MI – micronuclei, PM – paroral membrane, RM – right marginal row. Scale bars 30 µm.

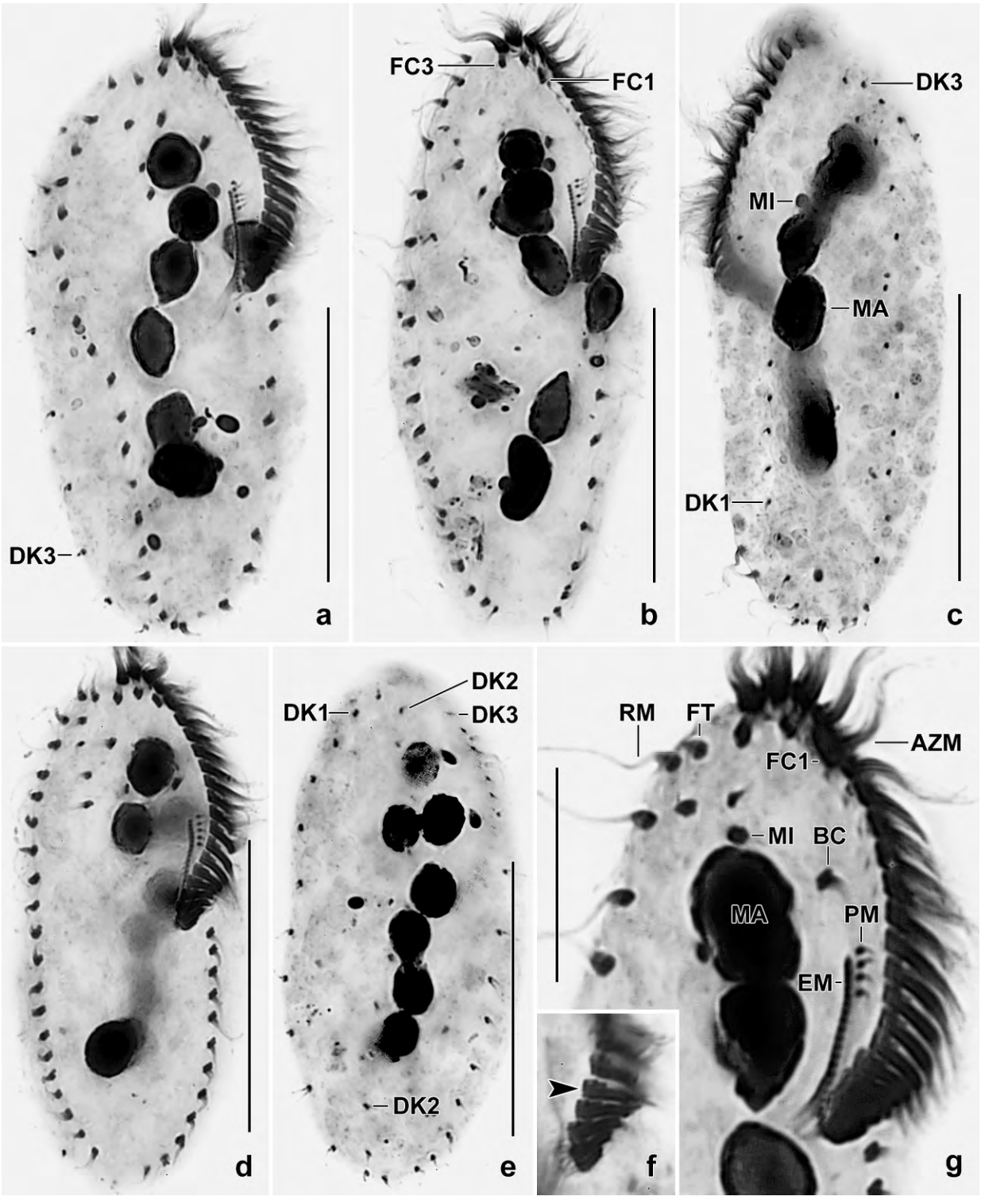

Fig. 211a–g. *Gonostomoides galapagensis*, infraciliature and nuclear pattern after protargol impregnation. **a, b, d, g:** Ventral views. Note absence of transverse cirri. **c, e:** Dorsal views. Note absence of caudal cirri. **f:** Shape of proximal adoral membranelles which consist of four rows of basal bodies (arrowhead). AZM – adoral zone of membranelles, BC – buccal cirrus, DK1–3 – dorsal kineties, EM – endoral membrane, FC1, 3 – frontal cirri, FT – frontoterminal cirri, MA – macronuclear nodules, MI – micronuclei, PM – paroral membrane, RM – right marginal row. Scale bars 15 μm (g) and 30 μm (a–e).

Table 77. Morphometric data on *Gonostomoides galapagensis* (upper line) and *G. bimacronucleatus* (lower line) based on mounted, protargol-impregnated, and randomly selected specimens from non-flooded Petri dish cultures. Measurements in µm. CV – coefficient of variation in %, M – median, Max – maximum, Mean – arithmetic mean, Min – minimum, n – number of individuals investigated, SD – standard deviation, SE – standard error of arithmetic mean.

Characteristics	Mean	M	SD	SE	CV	Min	Max	n
Body, length	60.7	61.0	7.7	1.7	12.7	48.0	76.0	21
	77.8	80.0	8.4	1.8	10.7	60.0	91.0	21
Body, width	24.0	24.0	3.4	0.7	14.2	18.0	30.0	21
	28.3	28.0	2.9	0.6	10.1	22.0	35.0	21
Body length:width, ratio	2.6	2.5	0.4	0.1	16.7	1.9	3.5	21
	2.8	2.7	0.4	0.1	12.7	2.1	3.3	21
Anterior body end to proximal end of adoral zone of membranelles, distance	26.0	26.0	1.4	0.3	5.4	24.0	29.0	21
	30.7	31.0	2.2	0.5	7.1	25.0	34.0	21
Adoral membranelles, number	20.3	20.0	1.2	0.3	5.7	18.0	22.0	21
	21.1	21.0	0.7	0.2	3.5	19.0	22.0	21
Largest adoral membranelle, width of base	4.5	4.0	0.6	0.1	13.4	4.0	6.0	21
	3.9	4.0	0.5	0.1	12.4	3.0	5.0	21
Anterior body end to right marginal row, distance	3.8	4.0	1.2	0.3	31.7	2.0	7.0	21
	4.0	4.0	1.1	0.3	28.5	2.0	6.0	21
Anterior body end to buccal cirrus, distance	10.9	11.0	1.5	0.3	13.6	7.0	14.0	21
	13.7	14.0	1.3	0.3	9.3	11.0	16.0	21
Anterior body end to paroral membrane, distance	15.1	15.0	1.4	0.3	9.0	12.0	17.0	21
	15.0	15.0	1.9	0.4	12.7	12.0	19.0	21
Anterior body end to endoral membrane, distance	15.8	16.0	1.3	0.3	8.0	13.0	17.0	21
	16.3	17.0	1.6	0.4	9.7	13.0	20.0	21
Anterior body end to last frontoventral cirrus, distance	16.4	16.0	3.2	0.7	19.5	10.0	26.0	21
	not investigated							
Posterior body end to right marginal row, distance	3.1	3.0	2.8	0.6	90.2	0.0	12.0	21
	3.2	3.0	1.9	0.4	57.7	0.0	7.0	21
Posterior body end to left marginal row, distance	2.0	1.0	3.6	0.8	182.0	0.0	15.0	21
	0.8	1.0	0.9	0.2	114.7	0.0	3.0	21
Paroral membrane, length	3.0	3.0	0.4	0.1	13.0	2.0	4.0	21
	3.8	4.0	1.1	0.2	28.3	2.0	6.0	21
Endoral membrane, length	9.9	10.0	0.9	0.2	9.2	9.0	12.0	21
	14.3	15.0	1.5	0.3	10.2	11.0	16.0	21
Macronuclear nodules, number	6.2	6.0	1.4	0.3	22.0	4.0	9.0	21
	2.0	2.0	0.0	0.0	0.0	2.0	2.0	21
Macronuclear nodules, length	8.4	9.0	2.1	0.5	24.6	5.0	12.0	21
	17.1	16.0	3.1	0.7	18.4	11.0	23.0	21
Macronuclear nodules, width	5.5	5.0	0.8	0.2	13.7	5.0	7.0	21
	7.3	7.0	0.8	0.2	10.9	6.0	9.0	21
Nuclear figure, length	not investigated							
	42.5	42.0	7.4	1.8	17.3	28.0	56.0	16
Macronuclear nodules, distance in between	not investigated							
	7.7	7.0	2.4	0.6	31.6	5.0	14.0	19

continued

Characteristics	Mean	M	SD	SE	CV	Min	Max	n
Micronuclei, number	1.9	2.0	0.7	0.2	36.8	1.0	3.0	21
	1.9	2.0	0.6	0.1	32.8	1.0	4.0	21
Micronuclei, length	2.1	2.0	0.3	0.1	14.3	1.7	3.0	21
	2.5	2.5	0.4	0.1	16.0	1.8	3.0	21
Micronuclei, width	1.9	2.0	–	–	–	1.7	2.0	21
	2.0	2.0	–	–	–	1.5	2.7	21
Paroral basal bodies, number	4.1	4.0	0.5	0.1	13.2	3.0	5.0	21
	5.9	6.0	1.0	0.2	17.3	4.0	8.0	21
Frontal cirri, number	3.0	3.0	0.0	0.0	0.0	3.0	3.0	21
	3.0	3.0	0.0	0.0	0.0	3.0	3.0	21
Frontoventral cirri, number (without frontal and buccal cirri)	5.8	6.0	0.9	0.2	16.4	5.0	8.0	21
	6.6	7.0	1.1	0.2	17.0	4.0	8.0	21
Buccal cirri, number	1.0	1.0	0.0	0.0	0.0	1.0	1.0	21
	1.0	1.0	0.0	0.0	0.0	1.0	1.0	21
Right marginal cirri, number	18.0	18.0	1.9	0.4	10.3	15.0	22.0	21
	22.7	23.0	2.1	0.5	9.3	19.0	28.0	21
Left marginal cirri, number	11.8	12.0	3.1	0.7	26.1	6.0	16.0	21
	16.6	16.0	2.1	0.5	12.4	14.0	20.0	21
Dorsal kineties, number	3.0	3.0	0.0	0.0	0.0	3.0	3.0	21
	3.0	3.0	0.0	0.0	0.0	3.0	3.0	21
Kinetids in dorsal kinety 1, number	8.3	9.0	2.4	0.5	29.0	5.0	13.0	21
	10.6	10.0	2.3	0.5	21.6	6.0	17.0	21
Kinetids in dorsal kinety 3, number	11.6	12.0	2.3	0.5	19.8	6.0	16.0	21
	15.8	16.0	1.5	0.3	9.5	11.0	18.0	21

On average two globular to broadly ellipsoid micronuclei attached to macronuclear strand at various sites (Fig. 210a, d, h, i, 211a–e, g; Table 77). Contractile vacuole in mid-body posterior to buccal vertex, with short, lacunar collecting canals. Cortex very flexible. Cortical granules inconspicuous because colourless, rather dispersed, and only 0.7–1 × 0.4–0.6 µm in size; moderately compact and bright (Fig. 210e, f). Cytoplasm turbid due to countless, minute organic granules, colourless, posterior region usually studded with lipid droplets 1–2 µm across. Feeds on bacteria and possibly also on humic material digested in vacuoles 4–6 µm across (Fig. 210a). Glides rather rapidly on microscope slides and soil particles.

Cirral pattern gonostomoid (for a review, see Berger 1999) but without transverse and caudal cirri checked in 50 specimens (Fig. 210a, c, d, g, h, 211a–e; Table 77). Frontal cirri in convex row, about 13 µm long in vivo, first frontal cirrus distinctly enlarged. Buccal cirrus far anterior of undulating membranes, 14 µm long in vivo; frontoventral cirri of various size and arrangement, restricted to anterior fifth of cell on average. Marginal cirri thick, about 12 µm long in vivo, rows widely open posteriorly.

Dorsal bristles about 3 µm long in vivo, arranged in three kineties, i. e., a row each along body margin and one in body midline; the latter frequently irregularly curved, possibly due to the

macronuclear strands and/or food vacuoles; number of bristles highly variable, e. g., coefficient of variation 29% in row 1 (Fig. 210h, l, 211c; Table 77).

Adoral zone extends 43% of body length on average, with typical *Gonostomum* shape (for a review, see Berger 1999), composed of an average of 20 membranelles having ciliary row 3 distinctly shortened, largest membranellar base about 4 µm long in protargol preparations, cilia up to 10 µm long in vivo (Fig. 210a–c, g, 211a, b, d, f, g; Table 77). Buccal cavity flat and narrow; buccal lip broadly convex covering proximal third of adoral zone. Undulating membranes side by side, straight, endoral composed of about 20 basal bodies with 5 µm long cilia; paroral composed of an average of four kinetids, of which one or two may lack the cilium, cilia highly mobile and about 10 µm long in vivo, distal half very fine and thus difficult to recognize (Fig. 210a–c, 211a, b, d, g; Table 77). Pharyngeal fibres distinct both in vivo and in protargol preparations, extend obliquely backwards (Fig. 210a–c, g, 211a).

Occurrence and ecology: As yet found only at type locality, became rather abundant in the non-flooded Petri dish culture two days after rewetting the sample, indicating a r-selected live strategy.

Remarks: Size and shape of *Gonostomoides galapagensis* highly resemble a small *Gonostomum affine*, one of the most common soil ciliates (Foissner et al. 2002). However, it is easily distinguished from *Gonostomum* spp., except of *G. kuehnelti*, by the moniliform macronucleus (vs. two nodules). *Gonostomum kuehnelti* has four macronuclear nodules (vs. six) and four (vs. absent) distinct transverse cirri. In the Galápagos preparations, *G. galapagensis* is easily confused with a *Gonostomum affine* population having only one transverse cirrus, just as the Saudi Arabian specimens studied by Foissner et al. (2001).

Another very similar species is *Paragonostomum simplex*, differing from *G. galapagensis* mainly by the presence (vs. absence) of caudal cirri and the average number of cilia (eight vs. four) comprising the paroral membrane (Foissner et al. 2005a).

Gonostomoides bimacronucleatus nov. spec. (Fig. 212a–d, 213a–g; Table 77)

Diagnosis: Size in vivo about 90 × 30 µm; slenderly ellipsoid to ellipsoid. 2 ovate to slenderly ovate macronuclear nodules with narrowed ends opposed. On average 3 frontal cirri, 7 frontoventral cirri, 1 buccal cirrus at level of anterior end of paroral membrane, 23 cirri in right marginal row and 16 in left. 3 dorsal kineties. Adoral zone extends an average of 39% of body length, composed of about 21 membranelles. Buccal cavity narrow and flat. Paroral membrane composed of 6 kinetids on average.

Type locality: Venezuelan site (57), i. e., moss on stones and soil from a small cave in the Golfete de Cuare del Indio, 67°13'W 11°33'N.

Type material: 1 holotype and 1 paratype slide with protargol-impregnated specimens have been deposited in the Biology Centre of the Upper Austrian Museum in Linz (LI). Relevant specimens have been marked with black ink circles on the coverslip.

Etymology: The species name is a composite of the numeral *bi* (two), the Greek adjective *macros* (large), and the Latin adjective *nucleatus* (with a nucleus), referring to the two macronuclear nodules (in contrast to *G. galapagensis* which has eight).

Description and Remarks: *Gonostomoides bimacronucleatus* is in vivo highly similar to several *Gonostomum* and *Paragonostomum* species, especially to the very common *G. affine*, except, of course, for the lack of transverse and caudal cirri. From → *G. fraterculus*, the sole congener with two macronuclear nodules, *G. bimacronucleatus* differs by body size (90 × 30 µm vs. 70 × 25 µm), the arrangement of the macronuclear nodules (close together vs. clearly distant), the number of frontoventral cirri (7 vs. 10 in specific pattern), the number of adoral membranelles (26 vs. 21), and the number of paroral kinetids (6 vs. 11, almost non-overlapping). Obviously, *G. fraterculum* and *G. bimacronucleatus* are rather similar. Very likely, the best separation is achieved by the frontoventral cirral pattern and the number of paroral kinetids.

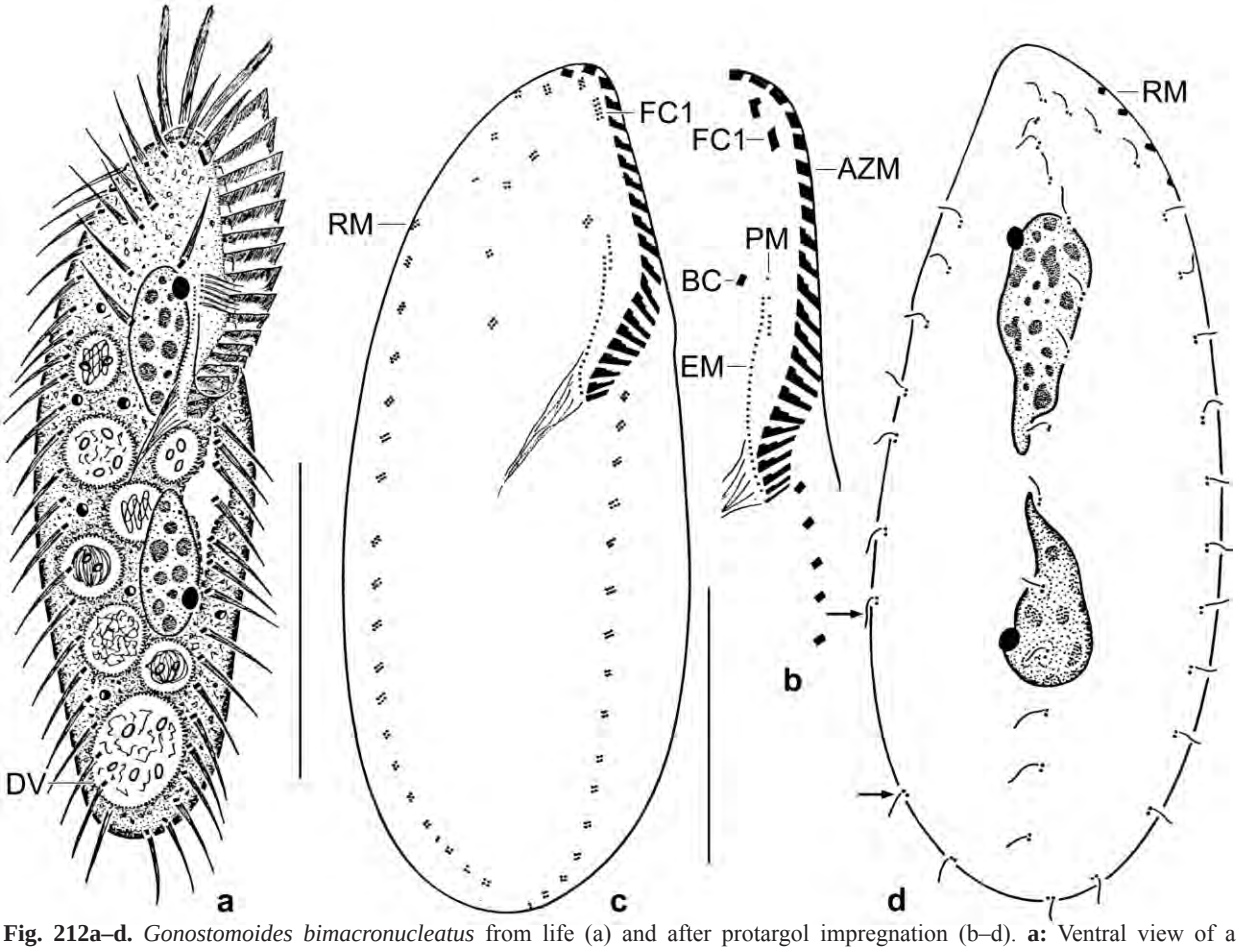

Fig. 212a–d. *Gonostomoides bimacronucleatus* from life (a) and after protargol impregnation (b–d). **a:** Ventral view of a representative specimen, length 90 µm. Note the ovate macronuclear nodules opposed with the narrow end. **b:** Oral apparatus of a paratype specimen. **c, d:** Ventral and dorsal view of holotype specimen, length 77 µm. Note the minute cirral bases and the elongate ovate macronuclear nodules with the narrow end opposed. Arrows in (d) mark a one-bristle-wide gap in dorsal kinety 1. Note the lack of transverse- and caudal cirri. AZM – adoral zone of membranelles, BC – buccal cirrus, DV – defecation vacuole, EM – endoral membrane, FC1 – frontal cirrus 1, PM – paroral membrane, RM – right marginal cirral row. Scale bars 25 µm (c, d) and 40 µm (a).

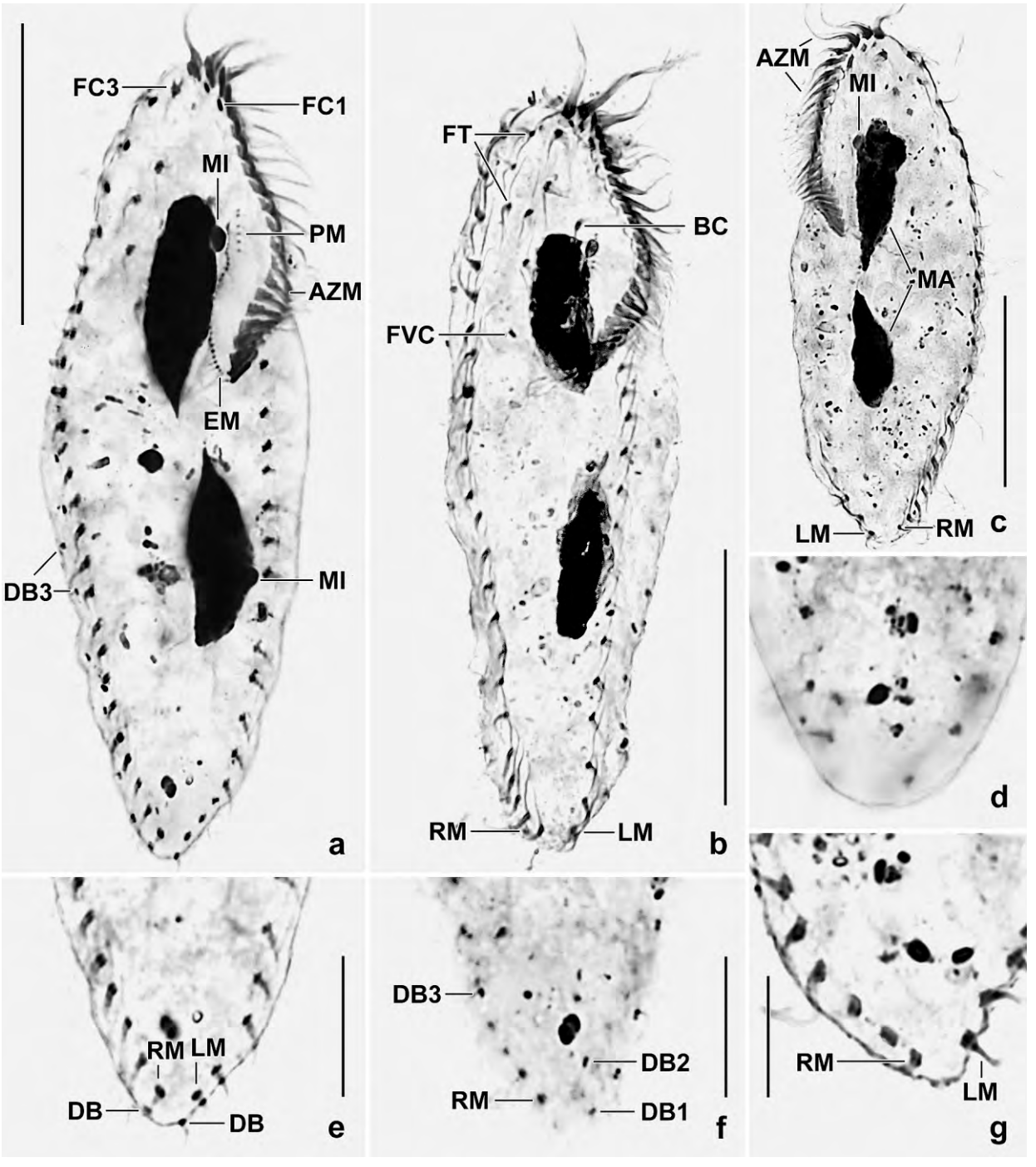

Fig. 213a–g. *Gonostomoides bimacronucleatus* after protargol impregnation. **a, e, f:** Ventral (a, e) and dorsal (f, focused through) view, showing the lack of transverse and caudal cirri. **b:** Ventral view of a specimen with elongate ellipsoid macronuclear nodules. Note the absence of transverse and caudal cirri. **c:** Optical section of a specimen with typical macronuclear nodules, i. e., elongate ovate with narrowed ends opposed. **d, g:** Dorsal and ventral posterior end, showing the absence of caudal and transverse cirri. AZM – adoral zone of membranelles, BC – buccal cirrus, DB1–3 – dorsal kineties and bristles, EM – endoral membrane, FC1, 3 – frontal cirri, FT – frontoterminal cirri, FVC – frontoventral cirri, LM – left marginal cirral row, MA – macronuclear nodules, MI – micronuclei, PM – paroral membrane, RM – right marginal cirral row. Scale bars 10 µm (d–g) and 30 µm (a–c).

Thus, we do not provide an ordinary description, which would be a repetition of that of → *G. galapagensis*, but refer the reader to the diagnosis, the detailed morphometric analysis, the figures, and the figure explanations (Fig. 212a–d, 213a–g; Table 77). As concerns *Gonostomum affine*, a highly variable species (Berger 1999, Foissner et al. 2001), the numbers of adoral membranelles (21 vs. ≥ 25) and paroral kinetids (6 vs. 11 on average) are lower in *G. bimacronucleatus*.

Occurrence and ecology: As yet found only at the slightly saline (~ 10‰) type locality. In the non-flooded Petri dish culture, *G. bimacronucleatus* became numerous six days after rewetting the sample.

Gonostomoides caudatus nov. spec. (Fig. 214a–e, 215a–d; Table 78)

Diagnosis: Size in vivo about 85 × 20 µm; pisciform and slightly sigmoid. Usually 4 ellipsoid macronuclear nodules and 2 micronuclei in anterior thirds of body. On average 3 frontal cirri, 1 buccal cirrus at level of anterior end of paroral membrane, 9 frontoventral cirri including 4 frontoterminal cirri, 30 cirri in right marginal row and 22 in left. 3 dorsal kineties. Adoral zone extends an average of 27% of body length, composed of about 16 membranelles. Buccal cavity very narrow and flat. Paroral membrane composed of 6 kinetids on average.

Type locality: Soil from the Isla Robinson Crusoe, Archipelago Juan Fernandez, Chile 33°S 78°W.

Type material: 1 holotype and 3 paratype slides with protargol-impregnated specimens have been deposited in the Biology Centre of the Upper Austrian Museum in Linz (LI). Relevant specimens have been marked with black ink circles on the coverslip.

Etymology: The Latin participle *caudatus* refers to the tail-like posterior body end, a main feature of this species.

Description: This species is very fragile. Thus live observation was difficult and the tail usually incompletely maintained in the protargol preparations.

Size in vivo 70–115 × 15–25 µm, on average about 85 × 20 µm, as calculated from some in vivo measurements and the morphometric data in Table 78 adding 15% width and 25% length shrinkage due to insufficient tail preservation and general preparation shrinkage. Body in vivo pisciform and slightly sigmoid, laterally flattened up to 2:1, right margin more convex than left, length and distinctness of tail highly variable (Fig. 214a–d, 215b); in protargol preparations often elongate lenticular due to shrinkage or inflation of tail (Fig. 214d, 215a). Four to six, on average four ellipsoid macronuclear nodules in anterior thirds of body and left of its midline; nucleoli of ordinary number and size. One to four, on average two broadly ellipsoid micronuclei attached to various sites of macronuclear nodules (Fig. 214a, e, 215a, b). Contractile vacuole not found, possibly lacking. Cortex highly flexible, very likely without specific granules. Cytoplasm clear and colourless, contains some lipid droplets and barrel-shaped crystals concentrated in base of tail, both 2–4 µm in size; with some 2–3 µm long, deeply impregnating, lenticular inclusions (cortical granules?). Feeds on deeply impregnating bacteria digested in about 7 µm-sized vacuoles. Glides

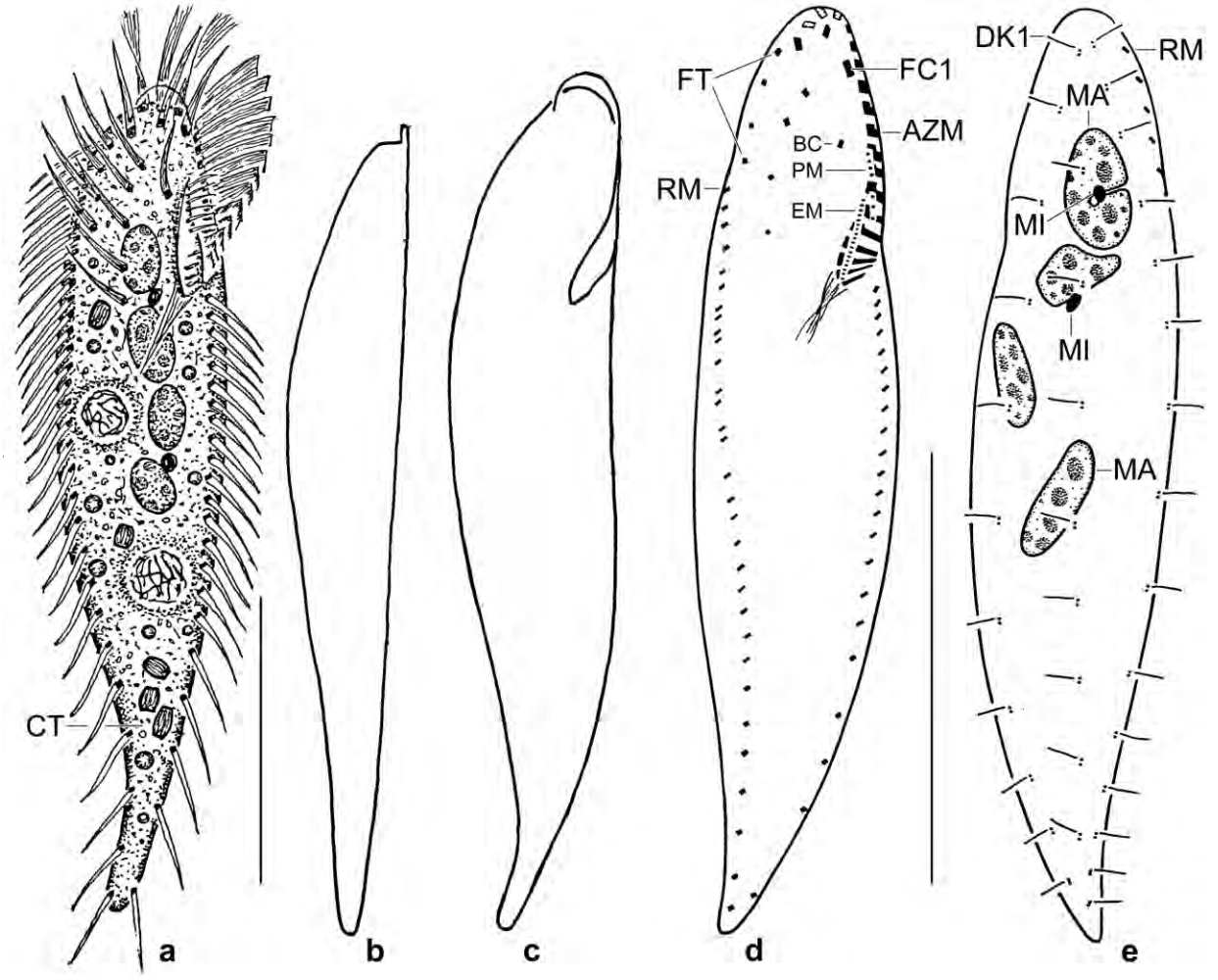

Fig. 214a–e. *Gonostomoides caudatus* from life (a–c) and after protargol impregnation (d, e). **a, b:** Ventral and lateral view of a representative specimen, length 85 µm. **c:** Shape variant. **d, e:** Infraciliature of ventral and dorsal side and nuclear apparatus of holotype specimen, length 68 µm. Note the very narrow buccal cavity. AZM – adoral zone of membranelles, BC – buccal cirrus, CT – crystals, DK1 – dorsal kinety 1, EM – endoral membrane, FC1 – frontal cirrus 1, FT – frontoterminal cirri, MA – macronuclear nodules, MI – micronuclei, PM – paroral membrane, RM – right marginal cirral row. Scale bars 30 µm.

slowly on microscope slide and soil particles, showing much flexibility (Fig. 214a, 215a–c).

Cirri fine and about 8 µm long in vivo, except of thickened and 10 µm long frontal cirri, arranged in gonostomoid pattern (Berger 1999, 2011) but without transverse and caudal cirri (Fig. 214a, d, e, 215a–c; Table 78). Frontal cirri in strongly convex pattern, first slightly enlarged, second thinner than first and third. Buccal cirrus at level of anterior end and distinctly right of paroral membrane. Four frontoterminal cirri in a row near right body margin, other frontoventral cirri in one or two rough rows right of and in body midline. Marginal cirri comparatively numerous, intracirral distances greatly increase in tail area (Fig. 214a, d, 215a–d; Table 78).

Three almost bipolar dorsal kineties with bristles 3–4 µm long in vivo and 2–3 µm in protargol preparations; on average nine bristles in row 2 (Fig. 214e; Table 78).

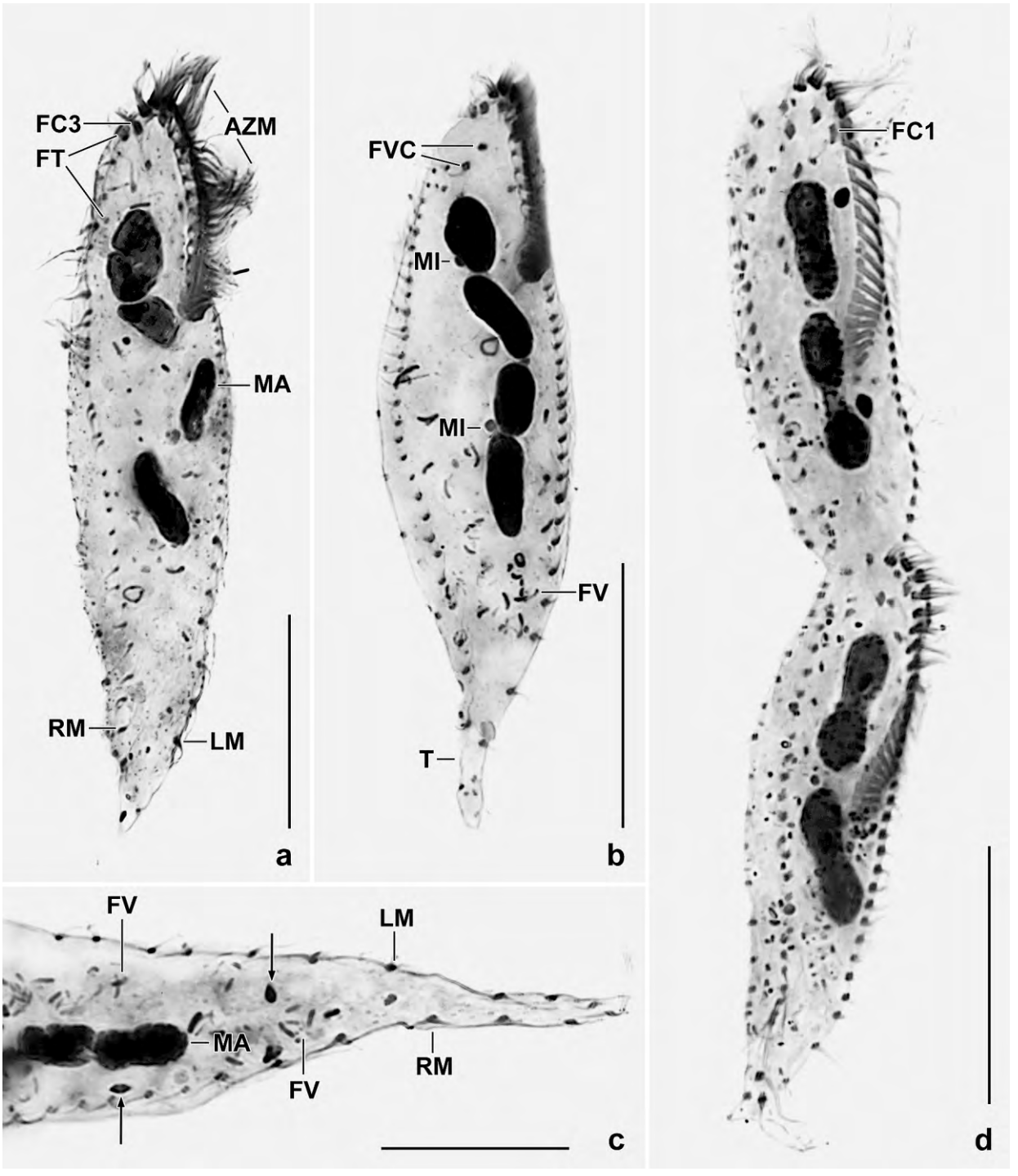

Fig. 215a–d. *Gonostomoides caudatus*, infraciliature and nuclear apparatus after protargol impregnation. Note the four macronuclear nodules, an important feature of this species. **a:** Ventral view of holotype specimen in which the tail shrunk to an "acute end" due to the preparation procedures, length 68 µm. **b:** Ventral view of a paratpye specimen with preserved tail and deeply impregnated bacteria in the food vacuoles. **c:** Ventral view of tail, showing the absence of transverse and caudal cirri. The arrows mark lenticular inclusions. **d:** Ventral view of a very late divider. AZM – adoral zone of membranelles, FC1, 3 – frontal cirri, FV – food vacuoles, FVC – frontoventral cirri, FT – frontoterminal cirri, LM – left marginal cirral row, MA – macronuclear nodules, MI – micronuclei, RM – right marginal cirral row, T – tail. Scale bars 20 µm (a, c) and 30 µm (b, d).

Adoral zone extends 27% of body length on average, with typical *Gonostomum* shape (for a review, see BERGER 1999), composed of an average of 20 membranelles with about 10 µm long cilia (Fig. 214a, d, 215a, b; Table 78). Buccal cavity very flat and narrow both in vivo and in protargol preparations; buccal lip inconspicuous, slightly convex, covers proximal region of adoral zone. Endoral and paroral membrane short, the latter comprising only six cilia on average. Pharyngeal fibres short, extend obliquely backwards (Fig. 214a, d, 215a, b; Table 78).

Occurrence and ecology: As yet found only at type locality, i. e., in soil of a very dry steppe grown with wild barley near the airport of the Juan Fernandez archipelago; pH 6.5 in water.

Remarks: *Gonostomoides caudatus* is easily distinguished from the congeners by the pisciform shape which, however, makes it similar to a variety of genera described *inter alia* by FOISSNER (1982) and FOISSNER et al. (2002), such as *Urosomoida*, *Erimophrya*, *Gonostomum* and, especially, *Paragonostomum* spp. which also lack transverse cirri but have caudal cirri. The most

Table 78. Morphometric data on *Gonostomoides caudatus* (upper line) and *G. fraterculus* (lower line) based on mounted, protargol-impregnated, and randomly selected specimens from non-flooded Petri dish cultures. Measurements in µm. CV – coefficient of variation in %, M – median, Max – maximum, Mean – arithmetic mean, Min – minimum, n – number of individuals investigated, SD – standard deviation, SE – standard error of arithmetic mean.

Characteristics	Mean	M	SD	SE	CV	Min	Max	n
Body, length	68.4	67.0	7.9	1.7	11.5	58.0	92.0	21
	58.3	58.0	4.7	1.0	8.1	52.0	69.0	21
Body, width	17.1	17.0	1.6	0.4	9.2	14.0	20.0	21
	22.5	22.0	2.9	0.6	13.1	17.0	30.0	21
Body length:width, ratio	4.0	3.9	0.4	0.1	9.6	3.4	5.1	21
	2.7	2.6	0.4	0.1	14.1	2.0	3.8	21
Anterior body end to proximal end of adoral zone of membranelles, distance	18.5	18.0	1.4	0.3	7.4	17.0	21.0	21
	25.7	26.0	1.9	0.4	7.4	21.0	29.0	21
Adoral zone of membranelles, percentage of body length	27.5	28.0	2.4	0.5	8.6	23.0	32.0	21
	44.2	45.0	3.6	0.8	8.1	36.0	48.0	21
Adoral membranelles, number	16.0	16.0	1.1	0.3	6.9	14.0	18.0	19
	25.6	26.0	1.2	0.3	4.9	23.0	28.0	21
Anterior body end to right marginal row, distance	2.9	3.0	0.6	0.2	22.0	2.0	5.0	19
	5.5	5.0	1.3	0.3	24.2	3.0	9.0	21
Anterior body end to buccal cirrus, distance	8.6	8.8	0.9	0.2	10.3	7.0	10.0	20
	12.3	13.0	1.4	0.3	11.4	10.0	15.0	21
Anterior body end to paroral membrane, distance	not measured							
	12.2	12.0	1.6	0.3	12.9	9.0	16.0	21
Anterior body end to endoral membrane, distance	not measured							
	13.4	14.0	1.6	0.3	11.6	10.0	16.0	21
Anterior body end to last frontoventral cirrus, distance	14.8	14.5	1.8	0.4	12.1	12.0	19.0	18
	21.3	21.0	1.6	0.4	7.5	19.0	25.0	21
Posterior body end to left marginal row, distance	2.8	3.0	1.3	0.3	45.6	1.0	5.0	16
	0.5	0.5	–	–	–	0.5	0.5	21

continued

Characteristics	Mean	M	SD	SE	CV	Min	Max	n
Paroral membrane, length	4.9	5.0	0.5	0.2	9.1	4.0	6.0	7
	not measured							
Endoral membrane, length	5.6	5.5	–	–	–	5.0	6.0	11
	not measured							
Macronuclear nodules, number	4.5	4.0	0.8	0.2	16.6	4.0	6.0	21
	2.0	2.0	0.0	0.0	0.0	2.0	2.0	21
Anterior macronuclear nodule, length	8.0	8.0	2.1	0.5	25.7	4.0	11.0	21
	11.1	11.0	2.3	0.5	20.5	8.0	17.0	21
Anterior macronuclear nodule, width	3.8	4.0	0.9	0.2	23.8	2.0	6.0	21
	5.6	6.0	0.6	0.1	9.8	5.0	7.0	21
Nuclear figure, length	33.7	33.3	3.8	0.9	11.4	28.0	41.0	20
	31.0	30.0	3.5	0.8	11.2	26.0	40.0	21
Macronuclear nodules, distance in between	not measured							
	8.6	8.5	2.1	0.5	24.5	5.0	12.0	21
Micronuclei, number	2.0	2.0	0.9	0.2	46.8	1.0	4.0	19
	2.5	2.0	0.7	0.2	26.9	2.0	4.0	21
Micronuclei, length	1.5	1.5	–	–	–	1.0	2.0	19
	1.7	1.5	–	–	–	1.5	2.0	21
Micronuclei, width	1.0	1.0	–	–	–	1.0	1.5	19
	1.4	1.5	–	–	–	1.0	1.5	21
Paroral basal bodies, number	5.6	5.0	0.8	0.3	14.1	5.0	7.0	7
	10.7	11.0	1.9	0.4	17.5	7.0	14.0	21
Frontal cirri, number	3.0	3.0	0.0	0.0	0.0	3.0	3.0	17
	3.0	3.0	0.0	0.0	0.0	3.0	3.0	21
Frontoventral cirri, number (frontal and buccal cirri excluded)	8.9	9.0	0.9	0.2	10.1	7.0	11.0	17
	10.3	10.0	0.9	0.2	8.8	8.0	12.0	21
Buccal cirri, number	1.0	1.0	0.0	0.0	0.0	1.0	1.0	21
	1.0	1.0	0.0	0.0	0.0	1.0	1.0	21

similar species is probably *Paragonostomum multinucleatum* which, however, has only two frontoterminal cirri and a bipartite paroral membrane.

Gonostomoides fraterculus nov. spec. (Fig. 216a–g; Table 78)

Diagnosis: Size in vivo about 70 × 25 µm; slenderly ellipsoid. 2 ellipsoid to ovate macronuclear nodules and an average of 2 broadly ellipsoid micronuclei. On average 3 frontal cirri, 10 frontoventral cirri, 1 buccal cirrus slightly anterior of paroral membrane, 23 cirri in right marginal row and 17 in left. 3 dorsal kineties. Adoral zone extends an average of 44% of body length, composed of about 26 membranelles. Buccal cavity narrow and flat. Paroral membrane composed of 11 kinetids on average.

Type locality: Soil under a *Pandanus* palm in the garden of the hotel San Fernando, Puerto

Ayora, Santa Cruz Island, Galápagos, 0°37'S 90°21'W.

Type material: 1 holotype and 5 paratype slides with protargol-impregnated specimens have been deposited in the Biology Centre of the Upper Austrian Museum in Linz (LI). Relevant specimens have been marked with black ink circles on the coverslip.

Etymology: The Latin species name is a composite of the noun *frater* (brother) and the diminutive *culus* (similar, small), referring to → *G. galapagensis*, a congener from Galápagos, and to the similarity with → *G. bimacronucleatus*.

Description: Size in vivo 60–80 × 20–35 µm, usually about 70 × 25 µm, as calculated from some in vivo measurements and the morphometric data in Table 78 adding 20% length and 15% width shrinkage due to ethanol fixation. Body slenderly ellipsoid with anterior end usually narrower than posterior (Fig. 216a, d, f, g); dorsoventrally flattened up to 2:1. Nuclear apparatus in *Gonostomum* pattern, i. e., macronuclear nodules slightly left of body`s midline and separated by an about 12 µm wide distance. Individual nodules broadly to slenderly ellipsoid or ovate, on average 11 × 6 µm in protargol preparations. Two to four, on average two broadly ellipsoid micronuclei attached to various sites of macronuclear nodules (Fig. 216a, b, e, g; Table 78). Contractile vacuole in mid-body posterior of buccal vertex, with short collecting canals. Cortex very flexible, possibly with colourless, inconspicuous granules. Cytoplasm not studied in detail. Feeds on bacteria, small heterotrophic flagellates, and fungal spores digested in vacuoles 4–7 µm across (Fig. 216a). Glides rather rapidly on microscope slides and soil particles.

Cirri about 10 µm long in vivo, except of 15 µm long frontal cirri. Frontal cirrus 1 slightly enlarged. Buccal cirrus at or slightly anterior of distal end of paroral membrane. Frontoventral cirri in characteristic pattern: three frontoterminal cirri posterior of rightmost frontal cirrus; left and slightly posterior of frontoterminal cirri three cirri; and an oblique row composed of three to five, usually four cirri posterior of frontoventral row. Absence of transverse and caudal cirri checked in over 30 specimens and in a late divider (Fig. 216a, c, d, e, f; Table 78).

Dorsal bristles about 3 µm long in vivo and in protargol preparations, arranged in three rows, i. e., a kinety each along body margin and one in midline of body (Fig. 216b, e).

Adoral zone extends 44% of body length on average, with typical *Gonostomum* shape in specimens fixed with Stieve`s solution while ethanol fixed cells become rather inflated making zone more or less convex. On average 26 adoral membranelles having row 3 distinctly shortened, cilia of frontal membranelles about 15 µm long, those in ventral region 10 µm (Fig. 216a, d, f, g; Table 78). Buccal cavity flat and moderately narrow; buccal lip slightly convex covering some proximal membranelles. Undulating membranes side by side, slightly curved, endoral membrane about 2.5 times longer than paroral composed of an average of 11 kinetids with about 8 µm long cilia. Pharyngeal fibres distinct, extend obliquely to right body margin (Fig. 216a, d; Table 78).

Occurrence and ecology: As yet found only at type locality.

Remarks: For comparison with related species, see → *G. bimacronucleatus*. Easily confused with *Gonostomum affine* (with transverse and caudal cirri)!

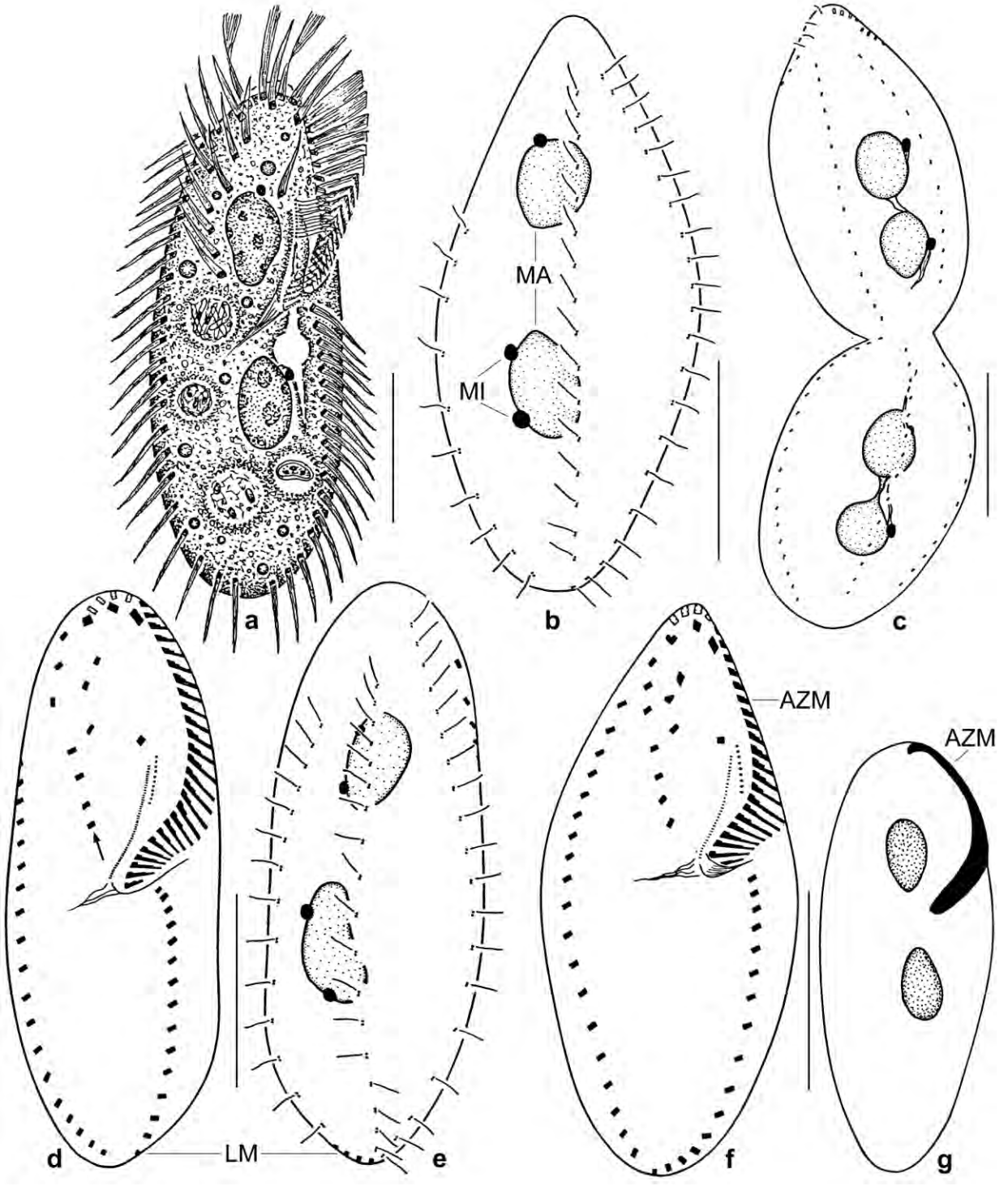

Fig. 216a–g. *Gonostomoides fraterculus* from life (a) and after protargol impregnation (b–g). **a:** Ventral view of a representative specimen, length 70 µm. **b, f:** Dorsal and ventral view of a paratype specimen with acute anterior end possibly caused by ethanol fixation. **c:** A very late divider, showing the absence of caudal cirri. **d, e:** Ventral and dorsal view of holotype specimen, length 60 µm. Note the oblique row of frontoventral cirri (arrow) and the absence of transverse and caudal cirri. **g:** A specimen with ovate macronuclear nodules and convex adoral zone of membranelles due to insufficient fixation. AZM – adoral zone of membranelles, LM – left marginal row, MA – macronuclear nodules, MI – micronuclei. Scale bars 30 µm.

Gonostomum strenuum (Engelmann, 1862) Sterki, 1878 (Fig. 217a–e, 218a–g; Tables 79, 80)

Material: We investigated a population each from the Dominican Republic (grassland soil from the airport area of Puerto Plata, pH 6.6) and Tanzania, Africa (dark brown to black soil and some litter from the margin of the Ngarongora crater, 3°10'S 35°34'E; sample kindly provided by Mr. Emmerich Petz). Two and four voucher slides from the Dominican and Tanzanian population, respectively, have been deposited in the Biology Centre of the Upper Austrian Museum in Linz (LI). Relevant specimens have been marked by black ink circles on the coverslip.

Remarks: *Gonostomum strenuum* has been reviewed and neotypified by Berger (1999) and Foissner et al. (2002). Thus, we restrict the description of the two new populations to some figures, a detailed morphometry (Tables 79, 80), and the most important features. The Dominican population has small body size and, like the Spanish specimens, one or two supernumerary cirri between frontoventral cirral row V and the pretransverse/transverse cirri. The Tanzanian specimens are almost as slender as the type specimen (Fig. 217a, c, 218f). They have more adoral membranelles and micronuclei but less cirri in frontoventral row V, which thus does not extend beyond the buccal vertex (Table 80).

The addition of two populations to the three known ones slightly increases the range of most features (Table 80). This is not unexpected and hardly can be used to split *G. strenuum* into subspecies. Now, molecular data are needed.

Notes on a Dominican population (Fig. 217e, 218a–e; Tables 79, 80): Size in vivo about 100 × 30 µm. Shape indistinguishable from that of *G. affine*. Two to four, usually three micronuclei. Contractile vacuole slightly posterior of buccal vertex, with lacunar collecting canals. Cortical granules in narrow rows forming a rather distinct fringe, colourless, in vivo about 1.5 × 1 µm in size, stain red with methyl green-pyronin. Cytoplasm with 4–7 µm-sized food vacuoles containing bacteria; posterior third crammed with barrel-shaped, about 3 µm long, bright inclusions (crystals?).

Frontal cirri in vivo 15 µm long, transverse cirri about 20 µm, marginal cirri 15 µm long and likely composed of three ciliary rows. On average 26 right marginal cirri and 19 left, 3 frontal cirri, 5 frontoterminal cirri, 13 frontoventral cirri, 1 buccal cirrus, and 4 pretransverse and transverse cirri; frontoventral row V composed of an average of seven cirri, slightly to distinctly surpasses buccal vertex; one or two supernumerary cirri between frontoventral row V and pretransverse/transverse cirri in 67% of specimens (34% with one cirrus, 33% with two cirri), either side by side or one after the other (Fig. 217e, 218a, b; Table 79). Dorsal bristles 4 µm long in vivo, arranged in three rows.

Adoral zone extends 46% of body length, composed of 29 membranelles on average; 12 paroral cilia on a convexity of buccal lip.

Notes on a Tanzanian population (Fig. 217a, b, d, 218f, g; Tables 79, 80): Size in vivo about 120 × 30 µm, i. e., elongate ellipsoid. Shape indistinguishable from that of *G. affine*. Five to eight, on average six ellipsoid micronuclei. Contractile vacuole slightly posterior of buccal vertex and

slightly left of body's midline, with two collecting canals. Cortical granules as in Dominican specimens. Cytoplasm with 4–7 µm-sized food vacuoles containing bacteria; posterior third studded with knotty, bright inclusions (crystals?).

Frontal cirri in vivo about 18 µm long, marginal cirri about 12 µm, transverse cirri about 20 µm; caudal cirri beat vividly, about 20 µm long. On average 27 right marginal cirri and 19 left, 3 frontal cirri, 4 frontoterminal cirri, 11 frontoventral cirri, 1 buccal cirrus, and 4 pretransverse and transverse cirri; frontoventral row V composed of an average of six cirri, does not surpass buccal vertex. Dorsal bristles 3 µm long in vivo, arranged in three rows (Fig. 217a, d, e, 218a, b, d, e–g; Tables 79, 80).

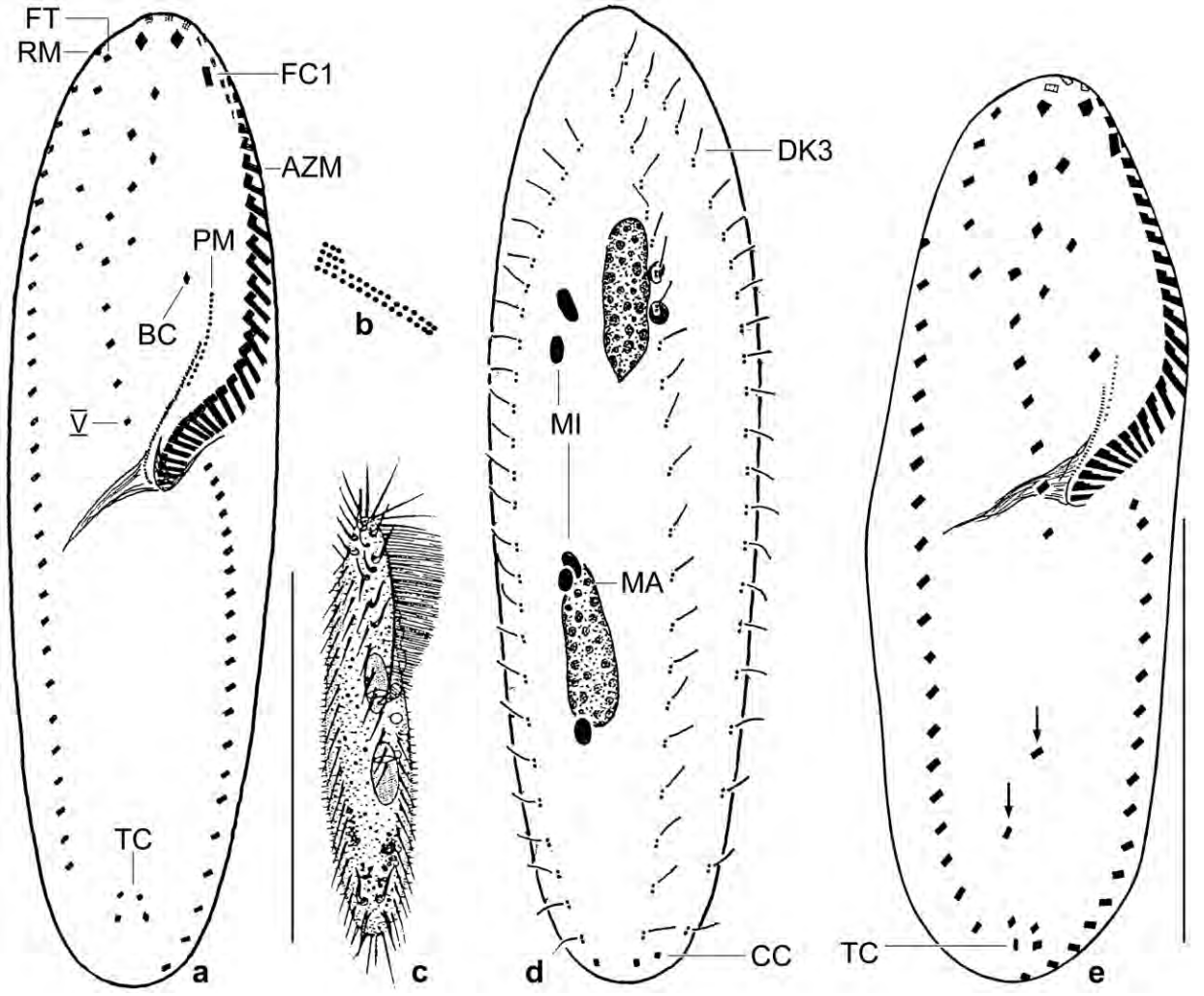

Fig. 217a–e. *Gonostomum strenuum* from Tanzania (a, b, d), Germany (c, from ENGELMANN 1862), and the Dominican Republic (e) from life (c) and after protargol impregnation (a, b, d, e). **a, b, d:** Infraciliature of ventral and dorsal side, length 103 µm. Note the similarity to the type specimen (c) in the length:width ratio (3.6:1 and 4.8:1) and body length (118 µm when 15% preparation shrinkage is added vs. 135 µm). Ciliary rows three and four of the adoral membranelles are strongly shortened (b). **c:** A specimen from the German type population, length 135 µm (for details, see explanation to figures (a, d). **e:** Ventral view of a specimen from the Dominican Republic, length 85 µm. Arrows mark supernumerary cirri occurring in 67% of specimens. AZM – adoral zone of membranelles, BC – buccal cirrus, CC – caudal cirri, DK3 – dorsal kinety 3, FC1 – frontal cirrus 1, FT – frontoterminal cirri, MA – macronuclear nodule, MI – micronuclei, PM – paroral membrane, RM – right marginal row, TC – transverse cirri, V – frontoventral cirral row V. Bars 40 µm.

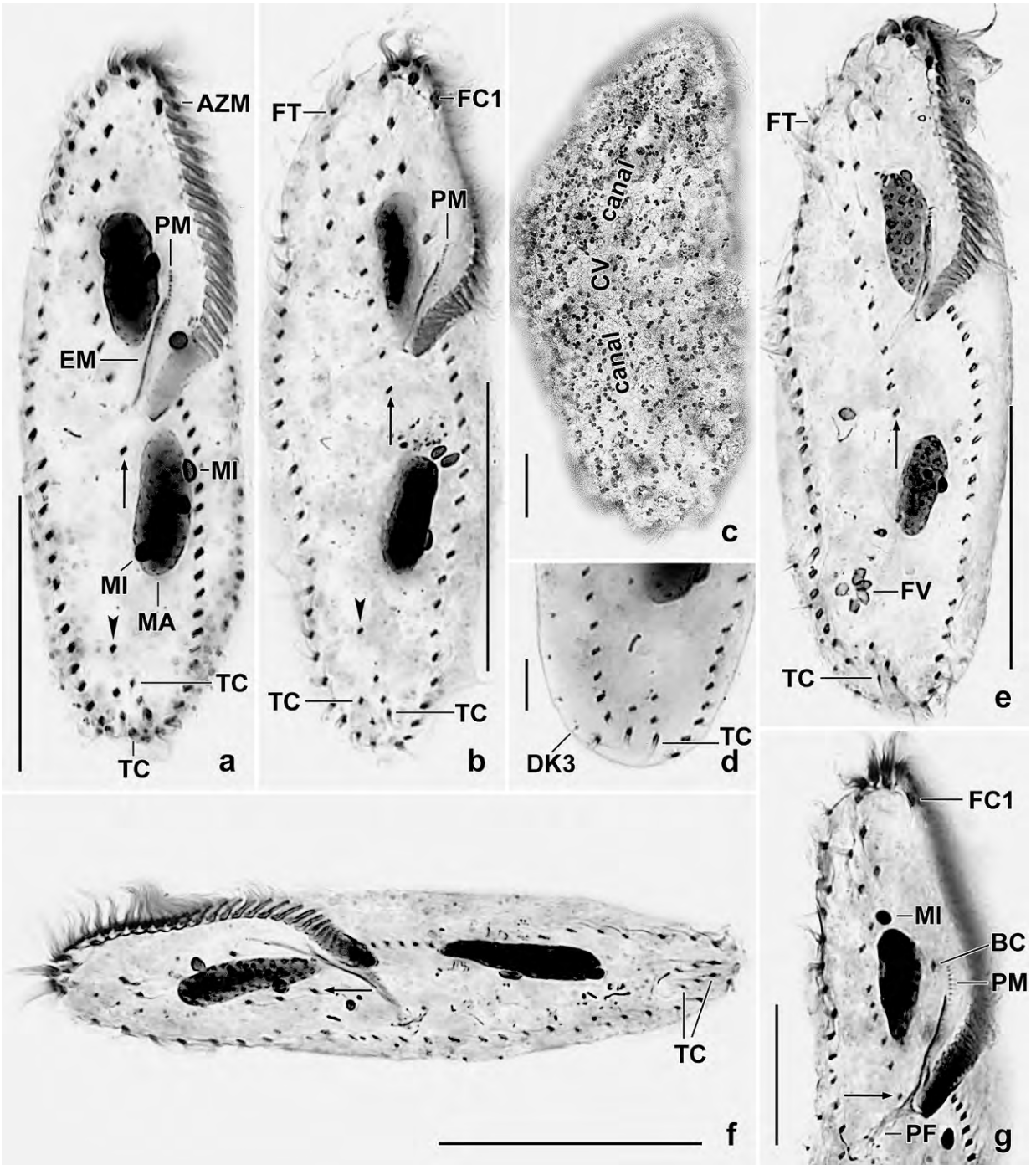

Fig. 218a–g. *Gonostomum strenuum* from the Dominican Republic (a–e) and from Tanzania (f, g) after methyl green-pyronin staining (c) and protargol impregnation (a, b, d–g). **a, b, d, e:** Ventral views, showing the low variability of the cirral and nuclear pattern. Arrows mark the last cirrus of frontoventral row V, which extends postorally. Arrowheads denote supernumerary cirri typical for this population. **c:** Dense cortical granulation. **f, g:** Ventral views, showing the slender body and the paroral membrane (g). Arrows denote last cirrus of frontoventral row V, which does not surpass the buccal vertex on average (Table 79). AZM – adoral zone of membranelles, BC – buccal cirrus, DK3 – dorsal kinety 3, EM – endoral membrane, FC1 – frontal cirrus 1, FT – frontoterminal cirri, FV – food vacuole, MA – macronuclear nodule, MI – micronuclei, PF – pharyngeal fibres, PM – paroral membrane, TC – transverse and pretransverse cirri. Scale bars 10 µm (c, d), 20 µm (g), and 40 µm (a, b, e, f).

Table 79. Morphometric data on *Gonostomum strenuum* from Tanzania, Africa (upper line) and the Dominican Republic, Caribbean area (lower line) based on mounted, protargol-impregnated (FOISSNER's method), and randomly selected specimens from non-flooded Petri dish cultures. CV – coefficient of variation in %, M – median, Max – maximum, Mean – arithmetic mean, Min – minimum, n – number of individuals investigated, SD – standard deviation, SE – standard error of arithmetic mean.

Characteristics	Mean	M	SD	SE	CV	Min	Max	n
Body, length	102.1	101.0	3.9	1.1	3.8	97.0	110.0	13
	83.6	83.0	6.3	1.4	7.5	73.0	100.0	21
Body, width	29.5	30.0	2.8	0.8	9.3	24.0	35.0	13
	27.3	27.0	2.0	0.4	7.3	22.0	31.0	21
Body length:width, ratio	3.5	3.4	0.4	0.1	11.2	2.8	4.5	13
	3.1	3.0	0.2	0.0	5.3	2.9	3.5	21
Anterior body end to end of adoral zone, distance	49.3	50.0	2.5	0.7	5.1	45.0	53.0	13
	38.4	38.0	2.0	0.4	5.3	34.0	41.5	21
Adoral membranelles, number	34.2	35.0	1.7	0.5	4.9	32.0	37.0	13
	29.2	29.0	1.4	0.3	4.8	26.0	32.0	21
Paroral kinetids, number	16.4	17.0	1.6	0.4	9.5	14.0	19.0	13
	12.3	12.0	1.5	0.3	11.8	10.0	15.0	21
Macronuclear nodules, length	18.7	18.0	2.2	1.6	11.6	15.0	22.0	13
	17.1	17.0	2.0	0.4	11.8	13.5	22.0	21
Macronuclear nodules, width	5.8	6.0	0.8	0.2	14.4	5.0	7.0	13
	5.8	6.0	0.7	0.2	12.5	4.5	7.5	21
Macronuclear nodules, number	2.0	2.0	0.0	0.0	0.0	2.0	2.0	13
	2.0	2.0	0.0	0.0	0.0	2.0	2.0	21
Micronuclei, length	3.3	3.0	0.5	0.1	15.8	2.5	4.0	13
	2.2	2.0	–	–	–	2.0	2.5	21
Micronuclei, width	2.3	2.0	–	–	–	2.0	3.0	13
	1.5	1.5	–	–	–	1.0	2.0	21
Micronuclei, number	6.1	6.0	1.1	0.3	18.4	5.0	8.0	13
	2.9	3.0	0.7	0.1	22.9	2.0	4.0	21
Anterior body end to end of frontoventral cirral row III, distance	17.5	16.0	3.1	0.9	17.7	15.0	25.0	13
	16.4	16.0	2.8	0.6	16.9	11.5	22.0	21
Frontoventral row III, number of cirri	2.1	2.0	–	–	–	2.0	3.0	13
	2.3	2.0	–	–	–	2.0	3.0	21
Anterior body end to end of frontoventral cirral row IV, distance	25.9	26.0	3.6	1.0	14.0	20.0	30.0	13
	23.5	23.0	3.5	0.8	15.0	18.0	31.0	21
Frontoventral row IV, number of cirri	3.1	3.0	0.6	0.2	20.8	2.0	4.0	13
	3.6	4.0	0.8	0.2	22.7	2.0	6.0	21
Anterior body end to end of frontoventral cirral row V, distance	47.2	47.0	4.1	1.1	8.6	40.0	55.0	13
	44.2	44.0	3.8	0.8	8.6	37.0	51.0	21
Frontoventral row V, number of cirri	5.7	6.0	0.8	0.2	13.2	4.0	7.0	13
	7.5	7.0	0.7	0.2	9.1	6.0	9.0	21
Fontal cirri, number	3.0	3.0	0.0	0.0	0.0	3.0	3.0	13
	3.0	3.0	0.0	0.0	0.0	3.0	3.0	21
Buccal cirri, number	1.0	1.0	0.0	0.0	0.0	1.0	1.0	13

continued

Characteristics	Mean	M	SD	SE	CV	Min	Max	n
	1.0	1.0	0.0	0.0	0.0	1.0	1.0	21
Frontoterminal cirri, number	4.1	4.0	0.6	0.2	15.6	3.0	5.0	13
	5.2	5.0	0.9	0.2	17.0	3.0	7.0	21
Pretransverse and transverse cirri, number	4.5	4.0	0.8	0.2	17.4	4.0	6.0	13
	4.5	4.0	0.6	0.1	13.3	4.0	6.0	21
Fronto-ventral-transverse cirri, total number	23.5	23.0	1.9	0.5	8.3	21.0	26.0	13
	24.1	24.0	2.3	0.5	9.4	21.0	30.0	21
Right marginal row, number of cirri	26.8	27.0	3.2	0.9	12.0	21.0	33.0	13
	26.1	26.0	2.9	0.6	11.0	22.0	33.0	21
Left marginal row, number of cirri	18.8	19.0	1.7	0.5	9.3	16.0	22.0	13
	18.9	19.0	1.6	0.4	8.4	16.0	22.0	21
Caudal cirri, number	3.0	3.0	0.0	0.0	0.0	3.0	3.0	13
	3.0	3.0	0.0	0.0	0.0	3.0	3.0	21
Dorsal kineties, number	3.0	3.0	0.0	0.0	0.0	3.0	3.0	13
	3.0	3.0	0.0	0.0	0.0	3.0	3.0	21

Adoral zone extends 48% of body length, composed of 34 membranelles on average; 16 paroral cilia on a convexity of buccal lip (Fig. 217a, e, 218a, b, e–g; Tables 79, 80).

Gonostomum halophilum nov. spec. (Fig. 219a–e, 220a–e; Table 81)

Diagnosis: Size in vivo about 80 × 30 µm; ellipsoid to elongate rectangular. 2 macronuclear nodules and 2 micronuclei. Cortical granules scattered, colourless, about 0.8 µm across. 3 frontal cirri; 4–5 frontoterminal cirri; 1 buccal cirrus far anterior of paroral membrane; 2 transverse cirri near posterior body end. 3 dorsal kineties and caudal cirri. Right marginal row composed of an average of 28 cirri, left of 20. Adoral zone flat, extends about 40% of body length, consists of an average of 26 membranelles. On average 2 paroral kinetids near anterior end of endoral membrane.

Type locality: Highly saline soil from a mangrove swamp in the outskirts of the town of Cairns, Australia, 145°E 17°S.

Type material: 1 holotype and 2 paratype slides with protargol-impregnated specimens have been deposited in the Biology Centre of the Upper Austrian Museum in Linz (LI). The holotype and other relevant specimens have been marked by black ink circles on the coverslip.

Etymology: *halophilum* (loving saline habitats) is a Greek adjective and refers to the habitat the species was discovered.

Description: Most features of *G. halophilum* have an ordinary variability (CV < 15%; Table 81); of those important for the diagnosis of the species, only the number of kinetids comprising the paroral membrane has a coefficient of variation of > 30%. However, the average is two and thus far away from the congeners, except of *G. algicola* (see **Remarks**).

Table 80. Comparison of main morphometrics in five populations of *Gonostomum strenuum* from Tanzania (Africa, original data, TA), Namibia (Southwest Africa, from FOISSNER et al. 2002, NA), China (from SONG 1990b, CH), Europe (Spain, OLMO & TÉLLEZ 1997, SP), and the Dominican Republic (original data, DO). Based on protargol-impregnated specimens, if not mentioned otherwise.

Characteristics	Pop	Mean	M	SD	SE	CV	Min	Max	n
Body, length (µm)	TA	102.1	101.0	3.9	1.1	3.8	97.0	110.0	13
	NA	81.5	80.0	7.8	2.2	9.6	72.0	98.0	13
	CH	103.8	?	7.9	2.4	7.6	88.0	119.0	11
	SP [a]	124.9	120.0	9.8	1.8	7.9	110.0	145.0	30
	DO	83.6	84.0	6.3	1.4	7.5	73.0	100.0	21
Body, width (µm)	TA	29.5	30.0	2.8	0.8	9.3	24.0	35.0	13
	NA	30.0	30.0	2.9	0.8	9.6	26.0	36.0	13
	CH	37.0	?	5.0	1.5	13.4	28.0	44.0	11
	SP [a]	51.4	51.0	6.4	1.2	12.5	40.0	65.0	30
	DO	27.3	27.0	2.0	0.4	7.3	22.0	31.0	21
Body length:width, ratio	TA	3.5	3.4	0.4	0.1	11.2	2.8	4.5	13
	NA	2.7	2.8	0.3	0.1	10.3	2.3	3.5	13
	CH	2.8	?	?	?	?	?	?	11
	SP	2.4	?	?	?	?	?	?	30
	DO	3.1	3.0	0.2	0.1	5.3	2.9	3.5	21
Anterior body end to proximal end of adoral zone of membranelles, distance (µm)	TA	49.3	50.0	2.5	0.7	5.1	45.0	53.0	13
	NA	42.3	43.0	4.9	1.4	11.6	32.0	49.0	13
	CH	54.5	?	7.2	2.2	13.2	41.0	69.0	11
	SP [a]	58.6	60.0	2.5	0.5	4.3	55.0	65.0	30
	DO	38.4	38.0	2.0	0.4	5.3	34.0	41.5	21
Adoral membranelles, number	TA	34.2	35.0	1.7	0.5	4.9	32.0	37.0	13
	NA	27.9	28.0	2.4	0.7	8.6	24.0	31.0	13
	CH	29.5	?	2.2	0.6	7.3	26.0	33.0	11
	SP	29.4	29.0	2.0	0.4	7.0	26.0	34.0	30
	DO	29.2	29.0	1.4	0.3	4.8	26.0	32.0	21
Fronto-ventral-transverse cirri, total number	TA	23.5	23.0	1.9	0.5	8.3	19.0	29.0	13
	NA	26.4	26.0	2.2	0.5	11.9	23.0	29.0	13
	CH	26.8	?	?	?	?	23.0	32.0	11
	SP	24.2	?	?	?	?	22.0	31.0	30
	DO	27.1	26.0	2.2	0.5	11.9	23.0	32.0	21
Paroral kinetids, number	TA	16.4	17.0	1.6	0.4	9.5	14.0	19.0	13
	NA	12.2	13.0	2.0	0.5	16.1	9.0	15.0	13
	CH	17.0, according to a single figure							
	SP	14.0, according to a single figure							
	DO	12.3	12.0	1.5	0.3	11.8	10.0	15.0	21
Right marginal row, number of cirri	TA	26.8	27.0	3.2	0.9	12.0	21.0	33.0	13
	NA	20.5	19.0	3.5	1.0	17.2	16.0	27.0	13
	CH	25.8	?	2.0	0.5	7.6	23.0	29.0	13
	SP	26.9	27.0	1.9	0.4	7.2	23.0	30.0	30
	DO	26.1	26.0	2.9	0.6	11.0	22.0	33.0	21
Left marginal row, number of cirri	TA	18.8	19.0	1.7	0.5	9.3	16.0	22.0	13

continued

Characteristics	Pop	Mean	M	SD	SE	CV	Min	Max	n
	NA	14.9	15.0	1.6	0.4	10.4	13.0	18.0	13
	CH	17.7	?	5.2	1.5	29.6	17.0	21.0	13
	SP	17.4	17.0	2.0	0.4	11.6	16.0	22.0	30
	DO	18.9	19.0	1.6	0.4	8.4	16.0	22.0	21

[a] From silver carbonate-impregnated specimens. Very likely, considerably inflated.

Size in vivo 67–93 × 23–37 µm, usually about 80 × 30 µm, as calculated from some in vivo measurements and the morphometric data in Table 81 adding 15% preparation shrinkage. Body shape very similar to that of *G. affine*, i. e., ellipsoid to elongate ellipsoid or elongate rectangular; anterior body end obliquely rounded, posterior narrowly to broadly rounded (Fig. 219a, c, d, 220a–c; Table 81). Nuclear apparatus left of body´s midline, one ellipsoid to elongate ellipsoid macronuclear nodule in oral portion of cell, the second postoral in third quarter; with many ordinarily-sized nucleoli. On average two broadly ellipsoid micronuclei attached to various sites of macronuclear nodules (Fig. 219a, e, 220a–c; Table 81). Contractile vacuole not recognizable, very likely due to the high salt concentration. Cortex very flexible, contains colourless, scattered granules about 0.8 µm across in vivo (Fig. 219c); granules difficult to recognize due to the opaque cytoplasm, do not impregnate with the protargol method used. Cytoplasm opaque because studded with food vacuoles and countless granules. Feeds mainly on spore-forming bacteria, rarely on small heterotrophic flagellates digested in vacuoles 4–10 µm across. Movement without peculiarities; very flexible.

Cirri of ordinary length and thickness, arranged as in → *G. strenuum,* i. e., with comparatively long frontoterminal row and long, slightly oblique anlage V, each composed of four to five cirri (Fig. 219a, d, 220a–c, e; Table 81). Three frontal cirri about 15 µm long in vivo; between frontal cirrus 2 and 3 a smaller, cirrus-like dot formed by three crossing fibres (Fig. 219d, 220b, e); basis of frontal cirrus 1 slightly enlarged in some specimens; second cirrus of anlage III slightly enlarged and at level of begin of right marginal row. Buccal cirrus far anterior of undulating membranes, composed of six cilia. Invariably two transverse cirri one upon the other and about 15 µm long in vivo. Marginal cirri each composed of two minute rows with about 10 µm long cilia; right marginal row commences subapically and ends subterminally, left row extends to body`s midline posteriorly (Fig. 219a, d, 220a–c, e; Table 81).

Dorsal bristle pattern without peculiarities, bristles about 3 µm long in vivo and in protargol preparations. Caudal cirri on posterior body end, difficult to recognize possibly because composed of only two cilia (Fig. 219a, e, 220d; Table 81).

Oral apparatus in *Gonostomum* pattern (Berger 2011), i. e., the adoral zone follows the anterior and left body margin to bend abruptly into the cell at about 40% of body length (Fig. 219a, b, d, 220a–c, e; Table 81). Adoral zone flat, on average composed of 26 gonostomoid membranelles with largest bases about 3 µm long in protargol preparations. Buccal cavity narrow, covered by a convex lip bearing paroral membrane composed of an average of only two kinetids (Fig. 219a, b, 220c, e; Table 81). Endoral membrane commences at paroral membrane, almost straight. Pharyngeal fibres extend slightly obliquely to right body margin.

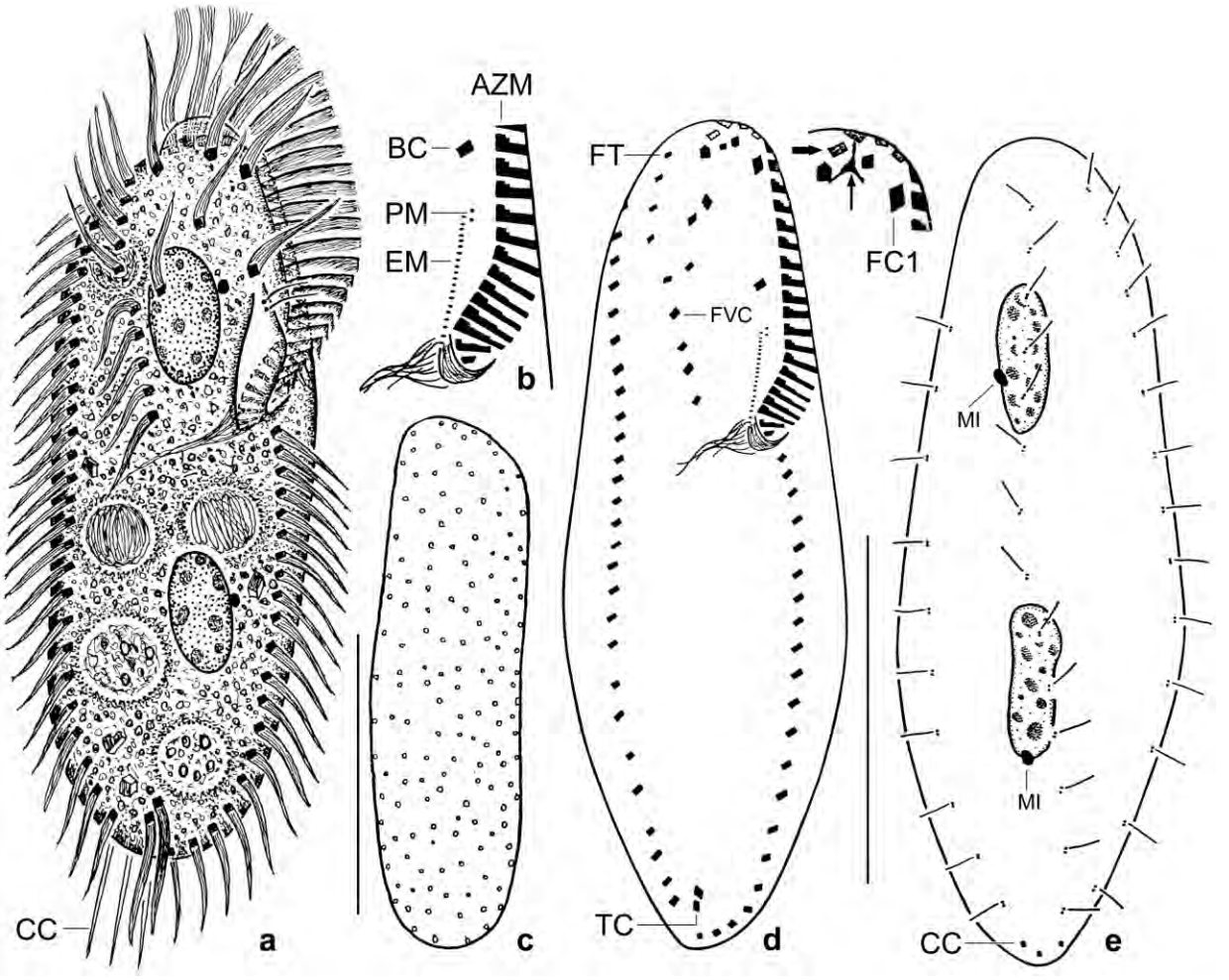

Fig. 219a–e. *Gonostomum halophilum* from life (a, c) and after protargol impregnation (b, d, e). **a:** Ventral view of a representative specimen, length 80 µm. **b, d, e:** Ventral and dorsal view of holotype specimen, length 72 µm. Note the main feature of this new species, viz., the paroral membrane which consists of an average of only two kinetids (b). The arrow marks a frontal cirrus-like structure produced by the crossing of three fibres. **c:** A slender, rectangular specimen showing the sparse cortical granulation. AZM – adoral zone of membranelles, BC – buccal cirrus, CC – caudal cirri, EM – endoral membrane, FC1 – frontal cirrus 1, FT – frontoterminal cirri, FVC – frontoventral cirri, MI – micronuclei, PM – paroral membrane, TC – transverse cirri. Scale bars 30 µm.

Occurrence and ecology: As yet found only at type locality, i. e., in highly saline (> 30‰) and slightly acidic (pH 6.4 in water) soil from a mangrove forest.

Remarks: *Gonostomum halophilum* has a clear identity because it has the lowest number (two) of paroral kinetids in the family, followed by *G. algicola* which possesses an average of four and has only one transverse cirrus (Berger 2011, Foissner et al. 2002). Other rare features are the low number of transverse cirri (two) and the location of the buccal cirrus far anterior of the undulating membranes. The cirral pattern of *G. halophilum* is more similar to that of → *G. strenuum* than to that of *G. affine* due to the frontoterminal cirral row and anlage V both composed of four to five cirri (for a review, see Berger 2011). For separation from → *G. salinarum* see that species.

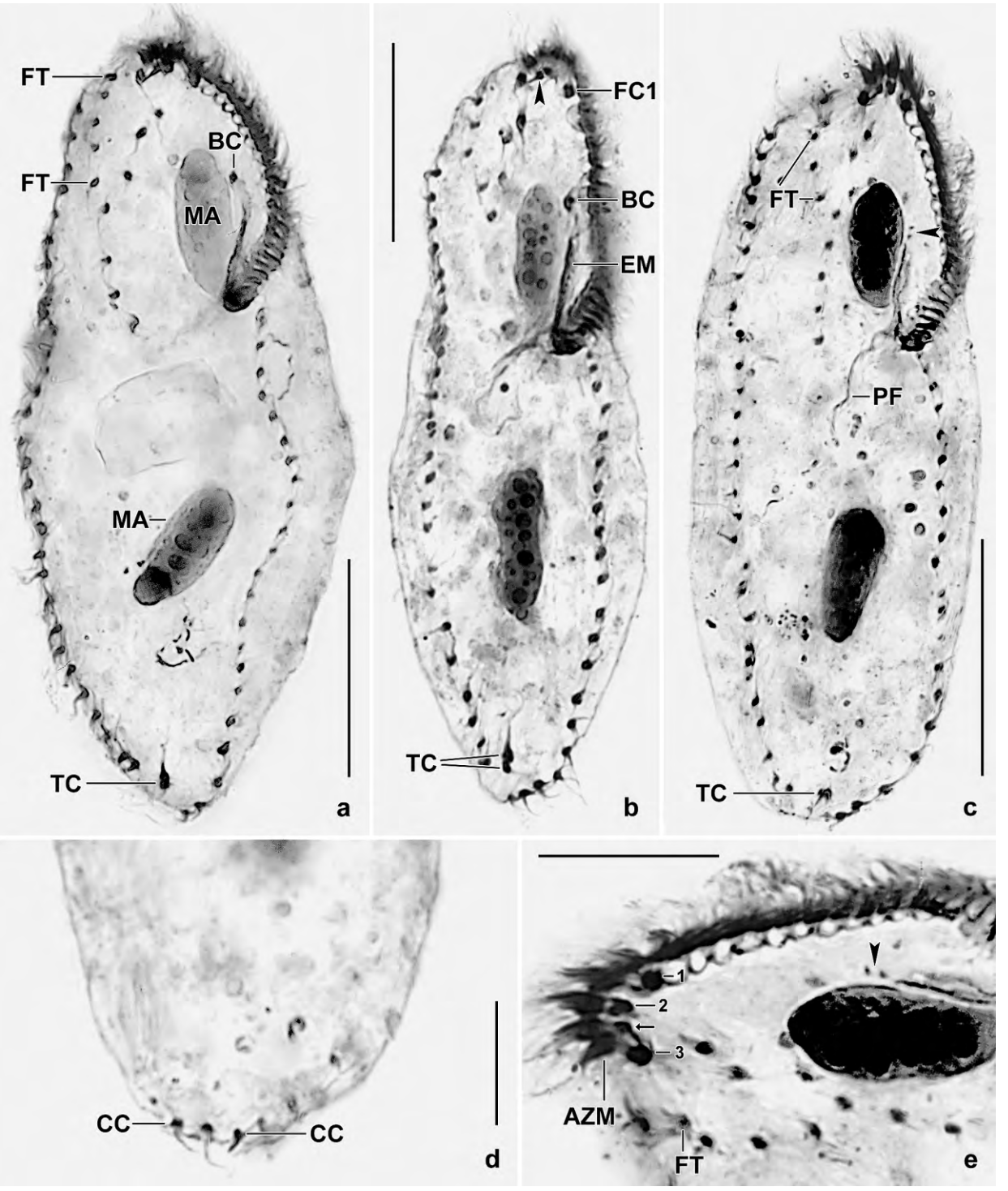

Fig. 220a–e. *Gonostomum halophilum*, infraciliature after protargol impregnation. **a, b:** Ventral overviews with frontal cirrus-like fibre crossing marked by arrowhead (b). **c, e:** Ventral views of same specimen, showing the paroral membrane composed of only two kinetids (arrowheads) and a cirrus-like fibrillar structure between frontal cirri 2 and 3 (arrow). **d:** Dorsal posterior region, showing the caudal cirri. AZM – adoral zone of membranelles, BC – buccal cirrus, CC – caudal cirri, EM – endoral membrane, FC1 – frontal cirrus 1, FT – frontoterminal cirri, MA – macronuclear nodules, PF – pharyngeal fibres, TC – transverse cirri. 1–3 – frontal cirri. Scale bars 10 μm (d, e) and 25 μm (a–c).

Table 81. Morphometric data on *Gonostomum halophilum* (GH) and *Gonostomum salinarum* (GS) based on mounted, protargol-impregnated, and randomly selected specimens from non-flooded Petri dish cultures. Measurements in µm. CV – coefficient of variation in %, M – median, Max – maximum, Mean – arithmetic mean, Min – minimum, n – number of individuals investigated, Pop – population, SD – standard deviation, SE – standard error of arithmetic mean.

Characteristics	Pop	Mean	M	SD	SE	CV	Min	Max	n
Body, length	GH	69.7	69.0	7.2	1.6	10.4	58.0	81.0	21
	GS	70.8	72.0	8.8	1.9	12.4	55.0	88.0	21
Body, width	GH	25.9	26.0	3.5	0.8	13.4	20.0	32.0	21
	GS	27.0	26.0	3.8	0.8	14.1	19.0	34.0	21
Body length:width, ratio	GH	2.7	2.8	0.3	0.1	10.5	2.0	3.0	21
	GS	2.6	2.6	0.3	0.1	9.4	2.3	3.3	21
Anterior body end to proximal end of adoral zone, distance	GH	27.5	28.0	1.4	0.3	5.2	25.0	30.0	21
	GS	36.6	36.0	2.6	0.6	7.1	32.0	43.0	21
Adoral zone of membranelles, percentage of body length	GH	39.7	40.0	3.4	0.8	8.7	35.0	50.0	21
	GS	52.1	51.0	4.6	1.0	8.9	43.0	63.0	21
Adoral membranelles, number	GH	25.6	26.0	1.0	0.2	4.0	24.0	27.0	21
	GS	28.0	28.0	1.1	0.2	3.8	26.0	30.0	21
Largest membranellar basis, width	GH	3.0	3.0	–	–	–	3.0	3.5	16
	GS	4.1	4.0	–	–	–	4.0	4.5	21
Anterior body end to paroral membrane, distance	GH	15.8	16.0	0.9	0.2	5.5	14.0	17.0	15
	GS	18.5	19.0	1.8	0.4	9.9	15.0	21.0	21
Paroral membrane, length	GH	1.2	1.0	0.4	0.1	31.6	0.5	2.0	14
	GS	7.9	7.0	1.7	0.4	21.9	6.0	12.0	21
Paroral membrane, number of kinetids	GH	2.6	2.0	0.9	0.2	33.5	1.0	4.0	21
	GS	10.0	10.0	1.6	0.4	16.0	8.0	13.0	21
Anterior body end to endoral membrane, distance	GH	17.0	17.0	0.7	0.2	4.3	16.0	18.0	16
	GS	23.0	23.0	1.9	0.4	8.2	20.0	27.0	21
Endoral membrane, length	GH	7.9	8.0	0.8	0.2	10.2	7.0	9.0	16
	GS	13.1	13.0	1.3	0.3	9.7	11.0	17.0	21
Anterior body end to first macronuclear nodule, distance	GH	12.0	12.0	1.6	0.4	13.7	8.0	15.0	21
	GS	13.8	14.0	2.1	0.5	15.1	9.0	16.0	21
Macronuclear figure, length	GH	40.6	41.0	4.8	1.2	11.8	32.0	48.0	16
	GS	41.6	42.0	5.8	1.3	14.0	33.0	53.0	21
Macronuclear nodules, distance in between	GH	15.1	16.0	3.1	0.8	20.6	9.0	20.0	16
	GS	11.3	11.0	3.0	0.7	26.6	6.0	16.0	21
Macronuclear nodules, length	GH	13.0	13.0	1.7	0.4	12.8	10.0	16.0	21
	GS	15.8	15.0	3.0	0.7	19.0	8.0	20.0	21
Macronuclear nodules, width	GH	5.1	5.0	0.6	0.1	12.4	4.0	6.0	21
	GS	6.3	6.0	0.9	0.2	14.4	5.0	8.0	21
Macronuclear nodules, number	GH	2.0	2.0	0.0	0.0	0.0	2.0	2.0	21
	GS	2.1	2.0	–	–	–	2.0	3.0	21

continued

Characteristics	Pop	Mean	M	SD	SE	CV	Min	Max	n
Micronuclei, length	GH	1.3	1.5	–	–	–	1.0	1.5	19
	GS	2.1	2.0	–	–	–	2.0	2.5	21
Micronuclei, width	GH	1.0	1.0	–	–	–	0.5	1.0	19
	GS	1.6	1.5	–	–	–	1.0	2.0	21
Micronuclei, number	GH	2.0	2.0	–	–	–	1.0	3.0	19
	GS	2.1	2.0	–	–	–	1.0	3.0	21
Frontal cirri, number	GH	3.0	3.0	0.0	0.0	0.0	3.0	3.0	21
	GS	3.0	3.0	0.0	0.0	0.0	3.0	3.0	21
Anterior body end to buccal cirrus, distance	GH	12.7	13.0	1.0	0.2	7.9	11.0	15.0	21
	GS	19.0	19.0	2.1	0.5	11.3	16.0	23.0	20
Buccal cirri, number	GH	1.0	1.0	0.0	0.0	0.0	1.0	1.0	21
	GS	1.0	1.0	0.0	0.0	0.0	1.0	1.0	21
Anterior body end to rearmost frontoterminal cirrus, distance	GH	12.8	13.0	2.1	0.5	16.7	10.0	16.0	16
	GS	20.1	19.0	4.0	0.9	19.9	15.0	29.0	21
Frontoterminal cirri, number	GH	4.5	4.5	–	–	–	4.0	5.0	16
	GS	4.4	4.0	–	–	–	4.0	5.0	21
Anterior body end to last frontoventral cirrus, distance	GH	26.9	27.0	2.1	0.5	7.9	23.0	30.0	16
	GS	36.9	35.0	5.1	1.1	13.8	27.0	46.0	21
Frontoventral cirri, number	GH	7.8	8.0	0.7	0.2	8.8	7.0	9.0	16
	GS	7.0	7.0	0.9	0.2	12.8	6.0	9.0	21
Posterior body end to rearmost transverse cirrus, distance	GH	2.8	3.0	0.7	0.2	25.9	1.0	4.0	20
	GS	3.6	3.0	0.8	0.2	23.3	2.0	5.0	20
Transverse cirri, number	GH	1.4	1.0	–	–	–	0.0	2.0	21
	GS	2.1	2.0	0.4	0.1	19.2	1.0	3.0	20
Anterior body end to right marginal row, distance	GH	6.3	6.0	1.3	0.3	21.4	4.0	9.0	21
	GS	4.8	5.0	1.0	0.2	20.4	2.0	6.0	21
Posterior body end to right marginal row, distance	GH	3.4	3.0	1.1	0.2	32.0	1.0	5.0	21
	GS	3.2	3.0	1.1	0.2	33.8	1.0	6.0	21
Right marginal row, number of cirri	GH	27.9	27.0	2.6	0.6	9.5	21.0	34.0	21
	GS	21.4	21.0	2.1	0.5	9.8	19.0	25.0	21
Posterior body end to left marginal row, distance	GH	1.0	1.0	–	–	–	0.5	2.0	21
	GS	not measured							21
Left marginal row, number of cirri	GH	20.4	21.0	2.1	0.5	10.2	15.0	24.0	21
	GS	14.9	15.0	1.3	0.3	8.7	13.0	17.0	21
Dorsal kineties, number	GH	3.0	3.0	0.0	0.0	0.0	3.0	3.0	21
	GS	3.0	3.0	0.0	0.0	0.0	3.0	3.0	21
Kinetids in dorsal kinety 2	GH	15.2	15.0	1.4	0.3	9.1	13.0	18.0	16
	GS	13.5	14.0	1.4	0.3	10.7	10.0	16.0	21
Caudal cirri, number	GH	usually 3, rarely 2, see text							
	GS	3.0	3.0	–	–	–	2.0	3.0	21

Gonostomum salinarum **nov. spec.** (Fig. 221a–f, 222a–c; Table 81)

Diagnosis: Size in vivo about 80 × 30 µm; slightly elongate ovate or elongate rectangular. 2 macronuclear nodules and 2 micronuclei. Cortical granules in loose rows, colourless, about 1 × 0.5 µm in size. 3 frontal cirri, 4–5 frontoterminal cirri, 1 buccal cirrus right of anterior end of paroral membrane, and 2 transverse cirri near rear end. 3 dorsal kineties and caudal cirri. Right marginal row composed of an average of 21 cirri, left of 15. Adoral zone flat, extends about 52% of body length, consists of an average of 28 membranelles. On average 10 paroral kinetids with 8–10 µm long cilia.

Type locality: Highly saline (> 30‰, pH 8) coastal soil from the Great Salt Lake in the surroundings of the town of Brigham, Utah, USA, 112°5'W 44°N.

Type material: 1 holotype and 4 paratype slides with protargol-impregnated specimens have been deposited in the Biology Centre of the Upper Austrian Museum in Linz (LI). The holotype and other relevant specimens have been marked by black ink circles on the coverslip.

Etymology: *Salinarum* (living in saline environments) is a noun in plural genetive and thus does not change the neuter when combined with a genus having another gender.

Description: Most features of *G. salinarum* have an ordinary variability (CV ≤ 15%), including those important for the diagnosis of the species (Table 81).

Size in vivo 60–100 × 20–40 µm, usually about 80 × 30 µm, as calculated from some in vivo measurements and the morphometric data in Table 81 adding 15% preparation shrinkage. Body shape very similar to that of *G. affine*, viz., usually slightly elongate ovate, rarely ellipsoid or elongate rectangular; anterior body end narrower rounded than posterior (Fig. 221a, b, 222a, b; Table 81). Nuclear apparatus left of body´s midline, consists of two, very rarely of three macronuclear nodules and two micronuclei. Macronuclear nodules ellipsoid to elongate ellipsoid, anterior nodule in second quarter of cell, posterior in third quarter, both with many ordinary nucleoli. Micronuclei attached to various sites of macronucleus, globular to ellipsoid (Fig. 221a, f, 222a–c; Table 81). Contractile vacuole slightly posterior to proximal end of adoral zone of membranelles. Cortex flexible, contains loose rows of colourless, lenticular granules not impregnating with the method used (Fig. 221c, d). Cytoplasm colourless, contains few to many lipid droplets mainly in posterior quarter of cell and 1–4 µm across. Food vacuoles scattered throughout body, about 7 µm across, contain bacteria. Movement without peculiarities.

Cirri of ordinary length and thickness, arranged as in → *G. strenuum* and → *G. halophilum*, i. e., with comparatively long frontoterminal row and long row V, each composed of four to five cirri (Fig. 221a, e, 222a, b; Table 81). Three slightly enlarged frontal cirri; buccal cirrus right of anterior end of paroral membrane; one to three, on average two transverse cirri about 18 µm long in vivo, project distinctly from body proper. Marginal cirri composed of two rows with three cilia each, about 12 µm long; right row commences subapically and ends terminally, left row extends to body´s midline posteriorly (Fig. 221a, e, 222a, b; Table 81).

Dorsal bristle pattern without peculiarities, bristles 3–4 µm long in vivo and in protargol preparations. Caudal cirri in mid of posterior end (Fig. 221a, f; Table 81).

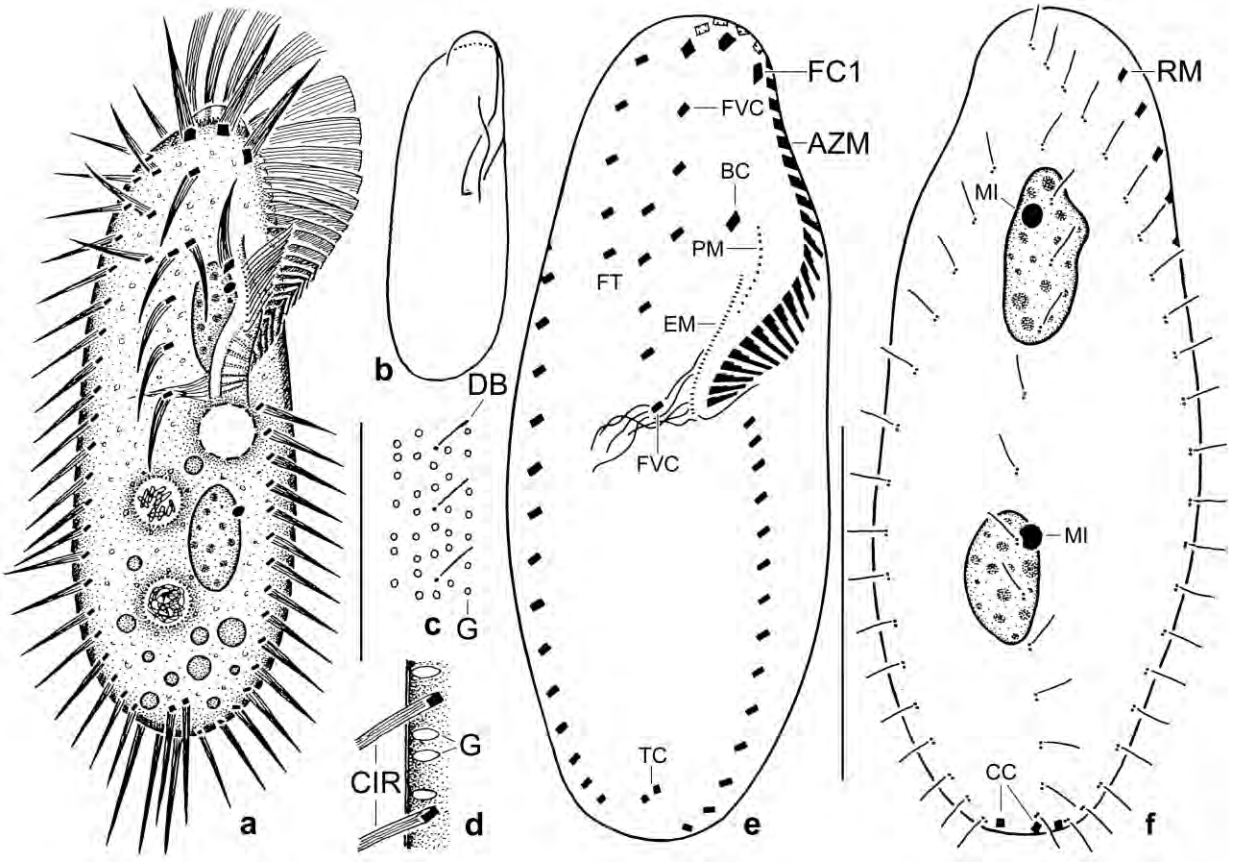

Fig. 221a–f. *Gonostomum salinarum* from life (a–d) and after protargol impregnation (e, f). **a:** Ventral view of a representative specimen, length 80 µm. **b:** Shape variant. **c, d:** Surface view and optical section of cortex, showing the cortical granulation. **e, f:** Ventral and dorsal view of holotype specimen, length 72 µm. AZM – adoral zone of membranelles, BC – buccal cirrus, CC – caudal cirri, CIR – cirri, DB – dorsal bristle, EM – endoral membrane, FC1 – frontal cirrus 1, FT – frontoterminal cirri, FVC – frontoventral cirri, G – cortical granules, MI – micronuclei, PM – paroral membrane, RM – right marginal cirral row, TC – transverse cirri. Scale bars 30 µm.

Oral apparatus in *Gonostomum* pattern (Berger 2011), i. e., the adoral zone follows the anterior and left body margin to bend abruptly into cell at about 52% of body length (Fig. 221a, e, 222a, b; Table 81). Adoral zone flat, composed of an average of 28 gonostomoid membranelles with largest bases 4–5 µm long in vivo and in protargol preparations. Buccal cavity narrow, covered by a convex lip bearing paroral membrane composed of an average of 10 kinetids with 8–10 µm long cilia. Endoral membrane commences near mid and right of paroral, extends to proximal end of adoral zone of membranelles. Pharyngeal fibres extend slightly obliquely to right body margin (Fig. 221a, b, e, 222a, b; Table 81).

Occurrence and ecology: As yet found only at type locality, viz., in soil mixed with halophyte litter from a dry, flat pond on the coast of the Great Salt Lake in the surroundings of the town of Brigham.

Remarks: *Gonostomum salinarum* is most similar to the Australian *G. halophilum* but differs distinctly in the following, non-connected features (Table 81): length of adoral zone of membranelles (52% vs. 40% of body length), number of marginal cirri (36 vs. 48), number of

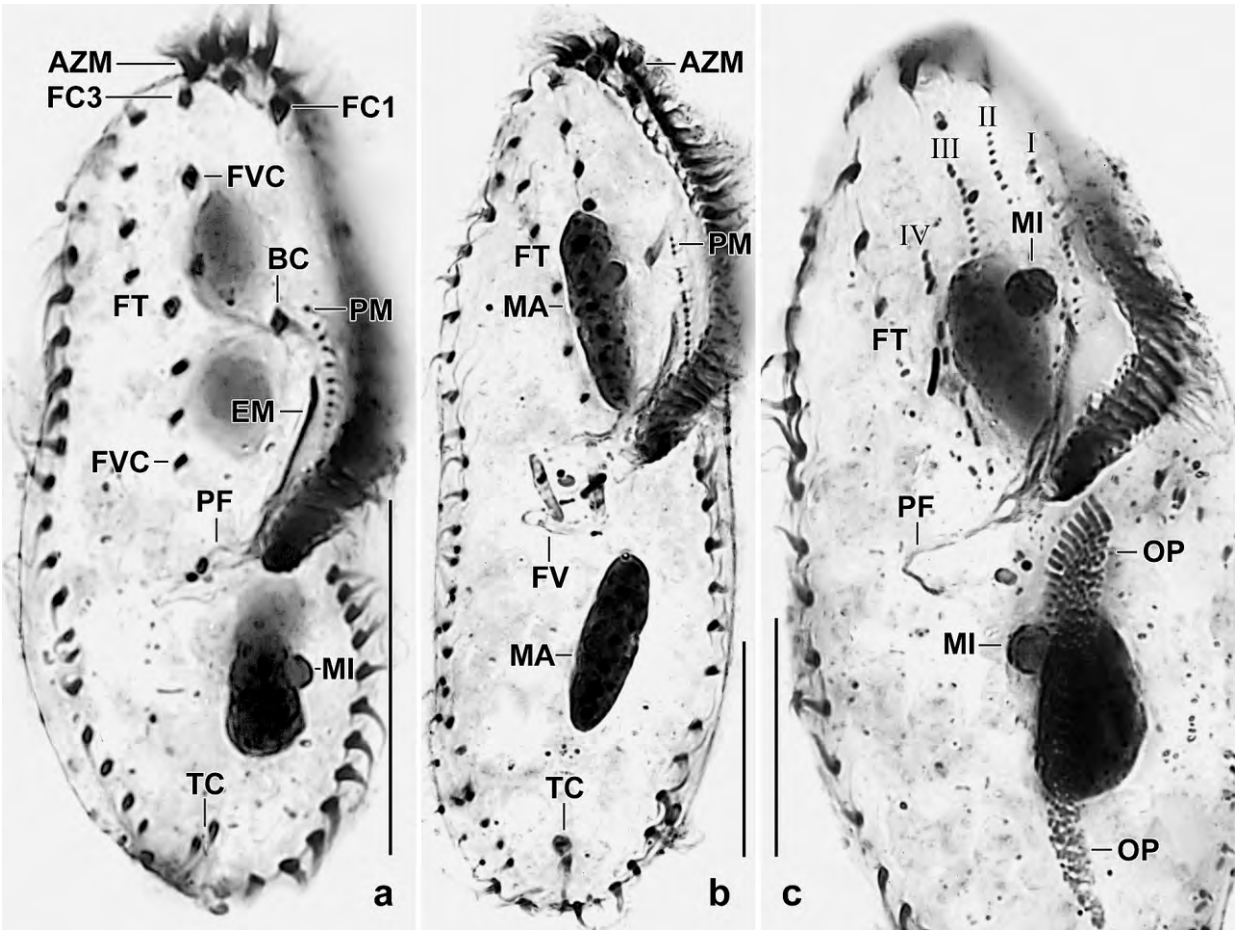

Fig. 222a–c. *Gonostomum salinarum*, ventral views after protargol impregnation. **a:** A specimen with three macronuclear nodules and ordinary cirral pattern. The paroral membrane consists of 10 kinetids with 8–10 µm long cilia. **b:** A specimen with 14 paroral kinetids in three groups. A food vacuole is just forming. **c:** An early divider, showing the large oral primordium, the inflated micronuclei, and four cirral anlagen in the proter. AZM – adoral zone of membranelles, BC – buccal cirrus, EM – endoral membrane, FC1, 3 – frontal cirri, FT – frontoterminal cirri, FV – food vacuoles, FVC – frontoventral cirri, MA – macronuclear nodules, MI – micronuclei, OP – oral primordium, PF – pharyngeal fibres, PM – paroral membrane, TC – transverse cirri, I–IV – cirral anlagen. Scale bars 20 µm (b, c) and 30 µm (a).

paroral kinetids (10 vs. 2), length of endoral membrane (13 µm vs. 8 µm), and location of buccal cirrus (right vs. far anterior of distal end of paroral membrane). The most important features are the number of paroral kinetids and the location of the buccal cirrus.

Gonostomum caudatulum Foissner & Heber **nov. spec.** (Fig. 223a–e, 224a–d; Tables 82, 83)

Diagnosis: Size in vivo about 85 × 30 µm. Outline roughly pisciform, posterior end narrowed to a short tail. 2 ellipsoid macronuclear nodules and 2 globular micronuclei. 3 frontal cirri, 2 frontoterminal cirri, 1 buccal cirrus right of anterior end of paroral membrane, on average 4 frontoventral cirri anterior of buccal vertex, and 5 subterminal transverse cirri. Right marginal row on average composed of 13 cirri, left of 9. Dorsal bristles gradually elongated from 3 µm

anteriorly to 8 µm posteriorly. Caudal cirri thin, about 20 µm long in vivo. Adoral zone extends about 58 % of body length, usually consists of 29 membranelles; paroral membrane about 1.2 times the length of endoral, on average consists of 12 wide-spaced (~ 1 cilium / µm) cilia.

Type locality: Sieved sand with much plant debris from the grass zone of a Resting area about 100 m off the sea, outskirts of Rio de Janeiro, Brazil, 22°54'S 43°12'W.

Type material: 1 holotype and 3 paratype slides with protargol-impregnated specimens have been deposited in the Biology Centre of the Upper Austrian Museum in Linz (LI). Relevant specimens have been marked by black ink circles on the coverslip.

Etymology: Diminutive of the Latin participle *caudatum* (having a tail, tailed), referring to the tail-like body end, an important feature of this species.

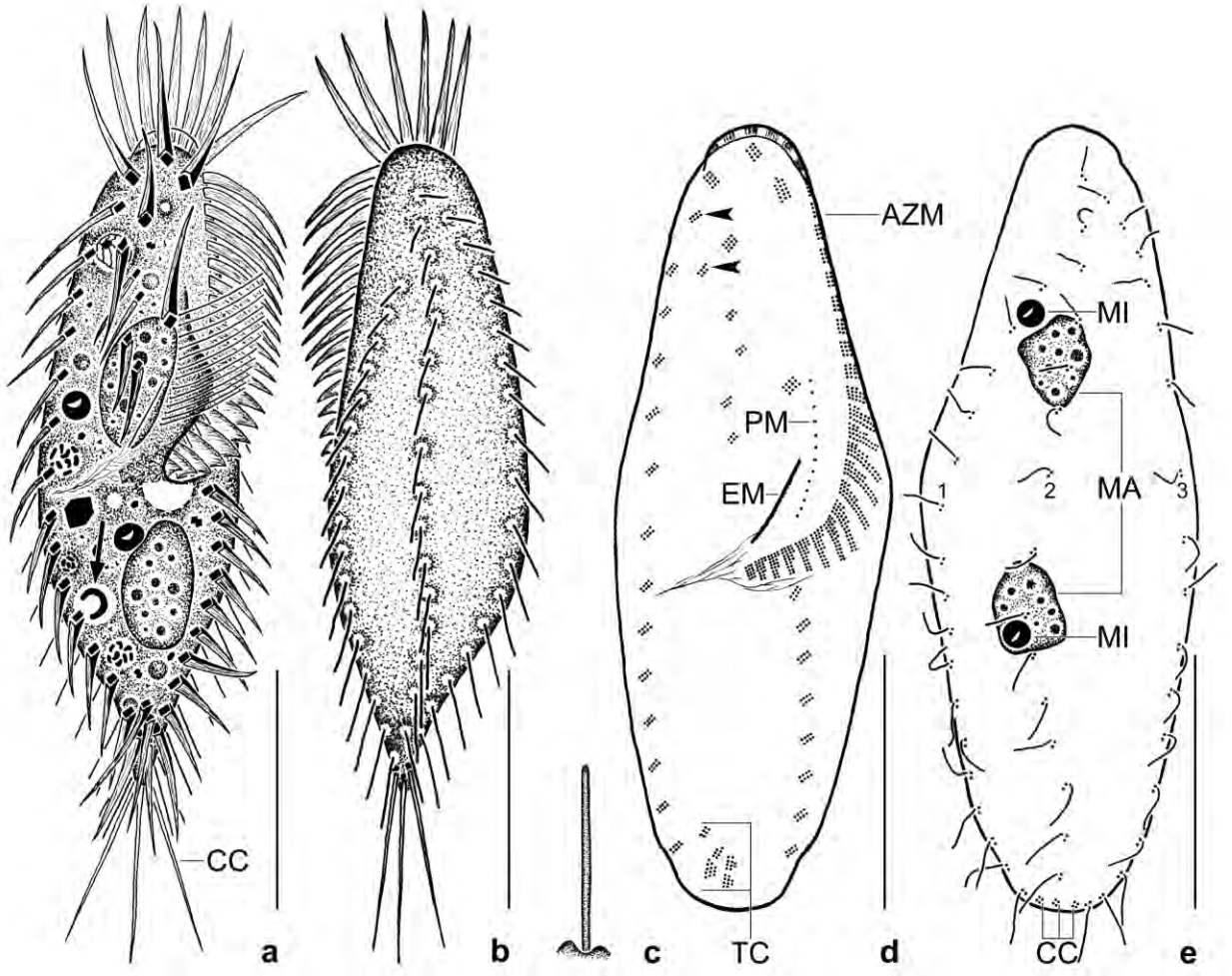

Fig. 223a–e. *Gonostomum caudatulum* from life (a–c) and after protargol impregnation (d, e). **a:** Ventral view of a representative specimen having ingested bacteria and a flagellate, length 70 µm. The arrow marks a single, semi-circular bacterium. **b:** Dorsal view, showing the dorsal bristles gradually elongated posteriorly. **c:** Dorsal bristle. **d, e:** Ventral and dorsal view of holotype specimen, showing the infraciliature, the nuclear apparatus, and the long paroral with wide-spaced cilia, length 77 µm. The arrowheads denote the frontoterminal cirri. 1–3 – dorsal kineties, AZM – adoral zone of membranelles, CC – caudal cirri, EM – endoral membrane, MA – macronuclear nodules, MI – micronuclei, PM – paroral membrane, TC – transverse and pretransverse cirri. Scale bars 25 µm.

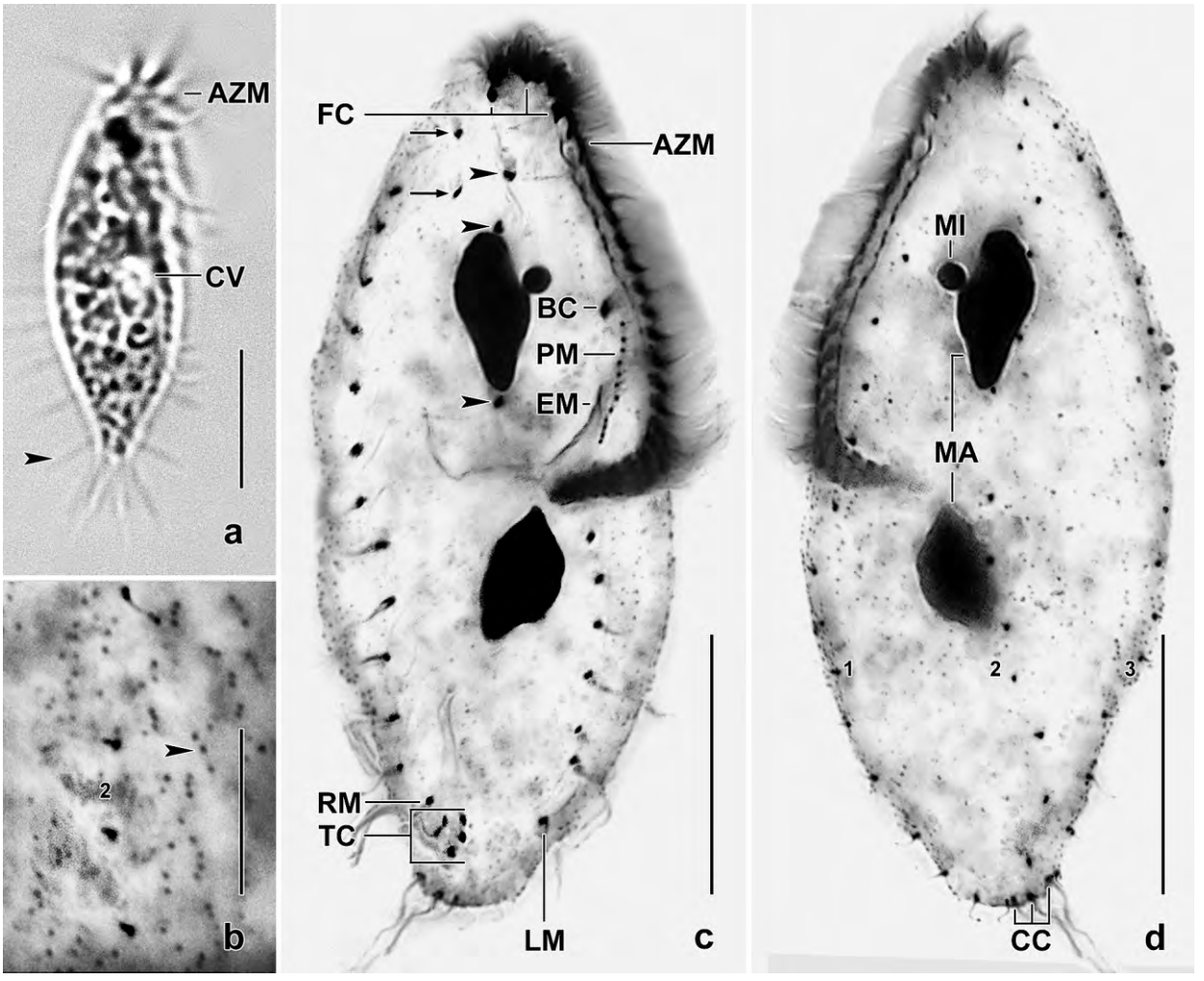

Fig. 224a–d. *Gonostomum caudatulum* from life (a) and after protargol impregnation (b–d). **a:** Ventral view of a representative specimen, length 70 µm. Although the micrograph is unsharp, it shows two important features clearly: the narrowed, tail-like posterior body region and the posteriorly elongated dorsal bristles (arrowhead). **b:** Surface view, showing the minute cortical granules (arrowhead). **c, d:** Ventral and dorsal view of an inflated specimen, showing the ciliature and the nuclear and oral apparatus, length 84 µm. Frontoterminal cirri marked by arrows, arrowheads denote the frontoventral cirri. One frontoventral cirrus and a micronucleus are hidden by the anterior, respectively, posterior macronuclear nodule. 1–3 – dorsal kineties, AZM – adoral zone of membranelles, BC – buccal cirrus, CC – caudal cirri, CV – contractile vacuole, EM – endoral membrane, FC – frontal cirri, LM – left marginal cirral row, MA – macronuclear nodules, MI – micronucleus, PM – paroral MEMBRANE, RM – right marginal cirral row, TC – transverse and pretransverse cirri. Scale bars 10 µm (b) and 25µm (a, c, d).

Description: Unfortunately, only 11 poorly fixed (see high CV of body width, Table 82) protargol-impregnated specimens were available for the morphometric analysis. However, the main features, i. e., the gradually elongated dorsal bristles and the tail-like posterior body end are well supported by the life observations (Fig. 224a).

Size about 85 × 30 µm in vivo. Body flexible and colourless. Outline narrowly to ordinarily pisciform with broadest region usually posterior to mid-body; left body margin in vivo less convex than right; anterior body end distinctly narrowed, tail-like posterior end hardly recognizable in the inflated, protargol-impregnated specimens (Fig. 223a, b, 224a). Nuclear apparatus slightly

left of main body axis within central quarters of cell, consists of two macronuclear nodules and usually two (0–4) micronuclei (Fig. 223a, e, 224d; Table 82). Individual nodules rotund to narrowly ellipsoid, on average 14 × 7 µm in protargol preparations; nucleoli up to 1.5 µm across. Micronuclei globular to ellipsoid, about 2.8 × 2.6 µm after protargol impregnation. Cortical granules not seen in vivo, but loose rows of minute (~ 0.5 µm) granules recognizable in 3 out of 11 protargol-impregnated cells. Contractile vacuole in mid-body slightly left of cell centre (Fig. 223a, 224a). Cytoplasm colourless, contains 1–4 µm-sized crystals. Food vacuoles scattered throughout cytoplasm, about 5 µm across, contain bacteria and flagellates (Fig. 223a). Hurries to and fro, frequently changing direction.

Cirral pattern as typical for *Gonostomum* (Berger 2011) and shown in Figures 223a, d, and 224c. Invariably three frontal cirri in convex pattern following anterior body margin, thickened and about 15 µm long in protargol preparations. Two frontoterminal cirri, anterior cirrus in gap between right marginal row and adoral zone, posterior cirrus at level of uppermost right marginal cirrus, in protargol preparations about 12 µm long. Usually four (three to five) frontoventral cirri in coarse row not extending beyond buccal vertex, anteriormost cirrus usually thickened, 8–10 µm long. Buccal cirrus right of anterior end of paroral, thickened and about 12 µm long. Five transverse/pretransverse cirri at base of tail and in gap between marginal rows, three cirri thickened, two ordinary, about 12 µm long in vivo and in protargol preparations. Marginal cirral rows end subterminally, right row commences at level of posterior frontoterminal cirrus, on average consists of 13 cirri, left of 9; cirri composed of two kineties with cilia 8–10 µm long in vivo and after protargol impregnation (Fig. 223d, 224c; Table 82).

About 51 dorsal bristles in three rows; row 1 slightly shortened anteriorly. Bristles carefully observed in vivo, stiff and obliquely directed backwards, gradually increase in length from 3 µm anteriorly to 8 µm posteriorly and from 2.5 µm to 6 µm in protargol preparations, respectively. Three caudal cirri, one at end of each bristle row, composed of only few basal bodies with cilia in vivo up to 20 µm long, about 12 µm in protargol preparations (Fig. 223a–c, e, 224a, d; Table 82).

Oral apparatus in *Gonostomum* pattern (Berger 2011), i. e., adoral zone follows body margin and bends abruptly into cell at about 58 % of body length; on average composed of 29 ordinary membranelles, bases of largest membranelles about 5 µm long in protargol preparations, cilia about 15 µm long in vivo and 12 µm after protargol impregnation (Fig. 223a, d, 224c; Table 82). Endoral membrane ordinary, proximal end near buccal vertex, about 11 µm long. Paroral membrane commences at level of buccal cirrus, on average 12 µm long after protargol impregnation, composed of comparatively widely spaced cilia (about 1 cilium / µm) with spacing often gradually increasing anteriorly; cilia about 10 µm long in vivo. Buccal lip covers buccal cavity, sometimes conspicuously enlarged and then projecting from body margin, hyaline, soon becoming undetectable under slight coverslip pressure. Pharyngeal fibres directed to right body margin, about 10 µm long in protargol preparations.

Occurrence and ecology: As yet found only at the sandy, slightly saline (10 ‰) and acidic (pH 5.2) type locality. The slender shape, the tail, and the long dorsal bristles and caudal cirri of *G. caudatulum* could be adaptations to the sandy habitat.

Table 82. Morphometric data on *Gonostomum caudatulum* based on mounted and protargol-impregnated specimens from a non-flooded Petri dish culture. Data should be used and interpreted with care because the specimens were poorly fixed. Measurements in µm. CV – coefficient of variation in %, M – median, Max – maximum, Mean – arithmetic mean, Min – minimum, n – number of individuals investigated, SD – standard deviation, SE – standard error of arithmetic mean.

Characteristics	Mean	M	SD	SE	CV	Min	Max	n
Body, length	72.6	71.0	11.2	3.4	15.5	57.0	95.0	11
Body, width	32.1	32.0	7.0	2.1	21.7	22.0	45.0	11
Body length:width, ratio	2.3	2.4	0.5	0.2	21.9	1.6	3.0	11
Macronuclear nodules, number	2.0	2.0	0.0	0.0	0.0	2.0	2.0	11
Micronuclei, number	1.5	2.0	1.1	0.3	73.0	0.0	4.0	11
Anterior macronuclear nodule, length	13.6	14.0	2.5	0.8	18.6	10.0	18.0	11
Anterior macronuclear nodule, width	6.8	7.0	1.0	0.3	14.4	5.0	8.0	11
Anterior macronuclear nodule length:width, ratio	2.0	2.2	0.5	0.2	24.8	1.3	2.8	11
Anterior micronucleus, length	2.8	2.8	–	–	–	2.4	3.2	9
Anterior micronucleus, width	2.6	2.8	0.6	0.2	24.1	1.2	3.2	9
Adoral zone of membranelles, length	42.0	43.0	4.3	1.3	10.3	34.0	47.0	11
Adoral zone of membranelles, percentage of body length	58.4	58.4	5.9	1.8	10.1	46.3	65.7	11
Adoral membranelles, number	28.6	29.0	2.5	0.9	8.8	24.0	32.0	7
Adoral membranelles, width of largest membranellar basis	4.6	5.0	–	–	–	4.0	5.0	11
Paroral membrane, number of cilia	12.3	12.5	1.9	0.6	15.4	9.0	15.0	10
Paroral membrane, length	12.4	12.5	2.0	0.6	15.8	9.0	15.0	10
Paroral, cilia per µm (calculated from the two features above)	1.0	1.0	–	–	–	0.9	1.1	11
Endoral membrane, length	10.8	11.0	1.5	0.5	13.8	8.0	12.0	8
Paroral:endoral length, ratio	1.2	1.2	0.1	0.1	11.9	1.0	1.4	8
Frontal cirri, number	3.0	3.0	0.0	0.0	0.0	3.0	3.0	9
Frontoterminal cirri, number	2.0	2.0	0.0	0.0	0.0	2.0	2.0	9
Anterior body end to last ventral cirrus, distance	29.3	30.5	3.8	1.2	13.1	22.0	34.0	10
Ventral cirri, number	4.4	4.5	0.7	0.2	15.9	3.0	5.0	10
Buccal cirri, number	1.0	1.0	0.0	0.0	0.0	1.0	1.0	9
Transverse and pretransverse cirri, number	5.0	5.0	0.0	0.0	0.0	5.0	5.0	7
Frontal-ventral-transverse cirri, total number	15.2	15.0	0.8	0.3	5.0	14.0	16.0	6
Right marginal row, number of cirri	13.4	13.5	1.1	0.4	7.9	12.0	15.0	8
Left marginal row, number of cirri	8.6	9.0	1.0	0.3	11.8	7.0	10.0	9
Caudal cirri, number	3.0	3.0	0.0	0.0	0.0	3.0	3.0	4
Dorsal kineties, number	3.0	3.0	0.0	0.0	0.0	3.0	3.0	11
Dorsal kinety 1, number of bristles	16.5	16.5	2.1	0.8	12.6	14.0	20.0	6
Dorsal kinety 2, number of bristles	14.7	15.0	2.1	0.8	14.0	12.0	17.0	7
Dorsal kinety 3, number of bristles	18.6	18.0	1.5	0.7	8.2	17.0	21.0	5
Dorsal bristles, total number	50.6	51.0	5.2	2.3	10.2	44.0	58.0	5

Remarks: The combination of a tailed posterior body end and gradually elongated dorsal bristles is unique within the genus. A tail occurs also in *G. namibiense* and *Urosoma macrostoma* (incertae sedis in Gonostomum, BERGER 2011) but G. namibiense lacks long dorsal bristles and differs in the cirral pattern while *U. macrostoma* stands out by its densely arranged paroral cilia, indicating that it does not belong to the genus.

Table 83. Comparison of main morphometrics of *Gonostomum caudatulum* from Brazil and of *Gonostomum affine* populations from Austria, Saudi Arabia, Namibia (sites 26 and 31), Venezuela, Brazil, and Galápagos (original data). Data based on mounted, protargol-impregnated, and randomly selected specimens from non-flooded Petri dish cultures. Measurements in µm: first value arithmetic mean; minimum and maximum in parentheses. Data of the Austrian, Saudi Arabian, Namibian, Venezuelan, and Brazilian *G. affine* are from FOISSNER et al. (2001).

Characteristics	Austria	Saudi Arabia	Namibia (site 26)	Namibia (site 31)	Venezuela	Brazil	Galápagos	*G. caudatulum*
Body, length	79.0 (63–100)	68.8 (50–85)	60.5 (50–75)	75.8 (67–97)	72.5 (60–82)	81.0 (70–93)	68.9 (58–79)	72.6 (57–95)
Body, width	34.7 (28–44)	28.6 (21–35)	29.2 (21–37)	31.8 (26–40)	29.9 (20–40)	32.8 (24–41)	42.3 (36–49)	32.1 (22–45)
Adoral zone, length	41.9 (29–55)	33.2 (26–40)	29.2 (25–42)	36.6 (34–40)	33.2 (29–38)	39.2 (36–44)	34.9 (31–38)	42.0 (34–47)
Adoral membranelles, number	28.8 (23–35)	21.5 (17–24)	22.0 (18–27)	25.9 (24–28)	24.7 (21–27)	27.1 (25–29)	27.8 (25–30)	28.6 (24–32)
Paroral, number of cilia	13.6 (8–19)	10.6 (5–14)	8.6 (6–12)	10.2 (6–14)	9.0 (6–11)	12.5 (6–16)	11.3 (8–15)	12.3 (9–15)
Paroral, length	9.9[a]	7.8[a]	7.2[a]	7.9[a]	4.9[a]	9.6[a]	8.4 (5–13)	12.4 (9–15)
Paroral, cilia per µm	1.1[a]	1.3[a]	1.4[a]	1.1[a]	1.6[a]	1.4[a]	1.4 (1.1–1.8)	1.0 (0.9–1.1)
Endoral, length	10.8[a]	15.6[a]	11.6[a]	12.8[a]	12.4[a]	13.1[a]	12.9 (10–14)	10.8 (8–12)
Paroral:endoral, length ratio	0.9[a]	0.5[a]	0.6[a]	0.6[a]	0.4[a]	0.7[a]	0.7 (0.4–1.1)	1.2 (1.0–1.4)
Anterior body end to last ventral cirrus, distance	33.6 (22–49)	25.9 (21–32)	17.6 (13–28)	21.7 (18–25)	26.5 (21–30)	26.2 (19–32)	26.4 (22–30)	29.3 (22–34)
Ventral cirri, number	5.5 (5–7)	5.9 (4–7)	3.8 (3–6)	4.8 (3–6)	5.0 (4–6)	3.1 (3–5)	5 (5–5)	4.4 (3–5)
Transverse cirri, number	4.7 (3–6)	1.0 (0–1)	2.6 (0–4)	4.0 (3–4)	4.0 (3–6)	3.9 (2–4)	4.8 (2–7)	5.0 (5–5)
Frontal-ventral-transverse cirri, total number	16.1 (14–18)	13.7 (11–15)	12.3 (10–15)	14.7 (13–16)	14.8 (14–17)	12.9 (10–15)	15.8 (13–18)	15.2 (14–16)
Right marginal row, number of cirri	16.6 (10–21)	17.8 (12–23)	16.5 (11–20)	19.5 (16–26)	17.7 (13–23)	18.8 (15–22)	21.2 (18–25)	13.4 (12–15)
Left marginal row, number of cirri	11.0 (7–15)	11.8 (6–16)	12.3 (8–22)	14.8 (12–17)	12.6 (10–16)	12.3 (11–15)	14.0 (12–16)	8.6 (7–10)
Specimens investigated, number	21	21	21	21	21	21	15	4–11

[a] According to Fig. 8 (Austria), 11 (Saudi Arabia), 7 (Namibian site 26), 10 (Namibian site 31), 12 (Venezuela), and 9 (Brazil) in FOISSNER et al. (2001).

Gonostomum caudatulum is morphologically and morphometrically (Table 83) possibly most closely related to *G. affine* because of the similar cirral pattern and the occurrence of G. affine populations with long dorsal bristles or a tail (for a review, see BERGER 2011). GELLÈRT (1956) reported long dorsal bristles for *G. bryonicolum* and *G. spirotrichoides*, and BUITKAMP (1977b) for *Trachelostyla affine*. However, these species are tailless and details about their dorsal bristles are lacking. A tail-like posterior body end has been reported also for *G. geleii* by GELLÈRT (1957), unfortunately without any information about the dorsal side. Nonetheless, synonymy with *G. caudatulum* seems unlikely because, according to his illustration, *G. geleii* has a lower number of

frontal-ventral-transverse cirri (11 vs. 15) and adoral membranelles (17 vs. 29).

The gradually elongated dorsal bristles and the tailed body end of *G. caudatulum* are best observed in vivo. A morphometric comparison of *G. caudatulum* with several *G. affine* populations (Table 83) reveals that only the spacing of the paroral cilia (0.9–1.1 cilia / µm vs. 1.1–1.8) and the paroral:endoral length ratio (1.0–1.4 vs. 0.4–1.1) are possibly of value for separating these species in protargol preparations.

Gonostomum singhii Kamra, Kumar & Sapra, 2008 (Fig. 225a–h, 226a–g, 227a–d, 228a–g; Table 84)

Improved diagnosis (for three populations, i. e., including the Indian type): Size in vivo about 70 × 26 µm or 100 × 32 µm; elongate ellipsoid. 2 ordinarily spaced macronuclear nodules. Cortical granules in loose rows, about 2 × 1 µm in size. 3 frontal cirri, 2 frontoterminal cirri, 1 buccal cirrus right of anterior end of paroral membrane, 2 frontoventral cirral pairs, 2 pretransverse cirri in special pattern, and 4 transverse cirri. Right marginal row composed of an average of 17–19 cirri, left of 13. Dorsal bristles 3–4 µm long; 3 thin caudal cirri. Adoral zone slightly sigmoid, extends about 53% of body length, consists of an average of 27 or of 34 membranelles; undulating membranes long, paroral composed of 15–19 kinetids on average.

Type locality: Soil from the Valley of Flowers National Park, India, 30°41’ to 30°48’N and 79°33’ to 79°46’E.

Voucher slides: 4 voucher slides with protargol-impregnated Australian specimens have been deposited in the Biology Centre of the Upper Austrian Museum in Linz (LI). The main voucher specimen and other relevant cells have been marked by black ink circles on the coverslip. Furthermore, 6 voucher slides from the Venezuelan population have been deposited in the same repository.

Etymology: The species name is derived from *singhi*, the local name of the common Indian food fish *Heteropneustus fossilis* whose long barbles resemble the frontal membranelles of the ciliate.

Redescription: We studied two populations, one from Australia where many specimens occurred, and another from Venezuelan site (24), where only seven cells were found in the protargol slides, one strongly inflated and thus excluded from width measurement (Table 84). Both populations are so similar that they are described together.

Size in vivo 80–115 × 30–45 µm, usually about 100 × 32 µm, as calculated from some live measurements and the morphometric data in Table 84 adding 15% preparation shrinkage. Body shape inconspicuous, i. e., elongate ellipsoid with anterior region more narrowed than posterior; laterally flattened up to 2:1 (Fig. 225a, d, f, 226a–d, 227a, 228b, g; Table 84). Two ellipsoid to very elongate ellipsoid macronuclear nodules with many ordinary nucleoli. Micronuclei highly variable in number, on average three and two in Australian and Venezuelan specimens, respectively; globular to ellipsoid, on average broadly ellipsoid (Fig. 226a–d, 227a, d, 228a–c, g; Table 84). Contractile vacuole posterior and right of buccal vertex, with long collecting canals

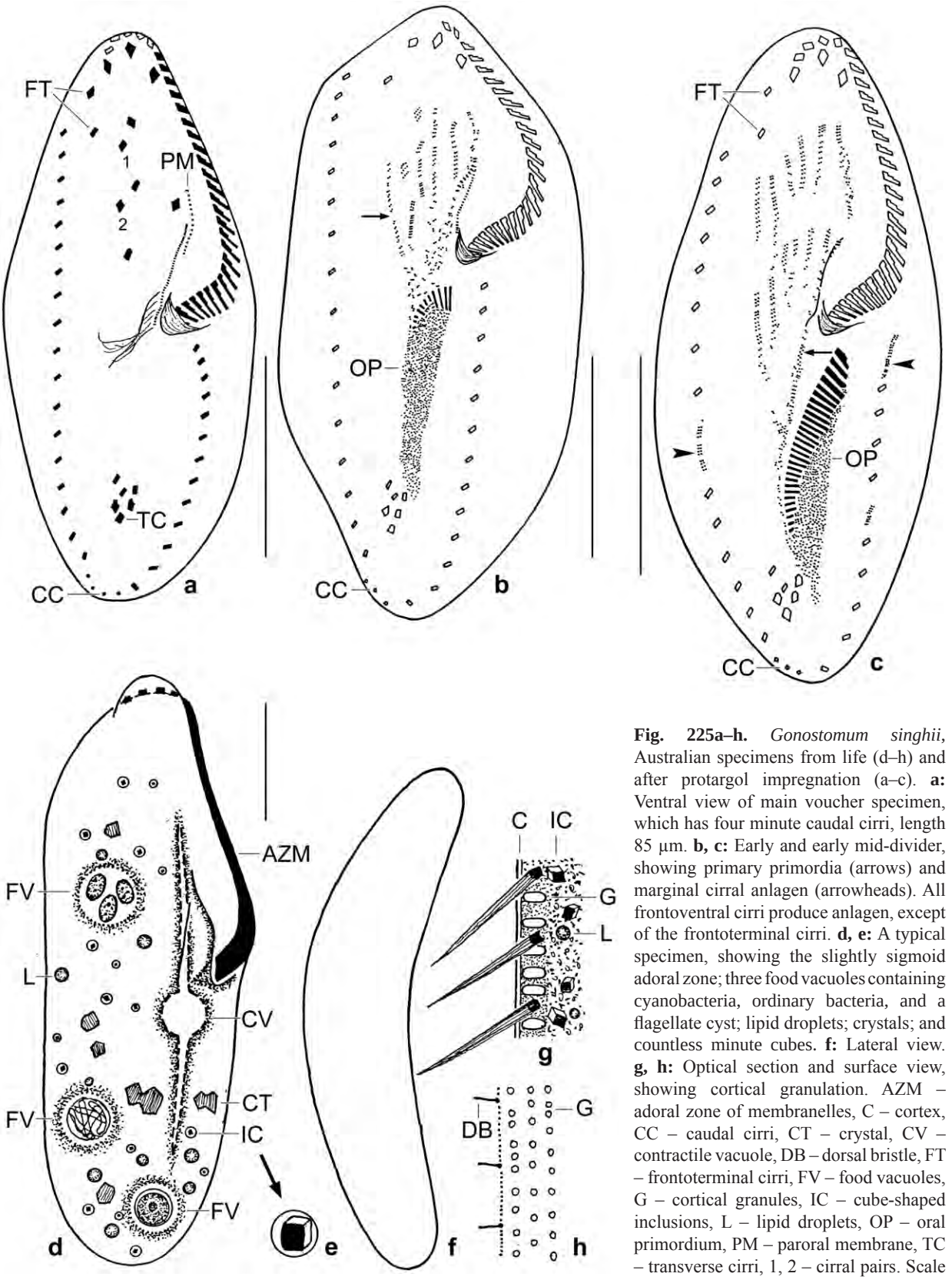

Fig. 225a–h. *Gonostomum singhii*, Australian specimens from life (d–h) and after protargol impregnation (a–c). **a:** Ventral view of main voucher specimen, which has four minute caudal cirri, length 85 µm. **b, c:** Early and early mid-divider, showing primary primordia (arrows) and marginal cirral anlagen (arrowheads). All frontoventral cirri produce anlagen, except of the frontoterminal cirri. **d, e:** A typical specimen, showing the slightly sigmoid adoral zone; three food vacuoles containing cyanobacteria, ordinary bacteria, and a flagellate cyst; lipid droplets; crystals; and countless minute cubes. **f:** Lateral view. **g, h:** Optical section and surface view, showing cortical granulation. AZM – adoral zone of membranelles, C – cortex, CC – caudal cirri, CT – crystal, CV – contractile vacuole, DB – dorsal bristle, FT – frontoterminal cirri, FV – food vacuoles, G – cortical granules, IC – cube-shaped inclusions, L – lipid droplets, OP – oral primordium, PM – paroral membrane, TC – transverse cirri, 1, 2 – cirral pairs. Scale bars 20 µm (d, e) and 30 µm (a–c).

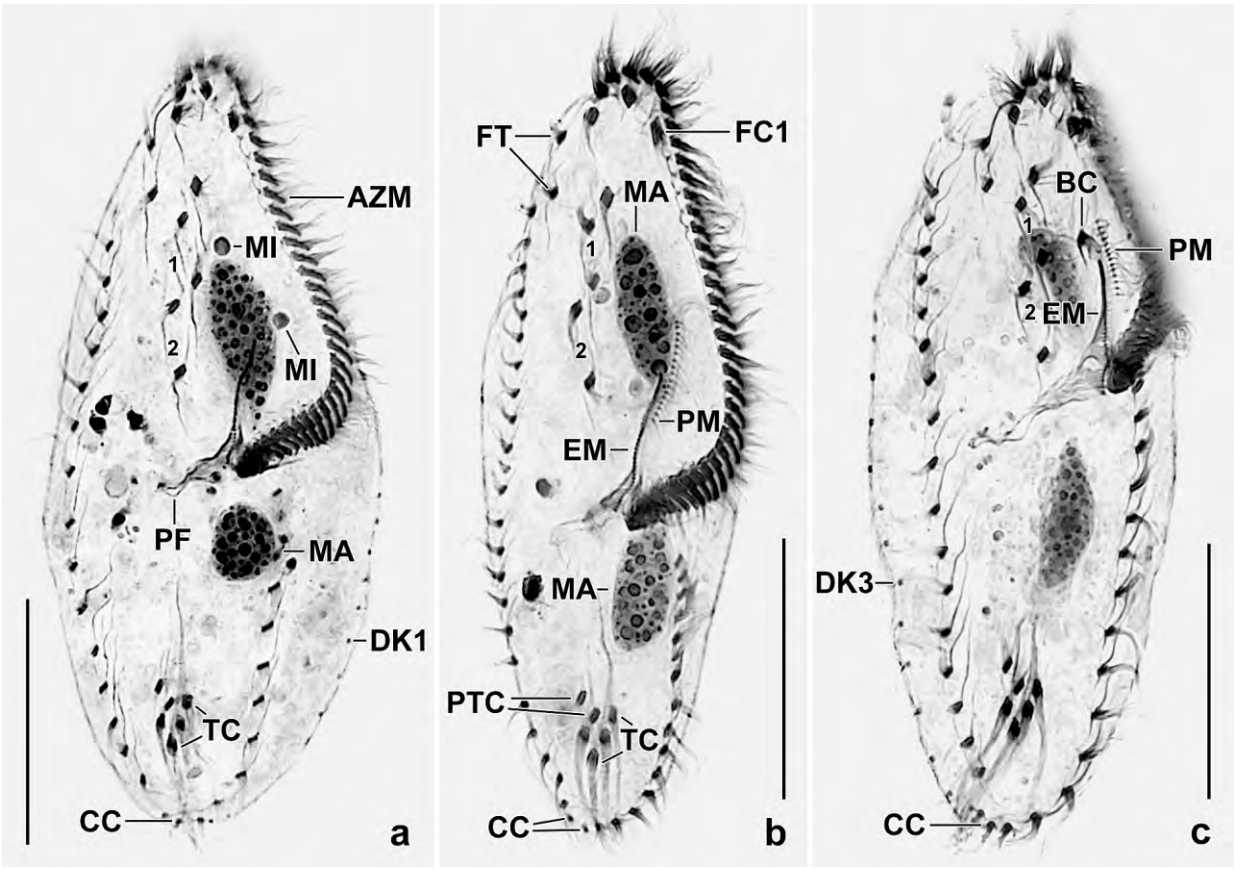

Fig. 226a–c. *Gonostomum singhii*, ventral views of Australian specimens after protargol impregnation. **a:** A specimen showing the slightly sigmoid adoral zone of membranelles. **b, c:** Note the long paroral membrane; the two pretransverse and the four transverse cirri, a very stable pattern. Figure (c) shows a specimen with short adoral zone of membranelles, i. e., 40% of body length. AZM – adoral zone of membranelles, BC – buccal cirrus, CC – caudal cirri, DK1, 3 – dorsal kineties, EM – endoral membrane, FC1 – frontal cirrus 1, FT – frontoterminal cirri, MA – macronuclear nodules, MI – micronuclei, PF – pharyngeal fibres, PM – paroral membrane, PTC – pretransverse cirri, TC – transverse cirri, 1, 2 – frontoventral cirral pairs. Scale bars 30 µm.

(Fig. 225d). Cortex very flexible, contains loose rows of colourless granules about 2 × 1 µm in size (Fig. 225g, h, 227a, b), elongate to about 50 µm long filaments after extrusion. Cytoplasm colourless, contains three types of inclusions: (i) a moderate number of crystals 2–10 µm in size; (ii) innumerable cube-shaped structures each in a vacuole and 1–2 µm in size, lacking in a second Australian population; (iii) a moderate number of lipid droplets 2–4 µm in size (Fig. 225d, e, 227a, b); in two out of the seven Venezuelan specimens occur lenticular, deeply impregnating structures, possibly bacteria (Fig. 228f). Food vacuoles 7–10 µm across, contain coccal cyanobacteria, ordinary bacteria, flagellate cysts, and a heterotrophic euglenid (*Peranema* sp.; Fig. 225d, 227a). Swims and creeps rather slowly.

Cirri arranged in *Gonostomum* pattern shown in Berger (1999, 2011) and in Figures 225a, 226a–d, 227a, c, 228b, g. Invariably three slightly thickened frontal cirri in strongly convex pattern following anterior body margin; frontal cirrus 1 not enlarged. Two frontoterminal cirri in gap between adoral zone and right marginal cirral row. Buccal cirrus subapical and right of paroral membrane (Venezuelan specimens) or right of its anterior end (Australian specimens). Usually

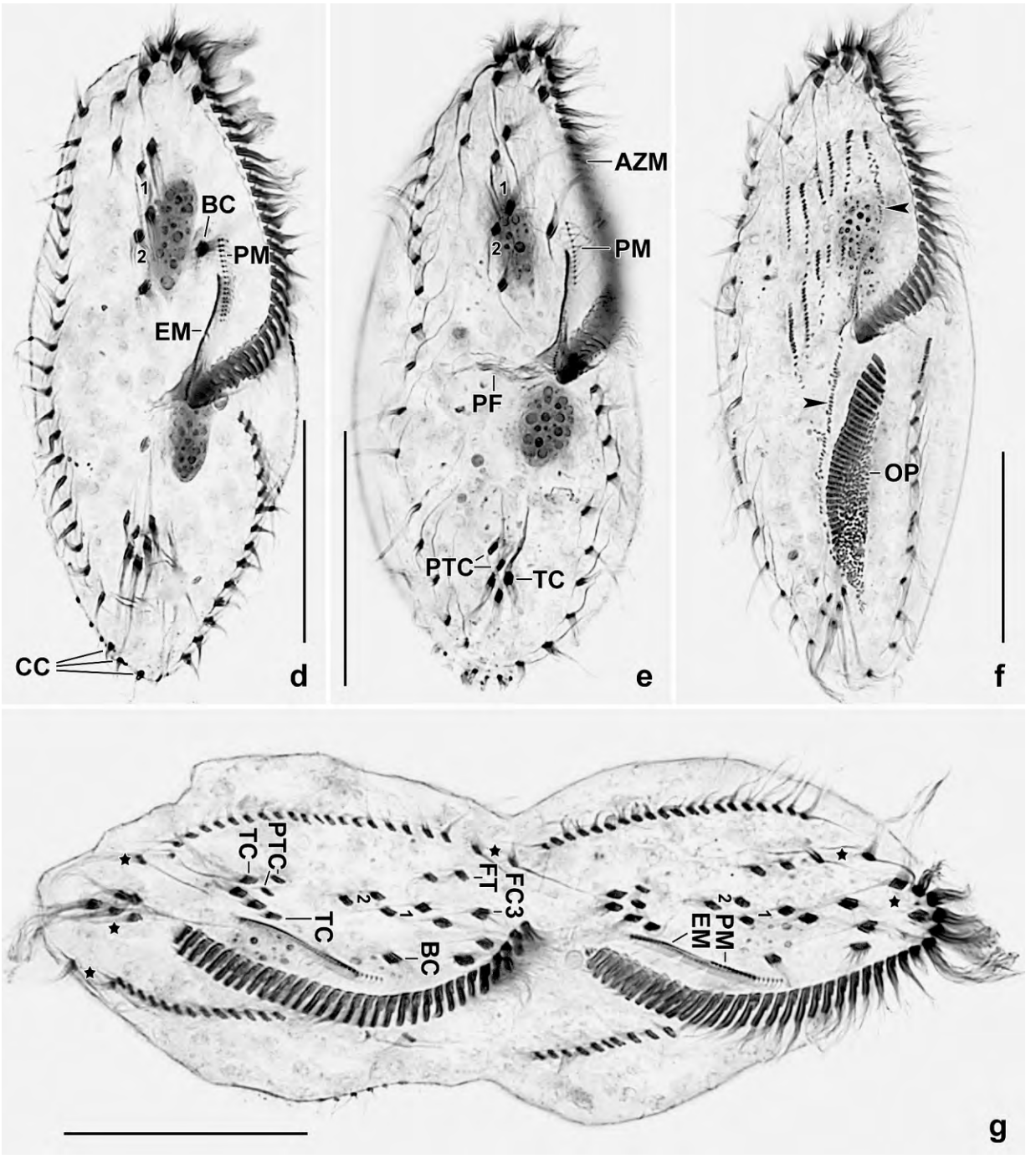

Fig. 226d–g. *Gonostomum singhii* (d, f, g) and a supposed *G. affine* (e), ventral views of morphostatic (d, e) and dividing (f, g) Australian specimens after protargol impregnation. **d:** A typical specimen. **e:** Possibly, this is a *G. affine* because it has a short paroral membrane and only three transverse cirri while the frontoventral cirral pattern is as in *G. singhii*. **f:** An early mid-divider with six cirral anlagen in proter and opisthe. The arrowheads mark a primary primordium producing the first frontal cirrus and the undulating membranes. **g:** A late divider with the new cirral pattern finished in the opisthe while it is still organizing in the proter. Asterisks mark not yet resorbed parental cirral bases. AZM – adoral zone of membranelles, BC – buccal cirrus, CC – caudal cirri, EM – endoral membrane, FC3 – frontal cirrus 3, FT – frontoterminal cirri, OP – oral primordium, PF – pharyngeal fibres, PM – paroral membrane, PTC – pretransverse cirri, TC – transverse cirri, 1, 2 – frontoventral cirral pairs. Scale bars 30 µm.

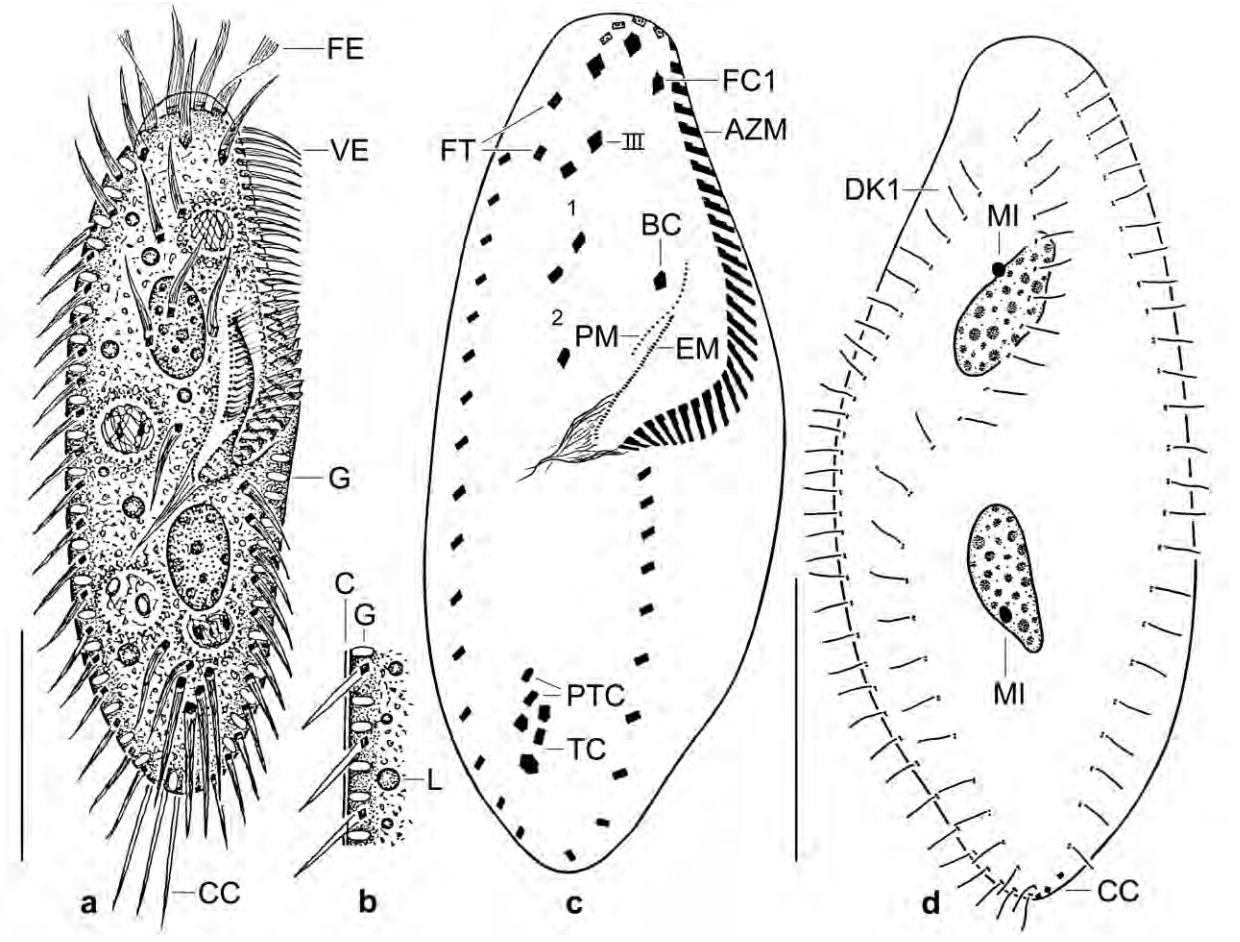

Fig. 227a–d. *Gonostomum singhii*, Venezuelan specimens from life (a, b) and after protargol impregnation (c, d). **a:** Ventral view of a representative specimen, length 90 µm. **b:** Cortical granulation. **c, d:** Ventral and dorsal view of infraciliature and nuclear apparatus of main voucher specimen, length 90 µm. Note the four transverse cirri and the thin bases of the caudal cirri. AZM – adoral zone of membranelles, BC – buccal cirrus, C – cortex, CC – caudal cirri, DK1 – dorsal kinety 1, EM – endoral membrane, FC1 – frontal cirrus 1, FE – frontal membranelles, FT – frontoterminal cirri, G – cortical granules, L – lipid droplet, MI – micronuclei, PM – paroral membrane, PTC – pretransverse cirri, TC – transverse cirri, VE – ventral membranelles, 1, 2 – frontoventral cirral pairs, III – second cirrus of anlage III. Scale bars 30 µm.

two oblique pairs of frontoventral cirri and a single cirrus posterior of second pair. Two thin pretransverse cirri and four more or less thickened transverse cirri slightly projecting from body proper; pretransverse cirri in unusual pattern, viz., one after the other in and above the V formed by the transverse cirri. Marginal cirri about 12 µm long each composed of two rows of basal bodies; right row shortened anteriorly and posteriorly, composed of an average of 19 cirri, left marginal row composed of 13 cirri on average, extends to mid of posterior body end (Fig. 225a, 226a–d, 227a, c, 228a–c, e, g; Table 84).

Usually three, very rarely four dorsal bristle rows, in Australian specimens occasionally short kinetofragments between ordinary rows; bristles 3–4 µm long, the last close to caudal cirri. Dorsal kineties associated with three, very rarely four fine, about 20 µm long caudal cirri in and right of body`s midline (Fig. 227d, 228a, f, g; Table 84).

Oral apparatus in *Gonostomum* pattern (Berger 1999, 2011), i. e., adoral zone slightly sigmoid

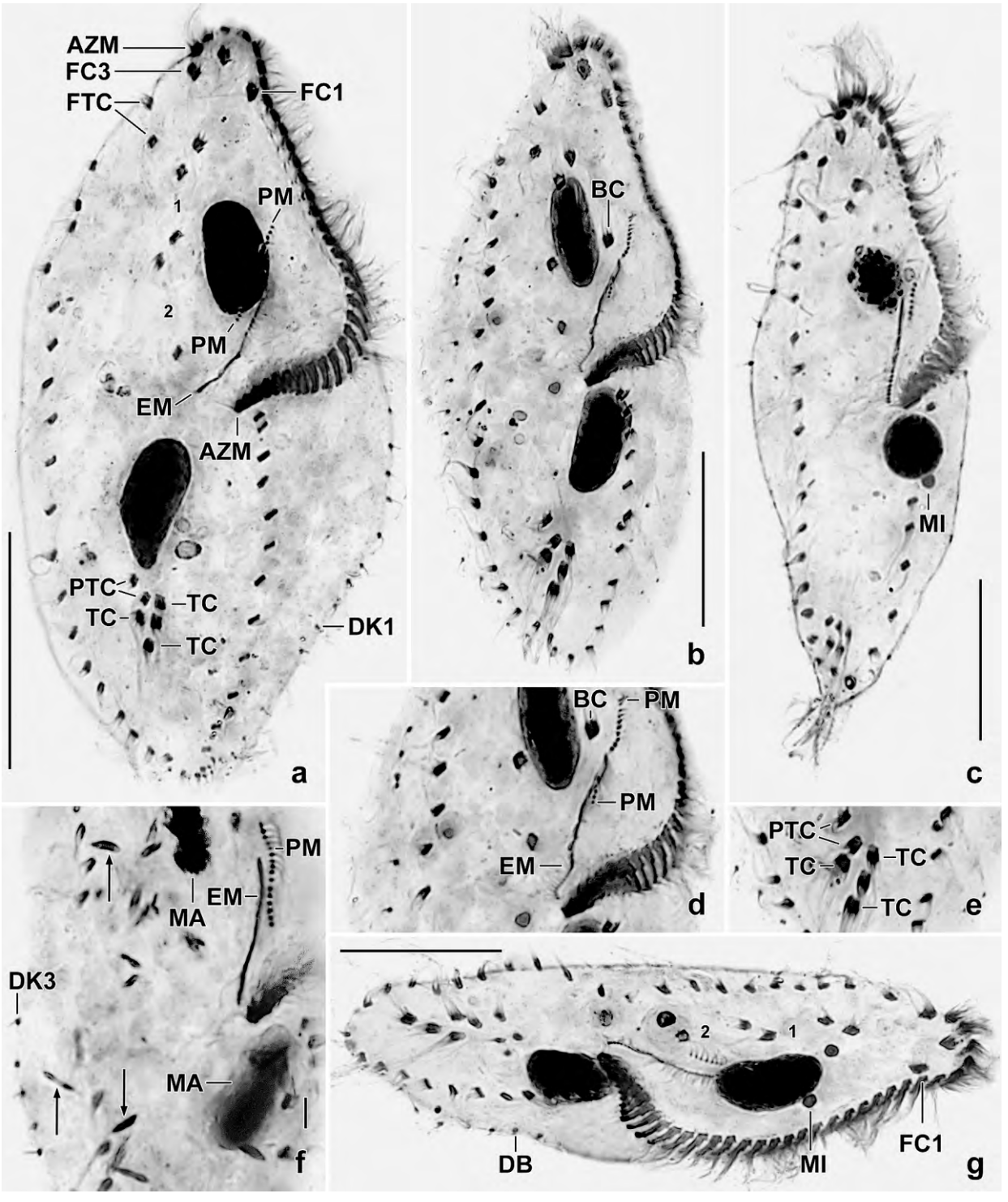

Fig. 228a–g. *Gonostomum singhii*, Venezuelan specimens after protargol impregnation. Note the long paroral membrane (a, d, f), the two pretransverse cirri (a, e), and the four transverse cirri (a–c, e, g). **a, c, g:** Ventral views of an inflated and two ordinary specimens. **b, d, e:** Overview and details of a representative specimen. **f:** Cortical granules (arrows)? AZM – adoral zone of membranelles, BC – buccal cirrus, DB – dorsal bristle, DK1, 3 – dorsal kineties, EM – endoral membrane, FC1, 3 – frontal cirri, FTC – frontoterminal cirri, MA – macronuclear nodules, MI – micronuclei, PM – paroral membrane, PTC – pretransverse cirri, TC – transverse cirri, 1, 2 – frontoventral cirral pairs. Scale bars 5 µm (f) and 25 µm (a–c, g).

and following left body margin before bending abruptly inwards at about 55% of body length; on average composed of 34 ordinary membranelles with largest bases 4–5 µm long in protargol preparations (Fig. 225a, d, 226a–d, 227a, c, 228a–d, g; Table 84). Buccal cavity of ordinary size, flat; buccal lip moderately convex, bears paroral membrane composed of an average of 15–19 narrowly spaced cilia 6 µm long in protargol preparations, with a minute gap in some specimens. Endoral membrane anteriorly distinctly shorter than paroral while distinctly longer posteriorly extending to buccal vertex; undulating membrane pattern depending on preparation and angle viewed, i. e., the paroral may be right or left of the endoral. Pharyngeal fibres about 20 µm long, extend obliquely to right body margin (Fig. 225a, d, 226a–d, 227a, c, 228a–d, f, g; Table 84).

Ontogenesis: This is highly similar to that of *G. algivora*, as described by Foissner et al. (2002), and of *G. affine* and *G. kuehnelti* as described by Eigner (1999). Thus, we show only some early stages with typical primary primordia (Fig. 225b, c, 226f) and a late stage where the frontoventral cirral pairs are organizing (Fig. 226g).

Occurrence and ecology: The Australian sample was composed of the upper 5 cm litter and soil under *Nothofagus* trees; pH 4.1, about 200 m above sea level. In Venezuela, *G. singhii* occurred at site (24), viz., in soil of a *Tachypogon* savannah. In India, it occurred also in soil treated with the non-flooded Petri dish method (see type locality above). Possibly restricted to Gondwana.

Remarks: Many features of *Gonostomum singhii* are between → *G. lajacola* and the *G. affine* complex (Table 84). It differs from → *G. lajacola* by the sparse (vs. dense) cortical granulation, the length of the dorsal bristles (3–4 µm vs. up to 10 µm), the number of transverse cirri (4 vs. 5), and the number of frontoventral cirral pairs (2 vs. 3). From → *G. affine*, as described by Berger (1999, 2011) and Foissner et al. (2001), it differs mainly by the specific location of the pretransverse cirri and the number of paroral cilia (~ 10 vs. 15–19). Additionally, *G. affine* rarely makes as distinct frontoventral cirral pairs as *G. singhii*, the caudal cirri are thicker, and the adoral zone of membranelles usually occupies 50% or less of body length.

When finishing the text for this "new species", we recognized that it has been described by Kamra et al. (2008). Unfortunately, their description is not very detailed and even partially incorrect. This concerns the pretransverse cirri which are one upon the other the anterior cirrus being slightly left of the posterior one while their photograph Figure 9d shows the opposite and matches our data (Fig. 225a, 226a–e, 227c, 228a, b, g). Further, we disagree that the cirri of *G. singhii* are hypertrophied. In our populations, cirral length is similar to the Indian specimens and the marginal cirri consist of two rows of basal bodies, as usual. Kamra et al. (2008) do not provide such data. Third, Kamra et al. (2008) place the caudal cirri in the centre of the posterior body end. Again, their photograph 9e shows that they are in and slightly right of body`s midline which matches our observations.

There is some indication that the Australian and the Venezuelan populations are sufficiently different from the Indian *G. singhii* to be classified as a subspecies: the adoral zone is longer (on average 55% vs. 49% of body length); the number of adoral membranelles is higher (on average 34 vs. 27), possibly due to the higher body length (100 × 32 µm vs. 70 × 26 µm in vivo); and the number of dorsal bristles is markedly higher, especially in the Venezuelan specimens (33 vs. 18 in row 1). The sole feature that hinders us is the very stable pattern of the pretransverse and transverse cirri in all populations.

Table 84. Morphometric data on *Gonostomum lajacola* (G. laj), *G. singhii* (G. sin, Venezuela; G. sing, Australia), and *G. affine* (G. aff) contained in the same slides as *G. singhii.* Data based on mounted, protargol-impregnated, and randomly selected specimens from non-flooded Petri dish cultures. CV – coefficient of variation in %, M – median, Max – maximum, Mean – arithmetic mean, Min – minimum, n – number of individuals investigated, SD – standard deviation, SE – standard error of arithmetic mean.

Characteristics	Species	Mean	M	SD	SE	CV	Min	Max	n
Body, length (µm)	G. laj	86.0	86.0	9.5	3.6	11.0	75.0	98.0	7
	G. sin	77.6	80.5	10.3	3.9	13.3	61.0	91.0	7
	G. sing	85.4	86.0	6.8	1.5	7.9	72.0	100.0	21
	G. aff	78.4	79.0	5.7	1.2	7.2	65.0	89.0	22
Body, width (µm)	G. laj	33.0	33.0	3.8	1.4	11.5	26.0	38.0	7
	G. sin	27.8	25.0	6.2	2.4	22.4	22.0	39.0	7
	G. sing	31.7	31.0	3.4	0.7	10.7	25.0	38.0	21
	G. aff	22.9	22.5	3.2	0.7	13.9	19.0	30.0	22
Body length:width, ratio	G. laj	2.6	2.7	0.4	0.1	14.4	2.1	3.2	7
	G. sin	2.8	2.8	0.4	0.1	12.8	2.2	3.2	7
	G. sing	2.7	2.7	0.3	0.1	9.6	2.2	3.1	21
	G. aff	3.5	3.5	0.4	0.1	10.6	2.7	4.3	22
Anterior body end to proximal end of adoral zone of membranelles, distance (µm)	G. laj	50.6	51.0	6.8	2.6	13.4	43.0	62.0	6
	G. sin	42.6	44.0	4.2	1.6	9.7	35.0	47.0	7
	G. sing	45.8	47.0	5.2	1.1	11.3	36.0	56.0	21
	G. aff	41.3	41.0	3.1	0.7	7.5	36.0	46.0	22
Adoral zone of membranelles, percentage of body length	G. laj	58.7	59.0	3.2	1.2	5.4	54.0	63.0	7
	G. sin	55.3	54.8	3.5	1.3	6.3	52.0	61.0	7
	G. sing	53.5	53.0	4.5	1.0	8.4	41.4	61.0	21
	G. aff	52.9	53.0	5.0	1.1	9.4	40.0	61.0	22
Anterior body end to paroral membrane, distance (µm)	G. laj	27.7	28.0	5.1	1.9	18.4	20.0	35.0	7
	G. sin	22.3	22.5	2.0	0.8	8.9	19.0	25.0	6
	G. sing	23.8	24.0	3.3	0.7	14.0	17.0	30.0	21
	G. aff	24.1	24.0	2.2	0.5	8.9	20.0	27.0	20
Anterior body end to endoral membrane, distance (µm)	G. laj	35.4	36.0	5.7	2.2	16.1	28.0	44.0	7
	G. sin	27.7	28.0	2.8	1.2	10.0	24.0	31.0	5
	G. sing	28.5	30.0	3.6	0.8	12.8	22.0	36.0	21
	G. aff	27.5	27.8	2.2	0.5	7.9	24.0	30.0	18
Anterior body end to first macronuclear nodule, distance (µm)	G. laj	not measured							
	G. sin	17.7	17.5	2.1	0.8	11.6	15.0	21.0	7
	G. sing	18.4	18.0	2.3	0.5	12.2	15.5	22.5	21
	G. aff	18.4	18.0	1.2	0.3	6.5	17.0	21.0	22
Anterior body end to buccal cirrus, distance (µm)	G. laj	not measured							
	G. sin	23.7	24.0	1.9	0.8	8.0	21.0	26.0	6
	G. sing	24.6	25.0	3.2	0.7	13.0	18.0	31.0	21
	G. aff	25.0	25.0	2.2	0.5	8.8	22.0	29.0	18
Anterior body end to rearmost frontoventral cirrus, distance (µm)	G. laj	not measured							
	G. sin	35.4	35.5	3.3	1.3	9.4	30.0	39.0	7
	G. sing	35.0	35.0	3.4	0.7	9.7	29.0	43.0	21

continued

Characteristics	Species	Mean	M	SD	SE	CV	Min	Max	n
	G. aff	36.6	37.0	2.4	0.5	6.6	31.0	40.0	22
Anterior body end to right marginal cirral row, distance (µm)	G. laj	not measured							
	G. sin	14.1	14.0	1.8	0.7	13.0	12.0	17.0	7
	G. sing	12.6	13.0	1.3	0.3	10.2	11.0	16.0	21
	G. aff	17.7	18.5	1.2	0.3	6.5	17.0	21.0	22
Posterior body end to right marginal cirral row, distance (µm)	G. laj	not measured							
	G. sin	2.9	2.0	1.1	0.4	37.4	2.0	4.0	7
	G. sing	5.7	6.0	1.3	0.3	23.4	4.0	9.0	21
	G. aff	4.2	4.0	1.0	0.2	24.4	2.0	7.0	22
Posterior body end to left marginal cirral row, distance (µm)	G. laj	not measured							
	G. sin	2.2	2.0	1.5	0.6	67.6	1.0	5.0	7
	G. sing	2.2	2.0	0.8	0.2	37.8	1.0	4.0	21
	G. aff	2.5	2.5	1.1	0.2	42.5	1.0	5.0	22
Posterior body end to rearmost transverse cirrus, distance (µm)	G. laj	8.2	9.5	2.8	1.1	34.1	3.0	10.0	6
	G. sin	8.1	6.0	3.5	1.3	42.9	4.5	14.0	7
	G. sing	10.3	10.0	1.6	0.4	15.9	8.0	14.0	21
	G. aff	10.3	10.5	2.5	0.5	24.7	5.0	15.0	22
Anterior macronuclear nodule, length (µm)	G. laj	16.3	16.0	3.5	1.3	21.2	13.0	21.0	7
	G. sin	13.7	13.0	1.7	0.6	12.3	12.0	17.0	7
	G. sing	16.3	16.0	3.5	0.8	21.6	8.0	23.0	21
	G. aff	14.0	14.0	1.4	0.3	10.1	12.0	17.0	22
Anterior macronuclear nodule, width (µm)	G. laj	6.6	6.0	0.8	0.3	12.0	6.0	8.0	7
	G. sin	5.7	5.5	0.8	0.3	13.2	4.5	7.0	7
	G. sing	6.7	7.0	0.8	0.2	11.9	5.0	8.0	21
	G. aff	4.9	5.0	0.6	0.1	12.2	4.0	6.0	22
Macronuclear nodules, number	G. laj	2.0	2.0	0.0	0.0	0.0	2.0	2.0	7
	G. sin	2.0	2.0	0.0	0.0	0.0	2.0	2.0	7
	G. sing	2.0	2.0	0.0	0.0	0.0	2.0	2.0	21
	G. aff	2.0	2.0	0.0	0.0	0.0	2.0	2.0	22
Anteriormost micronucleus, length (µm)	G. laj	2.2	2.0	–	–	–	2.0	2.5	7
	G. sin	1.9	2.0	–	–	–	1.5	2.0	7
	G. sing	2.3	2.5	–	–	–	2.0	3.0	21
	G. aff	1.8	1.8	–	–	–	1.5	2.0	18
Anteriormost micronucleus, width (µm)	G. laj	1.9	2.0	–	–	–	1.5	2.0	7
	G. sin	1.5	1.5	–	–	–	1.5	1.5	7
	G. sing	1.8	2.0	–	–	–	1.5	2.0	21
	G. aff	1.5	1.5	–	–	–	1.0	2.0	18
Micronuclei, number	G. laj	2.0	2.0	0.0	0.0	0.0	2.0	2.0	7
	G. sin	2.0	2.0	1.0	0.4	50.0	1.0	4.0	7
	G. sing	3.0	3.0	1.0	0.2	34.7	1.0	5.0	21
	G. aff	2.4	2.0	1.0	0.2	41.0	1.0	4.0	18
Adoral membranelles, number	G. laj	32.7	32.0	4.0	1.5	12.1	28.0	38.0	7
	G. sin	35.0	35.0	1.6	0.6	4.7	32.0	37.0	7
	G. sing	33.6	34.0	3.0	0.7	9.0	27.0	39.0	21
	G. aff	27.2	27.0	1.7	0.4	6.1	24.0	29.0	22

continued

Characteristics	Species	Mean	M	SD	SE	CV	Min	Max	n
Paroral kinetids, number	G. laj	23.0	23.0	1.1	0.5	4.8	21.0	24.0	6
	G. sin	19.0	19.0	1.7	0.7	8.8	16.0	21.0	6
	G. sing	15.2	16.0	2.2	0.5	14.6	10.0	19.0	21
	G. aff	10.4	10.0	1.3	0.3	12.6	9.0	13.0	20
Frontal cirri, number	G. laj	3.0	3.0	0.0	0.0	0.0	3.0	3.0	6
	G. sin	3.0	3.0	0.0	0.0	0.0	3.0	3.0	7
	G. sing	3.0	3.0	0.0	0.0	0.0	3.0	3.0	21
	G. aff	3.0	3.0	0.0	0.0	0.0	3.0	3.0	22
Buccal cirri, number	G. laj	1.0	1.0	0.0	0.0	0.0	1.0	1.0	4
	G. sin	1.0	1.0	0.0	0.0	0.0	1.0	1.0	6
	G. sing	1.0	1.0	0.0	0.0	0.0	1.0	1.0	21
	G. aff	1.0	1.0	0.0	0.0	0.0	1.0	1.0	22
Frontoventral cirri, number	G. laj	5.5	5.0	–	–	–	5.0	6.0	4
	G. sin	5.0	5.0	0.0	0.0	0.0	5.0	5.0	7
	G. sing	5.0[a]	5.0	0.0	0.0	0.0	5.0	5.0	21
	G. aff	5.1	5.0	0.4	0.1	8.4	5.0	7.0	22
Pretransverse cirri, number	G. laj	see transverse cirri							
	G. sin	2.1	2.0	–	–	–	2.0	3.0	7
	G. sing	2.0	2.0	0.0	0.0	0.0	2.0	2.0	21
	G. aff	2.0	2.0	0.0	0.0	0.0	2.0	2.0	22
Transverse cirri, number (+ pretransverse cirri in *G. lajacola*)	G. laj	6.4	7.0	0.9	0.4	14.0	5.0	7.0	5
	G. sin	4.0	4.0	0.0	0.0	0.0	4.0	4.0	7
	G. sing	4.0	4.0	0.4	0.1	9.7	3.0	5.0	21
	G. aff	4.0	4.0	0.0	0.0	0.0	4.0	4.0	22
Frontoterminal cirri, number	G. laj	2.0	2.0	0.0	0.0	0.0	2.0	2.0	3
	G. sin	2.0	2.0	0.0	0.0	0.0	2.0	2.0	7
	G. sing	2.0	2.0	0.0	0.0	0.0	2.0	2.0	21
	G. aff	2.0	2.0	0.0	0.0	0.0	2.0	2.0	22
Right marginal cirri, number	G. laj	18.4	17.0	4.3	1.9	23.3	14.0	25.0	5
	G. sin	17.9	18.0	1.4	0.5	7.5	16.0	19.0	7
	G. sing	18.8	18.0	2.5	0.5	13.0	16.0	24.0	21
	G. aff	14.0	14.0	1.7	0.4	11.9	10.0	18.0	22
Left marginal cirri, number	G. laj	12.2	11.0	2.6	1.2	21.2	10.0	15.0	5
	G. sin	11.3	11.0	1.1	0.4	9.9	10.0	13.0	7
	G. sing	13.0	13.0	1.5	0.3	11.3	10.0	16.0	21
	G. aff	9.6	9.0	1.0	0.2	10.1	8.0	12.0	22
Dorsal kineties, number	G. laj	3.0	3.0	0.0	0.0	0.0	3.0	3.0	5
	G. sin	3.0	3.0	0.0	0.0	0.0	3.0	3.0	7
	G. sing	3.0[b]	3.0	0.0	0.0	0.0	3.0	3.0	21
	G. aff	3.0	3.0	0.0	0.0	0.0	3.0	3.0	22
Bristles in dorsal kinety 1, number	G. sin	28.5	28.0	3.4	1.7	12.0	25.0	33.0	4
	G. sing	22.3	22.0	2.0	0.6	9.0	19.0	25.0	11
Bristles in dorsal kinety 2, number	G. sin	23.3	24.0	2.2	1.1	9.5	20.0	25.0	4
	G. sing	18.7	19.0	2.4	0.7	12.7	16.0	22.0	11
Bristles in dorsal kinety 3, number	G. sin	27.3	27.0	2.2	1.1	8.1	25.0	30.0	4

continued

Characteristics	Species	Mean	M	SD	SE	CV	Min	Max	n
	G. sing	22.6	22.0	1.8	0.5	8.0	22.0	25.0	11
Caudal cirri, number	G. laj	3.0	3.0	0.0	0.0	0.0	3.0	3.0	4
	G. sin	3.0	3.0	0.0	0.0	0.0	3.0	3.0	7
	G. sing	3.0[b]	3.0	0.0	0.0	0.0	3.0	3.0	21
	G. aff	3.0	3.0	0.0	0.0	0.0	3.0	3.0	20

[a] Only three in one out of 21 specimens.

[b] Four rows and four caudal cirri in one out of 21 specimens.

Gonostomum lajacola nov. spec. (Fig. 229a–d, 230a–c; Table 84)

Diagnosis: Size in vivo about 100 × 35 µm; ellipsoid. 2 ordinarily spaced macronuclear nodules. Cortical granules in rough rows, numerous, colourless, about 3 × 1 µm in size. 3 frontal cirri, 2 frontoterminal cirri, 1 buccal cirrus subapical of paroral membrane, 2 frontoventral cirral pairs, and 5–7 pretransverse and transverse cirri. Right marginal row composed of an average of 18 cirri, left of 12. Dorsal bristles gradually elongating from 3 µm anteriorly to 10 µm posteriorly. Three thin caudal cirri. Adoral zone extends 59% of body length, consists of an average of 32 membranelles; undulating membranes long, paroral composed of 23 cilia on average.

Type locality: Venezuelan site (32), i.e., soil under a carpet of Velosiacean plants in a lithotelma (Laja) between the Agricultural Research Station and the airport of Puerto Ayacucho, 67°36'W 5°41'N.

Type slides: 1 holotype and 2 paratype slides with protargol-impregnated specimens have been deposited in the Biology Centre of the Upper Austrian Museum in Linz (LI). The holotype and other relevant specimens have been marked by black ink circles on the coverslip.

Etymology: The species name is a composite of *Laja* (indigenous name for ephemeral puddles on granitic outcroppings) and the Latin verb *colere* (to live in) referring to the habitat the species was discovered.

Description: This species was very rare. One specimen was used for live observation and seven cells, most rather strongly inflated, were found in the protargol slides. However, the species has a clear identity by a combination of four features (see "**Remarks**"). Thus, we describe it but emphasize the need for further live observation and a more detailed morphometry.

Size in vivo 85–115 × 30–40 µm, usually about 100 × 35 µm, as calculated from a live specimen and the morphometric data in Table 84 adding 15% preparation shrinkage. Body shape inconspicuous, i. e., elongate ellipsoid and up to 2:1 flattened laterally (Fig. 229a, 230a). Nuclear apparatus in central quarters of body slightly left of midline (Fig. 229a, b, 230a–c; Table 84). Two ellipsoid to elongate ellipsoid macronuclear nodules with a distance of about 15 µm in protargol preparations; anterior nodule slightly larger than posterior; with many minute nucleoli. Usually two globular to broadly ellipsoid micronuclei near or attached to macronuclear nodules and about 2 µm in size. Contractile vacuole not observed. Cortex very flexible, conspicuous because studded with granules, forming a 3–4 µm wide fringe; individual granules in rather dense rows, colourless,

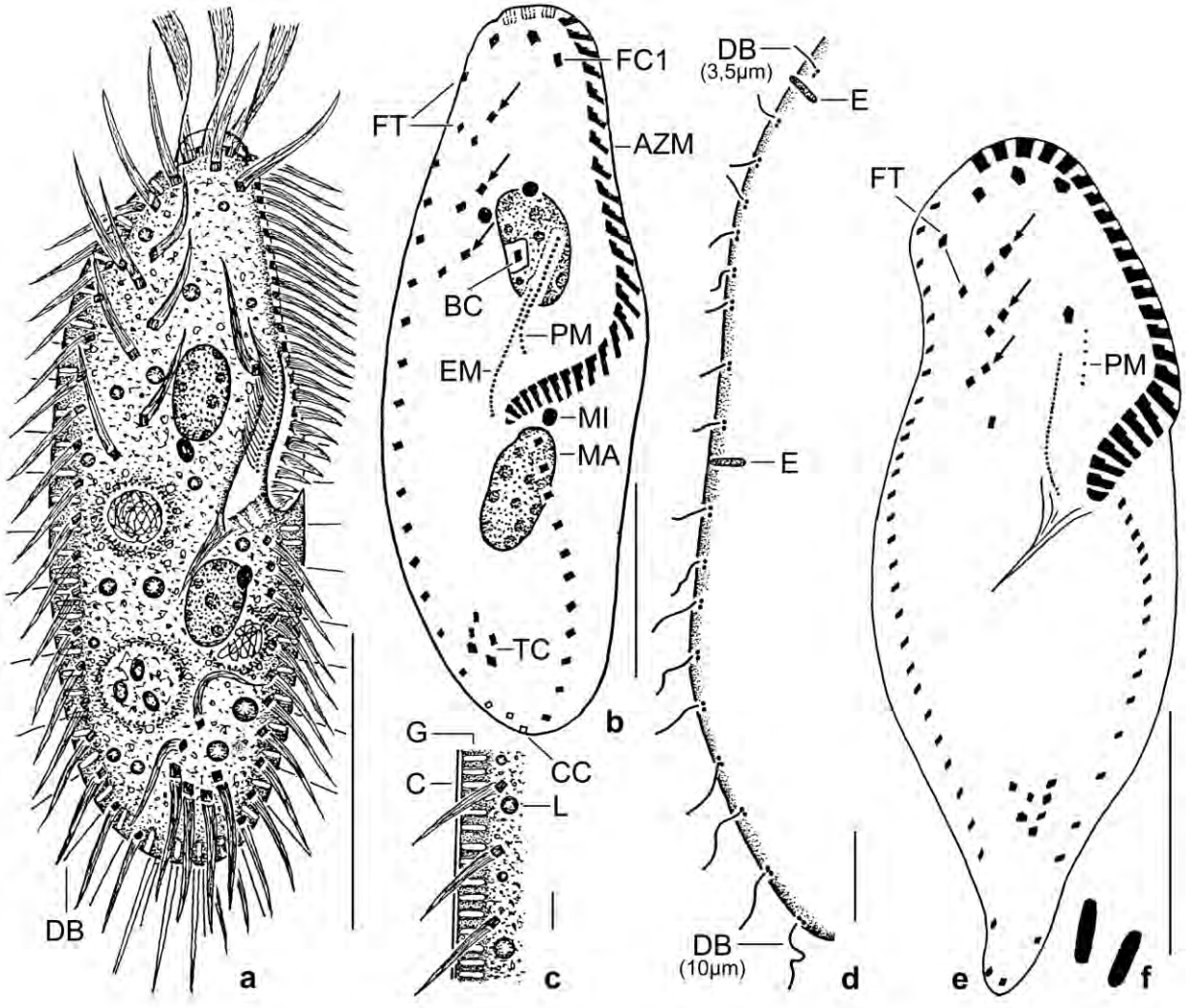

Fig. 229a–f. *Gonostomum lajacola* (a–d) and *G. namibiense* (e, f; from Foissner et al. 2002) from life (a, c, f) and after protargol impregnation (b, d, e). **a:** Ventral view of a representative specimen, length 100 µm. **b:** Ventrolateral view of infraciliature and nuclear apparatus of holotype specimen, length 76 µm. Note three pairs of frontoventral cirri (arrows) and the long paroral membrane, important features of this species. **c:** Optical section, showing the dense cortical granulation, an important feature of *G. lajacola*. **d:** Dorsal kinety 3, showing the gradual length increase of the dorsal bristles from 3.5 µm anteriorly to 10 µm posteriorly. **e:** *Gonostomum namibiense* is quite similar to *G. lajacola* in some features (e. g., body size; cortical granulation; three pairs of frontoventral cirri, arrows) but has a tailed (vs. broadly rounded) body, a short (vs. long) paroral membrane, five (vs. four) transverse cirri, and shorter (up to 4 µm vs. up to 10 µm) dorsal bristles. **f:** Cortical granules, about 1 × 0.3 µm. AZM – adoral zone of membranelles, BC – buccal cirrus, C – cortex, CC – caudal cirri, DB – dorsal bristles, E – extrusomes, EM – endoral membrane, FC1 – frontal cirrus 1, FT – frontoterminal cirri, G – cortical granules (extrusomes), L – lipid droplet, MA – macronuclear nodule, MI – micronucleus, PM – paroral membrane, TC – transverse cirri. Scale bars 5 µm (c), 10 µm (d), 20 µm (b, e), and 40 µm (a).

about 3×1 µm in size, impregnate lightly with the protargol method used (Fig. 229a, c, 230a–c). Cytoplasm colourless, contains some lipid droplets and up to 12 µm-sized food vacuoles with bacteria and their indigestible spores (Fig. 229a, c).

Cirri arranged in typical *Gonostomum* pattern (Berger 1999, 2011) shown in Figures 229a, b. Invariably three thickened frontal cirri in convex pattern following anterior body margin; frontal cirrus 1 not enlarged. Two frontoterminal cirri in gap between adoral zone and right marginal

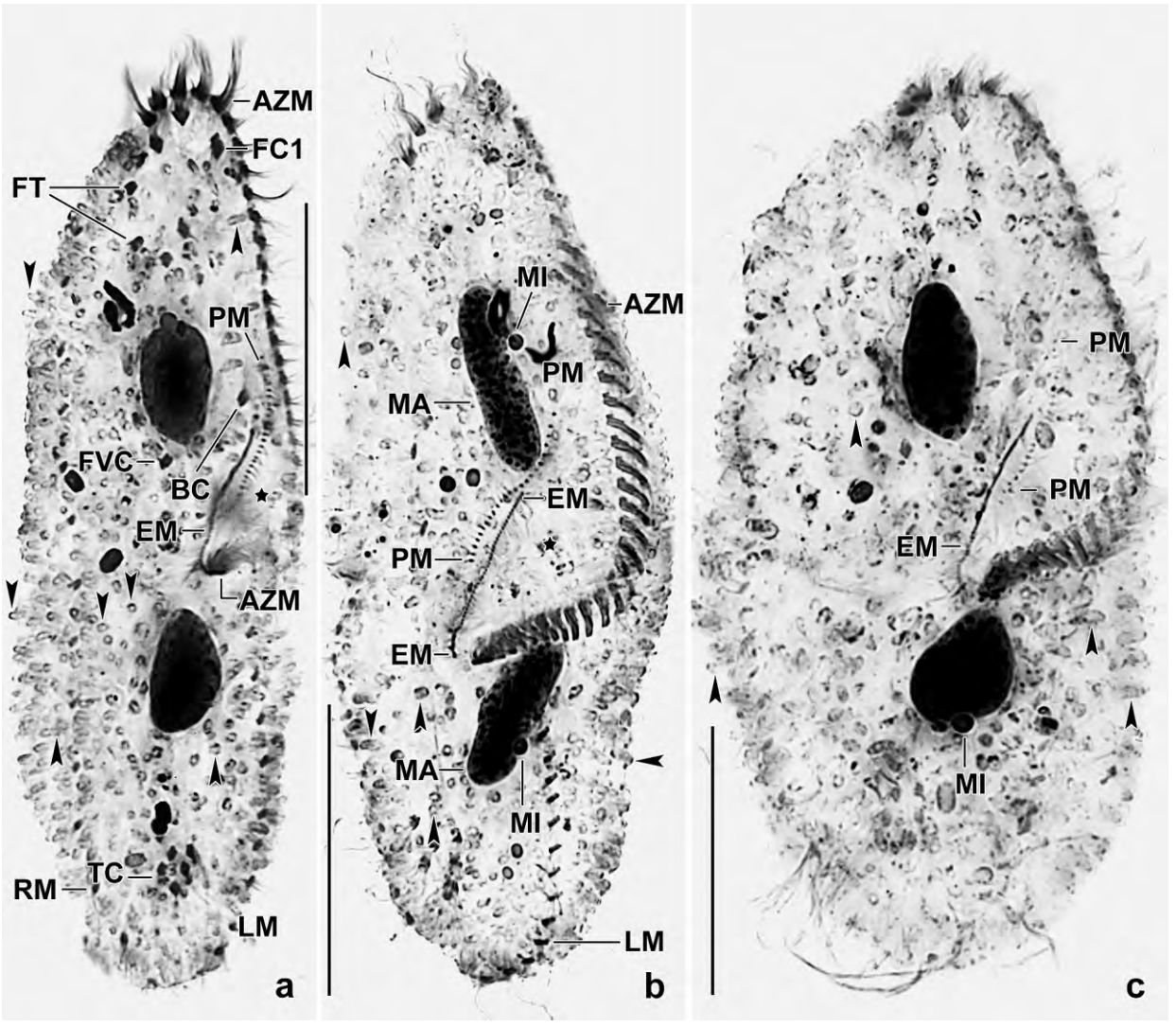

Fig. 230a–c. *Gonostomum lajacola*, ventral views after protargol impregnation. **a:** A well-preserved specimen with narrow buccal cavity (asterisk) and countless lightly impregnated cortical granules (arrowheads). Note the long undulating membranes. **b:** A moderately-preserved specimen in which the buccal cavity (asterisk) is greatly inflated. Note the cortical granules (arrrowheads), the long undulating membranes, and the long adoral zone of membranelles. **c:** A poorly-preserved, stongly inflated specimen, showing the long undulating membranes and countless, partially exploded cortical granules (arrowheads). AZM – adoral zone of membranelles, BC – buccal cirrus, EM – endoral membrane, FC1 – frontal cirrus 1, FT – frontoterminal cirri, FVC – last frontoventral cirrus, LM – left marginal cirral row, MA – macronuclear nodules, MI – micronuclei, PM – paroral membrane, RM – right marginal cirral row, TC – pretransverse and transverse cirri. Scale bars 30 µm.

cirral row. Buccal cirrus subapical and right of paroral membrane. Usually three oblique pairs of frontoventral cirri. Five to seven pretransverse and slightly thickened transverse cirri about 20 µm long in vivo and thus projecting from body proper. Marginal cirri about 17 µm long; right row commences far subapically, composed of an average of 18 cirri, ends subterminally; left marginal row composed of an average of 12 cirri, extends to mid of posterior body end.

Three rows of dorsal bristles, their length increasing from 3–4 µm anteriorly to about 10 µm posteriorly (Fig. 229d). Three fine and about 20 µm long caudal cirri in and right of body`s midline (Fig. 229a, b).

Oral apparatus in *Gonostomum* pattern (Berger 1999), i. e., the slightly sigmoidal adoral zone follows the body margin and bends abruptly into the cell at about 59% of body length, on average composed of 32 ordinary membranelles with largest bases 4–5 µm width in protargol preparations; cilia of frontal membranelles about 25 µm long, those of ventral membranelles up to 15 µm long in protargol preparations (Fig. 229a, b, 230a–c; Table 84). Buccal cavity narrow and flat; buccal lip slightly to moderately convex, bears paroral membrane composed of an average of 23 narrowly spaced cilia 6 µm long in protargol preparations. Endoral membrane anteriorly distinctly shorter than paroral while distinctly longer posteriorly extending to buccal vertex, cilia about 8 µm long in protargol preparations (Fig. 229a, b, 230a–c; Table 84).

Occurrence and ecology: As yet found only at type locality. Grew poorly in the non-flooded Petri dish culture, indicating that it could be a limnetic species.

Remarks: In vivo, the new species looks like the very common *Gonostomum affine* (Fig. 229a). However, *G. lajacola* and *G. affine* differ by four distinct features (for data on the latter, see Table 84; Berger 1999; and Foissner et al. 2001, who studied seven populations): length of the adoral zone of membranelles (59% vs. 49% of body length); the cortical granulation (granules in dense rows and ~ 3 µm long vs. lacking or dispersed and ~ 1 µm in size); the length of the dorsal bristles (gradually increasing to ~ 10 µm vs. 3–4 µm throughout); and, especially, the number of paroral cilia (on average 23 vs. 11). *Gonostomum bryonicolum, G. spirotrichoides*, and → *G. caudatulum* have also long dorsal bristles but their bodies are distinctly narrowed posteriorly and the number and arrangement of the FVT-cirri is different. As concerns G. *namibiense*, see explanation to Fig. 229e. For the separation from → *G. singhii*, see that species.

Gonostomum multinucleatum nov. spec. (Fig. 231a–i, 232a–m; Table 85)

Diagnosis (for two populations): Size in vivo about 80 × 20 µm; very slenderly ellipsoid and usually slightly sigmoid. On average 13 globular to ellipsoid macronuclear nodules and 3 broadly ellipsoid micronuclei. Cortical granules in rough rows, slightly yellowish, 0.5–0.9 µm across. 3 frontal cirri, 2 frontoterminal cirri, 1 buccal cirrus right of anterior end of paroral membrane, and 2 frontoventral cirral pairs. Right marginal row composed of an average of 16–23 cirri, left of 11–17. Dorsal bristles 3 µm long; 2 to 3 thin caudal cirri. Adoral zone gonostomoid, posterior half covered by the strongly convex buccal lip, extends about 38% of body length, consists of 20 membranelles on average; Buccal cavity very narrow and flat; paroral membrane composed of about 7 kinetids.

Type locality: Soil from an abandoned cacao plantago near Punta Pirikiki, about 54 km south of Limon, Caribbean Sea coast of Costa Rica, Central America, 82°40’W, 9°40’N.

Type slides: 1 holotype and 5 paratype slides with protargol-impregnated specimens have been deposited in the Biology Centre of the Upper Austrian Museum in Linz (LI). The holotype and other relevant specimens have been marked by black ink circles on the coverslip. Furthermore, 4 voucher slides from the Brazilian population have been stored in the same repository.

Etymology: The species name is a composite of the Latin quantifier *mult-* (many), the thematic vowel *-i-*, and the Latin participle *nucleatum* (having a nucleus). It refers to the multiple macronuclear nodules, a main feature of this species.

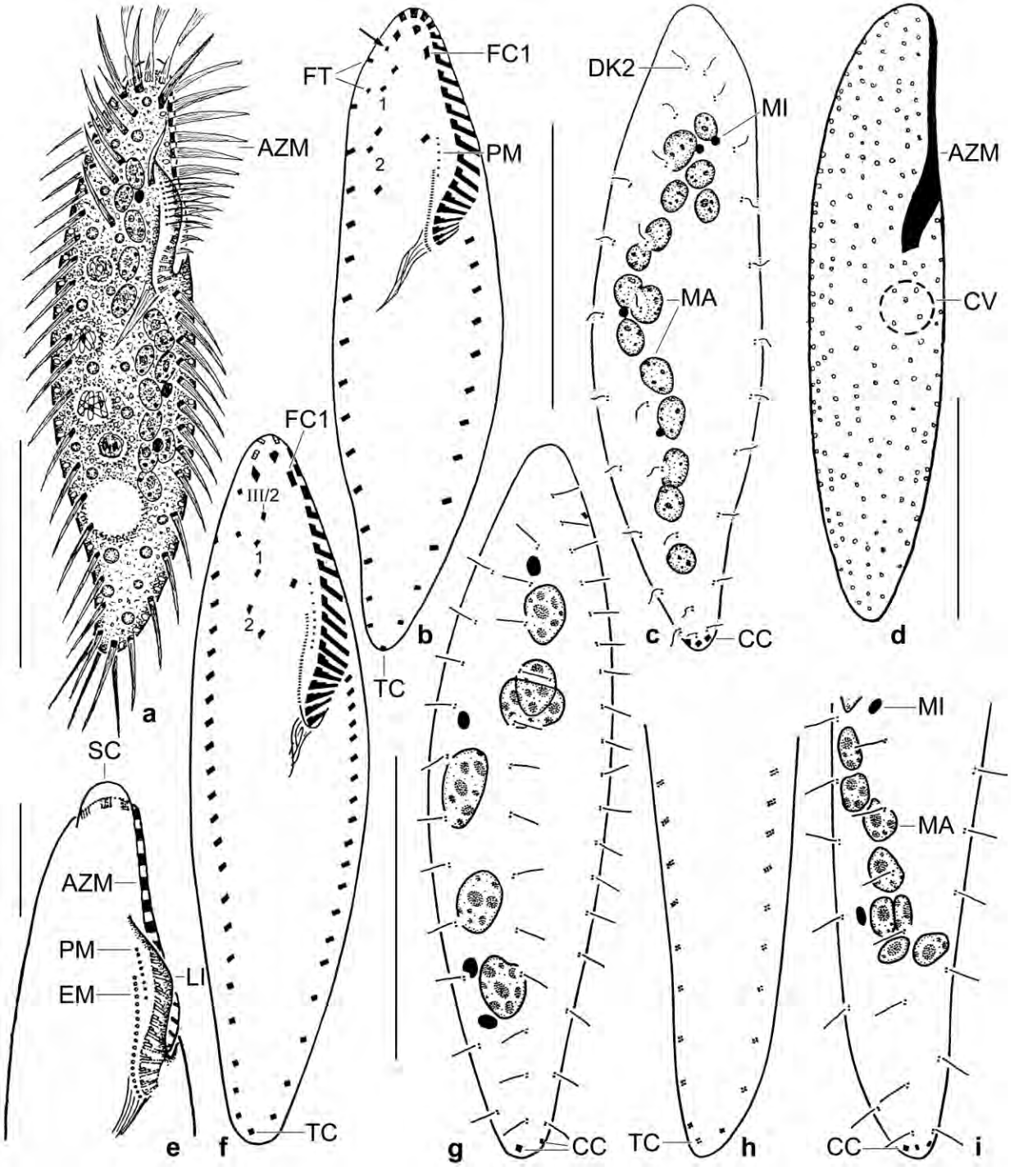

Fig. 231a–i. *Gonostomum multinucleatum* from Costa Rica (a–e) and Brazil (f–i) from life (a, d, e) and after protargol impregnation (b, c, f–i). **a, e:** Ventral views of a representative specimen, length 80 µm The buccal lip covers the proximal half of the adoral zone. **b, c, f–i:** Ventral and dorsal views of holotype (b, c) and of two voucher specimens (f–i); the arrow in (b) marks a minute cirrus, very likely a remnant from the last division. **d:** Shape of body and cortical granulation. AZM – adoral zone of membranelles, CC – caudal cirral bases, CV – contractile vacuole, DK2 – dorsal kinety 2, EM – endoral membrane, FC1 – frontal cirrus 1, FT – frontoterminal cirri, LI – buccal lip, MA – macronuclear nodules, MI – micronuclei, PM – paroral membrane, SC – scutum, TC – transverse cirrus, 1, 2 – frontoventral cirral pairs, III/2 – second cirrus of anlage III. Scale bars 15 µm (e) and 30 µm (a–d, f, g).

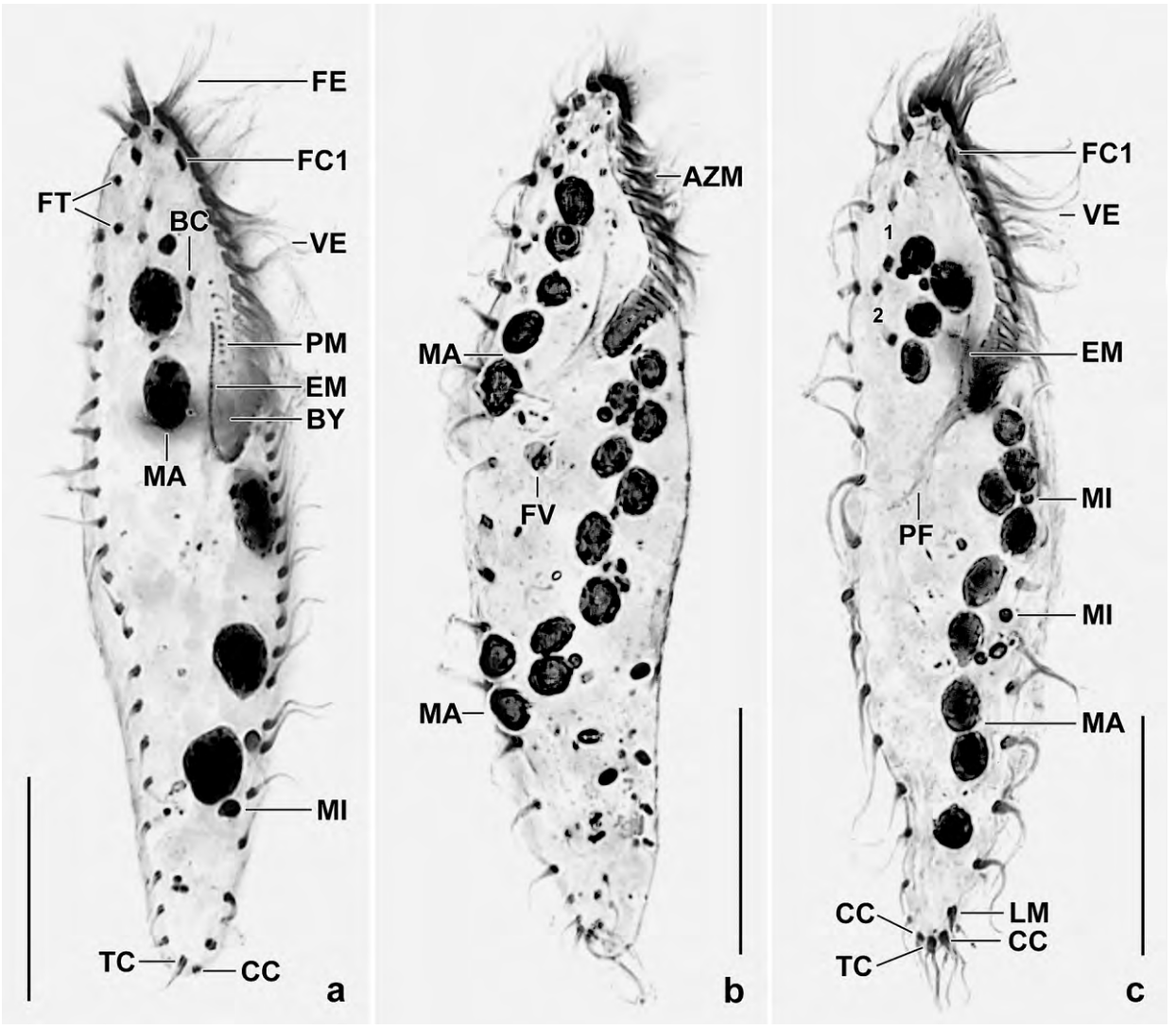

Fig. 232a–c. *Gonostomum multinucleatum*, ventral views of Costa Rican specimens after protargol impregnation. Note the very narrow buccal cavity and the slender body. The specimens have a single transverse cirrus and two or three caudal cirri. AZM – adoral zone of membranelles, BC – buccal cirrus, BY – buccal cavity, CC – caudal cirri, EM – endoral membrane, FC1 – frontal cirrus 1, FE – frontal adoral membranelles, FT – frontoterminal cirri, FV – food vacuole, LM – left marginal cirral row, MA – macronuclear nodules, MI – micronuclei, PF – pharyngeal fibres, PM – paroral membrane, TC – transverse cirrus, VE – ventral adoral membranelles, 1, 2 – frontoventral cirral pairs. Scale bars 20 µm.

Description: We investigated a Costa Rican and a Brazilian population. The specimens of the former are smaller than those of the latter by 12 µm (20%) on average. Very likely, this is not a preparation artifact because they have also less marginal cirri and bristles in dorsal kinety 2. However, the in vivo measurements of the Costa Rican specimens match well the protargol data of the Brazilian specimens: 70–90 × 17 –20 µm vs. 69–113 × 15–25 µm, $\bar{x}$ 87 × 18 when 15% preparation shrinkage is added. Thus, we calculated an overall in vivo size of 80 × 20 µm for the "representative specimen" (Fig. 231a). Size of protargol-impregnated Costa Rican specimens 53–87 × 14–25 µm, on average 72 × 20 µm when 15% preparation shrinkage is added; Brazilian specimens 69–113 × 15–25 µm, on average 87 × 18 µm (see above and Table 85). Body very slenderly ellipsoid (length:width ratio ~ 4:1) and

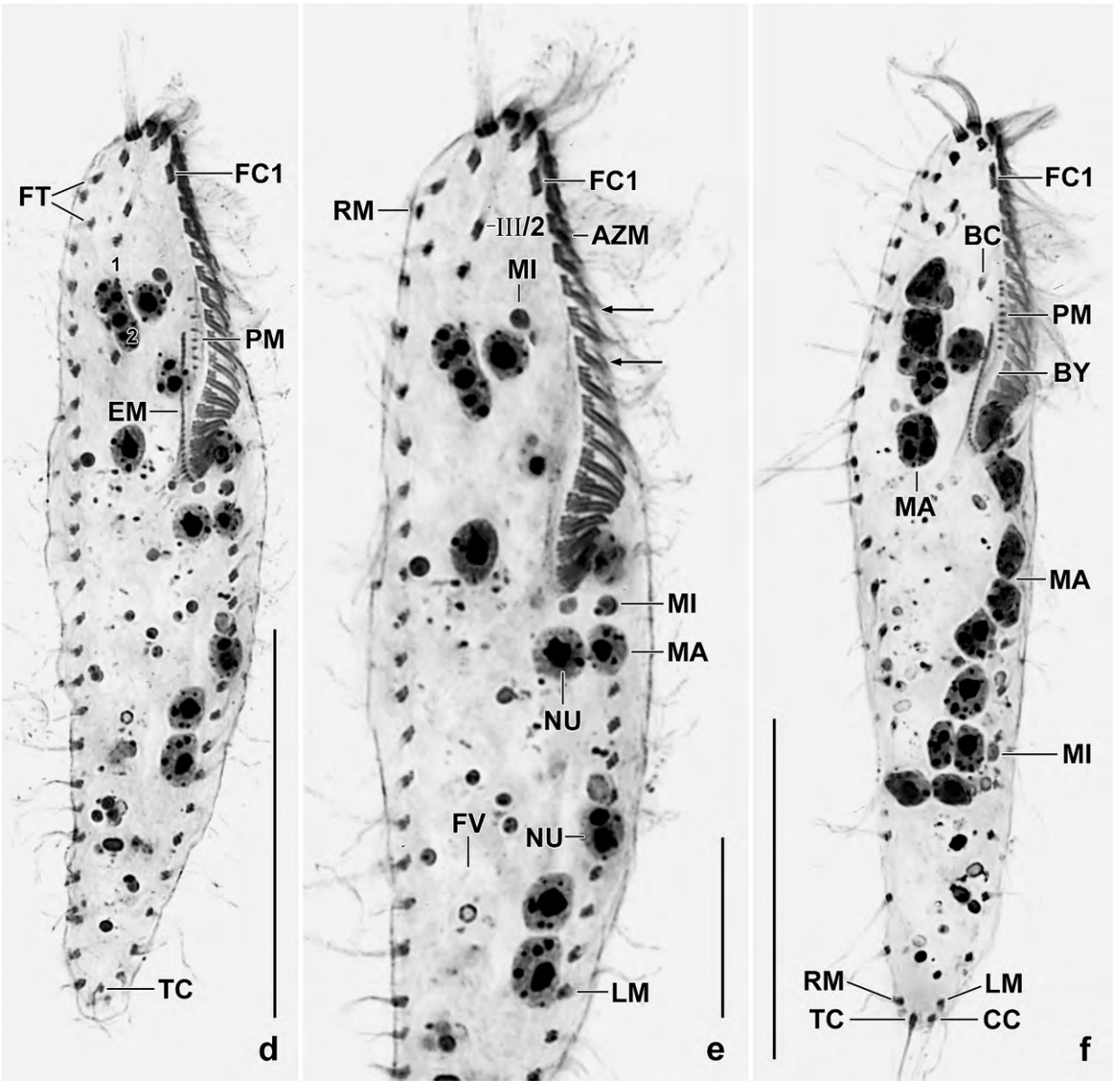

Fig. 232d–f. *Gonostomum multinucleatum*, ventral views of Brazilian specimens after protargol impregnation. **d, e:** Overview and detail, showing the gonostomoid adoral zone with membranelles having minute, equally long kineties 3 and 4 (arrows), the single frontoventral cirrus III/2, the two frontoventral cirral pairs (1, 2), and the distinctly enlarged frontal cirrus 1 (e). **f:** A very slender specimen, showing the very narrow buccal cavity, the enlarged frontal cirrus 1, and details of the ciliature on posterior body end. AZM – adoral zone of membranelles, BC – buccal cirrus, BY – buccal cavity, CC – caudal cirri, EM – endoral membrane, FC1 – frontal cirrus 1, FT – frontoterminal cirri, FV – food vacuole, LM – left marginal cirral row, MA – macronuclear nodules, MI – micronuclei, NU – nucleoli, PM – paroral membrane, RM – right marginal cirral row, TC – transverse cirrus, 1, 2 – frontoventral cirral pairs, III/2 – second cirrus of anlage III. Scale bars 10 µm (e), 30 µm (f), and 35 µm (d).

usually slightly sigmoid, inconspicuously flattened laterally (Fig. 231a, b, d, f, 232a–d, g; Table 85). Nuclear apparatus in central quarters of cell (Fig. 231a, c, g, i, 232a–i; Table 85). On average 13 macronuclear nodules in a rough row, about one third of nodules in oral region right of body`s midline, the others postoral left of midline. Individual nodules globular to ellipsoid, on average 5 × 4 µm after protargol impregnation, contain minute and comparatively large nucleoli; Brazilian

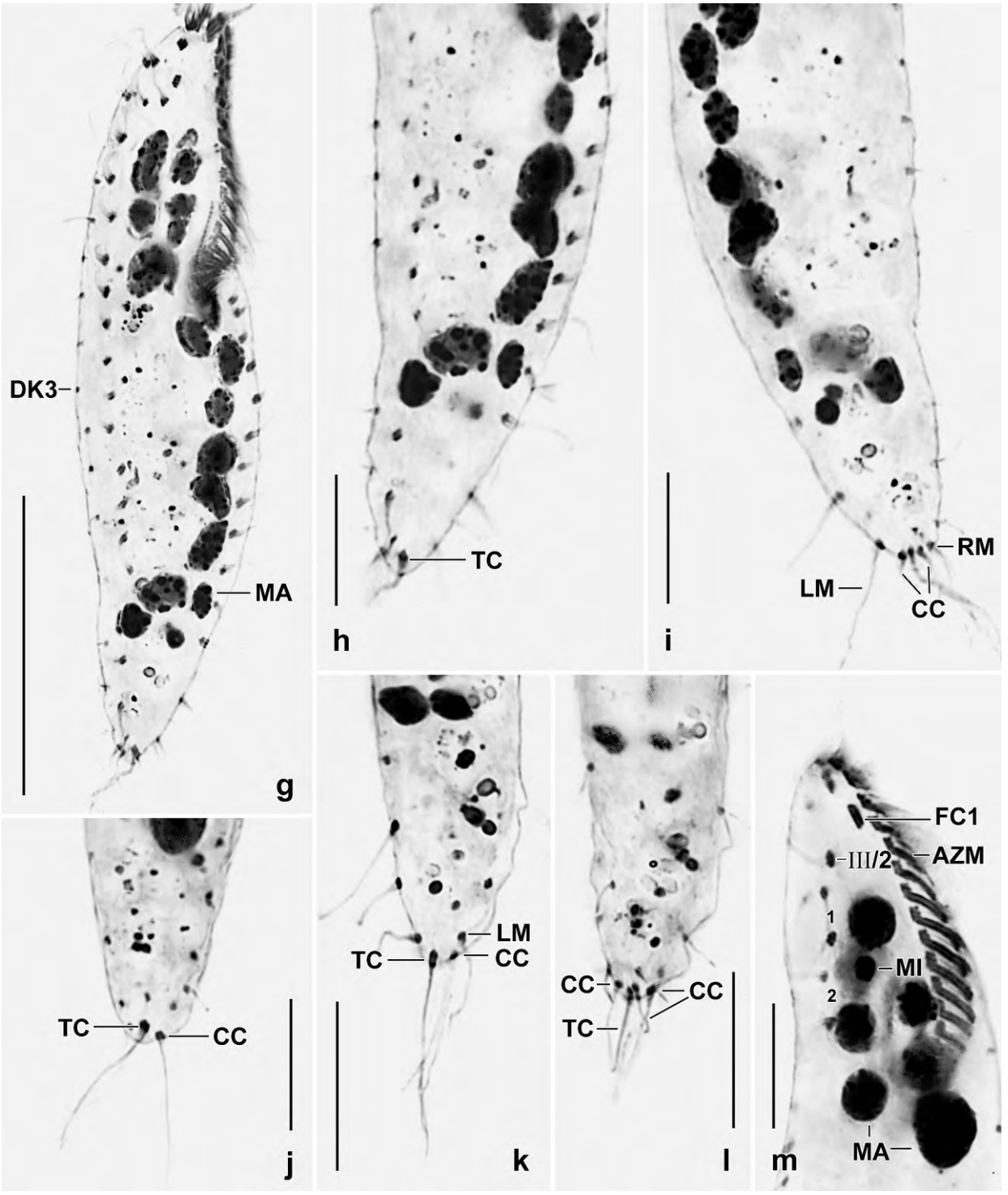

Fig. 232g–m. *Gonostomum multinucleatum*, Brazilian specimens after protargol impregnation. **g–i:** Overview and details of a single specimen, showing the single transverse cirrus and the three caudal cirri. **j–l:** As (g–i) but different specimens. **m:** Oral region, showing the frontoventral cirral pairs (1, 2) and the adoral membranelles in which rows 3 and 4 have the same length. AZM – adoral zone of membranelles, CC – caudal cirri, DK3 – dorsal kinety 3, FC1 – frontal cirrus 1, LM – left marginal row, MA – macronuclear nodules, MI – micronucleus, RM – right marginal row, TC – transverse cirrus, 1, 2 – frontoventral cirral pairs, III/2 – second cirrus of anlage III. Scale bars 10 µm (h–m) and 30 µm (g).

Table 85. Morphometric data on *Gonostomum multinucleatum* from Costa Rica (upper line, type) and Brazil (lower line). Data based on mounted, protargol-impregnated, and randomly selected specimens from non-flooded Petri dish cultures. Measurements in µm. CV – coefficient of variation in %, M – median, Max – maximum, Mean – arithmetic mean, Min – minimum, n – number of individuals investigated, SD – standard deviation, SE – standard error of arithmetic mean.

Characteristics	Mean	M	SD	SE	CV	Min	Max	n
Body, length	62.9	62.0	7.8	1.7	12.4	46.0	76.0	21
	75.6	74.0	9.8	2.1	13.0	60.0	98.0	21
Body, width	17.1	17.0	2.3	0.5	13.3	12.0	22.0	21
	16.0	16.0	1.9	0.4	11.6	13.0	22.0	21
Body length:width, ratio	3.7	3.8	0.4	0.1	11.4	2.9	4.3	21
	4.7	4.6	0.6	0.1	12.4	4.0	6.5	21
Anterior body end to proximal end of adoral zone of membranelles, distance	24.3	24.0	2.1	0.5	8.6	20.0	28.0	21
	29.1	29.0	2.8	0.6	9.7	22.0	35.0	21
Adoral zone of membranelles, percentage of body length	39.0	38.0	4.9	1.1	12.5	32.0	52.0	21
	38.5	38.0	3.5	0.8	9.0	31.0	43.0	21
Longest membranellar base, width	3.0	3.0	0.0	0.0	0.0	3.0	3.0	21
	not measured							
Adoral membranelles, number	19.1	19.0	1.0	0.2	5.3	18.0	21.0	21
	20.3	21.0	1.7	0.4	8.3	15.0	22.0	21
Anterior body end to paroral membrane, distance	12.0	12.0	1.4	0.3	11.9	10.0	14.0	21
	not measured							
Paroral membrane, length	4.9	5.0	0.8	0.2	15.7	3.0	6.0	21
	6.2	6.0	0.9	0.2	13.8	5.0	8.0	21
Paroral kinetids, number	6.6	7.0	0.9	0.2	13.2	5.0	8.0	21
	8.2	8.0	1.2	0.3	14.3	7.0	11.0	21
Anterior body end to endoral membrane, distance	15.0	15.0	1.9	0.4	12.5	13.0	18.0	21
	not measured							
Endoral membrane, length	9.0	9.0	1.0	0.2	11.1	7.0	10.0	21
	not measured							
Buccal cavity, width	1.9	2.0	1.2	0.3	64.0	0.0	5.0	21
	not measured							
Nuclear figure, length	39.3	38.0	5.2	1.1	13.2	32.0	50.0	21
	49.1	49.0	6.5	1.4	13.3	41.0	65.0	21
Anterior macronuclear nodule, length	4.6	4.0	1.4	0.3	31.5	3.0	8.0	21
	4.8	4.0	1.7	0.4	34.2	3.0	10.0	21
Anterior macronuclear nodule, width	3.3	3.0	0.7	0.1	19.7	2.0	5.0	21
	3.2	3.0	0.6	0.1	19.9	2.0	5.0	21
Macronuclear nodules, number	13.0	13.0	2.0	0.4	15.4	8.0	16.0	21
	11.9	12.0	3.4	0.7	28.6	6.0	19.0	21
Micronuclei, length	1.0	1.0	–	–	–	1.0	1.5	21
	1.9	2.0	–	–	–	1.5	2.5	21
Micronuclei, width	1.1	1.0	–	–	–	1.0	1.5	21
	1.4	1.5	–	–	–	1.0	1.5	21
Micronuclei, number	3.2	3.0	1.3	0.3	41.3	1.0	7.0	21
	2.6	3.0	1.1	0.2	43.6	1.0	4.0	21

continued

Characteristics	Mean	M	SD	SE	CV	Min	Max	n
Anterior body end to last frontoventral cirrus, distance	17.1	17.0	2.1	0.5	12.1	13.0	20.0	21
	20.0	20.0	2.4	0.5	12.0	14.0	25.0	21
Anterior body end to buccal cirrus, distance	11.9	12.0	1.5	0.3	12.3	10.0	14.0	21
	13.7	14.0	1.3	0.3	9.6	11.0	16.0	21
Anterior body end to right marginal cirral row, distance	4.2	4.0	0.8	0.2	19.6	3.0	6.0	21
	4.6	5.0	1.0	0.2	21.6	3.0	6.0	21
Frontal cirri, number	3.0	3.0	0.0	0.0	0.0	3.0	3.0	21
	3.0	3.0	0.0	0.0	0.0	3.0	3.0	21
Frontoterminal cirri, number	2.0	2.0	0.0	0.0	0.0	2.0	2.0	21
	2.0[a]	2.0	0.0	0.0	0.0	2.0	2.0	21
Buccal cirri, number	1.0	1.0	0.0	0.0	0.0	1.0	1.0	21
	1.0	1.0	0.0	0.0	0.0	1.0	1.0	21
Other frontoventral cirri, number	5.0	5.0	0.0	0.0	0.0	5.0	5.0	21
	5.3	5.0	0.9	0.2	16.1	4.0	7.0	21
Transverse cirri, number	1.0	1.0	0.0	0.0	0.0	1.0	1.0	21
	1.0	1.0	0.0	0.0	0.0	1.0	1.0	21
Right marginal row, number of cirri	16.7	16.0	1.5	0.3	9.0	15.0	20.0	21
	22.5	23.0	1.9	0.4	8.3	19.0	25.0	21
Left marginal row, number of cirri	11.1	11.0	1.1	0.2	9.8	9.0	13.0	21
	16.9	17.0	2.1	0.5	12.2	14.0	22.0	21
Dorsal kineties, number	3.0	3.0	0.0	0.0	0.0	3.0	3.0	21
	3.0	3.0	0.0	0.0	0.0	3.0	3.0	21
Kinetids in middle dorsal kinety, number	9.9	10.0	1.4	0.3	14.6	7.0	12.0	21
	13.0	13.0	1.3	0.3	9.7	11.0	15.0	21
Caudal cirri, number	3.0	3.0	0.0	0.0	0.0	3.0	3.0	21
	3.0	3.0	0.0	0.0	0.0	3.0	3.0	10

[a] Three in one out of 25 specimens.

nodules occasionally with a central, cube-shaped nucleolus surrounded by several granular nucleoli (Fig. 232d–f). One to four, on average 2.6 broadly ellipsoid micronuclei near and attached to macronuclear nodules. Contractile vacuole in or near mid-body posterior of buccal vertex (Fig. 231d). Cortex very flexible, contains loose rows of granules not impregnating with the protargol method used; individual granules globular to broadly ellipsoid, slightly yellowish, only 0.9 × 0.6 µm in size and thus difficult to recognize in vivo (Fig. 231a, d). Cytoplasm colourless, contains some lipid droplets about 2 µm across and 4–6 µm-sized food vacuoles with bacteria and their spores; does not contain crystals; in posterior body half occasionally a seemingly empty vacuole (Fig. 231a). Glides rapidly on microscope slides and soil particles, showing pronounced flexibility. Cirri arranged in *Gonostomum* pattern shown in Berger (1999, 2011) and in Figures 231a, b, f, h, 232a, c–h. Invariably three slightly thickened frontal cirri in strongly convex row following anterior body margin; base of frontal cirrus 1 about twice as long as that of cirri 2 and 3 (Fig. 231a, b, f, 232a, c–f, m). Two frontoterminal cirri in gap between adoral zone and right marginal cirral row. Buccal cirrus right of anterior end of paroral membrane, composed of six cilia. Invariably two oblique pairs of frontoventral cirri each composed of two rows each with four cilia; a single, very rarely two or three frontoventral cirri posterior of second pair. One, very rarely two transverse

cirri in mid of posterior cell margin, composed of four 12–16 µm long cilia; occurrence of only a single transverse cirrus confirmed by a late divider. Marginal cirri in vivo about 10 µm long, composed of six cilia in anterior quarters of rows and of only two to four cilia in posterior quarter; intracirral distance gradually and distinctly increasing from anterior to posterior. Three rows of dorsal bristles, 3 µm long in vivo and in protargol preparations; row 1 distinctly shortened anteriorly. Three, rarely only two caudal cirri each composed of two to four cilia 12 µm long in vivo. Marginal, transverse, and caudal cirri produce a rather distinct "brush" at posterior body end (Fig. 231c, g, i, 232a, c, f, i–l; Table 85). Oral apparatus in *Gonostomum* pattern (Berger 1999, 2011), i. e., adoral zone slightly sigmoid and following body margin before bending abruptly into cell proximally at 38% of body length; zone on average composed of 20 membranelles with cilia about 12 µm long in anterior half; membranellar ciliary rows 3 and 4 very short and of same length in few to many ventral membranelles providing them a hook-like appearance (Fig. 231a, f, 232a–g, m; Table 85). Buccal cavity very narrow and flat; buccal lip distinctly convex covering proximal half of adoral zone of membranelles (Fig. 231a, e), bears paroral membrane composed of about seven cilia 10 µm long in vivo. Endoral membrane right of paroral, anteriorly shorter then paroral while much longer posteriorly extending to end of adoral zone of membranelles. Pharyngeal fibres short, obliquely directed to right body margin (Fig. 231a, b, e, f, 232a, c, d, f, g, m; Table 85).

Occurrence and ecology: *Gonostomum multinucleatum* has been found in two soil samples from Costa Rica, in a sample from Brazil, and in Venezuelan samples (54, 61), indicating wide distribution in Central and South America. Costa Rican sample 2: Highly saline sand and soil from the Carribean coast at Punta Cocles, pH 7.6 in water. Costa Rican sample 3 (type locality): Soil and litter from an abandoned cacao plantago at Punta Cocles. Soil brown, pH 7.3 in water. Brazilian sample: Abandoned nest material of the termite *Anoplotermes* sp. on the Ilha de Marchantaria, i. e., an island in the Amazon River (sample kindly provided by Dr. Christopher Martius, Univ. Göttingen, Germany; for details, see Martius 1994).

Remarks: Among the congeners reviewed in Berger (1999, 2011) only *G. kuehnelti* is multinucleate. However, this species is easily distinguished from *G. multinucleatum* by the ellipsoid body (vs. slenderly ellipsoid, length:width ratio 2.5:1 vs. 4:1) and the number of transverse cirri (4 vs. 1). More difficult is the separation from *Paragonostomum simplex* Foissner et al. (2005a). This species has a stouter posterior body end, lacks transverse cirri (vs. one cirrus present), has four (vs. two) frontoterminal cirri and four (vs. one) cirri posterior of the two frontoventral cirral pairs. These differences are difficult to recognize in vivo, suggesting that identifications should be controled in protargol preparations.

Gonostomum bromelicola nov. spec. (Fig. 233a–l, 234a–m; Table 86)

Diagnosis: Size in vivo about 100 × 35 µm. Ellipsoid with distinctly narrowed oral region. 2 macronuclear nodules and 2 minute micronuclei about 1.5 µm in diameter. Cortical granules scattered and in loose rows, colourless, 3–4 × 1 µm in size. Cirri comparatively thick and long, except of three fine caudal cirri. 3 frontal cirri, first rarely slightly enlarged; 2 frontoterminal cirri; 1 buccal cirrus right of anterior end of paroral membrane; 2 pretransverse cirri in specific pattern; and 5 transverse cirri 16% distant from posterior body end. Right marginal row commences 20%

Table 86. Morphometric data on *Gonostomum bromelicola* (upper line) and *Gonostomum fraterculum* (lower line) based on mounted, protargol-impregnated, and randomly selected specimens from tank bromeliads and a non-flooded Petri dish culture. Measurements in µm. CV – coefficient of variation in %, M – median, Max – maximum, Mean – arithmetic mean, Min – minimum, n – number of individuals investigated, SD – standard deviation, SE – standard error of arithmetic mean.

Characteristics	Mean	M	SD	SE	CV	Min	Max	n
Body, length	85.6	85.0	5.7	1.2	6.7	75.0	95.0	21
	95.8	98.0	11.0	2.4	11.5	77.0	116.0	21
Body, width	32.9	32.0	3.5	0.8	10.5	26.0	39.0	21
	29.7	30.0	3.6	0.8	12.0	22.0	37.0	21
Body length:width, ratio	2.6	2.6	0.2	0.0	7.9	2.2	3.0	21
	3.2	3.2	0.3	0.1	9.7	2.8	3.9	21
Anterior body end to proximal end of adoral zone of membranelles, distance	47.3	47.0	2.4	0.5	5.1	43.0	52.0	21
	55.1	56.0	6.3	1.4	11.5	44.0	65.0	21
Adoral zone of membranelles, percentage of body length	55.4	56.0	3.9	0.8	7.0	48.0	64.0	21
	57.6	58.0	2.7	0.6	4.7	53.0	62.0	21
Largest membranellar basis, length	4.3	4.0	0.5	0.1	11.1	4.0	5.0	21
	4.6	5.0	0.5	0.1	11.1	4.0	5.0	21
Distance between endoral membrane and adoral zone of membranelles	7.3	7.0	1.5	0.3	20.5	5.0	13.0	21
	7.0	7.0	1.5	0.3	20.8	5.0	9.0	21
Anterior body end to right marginal row, distance	17.0	17.0	1.5	0.3	9.1	14.0	19.0	21
	12.7	13.0	2.1	0.5	16.5	9.0	17.0	21
Anterior body end to paroral membrane, distance	26.5	27.0	2.0	0.4	7.6	23.0	29.0	21
	29.3	30.0	3.6	0.8	12.4	21.0	35.0	21
Anterior body end to endoral membrane, distance	28.0	28.0	2.2	0.5	7.7	25.0	31.0	21
	37.1	38.0	4.9	1.1	13.2	28.0	45.0	21
Anterior body end to buccal cirrus, distance	26.9	27.0	1.8	0.4	6.5	24.0	30.0	21
	29.5	29.0	3.3	0.7	11.3	23.0	36.0	21
Anterior body end to first macronuclear nodule, distance	16.6	16.0	1.0	0.2	6.2	15.0	18.0	21
	21.8	22.0	2.8	0.6	13.1	15.0	26.0	21
Posterior body end to lowermost transverse cirrus, distance	14.0	14.0	1.8	0.4	13.2	10.0	18.0	21
	9.8	10.0	2.4	0.5	24.9	5.0	15.0	21
Posterior body end to right marginal row, distance	3.6	4.0	1.2	0.3	33.2	2.0	5.0	21
	4.0	4.0	0.9	0.2	22.7	2.0	5.0	21
Posterior body end to left marginal row, distance	1.8	2.0	1.0	0.2	56.5	0.0	4.0	21
	1.6	1.5	0.6	0.1	36.7	1.0	3.0	21
Anterior macronuclear nodule, length	17.4	17.0	2.0	0.4	11.4	13.0	21.0	21
	15.5	15.0	1.7	0.4	10.7	13.0	20.0	21
Anterior macronuclear nodule, width	6.0	6.0	0.7	0.2	12.2	5.0	7.0	21
	6.5	6.0	0.6	0.1	9.3	6.0	8.0	21
Macronuclear nodules, number	2.0	2.0	0.0	0.0	0.0	2.0	2.0	21
	2.0	2.0	0.0	0.0	0.0	2.0	2.0	21
Micronuclei, number	1.9	2.0	1.3	0.3	70.2	0.0	5.0	21
	2.8	3.0	0.7	0.1	24.2	2.0	4.0	21
Micronuclei, length	1.5	1.5	0.7	0.1	44.8	0.0	2.0	21
	2.5	2.5	0.7	0.1	26.3	2.0	4.0	21

continued

Characteristics	Mean	M	SD	SE	CV	Min	Max	n
Micronuclei, width	1.3	1.5	0.6	0.1	46.4	0.0	2.0	21
	2.1	2.0	0.3	0.1	14.4	1.5	3.0	21
Adoral membranelles, number	36.8	37.0	2.5	0.5	6.7	34.0	43.0	21
	38.8	39.0	3.7	0.8	9.4	31.0	43.0	21
Frontal cirri, number	3.0	3.0	0.0	0.0	0.0	3.0	3.0	21
	3.0	3.0	0.0	0.0	0.0	3.0	3.0	21
Frontoterminal cirri, number	2.0	2.0	0.0	0.0	0.0	2.0	2.0	21
	2.0	2.0	0.0	0.0	0.0	2.0	2.0	21
Buccal cirri, number	1.0	1.0	0.0	0.0	0.0	1.0	1.0	21
	1.0	1.0	0.0	0.0	0.0	1.0	1.0	21
Frontoventral cirral pairs, number	2.0	2.0	0.0	0.0	0.0	2.0	2.0	21
	2.0	2.0	0.0	0.0	0.0	2.0	2.0	21
Frontoventral anlage III, number of cirri	2.0	2.0	0.0	0.0	0.0	2.0	2.0	21
	1.0	1.0	0.0	0.0	0.0	1.0	1.0	21
Pretransverse and transverse cirri, number	7.0	7.0	0.0	0.0	0.0	7.0	7.0	21
	7.0	7.0	0.0	0.0	0.0	7.0	7.0	21
Caudal cirri, number	3.0	3.0	0.2	0.0	7.4	2.0	3.0	21
	3.0	3.0	0.0	0.0	0.0	3.0	3.0	21
Right marginal cirri, number	17.5	17.0	1.8	0.4	10.5	15.0	22.0	21
	23.4	23.0	3.3	0.7	14.0	17.0	30.0	21
Left marginal cirri, number	11.0	11.0	1.1	0.2	10.0	9.0	13.0	21
	15.6	16.0	2.3	0.5	14.7	12.0	21.0	21
Paroral kinetids, number	14.1	14.0	1.7	0.4	12.3	11.0	17.0	21
	21.7	22.0	3.5	0.8	16.1	17.0	28.0	21
Dorsal kineties, number	3.0	3.0	0.0	0.0	0.0	3.0	3.0	21
	3.0	3.0	0.0	0.0	0.0	3.0	3.0	21
Dorsal kinety 1, number of kinetids	35.3	35.0	4.5	1.0	12.6	26.0	44.0	21
	29.6	30.0	5.3	1.2	18.1	19.0	37.0	21
Dorsal kinety 2, number of kinetids	26.2	26.0	3.7	0.8	14.0	21.0	35.0	21
	26.0	27.0	3.8	0.8	14.6	18.0	32.0	21
Dorsal kinety 3, number of kinetids	32.7	33.0	4.4	0.9	13.3	18.0	38.0	21
	29.5	29.0	4.3	0.9	14.7	23.0	38.0	21
Resting cyst, length	37.6	38.0	3.4	0.8	9.0	30.0	45.0	17
	no data							
Resting cyst, width	36.5	36.0	2.5	0.6	6.8	30.0	42.0	17
	no data							

subapical, composed of an average of 17 cirri, left of 11. An average of 94 dorsal bristles up to 5 µm long, form 3 rows, middle row with distinct break/irregularity posterior of mid-body. Adoral zone flat to slightly sigmoid, preoral dish usually distinct; extends about 56% of body length and consists of an average of 37 membranelles. On average 14 paroral kinetids with cilia 15–20 µm long in vivo and in SEM micrographs. Resting cyst with thin, smooth wall.

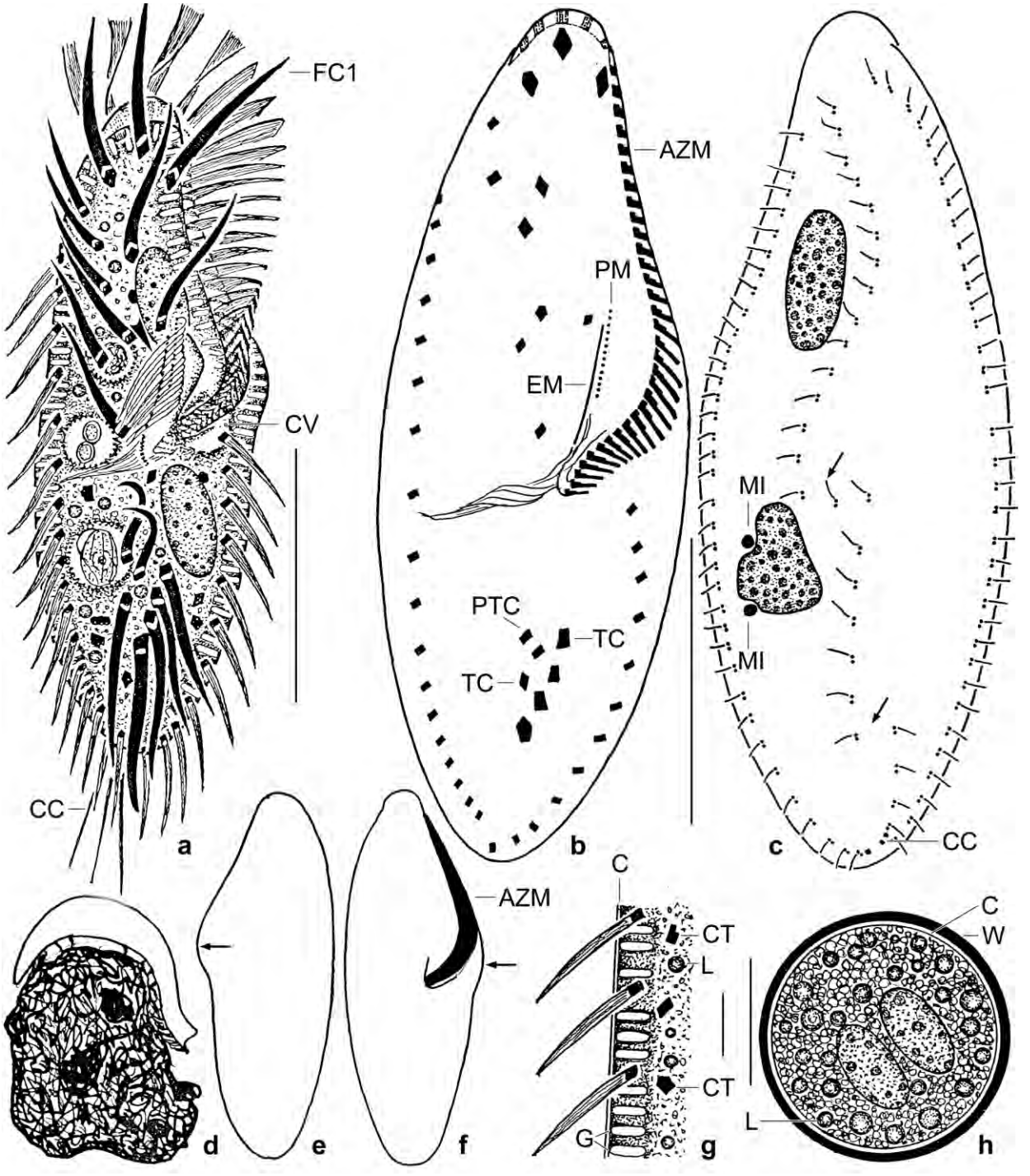

Fig. 233a–h. *Gonostomum bromelicola* from live (a, d, g, h), after protargol impregnation (b, c), and redrawn from scanning electron micrographs (e, f). **a, g:** Ventral view of a representative specimen (length 100 µm) and its cortical granules. The arrowhead marks the long paroral cilia. Note the thick cirri. **b, c:** Ventral and dorsal view of holotype specimen, length 90 µm. The arrows mark interruptions in dorsal kinety 2. **d:** Showing the high flexibility when crawling on a mud particle. **e, f:** The arrows mark the oral dish well recognizable in vivo and in the SEM. **h:** Resting cyst, 40 µm. AZM – adoral zone of membranelles, C – cortex, CC – caudal cirri, CT – crystals, CV – contractile vacuole, EM – endoral membrane, FC1 – frontal cirrus 1, G – cortical granules, L – lipid droplets, MI – micronuclei, PM – paroral membrane, PTC – pretransverse cirri, TC – transverse cirri, W – cyst wall. Scale bars 10 µm (g), 20 µm (h), 30 µm (b, c), and 40 µm (a).

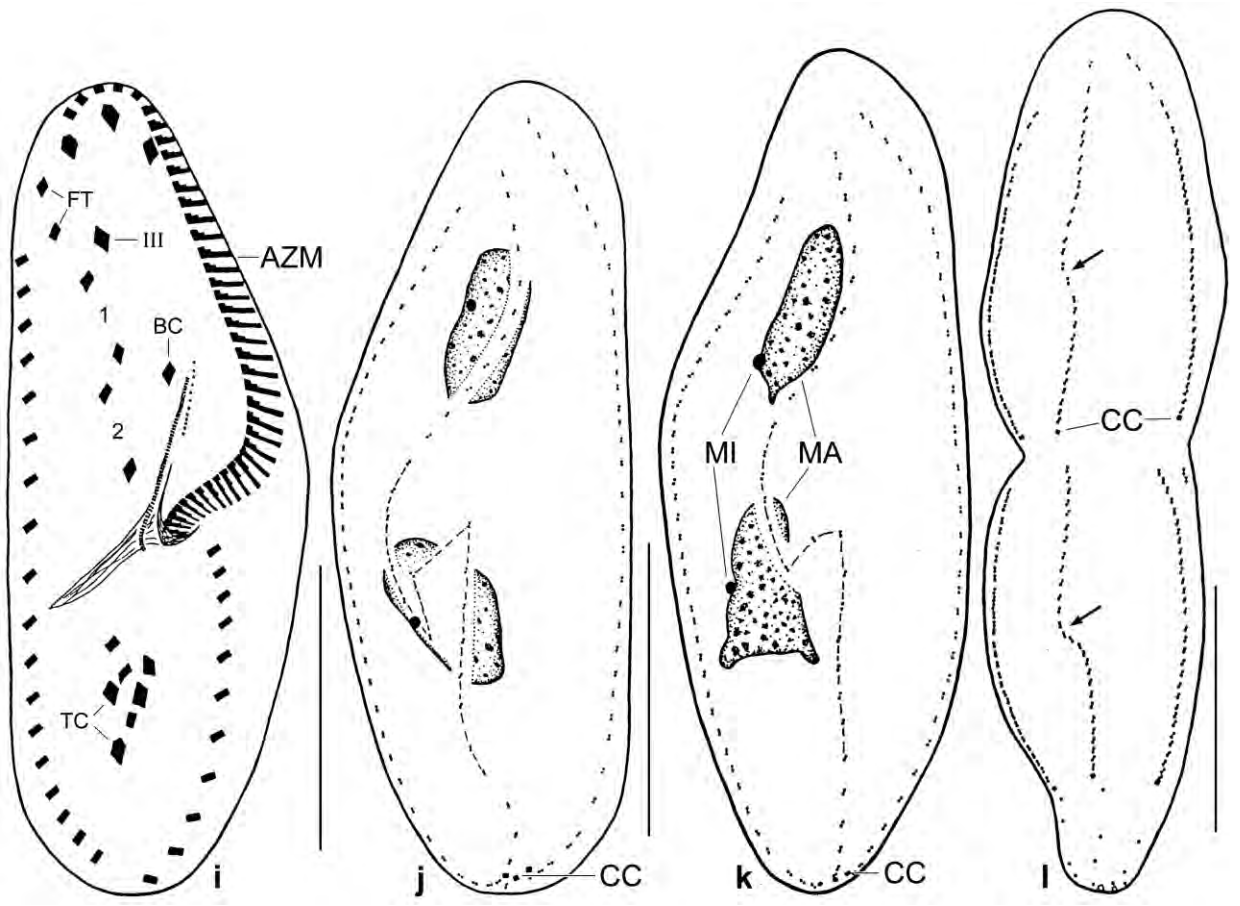

Fig. 233i–l. *Gonostomum bromelicola* after protargol impregnation. **i, j:** Ventral and dorsal view of a paratype specimen, showing the two ventral cirral pairs (numerals), the enlarged cirrus from anlage III, and the transverse cirri which are far subterminal. Note also the comparatively thick cirri and the bracket-shaped adoral zone of membranelles. The hatched portion in (j) marks the break in the middle dorsal kinety. **k:** Another paratype specimen, showing the break in dorsal kinety 2 (hatched portion). Note the comparatively large number of bristle dikinetids, another speciality of *G. bromelicola*. **l:** A late divider, showing the origin of the break in dorsal kinety 2 (arrows). AZM – adoral zone of membranelles, BC – buccal cirrus, CC – caudal cirri, FT – frontoterminal cirri, MA – macronuclear nodules, MI – micronuclei, TC – transverse cirri. Scale bars 30 µm.

Type locality: Tanks of *Achmea paniculigera* in Jamaica, 77°41'W 18°17'N.

Type material: 1 holotype and 5 paratype slides with protargol-impregnated specimens have been deposited in the Biology Centre of the Upper Austrian Museum in Linz (LI). The holotype and other relevant specimens have been marked by black ink circles on the coverslip.

Etymology: The species name is a composite of the genus group name *Bromelia* (the plant on which the ciliate lives), the thematic vowel *-i-*, and the Latin verb *colere* (to live in), referring to the habitat the species was discovered.

Description: Most features of ordinary variability, i. e., with coefficients of variability < 15% (Table 86), except of width of buccal cavity (CV = 24.2%) and posterior body end to right and left marginal cirral row (CV = 33.2% and 56.5%).

Size in vivo 85–110 × 30–45 µm, usually about 100 × 35 µm, as calculated from some in vivo measurements and the morphometric data in Table 86 adding 15% preparation shrinkage. Body

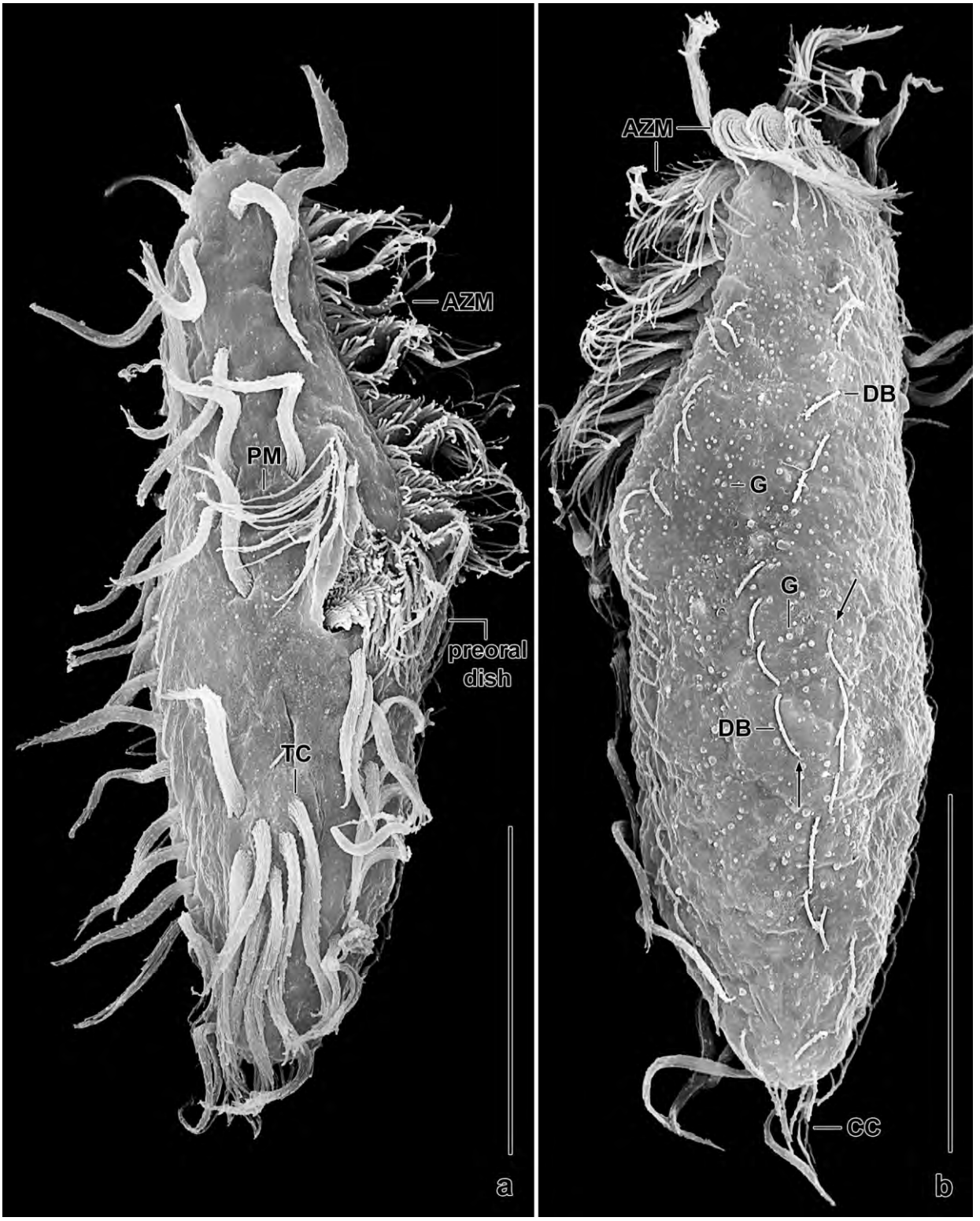

Fig. 234a, b. *Gonostomum bromelicola*, ventral and dorsal view in the SEM. Note the long paroral cilia, the sigmoid adoral zone, and the break in dorsal kinety 2 (b, arrows). AZM – adoral zone of membranelles, CC – caudal cirri, DB – dorsal bristles up to 5 µm long, G – cortical granules, PM – paroral membrane, TC – transverse cirri. Scale bars 30 µm.

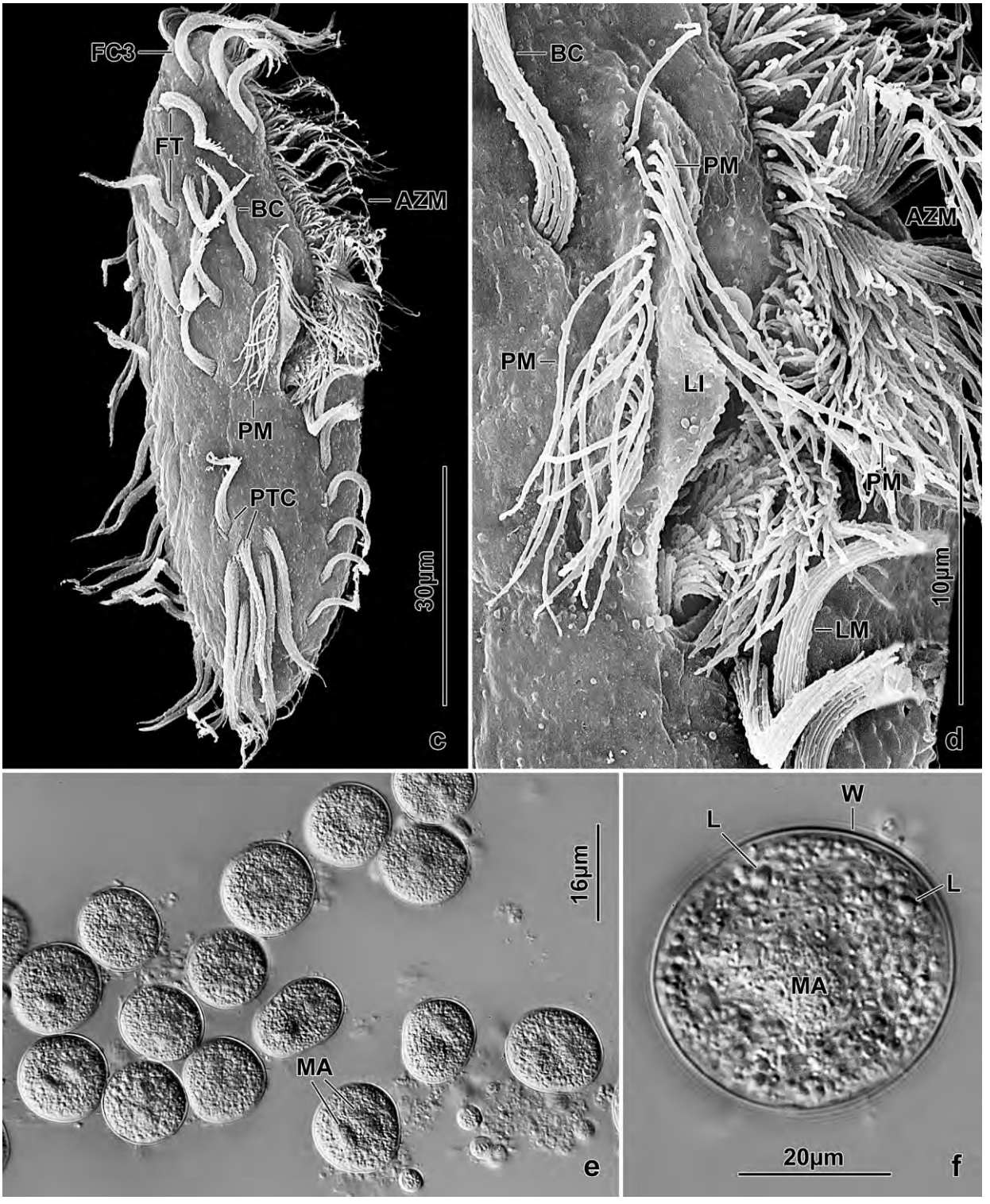

Fig. 234c–f. *Gonostomum bromelicola* in the SEM (c, d) and in vivo (e, f). **c, d:** Ventral overview and detail showing, especially, the about 15 µm long paroral cilia and the buccal lip**. e, f:** Resting cysts. The macronuclear nodules are not fused. AZM – adoral zone, BC – buccal cirrus, FC3– frontal cirrus 3, FT – frontoterminal cirri, L – lipid droplets, LI – buccal lip, LM – left marginal row, MA – macronuclear nodules, PM – paroral membrane, PTC – pretransverse cirri, W – wall.

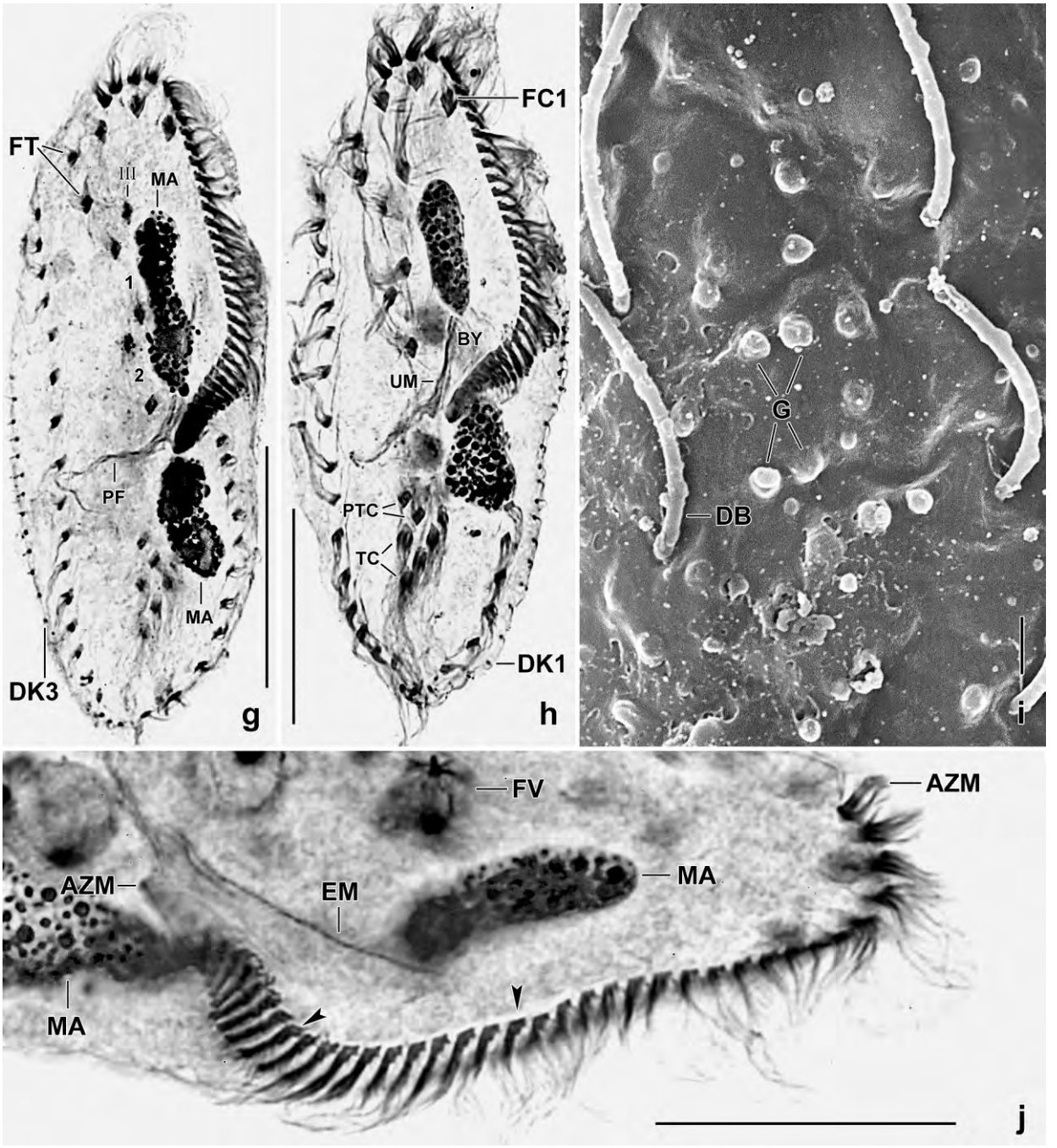

Fig. 234g–j. *Gonostomum bromelicola* in the scanning electron microscope (i) and after protargol impregnation (g, h, j). **g, h:** Ventral views, showing the elongate ellipsoid to globular macronuclear nodules, the bracket-shaped adoral zone of membranelles, the frontoventral cirral pairs (numerals), the posterior cirrus of anlage III, and the transverse cirri which are far subterminal and only slightly project from body proper. **i:** Dorsal cortex with emerging extrusomes (cortical granules). **j:** Oral apparatus of a specimen with slightly sigmoid adoral zone. The arrowheads mark a ventral and a proximal adoral membranelle, respectively; kineties 3 and 4 are very short in the ventral membranelles while kinety 3 elongated in the proximal membranelles. AZM – adoral zone of membranelles, BY – buccal cavity, DB – dorsal bristles, DK1, 3 – dorsal kineties, EM – endoral membrane, FC1 – frontal cirrus 1, FT – frontoterminal cirri, FV – food vacuole with the flagellate *Polytomella*, G – cortical granules, MA – macronuclear nodules, PF – pharyngeal fibres and endoral cilia, PTC – pretransverse cirri, TC – transverse cirri, UM – undulating membranes. Scale bars 1 µm (i), 20 µm (j), and 30 µm (g, h).

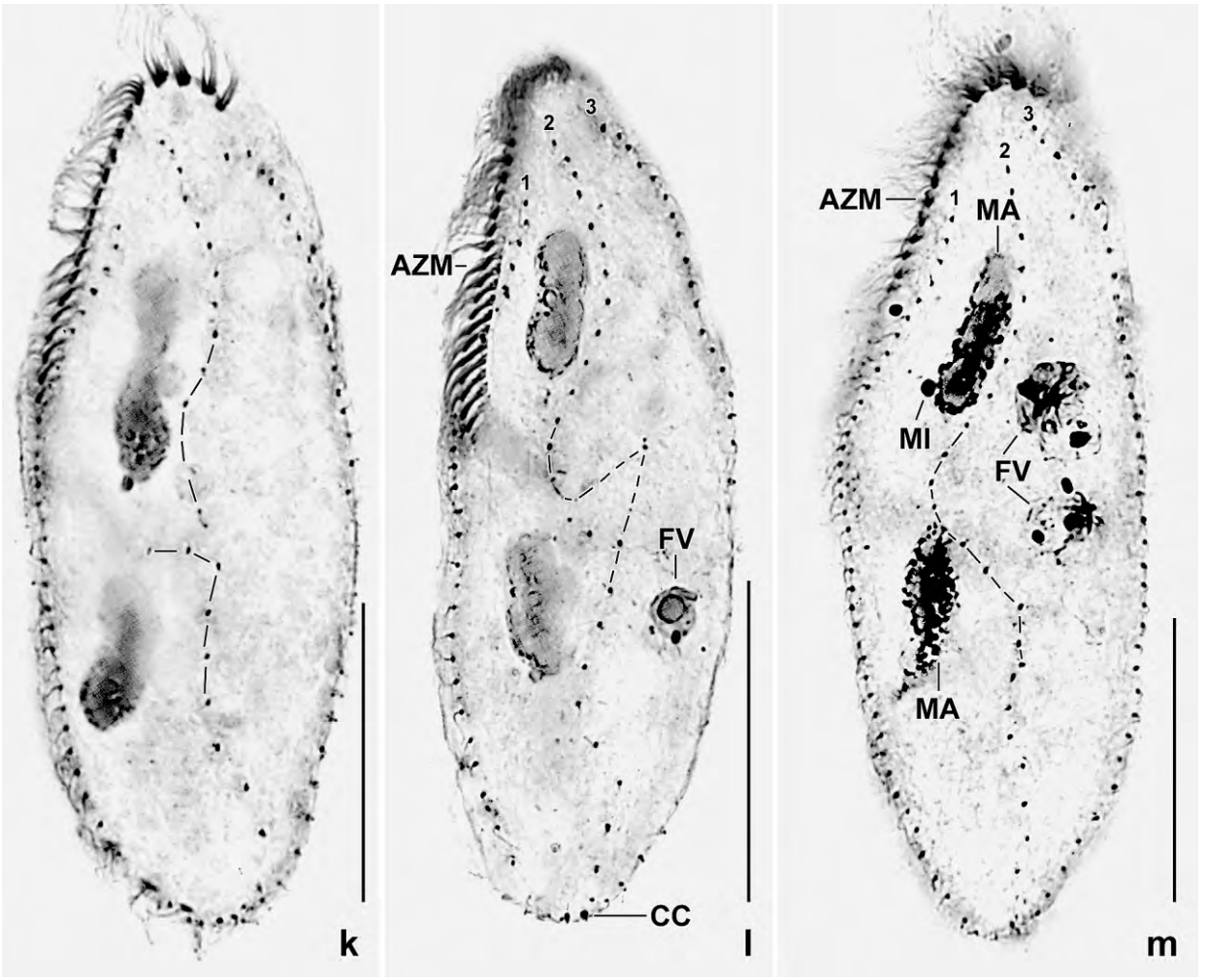

Fig. 234k–m. *Gonostomum bromelicola*, dorsal views after protargol impregnation to show the break or irregularity in the middle dorsal kinety (hatched lines). Note also the narrowly spaced dikinetids in the dorsal kineties and some variation in body shape. AZM – adoral zone of membranelles, CC – caudal cirri, FV – food vacuoles with the heterotrophic flagellate *Polytomella*, MA – macronuclear nodules, MI – micronucleus, 1, 2, 3 – dorsal kineties. Scale bars 30 µm.

ellipsoid, central part of adoral zone flat or slightly concave, preoral dish distinct to indistinct, both ends usually distinctly narrowed; laterally flattened up to 2:1 (Fig. 233a, e, f, i, k, 234a–c, g, j, l; Table 86). Nuclear apparatus in central quarters of cell slightly left of body`s midline. Two, very rarely three macronuclear nodules elongate ellipsoid on average; anterior nodule underneath of anterior half of paroral membrane, posterior close to proximal portion of adoral zone; with many minute nucleoli. Two to five, on average two micronuclei attached to or near to macronuclear nodules, small compared to size of cell, i. e., about 1.5 µm across (Fig. 233a, c, j, k, 234g, h, j, k–m; Table 86). Contractile vacuole underneath proximal portion of adoral zone (Fig. 233a). Cortex very flexible, studded with colourless granules forming a rather distinct fringe in vivo and in protargol preparations; individual granules in vivo about 3–4 × 1µm in size, scattered and in short rows (Fig. 233a, g, 234b, i). Cytoplasm colourless, usually packed with 5–10 µm-sized food vacuoles containing bacteria and small heterotrophic flagellates (*Polytomella* sp., *Anisonema* sp.); some lipid droplets 0.5–1.5 µm across; and rather many stout crystals 2–3 × 1–2

µm in size (Fig. 233a, g). Glides rapidly on microscope slides and creeps between mud particles, showing great flexibility (Fig. 233d).

Cirri comparatively thick and long, e. g., marginal cirri composed of three rows of cilia and about 15 µm long in vivo (Fig. 233a, b, 234a, c, h); arranged in typical *Gonostomum* pattern (Berger 2011) shown in Figures 233a, b, i, 234a, c, g, h. Three frontal cirri in strongly convex row following anterior body margin, thick and about 25 µm long in vivo, basis of first frontal cirrus slightly enlarged in some specimens. Two frontoterminal cirri and two frontoventral cirral pairs with cilia 20–25 µm long in vivo; posterior cirrus of anlage III slightly enlarged and at level of posterior frontoterminal cirrus. Buccal cirrus right of anterior end of paroral membrane. Two pretransverse and five transverse cirri far (16% of body length) subterminal and thus only slightly projecting from body proper although about 25 µm long in vivo; pretransverse cirri clearly separate, form an oblique pair in cavity of transverse cirri. Two marginal cirral rows with cirral distances gradually decreasing from anterior to posterior except of first two cirri of right marginal row slightly narrower spaced than the following; right marginal row commencing far (20% of body length) subapically and ends slightly subterminally; left marginal row extends to midline of body posteriorly (Fig. 233a, b, i, 234a, b, g, h; Table 86).

Three dorsal kineties with a total of 94 kinetids on average, a high number compared to most congeners; kineties 1 and 2 slightly shortened anteriorly. Cilia (bristles) 3–4 µm long in anterior and posterior third of rows while 4–5 µm in middle third. Middle row invariably with one, very rarely two breaks or irregularities posterior of mid-body, an outstanding feature resembling the ontogenetic break of dorsal kinety 3 in the oxytrichids s. str.; development of break seen in two late dividers (Fig. 233l). Three, very rarely only two fine caudal cirri each composed of four cilia about 20 µm long in vivo (Fig. 233a, c, j–l, 234b, k–m; Table 86).

Oral apparatus in *Gonostomum* pattern (Berger 2011), i. e., the adoral zone follows the anterior and left body margin and bends abruptly into the cell at about 56% of body length; bend associated with a slightly projecting concavity that we call "preoral dish" (Fig. 233a, e, f, 234b). Adoral zone flat to slightly sigmoid, on average composed of 37 gonostomoid membranelles with largest bases about 4 µm width in protargol preparations (Fig. 233a, b, i, 234a, c, d, g, h, j; Table 86). Buccal cavity flat and rather narrow, partially covered by a convex lip. Paroral membrane right of buccal lip, composed of an average of 14 kinetids with cilia 15–20 µm (!) long in vivo and in SEM micrographs (Fig. 233a, 234a, c, d), an outstanding length not reported from any other hypotrich. Endoral membrane commencing slightly posterior of paroral and extending to proximal end of adoral zone, cilia about 20 µm long and distinctly beating in the pharynx extending obliquely to right body margin.

Resting cyst: Resting cysts colourless, globular to slightly ellipsoid, on average 37.6 × 36.5 µm in size (Fig. 233h, 234e, f; Table 86). Wall smooth, without zonation, 1–1.5 µm thick. Macronuclear nodules not fused. Cytoplasm studded with lipid droplets or autophagous vacuoles up to 4 µm across and countless granules smaller than 1.5 µm.

Molecular phylogeny: The SS-rDNA of *G. bromelicola* has been sequenced by Dunthorn et al. (2012) where it has been named "*Gonostomum* (undescr. sp.?)"; the GenBank number is JQ

723970. *Gonostomum bromelicola* is in a well supported clade (ML99/BI/100) containing *G. strenuum* and *Cotterillia bromelicola* Foissner & Stoeck, 2011 while *G. namibiense* belongs to another clade that is poorly supported (–/62) but provides an indication that *Gonostomum* is not monophyletic.

Occurrence and ecology: As yet found only at type locality. A raw culture was obtained by adding some wheat grains to the sample distributed in a Petri dish. However, it grew slowly and only for a few days.

Obviously, *G. bromelicola* is a rare species but the common *G. affine* is also infrequent in tank bromeliads. We could not find a reason for the break in dorsal kinety 2 but it provides the species with a unique identity.

Remarks: There are three similar species all described in the present monograph: *G. lajacola*, *G. bromelicola*, and *G. fraterculus*. *Gonostomum fraterculus* differs from *G. bromelicola* by (i) the number of paroral kinetids (22 vs. 14), (ii) the length of the paroral cilia (~ 10 µm vs. 15–20 µm), and (iii) dorsal kinety 2 (without vs. with distinct break).

Gonostomum lajacola differs from *G. bromelicola* by (i) the number of paroral kinetds (23 vs. 14), (ii) the length of the paroral cilia (~ 6 µm vs. 15–20 µm), (iii) the length of the dorsal bristles (up to 10 µm vs. up to 5 µm), and (iv) dorsal kinety 2 (without vs. with distinct break).

Gonostomum fraterculus differs from *G. lajacola* by (i) the length of the paroral cilia (~ 6 µm vs. ~ 10 µm), (ii) the location of the buccal cirrus (at level of begin of paroral membrane vs. subapical of paroral membrane), (iii) the number of adoral membranelles (39 vs. 32), (iv) the length of the dorsal bristles (4–5 µm vs. up to 10 µm), and (v) the number of dorsal bristles in kinety 3 (29 vs. 18).

Gonostomum fraterculus nov. spec. (Fig. 235a–d, 236a–d; Table 86)

Diagnosis: As *G. bromelicola* but living in soil and without break in dorsal kinety 2.

Type locality: Surface litter and loamy soil up to 5cm depth on an island in the Amazon River, Janauari region, outskirts of the town of Manaus, Brazil, 60°W 4°S.

Type material: 1 holotype and 3 paratype slides with protargol-impregnated specimens have been deposited in the Biology Centre of the Upper Austrian Museum in Linz (LI). The holotype and other relevant specimens have been marked by black ink circles on the coverslip.

Etymology: The Latin species name is an apposite noun composed of *frater* (brother) and the diminutive *culum* (small, similar), referring to → *G. bromelicola* which is very likely derived from *fraterculus*.

Description and Remarks: *Gonostomum fraterculus* is very likely the ancestor of → *G. bromelicola*, differing mainly in having an ordinary dorsal kinety 2 and living in soil (vs. in tanks

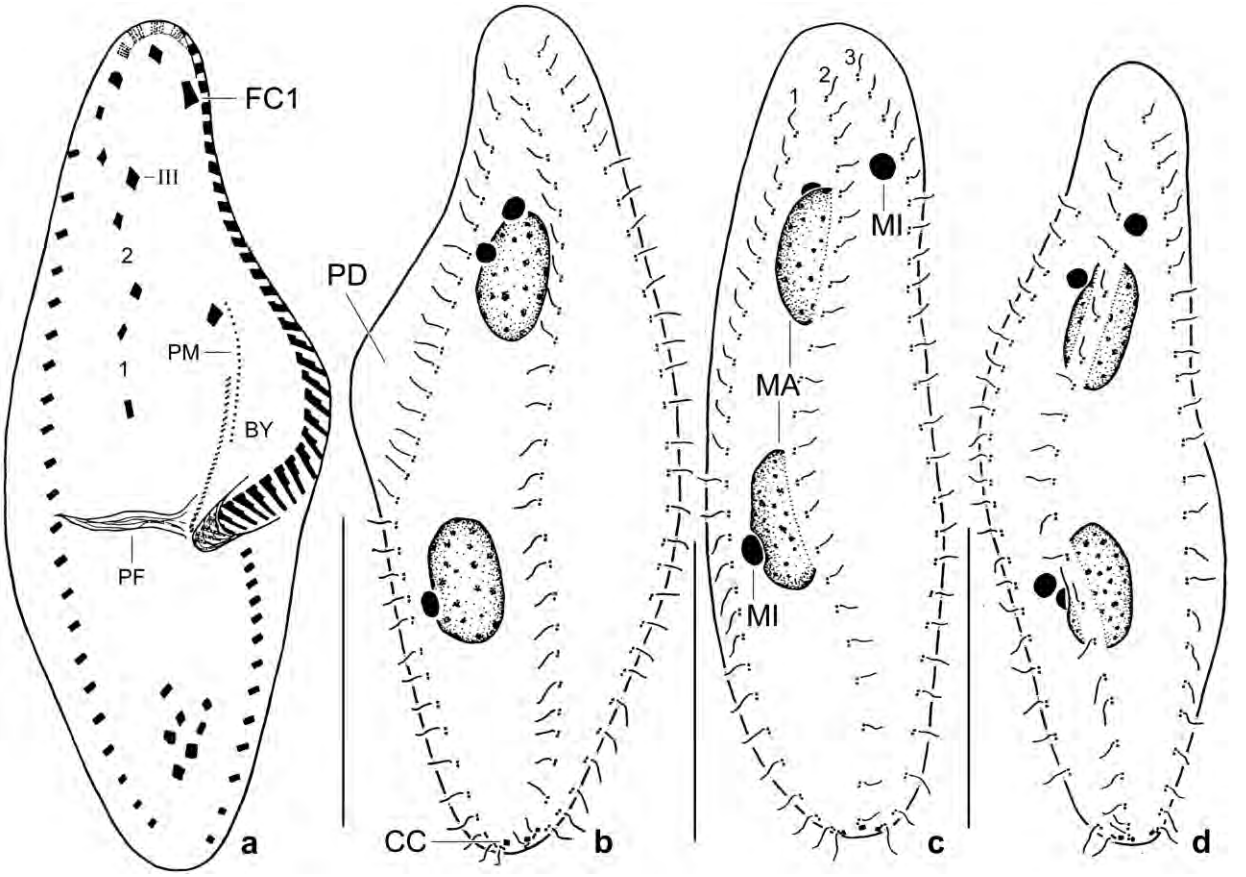

Fig. 235a–d. *Gonostomum fraterculus* after protargol impregnation. **a, b:** Ventral and dorsal view of holotype specimen, length 85 µm. Note the distinct preoral dish and the increased size of the first frontal cirrus. **c, d:** Dorsal views, showing the ordinary dorsal kinety 2. BY – buccal cavity, CC – caudal cirri, FC1 – frontal cirrus 1, MA – macronuclear nodules, MI – micronuclei, PD – preoral dish, PF – pharyngeal fibres, PM – paroral membrane, III – posterior cirrus of anlage III, 1, 2 – frontoventral cirral pairs, 1, 2, 3 – dorsal kineties. Scale bars 30 µm.

of bromeliads). However, the following features are also different, adding to the distinctness of this species (Fig. 235a–d, 236a–d; Table 86): (i) *fraterculus* is on average more slender than *bromelicola* (length:width ratio 3.2:1 vs. 2.6:1), (ii) the micronuclei are larger (on average 2.5 × 2.1 µm vs. 1.5 × 1.3 µm), (iii) the cirri are of ordinary thickness (marginal cirri composed of 2 vs. 3 ciliary rows) and length (e.g., transverse cirri 18 µm vs. 25 µm), (iv) the right marginal cirral row commences more anteriorly (13% vs. 20% of body length), (v) the number of paroral kinetids is higher by 7% relative to body length, and (vi) the cilia of the paroral kinetids are shorter (~ 10 µm vs. 20 µm). The shape of the adoral zone of membranelles is very variable (Fig. 236a–d). For separation from → *G. lajacola*, see → *G. bromelicola*.

Although these are a lot of differences, the first impression of a close relationship with → *G. bromelicola* is overwhelming because all differences are quantitative except of the lack of a break in dorsal kinety 2 and the terrestrial habitat. The break of dorsal kinety 2 of → *G. bromelicola* has heavy taxonomic weight because the dorsal ciliature is very stable in hypotrichs.

Occurrence and ecology: As yet found only at type locality. Considering the Amazon floods, a wide distribution is very likely.

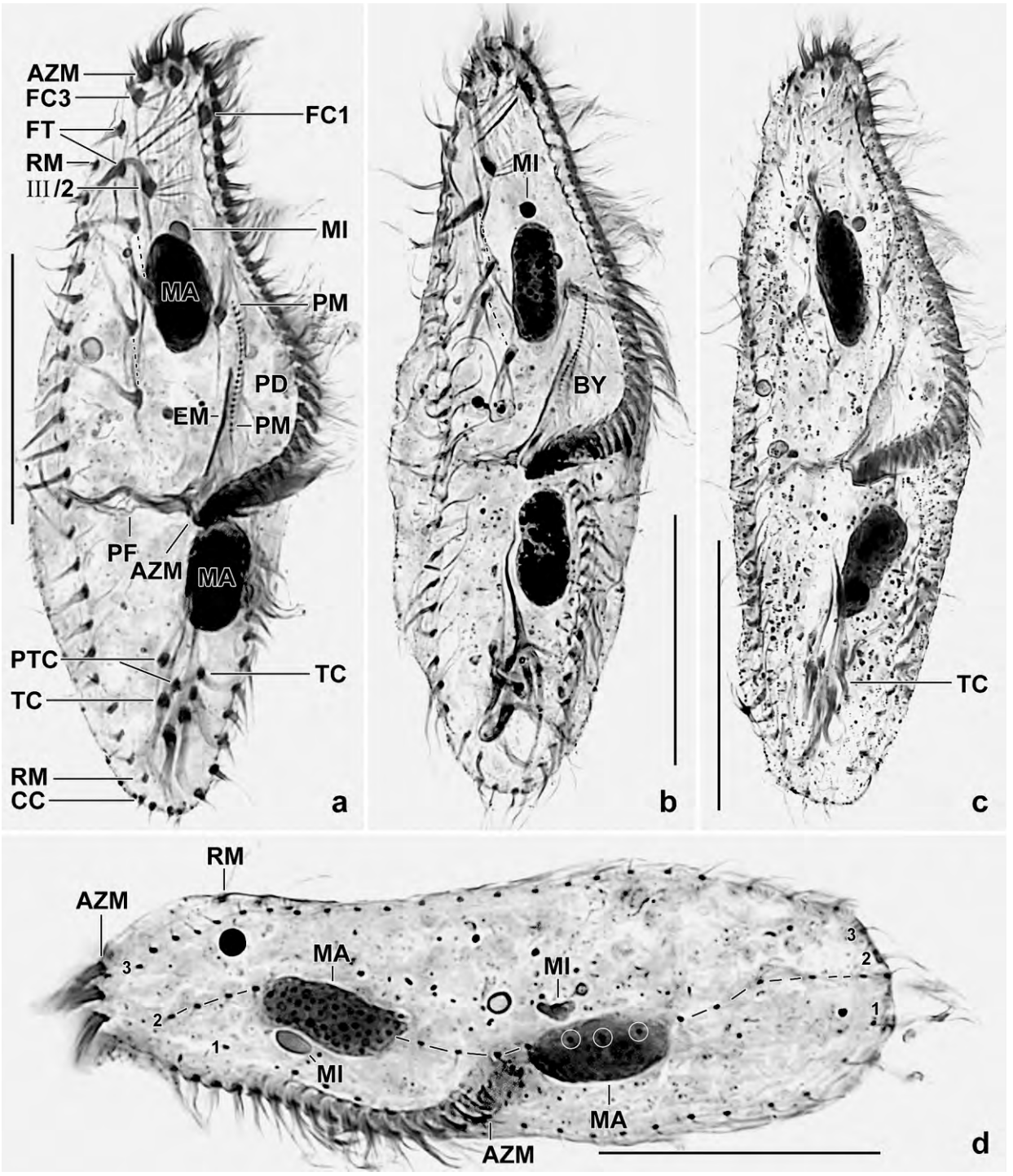

Fig. 236a–d. *Gonostomum fraterculus,* ventral (a–c) and dorsal (d) views after protargol impregnation. **a, b:** Holotype and a paratype specimen. Note the conspicuous preoral dish and the long paroral membrane. The cirri of the two frontoventral cirral pairs are connected by hatched lines. **c:** Surface view, showing the dense cortical granulation. **d:** Dorsal kinety 2 is sigmoid but lacks an irregularity or a break so typical for that of → *G. bromelicola*. AZM – adoral zone of membranelles, BY – buccal cavity, CC – caudal cirri, EM – endoral membrane, FC1, 3 – frontal cirri, FT – frontoterminal cirri, MA – macronuclear nodules, MI – micronuclei, PD – preoral dish, PF – pharyngeal fibres, PM – paroral membrane, PTC – pretransverse cirri, RM – right marginal cirral row, TC – transverse cirri, III/2 – cirrus 2 of anlage III, 1, 2, 3 – dorsal kineties. Scale bars 30 μm.

The sample was taken about 20 km east of the town of Manaus in the Janauari region where are many small islands. The islands are covered with a primary (?) rain forest and are flooded by the Rio Solimões during high water periods. The sample was a collection of litter, soil and roots from 0–5 cm: litter layer up to 2 cm thick, followed by a rather conspicuous root-carpet mixed with brown, humic soil; mineral soil under root-carpet loamy, brownish; pH 5.1.

Families Oxytrichidae and Urosomoididae

The huge morphologic diversity of these families is confirmed by their genetic diversity, especially the genus *Oxytricha* s. l. whose species are irregularly distributed over the molecular hypotrich tree (Schmidt et al. 2007a, Paiva et al. 2009, Foissner et al. 2014a, Singh & Kamra 2015). These indicates polyphyly possibly based on fast radiation events (Foissner et al. 2011). What hypotrich specialists formerly often considered as "high variation" is now frequently recognized as a new species or genus.

A first split of the time-honoured genus *Oxytricha* was performed by Berger (1999), using the absence vs. presence of transverse and caudal cirri. We continue and split *Oxytricha* and some relatives into eight new genera, using several distinct features, such as the structure of the resting cyst, the nuclear pattern, and the genesis of the dorsal ciliature. This split is not very radical, considering that there are very likely thousands of undescribed hypotrichs (we still have about 150 undescribed species in our notebook!).

Oxytricha lithofera nov. spec. (Fig. 237a–i, 238a–e; Table 87)

Diagnosis: Size in vivo about 70 × 25 µm; usually elongate ellipsoid. 2 abutting, ellipsoid macronuclear nodules and 2 globular micronuclei. 2 conspicuous lithosomes, one subapical the other subterminal. Cirri thick, right marginal row commences at level of buccal vertex. 6 rows of dorsal bristles gradually increasing in length from about 3 µm anteriorly to 10 µm posteriorly; distal bristle region with increased protargol affinity. Caudal cirri conspicuous because about 25 µm long. Adoral zone of membranelles extends about 36% of body length, composed of an average of 20 membranelles. Buccal cavity very narrow and shallow. Undulating membranes straight, optically side by side.

Type locality: Venezuelan site (57), i. e., moss on stones and soil from a small cave in the Golfete de Cuare del Indio, 69°W 11°N.

Type material: 1 holotype and 1 paratype slide with protargol-impregnated specimens have been deposited in the Biology Centre of the Upper Austrian Museum in Linz (LI). Relevant specimens have been marked with black ink circles on the coverslip.

Etymology: The species name is a composite of the Greek noun *lithos* (stone) and the Latin verb *fero* (carrying). It refers to the conspicuous lithosomes.

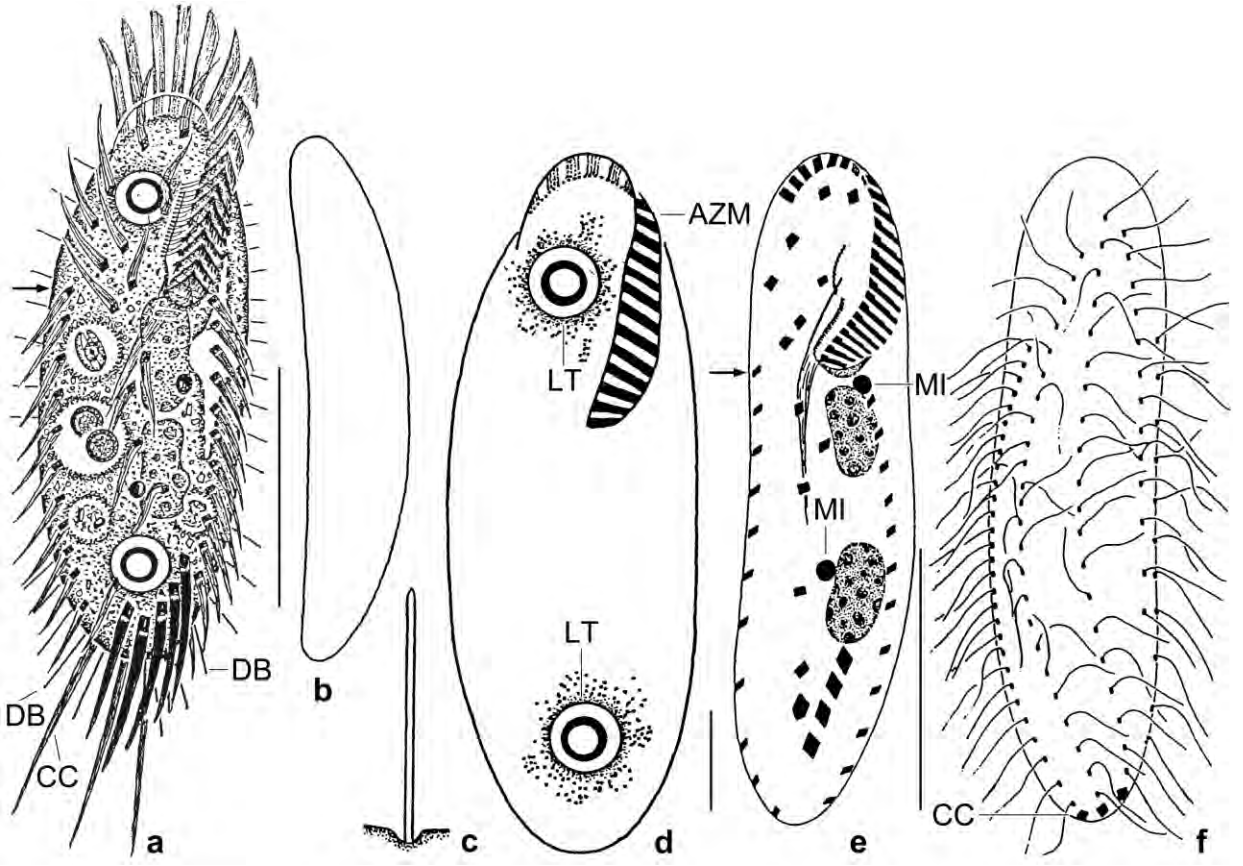

Fig. 237a–f. *Oxytricha lithofera* (a–d) and *O. siseris* (e, f; from Foissner 1982). **a, b:** Ventral and lateral view of a representative specimen, length 70 µm. The arrow marks the begin of the right marginal cirral row. Note the lithosomes and the long caudal cirri. **c:** Dorsal bristle, 10 × 0.4 µm. **d:** *Oxytricha lithofera* has two conspicuous lithosomes, each in a vacuole surrounded by rather refractive granules (lithosome precursors?). **e, f:** *Oxytricha siseris* resembles *O. lithofera* in many features (e. g. begin of the right marginal row at level of buccal vertex, arrowhead; nuclear apparatus) but lacks lithosomes and has another structure of the oral apparatus. AZM – adoral zone of membranelles, CC – caudal cirri, DB – dorsal bristles, LT – lithosomes, MI – micronuclei. Scale bars 10 µm (d) and 30 µm (a, b, e, f).

Description: Size in vivo 60–85 × 23–32 µm, usually about 70 × 25 µm, as calculated from some in vivo measurements and the morphometric data in Table 87 adding 15% preparation shrinkage. Body shape simple, viz., ellipsoid to elongate ellipsoid, on average 2.8:1; rarely elongate quadrangular; up to 2:1 flattened laterally (Fig. 237a, b, g, 238d; Table 87). Nuclear apparatus in mid-body slightly left of midline, remarkable because of abutting macronuclear nodules (Fig. 237a, h, 238a, d; Table 87). Anterior macronuclear nodule commences slightly anterior to buccal vertex on average, outline rather irregular, broadly to elongate ellipsoid, rarely very elongate ellipsoid, variation of nodule width thus high (20.4%), on average 15 × 7 µm in protargol preparations; many nucleoli up to 2 µm across. One or two, usually two globular micronuclei about 2 µm across and attached to various sites of macronuclear nodules, never in between. Contractile vacuole in or near mid-body at left cell margin, with short collecting canals (Fig. 237a). Cortex colourless, very flexible, without specific granules. Cytoplasm colourless, usually contains some food vacuoles and minute crystals, dominated by two highly refractive and thus conspicuous lithosomes, one subapical the other subterminal (Fig. 237a, d, 238a, c). Individual lithosomes hollow, 4–6 µm across, within a vacuole 6–8 µm in diameter and surrounded by many

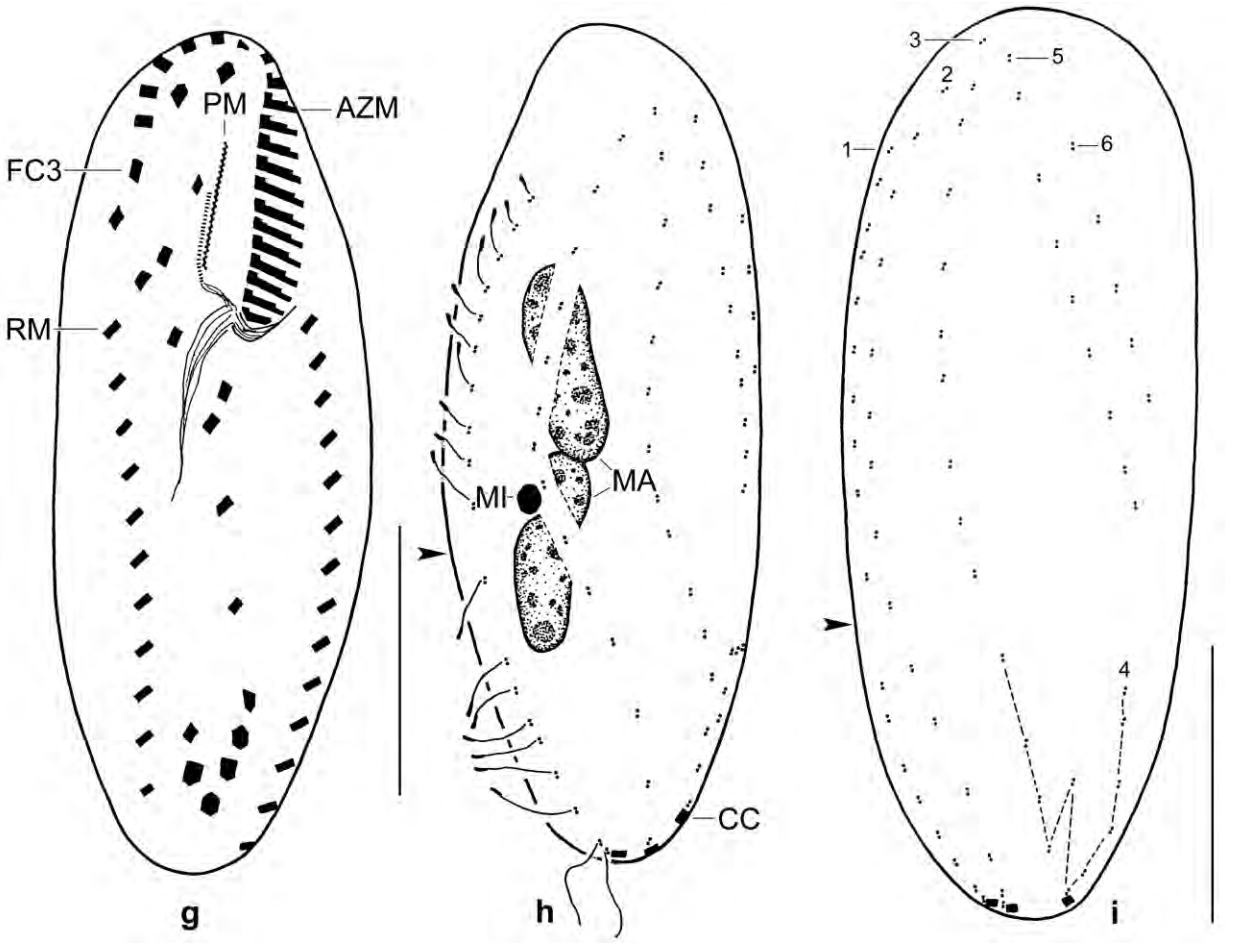

Fig. 237g–i. *Oxytricha lithofera* after protargol impregnation. **g, h:** Ventral and dorsal view of holotype specimen, showing the oxytrichid infraciliature, length 63 µm. The right marginal cirral row begins at level of buccal vertex and the dorsal bristles increase in length from about 3 µm anteriorly to 10 µm posteriorly. Note the thickened distal end of the dorsal bristles and the straight undulating membranes. The arrowhead marks a one-bristle-wide gap in dorsal kinety 1. **i:** Dorsal view of a paratype specimen, showing the six rows of dorsal bristles (numerals); row 4 originates from a posterior split of row 3, as typical for *Oxytricha* s. str. The arrowhead marks a one-bristle-wide gap in row 1. AZM – adoral zone of membranelles, CC – caudal cirri, FC3 – frontal cirrus 3, MA – macronuclear nodules, MI – micronucleus, PM – paroral membrane, RM – right marginal cirral row, 1–6 – dorsal kineties. Scale bars 20 µm.

rather refractive granules, very likely lithosome precursors; wall 1–1.5 µm thick, dissolves during protargol preparation and does not stain with methyl green-pyronin, showing its inorganic nature. Food vacuoles 5–15 µm across, contain heterotrophic euglenids and protist cysts. Swims rather rapidly and creeps on mud accumulations, showing great flexibility.

Ventral cirral pattern as typical for *Oxytricha* s. str., i. e., with 18 comparatively thick and thus conspicuous FVT-cirri (Fig. 237a, g, 238d; Table 87). Buccal cirrus at level of anterior end of endoral membrane; transverse cirri thick, in bowl-like pattern, about 20 µm long and distinctly projecting from body proper. Marginal cirri about 10 µm long, right marginal row commences at level of buccal vertex and ends subterminally.

Six rows of dorsal bristles in typical *Oxytricha* pattern, i. e., three bipolar rows left of midline of body, rows 1 and 2 each associated with a caudal cirrus, row 1 with a one-bristle-wide gap

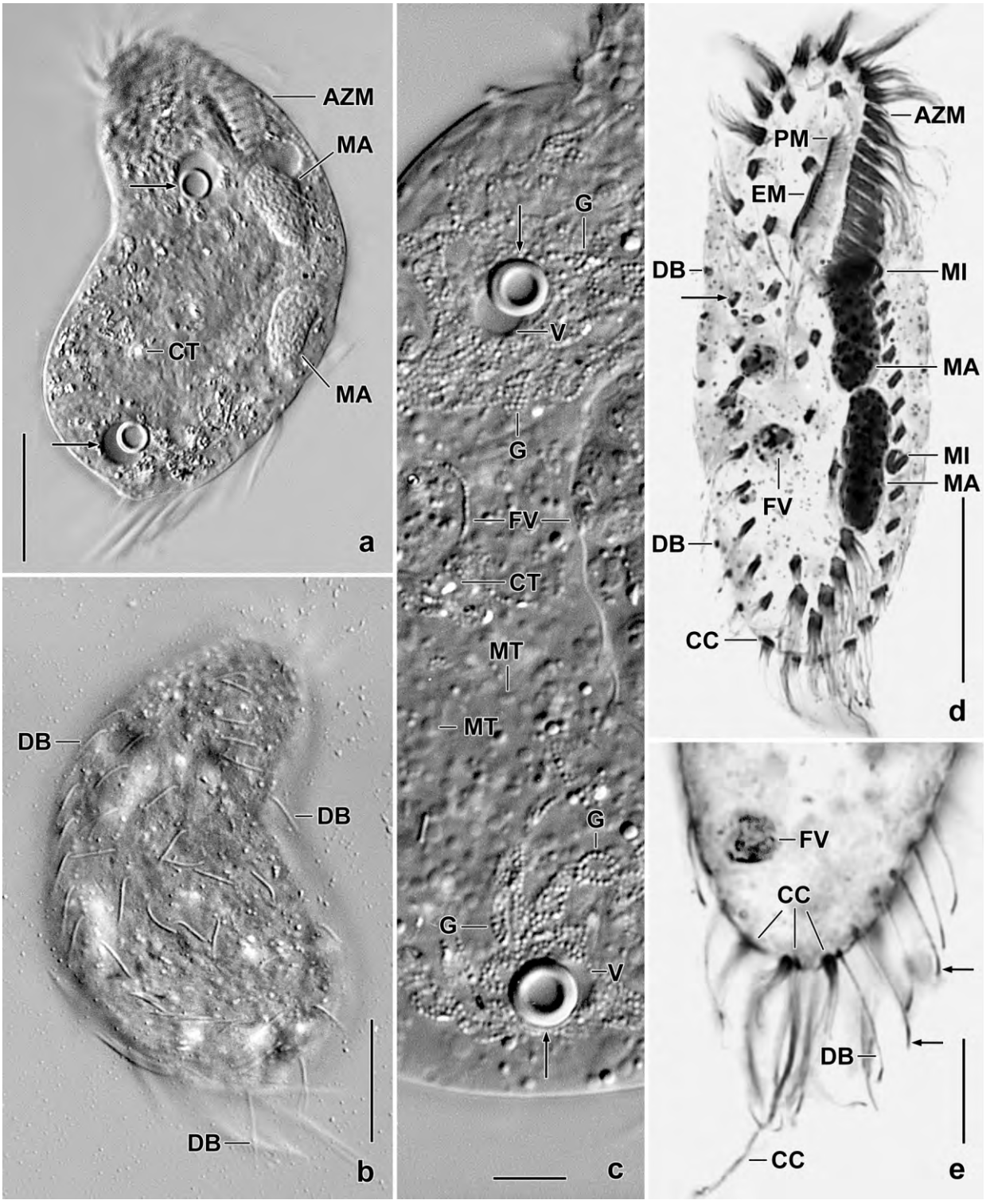

Fig. 238a–e. *O. lithofera* from life (a–c) and after protargol impregnation (d, e). **a–c:** Ventral and dorsal overview and detail with lithosomes (arrows). **d:** Ventral overview showing the right marginal row beginning at level of buccal vertex (arrow). **e:** Dorsal posterior region with dark end of bristles (arrows). AZM – adoral zone, CC – caudal cirri, CT – crystals, DB – dorsal bristles, EM – endoral membrane, FV – food vacuole, G – granules, MA – macronuclear nodules, MI – micronuclei, MT – mitochondria, PM – paroral membrane, V – vacuole. Scale bars 10 µm (c, e) and 20 µm (a, b, d).

Table 87. Morphometric data on *Oxytricha lithofera* based on mounted, protargol-impregnated, and randomly selected specimens from a non-flooded Petri dish culture. Measurements in µm. CV – coefficient of variation %, M – median, MA – macronuclear nodules, Max – maximum, Mean – arithmetic mean, Min – minimum, n – number of specimens investigated, SD – standard deviation, SE – standard error of mean.

Characteristics	Mean	M	SD	SE	CV	Min	Max	n
Body, length	60.6	59.0	6.1	1.3	10.1	53.0	75.0	21
Body, width	23.1	22.0	2.4	0.5	10.3	20.0	28.0	21
Body length: width, ratio	2.6	2.7	0.2	0.0	8.7	2.2	3.0	21
Adoral zone of membranelles, length [a]	21.7	22.0	1.5	0.3	7.0	19.0	24.0	21
Adoral zone of membranelles, percentage of body length	2.8	2.8	0.2	0.0	8.0	2.4	3.3	21
Largest membranellar basis, width	4.2	4.0	–	–	–	4.0	5.0	21
Buccal field, width [b]	4.1	4.0	0.6	0.1	15.3	3.0	5.0	21
Anterior body end to right marginal row, distance	20.0	21.0	2.2	0.5	11.2	15.0	23.0	21
Anterior body end to paroral membrane, distance	7.0	7.0	1.0	0.2	14.0	5.0	9.0	21
Anterior body end to endoral membrane, distance	9.5	10.0	2.2	0.5	22.7	6.0	13.0	21
Anterior body end to buccal cirrus, distance	8.9	9.0	1.1	0.2	12.6	7.0	10.0	21
Anterior body end to first MA nodule, distance	17.8	18.0	2.5	0.6	14.3	13.0	22.0	21
Posterior body end to transverse cirri, distance	3.6	4.0	0.8	0.2	20.9	2.5	5.0	21
Posterior body end to right marginal row, distance	4.5	5.0	0.8	0.2	17.2	3.0	6.0	21
Posterior body end to left marginal row, distance	2.0	2.0	0.7	0.1	33.6	1.0	3.0	21
Anterior macronuclear nodule, length	13.5	14.0	1.9	0.4	14.3	10.0	17.0	21
Anterior macronuclear nodule, width	5.9	6.0	1.2	0.3	20.4	3.0	8.0	21
Macronuclear nodules, number	2.0	2.0	0.0	0.0	0.0	2.0	2.0	21
Macronuclear nodules, distance in between	0.6	0.0	–	–	–	0.0	3.0	21
Micronuclei, number	1.7	2.0	–	–	–	1.0	2.0	21
Anterior micronucleus, length	2.1	2.0	–	–	–	2.0	3.0	21
Anterior micronucleus, width	2.0	2.0	–	–	–	2.0	2.5	21
Adoral membranelles, number	19.8	20.0	0.5	0.1	2.6	19.0	21.0	21
Frontal cirri, number	3.0	3.0	0.0	0.0	0.0	3.0	3.0	21
Buccal cirrus, number	1.0	1.0	0.0	0.0	0.0	1.0	1.0	21
Right marginal cirri, number	10.7	11.0	1.0	0.2	8.9	9.0	12.0	21
Left marginal cirri, number	13.4	13.0	0.9	0.2	6.9	12.0	15.0	21
Frontoventral cirri, number	4.0	4.0	0.0	0.0	0.0	4.0	4.0	21
Postoral ventral cirri, number	3.0	3.0	0.0	0.0	0.0	3.0	3.0	21
Transverse cirri, number	5.0	5.0	0.0	0.0	0.0	5.0	5.0	21
Pretransverse cirri, number	2.0	2.0	0.0	0.0	0.0	2.0	2.0	21
Caudal cirri, number	3.0	3.0	0.0	0.0	0.0	3.0	3.0	21
Dorsal kineties, number	6.0	6.0	0.0	0.0	0.0	6.0	6.0	21
Dorsal kinety 1, number of bristles	17.9	17.0	1.6	0.4	9.1	16.0	21.0	21
Dorsal kinety 2, number of bristles	14.7	14.0	1.6	0.3	10.6	12.0	17.0	21
Dorsal kinety 3, number of bristles	12.7	13.0	1.3	0.3	10.0	11.0	15.0	21
Dorsal kinety 6, number of bristles	4.5	5.0	1.3	0.3	28.8	2.0	7.0	21

[a] Anterior body end to proximal end of zone.

[b] Distance between centre of paroral membrane and right margin of adoral zone.

posterior of mid-body; row 4 originates by a posterior split of row 3, short, produces third caudal cirrus; rows 5 and 6 distinctly shortened, originate from right marginal row. Bristles of rows 1–3 anteriorly 3–5 µm long, gradually increase to 10 µm posteriorly; bristles of dorsomarginal rows 4–7 µm long (Fig. 237a, h, 238b); distal region of all bristles with increased protargol affinity, possibly slightly thickened (Fig. 237h, 238e). Caudal cirri conspicuous because comparatively thick and about 25 µm long in vivo (Fig. 237a, h, i, 238e; Table 87).

Oral apparatus extends 31–40%, on average 36% of body length in protargol preparations (Fig. 237a, d, g, 238a, d; Table 87). Adoral zone of ordinary shape and structure, composed of an average of 20 membranelles with cilia about 15 µm long in frontal membranelles; largest membranellar bases about 6 µm wide in vivo and 4.2 µm in protargol preparations. Buccal cavity very narrow and shallow, in three specimens about 2 µm wide in vivo, widens to 4.2 µm on average in protargol preparations (Table 87); buccal lip narrow, bears paroral membrane with cilia about 5 µm long in vivo (Fig. 237a). Undulating membranes straight, optically side by side or one upon the other, paroral distinctly longer than endoral anteriorly. Pharyngeal fibres distinct in vivo and in protargol preparations, extend posteriorly.

Occurrence and ecology: As yet found only at the moderately saline and circumneutral type locality. *Oxytricha lithofera* became numerous three weeks after rewetting the sample, indicating a k-selected life strategy. Recently found also in Australia.

Remarks: This is a highly distinct species with a combination of features not present in any other described *Oxytricha* s. l. (Berger 1999, Foissner et al. 2002): Two large lithosomes (unique for *Oxytricha*); abutting macronuclear nodules; right marginal cirral row commencing at level of buccal vertex; dorsal bristles increase in length from about 4 µm anteriorly to 10 µm posteriorly, their distal end with increased protargol affinity; a one-bristle-wide gap in dorsal kinety 1; and straight undulating membranes. There are several *Oxytricha* species which have one or more of these features, e. g., *O. siseris* (Fig. 237e, f) redescribed by Foissner (1982) but none has all the characteristics typical for *O. lithofera*. The composition and function of the lithosomes is not known.

Oxytricha pulvillus nov. spec. (Fig. 239a–k, 240a–r, 241a–o; Table 88)

Diagnosis: Size in vivo about 90 × 35 µm; ellipsoid. 2 almost abutting, broadly ellipsoid macronuclear nodules and 2 globular micronuclei. Cortical granules in rather narrowly spaced rows, colourless, about 0.5 µm across. Cirri of ordinary size and length, transverse cirri fringed distally. 6 rows of dorsal bristles 3–4 µm long; 3 caudal cirri. Adoral zone of membranelles extends about 38% of body length, composed of an average of 26 membranelles. Buccal cavity narrow, anterior of cavity a cushion-like convexity seemingly pushing membranellar scutum right to body`s midline; undulating membranes slightly curved, close together optically crossing in mid of buccal cavity. Resting cyst with thin, smooth wall and a compact slime layer 3–4 µm thick. Ontogenesis in typical *Oxytricha* pattern.

Type locality: Venezuelan site (65), i. e., highly saline (~ 50‰) soil from an abandoned field in the surroundings of the village of Chichiriviche, north coast of Venezuela, Morrocoy National Park, 67°13’W 11°33’N.

Type material: 1 holotype and 5 paratype slides with protargol-impregnated specimens have been deposited in the Biology Centre of the Upper Austrian Museum in Linz (LI). Relevant specimens have been marked with black ink circles on the coverslip.

Etymology: *Pulvillus* (a small cushion) is a Latin noun in apposition, referring to the pillow-like preoral area.

Description: Most and especially the important features of *O. pulvillus* have an ordinary variability (CV ≤ 15%). Of those having a higher coefficient of variation, the distance between the macronuclear nodules and the distance from the lowermost transverse cirrus to the body end should be mentioned (Table 88).

Size in vivo 80–100 × 30–45 µm, usually about 90 × 35 µm, as calculated from in vivo measurements and the morphometric data in Table 88 adding 20% preparation shrinkage due to ethanol fixation and 5% contractility of the anterior body half, resulting in a length:width

Table 88. Morphometric data on *Oxytricha pulvillus* based on mounted, protargol-impregnated, and randomly selected specimens from a non-flooded Petri dish culture. Measurements in µm. CV – coefficient of variation in %, M – median, Max – maximum, Mean – arithmetic mean, Min – minimum, n – number of individuals investigated, SD – standard deviation, SE – standard error of arithmetic mean.

Characteristics	Mean	M	SD	SE	CV	Min	Max	n
Body, length	70.4	70.0	5.2	1.1	7.4	63.0	80.0	21
Body, width	32.3	32.0	2.9	0.6	9.0	25.0	37.0	21
Body length:width, ratio (protargol)	2.2	2.2	0.2	0.1	8.9	1.9	2.6	21
Body length:width, ratio (in vivo, from micrographs)	2.8	2.8	0.2	0.1	6.8	2.4	3.1	11
Body length:width, ratio (scanning electron microscopy)	2.1	2.2	0.1	0.1	4.8	2.0	2.3	9
Anterior body end to proximal end of adoral zone of membranelles, distance	26.3	26.0	1.8	0.4	6.9	21.0	30.0	21
Adoral zone of membranelles, percentage of body length	37.6	38.0	3.4	0.7	8.9	32.0	43.0	21
Adoral membranelles, number	26.0	26.0	1.0	0.2	3.9	23.0	27.0	21
Anterior body end to paroral membrane, distance	7.5	8.0	1.1	0.2	14.3	6.0	11.0	21
Anterior body end to endoral membrane, distance	9.5	10.0	1.2	0.3	12.9	8.0	13.0	21
Anterior body end to upper macronuclear nodule, distance	23.2	23.0	2.2	0.5	9.6	18.0	27.0	21
Macronuclear nodules, distance in between	4.3	4.0	1.9	0.4	43.5	1.0	8.0	21
Nuclear figure, length	27.9	28.0	3.5	0.8	12.4	22.0	35.0	21
Anterior macronuclear nodule, length	11.2	11.0	1.5	0.3	13.8	10.0	15.0	21
Anterior macronuclear nodule, width	7.9	8.0	0.8	0.2	10.7	6.0	10.0	21
Macronuclear nodules, number	2.0	2.0	0.0	0.0	0.0	2.0	2.0	21
Micronuclei, length	2.1	2.0	–	–	–	1.5	2.5	21
Micronuclei, width	1.9	2.0	–	–	–	1.0	2.5	21
Micronuclei, number	2.1	2.0	0.8	0.2	37.0	1.0	4.0	21
Anterior body end to right marginal row, distance	14.0	14.0	1.7	0.4	12.1	12.0	18.0	21
Posterior body end to right marginal row, distance	2.6	2.5	1.0	0.2	39.3	1.0	5.0	21
Right marginal row, number of cirri	18.8	19.0	1.7	0.4	9.2	16.0	23.0	21

continued

ratio of 2.2:1 in protargol and SEM preparations while of 2.8:1 in vivo (Table 88), showing a considerable width inflation by the preparation procedures. Body outline elliptic to elongate elliptic, laterally flattened up to 2:1, ventral side flat, dorsal more or less convex, depending of nutrition state (Fig. 239a, g, 240a, b, d, e, i–k, m, o, r). Nuclear apparatus in mid-body slightly left of midline, remarkable because macronuclear nodules only 4 µm apart on average (Fig. 239a, 240p–r, 241b; Table 88). Macronuclear nodules globular to ellipsoid, on average broadly ellipsoid; many nucleoli up to 2 µm across. One to four globular to broadly ellipsoid micronuclei attached to or rather distant from macronuclear nodules. Contractile vacuole not recognizable, very likely due to the high salinity (50‰). Cortex colourless, moderately flexible (~ *Sterkiella*), studded with rows of colourless granules only about 0.5 µm across and not staining with methyl green-pyronin (Fig. 239c, d, f). Cytoplasm colourless or brownish when digesting many fungal spores, studded with (i) countless weakly refractive granules about 0.7 µm in size; (ii) highly refractive crystals 2–4 µm in size and with "doubled" ends (Fig. 239e); (iii) starch grains in raw cultures; (iv) lipid droplets 2–3 µm across; (v) 5–15 µm-sized food vacuoles containing small colonies of choanoflagellates, fungal spores, and globular inclusions likely from small ciliates and flagellates (Fig. 239a). Swims and creeps rather slowly.

Ventral cirral pattern as typical for *Oxytricha* s. str. (Berger 1999), i. e., with 18 fronto-ventral-transverse cirri of ordinary size and length (Fig. 239a, 240a–e, k, l, p–r, 241a; Table 88). Buccal cirrus subapical of paroral membrane; transverse cirri distinctly projecting from body proper, fringed distally, 20–25 µm long in vivo. Marginal cirral rows extend to near posterior body end, cirri composed of two to three rows of basal bodies, about 12 µm long in vivo.

Characteristics	**Mean**	**M**	**SD**	**SE**	**CV**	**Min**	**Max**	**n**
Posterior body end to left marginal row, distance	1.0	1.0	0.5	0.1	50.0	0.5	2.0	21
Left marginal row, number of cirri	21.7	22.0	1.7	0.4	7.9	17.0	25.0	21
Frontal cirri, number	3.0	3.0	0.0	0.0	0.0	3.0	3.0	21
Anterior body end to buccal cirrus, distance	9.0	9.0	1.2	0.3	13.6	7.0	12.0	21
Buccal cirrus, number	1.0	1.0	0.0	0.0	0.0	1.0	1.0	21
Anterior body end to last frontoventral cirrus, distance	23.1	23.0	1.7	0.4	7.4	20.0	27.0	21
Frontoventral cirri, number	4.0	4.0	0.0	0.0	0.0	4.0	4.0	21
Anterior body end to last postoral cirrus, distance	37.1	37.0	2.4	0.5	6.4	33.0	41.0	21
Postoral cirri, number	3.0	3.0	0.0	0.0	0.0	3.0	3.0	21
Posterior body end to posteriormost transverse cirrus, distance	4.9	5.0	1.1	0.2	22.0	3.0	7.0	21
Transverse cirri, number	5.0	5.0	0.0	0.0	0.0	5.0	5.0	21
Pretransverse cirri, number	2.0	2.0	0.0	0.0	0.0	2.0	2.0	21
Dorsal kineties, number	5.0	5.0	0.0	0.0	0.0	5.0	5.0	21
Kinetids in dorsal kinety 1, number	24.7	25.0	2.5	0.5	10.0	18.0	28.0	21
Kinetids in dorsal kinety 2, number	21.1	21.0	1.4	0.4	6.7	18.0	23.0	15
Kinetids in dorsal kinety 3, number	25.1	25.0	2.0	0.6	8.1	22.0	28.0	10
Kinetids in dorsal kinety 4, number	11.9	12.0	2.3	0.6	19.1	8.0	16.0	15
Kinetids in dorsal kinety 5, number	2.6	2.0	1.0	0.2	37.6	1.0	5.0	16
Caudal cirri, number	3.0	3.0	0.0	0.0	0.0	3.0	3.0	21
Resting cyst, diameter (without slime cover)	37.6	38.0	4.3	1.4	11.6	32.0	44.0	9

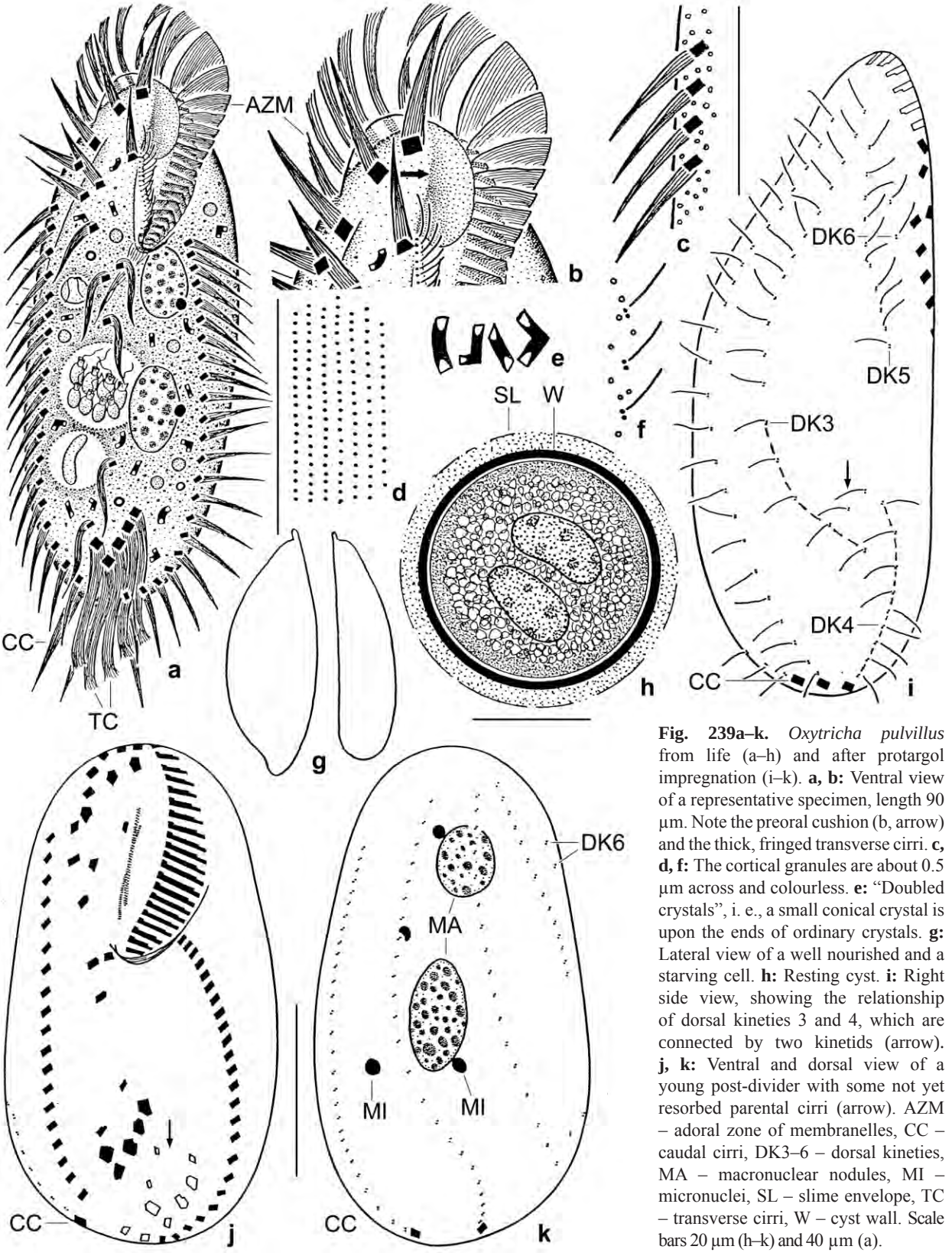

Fig. 239a–k. *Oxytricha pulvillus* from life (a–h) and after protargol impregnation (i–k). **a, b:** Ventral view of a representative specimen, length 90 µm. Note the preoral cushion (b, arrow) and the thick, fringed transverse cirri. **c, d, f:** The cortical granules are about 0.5 µm across and colourless. **e:** "Doubled crystals", i. e., a small conical crystal is upon the ends of ordinary crystals. **g:** Lateral view of a well nourished and a starving cell. **h:** Resting cyst. **i:** Right side view, showing the relationship of dorsal kineties 3 and 4, which are connected by two kinetids (arrow). **j, k:** Ventral and dorsal view of a young post-divider with some not yet resorbed parental cirri (arrow). AZM – adoral zone of membranelles, CC – caudal cirri, DK3–6 – dorsal kineties, MA – macronuclear nodules, MI – micronuclei, SL – slime envelope, TC – transverse cirri, W – cyst wall. Scale bars 20 µm (h–k) and 40 µm (a).

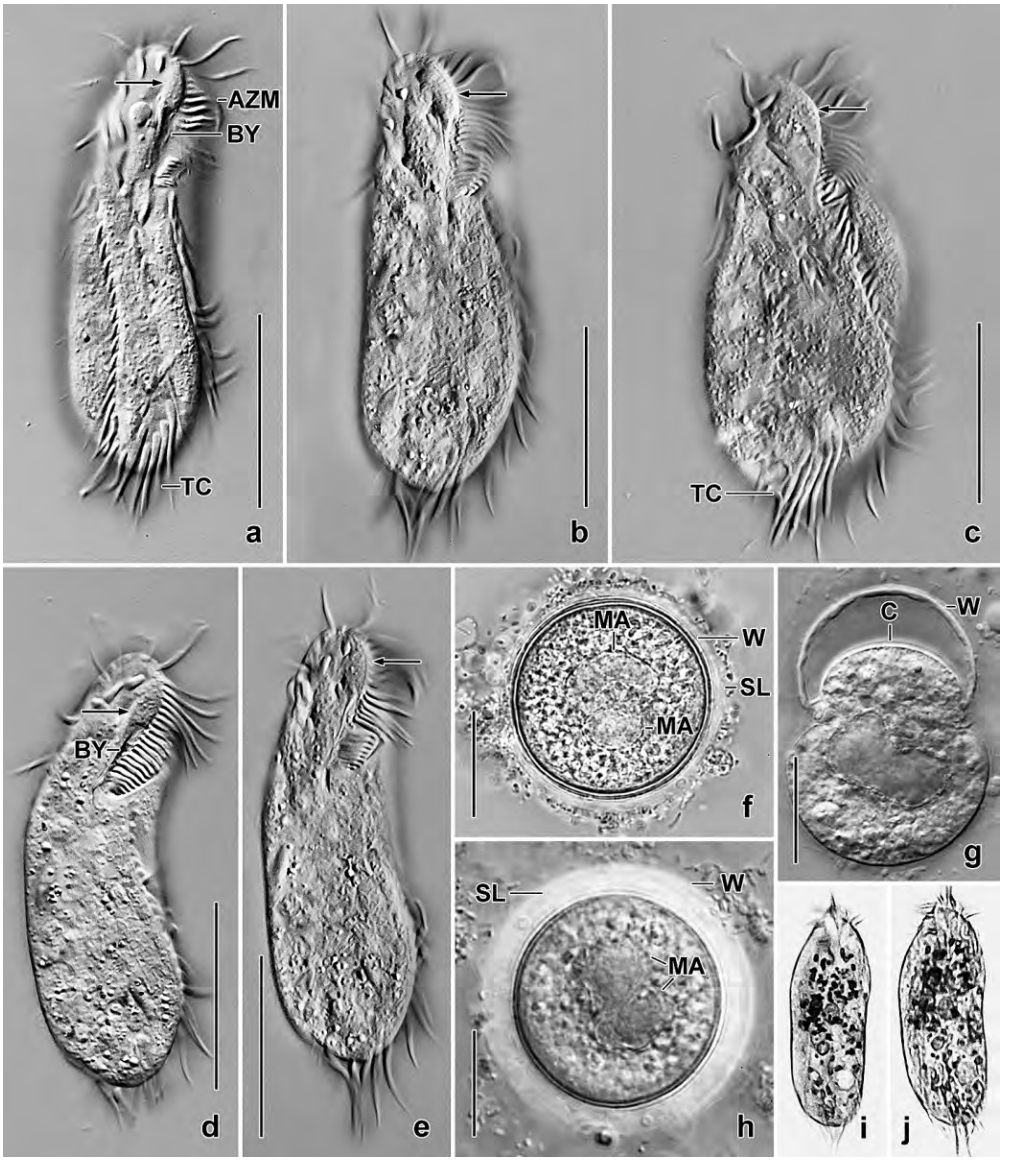

Fig. 240a–j. *Oxytricha pulvillus* from life. **a–e:** Ventral views of specimens slightly pressed by coverslip, showing the cushion-like preoral area (arrows), a main feature of this species. Note also the very narrow buccal cavity and the rather thick transverse cirri, two other important features. **f, h:** Resting cysts. Note the thin wall and the slime (?) envelope which can be prominent (h). **g:** A squashed cyst, showing the thin wall and the cortex of the cell. **i, j:** Body shape of freely motile specimens, length about 90 µm. AZM – adoral zone of membranelles, BY – buccal cavity, C – ciliate cortex, MA – macronuclear nodules, SL – slime envelope, TC – transverse cirri, W – cyst wall. Scale bars 20 µm (f–h) and 40 µm (a–e).

Dorsal ciliature also in typical *Oxytricha* pattern (Berger 1999). Bristle rows 3 and 4 connected by some scattered kinetids; rows 5 and 6 consist of only 1–5 and 2 bristles, respectively; bristles 4–5 µm long in vivo and in SEM preparations (Fig. 239i, 240m–o, 241b; Table 88).

Oral apparatus extends to 32–43% of body length, on average 38% in protargol preparations (Fig. 239a, b, 240a–e, k, l, p–r, 241a; Table 88). Adoral zone of ordinary shape and structure, composed of an average of 20 membranelles with frontal cilia about 15 µm long and largest bases about 7 µm wide in vivo. Buccal cavity flat, narrow to very narrow, anterior of cavity a cushion-like convexity including left half of membranellar scutum, right half hyaline, as usual (Fig. 239a, b, 240a–c, k). Buccal lip very narrow, bears paroral membrane having 5 µm long cilia in vivo. Undulating membranes slightly curved, close together optically crossing in or near mid of buccal cavity. Pharyngeal fibres inconspicuous.

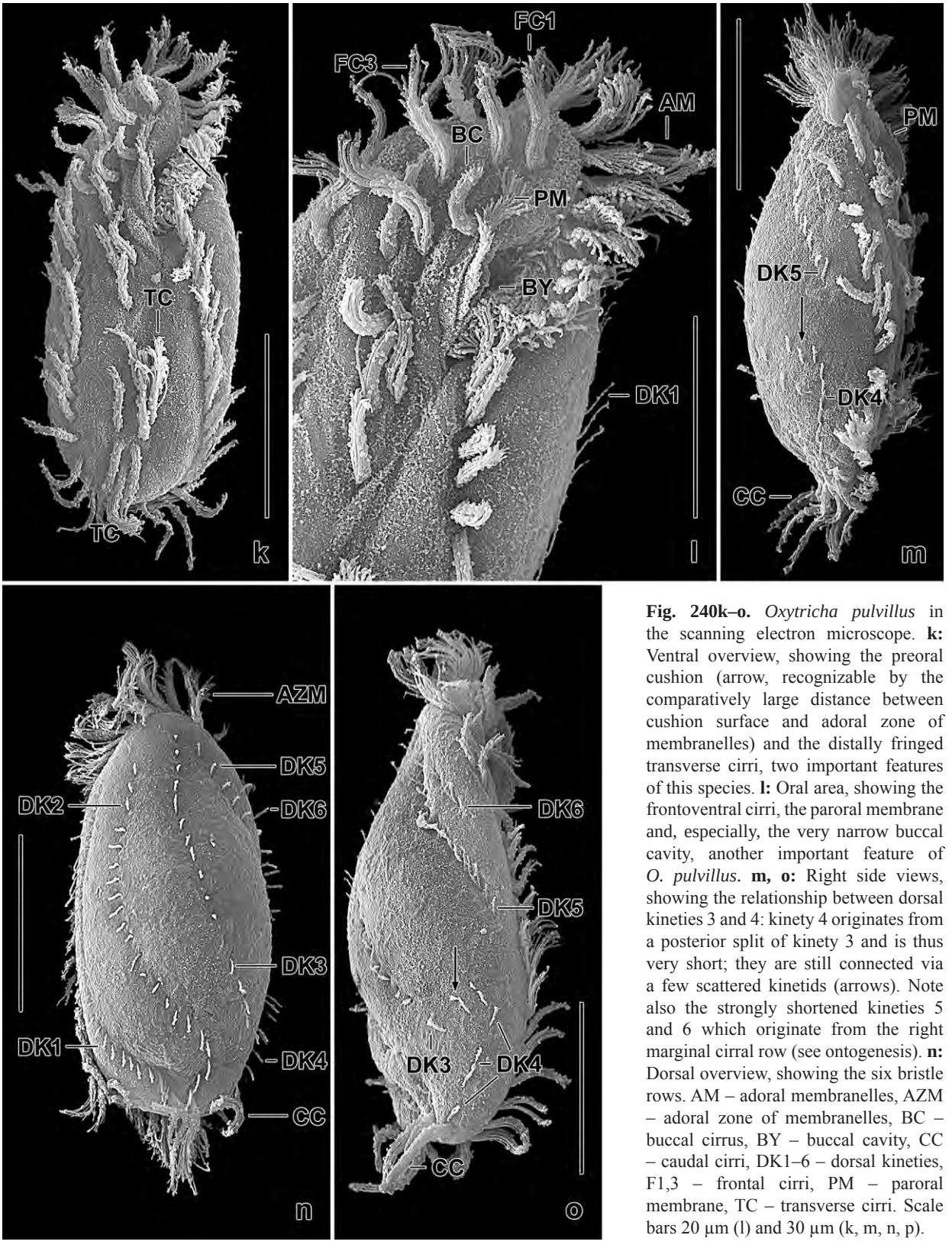

Fig. 240k–o. *Oxytricha pulvillus* in the scanning electron microscope. **k:** Ventral overview, showing the preoral cushion (arrow, recognizable by the comparatively large distance between cushion surface and adoral zone of membranelles) and the distally fringed transverse cirri, two important features of this species. **l:** Oral area, showing the frontoventral cirri, the paroral membrane and, especially, the very narrow buccal cavity, another important feature of *O. pulvillus*. **m, o:** Right side views, showing the relationship between dorsal kineties 3 and 4: kinety 4 originates from a posterior split of kinety 3 and is thus very short; they are still connected via a few scattered kinetids (arrows). Note also the strongly shortened kineties 5 and 6 which originate from the right marginal cirral row (see ontogenesis). **n:** Dorsal overview, showing the six bristle rows. AM – adoral membranelles, AZM – adoral zone of membranelles, BC – buccal cirrus, BY – buccal cavity, CC – caudal cirri, DK1–6 – dorsal kineties, F1,3 – frontal cirri, PM – paroral membrane, TC – transverse cirri. Scale bars 20 µm (l) and 30 µm (k, m, n, p).

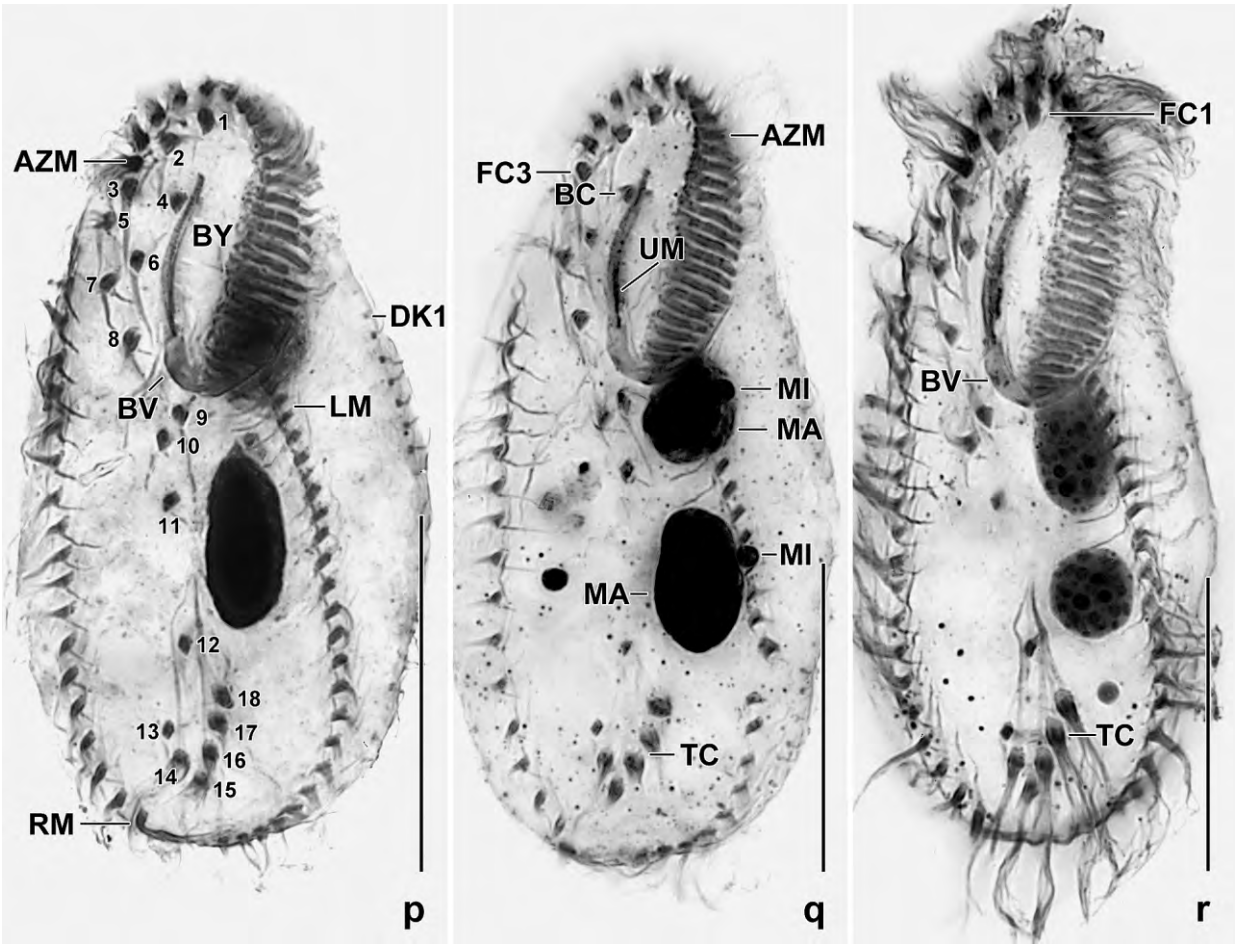

Fig. 240p–r. *Oxytricha pulvillus*, ventral views after fixation with ethanol and protargol impregnation. The rather poor fixation caused length shrinkage, width inflation and, especially, a distinct widening of the buccal cavity (cp. with Fig. 240a, d). Note the rather closely spaced macronuclear nodules, the rather thick transverse cirri, and the 18 fronto-ventral-transverse cirri (numerals). AZM – adoral zone of membranelles, BC – buccal cirrus, BV – buccal vertex, BY – buccal cavity, DK1 – dorsal kinety 1, FC1,3 – frontal cirri, LM – left marginal cirral row, MA – macronuclear nodules, MI – micronuclei, RM – right marginal cirral row, TC – transverse cirri, UM – undulating membranes. Scale bars 30 µm.

Resting cyst: Globular with an average diameter of 38 µm (Table 88); smooth and colourless. Wall composed of two distinct layers, viz., a very hyaline but compact slime (?) envelope 3–4 µm thick and an about 1 µm thick, moderately refractive wall possibly composed of two layers. Cortex of cell very thin, underlaid by a 2–3 µm thick, finely granular layer followed by a mass of rather hyaline globules 1–4 µm in size. Macronuclear nodules not fused (Fig. 239h, 240f–h; Table 88).

Ontogenesis: This is virtually as in *Oxytricha granulifera*, type of the genus (Foissner & Adam 1983b, Berger 1999) except for small differences in the temporal sequence of the processes, e. g., the production of adoral membranelles occurs slightly later while the postoral cirri develop to anlagen slightly earlier. Ontogenesis confirms two dorsomarginal kineties and a posterior split of dorsal kinety 3 to produce kinety 4. Further details, see figure explanations (Fig. 239j, k, 241c–o).

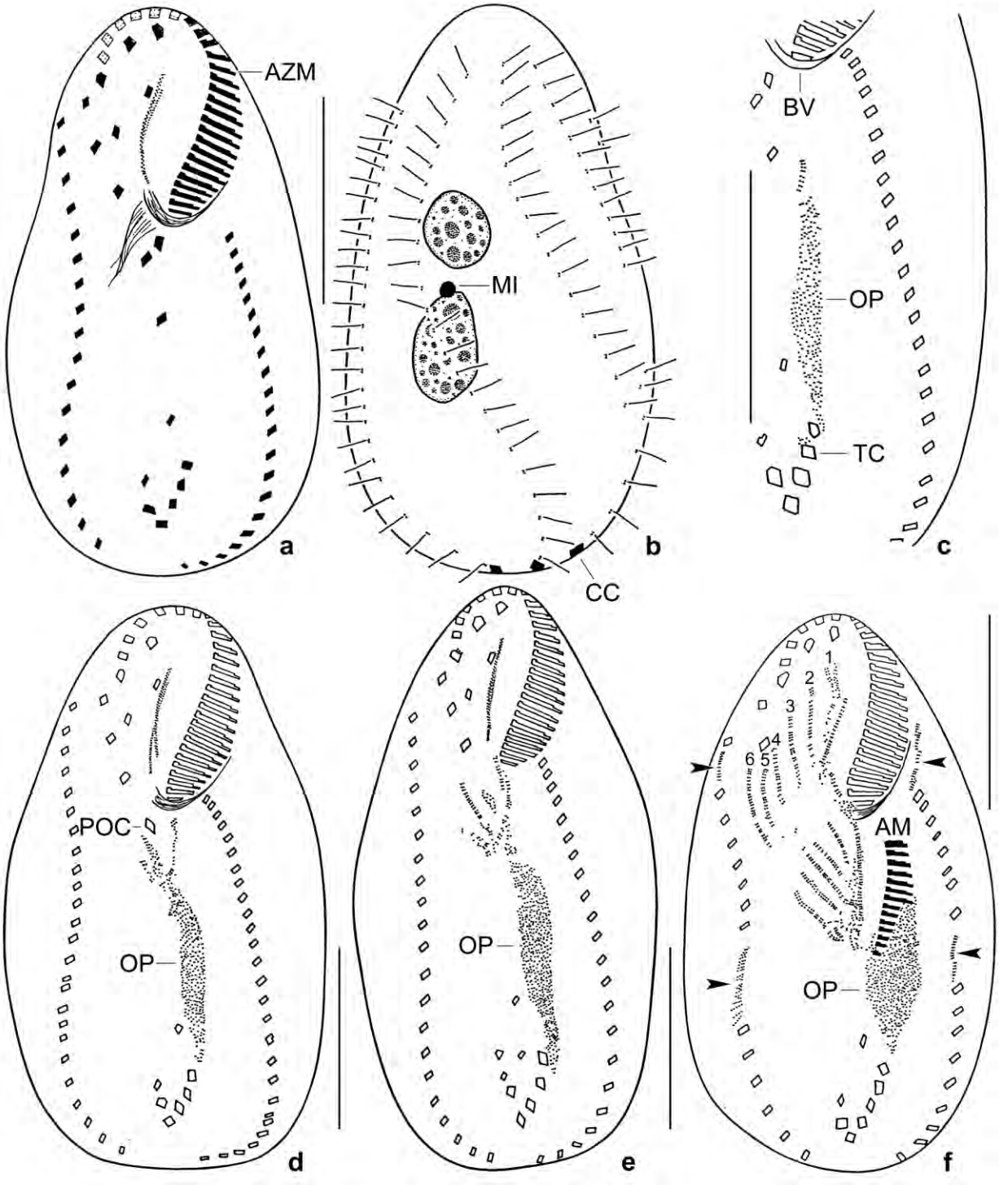

Fig. 241a–f. *Oxytricha pulvillus*, holotype (a, b) and early (c, e) to early mid-dividers (f) after protargol impregnation. **a, b:** Ventral and dorsal view, length 70 µm. Only one of the two micronuclei is recognizable. **c:** An anarchic field of basal bodies develops between buccal vertex and transverse cirri. **d:** Two of the three postoral cirri are modified to cirral anlagen. **e:** All postoral cirri became anlagen. **f:** Six fronto-ventral-transverse cirral anlagen (numerals) and four anlagen for the marginal cirral rows (arrowheads) developed in proter and opisthe. AM – adoral membranelles, AZM – adoral zone of membranelles, BV – buccal vertex, CC – caudal cirri, MI – micronucleus, OP – oral primordium, POC – postoral cirri, TC – transverse cirri. Scale bars 25 µm.

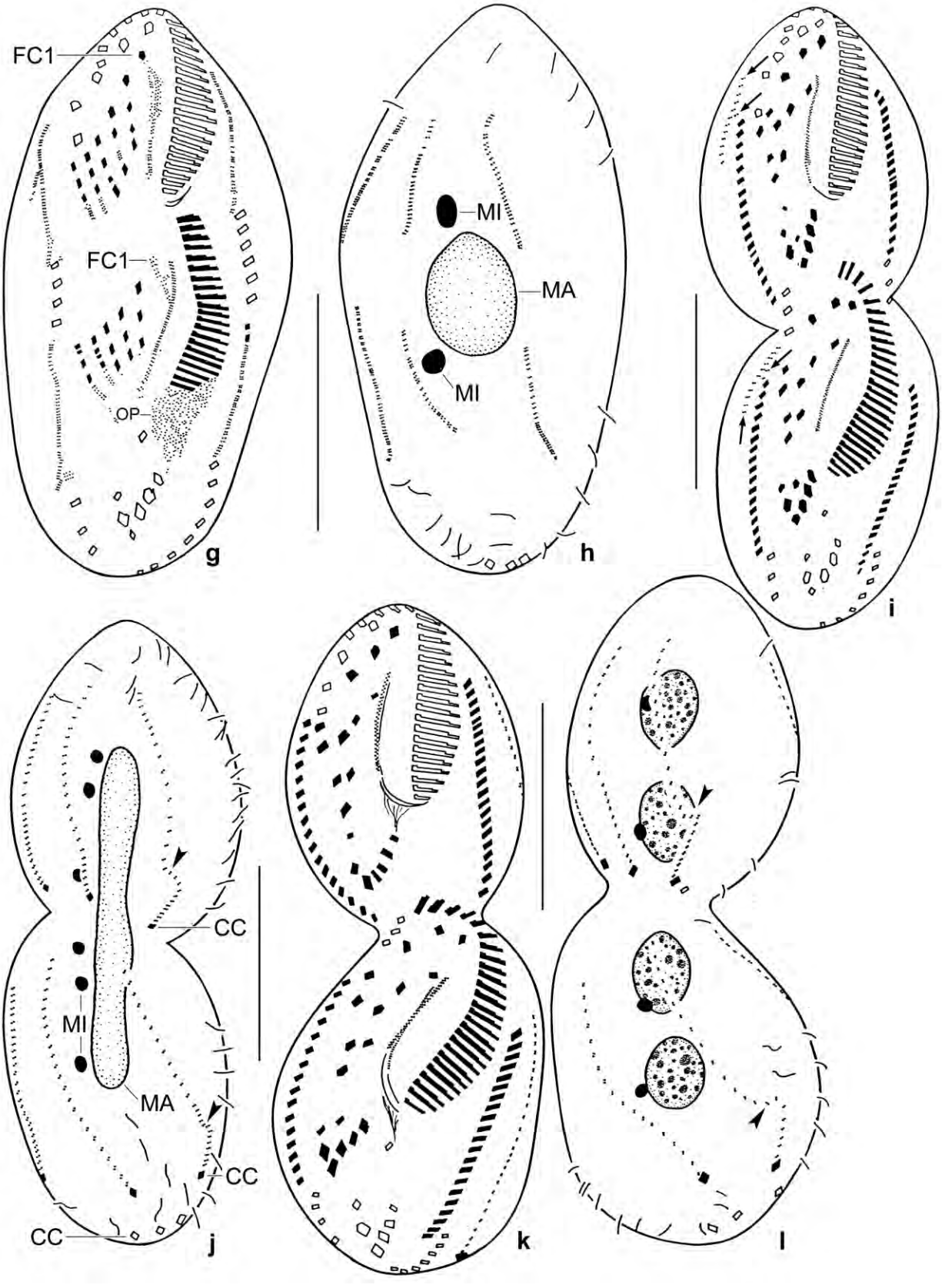
FC1
FC1
OP
g
MI
MA
MI
h
i
CC
MI
MA
CC
CC
j
k
l

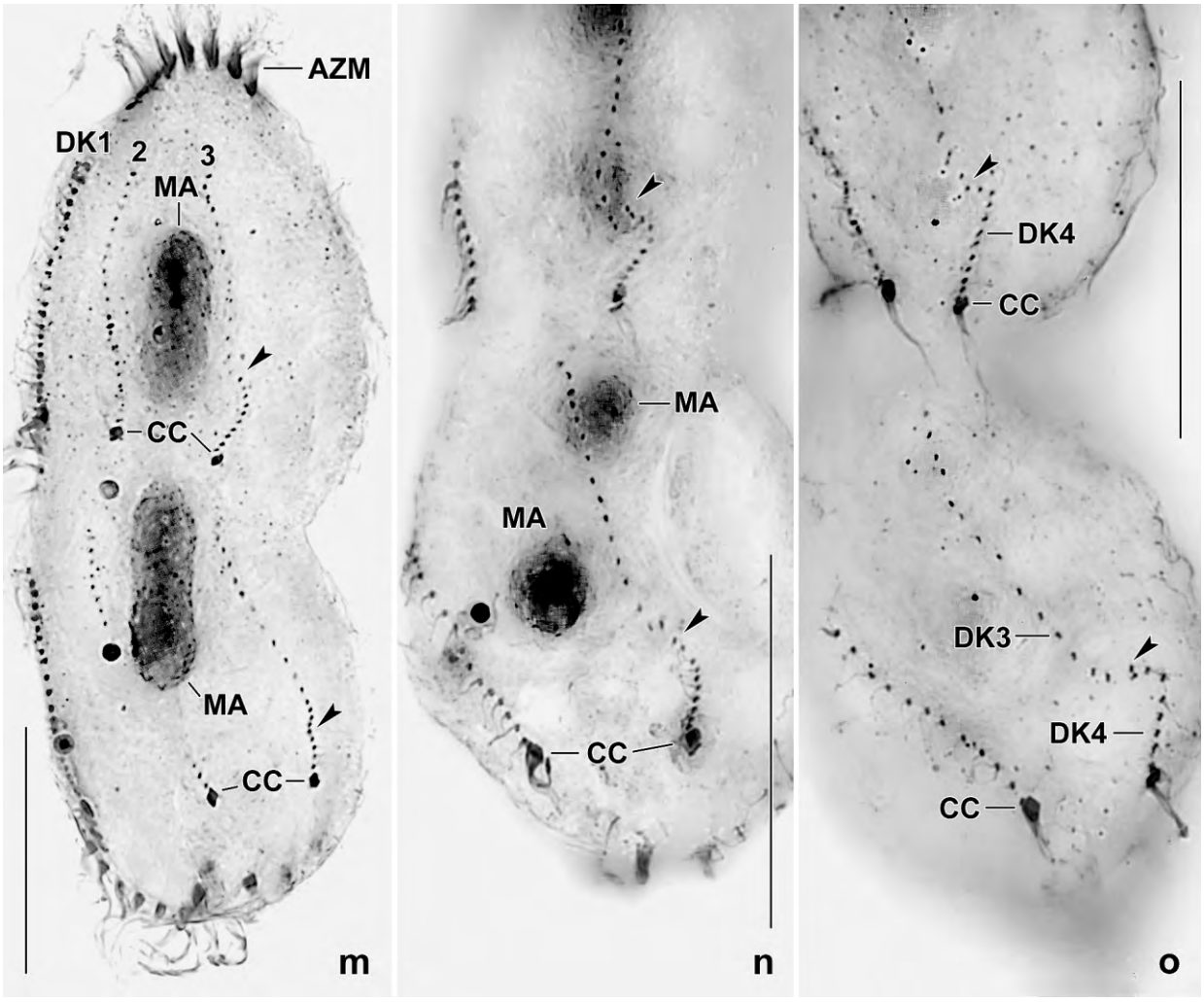

Fig. 241m–o. *Oxytricha pulvillus*, dorsal views of protargol-impregnated specimens, showing the genesis of dorsal kinety 4 by a posterior split of kinety 3 (arrowheads). AZM – adoral zone of membranelles, CC – caudal cirri, DK1–4 – dorsal kineties, MA – macronuclear nodules. Scale bars 30 µm.

Occurrence and ecology: *Oxytricha pulvillus* was discovered at Venezuelan site (65), i. e., in a highly saline (50‰) sample from the north coast. It occurred also at Venezuelan site (47), i. e., in a slightly saline sample (10‰) from the north coast of the Henri Pittier National Park. This shows that *O. pulvillus* is a euryhaline species from which we got raw cultures with artificial sea water and some squashed wheat grains.

Fig. 241g–l. *Oxytricha pulvillus*, dividers after protargol impregnation. **g, h:** Ventral and dorsal view of a mid-divider with macronuclear nodules fused to a central globular mass. Cirri are formed in the fronto-ventral-transverse anlagen and anlagen developed in dorsal kineties 1–3. Most of the parental cirri, shown by contour, that did not form anlagen, are still present. **i, j**: Late divider with rod-shaped macronuclear mass and divided micronuclei. The fronto-ventral-transverse cirri have been formed and migrate to their specific sites. The dorsomarginal kineties have been formed (arrows), and the newly generated dorsal kinety 3 begins to break subterminally (arrowheads). **k, l:** A very late divider with fully developed nuclear apparatus. The fronto-ventral-transverse cirri moved to their specific sites and most of the parental ciliature has been resorbed. Dorsal kinety 3 splits into a long anterior and a short posterior portion (arrowheads). A young post-divider is shown in Figure 239j, k. CC – caudal cirri, FC1 – frontal cirrus 1, MA – macronuclear mass, MI – micronuclei, OP – oral primordium. Scale bars 30 µm.

Remarks: *Oxytricha* spp. are difficult to identify because many of the old and also some of the more recent descriptions are very incomplete. We do not use the inconspicuous cortical granules and the preoral cushion as discriminating features because they are too sophisticated for the old descriptions. Then, *O. pulvillus* has seven features not combined in any previous description: (i) size about 90 × 35 µm; (ii) macronuclear nodules rather close together, each with a micronucleus; (iii) transverse cirri rather thick and fringed distally; (iv) caudal cirri well recognizable; (v) buccal cavity narrow; (vi) dorsal bristles not longer than 5 µm; (vii) saline habitat. Using these features, *Oxytricha oxymarina* Berger, 1999 (formerly *O. marina* Kahl, 1932) is probably the most similar species, viz., it is 100–120 µm long, has rather close macronuclear nodules, a narrow buccal cavity, a saline habitat, and more than three frontal adoral membranelles, a distinct feature present also in *O. pulvillus*. There are, however, also some differences that suggest *O. pulvillus* as a different species: transverse cirri thin (vs. rather thick and fringed distally), caudal cirri, although conspicuous, not mentioned by Kahl, and the length:width ratio of the body in vivo (~3.8:1 vs. 2.8:1). A second similar species is *Oxytricha procera* Kahl, 1932. However, this species is much more slender than *O. pulvillus* (5–6:1 vs. 2.8:1 in vivo) and its transverse cirri are thin and not fringed (vs. rather thick and fringed).

The following species differ more distinctly from *O. pulvillus* than *O. oxymarina* and *O. procera* (see Berger 1999 for authors and dates): *O. kahlovata, O. longa, O. minor, O. similis, O. parahalophila, and O. tenella.*

Notohymena antarctica Foissner, 1996a (Fig. 242a–k, 243a–h; Tables 89, 90)

Material: Over the years, we collected data from six soil populations belonging to four major biogeographic regions: Antarctica (type locality; holo- and paratype slide deposited in Linz (LI), reg. no.1997/48, 49); Brazil (material from a termite nest); Australian population 1 (Dinaro dam in the outskirts of the town of Cairns), two voucher slides deposited in Linz (LI), reg. no. 2000/91, 92; Australian population 2 (dry basin of the Fogg Dam near to the town of Darwin); Austrian population 1 (Johannser Kogel in the outskirts of the town of Vienna; for detailed site description, see Foissner et al. 2005), four voucher slides deposited in Linz (LI), reg. no. 2007/634–637; Austrian population 2 (junction area of the Enns River and the Danube River near to the town of Linz, Upper Austria; for details, see Foissner 2004), two voucher slides deposited in Linz (LI), reg. no. 2007/599, 600. Thus, it is possible to evaluate three important features: the cortical granules, major morphometrics, and the distribution.

Cortical granules (Fig. 242f, h, 243b–d; Table 90): The arrangement, size, and colour of the cortical granules, likely a kind of extrusomes, are important features in the α-taxonomy of hypotrichs (Kahl 1932, Foissner 1982, Berger 1999). The arrangement and size of the cortical granules of *N. antarctica* are little variable while their colour varies from colourless over yellow to orange (Table 90).

The morphometric and morphological data indicate that the colour differences are not due to different species. Thus, we conclude that the colour of the cortical granules is a poor feature in this species, especially when not supported by another "strong" character, for instance, the

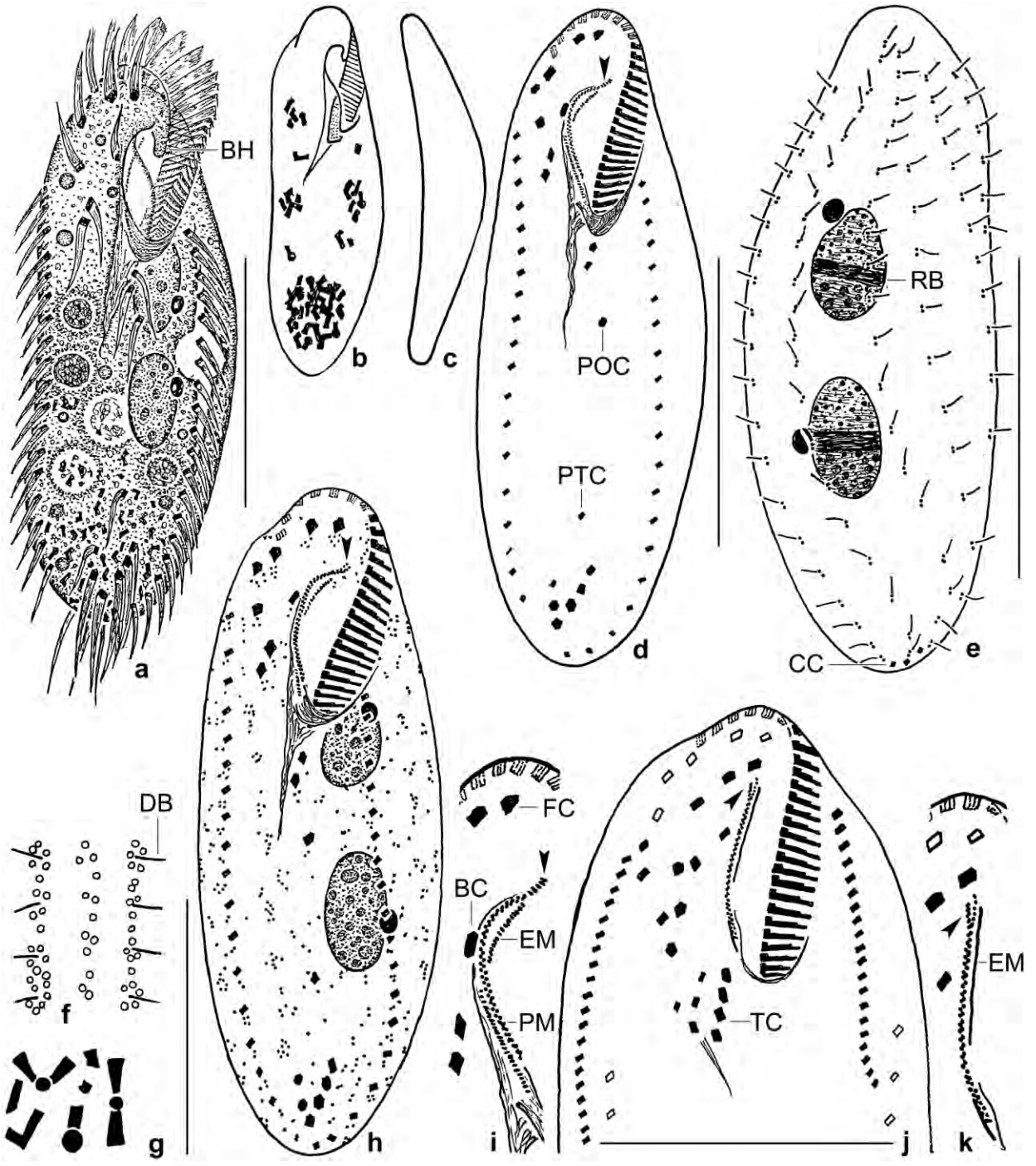

Fig. 242a–k. *Notohymena antarctica*, Austrian population 1 (a–g, i) and 2 (h), and Australian population 1 (j, k) from life (a–c, f, g) and after protargol impregnation (d, e, h–k). The arrowhead in figures (d, h–k) marks the curved anterior end of the paroral membrane. **a:** Ventral view of a representative specimen, length 110 µm. Note the buccal horn (BH). **b:** Ventral view of a slender specimen, showing the distribution of cytoplasmic crystals. **c:** Lateral view. **d, e, i:** Ventral and dorsal view of main voucher specimen. **f:** Cortical granulation on dorsal side. **g:** Cytoplasmic crystals. **h:** Ventral view, showing the distribution of the cortical granules. **j, k:** Ventral view of a late proter divider, showing that the anterior end of the paroral consists of paroral dikinetids and a short row of monokinetids (k). BC – buccal cirrus, BH – buccal horn, CC – caudal cirri, DB – dorsal bristle, EM – endoral membrane, FC – frontal cirrus 1, RB – reorganization band, PM – paroral membrane, POC – last postoral cirrus, PTC – upper pretransverse cirrus, TC – transverse cirri. Scale bars 30 µm (h, j) and 50 µm (a, d, e).

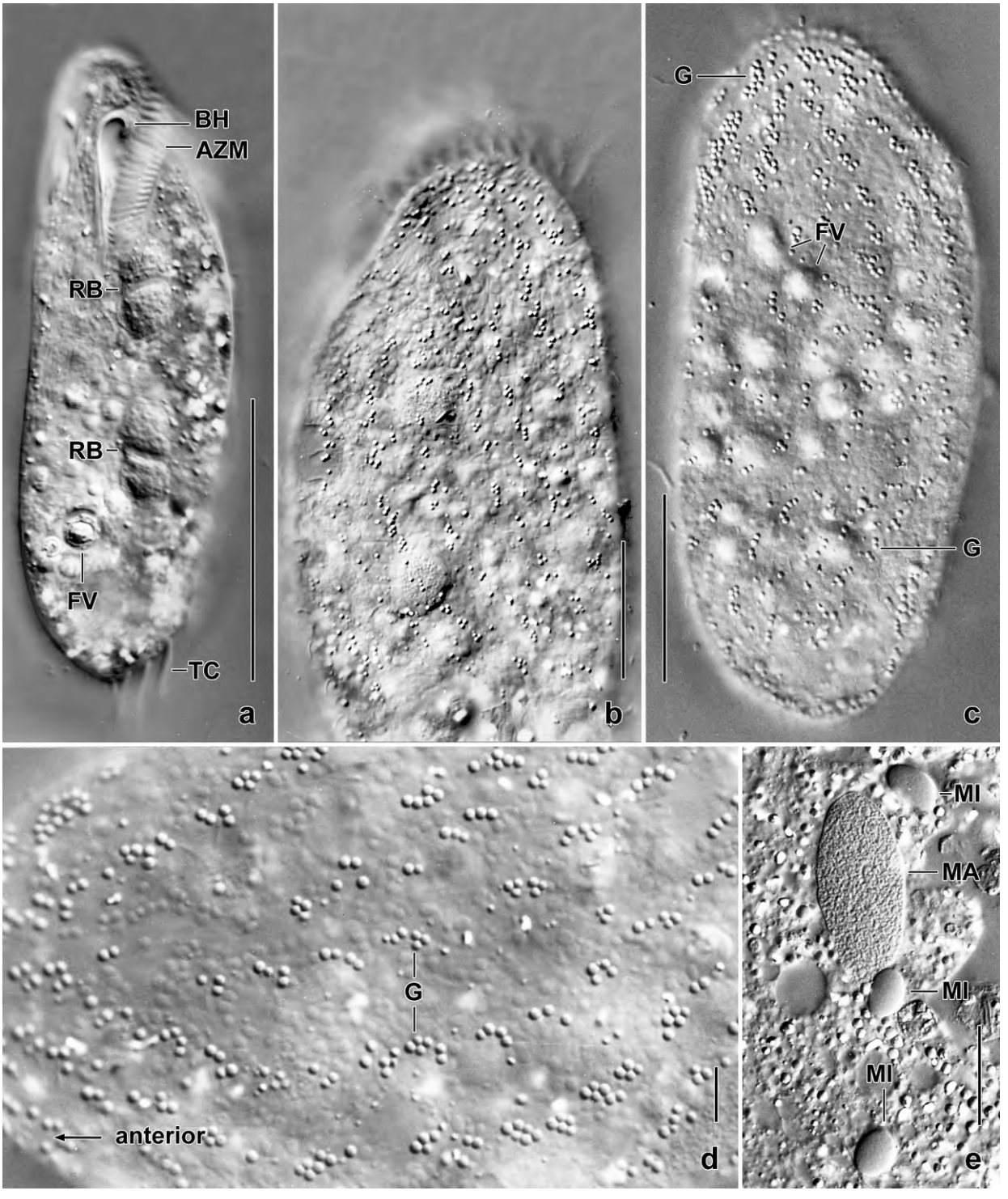

Fig. 243a–e. *Notohymena antarctica*, Austrian population 1 (a, b) and Australian population 1 (c–e). **a:** Ventral view of a slender specimen, showing the conspicuous buccal horn (BH). **b–d:** Dorsal views, showing the cortical granulation. The granules, which form loose rows, are colourless to slightly yellowish and have a diameter of about 1 µm. **e:** Anterior macronuclear nodule and three large (~ 5 × 4 µm), compact micronuclei. AZM – adoral zone of membranelles, BH – buccal horn, FV – food vacuole, G – cortical granules, MA – macronucleus, MI – micronuclei, RB – reorganization bands, TC – transverse cirri. Scale bars 5 µm (d), 10 µm (e), 30 µm (b, c), and 50 µm (a).

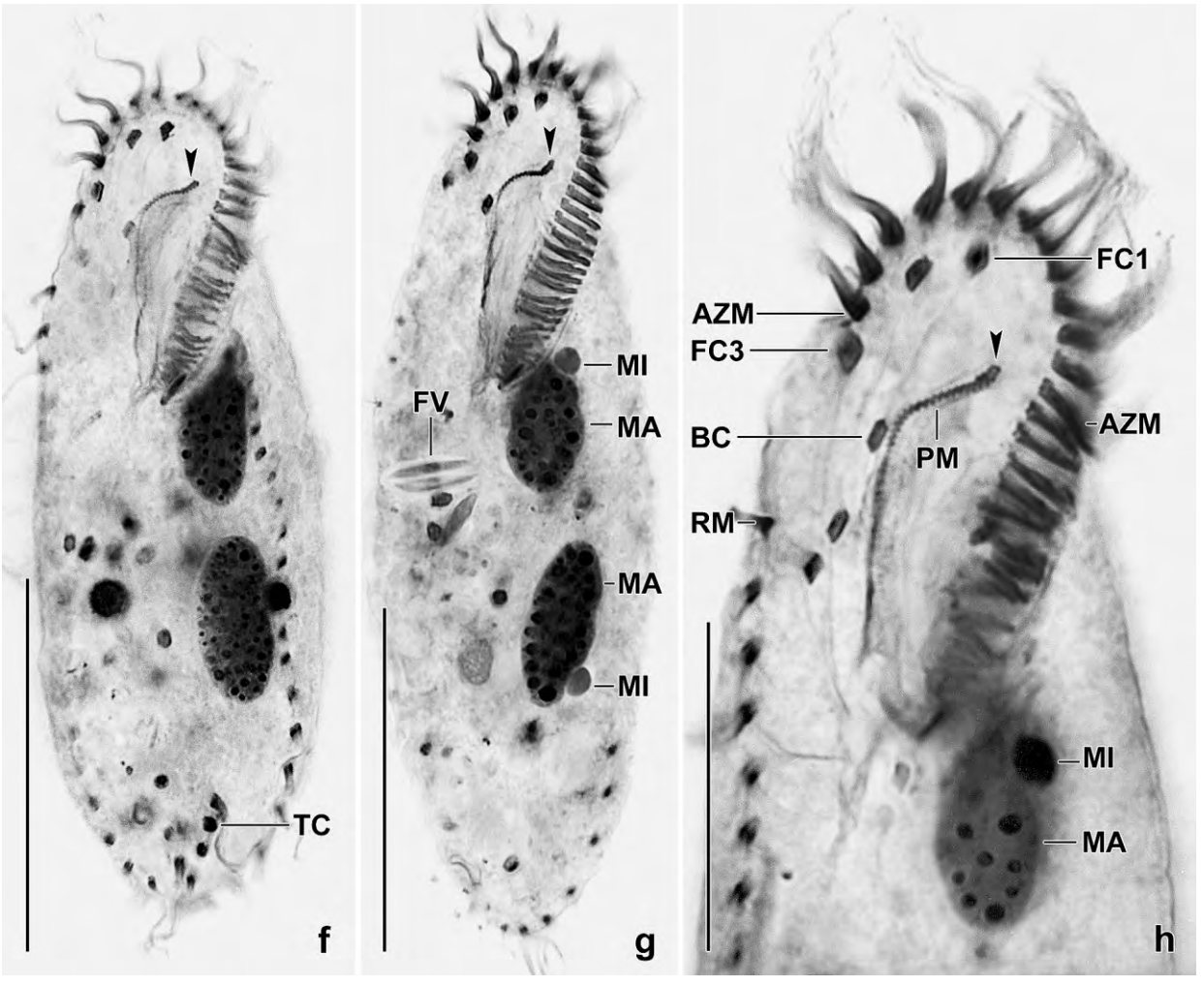

Fig. 243f–h. *Notohymena antarctica*, ventral views of Austrian population 1 after protargol impregnation. The arrowheads mark the curved and thickened anterior end of the paroral membrane, i. e., the character defining the genus *Notohymena*. AZM – adoral zone of membranelles, BC – buccal cirrus, FC1, 3 – frontal cirri, FV – food vacuole, MA – macronuclear nodules, MI – micronuclei, PM – paroral membrane, RM – right marginal row, TC – transverse cirri. Scale bars 20 µm (h) and 40 µm (f, g).

number of adoral membranelles.

Morphometric analyses (Table 89): The four populations are highly similar in most morphological and morphometric features, suggesting conspecificity. The average variability coefficients (CV) are ≤ 10% for the following important features: body length 76–94 µm, CV 6.7–8.6%; length of the adoral zone of membranelles 28–34 µm, CV 3.4–11.7%; number of adoral membranelles 28–30, CV 2.6–6.4%; and the number of cirri in the right (17–19, CV 3.4–9%) and left (18–20, CV 3.7–8%) marginal row. Further, the median is invariable for many features: two macronuclear nodules, two micronuclei, three frontal cirri, four frontoventral cirri, one buccal cirrus, three postoral cirri, two pretransverse cirri, five transverse cirri, three caudal cirri, and six dorsal kineties. However, the Upper Austrian population is rather variable: one to two micronuclei, two to four frontoventral cirri, four to five transverse cirri, three to five caudal cirri, and 6–7 dorsal kineties.

Table 89. Morphometric data on *Notohymena antarctica* (ANT) from Antarctica (type locality; from FOISSNER 1996); Australia, population 1 (AUT); Austria, population 2 (AUE); and Austria, population 1 (AUV). Data based on mounted, protargol-impregnated (FOISSNER's method), and randomly selected specimens from non-flooded Petri dish cultures. CV – coefficient of variation in %, M – median, Max – maximum, Mean – arithmetic mean, Min – minimum, n – number of individuals investigated, SD – standard deviation, SE – standard error of arithmetic mean.

Characteristics	Pop	Mean	M	SD	SE	CV	Min	Max	n
Body, length (µm)	ANT	85.5	87.0	5.8	1.7	6.7	70.0	91.0	11
	AUT	85.2	86.0	6.6	1.8	7.7	77.0	97.0	13
	AUE	75.8	75.0	6.5	1.8	8.6	65.0	85.0	13
	AUV	94.1	94.0	6.3	1.5	6.7	82.0	105.0	19
Body, width (µm)	ANT	30.4	31.0	2.1	0.6	7.0	28.0	34.0	11
	AUT	34.6	33.0	3.1	0.9	9.1	30.0	40.0	13
	AUE	32.4	32.0	2.6	0.7	8.0	29.0	37.0	13
	AUV	34.3	35.0	2.7	0.6	8.0	29.0	38.0	19
Body length:width, ratio	ANT	2.8	–	–	–	–	–	–	11
	AUT	2.5	2.4	0.2	0.1	6.8	2.3	2.8	13
	AUE	2.4	2.3	0.2	0.1	7.1	2.2	2.7	13
	AUV	2.7	2.8	0.2	0.1	7.4	2.4	3.2	19
Anterior body end to proximal end of adoral zone of membranelles, distance (µm)	ANT	32.4	32.0	2.2	0.7	6.8	28.0	35.0	11
	AUT	27.9	27.0	3.2	0.9	11.5	25.0	36.0	13
	AUE	28.5	29.0	1.0	0.3	3.4	27.0	30.0	13
	AUV	33.7	34.0	2.4	0.6	7.1	30.0	40.0	19
Macronuclear nodules, distance in between (µm)	ANT	6.5	7.0	1.7	0.5	26.3	4.0	9.0	11
	AUT	6.1	6.0	2.5	0.7	41.7	0.0	9.0	13
	AUE	5.6	5.0	2.4	0.7	42.1	2.0	10.0	13
	AUV	3.1	3.0	1.9	0.4	63.2	0.0	6.0	19
Macronuclear nodules, length (µm)	ANT	12.9	13.0	2.1	0.6	16.0	11.0	18.0	11
	AUT	14.6	14.0	1.7	0.5	11.7	13.0	18.0	13
	AUE	12.0	12.0	1.4	0.4	11.3	9.0	14.0	13
	AUV	17.5	17.0	1.3	0.3	7.5	15.0	21.0	19
Macronuclear nodules, width (µm)	ANT	7.1	7.0	–	–	–	7.0	8.0	11
	AUT	8.2	8.0	0.9	0.3	11.3	7.0	10.0	13
	AUE	8.5	8.0	0.9	0.2	10.4	7.0	10.0	13
	AUV	8.8	9.0	0.8	0.2	9.4	7.0	10.0	19
Macronuclear nodules, number	ANT	2.0	2.0	0.0	0.0	0.0	2.0	2.0	11
	AUT	2.0	2.0	0.0	0.0	0.0	2.0	2.0	13
	AUE	2.0	2.0	0.0	0.0	0.0	2.0	2.0	13
	AUV	2.0	2.0	0.0	0.0	0.0	2.0	2.0	19
Micronuclei, length (µm)	ANT	3.2	3.0	–	–	–	3.0	4.0	11
	AUT	3.4	3.0	–	–	–	3.0	4.0	13
	AUE	3.5	4.0	–	–	–	3.0	4.0	13
	AUV	4.1	4.0	–	–	–	3.5	5.0	19
Micronuclei, width (µm)	ANT	2.8	3.0	–	–	–	2.5	3.0	11
	AUT	2.5	3.0	–	–	–	2.0	3.0	13
	AUE	3.0	3.0	–	–	–	3.0	4.0	13

continued

Characteristics	Pop	Mean	M	SD	SE	CV	Min	Max	n
	AUV	3.6	3.5	–	–	–	3.0	4.0	19
Micronuclei, number	ANT	2.4	2.0	0.7	0.2	28.5	1.0	3.0	11
	AUT	2.0	2.0	0.0	0.0	0.0	2.0	2.0	13
	AUE	1.9	2.0	–	–	–	1.0	2.0	13
	AUV	1.9	2.0	0.5	0.1	24.2	1.0	3.0	19
Anterior body end to first macronuclear nodule, distance (µm)	AUV	30.0	30.0	2.1	0.5	7.1	26.0	35.0	19
Anterior body end to right marginal cirral row, distance (µm)	AUV	19.7	20.0	2.9	0.7	14.6	14.0	27.0	19
Anterior body end to buccal cirrus, distance (µm)	AUV	13.2	13.0	1.4	0.3	10.6	10.0	16.0	19
Anterior body end to last postoral cirrus, distance (µm)	AUV	47.1	47.0	3.5	0.8	7.4	41.0	58.0	19
Anterior body end to paroral membrane, distance (µm)	AUV	9.5	10.0	1.3	0.3	13.8	7.0	12.0	19
Paroral membrane, length (µm)	AUV	18.0	18.0	1.5	0.3	8.3	16.0	20.0	19
Adoral membranelles, number	ANT	30.2	31.0	1.9	0.6	6.4	27.0	33.0	11
	AUT	28.2	28.0	0.7	0.2	2.6	27.0	30.0	13
	AUE	27.9	28.0	1.2	0.3	4.4	26.0	30.0	13
	AUV	28.6	29.0	0.9	0.2	3.2	27.0	30.0	19
Right marginal cirri, number	ANT	16.8	17.0	1.2	0.4	6.9	15.0	19.0	11
	AUT	18.9	19.0	0.6	0.2	3.4	18.0	20.0	13
	AUE	19.2	19.0	1.7	0.5	9.0	17.0	22.0	13
	AUV	18.1	18.0	1.2	0.3	6.7	16.0	21.0	19
Left marginal cirri, number	ANT	17.9	18.0	1.3	0.4	7.3	16.0	20.0	11
	AUT	19.0	19.0	0.7	0.2	3.7	18.0	20.0	13
	AUE	19.3	19.0	1.6	0.4	8.0	17.0	22.0	13
	AUV	20.2	20.0	1.0	0.2	4.8	18.0	22.0	19
Frontal cirri, number	ANT	3.0	3.0	0.0	0.0	0.0	3.0	3.0	11
	AUT	3.0	3.0	0.0	0.0	0.0	3.0	3.0	13
	AUE	3.0	3.0	0.0	0.0	0.0	3.0	3.0	13
	AUV	3.0	3.0	0.0	0.0	0.0	3.0	3.0	19
Frontoventral cirri, number	ANT	4.0	4.0	0.0	0.0	0.0	4.0	4.0	11
	AUT	4.0	4.0	0.0	0.0	0.0	4.0	4.0	13
	AUE	3.9	4.0	0.6	0.2	14.4	2.0	4.0	13
	AUV	4.0	4.0	0.0	0.0	0.0	4.0	4.0	19
Buccal cirri, number	ANT	1.0	1.0	0.0	0.0	0.0	1.0	1.0	11
	AUT	1.0	1.0	0.0	0.0	0.0	1.0	1.0	13
	AUE	1.0	1.0	0.0	0.0	0.0	1.0	1.0	13
	AUV	1.0	1.0	0.0	0.0	0.0	1.0	1.0	19
Postoral cirri, number	ANT	3.0	3.0	0.0	0.0	0.0	3.0	3.0	11
	AUT	3.2	3.0	0.6	0.2	17.6	3.0	5.0	13
	AUE	3.0	3.0	0.0	0.0	0.0	3.0	3.0	13
	AUV	3.0	3.0	0.0	0.0	0.0	3.0	3.0	19
Pretransverse cirri, number	ANT	2.0	2.0	0.0	0.0	0.0	2.0	2.0	11
	AUT	2.3	2.0	–	–	–	2.0	3.0	13
	AUE	2.0	2.0	0.0	0.0	0.0	2.0	2.0	13

continued

Characteristics	Pop	Mean	M	SD	SE	CV	Min	Max	n
	AUV	2.0	2.0	0.0	0.0	0.0	2.0	2.0	19
Transverse cirri, number	ANT	5.0	5.0	0.0	0.0	0.0	5.0	5.0	11
	AUT	5.2	5.0	–	–	–	5.0	6.0	13
	AUE	4.9	5.0	–	–	–	4.0	5.0	13
	AUV	5.0	5.0	0.0	0.0	0.0	5.0	5.0	19
Posterior body end to rearmost transverse cirrus, distance (µm)	AUV	3.6	4.0	0.8	0.2	21.0	2.0	5.0	19
Caudal cirri, number	ANT	3.0	3.0	0.0	0.0	0.0	3.0	3.0	11
	AUT	3.0	3.0	0.0	0.0	0.0	3.0	3.0	13
	AUE	3.5	3.0	0.7	0.2	19.1	3.0	5.0	13
	AUV	3.0	3.0	0.0	0.0	0.0	3.0	3.0	19
Dorsal kineties, number	ANT	6.0	6.0	0.0	0.0	0.0	6.0	6.0	11
	AUT	6.2	6.0	–	–	–	6.0	7.0	13
	AUE	6.1	6.0	–	–	–	6.0	7.0	13
	AUV	6.0	6.0	0.0	0.0	0.0	6.0	6.0	19
Kinetids in dorsal kinety 1, number	AUV	19.2	19.0	1.8	0.4	9.3	16.0	22.0	19
Kinetids in dorsal kinety 5, number	AUV	12.4	13.0	2.4	0.6	19.4	8.0	17.0	19

Basically, these data confirm those of Foissner (1982) that many morphological and morphometric characters of the hypotrichs are valuable or very valuable for defining species, especially those which are countable, such as the number of adoral membranelles, FVT-cirri, caudal cirri, dorsal kineties, and macronuclear nodules.

Distribution: Except of Africa, *N. antarctica* has now been recorded from all main biogeographic regions (Foissner 1996a, 2004; this study). The absence from Africa is surprising because we made several detailed studies on soil ciliates (Foissner 1999b, Foissner et al. 2002, 2008).

Improved diagnosis (based on four populations, Table 89): Size in vivo about 90–110 × 35–40 µm. 2 ellipsoid macronuclear nodules and 2 micronuclei. Cortical granules mainly around bases of cirri and dorsal bristles; 0.5–1.5 µm in diameter; colourless, yellow or orange. On average 18 FVT-cirri, 17–19 cirri in right marginal row and 18–20 in left row. Usually 6 dorsal kineties and 3 caudal cirri. Adoral zone extends 33–38% of body length on average, composed of 28–30 membranelles.

Description of Austrian population 1 (Fig. 242a–g, i, 243a, b, f–h; Tables 89, 90): Size in vivo 95–120 × 35–45 µm, usually about 110 × 45 µm, as calculated from some in vivo measurements and the morphometric data in Table 89 adding 15% preparation shrinkage. Length:width ratio 2.4–3.2:1, on average 2.7:1 in vivo and in protargol preparations, body shape thus slenderly ellipsoid, posterior end occasionally bluntly pointed, ventral margin usually slightly convex, dorsal margin straight to slightly concave, laterally flattened about 2:1 (Fig. 242a–e, 243a, e–g; Table 89). Nuclear apparatus in middle third of cell slightly left of body's midline, composed of two macronuclear nodules and one to three micronuclei (Fig. 242a, e, 243a, f, g; Table 89). Macronuclear nodules rather close together, ellipsoid (~ 2:1), contain many small nucleoli. Micronuclei in deep concavities of or near to macronuclear nodules, especially conspicuous in

Table 90. Cortical granules of six soil populations of *Notohymena antarctica*, according to live observations and the laboratory notebook.

Source	Description
Antarctica (FOISSNER 1996)	Arranged in groups around bases of cirri and dorsal bristles; yellow to yellow-green, give cells yellowish colour at low magnification (≤ ×100); do not impregnate with protargol.
Brazil (FOISSNER, unpubl.)	Arranged in groups around bases of cirri and dorsal bristles, rare on ventral surface; 1–1.5 µm in diameter; usually yellowish, rarely almost or entirely colourless.
Australia, population 1 (FOISSNER, unpubl.)	Arranged in groups around bases of cirri and dorsal bristles, on ventral side in loose rows; about 1 µm in diameter; colourless to slightly yellowish (Fig. 242j, k, 243b–e); do not impregnate with protargol.
Australia, population 2 (FOISSNER, unpubl.)	Occur mainly around the bases of cirri and dorsal bristles; about 1 µm in diameter; citrine, rarely with orange shimmer, give cells a yellowish shimmer; in a further population orange!
Austria, population 1 (FOISSNER, unpubl.)	Arranged in groups around bases of dorsal bristles plus a loose row between two bristle rows each, loosely arranged on ventral side, not grouped around cirri; 0.4–0.6 µm in diameter; colourless to yellow; stain red and burst with methyl green-pyronin (Fig. 242a–g, 243a, f–h).
Austria, population 2 (FOISSNER, unpubl.)	Similar to Antarctic population; impregnate with protargol (Fig. 242h).

vivo because about 5 × 3.5 µm in size and strongly refractive (Fig. 243e), as in the Antarctic type population. Contractile vacuole in or slightly anterior of mid-body, without distinct canals. Cortex very flexible, colourless to yellowish due to the cortical granules (Table 90). Cytoplasm colourless, contains food vacuoles and, usually, many crystals (Fig. 242a, b, g, 243a). Food vacuoles 5–12 µm across in vivo, contain the flagellate *Polytoma*, naked amoebae, fungal hyphae, and up to 20 µm long spores of *Fusarium*. Crystals of usual shape and size, frequently accumulate in posterior half, forming dark spots under bright field illumination at low magnification (≤ ×100; Fig. 242b). Glides slowly to rather rapidly on microscope slide, never rests.

Somatic and oral ciliature perfectly oxytrichid and as described in type population (Fig. 242a, d, e, 243f–h; Table 89). Cirri rather thick, except of last marginal cirri; transverse cirri about 25 µm long in vivo and thus distinctly projecting from body proper; caudal cirri thin and right of body's midline, indistinctly separate from left marginal cirri. Buccal horn and undulating membranes as conspicuous as in type specimens. Buccal lip broader than in type, thus covering most of buccal cavity, difficult to recognize because very hyaline (Fig. 242a, b).

Notes on Australian population 1 (Fig. 242j, k, 243c–e; Tables 89, 90). Size in vivo about 100 × 40 µm; ellipsoid to slenderly ellipsoid, frequently slenderly obovate; about 2:1 flattened laterally. Micronuclei in vivo conspicuous because about 5 × 4 µm in size and strongly refractive (Fig. 243e). Contractile vacuole in mid-body, with short collecting canals. Cortical granules described in Table 90. Cytoplasm with crystals and many lipid droplets up to 3 µm across in posterior body region. Feeds on *Polytoma* digested in food vacuoles 7–10 µm in diameter and, occasionally, on small cyanobacteria. Creeps and swims rather rapidly.

Somatic and oral ciliature very similar to that of type population (Table 89). Frontal cirri in vivo ~ 15 µm long, marginal cirri ~ 13 µm, transverse cirri ~ 23 µm, caudal cirri ~ 17 µm, dorsal bristles

~ 3 µm, bases of largest adoral membranelles ~ 8 µm wide, paroral cilia ~ 10 µm long.

A late divider shows the origin of the thickened anterior end of the paroral membrane from a minute fork composed of the dikinetal paroral and a short monokinetal row (Fig. 242j, k). This is possibly different from *Notohymena rubescens* in which only some dikinetids are added laterally to the anterior region of the paroral (Voss 1991).

Notes on Austrian population 2 (Fig. 242h, 243a, b; Tables 89, 90). The Upper Austrian specimens have a rather variable 18 FVT-cirral pattern, for instance, three to five caudal cirri sometimes difficult to distinguish from left marginal cirri (Table 89). Here, we illustrate the cortical granulation of the ventral side, showing that it is irregular but we cannot exclude that some granules did not impregnate (Fig. 242h). Granules in protargol preparations much smaller than in vivo (≤ 0.5 µm vs. ~ 1 µm). Feeds on a medium-sized *Peranema* and fungal conidia. Stomatogenesis commences at uppermost transverse cirrus.

Synonymy: The observations from six populations globally show a high variability in an important species feature, viz., the colour of the cortical granules that varies from colourless to orange (Table 90). Thus, *Notohymena pampasica* Küppers et al., 2007, whose main feature are the colourless cortical granules, is very likely synonymous with *N. antarctica*. The synonymy is emphasized by the highly similar morphometrics.

Notohymena quadrinucleata **nov. spec.** (Fig. 244a–g, 245a–f; Table 91)

Diagnosis: Size in vivo about 100 × 35 µm; ellipsoid to elongate ellipsoid. 4 macronuclear nodules and 2 micronuclei in line left of body`s midline. Cortical granules yellowish to citrine, 0.7–1 µm across. 18 ordinary fronto-ventral-transverse cirri; right marginal cirral row commences far subapically. 6 dorsal kineties with 3 µm long bristles, 3 caudal cirri. Adoral zone of membranelles occupies about 36% of body length, composed of an average of 28 membranelles. Buccal cavity narrow and deep; buccal horn conspicuous.

Type locality: Site (71), i. e., soil under a *Pandanus* palm in Santa Cruz Island, Galápagos, 0°37'S 90°21'W.

Type material: 1 holotype and 2 paratype slides with protargol-impregnated specimens have been deposited in the Biology Centre of the Upper Austrian Museum in Linz (LI). Relevant specimens have been marked with black ink circles on the coverslip.

Etymology: The species name is a composite of the Latin quantifier *quadr* (four), the thematic vowel *-i-*, and the Latin participle *nucleata* (having a nucleus). It refers to the four macronuclear nodules, a main feature of the species.

Description: *Notohymena quadrinucleata* has a surprisingly low variability, most variation coefficients being lower than 10% (Table 91).

Size in vivo 80–110 × 30–45 µm, usually about 100 × 35 µm, as calculated from some in vivo

measurements and the morphometric data in Table 91 adding 20% and 15% for length and width shrinkage, respectively, due to ethanol fixation; Columbian specimens in vivo up to 130 µm long and more slender than those from Galápagos (Fig. 245a, b). Body shape inconspicuous, i. e., ellipsoid to elongate ellipsoid or slightly ovate, laterally flattened up to 2:1 (Fig. 244a, b). Nuclear apparatus in central quarters left of cell`s midline (Fig. 244a, g, 245d–f; Table 91). Invariably four macronuclear nodules in line, rarely in two indistinct pairs, anterior nodule underneath proximal end of adoral zone of membranelles; studded with ordinary nucleoli. Usually two globular micronuclei attached to various sites of macronuclear nodules. Contractile vacuole slightly anterior of mid-body, with two long collecting canals (Fig. 244a). Cortex very flexible, contains loose rows of yellowish to citrine granules 0.7–1 µm across (Fig. 244c, d). Cytoplasm with a moderate number of lipid droplets up to 5 µm across and many colourless crystals scattered throughout postoral body portion, usually forming some aggregates in rear

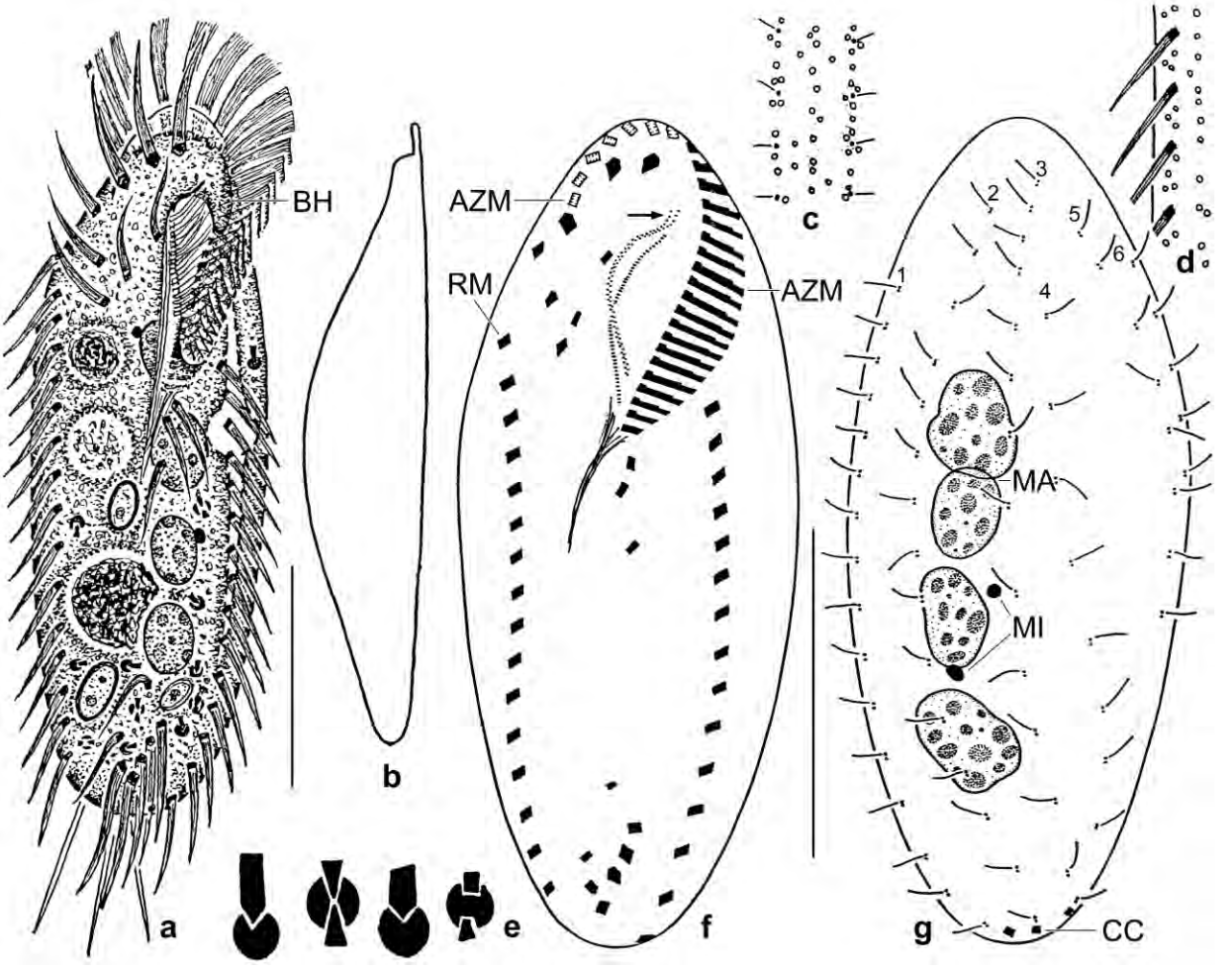

Fig. 244a–g. *Notohymena quadrinucleata,* Galápagos specimens from life (a–e) and after protargol impregnation (f, g). **a:** Ventral view of a representative specimen, length 95 µm. Note the conspicuous buccal horn. **b:** Lateral view. **c, d:** Cortical granulation on dorsal and ventral side. **e:** Cytoplasmic crystals, 3–5 µm. **f, g:** Infraciliature and nuclear apparatus of holotype specimen, length 76 µm. The right marginal cirral row commences far subapically and the macronucleus consists of four nodules, a main feature of this species. The arrow marks the notohymenid anterior curve of the paroral membrane. The numerals denote the dorsal kineties. AZM – adoral zone of membranelles, BH – buccal horn, CC – caudal cirri, DK1,6 – dorsal kineties, MA – macronuclear nodules, MI – micronuclei, RM – right marginal cirral row. Scale bars 30 µm (a, f, g).

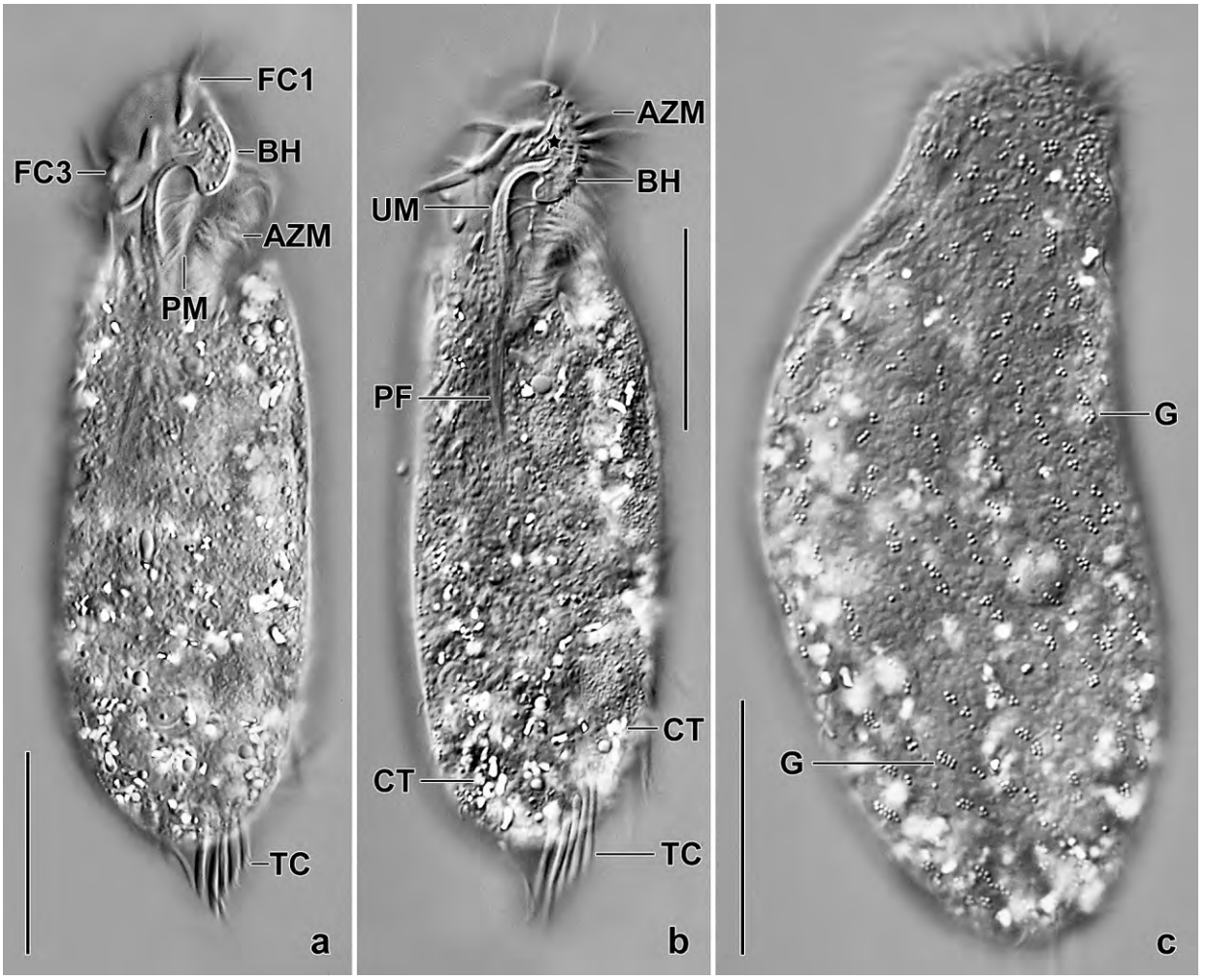

Fig. 245a–c. *Notohymena quadrinucleata,* Columbian specimens from life. **a, b:** Ventral view of a specimen at two focal planes, showing the complex oral apparatus, especially the conspicuous buccal horn. The asterisk (b) marks the sigmoid anterior region of the paroral membrane, as typical for *Notohymena.* **c:** Dorsal view, showing the loose cortical granulation slightly disturbed by mild coverslip pressure. AZM – adoral zone of membranelles, BH – buccal horn, CT – cytoplasmic crystals, FC1,3 – frontal cirri, G – cortical granules, yellowish to citrine, PF – pharyngeal fibres, PM – cilia of paroral membrane, TC – transverse cirri, UM – undulating membranes. Scale bars 30 µm.

end (Fig. 244a, e, 245a–c). Feeds on colourless and dark brown fungal spores and, possibly, on small ciliates digested in food vacuoles 5–20 µm across. Moves ordinarily, showing pronounced flexibility when creeping between soil particles.

Ventral cirral pattern as typical for *Oxytricha* s. str., i. e., with 18 ordinarily-sized fronto-ventral-transverse cirri (Fig. 244a, f, 245a, b, d, e; Table 91). Frontal cirri about 20 µm long in vivo; buccal cirrus at level of summit of paroral membrane, i. e., far distant from its anterior end; upper postoral cirri close together; transverse cirri about 20 µm long in vivo, project distinctly from body proper because posteriormost cirrus only 4 µm anterior of rear body end. Marginal cirri about 13 µm long in vivo, right row commences 17 µm distant from anterior body end, distance between first and second cirrus slightly enlarged; left marginal row extends to body`s midline posteriorly.

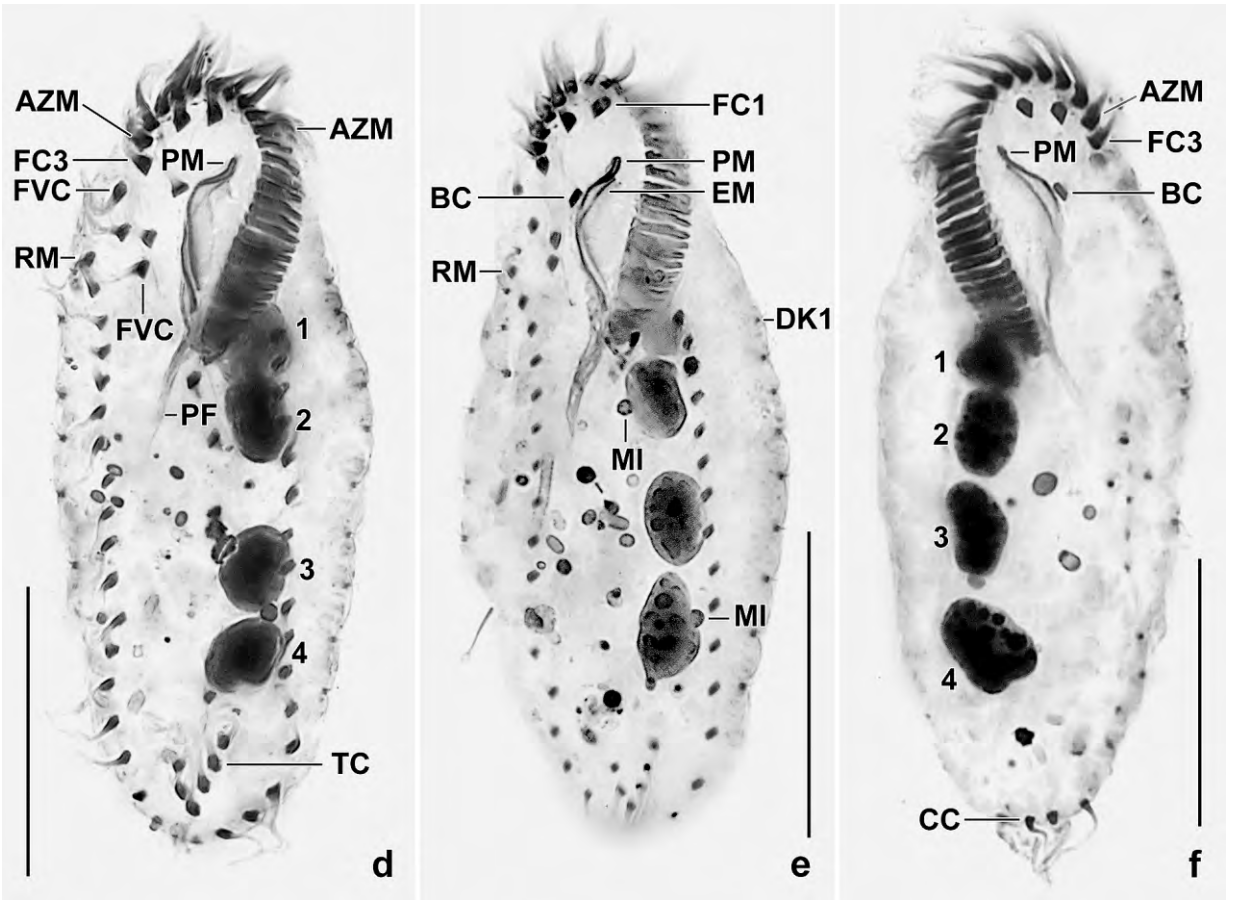

Fig.245d–f. *Notohymena quadrinucleata,* Galápagos specimens after protargol impregnation. The cells are rather inflated due to ethanol fixation. Numerals denote the four macronuclear nodules, a main feature of this species**. d, e:** Ventral views, showing the somatic and oral infraciliature as well as the nuclear apparatus. The right marginal row commences far subapically. **f:** Dorsal view, showing the inconspicuous caudal cirri, the four macronuclear nodules, and the oral apparatus. AZM – adoral zone of membranelles, BC – buccal cirrus, CC – caudal cirri, DK1 – dorsal kinety 1, EM – endoral membrane, FC1,3 – frontal cirri, FVC – frontoventral cirri, MI – micronuclei, PF – pharyngeal fibres, PM – paroral membrane, RM – right marginal cirral row, TC – transverse cirri. Scale bars 30 µm.

Six dorsal kineties in typical *Oxytricha* pattern, bristles 3 µm long in vivo (Fig. 244g, 245e; Table 91). Caudal cirri of ordinary thickness, about 20 µm long in vivo, insert in and left of body`s midline.

Oral apparatus extends 32–46%, on average 36% of body length in protargol preparations (Fig. 244a, f, 245a, b, d, e; Table 91). Adoral zone of ordinary shape and structure, composed of an average of 28 membranelles with longest bases about 8 µm wide in vivo and 6 µm after protargol impregnation. Buccal cavity narrow but deep, especially in anterior half; buccal horn conspicuous, covers part of adoral zone and proceeds as membranellar scutum; buccal lip narrow, bears paroral membrane with cilia about 8 µm long in vivo, those of endoral 20 µm long and extending into pharynx. Undulating membranes as typical for genus, paroral and endoral of similar length, optically intersect at level of mid buccal cavity. Pharynx distinct in vivo and in protargol preparations due to the long endoral cilia (Fig. 244a, f, 245a, b, d, e; Table 91).

Occurrence and ecology: As yet found in Galápagos (type), Columbia (San Andres Island; sandy soil covered with grass, palm litter, and banana litter; pH 7.5; not saline; sample kindly collected by Dr. W. Petz), and Japan (soil from a rice field in the surroundings of the Lake Biwa museum). This shows wide, probably cosmopolitan distribution and, possibly, a preference for immature soil environments.

Remarks: There is only one congener with four macronuclear nodules: *Notohymena saprai* Kamra & Kumar, 2010. This species has dark green cortical granules while those of *N. quadrinucleata* are yellowish to citrine. Further, *N. saprai* is twice as long as *N. quadrinucleata* (149 × 49 μm vs. 78 × 33 μm in protargol preparations). See Berger (1999) and Lv et al. (2013) for overviews of the species described.

Table 91. Morphometric data on *Notohymena quadrinucleata* based on mounted, protargol-impregnated, and randomly selected specimens from a non-flooded Petri dish culture. Measurements in μm. CV – coefficient of variation in %, M – median, Max – maximum, Mean – arithmetic mean, Min – minimum, n – number of individuals investigated, SD – standard deviation, SE – standard error of arithmetic mean.

Characteristics	Mean	M	SD	SE	CV	Min	Max	n
Body, length	78.5	80.0	6.4	1.4	8.1	66.0	90.0	21
Body, width	33.1	33.0	3.0	0.7	9.2	27.0	38.0	21
Body length:width, ratio	2.4	2.4	0.2	0.1	7.6	2.1	2.8	21
Anterior body end to proximal end of adoral zone, distance	28.4	29.0	1.1	0.2	3.8	26.0	30.0	21
Adoral zone of membranelles, percentage of body length	36.4	36.0	3.3	0.7	9.0	32.0	45.7	21
Adoral zone, number of membranelles	27.9	28.0	1.0	0.2	3.7	26.0	30.0	21
Largest adoral membranelle, base width	6.3	6.0	0.4	0.1	5.9	5.0	7.0	21
Anterior body end to paroral membrane, distance	7.6	7.5	0.7	0.2	9.7	6.0	9.0	21
Anterior body end to endoral membrane, distance	10.0	10.0	0.8	0.2	8.2	9.0	12.0	21
Buccal cavity, width	6.6	7.0	0.7	0.2	11.1	5.0	8.0	21
Anterior body end to first macronuclear nodule, distance	21.8	22.0	2.3	0.5	10.3	15.0	26.0	21
Nuclear figure, length	40.8	40.0	3.6	0.8	8.8	35.0	50.0	21
Macronuclear nodules, number	4.0	4.0	0.0	0.0	0.0	4.0	4.0	21
First macronuclear nodule, length	9.8	10.0	1.0	0.2	10.2	8.0	12.0	21
First macronuclear nodule, width	7.1	7.0	0.9	0.2	11.9	6.0	9.0	21
Micronuclei, number	2.0	2.0	0.9	0.2	47.2	0.0	4.0	21
Micronuclei, length	2.0	2.0	–	–	–	1.5	3.0	20
Micronuclei, width	1.6	1.5	–	–	–	1.0	2.0	20
Frontal cirri, number	3.0	3.0	0.0	0.0	0.0	3.0	3.0	21
Anterior body end to buccal cirrus, distance	11.1	11.0	0.8	0.2	7.3	9.0	12.0	21
Buccal cirrus, number	1.0	1.0	0.0	0.0	0.0	1.0	1.0	21
Anterior body end to first frontoventral cirrus, distance	10.3	11.0	1.1	0.3	11.1	8.0	12.0	21
Anterior body end to last frontoventral cirrus, distance	20.4	21.0	1.0	0.2	5.1	19.0	22.0	21

continued

Characteristics	Mean	M	SD	SE	CV	Min	Max	n
Frontoventral cirri, number	4.0	4.0	0.0	0.0	0.0	4.0	4.0	21
Anterior body end to first postoral cirrus, distance	28.6	29.0	1.8	0.4	6.2	23.0	31.0	21
Anterior body end to last postoral cirrus, distance	38.6	39.0	1.4	0.3	3.6	36.0	42.0	21
Postoral cirri, number	3.0	3.0	0.0	0.0	0.0	3.0	3.0	21
Anterior body end to right marginal row, distance	17.2	18.0	2.4	0.5	13.9	10.0	22.0	21
Posterior body end to right marginal row, distance	6.3	6.5	1.5	0.3	24.2	3.0	9.0	21
Right marginal row, number of cirri	15.7	16.0	0.8	0.2	5.1	14.0	17.0	21
Posterior body end to left marginal row, distance	1.3	1.0	–	–	–	1.0	2.0	21
Left marginal row, number of cirri	15.1	15.0	0.9	0.2	5.9	13.0	17.0	21
Posterior body end to lowermost transverse cirrus, distance	4.0	4.0	0.8	0.2	20.9	3.0	6.0	20
Transverse cirri, number	5.0	5.0	0.0	0.0	0.0	5.0	5.0	21
Pretransverse cirri, number	2.0	2.0	0.0	0.0	0.0	2.0	2.0	21
Dorsal kineties, number	6.0	6.0	0.0	0.0	0.0	6.0	6.0	21
Dorsal kinety 1, number of kinetids	15.7	16.0	1.3	0.3	8.1	14.0	18.0	20
Dorsal kinety 2, number of kinetids	17.8	18.0	1.6	0.4	8.9	14.0	21.0	19
Dorsal kinety 3, number of kinetids	13.1	13.0	1.0	0.3	7.5	12.0	15.0	15
Dorsal kinety 4, number of kinetids	11.5	12.0	1.5	0.4	12.7	9.0	14.0	14
Dorsal kinety 5, number of kinetids	9.3	10.0	1.0	0.2	10.6	8.0	11.0	17
Dorsal kinety 6, number of kinetids	5.2	5.0	1.5	0.3	28.4	3.0	8.0	19
Caudal cirri, number	3.0	3.0	0.0	0.0	0.0	3.0	3.0	21

Fragmospina nov. gen.

Diagnosis: Semirigid Oxytrichidae EHRENBERG, 1838 with 18 fronto-ventral-transverse cirri in *Oxytricha* pattern. Third postoral cirrus not involved in anlagen formation. 1 right and 1 left row of marginal cirri. 6 dorsal kineties, kinety 4 originates by a split of kinety 3. Buccal cavity moderately wide and deep, *Cyrtohymena*-like in vivo. Undulating membranes distinctly curved, but not recurved, i. e., in *Australocirrus* pattern. Resting cyst with conspicuous spines.

Type species: *Steinia candens depressa* GELLÉRT, 1942.

Etymology: *Fragmospina* is composed of the Latin nouns *fragmentum* (piece broken off) and *spina* (thorn), referring to the fragmentation of dorsal kinety 3 and the spinous resting cyst. Feminine gender.

Remarks: See BERGER (1999) for all species and authors mentioned. GELLÉRT (1942) stated that his population is a variety of *Steinia candens* and provided a precise diagnosis and description. FOISSNER (1989) transferred it to *Cyrtohymena*: *C. candens* var. *depressa* (GELLÉRT, 1942) FOISSNER, 1989. BERGER (1999), in contrast, supported synonymy with *C. inquieta* because *C. depressa* is less than 150 µm long and "it is impossible to separate it reliably from *C. inquieta* or *C. candens*". However, on page 317, BERGER (1999) states: "Synonymy with *C. inquieta* is uncertain because the full set (3) of postoral ventral cirri is present".

We know *C. depressa* since years and from soils globally. It is not a very rare species because it is present in seven out of the 71 neotropis samples (see species list). Our reinvestigation shows that *C. depressa* is not only a "good" species but also the representative of a new genus: *Fragmospina*.

Fragmospina is characterized by a combination of four features (Fig. 246a–d, g, 247a–f): 18 FVT-cirri, dorsal kinety 4 originates by a split of kinety 3, undulating membranes in *Australocirrus* pattern, and a spinous resting cyst. 18 FVT-cirri and a split of dorsal kinety 3 characterize *Oxytricha* s. str. while *Australocirrus* spp. have multiple fragmentation of kinety 3 (Berger 1999, Foissner et al. 2005a, Kumar & Foissner 2015). The shape and arrangement of the undulating membranes match *Australocirrus* while the paroral membrane of *Cyrtohymena* recurves distally (Kumar & Foissner 2015), and that of *Oxytricha* never touches the adoral zone of membranelles (Berger 1999, Kumar & Foissner 2015). The spinous resting cyst is of particular importance. Spinous cysts are rather common in stylonychine oxytrichids while those of *Australocirrus* spp. lack spines but have special crystals between ectocyst and mesocyst (Berger 1999, Foissner et al. 2005a, Kumar & Foissner 2015).

Fragmospina depressa (Gellért, 1942) nov. comb., nov. stat. (Fig. 246a–h, 247a–f; Table 92)

Improved diagnosis (based on three populations): Size in vivo about 100 × 40 µm; ellipsoid to broadly ellipsoid. 2 macronuclear nodules with a micronucleus each. About 19 and 17 cirri in right and left marginal row, respectively. Dorsal kinety 4 extends to mid-body; 3 caudal cirri. Adoral zone extends about 27–30% of body length, composed of approximately 30 membranelles.

Type locality: Algal film on tree bark in the surroundings of the town of Kolozsvár (Klausenburg), Hungary (now Rumania), 23°E 47°N.

Material investigated and deposited: 4 and 2 voucher slides with protargol-impregnated specimens from Rwanda and Venezuelan site (56), respectively, have been deposited in the Biology Centre of the Upper Austrian Museum in Linz (LI). Relevant specimens have been marked by black ink circles on the coverslip.

Etymology: Not given in the original description. Possibly, the epithet refers to the deepened buccal cavity.

Redescription: The morphometric data on the Rwandan and the Venezuelan population match almost perfectly, in spite of the large spatial distance, showing not only conspecificity but also the value of such analyses (Table 92).

Length 100–120 µm, according to Gellért (1942); specimens from Rwanda and Venezuela in vivo 80–115 × 30–50 µm, usually about 100 × 40 µm, as calculated from some in vivo measurements and the morphometric data in Table 92 adding 15% preparation shrinkage. Body shape highly similar in the three populations, i. e., ellipsoid to broadly ellipsoid (2–3:1), rarely quadrangular with rounded ends or elongate obovate; dorsoventrally flattened up to 2:1 (Fig. 246a, b, d–f, h, 247d, e). Nuclear apparatus in central quarters slightly left of body´s midline (Fig. 246a, c, h,

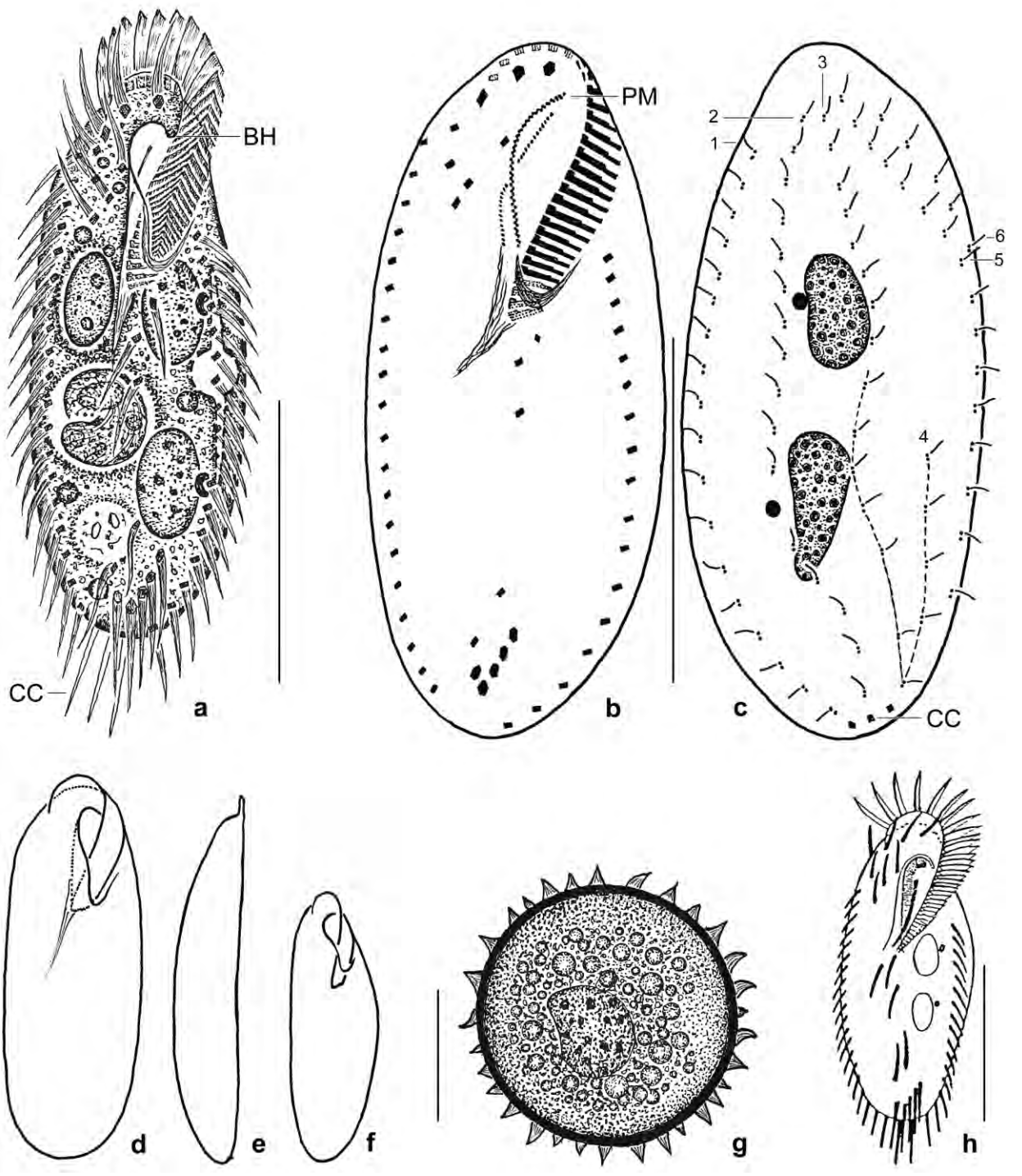

Fig. 246a–h. *Fragmospina depressa* from live (a, d–g), after protargol impregnation (b, c), and after mercuric chloride fixation and opalblue embedding (h). **a:** Ventral view of a representative specimen, length 100 µm. The cell is studded with food vacuoles containing an ellipsoid green algae and a *Colpoda maupasi*. **b, c:** Infraciliature of ventral and dorsal side and nuclear apparatus of main voucher specimen, length 90 µm. Note the short dorsal kinety 4, a main feature of this species. **d, e:** Ventral and lateral view of same specimen. **f:** Ventral view of a slender specimen. **g:** Resting cyst, 50 µm. **h:** Ventral view of type specimen, length 100 µm (from Gellért 1942). BH – buccal horn, CC – caudal cirri, PM – paroral membrane, 1–6 – dorsal bristle rows. Scale bars 25 µm (g) and 50 µm (a–c, h).

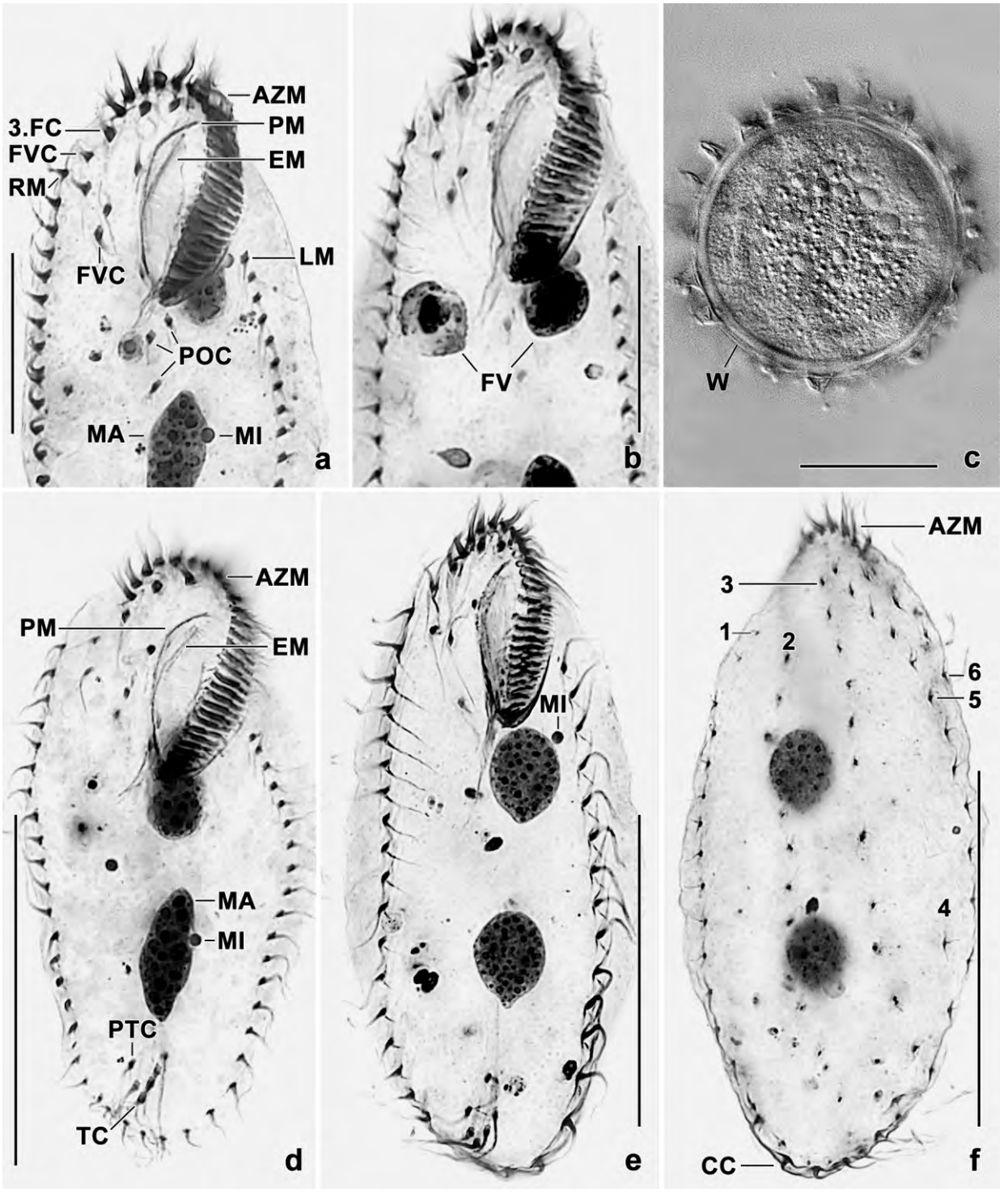

Fig. 247a–f. *Fragmospina depressa* from live (c) and after protargol impregnation (a, b, d–f). **a, b:** Ventral views, showing the cirral pattern and the comparatively narrow buccal cavity. The paroral membrane almost touches the adoral zone. **c:** Resting cyst, 50 µm. **d, e:** Ventral views, showing the 18 FVT-cirral pattern. **f:** Dorsal view, showing the short bristle row 4. AZM – adoral zone of membranelles, CC – caudal cirri, EM – endoral, 3.FC – third frontal cirrus, FV – food vacuoles, FVC – frontoventral cirri, L – left marginal row, MA – macronuclear nodules, MI – micronuclei, PM – paroral, POC – postoral cirri, PTC – pretransverse cirri, RM – right marginal row, TC – transverse cirri, W – cyst wall. Scale bars 25 µm (a–c) and 50 µm (d–f).

Table 92. Morphometric data on *Fragmospina depressa* from Rwanda (RW) and Venezuelan site 56 (VE). *Cyrtohymena candens* (CC) is from Venezuelan site (51). Data based on mounted, protargol-impregnated, randomly selected specimens from non-flooded Petri dish cultures (*F. depressa*) and a pure culture (*C. candens*). Measurements in µm. CV – coefficient of variation in %, M – median, Max – maximum, Mean – arithmetic mean, Min – minimum, n – number of individuals investigated, Pop – population, SD – standard deviation, SE – standard error of arithmetic mean.

Characteristics	Pop	Mean	M	SD	SE	CV	Min	Max	n
Body, length	RW	88.6	90.0	7.2	2.2	8.1	79.0	100.0	11
	VE	90.1	90.0	5.4	1.2	6.0	78.0	101.0	21
	CC	100.0	99.0	10.1	2.2	10.2	84.0	121.0	21
Body, width	RW	38.1	38.0	4.2	1.3	11.0	32.0	45.0	11
	VE	38.4	38.0	3.7	0.8	9.7	31.0	44.0	21
	CC	49.0	50.0	6.2	1.4	12.5	39.0	65.0	21
Body length:width, ratio	RW	2.4	2.4	0.3	0.1	11.3	1.9	2.8	11
	VE	2.4	2.4	0.2	0.1	8.0	1.9	2.8	21
	CC	2.0	2.0	0.2	0.1	8.9	1.8	2.4	21
Anterior body end to proximal end of adoral zone of membranelles, distance	RW	31.6	31.0	2.2	0.7	6.8	29.0	36.0	11
	VE	34.3	34.0	1.9	0.4	5.4	31.0	38.0	21
	CC	41.6	42.0	2.4	0.5	5.8	39.0	49.0	21
Adoral membranelles, number	RW	28.5	29.0	1.7	0.5	6.0	26.0	30.0	11
	VE	30.4	30.0	1.7	0.4	5.5	27.0	33.0	21
	CC	35.2	35.0	1.8	0.4	5.1	32.0	38.0	21
Adoral membranelles, widest base	VE	7.5	7.0	0.5	0.1	7.0	6.5	8.5	21
	CC	7.8	8.0	–	–	–	7.5	8.5	21
Anterior body end to macronucleus, distance	VE	28.9	28.0	2.8	0.6	9.8	26.0	39.0	21
	CC	31.5	31.0	3.2	0.7	10.1	26.0	38.0	21
Nuclear figure, length	VE	39.1	39.0	4.2	0.9	10.7	27.0	44.0	21
	CC	46.7	46.0	5.2	1.1	11.2	35.0	58.0	21
Macronuclear nodules, distance in between	RW	10.8	10.0	3.5	1.1	32.5	6.0	17.0	11
	CC	7.2	7.0	4.2	0.9	58.1	0.0	18.0	21
Macronuclear nodules, length	RW	16.9	17.0	1.8	0.5	10.7	15.0	20.0	11
	VE	16.6	17.0	2.1	0.5	13.0	13.0	20.0	21
	CC	18.8	19.0	2.0	0.4	10.6	14.0	23.0	21
Macronuclear nodules, width	RW	7.8	8.0	1.0	0.3	12.6	7.0	10.0	11
	VE	8.4	8.0	0.9	0.2	11.2	6.0	10.0	21
	CC	10.4	10.0	2.4	0.5	22.7	7.0	14.0	21
Macronuclear nodules, number	RW	2.0	2.0	0.0	0.0	0.0	2.0	2.0	11
	VE	2.0	2.0	0.0	0.0	0.0	2.0	2.0	21
	CC	2.0	2.0	0.0	0.0	0.0	2.0	2.0	21
Micronuclei, length	RW	2.2	2.2	–	–	–	2.0	2.3	11
	VE	2.0	2.0	–	–	–	1.5	2.0	21
	CC	2.4	2.5	–	–	–	2.0	2.5	21
Micronuclei, width	RW	2.2	2.2	–	–	–	2.0	2.3	11
	VE	1.7	1.5	–	–	–	1.5	2.0	21
	CC	2.1	2.0	–	–	–	2.0	2.5	21
Micronuclei, number	RW	2.3	2.0	–	–	–	2.0	3.0	11

continued

Characteristics	Pop	Mean	M	SD	SE	CV	Min	Max	n
	VE	2.2	2.0	0.5	0.1	23.4	2.0	4.0	21
	CC	2.9	3.0	1.0	0.2	36.0	1.0	5.0	21
Anterior body end to paroral membrane, distance	VE	5.5	5.0	1.3	0.3	22.8	3.0	7.0	21
	CC	7.3	7.0	0.7	0.2	9.6	6.0	9.0	21
Anterior body end to endoral membrane, distance	VE	8.7	9.0	1.2	0.3	13.7	5.0	10.0	21
	CC	10.5	10.0	1.3	0.3	12.5	8.5	14.0	21
Buccal cavity, maximum width	RW	6.3	6.0	0.9	0.3	14.4	5.0	8.0	11
	VE	8.5	8.0	1.3	0.3	14.9	7.0	11.0	21
	CC	12.8	13.0	1.5	0.3	11.8	10.0	17.0	21
Anterior body end to right marginal row, distance	VE	14.8	15.0	1.7	0.4	11.6	11.0	19.0	21
	CC	19.4	19.0	3.6	0.8	18.8	14.0	28.0	21
Posterior body end to right marginal row, distance	VE	4.6	4.5	1.3	0.3	27.1	2.0	7.0	21
	CC	5.4	5.0	2.0	0.4	37.1	2.0	10.0	21
Posterior body end to left marginal row, distance	VE	1.3	1.0	0.5	0.1	40.9	0.5	3.0	21
	CC	0.8	0.5	–	–	–	0.5	1.5	21
Posterior body end to transverse cirri, distance	VE	3.1	3.0	0.8	0.2	25.2	1.5	5.0	21
	CC	5.3	5.0	1.1	0.2	20.9	3.0	7.0	21
Anterior body end to buccal cirrus, distance	VE	11.7	12.0	1.3	0.3	10.9	9.0	16.0	21
	CC	15.6	15.0	1.5	0.3	9.5	13.0	19.0	21
Anterior body end to first postoral cirrus, distance	VE	36.7	37.0	2.4	0.5	6.7	32.0	41.0	21
	CC	44.5	44.0	4.1	0.9	9.3	39.0	53.0	21
Anterior body end to third postoral cirrus, distance	VE	48.3	49.0	2.3	0.5	4.8	45.0	54.0	21
	CC	63.2	63.0	6.7	1.5	10.6	52.0	75.0	21
Anterior body end to last frontoventral cirrus, distance	VE	23.3	23.0	1.7	0.4	7.3	20.2	27.0	21
	CC	30.8	29.0	3.9	0.8	12.5	26.0	39.0	21
Frontal cirri, number	RW	3.0	3.0	0.0	0.0	0.0	3.0	3.0	11
	VE	3.0	3.0	0.0	0.0	0.0	3.0	3.0	21
	CC	3.0	3.0	0.0	0.0	0.0	3.0	3.0	21
Frontoventral cirri, number	RW	4.0	4.0	0.0	0.0	0.0	4.0	4.0	11
	VE	4.0	4.0	0.0	0.0	0.0	4.0	4.0	21
	CC	4.0	4.0	0.0	0.0	0.0	4.0	4.0	21
Buccal cirri, number	RW	1.0	1.0	0.0	0.0	0.0	1.0	1.0	11
	VE	1.0	1.0	0.0	0.0	0.0	1.0	1.0	21
	CC	1.0	1.0	0.0	0.0	0.0	1.0	1.0	21
Postoral cirri, number	RW	3.0	3.0	0.0	0.0	0.0	3.0	3.0	11
	VE	3.1	3.0	0.5	0.1	16.3	2.0	5.0	21
	CC	3.0	3.0	0.0	0.0	0.0	3.0	3.0	21
Pretransverse cirri, number	RW	2.0	2.0	0.0	0.0	0.0	2.0	2.0	11
	VE	2.0	2.0	0.0	0.0	0.0	2.0	2.0	21
	CC	2.0	2.0	0.0	0.0	0.0	2.0	2.0	21
Transverse cirri, number	RW	5.0	5.0	0.0	0.0	0.0	5.0	5.0	11
	VE	5.0	5.0	0.0	0.0	0.0	5.0	5.0	21
	CC	5.0	5.0	0.0	0.0	0.0	5.0	5.0	21
Right marginal cirri, number	RW	18.8	19.0	1.0	0.3	5.2	18.0	21.0	11
	VE	19.6	20.0	1.2	0.3	5.9	18.0	22.0	21

continued

Characteristics	Pop	Mean	M	SD	SE	CV	Min	Max	n
	CC	17.3	17.0	1.2	0.3	6.6	15.0	19.0	21
Left marginal cirri, number	RW	16.9	17.0	1.3	0.4	7.7	15.0	20.0	11
	VE	18.4	18.0	1.0	0.2	5.3	17.0	21.0	21
	CC	17.0	17.0	1.3	0.3	7.7	15.0	19.0	21
Caudal cirri, number	RW	3.0	3.0	0.0	0.0	0.0	3.0	3.0	11
	VE	3.0	3.0	0.0	0.0	0.0	3.0	3.0	21
	CC	3.0	3.0	0.0	0.0	0.0	3.0	3.0	21
Dorsal kineties, number	RW	6.0	6.0	0.0	0.0	0.0	6.0	6.0	11
	VE	6.0	6.0	0.0	0.0	0.0	6.0	6.0	21
	CC	6.0	6.0	0.0	0.0	0.0	6.0	6.0	21
Dorsal kinety 1, number of bristles	VE	20.6	20.0	1.9	0.4	9.2	18.0	25.0	21
	CC	27.2	28.0	3.1	0.7	11.2	22.0	33.0	21
Dorsal kinety 2, number of bristles	VE	19.2	19.0	1.6	0.3	8.2	16.0	22.0	21
	CC	24.4	24.0	1.9	0.4	7.8	22.0	29.0	21
Dorsal kinety 3, number of bristles	VE	16.0	16.0	1.9	0.4	12.0	13.0	20.0	21
	CC	19.9	20.0	1.7	0.4	9.2	17.0	25.0	21
Dorsal kinety 4, number of bristles	VE	7.3	7.0	1.2	0.3	15.8	6.0	11.0	21
	CC	20.3	20.0	1.7	0.4	8.6	16.0	25.0	21
Dorsal kinety 5, number of bristles	VE	16.2	16.0	1.9	0.4	11.3	12.0	19.0	21
	CC	12.8	13.0	1.6	0.3	12.3	10.0	16.0	21
Dorsal kinety 6, number of bristles	VE	7.2	7.0	1.1	0.2	15.1	5.0	9.0	21
	CC	6.0	6.0	1.1	0.2	18.0	5.0	8.0	21

247a, d–f; Table 92). Macronuclear nodules slenderly to broadly ellipsoid, on average ellipsoid, about 20 × 10 µm in vivo; nucleoli numerous, up to 2 µm across. Usually one micronucleus near or attached to each macronuclear nodule, rarely three or four micronuclei; individual micronuclei globular to broadly ellipsoid, on average 2 µm in protargol preparations, in vivo about 4 × 3 µm. Contractile vacuole in or slightly anterior of mid-body at left margin of cell, with short collecting canals (Fig. 246a). Cortex semirigid, becomes flexible under slightest coverslip pressure; specific cortical granules absent. Cytoplasm colourless, studded with various inclusions, such as lipid droplets up to 10 µm across, ordinary crystals 2–5 µm in size, and many food vacuoles containing pieces of filamentous cyanobacteria, ordinary bacteria, green algae about 15 × 9 µm in size, heterotrophic flagellates, and middle-sized ciliates (*Protocyclidium terricola*, *Colpoda maupasi*) digested in food vacuoles up to 30 µm across (Fig. 246a). Swims and glides rather rapidly.

18 fronto-ventral-transverse cirri in *Oxytricha* pattern (for a review, see Berger 1999; Fig. 246a, b, h, 247a, b, d, e; Table 92). Marginal cirri about 15 µm long, left marginal row posteriorly slightly longer than right (Table 92). Transverse cirri inconspicuously thickened, about 20 µm long in vivo and thus distinctly projecting from body proper. Caudal cirri right of body´s midline, fine, beat lively, about 20 µm long in vivo. Dorsal bristles 3 µm long in vivo, arranged in six rows (Fig. 246c, 247f; Table 92): rows 1–3 almost bipolar; row 4 short, does not extend beyond mid-body; rows 5 and 6 dorsomarginal, row 5 slightly shortened posteriorly, row 6 very short, does not extend beyond first third of cell.

Adoral zone of oxytrichid shape and structure, extends approximately 1/3 of body length, composed of 29 membranelles on average (Fig. 246a, b, h, 247a, b, d, e; Table 92). Largest membranellar bases about 9 µm wide in vivo and 7 µm in protargol preparations. Buccal cavity of ordinary width but rather deep, anterior margin in vivo semicircularly curved, forming a distinct buccal horn (Fig. 246a). Buccal lip about 4 µm wide, covers proximal portion of adoral zone (Fig. 246a, d, f, h). Paroral membrane composed of zigzagging basal bodies, cilia about 10 µm long in vivo, in protargol preparations distinctly curved but never recurved, extends to left anterior corner of cell almost touching adoral zone. Endoral membrane curved, optically intersects paroral in mid-buccal cavity. Pharyngeal fibres inconspicuous, extend obliquely backwards (Fig. 246a, b, d, f, h, 247a, b, d, e; Table 92).

Resting cyst: The resting cysts of *F. depressa* are colourless and approximately 50 µm in diameter (Fig. 246g, 247c). The cyst wall is about 5 µm thick, yellowish, and studded with conical spines 3–5 µm long. The cyst contents is bipartite: the peripheral third is finely granular, the central area contains many lipid droplets up to 5 µm across and the very likely fused macronuclear nodules.

Ontogenesis: Some dividers showed that an anarchic field of basal bodies originates from the transverse and postoral cirri. The last postoral cirrus is not involved in anlagen formation.

Occurrence and ecology: *Fragmospina depressa* has been recorded from all main biogeographic regions (usually as *Cyrtohymena candens depressa*), except of Antarctica (Foissner 1998). It is rather frequent inhabiting a great variety of habitats (see species list). In Rwanda, we found it in a mixture of surface soil and moss from large stones on the coast of the Kibuye Lake, 29°40'E 2°26'S. The type locality is in Rumania, where Gellért (1942) discovered *F. depressa* in the algal film of tree bark.

Remarks: In protargol preparations, *F. depressa* is fairly easily recognizable by the special pattern of the paroral membrane described in the diagnosis of the genus, the distinctly shortened dorsal kinety 4, and the moderate body size (~ 100 × 40 µm). In vivo, the identification is difficult, although we usually recognize the species as a "*Cyrtohymena candens* with narrow buccal cavity" (Table 92). Beginners should check the identification in protargol preparations because *F. depressa* is easily confused with *Notohymena* spp., *Cyrtohymena* spp., *Oxytricha* spp., and certain populations of *Sterkiella histriomuscorum*.

Paroxytricha nov. gen.

Diagnosis: Flexible oxytrichids with 18 fronto-ventral-transverse cirri. Dorsal kinety 3 produces kinety 4 during ontogenesis. 2 or more macronuclear nodules and micronuclei. Resting cyst with separate macronuclear nodules and onion tower-shaped lepidosomes (scales) on surface.

Type species: *Paroxytricha quadrinucleata* nov. spec.

Etymology: *Paroxytricha* is a composite of the Latin prefix *para* (like, equal) and the Greek generic name *Oxytricha* (with sharp hairs = cirri), referring to the similarity with *Oxytricha*. Feminine gender.

Species assignable: According to our unpublished observations two further species fit the diagnosis: *Paroxytricha ottowi* (Foissner, 1997) nov. comb. (basionym: *Oxytricha ottowi* Foissner, 1997) and *Paroxytricha longigranulosa* (Berger & Foissner, 1989) nov. comb. (basionym: *Oxytricha longigranulosa* Berger & Foissner, 1989).

Remarks: When we discovered the species mentioned above, we supposed that they were close relatives of *Oxytricha granulifera* Foissner & Adam, 1983b because they differ morphologically only by the number of macronuclear nodules (four and eight vs. two) and the shape of the cortical granules (rod-like vs. globular). It was thus a surprise when the small subunit (SSU) rRNA placed *O. longigranulosa* in a distinct clade different from *O. granulifera* (Schmidt et al. 2007). This motivated us to look at the resting cysts. *Oxytricha granulifera*, type of the genus, has globular lepidosomes on the cyst surface (Foissner et al. 2007) while that of the three *Paroxytricha* species are onion tower-shaped (Fig. 248k, l, 249o–s). The fine structure, in contrast, is rather similar (Foissner et al. 2007 and unpubl.). A further difference concerns the macronuclear nodules: they fuse in the cyst of *Oxytricha granulifera* (Berger 1999) but remain separate in the three *Paroxytricha* species (Fig. 248k; Foissner unpubl.). Taking into account the differences in cyst morphology and molecular sequences, a distinct genus appears appropriate.

Paroxytricha quadrinucleata nov. spec. (Fig. 248a–n, 249a–s; Table 93)

Diagnosis: Size in vivo about 100 × 40 µm; ellipsoid. 4 broadly ellipsoid macronuclear nodules. Cortical granules in dense rows, colourless, rod-shaped, in vivo about 2 × 0.3 µm in size. Somatic and oral infraciliature in typical *Oxytricha* pattern. Resting cyst globular, lepidosomes 2–4 µm high.

Type locality: In tanks of *Tillandsia heterophylla* (Bromeliaceae) from a cloud mountain forest (1460 m above sea level) in Mexico, Veracruz province, surroundings of the town of Jalapa (Xalapa), 19°32’51’’N 96°57’36’’W.

Type material: The description and the type material are from pure cultures with tap water and some cracked wheat kernels for bacterial growth. The protargol slides have been deposited in the Biology Centre of the Upper Austrian Museum in Linz (LI). Unfortunately, the holotype and the paratype slide bleached almost completely for unknown reasons. Thus, we added 3 paratype slides with unbleached specimens from the same preparation series.

Etymology: The name is a composite of the Latin numeral *quadr-* (four) and the Latin adjective *nucleatus* (with a nucleus), referring to the main feature of the species.

Description: Ordinarily variable, i. e., most and all important features with a CV ≤ 15% (Table 93).

Size highly variable, likely mainly depending on culture conditions; average in vivo sizes between 80 × 30 µm and 110 × 40 µm observed in various culture dishes. Adding 15% preparation shrinkage, an in vivo size of 70–90 µm × 30–43 µm (mean: 80 × 35 µm) results for the culture

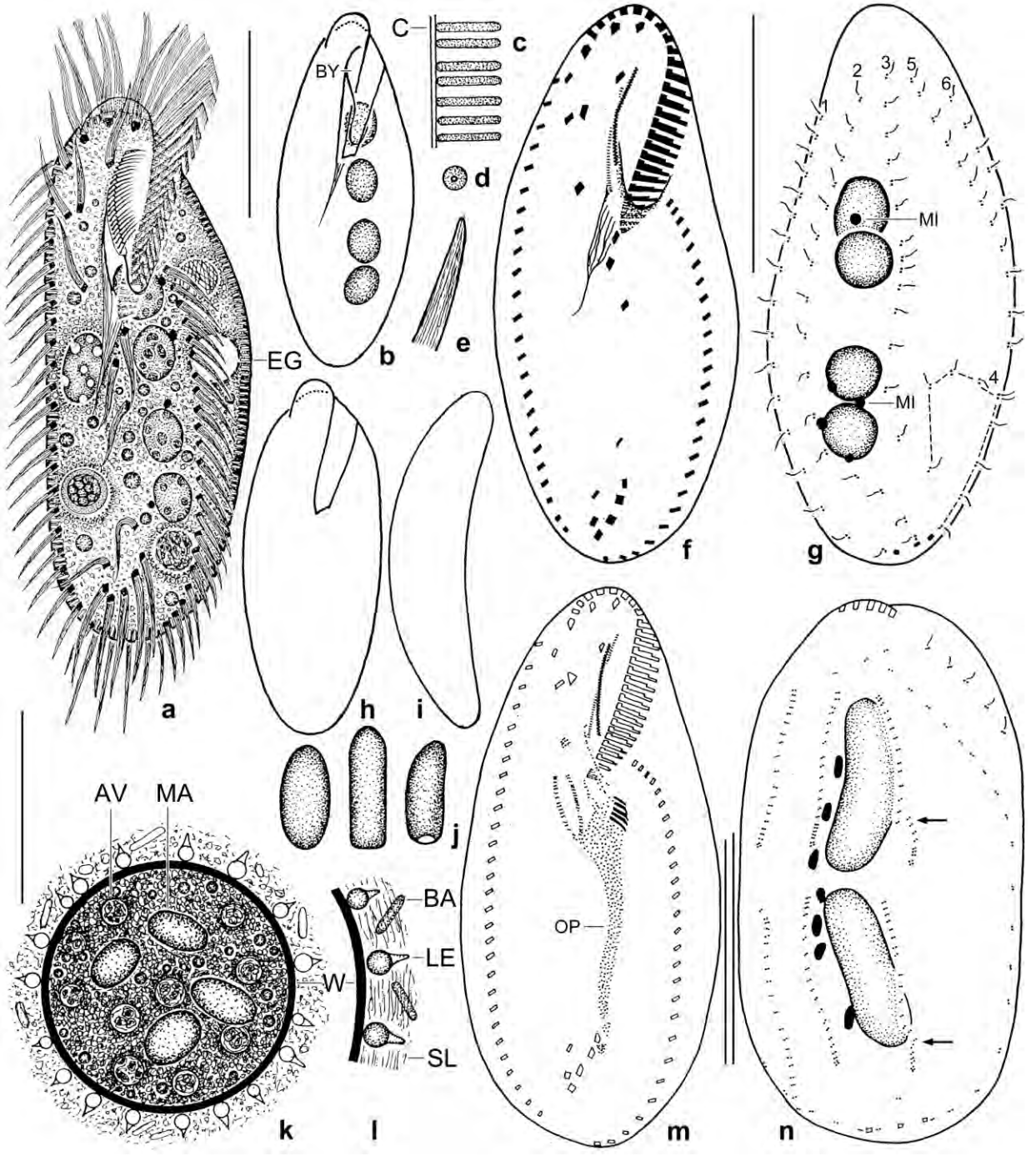

Fig. 248a–n. *Paroxytricha quadrinucleata*, cultivated specimens from life (a–d, h, i, k, l), after protargol impregnation (f, g, m, n), in a methyl green-pyronin stain (e), and in the SEM (j). **a:** Ventrolateral view of a specimen with stretched right margin, length 90 µm. **b:** A well-fed, lenticular specimen, showing the four macronuclear nodules and the narrow buccal cavity. **c, d:** The cortical granules are about 2 × 0.3 µm in size and have a bright centre (d). **e, j:** Extruded cortical granules, length 5 µm and 1.5–2 µm. **f, g, n:** Ventral and dorsal view of holotype specimen (f, g), length 66 µm. The broken line in (g) and the arrows in (n) show the origin of dorsal kinety 4 by a split of kinety 3. **h, i:** Ventral and lateral view of an ellipsoid specimen. **k, l:** The resting cyst is covered by onion tower-shaped lepidosomes embedded in a slimy matrix. **m:** An early divider. AV – autophagous vacuole, BA – bacterium, BY – buccal cavity, C – cortex, EG – extrusome fringe, LE – lepidosomes, MA – macronuclear nodules, MI – micronuclei, OP – oral primordium, SL – slime cover, W – cyst wall, 1–6 – dorsal kineties. Scale bars 30 µm.

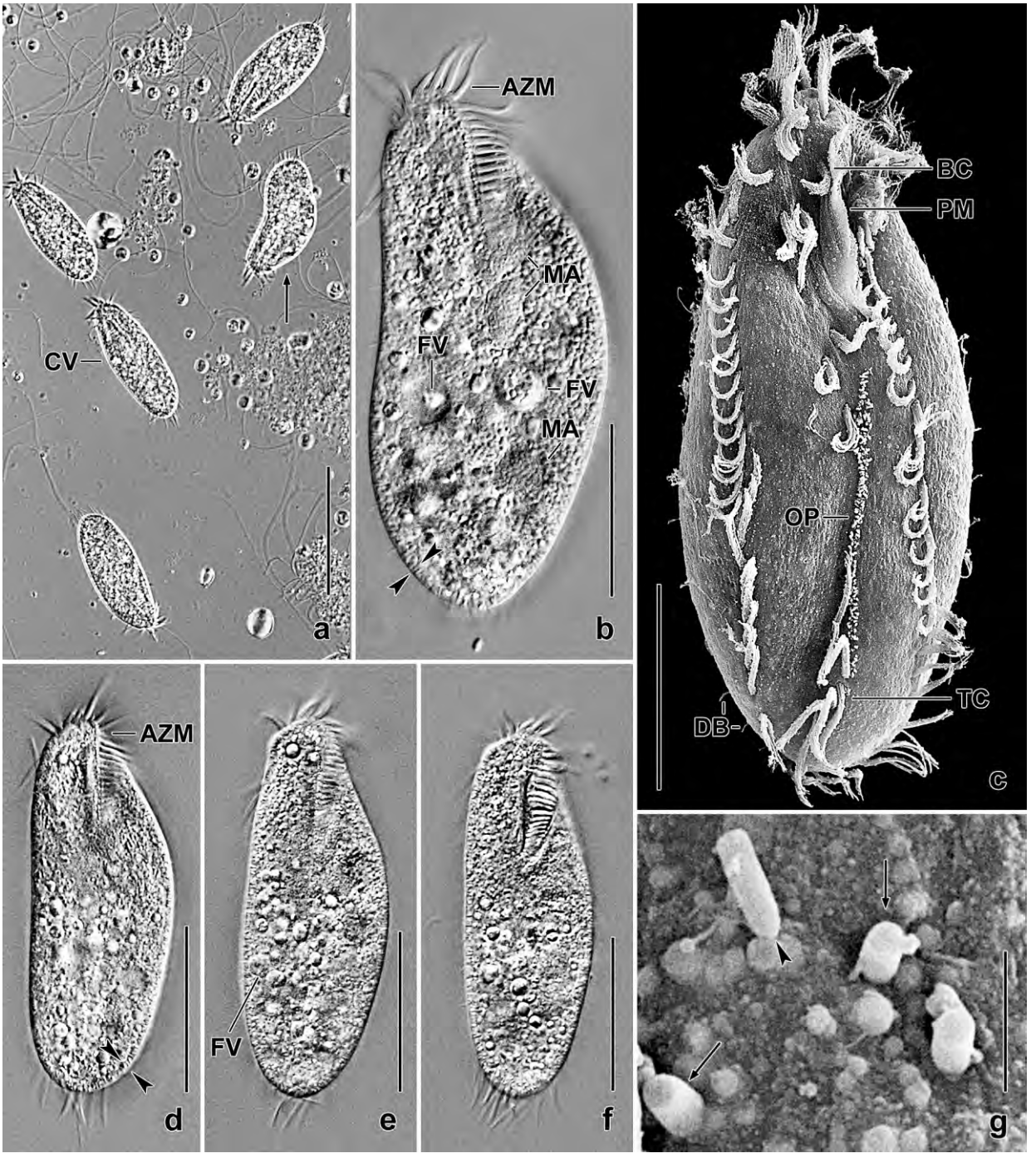

Fig. 249a–g. *Paroxytricha quadrinucleata*, cultivated specimens from life (a, b, d–f) and in the scanning electron microscope (c, g). **a:** Freely motile specimens, showing their inconspicuous shape. The arrow marks a cell performing an avoiding reaction. **b:** A slightly pressed (by coverslip) specimen, showing three of the four macronuclear nodules and the extrusome fringe (opposed arrowheads). **c:** A very early divider with oral primordium extending from uppermost transverse cirrus to near buccal vertex. **d–f:** Shape variability of well-fed, freely motile specimens. The opposed arrowheads mark the extrusome fringe. **g:** An extruded (arrowhead) and some emerging (arrows) extrusomes (see also next plate). AZM – adoral zone of membranelles, BC – buccal cirrus, CV – contractile vacuole, DB – dorsal bristles, FV – food vacuoles with starch grains and a flagellate cyst, MA – macronuclear nodules, OP – oral primordium, PM – paroral membrane, TC – transverse cirri. Scale bars 2 µm (g), 25 µm (b), 30 µm (c), 40 µm (d–f), and 95 µm (a).

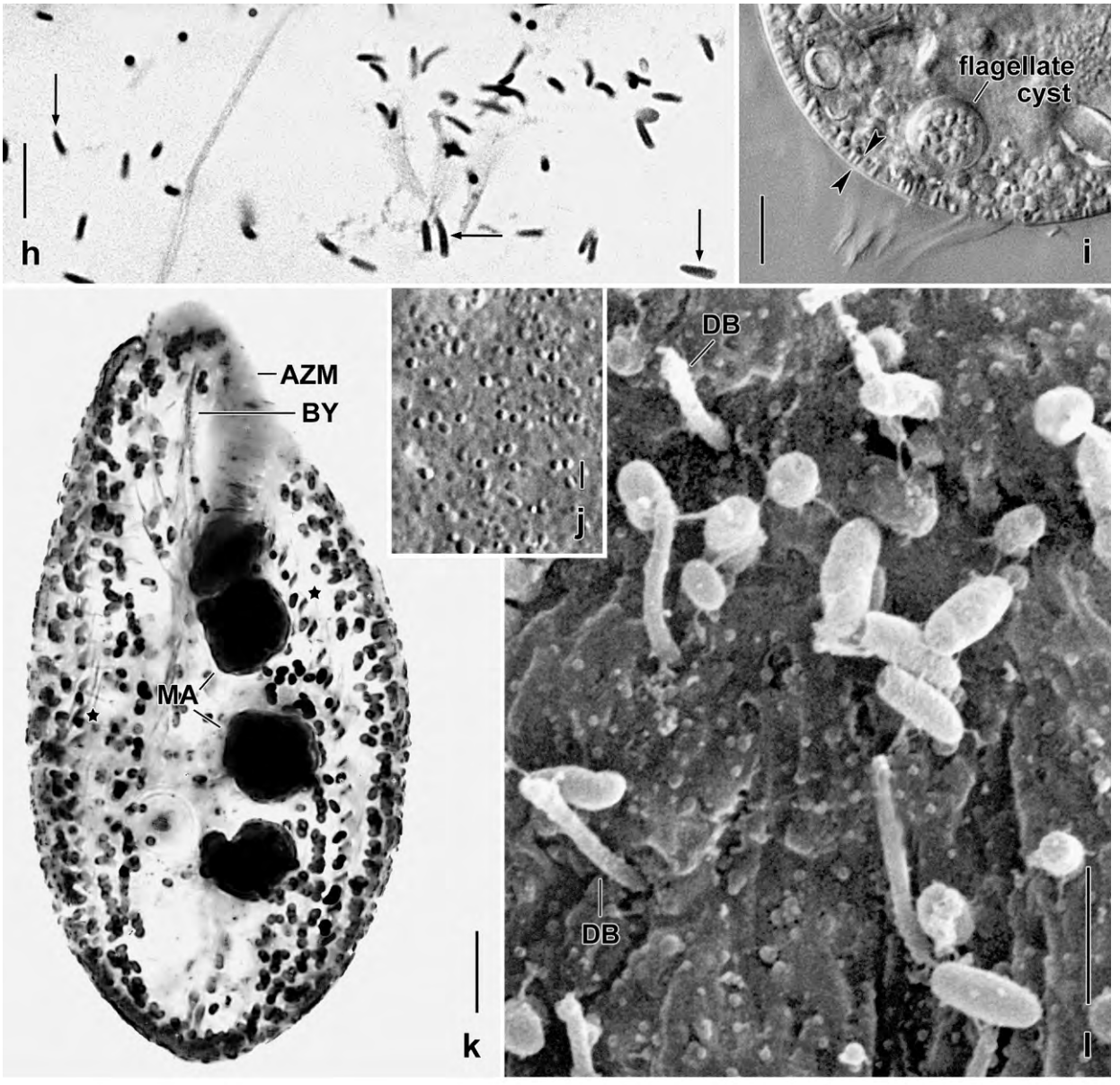

Fig. 249h–l. *Paroxytricha quadrinucleata* from life (i, j), after staining with methyl green-pyronin (h) and protargol (k), and in the scanning electron microscope (l). **h:** Extruded cortical granules (= extrusomes) are horn-shaped (arrows) or oblong and about 5 µm long. **i:** Optical section of posterior body end, showing the fringe (opposed arrowheads) produced by the 2 µm long cortical granules (= extrusomes). **j:** Surface view, showing the cortical granules. **k:** Ventral view, showing the deeply impregnated cortical granules forming rather dense rows. The granules are inflated and absent within the marginal cirral rows (asterisks). **l:** Extruded and emerging extrusomes on dorsal side of cell. AZM – adoral zone of membranelles, BY – buccal cavity, DB – dorsal bristles, MA – macronuclear nodules. Scale bars 1 µm (j), 2 µm (l), and 10 µm (h, i, k).

investigated (Table 93); specimens fixed with Bouin or Stieve´s solution differ by only 4 µm (68 vs. 72 µm; data not shown). Body shape usually ellipsoid (Fig. 248f, h), rather frequently with stretched right margin (Fig. 248a, 249b, d); rarely slightly obovate or, when overfed, lenticular (Fig. 248b); when disturbed with typical avoiding reaction becoming slightly reniform (Fig. 249a); laterally flattened up to 2:1 (Fig. 248a, b, f, h, i, 249a–f, m; Table 93). Nuclear apparatus in central quarters and left of midline of body (Fig. 248a, b, g, 249b, k; Table 93). Invariably four

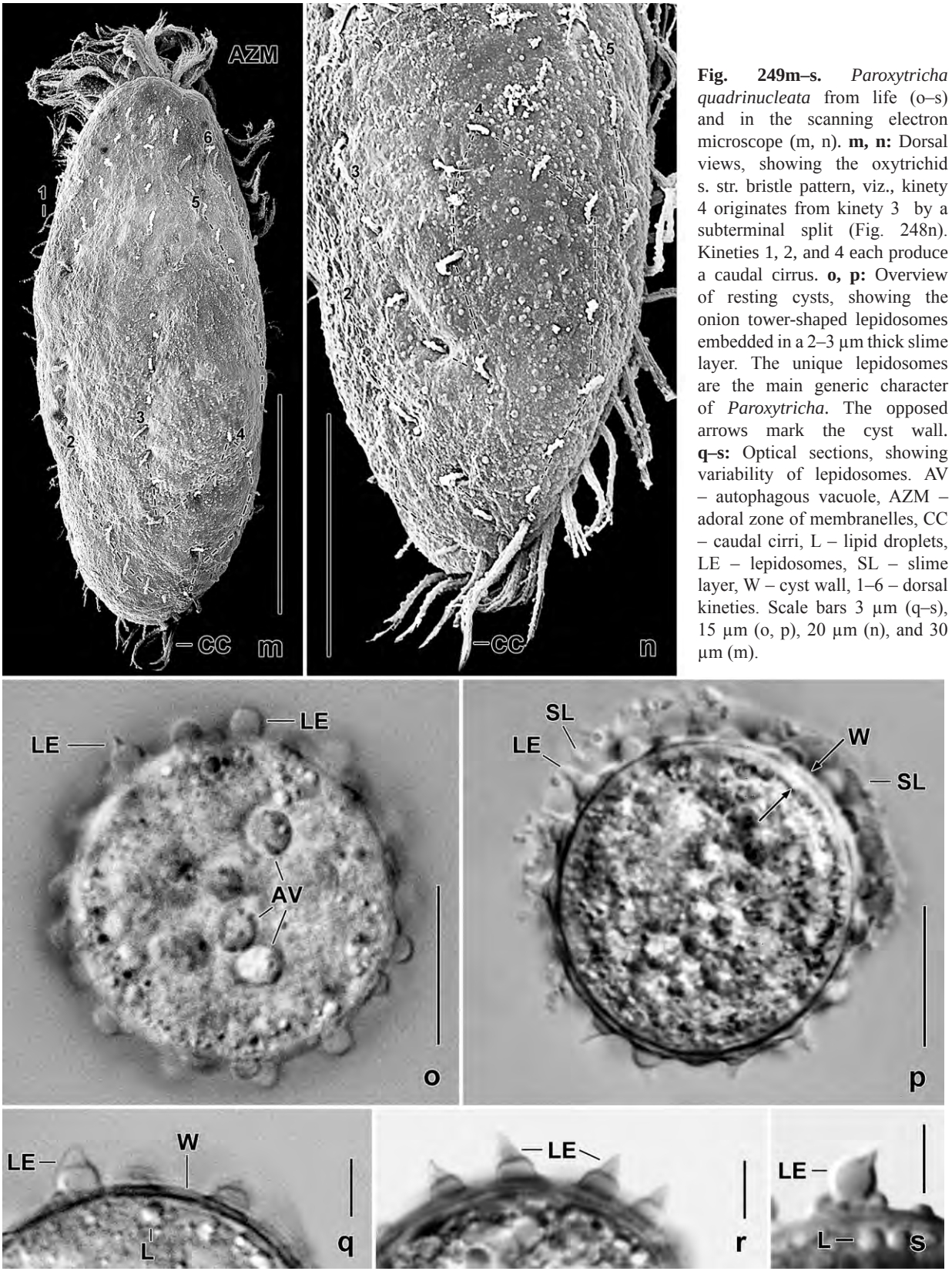

Fig. 249m–s. *Paroxytricha quadrinucleata* from life (o–s) and in the scanning electron microscope (m, n). **m, n:** Dorsal views, showing the oxytrichid s. str. bristle pattern, viz., kinety 4 originates from kinety 3 by a subterminal split (Fig. 248n). Kineties 1, 2, and 4 each produce a caudal cirrus. **o, p:** Overview of resting cysts, showing the onion tower-shaped lepidosomes embedded in a 2–3 µm thick slime layer. The unique lepidosomes are the main generic character of *Paroxytricha*. The opposed arrows mark the cyst wall. **q–s:** Optical sections, showing variability of lepidosomes. AV – autophagous vacuole, AZM – adoral zone of membranelles, CC – caudal cirri, L – lipid droplets, LE – lepidosomes, SL – slime layer, W – cyst wall, 1–6 – dorsal kineties. Scale bars 3 µm (q–s), 15 µm (o, p), 20 µm (n), and 30 µm (m).

Table 93. Morphometric data on *Paroxytricha quadrinucleata* based on mounted, protargol-impregnated, and randomly selected specimens from a non-flooded Petri dish culture. Measurements in µm. CV – coefficient of variation in %, M – median, Max – maximum, Mean – arithmetic mean, Min – minimum, n – number of individuals investigated, SD – standard deviation, SE – standard error of arithmetic mean.

Characteristics	Mean	M	SD	SE	CV	Min	Max	n
Body, length	68.3	68.0	5.4	1.2	7.9	61.0	80.0	21
Body, width	30.0	29.0	3.1	0.7	10.4	26.0	37.0	21
Body length: width, ratio	2.3	2.3	0.2	0.0	8.0	2.1	2.6	21
Adoral zone of membranelles, length[a]	26.8	27.0	1.6	0.3	5.9	24.0	29.0	21
Body length: adoral zone length, ratio	2.6	2.5	0.2	0.0	6.8	2.3	2.9	21
Largest membranellar basis, width	5.0	5.0	0.0	0.0	0.0	5.0	5.0	21
Buccal field, width[b]	3.5	3.5	0.5	0.1	13.6	3.0	4.0	21
Anterior body end to first MA nodule, distance	19.7	20.0	1.6	0.3	8.1	17.0	22.0	21
Anterior body end to paroral membrane, distance	5.9	5.5	0.8	0.2	13.8	5.0	8.0	21
Anterior body end to endoral membrane, distance	8.7	8.5	0.9	0.2	10.0	7.0	10.5	21
Anterior body end to right marginal row, distance	8.3	8.0	0.9	0.2	11.1	6.0	10.0	21
Anterior body end to buccal cirrus, distance	7.0	7.0	0.8	0.2	11.7	6.0	9.0	21
Nuclear figure, length	34.5	34.0	2.9	0.6	8.5	30.0	42.0	21
Posterior body end to right marginal row, distance	2.0	2.0	0.8	0.2	41.0	0.0	3.5	21
Posterior body end to left marginal row, distance	0.2	0.0	0.3	0.1	142.7	0.0	1.0	21
Posterior body end to transverse cirri, distance	3.7	4.0	1.2	0.3	32.4	2.0	6.0	21
Anterior macronuclear nodules, length	8.4	8.0	1.2	0.3	13.8	7.0	11.0	21
Anterior macronuclear nodules, width	6.8	7.0	0.7	0.2	10.6	5.5	8.5	21
Macronuclear nodules, number	4.0	4.0	0.0	0.0	0.0	4.0	4.0	21
Micronuclei, number	3.4	3.0	2.1	0.5	60.9	1.0	7.0	21
Micronucleus, length	1.6	1.5	0.2	0.0	12.6	1.5	2.0	21
Micronucleus, width	1.5	1.5	0.2	0.0	9.7	1.5	2.0	21
Adoral membranelles, number	26.1	26.0	1.0	0.2	3.9	25.0	28.0	21
Right marginal row, number of cirri	25.5	25.0	1.4	0.3	5.5	23.0	28.0	21
Left marginal row, number of cirri	24.4	24.0	1.4	0.3	5.7	22.0	27.0	21
Anterior frontal cirri, number	3.0	3.0	0.0	0.0	0.0	3.0	3.0	21
Posterior frontal cirri, number	4.0	4.0	0.0	0.0	0.0	4.0	4.0	21
Postoral cirri, number	3.1	3.0	0.5	0.1	15.2	3.0	5.0	21
Buccal cirri, number	1.0	1.0	0.0	0.0	0.0	1.0	1.0	21
Transverse cirri, number	5.0	5.0	0.0	0.0	0.0	5.0	5.0	21
Pretransverse cirri, number	2.0	2.0	0.0	0.0	0.0	2.0	2.0	21
Caudal cirri, number	3.0	3.0	0.0	0.0	0.0	3.0	3.0	21
Dorsal kineties, number	6.0	6.0	0.0	0.0	0.0	6.0	6.0	21
Dorsal kinety 1, number of bristles	20.1	20.0	1.7	0.4	8.2	17.0	24.0	21
Dorsal kinety 2, number of bristles	18.8	19.0	2.0	0.4	10.7	16.0	22.0	21
Dorsal kinety 3 + 4, number of bristles	16.3	16.0	2.4	0.5	14.4	10.0	20.0	21
Dorsal kinety 5, number of bristles	16.4	16.0	1.4	0.3	8.7	14.0	20.0	21
Dorsal kinety 6, number of bristles	5.0	5.0	0.9	0.2	18.6	4.0	7.0	21
Resting cyst (in vivo)								
Resting cyst, length	35.8	35.0	4.5	1.2	12.5	31.0	50.0	15

continued

Characteristics	Mean	M	SD	SE	CV	Min	Max	n
Resting cyst, width	33.2	34.0	2.5	0.6	7.4	30.0	38.0	15
Resting cyst, height of spines	5.6	6.0	1.0	0.3	17.6	4.0	7.0	15
Resting cyst, width of spines	3.2	3.0	0.6	0.2	17.4	2.5	4.5	15
Resting cyst, wall thickness without spines	1.6	1.5	0.3	0.1	18.6	1.0	2.0	14

[a] Anterior body end to proximal end of zone.

[b] Distance between centre of paroral membrane and right margin of adoral zone.

globular to ellipsoid, on average broadly ellipsoid macronuclear nodules with distinct nucleoli; anterior nodule usually underneath proximal region of adoral zone of membranelles; nodules frequently in two rather distinct pairs. One to seven, usually three to four globular micronuclei near or attached to macronuclear nodules. Contractile vacuole slightly anterior of mid-body, without collecting canals (Fig. 248a, 249a). Cortex and cell very flexible. Cortical granules in more or less dense rows, absent along marginal cirral rows, colourless, in vivo about 2 × 0.3 µm forming a rather distinct fringe; with bright central canal and minute concavity on anterior end; extruded when methyl green-pyronin is added, becoming up to 5 µm long rods or funnels (Fig. 248a, c–e, 249b, d, h–k); in the SEM ellipsoid or oblong with conical anterior region (Fig. 248j, 249g, l). Cytoplasm colourless, in cultures opaque because studded with countless minute lipid droplets and food vacuoles with bacteria, flagellate cysts, and corroded starch grains (Fig. 248a, 249a, b, d–f, i). Movement without peculiarities.

Somatic and oral infraciliature as in typical oxytrichids, e. g., as in *Oxytricha granulifera*, type of the genus (Berger 1999). Thus, the Figures, the detailed morphometry, and some notes should suffice (Fig. 248a, f, g, 249b, c, m, n; Table 93). Marginal cirri in vivo about 12 µm long, transverse cirri 20–25 µm and thus distinctly projecting from body proper. Buccal cavity in vivo 4–5 µm wide and flat; paroral cilia about 5 µm long in vivo. Dorsal kinety 3 produces kinety 4 by a subterminal split (Fig. 248n).

Resting cyst (Fig. 248k, l, 249o–s; Table 93): Globular to slightly ellipsoid, in vivo 30 × 27 µm on average. Cyst wall compact but only about 1 µm thick, covered by a 2–3 µm slime layer containing bacteria and many lepidosomes 2–4 µm high and staining pink with methyl green-pyronin; lepidosomes not recognizable in the scanning electron microscope because embedded in slime. Cyst studded with minute lipid (?) droplets, autophagous vacuoles, and the four macronuclear nodules.

Occurrence and ecology: Common in Central and South America because found in Mexico, Jamaica, Venezuela, Brazil, and Chile. Likely prefers semiterrestrial habitats, such as tank bromeliads and floodplain soils.

Remarks: *Paroxytricha quadrinucleata* is highly similar to only one species, viz., *Oxytricha islandica* which has similar shape and size and four macronuclear nodules but lacks cortical granules and has only four dorsal kineties (Berger 1999).

Paroxytricha longigranulosa (Berger & Foissner, 1989) nov. comb. (Fig. 252c, d; Table 95)

Improved diagnosis: Size in vivo about 90 × 35 µm, 170 × 55 µm or 80 × 25 µm. Ellipsoid to elongate ellipsoid. 2 narrowly or widely spaced, ellipsoid macronuclear nodules and 2 broadly ellipsoid micronuclei. Cortical granules arranged in loose rows, elongate ellipsoid or ellipsoid, colourless. Cirral pattern oxytrichid; buccal cirrus right or slightly anterior of distal end of paroral membrane; 4 or 5 transverse cirri on average 7%, 10% or 4% distant from posterior body end; right marginal row composed of 24, 37 or 17 cirri on average. Dorsal kinety pattern very likely as in typical *Oxytricha* species; 3 caudal cirri. Buccal cavity narrow and shallow. Adoral zone extends about 33% or 37% of body length, composed of an average of 24, 40 or 21 membranelles with largest bases 5–7 µm width. Undulating membranes side by side, paroral about 8% or 15% distant from anterior body end.

Remarks: See Berger (1999), Berger & Foissner (1989), and Blatterer & Foissner (1988) for descriptions of this species. We split *P. longigranulosa* into three subspecies based on the investigation of new populations from China and Venezuela.

Paroxytricha longigranulosa longigranulosa nov. stat. (Fig. 252c, d; Table 95)

Improved diagnosis: Size in vivo about 95 × 35 µm; ellipsoid. Macronuclear nodules widely spaced. Cortical granules elongate ellipsoid. 5 transverse cirri about 7% distant from posterior body end; right marginal row composed of 24 cirri on average. Adoral zone extends about 33% of body length, composed of an average of 24 membranelles with largest bases about 6 µm width. Paroral membrane about 8% distant from anterior body end.

Paroxytricha longigranulosa sinensis nov. sspec. (Fig. 250a–i, 251a, b; Tables 94, 95)

Diagnosis: Size in vivo about 170 × 55 µm; elongate ellipsoid or slightly obovate. Macronuclear nodules widely spaced. 5 transverse cirri about 10% distant from posterior body end; right marginal row composed of 37 cirri on average. Adoral zone extends about 33% of body length, composed of an average of 40 membranelles with largest bases about 7 µm wide. Paroral membrane about 15% distant from anterior body end.

Type locality: Litter and mud/soil from a dry river drain in the surroundings of the Wei Ming hotel, outskirts of the town of Beijing, China, 116°E 39°N.

Type material: 1 holotype and 3 paratype slides with protargol-impregnated specimens have been deposited in the Biology Centre of the Upper Austrian Museum in Linz (LI). The holotype and other relevant specimens have been marked by black ink circles on the coverslip.

Etymology: The Latin adjective *sinensis* (belonging to China) refers to the country the species was discovered.

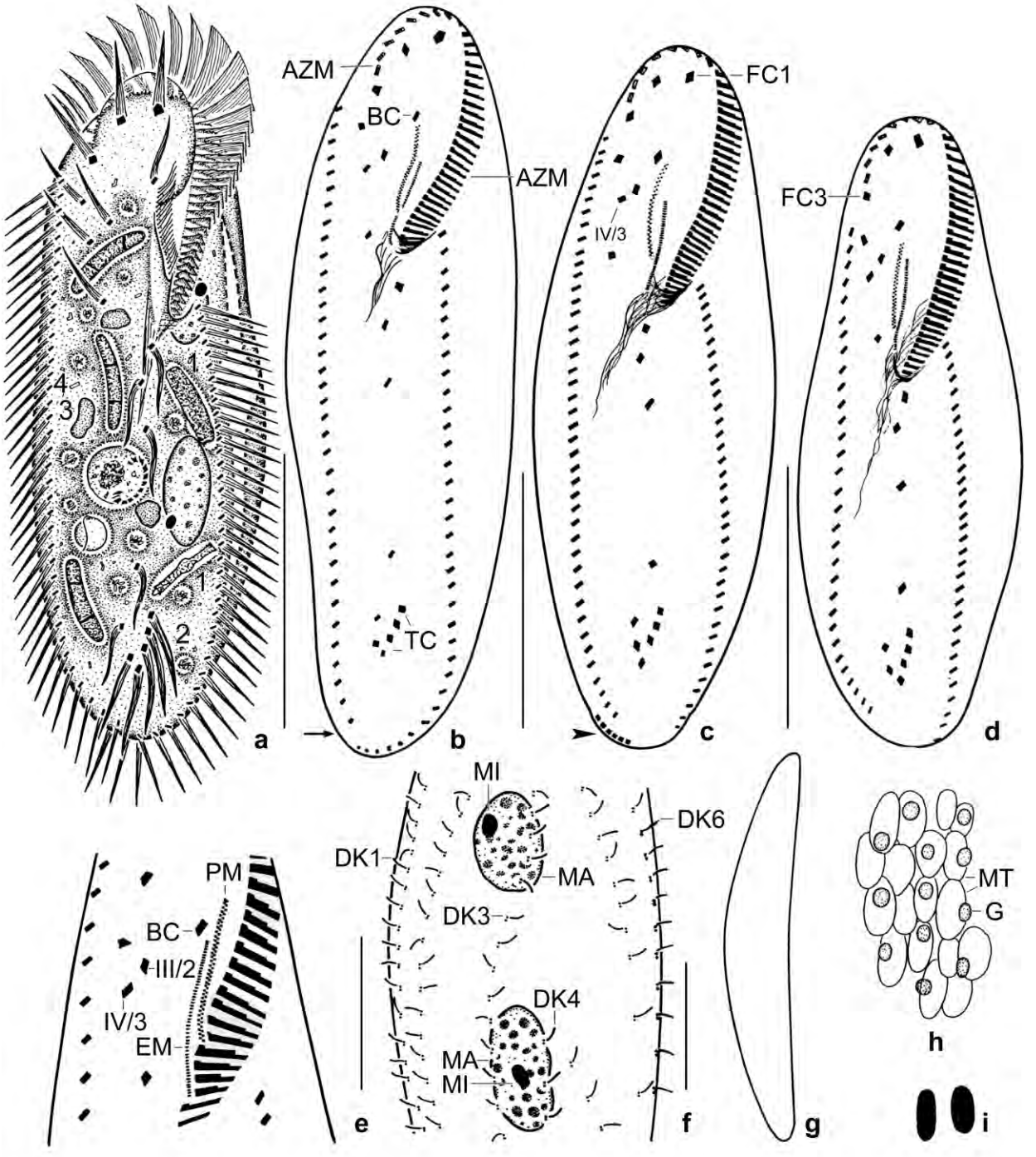

Fig. 250a–i. *Paroxytricha longigranulosa sinensis* from life (a, g–i) and after protargol impregnation (b–f). **a:** Ventral view of a representative specimen studded with food vacuoles containing pieces of fungal hyphae and fungal spores (1), bacteria (2), lipid droplets (3), and minute crystals (4); length 170 µm. **b:** Ventral view of holotype specimen, length 150 µm. Arrow marks site of caudal cirri on dorsal side. **c, d:** Ventral views of paratype specimens. The arrowhead in (c) denotes a remnant of the parental marginal cirral row. **e:** A specimen with buccal cirrus rather far posterior of begin of paroral membrane. **f:** Nuclear apparatus and dorsal kineties. **g:** Lateral view. **h:** Surface view, showing cortical granules and mitochondria. **i:** Cortical granules, 1.5 µm. AZM – adoral zone of membranelles, BC – buccal cirrus, DK1, 3, 4, 6 – dorsal kineties, EM – endoral membrane, FC1, 3 – frontal cirri, G – cortical granules, MA – macronuclear nodules, MI – micronuclei, MT – mitochondria, PM – paroral membrane, TC – transverse cirri, III/2, IV/3 – frontoventral cirri. Scale bars 20 µm (e), 25µm (f), 50 µm (b–d), and 70 µm (a).

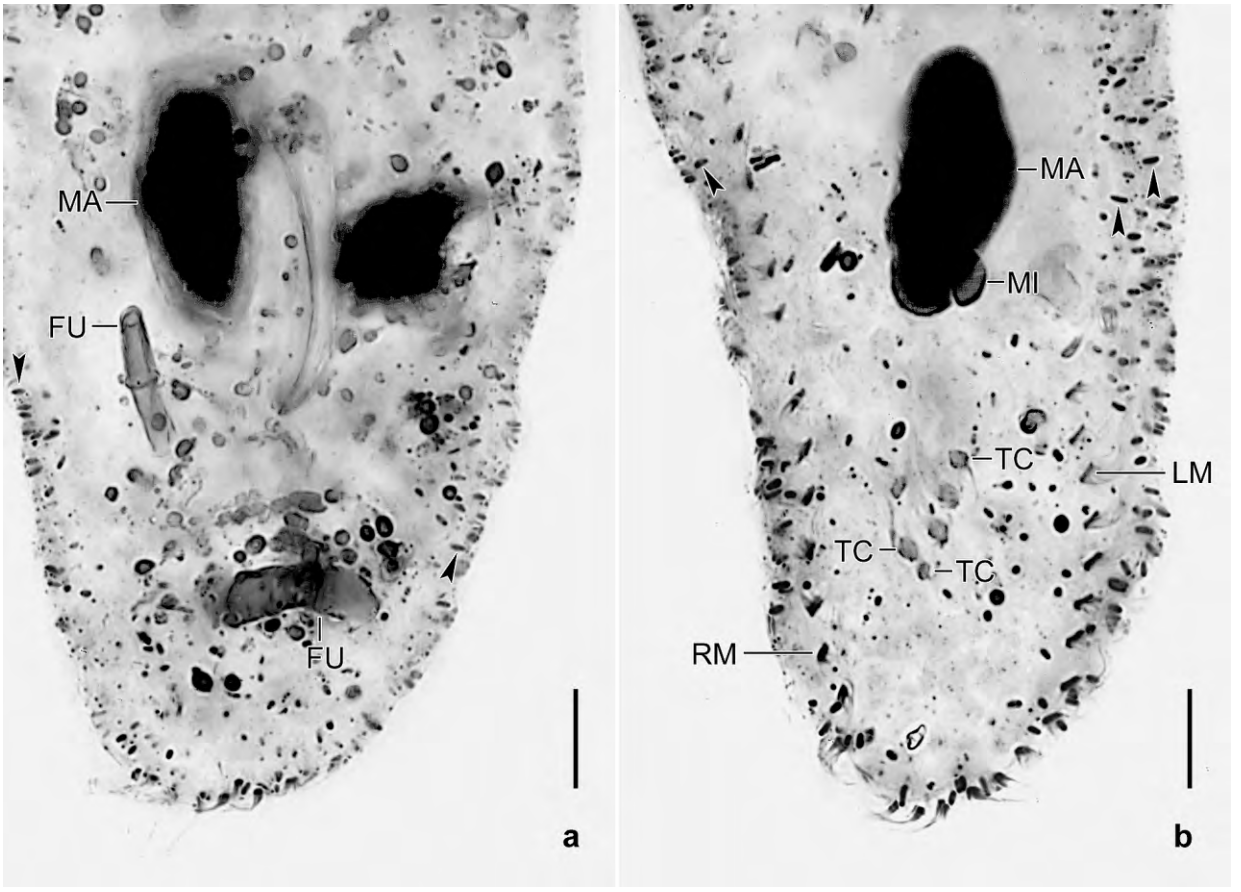

Fig. 251a, b. *Paroxytricha longigranulosa sinensis,* dorsal and ventral view of posterior body region after protargol impregnation. The arrowheads mark the 1.5–2 µm long, deeply impregnated cortical granules. The transverse cirri are far subterminal (b), an important feature. The cytoplasm contains pieces of fungal hyphae and fungal spores (FU). LM – left marginal cirral row, MA – macronuclear nodules, MI – micronucleus, RM – right marginal cirral row, TC – transverse cirri. Scale bars 10 µm.

Description: The protargol preparations are rather poor because the species is fragile and the cortical granules impregnate deeply, making the analysis of the dorsal ciliature almost impossible. There is indication that most of the largest specimens even disintegrated. Later and in another species of this constitution, we recognized that ethanol (~ 70%) stabilizes the cells properly and provides clear impregnations.

The insufficient fixation is very likely partially responsible for the high coefficients of variation (> 15%, Table 94), for instance, the width of the buccal cavity (36%), the distance of the posterior body end to the transverse cirri (20%), and the distance of the posterior body end to the right marginal cirral row (45%).

Size in vivo 145–185 × 35–75 µm, usually about 170 × 55 µm, as calculated from some in vivo measurements and the morphometric data in Table 94 adding 15% preparation shrinkage. Body shape inconspicuous, usually elongate ellipsoid, rarely ellipsoid or slightly elongate obovate; laterally flattened up to 2:1, ventral side flat, dorsal convex (Fig. 250a–d, g). Nuclear apparatus in middle third and left of midline of cell (Fig. 250a, f). Macronuclear nodules widely separate, anterior nodule in proximal region of adoral zone of membranelles, broadly ellipsoid to ellipsoid,

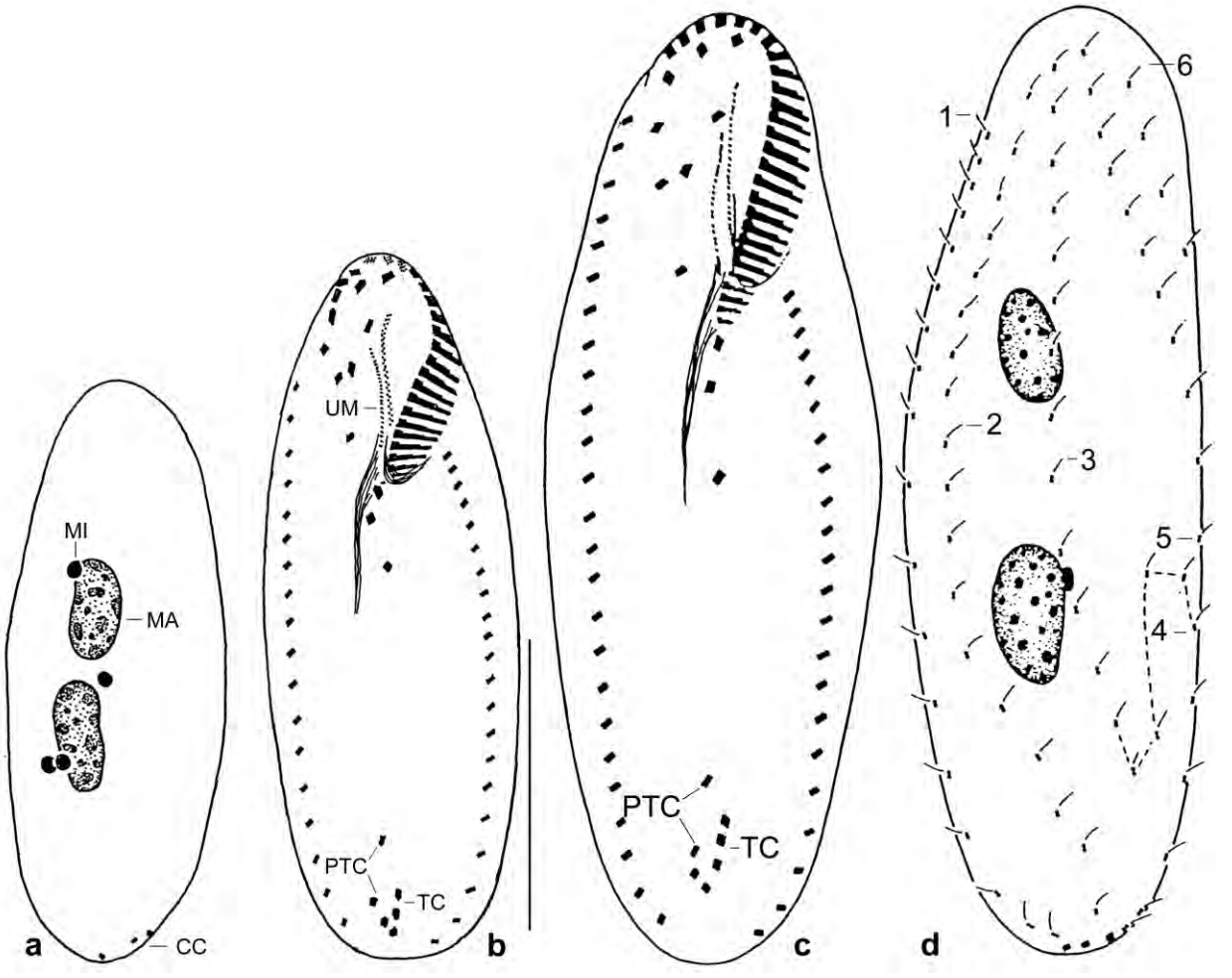

Fig. 252a–d. Comparison of *Paroxytricha longigranulosa imperfecta* (PLI, a, b) and *Paroxytricha longigranulosa longigranulosa* drawn to scale (PLL, c, d; from Berger & Foissner 1989). **a:** The macronuclear nodules are narrowly spaced in (PLI, a) and ordinarily spaced in (PLL, d). **b, c:** (PLI, b) and (PLL, c) have the same cirral pattern but the cells are smaller and have only four (vs. five in PLL, c) transverse cirri. Note also the V-like spread anterior portion of the undulating membranes in (PLI, b). **d:** (PLL) has six dorsal kineties of which kinety 4 originates by a posterior split of kinety 3. CC – caudal cirri, MA – macronuclear nodule, MI – micronucleus, PTC – pretransverse cirri, TC – transverse cirri, UM – undulating membranes (paroral, endoral), 1–6 – dorsal kineties. Drawn to scale = 30 μm.

on average 20 × 10 μm in protargol preparations; studded with small nucleoli. Usually, two globular to broadly ellipsoid micronuclei one each attached to macronuclear nodules. Contractile vacuole slightly anterior to mid-body, with two long collecting canals (Fig. 250a). Cortex very flexible and thin, underlain by a dense layer of mitochondria 2–3 μm long; loose rows of cortical granules between pellicle and mitochondrial layer (Fig. 250h, i, 251a, b); individual granules about 1.5 × 0.8 μm in size, colourless or with a yellowish shimmer, stain reddish with methylgreen-pyronin and deeply with protargol; difficult to recognize in vivo. Cytoplasm colourless, specimens however brownish under low magnification (≤ × 100) because crammed with (i) up to 20 brown pieces and spores of fungi, (ii) many food vacuoles only 3–5 μm across and containing bacteria, (iii) some up to 10 μm-sized globular and irregular lipid droplets, and (iv) rather many crystals 1–3 μm in size (Fig. 250a). Feeds mainly on bacteria, but fungi, flagellates, and ciliates (*Halteria grandinella*) occur also in the food vacuoles (Fig. 250a). Swims and creeps rather slowly.

Table 94. Morphometric data on *Paroxytricha longigranulosa sinensis* (upper line) and *Paroxytricha longigranulosa imperfecta* (lower line) based on mounted, protargol-impregnated, and selected (*P. l. sinensis*) or randomly selected (*P. l. imperfecta*) specimens from non-flooded Petri dish cultures. Measurements in µm. CV – coefficient of variation in %, M – median, Max – maximum, Mean – arithmetic mean, Min – minimum, n – number of individuals investigated, SD – standard deviation, SE – standard error of arithmetic mean.

Characteristics	Mean	M	SD	SE	CV	Min	Max	n
Body, length	145.6	146.0	11.1	2.4	7.6	124.0	161.0	21
	68.6	69.0	4.4	1.2	6.5	61.0	75.0	15
Body, width	48.2	48.0	7.2	1.6	15.0	32.0	68.0	21
	22.4	22.0	2.1	0.5	9.2	18.0	26.0	15
Body length:width, ratio	3.1	3.1	0.5	0.1	15.0	2.4	4.6	21
	3.1	3.0	0.3	0.1	9.6	2.7	3.8	15
Anterior body end to proximal end of adoral zone of membranelles, distance	50.2	51.0	5.3	1.2	10.6	37.0	57.0	20
	22.5	22.0	1.7	0.5	7.7	20.0	25.0	15
Adoral zone of membranelles, percentage of body length	37.0	38.0	5.2	1.1	14.0	25.0	46.0	21
	32.8	33.0	2.2	0.6	6.8	29.0	38.0	15
Largest membranellar bases, width	6.4	6.0	–	–	–	6.0	7.0	21
	4.7	5.0	–	–	–	4.0	5.0	15
Adoral membranelles, number	39.0	40.0	4.2	0.9	10.8	29.0	45.0	21
	20.7	21.0	1.4	0.4	6.7	18.0	22.0	15
Anterior body end to first macronuclear nodule, distance	37.6	37.0	3.1	0.7	8.1	31.0	43.0	21
	20.4	20.0	1.6	0.4	7.8	18.0	23.0	15
Anterior macronuclear nodule, length	19.8	20.0	1.9	0.4	9.5	17.0	24.0	21
	11.8	12.0	1.4	0.4	12.1	9.0	14.0	15
Anterior macronuclear nodule, width	10.8	10.0	1.5	0.3	13.8	8.0	14.0	21
	5.1	5.0	0.6	0.2	11.7	4.0	6.0	15
Macronuclear nodules, number	2.0	2.0	0.0	0.0	0.0	2.0	2.0	21
	2.0	2.0	0.0	0.0	0.0	2.0	2.0	15
Anterior micronucleus, length	3.9	4.0	0.7	0.2	17.9	3.0	5.0	21
	1.9	2.0	–	–	–	1.5	2.5	14
Anterior micronucleus, width	3.1	3.0	–	–	–	3.0	4.0	21
	1.8	2.0	–	–	–	1.5	2.0	14
Micronuclei, number	2.1	2.0	0.5	0.1	22.3	2.0	4.0	21
	2.8	3.0	0.7	0.2	25.1	2.0	4.0	14
Anterior body end to right marginal row, distance	19.0	20.0	4.1	0.9	21.6	10.0	26.0	21
	10.7	11.0	1.5	0.4	14.0	8.0	13.0	15
Posterior body end to right marginal row, distance	4.1	4.0	1.8	0.4	45.0	0.5	8.0	21
	5.0	5.0	1.4	0.4	27.2	3.0	7.0	14
Right marginal row, number of cirri	37.2	37.0	3.8	0.8	10.3	32.0	48.0	21
	17.0	17.0	2.0	0.6	11.8	14.0	20.0	13
Posterior body end to left marginal row, distance	1.3	1.0	1.0	0.2	73.4	0.5	4.0	21
	1.3	1.0	0.6	0.2	47.5	1.0	3.0	14
Left marginal row, number of cirri	34.9	34.0	3.5	0.8	10.0	28.0	42.0	21
	18.6	19.0	1.8	0.5	9.9	16.0	22.0	15
Anterior body end to buccal cirrus, distance	18.8	19.0	2.2	0.5	12.0	14.0	23.0	21

continued

Characteristics	Mean	M	SD	SE	CV	Min	Max	n
	6.9	7.0	1.1	0.3	15.9	5.0	10.0	15
Buccal cirri, number	1.0	1.0	0.0	0.0	0.0	1.0	1.0	21
	1.0	1.0	0.0	0.0	0.0	1.0	1.0	15
Posterior body end to transverse cirri, distance	14.8	15.0	3.0	0.7	20.1	9.0	21.0	21
	2.5	2.0	0.8	0.2	30.4	2.0	4.0	14
Transverse cirri, number	5.0	5.0	0.0	0.0	0.0	5.0	5.0	21
	4.0	4.0	0.0	0.0	0.0	4.0	4.0	15
Pretransverse cirri, number	2.0	2.0	0.0	0.0	0.0	2.0	2.0	21
	1.9	2.0	–	–	–	1.0	2.0	14
Frontal cirri, number	3.0	3.0	0.0	0.0	0.0	3.0	3.0	21
	3.0	3.0	0.0	0.0	0.0	3.0	3.0	15
Frontoventral cirri, number	4.0	4.0	0.0	0.0	0.0	4.0	4.0	21
	4.0	4.0	0.0	0.0	0.0	4.0	4.0	15
Postoral cirri, number	3.0	3.0	0.0	0.0	0.0	3.0	3.0	21
	3.0	3.0	0.0	0.0	0.0	3.0	3.0	15
Caudal cirri, number	3.2	3.0	–	–	–	3.0	4.0	21
	3.0	3.0	0.0	0.0	0.0	3.0	3.0	15
Buccal cavity, width	6.7	7.0	2.4	0.5	36.3	2.0	12.0	21
	4.8	5.0	1.3	0.3	27.5	3.0	8.0	15
Anterior body end to paroral membrane, distance	21.1	22.0	4.0	0.9	19.1	13.0	29.0	21
	5.7	6.0	0.9	0.2	15.4	4.0	7.0	15
Paroral membrane, length	17.9	17.0	3.4	0.8	18.9	12.0	23.0	19
	11.0	11.0	1.1	0.3	9.7	9.0	13.0	15
Anterior body end to endoral membrane, distance	26.6	27.0	4.4	1.0	16.5	18.0	33.0	21
	10.0	10.0	0.9	0.2	9.3	7.0	11.0	15
Endoral membrane, length	19.7	19.0	2.7	0.6	13.5	12.0	23.0	19
	8.8	9.0	1.1	0.3	12.3	7.0	10.0	15

Ventral cirral pattern as in *Oxytricha*, specifically, cirrus III/2 slightly anterior of cirrus IV/3 (Fig. 250c, e). Buccal cirrus on average 2 µm anterior of paroral membrane, rarely right of anterior end or some µm posterior of paroral. Frontal and transverse cirri slightly enlarged, the latter on average 10% (15 µm) distant from posterior body end and thus only slightly projecting from body proper. Marginal cirri about 17 µm long in vivo, their size gradually and distinctly decreasing near posterior end of rows (Fig. 250a–e; Table 95).

Dorsal bristles 3–4 µm long in vivo and in protargol preparations. Very likely arranged in *Oxytricha* pattern (Fig. 250f). Two dividers show two dorsomarginal kineties and one divider suggest split of kinety 3. Three thin caudal cirri slightly right of body´s midline, about 20 µm long and thus in vivo difficult to distinguish from marginal cirri.

Adoral zone of membranelles indistinctly *gonostomoid* and with membranellar bases only 6–7 µm width (13% of body width), i. e., small compared to body size producing a narrow stripe, especially in large specimens and compared to *P. longigranulosa longigranulosa* (cp. Fig. 250b–d with Fig. 252c); extends to 34% of body length and is composed of 39 membranelles on average

Table 95. Comparison of main morphometrics of *Paroxytricha longigranulosa longigranulosa* from Japan (PLLJ, from BERGER & FOISSNER 1989) and Australia (PLLA, from BLATTERER & FOISSNER 1988) as well as of *Paroxytricha longigranulosa sinensis* (PLS) from China (original) and of *Paroxytricha longigranulosa imperfecta* (PLI) from Venezuela (original). Data based on mounted and protargol-impregnated specimens from non-flooded Petri dish cultures. Measurements in µm. CV – coefficient of variation in %, M – median, Max – maximum, Mean – arithmetic mean, Min – minimum, n – number of individuals investigated, Pop – population, SD – standard deviation, SE – standard error of arithmetic mean.

Characteristics	Pop	Mean	M	SD	SE	CV	Min	Max	n
Body, length	PLLJ	87.6	91.0	8.5	2.3	9.6	72.0	98.0	13
	PLLA	75.7	79.0	6.3	2.0	8.3	65.0	83.0	10
	PLS	145.6	146.0	11.1	2.4	7.6	124.0	161.0	21
	PLI	68.6	69.0	4.4	1.2	6.5	61.0	75.0	15
Body, width	PLLJ	31.9	32.0	3.1	0.9	9.8	27.0	38.0	13
	PLLA	27.5	27.5	2.8	0.9	10.3	21.0	32.0	10
	PLS	48.2	48.0	7.2	1.6	15.0	32.0	68.0	21
	PLI	22.4	22.0	2.1	0.5	9.2	18.0	26.0	15
Adoral zone of membranelles, percentage of body length	PLLJ	32.0	–	–	–	–	–	–	13
	PLLA	35.0	–	–	–	–	–	–	10
	PLS	37.0	–	–	–	–	–	–	21
	PLI	32.8	33.0	2.2	0.6	6.8	29.0	38.0	15
Adoral membranelles, number	PLLJ	26.5	27.0	1.1	0.3	4.0	24.0	28.0	13
	PLLA	22.0	22.0	1.3	0.4	6.1	20.0	24.0	10
	PLS	39.0	40.0	4.2	0.9	10.8	29.0	45.0	21
	PLI	20.7	21.0	1.4	0.4	6.7	18.0	22.0	15
Macronuclear nodules, length	PLLJ	14.8	14.0	1.8	0.5	12.1	12.0	17.0	13
	PLLA	10.1	10.0	0.7	0.2	7.3	9.0	11.0	10
	PLS	19.8	20.0	1.9	0.4	9.5	17.0	24.0	21
	PLI	11.8	12.0	1.4	0.4	12.1	9.0	14.0	15
Posterior body end to transverse cirri, distance in % of body length	PLLJ	7.8 (from Figures)		–	–	–	–	–	2
	PLLA	not measured							
	PLS	10	–	–	–	–	–	–	21
	PLI	3.6	–	–	–	–	–	–	15
Right marginal row, number of cirri	PLLJ	25.9	26.0	1.6	0.4	6.1	23.0	28.0	13
	PLLA	19.1	19.0	1.5	0.5	8.0	17.0	22.0	10
	PLS	37.2	37.0	3.8	0.8	10.3	32.0	48.0	21
	PLI	17.0	17.0	2.0	0.6	11.8	14.0	20.0	13

(Fig. 250a–d; Table 94). Buccal cavity rather narrow and flat. Paroral and endoral membrane slightly staggered and side by side (± *Stylonychia* pattern), unusually short (12%) compared to body length because commencing 21 µm (= 58% of length of adoral zone) subapically. Paroral membrane usually slightly convex, endoral indistinctly concave (Fig. 250b–e; Table 94).

Remarks: In this sample occurred both, *Paroxytricha longigranulosa longigranulosa* and *Paroxytricha longigranulosa sinensis.* Thus, we selected for specimens longer than 120 µm, based on the Japanese type population which reaches around 100 µm in protargol preparations

and up to 135 µm in vivo (Table 95). We realize that this is a dangerous method because there is no gap between the size-classes and no indication of macrostomy. On the other hand, mixing all specimens would result in extreme variability, for instance, 65–161 µm body length and, especially, 20–45 adoral membranelles (Table 95) while the width of the membranellar bases (7 µm) is similar to that of *P. longigranulosa longigranulosa*. These data are in favour of classifying the large specimens as a distinct species; however, subspecies rank is possibly more appropriate considering the artificial size separation. The small specimens agree well with *P. longigranulosa longigranulosa*.

Paroxytricha longigranulosa sinensis is easily confused with *Urosoma gigantea* (for a review, see Berger 1999). Indeed, these species are almost inseparable in vivo, differing by the shape of the cortical granules (ellipsoid vs. globular) and the less subterminally arranged transverse cirri. In protargol preparations, they can be separated by the cirral pattern (oxytrichid vs. urosomoid) and the dorsal infraciliature (six vs. four kineties).

***Paroxytricha longigranulosa imperfecta* nov. sspec.** (Fig. 252a, b, 253a–g; Tables 94, 95)

Diagnosis: Size in vivo about 80 × 25 µm, ellipsoid. Macronuclear nodules narrowly spaced. 4 transverse cirri about 4% distant from posterior body end; right marginal row composed of 17 cirri on average. Adoral zone extends about 37% of body length, composed of an average of 21 membranelles with largest bases about 5 µm width. Paroral membrane about 8% distant from anterior body end.

Type locality: Venezuelan site (14), i. e., highly fertile field (Mahadja) soil from the outskirts of Pto. Ayacucho, 67°36'W 5°41'N.

Type material: 1 holotype and 1 paratype slide with protargol-impregnated specimens have been deposited in the Biology Centre of the Upper Austrian Museum in Linz (LI). The holotype and other relevant specimens have been marked by black ink circles on the coverslip.

Etymology: The Latin adjective *imperfecta* (incomplete) refers to the missing fifth transverse cirrus.

Description and Remarks: *Paroxytricha longigranulosa imperfecta* is most similar to the nominal subspecies differing mainly by the number (4 vs. 5) and location (3.6% vs. 7–8% distant from rear body end) of the transverse cirri (Tables 94, 95), an important feature in oxytrichid hypotrichs (Berger 1999). A feature not used in the diagnosis, but presumably important, is the V-like spread of the anterior half of the undulating membranes (Fig. 252b).

This small ciliate is difficult to identify the most important feature being the ellipsoid cortical granules guiding to *Paroxytricha longigranulosa* and the four transverse cirri characterizing the subspecies *imperfecta*. Very similar species are *Oxytricha lanceolata*, which lacks cortical granules and has five transverse cirri, and *O. granulifera quadricirrata* which has, like *P. longigranulosa imperfecta* four transverse cirri but globular cortical granules (for a review, see Berger 1999).

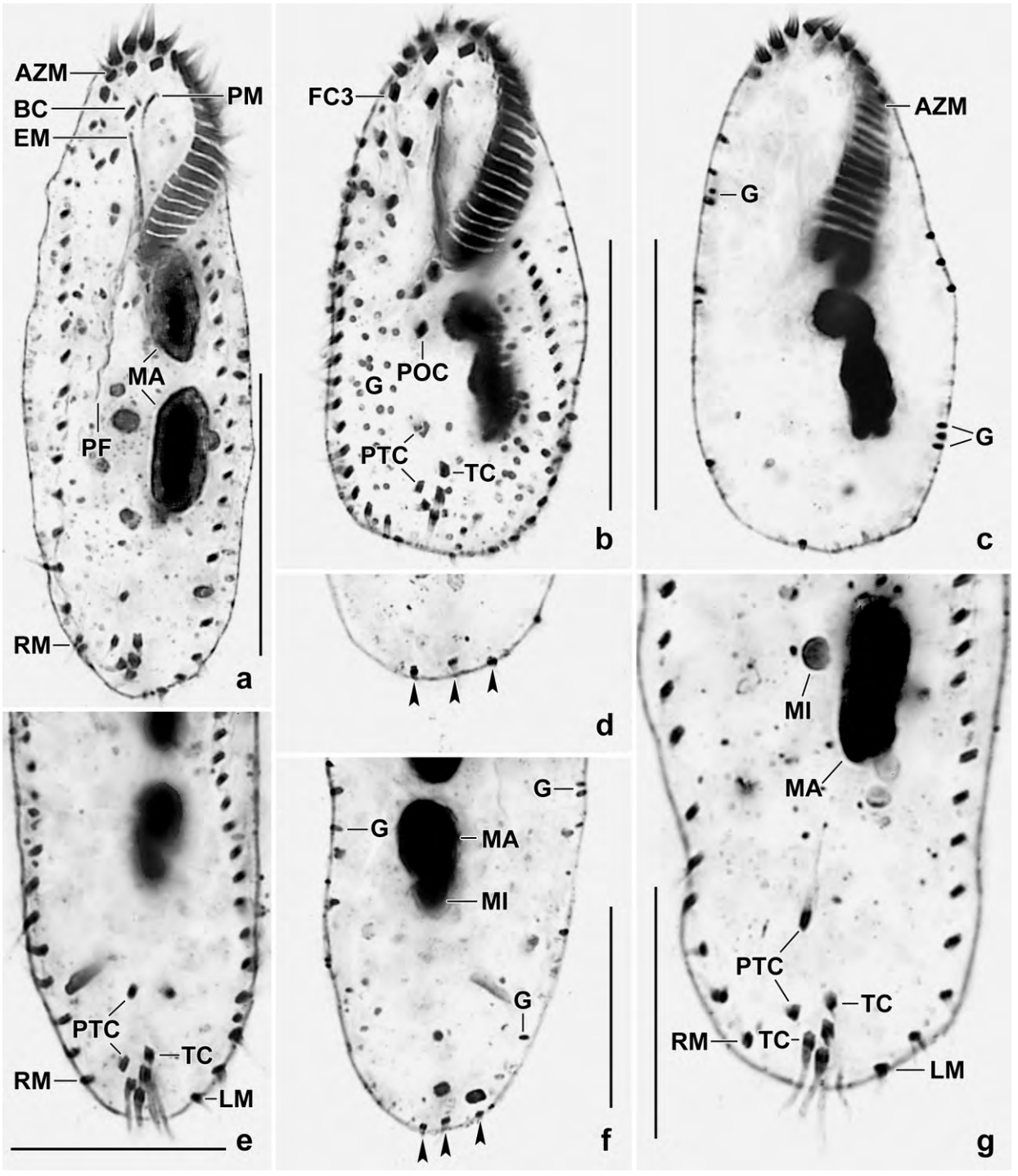

Fig. 253a–g. *Paroxytricha longigranulosa imperfecta* after protargol impregnation. **a, b, e, g:** Ventral views of infraciliature and nuclear apparatus. This species has only four transverse cirri. Note the V-like spread undulating membranes (a). **c:** Same specimen as in (b) but focused to the ellipsoid cortical granules. **d, f:** *Oxytricha l. imperfecta* has three caudal cirri (arrowheads). AZM – adoral zone of membranelles, BC – buccal cirrus, EM – endoral membrane, F3 – frontal cirrus 3, G – cortical granules, LM – left marginal cirral row, MA – macronuclear nodules, MI – micronuclei, PF – pharyngeal fibres, PM – paroral membrane, PTC – pretransverse cirri, RM – right marginal cirral row, TC – transverse cirri. Scale bars 20 µm (e–g) and 30 µm (a–c).

Both, *Paroxytricha longigranulosa imperfecta* and *Oxytricha granulifera quadricirrata* possibly belong to the Urosomoidae because they have only four transverse cirri. Possibly, sequence data can clear the matter.

Monomicrocaryon nov. gen.

Diagnosis: Flexible Oxytrichidae with 18 fronto-ventral-transverse cirri and two macronuclear nodules with a micronucleus in between. Usually 5 dorsal kineties and 3 caudal cirri; kinety 4 originates by a split of kinety 3.

Type species: *Monomicrocaryon granulatum* nov. spec.

Etymology: Composite of the Greek numeral *mono* (one), the adjective *mikros* (small), and the noun *karyon* (nucleus), referring to the single micronucleus characteristic for this type of oxytrichids. Neuter gender.

Remarks: Berger (1999) recognized 54 *Oxytricha* species. Some have been described recently, increasing the number to 57 (Foissner 1999b, Foissner et al. 2008a). Of these, 15 have the specific nuclear pattern described in the diagnosis of the genus while the others have at least two micronuclei and 2, 4 or 8 macronuclear nodules (Berger 1999). We assume that the specific nuclear pattern of *Monomicrocaryon* is usually based on a common ancestor (but see → *Quadristicha*), and thus we separate these species at genus level. The nuclear pattern has been used in several groups of ciliates as a generic or subgeneric character, for instance, in *Blepharisma* (Hirshfield et al. 1973) and dileptids (Vďačný & Foissner 2012).

Species assignable (according to the review of Berger 1999): *Monomicrocaryon balladyna* (Song &Wilbert, 1989) nov. comb. (basionym: *Oxytricha balladyna* Song & Wilbert, 1989); → *M. crassicirratum* nov. spec.; *M. elegans* (Foissner, 1999b) nov. comb. (basionym: *Oxytricha elegans* Foissner, 1999b), → *M. euglenivorum fimbricirratum* nov. sspec.; → *M. granulatum* nov. spec.; *M. opisthomuscorum* (Foissner et al. 1991) nov. comb. (basionym: *Opisthotricha muscorum* Kahl, 1932).

The following species have also the typical nuclear pattern but some might belong to the genus → *Quadristicha*: *Monomicrocaryon alfredi* (Berger, 1999) nov. comb. (basionym: *Oxytricha alfredi* Berger, 1999), *M. crassistilatum* (Kahl, 1932) nov. comb. (basionym: *Opisthotricha crassistilata* Kahl, 1932), *M. euglenivorum* (Kahl, 1932) nov. comb. (*Opisthotricha euglenivora* Kahl, 1932), *M. geleii* (Wilbert, 1986) nov. comb. (basionym: *Holosticha geleii* Wilbert, 1986), *M. halophilum* (Kahl, 1932) nov. comb. (basionym: *Opisthotricha halophila* Kahl, 1932), *M. kahlovatum* (Berger, 1999) nov. comb. (basionym: *Oxytricha kahlovata* Berger, 1999), *M. longicirratum* (Kahl, 1932) nov. comb. (basionym: *Urosoma longicirrata* Kahl, 1932), *M. parahalophilum* (Wang & Nie, 1935) nov. comb. (basionym: *Oxytricha parahalophila* Wang & Nie, 1935), *M. pseudofurcatum* (Berger, 1999) nov. comb. (basionym: *Tachysoma furcata* Gelei, 1954), *M. pseudofusiformis* (Dragesco & Dragesco-Kernéis, 1986) nov. comb. (basionym: *Oxytricha pseudofusiformis* Dragesco & Dragesco-Kernéis, 1986), *M. saprobia* (Kahl, 1932) nov. comb. (basionym: *Oxytricha saprobia* Kahl, 1932), *M. sphagni* (Kahl, 1932) nov. comb. (basionym: *Oxytricha sphagni* Kahl, 1932).

Monomicrocaryon granulatum **nov. spec.** (Fig. 254a–e, 255a–g; Table 96)

Diagnosis: Size in vivo about 70 × 25 µm; ellipsoid to slenderly ellipsoid. Cortical granules in loose rows, colourless, 0.5–1 µm across. Transverse cirri thick and protruding from body proper; buccal cirrus near anterior end of paroral. 6 dorsal bristle rows, rows 1, 2, and 4 bipolar; bristles about 7 µm long, last bristle of rows 1, 2, and 4 elongated to 10–15 µm. Three caudal cirri left of body´s midline, 20–25 µm long. Adoral zone extends about 33% of body length, composed of an average of 21 ordinary membranelles. Buccal cavity flat and narrow. Paroral and endoral membrane one upon the other.

Type locality: Upper soil layer of the rainforest in the Henri Pittier National Park, north coast of Venezuela, 67°37'W 10°30'N.

Type material: 1 holotype and 3 paratype slides with protargol-impregnated specimens have been deposited in the Biology Centre of the Upper Austrian Museum in Linz (LI). Relevant specimens have been marked by black ink circles on the coverslip.

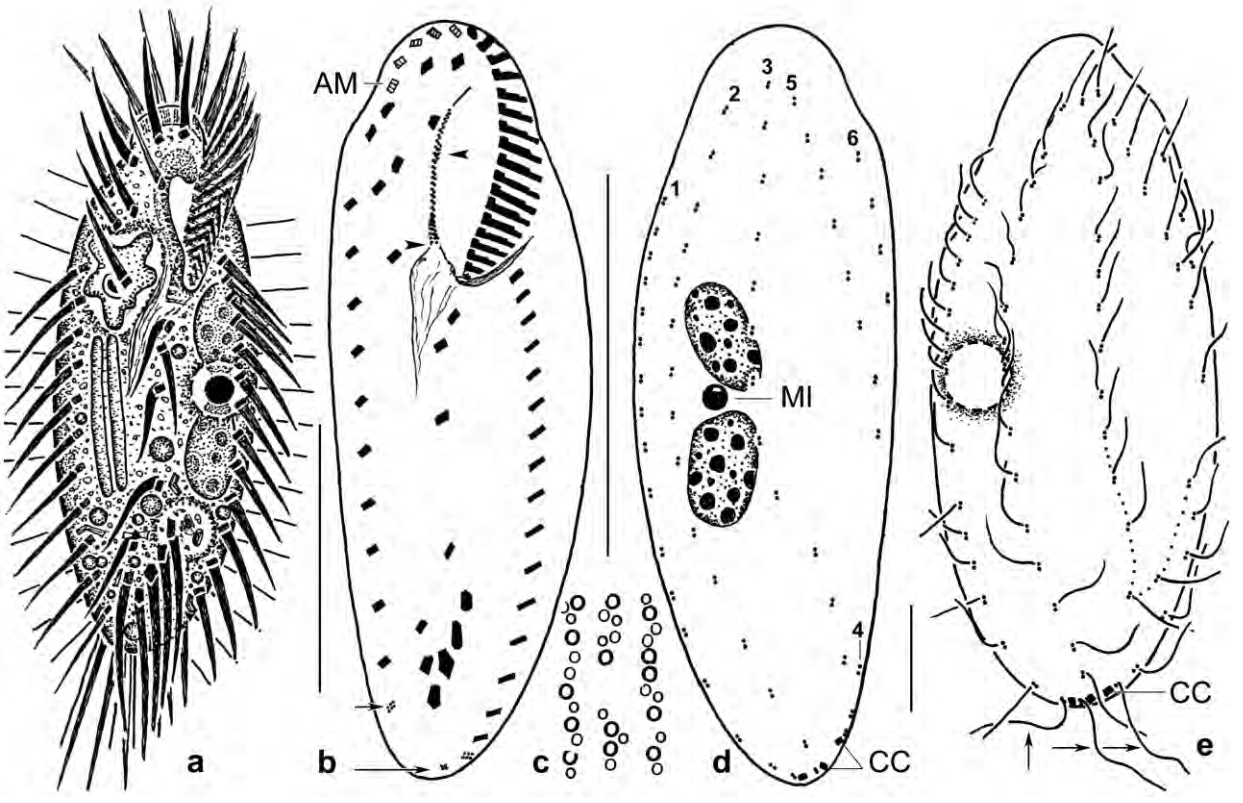

Fig. 254a–e. *Monomicrocaryon granulatum* from life (a, c) and after protargol impregnation (b, d, e). **a:** Ventral view of a representative specimen having ingested a naked amoeba and two fungal spores, length 70 µm. **b, d:** Ventral and dorsal view of holotype specimen, showing the infraciliature and the nuclear apparatus, length 60 µm. Arrows denote gap between right and left marginal row; this gap is occupied by the caudal cilia on dorsal side (d). The arrowheads mark the ends of the endoral membrane, which is underneath the paroral. **c:** Surface view, showing cortical granulation; the granules are colourless and have a size of about 0.5–1 µm. **e:** Dorsal view of a deeply impregnated specimen, showing the dorsal bristles. Arrows mark three bristles elongated to 12–15 µm. AM – distalmost adoral membranelle, CC – caudal cirri, MI – micronucleus. Scale bars 10 µm (e), 35 µm (a), and 50 µm (b, d).

Etymology: The Latin adjective *granulatus* refers to the cortical granules, a main feature of this species.

Description: Size in vivo 60–90 × 20–30 µm, usually about 70 × 25 µm, as calculated from some live measurements and the data in Table 96 adding 15% preparation shrinkage; not contractile but very flexible. Shape inconspicuous, i. e., ellipsoid to slenderly ellipsoid, thus easily confused with a variety of middle-sized oxytrichids, such as *Urosomoida* spp. and *Oxytricha* spp. (Fig. 254a, b, e, 255a–d; Table 96). Nuclear apparatus on average in mid-body and left of body´s midline, consists of two macronuclear nodules and a micronucleus in between (Fig. 254a, d, 255a–d; Table 96). Macronuclear nodules ellipsoid to broadly ellipsoid, on average 12 × 6 µm in protargol preparations and in vivo; nucleoli 0.5–2 µm across. Micronucleus about 3 µm across in vivo, in one specimen attached to mid of anterior macronuclear nodule. Contractile vacuole on average in mid of left body margin (Fig. 254a, d; Table 96). Cortical granules in loose rows, colourless, 0.5–1 µm across, do not stain with methyl green-pyronin and protargol (Fig. 254c). Cytoplasm colourless, rear portion frequently dark at low magnification (≤ × 100) because studded with lipid droplets and crystals 2–4 µm in size. Food vacuoles 5–8 µm across, 20 × 12 µm and with various inclusions in a protargol-impregnated specimen. Feeds on various, up to 30 µm long fungal spores (Fig. 254a, 255c), flagellates (*Anisonema*, *Polytoma*), and naked amoebae (Fig. 254a). Glides rapidly on microscope slide jumping when changing direction.

Cirral pattern oxytrichid, i. e., usually 18 cirri (Berger 1999): three frontal cirri, four frontoventral cirri, one buccal cirrus, three postoral cirri, two pretransverse cirri, and five thick transverse cirri about 20 µm long. Right marginal cirral row commences far posteriorly of anterior body end, viz., at level of mid-buccal cavity, cirri composed of three kineties with about 13 µm long cilia. Left marginal row extends to body´s midline posteriorly, cirral bases slightly longer than those of right row but composed of only two kineties (Fig. 254a, b, 255a–c, e, g; Table 96). Transverse cirri, last marginal cirri, and caudal cirri produce conspicuous tuft around posterior end of cell (Fig. 254a).

Six dorsal bristle rows in oxytrichid pattern (Fig. 254a, d, e, 255d; Table 96). Rows 1 and 2 bipolar; row 3 slightly shortened posteriorly and with or without some scattered kinetids guiding to row 4 composed of only a few dikinetids; row 5 extends beyond mid-body; row 6 composed of an average of four dikinetids. Bristles conspicuous because 7–8 µm long, last bristle of rows 1, 2, and 4 close to caudal cirri and up to 15 µm long. Caudal cirri right of body´s midline filling gap between ends of marginal cirral rows, conspicuous because up to 30 µm long, usually about 22 µm (Fig. 254a, d, e, 255c, d, g; Table 96).

Oral apparatus extends 33% of body length (Fig. 254a, b, 255a–c, e, f; Table 96). Adoral zone of ordinary shape, composed of an average of 21 membranelles of usual structure and cilia up to 15 µm long; largest membranellar bases about 5 µm width. Buccal cavity flat and narrow, in vivo about 4 µm width, anterior and right margin thickened (Fig. 254a). Paroral and endoral membrane one upon the other when viewed frontally, paroral composed of oblique dikinetids, anteriorly about 3 µm longer than endoral composed of monokinetids, both usually ending slightly anterior of buccal vertex; paroral with a short, fibrillar process anteriorly. Pharyngeal fibres ordinary (Fig. 254b, 255b, f).

Occurrence and ecology: As yet found only at type locality, i. e., a litter and soil sample from along the nature trail of Rancho Grande. The abundance was moderate in the non-flooded Petri dish culture.

Table 96. Morphometric data on *Monomicrocaryon granulatum* based on mounted, protargol-impregnated, and randomly selected specimens from a non-flooded Petri dish culture. Measurements in µm. CV – coefficient of variation in %, M – median, Max – maximum, Mean – arithmetic mean, Min – minimum, n – number of individuals investigated, SD – standard deviation, SE – standard error of arithmetic mean.

Characteristics	Mean	M	SD	SE	CV	Min	Max	n
Body, length	63.7	65.0	6.6	1.4	10.3	53.0	76.0	21
Body, width	23.6	24.0	2.0	0.4	8.5	20.0	27.0	21
Body length:width, ratio	2.7	2.7	0.3	0.1	9.4	2.3	3.5	21
Anterior body end to right marginal row, distance	15.0	15.0	1.2	0.3	8.0	13.0	18.0	21
Anterior body end to buccal cirrus, distance	7.5	8.0	0.6	0.1	8.0	6.0	8.0	21
Anterior body end to paroral membrane, distance	6.5	6.0	0.7	0.2	11.6	5.0	8.0	21
Anterior body end to proximal end of endoral, distance	17.8	18.0	1.3	0.3	7.5	15.0	20.0	21
Posterior body end to posteriormost transverse cirrus, distance	5.7	6.0	0.8	0.2	14.8	4.0	7.0	21
Posterior body end to right marginal row, distance	4.3	4.0	1.0	0.2	22.3	3.0	7.0	21
Anterior body end to upper margin of contractile vacuole, distance	29.0	30.0	3.8	1.0	13.2	23.2	36.0	16
Anterior body end to macronucleus, distance	20.5	20.0	1.7	0.4	8.5	18.0	24.0	21
Anterior macronuclear nodule, length	11.2	12.0	1.2	0.3	10.9	8.0	13.0	21
Anterior macronuclear nodule, width	5.9	6.0	0.8	0.2	14.2	5.0	8.0	21
Macronuclear nodules, number	2.0	2.0	0.0	0.0	0.0	2.0	2.0	21
Micronucleus, length	2.5	2.5	–	–	–	2.0	3.0	21
Micronucleus, width	2.4	2.5	–	–	–	2.0	2.8	21
Micronucleus, number	1.0	0.0	0.0	0.0	0.0	1.0	1.0	21
Anterior body end to proximal end of adoral zone, distance	21.0	21.0	1.0	0.1	5.0	20.0	23.0	21
Body length:length of adoral zone, ratio	3.0	3.1	0.2	0.0	7.2	2.7	3.4	21
Largest membranellar base, width	5.0	5.0	0.3	0.1	6.3	4.0	6.0	21
Adoral membranelles, number	20.5	21.0	0.9	0.2	4.5	18.0	23.0	21
Buccal cavity, width	4.8	5.0	1.0	0.2	20.1	3.5	7.0	21
Frontal cirri, number	2.8	3.0	–	–	–	2.0	3.0	23
Frontoventral cirri, number [a]	4.0	4.0	0.0	0.0	0.0	4.0	4.0	22
Buccal cirri, number	1.0	1.0	0.0	0.0	0.0	1.0	1.0	21
Postoral cirri, number [a]	3.0	3.0	0.0	0.0	0.0	3.0	3.0	22
Pretransverse cirri, number [a]	2.0	2.0	0.0	0.0	0.0	2.0	2.0	21
Transverse cirri, number [a]	5.0	5.0	0.0	0.0	0.0	5.0	5.0	21
Right marginal row, number of cirri	10.7	11.0	1.0	0.2	8.9	9.0	13.0	21
Left marginal row, number of cirri	16.9	17.0	1.3	0.3	7.7	15.0	20.0	21
Caudal cirri, number	3.0	3.0	0.0	0.0	0.0	3.0	3.0	21
Dorsal bristle rows, number	5.0	5.0	0.0	0.0	0.0	5.0	5.0	21
Bristles in dorsal row 1, number	16.6	16.0	1.2	0.3	7.0	15.0	19.0	21
Bristles in dorsal row 2, number	14.6	14.0	1.6	0.4	11.2	11.0	17.0	21
Bristles in dorsal row 3, number	12.0	12.0	0.9	0.2	7.2	10.0	13.0	21
Bristles in dorsal row 6, number	4.3	4.0	1.1	0.2	24.6	2.0	6.0	21

[a] Of 23 specimens analysed, one has 3 frontoventral cirri, another has 2 postoral cirri, and one has 4 transverse cirri.

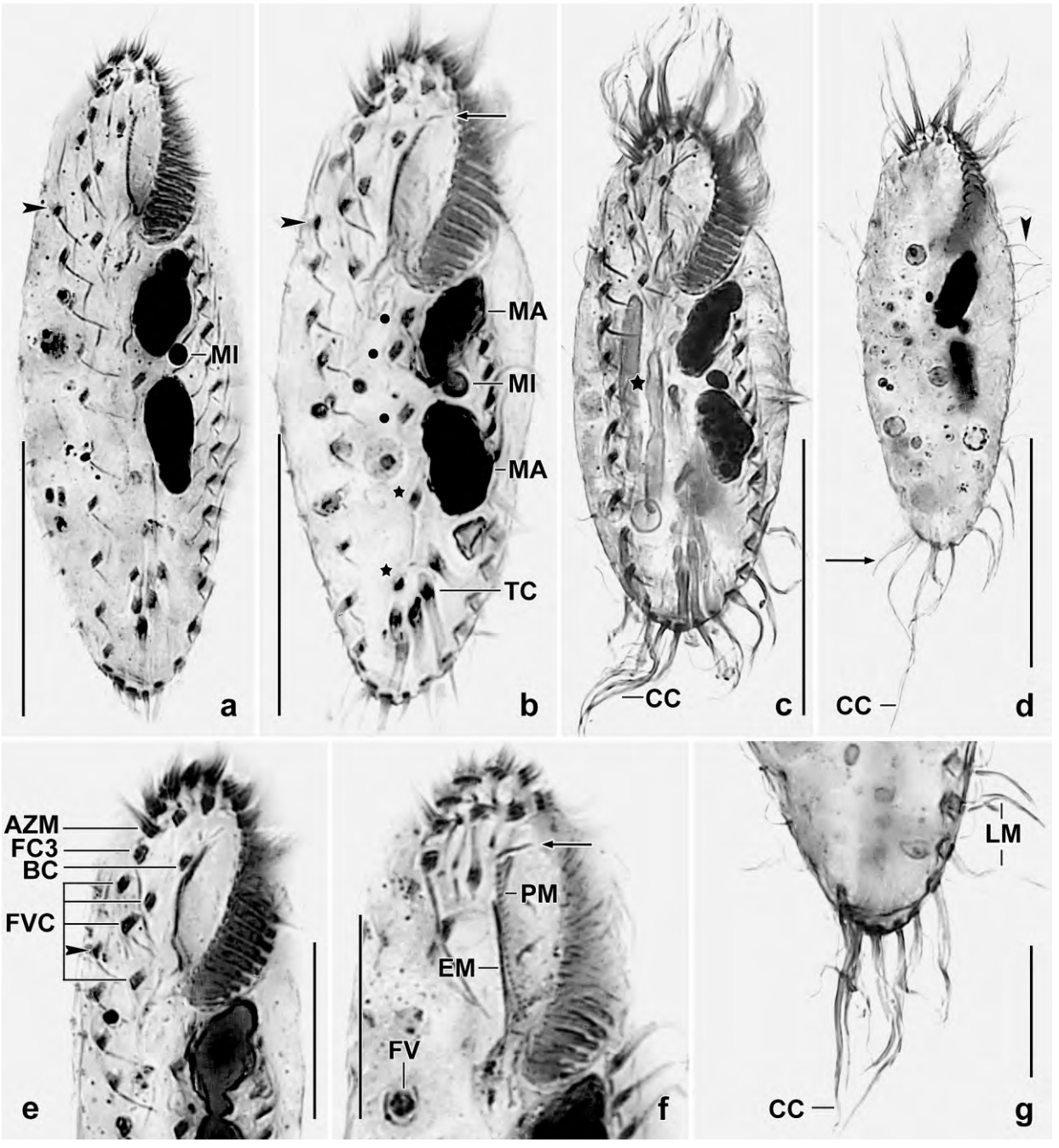

Fig. 255a–g. *Monomicrocaryon granulatum* after protargol impregnation. **a, b, e, f:** These figures show the 18FVT cirral pattern, the begin of the right marginal row (a, b, e, arrowheads), a short fibre originating from the undulating membrane (b, f, arrows), the two pretransverse cirri (b, asterisks), the three postoral cirri (b, dots), and the nuclear apparatus composed of two ellipsoid macronuclear nodules and a globular micronucleus in between. The paroral and endoral are one upon the other. **c:** A specimen having ingested two fungal conidia (asterisk). **d, g:** The cilia of the frontal adoral membranelles and the caudal cirri are very prominent. The arrow (d) marks a long dorsal bristle at end of row 4. The arrowhead marks the 8 µm long, "ordinary" dorsal bristles. AZM – first membranelle of adoral zone, BC – buccal cirrus, CC – caudal cirri, EM – endoral membrane, FC3 – frontal cirrus 3, FV – food vacuole, FVC – frontoventral cirri, LM – left marginal cirral row, MA – macronuclear nodules, MI – micronucleus, PM – paroral membrane, TC – transverse cirri. Scale bars 15 µm (e–g) and 30 µm (a–d).

Remarks: As mentioned above, the genus *Monomicrocaryon* contains 16 species, of which seven have long dorsal bristles, as has *M. granulatum*. Of these, → *M. euglenivorum* (KAHL, 1932) is highly similar to *M. granulatum*, except for the absence of cortical granules. All other species with long dorsal bristles differ from *M. granulatum* not only by the absence of cortical granules but also in other important features. *Monomicrocaryon balladyna* and *M. opisthomuscorum* have, inter alia, dorsal bristle row 4 distinctly shortened anteriorly. Interestingly, row 4 has a short break in *M. granulatum* in that area the row ends in *M. balladyna* and *M. opisthomuscorum*, indicating that the shortened state is apomorphic. *Monomicrocaryon crassistilatum* is considerably larger than *M. granulatum* (90–150 µm vs. 60–90 µm). *Monomicrocaryon kahlovatum* differs from *M. granulatum* by body shape (ovate vs. ellipsoidal) and the location of the transverse cirri (far subterminal so that they do not protrude from body proper vs. subterminal and protruding). *Quadristicha setigera* differs from *M. granulatum* by the location of the buccal cirrus (near posterior vs. anterior end of paroral membrane). *Monomicrocaryon sphagni* differs from *M. granulatum* by body shape (length:width ratio ~5:1 vs. 2.7:1) and the 15 µm long dorsal bristles (vs. 8 µm, except of three 15 µm long bristles at end of rows 1, 2 and 4).

Monomicrocaryon euglenivorum (KAHL, 1932) **nov. comb.**

Improved diagnosis: Size in vivo about 80–90 µm x 30–45 µm or 50–70 x 20–30 µm. Shape lenticular to ovoid or ellipsoid to slenderly ellipsoid. Buccal cirrus near anterior end of paroral membrane; transverse cirri acicular or rod-shaped with fringed distal end; right marginal row commences anterior or at level of buccal vertex; caudal cirri in mid of posterior end or left of body's midline. 5 dorsal kineties, bristles 7–10 µm long, posteriorly up to 15 µm; 3 caudal cirri. Adoral zone about one third of body length, composed of about 18 membranelles.

Remarks: The diagnosis is based on KAHL (1932) and the present investigations. We split *M. euglenivorum* into two subspecies because of distinct differences in some morphometrics and the fringed (vs. acicular) transverse cirri, a feature already used by XIN-BAI & AMMERMANN (2004) to distinguish *Stylonychia ammermanni* from *S. harbinensis*. BORROR (1972) synonymized *M. euglenivorum* with *M. crassistilatum* and *M. opisthomuscorum*; however, we agree with BERGER (1999), who follows KAHL (1932), considering them as valid species.

Monomicrocaryon euglenivorum euglenivorum (KAHL, 1932) **nov. stat.** (Fig. 256d)

Improved diagnosis: Size in vivo about 80–90 µm x 30–45 µm. Shape lenticular, ovoid when well-fed. Transverse cirri acicular; right marginal row commences anterior to buccal vertex; caudal cirri in body's midline.

Type locality: Not given in original description, very likely in Germany near to the town of Hamburg.

Descriptions: KAHL (1932) and BERGER (1999).

Monomicrocaryon euglenivorum fimbricirratum Foissner & Liebetreu **nov. sspec.** (Fig. 256a–c, e–i, 257a–g; Table 97)

Diagnosis: Size in vivo 50–70 x 20–30 µm. Shape ellipsoid to slenderly ellipsoid. Transverse cirri rod-shaped with fringed distal end; right marginal row commences at level of buccal vertex; caudal cirri right of body's midline. 5 dorsal bristle rows; row 1 with a one-kinetid-wide gap posterior to mid-body; row 4 distinctly shortened anteriorly; row 5 dorsomarginal, extends to mid-body.

Type locality: Venezuelan site (1), i. e., upper soil layer from the Orinoco floodplain at the village of Cabruta, Venezuela, 7°38'N 66°14'W.

Type material: 1 holotype and 2 paratype slides with protargol-impregnated specimens have

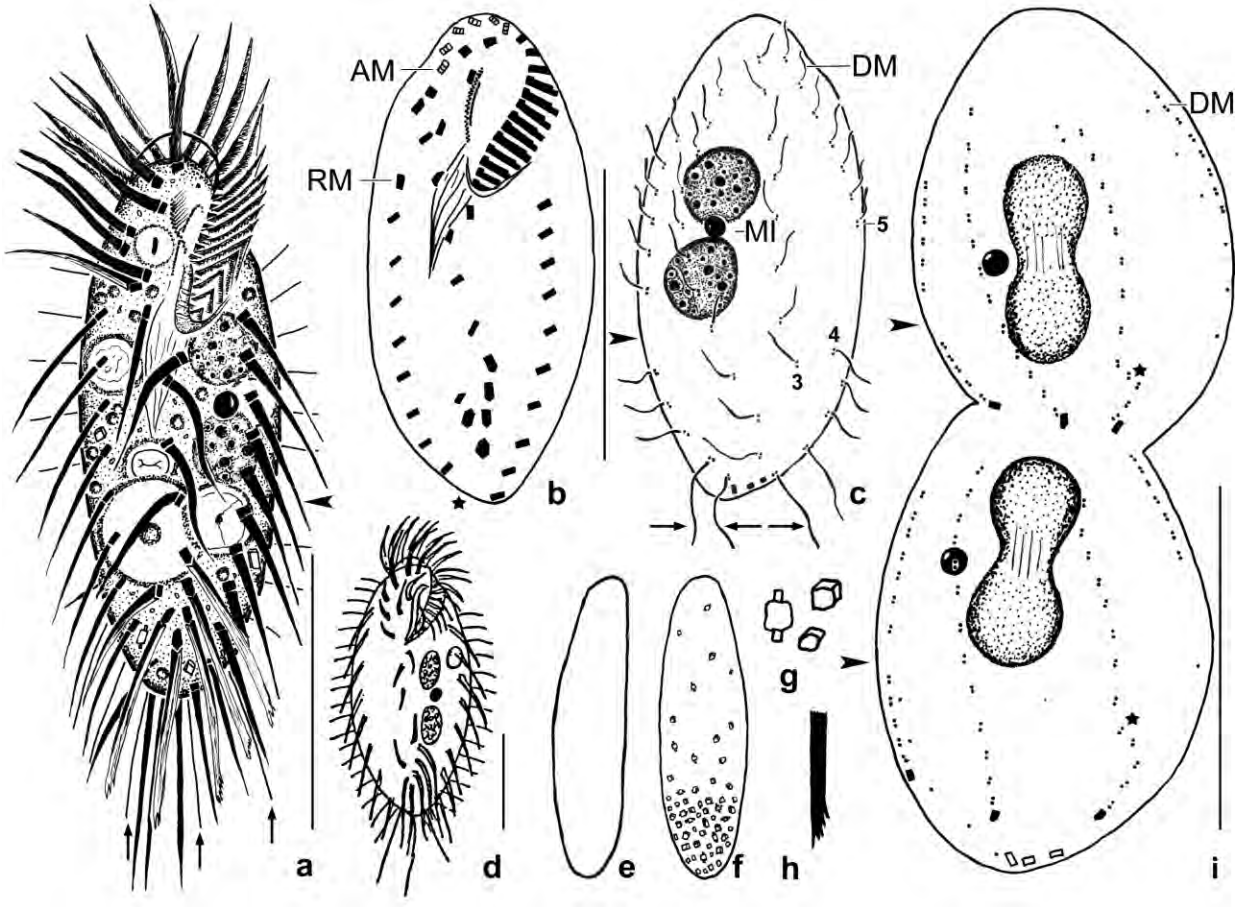

Fig. 256a–i. *Monomicrocaryon euglenivorum fimbricirratum* (a–c, e–i) and *M. euglenivorum euglenivorum* (d, from Kahl 1932) from life (a, d–h) and after protargol impregnation (b, c, i). Arrows mark the elongated dorsal bristles at posterior end of kineties 1, 2 and 4; arrowheads denote gap in dorsal kinety 1. **a:** Ventral view of a representative specimen, length 60 µm, having ingested a flagellate (*Polytoma*), a bacterial spore and wheat starch. A large vacuole appeared empty except of a bright globule in centre. **b, c:** Ventral and dorsal view of holotype specimen, showing the infraciliature and the nuclear apparatus, length 50 µm. In this specimen, the anteriormost cirrus of the right marginal row is misdirected. Asterisk denotes gap between right and left marginal row, occupied by caudal cirri on dorsal side. **d:** Ventral view of *Monomicrocaryon euglenivorum euglenivorum*, length 80 µm. **e-g:** Lateral and dorsal view of a slender specimen, showing cytoplasmic crystals (g) studded in posterior third. **h:** Fringed end of a transverse cirrus. **i:** Dorsal view of a late divider, length 75 µm. Asterisks mark beginning separation of kinety 4 from kinety 3. Old (parental) kinetids represented by single dots. New caudal cirri at end of kineties 1, 2 and 4 shaded black; parental caudal cirri depicted by contour. AM – distalmost adoral membranelle, CC – caudal cirri, DM – dorsomarginal row, RM – right marginal cirral row. Scale bars 30 µm.

been deposited in the Biology Centre of the Upper Austrian Museum in Linz (LI). Relevant specimens have been marked by black ink circles on the coverslip.

Etymology: Composite of the Latin noun *fimbria* (fringe) and the Latin adjective *cirratum* (cirri bearing), referring to the fringed ends of the transverse cirri.

Description: The species was rather rare in the non-flooded Petri dish culture but grew well in a semi-pure culture fed with some squashed wheat grains. The description is based on this material.

Size in vivo 50–70 x 20–30 µm, usually about 60 x 25 µm, as calculated from some in vivo measurements and the morphometric data in Table 97 adding 15% preparation shrinkage. Very flexible, slightly contractile in oral portion. Body length:width ratio in vivo 2.2–3:1, after protargol impregnation stouter, viz., 1.7–2.4, very likely due to some inflation during the preparation procedures (Fig. 256a, b, 257a, d, f; Table 97). Shape inconspicuous, i. e., ellipsoid to slenderly ellipsoid (Fig. 256a, f, 257a), thus easily confused with a variety of moderately small oxytrichids, such as *Monomicrocaryon* spp., *Oxytricha* spp., and *Urosomoida* spp. Hardly flattened laterally (Fig. 256e). Nuclear apparatus on average in mid-body and left of body's midline, anterior macronuclear nodule commences near level of buccal vertex (Fig. 256a, c, 257b, d, f; Table 97). Macronuclear nodules globular to broadly ellipsoid, on average 8 x 7 µm in protargol preparations; nucleoli 0.5–1 µm across. One out of 28 specimens with cordiform anterior macronuclear nodule; six out of 28 cells with a single, large, ellipsoid to reniform or dumbbell-shaped macronucleus about 15 x 7 µm in size. Micronucleus between macronuclear nodules, about 2 µm across after protargol impregnation; in one specimen attached to anterior half of anterior macronuclear nodule, in another to posterior half of posterior nodule; two specimens with two micronuclei: in one cell attached to anterior and posterior end of macronuclear nodules, respectively; in the other both left of the abutting macronuclear nodules. Contractile vacuole in or near mid-body at left cell margin, with inconspicuous collecting canals (Fig. 256a, 257b). No cortical granules. Cytoplasm colourless, studded with refractive (lipid?) granules 1–1.5 µm across; with or without cubic crystals 2–3 µm in size, make rear portion dark (refractive) at low magnification when numerous. Food vacuoles in vivo 6–12 µm across, contain flagellates (*Polytoma*), bacterial spores, indeterminable pale matter, and wheat starch grains when cultivated (Fig. 256a, f, g, 257b). Glides very rapidly on microscope slide, jumps after short resting periods and when changing direction.

Cirral pattern oxytrichid, i. e., usually 18 cirri (Berger 1999) most about 15 µm long (Fig. 256a, b, 257d, f; Table 97): three frontal cirri, four frontoventral cirri, one buccal cirrus near anterior end of paroral, three postoral cirri, two pretransverse cirri, and five transverse cirri. Transverse cirri conspicuous because rather thick, about 20 µm long and protruding from body proper, distally not tapered but fringed on left side (Fig. 256a, h, 257a). Frontal cirri and transverse cirri each composed of three kineties; other cirri of two. Right marginal row commences at level of buccal vertex, posteriorly slightly shortened, composed of an average of only nine cirri. Left marginal row extends to body's midline posteriorly, composed of 10 cirri on average. Transverse cirri, last marginal cirri, and caudal cirri form conspicuous tuft around posterior end of cell (Fig. 256a, 257a, b, d).

Five dorsal bristle rows in oxytrichid pattern (Fig. 256a, c, i, 257b, c, e; Table 97). Row 1 shortened

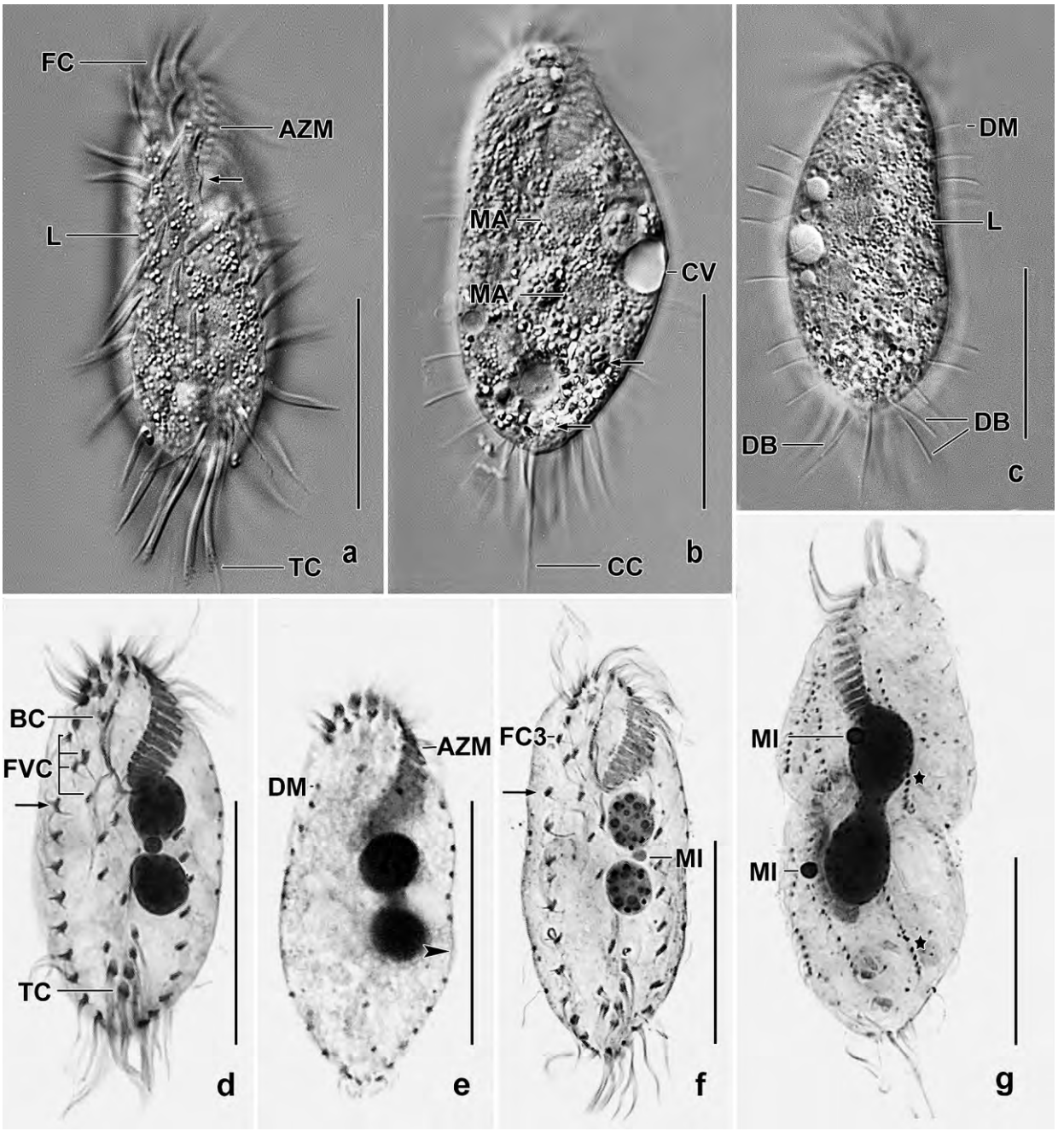

Fig. 257a–g. *Monomicrocaryon euglenivorum fimbricirratum* from life (a–c) and after protargol impregnation (d–g). **a, b:** Ventral view of a freely motile (a) and a slightly squashed (b) specimen. Note the rod-shaped, distally fringed transverse cirri (a) and a long caudal cirrus (b). Arrows mark buccal lip (a) and cytoplasmic crystals (b). **c:** Dorsal view, showing dorsomarginal bristle row and some of the elongated dorsal bristles at end of rows 1, 2 and 4. **d, e:** Surface view and optical section of holotype specimen, showing the 18 FVT cirral pattern, the nuclear apparatus, and the gap in dorsal kinety 1 (arrowhead). The right marginal row commences at level of buccal vertex (arrow). **f:** Ventral view of a slender specimen. Arrow marks first cirrus of right marginal row. **g:** A late divider with not yet separated dorsal kineties 3 and 4 (asterisks). AZM – adoral zone of membranelles, BC – buccal cirrus, CC – caudal cirri, CV – contractile vacuole, DB – dorsal bristles, DM – dorsomarginal row, FC – frontal cirri, FC3 – frontal cirrus 3, FVC – frontoventral cirri, L – lipid (?) granules, MA – macronuclear nodules, MI – micronucleus, TC – transverse cirri. Scale bars 30 µm.

Table 97. Morphometric data on *Monomicrocaryon euglenivorum fimbricirratum* based on mounted, protargol-impregnated, and randomly selected specimens from a semipure culture. Measurements in µm. CV – coefficient of variation in %, M – median, Max – maximum, Mean – arithmetic mean, Min – minimum, n – number of individuals investigated, SD – standard deviation, SE – standard error of arithmetic mean.

Characteristics	Mean	M	SD	SE	CV	Min	Max	n
Body, length	50.8	51.0	3.9	0.8	7.6	43.0	59.0	21
Body, width	24.0	23.0	2.0	0.4	8.4	21.5	28.0	21
Body length:width, ratio	2.1	2.1	0.2	0.0	7.7	1.7	2.4	21
Anterior body end to right marginal row, distance	20.6	20.0	1.5	0.3	7.3	19.0	25.0	21
Anterior body end to buccal cirrus, distance	8.3	8.0	1.0	0.2	11.5	7.0	10.0	21
Anterior body end to paroral membrane, distance	6.4	6.0	0.8	0.2	12.9	5.0	8.0	21
Anterior body end to proximal end of endoral membrane, distance	16.0	16.0	1.3	0.3	8.1	14.0	19.0	21
Posterior body end to posteriormost transverse cirrus, distance	5.1	5.0	1.1	0.2	22.3	3.0	7.0	21
Posterior body end to right marginal row, distance	3.7	4.0	1.1	0.2	28.4	2.0	6.0	21
Anterior body end to macronucleus, distance [a]	17.0	17.0	1.6	0.3	9.3	13.0	20.0	21
Anterior macronuclear nodule, length [a]	8.5	8.0	1.2	0.3	13.5	7.0	11.0	21
Anterior macronuclear nodule, width [a]	7.0	7.0	0.5	0.1	7.1	6.0	8.0	21
Anterior macronuclear nodule, length:width ratio	1.2	1.1	0.2	0.0	18.6	1.0	1.8	21
Macronuclear nodules, number	1.8	2.0	–	–	–	1.0	2.0	28
Micronuclei, length	2.2	2.0	–	–	–	2.0	2.5	21
Micronuclei, width	1.9	2.0	–	–	–	1.5	2.0	21
Micronucleus, number	1.0	1.0	0.0	0.0	0.0	1.0	1.0	21
Anterior body end to proximal end of adoral zone, distance	18.5	19.0	1.3	0.3	7.2	16.0	21.0	21
Body length:length of adoral zone, ratio	2.8	2.7	0.3	0.1	9.9	2.4	3.4	21
Largest membranellar basis, width	5.5	5.5	0.6	0.1	10.2	4.0	6.0	21
Adoral membranelles, number	17.5	18.0	0.8	0.2	4.6	16.0	19.0	21
Buccal cavity, width	4.2	4.0	0.6	0.1	14.4	3.0	5.0	21
Frontal cirri, number	3.0	3.0	0.0	0.0	0.0	3.0	3.0	21
Frontoventral cirri, number [b]	4.0	4.0	0.0	0.0	0.0	4.0	4.0	21
Buccal cirri, number	1.0	1.0	0.0	0.0	0.0	1.0	1.0	21
Postoral cirri, number [b]	3.0	3.0	0.0	0.0	0.0	3.0	3.0	21
Pretransverse cirri, number [b]	2.0	2.0	0.0	0.0	0.0	2.0	2.0	21
Transverse cirri, number	5.0	5.0	0.0	0.0	0.0	5.0	5.0	21
Right marginal row, number of cirri	9.0	9.0	0.7	0.2	8.3	8.0	10.0	21
Left marginal row, number of cirri	10.2	10.0	0.7	0.2	7.4	9.0	11.0	21
Caudal cirri, number	3.0	3.0	0.0	0.0	0.0	3.0	3.0	21
Dorsal bristle rows, number	5.0	5.0	0.0	0.0	0.0	5.0	5.0	21
Bristles in dorsal row 1, number	10.7	11.0	1.1	0.2	9.9	9.0	12.0	21
Bristles in dorsal row 2, number	10.1	10.0	0.9	0.2	8.4	8.0	11.0	21
Bristles in dorsal row 3, number	8.7	9.0	0.7	0.1	7.6	8.0	10.0	21
Bristles in dorsal row 4, number	4.1	4.0	0.6	0.1	13.8	3.0	5.0	21
Bristles in dorsal row 5, number	7.9	8.0	0.6	0.1	7.3	7.0	9.0	21

[a] Measured in cells with 2 distinct nodules.

[b] Of 24 specimens analysed, one has 3 frontoventral cirri, another has 2 postoral cirri, and one has 4 transverse cirri.

anteriorly, with a one-kinetid-wide break posterior to mid-body; row 2 bipolar and distinctly curved; row 3 shortened posteriorly, often indistinctly separated from row 4; row 4 strongly shortened anteriorly, consists of an average of only 4 kinetids; dorsomarginal row 5 terminates about mid-body. Most bristles in vivo 7–10 µm long, last bristles of rows 1, 2 and 4 gradually elongated to about 15 µm (Fig. 257c). Caudal cirri right of body's midline, fill gap between ends of marginal rows, associated with kineties 1, 2 and 4, very motile, 20–25 µm long in vivo.

Oral apparatus extends 36% of body length on average (Fig. 256a, b, 257a, d–f; Table 97). Adoral zone of ordinary shape, composed of an average of 18 membranelles of usual structure and with cilia up to 15 µm long in protargol preparations, proximal portion covered by buccal lip (Fig. 257a); largest membranellar bases on average 6 µm width. Buccal cavity in vivo moderately deep and about 4 µm wide. Membranellar scutum about 3 µm high. Paroral and endoral membrane slightly curved and almost one upon the other, both end far anteriorly of buccal vertex. Paroral composed of oblique dikinetids with about 4 µm long cilia, endoral of monokinetids. Pharyngeal fibres extend vertically to mid-body.

Notes on ontogenesis (Fig. 256i, 257g): The dorsal ciliature develops in *Oxytricha s.str.* pattern, i. e., kinety 5 is formed dorsomarginally and kinety 3 divides into two pieces: the longer anterior piece becomes kinety 3, the short posterior fragment kinety 4. However, the separation of kineties 3 and 4 is often incomplete, similar to *Oxytricha opisthomuscorum* (Petz & Foissner 1997). The fragmentation of kinety 3 occurs comparatively late, i. e., when the division furrow is already distinct (Fig. 256i, 257g). In other *Oxytrichinae*, e. g., *Oxytricha granulifera* Foissner & Adam, 1983b, *Allotricha antarctica* (Petz & Foissner 1996), and *Cyrtohymena muscorum* (Voss 1991), the separation of kineties 3 and 4 begins earlier, i. e., when the division furrow is hardly recognizable.

Occurrence and ecology: As yet found only at type locality where it appeared two weeks after rewetting the sample. Grew well in a semi-pure culture fed with some squashed wheat grains.

Remarks (for literature, see Berger 1999): *Monomicrocaryon euglenivorum fimbricirratum* and *M. euglenivorum euglenivorum* differ by the features given in their diagnoses, especially by the transverse cirri (fringed distally vs. acicular; Fig. 256a, d).

The genus → *Monomicrocaryon* contains 17 species, those well-known lack a one-kinetid-wide gap in the first dorsal bristle row, as to be found in *M. euglenivorum fimbricirratum*. Another conspicuous difference are the elongated posterior dorsal bristles, a feature as yet only found in *M. euglenivorum euglenivorum* and in → *M. granulatum*. However, → *M. granulatum* can be clearly distinguished by the cortical granule rows and the acicular transverse cirri.

The only other *Monomicrocaryon* species with fringed transverse cirri, so typical for *M. euglenivorum fimbricirratum,* is → *M. crassistilatum*. However, *M. crassistilatum* differs in body size (90–150 µm vs. 50–70 µm) and lacks elongated dorsal bristles posteriorly. *Monomicrocaryon balladyna* and *M. opisthomuscorum* also resemble *M. euglenivorum fimbricirratum* but have the last dorsal bristles not elongated and have acicular, distally not fringed transverse cirri.

Monomicrocaryon *crassicirratum* nov. spec. (Fig. 258a–g, 259a–j; Table 98)

Diagnosis: Size in vivo about 125 × 50 µm; more or less ovate. Cirri thick and long; buccal cirrus subapical of paroral membrane, transverse cirri projecting from body proper and fringed distally. 6 dorsal kineties with 5–10 µm long bristles. 3 thick, up to 30 µm long caudal cirri in and slightly left of body`s midline. Adoral zone extends about 42% of body length, composed of an average of 25 comparatively widely spaced, large membranelles with bases up to 16 µm width. Buccal cavity narrow and almost completely covered by buccal lip. Paroral and endoral membrane slightly curved and side by side.

Type locality: Soil from the rainforest in the outskirts of the village of Quillabamba, Peru, 72°41'W 12°51'S.

Type material: 1 holotype and 6 paratype slides with protargol-impregnated specimens have been deposited in the Biology Centre of the Upper Austrian Museum smuseum in Linz (LI). Relevant specimens have been marked by black ink circles on the coverslip. Further, we deposited 5 voucher slides from a Brazilian population.

Etymology: *Crassicirratum* is a composite of the Latin adjectives *crassus* (thick) and *cirratus* (tendrilled) and the thematic vowel *-i-*, referring to the long, thick cirri.

Description: We studied a population each from Peru (type) and Brazil (Table 98). They match well, except of body and adoral zone length which are larger by 12% and 25% in the Peruvian specimens, respectively; furthermore, the dorsal bristles are only 3–5 µm long in the Brazilian cells which grew poorly in the non-flooded Petri dish culture. We cannot exclude that the Brazilian population presents a distinct subspecies. Thus, the diagnosis and the following description contain only Peruvian specimens.

Size in vivo 100–150 × 32–60 µm, usually about 125 × 50 µm, as calculated from some in vivo measurements and the morphometric data in Table 98 adding 15% preparation shrinkage. Body more or less ovate, rarely ellipsoid or rectangular; laterally only slightly flattened; anterior end more or less conical because the adoral zone curves ventrally at distal end where two membranelles insert ventrolaterally (Fig. 258a, b, d, e, 259a–c, g; Table 98). Nuclear apparatus on average in central third of body slightly left of midline, consists of two macronuclear nodules and a micronucleus in between; nuclear figure usually slightly oblique, i. e., anterior macronuclear nodule under proximal end of buccal cavity, posterior nodule approaching left margin of cell. Individual macronuclear nodules globular to ellipsoid, on average broadly ellipsoid, contain many minute nucleoli. Micronucleus about 6 µm across in vivo (8 µm in Brazilian specimens), in one specimen attached to mid of anterior macronuclear nodule (Fig. 258a, c, d, 259a–c, e; Table 98). Contractile vacuole in or near mid of left body margin (Fig. 258a). Cortex flexible, without specific granules. Cytoplasm colourless but cells may look dark when studded with highly refractive crystals 3–10 µm in size, lipid droplets in 4 µm-sized vacuoles, and up to 15µm-sized food vacuoles containing small ciliates (*Vorticellides astyliformis*, *Protocyclidium terricola*) and flagellates (*Polytomella* sp., in Brazil an euglenid resembling *Peranema* and packed with paramylon grains). Glides rapidly on microscope slide, performing short, fast strokes to and fro.

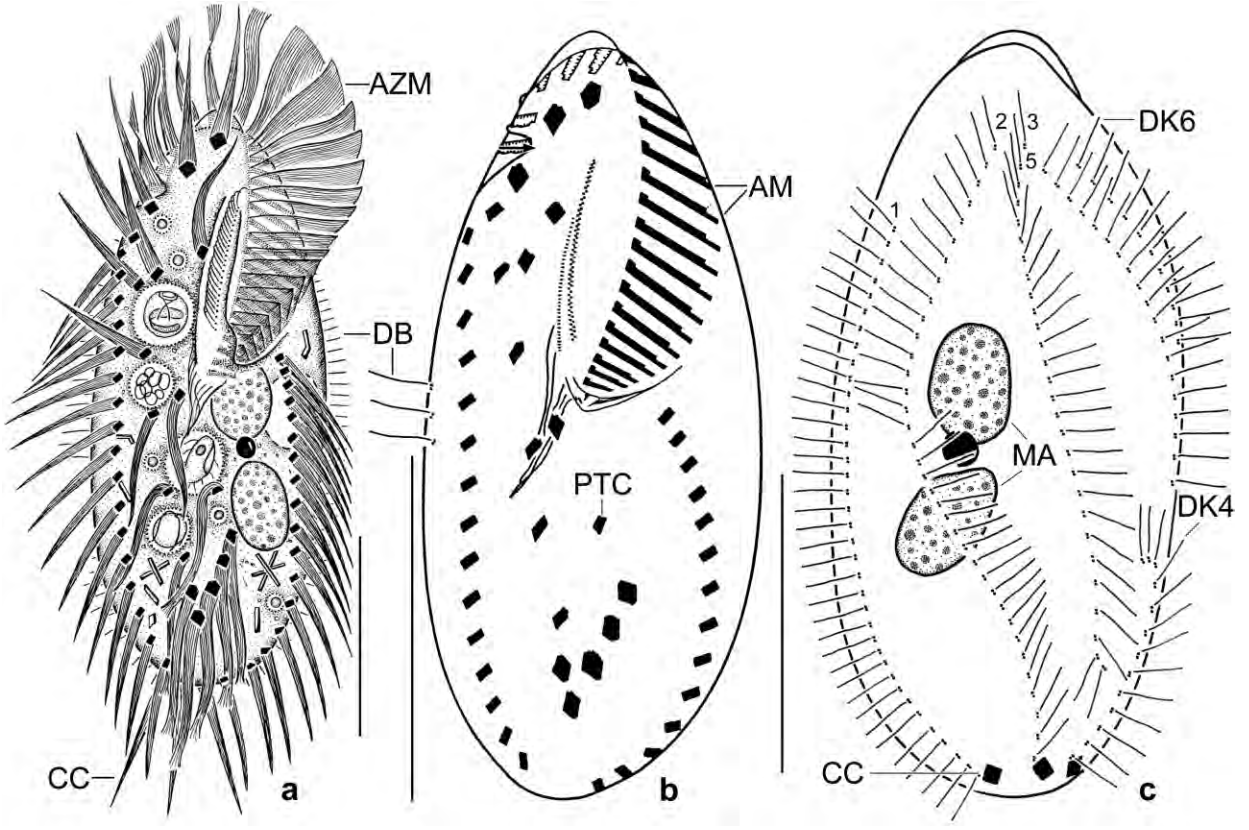

Fig. 258a–c. *Monomicrocaryon crassicirratum*, Peruvian specimens from life (a) and after protargol impregnation (b, c). **a:** Ventral view of a representative specimen, length 125 µm. Note the long, thick cirri and, especially, the massive adoral zone of membranelles. **b:** Ventral view of holotype specimen, length 95 µm. The arrow marks the distal end of the adoral zone two membranelles of which curve onto the ventral side. Note the up to 14 µm long and widely spaced adoral membranelles. **c:** Dorsal view of a paratype specimen with elongated bristles in the dorsomarginal kineties. Note the massive bases of the caudal cirri and the obliquely arranged nuclear apparatus. AM – adoral membranelles, AZM – adoral zone of membranelles, CC – caudal cirri, DB – dorsal bristles, DK1–6 – dorsal kineties, MA – macronuclear nodules, PTC – upper pretransverse cirrus. Scale bars 40 µm.

Cirral pattern oxytrichid, i. e., usually 18 fronto-ventral-transverse cirri (Berger 1999) all conspicuously long and thick, especially the frontal, transverse and, surprisingly, also the caudal cirri; last marginal cirri, transverse cirri, and caudal cirri form a rather distinct corona around posterior body end (Fig. 258a–c, f, 259a–c, g, i, j; Table 98). Invariably three about 25 µm long frontal cirri in strongly oblique row commencing in body´s midline and ending with frontal cirrus 3 posterior to last adoral membranelle. Cirrus III/2 close to second frontoterminal cirrus and posterior to buccal cirrus at level of begin of endoral membrane, i. e., distinctly subapical of paroral membrane. Left pretransverse cirrus far anterior at or near to level of last postoral cirrus. Transverse cirri in typical *Oxytricha* pattern, distal end fringed, about 30 µm long and thus distinctly projecting from body proper, rearmost cirrus about 12 µm anterior of body end. Marginal cirri in vivo about 15 µm long, composed of four ciliary rows, arranged in a right and a left row each comprising about 17 cirri, both rows end close to posterior body margin; right row commences far subapically (Fig. 258a, b, 259a, b, g, j; Table 98).

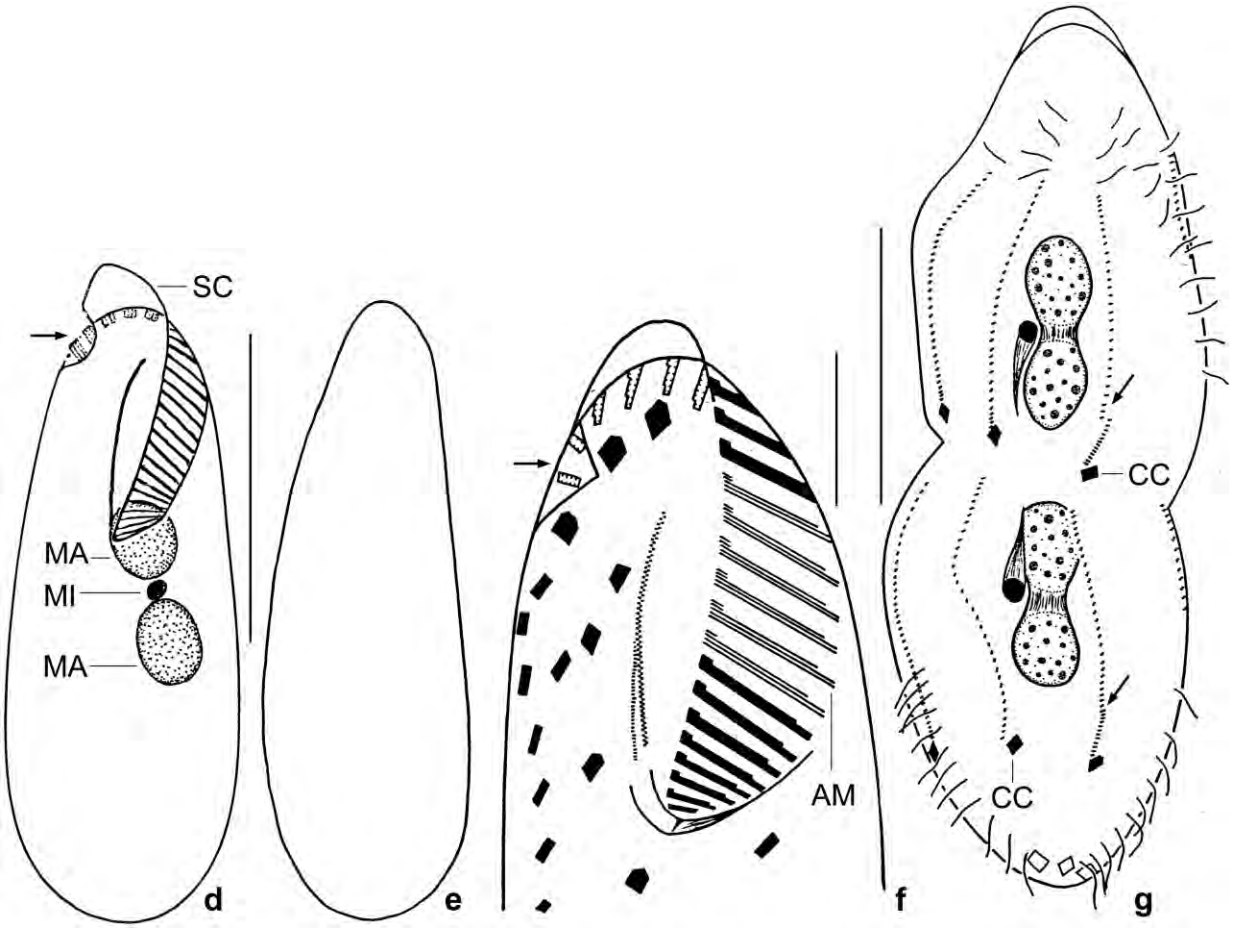

Fig. 258d–g. *Monomicrocaryon crassicirratum*, Brazilian (d, e) and Peruvian (f, g) specimens from life (d, e) and after protargol impregnation (f, g). **d, e:** Ventral and lateral view. The arrow denotes the site where the distal end of the adoral zone of membranelles approaches the ventral side. Note also the high, triangular scutum. **f:** Ventrolateral view, exposing the adoral zone of membranelles; the central membranelles are very likely composed of five rows of basal bodies. The arrow marks the site where the distal end of the adoral zone of membranelles approaches the ventral side. **g:** Dorsal view of a late divider, showing the origin of kinety 4 by a split (arrowhead) of kinety 3. Note the large bases of the caudal cirri. AM – adoral membranelles, CC – caudal cirri, MA – macronuclear nodules, MI – micronucleus, SC – scutum. Scale bars 15 µm (f), 50 µm (g), and 80 µm (d, e).

Dorsal bristles in six rows, row 1 begins subapically, rows 2 and 3 bipolar, row 4 short and originating from row 3, row 5 ends near mid-body and is generated dorsomarginally, row 6 ends distinctly anterior of mid-body and is also generated dorsomarginally. Length of bristles highly variable between populations but also within a single cell: 5–10 µm in Peruvian specimens, 3–5 µm in Brazilian cells. Three caudal cirri in and slightly right of body`s midline, insert very near to posterior body end, as thick or even slightly thicker than frontal cirri (Fig. 258a, c, 259a, c, d, i; Table 98).

Oral apparatus full of specific features (Fig. 258a, b, f, 259a, b, f–h, j; Table 98): (i) adoral zone of membranelles extends 42% of body length on average, as typical for stylonychids; (ii) its distal end curved ventrally; (iii) cilia of frontal membranelles about 25 µm long; (iv) membranellar distances wider than usual (~ 1.7 µm between membranelles 12 and 13), resembling *Australocirrus* Blatterer & Foissner, 1988; (v) membranellar bases as long as in large hypotrichs, viz. about 14 µm as, e. g., in *Afrokeronopsis* Foissner et al., 2010b; (vi) middle ventral membranelles very likely

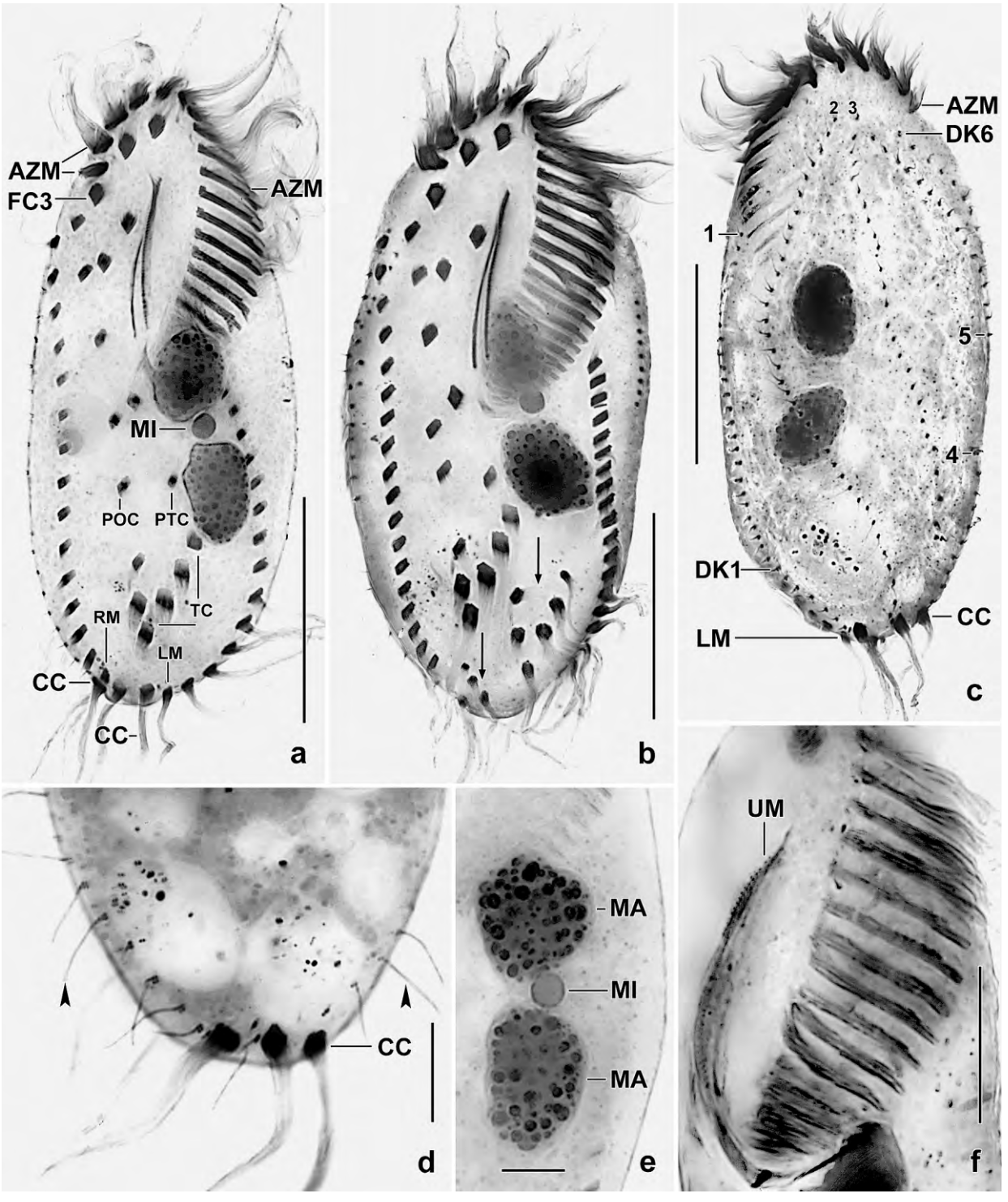

Fig. 259a–f. *Monomicrocaryon crassicirratum*, Peruvian specimens after protargol impregnation. **a:** Ventral view, showing two distal adoral membranelles on ventral side. **b:** A young post-divider with some parental cirri not yet resorbed (arrows). **c, d:** Dorsal views, showing the massive caudal cirri and the about 9 µm long dorsal bristles (arrowheads). **e:** Nuclear apparatus. **f:** Adoral zone with long and widely spaced membranelles. AZM – adoral zone of membranelles, CC – caudal cirri, DK1–6 – dorsal kineties, FC3 – frontal cirrus 3, LM – left marginal row, MA – macronuclear nodules, MI – micronucleus, RM – right marginal row, POC – last postoral cirrus, PTC – upper pretransverse cirrus, TC – transverse cirri, UM – undulating membranes. Scale bars 10 µm (d, e), 15 µm (f), 30 µm (b), and 40 µm (a, c).

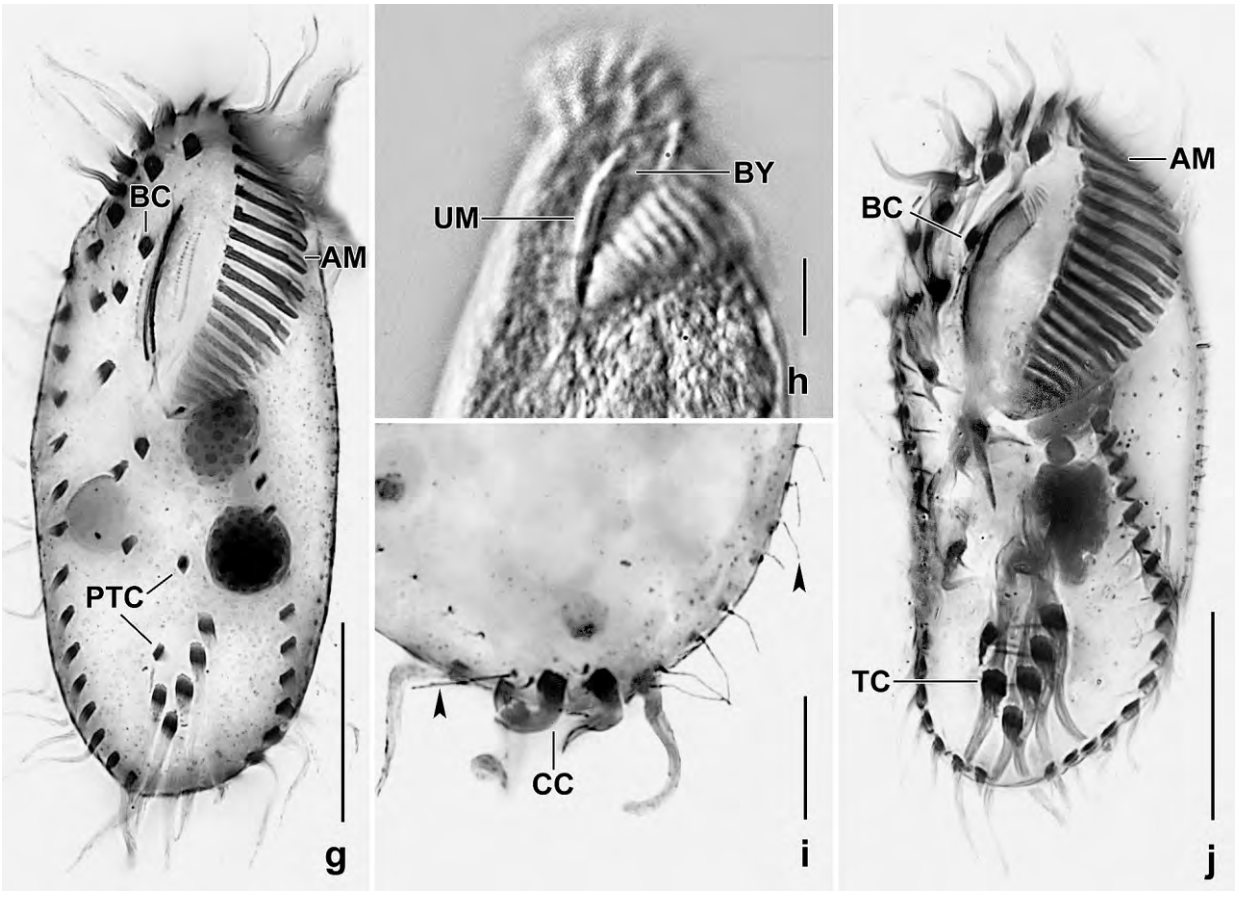

Fig. 259g–j. *Monomicrocaryon crassicirratum*, Brazilian (h, j) and Peruvian (g, i) specimens from life (h) and after protargol impregnation (g, i, j). **g:** Ventral view, showing a specimen with rather small cirral bases but widely spaced adoral membranelles. **h:** Oral body portion of a slightly pressed specimen, showing the narrow buccal cavity and the projecting distal part of the adoral zone. **i:** Dorsal view of posterior body portion, showing the massive caudal cirri and the dorsal bristles whose length varies from 5 µm (right) to 9 µm (left; arrowheads). **j:** Ventrolateral view, showing the massive adoral membranelles and the thick cirri. AM – adoral membranelles, BC – buccal cirrus, BY – buccal cavity, CC – caudal cirri, PTC – pretransverse cirri, TC –transverse cirri, UM – undulating membranes. Scale bars 10 µm (h, i) and 30 µm (g, j).

composed of five ciliary rows; (vii) buccal cavity narrow in live cells (Fig. 259h; width doubled in protargol preparations) and almost covered by buccal lip about 6 µm wide in vivo. Adoral zone composed of an average of 26 membranelles, its massiveness resembling *Australocirrus*, as mentioned above. Undulating membranes slightly curved, side by side diverging posteriorly; paroral membrane longer than endoral anteriorly, extends near left margin of buccal lip, cilia only 7 µm long in vivo. Pharyngeal fibres ordinary.

Occurrence and ecology: As yet found in Peru, Brazil, and at Venezuelan site (23), i. e., in fertile Mahadja soil. The Peruvian sample is from a rainforest and consisted of the upper 5 cm litter and soil layer. The site is occasionally flooded by a stream, and thus the soil is sandy and studded with fine grass roots; on the surface is some moss; pH 5.8 in water. The Brazilian sample, kindly collected by Mag. Birgit Weissenbacher, is from the floodplain of the Rio Claro in the northern Pantanal, 56°73’58’’W 16°62’10’’S. The soil was dusty, lightbrown, and contained few litter and roots.

Table 98. Morphometric analysis on *Monomicrocaryon crassicirratum* from Brazil (upper line) and Peru (lower line). Data based on mounted, protargol-impregnated, and randomly selected specimens from non-flooded Petri dish cultures. Measurements in µm. CV – coefficient of variation in %, M – median, Max – maximum, Mean – arithmetic mean, Min – minimum, n – number of individuals investigated, SD – standard deviation, SE – standard error of arithmetic mean.

Characteristics	Mean	M	SD	SE	CV	Min	Max	n
Body, length	92.8	95.0	8.6	2.9	9.2	78.0	104.0	9
	111.0	112.0	10.3	1.9	9.3	87.0	131.0	29
Body, width	41.3	40.0	5.3	1.8	12.8	34.0	50.0	9
	42.3	43.0	5.2	1.0	12.2	32.0	52.0	29
Body length:width, ratio	2.3	2.3	0.2	0.1	9.2	2.0	2.5	9
	2.6	2.6	0.3	0.1	11.6	2.1	3.2	29
Anterior body end to proximal end of adoral zone of membranelles, distance	38.9	39.0	2.7	0.9	7.1	34.0	43.0	9
	48.8	49.0	3.6	0.7	7.4	41.0	54.0	29
Adoral membranelles, number	25.2	25.0	0.8	0.3	3.3	24.0	27.0	9
	25.5	26.0	1.8	0.3	7.1	23.0	28.0	29
Largest adoral membranelle, width of base	14.5	14.0	0.9	0.3	6.0	13.0	16.0	9
	13.6	14.0	1.0	0.2	7.2	12.0	15.0	29
Adoral membranelles, distance between membranelles 12 and 13	1.1	1.0	–	–	–	1.0	1.5	9
	1.7	1.8	–	–	–	1.2	2.0	29
Anterior body end to buccal cirrus, distance	19.1	19.0	2.4	0.8	12.4	15.0	23.0	9
	25.9	26.0	2.4	0.5	9.3	21.0	32.0	28
Anterior body end to paroral membrane, distance	11.4	12.0	1.6	0.5	14.0	9.0	13.0	9
	17.7	17.3	2.4	0.5	13.7	14.0	24.0	28
Anterior body end to endoral membrane, distance	15.1	15.0	1.7	0.6	11.6	11.0	17.0	9
	19.0	19.0	2.3	0.5	12.0	15.0	23.0	22
Anterior body end to rearmost frontoventral cirrus, distance	35.8	36.0	2.8	0.9	7.9	31.0	40.0	9
	45.1	45.0	3.7	0.7	8.2	38.0	52.0	25
Anterior body end to rearmost postoral cirrus, distance	59.0	60.0	3.9	1.4	6.5	52.0	63.0	8
	71.0	71.0	7.1	1.5	10.1	49.0	82.0	23
Anterior body end to right marginal row, distance	19.4	19.0	1.9	0.7	9.7	16.0	22.0	8
	24.5	25.0	3.0	0.6	12.1	19.0	31.0	26
Posterior body end to right marginal row, distance	1.7	1.5	0.6	0.2	35.9	1.0	3.0	9
	2.5	2.5	0.7	0.1	27.7	1.0	4.0	26
Posterior body end to left marginal row, distance	1.2	1.0	0.4	0.2	36.1	0.5	2.0	9
	1.7	1.5	1.1	0.2	67.8	0.5	5.0	26
Posterior body end to rearmost transverse cirrus, distance	7.5	7.0	2.5	0.9	32.7	4.0	12.0	8
	10.9	11.0	2.1	0.4	19.0	8.0	16.0	24
Anterior body end to anterior macronuclear nodule, distance	31.7	33.0	3.4	1.1	10.8	25.0	35.0	9
	44.0	44.0	3.9	0.7	8.9	36.0	51.0	28
Macronuclear nodules, number	2.0	2.0	0.0	0.0	0.0	2.0	2.0	9
	2.0	2.0	0.0	0.0	0.0	2.0	2.0	29
Macronuclear nodules, length	15.2	15.0	2.2	0.7	14.4	12.0	19.0	9
	15.8	16.0	1.5	0.3	9.4	13.0	19.0	29
Macronuclear nodules, width	9.2	9.0	0.5	0.2	5.5	8.0	10.0	9
	11.4	11.0	1.3	0.2	11.2	10.0	14.0	29

continued

Characteristics	Mean	M	SD	SE	CV	Min	Max	n
Nuclear figure, length	31.4	30.0	4.2	1.4	13.3	27.0	41.0	9
	34.7	35.0	3.7	0.7	10.8	28.0	46.0	29
Macronuclear nodules, distance in between	2.1	2.0	1.1	0.4	52.2	0.5	4.0	9
	3.6	3.5	1.6	0.3	43.5	0.5	6.0	28
Micronuclei, number	1.0	1.0	0.0	0.0	0.0	1.0	1.0	9
	1.0	1.0	0.0	0.0	0.0	1.0	1.0	29
Micronuclei, length	3.6	3.5	–	–	–	3.0	4.0	9
	4.2	4.0	–	–	–	3.0	5.0	29
Micronuclei, width	3.5	3.5	–	–	–	3.0	4.0	9
	3.9	4.0	–	–	–	3.0	5.0	29
Frontal cirri, number	3.0	3.0	0.0	0.0	0.0	3.0	3.0	9
	3.0	3.0	0.0	0.0	0.0	3.0	3.0	28
Frontoventral cirri, number	4.0	4.0	0.0	0.0	0.0	4.0	4.0	9
	4.0	4.0	0.0	0.0	0.0	4.0	4.0	25
Buccal cirri, number	1.0	1.0	0.0	0.0	0.0	1.0	1.0	9
	1.0	1.0	0.0	0.0	0.0	1.0	1.0	28
Postoral cirri, number	3.0	3.0	0.0	0.0	0.0	3.0	3.0	8
	3.0	3.0	–	–	–	2.0	3.0	23
Transverse cirri, number	5.0	5.0	0.0	0.0	0.0	5.0	5.0	8
	5.0	5.0	0.0	0.0	0.0	5.0	5.0	22
Pretransverse cirri, number	2.0	2.0	0.0	0.0	0.0	2.0	2.0	8
	2.0	2.0	0.0	0.0	0.0	2.0	2.0	23
Caudal cirri, number	3.0	3.0	0.0	0.0	0.0	3.0	3.0	9
	3.0	3.0	0.3	0.1	9.3	2.0	4.0	27
Right marginal cirri, number	16.7	17.0	1.1	0.4	6.7	15.0	18.0	9
	16.9	17.0	1.6	0.3	9.3	13.0	20.0	26
Left marginal cirri, number	15.8	16.0	1.3	0.4	8.3	13.0	17.0	9
	16.6	17.0	1.6	0.3	9.7	13.0	19.0	25
Dorsal kineties, number	6.0	6.0	0.0	0.0	0.0	6.0	6.0	8
	6.0	6.0	0.0	0.0	0.0	6.0	6.0	23

Remarks: *Monomicrocaryon crassicirratum* has a unique combination of features, suggesting that it is a new species or even a new genus: (i) moderate size, (ii) cirri long and thick, especially the caudal cirri, (iii) transverse cirri fringed, (iv) adoral zone of membranelles occupies more than 40% of body length, as in stylonychids (Berger 1999), (v) distances between adoral membranelles wider than usual, resembling *Australocirrus*, (vi) bases of adoral membranelles comparatively width, viz., about 14 µm, (vii) dorsal bristles 5–10 µm long, (viii) buccal cavity narrow and covered by buccal lip. Two species have some similarity (Berger 1999): *Oxytricha hymenostomata* (similar size and shape, adoral zone occupies > 40% of body length) and *Oxytricha africana* Foissner, 1999b (similar size, shape, and oral apparatus, long dorsal bristles).

Quadristicha nov. gen.

Diagnosis: Flexible Oxytrichidae with 18 fronto-ventral-transverse cirri and two macronuclear nodules with a micronucleus in between. Dorsal kineties do not fragment during ontogenesis; 3 caudal cirri.

Type species: *Oxytricha setigera* Stokes, 1891.

Etymology: *Quadristicha* is a composite of the Latin numeral *quadri* (four) and the Latinized Greek noun *sticha* (row), referring to the four non-fragmenting dorsal bristle rows. Feminine gender.

Species assignable: As yet monotypic: *Quadristicha setigera* Stokes (1891) nov. comb. (basionym: *Oxytricha setigera* Stokes, 1891). Very likely, some of the insufficiently known *Oxytricha* species can be affiliated with the new genus as soon as they have been redescribed with modern methods.

Remarks: *Quadristicha* differs from → *Monomicrocaryon* by the genesis of the dorsal ciliature: intrakinetal and dorsomarginal vs. a fragmenting kinety 3 producing kinety 4. The type species of *Quadristicha* is well known (for a review, see Berger 1999).

Hemioxytricha nov. gen.

Diagnosis: Flexible Oxytrichidae with 18 fronto-ventral-transverse cirri and more than 3 caudal cirri associated with dorsal kineties 1–3; kinety fragmentation absent.

Type species: *Hemioxytricha isabelae* nov. spec.

Etymology: Composite of the Greek prefix *hemi* (half) and the generic name *Oxytricha*, referring to the similarity with the genus *Oxytricha*. Feminine gender.

Remarks: The ventral ciliature of *Hemioxytricha* is as in typical *Oxytricha* species (18 FVT-cirri) while the four non-fragmenting dorsal kineties resemble the new family → *Urosomoidae*. Thus, the classification of *Hemioxytricha* remains obscure. Except of the caudal cirri, *Hemioxytricha* matches the genus *Heterourosomoida* Singh & Kamra, 2015.

Most "typical" oxytrichids have two or three caudal cirri (Berger 1999) while *Hemioxytricha isabelae* has six because kineties 1–3 each produces usually two caudal cirri. An increased number of caudal cirri is found also in *Notohymena australis*, *Gastrostyla dorsicirrata*, and *Allotricha mollis*, all being "typical" oxytrichids producing dorsal kinety 4 by a split of kinety 3, in contrast to *Hemioxytricha*. This indicates that more than three caudal cirri evolved several times independently. Thus, we raise these species to genus rank.

Aponotohymena nov. gen.

Diagnosis: Flexible Oxytrichidae with 18 fronto-ventral-transverse cirri and more than 3 caudal cirri associated with dorsal kineties 1, 2, 4; kinety 3 produces kinety 4.

Type species: *Aponotohymena australis* (Foissner & O´Donoghue, 1990) nov. comb. (basionym: *Oxytricha australis* Foissner & O´Donoghue, 1990). Monotypic!

Etymology: The name is a composite of the Greek prefix *apo* (derived from) and the genus-group name *Notohymena.* Feminine gender.

Gastrostylides nov. gen.

Diagnosis: Flexible or semirigid oxytrichids with more than 18 fronto-ventral-transverse cirri and more than three caudal cirri associated with dorsal kineties 1, 2, 4; kinety 3 produces kinety 4.

Type species: *Gastrostylides dorsicirratus* (Foissner, 1982) nov. comb. (basionym: *Gastrostyla dorsicirrata* Foissner, 1982). Monotypic!

Etymology: The name is a composite of the Greek suffix *-ides* (similar to; related; deviating) and the genus-group name *Gastrostyla.* Masculine gender.

Remarks: Possibly, *Gastrostyla (Spetastyla) mystacea minima* Hemberger, 1985 also belongs to *Gastrostylides* because one third of the specimens have four caudal cirri (Foissner et al. 2002).

Allotrichides nov. gen.

Diagnosis: Flexible oxytrichids with 18 fronto-ventral-transverse cirri, multiple marginal cirral rows, and 3 caudal cirri produced by dorsal kineties 1, 2, 4; kinety 3 produces kinety 4.

Type species: *Allotrichides antarcticus* (Berger, 1999) nov. comb. (basionym: *Onychodromopsis flexilis* Petz & Foissner, 1996). Monotypic!

Etymology: The name is a composite of the Greek suffix *-ides* (similar to; related; deviating) and the genus-group name *Allotricha.* Masculine gender.

Remarks: *Allotricha mollis*, type of the genus, has more than three caudal cirri. Thus, a new genus has to be established for *A. antarctica* which has usually only three caudal cirri. See Berger (1999) for details of classification.

Hemioxytricha isabelae Foissner & Liebetreu nov. spec. (Fig. 260a–h, 261a–g; Table 99)

Diagnosis: Size in vivo about 100 × 25 µm; narrowly ellipsoid. Four macronuclear nodules and two large micronuclei. Cortical granules in closely spaced, discontinuous rows, colourless, 0.7–1 µm across in vivo. Transverse cirri protruding from body proper; buccal cirrus near anterior end of paroral. 4 dorsal kineties and an average six caudal cirri. Adoral zone extends 26% of body length on average, composed of about 20 membranelles.

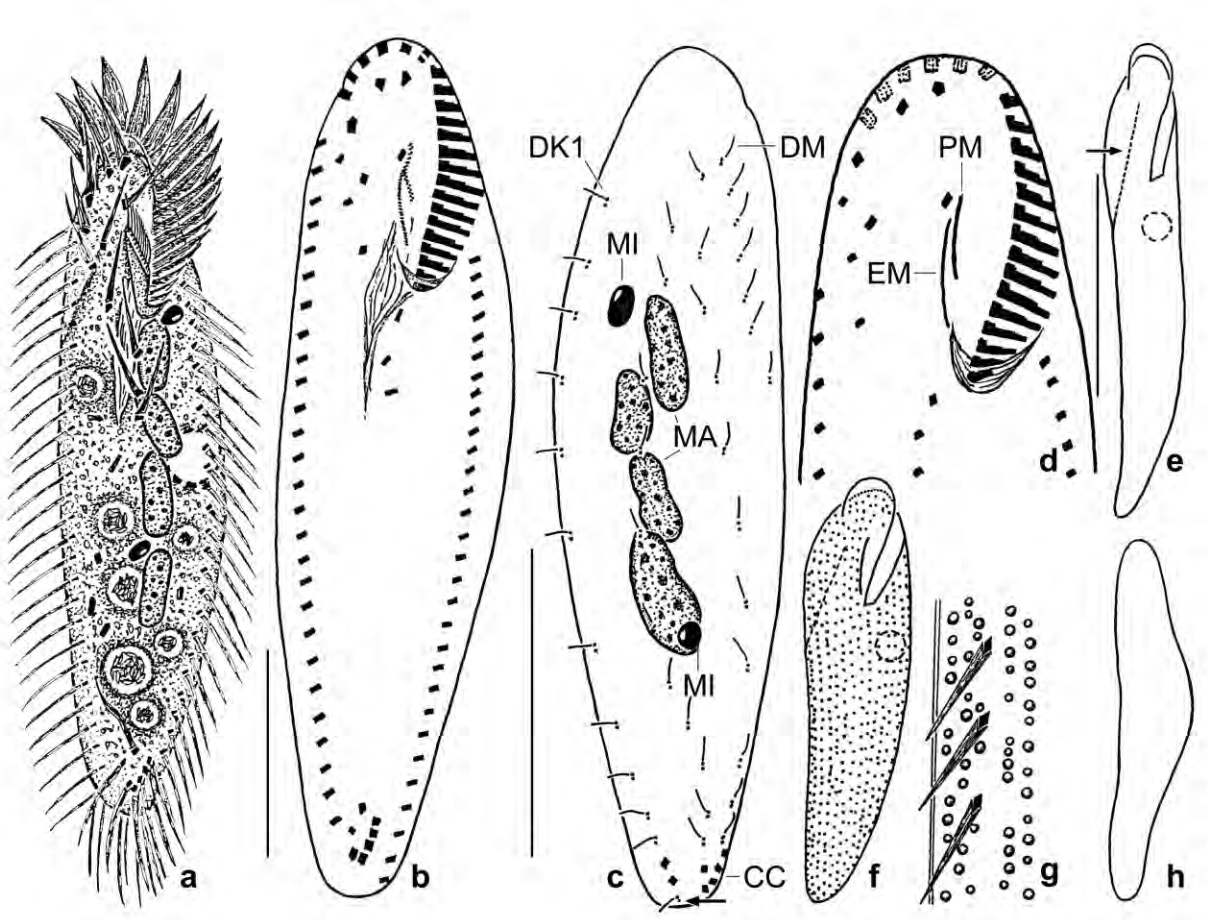

Fig. 260a–h. *Hemioxytricha isabelae* from life (a, e–h) and after protargol impregnation (b, c, d). **a:** Ventral view of a representative specimen, length 100 µm, having ingested many bacterial rods. **b, c:** Ventral and dorsal view of holotype specimen, showing the infraciliature and the nuclear apparatus, length 85 µm. In this specimen, the distance between the posterior end of the cell and the right marginal row is comparatively large (cp. Table 99). Arrow marks an additional kinetid posterior to the caudal cirri of kinety 1. **d:** Ventral view, showing details of the infraciliature. **e, f:** Shape variants. Arrow marks the furrow along the dorsomarginal kinety. In (f), the dense cortical granulation is indicated. **g:** The cortical granules are strongly refractive and 0.7–1 µm across. **h:** Lateral view. CC – caudal cirri, DK1 – dorsal kinety 1, DM – dorsomarginal kinety, EM – endoral membrane, MA – macronuclear nodules, MI – micronuclei, PM – paroral membrane. Scale bars 30 µm.

Type locality: Galápagos site (68), i. e., highly saline (~ 30‰) soil and bark from a mangrove forest near the village of Puerto Villamil, Galápagos, south coast of Isabela Island, 0°57'S 90°57'W.

Type material: 1 holotype and 2 paratype slides with protargol-impregnated specimens have been deposited in the Biology Centre of the Upper Austrian Museum in Linz (LI). Relevant specimens have been marked by black ink circles on the coverslip.

Etymology: Named after the island it was discovered, i. e., Isabela Island of the Galápagos archipelago.

Description: This species is rather fragile. Thus, Stieve's fixative was enriched with some drops of osmiumtetroxide (2%). Size in vivo 80–120 × 20–35 µm, usually about 100 × 25 µm, as calculated from some in vivo measurements and the morphometric data in Table 99 adding 15%

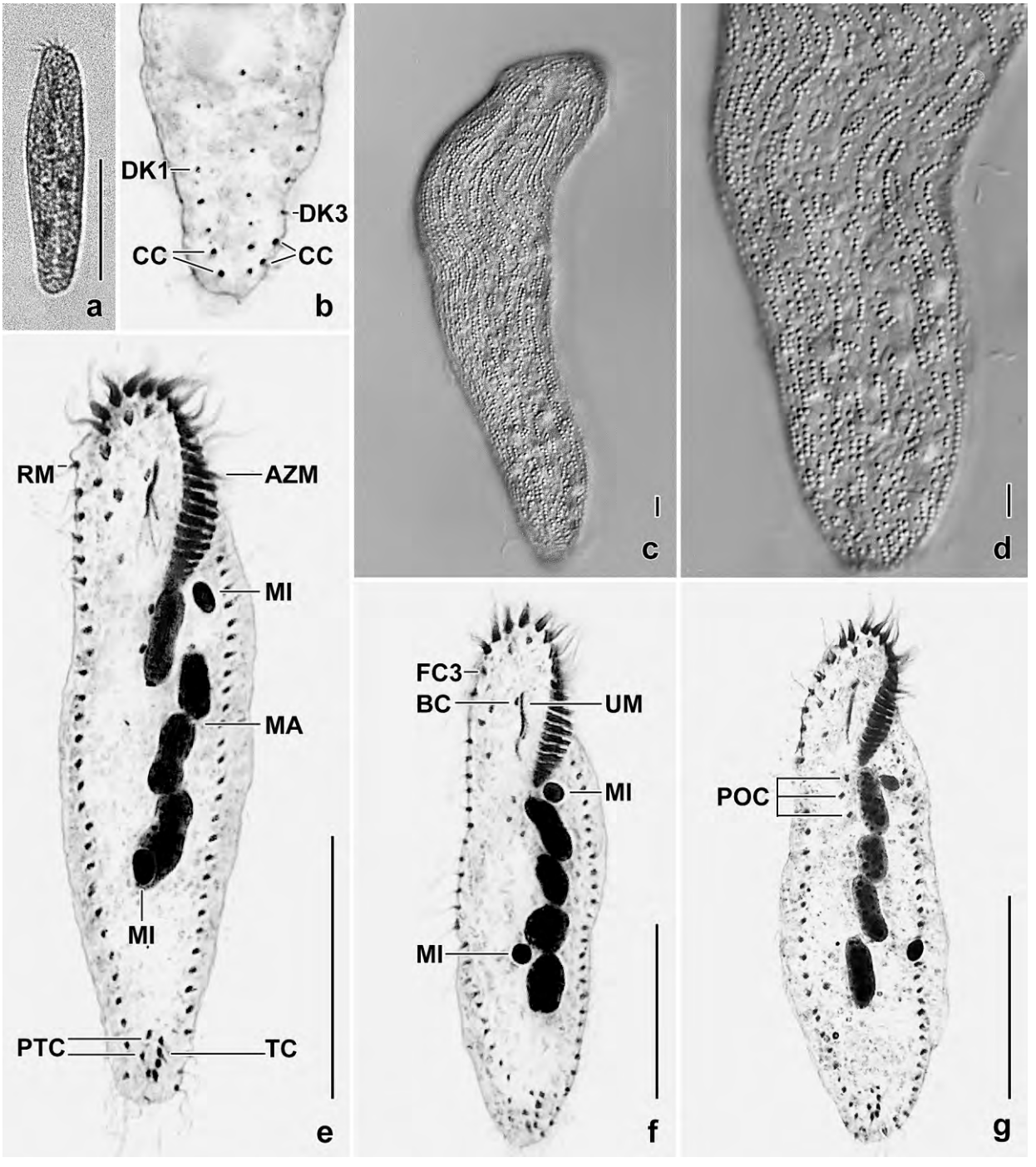

Fig. 261a–g. *Hemioxytricha isabelae* from life (a, c, d) and after protargol impregnation (b, e–g). **a:** Dorsal view of a freely motile specimen, showing the inconspicuous shape. **b:** Posterior body end, showing six caudal cirri. **c, d:** Surface views, showing the cortical granules which form discontinuous rows. The granules are rather refractive and thus easily to recognize although they are colourless. **e–g:** Ventral views, showing the infraciliature and the typical nuclear apparatus composed of four macronuclear nodules and two large micronuclei. AZM – adoral zone of membranelles, BC – buccal cirrus, CC – caudal cirri, DK1, 3 – dorsal kineties, FC3 – frontal cirrus 3, MA – macronucleus, MI – micronuclei, POC – postoral cirri, PTC – pretransverse cirri, RM – right marginal cirral row, UM – undulating membranes. Scale bars 3 µm (c, d), 30 µm (e–g), and 50 µm (a).

Table 99. Morphometric data on *Hemioxytricha isabelae* based on mounted, protargol-impregnated, and randomly selected specimens from a non-flooded Petri dish culture. Measurements in µm. CV – coefficient of variation in %, M – median, Max – maximum, Mean – arithmetic mean, Min – minimum, n – number of individuals investigated, SD – standard deviation, SE – standard error of arithmetic mean.

Characteristics	Mean	M	SD	SE	CV	Min	Max	n
Body, length	84.7	85.0	7.0	1.5	8.3	73.0	105.0	21
Body, width	22.4	21.0	2.9	0.6	12.9	19.0	29.0	21
Body length:width, ratio	3.8	3.9	0.4	0.1	11.7	2.8	4.6	21
Anterior body end to proximal end of adoral zone, distance	22.6	22.0	1.7	0.4	7.7	19.0	25.0	21
Body length:length of adoral zone, ratio	3.8	3.7	0.4	0.1	11.1	3.2	4.8	21
Anterior body end to first frontoventral cirrus, distance	11.8	12.0	1.5	0.3	12.6	9.0	14.0	21
Anterior body end to last frontoventral cirrus, distance	19.4	20.0	2.0	0.4	10.1	15.0	22.0	21
Anterior body end to buccal cirrus, distance	9.9	10.0	1.2	0.3	11.9	7.0	12.0	21
Anterior body end to right marginal row, distance	9.9	10.0	2.2	0.5	22.5	6.0	13.0	21
Anterior body end to left marginal row, distance	21.2	21.0	1.6	0.3	7.4	17.0	24.0	21
Anterior body end to first postoral cirrus, distance	25.2	25.0	1.6	0.3	6.2	23.0	29.0	21
Anterior body end to last postoral cirrus, distance	32.2	32.0	1.9	0.4	5.8	29.0	35.0	21
Anterior body end to last postoral cirrus:body length, ratio (%)	38.2	38.3	3.3	0.7	8.6	31.4	44.3	21
Posterior body end to rearmost transverse cirrus, distance	3.1	3.0	1.0	0.2	32.2	1.0	5.0	21
Posterior body end to right marginal row, distance	4.1	4.0	1.4	0.3	34.4	2.0	7.0	21
Posterior body end to left marginal row, distance	3.3	3.0	1.3	0.3	38.7	2.0	7.0	21
Anterior body end to paroral membrane, distance	9.0	9.0	1.3	0.3	14.2	7.0	11.0	21
Paroral membrane, length	7.6	8.0	1.0	0.2	12.9	6.0	10.0	21
Anterior body end to endoral membrane, distance	11.7	12.0	1.3	0.3	11.0	9.0	14.0	21
Endoral membrane, length	10.7	11.0	1.0	0.2	9.4	9.0	13.0	21
Anterior body end to first macronuclear nodule, distance	24.9	25.0	2.3	0.5	9.4	20.0	29.0	21
Nuclear figure, length	38.4	38.0	3.6	0.8	9.3	33.0	46.0	21
Anterior macronuclear nodule, length	9.6	10.0	1.4	0.3	14.2	6.0	12.0	21
Anterior macronuclear nodule, width	4.4	4.0	1.0	0.2	22.2	3.0	6.0	21
Macronuclear nodules, number	4.0	4.0	0.0	0.0	0.0	4.0	4.0	21
Anterior micronucleus, length	4.0	4.0	0.8	0.2	19.4	3.0	6.0	21
Anterior micronucleus, width	2.3	2.0	–	–	–	2.0	3.0	21
Micronuclei, number	2.0	2.0	0.0	0.0	0.0	2.0	2.0	21
Adoral membranelles, number	20.1	20.0	1.2	0.3	5.9	18.0	22.0	21
Largest membranellar basis, width	4.2	4.0	–	–	–	4.0	5.0	21
Frontal cirri, number [a]	3.0	3.0	0.0	0.0	0.0	3.0	3.0	21
Frontoventral cirri, number [a]	4.0	4.0	0.0	0.0	0.0	4.0	4.0	21
Buccal cirri, number	1.0	1.0	0.0	0.0	0.0	1.0	1.0	21
Postoral cirri, number	3.0	3.0	0.0	0.0	0.0	3.0	3.0	21
Pretransverse cirri, number [a]	1.8	2.0	–	–	–	1.0	2.0	21
Transverse cirri, number [a]	4.6	5.0	–	–	–	4.0	5.0	21
Right marginal row, number of cirri	26.8	28.0	2.7	0.6	10.2	21.0	31.0	21
Left marginal row, number of cirri	27.4	27.0	2.4	0.5	8.8	20.0	31.0	21
Caudal cirri, number	5.6	6.0	0.7	0.1	11.9	4.0	7.0	21
Dorsal bristle rows, number	4.0	4.0	0.0	0.0	0.0	4.0	4.0	21

continued

Characteristics	Mean	M	SD	SE	CV	Min	Max	n
Bristles in dorsal row 1, number	10.1	10.0	1.9	0.4	18.3	8.0	14.0	21
Bristles in dorsal row 2, number	11.5	11.0	1.9	0.6	16.3	8.0	14.0	11
Bristles in dorsal row 3, number	12.6	13.0	1.5	0.5	11.9	10.0	15.0	11
Bristles in dorsal row 4, number	6.7	7.0	1.1	0.2	16.7	5.0	8.0	21

[a] Of 22 specimens analysed, one has 2 frontal cirri, one has 3 frontoventral cirri, one has 3 pretransverse cirri, and one has 3 transverse cirri.

preparation shrinkage. Body length:width ratio in vivo 3–4.2:1, after protargol impregnation 2.8–4.6:1, on average 3.8:1. Narrowly ellipsoid and indistinctly sigmoid, left margin slightly convex, right straight; ventral side flat, dorsal slightly convex; right of kinety 4 flattened, producing a distinct ridge (Fig. 260a, e, f, h). Nuclear apparatus on average in middle quarters of cell, slightly left of midline, consists of four macronuclear nodules and two micronuclei. Macronuclear nodules arranged almost serially, anterior nodule commences near level of buccal vertex (Fig. 260a, c, 261e–g; Table 99); slenderly ellipsoid to almost globular, sometimes dumbbell-shaped, on average 10 × 4 µm in protargol preparations; nucleoli 0.5–1 µm across. One micronucleus close to left anterior half of anterior macronuclear nodule, the second in posterior half of posterior nodule or in vertex of third and fourth nodule (10 and 11 out of 21 specimens, respectively), conspicuously large, i. e., about 6 × 4 µm in vivo and 4 × 2 µm on average after protargol impregnation; three micronuclei in two out of 30 specimens investigated (Fig. 260a, c, 261e–g; Table 99). Contractile vacuole in or near mid-body at left cell margin (Fig. 260a, e); no activity observed, probably due to the highly saline environment. Cortex very flexible; cortical granulation conspicuous because in dense, slightly discontinuous rows and granules rather strongly refractive; individual granules colourless and 0.7–1 µm across (Fig. 260f, g, 261c, d). Cytoplasm colourless, with some scattered crystals 2–3 µm in size and many food vacuoles 4–8 µm across in vivo and containing bacteria (Fig. 260a, 261a). Glides rapidly.

Most cirri 12 µm long in vivo, cirral pattern ordinarily oxytrichid, i. e., usually 18 cirri (Berger 1999): three slightly enlarged frontal cirri, four frontoventral cirri, one buccal cirrus right of anterior end of paroral membrane, three postoral cirri, two pretransverse cirri, and five transverse cirri (Fig. 260a, b, d, 261e–g; Table 99); pretransverse and transverse cirri 15 µm long in vivo and thus distinctly projecting from body proper. Right marginal row commences at level of anterior frontoventral cirrus (= cirrus VI/4), composed of 28 cirri on average; left marginal row extends almost to body's midline posteriorly, composed of 27 cirri on average. Ontogenesis commences with an anlage close to the third postoral cirrus.

Dorsal bristles about 3 µm long in vivo, arranged in four rows (Fig. 260c, 261b; Table 99). Row 1 slightly shortened anteriorly, composed of 10 bristles on average; row 2 shortened anteriorly, slightly sigmoid, extends to right posterior end of cell, composed of 11 bristles on average; row 3 slightly shortened anteriorly, extends obliquely from anterior midline to right posterior end of cell, composed of 13 bristles on average; row 4 dorsomarginal, terminates distinctly anterior to mid-body, composed of 7 bristles on average. Four to seven, on average six caudal cirri associated with kineties 1, 2 and 3; about 12 µm long after protargol impregnation; in 4 out of 30 specimens an additional dikinetid posterior to caudal cirri (Fig. 260c; Table 99).

Adoral zone extends 20–32%, on average 26% of body length after protargol impregnation, of ordinary shape, composed of an average of 20 membranelles of usual structure and with cilia up to

12 µm long; largest membranellar bases about 5 µm width in vivo and in protargol preparations (Fig. 260a, b, d, 261e–g; Table 99). Buccal cavity narrow and shallow, buccal lip angularly projecting, bears paroral membrane in distinct cleft (Fig. 260a). Undulating membranes slightly curved and optically intersecting in anterior third or close together (Fig. 260b, d, 261e, f). Endoral and paroral 11 and 8 µm long on average, respectively; paroral cilia about 5 µm long in vivo. Pharyngeal fibres extend to mid-body.

Occurrence and ecology: As yet found only at the highly saline (~ 30‰) type locality 10 days after rewetting the sample.

Remarks: *Hemioxytricha isabelae* can easily be distinguished from most *Oxytricha* species by the four macronuclear nodules, a feature only shared with *Oxytricha islandica*, which, however, lacks cortical granules and has only three caudal cirri. → *Lepidothrix dorsiincisura* is fairly similar to *H. isabelae* due to its dorsal furrow, the four dorsal bristle rows, and the four macronuclear nodules, but it can be distinguished by the larger oral region, the arrangement of its cortical granules (reticulate vs. densely spaced discontinuous rows), and the number of transverse and pretransverse cirri (three vs. five and two).

Urosomoididae nov. fam.

Diagnosis: Flexible Oxytrichinae, as defined by Berger (1999), with less than 18 fronto-ventral-transverse cirri and 4 or 5 dorsal kineties of which kineties 4 and 5 originate dorsomarginally. Oral apparatus usually inconspicuous.

Type genus: *Urosomoida* Hemberger in Foissner, 1982.

Genera assignable: *Urosomoida* Hemberger 1985 in Foissner, 1982, with eight species: *U. agilis* (Engelmann, 1862) Hemberger in Foissner, 1982 (type species); *U. agiliformis* Foissner, 1982; *U. minima* Hemberger, 1985; *U. granulifera* Foissner, 1996a; *U. deserticola* Foissner et al., 2002; *U. namibiensis* Foissner et al., 2002; → *U. halophila* nov. spec., → *U. galapagensis* nov. spec. → *Lepidothrix* nov. gen. with *L. dorsiincisura* as type (basionym: *Urosomoida dorsiincisura* Foissner, 1982). → *Oxytrichella* nov. gen. (with four species mentioned below; type → *O. mahadjacola* nov. spec.); *Hemiurosomoida* Singh & Kamra, 2015 (type: *Oxytricha longa* Gelei & Szabados, 1950); *Paraurosomoida* Singh & Kamra, 2013 (monotypic with *P. indiensis* as type), and *Erimophrya* Foissner et al., 2002 with *E. glatzeli* as type and three further species: *E. arenicola* Foissner et al., 2002; *E. sylvatica* Foissner et al., 2005a; and *E. quadrinucleata* Foissner et al., 2005a. See Berger (1999) and Shao et al. (2015) for morphological descriptions. See also → *Hemioxytricha* and → *Quadristicha*.

Remarks: There are several *Urosomoida*-like genera with or without 18 FVT-cirri and only two or three dorsal kineties: *Apourosomoida* Foissner et al., 2002; *Vermioxytricha* Foissner et al., 2002; and *Heterourosomoida* Singh & Kamra, 2015.

The main differences between the Oxytrichidae and Urosomoididae are the number of FVT-cirri (18 vs. less) and dorsal kinety 3 (fragmenting vs. not fragmenting).

Unfortunately, molecular sequences are available only for a few genera and species classified into the new family. The most recent "*Urosomoida* tree" is flawed by low bootstrap values hardly providing reliable support for all flexible oxytrichids included (Singh & Kamra 2015). But this is common in hypotrichs (Schmidt et al. 2007, Paiva et al. 2009, Foissner et al. 2014a). Obviously, more genes must be studied because the hypotrichs are full of plesiomorphies (Foissner et al. 2004, Foissner & Stoeck 2011).

Oxytrichella nov. gen.

Diagnosis: *Urosomoidae* with a single micronucleus between two macronuclear nodules.

Type species: *Oxytrichella mahadjacola* nov. spec.

Etymology: The name is a composite of the generic name *Oxytricha* and the Latin diminutive *ellus*, meaning a small *Oxytricha*. Feminine gender.

Species assignable: *Oxytrichella buitkampi* (Dragesco & Dragesco-Kerneis, 1986) nov. comb (basionym: *Oxytricha setigera* Buitkamp, 1977a), *Oxytrichella perthensis* (Foissner & O`Donoghue, 1990) nov. comb. (basionym: *Urosomoida perthensis* Foissner & O`Donoghue, 1990); *Oxytrichella monostyla* (Foissner, Agatha & Berger, 2002) nov. comb. (basionym: *Urosomoida monostyla* Foissner, Agatha & Berger, 2002) nov. comb., and → *Oxytrichella mahadjacola* nov. spec. (type; see below).

Remarks: For reasoning of the new genus, see → *Monomicrocaryon*. The biogeographic distribution of the four species is remarkable (for data, see Berger 1999). *Oxytrichella perthensis* occurs in Australia and in South Africa, *O. monostyla* and *O. buitkampi* occur in Africa, and → *O. mahadjacola* was discovered in Venezuela, South America. All species are infrequent, i. e., have been found only at their type locality. Of course, further research might increase their range but not greatly because we did not find them in about 1000 other soil samples investigated.

Oxytrichella mahadjacola nov. spec. (Fig. 262a–c, 263a–f; Table 100)

Diagnosis: Size in vivo about 50 × 17 µm; elongate ellipsoid. 2 macronuclear nodules and 1 micronucleus in between. Buccal cirrus right of posterior end of undulating membranes; 4 frontoventral cirri, 3 posterior of buccal vertex; 3 postoral cirri in mid-body; 4 transverse and 2 pretransverse cirri. Right marginal cirral row commences in mid-body, composed of an average of 4 cirri. 4 dorsal kineties with up to 8 µm long bristles; kinety 1 with a one-bristle-wide gap posterior to mid-body; 3 caudal cirri. Adoral zone extends about 31% of body length, composed of an average of 15 membranelles.

Type locality: Venezuelan site (23), i. e., Mahadja soil from the surroundings of the village of El Sapo, about 50 km north of Pt. Ayacucho, 67°36'W 5°41'N.

Type material: 1 holotype and 3 paratype slides with protargol-impregnated specimens have been deposited in the Biology Centre of the Upper Austrian Museum in Linz (LI). The holotype

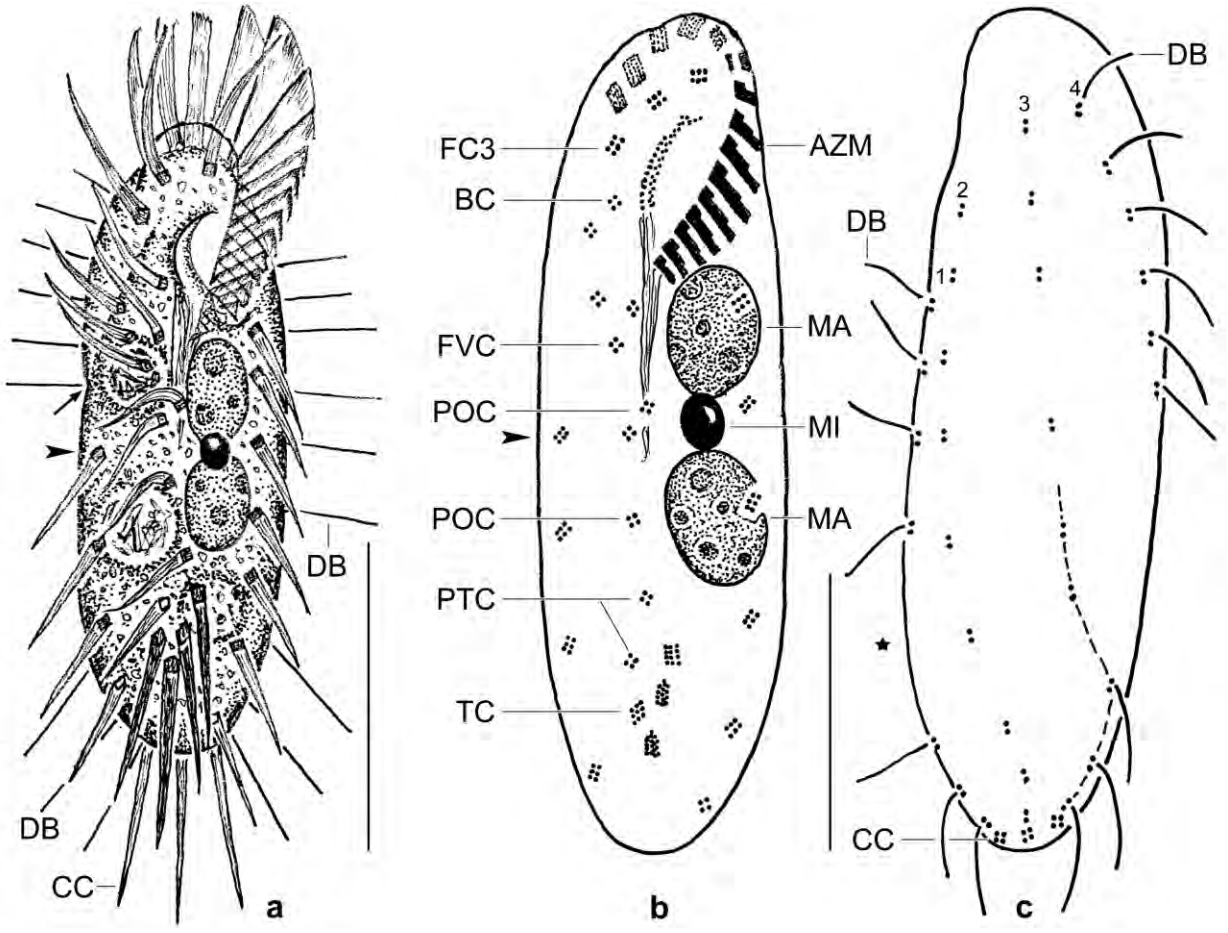

Fig. 262a–c. *Oxytrichella mahadjacola* from life (a) and after protargol impregnation (b, c). **a:** Ventral view of a representative specimen, length 50 µm. The arrow marks the posterior end of dorsal kinety 4, where the height of the dorsal body suddenly increases causing an oblique line. The arrowhead denotes the first cirrus of the right marginal row. **b, c:** Ventral and dorsal view of holotype specimen, length 45 µm. The arrowhead marks the first cirrus of the right marginal row. The asterisk denotes a gap in dorsal kinety 1. AZM – adoral zone of membranelles, BC – buccal cirrus, CC – caudal cirri, DB – dorsal bristles, FC3 – frontal cirrus 3, FVC – frontoventral cirri, MA – macronuclear nodules, MI – micronucleus, POC – postoral cirri, PTC – pretransverse cirri, TC – transverse cirri. Scale bars 25 µm (a) and 15 µm (b, c).

and other relevant specimens have been marked by black ink circles on the coverslip.

Etymology: The name is a composite of *Mahadja* (a special agricultural practice mixing excrements with soil) and the Latin verb *colere* (to live in), referring to the habitat the species was discovered.

Description: Size in vivo 40–65 × 14–20 µm, usually about 50 × 17 µm, as calculated from some in vivo measurements and the morphometric data in Table 100 adding 15% preparation shrinkage; up to 2:1 flattened, ventral side flat, dorsal more or less convex. Body elongate ellipsoid, rarely elongate quadrangular with rounded ends (Fig. 263c); right of dorsal kinety 4 a sudden elevation of dorsal body in anterior half of cell, producing a minute indentation in outline of body and an oblique line when viewed ventrally or dorsally (Fig. 262a, 263a, b). Nuclear apparatus in central third of body left of midline (Fig. 262a, b, 263a–d; Table 100). Macronuclear nodules almost abutting, globular to ellipsoid, on average broadly ellipsoid in protargol preparations;

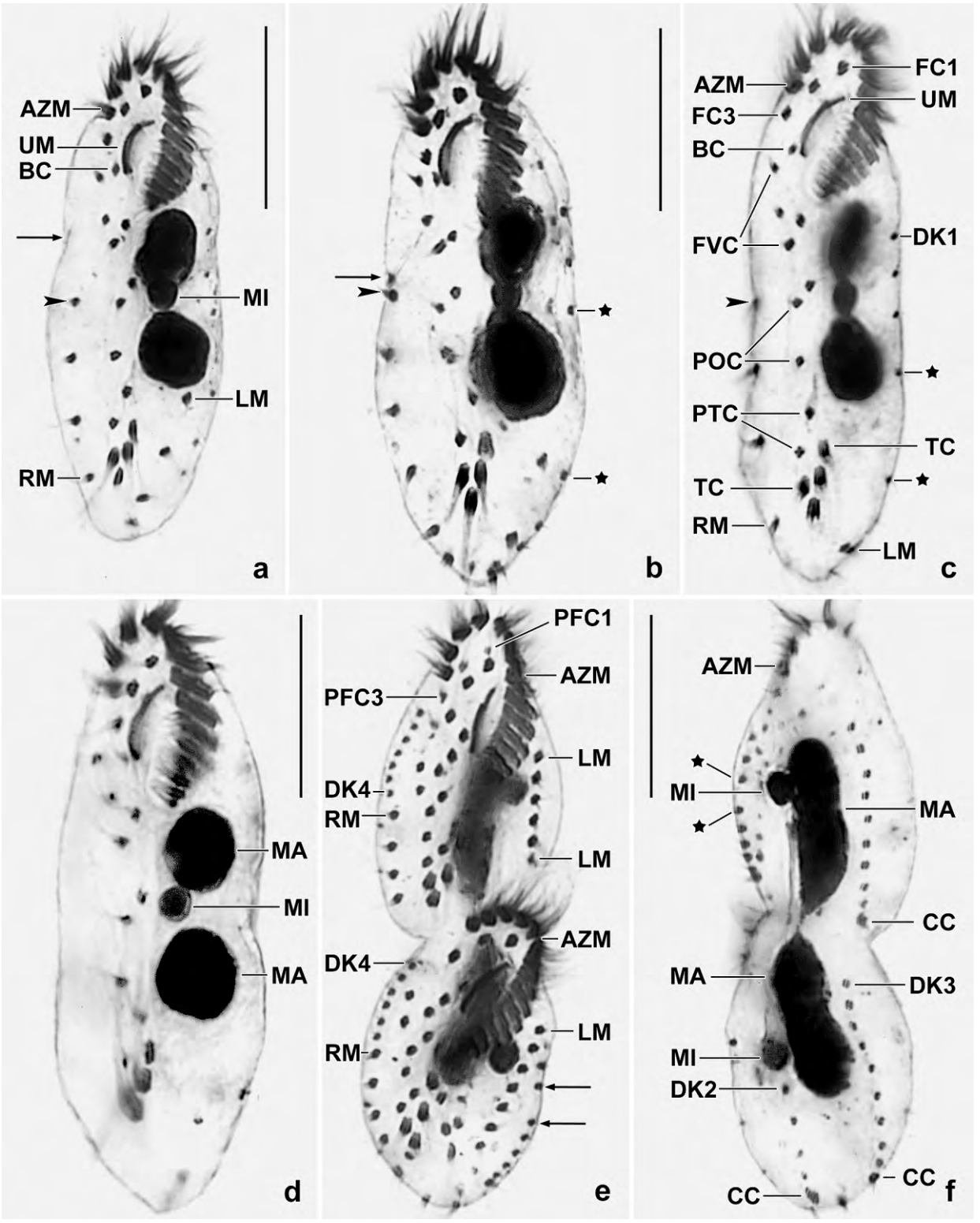

Fig. 263a–f. *Oxytrichella mahadjacola,* ventral (a–e) and dorsal (f) views. Asterisk mark gap in dorsal kinety 1, arrows denote indentation caused by dorsal kinety 4, and arrowheads denote begin of right marginal row. AZM – adoral zone, BC – buccal cirrus, CC – caudal cirri, DK1–4 – dorsal kineties, FC1, 3 – frontal cirri, FVC – frontoventral cirri, LM – left marginal row, MA – macronuclear nodules, MI – micronucleus, PFC1, 3 – parental frontal cirri, POC – postoral cirri, PTC – pretransverse cirri, RM – right marginal row, TC – transverse cirri, UM – undulating membranes. Scale bars 15 μm.

nucleoli scattered throughout macronuclear nodules, globular and of ordinary size. Micronucleus in between or in vertex of macronuclear nodules, globular to broadly ellipsoid, rather refractive and thus easily recognizable in vivo. Contractile vacuole in left body margin in or near mid-body. Cortex very flexible, colourless, without specific granules. Cytoplasm without peculiarities, food vacuoles up to 7 µm across and likely containing bacteria.

Cirral pattern urosomoid, i. e., only 17 FVT-cirri because one transverse cirrus is lacking (Fig. 262a, b, 263a–d; Table 100). Frontal cirri each composed of six, rarely of eight basal bodies, about 15 µm long in vivo, third cirrus comparatively distant from anterior body end, i. e., at level of mid buccal cavity; buccal cirrus right of posterior end of undulating membranes, composed of four basal bodies; four frontoventral cirri each composed of four basal bodies, the last three cirri posterior of buccal vertex, postoral cirri thus in mid-body each composed of four basal bodies; two pretransverse and four transverse cirri, the latter about 15 µm long in vivo and slightly projecting from body proper, composed of approximately nine basal bodies. Right marginal cirral row commences in or near mid-body, composed of an average of only four cirri each made of six basal bodies; left marginal row in ordinary pattern, composed of an average of six cirri each made of six basal bodies except of last cirrus composed of only four basal bodies (Fig. 262a, b, 263a–d; Table 100).

Four dorsal kineties with bristles up to 8 µm long in vivo (Fig. 262a, c, 263b, c, e, f; Table 100). Kinety 1 distinctly shortened anteriorly, with a one-kinetid-wide gap in posterior half, composed of an average of eight dikinetids; kineties 2 and 3 extend slightly obliquely, each composed of an average of nine dikinetids; kinety 4 originates dorsomarginally (Fig. 263e, f), extends to near mid-body, composed of an average of six dikinetids. Caudal cirri associated with dorsal kineties 1, 2, and 3, each likely composed of four basal bodies.

Adoral zone extends 31% of body length, composed of an average of 15 membranelles of usual structure, largest bases about 4 µm width (Fig. 262a, b, 263a–d; Table 100). Buccal cavity of ordinary width but short and deep. Undulating membranes oblique and moderately curved, of similar length, optically extend side by side or one upon the other crossing near anterior end. Pharyngeal fibres distinct, extend to mid-body.

Occurrence and ecology: As yet found only at type locality, i. e., in a mixture of soil and excrements of domestic animals. Very rare in the non-flooded Petri dish culture.

Remarks: The four species assigned to the new genus *Oxytrichella* are rather difficult to separate in vivo. See Dragesco & Dragesco-Kerneis (1986) and Berger (1999) for the species mentioned in this paragraph. *Oxytrichella buitkampi* differs from → *O. mahadjacola* mainly by the right marginal cirral row (commencing far subapically vs. in mid-body), frontal cirrus 3 (distinctly vs. slightly posterior to first adoral membranelle), the buccal cirrus (distinctly anterior to buccal vertex vs. at level of buccal vertex), and the site (Africa vs. Venezuela). *Oxytrichella perthensis* differs from → *O. mahadjacola* by the arrangement of the frontoventral and postoral cirri (ordinary *Oxytricha* pattern vs. *mahadjacola* pattern), the number of marginal cirri (up to 19 vs. up to 7 per row), and the length of the dorsal bristles (10–15 µm vs. up to 8 µm). *Oxytrichella monostyla* Foissner et al. (2002) differs from *O. mahadjacola* by the buccal cirrus (near anterior

Table 100. Morphometric data on *Oxytrichella mahadjacola* based on mounted, protargol-impregnated, and randomly selected specimens from a non-flooded Petri dish culture. Measurements in µm. CV – coefficient of variation in %, M – median, Max – maximum, Mean – arithmetic mean, Min – minimum, n – number of individuals investigated, SD – standard deviation, SE – standard error of arithmetic mean.

Characteristics	Mean	M	SD	SE	CV	Min	Max	n
Body, length	44.2	44.5	5.1	1.5	11.5	37.0	56.0	12
Body, width	15.0	15.0	1.4	0.4	9.4	12.0	17.0	12
Body length:width, ratio	3.0	2.9	0.4	0.1	13.6	2.5	3.7	12
Anterior body end to proximal end of adoral zone of membranelles, distance	13.7	13.5	1.4	0.4	10.0	11.0	16.0	12
Anterior body end to undulating membranes, distance	5.0	5.0	0.4	0.1	8.5	4.0	6.0	12
Undulating membranes, length	5.0	5.0	0.4	0.1	8.5	4.0	6.0	12
Anterior body end to anterior macronuclear nodule, distance	12.8	13.0	1.7	0.5	13.0	10.0	15.0	12
Anterior body end to right marginal cirral row, distance	21.5	21.0	3.3	1.0	15.6	17.0	28.0	12
Anterior body end to buccal cirrus, distance	9.4	9.0	1.2	0.3	12.4	7.0	12.0	12
Anterior body end to last postoral cirrus, distance	25.9	26.5	2.6	0.8	10.2	22.0	30.0	12
Posterior body end to right marginal row, distance	4.6	4.0	1.1	0.3	23.6	3.0	7.0	12
Posterior body end to left marginal row, distance	1.3	1.0	–	–	–	0.0	2.0	12
Nuclear figure, length	17.9	17.0	2.4	0.7	13.1	14.0	22.0	12
Macronuclear nodules, distance in between	1.8	1.8	–	–	–	0.0	3.0	12
Anterior macronuclear nodule, length	8.2	8.0	1.3	0.4	16.4	7.0	11.0	12
Anterior macronuclear nodule, width	5.3	5.0	0.6	0.2	11.8	4.0	6.0	12
Macronuclear nodules, number	2.0	2.0	0.0	0.0	0.0	2.0	2.0	12
Micronucleus, length	2.9	3.0	0.4	0.1	13.4	2.0	3.5	12
Micronucleus, width	2.7	2.7	–	–	–	2.0	3.0	12
Micronucleus, number	1.0	1.0	0.0	0.0	0.0	1.0	1.0	12
Adoral membranelles, number	14.6	15.0	0.8	0.2	5.4	13.0	16.0	12
Adoral membranelles, length of longest base	3.7	4.0	–	–	–	3.0	4.0	12
Frontal cirri, number	3.0	3.0	0.0	0.0	0.0	3.0	3.0	12
Frontoventral cirri, number	4.0	4.0	0.0	0.0	0.0	4.0	4.0	12
Buccal cirri, number	1.0	1.0	0.0	0.0	0.0	1.0	1.0	12
Postoral cirri, number	3.0	3.0	0.0	0.0	0.0	3.0	3.0	12
Pretransverse cirri, number	2.0	2.0	0.0	0.0	0.0	2.0	2.0	12
Transverse cirri, number	4.0	4.0	0.0	0.0	0.0	4.0	4.0	12
Right marginal cirri, number	4.3	4.0	0.6	0.2	14.6	3.0	5.0	12
Left marginal cirri, number	6.4	6.5	0.7	0.2	10.4	5.0	7.0	12
Dorsal kineties, number	4.0	4.0	0.0	0.0	0.0	4.0	4.0	12
Dorsal bristles, length	6.8	7.0	1.2	0.3	17.5	6.0	9.0	12
Dorsal kinety 1, number of bristles in anterior fragment	3.2	3.0	–	–	–	3.0	4.0	12
Dorsal kinety 1, number of bristles in posterior fragment	4.4	4.0	–	–	–	4.0	5.0	12
Dorsal kinety 1, distance between anterior and posterior fragment	8.3	8.0	2.5	0.7	29.8	6.0	13.0	12
Dorsal kinety 1, total number of bristles	7.6	8.0	–	–	–	7.0	8.0	12
Dorsal kinety 2, number of bristles	8.7	9.0	0.7	0.2	7.5	8.0	10.0	12
Dorsal kinety 3, number of bristles	8.9	9.0	0.7	0.2	7.5	8.0	10.0	12
Dorsal kinety 4, number of bristles	6.1	6.0	0.7	0.2	11.0	5.0	7.0	12
Caudal cirri, number	3.0	3.0	0.0	0.0	0.0	3.0	3.0	12

vs. posterior end of undulating membranes), the number of postoral cirri (1 vs. 3), and the number of caudal cirri (2 vs. 3).

In vivo, *Oxytrichella mahadjacola* is easily mixed with → *Quadristicha setigera* because the differences are inconspicuous: 4 vs. 5 transverse cirri; dorsal kinety 1 with vs. without a break posterior to mid-body; dorsal bristles up to 8 µm long vs. 10–15µm.

Lepidothrix nov. gen.

Diagnosis: Flexible Oxytrichidae Ehrenberg, 1838 with less than 18 fronto-ventral-transverse cirri in *Oxytricha* pattern. 1 right and 1 left row of marginal cirri. 4 dorsal kineties of which kinety 4 is dorsomarginal. Buccal cavity moderately wide and deep; undulating membranes distinctly curved but not recurved, intersect optically, almost touch adoral zone of membranelles in left anterior corner of cell. Resting cyst with 2 size-types of colourless to indistinctly yellowish, globular lepidosomes.

Type species: *Urosomoida dorsiincisura* Foissner, 1982.

Etymology: The name is a composite of the Greek adjective *lepido* (covered with small scales) and the Greek noun *thrix* (hair ~ ciliate), referring to the lepidosomes of the resting cyst and the hair-like cirri. Feminine gender.

Species assignable: *Lepidothrix dorsiincisura* (Foissner, 1982) nov. comb. (basionym: *Urosomoida dorsiincisura* Foissner, 1982) and *Lepidothrix reticulata* (Foissner, Agatha & Berger 2002) nov. comb. (basionym: *Urosomoida reticulata* Foissner, Agatha & Berger, 2002). The two species match in most features but differ in the number of macronuclear nodules (4 vs. 2).

Remarks: Hypotrichs as diagnosed above are usually classified in *Urosomoida* (for reviews, see Berger 1999 and Foissner et al. 2002). However, the resting cysts of *U. agilis*, type of the genus, and of *U. agiliformis* Foissner, 1982 lack lepidosomes (Foissner, unpubl.), which I consider as a generic and thus most important character of *Lepidothrix*. Unfortunately, the resting cyst of *L. reticulata* has not been described. A second important feature concerns the oral apparatus, which is large compared with other *Urosomoida* species. Actually, it is quite similar to that of → *Fragmospina*, which has spinous cysts. A further feature common to *L. dorsiincisura* and *L. reticulata* is the crystalline, subcortical reticulum. Possibly, it can serve as a third genus character when further such species are discovered. However, this feature occurs also in some other hypotrichs, e. g. in *Erimophrya* Foissner et al., 2005a.

Lepidothrix dorsiincisura (Foissner, 1982) **nov. comb.** (Fig. 264a–k, 265a–s, 266a–z; Table 101)

Improved diagnosis (based on two populations): Size in vivo about 95 × 30 µm or about 120 × 45 µm. Body ellipsoid to slenderly obovate, in right anterior quadrant a rather distinct, oblique line caused by the steep slope of the dorsal body along kinety 4. Usually 4 ellipsoid

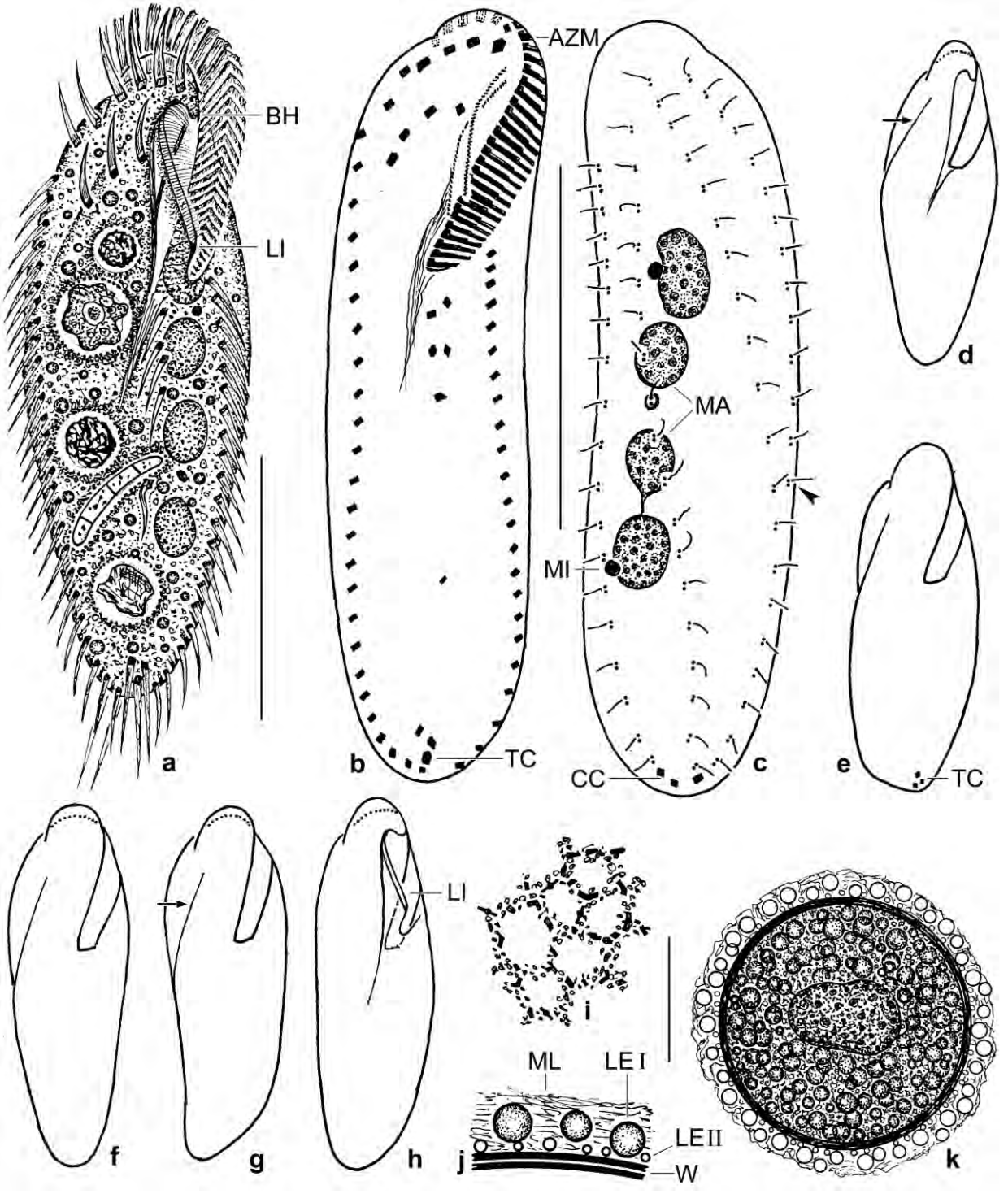

Fig. 264a–k. *Lepidothrix dorsiincisura* from life (a, d–k) and after protargol impregnation (b, c). **a:** Ventral view of a representative specimen, length 120 µm. Note the broad buccal lip. **b, c:** Ventral and dorsal view of a slender specimen with three caudal cirri. Arrowhead marks end of dorsal kinety 4. Note supernumerary cirri: 4 frontal instead of 3, 6 frontoventral instead of 5, 6 postoral instead of 3, and 3 caudal cirri instead of 2. **d–h:** Shape variability. Most but not all (h) specimens have a steep slope producing a more or less distinct line (arrows) right of dorsal kinety 4. **i:** Subcortical pattern of crystals and organic granules. **j, k:** Resting cyst, showing the thin wall covered with two types of lepidosomes. AZM – adoral zone of membranelles, BH – buccal horn, CC – caudal cirri, LE I, II – lepidosome types, LI – buccal lip, MA – macronuclear nodules, MI – micronucleus, ML – mucus layer, TC – transverse cirri, W – cyst wall. Scale bars 25 µm (k) and 50 µm (a–c).

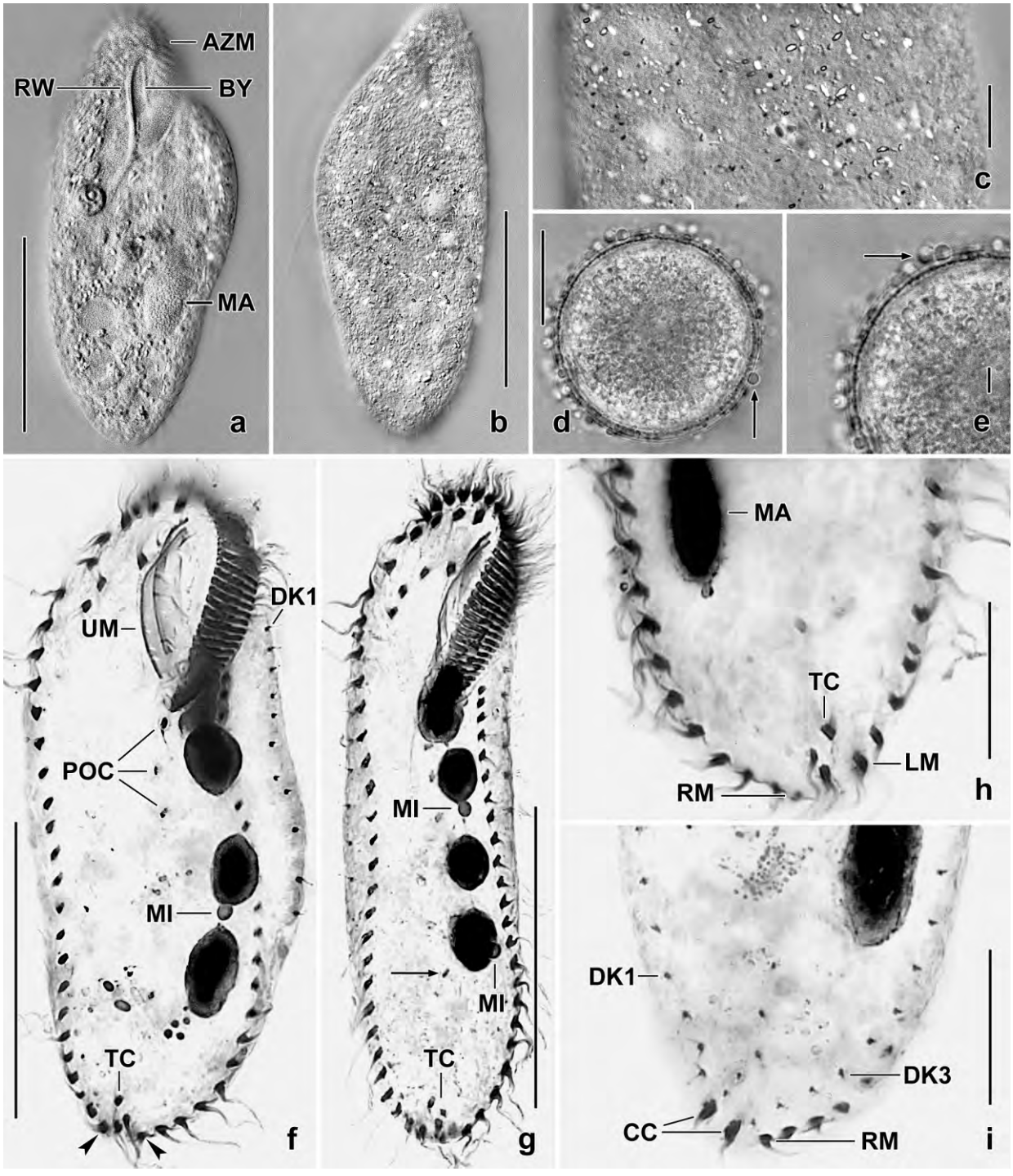

Fig. 265a–i. *L. dorsiincisura* from life (a–e) and after protargol impregnation (f–i). **a:** Ventral view of a slightly pressed specimen, showing the compact line produced by the dorsal wall of the buccal cavity. **b, c:** Minute crystals and organic granules form a subcortical reticulum. **d, e:** The resting cysts are covered by lepidosomes (arrows). **f, g:** Ventral view of an ordinary and of a slender specimen. Note the oxytrichid oral apparatus and the almost confluent marginal cirral rows (arrowheads). Arrow marks a supernumerary cirrus. **h, i:** *L. dorsiincisura* has three transverse cirri and two caudal cirri. AZM – adoral zone of membranelles, BY – buccal cavity, CC – caudal cirri, DK1, 3 – dorsal kineties, LM – left marginal row, MA – macronuclear nodules, MI – micronuclei, POC – postoral cirri, RM – right marginal row, RW – right wall of buccal cavity, TC – transverse cirri, UM – undulating membranes. Scale bars 5 µm (e), 10 µm (c, h, i), 25 µm (d), and 50 µm (a, b, f, g).

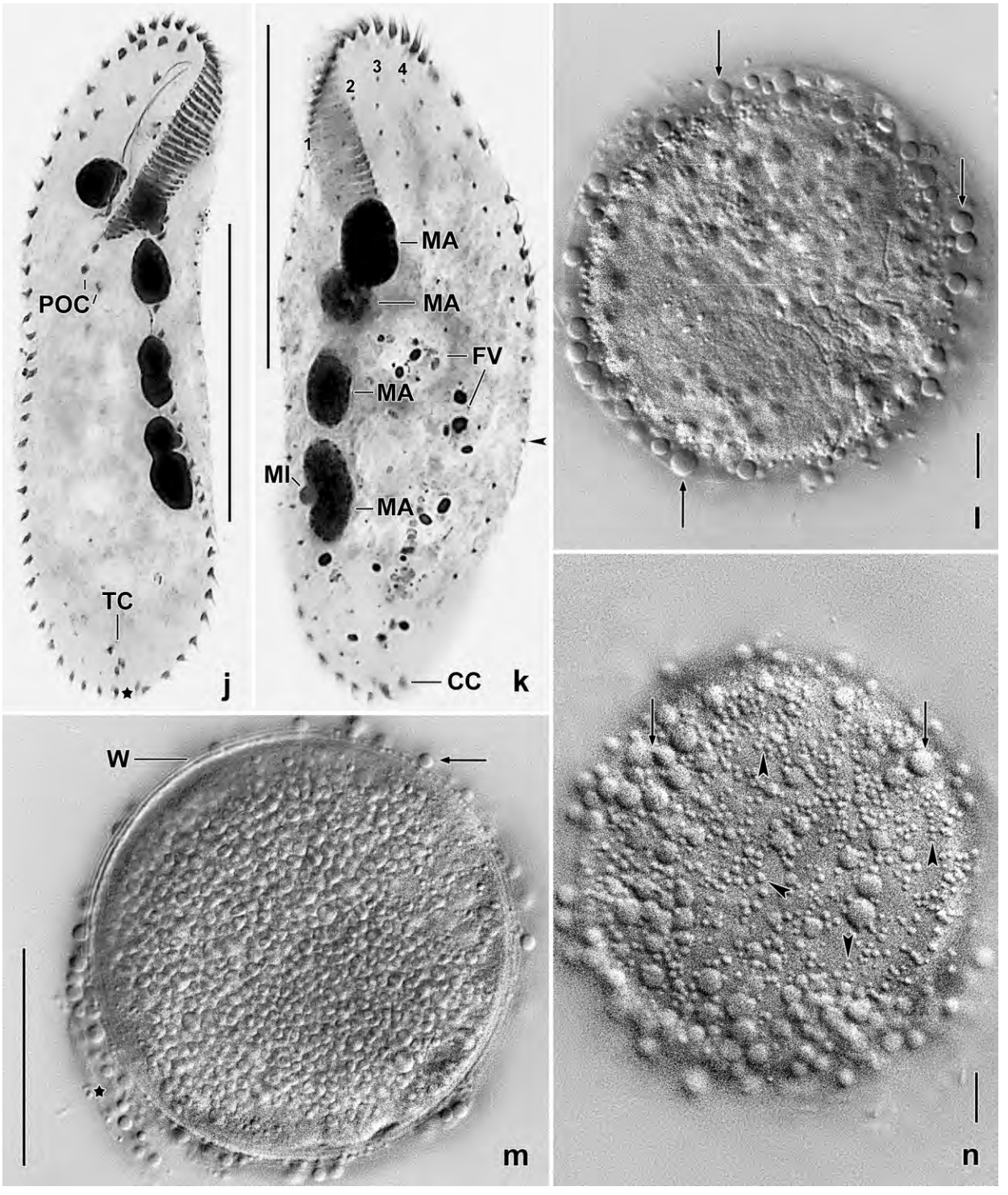

Fig. 265j–n. *Lepidothrix dorsiincisura* from life (l–n) and after protargol impregnation (j, k). **j:** Ventral view of a slender specimen. The marginal cirral rows are almost confluent (asterisk). **k:** Dorsal view of an ordinary specimen, showing the four bristle rows; row 4 is distinctly shortened (arrowhead). **l–n:** Resting cysts. Arrows mark large lepidosomes; arrowheads denote minute lepidosomes; asterisk (m) marks mucus and lepidosomes covering the cyst wall. CC – caudal cirri, FV – food vacuoles with spores of bazilli, MA – macronuclear nodules, MI – micronucleus, POC – postoral cirri, TC – transverse cirri, W – wall, 1–4 – dorsal bristle rows. Scale bars 5 µm (l, n), 25 µm (m), and 50 µm (j, k).

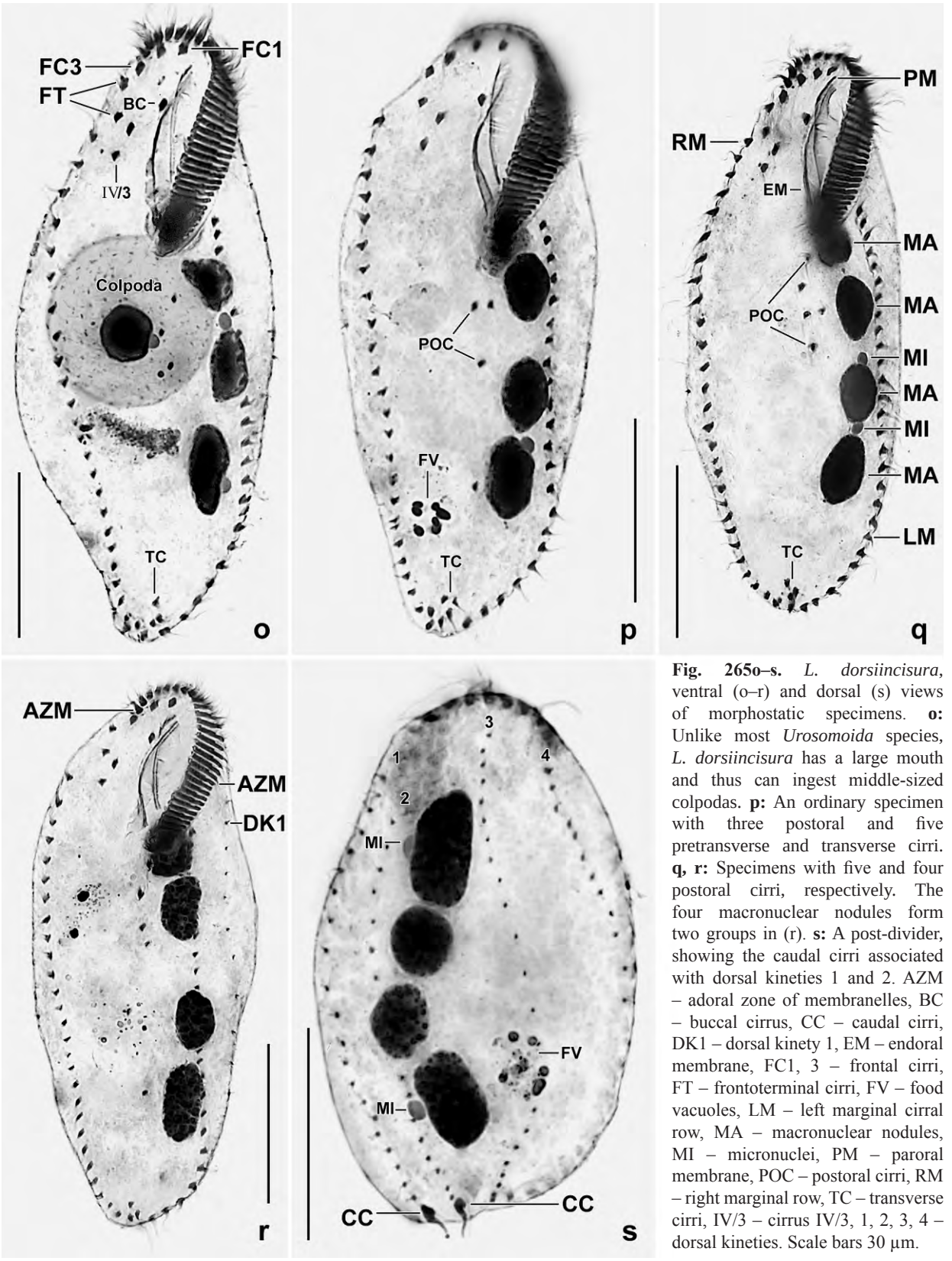

Fig. 265o–s. *L. dorsiincisura*, ventral (o–r) and dorsal (s) views of morphostatic specimens. **o:** Unlike most *Urosomoida* species, *L. dorsiincisura* has a large mouth and thus can ingest middle-sized colpodas. **p:** An ordinary specimen with three postoral and five pretransverse and transverse cirri. **q, r:** Specimens with five and four postoral cirri, respectively. The four macronuclear nodules form two groups in (r). **s:** A post-divider, showing the caudal cirri associated with dorsal kineties 1 and 2. AZM – adoral zone of membranelles, BC – buccal cirrus, CC – caudal cirri, DK1 – dorsal kinety 1, EM – endoral membrane, FC1, 3 – frontal cirri, FT – frontoterminal cirri, FV – food vacuoles, LM – left marginal cirral row, MA – macronuclear nodules, MI – micronuclei, PM – paroral membrane, POC – postoral cirri, RM – right marginal row, TC – transverse cirri, IV/3 – cirrus IV/3, 1, 2, 3, 4 – dorsal kineties. Scale bars 30 µm.

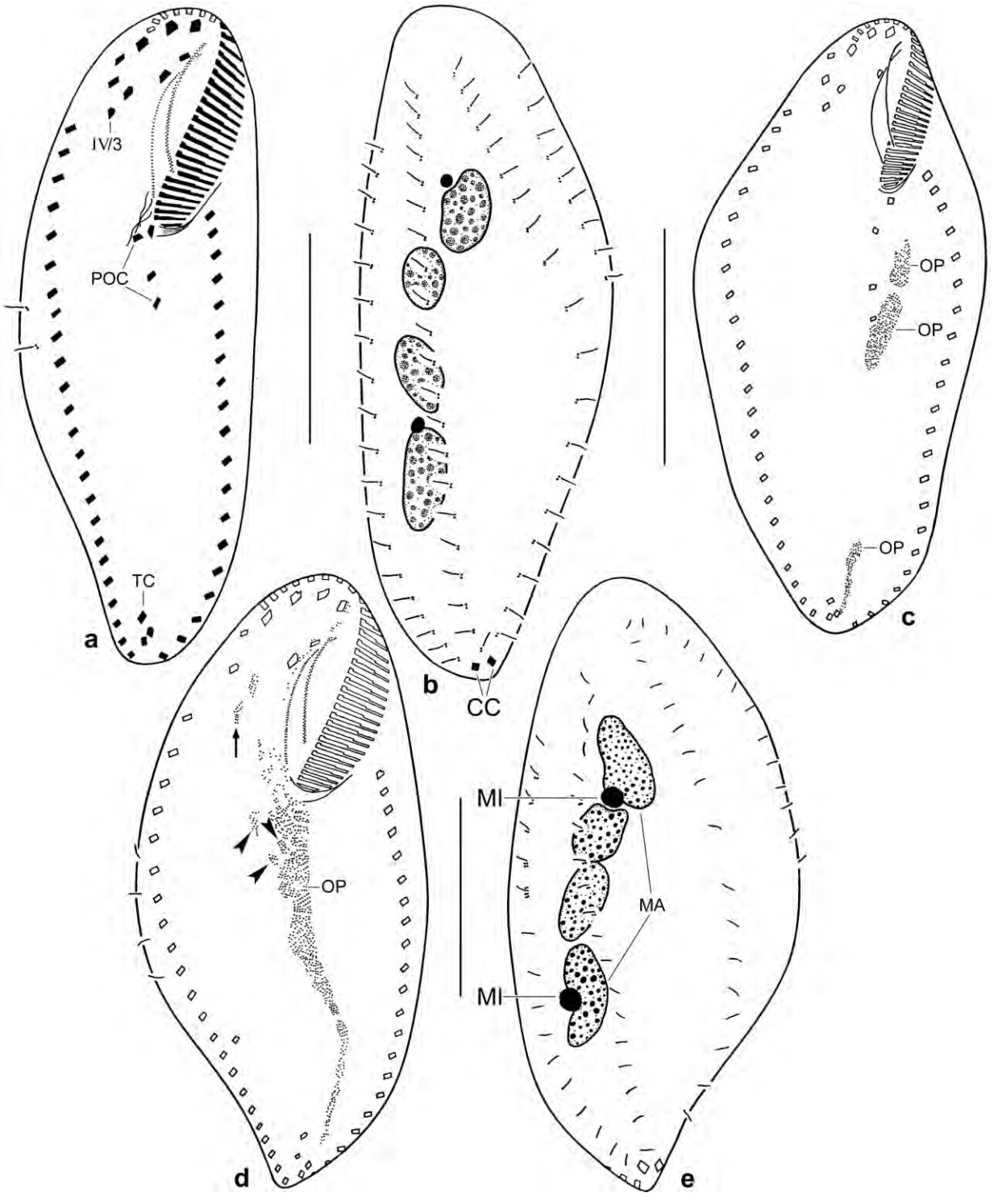

Fig. 266a–e. *Lepidothrix dorsiincisura*, morphostatic (a, b) and dividing (c–e) specimens; parental structures shown by contour in (c–e). **a, b:** Ventral and dorsal view of a "typical" morphostatic specimen with, however, four postoral cirri. **c–e:** Ontogenesis commences with the production of three anarchic fields of basal bodies (c) which soon develop to a large oral primordium by production of basal bodies and incorporation of the postoral cirri (arrowheads). Proter cirri III/2 and IV/3 develop to anlagen (arrow). CC – caudal cirri, MA – macronuclear nodules, MI – micronuclei, OP – oral primordium, POC – postoral cirri, TC – transverse cirri, III/2, IV/3 – cirral anlagen. Scale bars 30 μm.

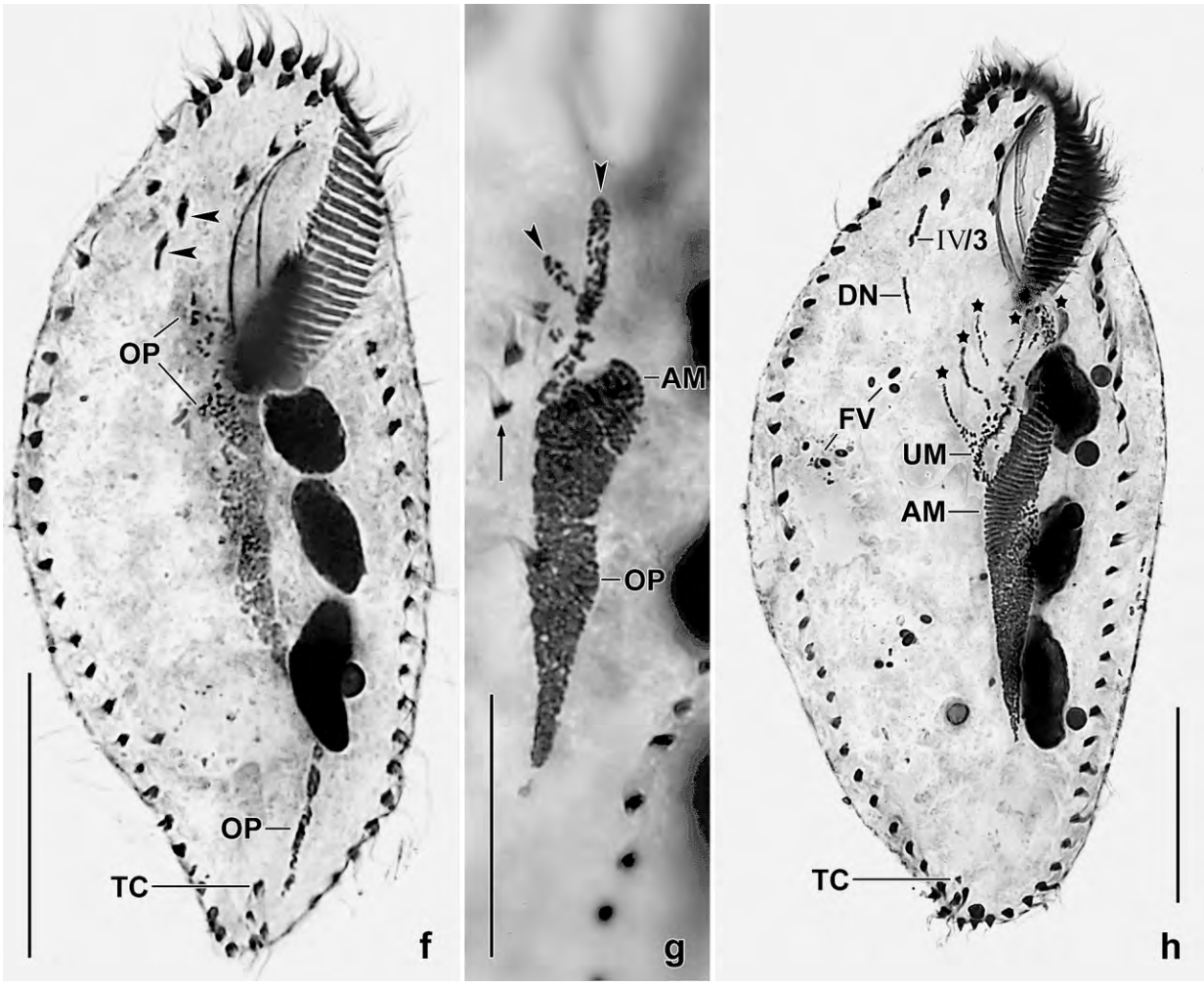

Fig. 266f–h. *Lepidothrix dorsiincisura*, ventral view of protargol-impregnated dividers. **f:** A very early divider with fully developed oral primordium which has incorporated the postoral cirri. The arrowheads denote cirrus III/2 and cirrus IV/3 which just develop to anlagen. **g:** An early opisthe divider which shortened the oral primordium and developed adoral membranelles and cirral anlagen streaks (arrowheads). The postoral cirri (arrow) were not included in the oral primordium. **h:** An early divider, showing that proter anlage VI originates de novo (DN). In the opisthe, the oral primordium transforms to adoral membranelles and five cirral anlagen streaks are developing (asterisks). AM – adoral membranelles, DN – de novo, FV – food vacuoles, OP – oral primordium, TC – transverse cirri, UM – anlagen for the undulating membranes of the opisthe, IV/3 – cirrus IV/3. Scale bars 30 µm.

macronuclear nodules and 2–3 micronuclei. A reticulate, subcortical accumulation of small crystals and organic granules. On average 26–34 cirri in right marginal row, 23–30 in left. 3–4 frontal cirri, 1 buccal cirrus at second quarter of paroral, 4 frontoventral cirri, 3 pretransverse and transverse cirri, and 2 caudal cirri. Dorsal kinety 4 ends slightly posterior to mid-body. Adoral zone extends about 31–37% of body length, composed of 32–35 membranelles on average.

Description of Galápagos sites (70, 71) population: Size in vivo 100–140 × 30–55 µm, usually about 120 × 45 µm, as calculated from some in vivo measurements and the morphometric data in Table 101 adding 15% preparation shrinkage. Body ellipsoid to obovate, rarely indistinctly sigmoid, usually slenderly obovate (~ 3:1), in right anterior quadrant a rather distinct, oblique

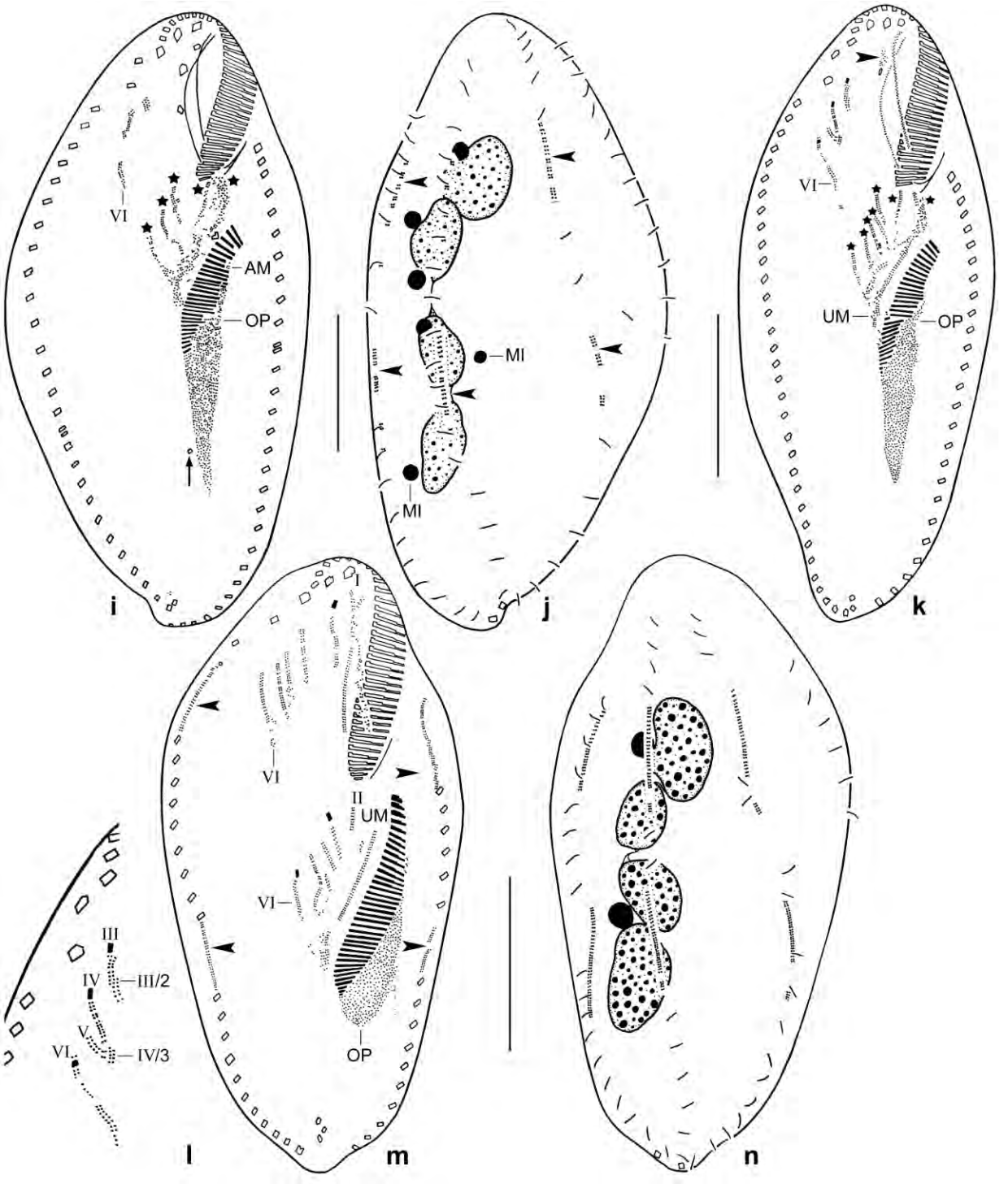

Fig. 266i–n. *Lepidothrix dorsiincisura*, dividers after protargol impregnation. **i, j:** Ventral and dorsal view of an early mid-divider, showing five cirral anlagen streaks in the opisthe (asterisks) and intrakinetal anlagen in dorsal kineties 1–3 (arrowheads). The arrow in (a) marks a supernumerary cirrus. **k, l:** Ventral view of an early mid-divider, showing seven cirral anlagen in the opisthe and cirrus IV/3 which produces proter anlagen IV and V. The buccal cirrus transforms to anlage II (arrowhead). **m, n:** Ventral and dorsal view of an early mid-divider, showing six cirral anlagen each in proter and opisthe. Anlagen developed in the marginal rows (arrowheads). AM – adoral membranelles, MI – micronuclei, OP – oral primordium, UM – primordium for the undulating membranes, II, III, III/2, IV, IV/3, V, VI – cirri and cirral anlagen. Scale bars 30 µm.

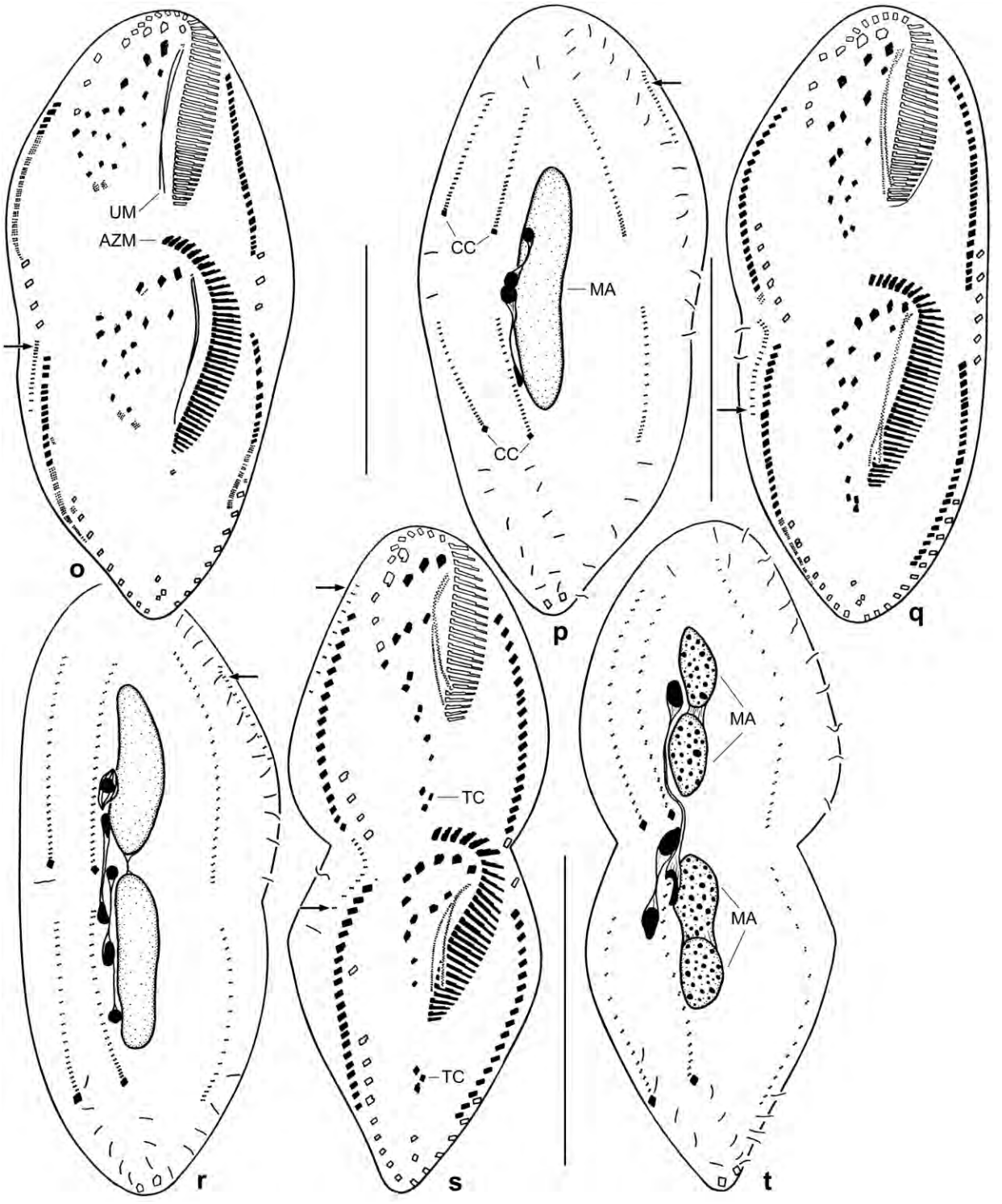

Fig. 266o–t. *Lepidothrix dorsiincisura*, protargol-impregnated dividers. Arrows mark the newly formed dorsomarginal kinety. **o, p:** Mid-divider with fused macronuclear nodules. Cirri formed in the anlagen, the undulating membranes (UM) reorganized, and the opisthe´s adoral zone (AZM) has been completed. **q, r:** Late divider with beginning cytokinesis. The new cirri migrate to their specific sites and the nuclear apparatus divides. **s, t:** A late divider with transverse cirri (TC) migrating posteriorly. The macronuclear nodules divide a second time. AZM – adoral zone of membranelles, CC – caudal cirri, MA – macronuclear nodules, TC – transverse cirri, UM – reorganized undulating membranes. Scale bars 50 µm.

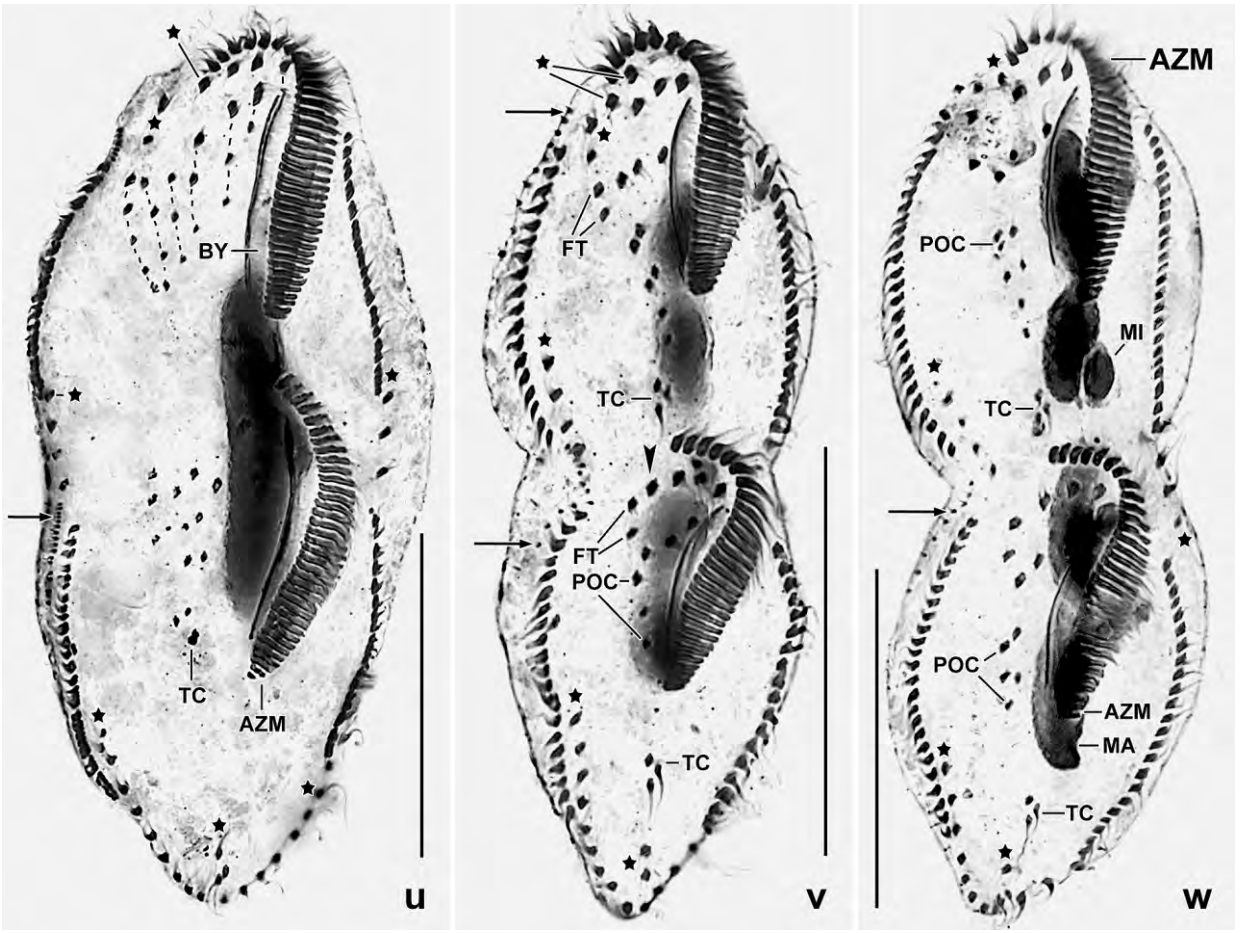

Fig. 266u–w. *Lepidothrix dorsiincisura*, ventral view of protargol-impregnated dividers. Arrows denote dorsomarginal kineties. Asterisks mark parental ciliature which will be resorbed in late and very late dividers**. u:** A mid-divider with fused macronuclear nodules and fully developed opisthe adoral zone of membranelles. Likely, the proter has seven anlagen streaks whose cirri are connected by broken lines. The buccal cavity of the proter is rather narrow indicating that it has been reconstructed. **v:** An early late divider with distinct division furrow. The new cirri are migrating to their specific sites. The new adoral zone of membranelles curved to the right anteriorly. The macronuclear mass divided. The arrowhead marks a supernumerary frontal cirrus. **w:** A late divider with cirral migration almost finished. Some parental cirri have been resorbed. The proter has seven postoral cirri, the opisthe has five (instead of the usual three). Although some of the supernumerary cirri will be possibly resorbed, the highly variable number of postoral and buccal cirri is maintained in the morphostatic specimens (Table 101). The macronuclear nodules divided a second time. AZM – adoral zone of membranelles, BY – buccal cavity, FT – frontoterminal cirri, MA – macronuclear nodules, MI – micronucleus, POC – postoral cirri, TC – transverse cirri. Scale bars 50 µm.

line caused by the steep slope of the dorsal body along kinety 4 (Fig. 264a, d–h, 265f, k; Table 101); slenderly rectangular (~ 4:1) in about 5% of specimens (Fig. 264b, 265g). Nuclear apparatus in central quarters of body and slightly left of cell's midline (Fig. 264a, c, 265a, f, g, j, k, 266a; Table 101). Four macronuclear nodules arranged in a slightly oblique series commencing near cell's midline and extending slightly obliquely posteriorly; individual nodules ellipsoid to broadly ellipsoid, studded with nucleoli 1–2 µm across. Two to three micronuclei attached to and/or between macronuclear nodules. Cortex very flexible, underlain by a curious reticulum (Fig. 264i, 265b, c) made of organic granules 0.2–0.5 µm across and 1–4 µm long crystals sparkling under interference contrast illumination, as in the Austrian type population (Foissner 1982). Cytoplasm colourless, in well-nourished specimens packed with up to 20 µm-

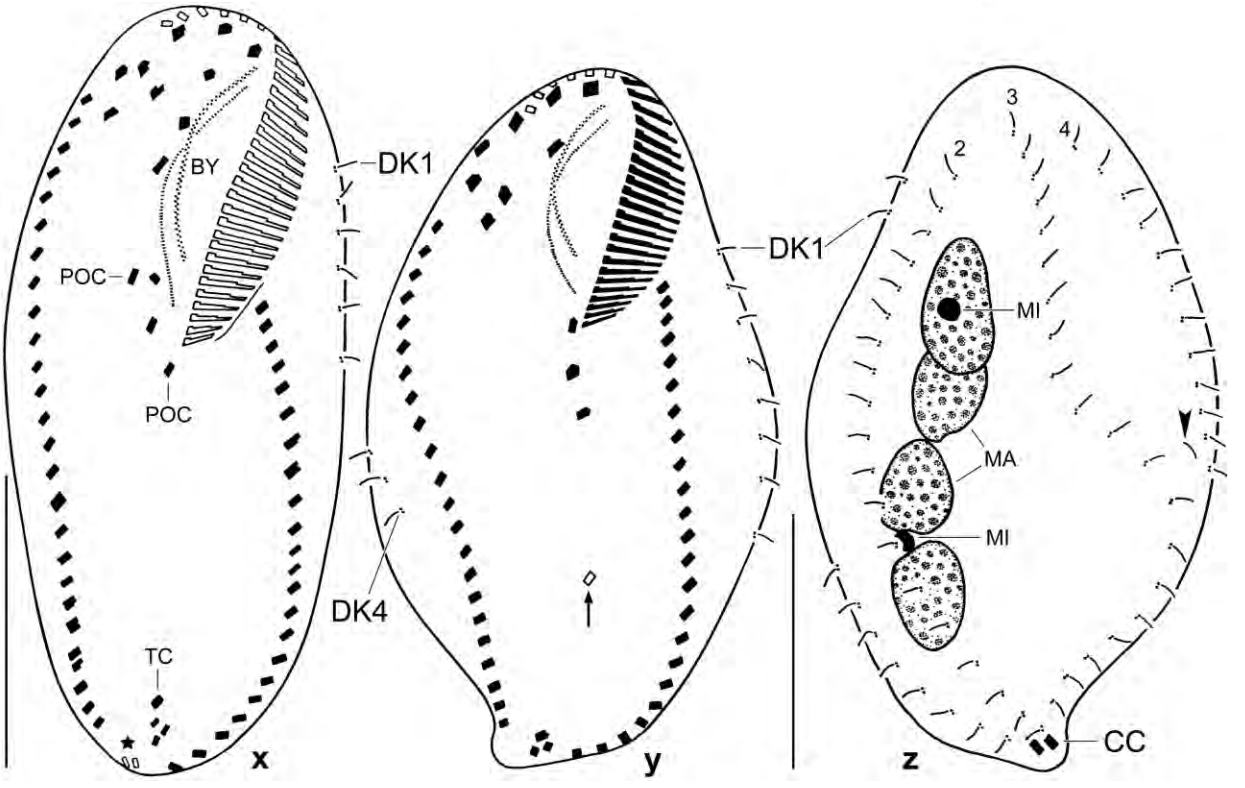

Fig. 266x–z. *Lepidothrix dorsiincisura*, protargol-impregnated post-dividers are smaller and wider than mature specimens. Parental structures shown by contour, new structures shaded black. **x:** Ventral view of a proter post-divider recognizable by the broadly rounded posterior end. It has four postoral cirri and four transverse cirri of which one is possibly parental. The parental cirri have been resorbed except of two cirri of the right marginal row (asterisk). Several cirri have small irregularities which will be corrected post-divisionally. Note the reconstructed proter buccal cavity which has now the ordinary width. **y, z:** Ventral and dorsal view of an opisthe post-divider recognizable by the bluntly pointed posterior end. The cirri obtained their specific pattern and lost their irregularities. The arrow marks a single, possibly parental cirrus. The dorsal bristle pattern is also finished expect of a single parental bristle (arrowhead). BY – buccal cavity, CC – caudal cirri, DK1–4 – dorsal kineties, MA – macronuclear nodules, MI – micronuclei, POC – postoral cirri, TC – transverse cirri. Scale bars 30 µm.

sized food vacuoles containing naked amoebae, fungal conidia, humus particles, and compact material, possibly flagellates and/or small ciliates (Fig. 264a). Movement without peculiarities. Most cirri thick but only about 15 µm long in vivo, arranged in typical *Urosomoida* pattern (Fig. 264a, b, 265f–j, o–r, 266a; Table 101; for a review, see Berger 1999). Number of FVT-cirri highly variable (13–23), especially the postoral cirri (3–7). One, rarely two buccal cirri at second quarter of paroral; three to four pretransverse and transverse cirri in body's midline and very near to its end, about 20 µm long in vivo and thus widely projecting from body proper. Marginal cirral rows frequently almost confluent, i. e., only one cirrus would be needed to close the gap (Fig. 264b, 265f–h, j, o–r, 266a); right row commences far away from anterior body end, i. e., near level of last frontoventral cirrus (Table 101). Dorsal bristles in vivo about 3 µm long, arranged in four rows (Fig. 264c, 265i, k, s, 266b; Table 101): rows 1–3 almost bipolar, row 3 does not split during ontogenesis; row 4 dorsomarginal ending slightly posterior to mid-body. Two, rarely three caudal cirri in or left of body's midline, as thick as marginal cirri, about 20 µm long (Fig. 264a, c, 265i, k, s, 266b; Table 101). Oral apparatus similar to that of → *Fragmospina depressa*. Adoral zone of oxytrichid shape

Table 101. Morphometric analysis of *Lepidothrix dorsiincisura* from Galápagos (LG) and Austria (LD; from FOISSNER 1982). Data based on mounted, protargol-impregnated, randomly selected specimens from non-flooded Petri dish cultures. Measurements in µm. AE – anterior body end. CV – coefficient of variation in %, M – median, Max – maximum, Mean – arithmetic mean, Min – minimum, n – number of specimens investigated, PE – posterior end of body, Pop – population, SD – standard deviation, SE – standard error of arithmetic mean.

Characteristics	Pop	Mean	M	SD	SE	CV	Min	Max	n
Body, length	LG	106.7	110.0	12.2	2.7	11.4	86.0	123.0	21
	LD	81.3	80.5	8.5	2.7	10.4	70.0	98.0	10
Body, width	LG	41.0	40.0	6.0	1.3	14.5	28.0	50.0	21
	LD	24.0	24.0	2.0	0.6	8.3	20.0	27.0	10
Body length:width, ratio	LG	2.7	2.9	0.5	0.1	18.3	1.8	3.7	21
	LD	3.4	–	–	–	–	–	–	10
Adoral membranelles, number	LG	35.3	36.0	4.2	0.9	12.0	27.0	42.0	21
	LD	31.6	31.5	2.2	0.7	7.0	28.0	36.0	10
Adoral membranelles, longest base	LG	8.1	8.0	0.8	0.2	9.7	7.0	10.0	21
Anterior body end to proximal end of adoral zone, distance	LG	39.6	39.0	4.1	0.9	10.3	30.0	45.0	21
	LD	25.6	25.0	3.3	1.0	13.0	20.0	33.0	10
Body length:length of adoral zone of membranelles, ratio	LG	2.7	2.8	0.4	0.1	15.3	2.0	3.7	21
	LD	3.2	–	–	–	–	–	–	10
AE to first frontoventral cirrus, distance	LG	12.9	14.0	4.3	0.9	33.4	1.0	19.0	23
AE to last frontoventral cirrus, distance	LG	23.9	25.0	4.5	0.9	18.9	12.0	32.0	23
AE to buccal cirrus, distance	LG	13.2	13.0	1.6	0.3	11.7	11.0	16.0	21
AE to right marginal row, distance	LG	24.2	25.0	6.8	1.5	28.2	1.0	33.0	22
AE to left marginal row, distance	LG	33.8	33.0	4.1	0.9	12.2	23.0	44.0	21
AE to first postoral cirrus, distance	LG	38.6	38.0	5.0	1.1	13.0	32.0	48.0	21
AE to last postoral cirrus, distance	LG	54.3	51.0	9.7	2.1	17.8	41.0	81.0	21
AE to paroral membrane, distance	LG	5.2	5.0	1.7	0.4	32.6	1.0	8.0	21
Paroral membrane, length	LG	28.4	28.0	3.6	0.8	12.6	21.0	35.0	21
AE to endoral membrane, distance	LG	6.7	7.0	1.6	0.4	23.6	4.0	10.0	21
Endoral membrane, length	LG	26.3	25.0	4.1	0.9	15.6	20.0	35.0	21
AE to first macronuclear nodule, distance	LG	26.1	26.0	4.2	0.9	16.3	17.0	32.0	21
Nuclear figure, length	LG	59.6	59.0	8.6	1.9	14.4	47.0	76.0	21
Macronuclear nodules, number	LG	4.0	4.0	0.0	0.0	0.0	4.0	4.0	21
	LD	4.7	4.5	0.8	0.2	16.6	4.0	6.0	10
Macronuclear nodules, length	LG	15.2	15.0	2.3	0.5	15.2	12.0	20.0	21
	LD	9.0	9.0	0.8	0.3	9.1	8.0	11.0	10
Macronuclear nodules, width	LG	8.1	8.0	1.2	0.3	15.1	6.0	11.0	21
	LD	5.0	4.7	0.9	0.3	18.9	4.0	7.0	10
Micronuclei, number	LG	1.6	2.0	0.9	0.2	55.4	0.0	3.0	21
Micronuclei, length	LD	2.9	3.0	0.5	0.1	17.6	2.0	4.0	21
Micronuclei, width	LG	2.2	2.0	–	–	–	2.0	3.0	21
PE to uppermost transverse cirrus, distance	LG	6.7	6.0	2.0	0.4	29.4	4.0	10.0	21
PE to lowermost transverse cirrus, distance	LG	2.4	2.0	1.4	0.3	57.1	1.0	5.0	21
PE to right marginal row, distance	LG	2.2	2.0	0.8	0.2	37.1	1.0	4.0	21
PE to left marginal row, distance	LG	2.1	2.0	1.0	0.2	47.3	1.0	5.0	21

continued

Characteristics	Pop	Mean	M	SD	SE	CV	Min	Max	n
Right marginal row, number of cirri	LG	26.0	26.0	2.8	0.6	10.7	22.0	31.0	21
	LD	34.1	34.0	1.9	0.6	5.6	32.0	39.0	10
Left marginal row, number of cirri	LG	23.4	23.0	2.4	0.5	10.2	20.0	29.0	21
	LD	29.7	29.5	2.4	0.8	8.1	26.0	34.0	10
Left and right marginal row, distance at posterior end	LG	4.1	4.0	1.7	0.3	40.5	1.0	8.0	24
	LD [a]	5.7	5.0	1.9	0.3	33.6	2.0	10.0	31
Postoral cirri, number	LG	4.2	4.0	1.3	0.3	30.7	3.0	7.0	21
	LD	3.0	3.0	0.0	0.0	0.0	3.0	3.0	10
Frontal cirri, number	LG	3.7	4.0	0.6	0.1	17.3	3.0	5.0	21
	LD	3.0	3.0	0.0	0.0	0.0	3.0	3.0	10
Buccal cirri, number	LG	1.3	1.0	–	–	–	1.0	2.0	32
	LD	1.0	1.0	0.0	0.0	0.0	1.0	1.0	10
Frontoventral cirri, number	LG	4.2	4.0	0.5	0.1	12.2	3.0	5.0	21
	LD	4.0	4.0	0.0	0.0	0.0	4.0	4.0	10
Transverse plus pretransverse cirri, number	LG	3.3	3.0	–	–	–	3.0	4.0	21
	LD	2.8	3.0	–	–	–	2.0	3.0	10
Caudal cirri, number	LG	2.1	2.0	–	–	–	2.0	3.0	21
	LD	2.2	2.0	–	–	–	2.0	3.0	10
Dorsal kineties, number	LG	4.0	4.0	0.0	0.0	0.0	4.0	4.0	21
	LD	4.0	4.0	0.0	0.0	0.0	4.0	4.0	10
Dorsal kinety 1, number of bristles	LG	19.4	19.0	3.2	0.7	16.6	14.0	26.0	21
Dorsal kinety 2, number of bristles	LG	19.1	19.0	2.7	0.6	13.9	16.0	24.0	21
Dorsal kinety 3, number of bristles	LG	20.7	20.0	2.1	0.5	10.0	16.0	24.0	21
Dorsal kinety 4, number of bristles	LG	13.0	13.0	1.7	0.4	13.3	9.0	16.0	21

[a] Taken from Austrian type population.

and structure, extends about 37% of body length, composed of an average of 35 membranelles with largest bases about 8 µm wide in protargol preparations (Fig. 264a, b, h, 265a, f, g, j, s–r, 266a; Table 101). Buccal cavity moderately wide and deep in ordinary specimens (Fig. 1a, 2f) while narrow and deep in slender cells (Fig. 264b, 265g, j), right wall in vivo straight and thick (Fig. 264a, 265a), anterior margin semicircularly curved, forming a distinct buccal horn (Fig. 264a, h). Buccal lip conspicuous because up to 10 µm wide, covers posterior half of buccal cavity and proximal region of adoral zone (Fig. 264a, h). Paroral membrane composed of zigzagging basal bodies, cilia about 10 µm long in vivo, in protargol preparations distinctly curved but never recurved, extends to left anterior corner of cell almost touching adoral zone. Endoral membrane as long as paroral, distinctly curved, optically intersects paroral in anterior third, cilia 30–40 µm long (!) and thus extending deep into the pharynx.

Resting cyst (Fig. 264j, k, 265d, e, l–n): The resting cysts are colourless and spherical to slightly ellipsoid with an average size of 49.6 × 46.2 µm (n = 10). The cyst wall is 1–1.5 µm thick and consists of two moderately refractive layers (Fig. 264j, 265m). It is covered by a 3–5 µm thick slime layer containing two types of lepidosomes, i. e., organic "scales" appearing structureless in the light microscope. The type I lepidosomes, which are colourless to very slightly yellowish, have a diameter of 2.5–3 µm and are scattered through the slime layer. Most type II lepidosomes,

which are colourless and have a diameter of ≤ 0.5 µm, lie on the cyst wall. The macronuclear nodules fused, forming a globular mass in cyst centre. The cytoplasm is packed with lipid droplets 2–4 µm across (Fig. 264k, 265m).

Ontogenesis (Fig. 266a–z): The ontogenesis of *Lepidothrix dorsiincisura* is identical with that of *Urosomoida agiliformis* which has been misinterpreted in an important detail by Foissner & Adam (1983a). Specifically, these authors stated that cirral anlage V originates de novo. However, their Figure 13 is quite similar to Fig. 266k, l of *Lepidothrix*, suggesting that cirral anlagen streaks IV and V are generated by cirrus IV/3; only anlage VI originates de novo. The other anlagen are generated as usual: anlage I originates from the undulating membranes, anlage II from buccal cirrus II/2, and anlage III from cirrus III/2. We could not clarify anlagen development in the opisthe due to the highly variable number of cirri. Likewise we could not determine the number of cirri produced by the individual anlagen. In both, *Lepidothrix dorsiincisura* and *Urosomoida agiliformis* the ontogenesis begins with three small anarchic fields of basal bodies (Fig. 266c) and all anlagen develop separately in proter and opisthe. For further details, see explanations to Fig. 266c–z.

The genesis of the dorsal ciliature is also identical in *U. agiliformis* and *L. dorsiincisura*. Kineties 1, 2, 3 develop anlagen but caudal cirri are generated only by kineties 1 and 2. Kinety 4 originates dorsomarginally.

Occurrence and ecology: *Lepidothrix dorsiincisura* has been recorded from many habitats but is possibly absent from Africa and Antarctica (Foissner 1998, Foissner et al. 2002, 2008a). In the Neotropis, it occurred at several quite different sites, indicating a wide ecological range (see species list).

Remarks: At first glance, the Galápagos population of *L. dorsiincisura* appears rather different from the Austrian one described by Foissner (1982). Specifically, the length:width ratio of the body is rather different (2.7 vs. 3.4), many specimens are narrowed posteriorly (vs. usually ellipsoid), the posterior distance of the marginal cirral rows appears narrower in the Galápagos than in the Austrian specimens, the in vivo structure of the oral apparatus, and the variability in the number of cirri, e. g., 3–5, on average 4 frontal cirri. Thus, we reinvestigated the protargol-impregnated Austrian specimens for some of these features. This showed both, specimens distinctly narrowed posteriorly and with a small distance between the marginal rows ($\bar{x}$ = 4.1 µm vs. 5.7 µm; Table 101). The finer resolution of the oral structures results from our increased knowledge of live observation. The high variability of most FVT-cirri could result from the rather high soil salinity (20‰, see site description). There are also rather pronounced differences in some morphometrics, especially in the number of frontal and marginal cirri. The high variability of the Galápagos specimens makes their classification difficult because it covers the pronounced overall similarity, suggesting that the Galápagos and Austrian populations are conspecific.

Material deposited: Nine voucher slides with protargol-impregnated specimens from Galápagos have been deposited in the Biology Centre of the Upper Austrian Museum in Linz (LI). Some relevant specimens have been marked by black ink circles on the coverslip.

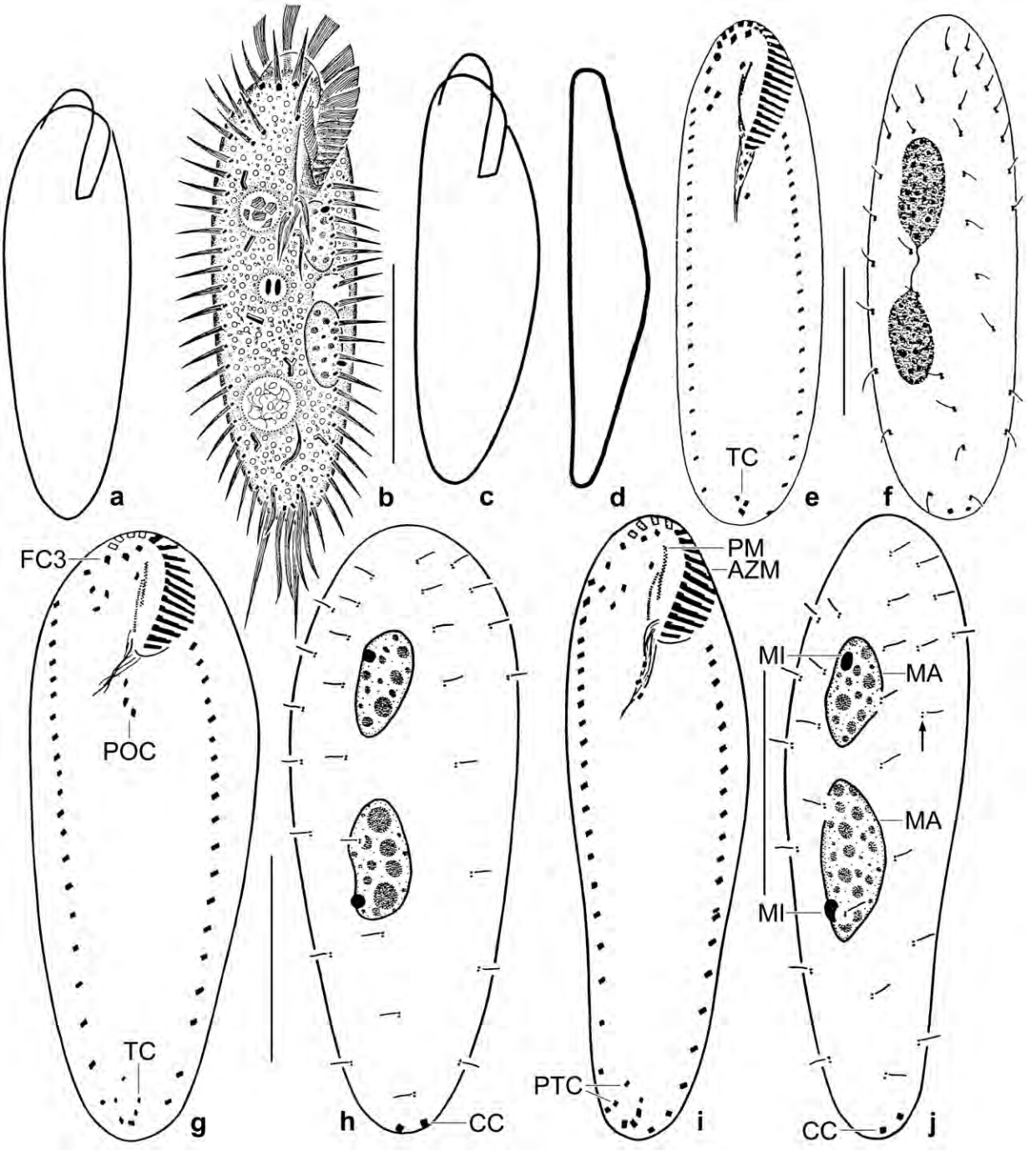

Fig. 267a–j. *Urosomoida halophila* (a–d, g–j) and *U. agiliformis* (e, f; from Foissner 1982) from life (a–d) and after protargol impregnation (e–j). **a, c:** Frequent body shapes. **b:** Ventral view of a representative specimen, length 70 µm. Note the short adoral zone of membranelles. **d:** Lateral view. **e, f:** Ventral and dorsal view of *U. agiliformis* for comparison with *U. halophila.* **g–j**: Ventral and dorsal view of holotype (g, h) and a paratype specimen with extra dorsal bristles (j, arrow). Note the short oral area. AZM – adoral zone of membranelles, CC – caudal cirri, FC3 – frontal cirrus 3, MA – macronuclear nodules, MI – micronuclei, PM – paroral membrane, POC – postoral cirri, PTC – pretransverse cirri, TC – transverse cirri. Scale bars 20 µm (g–j) and 30 µm (b, e, f).

Urosomoida halophila **nov. spec.** (Fig. 267a–j, 268a–h; Tables 102, 103)

Diagnosis: Size in vivo about 70 × 20 µm; ellipsoid to slightly obovate or elongate ellipsoid to elongate obovate. 2 macronuclear nodules and 2 micronuclei. 1 buccal cirrus subapical of paroral membrane, 3 postoral cirri, 5 to 7 ($\bar{x}$ = 6.2) pretransverse and transverse cirri. 4 dorsal kineties and 2 caudal cirri. Adoral zone extends 20% of body length, composed of an average of 16 membranelles.

Type locality: Venezuelan site (65), i. e., hypersaline (50‰) soil from the north coast, 67°13'W 11°33'N.

Type material: 1 holotype and 2 paratype slides with protargol-impregnated specimens have been deposited in the Biology Centre of the Upper Austrian Museum in Linz (LI). The holotype and other relevant specimens have been marked by black ink circles on the coverslip.

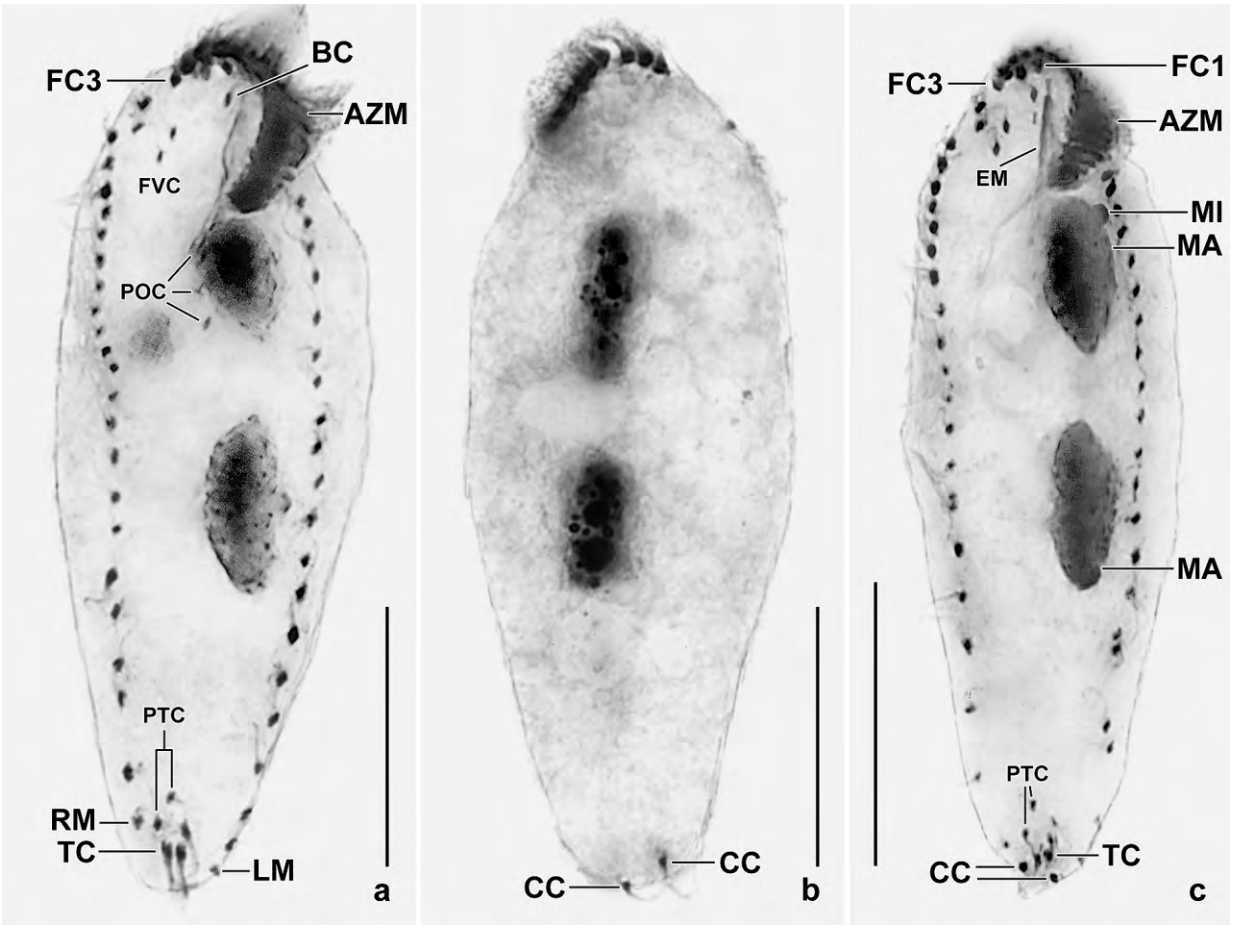

Fig. 268a–c. *Urosomoida halophila*, ventral (a, c) and dorsal (b) views after protargol impregnation. Note the elongate obovate body shape, the two macronuclear nodules, the very short adoral zone of membranelles, the rather distantly located pretransverse cirri, the reduced number of transverse cirri, and the two caudal cirri. AZM – adoral zone of membranelles, BC – buccal cirrus, CC – caudal cirri, EM – endoral membrane, FC1, 3 – frontal cirri, FVC – frontoventral cirri, LM – left marginal cirral row, MA – macronuclear nodules, MI – micronuclei, POC – postoral cirri, PTC – pretransverse cirri, RM – right marginal cirral row, TC – transverse cirri. Scale bars 20 µm.

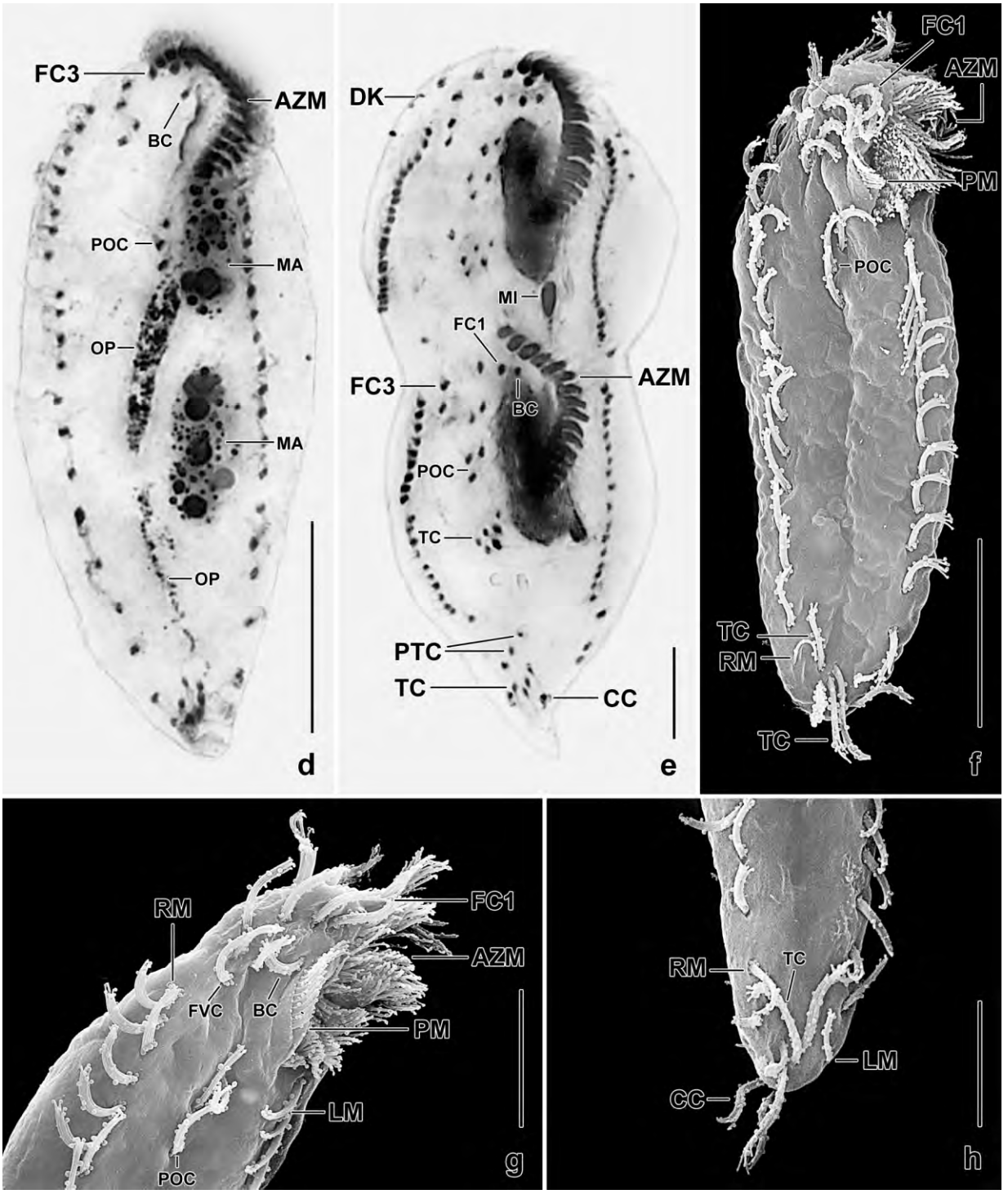

Fig. 268d–h. *U. halophila* after protargol impregnation (d, e) and in the SEM (f–h). **d:** Ventral view of an early divider with oral primordium. **e:** Ventral view of a late divider with parental and new cirri. **f–h:** Ventral overview and details, showing the very short adoral zone of membranelles. The pretransverse cirri are unciliated and thus not recognizable. AZM – adoral zone of membranelles, BC – buccal cirrus, CC – caudal cirri, DK – dorsomarginal kinety, FC1, 3 – frontal cirri, FVC – frontoventral cirri, LM – left marginal row, MA – macronuclear nodules, MI – dividing micronucleus, OP – oral primordium, PM – paroral membrane, POC – postoral cirri, PTC – pretransverse cirri, RM – right marginal row, TC – transverse cirri. Scale bars 10 μm (g, h) and 20 μm (d–f).

Table 102. Morphometric data on *Urosomoida halophila* based on mounted, protargol-impregnated, and randomly selected specimens from a non-flooded Petri dish culture. Measurements in µm. CV – coefficient of variation in %, M – median, Max – maximum, Mean – arithmetic mean, Min – minimum, n – number of individuals investigated, SD – standard deviation, SE – standard error of arithmetic mean.

Characteristics	Mean	M	SD	SE	CV	Min	Max	n
Body, length	56.8	56.0	5.5	1.2	9.7	45.0	67.0	21
Body, width	19.3	19.5	2.0	0.4	10.4	14.0	23.0	21
Body length:width, ratio	3.0	3.0	0.4	0.1	13.4	2.3	3.9	21
Anterior body end to proximal end of adoral zone, distance	11.5	11.5	0.8	0.2	7.2	10.0	13.0	21
Adoral zone of membranelles, percentage of body length	20.5	20.0	2.7	0.6	13.2	16.0	27.0	21
Adoral membranelles, number	16.5	17.0	0.8	0.2	4.5	15.0	18.0	21
Anterior body end to paroral membrane, distance	2.6	2.5	0.5	0.1	20.0	2.0	4.0	21
Anterior body end to endoral membrane, distance	4.3	4.0	0.6	0.1	14.1	3.0	6.0	21
Anterior body end to first macronuclear nodule, distance	11.0	11.0	0.9	0.2	8.3	9.0	13.0	21
Nuclear figure, length	26.6	26.5	2.5	0.5	9.2	22.0	32.0	21
Macronuclear nodules, distance in between	3.7	4.0	1.3	0.3	34.5	2.0	6.0	21
Anterior macronuclear nodule, length	10.8	11.0	1.5	0.3	13.4	9.0	14.0	21
Anterior macronuclear nodule, width	4.7	4.5	0.5	0.1	11.4	4.0	6.0	21
Macronuclear nodules, number	2.0	2.0	0.0	0.0	0.0	2.0	2.0	21
Anteriormost micronucleus, length	1.7	1.5	–	–	–	1.0	2.0	21
Anteriormost micronucleus, width	1.2	1.0	–	–	–	1.0	2.0	21
Micronuclei, number	1.6	2.0	0.6	0.1	36.4	1.0	3.0	21
Frontal cirri, number	3.0	3.0	0.0	0.0	0.0	3.0	3.0	21
Anterior body end to buccal cirrus, distance	3.4	3.5	0.5	0.1	13.4	2.0	4.0	21
Buccal cirri, number	1.1	1.0	–	–	–	1.0	2.0	21
Anterior body end to last frontoventral cirrus, distance	7.6	7.5	1.0	0.2	12.6	5.0	9.0	21
Frontoventral cirri, number	4.0	4.0	0.0	0.0	0.0	4.0	4.0	21
Anterior body end to last postoral cirrus, distance	18.1	18.0	1.4	0.3	7.8	16.0	21.0	21
Postoral cirri, number	3.0	3.0	0.0	0.0	0.0	3.0	3.0	21
Pretransverse cirri, number	2.1	2.0	–	–	–	2.0	3.0	21
Transverse cirri, number	4.1	4.0	0.5	0.1	11.5	3.0	5.0	21
Posterior body end to lowermost transverse cirrus, distance	1.9	2.0	0.7	0.1	34.6	1.0	4.0	21
Anterior body end to right marginal cirral row, distance	5.1	5.0	0.8	0.2	15.4	4.0	7.0	21
Posterior body end to right marginal cirral row, distance	3.7	3.5	1.2	0.3	31.8	2.0	7.0	21
Right marginal cirri, number	20.8	21.0	1.2	0.3	5.6	19.0	23.0	21
Posterior body end to left marginal row, distance	2.4	2.0	1.0	0.2	39.8	1.0	5.0	21
Left marginal cirri, number	20.4	20.0	1.8	0.4	8.7	17.0	24.0	21
Dorsal kineties, number	4.1	4.0	–	–	–	4.0	5.0	16
Caudal cirri, number	2.0	2.0	0.0	0.0	0.0	2.0	2.0	21

Etymology: *halophilum* (loving saline habitats) is a Greek adjective and refers to the habitat the species was discovered.

Description: *Urosomoida halophila* has an ordinary variability with most variation coefficients being < 15%, especially those of the important diagnostic features.

Size in vivo 55–84 × 15–25 µm, usually about 70 × 20 µm, as calculated from some in vivo measurements and the morphometric data in Table 102 adding 25% length and 15% width shrinkage, respectively (ethanol fixation plus about 10% contractility). Body usually slightly elongate obovate or elongate ellipsoid, rarely slightly obovate or ellipsoid; slightly flattened laterally; very flexible and up to 10% contractile (Fig. 267a–d, g, i, 268a–c, d, f; Table 102). Nuclear apparatus in central quarters of cell, composed of two macronuclear nodules and two micronuclei. Macronuclear nodules ellipsoid to elongate ellipsoid, on average about 11 × 4.5 µm in protargol preparations. Micronuclei usually attached to macronuclear nodules, globular to bluntly ellipsoid, in vivo about 2 µm in size (Fig. 267b, h, j, 268a–c; Table 102). Contractile vacuole in mid-body at left cell margin (Fig. 267b). Cortex very flexible, without specific granules. Cytoplasm colourless, studded with some ordinary crystals, food vacuoles and innumerable pale granules about 1 µm across (Fig. 267b). Feeds on sporulating bacteria, in raw cultures also on small starch grains. Glides slowly on microscope slide and bottom of Petri dish. Very flexible burrowing in mud and soil aggregates. Cirral pattern slightly unstable, i. e., extra marginal cirri occur rather frequently isolated or in short rows; otherwise as typical for genus but frontoventral cirri more close together due to the short oral area (Fig. 267b, g, i, 268a, c, f–h; Table 102). Three slightly thickened frontal cirri, one buccal cirrus subapical of paroral membrane, four frontoventral cirri, three narrowly spaced postoral cirri, two unciliated pretransverse cirri (thus not visible in the SEM, Fig. 268f, h) rather distant from three to five ($\bar{x}$ = 4) transverse cirri about 15 µm long in vivo and thus distinctly projecting from body proper. Marginal cirral rows end subterminally, intracirral distances gradually increase from anterior to posterior, both rows composed of about 20 cirri 10 µm long in vivo and usually composed of 2 × 3 basal bodies, rarely of mainly 2 × 2. Dorsal bristles 2.5–3 µm long in vivo and in protargol preparations, arranged in four rows (Fig. 267h, j, 268b; Table 102). Rows 1–3 almost bipolar, bristles widely spaced in posterior half; row 4 dorsomarginal, extends to second quarter of cell, composed of only three to five bristles. Caudal cirri about 20 µm long in vivo and comparatively thick each likely comprising nine cilia. Oral apparatus small, adoral zone extends only 20% of body length, composed of an average of 16 membranelles with largest bases about 4 µm width in vivo (Fig. 267b, g, i, 268a, c, f, g; Table 102). Buccal cavity flat and narrow, buccal lip covers proximal membranelles. Undulating membranes straight to slightly curved, staggered, i. e., posterior half of paroral side by side with anterior half of endoral; paroral cilia in vivo 3 µm long. Pharyngeal fibres inconspicuous.

Occurrence and ecology: As yet found only at type locality where it became rather numerous in the non-flooded Petri dish culture two weeks after rewetting the sample; a raw culture could be established with artificial sea water and some squashed wheat grains. With its small, slender body, the species is well adapted to soil life.

Remarks: *Urosomoida halophila* is most similar to *U. agiliformis* Foissner, 1982, a frequent cosmopolite (Fig. 267e, f). A comparison of the main features (Table 103) shows that these species differ significantly by the length of the adoral zone of membranelles (slightly overlapping), the number of adoral membranelles (non-overlapping), and the number of pretransverse and transverse cirri (non-overlapping). There might be further valuable features but the data from *U. agiliformis* are too incomplete. The two non-overlapping features are strong indicators for considering the hypersaline Venezuelan population as a distinct species.

Table 103. Comparison of main features in *Urosomoida halophila* and *U. agiliformis.* All based on protargol-impregnated specimens. Extreme values in parenthesis.

Characteristics	*U. halophila,* n = 21	*U. agiliformis,* n = 12 (Foissner 1982)	*U. agiliformis,* n = 25 (Foissner & Adam 1983a)
Body length (µm)	56.8 (45.0–67.0)	70.4 (64.0–77.0)	69.5 (55.0–87.0)
Adoral zone, percentage of body length	20.5 (16.0–27.0)	26.0 (24.0–30.0)	30.0 (26.0–35.0)
Adoral membranelles, number	16.5 (15.0–18.0)	21.7 (20.0–23.0)	22.2 (20.0–26.0)
Pretransverse and transverse cirri, number	6.2 (5.0–8.0)	3.1 (3.0–4.0)	2.9 (1.0–4.0)
Right marginal cirri, number	20.8 (19.0–23.0)	20.1 (19.0–22.0)	24.1 (20.0–29.0)
Left marginal cirri, number	20.4 (17.0–24.0)	19.6 (16.0–22.0)	21.6 (18.0–25.0)

Urosomoida galapagensis Foissner & Liebetreu **nov. spec.** (Fig. 269a–i, 270a–i; Table 104)

Diagnosis: Size in vivo about 90 x 30 µm; narrowly ellipsoid, rarely ellipsoid. 2 macronuclear nodules with a micronucleus each. Cortical granules in loose rows, colourless to yellowish, about 0.5 µm across. 3 postoral cirri, 4–6 pretransverse and transverse cirri, 4 dorsal kineties and 3 caudal cirri. Adoral zone extends 28% of body length, composed of an average of 22 membranelles.

Type locality: Galápagos site (68), i. e., saline (~ 30 ‰) soil and tree bark from a mangrove forest near to the village of Puerto Villamil, south coast of Isabela Island, 0°57'S 90°57' W.

Type material: 1 holotype and 2 paratype slides with protargol-impregnated specimens have been deposited in the Biology Centre of the Upper Austrian Museum in Linz (LI). Relevant specimens have been marked by black ink circles on the coverslip.

Etymology: Named after the archipelago where it was discovered, i. e., the Galápagos Islands.

Description: Size in vivo 80–110 × 25–45 µm, usually about 90 × 30 µm, as calculated from some in vivo measurements and the morphometric data in Table 104 adding 15% preparation shrinkage. Body length:width ratio in vivo 2.6–3.7:1, after protargol impregnation slightly stouter, viz., 1.9–3.3, very likely due to some inflation during preparation (Table 104). Usually narrowly ellipsoid, rarely ellipsoid with right margin typically less convex than left (Fig. 269a, b, e, f, 270d–f). Dorsoventrally flattened up to 2:1, ventral side flat, dorsal vaulted in mid-body. Nuclear apparatus on average in middle body third left of body's midline, anterior macronuclear nodule commences near level of buccal vertex, distance between macronuclear nodules highly variable (Fig. 269a, d, 270a, d-f; Table 104). Macronuclear nodules ellipsoid to slenderly ellipsoid, rarely irregulary reniform, pyriform or dumbbell-shaped, on average 15 × 6 µm in protargol preparations, occasionally connected by a fine strand; nucleoli irregularly ellipsoid to globular, up to 2 µm across. Usually one micronucleus attached to each macronuclear nodule, about 2 µm across after protargol impregnation; out of 30 specimens investigated three had no micronucleus attached to the posterior macronuclear nodule, one specimen was amicronucleate, and another had three micronuclei. Contractile vacuole in or near mid-body at left cell margin (Fig. 269a).

Cortex very flexible. Cortical granules in loose rows, about 0.5 µm across, slightly yellowish to colourless; conspicuous, even under brightfield illumination, because strongly refractive, in cultivated cells even more distinct; impregnate sometimes with protargol, appearing as sand-like grains (Fig. 269e, h, 270b, c). Cytoplasm colourless, with lipid droplets 1–3 µm across and some 3–5 µm large crystals of various shapes (Fig. 269a, g, 270a, c). Usually packed with food vacuoles 4–15 µm across in vivo, contain fungal spores (*Fusarium*) and rod-shaped bacteria; young food vacuoles with bacterial rods first ellipsoid and 4–7 µm long, later becoming globular and 10–15 µm in size (Fig. 269a, 270a). Glides moderately fast.

Cirral pattern constant, number of cirri rather variable (Fig. 269a, b, 270d–f; Table 104): three slightly enlarged frontal cirri; four frontoventral cirri, left cirrus (= cirrus III/2) usually in mid of frontoterminal cirri; one buccal cirrus right of anterior end of paroral membrane; three postoral cirri in usual pattern, 8 out of 32 specimens with two additional postoral cirri posterior to the

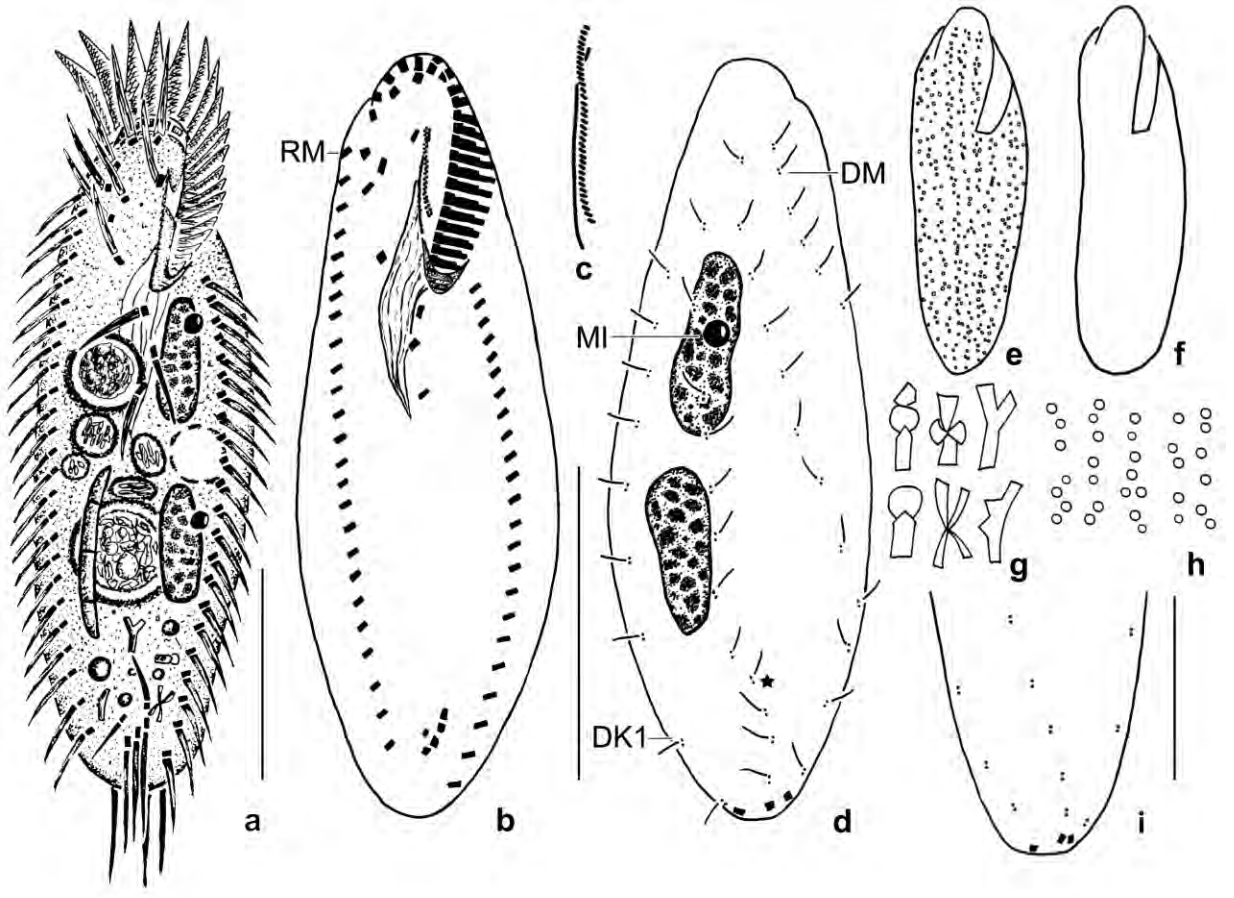

Fig. 269a–i. *Urosomoida galapagensis* from life (a, e–h) and after protargol impregnation (b–d, i). **a:** Ventral view of a representative specimen, length 90 µm, having ingested a fungal spore (*Fusarium*) and many bacterial rods. **b–d:** Ventral and dorsal view of holotype specimen, showing the infraciliature, the nuclear apparatus, and the undulating membranes at higher magnification, length 75 µm. In this specimen, dorsal kinety 2 shows a distinct bend in the posterior region (d, asterisk). Second micronucleus covered by posterior macronuclear nodule. **e, f:** Shape variants and cortical granulation (e). **g:** Cytoplasmic crystals, 3–5 µm long. **h:** Cortical granulation, granules yellowish and about 0.5 µm across. **i:** Posterior part of a specimen with straight kinety 2. DK1 – dorsal kinety 1, DM – dorsomarginal row, MI – micronucleus, RM – right marginal row. Scale bars 30 µm (a, b, d) and 20 µm (i).

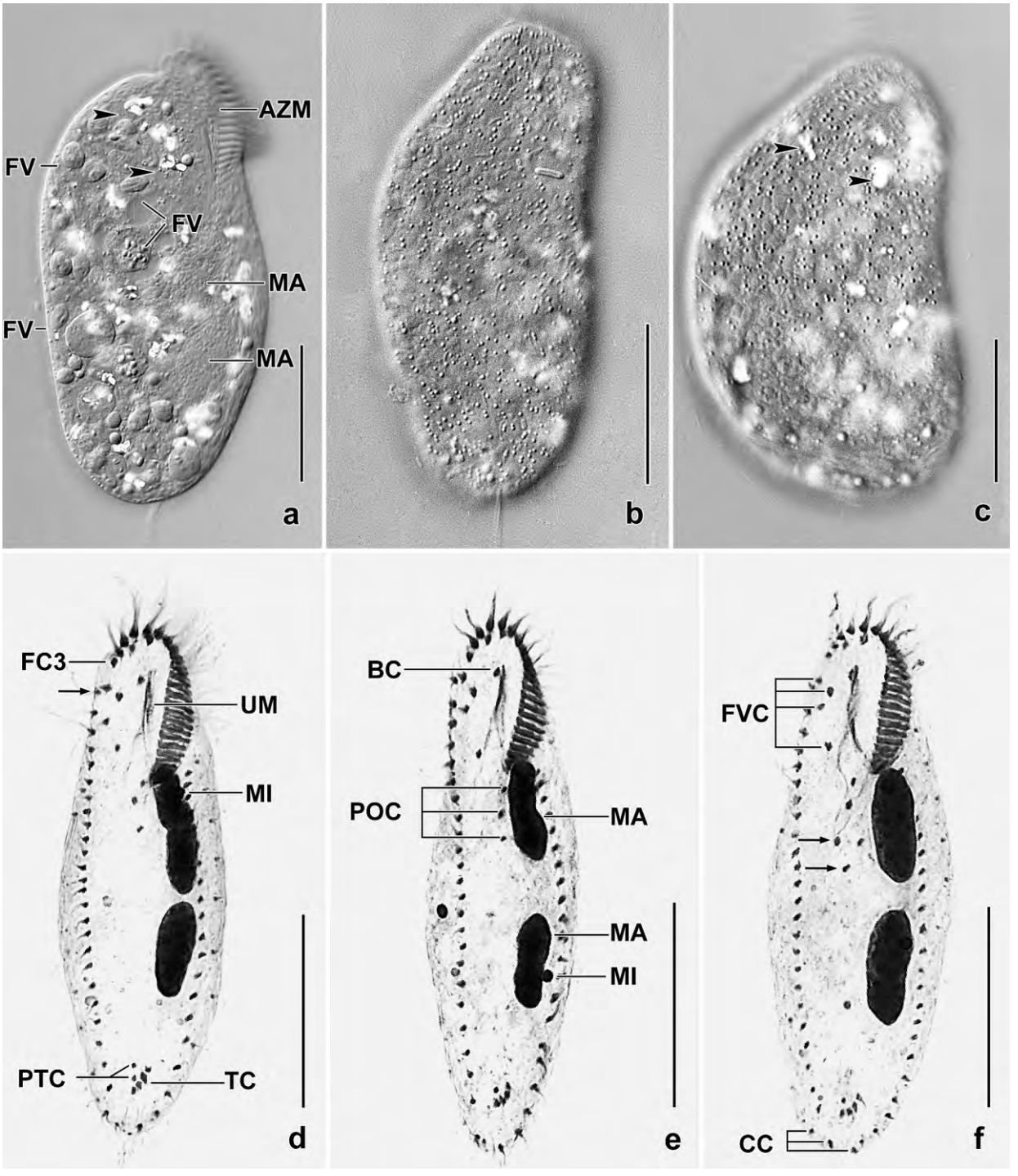

Fig. 270a–f. *Urosomoida galapagensis* from life (a–c) and after protargol impregnation (d–f). Arrowheads mark cytoplasmic crystals. **a:** Ventral view of a squashed specimen, showing the nuclear apparatus, crystals, and food vacuoles. **b, c:** Dorsal view of specimens slightly flattened by coverslip pressure, showing the loose rows of cortical granules. **d, e:** Ventral views, showing the infraciliature and the nuclear apparatus. Arrow (d) marks begin of right marginal row. Micronuclei partially or completely covered by macronuclear nodules. **f:** A specimen with five postoral cirri (arrows). AZM – adoral zone of membranelles, BC – buccal cirrus, CC – caudal cirri, FC3 – frontal cirrus 3, FV – food vacuoles, FVC – frontoventral cirri, MA – macronuclear nodules, MI – micronuclei, POC – postoral cirri, PTC – pretransverse cirri, TC – transverse cirri, UM – undulating membranes. Scale bars 30 μm.

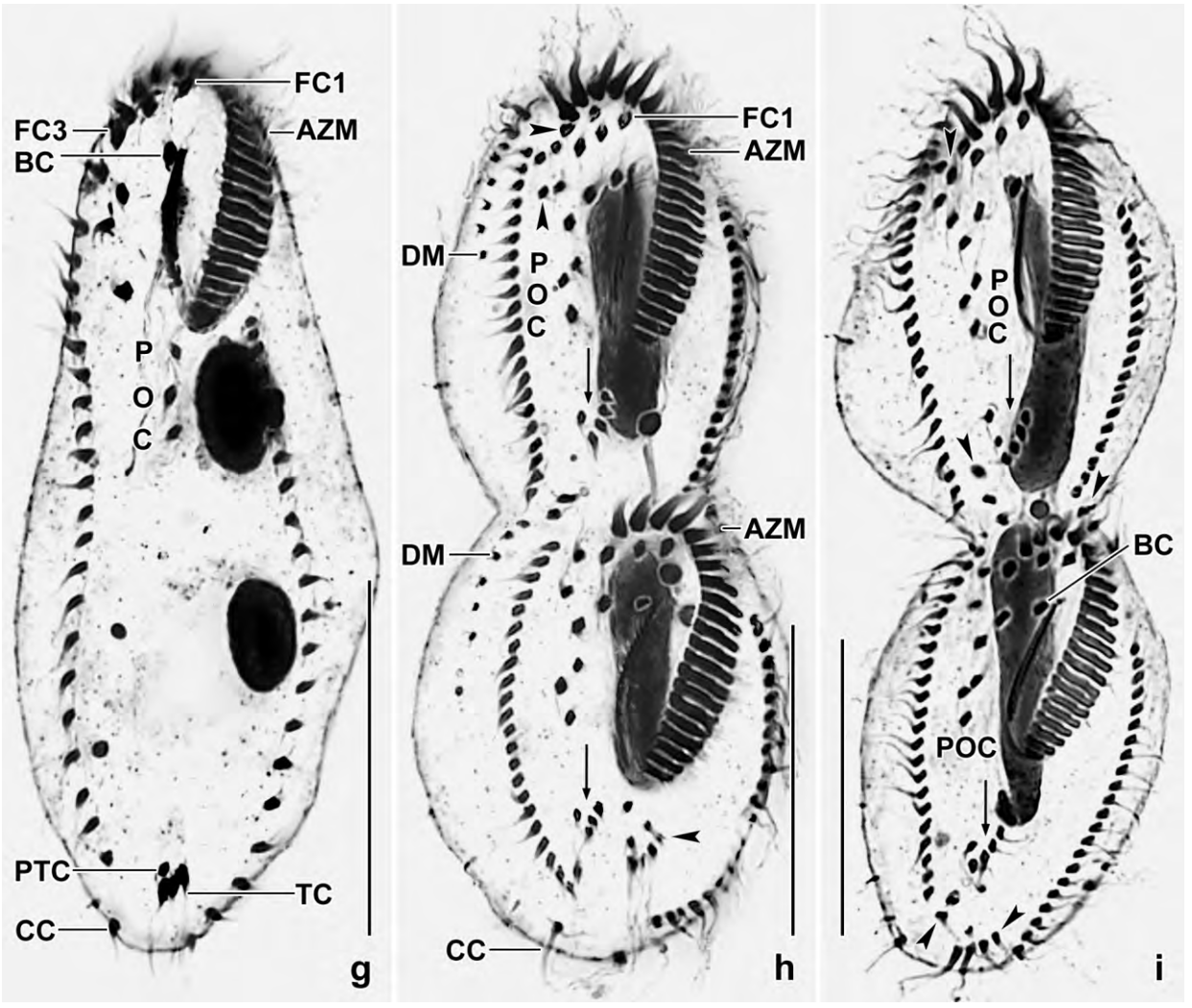

Fig. 270g–i. *Urosomoida galapagensis*, ventral views after protargol impregnation. **g:** A morphostatic specimen, showing the reduced number of transverse and pretransverse cirri. **h, i:** Ventral view of late dividers, showing the migrating cirri, the dorsomarginal kinety, and the dividing macronuclear nodules. Arrows mark the new pretransverse and transverse cirri. Arrowheads denote parental cirri which will be resorbed in very late dividers and early post-dividers. AZM – adoral zone of membranelles, BC – buccal cirrus, CC – caudal cirri, DM – dorsomarginal kinety, FC1,3 – frontal cirri, POC – postoral cirri, PTC – pretransverse cirri, TC – transverse cirri. Scale bars 30 μm.

Table 104. Morphometric data on *Urosomoida galapagensis* based on mounted, protargol-impregnated, and randomly selected specimens from a non-flooded Petri dish culture. Measurements in µm. CV – coefficient of variation in %, M – median, Max – maximum, Mean – arithmetic mean, Min – minimum, n – number of individuals investigated, SD – standard deviation, SE – standard error of arithmetic mean.

Characteristics	Mean	M	SD	SE	CV	Min	Max	n
Body, length	78.0	78.0	5.0	1.1	6.5	70.0	89.0	21
Body, width	28.7	27.0	4.6	1.0	16.2	22.0	40.0	21
Body length: width ratio	2.8	2.8	0.4	0.1	13.8	1.9	3.3	21
Anterior body end to proximal end of adoral zone, distance	22.4	22.0	1.5	0.3	6.8	20.0	25.0	21
Body length: length of adoral zone, ratio	3.5	3.5	0.3	0.1	7.7	3.0	4.0	21
Anterior body end to first frontoventral cirrus, distance	10.0	10.0	1.9	0.4	18.7	6.0	14.0	21
Anterior body end to last frontoventral cirrus, distance	19.6	20.0	1.7	0.4	8.8	15.0	22.0	21
Anterior body end to buccal cirrus, distance	7.5	7.0	0.9	0.2	12.3	5.0	9.0	21
Anterior body end to right marginal row, distance	11.2	11.0	1.6	0.3	14.0	9.0	15.0	21
Anterior body end to first postoral cirrus, distance	24.4	24.0	1.6	0.4	6.7	22.0	27.0	21
Anterior body end to last postoral cirrus, distance	31.3	31.0	2.1	0.5	6.8	28.0	35.0	21
Anterior body end to last postoral cirrus:body length, percentage (%)	40.3	40.5	3.3	0.7	8.1	34.9	45.8	21
Posterior body end to rear transverse cirrus, distance	5.6	6.0	1.2	0.3	21.7	4.0	8.0	21
Posterior body end to anteriormost pretransverse cirrus, distance	9.7	10.0	1.6	0.4	17.0	7.0	12.0	21
Posterior body end to anteriormost pretransverse cirrus:body length, percentage (%)	12.5	12.5	2.2	0.5	17.4	8.3	17.1	21
Posterior body end to right marginal row, distance	7.7	8.0	2.5	0.5	31.8	4.0	13.0	21
Posterior body end to left marginal row, distance	2.4	2.0	1.0	0.2	40.9	1.0	4.0	21
Anterior body end to paroral membrane, distance	8.0	8.0	1.5	0.3	18.4	6.0	11.0	21
Paroral membrane, length	8.3	8.0	1.5	0.3	17.9	6.0	12.0	21
Anterior body end to endoral membrane, distance	6.4	7.0	1.2	0.3	18.8	4.0	9.0	21
Endoral membrane, length	11.7	12.0	1.9	0.4	16.0	9.0	18.0	21
Anterior body end to first macronuclear nodule, distance	21.4	21.0	1.4	0.3	6.4	19.0	24.0	21
Nuclear figure, length	34.8	35.0	3.0	0.7	8.8	28.0	40.0	21
Nuclear figure:body length, percentage (%)	44.7	45.0	3.8	0.8	8.4	33.3	49.3	21
Macronuclear nodules, distance in between	5.0	5.0	2.8	0.6	55.5	1.0	13.0	21
Anterior macronuclear nodule, length	15.0	15.0	2.0	0.4	13.5	11.0	20.0	21
Anterior macronuclear nodule, width	5.7	6.0	1.0	0.2	17.0	4.0	7.0	21
Posterior macronuclear nodule, length	15.4	15.0	1.7	0.4	10.8	12.0	20.0	21
Posterior macronuclear nodule, width	5.3	5.0	1.0	0.2	19.1	3.0	7.0	21
Macronuclear nodules, number	2.0	2.0	0.0	0.0	0.0	2.0	2.0	21
Anterior micronucleus, length	2.1	2.0	0.3	0.1	12.2	2.0	3.0	21
Anterior micronucleus, width	1.8	2.0	0.3	0.1	17.1	1.0	2.0	21
Micronuclei attached to anterior macronuclear nodule, number	1.0	1.0	0.0	0.0	0.0	1.0	1.0	21
Micronuclei attached to posterior macronuclear nodule, number	0.7	1.0	–	–	–	0.0	1.0	21
Micronuclei, total number	1.7	2.0	–	–	–	1.0	2.0	21
Adoral membranelles, number	22.2	22.0	1.2	0.3	5.5	20.0	25.0	21

continued

Characteristics	Mean	M	SD	SE	CV	Min	Max	n
Largest membranellar basis, width	4.8	5.0	–	–	–	4.0	5.0	21
Frontal cirri, number	3.0	3.0	0.0	0.0	0.0	3.0	3.0	21
Frontoventral cirri, number	4.0	4.0	0.0	0.0	0.0	4.0	4.0	21
Buccal cirri, number	1.0	1.0	0.0	0.0	0.0	1.0	1.0	21
Postoral cirri, number	3.3	3.0	–	–	–	3.0	5.0	21
Pretransverse cirri, number	1.8	2.0	–	–	–	1.0	3.0	21
Transverse cirri, number	3.4	3.0	–	–	–	3.0	4.0	21
Pretransverse and transverse cirri, number	5.2	5.0	0.6	0.1	11.6	4.0	6.0	21
Right marginal row, number of cirri	23.6	24.0	2.2	0.5	9.4	20.0	28.0	21
Left marginal row, number of cirri	22.9	23.0	2.4	0.5	10.7	19.0	27.0	21
Caudal cirri, number	3.0	3.0	0.0	0.0	0.0	3.0	3.0	21
Dorsal bristle rows, number	4.0	4.0	0.0	0.0	0.0	4.0	4.0	21
Bristles in dorsal row 1, number	9.1	9.0	1.2	0.3	13.0	7.0	12.0	21
Bristles in dorsal row 2, number	10.2	10.0	1.3	0.3	12.3	8.0	13.0	21
Bristles in dorsal row 3, number	11.0	11.0	1.8	0.4	16.0	8.0	14.0	21
Bristles in dorsal row 4, number	5.8	6.0	0.9	0.2	15.4	4.0	7.0	21

ordinary ones (Fig. 270f); one to three pretransverse cirri; three to four transverse cirri in vivo 15 µm long and thus distinctly projecting from body proper. Bases of pretransverse cirri usually distinctly smaller than those of all other cirri, nevertheless sometimes difficult to distinguish from transverse cirri. Marginal cirri about 10 µm long in vivo, distance between cirri increases slightly from anterior to posterior end in both rows; right marginal row commences at level of anterior frontoventral cirrus (= cirrus VI/4), distance to posterior end of cell very variable (4–13 µm), composed of 24 cirri on average; left marginal row extends almost to body's midline posteriorly, composed of 23 cirri on average.

Dorsal bristles about 3 µm long in vivo, arranged in four rows (Fig. 269d; Table 104). Row 1 distinctly shortened anteriorly, composed of 9 bristles on average; row 2 slightly shortened anteriorly, composed of 10 bristles on average, in 15 out of 32 specimens straight in posterior part (Fig. 269i), in eight specimens with distinct (Fig. 269d) and in seven with a slight posterior bend, respectively, in two specimens with some scattered dikinetids close to posterior end of kinety; row 3 bipolar, extends obliquely from anterior midline to right posterior end of cell, composed of 11 bristles on average; row 4 dorsomarginal, terminates about mid-body, composed of 6 bristles on average. Three caudal cirri associated with kineties 1, 2 and 3, about 15 µm long in vivo (Fig. 269a, d, i, 270f; Table 104).

Oral apparatus extends 25–33%, on average 28% of body length after protargol impregnation (Fig. 269a, b, 270d–f; Table 104). Adoral zone of ordinary shape, composed of an average of 22 membranelles of usual structure and with cilia up to 13 µm long in vivo; largest membranellar bases about 6 µm and 5 µm width, respectively, in vivo and in protargol preparations. Buccal cavity very narrow but rather deep, lip 2–3 µm width. Undulating membranes slightly curved and optically intersecting in anterior third (Fig. 269c, 270d–f). Paroral composed of oblique dikinetids with about 3 µm long cilia in vivo. Pharyngeal fibres distinct in protargol preparations, extend obliquely to mid-body.

Notes on Ontogenesis: A few dividers show that the dorsal ciliature develops in *Urosomoida* pattern, i. e., dorsal kinety 3 does not fragment and only one dorsomarginal kinety develops.

Occurrence and ecology: As yet found only at the highly saline (~ 30 ‰) type locality one day after rewetting the sample.

Remarks: The genus *Urosomoida* contains 11 species, five of which have cortical granules (Berger 1999, Foissner et al. 2002), as *U. galapagensis*. However, only *U. namibiensis* has a similar granule pattern (loose rows) but can easily be distinguished by the number of macronuclear nodules (four vs. two in *U. galapagensis*). In *U. agilis* and *U. granulifera,* the granules are mainly around the cirral and bristle bases or form irregular patches, respectively. *Urosomoida granulifera* has only two caudal cirri compared to three in *U. galapagensis. Urosomoida agilis* has three transverse and pretransverse cirri while there are four to six in *U. galapagensis*.

Heterourosomoida salinarum nov. spec. (Fig. 271a–h, 272a–c; Table 105)

Diagnosis: Size in vivo about 100 × 35 µm; ellipsoid. 2 ellipsoid macronuclear nodules and 2 micronuclei. Cortical granules scattered, colourless, about 0.5 µm across. Cirri of ordinary size and length, transverse cirri fringed distally. 5 rows of dorsal bristles 5–6 µm long in vivo; 2 caudal cirri. Adoral zone of membranelles extends 36% of body length, composed of an average of 23 membranelles. Buccal cavity ordinary; paroral and endoral membrane moderately curved and optically one upon the other, paroral cilia 8 µm long in vivo.

Type locality: Highly saline (~ 100‰) soil from a dry, flat, small lagoon on the coast of the Santa Rosa National Park, Costa Rica, 85°38’ W 10°50’ N.

Type material: 1 holotype and 2 paratype slides with protargol-impregnated specimens have been deposited in the Biology Centre of the Upper Austrian Museum in Linz (LI). Relevant specimens have been marked with black ink circles on the coverslip.

Etymology: The species name is a noun in plural genitive and thus does not change the gender when combined with, e. g., a masculine genus; it refers to the environment, i. e., living and growing in highly saline habitats.

Description: Ordinarily variable, i. e., most and all important features with a CV ≤ 15% (Table 105).

In vivo measurements suggest about 100% preparation shrinkage! Thus, in vivo values for data in Table 105 increase to 85–140 × 35–50 µm with averages of about 115 × 40 µm. Body outline elliptic, laterally flattened up to 2:1 (Fig. 271a, f, 272b). Nuclear apparatus in central third and slightly left of midline of body (Fig. 271a, d, g, 272a, b; Table 105). Macronuclear nodules close together in most specimens, globular to elongate ellipsoid, on average ellipsoid, with many minute nucleoli. Two broadly ellipsoid micronuclei attached to various sites of macronuclear nodules, in vivo about 4 × 3 µm in size. Contractile vacuole near or in mid-body at left margin of cell (Fig. 271a). Cortical granules mainly within cirral and dorsal bristle rows, colourless, rather refractive and thus well recognizable although only 0.5 µm across (Fig. 271e). Cytoplasm

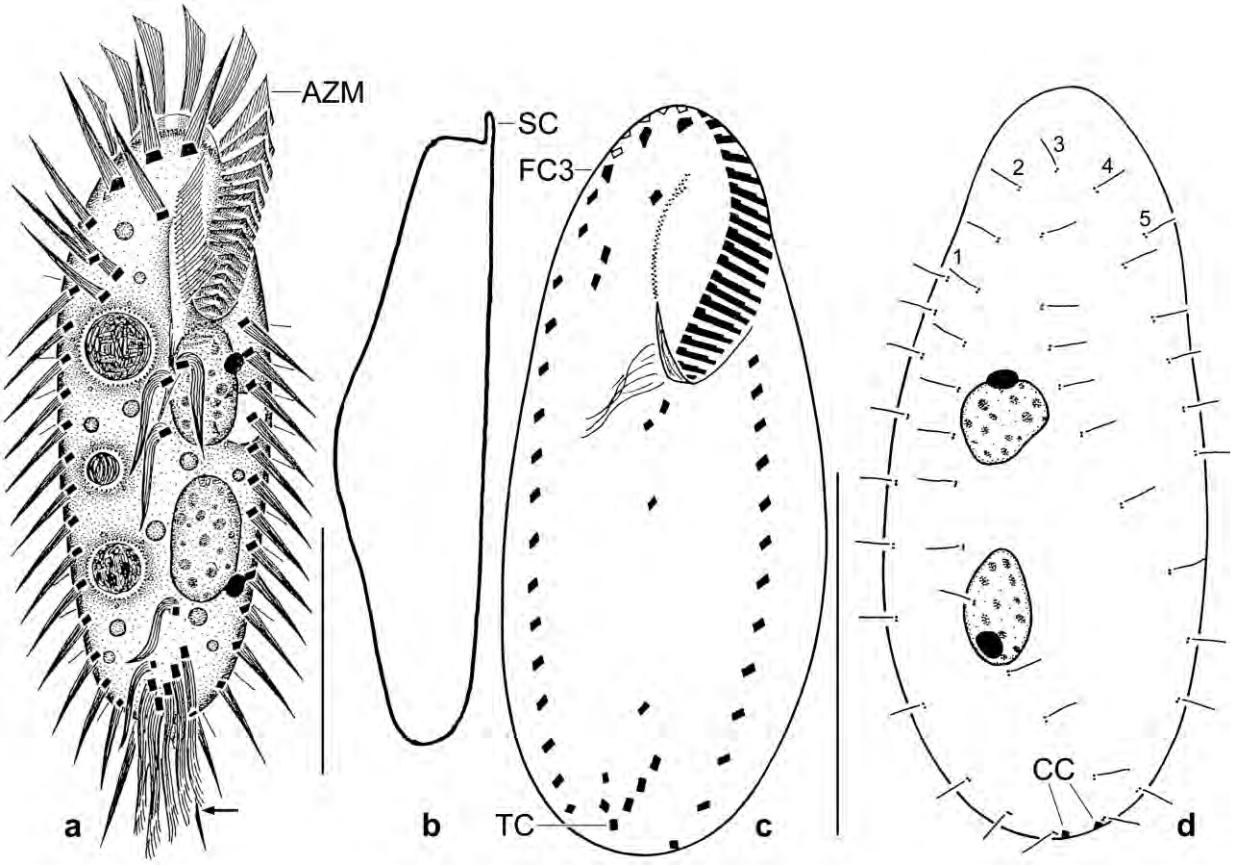

Fig. 271a–d. *Heterourosomoida salinarum* from life (a, b) and after protargol impregnation, which caused strong shrinkage (c, d). **a:** Ventral view of a representative specimen, length 100 µm. The arrow marks the fringed transverse cirri. **b:** Lateral view. **c, d:** Ventral and dorsal view of holotype specimen, length 63 µm. Dorsal kinety 5 consists of only one or two kinetids. Note the 18 fronto-ventral-transverse cirri, i. e., the typical *Oxytricha* pattern. The dorsal bristles, which are 5–6 µm long in vivo, shrunk to 3 µm. AZM – adoral zone of membranelles, CC – caudal cirri, FC3 – frontal cirrus 3, SC – scutum, TC – transverse cirri, 1–5 – dorsal kineties. Scale bars 30 µm (c, d) and 40 µm (a).

colourless, packed with few to many lipid droplets and food vacuoles up to 15 µm across. Likely feeds on bacteria and small protists. Swims and creeps rather rapidly, showing distinct flexibility.

Ventral cirral pattern as typical for *Oxytricha* s. str. (Berger 1999), i. e., with 18 fronto-ventral-transverse cirri of ordinary size, marginal cirri probably composed of three rows of cilia because appearing "thick" in vivo. Frontal and frontoventral cirri about 20 µm long in vivo; buccal cirrus distinctly subapical of paroral membrane; transverse cirri in vivo 25 µm long and thus conspicuously projecting from body proper, fringed distally. Marginal cirral rows extend to near posterior body end (Fig. 271a, c, f, 272a, b; Table 105).

Dorsal bristles 5–6 µm long in vivo, arranged in five rows the two rightmost originating dorsomarginally. Row 3 does not split subterminally as shown by a late divider; row 5 usually composed of only two kinetids; rows 1 and 2 each produces a caudal cirrus (Fig. 271d, g, h, 272c; Table 105).

Oral apparatus extends 30–44% of body length, on average 36% in protargol preparations (Fig. 271a, c, f, 272a, b; Table 105). Adoral zone of ordinary shape and structure, composed of an

Table 105. Morphometric data on *Heterourosomoida salinarum* based on mounted, protargol-impregnated, and randomly selected specimens from a non-flooded Petri dish culture. Measurements in µm. CV – coefficient of variation in %, M – median, Max – maximum, Mean – arithmetic mean, Min – minimum, n – number of individuals investigated, SD – standard deviation, SE – standard error of arithmetic mean.

Characteristics	Mean	M	SD	SE	CV	Min	Max	n
Body, length	56.5	55.0	6.7	1.5	11.9	43.0	69.0	21
Body, width	21.0	21.0	1.9	0.4	9.3	17.0	24.0	21
Body length:width, ratio	2.7	2.7	0.2	0.1	7.4	2.3	3.2	21
Anterior body end to proximal end of adoral zone of membranelles, distance	20.5	21.0	1.5	0.3	7.3	18.0	24.0	21
Adoral zone of membranelles, percentage of body length	36.5	36.0	3.8	0.8	10.4	30.0	44.0	21
Adoral membranelles, number	22.8	23.0	0.8	0.2	3.7	22.0	25.0	21
Largest basis of adoral membranelles, width	4.8	5.0	–	–	–	4.0	5.5	21
Anterior body end to paroral membrane, distance	5.1	5.0	0.9	0.2	16.9	4.0	7.0	21
Anterior body end to endoral membrane, distance	7.0	7.0	1.5	0.3	21.1	5.0	10.0	21
Anterior body end to first macronuclear nodule, distance	18.7	19.0	1.7	0.4	9.1	15.0	21.0	21
First macronuclear nodule, length	10.4	10.0	2.0	0.4	18.9	7.0	15.0	21
First macronuclear nodule, width	5.7	6.0	0.8	0.2	14.6	4.0	7.0	21
Macronuclear nodules, number	2.0	2.0	0.0	0.0	0.0	2.0	2.0	21
Anterior micronucleus, length	2.2	2.0	–	–	–	1.5	3.0	21
Anterior micronucleus, width	1.7	1.5	–	–	–	1.5	2.0	21
Micronuclei, number	2.0	2.0	0.0	0.0	0.0	2.0	2.0	21
Frontal cirri, number	3.0	3.0	0.0	0.0	0.0	3.0	3.0	21
Anterior body end to buccal cirrus, distance	7.1	7.0	0.8	0.2	11.4	6.0	9.0	21
Buccal cirri, number	1.0	1.0	0.0	0.0	0.0	1.0	1.0	21
Frontoventral cirri, number	4.0	4.0	0.0	0.0	0.0	4.0	4.0	21
Postoral cirri, number	3.0	3.0	0.0	0.0	0.0	3.0	3.0	21
Posterior body end to rearmost transverse cirrus, distance	2.4	2.5	0.7	0.2	28.2	1.0	4.0	21
Pretransverse cirri, number	2.0	2.0	0.0	0.0	0.0	2.0	2.0	21
Transverse cirri, number	5.0	5.0	0.0	0.0	0.0	5.0	5.0	21
Anterior body end to right marginal cirral row, distance	13.1	13.0	1.5	0.3	11.7	10.0	17.0	21
Posterior body end to right marginal cirral row, distance	3.1	3.0	1.1	0.2	34.0	1.0	6.0	21
Right marginal cirri, number	13.0	13.0	1.3	0.3	10.0	10.0	17.0	21
Posterior body end to left marginal cirral row, distance	1.0	1.0	–	–	–	0.5	3.0	21
Left marginal cirri, number	13.3	13.0	0.8	0.2	5.9	12.0	15.0	21
Dorsal kineties, number	5.0	5.0	0.0	0.0	0.0	5.0	5.0	21
Kinetids in dorsal kinety 1, number	10.4	10.0	0.8	0.2	7.8	9.0	13.0	21
Kinetids in dorsal kinety 2, number	12.0	12.0	1.0	0.2	8.6	10.0	15.0	21
Kinetids in dorsal kinety 3, number	10.7	11.0	1.0	0.2	9.4	9.0	14.0	21
Kinetids in dorsal kinety 4, number	4.1	4.0	0.5	0.1	11.5	3.0	5.0	21
Kinetids in dorsal kinety 5, number	2.1	2.0	0.4	0.1	18.8	1.0	3.0	21
Caudal cirri, number	2.0	2.0	0.0	0.0	0.0	2.0	2.0	21

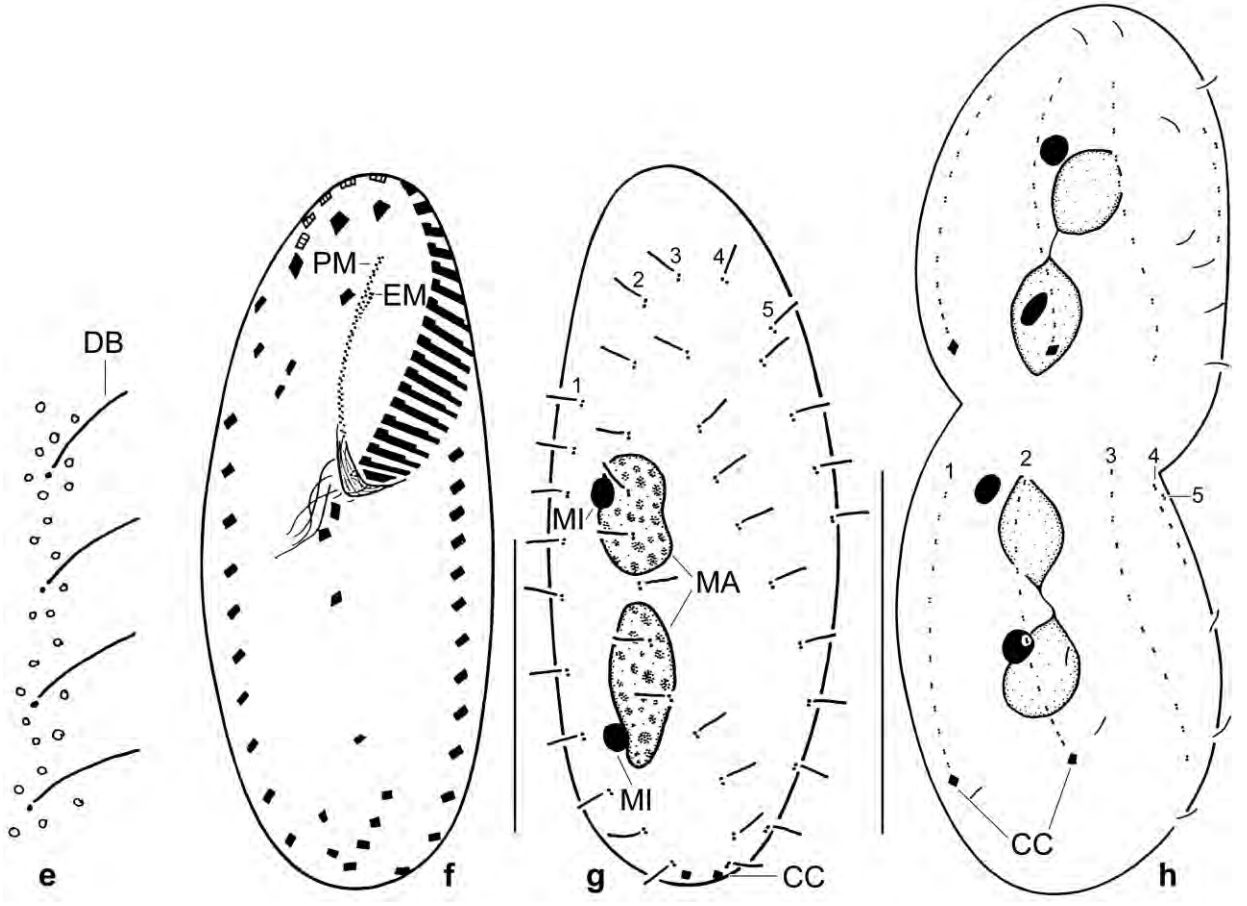

Fig. 271e–h. *Heterourosomoida salinarum* from life (e) and after protargol impregnation (f–h). **e:** Loose cortical granulation. The granules are difficult to recognize because they are colourless and only 0.5 µm in diameter. **f, g:** Ventral and dorsal view of a paratype specimen. The dorsal bristles, which are 5–6 µm long in vivo, shrunk to 3 µm. **h:** Dorsal view of a late divider, showing the absence of fragmentation of kinety 3 and the two caudal cirri produced by kineties 1 and 2. Kinety 5 consists of only one kinetid. CC – caudal cirri, DB – dorsal bristle, EM – endoral membrane, MA – macronuclear nodules, MI – micronuclei, PM – paroral membrane, 1–5 – dorsal kineties. Scale bars 20 µm (f, g) and 30 µm (h).

average of 23 membranelles with largest bases about 10 µm long in vivo. Buccal cavity ordinary; buccal lip narrow, bears paroral membrane with cilia about 8 µm long in vivo. Paroral and endoral membrane slightly curved, optically one upon the other. Pharyngeal fibres ordinary.

Occurrence and ecology: As yet found only at type locality, i. e., in a soil and litter sample from a flat, highly saline (~ 100‰) coastal lagoon.

Remarks: *Heterourosomoida salinarum* differs from *H. lanceolata*, type of the genus (Singh & Kamra, 2015), by the presence vs. absence of cortical granules, the location of the buccal cirrus (far subapical vs. near anterior end of paroral), the arrangement of the undulating membranes (optically one upon the other vs. side by side), and the number of dorsal kineties (5 vs. 4).

Of course, several *Oxytricha* species resemble *H. salinarum*. *Oxytricha nauplia* lacks (vs. possesses) cortical granules, has three (vs. 2) caudal cilia, and dorsal kinety 5 has more kinetids. *Oxytricha halophila* and *O. parahalophila* have very likely a single micronucleus between two

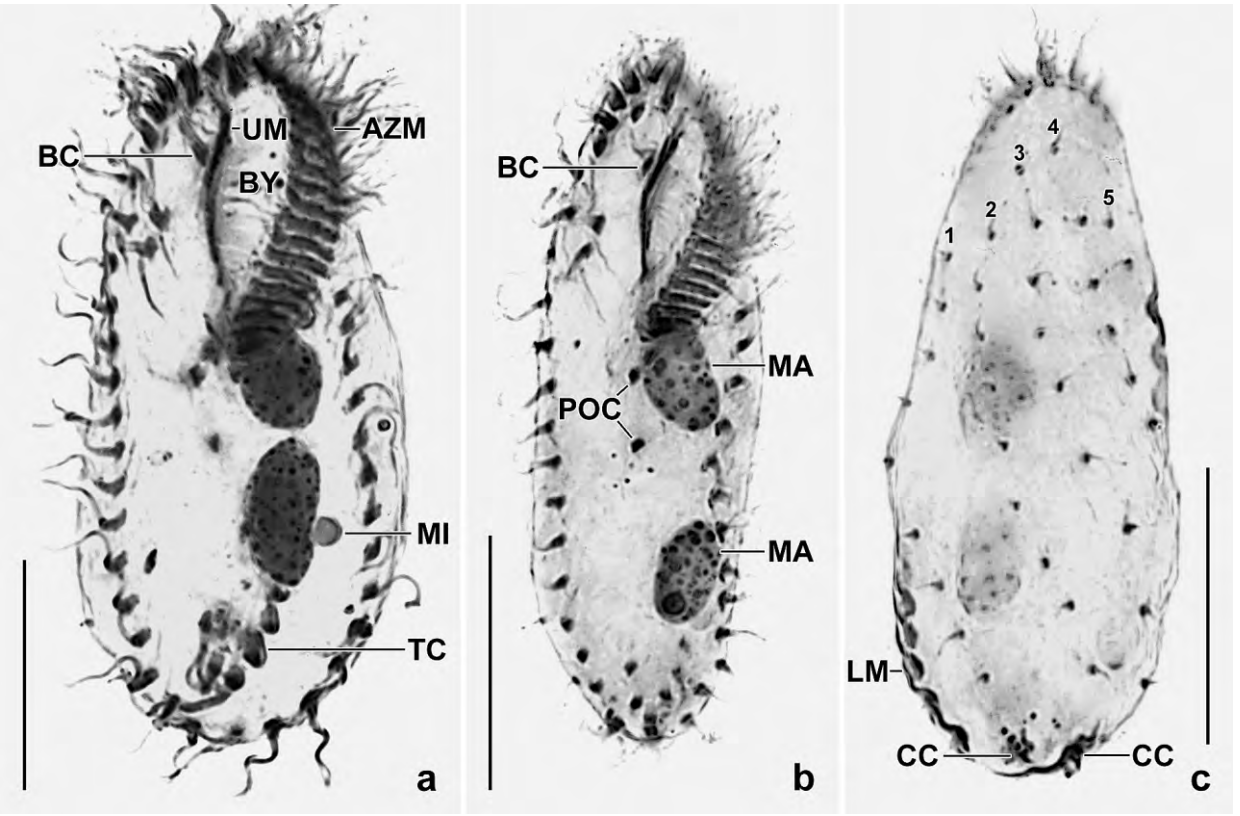

Fig. 272a–c. *Heterourosomoida salinarum* after protargol impregnation. **a, b:** Ventral views showing the high variability in the distance between the macronuclear nodules, the undulating membranes which are optically one upon the other, and the buccal cirrus which is far subapical of the undulating membranes. **c:** Dorsal view, showing the five dorsal kineties of which kinety 5 consists of only two kinetids. Kineties 1 and 2 produce a caudal cirrus each. AZM – adoral zone of membranelles, BC – buccal cirrus, BY – buccal cavity, CC – caudal cirri, LM – left marginal cirral row, MA – macronuclear nodules, MI – micronucleus, POC – postoral cirri, TC – transverse cirri, UM – undulating membranes, 1–5 – dorsal kineties. Scale bars 20 µm.

macronuclear nodules. *Oxytricha similis*, for which a modern redescription is not available, differs by rather vague features, such as the length:width ratio of the body (~3:1 vs. 4:1), the transverse cirri (fringed distally vs. acute), the cortical granules (present vs. absent), and the habitat (mud and soil from a highly saline coastal lagoon vs. freshwater). See Berger (1999) for a review of the species mentioned.

Sterkiella ecuadoriana Foissner & Heber **nov. spec.** (Fig. 273a–f, 274a–c; Tables 106, 107)

Diagnosis: Size in vivo about 145 × 75 µm; ellipsoid to ovate. Nuclear apparatus on average composed of two ellipsoid macronuclear nodules and three micronuclei. On average 19 frontal-ventral-transverse cirri, buccal cirrus between first and second third of paroral membrane. Left marginal row on average composed of 25 cirri, right of 26; rows slightly staggered and almost confluent at posterior end. Six dorsal kineties, kinety 2 with 32 bristles on average. Usually three narrowly spaced caudal cirri. Adoral zone extends about 48% of body length, on average composed of 43 membranelles.

Type locality: Litter and surface soil near the entrance to the El Pahuma Orchid Reserve 35 km northwest of Quito, Ecuador, 1800 m above sea level, 00°01'N 78°38'W.

Type material: 1 holotype slide and 4 paratype slides with protargol-impregnated specimens have been deposited in the Biology Centre of the Upper Austrian Museum in Linz (LI). Relevant specimens have been marked by black ink circles on the coverslip.

Etymology: The species name refers to the Republic of Ecuador, where *Sterkiella ecuadoriana* was discovered.

Description: Size in vivo 110–180 × 60–100 µm, usually about 145 × 75 µm, as calculated from some in vivo measurements and the morphometric data in Table 106 adding 15 % preparation shrinkage. Body semirigid, light brown at low magnification, ellipsoid to broadly ovate, both ends broadly rounded, rarely bluntly pointed posteriorly, dorsoventrally flattened about 2:1 (Fig. 273a–d, 274a, b; Table 106). Nuclear apparatus within central quarters of cell slightly left of body´s midline, on average composed of two macronuclear nodules and 3–4 micronuclei (Fig. 273a, e, 274b; Table 106). Macronuclear nodules broadly to narrowly ellipsoid, rarely dumbbell-shaped, on average 25 × 13 µm in protargol preparations; nucleoli 1–4 µm across. Micronuclei usually attached to macronuclear nodules, globular to ellipsoid, on average 3.2 × 2.5 µm in protargol preparations. Contractile vacuole in mid-body at left cell margin, collecting canals extend about one quarter of body length anteriorly and posteriorly (Fig. 273a). Cortical granules absent (checked with methyl green-pyronin). Food vacuoles scattered throughout body, in vivo up to 30 µm across, contain bacteria, small ciliates (*Protocyclidium terricola*), cysts, flagellates (*Polytomella*), unicellular green algae, and filamentous cyanobacteria. Usually creeps vividly on and between soil particles, showing considerable flexibility, rarely swimming appearing rigid like a board.

Cirral pattern oxytrichid (Berger 1999), number of fronto-ventral-transverse cirri, however, unusually variable (Table 106), causing an average of 19 cirri instead of 18 as typical (Fig. 273a, c, f, 274a, b). Usually three slightly thickened, in vivo about 22 µm long frontal cirri, right cirrus posterior of distal-most adoral membranelle, middle cirrus anterior of buccal cirrus, left cirrus anterior of distal end of undulating membranes; four frontal cirri in one out of 25 specimens. Invariably one slightly thickened buccal cirrus, in protargol preparations about 15 µm long, on average 6 µm posterior of distal end of endoral membrane; anterior of distal end of endoral in one out of 25 specimens investigated. On average five hook-like arranged frontoventral cirri, about 20 µm long in vivo, anterior-most cirrus usually at level of buccal cirrus. On average three postoral cirri in inverted L-shaped pattern slightly posterior to body centre, distance between cirrus V/4 and V/3 on average 13 µm in protargol preparations. Usually two obliquely arranged pretransverse cirri, about 15 µm long in protargol preparations. On average five hook-like arranged transverse cirri, slightly thickened and distally fringed, about 30 µm long in vivo and about 20 µm in protargol preparations, distal half projects from body proper. Marginal cirral rows posteriorly staggered and almost confluent in body´s midline, leaving an average space of 5.6 µm. Left marginal row difficult to separate from caudal cirri, composed of an average of 25 cirri, right of 26; cirri about 20 µm long in vivo, 15–16 µm in protargol preparations, composed of two to three ciliary rows, rarely of one or four, cirral size gradually decreasing posteriorly (Fig. 273a, c, f, 274a, b; Table 106).

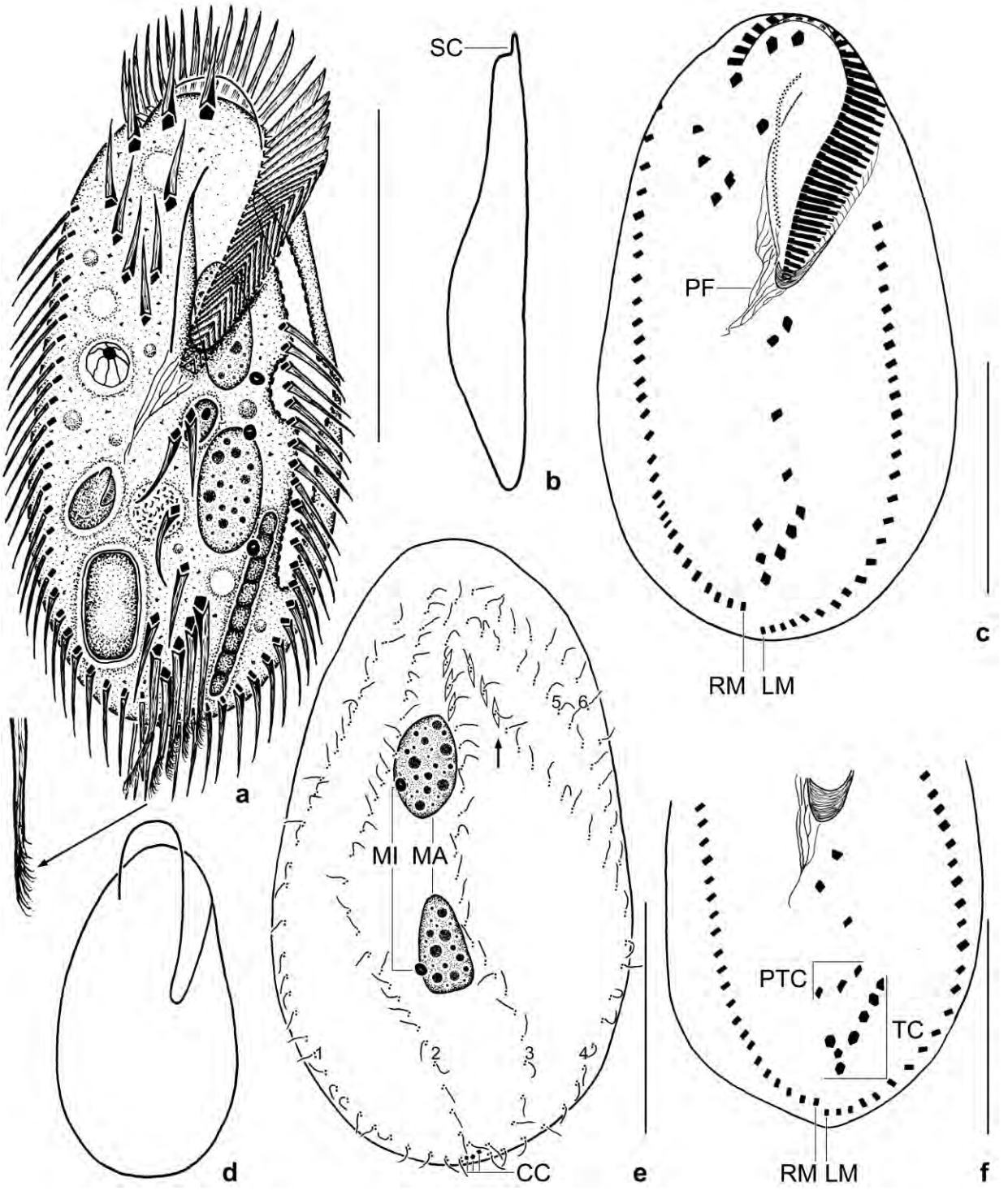

Fig. 273a–f. *Sterkiella ecuadoriana* from life (a, b, d) and after protargol impregnation (c, e, f). **a:** Ventral view of a representative specimen, length 145 µm. **b:** Lateral view. **c, e:** Ventral and dorsal view of holotype, length 135 µm. Arrow marks lenticular fibre bundles around the dorsal kinetids. **d:** Outline of an ovate specimen. **f:** Posterior body region of a specimen with a very narrow gap between the almost confluent marginal cirral rows. Note supernumerary pretransverse and transverse cirri. CC – caudal cirri, LM – left marginal row, MA – macronuclear nodules, MI – micronuclei, PF – pharyngeal fibres, PTC – pretransverse cirri, RM – right marginal row, SC – scutum, TC – transverse cirri, 1–6 – dorsal kineties. Scale bars 50 µm (c, e, f) and 75 µm (a).

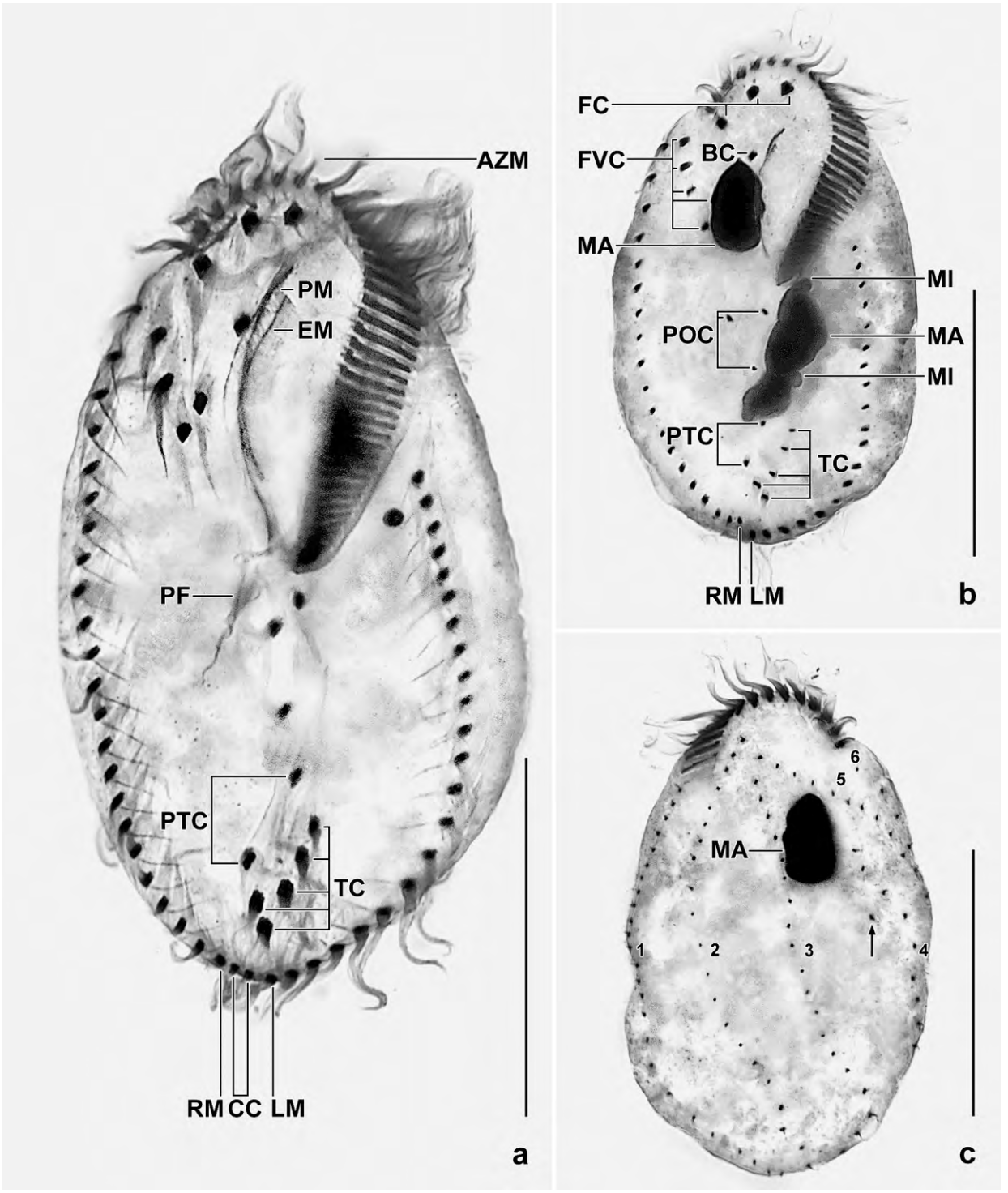

Fig. 274a–c. *Sterkiella ecuadoriana* after protargol impregnation. **a:** Ventral view of an ellipsoid specimen, showing caudal cirri in gap between marginal rows, length 113 µm. **b, c:** A broadly ovate specimen, showing the ventral and dorsal infraciliature and the almost confluent marginal rows, length 91 µm. Arrow marks a supernumerary dorsal bristle. AZM – adoral zone of membranelles, BC – buccal cirrus, CC – caudal cirri, EM – endoral, FC – frontal cirri, FVC – frontoventral cirri, LM – left marginal row, MA – macronuclear nodules, MI – micronuclei, PF – pharyngeal fibres, PM – paroral, POC – postoral cirri, PTC – pretransverse cirri, RM – right marginal row, TC – transverse cirri, 1–6 – dorsal kineties. Scale bars 50 µm.

Six dorsal kineties composed of a total of 137 bristles on average (Table 106). Kineties 1–3 bipolar, kinety 4 slightly shortened anteriorly, kineties 5 and 6 do not extend beyond mid-body (Fig. 273e, 274c). Dorsal bristles 3–4 µm long in vivo and in protargol preparations, some parental bristles occasionally preserved. Caudal cirri in or slightly right of body´s midline at end of bristle rows 1, 2, and 4, about 20 µm long in protargol preparations, conspicuously thin and very narrowly spaced (distance between first and third cirrus 3.5 µm, Table 106); easily confused with last cirri of marginal rows; only two caudal cirri in 10 out of 25 specimens investigated (Fig. 273e, 274a; Table 106).

Adoral zone extends about 48% of body length, on average composed of 43 ordinary membranelles with about 17 µm long cilia, bases of largest membranelles about 11 µm width in protargol preparations (Fig. 273a, c, 274a, b; Table 106). Buccal cavity rather flat and narrow, right wall straight and thickened. Buccal lip about 6 µm wide in vivo, covers proximal membranelles. Undulating membranes in body´s midline, slightly curved leftward in protargol preparations,

Table 106. Morphometric data on *Sterkiella ecuadoriana* based on mounted, protargol-impregnated, and randomly selected specimens from a non-flooded Petri dish culture. Measurements in µm. CV – coefficient of variation in %, M – median, Max – maximum, Mean – arithmetic mean, Min – minimum, n – number of individuals investigated, SD – standard deviation, SE – standard error of arithmetic mean.

Characteristics	Mean	M	SD	SE	CV	Min	Max	n
Body, length	124.0	120.0	15.2	2.9	12.2	91.0	150.0	27
Body, width	72.3	70.0	8.4	1.6	11.7	56.0	91.0	27
Body length:width, ratio	1.7	1.7	0.1	0.1	7.0	1.5	2.0	27
Macronuclear nodules, number [a]	2.3	2.0	–	–	–	2.0	3.0	23
Anterior body end to first macronuclear nodule, distance	34.0	33.0	6.4	1.3	18.9	17.0	45.0	23
Macronuclear figure, length	61.5	60.0	8.1	1.7	13.2	47.0	76.0	23
Anterior macronuclear nodule, length	23.7	24.0	3.9	0.8	16.7	15.0	33.0	23
Anterior macronuclear nodule, width	12.9	13.0	1.7	0.4	13.2	10.0	16.0	23
Micronuclei, number	3.5	3.0	1.5	0.3	44.0	1.0	7.0	25
Anterior micronucleus, length	3.2	3.3	–	–	–	2.6	3.9	25
Anterior micronucleus, width	2.5	2.6	–	–	–	2.0	3.3	25
Anterior end to proximal end of adoral zone, distance	60.0	60.0	8.5	1.7	14.2	42.0	73.0	25
Adoral zone of membranelles, percentage of body length	48.1	48.0	3.4	0.7	7.1	40.5	55.2	25
Adoral membranelles, number	42.6	44.0	4.7	0.9	11.1	32.0	49.0	25
Adoral membranelles, length of widest bases	11.0	11.0	1.2	0.2	10.9	9.0	13.0	25
Anterior body end to paroral, distance	12.3	12.0	1.8	0.4	14.6	10.0	16.0	25
Paroral, length	33.6	33.0	7.0	1.4	20.7	19.0	45.0	25
Anterior body end to endoral, distance	16.2	16.0	2.1	0.4	13.2	12.0	20.0	25
Endoral, length	38.0	40.0	6.9	1.4	18.2	22.0	47.0	25
Anterior body end to buccal cirrus, distance	22.2	22.0	4.1	0.8	18.6	14.0	31.0	25
Anterior end of endoral to buccal cirrus, distance [b]	6.4	6.5	2.8	0.6	42.8	1.0	12.0	24
Frontoventral cirri, number	4.6	4.0	1.0	0.2	20.8	4.0	8.0	25
Postoral cirri, number	3.3	3.0	1.0	0.2	29.8	1.0	6.0	25

continued

Characteristics	Mean	M	SD	SE	CV	Min	Max	n
Postoral cirrus V/4 and V/3, distance in between	13.0	13.0	3.2	0.6	24.7	7.0	20.0	25
Pretransverse cirri, number	2.0	2.0	0.4	0.1	17.2	1.0	3.0	25
Anterior body end to first transverse cirrus, distance	97.8	98.0	12.7	2.5	13.0	66.0	122.0	25
Posterior body end to last transverse cirrus, distance	9.2	9.0	2.7	0.5	29.1	6.0	14.0	25
Transverse cirri, number	5.3	5.0	0.6	0.1	11.6	4.0	7.0	25
Frontal-ventral-transverse cirri, total number	19.2	19.0	1.9	0.4	9.6	15.0	24.0	25
Right marginal row, number of cirri	25.9	26.0	2.7	0.5	10.5	19.0	30.0	25
Left marginal row, number of cirri	24.7	25.0	2.3	0.5	9.4	19.0	28.0	25
Posteriormost marginal cirri, transverse distance	5.6	5.6	2.2	0.4	38.3	2.0	11.0	25
Posteriormost marginal cirri, staggered (longitudinal) distance	2.0	2.0	1.1	0.2	54.5	0.4	4.0	25
Caudal cirri, number	2.6	3.0	–	–	–	2.0	3.0	25
Caudal cirri 1 and 3, distance in between	3.5	3.2	0.7	0.2	20.0	2.5	5.0	15
Dorsal kinety 1, number of bristles	36.0	36.0	4.7	1.0	13.2	27.0	45.0	21
Dorsal kinety 2, number of bristles	32.0	33.0	3.9	0.8	12.1	24.0	42.0	21
Dorsal kinety 3, number of bristles	24.2	24.0	2.3	0.5	9.4	20.0	28.0	21
Dorsal kinety 4, number of bristles	21.3	22.0	3.4	0.8	16.1	13.0	28.0	21
Dorsal kinety 5, number of bristles	14.9	15.0	3.6	0.8	24.0	6.0	21.0	21
Dorsal kinety 6, number of bristles	8.2	8.0	2.3	0.5	27.7	4.0	12.0	21
Dorsal bristles, total number	136.7	137.0	15.5	3.4	11.4	106.0	158.0	21

[a] Two specimens with only one nodule were excluded.

[b] One out of 25 specimens investigated has the buccal cirrus in front of the endoral and was thus excluded.

intersect optically near or slightly posterior to buccal cirrus. Paroral on average 34 µm long, commences 12 µm posterior of anterior body end, cilia about 12 µm long in vivo. Endoral commences 4 µm posterior of paroral and extends to buccal vertex, cilia in vivo likely more than 20 µm long, forming a dense pharyngeal bundle (Fig. 273c, 274a; Table 106).

Notes on ontogenesis: Very similar to that of *S. nova* (Foissner & Berger 1999), i. e., formation of dorsal kineties in *Oxytricha* pattern, adoral zone not reorganized, and separate cirral anlagen for proter and opisthe. Proter's cirral anlagen formed by undulating membranes and cirri II/2, III/2, VI/3; opisthe's anlagen generated by oral primordium and cirri IV/2, V/4. One out of eight dividers with seven proter cirral anlagen.

Occurrence and ecology: As yet found only at type locality. The clumsy body shape suggests that *S. ecuadoriana* is a litter species.

Remarks: Four species of the *S. histriomuscorum* complex have two macronuclear nodules: *S. ecuadoriana*, *S. histriomuscorum*, *S. nova*, and *S. tricirrata*. The first three species are easily distinguished from S. tricirrata by the increased number of transverse cirri (> 3 vs. 3) and dorsal kineties (6 vs. 5). The comparison in Table 107 reveals that *S. ecuadoriana* can be separated from the congeners by body size (124 × 72 µm vs. 74–99 × 39–47 µm), the fringed transverse cirri (vs. tapered), and the staggered, almost confluent marginal cirral rows (vs. not staggered and more separate); however, the two last mentioned features have high coefficients of variability (CV = 54.5 and 38.3) and must thus used with care. Furthermore, *S. ecuadoriana* differs from *S. nova*

Table 107. Comparison of *Sterkiella ecuadoriana*, *S. nova* (from FOISSNER & BERGER 1999), a *Sterkiella* population from activated sludge (AUGUSTIN & FOISSNER 1992), and combined values of nine *S. histriomuscorum* populations from Austria (FOISSNER 1982 and BERGER et al. 1985), Korea (SHIN & KIM 1994), USA (FOISSNER & BERGER 1999), and Antarctica (PETZ & FOISSNER 1997). Data based on mounted, protargol-impregnated (FOISSNER's method), and randomly selected specimens. Measurements in µm: first value arithmetic mean; minimum and maximum in parentheses.

Characteristics	***S. ecuadoriana***	**AUGUSTIN & FOISSNER 1992**	***S. nova***	***S. histrio-muscorum***
Body, length	124 (91–150)	99 (85–129)	98 (87–113)	74 (52–96)
Body width	72 (56–91)	47 (41–62)	47 (25–60)	39 (25–50)
Adoral zone of membranelles, percentage of body length	48 (41–55)	45[a]	41[a]	41[a] (38–44)[a]
Adoral membranelles, number	43 (32–49)	39 (34–44)	34 (30–39)	30 (24–35)
Transverse cirri fringed	yes	no	no	no
Marginal cirral rows staggered posteriorly	yes	no	no	no
Left marginal row, number of cirri	25 (19–28)	23 (18–25)	20 (17–23)	18 (12–21)
Dorsal kinety 2, number of bristles	32 (24–42)	32[b]	20 (16–22)	18 (17–26)
Posteriormost cirri of marginal rows, transverse distance	5.6 (2.4–11.2)	10.4[b]	5.5[b]	8.2[b] (5.0–10.4)[b]
Caudal cirri 1 and 3, distance in between	3.5 (2.5–4.8)	5.8[b]	3.5[b]	4.1[b] (3.1–5.0)[b]
Habitat	soil	activated sludge	limnetic	soil
Specimens investigated, number	15–27	20	29	> 100

[a] Calculated from arithmetic means.

[b] According to the related illustrations.

and *S. histriomuscorum* by the number of adoral membranelles (43 vs. 34 and 30) and by the number of bristles in dorsal kinety 2 (32 vs. 20 and 18). Interestingly, a *Sterkiella* population from activated sludge has some characters similar to *S. ecuadoriana* (AUGUSTIN & FOISSNER 1992). However, in other features, such as body size, the distance between the caudal cirri, and the distance between the marginal rows, the sludge population differs clearly from *S. ecuadoriana* (Table 107); very likely, it is another distinct species of the *S. histriomuscorum* complex and possibly the one most closely related to *S. ecuadoriana*.

Totothrix nov. gen.

Diagnosis: Oxytrichids with frontoterminal, transverse, and caudal cirri. Two or more rows each of right and left (marginal?) cirri; one or more curved cirral rows in body´s midline. 5 or 6 fronto-ventral-transverse cirral anlagen originating in *Oxytricha* pattern. Dorsal kineties generated by within anlagen, split of kinety 3, and dorsomarginally. Buccal cavity wide and deep. Adoral zone of membranelles formed like a question mark. Undulating membranes long, curved, and optically intersecting.

Table 108. Comparison of *Totothrix* with similar genera.

Features	*Toto-thrix*	*Anatolio-cirrus*	*Fragmo-cirrus*	*Allo-tricha*	*Parento-cirrus*	*Para-kahliella*	*Para-urostyla*
Transverse cirri	present	present	present	present	present	absent	present
Caudal cirri	present	present	present	present	present	present	present
Dorsal kinety fragmentation	present	absent	absent	present	present	present	present
Frontoterminal cirri	present	present	absent	absent	absent	absent	absent
References	This study	FOISSNER et al. (2000)	FOISSNER (2000b)	BERGER (1999)	BERGER (1999)	BERGER (2011)	BERGER (1999)

Type species: *Totothrix panamensis* nov. spec.

Etymology: Composite of the Latin adjective *totus* (complete) and the Greek noun *thrix* (hair ~ ciliature), meaning a "ciliate with complete cirral pattern". Feminine gender.

Remarks: The morphostatic and the dividing cirral pattern of *T. panamensis* indicate that it has frontoterminal cirri, five or six fronto-ventral-transverse cirral anlagen, and a split of dorsal kinety 3. Thus, it is very likely an oxytrichid (for a review, see BERGER 1999). Table 108 compares *Totothrix* with similar genera. Each of the features chosen is a genus character. *Totothrix* differs from the other genera in having all features while, e. g., *Anatoliocirrus* lacks fragmentation of dorsal kinety 3 (FOISSNER et al. 2002). Of course, there are also other important characteristics which, however, were excluded because they are not yet known in *Totothrix*.

Totothrix panamensis nov. spec. (Fig. 275a–g; Tables 108, 109)

Diagnosis: Size in vivo about 120 × 45 µm; ellipsoid to elongate ellipsoid. On average 7 globular macronuclear nodules and several globular micronuclei in a row left of body´s midline. 2 right (marginal?) cirral rows, 2–3 left rows, and 1 row in body´s midline composed of 12 cirri on average and extending about 60% of body length. 4 frontal cirri, 5 frontoterminal cirri, 1 buccal cirrus, 3 transverse cirri, 2 caudal cirri, and 5 dorsal kineties. Adoral zone of membranelles occupies about 36% of body length, composed of 41 membranelles on average. Paroral and endoral membrane intersect in or near mid of buccal cavity.

Type locality: Brownish surface soil (pH 8) from the foot of the Cerro Pirre mountain in the Darien Forest, Panama, 8°10'N 77°30'W.

Type material: 1 holotype and 4 paratype slides with protargol-impregnated specimens have been deposited in the Biology Centre of the Upper Austrian Museum in Linz (LI). Relevant specimens have been marked by black ink circles on the coverslip.

Etymology: Named after the country it was discovered, i. e., Panama, Central America.

Description: This species was very rare and thus only 10 useable specimens were found in the protargol preparations. Rather variable, i. e., coefficients of variation (CV) often near or above 15%.

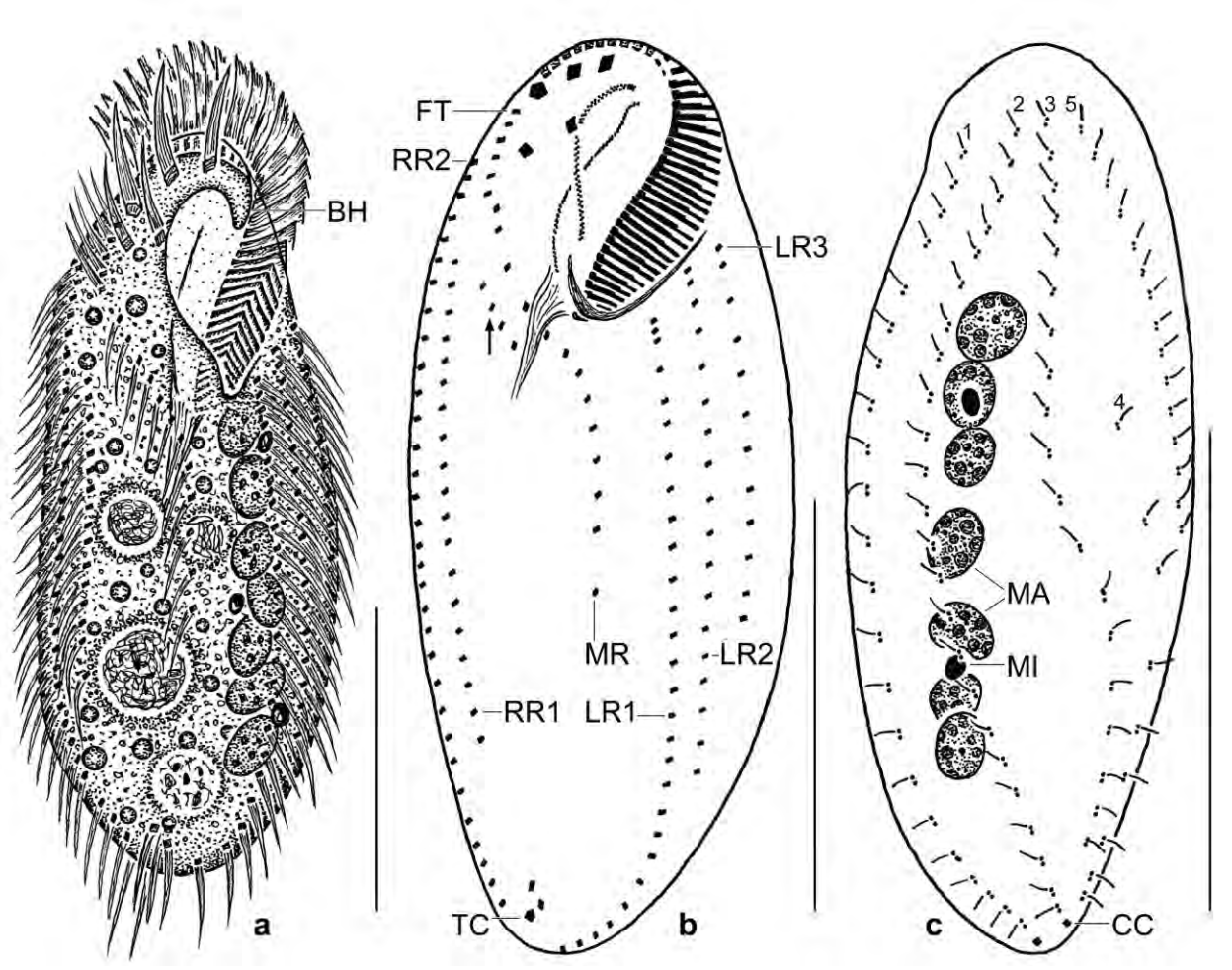

Fig. 275a–c. *Totothrix panamensis* from life (a) and after protargol impregnation (b, c). **a:** Ventral view of a representative specimen, length 120 µm. **b:** Infraciliature of ventral side of holotype specimen, length 110 µm. Arrow marks a very short cirral row. **c:** Dorsal view, showing the nuclear apparatus and the oxytrichid bristle pattern, that is, row 4 very likely originates from a split of row 3 and is thus distinctly shorter. BH – buccal horn, CC – caudal cirri, FT – supposed frontoterminal cirri, LR1–3 – cirral rows in left field, MA – macronuclear nodules, MI – micronucleus, MR – middle cirral row, RR1, 2 – cirral rows in right field, TC – transverse cirri, 1–5 – dorsal bristle rows. Scale bars 50 µm.

Size in vivo 80–140 × 40–55 µm, usually about 120 × 45 µm, as calculated from some live measurements and the morphometric data in Table 109 adding 15% preparation shrinkage. Body ellipsoid (~ 2:1) to elongate ellipsoid (~ 3:1) with both ends broadly rounded; flattened laterally about 2:1 and 3:1 right of dorsomarginal kinety, producing a rather sharp, oblique line when focused from ventral to dorsal (Fig. 275a, d; Table 109). Nuclear apparatus in left half of cell, composed of an average of seven macronuclear nodules and three micronuclei, forming a row between buccal vertex and body end (Fig. 275a, c; Table 109). Macronuclear nodules globular to broadly ellipsoid, with many ordinarily-sized nucleoli. Micronuclei globular to broadly ellipsoid, attached to macronuclear row at various positions. Contractile vacuole not studied. Cortex flexible, countless subcortical crystals in roughly longitudinal rows, individual crystals granular, oblong, dumbbell-shaped, or drumstick-shaped, up to 3 µm long (Fig. 275e). Cytoplasm colourless, contains lipid droplets and food vacuoles about 15 µm across (Fig. 275a). Feeds on bacteria, heterotrophic flagellates, cysts of naked amoebae, and likely also on small and middle-

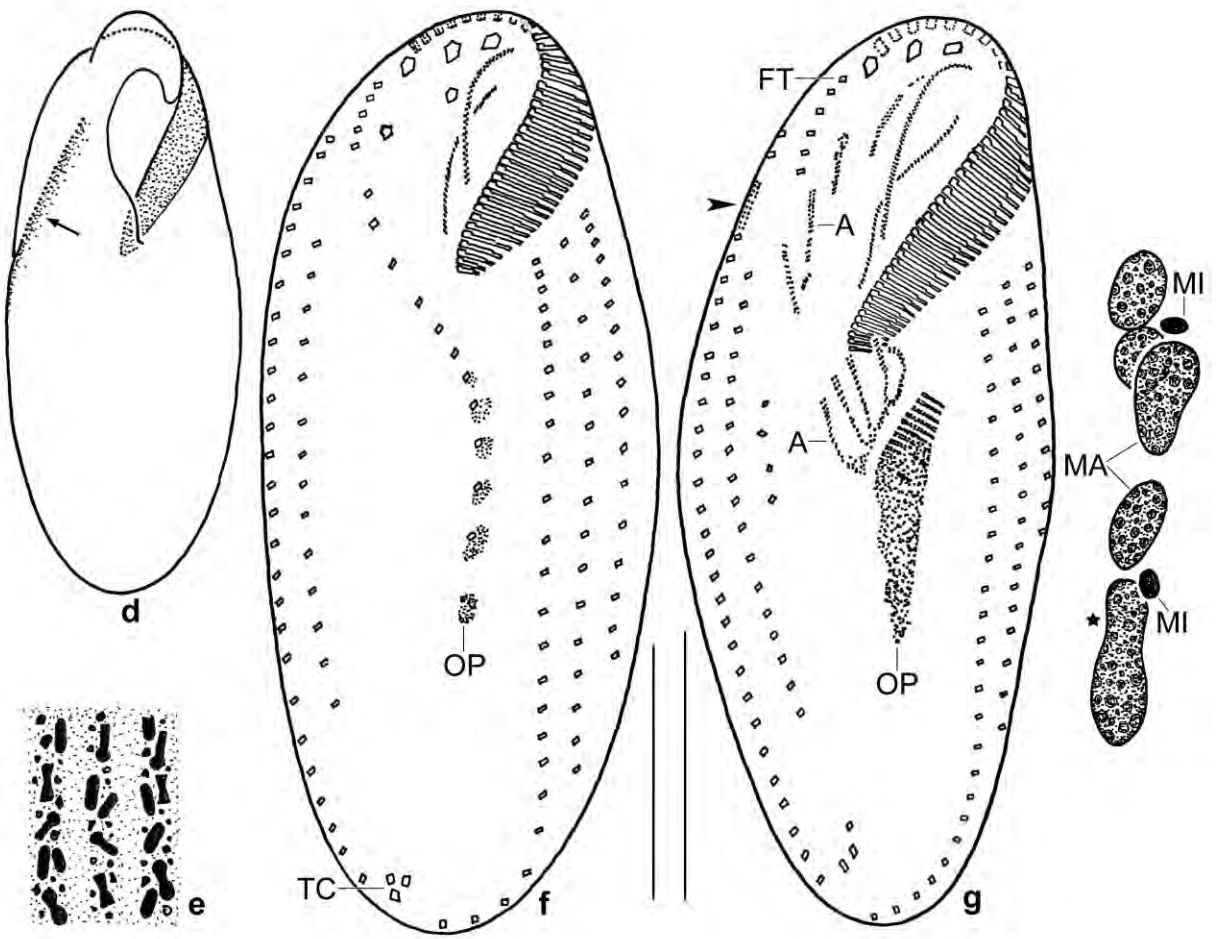

Fig. 275d–g. *Totothrix panamensis* from life (d, e) and after protargol impregnation (f, g). **d:** An ellipsoid specimen with a distinct line (arrow) along the dorsomarginal bristle kinety, where the body abruptly flattens. **e:** Subcortical crystal stripes, individual crystals up to 3 µm long. **f:** Ventral view of a very early divider, showing the oral primordium developing in the posterior half of the middle cirral row. **g:** An early mid-divider, showing fusing macronuclear nodules (asterisk), the forming opisthe adoral zone of membranelles, and cirral anlagen streaks. The arrowhead marks an anlage in row 2 of the right cirral field. A – cirral anlagen streaks, FT – frontoterminal cirri, MA – macronuclear nodules, MI – micronuclei, OP – oral primordium, TC – transverse cirri. Scale bars 30 µm.

sized ciliates. Glides rather rapidly on microscope slide.

Frontal cirri and buccal cirrus about 20 µm long in vivo and distinctly enlarged, third frontal cirrus at anterior end of adoral zone of membranelles, buccal cirrus slightly anterior of mid of paroral membrane. Other cirri thin, in vivo about 15 µm long, arranged as shown in Figures 275a, b, f: two cirral rows along right body margin, external row 2 almost bipolar, internal row 1 in central quarters of body, length and number of cirri highly variable (CV ~ 22%); three, rarely two cirral rows along left body margin, length of rows and number of cirri strongly decreasing from right to left; middle cirral row commences anterior to buccal vertex and ends posterior of mid-body, distinctly convex, number of cirri rather stable (CV 12%); frontoterminal cirri slightly right of anterior end of middle cirral row, composed of an average of five cirri forming a distinct row near right anterior margin of cell; transverse cirri comparatively inconspicuous because of

Table 109. Morphometric data on *Totothrix panamensis* based on mounted, protargol-impregnated, randomly selected specimens from a non-flooded Petri dish culture. Measurements in µm. CV – coefficient of variation in %, M – median, Max – maximum, Mean – arithmetic mean, Min – minimum, n – number of individuals investigated, SD – standard deviation, SE – standard error of arithmetic mean.

Characteristics	Mean	M	SD	SE	CV	Min	Max	n
Body, length	100.0	100.0	14.1	4.4	14.1	75.0	120.0	10
Body, width	40.6	39.5	4.8	1.5	11.9	35.0	49.0	10
Body length:width, ratio	2.5	2.4	0.3	0.1	10.5	2.1	3.1	10
Anterior body end to proximal end of adoral zone, distance	35.0	35.0	4.5	1.4	12.8	25.0	40.0	10
Adoral zone of membranelles, number of membranelles	35.5	35.7	5.5	1.8	15.6	27.0	45.0	10
Adoral zone, number of membranelles	40.7	40.5	4.2	1.3	10.4	35.0	48.0	10
Anterior body end to end of middle cirral row, distance	60.9	56.0	8.9	3.4	14.6	50.0	75.0	7
Middle row, number of cirri	11.7	11.5	1.2	0.5	10.4	10.0	13.0	6
Nuclear figure, length	55.6	55.5	8.2	2.6	14.8	42.0	70.0	10
Macronuclear nodules, length	8.5	8.0	1.7	0.5	19.4	7.0	11.0	10
Macronuclear nodules, width	7.3	7.0	1.2	0.4	15.9	6.0	10.0	10
Macronuclear nodules, number	7.3	7.0	0.8	0.2	9.2	6.0	8.0	10
Micronuclei, length	3.0	3.0	0.0	0.0	0.0	3.0	3.0	10
Micronuclei, width	2.6	2.3	–	–	–	2.0	2.5	10
Micronuclei, number	3.1	3.0	1.2	0.4	39.9	1.0	5.0	8
Right (marginal?) rows, number	2.0	2.0	0.0	0.0	0.0	2.0	2.0	10
Right (marginal?) row 1, number of cirri	15.9	16.5	3.5	1.1	21.9	7.0	19.0	10
Right (marginal?) row 2, number of cirri	31.0	31.0	1.8	0.6	5.9	28.0	33.0	10
Left (marginal?) rows, number	2.9	3.0	–	–	–	2.0	3.0	10
Left (marginal?) row 1, number of cirri	22.6	25.0	6.3	2.0	28.0	7.0	28.0	10
Left (marginal?) row 2, number of cirri	18.6	18.0	3.0	1.0	16.3	14.0	26.0	10
Left (marginal?) row 3, number of cirri	9.8	10.5	3.2	1.0	32.9	2.0	13.0	10
Frontoterminal cirri, number	5.1	5.0	0.9	0.3	18.2	4.0	6.0	9
Frontal cirri, number	3.0	3.0	0.0	0.0	0.0	3.0	3.0	10
Buccal cirri, number	1.0	1.0	0.0	0.0	0.0	1.0	1.0	10
Transverse cirri, number	3.0	3.0	0.0	0.0	0.0	3.0	3.0	10
Caudal cirri, number	2.0	2.0	0.0	0.0	0.0	2.0	2.0	10
Dorsal kineties, number	5.0	5.0	0.0	0.0	0.0	5.0	5.0	7

low number (3) and location between ends of lateral cirral rows.

Dorsal bristles about 3 µm long in protargol preparations, arranged in oxytrichid pattern, i. e., with fragmenting row 3 producing row 4: rows 1–3 almost bipolar; row 4 extends near right body margin, begins about mid-body with widely spaced bristles and ends near caudal cirri; row 5 dorsomarginal, ends about mid-body. Invariably two inconspicuous caudal cirri (Fig. 275c; Table 109).

Oral apparatus conspicuous because of wide and deep buccal cavity and a distinct buccal horn, similar as in the oxytrichid *Cyrtohymena* (Fig. 275a, b, d; Table 109). Adoral zone occupies 36%

of body length on average, of usual shape and structure, consists of an average of 41 very narrowly spaced membranelles. Paroral membrane distinctly convex, commences near anterior body end; endoral membrane slightly convex, crosses paroral near mid of buccal cavity. Pharyngeal fibres distinct in vivo and in protargol preparations.

Notes on ontogenesis: A very early divider (Fig. 275f) and an early mid-divider with fusing macronuclear nodules (Fig. 275g) were found in the preparations. They show the following processes: (i) the ontogenesis begins in the posterior half of the middle cirral row, where minute anlagen (anarchic fields of basal bodies) are generated left of the cirri (Fig. 275f); (ii) the posterior two thirds of the middle cirral row are incorporated into a large anarchic field that generates the anlagen for proter and opisthe, much later in the former than in the latter, which shows five anlagen streaks (Fig. 275g); (iii) the anterior portion of the middle cirral row does not form anlagen, suggesting that it consists of frontoterminal cirri; (iv) an anlage is recognizable in the external cirral row 2 of the right field. Thus, this is very likely a marginal row (Fig. 275g). Considering that the middle cirral row produces only anlagen for the proter and opisthe frontoventral cirri and the opisthe oral apparatus, the external row 2 of the right cirral field and row 1 of the left cirral field possibly produce several marginal rows, as, for instance, in *Allotricha, Parakahliella,* and *Fragmocirrus* (Berger 1999, 2011, Foissner 2000b).

Occurrence and ecology: As yet found only at type locality. Appeared four weeks after rewetting the sample, indicating a k-selected life strategy.

Remarks: We did not find a species in the literature that could be identical with *T. panamensis*. However, there are many species that are similar in size and cirral pattern; they belong to the genera compared in Table 108 and have been reviewed by Berger (1999, 2011). The following combination of features might be helpful for identifying *T. panamensis* in live: length approximately 120 µm; about 7 macronuclear nodules in a row left of body´s midline; countless subcortical crystals; transverse and caudal cirri inconspicuous; buccal cavity conspicuous, i. e., wide and deep as in *Cyrtohymena*; about 40 adoral membranelles.

Uroleptoides polycirratus (Berger & Foissner, 1989) Berger, 2008 (Fig. 276a–f)

Supplementary observations: The specimens from the mud of a tree fork in the Dominican Republic largely agree with previous descriptions (for a review, see Berger 2008). Specifically, the specimens match the Brazilian, South African, and Namibian populations in being about 200 µm long and having about 50 adoral membranelles. Further, about half of the specimens have one or two supernumerary frontoventral cirri (Fig. 276a, b), while the other half has the pattern shown in Berger (2008). Feeds on *Drepanomonas revoluta, Leptopharynx costatus,* medium-sized Colpodas, and heterotrophic flagellates.

Occurrence and ecology: Infrequent, as yet recorded from Madeira, various sites in tropical and subtropical Africa, and in the Neotropis (see species list). Thus, it is possibly a cosmopolitan, although records from Europe and Australia are still lacking.

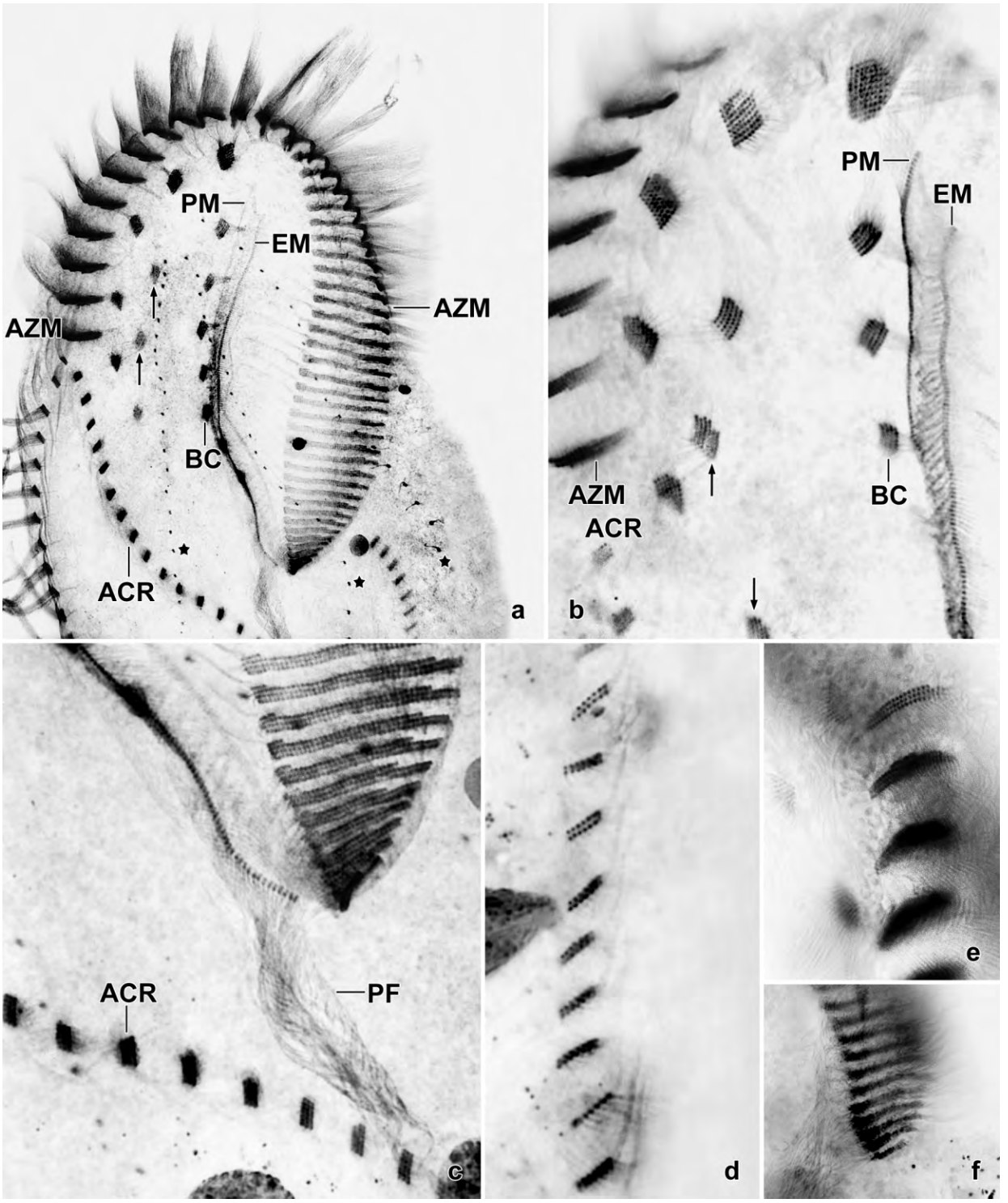

Fig. 276a–f. *Uroleptoides polycirratus* after protargol impregnation (from two heavily squashed specimens and thus without scale bars). **a, b:** Frontal and adoral ciliature. Arrows mark supernumerary cirri, asterisks denote the three dorsal bristle rows. **c, f:** Proximal end of adoral zone. **d:** Part of left marginal row, showing cirri to be composed of one or two rows of basal bodies, while those of the amphisiellid cirral row are composed of three rows (c). **e:** Distal end of adoral zone of membranelles. ACR – amphisiellid cirral row, AZM – adoral zone of membranelles, BC – buccal cirri, EM – endoral membrane, PF – pharyngeal fibres, PM – paroral membrane.

Nudiamphisiella interrupta Foissner, Agatha & Berger, 2002 (Fig. 277a–e)

The specimens from Venezuelan site (1) match the Namibian type population, except of body's length:width ratio (4.3:1 vs. 3:1) and body width ($\bar{x}$ = 150 × 35 µm, 120–170 × 25–40 µm, n = 9 vs. $\bar{x}$ = 150 × 50 µm, 120–170 × 35–55 µm in vivo). Further, body shape is slightly different, i. e., the posterior region is inconspicuously narrowed and curved to the left in about 70% of specimens (Fig. 277b–d). The macronuclear nodules sometimes contain a (protein?) crystal. The colourless cortical granules form rather widely spaced rows well recognizable because the granules are fairly refractive and 0.5–1 µm across (Fig. 277e). The cytoplasm usually contains many Y- and L-shaped crystals up to 10 µm long.

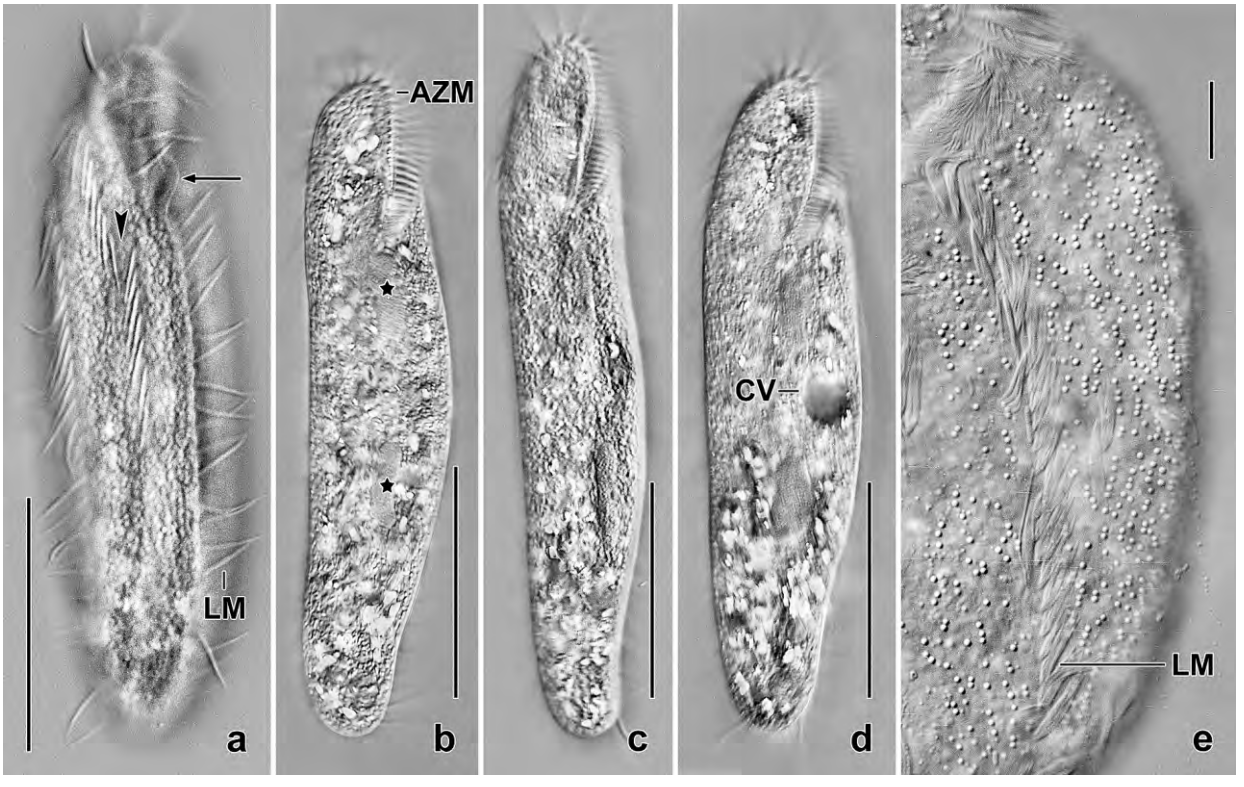

Fig. 277a–e. *Nudiamphisiella interrupta* from life (interference contrast). **a:** Surface view, showing the interruption (arrowhead) in the ventral cirral row. The arrow marks the distinctly curved buccal lip. **b–d:** Shape and size variability. The asterisks denote the elongate ellipsoid macronuclear nodules. The bright spots in the cytoplasm are caused by crystals up to 10 µm long. **e:** Surface view of a specimen slightly pressed by the coverslip, showing the cortical granules. AZM – adoral zone of membranelles, CV – contractile vacuole, LM – left row of marginal cirri. Scale bars 10 µm (e) and 50 µm (a–d).

Afroamphisiella abdita (Foissner, 1997) Foissner, Agatha & Berger, 2002 (Fig. 278a–d, 279a–g; Table 110)

Material and occurrence: Venezuelan site (21), i. e., a lithotelma of the Orinoco River while the type population was discovered in rainforest soil near to the town of Cairns, Australia. The Venezuelan record is the second at all, indicating that *A. abdita* is a rare species or does not grow well under the conditions provided by the non-flooded Petri dish method, where it appeared six days after rewetting the sample.

Table 110. Morphometric data on a Venezuelan population of *Afroamphisiella abdita* based on mounted, protargol-impregnated, and randomly selected specimens from a non-flooded Petri dish culture. Measurements in µm. ACR – amphisiellid cirral row, CV – coefficient of variation in %, M – median, Max – maximum, Mean – arithmetic mean, Min – minimum, n – number of individuals investigated, SD – standard deviation, SE – standard error of arithmetic mean.

Characteristics	Mean	M	SD	SE	CV	Min	Max	n
Body, length	73.5	72.0	8.2	1.8	11.1	57.0	90.0	21
Body, width	19.3	19.0	2.7	0.6	14.0	15.0	27.0	21
Body length:width, ratio	3.9	3.7	0.5	0.1	13.9	3.2	5.0	21
Anterior body end to proximal end of adoral zone, distance	15.5	15.5	0.9	0.2	6.0	14.0	17.0	20
Adoral zone of membranelles, percentage of body length	21.1	21.0	3.0	0.7	14.1	16.0	28.0	20
Adoral membranelles, number	18.0	18.0	1.0	0.2	5.7	16.0	20.0	21
Largest membranellar basis, width	4.7	5.0	0.6	0.1	13.6	4.0	6.0	21
Anterior body end to paroral membrane, distance	5.0	5.0	1.0	0.2	20.5	3.0	7.0	21
Anterior body end to endoral membrane, distance	4.2	4.0	0.7	0.2	16.2	3.0	6.0	21
Buccal cavity, width	2.8	3.0	0.6	0.1	20.1	2.0	4.0	20
Anterior body end to first macronuclear nodule, distance	15.6	16.0	1.6	0.4	10.5	12.0	19.0	21
Anterior macronuclear nodule, length	9.7	10.0	1.4	0.3	14.9	7.0	13.0	21
Anterior macronuclear nodule, width	4.7	4.5	0.8	0.2	17.0	4.0	7.0	21
Second anterior macronuclear nodule, length	7.5	7.0	1.2	0.3	16.5	5.0	11.0	21
Second anterior macronuclear nodule, width	4.3	4.0	0.7	0.1	15.3	3.0	6.0	21
Macronuclear nodules, number	4.0	4.0	0.4	0.1	9.7	3.0	5.0	21
Micronuclei, length	1.8	2.0	–	–	–	1.5	2.0	21
Micronuclei, width	1.6	1.5	–	–	–	1.5	2.0	21
Micronuclei, number	2.9	3.0	0.5	0.1	16.7	2.0	4.0	21
Frontal cirri, number	3.0	3.0	0.0	0.0	0.0	3.0	3.0	21
Anterior body end to first buccal cirrus, distance	5.3	5.3	0.9	0.2	17.3	3.0	7.0	20
Buccal cirri, number	1.4	1.0	–	–	–	1.0	2.0	21
Anterior body end to end of first cirral row left of ACR, distance	13.4	13.5	1.9	0.4	14.3	9.0	18.0	21
First row left of ACR, number of cirri	2.9	3.0	0.5	0.1	18.6	2.0	4.0	21
Anterior body end to end of second cirral row left of ACR, distance	8.3	8.5	1.2	0.3	14.2	6.0	11.0	21
Second row left of ACR, number of cirri	1.9	2.0	–	–	–	1.0	2.0	21
Anterior body end to ACR, distance	3.6	3.5	0.4	0.1	12.3	3.0	5.0	21
Anterior body end to end of ACR, distance	32.0	32.0	4.3	0.9	13.4	25.0	41.0	21
Amphisiellid cirral row (ACR), length	28.0	28.0	4.1	0.9	14.8	21.0	36.0	21
Amphisiellid cirral row (ACR), number of cirri	13.6	13.0	2.2	0.5	15.9	10.0	19.0	21
Anterior body end to right marginal row, distance	6.6	6.5	1.1	0.3	17.2	5.0	9.0	21
Right marginal row, number of cirri	29.6	29.0	3.3	0.7	11.3	25.0	39.0	21
Left marginal row, number of cirri	26.9	27.0	2.6	0.6	9.8	22.0	32.0	21
Dorsal kineties, number	3.0	3.0	0.0	0.0	0.0	3.0	3.0	21
Dorsal kinety 1, number of kinetids	7.7	8.0	1.3	0.3	16.5	5.0	11.0	21
Dorsal kinety 2, number of kinetids	13.1	13.0	0.9	0.2	6.6	10.0	14.0	21
Dorsal kinety 3, number of kinetids	12.6	12.0	1.5	0.3	12.2	10.0	16.0	21

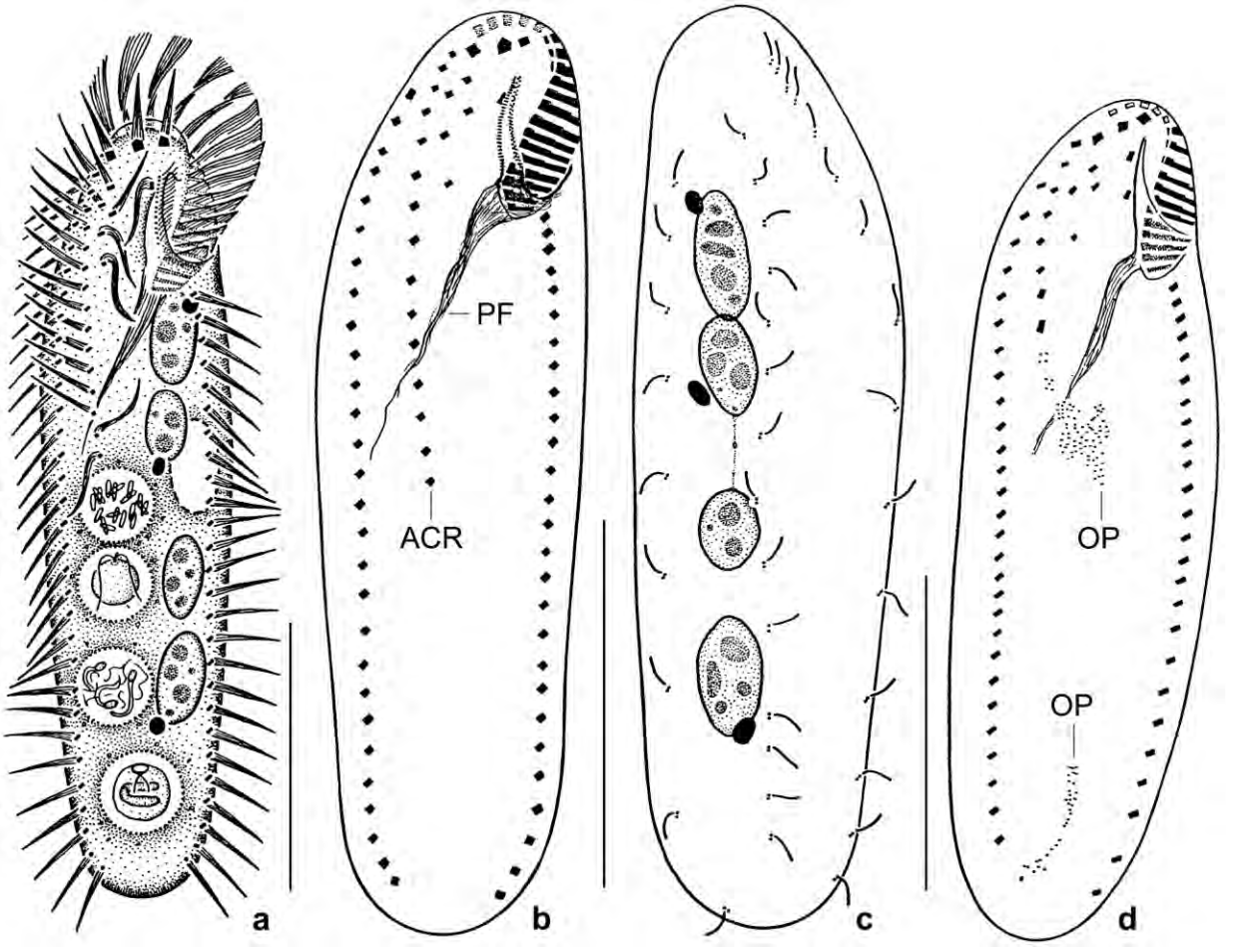

Fig. 278a–d. *Afroamphisiella abdita* from life (a) and after protargol impregnation (b–d). **a:** Ventral view of a representative specimen, length 85 µm. **b, c:** Ventral and dorsal view of main voucher specimen, showing the important features of the genus and species: four macronuclear nodules, absence of transverse and caudal cirri, the amphisiellid cirral row (ACR) extending to mid-body, the short adoral zone of membranelles, and the three dorsal kineties. **d:** An early divider with two oral primordia (OP) which later fuse and produce cirral streaks (Berger 2008). PF – pharyngeal fibres. Scale bars 30 µm.

Four voucher slides with protargol-impregnated specimens have been deposited in the Biology Centre of the Upper Austrian Museum in Linz (LI). Relevant specimens have been marked by black ink circles on the coverslip.

Morphology: The Venezuelan and the Australian cells are very similar both in morphology and morphometry (Fig. 278a–d, 279a–d; Table 110). Early dividers also look alike (Fig. 278d, 279e–g). Thus, we do not provide a redescription but refer the reader to the figures, the morphometric data (Table 110), and to the monograph of Berger (2008). The classification of the genus is uncertain.

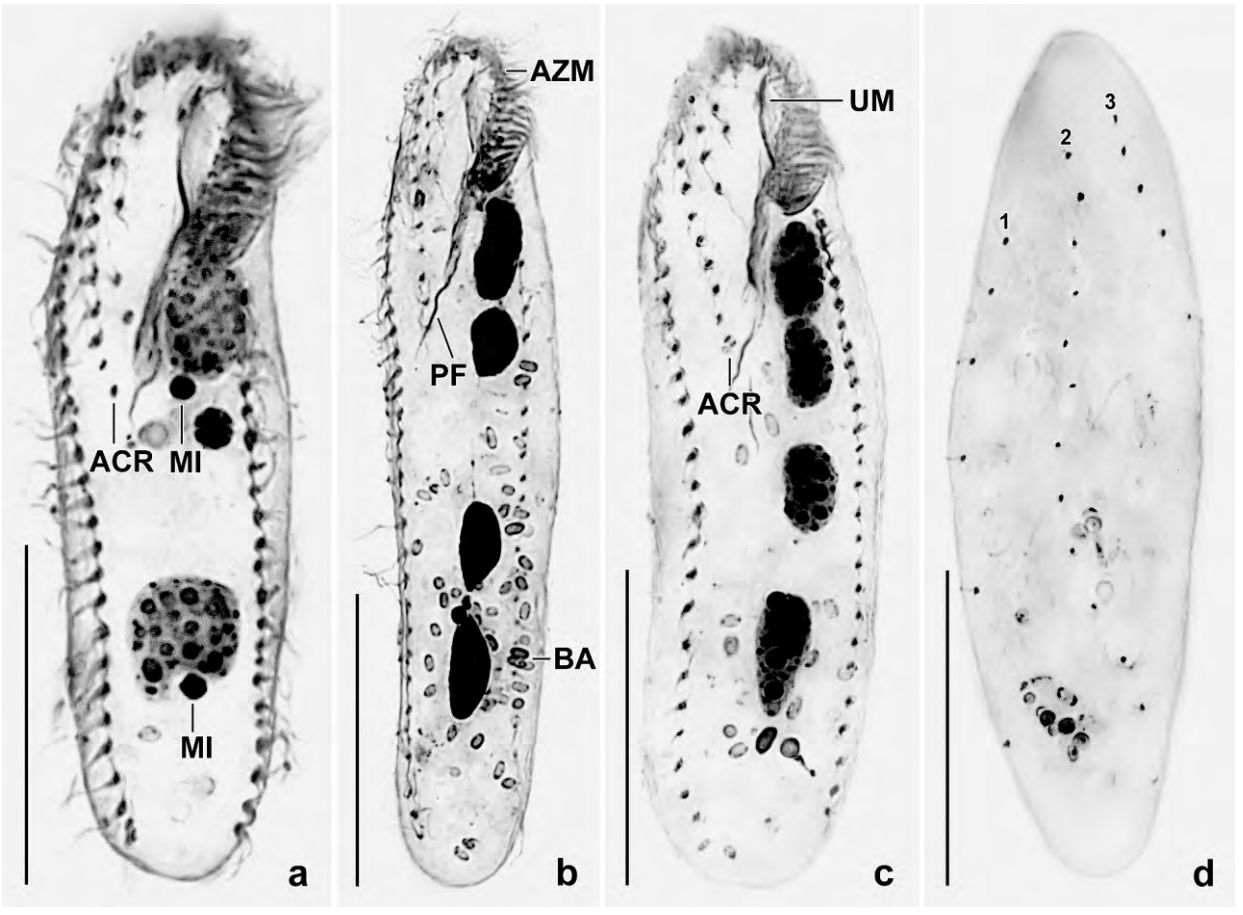

Fig. 279a–d. *Afroamphisiella abdita* after protargol impregnation. **a:** A specimen with only three macronuclear nodules. **b, c:** Ventral views of typical specimens, that shown in (b) has many bacterial spores in the food vacuoles. The buccal cirri are out of focus. **d:** Dorsal view, showing the three dorsal kineties (numerals). ACR – amphisiellid cirral row, AZM – adoral zone of membranelles, BA – bacterial spores, MI – micronuclei, PF – pharyngeal fibres, UM – undulating membranes. Scale bars 30 µm.

Amphisiellides illuvialis EIGNER & FOISSNER, 1994 (Fig. 280a–e, Table 111)

Material: Live observations and protargol-impregnated specimens from Venezuelan site (54). Two voucher slides, each containing only few specimens, have been deposited in the Biology Centre of the Upper Austrian Museum in Linz (LI). Relevant specimens have been marked by black ink circles on the coverslip.

Morphometry: This population is rather similar to the Austrian type from leaf litter, nameable differences occur in the following features (Table 111): average body length in protargol preparations (82.7 µm vs. 98 µm), average length of anterior macronuclear nodule (15.2 µm vs. 24.3 µm), average number of cirri right of amphisiellid cirral row (usually zero vs. 2.1), average number of cirri left of amphisiellid cirral row (1.3 vs. 2.1), average number of transverse cirri (1.5 vs. 2.3), and average number of caudal cirri (2 vs. 3.5). Some of these differences are rather distinct but possibly insufficient to ascribe subspecies status to the Venezuelan population because *A. illuvialis* is highly variable in these and other features, as shown by the high variation coefficients (Table 111).

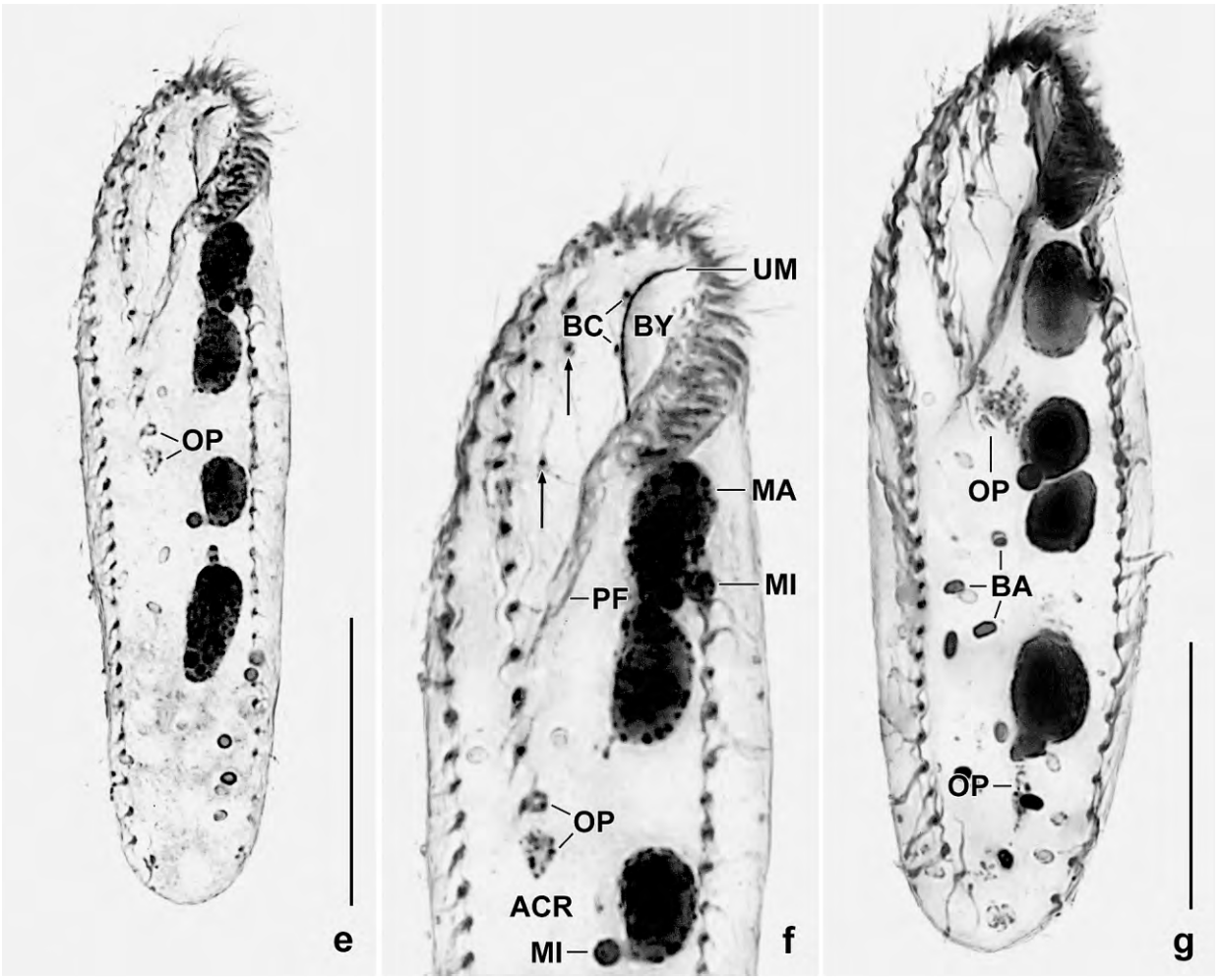

Fig. 279e–g. *Afroamphisiella abdita*, early dividers after protargol impregnation. **e, f:** Very early divider with oral primordium originating from the two last cirri of the amphisiellid cirral row. The arrows mark first and second cirral row left of the amphisiellid cirral row. **g:** Early divider showing an oral primordium not only at the proximal end of the amphisiellid cirral row but also near the posterior body end where usually are transverse cirri lacking, however, in *Afroamphisiella* (cp. Fig. 278d). ACR – amphisiellid cirral row, BA – bacterial spores, BC – buccal cirri, BY – buccal cavity, MA – macronuclear nodule, MI – micronuclei, OP – oral primordium, PF – pharyngeal fibres, UM – undulating membranes. Scale bars 30 µm.

Additional observations: Body shape elongate ellipsoid to elongate obovate (Fig. 280a–c); cortical granules absent (carefully checked in four specimens); cirri about 15 µm long; dorsal bristles 3–4 µm long; buccal cavity narrow and flat, covered almost completely by the buccal lip; feeds on bacteria.

Generic assignment: Berger (2008) transferred *A. illuvialis* to the genus *Nudiamphisiella,* without providing sufficient reasons. Briefly, *Nudiamphisiella* Foissner, Agatha & Berger (2002) is, inter alia, characterized by the absence of transverse cirri that doubtlessly are present in *A. illuvialis,* either one (as usual in the Venezuelan population) or more (one transverse cirrus plus one or several pretransverse cirri in Austrian population).

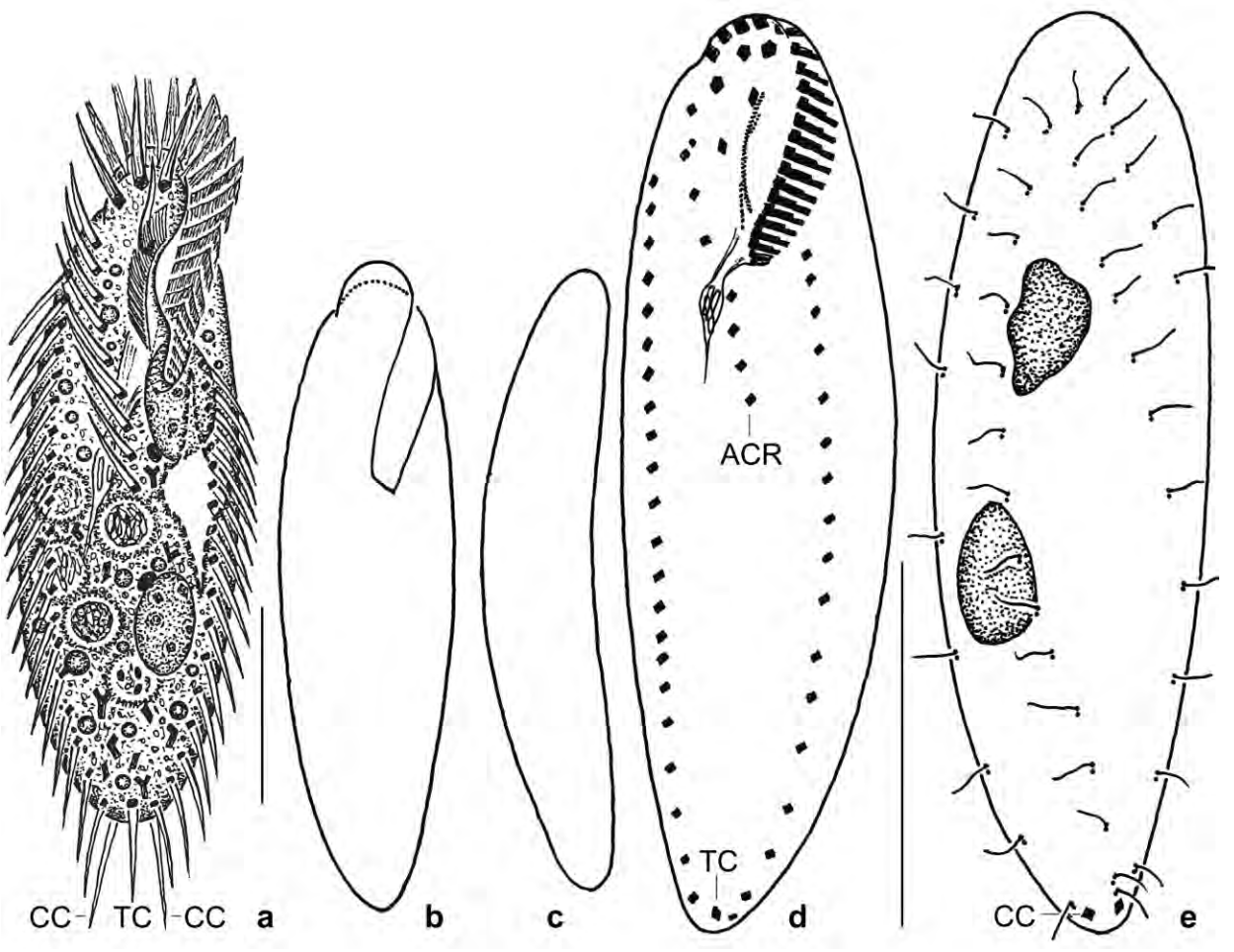

Fig. 280a–e. *Amphisiellides illuvialis* from life (a–c) and after protargol impregnation (d, e). **a:** An elongate ellipsoid specimen, length 100 µm. Note the narrow entrance to the buccal cavity, the single transverse cirrus, and the two caudal cirri. **b, c:** Ventral and lateral view of a slender specimen. **d, e:** Ventral and dorsal view of cirral and bristle pattern, length 75 µm. ACR – amphisiellid cirral row, CC – caudal cirri, TC – transverse cirrus. Scale bars 30µm.

Stylonychia gibbera Foissner & Heber **nov. spec.** (Fig. 281a–c, f, 282a–k; Table 112)

Diagnosis: Size in vivo about 100 × 55 µm. Outline elliptic to obovate; ventral side flat; convex dorsal side with two conspicuous humps. Cirral pattern, oral apparatus, and dorsal kineties stylonychid. Frontoventral cirri in V-pattern; postoral cirri in inverted L-pattern; pretransverse and transverse cirri in two distinct groups, forming a Y-like figure. Right marginal row on average consisting of 12 cirri, left of 10. Caudal cirri comparatively narrow-spaced, about 30 µm long. Adoral zone extends about 45% of body length, composed of an average of 27 membranelles.

Type locality: Venezuelan site (1), i. e., upper soil layer from the Orinoco floodplain at the village of Cabruta, Lower Orinoco, 66°14′W 7°38′N.

Type material: 1 holotype slide and 7 paratype slides with protargol-impregnated specimens have been deposited in the Biology Centre of the Upper Austrian Museum in Linz (LI). Relevant specimens have been marked by black ink circles on the coverslip.

Table 111. Morphometric data on *Amphisiellides illuvialis* based on mounted, protargol-impregnated, and randomly selected specimens from a non-flooded Petri dish culture (Venezuelan population) and from a pure culture (Austrian specimens; from EIGNER & FOISSNER 1994). Measurements in µm. AU – Austrian population, CV – coefficient of variation in %, M – median, Max – maximum, Mean – arithmetic mean, Min – minimum, n – number of specimens investigated, Pop – population, SD – standard deviation, SE – standard error of arithmetic mean, VE – Venezuelan population.

Characteristics	Pop	Mean	M	SD	SE	CV	Min	Max	n
Body, length	VE	82.7	80.0	10.4	2.7	12.6	70.0	107.0	15
	AU	98.0	103.0	14.3	0.7	14.6	56.0	132.0	28
Body, width	VE	29.5	29.0	4.6	1.2	15.7	22.0	38.0	15
	AU	26.7	26.5	6.8	1.3	25.6	16.0	46.0	28
Body length:width, ratio	VE	2.8	2.8	0.4	0.1	14.2	2.2	3.5	15
	AU	3.7	?	?	?	?	?	?	28
Anterior body end to proximal end of adoral zone, distance	VE	26.5	27.0	3.6	0.9	13.5	20.0	34.0	15
	AU	28.7	29.0	2.7	0.5	9.5	24.0	35.0	28
Anterior body end to proximal end of amphisiellid cirral row, distance	VE	43.0	44.0	8.1	2.1	18.9	32.0	61.0	15
	AU	53.6	51.0	12.3	2.3	23.0	19.0	80.0	28
Anterior macronucleus nodule, length	VE	15.2	13.0	3.9	1.0	26.0	10.0	24.0	15
	AU	24.3	27.0	7.0	1.3	28.0	9.0	32.0	27
Anterior macronucleus nodule, width	VE	8.4	9.0	1.1	0.3	13.3	6.0	10.0	15
	AU	7.2	7.0	2.0	0.4	27.6	4.0	12.0	27
Macronucleus nodules, number	VE	2.0	2.0	0.0	0.0	0.0	2.0	2.0	15
	AU	2.0	2.0	–	–	–	1.0	4.0	28
Adoral membranelles, number	VE	23.1	23.0	2.3	0.6	9.9	20.0	27.0	15
	AU	24.6	25.0	2.7	0.5	10.8	21.0	35.0	28
Right marginal row, number of cirri	VE	20.7	20.0	2.1	0.5	10.1	17.0	25.0	15
	AU	25.6	26.0	4.3	0.8	16.7	15.0	36.0	28
Left marginal row, number of cirri	VE	18.3	18.0	2.1	0.5	11.2	15.0	22.0	15
	AU	19.4	20.5	4.3	0.8	22.0	8.0	27.0	28
Frontal cirri, number	VE	3.0	3.0	0.0	0.0	0.0	3.0	3.0	15
Buccal cirri, number	VE	1.0	1.0	0.0	0.0	0.0	1.0	1.0	15
	AU	1.0	1.0	–	–	–	1.0	2.0	28
Amphisiellid cirral row, number of cirri	VE	9.1	9.0	1.5	0.4	16.4	7.0	11.0	15
	AU	13.0	12.0	3.6	0.7	27.6	5.0	27.0	28
Cirri right of amphisiellid cirral row, number	VE	0.1	0.0	–	–	–	0.0	2.0	15
	AU	2.1	0.0	–	–	–	0.0	13.0	28
Cirri left of amphisiellid cirral row, number	VE	1.3	1.0	0.6	0.2	46.9	1.0	3.0	15
	AU	3.0	3.0	1.5	0.4	50.0	1.0	6.0	14
Transverse cirri, number	VE	1.5	1.0	0.6	0.2	43.6	1.0	3.0	15
	AU	2.3	2.0	0.8	0.2	34.8	1.0	5.0	25
Dorsal bristle rows, number	VE	4.0	4.0	0.0	0.0	0.0	4.0	4.0	15
	AU	4.0	4.0	0.0	0.0	0.0	4.0	4.0	28
Caudal cirri, number	VE	2.0	2.0	0.0	0.0	0.0	2.0	2.0	15
	AU	3.5	3.0	1.1	0.2	31.4	2.0	7.0	28

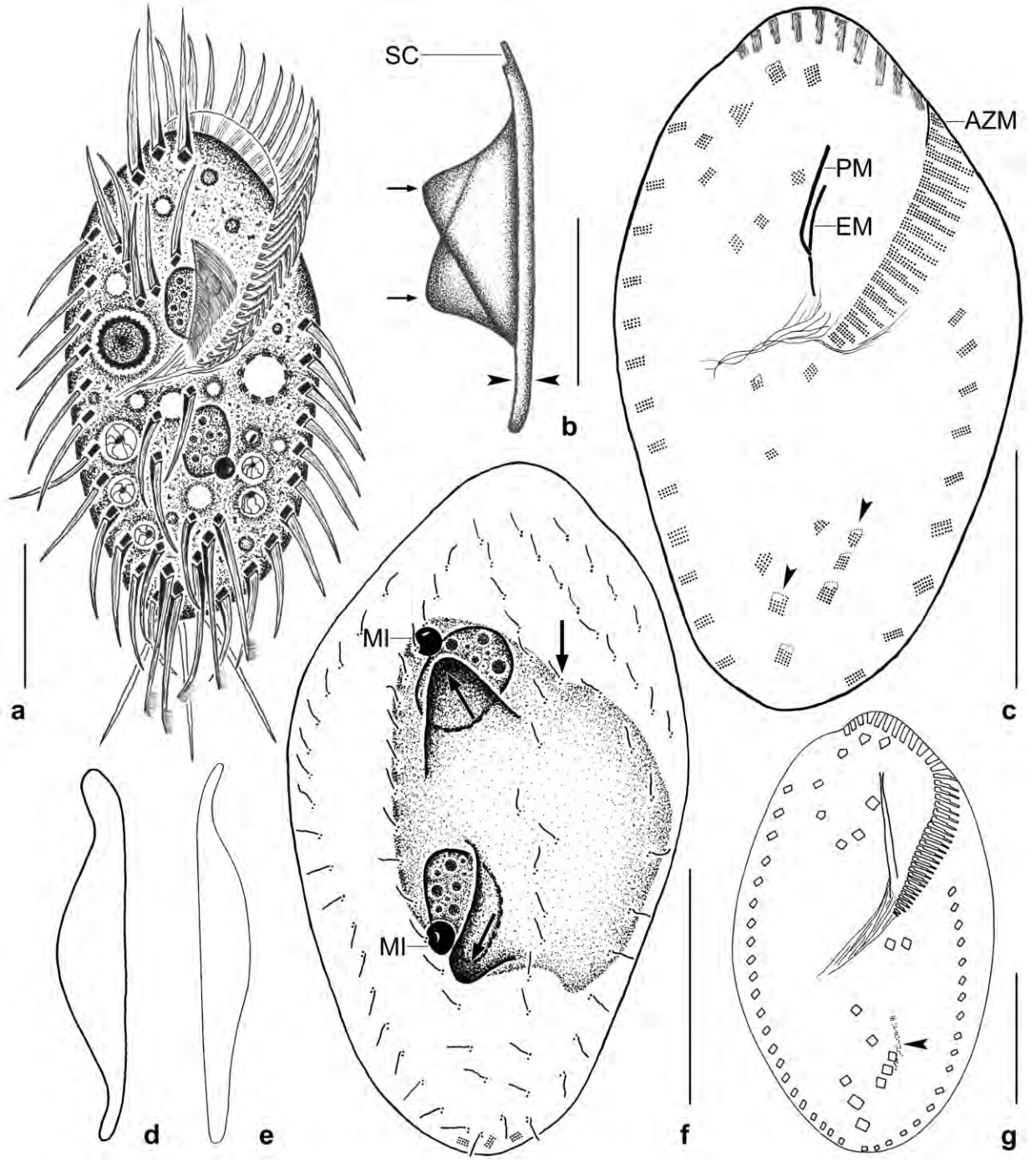

Fig. 281a–g. *Stylonychia gibbera* from life (a, b), after protargol impregnation (c, f), and in the scanning electron microscope (b). **a:** Ventral view of a representative specimen having ingested flagellates and a cyst, length 100 µm. Note the fringed transverse cirri. **b:** Lateral outline, showing the dorsal humps (arrows) and the flattened body margin (arrowheads), length 70 µm. **c, f:** Ventral and dorsal view of holotype specimen, showing the infraciliature, the nuclear apparatus, and the dorsal humps (arrows), length 88 µm. The arrow denotes the anterior end of dorsal kinety 4; the arrowheads mark the transverse cirri with barren anterior basal bodies. **d, e, g:** Lateral (d, e) and ventral (g) views of *Stylonychia bifaria* (d, from Moravcová 1962; e, g, from Wirnsberger et al. 1985) from life (d, e,) and after protargol impregnation (g). The arrowhead in (g) marks the oral primordium originating at the same site as in *S. gibbera.* AZM – adoral zone of membranelles, EM – endoral, MI – micronuclei, PM – paroral membrane, SC – scutum. Scale bars 30 µm.

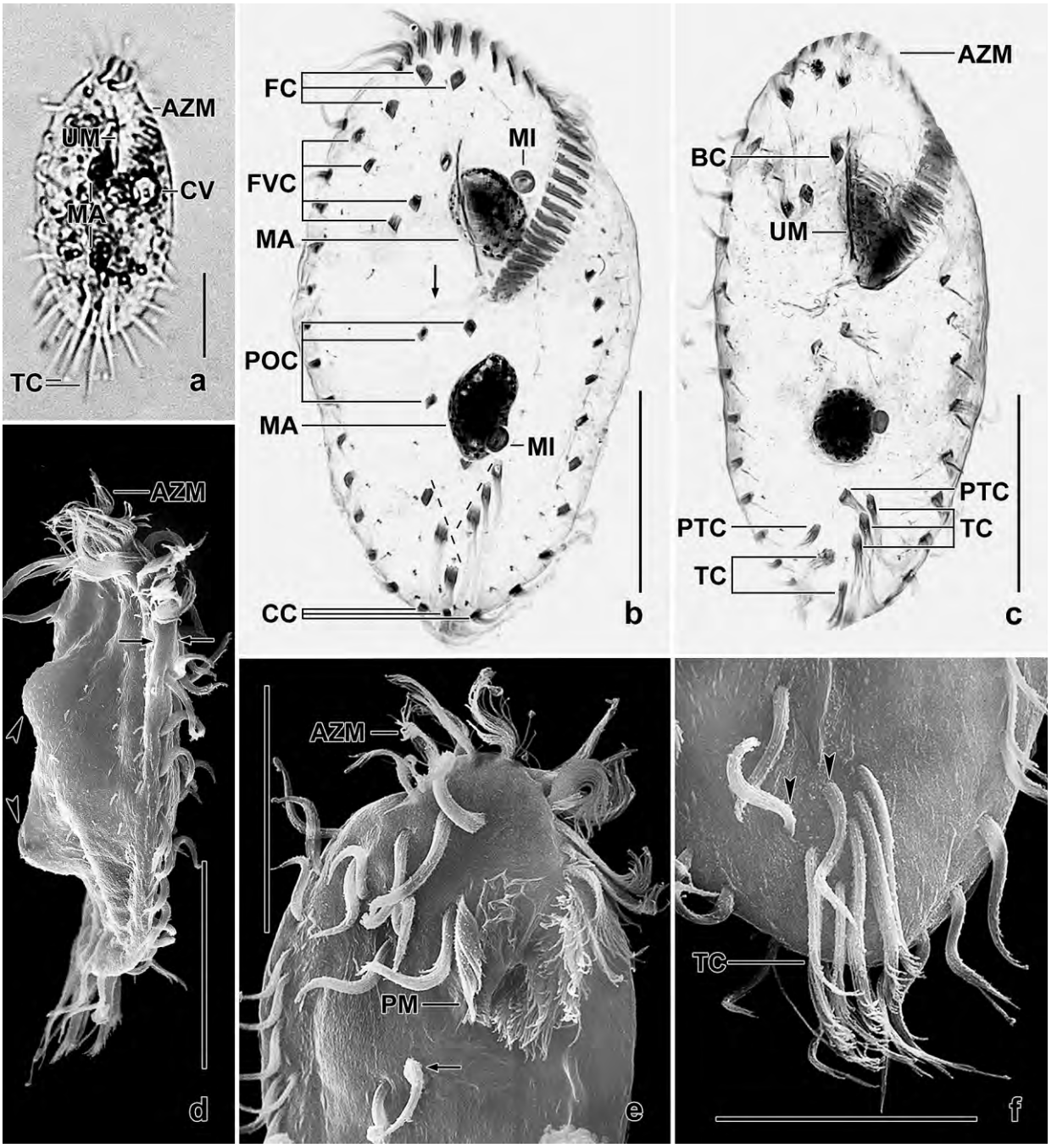

Fig. 282a–f. *Stylonychia gibbera* from life (a), after protargol impregnation (b, c), and in the scanning electron microscope (d–f). **a:** Ventral view, length 100 µm. **b:** Ventral view of the slightly obovate holotype, length 88 µm. The arrow marks the pharyngeal fibres. The Y-like arranged transverse cirri are connected by dashed lines. **c:** Ventral view of an ellipsoid paratype specimen, length 89 µm. **d:** Lateral view, showing the dorsal humps (arrowheads), the most important feature of this species; arrows denote the flattened body margin, length 60 µm. **e:** Ventral view of anterior body region, showing the inconspicuous paroral membrane, while the endoral is covered by the buccal seal. The arrow marks postoral cirrus IV/2. **f:** Ventral view of posterior body region, showing the fringed transverse cirri; arrowheads denote pretransverse cirri. AZM – adoral zone of membranelles, BC – buccal cirrus, CC – caudal cirri, CV – contractile vacuole, FC – frontal cirri, FVC – frontoventral cirri, MA – macronuclear nodules, MI – micronuclei, PM – paroral membrane, POC – postoral cirri, PTC – pretransverse cirri, TC – transverse cirri, UM – undulating membranes. Scale bars 30 µm.

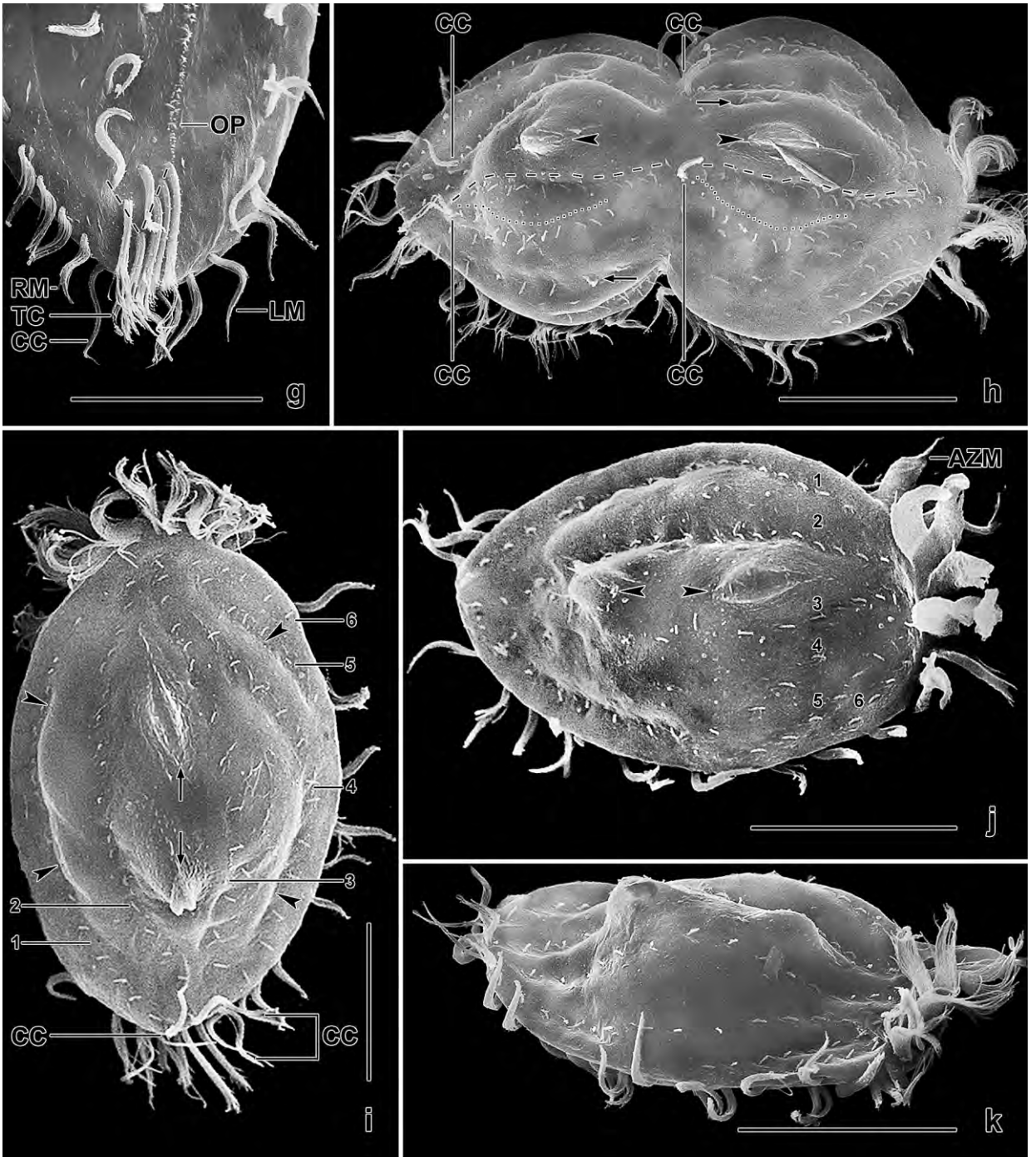

Fig. 282g–k. *Stylonychia gibbera*, scanning electron micrographs. **g:** Ventral view of posterior body region, showing the oral primordium originating close to and left of the uppermost transverse cirrus. Note the V-like arranged, fringed transverse cirri (dashed). **h:** Dorsal view of a late divider. Arrowheads denote the not yet duplicated parental humps; arrows mark parental bristles; dorsal kinety 4 (dotted) originates from kinety 3 (dashed), as typical for *Stylonychia*, length 100 µm. **i:** Dorsal view of a specimen with lip-like furrowed dorsal humps (arrows); the arrowheads denote the basal convexity of the dorsal surface, length 100 µm. **j:** Dorsal view of a post-divider with both dorsal humps developed (arrowheads), length 70 µm. **k:** Slightly oblique view of an individual with prominent dorsal humps, length 70 µm. 1–6 – dorsal kineties, AZM – adoral zone of membranelles, CC – caudal cirri, LM – left marginal cirral row, OP – oral primordium, RM – right marginal cirral row, TC – transverse cirri. Scale bars 30 µm.

Table 112. Morphometric data on *Stylonychia gibbera* based on mounted, protargol-impregnated, and randomly selected specimens from a non-flooded Petri dish culture. Measurements in µm. CV – coefficient of variation in %, M – median, Max – maximum, Mean – arithmetic mean, Min – minimum, n – number of individuals investigated, SD – standard deviation, SE – standard error of arithmetic mean.

Characteristics	Mean	M	SD	SE	CV	Min	Max	n
Body, length	88.2	88.0	7.2	1.5	8.1	74.0	104.0	23
Body, width	47.3	48.0	6.4	1.3	13.4	36.0	60.0	23
Body length:width, ratio	1.9	1.8	0.2	0.0	10.8	1.7	2.5	23
Body, width at level of middle transverse cirrus	30.7	29.0	4.5	0.9	14.7	24.0	40.0	23
Anterior macronuclear nodule, length	15.7	15.0	3.1	0.6	19.4	11.0	21.0	23
Anterior macronuclear nodule, width	9.7	10.0	0.9	0.2	9.4	8.0	12.0	23
Anterior macronuclear nodule, length:width ratio	1.6	1.6	0.3	0.1	18.4	1.1	2.1	23
Macronuclear nodules, distance in between	13.2	13.0	3,3	0.7	23.7	7.0	21.0	23
Anterior micronucleus, length	3.7	4.0	–	–	–	3.0	4.0	23
Anterior micronucleus, width	3.1	3.0	0.5	0.1	14.6	2.0	4.0	23
Anterior micronucleus, length:width ratio	1.2	1.3	0.2	0.0	15.0	1.0	1.5	23
Micronuclei, number [a]	2.0	2.0	0.0	0.0	0.0	2.0	2.0	23
Anterior body end to proximal end of adoral zone, distance	39.7	40.0	3.5	0.7	8.9	32.0	48.0	23
Adoral zone of membranelles, percentage of body length	45.2	44.4	3.9	0.8	8.5	38.9	54.1	23
Largest membranellar basis, width	6.4	6.0	0.6	0.1	9.1	6.0	8.0	23
Adoral membranelles, number	26.2	27.0	1.4	0.3	5.3	23.0	28.0	23
Anterior body end to proximal end of paroral, distance	31.4	31.0	2.9	0.6	9.3	27.0	38.0	23
Anterior body end to proximal end of endoral, distance	36.2	36.0	3.6	0.8	10.0	30.0	45.0	23
Paroral, length	14.6	15.0	2.2	0.5	14.9	10.0	18.0	23
Endoral, length	16.0	16.0	2.4	0.5	15.0	12.0	20.0	23
Anterior body end to uppermost postoral cirrus, distance	42.3	43.0	3.6	0.7	8.4	37.0	50.0	23
Posterior body end to lowermost transverse cirrus, distance	5.0	5.0	1.0	0.2	19.1	3.0	7.0	23
Caudal cirri, distance in between	5.9	5.0	1.5	0.3	24.9	5.0	11.0	23
Right marginal row, number of cirri	11.8	12.0	1.3	0.3	11.3	9.0	14.0	23
Left marginal row, number of cirri	9.8	10.0	0.9	0.2	8.7	8.0	11.0	23
Anterior body end to distal end of anterior hump, distance	22.7	23.0	2.6	0.5	11.4	18.0	28.0	23
Distal end of anterior hump to proximal end of posterior hump, distance	39.2	40.0	4.6	1.0	11.8	27.0	47.0	23
Hump summits, distance in between	32.0	32.0	3.0	0.6	9.2	26.0	39.0	23
Bristles in dorsal row 1, number	18.0	18.0	1.6	0.3	8.8	15.0	21.0	23
Bristles in dorsal row 2, number	17.5	18.0	1.2	0.3	6.9	15.0	19.0	23
Bristles in dorsal row 3, number	15.6	15.0	0.9	0.2	5.7	14.0	17.0	23
Bristles in dorsal row 4, number	11.7	12.0	1.3	0.3	10.9	10.0	14.0	23
Bristles in dorsal row 5, number	8.1	8.0	1.2	0.3	15.3	6.0	10.0	23
Bristles in dorsal row 6, number	4.4	4.0	0.8	0.2	17.8	3.0	6.0	23
Dorsal bristles, total number	75.3	75.0	4.1	0.9	5.5	68.0	84.0	23

[a] Of 24 specimens analysed, one has three micronuclei.

Etymology: The Latin adjective *gibber* (humpbacked, humpy) refers to the two dorsal humps, a key feature of this species.

Description: Size in vivo 80–110 × 40–70 µm usually about 100 × 55 µm, as calculated from some in vivo measurements and the morphometric data in Table 112 adding 15% preparation shrinkage. Body very rigid and colourless, outline narrowly obovate/elliptic to ordinarily obovate/elliptic (Fig. 281a, c, 282a–c, i; Table 112). Cell margin leaf-like flattened; ventral side flat; dorsal convexity more pronounced along right than left margin of body, with two lenticular, about 15 µm long and 8 µm high humps in central quarters of cell and in midline of dorsal convexity between kineties two and three; optically above macronuclear nodules; frequently with a longitudinal furrow and then appearing lip-like (Fig. 281b, f, 282d, h–k; Table 112). Nuclear apparatus usually in middle third of body slightly left of midline, consists of two macronuclear nodules each with a micronucleus attached to left margin of nodule (Fig. 281a, f, 282a–c; Table 112). Anterior nodule at level of buccal cavity, rear nodule on average 13 µm posteriorly; no distance between nodules in one out of 23 specimens. Individual nodules rotund to ellipsoid, on average 15 × 10 µm after protargol impregnation; nucleoli globular, 0.5–1.5 µm in diameter. Micronuclei globular to ovoid/broadly ellipsoid, on average 3 × 4 µm; three micronuclei in one out of 24 specimens. Contractile vacuole in mid-body near left body margin (Fig. 281a, 282a). Cortex rigid; cortical granules absent. Cytoplasm colourless, densely granulated, contains some lipid droplets and 1 µm-sized crystals. Food vacuoles scattered throughout body, 5–15 µm across, some appearing empty. Feeds on flagellates (*Polytomella*), protist cysts, and bacteria, the spores of which remain undigested. Movement erratic, often paused by jerky stops.

Cirral pattern oxytrichid (Berger 1999), i. e., 18 frontal-ventral-transverse cirri in six groups; 17–24 cirri in four out of 42 specimens; anterior basal bodies of cirral bases sometimes barren (Fig. 281c). Frontal cirri thickened, in convex pattern following body margin, in vivo about 30 µm long. Frontoventral cirri in V-pattern (Fig. 281a, c, 282b, c; Table 112). Buccal cirrus close to paroral membrane at level of anterior end of endoral. Postoral cirri in inverted L-pattern, cirrus IV/2 usually the most anterior one (Fig. 281a, c, 282b, c). Transverse cirri thickened and terminally fringed, both in vivo and in SEM preparations, in vivo about 30 µm long and thus considerably protruding from body proper, in two distinct groups forming Y-pattern together with right pretransverse cirrus: right group composed of three cirri in line ending close to posterior body margin; left group also composed of three cirri, commences left of middle cirrus of right group and extends obliquely to cell´s midline (Fig. 281a, c, 282b, c, f); rarely in V- pattern (Fig. 282g). Left pretransverse cirrus near body´s midline at or near level of uppermost transverse cirrus. Marginal cirral rows clearly separate posteriorly; cirri composed of three kineties, rarely of four, in vivo about 20 µm long. Right row commences at level of anterior end of paroral membrane, distance between foremost cirri usually slightly increased (Fig. 281a, c, 282b, c).

Six dorsal bristle rows in typical stylonychid pattern more or less disturbed by the dorsal convexities; kinety 4 shortened anteriorly, kineties 5 and 6 do not reach mid-body; bristles about 3 µm long in vivo and protargol preparations (Fig. 281f, 282h–j; Table 112). Caudal cirri rather narrowly spaced, in or right of body´s midline, optically between gap of marginal rows, in vivo conspicuous because about 30 µm long (Fig. 281a, f, 282b, g–i; Table 112).

Oral apparatus stylonychid (Berger 1999), i. e., with parallel undulating membranes and wide, flat buccal cavity. Adoral zone occupies about 45 % of body length, composed of an average of 27 ordinary membranelles, bases of largest membranelles about 7 µm width in vivo and 6–8 µm in protargol preparations (Fig. 281a, c, 282a–c, e; Table 112). Paroral membrane on average 15 µm long, posterior end optically often covering endoral, cilia in vivo gradually decreasing from 10 µm anteriorly to 5 µm posteriorly; endoral membrane of similar length as paroral, distal end at level of buccal cirrus, proximal end near buccal vertex (Fig. 281a, c, 282b, c; Table 112). Pharyngeal fibres of ordinary shape and structure, extend transversely to right body margin, 10–20 µm long (Fig. 281c, 282b).

Notes on ontogenesis: Stomatogenesis begins very close to and left of the uppermost transverse cirrus (Fig. 282g). The humps are generated in post-dividers (Fig. 282h, j). The dorsal ciliature develops in *Oxytricha* pattern as typical for *Stylonychia* (Berger 1999), i. e., dorsal kinety 4 originates from kinety 3 (Fig. 282h).

Occurrence and ecology: As yet found only at type locality. The floodplain habitat and the rare occurrence of stylonychids in soil habitats suggest *Stylonychia gibbera* as a limnetic species that excysted in the non-flooded Petri dish culture.

Remarks: Within the stylonychids, dorsal processes, one of the main features of *S. gibbera*, are known only from *Onychodromus grandis* (for a review, see Berger 1999) and *Styxophrya quadricornutus* (Foissner et al. 1987, 2004). These species can easily be distinguished from *S. gibbera* by the number of macronuclear nodules (> 2 vs. 2), frontal-ventral-transverse cirri (> 18 vs. 18), and dorsal kineties (> 6 vs. 6). The molecular data indicate a close relationship of *Styxophrya* and *Stylonychia* (Schlegel et al. 1991, Hammerschmidt et al. 1996); this is sustained by *S. gibbera*.

Stylonychia gibbera is probably most closely related to *S. bifaria* and *S. notophora* (for a review, see Berger 1999) because they share the same cirral pattern, specifically the V-like arranged frontoventral cirri, the inversely L-like arranged postoral cirri, and the Y-like pattern formed by the transverse cirri. *Stylonychia bifaria* and *S. gibbera* also share the origin of the oral primordium close to and left of the uppermost transverse cirrus and the shortened dorsal kinety 4 (Fig. 281g, 282g–j). Beside the absence of dorsal humps, *S. bifaria* and *S. notophora* differ from *S. gibbera* by the number of marginal cirri (*S. gibbera*: left row 8–11, right row 9–14 cirri; *S. bifaria*: 15–19, 14–22; *S. notophora*: 12–15, 18–22). After all, *Stylonychia gibbera* has the least number of cirri in the marginal rows within the genus, possibly except of *S. curvata*, which, however, likely does not belong to this genus (Berger 1999).

Stylonychia notophorides **nov. spec.** (Fig. 283a–c, 284a–c; Table 113)

Diagnosis: Size in vivo about 90 × 35 µm; elongate obovate. On average 18 fronto-ventral-transverse cirri, cirrus III/2 and buccal cirrus close together at same level subapical of paroral membrane; postoral cirrus IV/2 slightly anterior of cirrus V/4; transverse cirri in two groups. Right marginal row composed of an average of 13 cirri, left of 11. 6 dorsal kineties; caudal cirri narrowly spaced and about 30 µm long. Adoral zone extends about 47% of body length, composed of 28 membranelles on average.

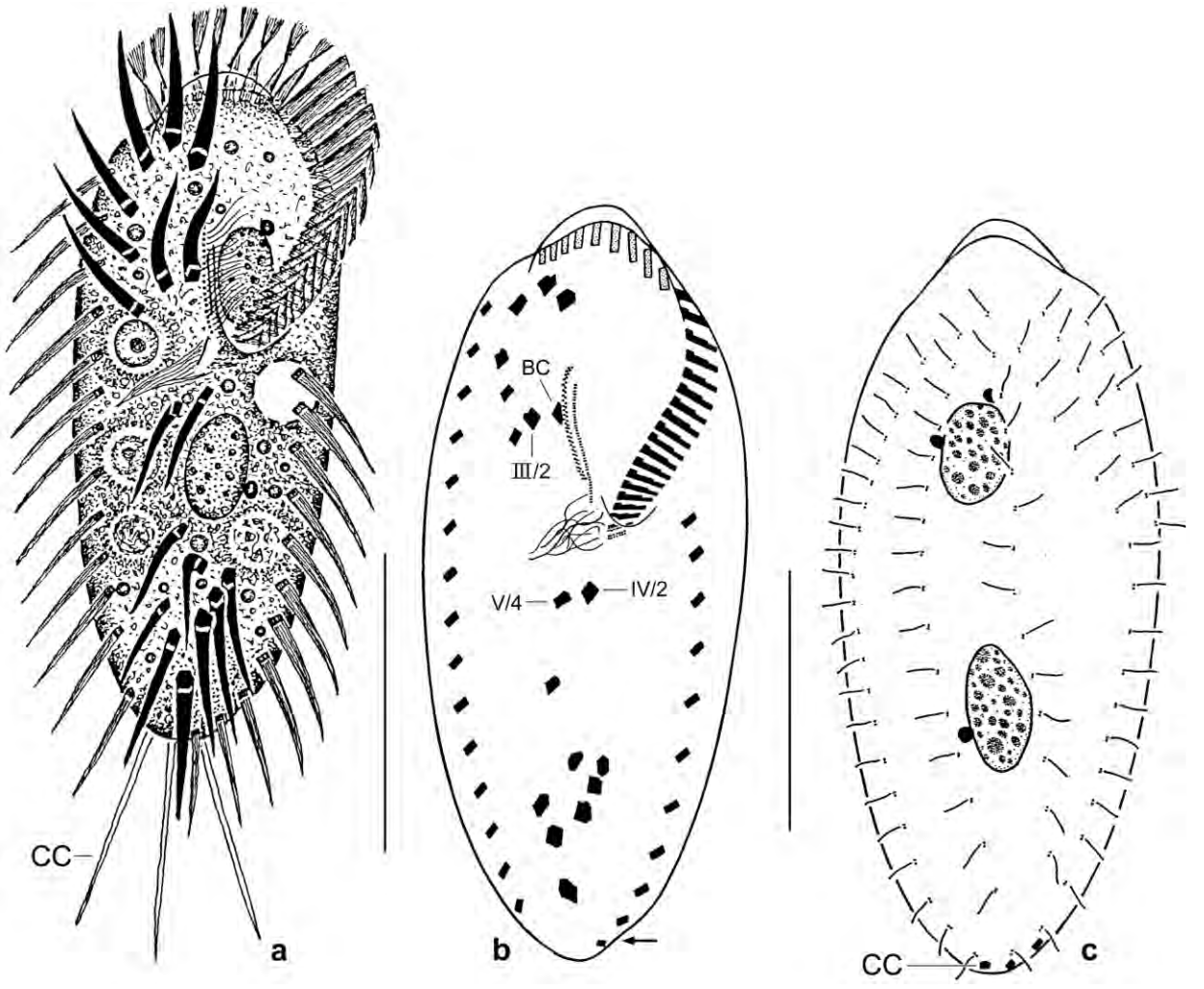

Fig. 283a–c. *Stylonychia notophorides* from life (a) and after protargol impregnation (b, c). **a:** Ventral view of a representative specimen with 18 fronto-ventral-transverse cirri shaded black, length 90 µm. **b, c:** Ventral and dorsal view of holotype specimen, length 86 µm. The arrow marks an inconspicuous emargination. BC – buccal cirrus, CC – caudal cirri, III/2, IV/2, V/4 – cirral names. Scale bars 30 µm (b, c) and 40 µm (a).

Type locality: Soil from Venezuelan site (24), i. e., a heavily used pasture in the outskirts of the town of Puerto Ayacucho, 67°36'W 5°41'N.

Type material: 1 holotype and 3 paratype slides with protargol-impregnated specimens have been deposited in the Biology Centre of the Upper Austrian Museum in Linz (LI). Relevant specimens have been marked by black ink circles on the coverslip.

Etymology: The name is a composite of the species group name *notophora*, the thematic vowel *-i-*, and the Greek suffix *-ides* (similar), indicating that *S. notophora* is probably the nearest relative.

Description: Size in vivo 70–105 × 28–36 µm, usually about 90 × 35 µm, as calculated from in vivo measurements and the morphometric data in Table 113 adding 15% preparation shrinkage. Body invariably moderately obovate, widest site in mid of adoral zone of membranelles, rarely with an inconspicuous terminal emargination on left margin; anterior and posterior quarter leaf-

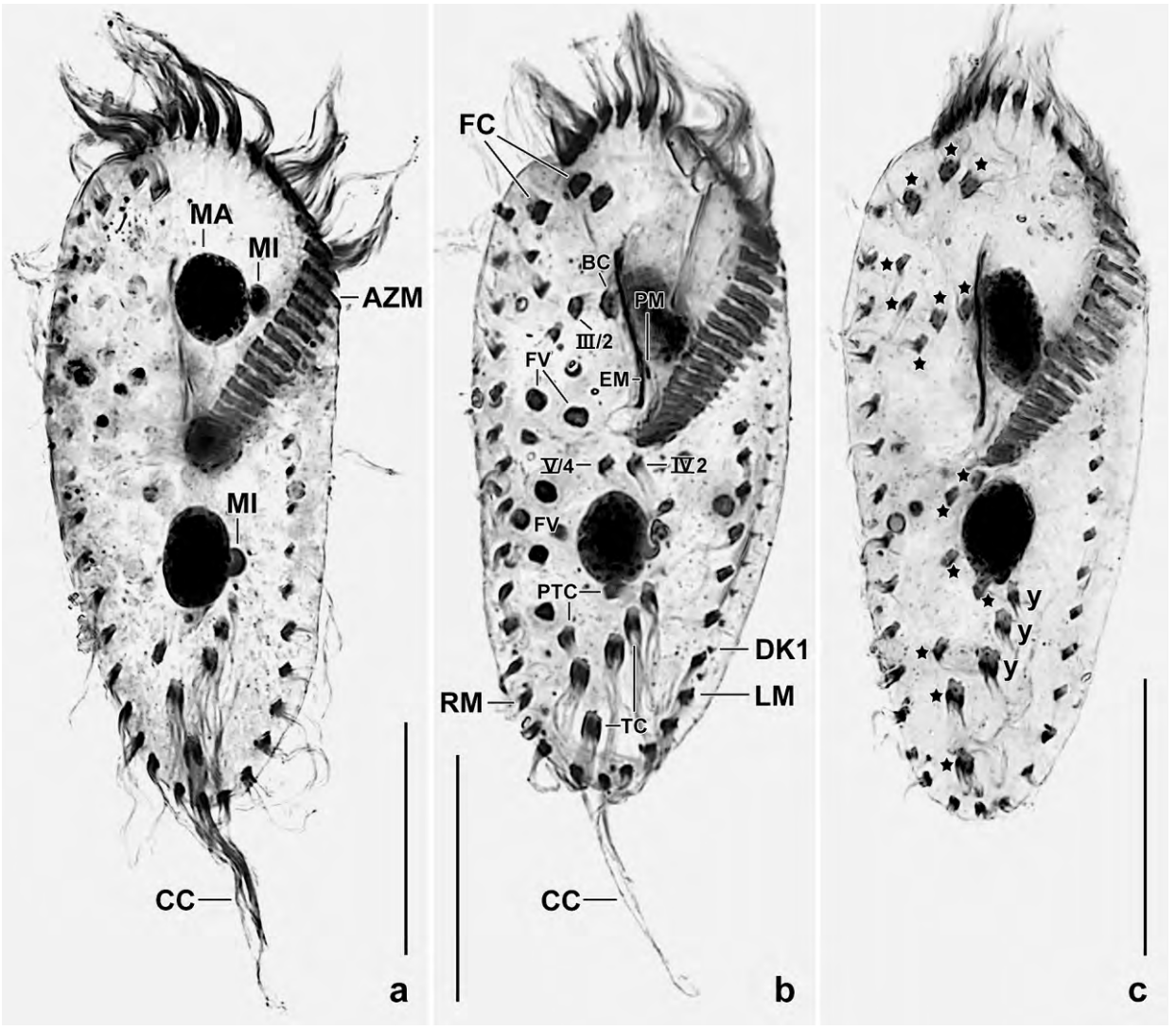

Fig. 284a–c. *Stylonychia notophorides*, ventral views after protargol impregnation. Asterisks in (c) mark 15 fronto-ventral-transverse cirri, and the (y) denote three further fronto-ventral-transverse cirri which form one of the two groups of transverse cirri. AZM – adoral zone of membranelles, BC – buccal cirrus, CC – caudal cirri, DK1 – dorsal kinety 1, EM – endoral membrane, FC – frontal cirri, FV – food, i. e., flagellates with deeply impregnated nucleus. LM – left marginal cirral row, MA – macronuclear nodule, MI – micronuclei, PM – paroral membrane, PTC – pretransverse cirri, RM – right marginal cirral row, TC – transverse cirri, III/2, IV/2, V/4 – cirral names. Scale bars 30 µm.

like flattened, dorsal central quarters more or less convex, depending on nutrition state (Fig. 283a, b, 284a–c; Table 113). Nuclear apparatus in central quarters and slightly left of body`s midline. Anterior macronuclear nodule underneath of buccal cavity, posterior nodule between buccal vertex and anteriormost transverse cirrus; individual nodules broadly to slenderly ellipsoid, on average 13 × 7 µm after protargol impregnation. One to four, on average two broadly ellipsoid micronuclei attached to various sites of macronuclear nodules (Fig. 283a, c, 284a–c; Table 113). Contractile vacuole left of buccal vertex, i. e., slightly anterior to mid-body. Cortex inflexible, bright, without specific granules. Cytoplasm colourless, central third usually studded with some lipid droplets and many food vacuoles containing a heterotrophic flagellate about 10 µm in size (Fig. 283a).

Table 113. Morphometric data on *Stylonychia notophorides* based on mounted, protargol-impregnated, and randomly selected specimens from a non-flooded Petri dish culture. Measurements in µm. CV – coefficient of variation in %, M – median, Max – maximum, Mean – arithmetic mean, Min – minimum, n – number of individuals investigated, SD – standard deviation, SE – standard error of mean.

Characteristics	Mean	M	SD	SE	CV	Min	Max	n
Body, length	80.1	80.0	5.4	1.2	6.7	68.0	90.0	21
Body, width	31.0	31.0	2.5	0.5	8.0	28.0	36.0	21
Body length:width, ratio	2.6	2.6	0.2	0.1	6.9	2.3	2.9	21
Anterior body end to proximal end of adoral zone, distance	37.2	37.0	2.2	0.5	5.9	32.0	41.0	21
Adoral zone of membranelles, percentage of body length	46.6	47.0	2.2	0.5	4.6	42.0	50.0	21
Largest membranellar basis, width	5.2	5.0	–	–	–	5.0	6.0	21
Adoral membranelles, number	27.5	28.0	1.4	0.3	5.1	24.0	29.0	21
Anterior body end to paroral membrane, distance	16.4	17.0	1.3	0.3	7.6	14.0	19.0	21
Paroral membrane, length	14.7	15.0	0.8	0.2	5.7	13.0	16.0	18
Anterior body end to endoral membrane, distance	19.0	19.0	1.4	0.3	7.2	17.0	22.0	21
Endoral membrane, length	13.9	14.0	1.1	0.3	7.6	12.0	16.0	18
Anterior macronuclear nodule, length	13.6	13.0	2.0	0.4	14.7	11.0	17.0	21
Anterior macronuclear nodule, width	7.5	7.5	0.9	0.2	12.2	6.0	9.0	21
Macronuclear nodules, number	2.0	2.0	0.0	0.0	0.0	2.0	2.0	21
Anterior micronucleus, length	2.3	2.0	–	–	–	1.5	3.0	21
Anterior micronucleus, width	1.8	1.5	–	–	–	1.5	2.5	21
Micronuclei, number	1.9	2.0	1.0	0.2	52.3	1.0	4.0	21
Frontal cirri, number	2.9	3.0	–	–	–	1.0	3.0	21
Anterior body end to buccal cirrus, distance	20.6	21.0	1.4	0.3	6.9	19.0	24.0	21
Buccal cirri, number	1.0	1.0	0.0	0.0	0.0	1.0	1.0	21
Anterior body end to last frontoventral cirrus, distance	26.6	27.0	1.9	0.4	7.2	24.0	30.0	21
Frontoventral cirri, number	4.0	4.0	–	–	–	3.0	4.0	21
Anterior body end to rearmost postoral cirrus, distance	51.9	52.0	3.5	0.8	6.7	45.0	58.0	21
Postoral cirri, number	3.0	3.0	0.0	0.0	0.0	3.0	3.0	21
Pretransverse cirri, number	2.0	2.0	0.0	0.0	0.0	2.0	2.0	21
Posterior body end to lowermost transverse cirrus, distance	6.4	6.0	1.3	0.3	20.3	4.0	11.0	21
Transverse cirri, number	5.0	5.0	–	–	–	4.0	5.0	21
Anterior body end to right marginal row, distance	10.5	10.0	1.5	0.3	14.6	8.0	14.0	21
Right marginal row, number of cirri	13.4	13.0	1.4	0.3	10.7	9.0	16.0	21
Left marginal row, number of cirri	10.7	11.0	0.7	0.2	6.9	9.0	12.0	21
Dorsal kineties, number	6.0	6.0	0.0	0.0	0.0	6.0	6.0	21
Bristles in dorsal row 1, number	22.1	22.0	1.5	0.3	6.9	20.0	27.0	21
Bristles in dorsal row 2, number	17.1	17.0	1.2	0.3	7.0	15.0	20.0	21
Bristles in dorsal row 3, number	12.9	13.0	1.0	0.2	7.9	11.0	14.0	21
Bristles in dorsal row 4, number	16.5	17.0	1.5	0.4	9.1	14.0	20.0	21
Bristles in dorsal row 5, number	7.4	7.0	0.7	0.2	9.2	6.0	8.0	21
Bristles in dorsal row 6, number	4.0	4.0	1.3	0.3	32.6	1.0	6.0	21
Caudal cirri, distance between cirrus 1 and 3	4.9	5.0	0.7	0.1	13.3	4.0	7.0	21
Caudal cirri, number	3.0	3.0	0.0	0.0	0.0	3.0	3.0	21

Cirral pattern as typical for genus (Berger 1999), i. e., usually 18 fronto-ventral-transverse cirri with some variation, such as a missing frontal or transverse cirrus (Fig. 283a, b, 284a–c; Table 113). Three moderately enlarged frontal cirri close together right of body´s midline. Frontoventral cirri in specific pattern, i. e., buccal cirrus and cirrus III/2 side by side anterior to mid of undulating membranes. Anterior postoral cirri close together, cirrus IV/2 slightly anterior or at level of cirrus V/4; third postoral cirrus 65% distant from anterior body end. Transverse cirri distinctly enlarged, in two groups, in vivo about 20 µm long and thus moderately projecting from body proper. Marginal cirri about 17 µm long, each composed of three ciliary rows, right row moderately shortened anteriorly and posteriorly, left row extends to body´s midline posteriorly (Fig. 283a, b, 284a–c; Table 113).

Dorsal bristles 3–4 µm long, arranged in typical *Stylonychia* pattern, i. e., in four almost bipolar rows and two strongly shortened dorsomarginal kineties; last bristle of rows 1, 2, 4 close to caudal cirri in vivo 25–35 µm long and obliquely spread in and right of body`s midline (Fig. 283a, c, 284a, b).

Oral apparatus in typical *Stylonychia* pattern, i. e., with comparatively short, almost straight undulating membranes and a large, obtriangular, flat buccal cavity (Fig. 283a, b, 284a–c; Table 113). Adoral zone occupies about 47% of body length, composed of an average of 27 ordinary membranelles with cilia 15–20 µm long in anterior half of zone. Undulating membranes side by side or one upon the other, straight or slightly curved. Pharyngeal fibres about 10 µm long.

Occurrence and ecology: As yet found only at Venezuelan sites (24) and (26), i. e., in soil of the *Tachypogon* Savannah in the outskirts of the town of Puerto Ayacucho and in the floodplain of the Orinoco River. Thus, *S. notophorides* is possibly a limnetic species. At site (24), it occurred two days after rewetting the sample; at site (26), it occurred after three weeks.

Remarks: *Stylonychia notophorides* has a unique combination of four important features: (i) narrowly spaced, about 30 µm long caudal cirri; (ii) transverse cirri in two groups; (iii) buccal cirrus and cirrus III/2 close together at same level; and (iv) postoral cirrus IV/2 at same level or slightly anterior to cirrus V/4. There are five congeners with long, narrowly spaced caudal cirri (Berger 1999): *Stylonychia notophora*, the most similar species, has a different frontoventral cirral pattern, specifically, the buccal cirrus is distinctly separate from cirrus III/2; further, it has more adoral membranelles (33–36 vs. 24–29) and marginal cirri (54 according to Stokes`illustration vs. 24; 32 vs. 24 in the population studied by Dragesco and Njine 1971); *S. putrina* and *S. vorax* differ from *S. notophorides* by the arrangement of the frontoventral cirri; *S. curvata* has a different oral apparatus and frontoventral cirral pattern; and *S. pusilla* has an unclear identity and might belong to the *S. mytilus* complex.

Body size and shape are highly similar to those of *S. bifaria*, *Tetmemena pustulata*, and *S. vorax*, i. e., about 100 × 30 µm and more or less obovate. Thus, be careful in identification.

Stylonychia ammermanni Gupta et al., 2001 (Fig. 285a–d, 286a–i; Tables 114, 115)

Observations on Venezuelan site (56) population (Fig. 285a–c, 286a, b, d–i): The main

characteristics are compiled and compared in Tables 114 and 115 and the Figures cited. Additionally, the following peculiarities should be mentioned: (i) outline usually asymmetric, right margin slightly to distinctly convex, left straight to slightly convex, i. e., similar to the type population (Fig. 285d, 286c), although GUPTA et al. (2001) described parallel body margins; (ii) posterior body end often truncate (vs. rounded; Fig. 285d, 286c); (iii) anomalies in the 18 FVT-cirral pattern not uncommon, i.e., 17–25 cirri in 31 out of 85 specimens, 18 of them with 21 cirri (not mentioned in Indian and Chinese populations); (iv) right caudal cirrus optically upon last cirrus of right marginal row (vs. last 2–3 cirri).

Notes on ontogenesis (Fig. 286b): Cell division follows the pattern of the *Stylonychia mytilus* complex (BERGER 1999, GUPTA et al. 2001). The oral primordium is formed close to and left of the unaltered anteriormost transverse cirrus II/1. The postoral cirrus V/4 and the frontoventral cirri III/2 and IV/3 are modified to primordia. The anterior parts of the undulating membranes are reorganized while the posterior regions remain unchanged.

Material deposited: 3 voucher slides with protargol-impregnated specimens have been deposited in the Biology Centre of the Upper Austrian Museum in Linz (LI). Relevant specimens have been marked by black ink circles on the coverslip.

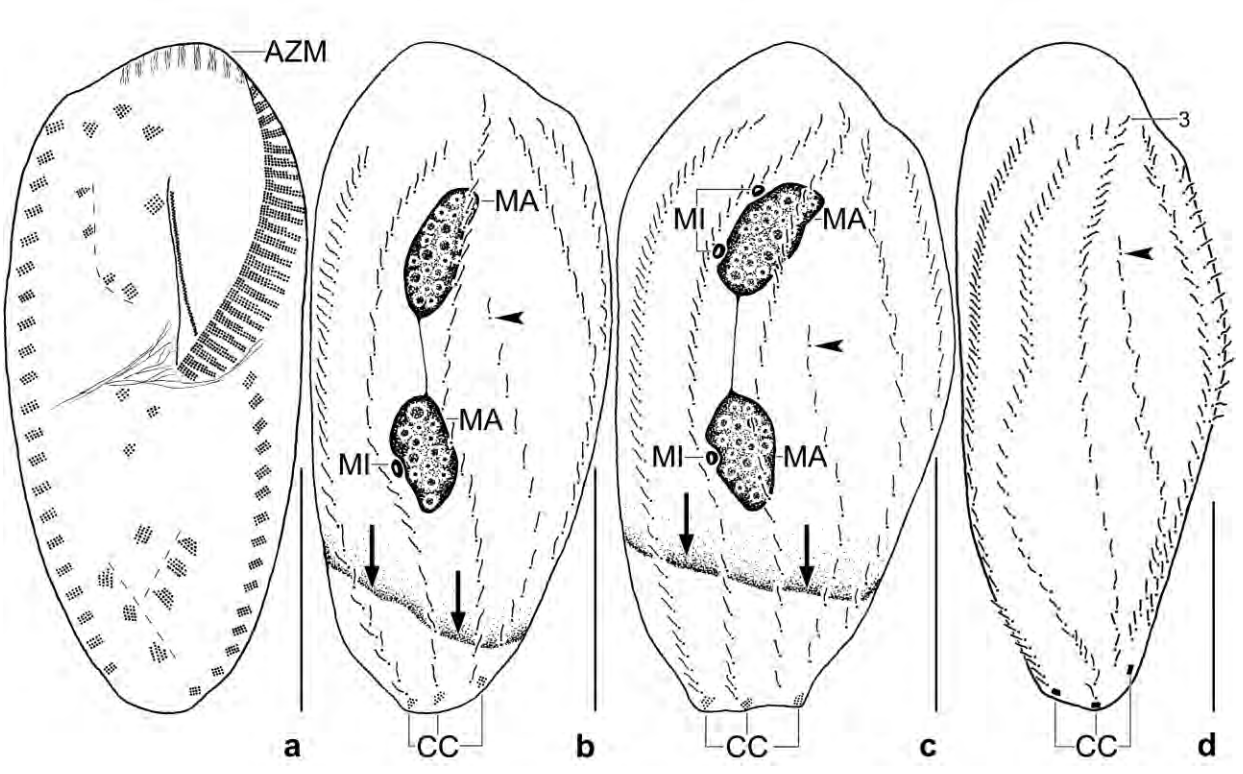

Fig. 285a–d. *Stylonychia ammermanni*, infraciliature of Venezuelan population (a–c) and Indian holotype (d, original) after protargol impregnation. Arrowheads denote the anterior end of dorsal kinety 4; arrows mark the anterior end of the flattened posterior body region; dikinetids in the dorsal bristle rows are illustrated as single dots. **a, b:** Ventral and dorsal view of a slender specimen with rounded body ends, length 110 µm. The J-shaped pattern of the frontoventral cirri and the Y-like arranged pretransverse and transverse cirri are indicated by dashed lines. **c:** Dorsal view of a broad specimen with truncate posterior body end, length 105 µm. **d:** Dorsal view of a slender specimen from Indian holotype slide, length 128 µm. Note the bipolar kinety 3. AZM – adoral zone of membranelles, CC – caudal cirri, MA – macronuclear nodules, MI – micronuclei. Scale bars 40 µm.

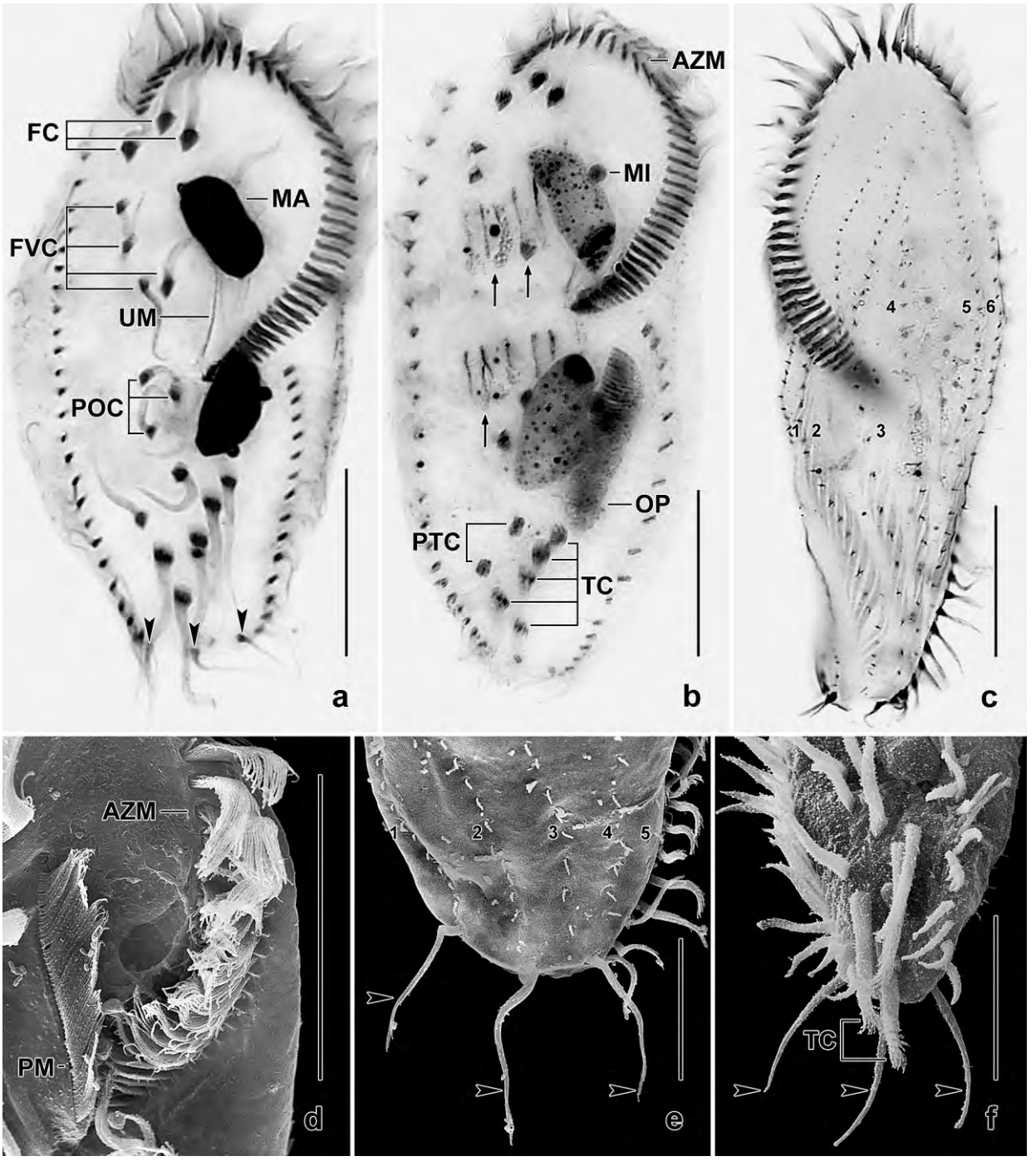

Fig. 286a–f. *Stylonychia ammermanni*, Venezuelan population (a, b, d–f) and a specimen from Indian holotype slide (c) after protargol impregnation (a–c) and in the scanning electron microscope (d–f). Arrowheads denote the conspicuous caudal cirri. **a:** Cirral pattern, length 100 µm. **b:** Ventral view of an early mid-divider, length 120 µm. Arrows mark the primordia produced by cirri V/4, IV/3, and III/2. **c:** Dorsal view, length 135 µm. Note bipolar kinety 3 (posteriorly distinctly shortened in Gupta et al. 2001). **d:** Oral region. **e:** Dorsal view of posterior body region, showing the wide-spaced caudal cirri. **f:** Ventral view of posterior body region. Note the tapered caudal cirri and the fringed transverse cirri, only two of which protrude from body proper. AZM – adoral zone of membranelles, FC – frontal cirri, FVC – frontoventral cirri, MA – macronuclear nodule, MI – micronucleus, OP – oral primordium, PM – paroral membrane, POC – postoral cirri, PTC – pretransverse cirri, TC – transverse cirri, UM – undulating membranes, 1–6 – dorsal kineties. Scale bars 20 µm (e) and 30 µm (a–d, f).

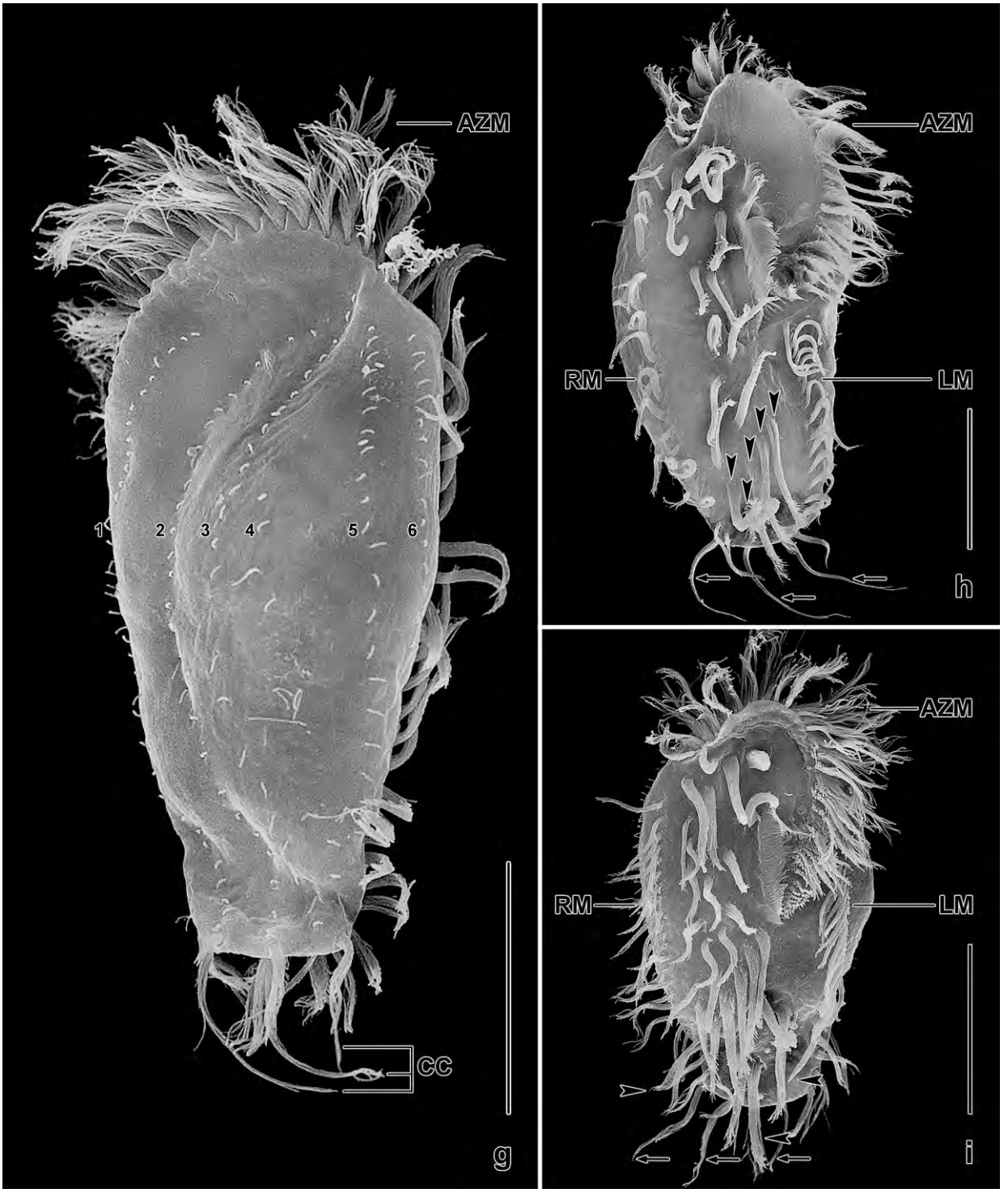

Fig. 286g–i. *Stylonychia ammermanni*, Venezuelan specimens in the scanning electron microscope. **g:** Dorsal view, showing the shortened bristle row 4 as well as the flattened and transverse-truncate posterior body region, length 88 µm. **h:** Ventral view, showing cirral pattern with fringed transverse cirri marked by arrowheads, length 100 µm. Arrows denote the long caudal cirri. **i:** Ventral view of an opisthe post-divider with some parental cirri still present (arrowheads), length 72 µm. Arrows denote caudal cirri. 1–6 – dorsal kineties, AZM – adoral zone of membranelles, CC – caudal cirri, LM – left marginal cirral row, RM – right marginal cirral row. Scale bars 30 µm.

Table 114. Morphometric data on *Stylonychia ammermanni* from Venezuela based on mounted, protargol-impregnated, and randomly selected specimens from a non-flooded Petri dish culture. Measurements in µm. CV – coefficient of variation in %, M – median, Max – maximum, Mean – arithmetic mean, Min – minimum, n – number of individuals investigated, SD – standard deviation, SE – standard error of arithmetic mean.

Characteristics	Mean	M	SD	SE	CV	Min	Max	n
Body, length	110.5	110.0	7.4	1.6	6.7	98.0	128.0	21
Body, width	50.1	49.0	4.3	0.9	8.6	42.0	58.0	21
Body length:width, ratio	2.2	2.2	0.2	0.0	6.8	1.9	2.4	21
Body, width at mid-transverse cirrus	34.8	36.0	3.3	0.7	9.6	28.0	39.0	21
Anterior macronuclear nodule, length	21.0	21.0	1.8	0.4	8.5	18.0	24.0	21
Anterior macronuclear nodule, width	10.4	10.0	1.2	0.3	11.2	9.0	14.0	21
Anterior macronuclear nodule, length:width ratio	2.0	2.0	0.3	0.1	13.8	1.5	2.7	21
Macronuclear nodules, distance in between [a]	14.2	15	2.7	0.6	19.0	10	20	21
Micronuclei, number [b]	2.7	3.0	1.0	0.2	37.1	1.0	4.0	21
Anterior micronucleus, length	2.5	2.5	–	–	–	2.0	3.5	21
Anterior micronucleus, width	2.1	2.0	–	–	–	1.5	2.5	21
Anterior body end to proximal end of adoral zone, distance	57.5	57.0	3.6	0.8	6.3	49.0	64.0	21
Adoral zone of membranelles, percentage of body length	52.1	52.6	2.7	0.6	5.2	47.8	57.7	21
Largest membranellar basis, width	7.7	8.0	–	–	–	7.0	8.0	21
Adoral membranelles, number	39.1	39.0	2.2	0.5	5.5	34.0	44.0	21
Anterior body end to proximal end of endoral, distance	51.0	51.0	4.2	0.9	8.3	43.0	60.0	21
Anterior body end to proximal end of paroral, distance	50.4	51.0	3.8	0.8	7.6	43.0	58.0	21
Endoral, length	27.7	27.0	3.0	0.6	10.7	23.0	35.0	21
Paroral, length	21.6	22.0	3.0	0.6	13.8	15.0	26.0	21
Anterior body end to uppermost postoral cirrus, distance	58.5	58.0	4.2	0.9	7.1	47.0	68.0	21
Posterior body end to lowermost transverse cirrus, distance	9.2	9.0	1.9	0.4	21.1	7.0	15.0	21
Strongly flattened posterior end, length	14.0	14.0	3.9	0.9	28.2	8.0	22.0	21
Caudal cirri, distance between number 1 and 3	12.9	13.0	1.6	0.3	12.1	10.0	16.0	21
Right marginal row, number of cirri	22.4	23.0	1.2	0.3	5.6	20.0	24.0	21
Left marginal row, number of cirri	15.9	16.0	1.3	0.3	8.0	13.0	18.0	21
Bristles in dorsal row 1, number	37.6	37.0	3.3	0.7	8.7	28.0	44.0	21
Bristles in dorsal row 2, number	27.9	28.0	1.6	0.4	5.7	25.0	31.0	21
Bristles in dorsal row 3, number	25.0	25.0	1.9	0.4	7.4	22.0	28.0	21
Bristles in dorsal row 4, number	12.0	12.0	1.4	0.3	11.3	10.0	15.0	21
Bristles in dorsal row 5, number	20.9	20.0	1.9	0.4	8.9	18.0	25.0	21
Bristles in dorsal row 6, number	12.9	13.0	2.0	0.4	15.6	10.0	17.0	21
Dorsal bristles, total number	136.3	137.0	6.2	1.3	4.5	122.0	147.0	21
Anterior body end to dorsal row 4, distance	45.0	44.0	5.9	1.3	13.2	34.0	59.0	21

[a] Of 85 specimens analysed, six have one macronuclear nodule.

[b] Of 21 specimens analysed, three have one micronucleus, five have two micronuclei, eight have three, and five have four.

Occurrence and ecology: As yet found in Asia, Europe and South America, i. e., in backwaters of the Yamuna river in the Delhi region, India, 28°34′N 76°07′E; in ponds and small rivers around Harbin, Heilongjiang province, China, 45°70′N 126°80′E; in the mould of a soil infusion of a *Caricetum curvulae* biotope near the Wallackhaus, Großglockner region, Austria, 47°04′N

Table 115. Comparison of main morphometrics of *Stylonychia ammermanni* populations from Austria (misidentified as *S. mytilus* by FOISSNER 1982), Venezuela (for more details, see Table 114), India (type population, GUTPA et al. 2001), and China (described as *S. harbinensis* by XIN-BAI & AMMERMANN 2004). Data based on mounted, protargol-impregnated, and randomly selected specimens. Measurements in µm: first value arithmetic mean; minimum and maximum in parentheses.

Characteristics	Austria	Venezuela	India	China[a]
Body, length	93 (89–100)	110 (98–128)	134 (126–146)/ 126[b] (106–150)[b]	142 (±6)
Body, width	40 (40–40)	50 (42–58)	52 (47–58)	58 (±3)
Body length:width, ratio	2.3	2.2 (1.9–2.4)	2.6 (2.3–3.0)	2.5 (±0.9)
Anterior body end to buccal cirrus, distance in % of body length	25[c]	26 (21–33)	28[b] (27–30)[b]	27 (±1.7)
Anterior body end to dorsal row 4, distance in % of body length	45[c]	41 (28–54)	33[b] (27–36)[b]	36[d]
Micronucleus, size	4.4 × 3.3[c]	2.5 × 2.1 (2.0–3.5 × 1.5–2.5)	2.6 (2.5–3.0)	5.0 (±0.25)
Micronuclei, % of cells with 1; 2; 3; 4 micronuclei	(–)[e]	14; 24; 38; 24	0; 33; 33; 33[f]	<5; 95; <5; <5[g]
Adoral membranelles, number	39 (38–41)	39 (34–44)	51 (46–55)/ 49 (44–53)[b]	45 (±4)
Left marginal row, number of cirri	14 (13–14)	16 (13–18)	17 (13–18)	19 (±2)
Right marginal row, number of cirri	18 (17–19)	22 (20–24)	24 (22–27)	27 (±4)
Dorsal bristle rows, number	5	6	6	6
Dorsal bristles, total number	116[c]	136 (122–147)	189 (176–200)	155 (±13)[h]
Caudal cirri	tapered[c]	tapered	no data	fringed
Material	soil infusion	non-flooded Petri dish culture	pure culture	clone culture
Specimens investigated, number	3	21	12–30	5–15

[a] Values in parentheses show standard deviation.
[b] Our measurements of 13 specimens from holotype slide.
[c] According to Fig. 30 in FOISSNER (1982).
[d] According to Fig. 3 in XIN-BAI & AMMERMANN (2004).
[e] No information given in publication, the illustrations show 1 micronucleus.
[f] From a personal communication of G.R. SAPRA to XIN-BAI & AMMERMANN (2004). Not recognizable in our reinvestigation of the holotype slide.
[g] 100 specimens investigated.
[h] Calculated from arithmetic means; kinety 6 not included.

12°50′E; and in slightly saline (4 ‰) soil and mud from ephemeral ponds on the north coast of Venezuela, 11°33′N 67°13′W. These records show *S. ammermanni* to be a limnetic, cosmopolitan species.

Remarks: The *Stylonychia mytilus* complex is composed of four species: *S. ammermanni*, *S. harbinensis*, *S. lemnae*, and *S. mytilus* (BERGER 1999, GUPTA et al. 2001, XIN-BAI & AMMERMANN 2004). Species of the complex share the same morphogenetic pattern, posteriorly separated marginal cirral rows, and widely spaced caudal cirri (Fig. 285a–d, 286a–c, e–h). *Stylonychia ammermanni*, *S. harbinensis*, the present Venezuelan population, and specimens from Austria (FOISSNER 1982) are easily separated from the other members of the complex by body length (<

150 µm) and the shortened dorsal kinety 4 (Fig. 285b–d, 286c, g; Table 115).

Important characters to distinguish *S. ammermanni* and *S. harbinensis*, such as a posteriorly shortened dorsal kinety 3 and a more anteriorly positioned buccal cirrus (XIN-BAI & AMMERMANN 2004) were disproved by our reinvestigation of the *S. ammermanni* holotype slide (Fig. 285d, 286c; Table 115). Other characters different between *S. ammermanni, S. harbinensis,* the populations from Venezuela and Austria are weak because they usually overlap (Table 115). For example, the Venezuelan population matches well *S. ammermanni* in the number of marginal cirri, while the number of adoral membranelles match better *S. harbinensis*. The data compiled in Table 115 suggest that all these populations belong to a single morphospecies, *S. ammermanni*.

Tetmemena pustulata (MÜLLER, 1786) EIGNER, 1999 (Fig. 287a–d, 288a–g; Tables 116, 117)

Observations on a Venezuelan population: Detailed morphometric data on the Venezuelan site (56) population of *Tetmemena pustulata* are presented in Table 116, and the main characteristics are compared with those from other populations in Table 117. The Venezuelan specimens differ rather markedly from other *Tetmemena pustulata* populations: generally, all features studied morphometrically are smaller. Of these, the number of adoral membranelles is perhaps the most important ($\bar{x}$ = 28 vs. ≥ 32). There is also a curious morphological peculiarity (Fig. 287a, b, 288a, d, e): about 60 % (n = 124) of the specimens have a fairly distinct emargination at right posterior body end, similar to that found in *Urosoma emarginata* (for a review, see BERGER 1999). None of the *T. pustulata* illustrations in FOISSNER et al. (1991), GSCHWINDT (1991), ROSATI et al. (1988), and WIRNSBERGER et al. (1985) shows such a peculiarity. The emargination is indistinct or even lacking in 39 % of the specimens (Fig. 287c, d, 288c, f, g). Thus, and because of the lack of molecular and cyst data, we hesitate to classify the Venezuelan population as a distinct species or subspecies.

Material deposited: 4 voucher slides with protargol-impregnated specimens have been deposited in the Biology Centre of the Upper Austrian Museum in Linz (LI). Relevant specimens have been marked by black ink circles on the coverslip.

Occurrence and ecology: According to BERGER (1999), *Tetmemena pustulata* is one of the most common freshwater ciliates and has already been reported from Venezuela, i. e., in moss infusions from the vicinity of Caracas (SCORZA & MONTIEL 1954). We found it in the same region, that is, in slightly saline (4 ‰) soil and mud from ephemeral puddles.

Euplotopsis incisa FOISSNER, AGATHA & BERGER, 2002 (Fig. 289a–e).

The specimens from Venezuelan site (54) match well the original description, except for a 10th frontoventral cirrus (Fig. 289a) present also in the Saudi Arabian population (FOISSNER et al. 2002). Here, we present SEM micrographs, showing two main features of *E. incisa* for the first time, viz., the incision at the right body margin and the three caudal cirri (Fig. 289a–c, e). Further, we observed, conjugation (Fig. 289d). See Figures 289a–e for more details.

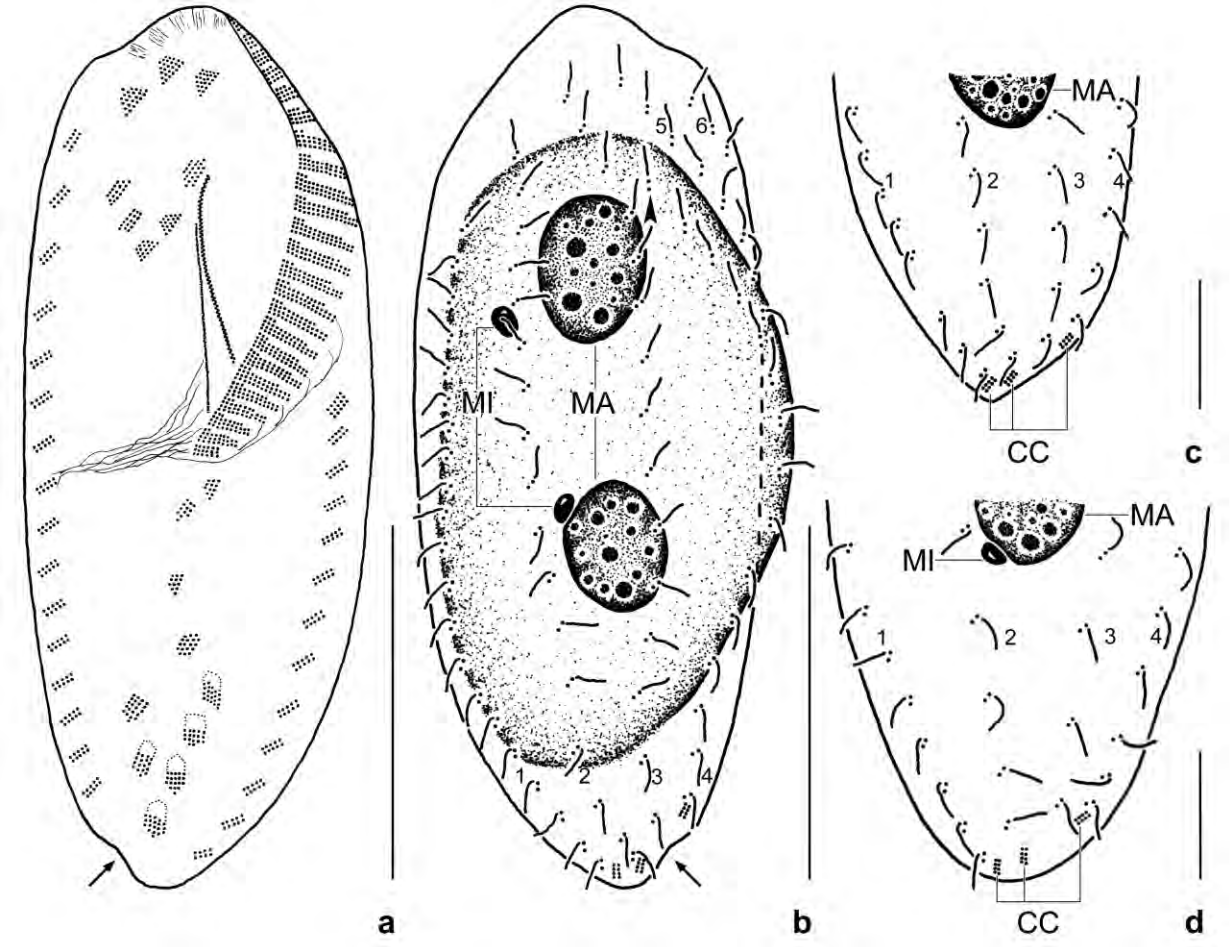

Fig. 287a–d. *Tetmemena pustulata* from Venezuelan site (56) after protargol impregnation. **a, b:** Ventral and dorsal view of a representative specimen, showing the infraciliature, the nuclear apparatus, and the emargination at the right posterior body end (arrows), a common peculiarity of the Venezuelan specimens; length 74 µm. The anterior part of the transverse cirri is not ciliated; the anterior end of the shortened dorsal kinety 4 is marked by an arrowhead. Further labels, see micrographs 2a, b. **c:** Dorsal posterior view of a specimen with acute body end. **d:** Dorsal posterior view of a specimen with rounded body end. CC – caudal cirri, MA – macronuclear nodules, MI – micronuclei, 1–6 – dorsal kineties. Scale bars 10 µm (c, d) and 30 µm (a, b).

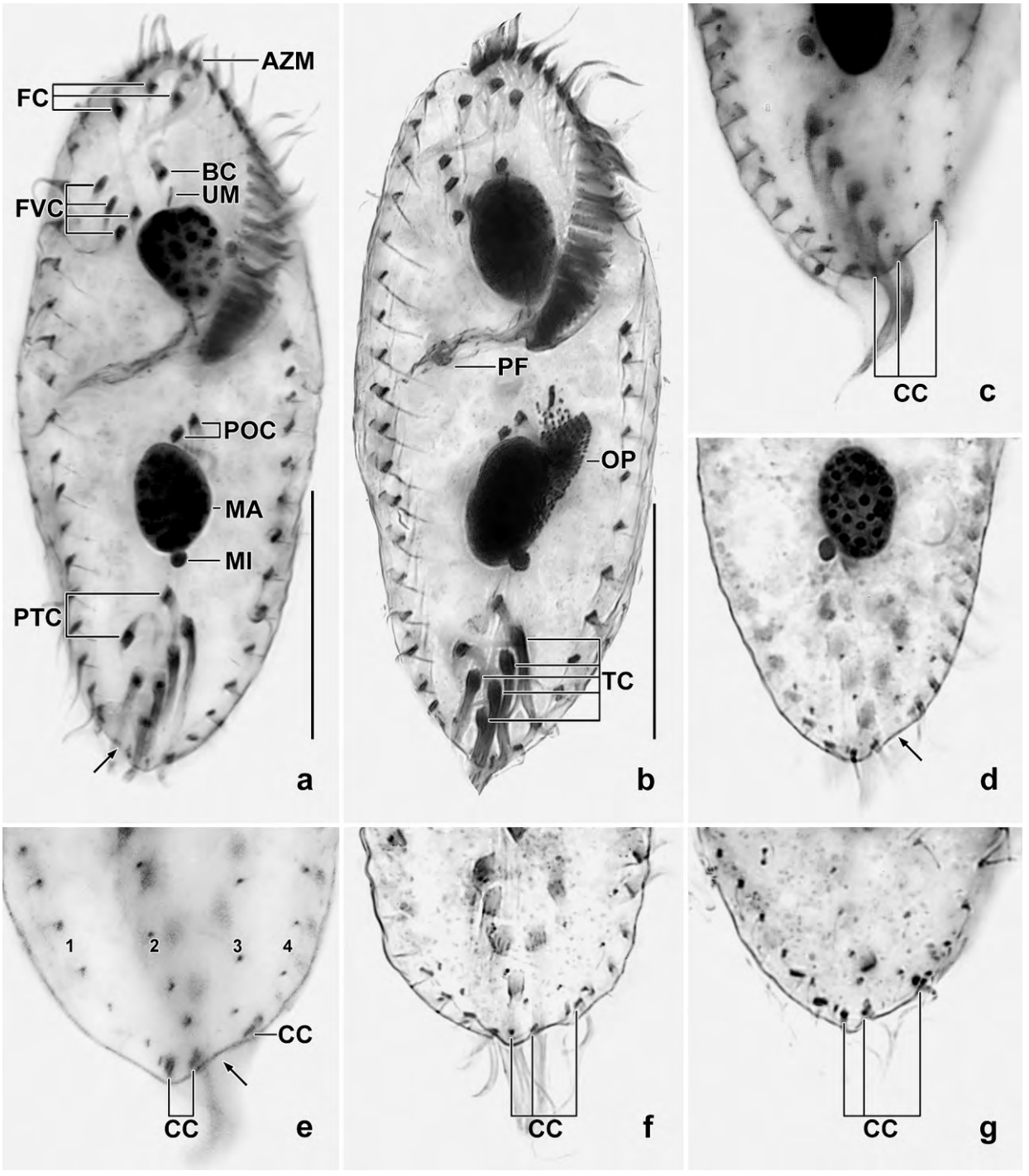

Fig. 288a–g. *Tetmemena pustulata* from Venezuelan site (56) after protargol impregnation. **a:** Ventral view of a representative specimen, length 86 µm. One postoral cirrus is invisible because it is over the macronuclear nodule. Arrow marks emargination. **b:** Ventral view of an early divider, length 91 µm. The oral primordium has been formed de novo left of the postoral cirri. **c–g:** Dorsal views, showing variations in the shape of the posterior body end. Arrows in (d, e) mark a fairly distinct emargination at right posterior body end. AZM – adoral zone of membranelles, BC – buccal cirrus, CC – caudal cirri, FC – frontal cirri, FVC – frontoventral cirri, MA – macronuclear nodule, MI – micronucleus, OP – oral primordium, PF – pharyngeal fibres, POC – postoral cirri, PTC – pretransverse cirri, TC – transverse cirri, UM – undulating membranes, 1–4 – dorsal kineties. Scale bars 30 µm.

Table 116. Morphometric data on a slowly growing culture of *Tetmemena pustulata* from Venezuelan site (56) based on mounted, protargol-impregnated, and randomly selected specimens from a semi-pure culture. Measurements in µm. CV – coefficient of variation in %, M – median, Max – maximum, Mean – arithmetic mean, Min – minimum, n – number of individuals investigated, SD – standard deviation, SE – standard error of arithmetic mean.

Characteristics	Mean	M	SD	SE	CV	Min	Max	n
Body, length	77.7	76.0	8.4	1.8	10.8	64.0	100.0	21
Body, width	32.7	31.0	4.5	1.0	13.7	26.0	45.0	21
Body length:width, ratio	2.4	2.4	0.2	0.0	8.2	2.1	2.9	21
Body, width at level of middle transverse cirrus	20.1	19.0	3.1	0.7	15.7	17.0	30.0	21
Anterior body end to anterior macronuclear nodule, distance	16.7	16.0	1.7	0.4	10.3	14.0	21.0	21
Anterior macronuclear nodule, length	13.8	13.0	1.8	0.4	13.1	10.0	18.0	21
Anterior macronuclear nodule, width	9.3	9.0	0.6	0.1	6.2	8.0	10.0	21
Macronuclear nodules, distance in between [a]	12.5	13.0	2.1	0.5	16.5	9.0	16.0	21
Micronuclei, number [b]	1.9	2.0	–	–	–	1.0	2.0	21
Anterior micronucleus, length	2.4	2.4	–	–	–	2.0	2.8	21
Anterior micronucleus, width	1.9	2.0	–	–	–	1.4	2.4	21
Anterior body end to proximal end of adoral zone, distance	37.6	38.0	2.1	0.5	5.7	33.0	41.0	21
Adoral zone of membranelles, percentage of body length	48.7	48.7	3.8	0.8	7.7	41.0	55.0	21
Largest membranellar basis, length	6.1	6.0	0.4	0.1	7.2	5.0	7.0	21
Adoral membranelles, number	27.5	28.0	1.6	0.3	5.7	24.0	30.0	21
Anterior body end to proximal end of paroral, distance	30.2	31.0	1.8	0.4	5.9	26.0	33.0	21
Anterior body end to proximal end of endoral, distance	33.3	34.0	2.4	0.5	7.1	28.0	38.0	21
Paroral membrane, length	15.4	16.0	1.4	0.3	8.8	12.0	18.0	21
Endoral membrane, length	15.5	16.0	2.2	0.5	14.1	10.0	21.0	21
Anterior body end to buccal cirrus, distance	13.0	13.0	0.8	0.2	6.2	11.0	14.0	21
Anterior margin of buccal cirrus to paroral, distance	1.8	2.0	0.7	0.1	38.7	0.5	3.0	21
Anterior body end to uppermost postoral cirrus, distance	40.0	40.0	3.2	0.7	8.0	34.0	46.0	21
Posterior body end to lowermost transverse cirrus, distance	4.2	4.0	0.6	0.1	14.7	3.0	6.0	21
Caudal cirri, distance between cirrus 1 and 2	1.4	1.6	–	–	–	1.2	1.6	21
Caudal cirri, distance between cirrus 2 and 3	3.9	4.0	–	–	–	3.2	4.8	21
Right marginal row, number of cirri	18.6	19.0	1.4	0.3	7.7	16.0	22.0	21
Left marginal row, number of cirri	13.0	13.0	1.5	0.3	11.9	8.0	15.0	21
Marginal cirral rows, difference in numbers of cirri	5.6	5.0	1.4	0.3	25.7	3.0	9.0	21
Bristles in dorsal row 1, number	19.2	19.0	1.7	0.4	8.8	16.0	22.0	21
Bristles in dorsal row 2, number	16.7	17.0	1.0	0.2	5.7	15.0	18.0	21
Bristles in dorsal row 3, number	14.0	14.0	1.1	0.2	7.6	12.0	16.0	21
Bristles in dorsal row 4, number	14.4	15.0	1.4	0.3	9.4	12.0	17.0	21
Bristles in dorsal row 5, number	7.7	8.0	0.6	0.1	7.3	7.0	9.0	21
Bristles in dorsal row 6, number	3.1	3.0	0.5	0.1	15.2	2.0	4.0	21
Dorsal bristles, total number	75.2	75.0	4.1	0.9	5.5	67.0	85.0	21
Anterior body end to dorsal bristle row 4, distance	15.0	15.0	2.0	0.4	13.1	11.0	19.0	21

[a] Of 128 specimens analysed, one lacks macronuclear nodules and three have only one nodule.

[b] Of 26 specimens analysed, one lacks micronuclei.

Table 117. Comparison of *Tetmemena pustulata* populations from Italy (ROSATI et al. 1988; according to BERGER 1999 misidentified as *Oxytricha bifaria*), Austria (Lunzer Lake, GSCHWINDT 1991; Lake Mondsee, WIRNSBERGER et al. 1985), and Venezuelan site (56). Data based on mounted, protargol-impregnated specimens (Austrian and Venezuelan populations) and scanning electron micrographs (Italian population). Measurements in µm: first value arithmetic mean; minimum and maximum in parentheses.

Characteristics	Italy, pure culture[a]	Lunzer Lake, natural population	Lake Mondsee, natural population	Lake Mondsee, small clone	Lake Mondsee, large clone	Venezuela, natural population
Body, length	80	53 (44–66)	65 (43–90)	79 (64–93)	94 (79–108)	78 (64–100)
Body, width	45	26 (21–31)	34 (22–50)	36 (27–48)	47 (35–62)	33 (26–45)
Body length: width, ratio	1.8[b]	2.0[b]	1.9[b]	2.2[b]	2.0[b]	2.4 (2.1–2.9)
Macronuclear nodules, length	no data	12 (9–14)	14 (9–17)	15 (10–20)	18 (10–28)	14 (10–18)
Macronuclear nodules, width	no data	6 (6–8)	7 (5–8)	7 (5–8)	9 (7–13)	9 (8–10)
Adoral zone of membranelles, length	no data	29 (24–37)	35 (25–44)	42 (31–48)	49 (40–56)	38 (33–41)
Adoral membranelles, number	no data	32 (27–39)	34 (24–42)	34 (31–37)	38 (34–42)	28 (24–30)
Left marginal row, number of cirri	no data	15 (12–18)	19 (12–22)	19 (16–22)	21 (18–24)	13 (8–15)
Right marginal row, number of cirri	28 (±2.3)	24 (20–29)	26 (18–32)	27 (25–30)	31 (28–34)	19 (16–22)
Dorsal kinety 4	bipolar[c]	slightly shortened	bipolar	no data	no data	slightly shortened
Bristles in dorsal row 1, number	20–30	24[d]	29[e]	no data	no data	19 (16–22)
Bristles in dorsal row 4, number	26 (±1.6)	16[d]	26[e]	no data	no data	14 (12–17)
Bristles in dorsal row 6, number	5[c]	4[d]	5[e]	no data	no data	3 (2–4)
Dorsal bristles, total number	105–147[f]	86[d]	111[e]	no data	no data	75 (67–85)
Specimens investigated, number	20–50	21	25	25	25	21

[a] Values in parentheses show standard deviation.

[b] Calculated from arithmetic mean.

[c] According to Figure 1 in ROSATI et al. (1988).

[d] According to Figure 8d in GSCHWINDT (1991).

[e] According to Figure 10 in WIRNSBERGER et al. (1985).

[f] Calculated from minimum and maximum, values of rows 5 and 6 taken from Figure 1 in ROSATI et al. (1988).

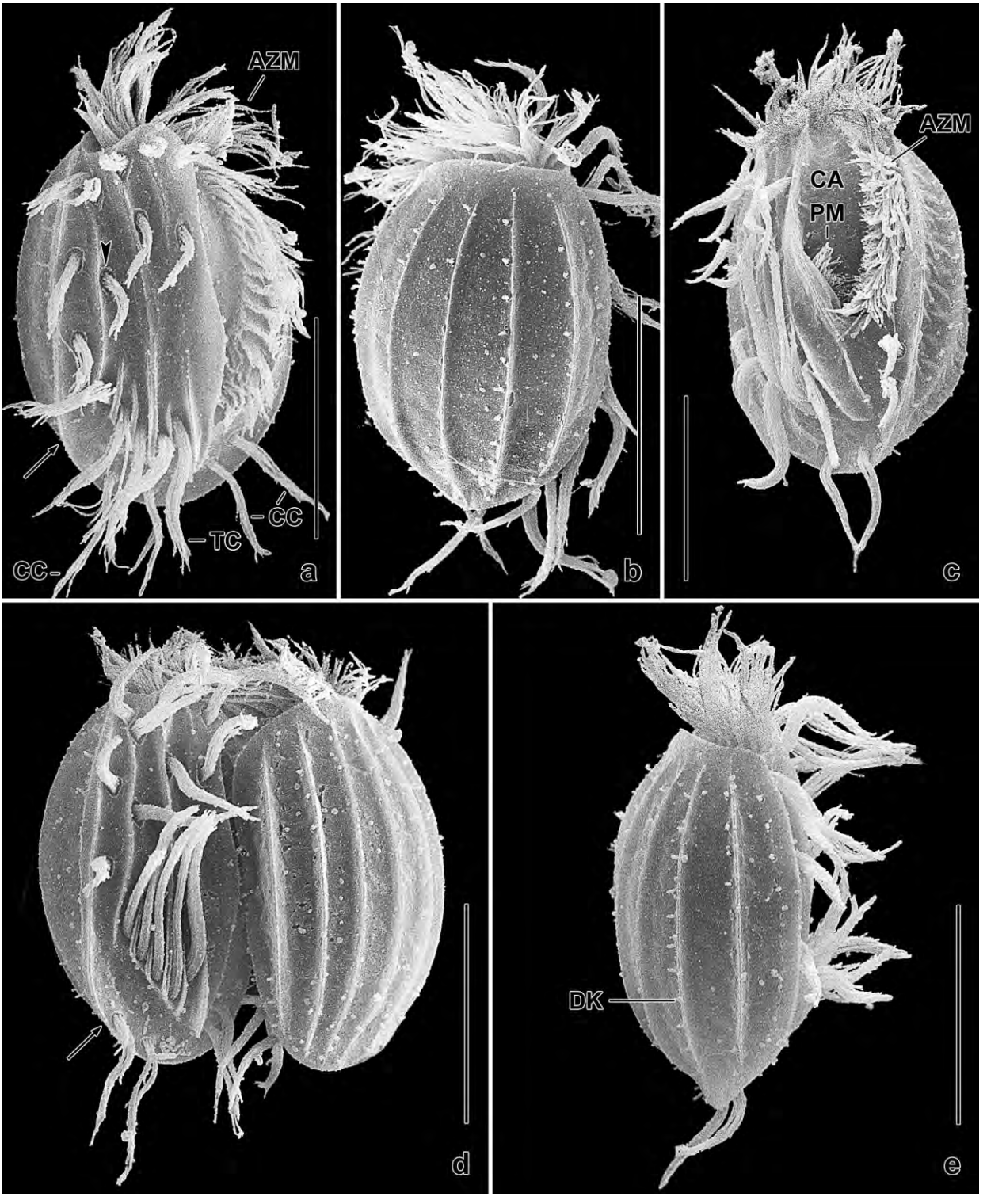

Fig. 289a–e. *Euplotopsis incisa* in the scanning electron microscope, showing the infraciliature and the cortical pattern. **a, b:** Ventral and dorsal view. The arrow marks the typical incision at the right body margin; the arrowhead denotes a 10th fronotventral cirrus. **c:** Ventral view, showing the flat buccal cavity. **d:** Conjugating specimens unite ventral to dorsal. The arrow marks the incision at right body margin. **e:** Lateral view. AZM – adoral zone of membranelles, CA – buccal cavity, CC – caudal cirri, DK – dorsal kinety, PM – paroral membrane, TC – transverse cirri. Scale bars 20 μm.

Condylostomides coeruleus nov. spec. (Fig. 290a–j, 291a–y, 292a–l, 293a–i, 294; Table 118)

Diagnosis: Size in vivo about 235 × 120 µm; ellipsoid. On average 9 macronuclear nodules in moniliform pattern, 39 ciliary rows, and 43 adoral membranelles. Conspicuously blueish or bluegreen due to bright cortical granules about 0.3 µm across and arranged in closely spaced rows. Resting cyst about 100 µm in diameter, greenish due to cortical granules scattered throughout cytoplasm and collected in large, polymorphic storages. Escape opening a small convexity. Macronuclear nodules not fused.

Type locality: Venezuelan site (56), i. e., slightly saline mud and soil from temporary grassland puddles in the surroundings of the village of Chichiriviche, Morrocoy National Park, 67°13'W 11°33'N.

Type material: 1 holotype and 13 paratype slides, including 4 slides with resting cysts, with protargol- and silver nitrate-impregnated specimens have been deposited in the Biology Centre of the Upper Austrian Museum in Linz (LI). Relevant specimens have been marked by black ink circles on the coverslip.

Etymology: The Latin adjective *coeruleus* (blue) refers to the colour of the cortical granules and of the body.

Description: All data are from cultures set up with Eau de Volvic and some slightly squashed wheat kernels to support bacterial and protist growth. Some ml from the non-flooded Petri dish culture were added to the medium providing food for *C. coeruleus*. Later, *Blepharisma americana* and *Colpidium colpoda*, both ingested by *C. coeruleus*, were added to obtain cleaner cultures. We cultivated *C. coeruleus* for 11 years without problems.

Condylostomides coeruleus has a profound variability with half of the coefficients of variation between 15% and 25%. However, two important features, viz., the number of ciliary rows and adoral membranelles have CVs < 10% (Table 118).

Size in vivo 150–315 × 85–155 µm, usually about 235 × 120 µm, as calculated from some in vivo measurements and the morphometric data Table 118 adding 5% preparation shrinkage (Champy´s fixative with osmium tetroxide); rarely occur smaller or larger specimens, especially in old cultures. Body shape inconspicuous, i. e., ellipsoid with a more or less distinct concavity in anterior third of oral apparatus; up to 2:1 flattened laterally (Fig. 290a, f, h, i, 291a, b, i, j; Table 118). Nuclear apparatus in central fifths of cell´s midline, composed of a moniliform macronucleus with an average of nine nodules and several micronuclei (Fig. 290a, g, 291k, l, n, t, 293h; Table 118). Macronuclear nodules globular to broadly ellipsoid, connected by short, argyrophilic strands; with many ordinary nucleoli; rarely form a loop anteriorly or posteriorly; first nodule usually distinctly enlarged (Table 118). Micronuclei globular, rarely impregnated with

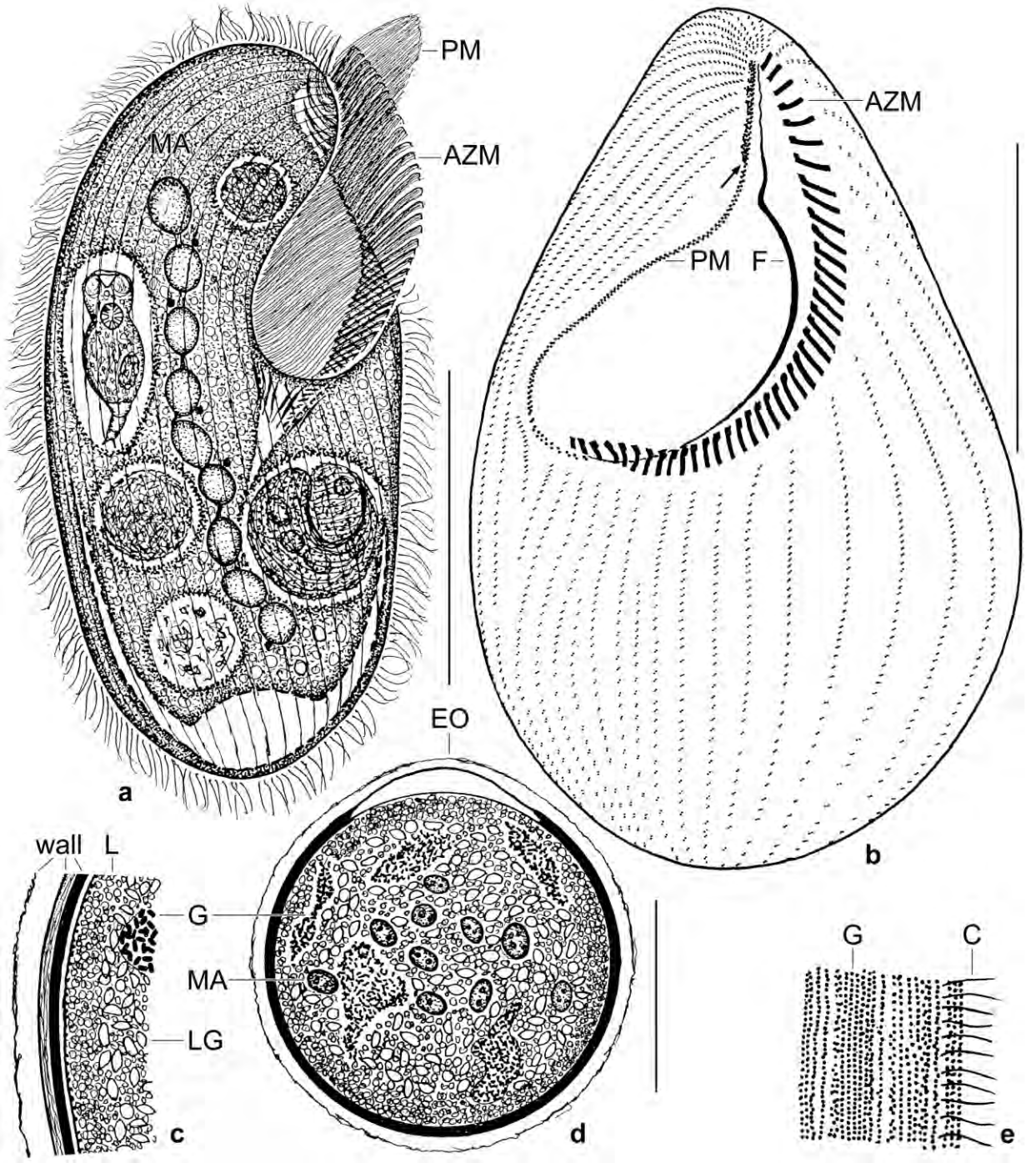

Fig. 290a–e. *Condylostomides coeruleus* from life (a, c–e) and after protargol impregnation (b). **a, e:** Right side view of a representative specimen, length 240 µm (a). This species is blueish or bluegreen due to innumerable cortical granules in dense rows (e). Note the moniliform macronucleus and large food vacuoles containing a rotifer and a *Blepharisma americana*. **b:** Ventral view of infraciliature. The arrow marks the frontal membranelles right of the paroral membrane. The thick fibre (F) is made of fine fibres originating from the adoral membranelles (see Fig. 291). **c, d:** The globular resting cysts have an inconspicuous escape opening. The complex wall is about 8 µm thick. The cytoplasm contains the macronuclear nodules; large, polymorphic accumulations of cortical granules making the cyst greenish; and innumerable lipid (?) droplets forming a finely granular layer under the wall; the cyst centre is studded with lenticular granules. AZM – adoral zone of membranelles, C – cilia, EO –escape opening, F – fibre, G – cortical granules, L – lipid droplets, LG – lenticular granules, MA – macronucleus (nodules), PM – paroral membrane. Scale bars 50 µm (d), 70 µm (b), and 100 µm (a).

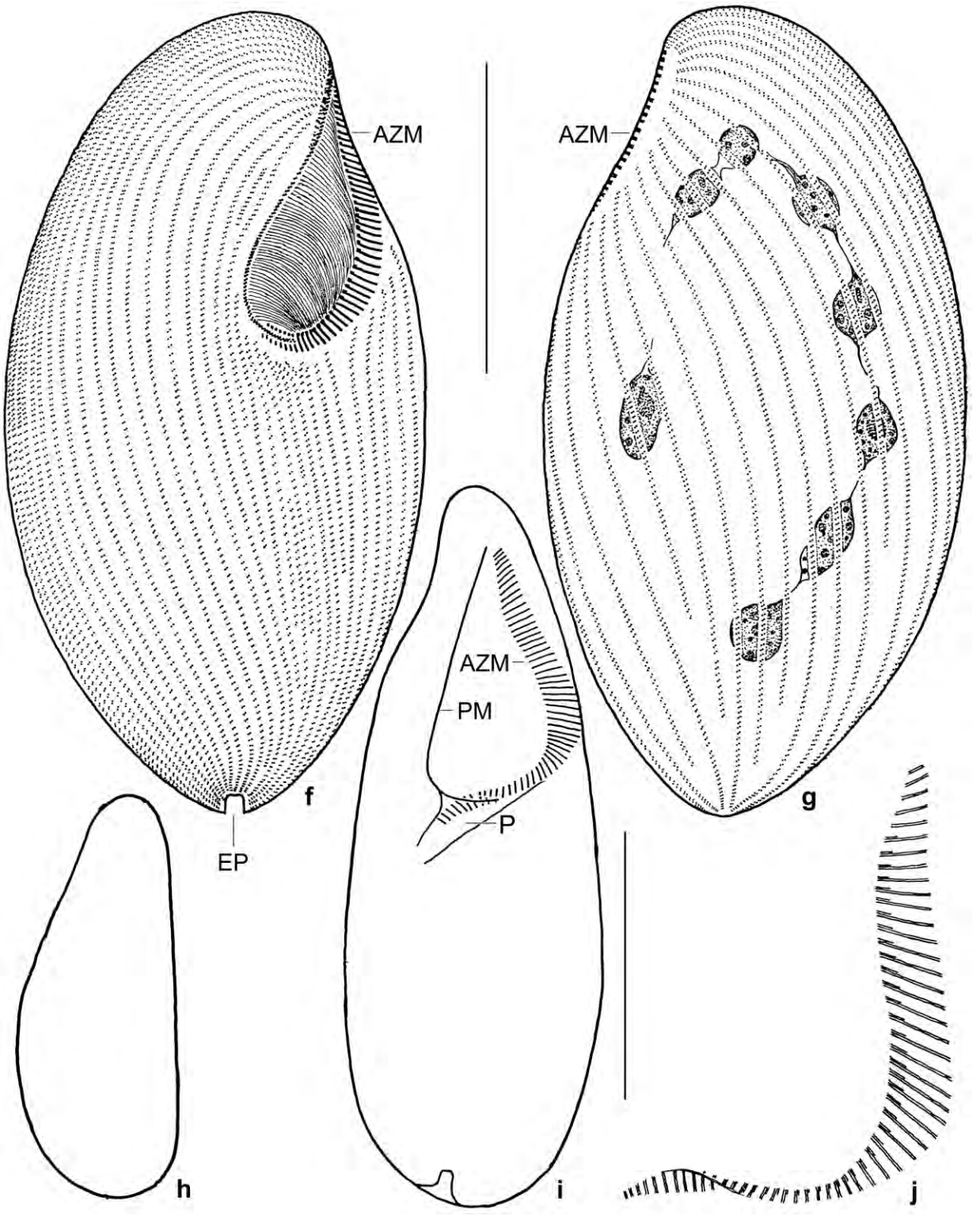

Fig. 290f–j. *Condylostomides coeruleus* from life (h), after protargol impregnation (f, g, j), and in a Chatton-Lwoff silver nitrate preparation (i). **f, g:** Right and left side view of holotype specimen, length 210 µm. **h–i:** Ventral views showing lateral flattening. **j:** Adoral zone. AZM – adoral zone of membranelles, EP – excretory pore, P – pharynx, PM – paroral membrane. Scale bars 80 µm (f, g, i).

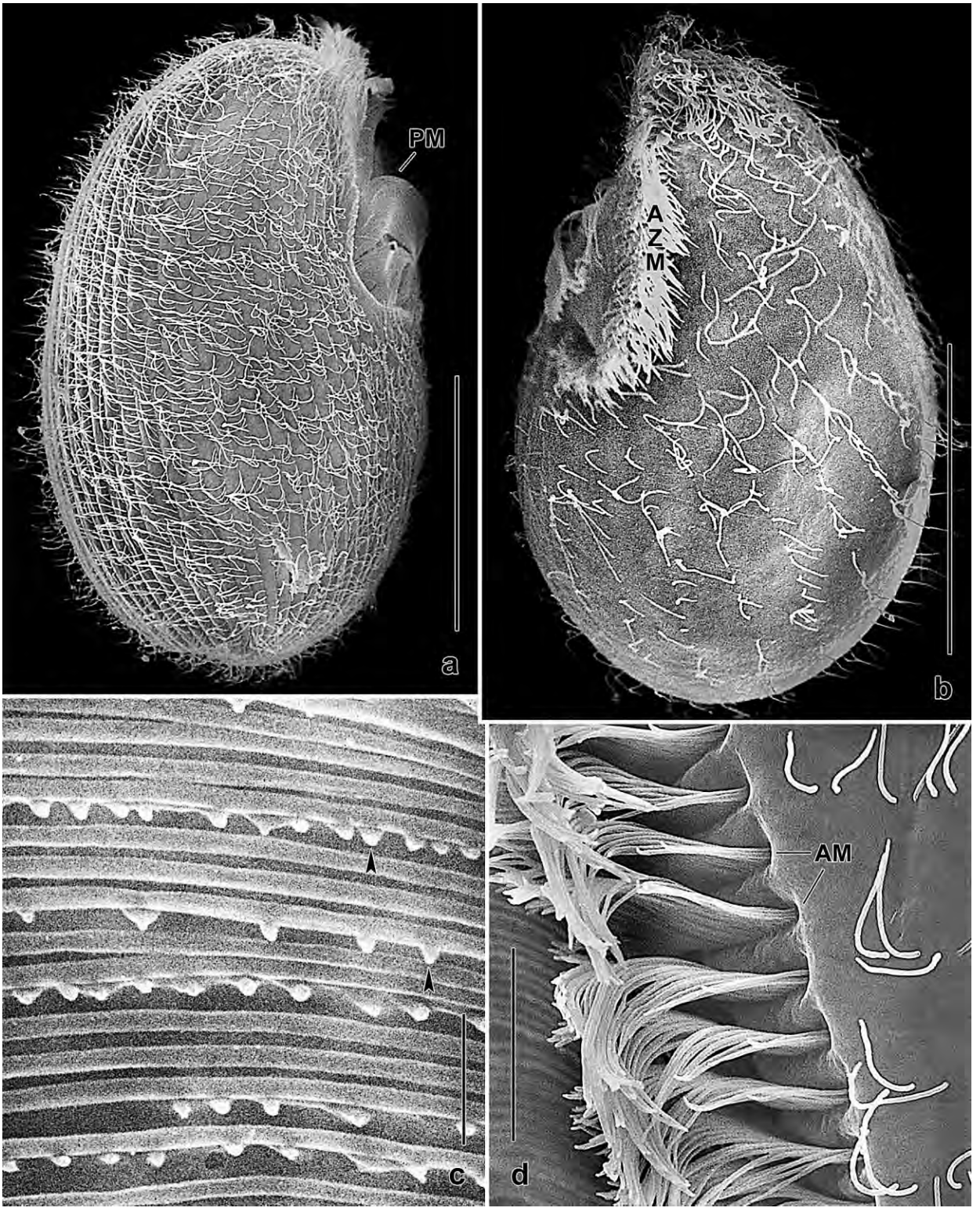

Fig. 291a–d. *Condylostomides coeruleus* in the scanning electron microscope. **a, b:** Right and left side overview, showing the right side more densely ciliated than the left. **c:** Special organelles (arrowheads) occur between the oral ribs on the bottom of the buccal cavity. **d:** Distal end of some adoral membranelles and somatic ciliature. AM – adoral membranelles, AZM – adoral zone of membranelles, PM – paroral membrane. Scale bars 2 µm (c), 10 µm (d), and 70 µm (a, b).

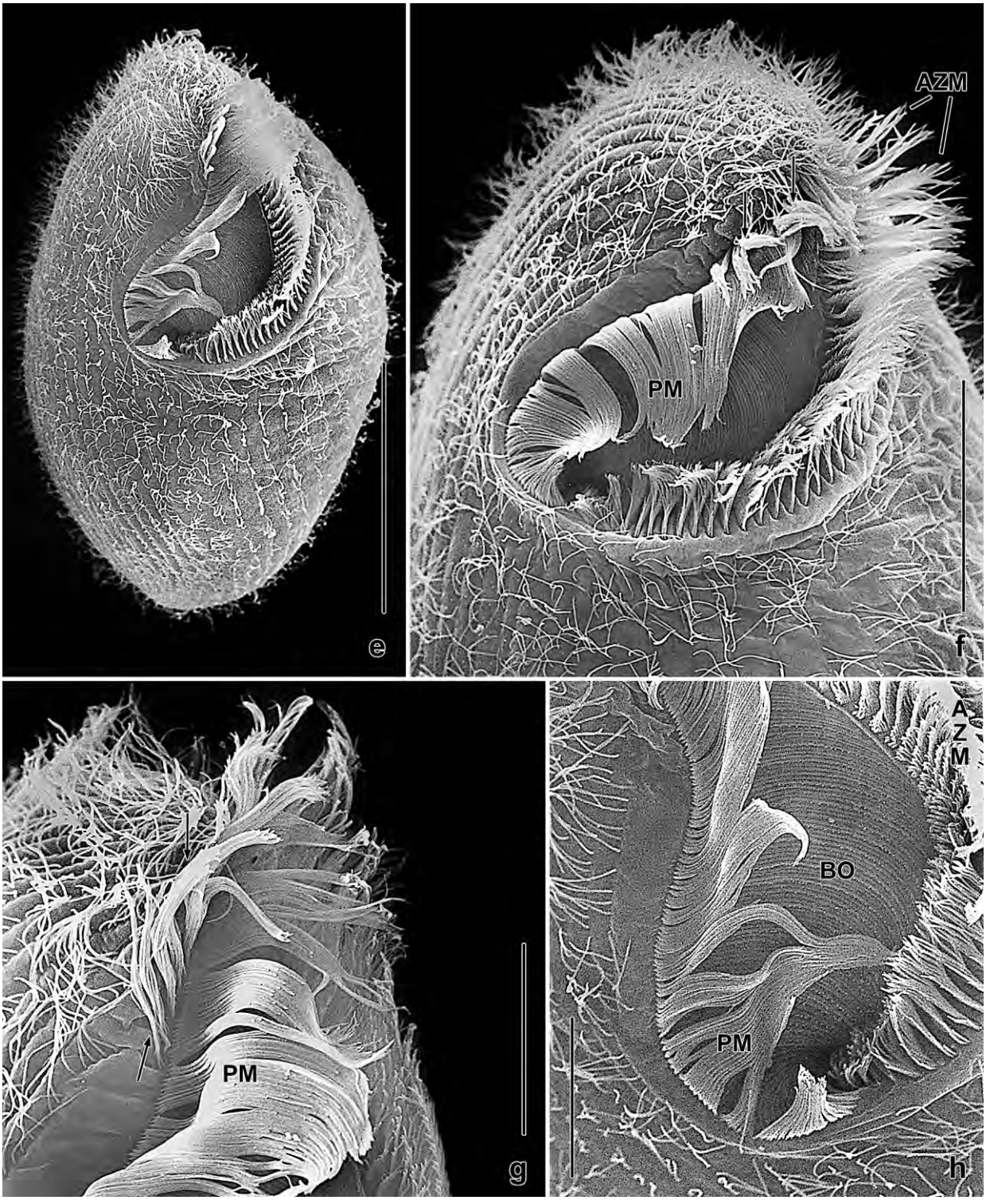

Fig. 291e–h. *Condylostomides coeruleus*, ventral views in the scanning electron microscope. **e:** Overview, showing the large, triangular oral apparatus (obtriangular in *Condylostoma*!). **f–h:** Details of oral apparatus with frontal membranelles marked by arrows. The striation of the buccal bottom is caused by fibre bundles originating from the paroral membrane. AZM – adoral zone of membranelles, BO – bottom of buccal cavity, PM – paroral membrane. Scale bars 20 µm (g, h), 40 µm (f), and 70 µm (e).

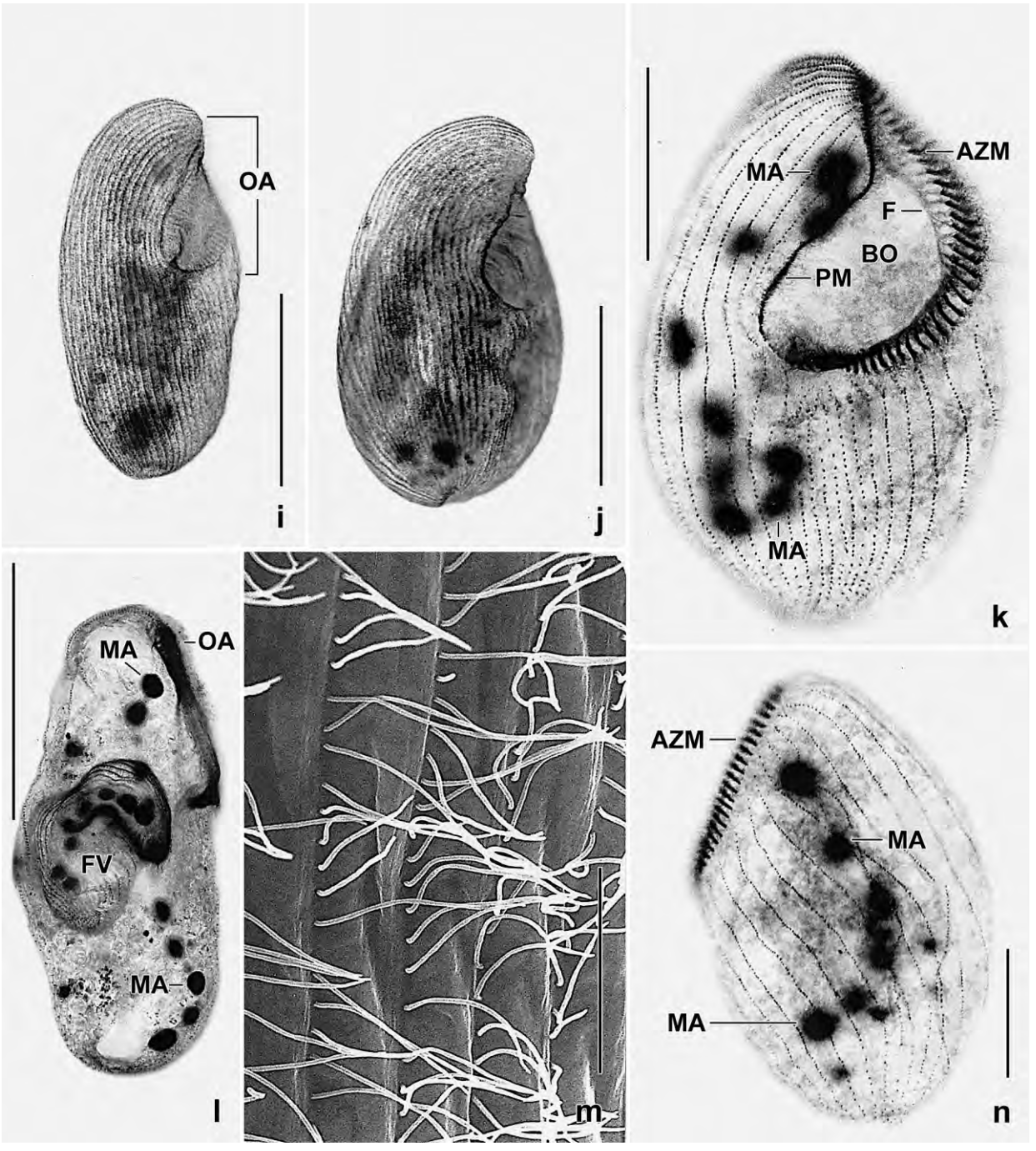

Fig. 291i–n. *Condylostomides coeruleus* after Chatton-Lwoff silver nitrate impregnation (i, j), protargol impregnation (k, l, n), and in the scanning electron microscope (m). **i, j:** Right side view of a slender and of a broad specimen both showing body shape perfectly (osmium fixation). **k:** Ventrolateral overview of infraciliature and nuclear apparatus. **l:** A specimen having ingested a large *Blepharisma americana*. **m:** The somatic ciliature consists of dikinetids throughout in protargol preparations. However, only the anterior basal body of the dikinetids has an about 10 µm long cilium. **n:** Left side overview, showing the wide spacing of the ciliary rows and the macronuclear nodules. AZM – adoral zone of membranelles, BO – bottom of buccal cavity, F – fibres, FV – food vacuole, MA – macronuclear nodules, OA – oral apparatus, PM – paroral membrane. Scale bars 10 µm (m), 50 µm (k, n), and 100 µm (i, j, l).

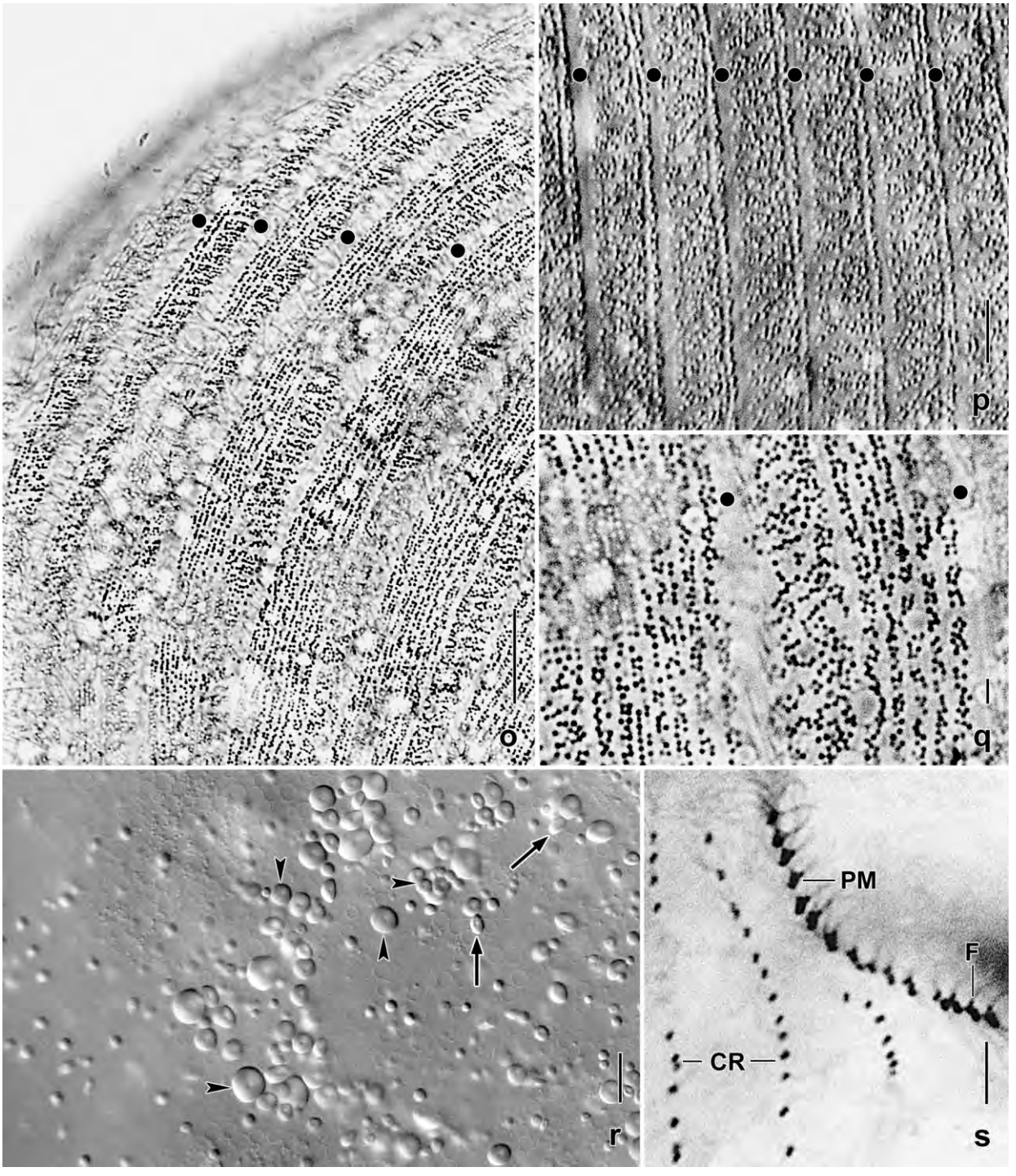

Fig. 291o–s. *Condylostomides coeruleus* from life (o–r) and after protargol impregnation (s). **o–q:** Cortical granulation of a pressed (by coverslip) specimen under bright field (o, q) and interference contrast (p) illumination. Although only about 0.3 µm across, the granules are very distinct because they are bluegreen. The dots mark ciliary rows where granules are absent. **r:** The cytoplasm of morphostatic cells and of the resting cysts is packed with globular (arrowheads) and lenticular (arrows) inclusions 1–5 µm across and having a concave centre. **s:** Buccal vertex with comparatively loosely spaced paroral dikinetids each associated with a fibre extending into the buccal bottom (cp. Fig. 291c, h). CR – ciliary rows, F –fibre, PM – paroral membrane. Scale bars 10 µm.

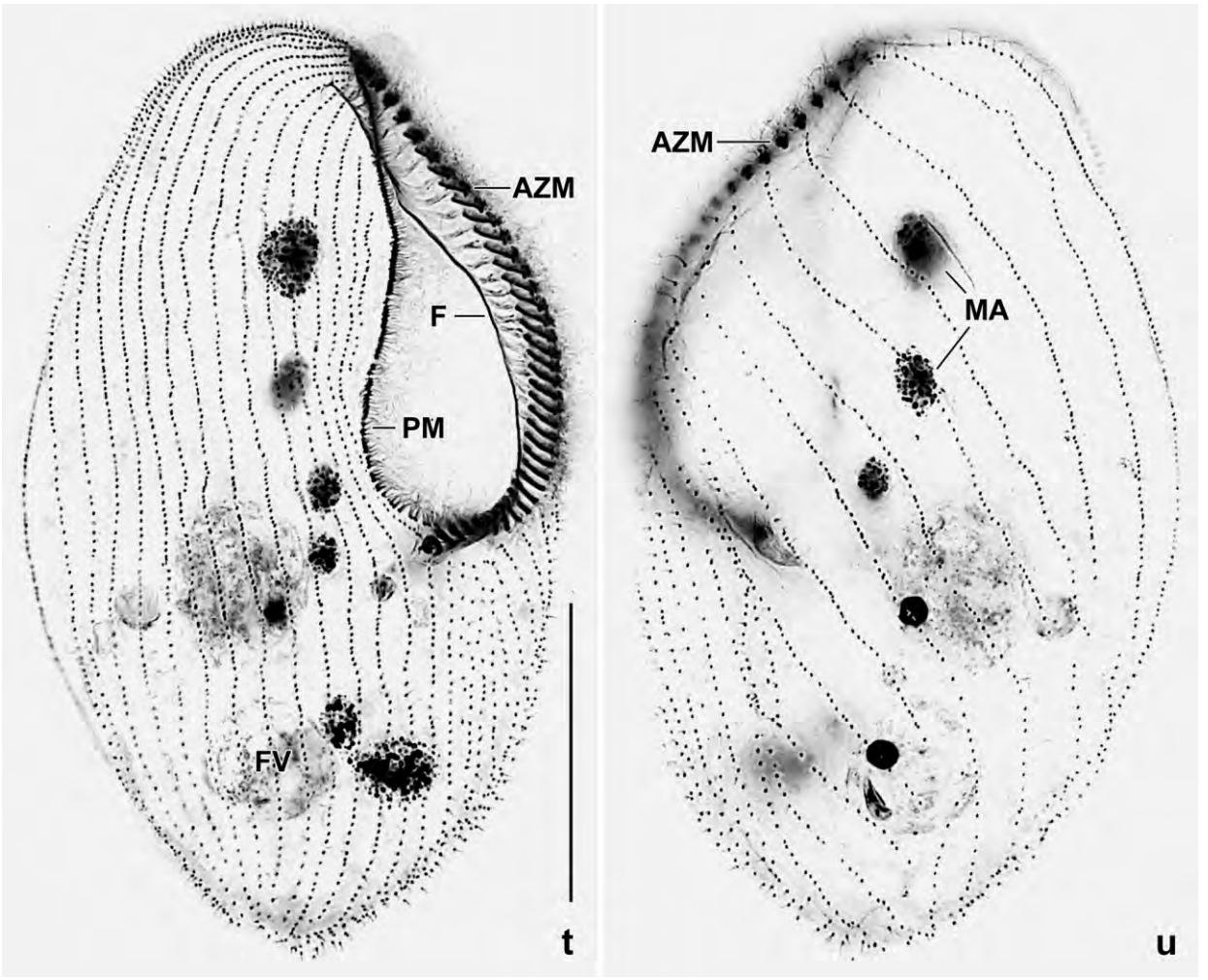

Fig. 291t, u. *Condylostomides coeruleus* after protargol impregnation. Right and left side view of a typical specimen more densely ciliated on the right than the left side. AZM – adoral zone of membranelles, F – thick fibre, FV – food vacuole, MA – macronuclear nodules, PM – paroral membrane. Scale bar 50 μm.

the protargol method used. Contractile vacuole in posterior body end, with two canals extending to mid-body and a large, central excretory pore (Fig. 290a, f, i). Cytopyge at site of contractile vacuole, fecal mass with brownish remnants, up to 50 μm in diameter. Cortex very flexible, dominated by closely spaced rows of pigment granules absent only within and along ciliary rows (Fig. 290e, 291o–q, 292h, i), overall colour in masses very similar to that of *Stentor coeruleus*. Individual granules 0.2–0.5 μm in size, broadly ellipsoid, greyish-green or light blue, at higher concentration (anterior body region) more greenish than blueish; do not change colour when cultivated in the dark. Cytoplasm colourless, usually studded with food vacuoles and globular or lenticular, 1–5 μm-sized granules with a central concavity, as in the resting cysts (Fig. 291r). Feeds on filamentous bluegreen bacteria, small (*Leptopharynx costatus*) and large (*Blepharisma americana, Colpidium colpoda*) ciliates, small rotifers, and starch grains from the wheat kernels added to the culture (Fig. 290a, 291l, t, 292e). Glides on bottom of culture dish and swims slowly rotating about main body axis.

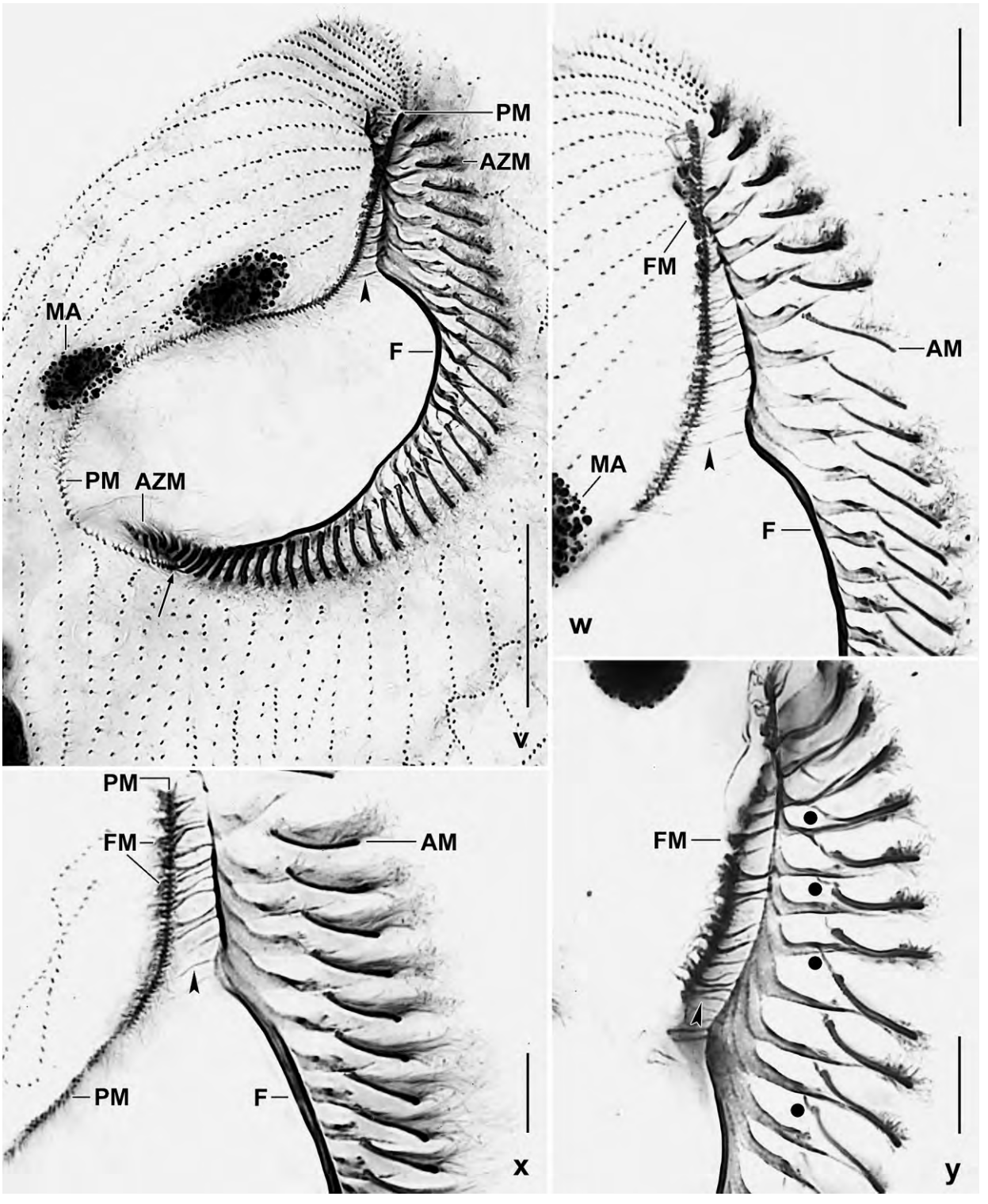

Fig. 291v–y. *Condylostomides coeruleus*, protargol-impregnated oral structures, overview (v) and details (w–y). The arrow in (v) marks proximal end of paroral membrane. The arrowheads denote transverse fibres connecting adoral membranelles with frontal membranelles. The dots (y) mark intermembranellar fibres. AM – adoral membranelles, AZM – adoral zone of membranelles, F – thick fibre made by the fibrous lamellae of the adoral membranelles, FM – frontal membranelles, MA – macronuclear nodules, PM – paroral membrane. Scale bars 10 μm (w–y) and 30 μm (v).

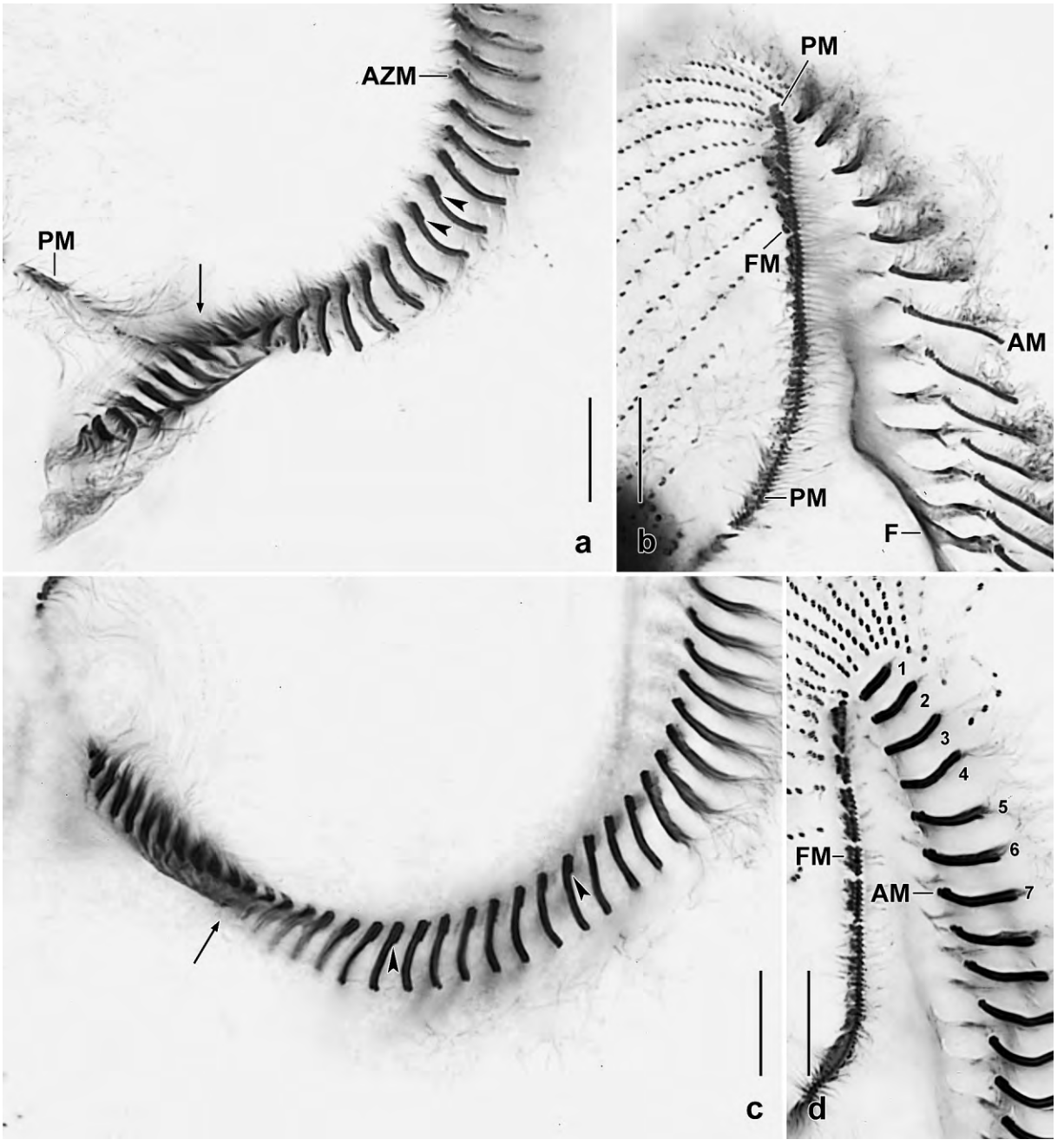

Fig. 292a–d. *Condylostomides coeruleus*, oral structures after protargol impregnation (see also Fig. 291v–y). **a, c:** Proximal region where the adoral zone of membranelles makes a helical turn (arrows). The individual membranelles are made of two long and a short row of basal bodies (arrowheads). **b, d:** Anterior region of oral apparatus where the paroral membrane is accompanied by small fields of anarchic basal bodies whose cilia form the "frontal membranelles" (cp. Fig. 291f, g). The adoral membranelles are associated with a fibrous lamella several of which unite and form a thick fibre (F; see also Fig. 291v, x) extending along the right margin of the membranellar zone. The anteriormost membranelles are short and consist of only two rows of basal bodies (numbers 1–4 in Fig. 292d). The further membranelles have a third row beginning with one basal body gradually increasing to up to six basal bodies (numbers 5–7 and Fig. a, c). AM – adoral membranelles, AZM – adoral zone of membranelles, F – thick fibre, FM – frontal membranelles, PM – paroral membrane, 1–7 – adoral membranelles. Scale bars 10 μm.

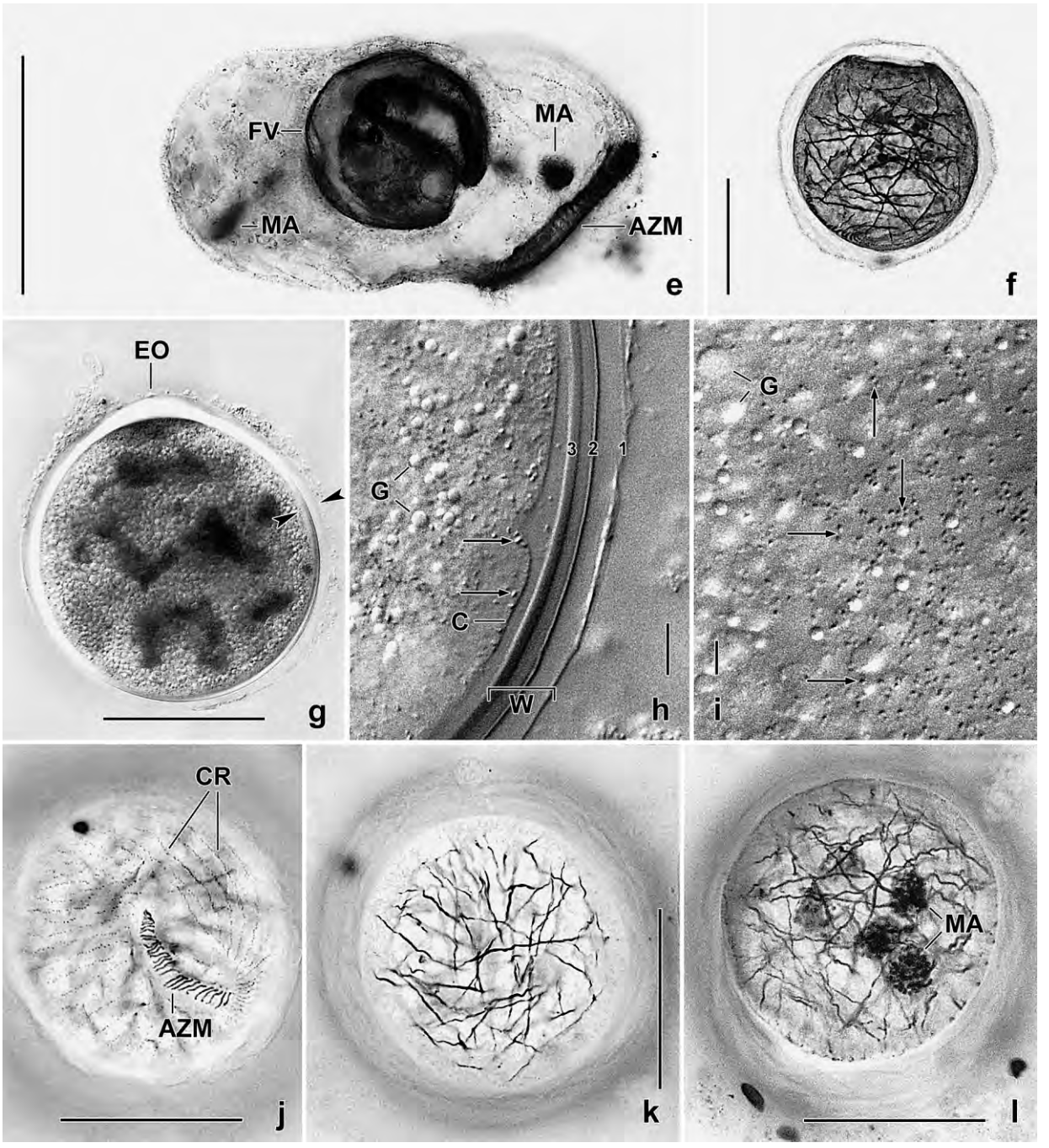

Fig. 292e–l. *Condylostomides coeruleus* from life (g–i) and after protargol impregnation (e, f, j–l). **e:** A specimen having ingested a *Blepharisma americana*. **f:** The cyst has a hyaline external layer 2–10 µm thick and contains, inter alia, many unsorted fibres (see also Fig. k, l). **g, i:** In vivo, the resting cysts are green or bluegreen because the cortex is still studded with pigment granules (i, arrows) most of which, however, form bluegreen, polymorphic aggregates appearing dark in the micrograph (g). The arrowheads delimit the cyst wall. Note the inconspicuous escape opening. **h:** A squashed cyst, showing wall details. The arrows mark cortical pigment granules. The wall consists of three distinct layers (numerals). **j–l:** A cyst at three focal planes, showing that the infraciliature is partially maintained (j), many unsorted fibres in the cytoplasm (k), and the macronuclear nodules (l). AZM – adoral zone of membranelles, C – cortex, CR – ciliary rows, EO – escape opening, FV – food vacuole, G – globular granules, MA – macronuclear nodules, W – cyst wall. Scale bars 5 µm (h, i), 50 µm (f, g, j–l), and 100 µm (e).

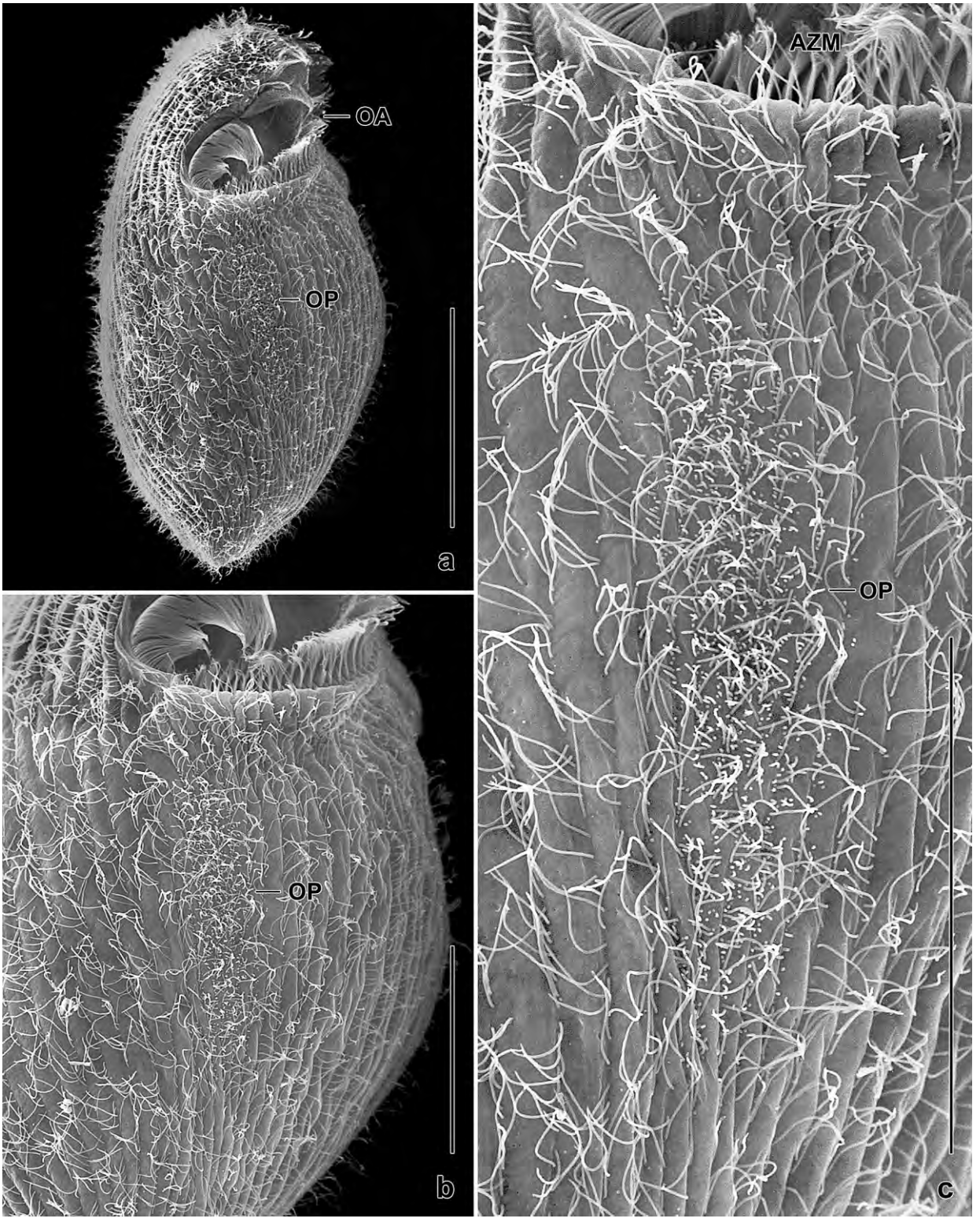

Fig. 293a–c. *Condylostomides coeruleus*, an early divider in the scanning electron microscope. The oral primordium originates polyparakinetally, i. e., several postoral kineties are involved and produce a large field of anarchic cilia. AZM – parental adoral zone, OA – parental oral apparatus, OP – oral primordium. Scale bars 50 µm (b, c) and 100 µm (a).

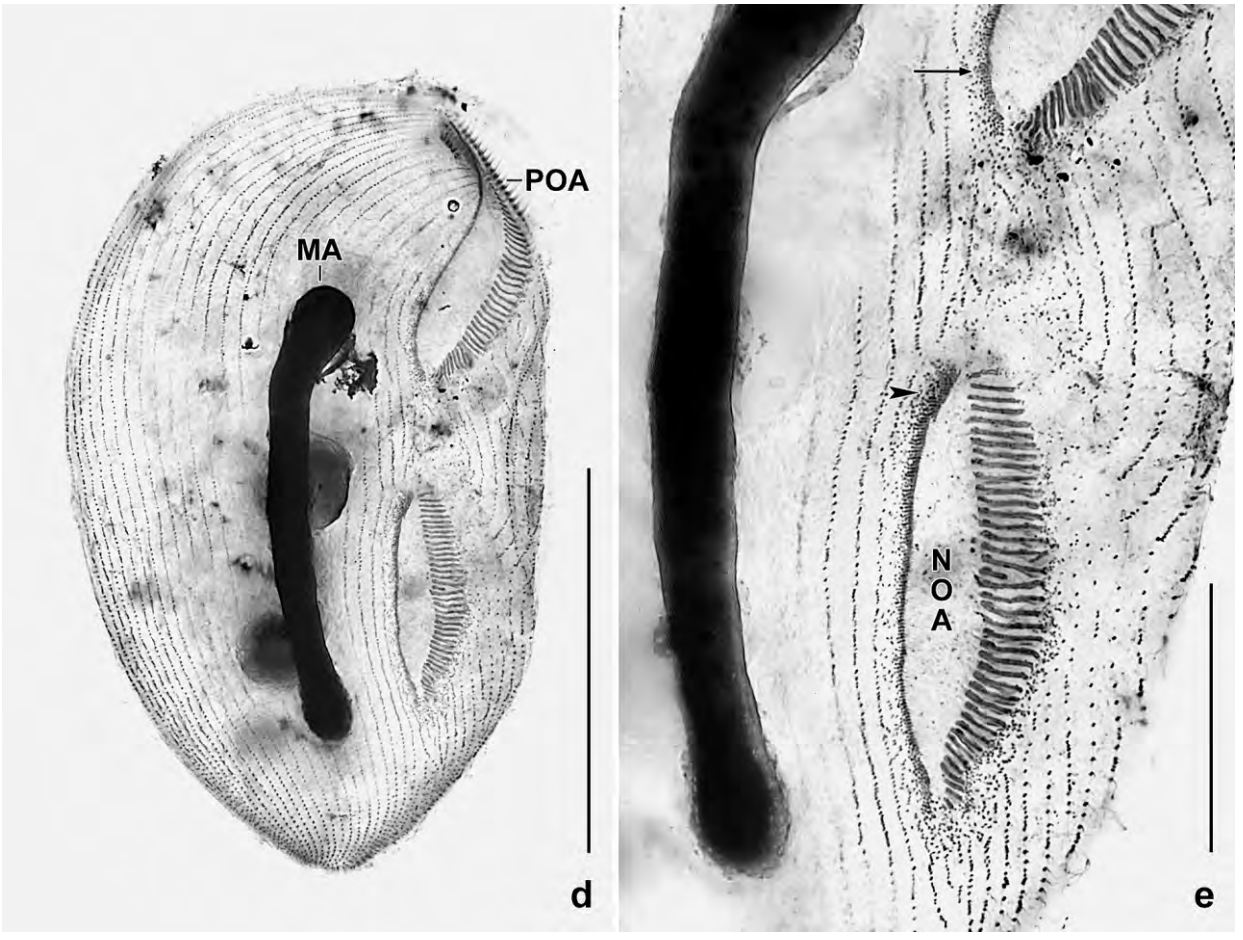

Fig. 293d, e. *Condylostomides coeruleus*, overview and detail of a mid-divider in a protargol preparation (cp. Fig. 293f, g). The macronuclear nodules fused to a rod and the new oral apparatus is almost finished. The arrowhead in (e) marks an anarchic field of basal bodies which will form the frontal membranelles of the opisthe. The arrow in (e) denotes the reorganizing parental paroral membrane. MA – macronucleus, NOA – new oral apparatus, POA – parental oral apparatus. Scale bars 30 µm (e) and 100 µm (d).

Somatic cilia about 12 µm long in vivo, arranged in an average of 39 rows twice as narrowly spaced on right than on left side of cell. Ciliary rows composed of narrowly spaced dikinetids having ciliated only the anterior basal body, bipolar on right and dorsal side, gradually shortened along left half of oral opening, irregularly shortened postorally on ventral side; usually a short kinety fragment right of paroral membrane (Fig. 290a, b, f, g, 291a, b, e, f, i–k, m, n, t, u; Table 118).

Oral apparatus conspicuous, extends on average to 44% of body length, that is, from anterior body end to near mid-body; oral opening triangular with tip anteriorly (Fig. 290a, b, f, i, 291a, b, e, f, i–l, t; Table 118). Buccal cavity large but only slightly concave and not contractile, thus always open, even in preserved specimens; buccal wall lined by long microtubule ribbons originating from paroral dikinetids, stripes of microtubule ribbons separated by rows of minute, non-extrusive, conical organelles (Fig. 291c, f, h). Pharynx comparatively small, surrounded by fusiform structures, likely membrane reservoirs for food vacuole formation (Fig. 290a).

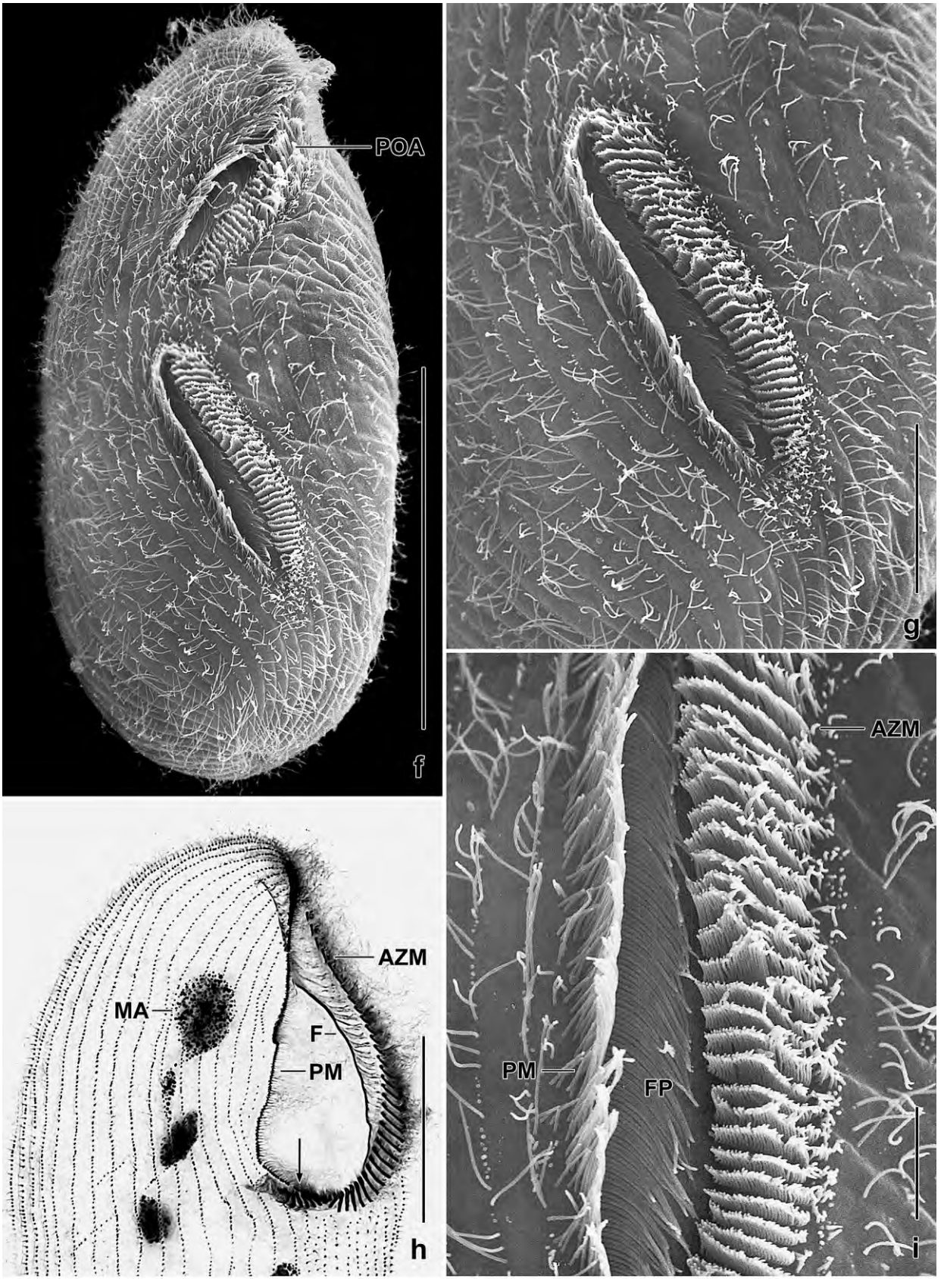
POA
f
g
AZM
MA
F
PM
h
PM
FP
AZM
i

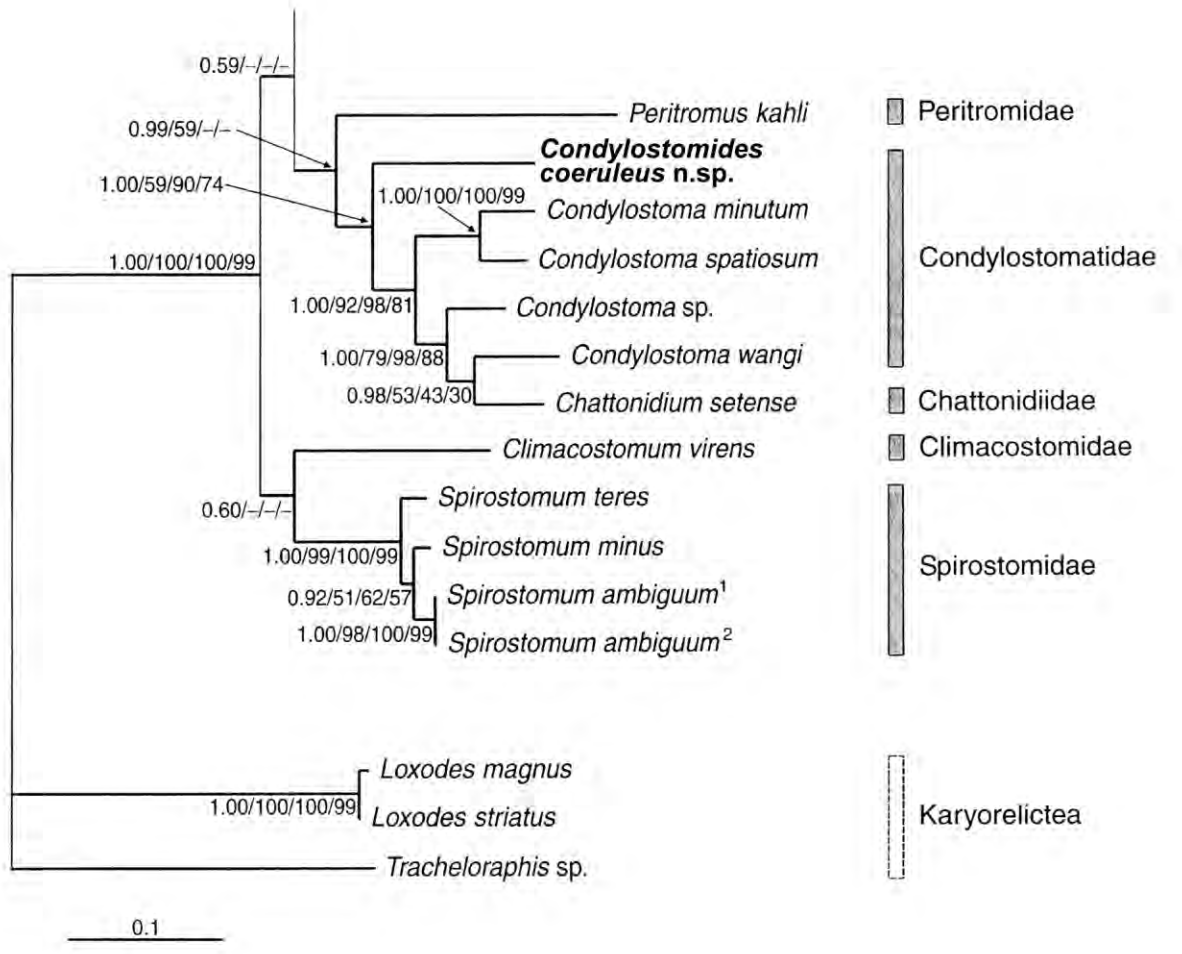

Fig. 294. Molecular phylogeny of *Condylostomides coeruleus* (from Schmidt et al. 2007b). The tree is based on the ribosomal small subunit (SSU) rDNA sequences and a Bayesian analysis. The numbers at the nodes represent in order the posterior probabilities from the Bayesian analysis (first number; 1.000.000 generations), the support values from the maximum likelihood analysis after 100 replication steps (second number), the bootstrap values from the neighbour joining analysis (third number; 10.000 resamplings), and bootstrap values from the maximum parsimony analysis (fourth number; 2.000 resamplings). *Condylostomides coeruleus* is very likely most closely related to *Condylostoma* spp.

Paroral membrane conspicuous, left of right margin of buccal cavity thus producing a barren stripe between somatic and oral infraciliature, inverted L-shaped, commences apically and extends to midline of proximal buccal vertex, composed of dikinetids having 40 µm (!) long cilia producing a giant velum. Frontal membranelles form a distinct stripe along right anterior quarter of paroral, composed of closely spaced, about 30 µm long cilia, indistinctly separate from each other forming cirrus-like structures (Fig. 290a, b, f, i, 291e–h, k, s, t, v–y, 292b, d, 293h; Table 118).

Fig. 293f–i. *Condylostomides coeruleus*, ventrolateral view of anterior body half of a protargol-impregnated morphostatic specimen (h) and of a mid-divider in the scanning electron microscope (f, g, i). The new (opisthe) oral apparatus is almost finished but the frontal membranelles and the proximal curve of the paroral membrane have not yet formed (cp. Fig. 291h, x, arrow). AZM – adoral zone of membranelles, F – thick fibre, FP – fibres originating from the paroral membrane and supporting the bottom of the buccal cavity, MA – macronucleus, PM – paroral membrane, POA – parental oral apparatus. Scale bars 10 µm (i), 30 µm (g), 50 µm (h), and 100 µm (f).

Table 118. Morphometric data on *Condylostomides coeruleus* based on mounted, protargol- or silver nitrate-impregnated specimens from pure cultures. Measurements in µm. CV – coefficient of variation in %, IV – in vivo, M – median, Max – maximum, Mean – arithmetic mean, Min – minimum, n – number of individuals investigated, P – protargol (ethanol fixation), SD – standard deviation, SE – standard error of arithmetic mean, SN – silver nitrate (CHATTON-LWOFF method).

Characteristics	Method	Mean	M	SD	SE	CV	Min	Max	n
Body, length	SN	224.9	224.0	48.7	10.6	21.7	144.0	300.0	21
Body, width in lateral view	SN	114.9	116.0	19.3	4.2	16.8	80.0	148.0	21
Body length:width, ratio	SN	2.0	2.0	0.4	0.1	20.7	2.0	3.0	21
Body, width in ventral or dorsal view	SN	72.7	76.0	11.6	2.5	15.9	56.0	100.0	21
Anterior body end to buccal vertex, distance	SN	97.2	96.0	19.2	4.2	19.7	55.0	129.0	21
Body length:anterior body end to buccal vertex, ratio	SN	2.4	2.0	0.3	0.1	13.5	2.0	3.0	21
Anterior body end to buccal vertex, percentage of body length	SN	43.6	44.0	4.7	1.0	10.8	30.0	51.0	21
Oral opening, maximum width	SN	53.5	52.0	11.9	2.6	22.2	25.0	82.0	21
Macronuclear figure, length	P	132.6	130.0	16.5	3.6	12.4	108.0	160.0	21
Macronuclear nodules, number	P	9.5	9.0	1.6	0.4	16.8	7.0	13.0	21
First macronuclear nodule, length	P	16.6	17.0	3.4	0.7	20.3	11.0	25.0	21
First macronuclear nodule, width	P	11.9	12.0	1.8	0.4	15.2	8.0	15.0	21
Fourth macronuclear nodule, length	P	12.5	12.0	2.4	0.5	18.8	10.0	19.0	21
Fourth macronuclear nodule, width	P	9.7	10.0	1.6	0.4	16.6	8.0	14.0	21
Ciliary rows on right side, number	P	15.0	15.0	1.2	0.3	8.3	13.0	17.0	21
Ciliary rows, total number	P	39.2	39.0	3.4	0.7	8.7	34.0	51.0	21
Ciliary rows, distance on right side	P	5.1	5.0	1.1	0.2	20.7	4.0	8.0	21
Ciliary rows, distance on left side	P	11.7	12.0	1.7	0.4	14.4	9.0	15.0	21
Kinetofragments right of paroral, number	P	1.0	1.0	–	–	–	0.0	2.0	21
Adoral membranelles, number	P	43.0	42.0	3.3	0.7	7.6	37.0	49.0	21
Largest adoral membranelle, length of base	P	8.6	9.0	0.7	0.2	8.6	7.0	10.0	21
Resting cysts, length	IV	106.0	104.0	7.9	2.0	7.4	88.0	120.0	15
Resting cysts, width	IV	93.0	92.0	5.7	1.5	6.1	84.0	104.0	15

Adoral zone of membranelles conspicuous, extends in a wide spiral from the thickened anterior left margin of buccal cavity to near mid-body, where it curves right and to body centre; composed of an average of 43 membranelles strongly decreasing in base length at both ends of zone; longest bases in mid of zone, 9 µm in protargol preparations, about 15 µm in vivo, and 10–13 µm in SEM preparations. Individual membranelles separated by inconspicuous intermembranellar ridges (Fig. 291d, f), composed of two long rows and one short row of basal bodies at right proximal end, except for three to six anterior membranelles consisting of only two long rows (Fig. 290a, j, 291y, 292a, c, d). The membranelles produce two major fibre systems, viz., a thin intermembranellar connective each and a broad lamella that unites with the neighbouring lamellae to a "thick fibre" extending along right margin of membranellar zone and contacting frontal membranelles via short transverse fibres (Fig. 290b, 291v–y, 292a–d).

Ontogenesis (Fig. 293a–i): *Condylostomides coeruleus* has a typical heterotrich ontogenesis demonstrated by the Figures cited (for a review, see Foissner 1996). However, we did not study it in all details some of which might be different.

Resting cysts (Fig. 290c, d, 291r, 292f–l; Table 118): Spheric to slightly elliptic, with a small convexity marking escape opening (Fig. 290d, 292g; Table 118). Bluegreen or greenish because cortical granules stored in large, polymorphic aggregates and throughout cortex and cytoplasm (Fig. 290c, d, 292g–i). Infraciliature partially maintained and macronuclear nodules not fused, checked in 30 old, protargol-impregnated cysts (Fig. 292j, l). Cyst contents bipartite in an external, finely granular layer 5–10 µm thick, and a central portion containing many unsorted fibres, the macronuclear nodules, countless lipid droplets 1–3 µm across, and globular or lenticular inclusions with a central concavity and 2–5 µm in size (Fig. 291r, 292h, i).

Cyst wall in vivo composed of three distinct layers (Fig. 290c, d, 292f–h): external layer 2–10 µm thick, hyaline, structureless, firm, does not impregnate with protargol (Fig. 292f) and thus very likely not a simple slime cover; middle layer 1–1.5 µm thick, rather refractive and attached to the internal, strongly compact and refractive layer 1.5–2 µm thick. Middle and internal layer about 3 µm thick, often difficult to distinguish, conspicuous in the bright field microscope.

Molecular phylogeny: Schmidt et al. (2007b) investigated the molecular phylogeny of *C. coeruleus* (*Condylostomides* n. sp. in their paper), using the ribosomal small subunit (Fig. 294). This shows that *C. coeruleus* forms a distinct, statistically rather well supported clade sufficient for genus rank. The nearest relatives are *Condylostoma* spp.

Occurrence and ecology: As yet found in Venezuela (type locality), Costa Rica, and the Dominican Republic (margin of a mangrove forest). Possibly, *C. coeruleus* is rather common in slightly to moderately saline habitats of Central and South America. The large size and blunt shape indicate that it is a litter or a limnetic species.

Remarks: *Condylostomides coeruleus* is fairly similar to *C. etoschensis* Foissner et al, 2002, which is rather common in saline inland habitats of Namibia, Southwest Africa. Actually, the morphostatic specimens differ mainly by the colour of the cortical granules (blueish or bluegreen vs. yellowish or brilliant citrine) and the number of adoral membranelles (56 vs. 43). Main differences occur in the resting cysts: macronuclear nodules not fused vs. fused; wall with three vs. two layers; escape opening an inconspicuous convexity vs. a distinct knob; with vs. without polymorphic cortical granule aggregates in the cytoplasm; size in vivo 106 vs. 44 µm.

Possibly, *Condylostomides nigra* Dragesco, 1960 should be mentioned because it is similar in many features to *C. coeruleus*, such as the blueish cortical granules, body size, and the number of macronuclear nodules, ciliary rows, and adoral membranelles. However, *C. nigra* has an obtriangular (vs. triangular) oral opening, several small contractile vacuoles, and blueish and colourless (vs. only blueish) cortical granules.

The huge size and the conspicuous colour make *C. coeruleus* a biogeographic flagship. It is highly remarkable that a different species occurs in Southwest Africa, Namibia, (see above). As yet, we did not find a similar species in Laurasian and Australian habitats although we studied many saline inland samples from Australia.

Apometopidae nov. fam.

Diagnosis: Pyriform Metopida with special kineties on ventral side of preoral dome and with almost circular perizonal stripe and adoral zone of paramembranelles.

Type genus: *Apometopus* nov. gen.

Remarks: The new genus *Apometopus*, described below, has a unique ciliary pattern, suggesting the need of a distinct family. As yet, the Metopida Jankowski, 1980 contain only two families (Lynn 2008): the Caenomorphidae Poche, 1913 and the Metopidae Kahl, 1927. Jankowski (2007) recognized a third family, the Ludioidea, whose ciliary pattern is not known in detail.

Few Metopida have been investigated with modern methods. Thus, we are convinced that intensified research will discover further families, genera, and species.

Apometopus nov. gen.

Diagnosis: Small to middle-sized Apometopidae with 4–5 ventral kineties and a perizonal stripe composed of 4 kineties. Caudal cilia in semicircular array, not matted or matted appearing like a cortical spine.

Type species: *Apometopus pelobius* nov. spec.

Etymology: *Apometopus* is a composite of the Greek prefix *apo* (derived from) and the genus-group name *Metopus* (a ciliate with distinct forehead). Masculine gender.

Species assignable: There is only one species in the literature that could belong to the genus because it has the same body shape and a matted bundle of caudal cilia (Fig. 295c): *Brachonella caenomorphides* Foissner, 1980b. Unfortunately, Foissner's description is entirely based on live observations, and thus details of the ciliary pattern are not known. A re-analysis of the original notes did not provide new insights. Thus, we do not transfer *B. caenomorphides* to *Apometopus*. As concerns → *Metopus pyriformis* see the following redescription.

Remarks: There is only one genus that looks similar to *Apometopus*: *Cirranter* Jankowski, 1964 (Fig. 295l, m). However, *Cirranter* has only a single special kinety in the dome centre and lacks both, ordinary dome kineties and a bundle of long, matted caudal cilia (Penard 1922, Kahl 1932, Jankowski 1964). However, the exact ciliary pattern is not known because it has been not yet investigated with modern methods. Considering the body shape and the circular adoral zone, *Cirranter* is classified into the Apometopidae.

Apometopus has four perizonal kineties while other Metopidae have five (Dragesco & Dragesco-Kerneis 1986, Foissner & Agatha 1999, Foissner et al. 2002), a remarkable difference the significance of which is not yet clear. The bundle of caudal cilia is thick and immobile, thus looking like a cortical differentiation.

We split *Apometopus* into two subgenera, according to the arrangement of the caudal cilia.

Apometopus (*Apometopus*) nov. subgen.

Diagnosis: Apometopids with matted caudal cilia appearing like a cortical spine.

Type species: *Apometopus pelobius* nov. spec.

Apometopus (*Apometopus*) *pelobius* nov. spec. (Fig. 295a–k, 296a–f, Table 119)

Diagnosis: Size in vivo about 50 × 40 µm. Pyriform, postoral width about half of dome width; ratio of dome height and cone length 1.7:1 on average. Macronucleus and micronucleus in preoral dome, globular. 2 ordinary dome kineties and an average of 17 cone kineties; caudal bundle composed of an average of 11 cilia about 45 µm long in vivo. On average 38 adoral paramembranelles.

Type locality: Mangrove swamp in the surroundings of the town of Puerto Plata, Punta Cana, Dominican Republic, 70°40'W 19°45'N.

Type material: 1 holotype and 2 paratype slides with protargol-impregnated specimens have been deposited in the Biology Centre of the Upper Austrian Museum in Linz (LI). Relevant specimens have been marked by black ink circles on the coverslip.

Etymology: The Greek *pelobius* refers to the habitat the species was discovered, viz., a Mangrove swamp.

Description: Size in vivo 45–60 × 35–50 µm, usually about 50 × 40 µm, as calculated from some in vivo measurements and the morphometric data in Table 119 adding 15% preparation shrinkage. Body shape fairly constant, pyriform, ratio of dome and cone length 1.7:1 on average; postoral width about half of dome width; ventral side flat to slightly convex, dorsal side distinctly convex. Dome conspicuous because semiglobular in lateral view, separated from narrowed cone by perizonal stripe; not campanulate (Fig. 295b, g, h, 296a, f). Nuclear apparatus frequently in right posterior portion of dome, usually deeply impregnated. Macronucleus and micronucleus broadly ellipsoid to globular; macronuclear nucleoli 1–2 µm across; micronucleus very lightly impregnated in about one third of specimens (Fig. 295b, f, h, k, 296a–c, e, f). Contractile vacuole in posterior body end (Fig. 295b). Cortex flexible, contains minute granules likely producing a thin, slimy cover in dying specimens (Fig. 295a). Cytoplasm colourless, contains some curious, argyrophilic, about 4 × 2 µm-sized bacteria with conical ends and a deeply impregnating central granule (Fig. 295b). Food vacuoles mainly in dome, contain bacteria, up to 10 µm across. Swims rapidly in wide spirals. Somatic ciliature dikinetal and complex, consists of five types of kineties: (i) two "ordinary" dome kineties, (ii) a perizonal kinety stripe, (iii) four curved ventral kineties, (iv) an average of 17 cone kineties, and (v) a bundle of caudal cilia originating from a distinct row of basal bodies (Fig. 295b, d, g–j, 296a–d, f, Table 119). Dome kineties commence and end on ventral side, slightly shorter than perizonal stripe, in fusiform pattern, i. e., rather narrowly spaced and close to perizonal stripe on ventral side becoming widely spaced, convex, and distinctly apart from perizonal kineties in middle third of dorsal side, dikinetids comparatively widely spaced bearing about 15 µm long cilia. Perizonal ciliary stripe near posterior margin of dome, almost circular, i. e., begins and ends on ventral side but at slightly different levels; consists of four rows of narrowly spaced, ciliated dikinetids more obliquely arranged in the upper two rows than in the two lower ones, cilia about 15 µm long in protargol preparations. Ventral dome surface dominated by four widely spaced, densely ciliated ventral kineties increasingly

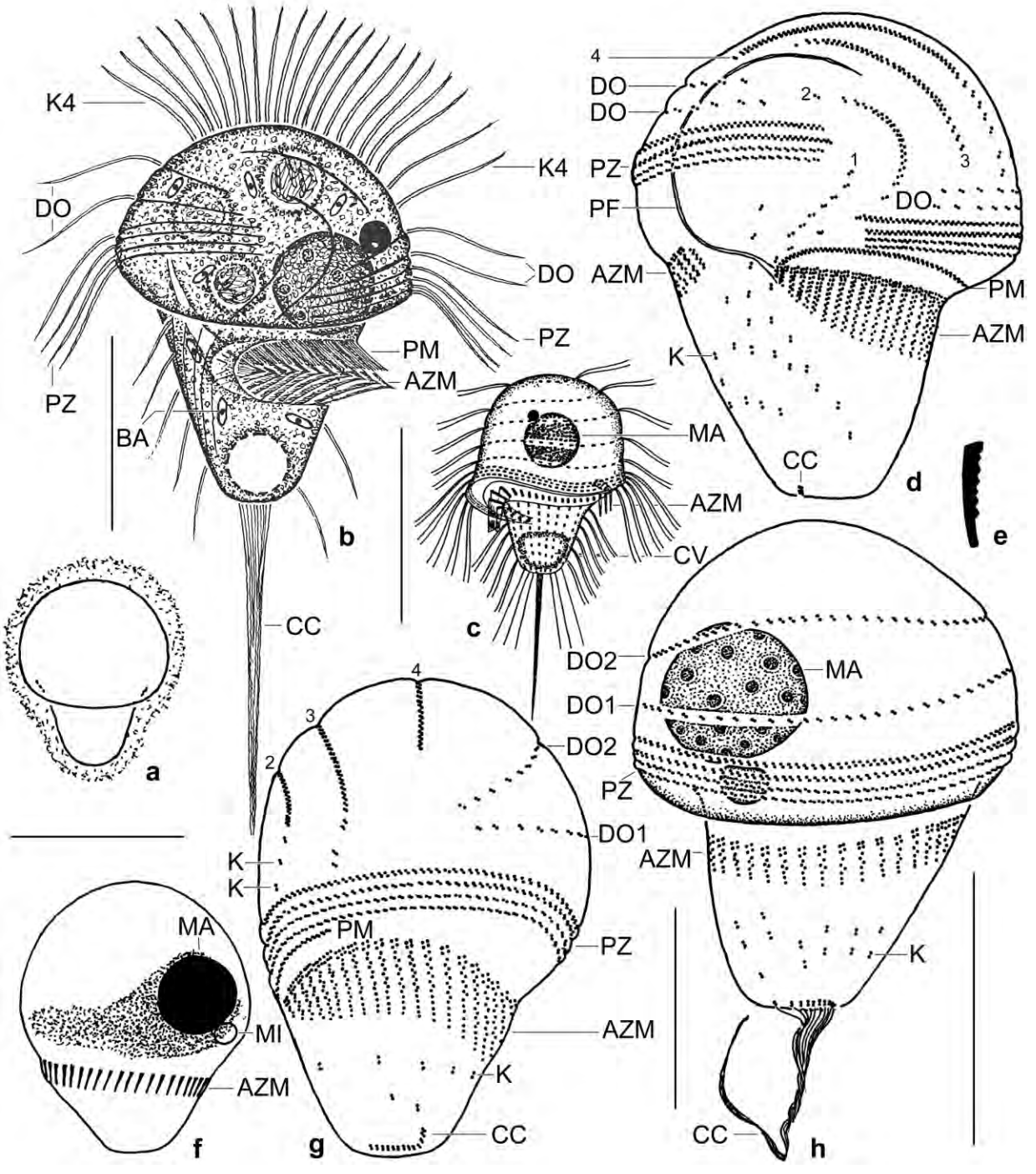

Fig. 295a–h. *Apometopus pelobius* (a, b, d–h) and *Brachonella caenomorphides* (c, from Foissner 1980b) from life (a–c) and after protargol impregnation (d–h). **a:** Dying cells release a slimy substance. **b:** Ventral view of a representative specimen, length 50 µm. Both basal bodies of the dome dikinetids are ciliated but only one cilium is shown for the sake of clarity. **c:** *B. caenomorphides*, length 30 µm. **d, h:** Ventral and dorsal view of ciliary pattern and nuclear apparatus of holotype specimen, length 50 µm. Numerals 1–4 designate the specific ventral kineties. **e:** Adoral paramembranelle. **f:** A mass with slightly increased argyrophily surrounds the nuclear apparatus and extends into the dome plasm. **g:** Left side view, showing ventral flattening. AZM – adoral zone of paramembranelles, BA – bacterium, CC – caudal cilia, CV – contractile vacuole, DO – dome kineties, K – ordinary kineties, MA – macronucleus, MI – micronucleus, PF – pharyngeal fibres, PM – paroral membrane, PZ – perizonal stripe, numerals 1–4 – ventral kineties. Scale bars 15 µm (g) and 30 µm (b, c, d, h, f).

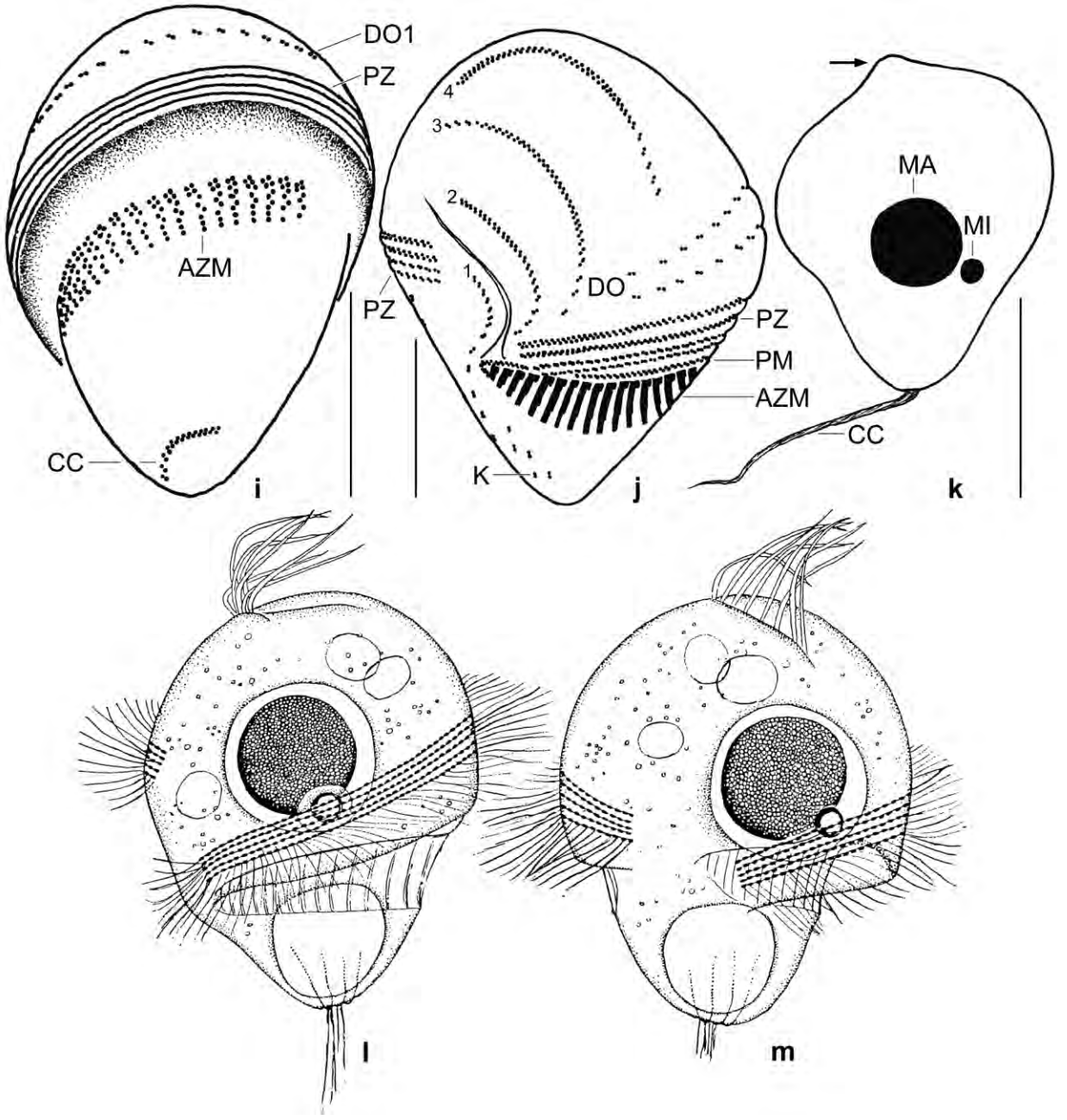

Fig. 295i–m. *Apometopus pelobius* after protargol impregnation (i, j, k) and *Cirranter mobilis* after mercury chloride fixation (l, m; from Jankowski 1964)**. i:** Oblique posterior polar view, showing the curved row of basal bodies associated with long caudal cilia. Cone ciliary rows insufficiently impregnated, and thus not shown. **j:** Oblique anterior polar view, showing the four curved ventral kineties and the arrangement of the perizonal ciliary stripe. Ventral kinety 4 extends on top of preoral dome. **k:** About one third of the specimens shows a characteristic preparation artifact, viz., a ridge where ventral kinety 4 extends (arrow). Note the long bundle of caudal cilia**. l, m:** Ventrolateral and ventral view of *Cirranter mobilis*, length about 50 µm. AZM – adoral zone of paramembranelles, CC – caudal cilia, DO – dome kineties, K – ordinary kineties, MA – macronucleus, MI – micronucleus, PM – paroral membrane, PZ – perizonal stripe, numerals 1–4 – ventral kineties. Scale bars 15 µm (i, j) and 30 µm (k).

curved from proximal to distal; kinety 4 in centre of anterior pole, dikinetids obliquely arranged, more widely spaced at ends of kineties. Cone kineties highly reduced, most consisting of only one to three dikinetids with cilia about 9 µm long in protargol preparations; anterior basal body of dikinetids not ciliated. On average 11 caudal cilia originating from a curved, dikinetal

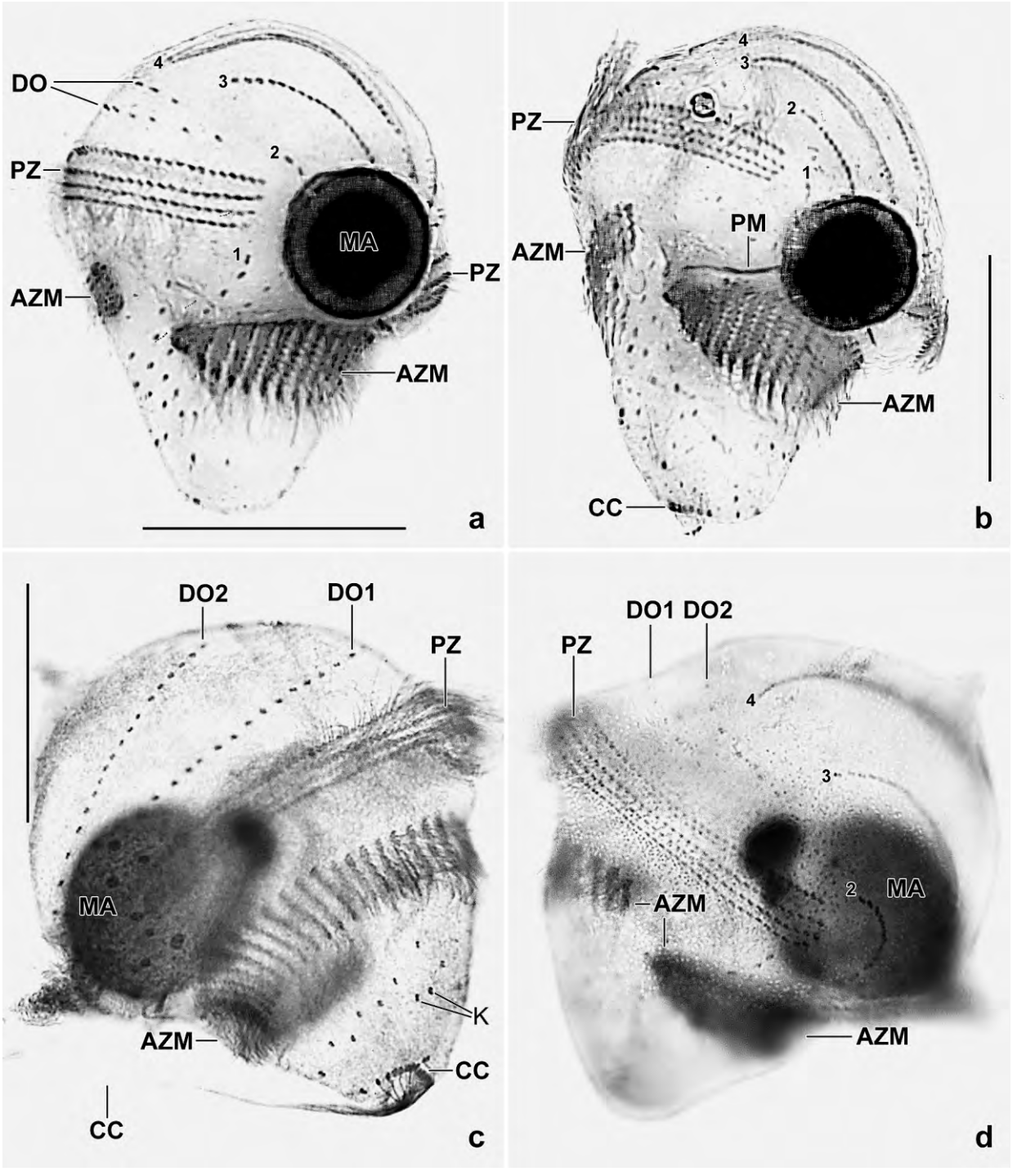

Fig. 296a–d. *Apometopus pelobius* after protargol impregnation. **a, b:** Ventral views, showing the somatic and oral ciliary pattern, specifically, the four characteristic ventral kineties (numerals). **c, d:** Dorsal and ventral view of same specimen, showing the almost circular adoral zone of paramembranelles and the long caudal cilia originating from a curved row of dikinetids having ciliated only one basal body. AZM – adoral zone of paramembranelles, CC – caudal cilia, DO – dome kineties, K – ordinary somatic kineties, MA – macronucleus, PM – paroral membrane, PZ – perizonal stripe, numerals 1–4 – ventral dome kineties. Scale bars 20 µm.

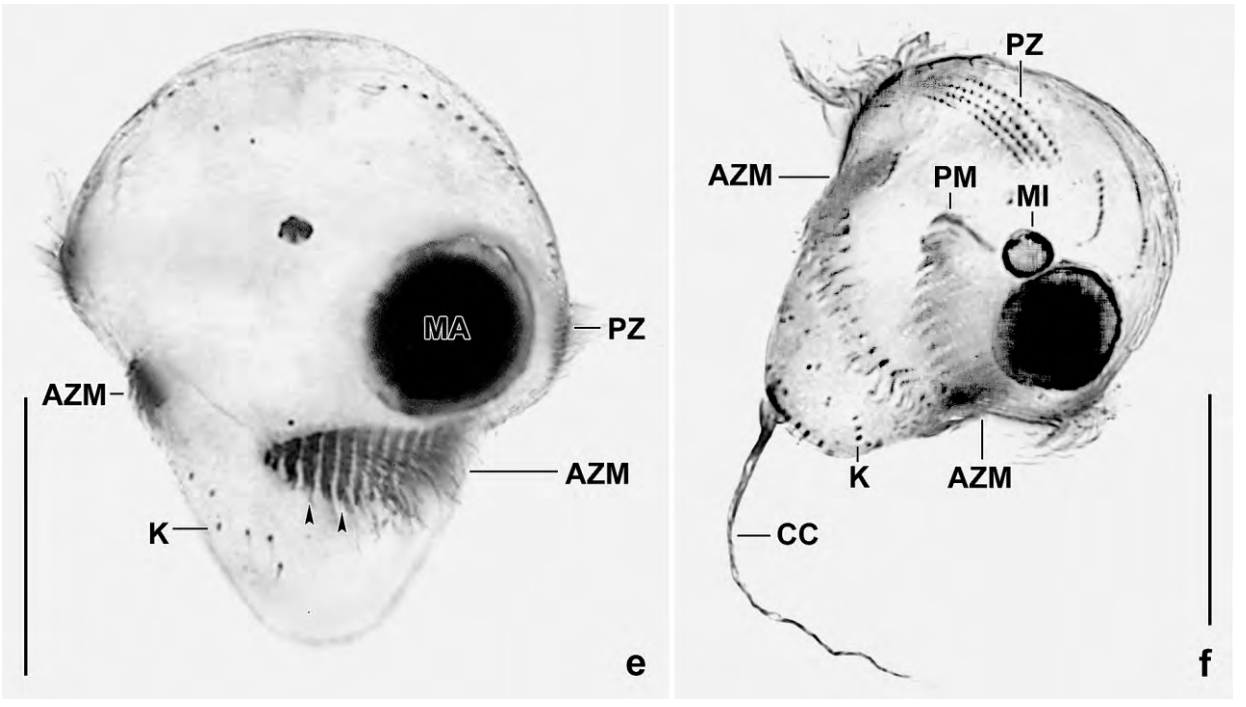

Fig. 296e, f. *Apometopus pelobius* after protargol impregnation. **e, f:** Ventral views, showing the almost circular adoral zone of paramembranelles, the thickened proximal paramembranelles (arrowheads), the nuclear apparatus, and the long bundle of caudal cilia. AZM – adoral zone of paramembranelles, CC – caudal cilia, K – ordinary somatic kineties, MA – macronucleus, MI – micronucleus, PM – paroral membrane, PZ – perizonal ciliary stripe. Scale bars 20 μm (e) and 30 μm (f).

row in posterior pole area, form a conspicuous bundle on average 40 μm long in protargol preparations; bundle immobile and obconical, individual cilia thus obviously gradually shortened distally, only one basal body of dikinetids ciliated (Fig. 295b, g–i, k, 296b, c, f; Table 119). Oral apparatus metopid, i. e., slightly posterior of dome and consisting of an adoral zone with an average of 38 paramembranelles; a dikinetal, short paroral membrane; and very long pharyngeal fibres extending along ventral side to top of dome (Fig. 295b, d, e, g–j, 296a–f; Table 119). Adoral zone almost circular with right end slightly anterior of left end, i. e., of mouth entrance; right side and dorsal paramembranelles shorter than ventral ones, except of 5 to 8 shorter and thicker paramembranelles at mouth entrance (Fig. 296e); left margin of paramembranelles serrate (Fig. 296a, b), exact structure difficult to recognize, possibly as shown in Figures 295d, g–i.

Occurrence and ecology: As yet found only at type locality, that is, in the anoxic, brackish mud at the margin of a mangrove swamp near Punta Cana, Dominican Republic, 18°38'N 68°28'W.

Comparison with similar species: *Apometopus pelobius* is easily identified by the special bundle of caudal cilia. There is only one other species having the same feature: *Brachonella caenomorphides* (Fig. 295c). Unfortunately, the description of *B. caenomorphides* is very incomplete, thus identity cannot be excluded (see **Remarks** to genus). However, *B. caenomorphides* is considerably smaller than *A. pelobius* (length about 30 vs. 50 μm), possibly has five (vs. two) "ordinary" dome kineties, and was discovered in the anoxic mud of an algae-rich pond in the Austrian Central Alps (Foissner 1980b, c).

Table 119. Morphometric data on *Apometopus pelobius* based on mounted, protargol-impregnated, and randomly selected environmental specimens. Measurements in µm. AZM – adoral zone of paramembranelles, CV – coefficient of variability in %, M – median, Max – maximum, Mean – arithmetic mean, Min – minimum, n – number of specimens investigated, SD – standard deviation, SE – standard error of arithmetic mean.

Characteristics	Mean	M	SD	SE	CV	Min	Max	n
Body, length	45.7	45.0	3.0	0.8	8.3	40.0	55.0	21
Body, dome width	37.1	37.0	2.7	0.6	7.2	33.0	43.0	21
Body, postoral width (posterior of AZM)	21.1	21.0	2.8	0.6	13.4	17.0	27.0	21
Anterior body end to proximal margin of AZM	27.4	27.0	3.1	0.7	11.5	21.0	36.0	21
Body length:width, ratio	1.2	1.2	–	–	–	1.2	1.3	21
Dome width:postoral width, ratio	1.8	1.8	0.2	0.1	9.2	1.6	2.0	21
Body length:cone length, ratio	1.7	1.7	0.1	0.1	6.6	1.5	2.0	21
Macronucleus, length	13.7	13.0	1.5	0.3	10.7	12.0	16.0	21
Macronucleus, width	13.0	13.0	1.4	0.3	10.9	11.0	16.0	21
Micronucleus, length	5.0	5.0	0.7	0.2	14.9	4.0	7.0	21
Micronucleus, width	4.4	4.0	0.7	0.2	16.3	3.5	6.0	21
Perizonal ciliary stripe, width	3.5	3.5	–	–	–	3.0	4.0	21
Perizonal cilia, length	13.8	15.0	1.3	0.3	9.4	12.0	15.0	19
Perizonal stripe, number of kineties	4.0	4.0	0.0	0.0	0.0	4.0	4.0	21
Postoral cilia, length	8.7	9.0	–	–	–	8.0	9.0	3
Cilia of ventral kinety 4, length	15.6	15.0	2.8	0.8	18.2	12.0	20.0	14
Caudal bundle, number of cilia	10.9	10.5	1.6	0.5	14.6	8.0	13.0	10
Cilia of caudal bundle, length	40.0	40.0	6.7	2.1	16.7	30.0	50.0	10
Special ventral kineties, number	4.0	4.0	0.0	0.0	0.0	4.0	4.0	21
Ordinary dome kineties, number	2.0	2.0	0.0	0.0	0.0	2.0	2.0	21
Cone kineties, number	17.4	17.0	1.3	0.5	7.3	16.0	20.0	7
Adoral paramembranelles, number	38.4	38.0	1.8	0.4	4.7	36.0	42.0	21
Adoral paramembranelles, length near mouth	7.1	7.0	1.0	0.2	13.6	5.0	9.0	20
Adoral paramembranelles, dorsal length	4.5	4.0	0.6	0.1	13.4	4.0	6.0	21
First adoral paramembranelle, length	3.8	4.0	0.6	0.1	16.6	3.0	5.0	21

Apometopides nov. subgen.

Diagnosis: Apometopids with comparatively widely spaced caudal cilia not forming a spine-like array.

Type species: *Metopus pyriformis* LEVANDER, 1894.

Etymology: Composite of the generic name *Apometopus* (see above) and the suffix *ides* (similar), referring to the similarity with *Apometopus*. Masculine gender.

Apometopus (*Apometopides*) *pyriformis* (LEVANDER, 1894) nov. comb. (Fig. 297a–g, 298a–i; Table 120)

1894 *Metopus pyriformis* LEVANDER, Acta Soc. Fauna Fl. Fenn., 9: 28, 36 (diagnosis of species).
1932 *Metopus pyriformis* LEVANDER, 1894 – KAHL, Tierwelt Dtl., 25: 426.

1964 *Metopus pyriformis* Levander, 1894 – Jankowski, Arch. Protistenk., 107: 221.
1995 *Brachonella pyriformis* (Levander, 1894) – Esteban, Fenchel & Finlay, Arch. Protistenk. 146: 139 (transfer not indicated).

Improved diagnosis: Size in vivo about 55 × 50 µm. Broadly pyriform, postoral width about two thirds of dome width; ratio of dome height and cone length 1.8:1 on average. Nuclear apparatus in dome, macronucleus globular, micronucleus broadly ellipsoid. 2 ordinary dome kineties and an average of 14 cone kineties; about 7 caudal cilia half as long as body. On average 46 adoral paramembranelles.

Type locality: River Warnow near to the town of Rostock, Germany.

Material: As far as we know, Levander (1894) did not deposit type material. We deposited 3 voucher slides with protargol-impregnated specimens from Australian site (98) in the Biology Centre of the Upper Austrian Museum in Linz (LI). Relevant specimens have been marked by black ink circles on the coverslip.

Etymology: Not provided by Levander (1894). The Latin adjective *pyriformis* (pear-shaped) obviously refers to the shape of the species.

Description of Australian population: Size in vivo 43–70 × 43–67 µm, usually about 55 × 52 µm as calculated from data in Table 120 adding 15% preparation shrinkage; some in vivo measurements show a size of 70–90 × 50–60 µm, indicating insufficient fixation and thus 25%–30% preparation shrinkage (see also macronucleus). Levander gives a length of 50–70 µm and emphasizes that cells could be not well preserved not even with osmic acid. Body shape fairly constant, broadly pyriform, ratio of dome height and cone length highly variable (CV = 20%), on average 1.8:1, as in *A. pelobia*; postoral width about two thirds of dome width; transverse outline broadly elliptic in vivo; dome conspicuous because semiglobular, separated from narrowed cone by perizonal stripe; not campanulate; posterior end transverse-truncate, frequently rugged by contractile vacuole contained (Fig. 297c, f, 298b, c, e; Table 120). Nuclear apparatus in posterior half of dome, very rarely in upper half of cone, usually closer to ventral than to dorsal side of cell (Fig. 297c, g, 298b, c; Table 120). Macronucleus globular to broadly ellipsoid, studded with nucleoli (?) about 1 µm across; macronuclear membrane in most specimens split, possibly due to insufficient fixation, producing a kind of coat 1–10 µm distant from internal membrane covering central mass, inner surface of external membrane covered by many granules and filaments forming reticulate structures. Micronucleus attached to external membrane of macronucleus, globular to ellipsoid, size rather variable, 5.4 × 3.4 µm in protargol preparations on average (Fig. 297c, g; Table 120); not recognizable in about one quarter of specimens.

Contractile vacuole in posterior body end; excretory pore in pole centre and surrounded by caudal cilia, gives rise to many fibres extending anteriorly half of cone length (Fig. 297e). Cortex flexible, contains many extrusomes which elongate to about 10 µm long rods during extrusion and then to long filaments forming a reticulate envelope (Fig. 297c, 298g); resting extrusomes not observed. Levander (1894) describes the cortex as ”a rather broad and bright zone showing a radial striation”, indicating that the extrusomes are fine rods. Cytoplasm clear, with some food vacuoles possibly containing bacteria and small flagellates. Possibly no symbiotic bacteria that, when present, usually deeply impregnate with protargol.

Somatic ciliature dikinetal and complex, consists of five types of kineties: (i) two “ordinary”

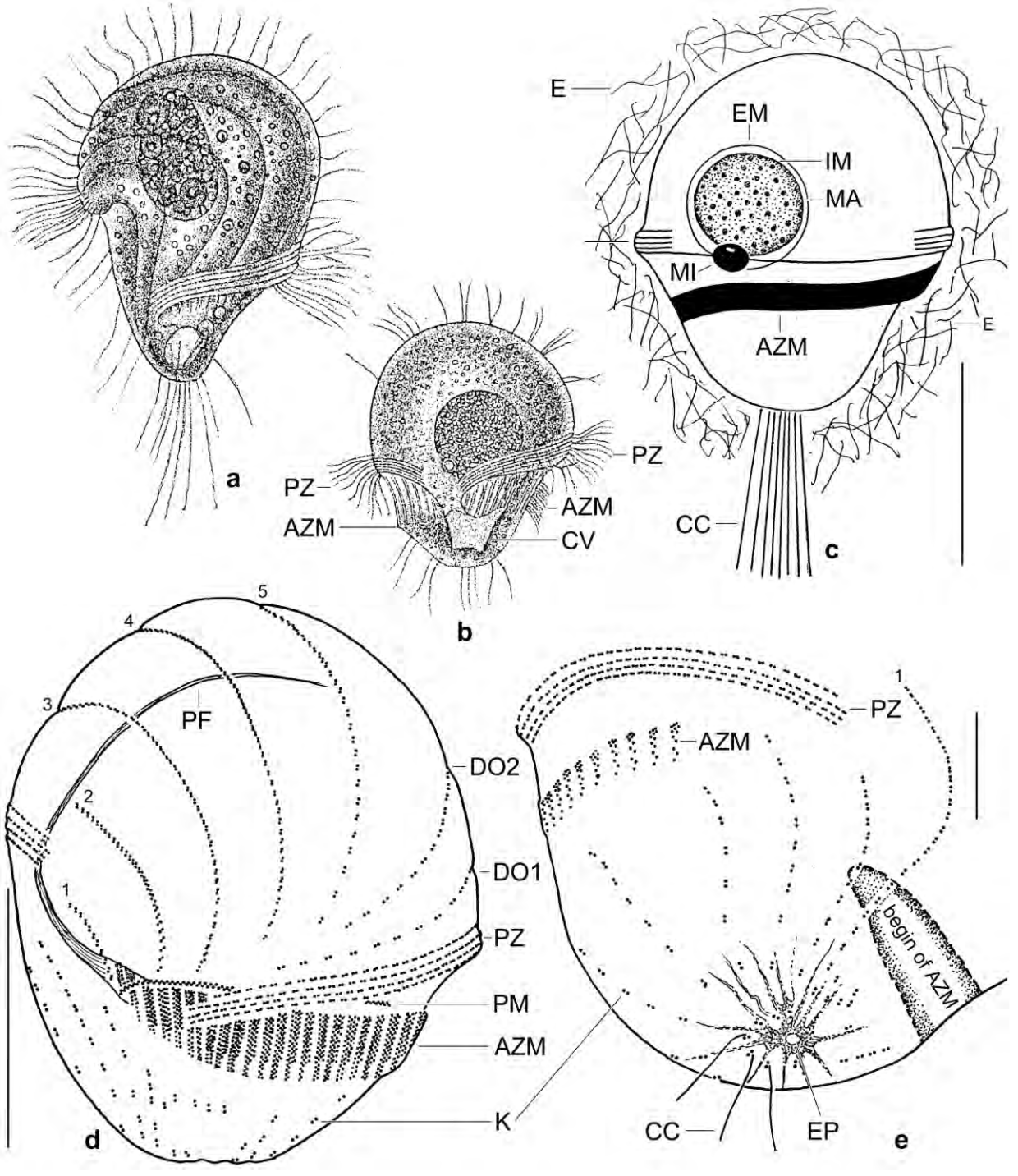

Fig. 297a–e. *Apometopus (Apometopides) pyriformis* from life and various preparation methods (a–c), and after protargol impregnation (d, e). **a, b:** German specimens from Levander (1894). Figure 297b has been selected as type because Fig. 297a probably shows another species. **c:** Scheme of Australian species, dorsal view. **d:** Oblique ventral view of an Australian specimen, showing the dome ciliature. **e:** Posterior polar view of an Australian cell, showing the semicircular array of seven dikinetids each with an elongated caudal cilium not shown in full length. AZM – adoral zone of paramembranelles, CC – caudal cilia, CV – contractile vacuole, DO1,2 – dome kineties, E – extrusomes, EM – external membrane, EP – excretory pore of contractile vacuole, IM – internal membrane, K – cone kineties, MA – macronucleus, MI – micronucleus, PF – pharyngeal fibres, PM – paroral membrane, PZ – perizonal ciliary stripe, 1–5 – ventral kineties. Scale bars 10 µm (e) and 25 µm (c, d).

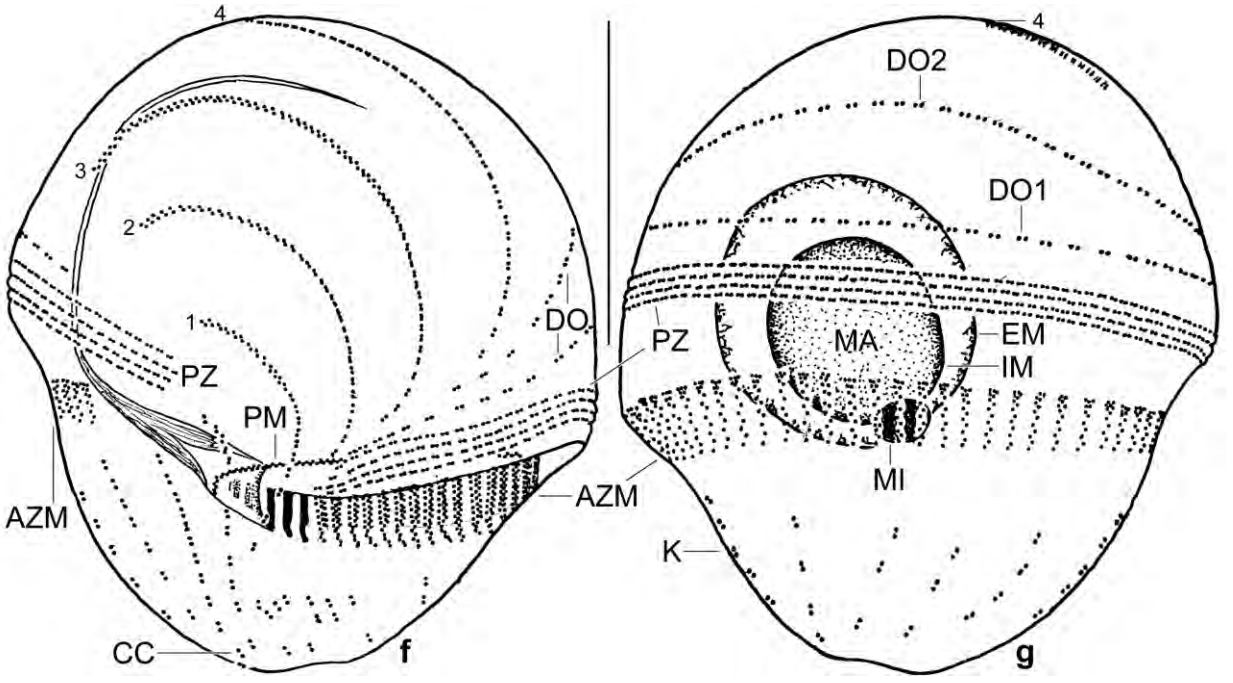

Fig. 297f, g. *Apometopus (Apometopides) pyriformis*, ventral and dorsal view of Australian holotype specimen after protargol impregnation, length 50 µm. The most important features of *Apometopus* are the almost circular adoral zone of paramembranelles and of perizonal kineties. Further, there are four to five (Fig. 297d) unique, curved kineties which are very densely ciliated and occupy the ventral side while the dorsal side bears only two dome kineties. AZM – adoral zone of paramembranelles, CC – dikinetids of caudal cilia, DO1,2 – dome kineties, EM – external membrane, IM – internal membrane, MA – macronucleus, MI – micronucleus, K – cone kineties, PM – paroral membrane, PZ – perizonal ciliary stripe, 1–4 – ventral kineties. Scale bars 25 µm.

dome kineties, (ii) a perizonal kinety stripe, (iii) four to five ventral kineties, (iv) an average of 14 cone kineties, and (v) eight caudal cilia (Fig. 297c–g, 298a–f, h, i; Table 120). Dome kineties commence and end on ventral side, slightly shorter than perizonal stripe, in fusiform pattern, i. e., kinety 1 rather close to perizonal stripe while kinety 2 curves anteriorly on dorsal side and posteriorly on right side; dikinetids comparatively widely spaced. Perizonal ciliary stripe near posterior margin of dome, almost circular, i.e., begins and ends on ventral side but at slightly different levels; consists of four rows of narrowly spaced, ciliated dikinetids oriented in or slightly obliquely to main kinety axis; anterior kinety separated from posterior kineties by a slightly increased distance. Ventral dome surface dominated by four to five widely spaced, densely ciliated ventral kineties increasingly curved from proximal to distal dome surface; most dikinetids obliquely arranged, more widely spaced at ends of kineties; number of ventral kineties depending on shape: first curved row is kinety 1 (Fig. 297d, f, 298a–d, f). Cone kineties highly reduced, half consisting of only one to three dikinetids. On average eight comparatively widely spaced caudal cilia in semicircular pattern, in vivo about half as long as body; very likely originate from posterior basal body of last dikinetid of dorsal cone kineties (Fig. 297c, e, f, 298a, b, d; Table 120).

Silverline pattern finely reticulate with meshes about 1 µm in size, as in other metopids (Klein 1930).

Oral apparatus metopid, i. e., slightly posterior of dome and consisting of an adoral zone with 49 paramembranelles on average; a dikinetal, short paroral membrane; and very long pharyngeal

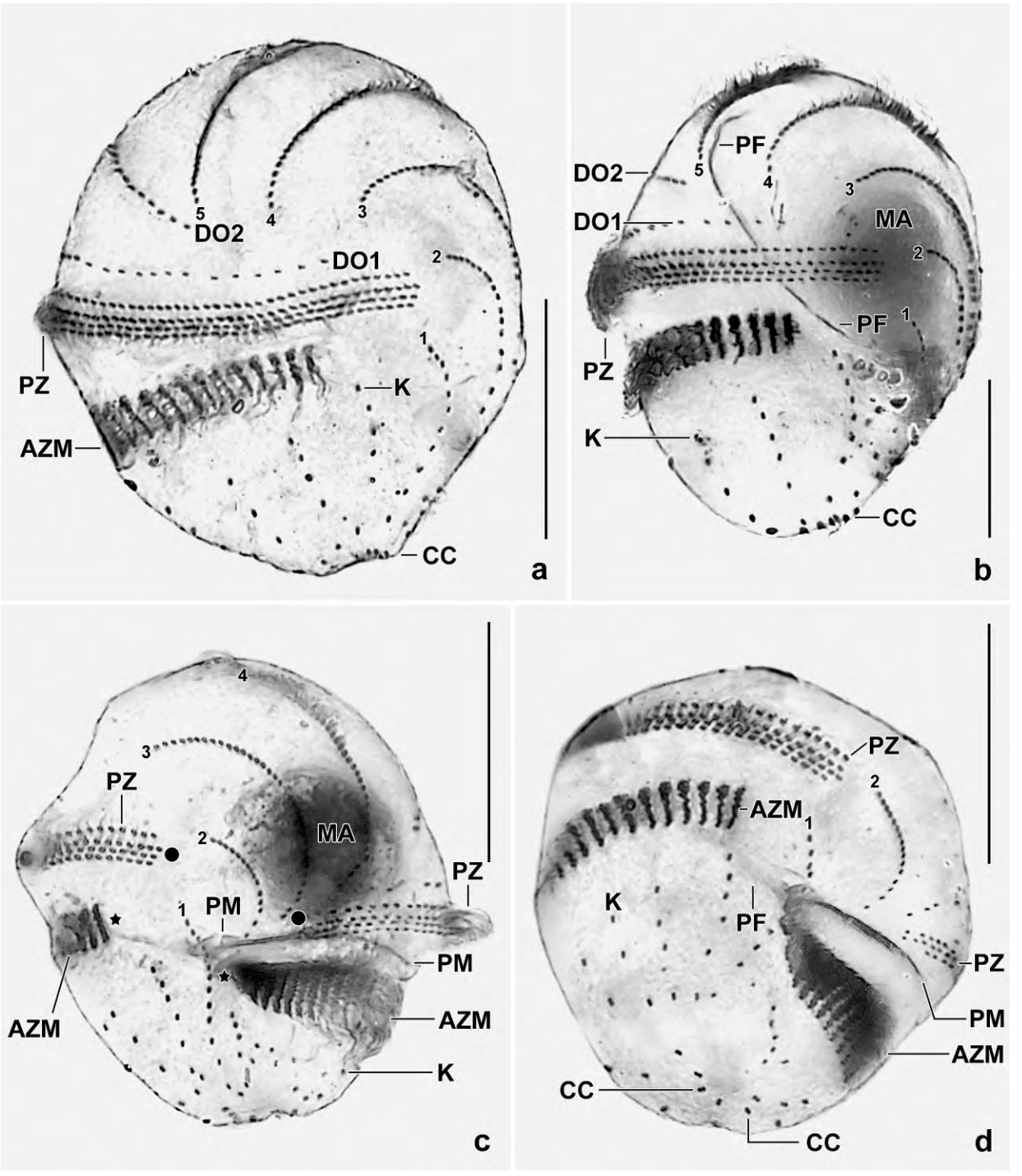

Fig. 298a–d. *Apometopus (Apometopides) pyriformis*, Australian specimens after protargol impregnation. **a, b:** Right side views, showing five special ventral kineties. The two dome kineties are slightly shorter than the perizonal stripe. **c:** Ventral view, showing the main characteristics of *Apometopus*, viz., the almost circular perizonal stripe (ends marked by dots) and adoral zone of paramembranelles (ends marked by asterisks). **d:** Oblique posterior polar view, showing dikinetids possibly associated with caudal cilia, the sparse cone kinetids, and the almost circular adoral zone of paramembranelles. AZM – adoral zone of paramembranelles, CC – dikinetids possibly associated with elongated caudal cilia, DO1,2 – dome kineties, K – cone kineties, MA – macronucleus, PF – pharyngeal fibres, PM – paroral membrane, PZ – perizonal ciliary stripe, 1–5 – ventral kineties. Scale bars 25 µm.

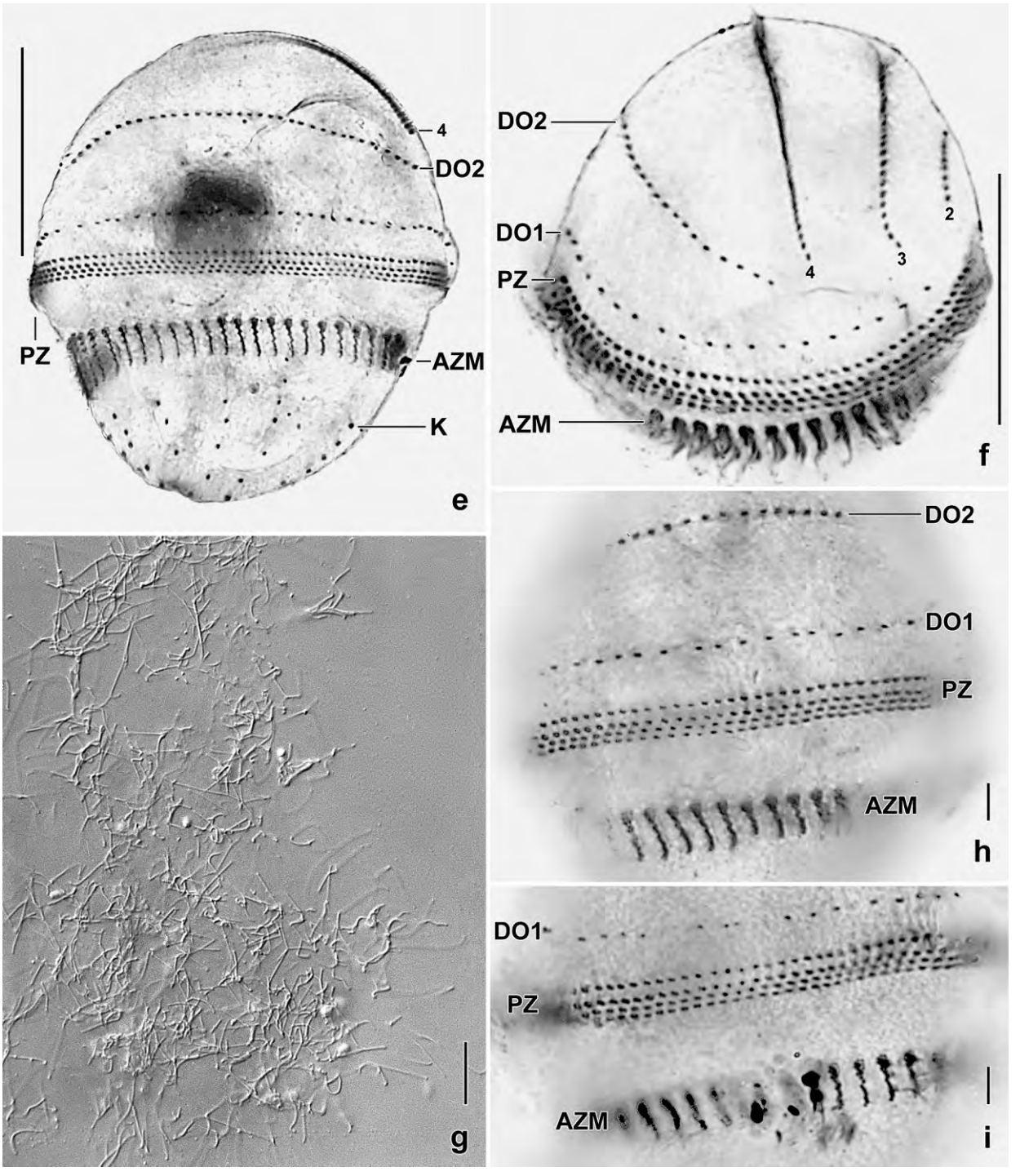

Fig. 298e–i. *Apometopus (Apometopides) pyriformis,* Australian specimens from life (g) and after protargol impregnation (e, f, h, i). **e:** Dorsal view, showing the dome kineties and the slender paramembranelles. **f:** Oblique anterior polar view, showing the relationship of adoral paramembranelles, perizonal ciliary stripe, dome kineties, and ventral kineties. **g:** When the extrusomes are released, they elongate and form a reticulate coat. **h, i:** Dorsal views, showing the dome kineties and the perizonal ciliary stripe composed of dikinetids. The adoral paramembranelles are possibly composed of very oblique dikinetids and a patch of basal bodies anteriorly. AZM – adoral zone of paramembranelles, DO1,2 – dome kineties, K – cone kineties, MA – macronucleus, PZ – perizonal ciliary stripe, 2–4 – ventral kineties. Scale bars 5 µm (h, i), 10 µm (g), and 25 µm (e, f).

Table 120. Morphometric data on *Apometopus pyriformis* based on mounted, protargol-impregnated, and randomly selected specimens from a non-flooded Petri dish culture. Measurements in µm. AZM – adoral zone of membranelles, CV – coefficient of variation in %, M – median, Max – maximum, Mean– arithmetic mean, Min – minimum, n – number of individuals investigated, SD – standard deviation, SE – standard error of arithmetic mean.

Characteristics	Mean	M	SD	SE	CV	Min	Max	n
Body, length	49.5	48.0	7.2	1.6	14.4	37.0	62.0	21
Body, dome width	45.1	44.0	5.9	1.3	13.1	37.0	58.0	21
Body, postoral width (posterior of AZM)	31.4	31.0	5.4	1.2	17.1	24.0	43.0	21
Anterior body end to proximal margin of AZM, distance	31.3	30.0	5.5	1.2	17.7	21.0	40.0	21
Body length:width, ratio	1.1	1.1	0.1	0.1	7.6	1.0	3.0	21
Dome width:postoral width, ratio	1.5	1.4	0.1	0.1	5.2	1.3	1.6	21
Body length:cone length, ratio	2.8	2.8	0.5	0.1	17.2	1.9	4.0	21
Anterior body end to proximal margin of adoral zone of membranelles:cone length, ratio	1.8	1.8	0.4	0.1	20.5	1.0	2.7	21
Macronucleus, length	14.3	14.0	1.5	0.3	10.4	12.0	18.0	21
Macronucleus, width	14.1	14.0	1.6	0.3	11.0	12.0	18.0	21
Micronucleus, length	5.4	5.0	0.8	0.2	15.4	4.5	8.0	21
Micronucleus, width	3.4	3.0	0.6	0.1	17.4	2.5	5.0	21
Perizonal ciliary stripe, width	3.1	3.0	–	–	–	3.0	4.0	21
Perizonal stripe, number of kineties	4.0	4.0	0.0	0.0	0.0	4.0	4.0	21
Cilia of ventral kinety 4, length	12.4	11.0	3.5	1.3	28.6	10.0	20.0	8
Caudal cilia, number	7.9	8.0	1.4	0.3	18.2	6.0	10.0	20
Special ventral kineties, number	4.5	4.5	–	–	–	4.0	5.0	21
Ordinary dome kineties, number	2.0	2.0	0.0	0.0	0.0	2.0	2.0	21
Cone kineties, number	14.3	14.0	1.9	0.4	12.9	10.0	18.0	21
Adoral paramembranelles, number	45.8	46.0	2.6	0.6	5.6	40.0	50.0	19
Adoral paramembranelles, length near mouth	6.7	7.0	–	–	–	6.0	7.0	17
Adoral paramembranelles, dorsal length	4.7	5.0	–	–	–	4.0	5.0	21
First adoral paramembranelle, length	3.8	4.0	0.7	0.2	18.3	3.5	5.0	21
Paroral membrane, length	22.5	22.0	2.2	0.6	10.0	18.0	25.0	14

fibres extending along ventral side to top of dome (Fig. 297d–g, 298a–d; Table 120). Adoral zone almost circular with right end slightly anterior of left end; right side and dorsal paramembranelles shorter than ventral ones, except of some short paramembranelles at mouth entrance (Fig. 297d, f, 298c, d); margin of paramembranelles indistinctly serrate due to strongly oblique dikinetids, exact structure not recognizable.

Occurrence and ecology: As yet found only in the upper 10 cm litter and soil layer from the dry Fogg Dam in northern Australia, surroundings of the town of Darwin; pH 5.0. Thus, *Apometopus pyriformis* makes resting cysts which were activated in the non-flooded Petri dish culture. It appeared three weeks after rewetting the sample and anaerobic or microaerobic conditions prevailed in the lower zones of the culture. We did not find cytoplasmic bacteria so common in anaerobic metopids and present in some other metopids of this sample. Thus, *A. pyriformis* can possibly survive in microaerobic conditions.

Remarks: *Metopus pyriformis* has the typical ciliary pattern of *Apometopus*, viz., special ventral kineties on the preoral dome and an almost closed adoral zone of membranelles. Thus, we transfer *Metopus pyriformis* to *Apometopus* (*Apometopides) pyriformis* (Levander, 1894) nov. comb.

We identify the Australian population as *Metopus pyriformis* which Levander (1894) discovered in a sapropelic river in northern Germany. This species has been never redescribed but was mentioned in the reviews of Kahl (1932), Jankowski (1964), and Esteban et al. (1995) who referred it to the genus *Brachonella*.

Levander (1894) describes and illustrates two specimens, according to live observations and fixation with osmium acid (Fig. 297a, b). They differ considerably in body and macronucleus shape and the presence vs. absence of caudal cilia. However, the description of Levander (1894) is rather vague and gives the impression that he was uncertain about the conspecificity of the two "forms". Our identification is based on a character emphasized by Levander (1894), viz., the almost closed perizonal stripe and adoral zone of membranelles, a feature we use for defining the new family Apometopidae. Further, body size and shape are quite similar when the specimen shown in Fig. 297b is fixed as type for *M. pyriformis*, using articles 67, 69 and 70 of the International Code of Zoological Nomenclature. However, we do not neotypify *M. pyriformis* because of the large spatial distance, i. e., we want not exclude the possibility that the Australian and the German populations are different species.

There are at least two species that are similar to *Apometopus pyriformis*: *M. campanula* and *M. galeatus* both described by Kahl (1927, 1932). *Metopus campanula* matches *M. pyriformis* in many features but might have a different ciliary pattern, i. e., the five dome kineties possibly extend to posterior end (Jankowski, 1964) while Kahl (1932) supposed that the cone is unciliated. We cannot exclude that *M. campanula* is a junior synonym of M. *pyriformis* especially because Kahl (1932) did not compare these species. Similar problems exist with *M. galeatus* but this might be a distinct species because the dome margin is protruding as in a steel helmet.

***

4. References

Aescht E. (2001): Catalogue of the generic names of ciliates (Protozoa, Ciliophora). — Denisia (Linz) **1**: 1–350.

Agatha S. & Foissner W. (2000): 3,000 or 30,000 free-living ciliates? An investigation on Namibian soil ciliates. — XVIIIth Int. Congr. Zool., Athens, Book of Abstracts: 159 pp.

Aladro-Lubel M. A. & Martinez-Murillo M. E. (1999): First description of the lorica of *Metacystis truncata* and its occurrence on *Thalassia testudinum*. — J. Eukaryot. Microbiol. **46:** 311–317.

Aladro-Lubel M. A. & Martinez-Murillo M. E. (2003): *Metacystis borrori* n. sp. (Ciliophora: Metacystidae) on the seagrass *Thalassia testudinum.* — J. Eukaryot. Microbiol. **50:** 204–209.

Alekperov I. K. (2005): Atlas of Free-Living Infusoria. — Baku: 310 pp. (in Russian).

Arregui L., Pérez-Uz B., Zornoza A. & Serrano S. (2010): A new species of the genus *Metacystis* (Ciliophora, Prostomatida, Metacystidae) from a wastewater treatment plant. — J. Eukaryot. Microbiol. **57:** 362–368.

Augustin H. & Foissner W. (1992): Morphologie und Ökologie einiger Ciliaten (Protozoa: Ciliophora) aus dem Belebtschlamm. — Arch. Protistenk. 141: 243–283.

Beers C. D. (1952): Observations on the ciliate *Bursaria ovata*, n. sp. — J. Elisha Mitchell scient. Soc. **68:** 184–190.

Berger H. (1999): Monograph of the Oxytrichidae (Ciliophora, Hypotrichia). — Monographiae biol. **78**: xii + 1080 pp.

Berger H. (2003): Redefinition of *Holosticha* Wrzesniowski, 1877 (Ciliophora, Hypotricha). — Eur. J. Protistol. **39:** 373–379.

Berger H. (2006): Monograph of the Urostyloidea (Ciliophora, Hypotricha). — Monographiae biol. **85:** xvi + 1–1303 pp.

Berger H. (2008): Monograph of the Amphisiellidae and Trachelostylidae (Ciliophora, Hypotricha). — Monographiae boil. **88:** xvi + 1–737 pp.

Berger H. (2011): Monograph of the Gonostomatidae and Kahliellidae (Ciliophora, Hypotricha). — Monographiae biol. **90**: xiv + 741 pp.

Berger H. & Foissner W. (1987): Morphology and biometry of some soil hypotrichs (Protozoa: Ciliophora). — Zool. Jb. Syst. **114:** 193–239.

Berger H. & Foissner W. (1989): Morphology and biometry of some soil hypotrichs (Protozoa, Ciliophora) from Europe and Japan. — Bull. Br. Mus. nat. Hist. (Zool.), **55:** 19–46.

Berger H., Foissner W. & Adam H. (1985): Morphological variation and comparative analysis of morphogenesis in *Parakahliella macrostoma* (Foissner, 1982) nov. gen. and *Histriculus muscorum* (Kahl, 1932), (Ciliophora, Hypotrichida). — Protistologica **21**: 295–311.

Berger H., Al-Rasheid K. A. S. & Foissner W. (2006): Morphology and cell division of *Saudithrix terricola* n. gen., n. sp., a large, stichotrich ciliate from Saudi Arabia. — J. Eukaryot. Microbiol., **53:** 260–268.

Blatterer H. & Foissner W. (1988): Beitrag zur terricolen Ciliatenfauna (Protozoa: Ciliophora) Australiens. — Stapfia, Linz **17:** 1–84.

Borror A. C. (1972): Revision of the order Hypotrichida (Ciliophora, Protozoa). — J. Protozool. **19**: 1–23.

Borror A. C. & Evans F. R. (1979): *Cladotricha* and phylogeny in the suborder Stichotrichina (Ciliophora, Hypotrichida). — J. Protozool. **26:** 51–55.

Bory de Saint-Vincent J.B. (1824): Encyclopédie Méthodique. Histoire Naturelle des Zoopytes, ou Animaux Rayonnés, Faisant Suite a l'Histoire Naturelle des Vers de Bruguière. Tome second. — Agasse, Paris: 819 pp.

Buitkamp U. (1977a): Die Ciliatenfauna der Savanne von Lamto (Elfenbeinküste). — Acta Protozool. **16:** 249–276.

Buitkamp U. (1977b): Über die Ciliatenfauna zweier mitteleuropäischer Bodenstandorte (Protozoa, Ciliata). — Decheniana (Bonn) **130**: 114–126.

Bütschli O. (1887–1889): Protozoa. III. Abteilung: Infusoria und System der Radiolaria. — In: Bronn H. G. (ed.): Klassen und Ordnungen des Thier-Reichs. Erster Band. C. F. Winter, Leipzig: 1098–2035.

Certes A. (1891): Note sur deux infusoires nouveaux des environs de Paris. — Mém. Soc. zool. Fr. **4:** 536–541.

Chao A., Li P. C., Agatha S. & Foissner W. (2006): A statistical approach to estimate soil ciliate diversity and distribution based on data from five continents. — Oikos **114:** 479–493.

Chorik F. P. [Čorjk F. P.] & Vikol M. M. [Vikol M. M.] (1973): Fauna donnyh svobodnoživuših infuzorij Kučurganskogo linana–ohlacitelâ moldavskoi RRÈS [Fauna of bottom-dwelling free-living infusoria of the Kuchurgansk cooling plant of Moldavian RRÈS]. — In: Biologičeskie resursy vodoemov Moldavii [Biological resources of water bodies of Moldavia]. Izdatel´stvo, "Štinica", Kišinev: 56–72 [in Russian].

Claparède E. & Lachmann J. (1859): Études sur les infusoires et les rhizopodes. — Mém. Inst. natn. génev. **6** (year 1858): 261–482.

Corliss J. O. (1952): Le cycle autogamique de *Tetrahymena rostrata*. — C. R. Acad. Sci., Paris **235**: 399–402. Corliss, J. O. (1973): History, taxonomy, ecology and evolution of species of *Tetrahymena*. — In: Elliott A. M. (ed.): Biology of *Tetrahymena*. Dowden, Hutchinson, & Ross, Stroudsburg, Pa: 1–55.

Cotterill F.P.D., Augustin H., Medicus R. & Foissner W. (2013): Conservation of protists: the Krauthügel pond in Austria. — Diversity **5:** 374–392.

Dingfelder J. H. (1962): Die Ciliaten vorübergehender Gewässer. — Arch. Protistenk. **105**: 509–658.

Dragesco J. (1960): Ciliés mésopsammiques littoraux. Systématique, morphologie, écologie. — Trav. Stn biol. Roscoff **122**: 1–356.

Dragesco J. & Njine T. (1971): Compléments à la connaissance des ciliés libres du Cameroun. — Annls Fac. Sci. Univ. féd. Cameroun **7-8**: 97–140.

Dragesco J. & Dragesco-Kernéis A. (1986): Ciliés libres de l'Afrique intertropicale. Introduction à la connaissance et à l'étude des ciliés. — Faune tropicale (Éditions de l'Orstom, Paris) **26**: 1–559.

Dragesco J., Iftode F. & Fryd-Versavel G. (1974): Contribution a la connaissance de quelques ciliés holotriches rhabdophores; I. Prostomiens. — Protistologica **10:** 59–76.

Dunthorn M., Stoeck T., Wolf K., Breiner H.-W. & Foissner W. (2012): Diversity and endemism of ciliates inhabiting neotropical phytotelmata. — Systematics and Biodiversity **10:** 195–205.

Ehrenberg C. G. (1838): Die Infusionsthierchen als vollkommene Organismen. Ein Blick in das tiefere organische Leben der Natur. — L. Voss, Leipzig: xviii + (4) + 548 pp.

Eigner P. (1995): Divisional morphogenesis in *Deviata abbrevescens* nov. gen., nov. spec., *Neogeneia hortualis* nov. gen., nov. spec., and *Kahliella simplex* (Horváth) Corliss and redefinition of the Kahliellidae (Ciliophora, Hypotrichida). — Eur. J. Protistol. **31**: 341–366.

Eigner P. (1999): Comparison of divisional morphogenesis in four morphologically different clones of the genus *Gonostomum* and update of the natural hypotrich system (Ciliophora, Hypotrichida). — Eur. J. Protistol. **35:** 34–48.

Eigner P. & Foissner W. (1992): Divisional morphogenesis in *Bakuella pampinaria* nov. spec. and reevaluation of the classification of the urostylids (Ciliophora, Hypotrichida). — Eur. J. Protistol. **28:** 460–470.

Eigner P. & Foissner W. (1994): Divisional morphogenesis in *Amphisiellides illuvialis* n. sp., *Paramphisiella caudata* (Hemberger) and *Hemiamphisiella terricola* Foissner, and redefinition of the Amphisiellidae (Ciliophora, Hypotrichida). — J. Euk. Microbiol. **41**: 243–261.

Engelmann T. W. (1862): Zur Naturgeschichte der Infusionsthiere. — Z. wiss. Zool. **11:** 347–393.

Esteban G., Fenchel T. & Finlay B. (1995): Diversity of free-living morphospecies in the ciliate genus *Metopus*. — Arch. Protistenk. **146**: 137–164.

Esteban G. F., Finlay B. J., Olmo J. L. & Tyler P.A. (2000): Ciliated protozoa from a volcanic crater-lake in Victoria, Australia. — J. Nat. Hist. **34**: 159–189.

Fan Y., Hu X., Gao F. & Al-Rasheid K. A. S. (2014): Ontogenetic features and SSU rRNA gene-base phylogeny of a new soil ciliate, *Bistichella encystica* spec. nov. (Ciliophora, Stichotrichia), with establishment of Bistichellidae fam. nov. — J. Eukaryot. Microbiol. (in press).

Fenchel T. (1987): Ecology of Protozoa. The Biology of Free-Living Phagotrophic Protists. — Science Tech. Publishers, Madison: x + 197 pp.

Finlay B. J. & Esteban G. F. (1998): Freshwater protozoa: biodiversity and ecological function. — Biodiv. Conserv. **7**: 1163–1186.

Finlay B. J., Esteban G. F., Olmo J. L. & Tyler P. A. (1999): Global distribution of free-living microbial species. — Ecography **22**: 138–144.

Finlay B. J., Esteban G. F., Clarke K. J. & Olmo J. L. (2001): Biodiversity of terrestrial protozoa appears homogeneous across local and global spatial scales. — Protist **152:** 355–366.

Foissner I. & Foissner W. (1986): *Ciliomyces spectabilis*, nov. gen., nov. spec., a zoosporic fungus which parasitizes cysts of the ciliate *Kahliella simplex* I. Infection, vegetative growth and sexual reproduction. — Z. Parasitenk. **72:** 29–41.

Foissner I. & Foissner W. (1995a): *Ciliatomyces* nom. nov. for *Ciliomyces* Foissner & Foissner 1986 (Lagenidiaceae, Oomycota). — Phyton (Horn, Austria) **35:** 115–116.

Foissner I. & Foissner W. (1995b): *Ciliatosporidium platyophryae* nov. gen., nov. spec. (Microspora incerta sedis), a parasite of *Platyophrya terricola* (Ciliophora, Colpodea). — Eur. J. Protistol. **31:** 248–259.

Foissner W. (1975a): Der elektronenmikroskopische Nachweis der fibrillären Natur des Silberliniensystems bei peritrichen Ciliaten. — Z. Naturf. **30c:** 818–822.

Foissner W. (1975b): Opisthonectidae (Ciliata, Peritrichida) nov. fam. und Revision der Genera *Telotrochidium* (Kent) und *Opisthonecta* (Fauré-Fremiet). — Protistologica **11:** 395–414.

Foissner W. (1976): Eine Neubeschreibung von *Telotrochidium johanninae* Faurè-Fremiet 1950 (Ciliata, Opisthonectidae). — Protistologica **12:** 263–269.

Foissner W. (1977): Revision der Genera *Astylozoon* (Engelmann) und *Hastatella* (Erlanger) (Ciliata Natantina). — Protistologica **13:** 353–379.

Foissner W. (1978a): Morphologie, Infraciliatur und Silberliniensystem von *Plagiocampa rouxi* Kahl, 1926 (Prostomatida, Plagiocampidae) und *Balanonema sapropelica* nov. spec. (Philasterina, Loxocephalidae). — Protistologica **14:** 381–389.

Foissner W. (1978b): *Opisthonecta bivacuolata* nov. spec., *Telotrochidium cylindricum* nov. spec. und *Epistylis alpestris* nov. spec., drei neue peritriche Ciliaten aus dem Hochgebirge (Hohe Tauern, Österreich). — Annln naturh. Mus. Wien **81:** 549–565.

Foissner W. (1980a): Colpodide Ciliaten (Protozoa: Ciliophora) aus alpinen Böden. — Zool. Jb. Syst. **107:** 391–432.

Foissner W. (1980b): Taxonomische Studien über die Ciliaten des Grossglocknergebietes (Hohe Tauern, Österreich). IX. Ordnungen Heterotrichida und Hypotrichida. — Ber. Nat.-Med. Ver. Salzburg **5**: 71–117.

Foissner W. (1981a): Morphologie und Taxonomie einiger neuer und wenig bekannter kinetofragminophorer Ciliaten (Protozoa: Ciliophora) aus alpinen Böden. — Zool. Jb. Syst. **108:** 264–297.

Foissner W. (1981b): Die Gemeinschaftsstruktur der Ciliatenzönose in alpinen Böden (Hohe Tauern, Österreich)

und Grundlagen für eine Synökologie der terricolen Ciliaten (Protozoa, Ciliophora). — Veröff. Österr. MaB-Programms **4**: 7–52.

Foissner W. (1982): Ökologie und Taxonomie der Hypotrichida (Protozoa: Ciliophora) einiger österreichischer Böden. — Arch. Protistenk. **126:** 19–143.

Foissner W. (1983): Taxonomische Studien über die Ciliaten des Großglocknergebietes (Hohe Tauern, Österreich) I. Familien Holophryidae, Prorodontidae, Plagiocampidae, Colepidae, Enchelyidae und Lacrymariidae nov. fam. — Annln naturh. Mus. Wien **84B**: 49–85.

Foissner W. (1984): Infraciliatur, Silberliniensystem und Biometrie einiger neuer und wenig bekannter terrestrischer, limnischer und mariner Ciliaten (Protozoa: Ciliophora) aus den Klassen Kinetofragminophora, Colpodea und Polyhymenophora. — Stapfia (Linz) **12:** 1–165.

Foissner W. (1985): Klassifikation und Phylogenie der Colpodea (Protozoa: Ciliophora). — Arch. Protistenk. **129:** 239–290.

Foissner W. (1987a): Neue und wenig bekannte hypotriche und colpodide Ciliaten (Protozoa: Ciliophora) aus Böden und Moosen. — Zool. Beitr. N. F. **31:** 187–282.

Foissner W. (1987b): Soil protozoa: fundamental problems, ecological significance, adaptations in ciliates and testaceans, bioindicators, and guide to the literature. — Progr. Protistol. **2:** 69–212.

Foissner W. (1987c): Neue terrestrische und limnische Ciliaten (Protozoa, Ciliophora) aus Österreich und Deutschland. — Sber. Akad. Wiss. Wien **195** (year 1986): 217–268.

Foissner W. (1987d): Faunistische und taxonomische Notizen über die Protozoen des Fuscher Tales (Salzburg, Österreich). — Jber. Haus Nat. Salzburg **10:** 56–68.

Foissner W. (1988a): Gemeinsame Arten in der terricolen Ciliatenfauna (Protozoa: Ciliophora) von Australien und Afrika. — Stapfia, Linz **17**: 85–133.

Foissner W. (1988b): Taxonomie und Ökologie einiger Ciliaten (Protozoa, Ciliophora) des Saprobiensystems. II. Familie Chilodonellidae. — Hydrobiologia **162:** 21–45.

Foissner W. (1989): Morphologie und Infraciliatur einiger neuer und wenig bekannter terrestrischer und limnischer Ciliaten (Protozoa, Ciliophora). — Sber. Akad. Wiss. Wien **196** (year 1987): 173–247.

Foissner W. (1992): Estimating the species richness of soil protozoa using the "non-flooded petri dish method". — In: Lee J. J. & Soldo A. T. (ed.): Protocols in protozoology. Society of Protozoologists, Lawrence, Kansas: B-10.1 to B-10.2.

Foissner W. (1993a): Colpodea (Ciliophora). — Gustav Fischer, Stuttgart, Germany, Protozoenfauna **4:** x + 798 pp.

Foissner W. (1993b): *Idiocolpoda pelobia* gen. n., sp. n., a new colpodid ciliate (Protozoa, Ciliophora) from an ephemeral stream in Hawaii. — Acta Protozool. **32:** 175–182.

Foissner W. (1994): *Spetazoon australiense* nov. gen., nov. spec., ein neues Wimpertier (Protozoa, Ciliophora) von Australien. — In: Aescht E. (ed.): Die Urtiere, eine verborgene Welt. Kataloge des OÖ. Landesmuseums N. F., Linz, Austria. **71:** 267–278.

Foissner W. (1995): Tropical protozoan diversity: 80 ciliate species (Protozoa, Ciliophora) in a soil sample from a tropical dry forest of Costa Rica, with descriptions of four new genera and seven new species. — Arch. Protistenk. **145**: 37–79.

Foissner W. (1996a): Faunistics, taxonomy and ecology of moss and soil ciliates (Protozoa, Ciliophora) from Antarctica, with description of new species, including *Pleuroplitoides smithi* gen. n., sp. n. — Acta Protozool. **35:** 95–123.

Foissner W. (1996b): Ontogenesis in ciliated protozoa, with emphasis on stomatogenesis. — In: Hausmann K. & Bradbury P. (ed.): Ciliates: cells as organisms. Gustav Fischer, Stuttgart: 95–177.

Foissner W. (1997): Soil ciliates (Protozoa: Ciliophora) from evergreen rain forests of Australia, South America and

Costa Rica: diversity and description of new species. — Biol. Fertil. Soils **25:** 317–339.

Foissner W. (1998): An updated compilation of world soil ciliates (Protozoa, Ciliophora), with ecological notes, new records, and descriptions of new species. — Eur. J. Protistol. **34:** 195–235.

Foissner W. (1999a): Description of two new, mycophagous soil ciliates (Ciliophora, Colpodea): *Fungiphrya strobli* n. g., n. sp. and *Grossglockneria ovata* n. sp. — J. Eukaryot. Microbiol. **46:** 34–42.

Foissner W. (1999b): Notes on the soil ciliate biota (Protozoa, Ciliophora) from the Shimba Hills in Kenya (Africa): diversity and description of three new genera and ten new species. — Biodivers. Conserv. **8**: 319–389.

Foissner W. (1999c): Protist diversity: estimates of the near-imponderable. — Protist **150**: 363–368.

Foissner W. (1999d): Soil protozoa as bioindicators: pros and cons, methods, diversity, representative examples. — Agric. Ecosyst. Environ. **74**: 95–112.

Foissner W. (2000a): A compilation of soil and moss ciliates (Protozoa, Ciliophora) from Germany, with new records and descriptions of new and insufficiently known species. — Eur. J. Protistol. **36:** 253–283.

Foissner W. (2000b): Notes on ciliates (Protozoa, Ciliophora) from *Espeletia* trees and *Espeletia* soils of the Andean Páramo, with descriptions of *Sikorops espeletiae* nov. spec. and *Fragmocirrus espeletiae* nov. gen., nov. spec. — Stud. Neotrop. Fauna & Environm. **35:** 52–79.

Foissner W. (2003a): *Pseudomaryna australiensis* nov. gen., nov. spec. and *Colpoda brasiliensis* nov. spec., two new colpodids (Ciliophora, Colpodea) with a mineral envelope. — Eur. J. Protistol. **39:** 199–212.

Foissner W. (2003b): Two remarkable soil spathidiids (Ciliophora: Haptorida), *Arcuospathidium pachyoplites* sp. n. and *Spathidium faurefremieti* nom. n. — Acta Protozool. **42:** 145–159.

Foissner W. (2003c): The Myriokaryonidae fam. n., a new family of spathidiid ciliates (Ciliophora: Gymnostomatea). — Acta Protozool. **42:** 113–143.

Foissner W. (2004): Some new ciliates (Protozoa, Ciliophora) from an Austrian floodplain soil, including a giant, red "flagship", *Cyrtohymena* (*Cyrtohymenides*) *aspoecki* nov. subgen., nov. spec. — Denisia **13:** 369–382.

Foissner W. (2005): Two new "flagship" ciliates (Protozoa, Ciliophora) from Venezuela: *Sleighophrys pustulata* and *Luporinophrys micelae*. — Eur. J. Protistol. **41:** 99–117.

Foissner W. (2006): Biogeography and dispersal of micro-organisms: a review emphasizing protists. — Acta Protozool. **45:** 111–136.

Foissner W. (2007): Dispersal and biogeography of protists: recent advances. — Jpn. J. Protozool. **40**: 1–16.

Foissner W. (2008a): Protist diversity and distribution: some basic considerations. — Biodivers. Conserv. **17:** 235–242.

Foissner W. (2008b): Notes on soil ciliates from Singapore, with description of *Suturothrix monoarmata* nov. gen., nov. spec. (Protozoa, Ciliophora). — Soil Organisms **80:** 81–97.

Foissner, W. (2009): The stunning, glass-covered resting cyst of *Maryna umbrellata* (Ciliophora, Colpodea) — Acta Protozool. **48:** 223–243.

Foissner W. (2010a): Life cycle, morphology, ontogenesis, and phylogeny of *Bromeliothrix metopoides* nov. gen., nov. spec., a peculiar ciliate from tank bromeliads. — Acta Protozool. **49:** 159–193.

Foissner W. (2010b): *Enchelys micrographica* nov. spec., a new ciliate (Protista, Ciliophora) from moss of Austria. — MittBl. Mikroskop. Ges. Wien, Festschrift: 71–79.

Foissner W. (2011): Dispersal of protists: the role of cysts and human introductions. — In: Fontaneto D. (ed): Biogeography of microscopic organisms. Is everything small everywhere? Cambridge Univ. Press, Cambridge, UK: 61–87.

Foissner W. (2012a): *Schmidingerothrix extraordinaria* nov. gen., nov. spec., a secondarily oligomerized hypotrich (Ciliophora, Hypotricha, Schmidingerotrichidae nov. fam.) from hypersaline soils of Africa. — Eur. J. Protistol.

48: 237–251.

Foissner W. (2012b): Ein Ciliat als Altarbild und Protisten in der Oper. — Mikrokosmos **101**(2): 82–84.

Foissner W. (2014): An update of 'basic light and scanning electron microscopic methods for taxonomic studies of ciliated protozoa'. — Int. J. Syst. Evol. Microbiol. **64:** 271-292.

Foissner W. & Adam H. (1983a): Die Morphogenese von *Urosomoida agiliformis* Foissner, 1982 (Ciliophora, Oxytrichidae). — Zool. Anz. **211:** 161–176.

Foissner W. & Adam H. (1983b): Morphologie und Morphogenese des Bodenciliaten *Oxytricha granulifera* sp. n. (Ciliophora, Oxytrichidae). — Zool. Scr. **12**: 1–11.

Foissner W. & Agatha S. (1999): Morphology and morphogenesis of *Metopus hasei* Sondheim, 1929 and *M. inversus* (Jankowski, 1964) nov. comb. (Ciliophora, Metopida). — J. Eukaryot. Microbiol. **46**: 174-193.

Foissner W. & Al-Rasheid K. (2006): A unified organization of the stichotrichine oral apparatus, including a description of the buccal seal (Ciliophora: Spirotrichea). — Acta Protozool. **45:** 1–16.

Foissner W. & Berger H. (1999): Identification and ontogenesis of the nomen nudum hypotrichs (Protozoa: Ciliophora) *Oxytricha nova* (= *Sterkiella nova* sp. n.) and *O. trifallax* (= *S. histriomuscorum*). — Acta Protozool. 38: 215–248.

Foissner W. & Foissner I. (1988): The fine structure of *Fuscheria terricola* Berger et al., 1983 and a proposed new classification of the subclass Haptoria Corliss, 1974 (Ciliophora, Litostomatea). — Arch. Protistenk. **135:** 213–235.

Foissner W. & Kreutz M. (1998): Systematic position and phylogenetic relationships of the genera *Bursaridium, Paracondylostoma, Thylakidium, Bryometopus,* and *Bursaria* (Ciliophora: Colpodea). — Acta Protozool. **37**: 227–240.

Foissner W. & O'Donoghue P. J. (1990): Morphology and infraciliature of some freshwater ciliates (Protozoa: Ciliophora) from Western and South Australia. — Invertebr. Taxon. **3**: 661–696.

Foissner W. & Pfister G. (1997): Taxonomic and ecologic revision of urotrichs (Ciliophora, Prostomatida) with three or more caudal cilia, including a user-friendly key. — Limnologica **27**: 311–347.

Foissner W. & Schiffmann H. (1975): Vergleichende Studien an argyrophilen Strukturen von vierzehn peritrichen Ciliaten. — Protistologica **10:** 489–508.

Foissner W. & Schubert G. (1977): Morphologie der Zooide und Schwärmer von *Heteropolaria colisarum* gen. nov., spec. nov. (Ciliata, Peritrichida), einer symphorionten Epistylidae von *Colisa fasciata* (Anabantoidei, Belontiidae). — Acta Protozool. **16:** 231–247.

Foissner W. & Song W. (2002): *Apofrontonia lametschwandtneri* nov. gen., nov. spec., a new peniculine ciliate (Protozoa, Ciliophora) from Venezuela. — Eur. J. Protistol. **38:** 223–234.

Foissner W. & Stoeck T. (2006): *Rigidothrix goiseri* nov. gen., nov. spec. (Rigidotrichidae nov. fam.), a new "flagship" ciliate from the Niger floodplain breaks the flexibility-dogma in the classification of stichotrichine spirotrichs (Ciliophora, Spirotrichea). — Eur. J. Protistol. **42:** 249–267.

Foissner W. & Stoeck T. (2009): Morphological and molecular characterization of a new protist family, Sandmanniellidae n. fam. (Ciliophora, Colpodea), with description of *Sandmanniella terricola* n. g., n. sp. from the Chobe floodplain in Botswana. — J. Eukaryot. Microbiol. **56:** 472–483.

Foissner W. & Stoeck T. (2011): *Cotterillia bromelicola* nov. gen., nov. spec., a gonostomatid, bromeliad-inhabiting ciliate (Ciliophora, Hypotricha) with *de novo* originating dorsal kineties. — Eur. J. Protistol. **47:** 29–50.

Foissner W. & Wenzel F. (2004): Life and legacy of an outstanding ciliate taxonomist, Alfred Kahl (1877–1946), including a facsimile of his forgotten monograph from 1943. — Acta Protozool. **43** (Suppl.)**:** 3–69.

Foissner W. & Wolf K. (2009): Morphology and ontogenesis of *Platyophrya bromelicola* nov. spec., a new macrostome-forming colpodid (Protists, Ciliophora) from tank bromeliads of Jamaica. — Eur. J. Protistol. **45:**

87–97.

Foissner W. & Xu K. (2007): Monograph of the Spathidiida (Ciliophora, Haptoria). Volume I: Protospathidiidae, Arcuospathidiidae, Apertospathulidae. — Monographiae biol. **81:** 1–485.

Foissner W., Czapik A. & Wiackowski K. (1981): Die Infraciliatur und das Silberliniensystem von *Sagittaria hyalina* nov. spec., *Chlamydonella polonica* nov. spec. und *Spirozona caudata* Kahl, 1926 (Protozoa, Ciliophora). — Arch. Protistenk. **124:** 361–377.

Foissner W., Hoffmann G. L. & Mitchell A. J. (1985a): *Heteropolaria colisarum* Foissner & Schubert, 1977 (Protozoa: Epistylididae) of North American freshwater fishes. — J. Fish Deseases **8:** 145–160.

Foissner W., Peer T. & Adam H. (1985b): Pedologische und protozoologische Untersuchung einiger Böden des Tullner Feldes (Niederösterreich). — Mitt. öst. bodenk. Ges. **30**: 77–117.

Foissner W., Schlegel M. & Prescott D. M. (1987): Morphology and morphogenesis of *Onychodromus quadricornutus* n. sp. (Ciliophora, Hypotrichida), an extraordinarily large ciliate with dorsal horns. — J. Protozool. **34**: 150–159.

Foissner W., Blatterer H. & Foissner I. (1988): The Hemimastigophora (*Hemimastix amphikineta* nov. gen., nov. spec.), a new protistan phylum from Gondwanian soils. — Eur. J. Protistol. **23:** 361–383.

Foissner W., Blatterer H., Berger H. & Kohmann F. (1991): Taxonomische und ökologische Revision des Saprobiensystems. – Band I: Cyrtophorida, Oligotrichida, Hypotrichia, Colpodea. — Informationsberichte des Bayer. Landesamtes für Wasserwirtschaft **1/91**: 478 pp.

Foissner W., Berger H. & Kohmann F. (1994): Taxonomische und ökologische Revision der Ciliaten des Saprobiensystems – Band III: Hymenostomata, Prostomatida, Nassulida. — Informationsberichte des Bayer. Landesamtes für Wasserwirtschaft **1/94:** 548 pp.

Foissner W., Berger H., Blatterer H. & Kohmann F. (1995): Taxonomische und ökologische Revision der Ciliaten des Saprobiensystems – Band IV: Gymnostomatea, *Loxodes*, Suctoria. — Informationsberichte des Bayer. Landesamtes für Wasserwirtschaft **1/95:** 540 pp.

Foissner W., Berger H. & Schaumburg J. (1999): Identification and ecology of limnetic plankton ciliates. — Informationsberichte des Bayer. Landesamtes für Wasserwirtschaft **3/99**: 793 pp.

Foissner W., Stoeck T., Schmidt H. & Berger H. (2001): Biogeographical differences in a common soil ciliate, *Gonostomum affine* (Stein), as revealed by morphological and RAPD-fingerprint analysis. — Acta Protozool. **40:** 83–97.

Foissner W., Agatha S. & Berger H. (2002): Soil ciliates (Protozoa, Ciliophora) from Namibia (Southwest Africa), with emphasis on two contrasting environments, the Etosha region and the Namib Desert. — Denisia **5:** 1–1459.

Foissner W., Moon-van der Staay S. Y., van der Staay G. W. M., Hackstein J. H. P., Krautgartner W.-D. & Berger H. (2004): Reconciling classical and molecular phylogenies in the stichotrichines (Ciliophora, Spirotrichea), including new sequences from some rare species. — Eur. J. Protistol. **40**: 265–281.

Foissner W., Berger H., Xu K. & Zechmeister-Boltenstern S. (2005a): A huge, undescribed soil ciliate (Protozoa: Ciliophora) diversity in natural forest stands of Central Europe. — Biodivers. Conserv. **14:** 617–701.

Foissner W., Mueller H. & Weisse T. (2005b): The unusual, lepidosome-coated resting cyst of *Meseres corlissi* (Ciliophora, Oligotrichea): light and scanning electron microscopy, cytochemistry. — Acta Protozool. **44:** 201–215.

Foissner W., Xu K. & Kreutz M. (2005c): The Apertospathulidae, a new family of haptorid ciliates (Protozoa, Ciliophora). — J. Eukaryot. Microbiol. **52:** 360–373.

Foissner W., Pichler M., Al-Rasheid K. & Weisse T. (2006): The unusual, lepidosome-coated resting cyst of *Meseres corlissi* (Ciliophora: Oligotrichea): encystment and genesis and release of the lepidosomes. — Acta Protozool. **45:** 323–338.

Foissner W., Müller H. & Agatha S. (2007): A comparative fine structural and phylogenetic analysis of resting cysts

in oligotrich and hypotrich Spirotrichea (Ciliophora). — Eur. J. Protistol. **43:** 295–314.

Foissner W., Quintela-Alonso P. & Al-Rasheid K. (2008a): Soil ciliates from Saudi Arabia, including descriptions of two new genera and six new species. — Acta Protozool. **47:** 317–352.

Foissner W., Chao A. & Katz L. A. (2008b): Diversity and geographic distribution of ciliates (Protista: Ciliophora). — Biodivers. Conserv. **17:** 345–363.

Foissner W., Blake N., Wolf K., Breiner H.-W. & Stoeck T. (2009a): Morphological and molecular characterization of some peritrichs (Ciliophora: Peritrichida) from tank bromeliads, including two new genera: *Orborhabdostyla* and *Vorticellides*. — Acta Protozool. **48:** 291–319.

Foissner W., Weissenbacher B., Krautgartner W.-D. & Lütz-Meindl U. (2009b): A cover of glass: first report of biomineralized silicon in a ciliate, *Maryna umbrellata* (Ciliophora: Colpodea). — J. Eukaryot. Microbiol. **56:** 519–530.

Foissner W., Kusuoka, Y. & Shimano, S. (2009c): Morphological and molecular characterization of *Histiobalantium natans viridis* Kahl, 1931 (Ciliophora, Scuticociliatia). — Eur. J. Protistol. **45**: 193–204.

Foissner W., Hess S. & Al-Rasheid K. A. S. (2010a): Two vicariant *Semispathidium* species from tropical Africa and central Europe: *S. fraterculum* nov. spec. and *S. pulchrum* nov. spec. (Ciliophora, Haptorida). — Eur. J. Protistol. **46:** 61–73.

Foissner W., Shi X., Wang R. & Warren A. (2010b): A reinvestigation of *Neokeronopsis* populations, including the description of *N. asiatica* nov. spec. (Ciliophora, Hypotricha). — Acta Protozool. **49:** 87–105.

Foissner W., Stoeck T., Agatha S. & Dunthorn M. (2011): Intraclass evolution and classification of the Colpodea (Ciliophora). — J. Eukaryot. Microbiol. **58:** 397–415.

Foissner W., Jung J.-H., Filker S., Rudolph J. & Stoeck T. (2013): Morphology, ontogenesis and molecular phylogeny of *Platynematum salinarum* nov. spec., a new scuticociliate (Ciliophora, Scuticociliata) from a solar saltern. — Eur. J. Protistol. **50:** 174–184.

Foissner W., Filker S. & Stoeck T. (2014a): *Schmidingerothrix salinarum* nov. spec. is the molecular sister of the large oxytrichid clade (Ciliophora, Hypotricha). — J. Eukaryot. Microbiol. **61:** 61–74.

Foissner W., Bourland W. A., Wolf K. W., Stoeck T. & Dunthorn M. (2014b): New SSU-rDNA sequences for eleven colpodeans (Ciliophora, Colpodea) and description of *Apocyrtolophosis* nov. gen. — Eur. J. Protistol. **50**: 40–46.

Foissner W., Quintela-Alonso P., Kumar S. & Wolf K. W. (2014c): Five new spathidiids (Ciliophora: Haptoria) from Caribbean tank bromeliads. — Acta Protozool. **53:** 159–194.

Fontaneto D. (ed.) (2011): Biogeography of Microscopic Organisms. Is Everything Small Everywhere? — Cambridge Univ. Press, The Systematics Association, Special Volume **79:** x + 265 pp.

Gabilondo R. & Foissner W. (2009): Four new fuscheriid soil ciliates (Ciliophora: Haptorida) from four biogeographic regions. — Acta Protozool. **48:** 1–24.

Gaievskaïa N. (1925): Sur deux nouveaux infusoires des mares salées – *Cladotricha koltzowii* nov. gen. nov. sp. et *Palmarium salinum* nov. gen. nov. sp. — Russk. Arkh. Protist. **4:** 255–288.

Gelei G. v. (1940): *Cinetochilum* und sein Neuronemensystem. — Arch. Protistenk. **94**: 57–79.

Gelei J. v. (1950): Die Marynidae der Sodagewässer in der Nähe von Szeged. — Hidrol. Közl. **30**: 107–119.

Gelei J. v. (1954): Über die Lebensgemeinschaft einiger temporärer Tümpel auf einer Bergwiese im Börzsönygebirge (Oberungarn) III. Ciliaten. — Acta biol. hung. **5**: 259–343.

Gellért J. (1942): Életegyüttes a fakéreg zöldporos bevonatában. — Acta Sci. math.-nat. Univ. Kolozsvár (N. S.) **8**: 1–36 (in Hungarian).

Gelei J. & Szabados M. (1950): Tömegprodukció városi esövizpocsolyában (Massenproduktion in einer städtischen Regenwasserpfütze). — Annls biol. Univ. szeged. **1**: 249–294 (in Hungarian with Russian and

German summaries).

Gellért J. (1956): Ciliaten des sich unter dem Moosrasen auf Felsen gebildeten Humus. — Acta biol. hung. **6**: 337–359.

Gellért J. (1957): Néhány hazai lomblevelü és tülevelü erdö talajának ciliáta-faunája (Ciliatenfauna im Humus einiger ungarischer Laub- und Nadelholzwälder). — Annls Inst. biol. Tihany **24**: 11–34 (in Hungarian with German summary).

Gong J. & Song W. (2008): Morphology and infraciliature of a new marine ciliate, *Cinetochilum ovale* n. sp. (Ciliophora: Oligohymenophorea). — Zootaxa **1939**: 51–57.

Grain J. (1994): Classe des Litostomatea Small & Lynn, 1981. — Traité Zoologie **2** (2): 267–310.

Grandori R. & Grandori L. (1934): Studî sui protozoi del terreno. — Boll. Lab. Zool. agr. Bachic. R. Ist. sup. agr. Milano **5**: 1–341.

Gschwindt K. (1991): Morphologie und Infraciliatur einiger limnischer Ciliaten (Protozoa: Ciliophora). — Diplomarbeit Universität Salzburg: 115 pp.

Gupta R., Kamra K., Arora S. & Sapra G. R. (2001): *Stylonychia ammermanni* sp. n., a new oxytrichid (Ciliophora: Hypotrichida) ciliate from the river Yamuna, Delhi, India. — Acta Protozool. **40**: 75–82.

Hammerschmidt B., Schlegel M., Lynn D. H., Leipe D. D., Sogin M. L. & Raikov I. B. (1996): Insights into the evolution of nuclear dualism in ciliates revealed by phylogenetic analysis of rRNA sequences. — J. Eukaryot. Microbiol. **43**: 225–230.

Heber D., Stoeck T. & Foissner W. (2014): Morphology and ontogenesis of *Psilotrichides hawaiiensis* nov. gen., nov. spec. and molecular phylogeny of the Psilotrichidae (Ciliophora, Hypotrichia). — J. Eukaryot. Microbiol. **61:** 260–277.

Hemberger H. (1982): Revision der Ordnung Hypotrichida Stein (Ciliophora, Protozoa) an Hand von Protargolpräparaten und Morphogenesedarstellungen. — Dissertation Universität Bonn: iv + 296 pp.

Hemberger H. (1985): Neue Gattungen und Arten hypotricher Ciliaten. — Arch. Protistenk. **130:** 397–417.

Hirschfield H. I., Isquith I. R. & Di Lorenzo A. E. (1973): Classification, distribution, and evolution. — In: Giese A. C. (ed.): *Blepharisma*. Stanford Univ. Press, Stanford, California: 304–332.

International Commission on Zoological Nomenclature (1999): International Code of Zoological Nomenclature. 4th ed. — Tipografia La Garangola, Padova: xxix + 306 pp.

Jankowski A. V. (1964): Morphology and evolution of Ciliophora. III. Diagnoses and phylogenesis of 53 sapropelebionts, mainly of the order Heterotrichida. — Arch. Protistenk. **107:** 185–294.

Jankowski A. V. (1980): Conspectus of a new system of the phylum Ciliophora. — Trudy zool. Inst., Leningr. **94**: 103–121 (in Russian).

Jankowski A. V. (2007): Phylum Ciliophora Doflein, 1901. Review of taxa. — In: Alimov A. F. (ed.) Protista: Handbook on zoology. Nauka, St. Petersburg, Part **2**: pp 415–993 (in Russian with English summary).

Jiang J., Huang J., Li L., Shao C., Al-Rasheid K. A. S., Al-Farraj S. A. & Chen Z. (2013): Morphology, ontogeny, and molecular phylogeny of two novel bakuellid-like hypotrichs (Ciliophora: Hypotrichia), with establishment of two new genera. — Eur. J. Protistol. **49**: 78–92.

Johnson W. H. & Larson E. (1938): Studies on the morphology and life history of *Woodruffia metabolica*, nov. sp. — Arch. Protistenk. **90**: 383–392.

Kahl A. (1926): Neue und wenig bekannte Formen der holotrichen und heterotrichen Ciliaten. — Arch. Protistenk. **55**: 197–438.

Kahl A. (1927): Neue und ergänzende Beobachtungen holotricher Ciliaten. I. — Arch. Protistenk. **60**: 34–129.

KAHL A. (1928a): Die Infusorien (Ciliata) der Oldesloer Salzwasserstellen. — Arch. Hydrobiol. **19:** 50–123.

KAHL A. (1928b): Die Infusorien (Ciliata) der Oldesloer Salzwasserstellen. — Arch. Hydrobiol. **19**: 189–246.

KAHL A. (1930a): Urtiere oder Protozoa I: Wimpertiere oder Ciliata (Infusoria) 1. Allgemeiner Teil und Prostomata. — Tierwelt Dtl. **18**: 1–180.

KAHL A. (1930b): Neue und ergänzende Beobachtungen holotricher Infusorien. II. — Arch. Protistenk. **70:** 313–416.

KAHL A. (1931): Urtiere oder Protozoa I: Wimpertiere oder Ciliata (Infusoria) 2. Holotricha außer den im 1. Teil behandelten Prostomata. — Tierwelt Dtl. **21**: 181–398.

KAHL A. (1932): Urtiere oder Protozoa I: Wimpertiere oder Ciliata (Infusoria) 3. Spirotricha. — Tierwelt Dtl. **25**: 399–650.

KAHL A. (1933): Ciliata libera et ectocommensalia. — In: GRIMPE G. & WAGLER E. (eds.): Die Tierwelt der Nord- und Ostsee. Akad. Verlag-Ges., Leipzig, Germany **23** (Teil II, c_3): 29–146.

KAHL A. (1934): Ciliata entocommensalia et parasitica. — In: GRIMPE G. & WAGLER E. (eds.): Die Tierwelt der Nord- und Ostsee. Akad. Verlag-Ges., Leipzig, Germany **26** (Teil II, c_4): 147–183.

KAHL A. (1935): Urtiere oder Protozoa I: Wimpertiere oder Ciliata (Infusoria) 4. Peritricha und Chonotricha. — Tierwelt Dtl. **30**: 651–886.

KAHL A. (1943): Infusorien (1. Teil). Ein Hilfsbuch zum Erkennen, Bestimmen, Sammeln und Präparieren der freilebenden Infusorien des Süßwassers und der Moore. Buchbeilage zum *Mikrokosmos* Jahrgang 1942/43, d. h., erschienen in der Reihe „Handbücher für die praktische naturwissenschaftliche Arbeit", Band 31/32, 52 pp. Franckh´sche Verlagsbuchhandlung, W. KELLER & Co., Stuttgart. Reprinted in FOISSNER W. & WENZEL F. (2004): Life and legacy of an outstanding ciliate taxonomist, ALFRED KAHL (1877–1946), including a facsimile of his forgotten monograph from 1943. — Acta Protozool. **43** (Suppl.)**:** 3–69.

KAISER D. & GORDONES O. (1994): Venezuela, Reisehandbuch. — Därr-Reisebuch-Verlag, Hohenthann, Deutschland: 522 pp.

KAMRA K. & KUMAR S. (2010): *Notohymena saprai* sp. nov, a new oxytrichid (Protozoa: Ciliophora) from the Valley of Flowers, a Himalayan bioreserve region; description and morphogenesis of the new species. — Indian J. Microbiol. **50:** 33–45.

KAMRA K., KUMAR S. & SAPRA G. R. (2008): Species of *Gonostomum* and *Paragonostomum* (Ciliophora, Hypotrichida, Oxytrichidae) from the Valley of Flowers, India, with descriptions of *Gonostomum singhii* sp nov, *Paragonostomum ghangriai* sp nov and *Paragonostomum minuta* sp nov. — Indian J. Microbiol. **48**: 372–388.

KENT W. S. (1880-1882): A manual of the infusoria: including a description of all known flagellate, ciliate, and tentaculiferous protozoa, British and foreign, and an account of the organization and affinities of the sponges. — Volumes I–III. David Bogue, London: 913 pp. (Vol. I 1880: 1–432; Vol. II 1881: 433–720; Vol. II 1882: 721–913; Vol. III 1882: Plates).

KLEIN B. M. (1930): Das Silberliniensystem der Ciliaten. Weitere Ergebnisse. IV. — Arch. Protistenk. **69:** 235–326.

KREUTZ M. & FOISSNER W. (2006): The *Sphagnum* ponds of Simmelried in Germany: a biodiversity hot-spot for microscopic organisms. — Protozool. Monogr. **3:** 1–267.

KREUTZ M. & MAYER P. (2000): *Ileonema simplex* – ein Ciliat mit einem außergewöhnlichen Mundorganell. — Mikrokosmos **89**: 193–196.

KUMAR S. & FOISSNER W. (2015): Biogeographic specializations of two large hypotrich ciliates: *Australocirrus shii* and *A. australis* and proposed synonymy of *Australocirrus* and *Cyrtohymenides*. — Eur. J. Protistol. **51**: 210–228.

KÜPPERS G. C., CLAPS M. C. & LOPRETTO E.C. (2007): Description of *Notohymena pampasica* n. sp. (Ciliophora, Stichotrichia). — Acta Protozool. **46:** 221–227.

LEPSI I. (1957): Protozoen aus dem anmoorigen Gebirgssee St. Anna in Rumänien. — Trav. Mus. Hist. nat., "Gr. Antipa" **1**: 73–109.

Levander K.M. (1894): Beiträge zur Kenntniss einiger Ciliaten. — Acta Soc. Fauna Flora fenn. **9:** 1–87.

Lom J. & Dyková I. (1992): Protozoan Parasites of Fishes. — Elsevier, Amsterdam, London, New York, Tokyo: xi + 315 pp.

Lüftenegger G., Foissner W. & Adam H. (1985): r- and K-selection in soil ciliates: a field and experimental approach. — Oecologia **66**: 574–579.

Lv Z., Chen L., Chen L., Shao C., Miao M. & Warren A. (2013): Morphogenesis and molecular phylogeny of a new freshwater ciliate, *Notohymena apoaustralis* n. sp. (Ciliophora, Oxytrichidae). — J. Eukaryot. Microbiol. **60:** 455–466.

Lynn D. H. (2008): The Ciliated Protozoa. Characterization, Classification and Guide to the Literature, 3rd ed. — Springer, Dordrecht: xxxii + 605 pp.

Maddicks R. (2011): Venezuela Travel Guide, fifth edition. — Bradt Travel Guides, England & USA: x + 438 pp.

Martin-Cereceda M., Guinea A., Bonaccorso E., Dyal P., Novarino G. & Foissner W. (2007): Classification of the peritrich ciliate *Opisthonecta matiensis* (Martin-Cereceda et al. 1999) as *Telotrochidium matiense* nov. comb., based on new observations and SSU rDNA phylogeny. — Eur. J. Protistol. **43:** 265–279.

Martius C. (1994): Termite nests as structural elements of the Amazon floodplain forest. — Andrias **13:** 137–150.

Moravcová V. (1962): The cultivation and sequence of protozoa from the polluted streams. — Sb. vys. Šk. chem.-technol. Praze **6**: 345–435.

Mueller O. F. (1786): Animalcula Infusoria Fluviatilia et Marina, quae Detexit, Systematice Descripsit et ad Vivum Delineari Curavit. — N. Mölleri, Hauniae: lvi + 367 pp.

Muecke G. (1979): Ökologische Untersuchungen der Ciliaten in Gewässern des Naturschutzgebietes "Heiliges Meer" unter besonderer Berücksichtigung zönologischer Gesichtspunkte. — Arb. Inst. landw. Zool. Bienenkd. **5**: 1–275.

Nauwerck A. (1996): Trophische Strukturen im Pelagial des meromiktischen Höllerersees (Oberösterreich) — Ber. Nat.-Med. Ver. Salzburg **11**: 147–178.

Netuzhilin I., Cerda H., López-Hernández D., Torres F., Chacon P. & Paoletti M. G. (1999): Biodiversity tools to evaluate sustainability in savanna-forest ecotone in the Amazonas (Venezuela). — In: Reddy M. V. (ed.): Management of tropical agroecosystems and the beneficial soil biota. Science Publishers, Enfield, New Hampshire: 291–352.

Nicholls K. H. & Lynn D. H. (1984): *Lepidotrachelophyllum fornicis*, n. g., n. sp., a ciliate with an external layer of organic scales (Ciliophora, Litostomatea, Haptoria). — J. Protozool. **31**: 413–419.

Oertel A., Wolf K., Al-Rasheid K. & Foissner W. (2008): Revision of the genus *Coriplites* Foissner, 1988 (Ciliophora: Haptorida), with description of *Apocoriplites* nov. gen. and three new species. — Acta Protozool. **47:** 231–246.

Omar A. & Foissner W. (2014): Three new microthoracids (Ciliophora, Nassophorea) from Austria and Venezuela. — Acta Protozool. **53**: 295–311.

Olmo J. L. & Téllez C. (1997): New aspects of the morphology and morphogenesis of *Gonostomum strenua* Engelmann, 1862 (Ciliophora, Hypotrichida). — Arch. Protistenk. **148:** 191–197.

Omar A. & Foissner W. (2012): Description of *Leptopharynx brasiliensis* nov. spec. and *Leptopharynx costatus gonohymen* nov. subspec. (Ciliophora, Microthoracida). — Eur. J. Protistol. **48:** 30–47.

Omar A. & Foissner W. (2013): Description of two new *Drepanomonas* taxa and an account on features defining species in *Drepanomonas* Fresenius, 1858 (Ciliophora, Microthoracida). — Eur. J. Protistol. **49:** 420–437.

Paiva T. S., Borges B. N., Harada M. L. & Silva-Neto I. D. (2009): Comparative phylogenetic study of Stichotrichia (Alveolata: Ciliophora: Spirotrichea) based on 18S-rDNA sequences. — Genet. Mol. Res. **8:** 223–246.

Paoletti M. G. (1980): Le strategie di vita nella foresta neotropicale: interesse teorico ed applicativo anche per gli

ecosistemi delle regioni temperate. Il paradosso della fauna pensile del suolo. Alcune riflessioni. — Boll. Mus. civ. St. nat. Venezia. Year 1980: 115–128.

Paoletti M. G., Taylor R. A. J., Stinner B. R., Stinner D. H. & Benzing D. H. (1991): Diversity of soil fauna in the canopy and forest floor of a Venezuelan cloud forest. — J. Trop. Ecol. **7**: 373–383.

Peer T. & Foissner W. (1985): Protozoologische Untersuchungen an Almböden im Gasteiner Tal (Zentralalpen, Österreich). II. Bodenkundliche Analysen mit besonderer Berücksichtigung der stark belebten Zone. — Veröff. Österr. MaB-Programms **9:** 51–63.

Penard E. (1914): Les cothurnidés muscicoles. — Mém. Soc. Phys. Hist. nat. Genève **38:** 19–66.

Penard E. (1922): Études sur les Infusoires d´Eau Douce. — Georg & Cie, Genève: 331 pp.

Pérez-Hernández R. & Lew D. (2001): Las clasificaciones e hipótesis biogeográficas para la Guyana Venezolana. — Interciencia, **26**: 373–382.

Perty M. (1852): Zur Kenntniss kleinster Lebensformen nach Bau, Funktionen, Systematik, mit Specialverzeichniss der in der Schweiz beobachteten. Jent & Reinert, Bern: 228 pp.

Petz W. & Foissner W. (1996): Morphology and morphogenesis of *Lamtostyla edaphoni* Berger and Foissner and *Onychodromopsis flexilis* Stokes, two hypotrichs (Protozoa: Ciliophora) from Antarctic soils. — Acta Protozool. **35**: 257–280.

Petz W. & Foissner W. (1997): Morphology and infraciliature of some soil ciliates (Protozoa, Ciliophora) from continental Antarctica, with notes on the morphogenesis of *Sterkiella histriomuscorum*. — Polar Record **33**: 307–326.

Poche F. (1913): Das System der Protozoa. — Arch. Protistenk. **30**: 125–321.

Pomp R. & Wilbert N. (1988): Taxonomic and ecological studies of ciliates from Australian saline soils: colpodids and hymenostomate ciliates. — Aust. J. Mar. Freshw. Res. **39**: 479–495.

Pratt J. R., Horwitz R. & Cairns Jr. J. (1987): Protozoan communities of the Flint River-Lake Blackshear ecosystem (Georgia, USA). — Hydrobiologia **148**: 159–174.

Puytorac P. De, Didier P., Detcheva R. & Glorlière C. (1974): Sur la morphogenèse de bipartition et l´ultrastructure du cilié *Cinetochilum margaritaceum* Perty. — Protistologica **10**: 223–238.

Quennerstedt A. (1867): Bidrag till sveriges infusorie-fauna. — Acta Univ. lund. **4**: 1–48 (in Swedish).

Ramirez De Guerrero M. A. (1970): Sistematica y morfologia de algunas especies de protozoarios del estado de puebla, Mexico. — Revta Soc. mex. Hist. nat. **31**: 69–93.

Rosati G., Giari A. & Ricci N. (1988): *Oxytricha bifaria* (Ciliata, Hypotrichida) general morphology and ultrastructure of normal cells and giants. — Eur. J. Protistol. **23**: 343–349.

Roux J. (1899): Observations sur quelques infusoires ciliés des environs de Genève avec la description de nouvelles espèces. — Revue suisse Zool. **6:** 557–636.

Roux J. (1901): Faune infusorienne des eaux stagnantes des environs de Genève. — Mém. Inst. natn. génev. **19:** 1–148.

Ruinen J. (1938): Notizen über Ciliaten aus konzentrierten Salzgewässern. — Zoöl. Meded, Leiden **20:** 243-256.

Ruthmann A. & Kuck A. (1985): Formation of the cyst wall of the ciliate *Colpoda steinii*. — J. Protozool. **32:** 677–682.

Schewiakoff W. (1893): Über die geographische Verbreitung der Süsswasser-Protozoën. — Zap. imp. Akad. Nauk. SSSR (Series 7) **41**: 1–201.

Schlegel M., Elwood H. J. & Sogin M. L. (1991): Molecular evolution in hypotrichous ciliates: sequence of the small subunit ribosomal RNA genes from *Onychodromus quadricornutus* and *Oxytricha granulifera* (Oxytrichidae, Hypotrichida, Ciliophora). — J. Mol. Evol. **32**: 64–69.

Schmähl O. (1926): Die Neubildung des Peristoms bei der Teilung von *Bursaria truncatella*. — Arch. Protistenk. **54:** 359–430.

Schmidt S. L., Bernhard D., Schlegel M. & Foissner W. (2007a): Phylogeny of the Stichotrichia (Ciliophora; Spirotrichea) reconstructed with nuclear small subunit rRNA gene sequences: discrepancies and accordances with morphological data. — J. Eukaryot. Microbiol. **54**: 201–209.

Schmidt S. L., Foissner W., Schlegel M. & Bernhard D. (2007b): Molecular phylogeny of the Heterotrichea (Ciliophora; Postciliodesmatophora) based on small subunit rRNA gene sequences. — J. Eukaryot. Microbiol. **54**: 358–363.

Schwerdtfeger R. (1975): Synökologie. — P. Parey, Hamburg und Berlin: 451 pp.

Scorza J. V. & Montiel B. O. N. (1954): Estudio experimental sobre la sucesion de protozoarios que se dessarrolle en las infusions de musgo yde las variaciones de pH que la accompanan. — Acta biol. venez. **1**: 213–230.

Senler N. G. & Yildiz I. (2003): Infraciliature and other morphological characteristics of *Enchelyodon longikineta* n. sp. (Ciliophora, Haptoria). — Eur. J. Protistol. **39**: 267–274.

Sergejeva G. I. (1989): Ciliates of the genus *Bursaria* and "reality" of a species *Archiastomata adami* Foissner 1976. — In: Poljansky, G. I., Zhukov, B. F. & Raikov, I. B. (eds.): Ecology of marine and fresh-water protozoans: 62 (Abstract; in Russian, translated by A. V. Jankowski).

Sergejeva G. I., Livolant F., DaConceicao M., Samoshkin A. A., Bolshakova N. N. & Raikov I. B. (1995): Ciliates of the genus *Bursaria* in TNE state of cryptobiosis. — Tsitologija **37:** 1189–1213.

Shao C., Lu X. & Ma H. (2015): A general overview of the typical 18 frontal-ventral-transverse cirri Oxytrichidae s. l. genera (Ciliophora, Hypotrichia). — J. Ocean. Univ. China **14**: 1–11.

Shen Y., Liu J., Song B., Gu M. (1992): Protozoa. — In: Yin W. et al. (eds.): Subtropical soil animals of China. Science Press, Beijing: 97–156 (in Chinese).

Shin M. K. & Kim W. (1994): Morphology and biometry of two oxytrichid species of genus *Histriculus* Corliss, 1960 (Ciliophora, Hypotrichida, Oxytrichidae) from Seoul, Korea. — Korean J. Zool. 37: 113–119.

Shizheng W. & Zhengxue M. (1994): The ciliates from industrial wastewater of Xining and three indicative species of Rhizopoda on high mountains and subhigh mountains. — J. Northwest Normal Univ. (Nat. Sci.), China **30**: 60–65 (in Chinese with English summary).

Singh J. & Kamra K. (2013): *Paraurosomoida indiensis* gen. nov., sp. nov., an oxytrichid (Ciliophora, Hypotricha) from Kyongnosla Alpine Sanctuary, including note on non-oxytrichid Dorsomarginalia. — Eur. J. Prostistol. **49:** 600–610.

Singh J. & Kamra K. (2015): Molecular phylogeny of *Urosomoida agilis*, and new combinations: *Hemiurosomoida longa* gen. nov., comb. nov. and *Heterourosomoida lanceolata* gen. nov., comb. nov. (Ciliophora, Hypotricha). — Eur. J. Protistol. **51**: 55–65.

Siqueira-Castro I. C. V., Paiva T. S. da & Silva-Neto I. D. da (2009): Morphology of *Parastrongylidium estevesi* comb. nov. and *Deviata brasiliensis* sp. nov. (Ciliophora: Stichotrichia) from a sewage treatment plant in Rio de Janeiro, Brazil. — Zoologia **26**: 774–786.

Small E. B. & Lynn D. H. (1985): Phylum Ciliophora Doflein, 1901. — In: Lee J. J., Hutner S. H. & Bovee E. C. (eds.): An illustrated guide to the protozoa. Society of Protozoologists, Lawrence, Kansas: 393–575.

Smith J. C. (1897): Notices of some undescribed infusoria, from the infusorial fauna of Louisiana. — Trans. Amer. micros. Soc. **19**: 55–68.

Snell H. M., Stone P. A. & Snell H. L. (1996): A summary of geographical characteristics of the Galápagos Islands. — J. Biogeo. **23**: 619–624.

Song W. (1990a): Infraciliature and silverline system of the ciliate *Pseudotrachelocerca trepida* (Kahl, 1928), nov.

gen., nov. comb., and establishment of a new family, the Pseudotrachelocercidae nov. fam. (Ciliophora, Haptoria). — Eur. J. Protistol. **26**: 160–166.

Song W. (1990b): A comparative analysis of the morphology and morphogenesis of *Gonostomum strenua* (Engelmann, 1862) (Ciliophora, Hypotrichida) and related species. — J. Protozool. **37:** 249–257.

Song W. & Wilbert N. (1989): Taxonomische Untersuchungen an Aufwuchsciliaten (Protozoa, Ciliophora) im Poppelsdorfer Weiher, Bonn. — Lauterbornia **3**: 2–221.

Song W., Warren A. & Hu X. Z. (2009): Free-living Ciliates in the Bohai and Yellow Seas, China. — Science Press, Bejing: 518pp.

Stein F. (1859): Der Organismus der Infusionsthiere nach eigenen Forschungen in systematischer Reihenfolge bearbeitet. I. Abtheilung. Allgemeiner Theil und Naturgeschichte der hypotrichen Infusionsthiere. — W. Engelmann, Leipzig: xii + 206 pp.

Stein F. (1867): Der Organismus der Infusionsthiere nach eigenen Forschungen in systematischer Reihenfolge bearbeitet. II. Abtheilung. 1) Darstellung der neuesten Forschungsergebnisse über Bau, Fortpflanzung und Entwickelung der Infusionsthiere. 2) Naturgeschichte der heterotrichen Infusorien. — W. Engelmann, Leipzig: viii + 355 pp.

Sterki V. (1878): Beiträge zur Morphologie der Oxytrichinen. — Z. wiss. Zool. **31:** 29–58.

Stiller J. (1971): Szájkoszorús Csillósok — Peritricha. Fauna Hungariae **105**: 1–245.

Stokes A. C. (1884a): Notices of new fresh-water infusoria. — Am. mon. microsc. J. **5**: 121–125.

Stokes A. C. (1884b): Notes on some apparently undescribed forms of freshwater infusoria. — Am. J. Sci. **28**: 38–49.

Stokes A. C. (1885): Some new infusoria. — Am. Nat. **19**: 433–443.

Stokes A. C. (1891): Notes of new infusoria from the fresh waters of the United States. — JI R. microsc. Soc. year 1891: 697–704.

Tuffrau M. (1979): Une nouvelle famille d'hypotriches, Kahliellidae n. fam., et ses consequences dans la repartition des Stichotrichina. — Trans. Am. microsc. Soc. **98**: 521–528.

Vďačný P. & Foissner W. (2008): Morphology, conjugation, and postconjugational reorganization of *Dileptus tirjakovae* n. sp. (Ciliophora, Haptoria). — J. Eukaryot. Microbiol. **55:** 436–447.

Vďačný P. & Foissner W. (2012): Monograph of the dileptids (Protista, Ciliophora, Rhynchostomatia). — Denisia **31:** 1–529.

Vďačný P., Breiner H.-W., Yashchenko V., Dunthorn M., Stoeck T. & Foissner W. (2014): The chaos prevails: molecular phylogeny of the Haptoria (Ciliophora, Litostomatea). — Protist **165:** 93–111.

Voss H.-J. (1991): Die Morphogenese von *Cyrtohymena muscorum* (Kahl, 1932) Foissner, 1989 (Ciliophora, Oxytrichidae). — Arch. Protistenk. **140**: 219–236.

Vuxanovici A. (1959): Contributii la studiul unor infuzori holotrichi. — Studii Cerc. Biol. (Biol. Anim.) **11:** 307–335 (in Roumanian with Russian and French summaries).

Vuxanovici A. (1962): Contributii la sistematica ciliatelor (Nota III). — Studii Cerc. Biol. (Biol. Anim.) **14**: 549–573 (in Roumanian with Russian and French summaries).

Wang C. C. & Nie D. (1935): Report on the rare and new species of freshwater infusoria, part II. — Sinensia, Shanghai **6**: 399–524.

Wang H., Clamp J. C., Shi X., Utz L. R. P. & Liú G. (2012): Evolution of variations in the common pattern of stomatogenesis in peritrich ciliates: evidence from a comparative study including a new description of stomatogenesis in *Pseudepistylis songi* Peng et al., 2007. — J. Eukaryot. Microbiol. **59**: 300–324.

Weisse T. (2014): Ciliates and rare biosphere – community ecology and population dynamics. — J. Eukaryot. Microbiol. **61:** 419–433.

Weisse T., Strüder-Kypke C., Berger H. & Foissner W. (2008): Genetic, morphological, and ecological diversity of spatially separated clones of *Meseres corlissi* Petz & Foissner, 1992 (Ciliophora, Spirotrichea). — J. Eukaryot. Microbiol. **55**: 257–270.

Wenzel F. (1953): Die Ciliaten der Moosrasen trockner Standorte. — Arch. Protistenk. **99:** 70–141.

Wilbert N. (1986): Ciliates from saline lakes in Saskatchewan. — Symposia Biologica Hungarica. **33**: 249–256.

Wilbert N. (1995): Benthic ciliates of salt lakes. — Acta Protozool. **34**: 271–288.

Wirnsberger E., Foissner W. & Adam H. (1985): Morphological, biometric, and morphogenetic comparison of two closely related species, *Stylonychia vorax* and *S. pustulata* (Ciliophora: Oxytrichidae). — J. Protozool. **32**: 261–268.

Xin-Bai S. & Ammermann D. (2004): *Stylonychia harbinensis* sp. n., a new oxytrichid ciliate (Ciliophora, Hypotrichia) from the Heilongjiang Province, China. — Protistology **3**: 219–222.

Yi Z. Z. & Song W. (2011): Evolution of the order Urostylida (Protozoa, Ciliophora): new hypotheses based on multi-gene information and identification of localized incongruence. — Plos ONE **6:** e17471.

Yi Z. Z., Clamp J. C., Al-Rasheid K. A. S., Al-Khedhairy A. A., Chen Z. G. & Song W. (2009a): Evolutionary relationship and species separation of four morphologically similar stichotrichous ciliates (Protozoa, Ciliophora) inferred from PCR-RFLA patterns, ITS2 region sequence, and ITS2 secondary structures. — Prog. Nat. Sci. **19:** 581-586.

Yi Z. Z., Song W, Clamp J. C, Chen Z. G., Gao S. & Zhang Q. Q. (2009b): Reconsideration of systematic relationships within the order Euplotida (Protista, Ciliophora) using new sequences of the gene coding for small-subunit rRNA and testing the use of combined data sets to construct phylogenies of the *Diophrys*-complex. — Molec. Phylogenet. Evol. **50:** 599-607.

Yi Z. Z., Katz L. A. & Song W. (2012): Assessing whether alpha-tubulin sequences are suitable for phylogenetic reconstruction of Ciliophora with insights into its evolution in euplotids. — Plos ONE **7**: e40635.

5. Systematic Index

Bolded names are species described or redescribed in this monograph. All other names concern described species in the 71 samples or synonyms (see species list in chapter 3.1.1). Suprageneric names are in s p a c e d t y p e .

Impressum [Imprint]
Denisia 35: 912 pp.

Eigentümer, Herausgeber und Verleger [Copyright, editor & publisher]: Land Oberösterreich, Biologiezentrum/Oberösterreichisches Landesmuseum; J.-W.-Klein-Str. 73, A-4040 Linz, Austria, Tel.: +43-(0)732-7720-52114, Fax: +43-(0)732-7720-252199, E-Mail: bio-linz@landesmuseum.at, URL: http://www.biologiezentrum.at

Redaktion [Editorial staff]: Dr. Erna Aescht; Computerlayout, Druckorganisation [Layout, printing organisation]: Dr. Erna Aescht, Michaela Minich

Bestellung [Ordering]: katalogbestellung@landesmuseum.at

Das Werk einschließlich aller seiner Teile ist urheberrechtlich geschützt. Jede Verwertung außerhalb der engen Grenzen des Urheberrechtsgesetzes ist ohne Zustimmung des Medieninhabers unzulässig und strafbar. Das gilt insbesondere für Vervielfältigungen, Übersetzungen, Mikroverfilmungen sowie die Einspeicherung und Verarbeitung in elektronischen Systemen. Schriftentausch ist erwünscht! [All rights reserved. No part of this publication may be reproduced or transmitted in any form or by any means without prior permission from the publisher. We are interested on an exchange of publications.]

Druck [Printing]: Plöchl Druck GmbH, Werndlstr. 2, A-4240 Freistadt, Austria

ISSN-Nr. 1608-8700; Erscheinungsdatum [Delivery date]: 30. 10. 2015

Umschlag [Cover]: Lepidosome types in the Trachelophyllina.